SAE TRANSACTIONS

TL
1
S6
vol. 64

Society of Automotive Engineers, Inc.
29 West 39th Street New York 18, New York

George A. Delaney
President

John A. C. Warner
Secretary and General Manager

B. B. Bachman
Treasurer

E. D. Allen
Editor

All articles appearing in SAE Transactions are indexed in "Engineering Index."

Copyright 1956, Society of Automotive Engineers, Inc.

Price: $3 to members, $7 to public and college libraries and U. S. Government Agencies, $10 to nonmembers. Foreign: $3 to members, $8 to public and college libraries, $11 to nonmembers.

Photolithographed reproductions can be had of any article published in SAE Transactions. Prices, on quantities of 100 copies or more, varying with number of pages and illustrations, can be obtained upon request from SAE Special Publications Department, 29 West 39th Street, New York 18, N. Y.

CONTENTS—VOL. 64, 1956

(Complete Author and Subject Index Starts on p. 812)

Page

Application of Metallic Materials for Aircraft Structures in the Temperature Range 600 to 1100 F – JAMES W. HUFFMAN 5

Automobile Body Loads – PHILIP O. JOHNSON 12

Creativity in Engineering – JOHN E. ARNOLD 17

High-Temperature Problems Associated with the Use of Rubber in Aircraft – FREDERICK E. CLARK 24

Fatigue and Its Relation to the Mechanical and Metallurgical Properties of Metals – GEORGE R. GOHN 31

Flexible Suspension Systems for Equipment in Transit – JOHN J. GOODILL 41

Pneumatic and Sonic Measurement of Combustion-Chamber Volume – G. A. WEINERT 50

Steels and Protective Treatments For Use up to 1000 F – H. J. NOBLE and W. H. SHARP 59

Mechanical Octanes for Higher Efficiency – D. F. CARIS, B. J. MITCHELL, A. D. McDUFFIE, and F. A. WYCZALEK 76

Some Experiments in the Application of Boundary-Layer Control – JOSEPH FLATT 101

Wing-Lift Augmentation Methods for the Improvement of Low-Speed Performance of High-Speed Aircraft – JOHN S. ATTINELLO 108

New and Improved Synthetic Elastomeric Materials for Automotive Use – W. J. SIMPSON 123

The Selection of Metals for Airframe Components as Affected by Operation at Elevated Temperatures up to 600 F – M. TIKTINSKY 131

Considerations Affecting the Life of Automotive Camshafts and Tappets – M. F. GARWOOD, D. R. KINKER, and J. J. MANGANELLO 138

Camshaft-Tappet Problems in Ford Overhead Valve Engines – J. S. LAIRD, C. L. STEVENS, and V. L. ILES 153

Interrelationship of Design, Lubrication, and Metallurgy in Cam and Tappet Performance – E. B. ETCHELLS, R. F. THOMSON, G. H. ROBINSON, and G. K. MALONE 161

The Supercharged Turboprop – S. G. HOOKER 185

The New Plymouth V-8 Engine – H. L. WELCH 195

The New Packard V-8 Engine – W. E. SCHWIEDER 205

A Study of Nonprotective Rust Formation on Auto-Body Sheet Steel – J. C. HOLZWARTH, R. F. THOMSON, and A. L. BOEGEHOLD 221

A Practical Stopping-Ability Regulation – CARL C. SAAL 229

Cushion Design From Fragility Rating – H. E. NIETSCH 241

Evaluation of Reaction Kinetics Eliminates Diesel Knock – The M-Combustion System of MAN – J. S. MEURER 250

Passenger-Car Suspension Analysis – A. C. BODEAU, R. H. BOLLINGER, and L. LIPKIN 273

The New Packard Torsion Level Suspension – FOREST R. McFARLAND 284

A Jet Exhaust Silencer – J. M. TYLER and G. B. TOWLE 294

How High Should We Fly? – SCHUYLER KLEINHANS 300

Practical Tire Research – V. E. GOUGH 310

Tires for High-Performance Cars – T. J. P. JOY, D. C. HARTLEY, and D. M. TURNER 319

High-Speed Cornering Forces – J. J. ROBSON 334

Page

Operation of Passenger Tires at High Speeds – E. H. WALLACE and S. A. LIPPMANN 338

Shaft Gas Turbines for Helicopters – W. S. MILLER, JR., R. P. KREBS, and T. C. BLASCHKE 348

Instrumentation for Valve-Burning Studies – W. D. SIMS 356

Application of High-Temperature Materials to Aircraft Powerplants in the Temperature Range 1200-2400 F – ALAN V. LEVY 366

The Low Silhouette Drive Line – R. BURKHALTER and P. J. MAZZIOTI 379

Farm Tractors and Their Tires – F. C. WALTERS and W. H. WORTHINGTON 394

The Napier Deltic Diesel Engine – ERNEST CHATTERTON 408

Fatigue and Fail-Safe Airframe Design – J. F. McBREARTY 426

Human Problems in Jet Air Transportation - DR. ROSS A. McFARLAND 437

Lightweight Springs for Limited Life – E. H. SPAULDING 453

Automotive Gasoline Injection – SIDNEY E. MILLER 458

A New Approach to Turbojet and Ramjet Engine Control – WENDELL E. REED 472

Principles and Application of Bypass Turbojet Engines – GEORGE F. WISLICENUS 486

Tire Design – Present and Future – L. L. BALDWIN 502

The Differential Gas Turbine – DAVID W. HUTCHINSON 510

Some Elevated Temperature Structural Problems of High-Speed Aircraft – RICHARD R. HELDENFELS 524

Effect of Rapid Load Changes on Torque-Converter Performance – P. J. SWANSON and J. H. MEIER 534

NACA Investigation of Thrust-Reversal Techniques – JOHN H. POVOLNY and JACK G. McARDLE 542

Knocking Behavior of Fuels and Engines – R. V. KERLEY and K. W. THURSTON 554

Flight Research at High Altitudes and High Speeds with Rocket-Propelled Research Airplanes – WALTER C. WILLIAMS 570

A Radioactive Method for Measuring Engine Deposits – J. G. MINGLE, H. W. SIGWORTH, and B. A. FRIES 577

New Alloys for Automotive Turbines – DONALD N. FREY 582

Nuclear Power and the Machinery Builder – R. C. ALLEN 589

Relationship of Low-Temperature Cranking Resistance to Viscosity Characteristics of Multigrade Engine Oils – G. K. MALONE and T. W. SELBY 602

Cold Starting with V. I. Improved Multigrade Oils – F. B. FISCHL, H. H. HOROWITZ, and T. S. TUTWILER 608

Human and Environmental Factors of Automobile Safety – DR. ROSS A. McFARLAND 625

Design Factors in Automotive Safety – A. L. HAYNES 644

A Billion Engine Hours on Aluminum Bearings – R. S. FRANK and W. J. LUX 655

New Instrumentation for Engine Combustion Studies – J. A. WARREN and J. B. HINKAMP 665

Diesel Smoke Measurement (Progress Report of the Smokemeter Group of the Diesel Fuels Division, Coordinating Fuel and Equipment Research Committee, CRC) – H. C. HUNTER 680

Physical and Chemical Ignition Delay in an Operating Diesel Engine Using the Hot-Motored Technique – T. C. YU, O. A. UYEHARA, P. S. MYERS, R. N. COLLINS, and K. MAHADEVAN 690

Fuel Heat Gain and Release in Bomb Autoignition – R. W. HURN, J. O. CHASE, C. F. ELLIS, and K. J. HUGHES 703

Fuel Vaporization and Ignition Lag in Diesel Combustion – M. M. EL WAKIL, P. S. MYERS, and O. A. UYEHARA 712

Human Factors in Highway Transport Safety – DR. ROSS A. McFARLAND 730

Stop Sludge and Go Clean – R. H. ALBRECHT, R. I. POTTER, and KENT HYATT 751

Learning Curve Theory as Applied to Production Costs – ROBERT H. LUNDBERG 775

Mechanism of Engine Sludge Formation and Additive Action – D. T. ROGERS, W. W. RICE, and F. L. JONACH 782

Nitrogen Oxides, Combustion, and Engine Deposits – R. S. SPINDT, COURT L. WOLFE, and DONALD R. STEVENS 797

Application of Metallic Materials for Aircraft Structures in the Temperature Range 600 to 1100 F

James W. Huffman, North American Aviation, Inc.

This paper was presented at the Aircraft Research Seminar held by the SAE Southern California Section at the University of California, Los Angeles, Dec. 8, 1954.

A BRIEF review is presented of a portion of the available strength property data for a few representative alloys which find use in airframe structural components in the range from 600 to 1100 F. Several modes of behavior are illustrated, and some general principles regarding the interpretation and use of said data for design purposes are discussed.

IN this paper are reviewed the available data on the properties of metals most useful for airframe structures in the temperature range 600 to 1100 F. Some general principles governing the use of the data for design purposes will be discussed.

The extent of the available information on metal properties in the temperature range 600 to 1100 F is surprisingly small in view of the fact that the incidence of such temperatures in airframe structures is expected to increase with increased flight speeds. Fortunately, the lack of such information has been generally realized and programs have been initiated in a number of research organizations to develop the necessary data.

In spite of the present deficiencies, more data are available than can be presented in a short paper. In order, therefore, to present a broad picture of the available alloys and to allow space for discussion of principles, property data are given for a few representative materials and are sufficient to exemplify certain kinds of behavior only. Sources of more detailed data are found in references given at the end of this paper.

In general, all of the data presented here are tentative in that they have not been established as representative of a large number of heats. Certain property data given are based on a few direct tests or have been established by an examination of data related to, but not a direct measurement of, the property in question. In those cases the data are indicated in the figures by dotted lines.

Materials

The structural metals discussed here for the range 600 to 1100 F can be classified into the following four types: (1) martensitic steels, (2) austenitic steels, (3) precipitation-hardening alloys, and (4) titanium alloys.

The nominal compositions of the alloys are given in Table 1. Discussion of the titanium alloys has been limited to the one sheet alloy currently available in quantity. The behavior of titanium alloys differs markedly in many respects from that of the other metals that are suitable for use at elevated temperatures, and even a superficial discussion of the general characteristics of the titanium alloys would require more space than is available. For this

Table 1 – Nominal Chemical Composition

Type	Alloy	Element, % C	Cr	Ni	W	Mo	Ti	Al	Fe	Others
1	4130	0.30	0.95			0.20			Balance	
	4340	0.40	0.8	1.8		0.25			Balance	
	422	0.20	13.00	0.75	1.05	1.05			Balance	V 0.25
	HWD[a]	0.33	5.00		1.25	1.45			Balance	Si/0.85; V/0.23
	AMS 5616	0.15	13.00	2.00	3.00				Balance	
2	301	0.15	17.00	7.00					Balance	
	321		18.00	10.00			0.50		Balance	
	19-9DX	0.30	19.00	9.00		1.50	0.60		Balance	
3	17-7PH		17.00	7.00				1.15	Balance	
	A286		15.00	25.00		1.25	2.10	0.35	Balance	V 0.25
	Inconel X		15.00	Balance			2.30	1.20	7.00	Cb 1.00
4	AMS 4908						Balance			Mn 8.00

[a] A hot-work die steel.

reason, and since titanium and its alloys are treated in other papers, sufficient data on one such alloy only will be given to indicate its strength in relation to that of the other metals.

The outstanding characteristics of the above types of metals are as follows: (1) The martensitic steels can be heat treated to very high short-time strengths, are unstable under prolonged heating, and have relatively poor corrosion resistance. (2) The austenitic steels in general have relatively low short-time properties, do not respond to heat treatment, and are stable under prolonged heating, with the exception of some types exhibiting a microstructural instability at certain temperatures that leads to serious corrosion effects. Otherwise, the austenitic steels are highly corrosion resistant. (3) The precipitation-hardening alloys have high strength properties, are generally stable under prolonged heating, and are highly corrosion resistant. (4) The titanium alloys are much lighter in weight than the other alloys discussed, have high strength in proportion to their weight, and are highly corrosion resistant.

General Effects of Time Nomenclature

In general, the element of time must be considered when measuring the properties of metals at elevated temperatures. The effects of stress and high temperature on metals are functions of the length of time the stress and heat are applied. In discussions of elevated temperature phenomena certain terms are often used to indicate in a general way the nature of the time element.

The term "short-time property" is used when the effects of stress and temperature are measured during a very short period, such that the effects may be said to occur immediately. An example of a short-time property is the tensile ultimate stress, which is measured by a rapid application of stress after heat has been applied for only a short time. The term "long-time property" denotes a property that is measured throughout a long period of time. In such cases the combined effects of stress and temperature are considered during the passage of time. Creep, or the increase in elongation of a metal under a constant stress, is a long-time property. The terms "stability" and "instability" denote the maintenance of loss of some specific property during exposure to stress and/or temperature. Generally, a comparison is made of the property before and after an interval of time; for example, the tensile ultimate strength can be measured before and after a period of heating. It is considered that the property is "maintained" under such conditions if it does not change significantly.

Short-Time Tensile Properties

The most commonly determined properties are the short-time tensile properties. In Fig. 1 are compared the tensile ultimate strengths at elevated temperatures of several alloys following a short exposure at each temperature. The values in parentheses in this and in succeeding figures indicate the tensile ultimate strengths at room temperature. The information given by these curves is useful when high stresses are applied for short periods of time and at infrequent intervals. From the tensile ultimate strength curves, tentative inferences can be drawn concerning other properties. Consider the slopes of those curves, for example. In general, those alloys whose curves fall rapidly with increasing temperature, as for some martensitic steels and 17-7PH stainless steel, are relatively unstable at higher temperatures and may exhibit relatively low creep strengths at higher temperatures. A flat curve on the other hand, which obtains for the precipitation hardening alloys and the austenitic alloys, indicates stability and good long-time properties at higher temperatures. Such deductions from the short-time data are rough and ready approximations.

The effect of alloy content is seen by comparing the ultimate strength of the three martensitic steels. Addition of tungsten and molybdenum improves this property, particularly at higher temperatures. The high carbon content of the hot-work die steel as compared to the 422 permits achieving very high strengths. The potentialities of steels of the type represented by the hot-work die steel for elevated temperature structural use have not been sufficiently explored.

To compare the titanium-manganese alloy with the heavier alloys on a strength/weight basis, the values for the titanium-manganese alloy must be increased by a factor of approximately 1.7. If the tensile ultimate strength values for the titanium-manganese alloy are multiplied by 1.7 and plotted on Fig. 1, they would lie on a curve just above the 17-7PH curve at 600 F and slightly below the 4340 curve at 900 F. The curve for the titanium-manganese alloy is omitted from this and other figures for the sake of clarity inasmuch as it nearly coincides with the curves for the other alloys.

The tensile yield strengths are shown in Fig. 2. The yield strength is used less frequently than the ultimate strength for design purposes. When the yield strength is less than two-thirds of the ulti-

mate strength the former may be the limiting factor since it is often required that aircraft structures shall not deform permanently at the highest stress expected in service. The yield strength may be used also as an indication of the proportional limit in designs where the elastic properties are important, such as springs. The yield strength curve of the titanium-manganese alloy multiplied by 1.7, if plotted in Fig. 2, would lie almost on the 4340 curve from 600 to 900 F. Note in comparing Figs. 1 and 2 that the martensitic steels exhibit much higher relative strengths at the lower temperatures on the basis of tensile yield strength.

Effects of Prolonged Heating

If exposure to temperature has been short, Figs. 1 and 2 present a useful comparison of the short-time properties of alloys. Throughout a certain temperature range which is characteristic for each alloy, the properties are maintained during very long exposure. At higher temperatures the strengths decrease with time. Data are not available to enable prediction of strengths after exposure for a given time at any temperature, although such information would be very useful. It is possible, however, to establish temperature ranges in which the properties will remain constant for a certain time.

In Fig. 3 are shown curves for tensile ultimate strength versus temperature for 4340 at several heat-treat levels. Above a certain temperature, an exposure of 1000 hr lowers the strength appreciably. The curves indicate roughly the decrease in tensile ultimate strength that would be detected in a test conducted at a given temperature if the metal were exposed for 1000 hr at that temperature. This is representative of a common service condition in which the metal is heated for extended periods and intermittently subjected to high loads of short duration.

For a number of alloys, Fig. 4 shows the temperature ranges in which tensile ultimate strength is maintained for 1000 hr. 301 ½H is not shown. At temperatures considerably below those affecting strength, the micro-structure of unstabilized 18-8 type steels is altered in such a manner that damaging intergranular corrosion will subsequently develop in certain environments. For heat-treated materials, the upper limit of the stable range is usually related to the heat-treat temperature. For low-alloy steels, of which 4340 may be considered typical, the upper limit of stability for about 1000 hr is about 150 to 200 F below the tempering temperature. The ductility of an alloy can be adversely affected by prolonged heating within the temperature range where the tensile ultimate strength is maintained in smooth test specimens. The loss of ductility is reflected in an increase in notch sensitivity. Practically, this means that the strength may be lowered in a part where a stress concentration exists. Unfortunately, no data are available at this writing on the effect of heating on the short-

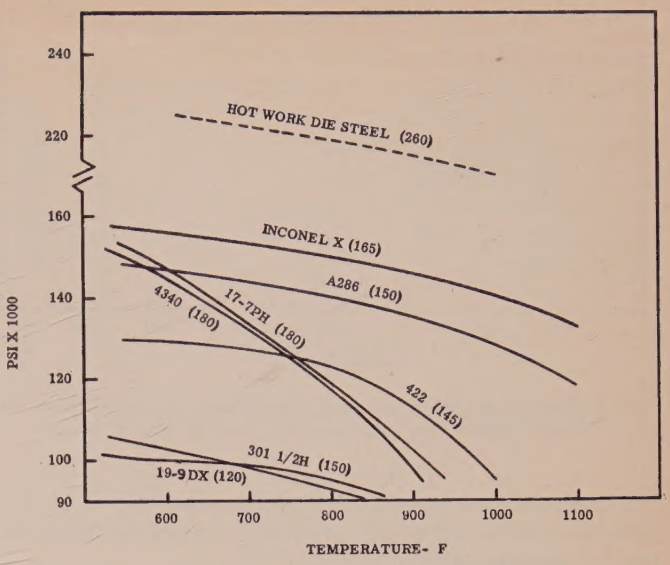

Fig. 1 – Variation of tensile ultimate strength with temperature for short-time exposure at temperature (see references 1-7, 10, 29 at end of paper)

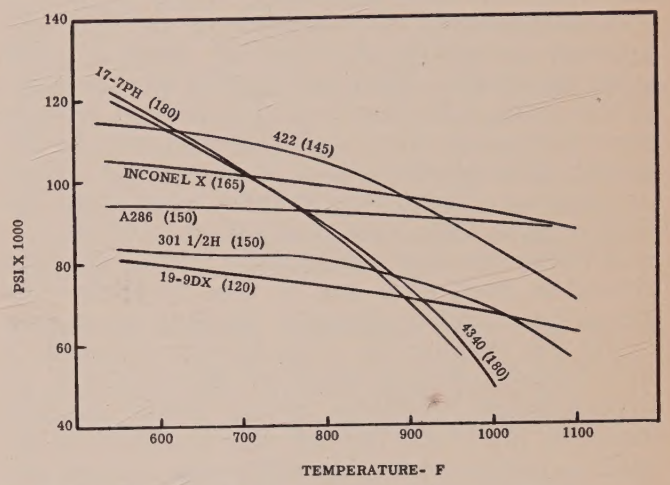

Fig. 2 – Variation of tensile yield strength with temperature for short-time exposure at temperature (see references 1-7, 10, 29 at end of paper)

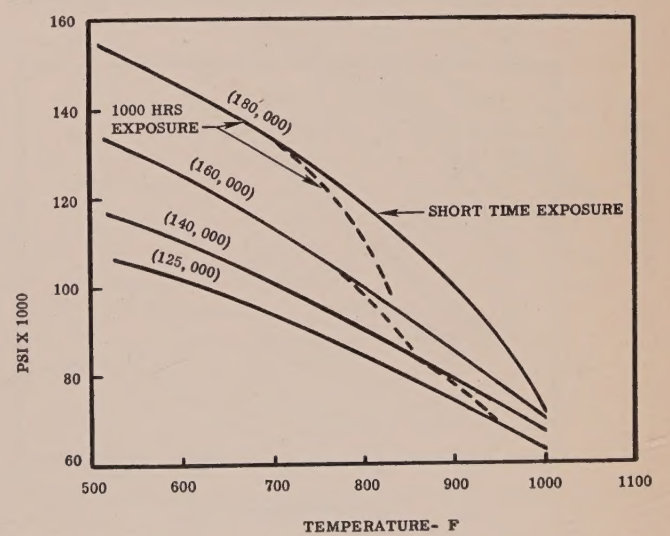

Fig. 3 – Variation of tensile ultimate strength of 4340 steel with temperature for several lengths of exposure time at temperature (see references 5, 22, 23 at end of paper)

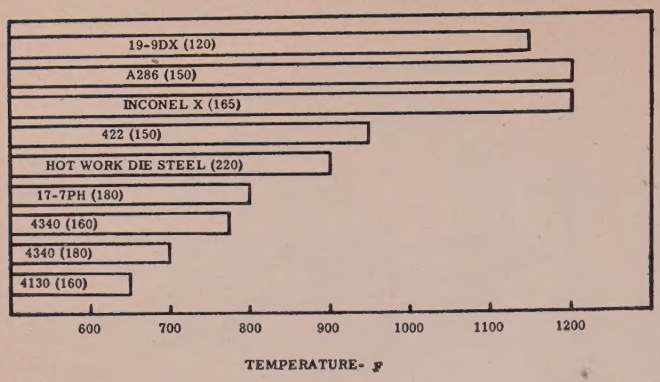

Fig. 4 – Relative maximum exposure temperatures of several alloys for 1000-hr stability (see references 4, 22-24 at end of paper)

time properties of notched parts. The effect of decreased notch strength will be illustrated further on by stress-rupture tests.

Short-Time Compression, Shear, and Bearing Elastic Moduli

A small amount of data exists on elevated temperature properties of materials under stresses other than tensile. When information on some property is scant, it is often helpful to relate it to some more commonly determined property, such as the tensile ultimate strength or yield strength. Shear and bearing ultimate strengths for a few alloys are illustrated in Figs. 5 and 6 as a fraction of the corresponding elevated temperature tensile ultimate strengths. Such plots can be used to predict the strengths of similar alloys for which no direct data exists. For example, the shear ultimate strength of heat-treated low-alloy steels can be assumed to be approximately six-tenths of the tensile ultimate strength. Shear and bearing data are likely to exhibit variations reflecting differences in test setups. Variations in rigidity of test fixtures and in specimen dimensions will cause variations in the strength values obtained. Characteristically, shear

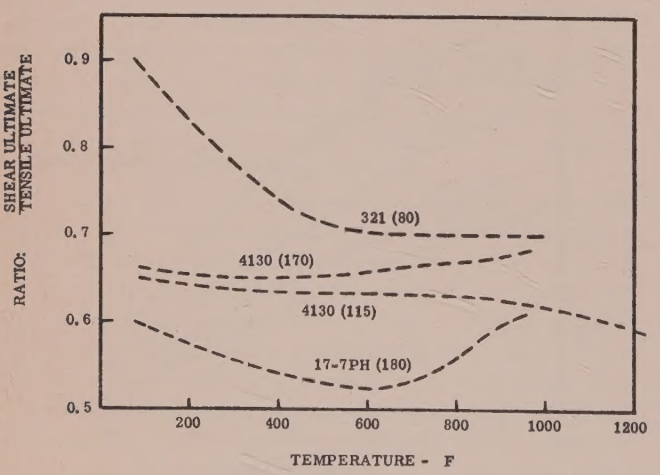

Fig. 5 – Variation of shear ultimate strength with temperature for short-time exposure at temperature (see references 3, 16, 25 at end of paper)

and bearing tests produce areas of stress concentration in the test specimens; hence, the results can be influenced by ductility variations. The effect of low ductility is shown in the shear data on 17-7PH stainless steel, Fig. 5. In the temperature range where the shear strength dips, low values of elongation are obtained in tensile tests. Because of such effects, stability data determined for tensile strengths in Fig. 4 should be applied cautiously to shear and bearing strengths until the effect of exposure on ductility is determined.

A few tests indicate that the compression yield strength is close to the tensile yield strength except in those cases where anisotropy exists, as in work-hardened stainless steel. No data exist on bearing yield strength at elevated temperatures.

Tension moduli versus temperature are given in Fig. 7. Moduli of elasticity are not generally affected by heat treatment, although cold-working may produce anisotropism in the moduli. The curve shown in Fig. 7 for 301 ½H represents values from specimens loaded parallel to the direction of rolling. Moduli obtained from specimens of 301 ½H or annealed loaded transverse to the direction of rolling are higher, lying near the 4340 steel curve in Fig. 7.

Values obtained for moduli are dependent on the test method employed, and because of creep effects, lower moduli values can be obtained at high temperatures when determined by stress-strain tests than when calculated from vibration data (tuning fork). The latter method is usually assumed to give the "true" modulus, while the stress-strain data more nearly represent the usual loading conditions. The curves in Fig. 7 are based on calculations from both stress-strain and vibration data. Vibration data were used only in regions where creep effects should not significantly influence the results. Compression modulus values are usually close to the tensile modulus values.

Creep and Stress-Rupture

The significance of creep and stress-rupture properties in aircraft structural design have not yet been evaluated fully. In many applications these properties are not critical because the parts are designed to withstand high emergency loads of short duration. In such cases the steady loads are often below those that will produce appreciable creep.

Tensile stresses causing rupture in 100 and 1000 hr are shown in Fig. 8. The 1000-hr rupture curve for the titanium-manganese alloy multiplied by 1.7 for weight adjustment lies almost directly upon the 100 hr curve for 4340.

The information given by stress-rupture curves is valid although the temperatures may be above the stable range since the effect of exposure is evaluated by the nature of the test. If much higher loads than those shown are applied momentarily, however, consideration must be given to the possible effect of exposure on the short-time strength. Under stress-rupture conditions the metal is ex-

posed for long periods to both stress and heat. Generally, a sufficiently accurate estimate of the effect on the metal is obtained by consideration of the heat effect only, for it has been found that the effect of stress is minor in comparison to that of heat.

Fig. 8 shows stress-rupture data obtained by continuous loading at each temperature. It must be remembered, however, that during its service life, an airframe part will be subjected to various combinations of stress and heat.

In a limited number of tests, a reasonably accurate estimate of the sum effect of n various stress and temperature combinations is given by the following formula:

$$\sum \left(\frac{N_1}{L_1} + \frac{N_2}{L_2} + \frac{N_3}{L_3} + \cdots + \frac{N_n}{L_n}\right) = F \qquad (1)$$

where N_1 represents the total time in service that the metal is subjected to stress 1 and temperature 1, and L_1 represents the time required for rupture to occur at stress 1 and temperature 1. F must be less than unity in order that failure will not occur during service. The margin of safety, M_s, under such conditions may be represented by:

$$M_s = \frac{1}{F} - 1 \qquad (2)$$

Formula (2) assumes that fractions of stress-rupture life obtained under various conditions are additive. This assumption has no basis in theory and its applicability to specific materials and stress and temperature ranges should be verified by tests. Use of formula (2) most certainly will not give accurate results if any of the stress and temperature combinations causes a significant change in the strength of the material.

Notch Effects and Creep

The effects of notches at elevated temperatures are similar to those met at ordinary temperatures. In their initial conditions most metals show notch strengthening in static tests. As previously noted, however, prolonged exposure to heat may result in loss of ductility, which loss may then proceed to the point where the material is weakened by notches. These principles are illustrated in stress-rupture tests on two martensitic steels, Fig. 9. In short-time tests the notched specimens were stronger. After long times at low stresses, the notch no longer had a strengthening effect in 4340 and became a weakening element in the highly alloyed AMS 5616. Relative differences in loss of ductility such as those illustrated in Fig. 9 have been correlated with the amount and kind of alloying elements present.

Most of the creep data determined so far for the range 600 to 1100 F have been reported only in terms of the stress necessary to produce a specified constant rate of creep, for example, one per cent

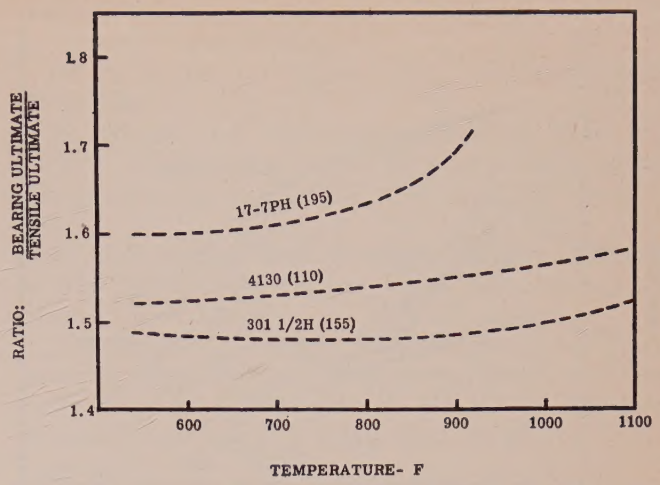

Fig. 6 – Variation of bearing ultimate strength with temperature for short-time exposure at temperature ($e/d = 1.5$), (see references 3, 4, 16, 26 at end of paper)

per 10,000 hr. For airframe structural design it is usually necessary to know the total amount of deformation which takes place from the time stress and heat are first applied. At the present time the data available on total deformation are not complete enough to allow construction of curves showing stresses producing a specified amount of deformation in a given time. Such curves would present a picture of creep similar to that presented for stress-rupture in Fig. 8. In general, the principles set forth above regarding the use of stress-rupture data apply to creep data as well.

Long-Time Properties Under Stress Other Than Tension

Work was begun only recently on the determination of creep and stress-rupture properties under compression, shear, and bearing for a number of

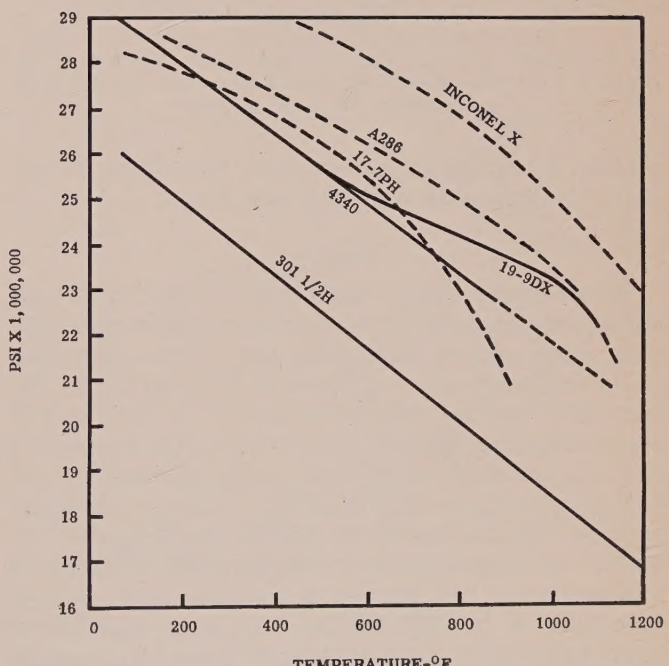

Fig. 7 – Variation of tensile moduli of elasticity with temperature for several alloys (see references 1, 10, 16-18, 27 at end of paper)

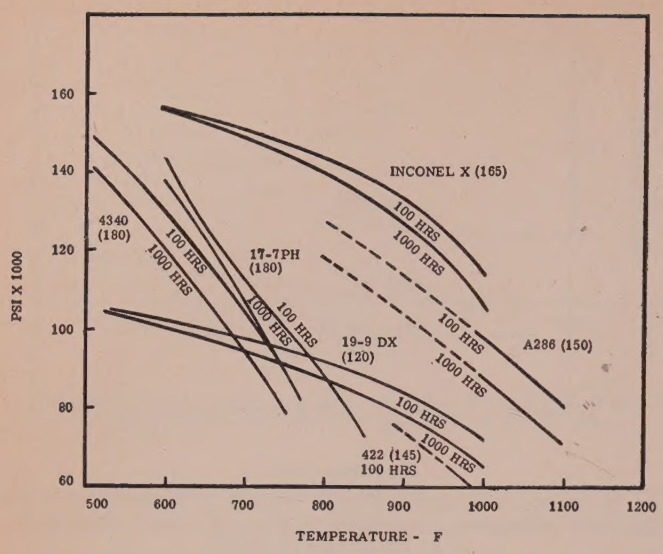

Fig. 8 – Variation of tensile stress to cause rupture with temperature for several alloys held at temperature for different lengths of time (see references 1, 2, 4, 5, 10-13, 16, 28 at end of paper)

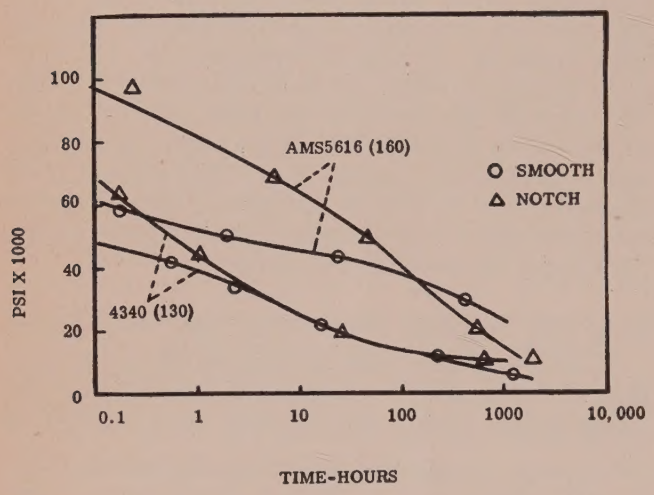

Fig. 9 – Variation of tensile stress to cause rupture with time of exposure at 1100 F for smooth and notched specimens of several alloys (see reference 14 at end of paper)

metals. The data so far obtained have been principally for aluminum and titanium alloys.

Fatigue

When cyclic stress tests are conducted at elevated temperatures, it is often found that considerable creep occurs during the test. This creep may be a factor in producing eventual failure; hence, the test takes on the combined aspects of fatigue and stress-rupture. The amount of creep that occurs is a function of both amplitude and frequency of the stress cycles as well as the value of the mean stress applied. Establishment of general rules for the behavior of metals under cyclic stresses at elevated temperatures has proved a complex task. Alloys classified as having similar fatigue properties at room temperature can show widely dissimilar properties in fatigue tests at higher temperatures owing to dissimilar creep characteristics.

Fig. 10 shows the variation in creep for a fatigue test resulting from variations in both the amplitude of the stress cycles and the absolute value of the stresses. The frequency in these tests was between 2000 and 2500 cpm. The creep was very small when the mean stress was zero; that is, when maximum tensile stress equaled maximum compressive stress. Creep was maximum when the maximum and mean stresses were equal; that is, when the test was conducted as a standard creep test.

Fabrication Characteristics

Final selection of a material for a particular use frequently depends as much upon fabrication characteristics as upon strength. The following comparisons of alloys are general in nature since relative ease of fabrication varies for each type of operation.

All the alloys discussed in this paper are worked by the ordinary machining and forming operations. The austenitic steels are generally among the more readily formed of the several alloy types. Stainless steel 17-7PH is equal in formability to the austenitic steels in most respects. Representative alloys such as Inconel X and A286 are somewhat more difficult to form. The martensitic steels are intermediate between the other two types in formability. From the standpoint of machinability, martensitic steels rate highest, austenitic grades and 17-7PH stainless steel are intermediate, and the other two precipitation-hardening alloys are the most difficult to machine of the alloys discussed.

All the alloys discussed can be hot-worked satisfactorily. Maximum strengths cannot usually be achieved after hot-working in alloys such as 301 ½H or 19-9DX, which require a certain amount of cold- or hot-cold-working for strength. All the other alloys can be heat-treated to normal strengths after hot-working.

Problems arising in heat-treating or joining can be decisive factors in the selection of an alloy. Other things being equal, low heat-treat temperatures are desirable since problems arising from warping and oxidation are thereby minimized. Precipitation-hardening alloys such as Inconel X and A286 require only relatively low ageing temperatures for maximum strength properties. Dimensional changes during heat-treatment are very small in these two alloys and warpage is not usually a problem. The martensitic steels require heating to higher hardening temperatures and can change dimensionally during hardening by various amounts, depending upon the size and shape of the part. Consequently, considerable trouble from warpage is experienced in fabricating parts from these alloys. Alloy 17-7PH grows about 0.5% in all directions during its final heat-treatment, and therefore may warp considerably.

In alloys that warp excessively, elimination or removal of warpage may be accomplished by restraint during heat-treating or by cold or hot

straightening after heat-treatment. Generally, the higher the final strength of the alloy the more difficult it is to remove warpage.

Joining by fusion welding can be satisfactorily accomplished on all the alloys discussed. Welds may be heat treated to high strengths except in the austenitic steels. Welding of highly hardenable martensitic steel requires special care to prevent cracking.

References

1. International Nickel Co., Inc. data manual, "Inconel X," January, 1949.
2. Universal-Cyclops Steel Corp. data manual, "Super Alloys, Physical Properties and Processing Data," 1954.
3. Air Force Report, AFTR 6517, Part 2, "Determination of Physical Properties of Ferrous and Nonferrous Structural Sheet Materials at Elevated Temperatures," December, 1952.
4. Armco Steel Corp., "Technical Data Manual – Armco Precipitation Hardening Stainless Steels," Feb. 15, 1954.
5. North American Aviation Report, NA-48-1316, "High-Temperature Properties of Low-Alloy Steels," Dec. 3, 1948.
6. North American Aviation Report, NA-47-825, "Short-Time Tensile Properties of Low-Alloy Steels at Elevated Temperatures," Oct. 15, 1947.
7. Universal-Cyclops Steel Corp., "Technical Data on Uniloy 19-9DX," Oct. 26, 1953.
8. North American Aviation, "Mechanical Properties of RC-130A" Engineering Research Project CP 2253 (unpublished).
9. Rem-Cru Titanium Inc., "Rem-Cru Titanium Manual," 1954.
10. Alleghany Ludlum Steel Corp., "Technical Data on Alleghany Ludlum Alloy A286," Jan. 9, 1952.
11. ASTM-ASME Aviation Panel Project AP-2 Report, "Exploratory Investigation on High-Temperature Sheet Materials," Nov. 13, 1951.
12. United States Steel Corp. Report No. 623, "Strength of Two Hardened Alloy Steels in the Temperature Range 75 to 700 F," August, 1949.
13. Naval Air Material Center, Philadelphia, Report No. AML NAM AE 411022, "Investigation of the Properties of Steels at Intermediate Temperatures," January, 1950.
14. W. F. Brown, Jr., M. H. Jones, and D. P. Newman, "Influence of Sharp Notch on the Stress-Rupture Characteristics of Heat-Resisting Alloys: Part II," Proceedings, ASTM, Vol. 53, 1953.
15. ASTM Special Technical Publication No. 128, "Symposium on Strength and Ductility of Metals at Elevated Temperatures with Particular Reference to Effects of Notches and Metallurgical Changes," June 23, 1952.
16. Armour Research Foundation Report No. 50, "Determination of Physical Properties of Ferrous and Nonferrous Structural Sheet Materials at Elevated Temperatures," Sept. 24, 1954.
17. Universal-Cyclops Steel Corp., "Data Sheets on 19-9DL," Aug. 7, 1944.
18. S. L. Hoyt, "Metal Data," Reinhold, New York, 1952.
19. Wright Air Development Center Technical Report 52-325, Part I, "Elevated-Temperature Fatigue Properties of SAE 4340 Steel," December, 1952.
20. T. J. Dolan, "Past Work on Fatigue of Metals in the High-Temperature Field," University of Illinois, June, 1950.
21. Cornell University, "Investigation of Compressive, Bearing, and Shear Creep-Rupture Properties of Aircraft Structural Metals at Elevated Temperatures" (work being done on an Air Force contract).
22. North American Aviation, "Room-Temperature Mechanical Properties of Metals after Prolonged Heating," Engineering Research Project CP 3122 (to be published).
23. North American Aviation Report No. NA-54-358, "Stability of Steels and Heat-Resistant Alloys at Elevated Temperatures," April 1, 1954.
24. Crucible Steel Co. of America Data Sheet, "Resistal 422 Stainless Steel," February, 1952.
25. North American Aviation Report No. NA-48-1386, "Elevated-Temperature Shear Properties of AISI 4130 Steel and AISI 302 Stainless Steel," Dec. 23, 1948.
26. North American Report No. NA-52-854, "Corrosion-Resistant Steel Sheet, Bearing Strengths," Aug. 18, 1954.
27. International Nickel Co., "Nickel Alloy Steels," second edition.
28. North American Aviation, Engineering Research Project CP 3120, "Creep-Rupture Properties of 17-7PH" (to be published).
29. Alleghany Ludlum Steel Corp., "Data Sheets, Special Steels – Tool, Stainless, Electrical."

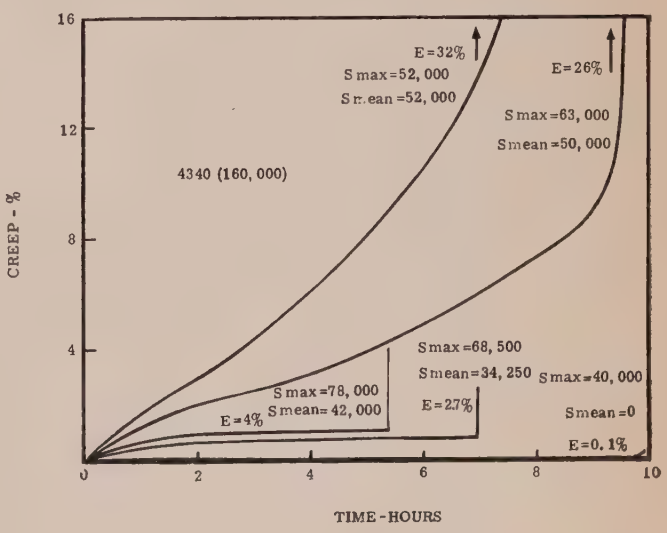

Fig. 10 – The effect of the character of stress cycle on the variation of creep with time of exposure at 1000 F for 4340 steel (see reference 19 at end of paper)

SINCE passenger-car bodies cannot practically be designed to meet the abnormal stresses of collision, normally needed rigidity is a major design criterion for the modern body.

Bodies must be stiff enough, the author points out, not to respond easily to the excitation caused by vibration of the unsprung mass of wheels and suspensions, but not too stiff to ride comfortably.

Recent trends toward more glass area and lower body height have increased the importance of determining body loads and structural requirements. Discussed here are some of the ways in which these factors are investigated, and the results which have been achieved.

Automobile

A TECHNICAL understanding of the loads imposed, and an understanding of the way the body reacts to these loads, is necessary in order to design a modern and efficient passenger-car body structure. This is evidenced by the fact that very successful bodies are being produced today which were not considered feasible from a structural standpoint just a few years ago. Further improvements in style, comfort, and safety can be accomplished through a better knowledge of the actual structural requirements of a passenger-car body.

What is known, then, about the loads a body is required to carry? Can specific design conditions be established? A little thought will quickly reveal that few failures of basic body structure ever occur. Did you ever see a rocker panel, pillar, or roof rail completely buckle or collapse because of carrying too much load in the car, or because of bouncing over a dip in the road at too great a speed? Complete failures apparently happen only as a result of collisions. Naturally, considerable strength is built into the body to afford adequate protection in collisions. New models are frequently tested under simulated roll-over and collision conditions to actually prove the structure and safety of the body, but to establish a degree of collision as a design condition for the structure hardly seems practical. We do know the maximum accelerations to which a body is subjected during normal operation, but no normal operation causes loads great enough to cause failure or to be considered as design criteria.

Some other type of condition, then, must provide the major design criterion for a body. This criterion is rigidity or stiffness. There are two major reasons why a body must be rigid. First, it is a well-known principle of dynamics that the stiffer a beam or structure, the higher the frequency of vibration and the lower the amplitude of vibration. Further, the amplitude of vibration is greatly affected by how closely the natural frequency of the structure corresponds to the frequency of excitation.

The major source of shake and vibration in a passenger-car body is the excitation caused by the vibration of the unsprung mass of the wheels and suspensions. The frequency of vibration of the unsprung mass is dependent on its weight and the spring and tire rates, but is usually in the order of 10 to 15 cps. Bodies must therefore be stiff enough not to respond readily to this excitation. On the other hand, too stiff a body can produce an uncomfortably harsh ride in the completed car. Largely by experience, the most acceptable range of stiffness for bodies has been determined. No single value for this stiffness can be stated, for it will vary somewhat with car weight, wheelbase, type of suspension, and the type of performance desired by each manufacturer. The total range of stiffness for all cars on the market is not too great, and for cars in the same price class is surprisingly narrow.

The second requirement for stiffness or rigidity is that the body openings cannot accommodate any large amount of distortion. The doors and deck lid fit into these openings with little metal-to-metal clearance, and must fit tightly against the weatherstrip in order to maintain an air and water-tight seal at all times. Also, large pieces of glass must be retained in the windshield and backlight openings without breaking due to body distortion.

While overall body stiffness is the major design criterion, it would be well to look briefly at some of

Body Loads

Philip O. Johnson, Fisher Body Division, GMC

This paper was presented at the SAE Golden Anniversary Passenger-Car, Body, and Materials Meeting, Detroit, March 2, 1955.

the other design conditions. All design criteria for body structure fit rather nicely into the following three subdivisions:

1. Stiffness: In addition to the need for overall body stiffness required to control shake and to prevent excessive distortion of the body openings, as already described, there are other specific conditions which dictate a degree of stiffness in the passenger-car body. One of the most important of these is recognition of the fact that the present-day cars are jacked by their bumpers to change tires. It is essential that doors do not jam in the openings when the car is on a bumper jack. Not only is it very objectionable not to be able to open or close a door, but a door jammed in the opening will usually result in damage to the painted surfaces.

It is also current practice to tow cars with one end hoisted by the bumper. Not only does this redistribution of supports tend to cause distortion, but consideration must be given to the dynamic accelerations involved while the car is being towed in this manner.

The tendency for squeaks and rattles to develop is probably also related to the stiffness of the body.

2. Strength: It has been found that the maximum vertical acceleration of a car encountered during normal operation (that is, something short of actual collision or rolling over) is in the order of 3*g*. As stated previously, however, the requirement for stiffness insures this degree of strength to the extent that the overall body structure, if well engineered, will normally carry several times this loading without failure.

Many individual components of the body are, of course, designed for strength rather than, or in addition to, stiffness. Seats, seat adjusters, hinges, many of the mechanisms, shock absorber, and bumper attachments are a few examples.

3. Durability: The continual shake and distortion of a passenger-car body due to operating the car under all kinds of conditions, and the resulting reversal of loading, can cause a gradual weakening of the structure. This is particularly true at spotwelded joints, and adequate welding must be provided.

All mechanisms must be designed and checked to withstand the maximum number of cycles of usage expected during the life of the car.

In designing a new body, the general practice is to summarize and review the structural performance of the most similar existing models. These data are available from the extensive proof tests conducted before the actual introduction of each new model, and from the continual tests conducted during the model year. With a thorough understanding of the structure in the existing models, and with the application of some theory and some good common sense, the structure of the new model is determined and roughly evaluated. It should be completely and immediately understood that even if a complete and detailed theoretical analysis of the structure for a new model were entirely practical, that the analysis has to follow after the design. This is not true of simple structures. For example, it is practical to determine by analysis the size of the seat members, a door hinge, or a rear axle before the parts are designed. However, in a more complex structure made up of framing, such as a body, the distribution of load throughout the structure is dependent on the relative stiffness of each

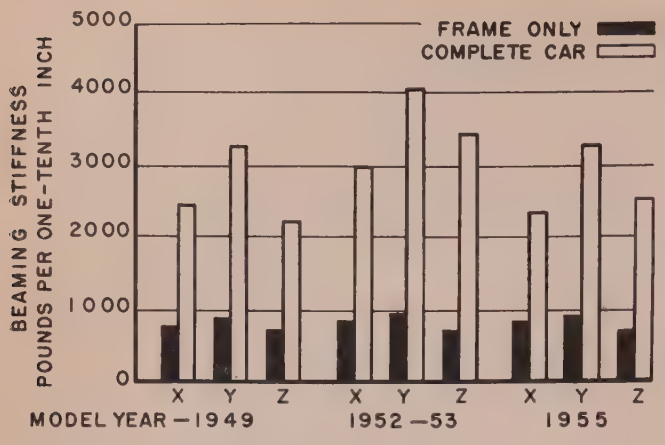

Fig. 1 – Beaming stiffness for three high-production cars for last three basic body model change years

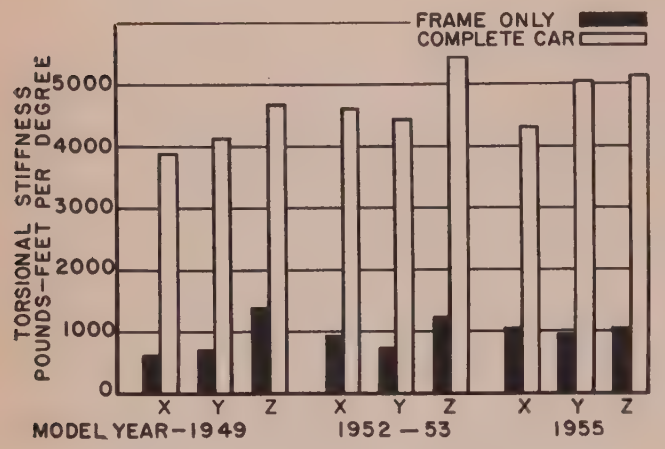

Fig. 2 – Torsional stiffness for three high-production cars for last three basic body model change years

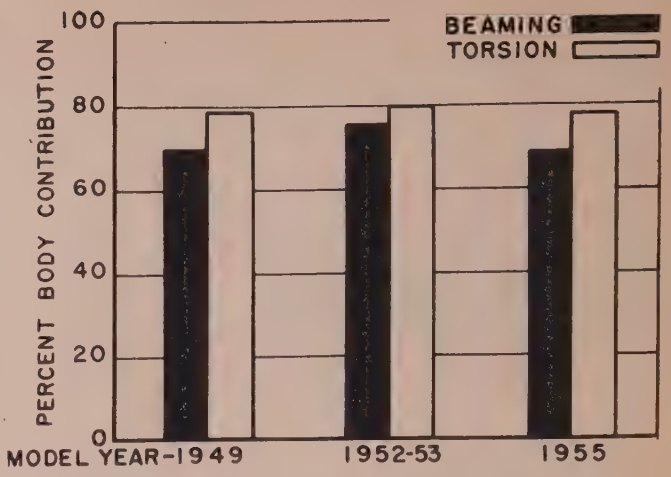

Fig. 3 – Average body contribution to complete car stiffness

part of the structure. If a pillar is made less stiff it will carry less load, with some part of the remaining structure absorbing more load. This type of analysis is lengthy and difficult, since the structure is to be established by the analysis, but the analysis cannot be made until the structure is established.

The determination of passenger-car body loads and the structural requirements of each member is not a completely developed or exact science. A complete set of design conditions necessary for a mathematical analysis is difficult to establish. For these reasons, the complete application of an analytical approach to design is somewhat impractical.

The real purpose of this paper, then, is to try to present information leading to a better understanding of how a body structure really works. There are several excellent methods for obtaining this type of information. In addition to the theoretical analysis already described, excellent information can be obtained by testing. The distribution of loading in the structure can be related to an accurate determination of the distortion of the structure. For example, if the joint of a pillar with the rocker bends backward when the body is subjected to an overall beaming load, the type and direction of loading is readily apparent. This same joint might then be isolated, or cut out, from the body and subjected to the type and direction of loading already deduced. If the deflections can be duplicated, the actual magnitude of the load has been nicely approximated.

With accelerometers, strain gages, and displacement gages, used with a recording oscillograph, quite detailed analysis of the structure can be made even under actual operating conditions. Brittle lacquer stresscoat is another tool that can be used to determine the type and approximate magnitude of load at any part of the structure.

The importance of stiffness or rigidity leads to two very important tests for evaluating body structure – the beaming and torsional-stiffness tests. The procedure for conducting these tests is generally familiar and has been adequately described in other SAE papers. Briefly, the beaming test consists of applying a known arbitrary load in the car and measuring the resulting deflections of the chassis frame caused by this bending load. The torsion test consists of applying a twisting moment to the car and measuring the resulting angle of twist at various stations along the chassis frame. It is most convenient to express the stiffness data obtained in the same manner that a spring would be rated – that is, pounds per inch deflection in beaming and pounds-feet per degree rotation in torsion.

Fig. 1 shows beaming stiffness data obtained from three competitive high-production cars of

approximately the same wheelbase. The data were obtained from different sources, and are not identified by car in the graph, as it would serve no useful purpose in this paper. The three periods shown represent the years in which basic model changes were made to the bodies. The short, solid bars represent the chassis frame stiffness. The longer open bars show the stiffness of the complete cars. The slight change in stiffness from year to year cannot be assumed to be either an improvement or loss in body efficiency. Changes or improvements in suspensions, or in the type and number of shims used between the body and chassis frame, can make some change in complete car stiffness desirable or totally acceptable. The chart clearly shows that the body accounts for a major portion of the complete car stiffness.

Fig. 2 shows the same type of comparison for torsional stiffness. In this case, both frame and complete car stiffnesses show a gradual increase. These charts show that desirable limits for beaming and torsional stiffness for a proposed new model can be fairly well defined.

Fig. 3 is a summary of the first two charts, and shows the average body contribution to complete car stiffness. About 70% of the beaming stiffness and about 80% of the torsional stiffness are provided by the body.

It has been shown that the body does provide a very high percentage of the total strength and stiffness of the complete car. But just how does a body actually work as a load-carrying member? Fig. 4 shows the basic framing making up the side of a typical 4-door sedan. When the chassis frame and body are bent as a beam, the body side frame is loaded primarily by the reactions in the front from the cowl and front-end sheet metal, and by the reactions in the rear from the quarter and wheelhouse panels. Some additional bending may be introduced when the rocker is forced to follow the bending of the chassis frame because of intermediate attachments along the rocker.

The line drawing shows, in exaggerated form, typical displacement of the side frame due to body beaming. Since the doors are hinged to the lower portion of the pillars, the pillar rotation in this area determines the door displacement. The horizontal distance across the opening will normally close, and the doors will normally rise with respect to the lock pillars, when the body is subjected to a vertical beaming load.

Jacking or hoisting the car from the rear will normally cause a rather similar side-frame distortion, with the doors moving in these same directions. Jacking from the front, however, may cause the doors to drop instead of rise.

Remembering that points of inflection in the deflection curve correspond to zero bending moment on a moment diagram, the general nature of the bending moment curve can be estimated. In the area of the windshield pillar, for example, the bending moment is obviously zero at some point near the middle of the pillar, while very high bending moments exist at the joints of the pillar with the cowl and roof. Direct axial-tension or compression loads in any of the side-frame members are so small that they can be omitted from any consideration.

It has been found that the vertical accelerations experienced on the road, which cause beaming

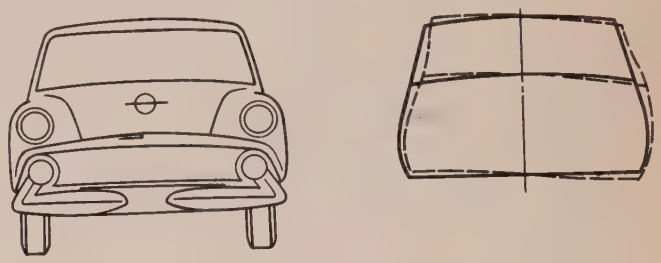

Fig. 5 – Torsional load deflection diagram

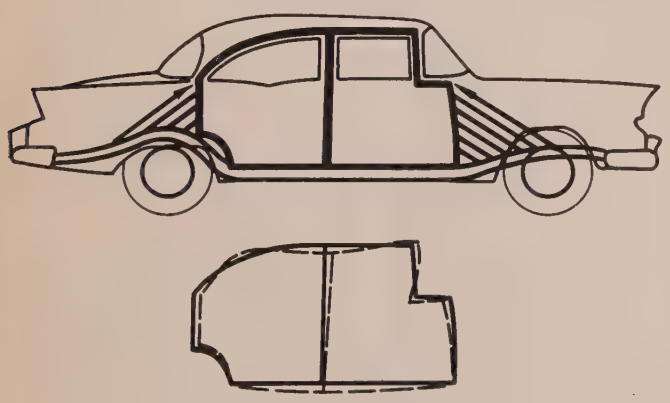

Fig. 4 – Beaming load deflection diagram

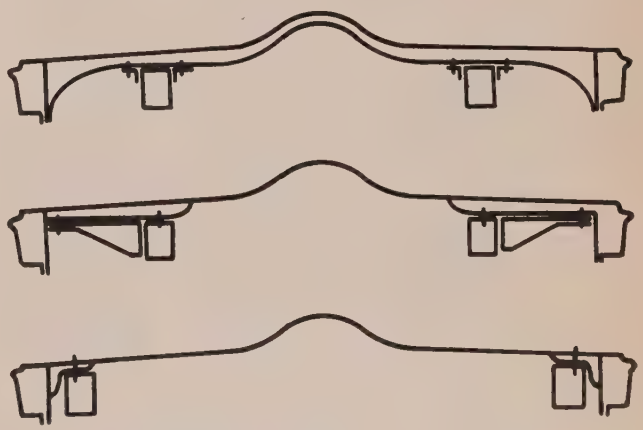

Fig. 6 – Typical methods of transferring load from chassis frame to body

deflections in the body, are approximately equal up or down. For this reason, the indicated deflections and bending moments in the diagram should all be considered plus or minus.

Since the essential requirement for the windshield pillar is bending stiffness, and since the direct load is negligible, the vertical windshield pillar design offers no major structural problem. Close attention to design, particularly in the joints, can produce a pillar matching the bending stiffness of the older sloping pillars.

When the car is subjected to torsional loading, the body side frame and doors deflect in the same manner as already illustrated for beaming and, in addition, in a lateral direction. Fig. 5 shows the distortions experienced in the windshield frame due to body torsional loading. Below the windshield opening the loading is carried in part by shear in the dash panel. Again the general nature of the bending moments can be estimated. There is zero bending moment at some point near the middle of the pillars, while very high bending moments exist at the joints of the pillars with the cowl and roof. Zero bending moment also occurs near the middle of the windshield header. The direct tension-compression loads can be neglected. Note that these bending moments add to those in the plane of the side frame. Note the importance of adequate stiffness between the windshield header and pillar.

A similar analysis can be made of the backlight opening. Below the opening, the loading is usually carried by large gussets or diagonals in the plane of the rear seat back.

It has been shown that, for both beaming and torsional loading, the side framing is the essential structure providing body stiffness. For this structure to be effective, it must be adequately tied to the chassis frame. Fig. 6 shows several typical methods of transferring load from the chassis frame to the side frame. Any of these methods, when efficiently designed, will provide an adequate tie between the two frames. It is considered of utmost importance that a good tie be provided at each end of the side frame (at each end of the rocker). The intermediate connections are of less importance in affecting the overall rigidity of the body. Since the chassis frame must be narrowed at each end to clear the front and rear wheels, a considerable overhang is usually necessary at each end of the rocker.

Two major factors are influencing the type of body structure that must be designed for our present and future cars. Fig. 7 shows that there has been a definite trend toward greater glass areas. There is about 30% more glass in the current bodies than in the 1949 models. This has meant less available space to provide upper structure.

Fig. 8 shows that there has been a definite trend toward reduced overall car height. This reduction was largely accomplished by lowering the floor in the body, while maintaining the same ground clearance to the bottom of the chassis frame. Any further reduction in car height must certainly be accomplished in this manner. This also means less space available to provide body structure.

The charts presented earlier (Figs. 1, 2, and 3) showed that basic body structure has been maintained or improved over the last three basic body models, while allowing the full styling development of the bodies. A slight indication of future problems was indicated in the last two charts (Figs. 7 and 8).

This continual challenge to the body engineer to design and build new and better bodies can and will be met. It is hoped that this paper will lead to a better understanding of body loads, and in this way play a part in the development of new bodies for tomorrow's cars.

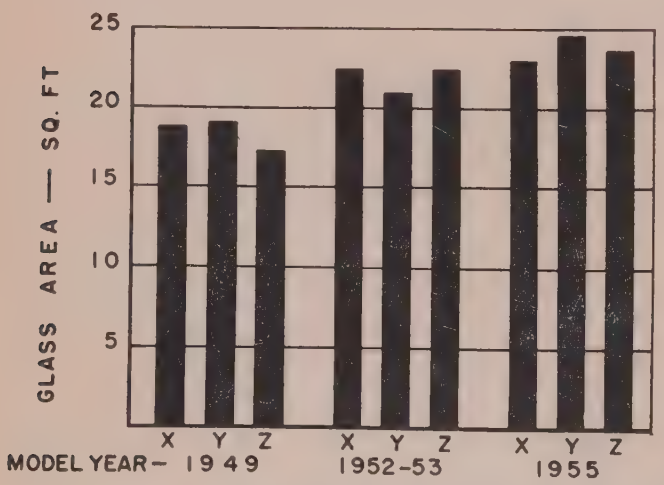

Fig. 7 – Total glass area for three different high-production cars for last three body model change years

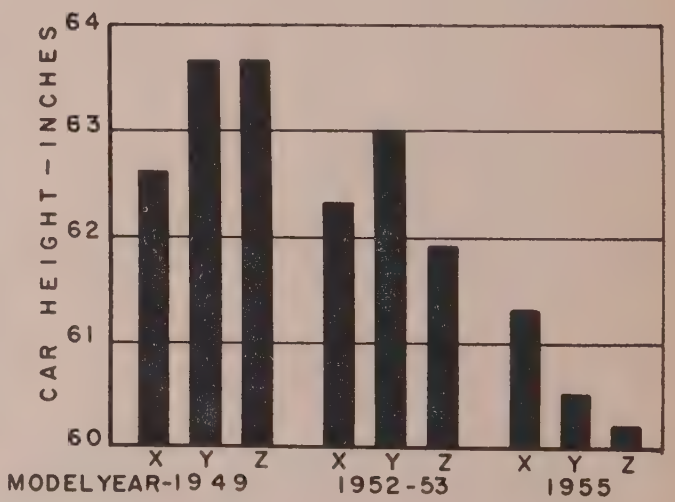

Fig. 8 – Total car height for three different high-production cars for last three body model change years

Creativity In Engineering

John E. Arnold, Massachusetts Institute of Technology

This paper was presented at SAE Mid-Michigan Section, Flint, Mich., Nov. 15, 1954.

OCCASIONALLY when I mention the words "Creative Engineering," or when I give a talk describing the work that we do at M.I.T. in a course by the same name, someone points out the apparent redundancy in the phrase. Engineers, by definition, are creative; at least they are supposed to be. Why, then, give a special course in creative techniques? I will try to answer this question here. After defining creative problems and the creative process, I will try to show briefly some of the factors that are essential to the creative person, and some of the factors that seem to inhibit him. I will try to show that there are various levels of creative activity, and that it is possible to realize to a greater extent one's own imaginative potential. I will try to point out the reasons for the increased activity in this area today, and to give my idea of what the creative engineer of the future will be like.

Some Definitions

Some definitions, then: What is a creative problem? I like to define the creative problem by contrasting it with another type of problem that we are all more familiar with, that of the analytical type. I distinguish between these two different problems in three ways. First of all, the way the problem is stated; second, the type and number of approaches used to reach a solution; and third, the number of resulting solutions. The analytical problem is usually stated quite precisely and very exactly. Frequently, the answer is contained, or certainly hinted at, in the problem statement. There are two approaches that you can use to arrive at the answer.

1. The approach involving the use of symbolic logic or mathematics.
2. The approach involving experimentation. Both of these approaches lead to one, and only one, right answer.

The creative problem, on the other hand, usually has a very broad and general problem statement. There are a great many different approaches that can be used in arriving at a solution. Finally, there is no one right solution. The many different approaches used lead to many different answers, and these answers usually form a complete spectrum from bad to good. I believe that the number of answers arrived at is the best way of distinguishing between the analytical and the creative problem. The analytical problem has only one right answer. The creative problem has many, many adequate answers. You may think that you have arrived at the best possible solution today, but tomorrow someone else may find a better one. Creative problems, then, not only involve analysis

ANALYZED in this paper are the creative problem, the creative process, and the creative person.

Among factors essential to the creative individual, the author says, are:

1. More ideas per unit of time.
2. Ability to rule out judgment during the idea-forming stage.
3. Lack of barriers between the subconscious and conscious mind.
4. Fluency of ideation.
5. Flexibility.
6. Originality.
7. Sensitivity to existence of problems.

Most encouraging, he feels, is the fact that exercise and practice can develop most of these factors in most people. He urges greater interest and endeavor in this direction throughout American industry.

and synthesis, but also draw very heavily on evaluation. I should also like to add one more specification, and that is that creative problems are always oriented forwardly in time.

One more definition – that of the creative process. I believe that the creative process is a process of mental activity in which one combines past experience with present experience, with possibly some distortion, in such a fashion that one arrives at new combinations, new patterns, and new configurations that better satisfy some need of man. This need may be an implied need just as well as an expressed one; but in every case the creative process is not completed until one produces some tangible evidence that the need has been satisfied. Some may question the inclusion of the word "better" in my definition, and insist that any new and different combination that is accepted by the public be specified as creative. I prefer not to, but maybe the "better satisfaction" phrase should be reserved for only high-level creative work.

Creative Process versus Creative Problems

Note, at this point, that there is a distinction between the creative process and creative problems. The creative process may play a very vital role in the activity of the scientist in his search for the one right answer from nature, so that men like Pasteur, Poincaré, Newton, and Einstein would be classified as past masters of the creative process, even though they were seeking the one right, truthful solution. The processes of scientific discovery and invention are the same. The one discloses new combinations that always existed, the other forms new combinations that did not previously exist. In the same manner, you cannot look at the solution of a problem alone and say with any certainty whether or not it was arrived at through creative activity. Chance may solve creative problems. I am talking about pure chance now, the 50,000,000-monkeys-and-typewriters kind of thing, not the chance that Pasteur said "favors the prepared mind," or even the chance that is associated with the process of serendipity.

The limitation on the creative problem, that it must be forwardly oriented in time, might also be applied to the creative process. There is a great deal of mental activity that involves new combinations of past and present experience that is primarily, if not wholly, backward-looking. I am thinking now of problems of a judicial nature, those concerned primarily with evaluation. I have, however, known some very creative judges and lawyers, and it might well be that their creativeness was a result of their concern as to the effect that their decisions on past events would have on man's behavior in the future.

One other point should probably be made before I leave this matter of definitions. I am quite convinced that the creative process which I have just defined is a unique process, wholly independent of the human activity area in which it is being exercised. In other words, the artist, the poet, the composer, and the businessman, as well as the engineer, use the same process but with different tools. This may account for the fact that a great many highly creative people exercised their talent in more than one field. Albert Schweitzer is an outstanding example of this.

We're All Born with Imagination

With the definitions out of the way, we can now look briefly at some of the factors that seem to be essential to the person who is trying to be efficient and productive in the solution of creative problems through the creative process. Let me start off with two hypotheses: first, that all people are born with certain potential for creative activity; and second, that it is possible and probable that creative potential and intellectual potential are two distinct mental capacities, at least partially independent of each other. Almost all children are born with and exhibit a high order of curiosity and imagination, two prime requisites of the creative adult. This establishes the existence of the potential. Unfortunately, somewhere between childhood and adulthood, the great majority of us lose or fail to use or exercise these capacities, and we end up un-

imaginative and conventional, though still useful members of society. We'll discuss this more later.

There seems to be very good evidence that people can be highly intellectual, highly analytical, and judicial, without being productive in a creative fashion. A followup study on the 1000 gifted children with IQ's of 140 or higher did not reveal very many highly creative adults. It is true that a great majority were highly successful in their businesses and professions, but the creative genius expected did not materialize. On the other hand, there is a great deal of evidence that students with average or less-than-average intellectual ability, as measured by their grades in school, have developed into highly creative people in all the areas of human activity. I am sure you realize that I am not trying to say that the highly intellectual person cannot be creative, nor that the one with lower intellectual capacity is bound to be. At this point, I am merely trying to show that the two potentials are probably independent of each other. There is no question in my mind that the combination of high intelligence and imagination is the most desirable one. F. A. Magoun, who taught for many years at M.I.T., wrote an interesting paper on the selection of men with creative ability, and he pointed up the problem that we have just been discussing quite well:

"Out of the 497 men listed in *Who's Who* and also in *Who's Who in Engineering* or in *American Men of Science,* ranked in order scholastically, most are in the top or the bottom tenth of their graduating class, fewest in the middle portions. Is a poor school record sometimes the very result of creative ability, a restless appetite? One conclusion seems certain: mediocrity always seems mediocre."

Dr. J. P. Guilford, of the University of Southern California, has been carrying out for a number of years now some very interesting and important factorial studies on the three major mental capacities – analytical, creative, and judicial thinking. One of his original hypotheses was the independence of the three. The results of his investigation seemed to verify this hypothesis, and his results show that these potentials are more dependent on more basic mental attributes, some of which are common to all three, but many of which are uniquely associated with only one.

Factors Peculiar to Creative Person

Let us look at a few of these factors that are peculiar to the creative person. Guilford isolated certain fluency factors that varied with the complexity of the test situation and the restriction placed on the goal. Regardless of the limiting conditions, the creative person has more ideas per unit time than the noncreative. He is somehow able to rule out judgment during the idea-forming stage so he can get many ideas, both good and bad. There seem to be no blocks to prevent the associations made in the subconscious to permeate up into the conscious, and he has no inhibitions or difficulties in communicating them to others. Fluency of ideation, then, is an important attribute of the creative individual.

Flexibility is another. The creative person is more flexible in his thinking than the noncreative person. He has the ability to jump from one approach to another without difficulty or without losing sight of the main goal. He can search through widely scattered fields following the many paths that lead to the multiple solutions that he knows exist. Dr. Jerome Bruner of Harvard, speaking at my recent summer seminar in Creative Engineering, spent considerable time going over some of the prices we pay for conventional or rigid thinking. He listed three.

The first, he said, was "functional fixedness," and this deals with the meaning that the ideas and things that we work with have for us. He gave an example: Students who had been well trained in the use of knife switches in problems of electrical circuitry had great difficulty in seeing the knife switch as anything but a switch. When they were faced with a problem of constructing a pendulum out of the materials on hand, and the knife switch was the only relatively heavy piece of equipment available, many of them failed. A knife switch is used on electrical problems. It is not used in making a pendulum.

There is a second kind of rigidity, according to Bruner, which deals with the method of proceeding in problem-solving situations. It is called "Einstellung." His example was that people long trained to solve certain kinds of mathematical problems by a subtractive procedure do not readily shift over to additive methods, even when they are obviously more efficient in special cases.

Dr. Bruner gave the last type of conventionalization the name of "problem set." This deals with the way in which different people behave in problem situations when they know something about the type of answer expected or the method to be used in arriving at a solution. The behavior of a person who knows that a problem has a unique solution is quite different from that of the person who thinks that a problem must be solved by cut-and-try methods, by pure chance, or by the application of logical reasoning.

A creative person, then, is not bound by these three types of rigidity, but is able to apply "multipath-low-probability" thinking to the solution of his problem. He is flexible.

The creative person is more original in his thinking. He can penetrate into divergent areas and find remote relationships that the noncreative person cannot see or recognize until they are pointed out to him. He is always on the lookout for unusual combinations, and these spring into his mind with greater rapidity than commonplace and prosaic

solutions appear to the less imaginative. The originality factor ties in very closely with another factor Guilford calls "re-definition." Bruner would call this the ability to be generic, to be able to abstract the fundamental attributes of all things learned so that the information obtained is easily retained and, almost more important, easily alterable.

The last Guilford factor that I want to mention at this time is probably the most important one. He calls it "problem sensitivity." In order to solve a problem, one must be aware of its existence. You must be aware of the gaps in your environment. You must be able to read between the lines and define the really important problem, no matter how well it is disguised. The truly creative person has this ability to a high degree. He is highly sensitive to all the situations where there is a lack of closure. Yet, as Dr. Morris Stein of Chicago points out, he is able to tolerate a higher degree of ambiguity than the noncreative person. This is only one of the many apparent contradictions that seem to exist side by side in the creative person's personality. Problem sensitivity gives rise to another seeming contradiction. The creative person must question everything that he perceives or develops by thought processes but, at the same time, believe that everything and anything is possible. Another is that he cannot be happy without being unhappy. He must experience some condition of disequilibrium, irritation, and frustration to motivate him into seeking closure. He finds his greatest happiness in doing productive work in extremely frustrating conditions.

These Factors Are Trainable

Although I have now mentioned briefly a number of the factors that are essential to the creative person, I have not as yet told you anything about the very important things that we have discovered in working with these factors in the Creative Engineering Laboratory at M.I.T. The most exciting and comforting thing is that these factors are trainable. We can show in a subjective way at the present time, and before long I hope that we can offer more objective proof, that one can, through exercise and practice, become more flexible and fluent in one's thinking. Problem sensitivity can be increased. Deep penetration and originality can be developed, and the ability to re-define greatly improved. We have condensed the steps in the creative process down to "question, observe, associate, and predict" – and our work with case studies and in the seminar definitely indicates that one's efficiency in carrying out these steps can be improved. I do not believe that we are creating talent where there is none, but we are helping our students to realize their creative potential to a greater degree.

So much for some of the factors that are essential to the creative individual. Even with these factors, however, a person may be prevented from doing productive work. Blocks to creative activity may be categorized into three groups: perceptual, cultural, and emotional. We must gather information about the real world in which we live before we can apply that information to the solution of creative tasks. Sir Joshua Reynolds stated this fact very precisely:

"A great part of every man's life must be employed in collecting materials for the exercise of genius. Invention, strictly speaking, is little more than new combinations of those images which may have been previously gathered and deposited in the memory. Nothing can come of nothing. He who has laid up no material can produce no combinations. The more extensive your acquaintance is with the works of those who have excelled, therefore, the more extensive will be your powers of invention and, what may appear still more like a paradox, the more original will be your conceptions."

Perceptual Blocks

Those things that prevent us from getting true information about the outside world are the perceptual blocks. They are closely tied in with the theories of the Gestalt psychologists, and the best examples of these blocks can be found in their writings. I recommend very highly a little book by Max Wertheimer called "Productive Thinking," in which he describes a number of learning and problem-solving situations, including that of Albert Einstein as he developed his general theory of relativity.

I am sure that we are all well aware that perceptual blocks do exist. We have either experienced or observed cases where we have seen or heard the things we wanted to or expected to see and hear. If this weren't true, magicians, confidence men, and even salesmen would have a much more difficult job.

Cultural Blocks

The next large group of inhibiting blocks are those in the cultural area. As living, gregarious organisms, we cannot help but be influenced by the products of the minds and hands of our fellow men, both living and dead. The great majority of our experience is vicarious, handed down to us by others: our parents, brothers and sisters, school teachers, playmates, wives, co-workers, employees, and so forth. Morris Stein, in his paper on creativity and culture, explores this area quite thoroughly, and he points out many of the problems that exist.

For example, "Does the culture tolerate devia-

tion from the traditional, the status quo, or does it insist upon conformity whether in politics, science, or school? Does the culture permit the individual to seek new experiences on his own, or do the bearers of culture (parents, teachers, and so forth) spoon-feed the young so that they constantly find ready-made solutions available to them as they come upon a situation that is lacking in closure? Furthermore, to what extent do the adults accept or reward, and thus reinforce, the creative experience that the individual has had?"

Emotional Blocks

The third classification of blocks is designated as emotional, and it includes all of the things that we inadvertently do to prevent our most productive and efficient work. It is the largest group, and by far the most devastating. The influence of our unconscious mind and our emotions on our creative work is tremendous, and could easily command the attention of a number of books rather than a paragraph or two in a short paper.

An important emotional block is overmotivation. It is obvious that one must be motivated in order to enter a problem-solving situation, but it may not be quite so obvious that overmotivation or just plain high motivation can inhibit creative activity. What are the prices that one pays for high motivations? Dr. Bruner lists four.

The first one he calls narrowing of the field for the person who is highly motivated. In order to maximize speed of goal attainment, the person takes in a minimum number of clues from the situation. He looks for just certain specific clues that will give him the information about the problem, and a lot of general things he lets pass by.

The second price one pays is that of giving up vicarious trial and error for the sake of speed and sure success, so that only the most obvious paths are taken. No consideration of alternate routes is given. Vicarious trial and error is given up.

The third thing that is given up is the ability to be generic. General principles are forgotten. Information picked up in one field that might be very useful in the present case cannot be transferred.

The fourth price is associated with the redundancy present in the information available to the problem solver. Either one of two extremes can occur. The highly motivated person can either make excessive use of the redundancy, make snap judgments because he believes that there is more information present than there really is, or else become highly literal and refuse to use even the information present. You have probably noticed that some of the effects of overmotivation should be classed as perceptual blocks. This is not unusual, for the emotions have considerable influence over our physical health as well as our mental health. They influence the way in which we receive information as well as affecting the way in which we react to others.

Dr. Dana Farnsworth, former head of the medical department at M.I.T., summed up a paper that he delivered to my group on the emotional blocks to creative activity in this fashion:

"So the creative thinker, or the one who is trying to be a creative thinker, is the one who can go back into the wellsprings of his own existence, who can understand himself, see what these motives are, who can accept himself for what he is, who can recognize when he is becoming fearful, angry, jealous, suspicious, or what have you, and then direct all his energies over into the daring side of things. When he has learned that technique, then he is in a position to learn to be creative."

Levels of Creative Activity

I have already indicated that I believe there are various levels of creative activity. These levels can be distinguished on the basis of the complexity of the problem itself, on the basis of the value the solution has for society, or on the basis of the types of approach used in arriving at a creative solution. I prefer the last method, primarily because it is the simplest of the three and it avoids the problems associated with making value judgments. I make two general classes of creative activity: the "organized" approach and the "inspired" approach. The "organized" classification is a step-by-step building-block type of activity. One starts with a given problem or need-area, and then gradually, little by little, makes improvements. This process continues until finances or time call a halt. The "inspired" approach is quite the opposite. It starts by dreaming the biggest dream possible, thinking the biggest thought possible, and then devoting all of one's energies to making that dream come true. It is a much more difficult approach, but it results in much greater progress.

Organized Approach

The "organized" approach probably accounts for the great majority of creative industrial work. It is probably the only way in which teams can operate efficiently and without too much friction, unless they have an outstanding leader. It is also the easiest kind of approach to teach, for there are any number of tricks or aids that make for greater productiveness. Alex Osborn lists many of them in his latest book, "Applied Imagination." His most important and successful contribution is probably that of "brain storming" – group activity in idea formation. The procedure is relatively simple, yet

very effective. Groups of from 5 to 10, operating with a leader and recorder and with a very simple set of rules, can, in an hour or two, come up with an amazingly long list of ideas on almost any conceivable problem. Some of Osborn's rules are:

"1. *Judicial judgment is ruled out.* Criticism of ideas must be withheld until later.

"2. *Free wheeling is welcomed.* The wilder the idea, the better; it is easier to tame down than to think up.

"3. *Quantity is wanted.* The greater the number of ideas, the more likelihood of winners.

"4. *Combinations and improvements are sought.* In addition to producing ideas of their own, participants should suggest how ideas of others can be turned into better ideas or how two or more ideas can be joined into still another idea."

Osborn suggests that care be used in selecting the topics used for brain storming, and recommends that precisely stated and well-defined problems having a relatively narrow goal be used, so that all members of the group can aim their ideas at one target. This is an important warning, and should be heeded by inexperienced or heterogeneous groups. I have, however, seen some unusual groups handle, and very effectively too, problems of very broad scope.

Within the organized approach to creative activity, there are two extremes. One is called the Baconian or Edisonian approach, in which one systematically tries every conceivable combination until the most satisfactory one is found; the other is called the Aristotlean method, and is typified by more vicarious trial and error and a limited amount of physical experimentation. More time is devoted to hypothesis formation in this last method, and it is so close to the inspired type of approach that it is very difficult to draw a boundary line between them. Most men follow combinations of these two extremes, although a few are archtypes of the limits. Rare individuals like the late Thomas Midgley, Jr., can operate efficiently at either extreme. His development of tetraethyllead is a typical example of the Edisonian method, while his research leading to the use of fluorinated hydrocarbons as safe refrigerants was accomplished in three days by means of his creative imagination, careful analysis, the observation of the periodic table, and a minimum of experimentation.

Product Improvement

In our creative engineering work at M.I.T., we use product design as the vehicle for demonstrating the various techniques of the creative process. We believe that product improvement can be carried out in four major areas:

1. Increased function.
2. Higher performance level.
3. Lower cost.
4. Greater salability.

Increased function is making the product do more things than it did before, or satisfying the original need by an entirely new approach. Higher performance level includes all of the improvements that result in longer life, greater efficiency, increased accuracy, easier maintenance and repair, more convenient and safer operation, and so forth. Design for lower cost involves selection of cheaper materials and manufacturing methods, elimination of unnecessary parts, design for subassemblies, and eventual automatic manufacture. The area of increased salability includes all of the design activity associated with improved appearance and market surveys and consumer analysis.

Lack of Activity on Increased Function

As I travel over the country and work with various industries, I am amazed at the lack of design activity in the area of increased function. Group after group that I have visited has admitted that the great majority of its "creative activity" was in the field of higher performance level, and usually at the expense of higher cost. In certain industries, design for greater salability got equal, if not greater, attention. The automobile industry is, I believe, a typical example. "Designed for obsolescence" is the battle cry. A large share of American industry today is devoting the major portion of its research and development time to the improvement of functional change conceived by its founders. When new ideas do crop up in these industries, they are frequently the result of suggestions or purchases from the outside. One large company was greatly concerned over the fact that they had what they considered to be an ideal research and engineering group, almost 3000 strong. Yet very few new functional changes were being made. At the same time, they were being pressed by small companies formed by energetic and imaginative young men who were coming out with new approaches that threatened to make their equipment obsolete. Their only recourse was to buy up these outsiders.

Why should this condition prevail, and what can be done to change it? Changes can be and must be made in our educational methods so that imagination and curiosity will be fostered rather than stifled; so that the schools of higher education can turn out more young people excelling in the creative process. Emphasis must be placed on the integrity and dignity of each individual. He must not extend into the realm of ideas the mass method technique which is so useful in industry. John Steinbeck has said that:

"It is true that two men can lift a bigger stone than one man. A group can manufacture automobiles quicker and better than one man, and bread from a huge factory is cheaper and more uniform" . . . but that it does not follow that two men can

write a better poem than one man, or that two men can paint a better picture than one man, or that a group can invent a better machine than one man.

I am a firm believer that the only creative tool man has is the "individual" mind and spirit of a man. Individuals and groups can and do exercise the creative process, and the group is frequently a wonderful stimulus to imaginative thinking. But the group is not the creative unit; it is the individual in the group.

Proper Environment Needed

Even if schools are highly successful in turning out the creative engineers and so on, management must then provide the proper environment so that the creative process can flourish. Management's responsibility to its creative personnel is to stimulate, encourage, assist, recognize, and reward their creative efforts. Unfortunately, little information is known that is useful in these areas. What little is available is quite contradictory or poorly validated. The ways in which management can meet its responsibilities require a great deal of research work, some of which we are trying to do in our Creative Engineering Laboratory. Many other schools are carrying out similar projects. A number of industries are making valuable contributions in this field. The work that GMC's AC Spark Plug Division is doing to implement all five of the above responsibilities should be singled out for special praise. I sincerely hope that more industrial groups will become interested in this same problem, and if they are not equipped to do the work themselves, I hope that they will financially assist educational groups to do the job for them.

Conclusion

In conclusion, let me summarize the points that I have talked about and make one additional point. I have defined the creative problem and the creative process, and have tried to show the difference between them. Creative problems are primarily multisolutional, and they can be solved, although not preferably so, by noncreative processes. The creative process is one which combines existing information into new patterns that did not previously exist, and that better solve some expressed or implied need of man. I have outlined briefly some of the factors that seem to be essential to the creative individual and, what is more important, have indicated that I firmly believe these factors to be trainable. I have mentioned the areas in which inhibiting blocks occur, and I have frequently found that the mere mention of some of these blocks is sufficient to release their hold on the creative person. This is, of course, not true of all. For some are deeply ingrained negative habits that can only be erased by substituting properly oriented positive ones in their place.

I have sketched some of the ways in which the creative person works, and have indicated that the establishment of a higher creative level in American industry is a joint responsibility of education and industry.

Now for the last point. I did not discuss to any extent the inspired approach to creative activity. A great deal could be said about it, just as all the topics I have mentioned could be greatly expanded. I believe, however, that a culmination of the inspired approach lies in what I call the comprehensive designer. This term was first used by R. Buxminister Fuller, who describes this individual as "the emerging synthesis of artist, inventor, mechanic, objective economist, and evolutionary strategist." I like to define him by listing the five attributes or qualities that he must possess.

First, the comprehensive designer must be motivated by very broad concepts of human thought and behavior. These concepts are not local or even national in scope, but worldwide. He should be concerned by the fact that two-thirds of the world's population is constantly hungry; that 80% of the world copper supply is utilized by 8% of the world's population; and that 100% of the world's logistics, as Bucky Fuller points out, are grown, mined, modified, and transported by 100% of the world's population, but wind up to increase the comfort and enjoyment of only 25%.

Second, the comprehensive designer must have complete knowledge of the people for whom he is designing and the total environment in which his product must be manufactured, sold, and operated. The new field of human engineering, or the application of psychology to design, must be encouraged.

Third, he must be articulate in all types and levels of communication. The types I refer to are the languages of the written and spoken word, the language of symbolic logic, and the language of vision. In order to conceive, record, and transmit his ideas, he should be able to use all three of these languages equally well, always using the most efficient one for the communication problem on hand. The levels of communication refer to the interchange of information that takes place, first, within man himself; second, between man and man; third, between man and machine; and fourth, between machine and machine.

The fourth attribute of the comprehensive designer is that he be able to maintain a delicate balance between his ability to analyze, synthesize, and evaluate.

Fifth, and last, he must be thoroughly familiar with, and a past master in the use of, the creative process.

It is probably very obvious that the person I have described is a rather rare one in our society. We probably don't need a great many of these men, but let's hope we get some.

High-Temperature Problems Associated with the Use

HIGH-temperature-resistant rubber is desperately needed for tomorrow's aircraft. It has been estimated that an airplane flying at 15,000 ft above sea level at a speed of Mach 2.5 will develop a skin temperature of 600 F. Add to this aerodynamic heating the heat developed by an engine powerful enough to propel the airplane at Mach 2.5, plus the heat rejection of other power dissipating systems such as the hydraulic system, and it is obvious that the aircraft of the future will not have many cool spots.

It is an unfortunate fact that materials deteriorate at elevated temperatures. This is particularly so for organic materials like rubber, for which each 10 C increase in temperature approximately doubles the reaction rates of the chemical processes responsible for degradation and loss of useful properties.

NATURAL and synthetic rubbers of several types are described briefly, together with their suitability for use in modern aircraft under conditions of exposure to high temperature. Application of the several rubber compounds for aircraft components, as affected by strength considerations, stress cycle, exposure to fuels, oils, hydraulic fluids, and hot gases is discussed.

The author lucidly states that to achieve speeds of the order of Mach 2.5, either a rubber suitable for service at around 600 F must be developed in the very near future, or aircraft designers shall face the possibility of having to eliminate rubber in aircraft components.

It is the purpose of this paper to explore in a general fashion the effect of heat on rubber. Specific topics of discussion will include a description of rubbers in general use, high-temperature effects on rubber, high-temperature test methods, new high-temperature rubbers, rubber components, and finally, the outlook for the future. Before considering specific rubber problems, however, it is worth while to review briefly some basic facts pertinent to rubber technology.

Chemically speaking, vulcanized rubber consists of flexible long-chain molecules tied together at a few points by cross-links. Physically, three properties define a rubber:

1. Large deformation is possible, followed by nearly complete recovery of original dimensions when the deforming force is removed.

2. Low initial modulus, which at first decreases and then increases up to several hundred times its initial value, is apparent during extension.

3. The elastic modulus, over a long range of extension, changes rapidly with absolute temperature.

These three physical properties, collectively known as elasticity but not to be confused with elasticity of metals, are so different from those encountered in other systems, that is, gases, liquids, and crystals, that rubber is now considered a separate and distinct state of matter. The designer con-

# of Rubber in Aircraft

Frederick E. Clark, North American Aviation, Inc.

This paper was presented at the Aircraft Research Seminar held by the SAE Southern California Section at the University of California, Los Angeles, Dec. 7, 1954.

sciously or unconsciously thinks of elasticity when he specifies an aircraft part to be made of rubber.

The energy-storing capacity of rubber, which is associated with its elasticity, as compared to a few common structural materials is shown in Table 1. The ability to absorb tremendous energy places rubber in a unique position.

Rubbers in General Use

There are six classes of rubber widely used in aircraft: (1) natural, (2) neoprene, (3) buna N, (4) Thiokol, (5) butyl, and (6) silicone. Each class has one or more outstanding properties which makes it desirable for a specific application. The chemical structures of these polymers are given in Table 2 and described briefly as follows:

1. Natural rubber: Natural rubber is a polymer of isoprene and is vulcanized, or cross-linked, by sulfur, which reacts at a few of the double bonds of adjacent chains. Natural rubber has the best combination of physical properties of available rubbers. However, it has poor resistance to oils, weathering, ozone, and cannot be used at high temperatures.

2. Neoprene: Neoprene is a polymer of 2-chloro butadiene. The polymer is vulcanized by basic metallic oxides such as magnesium oxide which react with a few of the chlorine atoms rather than at the double bonds. Neoprene has good resistance to ozone, sunlight and weathering, and fair resistance to oils. It has good mechanical properties and it is the nearest to natural rubber of any of the synthetics. The useful temperature range is from — 50 to 250 F, although certain compounds can be plasticized to –65 F.

3. Buna N: Buna N is a copolymer of butadiene and acrylonitrile. The acrylonitrile content of commercial compounds varies between 18 and 45% approximately. Oil resistance and heat resistance are roughly proportional to the acrylonitrile content, whereas low-temperature flexibility is adversely affected by increasing the acrylonitrile portion of the polymer. Buna N is commonly vulcanized with sulfur and in this respect is similar to natural rubber. The most important characteristic of buna N rubber is its resistance to oils and other solvents. It has good abrasion and age resistance characteristics, but is greatly inferior to natural rubber in resilience and heat buildup. Buna N has rather mediocre ozone resistance and for this reason it is not advisable to use it for access door and other external seals. Properly compounded stocks may be used in oil from —65 to 350 F, but resis-

Table 1 – Energy-Storing Capacity

	Energy, ft-lb per lb
Gray Cast Iron	0.37
Extra Soft Steel	3.07
Phosphor Bronze	4.08
Rolled Aluminum	7.56
Hardened and Tempered Spring Steel	95.30
Hickory Wood	122.50
Vulcanized Rubber	14,600.00

Table 2 – Chemical Structure of Commercial Rubbers

	Segment
Natural Rubber	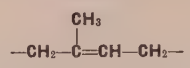
Neoprene	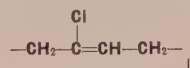
Buna N	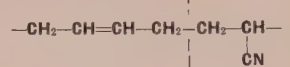
Thiokol FA	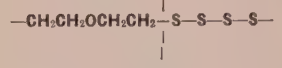
Butyl	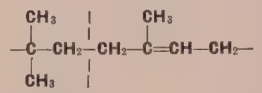
Silicone	

tance to both temperature extremes is not available in the same compound.

4. Thiokol: Thiokol rubber is made by condensation of an organic dichloride with sodium polysulfide. Ethylene dichloride was used in producing the first Thiokol, appropriately called Thiokol A. Thiokol rubber is vulcanized with oxidizing agents such as lead peroxide, zinc oxide, or p-quinone dioxime (GMF). Thiokol has excellent resistance to oils, solvents, and aromatic fuels, and good resistance to weathering and ozone. It is a thermoplastic and softens at moderate temperatures. Physical properties are quite low and resistance to cold flow is poor at all temperatures.

5. Butyl: Butyl rubber is a copolymer of isobutylene and just enough isoprene to permit vulcanization. The ratio of isobutylene to isoprene is usually 97 to 3. Vulcanization is accomplished with either sulfur or an oxidizing agent such as p-quinone dioxime (GMF). Because the vulcanizate is completely saturated, it is unusually resistant to weathering and ozone, and is approximately ten times as impermeable to gases as natural rubber. Butyl rubber is not ordinarily considered an oil-resistant rubber, but it has better resistance to phosphate ester fluids (Skydrol) than most other rubbers. It can be compounded to have good mechanical properties with the exception of resilience and creep characteristics. Butyl rubber can be used over the temperature range —65 to 225 F.

6. Silicone: Silicone rubber is relatively a newcomer to the family of synthetic elastomers and its possibilities have not been fully explored. It is basically a dimethyl silicone polymer with a small percentage of phenyl branches included for low-temperature flexibility. Since silicone appears in the chain, silicone rubber cannot be classed as an organic rubber. On the other hand, silicone rubber is not strictly an inorganic polymer because the chain branches are organic. The rubber is vulcanized by benzoyl peroxide and requires a long after-cure of 24 hr at 480 F in an open oven to free the polymer of benzoic acid, an undesirable reaction product. The most interesting feature of silicone rubber is the wide temperature range over which it retains its rubbery properties, that is, from —100 to 500 F. Silicone rubber is almost completely resistant to weathering and ozone. It has poor oil and solvent resistance except in low swell fluids. In general, silicone rubber rates poor in tensile strength, tear resistance, abrasion resistance, and resilience. High-pressure steam hydrolyzes silicone rubber to a low molecular weight polymer.

The properties of the rubbers discussed above are summarized in Table 3 and typical physical properties are shown in Table 4.

High-Temperature Effects on Rubber

Deterioration of rubber by heat is an oxidation phenomenon, for all practical purposes. The mechanism of oxidation is complex and has not been fully explained. Physically, there is a reduction in chain length, or chain scission, and an increase in cross-linking. Chain scission leads to a softening of the polymer while increased cross-linking causes hardening and loss of flexibility. Both effects occur simultaneously, but not necessarily at the same rate. Either chain scission or cross-linking, if carried far enough, results in loss of all useful proper-

Table 3 – Property Relation of Natural and Synthetic Rubbers

	Natural Rubber	Neoprene	Thiokol	Buna N	Butyl	Silicone
Resistance to Lubricating Oil	Poor	Good	Excellent	Excellent	Poor	Poor-fair
Resistance to Aromatic Hydrocarbons	Poor	Poor	Good	Fair	Poor	Poor
Resistance to Diester Lubricants	Poor	Fair	Excellent	Good	.....	Fair
Resistance to Silicate Esters	Poor	Fair	.....	Fair-good	.....	Poor
Gas Diffusion	Fair	Good	Excellent	Good	Excellent	Fair
Electrical Properties	Good	Fair	Fair	Fair	Fair	Fair
Tensile Strength	Excellent	Good	Poor	Excellent	Fair	Poor
Elongation	Excellent	Excellent	Fair	Excellent	Excellent	Poor
Rebound Elasticity	Excellent	Good	Good	Fair	Poor	Poor
Abrasion Resistance	Excellent	Good	Poor	Excellent	Fair	Poor
Tear Resistance	Excellent	Good	Poor	Good	Good	Poor
Flame Resistance	Poor	Good	Poor	Poor	Poor	Fair
Aging Resistance	Fair	Good	Good	Good	Good	Excellent
Ozone Resistance	Poor	Fair-good	Good	Fair	Good	Excellent
Temperature Range, F	—65 to 200	—50 to 250	—50 to 250 —65 to 200	—40 to 350 —65 to 300	—65 to 225	—100 to 500
Approximate Specific Gravity	0.93	1.25	1.35	1.00	0.91	1.2 to 2.6

ties. Chain scission predominates with natural rubber compounds, whereas cross-linking predominates with most synthetic rubber compounds.

Rubber will still deteriorate in the complete absence of air, but at a considerably higher temperature since enough energy must be supplied to rupture the C-C bond or, in the case of Thiokol and silicone rubber, the S-S and the Si-O bonds, respectively.

Antioxidants inhibit the oxidation of rubber for relatively long periods of time at moderate temperatures. No antioxidant has been found which is effective above approximately 300 F.

Immersion in oil, unless the oil specifically attacks and swells the rubber, is beneficial in that it limits the access of oxygen. In addition, rubber is plasticized by the oil and tends to retain its low-temperature properties for a longer period than an equally cross-linked polymer which has been aged in air.

The application of stress accelerates the heat-aging of rubber. Any strain on the rubber molecules, whether from tension, compression, or shear, makes the rubber more subject to chemical attack. Dynamic loading in the form of rapid flexing is much more deleterious than static loading because it introduces the factor of hysteresis or heat build-up, and inasmuch as rubber is a poor conductor, it cannot dissipate the additional heat developed.

The considerations above lead to the conclusion that it is impossible to predict on the basis of physical properties alone how long a given rubber will last in a given application. Each application must be tested under conditions simulating as nearly as possible the conditions prevailing in service.

High-Temperature Test Methods

In casually inspecting the rubber literature, one is confronted by the lack of reliable high-temperature test data for both standard commercial rubbers and newer rubbers which were developed specifically for use at elevated temperatures.

Almost without exception, the data available were obtained at room temperature after an exposure period at elevated temperature. This kind of information is useful in showing how fast rubber deteriorates but it doesn't indicate whether or not the rubber should have been used at high temperature in the first place. Measurements should be made at the temperature at which the material is expected to be used. Table 5 illustrates how rapidly tensile strength and elongation decrease from room-temperature values with an increase in temperature to 200 F. Other properties decrease proportionately.

Another testing factor which needs standardization is the amount of oxygen which is permitted to contact the rubber during oil-aging. It is pointed out in the discussion on high-temperature effects that oxygen is the most important contributor to deterioration. Some investigators have used tightly sealed containers while others obtained radically different results with loosely sealed or open containers. Limited ingress of air most closely simulates most aircraft applications involving oil-resistant rubber.

Table 4 – Physical Properties of Typical Channel Black Stocks

	Hardness Shore A	Tensile Strength, psi	Elongation, %	Tear Resistance, lb per in.	Heat Buildup[a]
Natural Rubber	20–100	3500–4500	550–650	650	100
Neoprene	20–90	3000–3500	500–600	450	90
Butyl	15–75	2500–3000	650–850	400	60
Buna N, H.A.	20–100	4000–4500	500–650	300	75
Buna N, L.A.	20–100	3000–3500	450–600	300	75
Thiokol	25–80	1300–1700	600–700	250	70
Silicone[b]	40–90	400–800	50–300	25–100	.....

[a] Percentage rating based on temperature rise.
[b] Gum stocks.

Table 5 – Retention of Physical Properties of Typical Channel Black Stocks at 200 F

	Tensile Strength, % of room temperature value	Elongation, % of room temperature value	Resilience, % of room temperature value
Natural Rubber	65	110	100
Neoprene	40	70	110
Butyl	40	120	65
Buna N, H.A.	25	65	85
Buna N, L.A.	33	65	90
Thiokol FA	33	65	85

New High-Temperature Rubbers

Several new rubbers or flexible plastics have appeared on the market very recently which definitely are of interest from a high-temperature standpoint. Among these may be mentioned new silicone rubbers, polyacrylate rubber, poly FBA rubber, Kel-F elastomer, Teflon, and Kel-F plastics. Structural formulas are shown in Table 6.

New Silicones – A modified silicone rubber appears to have much better resistance to MIL-O-5606 hydraulic fluid than previous silicones. Resistance to other fluids and temperature is being investigated at present.

Another new silicone rubber, X-96, is reported to have excellent compression set characteristics at 350 F (15% after 22 hr). This rubber can be vulcanized in thick sections without porosity with di-tertiary-butyl peroxide.

Two companies are producing silicone rubbers which can be vulcanized with sulfur instead of benzoyl peroxide. These silicones can be mixed with organic rubber; that is, buna N, and as such it would be expected that the mixture would extend the useful temperature range of buna N with some sacrifice in physical properties and oil resistance.

A high-tensile-strength silicone rubber, COHR-lastic HT, is on the market. Tensile strengths of 1000-2000 psi are obtained by reinforcing with a finely divided silica. Tear strength is increased proportionately. However, the upper temperature

limit appears to be approximately 350 F and compression set is high (25% at 212 F).

Polyacrylate – Polyacrylate rubber (Hycar 4021) has been known for several years but was not used extensively until very recently. It is basically a polymer of ethyl acrylate and is usually vulcanized with an amine (triethylene tetramine).

Polyacrylate rubber is resistant to hot oils of low aniline point and dry air up to 350 F. Resistance to flex cracking, oxidation, ozone, and sunlight is good. Compression set, cold flow, water resistance, and resistance to high aniline point oils are poor. The brittle point of polyacrylate rubber is about 0 F.

Poly FBA – Poly 1, 1 – dihydroperfluoro butyl acrylate, better known as poly FBA, is quite similar to polyacrylate rubber except that most of the hydrogen atoms are replaced by fluorine atoms. Poly FBA is much more oil resistant than polyacrylate rubber but the useful temperature range is the same, from 0 to 350 F. Poly FBA has excellent resistance to the di-2-ethyl hexyl sebacate type of lubricating oils. Physical properties are rather low, however. At present poly FBA is available in small quantities only.

Kel-F Elastomer – Kel-F elastomer is the most promising rubber for high-temperature use which has been developed to date. It is stated to be a saturated copolymer of chlorotrifluoroethylene containing more than 50% fluorine. The other ingredient has not been revealed. Vulcanization is carried out with benzoyl peroxide, polyamines, or diisocyanates. Excellent physical properties with the exception of compression set are obtained. Kel-F elastomer is outstanding for its resistance to heat, solvents, chemicals, ozone, and weathering. The high-temperature resistance of Kel-F elastomer approaches that of silicone rubber. It resists white fuming nitric acid for weeks. Strangely enough,

Table 6 – Chemical Structure of High-Temperature Rubbers

	Segment
Polyacrylate	$-CH_2CH-$ $\quad\quad\quad

Kel-F elastomer is soluble in ketones, esters, and cyclic ethers and for this reason it cannot be used with synthetic diester lubricating oils.

The brittle point of Kel-F elastomer is —60 F, but it becomes very stiff at temperatures below 20 F. However, for many applications where rapid flexing is not required, it should be possible to use the rubber down to temperatures approaching the brittle point.

Kel-F elastomer has been made in experimental quantities only up to the present time. It is expected that a large pilot plant will go into operation in the spring of 1955.

Teflon and Kel-F – Teflon is a polymer of tetrafluoroethylene and Kel-F is a polymer of monochlorotrifluoroethylene. Teflon and Kel-F are not rubbers in the sense that they can be vulcanized. However, in thin sections, they possess considerable flexibility and for this reason they show great promise as high-temperature hose liners. Both polymers are completely resistant to nearly all chemicals, oils, and solvents. Teflon is preferable to Kel-F because it is thermally stable from below —100 to 550 F. Cold flow of Teflon has been a real problem at temperatures above 275 F, but one manufacturer appears to have had considerable success in solving this problem. More will be mentioned about the cold flow of Teflon in the section on flexible hose.

The effect of aging in air on the tensile strength and elongation of several high-temperature rubbers is shown in Figs. 1 and 2. A few data on oil resistance are listed in Table 7.

Rubber Components

This section will deal with the application of high-temperature rubbers to specific rubber components. The treatment intended is illustrative rather than exhaustive.

Tires and Tubes – Present-day high-speed landings demand a high-strength tire with low hysteresis. Qualification testing is carried out simulating landing speeds of 200 mph. To date, natural rubber reinforced with nylon plies is the only rubber available for tires with the necessary combination of high physical properties and low hysteresis. Tubes are usually constructed of natural rubber also, although butyl rubber has been used to some extent because of its superior air retention properties. As long as aircraft continue to use tires, it appears necessary to cool the landing gear area to 200 F or less in order to prevent premature failures.

Fuel Cells – Fuel cells are constructed of buna N rubber reinforced with nylon fabric. Until the present time the fuel system has been regarded as a large heat sink which could be depended upon to cool other systems but remain cool itself. Now, however, because of increased speed and cooling demands, it is expected that the temperature of the fuel system will reach 400 F within the next few years.

Present buna N fuel cells are expected to be satisfactory to 250 F. With improved compounding it should be possible to construct a buna N fuel cell which will function at 300 F. Above 300 F it will be necessary to use a new combination of materials. An interesting possible combination is Kel-F elastomer reinforced with glass fabric.

There is a trend toward replacing fuel cells with integral fuel tanks to make it possible to carry more fuel per plane. As far as high-temperature service is concerned, this merely exchanges one set of difficult problems for another.

Flexible Hose – Flexible hose is used to convey fuel, oil, hydraulic fluid, air, and oxygen under pressures ranging from a few psi to as high as 3000 psi.

Oxygen hose does not present any particular problem since it is used in the cockpit area which must be kept cool for obvious reasons.

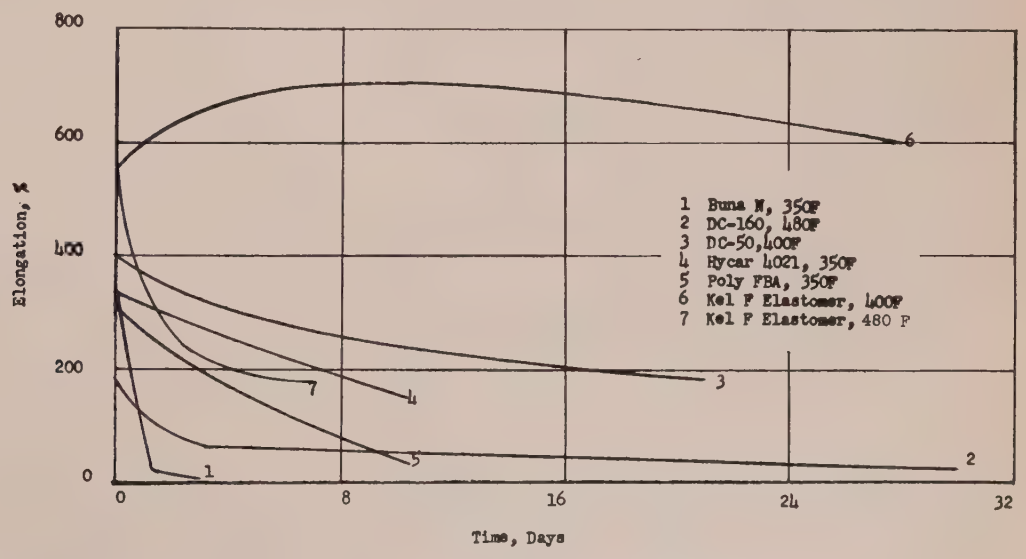

Fig. 2 – Variation of elongation with time of air aging at elevated temperatures for several types of rubber

Present fuel and oil hose (buna N and neoprene) is satisfactory to about 275 F, although the life at 275 F is considerably reduced over the life at 160 F. Neoprene hose cannot be used with some of the new synthetic lubricating oils and hydraulic fluids. Teflon-lined, stainless-steel wire-braided hose appears satisfactory over the range —100 to 450 F and will probably replace rubber hose at higher temperatures. Teflon hose is somewhat stiffer than rubber hose when installed, but it doesn't stiffen with age as does rubber hose. The manufacturer has apparently solved the cold-flow problem with Teflon because the hose seldom fails at the end fittings. Hose is available to withstand a working pressure of 1000 psi, and a 3000-psi hose is in the process of development.

Ducting – Flexible ducting is used to convey hot gases about the airplane. Silicone impregnated glass cloth has been used from —100 to 550 F with considerable success. Incidental contact with oil and fuel has created problems and it is hoped that a more oil-resistant silicone rubber will be available soon. Glass cloth impregnated with Teflon may be an answer to the question of occasional oil contact.

Seals – A wide variety of seals is used throughout the airplane to seal against oil, fuel, air, oxygen, dust, and moisture, the two common types being O-rings and bulb seals.

O-rings are used to seal both moving and static parts. O-rings used to seal high-pressure systems of 1500 to 3000 psi are supported by Teflon backup rings.

Silicone O-rings are used to seal air to 500 F, although the seal may not be perfect above 400 F because of high compression set.

Buna N hydraulic O-rings are satisfactory to 275 F. O-rings are needed which will resist silicate ester hydraulic fluids to 400 F. Although poly FBA rubber is resistant to silicate ester fluids, cyclic tests have shown that it does not have the necessary physical properties at 400 F to be considered for dynamic seals. One difficulty in testing O-rings at high temperature has been that the Teflon backup rings usually fail before the O-rings. Metal backup rings are being considered as a replacement for Teflon backup rings. Kel-F elastomer has not been tested in silicate ester fluid as yet.

Buna N O-rings are satisfactory fuel seals to about 225 F. Kel-F elastomer appears promising for this application at high temperatures.

Special buna N O-rings have been developed which seal MIL-L-7808 diester lubricating oil to 350 F. Poly FBA, which has excellent resistance to this fluid, can possibly serve as a static seal to 400 F.

Bulb or P-section seals are formed from extruded rubber, fabric-covered extrusions, rubber impregnated fabric, and other combinations. Each bulb seal application is a specific problem and cannot be generalized. The use of high-temperature resistant rubber will extend the range over which bulb seals may be used.

Sealants – Sealants are required to seal off openings to air, oil, fuel, moisture, and hydraulic fluid. Physical property requirements are low, but since sealants are frequently applied in inaccessible areas they are expected to last the lifetime of the airplane. They should be easily spread and it should be possible to vulcanize them at room temperature or slightly above. A sealant based on Thiokol rubber has been the most popular to date. Small quantities of a polyacrylate sealant are being used at elevated temperature. It should be possible to adapt Kel-F elastomer as a sealant. Suitable test conditions for a high-temperature sealant have been recommended as 100 hr at 500 F followed by 2300 hr at 400 F.

Miscellaneous – High-temperature resistant rubber is needed for numerous other aircraft applications not previously mentioned, such as rain-erosion resistant coatings, electrical insulation, vibration absorbers, cements, valve seats, and gaskets.

Outlook for the Future

The rubber industry has come a long way toward developing a high-temperature rubber. Today, rubber is used at temperatures which are above the accelerated aging temperatures of ten years ago. However, much more must be accomplished. Efforts must be doubled and redoubled because time is short. Problems for which there are no readily apparent solutions are crying to be solved. The plane of today and of the near-tomorrow requires an oil-resistant rubber with high physical properties over the range —65 to 400 F. The plane to come certainly will require a rubber to withstand 600 F.

Of the available commercial rubbers, only silicone rubber can be classed as a high-temperature rubber. Greater efforts should be exerted toward improving its physical properties and oil resistance.

More work must be done on Kel-F elastomer, particularly from the standpoint of improving its low-temperature properties. More important, sizable samples of this interesting rubber must be placed in the hands of the fabricators at the earliest opportunity so the details of compounding and processing can be worked out quickly. Other polymers must be synthesized as rapidly as possible in case Kel-F elastomer does not provide the answer.

If it becomes impossible to develop a suitable high-temperature rubber, and design engineers are not successful in eliminating rubber from the airplane, then truly, it may be said that the speed of the airplane will be limited by the rubber it carries.

Acknowledgment

The information contained in this paper was drawn from sources too numerous to mention individually, and include published reports, manufacturers' recommendations, and laboratory reports.

Fatigue and Its Relation to the Mechanical and Metallurgical Properties of Metals

George R. Gohn, Bell Telephone Laboratories, Inc.

This paper was presented at a meeting of Division XX-Shotpeening, of the SAE Iron and Steel Technical Committee, Hot Springs, Va., Sept. 28, 1954.

NO PROBLEM relating to the strength of materials has been studied more extensively than that of fracture by fatigue. Peterson[1] has pointed out that, as early as 1849, fatigue of metals was the subject under discussion at a meeting similar to this held by the Institution of Mechanical Engineers in Birmingham, England. At that time the Institution (then only two years old), was greatly concerned over the deterioration of railway axles which was attributed to a change in the material from a fibrous to a crystalline structure. Today that conclusion is rejected because metallographic and X-ray studies have conclusively revealed that, from the instant of solidification, all metals have a crystalline structure.

[1] See *ASTM Bulletin*, No. 164, February, 1950, pp. 50-53: "Discussions of a Century Ago Concerning Nature of Fatigue, and Review of Some of Subsequent Researches Concerning Mechanism of Fatigue," by R. E. Peterson.

[2] See National Bureau of Standards LC 486 (1937), "Metals Do Not 'Crystallize' under Vibration."

[3] See Proceedings of Institution of Mechanical Engineers, Oct. 24, 1849, pp. 13-21: "Report of General Meeting Held in Birmingham, England."

[4] p. 923, "Webster's New International Dictionary of English Language." Pub. by G. and C. Merriam Co., Springfield, Mass., second edition (unabridged), 1941.

The belief, however, that metals fail from crystallization caused by vibration is a hardy perennial, and as recently as 1937, the National Bureau of Standards found it desirable to issue a letter circular[2] pointing out that metals do not "crystallize" under repeated vibration. A second point to be remembered from that early discussion is that one of the participants, James E. McConnell,[3] stated that all his experience had proved the desirability of maintaining the journals of railway axles as free as possible from sharp, abrupt corners and sudden alterations in diameter and sectional strength in order to obtain satisfactory service life. Such sound advice, if heeded during the intervening years, would have prevented many fatigue failures.

What Is Fatigue

Fatigue is defined by Webster[4] as: "exhaustion of strength from labor, toil, or exertion of any kind." This is not an engineering definition but it does indicate surprisingly well what happens when a structural part or a machine element fails from

A COMPARISON of the fatigue strength of metals with the other mechanical and metallurgical properties shows no precise correlation by which the fatigue strength can be evaluated with sufficient accuracy for engineering use from the more readily determined properties.

It is shown that fatigue is a discrete property of metals which must be established on the basis of independent laboratory tests.

Several theories of the mechanism of fatigue are discussed and an explanation is offered for the beneficial effects of surface treatments such as cold-rolling, shotpeening, and electroplating.

fatigue; namely, the complete loss of strength as the result of a part being worked. In the engineering sense, however, fatigue occurs only as a result of a special type of working called cyclic stressing. The cyclic stress may be applied very slowly, very rapidly, intermittently, or as a stress spectrum which is difficult to reproduce experimentally. These stresses may be caused by either vibration, rotation, reciprocating motion of machine elements, alternate loading and unloading, thermal changes, magneto-striction, or otherwise. Nevertheless, irrespective of the source of cyclic stress, the phenomenon of progressive fracture of metal by means of a crack which is propagated by repeated cycles of stress or strain is called fatigue. This is a discrete property of metals, and despite many attempts to prove otherwise, no one has been able to show a precise correlation between fatigue and any other physical property.

What Causes Fatigue Failure

Fatigue failures are probably due primarily to progressive strain hardening, particularly in areas of high stress-concentration which can arise from material defects, design features, fabrication accidents or surface damage during use. In service, an infinitely small amount of metal usually at or near the surface is subjected to stresses above the fatigue strength of the metal and fails. The volume of metal originally affected at the start of fatigue failure is so small that up to the present time, it has not been detectable by either metallographic examination, X-ray, sonic or ultrasonic methods, dilatometry, loss in stiffness, treatment with magnetic particles, or any other method until after irreparable damage has been done. Bennett,[5] working at the National Bureau of Standards, developed a technique for microscopically detecting the early appearance of circumferential cracks in rotating-beam steel specimens. His technique indicated that cracks could not be detected until their length was at least sufficiently long to cover 6 deg of arc, and that no significant changes in properties could be detected from load-deflection tests on such specimens until the cracks were sufficiently long to cover approximately 60 deg of arc. More recently, Hunter and Fricke[6] have used both the metallographic microscope and the electron microscope to determine the beginning of slip and the point of slip saturation on polished and etched aluminum alloy fatigue specimens. Curves of these values plotted against the log of cycle life are similar to the conventional *S-N* diagrams and there appears to be a definite correlation between the two, although the slip saturation curve tends to become asymptotic at a lower stress value than does the *S-N* curve.

While present test methods will not detect the failure of such an infinitesimal amount of metal which marks the beginning of fatigue, it appears quite plausible to assume that local failure at the submicroscopic level automatically increases the stress at that point. As the stress increases, the crack progresses until the section becomes too weak to withstand the load, after which complete failure occurs. The fatigue failure occurs with little or no deformation and seldom with any warning. The fracture itself is generally transcrystalline and may show two or more distinct zones: first, a smooth area showing concentric or oyster-scale markings starting from a nucleus or stress-raiser, and second, a rougher area which frequently shows bright crystalline facets. There may also be present a discolored area where, under progressive fracture, the two surfaces have rubbed together. In the absence of corrosion, usually only one crack is observed, but where corrosion is a factor, many cracks starting from microscopic corrosion pits are present.

For most metals the frequency of the applied stress has but little effect on fatigue life in the absence of creep or corrosion. However, when one or both of these two factors are present, more cycles-to-failure are usually observed at faster testing speeds because both corrosion and creep are time-dependent functions and their effects are less pronounced at high testing speeds.

Since fatigue failure occurs as a result of extreme stress-concentration, in this respect it resembles the failure of a notched impact bar. The only difference – but a most important one – is that of time. In the fatigue test the specimen will hold

---

[5] See *Journal of Research of National Bureau of Standards*, Vol. 37, No. 2, 1946, pp. 123-139: "Study of Damaging Effect of Fatigue Stressing on SAE X4130 Steel," by J. A. Bennett.

[6] See Proceedings of ASTM, Vol. 54, 1954, pp. 717-736: "Metallographic Aspects of Fatigue Behavior of Aluminum," by M. S. Hunter and W. G. Fricke, Jr.

[7] See Proceedings of ASTM, Vol. 50, 1950, pp. 1071-1081: "Reverting of Hard-Drawn Copper to Soft Condition under Variable Stress," by J. N. Kenyon.

together for a period of time after initiation of the first crack. This time interval may be relatively long or short in the case of fatigue, depending upon the properties of the material, magnitude of the localized stress, and frequency of the stress fluctuation, whereas in the impact test failure takes place almost immediately because of higher stresses and greater stress gradient; thus the impact crack is propagated faster than the fatigue crack. In neither case is there any appreciable deformation nor any warning prior to failure.

While the progressive strain-hardening theory explains many of the phenomena observed in fatigue, there are some which this theory does not explain. Kenyon[7] observed that hard-drawn copper wire subjected to reversed bending stresses in rotating beam fatigue tests developed "islands" of soft copper at the periphery. Polakowski and Palchoudhuri[8] reported a similar softening in cold-worked copper, Grade A (5% tin) bronze, 80-20 cupro-nickel, 2S and 3S aluminum alloys and low carbon-titanium steel rods tested in alternate tension and compression. These investigators have suggested, therefore, that the progressive strain-hardening theory applies only to soft or unworked metals; for cold-worked metals, and by implication, for heat-treated metals, they suggest further that the formation of fatigue cracks is associated with the semiplastic condition developed by the action of alternate strains.

Fatigue is a Statistical Phenomenon

Two recent symposia[9, 10] have shown that fatigue is a statistical phenomenon. At high stresses, that is, in the finite life range, our own tests indicate that the number of cycles-to-failure has a log-normal distribution for any given stress. At lower stresses approaching or corresponding to the infinite life range, the distribution of the number of cycles-to-failure is no longer log-normal, and as yet, the probable nature of the distribution has not been established.

Dislocation Theory

An explanation has been suggested for the mechanism of crack formation in fatigue based upon the recently developed concept of dislocations. Slip, which appears to precede the formation of a fatigue crack, is conceived to take place by the propagation of dislocations. This lattice defect in its simplest form consists of a missing half-plane of atoms in a part of a crystal. Thus, on one side of the slip plane the lattice is compressed so that $n + 1$ atoms are opposite n atoms on the other side. This causes a distortion over a limited distance in the lattice, which distortion can be moved along the slip plane with relative ease, producing microscopic slip. Orowan[11] has shown how the piling up of dislocations against an obstruction – a precipitate particle, for instance – can lead to the formation of a crack perpendicular to the slip plane. The same author has explained how a grouping of dislocations can result in a stress pattern which will tend to open up a crack along the slip plane.

While dislocation theory has not been successful in providing a complete theory of fatigue failure, there is justification for applying it in a somewhat speculative form. Increasing evidence indicates that metals do deform by means of dislocations; therefore any theory of fatigue must take them into account. Indeed, it is possible that only when the behavior of dislocations under cyclic stressing is understood will the theory of fatigue failure be in a satisfactory state.

The importance to the machine designer of a thorough understanding of the behavior of metals subjected to fatigue is indicated by the fact that no less an authority than H. W. Gillett, who died a few years ago, has stated that 90% of all service failures result from fatigue. In England, an extensive survey made by George, Grover, and Chalmers[12] of the Royal Aircraft Establishment indicated that 60-90% of all aircraft failures during World War II could be attributed to fatigue. (The recent failures of the British Comets have likewise been officially attributed to fatigue.) Such fatigue failures originated at positions where there was either an abrupt change in cross-section or a sharp re-entrant angle resulting either from the design of the component or from the method of manufacture, such as unduly rough machining in a region of high stress. In general, they concluded that the most usual cause of fatigue in aircraft was the coincidence of high stress due primarily to stress-concentration and fluctuating or alternating stress. Such stress-concentration may arise from either faulty design resulting from lack of adequate engineering data, inability to analyze stress conditions accurately, or failure to correctly apply engineering data that are available. The latter two are problems for the machine designer to resolve; the former is a problem for the metallurgist and the materials engineer.

Many mechanical properties, including the fatigue characteristics of metals, have been determined and are available to the designer. Some of these properties are constant, while others vary from lot to lot with slight changes in composition,

---

[8] See Proceedings of ASTM, Vol. 54, 1954, pp. 701-716: "Softening of Certain Cold-Worked Metals under Action of Fatigue Loads," by N. H. Polakowski and A. Palchoudhuri.

[9] See ASTM STP 121 (1951), "Symposium on Special Aspects of Fatigue."

[10] See ASTM STP 137 (1952), "Fatigue with Emphasis on Statistical Approach—Part II."

[11] See pp. 188-192: "Ductile Fracture and Fatigue," in "Dislocation in Metals," by J. S. Koehler, F. Seitz, W. T. Read, Jr., W. Shockley, and E. Orowan. Pub. by AIME, New York City, 1954.

[12] See pp. 56-61: "Factors Contributing to Fatigue Failure in Aircraft," by C. W. George, S. F. Grover, and B. Chalmers, in "Failure of Metals by Fatigue," Proceedings of Symposium, University of Melbourne, Melbourne University Press, 1947.

variations in heat-treatment, or amount of cold-working. Those which vary to any extent must be determined for each lot of material; other more constant properties need be determined only occasionally. Unfortunately, those properties which are usually determined during inspection are of little use to designers, while the determination of those properties which are required for sound design involve either precise laboratory equipment and techniques not generally available in the routine inspection laboratory or take long periods of time for their evaluation. The properties normally used for inspection include hardness or tensile strength, elongation or reduction in area, and yield strength. Occasionally, electrical resistivity or conductivity and notch impact strength are also acceptance requirements. Useful engineering properties which are usually determined in the research laboratory include the modulus of elasticity, creep strength and fatigue. Any appraisal of the adequacy of the material for use in engineering design should be made in terms of stress or strain and resistance to stress or deformation. Obviously, hardness, the most commonly used acceptance test, does not meet this criterion. The hardness value, while it may convey useful information about machinability and wear, is not itself directly applicable in design because like tensile strength, it involves deformation far greater than can be permitted in service. Furthermore, hardness cannot be used as a ready means for evaluating fatigue strength because materials may have the same hardness but exhibit widely different fatigue properties (see Figs. 1 and 2).[13, 14]

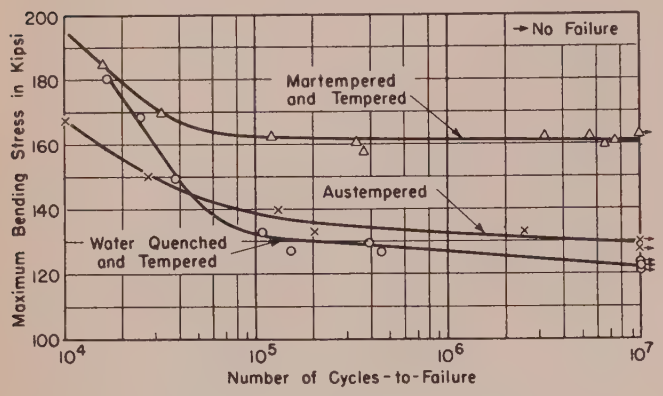

Fig. 1 – *S-N* diagrams for SAE 1095 steel hardened to RC 53[13]

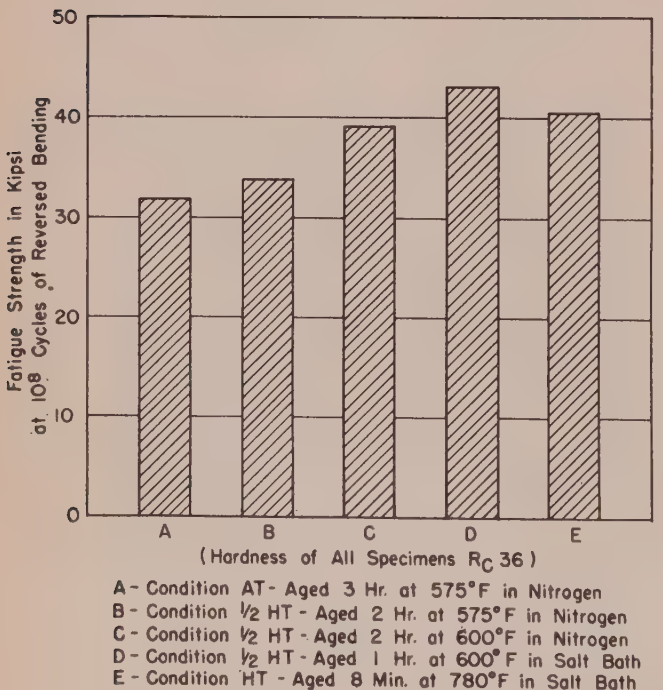

Fig. 2 – Variation in fatigue strength of heat-treated beryllium-copper strip with aging conditions[14]

The tensile strength test, which is the basic acceptance test for practically all metals, is measured in terms of stress, but since it is a measure of failure, it is a value which seldom can be used in design. Complete rupture in engineering applications occurs only in protective devices such as shear pins, fuses, and bursting discs and such things as high explosive shells. Everywhere else the engineer designs for life, not failure.

Tensile Strength versus Fatigue Properties

Because the tensile test is so widely used in the inspection of materials, considerable effort has been made to correlate tensile strength with fatigue properties. For low carbon steels the correlation is fair. In Fig. 3 Bullens[15] has shown graphically that the endurance limits of polished specimens of carbon steel are approximately 50% of the tensile strength up to values of about 180,000 psi, after which the ratio decreases rapidly. However, there is a wide scatter band on both sides of the average line which makes the use of this relationship for intelligent design dangerous. This tensile strength-fatigue relationship also applies only to polished specimens which have had all grinding marks removed by a final longitudinal polishing operation. In the presence of notches the fatigue strength may be much lower, and in the presence of corrosion, a still greater loss in fatigue strength may be anticipated.

Greenall and Gohn[16] in 1937, and, more recently, Burghoff and Blank[17] in 1948, have shown that

---

[13] See *Metal Progress*, Vol. 54, November, 1948, pp. 683-685: "Fatigue Limit of SAE 1095 after Various Heat-Treatments," by A. C. Forsyth and R. P. Carreker.

[14] See Proceedings of ASTM, Vol. 46, 1946, pp. 741-775: "Fatigue Properties of Beryllium-Copper Strip and Their Relation to Other Physical Properties," by G. R. Gohn and S. M. Arnold.

[15] See p. 37 of Vol. 1, "Steel and Its Heat-Treatment," by D. K. Bullens. Pub. by Wiley, New York, 1938.

[16] See Proceedings of ASTM, Vol. 37, 1937, pp. 160-191: "Fatigue Properties of Nonferrous Sheet Metals," by C. H. Greenall and G. R. Gohn.

[17] See Proceedings of ASTM, Vol. 48, 1948, pp. 709-732: "Fatigue Properties of Some Copper and Copper Alloys in Strip Form," by H. L. Burghoff and A. I. Blank.

the bending fatigue strength of as-rolled copper-base alloys in the form of strip varies from as little as 14 to as much as 44% of the ultimate tensile strength for cold-rolled or cold-rolled and annealed materials (Fig. 4). Whereas the tensile strength of these materials could be more than doubled by cold-rolling alloys 8 to 10 numbers hard (60.5-68.0% reduction), the fatigue properties were increased only 30 to 50% by such cold-working. This is also true, in general, for the aluminum alloys in so far as the effect of cold-working is concerned, but in the case of some of the heat-treated aluminum alloys, the improvement in fatigue properties resulting from heat-treatment more nearly approximates the gain in tensile strength. Gohn and Arnold,[14] in studies on beryllium copper, showed that by heat-treatment the tensile strength could be more than doubled while the increase in bending fatigue strength was less than 20%. A similar lack of correlation between fatigue and tensile strength for machined and polished specimens of various nonferrous materials is reported by Anderson, Swan, and Palmer.[18] Thus, while it appears that the fatigue strength is somewhat related to the tensile strength of the material, it would be dangerous from a design standpoint to assume that the fatigue strength can be estimated from the tensile strength.

Elongation and Reduction of Area

Ductility values in the nature of elongation and reduction of area, which are frequently determined during the tensile test, cannot be used in design by the engineer to measure resistance to stress or strain, nor can they be used directly by the manufacturer to evaluate the cold-forming or drawing properties of a material. According to Gillett[19] both are used for what they connote rather than what they state. While elongation or reduction of area cannot be used even indirectly to measure toughness, they do give some idea of the reserve of plasticity available for insurance against shattering fracture in case of accident. Some ductility is beneficial in fatigue because under conditions of repeated stress, local yielding at the base of notches permits a redistribution of stress which may prevent or delay fatigue failure. For example, a hardened steel used as a shaft or bolting material may have a fatigue life no greater than that of a mild steel part because of its increased notch sensitivity. In the case of low ductility materials such as hardened steels, stress-concentration at rough-machined surfaces, re-entrant angles, keyways, and threads, may start microscopic cracks which then develop further until failure results. In the case of parts made from a more ductile material, stress-concentration may result only in local yielding and redistribution of stress. This is particularly evident in redundant, built-up structures such as welded, riveted or bolted assemblies, where the more ductile materials may yield sufficiently to redistribute the stress in the entire structure, whereas high-strength materials of low ductility fail. This point should be kept in mind, particularly in aircraft design where there is an increasing tendency to use light alloys of higher and higher tensile and yield properties gained at the expense of ductility.

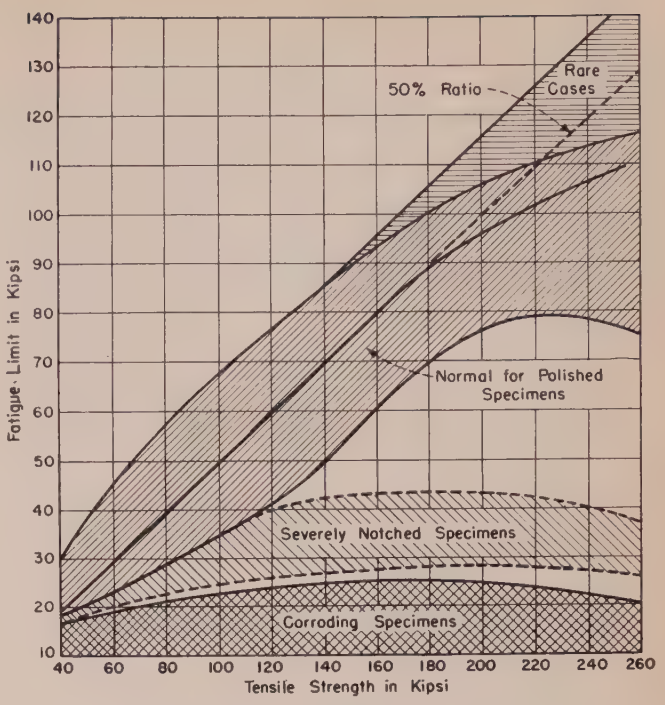

Fig. 3 – Behavior of wrought steel in fatigue[15]

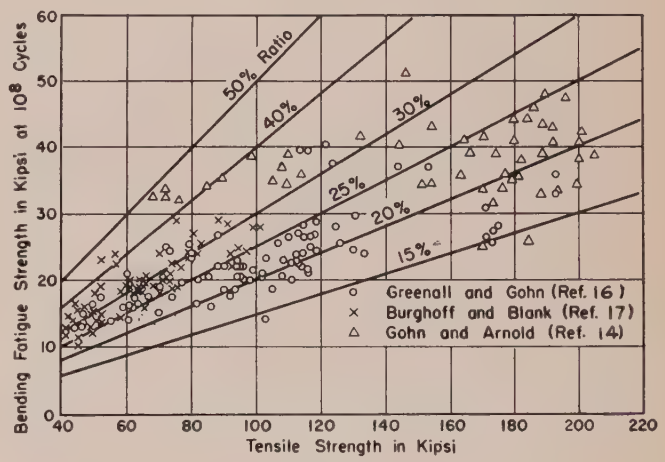

Fig. 4 – Behavior of nonferrous alloys in fatigue

[18] See Proceedings of ASTM, Vol. 46, 1946, pp. 678-690: "Fatigue Tests on Some Additional Copper Alloys," by A. R. Anderson, E. F. Swan, and E. Palmer.

[19] See p. 43, "An Engineering Approach to Selection, Evaluation, and Specification of Metallic Materials," by H. W. Gillett. Pub. by Penton Publishing Co., Cleveland, 1944.

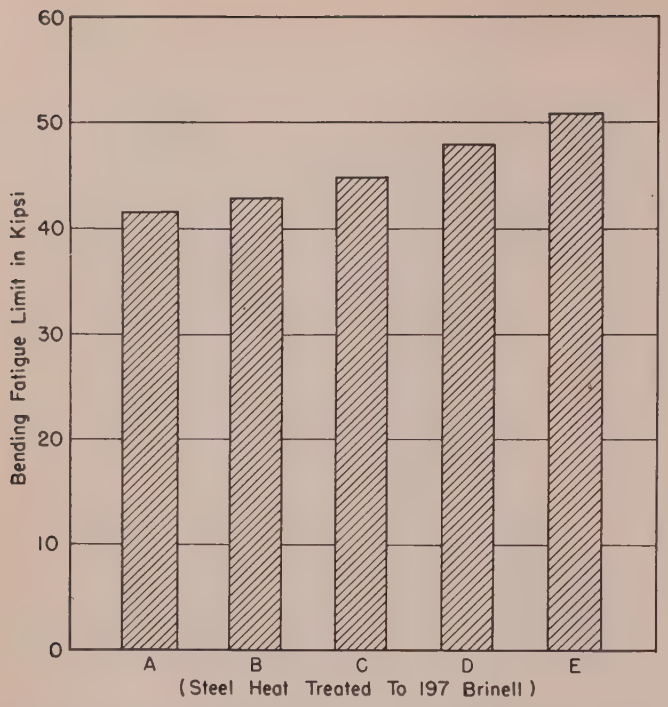

Fig. 5 – Effect of surface finish on fatigue limit of 0.49% carbon steel (data obtained from rotating beam tests). A – Rough turned; B – Smooth turned; C – Ground; D – 00 Emery; E – High polish-longitudinal

In general the primary criterion of load-carrying ability is yield strength, or the maximum stress that can be carried safely by the machine element without any permanent deformation. While this property is frequently determined during inspection, except for mild steels and a few similar materials, this property is an arbitrary value based upon a given offset of the load-strain curve from the extension of the straight-line portion of the curve, or upon a specified total elongation under load. Little work has been done to establish the relationship between the yield strength and fatigue. In his recent Gillett Memorial Lecture, Templin[20] showed that the yield strength of aluminum alloys could be increased from 5000 psi for 2 SO to more than 70,000 psi for 75 ST as a result of alloying, heat-treatment, and cold-working. For the same alloys the fatigue strength increased from 5000 psi to only 24,000 psi—a five-fold increase in fatigue strength compared to a 14-fold increase in yield strength. About all that can be said is that under conditions of completely reversed stress, with few exceptions, the fatigue limit is considerably less than the yield strength, and for conditions of alternating or fluctuating stress superimposed upon a mean stress other than zero, the maximum stress amplitude in the cycle is limited by the yield strength. A similar lack of correlation exists between the elastic limit and the fatigue strength of metals.

Attention has been previously called to the fact that both fatigue and impact failures produce brittle, nonductile fractures. The similarity in the type of fracture might indicate some correlation between these two properties. It should be remembered that the notch brittleness of a material depends upon the geometry of the piece and the restraint this geometry of size and shape imposes upon plastic deformation and upon the ability of the material to deform in a plastic fashion. Furthermore, the fatigue strength generally increases with decreasing temperature, whereas the impact value of many ferrous alloys decreases under similar conditions. It should be observed that cast iron, which has very poor impact strength, not only has fatigue ratios approximating those of some steels of the highest impact strengths, but also exhibits less notch sensitivity than any other ferrous metal. The significance of the impact test itself is still the subject of much controversy and it is doubtful if any correlation can be established between impact and fatigue strength.

Modulus of Elasticity

The modulus of elasticity of the material, which measures the elastic deformation per unit stress, is seldom determined in routine inspection because it is essentially constant for a given class of material and is not subject to control by the metallurgist or the metal manufacturer. While variations in composition, cold-working, or heat-treatment may cause slight variations in modulus, in most cases the values are so nearly constant for any given class of material that previously determined values can be used by the designer to calculate the stiffness of his structure without the introduction of serious errors. For example, the modulus of elasticity of carbon steels and most alloy steels is 29 or 30 million psi; for aluminum alloys, 10.3 million psi; for the magnesium alloys, 6.5 million psi; for brasses and bronzes, about 15 million psi. The modulus values are affected slightly by things such as changes in composition, heat-treatment, and cold-working, but the effect is small compared to the effect of these variables on the fatigue strength. On the other hand, grain direction generally has a far greater effect on the modulus of elasticity than it does on fatigue strength. It has been shown that composition and heat-treatment markedly affect the fatigue properties of steels but not the modulus of elasticity, and that cold-working, composition and, sometimes, heat-treatment affect the fatigue strength of nonferrous alloys without affecting the modulus of elasticity. Hence it would appear that there can be no relation between the modulus of elasticity and the fatigue strength.

Creep and fatigue have been related in some of the work done at the National Advisory Committee

[20] See Proceedings of ASTM, Vol. 54, 1954, pp. 641-699: "Fatigue of Aluminum," by R. L. Templin.

for Aeronautics by Machlin and others. However, the determination of creep properties is a far more time-consuming and critical operation than fatigue testing and it may be said, that at the present time creep properties are not sufficiently well established to permit their use as a basis upon which to estimate fatigue life.

Rather fruitless attempts have also been made to correlate damping capacity with fatigue. However, in the case of structures such as line wire and cable, a high damping capacity may prevent buildup of dangerous stress amplitudes under external forces such as wind or vibration which would lead to premature failure of the structure.

Comparison of fatigue strength with more readily determined mechanical properties of metals indicates that fatigue may not be evaluated except by independent tests upon the materials themselves. The basic fatigue properties of any metal can be portrayed by an *S-N* diagram in which stress, *S*, is plotted against the cycle life, *N*. If the *S-N* curve becomes asymptotic to the cycle axis, the material is said to have a fatigue limit. For most materials this condition is never realized – at least not within a reasonable finite time. In the case of aluminum and magnesium alloys, this limit is not reached even after 500 million cycles. For copper-base alloys the curve is essentially horizontal after 100 to 300 million cycles of repeated stress, although here again, a true fatigue limit is seldom realized. In the case of wrought steels, however, the fatigue limit is approached in conventional tests after about 12 to 20 million cycles, but in corrosive media even these steels show no fatigue limit. Nevertheless, it is well to remember that while few materials have a fatigue limit, they all possess a definite fatigue strength corresponding to a specified cycle life.

Grain Size

Grain size, particularly the grain size in the ready-to-finish anneal, markedly affects fatigue. Higher values of fatigue are usually associated with small grain size material. It should be noted that the effect of grain size on creep is just the opposite. For the latter, best results are obtained with large grain size material. Hence in a structure such as a gas turbine or jet engine, where both creep and fatigue are factors, the optimum grain size must be a compromise.

Work-hardening processes such as cold-rolling, cold-drawing and shotpeening have all been used to increase the fatigue properties of metals, but too heavy reductions or excessive shotpeening may exhaust the ductility of the metal to the point where cracks are formed or where a low stress may start a fatigue crack. While most fatigue cracks start in areas where tensile stresses predominate, torsion fatigue cracks have been known to start in areas where shear stresses predominate, and Moore[21] has shown some rail heads where failure appears to have started in areas where compressive stresses predominated. Nevertheless, it is generally concluded that cold-working is beneficial, particularly so when it induces compressive stresses in areas subjected to fatigue stress.

Since practically all fatigue failures originate at or near the surface, surface finish is bound to have a marked effect on fatigue. The effect of surface finishes used to prepare fatigue specimens for test is shown in Fig. 5. Surface treatments such as anodizing or pickling may also have an adverse effect on fatigue life. This is illustrated in Fig. 6, which shows the effect of various standard surface treatments on the fatigue life of some forged magnesium bars. As shown in Fig. 7, protective finishes, particularly those with high residual tensile stresses, may also affect fatigue life.

The size of the fatigue specimen also affects fatigue life. Moore,[22] in tests on a series of steels, showed that fatigue limits decreased 15-20% as the size of the test specimen increased from ⅛ to about 1 in. in diameter but showed no further decrease up to 2-in. diameter sections. Much larger sections have been shown by Horger[23, 24] and others to have

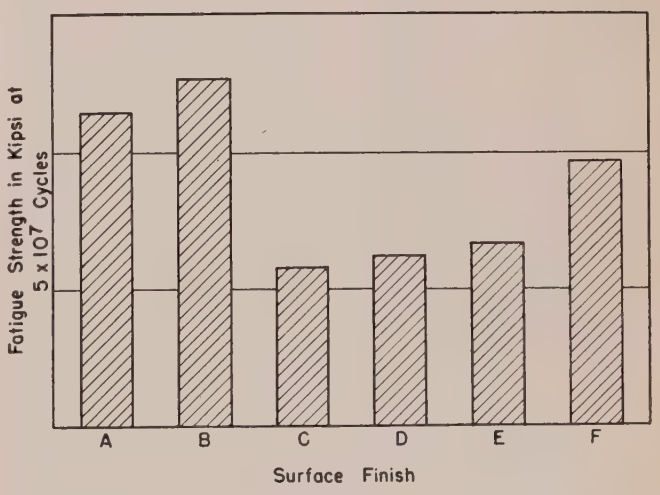

Fig. 6 – Effect of surface finish on fatigue strength of extruded magnesium-alloy bars of following composition: 10% Al, 0.15% Mn, balance Mg. A – Smooth machined; B – Polished; C – Nitric acid etched; D – Sulfuric acid etched; E – Caustic soda cleaning; F – Nitric acid etched and hot chromate treatment for ½ hr (all specimens initially smooth machined)

[21] See pp. 8-24: "Metallography, Fatigue of Metals, and Conventional Stress Analysis," by H. F. Moore, in "Failure of Metals by Fatigue," Proceedings of Symposium, University of Melbourne, Melbourne University Press, 1947.

[22] See Proceedings of ASTM, Vol. 45, 1945, pp. 507-521; "A Study on Size Effect and Notch Sensitivity in Fatigue Tests on Steel," by H. F. Moore.

[23] See Proceedings of ASTM, Vol. 39, 1939, pp. 723-737: "Fatigue Strength of Machined Forgings 6-7 In. in Diameter," by O. J. Horger and H. R. Neifert.

[24] See *Journal of Applied Mechanics*, Vol. 12, September, 1945, pp. A149-A155: "Fatigue Strength of 5¼-In. Diameter Shafts as Related to Designs of Large Parts," by O. J. Horger, T. V. Buckwalter, and H. R. Neifert.

lower fatigue strengths, which may be attributed to variations in the steel throughout large sections.

The type of machine used to determine the fatigue properties may likewise affect the results. For example, direct axial stress machines may give results that are as much as 30% lower than the results obtained in rotating beam tests, while the results of flexural tests are usually somewhat higher than those obtained in rotating beam tests. The low results of axial fatigue tests may be due to difficulties in avoiding some eccentricity in loading.

The speed of test has but little effect on the fatigue limit of most metals tested at room temperature. On the other hand, metals like lead, which are plastic at room temperature, are markedly affected by the speed of test. In such cases high testing speeds usually result in greatly increased cycle-life, as shown in Fig. 8. At elevated temperatures such as used in gas turbines, the fatigue properties of other metals are undoubtedly affected in a similar manner.

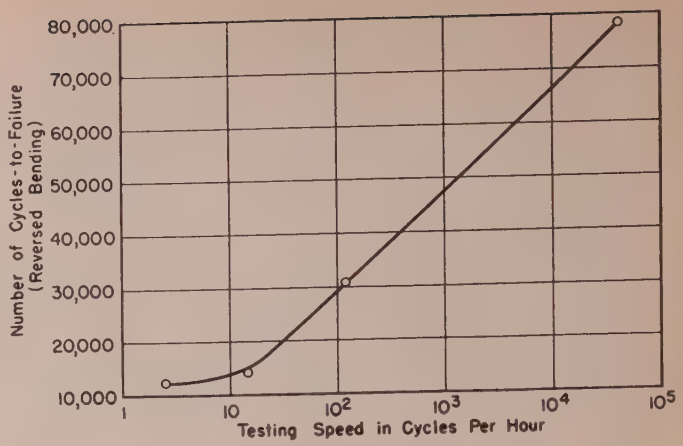

Fig. 8 – Effect of testing speed on fatigue test results using cantilever beam specimens for 1% Sb lead cable sheath. Temperature: 85 F and deflection: 0.300 in.

Corrosion

The effect of corrosion has been shown to be associated with the formation of corrosion pits, the result being similar to notch sensitivity in uncorroded specimens. The effect of notches and notch sensitivity has been studied intensively and

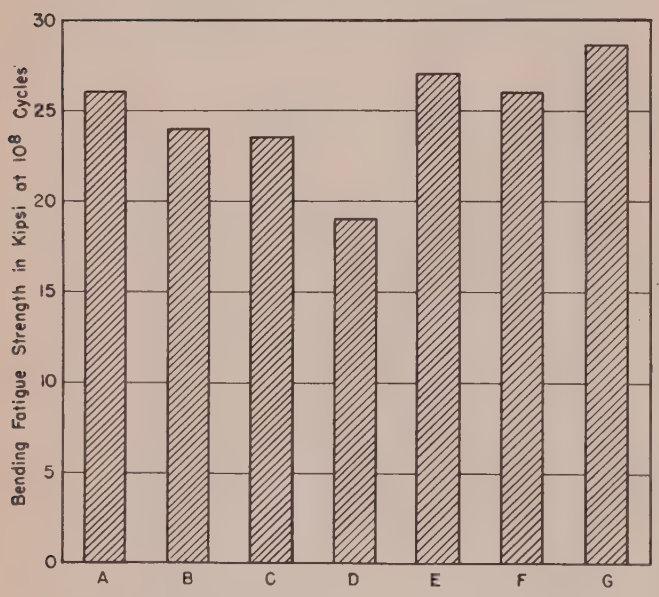

Fig. 7 – Effect of electroplated finishes on fatigue life of spring temper, Grade C, phosphor-bronze strip[16]

stress-concentration nomograms have been developed by Neuber[25] for evaluating the effect of notches on round shafts, either solid or hollow, when used in torsion, bending, or tension.

The effect of mean stress on the stress range is of primary importance. In most cases the range of stress decreases with increasing mean stress, but as Gohn and Ellis[26] have demonstrated, this is not true of bending tests on nonferrous sheet metals, nor is it true for torsional tests on ferrous metals. Since stress conditions may vary, it is essential that fatigue properties be established for various mean stresses by obtaining fatigue diagrams like those shown in Fig. 9.[27]

The influence of stress cycles of different magnitudes applied in succession and after rest periods is important, but few studies of this type have been made for this typical service condition.

To sum up, our present knowledge of fatigue is largely determined from laboratory tests on highly polished specimens tested either in bending (rotation or flexure), tension-compression, or torsion under conditions of constant deflection or constant load until failure occurs. The standard specimen is an ideal one, however, and seldom simulates service conditions. The surface of the test specimen is usually very carefully ground or longitudinally polished to eliminate stress-raisers. Since the latter are nearly always present in machine parts due to machining, grinding or other fabricating operations, or from the use of threads, collars, or splines, we must allow for a factor of ignorance when the results of laboratory fatigue tests are applied to our designs. Furthermore, allowance must be made for differences in size

[25] "Theory of Notched Stresses," by H. Neuber. Translated from 1937 German edition by F. A. Raven. Pub. by J. D. Edwards, Ann Arbor, Mich., 1946. (Also pub. as David W. Taylor Model Basin, Translation No. 74, November, 1945.)

[26] See Proceedings of ASTM, Vol. 47, 1947, pp. 713-721: "Fatigue Characteristics of Copper-Nickel-Zinc and Phosphor-Bronze Strip in Bending under Conditions of Unsymmetrical Loading," by G. R. Gohn and W. C. Ellis.

[27] P. 69 ASTM Manual on Fatigue Testing, STP 91 (1949).

between test specimen and machine elements, which introduces still another variable. Hence it must be concluded that even when used as an evaluation test, a fatigue test yields an ideal fatigue strength which cannot be used in design without a factor of safety, the magnitude of which can be determined only from valid life test data.

While it has been shown that it is possible to increase the fatigue strength of a metal by heat-treatment or cold-working, it should be remembered that the harder materials are usually more notch-sensitive and hence, under corrosive conditions, they may be no better than a softer, more ductile material.

The fatigue life of a material is not a constant. Its value frequently depends upon whether it is determined in bending, in alternate tension-compression tests, or in torsion. How, then, can it be expected that the fatigue strength will be precisely related to the other more commonly determined physical properties? Furthermore, it has been shown that the fatigue strength is a function of the surface finish, and for a given finish the fatigue strength may be raised by understressing or lowered by overstressing. Finally, since it has been pointed out that fatigue starts at areas of high local stresses, the fatigue life of a metal may be affected by many things such as nonmetallic inclusions, internal cracks, blowholes or porosity, surface defects resulting either from manufacture of the material or from fabrication such as machining, grinding or polishing, screw threads, sharp or re-entrant angles, keyways and oil grooves, press fits, cracks resulting from heat-treatment, and identification or inspection marks. All of these act as stress-raisers and tend to reduce fatigue life, but the effect is rarely as great as that estimated from mathematical theory, probably because of the existence of high localized stresses well above those which cause slip. These may cause considerable yielding under repeated stress and tend to relieve the high points of stress-concentration rather than cause the formation of cracks.

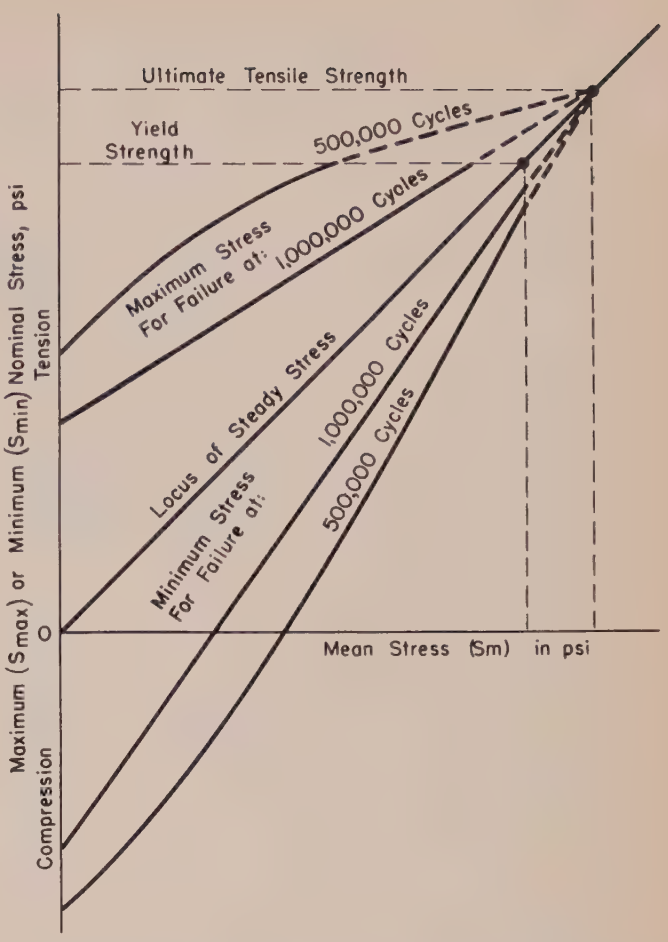

Fig. 9 – Diagram for representation of failure at constant number of cycles. Note that if both axes are to same scale, locus of steady stress is inclined at 45 deg to horizontal[27]

Elimination of Stress-Raisers

One of the most important steps in reducing the number of fatigue failures in moving parts would be to eliminate stress-raisers. That is true; yet Zimmerli, Moore, and Almen have all shown that by roughening a surface by shotpeening, the fatigue life of a part may be greatly increased.

The effectiveness of shotpeening in improving the fatigue resistance of manufactured parts has been summarized by the ASM Committee on Shotpeening.[28] This article, which was prepared to aid in selecting the most suitable process, evaluates shotpeening, surface rolling, hand and mechanical peening, and prestressing. Among the data presented, some show that the fatigue strength of phosphor-bronze sheet can be increased from 31,600 psi at 10^7 cycles of reversed stress to 47,000 psi by shotpeening, a gain of 52%. Our own data, presented in Fig. 10, for two tempers of Grade A (5% tin) phosphor-bronze, show that under certain circumstances even greater resistance can be imparted by shotpeening. However, the commercial application of such shotpeening to thin sheet-metal springs of low section modulus used in communication equipment is rather difficult because of close engineering requirements which frequently necessitate spring adjustments after assembly or during service. Such adjustments materially reduce the effectiveness of shotpeening.

The data presented in Fig. 10 are significant not only because they show that fatigue resistance can be increased by *adding* surface stresses of the proper kind, but also because they show that *elimination* of residual stresses by stress-relief annealing will also be beneficial. In the examples shown, the gain in fatigue resistance resulting from the elimination or reduction of residual stress by low-

[28] See *Metal Progress*, Vol. 66, July 15, 1954, pp. 104-108: "Shotpeening and Other Surface Working Processes," by ASM Committee on Shotpeening.

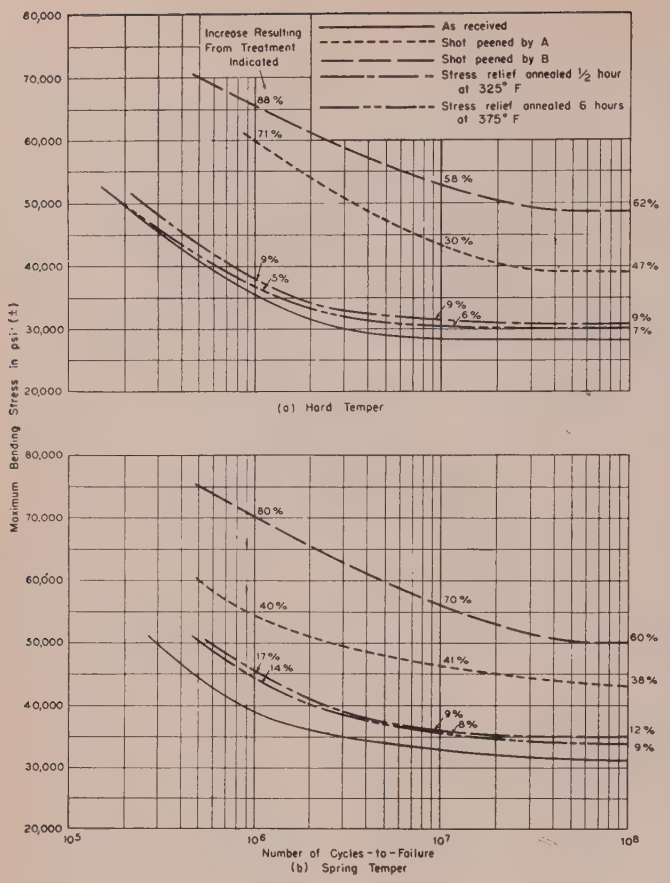

Fig. 10 – Effect of shotpeening and stress-relief annealing on average bending fatigue properties of Grade A (5% Sn) phosphor-bronze strip

temperature annealing is not as great as that resulting from the introduction of added compressive stresses by shotpeening. This apparent anomaly on the effect of residual stresses clearly shows the danger inherent in attempting to draw general conclusions from any given set of fatigue data.

Vitovec[29] offers a possible explanation of the beneficial effect of shotpeening as well as other forms of cold-working, case-hardening, and the like. According to his theory, the deformation of a polycrystalline material is inhomogeneous, and due not only to the statistical orientation of the grains, but also to the influence of the free surface. Because of the statistical crystallographic orientation of the grains, slip planes do not coincide. When the material is stressed, this causes lattice distortions and a mutual hindering of slip of the grains. Any interior grain is strengthened by the hindering effect of the surrounding grain. For an interior grain, Vitovec[29] shows mathematically that the total hindering effect is theoretically twice the relative hindering effect on a surface grain. From this it follows that if fatigue is caused by slip, then fatigue in a homogeneous material is a surface phenomenon and the fatigue of metals must be intimately related to the surface effect on plastic deformation. The fatigue strength of metals, therefore, can be increased by increasing the yield strength of the layer which is influenced by the free surface. Various processes such as electroplated finishes having residual compressive rather than tensile stresses, cold-working by shotpeening, aging, case-hardening, carburizing, nitriding, and precipitation-hardening will increase the yield strength in this surface layer. According to Vitovec, this increase in yield strength will result in an increase in fatigue, but the increase is only effective up to the fatigue strength of the material inside the specimen.

Conclusion

In conclusion, it should be pointed out that in any case, the fatigue properties of a metal are dependent upon the general quality of the material. This is undoubtedly one of the major factors contributing to reliable performance in fatigue. Without material of good quality the most careful design and fabrication will not produce the desired quality and reliability in the final product. Coordination of effort between the metal producer and user is necessary to obtain the most efficient result, and seldom can the one rectify the mistakes of the other. For best results it is necessary to maintain proper standards of composition as regards constituents and impurities, and the application of the proper techniques in melting, casting and method of manufacture. In the case of heat-treatment, the use of correct heat-treating techniques must be vigorously observed. The machine elements themselves must be designed to withstand previously calculated static and dynamic stresses with full allowance made for all known stress-raisers, and the parts must be made by manufacturing processes which will not add unknown stresses to those used in design. It should also be remembered that despite the fact that fatigue testing is now over 100 years old, the study of fatigue is still relatively young and great advances in the knowledge of fatigue are apt to be made in future years. For the present, at least, there is no substitute for a fatigue test except a service test, which is itself a fatigue test.

Acknowledgment

The author is indebted to the Bell Telephone Laboratories, Inc., for permission to publish this paper. Many helpful suggestions and criticisms have been received from E. E. Schumacher, W. C. Ellis, and F. L. Vogel, Jr. with respect to the theoretical aspects of the paper. I. V. Williams and G. J. Herbert have assisted materially by reviewing the manuscript. Miss A. V. Jastram prepared the various sketches used in the paper.

[29] See Wright Air Development Center Report 53-167 (1953), "Effect of Specimen Surface as Discontinuity in Fatigue Phenomena," by F. H. Vitovec.

Flexible Suspension Systems for Equipment in Transit

John J. Goodill, Lord Mfg. Co.

This paper was presented at the SAE Golden Anniversary Aeronautic Meeting, New York, April 18, 1955.

DURING the last ten years, a revolution in the packaging field has been taking place. The cause of this is the engineered internal flexible suspension system for the protection of equipment from shock and vibration during shipment. These systems are specifically designed to limit the forces which may act on the equipment they protect to values it can stand without being damaged. They are composed of individual resilient mountings, and dampers if necessary, so arranged to produce the calculated required spring rate and damping force in every direction. These suspension systems represent the engineering solution to the problem of damage in shipment because their design is based on the known fragility of the packaged equipment and the known hazards of shipment.

These suspension systems are very economical to use, for not only do they protect equipment from shipping damage, but also they reduce shipping rates and increase customer satisfaction. They may be incorporated either into reusable or disposable shipping containers. When used in disposable containers, the basic elements of the suspension system may be salvaged and reused many times, thus making the actual cost per shipment very nominal.

The fundamental component of a flexible suspension system is the resilient mounting, of which there are three basic types.

The first type is the plate-form mounting shown in Fig. 1. This type of mounting consists of a metal plate and tube bonded to an elastomer in the shape illustrated. The mounting is designed to have a low initial spring rate in order that good isolation of a wide range of disturbing frequencies is obtained, and a gradually increasing spring rate to secure protection from shock loads. These objectives are realized in this design by having the static weight of the mounted mass carried by rubber in shear and shock loads by rubber in compression.

The load-deflection curve for this mounting is shown in Fig. 2. The energy-absorbing capabilities of this type of mounting can be increased, and greater protection afforded the mounted mass, by

SEVERAL types of mountings and friction dampers used in flexible suspension systems for shipping containers, and their characteristics, are discussed and illustrated.

For a particular piece of equipment, a method for selecting the proper mounting and determining its correct location in the shipping container is presented.

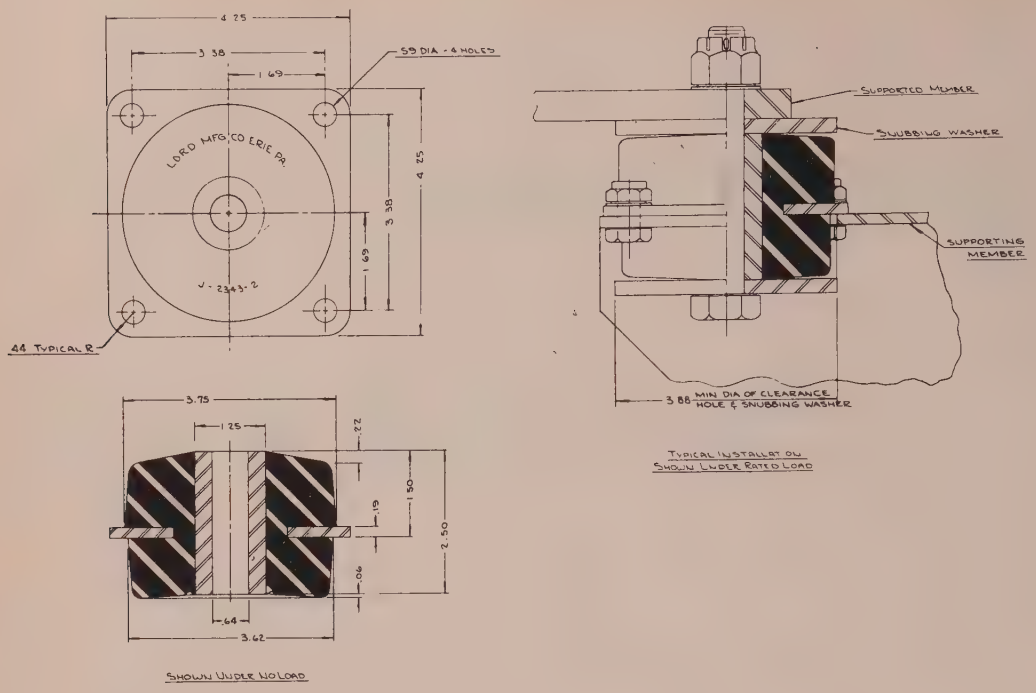

Fig. 1 – Typical plate-form mounting

using spacers between the inner member and snubbing washers to increase the shear travel before snubbing takes place. For comparison purposes, the load-deflection curve for this mounting with 5/8-in. spacers between the inner member and snubbing washers is shown in Fig. 3.

A typical installation of this type of mounting in a shipping container is shown in Fig. 4. The business machine in this illustration is clamped to a plywood base flexibly mounted on four plate-form mountings. The plates of the plate-form mountings are bolted to the plywood base and the inner members are bolted to the container. Spacers are used between the inner members and snubbing washers to provide greater travel and more protection before snubbing takes place. The mountings are located beneath the center of gravity of the machine to induce rotation of the machine on the shock mountings when the container is dropped on its side or end. In this manner, the machine is given greater lateral protection than it would receive if it were

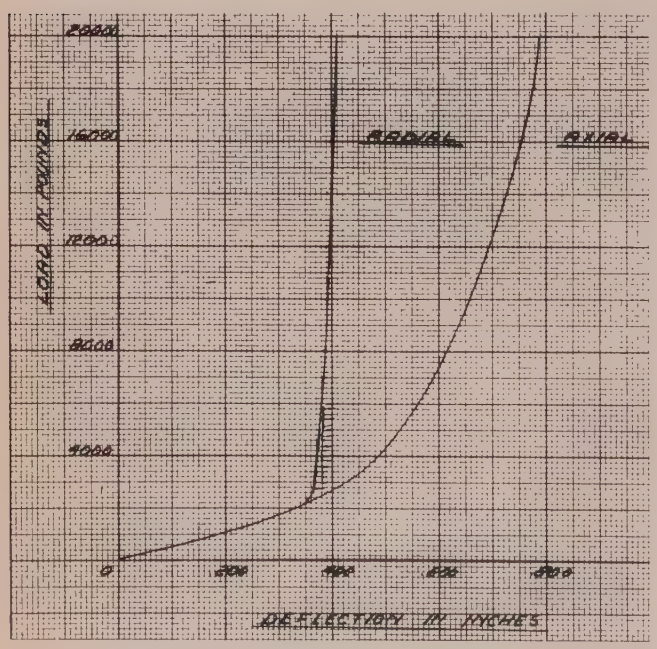

Fig. 2 – Load-deflection curves for typical plate-form mounting

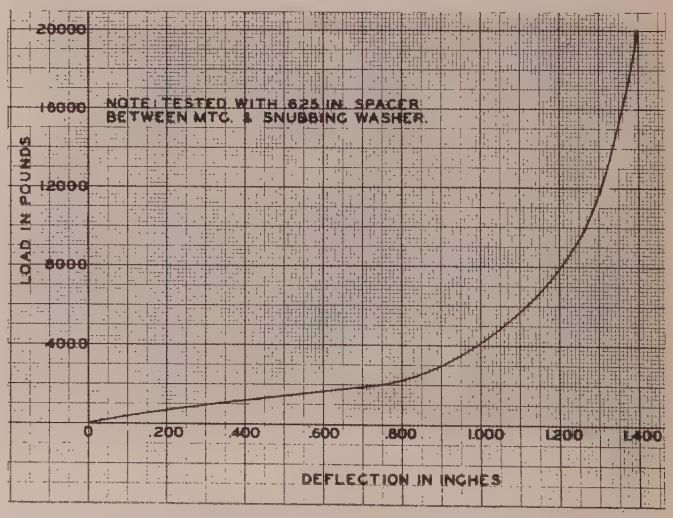

Fig. 3 – Load-deflection curve for typical plate-form mounting with 5/8-in. spacer between inner member and snubbing washer

limited to pure translation. Locating the mountings beneath the machine simplifies the installation because attachment to the cradle can be accomplished without additional bracketing, and does not require the container to be made larger to accommodate the mountings since they are out of the way of the deflecting machine. The size of the container, therefore, is dependent upon only the size of the shock-mounted machine and the movement it is permitted to take. The use of this suspension system eliminated all servicing on this machine, which had been running 10 hr per machine after each shipment, and cut damage claims to 0.5%.

The second type is the shear sandwich mounting shown in Fig. 5. This type mounting is composed of two metal plates bonded to an elastomer between them. Some means of attachment must be provided in the design of the metal plates. In the illustrated mounting, this is accomplished by dome nuts which are locked into the plates and protrude into the rubber section. The shear sandwich mounting has essentially a linear load-deflection curve and can be designed to provide a wide range of spring rates and deflections. Those commercially available at the present time have spring rates varying from 20 to 4200 lb per in., and some are capable of deflecting 12 in. linearly.

The linear load-deflection curve and large deflection of the shear sandwich mounting make it the ideal resilient member of a shipping container suspension system. Because of these two characteristics, a suspension system composed of shear sandwich mountings will permit only relatively small forces to act on the protected equipment even though large amounts of energy are being exchanged between the equipment and the shear sandwich mountings. This can best be understood by comparing the parabolic load-deflection curve of a compression mounting with the linear load-deflection curve of a shear sandwich mounting. Since the area beneath these curves is directly proportional to the amount of energy which the mountings are capable of storing and dissipating, the shear sandwich mounting with the straight line load-deflection curve will require a much smaller force to absorb a given amount of energy than will the compression mounting with a parabolic load-deflection curve. Of course, the shear mounting must deflect farther than the compression mounting to do this. Fig. 6 shows the linear load-deflection curve of the shear sandwich mounting illustrated in Fig. 5. The parabolic curve represents the load-deflection characteristic of a compression mounting of equal spring rate. The shaded portions beneath these curves represent equal amounts of energy. From these curves, it is seen that the shear sandwich mounting deflects 3.5 in. to absorb the energy at a force of 6000 lb. The compression mounting, however, deflects 2.88 in. at a force of 11,250 lb, or nearly twice that of the shear sandwich mounting. An equipment mounted alternately on the compression mountings and on the shear sandwich mount-

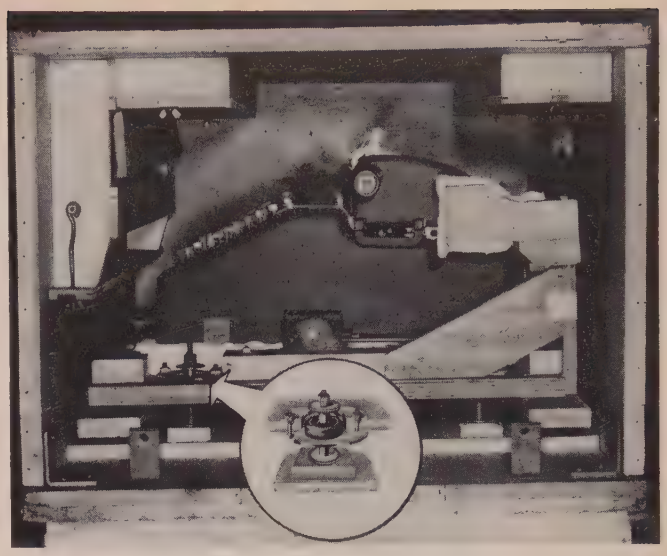

Courtesy, Burroughs Corp.

Fig. 4 – Typical installation of plate-form mountings in shipping container

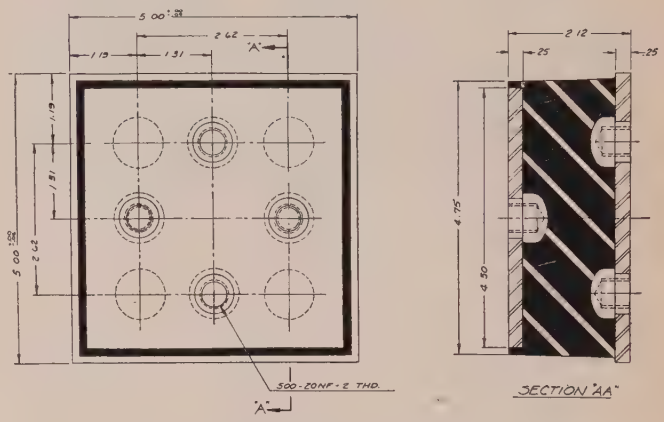

Fig. 5 – Typical shear sandwich mounting

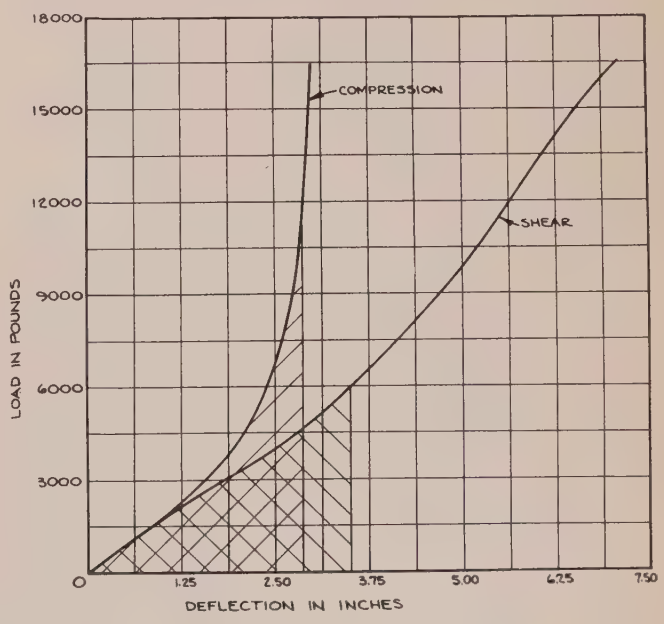

Fig. 6 – Load-deflection curves for compression and shear sandwich mountings. Shaded areas indicate equal amounts of energy

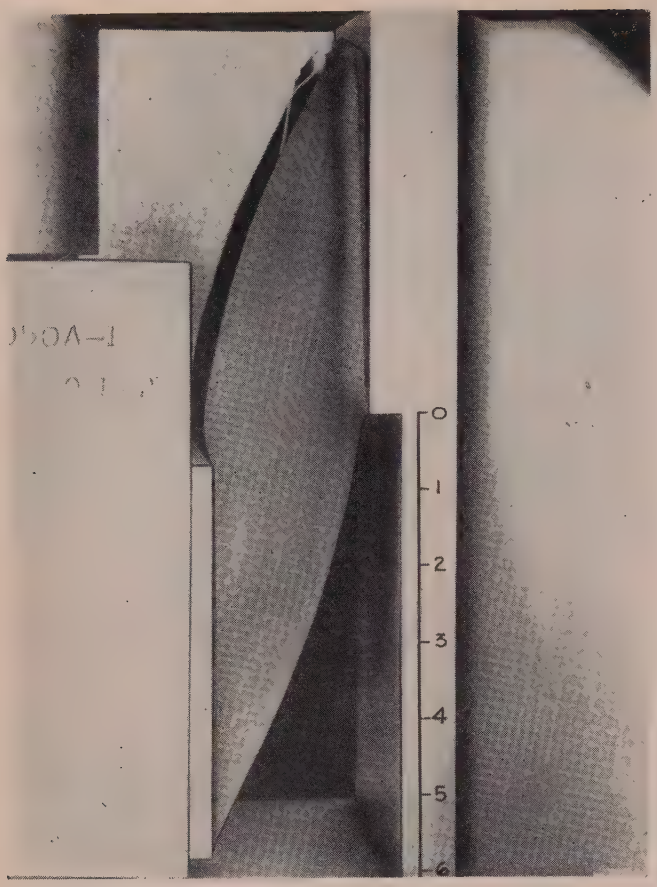

Fig. 7 – Shear sandwich mounting in deflected position

ings represented by these curves, and possessing the energy represented by the areas beneath these curves, would experience approximately twice the deceleration in being brought to rest on the compression mountings as it would on the shear mountings.

Besides possessing the type of load-deflection curve necessary to protect delicate equipment in transit, the shear sandwich mounting is very compact and requires little room in the container. As can be seen in Fig. 5, this shear mounting is only 5 x 5 x 2⅛ in.; yet it will produce a spring rate of 1700 lb per in. and will deflect over 7 in. Fig. 7 shows this mounting in a deflected position. Its very shape lends it ideally to container installations. It is thin, so that it can be located between the protected equipment and the container and not increase the width of the container over that which would be required for clearance due to motion of the equipment on its suspension system during shock.

The shear sandwich mounting is easy and simple to install. In the container, it is bolted to a flat plate welded to the container side if the container is metal, or to a metal or wooden bracket if the container is wooden. The other plate of the mounting is bolted to a structural member such as an angle or 2 x 4, forming a cradle to which the protected equipment is attached. Shear sandwich mountings have been used even in corrugated boxes by bolting them to V board liners which slip inside the corrugated exterior box.

Shear sandwich mountings are installed in horizontal round containers with their shear planes vertical and paralleling the longitudinal axis of the container. In this manner, they give excellent protection in the vertical and longitudinal directions; in the lateral direction, they act as compression mountings. They are so located because the container dimensions dictate that the major shipping shocks will be along its vertical and longitudinal axes. Also, the container itself, being round, offers protection laterally, for, if tipped on its side, it rolls like a cylinder and produces little acceleration on the equipment mounted inside. Fig. 8 illustrates a container and suspension system of this type. This suspension system will limit to 12*g* the acceleration imposed on the aircraft turbine it is designed to protect when either end of the container is dropped from a height of 36 in.

Shear sandwich mountings which must protect equipment in containers likely to be subjected to shock forces in all directions are located beneath the center of gravity of the equipment to induce rotation of the equipment when the container is shocked along the compression axis of the shear mountings. Sometimes they are located at a 45-deg angle to the side of the container to provide the same deflection in all lateral directions. This type of design is illustrated in Fig. 9. The typewriter, suspended in the wooden container on four shear sandwich mountings, was dropped along its three principal axes from a height of 60 in. and experienced no damage.

In those extreme circumstances which require more protection than can be obtained by locating

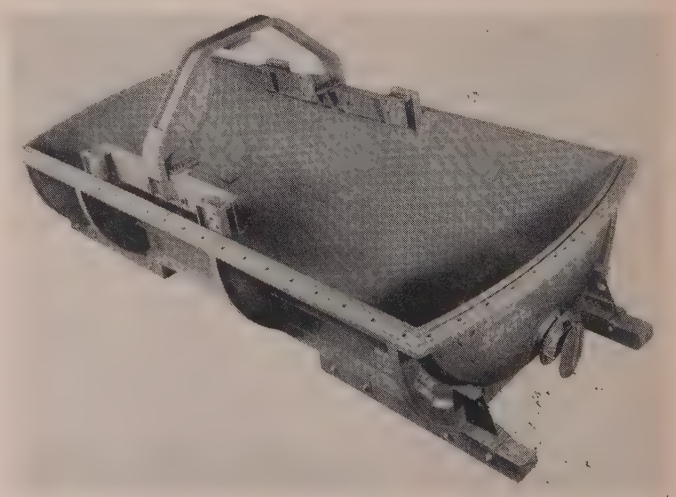

Courtesy, Champion Co.

Fig. 8 – Installation of shear sandwich mountings in horizontal cylindrical container

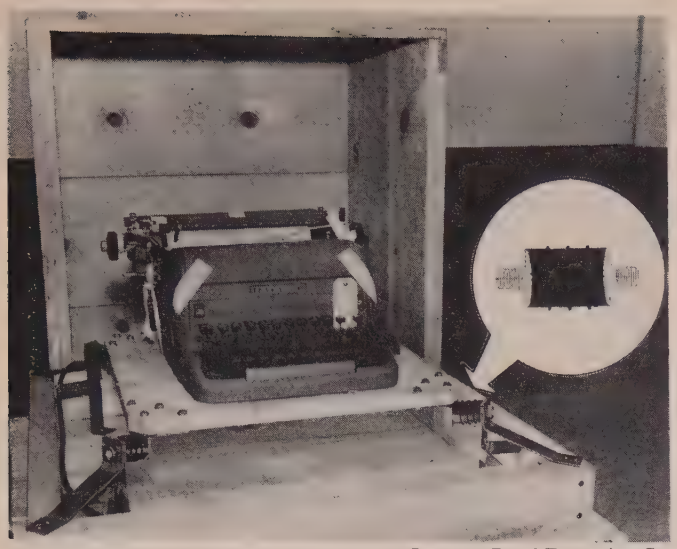

Courtesy, Royal Typewriter Co.

Fig. 9 – Installation of shear sandwich mountings in wooden shipping container

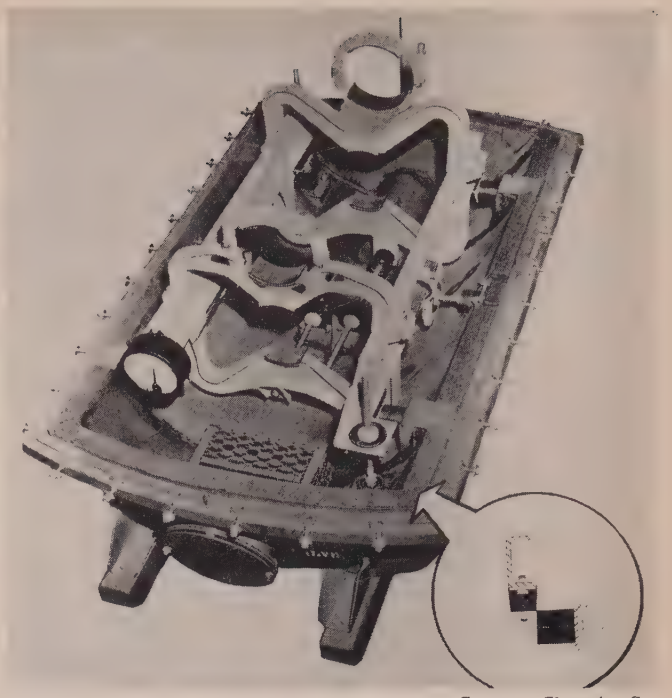

Courtesy, Champion Co.

Fig. 10—Installation showing shear sandwich mountings compounded to deflect in shear simultaneously along three coordinate axes

the shear sandwich mountings below the center of gravity of the equipment or at 45-deg to the principal axis of the equipment, the additional required protection can be obtained by compounding shear sandwiches so that one set will be in shear in a horizontal plane while the second set will be in shear in the vertical plane. Fig. 10 illustrates this principle. Four shear mountings, with shear planes vertical, support brackets to which are bolted four shear mountings with shear planes horizontal. The cradle in which the protected equipment is clamped is bolted to the top plates of the horizontal shear mountings. The mountings with shear planes vertical afford excellent protection from vertical shocks, and the mountings with shear planes horizontal offer excellent protection from horizontal shocks. This excellent multidirectional protection is obtained at little sacrifice in container size due to the compactness inherent in shear sandwich mountings of good design.

Most equipments will withstand g loads which permit the use of suspension systems that impart natural frequencies to the mounted mass outside the range of frequencies normally encountered in shipment. For those extremely delicate equipments, however, which require very soft suspension systems for protection and must, therefore, be mounted in the low range of forcing frequencies encountered in shipment, some provision must be made to prevent large amplification factors at resonance. This has been accomplished successfully by the use of friction dampers, one of which is shown in Fig. 11. This damper dissipates energy by sliding a nylon bushing up and down an aluminum rod. The bushing is in three segments and is pressed against the rod by the force of the elastomer compressed between the bushing and outer holder. Attachment to

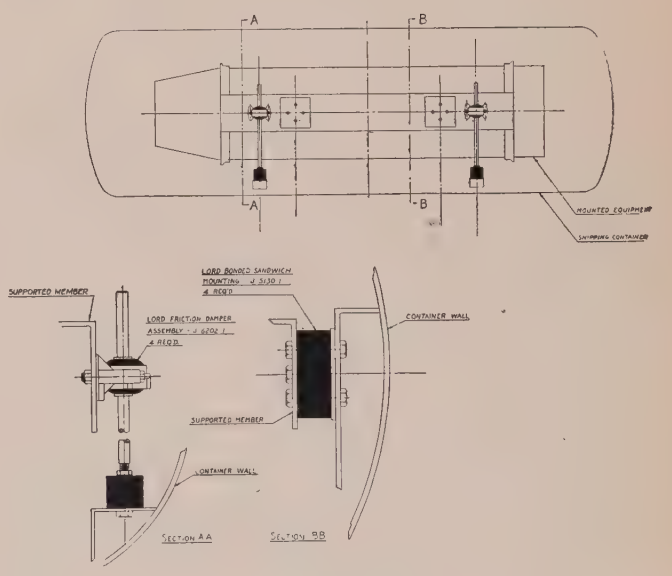

Fig. 11 – Typical friction damper and its installation in shipping container

the end of the rod is made through a flexible mounting so that the rod is free to cock in all directions and not limit the travel of the mounted equipment during shock. These dampers are designed to limit the amplification factor of a shipping container suspension system at resonance to 3 or less, and because of the size of the friction force generated, they have little effect on the shock characteristics of the system.

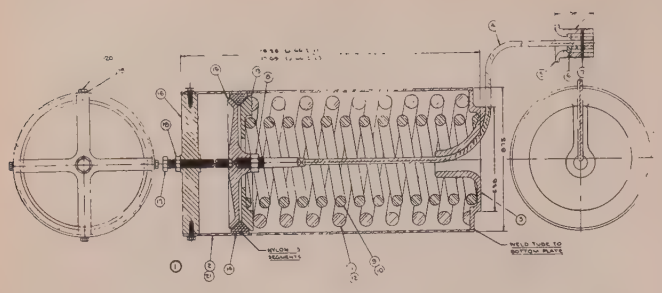

Fig. 12 – All-metal mounting

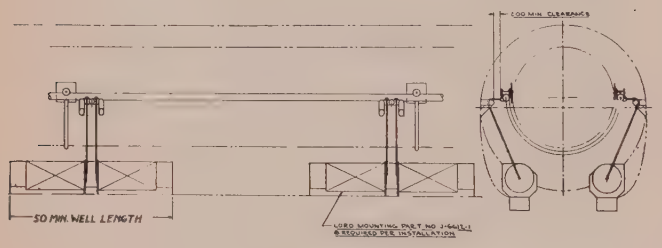

Fig. 13 – Schematic drawing of all-metal mountings installed in shipping container

The installation of this damper is shown in Fig. 11. The housing containing the nylon bushing is bolted to the cradle to which the equipment is clamped, and the rod is attached to the container through its flexible mounting. Many sizes of this type damper are now commercially available, producing friction forces of from a few pounds to over 100 lb.

The mountings discussed so far can be used in the majority of applications for shipping container suspension systems. Occasionally, however, it is required to provide a flexible mount for an equipment which will afford the same protection at –65 F as well as at more normal temperatures. This means that the equipment is not merely stored at –65 F, in which case the mountings previously discussed would be perfectly satisfactory, but that it is actually subjected to all of the shipping shocks and vibrations that it will receive at room temperature, which can happen only if transport vehicles, handling equipment, and men operate at those same temperatures. The necessity and practicality of this requirement should be studied very closely before being specified.

An all-metal mounting is the only practical one which will operate at these abnormal temperatures at the present time and is the third type to be discussed. This mounting poses two very difficult problems. First, the size of the mounting required to produce the necessary spring rate and deflection. Its excessive size, and the fact that heretofore it had to be positioned in the container at calculated locations to provide the required accelerations and stability, increased the size and cost of the container considerably. Second, the difficulty in making a multidirectional mounting out of a unidirectional spring.

The simplest mounting which will meet the cold temperature requirement and overcomes these major problems is shown in Fig. 12. It is actuated by a flexible cable which compresses a nest of coil springs between two plates. This method of loading the springs was chosen to permit the mountings to be located in the container in space that would not otherwise be used. Through the flexible cables, the mountings are made to support the equipment at the calculated support points although not located there. Further, only one set of mountings is required, no matter in which direction the equipment is forced to deflect, for the flexible cable will always compress the springs regardless of the direction from which the cable is pulled. By placing the mountings remotely from the protected equipment and utilizing the same mountings to absorb shocks in all directions, the all-metal suspension system is greatly simplified and the container size kept nominal.

The all-metal mounting illustrated has a built-in damper which provides a friction force proportional to the deflection. This is an advantage for it does not impede the isolation of vibrations of small amplitude, and yet is effective if the amplitude tends to increase at a resonant frequency. The friction force is obtained by wedging a split ring between the plate to which the cable is attached and the plate against which the springs seat and forcing the ring to bear against the ID of the mounting shell. The split ring is drawn along the mounting shell. Since the normal force on the split ring is determined by the force of the spring nest, a frictional force is generated which is proportional to the deflection of the mounting. If the natural frequency of the mounted mass can be made high enough so that friction damping is not required, this mounting can be furnished without it.

This mounting is quite readily installed in the container and no special preloading devices are required. The mounting is butted against a flat plate with a hole large enough to permit the neck on the front plate of the mounting to pass through. The cable is then looped over a pulley or bearing and its end attached to the equipment cradle at the calculated location with a fitting provided. The mounting is supplied precompressed to provide enough cable slack to make this attachment, and the bolt at the end of the mounting is backed out after installation to permit the springs to take up the cable slack. No other attachment of any kind is necessary to hold this mounting in position since the force of the spring nest against the front plate will hold it in position.

A schematic drawing of the installation of this mounting is shown in Fig. 13. The mountings are located in pockets in the container directly over the skids and are out of the way of the equipment. The cables are strung upward, over pulleys, and horizontally to the equipment cradle.

It should be noted that the all-metal shock mounting shown in Fig. 12 was designed to produce a spring rate of 700 lb per in. and a deflection of 8 in. A shear mounting with the same characteristics would be approximately 5 x 5 x 4 in. and would weigh appreciably less.

Now let us examine a typical problem to illustrate how the correct mountings are chosen and their proper position in the container determined. Suppose we have an equipment that can safely take N number of g's with no damage and is to be packed in a container and tested by dropping one end of the container on a solid floor from a height H while the other end rests on a wooden block. The data on the equipment follow:

W = Weight of equipment, lb
M = Mass of equipment, lb-sec^2 per in.
L_1 = Length of equipment, in.
I_1 = Moment of inertia of equipment in pitch, in.-lb-sec^2
$L_{1/2}$ = Distance from end of equipment to the c.g.

Step one in the solution of this problem is to assume a container for the equipment. Our assumption follows (see Fig. 14):

L = Length of container, in.
Y = Height of c.g. of mounted equipment above ground, in.
X = Distance from end of container to c.g. of mounted equipment, in.

Step two is to calculate the rotational velocity of the equipment at the instant of impact (refer to Fig. 15):

I_0 = Moment of inertia of missile about pivot point 0, in.-lb-sec^2
$= I_1 + MR^2$
R = Distance from pivot point to c.g., in.
$= \sqrt{X^2 + Y^2}$
R_1 = Radius of gyration of missile about pivot point, in.
$= \sqrt{I_0/M}$
α = Rotational acceleration of missile about pivot point, radians per sec^2
T = Torque acting on missile, in.-lb
C = Constant of integration
h_1 = Dimension as defined in Fig. 15, in.
h_2 = Dimension as defined in Fig. 15, in.
θ = Angle between vertical line containing pivot point and line containing pivot point and c.g., radians
θ_1 = Angle as defined in Fig. 15, deg
$= 90 \text{ deg} - \tan^{-1} Y/X - \sin^{-1} (h_1 - h_2)/L$
θ_2 = Angle as defined in Fig. 15, deg
$= 90 \text{ deg} - \tan^{-1} Y/X + \sin^{-1} h_2/L$
g = Acceleration due to gravity, in. per sec^2
ω_0 = Angular velocity of equipment about pivot point, radians per sec

$$T = I_0 \cdot \alpha \quad (1)$$

$$T = W \cdot R \cdot \sin\theta \quad (2)$$

$$\alpha = \frac{d^2\theta}{dt^2} = \omega_0 \frac{d\omega_0}{d\theta}$$

Substituting $\omega_0 \dfrac{d\omega_0}{d\theta}$ for α in equation (1) and equating equation (1) and (2), we have:

$$I_0 \cdot \omega_0 \frac{d\omega_0}{d\theta} = W \cdot R \cdot \sin\theta$$

$$I_0 \omega_0 \cdot d\omega_0 = W \cdot R \cdot \sin\theta \cdot d\theta$$

$$\frac{I_0 \omega^2}{2} = -W \cdot R \cdot \cos\theta + C$$

$$\omega_0 = \sqrt{\frac{-2W \cdot R \cdot \cos\theta}{I_0} + C}$$

when:

$$\omega_0 = 0, \theta = \theta_1$$

$$0 = \sqrt{\frac{-2W \cdot R \cdot \cos\theta_1}{I_0} + C}$$

$$C = \frac{2W \cdot R \cdot \cos\theta_1}{I_0}$$

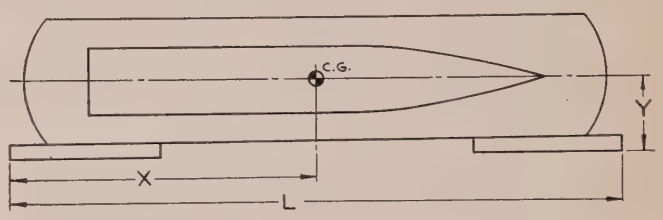

Fig. 14 – Sketch of assumed container

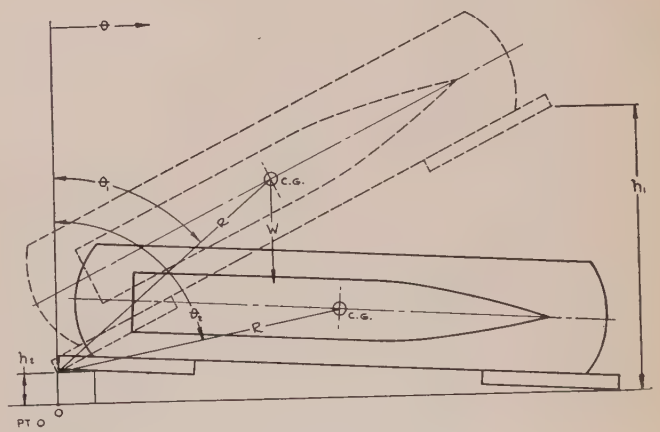

Fig 15 – Rotational drop test

$$\omega_0 = \sqrt{\frac{2W \cdot R}{I_0} (\cos \theta_1 - \cos \theta)}$$

when:

$$\omega_0 = \text{maximum}, \theta = \theta_2$$

$$\omega_0 = \sqrt{\frac{2W \cdot R}{I_0} (\cos \theta_1 - \cos \theta_2)}$$

$$\omega_0 = \sqrt{\frac{2W \cdot R}{\frac{W R_1^2}{g}} (\cos \theta_1 - \cos \theta_2)}$$

$$\omega_0 = \sqrt{\frac{2R \cdot g}{R_1^2} (\cos \theta_1 - \cos \theta_2)} \qquad (3)$$

Step three is to calculate the instantaneous vertical[1] acceleration and deflection at the center of gravity, and from this, obtain the vertical spring rate of a suspension system to yield a specified g load at the center of gravity.

a_1 = Vertical instantaneous acceleration at c.g. of equipment, in. per sec^2

A = Maximum vertical acceleration at c.g. of equipment, in. per sec^2

v_1 = Vertical instantaneous velocity at c.g. of equipment, in. per sec

s_1 = Vertical instantaneous deflection at c.g. of equipment, in.

t = Time, sec, starting at the instant of impact

ω_1 = Vertical translational circular frequency

C_1 = Constant of integration

C_2 = Constant of integration

G_1 = Maximum vertical acceleration in "G" units at c.g. of equipment

K = Total vertical spring rate of suspension system, lbs per in.

K_1 = Vertical spring rate of one mounting, lbs per in.

S_1 max = Maximum vertical deflection at c.g. of equipment

$$a_1 = \frac{d^2 s_1}{dt^2} = -A \cdot \sin \omega_1 t$$

$$v_1 = \frac{ds_1}{dt} = \frac{A}{\omega_1} \cdot \cos \omega_1 t + C_1$$

when:

$$t = 0, v_1 = R \cdot \omega_0 \cdot \cos (\tan^{-1} Y/X)$$

Therefore:

$$R \cdot \omega_0 \cdot \cos (\tan^{-1} Y/X) = \frac{A}{\omega_1} + C_1$$

$$C_1 = R \cdot \omega_0 \cdot \cos (\tan^{-1} Y/X) - \frac{A}{\omega_1}$$

$$v_1 = \frac{A}{\omega_1} \cdot \cos \cdot \omega_1 t + R \cdot \omega_0 \cdot \cos (\tan^{-1} Y/X) - \frac{A}{\omega_1}$$

$$s_1 = \frac{A}{\omega_1^2} \cdot \sin \omega_1 t + R \cdot \omega_0 \cos (\tan^{-1} Y/X)\, t - \frac{A}{\omega_1} t + C_2$$

when:

$$t = 0, s_1 = 0 \text{ and } C_2 = 0$$

$$s_1 = \frac{A}{\omega_1^2} \cdot \sin \omega_1 t + R \cdot \omega_0 \cos (\tan^{-1} Y/X)\, t - \frac{A}{\omega_1} t$$

when:

$$\omega_1 t = \frac{\pi}{2}, v_1 = 0$$

Therefore:

$$R \cdot \omega_0 \cdot \cos (\tan^{-1} Y/X) = \frac{A}{\omega_1}$$

$$A = \omega_1 \cdot R \cdot \omega_0 \cdot \cos (\tan^{-1} Y/X)$$

$$a_1 = -\omega_1 \cdot R \cdot \omega_0 \cos (\tan^{-1} Y/X) \sin \omega_1 t \qquad (4)$$

$$s_1 = \frac{R \cdot \omega_0}{\omega_1} \cos (\tan^{-1} Y/X) \sin \omega_1 t \qquad (5)$$

$$G_1 = \frac{-A}{g} = \frac{-\omega_1 \cdot R \cdot \omega_0 \cdot \cos (\tan^{-1} Y/X)}{g} \qquad (6)$$

$$\omega_1 = \frac{G_1 \cdot g}{R \cdot \omega_0 \cdot \cos (\tan^{-1} Y/X)} \qquad (7)$$

$$K = \omega_1^2 M \qquad (8)$$

If four mountings are used:

$$K_1 = \frac{\omega_1^2 M}{4} \qquad (9)$$

$$S_1 \text{ max} = \frac{R\omega_0}{\omega_1} \cos (\tan^{-1} Y/X) \qquad (10)$$

Step four is to calculate the instantaneous vertical acceleration and deflection at the end of the equipment due to its rotation about the center of gravity, and from this, obtain the rotational spring rate of the suspension system to yield the proper spacing of the mountings about the center of gravity.

a_2 = Vertical instantaneous acceleration at end of equipment due to its rotation about c.g., in. per sec^2

B = Maximum vertical acceleration at end of equipment due to its rotation about c.g., in. per sec^2

v_2 = Vertical instantaneous velocity at end of equipment due to its rotation about c.g., in. per sec

s_2 = Vertical instantaneous deflection at end of equipment due to its rotation about c.g., in.

ω_2 = Rotational circular frequency, radians per sec

C_3 = Constant of integration

Z = Distance from c.g. to end of equipment, in.

C_4 = Constant of integration

G_2 = Maximum acceleration at end of equipment due to rotation, "G" units

K_R = Total rotational spring rate of the suspension system in.-lb per radian

d = Distance from c.g. to mounting location, in.

S_2 max = Maximum vertical deflection at end of equipment due to rotation, in.

$$a_2 = \frac{d^2 s_2}{dt^2} = -B \cdot \sin \omega_2 t$$

$$v_2 = \frac{dS_2}{dt} = \frac{B}{\omega_2} \cos \omega_2 t + C$$

when:

$$t = 0, v_2 = Z \cdot \omega_0$$

$$Z \cdot \omega_0 = \frac{B}{\omega_2} + C_3$$

$$C_3 = Z \cdot \omega_0 - \frac{B}{\omega_2}$$

[1] Vertical here refers to the container only, with the base of the container determining the horizontal plane.

$$v_2 = \frac{B}{\omega_2} \cos \omega_2 t + Z \cdot \omega_0 - \frac{B}{\omega}$$

$$s_2 = \frac{B}{\omega_2^2} \sin \omega_2 t + Z \cdot \omega_0 t - \frac{B}{\omega_2} t + C_4$$

when:

$$t = 0, S_2 = 0 \text{ and } C_4 = 0$$

$$0 = Z \cdot \omega_0 - \frac{B}{\omega_2}$$

$$B = \omega_2 \cdot Z \cdot \omega_0$$

Therefore:

$$a_2 = -\omega_2 \cdot Z \cdot \omega_0 \cdot \sin \omega_2 t \quad (11)$$

$$S_2 = \frac{Z \cdot \omega_0}{\omega_2} \sin \omega_2 t \quad (12)$$

$$G_2 = \frac{-B}{g} = \frac{-\omega_2 \cdot Z \cdot \omega_0}{g} \quad (13)$$

$$\omega_2 = \frac{G_2 \cdot g}{Z \cdot \omega_0} \quad (14)$$

$$K_R = \omega_2^2 I_1 \quad (15)$$

$$d = \sqrt{\frac{K_R}{K}} \quad (16)$$

$$S_2 \max = \frac{Z \cdot \omega_0}{\omega_2} \quad (17)$$

Now we know the location of the mountings in the container based on the known additional acceleration which the equipment can take due to its rotational velocity.

Step five is to calculate the total acceleration and deflection at the end of the equipment and the maximum deflection at the mounting locations.

G_T = Total acceleration at end of equipment, g units
S_T = Total deflection at end of equipment, in.
S_0 = Maximum deflection at the mounting location, in.

$$G_T = \frac{-A}{g} \sin \omega_1 t - \frac{B}{g} \sin \omega_2 t \quad (18)$$

$$S_T = \frac{A}{\omega_1} \sin \omega_1 t + \frac{B}{\omega_2} \sin \omega_2 t \quad (19)$$

$$S_0 = \frac{A}{\omega_1} \sin \omega_1 t + \frac{a}{z} \frac{B}{\omega_2} \sin \omega_2 t \quad (20)$$

Step six is to choose a mounting having the calculated spring rate and capable of deflecting the distance S_0 in shear linearly.

Finally, step seven is to compute the vertical natural frequency of the system.

f_n = Vertical natural frequency, cps (21)

$$f_n = \frac{\omega_1}{2\pi}$$

For this computation, the dynamic modulus of the elastomer in the mounting is used. If this results in a natural frequency out of the range of forcing frequencies normally encountered in shipment, no additional damping is required.

The dynamic modulus of elastomers varies greatly with the dynamic strain, decreasing as the strain increases. For this reason the same spring rate of a mounting should not be used for both natural frequency and shock calculations. The change in dynamic modulus is of particular importance in shipping container mountings; for ordinary applications it permits a mounting to impart to the protected equipment a natural frequency out of the range of the very low forcing frequencies encountered in shipment, and maintains a low spring rate which affords excellent shock protection.

It should also be borne in mind that any mounting used to protect an equipment in shipment should offer as much protection in the rebound direction as in the direction of the initial shock. This is important since the containers themselves sometimes become as massive as the equipment they hold. If the rebound protection of a mounting is sacrificed, the rebound shock could be greater than the initial shock.

We have now completely defined the performance of the flexible suspension system, and the container can be built around it.

In conclusion, it is pointed out that the foregoing analysis assumes the equipment to be a rigid body. Actually, this is not so, for the equipment is made up of many components, all of which have their own natural frequencies. Fortunately, all these natural frequencies are usually appreciably above those at which the equipment normally is mounted. If at all possible, however, the lowest natural frequency of any component in the equipment should be determined first, and the suspension system designed accordingly to isolate all frequencies near that lowest resonant point.

ORAL DISCUSSION

Reported by Stanley M. Birnbaum
Wright Air Development Center

Question: What is the reason for mounting the suspension system below the center of gravity of the equipment?

Answer: It results in lower accelerations. Care should be taken, however, to ensure that there is sufficient room between the container and the equipment to permit the translatory motion of the item.

Question: What is the life of the friction dampers?

Answer: The information available at this time is incomplete.

Question: What determined the need for the 7-cps limitation requirement for damping?

Answer: The primary frequencies encountered in both rail and truck transportation were between 2 and 7 cps.

Question: Will you please give some information on the transmissibility of natural rubber?

Answer: The transmissibility of natural rubber is about 10. Some of the buna rubbers have transmissibilities of about 4, and for neoprene it is slightly less than 10. If possible, all rubber shock mounts should be designed so that they operate out of the resonant range. The transmissibility is, therefore, not a critical factor. If it is necessary to operate below 7 cps, friction dampers should be used.

Question: What is the effect of temperature rise when using friction dampers incorporating nylon, which has a temperature limit of 400 F?

Answer: No damage has been noted in vibration tests conducted for as long as 6 hr.

Pneumatic and Sonic Measurement of

TO a large degree, the performance of current automotive engines has been the result of a steady rise in compression ratio. As a result the accurate measurement of combustion-chamber volume has become a prime necessity in many types of automotive engines and vehicle testing. This is particularly true in the determination of engine octane requirement and deposit buildup in combustion chambers.

Limitations of Conventional Methods

Usually, measurements of volume do not present any particular difficulties because such measurements can be accomplished by filling the volume with a liquid from a calibrated burette or an initially weighed quantity of liquid. However, as applied to combustion chambers and deposits, a number of serious difficulties arise when volume measurements are made using liquids. The following limitations are encountered:

1. To avoid air entrapment an engine usually must be taken from the vehicle, cylinder heads removed, top dead-center located, ring gap sealed, and unventable regions of the chamber filled with modeling clay. Actual clearance volume must then be determined by adding the measured residual clearance volume to the volume of the modeling clay.

2. The process results in the loss of deposits from some parts of the quench area and contamination of the remaining deposits with measuring liquid and modeling clay.

3. Accuracy is limited by the inherent tendency of volume readings to be in error by the amount of liquid retained on the wall of the burette.

To determine the volume of combustion-chamber deposits additional difficulties are presented:

1. If deposit volume is found by the difference in chamber volume, even nominal errors in the latter can easily amount to a 50% error in deposit volume due to the high ratio of combustion chamber size to deposit volume.

2. The measurement of volume of carbon deposits removed from the combustion chamber is difficult due to the small physical size of the samples and the tendency of deposits to absorb air and resist wetting by the measuring liquid.

"Dry" Methods of Volume Measurement

The use of a compressible fluid such as air to

Combustion-Chamber Volume

G. A. Weinert, Ford Motor Co.

This paper was presented at the SAE Golden Anniversary Summer Meeting, Atlantic City, June 14, 1955.

AMONG the difficulties usually associated with measurement of combustion-chamber volume by liquid methods are amount of time required, contamination of combustion-chamber deposits, and inaccuracies arising from entrapped air.

Use of a gaseous fluid such as air as the measuring medium eliminates most of the objectionable features of volume measurement with liquids. Techniques utilizing air for volume measurement fall into two basic classifications: dynamic or sonic methods, and static or pneumatic systems.

Cylinder leakage and acoustic damping by engine deposits affect the accuracy of volume measurements based on dynamic properties of combustion-chamber volume, hence small volumes occupied by combustion-chamber carbon deposits must be measured separately by static or pneumatic means.

replace the measuring liquid is not a new idea. Pneumatic systems have been used in the past, but the most recent approach has been the development of volume-sensing instruments which use air under a dynamic or periodically varying pressure instead of a change in static pressure.

Dynamics of Compressible Fluids

In order to understand fully the various resonant or alternating pressure systems which are in use today, it is necessary to consider the nature of the air motion that results when a system consisting of a typical combustion chamber and spark-plug hole is subjected to a periodic pressure. The equation of motion for an ideal compressible fluid is shown in Fig. 1 below a simplified schematic diagram of a combustion chamber. The solution of this equation may be obtained easily if its similitude to the basic equation for electron motion (Fig. 1) is noted and the coefficients equated as indicated. Translation into an analogous electric circuit is valid provided the physical dimensions of the chamber are smaller than one-quarter wavelength of the frequency employed. Combustion chambers fall well within the latter limitation and full advantage may be taken of electric theory,

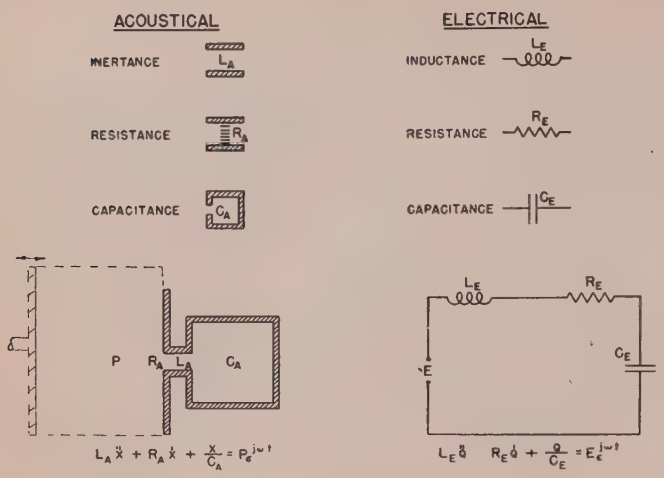

Fig. 1 – Analogies of an acoustic cavity and a series electric circuit under forced excitation

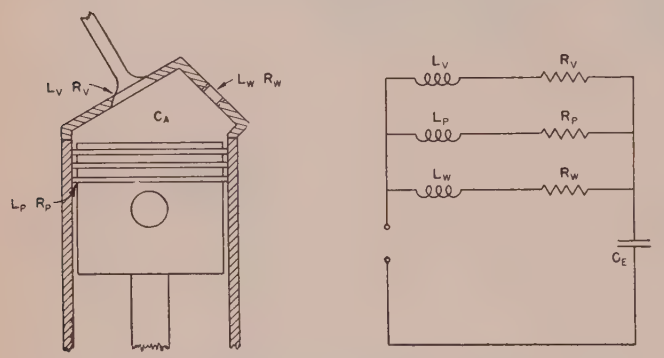

Fig. 2 – Electric analog of an actual engine combustion chamber

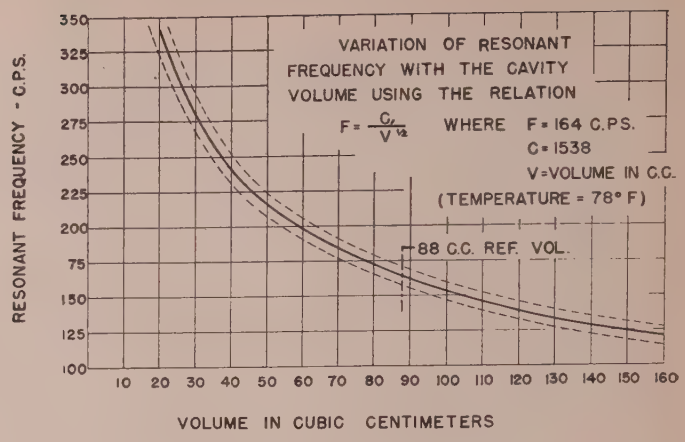

Fig. 3 – Variation of resonant frequency with combustion-chamber volume

including the use of dynamic electric models or analogues to determine design parameters.

In Fig. 2 the elements of the acoustic circuit formed by an engine combustion chamber, spark-plug-opening volume, and piston rings are shown in the form of a dynamically equivalent electric circuit for a chamber without carbon. If carbon deposits are present they may be represented by an additional resistance in series with the capacitance, C_E. The resulting series-parallel circuit can be reduced easily to the three element series circuit of Fig. 1. A combustion chamber will, therefore, behave dynamically as a simple series circuit in which the spark-plug opening and leakage passages are the inductive element, the chamber volume is the capacitive element, and the viscous and radiation loses the resistive element.

The complete solution (when $R^2/4L^2 < 1/LC$) for the equation of motion is:

$$i = \frac{E}{Z}(\sin \omega t + \lambda - \theta) + Ke^{-\alpha t} \sin (\beta t - \sigma)$$

(steady-state term) (transient term)

where:

K = Initial transient current

$e^{-\alpha t}$ = Dampening factor

The frequency β of the transient term is obtained from:

$$\beta = \sqrt{\frac{1}{LC} - \frac{R^2}{4L^2}}$$

and the natural excitation frequency in equivalent acoustic notation is:

$$F_R = \frac{1}{2\pi}\sqrt{\frac{1}{L_A C_A} - \frac{R_A^2}{4L_A}} \qquad (1)$$

Let:

$L_A = \frac{4\rho H}{D^2}$ = Equivalent acoustic inductance

$C_A = \frac{V}{\rho S^2}$ = Equivalent acoustic capacitance

D = Diameter of chamber throat

ρ = Air density

S = Speed of sound

H = Effective length of throat

V_x = Chamber volume

R_A = Total energy dissipation (damping)

F_R = Resonant frequency

Substituting in (1) we have:

$$F_R = \frac{1}{2\pi}\sqrt{\frac{1}{L_A \frac{V}{\rho S^2}} - \frac{R^2}{4L_A^2}} \qquad (2)$$

Squaring both sides:

$$F_R^2 = \frac{\rho S^2}{4\pi^2 L_A} \cdot \frac{1}{V_x} - \frac{R^2}{16\pi^2 L_A^2} = \frac{C_1}{V_2} - C_2 \qquad (3)$$

If R is negligible, then:

$$F_R = \frac{C_1}{V_x^{\frac{1}{2}}}$$

where:

$$C_1 = \frac{\rho S^2}{4\pi^2 L_A}$$

$$C_2 = \frac{R^2}{16\pi^2 L_A^2}$$

When the $\frac{R^2}{4L^2}$ term in equation (1) is less than $\frac{1}{L_A C_A}$, a freely oscillating system is obtained and a simple air jet applied to the throat opening is sufficient to maintain oscillation. Alternately an acoustic transducer can be used to drive the system as in Fig. 1, but the instrumentation is complicated by the necessity for providing power for the transducer and a phase-sensitive indicator to indicate resonance. Also, in a forced-excitation system the external chamber must have a low reactance (large volume) relative to the chamber being measured, which results in an adaptor whose physical bulk is too large for vehicle test work. In many o-h valve V-8 cars practically the only space available is that which is occupied by the spark plug itself.

Fig. 3 is the result of plotting volume versus the resonant frequency of a chamber using a fixed throat size, constant leakage factor, constant temperature, and constant dissipation or energy loss. Air temperature changes shift the basic curve as indicated by the dashed lines.

In the measurement of actual combustion chambers however, neither leakage nor energy absorption are constant values. The "constant" C_1 in equation (3) is a variable since L_A, the equivalent acoustic inductance in the simplified circuit, represents the parallel combination of fixed throat inductance and variable leakage inductance. In addition, to the degree that carbon deposits increase the energy dissipation of the system (namely, resistance), the "constant" C_2 also becomes a variable. To determine the magnitude of frequency shift under realistic conditions an actual engine cylinder was employed (Fig. 4), and the results in Figs. 5 and 6 show theoretical expectations and experimental results.

Since leakage produces a positive frequency shift and carbon a negative frequency shift, cancellation may take place and promote a false impression of possible accuracy of volume measurement.

An investigation was made to determine the possibility of a relationship between static cylinder-leakage flow and volume error. It was found that even though there was no direct correlation, the value of cylinder-leakage flow did define an upper limit for volume error and therefore indicated the possible range – if not the actual amount – of error in the volume measurement (Fig. 7).

Practical Sonic Volume Instrumentation

The general arrangement of instrumentation necessary for sonic volume comparison is presented in Fig. 8. The compressed air source is used to precheck the combustion chamber for leakage and to excite the resonant oscillation of the combustion chamber and throat inertance. The sound produced (100 to 300 cps, depending on the throat

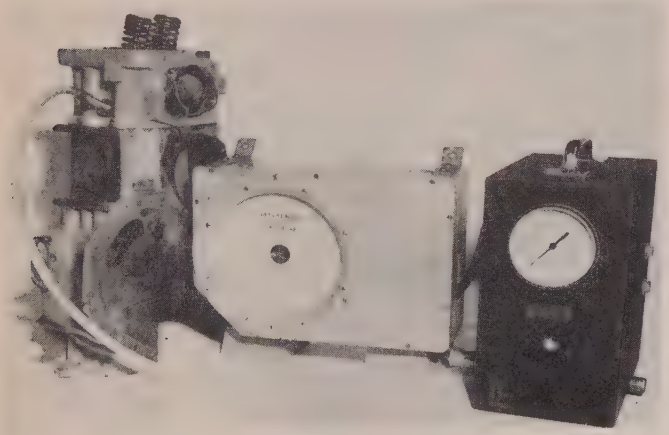

Fig. 4 – Actual combustion chamber used to determine frequency shift due to leakage and chamber deposits

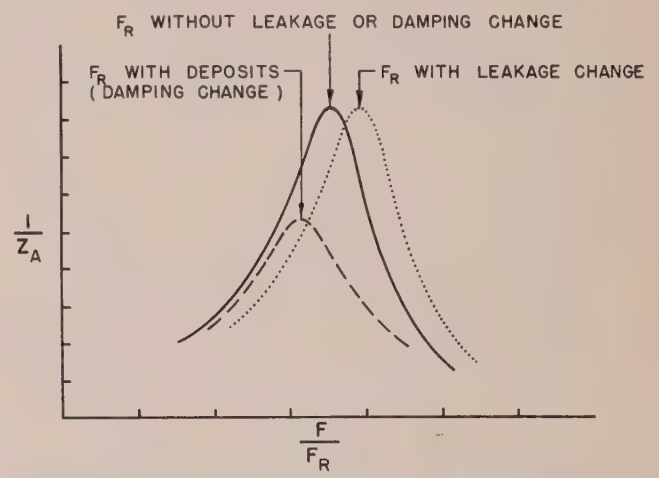

Fig. 5 – Theoretical frequency shifts due to leakage and chamber deposits – F = applied frequency, F_R = resonant frequency, Z_A = acoustic impedance

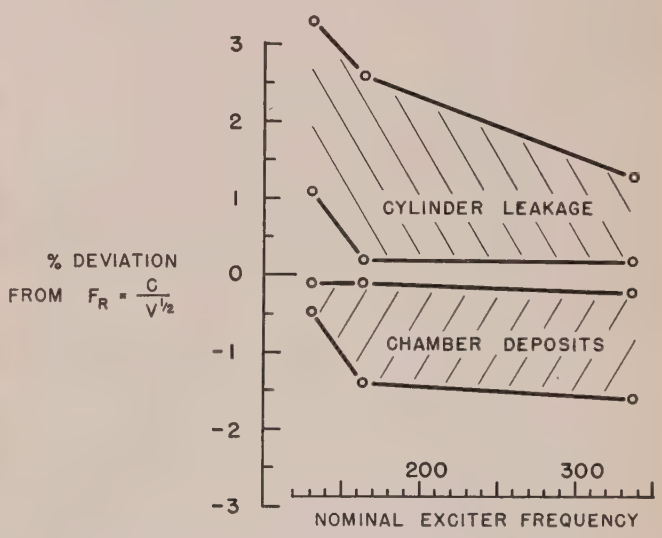

Fig. 6 – Actual frequency shifts due to leakage and chamber deposits

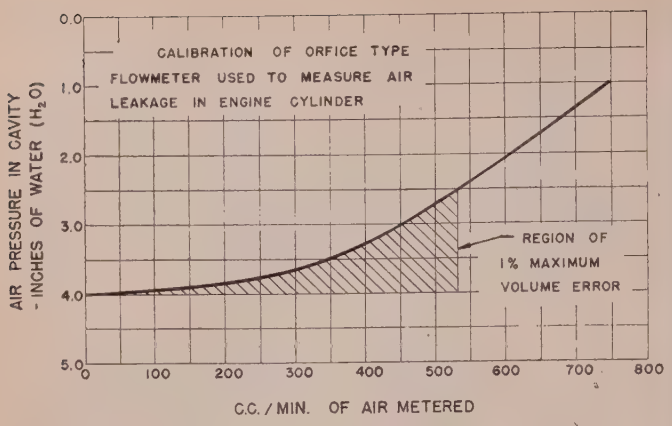

Fig. 7 – Relationship between cylinder leakage and maximum volume error

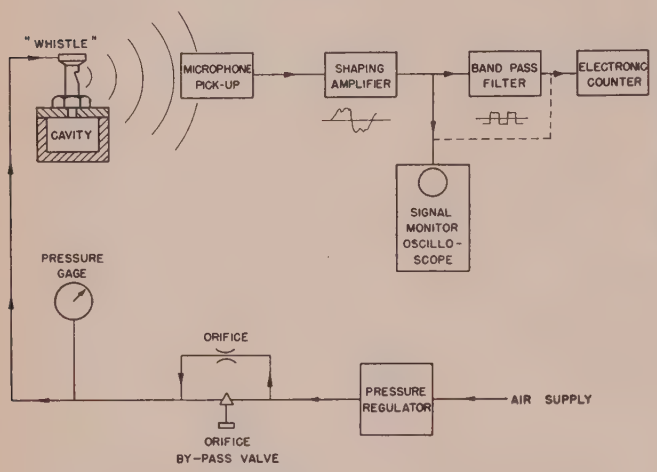

Fig. 8 – Schematic diagram of sonic volume comparator

dimensions and chamber size), is picked up by microphone, and is filtered, amplified, and shaped into a series of square voltage pulses. The electronic counter totals the number of pulses occurring in a 1-, 10-, or 100-second interval of time.

The advantages of measuring frequency of chamber oscillation by an integration or counting technique are the following:

1. A completely stable indication is automatically rendered in numerical form to an accuracy of ± one digit in the total number of cycles counted.
2. By varying the counting period, any desired number of digits in the value of the resonant frequency may be secured.
3. All major electronic components are standard commercial laboratory units requiring no design or development time.

The physical nature of the instrumentation is illustrated in Fig. 9 and the air jet exciter in Fig. 10. The physical dimensions of the exciter are such that it can replace either a 14- or 18-mm spark plug and its throat dimensions (length/area ratio) were designed to yield maximum freedom from leakage and end effects due to surrounding obstructions.

Fig. 9 – Instrumentation used in sonic volume comparator

Sonic Comparator Characteristics

The precision-ground master reference volume of Fig. 10 must be used to establish the constant C_1 of equation (3) since the ambient air temperature may easily vary between measurements. In practice however, the necessity for calculating C_1 or the preparation of curves or tables relating frequency and volume is eliminated by adding wafer-shaped precision-volume masters to the reference cavity until its volume is within 1 cc of the combustion chamber being measured. Over a 1 cc range the difference in counter readings is then nearly a linear function of the volume difference between the chamber and reference cavity.

In using cylindrical reference volumes care must be taken to establish a shape correction factor for the particular design or combustion chamber being measured (Fig. 11). Shape sensitivity is due to the change in the effective length of the exciter throat due to differences in the rate of change of cavity cross-section in the region adjacent to the exciter in the combustion chamber and the reference master. Once established (by independently determining the chamber volume), the shape correction factor is constant for a specific design of combustion chamber.

The sensitivity of the sonic volume comparator is demonstrated by measuring the resonant frequency of the master chamber before and after enlarging it 0.04 cc (Fig. 11). The change in resonant frequency is 12 cycles in 16,400, or sufficient to sense volume changes of the order of 0.02 cc.

Temperature sensitivity resulting in a volume error of approximately 1% exists for every 5 F difference between combustion chamber and reference master. In practice, however, such differences are easily eliminated by allowing sufficient time for temperature equalization in a stable thermal environment.

Limitations of Sonic Volume Comparison

In spite of the great potential stability and accuracy of comparing volume by acoustic resonance, it can be seen clearly that the frequency shift caused by cylinder leakage and carbon deposits will generally introduce an average uncertainty of volume data of ± 1%. For the precise determination of amount of carbon buildup, this uncertainty in total combustion-chamber volume cannot be tolerated because, as previously noted, carbon buildup is found by volume difference and the amount of buildup is of the order of only a few cc. Furthermore, since the density of carbon deposits as well as deposit volume is often required, additional methods for accurate volume measurements of carbon deposits when removed from combustion chambers are needed.

Theory of "Pneumatic" Volume Measurement

To measure volume without recourse to the dynamic properties of resonant chambers requires the ability, basically, to add (or remove) a definite weight of air to an unknown space or cavity. The resulting pressure change in the cavity will be a function of the volume. From the equation of state for a perfectly elastic gas (Fig. 12), it can be seen that if the temperature and weight of a gas occupying a space are either constant or a known quantity, the volume occupied is a function of the absolute pressure. For example, an unknown volume V_x (Fig. 12), could be determined by subtracting a definite weight of air from V_x and measuring the pressure of this gas in a chamber of known size, V_y. Thus if the pressure P_1 in V_x is initially greater than pressure P_2 in V_y, a definite weight of gas W_1 could be transferred from V_x to V_y. W_1 initially occupied V_x at a partial pressure equal to $P_1 - P_3$. Applying the equation of state for W_1 pounds of gas at a partial pressure equal to $P_1 - P_3$ in V_x allows a direct solution for the desired unknown volume V_x if the temperature T_1 remains constant.

Internal Temperature Change

One of the problems of previous pneumatic volume-measuring instruments has been internal temperature changes due to compression of air in the system. Note that in the process described above the expansion taking place is thermodynamically a constant enthalpy throttling process. From the Joule-Johnson experiment in classical physics it was found that temperature change is practically zero for gases with low boiling points which expand without doing external work – air, for example. Thus T_1 in the above process can be considered constant.

Practical "Pneumatic" Volume-Measurement Instrumentation

From the equation for V_x (Fig. 12), it can be seen that a solution for V_x would require the pre-

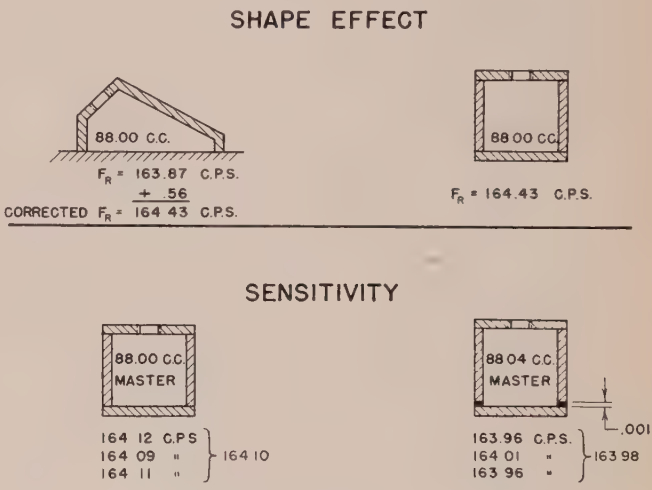

Fig. 11 – Illustration of shape effect and sensitivity

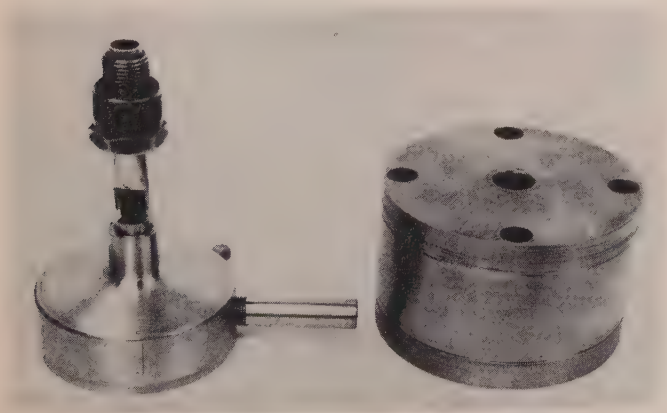

Fig. 10 – Exciter and master reference chamber

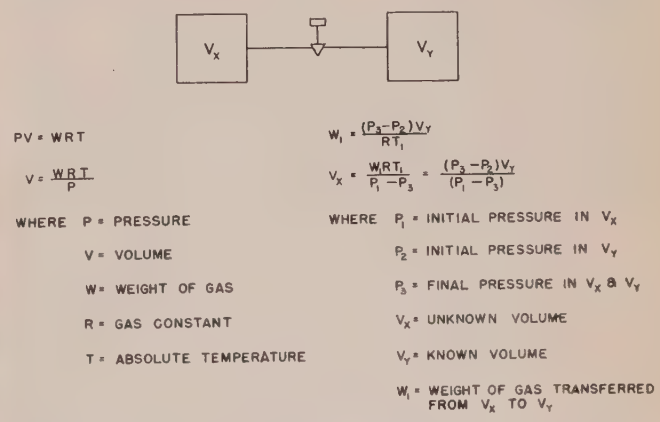

Fig. 12 – Development of pneumatic method of volume measurement

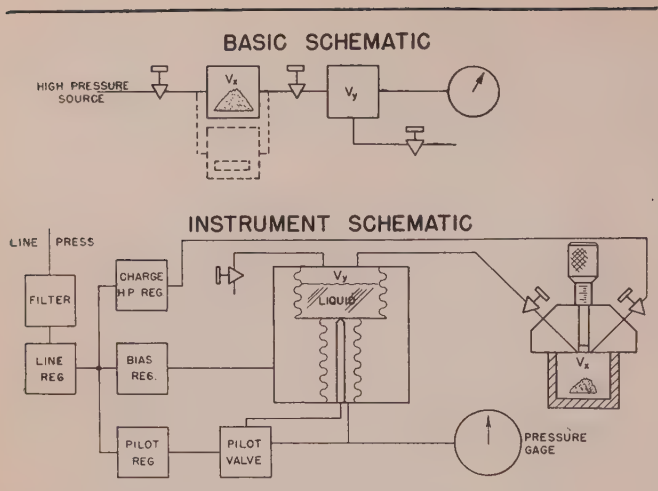

Fig. 13 – Schematic of pneumatic volume comparator

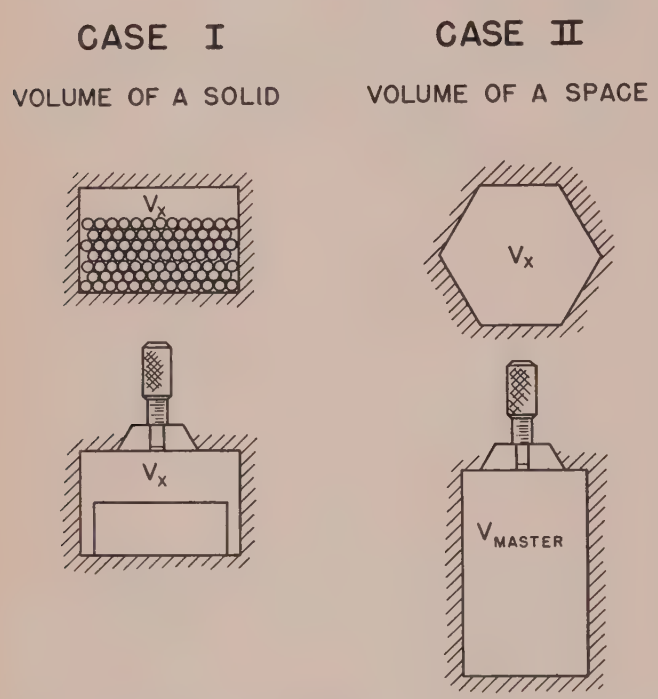

Fig. 14 – Measurement of a solid volume or a cavity by the pneumatic method

cise measurement of three pressures and one reference volume V_y. A more practical scheme is illustrated in Fig. 13. The space or object whose volume is being measured is placed in series with an arbitrary reference volume V_y. After charging the space or volume surrounding a solid material with air, the supply is cut off and the air allowed to expand into V_y. A sensitive pressure indicator is set to indicate the level of the equilibrium pressure. The process is repeated using a precise master to replace the unknown volume and adjusting the effective size of this master until the same final pressure reading is obtained. Thus, by using a strictly comparative process, the necessity for precise measurement of both initial pressures P_1 and P_2 and the reference volume V_y is eliminated. The final or equilibrium pressure indicator can be made highly sensitive since it acts only as a comparison gage in which calibration or range is unimportant.

The lower section of Fig. 13 shows the actual pneumatic circuit used in the instrument. The charging pressure is adjustable to any level from 0 to 45 psi. After selecting an arbitrary charging pressure, the charging regulator maintains the pressure P_1 to within 0.0004 psi. The reference volume is actually a bellows loaded on the exterior by an adjustable preload or bias pressure set slightly below the expansion pressure P_3. Air from the automatic pilot valve adjusts the pressure in the small balancing bellows until a force balance exists between the force exerted by the equilibrium pressure P_3 and the sum of forces due to bias and balancing bellows pressures. Due to the fixed area ratio of the bellows, the gage sensitivity is amplified to 59 times its normal value of 0.05 in. of Hg. The pressure sensing ability of the indicator is of the order of 0.0003 psi over a range from 0 to 20 psi.

Fig. 14 shows schematically the two basic types of volume measuring problems solvable by pneumatic comparison methods. Case I represents the measurement of a solid material by comparing the space surrounding the solid matter with the space surrounding a precise master. Case II illustrates the measurement of any air tight cavity by comparison to a precision cylinder. The accuracy of measurement is enhanced in Case I by the ratio of the volume occupied by the solid material to the volume of the residual space, or, in the case of powdered material, the interstitial space.

Fig. 15 illustrates the pneumatic volume-comparator indicator unit, test cavity stand, and precision-wafer type cylindrical reference masters. The indicator unit contains all pneumatic circuit components and controls with the exception of the test chambers, which are located externally to facilitate design changes arising from special test conditions.

Fig. 16 is an internal view of the indicator unit showing line pressure and pilot pressure regulators and the pneumatic amplifier. Regulators, amplifier, and pilot valve are standard commercially available pneumatic-control components.

A photograph of a test chamber and typical sample of combustion chamber deposits are shown in Fig. 17.

Pneumatic Comparator Characteristics

The basic sensitivity of pneumatic volume comparator when used to measure a cavity is 0.01% (see Fig. 18), or one part in 10,000. This sensitivity is constant regardless of the magnitude of volume measured, a condition which allows high accuracy when measuring small amounts of material encountered in analyzing combustion-chamber deposits.

The lower section of Fig. 18 defines the relationship between a change in final pressure per unit

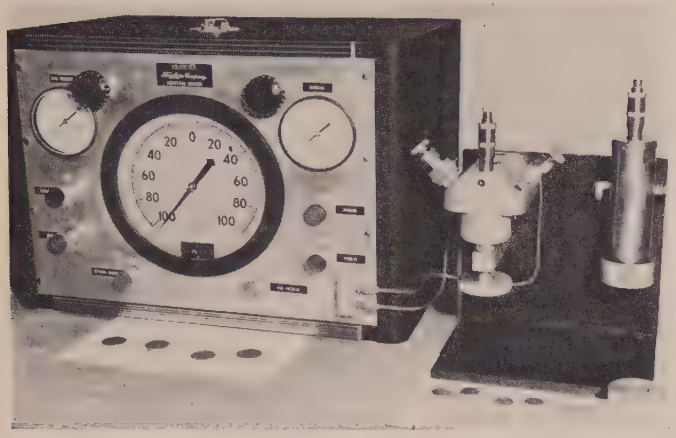

Fig. 15 – Pneumatic volume comparator, indicator unit, test chamber, and wafer-type volume masters

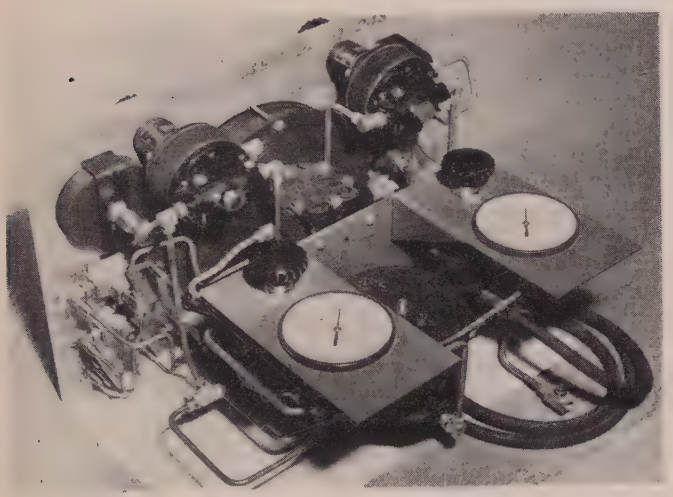

Fig. 16 – Interior of indicator unit

Fig. 17 – Test chamber and deposit sample

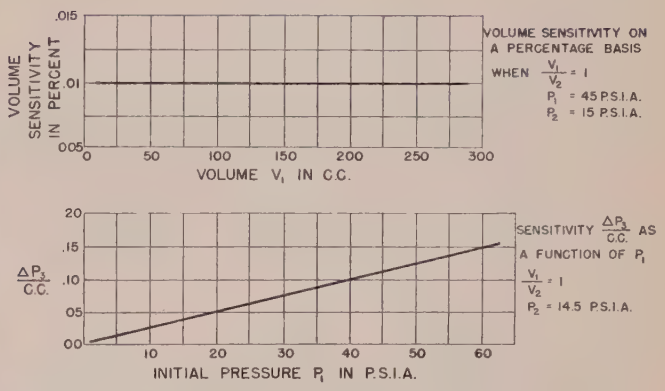

Fig. 18 – Sensitivity curves for pneumatic comparator

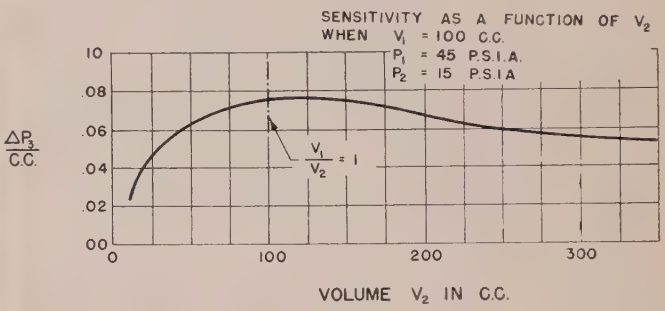

Fig. 19 – Optimum volume ratio between unknown volume and indicator volume for pneumatic volume comparator

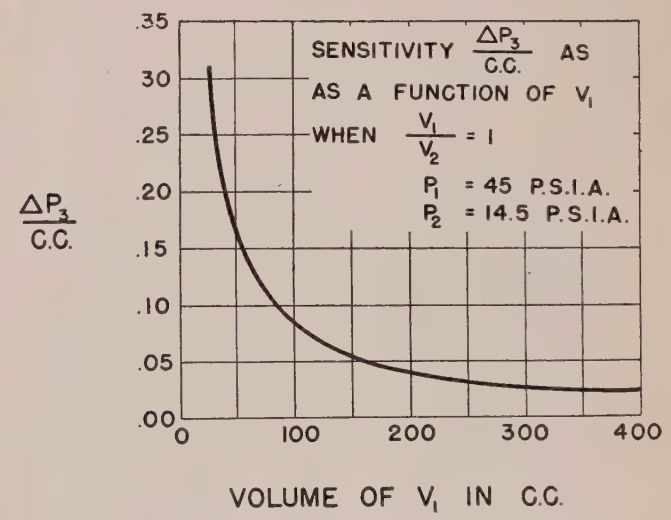

Fig. 20 – Response of pneumatic volume comparator to changes in magnitude of the unknown volume

change in measured volume. The data indicate that the absolute sensitivity P_3/cc is a linear function of the initial pressure P_1.

In Fig. 19 the effect of the relative size of the reference volume V_2 (V_y of Fig. 13), has been explored. The optimum relationship is a volume ratio of 1 to 1. If V_2 is either zero or infinite, sensitivity is zero. However, a practical operational range exists in the region where V_2 is not larger than 2 to 3 times the size of the volume under measurement, V_1 (V_x of Fig. 13).

The data in Fig. 20 reveal that the sensitivity per unit volume becomes very high for small volumes, or that we are able to measure easily 1/1000 cc in the small volume region.

Relative Merits of Sonic and Pneumatic Methods

Summarizing the merits of the pneumatic volume comparator and the sonic volume measuring technique, we note the following:

1. Because it uses a dry, low-viscosity fluid, the nondynamic pneumatic method can measure the volume of any solid material (carbon deposits, for example) or cavity (without leakage) regardless of size or complexity of shape. When leakage is present as in combustion chambers the dynamic or sonic technique must be employed.

2. The sensitivity of the pneumatic method is equal to or better than the sonic method and is roughly 20 times as accurate as the usual 100 cc burette.

3. The pneumatic comparator practically eliminates calibration error since the wafer-type volume masters can be checked by means of gage blocks. "Shape" corrections and other restrictions inherent in sonic methods are also avoided.

4. The pneumatic method is especially adaptable to measurement of combustion chamber deposits since wetting and flotation problems of liquid measurement are eliminated and the damping problem of the sonic method is avoided.

The rapidity of volume measurement offered by both the sonic and pneumatic methods so far exceeds conventional techniques that many areas of combustion research requiring volume determinations are opened because of the increased ability to gather data. The typical overall accuracies that can be reasonably expected for the most common applications are as follows:

Carbon deposits	± 0.01%	(pneumatic)
Cylinder-head chamber	± 0.1%	(sonic)
Combustion-chamber volumes	± 1.0%	(sonic)
Engine timing (top dead-center determination)	± 0.25 deg	(sonic)

Conclusions

Sonic and pneumatic instrumentation for measurement of volume have provided a highly accurate and efficient solution to special problems in volume measurement encountered in combustion-chamber research. Each of the instruments and techniques discussed can be used effectively if the characteristic limitations of the method, whether sonic or pneumatic, are clearly appreciated. Undoubtedly there are applications other than those associated with combustion-chamber research in which the unique characteristics of "dry" volume measurement can be successfully employed.

Acknowledgment

The author wishes to acknowledge the aid received from W. G. Moline, R. L. Dennis, J. Kovacs, and B. Mandel of the Research Instrumentation Section, and A. E. Cleveland and H. T. Niles of the Research Engine Section in the development of the instruments discussed in this paper.

References

1. NACA TN-27 (1920), "Instrument for Measuring Clearance Volumes," by S. W. Sparrow.

2. "Introduction to Principles of Pneumatic Gaging," by D. B. Kirk. Paper presented at ASME Annual Meeting, New York, Nov. 30-Dec. 5, 1952.

3. *Instruments,* Vol. 18, September, 1945, pp. 598-603: "Solution of Instrumentation Problems by Pneumatic Null Balance Method," by C. B. Moore.

4. "Elements of Acoustical Engineering," by H. F. Olson. Pub. by Van Nostrand, New York, 1940.

5. "Acoustic Measurements," by L. L. Beranck. Pub. by Wiley, New York, 1949.

6. *Physical Review,* Vol. 28, November, 1926, pp. 1038-1047: "Direct Absolute Measurement of Acoustic Impedance," by G. W. Stewart.

7. "Fundamentals of Acoustics," by L. E. Kinsler and A. R. Frey. Pub. by Wiley, New York, 1950.

8. *Journal of Acoustical Society of America,* Vol. 25, November, 1953, pp. 1068-1083: "Study of Factors Influencing Damping of Acoustic Cavity Resonator," by R. F. Lambert.

9. *Journal of Acoustical Society of America,* Vol. 25, January, 1953, pp. 138-146: "Characteristics of Jet-Edge-Resonator Whistles," by W. L. Nyborg, C. L. Woodridge, and H. K. Schilling.

10. *Journal of Acoustical Society of America,* Vol. 25, November, 1953, pp. 1037-1061: "On Theory and Design of Acoustic Resonators," by U. Ingard.

Steels and Protective Treatments For Use up to 1000 F

H. J. Noble and W. H. Sharp,
Pratt & Whitney Aircraft, Division of United Aircraft Corp.

This paper was presented at the SAE Golden Anniversary Summer Meeting, Atlantic City, June 14, 1955.

THIS discussion of steels and protective treatments for use up to 1000 F is divided into three parts.

First, the factors involved in the selection of appropriate steels are covered, emphasis being placed on the role of martensitic chromium steels, which combine strength with rust resistance. The effects of rusting of these steels and its prevention, as well as elevated-temperature considerations, are discussed.

Second, stress-corrosion of martensitic chromium steels is covered, and ranges are established in which these steels are prone to failure by this mechanism.

Third, the authors deal with protective coatings and set down the temperature ranges in which the protective coatings are used to advantage.

IN selecting steels for use up to 1000 F, a number of factors may come into play. All factors may be significant, and it would be difficult indeed to list them in order of importance. The physical properties such as resistance to oxidation and corrosion, resistance to erosion and wear, modulus of elasticity, coefficient of thermal expansion, and thermal conductivity may either all or in part come in for early consideration. Some of the following mechanical properties at room and elevated temperature, in all likelihood, will be involved: tensile properties including ductility, hardness, hardenability, creep and rupture strength, and fatigue strength. Resistance to stress-corrosion, which bridges the gap between physical and mechanical properties, has recently taken on new significance and may require consideration. Then, inevitably, we must take into account castability, forgeability, machinability, formability, and ability to be welded or brazed. Last, but certainly not least, we must consider alloy content as it affects the strategic index and the associated factors of cost and availability.

In selecting steels for use in aircraft engines,

and particularly in engines for military aircraft, it has become highly important to employ steels with the lowest possible strategic index. Without actually assigning values to the strategic elements, we can mention that columbium, tantalum, cobalt, tungsten, chromium, molybdenum, and nickel are all limited in supply, and that the use of these elements must be held to a minimum. Requirements of high percentages of cobalt, chromium, tungsten, and nickel in the alloys used for parts operating at temperatures above 1000 F, for example, turbine blades, stators, and discs of turbine engines, have necessitated stringent curtailment of use of these elements in the compressor sections and in lower-temperature parts of the turbines.

In general, selection of steels for use below 1000 F has been made from among the hardenable low-alloy constructional steels, the martensitic chromium steels and the austenitic stainless steels. Steels in greatest use at Pratt & Whitney Aircraft are listed under each of these three categories in Table 1.

Low-Alloy Steels – The practice of selecting a conventional hardenable low-alloy steel wherever practicable is adhered to, but there are a number of considerations coming under "practicability" which require explanation. Parts of relatively simple design may be made of heat-treated AMS 6280 (AISI 8630), AMS 6322 (AISI 8740), or AMS 6415 (AISI 4340) steels suitably protected by cadmium plate, provided that operating temperatures are in the useful temperature range for these types of steel, and that the protective coating (a) does not melt or otherwise break down at operating temperatures, (b) has resistance to abrasion by small particles frequently present in the air, and (c) does not seriously reduce fatigue strength of the part or otherwise jeopardize its life by reason of inducing high residual tensile stresses near surfaces.

When parts are complex in shape – for example, hollow struts welded onto skin sections – it usually is impractical to use any of the electrolytically plated coatings because of the limitation on throwing power. In such cases one must consider alternates such as electroless nickel or a paint, both very good protective coatings in the right location, but subject to limitations to be discussed subsequently in this paper.

In our various turbojet and turboprop engines, many parts are made of low-alloy constructional steels suitably protected by plated coatings, sprayed aluminum or paints. The low compressor cases of the J-57 turbojet engine, for example, are fabricated from AMS 6280 (AISI 8630) flash butt-welded flanged rings fusion-welded to AMS 6355 (AISI 8630) sheet, and the assemblies cadmium plated for corrosion protection. The turbine shaft of the J-57 engine is an AMS 6415 (AISI 4340) steel forging protected by an aluminum-pigment silicone resin paint having good resistance to heat and to hot engine oil.

Chromium Martensitic Steels – It is obvious that either because of the conditions under which a part operates or its complexity, the designer and metallurgist frequently will be forced to consider one of the martensitic chromium steels, for this class of steels combines the heat-treatability of low-alloy hardenable steels with a fair amount of rust and oxidation resistance. It is seldom that the designer and metallurgist can pass up consideration of the martensitic chromium steels for the lower strength austenitic stainless steels for applications under approximately 800 F, except in instances where the requirement is for the optimum in corrosion and oxidation resistance or for a large coefficient of thermal expansion. Alternatives to the use of martensitic chromium steels lie in the possible application of the precipitation-hardening stainless grades, such as AMS 5643 (AISI 17-4PH)

Table 1 – Steels Used at Temperatures below 1000 F

AMS or PWA Specification			Nominal Composition, %								
Bar, Forging	Sheet, Strip	SAE Type or Brand	C	Cr	Ni	Mo	Si	W	V	S	Ti
Low-Alloy Constructional Steels:											
6280	6355	8630	0.30	0.5	0.55	0.2	....	....	....	....	..
6322	....	8740	0.40	0.5	0.55	0.25	....	....	....	....	...
6415	....	4340	0.40	0.8	1.8	0.25	....	....	....	....	..
6302	....	Timken 17-22A(S)	0.30	1.25	....	0.5	0.65	....	0.25	....	.
PWA 722	....	Bethlehem Templex or Timken 17-22A	0.45	0.95	....	0.55	....	....	0.3	....	. .
Martensitic Chromium Steels:											
5613	5504	51410	0.12	12.5	....	....	....	..	.	....	...
5610	....	51416F	0.12	12.5	....	....	....	....	....	0.25	..
5615	....	51414	0.12	12.5	2.0	....	....	...		....	.
5616	....	Greek Ascoloy	0.15	13.0	2.0	....	....	3.0		..	.
5630	....	51440C	1.10	17.0	....	0.5	....	...		..	. .
Austenitic Stainless Steels:											
5637	5515-5517	30302	0.15 max	18.0	8.5	....	....	....	....	....	...
5640	....	30303F	0.15 max	18.0	9.0	....	....	....	....	0.25	....
5645	5510	30321	0.08 max	18.0	10.0	....	....	....	....	....	0.60
5648	5524	30316	0.08 max	18.0	13.0	2.3	....	...	....	....	.. .

or AMS 5644 (AISI 17-7PH) steels which have been employed successfully in aircraft in highly stressed low-temperature applications. However, these steels have the disadvantages of increased alloy content and elevated-temperature instability. These steels usually are restricted to temperatures below 600 F because of their instability.

Design of the compressor and diffuser sections of our axial flow turbojet and turboprop engines is based substantially upon utilization of one of the martensitic chromium steels, AMS 5613 or 5504 (Table 1). This steel was chosen for many details and assemblies because of its rust-resistant property coupled with the high strength available in the hardened and tempered condition. In a few instances AMS 5613 is used in the annealed condition, or hardened and tempered to a low-hardness range of Rockwell B 90-100, but in the majority of applications it is employed in the hardness ranges Rockwell C 25-33 for moderately stressed parts, and RC 30-38 for highly stressed parts. In one unusual instance, a compressor stator vane is hardened to RC 35-40 to permit the vane to be used to punch its own slot in the compressor outer shroud, which is left in the annealed condition to facilitate punching. Cold rolling the heat-treated vane stock has been employed in this case to maintain hardness consistently near the upper limit of RC 40.

Another chromium martensitic stainless steel used for numerous applications is AMS 5616 (Table 1), containing 2% nickel and 3% tungsten in addition to the chromium. This steel is familiarly known as Greek Ascoloy. We have employed this steel successfully for highly stressed parts such as bolts, compressor blades, and turbine discs. Normally, for use at temperatures up to 800 F or slightly higher, we specify a hardness range of RC 30-38 for this steel. By virtue of its higher carbon content and its resistance to tempering, we have found that this steel can be employed up to a hardness range of RC 45-50, where it displays ductility of a relatively high order contrasted to steels of types 420, 440A, or 440C, which are brittle at high hardness.

Figs. 1 and 2 show the various mechanical properties of AMS 5613 steel in the quenched, quenched and tempered, and annealed conditions. The sharp downward break in the hardness curve in the tempering range of 950 to 1100 F is well known. Brittleness between tempering temperatures of 750 to 1000 F is reflected in the dip of the Izod impact curve in this range. Although manufacturers of this grade have long recommended that this steel be used hardened and then stress-relieved below 700 F to assure maximum rust resistance with good impact ductility, it has generally been considered undesirable to employ this heat-treatment for jet-engine applications entailing operating temperatures above 700 F, which may cause possible embrittlement during service. Stress-relief below 700 F, furthermore, leaves parts with high residual

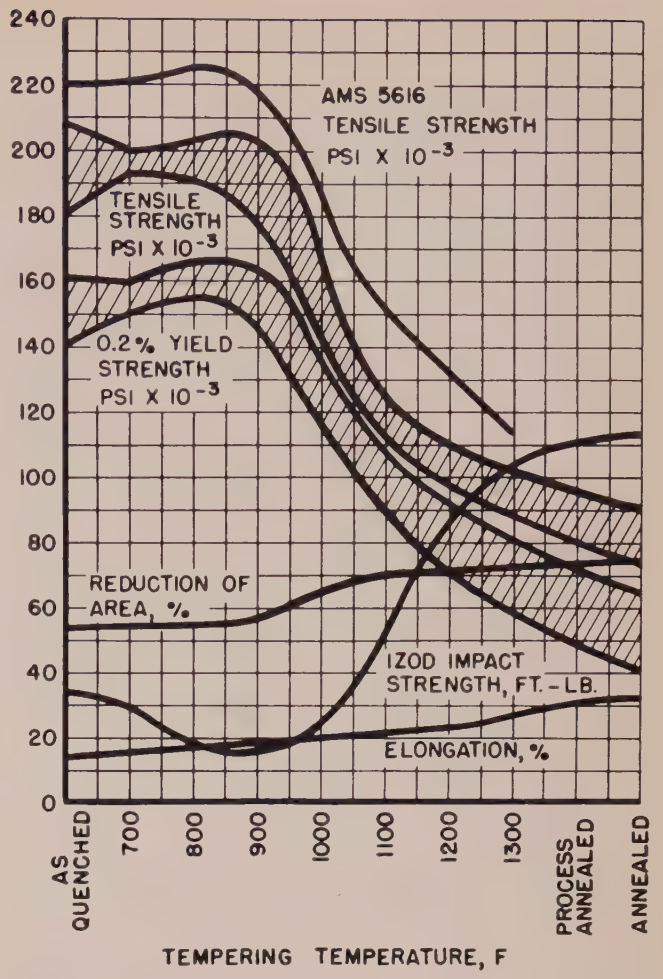

Fig. 1 – Effect of 2-hr tempering at various temperatures on tensile properties of AMS 5613 (AISI 410) steel and on tensile strength of AMS 5616 (Greek Ascoloy) steel

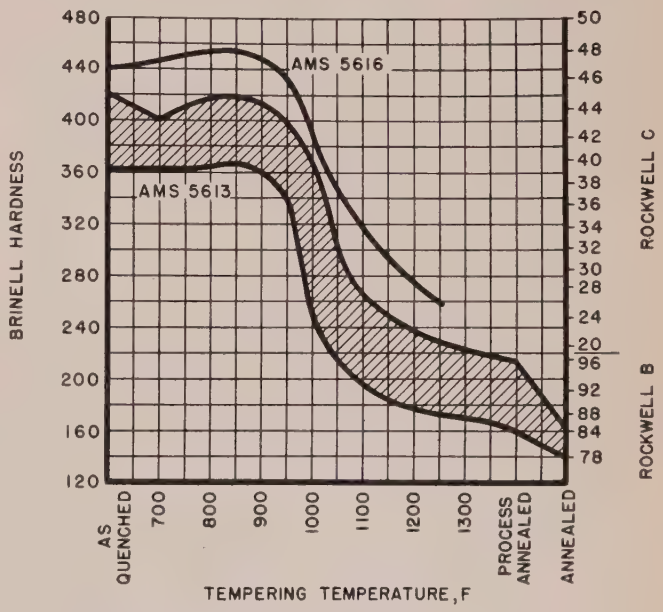

Fig. 2 – Effect of 2-hr tempering at various temperatures on the hardness of AMS 5613 (AISI 410) and AMS 5616 (Greek Ascoloy) steels

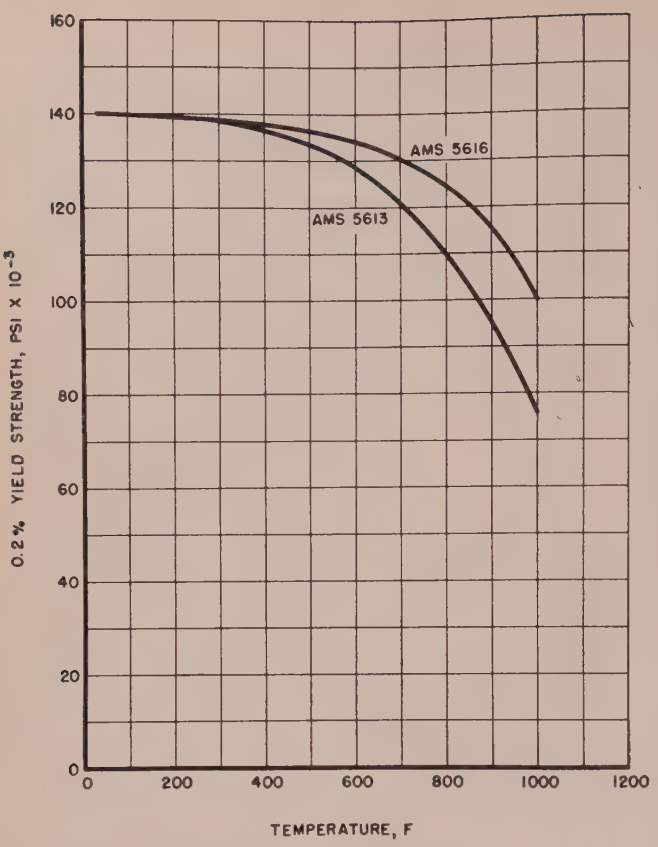

Fig. 3 – Effect of temperature on yield strength of AMS 5613 and AMS 5616 steels at hardness of RC 36

stresses which may cause distortion during machining, fabrication, or during engine operation. Thus, the hardness ranges of RC 25-33 and RC 30-38 were selected because they necessitate tempering at 950 to 1100 F, which range stabilizes the steel for use up to 800 F and provides adequate stress-relief.

For purposes of comparison, the effects of tempering temperature on tensile strength and hardness, respectively, of AMS 5616 are included in Figs. 1 and 2. Although the curves represent the typical condition, it should be added that tensile strength and hardness have been observed to be less subject to scatter in AMS 5616 than in AMS 5613. This is due to the presence of 2% nickel and the higher (0.12-0.17%) carbon content, which reduce the amount of delta ferrite in this grade. Note that above 1000 F, AMS 5616 may be tempered 100 F or more higher than AMS 5613 to obtain the same strength and hardness, a fact which suggests better properties at elevated temperature for AMS 5616.

Fig. 3 shows tensile yield strength from room temperature to 1000 F of AMS 5613 and AMS 5616 steels hardened and tempered to RC 36. The curve for AMS 5616 has the same general shape as that for AMS 5613, but maintains considerably higher strength above 600 F. It is obvious that AMS 5616 steel can be used at temperatures at least 50 F higher than AMS 5613, at this hardness and under the same stress.

Table 2 shows the effect of testing temperature on fatigue strength of AMS 5613 and AMS 5616 steels, both heat-treated to room-temperature hardness of RC 34. At room temperature both steels show a fatigue strength (R. R. Moore rotating-beam) of 78,000 psi, while at 1000 F the fatigue strength of AMS 5616 is 53,000 psi in contrast to 42,000 psi for AMS 5613. The latter values were obtained on Westinghouse-type (reverse bending) machines.

These figures indicate why AMS 5616 is a far better choice for compressor blades and other applications where engine operating temperatures may reach 800 F or higher. Although no direct comparisons are available for creep at elevated temperature for the same level of hardness for the two steels, there is no doubt that AMS 5616 shows definite superiority in this respect too. Limited testing indicates that Greek Ascoloy has an advantage of about 100 F in creep strength.

Low-Alloy Heat-Resistant Steels – Two steels currently used for highly stressed engine parts operating up to about 800 F are AMS 6302 and PWA 722 (Table 1). Both develop high creep strength at temperatures up to 900 F or above when heat-treated to develop the ferrite-carbide structure familiarly known as Widmanstätten structure, usually obtained by normalizing from about 1750 F and tempering at about 1100 F to RC 32-38 or 35-40. The lower carbon AMS 6302 is used mainly for bolting applications, while the higher carbon PWA 722 is used for parts with heavier sections such as high-pressure compressor discs, spacers, and shafting. Oxidation and corrosion protection for both steels is obtained by a diffused nickel-cadmium plate, which affords good protection up to about 1000 F. Although comparison of elevated temperature tensile and yield strengths of AMS 5616 and PWA 722 steels, both at a hardness level of RC 36-38, indicates little, if any, advantage for the latter steel up to 1000 F, comparison of creep properties shows a marked difference. Fig. 4 shows the decided advantage of PWA 722 over AMS 5616 with respect to creep strength. Stress to produce 0.1% creep in 150 hr is substantially higher for PWA 722 steel from 700 to 1000 F. These curves demonstrate why PWA 722 is preferred for compressor discs and other

Table 2 – Fatigue Strength at 10^7 Cycles of AMS 5613 and AMS 5616 Steels at Hardness of Rockwell C34
(Values given in psi)

Temperature, F	AMS 5613	AMS 5616
Room temperature	78,000	78,000
1000	42,000	53,000

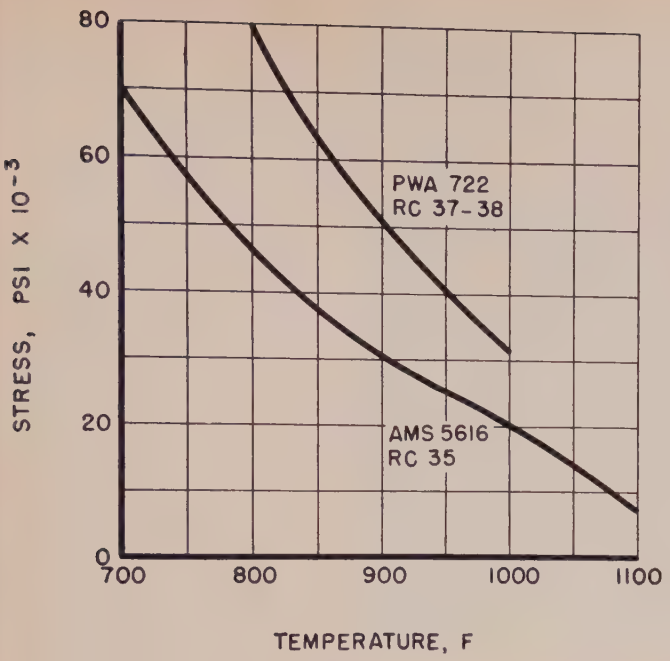

Fig. 4 – Stress to produce total plastic creep of 0.1% in 150 hr for AMS 5616 and PWA 722 steels as function of temperature

parts operating within this temperature range. The slight hardness advantage enjoyed by PWA 722 steel, RC 37.5 as opposed to RC 35 for AMS 5616, is not significantly relative to creep strength, although this hardness advantage would have a definite effect on tensile and tensile yield strengths at elevated temperature.

Structure versus Strength of Martensitic Chromium Steels – Aircraft-engine manufacturers for many years have employed low-alloy hardenable steels manufactured to high standards of cleanliness. It has long been the practice, furthermore, to exercise rigorous control over heat-treatment of these steels to obtain a consistent structure and absence of free ferrite. There can be little question that nonmetallic inclusions and free ferrite can reduce fatigue strength of engine parts, particularly where end-grain is present on a surface that is moderately or highly stressed. We have observed that inclusions and free ferrite impart to various steels serious directional effects for properties other than fatigue. Where the principal stress is normal to the grain flow, parts will be more prone to fracture under static or impact loading with inclusions or ferrite present. When the direction of stress and grain flow is the same, little effect, if any, on fatigue and tensile properties has been found.

It is well known that the high chromium and low carbon in martensitic chromium steels such as AMS 5613 and AMS 5610 (AISI 416) favors formation of delta ferrite which cannot be removed by ordinary heat-treatment. AMS 5615 (AISI 414) and AMS 5616 contain less ferrite by virtue of 2% nickel and, in the latter steel, higher carbon.

To determine the effect of ferrite as opposed to the effect of inclusions upon fatigue endurance, two heats of free-machining AMS 5610 steel with approximately 1 and 10% ferrite by volume, respectively, a heat of AMS 5613 with less than 1% free ferrite, and a heat of AMS 5615 with less than 1% ferrite were subjected to room-temperature rotating-beam R. R. Moore fatigue tests. All specimens were hardened and tempered to RC 25, then machined and polished. The AMS 5610 steels were tested with longitudinal and transverse grain flow, whereas the AMS 5613 and AMS 5615 steels were tested only with transverse grain flow, for it was found that effects of ferrite were not significant with grain flow parallel to the axis of the specimens. Scatter bands are shown in Fig. 5. It is obvious that the effect of high ferrite upon fatigue endurance for specimens with transverse grain flow is far more pronounced than that of transversely oriented inclusions. We do not interpret these results as suggesting that inclusions are not important, for we believe they are, but reduction in fatigue strength by ferrite, a weak ductile phase, far overshadows the effect of inclusions.

In another study, a heat of AMS 5616 with an abnormal amount of free ferrite was impact-tested employing Charpy vee-notch test specimens. The photomicrograph of a longitudinal section (Fig. 6) shows clearly why impact strength was only 3 ft-lb where the grain flow was split, as opposed to 40 ft-lb or more with grain flow normal to the applied load.

These studies demonstrate the need for development of martensitic chromium steels that are ferrite-free. Unfortunately, the martensitic chromium steels currently employed for moderate temperature applications up to 800 F, such as AMS 5613, AMS 5616, and other 12% chromium steels containing tungsten, molybdenum, and vanadium contain delta ferrite which may have serious adverse effects upon mechanical properties. We are currently working on compositions which include

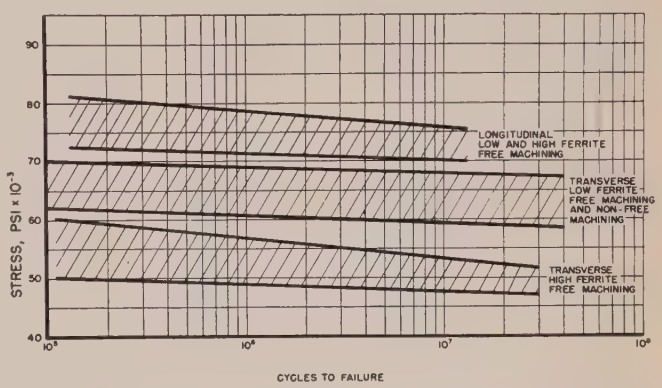

Fig. 5 – Endurance limit of free-machining and non-free-machining 13% chromium steels containing low and high delta ferrite

Fig. 6 – Brittle impact fracture along delta ferrite grains in AMS 5616 steel at hardness of RC 35. Original magnification: 500X

nickel and somewhat increased carbon to counteract the ferrite-forming chromium, tungsten, molybdenum, and vanadium. Chromium is desirable for rust resistance while tungsten, molybdenum, and vanadium, singly or in combination, tend to increase strength at elevated temperature.

Rusting of Martensitic Chromium Steels – Steel manufacturers have long recommended that martensite chromium steels be stress-relieved below 700 F after hardening in order to maintain optimum rust resistance. There is little argument with this recommendation, but such low-temperature stress-relief cannot be rationalized for these steels because of operating temperatures and residual-stress considerations.

When tested in a humidity cabinet, we have found that AMS 5613 and AMS 5616 steels with good surface finish do not rust in the hardened and stress-relieved, hardened and tempered (to RC 25-33 or 30-38), or annealed conditions. In salt spray, however, these steels show better rust resistance in the hardened and stress-relieved condition than in the highly tempered or annealed conditions. We have observed that AMS 5616 is generally slightly better than AMS 5613 with respect to rust resistance. It is well known that the best rust resistance is obtained if the martensitic chromium steels have a high surface finish.

While heat-treatment and surface finish both play a role in rust resistance, the most significant factor affecting rust resistance of type 400 steels of similar composition is the presence of contaminants on the steel surface. Traces of iron on the surface originating from rolling, forming, or machining operations constitute one factor, while oxides, whether embedded in the surface during rolling or produced during heat-treatment, constitute another. It is mandatory that sheet and strip be supplied in the pickled condition to assure material that is free from iron pickup and oxide. We have observed wide variations in rust resistance of these steels due to differences in processing of sheet and strip.

Other than polishing, we employ three processing treatments to assure optimum rust resistance of martensitic chromium steels. These are: (1) bright-hardening, (2) acid cleaning, and (3) abrasive blasting. Bright-hardening is normally applicable to parts which can be machined to finished dimensions prior to heat-treatment. Hardening is usually carried out in a cracked ammonia or hydrogen atmosphere. We have observed that bright-hardening of AISI type 400 steels in cracked ammonia or nitrogen is accompanied by nitriding if the atmosphere is dry enough to produce bright work. Nitriding lowers the ductility of the surface metal, and this may be serious when hardening martensitic chromium steels to hardness levels above RC 40, where ductility is at a premium. It has also been observed that retained austenite near the surface may increase when nitrogen pickup occurs. We have, therefore, discontinued the use of cracked ammonia for this purpose, and use hydrogen atmosphere only for bright-hardening.

Tempering after bright-hardening is carried out either in a nonoxidizing atmosphere or in air. The maximum tempering temperature in air is 800 F, up to which temperature we have found temper oxide to have negligible effect upon rust resistance. It is possible, however, to temper above 800 F and

restrict oxidation to the thinner oxide films by using argon or high-nitrogen atmospheres.

Acid cleaning, as used to remove iron contamination due to machining or forming, or to remove heat-treating oxide, is accomplished according to the following cycle:

1. Ten minutes in inhibited concentrated hydrochloric acid at 160 F, followed by a water rinse.
2. Five minutes in a solution of 20 parts concentrated nitric acid, 1 part concentrated hydrofluoric acid, and 79 parts water at room temperature, followed by a water rinse.
3. Five minutes in inhibited concentrated hydrochloric acid at 160 F, followed by a water rinse.
4. Two minutes in an alkaline neutralizing solution, followed by a water rinse.

Fig. 7 shows five types of martensitic chromium steels in the bright-hardened and tempered condition versus the hardened, tempered, and acid-cleaned condition after humidity testing for 100 hr. All specimens were bright-hardened from 1850 F and tempered in air at 600 F for 2 hr. The results demonstrate that the thin oxide coating produced at 600 F has no harmful effect upon rust resistance, compared to steels given the acid cleaning treatment to remove the oxide. There is also a clear cut case for the superior rust resistance of the low-carbon over the high-carbon grades, at least under the conditions of hardening and tempering imposed. Tempered above 800 F with temper oxide present, the five steels show severe rusting. Removal of the 800 F oxide by acid cleaning, however, provides about the same rust resistance as shown for the acid-cleaned specimens in Fig. 7.

Fig. 8 shows the pronounced effect of heavier oxide coatings on the rust resistance of AMS 5613 steel. The six hollow airfoil sections were hardened and then tempered at 1020 F for 3 hr, and all sections except *E* were acid cleaned to remove oxide. Parts were then stress-relieved at 1000 F for 4 hr. Sections *A*, *B*, and *C* were subjected to humidity cabinet testing with the oxide coating present, whereas *D*, *E*, and *F* were acid cleaned to remove oxide produced by the stress-relief treatment before humidity testing. The superior rust resistance of *D* and *F*, sections given two acid-cleaning treatments, is obvious. Section *E*, given only one acid-cleaning treatment, has somewhat inferior rust resistance as a result of inadequate oxide removal.

While bright-hardening and acid cleaning are by far the best methods of assuring optimum rust resistance for heat-treated martensitic chromium steels, it is not always possible to employ these protective treatments. Some welded assemblies frequently cannot be easily bright-hardened because of their large size, or consideration of distortion of large weldments may necessitate hardening of details prior to joining. In the latter instance, weldments will be given a final stress-relief treatment after welding and then cleaned to remove the oxide. Frequently, acid cleaning cannot be considered on complex weldments because of the hazard of acid entrapment and subsequent corrosion.

For many applications we have employed abrasive blasting with alumina to remove heat-treating oxide. While this method is not as satisfactory as

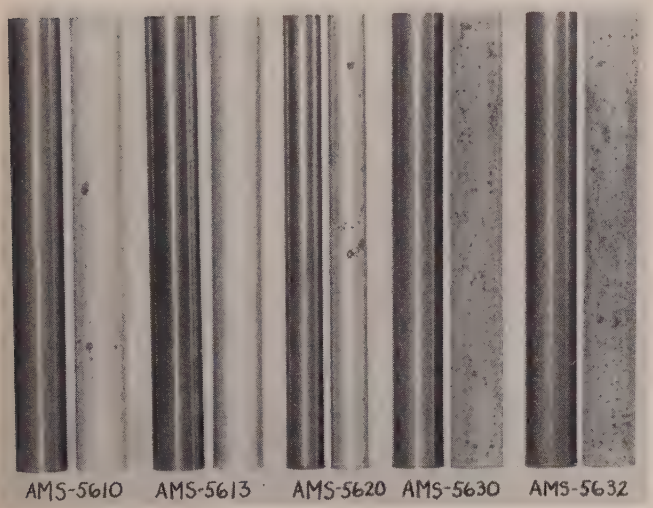

Fig. 7 – Stainless-steel test specimens after 100-hr exposure in humidity cabinet. Left-hand specimens of each pair are as heat-treated and tested; right-hand specimens were acid cleaned following heat-treatment

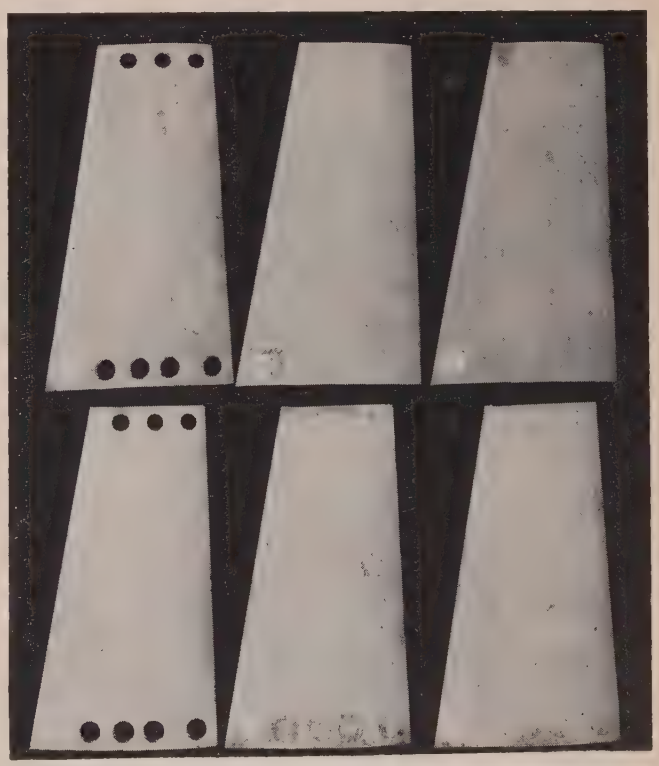

Fig. 8 – Effect of oxide removal by acid cleaning on rust resistance of hardened and tempered AMS 5504 steel. Lower airfoil sections were acid cleaned after tempering at 1020 F and after stress-relief at 1000 F, except *E*, which was cleaned only after stress-relief at 1000 F

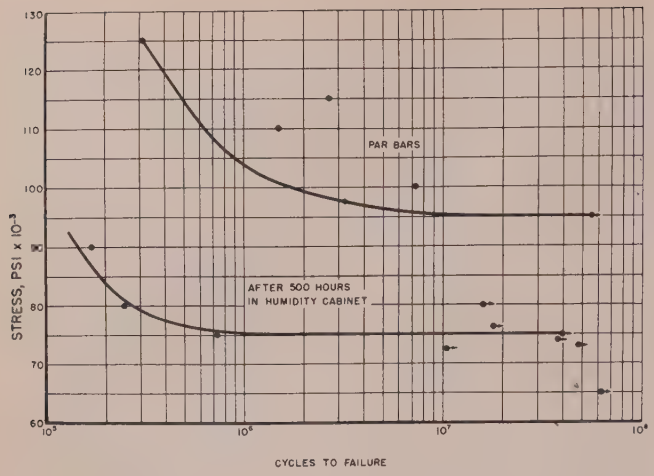

Fig. 9 – Endurance limit of AMS 5615 steel at RC 39-40 before and after 500 hr in humidity cabinet. Data were obtained with R. R. Moore-type fatigue specimens

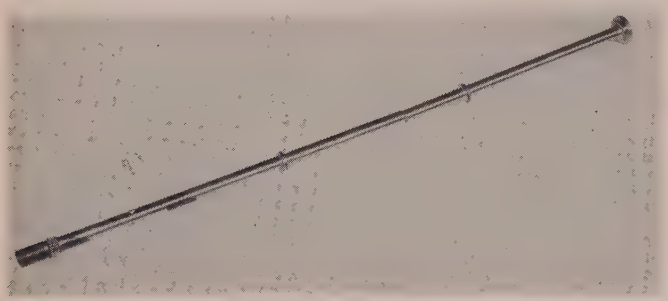

Fig. 10 – View of tie-rod showing location of fracture caused by stress-corrosion. Original magnification: ¼X

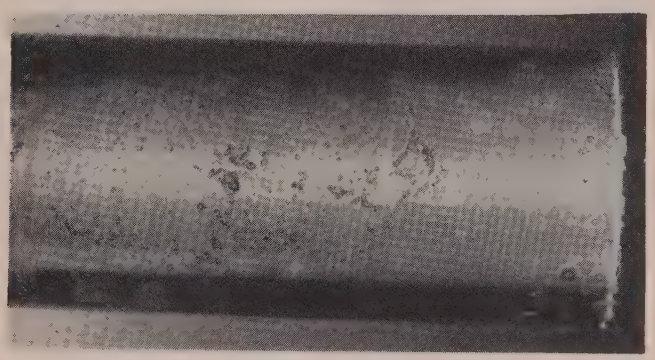

Fig. 11 – Enlarged view of tie-rod of Fig. 10, showing corroded area adjacent to fracture. Original magnification: 2½X

acid cleaning, it provides a surface with good rust resistance if the abrasive blasting is carried out thoroughly. Alumina is a relatively cheap and pure inert abrasive. Steel grits cannot be used because iron pickup causes as much rusting as blasting is supposed to prevent. Sand normally contains iron impurities, and we have learned that it is not a

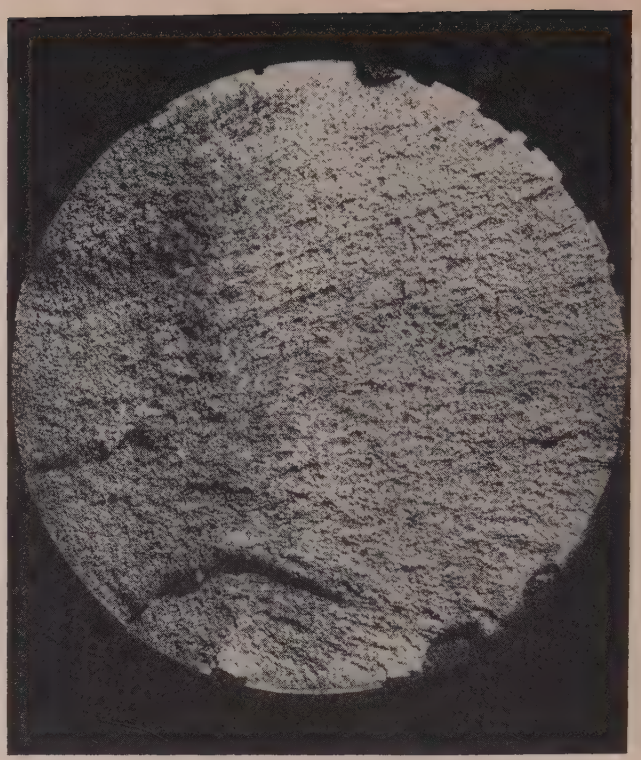

Fig. 12 – View of tie-rod fracture. Note discolored thumbnail patterns at OD. Original magnification: 4X

satisfactory abrasive for cleaning of rust-resistant steels.

That rusting of type 400 steels produces serious loss of fatigue strength was shown initially in AMS 5615 steel, a grade formerly chosen for compressor blades and discs because of freedom from ferrite. R. R. Moore fatigue-specimen blanks were hardened and tempered to RC 39-40 and then ground and polished. Half of the specimens were exposed to 95-100% humidity at 120 F for 500 hr, and after exposure there was at least one pinpoint of corrosion in the gage length per specimen. Fig. 9 shows that this amount of corrosion caused a decrease in the endurance limit of 20,000 psi, or 21%.

Summary – Chromium martensitic steels combine high strength with moderate rust resistance, but their use should be predicated on an understanding of heat-treatment as it affects mechanical properties and corrosion resistance. For temperatures up to about 800 F, AMS 5616 (Greek Ascoloy) is to be preferred over AMS 5613 (AISI 410). At higher temperatures, PWA 722 (AISI 17-22A) with suitable protection is definitely superior to available martensitic chromium steels. Rusting may seriously reduce fatigue strength of martensitic chromium steels, and delta ferrite can also markedly impair some properties of these steels.

Stress-Corrosion

Our first experience with stress-corrosion was with a tie-rod of AISI 414 steel (13Cr-2Ni) used for bolting together the compressor discs and

spacers of an early T-34 engine (Fig. 10). After engine operation, the compressor assembly had been cleaned in hot alkali, rinsed in hot water, and dried in live steam. Failure occurred after standing still for about two weeks in the assembled condition in shop atmosphere in late summer. This fracture was of the brittle type (Figs. 11 and 12), and was accompanied by numerous corrosion pits and small circumferential cracks which microscopic examination disclosed to be intergranular (Fig. 13). Bolting plus operating stresses in the tie-rod were established to be in the range of 100,000 psi. By statically loading 0.250-in. diameter tensile specimens machined from the tie-rod at this stress and exposing them to salt fog, we were able to reproduce the failure. At first we were inclined to blame the failure on the type of steel, but subsequent testing of other steels demonstrated that stress-corrosion is a design consideration for all type 400 steels.

Laboratory Test Procedure – After the first makeshift tests, a loading fixture was designed and several investment castings of the fixture were made of a heat- and corrosion-resistant material (Fig. 14). The tensile specimen was 0.250 in. in diameter for a 2-in. gage length. The threaded ends were 1 in. long, which permitted loading the specimen in a tensile machine and then tightening the nuts to maintain the load without introducing torsional strain. Bonded wire strain gages were used both as a means for getting accurate load readings and for calibrating measurements of extension under load. These calibrations later revealed that sufficiently accurate stressing with negligible torsion effect could be obtained without using a tensile machine by simply tightening the nuts on the specimen and measuring extension with a micrometer. After loading, the sides and ends of the fixture were dipped in hot wax, so that only the gage section was exposed to salt fog and the specimen was isolated from the fixture. Unless otherwise stated, all tests were conducted in salt fog according to ASTM B117-49T.

Mechanism of Failure – A survey of the literature revealed that stress-corrosion had been rarely recognized in other than austenitic steels and was transgranular in nature. This led to our first theory that galvanic corrosion was the mechanism of this failure, since a low-alloy steel part which was badly corroded was in close proximity to the failure. Additional tests were run with various metals in contact with the specimens. It was found that fail-

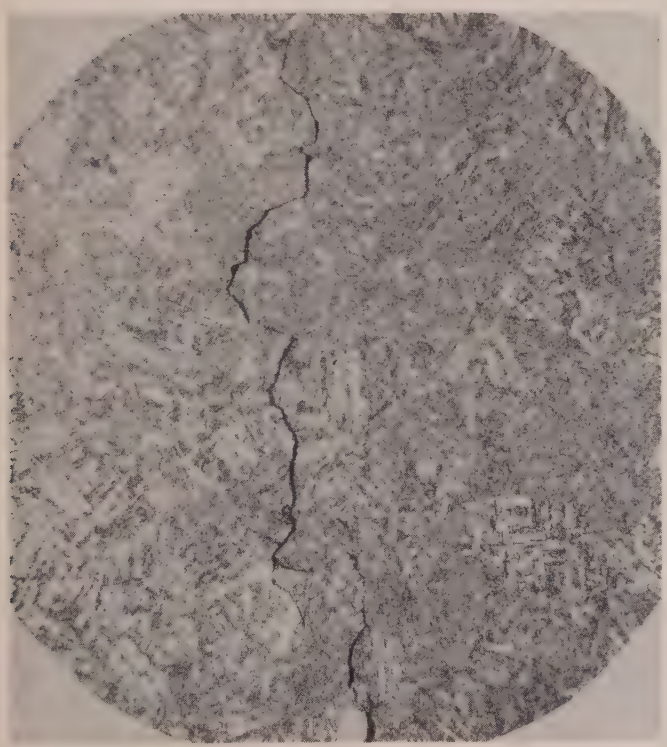

Fig. 13 – Photomicrograph of section through small crack adjacent to tie-rod. Original magnification: 250X

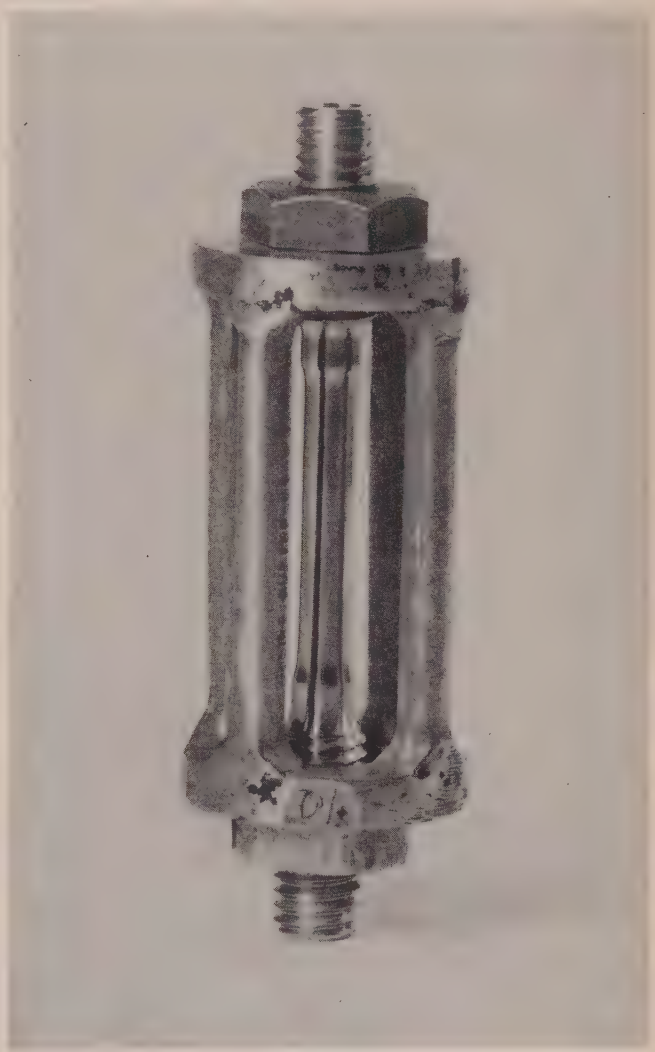

Fig. 14 – Photograph of tension-type stress-corrosion specimen in test fixture

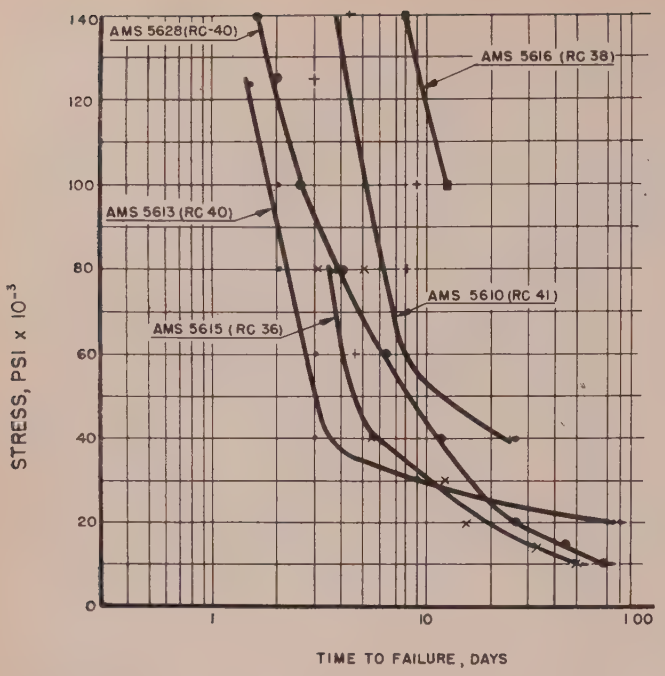

Fig. 15 – Effect of stress at constant hardness on time to failure for several steels

ure of AMS 5615 did not occur within the original maximum test time of 50 days when in contact with either magnesium or aluminum, that iron wire extended the time to failure to 27 days, and that copper wire diminished failure time to 0.6 days, compared to an expected time of two to three days with no couple. These results were more or less expected when considering the position of chromium stainless steels in the galvanic series.

In an effort to determine the part hydrogen embrittlement played in the failure mechanism, a specimen was stressed in the normal way, immersed as the anode in a 20% sodium chloride solution, and a 3-milliamp current passed through the solution. Under these conditions no hydrogen was released around the specimen, but the corrosive attack was quite severe, producing failure in 1½ days. When the specimen was made cathodic and hydrogen released on its surface, there was no visible corrosion, but failure occurred in 4½ days. This experiment was repeated in a sodium dichromate solution, which is a mild oxidizing agent and is frequently used as a corrosion inhibitor. When the specimen was made cathodic and hydrogen released on the surface, there was no corrosion, and failure time was approximately the same as for the sodium chloride solution. On reversing the current and making the specimen anodic, no hydrogen was released on the surface of the specimen and there was no visible corrosion. Failure time was extended to 48 days minimum. These data indicated that factors other than hydrogen embrittlement are important considerations.

Test Consistency – Our principal interest in this phenomenon was to find a solution to the trouble. It was not our intent to make a research project out of it. Various ideas on heat-treatments, surface treatments, stress levels, and variations in composition of the martensitic chromium steels were tried, producing a conglomeration of miscellaneous data difficult to present in concise graphic form. Considerable testing had been done before it was appreciated that various heats of the same analysis did not give consistent results when tested under the same conditions of heat-treatment and stress. However, specimens of the same heat when heat-treated together and tested under similar conditions, showed good consistency, validating the test method. For example, four specimens from one heat of AMS 5615 at RC 36 and 80,000-psi stress failed in the salt fog cabinet in 3, 3.5, 3.5, and 5 days; 10 specimens from one heat of AMS 5616 at RC 43 and 100,000-psi stress all failed in two to three days; 10 others from the same heat at RC 38 and 100,000 psi all failed between 10 and 14 days.

Effect of Hardness – Fig. 15 shows the effect of stress at constant hardness for five different martensitic chromium steels, each curve representing a series of specimens from the same heat, heat-treated together. Subsequent testing showed that the relative position of any of these curves with respect to the others has little significance. Heat characteristics and hardness levels may shift individual curves to the left, right, or vertically.

Fig. 16 shows the effect of hardness on stress-corrosion resistance of each of two steels at a constant stress level of approximately 100,000 psi. One heat of AMS 5616 is bracketed between the curved lines to show the consistency of a single heat. Other points show the scatter of several miscellaneous tests on different heats of the same material. Points of three different heats of Crucible 422 (0.20C, 13.0Cr, 0.75Ni, 1.0W, 1.0Mo, 0.3V) are also plotted.

Effect of Tempering Temperature – We con-

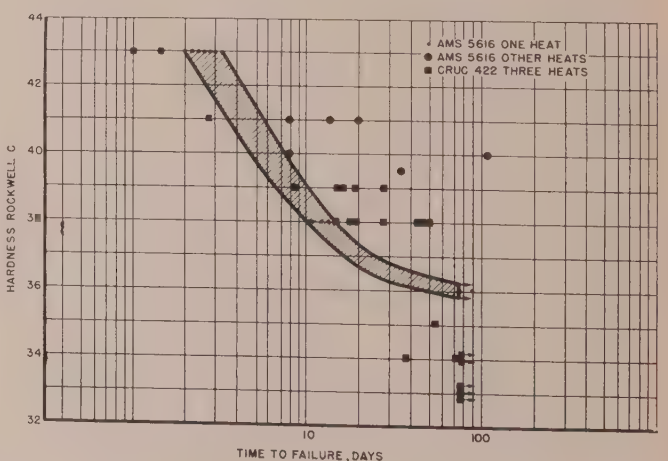

Fig. 16 – Effect of hardness at constant stress on time to failure for several steels

ducted a series of tests to investigate the effect of tempering temperature, the most significant observation being that no failures occurred at tempering temperatures of 300, 400, and 500 F. Additional specimens martempered in a salt bath at 500 or 650 F, either with or without subsequent tempering at 500 F, did not fail. Martempering in a 650 F salt bath followed by a 1000 F temper produced failure in a very short time. This stress-corrosion-insensitive tempering range of 300-500 F has no application in our work since it is expected that most parts made of these materials will undoubtedly reach temperatures above 500 F in service use. It did raise an interesting point as to which was the more important factor, hardness or tempering temperature. Additional tests were run to verify the presence of this insensitive tempering range. In all, 18 specimens of AMS 5613, 5615, and 5616 steels were tempered in the range from 300 to 500 F, and all but two ran from 75 to 95 days, at which time the tests were discontinued. The two failures occurred at 70 and 74 days. Fig. 17 shows the results of several heats of AMS 5613 and AMS 5615 stressed at 80,000 psi or above, plotted against tempering temperature, the shaded area indicating stress-corrosion susceptibility.

Fig. 18, in which some of the data in Fig. 16 are replotted against tempering temperature, shows that results for AMS 5616 and Crucible 422 conform well with the general S-curve of Fig. 17 derived from AMS 5613 and AMS 5615.

Limited data indicate that double tempering just about doubles the average time to failure.

Effect of Composition – Since our first interest in stress-corrosion we have completed more than 400 tests of the type described. Most of them have been on 13% chromium steels exposed to salt spray. We assumed first that compositions of steel were fairly important. We have tested 22 variations of the martensitic chromium steels in addition to a few austenitic and low-alloy steels. Various proprietary steels, as well as a few special compositions, were evaluated. As additions to the basic AISI 410-type composition, the following elements in various combinations and percentages were tried: nickel to 2%, vanadium to 0.4%, molybdenum and tungsten to 3% each, and nitrogen to 0.06%. Various hardnesses and tempering temperatures were employed.

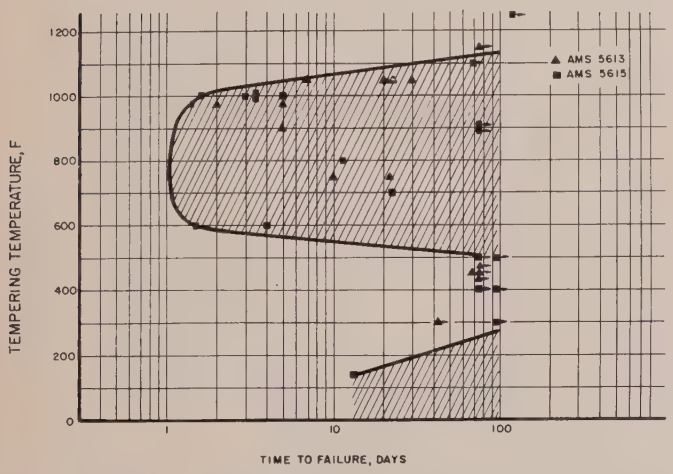

Fig. 17 – Effect of tempering temperature at high stress on time to failure for AMS 5613 and AMS 5615 steels

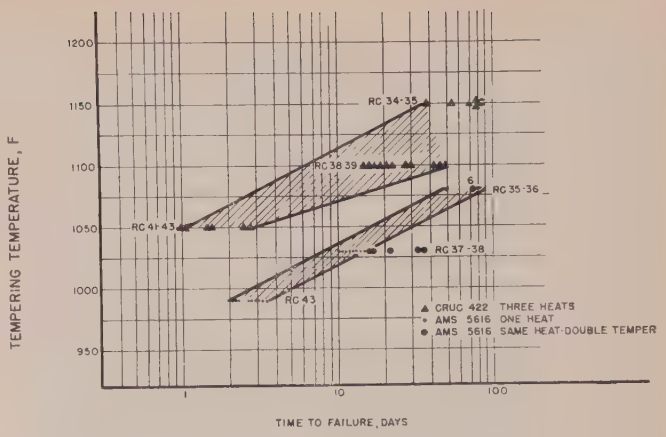

Fig. 18 – Effect of tempering temperature at high stress level on time to failure for two steels

All of these martensitic stainless steels showed decided susceptibility to stress-corrosion failure under certain conditions. In general, it appears that, for a given hardness level, a material which has the highest tempering temperature above 900 F is the most resistant to failure. However, AMS 5616 and Crucible 422 are exceptions to this rule. Under the conditions of our test, we have experienced no failure of AMS 5616 at RC 36 or below. We experienced three failures of Crucible 422 at RC 34 even though the tempering temperature was higher than that required for the RC 36 hardness level of AMS 5616. No failures were encountered in Crucible 422 at RC 33 or below. For the entire group of hardenable martensitic stainless steels, no failures were experienced at RC 26 or below. It also appears that an 1150 F temper will make them all fairly resistant to stress-corrosion.

Austenitic and Low-Alloy Steels – Three austenitic steels were investigated: cold-drawn AMS 5624 – a high-expansion bolting steel (12% Ni, 4½% Mn, 4% Cr), cold-drawn AMS 5637 (AISI 18-8) at approximately RC 32, and precipitation-hardened AMS 5643 (AISI 17-4 PH). AMS 5624 is not as corrosion resistant as the 13% Cr steels and failed in 15 days, showing numerous cracks on the surface. The 18-8 did not fail in the 50-day duration of the test. The 17-4 PH in the fully hardened condition and aged at 900 F to produce RC 40, failed in 14 to 50 days when stressed at 100,000 to 125,000 psi, but when overaged at 1100 F to RC 35 did not fail within a 75-day period.

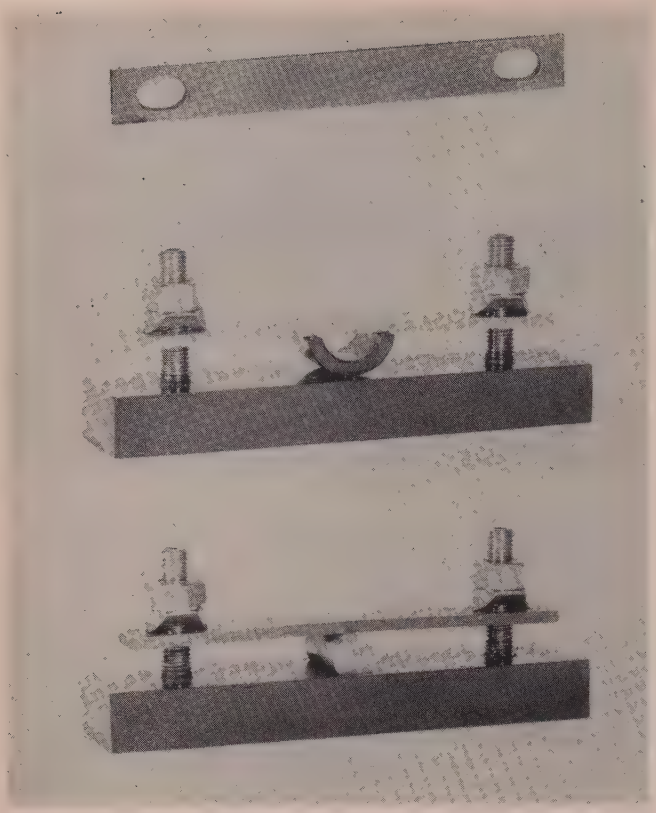

Fig. 19 – Views of strip-type stress-corrosion specimens in loading fixture

Fig. 20 – Photomicrograph showing typical intergranular stress-corrosion failure from corrosion pit in AMS 5613 steel. Original magnification: 250X

Several low-alloy and carbon steels, including SAE 4340, 6150, 8740, 1137, and 1095 were tested in the RC 30 to 40 hardness range with no failures. SAE 6150 at RC 50 failed in a very few days. This hardness, however, was produced by tempering in the so-called blue-brittle range at 550 F, and failure occurred in the threads as well as the gage length. This high hardness was not explored in any other material.

Surface Treatments – Passivation or other acid cleaning showed no significant effect. Shotpeening did have a beneficial effect provided the external stress was definitely below the compressive prestress produced by peening. Peening plus passivation prevented failure within the 75-day period at 60,000 psi in spite of numerous pits which appeared all over the test section. Peening with or without passivation at higher stress levels appeared to contribute very little. The use of vacuum for either melting or heat-treating did not appear to improve stress-corrosion resistance. Tests run in a humidity cabinet at 100% humidity and 120 F produced failure in a manner similar to that experienced in the salt-fog cabinet, except that time to failure was increased five to ten times. The average time to failure of four specimens exposed to marine atmosphere (Kure Beach) was 90 days, compared to four days for similar specimens in laboratory salt spray.

Strip-Type Tests – After considerable testing had been done on this tensile-type specimen, it came to our attention that other investigators were using a simple stressed-beam method. In some cases this test was run in an acid with or without an accelerator to produce early failure. Others have used this type of test because it represents conditions to which the material might be exposed in service. Fig. 19 shows two versions of this method of testing. Stress was determined in each case with a bonded-wire strain gage before the stressed specimen was placed in the salt-fog cabinet. Our results did not correlate very well with data previously obtained by the tensile method. Several beam-type specimens cracked but did not fail, which made it impossible to determine the actual failure time. After about 25 tests we discontinued use of this method.

Metallographic examination of failed specimens of the hardenable chromium stainless steels indicated that cracks usually start from corrosion pits and progress intergranularly. Fig. 20 is a typical

example of stress-corrosion cracking in AMS 5613 (AISI 410), showing corrosion pits and intergranular cracks. Fig. 21, a specimen of AMS 5616, shows greater subsurface corrosion, but the fracture is still primarily intergranular.

We do not believe that failure must necessarily start from a pit. Fig. 22 shows cold-drawn AMS 5624 austenitic steel used for high-expansion bolting applications. Numerous cracks can be seen at the surface with no evidence of pitting. These cracks progressed primarily through the grains, thus following the general concept that austenitic steels fail transgranularly.

Summary of Tests on Stress-Corrosion – A recapitulation of the more important observations from this investigation follows:

1. For a given hardness, the martensitic stainless steel having the highest tempering temperature appears to be the most resistant to stress-corrosion.
2. No failure was experienced in any of the martensitic stainless steels at RC 26 or below.
3. Of the martensitic stainless steels, AMS 5616 had the highest hardness, RC 36, at which no failure was experienced.
4. Tempering in the 300 to 500 F range or above 1150 F appears to make these steels resistant to stress-corrosion.
5. Stress-corrosion cracking occurs intergranularly in martensitic stainless steels.

Protective Treatments

Organic Coatings – Protection of low-alloy steel against corrosion may be accomplished by various methods which are governed by end-use requirements and limitations of the coatings themselves. Organic coatings have little service application for heat and corrosion protection of low-alloy steels. Our evaluation of them may be briefly summarized as follows:

1. Clear phenolic resins are good in air up to 400

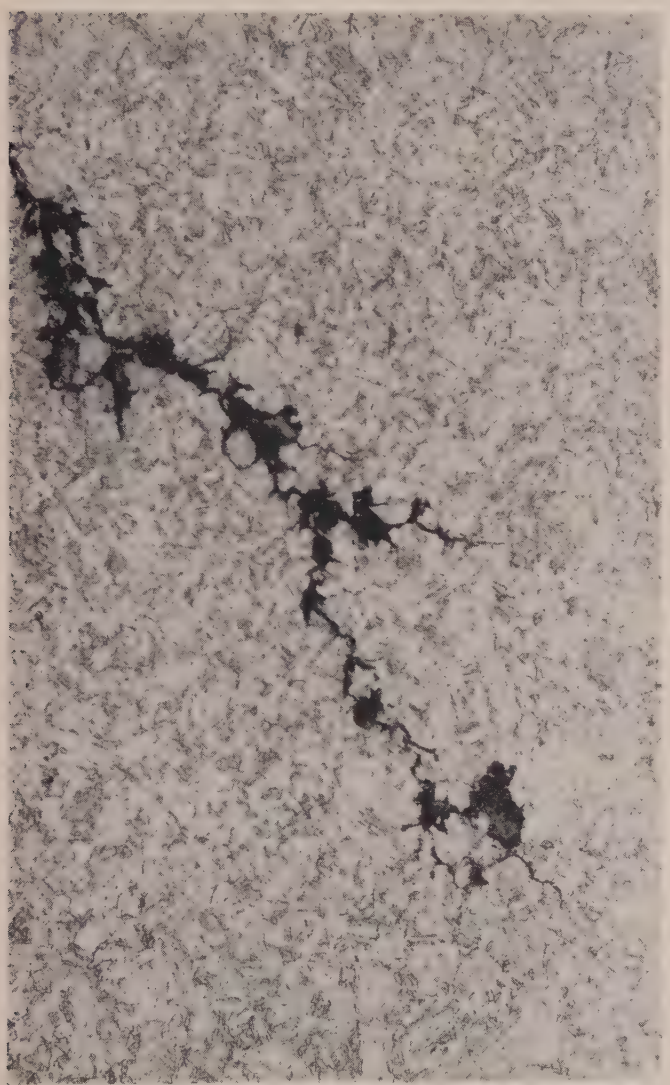

Fig. 21 – Photomicrograph showing heavy corrosive attack following intergranular stress-corrosion cracks in AMS 5616 steel. Original magnification: 250X

Fig. 22 – Photomicrograph showing transgranular stress-corrosion cracks in austenitic AMS 5624 steel (12.5 Ni, 4.5 Mn, 4.0 Cr, 0.55 C). Original magnification: 250X

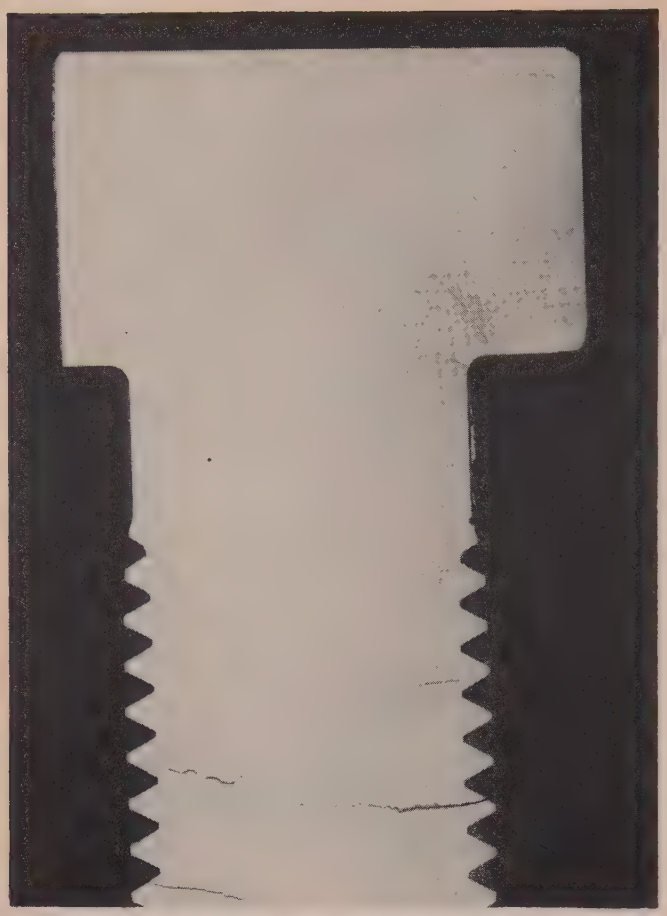

Fig. 23 – Section through indium-plated AMS 6322 steel bolt showing stress-alloying cracks after heating at 825 F under high stress. Original magnification: 10X

F for short duration (1 hr), at 325-350 F for 1 day, or at 250-300 F for an extended time of a month or more. Coatings fail by embrittlement and flaking.

2. Special pigmented phenolic resins are good up to 500 F for 1 hr, 400-450 F for 1 day, or 350-400 F for one month plus. For best performance these coatings require thickness of 0.005-0.007 in., which restricts their use to special applications.

3. Pigmented glycerol phthalate is good at 500, 400, and 300 F, respectively, for the periods mentioned above when used with a conventional zinc chromate primer. The temperature for extended service may be increased to 400 F if lithopone is substituted for the zinc chromate primer.

4. Innumerable aluminum-pigment silicone resins, all of which claim to have heat and corrosion resistance at temperatures in excess of 1000 F, have been marketed during the past few years. Most of these fall far short of the manufacturers' claims even though applied according to instructions. One such coating, developed through the collaboration of our laboratory with one of the paint manufacturers, has good heat resistance up to 1000 F and still withstands salt fog, solvents, and hot engine oil. This paint, purchased to PWA Specification 578, has given good service experience on turbine shafts operating up to 700 F with occasional short-time exposures to 900-1000 F. Its scratch and abrasion resistance is relatively poor, being somewhat inferior to the phenolics or baking enamels for equal thicknesses.

Organic coatings rely on a mechanical bond for adhesion which is a function of surface finish and cleanliness at the time of application. Furthermore, protection against corrosion is also physical, contrasted to galvanic protection offered by some of the sacrificial plates such as cadmium or zinc.

Electroplates – Electroplates offer a wide range of properties and give excellent service if properly selected.

Cadmium or zinc plate provides good corrosion protection, but both tend to oxidize at about 500 F, which reduces their effectiveness. Erosion and scratch resistance of these plates is not much better than that of organic coatings, but, because of their sacrificial nature, the former can tolerate considerable abuse before corrosion of the base metal occurs.

Stress-Alloying Failure – One deterrent to the use of cadmium or zinc plate is the possibility of stress-alloying if the temperature happens to rise above the melting point of the coating. Stress-alloying may be described as a catastrophic intergranular penetration of molten metal in contact with steel under stress, resulting in almost immediate failure or rupture. Although this phenomenon has not been investigated thoroughly, our laboratory data indicate that initial hardness of the base steel is the most important factor. No failures occurred on low-alloy heat-treated bolts at or below RC 35 regardless of the type of electrodeposited metal and applied stresses up to the yield strength. At RC 38 and above, electrodeposits of zinc, tin, indium, and cadmium, as well as hot-dipped cadmium, caused stress-alloying failures at stresses of 120,000 to 190,000 psi (Fig. 23). Failures of this type also occurred with plate combinations such as cadmium on tin, indium on silver, and tin on nickel. Frequency of failure increased with hardness; approximately 50% of the samples tested failed at RC 38, and almost 100% failed at RC 45. The effect of stress as a variable was not investigated below 120,000 psi, so that the minimum stress causing failure was not determined.

Service experience indicates that stress-alloying is not as straight-forward as laboratory tests would indicate. Deep-drawn SAE 1020 sheet failed by this mechanism when a small fitting was silver-brazed to it. Cold-drawn AISI 321 stainless steel wire used for reinforced flexible hose cracked when end fittings were brazed on. Silver-brazed cold-formed Monel sheet and Monel tubing not completely cleaned of Cerrobend after bending and subsequently brazed, also failed. Nickel-base alloy heat- and corrosion-resistant sheet which had been perforated with small, closely spaced holes, formed, and silver-brazed, cracked between the holes. All these materials had been cold-worked. They cracked in contact with a molten metal containing cadmium,

tin, or zinc.

The presence of a low-melting constituent is not necessary for stress-alloying. It has also been observed in copper-brazing. Proper stress-relieving before brazing and fixturing so that little external load is imposed during brazing will eliminate the trouble.

Electroplated Nickel – Nickel plate may have a wide variation in properties depending on the bath composition and plating conditions. A plate 0.0003-0.0005 in. thick from a modified Watts-type bath provides fair corrosion resistance in the as-plated condition as well as after heating at 375 F. Heating at 600 F lowers corrosion resistance. Heating to 900-1000 F improves corrosion resistance to a point where it can be considered better than in the as-plated condition or after the 375 F heating. Where elevated temperatures are not involved, 0.002-in. plate is recommended by AMS 2403.

Organic addition agents are frequently used with various nickel-plating baths for stress control or to obtain increased hardness and brightness. Stress in electrodeposited nickel of from 50,000 psi or more in tension to 10,000 psi in compression may be obtained by altering bath composition and by the use of addition agents. Tension stress adversely affects fatigue properties of the underlying steel practically in proportion to the stress measured in the plate, whereas compressive stress in the plate has no detrimental effect and may, in fact, increase fatigue strength slightly. Hardness of nickel plate may be varied from DPH 150 to over 600. Hard nickel plate has excellent abrasion resistance. In the past, brittleness has been associated with hard nickel deposits, but recent work has produced high hardness with very good ductility. So far there has been no noticeable effect on oxidation or corrosion resistance resulting from the use of these addition agents.

Heating reduces the high hardness and/or beneficial stress obtained by addition agents. When the bath is adjusted to produce a compressively stressed plate, the stress changes to tension when the plated part is heated to around 400 F. The tensile stress at room temperature after heating increases with increasing heating temperature, so that after heating at 900-1000 F the stress is considerably higher than if no addition agent were used. For one bath investigated with and without an addition agent, the room-temperature stress versus heating-temperature curves crossed at approximately 600 F. Also, high-hardness plated nickel softens upon heating above 400 F and does so very rapidly above 500 F. The hardness advantage at 1000 F due to an addition agent is less than 100 DPH units after heating.

Electroless Nickel Plate – A new type of nickel plate, generally termed electroless nickel plate but also known under several proprietary trade names, has been introduced during the past few years. This, as the name implies, does not require the use of current but is a chemical reduction process which is self-catalyzing as long as the proper bath composition is maintained. The deposited plate is not pure nickel but a nickel-phosphorous alloy inasmuch as a hypophosphite is the triggering agent. The rate of deposition is a function of the hypophosphite content, which has an effect on the amount of phosphorous in the end product, the latter varying from 4 to 12%. Hardness as well as brittleness increases with phosphorous content, ranging from approximately DPH 450 to 650 as deposited. Being a precipitation-hardening alloy, the deposit increases in hardness on heating. Maximum hardness, which may exceed DPH 1000, is obtained by heating to 750 F. Some investigations show no loss in hardness on continued heating up to 1000 F, but others show gradual reduction in hardness after reaching a peak. It has been reported that heating up to 1400 F seems to lower hardness to the order of its initial level, but we have not investigated the effect of temperature above 1000 F.

Although electroless nickel plate is more expensive than electrodeposited nickel plate because of the cost of reagents, its one large advantage lies in the very uniform thickness obtained in recesses and sharp edges, provided there is sufficient agitation to keep fresh solution in contact with areas to be plated. Complicated or irregularly shaped parts which would be practically impossible to plate by any electrodeposition method may be satisfactorily plated by this method. The electroless nickel deposit appears at least as free from porosity as electrodeposited nickel of the same thickness. Limited experience indicates good oxidation and corrosion resistance can be expected at least up to 1000 F.

Hydrogen embrittlement exists in the as-plated condition to about the same extent expected from electrodeposited plate, so that similar relief heat-treatments are recommended. Our test results show that electroless nickel behaves in the same manner as electrodeposited nickel with respect to corrosion resistance. When heated for an hour or more in the 600 F range, corrosion resistance of both types is definitely poorer than in the as-plated condition or after heating at 375 F or 900-1000 F. Fatigue strength of the base metal appears to be more adversely affected by electroless than by Watts-type nickel plate, even with no addition agent. Within the range of our test data, heating up to 900 F does not improve fatigue strength as it does on the Watts-type electrodeposited nickel. This can be attributed to age-hardening rather than to the annealing effect. Conceivably, overaging could have a beneficial effect, but the time and temperature required for this would lower the properties of the base metal below useful values.

Chromium Plate – Chromium plate has good abrasion resistance, and in adequate thicknesses, good oxidation and corrosion resistance up to 1000 F. AMS 2406 recommends a 0.002 in. thickness where protection against corrosion is required. This plate has been used very little for elevated

temperature applications, possibly because of widespread belief that it is hard and brittle and has a detrimental effect on fatigue. Actually, room-temperature fatigue tests on chromium-plated low-alloy steel specimens previously heated at 750 F or 1000 F show practically no loss in fatigue strength. Hardness after heating to 750 F is not significantly lowered and is still in excess of DPH 800. Continued heating up to 1000 F produces loss in hardness of plated chromium, but its effect on abrasion or galling resistance is not known.

Silver Plate – Silver plate is frequently used with good success for galling or wear resistance under dry-heat conditions up to 700-800 F. At temperatures around 1000 F oxygen diffuses through the plate and deteriorates the bond, causing blistering and ultimately bare spots. Under moderate loads this deterioration does not appear to be deleterious in so far as galling and wear are concerned, but of course the protection against corrosion is lost.

Nickel-Cadmium Plate – In a search for a more desirable coating, several dual plates were investigated. The combination which offered the most promise was nickel plus cadmium followed by heating to 620 F slightly above the melting point of cadmium, for ½ hr, during which cadmium diffuses into the nickel. This diffused nickel-cadmium plate has been in production use for more than 2 years with excellent results.

The principal advantages of diffused nickel-cadmium plate over other metallic-plate coatings on steel are:

1. The final thickness of the combined coatings is less than 0.0005 in., which is highly desirable for applications involving close dimensional tolerances. PWA specification requires 0.0002-0.0004-in. nickel and 0.0001-0.0002-in. cadmium on significant surfaces. A minimum of 0.002-in. nickel without cadmium is necessary for equal corrosion protection when used without heating.

2. It is effective, after heating to 620 F, in preventing corrosion up to 1000 F. A minimum of 0.0005-in. nickel without cadmium requires heating up to 950-1000 F to provide adequate corrosion resistance in the 500-600 F range.

3. Where scratches expose the base metal, it affords galvanic protection practically to the same extent as ordinary cadmium plate.

4. It does not cause stress-alloying.

5. It prevents stress-corrosion on martensitic stainless steels.

6. It has fair to good anti-galling properties.

7. On complex parts which are extremely difficult to plate uniformly, nonuniformity of plate thickness may be tolerated to the extent that as little as 0.00005-in. nickel, when covered by cadmium and diffused, is sufficient to guarantee freedom from stress-alloying and stress-corrosion and still provide adequate corrosion protection.

Diffused nickel-cadmium requires good control of the plating baths and procedures to guarantee satisfactory performance. Fixtures and conforming anodes, where necessary, are designed to produce as uniform a nickel-plate thickness as possible. Our procedure requires that the setup used for each highly stressed part be laboratory approved before production plating of the part is permitted. This applies to plating within our plant as well as by outside vendors who have been qualified on the basis of equipment and general procedures.

Early experience indicated that stress-alloying could be a real hazard if proper control were not maintained. Although considerable corrosion testing had been done on nickel-cadmium plated test pieces, both in the as-plated and in the diffused condition, the full import of stress-alloying was not

Fig. 24 – Test specimens showing roughness and balling of fused surface with 0.0001-in. cadmium plated on steel (left), or on 0.00001-in. nickel (center), and showing smooth surface when plated on 0.00005-in. nickel (right). Original magnification: 1.5X

appreciated. It was assumed that if operating temperatures were high enough to produce diffusion, a special heating operation during processing would be unnecessary. It was found, however, that diffusion had to be accomplished with the part unstressed, especially if the nickel plate was on the low side of thickness requirements. Diffusion produces a very smooth surface. If there is insufficient nickel present, the cadmium tends to ball, producing a rough surface quite noticeable to the touch as well as to the eye (Fig. 24). Consequently, inspection of the texture of the diffused coating is an added safety measure. No failures attributed to stress-alloying have occurred on production parts with diffused nickel-cadmium plate.

Summary – Our practice in the use of protective coatings for low-alloy steel has shown that the most important consideration is the temperature to which the part will be subjected. Where cadmium plate is ruled out because of temperature limitations, an aluminum-pigment silicone resin is used if resistance to abrasion is not considered critical, otherwise diffused nickel-cadmium plate is specified. Electroless nickel plate meets our requirements for both corrosion and abrasion resistance, but because of its adverse effect on fatigue strength is used only on relatively low-stressed parts. Under conditions of heavy wear or abrasion, chromium plate with a 750 F bake is specified. Silver against chromium, each plate 0.0001-0.0002 in. thick, has given about the best service where heavy galling may be expected.

DISCUSSION

Questions Concerning Cleaning and Welding Of Martensitic Stainless Steels

– Merle F. Valade
Aircraft-Engine Division, Ford Motor Co.

THE data are presented in a very concise and complete manner. I have a few questions on the subject, however, and would appreciate receiving your comments.

1. What has been your experience with the use of hot salt baths (for example, Kolene, Virgo, and sodium hydride) for cleaning martensitic stainless steel?

2. Do you perform any cleaning operation on parts that are tempered in air at 800 F?

3. Have you any test data on the effects of stress-corrosion on fusion-welded martensitic stainless steel when the weld is an inherent part of the test specimen? If so, were the welds made with martensitic or austenitic rod?

Has Also Noted Nitrogen Pickup When Treating AISI 440C Stainless

– Raymond C. Kopituk
Reaction Motors, Inc.

IN connection with the authors' discussion of the use of atmospheres containing nitrogen in relation to the presence of retained austenite with nitrogen pickup, I would like to add that we have also found this condition to exist. We have observed this condition particularly when treating AISI 440C stainless steel with carbon content on the high side. On the other hand, care should be taken that the dewpoint of the straight hydrogen atmosphere should not be higher than about −10 F, since decarburization occurs.

Note was made of the fact that the authors prefer to use chromium plate for heavy wear or abrasion. We would like to know if they have compared electroless nickel plate in its fully hardened condition with chromium plate, and if so, what results they have obtained. The 1400 F heat-treatment for electroless nickel plating is of particular interest since there is at least one vendor of this process now requesting the latter treatment in a proposed AMS specification. They have indicated that both ductility and abrasion resistance have been improved. Any further information regarding this subject would be appreciated.

Authors' Closure To Discussion

IN reply to Mr. Kopituk, we have no data that would substantiate any answer to his question.

In reply to Mr. Valade:

1. We have had no experience with any of the salt baths in cleaning martensitic stainless steels.

2. No cleaning is performed on parts bright hardened and tempered up to an including 800 F. Acid cleaning is usually used where the tempering temperature is above 800 F.

3. We have not investigated the effects of stress corrosion on fusion-welded martensitic steels.

ORAL DISCUSSION

Reported by O. W. McMullan
Bower Roller Bearing Co.

J. C. Holzwarth, General Motors Research: Why does less rusting occur on acid-treated airfoil shapes than on surfaces in the oxidized condition?

Mr. Sharp: On surfaces of parts heated to 800 F, there was no effect of the oxide but when heated at 1000 F oxidation of chromium on the surface occurs. The chromium oxide contributes to rusting and this oxide is removed by pickling and the surfaces become more rust resistant.

O. W. McMullan, Bower Roller Bearing Co.: I would like to refer to data showing two alloys of equal hardness and equal endurance limits when treated at room temperature but with one showing a higher endurance limit at 1000 F. Would hot hardness (at the temperature tested) be a reliable measure of the difference in endurance limits? Also, is there a relationship between recovery hardness (after return to room temperature) and hot hardness of a given alloy?

Mr. Sharp: These relationships would be hard to predict because of structural changes that might take place at elevated temperatures. We have studied only the effects on tensile and creep properties.

R. W. Seniff, Baltimore & Ohio Railroad: Is stress alloying or corrosion a matter of a metal of lower melting point penetrating into another metal of higher melting point?

Mr. Noble: I believe this might be the general pattern. We have observed that other metals, such as carbon steels, when silver brazed, may exhibit penetration of the brazing alloy (melting point 1175 F) if forming stresses are present in the steel. We have not determined the minimum stress necessary, but probably it would be below 50,000 psi on steel.

HIGHER compression ratios, the main key to better passenger-car engine efficiency, can be increased by two main factors: chemical and mechanical octane numbers. Although remarkable gains have been made in the former in recent years, the limits in improvements have about been reached. Thus the current emphasis on means of improving mechanical octane numbers.

The authors tell here of important experiments and developments in ignition control, valve timing, carburetion, engine-transmission relationship, and combusion-chamber design—the five factors most important in achieving mechanical octane numbers.

Presented also are 25-year charts of trends in passenger-car weight, length, horsepower, engine speed/car speed, compression ratio, acceleration time, fuel economy, and efficiency.

Mechanical Octanes

THE last half-century has seen the automobile industry develop from a struggling infant into one of the world's most important manufacturing enterprises. The automotive industry is an important factor in world economy, not only from the manufacturer's viewpoint, but because of the impact of the transportation which it makes available. It has changed the pattern of living beyond anything which could have been foreseen 50 years ago.

Today there are over 58,000,000 passenger cars, trucks, and buses in the United States alone, while annual production runs close to 8,000,000 units. At a conservative 125 hp per unit, this amounts to an annual production of 1,000,000,000 hp, or 40 times the installed horsepower of all the hydroelectric generating plants in the United States.

In 1954, American motorists burned 44,000,000,000 gal of gasoline, which cost them close to $13,000,000,000. When we look at internal combustion engine efficiency on a national scale, it is easy to see why automotive engineers consider its improvement one of their most important undertakings. An improvement in economy of only 10% would mean a saving of $1,300,000,000 each year.

Efforts to improve the efficiency of passenger car engines have been in progress since the industry began more than a half-century ago. Under the compelling urge of a healthy competition, research laboratories and engineering departments of the industry have studied practically every conceivable type of powerplant which might be suitable for passenger cars.

The result is, as C. L. McCuen[1] stated in 1951, "The most promising field for future improvement still seems to be further development of the spark-ignition 4-cycle engine. The most fundamental way in which we can improve the engine is to continue increasing the compression ratio. These conclusions have been reached only after a thorough study of proved test results. This means, of course, the development of the higher octane fuels which these engines will require."

This statement applies today, just as well as it did in 1951. Both compression ratio and octane quality have increased substantially, with resulting improvement in efficiency.

Mr. McCuen's paper showed a series of curves prepared from the General Motors Proving Ground Engineering Department showing the trends in the automotive industry over a 20-yr period from 1930 to 1950. We have received many requests to bring

[1] See SAE *Quarterly* Transactions, Vol. 6, April, 1952, pp. 290-303; "Economic Relationship of Engine-Fuel Research," by C. L. McCuen.

for Higher Efficiency

D. F. Caris, B. J. Mitchell, A. D. McDuffie, and F. A. Wyczalek
Research Laboratories Division, GMC

This paper was presented at the SAE Golden Anniversary Summer Meeting, Atlantic City, June 13, 1955.

these curves up to date, and are therefore including them together with additional data in this paper. It is helpful occasionally in bringing the picture into better perspective to examine past progress of the industry as an indication of what the future may hold. The curves represent data from 38 models from the following 18 manufacturers, and in many cases show not only the average values but also the spread between the models studied:

Buick	Ford	Oldsmobile
Cadillac	Hudson	Packard
Chevrolet	Imperial	Plymouth
Chrysler	Lincoln	Pontiac
DeSoto	Mercury	Rambler
Dodge	Nash	Studebaker

The first curve, Fig. 1, shows the trends in curb weight for the 38 models over the period from 1930 to 1955. It will be noted that while there is considerably less spread in the weight of the heaviest and lightest cars in recent years, the average weight of passenger cars is definitely greater in 1955 than it has ever been in the last 25 years. The average weight has increased from 3500 lb in 1930 to 3950 lb in 1955.

The data in Fig. 2 show the trend in wheelbase over the 25-year period. It is not surprising to find that the curb weight and wheelbase show similar trends over the years. The large cars are shorter and the small cars are longer than they were in the 1930's. However, on the average, passenger cars have increased only about 4 in. in wheelbase in the last 25 years.

The trend in rated horsepower, as shown by Fig.

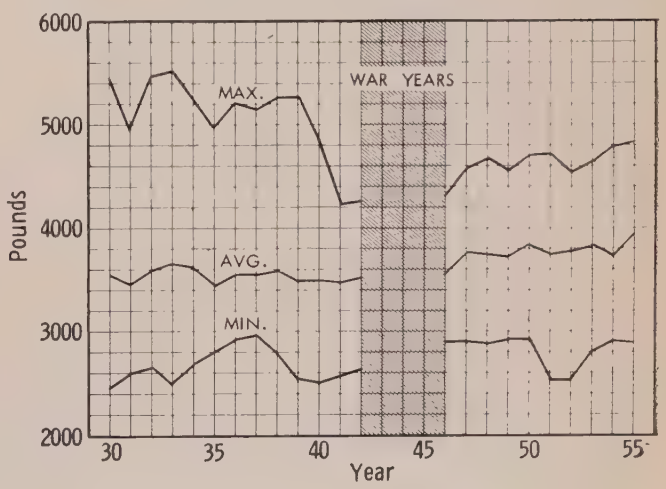

Fig. 1 – Trend in curb weight for 38 vehicles over past 25 years

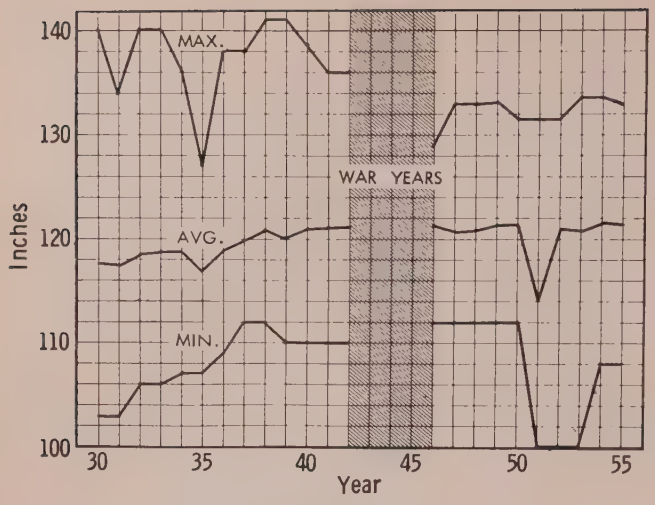

Fig. 2 – Trend in wheelbase

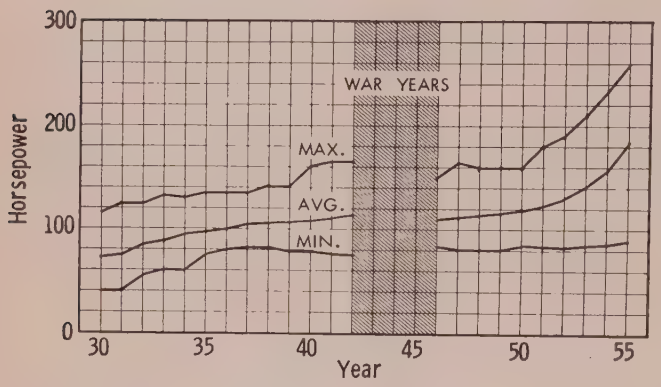

Fig. 3 – Trend in rated horsepower, up sharply over 25-year period

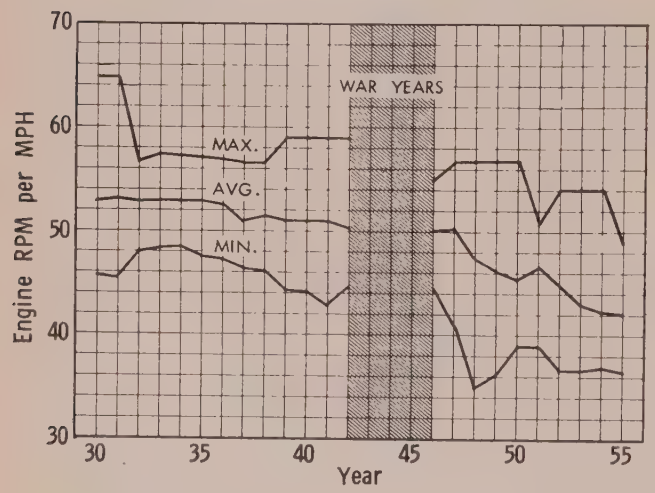

Fig. 4 – Decrease in engine rpm/mph relationship

3, has been up sharply over the 25-year period as automobile users have demanded better and better performance. From a little less than 75 in 1930, average rated horsepower has increased to 160 in 1955. It will be noted that the spread between the lowest- and highest-powered car is much greater

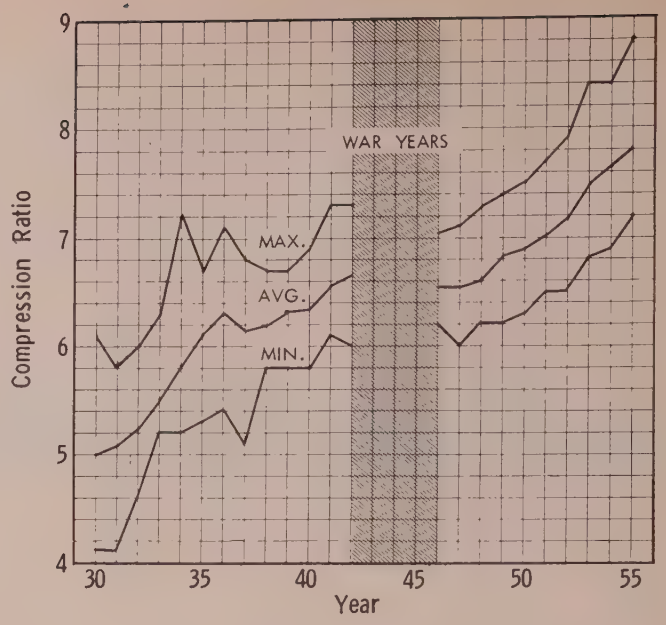

Fig. 5 – Increase in compression ratio

today than it was in 1930.

N/V (engine revolutions per minute per mile per hour) ratio, as shown by Fig. 4, has decreased on the average from about 53 in 1930 to 42 in 1955. The N/V relationship is an important one to automotive engineers because the lower it is, in general, the better the overall efficiency. The fact that the N/V ratio has decreased over the years in spite of demands for increased performance has been due to higher compression ratio, better mechanical efficiency, improved engine breathing, automatic transmissions, and in some cases, larger engines.

Higher power and better economy have been made possible to a large extent by the increase in compression ratio over the years, as shown by Fig. 5. You will note that the average compression ratio increased from 5/1 in 1930 to 7.8/1 in 1955. Practically all the new engines brought out since the war have been designed to operate at much higher compression ratios on the fuels of the future, and the sharp up-trend in compression ratio noted during the last five years may be expected to continue. These increases in compression ratio have been made possible by emphasis on better engine efficiency in all of our research and development programs. This would have been impossible without the cooperation of the petroleum industry in supplying the higher octane fuels which are required.

The trends in performance over the years, as indicated by the time to accelerate from 10 to 60 mph, are shown by Fig. 6. There is a wide spread in the performance of passenger cars, because some models emphasize performance while others emphasize economy. However, it is interesting to note that in recent years, as highways have become more congested and increased performance is required for safer passing ability, the trend in all cars is toward better performance.

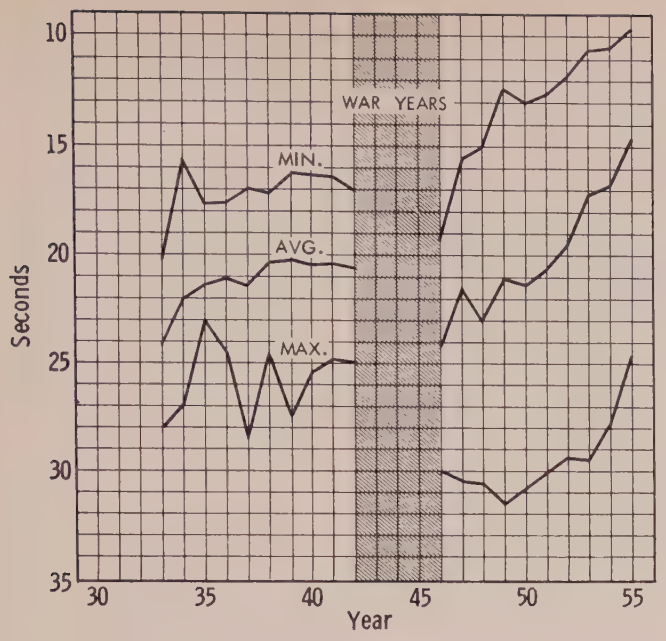

Fig. 6 – Performance trends, indicated by time needed to accelerate from 10 to 60 mph.

Higher horsepower and increased performance have not been accomplished over the years at a sacrifice in economy. Fig. 7 shows level-road, constant-speed economy in miles per gallon at 40 mph. While the spread between the highest and lowest economy cars is great, the trend in all cases is to higher economy over the 25-year period. The average of all cars studied increased from about 15 mpg in 1930 to 20 mpg in 1955.

From an overall vehicle efficiency standpoint, it is interesting to note the trend in ton-miles per gallon at 20, 40, and 60 mph, shown in Fig. 8. At 40 mph cruising speed, ton-miles per gallon has increased from 29 in 1930 to 45 in 1955. This represents a gain of 50% in the ability to move a ton a mile with a given quantity of fuel.

The spread in ton-miles per gallon has been plotted at 40 mph in Fig. 9, where it can be seen that the best 1930 model gave 35 ton-mpg while the poorest of the 1955 models gave 38. The spread from the poorest in 1930 to the best in 1955 was from 24 to almost 60 ton-mpg.

We have talked a lot about horsepower and performance during the last few years, and it may come as a surprise to some that miles per gallon in highway service has increased substantially during this period. The trend in highway fuel economy is shown in Fig. 10. These curves represent actual highway trips of over 300 miles, representing both city and country driving. A large number of makes and models was run on a selected schedule each year to obtain the average, maximum, and minimum points. The curve therefore represents a true picture of the tank mileage to be expected by the average car owner. These data are available only since the 1948 model year. While there is a spread of 4 to 10 mpg between the poorest and best economy cars, all three curves show definite improvements in highway economy since 1948. The average highway economy has increased from a little over 15 mpg in 1948 to 18.6 mpg in 1954, an improvement of 20%. Highway fuel economy data for 1955

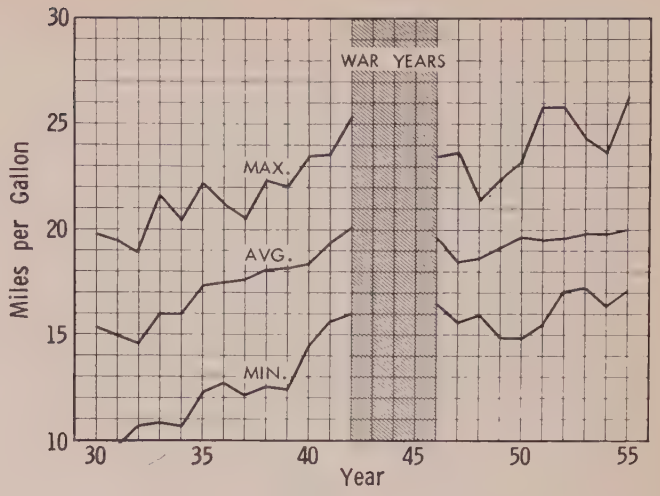

Fig. 7 – Level-road, constant-speed economy in mpg at 40 mph

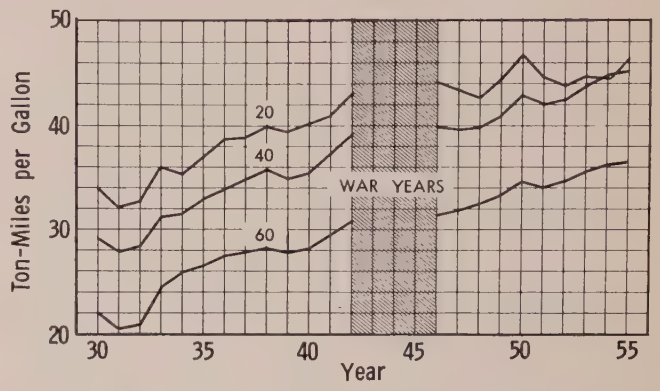

Fig. 8 – Trend in average automobile efficiency, as shown by ton-mpg at 20, 40, and 60 mph

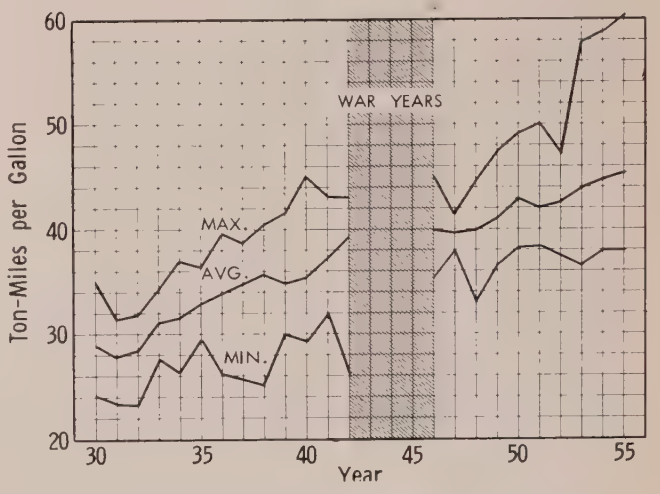

Fig. 9 – Increase in efficiency as shown by ton-mpg at 40 mph

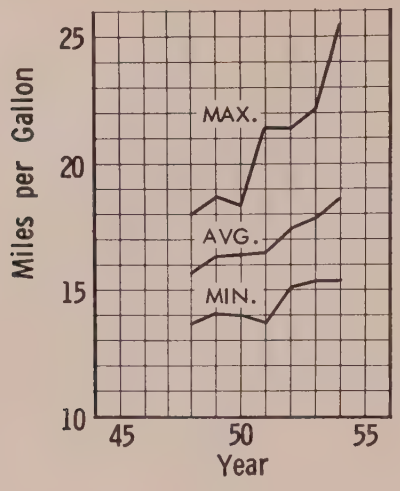

Fig. 10 – Seven-year trend in highway fuel economy

were not available in time for inclusion in this paper.

Compression Ratio – Key to Higher Efficiency

There are, of course, many factors besides compression ratio which can contribute to the overall efficiency of the automotive engine, such as mechanical efficiency, volumetric efficiency, carburetion, spark advance, and many others. Although all these factors are important, the key to further improvement in efficiency lies primarily in higher compression ratios.

There are two main factors which permit compression ratio to be increased:

1. Chemical octane numbers (built into the fuel at the refinery).
2. Mechanical octane numbers (built into the engine by the engine designer).

Chemical Octane Numbers

First, let us take a closer look at the methods of raising compression ratio. Higher compression ratio can be achieved by using the higher octane fuel which the petroleum industry makes available. Petroleum technologists have learned over the years how to rearrange the molecular structure of the gasoline and improve its antiknock quality. The octane quality of gasoline in the United States has improved on the average of about one octane number a year over the last 20 to 30 years. That this record of accomplishment has been achieved at no appreciable increase in cost to the customer is a remarkable tribute to the progressive efficiency of the petroleum industry. How effectively the automotive industry has used this improvement in fuel quality over the years is illustrated dramatically by Figs. 1 through 10. The full impact of this accomplishment can only be appreciated when it is recognized that it represents an improvement of approximately 50% in the utilization of gasoline. Since 3,000,000 bbl are consumed daily in the United States alone, this represents a tremendous saving in the cost of motor transportation.

Mechanical Octane Numbers

The compression ratio of automotive engines can also be increased by developing what we have chosen to call "mechanical octane numbers," which is simply the art of designing an engine to operate at higher compression ratios on fuels now available.

The following factors are important in the development of mechanical octane numbers, and will be discussed in some detail:

1. Ignition control.
2. Valve timing.
3. Carburetion.
4. Engine-transmission relationship.
5. Combustion-chamber design.

While exploitation of these factors in favor of mechanical octane numbers has been in progress for a long time, there has been intensive development in this field since the end of World War II. It is the purpose of this paper to describe some of these developments.

Ignition Control

The determination of the best compromise of power output and spark advance to establish the highest useful compression ratio for the most efficient utilization of available fuels involves a number of factors which must be considered collectively. The distributor spark curve must be determined by analyzing the relationship between power, spark advance, compression ratio, and fuel. The curves presented in Fig. 11 show a plot of full-throttle bmep for several engine speeds against spark advance using a nonknocking fuel. From these curves a spark advance grid (shown by Fig. 12) of spark advance versus engine speed is obtained at 100%, 99%, 95%, and 90% of maximum power.

Included in Fig. 11 are the borderline knock power points using four gasoline-type fuels at speeds of 800 and 2000 rpm. It will be noted that at 2000 rpm the engine requires a 98/85 (98 Research/85 Motor) octane fuel for borderline knock to develop maximum power, whereas for a 1% power loss the fuel requirement is reduced to a 93/83 octane fuel, a gain of five Research octane numbers for this slight loss in full-throttle power. At 800 rpm, a loss of 8% is the result of using 93/83 octane fuel. If this engine were installed in an automobile with an automatic-type transmission which permits full-throttle operation at speeds down to 800 rpm, a fuel with an octane rating of 93/83 would operate knock-free over the speed range with the spark setting indicated by the distributor spark curve in Fig. 12.

Fig. 13 summarizes the results of tests made on

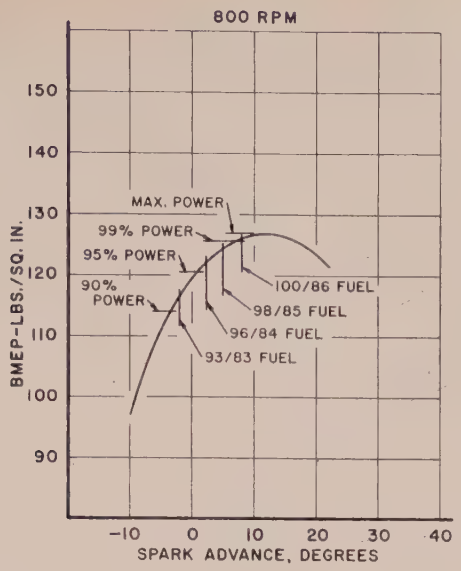

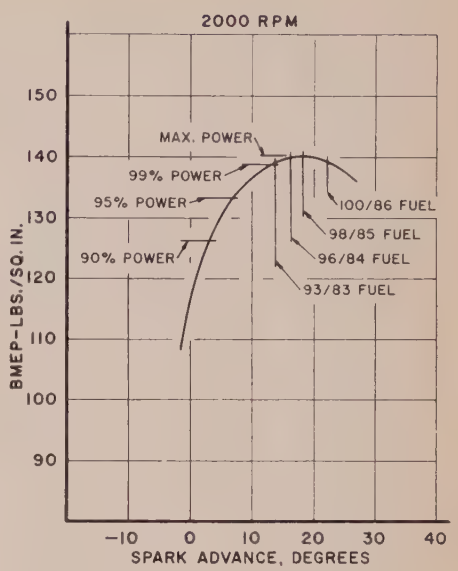

Fig. 11 – Full-throttle bmep versus spark advance at several speeds, with borderline knock values shown for several fuels

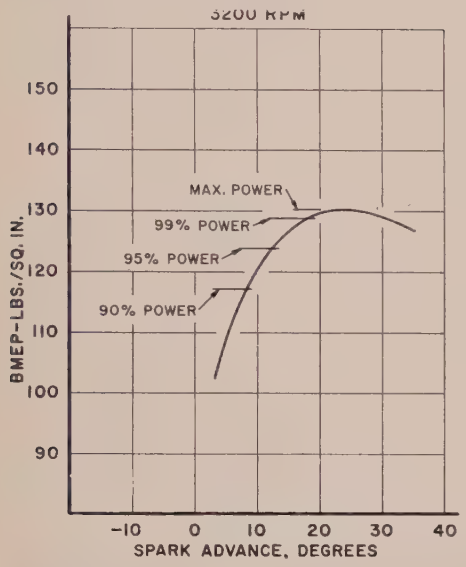

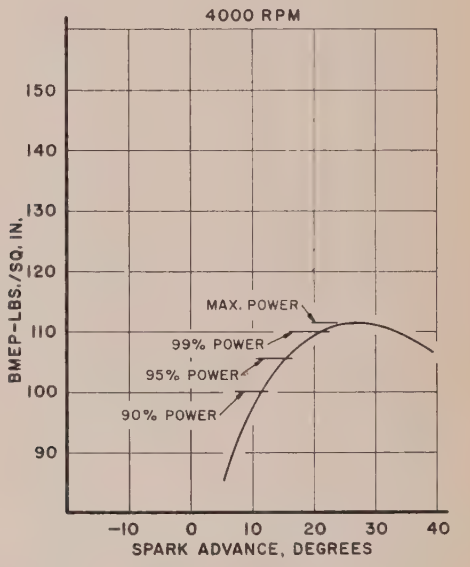

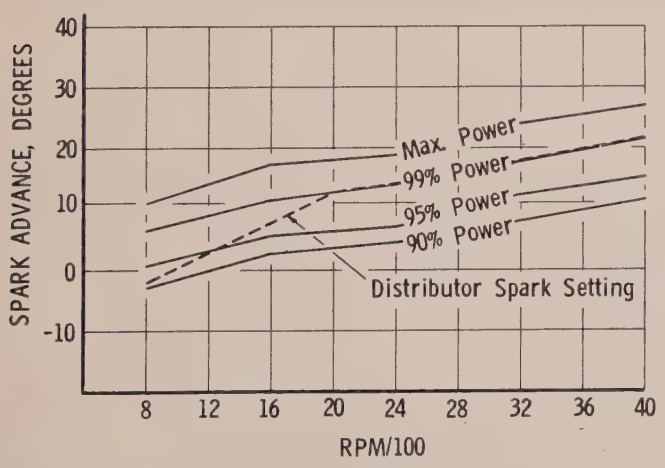

Fig. 12 – Spark-advance curves indicating spark-advance requirements of corresponding full-throttle power valves

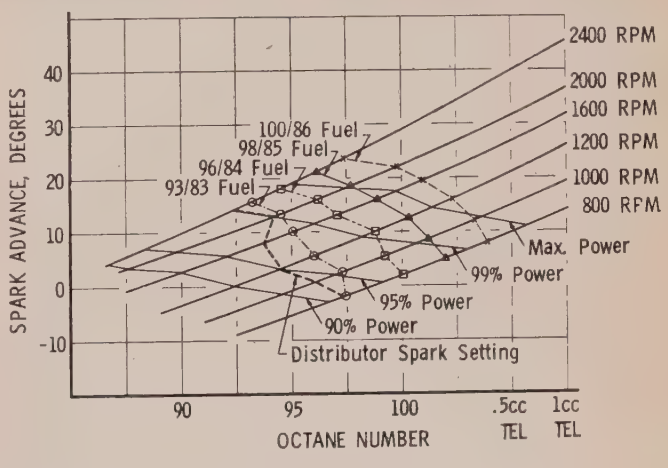

Fig. 13 – Full-throttle fuel octane requirement for typical car installation

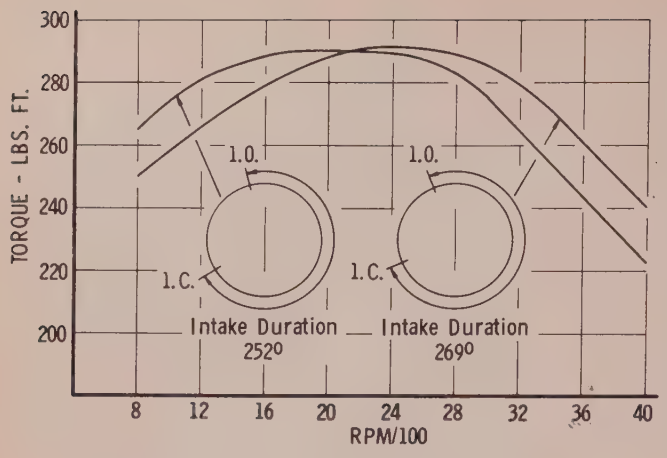

Fig. 14 – Effect of valve timing on engine torque

the same engine in a typical automotive installation, as follows:

1. A grid of borderline knock spark advance plotted against octane number of primary reference fuels at six different engine speeds.

2. Spark advance for 100%, 99%, 95%, and 90% of maximum power at each engine speed.

3. The distributor spark setting obtained from Fig. 12.

4. Spark advance for borderline knock at the six speed levels using four different gasolines.

The speed curves give the spark advance for borderline knock using primary reference fuels. For example, at 1200 rpm, the 95 octane number primary reference fuel developed borderline knock when the spark was set at 3½ deg btdc and 100-octane-number primary reference fuel gave borderline knock with the spark advance at 12 deg. The intersection of the 1200-rpm curve with the curve marked "maximum power" indicates that the spark advance for maximum power is 14 deg, and that a primary reference fuel of 100 plus 0.1 cc tel is required to operate at borderline knock under these conditions.

The curves labeled "max power," "99%," "95%," and "90%" are obtained from the data presented in Figs. 11 and 12, and indicate the primary reference fuel requirements that produce borderline knock for these values at each speed.

Included with these curves of the relationship of spark advance, power, and primary reference fuel octane requirements are the octane ratings of four gasolines in the engine used in these tests. These gasoline curves are labeled 100/86, 98/85, 96/84 and 93/83. The 96/84 gasoline, for example, had a Research rating of 96 and a Motor rating of 84. At 800 rpm this 96 Research octane number gasoline was rated by the engine to be equivalent to 100 octane primary reference fuel, while at 2400 rpm it was rated as 94.5 octane primary reference fuel.

The distributor spark curve was obtained from Figs. 11 and 12, and, when applied to Fig. 13, illustrates the fuel octane requirement to satisfy the engine. It can be seen that 93/83 gasoline comes very close to satisfying this requirement. Further examination of the curves reveals that to operate at maximum output spark advance the engine would require 100/86 fuel at speeds from 1000 to 2000 rpm and 98/85 above 2000 rpm. Two important observations might be pointed out here:

1. The octane requirement decreases rapidly for a relatively small loss in power due to retarded spark.

2. The importance of knowing the power output-spark advance relationship when comparing the octane requirement of engines.

With an automatic transmission the engine cannot operate at full throttle below 800 rpm, and it is unnecessary to consider full-throttle octane requirement below this speed. Therefore, choice of a small power loss in favor of octane numbers makes it possible to operate at a considerably higher compression ratio on available fuel. This increase in compression ratio results in a substantial increase in part-throttle fuel economy. Since an automobile is operated very little of the time at low-speed full throttle, the gain in favor of lower octane requirement, increased compression ratio, and better fuel economy justifies the sacrifice in full throttle power.

Valve Timing

Another important factor to consider as a source of mechanical octane numbers is the influence of valve timing.

It was shown by Fig. 13 that the low-speed range determines the octane requirement of overhead-valve engines. Valve events can be altered to change the characteristic shape of the torque curve as illustrated in Fig. 14. By delaying the closing of the intake valve, for example, the torque curve can be tailored to reduce the low-speed torque with a corresponding increase in torque in the higher speed range. In an engine with all other factors remaining constant, a reduction in torque by a change in valve timing results in a reduction in octane requirement, and, conversely, an increase

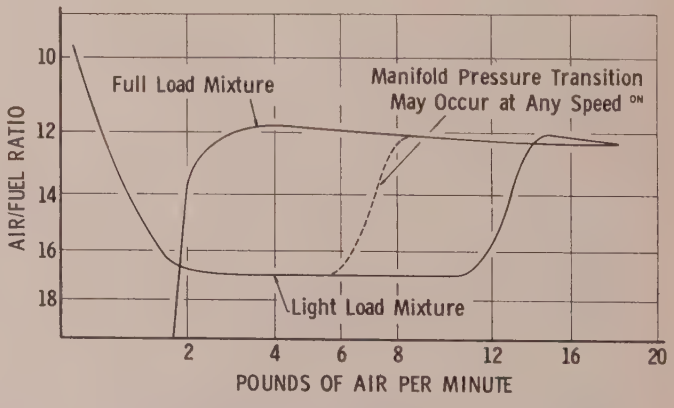

Fig. 15 – Carburetor metering curve, indicating that transition from lean to rich mixture may occur at any airflow

in torque results in an increase in octane requirement at a specific engine speed. Consequently, by suitably adjusting the valve timing, an engine can be more closely tailored to the characteristics of both the available fuel and the type of transmission coupled to the engine.

Carburetion

Most modern automotive engines are supplied with a combustible mixture of gasoline and air by means of a venturi tube carburetor. Its function is to meter the fuel at a rate that is in the proper proportion to the air flow through the carburetor to suit the conditions of operation of the engine. Although the role the carburetor plays in mixing fuel and air in the proper proportions is familiar to all automotive engineers, less is known about the part that this device can play in determining the mechanical octane characteristics of the automobile engine.

First, consider the vacuum enricher as a mechanical octane device. Modern engines will operate on a lean mixture ratio to produce maximum economy, provided the ignition timing is properly adjusted to suit the mixture being used. However, for obtaining the maximum power output of the engine at any given speed, the mixture and spark advance have to be simultaneously adjusted to meet this condition. This adjustment is accomplished by using the change in manifold pressure to increase the mixture strength and at the same time retard the spark to conditions that give maximum power. Figs. 15 and 16 show this manifold pressure transition that may occur at any car speed. The result of the use of this mechanism on modern high-performance passenger-car engines is that a very large part of the fuel is used at lean mixtures, with only an occasional dip into the rich mixture region for acceleration. This being true, it then becomes entirely feasible to gain in mechanical octane numbers by using a richer-than-best

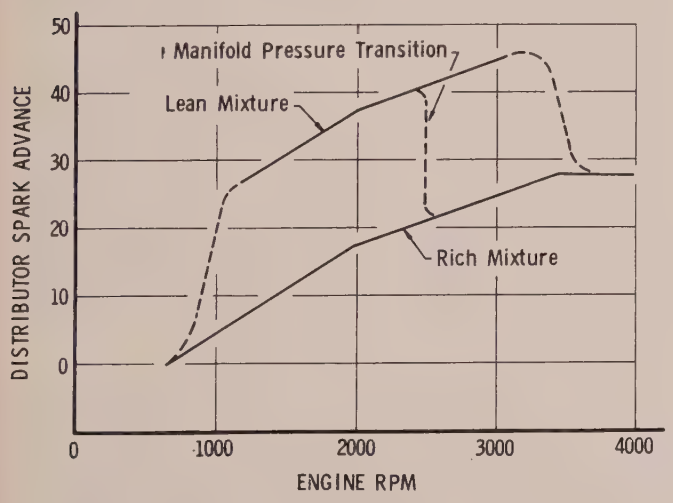

Fig. 16 – Distributor spark curve, indicating that spark retard to full-throttle value must occur at any engine speed

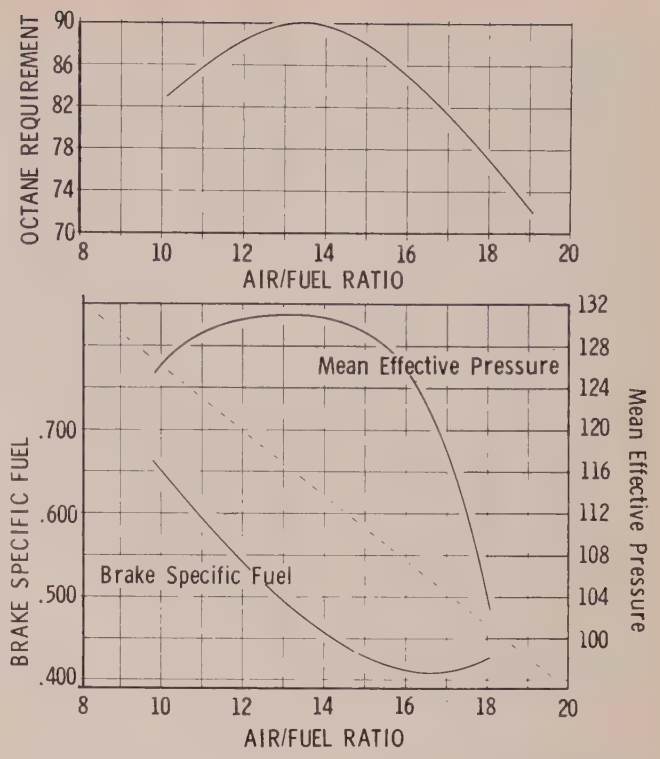

Fig. 17 – Upper curve indicates octane requirement of engine relative to mixture ratio

power mixture during the interval in which detonation or knock would occur (Fig. 17). In other words, use of an overrich mixture and slightly retarded spark at full throttle, low engine speed is justified because an automobile is driven under these conditions only a small percentage of the time. As a result of these compromises in favor of mechanical octane numbers, the vehicle may be operated at a higher compression ratio, which results in a substantial overall improvement in economy.

Mixture distribution plays a large part in the ability to take advantage of richer mixtures for improvement in mechanical octane numbers. The upper curve of Fig. 17 shows that, for any one cylinder, the tendency to knock is maximum at a mixture ratio of 13.5/1, and that any change from this value produces less knock.

At low engine speeds, the spread in air/fuel ratio due to distribution in the case of some multicylinder engines may be as much as three ratios between the individual cylinders, as shown in Fig. 18. It is obvious that under the conditions illustrated in Fig. 18 maximum knock would exist over a range of average mixture ratios from 12/1 to 15/1. This means that when the leanest cylinder is operating at 13/1, the richest cylinder will be operating at an air/fuel ratio of 10/1. If the engine is operated on the rich side in the interest of mechanical octane numbers, the air/fuel ratio of the leanest cylinder will be 11/1 and the richest cylinder 8/1, which is close to the limit of flammability.

The incentive for improving the mixture distri-

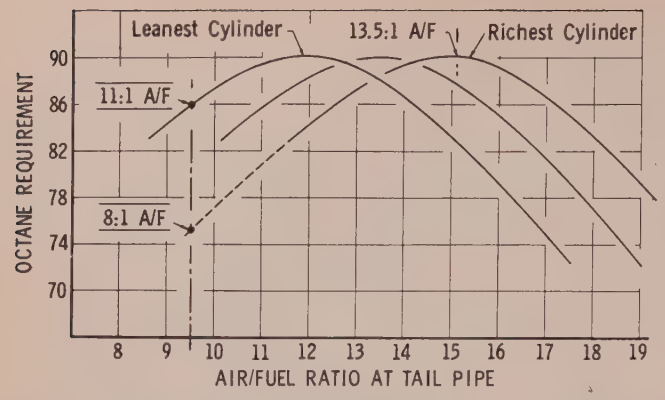

Fig. 18 – Relationship of octane requirement to average mixture ratio for several individual cylinders

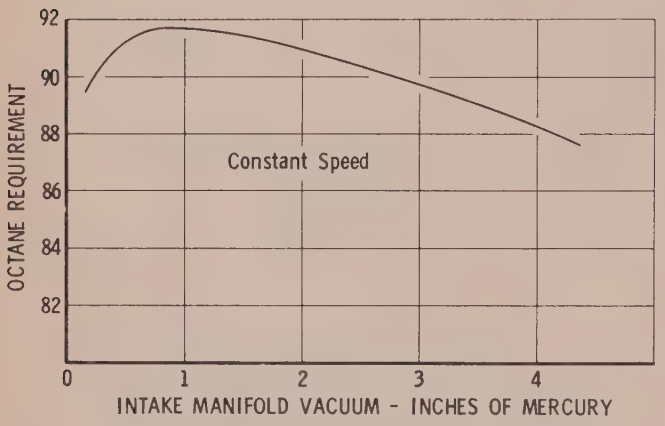

Fig. 19 – Octane requirement versus intake depression at constant speed for typical engine

bution in the lower speed portion of the operating range is much greater today than it has been in the past where power was the principal concern, because additional chemical octane numbers are now so much more difficult to obtain.

The improvement of distribution and carburetion with better engine and carburetor design has introduced a relatively new problem called part-throttle knock. This is experienced as a knock at low speed when the throttle is closed enough to lower the manifold pressure to ½-2 in. of Hg (Fig. 19). The following factors are involved.

1. The simple venturi carburetor has a tendency to lean out, due to a loss of pulse effect on the nozzle when the throttle is partly closed.

2. Distribution may be disturbed by throttle angle and the current tendency to crowd the carburetor down into the manifold to accommodate lower hood lines.

3. The reduction in manifold pressure increases exhaust dilution and results in higher temperatures in the combustion chamber.

Control of part-throttle knock offers a fertile field for mechanical octane numbers in some of the engines being built today.

Engine – Transmission Relationship

The transmission[2] is obviously not a part of the engine, but since it determines the relation between engine speed and wheel speed it has a direct and important bearing on the octane requirement. It should be kept in mind that all work on mechanical octane number improvement, except for that which results from combustion-chamber design, is directed toward allowing the engine to take full advantage of the fuel quality over the engine operating range. If the octane requirement of the engine matches the fuel rating over the speed range, a torque converter would not show any octane advantage.

Fig. 20 shows the full-throttle octane requirement of a typical overhead-valve engine over the speed range, together with the octane rating of a commercial fuel. If a transmission such as a torque converter is used, there could be no full-throttle operation below the stall speed of the transmission. For example, if the stall speed of the transmission is 2000 rpm, there would be a saving of 4 octane numbers. This would allow the compression ratio to be raised, permitting more efficient utilization of the fuel in the light-load range of operation where the majority of the fuel is used.

Combustion – Chamber Design

In an automotive engine, although less than 10% of the cycle is devoted to burning of the fuel-air mixture, this process and the manner in which it occurs has a profound influence upon engine efficiency. The charge can either burn uniformly and progressively from the point of ignition out to the confines of the combustion space, resulting in efficient conversion of the fuel's chemical energy into mechanical power, or it can detonate spontaneously and result in lost power and mechanical harm to the engine.

Detonation has been defined as the instantaneous burning of a large portion of the end gas. Whether detonation will or will not occur has been shown by many investigators[3, 4, 5, 6] to be dependent on fuel quality, pressure, temperature, and time history of the end gas. Since the objective is to produce maximum power from a given charge, the pressure and temperature are fixed. Under specific conditions of pressure and temperature, a critical period of time is required to complete certain chemical preparations before detonation can occur with any given fuel. As a result, detonation can

---

[2] See SAE Transactions, Vol. 61, 1953, pp. 81-96: "Engine-Transmission Relationship for Higher Efficiency," by D. F. Caris and R. A. Richardson.

[3] See SAE *Quarterly* Transactions, Vol. 4, April, 1950, pp. 232-274: "Ignition of Fuels by Rapid Compression," by C. F. Taylor, E. S. Taylor, J. C. Livengood, W. A. Russell, and W. A. Leary.

[4] See SAE Transactions, Vol. 61, 1953, pp. 402-408: "Effect of Combustion Time on Knock in Spark-Ignition Engine," by D. R. Diggs.

[5] See British Aeronautical Research Committee R&M 1324 (1929), "Experiments on Ignition of Gases by Sudden Compression," by R. W. Fenning and F. T. Cotton.

be controlled chemically by using higher-octane fuels which require more time to reach these critical conditions. On the other hand, it can be controlled mechanically by combustion-chamber designs which speed up the rate of burn and complete the combustion process before detonation has time to occur. This is the principle upon which combustion-chamber design for mechanical octane numbers is based.

Studies of the combustion periods of experimental chambers have established a relationship between combustion time and octane requirement. The results show that it is possible to reduce combustion time by more than 50%, and thereby achieve an important gain in mechanical octanes.

Such design factors as "compactness" and "piston coverage" are some of the physical characteristics possessed by chambers which have short combustion periods and thus low octane fuel requirements. In these cases, the clearance volume is concentrated around the point of ignition as "compactly" as permitted by ingenuity and the necessary practical compromises considering valves, piston, and spark plug. This physical arrangement of the clearance volume results in the optimum use of such factors as short flame travel, charge turbulence, and concentration of the mass of the charge at the point of ignition. Other investigators[7, 8, 9] have also shown that these factors increase the rate of combustion.

The work was not limited by the necessity for adhering to good chamber design practice. Some of the experimental setups were devised solely as an attempt to investigate the maximum potential effects of a particular variable. However, the ultimate objective was a chamber which combined all the desirable features in an overhead-valve arrangement without impairing high-speed breathing or sacrificing sound principles of design.

Detonation – Limited Tests of Clean Combustion Chambers

The effects of combustion-chamber design upon detonation must be studied by comparing the fuel requirements of each design under fixed test conditions. This includes control of such carburetor air entrance variables as temperature, pressure, and humidity. For each individual chamber design comparison, all physical and mechanical variables such as cams, cam timing, valve and port sizes were fixed in so far as possible so that combustion-chamber design was the only variable. Except when otherwise noted, the tests were performed with the chamber in a relatively clean state, since no direct attempt was made to accumulate deposits in these initial studies. Care was exercised to insure that each chamber had approximately the same amount of running prior to each test. This step was taken to minimize the many additional variables which are introduced by the presence of deposits which would tend to mask the results of this basic study. After the screening tests were completed, deposit effects on selected designs were studied as a separate and distinct problem.

In the case of overhead-valve combustion-chamber designs, increased engine speed usually results in a decrease in octane requirements. This characteristic effect is shown by Fig. 21, which compares two designs at speeds up to 3000 rpm. In general, no significant variation in the relative comparisons of combustion chambers was noted at different engine speeds. Therefore, for simplicity, the comparisons presented in this paper are shown only at

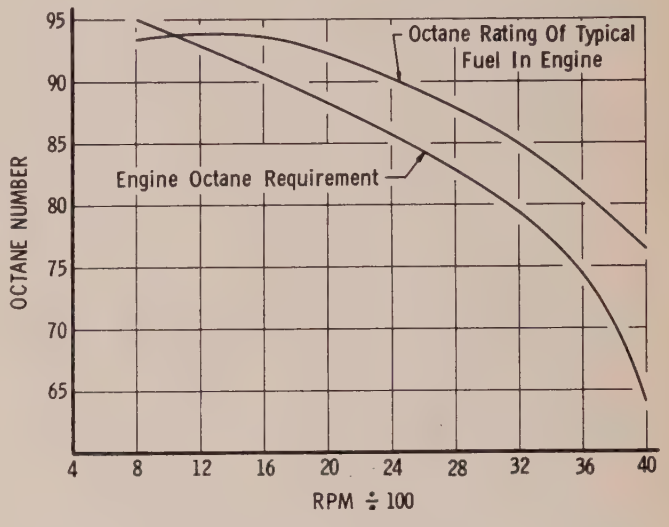

Fig. 20 – Full-throttle octane requirement of typical overhead-valve engine over speed range, together with octane rating of commercial fuel

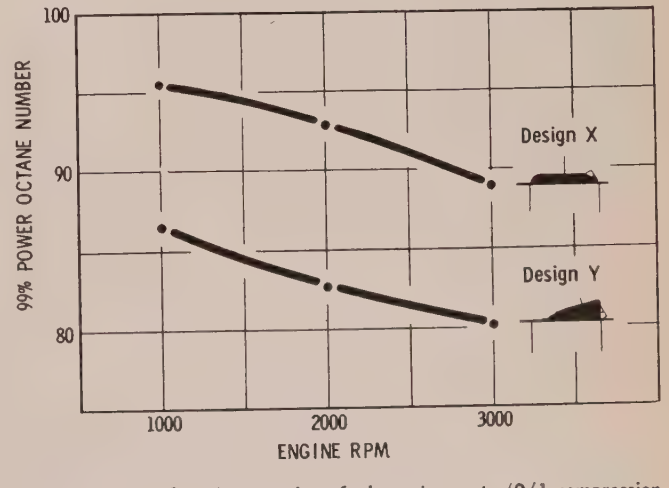

Fig. 21 – Effect of engine speed on fuel requirements (9/1 compression ratio)

[6] See *Philosophical Magazine* (London), Vol. 44, Series 6, July, 1922, pp. 79-121: "Experiments on Ignition of Gases by Sudden Compression," by H. T. Tizard and D. R. Pye.

[7] See *Journal of Aeronautical Sciences*, Vol. 3, July, 1936, pp. 313-315: "Notes on Effect of Cylinder-Head Design on Detonation," by C. F. Taylor and G. L. Williams.

[8] See *Automobile Engineer*, Vol. 19, July, August, 1929, pp. 257-261, 284-286: "Cylinder-Head Design," by H. R. Ricardo.

[9] See Ethyl Corp. Report AR-216: "Cylinder Performance – A Study of Turbulence, Quench, and Flame Travel Effects," by S. D. Heron and A. E. Felt.

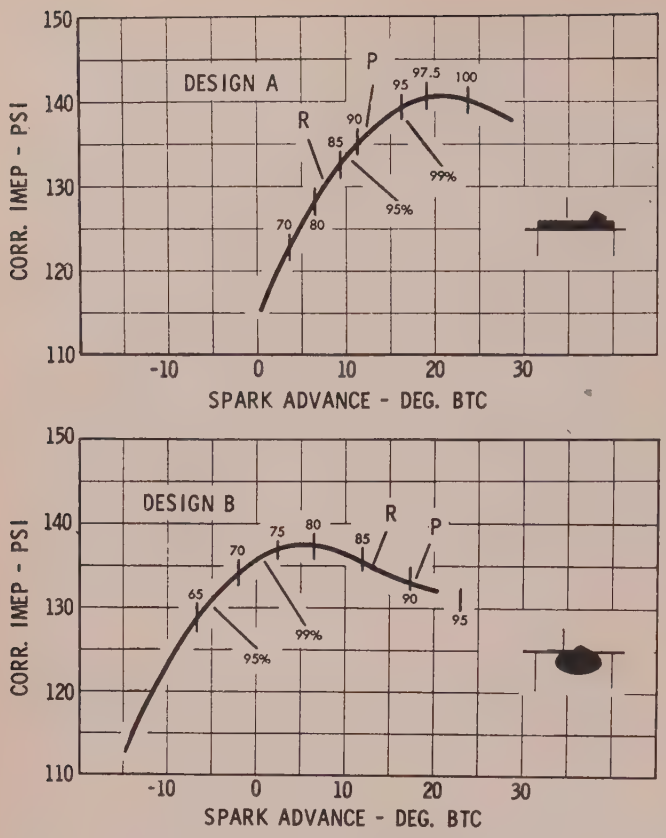

Fig. 22 – Comparison of typical fuel requirements tests (1000 rpm, 9/1 compression ratio)

the engine speed of 1000 rpm.

Fig. 22 shows two examples of the type of test which is made to obtain basic information about a combustion chamber at any given engine speed. This test shows three important facts.

1. The maximum potential power output with nonknocking fuel in terms of corrected imep.

2. The distributor spark advance setting required to obtain this power output.

3. Spark timing and power at borderline knock on various primary reference fuels and commercial gasolines.

As an example, a comparison of curves for chambers A and B of Fig. 22 shows how fuels of different octane number control the power output of an engine. Design A has a 99% maximum power octane requirement of 95.5, while design B shows a requirement of 73 octane numbers at 99% of maximum power. The most important fact obtainable from these curves is the borderline knock power output on commercial fuels. Commercial regular (R) and premium (P) fuels are shown for both combustion chambers. However, in this case the borderline knock power outputs cannot be compared because both fuels are of much higher octane quality than is required by design B. The fuel common to both designs on the retarded side of the curve is 70 octane. Using 70-octane primary reference fuel, design A produces borderline knock output of 123 imep, while design B produces 134 imep.

In some cases, depending upon the fuel requirements of the designs to be evaluated, the borderline knock power of several different fuels can be compared. However, all fuels show the same relative story. For simplicity, the comparisons shown later in this paper are made with one fuel which is common to the 90% to 99% maximum-power portion of the spark fishhooks.

Combustion Periods

In order to help interpret the effect of chamber design on octane requirement, indicator cards were taken on many combustion chambers. As an example, Fig. 23 compares the combustion portion of balanced diaphragm pressure cards for two representative chambers at 1000 rpm and 9/1 compression ratio. As was previously shown by Fig. 22, chamber A is a high-requirement design, while chamber B is a low-octane-requirement design. Both indicator cards were obtained at maximum-power spark settings. These were 21 deg btc for chamber A, and 6 deg btc for chamber B. The major differences which can be observed are: the charge for chamber B is ignited later than for design A; and the rate of pressure rise is higher for design B.

The actual combustion times of various chambers were also calculated from these balanced diaphragm pressure cards using the method outlined by Rassweiler and Withrow.[10] The method consists essentially of algebraically subtracting the pressure changes due to piston movement from the pressure card. The remaining pressure changes are due to combustion, and can be reduced to per cent mass of the charge which has been burned at any instant.

[10] See SAE Transactions, Vol. 33, 1938, pp. 185-204· "Motion Pictures of Engine Flames Correlated with Pressure Cards," by G. M. Rassweiler and L. L. Withrow.

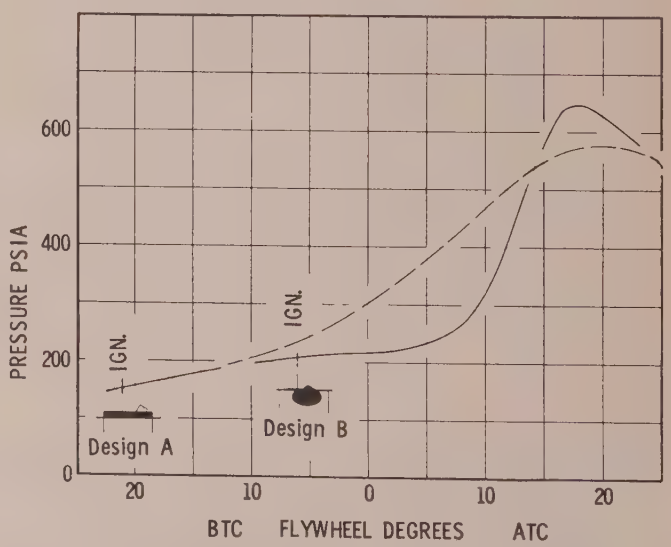

Fig. 23 – Effect of chamber design on combustion portion of pressure-time trace (1000 rpm, 9/1 compression ratio)

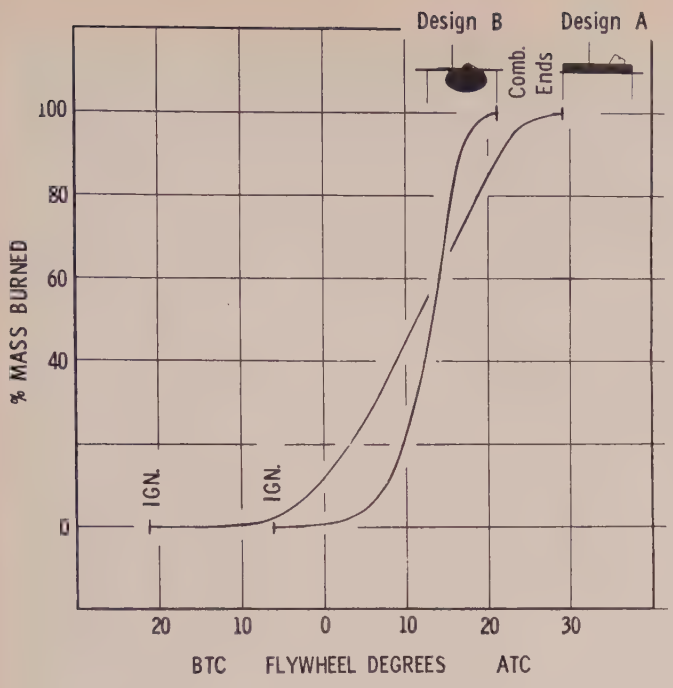

Fig. 24 – Effect of chamber design on rate of burn (1000 rpm, 9/1 compression ratio)

The mass burn curves calculated from the indicator cards of Fig. 23 are shown by Fig. 24. These curves show that the combustion times are 50 flywheel deg for the 95.5-octane- and 27 deg for the 73-octane-requirement chamber. The combustion time is reduced almost one-half for low-octane design B.

Fig. 25 summarizes the effects of combustion-chamber design upon the three factors: end gas pressure, end gas temperature, and total combustion time. These values were computed from experimental data obtained from balanced diaphragm indicator cards, and are plotted against chamber design as represented by its octane requirement at 99% of maximum power. This figure shows that combustion chambers which have a low-octane requirement exhibit somewhat higher end gas pressures and temperatures, as would be expected from the faster rates of burn, but show a substantial reduction in combustion time. Since higher pressures and temperatures tend to promote knock rather than suppress it, combustion time must be the dominant controlling factor which allows a reduction in octane requirements to be obtained through combustion chamber design. Diggs[4] has also studied the pressure, temperature, and time parameters, and reports similar effects.

Short combustion time resulting from faster burning of the mixture appears to be the fundamental consideration which allows some designs to operate satisfactorily on low octane fuels. However, there are a large number of associated factors such as flame travel, turbulence, and mass distribution, and the manner in which they are best obtained, which must be understood before an engine designer can produce a design that will yield the desired result. The subsequent paragraphs are devoted to a consideration of these variables.

Flame Travel Effects

Flame travel is one of the factors which influence the rate of combustion. The maximum flame travel is fixed by the distance from the spark plug to the most remote portion of the combustion space. In the case of the overhead-valve engine, where the valves are arranged to clear the cylinder bore, moving the ignition point as near the cylinder axis as will be allowed by the necessary considerations of casting and shop practices represents the minimum flame travel that can be accomplished without multiple ignition.

In order to show that the flame front burns out to the cylinder wall, the per cent of the mass of the charge which is burned at any instant during combustion was calculated for several representative experimental chambers. The results show that, depending upon the total combustion time, 90-99% of the charge is burned with the piston moving on the downstroke at the beginning of the expansion process. This is illustrated by Fig. 26, which shows the per cent of the mass of the charge which is burned at 1000 rpm and 9/1 compression ratio at the start of the expansion stroke, and how it varies with chamber design as represented by the 99% maximum-power octane requirements. Fig. 26 also shows the piston position at any instant during combustion. From this information it is apparent that by the time the last 2% of the charge is being consumed, even in the case of chambers with high rates of burn, the cylinder wall is exposed so that it becomes the actual confining limit of the combus-

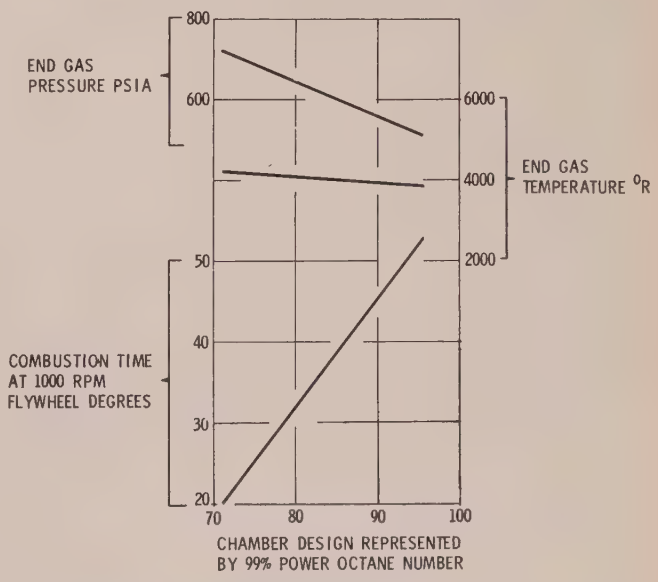

Fig. 25 – Summary of effect of combustion-chamber design on end gas pressure, calculated end gas temperature, and combustion time (1000 rpm, 9/1 compression ratio)

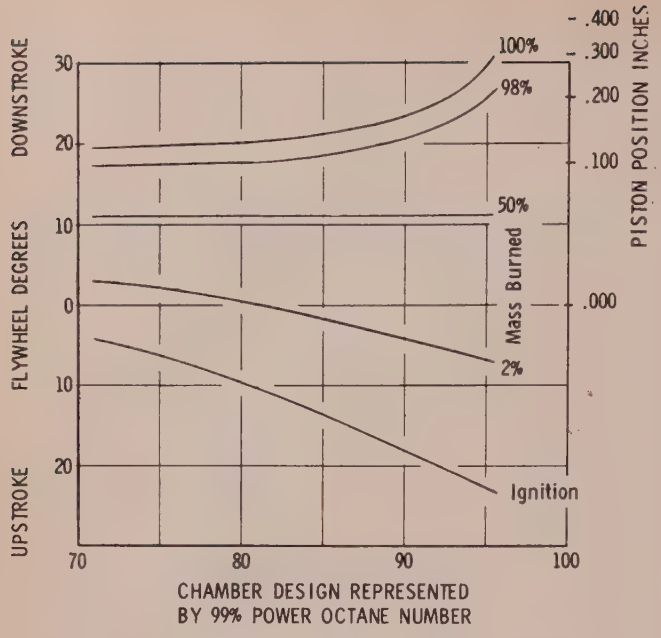

Fig. 26 – Summary of effect of combustion-chamber design on combustion periods and piston position at end of combustion (1000 rpm, 9/1 compression ratio)

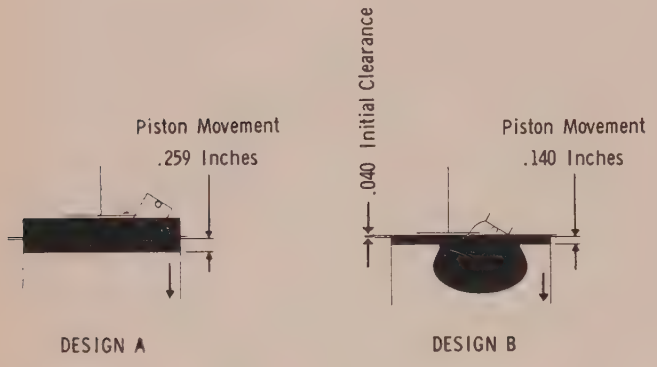

Fig. 27 – Effect of combustion-chamber design on piston position at end of combustion (1000 rpm, 9/1 compression ratio)

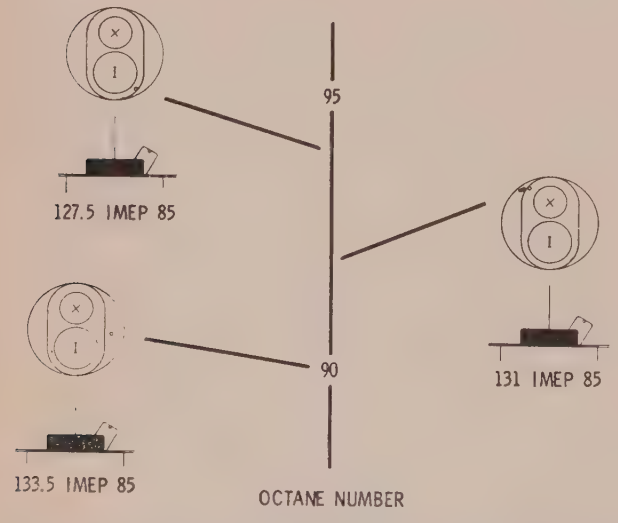

Fig. 28 – Effect of spark-plug location for design with moderate piston coverage on 99% power octane requirements (1000 rpm, 9/1 compression ratio)

tion space. This is illustrated clearly for two chambers by Fig. 27. Design A has already been shown to be a slow-burning high-octane-requirement design, while design B is a fast-burning low-octane chamber. Both chambers are shown with the pistons on the downward stroke at the end of the combustion process. The dimensions in inches show the calculated piston position at the instant when the last part of the charge has burned, which is also the time when the flame front has just reached the left-hand cylinder wall.

It is quite apparent from this illustration, based upon combustion periods calculated from balanced diaphragm pressure cards, that the cylinder wall will always be the confining limit of the combustion chamber. The flame front must burn out to this boundary if all of the charge is to be consumed.

Fig. 28 shows the effect of spark-plug location for a design which has moderate piston coverage. The plug location which results in the lowest octane requirement is the conventional position which is nearest the cylinder bore centerline.

In order to be certain that the improvement in fuel requirement has not been obtained at a sacrifice of power, the borderline-knock imep using a regular gasoline of 85/75 octane is shown beneath each design. As can be observed, the borderline-knock power is highest for the chamber which has the lowest fuel requirement.

Fig. 29 shows the results of a study of the effect of spark-plug location conducted during the development of the 1954 Buick combustion chamber.[11] As can be observed, the central plug location near the bore center results in a substantial reduction in octane requirements. The last chamber with the three plugs firing simultaneously results in an ad-

[11] See SAE Transactions, Vol. 61, 1953, pp. 478-502: "New Buick V-8 Engine Offers Many Advantages," by V. P. Mathews and J. D. Turlay.

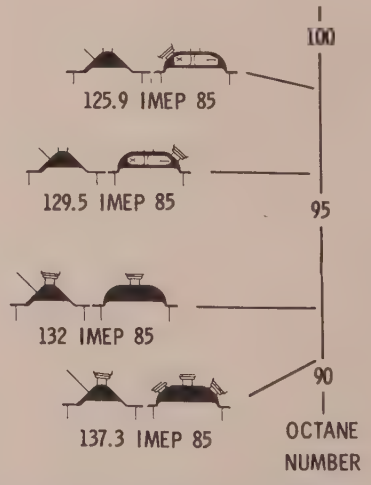

Fig. 29 – Effect of spark-plug location on 99% power octane requirements as observed during development of 1954 Buick combustion chamber (1000 rpm, 9/1 compression ratio)

Fig. 30 – Examples of shrouded intake valves

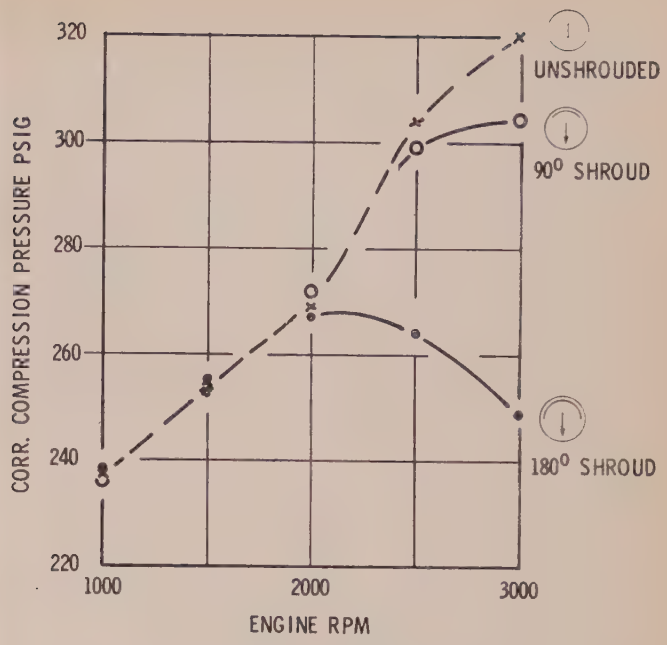

Fig. 31 – Effect of intake valve shrouding on compression pressures (9/1 compresson ratio)

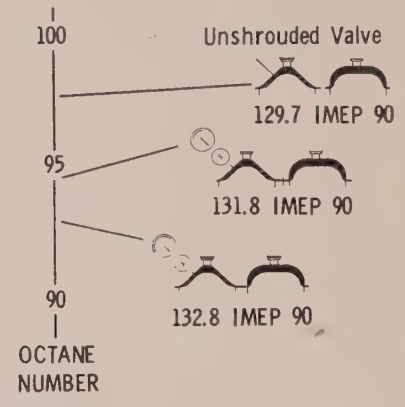

Fig. 32 – Effect of intake valve shrouding on 99% power octane requirements (1000 rpm, 9/1 compression ratio)

ditional improvement. Once again, examination of the power output on a regular-grade fuel shows the highest value for the chamber with the lowest fuel requirement.

In summarizing the results of this section, it is concluded that the flame travel length should be measured from the point of ignition to the most remote point in the chamber, with the piston in the position it actually occupies when the last part of the charge is burned. Moving the spark plug toward the center of the bore, which effectively shortens flame travel and also shortens the combustion period, results in a reduction in fuel requirement. This design change also increases the borderline-knock power output on a gasoline which knocks below the peak-power spark setting.

Turbulence Effects

Turbulence is another important factor which influences the rate of combustion. This factor is present in varying degrees during the intake, the compression, and the combustion periods. We know of no method for accurately gaging the degree of turbulence involved, and therefore the experiments performed are described in terms of various engine and combustion-chamber design features and their influence on mechanical octane numbers.

As an example, properly directing the intake passage or shrouding the intake valve, that is, masking the valve on one side so as to block mixture flow in one direction and force it to deflect (Heron and Felt[9] call it swirl) in the opposite direction, are descriptions of the physical changes which can be made on the intake system. Two shrouded valves are shown in Fig. 30. From a practical standpoint, it would be difficult to devise such a means of influencing the fuel requirements at low engine speeds, where knock is a problem, and still allow normal breathing at high engine speeds where power is desired. As an example, the effect upon breathing of shrouding the intake valve is shown by Fig. 31. This chart shows compression pressures for three cases: a normal intake valve which allows mixture flow in all radial directions, a valve with a 90 deg shroud, and a valve with a 180 deg shroud. By comparing compression pressures of both shrouded valves to the normal valve, it is apparent that this method of reducing the fuel requirements restricts breathing above 1800 rpm. At speeds below 1800 rpm, breathing is normal, as indicated by identical compression pressure valves.

However, in order to explore this approach, and

also as a means of determining the potential effects of the intake turbulence factor, without regard for practical applications of the system, a shrouded intake valve was installed in a combustion chamber and tests were run only at 1000 rpm where breathing, as represented by Fig. 31, is still normal.

As an example, Fig. 32 shows the effects of the intake shrouds described above for a combustion chamber with no piston coverage. The shrouds were fixed so that they direct the incoming charge toward the exhaust valve. It is apparent that a substantial reduction in octane requirement results as the degree of shrouding is increased. To be assured that power has not been sacrified, a comparison of borderline knock power on 90-octane fuel shows a higher value for the valve with the 180-deg shroud.

The investigation of the effects of shrouding was carried still further by exploring the influence of direction of the intake charge upon the octane requirements. For this purpose, the intake valve was fixed in the desired positions so that the shrouds would be located as shown by Fig. 33. This chart shows that the direction of the intake charge is very influential in determining the extent of the reduction in octane requirements. However, in every case, shrouding results in an improvement over the unshrouded intake system, regardless of direction. Once again, a comparison of borderline knock power on 70-octane fuel shows that power has not been sacrificed to obtain the gain in fuel requirement.

In summarizing these shrouded intake valve experiments, it is apparent that turbulence produced by this mechanical means is very effective in reducing the fuel requirements. Therefore, the effects of turbulence which are produced at this early stage in the engine cycle must persist throughout the combustion period to produce the results observed. However, it is apparent that this method also restricted engine operation above 1800 rpm, when the shrouding was increased to the point necessary to produce a measurable effect

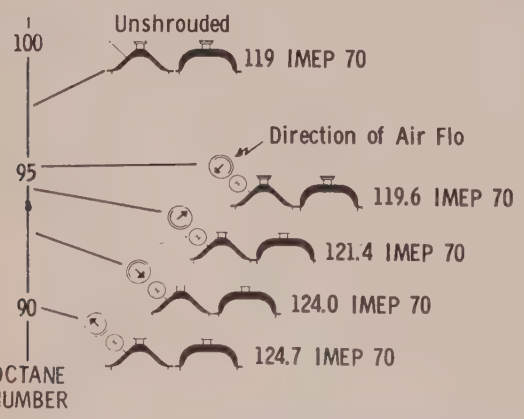

Fig. 33 – Effect of direction of intake valve shrouding on 99% power octane requirements (1000 rpm, 9/1 compression ratio)

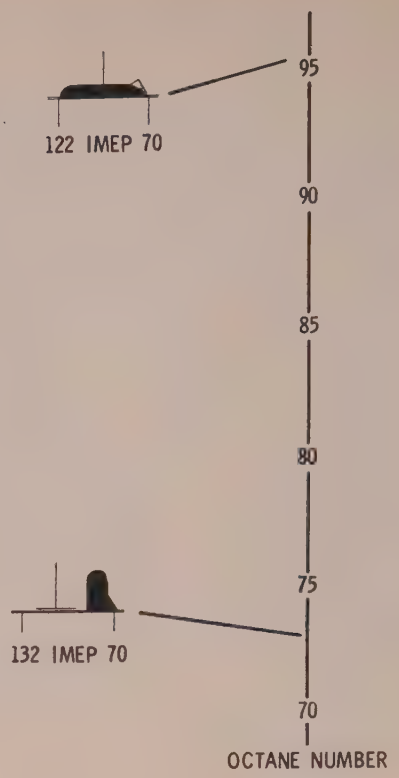

Fig. 34 – Effect of piston coverage with proper mass distribution of charge on 99% power octane requirements with two different chamber designs (1000 rpm, 9/1 compression ratio)

upon fuel requirements. Directed intake ports are not likely to be effective in producing turbulence at low engine speed where knock is a problem, unless the port areas are small enough to produce the necessary high velocities. Small port areas are impractical because of high-speed breathing requirements.

Although the designer is somewhat restricted in the gains he can achieve by means of intake turbulence, fortunately a more practical approach is available. This approach to turbulence is through piston coverage, which has the effect of physically displacing the charge from one side of the chamber to another as the piston approaches top dead center. To accomplish this, the piston is shaped so that part of it matches the head at top dead center, with only enough clearance to prevent interference. It is generally believed that this physical arrangement of the chamber results in some form of compressive turbulence. (Heron and Felt[9] call this effect squish.)

Presumably, the relative magnitude of compressive turbulence is proportional to the per cent coverage. However, no attempt was made to establish a relationship between turbulence and coverage by measuring mixture velocities. In addition, it was found that although the fuel requirements are reduced as per cent coverage is increased, the mass distribution of the charge is also an essential parameter. Combined with proper mass distribution, which is obtained by concentrating the ma-

Fig. 35 – Effect of piston coverage and mass distribution of charge on 99% power octane requirements with same cylinder head, changing only the pistons (1000 rpm, 9/1 compression ratio)

jority of the clearance volume around the spark plug, this method provides an effective means of influencing fuel requirement, since its beneficial effects occur just prior to and during ignition of the charge. It has the added advantage of having no limiting effects upon the normal breathing or functioning of the engine, as might be the case with intake shrouds or angled intake ports.

The effect of piston coverage with proper mass distribution of the charge is illustrated by Fig. 34, which compares two chamber designs. It will be noted that both chambers have the same distance from point of ignition to the cylinder bore. In short, the distance the flame front must traverse during combustion is the same for both cases. Therefore, the reduction of 23 numbers in octane requirement can be considered a result of piston coverage and the manner in which the majority of the charge is concentrated around the point of ignition. It is quite apparent from this illustration that this physical change in chamber design is extremely effective in reducing fuel requirements. It actually is the most important single design change which can be used to produce an improvement in fuel requirements. Examination of the borderline knock-limited power values obtained using 70-octane fuel shows that the lower octane requirement chamber produces 8% more knock-limited power than the high octane requirement design.

Another example of the beneficial effects of high piston coverage is shown by Fig. 35. In this example the spark-plug location is identical for both chambers, because the same cylinder head was used. Therefore, flame travel distances to the cylinder bore are the same in both cases. The effect observed was obtained by changing only the pistons. The design of the piston, which distributes the clearance volume around the spark plug concentrating as much of the mass of the charge as possible at the point of ignition, together with the high piston coverage which results from this arrangement, illustrates the ultimate objective of chamber design. This piston design change produces a 19-octane reduction in fuel requirements. A check of the knock-limited power on 70-octane fuel shows a 5% improvement in output.

Another design variable which was found to produce a profound effect upon octane requirement is the clearance between the head and piston at top dead center. This is often referred to as "quench thickness," implying that quenching is the beneficial mechanism involved. However, it is very difficult to separate the "quench" effect from the other factors involved. In order to evaluate this factor properly, quenching must be varied while all other variables are held constant. Heron and Felt[9] also discuss the difficulties of isolating this effect. Fig. 36 shows the two designs which are identical except for the clearance between the head and piston. Reducing the clearance results in a 12-number improvement in octane requirement with a corresponding increase in borderline-knock power on 70-octane fuel.

It is difficult to understand how such a minor change in design can have such a large effect. Since it has already been shown by Figs. 26 and 27 that the piston is on the down stroke when the last part of the charge is burning, quenching action at this time is not very likely to be effective. Therefore, it can be concluded that a reduction in clearance must

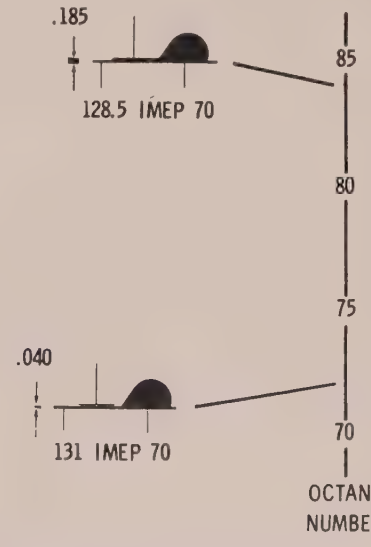

Fig. 36 – Effect of reducing clearance between cylinder head and piston on 99% power octane requirements (1000 rpm, 9/1 compression ratio)

result in a substantial increase in turbulence. Heron and Felt[9] have also studied this particular effect, and discuss it in detail. They show that reduced clearance results in increased borderline-knock output, and attribute the improvement to increased squish velocities resulting as the piston approaches top dead center.

Another factor, however, which the authors feel contributes importantly to this effect is the rapid change in mass distribution of the last part of the charge to burn due to piston motion. As the piston moves down, the flame front is accelerated toward the cylinder wall, resulting in shorter combustion time. Both increased piston coverage and reduced quench thickness accentuate this effect.

The effect of reduced clearance between piston and cylinder head is further illustrated in Fig. 37. In this case, the clearance is reduced from 0.100 in. to 0.040 in., and a substantial reduction is obtained in octane requirement. An increase in borderline knock output is obtained for the low requirement chamber.

Fig. 38 shows the effect of another combustion-chamber design which apparently enhances the effectiveness of the factors which piston coverage generates. The small design differences shown by Fig. 38 result in a remarkable reduction in octane requirement. In both designs the cylinder heads and the piston clearance at top dead center are identical. Therefore, this difference in construction of the piston must result in a substantial increase in the utilization of turbulence, and better mass distribution of the charge, to account for the large gains which result. Again, examination of the borderline knock-limited power values shows an increase in power on 70-octane fuel for the low-octane-requirement case.

In summarizing, it appears that turbulence can be introduced at any time during the intake and compression periods to produce a gain in mechanical octanes. The best results are obtained by arranging the clearance volume at the point of ignition so that the largest possible percentage of the mass of the charge will be concentrated at this point. In addition, the clearance between the piston

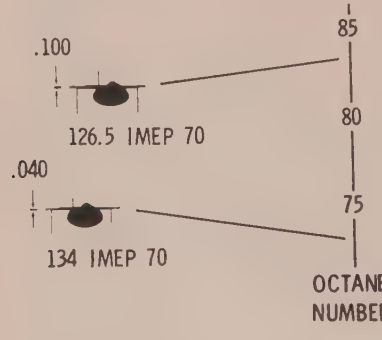

Fig. 37 – Further example of reduction in octane requirement through reduction of clearance between cylinder head and piston (1000 rpm, 9/1 compression ratio)

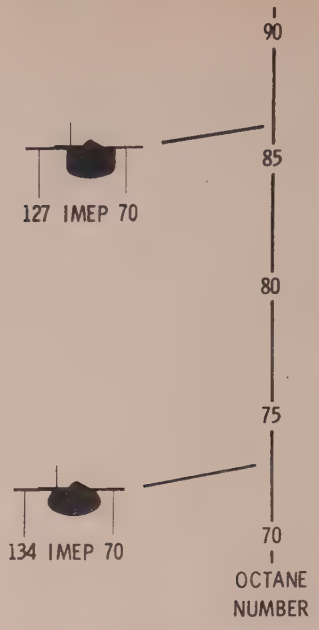

Fig. 38 – Effect of mass distribution of charge and piston coverage on 99% power octane requirements with another chamber design (1000 rpm, 9/1 compression ratio)

and cylinder head formed by the remainder of the chamber surfaces should be held to minimum practical values to effectively utilize piston coverage.

It is also apparent that power output must be considered when comparing designs, because the final objective of mechanical octanes is to increase the thermal efficiency by increasing the borderline-knock output per octane number.

Detonation – Limited Tests of Chambers with Deposits

Deposits were recognized early as a special problem which must be treated separately. Therefore, before the initial screening process was completed, preparations were made to study deposit effects on representative designs which spanned the octane scale.

Deposits on the combustion-chamber surfaces result in three main effects:[12, 13, 14] the compression ratio is increased, the power output decreases, and the fuel requirement is increased. The engine designer recognizes this last effect, and designs the engine with a lower compression ratio than would be possible with a clean engine. The increase in compression ratio is, of course, a result of the decrease in clearance volume due to the presence of the deposits. However, the decrease in power in spite of the increase in compression ratio is due to a reduction in charge density. The mechanism by which deposits reduce charge density is not by

[12] See SAE *Quarterly* Transactions, Vol. 5, October, 1951, pp. 565-576: "Possible Mechanisms by Which Combustion-Chamber Deposits Accumulate and Influence Knock," by L. F. Dumont.

[13] See SAE *Quarterly* Transactions, Vol. 5, October, 1951, pp. 577-583: "Effect of Combustion-Chamber Deposits on Octane Requirement and Engine Power Output," by J. B. Duckworth.

[14] See SAE Transactions, Vol. 61, 1953, pp. 361-377: "Combustion-Chamber Deposition and Knock," by H. J. Gibson, C. A. Hall, and D. A. Hirschler.

means of a mechanical restriction of breathing, but a thermal restriction. That is, deposits preheat the incoming mixture, thus reducing the charge density, and since an engine breathes volumetrically but produces power as a function of charge weight, the power decreases. On the other hand, fuel requirements increase with deposits in spite of the reduced charge density – in part due to increased compression ratio, but mainly because of preheating of the incoming mixture by the deposits during most of the intake process. The effect is quite similar to the events which occur when the incoming mixture is heated by adding heat to the carburetor air or to the mixture in the intake manifold. Fig. 39 shows the effects of raising the carburetor air temperature to 250 F. The air rate decreased 11.5% and the octane requirement increased from 86 to 94 octane numbers at 95% of the maximum power remaining at each temperature. However, because of the maximum-power loss with increased temperature, the fairest way to compare fuel requirements is to examine the borderline-knock output on a given fuel. As an example, Fig. 39 also shows the borderline-knock power obtained using 80-octane fuel. As can be seen, this value decreases very rapidly as temperature is increased. Increased carburetor inlet temperature also increased mixture temperature, but this value is not given because the mixture temperature recorded depends upon thermocouple location. Measurement of true mixture temperature by conventional methods is difficult.

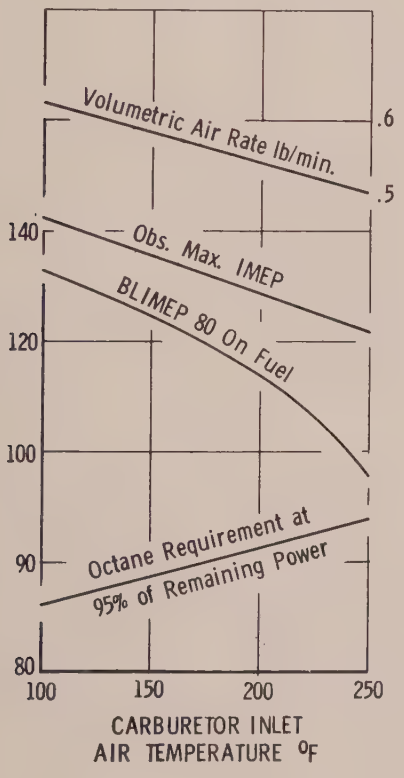

Fig. 39 – Effect of carburetor air temperature on several engine characteristics (1000 rpm, 9/1 compression ratio)

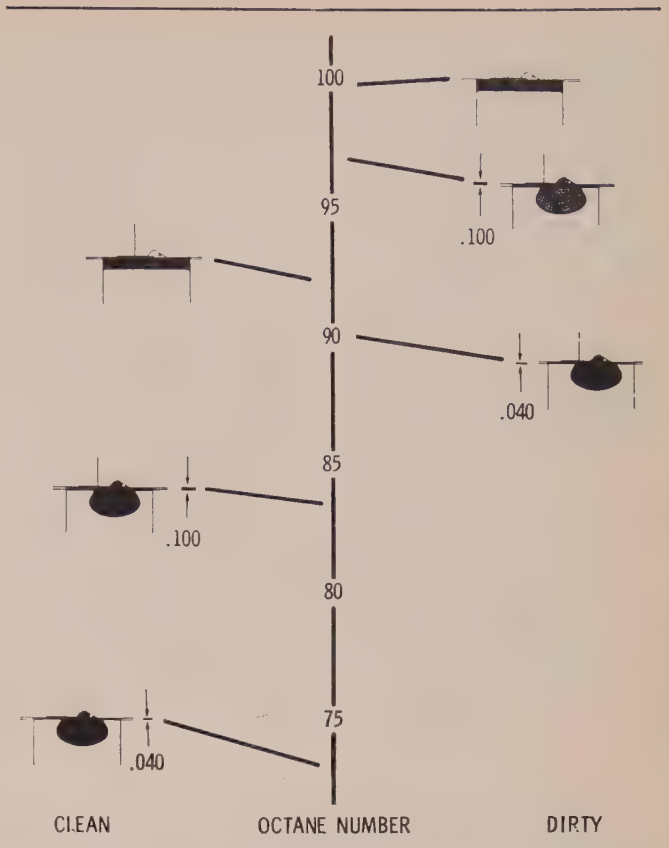

Fig. 40 – Effect of combustion-chamber deposits on 99% power octane requirements (9/1 compression ratio)

Fig. 40 shows the octane requirement increase caused by deposits. The three designs used in this test are shown together with the clean octane requirements to the left of the figure. The results with deposits present are shown by the right-hand chambers. The important point illustrated by Fig. 40 is that, although deposits increase the octane requirements of each design, the chamber shape which has the lowest requirement when clean still has the lowest requirement with deposits present.

The procedure used to obtain this information consists of building up deposits by alternately cycling the engine for 72 hr from 1 min of idle at 600 rpm up to 3 min of full-throttle operation at 1500 rpm. After this heavy-duty deposit buildup procedure is completed, the procedures described earlier in the paper were used to evaluate the fuel requirements.

In evaluating these data, it should be remembered that the octane scale is not linear. Octane numbers in the 95-100 range are much larger in terms of their effect on compression ratio than those in the 80-85 range. This nonlinearity has the effect of crowding the combustion chambers which have accumulated deposits together near the top of the scale.

Effects of Combustion-Chamber Design on Surface Ignition

Combustion-chamber design implies a controlled initiation of the combustion process and a regulated propagation of the flame front out from the

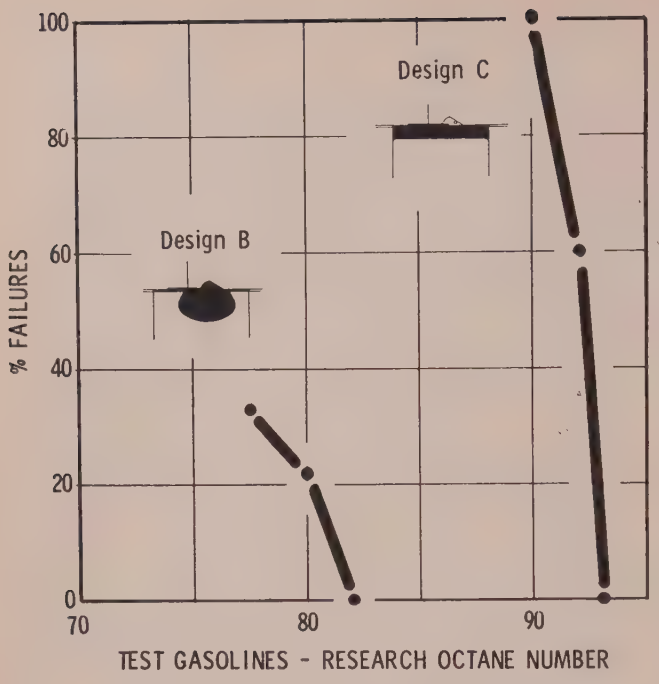

Fig. 41 – Effect of combustion-chamber design on surface ignition tendency (9/1 compression ratio)

encountered during prolonged road load operation of an automobile. A commercial premium gasoline of 93/85-octane rating was used for the deposit buildup. The engine is then operated at full throttle on a test gasoline – as an example, 90/82-octane gasoline. Aural observations are made and recorded regarding abnormal combustion noises such as wild ping, preignition, and autoignition. This full-throttle acceleration is repeated every 2 hr during the light-duty cycling procedure. The same test gasoline is used until sufficient observations have been made to establish the percentage of tests which result in failure. This procedure is then repeated, using other test gasolines, until the curves presented by Fig. 41 are obtained.

In order to allow each design equal opportunity for the occurrence of surface ignition and to eliminate detonation effects, the distributor spark setting was retarded so that ignition starts after the piston has passed top center. At the same compression ratio, and with all other factors equal, the compression processes of both designs are identical. Therefore, the deposits are subjected to the same pressure, temperature, and time stresses

point of ignition. In the presence of certain types of deposits, the initiation and the propagation of the combustion period becomes subject to the whims of the deposits. Under such conditions, combustion is no longer spark-controlled to secure the desired power and economy.

According to Withrow and Bowditch,[15] this problem is the direct result of ignition by deposit particles from the chamber surfaces. Since the deposit particles can ignite the charge at almost any location or number of locations on the chamber surfaces, and the ignitions can occur simultaneously or in some varying sequence at any time during the compression and combustion periods, abnormal combustion is a random event subject to the laws of probability. Events which occur at random can be classified by statistical techniques. Therefore, this is the basis of the method used to study the probability of occurrence of surface ignition for different combustion-chamber designs. As an example, Fig. 41 illustrates the results of a comparison between the two chamber designs shown at 9/1 compression ratio. For each design, the chart presents a curve of probability of occurrence of surface ignition when operating on gasolines of increasing research octane number. For design C, surface ignition will be controlled completely by 93-Research-octane gasoline and for design B, 82-Research-octane gasoline is required. This is a clear advantage of 11 Research octanes for design B.

The procedure used to obtain these curves consists of building deposits in the chamber under part-throttle, light-duty conditions such as are

[15] See SAE *Quarterly* Transactions, Vol. 6, October, 1952, pp. 724-752: "Flame Photographs of Autoignition Induced by Combustion-Chamber Deposits," by L. L. Withrow and F. W. Bowditch.

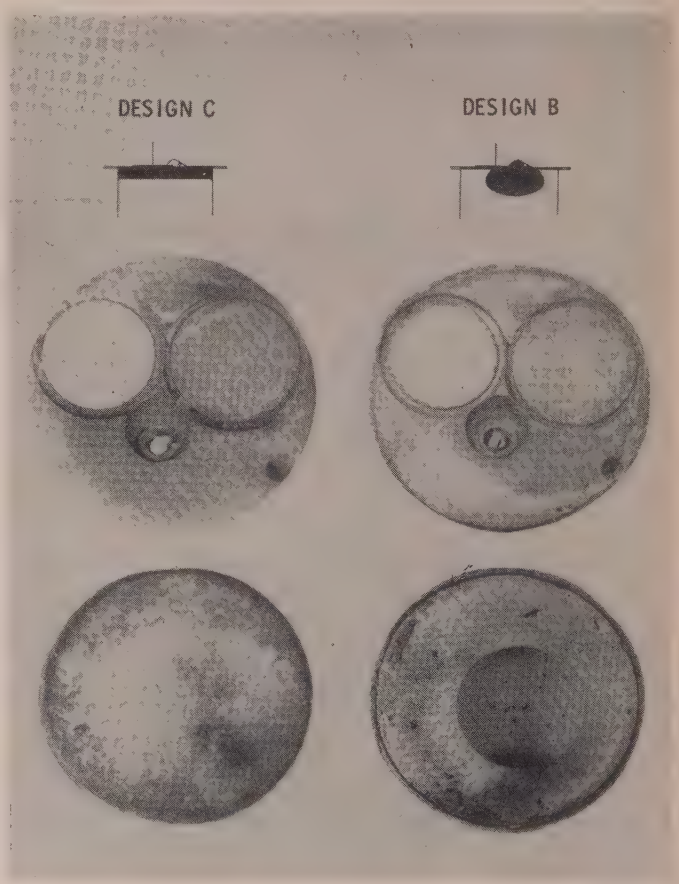

Fig. 42 – Effect of combustion-chamber design on deposit formation (surface ignition deposit accumulation schedule)

during each full-throttle acceleration test. As a result, the influence of chamber design upon the probability of occurrence of surface ignition must occur as a result of some difference in deposits. This is, in turn, controlled for the most part through the manner in which the chamber design influences the formation of deposits. As an example, Fig. 42 shows the deposits obtained during the comparison of designs B and C. The deposits obtained for design B were more or less firm and lava-like in nature rather than loose and crumbly as was the case for design C. It is apparent that the factors which result from design B stabilize the type of deposits which form in the chamber, and it is through this mechanism that surface ignition is controlled in this particular type of cycling test. It is probable that the presence of high turbulence provided by piston coverage sweeps out the loose deposits as they are formed, and leaves behind only the firm deposits.

An example of the influence of deposit character upon surface ignition is shown by Fig. 43. This chart compares the effects of deposits obtained with a commercial premium gasoline of 93/85 rating and two paraffin-base lubricating oils. Oil A contains bright stock, while oil B is a carefully selected distillate oil which contains no residual material. As can be observed, there is at least a 5 octane number advantage for oil B. Once again, examination of the deposit photographs shown by Fig. 44 indicates a difference in deposits. Oil B results in firmer deposits than those obtained using oil A.

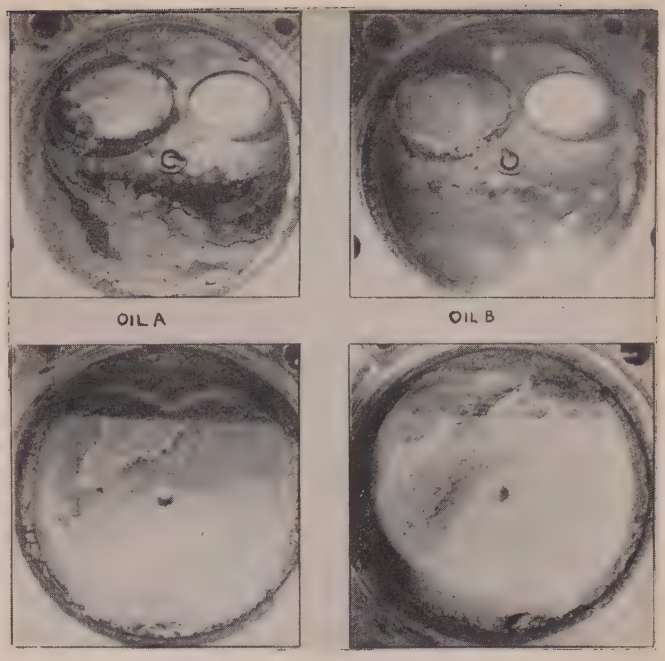

Fig. 44 – Effect of lubricating oils on deposit formation (surface ignition deposit accumulation schedule)

[16] See *SAE Journal*, Vol. 62, January, 1954, pp. 41-52: "Investigations of Preignition Are Bringing Results."
[17] See API Proceedings, Vol. 33, Sec. 3, 1953, pp. 137-150: "Preignition in Automotive Engines," by J. R. Sabina, J. J. Mikita, and M. H. Campbell.
[18] See SAE Transactions, Vol. 62, 1954, pp. 32-39: "Investigation of Preignition in Engines," by A. O. Melby, D. R. Diggs, and B. M. Sturgis.

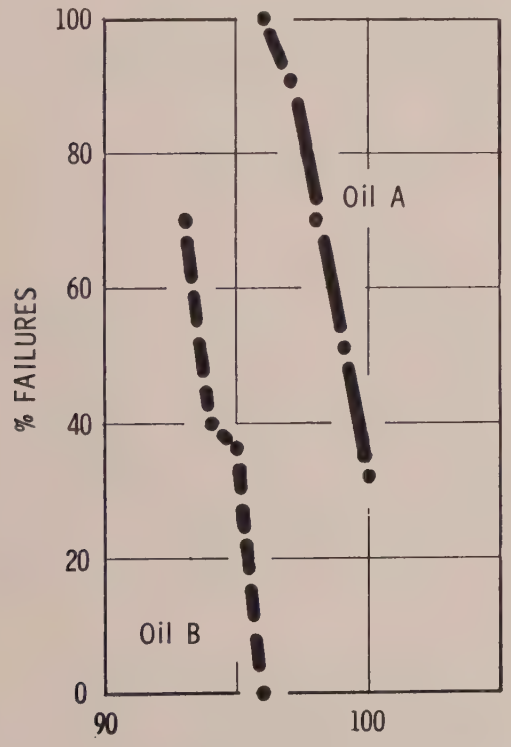

Fig. 43 – Effect of lubricating oils on surface ignition tendency

Other investigators[16, 17, 18] have suggested that the carbonaceous residue is the portion of chamber deposits which causes surface ignition. They show that the elimination of this portion of the deposits seems to make the problem of surface ignition less critical, and that the presence of the noncarbonaceous part of the deposits due to oil or gasoline additives serves in the capacity of binders or catalizers, rather than participating directly in the surface ignition processes.

The petroleum industry has long recognized these deposit effects, and has responded to the challenge by developing lubricating oils and oil additives which have resulted in the beneficial effects noted by Fig. 43. In addition, gasoline additives such as tri-cresyl-phosphate (TCP), ignition control compound (ICC), multi-propyl-phosphate (MP), and many others have been developed and are being marketed to aid in the control of these abnormal surface ignition effects. The ultimate result of these efforts by the petroleum industry will enable the automotive engine designer to take full advantage of the potential mechanical octanes shown to exist by the study of clean combustion chambers.

In summary, combustion-chamber design is a promising approach to increased mechanical octane numbers, and the results of the work described in

this paper indicate that short combustion time is generally associated with low-fuel-requirement chambers. A high rate of burn to obtain short combustion time is controlled principally by flame travel, turbulence, and proper mass distribution of the charge. Careful coordination of these factors is necessary in order to obtain the lowest octane requirement. The same principles apply whether the chamber is operated with or without deposits, even though their presence results in an increase in fuel requirements. This increase forcefully demonstrates the extent to which the deposits are penalizing the automotive engine designer.

Deposits also present another problem called surface ignition. Surface ignition studies show that its occurrence is determined by the character of the deposits. Combustion-chamber design has an important controlling influence on this problem because it determines, to some extent, the type of deposits which are formed.

DISCUSSION

Compares Own Results With Those of Authors

– H. A. Toulmin, Jr.
Ethyl Corp.

THE authors have presented some important ground rules for designing mechanical octane numbers into higher compression ratio engines. Some of the work reported parallels work that we have done at our laboratory, and we would like to compare some of our results with those reported by the authors.

Our work on mixture distribution to the cylinders of a multicylinder engine confirms the authors' conclusions that improvements in part-throttle mixture distribution would be one source of gaining mechanical octane numbers. A plot of the spark advance for trace knock against manifold vacuum for a typical V-8 engine is shown in Fig. A. It can be seen that in this engine the highest octane requirement (minimum spark advance on a given fuel) occurs at 1½-in. manifold vacuum, and at this point as much as 4 to 6 deg less spark advance can be tolerated than at full throttle. If the higher part-throttle requirement could be eliminated by improvements in mixture distribution, a gain of 2-3 octane numbers could be obtained at a given compression ratio, or the compression ratio could be increased approximately ½ ratio on a given quality fuel.

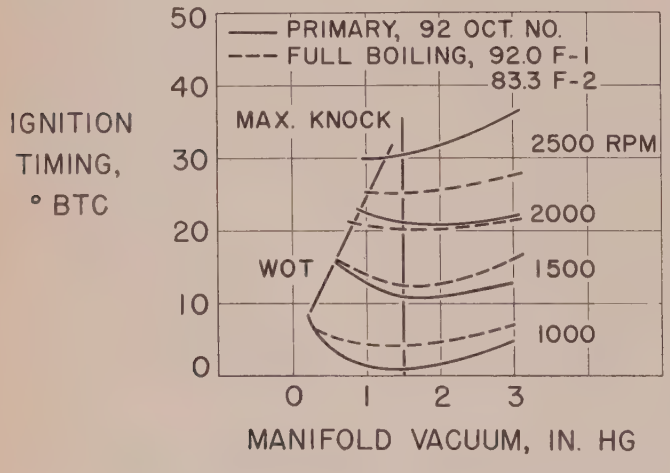

Fig. A – Ignition timing for trace knock in typical 1955 V-8 engine

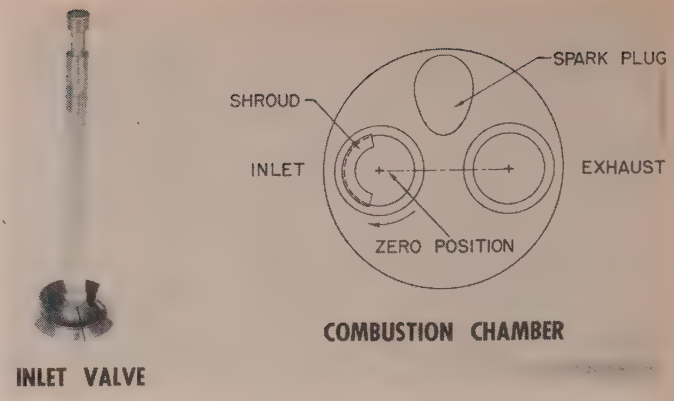

Fig. B – Plan view of combustion chamber and shrouded intake valve used in studying effectiveness of short combustion time in reducing octane requirement

The authors have pointed out the effectiveness of a short combustion time in reducing the octane requirement of engines. Our studies are in close agreement with these principles, and also show two other advantages which were not mentioned. As combustion time is decreased due to an increase in turbulence, the engine is able to make relatively better use of sensitive than insensitive fuels. This factor is rapidly becoming more and more important with the trend to more sensitive commercial fuels as the gasoline antiknock quality is improved. Fig. B shows the plan view of the combustion chamber and the shrouded intake valve that we used on this study. The engine was supercharged to maintain a constant air consumption, and the compression ratio was adjusted to the point of trace knock for each position of the shroud as the valve was rotated into various angular positions in the combustion chamber. Fig. C illustrates the type of data obtained. The lower curve indicates the variation in spark advance required for maximum power. The range of advance is from a maximum of 38 deg to a minimum of 20 deg. Also included are curves showing the variation in maximum permissible compression ratio for a sensitive and an insensitive fuel as the position of the shroud was changed. It will be noted that the positions of the shroud resulting in the lowest maximum-power spark advance allowed the highest permissible compression ratio, and that the sensitive fuel is rated at its highest value in terms of the insensitive fuel with the valve in this position. Also in our studies the highly turbulent fast-burn chambers showed the advantage of lower part-throttle fuel consumption than the nonturbulent chambers. We wonder if the authors would comment on these two trends?

A comparison of the two designs in Fig. 22 shows that two chambers of the same compression ratio but of different design do not give the same output at maximum power spark advance. The work of Drinkard and Carpentier,[a] and our work reported by Heron and Felt,[b] have also shown these same differences. Since the chambers do not all produce the same power and, therefore, thermal efficiency at the same compression ratio, it seems to us that the best comparison of the mechanical octanes contributed

[a] See SAE *Quarterly* Transactions, Vol. 5, July, 1951, pp. 346-358: "Development Highlights and Unique Features of New Chrysler V-8 Engine," by W. E. Drinkard and M. L. Carpentier.

[b] See SAE *Quarterly* Transactions, Vol. 4, October, 1950, pp. 445-499: "Cylinder Performance – Compression Ratio and Mechanical Octane-Number Effects," by S. D. Heron and A. E. Felt.

by a given chamber design would be a comparison of the fuel requirements of the chambers on sensitive fuels at a compression ratio adjusted to give the same thermal efficiency on both combustion chamber designs. We believe that this would give a better comparison than a comparison of the imep that can be obtained on the two chambers by setting the ignition timing for trace knock for a common fuel, since the values obtained in this latter comparison would depend on the antiknock quality of the fuel chosen. It is realized, however, that this would greatly complicate the study, since more combustion chambers would have to be made.

The authors have pointed out that their high-turbulence, fast-burn chamber was considerably better from a surface ignition standpoint than their slow-burn, nonturbulent chamber, and have attributed the difference in performance to the high turbulence sweeping out the loose deposits and thereby reducing the surface-ignition tendency. Our own experience with two multicylinder engines, one with a highly turbulent chamber somewhat similar to the authors' design Y and the other having a nonturbulent chamber with the spark plug located very close to the axis of the cylinder, indicates that, even though the combustion time as measured by the spark advance requirement for maximum power is very similar for these two chambers, their surface ignition tendencies vary considerably. Under conditions where the highly turbulent chamber is surface-ignition limited, that is, the octane number to satisfy the surface ignition requirement is higher than the knock requirement, the nonturbulent chamber cannot be made to surface ignite even when the fuel quality is lowered to that for medium knock. It would be very interesting to know whether the authors conducted surface ignition investigations on some of their intermediate combustion-chamber designs, and are able to separate the effects of turbulence, charge mass distribution, and flame travel on surface ignition.

Another Approach to Reducing Combustion Time

– D. R. Diggs
E. I. du Pont de Nemours & Co., Inc.

WE have also given considerable attention to the concept of reducing combustion time as a means of lowering an engine's fuel requirement. Our investigation was carried out employing multiple ignition in chambers of fixed design, rather than by altering chamber design as the authors did. This technique emphasizes flame travel and mass distribution as the controlling factors, with little attention to turbulence. As the authors have pointed out, careful coordination of all three of the factors just mentioned is necessary to achieve the optimum design. Therefore, multiple ignition may not be the most elegant experimental approach. Nevertheless, it is believed to give results which indicate reasonably well the effects which can be achieved by reducing combustion time.

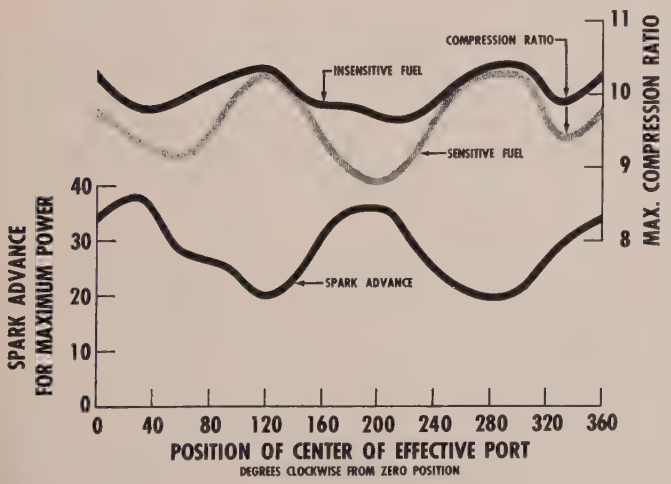

Fig. C – Effect of position of intake valve shroud on maximum power spark advance and fuel antiknock quality

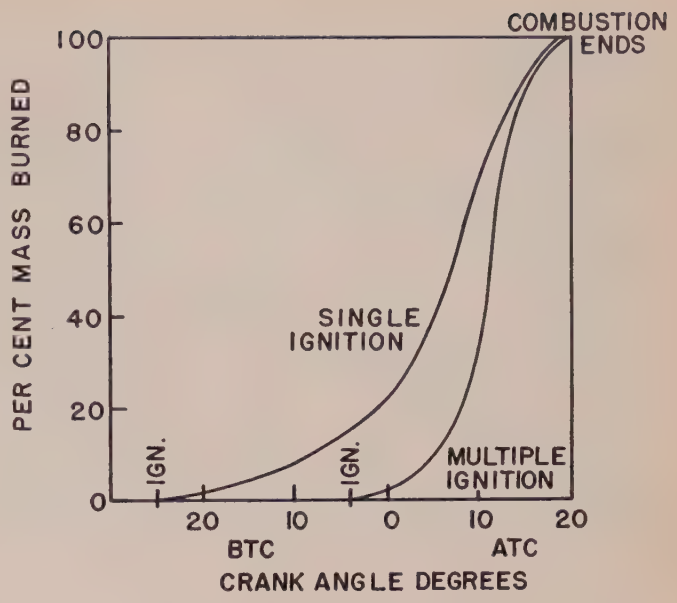

Fig. D – Effect of multiple ignition on the burning rate in a single-cylinder engine (1800 rpm)

Fig. D shows the decrease in combustion time which was achieved through the use of multiple ignition in a single cylinder laboratory engine. This figure shows the per cent mass burned, calculated by the same method used by the authors, as a function of engine crank angle. It can be seen that these curves are of the same type as shown in Fig. 24, where reduced combustion time was achieved by a change in chamber design. The decrease in combustion time shown in Fig. D was accompanied by a substantial reduction in octane requirement. At maximum-power spark timing the requirement was 78 octane number with single ignition and only 70 octane number with multiple ignition.

As was done by the authors, it was ascertained that the decrease in octane requirement accompanying faster burning rates could be translated into an increase in knock-limited output. Fig. E compares the knock-limited imep with single and multiple ignition at one engine operating condition using isooctane as fuel. These curves were obtained by boosting the manifold pressure until knock occurred. It can be seen that throughout the fuel/air ratio range there is a clear gain in performance with reduced burning time.

One interesting observation was made during our tests with respect to the fuel type employed for octane requirement determination. To determine if any effect would attend the use of temperature-sensitive fuels, reference fuels were blended containing an appreciable percentage of benzene together with isooctane and n-heptane. It was found that the reduction in octane requirement accompanying multiple ignition was somewhat greater in terms of the reference fuels containing benzene than in terms of primary reference fuels. For the data of Fig. D, for example, the octane requirement reduction was 8 octane numbers

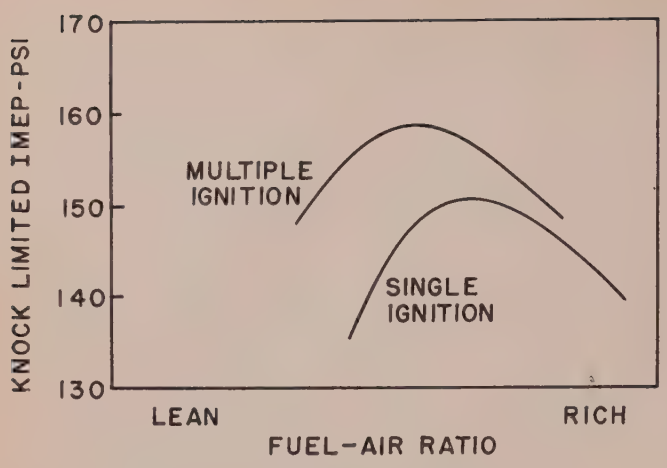

Fig. E – Effect of combustion time on knock-limited output in a single-cylinder engine (1800 rpm, fuel isooctane)

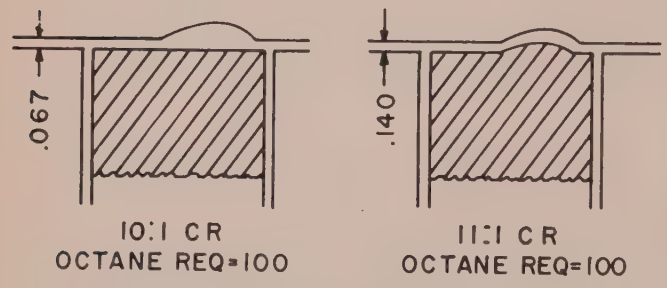

Fig. F – Effect of turbulence and squish on mechanical octanes in a multicylinder engine

with primary reference fuels, but 12 octane numbers with the benzene reference fuels. The authors state that all fuels showed the same relative effect in their tests as far as borderline-knock power was concerned. In our tests, knock-limited outputs were not determined with the temperature-sensitive reference fuels, and on this basis perhaps no difference would have been noted. The authors' comments on this point would be appreciated.

Some confirmatory evidence as to the authors' observation on the role of turbulence and mass distribution has been obtained in a multicylinder engine. Fig. F shows two configurations of a modified production overhead-valve engine. It will be noted that in one case a flat-top piston was used with a quite small clearance between the piston and the head in the quench or squish area. The compression ratio was 10/1, and the fuel requirement just about 100 octane. In the other case a modified piston with a builtup dome corresponding to the contour of the combustion chamber was used with the engine's normal squish area clearance. Here the compression ratio was 11/1, and the octane requirement was 100, the same as with the lower compression ratio chamber. Although a direct comparison of these two designs on the basis of the criteria listed in the authors' paper is not possible, the data demonstrate that mechanical octanes really work. An increase in compression ratio of 1 unit, with the accompanying gain in efficiency and performance, has been realized with the same fuel quality. Incidentally, the 11/1 compression ratio design shown in Fig. F operates quite satisfactorily in normal road service.

The data given so far in this discussion were obtained in clean combustion chambers. Experiments with multiple ignition in the single-cylinder engine also were conducted

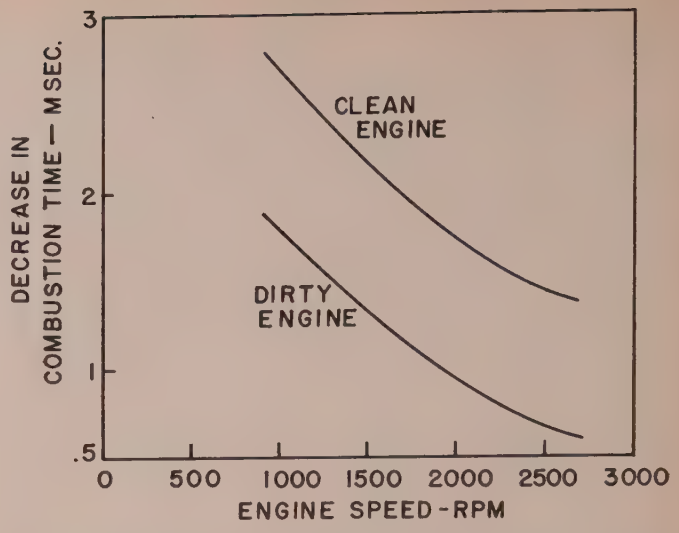

Fig. G – Effect of combustion-chamber deposits on reduction in combustion time obtained by multiple ignition in a single-cylinder engine

in the presence of deposits which had been accumulated during a number of hours of operation. It was found that multiple ignition was less effective in reducing burning time with a dirty engine than with a clean engine. These data are shown in Fig. G as a function of engine speed. As might be expected, the octane requirement reduction with multiple ignition was also smaller when deposits were present. At a representative engine operating condition where the reduction was 8 octane numbers in the clean engine, it was only 4 octane numbers in the dirty engine. These data are in agreement with Fig. 40. It would be interesting to know if the presence of deposits affected the relative burning times observed with the chambers shown in Fig. 40.

The authors' paper should provide many ideas for the consideration of the engine designer. The application of some of the concepts can be seen in present-day engines, and it is hoped that even more of them will be translated to actual practice in the not-too-distant future.

Tells Effects of Spark Setting, A/F Ratio and Compression Ratio

– Otto Enoch
Ford Motor Co.

WE ARE particularly interested in the authors' test results on piston coverage and quench thickness, which shed some more light on the controversial question: Is quench or squish affecting knock?

We have done some experimental work to study the combined effect of spark setting, air/fuel ratio, and compression ratio on octane requirement, maximum knock-limited power, and optimum thermal efficiency for a given combustion chamber and fuel.

In Fig. H are plotted power output versus octane requirement curves for a 1953 overhead-valve engine at 2000 rpm. Curve 1 was obtained by retarding the spark step-by-step with the overall air/fuel ratio kept constant at 13/1. Curves 2 and 3 are similar curves at 12/1 and 11/1 air/fuel ratio, respectively. The curves show at each point the relationship of power loss and gain in mechanical octane numbers when the spark is retarded. This relationship is indicated by the slope of the curves. We call it power-octane ratio. Power-octane ratios usually are low near mbt spark, and become gradually higher as the spark is more retarded. Power-octane ratios also were lower at richer mixtures.

Curves 4-7 were obtained by richening the mixture at con-

stant spark. The effect of richening is very favorable. For instance, curve 6 shows at its intersection with curve 2 (for 12/1 air/fuel ratio) not only additional gains of two mechanical octane numbers, but also of 1% power. Richening to 11/1 air/fuel ratio brought further gains in mechanical octane numbers, but the power fell off. The mixture-richening curves 4 and 5 at 8- and 12-deg spark show no gain in power, but gains in mechanical octane numbers. The mixture-richening curves have lower slopes than the spark-retard curves, but they do not reach very far. If we need only a few mechanical octane numbers, we can get them with a much smaller power loss or even sometimes with power gain by mixture richening rather than by spark retarding. By plotting a grid of spark retard and mixture-richening curves, we can easily find the optimum combination of air/fuel ratio and spark for maximum power for a given fuel octane rating.

Curve 8 on the graph shows knock-limited power of Indolene gasoline plus 1 cc of tel per gal, representative of a commercial sensitive fuel, at various air/fuel ratios, plotted against the rating of that commercial fuel in the engine. The curve peaks at approximately 11/1 air/fuel ratio. At 13/1 air/fuel ratio, Indolene rates 86.7, at 11/1 it drops to 85, and the knock-limited power is 97.4% of mbt power. A not-sensitive fuel of 86.7 octane number would follow a vertical straight line through the 86.7 abscissa and yield 98.2% of mbt power at 11/1 air/fuel ratio.

In Fig. I, we have added compression ratio as a third variable. Curves 1-4 in this graph show the effect of spark retarding at 13/1 air/fuel ratio at 7.3, 8.1, 8.7, and 9.1 compression ratios. Curves 5-8 show the effect of mixture richening, and curves 9-12 show knock-limited power of Indolene. Mbt power at the original compression ratio of 7.3 is given a 100% rating. Mbt octane requirement was 86. The peaks of curves 1-4 show mbt power and octane requirement increasing at increased compression ratios. Maintaining 86-octane requirement, we could increase the power output by 4% by raising the compression ratio to 8.1 and retarding the spark. At 8.7 compression ratio, power was down 4%. This means that maximum power at 13/1 air/fuel ratio was somewhere between 8.1 and 8.7 compression ratio. If, in addition to spark retarding, we richened the mixture as shown by curves 5-8, we still gained some power at each compression ratio. We agree with the authors that even with richening we can improve overall fuel economy because of high-efficiency part-load operation at high compression ratios.

Indolene rated 86 at 7.3 compression ratio and 13/1 air/fuel ratio, as shown by curve 9, and therefore yielded practically full mbt power. As the compression ratio increased, Indolene rated higher, up to 90 at 9.1 compression ratio. Therefore, knock-limited power was much higher than with a not-sensitive 86-octane fuel. Maximum power was still between 8.1 and 8.7 compression ratio, but at 9.1 we still had more power than at 7.3 compression ratio. Mixture richening brought further gains, although the fuel rating decreased.

As changes in compression ratio do affect octane rating of sensitive fuels, so do changes in combustion-chamber design. It seems as important to consider the combustion-chamber effect on fuel octane rating as on octane requirement.

We can illustrate this point in Fig. J. Mbt octane requirements and Indolene ratings are plotted for three experimental combustion chambers for engine speeds from 800 to 2000 rpm. The top curves show octane requirement, the bottom curves fuel octane ratings, and the areas between these curves octane deficiencies of the combustion chambers when run on Indolene. Chamber B has a high requirement, but much less deficiency than chamber A. Chamber C approximately equals chamber A in requirement, but can practically run knock-free on Indolene, while chamber A has a high octane deficiency.

We can illustrate this point further in Fig. K: We plotted

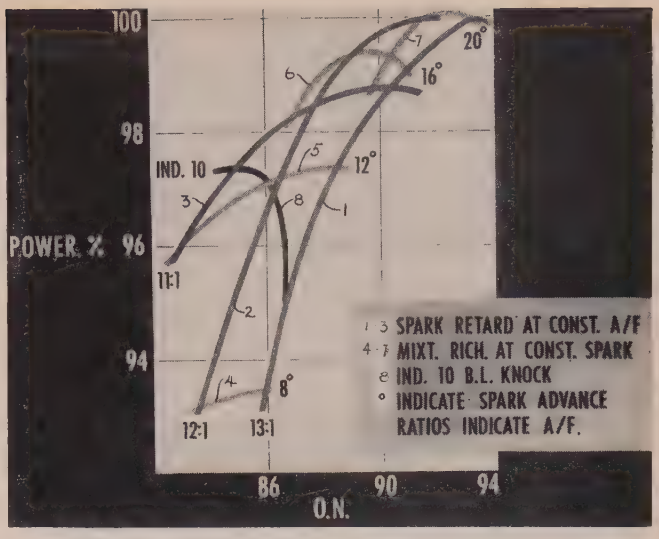

Fig. H – Octane requirement gain and power loss by spark retarding and mixture richening (2000 rpm, 8.7/1 compression ratio)

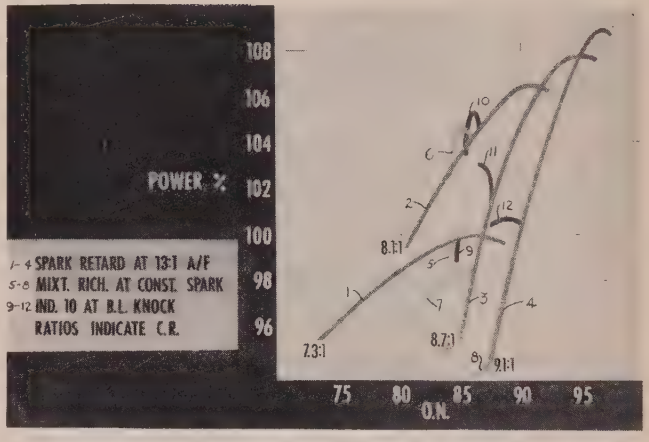

Fig. I – Effect of spark retarding and mixture richening on octane requirement and power at various compression ratios (1500 rpm)

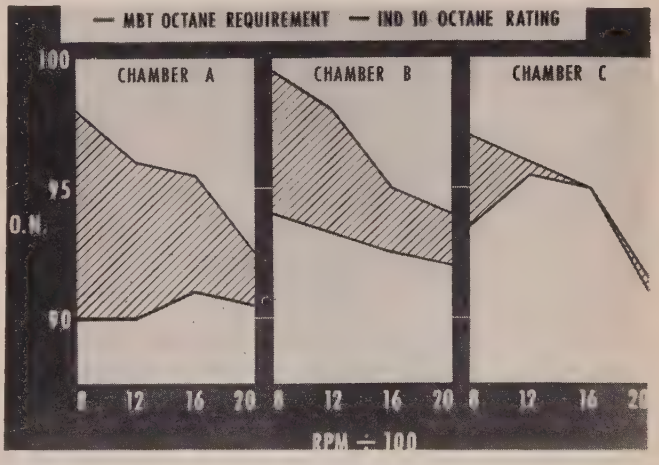

Fig. J – Mbt octane requirement (upper curves) and fuel octane ratings (lower curves) of three combustion chambers

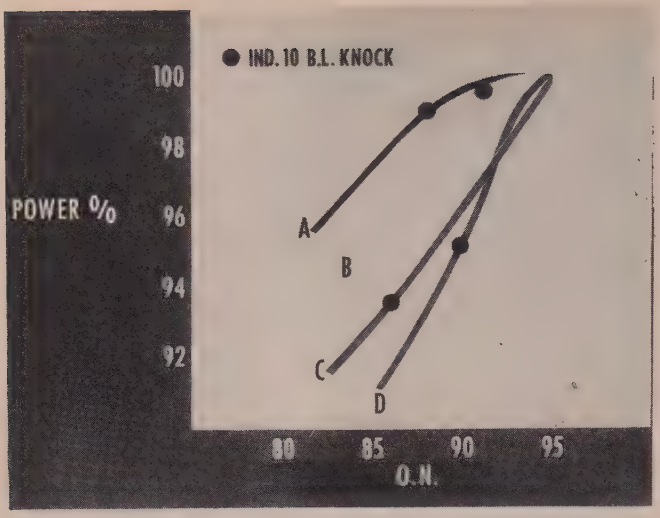

Fig. K – Power-octane ratio and Indolene 10 knock-limited power of 1953 competitive engines (1000 rpm)

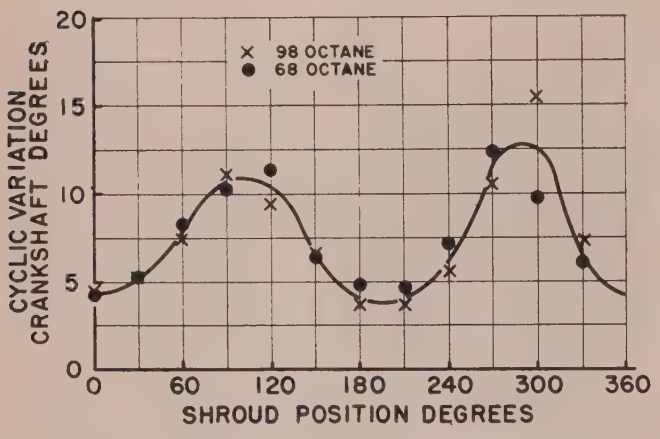

Fig. L – Cyclic variation versus shroud position

the spark-retard curves of four 1953 competitive engines. Mbt octane requirements of these engines did not differ much, but knock-limited power on Indolene did. This is partly due to differences in slope of these curves. It is greatly due to differences in Indolene rating in these engines. For instance, engine D shows higher power-octane ratios than engine C. That would mean lower knock-limited power for engine D than for engine C if the fuel rating would be the same. But actually knock-limited power of engine D is higher than that of engine C, because it rates Indolene so much higher.

Discusses Result of Turning Shrouded Valve

– Neil MacCoull
Texas Co.

THE data given by the authors in Figs. 32 and 33, on the effect of directed turbulence on detonation, confirm somewhat similar results in my unpublished paper, "The CFR Shrouded Intake Valve," presented before the SAE World Automotive Engineering Congress in 1939. One very interesting result of turning the shrouded valve, which has not been referred to by the authors, was the effect on "cyclic variation" as indicated by Fig. L (Fig. 12 in that paper). The greatest cyclic variation was developed at shroud positions permitting the highest compression ratios. Cyclic variation appears to be a feature of combustion which might well receive more attention because of its probable connection with engine roughness.

Authors' Closure To Discussion

MR. TOULMIN brought up the question of the effect of combustion-chamber design upon sensitive and insensitive fuels.

We have been vitally concerned with this problem throughout our investigations, because it means that this is an additional source of mechanical octane numbers. However, the results of our dynamometer and road tests have not always established a consistent relationship between sensitive fuels and chamber design. This is an area where future work will be necessary.

Mr. Toulmin also asked, "What is the effect of chamber design upon part-throttle fuel consumption?"

In our automotive installations we usually operate the fast-burn designs at higher compression ratios to take advantage of the mechanical octane numbers which they possess. As a result, these chambers show substantial gains in economy and power over the slow-burn designs. We have not made part-throttle fuel consumption comparisons of nonturbulent and turbulent designs at the same compression ratios.

Mr. Toulmin's third question was, "What is the effect of chamber design upon surface ignition?"

We are conducting an extensive research program to determine the effects of turbulence, mass distribution, and flame travel upon surface ignition. The results of this work with a variety of chamber designs indicated that the controlling factors involved are the quantity and nature of the deposits. As examples, our work shows that:

1. Oil type has a definite influence upon surface-ignition ratings.

2. High oil consumption produces high surface-ignition ratings.

3. As we stated in the paper, once the deposits have taken over the initiation and propagation of the flame front, chamber design no longer has a controllable influence upon the fuel requirements through the fundamental mechanisms described in the paper. Therefore, the design which leaves behind the firmest and the least deposits shows the lowest tendency to surface-ignite. The turbulent, compact chambers exhibit this characteristic, and as a result show a lower surface ignition tendency in addition to low detonation fuel requirements.

Mr. Diggs asked a question regarding the effect of chamber design upon the knock-limited outputs when compared with temperature-sensitive reference fuels.

We have compared the knock-limited outputs of the combustion chamber not only with primary reference fuels, but also with the sensitive gasoline-type fuels. As we have stated in our paper, our experience has shown that the same relative picture is always obtained. We generally obtain somewhat higher knock-limited outputs with the gasoline-type fuels because their higher latent heat of vaporization effectively increases the mixture density through the greater refrigerating effect of the gasoline.

Mr. Diggs states that it would be interesting to know if the presence of deposits affected the relative burning times observed with the chambers shown in Fig. 40.

During the course of our investigation, we calculated the burning times for many combustion chambers. However, all of our work was done on engines relatively free of deposits. We did not at that time carry out investigations of combustion time after deposits had accumulated. We are in the process of studying this effect at the present time, and we do not have sufficient information to answer this question.

Some Experiments in the Application of Boundary-Layer Control

Joseph Flatt, USAF, Wright Air Development Center

This paper was presented at the SAE Golden Anniversary Aeronautic Meeting, New York, April 20, 1955.

THE physical concepts of how boundary-layer control can be used to increase lifting capabilities of aircraft are reviewed. The development of boundary-layer control installations for high lift on an F-86 and a C-123 airplane are described, including background, wind tunnel test results, and flight test findings.

These two developments are historical "firsts" and are indicative of the influence that boundary-layer control is likely to have on future aircraft design.

IT was just 50 years ago that Prandtl conducted the first experiments on the application of boundary-layer control. Since that time a great deal of information has been accumulated in this field because of its potential for improving aircraft performance. Until fairly recently, however, the subject has been of interest only in an academic sense, primarily because little success was attained in trying to apply this interesting innovation in a practical manner. The results of recent work, especially that undertaken since 1949, have been more promising in connection with practical application.

In general, boundary-layer control can be used to effect significant improvement in aircraft performance in two ways: for achieving high lift for reduced take-off and landing speeds, and reducing aircraft skin-friction drag for improved range and speed. This paper will deal only with the high-lift aspects. I would like to review for you some of the fundamental physical considerations in connection with high-lift type boundary-layer control and acquaint you with two specific applications to Air Force aircraft. As a matter of interest, this will be the first time that either of these Air Force projects has been publicly disclosed.

Physical Considerations

One of the more basic forms of boundary-layer control is illustrated in Fig. 1. This deals with the delay of separation at high angles of attack on a

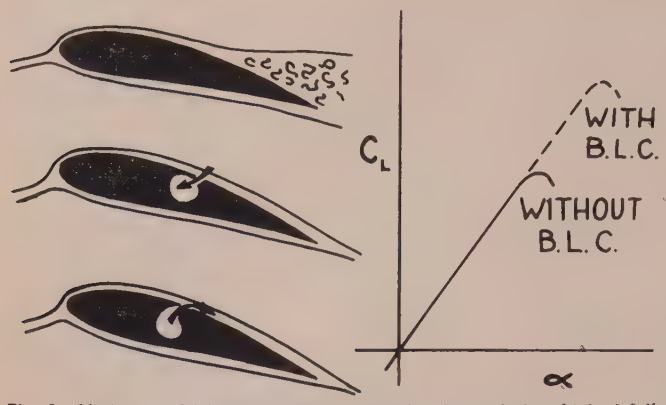

Fig. 1 – Variation of lift coefficient with angle of attack for thick airfoil showing effect of boundary-layer control

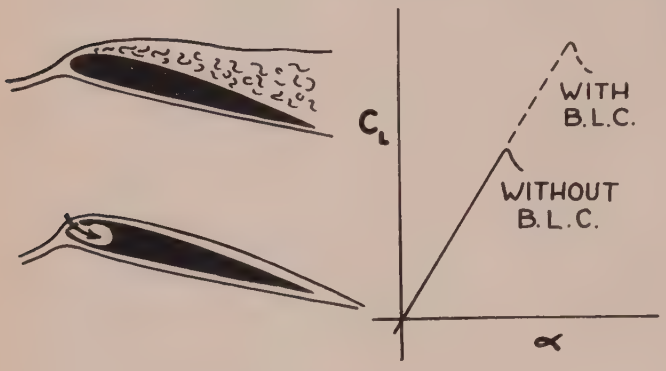

Fig. 2 – Variation of lift coefficient with angle of attack for thin airfoil showing effect of boundary-layer control

moderately thick airfoil section. In this instance the flow separation starts at the rear of the airfoil and progresses forward with further increase in incidence. The maximum lift and stall angle are limited by this separation, as indicated by the solid line on the lift coefficient (C_L) – angle of attack (α) curve. By delaying separation over the rear portion of the airfoil it is possible to obtain higher lift with increasing angle of attack, as illustrated by the dashed portion of the curve. Loss of energy within the boundary layer is responsible for the flow separation. This separation can be prevented by the application of either suction or blowing type boundary-layer control ahead of the normal separation point. In the case of suction, part of the low energy boundary layer air is withdrawn through a suction slot upstream of the separation point enabling the main flow to remain attached to the wing. The mechanics of the blowing type boundary layer control are somewhat different. The low energy boundary layer air is re-energized by a high velocity jet. The aerodynamic effect is similar – the main flow remains attached and higher lift is possible at higher angles of attack. By imparting very large energies in the blowing jet, the main flow about the wing can be altered to produce additional lift at a given angle of attack. This approach is very costly from a power standpoint, however, and will not be discussed further in this paper.

Another type of boundary-layer control is that associated with separation at high angles of attack on thin airfoil sections as illustrated in Fig. 2. The flow breaks away rather suddenly near the leading edge of the airfoil because of very high pressure gradients around the nose of the airfoil associated with the small leading-edge radius. Although the boundary layers at the nose of the airfoil are quite thin, they represent energy loss sufficient to cause separation in the presence of the high pressure gradients. Separation in this case can be avoided by the application of suction through slots or porous areas at the leading edge just ahead of the normal separation point. The effect on the wing lift coefficient – angle of attack relationship as shown on the right of Fig. 2 is very similar to the case just previously discussed – that is, by maintaining attached flow the wing is capable of higher lift at an increased angle of attack.

Boundary-layer control for increased lift can be of great value in connection with other types of high lift devices such as trailing edge flaps. Flaps are an effective device for producing higher lift without an increase in wing incidence by virtue of their ability to change wing camber. Fig. 3 illustrates how boundary-layer control can be used in conjunction with a flap to further increase its effectiveness. The flow over a wing with a flap is nor-

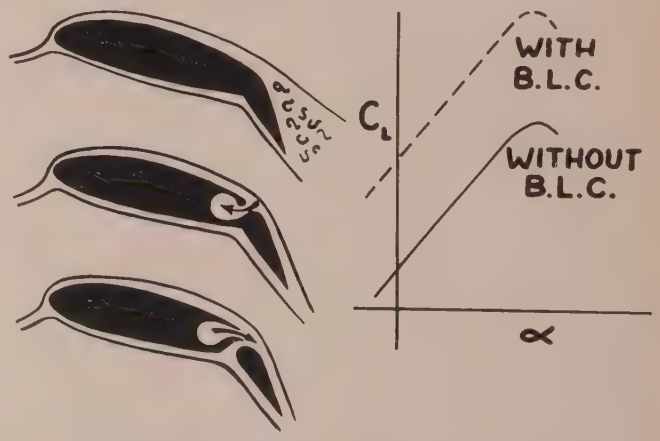

Fig. 3 – Variation of lift coefficient with angle of attack for thick airfoil with flap showing effect of boundary-layer control

mally separated to a large extent over the rear of the flap. By the use of suction or blowing type boundary-layer control, the flow can be made to adhere over the flap and provide a further increase in flap effectiveness. This increase in lift at a given angle of attack, as indicated on the right of Fig. 3, is an important consideration in aircraft design, particularly as it affects the landing gear geometry and pilot visibility. Because of its great importance, the use of boundary-layer control with flaps will be discussed in further detail.

The mechanics of flap type boundary-layer control at a given wing angle of attack are illustrated in Fig. 4. The variation of lift coefficient increment (C_L) with flap angle for a plain flap is not nearly linear as theory would predict because of flow separation over the flap. By applying boundary-layer control to prevent the flow separation, the theoretical flap effectiveness can be realized. Thus it is possible not only to obtain more lift at a given flap angle but to effectively utilize higher flap angles. Experimental results indicate that flap effectiveness can roughly be doubled through boundary-layer control.

The concepts just reviewed form the basis for practically all types of high lift boundary-layer control applications.

F-86 Leading Edge Suction Project

One of the first Air Force efforts in the application of boundary-layer control was that of applying leading edge suction to a swept-wing jet fighter. This project was initiated in 1949 by the Wright Air Development Center Aircraft Laboratory. This application was based on the principle previously illustrated in Fig. 2 – delay of separation at the leading edge of a thin airfoil. The purpose of this project was to determine if this form of boundary-layer control could be used as a substitute for slats or leading edge flaps and to gain some experience with the practical problems and limitations of boundary-layer control systems in flight. The fundamental data upon which this application was based were published in NACA Technical Note 1741. In that report Nuber and Needham of the NACA Ames Laboratory reported the results of two-dimensional tests on the effectiveness of area suction in eliminating leading edge separation over a 12% thick airfoil. Based on the promising nature of these results, particularly with regard to very low indicated pumping power requirements, a pro-

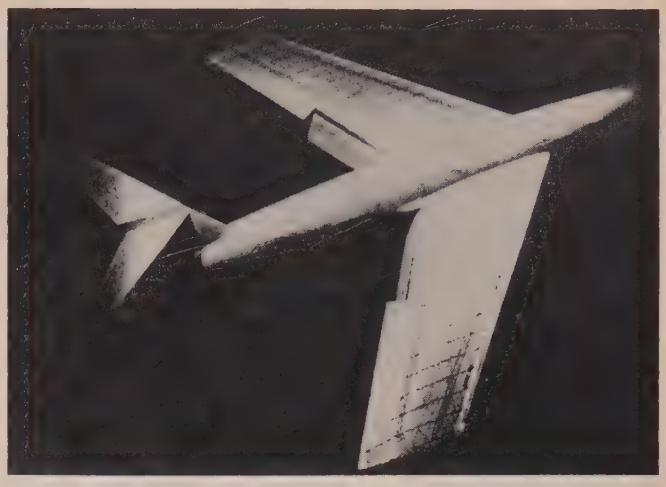

Fig. 5 – F-86 leading edge suction wind tunnel model

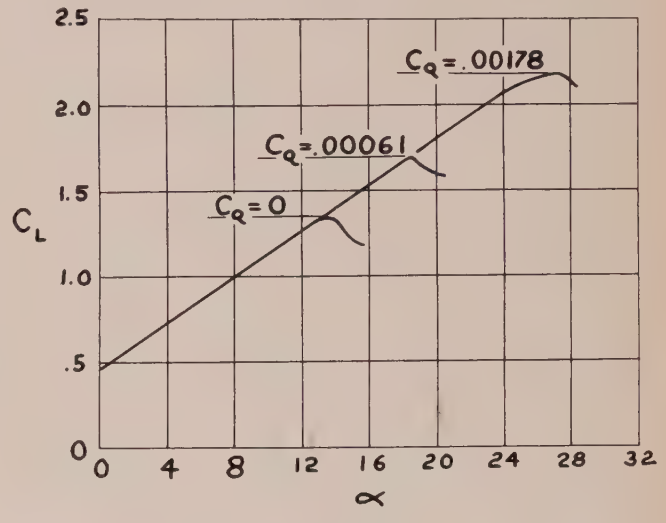

Fig. 6 – F-86 leading edge suction boundary-layer control wind tunnel test results

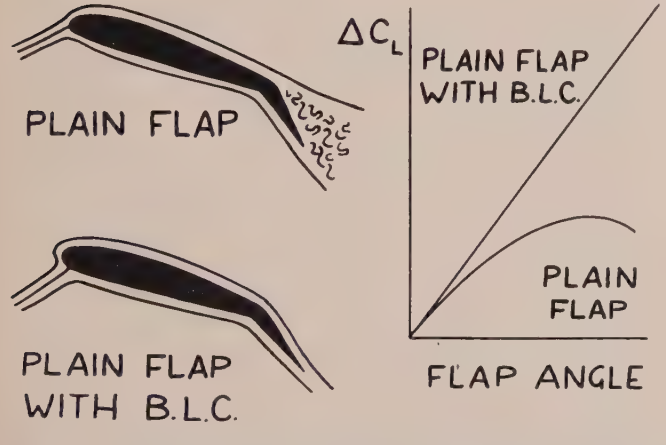

Fig. 4 – Change of lift coefficient with angle of attack illustrating flap effectiveness with boundary-layer control

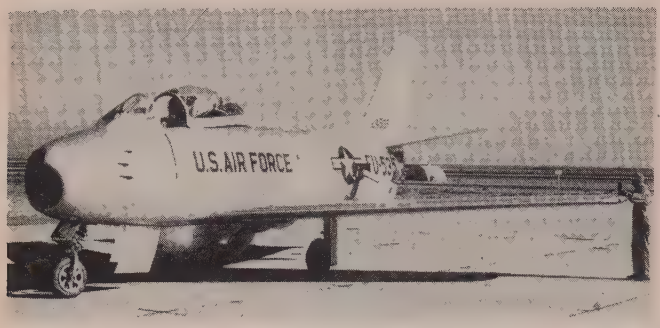

Fig. 7 – View of F-86F equipped with leading edge suction boundary-layer control

gram was initiated to apply this form of boundary-layer control to an F-86F airplane. In cooperation with the Air Force, the NACA Ames Aeronautical Laboratory conducted tests on a set of F-86 wing panels in the Ames full-scale wind tunnel for the purpose of developing the proper aerodynamic configuration and determining the pumping requirements for a full scale installation. Fig. 5 is a photograph of the test panels taken from some of the tuft-study motion pictures. The panels were attached to a fuselage model that was available from other tests. Leading edge suction strips covered the entire span of both wing panels and were constructed in such a manner so that a variety of chordwise area and porosity distribution could be investigated. The wind tunnel tests were quite successful. Fig. 6 shows the results of some of these tests. The data are presented in the form of lift coefficient versus angle of attack of the wing with flaps deflected. C_q is the suction flow coefficient, volume of sucked air divided by the free stream velocity and wing area. With zero C_q, or no boundary-layer control, the maximum lift coefficient was 1.3 at an angle of attack of 14 deg. With a small amount of suction, $C_q = 0.00061$, the maximum lift coefficient was increased to 1.57 at an angle of attack of 18½ deg. With a further increase in suction flow, $C_q = 0.00178$, a lift coefficient of 2.2 was obtained at 27-deg angle of attack. Thus in the wind tunnel it was possible to show a 70% increase in lift coefficient for the F-86 wing with the application of leading edge suction type boundary-layer control. The indicated pumping power requirement varied from 30 hp to 250 hp depending upon the suction area geometry and lift coefficient.

As a result of these favorable wind tunnel findings, North American Aviation, Inc., was given a contract to design and fabricate a flight installation of this arrangement on an F-86F airplane. The airplane fabrication was completed in September 1953. An illustration of the modified airplane is shown in Fig. 7. The full span leading edge modification consisted of replacing the standard leading edge skin with a porous sintered stainless steel sheet. Pumping was provided by a modified turbo-supercharger located in a housing underneath the fuselage of the aircraft. Air was bled from the jet engine compressor to drive the supercharger, which performed as a suction compressor. The suction air was ducted through a channel in the leading edge behind the porous area through the wing fuselage junction to the suction compressor. The supercharger was considerably larger in capacity than the wind tunnel tests indicated would be necessary, but was used as a matter of expediency to avoid development time and costs of a special pump and to provide extra power for a wider range of test conditions. The unit was housed externally to simplify installation and maintenance. On Sept. 18, 1953 the first flight was made with this installation by North American Aviation at the Los Angeles International Airport. It was somewhat of a historic occasion in that it marked the first time that either a jet aircraft or fighter equipped with boundary-layer control was flown in this country.

After a short interval of functional checkout the aircraft was transferred to the NACA Ames Aeronautical Laboratory, where the development flight-test program was conducted. The improvement in low-speed handling characteristics and reduction in minimum speeds due to boundary-layer control were quite noticeable to the pilots. Fig. 8 summarizes the results of the minimum speed portion of this flight test program. Lift coefficient versus airplane angle of attack are shown for three conditions.

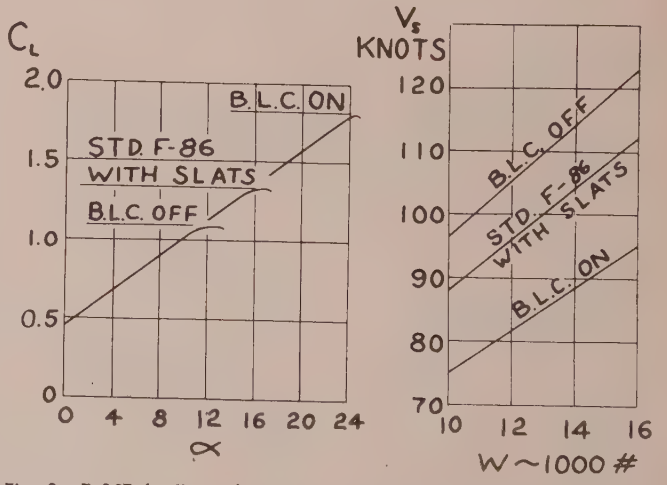

Fig. 8 – F-86F leading edge suction boundary-layer control flight test performance data

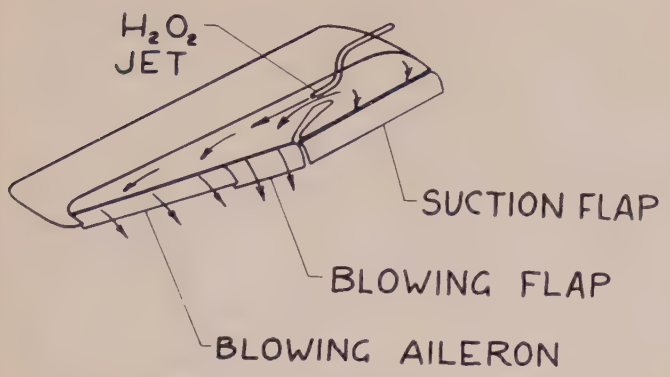

Fig. 9 – Schematic of AR 232A boundary-layer control system

With boundary-layer control off, a maximum lift coefficient of 1.1 was obtained at an angle of attack of 12 deg. With boundary-layer control on, a lift coefficient of 1.8 was obtained at an angle of attack of 24 deg. The standard F-86 airplane with full span leading edge slats has a lift coefficient of 1.35 at an angle of attack of 17 deg. In terms of minimum speeds, substantial reductions are apparent, as shown in the right portion of Fig. 8. At a gross weight of 14,000 lb the stalling speed was reduced from 114 knots for the boundary-layer control off condition to 88 knots with boundary-layer control on – a 23% reduction. Comparing the boundary-layer control on condition with the slatted F-86, the speed reduction was 16 knots, or 15%. The maximum values of C_L obtained from flight did not agree qualitatively with the wind tunnel results, probably because of the large difference in configurations. The percentage improvements, however, compared quite well.

The results of this program were quite gratifying in other respects. In addition to demonstrating that this type of boundary-layer control system can be successfully operated, much was learned regarding the requirements for a successful boundary-layer control installation. One very interesting finding was that although the minimum speed with boundary-layer control occurred at angles of attack considerably above the static ground angle of the airplane, the pilot would nonetheless make use of the increased lift to make his approaches for landing at lower speeds than he would for the airplane with slats. Considering the unique nature of this experiment, surprisingly little difficulty was experienced with the mechanical functioning of the system.

The performance of the NACA Ames Aeronautical Laboratory in the wind tunnel development and flight evaluation of this program cannot be too highly commended. C. W. Harper and his staff in the Full-Scale Tunnel were primarily responsible for the successful development of the aerodynamic configuration. Mr. Belsley and his staff in the Flight Division performed in a most thorough manner in developing and evaluating the flight article.

XC-123D Program

Shortly after World War II, information was received on a boundary-layer control arrangement which the Germans had proposed for use on the Arado 232A heavy transport airplane. This system made use of boundary-layer control in conjunction with trailing edge flaps to provide very high lift using the aerodynamic approach previously shown in Fig. 3. A combination of suction and blowing, more commonly referred to as a compound system, was proposed. A schematic of this system is shown in Fig. 9. Suction slots were located ahead of the inboard flap and blowing slots over the outboard flap and drooped aileron. Pumping was accomplished by a hydrogen peroxide rocket ejector located within the wing between the suction and blowing compartments. Ejector action of the rocket provided the necessary suction and the mixed flow exhaust provided the blowing. This system was appealing from the standpoint of relatively small amount of complexity, weight and plumbing required. In 1949 the Air Force contracted with the Cornell Aeronautical Laboratory to translate and study the documents associated with this development to determine whether or not this type of installation was feasible and worthy of further consideration. In connection with this study they were also to make an analysis of how effective this type of installation would be on a typical transport type airplane. The results of the Cornell study have been reported in Air Force Technical Report 6288. An interesting comparison was made in this study of how effectively the jet fuel could be used for boundary-layer control against its use as direct take-off

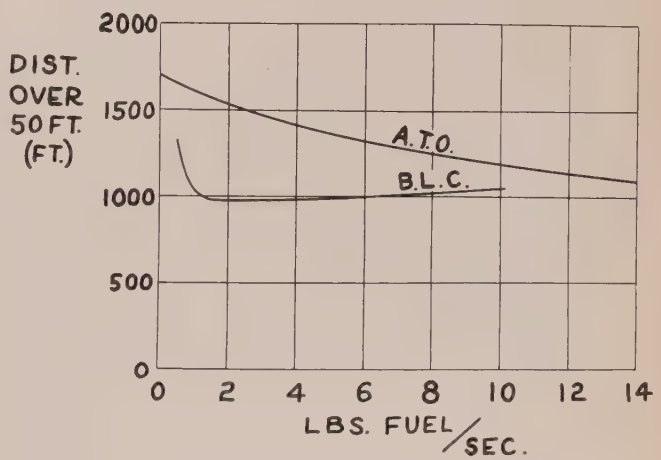

Fig. 10 – Comparison of boundary-layer control and assisted take-off

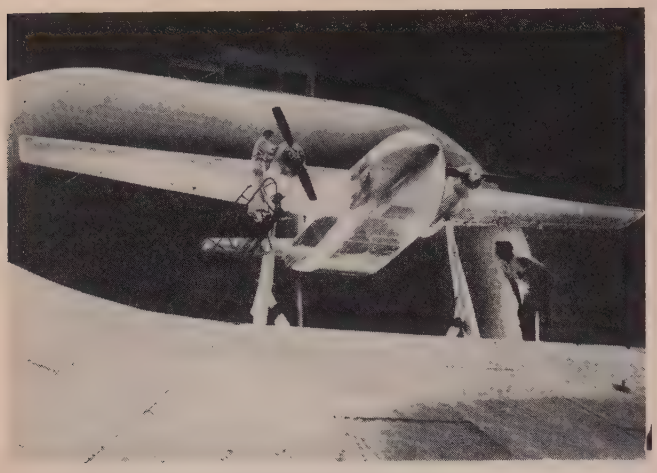

Fig. 11 – XC-123D wind tunnel model

thrust assist. The result of this analysis is shown in Fig. 10. Take-off distance over a 50-ft obstacle is plotted as a function of pounds of rocket fuel burned per second. This study was made for a C-46 airplane. The analysis showed that it was much more efficient to use rocket fuel for boundary-layer control than for direct thrust by a factor of better than 8 to 1. Using the rocket fuel for boundary-layer control, a take-off distance slightly less than 900 ft could be obtained with the use of 2 lb per sec of fuel, whereas using the rocket fuel for direct thrust, better than 15 lb per sec would be required to give the same take-off distance. The study also indicated that the weight penalty should not be excessive for a practical installation of this type.

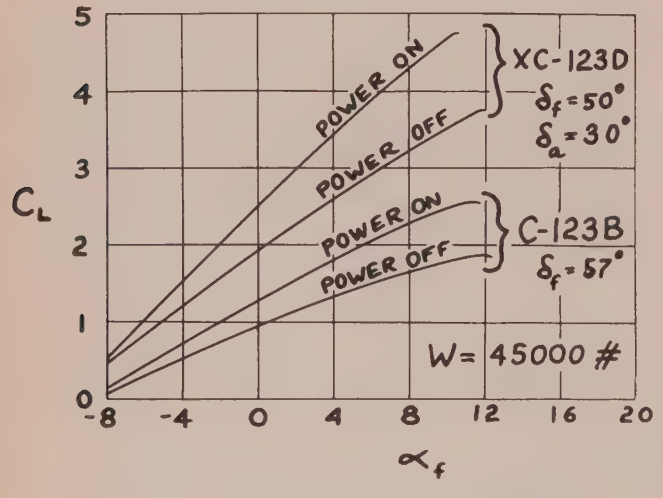

Fig. 12 – XC-123D wind tunnel test results

As a result of this study and more detailed considerations of the factors involved, it was decided to develop a full scale installation of such a compound boundary-layer control system for an Air Force cargo type airplane. The experimental article was to be built as close to a prototype version as possible, completely equipped for service use so that if it showed real promise, a production installation could be made with a minimum of delay. This is probably the first time that consideration was ever given to the use of boundary-layer control on a prototype basis. The aircraft chosen for this development was the C-123. This airplane was chosen because its basic mission, that of an assault type airplane, required the shortest possible take-off and landing distances and its wing planform was such that it would accommodate such an installation in a straightforward manner.

In 1951, a contract was let to the Chase Aircraft Co. in Trenton, N. J., for the design, fabrication and flight test of a compound boundary-layer control system for the C-123 airplane. This airplane was to be designated the XC-123D. One phase of this program was to conduct wind tunnel tests on a large scale power-on model of the airplane with complete aerodynamic simulation of the boundary-layer control system. The wind tunnel model for this development is shown in Fig. 11 mounted in the full scale wind tunnel at the NACA Langley Field Laboratory. The model was quite large as can be seen from the photograph. It had a wing span of 45 ft – larger, perhaps, than a number of our fighter aircraft. The tests were started in June, 1953, and completed in October, 1953. A brief resumé of wind tunnel test results is shown in Fig. 12. Comparable data for the C-123B airplane are also shown. The results are presented in terms of lift coefficient versus angle of attack of the fuselage. A 45,000-lb weight is noted because weight has a direct influence on lift coefficient when propeller effects and boundary-layer control are considered. The C-123B data are based on available wind tunnel and flight test information. The results indicated that it should be possible to increase the power-off lift coefficient from 1.85 for the standard C-123B to 3.75 for the boundary-layer control version. Power-on lift coefficient increments were somewhat larger, increasing from 2.6 to 4.7.

Based on these favorable results, construction of a test airplane was initiated. Design and fabrication of the flight article was accomplished by the Stroukoff Aircraft Corp., Trenton, N. J. Re-evaluation of the pumping arrangement using the rocket-type ejector nozzles indicated that it would be more desirable if a means for powering the boundary-layer control system could be found using gasoline rather than jet fuel. It was found that a small ducted-fan turbojet engine was available which could meet the pumping requirements for the system, operate on gasoline and have a greater

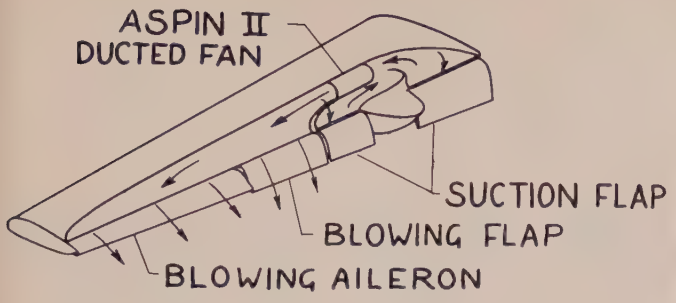

Fig. 13 – Schematic of XC-123D boundary-layer control system

Fig. 14 – View of XC-123D boundary-layer control airplane

efficiency than the rocket system. This was the French Turbomeca Aspin II unit. The design arrangement was revised to incorporate the ducted-fan as a basic pumping unit in place of the rocket. A schematic drawing of this installation is shown in Fig. 13. The Aspin II is located so that its inlet provides suction over the inboard flaps and its exhaust and fan output provide blowing over the outboard flap and aileron in a manner very similar to that originally considered for the rockets.

Fabrication of the XC-123D airplane was completed in November, 1954. A photograph of the airplane is shown in Fig. 14. The suction slots for the inboard flaps can be seen on either side of the nacelle tailcone. Blowing slots exit over the outboard flap and drooped aileron. The airplane was flown with boundary-layer control in operation for the first time on Dec. 7, 1954, by the Stroukoff Aircraft Corp. It is now undergoing a complete flight evaluation at the Air Research and Development Command, Wright Air Development Center.

Preliminary flight test indications are very encouraging concerning confirmation of the wind tunnel maximum lift results. To date no serious flight deficiencies have been found. Fig. 15 shows the predicted improvement in take-off and landing performance of the XC-123D due to boundary-layer control. Total distances over a 50-ft obstacle are shown as a function of airplane gross weight. At a weight of 50,000 lb, which is near the airplane design gross weight, take-off distance reduction from 1950 to 850 ft is indicated. Landing distance at the same weight should be reduced from 1200 to 775 ft. The minimum required field size at this weight, then, should be reduced to less than one-half by using boundary-layer control.

The assistance of the NACA again contributed significantly to the success of this program. In particular, the aid of Mr. Brewer and his staff in the Full-Scale Wind Tunnel at Langley Field in conducting the wind tunnel tests on the XC-123D model is acknowledged.

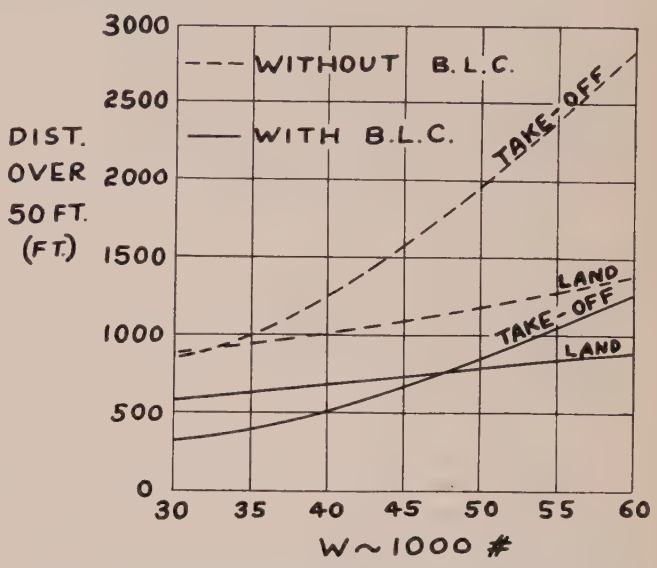

Fig. 15 – Variation of XC-123D landing and take-off distance with and without boundary-layer control

Closing Remarks

In summary, the physical concepts of boundary-layer control for high lift have been reviewed and the successful flight application of two of these concepts to Air Force aircraft has been described. The results of these and other programs now underway in the field of boundary-layer control will undoubtedly have a pronounced influence on the design of future aircraft. There is little question that boundary-layer control has arrived and is here to stay.

DISCUSSION . . .

. . . of this article on pp. 119-122.

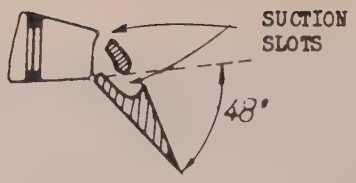

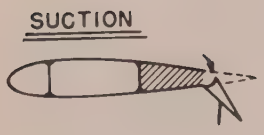

Wing-Lift Augmentation

for the Improvement of Low-

THE flight of any aircraft, whether it be a light plane or a multiton supersonic bomber, is bounded by the take-off and landing. Whether high-powered catapult and arresting gear or specially prepared long runways are available, it can be appreciated that the lower the speed at which landing and take-off occur, the greater the safety to man and machine. Although not always obvious in the resulting product, the designers' consideration for acceptable landing and take-off speed often compromises the high-speed performance for both military and commercial aircraft. For the fixed-wing aircraft, other things being equal, the stall speed is directly proportional to the square root of the wing loading and inversely proportional to the square root of maximum lift coefficient:

$$V_S = \sqrt{W/S\, C_{L_{max}}}$$

At first glance it would appear that a ready solution to the low-speed problem would be to increase the wing area. A preliminary layout will prove that aircraft size and weight will spiral rapidly upward, and in addition to compromising the remaining design requirements, the low-speed performance may very well be impaired rather than improved. The results of a study made on a turboprop aircraft of approximately 28,000-lb design gross weight illustrates this point. In Fig. 1, altering wing area to achieve low-speed performance is examined first in relation to its effect on V_{max}. The dashed line represents the original design and the high-lift boundary-layer control (BLC) version, the latter having take-off and landing speeds reduced 20 knots due to BLC. If wing area is increased to obtain the reduced speeds of the BLC version, a 20-knot reduction in V_{max} up to 35,000 ft is the first penalty. If the original take-off and landing speeds are acceptable, reducing wing area by holding span or aspect ratio equal to the original design, and adding BLC, up to 40 knots increase in V_{max} can be realized at altitudes up to 20,000 ft, and 20 knots at 30,000 ft. Above 35,000 ft, for this configuration, little gain was realized because of the onset of drag rise. For the same aircraft, the effect of these design changes on the range is reflected in Fig. 2. The lowest bar shows the original design range to be approximately 1400 nautical miles. Holding gross weight

Methods

Speed Performance of High-Speed Aircraft

John S. Attinello, Bureau of Aeronautics, Navy Department

This paper was presented at the SAE Golden Anniversary Aeronautic Meeting, New York, April 20, 1955.

FOR more than half a century, aeronautical researchers have attempted to augment wing-lift beyond the capabilities of mechanical flaps, slots, and the like. Theoretical studies and wind tunnel tests promised large gains in aircraft performance, but flight installations all over the world proved a long series of failures. Because of the problems inherent in the operation of high-speed jet aircraft, the Department of Defense revived interest in lift-increase systems.

A development of the Bureau of Aeronautics recently flight-tested on a Grumman jet fighter demonstrated what is considered the first practical, operationally suitable lift-augmentation system. Under the name of the BuAer Supercirculation System, whereby engine power was successfully diverted to create lift, it has provided new impetus for industry-wide research in the field.

constant, increasing wing area to achieve the 20 knots reduced take-off speed, and reducing the fuel load by the amount of weight increase reduces range to 538 nautical miles. This is only 38% of the original design range. Assuming a very conservative BLC system weight of 325 lb, the same reduced speeds could be obtained as in the case of increased wing area, but the range decreases only 7% for this improved low-speed performance. For the area-reduction configurations having the same landing and take-off speeds as the original design, small increases in range (5 to 10%) over the original design were realized. Since wing area increase results in large performance penalties, the parameter to consider in an attempt to influence the low-speed performance will therefore be limited to the wing lift coefficient.

The mechanism of lift for an airfoil or wing is intimately connected with the behavior of the thin layer of fluid (air) in the immediate vicinity of the solid boundary. This relatively slow-moving layer is called the boundary layer and is of importance because its behavior catalytically influences the flow field about the airfoil. Considering the flow over a flat plate (Fig. 3), the boundary layer which devel-

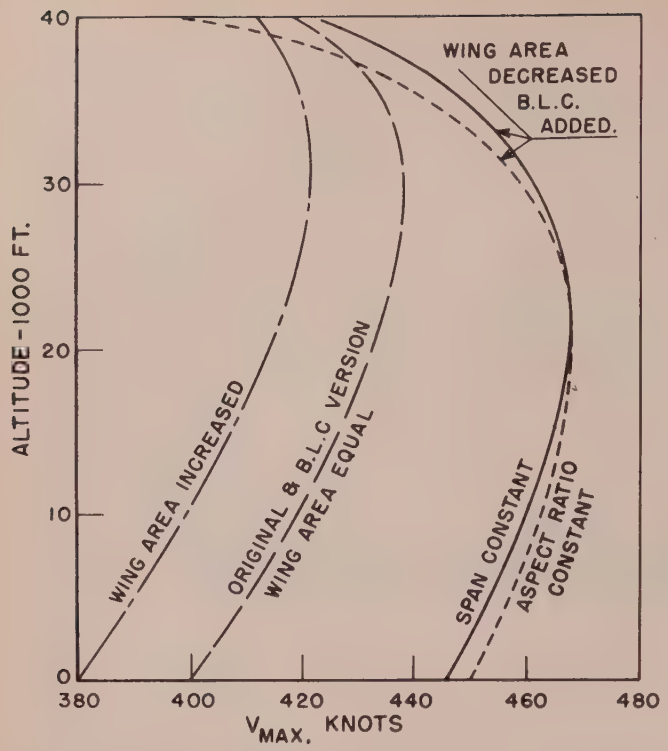

Fig. 1 – Variation of maximum velocity with altitude for turboprop aircraft illustrating effect of boundary-layer control

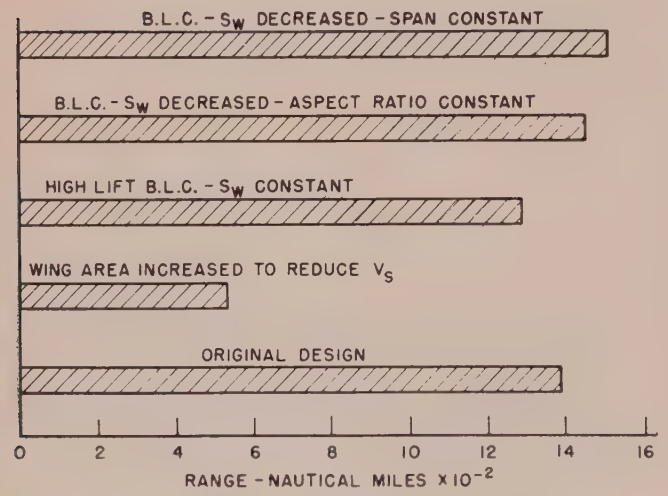

Fig. 2 – Effect of modifications on range of turboprop aircraft (assumed weight of boundary-layer control 325 lb)

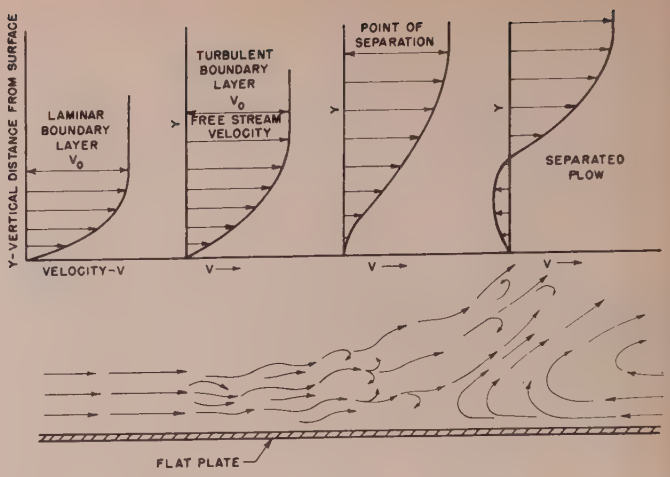

Fig. 3 – Boundary-layer velocity profiles and corresponding streamlines for flow over flat plate

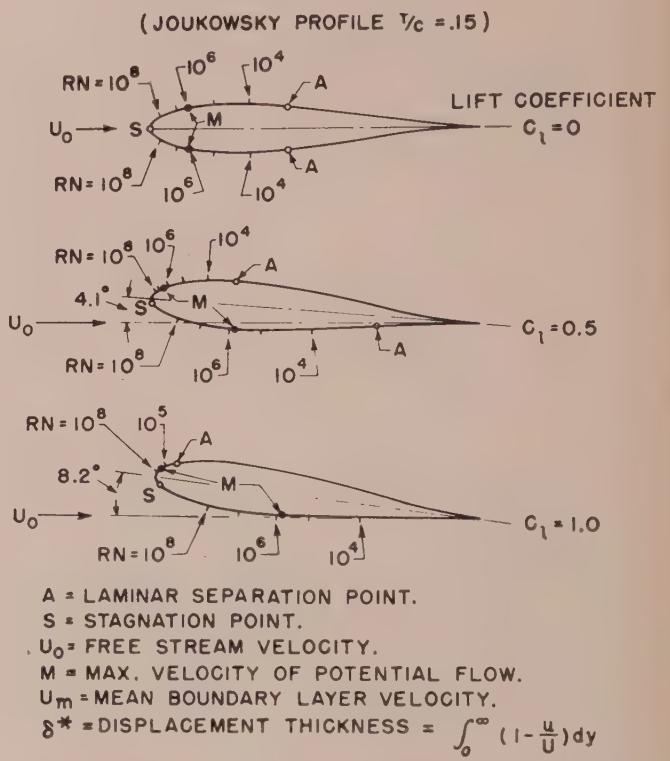

Fig. 4 – Instability points as function of Reynolds number $\left(\frac{U_m S^*}{\nu}\right)$

ops near the plate would normally be laminar. This laminar boundary layer is characterized by an orderly flow of distinct layers of fluid. The local velocities in this layer are zero at the body surface, and through the shear forces developed by the fluid viscosity, there is a gradual increase in local velocity at each point measured vertically away from the surface until the free stream velocity is reached.

Because of the deceleration of the thin layer of fluid near the solid boundary, the boundary layer thickens progressively along the surface. A point is reached when the disturbances in the boundary layer are amplified rather than damped, and a so-called transition area develops. In this area (erroneously called *point* of transition), the laminar flow is altered. Following the transition area, considerable small-scale turbulence or interlayer mixing occurs within the boundary layer.

This is the turbulent boundary layer and is characterized by a large increase in boundary-layer thickness and an altered velocity gradient. The velocity profiles of a boundary layer moving over a

flat plate – a surface of zero pressure gradient – are shown above the schematic sketch of the streamlines. Although separation is only illustrated for the turbulent layer it is equally common for such separation to take place for the laminar case. For the airfoil, the boundary layer must traverse a surface designed to produce a distinct pressure gradient. At the leading edge of the airfoil, this pressure gradient is first favorable; that is, the pressures change from the highest at the stagnation point to a low pressure some distance along the chord, depending upon the airfoil design. The boundary layer is then required to move through a region of adverse pressure gradient; that is, from the low-pressure area to the high-pressure area of the trailing edge. Unfortunately, the boundary layer has difficulty negotiating the adverse pressure gradient and usually separates from the airfoil surface when some critical Reynolds number is reached.

The prenomenon of separation is of great importance in the field of fluid flow, but unfortunately, it still remains one of the unsolved problems of fluid mechanics. Similarly, the methods for treating turbulent flow – and nearly all practical cases come under this category – are still unsolved. Schlichting[1, 2] has shown that for the laminar boundary layer, theory can predict separation

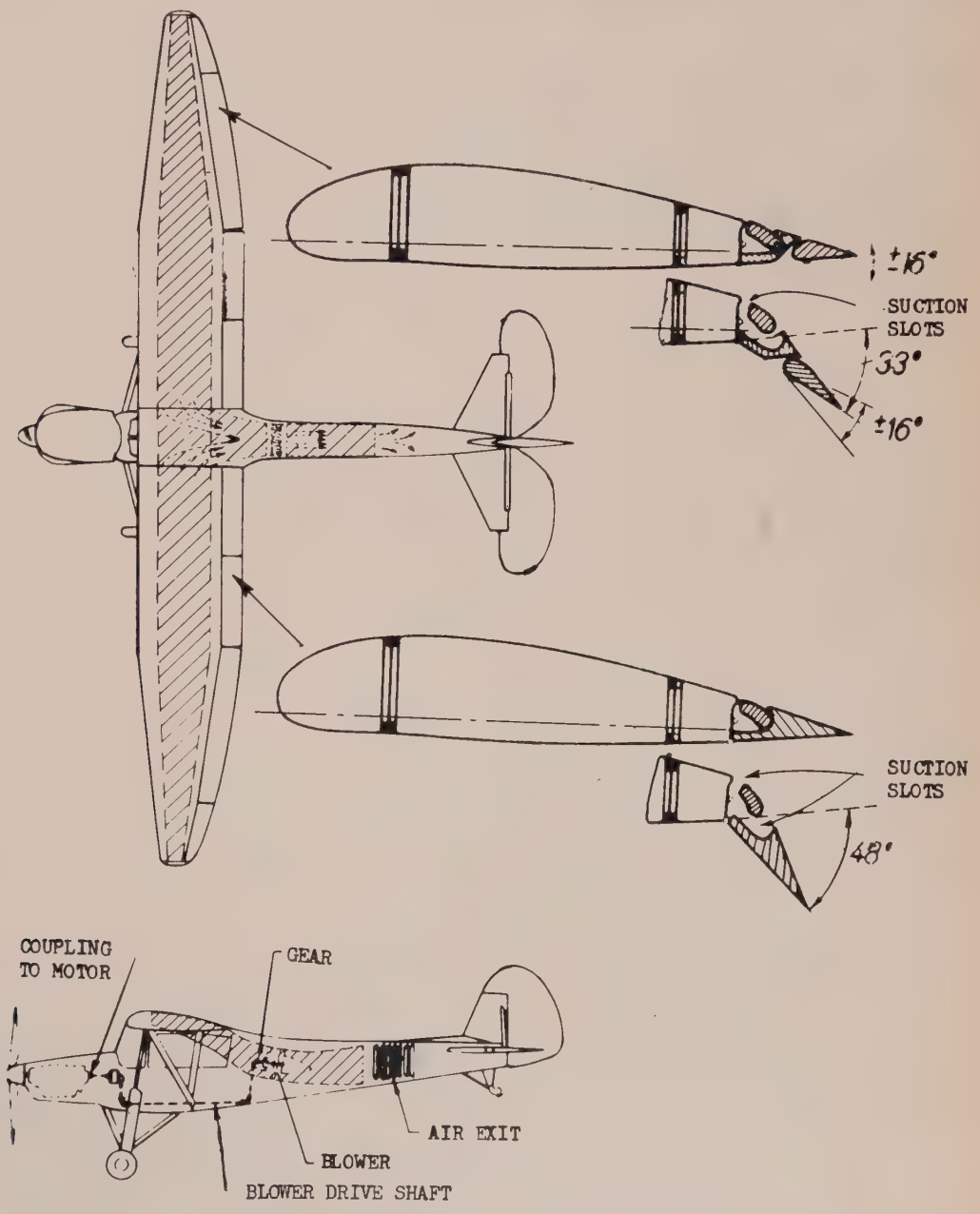

Fig. 5 – The German AF-2 boundary-layer control airplane

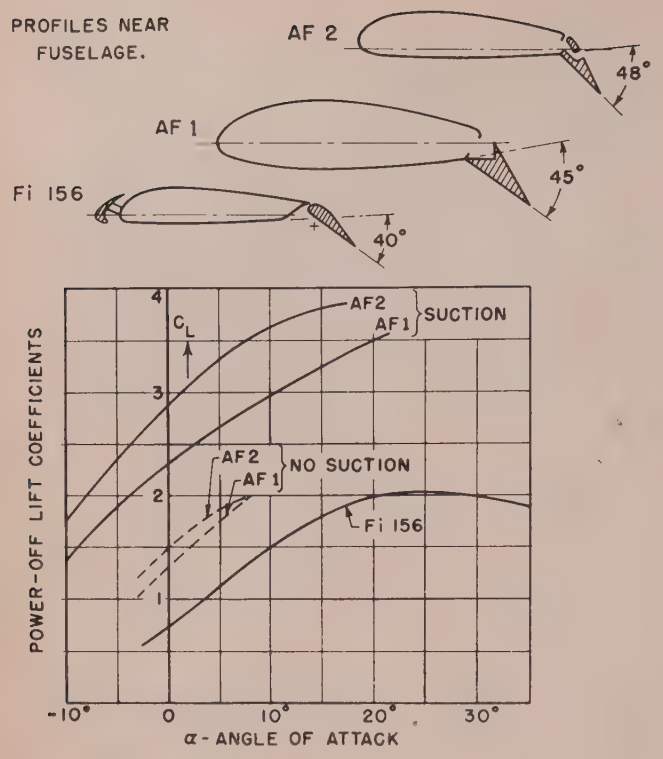

Fig. 6 – German high-lift light plane profiles and characteristics

points with acceptable accuracy. In Fig. 4 the *laminar* separation points are plotted for an airfoil at increasing lift coefficients to illustrate the forward movement of separation with increased lift coefficients. For the flapped airfoil, deflections greater than 20 deg preclude attached flow over the flap. It is apparent that such flow separation over the upper surface of the wing is accompanied by a loss in lift and eventual stall. The lift actually obtainable from a practical airfoil falls far short of that theoretically possible because of the behavior of the boundary layer. Since the formulation of the concept of the boundary layer by Prandtl some fifty years ago, aerodynamicists have searched for means for effectively influencing the behavior of the boundary layer so that theoretical lifts could be realized and drag reduced. This phase of aerodynamics is appropriately called boundary-layer control, and that category concerned with the improvement of the lifting properties of wings will be considered in this paper.

Nearly every country in the world engaged in aeronautical research has attempted practical boundary-layer control applications to aircraft. Probably the largest pre-World War II effort was concentrated under Prandtl, in the so-called "Goettingen Boundary Layer Control Group." This group included such outstanding men as Betz, Schrenk, Schlichting, Schweir, Regenscheit and others. The two outstanding attempts to apply a form of boundary-layer control for high lift by this group were the AF-1 and AF-2.[3] In Fig. 5 a general arrangement of the AF-2 and the suction slot installations of the -1 and -2 are shown for comparison. In both cases, however, as the flap was lowered to the take-off or landing position, slots opened at the flap-break. In this region of high negative peak pressures separation normally occurs for virtually all flap deflections greater than approximately 20 deg. The slots led into a large duct which occupied the space between the front and rear spars of the wing. Pumping power was supplied by an axial fan located in the fuselage and connected to the main power plant by means of shafting. A duct led from the wing to the fan and the air sucked off the wing was exhausted overboard at the sides of the fuselage.

The aerodynamic differences between the two AF installations were essentially the wing section and flap slot design. In Fig. 6 the curves of the lift coefficient versus angle of attack for the AF-1 and AF-2 are compared with the Fischler Storch, Fi-156. The Fi-156 was a well-known slow-flying, high-wing monoplane of the Thirties, incorporating full-span leading edge slat and as much flap as physically possible. Its slow flight performance was considered spectacular. As shown by the curves, however, the maximum lift coefficient available to the Fi-156 was 2.0 while the high-lift AF machines produced a marked improvement in demonstrating lift coefficients of 3.8. Unfortunately, in addition to the weight, space, and complexity of the installation, adverse lateral control characteristics were encountered at the low speeds obtained. The AF series could not be considered practical installations as aircraft designers made no attempts to duplicate the BLC installations of the AF series in new aircraft.

In America in 1944, Stalker,[4] with the Dow Chemical Co. under an Army Air Force contract, attempted to apply suction slots to a full-span multihinged flap, Fig. 7. Again, the installation

[1] See NACA TM 1217 (1949), "Boundary-Layer Theory – Part I – Laminar Flows," by H. Schlichting.

[2] See NACA TM 1218 (1949), "Boundary-Layer Theory – Part II – Turbulent Flows," by H. Schlichting.

[3] See NACA TM 1232 (1950), "Flight Experience and Tests on Two Airplanes with Suction Slots," by J. Stuper.

[4] See Fairchild Engine & Airplane Corp. Report RR-1 (April, 1954), "Aircraft Manufacturer Looks at Boundary-Layer Control," by R. Darby.

Fig. 7 – Stackler-Dow Chemical Co. BLC plane, 1944

complexities and weight left much to be desired. Before engineering improvements could be realized, the aircraft crashed, killing both the pilot and much of the enthusiasm for supporting BLC research in America.

In the Thirties, Bamber in the United States, Toussaint (Saint-Cyr) in France,[5] and Von Ehlers, Regenscheit, Bauman and Schweir[6] in Germany, attempted to increase the airfoil lift by ejecting air from slots placed on the upper wing surface. In the case of the suction slot, the boundary layer which was retarded by fluid viscosity is drawn within the airfoil, thereby suppressing separation at points of adverse pressure gradients. In the case of the blowing slot, kinetic energy of the jet is imparted to the retarded boundary layer, suppressing separation. Flow of the suction and blowing systems and the corresponding velocity profiles of the boundary layer are shown in Fig. 8. The suction slot acts as a sink and influences the circulation about the airfoil to a small extent in acting on the potential flow and giving rise to greater velocities upstream of the slot.[7] The parameter which defines the amounts of air which must be withdrawn through the suction slot is the flow coefficient, C_Q. This parameter is defined as the quotient of the flow quantity in cfs and the product of wing area and free stream velocity, Q/V_0S. Tests of suction slots show that there is a rapid increase in lift coefficient for small values of C_Q, but large values of C_Q do not result in more than a small increase in circulation. Little or no gain is accomplished by suction for C_Q's greater than 0.02.

Recent research conducted by the NACA in replacing the slot type of suction by porous material[8] has proved of considerable interest in producing the theoretical increments due to flap deflection up to 40 deg. In Fig. 9 the effect of such

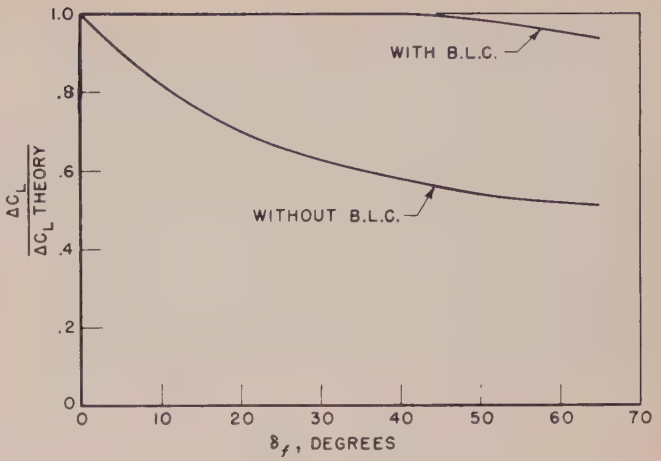

Fig. 9 – Lift increments for a range of trailing-edge flap deflections

Courtesy, NACA

Fig. 10 – View of the NACA suction flap F-86A

porous suction in obtaining theoretical flap effectiveness to large deflections is illustrated. Of prime importance in the porous suction research has been the reduction in power necessary for establishing attached flows over the flap. The NACA research F-86 equipped with a porous flap installation is shown in Fig. 10. The suction pump is shown fitted externally under the fuselage. Substantial improvements in $C_{L\max}$ have been demonstrated by this research aircraft. Unfortunately, experience in both America and in England with the porous materials used has indicated that they are readily clogged by the usual contaminants found in air and the effectiveness of porous suction rapidly deteriorates. Further research with porous metals may solve this practical problem.

The second method for exercising control over the behavior of flow over a lifting surface is by means of a blowing jet directed tangentially to the surface usually in the same areas occupied by the suction slots. The blowing jet performs the following functions:

1. It suppresses separation by imparting energy to the boundary layer.
2. It acts on the potential flow by accelerating each of the outer layers of flow, thereby increasing the circulation at a given airfoil incidence.[9]
3. It produces a reaction effect which causes a propulsive component and a lifting component when the jet is directed inclined to the free stream direc-

[5] See Librairie Polytechnique Beranger (Paris), 1950, pp. 454-463: "Aerodynamique Experimentale," by P. Rebuffet.

[6] See NACA TM 1148 (1947), "Lift Increase Produced by Blowing on Wing of Profile Thickness of 9% Equipped with Slot and Slotted Flap," by W. Schweir.

[7] "Sur le mechanism et l'application du controle de la couche limite aux avions," by P. Poisson-Quinton. Extract from Proceedings of International Colloquim on Mechanics (Poitiers), Vol. II, 1950.

[8] See "NACA University Conference on Aerodynamics, Construction, and Propulsion," Oct. 20-21, 1954, Vol. II, "Aerodynamics," Paper No. 12, "Boundary-Layer Control for High Lift," by W. L. Cook.

[9] See *Aeronautical Engineering Review*, Vol. 12, September, 1953, pp. 24-30: "Boundary-Layer Control and Supercirculation," by J. S. Attinello.

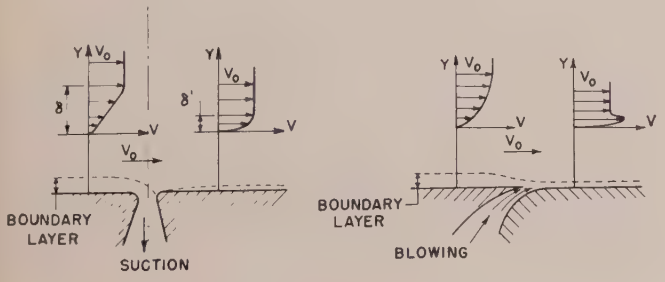

Fig. 8 – Effect of suction and blowing on boundary-layer profile

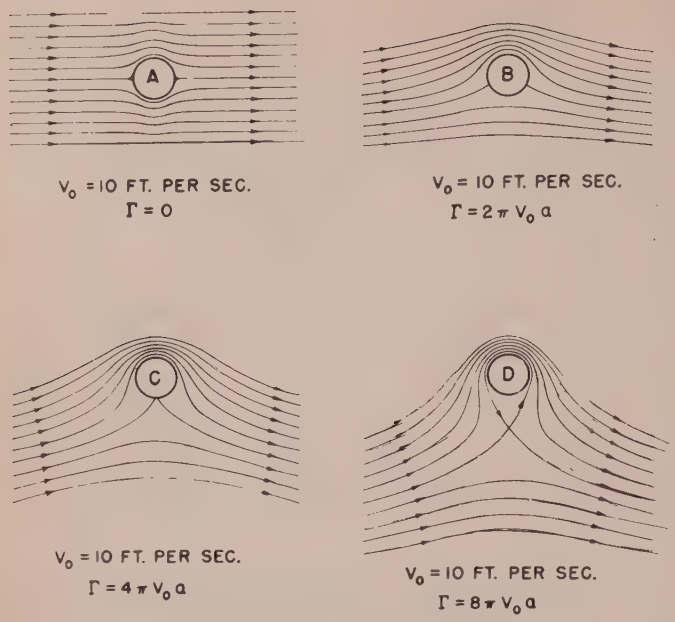

Fig. 11 – Ideal circulation about circular cylinder

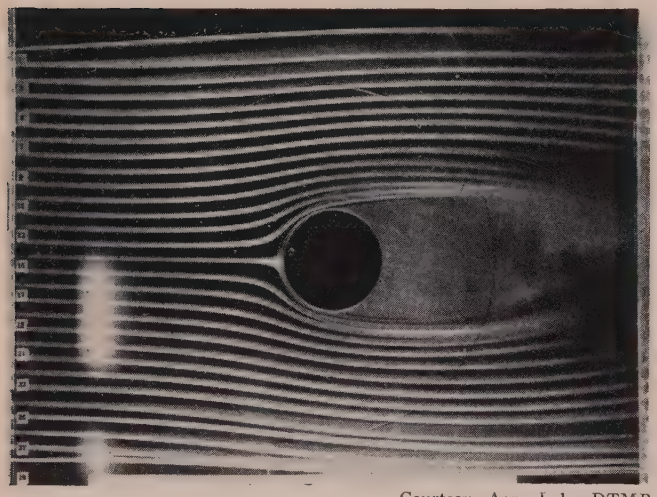

Courtesy, Aero Lab., DTMB

Fig. 12 – Smoke tunnel photo of flow about cylinder

tion, as in the case of blowing over a deflected flap.

4. An effective increase in flap chord is obtained at larger values of blowing coefficients.

The parameter corresponding to the flow coefficient for jet blowing is the momentum coefficient, defined as the quotient of the product of mass flow and jet velocity and the product of free stream dynamic pressure and reference area:

$$C\mu = Q_m V_j / q_0 S$$

For the ideal fluid of zero viscosity – and hence no boundary layer – the lifting ability of airfoils calculated from theory would be realized in practice. This theoretical flow about a cylinder positioned transversely to the free stream direction is shown in A of Fig. 11. The symmetrical pattern about the flow axis results in zero lift on the cylinder. If the flow field is distorted by the addition of some circulation strength, Γ, a positive lift will develop. In B of Fig. 11, a circulation strength of $2\pi V_0 a$, where a is the cylinder radius, has been superimposed on the symmetrical flow field of A. Since the lift coefficient is defined by $C_L = \pi / a V_0$, for case B ($\Gamma = 2\pi V_0 a$) the lift coefficient will be 2π, a large value. The characteristic downward shift of the stagnation point, which accompanies the increase in circulation and resulting positive lift, should be noted for future comparisons. Of interest are the flow fields plotted about cylinders B, C, and D, wherein increasing circulation strengths have been added to the flow. Since the time of Kutta and Joukowski, who independently are credited with the circulation concept, the generation of lift by imparting circulation to the flow field mechanically has occupied many researchers. One of the best known examples is the Flettner Rotor, which demonstrates that by mechanically rotating the cylinder at high speeds, through the viscous forces in the *real fluid,* a similarity to the *ideal flow field* of *no viscosity* could be produced. Because of the large power required and the relatively low lift-drag ratios of such an arrangement, no practical application of the Flettner Rotor has yet been made, as far as the writer knows.

If a cylinder is placed in a real fluid moving at a finite velocity, the streamline pattern more nearly assumes that shown by the smoke tunnel photo[10] of Fig. 12, though some variations occur with Reynolds numbers and flow turbulence levels. The flow has detached itself from the surface of the cylinder at some critical Reynolds number, resulting in a large region of separated flow behind the cylinder. In Fig. 13 the flow about the same cylinder has been radically altered, and is very similar to the theoretical flow field of cylinder B of Fig.

[10] See Navy Department, DTMB, Aero. Lab. Report Aero-872 (November, 1954), "Tangential Blowing on Surface of Airfoil as Boundary Value Problem," by S. T. de los Santos.

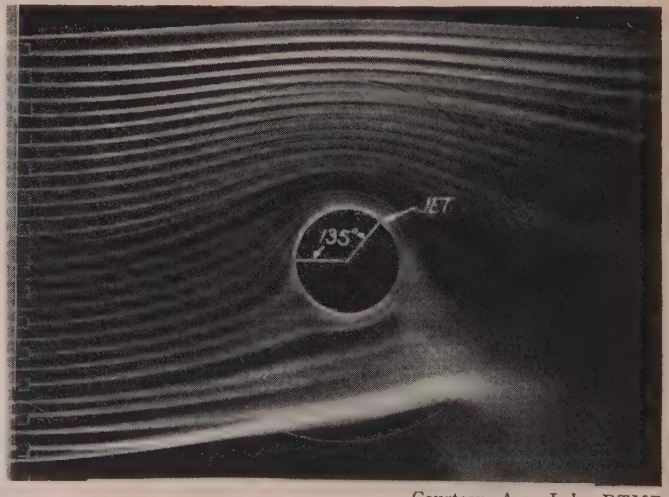

Courtesy, Aero Lab., DTMB

Fig. 13 – Smoke tunnel photo of flow about cylinder with blowing jet

11. This flow field distortion was accomplished by blowing a jet of air tangential to the surface at a point 135 deg from the original stagnation point. This slot position is well aft of the original separation point and serves to illustrate the upstream effect of the jet. Not only has attached flow been realized, but the flow field distortion and downward movement of the stagnation point evidence the increase in circulation achieved. It should be pointed out that the conditions necessary for good smoke tunnel photographs make only qualitative assessment possible at this time. Nevertheless such photos serve as a powerful research tool for examining unorthodox flow control methods.

The effect of a blowing jet on the flow field about the flapped airfoil section of a modern aircraft is illustrated by smoke tunnel photos. In Fig. 14, flow about the flapped airfoil at high angles of incidence shows relatively small distortion of the flow field and a large separated region of flow which indicates drag. In Fig. 15, the favorable effect of the blowing jet on the airfoil is immediately evident. The downward movement of the stagnation point illustrates the increase in circulation to produce lifts at low angles of incidence and the attached flow over the flap fills the previous highly turbulent separated region normally associated with large flap deflections. An effective chord extension is further illustrated.

As stated previously, smoke tunnel tests provided qualitative research information. A quantitative measure of the increases in lift coefficients obtainable by the blowing jet over the flap of a 9% thick airfoil, is illustrated in Fig. 16.[11] These are results of early German tests. Recent research in this field has resulted in much improved performance. In Fig. 17 the section lift coefficient of a plain flap at various flap deflections is compared to the theoretical lift line and a family of the same section equipped with blowing over the flap.[12] For these tests the flow coefficient, C_q, was held constant, and slot width, s/c, was altered.

The intriguing possibility of achieving the theoretical lift from practical wings has challenged most people associated with aircraft since the time of Prandtl,[13] who first demonstrated by means of water tunnel experiments the possibility of influencing the boundary layer favorably by suction through slots. The introduction of flaps in their

[11] See National Physical Laboratory, Aerodynamics Division, 17,027, Perf. 1272 (Sept. 6, 1954), "Analysis of Aerodynamic Data on Blowing over Trailing-Edge Flaps for Increasing Lift," by J. Williams.

[12] See University of Wichita, Engineering Study No. 139 for Office of Naval Research (September, 1954), "Boundary-Layer Control by Blowing – Method of Increasing Flap Effectiveness," by K. Razak.

[13] "Upon Fluid Motion with Very Small Friction," by L. Prandtl. Symposium of Third International Mathematics Congress, Heidelberg, 1904.

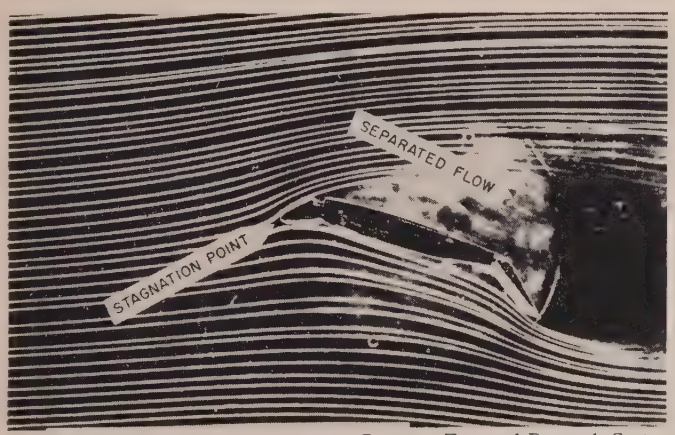

Courtesy, Forrestal Research Center

Fig. 14 – Smoke tunnel photo of flow about flapped airfoil

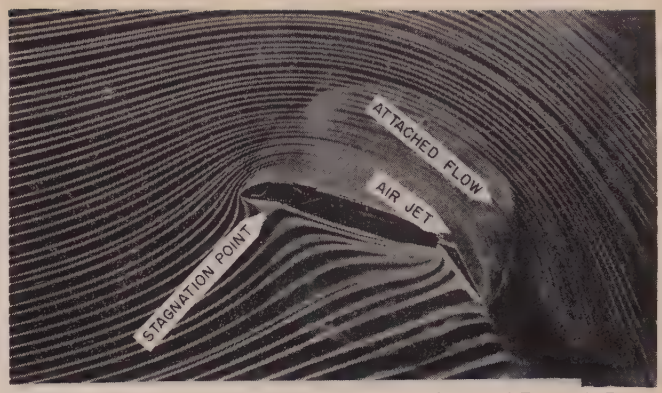

Courtesy, Forrestal Research Center

Fig. 15 – Smoke tunnel photo of flow about flapped airfoil with Supercirculation System

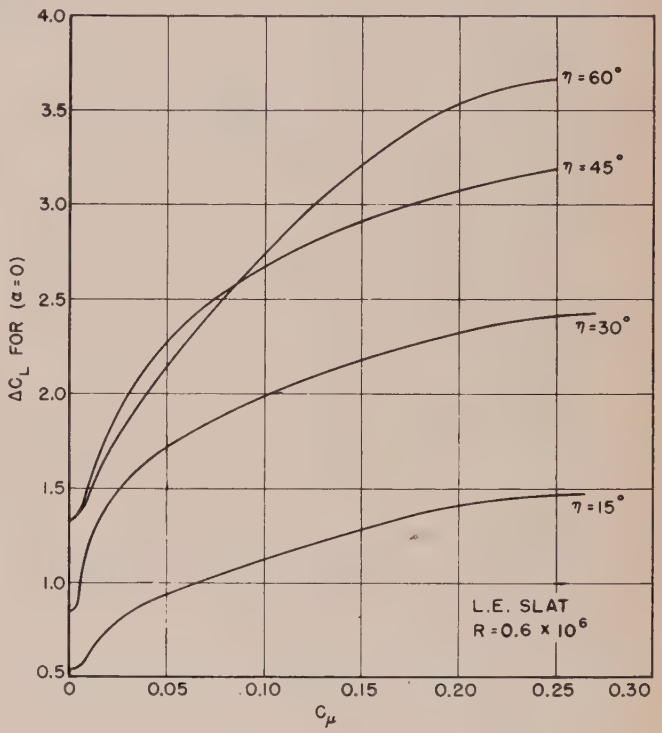

Fig. 16 – Two-dimensional tests of NACA 0009 with blowing over 25% flap

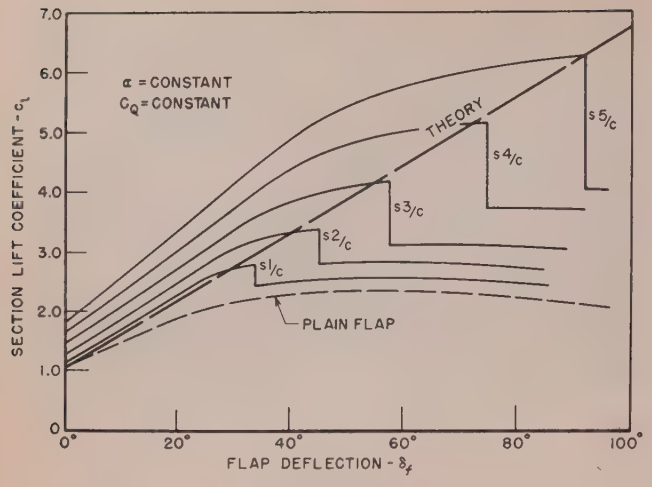

Fig. 17 – Illustration of flap effectiveness

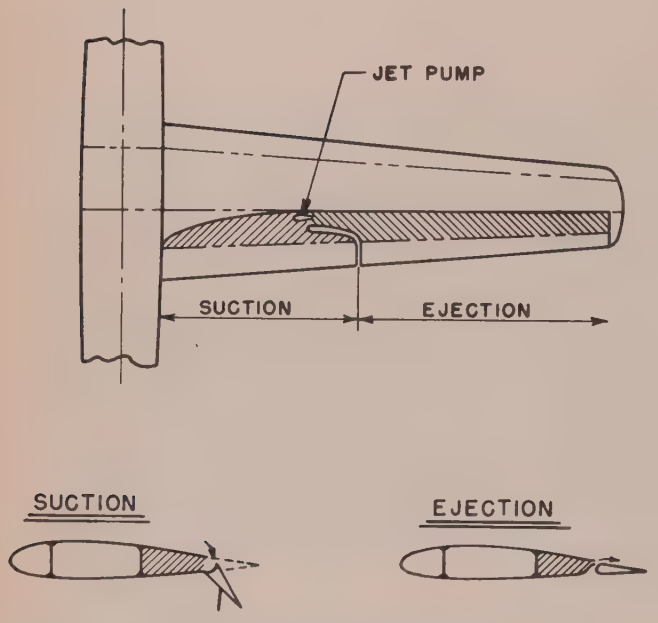

Fig. 18 – Arado 232 BLC showing combined suction and blowing arrangement

various well-known forms served to satisfy to a large extent the needs for lower take-off and landing speeds for many years. However, the gains from improving flap effectiveness to that theoretically possible served to spur on the researchers in high-lift BLC. Attempts to apply various forms of boundary-layer control to actual aircraft through the years have, until recently, been plagued by continued discouragement. The previous near misses, however, did not discourage Prandtl or his so-called "Goettingen Boundary-Layer Control Group." Although during World War II little or no research was conducted by the Allies, the Germans on the other hand conducted high-priority, top-secret research in this field with specific systems and aircraft applications in mind.[14, 15, 16]

From captured German documents it has been established that high-lift systems were being studied and engineered for the following aircraft:

1. Mescherschmitt ME-109 – Fighter of 7000-lb gross weight. All-blowing system. Two blowers imbedded in the wings driven by extension shafts from main engine. Model designation with BLC changed to ME-209.
2. Junkers Ju-109 – Four-engine transport of 40,000-lb gross weight. Fans driven by main engines.
3. Dornier DO-24-Flying Boat of 33,000-lb gross weight. Suction and blowing. Water, hydrogen peroxide jet pump.
4. Arado 232 – Troop Transport of 36,000-lb gross weight. Combined suction and blowing. Water, hydrogen peroxide jet pump.
5. Arado 234 – Jet Bomber. Studies only.

In 1947 the Air Branch of the Office of Naval Research, in its search for methods for improving the low-speed performance of Navy aircraft, uncovered many of the German documents concerning the high-lift BLC applications and began a research program to determine the effectiveness of such systems in modern aircraft. The most promising of the proposed German installations was believed to be the Arado 232 installation, shown schematically in Fig. 18. As can be seen, a combination of suction and blowing was utilized and an ingenious jet pump provided the necessary air moving machinery. The combined system reduced the amount of air pumped to approximately half that of an all-suction or an all-blowing system. More important, this arrangement reduced the duct sizes considerably. With a rear spar location only slightly forward of the normal position, all the ducting was housed outside the wing torque box. The jet pump utilized high-pressure steam generated by the decomposition of hydrogen peroxide. Blowing over the aileron appeared to solve the lateral control problem prevalent in the earlier AF series which utilized a suction system.

After exploratory wind tunnel tests under ONR sponsorship at the University of Wichita, evidence of the effectiveness of the Arado system was submitted. Plans for duplicating the system with an inexpensive light plane led to its application in a Cessna 170 airplane by the Cessna Aircraft Co., under ONR and BuAer sponsorship. Because of certain handling difficulties inherent in the use of concentrated hydrogen peroxide, the Arado pumping system was altered slightly (Fig. 19). Bleed air from an AiResearch turbine unit supplied high-

[14] "Boundary-Layer Control and Application to Aircraft," by A. Satin. Office of Naval Research Air Branch Memo, June 29, 1952.

[15] See Monthly Research Report, Office of Naval Research, Feb. 1, 1951, pp. 13-27: "Lower Minimum Speeds for Fixed-Wing Aircraft," by P. E. Mullowney.

[16] See James Forrestal Research Center, Princeton University, Literature Search No. 6 (Jan. 14, 1955), "Bibliography on Boundary-Layer Control," by M. Smith.

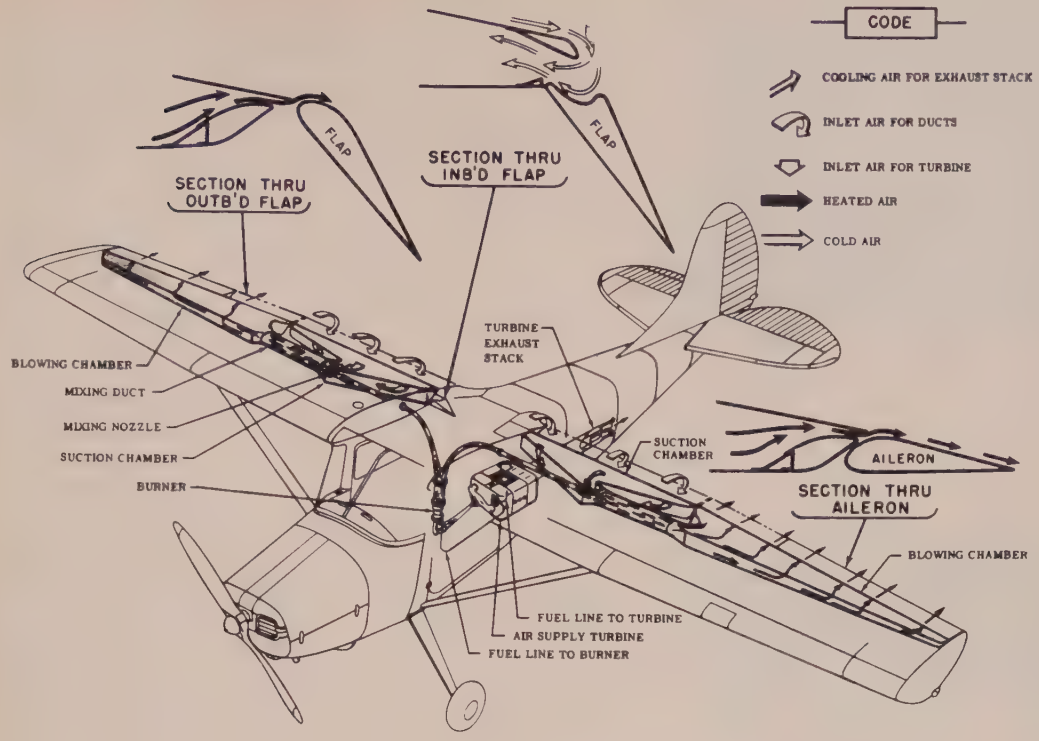

Fig. 19 – Application of modified Arado system to Cessna 170

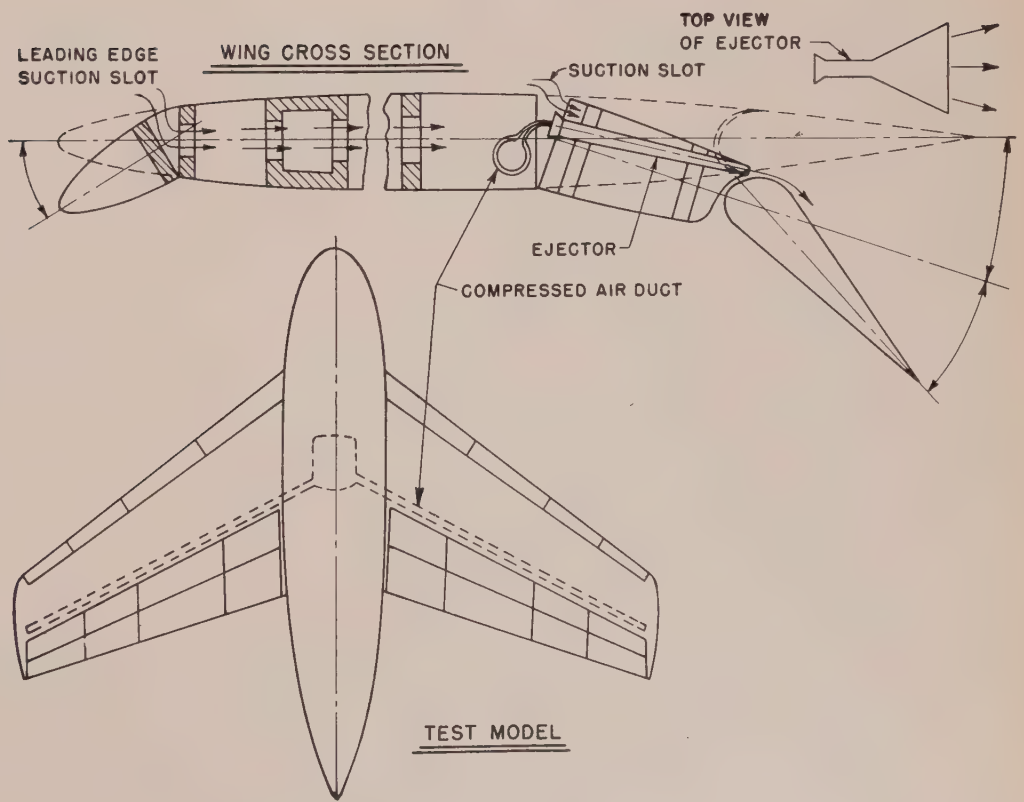

Fig. 20 – French Poisson-Quinton high-lift system on wing of S.O. 6020 fighter as tested at Chalais-Meudon full-scale wind tunnel

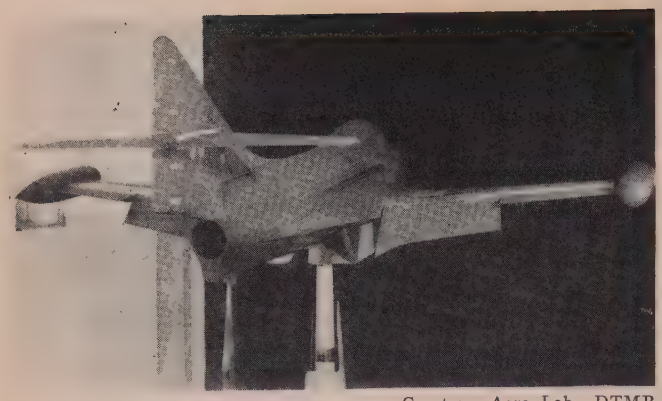

Courtesy, Aero Lab., DTMB

Fig. 21 – Grumman F9F-4 model in 8 x 10-ft wind tunnel

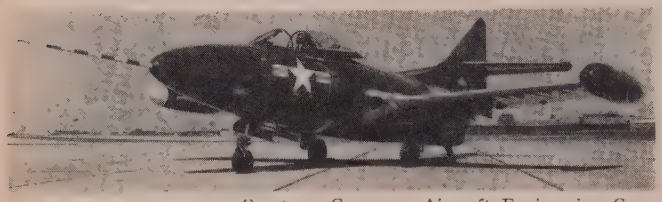

Courtesy, Grumman Aircraft Engineering Corp.

Fig. 22 – View of the Grumman F9F-4 "Panther" equipped with BuAer Supercirculation BLC System

pressure air to a burner-can (from a Boeing 501 turbine) in which fuel was injected and burned. The resulting hot, high-pressure gases served as the primary gas in the jet pumps located in each wing. Demonstrations of this machine,[17] now designated the Cessna 309, showed take-off reductions of 40%, the stall speed being some 15 mph slower than the production Cessna 170. Understandably, all the personnel connected with this project were pleased with the first results. The system was admittedly a research installation and not a prototype. The mechanism for accomplishing the increased lift weighed some 350 lb for a machine of approximately 2000-lb gross weight, but it was felt that engineering design could greatly improve the installation. Immediate investigations directed towards application of the Arado system to modern high-speed military aircraft, however, proved disheartening. An examination of the pumping power and the air quantities required for high-wing-loading aircraft with modern thin airfoil sections and high structural density proved the Arado system incompatible with modern military machines. Unfortunately, it is this class of aircraft which is in greatest need for assistance at the low-speed end of the flight spectrum.

An examination of French research[18] in the field of lift-augmentation systems reported in 1951 showed rather impressive lift increments for full scale swept wings. This system, shown diagrammatically in Fig. 20, required rather complex internal structure and elaborate flaps. Navy engineers and airframe contractors agreed that the structural and weight penalties for applying such a system to existing aircraft were prohibitive, and the application to future designs, highly questionable. The use of a main jet engine as a pumping source, as suggested by many and applied by the French, intrigued the writer. Preliminary calculations were initiated for utilizing this pumping power in a manner heretofore untried in the half century of BLC research. Grumman Aircraft Engineering Corp. personnel expressed interest in the system but required substantiation of the calculations by tests. The Navy's Aero Laboratory of DTMB conducted two-dimensional and then three-dimensional wind tunnel tests of the system, corroborating the calculations, Fig. 21. Grumman, under a BuAer contract and with the cooperation of the Allison Engine Division of General Motors Corp., installed the new system on an F9F-4 Navy jet fighter (Fig. 22). The machine first flew on Dec. 3, 1953, successfully demonstrating a decrease in take-off and landing distances as well as improved low-speed handling characteristics during simulated wave-offs. Inasmuch as the Navy is concerned with carrier operations, the Panther, after necessary carrier-suitability tests conducted at the Naval Air Test Center, Patuxent River, was tested aboard the aircraft carrier USS Bennington, CVA-20. At reduced carrier speeds, reduced catapult settings, and reduced arresting gear settings, the Panther made 32 landing and catapult take-offs with smoothness and without incident.

The lift increase due to the new system was equivalent to a 25% increase in wing area. The weight penalty for the installation was 50 lb. It takes little calculation to realize that for this 50 lb, the increase in lifting effectiveness would permit carrying more than 3000 lb of additional payload at the same take-off speed. As with all new devices, the BuAer Supercirculation system is not a panacea for all ills, and is not directly applicable to all existing aircraft. However, since both the Air Force and Navy are placing this high-lift system into production aircraft, it can be said that this is the first practical application of high-lift BLC to aircraft since Prandtl's original concept a half century before. The BuAer high-lift system is a step in the right direction. As further research and

---

[17] See University of Wichita, Engineering Report No. 032 (June, 1951), "Wind Tunnel Investigation of Method of BLC as Applied to Reflection Plane Model at Full-Scale Reynolds Number," by K. Razak, V. Razak, and R. J. Bondie.

[18] See NACA TM 1331 (1952), "Investigations of Boundary-Layer Control on Full-Scale Swept Wing with Air Bled off from Turbojet," by P. Rebuffet and P. Poisson-Quinton.

[19] "Flow Control – Integrations of Powerplant and Airframe for Future Aircraft," by J. S. Attinello. Paper presented at ASME Diamond Jubilee Spring Meeting, Baltimore, April, 1955.

[20] "Boundary-Layer Control," by G. Lachman. Paper presented before Royal Aeronautical Society, Nov. 11, 1954. Digested in *Flight*, Vol. 66, Nov. 12, 1954, pp. 711-714; *Aeroplane*, Vol. 87, Dec. 3, 1954, pp. 808-811.

experience is gained in its use on operational aircraft, not only will further lift gains be realized, but other uses for this powerful method of flow control[19, 20] will be developed.

Note: The opinions and assertions expressed herein are the private ones of the writer and are not to be construed as official or reflecting the views of the Navy Department or the Naval establishment at large.

DISCUSSION

Of Flatt and Attinello Papers

Effect of BLC On Performance Equations

– R. A. Darby
Fairchild Engine & Airplane Corp.

IN 1934, as an unemployed engineering graduate, I had fun helping a German inventor at nearby Hadley Field complete a small airplane which incorporated a system of boundary-layer control. This untimely prophet had worked on less than a shoestring, and, as a result of endless component breakdowns, his airplane failed, although its BLC system would be considered good, in concept, today. So I have taken unusual satisfaction from these excellent papers describing successful applications of BLC. My only question is why it took 19 years for American aviation to interest itself in and succeed at something so valuable and so much needed.

It is sometimes helpful, in trying to apply BLC, to review how it operates on the performance equations. Fig. A shows the essentials of take-off. Short ground roll and a steep angle of climb are desired. The speakers this morning have stressed the effectiveness of BLC in increasing the lift coefficient, C_L, and have indicated that it also reduces, or can reduce, the form drag coefficient, C_{Do}. The beneficial effect of BLC on ground roll is clear; essentially, the take-off speed is reduced. Its benefit to the angle of climb is less clean-cut because of the induced drag term at the far right. A very high C_L with a low aspect ratio, R, could actually flatten the climb angle and lengthen the air distance over an obstacle. If, however, C_L is kept moderate – but higher than without BLC – and the aspect ratio, R, is high, this term may be small enough that its increase is less than the increase in $T/W - C_{Do}/C_L$. Then BLC has the desired net effect of increasing sin Θ. The propeller thrust, T, is increased appreciably by the lower climb-out speed made possible by BLC.

Fig. B shows the most elementary, but still very basic, considerations of landing. Again, the glide should be steep and the ground roll short. With very high C_L the second term increases faster than the first decreases; hence, tan Θ is increased and the path is steepened. At more moderate values of C_L the glide angle might be flattened. Air brakes or very large flap deflections with BLC will insure steep, slow approaches.

Fig. C, attributable to P. E. Mullowney, shows very clearly the value of BLC in making possible higher cruise speeds for a given field length, weight and power. Here, the equation of level flight is solved to show that cruise speed is proportional to the cube root of the wing-loading, W/S, and inversely proportional to that of the parasite drag coefficient, C_{Do}. Since aviation began, wing loadings have been pushed up, at the expense of airport size and safety. Now, BLC enables the high wing-loadings, which are essential, without further increase in field size – indeed, with reduced field length – and will soon offer further increase in cruise speed through continuous use in cruise to reduce C_{Do}.

Use of BLC Depends on Aircraft Type and Application

– David Hazen
Princeton University

IT IS unfortunate that, in the BLC business, we have no method of computing the merit of a system similar to the one a friend of mine who works for Radio Corp. of America developed for computing the cost of electronic instruments. His system, which has been checked out on various bits of equipment ranging from an analog computer to my television set, is simply to count the number of knobs and multiply by 100.

In the BLC field, life is not nearly this simple because cost of a system is only a very small fraction of its merit. Were one exceptionally cost conscious, he probably wouldn't consider aircraft in the first place. Some far more complicated measure of value is necessary and it will not be found in the form of a single number or ratio regardless of how tempting it may be to correlate performance against some magic number such as the lift increment produced times the power required times the weight of the system, divided by the gross weight of the airplane, all raised to the number of man hours required for design.

The important thing to keep in mind is the final application of the aircraft being considered. Systems that would be highly acceptable and satisfactory for a fighter airplane may not even be feasible for a cargo plane.

For example, a typical fighter airplane employed by the Air Force would set a considerable premium upon short-field landing and take-off operation. This means the system desired should produce high lift and low drag on take-off and would produce high lift and high drag on landing. On the other hand, a Naval aircraft of the same variety would be interested primarily in achieving the lowest possible flight speeds but would not be as concerned about rates of climb and descent in the low-speed regime as the Air Force airplane.

Yet another complication is introduced in the application of such systems to larger aircraft of the cargo variety, for example. Presumably this type of airplane would utilize the BLC system to increase the cargo load that could be successfully operated from a given field. Hence one would be interested in maximizing its climb and descent performance in the low-speed flight configuration, and it would, in this respect, be similar to the Air Force fighter plane. But unlike the fighter airplane which can be characterized as having very thin wings with a minimum of ducting space available, combined with very high powers generally in the form of compressed air taken directly from the main power plants, the cargo airplane has thick wings allowing the use of large ducts and must generally rely upon auxiliary power units since the power plants are struggling, at least during the take-off maneuver, under conditions of maximum rated power. For this reason, a system moving small quantities of air at high pressure and powers, although very attractive to fighter aircraft, may be totally out of the question for cargo aircraft. Conversely, the ducting system utilized by a cargo machine to move large quantities of air at low pressures probably would not even fit into the wings of the fighter.

I wish to give these words of warning because there is a tendency to extend the application of any given BLC system to the entire range of aircraft, while the end result desired and the type of aircraft considered will very greatly influence the system selected.

I should also like to urge people not to fall into the trap of comparing the effectiveness of BLC systems solely on the increment of lift produced, since, in the final analysis, the airplane responds to its lift-drag polar. Experience has shown that very great care in tailoring spanwise load distributions is necessary to maintain the spanwise efficiency factor at a value sufficient to avoid the situation of creating large lift coefficients but not having sufficient

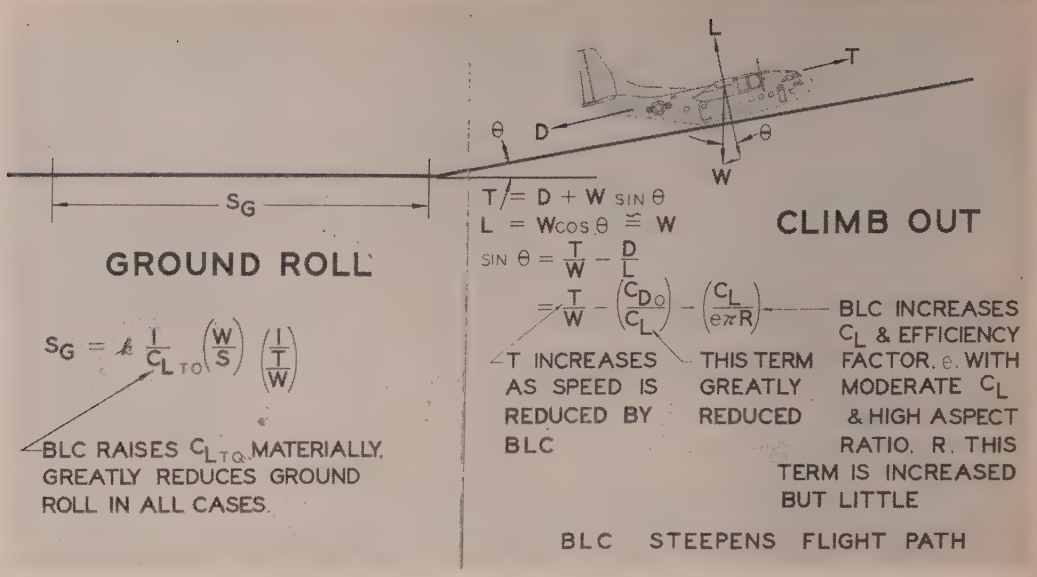

Fig. A – BLC can shorten take-off

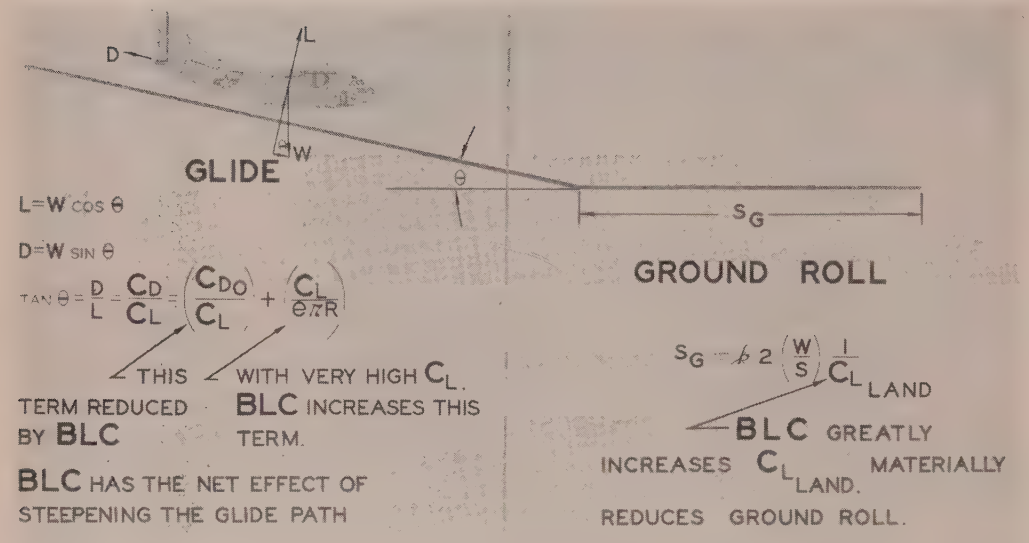

Fig. B – BLC can shorten landing

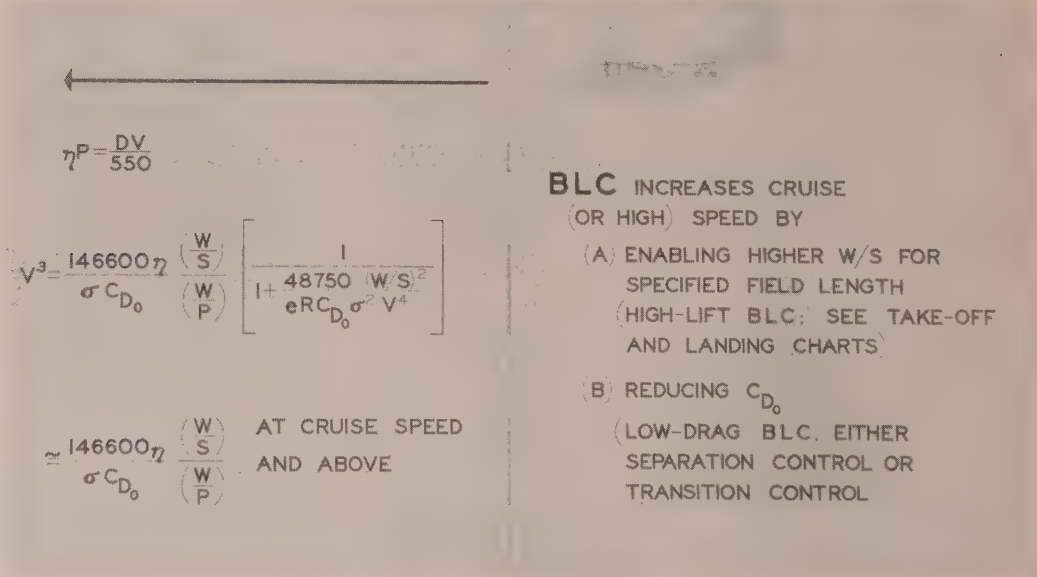

Fig. C – BLC can increase cruise speed

power to maintain level flight under these conditions.

Application of BLC to Jet and Propeller-Driven Aircraft

– Leo A. Geyer
Grumman Aircraft Engineering Corp.

AS Mr. Attinello mentioned in his paper, the application of BLC is not a direct process in all existing aircraft. Some of the reasons why the engine-bleed air system cannot be applied to a particular jet aircraft can be the existing wing structure and flap arrangement, the limited tail power or tail effectiveness to handle the increased pitching moments resulting from the increased lift, and the fact that the aircraft may become thrust limited. This last item can occur on take-off as a result of bleeding air from the main engine and requires much further development by both the airframe and the engine people. The airframe people must further improve the efficiency of the blowing system so that the same lift can be achieved with less bleed air. In turn, the engine people must supply the required bleed air with negligible thrust loss at least for limited periods of operation. It is encouraging that progress is being made along these lines.

Mr. Attinello mentioned that the F9F-4 installation weighed approximately 50 lb. It is necessary to mention further that the -4 was a "natural" for this installation. This weight is most attractive but could be cause for over optimism. In applying similar systems to more modern jet aircraft equipped with thinner wings and with higher thrust engines giving higher bleed-air temperatures and pressures, the weight penalty can be four or five times as great.

The BLC system to be used in propeller-driven aircraft can be of the high-pressure, Arado or suction type. All of the systems discussed here have good and bad points. In propeller-driven aircraft application one immediately runs into the problem of overall system reliability; that is, is it best to derive the BLC air supply from the main engines driving compressors and the like, or is it possible to use one or more separate power supplies for BLC air? I do not pretend to know the answer to this problem. It certainly requires considerable thought and development before reliable application of BLC to propeller-driven aircraft can be achieved.

We Still Don't Know What Type of BLC Is Best

– R. L. McManus
General Electric Co.

THE authors have failed to prove, in spite of diligent efforts for some time, *in what form* BLC is here to stay. The most important question to which we still have no answer is this: Do we implement the BLC concept with a blowing system, a suction system, or a compound system?

It is important to note that on no single airplane program to date have all three methods been evaluated comparatively. The question has not been reduced to a common denominator.

Until we have an answer to this question, two important members of the implementation team – the engine manufacturer and the accessory manufacturer – are left out.

If we go to the blowing system, large amounts of engine-bleed air will be required for an optimum system. This will necessitate radical changes in the design plane of the engine manufacturer.

If we're going to the suction or compound system requiring an auxiliary air source, indications are that a new one of higher flow and pressure ratio must be developed. Existing APU's will not allow an optimized BLC system.

Even if the old workhorse turbosupercharger is used (as on the F-86), important modifications will be necessary for an optimized system.

Now the prime consideration is this: No one is going to do anything – the engine manufacturer isn't going to design high-bleed flows into the new engines, the accessory manufacturer isn't going to develop a high-capacity APU – until we have a better answer than exists today.

We're not sure how to answer this question. Perhaps it can be answered by reducing the excellent work already accomplished by Messrs. Flatt and Attinello to one common denominator – a single airplane on which would be evaluated all the alternate systems – first by an analytical study and then by a flight test program.

We feel strongly that responsibility for answering this question rests with the Air Force, Navy, and Air Force manufacturers who are concerned with the problem. It has taken us 50 years to get from Prandtl's initial concept to today's sharp increase in operational progress. It appears that the single most important obstacle in the road of continued progress is in deciding whether the air should be coming, going, or both. Let's somehow reduce present knowledge to a most needed common denominator so that the sharp progress curve of BLC will continue upward.

Airplane Designer Has Problems In Application of BLC

– Kenneth Razak
University of Wichita

MR. FLATT has described two distinctly different methods of BLC application. The effort on the F-86 was to delay the leading-edge separation while the purpose of the XC-123D program was to increase the effectiveness of a deflected trailing-edge flap. The common feature of these two applications is that both were operations performed upon existing aircraft in an attempt to relieve a particular problem. The airplane designer is sufficiently aware of the fine balance that exists between the various elements of airplane design to realize that a disturbance of any element on an existing design can perhaps seriously unbalance the remainder of the design. This is another way of saying that the full value of either leading-edge control or improvement of the effectiveness of trailing-edge flaps may not have been secured in these two applications. For example, the engine and propeller system on the XC-123D is the same as the standard airplane. With the increased maximum lift coefficient, however, the airplane is capable of flying at a lower speed and the shape of the thrust horsepower available curve should be examined at this lower speed. A possibility exists that the excess thrust horsepower may be falling faster at the low-speed end than the thrust horsepower required for propulsion is being reduced by BLC. Although a net performance improvement was secured, a still further improvement would be possible if the engine-propeller combination were designed specifically to operate efficiently over the wider speed range.

It is very interesting to note that in neither of these programs have any peculiar or uncertain flight characteristics been encountered. Those who have been working in the field have long predicted that the act of preventing boundary-layer separation would not produce unusual flight characteristics but might actually relieve some of the existing problems, particularly those associated with the high drag that occurs immediately preceding airfoil stall.

It is quite evident that the next step in the true utilization of BLC is for the aerodynamicist and the designer to deter-

mine the particular problem that is to be relieved on the individual design and utilize the rapidly increasing supply of experimental data to make a particular application.

The historical review that Mr. Attinello has presented effectively demonstrates that the significance of BLC has long been recognized. The utilization of BLC, however, has waited until both a specific requirement existed for its application and a practical procedure was available. The use of direct engine-bleed has been found to be a practical approach in spite of the fact that the power that is being expended for the pumping is many times greater than that which is required with other methods. Unfortunately, any device that would reduce the required power would make the system so much heavier and more complex that it becomes almost impractical. Research is now continuing, however, on methods to reduce the amount of bleed air for a given lift increment to make this system even more practical.

The illustration of the effectiveness of BLC, as contrasted with adding wing area to produce a given landing speed, is merely an extension of the reason that high-lift flaps are justified on high-performance aircraft rather than larger wings. The effort that is now being exerted by the manufacturers of transport aircraft to improve, by even a small increment, the lifting effectiveness of conventional flaps is an indication of the importance of flap effectiveness. As soon as the results of additional research programs that are now being conducted become available to the industry, the manufacturers may see a method by which they can secure a distinct improvement in flap effectiveness over the best flap that is now available. Additional increments in aircraft performance from the standpoints of increased payload, increased range, or reduced landing and take-off speeds will then be available. Each designer will determine the combination of circumstances that must be examined to determine the actual result that he will attain by applying BLC.

Previous Experimentation With Vane Configuration for BLC

– Kurt P. H. Frey
Armour Research Foundation

MR. ATTINELLO shows that there has been remarkable progress in the development of high-lift vanes as compared to the conventional methods.

One naturally compares the lift and drag coefficients of a newly developed device with those of conventional vanes in a viscous flow. Small gliding angles and high-lift coefficients always present the problem of finding an appropriate compromise. Thus, the achievement of a lift coefficient of 3 to 3.8 is remarkable progress, provided this coefficient includes a fair magnitude of the gliding angle at the low-lift coefficient range. However, after measurements taken on rotating cylinders in Goettingen revealed that flow patterns similar to the ideal nonviscous flow and a lift coefficient of 10 could be achieved even in viscous flow, the judgment changed. Then the effort focused on finding vane configurations which would result in a deflection of the approaching flow, or in a lift coefficient, of the order of magnitude experienced with the rotating cylinder. Moreover, the gliding angles must be of approximately the same order of magnitude as the vanes at the range of low lift coefficient.

Two German investigations arrived at an initial solution of these problems, carried out independently by K. Frey about 25 years ago, and by L. Prandtl and B. Regenscheit about 10 to 15 years ago. In an unpublished study, Frey found a suitable combination of the vane and the rotating cylinder which achieved the desired deflection of the approaching flow. L. Prandtl and B. Regenscheit found a suitable combination of the vane and suction, which resulted in the desired order of magnitude of the lift coefficient. Their results were published as classified information during Wolrd War II, which like other interesting developments, have been made available to the public in the "Bibliography of Scientific and Industrial Reports" (since July 1949, "Bibliography of Technical Reports"), Department of Commerce, Office of Technical Services. L. Prandtl has briefly referred to the discussed investigations in his book "Essentials of Fluid Dynamics," p. 202, Fig. 3.87 (Hafner Publishing Co., New York).

The vane used by Prandtl and Regenscheit has a specially designed trailing edge at which suction has been applied. With a symmetrical vane and a stationary angle of attack of zero deg, a lift coefficient of ten has been achieved. The entire range, therefore, is $c_l = 0$ to $\pm$ 10. L. Prandtl told me in 1951 that he had originally thought to recommend this method as a stationary ship rudder, but he agreed that his method might also be useful in combined applications.

K. Frey obtained the deflection of flow he desired with the system shown in Fig. D. A wedge profile was attached to a rotating cylinder in such a way that it could be adjusted around the cylinder to any radial position witnin 360 deg. In the figure, the dark line crossing the cylinder is a support bar, and the white lines are strings to rotating the cylinder. The model is shown in slowly moving water, with a free surface on which aluminum powder has been sifted in order to obtain the flow pattern. Beneath the edge of the wedge at the location of the arrow, a wire and its shadow are seen. This wire, therefore, is a reference line for the angle of attack. The position of the vane shown represents a considerable negative angle of attack. The cylinder has been rotated in a clockwise direction, causing the flow to turn smoothly around the trailing edge of the device. The deflection shown corresponds to that which would be expected at a positive lift and a positive angle of attack; however, it cannot be raised to such a magnitude at a positive angle of attack. This is particularly true when using a sharp leading edge. An unusually efficient deflection of the approaching flow is obtained when the wedge profile is lined up with the oncoming subdividing streamline.

In the light of the facts just presented and the potentialities speculated upon, I would like to know whether such considerations have been taken into account by Mr. Attinello and what his conclusions may be.

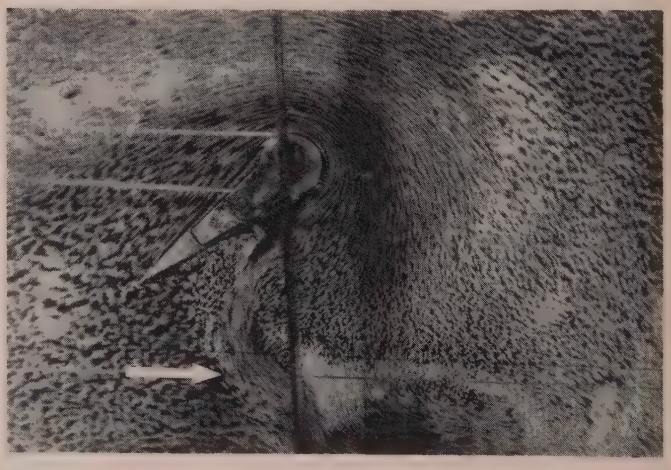

Fig. D – Flow pattern of wedge profile with a clockwise rotating cylinder at trailing edge at large negative angle of attack. Water moves in direction of the arrow. Order of magnitude of Reynolds number is about 3000. Streamlines are formed by sifting aluminum dust on water surface upstream from model

New and Improved Synthetic Elastomeric Materials for Automotive Use

W. J. Simpson, Rubber and Plastics Laboratory,
Central Engineering Division, Chrysler Corp.

This paper was presented at the SAE Golden Anniversary Passenger-Car, Body, and Materials Meeting, Detroit, March 1, 1955.

APPROXIMATELY twenty years ago, compounds made from oil-resistant specialty synthetic rubbers, Thiokol and neoprene, began to appear and the practical application of these new materials began. In this paper, the author presents some of the results of research and development that have been and are now going on to produce new types of synthetic rubbers for specialized applications.

The many new types of elastomers now being developed and examined in research laboratories have indicated that eventually elastomers may be handling jobs for which they are not now considered.

A FEW years ago most rubber technologists were building rubber compounds for automotive or any other use upon two basic materials – natural rubber and reclaimed rubber. Somewhat over twenty years ago, compounds made from the oil resistant specialty synthetic rubbers, Thiokol and neoprene began to appear, and the art of applying these new materials started to develop. Since that time the increase in available synthetic elastomers which technologists can use to make compounds for a variety of applications has been tremendous. The synthetic rubber materials now available include a great variety of types, each of which has its own specialized scope of application. It is the purpose of this paper to point out a few of the more recently developed elastomers and also to describe some of the improvements and new applications of the older types of synthetic polymers.

Buna S (GR-S)

Buna S or GR-S synthetic rubber manufactured by the Federal Facilities Corp. has been available, of course, for some time. Tremendous strides have been made recently in the art of compounding buna S, particularly in the use of super fine furnace proc-

Table 1 – Some Advantages and Disadvantages of Buna S Compared to Natural Rubber

Advantages	Disadvantages
More stable price	Greater heat buildup under dynamic loads
Better tread wear (passenger sizes)	Slightly lower tensile strength
Less set under load	Less surface tack for "plying up" operations
Greater heat resistance	Poorer properties in nonblack compounds
Greater variety of polymers for specific applications	

ess carbon blacks and also in the use of so called "oil extended" polymers. The development of the "cold rubber" process of polymerization (polymerizing at temperatures just above the freezing point of water) has resulted in the production of stronger and more abrasion resistant rubbers, so that now, practically all passenger tire treads are made from GR-S. The art of blending substantial quantities of low-cost petroleum plasticizers with the latex of high-viscosity polymers has resulted in the development of the "oil extended" GR-S elastomers, achieving not only a saving of cost, but an actual improvement in quality in some cases.

Improvements in the art of compounding have considerably extended the use of GR-S in products other than tires. For instance, many engine mountings are now being made from "cold rubber" GR-S compounds, if the greater hysteresis of GR-S (compared to natural rubber) can either be tolerated, or is actually desired for its damping characteristics. This has been particularly true since softer, high strength GR-S compounds have become available. With braking temperatures constantly increasing, the use of GR-S in wheel cylinder cups or seals, and even in master cylinder cups is increasing. This has been done to take advantage of the greater heat resistance and better high-temperature set characteristics of this material compared to natural rubber.

The development of so-called "arctic rubbers," that is, butadiene-styrene copolymers with greatly enhanced low-temperature properties has resulted in increased use of the special GR-S elastomers in military aircraft applications requiring serviceability at –65 F. Elastomers such as GR-1015 (95% to 5% butadiene-styrene ratio) and GR-S-1505 (90% to 10% ratio) are being used to advantage in producing a number of mechanical goods products for ordnance vehicles and military aircraft.

Table 1 lists some comparative characteristics of natural rubber and GR-S in order to suggest where the use of one may be more advantageous.

Butyl Rubber

The use of butyl rubber in the automotive industry is not new because it has been used in inner tubes for some time. There have been some problems in its application which have been overcome by the development of improved polymers, and by advances in the art of compounding and processing of butyl. Its preeminence in the manufacture of tubes, of course, has been due to its outstanding ability to resist diffusion of air. Lately the use of butyl rubber has been increasing in other automotive products, partly because it is the lowest priced elastomer available, and also because it has good weather resistance, flexing properties, and tear resistance. The use of tubeless tires on many of the 1955 model automobiles will certainly have an effect upon the consumption of butyl rubber in applications other than tubes because the supply of this very advantageous synthetic rubber will increase. This will undoubtedly lead to the development of more specialty types for "nontube uses" by the manufacturers of butyl polymer. A considerable amount of radiator hose is now being made from butyl rubber taking advantage of its good weathering and low diffusion properties. Because of the good tear resistance of this material, butyl rubber is being used to advantage in shims and similar products which are fastened in place by bostitching. The use of this elastomer in parts such as boots, spring and axle bumpers, and weatherstrips is constantly increasing because it has good resistance to heat, tearing, and weather.

The increased emphasis on the use of color in automotive styling will affect the application of butyl rubber in exposed parts. Compounds made from GR-S and natural rubber for parts exposed to weather, must of necessity contain large amounts of wax, which migrates to the surface to form a film to protect these materials against the effects of weather. Butyl rubber compounds, on the other hand, can be made resistant to weather or ozone with only small amounts of wax present. Thus, it is possible to apply color coatings to weather resistant butyl parts and obtain much better adhesion than with the same type of coatings applied to GR-S or natural rubber compounds.

The development of solid colored butyl rubber compounds is much more feasible than the development of similar compounds in either natural rubber or GR-S because the use of carbon black to enhance physical properties is not nearly so mandatory in this material. Colored butyl compounds seem to possess greater depth of color than do the compounds of either natural rubber or GR-S. The speed of the application of this material to colored parts will be dependent upon the availability of nonstaining types of butyl polymers, that is, polymers that do not contain antioxidants that tend to discolor the compound itself, or painted surfaces in contact with it. At the present time, nonstaining butyl rubber polymer can be obtained only from the Polymer Corp. at Sarnia, Ontario. The Federal Facilities Corp. does not make a nonstaining type of butyl because this type is not required in the manufacture of tubes. The Federal Facilities Disposal Commission has just announced

that a successful private bid has been made for at least one of the Government-owned butyl plants. Therefore, unless Congress overrules the bid tentatively accepted by the Disposal Commission, it may be assumed that this plant will soon be privately operated. Private bidders for the butyl facilities have indicated that they will produce nonstaining butyl rubber when the plants are turned over to them. Therefore, it appears likely that nonstaining type butyl rubber will be available in this country eventually, and that this elastomer can then be applied to the manufacture of colored products. In Table 2 are listed some of the characteristics of butyl rubber including its color possibilities that control its use in automobiles.

A new type of butyl polymer was announced at the last meeting of the Rubber Division of the American Chemical Society.[1] This is a polymer that has been modified by introducing 1-3½% bromine. This elastomer is produced by the B. F. Goodrich Chemical Co. under the commercial name "Hycar 2202." One of the disadvantages of butyl rubber is that it can be contaminated when even small amounts of ordinary sulphur vulcanizable rubbers such as natural rubber, buna S and buna N become mixed with it. This is due to the fact that the other rubbers contain much more chemical unsaturation than butyl rubber and, therefore, absorb the vulcanizing materials before they have a chance to react with the butyl rubber. This phenomenon is so pronounced that it is even impractical to make products in which a portion of the part made from butyl is cured adjacent to other rubbers. For instance, it is not possible to prepare a hose with a butyl tube and a cover made from one of the other rubbers. The bromine modified butyl, however, can be mixed with other polymers or vulcanized adjacent to them and still be satisfactorily cured. The new type butyl rubber is still too new to have been thoroughly evaluated, but it should prove to be advantageous in parts where it might be desirable to blend it with other elastomers or to make assemblies containing both brominated butyl and other elastomers, provided its ultimate price is not too high.

Table 2 – Some Comparative Characteristics of Butyl Rubber Affecting Its Use in Automotive Applications

Advantages	Disadvantages
Low price	Poor oil and fuel resistance
Good heat resistance	Relatively poor set characteristics
Good weathering characteristics	Fair low-temperature properties
Colored products available, either painted or solid color	More difficult to process than GR-S or natura rubber
Low gas permeability	
Good flex resistance	
Good tear resistance	

Table 3 – Some Advantages and Disadvantages of Neoprene for Automotive Uses

Advantages	Disadvantages
Fairly good resistance to most oils, greases, acids, and alkalies	Poor resistance to fuels with substantial aromatic content
Excellent resistance to flexing	Poor resistance to low aniline point oils
Low permeability to most gases	Low-temperature flexibility somewhat questionable after long exposure
Low heat buildup under dynamic loads	
Excellent resistance to weathering and/or ozone	

Neoprene

A large number of automotive parts have been made from neoprene for a long time and its advantages are well known. This material has been very valuable in a number of applications because it has very good weather resistance, flex cracking resistance, low permeability to gases, along with fairly good oil resistance. These properties have made neoprene a valuable base material for hose covers, hydraulic system diaphragms, some types of seals, and skin compounds for sponge rubber door weatherstrips. Table 3 lists both good and undesirable characteristics of this material that should be remembered when specifying neoprene for automotive use.

During the past two or three years the use of some new types has developed. One of these, known as type W, possesses the advantage of much lower compression set than the former neoprene GN without losing the advantages of good weather resistance, flexing resistance, and many of the other desirable qualities of neoprene. The development of this new type of neoprene has resulted in an extended application of neoprene seals requiring good set characteristics when used with fluids for which this elastomer has adequate resistance.

It is a well-known fact that both neoprene GN and neoprene W tend to crystallize when exposed to low temperatures for fairly long periods of time. The effect of this tendency has been greatly reduced by the development of the so-called RT types of neoprene. Rubber technologists can use neoprene GRT in place of neoprene GN or neoprene WRT in place of type W in applications where the hardening of compounds must be avoided during low-temperature exposure.

Recently, another new type of neoprene known as WHV has been developed. This is a high-viscosity W-type neoprene, to which very large quantities of low-cost petroleum-type plasticizer may be added during the mixing operation. Compounds made from this elastomer containing large quantities of plasticizer and dry fillers have physical properties that are adequate for a number of

[1] "Butyl-Type Polymers Containing Bromine," by R. T. Morrissey. Paper presented before Division of Rubber Chemistry, American Chemical Society, New York, Sept. 16, 1954.

Table 4 – Some Advantages and Disadvantages of Buna N for Automotive Products

Advantages	Disadvantages
Excellent resistance to most oils and fuels	Deteriorates in some extreme-pressure lubricants at elevated temperatures (250 F–300 F)
Excellent compression set characteristics	Rather poor resistance to fluids containing active sulfur and to di-ester hydraulic fluids
Heat resistance up to 300 F in most fluids	Only fair flex resistance
Dry heat resistance up to 250 F	Fairly poor resistance to fluids at temperatures over 300 F
Low-temperature flexibility good if properly compounded	
Abrasion resistance good in moving seals	

applications, and at the same time have the advantage of lower cost than standard neoprene compounds. Their use should be advantageous in applications where possible plasticizer extraction from the neoprene compound by fluids is not a problem, or in applications where fluid resistance is not required. These types of compounds are being used in parts such as dust seals and other seals where any occasional splashing with oil or other fluids is encountered, and in applications where the excellent weather resistance of neoprene is desirable.

Buna N

Buna N compounds have been available for use in seals and other applications requiring excellent resistance to oils and fluids since shortly before World War II. By varying the ratio of butadiene and acrylonitrile (co-monomers of this very versatile copolymer) it is possible to produce a number of varieties of buna N with varying degrees of resistance to oils and fuels and with varying degrees of low-temperature flexibility. The art of compounding buna N has been improving and compounds are now available for seal applications requiring resistance to oils at temperatures up to 300 F.

A tremendous amount of O-rings, lip type seals, rotating shaft seals, and other types of seals are being made from buna N for use in engines, transmissions, differential carriers, power steering units, and many other hydraulic applications. Satisfactory results are being obtained from buna N compounds in these applications as long as its limitations (listed in Table 4) are recognized.

Polyacrylic Rubbers

As performance of automotive vehicles is improved, various synthetic rubber seals used in engines, transmissions, and other places are expected to operate satisfactorily at temperatures which are continually increasing. Until recently, seals made from neoprene and buna N performed very satisfactorily in many of these applications. However, as temperatures have increased to 300 F, and even to 350 F, less life can be expected from seals made from these materials. There have been continual improvements in the art of compounding the various buna N polymers, and in some cases, buna N compounds stand up as long as 300 hr when completely immersed in lubricating oils at 300 F, and can be expected to last perhaps 75 hr in petroleum-type lubricants at 350 F.

For some time considerable effort has been expended to develop seals from a newer type of synthetic rubber known as polyacrylic rubber which is marketed under the trade names Hycar 4021 and Acrylon. Chemically these materials are copolymers of either butyl or ethyl acrylate with either vinyl ether or acrylonitrile. Compounds made from these rubbers will withstand 300 F dry heat for indefinite periods, whereas the best buna N compounds usually remain flexible for only one or two days at this temperature. In most lubricating oils or hydraulic fluids, polyacrylic elastomers will withstand temperatures up to 350 F and possibly 400 F for reasonably long periods. Compounds made from this material are also outstanding in their resistance to extreme-pressure lubricants, especially those containing active sulfur. On the other hand the extra heat and chemical resistance is obtained at some sacrifice in tensile strength, abrasion resistance, and tear resistance over the buna N materials as indicated in Table 5.

The use of polyacrylic seals is increasing, especially in static applications where heat resistance greater than that possible with buna N seals is required. One of the drawbacks to a more rapid development of its use has been difficulty in processing operations, although this is being gradually overcome as the art of compounding and processing this material progresses.

At the last meeting of the Rubber Division, American Chemical Society, a new type of polyacrylic rubber was announced.[2] This material is known as "Poly F.B.A." and is reported to be a polymer of 1,1-dihydroperfluorobutyl acrylate. The

[2] "Poly F.B.A. Fluorine Containing Polyacrylic Rubber," by P. J. Stedrý and J. F. Abere. Paper presented before Division of Rubber Chemistry, American Chemical Society, New York, Sept. 16, 1954.

Table 5 – Characteristics of Polyacrylic Rubber Affecting Its Use in Automotive Parts

Advantages	Disadvantages
Excellent dry heat resistance (300 F for indefinite time) (350 F for shorter periods)	Poor resistance to hot water or steam
Excellent resistance to hot oil (350 F for long periods) (400 F for short periods)	Poor resistance to glycol-type brake fluids
Excellent resistance to e-p lubricants	Abrasion resistance questionable
	Poor low-temperature resistance
	Minimum hardness for best properties is 60 durometer

addition of fluorine seems to have produced a rubber with low swelling characteristics in oils and fuels with substantial aromatic content, along with low shrinkage in high aniline point oils. Like standard polyacrylic rubbers, the new fluorinated type also has the drawback of rather poor low-temperature properties. A few preliminary tests in our laboratory have indicated that this material possesses remarkable resistance to oils (both low and high viscosity), extreme-pressure lubricants, fire-resistant hydraulic fluids, and dry heat. Not enough data have been accumulated to evaluate fully the new material, but it certainly looks promising. Its present price is extremely high because it is being made in the pilot plant, and to some extent its acceptance will be determined by its ultimate production price.

Recently, another type of polyacrylic rubber known as N5400 elastomer has appeared. This is an exploratory material of an acrylate type recently developed by the Monsanto Chemical Co. It was developed specifically to withstand fire-resistant hydraulic fluids such as Skydrol. Like other acrylate type rubbers it is not flexible at temperatures much lower than 0 F. It is being used in specialized aircraft applications where its ability to withstand fire resistant hydraulic fluids is valuable.

Silicone Rubber

The silicone rubbers have been available for quite a while, and their uses keep expanding. When these elastomers were first introduced, the suppliers sold only premixed compounds which rubber fabricators merely prepared and cured into parts. During the past two or three years the suppliers of silicone rubbers have supplied silicone gums as well as completely prepared compounds to rubber fabricators. This has given the rubber companies greater latitude in developing formulations to meet the requirements of specific applications and has resulted in considerable development effort toward the intelligent use of this material. The suppliers of silicone polymers have been constantly improving the physical properties of this unusual material, while at the same time the price has been going down somewhat, because of increased production.

Silicone rubber, of course, is valuable because of its great useful temperature range. Compounds, flexible as low as –130 F, are available, and in many applications parts made from these elastomers are exposed to temperatures up to 500-600 F. Although considerable improvement in tensile strength, tear resistance, and abrasion resistance has been made, silicone rubbers are still more deficient in these properties than organic type polymers, such as buna N and neoprene. Silicone rubber-glass fabric laminates are being fabricated into boots and other parts requiring some strength and resistance to flexing. The improvements made lately in the compression set of this type of elastomer, especially at higher temperatures (300-400 F) has increased its use in seals. Although silicone rubbers possess adequate oil resistance to make their use successful in a number of types of seals, further improvement in oil resistance would extend the use of these polymers to many more seal applications. Silicone rubber seal compounds also exhibit lower coefficient of friction against metal surfaces than do a number of the other synthetic rubbers, and this characteristic is beginning to be used to advantage in moving seals.

In the past, it has been practically impossible to blend silicone rubbers with other synthetic elastomers such as buna N, buna S and others, in an attempt to achieve compromise properties between the two types of rubbers. At a recent meeting of the Division of Rubber Chemistry, American Chemical Society, a new experimental silicone rubber was announced.[3] This experimental silicone polymer, because of its chemical make-up, can be blended with buna N, buna S, or other elastomers. It is anticipated that this feature may be used to enhance the low-temperature flexibility and increase the maximum high-temperature serviceability of compounds made from the lower-priced and stronger organic-type rubbers. A silicone rubber of this type is available under the trade name Dow Corning No. 410 Silicone Gum.

The use of silicone rubber in automotive parts is, of course, restricted to applications where its advantages overcome its rather high cost. If parts can be designed so that a minimum amount of silicone rubber polymer is used, the cost will be offset to some extent. The relatively low strength, tear resistance, and abrasion resistance must also be borne in mind when this material is applied to automotive use. Table 6 lists some of the advantages and disadvantages of silicones to guide the

Table 6 – Characteristics of Silicone Rubber Affecting Its Use in Automotive Parts

Advantages	Disadvantages
Best heat-resistant rubber available (withstands temperatures up to 500–600 F)	High cost
Best cold-resistant rubber available (many compounds have flexibility to –130 F)	Fairly poor tensile strength
Lower coefficient of friction against metals than most other rubbers	Fairly poor tear resistance
Very good compression-set characteristics, especially at high temperatures (300-400 F)	Fairly poor abrasion resistance
	Further improvement in oil and solvent resistance is needed, although it is satisfactory in many seal applications

[3] "Sulfur-Curable Silicone Rubber Compositions and Blends with Hydrocarbon Elastomers," by D. T. Hurd and R. C. Osthoff. Paper presented before Division of Rubber Chemistry, American Chemical Society, New York, Sept. 16, 1954.

potential user in the application of this elastomer.

Kel-F Elastomer

This is another brand-new synthetic rubber recently announced and available only in pilot-plant quantities.[4] Kel-F elastomer is a copolymer of chlorotrifluroethylene containing more than 50% fluorine. It has unusual resistance to corrosive chemicals, oils, fuels, extreme pressure lubricants, and many other fluids. It can be vulcanized to form compounds with high tensile strength (up to 3800 psi) and good tear resistance. It is reputed to have exceptional heat resistance, and excellent weather and ozone resistance. These characteristics, combined with its outstanding resistance to many fluids, should make it a very valuable material for seals of many kinds. (See Table 7.)

Because this material is so new, and because the supply of samples has been so limited, it has not been possible to evaluate it fully. Therefore, one cannot say just now how widely it will be accepted for use in automotive applications. Since it does possess such unusual resistance to a great variety of fluids and aging conditions, it seems safe to say that it will prove to be a very valuable synthetic rubber material, especially in applications where its advantages offset its high cost.

Carboxylic Elastomers

These rubbers form an entirely new class of synthetic elastomers that have just been announced by B. F. Goodrich Chemical Co.[5] They are made by chemically introducing small percentages of carboxyl groups into some of the standard type synthetic rubber monomers. These types of rubbers can then be vulcanized by cross-linking the carboxyl groups or by vulcanizing with sulfur. Samples of solid type carboxylic elastomers are not available. However, a buna N type of carboxylic elastomer in latex form is available.

The modification of standard buna S and buna N synthetic rubber by this means is said to produce elastomers with greatly enhanced physical properties, improved oil and fuel resistance, and increased useful temperature range. Since so little is known about this class of synthetic rubbers, it might be considered unwise to mention them in a paper such as this. Their development is being pointed out because this type of polymer modification seems to hold tremendous possibilities for improving the overall physical properties and serviceability of synthetic rubbers. It also emphasizes the enormous amount of research that is now going on to produce synthetic elastomers of improved quality.

Philprene VP

Philprene VP is one of a new polymer family that will soon be competing for a share of the market for oil-resistant synthetic rubbers. This material is known as "Philprene VP" and was developed by the Phillips Petroleum Co. These elastomers are copolymers of butadiene and methyl-vinylpyridine.[6] The manufacturer claims that these new polymers are unique in their ability to cope with cold, heat, and most types of oils and fuels. It probably will be at least a year before a full evaluation of the commercial possibilities of these rubbers can be made.

These synthetic rubbers are interesting because they utilize a chemical reaction known as quaternizing to assist the regular vulcanization. This is done by reacting an organic halide such as benzotrichloride with the nitrogen in the pyridene portion of the polymer to form a type of structure which apparently makes the polymer oil resistant. The organic halide is added during the regular mixing operation on the mill and the reaction takes place during the regular vulcanization. According to the manufacturers of this material, sulfur vulcanization does not enhance the oil and fuel resistance of Philprene VP to any great extent, but the quaternizing reaction definitely changes the mixture to an oil-resistant compound. Quaternizing does not eliminate the need for sulfur vulcanization but rather supplements it. Whether or not this new class of rubbers will find wide acceptance remains to be seen. However, their development illustrates again the fact that the types of synthetic elastomers that can be developed is almost unlimited.

Vinyls

In reviewing the increased use of synthetic elastomers in automotive applications, one must also consider the rubber-like plastics. In fact, the use of synthetic rubbers and rubber-like plastic materials is gradually becoming so interwoven, that eventually it probably will be impossible to draw any line between rubbers and plastics. Vinyl poly-

Table 7 – Probable Advantages and Disadvantages of Kel-F Elastomer

Advantages	Disadvantages
Good heat resistance	High cost
Excellent weather and ozone resistance	Somewhat difficult to process
Flame resistant	
Inert to most chemicals	
Inert to oils, fuels, e-p lubricants, and transmission lubricants	
Good tensile strength	
Unlimited colors available	

[4] "'Kel-F' Elastomer – New Fluorocarbon Rubber," by M. E. Conroy, L. E. Roble, D. R. Wolf, and F. J. Honn. Paper presented before Division of Rubber Chemistry, American Chemical Society, New York, Sept. 16, 1954.

[5] "Carboxylic Elastomers," by H. P. Brown and C. F. Gibbs. Paper presented before Division of Rubber Chemistry, American Chemical Society, New York, Sept. 16, 1954.

[6] See *Chemical Week*, Oct. 16, 1954, p. 54, "Linked for Resistance."

Table 8 – Characteristics of Vinyl Polymers Affecting Their Use in Automotive Parts

Advantages	Disadvantages
Variety of colors	High price (40¢ per lb or more)
Excellent color depth	Limited useful temperature range – 180 F max
Can be injection molded on short cycles	Takes set under load
Excellent weathering characteristics	
Excellent electrical insulating properties	
Smooth, easily cleaned surface	
Good abrasion resistance	

mers (polyvinyl chloride, polyvinylidene chloride, polyvinyl chloride acetate, and others) are now being used in a number of applications that were formerly filled by natural or synthetic rubber compounds as well as in many trim and upholstery parts formerly made from cloth or leather. The good weathering properties of vinyls as well as the great varieties and depth of color that can be obtained in products made from this material have led to its use in applications where appearance is important. Vinyl compounds are being successfully used in the production of fender welts, seat welts, upholstery materials, window weatherstrips, door locking knobs, and interior insulators. The excellent electrical properties and corona resistance lead to the use of vinyl compounds in distributor cap nipples and other electrical system parts. Some production weatherstrips are now being made from vinyls to take advantage of its good weathering properties and its excellent color characteristics.

A new application for this very versatile material has been the manufacture of arm rests using foamed vinyl integrally molded with an embossed vinyl skin to form a very attractive interior part. This has eliminated the necessity of trimming the sponge arm rest in a separate operation. In another new application, a vinyl coating applied to rubber mats during the manufacturing process produces very beautiful mats enhancing the interior styling. It also gives a surface with very good wearing qualities and one that can be easily cleaned to maintain its good appearance for a long time. Some of the advantages of this material utilized in the products mentioned are listed in Table 8. Some of its disadvantages are also listed there to assist in preventing its use in applications where it would be misapplied if its unfavorable properties were not also considered.

Hypalon

This is a synthetic rubber or rubber-like plastic (another borderline material) which is relatively young, having been commercially available only for two or three years. It is a polymer somewhat similar to neoprene that has the chemical name "chlorosulfonated polyethylene," and is made by treating polyethylene with chlorine and sulfur dioxide. Hypalon has unusual resistance to ozone and a great variety of chemicals (acids, alkalies, and the like). Since compounds with good properties can be made without the use of carbon black, it is possible to produce almost any desired color. The material has been applied to the manufacture of spark-plug covers where considerable corona discharge and heat are encountered. Much development work is being undertaken to produce flexible colored coatings from Hypalon for use on products made from other elastomers. Table 9 lists some of the good and adverse characteristics of this material that will affect its use in automotive applications.

Polyester – Isocyanate Elastomers

This class of material is another that is difficult to classify as rubber or plastic. The so-called isocyanates are the result of German research effort on plastics during and after World War II. Chemical reactions of isocyanates have been known for 50 years, but the intensified research of the last few years has led to the creation of this unique class of elastomeric materials.

The earliest application of isocyanates in this country was their use to assist the bonding of rayon cords to tire carcass rubber. This led to the use of isocyanates in cements for adhering nylon fabric to synthetic rubber compounds. From this beginning the use of isocyanates in adhesives of many kinds has developed till it now can be used in bonding elastomers to many other materials (wood, paper, metal, and others).

In Germany, during and just after World War II, scientists at the Bayer Co., working on research to develop plastic materials studied the isocyanate reactions and out of this developed polyester-isocyanate reaction products. This research ultimately led to the development of a solid rubber known as Vulcollan and a rubber-like foam known as Moltoprene. Using the same type of reactions it was found that it was possible to produce rigid "foamed-in-place" plastics.

The isocyanate foams are already being used in this country. They are made by blending polyester resins, water, emulsifying agents, catalyst, and isocyanate in either a single or two-stage process and allowing the resultant mixture to foam in mold cavities. With this process no heat is required as with sponge rubber. Thus, the manufacturing

Table 9 – Characteristics of Hypalon Important to Automotive Application

Advantages	Disadvantages
Excellent variety and depth of color possible	Price (95¢ per lb)
Excellent resistance to many chemicals	Minimum hardness – 50 durometer
Very good heat resistance	Only fair set characteristics
Excellent resistance to weather, ozone, and corona discharge	Moderate oil resistance (same as neoprene)

process is rather simple, even though the chemical reactions involved are complicated. Isocyanate foams have low density, excellent strength, and resistance to oils and weather. Because of its good tear resistance trim pads made from isocyanate foam can be sewn together. (Foamed rubber tears readily when attempts are made to stitch it in place.) Some of the disadvantages of this new material (as shown in Table 10) are its limited heat resistance and its relatively poor resistance to steam and hot water.

Considerable publicity[7] has been given to the solid type of polyester-isocyanate rubber known in Germany as Vulcollan and in this country under various trade names (such as Chemigum SL and Estane). The isocyanate foams have gained commercial use faster than the solid rubber because the manufacturing process is simpler, but the solid type of rubber also has great potential possibilities. The development of solid Vulcollan-type rubbers has been slower than that of the foam because the manufacturing processes are difficult to control, but the engineers and scientists working to develop this new type of "super" elastomer seem confident that the processing problems now present will eventually be overcome. (See Table 11.)

The characteristics of this new elastomer that have caused so much excitement among rubber manufacturers and consumers are greatly increased tensile strength (measurements up to 7000 psi have been made) and greatly increased resistance to abrasion as measured by tire tread wear. In addition, the new rubber has good resistance to flexing and weather, along with reasonably good oil resistance. While the good properties of this new material are being considered, one must not forget that it still has some deficiencies. Under steady load (such as in mountings) solid isocyanate rubber exhibits considerable cold flow and deformation. Its strength drops off considerably at 200 F, or higher, as does its oil resistance. Also, the resistance of the new elastomer to steam and hot water is poor. The people working to improve the processing and properties of isocyanate rubbers feel that some or all of these undesirable properties will be improved with continued research.

Whether or not the polyester-isocyanate elastomers will completely live up to the expectations of their most enthusiastic advocates remains to be seen. Certainly, the isocyanate foams are already here for some applications, and are causing considerable concern among producers of latex foam rubbers because of the strength, durability, and simple processing methods of the isocyanate material. The use of the new foam material is increasing rapidly and will probably continue to do so. Large scale commercial use of the solid isocyanate rubber is still at least five years away, but its physical properties are so attractive that enormous research time is being expended to get this elastomer ready for production and to improve its undesirable characteristics.

In a paper of this length it has been impossible to completely describe the important characteristics of each of the various synthetic elastomers discussed. This is especially true because there are so many different types of rubber to consider. It is the hope of the writer that this presentation has pointed out the tremendous amount of research and development that is now going on to produce new types of synthetic rubber for specialized applications. It is well-known that limitations of available rubbers (temperature range, resistance to various fluids, friction properties) have prevented their use in many applications where elastic materials would be desirable, or have prevented engineers from realizing the maximum benefits that rubber parts would produce if some of these limitations were overcome. The very fact that so many new types of elastomers have already been developed and that so many others are being examined in research laboratories leads us to conclude that, eventually, elastomers will be available to handle jobs for which synthetic rubber is not considered now, or for which it does not perform as well as it would if its properties were improved. Certainly, the strides made by the rubber industry in the past two or three decades have been tremendous, and it appears that the program in the immediate future will be fully as great.

Table 10 – Advantages and Disadvantages of Polyester-Isocyanate Foamed Rubbers

Advantages	Disadvantages
Excellent strength	Fairly poor heat resistance
Excellent tear resistance (can be sewn)	Poor resistance to steam
Flame resistant	Fairly poor resistance to hot water, alcohols, and glycols
Very low density	
Simple manufacturing methods	

Table 11 – Potential Advantages and Disadvantages of Polyester-Isocyanate Solid Rubber

Advantages	Disadvantages
High tensile strength (up to 7000 psi)	Cold flow under load
Excellent tear resistance	Fairly poor heat resistance
Outstanding abrasion resistance (tread wear, and so on)	Poor resistance to steam
Good resistance to flexing	Fairly poor resistance to hot water, hot oil, hot glycols, and the like
Good oil resistance (at low temperature)	Present high price
Good ozone and/or weather resistance	
Unlimited color possibilities	
High impact strength	

[7] See *Chemical Week*, July 4, 1953, p. 50, "New Life from Death Gas."

The Selection of Metals for Airframe Components as Affected by Operation at Elevated Temperatures up to 600 F

M. Tiktinsky, Lockheed Aircraft Corp.

This paper was presented at the Aircraft Research Seminar held by the SAE Southern California Section at the University of California, Los Angeles, Dec. 8, 1954

THE effects of elevated temperatures up to 600 F on the mechanical properties of common aircraft structural materials are treated briefly.

The shortcomings of both short- and long-time exposure data are set forth, as are the inadequacies of present methods of analyzing certain members of aircraft structures. The changes in material properties at the higher temperatures and the manufacturing considerations relevant to material selection, such as cost, formability, and availability, are mentioned as a part of the design problem in general as regards aircraft structures.

THE aircraft engineer's selection of a material for a structural component in an airplane is primarily a problem of selecting the lightest material which will satisfactorily perform the desired function. This emphasis on lightness, which is not evidenced in any other field of engineering, can be understood readily when some data on the ratio of basic airplane weight to disposable load is studied.

Basic airplane weight includes weight of the airframe, engines, landing gear, and the like, while the disposable load includes the weight of cargo, passengers, crew, fuel, and so on. For many modern commercial airplanes this ratio ranges from 0.92 to 1.90 lb of basic weight per lb of disposable load.

A recent study of fighter-type airplanes[1] indicates the existence of an even higher ratio. This study estimates that only approximately 32% of the gross weight of a fighter-type airplane is useful load. In terms of the ratios discussed above, this indicates that, for a fighter-type airplane, 2 lb of basic weight is required for 1 lb of disposable load.

The paramount importance of weight to the air-

[1] "Selection of Aircraft Construction Materials," by S. L. Shaw. Paper presented at the SAE National Aeronautic Meeting, Los Angeles, Oct. 7, 1954.

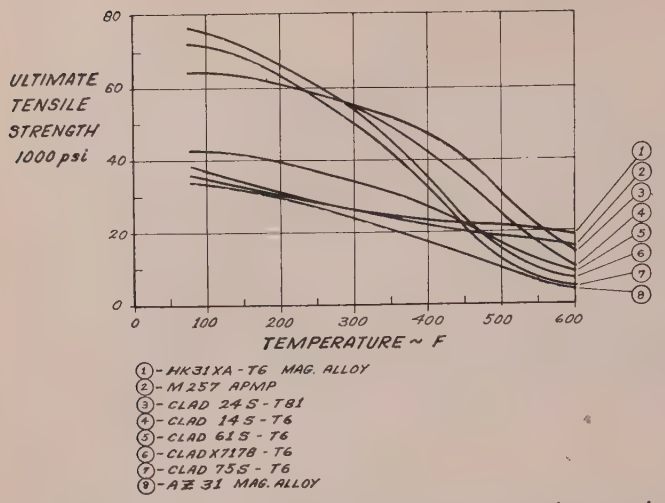

Fig. 1 – Effect of elevated temperatures on ultimate tensile strength for several alloys

plane designer and user is, therefore, self-evident. Thus high-strength light metals such as the heat-treatable aluminum alloys have long been used extensively in airplane manufacture, except for those special cases where other factors had to be considered. For items such as landing gear, where toughness, wear resistance, high unit strength, stiffness, and fatigue strength is required, heat-treated alloy steel has been the material employed throughout the entire airplane industry.

Materials other than aluminum alloys also had to be used for those parts which operated at elevated temperatures, such as engine exhaust systems and heating and de-icing systems. Fortunately, the stresses involved were low and the ordinary stainless steels were used, primarily for their oxidation and corrosion resistance and good formability rather than their high strengths at elevated temperatures.

The advent of the supersonic airplane, however, is rapidly changing this picture because of the heating of the airplane's basic structure. This heat comes from two sources: first and foremost, the higher operating temperature of the powerplants, and second, the adiabatic heating of air to high temperature levels at supersonic speeds. The net result is that the basic structure operates at ever-increasing temperatures. For purposes of this discussion, it is assumed that insulation and/or refrigeration is not compatible with the structural components of the airplane and that design will be based primarily on the elevated-temperature properties of the materials involved.

Short-time Exposure

To see why heated basic structures are a problem, let us look at some of the effects of heat on mechanical properties. Fig. 1 shows the effect of elevated temperatures on the tensile strength of some common airplane structural materials has been prepared.[2-9] Note the decrease in tensile strength of the more common heat-treatable aluminum alloys, clad XA78S-T6 (X7178), clad 75S-T6 (7075-T6), clad 24S-T81 (2024-T81), and clad 61S-T6 (6061-T6), two magnesium alloys-AZ31 and a new zirconium-thorium-magnesium alloy HK31XA-T6, and an aluminum-aluminum oxide powdered sintered material M-257 (approximately 7.5% oxide). Examination of Fig. 1 reveals first, the rapid decrease in tensile properties of AZ31, 75S, and 78S, particularly above 200 F for the Zn-Al alloys; second, the relatively flat shape of the 24S-T81 curve up to 300 F typical of other aged 24S products; and third, the relatively good properties of HK31XA-T6 and M-257 in the higher temperature ranges.

Of course, other metals have been proposed and are coming into prominence for use at temperatures above those recommended for the aluminum alloys. A comparison of these materials and three of the materials shown in Fig. 1 on a strength-weight basis is made in Fig. 2.[3, 4, 6-12] It is evident from Fig. 2 that the titanium alloys, the precipitation-hardening steels such as 17-7PH, and the normal aircraft steel alloys heat-treated to high strength levels offer a better hope for obtaining the lightest structures than either the aluminum alloys, the zirconium-thorium-magnesium alloys, or the new sintered aluminum products.

Effect of Rapid Heating Times

Unfortunately, Figs. 1 and 2 do not tell the whole story. The data reported in Figs. 1 and 2 are based on exposure times at temperature prior to testing of approximately ½ hr. Engineers concerned with the design of structures in which are encountered heating rates of hundreds of degrees per second and exposures of the order of minutes realize that those data are of little value, except to indicate trends in material behavior. Unfortunately, very limited work has been done in this field. However, based on the limited data available, it is evident that at extremely rapid heating rates the strength properties are considerably higher than those shown here. Sufficient data are not available on all of these materials to permit making any comparative evaluations.

Effect of Extended Exposures

On the other hand, engineers working with airplanes that are anticipated to have service lives of thousands of hours must know a great deal more about the effect of service conditions on mechanical

---

[2] See "ANC-5, Strength of Metal Aircraft Materials," issued by Subcommittee on Air Force-Navy-Civil Aircraft Design Criteria, Munitions Board Aircraft Committee, 1951.

[3] See AFTR 6517, Parts 1-3, (1951, 1954), "Determination of Physical Properties of Ferrous and Nonferrous Sheet Materials at Elevated Temperatures," by D. E. Miller and D. D. Doerr.

[4] See USAF Project Rand Report R-104 (1949), "Appraisal of Usefulness of Aluminum Alloys for Supersonic Aircraft and Guided Missile Construction."

[5] See USAF Project Rand Report R-146 (1949), "Effect of Temperatures on Mechanical Properties of Magnesium Alloys."

[6] LAC Report 8653 (1952), "Evaluation of Mechanical Properties of Aluminum Alloy XA78S."

[7] ALCOA Data Sheet Alloy M-257, "Tensile Properties of Aluminum Alloys as Function of Testing Temperature."

properties. First, some knowledge is desired of the mechanical properties after elevated-temperature exposure for various times.

Recent work by Armour Research Institute[3] and others[4, 5, 7, 8, 9] has begun to supply the desired data. These data can be summarized briefly as follows:

1. Extended exposure times will cause a drop in the elevated-temperature properties of the wrought aluminum alloys. For example, aged 24S undergoes a drop in elevated-temperature ultimate tensile strength ranging from 25% for 1000 hr exposure at 300 F to over 50% for a similar exposure period at 600 F.[3]

2. Extended exposure times up to 1000 hr do not greatly affect the mechanical properties of zirconium-thorium-magnesium alloys until temperatures of 600 F are reached. At 600 F, however, this alloy loses over 50% of its ultimate tensile strength and approximately 75% of its tensile yield strength in 1000 hr.[9]

3. The sintered aluminum powder products do not exhibit any change in properties with increased exposure times.[7, 8]

4. Annealed commercially pure titanium exhibits only slight changes in mechanical properties with exposure times of 1000 hr.[3]

5. The only titanium alloy about which there are extensive data is the 8% Mn sheet alloy tested by Armour Research Foundation.[3] This alloy, of the combined alpha-beta type, exhibits softening and then hardening characteristics at temperatures in the neighborhood of 300 F. At higher temperatures, that is, 500-600 F, aging begins immediately and reaches a maximum in approximately 100 hr, evidenced by the increase in tensile properties. Overaging, or softening, then begins and at the end of approximately 1000 hr, the tensile strength of the overaged 8% Mn titanium alloy is approximately the same as that of the annealed material tested after only short exposure time.[3] No evidences of embrittlement were reported occurring with this alloy. However, the writer has received unconfirmed verbal reports that other titanium alloys have exhibited marked embrittlement after elevated-temperature service which would indicate that extreme care must be exercised in obtaining complete design data before use is made of these alloys.

6. The cold-worked stainless steels exhibit slight aging tendencies with corresponding slight increases in ultimate tensile strength.[3, 6] However, the major portion of the data is for 100-hr exposure time and the effect of exposure times over 100 hr on the cold-worked stainless steels remains to be determined.

7. The effect of continued exposure time on the mechanical properties of heat-treated steels has not yet been completely determined. It has long been felt that temperatures under the tempering temperatures would not produce any significant change in mechanical properties. A recent Bureau of Standards study[13] on 4340 steel heat-treated to 260,000-280,000 psi in which practically no change in hardness was observed after 200-hr exposure to 400 F would seem to bear out this theory. How-

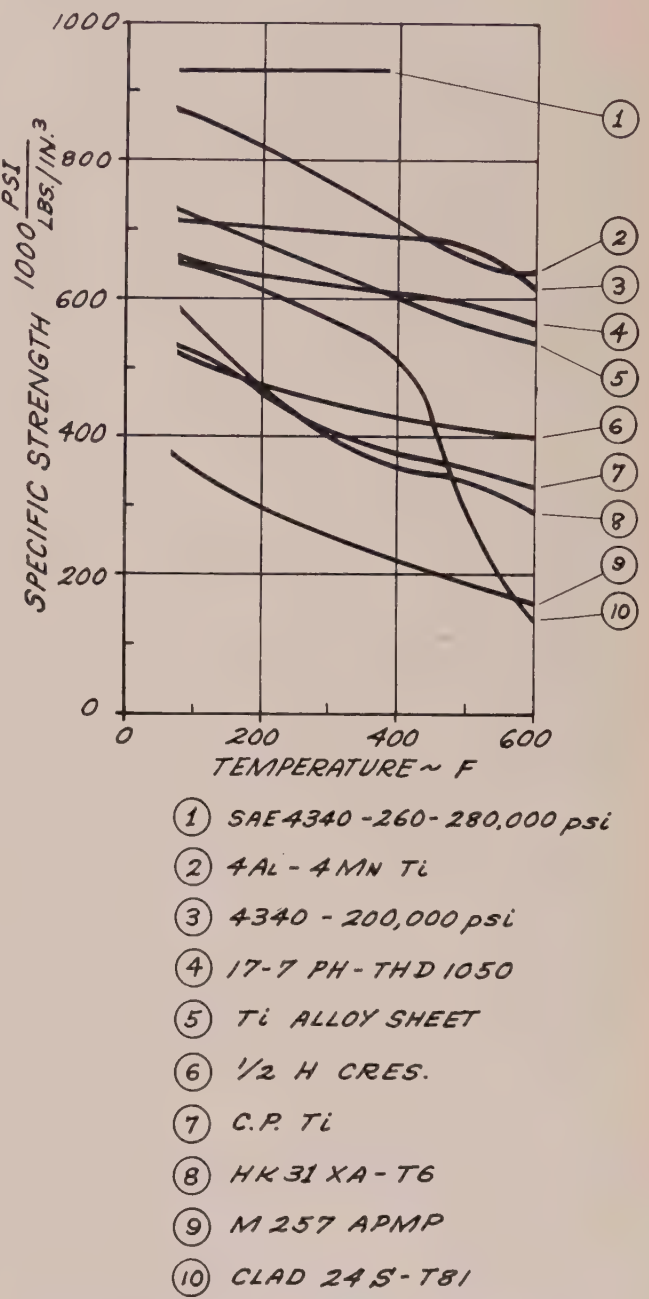

Fig. 2 – Tensile strength/weight ratios at elevated temperatures for several alloys

[8] See *Metal Progress*, Vol. 62, December, 1952, pp. 109-112: "Excellent Products of Aluminum Powder Metallurgy," by J. P. Lyle, Jr.

[9] Letter, 11/3/54, with data sheets attached, from John C. Mathes, Dow Chemical Co., to author.

[10] USS Steel Research Laboratory Report G23 (1949), "Strength of Two Hardened Alloy Steels in Temperature Range 75-700 F." (Supplement to Report 623.)

[11] Lockheed M&P Report 60-224 (1954), "Effect of High Temperatures upon Titanium and Its Alloys."

[12] See "Armco Precipitation Hardening Stainless Steels Technical Data Manual," pub. by Armco Steel Corp., Middletown, Ohio.

[13] See National Bureau of Standards Report TED-NBS-AE-4122 (1954), "Determination of Retained Austenite in Heat-Treated 4340 Steel."

ever, Armour Research Foundation, working with SAE 8630 steel heat-treated to approximately 160,000 psi tensile strength,[3] finds that at 400 and 600 F, an increase in strength occurs up to 10-hr exposure and some softening occurs between 10 and 100 hr. This would seem to indicate that further work must be done to determine the stability of steels, particularly the higher strength heat-treated steels exposed to temperatures somewhat below their tempering temperatures.

8. Based on the absence of any structural changes or precipitants in 17-7PH below 600 F, Armco[12] states that extended exposure time in this temperature range will not affect the elevated-temperature material properties.

Effect of Long-time Exposure

For those applications where maximum loads do not occur at maximum temperatures, but may, in fact, occur at ambient or closely related temperatures, some data are required on room-temperature mechanical properties after elevated-temperature exposure. Outside of the extensive work done on the aluminum and magnesium wrought alloys[4, 5, 9] there is little such data for other materials. Aluminum and magnesium alloys suffer permanent losses in room-temperature properties if exposure temperatures and times deviate from a rather narrow range. Probably every aircraft company which has done some hot forming has carefully established the safe times and temperatures to use in their shop for the common aircraft materials and has built up a library of data on what happens when these conditions are exceeded. There is no reason why these data cannot also be used to signify airplane service conditions and thus guide designers in their choice of materials.

For other materials the data available are very limited. Armco[12] has performed some tests which indicate, as before, that 17-7PH does not undergo any microstructural changes below 600 F, and therefore, the room-temperature properties remain unaffected. The same conclusions can be drawn for annealed commercially pure titanium and the stainless steels, including cold-worked ones. However, no data of this type are available for titanium alloys or the heat-treated alloy steels. Changes in tensile strength of these materials reported in the elevated-temperature tests discussed above indicate that some microstructural changes occur. There is need for more exact data in this field.

Creep

Some knowledge is necessary concerning the behavior of the metals involved under the combined conditions of load, temperature, and time – or, in more common terminology, its creep characteristics. Here a great deal of confusion exists. This may be due in large part to the uncertainty concerning the permissible amount of creep deformation that can be tolerated in various aircraft structures. For example, it has been estimated that ¼ of 1% total creep deformation in the materials used in the construction of a wing may cause sufficient change in the wing contours and angles to affect its aerodynamic performance. Others have recommended 0.2% total deformation as a criterion primarily because of its correlation with room-temperature yield strength. Whether other structures in the airplane can tolerate deformations as large as this or larger is not known yet. However, in the event somewhat larger creep deformations can be tolerated, it is the opinion of many designers that the largest permissible total deformation will probably not exceed 1%. Until such time as more exact information is developed on the total deformations which various parts of the airplane structure can safely tolerate, the above figures are the only ones available for analysis.

Another factor causing some confusion in connection with creep is the many different ways in which creep data are presented. Because a fundamental theory relating microstructure and prior processing to creep phenomena does not exist, a phenomenological approach is used in reporting actual test data for creep behavior. The methods of reporting creep data, therefore, are almost as numerous as the people doing the testing! To illustrate, a few of the methods of reporting creep data are repeated below:

1. Minimum creep rate.
2. Stress to obtain nominal creep rates, such as 0.00001, 0.0001, or 0.001 in. per in. per hr for specified temperatures.
3. Stress to obtain a nominal total deformation, either with or without the initial thermal expansion subtracted at a specific temperature. Furthermore, for some materials the deformation reported is 0.1, 0.2, 0.3, and 0.5%, whereas for other materials, deformation in the order of 1, 2, 3, and 5% are commonly reported.
4. Per cent deformation reached in various time intervals for a given stress through a range of temperatures.

Often, these data are reported in the form of curves, that is, semilog plots of stress to give desired deformation in definite time intervals at a specific temperature, or stress-creep rates at various temperatures or for other combinations of the desired data. Obviously, to obtain a complete set of data on any one material, at all the temperatures involved, is an expensive, time-consuming procedure. It is, therefore, understandable that those involved in creep testing tend to limit their programs to obtain primarily the data that interest them.

In many cases, then, only limited data on any one material are presented, while in a few cases, summary data reports are attempted. In a few cases where different laboratories test similar materials, different lots of materials and minor variations in test procedure or reporting methods, among other things, make such compilations ex-

tremely difficult.

Faced with this situation, that is, data reported in different manners and often irreconcilable, missing or meager data on the materials and temperatures involved, and incomplete testing of normal variations in material composition, the aircraft engineer is extremely hard put to find a basis for analysis and/or selection of the most suitable material for use under creep conditions.

The development of a time-temperature parameter by Larson and Miller[14] with a seemingly universal constant was a step in the right direction. This method allows plotting on one graph, for all temperatures and times, all the desired curves, that is, time to ¼% deformation, time to 1% deformation, creep rates, and the like. The amount of testing to establish the desired curve, the high cost, and long times involved can be greatly reduced. Furthermore, by taking any one desired characteristic such as stress and time to 1% deformation or creep rate, it is possible to plot data for all the relevant materials on one graph. In fact, by using stress divided by density instead of just stress, some sort of creep-stress weight evaluation could be made.

Further work has disclosed some difficulties with this method of attack. Primarily, the use of a universal constant does not always give results which correlate with experimental data.

Other parameters in closer agreement with experimental data have been proposed[15, 16] based upon constants which would be determined for each material from experimental data. A recent report by Heimerl[17] on the relationships between creep time-temperature parameters and creep data of aluminum alloys indicates that the Larson-Miller parameter can be used if the constant is adjusted for each material on the basis of experimental data. Obviously, differences in constants would eliminate strict use of creep-stress-weight ratios for evaluation but it would not preclude their use for rough comparisons.

An attempt was made to provide such a graph for the materials shown in Fig. 2. Unfortunately, the difficulties discussed above were encountered here again, namely:

1. Excellent data on clad 24S-T81.[16]

2. Stress to give nominal creep rates at 2 or 3 temperatures only are available on the zirconium-thorium-magnesium alloy and the aluminum sintered products.

3. Sufficient data on titanium and titanium alloy materials are not available to determine constants which will yield a single curve according to Larson and Miller.

4. Armco[12] states that the creep strength of 17-7PH below 600 F is equal to the elevated-temperature yield strength.

5. Data on heat-treated alloy steels just sufficient to draw a minimum creep rate curve only.

Based on available data, minimum creep rates of clad 24S-T81 and heat-treated 4340 steel were drawn (Fig. 3). Obviously, to make any comparisons between these two materials will require selection of pertinent times and temperature to determine the correct parameter and the desired creep strength/weight ratio.

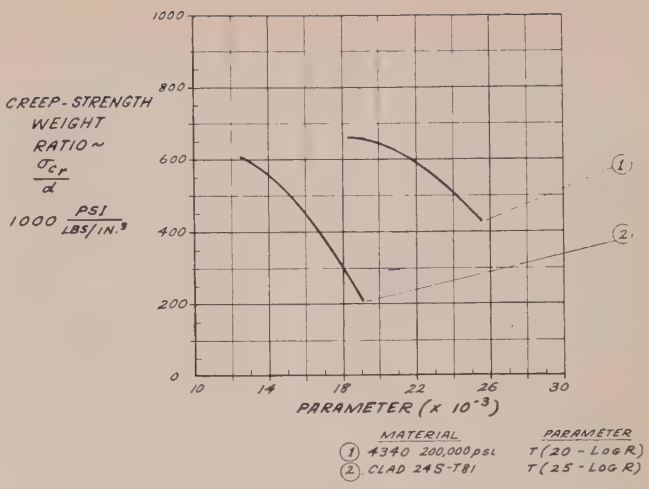

Fig. 3 – Minimum creep strength/weight ratios for two alloys

Intermittent Creep Loadings

So far we have discussed creep data obtained from tests at constant temperature and load. The aircraft designer is cognizant of the cyclic nature of the loads encountered during the service life of an airplane and must know whether the isothermal-constant load data can be directly applied to cyclic conditions, or if there will be either some recovery and/or relief of creep deformation or acceleration of creep damage during the period when the load or the temperature or both are removed. Obviously if some relief does occur during a portion of the cycle, use of isothermal data will be conservative and possibly some advantage could be taken of these effects to provide a more efficient design. On the other hand, if acceleration of creep occurs some allowance must be made in order to prevent any service failure. As pointed out above, unfortunately there is no theory which correlates microstructure, chemical composition, and the like, and creep which can be modified to allow for cyclic conditions. Again, the phenomenological approach in compiling large masses of data must be used.

It is only within the past 6 years and with the advent of the jet-type aircraft engine that this field has received some serious attention. A major portion of the work has, of course, been devoted to the effects of cyclic temperatures and/or loads at temperatures and on materials usually encoun-

[14] See ASME Transactions, Vol. 74, July, 1952, pp. 765-771: "Time-Temperature Relationship for Rupture and Creep Stresses," by F. R. Larson and J. Miller.

[15] See NACA TN-2890 (1953), "Linear Time-Temperature Relation for Extrapolation of Creep and Stress-Rupture Data," by S. S. Manson and A. N. Haferd.

[16] See ASTM Proceedings, Vol. 53, 1953, pp. 693-711: "Time-Temperature-Stress Relations for Correlation and Extrapolation of Stress-Rupture Data," by S. S. Manson and W. F. Brown.

[17] See NACA TN-3195 (1954), "Time-Temperature Parameters and Application to Rupture and Creep of Aluminum Alloys," by G. J. Heimerl.

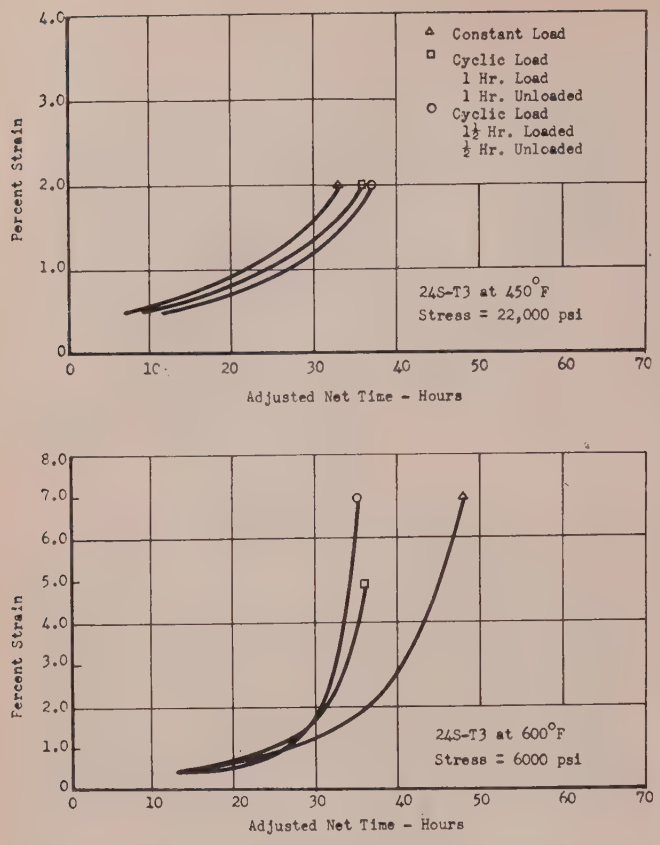

Fig. 4 – Composite curves of strain versus adjusted net time under load for constant and intermittent loading on 24S-T3 aluminum alloy

tered in jet-engine powerplants.[18] The data for metals, temperatures, and times typical of conditions which will be encountered in aircraft structures in the near future are very limited. A recent study by Shepard, Starr, Wiseman, and Dorn[19] emphasizes the need for more exact information in this field.

From their tests, Shepard, Starr, Wiseman, and Dorn concluded that on the basis of total test time, creep was more rapid under constant-load conditions than under either of the two cyclic conditions they used. However, a review of their data, particularly of creep under net times under load does not indicate a consistent pattern. For example, Fig. 4 (reproduced from Fig. 51 of their report) indicates that 24S-T3 at 450 F and at a stress of 22,000 psi has a greater rate of creep under constant load conditions than under cyclic conditions. At 600 F and 6000 psi, however, the cyclic conditions produce a greater creep deformation. The need for more detailed information on the behavior of all materials considered for aircraft structures under cyclic condition in pertinent ranges of temperature and load conditions is evident.

Compression-Type Loading

Heretofore, all our discussion has been based on tensile comparisons. However, tensile design occupies a small portion of load-carrying members of a modern airplane, that is, about one-third to one-half. Approximately one-third to two-fifths of the load-carrying members are designed as compression members, that is, columns, plates, and the like. For this type of loading two mechanical properties, the elastic modulus and the compression yield strength, plus the geometry of the members complicate the design study.

Some attempts have been made to analyze the structural efficiency of various materials, as columns and plates, both at room and elevated temperatures, by the use of dimensionless parameters to offset geometrical effects. Thus Heimerl and Hughes[20] have been able to show, for various types of members, that is, short and long columns and narrow and wide plates, the temperature ranges in which each of the materials analyzed, that is, 8% Mn titanium alloy, 4Al-4Mn titanium alloy, precipitation-hardening steel, heat-treated 4340 steel, and Inconel X, have the highest structural index.

The analysis performed by Heimerl and Hughes is based on the short-time elevated-temperature properties only with no attempt to consider creep effects. The methods of analyzing compression members under creep conditions to enable prediction of allowable loads, deformations or life under load has received considerable attention in the past few years.[21-27] The procedures presented in these studies do not agree completely with the limited tests which have been run to illustrate some of the theories developed. Considerable hope has been expressed that the use of the "isochronous stress-strain curves," wherein stress is plotted against values of creep strain for constant values of time, and the corresponding "isochronous tangent modulus curve" can be developed to a usable level. This would permit the use of techniques similar to the current methods for room temperature compression study and design. The conservative values obtained by using this technique reported by Baer[27] indicate that probably this method, too, will require some modification in order to be applicable. However, until sufficient test data are developed which indicate an accurate method of analysis, any comparison of the structural efficiencies of materials in this type of application seems out of the question.

Almost no attention has been paid to plates or to those members where stiffness is a factor (note – approximately 24% of the structure of a modern airplane is designed on this basis), or where both tension and compression loads act together.

---

[18] See Cornell Aeronautical Laboratory Report KH-702M-6 (1952), "Effects of Overheating and Overstressing of Metals."

[19] See WADC Technical Report 53-336 (1954), "Part 1—Creep Properties of Metals under Intermittent Stressing and Heating Conditions," by L. A. Shepard, C. D. Starr, C. D. Wiseman, and J. A. Dorn.

[20] See NACA TN-2975 (1953), "Structural Efficiencies of Various Aluminum, Titanium, and Steel Alloys at Elevated Temperatures," by G. J. Heimerl and P. J. Hughes.

[21] See WADC Technical Report 52-251 (1952), "Investigation of Compressive-Creep Properties of Aluminum Alloys at Elevated Temperatures," by R. L. Carlson and A. D. Schwope.

[22] See NACA Research Memorandum L53EO4a (1953), "Preliminary Investigation of Strength Characteristic of Structural Elements at Elevated Temperatures," by E. E. Mathauser and C. Libove.

It should be noted that all the techniques for compression analysis discussed above assume that tension creep data can be used in compression design. This assumption is based on the fact that a metal deforms as a result of the resultant stress and it does not know or care whether the resultant stress acts in a tensile or compressive manner. This explanation usually does not satisfy the aircraft engineer, for he is only too familiar with the numerous materials he commonly uses in aircraft design which have different tensile and compressive yield strengths at room temperature. Thus, until some experimental data are obtained to show that the behavior of materials under tensile and compressive creep is sufficiently similar to permit their interchangeability, any methods of computing compression creep behavior with tensile creep data will be skeptically received.

Thermal Stresses

Up to now this discussion has dealt mainly with the effects of mechanical properties and structural requirements upon material selection. No elevated-temperature design study can be considered complete until some consideration is given to those stresses induced by thermal expansion and thermal gradients. Obviously this will be a factor regardless of which material is used, unless a structural material is developed which has a zero coefficient of expansion throughout the temperature range involved. A discussion of thermal stresses, however, is beyond the scope of this paper and will not be undertaken.

Manufacturing Influences

The influence of manufacturing considerations on the selection of a material must be added to the factors already discussed. A few of the major manufacturing problems which may influence the selection of a material are discussed briefly:

1. Formability: The ability to form a material to the contours and shapes of a modern airplane is of prime concern, not only to the manufacturing division of an airplane company but also to the cost-conscious design engineer. If techniques and processes already developed cannot be used, the development of new techniques and/or equipment is a costly procedure. It is readily understandable why, for example, there is such a reluctance to engage in large-scale hot-forming operations with the attendant costly handling and equipment problems. Instead, room-temperature forming of relatively ductile materials which can be hardened with relatively low-temperature processing is usually preferred.

Furthermore, the introduction of a new material with entirely new formability characteristics requires the costly development of new design limitations. On the other hand, a new material which in its formable stage has forming limitations almost identical with an already established material is usually desired. This preference is due to two factors: first, the ability to use existing design criteria and thus minimize the costs attendant with developing new design limits, and second, the familiarity of the aircraft designer with the existing design limits which permits him to design a component without having to learn a whole new set of rules.

The choice of a material for a longeron operating at an elevated temperature will serve to illustrate the effect of formability upon the selection of a material. The operating temperature was one at which 17-7PH and the 8% Mn titanium alloy had approximately the same strength-weight ratio. However, to obtain the desired bend radius, the titanium alloy would have to be hot-formed, whereas the 17-7PH could be formed at room temperature in the solution-quenched condition and then aged to obtain the required mechanical properties. The final choice was 17-7PH.

2. Availability: There is great reluctance to incorporate a new material into the design of a production airplane unless some assurance is given that not only can the total quantity of material required be produced, but also that it can be produced in sufficient quantities in the time required to meet production schedules. Furthermore, production of this material must be such that in the event of an unusual jump in production quantities and/or schedules, there will be enough material available to avoid the necessity of suddenly finding acceptable substitutes.

3. Cost: Normally, the cost of the material is a small fraction of the cost of a finished part and receives only nominal attention except to assure the avoidance of unusually expensive items. However, when a material costs many times per pound as much as a competitive material, the comparative cost of a finished part may be further increased because of scrap, die trim, fabricating costs, etc. Despite large weight savings which might be achieved through the use of the more expensive material if the cost per pound of weight saved is high, its use might be discouraged.

It will be worth while to digress for a moment to mention what an aircraft company might be willing to pay in order to save a pound of weight. A figure of $20 per lb of weight saved is usually quoted. However, it must be remembered that this is a fictitious number depending upon many factors, among which are the status of design, the relationship of airplane weight to design weight, and the effect of lower weight on airplane performance. Thus at any specific time, a pound of weight saved may be worth from zero to several hundred dollars.

---

[23] See NACA TN 3139 (1954), "Time-Dependent Buckling of Uniformly Heated Column," N. Ness.

[24] See NACA TN 3137 (1954), "Creep Bending and Buckling of Nonlinearly Viscoelastic Columns," by J. Kempner.

[25] See NACA TN 3204 (1954), "Investigation of Creep Lifetime of 75S-T6 Aluminum-Alloy Columns," by E. E. Mathauser and W. A. Brooks, Jr.

[26] Rand Corp. Report P-498 (1954), "Method for Determining Effects of Elevated Temperature on Structural Design and Weight," by W. R. Nicks.

[27] Hughes Aircraft Co. Research & Development Laboratories Technical Memorandum 306 (1953), "Very-Short-Time Creep Buckling," by H. W. Baer.

Considerations Affecting the Life of

WORK done in a development program relative to camshafts and tappets in the design of the Chrysler overhead-valve V-8 engine is described. The types of failure encountered are categorized as wear, scuffing, and fatigue.

An accelerated test procedure was designed to promote early cam-tappet failures, and the development work was predicated upon the results obtained therefrom.

Among the variables affecting the failure conditions, major emphasis was placed on material development. Specifically, the greater amount of time was spent in determining the optimum tappet material, while some time was devoted to the camshaft material. A combination of adjusted chemical composition and heat-treatment of hardenable cast iron for camshaft and tappets provided the best solution to the failure problems.

DURING our development program to produce overhead-valve V-8 engines as opposed to the in-line engines formerly offered, considerable attention was focused on the performance of such engines. Unfortunately, the information available was meager since only two V-8 overhead-valve engines were then in production and both had been produced for a relatively short time. Due to the greater valve gear load requirements inherent in the design, it was recognized early that camshaft and valve tappet durability should be carefully evaluated.

Preliminary tests indicated that performance of both valve lifters and camshaft could be intensely sensitive to slight variations in design, material, lubrication, surface finish, surface coatings, and other factors. These prophecies were later fulfilled, and it was found that this tendency was generally common to V-8 overhead-valve engine designs.

The design was dictated largely by performance and test results. Initial selection of surface finishes and surface coatings was based not only on the results of tests, but also reflected experience on other

Automotive Camshafts and Tappets

M. F. Garwood, D. R. Kinker, and J. J. Manganello, Chrysler Corp.

This paper was presented at the SAE Golden Anniversary Passenger-Car, Body, & Materials Meeting, Detroit, March 2, 1955.

production engines. Initial material selection was influenced by design, test, experience, and somewhat by availability.

Introductory engines contained an alloy cast-iron camshaft and hydraulic valve tappets whose bodies were fabricated from chilled cast iron. Complete specifications for the pertinent engine components are shown in Table 1.

These specifications were quite satisfactory for the introductory engine. However, constant demands for increased engine performance demanded greater valve gear durability. A program designed to improve the durability of both camshaft and valve tappets was therefore inaugurated early in 1951.

Characteristics of Failures

In severe test-car operation, failures were most often encountered at less than 10,000 miles and occasionally at less than 5000 miles. In our experience those occurring at mileages above 15,000 miles were infrequent.

Camshaft distress was normally evidenced by several symptoms of improper operation:

1. Valve-seating (tappet) noise.
2. Reduced engine power.
3. Engine misfire.
4. Backfiring through intake system.
5. Reduced top engine speed.

Exhaust cam lobe failures can produce any of

Table 1 – 1951 Production Camshaft and Lifter Specifications

	Camshaft	Lifter
Material	Alloy cast iron	Chilled iron
Total Carbon, %	3.10 to 3.40	3.30 to 3.55
Manganese, %	0.50 to 0.80	0.85 to 1.10
Silicon, %	2.10 to 2.40	2.40 to 2.90
Chromium, %	0.60 to 1.00	—
Molybdenum, %	0.40 to 0.60	—
Hardness, Rc (min)	50	52
Surface Coating	Lubrite	Lubrite
Surface Finish, microin.	50 max	4 prior to coating
Cam Taper	0° 4′ 35″ to 0° 7′ 38″	—
Lifter Radius, in.	—	30
Offset, in.	0.050 nominal	
Valve Spring Load, lb	60 (valve closed)	165 (valve open)

these symptoms, while intake cam lobe wear does not cause backfiring. This probably accounted to a large degree for the discovery of nearly two exhaust cam failures for every intake cam failure. Laboratory testing actually showed a lower ratio of exhaust to intake cam lobe failures.

Before going further it should be mentioned that all failures could be roughly grouped into three classifications: those resulting from wear, those initiated by scuffing, and those caused by fatigue.

Wear was considered to be gradual deterioration by friction, and in this paper is considered the gradual and smooth loss of surface metal by friction. This definition is, for practical purposes, identical to that stated by Ambrose and Taylor.[1]

Scuffing was considered more severe than wear. The deterioration was not in the same sense gradual and uniform, but was characterized by deep grooves, rapid surface roughening, welding, and tearing away of surface metal. This was the most common failure encountered and the most important to correct.

Fatigue was construed as the tendency of a metal to chip or break up under conditions of repeated cyclic stressing considerably below the ultimate strength of the material. This failure has alternately been described as pitting, spalling, and flaking, and is typical of those found on chilled cast-iron tappets tested.

Examples of these types of failure are shown in Fig. 1. Representative photographs of wear, scuffing, and fatigue, respectively, are shown from left to right and identified as *A, C,* and *E*. Directly below each photograph is a photomicrograph showing more details of the characteristic failure. The photomicrographs are identified as *B, D,* and *E*.

When considering engines equipped with automatic-adjusting tappets, the only distress of consequence to engine operation is recognized to be cam lobe wear. Such a condition invariably results from a mutual scuffing of cam and tappet contact surfaces; the tappet deterioration, however, is not always severe.

Although generally manifested as a low-mileage failure, test-car operation showed that scuffing of cam and tappet surfaces can occur at any mileage and from various causes. Usually, only two or three cams on a shaft will show any distress, the remaining cams and tappets being in good condition. Fatiguing or spalling of either or both of the components may produce eventual failure by scuffing and often precede such a failure.

Other factors affecting the scuffing tendency are unit stress, geometry, surface finish, antiscuff coatings, material processing or structure, lubrication, and lubricant types.

In addition to failure by scuffing and the closely associated fatigue-type failure, a condition of abnormally high smooth wear on all cam lobes occasionally occurs. This latter condition causes a lowering of engine performance and usually results from a combination of unfavorable operating conditions and lubricant.

In some instances it appeared that metal fatigue was enhanced by chemical attack and might better be described as a type of corrosion fatigue. This type of fatigue has also been referred to as "oil fatigue." It is a spalling condition similar to normal-appearing metal fatigue with the following exceptions:

1. Pieces breaking out of the surface are generally smaller and shallower in depth.

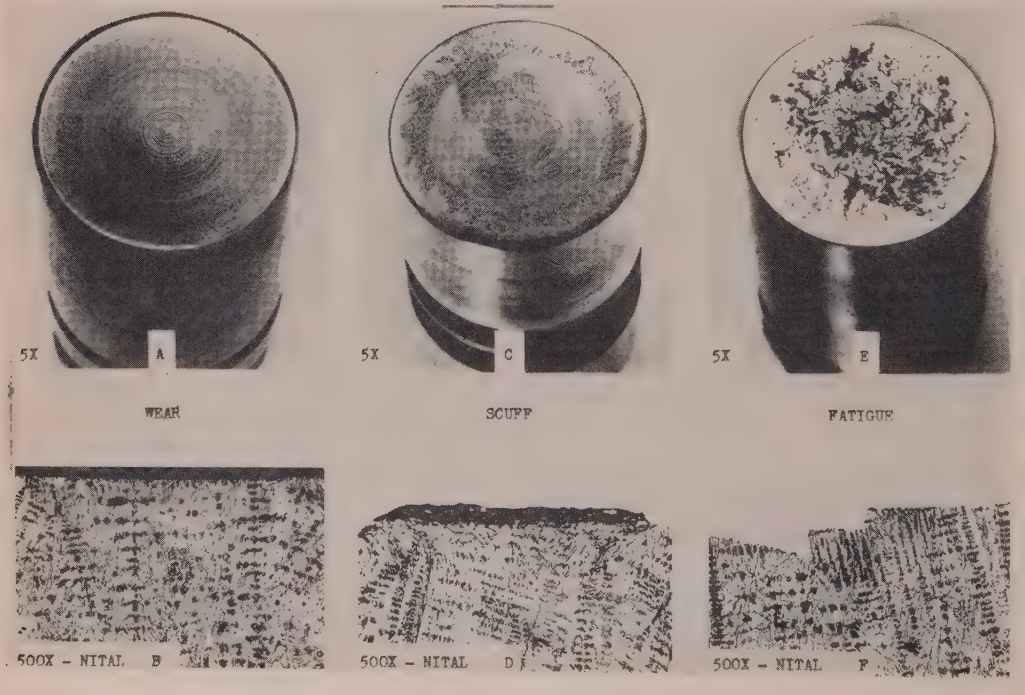

Fig. 1 – Examples of typical failure types discussed (photo micrographs reduced)

2. Edges around the fatigued area are rounded and smooth, as if healing.

3. When fatigue progresses to a severe state (covering one-half of the face or more), it forms a swirl-type pattern in the fatigued area.

4. A lightening in color of the tappet face usually precedes the fatigue condition and tends to surround the failed area after fatigue begins.

The name "oil fatigue" was coined because the condition of failure described was promoted entirely by specific oils and oil additives. This failure was obtained only with chilled cast iron and was never evidenced when using identical oils with hardenable cast-iron tappet material.

Description of Engine Test Procedure

Primary testing was carried out on engines incorporating the design and materials shown in Table 1, which were standard at that time. These engines operated on a schedule covering a wide speed range. Occasional failures were produced; however, results were inconsistent and slight improvements appeared to eliminate failures completely. Inconsistencies between laboratory and road tests prompted the initiation of modified schedules. These test schedules incorporated exaggerated requirements designed to promote early cam-tappet failures.

After testing a variety of operating conditions, a form of standard accelerated-failure schedule was developed. The provisions of this test are shown in Table 2, schedule *a*.

As shown, it includes an engine speed of 1200 rpm, no load engine output, 200 F oil temperature, and 180 F water temperature. The oil employed was Shell X-100 5W, their 1952 formulation. The valve spring load was 150% of standard, and the engine was run for 2 hr and then shut down 1 hr, during which time cold water was circulated through the block to cool both the engine and oil as much as possible. Inspection periods were established after each 40 hr of running, or 60 hr total time.

Later a second test schedule, *b* in Table 2, was attempted which provided an even more severe scuffing tendency. This schedule included an engine speed of 3600 rpm, no load engine output, 200 F oil temperature, and 180 F water temperature. The oil and valve spring loads were not changed. The operating schedule was to run 2 hr and then shut down 1 hr, during which time the engine and oil were cooled by circulating cold water through the block. Inspection periods were established after each 6 hr of running, or every 9 hr total time.

Important features of the test schedules shown in Table 2 are the increased valve spring load, operating speed and load, and the lubricant.

Table 2 – Accelerated Test Schedules

Break-in Time – None

Conditions:

Schedule	(a)	(b)
Engine Speed, rpm	1200	3600
Engine Output Load	0	0
Oil Temperature, F	200	200
Water Temperature, F	180	180
Lubricant	Shell X-100 5W (1952)	Shell X-100 5W (1952)
Valve Spring Load, % of standard	150	150

Operation:

Run 2 hr at specified conditions. Shutdown 1 hr during which time engine is cooled to 60 F oil and 50 F water temperatures. Repeat cycle.

Duration of Test:

When using 1200-rpm schedule, inspections of camshaft and tappets were made after each 40 hr of running (60 hr total time). With 3600-rpm schedule, inspections were made after 6 hr running (9 hr total time).

The valve spring load of 150% of standard at valve-open position provided a proportional increase in stress at critical contact areas. Speeds of 1200 and 3600 rpm were selected after tests at a variety of speeds showed those to exhibit the most desirable results. Engine output load was found to be inconsequential. Shell X-100 5W was selected as the test lubricant because it was the lowest viscosity oil available at that time.

The 1200-rpm accelerated engine-test schedule consistently produced failures which were judged to be equivalent to and typical of test-car failures we had witnessed. Severe cam-tappet scuffing with and without tappet fatigue, and tappet fatiguing without scuffing were readily created, generally within the first 40 hr of the test cycle. Approximately three out of four test runs produced a failure within 40 hr, and the majority of the remainder did so in 80 hr, only infrequent runs lasting past a total of 80 hr. These data are based on a total of approximately 43 test runs, of which 10 resulted in scuffing failure without tappet fatigue, 9 in failure with tappet fatigue, and 4 in tappet fatigue only in 40 hr. Similar failures occurred in 11 shafts after 80 hr, except that a larger number were fatigue-type failures. A total of only 3 shafts showed no signs of failure at 80 hr.

The 3600-rpm accelerated-failure schedule was consistently more severe than the 1200-rpm schedule. Fatiguing of tappets seldom occurred due to the short period of running and the high wear rate brought about by this very severe schedule. Because of its severe scuffing tendency, this procedure was never considered to be equivalent to field test operation; however, it did provide a good means of short time comparison.

Except as noted, the evaluation of all variables was performed using the 1200-rpm test schedule for comparison. Although physical measurements were obtained and recorded for all important tests, the criterion for judging performance was primarily visual inspection. This procedure was the most

[1] See SAE Transactions, Vol. 63, 1955, pp. 192-203: "Wear, Scuffing, and Spalling in Passenger-Car Engines," by H. A. Ambrose and J. E Taylor.

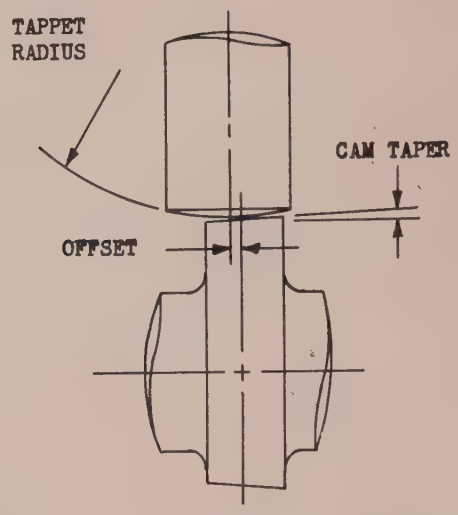

Fig. 2 – Cam-tappet contact geometry

	TAPPET DESIGN	NOMINAL CAM TAPER	CONTACT OR CENTERLINE OFFSET	RELATIVE UNIT PRESSURE
A (STD.)	30" SPHERICAL RADIUS	0° 6'	.050 IN.	1.00
B	60" SPHERICAL RADIUS	0° 3'	.050 IN.	0.88
C	FLAT FACE (FULL CONTACT)	NONE	1/32 IN.	0.58
D	30" CROWN – FLAT	0° 6'	.050 IN.	—

satisfactory because of the nature of the failures produced by the severe test schedules employed.

Evaluation of Variables

Effect of Increased Lubrication – Initial investigations included a brief study of the effect produced by varying only the amount of lubrication. In one type of test, the effect of pre-assembly lubrication was evaluated by oiling only one half of the camshaft by dipping it into the Shell X-100 5W crankcase fill oil before installation in the engine. The other half of the camshaft was left dry. Approximately 10 engine test runs in which this procedure was followed failed to show any distress pattern that would correlate with the oiling procedure. Failures occurred indiscriminately on the oiled and dry portions of the camshafts alike.

In the second type of test, the effect of increased lubrication during engine operation was evaluated. This was accomplished by means of an accessory oil manifold having individual "squirt" tubes aimed at each cam and tappet location so that the cam and tappet face areas were flooded with lubricant. Again no appreciable improvement in failure tendency was noted as a result of increased lubrication in the two test runs made.

Effect of Camshaft Surface Finish – Camshaft surface finish was found to be a very significant factor influencing the cam scuffing tendency. It was observed never to have any effect on tappet fatigue tendency. As shown in Table 1, the original specification for cam surface finish was 50 microin. maximum. A series of comparison test runs readily demonstrated an appreciable improvement by reducing the maximum allowable surface finish to 30 microin. Later testing and investigation of production procedures showed that a further reduction was both possible and practical, and a specification of 20 microin. maximum surface finish was adopted. A total of 26 test runs were made in reaching these conclusions. Of those, 16 were made using cams having 40-60 microin. finish, of which nine suffered a cam failure, and ten test runs were made using cams having 10-25 microin. finish, of which only three resulted in cam failures. Subsequent attempts to improve the scuffing resistance by additional surface finish modification were without benefit.

Effect of Design Modifications – Modifications in the cam-tappet contact geometry were tested extensively. Standard geometry and changes included in this test program are shown in Fig. 2.

A will be recognized as the standard 30-in. radius spherical tappet originally adopted

B is a 60-in. radius spherical crown tappet

C is a "full contact" flat-faced tappet used to provide minimum unit pressure, and many modifica-

tions of this basic design were evaluated for the purpose of increasing rotation. Edge loading was prevented by either hyperbolic tappet body contour or increased tappet bore clearance.

D is a combination crown-flat design tappet face. Basically it is a 30-in. radius spherical design with a ½-in. diameter flat in the center of the tappet face.

Although tested on several occasions using various material combinations and in different engines, the 60-in. radius crown tappets used to promote reduced unit pressure never provided any benefit. Actually, when tested with a hardenable cast-iron tappet and camshaft combination, the 60-in. crown was judged to be inferior to the 30-in. crown with identical materials. This comparison was especially noticeable when made using the 3600-rpm accelerated-test schedule. Appearance of tested components and type of failure indicated the possibility of poorer lubricant-film-forming characteristics with the 60-in. design as the cause of its inferior performance.

The combination crown-flat tappet face design was tested once but showed no benefit in the single test.

The "full contact" geometry was tested on a large scale. Preliminary tests showed it to have excellent possibilities for providing a practical solution to the cam distress problem. Both scuffing and fatigue tendencies appeared to be materially reduced. Several test runs were made in which time to failure was increased from an average of 40 hr using standard geometry, to approximately 200 hr with "full contact" geometry.

Following the preliminary runs, extensive testing of the "full contact" design was begun employing a group of six DeSoto V-8 engines. Conclusions drawn from the results obtained follow:

1. Tappet rotation was poor, and an unsatisfactory wear pattern developed whenever the tappet did not rotate. Occasionally a cam failure originated from non-rotation.

2. Improved tappet rotation could be obtained by providing a cam tappet centerline offset of a minimum of 1/16 in. The 1/16-in. offset was obtained partially by narrowing the cam lobe, which reduced the benefits of this design because it increased unit pressures.

3. With chilled cast-iron tappet material, the "full contact" design, although theoretically reducing the maximum tappet-face stress, was unsuccessful in reducing tappet-face fatigue and showed very little improvement in scuffing tendency.

4. Two tappet body designs were found to provide satisfactory aligning characteristics. The hyperbolic or barrel shape design retained the normal 0.0005-0.0015-in. tappet bore clearance as a minimum value, was capable of maintaining alignment with the cam lobes, and cancelled the effect of any nonsquareness that might exist. Reducing the tappet body diameter also allowed for misalignment correction by means of a 0.0015-in. additional tappet bore clearance.

5. Rounding of the cam lobe edges was not found to be absolutely necessary; however, results indicated that this feature was desirable if it could be satisfactorily incorporated in the design.

6. The outstanding deficiency which most discouraged a further evaluation of the "full contact" design was the excessive tappet-face fatigue tendency. Such a result was, of course, completely unexpected and without explanation. Every means possible was used to eliminate this difficulty, but none was successful.

The introduction of new tappet materials having reduced fatigue tendency might solve the problem

Table 3 – Tappet Body Materials

Steels:	Treatment	Case Depth, in.	Face Hardness, Rc	Face Coating	Results
Nitralloy Type 135G	Nitrided 12 hr at 975 F	0.015	60/68	Electrofilm	Increased scuff
Graphitic Steel	Induction hardened	0.080	58/63	Cadmium plate or lubrite	Increased scuff
51410 Stainless	Unknown	—	61/62	Electrofilm	Increased scuff
SAE 5120	Gas carburized at 1700 F, oil quenched, tempered at 350 F	0.060	57/59	Electrofilm or lubrite	Increased scuff
SAE 1137	Gas carburized at 1700 F, oil quenched, tempered at 350 F	0.080	61/64	Electrofilm or lubrite	Increased scuff
Cast Irons:					
Pearlitic Malleable	Induction hardened	0.080	54/58	Electrofilm	No change
Acicular	As cast	—	260 Bhn	Cadmium	Slight increased fatigue
Hardenable Alloy	Furnace hardened at 1550 F, oil quenched, tempered at 350 F	—	55/60	Lubrite	Decreased fatigue and scuff
Hardenable Alloy	Induction hardened	0.080	55/60	Lubrite	Decreased fatigue and scuff
Chrome-Vanadium Chill	—	—	56/58	Steam treated	No change
Chrome-Moly Chill	—	—	59/61	Steam treated	Increased fatigue
Chrome-Moly Chill	Stress relieved	—	59/61	Steam treated	No change
Standard Chill	Stress relieved	—	56/58	Steam treated	No change
Standard Chill	Shotpeened	—	56/58	Cadmium	Increased fatigue
Standard Chill	Reduced grinding feed	—	56/58	Steam treated	No change
Hard Facing:					
Colmonoy	Puddled	0.010/0.015	56/60	—	Increased scuff

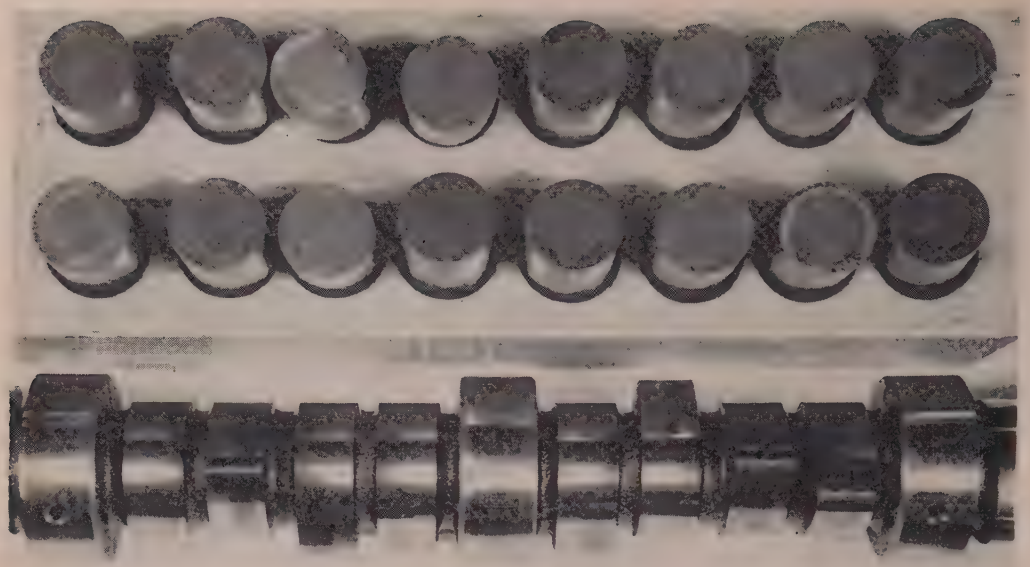

Fig. 3 – Scuff-type failure obtained using commercial oil No. 1 containing additive A. Running time: 40 hr

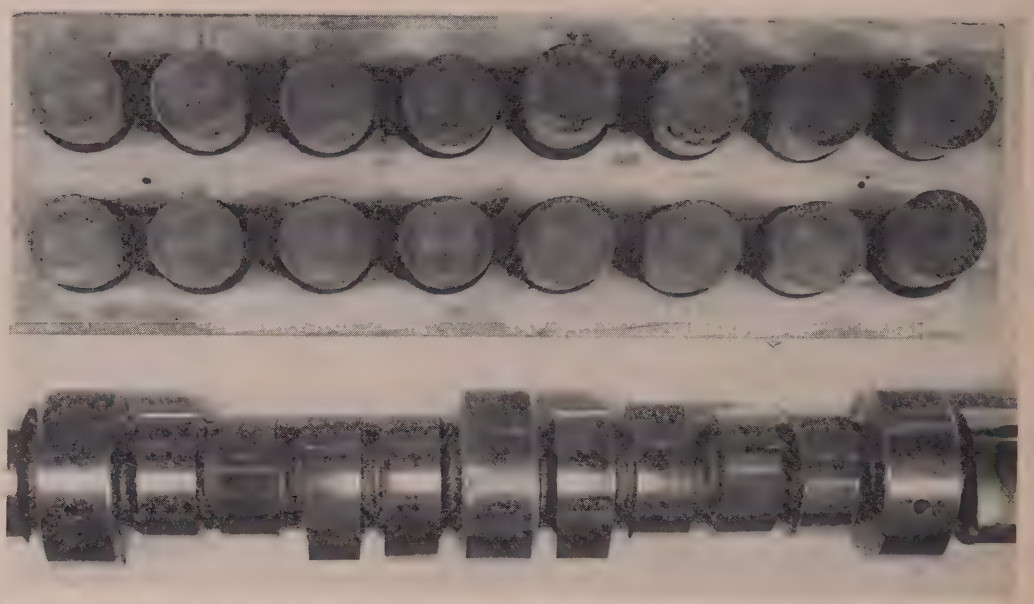

Fig. 4 – Scuff-type failure obtained using test oil No. 1 containing additive A only. Running time: 20 hr

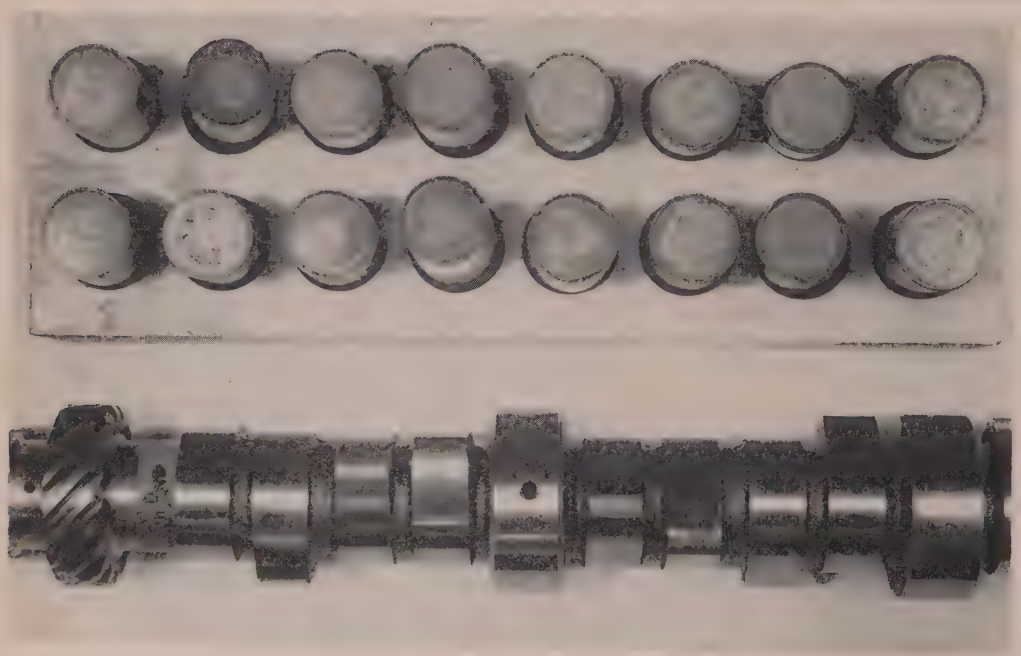

Fig. 5 – Fatigue-type failure obtained using commercial oil No. 2 containing additive B. Running time: 40 hr

of fatigue associated with the "flat face" geometry. A single test run which showed merit from the standpoint of promoting tappet rotation incorporated the use of a slight amount of cam taper instead of large values of centerline offset.

Tappet rotation is a variable frequently discussed with regard to its effect on cam-tappet distress. The observations we have made of both laboratory and road-test engine operation have impressed us of its importance. When non-rotation of the tappet occurs, both the low- and high-mileage scuffing tendencies are increased. A satisfactory "wearing in" is far less likely without tappet rotation, and the commonly observed non-rotation "ditch," which develops after increased running or at higher mileage, has been observed to cause cam scuffing failures.

Effect of Material Modifications – Testing of material modifications dominated a large portion of the nearly 4-yr test program. After it was determined that, among other things, the amount of lubrication, surface finish, and surface coatings did not offer the desired improvement, the possibility of realizing such improvement by means of material changes was introduced. Test results clearly show that material changes were major improvements and offered the greatest benefits of any modification considered.

Only a comparatively limited amount of testing was done on camshaft material evaluation. Materials tested included higher as-cast hardness hardenable cast iron and steel.

The higher hardness cast iron provided the anticipated benefits of increased fatigue and wear resistance but did not affect scuffing resistance.

Steel camshafts were tested with chilled and hardenable cast-iron and steel tappets. In combination with chilled cast-iron tappets, steel camshafts showed an increased resistance to scuffing and wear and no tendency towards cam fatigue. Steel camshafts with hardenable cast-iron tappets were unsatisfactory due to a greatly increased scuffing tendency; however, the high wear resistance of steel cams allowed little lift loss to result. Steel tappets on steel camshafts were also unsatisfactory due to increased scuffing tendency, but again, the amount of cam lobe wear was actually slight.

Table 3 shows a detailed list of tappet body materials, conditions tested, and results obtained when their performance is compared with that of chilled cast-iron tappets.

A careful study of Table 3 will show that the only tappet materials among approximately 15 types tested which showed any improvement over standard chilled cast iron was hardenable cast iron. The improved resistance to fatigue and scuffing demonstrated in preliminary tests prompted a more extensive evaluation of the hardenable cast iron material, and a development program ultimately totaling 40 runs and a total of approximately 6000 hr followed. From these data a general performance evaluation similar to that already described for chilled cast iron can be provided. Approximately one out of 20 test runs produced a failure within 40 hr, three out of 20 in 80 hr, and four out of 20 in 120 hr. Thus, only one out of five failed while running 40 hr longer than the time in which four out of five chilled iron sets failed. Of the remaining four out of five hardenable cast iron runs made without failure, the majority ran over 120 hr, with total test time running as high as 1000 hr on one run.

Table 4 – Effect of Coatings on Camshafts and Tappets

	Results
Tappet Coatings:	
Steam-Treated Chilled Cast Iron	Decreased scuff
Lubrite Coated Hardenable Cast Iron	Decreased scuff
Uncoated Hardenable Cast Iron	Slightly decreased scuff
Cadmium-Plated Hardenable Cast Iron	Decreased scuff
Electrofilmed Hardenable Cast Iron	Slightly decreased scuff
Steam-Treated Hardenable Cast Iron	Increased fatigue and slightly decreased scuff
Camshaft Coatings:	
Uncoated	Decreased scuff
Brass Plated	Decreased scuff
Chrome Plated	Decreased scuff
Copper Plated	Decreased scuff

It can also be seen readily from Table 3 that tappets made of steel generally suffered scuff-type distress, while iron materials other than hardenable cast iron were poorer due to increased fatigue tendency.

Effect of Coatings – Several coatings were tested on camshafts and on tappets using both chilled cast iron and hardenable cast iron.

Original specifications provided a lubrite coating on both the hardenable cast-iron camshaft and the chilled cast-iron tappet face. Table 4 compares the performance of various cam and tappet coatings with this standard combination.

The brass, chromium, and copper-plated camshafts were tested briefly and on a mild schedule (standard spring load and short duration), which tends to make those results less valid.

It is evident that an uncoated camshaft combined with either a steam-treated chilled cast-iron tappet or lubrite-coated hardenable cast-iron tappet provides the best performance.

Effect of Lubricants – The investigation of lubricant effects was carried out on a systematic basis in an effort to provide information on specific questions. Results will be discussed in groups as follows:

1. Base oils and factory fill oils.
2. Commercial oils and specific additives.
3. Tappet material.
4. Break-in oil.
5. Oil viscosity.
6. Oil sample analysis.
7. Laboratory bench tests.
8. Leaded gasoline.

1. Base oils and factory fill oils: This phase of the testing was concerned with oils containing little or no additive. In general, oils in this category

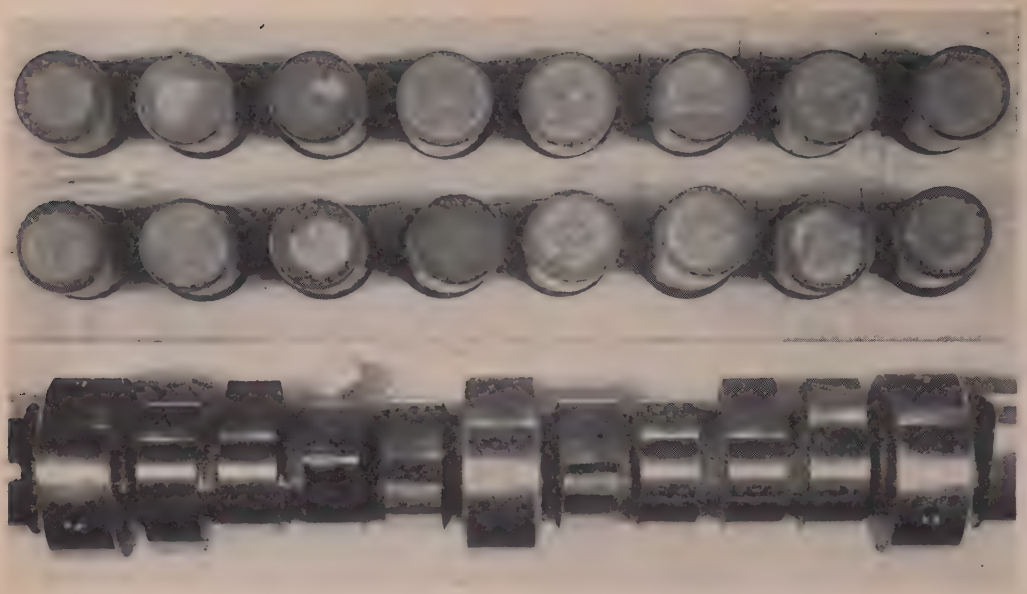

Fig. 6 – Fatigue-type failure obtained using test oil No. 2 containing additive B only. Running time: 40 hr

Fig. 7 – Neutral-type condition obtained using commercial oil No. 3 containing additive contents equivalent to oils Nos. 1 and 2. Running time: 120 hr

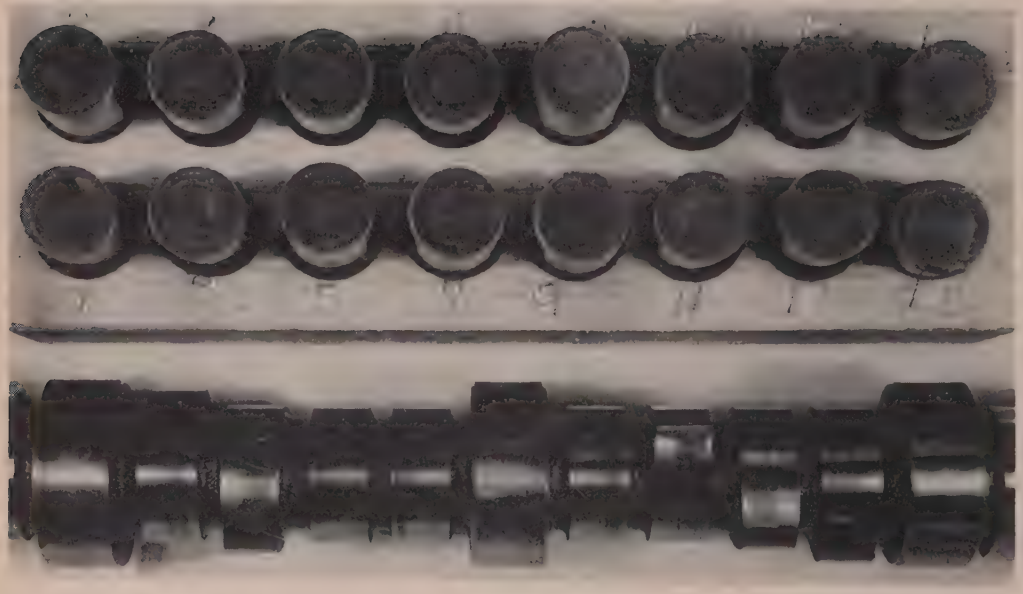

Fig. 8 – Neutral-type condition obtained using test oil No. 3 containing no additives. Running time: 160 hr

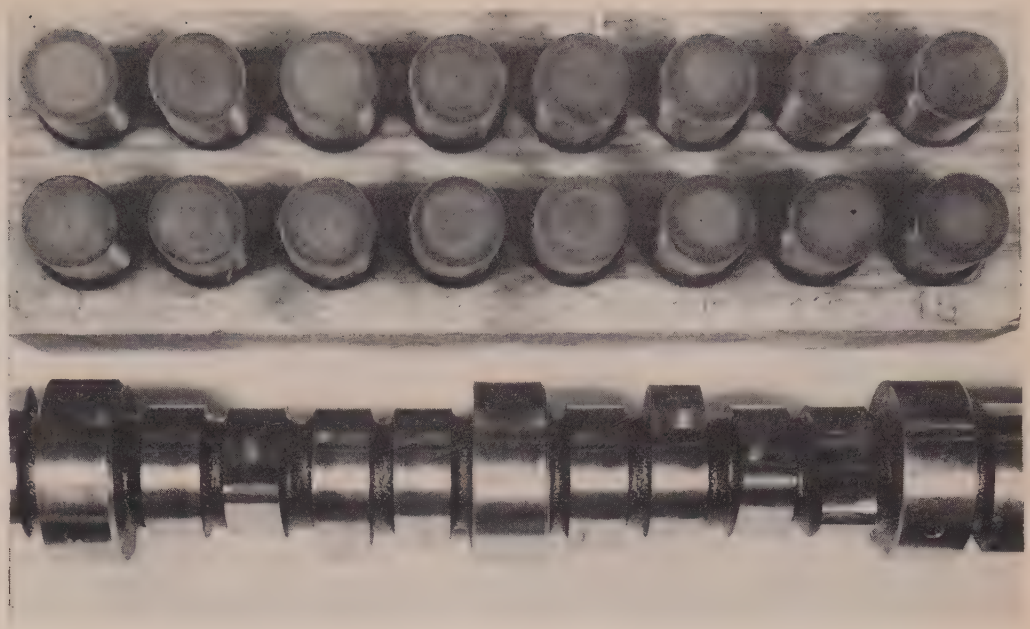

Fig. 9 – Results obtained using hardenable cast-iron tappet material and scuff-type test oil No. 1 containing additive A only. Running time: 140 hr

provided a good basis for comparison because their performance was consistent and not indicative of any peculiar oil effects, as was the case with many high-additive content oils. No tappet-face fatiguing was experienced with any of the six oils tested, and a condition of incipient to slight scuffing prevailed in all tests.

2. Commercial oils and specific additives: Sufficient testing was performed in this portion of the program to reach some definite conclusions regarding the affect of various commercial oils on cam-tappet distress. Furthermore, excellent correlation was obtained between the performance of test oils having a single additive and that of commercial oils known to contain similar amounts of the identical additive.

In general, it was easily possible to segregate both commercial and test oils into one of three categories by describing their influence on the cam-tappet deterioration. The basis of comparison was with chilled cast-iron tappets and hardenable cast-iron camshaft, the three categories being:

a. Scuff-type oil.
b. Fatigue-type oil.
c. Neutral-type oil.

Photographs demonstrating the appearance and results are shown in Figs. 3 to 8 inclusive.

A careful and fairly extensive study of road-test failure types also revealed a good correlation with the laboratory results on oil additive effects. In approximately 20% of the test car failures inspected, a reaction similar to that shown in labora-

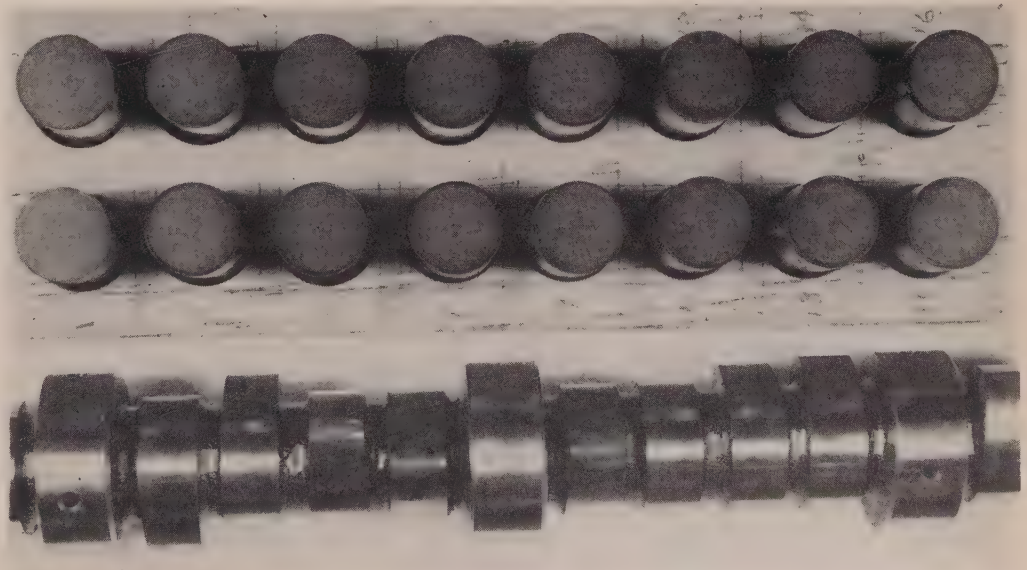

Fig. 10 – Results obtained using hardenable cast-iron tappet material and fatigue-type test oil No. 2 containing additive B only. Running time: 160 hr

tory tests was observed.

3. Tappet material: Hardenable cast-iron tappet material demonstrated a much different reaction to oil additives than did chilled cast iron. When tested with scuff-type oils, the wear rate was affected very little and scuffing did not take place. Use of fatigue-type oil did not create even a slight fatiguing tendency and scuffing resistance was increased noticeably.

Photographs illustrating these results are shown in Figs. 9 and 10.

This characteristic of hardenable cast iron has also been demonstrated in road test operation.

4. Break-in oil: A series of tests were run to determine the effect of using a low-additive neutral-type oil for a short period and then switching to a high-additive scuff- or fatigue-type oil. Test results indicated that breaking-in with a neutral-type oil would reduce the effect of a fatigue-type oil, whereas no influence was shown on the effect of a scuff-type oil.

5. Oil viscosity: Brief tests only have been made in this phase of the program. The conclusion indicated by the results is that the scuffing tendency did increase with reduction in viscosity, while fatiguing tendency was not affected.

6. Oil sample analysis: Although tried repeatedly, no satisfactory correlation was ever obtained between the elements found in an oil sample analysis and the category of effect on chilled cast-iron tappets into which an oil would fall. The wide variety of compounds, neutralizing effects of additives, and variations in base stock all contributed toward disturbing the correlation.

7. Laboratory bench tests: Application of the Almen load test on each of the commercial and test oils evaluated in engine tests failed to show any correlation with the oil's effect on chilled cast-iron tappets. This is illustrated by the graphs in Fig. 11.

8. Leaded gasoline: In tests using oils with high additive content, the apparent effect of the oil was not altered by the use of either leaded (3 cc per gal) or unleaded gasoline.

Material Development

Because engine tests had demonstrated that major improvements in cam-tappet life were possible through material changes, emphasis was placed on material development. Improvements in the camshaft were difficult to realize, were less effective, and were accomplished only by the introduction of other complications. The majority of our effort was therefore confined to development of an optimum tappet material. Only limited effort was devoted to camshaft material modifications.

Camshafts – Preliminary investigations into the effects of increasing the as-cast hardness of the cam noses to 35 Rc indicated this hardness would ensure the presence of an abundance of primary carbides, and consequently, a camshaft that generally possessed better wear properties. This increase in hardness was obtained by adjustment of carbon-silicon ratio and increasing the chromium content. However, as expected, this increase in cam nose hardness caused a proportional increase in bearing and gear blank hardness to 302/341 Brinell. The decrease in machinability was intolerable without a change in camshaft design.

Fig. 12 is a photomicrograph of a cam nose of one of the experimental, high-hardness camshafts with modified chemistry. The abundance of primary carbides is readily evident in this photograph taken prior to heat-treatment by flame-hardening.

Engine tests with the heat-treated experimental camshafts revealed several interesting facts. As mentioned in the discussion of effect of material modifications, an increase in hardness of the cam nose increased the resistance to fatigue and wear but did not appreciably affect scuffing tendency. This can be seen in Fig. 13, which is a photograph of a split set of hardenable cast-iron and chilled cast-iron tappet bodies after having been run 18 hr on the 3600-rpm test schedule. In an effort to obtain indicated benefits, foundry practice was adjusted to obtain camshafts on the higher side of the hardness specification of 269/302 Brinell. This was accomplished by a modification in chemistry referred to earlier. Specifically, the chromium content was increased from 0.80/0.90 to 1.00/1.10%.

Several unhardened camshafts were tested in engines. Although every effort was made to obtain the best possible structure in the cam nose, these tests showed that such camshafts had greater fatiguing tendency than heat-treated cams tested under identical conditions.

No method was found to appreciably decrease scuffing tendency. Further efforts to improve the camshaft metallurgically were concentrated, therefore, on heat-treatment of the cam nose. The production heat-treatment of the camshaft consists of flame-heating the cam noses to approximately 1550-1600 F and oil quenching without subsequent tempering. If caution is not exercised, it is possible to overheat the nose. The overheating with which

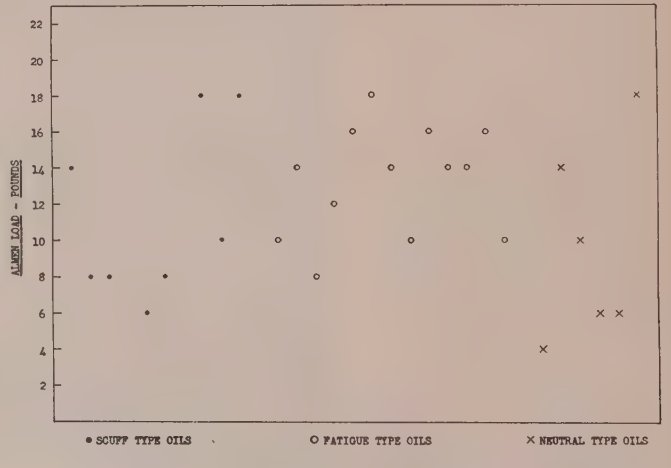

Fig. 11 – Results of Almen load test applied to various commercial and test oils

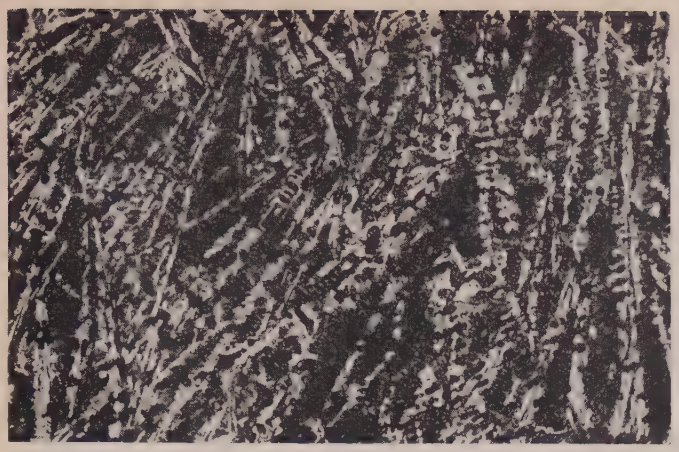

Fig. 12 – Photomicrograph of nose of experimental high-hardness camshaft (nital etch)

we were concerned was not only the actual melting of the metal, but also heating of the cam nose to the temperature range 1700-1800 F or above, which resulted in an undesirable microstructure. It had been proved that heating to this temperature and subsequently oil quenching produced appreciable amounts of retained austenite in the cam nose. The presence of retained austenite in the matrix lowers the nose hardness and makes it susceptible to failure by scuffing.

Tappet Bodies – One of the metallurgical problems concerned with the use of chilled cast-iron tappets was that of identifying the differences in quality which were apparently distinguishable from engine tests. On many occasions, examination and comparison of failed tappets with those that did not fail indicated it was practically impossible to identify the cause of failure other than to report it as a fatigue failure. The chills all consisted of a mixture of carbide, ferrite, and pearlite in various amounts.

Hardenable cast iron did not present this problem. There appeared to be very excellent correlation between material structure and engine performance of tappet bodies. This enabled us to successfully account for all failures observed and provided us with a method for predicting performance.

The initial hardenable cast-iron tappet body tests were made on samples machined from 1.2-in. diameter x 21-in. long arbitration test bars poured from a ladle of camshaft iron. The bodies were either induction- or flame-hardened, lubrite-coated, and then submitted to engine test. These tappets accumulated 733 hr of testing under normal operating conditions, that is, standard spring load, etc. While visual examination of the faces revealed that some fatiguing had occurred, closer examination showed that the microstructure lacked the primary carbides and graphite-type flakes which we now recognize to be of vital importance in resisting fatigue.

Further testing with blanks cast to size indicated that the as-cast hardness was directly proportional to susceptibility of the metal to fatigue. However, hardness was important if due only to the presence of carbides and not as the result of a very fine pearlite matrix. We have found that it is quite possible to meet the minimum hardness requirements of the specification (302 Brinell) and still have a material that is unsatisfactory because of carbide deficiency.

Fig. 14 is a typical illustration of the face of a hardenable cast-iron tappet that failed in fatigue during test.

Fig. 15 is a photomicrograph of the microstructure of this face showing the lack of primary car-

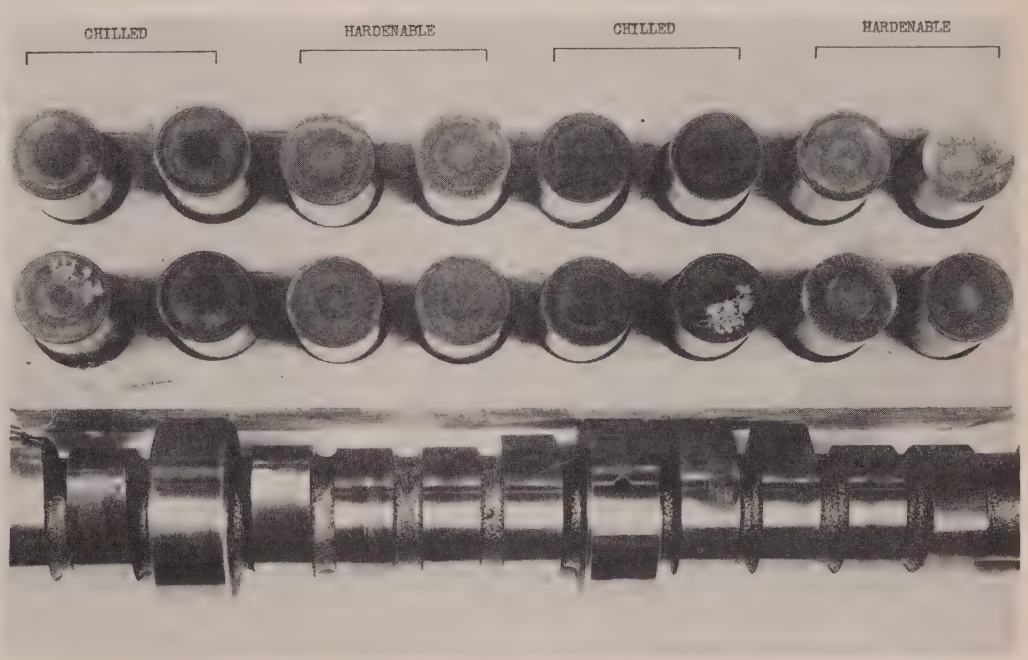

Fig. 13 – High-hardness heat-treated experimental camshaft with hardenable and chilled cast-iron tappets

Fig. 14 – Hardenable cast-iron tappet face showing fatigue failure (nital etch)

bides which are mandatory to resist fatigue.

Engine tests conducted on high-hardness tappet bodies (360/400 Bhn) also showed such tappets, whose microstructure approached that of chilled cast iron, to have increased scuffing failure tendencies. The tendency of low-hardness tappets to fatigue and high-hardness tappets to scuff bracketed the permissible as-cast hardness range for satisfactory castings.

As a result of the experience gained in early engine tests, samples of hardenable cast-iron tappets in the hardness range 302/341 Brinell were obtained and tested. Metallurgical examination indicated that these blanks possessed adequate carbides. Subsequently, the samples were subjected to engine tests with highly favorable results. Under the controlled conditions of this investigation, hardenable cast iron was definitely capable of withstanding more severe service than any of the other materials examined.

As a further illustration of the superiority of this material, Table 5 gives the results of 21 engine test runs made on split sets of hardenable cast-iron and chilled cast-iron tappet bodies. The superiority of hardenable cast-iron's resistance to fatigue and scuffing at low-speed operation is clearly evident.

With these test results as a basis, a material specification was established to provide a production material that would have minimum tendencies to either fatigue or scuff. It was decided that the specifications should be as exacting as possible, but still realistic and practical.

Since engine tests indicated that primary carbides at the face were of utmost importance in the successful performance of a hardenable cast-iron tappet, it was only logical that the material specification should be essentially based on microstructure. Most desired results dictated that the microstructure at the center of the face of the machined tappet body prior to hardening be a mixture of acicular-cellular carbides and graphite flakes in a matrix of pearlite.

Table 5 – Results of Engine Tests on 21 Split Sets of Lifters

Schedule	Material	Fatigue		Scuff		No. of Tappets Okay
		Incipient	Severe	Incipient	Severe	
a	Chill	18	13	48	3	12
	Hardenable	0	0	9	1	86
b	Chill	2	0	33	22	15
	Hardenable	0	0	34	12	26

The graphite flakes were specified as Type A or a mixture of Types A and E. The allowable graphite size ranged from 5 to 7, as measured by ASTM Specification No. A247 of latest issue. It was found that graphite flakes of Types B and D tended to permit early fatigue. Because of the importance of the amount and distribution of the carbides and graphite flakes on the performance of the tappet body, it was necessary to state that the end opposite the gated end of the cast blank be used as the face and have a hardness of 302/341 Brinell at the center. A maximum hardness of 321 Brinell was specified at the gated end. The face-end hardness was indicated to ensure satisfactory perform-

Fig. 15 – Microstructure of hardenable cast-iron tappet face illustrating the lack of primary carbides (nital etch)

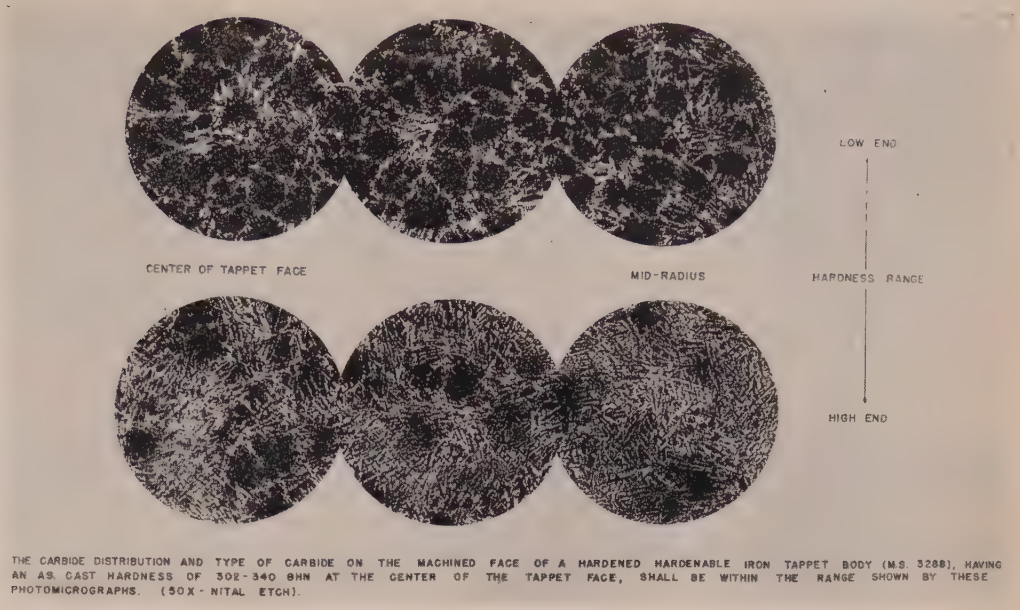

Fig. 16 – Microstructures of hardened hardenable cast-iron tappet body material falling within the acceptable range

ance, while the gated-end hardness ensured satisfactory machinability.

The allowable carbide distribution on the face was described by photomicrographs and is shown in Fig. 16.

It was further decided that under no circumstances should the casting be heat-treated prior to machining. This restriction made certain that the primary carbides would not be destroyed or altered in any way. Perhaps it is permissible to subcritically anneal the castings prior to machining without damage to the primary carbides; however, it was believed the small gain in machinability would not compensate for the cost of such an operation.

Optimum heat-treatment for acceptable blanks was performed after rough machining according to the following schedule: heat to 1575 F for 30 min, oil quench, temper for 1 hr at 300-325 F to a minimum hardness of 55 RC. This minimum hardness requirement can be obtained readily provided the cast blank possesses the specified carbide content.

Proper heat-treatment plays an important part in the performance of a tappet body. If the heat-treatment is not proper, failure is almost certain to occur. Improper heat-treatment includes decarburization, overheating, and underheating of the face. For example, investigations proved that if the heat-treating furnace atmosphere had a decarburizing potential, a breakdown of the carbide occurred. The carbides and graphite flakes on the face were destroyed, and this resulted in a tappet body with scuffing tendencies similar to steel.

To illustrate this, Fig. 17 shows the microstructure of a machined tappet body that has been decarburized during treatment. An affected layer of

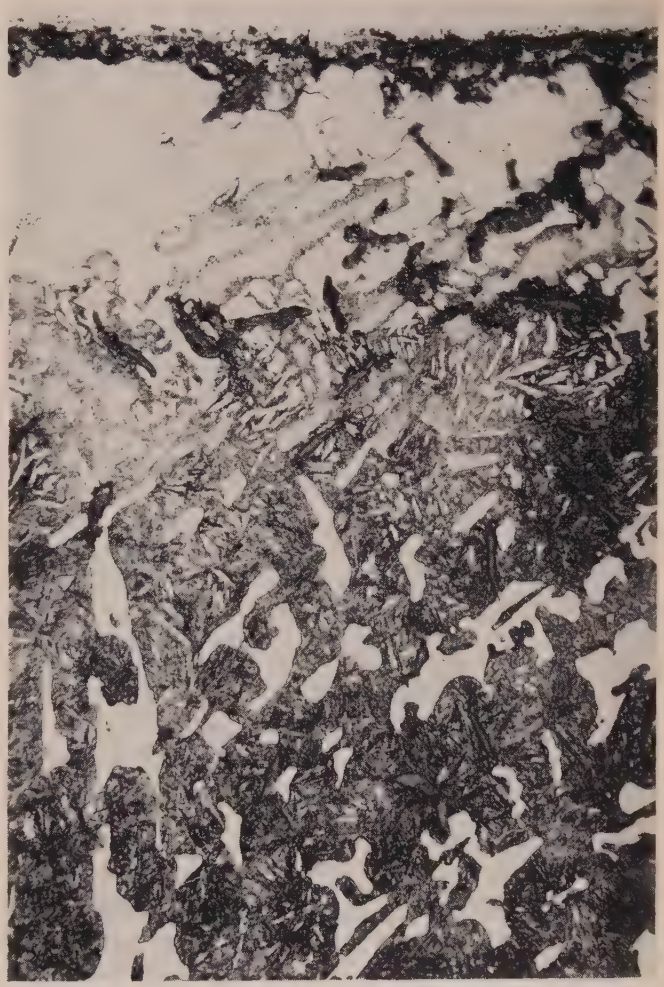

Fig. 17 – Microstructure of decarburized hardenable cast-iron tappet body (nital etch)

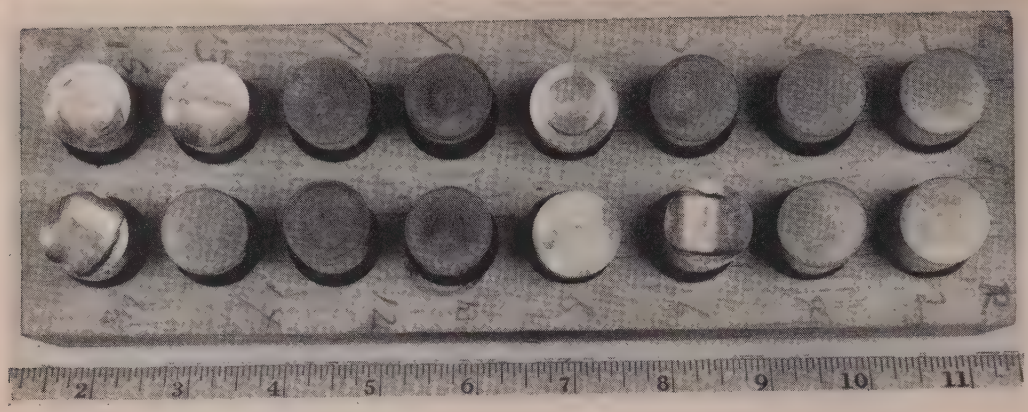

Fig. 18 – Results of engine tests on a split set of properly and improperly heat-treated lifters. Scuffed lifters were decarburized during heat-treatment

approximately 0.011 in. is present on the face of the tappet. Ferrite predominates the face surface area; directly beneath is an intermediate zone containing a mixture of partially-destroyed carbides and ferrite, and finally, below this the unaffected core is shown.

If this decarburized area is not removed in final grinding an early scuffing failure, shown in Fig. 18, is sure to result.

Difficulties can also be experienced as a result of improper flame- and induction-hardening. Such troubles are normally confined to overheating the tappet face, which produces an undesirable microstructure. Typical overheated structures have been determined to be partially dissolved carbide in a matrix of retained austenite and coarse martensite, a condition proved by engine tests to be very susceptible to scuffing.

Conclusions

1. Engine and road test results show that cam-tappet distress occurs most frequently between 5000 and 10,000 miles of operation and may take several forms: scuffing, fatigue, smooth wear, and "oil" fatigue.

2. A test procedure was developed which satisfactorily reproduced all forms of distress in greatly reduced time. Thus it was possible to evaluate all variables on an accelerated basis.

3. Increased lubrication showed no appreciable improvement in failure tendency. Both preassembly lubrication and additional lubrication during engine operation were evaluated.

4. Cam lobe surface finish was found to be a very significant factor influencing the cam scuffing tendency. Tests have shown the optimum range to be 10-20 microin. Surface finishes below 10 microin. proved to be less desirable.

5. A "full contact" cam-tappet geometry initially showed promising results; however, more extensive testing revealed a tendency for tappet nonrotation and fatigue. This design utilized a flat-face tappet having either a hyperbolic body contour or increased tappet bore clearance to provide satisfactory aligning characteristics.

6. Higher hardness cast-iron camshaft material provided increased wear resistance and decreased fatigue tendency but did not affect the scuffing tendency. Steel camshafts had a high resistance to wear and fatigue. The use of hardenable cast-iron tappet material in place of chilled cast iron was a major improvement and offered the greatest benefit of any change considered. Increased resistance to fatigue, scuffing, and lubricant additive effects was demonstrated by the hardenable cast-iron material.

7. Camshaft and tappet face coatings were found to have only relatively slight effect on cam-tappet distress. An uncoated camshaft combined with either a steam-treated chilled cast-iron tappet or a lubrite-coated hardenable cast-iron tappet provided the best performance.

8. Lubricant additives were found to be a very significant factor in the study of cam-tappet distress, particularly when chilled cast-iron tappets are employed. Certain additives were determined to be the cause of either high wear or corrosion fatigue. Hardenable cast-iron tappets were affected very little by oil additives.

9. Optimum performance of hardenable cast-iron tappet material was obtained when a hardness range of 302/341 Brinell was maintained on the face end in the as-cast condition. A lower hardness showed increased fatigue and wear tendencies, while a higher hardness showed increased scuffing tendency. A specific microstructure range was also found necessary for satisfactory performance. Both furnace- and induction-hardening procedures were satisfactorily employed.

Acknowledgment

The authors wish to express their gratitude to E. W. Beckman and A. J. Tache, and other engineers in the Engine Development and Metallurgical Laboratories who contributed to this paper. Their expression of thanks is also extended to the management of the Engineering Division of Chrysler Corp. for permission to publish the information contained herein.

DISCUSSION . . .

. . . of this paper starts on p. 181

Camshaft-Tappet Problems in Ford Overhead-Valve Engines

J. S. Laird, C. L. Stevens, and V. L. Iles,
Ford Motor Co.

This paper was presented at the SAE Golden Anniversary Passenger-Car, Body, and Materials Meeting, Detroit, March 2, 1955.

IN THE first part of this paper dealing with the metallurgical aspects of the camshaft-tappet problems met with in the design of the new Ford overhead-valve V8 engines, Messrs. Laird and Stevens describe the events which led to the adoption of the as-cast alloy-iron camshaft, nitro-carburized martensitic tappet combination. The combination cited works well in the engines described, but it is not implied that it will perform satisfactorily elsewhere.

In the second portion of the paper, Mr. Iles discusses the test schedule devised in connection with the development of the camshaft-tappet materials in the new engines. It is stated that important findings will occur when such tests involve a large number of parts, making possible the study of results on a frequency basis. Tests have shown that a predominantly martensitic tappet structure results in superior performance in combination with the as-cast alloy-iron camshaft used.

COMPLETELY new and more powerful engines are the order of the day. But to a large degree, these new engines must be made from the same materials as their less powerful predecessors. New materials are rarely available, and even marked improvements in old materials are few and far between. It then becomes a problem of juggling the old materials to meet the new operational demands. This problem has been aggravated in the case of the camshaft-tappet train due to the steeper, higher cam lobes needed for improved engine performance. Ford engineers have met the requirement for some engines by a combination that seems to be unique in the industry; namely, carburized steel tappets used with an alloy-iron camshaft in the as-cast condition.

It might be expected that from the countless hours of experimentation and testing that have gone into past engine building, that one combination of materials would have been demonstrated to be the most desirable, and that would have become standardized in the industry. However, for camshafts, there still are carburized steel, alloy

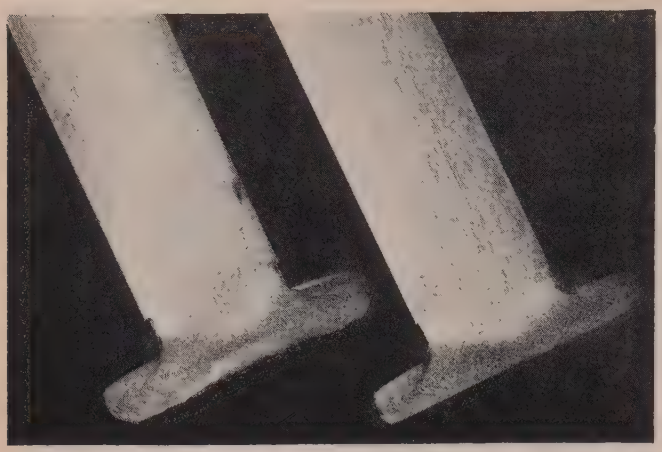

Fig. 1 – Etched sections of tappets after upsetting and grinding

iron – usually hardened, and chilled iron; for lifters, carburized steel, chilled iron, and hardened iron. Ambrose and Taylor[1] have suggested the general adoption of hardenable iron for valve lifters, this material being nonspalling and permitting the addition of antiwear agents to oils to minimize engine wear and scuffing. We cannot subscribe even to this degree of standardization, for what is satisfactory in one engine may be completely unsuitable in another.

For many years Ford has used cast-iron camshafts. Initially, a low-silicon iron, cast in green sand, was used. Its analysis follows:

Silicon: 0.60-0.90%

Carbon: 3.50-3.75%

Manganese: 0.50% max

Chromium: 0.50% max

Copper: 2.00-2.50%

Sulfur: 0.10% max

Phosphorus: 0.10% max

Naturally, the sharp camshaft lobes tended to chill when cast in this iron. A thin tab on each lobe extending into the sand increased the rate of cooling and insured that the lobe chilled hard. Several types of tappets, varying from iron cast in permanent molds to carburized SAE 5120 steel, were used with these camshafts with apparently equal success, the choice being based on economic factors rather than comparative performance.

The earlier camshafts were finished by grinding, so that hardness was no problem. Later changes in design made it necessary to do considerable machining on the cast camshafts. Since their sections and corners tended to chill to a hardness which made machining difficult, there were frequent complaints of flanges too hard to drill, and bearings too hard to finish. There were foundry problems also, for the analysis had to be controlled very closely and chill tabs were a nuisance. If chill tabs were knocked off, the lobe tip was frequently shattered, whereas grinding them off was costly in labor and grinding wheels. It was suggested that the shafts be cast with soft lobes to be hardened later by flame- or induction-heating.

This iron was not suitable for this method, giving poor wear resistance when hardened. A hardenable alloy iron, similar to that used by Campbell, Wyant and Cannon, and possibly others, was adopted. The analysis of this iron follows:

Silicon: 2.15-2.45%

Manganese: 0.60-0.90%

Chromium: 0.85-1.20%

Molybdenum: 0.45-0.70%

Carbon: 3.30-3.60%

Sulfur: 0.15% max

Phosphorus: 0.20% max

The lobes of these camshafts were flame-hardened to Scleroscope 65, and in L-head engines, had good wear characteristics with carburized and hardened SAE 5120 steel tappets. At first, these camshafts were cast in green sand. Later, they were produced by a shell-molding process. This process gave better dimensional accuracy with no noticeable change in properties of the shafts after heat-treatment or in their performance in engines.

The same type of camshaft was used during the development of the Ford 6-cyl overhead-valve engine, but this engine design called for production of an entirely different kind of tappet from that used in the L-head engines; namely, the mushroom-type with a thin head and solid, slender body. Tappets of this type have commonly been made of chilled iron or heat-treated alloy-iron castings. Our production facilities would be used to better advantage, however, if these tappets were made by upsetting steel bar stock. While a suitable upsetting machine was being developed, both hardened-iron and carburized-steel tappets were purchased for trial from outside sources. The hardened-iron tappets were reasonably satisfactory and showed wear characteristics distinctly better than the purchased steel tappets, but no better than those of the steel tappets ultimately produced in our own plant.

In our production, tappets are formed in a cold-upsetting machine from ½-in. SAE 5120 steel rod. This fully automatic machine draws the rod to size,

[1] See SAE Transactions, Vol. 63, 1955, pp. 192-203: "Wear, Scuffing, and Spalling in Passenger-Car Engines," by H. A. Ambrose and J. E. Taylor.

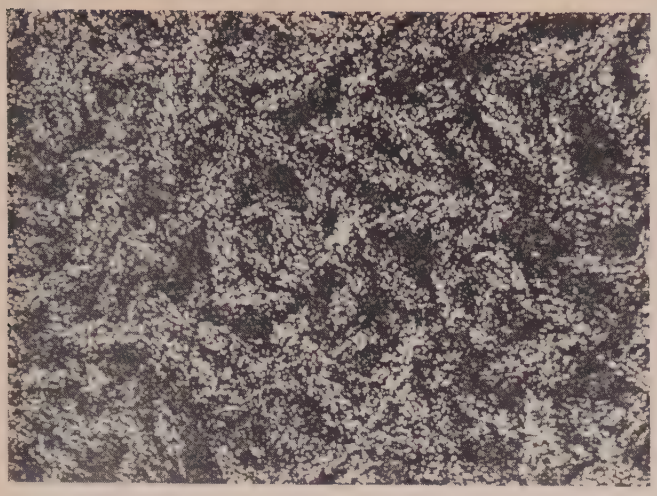

Fig. 2 – Tappet face containing 50% free cementite (Reduced from photomicrograph taken at 100X)

cuts to length, upsets and trims the head, coins a hemispherical recess in the foot, and rolls an undercut beneath the head. The heads are ground to a 60-in. radius with removal of not less than 0.020 in. of stock. In the upsetting process, folding or fracturing of fibers occurs to a depth of 0.010 to 0.015 in. Removal of 0.020 in. of stock insures the development of a solid face.

After grinding (Fig. 1), the tappets are fed automatically and continuously into the retort of a rotary carburizing furnace. The retort rotates alternately right and left, so that the stock moves forward for 2 min 42 sec, and then is reversed for 2 min 18 sec. In this way, the stock is constantly in motion while exposed to the carburizing gases and passes through the retort in seven hours. A temperature of 1700 F is held at the charge end and drops to 1500 F at the discharge end, where the carburized stock is quenched in oil without exposure to the atmosphere. The carburizing gas consists of a mixture of endothermic carrier gas, propane, and ammonia, adjusted to give the desired microstructure in the carburized tappets.

The quenched tappets are drawn at 350-375 F and the stems are then ground to final dimensions. Heads are honed to a surface finish of six microinches, only 0.002 to 0.003 in. of stock being so removed, so that the working face is held practically as carburized.

When carburized to an essentially eutectoid carbon concentration, these tappets gave only mediocre wear results with hardened-iron camshafts. Better results were obtained with higher carbon concentrations and microstructures showing islands, or nodules, of free cementite covering at least 50% of the surface. (See Fig. 2.)

While this tappet was being developed and subjected to merciless testing, the camshaft came in for further study. It was noted that camshafts whose lobes showed a marked development of acicular carbide needles gave the best wear results.

Methods were worked out by which the development of this preferred structure could be controlled with considerable precision. Our success in this control appears to be due, in some degree, to the shell-molding process which had been adopted. The cooling rate of the cams in shell molds appears to be more favorable to the development of acicular carbides than that in green sand.

This development led to further study of the heat-treatment of these camshafts. How essential was this troublesome process? Could the quench be made less drastic, thereby decreasing the amount of warping which occurred?

To obtain a base line for evaluation of the heat-treatment, some camshafts were run in the as-cast condition. To the surprise of all concerned, the unheat-treated camshafts gave a good account of themselves. As long as the cams had the acicular cementite structure (Fig. 3), the unheat-treated cams ran at least as well as the heat-treated cams with carburized-steel tappets. Results were not so favorable when the unheat-treated shafts were run with hardened-iron tappets, but various batches of iron tappets showed little consistency, some showing very little wear and other batches showing considerable wear. Extensive engine testing confirmed the desirability of the combination of an as-cast camshaft and carburized and hardened steel tappets. The as-cast camshaft also worked well with chilled cast-iron tappets in a larger overhead-valve engine. Therefore, it was adopted for production, the heat-treating process was abandoned, and the equipment was made available for other uses.

The combination of an as-cast camshaft with hardened-steel tappets containing a high percentage of cementite was used with success during a year's production of the 6-cyl overhead-valve engine. During this period, development of the Ford

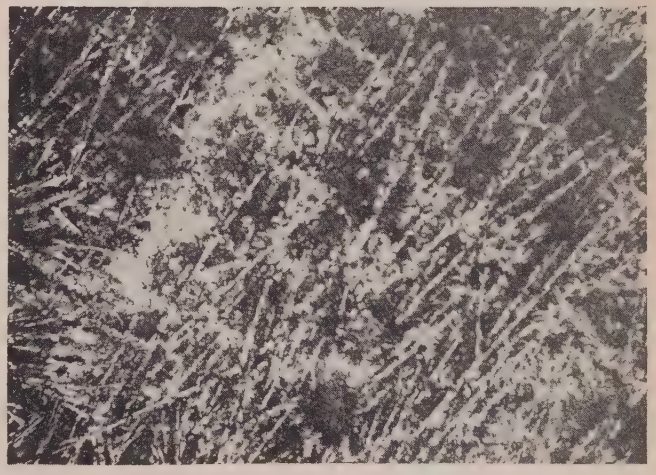

Fig. 3 – Section of cam lobe containing cementite needles (Reduced from photomicrograph taken at 50X)

8-cyl overhead-valve engine was being concluded. The same tappets were used with as-cast camshafts in the prototype V8 engines. Performance of this combination was satisfactory in the extensive dynamometer and road testing of this engine and, accordingly, it was released for production.

After this engine was introduced, some camshaft distress was reported from the field at very low mileages. The extensive testing which had been done prior to production had not indicated the likelihood of such difficulties. Usually, only a single camshaft lobe was involved, but, in some cases, this lobe was wiped out completely in a few miles of operation, with the corresponding tappet pitted and spalled.

Failures were infrequent and could not be reproduced at will with normal engine operation, or with a variety of abnormal operating conditions. This indicated some uncontrolled variation in manufacture which produced a small percentage of abnormal parts.

As described previously, tappet faces were finely honed. The camshaft lobes were left rougher and were etched by phosphate treatment, since it had been found that lobes with a finish as fine as 10 microin. running against 5-microin. tappets had distinctly more tendency to gall than somewhat rougher cams. The phosphate treatment was found to be highly critical, and only a properly etched and coated cam would hold the film of lubricant so essential at break-in. Rigid controls were set up to insure that on every camshaft, a coating 0.00012 in. thick was developed. The elimination of thin and spotty phosphate coating was highly beneficial, but did not, in itself, insure against early failures.

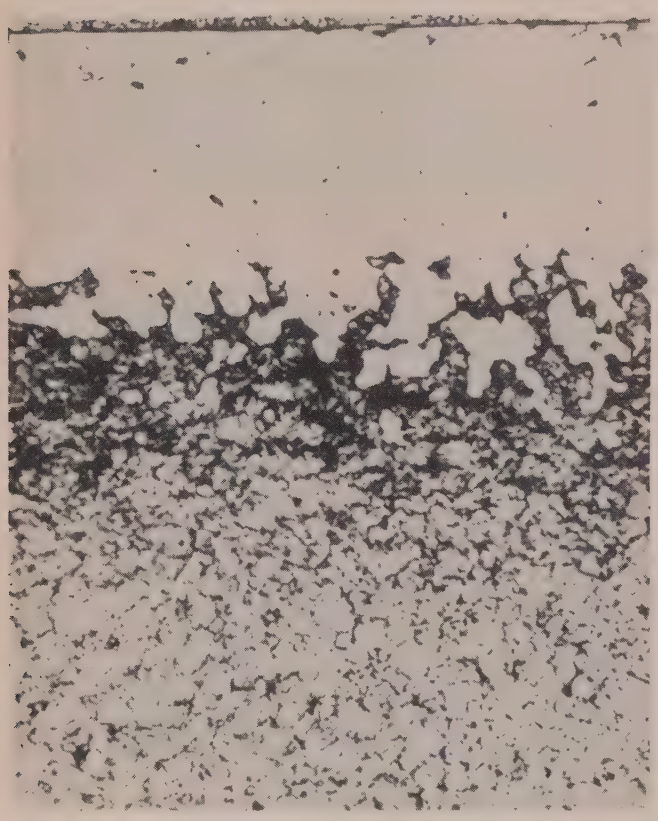

Fig. 4 – Section of tappet face with solid cementite layer (Reduced from photomicrograph taken at 500X)

In studying these camshafts, no one cam appeared to be more susceptible to failure than any other. No relationship existed between position of the cam with reference to gating or position in the engine and frequency of failure. However, it was noted that a high percentage of tappets which had run against the galled cams had cases containing exceedingly high carbon concentrations.

As noted, in developing tappets to run against flame-hardened cams, a case containing a considerable amount of free cementite had been found desirable. This was continued with the as-cast shafts, the preferred structure being one in which 50-80% of the surface was covered with cementite. To produce this, the furnace had to be operated under extreme carburizing conditions, with 65 and 180 cu ft per hr of propane and ammonia, respectively, added to 800 cu ft per hr of endothermic carrier gas. Control was very difficult, and the tappets produced showed considerable variations in structure from time to time. Carburization was most active immediately after the furnace had been cleaned and freed from deposited carbon. Under these conditions, the cementite nodules would coalesce into a solid white layer 0.002 to 0.003 in. deep. It was noted that a high percentage of the early failures involved tappets showing this white layer.

Our knowledge of this white layer is incomplete. Metallographic tests indicate, and X-ray diffraction examination confirms that it is cementite (Fig. 4). If it is cementite (Fe_3C), the carbon content must be over 6% – a surprisingly high concentration. Since ammonia was introduced into the retort, the case may contain some nitrogen, although, at the carburizing temperatures used, iron nitride would be unstable and little nitrogen would be expected to remain in the case. Some tappets with this structure have worn extremely well; a great many have been satisfactory, and some have been completely unsatisfactory. We have reached the conclusion that this structure is probably subject to variations in both composition and properties, and that under the least favorable conditions, it may be very brittle. We failed to demonstrate this brittleness by impact tests probably because the number of specimens tested was not large and we did not happen to include a tappet of the very brittle type. It was obvious, however, that this structure was to be avoided as unreliable.

Up to this time, dynamometer testing had not produced wear patterns which could be considered comparable to those occurring in the field. This anomaly led to an intensive study of test conditions. Ultimately, as will be described later, a test procedure was developed which gave results suffi-

Table 1 – Tappets Used in Ford Overhead-Valve Engines with As-Cast Iron Camshafts

V8 Engine Displacement, cu in.	Tappet
317	Iron – chilled
256	Steel – 5120, nitrocarburized
239	Steel – 5120, nitrocarburized
223	Iron – hardened

ciently consistent with field results to be considered significant.

From a long series of tests, it was concluded that high carbon concentration in the case was not desirable for the Ford V8 engine, that a eutectoid case gave at least as good results as a higher carbon case, and that the easiest way to make sure that no tappets with the solid cementite layer were produced was to carburize only to a eutectoid composition. This was accomplished by drastically reducing the input of both propane and ammonia, the temperatures remaining the same. This results in a case which, after quenching, is essentially martensitic. Field results with martensitic tappets and as-cast camshafts have been entirely satisfactory.

At this time, hardened-iron tappets were tested in the V8 engine with the as-cast camshaft. This combination was not satisfactory, producing a high rate of wear on both tappets and cam lobes. On the other hand, steel tappets, carburized and hardened to a martensitic case, wore satisfactorily with the as-cast camshaft in the 6-cyl and 8-cyl engines. An adequate explanation of the apparently greater wear resistance of the 6-cyl engine is being developed.

The combination of as-cast alloy camshaft and martensitic tappets appears to be rather insensitive to variations in oil. On the other hand, surface treatment of the camshaft must be carefully controlled. As noted, the camshafts are given a rigidly-controlled phosphate treatment after complete machining. At assembly, the camshafts are carefully oiled so that when engines are started on the hot test, there is no possibility of even momentary dry contact between tappets and camshaft. Slight scuffing at this point can lead to ultimate failure.

Continued development has led to incorporation of copper in the iron analysis. This diminishes the tendency to slight pitting shown when as-cast camshafts with still steeper lobes are run against martensitic eutectoid-steel tappets. The as-cast alloy camshaft is also being used with chilled-iron tappets in a larger V8 engine with excellent results.

As cast, the camshafts present a good structure of acicular carbide in a matrix of fine pearlite and graphite. This structure, combining hard and soft materials, tends to adjust and heal over slight abrasions. If these camshafts are heat-treated, the pearlite is converted to hard martensite, which, once abraded, tends to cut and score to destruction. It is obvious that the use of camshafts in the as-cast condition is desirable from a purely economic standpoint. They work well in the engines described, but it is not expected that they will work well in all engines.

This paper is not intended to provide a general answer to the camshaft-tappet problem, but merely to highlight the complexity of the problem by reference to our experience. That we produced a more desirable camshaft by omitting a supposedly essential heat-treatment is surprising, but it goes to show that, now and then, even metallurgists have a little luck.

Fitting the Tappet to the Camshaft

Tappet and cam-lobe wear problems became a common topic in technical papers in automotive literature during the winter of 1953-1954. Authors of technical papers were stressing the merits of hardened-iron tappets and almost totally disregarding other factors affecting the tappet-cam relationship.

Past experience at Ford had indicated that chilled-iron or steel tappets were preferred to hardened-iron tappets in some cases. A study and test program was initiated to review and modernize reference data for engine design, test, and production quality control. When this program was started, Ford engines were equipped with alloy-iron camshafts in combination with three types of tappets, as shown in Table 1.

In each case, the materials had been selected on the basis of experimental tests, "make-or-buy" considerations, economics, and service records. The reasons for the wide use of an as-cast iron camshaft have been discussed in the earlier portion of this paper. One reason for the use of a variety of tappet materials was the outcome of previous test results, which showed that although a particular cam and tappet material combination might be satisfactory in one engine model, it could be entirely unsatisfactory in another engine model.

The 239- and 256-cu in. V8 engines were selected for study because these two engine models were in highest production. The same tappet made by Ford was used in both engines. Design, metallurgical, and quality control personnel would, therefore, be vitally interested in knowing the effects of variables in material, heat-treatment, and manufacturing process.

The service department furnished camshafts and tappets from the field to serve as a reference basis for product improvement. A committee of Engineering Staff and Quality Control personnel was assigned to the task of reviewing the parts, discarding incidental items, and developing criteria for evaluation of the poorest performance cases. The following observations were made:

1. Poorest performance cases included wiped

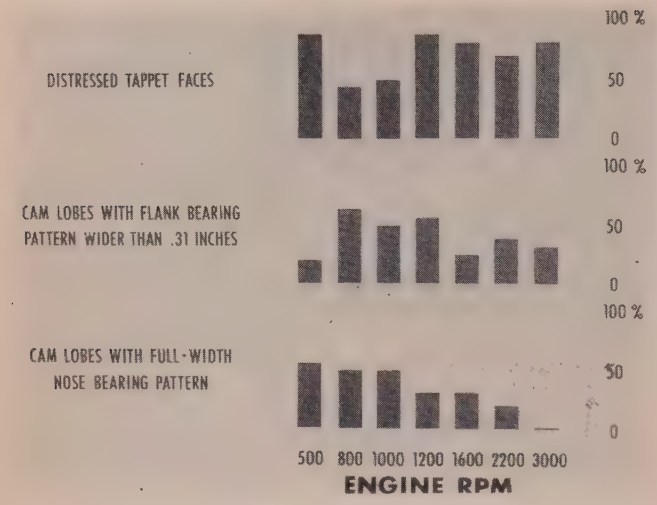

Fig. 5 – Cam and tappet distress related to engine speed

cam lobes. Usually, the mating tappet face showed pitting and spalling.

2. Poor tappets were occasionally found with a good mating cam lobe. This situation indicated that tappet-face distress preceded cam-lobe distress.

3. The frequency of cam or tappet distress was greater in passenger car engines than in truck engines.

4. Poor performance of tappets and cam lobes was evident in some engines after only 500 miles of operation.

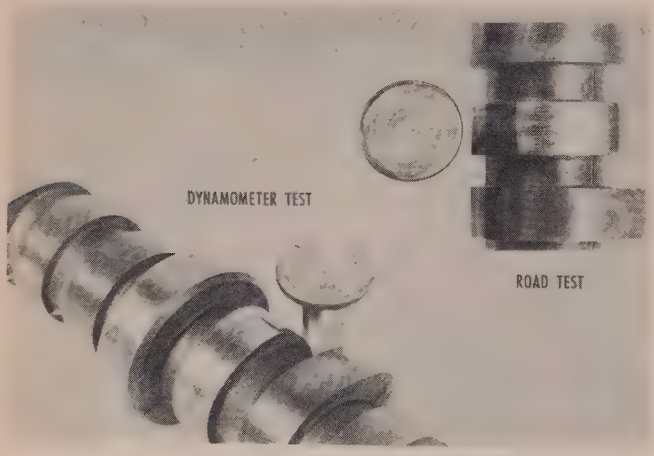

Fig. 6 – Cam and tappet wear-test correlation

Table 2 – Basic Test Cycle

1. Set valve lash cold to high-production limit.	
2. Crank engine for two minutes, then stop for one minute.	Repeat three times.
3. Run engine at following speeds and loads:	
400 rpm at manifold vacuum of 12 in. Hg for	15 min
4200 rpm at wide-open throttle for	5 min
500 rpm at manifold vacuum of 12 in. Hg for	10 min
1200 rpm at wide-open throttle for	5 min
Total	35 min

Water temperature maintained at 160-170 F
Oil temperature uncontrolled

5. There was no relationship between cam or tappet distress and the positions of these parts in the engine.

6. The frequency and types of distress were similar in both the 239- and 256-cu in. engines.

7. Distress of tappets and cam lobes showed no pattern varying with climate. Hence, corrosion could probably be discounted.

After the review of distressed tappets and camshafts, the objectives of a study and test program were defined. Keeping in mind that one defective tappet in a lot of 1600 would correlate with approximately 1% of production, a large number of parts with a short test was preferred over a small number of parts with a longer test. A short dynamometer test schedule had to be developed to duplicate the tappet-face distress observed on some parts received from the field. Since cam and tappet distress occurred in engines with standard valve spring loads and standard clearances, an acceptable test engine must remain standard in all specifications.

A logical program would consist of a test schedule development followed by an evaluation of the tappets being used in the field and subsequent tappet improvement.

Seven hundred tappets were used to establish firmly the desired scheme of test speeds for reproducing the typical distress patterns of tappets and cam lobes. Cycle testing was found more effective than constant-speed running, since changes in speed resulted in fatigue of the casehardened section of the tappet face. It was also obsereved that the typical distress pattern could be most readily induced at very low engine speeds (400-500 rpm). Therefore, it was decided to devote a large percentage of the allotted test time to low speed operation. Incidentally, it was found that if high-speed running preceded low-speed running, cam and tappet distress was not so easily reproduced.

Before proceeding further, it may be well to justify the use of as many as 700 tappets in establishing the test procedure. In 1952, we completed an extensive test program of a similar nature, the only

differences being in the camshaft-iron metallurgy and the fact that the engine was a 6-cyl model instead of a V8. At first, therefore, it was anticipated that tappet-distress response to a particular test condition would be the same in 1954 as it was in 1952. After repeated tests it became clear that the 1952 6-cyl engine data had little or no validity when applied to the 1954 V8.

Continuing with the development of the 1954 test schedule, the test speeds were determined by observing tappet-face and cam-lobe distress after a number of sets of new parts had undergone a 15-hr run at one of several speeds. The pattern of tappet-face and cam-lobe distress as a function of speed is shown in Fig. 5.

By this time, the data on desired test procedure was considered complete enough to establish the basic routine test cycle shown in Table 2. Table 3 shows how this basic test cycle was used to evaluate both experimental and production tappets.

Five hundred tappets of September, 1953 vintage were run on the dynamometer to evaluate tappets which were similar to those specified in production engines. The type of tappet-cam lobe distress obtained on the dynamometer was accepted as a duplication of the poorest performance cases received from the field. A comparison is shown in Fig. 6. The test revealed a considerable variation in performance among the 500 tappets in this lot.

A study was undertaken immediately to correlate the tappet performance variable with fits, clearances, material analysis, and heat-treatment. There seemed to be no single factor or simple combination of factors which would serve as a complete guide. However, it was noted that a fair correlation existed between tappet performance and cementite richness on the tappet face in about 60% of the cases.

The metallurgical department made reference photographs for cementite classification. These are illustrated in Fig. 7. Class 10 was predominantly cementite (white) with small blotches of martensite (black). Class 0 was essentially martensite. September, 1953 tappets fell into Classes 6 to 10, this having been the desired production range resulting from tests on the 1952 6-cyl engine. Contrary to 1952 data, however, the 1954 V8 engine gave better performance with Class 6 tappets than

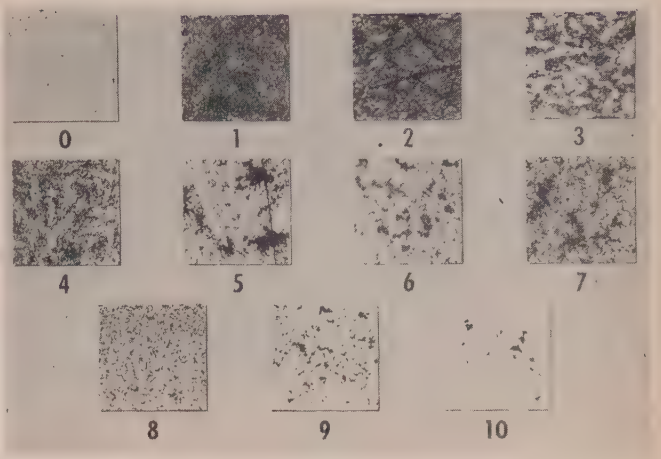

Fig. 7 – Classification of tappet-face microstructure according to cementite concentration (Reduced from photomicrograph taken at 100X)

with Class 10 tappets, on a frequency basis.

Because frequency analysis was required to differentiate the general performance between Classes 6 and 10, it was acknowledged that there were variables in the production of 150,000 tappets per day which were not understood in terms of current mechanical and metallurgical knowledge. Hence, test data on small lots of tappets with nonproduction heat-treatment would be of questionable value.

It was decided to gradually lower the amount of cementite in production tappets, during which time the Engineering Staff would test 100 tappets per day and quality control would inspect 15 production engines (after hot-test) per day.

At the stage in production where the reduction of cementite had resulted in a change from Class 10 to Class 1, 800 tappets were subjected to 11 hr and 40 min of cycle-testing. Following the tests, the tappets were visually screened and 33 of the best-looking were checked for cementite classification. The results of this classification are shown in Table 4.

It is unfortunate that there was no explanation for the fact that most Class 7 and Class 8 tappets were poor while a few were good. However, the data indicated that production of Class 0 tappets was preferred to any higher-cementite class. Thirty days of continued observation of Class 0 tappets in production and subsequent surveys of performance in the field have confirmed the choice of Class 0 tappets.

Tappet performance, in general, experienced with the respective cementite classifications, is shown in Fig. 8. A Class 10 tappet was characterized by spalling, and a Class 5 tappet was characterized by wear and porosity on the tappet face, whereas a

Table 3 – Breakdown of Tests

Dynamometer test engines:
1. 95% of tappets were run for 20 cycles (11 hr, 40 min).
2. 5% of tappets were run for 172 cycles (100 hr, 20 min).

Dynamometer verification on new production engines:
1. 24 production engines (as received) were run for 63 cycles (36 hr, 40 min).

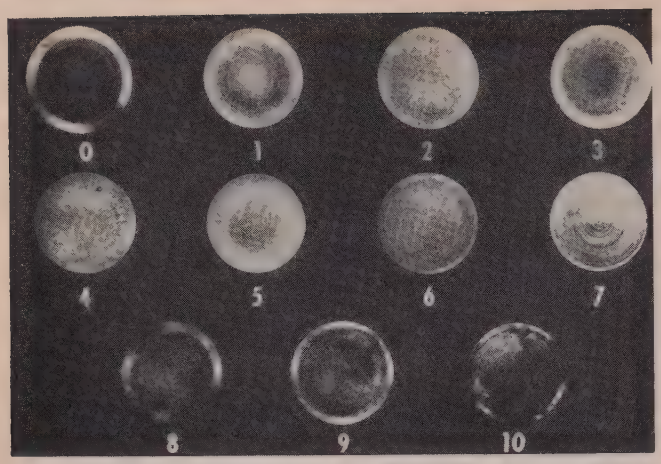

Fig. 8 – Physical appearance of tappets graded according to cementite concentration

Table 4 – Cementite Classification of 33 Good-Performance Tappets

Class 1 – 25	Class 6 – 0
Class 2 – 3	Class 7 – 1
Class 3 – 2	Class 8 – 1
Class 4 – 1	Class 9 – 0
Class 5 – 0	Class 10 – 0

Table 5 – Properties of Oils Selected for Evaluation

API Classification	Oil	SAE Grade	SUS Viscosity at 100 F	SUS Viscosity at 210 F	V. I.	S	P	Ca	Ba	Zn	Choice[a]
ML	A	10W	171	44.6	100	0.38	—	—	—	—	First
MS	B	10W	190	46.5	107	0.17	0.07	—	0.26	0.06	
MS	C	20	349	55.3	98	0.48	0.065	—	0.15	—	Second
MS	D	10W	185	45.9	105	0.44	0.06	—	0.18	—	
MS	E	10W	188	45.9	102	0.20	0.07	—	0.44	0.04	Third
MS	F	5W-20	168	50.5	154	0.51	0.06	0.03	0.27	0.03	

[a] Based on severity of cam and tappet wear observed.

typical Class 0 tappet exhibited the original honed pattern on its face, even after the test.

Because of current efforts to associate the tappet and cam wear problem with available types of lubricating oil, six oils were evaluated for comparative purposes. These types resulted in measurable, but relatively small, variations in tappet and cam lobe performance. A change of two cementite classes in the tappets would offset the variation among the six oils tested. Tappets used for oil evaluation tests had cementite classifications ranging from 1 to 5. The properties of the oils used in the test are shown in Table 5.

It should not be inferred from the classification of oils into first, second, and third choice that this means anything except a choice based on this particular tappet-cam wear study as applied to the two engine models tested. Moreover, none of the oils was tested for any other lubricant function.

In conclusion, the following were observed:

1. A particular combination of materials in camshaft and tappets can be satisfactory for one engine model and completely unsatisfactory for another engine model, even though both are of the same type. Most certainly, data derived in the development of one engine design should not be assumed arbitrarily to apply to another engine design.

2. Quality control in tappet production is very important. One defective tappet results in an unsatisfactory engine, even though the other 15 are perfectly good tappets.

3. Experimental tappet and camshaft tests which are intended to reproduce engine operating conditions in the vehicle must retain standard valve spring loads and standard clearances. While such deviations as abnormal valve spring loads are useful for research work, these variations are likely to create problems other than those encountered in the normal operation of the engine.

4. It has been shown that the particular test cycle presented in this paper was an efficient evaluation procedure for the particular engine models involved, as well as for the particular type of problem that was encountered. However, the value of this same test cycle would be highly questionable for any other combination at any other time.

5. Important findings in tappet testing are most likely to occur when the tests involve a large number of parts, since only large numbers will permit the study of trends on a frequency basis.

6. Tappet material and camshaft material have intangible qualities as individual parts; the compatibility between the two mating parts is what counts.

The present trend in the automotive industry seems to be toward a general change from chilled-iron and steel tappets to hardened-iron tappets. On the other hand, as the work outlined in this paper has shown, good performance may be obtained from the combination of an as-cast iron camshaft and steel tappets. Good performance potential requires a cam and tappet combination that is compatible from both metallurgical and mechanical standpoints.

DISCUSSION . . .

. . . of this paper starts on p. 181

Interrelationship of Design, Lubrication, and Metallurgy in Cam and Tappet Performance

E. B. Etchells, R. F. Thomson, G. H. Robinson, and G. K. Malone
General Motors Corp.

This paper was presented at the SAE Golden Anniversary Passenger-Car, Body, and Materials Meeting, Detroit, March 2, 1955.

A PROGRAM was undertaken to evaluate the performance of cams and tappets as influenced by design, lubrication, and metallurgical techniques. Car and dynamometer tests and a newly developed bench test are described. The latter shows promise in lending itself to the determination of the effects of single variables in a practical, short, and economic fashion, while the former do not.

For the conditions of high contact stress and boundary lubrication experienced in cam and tappet operation, the authors draw several conclusions from the test work described, categorically related to the design, lubrication, and metallurgical problems present.

RECENT developments in automotive passenger-car and truck engines and concurrent developments in the field of lubricants have posed an extremely difficult problem with regard to cam and tappet performance. At the present time there are more than 25 passenger-car engines in appreciable volume production. In these engines there are at least five commonly used camshaft materials and at least three commonly used tappet materials. There are more than 75 commercially available crankcase oils in the United States with a long list of additives of various types. The problem facing the engine builder and oil producer is one of developing an engine and a lubricant with such characteristics that satisfactory customer performance is ensured for all combinations. Without including infinitely variable operating conditions found in service, the more than 25,000 possible combinations of design, metallurgical materials, and lubricants make the selection of a suitable test method for the

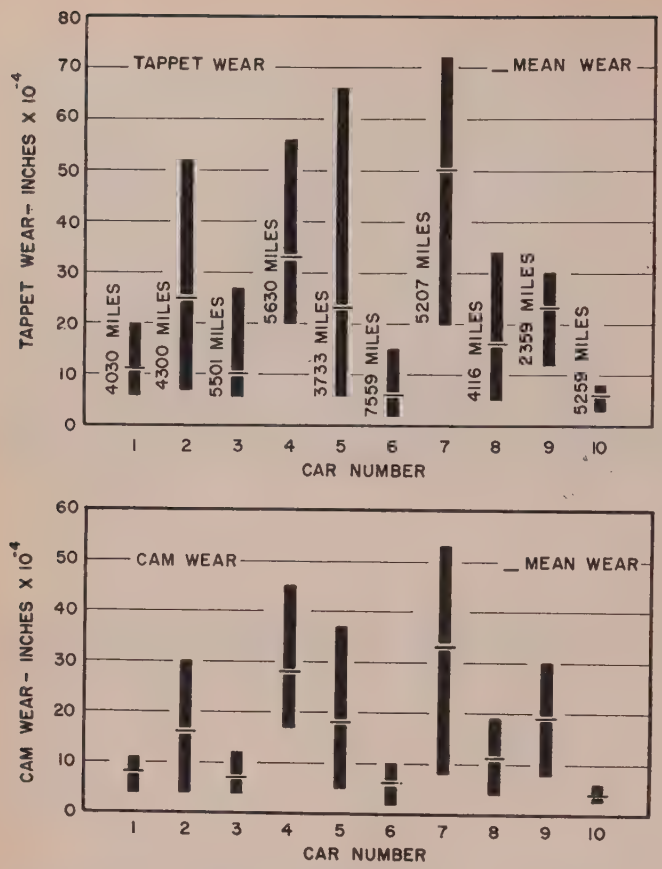

Fig. 1 – Tappet and cam wear variation for 10 cars of make No. 1 using SAE 5W-20 oil (Oil *M*)

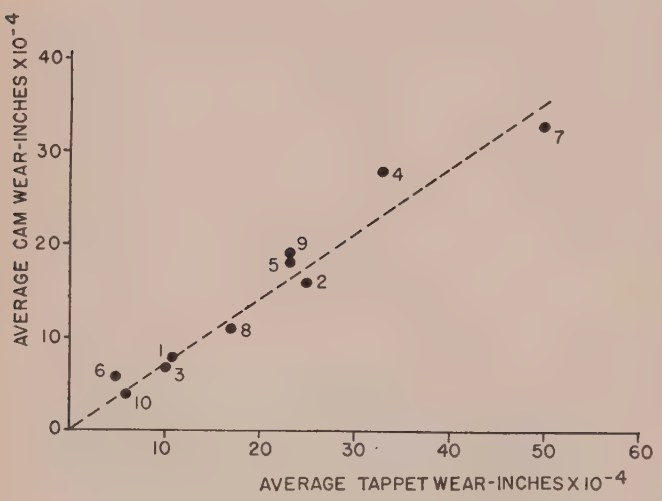

Fig. 2 – Average cam wear versus average tappet wear for cars of Fig. 1 (oil *M*)

evaluation of a single variable very important. Many data have been obtained in controlled car tests, dynamometer tests, and bench tests. The problem of evaluating crankcase lubricating oils is especially difficult under existing test methods.

This paper will recite some of the difficulties encountered in various testing techniques, illustrate some things we think we know, and point out the great need for a reliable, fast, and reproducible bench test to enable all concerned to monitor their efforts and so bring greater automotive performance and reliability to the consuming public. Some work being done in our laboratories on the development of a simple, accelerated bench test to help resolve this problem will also be described.

Testing Methods

Car Tests – The principal advantage of attempting to resolve wear and spalling problems by car testing is that the degree of attainment of success will be judged ultimately by performance in the hands of car owners in the field. Therefore, one can logically argue that since this is the final acceptance test, the solution will be successful if all testing is carried out in a similar manner. While this type of testing is necessary to determine general overall performance, it does not economically lend itself to the evaluation of a single variable.

Let us look at what happens when one attempts to evaluate reproducibility in such tests. In one series of tests run with 10 cars of the same make and year using a common oil with 10 different sets of uncontrolled driving conditions, the results shown in Fig. 1 were obtained. All cars were operated for about the same length of time, and the number of miles driven in each is indicated on the figure.

The results show a spread from satisfactory to unsatisfactory performance. There can be several reasons for this:

1. Driving conditions were different.
2. The metallurgical characteristics of cam and tappet materials were not identical.
3. Accumulations of manufacturing tolerances were sufficiently different to cause differing wear conditions.
4. A combination of any or all of the above.

This indicates that one must run a sufficient number of tests to encompass that combination of variables producing most severe wear conditions. Thus, a rather large number of cars must be included in the sample, and since the degree of variation in individual test cars is unknown, useful analysis of the data becomes difficult.

Some useful results are obtained either if the data are treated statistically or if one variable under control overshadows all others in degree of intensity. For example, in the above tests, two useful conclusions were deduced. First, it was found that under these conditions average cam wear for each car followed the trend of average tappet wear rather closely, as shown in Fig. 2. Second, it was shown that the type of operating conditions were a significant factor, as shown in Table 1, where one of the conclusions of a statistical analysis is obvious.

When one begins to separate these kinds of variables, the number of samples in each group becomes very small, even in a test using 10 cars.

If one attempts to evaluate various oils by running car tests, for example, the magnitude of the

Table 1 – Relationship of Type of Service to Cam and Tappet Wear
(10 Cars – Make No. 1 – Oil *M*)

	Mean Wear, in.		
	Short Trips	Mixed Trips	Long Trips
Cam	0.0021	0.0012	0.0006
Tappet	0.0028	0.0017	0.0006

job becomes staggering. In 1954 a spot check of 17 commercially available oils was made by observing the wear rate under carpool-type driving conditions. The results are shown in Fig. 3.

About the only conclusions to be drawn from this kind of test are that (1) multigraded oils show the same type of variation as single-grade oils and (2) some of the oils appear unsatisfactory.

Under these kinds of testing conditions one cannot determine which oil is satisfactory. The best one can do is say that oils of types *H, E,* and *P* tend to be unsatisfactory. One cannot conclude that oils *B, O,* and *U* are satisfactory, unless used under conditions which embrace the most unfavorable combination of variables. This means very extensive testing of the oils which look promising.

In the tests cited, the evaluation of a single variable is difficult even though tests were carefully controlled in that they encompassed only one engine model with one combination of tappet and camshaft materials. If one attempts to include all commercial engines and all metallurgical combinations, the scope of testing becomes impractical.

Dynamometer Tests – Since field testing seems to offer such difficulty and combines so many uncontrolled variables, a better degree of control can be obtained in dynamometer testing. The disadvantage of this type of testing lies in the necessity for developing an accelerated test which reproduces field-type failures in a suitably short time. The test should be reproducible and accentuate severely those conditions which cause failure, so that if materials pass the dynamometer test, the frequency of field operations exceeding those severe conditions is exceedingly small.

While many useful data have been obtained from this type of test, considerable scatter is encountered. (See Fig. 4.) The tests were initially run to determine a base line for the wear characteristics of hardened alloy-iron tappets and cams.

All these tests were run in one engine with the same batch of oil under the test conditions indicated. It is usually considered that under these test conditions any wear exceeding 0.001 in. is cause for concern.

It will be noted that in using the maximum wear figures for any single test one could conclude:

1. The oil is very good as measured by test 22.

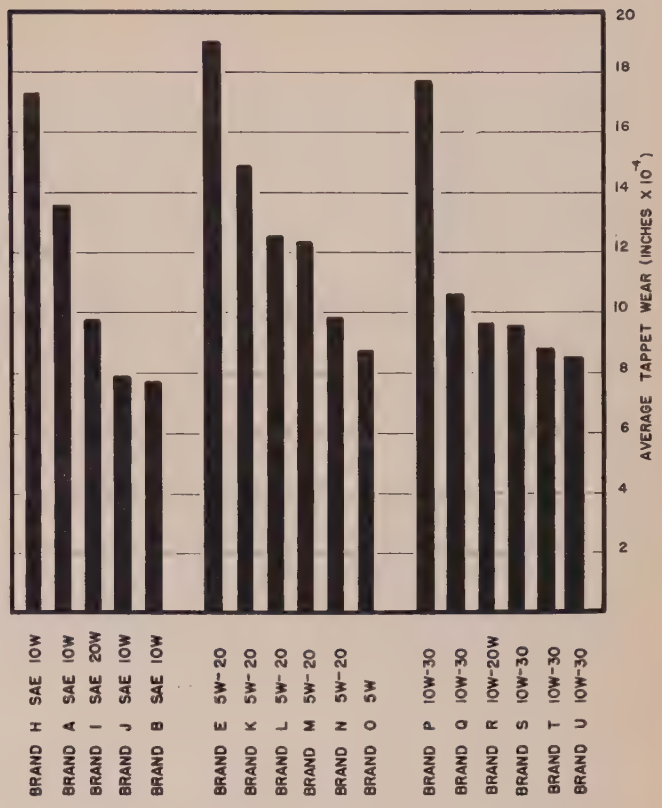

Fig. 3 – Average tappet wear for car make No. 2 after 10,000 miles of operation in car pool service

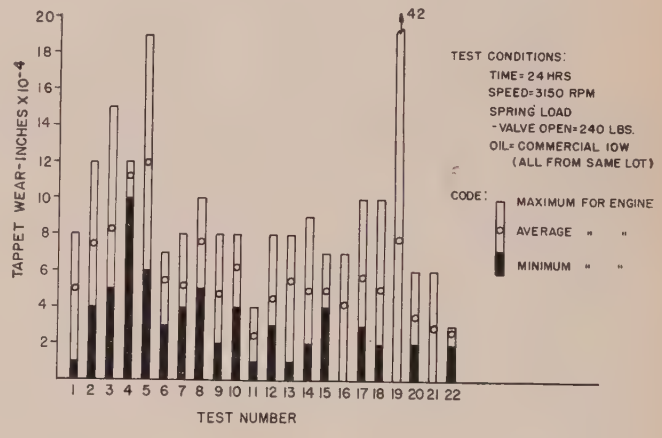

Fig. 4 – Variation of tappet wear in dynamometer tests. All tests were run in same engine with same oil and had hardened alloy-iron cams and tappets

2. The oil is very poor as measured by test 19.
3. Anything else one cared to.

One can presume only that the variation is due to varying metallurgical structure, accumulation of manufacturing tolerances between camshaft and tappet, or unequal reproduction of wearing surfaces.

Bench Tests – To the best of our knowledge, no satisfactory bench test has been developed to date

for achieving the objectives set forth in the first part of this paper.

Influence of Design Factors on Valve-Gear Performance

The barrel-or mushroom-type valve tappet has become almost standard construction in modern passenger-car and truck engines, and recently, attention has been drawn to cam and tappet combinations primarily because of:

1. Increased engine output and higher speeds.
2. Improvement in oils to reduce sludge and varnish.
3. Improper use and/or manufacture of cam and tappet materials.

One simple way to increase maximum engine hp is to lift the valves higher. A review of recent engine specifications shows that this has become rather standard practice. To do this and retain satisfactory idle conditions without accentuating carburetion problems, the valve opening and closing points must be maintained. To accomplish these aims of higher lift and satisfactory valve timing, cam contour velocities and accelerations are increased, and instantaneous nose radii commonly reduced. The natural result of increased cam accelerations and greater engine speeds is higher valve-spring opening loads. All these factors increase the stress on tappet and cam faces and the tendency to scuff, wear, and spall (or flake) from shear fatigue. Paradoxically, the changes that result from higher engine speed do not cause the trouble, for at high speed, inertia effects lower the contact stress at the critical point of dwell. Failures generally result from low speeds.

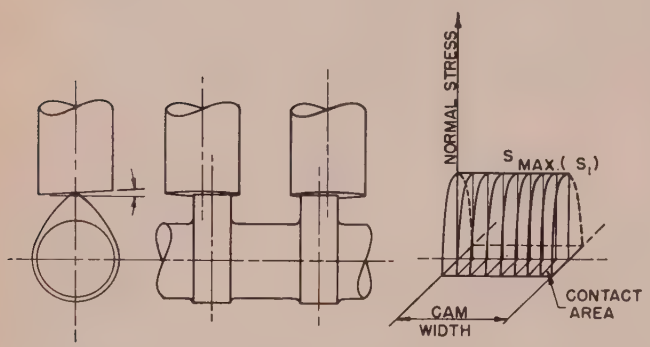

Fig. 5 – Flat cam and tappet with cam and tappet axes parallel

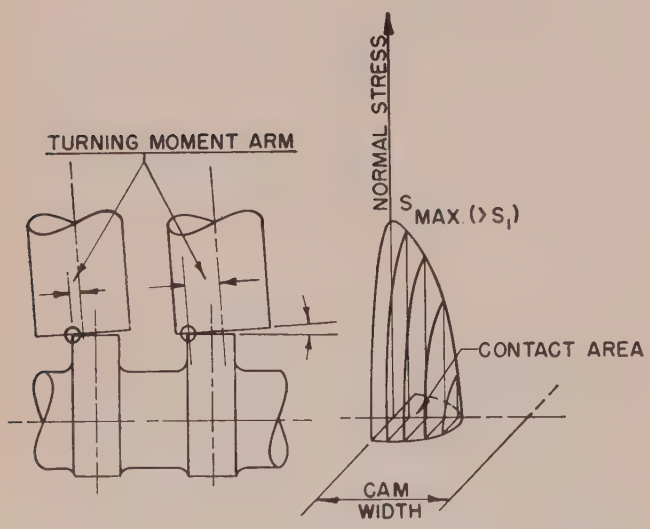

Fig. 6 – Flat cam and tappet with cam and tappet axes not parallel

At present there is apparent general agreement that cam-tappet face failures occur by:

1. Scoring or scuffing.
2. Wear.
3. Spalling or flaking.

The reasons for these failures are as numerous as they are varied. It is believed they can be condensed as follows, not necessarily in order of importance.

1. Contact stresses are too high.
2. Velocity of rubbing contact is too high.
3. Finish and/or treatment of contact surfaces is not adequate.
4. Lubrication and type of oil are not suitable.
5. Materials are not compatible.

Contact Stress – Stresses may be calculated according to the mathematical work of Hertz. However, the stresses that are difficult, if not impossible, to calculate are usually the ones that lead to failure.

For instance, referring to Fig. 5, for a flat-face tappet on flat cam, the normal stress, according to Hertz, may be calculated as follows:

$$S = 0.591 \sqrt{\frac{P}{WR\,(1/E_1 + 1/E_2)}}$$

where:

S = Stress, psi
P = Load, lb
W = Cam width, in.
R = Instantaneous nose radius, in.
E_1, E_2 = Moduli of elasticity of contacting materials, psi

In practice these parts do not always run to-

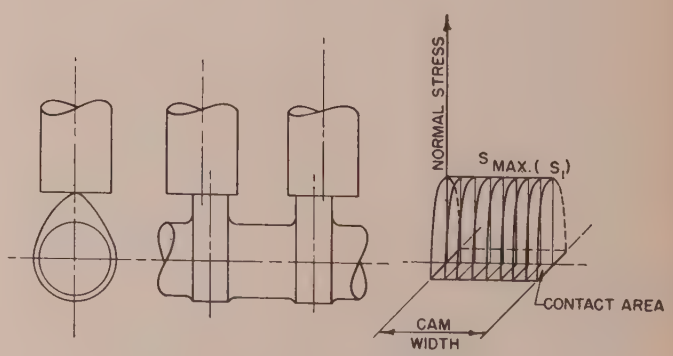

Fig. 7 – Tapered-face tappet on flat cam

Table 2 – Effect of Tappet Rotation on Spalling Tendency[a]

Test No.	Tappets	Camshaft	Engine No.	Rpm	Condition
93049	Chilled flat-face gray iron (not phosphate treated)	Heat-treated forged steel SAE 1039 phosphate treated	150C 150D 150E	2550 2150 2550	3 spalled 1 spalled 4 spalled 8 total spalled
100650	Chilled face gray iron 0.003 in./in. taper (not phosphate treated)	Heat-treated forged steel SAE 1039 phosphate treated	150C 150D 150E	2550 2150 2550	1 spalled (turned) 0 spalled 1 spalled (turned) 2 total spalled

Valve-Spring-Open Load, lb 160-170
Engine Oil X (SAE 10)
Hours Run 150

[a] While only one set of data is presented in many of the comparisons in this paper, the results are typical of those obtained in a considerable number of tests. However, the authors warn against extrapolation of the data to engines other than the types used in the tests.

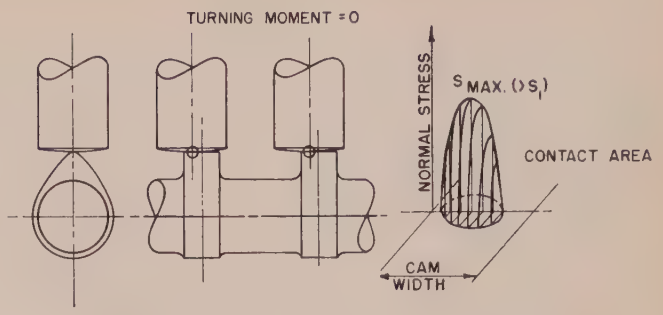

Fig. 8 – Straight-face cam and spherical-face tappet

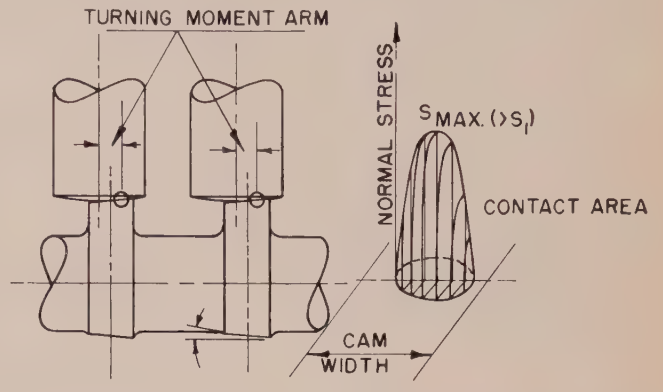

Fig. 9 – Tapered-face cam and spherical-face tappet

gether in this manner due to misalignments and deflections, and we are likely to get an assembly similar to that shown in Fig. 6. The sketches at the right of the figures qualitatively illustrate the stresses, and, as previously stated, the calculations for the misaligned or deflected case would be very difficult.

Note also from Figs. 5 and 6 that in this particular engine each pair of tappets is offset to provide for desired tappet rotation, but that they are offset in opposite directions to make room for the connecting-rod throw. It was observed that when misalignments or deflections were as shown, the right-hand tappet of each pair failed, whereas the left-hand one did not. It was also observed that the failed tappet was spinning in operation while the satisfactory one on the left turned very slowly, if at all. (It would seem that the same material stress conditions existed in both contacting surfaces, but this does not consider oil film buildup, which could help to distribute the stress in the case of the nonrotating tappet.) To study this effect further, a test was instituted with a tappet incorporating a 0.003 in. per in. tapered face (Fig. 7), in an attempt to prevent rotation.

The test conditions and results are shown in Table 2.

It will be observed that with a flat-face tappet, eight tappets were spalled, whereas with the tapered tappet only two were spalled, and examination indicated both of these had been rotating. In this test, those tappets which did not rotate had wear marks on the surface from 0.0008 to 0.0012 in. deep, which is thought to be undesirable.

With flat-face tappets, normal tappet rotation may be analyzed as the moment equal to the product of the offset and friction force. In the case of the cam and tappet face inclined at a small angle due to deflection or misalignment, the moment is somewhat greater, contact area for oil film buildup is substantially less, and the tendency for oil throw-off is greater, all of which are conducive to generating high stresses and consequent failure.

Spherical-face tappets will eliminate difficulties from deflection and misalignment, provided the radius is not so large as to produce excessive spinning of the tappet and edge contact under adverse conditions, although the theoretically normal stress is higher than for the flat-face tappet. The cams must be slightly tapered, or the axis of tappet and cam deliberately tilted, to provide some rotation and partial oil film. (See Figs. 8 and 9.)

Several tests were run to evaluate the effect of tappet-face radius and tapered cams. The minimum and maximum manufacturing tolerances were also evaluated, with the results shown in Tables 3 and 4.

It will be observed in Table 3 that there is a greater tendency to pit with less actual wear of mating surfaces with maximum-radius tappet face and maximum cam tapers. This is similar to tests with flat-face chilled-iron tappets and flat-face cams, which showed that when the tendency for the tappet to turn (or spin) is greater, the results are not as satisfactory. In this case, with spherical-face alloy-iron tappets and tapered cams, the calculated contact stress on the large-radius spherical face can be shown to be some 25% less than that on the minimum-radius face, but the tendency to

Table 3 – Effect of Tappet Crown and Cam Taper on Wear

Test No.	Tappets	Camshaft	Engine No.	Rpm	Condition
42050	Hardenable alloy cast iron. Phosphate-treated face. Tappets Nos. 1 to 8 with 50-in. radius. Tappets Nos. 9 to 16 with 80-in. radius	Hardenable alloy cast iron. Cams Nos. 1 to 8 with 0-4-min taper. Cam Nos. 9 to 16 with 0-7-min taper. Phosphate treated	741A	1150 to 2550[a]	Very slightly pitted on tappets Nos. 1 to 8. Crown wear averaged 0.0011 in. Cam nose wear averaged 0.0023 in. Very slight degree more pitting on tappets Nos. 9 to 16. Crown wear averaged 0.0005 in. Cam nose wear averaged 0.001 in.
Valve-Spring-Open Load, lb		167-170			
Engine Oil		*Y* (SAE 10) for 10 hr with e-p additive, then *Z* (SAE 10) for remainder[b]			
Hours Run		300			

[a] 1 hr each at 1150, 1350, 1850 and 2150 rpm and 6 hrs at 2550 rpm. All with *Y* oil plus e-p additive. 290 hr at 2550 rpm with *Z* oil.

[b] Oil *X*: medium e-p content. Oil *Y*: high e-p content. Oil *Z*: low e-p content.

Table 4 – Effect of Tappet Crown and Cam Taper on Wear

Test No.	Tappets	Camshaft	Engine No.	Rpm	Conditions
43054	Hardenable alloy cast iron. Phosphate-treated face. Random tappets crown 50 to 80 in.	Hardenable alloy cast iron. Cams with 0-6 min to 0-7-min taper. Phosphate treated	741G	1150 to 2550	No spalling or pitting. Cam nose wear range 0.0004 to 0.0014 in.
			741K	1150 to 2550[a]	No spalling or pitting. Cam nose wear range 0.0006 to 0.0015 in.
Valve-Spring-Open Load, lb		167-170			
Engine Oil		*Y* (SAE 10) for 10 hr with e-p additive, then *Z* (SAE 10) for remainder			
Hours Run		300			

[a] Oil *X*: medium e-p content. Oil *Y*: high e-p content. Oil *Z*: low e-p content.

Table 5 – Effect of Cam Width on Wear

Test No.	Tappets	Camshaft	Engine Oil	Engine No.	Rpm	Condition
9853	Hardenable alloy cast iron. Flat face. Phosphate treated	Hardenable alloy cast iron. High lift. Flat face. Phosphate-treated cam with minimum radius of curvature 0.187 in. Cam width 7/16 in. Lifter offset 1/8 in.	*X* SAE 10	92J34	2550	No tappets spalled. Cam-nose-wear range 0.0016 to 0.0102 in.
				92K34	2550	No tappets spalled. Cam-nose-wear range 0.0011 to 0.0106 in.
				92L34	2550	No tappets spalled. Cam-nose-wear range 0.0011 to 0.0085 in.
11254	Hardenable alloy cast iron (same as above)	Hardenable alloy cast iron. Same as above except cam width 5/16 in. lifter offset 1/8 in.	*Y* with e-p additive for 10 hr, then *Z* oil remainder of test[a]	0052A	1150 to 2550	No tappets spalled. Cam-nose-wear range 0.001 to 0.0016 in.
				0052B	1150 to 2550	No tappets spalled. Cam-nose-wear range 0.0012 to 0.0031 in.
				0052C	1150 to 2550[b]	No tappets spalled. Cam-nose-wear range 0.0009 to 0.0021 in.
Valve-Spring-Open Load, lb		222 to 229				
Hours Run		300				

[a] See Table 3 for detail.

[b] See Table 3 for detail.

Table 6 – Effect of Cam Contour on Spalling Tendency

Test No.	Tappets	Camshaft	Engine No.	Rpm	Condition
21050	Chilled gray iron – flat face (not phosphate treated)	Hardenable alloy cast iron. Phosphate-treated cams 0.070-in. minimum radius of curvature	150C	2550	2 spalled
			150D	2150	2 spalled
			150E	2550	2 spalled
					6 total spalled
32850	Chilled gray iron – flat face (not phosphate treated)	Same as above except new contour with 0.212-in. minimum radius of curvature cams	150C	2550	1 spalled
			150D	2150	0 spalled
			150E	2550	0 spalled
					1 total spalled
Valve-Spring-Open Load, lb		160 to 170			
Engine Oil		*X* (SAE 10)			
Hours Run		150			

pit is increased.

At least one important engine builder deliberately attempts to prevent rotation and utilizes the distribution-of-stress idea by centrally locating the axis of the flat-face tappet on the cam centerline (Fig. 10). Highly controlled manufacture is known to keep them from rotating. The small wear pattern near the center of the tappet face seems to do no harm after many miles of operation in this particular case, primarily because the loads are low.

It will be noted in the Hertz formula that the stress produced is inversely proportional to cam width. This has been confirmed, as shown in Table 5. It is observed that by increasing the cam width from 7/16 to 9/16 in. there is an appreciable reduction in maximum cam-nose wear from 0.0106 in. for the 7/16-in. width to 0.0031 in. for the 9/16-in. width.

An important way of reducing contact stress, probably not well understood, is to provide for a substantial radius of curvature on the cam at the maximum stress point. There is a feeling in some

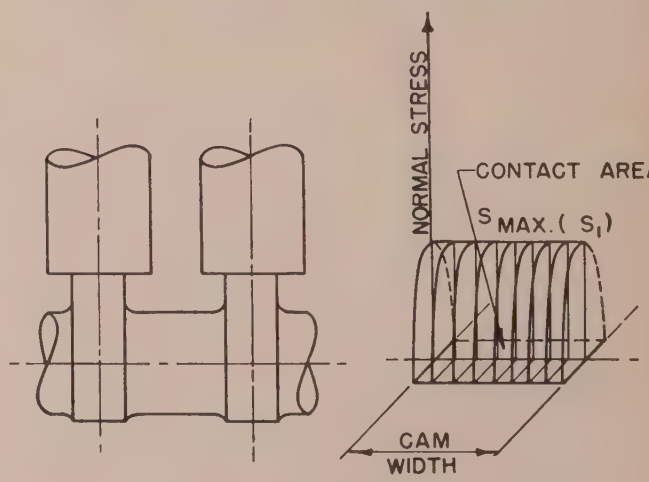

Fig. 10 – Centered tappet on flat cam

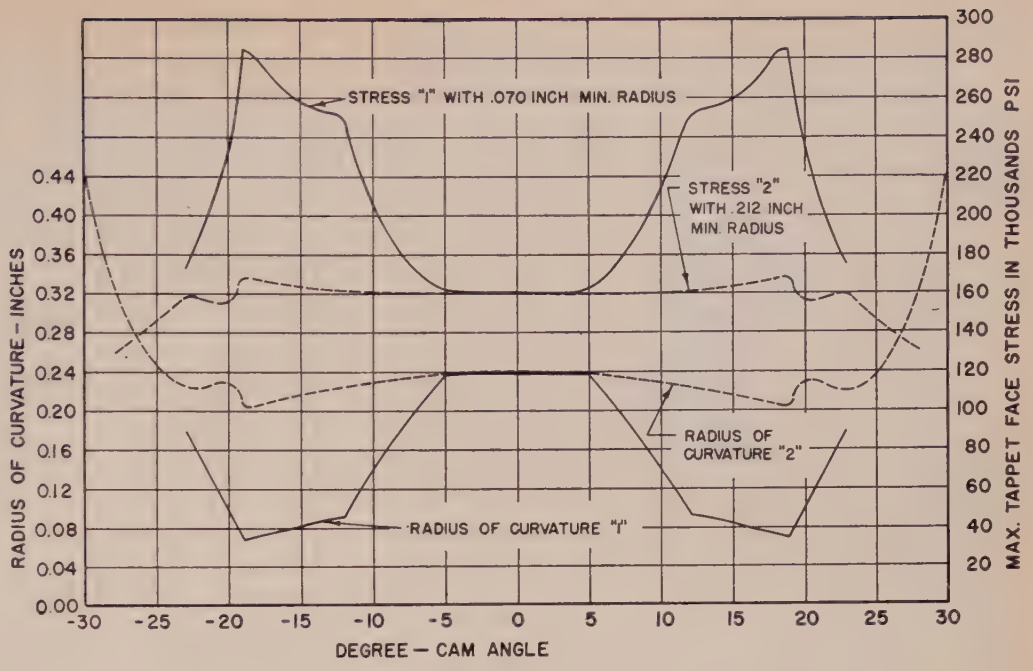

Fig. 11 – Variation of contact stress with cam radius of curvature. Stress is calculated on basis of spring force only, using manufacturer's maximum load limit on 30-in. radius spherical tappet face

quarters that a large nose radius is harmful, due to a tendency toward increased scuffing and wear. From a strict standpoint of stress computation, the minimum radius of curvature is not necessarily at the cam nose. This is illustrated in Fig. 11, where the relation between radius of curvature and stress for various cam angles is shown for 0.070- and 0.212-in. minimum-radii cams. It should be noted that for the 0.070-in. minimum-radius cam particularly, the maximum calculated stress does not occur at zero cam angle.

The radius of curvature of a cam contour at any point is proportional to the lift, acceleration, and base circle radius.[1]

$$R_c = 3283\left(\frac{d^2y}{dx^2}\right) + Z + r$$

where:

R_c = Radius of curvature, in.

$\frac{d^2y}{dx^2}$ = Acceleration at point of lift, in. per deg per deg

Z = Cam lift, in.

r = Base circle radius, in.

Once the minimum radius of curvature is known, the stress may be readily computed from charts available for this purpose.[2] Table 6 illustrates the decreased tendency for spalling by increasing the minimum radius of curvature of the cam contour. It will be observed that there is less spalling with a 0.212-in. minimum radius than with a 0.070-in. minimum radius. This is consistent with the Hertz equation, which shows the stress to be inversely proportional to the radius.

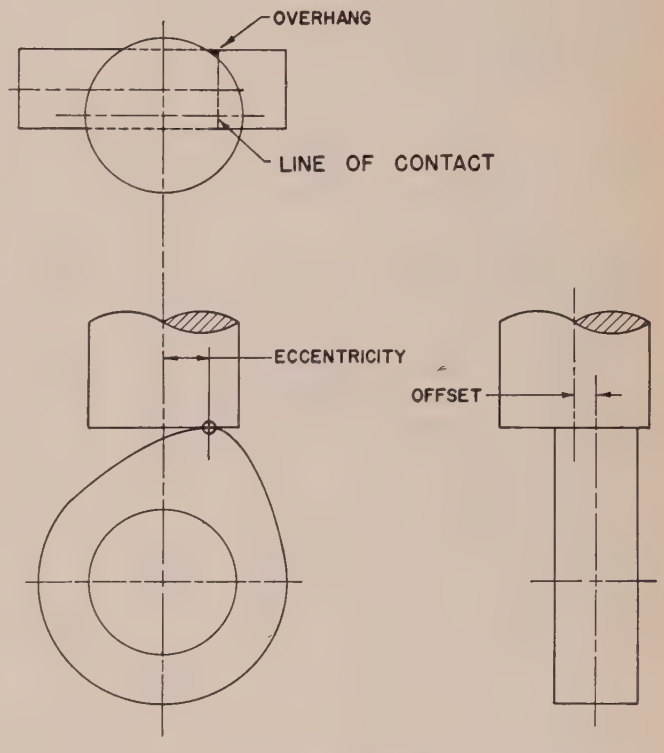

Fig. 12 – Cam eccentricity

Rubbing Velocity – An important factor in tappet performance is the manner in which the cam traverses the tappet face as the cam rotates.

The distance from the axis of the tappet to the

[1] See SAE *Quarterly* Transactions, Vol. 2, January, 1948, pp. 19-33, 51: "New Methods in Valve Cam Design," by W. M. Dudley.

[2] "Valve-Gear Design," by M. C. Turkish, Eaton Mfg. Co., 1946.

Table 7 – Representative Test Results Obtained with Phosphate-Treated Cams and Plain Chilled Face Tappets

Test No.	Tappets	Camshaft	Engine No.	Rpm	Condition
3250	Chilled flat-face gray iron. No phosphate treatment	Heat-treated forged steel cams with phosphate treatment 0.212 minimum radius of curvature[a]	150C	2550	2 spalled
3250	Chilled flat-face gray iron. No phosphate treatment	Heat-treated forged steel cams with phosphate treatment 0.212 minimum radius of curvature[a]	150D	2150	2 spalled
3250	Chilled flat-face gray iron. No phosphate treatment	Heat-treated forged steel cams with phosphate treatment 0.212 minimum radius of curvature[a]	150E	2550	2 spalled
					6 total spalled
Valve-Spring-Open Load, lb		165 to 170			
Engine Oil		*X* (SAE 10)			
Hours Run		150			

[a] Previous experience with omitting the wear-resistant phosphate coating from the cam surfaces, was entirely unsatisfactory.

point of contact with the cam is called the eccentricity (Fig. 12), and is proportional to the velocity of lift. This important theorem, which does not seem to appear in texts on cam design,[1] is expressed by:

$$e = \frac{180}{\pi} v$$

where:

e = Eccentricity, in.

v = Velocity of cam, in. per deg

It is obvious that the maximum eccentricity should be smaller than the tappet-face radius. The use of either an offset to induce tappet rotation, cams that are too wide, or tappets with too large a spherical-face radius when run with tapered cams, will often cause the resultant overhang to scrub the cam edge when excessive deflections or misalignments are present. (See upper left of Fig. 12.) Large eccentricities serve to distribute wear but increase rubbing velocity. Although rubbing velocity is ignored in stress computations, its effect should be considered in the tests of a final design. Our original hydraulic tappet durability investigation indicated that this effect was appreciable. Of 112 failures, it was found that 68.7% occurred at 2150 to 2550 rpm, whereas only 31.3% failed at 1350 rpm. (Approximately equal numbers of tests were run at each of the two levels of speed.) Rubbing velocity increases with increased engine rpm, while contact load tends to decrease at higher speeds because of inertia effects. Since total stress is a function of rubbing velocity and cam load, it appears that at some critical speed, the combination of some intermediate magnitude of each factor is more detrimental than the maximum of either.

Surface Finish and Surface Treatments – With a maximum calculated contact stress of the order of 150,000 psi or more, it is imperative that surfaces be properly finished and as accurate as possible. Roughness and inaccuracies that rupture the boundary oil film will produce relatively higher stresses, which may result in scuffing and rapid wear. Even though early scuff and wear do not show up, due to improved materials, these factors break the oil film and impose increased stress, which results in spalling (or flaking) from shear fatigue. Often a simple operation of lapping both cam- and tappet-face edges will eliminate the tendency toward scuffing and rapid wear.

In overhead-valve systems, other parts of the valve operating mechanism should be considered for finish, clearances, and compatibility of contacting surfaces, so that scuffing and wear of these parts do not increase tappet face and cam contact loads, with resultant higher stresses.

The value of phosphate-type surface treatments to inhibit scuffing at first contact and aid the breaking-in process is well known. In addition, this process produces a pock-marked surface similar in cross-section to hills and valleys, the hills having smooth plateaus. Oil carried in the valleys helps distribute the stresses of the partial or boundary oil film. The process must be rigidly controlled and the initial surface to be treated must be smooth enough to carry the load, otherwise early failure will result from scuffing and wear.

When attempts were made to run an SAE 1039 heat-treated steel camshaft with chilled-face gray-iron tappets using 0.212-in. minimum radius of curvature cams, excessive spalling was observed. Phosphate-treating the camshaft was a distinct improvement and typical data shown in Table 7 were obtained. When both camshaft and tappets were phosphate-treated and operated under the same conditions as above, complete freedom from spalling was observed. (See Table 8.)

With the minimum nose radius decreased to 0.070 in., the engines could be run 150 hr. There

Table 8 – Performance of Chilled Face Tappets with Both Cam and Tappet Face Phosphate Treated

Test No.	Tappets	Camshaft	Engine No.	Rpm	Condition
52250	Chilled flat-face gray iron with phosphate treatment	Heat-treated forged steel cams with phosphate treatment, 0.212-in. minimum radius of curvature	150C	2550	0 spalled
52250	Chilled flat-face gray iron with phosphate treatment	Heat-treated forged steel cams with phosphate treatment, 0.212-in. minimum radius of curvature	150D	2150	0 spalled
52250	Chilled flat-face gray iron with phosphate treatment	Heat-treated forged steel cams with phosphate treatment, 0.212-in. minimum radius of curvature	150E	2550	0 spalled
					0 total spalled
Valve-Spring-Open Load, lb		165 to 170			
Engine Oil		*X* (SAE 10)			
Hours Run		150			

Table 9 – Effect of Decreased Cam Nose Radius on Spalling of Chilled Face Tappets

Test No.	Tappets	Camshaft	Engine No.	Rpm	Hours Run	Condition
93049	Chilled flat-face gray iron. No phosphate treatment	Heat-treated forged steel cams with phosphate treatment, 0.070-in. radius of curvature	150C	2550	150	3 spalled
			150D	2150	150	1 spalled
			150E	2550	150	4 spalled
						8 total spalled
111649	Chilled flat-face gray iron blasted with fine shot	Heat-treated forged steel cams with phosphate treatment, 0.070-in. radius of curvature	150C	2550	120	1 spalled
			150D	2150	120	4 spalled
			150E	2550	120	6 spalled
						11 total spalled
102149	Chilled flat-face gray iron with phosphate treatment	Heat-treated forged steel cams with phosphate treatment, 0.070-in. radius of curvature	150C	2550	150	3 spalled
			150D	2150	150	2 spalled
			150E	2550	150	2 spalled
						7 total spalled
Valve-Spring-Open Load, lb		165 to 170				
Engine Oil		*X* (SAE 10)				

was significant spalling, however, as shown in Table 9, for the following:

1. Phosphate treatment of camshaft only.
2. Phosphate treatment of camshaft only with fine shotblast surface on tappets.
3. Phosphate treatment of both camshaft and tappets.

These representative tests on flat-faced chilled gray-iron tappets and heat-treated forged-steel flat-face cams have indicated that when calculated contact stresses exceed 150,000 psi, surface treatments will not ensure satisfactory performance.

Summary on Design Factors – From the foregoing discussion, there appear to be several practical methods of improving tappet-cam durability by design, as follows:

1. Design for low contact stresses.
2. Where deflecting mating parts cause edge contact and high stresses difficult to calculate, design for low deflection.
3. Design for low rubbing velocities with minimum overhang to prevent possible edge contact.
4. Specify the best finish and alignment possible consistent with volume production.

Influence of Lubrication on Valve-Gear Performance

Lubrication of the cam and tappet face is another factor affecting valve-gear performance. Due to the nature of the required design geometry, the oil film at best is only partial and a boundary film. However, these parts will not run together without oil, and they seem to operate much more satisfactorily if the oil has a higher e-p content. Recently, the breakin run of an engine was started three times (using new tappets and camshaft each time), before it was determined that a new barrel of oil was not breakin oil containing specified e-p additive, as marked. With higher loads and speeds, the situation is becoming more nearly comparable to that of hypoid gears.

Some time ago, when the automatic tappet was first investigated, there was noted an increased tendency of the tappet face to spall. An increased tendency for the rocker-arm bearings to score and push-rod seats to wear was also observed. It was felt this was due to the spring in the tappet, which although light (10-12 lb), keeps the contacting parts together (essential for automatic operation), as opposed to slack in the system 50% of the time with mechanical tappets. The latter allows for a more substantial oil film buildup.

The influence of lubricating oils on cam and tappet performance as determined at our laboratories has been previously reported.[3, 4] In addition to those data, considerable experience has been obtained during the past two years on the performance of various oils in car tests under two different conditions of driver operation. The first, car pool service, includes many different drivers in the same car, and in the second, owner-driver service, most of the mileage is accumulated by one driver. The procedure for evaluating these conditions is discussed below.

Car Pool Service – 1. Preparation of cars for test: The cars are drained upon delivery. The tappets and camshafts are measured, and test oils are installed, after which the cars are placed in the garage pool service.

2. Fuels and oils: The car is supplied with fuel and oil from a single source. The oil is changed at 2000-mile intervals.

3. Type of operation: The operation is a mixed one consisting largely of city driving with some interurban trips. The cars are stored at night in the company garage and each car is used by many different drivers. The extent of the operation is 12,000-20,000 miles per year.

4. Final inspection: Previous to sale of the cars the valve-gear parts are again inspected.

Owner-Driver Service – The procedure for handling the owner-driver cars employed is identical to that for the pool cars with two exceptions:

1. No effort is made to control the fuel.
2. No effort is made to control operating conditions.

Table 10 shows the comparative wear and spall-

Table 10 – Tappet Wear – 13,000 Miles of Operation – Car Pool Service – Make No. 2

Oil	No. of Cars	Tappet Wear, in. Maximum	Minimum	Average	Spalled Tappets, %
Brand *A* 10W	2	0.00410	0.00030	0.00106	12.5
Brand *B* 10W	2	0.00300	0.00050	0.00154	12.5
Brand *C* 10W	3	0.00492	0.00090	0.00261	52.5
Brand *C'* 5W	2	0.00580	0.00145	0.00265	50.0
Brand *D* 5W-20	3	0.00404	0.00090	0.00278	80.0
Brand *E'* 10W	2	0.01570	0.00140	0.00464	45.8
Brand *E* 5W	2	0.01020	0.00180	0.00464	45.8

[3] See SAE Transactions, Vol. 63, 1955, pp. 211-220: "Lifters and Lubricants," by J. B. Bidwell and P. Vermaire.

[4] See SAE Transactions, Vol. 63, 1955, pp. 349-361: "New Look in Lubricating Oils," by J. B. Bidwell and R. K. Williams.

Fig. 13 – Appearance of scuffed foot surface of steel tappet after running against alloy cast-iron cam. Tappet wear: 0.0008 in.; cam wear: 0.0670 in. (original photograph taken at 2X)

ing data for seven different engine oils in car make No. 2 operated under car pool conditions for 13,000 miles. Car make No. 2 employs a flat-face chill-cast tappet and a forged-steel camshaft.

While the data themselves do not conclusively rate the oils in order of satisfactory performance we can draw the following conclusions:

1. There are some oils on the market, such as *E*, which will cause serious distress in a relatively low number of miles under conditions approximating normal customer service for the combination of camshaft and tappet materials used in this test.

2. There is a considerable variation in the ability of commercial oils to prevent wear and spalling. (We have considerable other data on oil *A* that indicates that this oil gives consistently good results.)

3. The data indicate there is not a gross difference in performance between 5W and 10W oil given the same additive treatment.

When these same oils were tested in an engine of different design but using a chill face cast-iron tappet and a carburized steel camshaft, oil *E* still gave poor results from a spalling standpoint, as shown in Table 11.

Table 11 – Tappet Wear and Spalling – Car Pool Service – Make No. 4

Oil	Test Miles	Tappet Wear, in.			Spalled Tappets, %
		Maximum	Minimum	Average	
Brand *E*	8,850	0.00430	0.00040	0.00129	37.5
Brand *E*	10,885	0.00160	0.00080	0.00120	31.2

Table 12 – Tappet Wear – 10,000 Miles of Operation – Car Pool Service – Make No. 2

Oil	Maximum	Minimum	Average
Brand H SAE 10W	0.00764	0.00019	0.00175
Brand A SAE 10W	0.00260	0.00050	0.00136
Brand I SAE 20W	0.00277	0.00050	0.00095
Brand J SAE 10W	0.00196	0.00010	0.00079
Brand B SAE 10W	0.00158	0.00011	0.00077
Brand E 5W-20	0.00214	0.00133	0.00190
Brand K 5W-20	0.00206	0.00088	0.00147
Brand L 5W-20	0.00224	0.00075	0.00128
Brand M 5W-20	0.00326	0.00086	0.00125
Brand N 5W-20	0.00649	0.00058	0.00097
Brand O 5W-20	0.00331	0.00051	0.00086
Brand P 10W-30	0.00282	0.00102	0.00178
Brand Q 10W-30	0.00142	0.00057	0.00108
Brand R 10W-30	0.00152	0.00035	0.00096
Brand S 10W-30	0.00198	0.00059	0.00095
Brand T 10W-30	0.00129	0.00059	0.00087
Brand U 10W-30	0.00130	0.00065	0.00084

In 1953 and 1954 many new lubricating oils were introduced, and in addition to these innovations, camshaft and tappet materials were changed to hardened-iron shaft and hardened-iron tappets in the new models of car makes Nos. 1 and 2. In view of these modifications, it seemed desirable to make a spot check of the relationship between the newly formulated oils and the modified metallurgical compositions. These data were shown first in Fig. 3. They are shown in more detail in Table 12, which shows the average tappet wear with car make No. 2, using hardened alloy-iron camshaft and tappets, with 15 new oils and two oils (*B* and *E* from Tables 10 and 11), selected as good and poor reference oils from our previous experience in 10,000 miles of operation under pool-type conditions.

It will be noted that the 17 oils are divided into three groups: the conventional single-grade oils, the 5W-20 multigrade oils, and the 10W-30 multigrade oils. The important modifications introduced in the new oils were, in general, a change in the direction of increased detergency, an incorporation of antiwear agents, and a trend toward the development of all-purpose or multigrade oils. It is interesting to note the following:

1. There is the same type of variation in antiwear properties in each of the three groups. This suggests that whatever differences may exist as a result of differences in viscosity are overshadowed by larger differences in additive treatment.

2. Even with a different combination of materials, the oil selected as a good oil (oil *B*) and the oil selected as a poor oil (oil *E*) bracketed the entire range of wear experienced by all the oils tested.

Summary on Lubrication – Evaluation of a number of commercial oils by car tests has shown that crankcase oils vary considerably in ability to prevent wear and spalling of tappets. Differences in additive treatment appear to be more important in this respect than differences in viscosity. Excep-

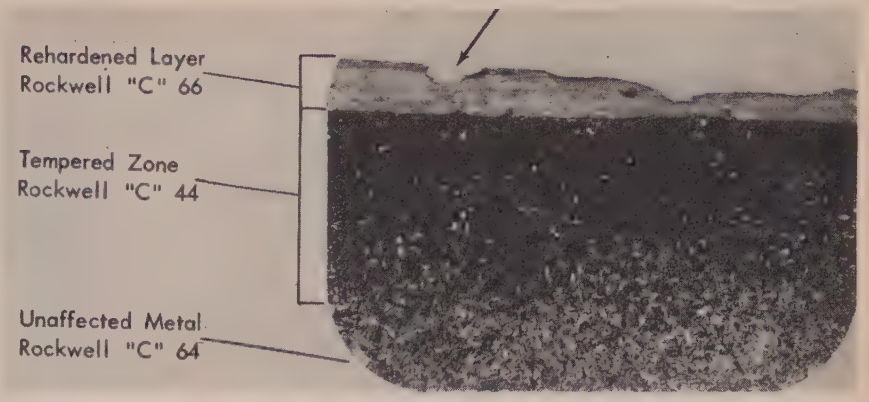

Fig. 14 – Cross-section of scuffed foot surface of steel tappet, showing rehardened surface and embedded material (arrow) (original photograph taken at 500X) (2% nital etch)

tionally poor and exceptionally good oils could be distinguished, and the order of this rating was apparently not affected by changes in design or metallurgy. A more quantitative evaluation of the various oils was not possible with the car test data.

Influence of Metallurgy on Valve-Gear Performance

The third major factor influencing valve-gear operation is the material used for tappets and camshafts. As with design, no one metallurgical combination has been recognized as superior by all engine manufacturers. An example of this variation in preference of materials for tappets and cams is shown in Table 13, which lists some typical combinations used by several manufacturers.

Although some combinations appear to be better than others, at least occasional failures have been observed with all, indicating that if valve gear loads are to be increased in the future, a further modification in metallurgy may be necessary.

A. Engine Experience – Types of failure: The types of tappet failures observed in engines are primarily related to tappet material.

Chilled cast-iron tappets ordinarily fail in fatigue, evidenced by spalling of the foot surface. The resultant roughened surface sometimes leads to damage of the cam with consequent loss in engine performance. The mode of failure of chilled-iron tappets is quite well understood and was discussed in detail in a recent paper.[4]

Failure of steel tappets can generally be classified as either wear or scuffing. Occasionally, a slight degree of spalling or pitting of the foot surface is also observed on this type of tappet. Scuffing, which appears as an irregular roughening of the foot surface, is by far the most serious type of failure since it almost invariably results in severe wear of the mating cam.

A considerable number of carburized steel tappets, representing both engine tests and actual service in automobiles, were examined in an effort to determine the nature of the failures. Fig. 13 shows the foot surface of a typical scuffed tappet. Although the tappet wear was quite low (0.0008 in.), cam wear was excessive (0.0670 in.). Fig. 14 shows a cross-section of the foot surface of this tappet. It is evident that a pronounced change has occurred in the material adjacent to the surface, with the formation of a thin, light-etching surface layer and a dark-etching region immediately below. The microstructure shown at the bottom of the figure is the normal structure ordinarily observed in this type of tappet.

The approximate hardness of the various regions, determined with a Bergsmann microhardness tester and converted to RC units, is indicated on the figure. The appearance of the surface layer and its high hardness, RC 66, indicates untempered martensite probably formed by rehardening of the original surface during operation in the engine. The minimum temperature at which such rehardening could occur, under equilibrium conditions, is approximately 1350 F. In the dark-etching region, the temperature reached was not sufficient to produce rehardening, but the original martensitic structure was appreciably tempered.

The photomicrograph shows spalling, which tends to originate in the rehardened layer, and some large white particles in the surface. These particles appear to be carbides, broken from the surface of the alloy cast-iron cam and embedded in the tappet foot surface during the momentary overheating. Fig. 15 shows the appearance of one of these rehardened areas on the actual tappet foot surface. The large embedded carbides are clearly visible. The foot surface was cleaned and etched only to

Table 13 – Tappet and Camshaft Material Specifications

Tappets	Camshaft
Chilled cast iron	Carburized low carbon steel
Chilled cast iron	Alloy cast iron
Chilled cast iron	Spray quenched medium carbon steel
Carburized steel	Alloy cast iron
Alloy cast iron	Alloy cast iron

obtain this photomicrograph.

Rehardening observed on scuffed tappets is presumably the result of a momentary breakdown of the lubricating oil film which permitted metal-to-metal contact and attendant heat generation. The severe cam wear observed in connection with scuffing is expected with this type of failure because spalling of the rehardened layer produces a hard, rough surface which tends to abrade the cam. The large carbide particles embedded in the rehardened material may also contribute to the cutting action.

Surface overheating of steel tappets does not always result in failure by scuffing and extreme cam wear. Fig. 16 shows a tappet which failed by wear, with little wear on the mating cam. Microexamination of the foot cross-section (Fig. 17) showed a shallow tempered surface layer. The surface temperature attained apparently was not enough to cause the rehardening observed on scuffed tappets, but the superficial tempering could presumably lower the wear resistance of this material enough to promote accelerated tappet wear. Reduced hardness produced by tempering would also result in lowering the fatigue endurance limit of the material and thus lead to spalling if the tempered material was not removed rapidly enough by wear. Fig. 18 shows a steel tappet where this type of failure has apparently occurred. The photomicrograph (Fig. 19) taken on a cross-section of this tappet, shows one of the spalled areas in a tempered layer. Again, cam wear was quite low.

The sensitivity of steel tappets to type of lubricating oil is not surprising in view of the suscepti-

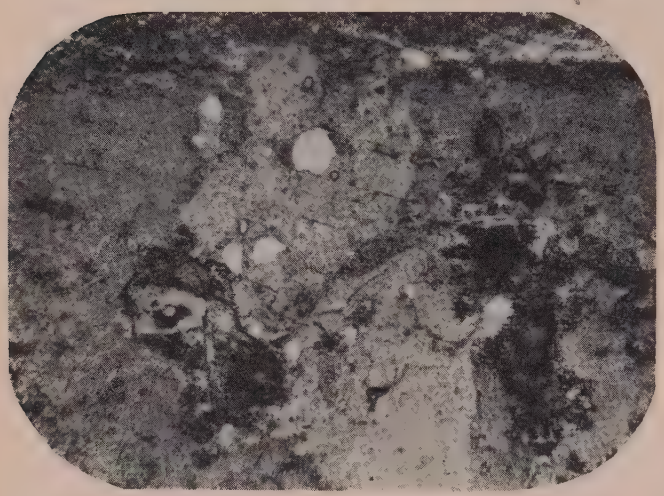

Fig. 15 – Appearance of steel tappet foot surface in rehardened area, showing spalling and embedded carbides (large white particles) (original photograph taken at 500X) (2% nital etch)

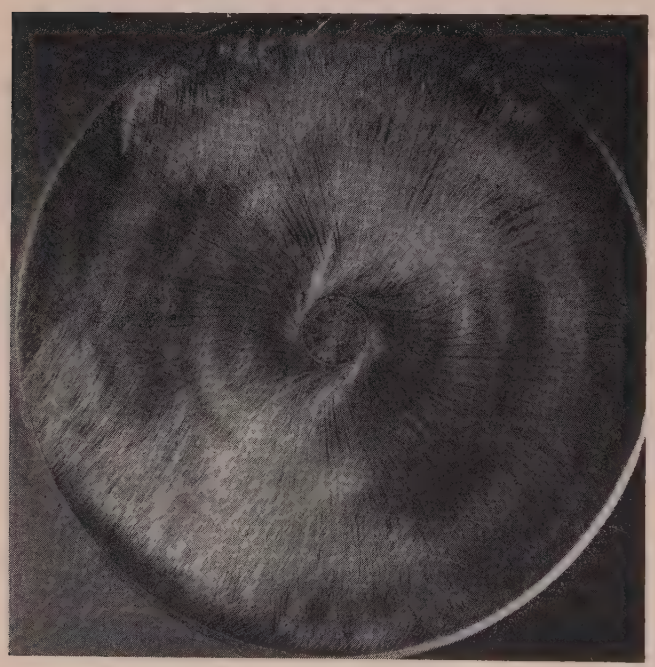

Fig. 16 – Appearance of foot surface of worn steel tappet after running against an alloy cast-iron cam. Tappet wear: 0.0073 in.; cam wear: 0.0008 in. (original photograph taken at 2X)

Fig. 17 – Cross-section of foot of worn steel tappet showing tempered surface (original photograph taken at 500X) (2% nital etch)

Table 14 – Summary of Engine Tests on Various Material and Design Combinations

Minimum Radius of Curvature, in.	Camshaft	Phosphate Treatment	Tappet	Phosphate Treatment	No. of Failed Tappets	Location of Data in Appendix
0.212	Steel[a]	Yes	Chilled iron[b]	No	6 spall	Note[b]
0.212	Steel	Yes	Chilled iron	Yes	0	Note[c]
0.212	Steel	Yes	Alloy iron[d]	Yes	9 worn[e]	Table A-1
0.212	Steel	Yes	Steel[f]	Yes	18 worn	Table A-2
0.212	Alloy iron[d]	Yes	Chilled iron	No	1 spall	Table A-3
0.212	Alloy iron	Yes	Alloy iron	Yes	0	Table A-4
0.212	Alloy iron	Yes	Steel[f]	Yes	0	Table A-5
0.187[g]	Alloy iron	Yes	Chilled iron	No	14 spall	Table A-6
0.187	Alloy iron	Yes	Alloy iron	Yes	0	Table A-7

[a] 1039 steel hardened – heat-treatment and hardness in Appendix Table A-8.
[b] Summary of results shown in Table 7. Chemical composition and hardness in Appendix Table A-8.
[c] Summary of results shown in Table 8.
[d] Chemical composition and hardness in Appendix Table A-8.
[e] 1/8-in. wear in 2 hr, 40 min.
[f] 5120 steel carburized – heat-treatment and hardness in Appendix Table A-8.
[g] Valve spring load increased to 207-212 lb with high-lift cam contour.

Table 15 – Relationship of Cam Lobe Position to Frequency of Failure (Alloy-Iron Cams and Tappets – 31 sets)

Odd Cams		Even Cams	
Lobe Position[a]	No. of Failed Cams[b]	Lobe Position	No. of Failed Cams
1	2	2	6
3	0	4	4
5	1	6	3
7	0	8	4
9	2	10	11
11	0	12	21

[a] Starting front of engine.
[b] Cam nose worn 0.007 in. or more.

bility of this material to surface overheating. Slight variations in oil film conditions would be expected to produce profound differences in tappet operation.

Alloy cast-iron tappets do not appear to be as prone to overheating as steel tappets. Scuffing of alloy-iron tappets is observed only occasionally, and then usually under abnormally severe operating conditions. Alloy iron does not exhibit the sensitivity to type of lubricant which has been observed with steel tappets.

Material compatibility: The compatibility of various camshaft and tappet materials has been investigated extensively. Since design and lubrication are such important factors, it has long been obvious there can be several correct material combinations under different design and lubrication conditions.

Data from one engine point out some general trends.

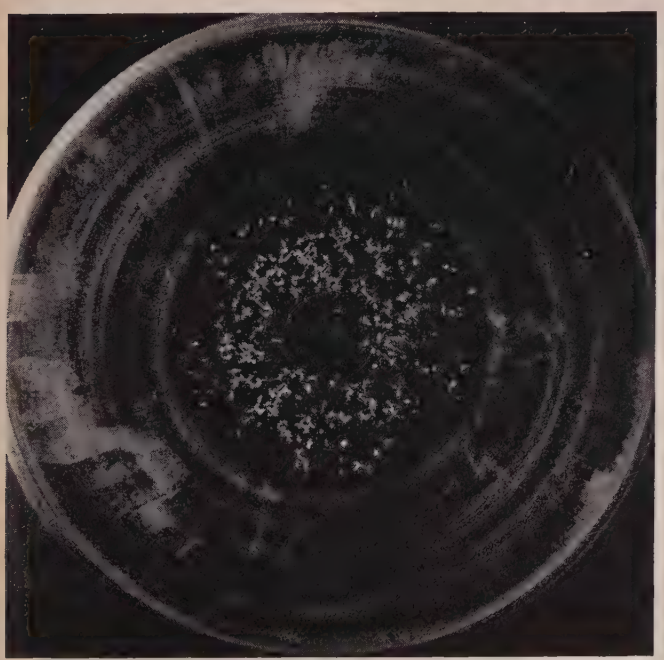

Fig. 18 – Appearance of foot surface of worn steel tappet showing light spalling after running against an alloy cast-iron cam. Tappet wear: 0.0013 in.; cam wear: 0.0005 in. (original photograph taken at 2X)

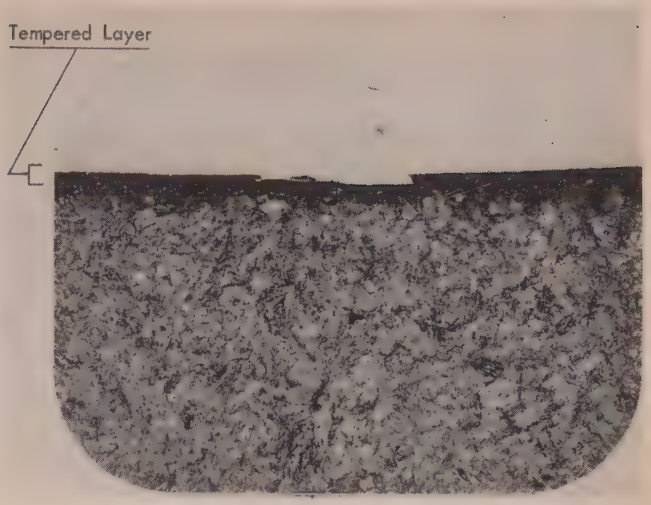

Fig. 19 – Cross-section of steel tappet foot showing spalling in tempered layer (original photograph taken at 500X) (2% nital etch)

With a normal valve-spring-open load of 165-170 lb and an SAE 10 medium e-p content oil, the summary shown in Table 14 was obtained from 150-hr tests on three engines. (Detailed data are shown in the Appendix.)

Previous experience had shown entirely unsatisfactory operation unless the camshaft was phosphate-treated. Several interesting conclusions may be drawn for this engine from these data:

1. Surface treatment improves the compatibility of materials.
2. Alloy cast-iron camshafts are generally more compatible with other materials than are hardened SAE 1039 camshafts.
3. An alloy-iron camshaft will run with hardened-steel tappets but a hardened-steel shaft will not run with alloy-iron tappets.
4. The incidence of spalling with chilled-iron tappets on an alloy-iron shaft increases with increased contact stress resulting from higher spring load and smaller radius of curvature.

Although the general properties of various metallurgical combinations can be evaluated roughly by engine tests, the variation in results from test to test makes quantitative comparisons impossible. The scatter in results is apparently due to

Table 16 – Distribution of Cam Carbide Rating

	Carbide Rating						
Lobe No.	(Dendritic)	1	2	3	4	5	(Cellular)
	% of Cams with Given Carbide Rating						
1		0	6	49	45	0	
12		0	0	13	47	40	

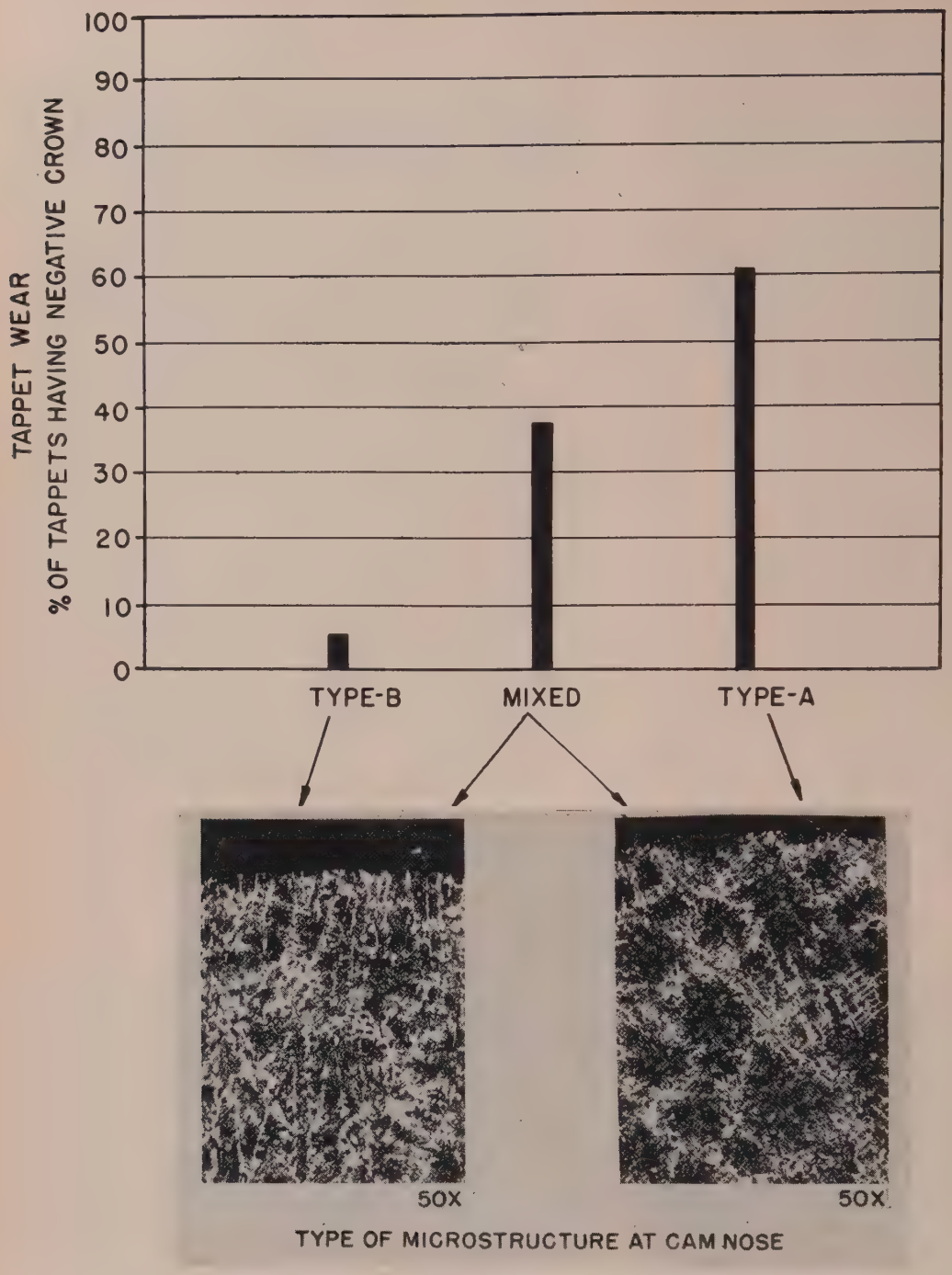

Fig. 20 – Effect of alloy cast-iron camshaft microstructure on tappet wear

the presence of a number of uncontrolled or only partly controlled variables which exert a considerable influence on tappet wear.

For example, experience over a number of tests has shown a consistent variation in wear rate of cam lobes from position to position as shown in Table 15.

It is apparent that the incidence of cam failure is greater on the even-numbered cams than on the odd-numbered ones, which probably relates to deflections and misalignment previously described.

The high incidence of failure at the No. 12 position correlates with the metallurgical facts shown in Table 16. This table shows the distribution of the cam carbide rating at the Nos. 1 and 12 positions determined from a large number of camshafts destructively examined without running. (The lower the carbide rating number, the denser

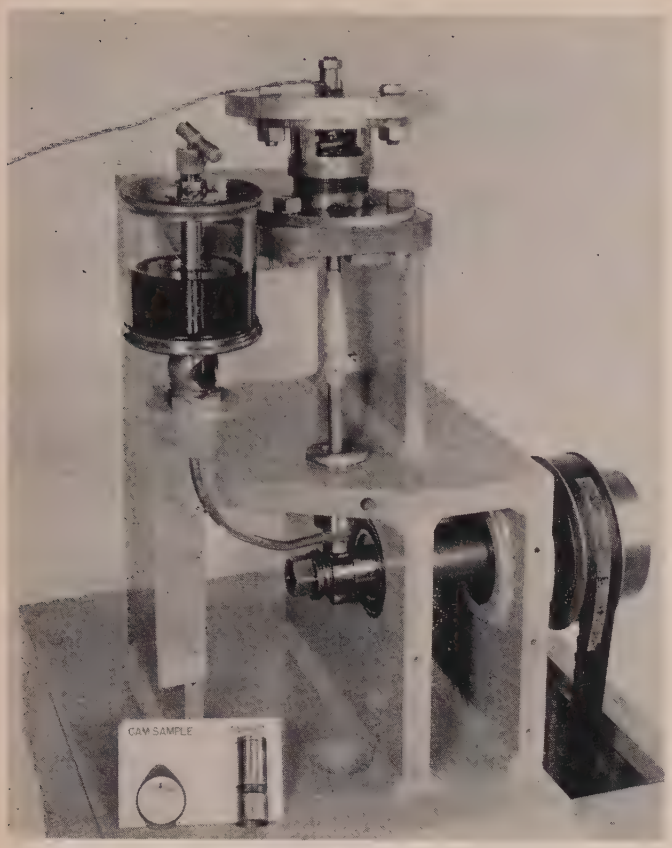

Fig. 21 – General view of test machine

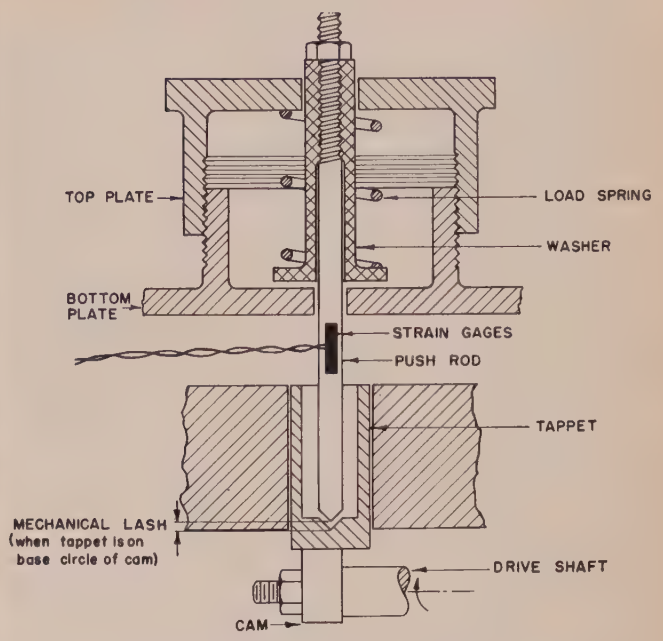

Fig. 22 – Cross-section of test machine showing method of loading. As shown, cam is in position of maximum lift

and more dentritic the carbide.) Observe that the carbide rating tends to be more cellular and less dense at the No. 12 position, which position showed the greatest incidence of failure.

Further substantiation of the correlation of carbide rating with performance is shown in Fig. 20, which summarizes the results of an examination of 20 sets of camshafts and tappets taken from service and dynamometer tests on another type of engine.

Both steel and alloy-iron tappets are represented, and all camshafts were alloy cast iron, flame-hardened. Since the wide variety of tests or service histories represented by these samples did not permit comparing actual wear figures, tappet wear was expressed as the percentage of tappets having a negative crown – that is, a concave foot surface. (These tappets are designed with a positive spherical crown of approximately 0.0010 in. on the foot surface.)

The photomicrographs at the bottom of Fig. 20 are representative of the two general types of microstructure observed at the cam noses of the cast-iron camshafts. The structure termed type *A* (carbide rating number = 5), shows a network distribution of "lake" carbide, while the type *B* structure (carbide rating number = 2 to 3) has needle-shaped carbides suggestive of a chilled iron. In the samples listed as *mixed,* the cam microstructure varied from one type to the other along the length of the shaft. The figure indicates that 60% of the tappets run against type *A* camshafts developed negative crowns, compared to only 5% for type *B* shafts. This amount of variation in microstructure, unfortunately, is very difficult to eliminate in a production operation, and this factor adds to the difficulty in interpreting engine test results.

B. *Laboratory Test Experience* – The observed scatter in engine test data has emphasized the need for a relatively simple bench test which could be used to evaluate materials more quantitatively. To be practical, the test conditions must not be too far removed from actual cam and tappet operation, and must permit closer control of conditions than can be attained in an engine. Our laboratory has developed such a test method, and preliminary results have been encouraging.

Description of test machine: Essentially, the test machine consists of a tappet held against a rotating cam by a spring-loaded push-rod, as shown in Fig. 21. Strain gages attached to the push-rod permit static measurements of loads with an estimated accuracy of ±3% of the indicated load. The cam is mounted on a shaft driven by an electric motor, and an oil cup supplies oil to the cam and tappet at a controlled rate. The cam samples were obtained

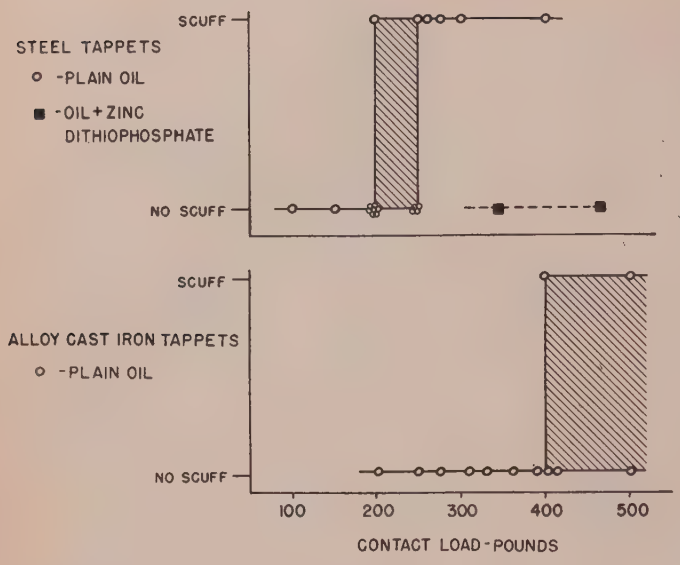

Fig. 23 – Difference in scuffing tendency of steel and alloy-iron tappets using oil *F*

by cutting individual cams from production camshafts and drilling to fit the drive shaft, as shown in Fig. 21.

The method of loading the tappet is shown schematically in Fig. 22. The load is applied by a high-strength coil spring and is adjusted by turning the threaded top plate. This preloads the spring in the same manner as shimming the valve springs in an engine. Since the tappet sample in this arrangement is a hydraulic tappet body operated as a mechanical tappet, there is some lash in the system. It is adjusted by turning the threaded washer and causing the push-rod to move up or down with respect to the tappet. The constant factors in these tests are summarized in Table 17.

The variable of cam microstructure was controlled indirectly by using adjacent cams from the same camshaft for each group of tests. (As was pointed out earlier, the microstructure of an alloy cast-iron camshaft appears to be either similar for all the cams in a given shaft, or varies uniformly from one end of the shaft to the other. Adjacent cams, therefore, would be expected to have quite similar microstructures.)

The primary objective of this first series of tests was to determine whether or not the test machine could distinguish between two tappet materials with regard to scuffing tendency, wear, and sensitivity to type of lubricant, in conformance with our engine test experience. A considerable number of engine tests had established the following:

1. Carburized-steel tappets are more prone to scuffing failure than alloy cast-iron tappets.

2. Steel tappets are quite sensitive to type of lubricant. Addition of a zinc dithiophosphate additive[5] to the lubricating oil produces an appreciable improvement in performance of steel tappets.

3. Alloy cast-iron tappets are relatively insensitive to type of lubricant.

The test machine was evaluated by comparing the test results with this engine test experience.

Tests to evaluate scuffing tendencies of materials: The results of a series of tests to determine

Table 17 – Bench Test Conditions

Type of Tappets	Carburized steel Alloy cast iron, flame hardened
Type of Cam	Alloy cast iron, flame hardened
Tappet Offset, in.	1/16
Direction of Rotation	Same as in normal engine operation
Mechanical Lash, in.	0.008-0.010
Lubricant	Commercial 10W motor oils, diluted 1:1 with kerosene[a]
Lubrication Rate	Two drops per second
Cam Speed, rpm	1240[b]

[a] The oils were diluted with kerosene to increase the severity of the test conditions.
[b] Equivalent to 2480 engine rpm.

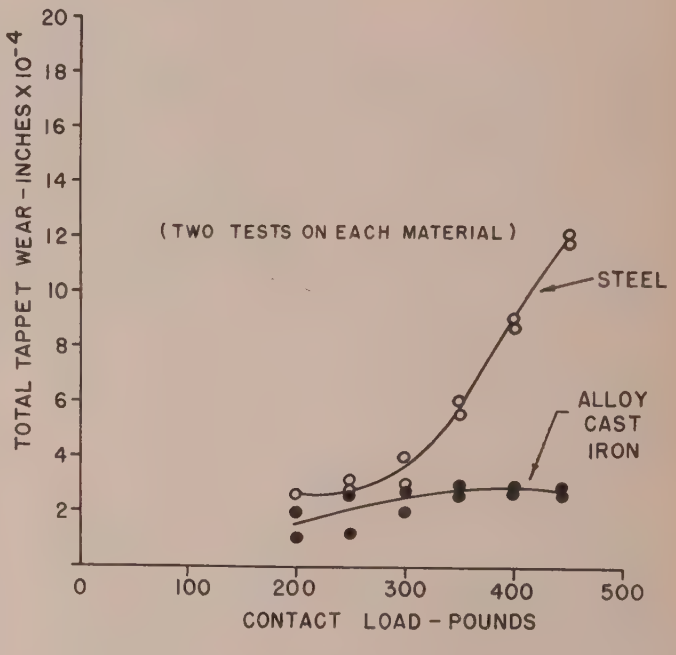

Fig. 24 – Comparison of wear behavior of steel and alloy-iron tappets using oil *F*

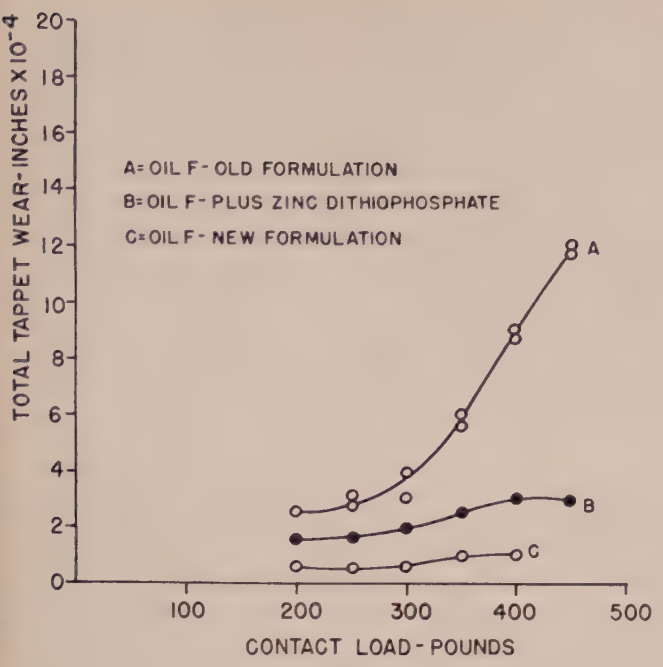

Fig. 25 – Effect of type of lubricant on wear behavior of steel tappets

scuffing tendencies are summarized in Fig. 23. The oil used (oil *F*) contained no zinc dithiophosphate and had shown poor results in engine tests. The tests were conducted by running each cam and tappet set at one load for 10 min. If no scuffing failure occurred, a new set of samples was assembled and run 10 min at a higher load. As shown in the figure, there is a critical range of loads for this type of failure. Tappets operated below this range did not scuff, while those run above the critical load scuffed in from 3 to 5 min after starting. The critical range for steel is considerably lower than that for alloy cast iron. The addition of 1% of a zinc dithiophosphate additive to the oil, however, prevented scuffing of the steel tappets at loads considerably over the critical. Both of these observations are in good agreement with engine test experience.

Tests to evaluate wear tendencies of materials: In the course of running scuffing tests, it was observed that when a cam-tappet set was operated below the critical load so that no scuffing occurred, the load then could be increased in increments of 50 lb with a 10 min run at each load, and loads considerably above the critical were attained without scuffing failure. Steel tappets operated in this manner showed a measurable amount of wear after each 10-min run at successively higher loads, this behavior suggesting another possible means of material evaluation. Accordingly, a series of tests was run with steel and alloy cast-iron tappets, using adjacent cams from the same shaft to minimize the effects of variables in the cam. Fig. 24 shows the comparison of steel and alloy iron obtained using oil *F*. A definite separation of the two materials is evident with respect to both total wear and general shape of the wear versus load curve. Rapid wear of the steel is due possibly to a continual tempering and subsequent removal by wear of the surface material.

The effect of a zinc dithiophosphate additive in the lubricating oil on the behavior of steel tappets may be seen in Fig. 25. Curve *A* is the average curve for steel with plain oil *F*.

Curve *B*, obtained by adding 1% of zinc dithiophosphate additive to the oil, looks very much like that obtained with alloy-iron tappets run with plain oil. Curve *C* was run to check these results, using a new lot of oil *F* because of depletion of the original supply. The shape of this curve is similar to that obtained using the original lot of oil *F* with zinc dithiophosphate added. Information subsequently obtained from the oil company confirmed this observation. Oil *F* had been modified by the addition of zinc dioctyl-dithiophosphate in the interval between the purchase of the two lots of oil *F*.

In addition to the wear versus load relationship, the test machine can be used to compare tappet materials and lubricants with respect to wear rate (wear versus time), as shown in Fig. 26. The lubri-

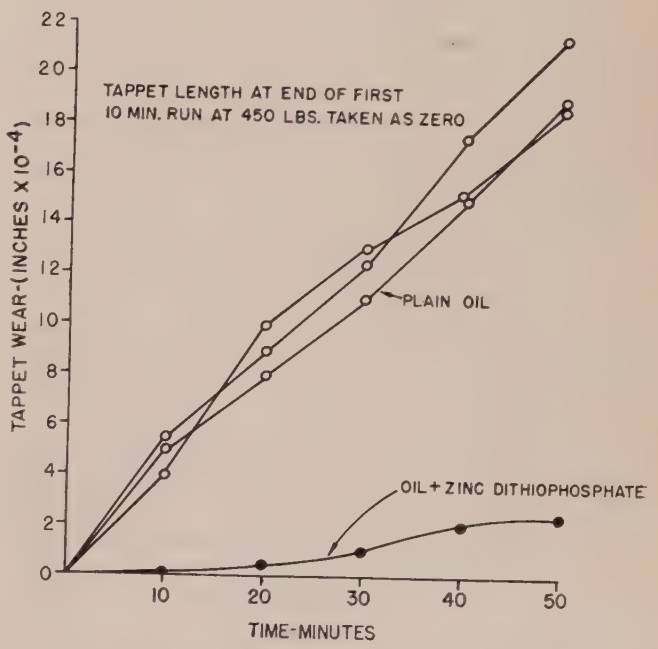

Fig. 26 – Wear of steel tappets at 450-lb load using oil *G*

[5] The zinc dithiophosphate additive referred to here and in the following sections is zinc dioctyl-dithiophosphate.

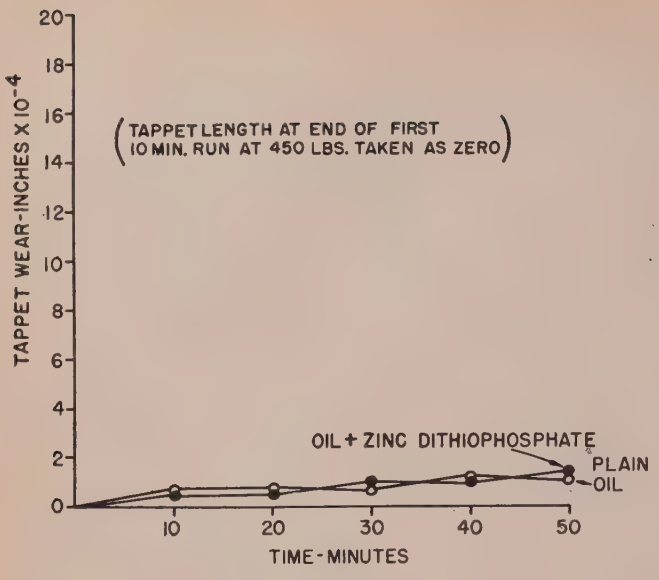

Fig. 27 – Wear of alloy cast-iron tappets at 450-lb load using oil *G*

cant used (oil *G*) was similar to the original lot of oil *F* in composition, and had also been rated poor in engine tests. These tests were conducted by first increasing the contact load to 450 lb in 50-lb increments, as done previously to determine the wear versus load relationship. The tappets were then operated at the 450-lb load and periodic measurements were made of tappet wear. The results again show a pronounced influence of zinc dithiophosphate additive on the wear tendency of steel tappets.

Fig. 27 summarizes the results of similar tests made with alloy cast-iron tappets. The addition of zinc dithiophosphate to the oil appeared to have no effect on the wear tendency of this material. However, the wear obtained with plain oil was so low that any beneficial effects of the zinc additive would probably not be detected under these test conditions.

The good reproducibility obtained with this type of test, evidenced by the agreement of the three wear curves for plain oil *G* in Fig. 26, indicates that the important variables affecting tappet performance were under adequate control. Considerable information can thus be obtained from a relatively small number of tests.

Severity of the test conditions must be increased before more wear-resistant materials can be evaluated. The results obtained with steel and alloy cast-iron tappets, however, have indicated the suitability of the general manner of testing. The method may also be useful for the rapid evaluation of lubricating oils.

Summary on Metallurgy – Examination of tappets after operation in engines has indicated that the performance of steel tappets is limited primarily by the production of high surface temperatures on the tappet foot, which results in either tempering of the surface to promote tappet wear, or local rehardening, which results in extreme cam wear.

Tappet performance in the engine is influenced appreciably by the microstructure of the mating cam.

Some progress has been made toward the development of a laboratory test for evaluating scuffing and wear tendencies of tappets and cams. The test results are in agreement with engine test experience with regard to the performance of both steel and alloy cast-iron tappets. Relative sensitivity of the tappet materials to type of lubricant can also be determined by the test, and the presence of 1% of a zinc dioctyl-dithiophosphate additive in lubricating oil can be easily detected.

Conclusions

The tappet-cam performance problem is so complex that it is difficult to draw many general conclusions at this time, even though a relatively large amount of test and service data have been accumulated. This discussion, however, has indicated some of the more important design, lubrication, and metallurgical factors influencing valve gear operation and the difficulties encountered in properly evaluating the effects of these variables. Consideration of these factors, and others which may subsequently

Table A-1

Test No.	Tappets	Camshaft	Engine No.	Rpm	Hours Run	Condition
4450	Hardenable alloy cast iron. Phosphate-treated face	Hardened forged steel. Cams with flat face, 0.212-in. minimum radius of curvature, phosphate treated	150C 150D 150E	2550 2150 2550	2⅔ 2⅔ 2⅔	Total of 9 tappets very badly worn (approximate ⅛ in.). Test stopped at 2⅔ hr

Table A-2

Test No.	Tappets	Camshaft	Engine No.	Rpm	Hours Run	Condition
6750	Hardened steel (5120). Phosphate-treated face	(Same as test No. 4450)	150C 150D 150E	2550 2150 2550	30 30 30	7 badly worn 1 badly worn 10 badly worn 18 total badly worn

Table A-3

Test No.	Tappets	Camshaft	Engine No.	Rpm	Hours Run	Condition
32850	Flat chilled-face gray iron. No phosphate treatment	Hardenable alloy cast iron. Cams with flat face, 0.212-in. minimum radius of curvature, phosphate treated	150C 150D 150E	2550 2150 2550	150 150 150	1 spalled 0 spalled 0 spalled 1 total spalled

be discovered, should increase our understanding of the conditions actually present at the tappet-cam interface and thereby lead to improvements in material, design, and lubricants, not only for tappets and cams, but perhaps for other components which must also operate under conditions of boundary lubrication and high contact stress.

From the available test methods at the present time we can draw the following conclusions:

1. While car field tests are necessary to evaluate ultimate car performance they do not generally lend themselves to a precise determination of the effect of a single variable, keeping in mind practical economy of time and test expense.

2. Dynamometer tests are more useful than car field tests for single variable evaluation but are not completely reproducible.

3. A suitable bench test is urgently needed for single variable evaluation. No previously known test is satisfactory.

4. A bench test developed at our laboratories has shown some exceptional promise.

5. Every effort should be made as far as possible to design for minimum contact stresses, minimum deflection of mating parts, and minimum rubbing velocities.

6. Surface finish and surface treatment are important factors.

7. There is considerable variation in the ability of commercial oils to minimize tappet-camshaft distress.

8. Different materials have different degrees of compatibility with various designs and lubricants.

9. Hardened alloy-iron tappets and camshafts appear better able to accommodate borderline lubricants than most other combinations in the engines tested.

10. Steel tappets appear to be less resistant to overheating from contact friction than hardened alloy-iron tappets.

Acknowledgments

The authors wish to express their appreciation to

Table A-4

Test No.	Tappets	Camshaft	Engine No.	Rpm	Hours Run	Condition
7650	Hardenable alloy cast iron. Phosphate treated	(Same as test No. 32850)	150C	2550	150	0 spalled
			150D	2150	150	0 spalled
			150E	2550	150	0 spalled
						0 total spalled

Table A-5

Test No.	Tappets	Camshaft	Engine No.	Rpm	Hours Run	Condition
42650	Hardened steel (5120). Phosphate treated	Hardenable alloy cast iron. Cams with flat face, 0.212-in. minimum radius of curvature, phosphate treated	150C	2550	150	0 spalled
			150D	2150	150	0 spalled
			150E	2550	150	0 spalled
						0 total spalled

Table A-6

Test No.	Tappets	Camshaft	Engine No.	Rpm	Hours Run	Condition
2253	Flat chilled-face gray iron. No phosphate treatment	Hardenable alloy cast iron. New high-lift cam contour. 0.187-in. minimum radius of curvature. Flat face. Phosphate treated	15E	2150	300	3 spalled
			15F	2550	300	6 spalled
			15G	2550	300	5 spalled
						14 total spalled

Table A-7

Test No.	Tappets	Camshaft	Engine No.	Rpm	Hours Run	Condition
32453	Hardenable alloy cast iron. Phosphate treated	(Same as test No. 42650)	15E	2150	300	0 spalled
			15F	2550	300	0 spalled
			15G	2550	300	0 spalled
						0 total spalled

Table A-8 – Tappet and Camshaft Materials

Material	Typical Chemical Composition, % Carbon	Manganese	Silicon	Nickel	Chromium	Molybdenum	Heat-Treatment	Hardness
Tappets:								
Chilled cast iron	3.35	1.10	2.40	0.20	0.30	....	.....	52 Rockwell C
Alloy cast iron	3.10	0.80	2.25	0.50	1.00	0.50	Oil quenched	60 Rockwell C
SAE 5120 steel	....	....	....	....	....	....	Carburized and reheated, oil quenched	62 Rockwell C
Camshafts:								
SAE 1020 steel	....	....	....	....	....	....	Carburized – water quenched	70 scleroscope
SAE 1039 steel	....	....	....	....	....	....	Water quenched	70 scleroscope
Alloy cast iron	3.30	0.75	2.25	0.30	1.00	0.50	Flame or induction hardened	70 scleroscope

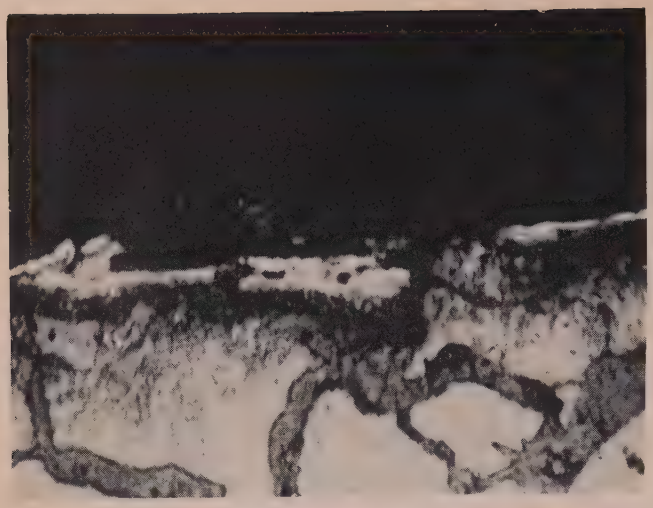

Fig. A – Fresh austenite martensite layer at worn cam face. Test conditions: 4400 rpm, 50% spring overload, SAE 5W oil, 40-hr duration (original photograph taken at 1000X) (2% nital etch)

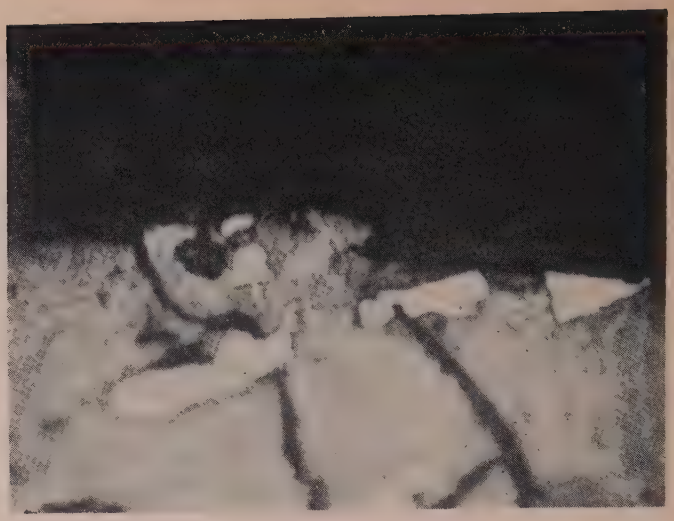

Fig. D – Satisfactory tappet surface (mating face to the cam in Fig. C) (original photograph taken at 1000X) (2% nital etch)

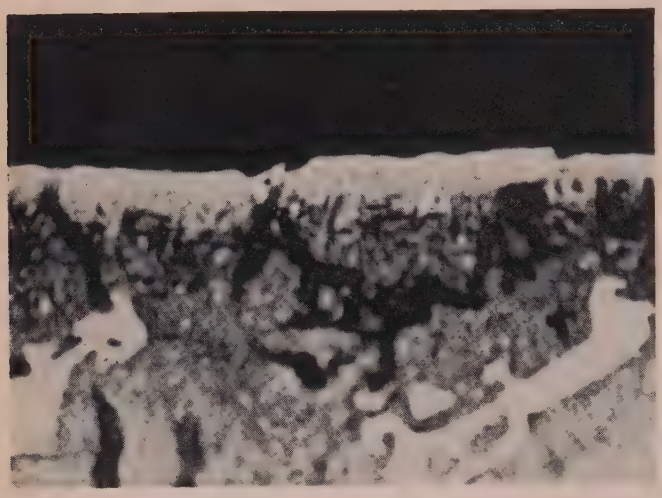

Fig. B – Fresh austenite martensite layer at worn tappet face (mating face to the cam in Fig. A) (original photograph taken at 1000X) (2% nital etch)

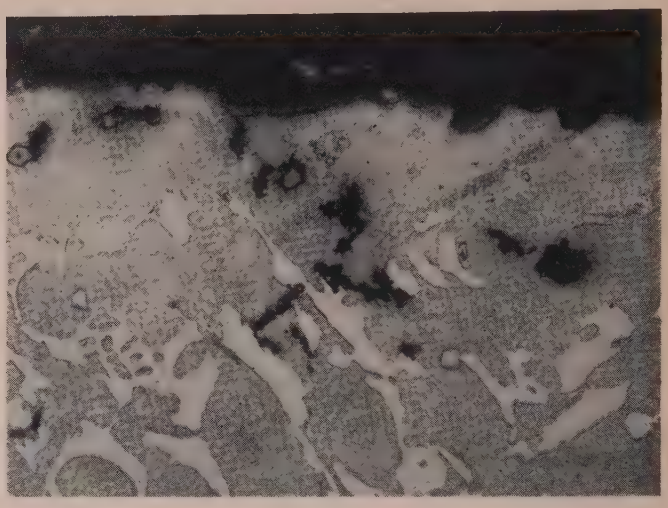

Fig. E – Decarburized tappet surface. Note the absence of massive carbides (original photograph taken at 1000X) (2% nital etch)

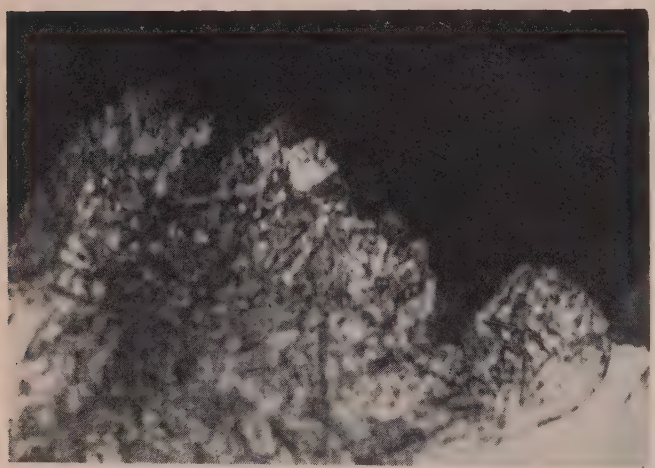

Fig. C – Satisfactory cam surface after undergoing same test as cam in Fig. A (original photograph taken at 1000X) (2% nital etch)

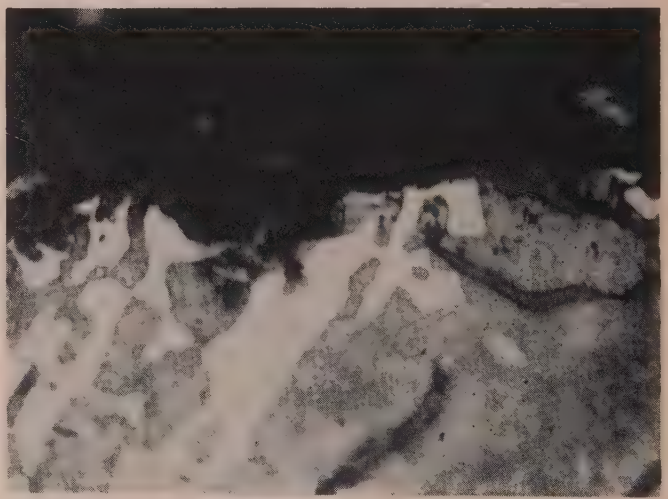

Fig. F – Satisfactory tappet surface before test. Note the massive carbides and graphite at surface (original photograph taken at 1000X) (2% nital etch)

E. R. Mantel of the Research Laboratories Division for his contribution to the design and operation of the tappet bench test and to J. B. Bidwell and others for many helpful suggestions. Unfortunately, space does not permit individual acknowledgment of the efforts of many who aided in obtaining the car and dynamometer test data.

APPENDIX

Tables A-1 through A-7: Engine test data which are summarized in Table 14.

In Tables A-1 through A-7, valve-spring-open load was 165-170 lb, engine oil was *X*, SAE 10.

Fig. H – Free ferrite plus carbide in tappet of hardenable iron after heating in lead at 1560 F for 15 min, followed by oil quench

DISCUSSION

of Garwood, Laird, and Etchells papers

Several Causes of Variation of Hardenable-Iron Structure

– R. A. Flinn
University of Michigan

THE mechanical engineer generally believes he can obtain reproducible engine performance if only the metallurgists will give him materials that are really the same. On the other hand, the metallurgical engineer considers that his materials will give the same service if only the mechanical engineer will build the engines the same.

In their more honest moments, both will admit that there is a generous splash factor in each field. Tolerances can build up to give an occasional engine that is a real groaner. On the other hand, unevaluated differences in the so-called "same" material can and do develop. This discussion is directed toward the second of these possible variables, the materials.

Hardenable iron can be a particularly difficult material to control if the user attempts to apply only the simple tests of chemical analysis and hardness that are often sufficient in the case of steel. It is essential in hardenable-iron production to reproduce certain metal structures to insure consistent service.

Three illustrations of variations in metal structure which provided difficulty in the development of hardenable iron as a tappet material may be of interest.

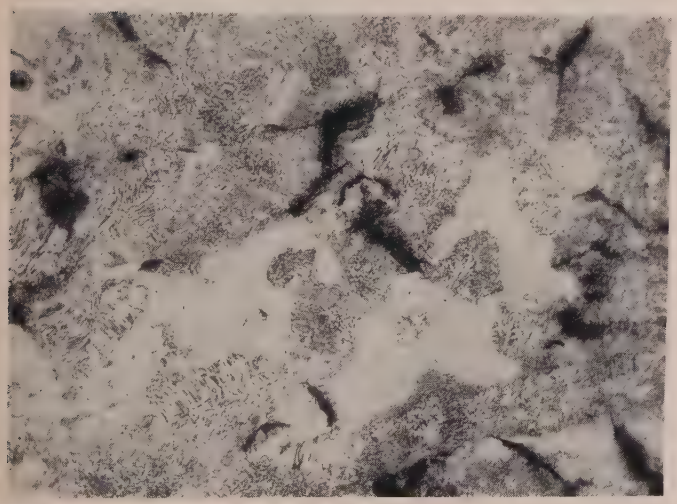

Fig. G – Pearlitic structure in tappet of hardenable iron after heating in lead at 1440 F for 15 min, followed by oil quench (original photograph taken at 500X) (2% nital etch)

Variation in Foundry Practice

As mentioned by Messrs. Garwood, Kinker, and Manganello, variations in carbide distribution are not reflected in either hardness variation or in chemical analysis. Figs. A-D show unsatisfactory and satisfactory cam tappet pairs from the same engine. The unsatisfactory pair (Figs. A and B) show the structures resulting from scuffing failure. The interface temperature must have exceeded 1500 F since a fresh austenite martensite layer was formed at the cam and tappet faces. This structure is generally found in badly worn hardenable-iron tappets, particularly in those where galling or scuffing has been encountered. It can result from either improper starting surfaces, such as those discussed next, or from undesirable base structure. This action is absent in the satisfactory pair (Figs. C and D).

Variation in Heat-Treatment and Grinding

In the paper, a severe case of decarburization is illustrated. Unfortunately, equally disastrous effects can appear unnoticed in the finished tappet as shown in Fig. E. This surface does not contain free ferrite, which may have been removed by grinding after heat-treatment, but notice the absence of graphite and free carbide at the surface.

Unfortunately, once scuffing begins it does not stop when the graphite and carbide are reached. Instead, high friction continues to wear away both mating surfaces and the fresh austenite martensite layer is encountered in tappets worn ⅛ in. deep. A good starting surface is illustrated in Fig. F.

Variation in Heat-Treatment Temperature

In the selection of proper heat-treatment time and tem-

Table A – Overhead-Valve V-8 Passenger-Car Lifter and Cam Materials

Engine	Lifter		Cam	
	1953	1955	1953	1955
1	CCI	HCI	S	HCI
2	HCI	HCI	HCI	HCI
3	CCI	CCI	HCI	HCI
4	CCI	HCI	HCI	HCI
5	S	HCI	HCI	HCI
6	CCI	CCI	S	S
7	CCI	HCI	HCI	HCI
8	HCI	HCI	HCI	HCI
9	—	HCI	—	HCI
10	—	S	—	ACI
11	—	S	—	ACI
12	—	HCI	—	HCI
13	—	HCI	—	HCI
14	—	HCI	—	HCI

Notation:
CCI = Chilled cast iron
HCI = Hardenable cast iron
ACI = Alloy cast iron
S = Steel

perature, the engineer should not be misled by the fact that the as-cast structure is largely pearlitic. In a steel this would generally indicate that the pearlite-to-austenite transformation would take place at around 1350 F. However, in this complex iron-carbon-silicon alloy, the transformation does not begin until about 1450 F and is not complete until about 1550 F. Figs. G and H show these effects.

Superchilled Cast Iron Shows Promise as Lifter Material

– A. C. Pilger
Tide Water Associated Oil Co.

THE results of two years of our cam and tappet road testing are in good agreement with the findings presented by Messrs. Garwood, Kinker, and Manganello. We have found that three major factors, each with many ramifications, influence the problem. They are engine design, type of service, and lubricating oil.

Our field data tend to support the Chrysler position that extreme-pressure properties, as now understood and measured by the Almen and similar bench test machines, appear poorly related to cam and tappet durability. In these tests, the addition of ½% of a particular e-p material to an oil having good cam and tappet wear properties markedly depreciated its performance.

The bulk of our work corroborates the authors' contention that hardenable cast iron is a superior tappet material. However, some of the data indicate that hardenable cast iron is not a cure-all or the best lifter material for all circumstances. Occasionally, as much as 0.120-in. dishing of the tappet face along with 0.140-in. loss of cam lift has been observed with hardenable cast iron in less than 1000 miles of operation. With at least one oil, hardenable cast-iron lifters produced nearly twice as much cam lobe wear as chilled cast iron when run in conjunction with a hardenable-iron camshaft. Also, it should be recognized that hardenable cast-iron lifters are unsuited for use with steel camshafts.

A new development in cast-iron lifter material known as superchilled cast iron was recently evaluated with excellent results. Six road tests were conducted using split lifter sets and different oils. Superchilled cast iron gave tappet face wear of the same magnitude as hardenable cast iron, but in all cases caused substantially less wear on the hardenable-iron camshafts. This may be of particular interest to manufacturers who wish to use steel camshafts but are encountering problems with chilled cast-iron lifters. Because hardenable cast-iron tappets are not compatible with steel camshafts, use of superchilled cast-iron lifters may be attractive.

There seems to be a growing tendency to classify various materials used in lubricating oils and engines as either good or bad. While this may be a convenience, our field tests indicate that the practice constitutes an over-simplification of an extremely complex problem.

Insufficient field data have been accumulated to date on the cam and lifter problem to properly establish significance and service correlation of existing laboratory engine test procedures. Differences in opinions regarding the merits of certain lubricating oil additives are known to be occasioned by divergence in results between laboratory and road tests. For the present at least, it still appears necessary to see what the engines say in service.

Questions Validity of Test Techniques Used

– T. W. Havely
Shell Oil Co.

THE most obvious and interesting point brought out by Messrs. Garwood and Laird and associates is that there exist two different material combinations for cams and lifters that are relatively insensitive to lubricants and which give good service life in the field.

We have had no laboratory test experience with steel tappets and as-cast alloy-iron cams discussed by Laird, Stevens, and Iles, but we can agree with Garwood, Kinker, and Manganello that hardenable cast iron gives good performance. It will be recalled that the superior characteristics of this material were reported in our paper of last year[a]. At that time there were eight overhead-valve V-8 engines and seven combinations of lifter and cam materials and surface treatments. As shown in Table A, there are now 14 overhead-valve V-8 engines and all but four have hardenable cast-iron lifters and cams. Of these four, two are equipped with metal combinations reported by Messrs. Laird, Stevens, and Iles to be little affected by lubricants. Thus, it is clear that the problem of supplying a motor oil suitable for the lubrication of cams and tappets

Table B – Influence of Lubricant Viscosity on Pitting[a]

Engine B	Viscosity at 185F, centistokes	Pitting Rating
SAE 10 with detergent + sulfur-phosphorus	6.0	Heavy/100
SAE 30 with detergent + sulfur-phosphorus	17.0	Light/12 Incipient/25
Engine C		
SAE 10 undoped mineral oil	6.0	Heavy/69
SAE 30 undoped mineral oil	17.0	None

[a] For test conditions and rating system, see paper mentioned in footnote a.

in passenger-car engines has been considerably simplified by the advent of the 1955 models.

Test Techniques

In our previous paper we expressed some doubt regarding the validity of pitting tests conducted with overloaded valve springs. In his discussion of the papers, Mr. Raviolo also expressed some concern about this technique, as do Messrs. Laird, Stevens, and Iles in their current paper. Messrs. Garwood, Kinker, and Manganello, on the other hand, state that they obtain good correlation with service using this technique to shorten the test time. We should like to add that we have made laboratory tests at normal spring load which show the same trends of lubricant performance as do tests with overloaded springs. The test time, however, is greatly increased. From a summary of this experience, then, it appears that as far as laboratory tests are concerned, the use of overloaded springs is a satisfactory technique.

Acceleration of laboratory pitting tests, incidentally, may be achieved by running at lower engine speeds. It now seems to be the general consensus that decreasing engine speed increases severity of pitting of chilled cast-iron lifters. This, of course, agrees with theory in that surface stresses at the nose of the cam increase with decreased speed. Regarding scuffing and wear, however, there is some disagreement in results. Mr. Yowell[b] reported that both steel and chilled cast-iron lifters are subject to less distress at high speeds than at low speeds, while Messrs. Garwood, Kinker, and Manganello have reported that at high speeds (3600 rpm) chilled cast-iron lifters are badly worn and scuffed.

Influence of Lubricant Viscosity on Surface Distress

In our paper last year it was stated that lubricant viscosity had no apparent effect on the scuffing of steel lifters. This work has been expanded to include chilled cast-iron lifters and it is found that increasing viscosity decreases the tendency of these lifters to pit. A typical example is shown in Table B. Here one of the lubricants contains an additive which promotes the pitting of chilled cast-iron lifters and the other is an undoped mineral oil. Comparing the SAE 10 and SAE 30 grades it was observed that considerably less pitting was obtained with the SAE 30 grade. As stated in our previous paper, this would be expected from results of fundamental investigations of pitting.

Our findings seem to be at variance with those of Messrs. Garwood, Kinker, and Manganello, who report that the scuffing tendency increased with reduction in viscosity, whereas the pitting tendency of lifters was not affected.

Concept of "Oil Fatigue"

Messrs. Garwood, Kinker, and Manganello introduce the concept of "oil fatigue" as a phenomenon different from normal metal fatigue. It is our opinion that early fatigue failures brought about by the lubricant are in no way fundamentally different from so-called normal metal fatigue. It is our opinion that some lubricant additives merely accelerate the process of fatigue and in doing so must give rise to the differences in appearance observed by Messrs. Garwood, Kinker, and Manganello. The view generally held is that these additives accelerate fatigue by corrosive action. This explanation, however, to our knowledge has not yet been substantiated. In fact, Bidwell and Vermaire's[c] finding that a phenate was extremely active in promoting pitting does not support the theory that corrosion is the major factor. The alkaline nature of phenates makes them good corrosion inhibitors and if pitting was caused solely by corrosive attack one would expect phenates to be beneficial.

---

[a] See SAE Transactions, Vol. 53, 1955, pp. 204-210: "Influence of Lubricant and Material Variables on Cam and Tappet Surface Distress," by T. W. Havely, C. A. Phalen, and D. G. Bunnell.
[b] P. 221, SAE Transactions, Vol. 53, 1955.
[c] See footnote 3 of main paper.

Suggests Improved Design to Answer Present Cam-Tappet Material Problems

– W. E. Day, Jr.
Spicer Mfg. Division, Dana Corp.

IT seems obvious that the requirement of higher velocities and greater acceleration rates in cams and tappets of our modern engines, the accompanying higher valve spring pressures, and the increased inertia loading by the valve mechanism in general have reached a point where the material in both the cam and the tappet is stressed very close to the ultimate. I believe it is for this reason that slight changes, often hardly discernible in microstructure, lead either to success or failure.

I see in these papers no references to the probable compressive stress in cams and tappets. Unquestionably it is extremely high—much higher, I believe, than most tests and calculations indicate. In this connection it might be interesting to test cam and tappet material on Amsler or similar machines which permit compressive loading under various conditions. Scuffing tendencies could also be determined on the same equipment. Of course, the final answer must come from engine tests.

It is interesting that although the testing procedure at Ford, relative to engine speeds, was different from that at Chrysler (one using a speed of 400-500 rpm and the other speeds of 1200 and 3600 rpm), the types of failure were the same, the exception being the 3600 rpm test, which produced more scuffing probably due to higher rubbing velocity.

The effect of different oils on fatigue shown by the Chrysler tests is worthy of further consideration by the oil companies. However, I do not believe that outside of the avoidance of a detrimental additive, too much significance can be placed on the effect of oil. In other words, a cam-tappet combination should perform satisfactorily with the regular standardized engine lubricants.

The finish necessary for good performance brought out by Chrysler's tests is important in my opinion, and this has also been found to be true in other applications such as cylinder bore finishes, where too smooth a finish promotes scuffing.

Messrs. Laird, Stevens and Iles reported that when carburizing 5120 to high surface-carbon content a layer 0.002-.003 in. thick was found which apparently was cementite, and further, that tappets with this structure often proved unsatisfactory. This is of interest to me, having observed a similar condition in carburized 5120 which was in no way connected with the tappet problem. In taking Knoop and 5 kg Vicker hardness measurements on this constituent, a much lower hardness was found than that attributed to iron carbide, Fe_3C.

In the tests at Ford and Chrysler, certain combinations of material have been used in different states and certain test procedures followed. The results of tests on cams and tappets in our laboratory, although involving materials and procedures different from those reported in these papers, still have a very similar note.

From our tests we recognize two types of failure; that due to pitting fatigue and that due to scuffing. No condition such as the smooth wear reported by Chrysler has been experienced which was not preceded by scuffing. I believe fatigue is associated with the low endurance constituents such as austenite, bainite, and ferrite, although a full martensitic surface will fail by pitting if sufficiently

stressed in compression (325,000 psi Hertzian stress or higher). Scuffing is primarily caused by welding of those surface asperities in contact in which the orientation and composition is the most suitable. Thus, for the proper combination of materials for tappets and cams, those of high endurance limit under compression with extremely poor welding qualities should be chosen.

In conclusion, I might say that the possibilities of improved design should not be overlooked, for it appears we are fast approaching the limit of what can be expected of the present materials commonly used when subjected to high stress and high rubbing velocities.

ORAL DISCUSSION

Reported by Vincent C. Ayres
Eaton Mfg. Co.

J. A. Hunter, G. M. Truck and Coach Division: Which produce the best tappet face condition, having tappets rotate, or not having them rotate?

Mr. Etchells: Spalling is often associated with rotation even though complete failure does not necessarily follow, although in some cases spalling of the tappet will produce a cam failure. One manufacturer used a geometrical design of cam and tappet contact which prevented rotation, and though a small ditch was worn into the tappet face, this was not considered failure. Without rotation spalling did not occur.

The foregoing pertains to chilled-iron tappets. Where alloy cast iron was used in an alloy-iron camshaft, there was, in general, less sensitivity to operational differences and a great reduction in the failure was experienced.

Michael Furey, Esso Research and Engineering Co.: Will Mr. Etchells please explain further the relationship of rubbing velocity versus spalling. In his paper, he stated one reason for failure is high rubbing velocity. What does this mean?

Mr. Etchells: Speed is very important, and while loads are higher at low speed, the rubbing velocity is low. At high speed the rubbing velocities are high and the loads are low. We felt that an intermediate speed was most desirable for testing because it provided an optimum relation between load and rubbing velocity.

Mr. Furey: Was tappet wear on long trips worse than on short trips?

Mr. Etchells: It was a function of speed and the previous answer covers the situation.

Mr. Furey: At a recent meeting of the ASLE, a Mr. Davis presented a paper in which the hydrodynamic effect of lubrication was discussed. I wonder whether the thicker oil film, as a result of high-speed operation, was the cause for the reduction in the failures at high speed, or was the thickness of the oil film greater due to separation of the valve train.

Dr. Thomson: In high-speed laboratory tests, failures sometimes resulted due to changes which take place in the valve gear motion. These were unique to the laboratory tests, however, and were not reproduced in the field.

Mr. Kinker: Does scuffing bear any relationship to the microstructure of hardenable iron?

Richard Flinn, University of Michigan: Yes, but these data are not yet available for presentation. There can be quite a variation in the structure of chilled cast iron, and I am assembling data on this subject as well.

William J. Harris, Studebaker-Packard Corp.: I agree that camshaft finish is a very important factor. Studebaker use cams which are lapped to a finish of 10 microin. maximum. This was the most successful in their test results, and is used without any coating on the camshaft in conjunction with hardenable-iron tappets.

When chilled tappets were used, spalling has been seen when the tappet did not rotate. However, it did seem to be less than when the tappets did rotate. It was concluded that the most desirable combination would be the least taper on the cams with the greatest radius on the tappet which would produce rotation.

The relationship between the unit loading of the tappet face in relation to the material combination is important. If the tappet loads are high, chilled-iron tappets on the cast-iron camshaft would fail by spalling or wear, and the camshaft nose would be rubbed off. Under high-load conditions improvement would result if a steel camshaft were used because the cam would not necessarily fail, even though the tappets spalled or wore. The Studebaker valve train has been redesigned to lower the tappet face load, and they are now using a hardenable cast-iron camshaft and tappet. The tappet has an RC 52-58 hardness requirement.

We have also conducted limited testing on higher alloy chilled cast-iron tappets with flame-hardened alloy cast-iron camshafts. The results indicate that this combination will stand up under higher loads than the flame-hardened camshaft and heat-treated cast-iron lifters.

Mr. Etchells: I would like to add something more in regard to lubrication. In 1949 when we were in the process of developing the use of automatic tappets in our engines, we noticed that in addition to the increased tendency of the tappet faces to spall, the rocker arm bearings would score badly and seize. By adding a simple oil groove on the rocker shaft, so that available oil at this point could be wiped into the effective loaded area, the problem was solved. We believe the trouble was due to the fact that the load did not reduce to zero as it did with valve lash and mechanical tappets used in prior engine models.

It is not so simple a lubrication problem to resolve with the rubbing contact of the tappet face on the cam. Yet, we know that these parts will not run well together without oil, and they seem to perform much more satisfactorily if the oil exhibits an e-p quality, either inherent or added. I wonder how many fully realize that the tappet-cam is the most highly stressed point in the engine. We have tried to point out in the paper how it may be relieved and made to live using proper techniques.

Once we ran a 25,000-mile test on five identical engines using five different types of oils. Although the tests were made for another purpose, it seemed curious to us that the oil with the highest viscosity index produced the highest overall engine wear. In addition, all the tappets were spalled, as against only one or two spalled and pitted tappets in the other four engines. Of course, it could be concluded that perhaps the additive had something to do with the poor performance of this particular oil. We don't know. However, lately we have come to be increasingly suspicious of oils with V.I. improvers, since engine parts do not appear to react to the oil as does the measurement in Saybolt viscometers.

What I am trying to get at is this:

1. We do not have a good oil test for e-p characteristics as related to the cam and tappet face.

2. We do not have a good viscosity test for an oil as related to parts in a running engine.

The Supercharged Turboprop

S. G. Hooker, Bristol Aeroplane Co., Ltd.

This paper was presented at the SAE Golden Anniversary Aeronautic Meeting, New York, April 18, 1955.

THIS paper outlines the experience gained on flight trials of the Bristol Proteus turboprop engine in the Britannia Civil Transport. The shortcomings of the conventional turboprop engine as regards take-off power at high-altitude airports and in the tropics are analyzed.

The simplest way of improving the specific fuel consumption of the turboprop engine is, says the author, to increase the compression ratio. To this end, a low- and high-pressure compressor arrangement is desirable, and the concept of the former supercharging the latter is obvious. Furthermore, there is the advantage in throttling the engine at take-off, as with a supercharged piston engine, thus having power to spare to cope with tropical or high-altitude conditions.

The consequences of this approach are examined in relation to the design of the Bristol B.E. 25 supercharged turboprop engine.

THE name "supercharged turboprop" seems to have caused much argument in some circles, and has even been described as "technical nonsense designed to confuse." Other writers have referred to it as "a derated engine" and as a consequence, have inferred that it will be heavy.

The idea and the name have first been applied to the Bristol B.E.25 turboprop engine, and hence the design of this engine will be used to illustrate this paper. Going back to the conception of this engine some 2½ years ago, the underlying thoughts were:

1. To produce a turboprop with a specific fuel consumption equal to the best compounded piston engine. This implied a pressure ratio greater than 10/1, and necessitated the 2-spool arrangement of compressors.

2. To produce a turboprop engine having a cruising power of the order of 3500 hp at 30,000 ft, with the lowest possible weight per hp. At full throttle such an engine would naturally give more than 8000 hp at sea level, and it was desirable to restrict this power to 4000-5000 hp in order to lighten materially the reduction gear and propeller, and thus achieve an appreciable improvement in the

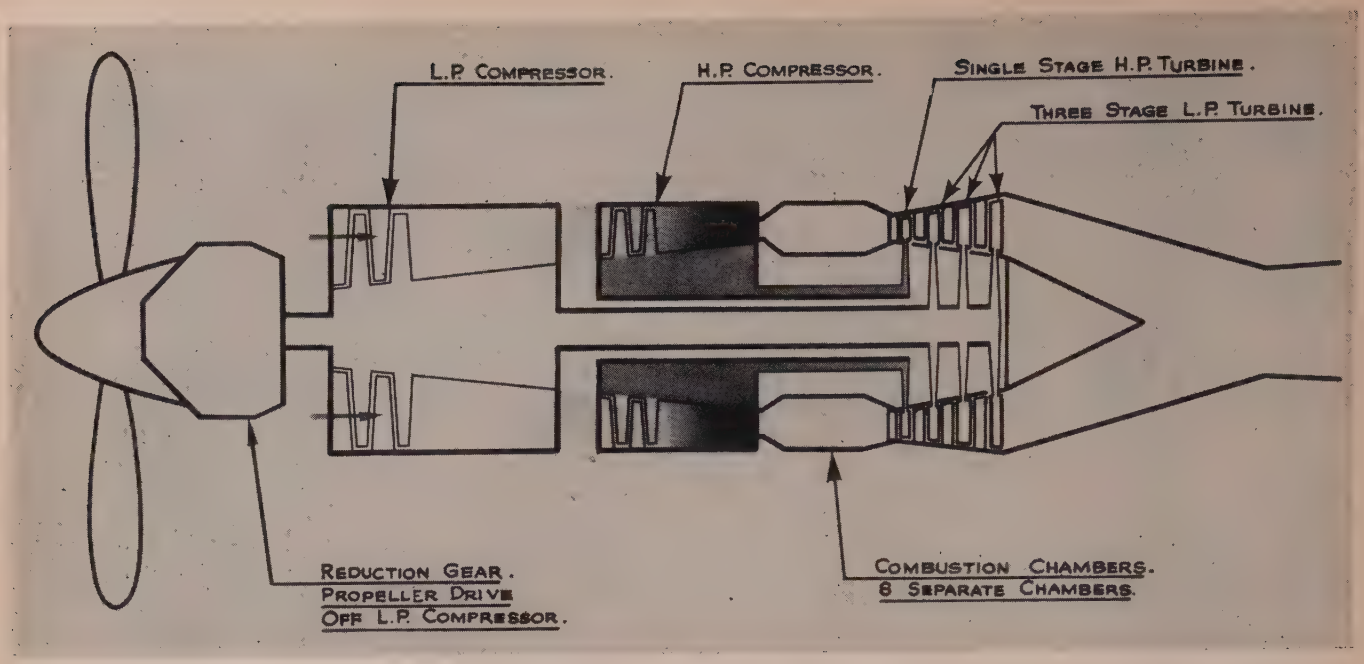

Fig. 1 – Diagram of arrangement of B.E. 25 engine

specific weight under cruising conditions. There is no satisfaction to be derived in towing a propeller and reduction gear designed to absorb 8000 hp at sea level through the sky at 30,000 ft, attached to an engine incapable of giving more than 3500 hp at that altitude. Nonetheless, this state of affairs applies in degree to all turboprop engines available today.

3. To produce a turboprop engine whose take-off power is independent of the altitude and air temperature at the world's airports. Present-day "naturally aspirated" turbine engines (to coin another name!) suffer badly at the higher and hotter airports, and, although the air temperature in the tropics can be partially mitigated by water-methanol injection, this method is at best messy and complicated, with a high nuisance value and economic cost.

4. To exploit to the fullest the known advantage of the turbine engine relative to piston engines, namely, its ability to produce large power for a small bulk and weight.

It would be practically impossible – and certainly no engine firm would attempt to do it – to produce a piston engine for transport purposes having a conservative cruising power of 3500 hp at 30,000 ft.

The very desirable properties outlined in 1, 2, and 3 above are enjoyed by the supercharged piston engine, and they are, of course, the fundamental reasons why this type of engine eventually entirely displaced the naturally aspirated piston engines of the early days of flying.

Realizing that the purpose of supercharging an engine, piston or turbine, is to maintain power at altitude, and to ensure the best thermal efficiency at cruising conditions by producing the highest possible compression, we find that the 2-spool turboprop engine is an admirable arrangement for achieving just this. A diagrammatic arrangement of the supercharged turboprop engine of this type is shown in Fig. 1.

The engine consists of a high-pressure compressor, combustion chamber, and high-pressure turbine which form an independent unit analogous to a single-spool jet engine. The high-pressure compressor is supercharged by a low-pressure compressor which, in turn, is driven by a 3-stage low-pressure turbine driven by the exhaust from the high-pressure system. The propeller is geared directly to the low-pressure compressor.

The engine is basically controlled by two levers, one of which is a fuel throttle governing the power and speed of the high-pressure system, the other being connected to a constant-speed unit controlling the propeller pitch, and hence the speed of the low-pressure or supercharging unit. The division of compression between the two compressors must be carefully chosen so that whatever the speed ratio between the two, neither runs into a surging condition.

The engine incorporates a compound epicyclic reduction gear in which the torque transmitted is measured on the final floating annulus gear by oil pressure on a piston balancing the torque reaction. It is arranged to limit the torque transmitted by balancing this torque pressure against the engine burner pressure. In other words, if the torque developed by the engine tends to exceed the limit value, a valve is opened, which reduces the flow from the fuel pump and thus throttles the engine

back. This control is analogous to the manifold-pressure control on piston engines, except that the torque controller ensures that the reduction gear is never called upon to transmit a torque greater than its tested value, whatever the ambient air conditions at which the engine is operating.

A study of the arrangement in Fig. 1 will show the great similarity between this engine and the exhaust-blown piston engine, and with the torque limiter controlling the power to part value at sea level, the analogy to the supercharged piston engine is complete.

Thermo and Aerodynamic Considerations

One of the prime objectives of long-range transport engines is to obtain the best specific fuel consumption under cruising conditions.

It is a property of turboprops that their specific fuel consumption decreases as the turbine inlet temperature is increased, but experience has shown that the reliability and durability of the combustion chambers, turbine blades and wheels, and other components at the "hot" end of the engine fall rapidly as their temperature is increased. A compromise should be struck with temperatures on the low side, despite the disadvantages in performance, in order to achieve a high order of reliability and durability, although little advantage will be obtained by reducing the inlet temperature much below 1000 K (1300 F). This, then, was the cruising temperature chosen for the B.E.25 engine, and Fig. 2 shows the sfc obtaining at 25,000 ft and 300 knots for engines of various compression ratios.

Note that at 1000 K turbine inlet or peak temperature, and with a cruising pressure ratio of 10/1, a sfc of 0.37 lb fuel per hp-hr is indicated. Higher compression ratios would be an advantage,

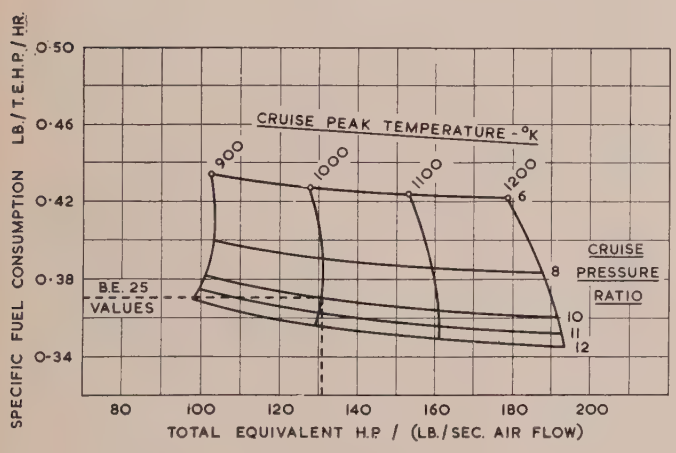

Fig. 2 – Generalized turboprop performance. Distribution of power between power turbine and jet, chosen to give maximum propulsive efficiency. ISA: 25,000 ft, 300 knots; compressor efficiency: 0.90 polytropic; turbine efficiency: 0.90 polytropic; duct losses: 5%; propeller efficiency: 0.85; reduction gear efficiency: 0.98; air intake efficiency: 0.90

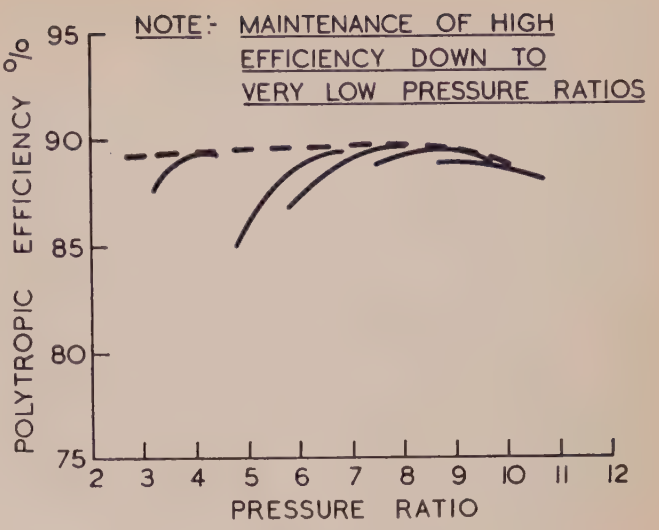

Fig. 3 – Overall compressor performance showing typical results from 2-spool compressor arrangement

but the best piston engine can be beaten at 10/1, which is well within experience on 2-spool compressors.

Turboprop engines so far have lagged behind the turbojet in aerodynamic performance due to the great advantage of jet propulsion for military purposes and the relative simplicity of such engines. Now that the first phase is over, turboprops are being designed equal to jets thermodynamically and greatly their superior in propulsive efficiency under appropriate flight conditions. In fact, the turboprop responds better to improvement in the air-thermal cycle than does the turbojet, for any improvement in the compressor or turbine performance of the latter provides more energy in, and thus more velocity to, the jet, resulting in decreased propulsive efficiency which considerably reduces the overall gain. On the other hand, similar improvements in the turboprop cycle provide an increase in power to the propeller which is transformed into useful thrust on the aircraft without loss in propulsive efficiency.

Returning to Fig. 2, the curves postulate polytropic efficiencies of 90% for both turbine and compressor. This figure is high, but has been achieved on component test, as Figs. 3 and 4 indicate. Slightly lower figures, varying with Reynolds number in the case of the compressor, have actually been used in the design of the B.E.25.

The ability of the 2-spool compressor to maintain high efficiency at both high and low pressure ratios is worthy of note, and is a feature which leads to great flexibility and stability in engine operation. It is, perhaps, worth emphasizing the obvious fact that the higher the overall efficiency of any engine, the wider the range of operating conditions over which it can be used with advantage. Thus, an efficient turboprop will be much less

sensitive to aircraft speed and altitude than a turbojet.

Engine Performance

The great merit of the gas turbine is its ability to produce large power for a relatively small weight and bulk. This feature has been exploited to the utmost in jet engines, which have grown tenfold in thrust since the Whittle engines of 1940. In comparing various engines, a convenient quantity to examine is the engine airflow at maximum sea level static conditions. This quantity is akin to the cubic capacity of piston engines and can be used as a rough indication of the relative powers of various engines. On the test bed a jet engine will give roughly 60 lb thrust for every lb per sec of airflow, while the corresponding figure for a turboprop engine is roughly 100 hp for every lb per sec airflow.

Jet engines are now flying with airflows approaching 200 lb per sec, whereas today's turboprops operate at about one-quarter of this value. It is not surprising, therefore, that when the two engine types have been compared, the jet engine has shown up to greater advantage in so far as high-altitude power is concerned. Despite the better propulsive efficiency of the propeller, the power of the jet greatly exceeds that of the turboprop at high altitude because of the far greater capacity of the jet engines relative to the turboprop engines which exist.

Any attempt to correct this deficiency on the part of the turboprop leads to an engine with an exceptionally high sea level power. This, in turn, brings about the great problem of transmitting

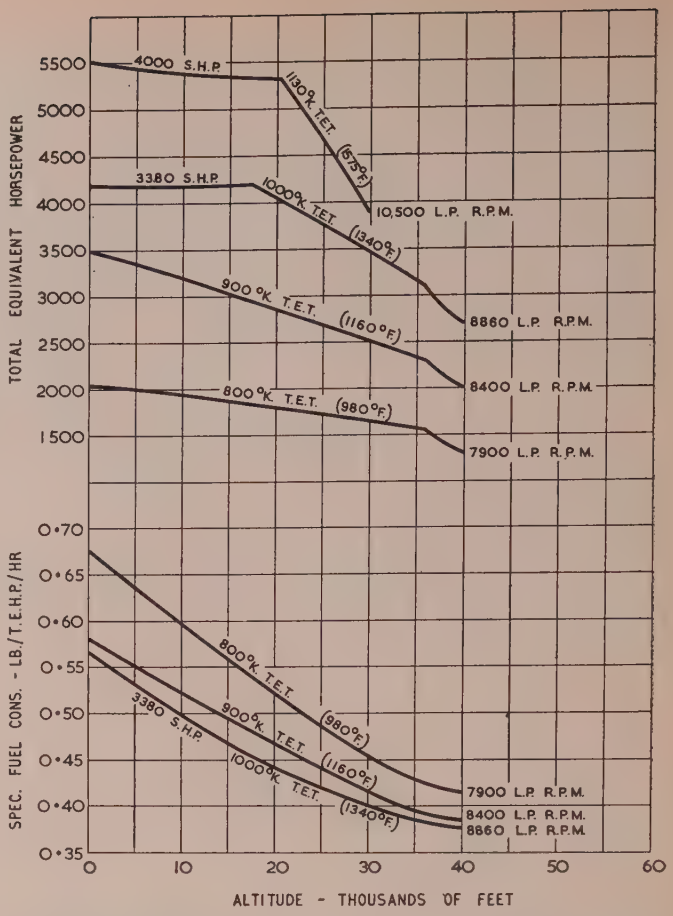

Fig. 5 – Total equivalent hp and specific fuel consumption for B.E. 25 turboprop at asssumed equivalent air speed of 220 mph, no intake loss, no power take-off

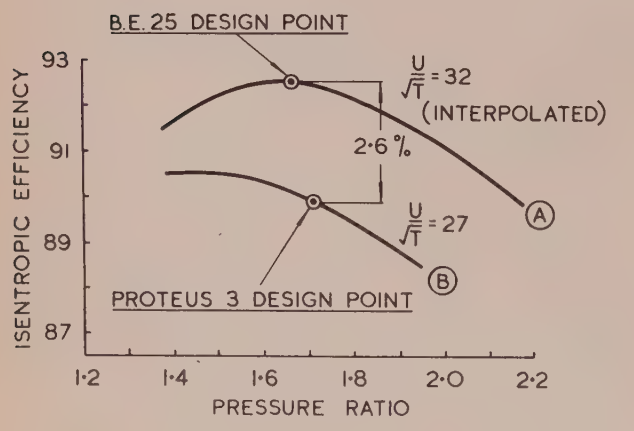

Ⓐ - LOW LOADING TURBINE TEST
(LASH-UP BY RESTAGGERING A PROTEUS 2. 1ST. STAGE BLADE)
CONTRACT REPORT P.C.T./44

Ⓑ - PROTEUS 3. 1st. STAGE TURBINE TEST
CONTRACT REPORT P.3 C.T./4. (WITH CORRECTION OF P.3 C.T./6)

Fig. 4 – Turbine test-rig results for B.E. 25 and Proteus 3 engines

power through a reduction gear to a propeller adequate in size for its absorption. Furthermore, transport aircraft will achieve their best overall cruising performance when flying at 25,000 to 35,000 ft with turboprops, at which altitudes the power output will be approximately one-half of the sea level maximum. It is desirable, therefore, in the interests of lowest possible powerplant weight, to restrict the take-off power to roughly the same value as that used for cruising at altitude.

In order to avoid detonation at lean-mixture cruising strength, it is necessary to reduce the cruising power of a supercharged piston engine to about 60% of its take-off power, but no such limitation occurs in the turboprop, and subject to the remarks made earlier on the effect of turbine inlet temperature upon reliability and durability, the turboprop engine can be operated at constant power.

A typical series of power curves for the B.E.25 is shown in Fig. 5. In this diagram, the top curve labeled 10,500 L.P.R.P.M. corresponds to maximum conditions, and will in fact be used only for take-off. The continuous cruise rating is 8860 L.P.R.P.M.,

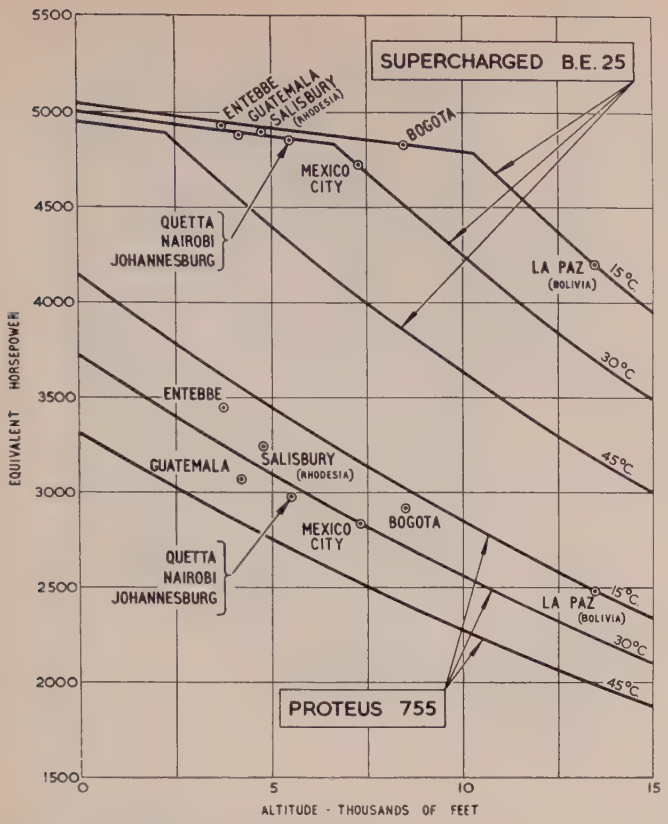

Fig. 6 – Comparison of effect of altitude and temperature on take-off power for Proteus 755 and the B.E. 25

which yields 3380 hp in the propeller up to 17,500 ft, the additional power up to 4150 hp shown being due to jet thrust. Thus, at 30,000 ft and 220 mph equivalent air speed (corresponding to a true speed of 360 mph), the engine gives 3500 equivalent hp with a sfc of 0.40 lb per hp-hr. Note that the turbine inlet temperature is constant at 1000 K (1340 F) at full throttle above 17,500 ft. Below this altitude the cruising power is restricted by the torque limiter, and the turbine inlet temperature falls to lower values as sea level is approached. Note that the engine can be throttled to less than half power at 7900 L.P.R.P.M. at 30,000 ft with a specific fuel consumption of 0.45 lb per hp-hr, and also that at 25,000 ft and 8400 L.P.R.P.M., 2700 hp can be obtained at a sfc of 0.44 lb per hp-hr, although at this speed the engine will be at full throttle from sea level upwards.

The curves in Fig. 5 are only illustrative of the engine performance, which will vary with true aircraft speed because of the ram effect and jet thrust available. At speeds higher than 220 mph equivalent air speed the specific fuel consumption will be lower because of the greater value of jet thrust when flying faster.

Turning to the conditions at take-off, Fig. 6 shows a comparison between the supercharged engine and a normal turboprop, the Bristol Proteus 755 serving as the latter for illustrative purposes. The curves show the equivalent hp for take-off as a function of altitude and are plotted for three ambient air temperatures, 15, 30, and 45 C. (Note: equivalent hp is defined as propeller hp plus jet thrust divided by 2.6).

Some of the higher, hotter, and thus more difficult airports of the world are indicated in altitude and temperature, and the great loss of power suffered by the normal turboprop (lower three curves) is obvious. Take Mexico City for example. The power of the Proteus is reduced from its normal value of 4150 hp to 2800 hp – a loss of more than 30% – and in this respect it is no worse than any other turboprop of today. Even if water-methanol injection were employed, thereby reducing the air temperature entering the compressor from 30 to 15 C, the power would increase only to 3150 hp, since nothing can compensate for the altitude effect. The picture with the supercharged turboprop engine (upper three curves) is entirely different. There is some small loss in power with temperature and altitude due to a reduction of jet thrust, but the great advantage of the supercharged concept is obvious, the loss in power even at La Paz being only 16%.

After studying Figs. 5 and 6, one will certainly agree that the B.E.25 is a supercharged engine in the same sense that we have known supercharged piston engines for the past 30 years.

Component Development

One of the great mechanical problems in the development of turboprops has been the reduction gear. In the case of piston engines, a reduction ratio of 2/1 or 3/1 is adequate, but with the higher speed of rotation of turbine engines, reduction ratios greater than 10/1 are necessary. In the case of the B.E.25 engine, the actual ratio is 11.1/1, necessitating two stages of epicyclic gearing. The problem with turboprop reduction gears has usually been one of failure in the gear teeth or webs of the wheels excited mainly by vibration due to the high rate of tooth contact which prevails on these faster rotating engines. The cure for this, as

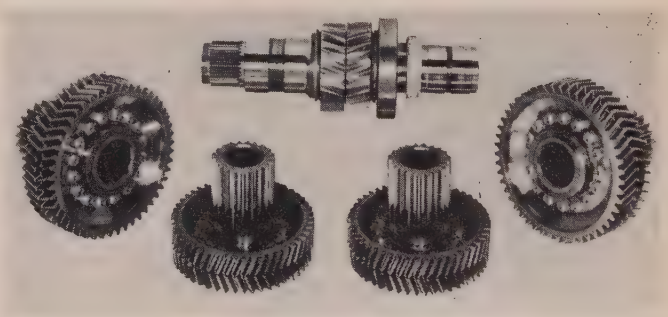

Fig. 7 – Proteus helical reduction gears

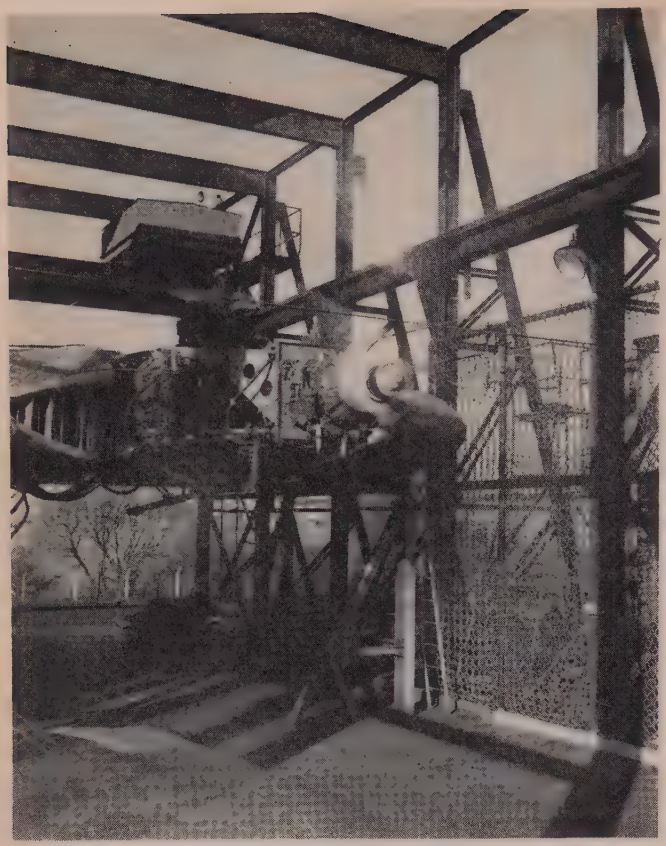

Fig. 8 – Endurance testing B.E. 25 reduction gears

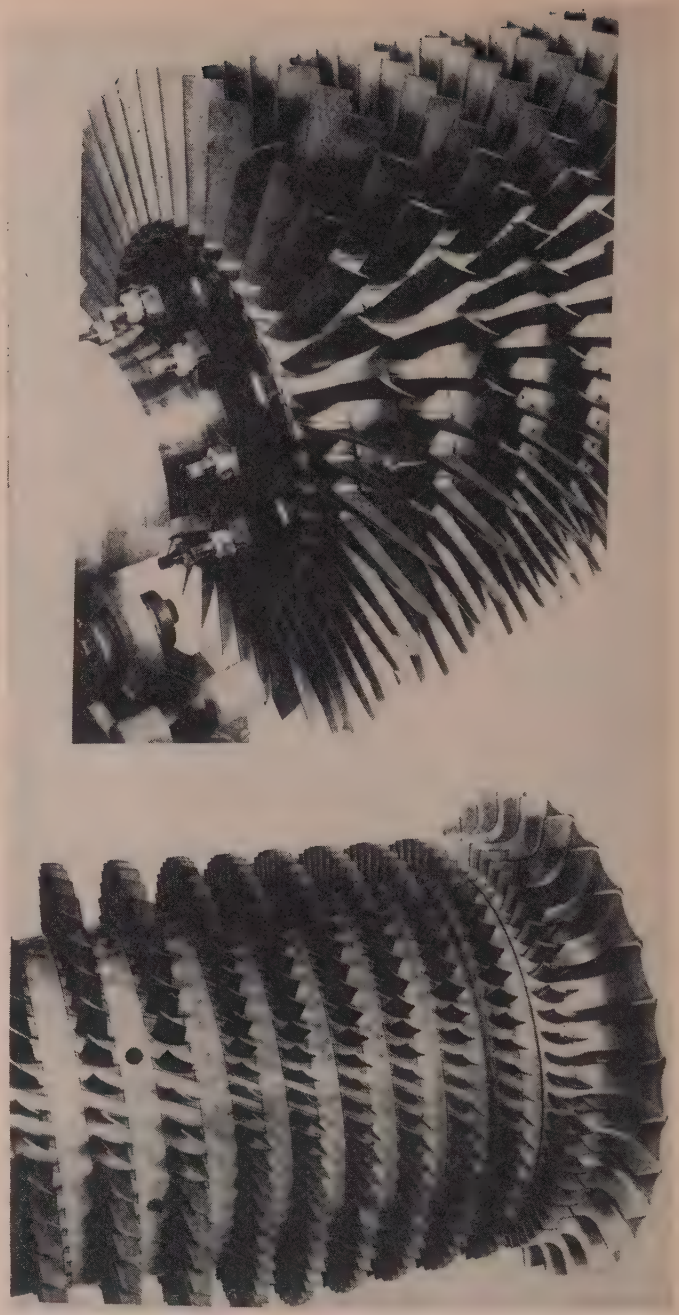

Fig. 9 – Damage to steel-bladed Proteus compressor due to passage of steel pin

all marine engineers know, is to use helical gears, typical examples of which are shown in Fig. 7.

The actual gears shown are used in the Proteus 755 engine, where they are rated at 3650 shaft hp for take-off. These gears will also be used on the B.E.25 engine, since the latter has been designed to have the same reduction gear ratio as the Proteus, 11.1/1. It is proposed, however, to rate the reduction gear at 4000 shaft hp for take-off in the case of the B.E.25. Fig. 8 shows the reduction gear under endurance test at 4250 shaft hp. In this particular rig, two Proteus engines are coupled together and their joint output passed through the reduction gear under test. In this way it will be possible to test the reduction gear up to 7000 hp if necessary; naturally, for the time being testing is concentrated in the 4000-4500 hp range. The fact that an existing gear with many thousands of hours of experience behind it is already available for the B.E.25 should prove of immense advantage in the development of this engine.

The B.E.25 low-pressure compressor is aerodynamically identical with one which has already been rig-tested and run some 500 hr. When the first B.E.25 engine runs in September or October, 1955, the low-pressure compressor is expected to have accumulated some 2000 hr of testing. This, too, will be a valuable advantage.

Both l-p and h-p compressors on the B.E.25 are constructed entirely of steel – discs, blades, and casings. Experience with the Proteus has shown that steel blades are capable of "eating" quite large pieces of ice, and that no catastrophic failure results even when a nut or bolt passes through the compressor. Quite recently, in flight on the Britannia, a drop in power of some 300 hp was noticed on one engine; on subsequent examination it was found that a steel pin had passed through the compressor. The result is shown in Fig. 9, where the small damage to the steel blades is evident. On the other hand, a similar accident happened in the past

to a compressor with aluminum blades, with the resultant damage shown in Fig. 10.

Large chunks of ice have passed through the steel-bladed compressor without damage, and all our experience points to the fact that steel blades are the most reliable proposition for civil and military transport aircraft.

The combustion chamber of the B.E.25 engine will be tubo-annular or cannular, the chambers themselves being based on the Proteus design shown in Fig. 11. The particular chambers shown were taken from an engine after the completion of a 500 hr endurance test on the test bed and were run during this whole period without servicing of any kind. The total life of the chambers at this point was, in fact, 580 hr, and they were fit for further service after minor repairs.

The turbine mechanical design will again be based on the Proteus, where shrouded blades are used on the first three stages and open blades on the last wheel. (See Fig. 12.) The particular wheels shown in Fig. 12 had completed 1230 hr endurance running on the test bed without servicing or reblading at a cruising temperature some 75 C hotter than will be employed on the B.E.25.

B.E.25 Powerplant

It is proposed to supply the B.E.25 engine as a complete powerplant, a photograph of a mockup of which is shown in Fig. 13.

In the first place, the B.E.25 engine will be applied to the Bristol Britannia Civil Aircraft, and since the powerplant requirements for this aircraft are entirely known, it has been possible to design all the required features into the engine from the beginning.

The propeller used will be the existing De Havilland 4-bladed, 16-ft diameter airscrew used on the Proteus 755 in the present aircraft. At the moment, this propeller is undergoing endurance testing at more than 4000 hp in conjunction with the reduction gear on the rig shown in Fig. 13. The performance for this propeller is illustrated in Fig. 14. With a maximum take-off rpm of 945 on the propeller (corresponding to 10,500 L.P.R.P.M. on the engine with the 11.1/1 reduction gear ratio), some static thrust is sacrificed, but at 120 knots the propeller

Fig. 11 – Proteus combustion chambers after 500-hr endurance test

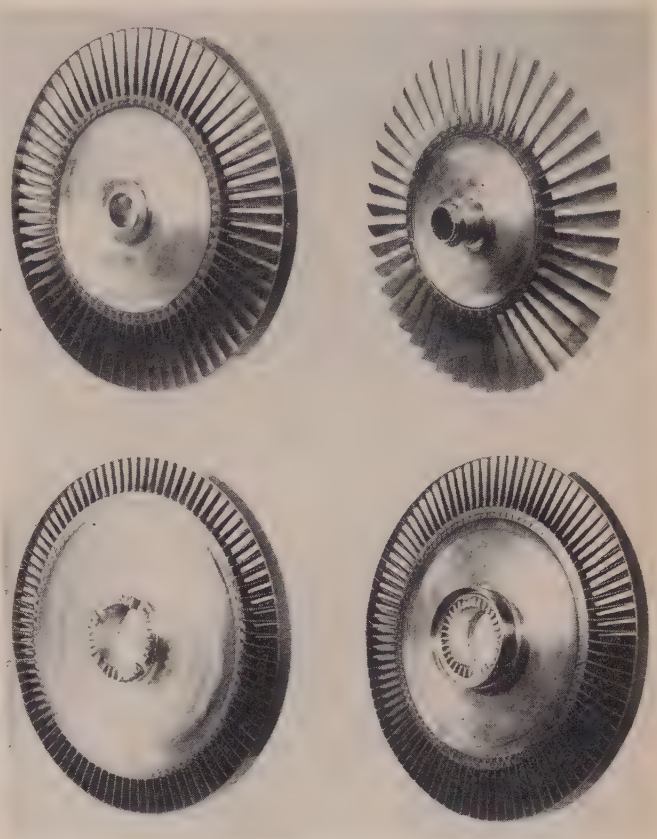

Fig. 12 – Proteus turbine wheels

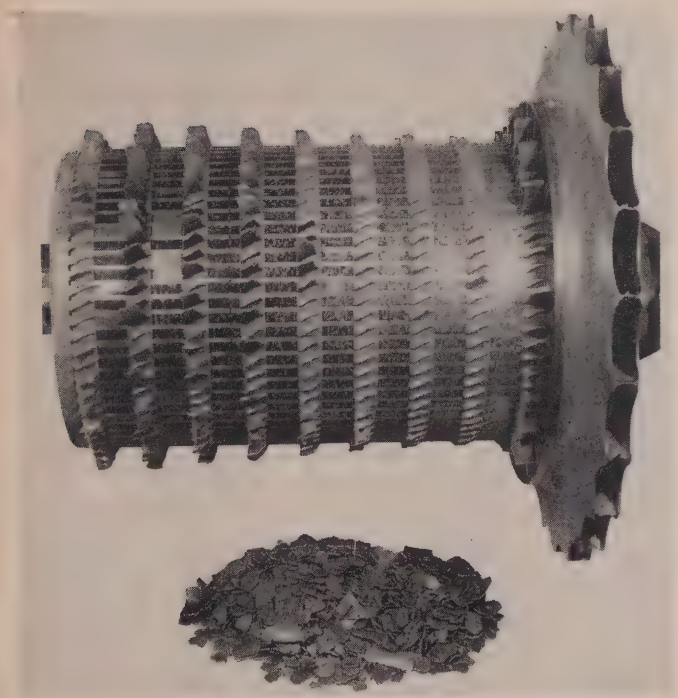

Fig. 10 – Damage to aluminum-bladed compressor due to passage of steel bolt

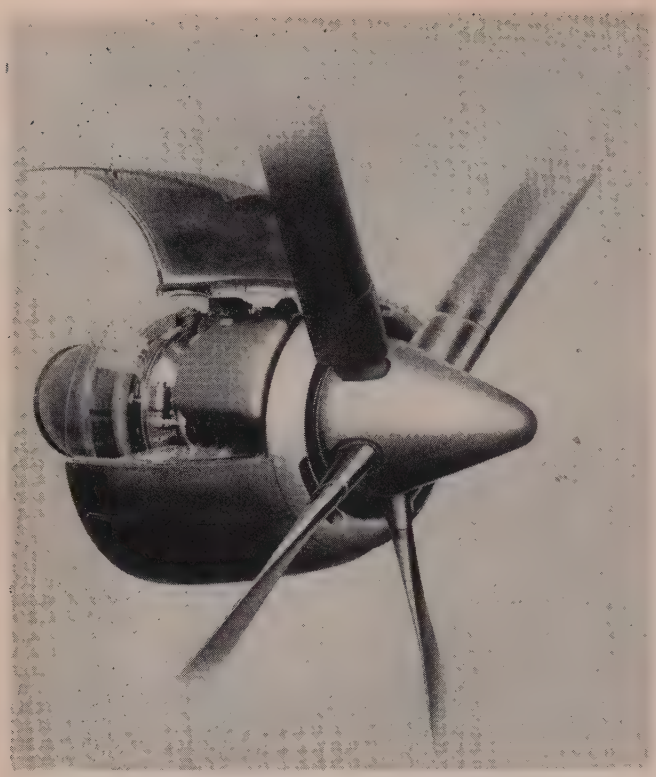

Fig. 13 – Bristol B.E. 25 powerplant mockup

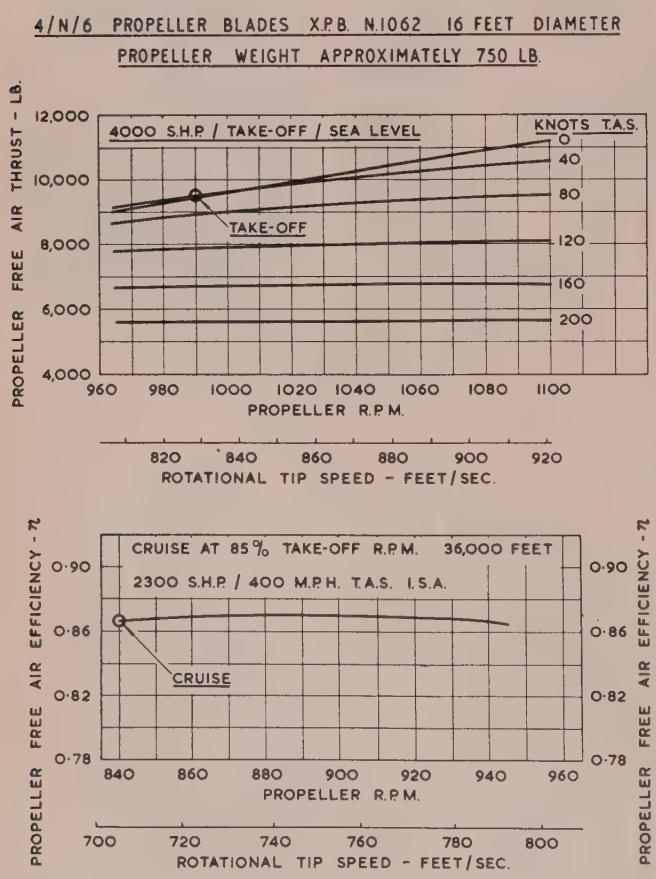

Fig. 14 – Performance of 4-bladed, 16-ft diameter De Havilland propeller on B.E. 25 turboprop engine

thrust is sensibly independent of the rpm. It should be remembered that in addition, the engine gives 2400 lb of jet thrust under the torque limited take-off conditions. Under cruising conditions at altitude, the propeller will be 800 (corresponding to 8860 L.P.R.P.M.), and the rotational tip speed rather less than 700 fps, which should make for a very low noise level. A free air efficiency of 86% is computed at 400 mph true air speed.

In addition to driving the aircraft, a modern power plant is called upon to supply a variety of other services to the aircraft. In the case of the B.E.25 in the Britannia the following additional services will be provided:

(1) 47-kva generator for electric supply. This will be driven by the high-pressure compressor, and will run at almost constant speed. It will not be necessary to employ superfine pitch operation on the propeller in order to maintain operation of the electric generator while taxiing.

(2) Cabin-pressure air direct from the low-pressure compressor, which is capable of maintaining sea-level pressure up to more than 35,000 ft.

(3) Air from the low-pressure compressor for direct wing de-icing. The temperature of this air will be approximately 180 C and is therefore suitable for introduction directly into the wing de-icing ducts. It should be noted that items 2 and 3 above are taken directly from the low-pressure compressor and will have no effect upon the operating temperature of the engine, other than to reduce the power available to the propeller. Over the range of operation of the engine (that is, while climbing), during which the torque limiter is in operation, bleeding air from the l-p compressor will have no effect on the power output. It must, of course, be paid for by increased fuel consumption.

(4) An air bleed is provided to operate an ejector for cooling the rectifiers.

(5) Propeller reversing will be used for braking purposes.

A picture of the engine mockup is shown in Fig. 15. It will be seen that all the powerplant items are grouped around the low-pressure compressor, and ahead of the built-in firewall. In general, the electric items are mounted at the top of the engine, the fuel-control system at the side, and the oil system at the bottom. Great attention has been paid to precautions against fire, and it should be impossible for fuel to come into contact with metal at a temperature higher than 150 C.

The engine is mounted on four dynamic suspension units focused on the center of gravity.

Table 1 summarizes the powerplant weights. The weights given in Table 1 do not account for the use of titanium, which will be incorporated as a weight saving during development.

Aircraft Performance

The B.E.25 engine is intended as a replacement engine for the Proteus 755. Power and fuel con-

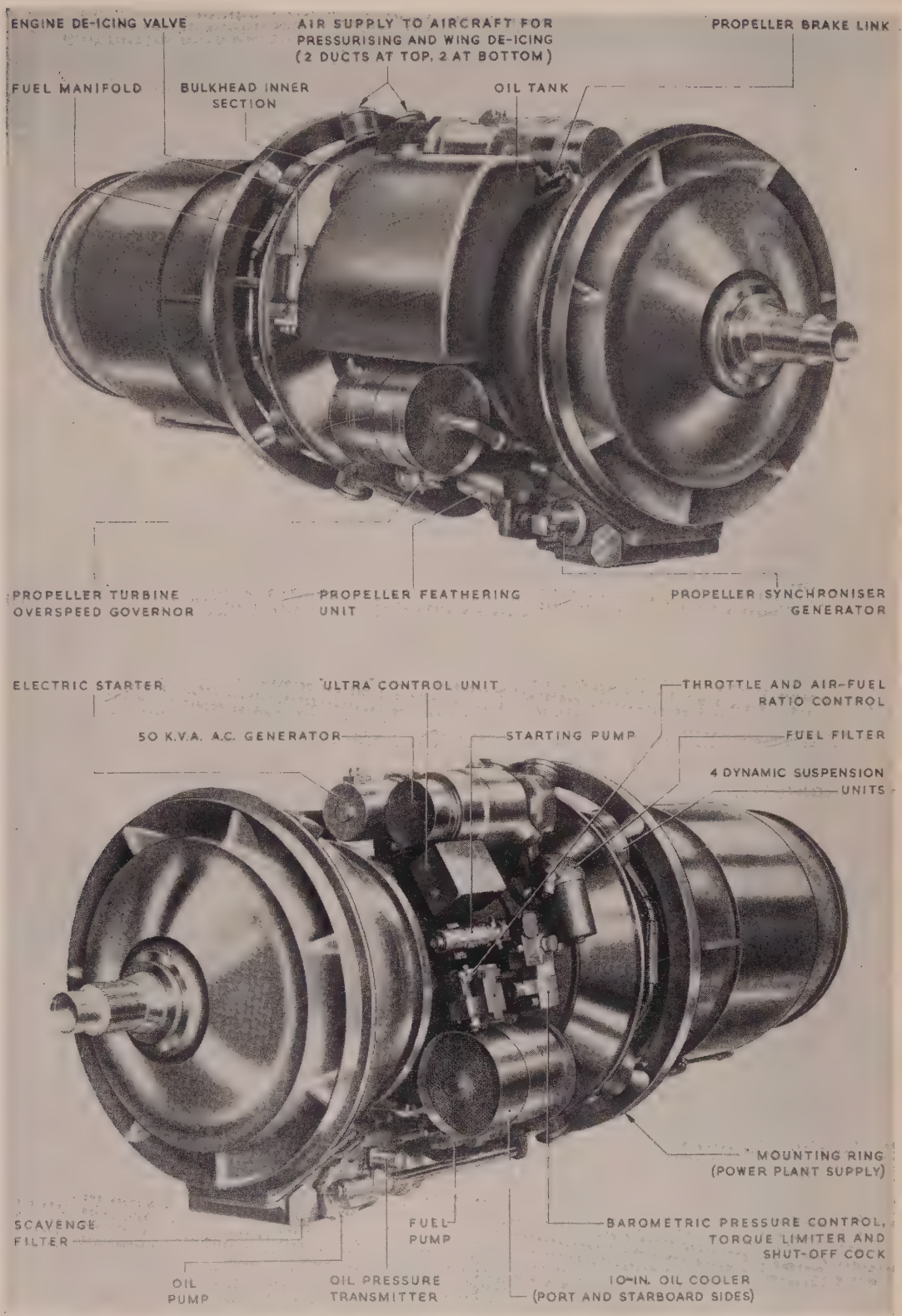

Fig. 15 – Mockup of B.E. 25 supercharged turboprop engine

Table 1 – B.E.25 Powerplant Weight

Component	Weight, lb
Engine (dry) complete, including oil tank, coolers, and dynafocal units	3200
Electrical systems	248
Cowlings and mountings	422
Cooling ducting, fire extinguishing system, and sundries	220
Propeller and spinner	870
Total	4960

sumption of the two engines are compared in Fig. 16.

It will be seen that at 30,000 ft the B.E.25 engine gives 3500 total equivalent hp for continuous cruising, compared to 2000 for the Proteus 755. At the same time the relative sfc are 0.405 for the B.E.25 and 0.50 for the Proteus, both engines assumed to be in an aircraft traveling at an indicated speed of 220 mph (360 mph true air speed).

On the Britannia the effect of an increase of 75% in cruising power per engine would be very great and would produce an aircraft speed in excess of the limiting Mach number for which the wing has been designed, $M = 0.63$. Consequently the full cruising power of the B.E.25 will not be used in the case of the Britannia, and almost for the first time in history there will be available a transport aircraft with excess power. There will be no question of scraping the bottom of the bucket for the 100-odd hp, and the surplus power available will be a great advantage in case of loss of one or even two engines en route.

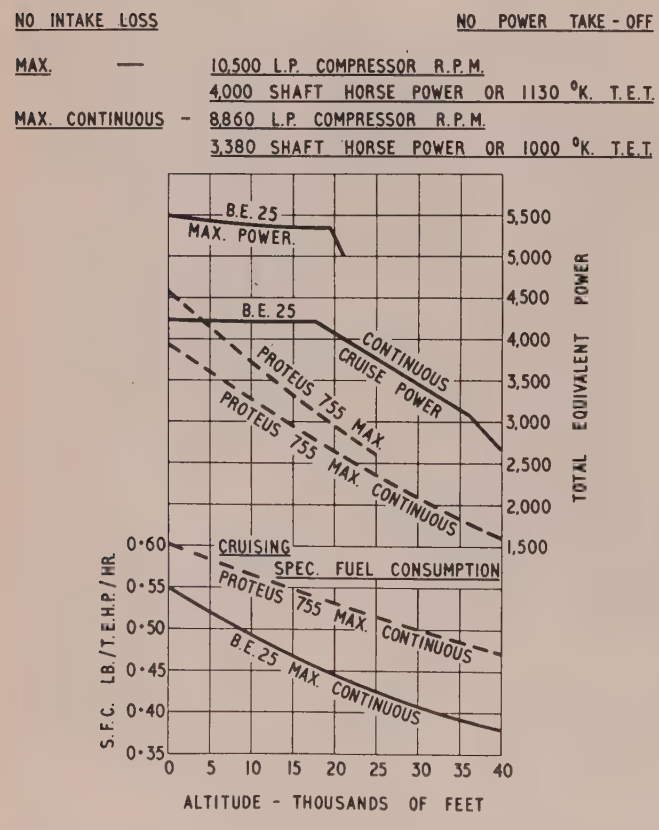

Fig. 16 – Comparison of equivalent power and fuel consumption for Proteus 755 and B.E. 25 turboprop engines at assumed equivalent air speed of 220 mph

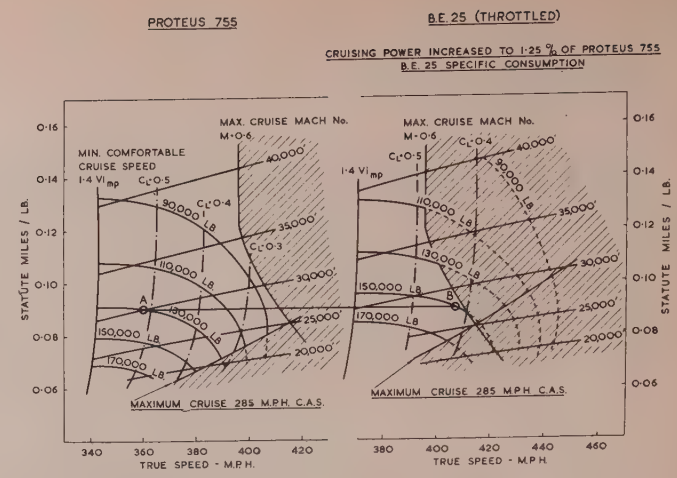

Fig. 17 – Performance comparison of aircraft equipped with Proteus 755 and B.E. 25 turboprop engines

The overall effect on the performance of an aircraft of roughly the Britannia specification is shown in Fig. 17. Taking point *A* on the left-hand series of curves as a typical point corresponding to 360 mph at 30,000 ft altitude with an aircraft weighing 130,000 lb, we see that the statute miles per lb of fuel are 0.09. Moving to the right-hand set of curves and considering point *B*, which also gives 0.09 statute miles per lb of fuel, we see that the aircraft speed has increased to 407 mph at about 28,000 ft, but under these conditions, the total weight can be increased to 150,000 lb, that is, an increased payload of 20,000 lb can be carried the same distance 47 mph faster. Even in this case the power required from the engine is only 25% greater than that given by the Proteus 755. On the other hand, if the total weight is maintained constant at 130,000 lb, the aircraft will travel 400 mph at about 33,000 ft with a range of 0.11 statute miles per lb of fuel, that is, an increase of 20% in range at the same total weight with a 40 mph increase in speed.

If the Mach number limitation on the wing can be lifted, then much greater cruising speeds in the order of 460 to 470 mph could be realized. Thus, we are left with the situation that in order to exploit the full potentialities of this new engine a new airframe must be made available.

Acknowledgments

The author is indebted to the Ministry of Supply for permission to publish this paper, to the De Havilland Propellers, Ltd. for the propeller data, and to his many colleagues for the help they have given him.

The New

PLYMOUTH

Engine

H. L. Welch, Chrysler Corp.

This paper was presented at the SAE Golden Anniversary Passenger-Car, Body, and Materials Meeting, Detroit, March 2, 1955.

A HIGH-PERFORMANCE V-8 engine with modified hemispherical combustion chamber has been designed and developed for the 1955 Plymouth passenger car. This new engine brings to the lowest-priced line of Chrysler Corp. automobiles the operating characteristics and advantages usually associated with engines of expensive, or even luxury-priced, cars.

This paper will cover a brief account of (1) the reasons for the selection of this type of engine, (2) a description of the engine, and (3) performance characteristics.

Reasons for Design

The choice of this type of engine was carefully made in the light of years of exhaustive study of a wide variety of combustion chambers and cylinder arrangements, as well as scores of combinations of mechanical components.

The most important qualities being sought in combination were:

PLYMOUTH'S new V-8 engine has a specific output of 0.65 bhp/cu in. and 145-psi bmep – obtained through a combination of high thermal, volumetric, and mechanical efficiencies.

Good design, the author points out, has achieved this high output despite the dual-venturi carburetor and the 7.6/1 compression ratio, selected for satisfactory operation on regular-grade fuels.

The engine has a bore and stroke of 3.563 x 3¼, weighs 568 lb without flywheel, is 29⅜ in. long, and is designed for optimum response to future compression ratio increases.

(A report of oral discussion following presentation of this paper appears on p. 220, following "The New Packard V-8 Engine," by W. E. Schwieder.)

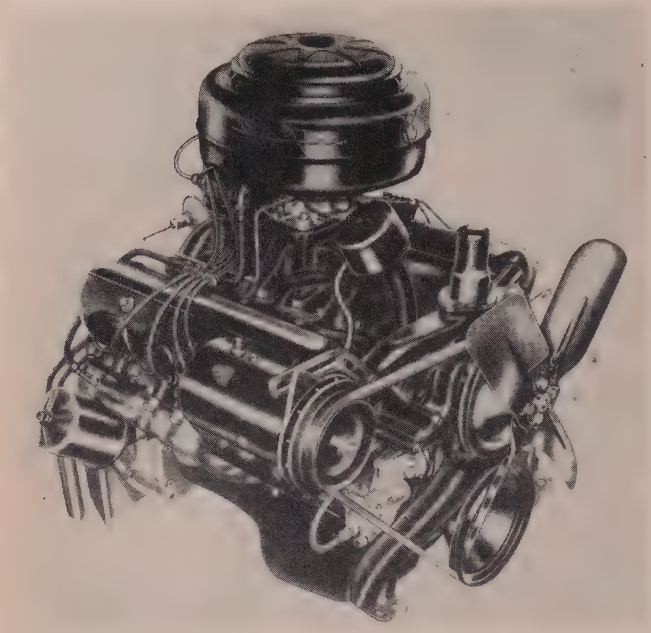

Fig. 1 – Plymouth V-8 engine

1. Effortless smoothness and quietness at all speeds.
2. Outstanding performance and fuel economy on regular-grade fuel.
3. Good adaptability for future requirements.
4. Low weight and bulk.
5. Long life and good reliability.
6. High degree of accessibility and simplicity for ease of servicing.
7. Low manufacturing cost.

Evaluation of experimental engines of in-line 6, flat or horizontal opposed 6, V-6, and V-8 cylinder arrangements revealed that most of the desired qualities could be met by the V-6, in-line 6, or V-8 engine types. However, it was found that the V-8 with five main bearings was significantly smoother under some operating conditions than the 6-cyl engines. It was felt that in the years ahead the discriminating car buyers will place increasing emphasis upon smoothness of a high order. In this regard, therefore, anything less than a V-8 would be a compromise considered unworthy of a new Plymouth engine. The V-8 engine also satisfied the weight and size requirement, and was found to be well adapted to producing high specific power, with long life.

As compared to a six, any V-8 engine presents a challenge to the engineers to achieve sufficient simplicity and low manufacturing cost. Nevertheless, there was a resolute desire to adhere as closely as possible to the ideals determined during the company's previous V-8 engine development programs.

An excellent case in point was in the choice of combustion chamber. Exhaustive studies of combustion-chamber types led to the adoption of the hemispherical chamber for the Chrysler, DeSoto, and Dodge V-8 engines.[1, 2] With the exceedingly satisfying results obtained from the hemispherical chamber in the company's existing V-8 engines, there was, naturally, a strong desire to employ this top-quality feature in the new Plymouth engine. It was recognized that the laterally positioned valves of the hemispherical chamber posed additional design problems in the form of valve operating means, compared to the conventional valve-in-line overhead-valve engines.

In consideration of the simplicity of the conventional overhead-valve engines, the advantages of the hemispherical combustion chamber were critically reviewed and analyzed. Briefly, some of these advantages are:

1. Maximum thermal efficiency for a given compression ratio.
2. Maximum volumetric efficiency.
3. Excellent valve-seat cooling and freedom from distortion.
4. Lowest loss to carbon deposits.
5. Lowest heat loss to cooling system.
6. Excellent detonation control and freedom from deposit-inspired preignition.
7. Excellent response to increases in compression ratio.

Without attempting to explain fully the characteristics of this type of combustion chamber, it is believed that the main reasons for superiority may be summarized by:

1. A compact chamber having the smallest surface/volume ratio.
2. Good spark-plug location, giving short flame travel.
3. Capacity for large valves, and proper disposition of valves and ports to augment volumetric efficiency.

Strong consideration was given to use of a conventional chamber with rather small, closely spaced valves, making it compact, and similar in shape to a hemispherical chamber. This would have resulted in restricted power potential and questionable valve durability. When combined with a large bore and very short stroke, it looked more attractive for valve size, but automatically meant a less compact chamber with lower thermal efficiency.

Through diligent design study, it was devised that by reorienting the exhaust valve, and placing it parallel to the cylinder axis, slightly off the transverse center plane of the cylinder, a combina-

[1] See SAE *Quarterly* Transactions, Vol. 5, July, 1951, pp. 346-358: "Development Highlights and Unique Features of New Chrysler V-8 Engine," by W. E. Drinkard and M. L. Carpentier.

[2] See SAE *Quarterly* Transactions, Vol. 6, October, 1952, pp. 677-688, 723: "New Horizons in Engine Development," by James C. Zeder.

tion was possible that closely approximated the compactness, with large valves, so characteristic of the hemispherical chamber. Of great significance in this study was the fact that both the valves could be operated from a single rocker shaft, and the spark plug could be placed outside the rocker cover, but still in a very desirable position within the chamber. This modified hemispherical-chamber design seemed to combine the simplicity of the conventional overhead-valve types with most of the characteristics of the sought-after hemispherical chamber.

Actual engines built to this design verified the expectation. It became possible, therefore, to design an engine for the Plymouth that embodied the desired performance features, without a cost penalty compared to less ideal types.

Experience with engines of widely varying stroke/bore ratio indicated very little change in mechanical efficiency over the range of 0.8 to 1.0. A noticeable trend was observed of a *decrease* in thermal efficiency as the stroke/bore ratio was decreased. Thus, while an ultra-short stroke/bore ratio favors maximum attainable valve size, and minimum width, height, and weight, a longer stroke/bore ratio enhances thermal efficiency and reduces length. When combined with the modified hemispherical combustion chamber, a stroke/bore ratio of 0.91 provided a light, compact, low-friction design, together with excellent thermal efficiency and performance.

Regardless of how sound the basic design of an engine may be, the true quality of an engine also depends heavily upon the meticulous and successful attention to all details of mechanical design, including the components and the combination of the parts as a whole. The experience gained from designing and developing the Chrysler, DeSoto, and Dodge V-8 engines proved extremely valuable, and was particularly useful in the mechanical component design of the Plymouth V-8 engine.

Description of the Engine

General – The new Plymouth engine is a 90-deg V-8, having a bore and stroke of 3.563 x 3¼, or a piston displacement of 259.2 cu in. Compression ratio is 7.6. The dry weight of the engine, including air intake silencer, starter, generator, and fan, but less flywheel, is 568 lb. Overall length of the engine, from the forward edge of the fan to the rear of the crankshaft flange, is 29⅜ in.

Fig. 1 shows the functional arrangement of the engine with the all-downward-flowing intake system in the center of the V, and the exhaust manifolds located low on the outside of the V. Generator, distributor, and spark plugs are easily accessible from the top of the engine. Secondary spark-plug leads are inherently well protected from exhaust heat and road splash. The oil-filler pipe and oil-level indicating stick are conveniently located near the front of the engine, and the pad-mounted oil filter is on the right side, accessible for service. The fuel pump is located on the side of the timing-chain cover at the front of the engine, in the interest of avoiding vapor-lock problems.

Belt Drive – The single belt driving the generator and water pump has 87 deg of wrap around the water pump pulley, thereby enhancing the capacity of the drive. Engines equipped with a power-steering pump mount the generator on the front left corner of the intake manifold, and utilize a short belt to drive the water-pump pulley, with a second short belt to drive the generator. This latter arrangement shortens the hydraulic lines between the power-steering pump and the steering gear.

Engine Mountings – Engine mountings are of the Floating-Power type, with the water-pump housing forming the seat for the front bonded-rubber mount. The stamped steel A frame carries the load of the front mounting down to the car frame. The two rear-engine mountings are attached to the under side of the automatic transmission where used, or the clutch housing where the manual-shift transmission is used.

Piston and Rings – Fig. 2 shows a transverse section of the engine. This view shows the compact crankshaft, connecting rod, piston, and cylinder-block structure. Pistons are especially robust, having very heavy vertical ribs between the pin bosses and head. Full-floating piston-pin construction with a steel-backed bronze bushing in the upper end of

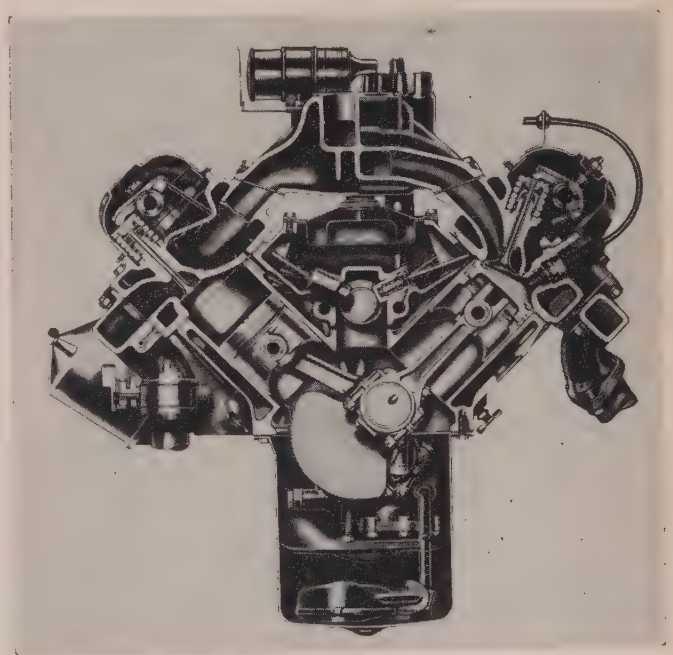

Fig. 2 – Transverse section of engine

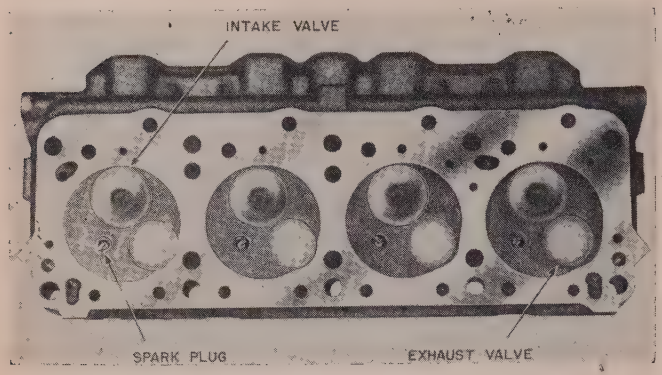

Fig. 3 – Cylinder head

the connecting rod is employed for optimum piston performance and ease of servicing. A steel band is cast into the piston skirt just below the ring belt, to provide excellent skirt clearance control under all operating conditions. As a further aid to quiet operation, the piston pin is offset 1/16 in. toward the thrust side of the piston. Pistons are tin-coated to prevent scuffing.

No unusual problems of oil control were encountered with this piston, the rather conventional piston ring lineup proving very effective. Compression rings are 5/64 in. wide, and are of the taper-twist type. The cast-iron oil ring is 3/16 in. wide, and uses a hump-type expander. One of the functions of the expander is to hold the oil-ring gap in its installed position, toward the center of the V.

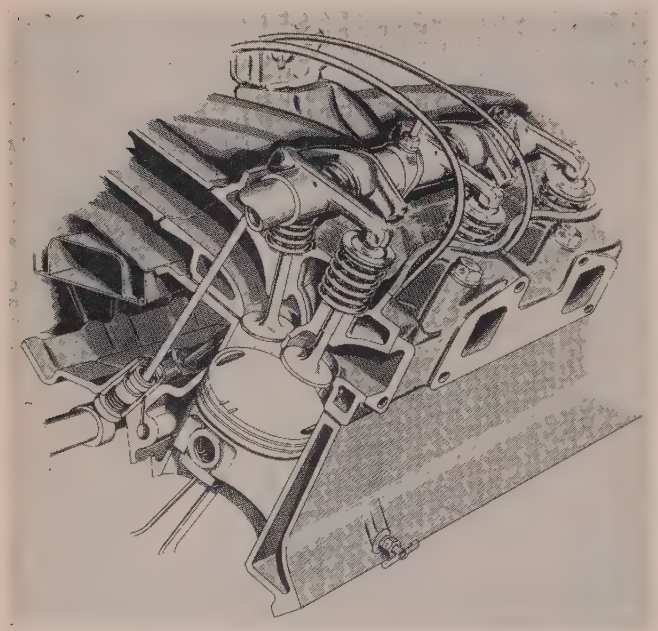

Fig. 4 – Valve actuation

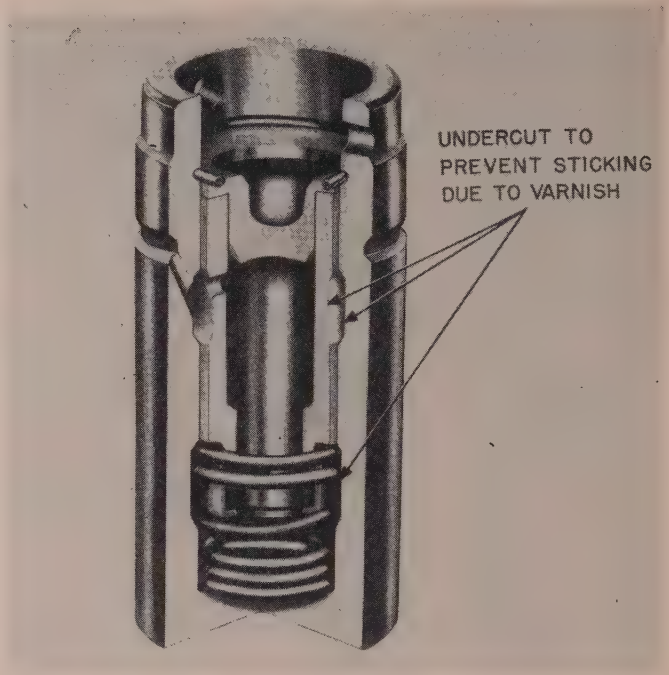

Fig. 5 – Hydraulic tappet

The two main oil galleries and feed to the hydraulic tappets may also be seen in Fig. 2.

Intake Manifold – The two-level intake manifold contains no pockets or sump in the intake passages, which eliminates puddling and "flash" problems. The exhaust crossover passage connects the exhaust port of cylinder No. 4 in the right bank with the port of cylinder No. 5 in the left bank. This feature is for the purpose of minimizing exhaust interference with induction, with the firing order 1-8-4-3-6-5-7-2. A thermostatic control valve at the outlet of the right bank exhaust manifold regulates the exhaust heat to the intake manifold.

Combustion Chamber and Valve Train – Fig. 2 also shows the modified hemispherical combustion chamber with streamlined intake and exhaust ports and the single-rocker-shaft valve-operating mechanism. A saving in engine weight of 35 lb was achieved by this simplified cylinder-head construction. The close similarity to the hemispherical chamber, including port shape and relative position of the valves and spark plug within the chamber,

[3] For a complete description of this material, and reasons for its selection, see pp. 138-152 of this issue: "Considerations Affecting the Life of Automotive Camshafts and Tappets," by M. F. Garwood, D. R. Kinker, and J. J. Manganello.

is plainly visible in this view and in Fig. 3. The valve drive train is shown in more detail in Fig. 4. Intake and exhaust valves are on opposite sides of the rocker shaft, as are the respective push-rods. Valve stems operate directly in the cylinder-head iron, and all valve seats are integral. Cylinder heads are cast of iron, with chromium added to insure a good wear-resistant structure of the integral valve-seat material. Right and left cylinder heads are identical for the convenience of service and manufacturing.

Intake valves, of 8440 steel, have a head diameter of 1 23/32 in., and are of modified tulip shape to conserve weight. Exhaust valves are made of Silchrome XCR, and have a head diameter of 1 15/32 in. Stems of both valves are $\frac{3}{8}$ in. in diameter for added strength and bearing area.

Push-rods are solid, made from $\frac{1}{4}$-in.-diameter drawn steel wire. The machined spherical ends are induction-hardened to give long life. This type of push-rod was selected on the basis of durability, and of valve-gear dynamic tests which showed these push-rods to be the simplest and lightest that gave adequate linear stiffness.

Single valve springs are employed. The cam design is the culmination of years of mathematical analysis coordinated with physical engine tests with electronic instrumentation. The resulting cams provide quiet and smooth valve operation to 5000 rpm with moderate valve-spring loads of 53 to 140 lb at valve closed and open positions, respectively.

Hydraulic tappets provide the important function of maintaining zero lash in the valve train for quiet operation and long trouble-free valve life. A sectional view of the tappet is shown in Fig. 5. The body of the tappet is made of hardenable cast iron held to rigid specifications of chemistry, structure, and hardness.[3] The spring-loaded flat check valve reduces takeup lift loss to virtually zero, but still exhibits good manners with regard to pump-up. The oil grooving in the body and reservoir in the plunger provide excellent quiet starting characteristics. The tappet has been made impervious to normal oil deposits, even where detergent oil is not used, by undercutting all critical areas of the plunger and tappet body bore.

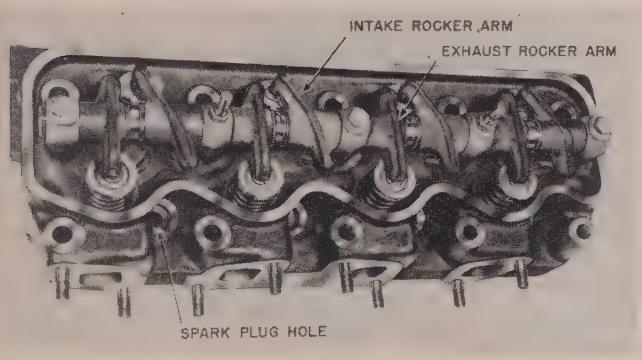

Fig. 6 – Top view of cylinder head

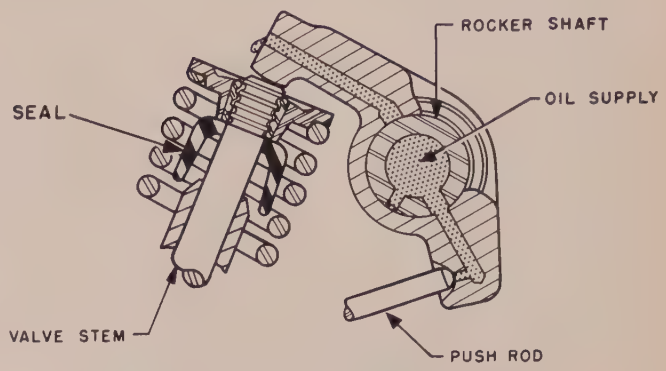

Fig. 7 – Intake valve rocker lubrication

Fig. 6 shows the top view of the cylinder-head assembly, with rocker cover removed. The entire rocker and shaft assembly, with five die-cast, aluminum support brackets, make a convenient bench assembly which is then assembled to the cylinder head as a unit. The proved reliability of the rocker and shaft mechanism scarcely needs mentioning, but has been further enhanced by very reliable lubrication plus generous bearing areas provided in the phosphate-coated cast malleable iron rockers. The easily accessible but well protected location of the spark plugs may be seen in Fig. 6.

Valve-Train Lubrication – Adequate lubrication of valve train parts without contributing to oil consumption is a worthy objective in all engines. Part of the method for accomplishing this in the Plymouth V-8 engine is shown in Fig. 7. Oil at pressure less than main gallery pressure is delivered to the hollow rocker shaft, from which it is admitted to the push-rod socket and valve-stem end of the rocker through drilled holes. To prevent oil from entering the combustion chamber past the intake valve stems, a synthetic rubber cup-type seal is used on all intake valves, as shown.

Low-Friction Valve Lock – As an aid to long valve life, a new type of low-friction valve lock has been developed. Shown in Fig. 8, it may be seen that the conventional valve-spring retainer is used, but that the lock and valve-stem tip grooving have been changed. The new lock is made to have radial clearance with the valve stem with the two halves of the lock butted together, permitting the valve to turn freely with respect to the valve spring re-

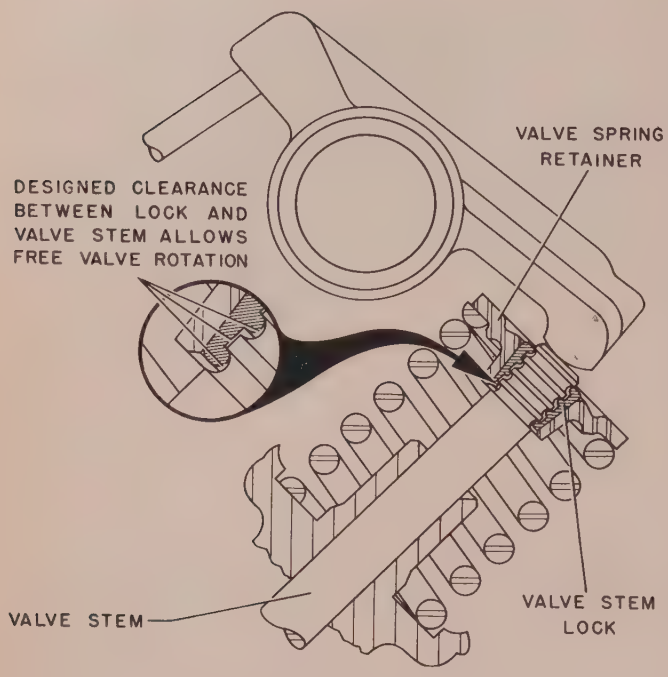

Fig. 8 – Low-friction valve lock

tainer. Four lands are provided to give long wearing life and high strength. Since contact between lock and valve stem is at a smaller diameter even than the valve stem itself, the torque required to turn the valve is very low.

Block and Crankshaft – In Fig. 9, the longitudinal section of the engine reveals the very rigid cylinder block and crankshaft structure. The crankshaft is only 25 in. long and has 2⅜-in. main journals, and 1 15/16-in.-diameter crankpins. Made from a steel forging, the crankshaft has a natural frequency in torsion of 293 cps, and weighs 50 lb. All fillets between bearing journals or crankpins and cheeks are turned by a formed tool, and shot-peened before the final grinding operation. By this means these all-important fillets are accurately controlled for both size and shape, as well as being work-hardened and residually stressed in compression for greater fatigue strength. Being undercut, they also facilitate obtaining very accurate crankpin and journal surfaces.

Bearings – All connecting-rod and crankshaft main bearings are microbabbitt, with steel backs. Lead-base babbitt is employed except for the flanged No. 3 main bearing, which takes thrust. This particular bearing is made of tin-base babbitt, which has excellent resistance to wear under thrust loading. By locating the thrust bearing in the No. 3 position, it is practical to lubricate the flanges generously without affecting the performance of crankshaft oil seals.

Crankshaft Seals – The front crankshaft oil seal is a very positive design comprising a slinger, internal trough, and spring-loaded, lip-type seal. To ensure long life of the seal, a rotating felt and slinger on the crankshaft pulley hub keep water and abrasive material from entering from the outside. The rear crankshaft oil seal is equally effective. A circumferential drainage groove near the rear edge of the No. 5 crankshaft bearing returns to the crankcase almost all of the oil that would otherwise flow out the rear of the No. 5 main bearing. The crankshaft slinger and ample slinger cavity further divert oil at this point, leaving the rope-type rear seal with very little oil to handle. Diagonal knurling on the crankshaft at the location of the rope seal adds a pumping action that makes the rope seal very effective.

Floating Oil Pump Intake – The floating type of oil pump intake screen, used for many years in Chrysler Corp.'s engines, is again selected for its added protection. Its location and that of the oil pump, beneath the rear main bearing cap, are shown in Fig. 9.

Camshaft and Timing Chain – The cast-alloy-iron camshaft is made exceptionally stiff in the interest of good valve-gear dynamics. The cams are ground with a taper to produce reliable tappet-body rotation. An extra-wide 1⅛-in. timing chain is employed, together with means for reliable, directed

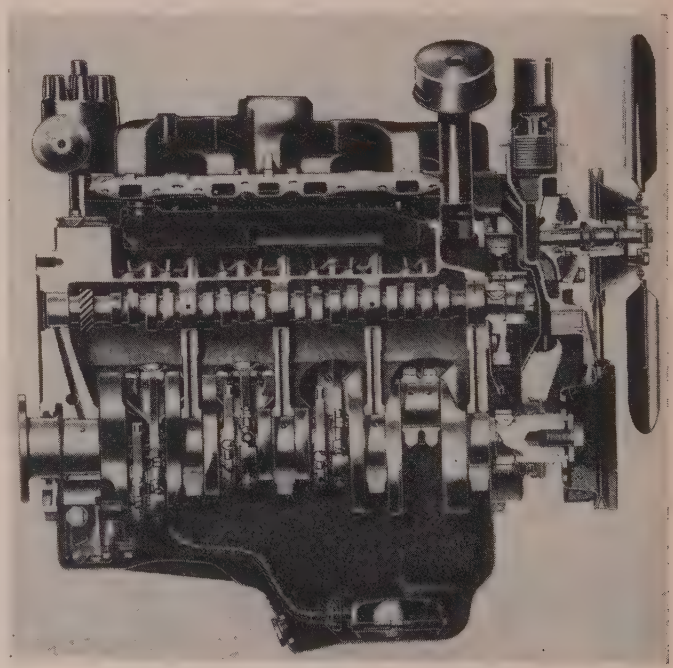

Fig. 9 – Longitudinal section of engine

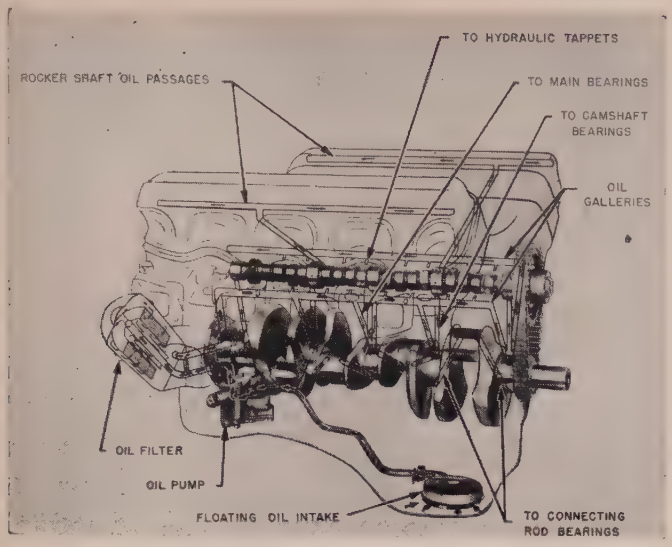

Fig. 10 – Lubrication system

lubrication to ensure long life of the timing drive under all driving conditions. The separate fuel pump drive eccentric is mounted on the front end of the camshaft, and is doweled to the camshaft sprocket hub. It is lubricated by spray from the timing chain.

Coolant Circulation – The water pump is fitted with ball bearings for long life and quiet operation. The pump delivers coolant into each bank of the cylinder block, from which it flows into the cylinder heads through calibrated holes in the deck. By thus regulating the flow pattern, very uniform coolant temperatures have been attained. Coolant leaves each cylinder head at the front, and is conveyed to the choke-type thermostat pocket through passages in the water-pump-housing casting. A permanent bypass provides good coolant circulation through the engine, even when the thermostat is closed.

Crankcase Ventilation – The engine is ventilated by air drawn through the filter cap on top of the oil filler pipe. The cavity in the block at the bottom of the oil filler pipe communicates with the timing chain housing and thence with the crankcase. The stamped-steel cover over the center of the cylinder block contains a low-velocity baffle to separate oil droplets from the ventilation air before it leaves via the conventional road draft tube.

Lubrication System – In Fig. 10 is shown a phantom view of the lubrication system. The pressure-regulating valve is located within the oil pump housing, the excess pump capacity being recirculated. Oil from the pump travels through the pad-mounted filter or through the shunt to arrive at the main oil gallery, to the right of the camshaft. This main oil gallery supplies oil to crankshaft and connecting-rod bearings, as well as camshaft bearings and the hydraulic tappets in the right bank. The parallel, secondary oil gallery located to the left of the camshaft is fed from the front crankshaft bearing. The secondary oil gallery supplies oil to the hydraulic tappets in the left bank.

Lower pressure oil for the rocker shaft lubrication is obtained without resorting to small metering holes, by utilizing intermittent partial registration of 5/32-in. drilled holes in the camshaft bearing journals with drilled passages in the cylinder block. As indicated in Fig. 10, drilled passages in the cylinder block and cylinder heads deliver oil from the No. 2 and No. 4 camshaft bearings to the hollow rocker-shaft support of the left and right banks, respectively. This is the same basic lubrication system that has been used very successfully on the Chrysler, DeSoto, and Dodge V-8 engines.

Carburetor – The standard carburetor (shown in Fig. 11) is a Ball & Ball dual-venturi design, having 1 3/16-in.-diameter main venturis and 1 7/16-in.-diameter throttle bores. As a result of the cooperative development efforts of our carburetor engineers and engineers skilled in die-casting techniques, this carburetor is being die-cast of aluminum. It weighs 3.2 lb, and is only 4½ in. tall. The float bowl is vented into the air horn in the interest of cleanliness and relative insensitivity to air-cleaner restriction. The remarkable simplicity of the carburetor is advantageous for both reliability and ease of servicing. For example, the stroke of the accelerator pump is easily adjusted by means of an external link, to suit extreme ambient temperature or fuel volatility conditions. Similarly, the float valve and seat can be removed and replaced

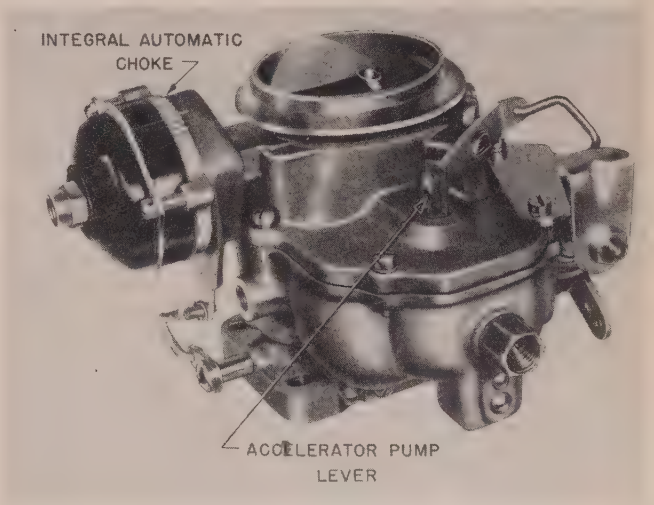

Fig. 11 – Carburetor

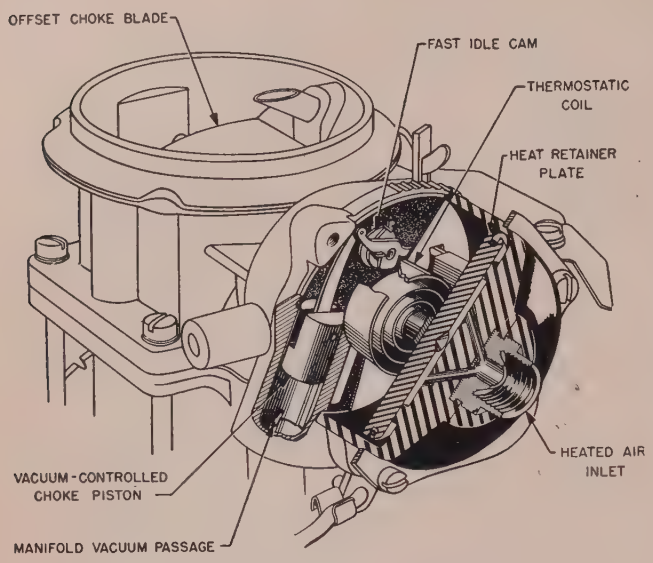

Fig. 12 – Carburetor integral automatic choke

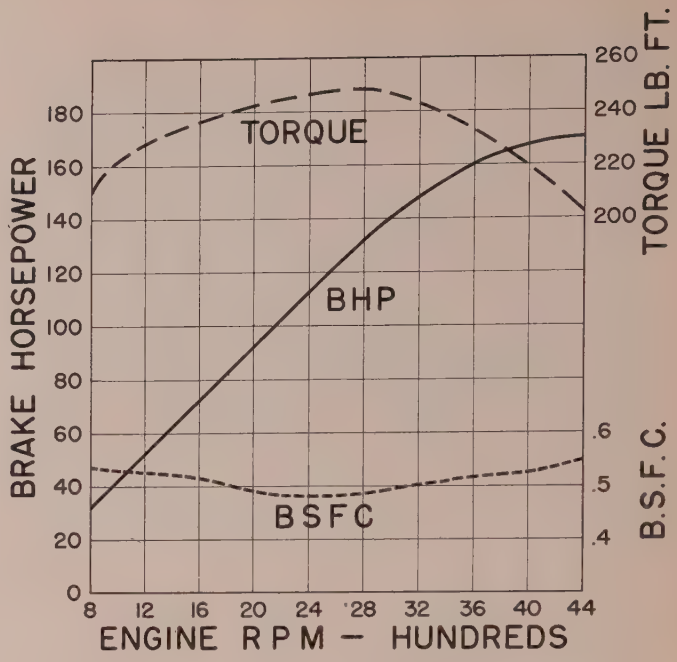

Fig. 14 – Gross power and brake specific fuel consumption

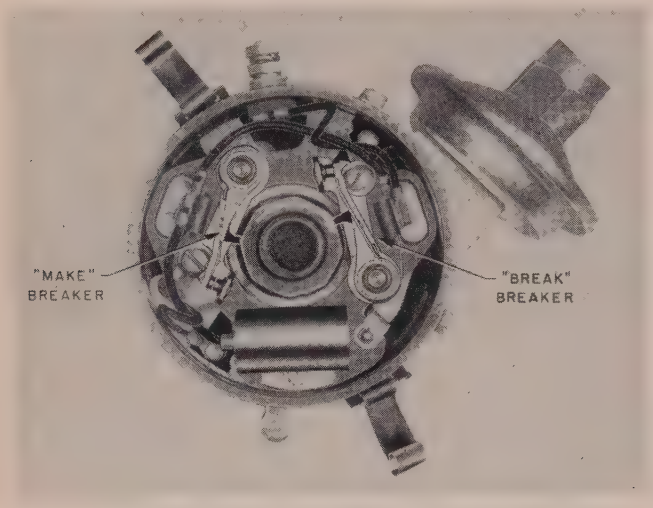

Fig. 13 – Double-breaker ignition distributor

without having to disassemble the carburetor or reset the float level.

Automatic Choke – An integral automatic choke is bolted to the outside of the air horn, having virtually all operating mechanism enclosed. The phantom view in Fig. 12 shows the heat-retainer plate which is incorporated to enable the thermostat to better provide the correct amount of choke during warming up and cooling periods. The choke stove for heating the air pulled past the choke thermostat is composed of an Inconel tube pressed into the right bank exhaust manifold. The location in the exhaust manifold assures that the stove receives ample heat when the engine is running.

Air Cleaner – A concentric oil bath air cleaner and intake silencer is used, as this type is efficient, simplest, generally of lowest restriction, and the least prone to affect fuel distribution. A convenient V-type clamp with a gasket is used to seal the joint positively between air cleaner and carburetor air horn.

Distributor – A double breaker distributor is provided to assure adequate secondary voltage at all speeds. Fig. 13 shows the two sets of contact points which operate in parallel, giving about 20% longer dwell time, with a consequent much higher secondary voltage at high engine speeds. For precise ignition timing control, a mechanical governor is used for the automatic advance at wide-open throttle, supplemented by a vacuum diaphragm to give extra advance at part throttle.

Resistor-Type Spark Plugs – Fourteen-millimeter resistor-type spark plugs are used, which give much longer electrode life, as well as built-in suppression of radio and television interference. The preignition rating of the specified Auto-Lite 4S-165 plug is 165-psi imep in the 17.6-cu-in. spark-plug rating engine.

Performance Characteristics

Of the many ways to evaluate an engine, one of the most significant and interesting means is to

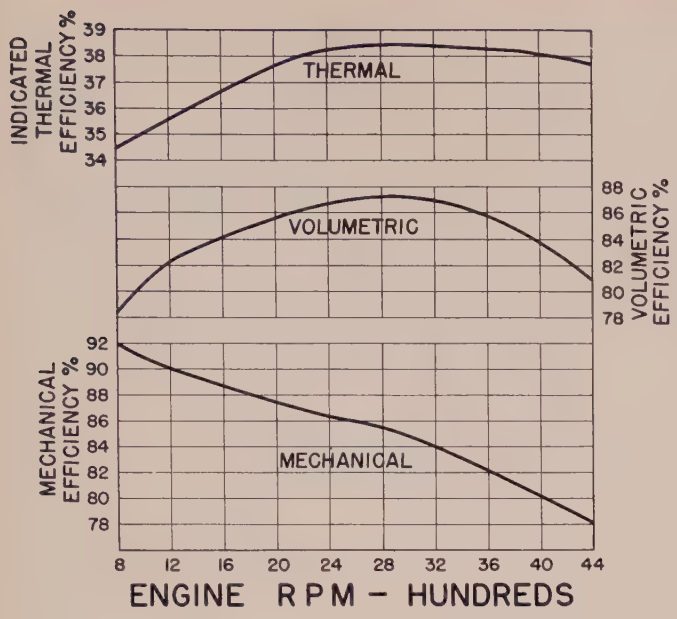

Fig. 15 – Gross efficiency (wide-open throttle)

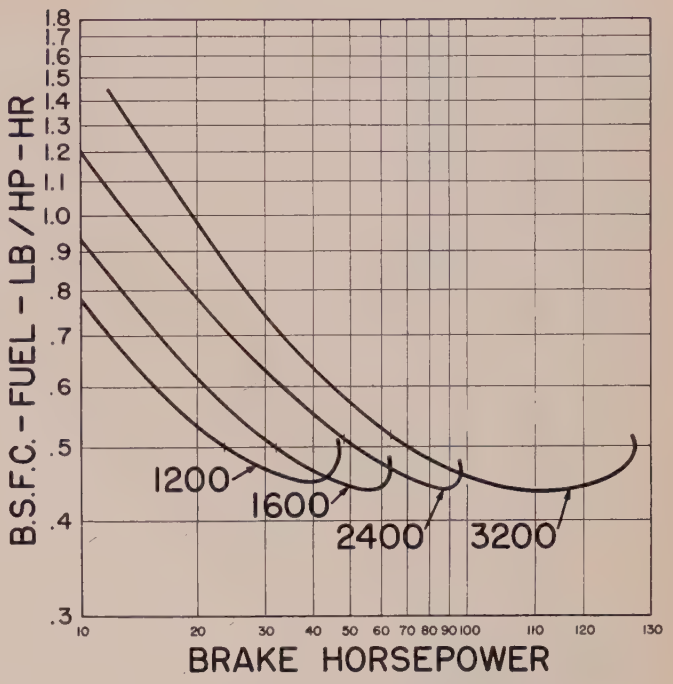

Fig. 16 – Part-throttle brake specific fuel consumption

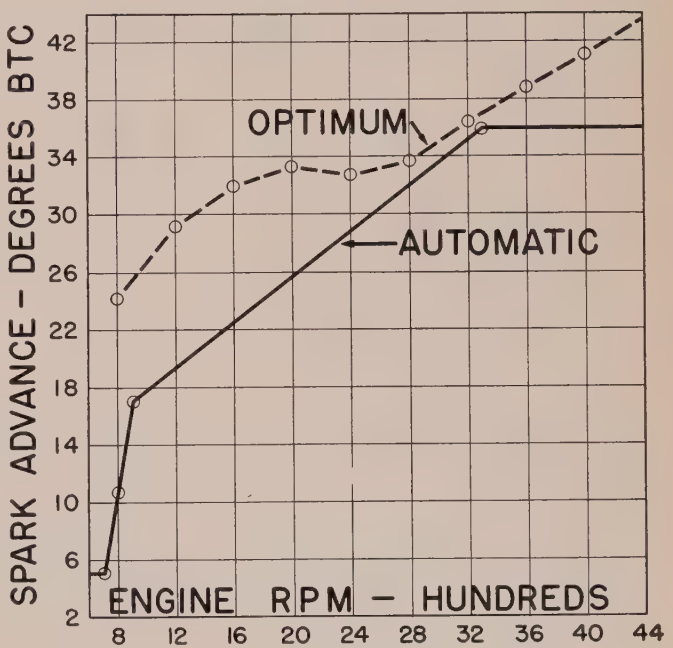

Fig. 17 – Optimum and automatic full-throttle ignition timing

measure its output. The new Plymouth engine is rated at 167 hp and 231 lb-ft torque. Using test conditions which are more directly comparable to other published ratings, namely, blocking off the exhaust heat from the intake manifold, the output is increased to 170 bhp at 4400 rpm, and 249 lb-ft torque at 2800 rpm, as shown in Fig. 14. This specific output of 0.65 bhp/cu in. and 145-psi bmep is believed to be very creditable for an engine with a dual-venturi carburetor. It should be noted that this output is developed with a modest compression ratio of 7.6, which was selected to give assured satisfactory operation on regular-grade fuels.

Efficiency – The high specific output of the engine is a combined result of high thermal, volumetric, and mechanical efficiency, as shown in Fig. 15. The indicated thermal efficiency is calculated from the specific air consumption,[4] and excels that of some competitive engines having 0.4 higher compression ratio. The volumetric efficiency is a natural result of ample valve sizes and well-disposed ports, together with a moderately high lift camshaft (0.365 at valve) and a fairly free induction system. The high mechanical efficiency is visible proof of a satisfactory stroke/bore ratio and careful mechanical design.

Part-throttle brake specific fuel consumption is shown in Fig. 16. In this graph, bsfc in lb of fuel per bhp-hr is plotted against observed bhp for four different speeds. A logarithmic scale is used for both coordinates, in order to facilitate reading the light-load part of the graph. Of great significance

[4] Based on heat input of 1240 Btu per lb of air.

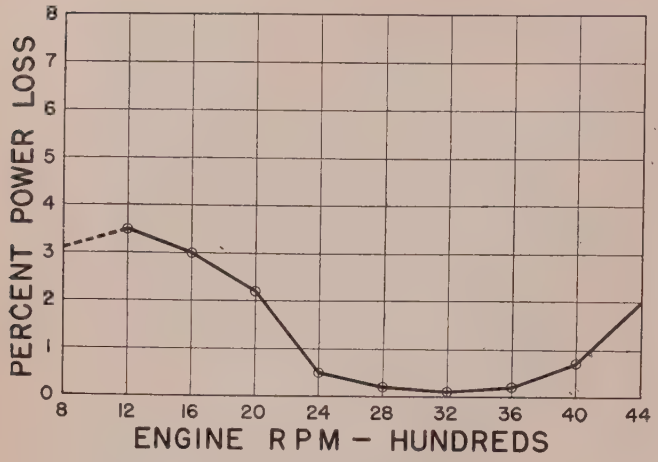

Fig. 18 – Power loss at automatic ignition timing

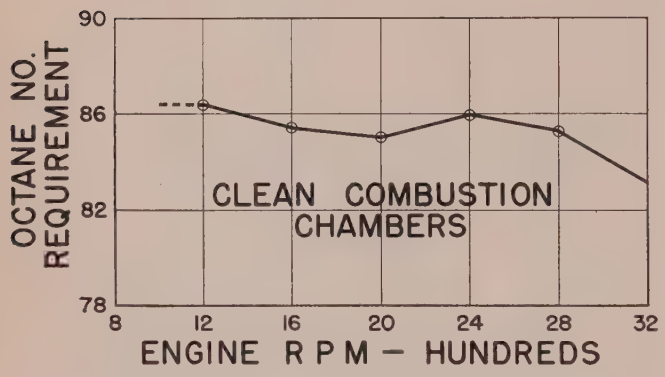

Fig. 19 – Fuel octane-number requirement at automatic ignition timing

is the remarkably low specific fuel consumption at light loads. At half load, for example, the specific fuel rate at 1200 to 3200 rpm is 0.50 to 0.52 lb per bhp-hr. This "flat" characteristic of the part-throttle specific fuel consumption is important to road load fuel economy, and is the result of high mechanical efficiency as well as high thermal efficiency.

Octane-Number Requirement – The Plymouth V-8 engine was developed for use of regular-grade fuel. Fig. 17 shows a comparison of the optimum wide-open-throttle ignition timing at each speed, and the specified automatic ignition timing. The per cent power loss at each speed resulting from the automatic ignition timing is shown in Fig. 18. With the automatic timing, the average octane-number requirement observed in the laboratory is as shown in Fig. 19. The test conditions include clean combustion chambers with the vehicle exhaust system installed.

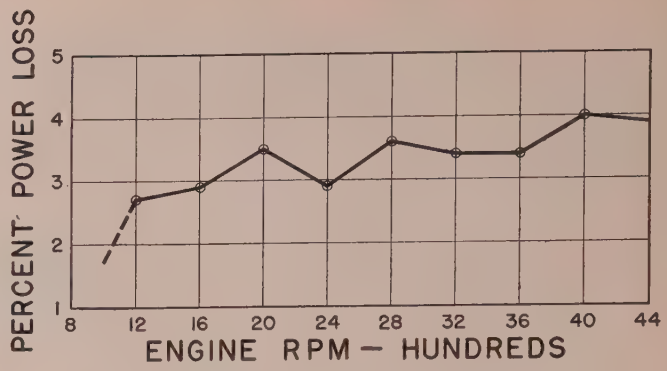

Fig. 20 – Power loss from combustion-chamber deposits

Effect of Combustion-Chamber Deposits – The engine has shown good behavior in the carboned state as well. Some background of the effects of combustion-chamber deposits has been accumulated in the laboratory by using a 30-hr part-load run with 1% of paraffin-base oil added to the fuel. The Plymouth V-8 engine has shown an octane-number requirement increase of about five numbers by this technique, which compares closely with that observed on the company's engines with the pure hemispherical combustion chamber. Of further significance is the absence of wild ping and other surface ignition phenomena resulting from chamber deposits. In this characteristic, too, it closely resembles the hemispherical combustion chamber.

Power loss from deposits is also a part of the laboratory carbon-accumulation test. As shown in Fig. 20, the loss has averaged from 2 to 4% through the speed range. This compares favorably with other types of chambers tested, and is very close to the hemispherical type, which has consistently shown the least loss from deposits.

Conclusion

This new V-8 engine brings to the Plymouth line of cars a new high level of performance. Equally significant is the inherent smoothness and quiet operation at all speeds. The other objectives of outstanding fuel economy, reliability, low maintenance, and long life have been achieved. The physical weight and size, together with the performance potential, make the engine highly adaptable for future requirements.

Finally, we believe that the modified hemispherical combustion chamber, as employed in the new Plymouth V-8 engine, offers a highly satisfactory solution to the problems of producing an engine that combines high efficiency and simplicity.

The New

Packard V-8 Engine

W. E. Schwieder, Packard Division, Studebaker-Packard Corp.

This paper was presented at the SAE Golden Anniversary Passenger-Car, Body, and Materials Meeting, Detroit, March 2, 1955.

AS a result of looking ahead and analyzing future requirements, an intensive engine-development program was undertaken shortly after World War II. Its objectives were twofold: 1. To exploit fully the potentialities of the Packard L-head, straight-8 engine for use during the interim. 2. To pursue vigorously the exploration of new and novel engine types and to evaluate their suitability for use some time in the future.

In 1949, it was becoming increasingly evident that the time was approaching when the familiar L-head engine would reach its limit of efficient utilization of high-octane premium fuels. Studies indicated that an engine of valve-in-head design offered the most promise of meeting future requirements. The feasibility of redesigning the existing straight-8 was considered, but this approach was discarded, since any change would require a major design and tooling program. Moreover, the trend throughout the industry was toward V-8's, and the public was being educated to expect V-8's.

When the decision was made to proceed with the design and development of the new valve-in-head V-8, an important turning point was reached. Substantial sums of money had to be budgeted for engineering this new engine, as well as for its manufacture. Once the outlay has been made for such a program, the plant facilities and tooling must be

ALTHOUGH its displacement and compression ratio are about the same as those of the 1954 straight-8 engine, the new Packard V-8 develops 22% more bhp, 7% higher torque, 29% less fhp at 4000 rpm, and 10% lower bsfc over the normal driving speed range. Its 0.875 stroke-bore ratio reduces piston travel 22%.

The mechanical and functional simplicity of the new configuration, the author says, increases flexibility for future styling trends and provides accessibility for servicing; its greatly increased rigidity provides for future operation on improved fuels at compression ratios over 12/1.

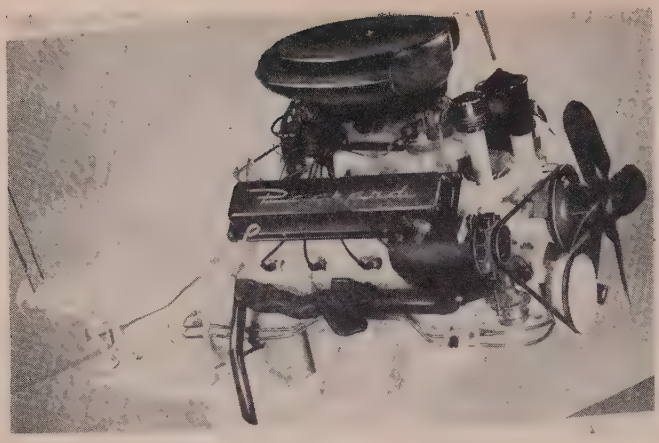

Fig. 1 – New Packard V-8 engine

usable without obsolescence and without much significant change for a long time to come. As a result, any new engine design must be approached on the basis of long-range planning and looking ahead.

In planning the Packard V-8, the primary objective was to design into this new engine the best features that present technical knowledge and the state of the art permit, providing sufficient flexibility to incorporate future changes as better fuels become available and increasingly higher compression ratios become practicable. Instead of being concerned about designing to meet minimum requirements, the contrary approach was taken to ensure that changing requirements could be satisfied without major retooling. Tentative specifications were first established for an engine that would meet these requirements, as well as those of the cars planned for 1955 production. Other major design objectives were as follows:

1. Basic design – Valve-in-head type to permit free-breathing and maximum volumetric efficiency.

2. Physical characteristics – Size and weight consistent with long life; adequate structural rigidity to provide smoothness and quietness despite future operation at higher compression ratios.

3. Displacement – Approximately the same as the L-head, straight-8 engine being superseded, and adaptable for enlargement without major changes in tooling.

4. Combustion system – Combustion control during the burning cycle to minimize octane requirements and to utilize efficiently improved fuels at increasingly higher compression ratios.

5. Stroke-bore ratio – Short stroke and large bore to increase mechanical and thermal efficiencies.

6. Performance – Capable of high specific output, maximum effective torque, and improved fuel economy.

7. Durability – Exceptionally long life, providing a new standard for passenger-car application.

8. Producibility – Basic simplicity for ease of assembly and economy of manufacture.

Background

Vast experience and know-how have been gained since Packard began building automotive engines back in 1899. Over the 56 years, Packard has designed and developed nearly every conceivable type of internal-combustion engine, including L-head, valve-in-head, overhead camshaft, and rotary-valve types with radial, horizontal, vertical, in-line, V, W, and X cylinder configurations.

For more than 40 years, Packard has built V-type engines, starting with the Packard 299, 905, the twin-six of the 1915 to 1923 era, the renowned Liberty engine of World War I, and the more recent classic 12 produced from 1932 to 1939. During World War II, Packard built the famous Rolls-Royce Merlin V-12 aircraft engine, and the equally famous Packard 4M-2500 V-12 marine engine which established such a fine reputation in torpedo boat operation. Being able to draw upon the vast reservoir of knowledge gained from the work conducted on these various types of engine has been invaluable during the design and development of the new Packard engine.

In planning the new engine, the performance requirements were projected into the future on the basis of existing scientific knowledge, as well as the predicted improvements in fuels over the years. For example, when work was first initiated back in 1949 on the design of the new Packard V-8 engine, it was anticipated that an engine having a displacement of 269 cu in. would be sufficiently powerful. Subsequently, the displacement was increased first to 303, then to 333, and finally to the present 352 cu in., as it became increasingly evident that greater torque was required to satisfy the higher performance requirements of the new models planned for future production. Although horsepower ratings can be increased in smaller displacement engines by increasing the volumetric and thermal efficiencies, the only way to get adequate torque is by starting

Table 1 – General Engine Specifications

Type	Overhead-valve, 90-deg V-8
Bore and Stroke, in.	4.0 x 3.5
Stroke-Bore Ratio	0.875
Displacement, cu in.	352
Compression Ratio	8.5/1
Designation of Cylinders	
Left Bank, Front to Rear	1-3-5-7
Right Bank, Front to Rear	2-4-6-8
Firing Order	1-8-4-3-6-5-7-2
Maximum Gross Brake Horsepower[a] at 4600 Rpm	280
Maximum Gross Torque[a] at 2400-2800 Rpm lb-ft	355
Maximum Bmep at 2600 Rpm, psi	152.1
Piston Travel, ft/mile	1480
Engine Weight, lb	698

[a] Corrected to SAE standard conditions of 29.92 in. of Hg atmospheric pressure and 60 F dry air.

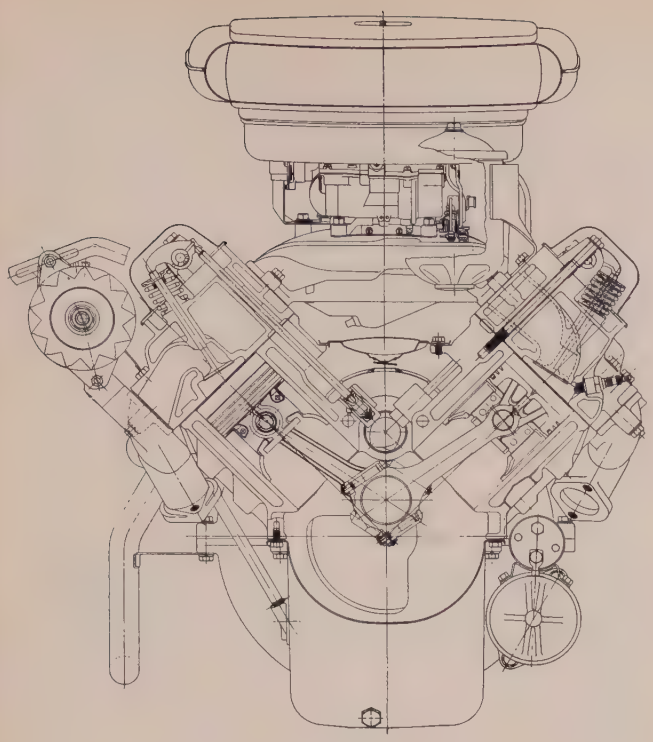

Fig. 2 – Transverse section of engine

with an engine of the right size. The new Packard V-8 engine has more displacement, and offers higher torque ratings, than any other engine in current automotive production. In addition, by providing extra spacing between the cylinder bores, ample provision exists for even greater displacement without changing foundry or production equipment materially.

During the continuing development, the promise of unusually high performance offered by the new engine generated a great deal of interest in its potentialities. As a result, sufficient preliminary work was conducted to explore the most practical methods of obtaining still greater performance. To improve the breathing characteristics of the engine, changes were made in the combustion chamber to accommodate even larger valves than used in the production engine, various types of intake manifolds were investigated, special camshafts were tested, and the exhaust system was modified to minimize restriction. After determining the individual improvements obtainable by making these modifications, an investigation was made of the influence of variations in combustion-chamber design and compression ratio.

Improvements in performance obtained during this work were sufficient to indicate that the new engine offers adequate capabilities of meeting future requirements for still greater horsepower and torque. An improvement of over 45% in power and 15% in torque is entirely feasible without major alteration of the basic engine. As work continues to extract still higher performance, the advanced designs resulting from these exploratory investigations will become future production realities.

Description and General Arrangement

As illustrated by Fig. 1, the new Packard engine has a valve-in-head, 90-deg V-8 configuration, and a large bore and short stroke, providing improved volumetric, mechanical, and thermal efficiencies. Superseded by the new engine is the L-head straight-8 engine, having a displacement of 359 cu in. and a rating of 212 bhp, which was used in the 1954 Packards. Brief specifications for the new engine are given in Table 1.

After establishing the basic design of the engine, considerable effort was devoted to locating the various engine components and accessories. The general arrangement and details of construction are shown by the transverse and longitudinal cross-sections of the engine, Figs. 2 and 3, respectively.

As will be discussed later in this paper, such major components as the cylinder block, cylinder head, and intake manifold were all designed to facilitate casting, machining, and assembly. In the location and arrangement of these items, as well as the various accessories, maximum mechanical and functional simplicity were considered extremely important to allow for ease of servicing and economy of manufacture.

1. Size: The reduced height and length of the 90-deg V-8 engine greatly simplifies the chassis design, and offers the body stylist somewhat more flexibility than was permissible with the 1954 straight-8 engine. However, the increased width of the 90-deg V-type of engine poses some clearance problems, particularly on the steering side of the engine com-

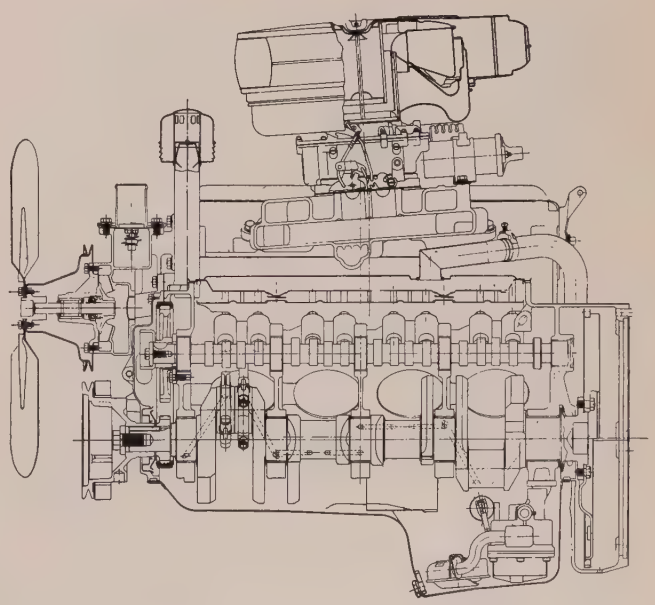

Fig. 3 – Longitudinal section of engine

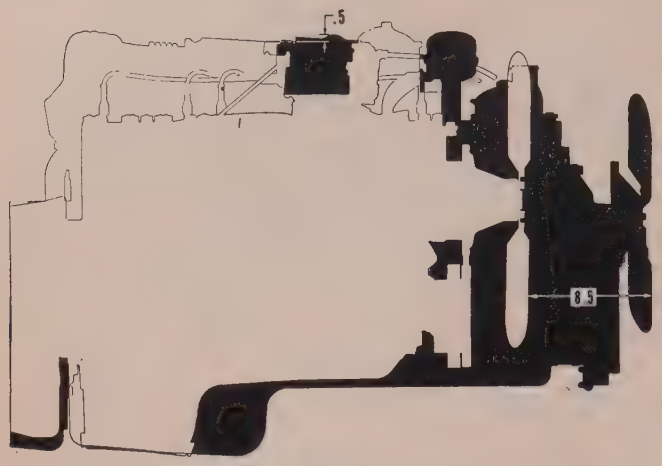

Fig. 4 – Size comparison of new V-8 engine with larger 1954 straight-8 engine

Table 2 – Comparison of 1954 and 1955 Engine Weights
(All weights are in pounds)

	1955 V-8	1954 Straight-8
Cylinder Block, Bare	210	283
Cylinder Head(s), Bare	128 (cast iron)	25 (Al)
Crankshaft	56	109
Ultramatic Flywheel and Ring Gear Assembly	8	9
Connecting-Rod Assembly, Complete Set	14	19
Intake Manifold	28	24
Exhaust Manifold(s)	23	28
Camshaft	10	13
Valve Train without Camshaft	27	11
Engine, Complete Assembly, including all Accessories Except Air Cleaner, Dry	698	752
Radiator, Complete with Core and Tank	22	32
Engine and Radiator, Dry, Total Weight	720	784

partment. Fig. 4 shows a comparison of the 1955 V-8 engine and the 1954 straight-8 engine. The new engine is ½ in. lower and 8½ in. shorter than the 1954 engine. Although the 90-deg V-8 is somewhat wider, judicious arrangement of the other items also housed in the engine compartment eliminated any real difficulty from this standpoint.

2. Weight: Studies and investigations were conducted to insure that full advantage was taken of the inherently lighter 90-deg V-8 design. As shown by the weight comparison of the major components tabulated in Table 2, a reduction of over 8% resulted from the introduction of the new engine. An even greater reduction in weight could have been obtained if compromises had been acceptable in the life and durability of this engine. Even so, it is evident that the new Packard V-8 engine compares very favorably with competitive V-8 engines on the basis of pounds-per-cubic-inch of displacement.

In addition to the direct savings resulting from the weight reduction, the new engine permits a somewhat more favorable weight distribution between the front and rear wheels of the car. Hence, by reducing the engine weight, an improvement has also been obtained in the amount of effort required for handling and steering the car.

Combustion Chamber

After extensive testing of the various types of combustion chambers and evaluation of their respective features, the high-turbulence, wedge-type combustion chamber, having an elliptical shape in the plan view (Figs. 5 and 6), was selected as being the most satisfactory for passenger-car application. This design provides a lower burning rate of the charge and avoids a high rate of pressure rise, resulting in freedom from objectionable combustion roughness. By cooling the last part of the charge to burn in the shallow section of the combustion chamber, called the quench area, combustion can be effectively controlled, and the octane requirements are minimized. Another important factor in favor of this type of combustion chamber is its adaptability for increasingly higher compression ratios without sacrificing smoothness.

The development of the combustion chamber for the new Packard engine is based on studies of combustion phenomena and the influence of turbulence, quench area, squish, spark advance, and other related factors. This work has culminated in a design remarkably insensitive to combustion-chamber deposits which are so troublesome in other designs, particularly under light-load city-driving conditions, causing knock, autoignition, preignition, and running-on. The combustion-chamber shape finally

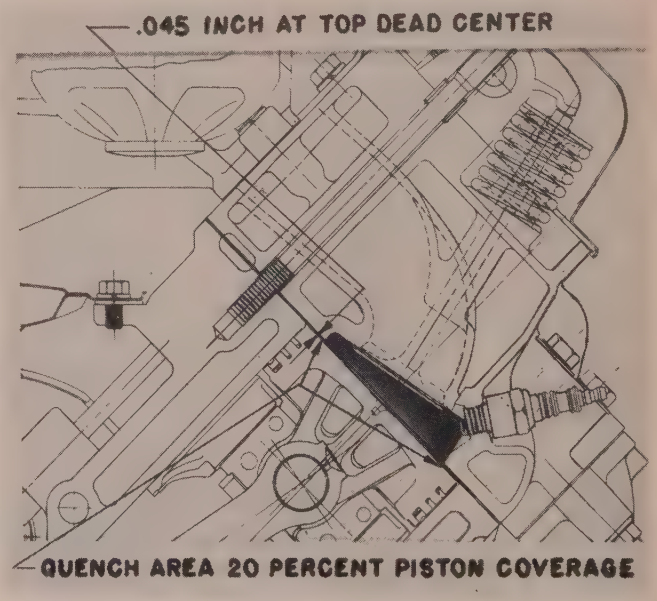

Fig. 5 – Cross-section of combustion chamber

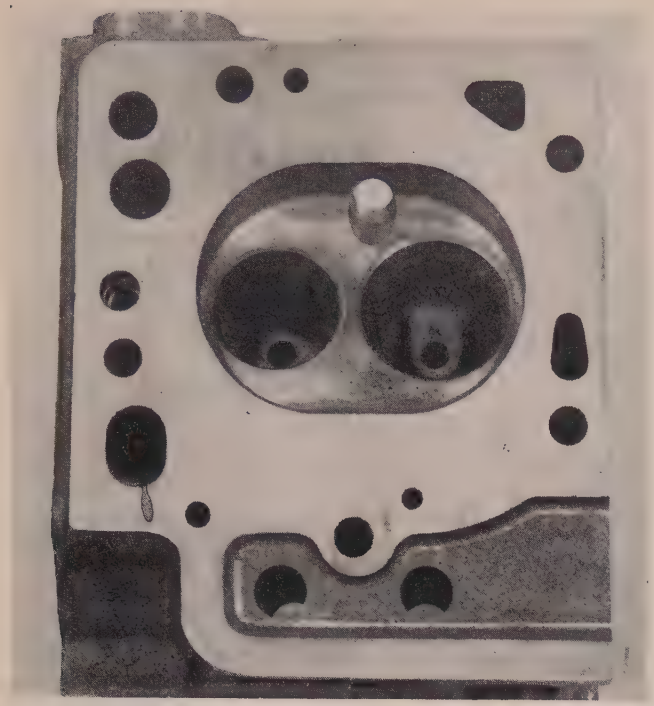

Fig. 6 – Completely machined, high-turbulence, wedge-type combustion chamber, showing side-by-side relationship of valves and spark-plug location

evolved is machined for accurate volume control, and now gives outstanding performance. The quench area amounts to 20% of the piston coverage, and the nominal squish clearance is 0.045 in. with the piston at top dead center (Fig. 5).

Compression Ratio

After working with engines at various compression ratios all the way up to 12/1, a compression ratio of 8.5/1 has been established for the new Packard engine, based on the octane rating of the premium-grade fuels now available throughout the country. At this compression ratio, continued satisfactory performance can be obtained even in the presence of substantial combustion-chamber deposits. Retarding the spark to permit acceptable operation after a few thousand miles of driving was not considered a suitable approach in establishing the compression ratio for the new engine, simply to be able to offer a somewhat higher compression ratio. The octane requirements were established during operation of cars at the Packard Proving Grounds under a variety of driving conditions. Their data indicated that the Ultramatic-equipped cars could be satisfied with 94-octane fuel, even under the most severe prolonged light-load city-driving conditions. Obviously, the compression ratio has been conservatively established to avoid having to specially adjust or service the engine in those parts of the country still lacking, at this time, the super fuels required to obtain successful performance at somewhat higher compression ratios.

Induction System

Since the power output of the engine is so largely dependent upon volumetric efficiency, considerable effort was devoted to the design and development of the induction system. Studies were made of the aerodynamic flow of the air/fuel charge through the induction system, resulting in the development of an exceptionally free-breathing engine. Extensive work was conducted to obtain equal distribution to all cylinders, to minimize restriction, and to promote turbulence only where desired for proper mixture of the charge entering the combustion chamber.

Early intake manifold designs were constructed out of wood, so that variations could readily be made to determine their influence on fuel distribution and general performance. As illustrated by Fig. 7, the intake manifold finally evolved for the new engine has a 90-deg T-shaped configuration at the intersection of the branches. The passages are smoothly contoured and equal in cross-section area throughout, and generous radii are provided at all junctions.

The carburetor choke stove is located in the center exhaust cross-over passage of the intake manifold. The flow of the exhaust gases through this passage connecting the cylinder banks is controlled by the action of the heat valve located at the junction of the left-hand exhaust manifold and the exhaust pipe. By forcing exhaust gases through the cross-over passage underneath the risers during warmup,

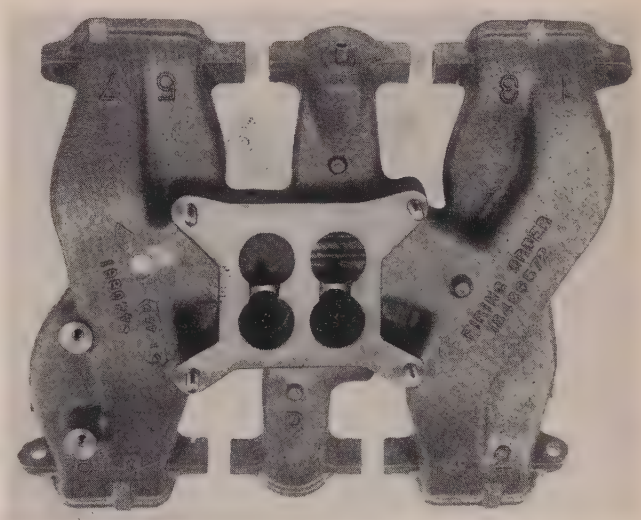

Fig. 7 – Intake manifold

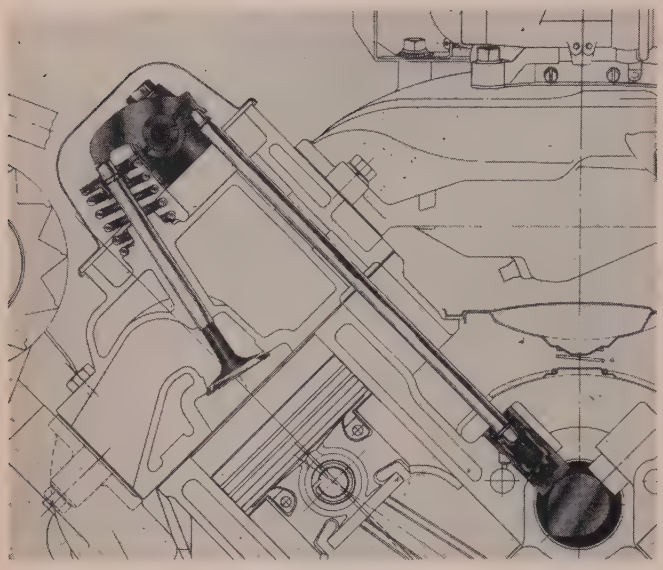

Fig. 8 – Valve train

sufficient heat is transferred to vaporize rapidly the fuel flowing through the intake manifold, and to the air being supplied the thermostatically controlled choke for positive operation. Adequate heat is applied to the intake manifold passages not only so that the choke comes off promptly during warmup, but also to avoid a noticeable transition thereafter in the performance of the engine. However, the charge is only sufficiently preheated in the intake manifold to provide for successful ignition of somewhat leaner mixtures at part-throttle operation, without adversely sacrificing octane requirements at full-throttle operation.

The passages in the cylinder head are likewise equal in cross-section throughout, possess generous radii at all junctions, and are contoured to minimize restriction, control flow, and provide optimum turbulence as the charge enters the combustion chamber. By taking advantage of the large bore offered by the new design, exceptionally large valves could be used, making an important contribution to the free-breathing characteristics of the engine.

Valve Train

As a result of studies made during the development of the new engine to obtain satisfactory dynamic valve motion, the cam profile was changed to decrease acceleration rates on both the opening and closing sides, and a lower-rate valve spring was developed to reduce the cam nose loading. By using tubing with a heavier wall and larger diameter, the push-rod rigidity was substantially increased, thereby minimizing deflection in the valve train. After making these changes, considerable improvement was obtained in the erratic behavior of the valve train formerly occurring at 4200 rpm, and the critical lifter "pump-up" speed was increased to over 5000 rpm. The valve train now used in the new engine is shown in Fig. 8, and its design specifications are given in Table 3.

Considerable work was conducted to obtain compatibility between the camshaft and lifters. Various types of materials and surface treatments were investigated in an effort to obtain freedom from excessive wear during the break-in period, and sufficiently high fatigue strength for long life under subsequent operating conditions.

The precision-molded alloy-iron camshaft is hardened after casting, phosphate coated all over, mounted on five bearings, and chain driven. The cams are ground with a taper of 6 min, and are positioned 0.062 in. to the rear of the lifter centerline to avoid lifter overrun and insure positive lifter rotation.

The lifters are of the hydraulic type, having hardenable iron bodies. The lifter faces are ground to a spherical radius of 30 in., hardened to a minimum of 54 Rockwell C, and Lubrited for improved break-in.

As a result of extensive testing, valves were de-

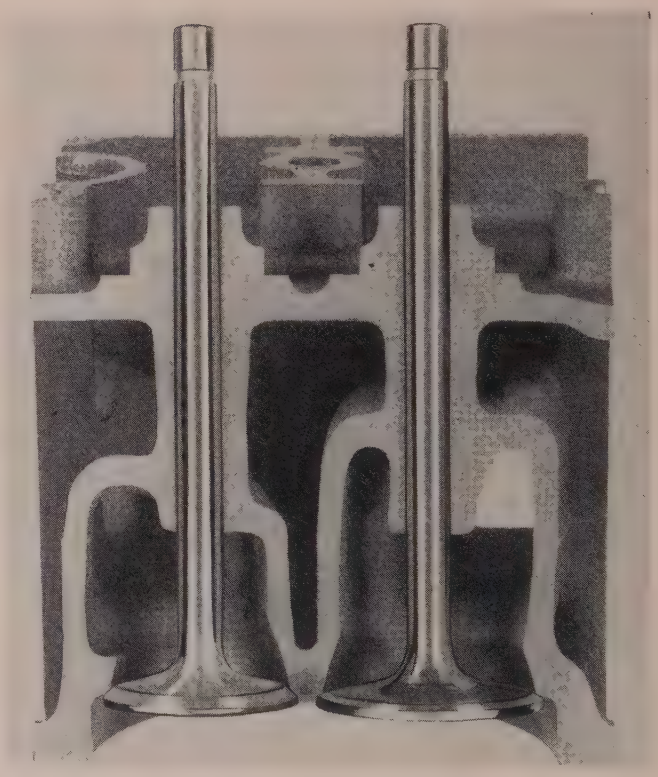

Fig. 9 – Valves and valve guides

Table 3 – Valve Train Specifications

Camshaft	
Material	Hardenable alloy iron
Bearings, No.	
Drive, type	Chain
Width, in.	1.000
Pitch, in.	0.375
Cams	
Width, in.	0.500
Taper, min	6
Lifters	
Type	Hydraulic
Body	
Material	Hardenable alloy iron
Diameter, in.	0.904
Face, Spherical Radius, deg	30
Push-Rods	
Material	Steel tubing
Size	
Diameter and Wall Thickness, in.	0.375 x 0.065
Length, in.	10.506
Ends, Spherical Radius, in.	0.250
Valve, Intake	
Material	Silchrome No. 1 steel
Head Diameter, in.	1.937
Stem Diameter, in.	0.3725
Seat Angle, deg	30
Valve, Exhaust	
Material	2112 austenitic steel
Head Diameter, in.	1.687
Stem Diameter, in.	0.3715
Seat Angle, deg	45
Rocker Arm	
Material	Pearlitic malleable iron
Ratio	1.60
Valve Lift, in.	0.375
Valve Spring Load	
Closed, lb	82
Open, lb	165
Valve Timing	
Intake Opens, deg btdc	14
Intake Closes, deg abdc	56
Exhaust Opens, deg bbdc	52
Exhaust Closes, deg atdc	18

veloped for this engine that possess life equivalent to the other components in the engine. The exhaust valve, for example, is of the special flexible-head design to assure maximum conformability of the valve face and seat. Fig. 9 shows the 2112 austenitic steel exhaust valve which has a 1.687-in. head diameter and a 45-deg seat angle. Also shown in Fig. 9 is the hardened and tempered Silchrome No. 1 steel intake valve, which has a 1.937-in. head diameter and a 30-deg seat angle. These large valves in combination with the lift of 0.375 in. are important factors in the high performance of the new engine.

Close coordination with the foundry resulted in obtaining generous cored passages around the valve seats, thereby assuring rapid and uniform heat dissipation to the coolant. Valve temperatures were further reduced by incorporating integral valve guides, which eliminate the thermal barrier normally encountered with the separate valve guides (Fig. 9). During the testing, it was found that the stem-to-guide clearances were extremely critical. As a result of this work, the stem-to-guide clearances were established at 0.001-0.002 in. for the inlet valves, and 0.002-0.003 in. for the exhaust valves, requiring selective assembly in manufacture. Valve sticking results from deviation from the minimum limits, whereas inadequate oil control exists, particularly on the inlet valve, when the clearances are excessive.

The fuel pump is actuated by a hardened, chrome-plated, stamped, steel eccentric bolted onto the front of the camshaft sprocket. The unbalance resulting from the eccentric has been compensated for by the nonsymmetrical location of the openings in the camshaft sprocket.

Cylinder Heads

The cylinder heads are conservatively designed, having greater height, width, and length than other competitive designs using a similar type of combustion chamber (Fig. 10). Generous water jackets have been provided for adequately cooling the valve seats, valve guides, and gas passages (Fig. 11). Conventional casting methods are used in making

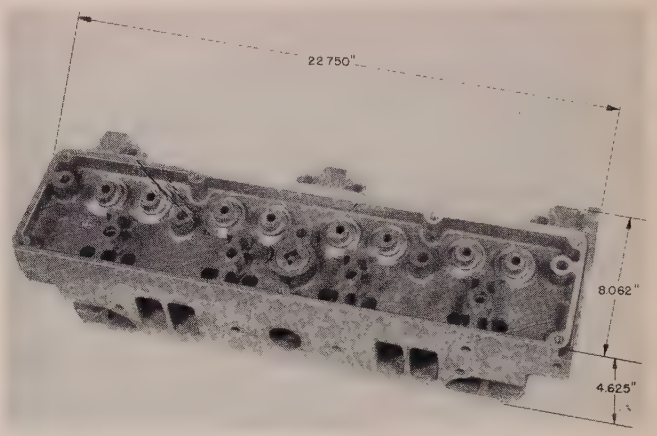

Fig. 10 – Cylinder head

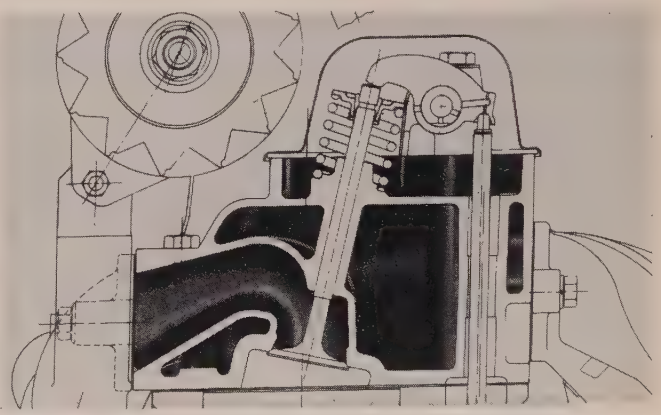

Fig. 11 – Cross-section of cylinder head

the cylinder heads, and the experimental design has been successfully translated into production. The cylinder heads are interchangeable, and are attached to the cylinder block by 15 screws, appropriately spaced so that five screws surround each bore (Fig. 12). Tension loads are transferred to the bulkheads in the cylinder block by this arrangement, permitting the use of a thin, one-piece, embossed, steel gasket.

Cylinder Block

Taking full advantage of one of the inherent characteristics offered by the 90-deg V-8, we developed an exceptionally rugged, durable cylinder block for this engine, providing adequate rigidity to support the loads (Fig. 13). The loads are distributed evenly throughout the entire structure by five transverse bulkheads, which tie the two blocks into a single rigid unit, made from a one-piece casting of high-grade alloy iron. After various stresscoat and strain gage studies, as well as dynamic tests, it was not considered necessary to extend the casting below the centerline of the crankshaft. To locate the main bearing caps satisfactorily, however, longitudinal rabbets are broached 0.125 in. above the oil pan gasket surface (Fig. 14). The cylinder-head screw bosses are tied into the water-jacket wall structure by vertical ribs to avoid stressing the individual cylinder barrels. Substantially larger water jackets have been provided around the full-length cylinder walls than offered by any other competitive design, lowering the temperature of the working parts and giving unusually long life. The center-to-center distance of the cylinder bores is 5 in., and the overall length of the block is 27.750 in. The upper half of the flywheel housing is cast integrally with the cylinder block, offering improved support for the transmission and propeller shaft by minimizing the deflection resulting from the attachment of these items (Fig. 12).

Crankshaft

As a result of an unbiased evaluation of the relative merits of both the cast and forged types of crankshafts, a cast-steel crankshaft is used in the new Packard V-8 engine (Fig. 15). Cast steel offers a sufficiently high modulus of elasticity, as well as density, to provide substantial savings in weight without sacrificing rigidity or stiffness. This type of crankshaft also permits disposition of the counterweights for maximum balancing effectiveness, and allows coring of the crankpins to minimize the amount of unbalance that must be compensated for

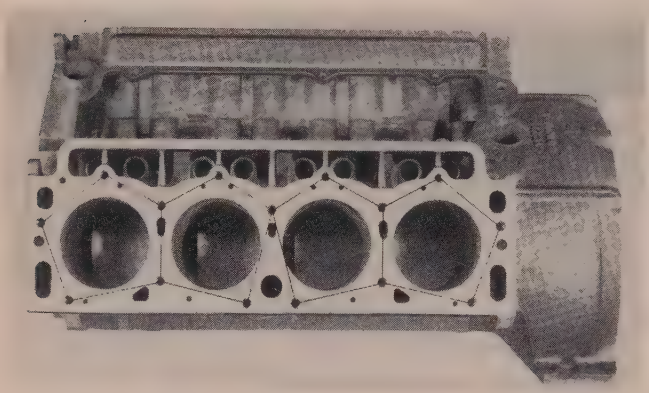

Fig. 12 – Right side of cylinder block

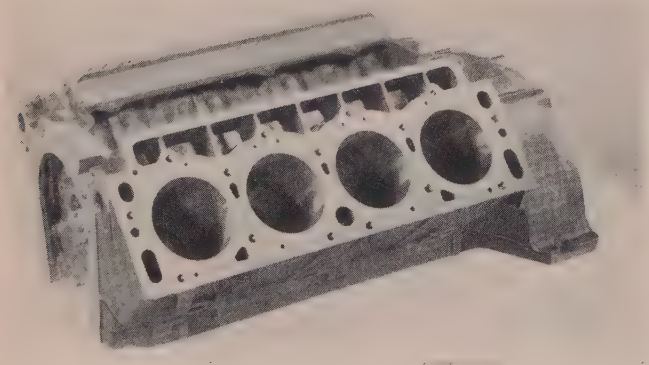

Fig. 13 – Cylinder block

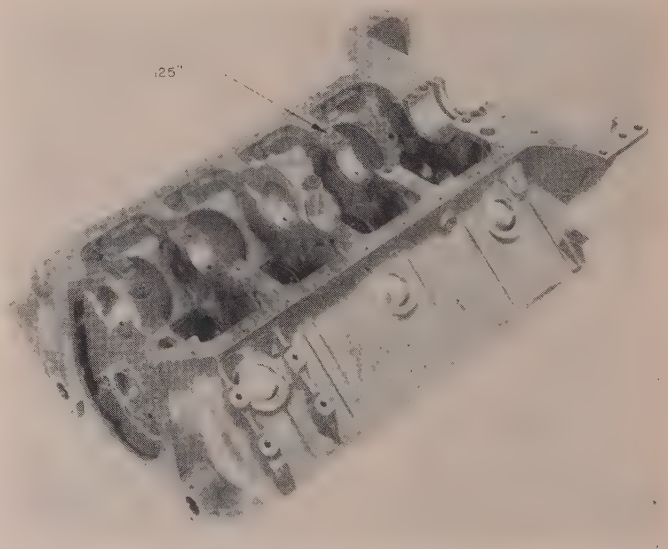

Fig. 14 – Underside of cylinder block

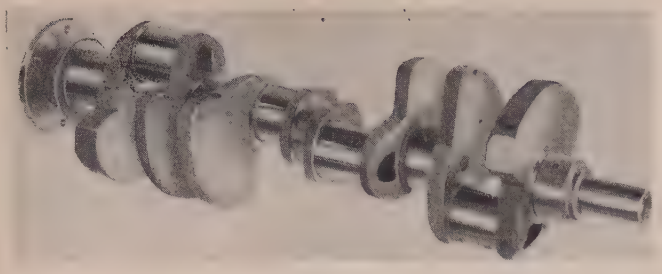

Fig. 15 – Crankshaft

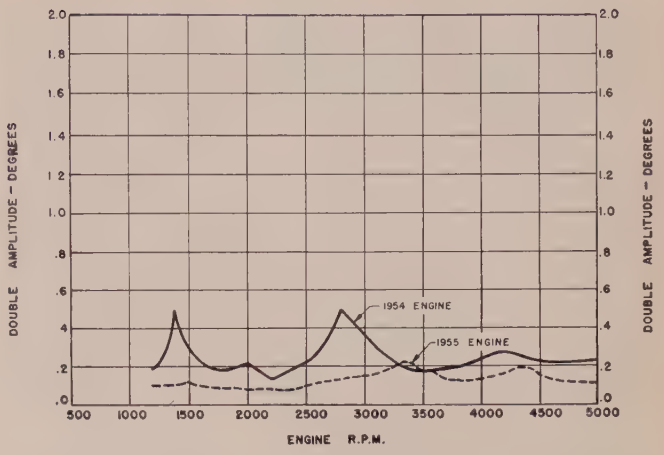

Fig. 16 – Comparison of crankshaft torsional vibration characteristics

by the counterweights. A physical description of the crankshaft is given in Table 4.

Either type of crankshaft could have been selected without the penalty of increased overall length, since the conservatively designed cylinder block already offered adequate spacing to accommodate the uncheeked counterweights and still provide grinding wheel clearance at each crank arm. As indicated by Table 4, only 9 lb of metal are removed during the processing of the cast crankshaft, or less than half the amount that would have to be removed from the forged type. By using the cast crankshaft, not only has a substantial weight reduction been obtained, but excellent manufacturing economies have also been realized.

By using a nonbonded rubber harmonic balancer, a suitable reduction has been obtained in the amplitude of crankshaft deflection, providing satisfactory performance throughout the normal operating speed range. Although a fifth order occurs at approximately 3400 rpm, its amplitude has been dampened to 0.22 deg double amplitude, and is imperceptible in the car. Other torsional disturbances do not occur in the normal driving speed range. As shown by Fig. 16, the torsional vibration characteristics of the new engine are greatly superior to those of the 1954 engine. The increased stiffness

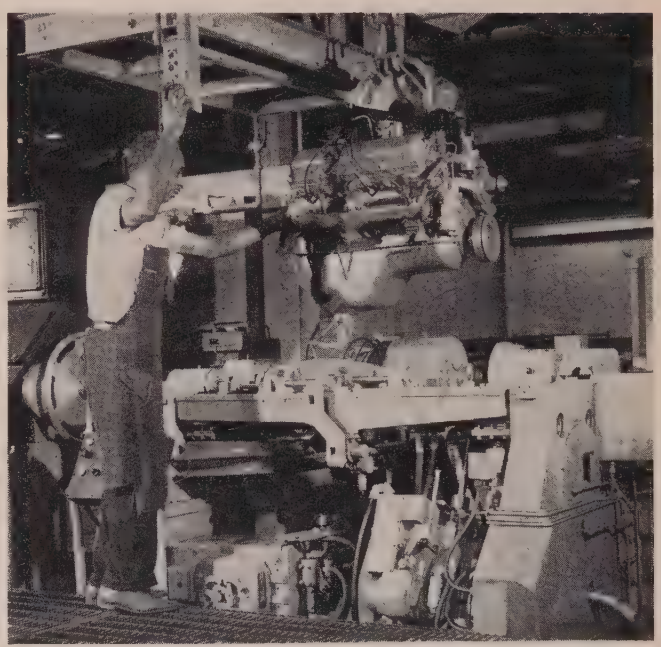

Fig. 17 – Lowering engine for final assembly balancing

Table 4 – Crankshaft Specifications

Main Bearings, no.	5
Counterweights, no.	6
Overall Length, in.	27.344
Connecting-Rod Journal Diameter, in.	2.250
Connecting-Rod Effective Bearing Area, sq in.	52.8
Main Bearing Journal Diameter, in.	2.500
Main Bearing Journal Effective Area, sq in.	38.6
Bearing Journal Overlap, in.	0.625
Rough Casting Weight, lb	65
Machined Casting Weight, lb	56

offered by the shorter crankshaft accounts primarily for the improvement, despite the higher output of the new V-8.

After assembly of all the components, which have been individually balanced for use in production or in service, the engine is mounted on a specially designed machine and balanced as a unit (Fig. 17). In performing this operation, the engine

Table 5 – Connecting-Rod Specifications

Center-to-Center Distance, in.	6.781
Length-Stroke Ratio	1.937
Material	SAE 1041
Weight with Piston-Pin Bushing, g	757

is motored sufficiently to indicate the amount of unbalance, at which point rotation stops and the prescribed amount of unbalance is compensated for by automatically drilling into the crankshaft pulley and welding a slug onto the flywheel (Fig. 18). As a result, the stackup of tolerances that otherwise might accumulate during the assembly of the engine is reduced to not more than ¼ in.-oz, thereby insuring precision balancing of every engine.

Bearings

All the main bearings are of the same diameter. The thrust load of the crankshaft is taken on the rear main bearing. Steel-backed micro lead-babbitt is used for the connecting-rod bearings, and over-plated copper-lead is used for the main bearings. Both types of bearing material perform equally as well on the cast-steel crankshaft without hardening of the journals. Both connecting-rod and main bearing loads are sufficiently low so that the bearing materials now used give exceptional durability and long life.

Connecting Rod

The connecting rod now used in the new V-8 has been conservatively designed and extensively tested under loads substantially in excess of those imposed under any driving condition (Fig. 19). Table 5 gives brief specifications for the connecting rod.

In an effort to reduce the reciprocating and rotating weight, the original connecting rod was redesigned by reducing the column section and crankpin journal end of the rod. Subsequent testing indicated that some improvement was obtained in the natural frequency of the mass elastic system without sacrificing any of the structural rigidity of the connecting rod. Balancing lugs are located at each end of the rod assembly.

Piston and Rings

Following previous Packard practice, the new V-8 also uses autothermic aluminum-alloy pistons (Fig. 20). Brief specifications for the piston and rings are given in Table 6.

Piston slap has been eliminated by study of the various factors related to the piston-to-bore clear-

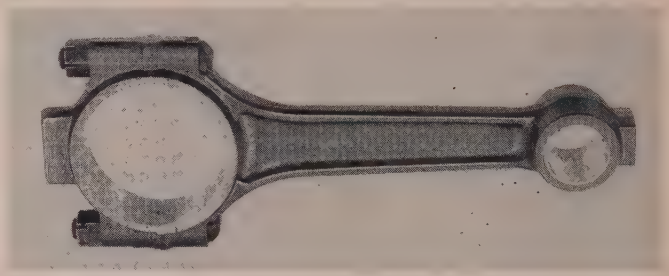

Fig. 19 – Connecting rod

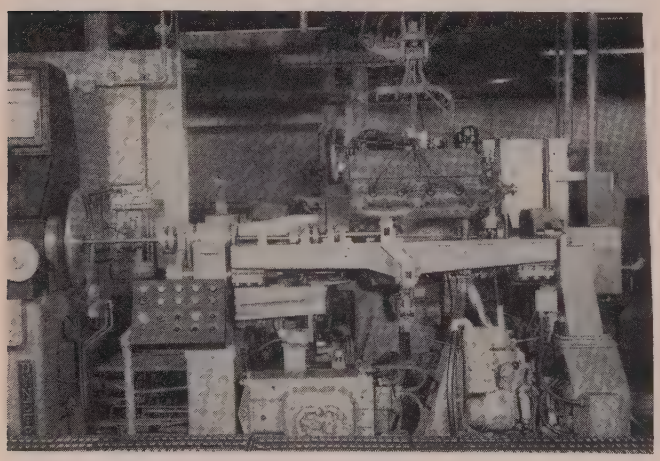

Fig. 18 – Engine mounted on final assembly balancing machine

Table 6 – Specifications of Piston, Rings, and Pins

Piston	
Type	Autothermic, cam ground, slipper skirt
Material	Aluminum alloy
Weight, g	702
Piston Rings, Compression	
Number	2
Type	Thick wall, taper-face
Material	
Top	Alloy iron, chrome-plated
Intermediate	Alloy iron, Ferrox-coated
Width, in.	0.078
Piston Rings, Oil	
Number	1
Type	Open slot, ventilated, with expander
Material	Alloy iron
Width, in.	0.186
Piston Pin	
Type	Full floating
Material	SAE 1117
Size, Diameter, and Length, in.	0.980 x 3.250

Table 7 – Specifications of Lubrication System

Lubrication System Type	Full pressure
Oil Pump Type	Gear
Oil Intake Type	Floating
Oil Pressure (Max), psi	50
Oil Filter Type	Partial flow
Crankcase Capacity (Less Filter), qt.	5

ance and the manner in which the piston moves across the bore near the top of the firing stroke, resulting in an offset of the piston pin of 0.062 in. toward the major thrust face. The fire-wall or top of the piston is 0.280 in. thick, allowing for trouble-free operation at compression ratios well above the currently used 8.5/1. Extensive tests were conducted to establish the camming and surface finish of the piston skirt, and complete freedom from scoring has resulted.

As shown in Fig. 20, two thick-wall, alloy-iron, 5/64-in.-wide, taper-face compression rings are used in combination with an open-slot, ventilated, alloy-iron, 3/16-in.-wide oil ring equipped with a hump-type expander. Complete freedom from scuffing during initial engine operation has been obtained by using a 0.004-0.007-in. chrome-plated top compression ring along with the Ferrox-coated second compression ring. No undue difficulty was encountered in obtaining satisfactory oil control under various driving conditions, both in urban and rural traffic. As the manifold vacuum increased, oil control became somewhat more troublesome; however, the variation in oil consumption between high and moderate vacuum conditions was relatively small. Although smoking from the exhaust may be observed under certain driving conditions, for example after long periods of idling, comparison with competitive engines has been quite favorable.

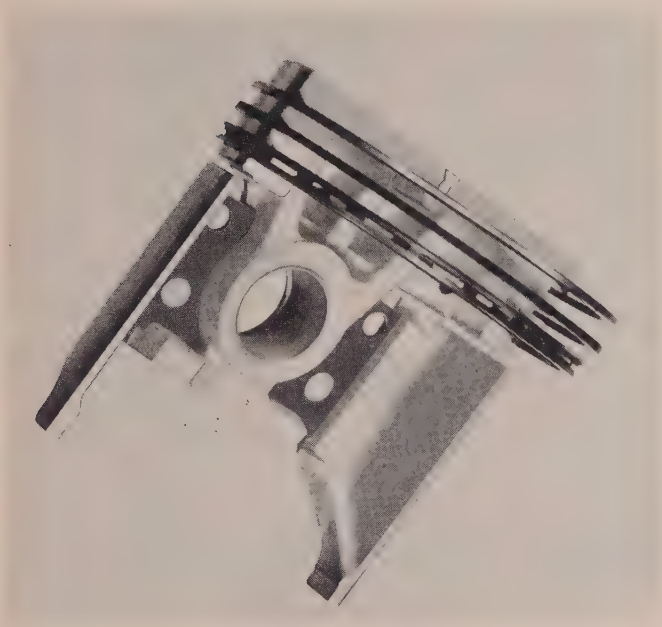

Fig. 20 – Piston assembly

The full-floating type of piston pin was selected, since past experience with the combination of the autothermic piston and this type of piston pin has been unusually satisfactory. Table 6 gives additional information on the piston pin.

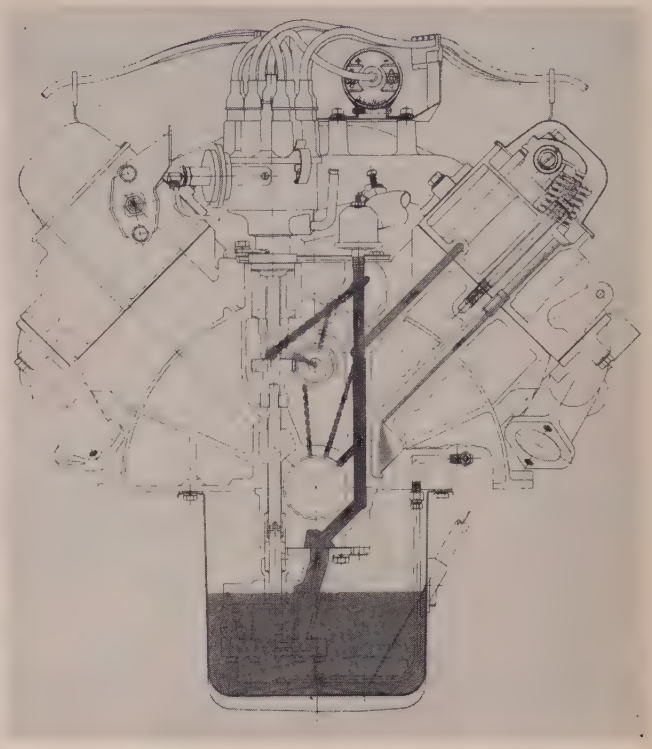

Fig. 21 – Transverse cross-section of lubrication system

Lubrication System

As illustrated by Figs. 21 and 22, lubrication for the new engine is provided by a full-pressure system. Brief specifications for this system are given in Table 7.

After entering the pump through a screened floating inlet at a controlled distance beneath the top of the oil level, oil is delivered through the rear bearing cap to a vertical oil header. From this vertical header, oil is forced (1) through drilled passages to lubricate the rear main bearing and adja-

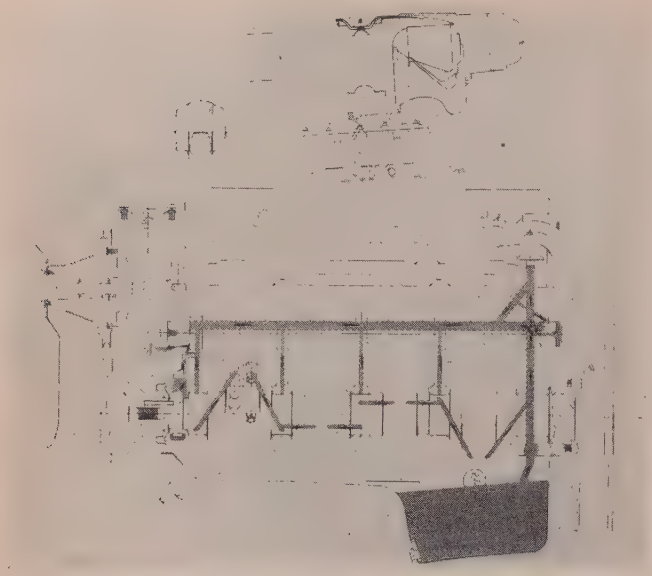

Fig. 22 – Longitudinal cross-section of lubrication system

and rocker arms. The filtered oil returns through a tapped hole, located in the cylinder block near the oil filler tube, to the timing chain compartment, and thence to the sump.

Fig. 21 shows the method of lubricating the distributor and oil pump drive. The distributor drive gear is splash-lubricated, and its thrust face is lubricated by a combination of splash and gravity feed. Oil flowing through a 5/16-in.-diameter hole in the distributor housing provides splash lubrication of the distributor gear bearing.

The oil pump is driven by an intermediate floating shaft coupled to the distributor drive gear (Fig. 21). A tongue-and-groove arrangement on the oil pump end of the drive shaft allows for slight misalignment. Continuing previous Packard practice, the oil pump uses coarse-pitch straight gears, providing freedom from pulsation and quiet operation. Variation in oil pressure has been reduced throughout the speed range, as a result of work on the relief valve, which recirculates the oil whenever the pressure rises above the predetermined maximum of 50 psi.

To control cold scuffing and piston slap, the cylinder walls are lubricated by spraying a fine stream of oil from the connecting rod of the corresponding cylinder in the opposite bank (Fig. 23). By pro-

cent connecting-rod bearings, (2) through an intersecting right longitudinal gallery, and (3) through a connecting header to feed the rear camshaft bearing and the left longitudinal gallery.

Through connecting drilled passages, oil flows from the right main gallery to the rocker-arm shaft and the valve-lifter guides on the right bank, and also to the center and front main bearings. The center and front camshaft bearings, respectively, are lubricated from the center and front main bearings, as well as the adjacent connecting-rod journals.

Oil flowing through the left main gallery lubricates the valve-lifter guides and the rocker-arm shaft on the left bank, the two intermediate main bearings, and all adjacent connecting-rod bearings. The two intermediate camshaft bearings are lubricated through drilled holes from the intermediate main bearings.

Forty-five-degree angular headers, located at the rear of the right main gallery and at the front of the left main gallery, supply oil upward through the cylinder block and head to the rocker shafts (Fig. 23). From the rocker shafts which act as oil galleries, oil is metered to the rocker arms and thence flows onto the valve stems and pushrod sockets. The surplus oil collects in the deep trough adjacent to the rocker cover rail, and returns through the cylinder-head drain-back passages and hollow cylinder-head dowels into the crankcase.

Oil is delivered to the partial-flow filter through a drilled and tapped hole that intersects the angular header which lubricates the left rocker shaft

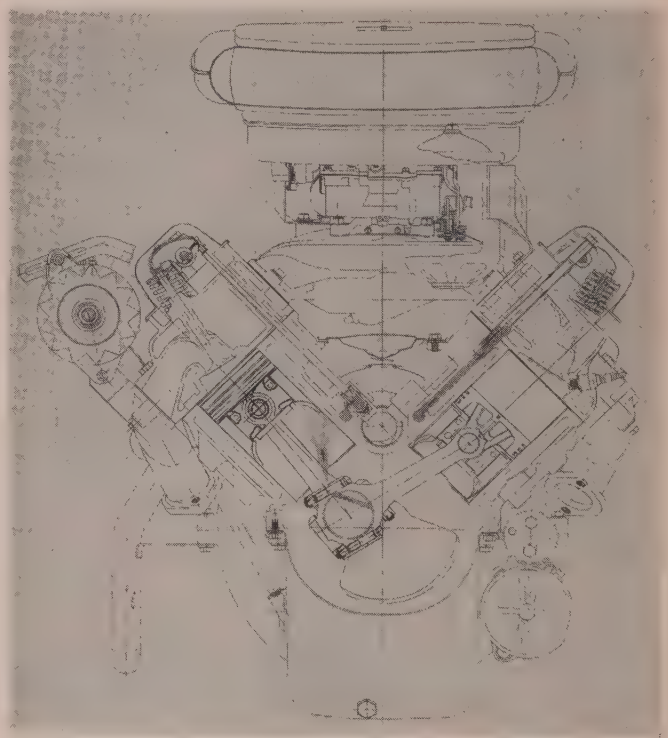

Fig. 23 – Lubrication of cylinder walls and valve train

viding a groove at the split line of the connecting rod, the best trajectory of the oil stream can be obtained without incurring objectionable stress risers in the highly loaded tension section of the rod. Ample lubrication is thereby provided on the critical areas of the upper sides of the cylinders, whereas gravity supplies oil to the lower sides. In addition to providing beneficial lubrication of the cylinder walls during cold starting, the oil sprayed from the connecting rod lubricates the piston pin and effectively cools the piston under hot operating conditions.

As illustrated by Fig. 22, lubrication of the timing chain is accomplished by oil supplied from the left main gallery to a groove in the camshaft thrust plate. Oil passes through a radial hole, intersecting this groove, which directs a continuous stream of oil downward onto the timing chain. The fuel-pump eccentric is lubricated by oil passing through a hole in the camshaft thrust plate, which communicates with the right main gallery and registers with a hole in the camshaft sprocket, allowing an intermittent stream of oil to spray onto its surface.

Ventilation System

Positive circulation has been provided to insure thorough ventilation of the engine under all driving conditions. With this system, air enters the engine through the combined crankcase-ventilator inlet and oil filler cap which is located at the front of the engine, directly in line with the fan blast.

After passing downward through the timing-gear compartment into the crankcase, the fresh filtered incoming air becomes thoroughly intermixed with the corrosive blowby gases. The air then passes upward through the pushrod clearance slots in the stamped steel baffle, designed to separate the crankcase from the valve lifter compartment and to prevent oil pull-over. As the air flows through this relatively large, low-velocity chamber, oil vapors are encouraged to condense before entering an opening near the front of, and leading into, a channel in the valve lifter compartment cover. From this channel, the air flows into the road draft tube, located at the rear of the valve-lifter compartment cover.

During idling of the engine, the exhaust from the windshield wiper rotary vacuum booster pump, attached to the underside of the oil pump, creates a pressure difference which assists in the circulation of the air through the crankcase. When the car is in motion, vacuum created by the air flowing past the road draft tube increases the circulation of air, thereby assuring positive ventilation of the engine under all operating conditions.

Cooling System

The cooling system employs a single, high-capacity water pump, centrally mounted at the front of the cylinder block. The pump discharges directly into an equalizing chamber, supplying a balanced flow and assuring even distribution of coolant to both cylinder banks. Upon entering the cylinder banks, the coolant circulates through the passages around the cylinders and upward through cored holes to the cylinder heads. As the coolant flows through the large, generous passages permitted by the conservative spacing of the cylinder bores, the critical regions around the cylinders, combustion chambers, valves, and spark plugs are thoroughly and adequately cooled. After leaving the cylinder heads through the outlet at the front, the coolant flows through a header, which houses the single thermostat. By restricting flow when the engine is cold, the thermostat controls the temperature of the coolant for prompt warmup.

In comparison with the 1954 engine, the heat rejection of the new engine to the coolant was greatly reduced, as shown by Fig. 24. At 4000 rpm, for example, the heat rejection amounted to 6900 Btu/min for the 1954 engine, and 5400 Btu/min for the 1955 engine, providing a 21% improvement. As indicated in Table 2, the reduction in the heat losses to the cooling system permitted a saving of 10 lb, or 31%, in the weight of the radiator required for the new engine.

Electrical System

Although early development of the new engine was conducted with the 6-v electrical system, it

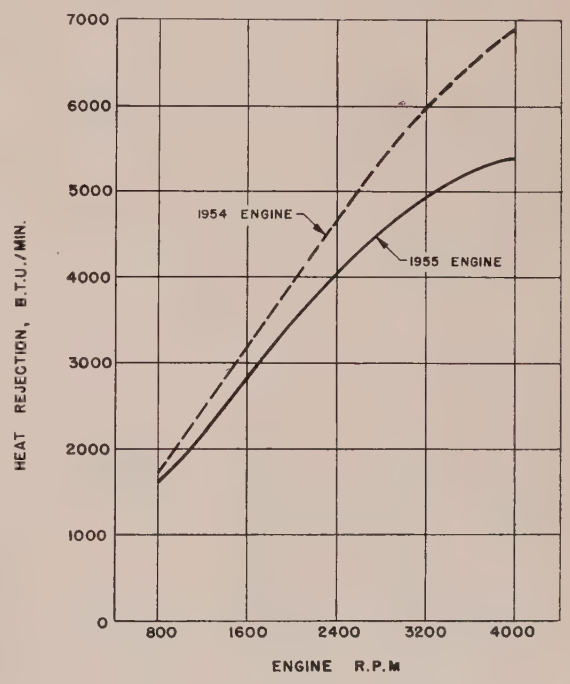

Fig. 24 – Comparison of full-load heat rejection

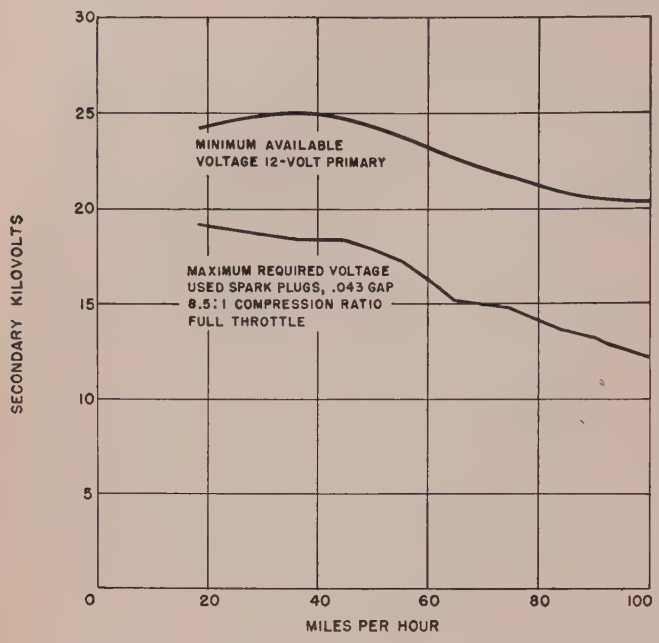

Fig. 25 – Full electrical load comparison of secondary voltages

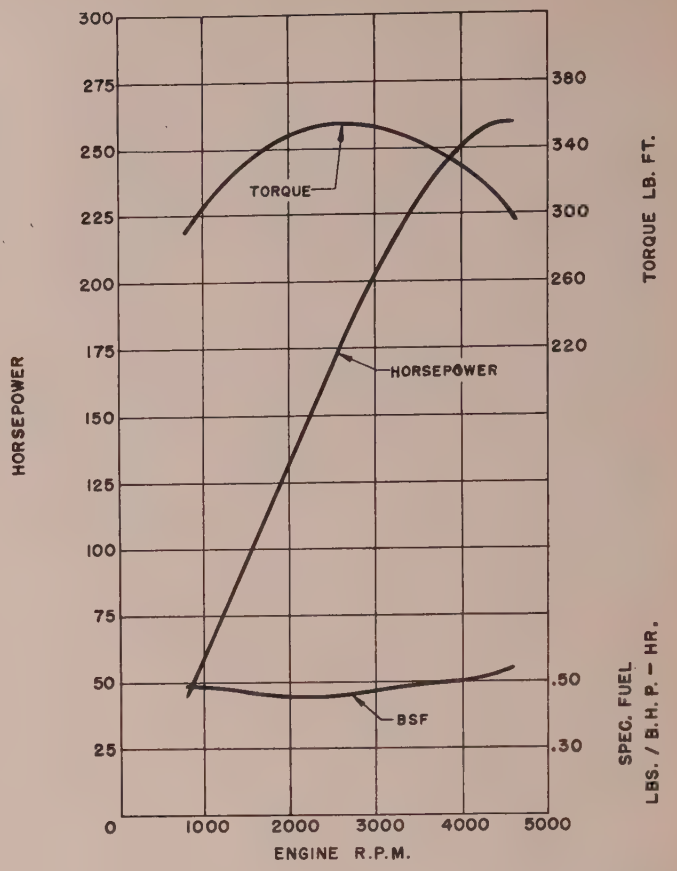

Fig. 26 – Full-throttle gross engine performance with single 4-barrel carburetor

became evident that higher voltages were necessary to satisfy the demands of the engine as the compression ratio was progressively increased and the general overall performance was improved. However, prior to the final selection of the electrical system, an analysis was made of the electrical requirements of the new engine, as well as those of the cars planned for 1955 production. As a result, the 12-v electrical system was adopted for the new engine, since its higher output was considered essential for both the present and long-range requirements. With this system, adequate voltage is always available to satisfy the requirements of the engine, as indicated by the comparison of the available voltage and the required voltage under the conditions shown by Fig. 25.

Adoption of the 12-v system offered the following major benefits:

1. Increased available voltage, providing an adequate reserve to fire the spark plugs under all driving conditions, and permitting greater gap growth before servicing is required.
2. Higher generator output to meet the ever increasing loads, particularly at slow engine speeds.
3. Improved cranking-motor performance to satisfy the cranking requirements under both cold- and hot-weather starting and operating conditions.

Performance

Considerable improvement in the performance characteristics of the new engine was obtained as a result of continuing development since the inception of its design. Through close coordination of the design, development, and testing, the outstanding performance now offered by this engine has been realized.

Fig. 26 shows the full-throttle gross performance of the new Packard V-8 engine equipped with a single 4-barrel carburetor. The gross performance of the engine is based on the test results obtained with manual fuel and optimum spark, corrected to SAE standard conditions of 29.92 in. of Hg atmospheric pressure and 60 F air temperature.

The new V-8 develops 260 bhp and 355 lb-ft torque, whereas the L-head straight eight developed 212 bhp and 330 lb-ft torque. Although a substantial gain in horsepower has been obtained, the really significant achievement is the improvement in effective torque, which, after all, means the translation of engine output into actual car performance. For the new engine, the maximum specific output is 0.739 bhp per cu in. of displacement, and the maximum bmep is 152.1 lb per cu in.

at 2600 rpm. The friction horsepower has been reduced from 76 at 4000 rpm for the 1954 engine to 54 at the same speed for the 1955 engine, giving an improvement of 29%. The specific fuel consumption of the new engine is lower over the entire speed range, reaching a minimum of 0.452 lb per bhp-hr.

For still greater output, the new engine equipped with dual 4-barrel carburetors is available in the Packard Caribbean models. As shown by Fig. 27, this combination develops 275 bhp at 4800 rpm. The torque remains unchanged at a maximum of 355 lb-ft, although it is available over a broader speed range, namely, 2400 to 3200 rpm. Both engine friction and specific fuel consumption are slightly higher, however.

Durability

From the inception of the design, outstanding durability was considered a basic requisite for the new engine. This objective was achieved primarily through the somewhat more conservative criteria used in designing the cylinder block and cylinder head, thereby providing exceptionally generous cooling for the critical regions in the engine. Rather than satisfy only minimum requirements, the contrary approach was made in an effort to achieve durability and life hitherto unknown for passenger-car application. During the development of this engine, thorough investigations and tests were undertaken to prove out the durability of the components, both in the laboratory and on the road. Information and data obtained from this work resulted in various changes in design to provide still greater improvement. Subsequent testing indicated that the new engine was capable of successfully completing a full-throttle, high-speed dynamometer test of 250-hr duration. Based upon these unusually favorable results, the next step was to determine the engine life on the road. As demonstrated during the recently completed 25,000-mile endurance run on the 2½-mile track at the Packard Proving Grounds, which was supervised by the American Automobile Association Contest Board, the new engine offers greatly improved performance and exceptional durability. According to the AAA certification, the prototype 1955 Packard V-8 powered sedan averaged 104.737 mph for the 25,000-mile run, including all stops, thereby surpassing every recognized stock car record.

Acknowledgments

Since work was first initiated on the new Packard V-8 engine, various individuals have been responsible for making a significant contribution to its design and development. Naturally, any undertaking as important to management as the design and development of a new engine, with the large expenditures required for its manufacture, involves the team play of many people in a large organization. Although a number of men might be mentioned for the value of their work, the two who most certainly deserve special recognition for their invaluable contributions are J. R. Ferguson, retiring chief engineer, and E. A. Weiss, assistant chief engineer, Packard Division, Studebaker-Packard Corp.

Summary

After the original objectives were established, work was initiated in the fall of 1949 and thousands of hours have since been expended on the design and development of the new Packard V-8 engine (Fig. 1). Prior to production, experimentally built engines were exhaustively tested, not only on dynamometers in the laboratory, but also in cars on the road at the Proving Grounds and elsewhere throughout the country. Since the initiation of production, testing has continued, of course, on production-built engines. How successfully the new Packard V-8 engine meets the original objectives is summarized as follows:

1. Basic design: Exceptionally free breathing is obtained through painstakingly designed passages, and overhead valves 25% larger in head area than those used in the 1954 engine provide maximum volumetric efficiency; incorporates short stroke, low friction characteristics to increase mechanical and thermal efficiencies, culminating in higher per-

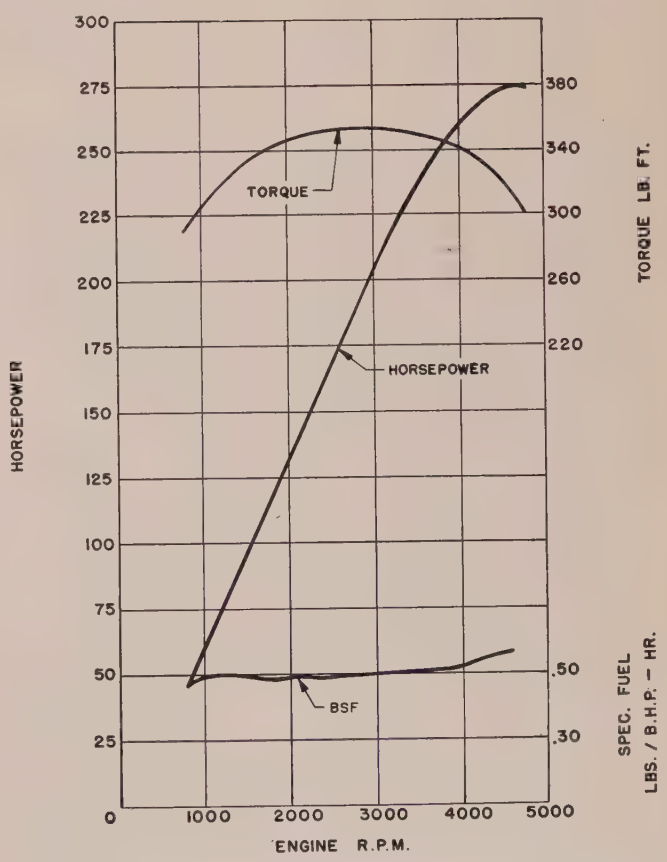

Fig. 27 – Full-throttle gross engine performance with optional dual 4-barrel carburetors

formance, greater economy, and longer life.

2. Physical characteristics: New configuration offers mechanical and functional simplicity, allowing more flexibility for future styling trends, and providing accessibility for servicing; and greatly increased rigidity, amply providing for future operation on improved fuels at compression ratios above 12/1.

3. Displacement: About the same as its predecessor, and potentially capable of being enlarged beyond the displacement obtainable with any other 1955 automotive engine, indicating extremely conservative design in anticipation of possible future requirements for still greater power and torque.

4. Combustion system: Highly turbulent, wedge-type, elliptically shaped combustion chamber, permitting knock-free operation on improved fuels at compression ratios over 12/1.

5. Stroke-bore ratio: Extremely favorable stroke-bore ratio of 0.875 gives a reduction in piston travel of 22% and accounts primarily for the higher power output of the 1955 Packard engine, since the displacement and compression ratio are about the same as the 1954 engine.

6. Performance: Overall performance greatly improved in comparison with the 1954 engine of essentially the same displacement and compression ratio, as follows: maximum bhp 22% higher and torque 7% higher, fhp 29% less at 4000 rpm, and bsfc 10% lower over the normal driving speed range – potentially capable of meeting future requirements for higher output and more efficient operation without major alteration.

7. Durability: Ruggedness and durability proved under every conceivable condition, including a 25,000-mile endurance run during which all previous stock car records were eclipsed, setting a new standard for automotive engines.

8. Producibility: Designed for manufacture by the most modern, efficient, and economical methods, including automated machining, assembly, and testing.

ORAL DISCUSSION

of Welch and Schwieder papers

Reported by H. R. Johnson, Jr.
Studebaker-Packard Corp.

R. M. Adsit, Detroit Diesel-Engine Division, GMC: Does the use of integral valve guides in both the Plymouth and Packard engines pose both manufacturing and servicing problems? How are worn valve guides serviced in the field?

Messrs. Welch and Schwieder: Integral valve guides do present machining and servicing problems. Machining problems were overcome by careful design of both the cylinder head and the automatic equipment that performs the various machining operations. Servicing worn guides in the field requires special reamers, and also makes it necessary for service departments to carry stocks of valves in predetermined valve-stem sizes.

The advantages gained by the use of integral guides (that is, lower manufacturing cost and better valve cooling) justified their use.

Jorma O. Sarto, Chrysler Corp.: Please explain the secondary operation of the Packard 4-barrel carburetor.

Mr. Schwieder: The secondary is mechanically operated, but I feel an increasing trend toward a different type.

Walter D. Appel, consultant: Why was the particular combustion-chamber design selected?

Mr. Welch: Chrysler tests and investigations favored the hemispherical-type chamber. We found that its combustion roughness characteristics were quite low, and that it gave good detonation control. In addition, the hemispherical chamber was found to be very efficient thermally, and capable of highest volumetric efficiency. The combustion-chamber design in the Plymouth engine was a modified hemispherical type, which retained most of the advantages of the true hemispherical chamber. It was modified for the sake of simplicity and weight reduction.

Mr. Schwieder: Packard had selected a design that tests had shown best satisfied driver requirements. It had the best low-range torque characteristics of the various types investigated. It also proved to be very efficient and to have good detonation control.

Mr. Appel: Is bore size a factor in determining this particular design?

Mr. Schwieder: It was not the particular influence on combustion-chamber design, as we had investigated a number of bore sizes in developing the new Packard engine.

Mr. Welch: Stroke-bore ratio is a factor. As the stroke is increased, the advantage of the hemispherical chamber is increased.

Mr. Appel: Is there a great similarity between the Chrysler and Plymouth combustion chambers?

Mr. Welch: There is a great deal. Although the Plymouth chamber was modified for simplicity, it retains the basic features of the Chrysler type. The spark-plug and valve locations are very similar, and, although the chamber is very compact, there is ample room for 1 23/32-in.-diameter inlet valves and 1 15/32-in.-diameter exhaust valves for a bore size of 3 9/16-in. diameter.

Achilles C. Sampietro, Thompson Products, Inc.: Since the swept volume varies as the square of the bore and directly as the stroke, while valve area varies directly with valve diameter, isn't the combustion-chamber design somewhat dependent on cylinder size?

Mr. Welch: It is. The greatest factor was the stroke-bore ratio for usual automotive-size engines. A low stroke-bore ratio, or small cylinder size for a given stroke-bore ratio, makes it easier to obtain adequate valve sizes with valve-in-line combustion-chamber designs. The hemispherical chamber provides room for larger valves, which become increasingly beneficial as cylinder size or stroke-bore ratio is increased.

A Study of Nonprotective Rust Formation On Auto-Body Sheet Steel

J. C. Holzwarth, R. F. Thomson, and A. L. Boegehold
Research Laboratories Division, GMC

This paper was presented at the SAE Golden Anniversary Summer Meeting, Atlantic City, June 14, 1955.

ALTHOUGH average car life has jumped in 30 years from 6½ to 13½ years, improvements in service life of body structures have not kept pace with increased durability of engines and other mechanical parts. Hence the growing interest in improving corrosion resistance of the sheet steels used in auto bodies.

This paper reports results obtained in cyclic humidity accelerated corrosion tests aimed at finding a cheap, easily formed sheet steel with better resistance against the sheltered corrosion which causes the most serious body damage. The test produces in 20 days the same kind of nonprotective rust formed in years of outdoor exposure.

Since high-carbon steels, shown in the tests to be the most potent corrosion reducers, cannot be used in auto bodies because of their poor forming characteristics, efforts are now being directed toward finding a combination of elements that will produce the same results without a cost or forming penalty.

IN A highly competitive industry like automobile manufacturing, one is much concerned with product corrosion, for this condition is extremely annoying to the customer and, hence, reflects unfavorably on the manufacturer. From time to time since 1940, the automotive industry has experienced a number of corrosion problems with automotive bodies, and in varying degrees of severity. While many improvements have been made to diminish the intensity of this problem, there would be considerable advantage to all if auto-body sheet steel, in addition to its present satisfactory properties, had improved corrosion resistance.

According to industry reports[1] passenger cars are being scrapped at the rate of about 3,000,000 per year. Except for the small number scrapped as total wrecks, nearly all are rusted beyond economic repair. AMA figures further show that the average life of cars scrapped in 1925 was 6½ years, while the average age of cars scrapped in 1951 had in-

[1] p. 17, "Automobile Facts and Figures." Pub. by Automobile Manufacturers Association, Detroit, 1952.

Fig. 1 – Perforation failure of a rocker panel by internal corrosion

creased to 13½ years. Longer life was primarily the result of improved durability of engines and other mechanical parts. In order that the service life of the body structure could be extended to keep pace with mechanical improvements, considerable emphasis has been placed on improving design and protective coatings. However, there has not been any significant improvement in corrosion resistance of the auto-body sheet steel in the past quarter of a century.

This paper reports some of our recent observations on the rusting of low-alloy steels in auto bodies and other environments where protective rust formation is not realized. The information, we feel, gives some new insight into the nature of auto-body corrosion failure, and may ultimately lead the way to the development of a better steel, or perhaps at least stimulate new ideas for improving design and protective coatings.

Service Experience

Sheltered Corrosion – Corrosion of automobile bodies is generally characterized by two types of rust: (1) that which causes unsightly discoloration of exterior body surfaces where protective finishes have been chipped or abraded from the steel, and (2) that which causes rapid deterioration and perforation of body components. The first type of rust, though a nuisance, is usually conspicuous during its early formation and is, therefore, readily controllable by accepted methods of polishing, waxing, and touchup painting. The second type is more insidious, occurring most often in sheltered areas such as interiors of rocker panels, inside doors and window wells, or in crevices of the underbody. In these inaccessible locations, rusting may proceed undetected until severe damage or complete perforation of the steel occurs. Furthermore, corrosion in these sheltered regions is greatly accelerated, since the rust formed is nonprotective.

Several investigators have shown that sheltering action greatly accelerates corrosion by retarding protective rust formation. Copson[2] points out that the washing action of rain on steel exposed outdoors aids protective rust formation by removing soluble corrosion products. If the soluble corrosion products are not washed away, they remain in the

[2] See ASTM Proceedings, Vol. 45, 1945, pp. 554-590: "Theory of Mechanism of Rusting of Low-Alloy Steels in Atmosphere," by H. R. Copson.

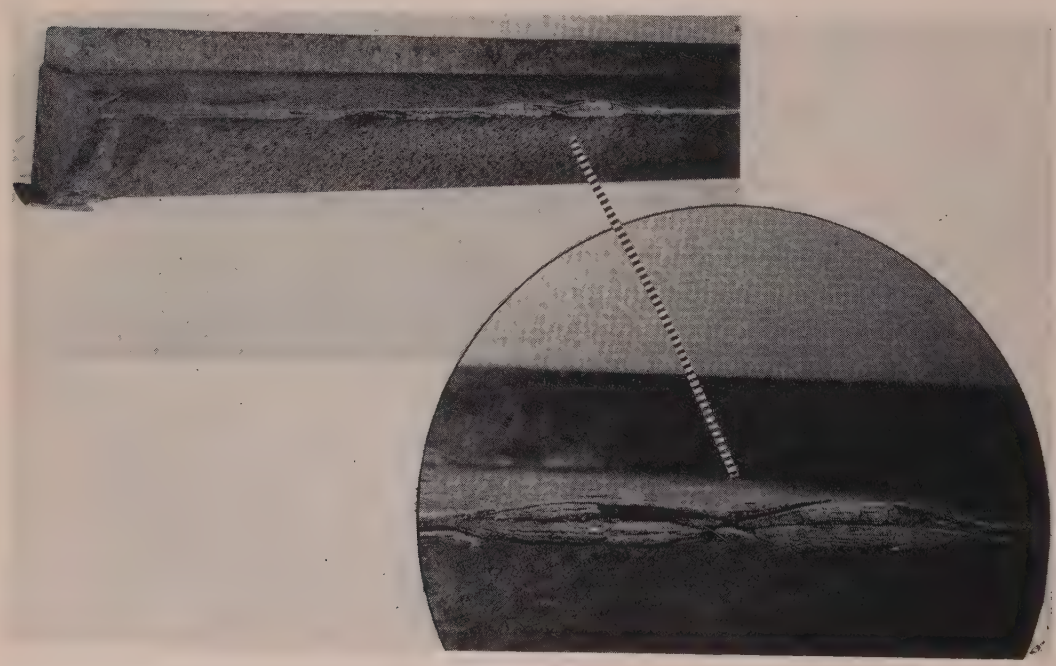

Fig. 2 – Rocker panel exposed 80 ft from ocean at Kure Beach, N. C. Heavy rust (inset) was cause by retention of moisture in crevice

rust, causing high porosity. In the sheltered areas of car bodies where washing action by waters is limited, one can reason that the soluble products are not likely to be removed and the rust remains porous. LaQue and Hergenroether[3] point out that complete and rapid drying is important to the formation of protective rusts. In the interior of auto-body components, where the steel remains wet for long periods without benefit of drying, the rust remains nonprotective, and the constant presence of moisture greatly accelerates corrosive attack. Fig. 1 shows a rocker panel on a car which corroded through from the inside. Retention of moisture within this enclosure caused rapid failure by perforation in less than four years of service.

Several methods of overcoming this situation are apparent. Improved design to eliminate crevice areas would, of course, eliminate the cause. However desirable this may be, it is many times not convenient and many times impractical to completely eliminate crevice areas. Likewise, continuous coating of the crevices with mastic materials to protect against moisture is not always possible, since the areas are by nature inaccessible. Obviously, then, one of the best places to reduce corrosion is where it starts – in the steel itself.

Requirements of an Improved Steel – On various occasions, the proprietary high-strength, low-alloy steels have been recommended for use in auto-body construction. However, the base price of these low-alloy steels is 1.5 times the cost of presently used rimmed steel. To date, no conclusive evidence has been presented to show that high-strength, low-alloy steels will sufficiently increase corrosion durability to justify this price increase.

The goal of the present authors is the development of a cheap, readily formed sheet steel having markedly improved resistance against sheltered corrosion. A material which corrodes at about one-fourth to one-half the rate of presently used rimmed auto-body sheet would show the improvement we require. However, such an improvement would need to be accomplished without the addition of large amounts of alloying elements which affect the forming characteristics and cost of the steel.

Selection of Suitable Test – The development of a more corrosion-resistant auto-body steel requires extensive testing of a vast number of different alloy compositions. To accomplish this, a rapid test method is needed to weed out the large number of low-corrosion-resistant materials and select the few most promising steels for a further program of service testing.

Of course, service testing is the final method of evaluating corrosion resistance. However, for use as a rapid exclusion test, it has several disadvantages. It requires a long time to obtain results, it is expensive, and it does not always give reproducible answers. While controlled atmospheric exposure tests may permit better reproducibility, the length of time to obtain results is still a disadvantage; and, more important, such tests do not indicate what corrosion rate to expect in sheltered areas. Yet sheltered corrosion is the most serious type to be encountered in auto bodies. We wish to emphasize that the rust formed under such conditions is more porous and less protective than the rust formed on openly exposed areas of the car or on outdoor exposure test specimens. Therefore, an entirely different type of test is required.

Table 1 – X-Ray Analysis of Rust Associated with Auto-Body Service Failure

Rust Removed from	Model	Manufacturer[a]	Composition	
			Fe_3O_4, %	$\alpha Fe_2O_3 \cdot H_2O$, %
Rocker panel	1939	L	80	20
Fender welt	1941	M	85	15
Inner door	1942	L	80	20
Fender welt	1942	N	85	15
Window well	1942	L	85	15
Fender welt	1946	M	90	10
Rocker panel	1946	M	85	15

[a] L, M, and N represent the three largest manufacturers of auto bodies.

Perhaps the types of rust formed under the different conditions are better exemplified by Fig. 2. The unpainted rocker panel shown here was exposed until failure on an outdoor test rack at Kure Beach, N.C., 80 ft from the ocean. The openly exposed surface is covered with a fairly even, uniform rust. However, in the center of the rocker panel, a spot welded seam may be observed, wherein two sheets of steel overlap to form a crevice. Here the steel between welds (inset, Fig. 2) is bulged by the voluminous, lamellar rust. Accelerated corrosion was caused by retention of moisture in the crevice area. The rust in this crevice is apparently less protective than the rust on the open surface, since the steel on which the heavy rust was formed is almost completely corroded away and is perforated in spots, while the boldly exposed area of steel has lost less than 10% of its original thickness on the average, and a maximum of 20% in the area of deepest pits.

Study of Corrosion Products

Auto-Body Corrosion Products – Various auto-body components removed from scrapped cars after 8-12 years' service were similarly found to be covered with heavy lamellar corrosion products on interior surfaces where protective rust formation was not realized. A series of rust samples collected from these perforated components in the area of

[3] "Corrosion Problems of Automotive Engineer," by F. L. LaQue and E. J. Hergenroether. Paper presented at SAE Summer Meeting, French Lick, Ind., June 7, 1949.

Table 2 – X-Ray Analysis of Rust Formed on Outdoor-Test-Rack Samples Exposed at Kure Beach, N. C.

Identification	Steel	Fe_3O_4, %	$\alpha Fe_2O_3 \cdot H_2O$, %	$\gamma Fe_2O_3 \cdot H_2O$, %
A	Rimmed body sheet[a]	None	50	50
A^1	Crevice – rimmed[a]	85	15	None
U	Open-hearth iron		No sample available	
V	Open-hearth steel	None	50	50
W	High-strength, low-alloy	None	40	60
X	SAE 2115	None	50	50
Y	SAE 2515	None	60	40
Z	3% Cr steel	None	50	50

[a] Sample A rust was removed from the openly exposed surface of the rocker panel shown in Fig. 2, while Sample A^1 was removed from the crevice of this same rocker panel.

failure was analyzed by X-ray diffraction techniques. Results of the study are shown in Table 1.

Regardless of make, model, or body location, rust associated with each body failure was found to be 80-90% Fe_3O_4 and 10-20% $Fe_2O_3 \cdot H_2O$. A magnified cross-section of rust associated with auto-body service failure is shown in Fig. 3. It is built up in alternate layers of Fe_3O_4 (blue-black) and $Fe_2O_3 \cdot H_2O$ (red-yellow), but the blue-black constituent is predominant.

Atmospheric Test Rusts – In contrast to the nonprotective type of rust associated with auto-body failure (sheltered corrosion), the rust formed on steel sheets exposed on outdoor test racks is quite different. Fig. 4 shows corrosion rate curves for several steels, exhibiting a wide range of corrosion susceptibility on test-rack exposure. These rate curves, reproduced from data supplied by the Corrosion Engineering Section, International Nickel Co., show that steel of very moderate alloy content (open-hearth steel) as well as steel of considerable alloy content (SAE 2515) forms protective rust to some degree on test-rack exposure. Open hearth iron, a material of very low alloy content, was the only steel which did not form a protective rust outdoors. In fact, when this investigation was begun, it was discovered that all test specimens of open hearth iron had completely corroded away, so that no rust samples were available for analysis.

X-ray identification of rusts formed on available samples of these steels and on several other steels exposed at Kure Beach, N.C., are given in Table 2. All of these rusts were found to be composed entirely of Fe_2O_3 hydrates, except rust from the crevice of the rocker panel shown in Fig. 2. Rust formed in this sheltered area was again found to be 85% Fe_3O_4 and 15% $Fe_2O_3 \cdot H_2O$.

The presence of 85% Fe_3O_4 in the crevice rust of this fabricated steel component suggests that nonprotective rusts are characterized by large percentages of magnetite, while protective rusts are predominantly Fe_2O_3 hydrates.

Corrosion products formed on several steels exposed to the industrial atmosphere at Bayonne, N.J., by the International Nickel Co. were also found to be composed largely of ferric oxide hydrates. Two steels, similar to steels V and X, formed rusts which contained larger amounts of α $Fe_2O_3 \cdot H_2O$ (90%) and smaller amounts of γ $Fe_2O_3 \cdot H_2O$ (10%) than their Kure Beach counterparts. Again, no Fe_3O_4 was detected by X-ray.

A magnified cross-section of rust formed on the openly exposed surface of rimmed body steel (steel A, Table 2) during outdoor exposure is shown in Fig. 5. Apparently, this rust is more protective and adherent than the rust associated with auto-body service failure, since it still clings tenaciously to the steel on which it was formed. Grains of ferrite in the steel are clearly defined in the bottom of the photograph. Here, only red-yellow constituents are visible in the rust layers. X-ray investigation tells us that this rust is entirely $Fe_2O_3 \cdot H_2O$. No blue-black magnetite can be seen, and none was detected by X-ray.

GM Research Test Rusts – In order to reproduce the sheltered type of corrosion experienced in auto bodies, GM Research developed a cyclic humidity accelerated corrosion test which appears to give the answers we are seeking. This 20-day laboratory

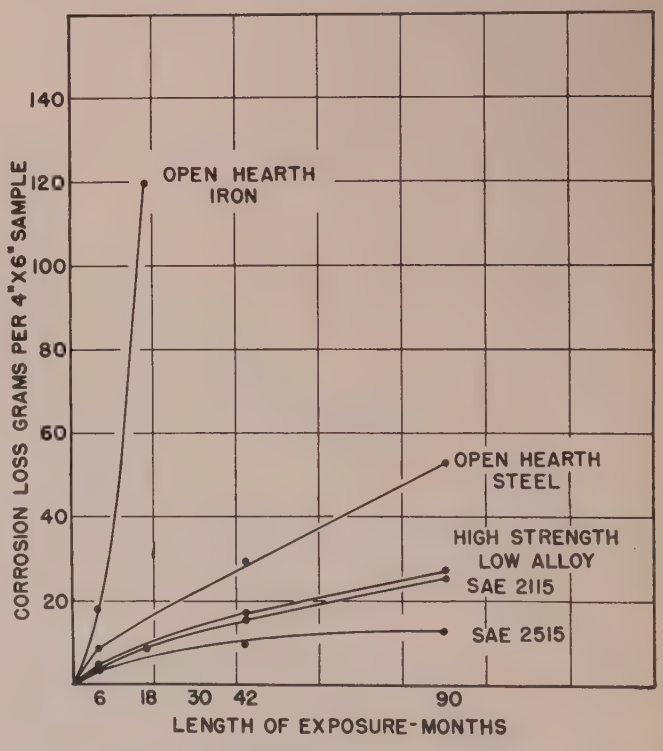

Fig. 4 – Corrosion rates for various low-alloy steels exposed 800 ft from ocean, Kure Beach

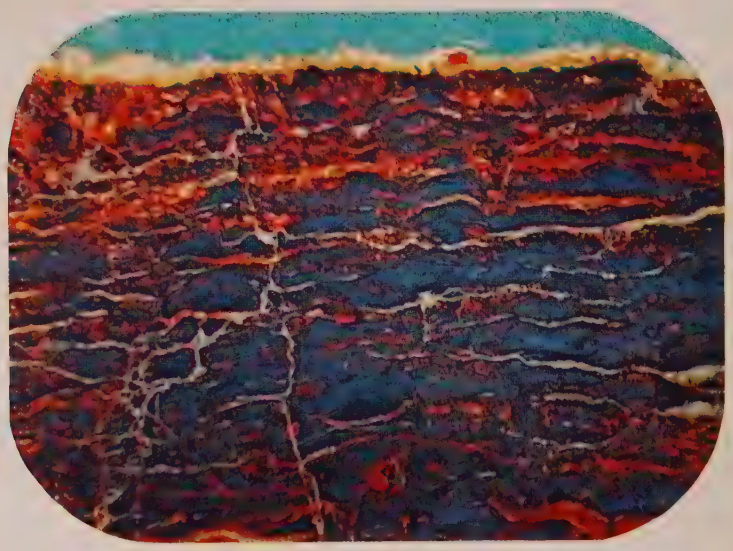

Fig. 3—Cross-section of rust removed from rocker panel which failed in service (50X)

Fig. 5—Cross-section of rust formed on rimmed auto-body steel during atmospheric exposure test (50X)

Fig. 7—Cross-section of rust formed on rimmed steel in 20-day GMR corrosion test (50X)

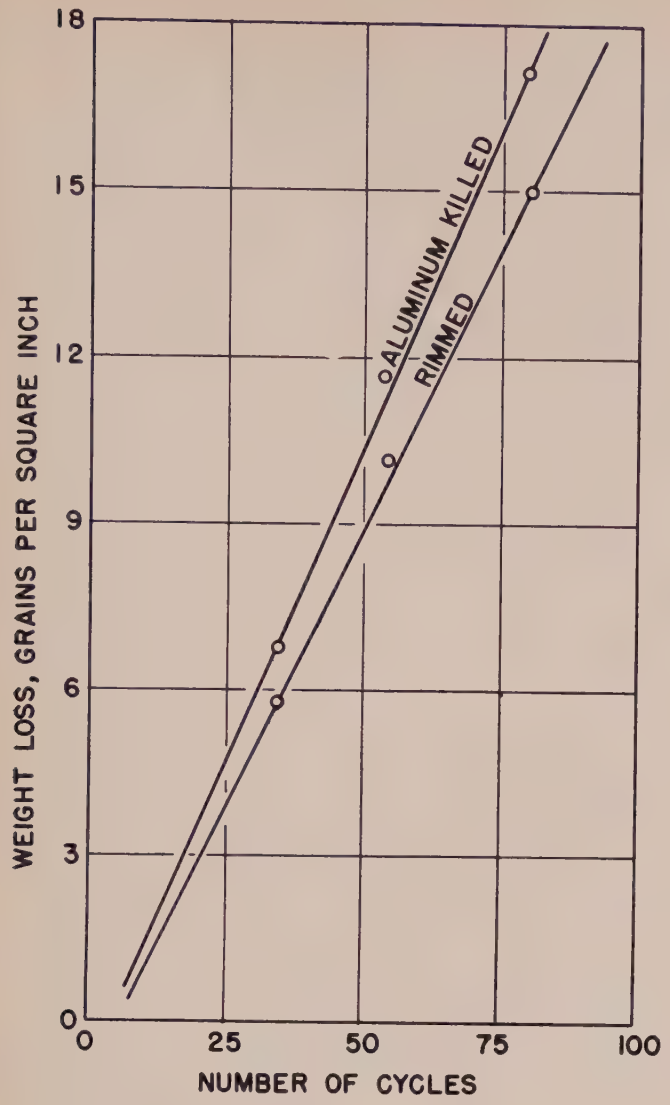

Fig. 6 – Linear behavior of corrosion loss with number of cycles

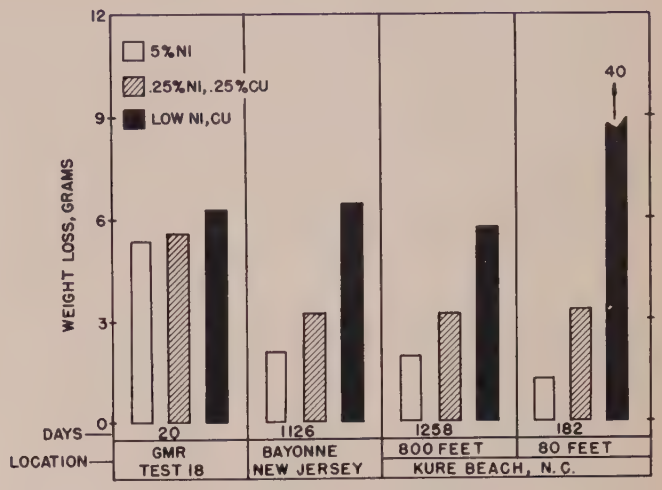

Fig. 8 – Comparison of GMR test with atmospheric exposure tests

test has been covered in detail in a previous publication,[4] and will be described only briefly here. Bare steel panels, suspended in a constant temperature cabinet at 125 F, are corroded by humid air passing over them. The relative humidity of this air is cycled between 100% and about 10%, each cycle requiring about 8 hr. Once each day the samples are wetted with a dilute salt solution.

This alternate moistening and partial drying of samples in the presence of the electrolyte produces a rust which is nonprotective. On each humidity cycle, a new layer of rust is produced under the corrosion products formed during previous cycles. The nonprotective nature of the rust is illustrated graphically by Fig. 6. Since rust formation on auto-body steels is linear with the number of cycles, it can be seen that this environment tests the corrosion resistance of the base metal, and not the protective characteristics of the rust which forms on the steel.

A micrographic cross-section of rust formed on rimmed auto-body steel in the GM Research test is shown in Fig. 7. It is built up in alternate layers of $Fe_2O_3 \cdot H_2O$ (red-yellow) and Fe_3O_4 (blue-black), and has the same appearance as auto-body service rust (Fig. 3). X-ray identification of rusts formed on auto-body steel and several alloy steels by the GMR test is listed in Table 3.

It is to be noted that the rust formed on auto-

Table 3 – X-Ray Analysis of Rust Produced in 20-Day GM Research Test

Identification	Steel	Fe_3O_4, %	$\alpha Fe_2O_3 \cdot H_2O$, %	$\gamma Fe_2O_3 \cdot H_2O$, %	Corrosion Loss – GM Research Test, %[a]
C	Rimmed auto body	85	15		100
D	High-strength, low-alloy	90	10		125
U	Open-hearth iron	85	15		173
V	Open-hearth steel	85	15		107
W	High-strength, low-alloy	80	15	5	77
X	SAE 2115	90	10		105
Y	SAE 2515	85	15		104
Z	3% Cr	85	15		140
C[1]	Carburized rimmed	40	30	30	37

[a] GM Research test corrosion performance is expressed as the per cent corrosion weight loss with respect to the weight loss of rimmed auto-body steel:

$$\frac{\text{Corrosion loss of steel in question}}{\text{Corrosion loss of standard rimmed steel}} \times 100$$

[4] See *ASTM Bulletin*, No. 187, January, 1953, pp. 47-53: "General Motors Research Corrosion Test: Cyclic Humidity Accelerated Corrosion Test for Sheet Steel," by A. J. Opinsky, R. F. Thomson, and A. L. Boegehold.

body steel by this test is nearly identical in composition and crystalline form to corrosion products associated with auto-body service failure (Table 1). Therefore, it appears that the GMR test produces in 20 days the same kind of nonprotective rust which contributes to auto-body failure after a number of years. Conventional outdoor tests, on the other hand, produce corrosion products which are usually, to some degree, protective. Furthermore, the alloy steels (V through Y), which formed protective rusts outdoors, yield largely nonprotective rusts in the GM Research test the same as auto-body sheet.

Several notable exceptions to this last observation are indicated in Table 3. The two steels, W and C[1], which performed better than rimmed steels in the GM Research test as indicated by the last column of Table 3, have less Fe_3O_4 content in the rust and show the presence of $\gamma Fe_2O_3 \cdot H_2O$. This would indicate that partially protective rusts are being formed, even under conditions which are not normally conducive to protective rust formation – that is, sheltered corrosion.

Effect of Alloying Elements – Several steels exposed in the cyclic humidity test and on outdoor test racks are compared in Fig. 8. In 20 days, the GMR test produces as much corrosion of auto-body type steel as three years of atmospheric exposure at Bayonne, N. J., or 3½ years in the 800-ft test lot at Kure Beach, N. C. This shows that the laboratory test is greatly accelerated.

The GMR test shows only small differences in weight loss among the three steels, while the outdoor tests show much greater differences. Probably the reason for wide differences among steels exposed outdoors is that the nickel and nickel-copper steels develop more protective rusts in atmospheric exposure tests, while under the conditions of sheltered corrosion produced in the GMR test, nickel and copper are less capable of developing protective corrosion products.

The effectiveness of chromium in promoting protective rusts on outdoor test samples has been demonstrated by Binder and Brown.[5] However, Larrabee[6] found that in a wet railroad tunnel where steels remained continually moist, corrosion rates for a copper steel and a high-strength, low-alloy steel of the Cr-Si-Cu-P type were nearly linear with time, and corroded at about the same rate as a low-carbon steel which had no special additive. His results further show that the copper steel was slightly superior to the more highly alloyed high-strength, low-alloy steel in this environment. The inability of nickel and chromium to form protective rusts under conditions of sheltered corrosion is exemplified in Fig. 9. In this chart, a number of low-alloy, high-strength steels and several nickel and chromium steels are compared with rimmed and aluminum-killed auto-body sheet. Since rimmed steel comprises 80% or more of all auto-body sheet, comparison is made by ratio of corrosion loss to rimmed steel. The two alloys containing 1% and 5% nickel show the same corrosion loss as rimmed steel; therefore, no benefit can be attributed to nickel additions under the environment of this test. Chromium additions up to 5% actually increased corrosion by as much as 50%. This indicates that under conditions where protective rust formation is retarded, small chromium additions to low-alloy steels may actually be harmful. Incidentally, steels containing 16% or more chromium show almost no corrosion in the 20-day GMR test.

The best of the high-strength, low-alloy steels show about 35% less corrosion than rimmed steel in the GMR test. At a base price increase of 50%, this small improvement can hardly be justified. Although these steels show up much better in outdoor exposure than unalloyed steels, they generally tend to form porous, lamellar, nonprotective rusts in the GMR test the same as auto-body steel.

A tentative evaluation of the effect of the more common alloying elements in steels is shown in Table 4. The elements are listed in decreasing order of effectiveness as measured by outdoor exposure and GMR test exposure. Nickel and chromium, as previously discussed, form protective rusts outdoors but do not contribute to protective rust formation under the conditions of sheltering action experienced in the GMR test environment. Carbon, which contributes no noticeable improvement in outdoor tests, has been found to be the most potent element in reducing corrosion, according to the

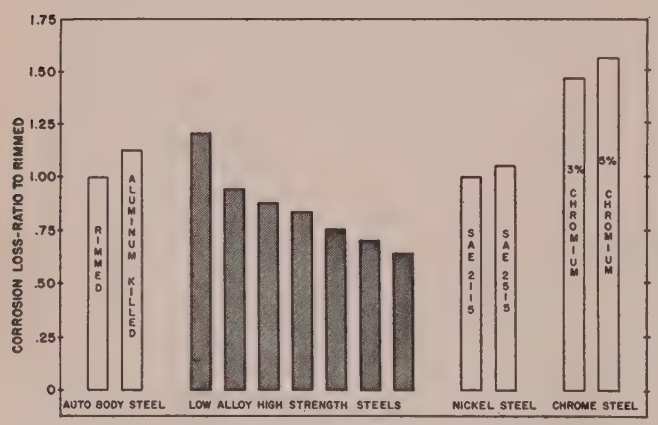

Fig. 9 – Comparison of corrosion resistances of low-alloy steels by GMR corrosion test

[5] See ASTM Proceedings, Vol. 46, 1946, pp. 593-609: "Atmospheric Corrosion Tests on High-Chromium Steels," by W. O. Binder and C. M. Brown.
[6] See *Corrosion*, Vol. 9, August, 1953, pp. 259-271: "Corrosion Resistance of High-Strength Low-Alloy Steels as Influenced by Composition and Environment," by C. P. Larrabee.

cyclic humidity test. The effectiveness of carbon in reducing corrosion under these conditions is shown in Fig. 10. Here, two auto-body materials and a typical high-strength, low-alloy steel, each containing about 0.10% carbon, were gas-carburized to about 1% carbon. Each material showed a decrease of more than 50% in corrosion due to the carburizing treatment.

Unfortunately, high-carbon steels cannot be used for auto bodies because of their poor forming characteristics. Therefore, present work is being directed toward finding an additive or combination of elements which, like carbon, will produce increased resistance to sheltered corrosion at low cost, but not affect forming characteristics.

Conclusions

1. Corrosion failure of auto bodies is generally the result of nonprotective rust formation. Nonprotective rusts, produced in sheltered areas of the car body, are composed of large amounts (80 to 90%) of magnetite, and small amounts (10 to 20%) of Fe_2O_3 hydrates.

2. On the samples investigated, protective rusts formed on low-alloy steels exposed on outdoor test racks are essentially all Fe_2O_3 hydrates. Under the influence of sheltering action, rust formed outdoors may be nonprotective, occurring as porous rust containing high percentages of magnetite and small percentages of Fe_2O_3 hydrates.

3. Nonprotective rusts having the same physical characteristics and composition as those associated with auto-body service failure are produced by the GMR corrosion test. Both auto-body steel and some low-alloy steels form corrosion products in this test which are nonprotective.

4. Alloying elements which aid protective rust formation outdoors do not necessarily contribute to protective rust formation under the conditions of sheltered corrosion experienced in the GMR test. On the other hand, some elements such as carbon, which are reported to have little effect on corrosion resistance of steels in outdoor tests, appear to reduce corrosion under the sheltering environment produced in this test.

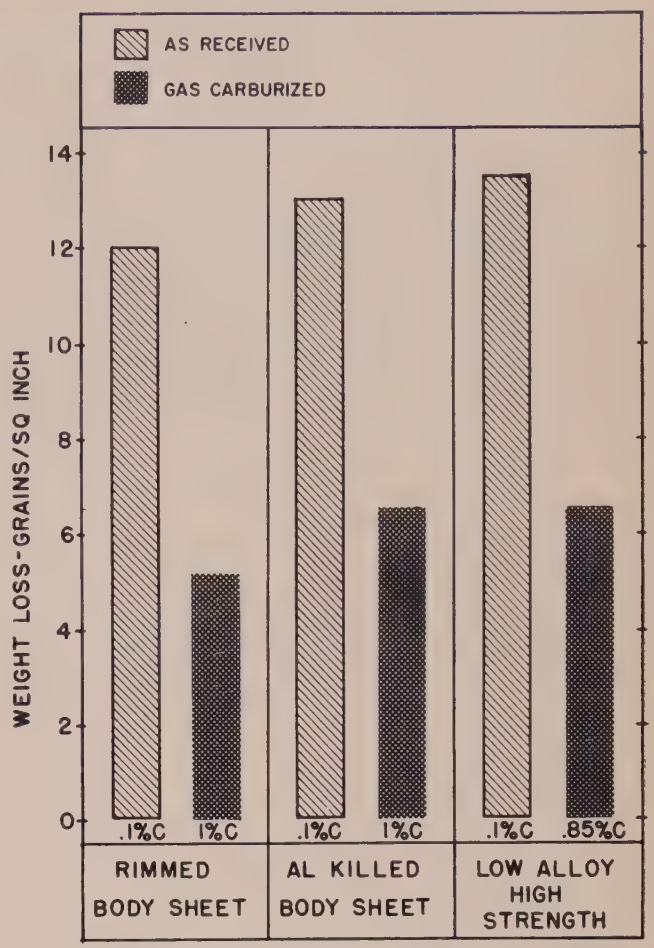

Fig. 10 – Effect of carbon on corrosion loss of some low-alloy steels – GMR corrosion test

Table 4 – Effect of Common Alloying Elements on Corrosion Resistance of Low-Alloy Steels as Determined by Outdoor Exposure and the GMR Test

	Outdoor Exposure			GM Research Test		
	Decreases Corrosion	No Effect	Increases Corrosion	Decreases Corrosion	No Effect	Increases Corrosion
1	Chromium	Carbon	Sulfur	Carbon	Nickel	Chromium
2	Nickel	Silicon		Phosphorous		
3	Copper			Manganese		
4	Phosphorous			Copper		
5	Manganese			Silicon		

Acknowledgments

The authors wish to express their appreciation to the Development and Research Division of the International Nickel Co., Inc., for many of the corrosion test samples which they supplied, and for permission to publish some of their results. The authors also wish to thank the Electrometallurgical Co. for supplying materials for testing. Finally, they are grateful to D. P. Koistinen who performed the X-ray determinations, and to J. L. Greene who carried out much of the experimental work.

DISCUSSION ON FOLLOWING PAGE →

DISCUSSION

Urges Better Draining and Ventilating Facilities

by F. L. LaQue

International Nickel Co.

THE present paper is a welcomed extension of the earlier description[a] of the testing device developed by these authors and of its use in predicting the abilities of steels to resist atmospheric corrosion. In the earlier paper, the authors suggested that this test was reasonably satisfactory for predicting the relative merits of steels in resisting atmospheric corrosion as experienced by specimens exposed outdoors on conventional test racks. In the present authors' discussion of this earlier paper, they emphasize the necessity of making a distinction between behavior under exposure conditions that would permit frequent drying of the rust, and behavior when the rust had little opportunity to dry. It was suggested that the GM test might readily achieve a proper rating of steels under the latter conditions, but would be much less useful in matching the behavior of steels when they could develop more protective rusts by frequent drying.

Since there are many surfaces of automobile bodies where rusts have limited opportunity for drying, it is probable that results of the GM test would be more indicative of performance in such service than the results obtained in conventional tests in natural atmospheres where frequent drying occurs.

It should be remembered, however, that the opportunity to improve the resistance of steels towards progressive rusting is much greater under conditions where the rusts can dry than when they are wet most of the time. This point was illustrated by the data covered by Fig. 8. It is, therefore, suggested once more that, in attacking the overall problem of reducing corrosion of automobile bodies, appropriate attention should be given to means of draining and ventilating the critical surfaces so that there will be a much better opportunity for steels, and especially those containing small amounts of nickel and copper, to form the protective rusts that account for their well-known superiority over ordinary steels in resisting atmospheric rusting.

The results of the X-ray studies which showed that the nonprotective rusts that formed under natural conditions of partially sheltered exposure and in the GM accelerated tests consisted predominantly of Fe_3O_4, while protective rusts formed under conditions of bold exposure consisted of ferric oxide hydrates, are quite interesting. Of the possible conclusions from these observations, probably the most reliable is that atmospheric rust containing much Fe_3O_4 is not likely to be protective. One consisting of ferric oxide hydrates may or may not be protective, depending on other characteristics of the rust not disclosed by the X-ray analysis. The influence of rust composition on the corrodibility of steels in the atmosphere has been discussed in detail by H. R. Copson.[b]

Since this test permits a comparison of steels under conditions frequently encountered in the automobile bodies, it should prove to be useful for preliminary screening in the search for steels such as the high carbon compositions described in the paper, which may have the desirable property of developing protective rusts even under conditions where there is little opportunity for the rusts to dry.

Some recent tests have indicated that some special steels containing small amounts of nickel and copper may demonstrate the required properties without sacrificing others required for automobile-body fabrication.

ORAL DISCUSSION

Reported by O. W. McMullan

Bower Roller Bearing Co.

L. H. Nagler, American Motors Corp: Can protective coating such as phosphates be applied to retard or prevent early damage from rust? If so, what are the relative merits of such coatings?

Mr. Holzwarth: Paint evaluation in this test is not successful, because paint does not adhere well enough in the 20-day test to make a valid appraisal. The test method can evaluate chromium plate and various metallic coatings as far as rust prevention is concerned, but these coatings may not be economical for body sheet. An aluminum coating was found to be superior to hot-dip galvanizing.

Question: Why is sheet metal not pretreated with rust-preventive-type materials preferably before assembly?

Mr. Holzwarth: Before assembly, pretreatment is not usually satisfactory for welded assemblies since the coating at and adjacent to welds interferes with bonding. Pretreatment such as phosphate coating is given, but generally after assembly. Such treatment is difficult because of inaccessible regions where close control is required to provide effective protection.

O. W. McMullan, Bower Roller Bearing Co.: What is the effect of temperatures in causing early muffler failures?

Mr. Holzwarth: Mufflers operate above the temperature range of our investigations. Many times they fail internally from the action of hydrobromic acid and other corrosive exhaust gases. We would hesitate, therefore, to predict performance of muffler materials on the basis of this test.

R. D. Chapman, Chrysler Corp.: What is the effect of adding inhibitors to salt used in the evaluation tests? Some cities use dichromates in salts applied to streets.

Mr. Holzwarth: Polyphosphates gave an improvement of about 15%, and dichromates somewhat more. But the values were below expectations, and we do not consider the result of this test alone would justify their use.

---

[a] See footnote 4 of main paper.
[b] See footnote 2 of main paper.

A WORKABLE, effective regulatory measure to assure minimum brake-performance requirements requires:

1. Commercially available instruments which facilitate rapid testing.
2. Statement of the requirement in units which allow most effective evaluation of braking performance.
3. Compliance with the requirement must be possible in both road and inspection-station tests.

The conclusions led to the final recommendation which was adopted for the Uniform Vehicle Code of 1954. A recommended enforcement program and testing requirements for the several vehicle classes are set forth.

A Practical Stopping-Ability Regulation

Carl C. Saal, Bureau of Public Roads

This paper was presented at the SAE Golden Anniversary West Coast Meeting, Portland, Ore., Aug. 17, 1955.

FOR more than 15 years, establishment of a practical stopping-ability regulation for all types of motor vehicles has been the common goal of vehicle operators, manufacturers of vehicles and braking equipment, and public officials responsible for highway design and regulation and control of vehicle operation. All agreed that the regulation should provide for maximum safety of operation and maximum economy in highway design, while avoiding undue penalties on operators and manufacturers of motor vehicle equipment. However, there was considerable disagreement as to what constituted adequate performance and what methods and instrumentation should be used to insure that this adequate performance would be observed by vehicles operating in everyday traffic.

It became evident very early that the differences of opinion among the varied interests could not be resolved with the basic data available on the subject. Consequently, at the behest of government, trade, and industrial representatives, a rather broad research program on motor-vehicle brakes was initiated in 1941 by the Bureau of Public Roads. The program was halted in 1942 by World War II, reorganized in 1947, and successfully concluded by the publication of a comprehensive report[1] in 1954.

Joint efforts of industry and government were pooled to produce the results in that report. This was accomplished through a committee of interests called the Advisory Committee on Brake Research to the Bureau of Public Roads, composed of representatives of 16 private organizations and 2 government agencies.

The primary function of this committee was to advise and assist in procedural matters and to approve the final report. However, the various

[1] See "Braking Performance of Motor Vehicles," by C. C. Saal and F. W. Petring. Pub. by U. S. Government Printing Office, Washington, 1954.

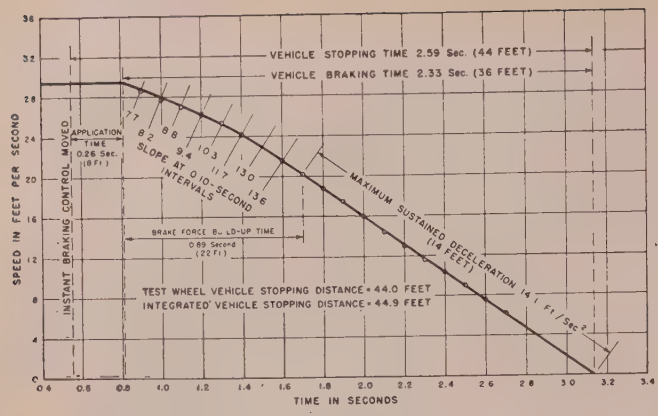

Fig. 1 – Time-speed curve for test vehicle No. 1 stopping from 20 mph, showing differentiation for deceleration and various phases of stopping

interests contributed far more than advice, furnishing instrumentation, test vehicles, test drivers, mechanics, police protection, and personnel for conducting the several test phases.

Early in 1954, the National Committee on Uniform Traffic Laws and Ordinances appointed a Brake Subcommittee which was asked "to review the brake requirements set forth in Section 150 of Act V of the Uniform Vehicle Code,[2] particularly subsection (b) which sets forth the performance requirements in terms of stopping distance and deceleration." This subcommittee recommended a revision of the brake requirement which was adopted by the parent committee and which is now included in the consolidated Uniform Vehicle Code.[3]

The bases for this revision were the conclusions and recommendations contained in the report[1] published by the Bureau of Public Roads. It is the purpose of this paper to show how the results of our study were applied to produce a practical stopping-ability regulation.

Terminology

Before proceeding with the discussion it is imperative that there be a clear understanding of the terms used in this paper:

1. Vehicle-stopping time or distance: Time elapsed or distance traveled between the instant or point at which the driver starts to move the braking controls and the instant or point at which the vehicle comes to rest.

2. Brake-system application time or distance: Time elapsed or distance traveled between the instant or point at which the driver starts to move the braking controls and the instant or point of first retardation by the brakes.

3. Braking time or distance: Time elapsed or distance traveled between the instant or point of first retardation by the brakes and the instant or point at which the vehicle comes to rest.

4. Brake-force-buildup time or distance: Time elapsed or distance traveled between the instant or point of first retardation by the brakes and instant or point maximum braking force is attained.

5. Maximum sustained deceleration: Rate of deceleration sustained from the instant maximum vehicle braking force is attained until the instant the vehicle comes to rest.

6. Maximum deceleration: Greatest rate of deceleration measured during the stop regardless of the time it is sustained.

7. Brake efficiency: Ratio of the sum of wheel braking forces to gross vehicle weight, multiplied by 100; or, rate of deceleration divided by the deceleration of gravity, 32.2 ft per sec per sec.

Misuse of terms has led to considerable confusion in the enforcement of brake requirements. Fig. 1 shows clearly what actually takes place during stopping of a commercial vehicle with power brakes. During one period immediately following the instant the braking controls are operated, called application time, the vehicle is not retarded appreciably. This time or distance is required to transmit power to the brake chambers and to overcome frictional resistance in the linkage between brake chamber and shoe and resistance in the brake-shoe return springs. Application time is followed by a second period, called the brake-force-buildup time, during which braking force at the wheels builds up to a maximum value. The phenomena of application and buildup times are complicated by the fact that they are usually different to some degree on each axle of a vehicle. The time-speed record shows the composite effect of the timing of forces at the individual axles. The final period of the braking cycle is indicated as maximum sustained deceleration on Fig. 1. During this period, the maximum braking force is acting to stop the vehicle.

For the example shown in Fig. 1, application time was 0.26 sec, buildup time 0.89 sec, and period of maximum sustained deceleration 1.44 sec. These times were equivalent to 8, 22, and 14 ft, respectively. It is significant that combined application and buildup constituted only 44.4% of vehicle stopping time of 2.59 sec, but 68.2% of vehicle stopping distance of 44.0 ft. Obviously it is important in regarding vehicle stopping distance to reduce application and buildup time to a minimum. Had the maximum sustained deceleration of 14.1 ft per sec per sec been sustained from the instant of moving the brake control, vehicle stopping distance would have been 30.5 ft.

The time-speed relation shown in Fig. 1 is representative for most combination units, some having shorter and others longer application and buildup

---

[2] See "Uniform Vehicle Code: Act V – Uniform Act Regulating Traffic on Highways." Revised and approved by National Committee on Uniform Traffic Laws and Ordinances. Pub. by U. S. Government Printing Office, Washington, 1952.

[3] See "Uniform Vehicle Code." A consolidation and rearrangement of Acts I-V, heretofore published separately. National Committee on Uniform Traffic Laws and Ordinances, Washington, revised 1954.

times. Curves for passenger cars and straight trucks take the same shape, although both application and buildup times are negligible in some instances. Fig. 1 indicates that measurement of deceleration alone will not give a true picture of brake performance for many commercial vehicles, for it is possible ultimately to develop sizable braking forces which result in high rates of deceleration but still provide poor overall brake performance.

Vehicle stopping distance must not be confused with the distance indicated by inertia-type decelerometers and other existing brake testers which often are wrongly purported to measure vehicle stopping distance. Actually these instruments are designed to measure deceleration or braking force occurring *after* application and buildup times. The distance they indicate is a mathematical conversion based on the assumption that deceleration or force is averaged for the entire braking period. As demonstrated in Fig. 1, this assumption is not valid. If the brake-force-buildup time is negligible the distance computed will correspond closely to vehicle-braking distance; if both brake-application and force-buildup times are negligible, it will correspond closely to vehicle-stopping distance. The latter possibilities depend on accuracy of the instrument measuring sustained deceleration or braking force.

Need for Revision of Old Code

The necessity for revising the old code can best be illustrated by comparing the requirements prevailing prior to the recent revision with actual levels of performance measured for various types of vehicles.

Act V, section 1506 of the Uniform Vehicle Code[2] states: "Every motor vehicle or combination of motor-drawn vehicles shall be capable at all times and under all conditions of loading of being stopped on a dry, smooth, level road free from loose material, upon application of the service (foot) brake, within the distances specified below, or shall be capable of being decelerated at a sustained rate corresponding to these distances:"

	Ft to Stop from 20 mph	Deceleration, ft per sec per sec
Vehicles or Combinations of Vehicles Having Brakes on All Wheels	30	14
Vehicles or Combinations of Vehicles Not Having Brakes on All Wheels	40	10.7

The following is footnoted:

"It is recommended that the means used for enforcement purposes to determine whether a motor vehicle or combination of motor vehicles is in compliance with the provisions of the above section should be by approved instrument or machine."

Stopping-distance requirements similar to the above are in force in most of the States and have been commonly enforced on the basis of the equivalent deceleration requirement using inertia-type decelerometers and drive-on-and-stop brake testers. Thus, feet to stop has generally been interpreted to be a distance indicated by such instruments which more closely approximates what has been defined as vehicle braking distance rather than vehicle stopping distance. However, in many instances the feet to stop has been interpreted as vehicle stopping distance and enforced as such.

The level of performance for all vehicles selected from everyday traffic is shown in Fig. 2. The curves plotted indicate the percentage of all vehicles of each type that can stop in a given distance or less from a speed of 20 mph. In studying these general results keep in mind that the sample of each vehicle type is made up of various gross weights, capacities, brake types and conditions of maintenance. The most striking point is the wide variation in performance of the several types of vehicles. For example, 50% values were approximately 21 ft for passenger cars, 28 ft for 2-axle trucks, 37 ft for 3-axle trucks, 39 ft for 2-axle truck-tractors with 1-axle semitrailers, 43 ft for 2-axle truck-tractors with 2-axle semitrailers, and 53 ft for other combination units. Obviously, a very large percentage of commercial vehicles now operating on highways cannot meet present requirements if

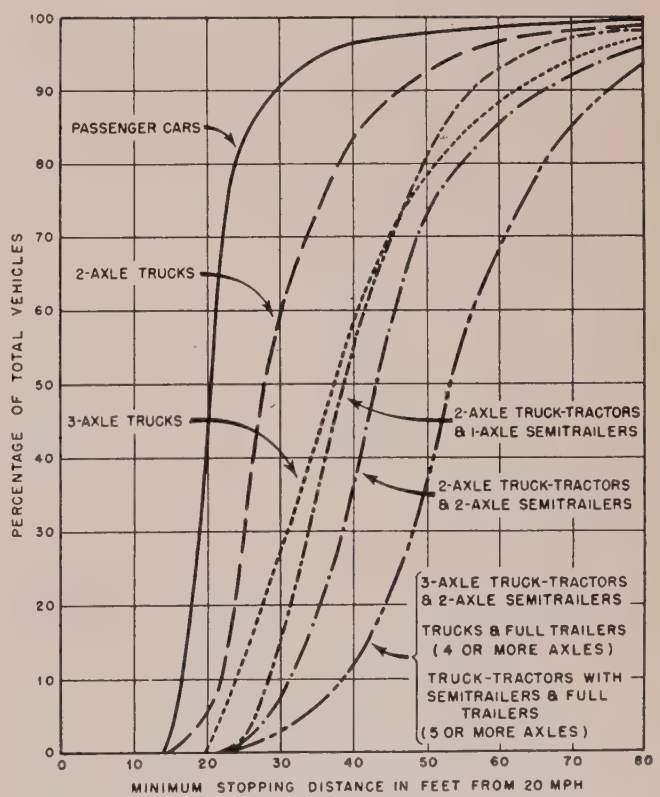

Fig. 2 – Cumulative frequency distribution of vehicle stopping distances for motor vehicles selected from everyday traffic

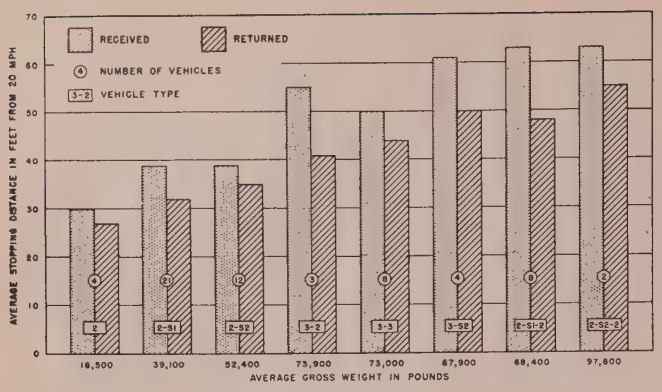

Fig. 3 – Comparison of average brake performance observed for various vehicle types as received from and as returned to service

interpreted in terms of vehicle stopping distance.

The results of brake tests made by manufacturers on new vehicles showed that 70% of new 2-axle trucks loaded to rated gross weight stopped in 30 ft or less. In other words, 30% of these new models could not meet the present common requirement when expressed in terms of vehicle-stopping distance. The 70% value compares with 59% read from the curve for 2-axle trucks plotted on Fig. 2, indicating that new models in the best condition, as expected, performed better than vehicles tested at random from everyday traffic. New models loaded 25% over rated gross vehicle weight, which is not uncommon, only 60% could stop in 30 ft or less.

In addition to measuring vehicle stopping distance, manufacturers also measured the rate of deceleration of 2-axle trucks with portable inertia-type decelerometers. It is of interest that about 95% of vehicles with a weight-rating ratio of 1.00 and about 81% of vehicles with a weight-rating ratio of 1.25 could meet a requirement of 14 ft per sec per sec or better.

Manufacturers also supplied data for nine new combination units. Performance was remarkably good compared with that indicated in Fig. 2 for combination units selected from everyday traffic. For seven vehicles loaded to gross combination-weight ratings ranging from 39,000 to 72,900 lb, vehicle stopping distances were 35 ft or less from an initial speed of 20 mph. Two other vehicles with a rated weight of 90,000 lb stopped in 38 and 42 ft from 20 mph.

From results of manufacturers' tests on new vehicles, it could be concluded that there should not be the wide variation in stopping ability between straight trucks and combination units as evidenced by the results shown in Fig. 2 for vehicles selected from everyday traffic. However, general performance of vehicles obtained from normal service of selected operators, shown in Fig. 3, also indicated a fairly wide difference between the stopping ability of various types of vehicles. When tested as received from service, average vehicle stopping distances varied from 30 ft for the 2-axle trucks to slightly over 60 ft for three of the vehicle types. Variation was not quite so great after maintenance had been performed, being from 27 ft for 2-axle trucks to 55 ft for 2-axle truck-tractors with 2-axle semitrailers and 2-axle full trailers. These tests were made with gross weights approximating full-volume loads of the particular operator's service.

Cumulative frequency distributions of vehicle stopping distances determined for vehicles obtained from normal service of selected operators are shown in Fig. 4. For vehicles received from service only about 12% could stop in 30 ft or less. After maintenance and repair about 27% could stop in 30 ft or less.

Curves showing cumulative frequency distribution of maximum sustained deceleration, obtained by the time-distance method for vehicles from normal service, are shown in Fig. 5. Had the vehicles been tested with a decelerometer having the accuracy of the time-distance method, approximately 39% in the original condition and 22% in the condition as returned to service would have failed to comply with the requirement of 14 ft per sec per sec. However, for combination units which comprise 92% of the sample, it was developed that a deceleration of 11 ft per sec per sec determined by the time-distance method was equivalent, on

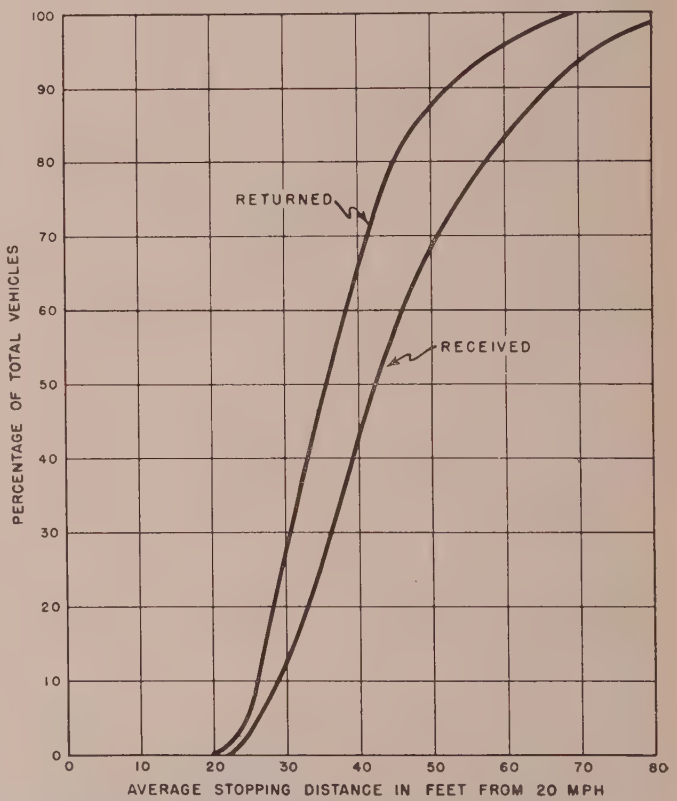

Fig. 4 – Cumulative frequency distribution of vehicle stopping distances measured for all types of trucks and combination units selected from service

the average, to about 14.0 ft per sec per sec determined by portable decelerometers of the pendulum type. Based on this correlation, 13% of vehicles as taken from service and only 2% as returned to service would have failed to meet the requirement of 14 ft per sec per sec when tested with the instrument now in common use for enforcement purposes.

Considering the results shown in Figs. 4 and 5, it is evident that present requirements in terms of deceleration can be met by practically all combination units in fleet service, whereas present requirements interpreted in terms of vehicle stopping distance can be met only by a small percentage of vehicles, even after considerable brake adjustment and repair work has been performed.

This discussion of the general level of performance is intended to give a broad picture of what braking ability can be expected of vehicles operating in everyday traffic, of new model performance in the manufacturers' hands, and of operation in normal fleet service. It has been shown clearly that there is a wide variation in average performance of several types of vehicles now operating on the highway, but results of new truck tests suggest that some of this gap can be closed in the near future. An important consideration is the fact that most commercial vehicles can meet present requirements in terms of deceleration of 14 ft per sec per sec when measured with available inertia-type instruments. Of equal importance is the fact that a large percentage of all types of vehicles in service, except passenger cars and very light trucks, did not meet the specification for a 30-ft stop from 20 mph if interpreted in terms of vehicle stopping distance.

One reason for a revision of the braking provisions of the Code[2] was the confusion that existed as to whether a measurement of vehicle stopping distance as defined in this report or an indication of the feet-to-stop, as shown by inertia-type brake testers was implied. Another important reason was that the findings just discussed showed that enforcement of the old requirement in terms of vehicle stopping distance would impose restrictive and unfair penalties on operators and manufacturers of commercial vehicles. It was most evident that a fair requirement should be written; one very explicit as to what portions of the braking event were to be measured and what instruments were to be used in the enforcement of the requirement.

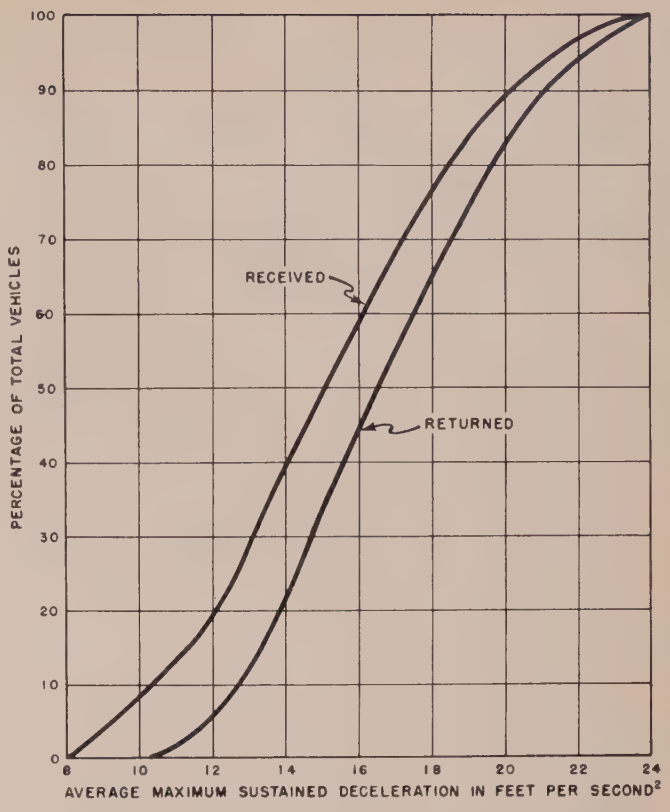

Fig. 5 – Cumulative frequency distribution of deceleration determined by time-distance method for all types trucks and combination units selected from service

Major Prerequisites for Brake Requirement

To be both workable and effective, any regulatory measure must meet certain qualifications. Three major prerequisites for formulation of a minimum brake-performance requirement are:

1. There must be commercially available, reasonably effective instruments which provide for rapid testing of vehicles to determine compliance with the specified requirement.

2. The requirement must be stated in a unit or units of measure that will give the most practical evaluation of braking performance from the viewpoint of highway safety.

3. It must be possible to determine compliance with the specified requirement by both road and inspection-station tests.

Availability of instruments currently limits the units of any requirement to stopping distance, deceleration, and braking force. Test wheels and decelerometers are available for measuring stopping distance and deceleration for road tests. Decelerometers, drive-on-and-stop type testers, and brake-chassis dynamometers (roller-type testers) are available for measuring deceleration and braking force in inspection stations. So far as the inspection station is concerned, deceleration and braking force are analogous, there being a mathematical relation between the two which converts one to the other. Logically, then, a regulatory measure may be formulated at present about either vehicle-stopping distance or deceleration, or a combination of the two.

Evaluation of Brake Testers

The first prerequisite was believed to be the most important, for any brake requirement or enforcement program must be built around the capabilities of brake testers. For that reason, the Bureau of Public Roads conducted extensive tests to evaluate

existing brake testers, and for the same reason the findings will be reported rather extensively in this paper.

Stopping tests were run on selected vehicles, measuring braking ability concurrently with several types of instruments. Each vehicle was tested first in an inspection station and then stopped from an initial speed of 20 mph on a highway test course. In the inspection station, deceleration was measured with three decelerometers (two of the pendulum type and one of the U-tube type), and braking force with a drive-on-and-stop brake tester. On the highway test course, deceleration was measured with the same three decelerometers and by the time-distance method, and vehicle stopping distance by a calibrated test wheel.

The data fell logically into four groups according to vehicle type and brake type. They are: (1) passenger cars, (2) single-unit trucks with hydraulic and vacuum-booster hydraulic brakes, (3) single-unit trucks and buses with air-mechanical brakes, and (4) truck-tractors with semitrailers.

In order to compare the performance of one instrument with that of another, the percentage variation between the indicated performances of both were computed for each stop for which there was a simultaneous recording of braking ability.

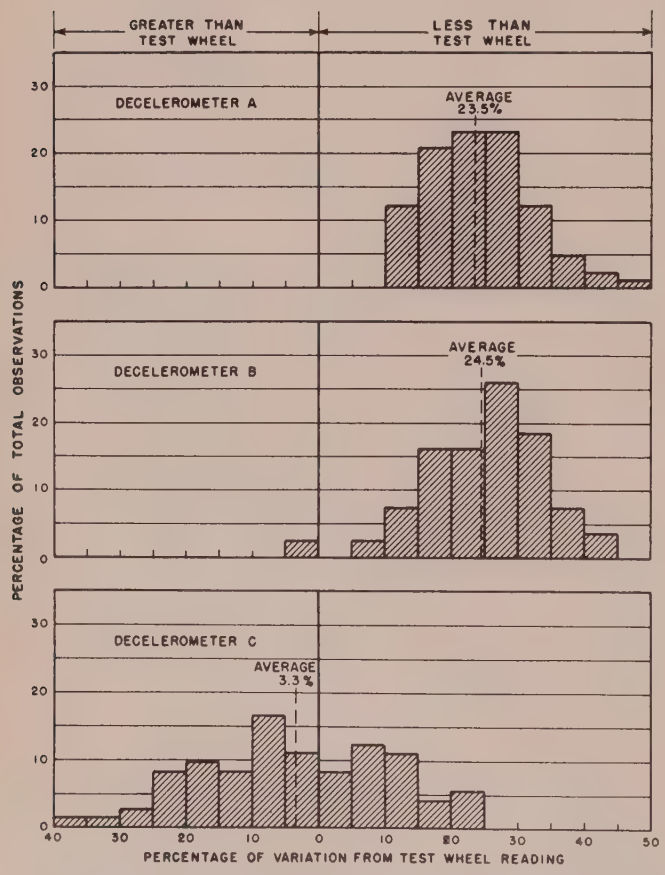

Fig. 6 – Variation of braking distances for passenger cars indicated by decelerometers from stopping distances measured by test wheel

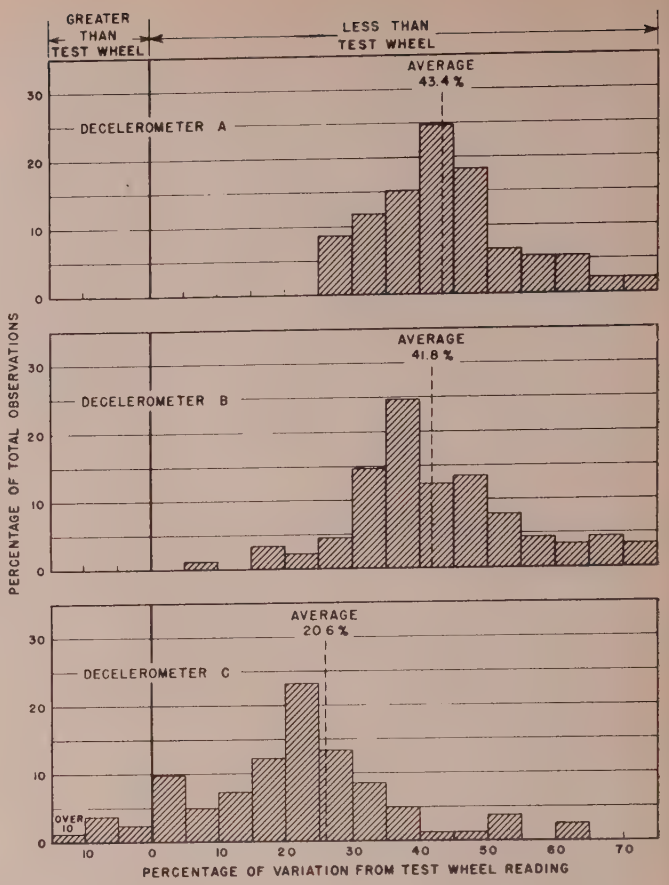

Fig. 7 – Variation of braking distances for truck-tractors with semitrailers indicated by decelerometers from stopping distances measured by test wheel

These percentage variations for a particular group of vehicles were then classified into percentage groups with a range of 5%. Bar graphs will be used to show the percentage of total observations falling in each group.

Fig. 6 indicates the ability of each of three decelerometers to predict vehicle stopping distance of passenger cars. Note that the average variation for decelerometers A and B are, respectively, 23.5 and 24.5% less than the test wheel, while that for decelerometer C is 3.3% greater than the test wheel. If average variation only is considered, C appears to be vastly superior to the other two in predicting brake performance of passenger cars. When the scatter of data about the average variation is considered, however, the picture changes, for the scatter was considerably more for C than for A and B. Standard deviations from average variations for A, B, and C were 7.7, 9.1, and 14.1, respectively. It follows that though average variation of decelerometer C from the test wheel was small, consistency of readings was considerably poorer than for the other two decelerometers.

Ability of decelerometers to predict vehicle stopping distance of 3- and 4-axle truck-tractors with semitrailers is shown in Fig. 7. Decelerometers again indicated distances considerably less than

Table 1 – Average Variations of Braking Distances Indicated by Decelerometers and Drive-on-and-Stop Tester from Stopping Distances Measured by Test Wheel, and Standard Deviations from These Averages.

	Average Variations, %[a]					Standard Deviations, %				
	Decelerometers				Drive-on-and-Stop Tester	Decelerometers				Drive-on-and-Stop Tester
	A	B	C	A[b]		A	B	C	A[b]	
Passenger Car	−23.5	−24.5	+3.3	—	−8.3	7.7	9.1	14.1	—	11.5
Single-Unit Trucks with Hydraulic and Vacuum-Booster Hydraulic Brakes	−35.0	−35.4	+0.3	−31.0	−19.6	12.2	12.4	22.5	18.0	12.3
Single-Unit Trucks and Buses with Air Brakes	−28.9	−28.9	−20.2	−33.0	−24.1	7.3	9.0	11.3	10.3	13.7
Truck-tractors with Semitrailers	−43.4	−41.8	−20.6	—	−30.6	10.8	13.1	15.4	—	9.4

[a] A minus sign denotes the instrument indicated a distance shorter than measured with a test wheel; a plus sign denotes the instrument indicated a longer distance.
[b] New truck tests by manufacturers.

those measured by the test wheel. Average variations of decelerometer readings from test wheel readings were 43.4, 41.8 and 20.6%, respectively, for A, B, and C, with corresponding standard deviations of 10.8, 13.1, and 15.4, respectively.

Data in Table 1 show that decelerometers A and B, both of the pendulum type, performed practically the same regarding their capabilities for predicting vehicle stopping distance on road tests. Average variations were approximately 24% for passenger cars, 32% for single-unit trucks, and 42% for 3- and 4-axle combination units. There was a wide dispersion of percentage variations about the average variation. For practically all stops, A and B indicated a distance less than the actual distance required to stop.

Decelerometer C, the U-tube type, did a better job on the average than A and B in predicting vehicle stopping distance, but was very unreliable, as shown by a wide deviation of the percentage variations about the average variation. A U-tube type decelerometer like C, with a high degree of damping designed into it, does not appear suitable for testing vehicles on the highway from 20 mph. The U-tube type can probably be designed to perform as well as the pendulum type if means are provided for holding the liquid at the maximum level.

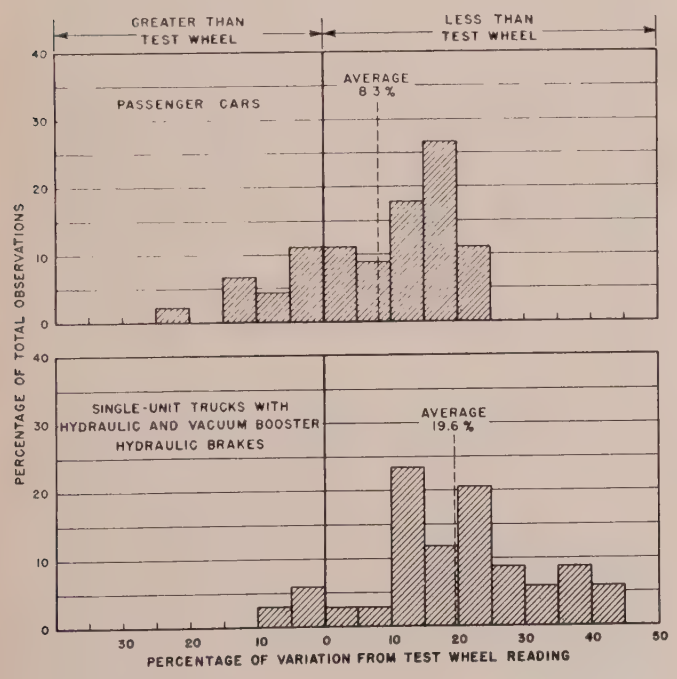

Fig. 8 – Variation of braking distances indicated by drive-on-and-stop brake tester from stopping distances measured by test wheel

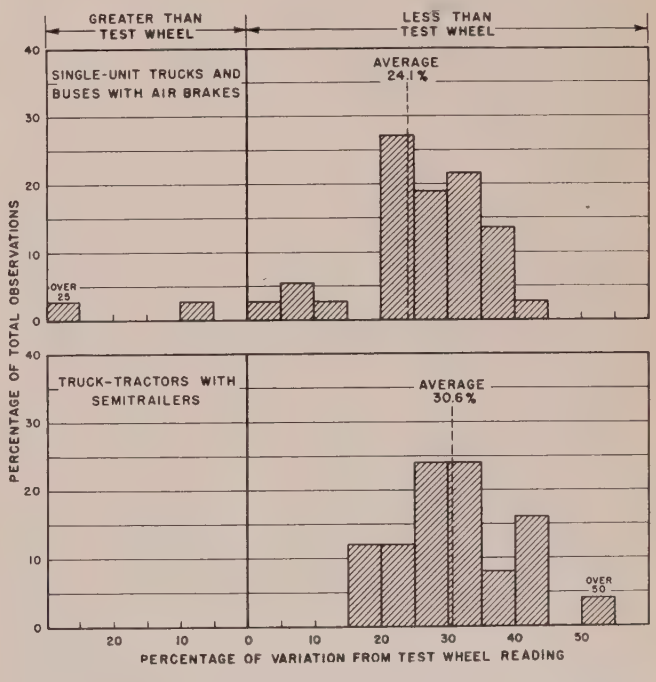

Fig. 9 – Variation of braking distances indicated by drive-on-and-stop brake tester from stopping distances measured by test wheel

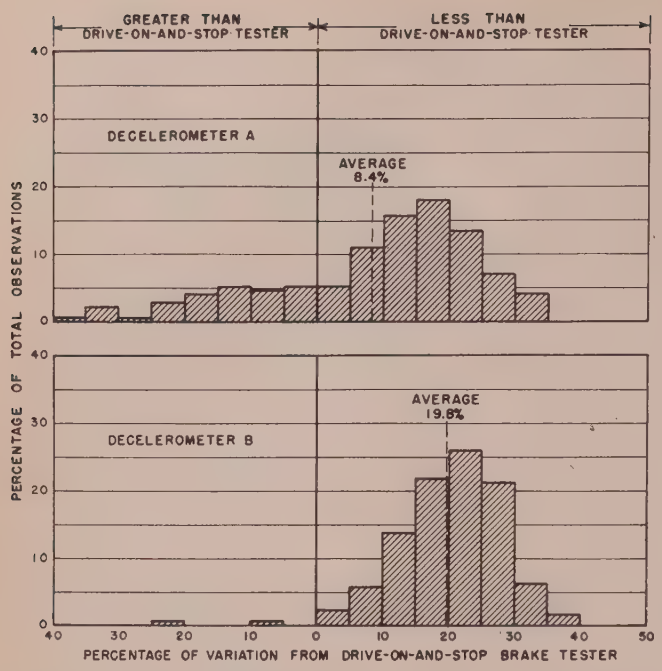

Fig. 10 – Variation of braking distances for passenger cars indicated by decelerometers from those indicated by drive-on-and-stop brake tester

Variations between braking distances indicated by the drive-on-and-stop tester and the vehicle-stopping distances measured by the test wheel are shown in Fig. 8 for passenger cars and trucks with hydraulic brakes, and in Fig. 9 for single-unit vehicles with air brakes and truck-tractors with semitrailers. Study of data in these figures reveals that average variations increased as the size and number of axles increased. This increase in average variation was due largely to an increase in application and force buildup times, which were shown previously to become greater as the size and number of axles increases. For all groups of vehicles except the combination units, the drive-on-and-stop tester indicated a distance on some stops greater than the vehicle stopping distance. This occurred in about 24, 9, and 5% of stops for passenger cars, trucks with hydraulic brakes, and trucks with air brakes, respectively.

For the four vehicle groups, Table 2 shows average variations of braking distance indicated by the drive-on-and-stop brake tester from vehicle stopping distances measured by the test wheel, and standard deviations from these averages. A comparison of these data with those for the decelerometers, also in Table 1, indicates that on the average, the drive-on-and-stop brake tester did a much better job in inspection-station tests than decelerometers A and B did in road tests in predicting vehicle stopping distance. Average variations for the drive-on-and-stop tester were 8.3, 19.6, 24.1, and 30.6% for the four vehicle groups in the order shown in the tables; for decelerometers A and B they averaged 24.0, 35.2, 28.9, and 42.6% for the corresponding groups of vehicles.

Decelerometers A and B and the drive-on-and-stop brake tester were tested simultaneously in the inspection station. At first, decelerometer C was also included, but its use in the inspection station was found to be impractical. Braking time was so short that the decelerometer, a highly damped instrument, had no time to respond fully to the braking forces.

Fig. 10 shows the variation of braking distances indicated by the decelerometers from those indicated by the drive-on-and-stop brake tester for passenger cars. The graph shows there were some stops for which decelerometers indicated a greater distance than the drive-on-and-stop tester, and that there was a wide dispersion of variations. It also reveals that, on the average, decelerometers indicated less distance than the drive-on-and-stop tester. A summary of average variations and standard deviations from those averages is contained in Table 2 for the four groups of vehicles.

Average variation of decelerometer A from the drive-on-and-stop brake tester was considerably less than that of B for passenger cars, single-unit trucks with hydraulic and vacuum-booster hydraulic brakes, and truck-tractors with semitrailers. This, no doubt, is due to the difference in damping in the two instruments. Decelerometer B, damped the least, was frequently thrown off-scale, particularly when testing passenger cars and unladen commercial vehicles. Although decelerometer A was thrown off-scale on the most severe stops, it did so less frequently than B. On inspection-station stops which were not severe enough to throw either instrument off-scale, B almost always indicated a shorter braking distance than A.

From the results in Fig. 10 and Table 2, it is seen that performance of decelerometer A compared favorably with that of the drive-on-and-stop tester for testing in an inspection station, the average variation of A from the tester being less than 10% for each group of vehicles. It was determined that, on the average, decelerometer A did a better job of predicting vehicle stopping distance in the inspection station than it did on the road tests.

Table 2 – Average Variations of Braking Distances Indicated by Decelerometers from Those Indicated by Drive-on-and-Stop Brake Tester, and Standard Deviations from These Averages

	Average Variation[a] of Decelerometer, %		Standard Deviation of Decelerometer, %	
	A	B	A	B
Passenger Car	−8.4	−19.8	15.4	8.1
Single-Unit Trucks with Hydraulic and Vacuum-Booster Hydraulic Brakes	−8.8	−15.8	9.7	7.5
Single-Unit Trucks and Buses with Air Brakes	−5.4	− 7.0	11.8	13.5
Truck-Tractors with Semitrailers	−3.7	−12.2	13.0	9.9

[a] A minus sign denotes the decelerometer indicated a distance shorter than that indicated by the drive-on-and-stop brake tester.

Table 3 – Average Variations of Maximum Decelerations Indicated by Decelerometers from Maximum Sustained Decelerations Determined from Time-Distance Records, and Standard Deviations from These Averages

	Average Variation[a] of Decelerometer, %			Standard Deviation of Decelerometer, %		
	A	B	C	A	B	C
Passenger Car	+10.8	+16.2	−16.3	11.7	16.5	10.6
Single-Unit Trucks with Hydraulic and Vacuum-Booster Hydraulic Brakes	+14.2	+16.1	−23.3	17.3	15.9	9.7
Single-Unit Trucks and Buses with Air Brakes	− 0.3	− 1.5	− 8.9	12.1	12.7	11.2
Truck-Tractors with Semitrailers	+21.7	+23.1	−14.3	16.8	24.4	15.3

[a] A minus sign denotes the decelerometer indicated a deceleration rate less than the maximum sustained deceleration determined from the time-distance record; a plus sign denotes the decelerometer indicated a greater rate of deceleration.

Decelerometers B and C appear to be unsuitable for inspection-station testing because of the degree of damping; B is damped too little and C too much. The key factor in the reliability of inertia brake-testers is definitely the degree of damping. Action should be taken to establish a standard for the damping in such instruments.

Relative effects of different degrees of damping found in the three decelerometers is clearly demonstrated by comparing maximum decelerations indicated by the decelerometers with maximum sustained decelerations determined from time-distance records. Fig. 11 shows (for passenger cars) variations of maximum decelerations indicated by each of the three decelerometers from the corresponding maximum sustained decelerations determined from time-distance records. Average variations and standard deviations for the four vehicle groups are listed in Table 3.

Results indicate that the decelerometers tested were unsatisfactory for accurately determining maximum sustained decelerations. Except for relatively low deceleration rates observed for single-unit trucks and buses with air-mechanical brakes, the rates indicated by A and B, on the average, can be expected to be from about 10-20% greater than the true rate. Deceleration rates indicated by C were always from about 10-20% less than the true rate. A wide dispersion of percentage variations from average variation existed for each tester.

Practical Limitations of Brake Testers

It was concluded from findings of comparative tests on brake testers that neither portable inertia-type decelerometers nor the drive-on-and-stop brake tester used in inspection stations is very reliable in predicting vehicle stopping distance of any type vehicle. Drive-on-and-stop testers, when gross vehicle weight is known, and adequately damped decelerometers (to a lesser degree), are presently most practical for use in testing passenger cars and very light trucks in inspection stations. Effectiveness of decelerometers in highway testing of any class of vehicle and of either type of instrument for testing large trucks and combinations in an inspection station, is questionable. Use of these brake testers appears to be definitely ineffective at the present time in singling out heavy trucks and combination units with unsafe brakes.

Feasibility of using decelerometers and drive-on-and-stop testers for enforcement purposes must be carefully considered in terms of whether the instrument readings will be accepted in court as evidence of a violation of a brake code. The wide dispersion of percentages of variation between distances indicated by uncalibrated existing testers of all types and those measured by the test wheel is not conducive to the establishment of their reliability in court. However, there is a saving feature in that use of such instruments, except when highly damped, can be shown to give the operator the benefit of any doubt in practically all instances, if the requirement is predicated on vehicle stopping distance or maximum sustained deceleration. It can be shown that where benefit of doubt is not given the operator, the vehicle's brakes are usually in very poor condition.

Existing brake testers can be calibrated to give

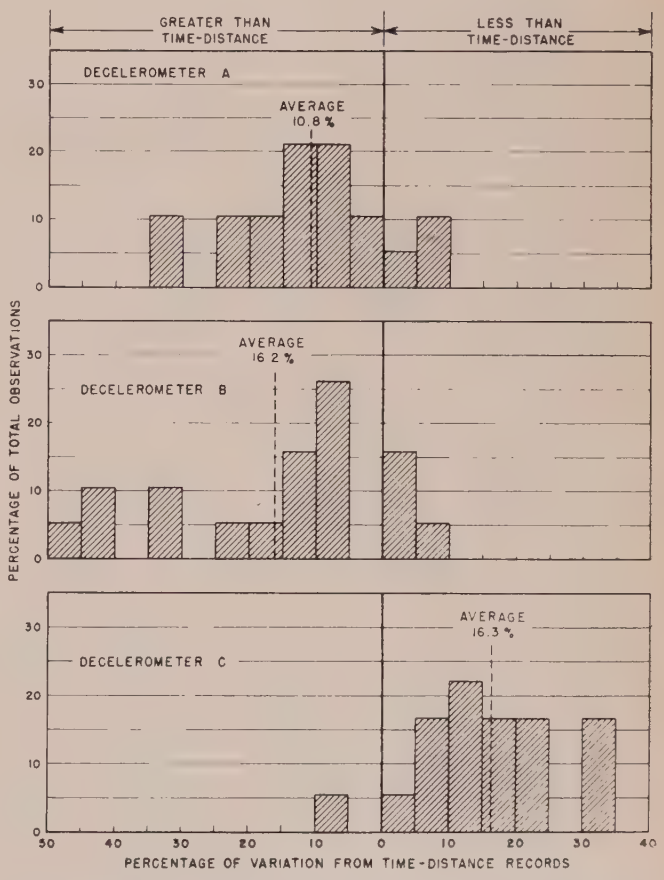

Fig. 11 – Variation of maximum decelerations for passenger cars indicated by decelerometers from maximum sustained decelerations determined from time-distance records

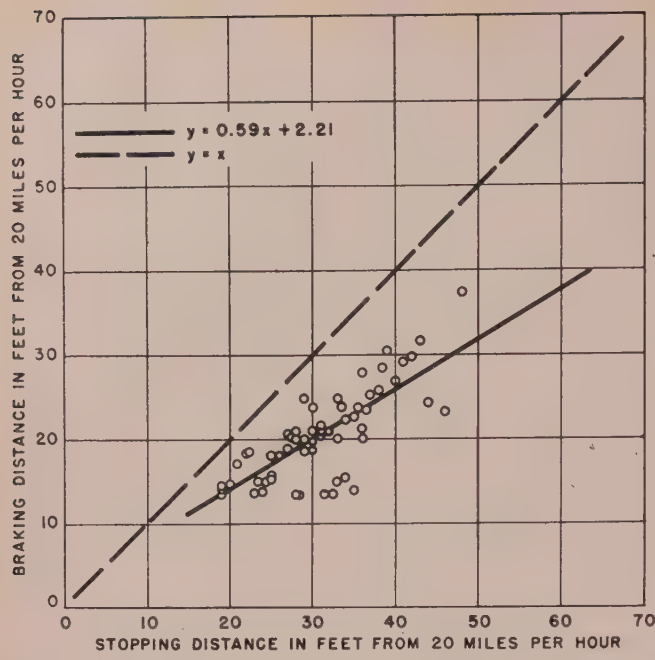

Fig. 12 – Correlation between braking distance indicated by decelerometer A and stopping distance measured by test wheel. Data are for single-unit trucks with hydraulic and vacuum-booster hydraulic brakes

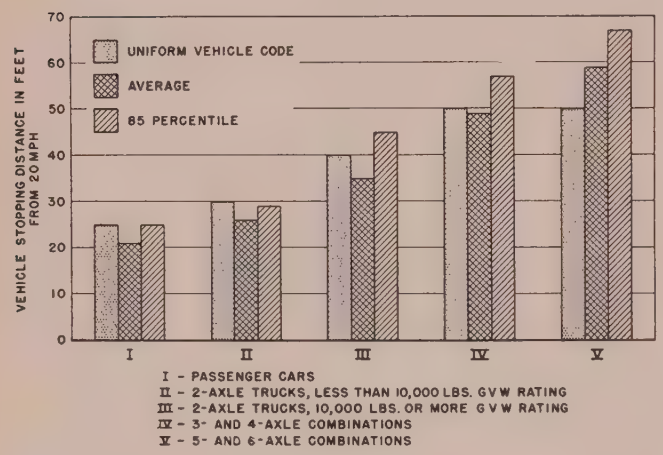

Fig. 13 – Comparison of Uniform Vehicle Code requirement with vehicle-stopping distances for passenger cars and loaded commercial vehicles operating in everyday traffic

a more accurate indication of true stopping ability. However, after an instrument has been calibrated, dispersion of data about the calibration line is significant, and benefit of doubt is no longer so frequently in favor of the vehicle operator.

If calibrated for enforcement purposes, strict adherence to values indicated by the calibration line would tend to fail a few vehicles which could meet the requirement when tested by a test wheel. For example, from Fig. 12, a requirement specifying a stopping distance of 30 ft from 20 mph would be equivalent to a braking distance of 20 ft indicated by decelerometer A when testing single-unit trucks with hydraulic brakes. Fig. 12 shows several points which indicate stopping distances less than 30 ft and braking distances greater than 20 ft. These points represent vehicles which would have been failed by the decelerometer but passed by the test wheel. Conversely, a cluster of points represents vehicles which would be failed by the test wheel but passed by the decelerometer. Those points indicate stopping distances greater than 30 ft and braking distances less than 20 ft.

It would seem unjust to enforce a brake requirement based on calibration which might fail vehicles that would be passed by a test wheel. For this reason calibration of inertia-type brake testers for enforcement purposes is not recommended. It is also impractical because each instrument must be calibrated separately for each vehicle type.

Vehicle-Stopping Distance or Deceleration as Unit of Measure

A requirement based solely on vehicle stopping distance would be ideal from the viewpoint of highway safety. Vehicle stopping distance is the most positive measure of stopping ability so far as the vehicle is concerned, since periods of application, brake-force-buildup, and maximum sustained force or deceleration are all included. There are two serious objections, however, to the use of vehicle stopping distance as the sole criterion: (1) it is not adaptable to inspection-station testing, and (2) it requires an accurate measurement of speed, necessitating use of a test wheel. Use of a test wheel is costly, requires skilled operators, and does not lend itself to mass testing of vehicles on the highway, for considerable time is consumed and occasional difficulty is experienced in attaching it to the vehicle. Since the test wheel is needed to measure speed in stopping-distance tests, it is most advantageous from the standpoint of time saved to equip it to measuring distance. A detonator may be used in measuring stopping distance, but additional time is consumed in attaching it to the vehicle and in taping the distance.

Development of a regulation based only on deceleration would be advantageous in some respects. Deceleration or its equivalent, braking force, can be measured both on the highway and in an inspection station. Since an accurate measurement of speed is not required, delays incidental to attaching a test wheel to the vehicle would be eliminated, making it possible to accelerate the rate of testing vehicles. The advantages, however, are more than offset for some types of vehicles by failure of the available instruments to give a true measure of stopping ability.

In this respect, previous discussion of limitations of existing brake testers indicates that typical decelerometers and inspection-station testers are now most practical for testing passenger cars

and very light single-unit trucks. Since these two types of vehicle comprise the greatest portion of those on the highway, instruments measuring deceleration or braking force should have an important role in the enforcement programs. For the same reason, deceleration and braking force should be an important term in any requirement. However, it is believed that brake performance of the remaining commercial vehicles can be effectively regulated only through enforcement of a vehicle stopping distance requirement.

Recommended Form

In light of the three prerequisites set forth above and the practical limitations of existing brake testers, the Bureau of Public Roads, with the approval of its Advisory Committee, recommended that a requirement should specify deceleration, braking force, and vehicle stopping distance. Values of deceleration and braking force to be specified would be equivalent to each other but would not correspond to any stopping distance, assuming that deceleration or braking force remains constant for the complete stop. Values for deceleration and vehicle stopping distance would be selected independently of each other on the basis of performance of existing vehicles.

A classification of vehicles by type was recommended, since findings of our study showed conclusively that there is a wide range in the vehicle stopping ability of the various types of vehicles now operating on the highway. Although this range may be narrowed, it will remain appreciable in the foreseeable future. For this reason, it appeared that any one requirement for vehicle stopping distance from 20 mph that would not unduly penalize combination units would permit passenger cars and single unit trucks to operate with poor brakes.

Such a requirement would not preclude use of any existing brake tester. However, an enforcement program should be built around the practical limitations of brake testers. All vehicles could be expected to meet either the requirement of deceleration, braking force, or vehicle-stopping distance, but would not necessarily be required to do so in the practical enforcement.

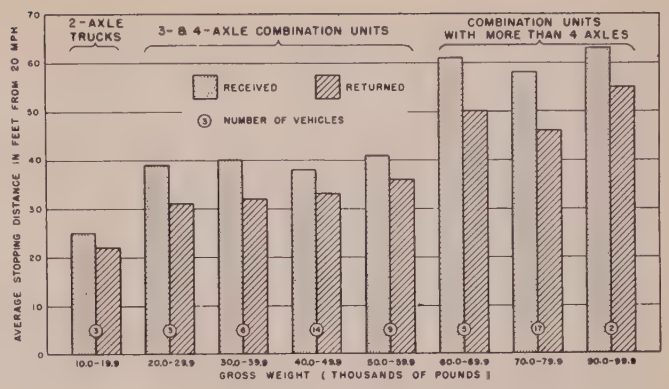

Fig. 14 – Variation of average vehicle stopping distances with gross weight for commercial vehicles selected from service

Adopted Requirement

The requirement adopted for the Uniform Vehicle Code[3] is shown in Table 4. It follows our recommendations to the letter. The basis for the selection of values for the vehicle stopping distance is shown in Fig. 13. Values selected are reasonable, except possibly for group V vehicles which appear to be penalized.

These 5- and 6-axle combination units must be well maintained, and in some cases major repairs will be necessary, in order to meet the requirement. However, the results in Fig. 14 indicate that the 50-ft stop can be met with reasonable maintenance and repair. To lower the requirement for this group would have necessitated splitting the combination units into two classes. Otherwise, a requirement (say 60 ft), for all combination units would have permitted 3- and 4-axle combination units to operate with unsafe brakes.

The requirement for deceleration or equivalent braking force was retained at 14 ft per sec per sec, except for passenger cars. Here, the requirement was raised to 17 ft per sec per sec to be commensurate with stopping capabilities of passenger cars. The 14 ft per sec per sec rate is practical in view of observed performance of commercial vehicles, especially when characteristics of existing brake testers are considered.

Table 4 – Uniform Vehicle Code (Sec. 12-302) – Performance Ability of Brakes

	Stopping Distance, ft	Deceleration, ft per sec per sec	Equivalent Braking Force, Percentage of Vehicle or Combination Weight
Passenger Vehicles, Excluding Buses	25	17	53.0
Single-Unit Vehicles with Manufacturer's Gross Vehicle Weight Rating of Less than 10,000 lb	30	14	43.5
Single-Unit, 2-Axle Vehicles with Manufacturer's Gross Vehicle Weight Rating of 10,000 lb or More	40	14	43.5
All Other Vehicles and Combinations with Manufacturer's Gross Vehicle Weight Rating of 10,000 lb or More	50	14	43.5

Recommended Enforcement Program

Consideration of the following points is necessary for formulation of a satisfactory enforcement procedure:

1. Operation of inspection stations is the only feasible means for brake testing all vehicles licensed in a State or its subdivisions. Road testing with either a test wheel or decelerometer requires

so much time that only a spot-check of either passenger cars or commercial vehicles is practical.

2. Effectiveness of brake testers which measure braking force or deceleration in testing vehicles other than passenger cars or very light trucks, either on the highway or in an inspection station, is very questionable. Spot checking of commercial vehicles on the highway for vehicle stopping distance is therefore highly desirable.

3. Brakes on commercial vehicles, because of their greater annual mileage and greater weight in proportion to engine braking, require more frequent attention, another reason for spot checking those vehicles on the highway.

In view of these considerations, it is believed that the most practical approach is outlined in Table 5.

Table 5 – Recommended Brake Performance Requirement Enforcement Programs in Order of Effectiveness

Programs, in Order of Effectiveness	Method of Inspection[a]			
	Passenger Cars and Very Light Trucks		Other Commercial Vehicles[b]	
	Station Inspection	Highway Spot-check	Station Inspection	Highway Spot-check
Alternate A	B or D	D	B or D	S
Alternate B	B or D	—	B or D	S
Alternate C	B or D	D	B or D	D
Alternate D	—	D	—	S
Alternate E	—	D	—	D

[a] B = Braking-force test. D = Deceleration test. S = Vehicle stopping distance test.
[b] Except buses in the public service.

Recommended Testing Requirement

The manner in which the performance requirement will be enforced is extremely important if confusion and unfairness are to be avoided. Based on results and conclusions of the Bureau of Public Roads' study[1] and experience gained in systematic testing of about 7000 vehicles of all types, the following specific test requirements are recommended:

1. Deceleration shall be measured with an inertia-type portable decelerometer, braking force with a drive-on-and-stop type tester or brake-chassis dynamometer (roller-type tester), and vehicle stopping distance with the gun method or a device that measures within plus or minus..... per cent of the gun method.

2. Road testing shall be conducted on a substantially level (grade not to exceed plus or minus 1%), dry, smooth, hard-surfaced road, free from loose material, and with a coefficient of friction of not less than..... The driver shall stop the vehicle from a speed of approximately 20 mph in the shortest possible distance and in the customary manner, using service brakes only. A means for accurately measuring vehicle speed to within plus or minus .....% shall be used in connection with measuring vehicle-stopping distance.

3. Stops in the inspection station shall be made by a test driver from an initial speed within the range from . . . to . . . mph, and from the highest possible speed in the case of commercial vehicles with power braking systems.

4. To meet the requirement, a minimum of ..... stops and a minimum of ..... minutes between stops shall be permitted.

5. Portable decelerometers shall be located as near the center of gravity of the vehicle as practical.

6. Tests conducted with inertia-type brake testers shall be invalidated if there is a sudden increase in braking force near the end of the stop.

7. Buses while in actual operation in public service, regardless of whether passengers are being carried or not, shall not be required to submit to brake tests.

8. If practical, public service and school buses (not in the service of the public) and property-carrying vehicles shall be tested in a loaded condition. Because of the difficulty in obtaining and loading suitable test weights, the testing of buses in a loaded condition must be limited practically to special tests on a very small sample of any fleet. Testing of loaded property-carrying vehicles in inspection stations may also prove impractical, except in special cases, because of loading difficulties.

9. Property-carrying vehicles loaded in a manner that might result in injury to persons, equipment, or load shall be excused from test until a later date to be designated by the enforcement officer.

Conclusion

The first step toward setting up practical procedures for regulating braking ability has been taken by the proposal of a model stopping-ability regulation for all types of vehicles providing for maximum safety of operation while avoiding undue requirements of operators and manufacturers of motor vehicle equipment. The next step is to get the new brake code adopted by the States and to be sure that standard testing requirements are clearly specified. The final step is to obtain adoption of an effective enforcement program in each State. The means definitely have been provided for reaching our common goal.

It has not been intended to indicate that classification of vehicles or requirement levels is the last word. They will be subject to change at a later date as vehicle stopping distances of commercial vehicles improves.

Cushion Design From Fragility Rating

H. E. Nietsch, Robinson Aviation, Inc.

This paper was presented at the SAE Golden Anniversary Aeronautic Meeting, New York, April 18, 1955.

GENERAL problems which arise in packaging design are treated, including a discussion of cushioning characteristics, fragility rating, and the energy concept of static and dynamic testing of cushion material.

A nomogram is presented which can be of use in designing cushioning installations.

The author suggests the following:

1. For maximum vibration protection, the natural frequency of the cushioned package should be at least one-third of the lowest critical-component natural frequency in the equipment shipped.

2. For necessary protection of equipment such as guided missiles, all-metal mounting systems of nonlinear design combined with a damping ratio of 20% should be employed.

PACKAGING covers a multitude of sins! There have been many general statements made about packaging and nearly everyone, from the layman to the packaging engineer, bemoans the fact that the science is apparently not too well coordinated. SAE Committee S-8 (Aircraft Equipment Shock and Vibration Isolation) hopes to funnel basic information into the proper channels where an accounting can be made of the progress to date and the future work which must be done. This paper is another step in that direction.

The following discussion pertains to the types of resilient materials available to the packaging engineer, characteristic load-deflection shapes, the energy concept for cushion design, and the problems associated with packaging large masses such as shipping containers for guided missiles. No attempt will be made to discuss the individual detailed properties of various cushioning materials. The importance of the correlation between fragility ratings for sensitive pieces of equipment and the various types of cushions available is taken into

consideration throughout the text.

Types of Cushioning Materials

SAE Committee S-8 has made a list of various types of cushioning materials. An expanded version of this list is shown in Table 1. These are the major classifications and do not include the many variations available within each classification. A detailed list of cushioning material suppliers classified by structure and basic material is available.[1] To this major list there have been added shock mounts, since they are playing an ever increasingly important part in solving today's problems of packaging.

There is an overall lack of coordinated knowledge concerning the design characteristics of cushioning materials. Although a particular manufacturer may have a pretty good idea of the technical properties of his product, little attempt has been made to utilize a standard set of parameters by which cushioning materials may be defined. Outstanding exceptions to this statement, however, are reflected in the work of Lassen, Kellicutt, and Sanderson[2]; U. S. Department of Commerce, Containers and Packaging Division, Business and Defense Services Administration; National Safe Transit Committee; and Container Laboratories, Inc.

The problem of correlating design data for the many types of packaging materials is difficult. The following variables lend to this complexity:

1. Material composition.
2. Load-deflection characteristics.
3. Damping.
4. Environmental tolerance.
5. Resistance to shock (dusting).
6. Static versus dynamic performance.
7. Returnability.
8. Acidity and *pH* tests.

Test Criteria

In order to establish a common ground upon which a choice of packaging materials may be made, static and dynamic loading tests of materials of different composition are recommended. The effectiveness of this approach has been pointed out by others.[2, 3] These two tests are necessary to determine the quality of the cushioning.

A measure of the quality of cushioning material may be put in terms of the amount of energy dissipated within the cushion when subjected to loading. Testing is required to determine the force performing work on the cushion when a package is dropped or subjected to shock under rough handling conditions. The static loading test establishes relationships between the force and the amount of cushion deflection or penetration and the work relative to the depth of penetration. The dynamic load-

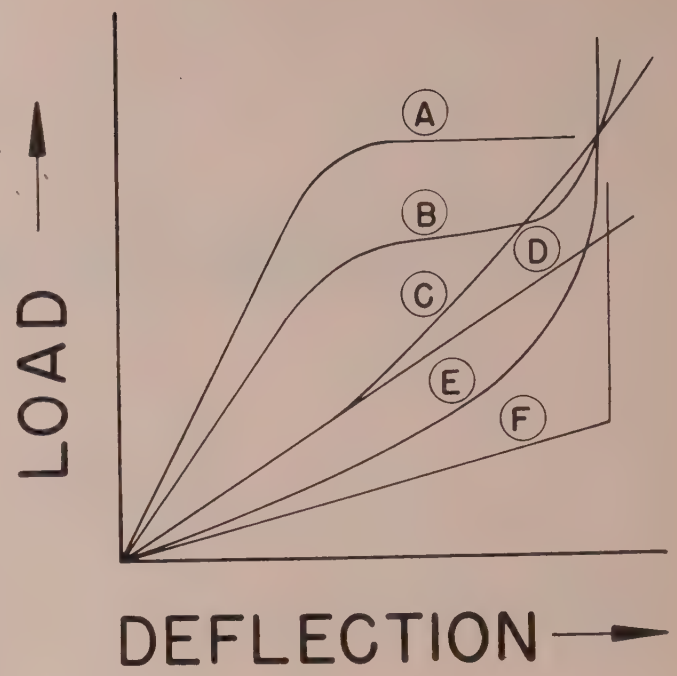

Fig. 1 – Typical load-deflection characteristics of cushioning materials[5]

Curve	Type of Elasticity
A	Hyperbolic tangent
B	Anomalous
C	Cubic
D	Linear
E	Tangent
F	Linear with abrupt snubbing (spring bottomed out)

Table 1 – Types of Cushioning Materials

- Excelsior (Curlex)
- Corrugated fiberboard
- Paper, shredded
- Crepe (paper) wadding
- Molded pulp
- Cotton wadding
- Felt, cellulose
- Felt, hair
- Cellulose fiber and latex
- Animal hair and latex
- Glass fibers and resin
- Latex foam
- Blown sponge
- Molded shredded foam or sponge
- Plastic derivatives
- Shock mounts:
  - Rubber
  - Spring
  - Knitted wire (Met-L-Flex)

[1] See *Industrial Packaging*, Vol. 1, March 15, 1955, pp. 28-33: "Cushioning—In Packing and Packaging," by A. B. Clunan.

[2] See United States Department of Agriculture, Forest Products Laboratory Report R1489 (1945), "Development of Procedure for Determination of Properties of Cushioning Materials and Their Application in Design of Cushions," by L. Lassen, K. Q. Kellicutt, and W. J. Sanderson.

ing test establishes the relationship between energy and depth of penetration. Details of this method of testing are covered in the literature.[2, 3] It is interesting to note further that Muller[4] has applied a theoretical approach to the problem of determining desirable characteristics of cushioning materials. He has also suggested a method of dynamic testing whereby a body is driven into a resilient material and the displacement and force compared to a calculated pulse.

Load-Deflection Shapes

The problem of correlating standardization procedures for cushioning materials is further aggravated by the variety of deflection shapes possible.

Fig. 1 illustrates typical load-deflection characteristics possible.[5] Curve A is indicative of a method employed for maximum energy absorption, where beyond a certain loading, a large deflection takes place. Although this principle is sound, careful consideration should be given to the returnability of the material after deflection. In the case of mechanical shock mounts it is imperative to prevent abrupt snubbing after the extended deflection in order to reduce the dynamic load effects. Curve B tends to correct this problem by additional resistance to loading. Curves C and E are typical nonlinear shapes and cover the deflection characteristics most common to available cushioning materials. Curve D is linear while curve F shows a typical load-deflection curve of a linear spring abruptly bottomed out.

The nonlinear load-deflection characteristics for packaging materials appear to be essential to dissipate the maximum amount of energy within the cushion. The ability of a material to progressively resist loading is the basis for the prevention of large dynamic loads and resulting transient vibration.

Cushioning materials should be noncorrosive for added protection of the packaged article. Adequate laboratory test procedures should be followed to determine the hydrogen ion concentration (*pH*) and acid content of each material.

Cushioning Characteristics and Fragility Rating

The fragility rating established for a piece of equipment is a measure of the sensitivity to transient vibration resulting from dynamic loads due to abrupt snubbing. The infinite number of natural frequencies of a piece of equipment subjected to in-transit or handling loads suddenly come into play in cushioning materials which allow secondary accelerations. The magnitude and persistence of the resulting natural frequencies is a function of the damping not only in the cushion material, but also within the resonating component of the equipment itself. The fragility rating defines the principal component frequencies most likely to result in damage to the equipment.

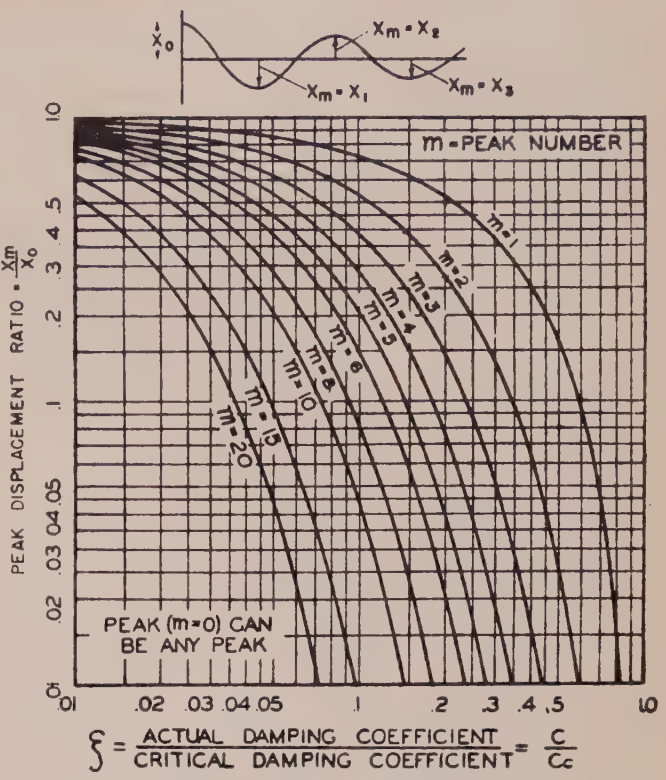

Fig. 2 – Peak-displacement ratios of oscillatory transients as a function of damping ratio for a one-degree-of-freedom system

Damping

Damping within a cushioning material is necessary to prevent amplification of vibratory displacements of the suspended mass due to intermittent periodic disturbances. The amount of damping also has an effect on the maximum acceleration that is attained in the dynamic load tests. Mindlin[5] points out that there is an optimum amount of damping that should not be exceeded. Damping has the effect of changing the slope of the acceleration-time curves, and reduces the natural frequency. Damping is especially effective in reducing the amount of rebound. As an example, with 50% damping, the tendency to rebound is reduced by a factor of 6. For the majority of conditions, however, the optimum amount of damping for the most

[3] See United States Department of Agriculture, Forest Products Laboratory, Report R1627 (1952), "Application of Properties of Cushioning Materials in Design of Cushions," by K. Q. Kellicutt.

[4] "Optimum Properties of Packaging Material," by J. T. Muller. Paper presented at SAE National Aeronautic Meeting, Los Angeles, Oct. 7, 1954.

[5] See *Bell System Technical Journal*, Vol. 24, July-October, 1945, pp. 353-461: "Dynamics of Package Cushioning," by R. D. Mindlin.

effective overall cushioning characteristics is between 25 and 30%.

An excellent method of measuring the amount of damping possessed by a cushioning material is shown in Fig. 2.[6]

Damping efficiency is generally measured in terms of % of critical damping, where C/C_c is the ratio of the actual damping coefficient to the critical damping coefficient. The simplest and most reliable method of measuring the damping ratio is to record the wave form of the cushioning material or the oscillatory transients set up after an initial shock loading. Noting the peak displacement ratios of successive peaks the damping ratio may be determined. Dynamic methods of instrumentation are necessary to obtain these data.

Environmental Tolerance

More and more in the commercial packaging field and certainly in the military, there is an ever-growing demand for materials which have environmental tolerance. Resistance to high and low temperatures, moisture, and dusting are but a few of the points to be considered. In fact, a packaged item is subjected to more methods of transportation than anything else. Besides, the effectiveness of cushioning is always being challenged by the rough treatment between the various methods of transportation. A well-designed package for railroad transportation may be entirely unsuitable for airline shipment in cases where the ambient temperature drops below the design limits of the cushioning material.

Energy Concept

Static and dynamic testing of cushion materials is essential in setting up cushion design criteria. It is possible to derive an energy curve from the static loading curve that can be used in the evaluation of the quality of cushioning material.[2]

The energy curve is derived simply. Under the static load tests of a cushion material, the work done on the test cushion is determined from the product of force and compression. Knowing the magnitude of the load and the corresponding compression, we can plot a stress-compression curve. The area under the stress-compression curve represents the energy expended in performing work on the cushion.

This method of approach has been applied extensively in the work of Kellicutt.[2, 3] To apply these basic principles to cushion design, the following information is necessary: (1) maximum shock that the packaged item can stand without damage (fragility g), (2) weight and size of the item, and (3) maximum shock expected to be encountered. Although the term g-factor has been used as a measure of the maximum shock noted in (1), the liberty has been taken to substitute fragility g as a basic parameter of fragility rating. Again it must

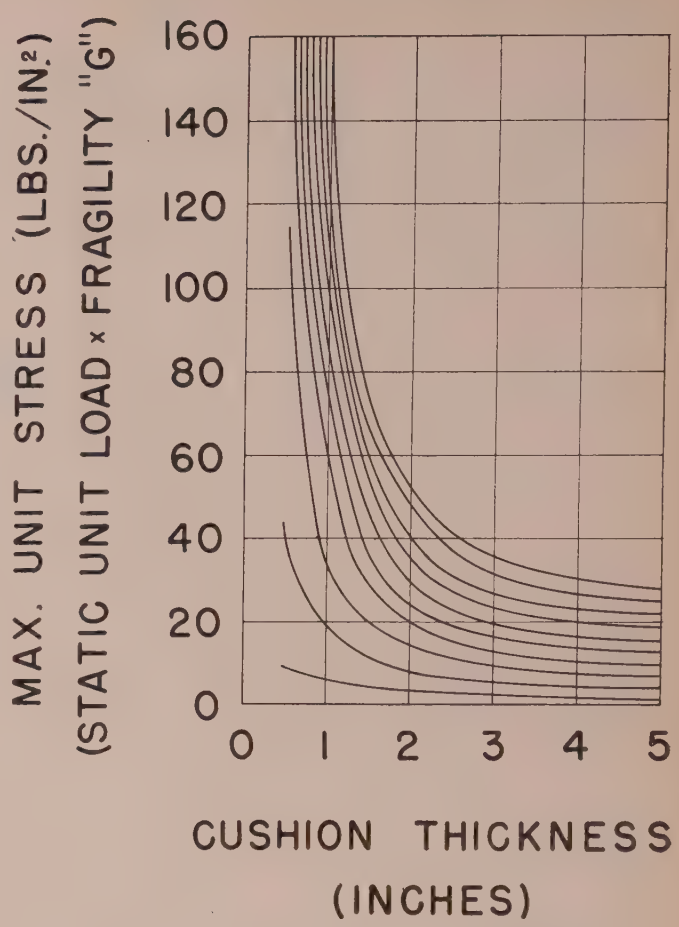

Fig. 3 – Design curves of equal energy levels for determination of thickness of cushioning material when maximum stress is known

be remembered that the fragility g of an item is in reference to the most fragile and sensitive component subjected to shock loading.

From the stress-compression and energy-compression data, so called design curves[3] are plotted for various types of cushioning materials. Fig. 3 is a typical example of a design curve. The product of static unit load and fragility g is plotted against the thickness of required cushioning. Each curve of the family represents a definite magnitude of energy.

The work which has been accomplished in the past, and specifically in reference to this energy concept, now becomes valuable design data for the choice of some cushioning materials. Its value is enhanced by the fragility rating information for products to be packaged. Heretofore it has been necessary to assume a g-factor or fragility g; it

[6] See *Design News*, Vol. 8, March 15, 1953, pp. 61-65; and April 1, pp. 51-53: "Design and Performance Characteristics of All-Metal Shock Mounts," by H. E. Nietsch.

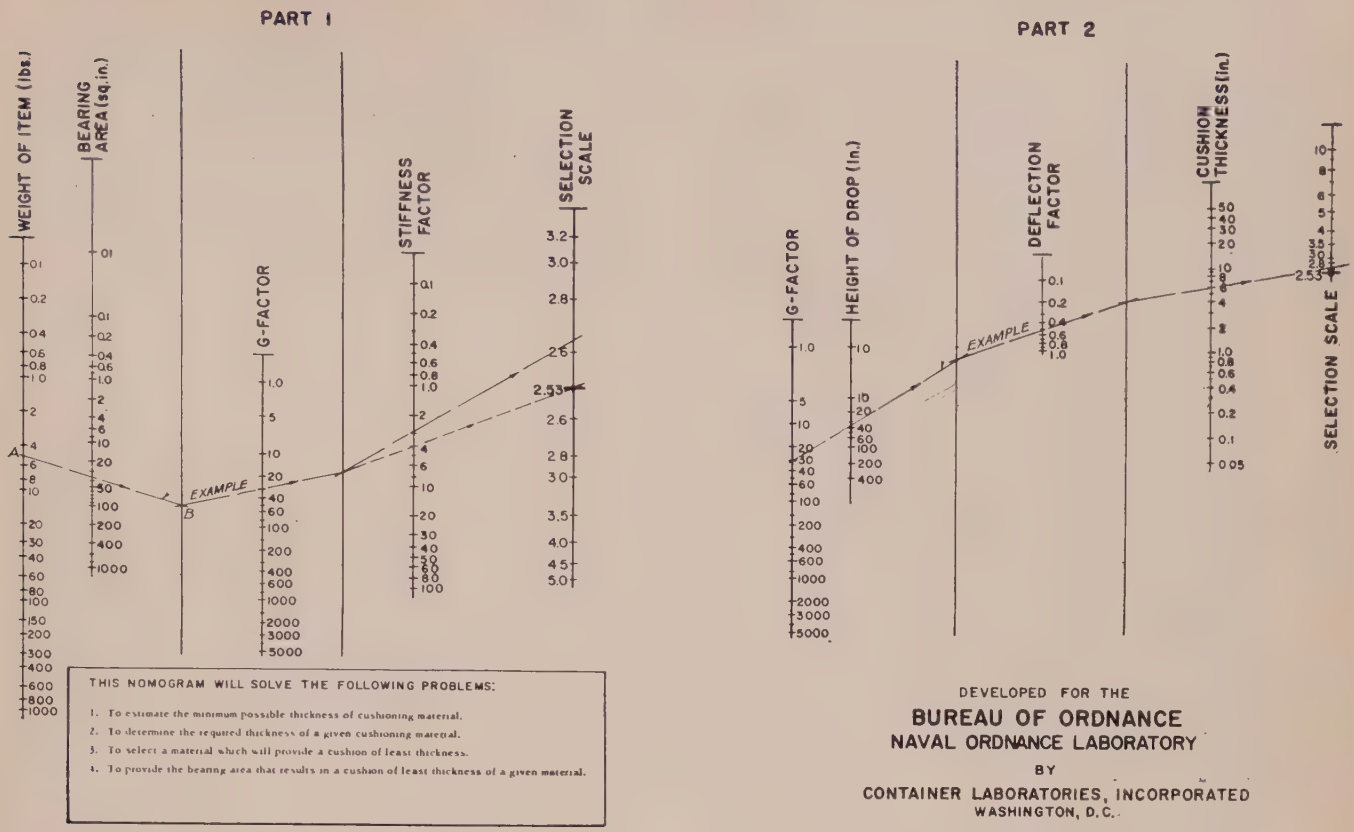

Fig. 4 – Cushioning nomogram

now becomes practical to apply the data from the fragility rating directly.

Cushioning Nomogram

Container Laboratories, Inc. has developed a cushioning nomogram for the Bureau of Ordnance, Naval Ordnance Laboratory, shown in Figs. 4 and 5. This nomogram will solve the following problems:

1. Estimate the minimum possible thickness of cushioning material.

2. Determine the required thickness of a given cushioning material.

3. Select a material which will provide a cushion of least thickness.

4. Provide the bearing area that results in a cushion of least thickness for a given material.

Natural Frequency Considerations

The problem of identifying and measuring the critical-component natural frequencies of an equipment to be packaged is quite difficult in some cases. These components may be subjected to multidirectional shock loads, requiring that their sensitivity to resonance be studied in all planes of loading. For maximum protection the cushioned-package natural frequencies must be at least one-third of the lowest critical-component natural frequency in the equipment being shipped.

It is generally advisable to design a packaged system such that equivalent stiffnesses are present in all planes. For small packages the formed cushions of rubberized curled hair represent an excellent means of forming a package of equivalent multidirectional stiffness. Such applications have also been successfully applied to paper, felt, cellulose, glass fiber, latex, plastic, and sponge-rubber cushioning products.

Design of Cushioning Material

The design of cushioning material based upon the fragility rating is subject to important limitations such as physical size and weight of the pack-

GENERAL

This nomogram is an alignment chart which is read by connecting known points on adjacent vertical scales with a straight line and extending this line until it intersects the adjacent vertical line. (See line A-B on example.) Another straight line is then drawn from this intersection through a known point on the next vertical scale and extended to the next vertical line. This procedure is continued across the chart in either or both directions until a line is drawn to intersect the vertical scale whose value is to be found. (See example on nomogram.)

To use this nomogram it is necessary to know the stiffness factor and deflection factor of the cushioning materials being considered. These factors are derived from the load-deflection curve for the material in accordance with a prescribed procedure and must be furnished by the manufacturer or a testing laboratory.

INSTRUCTIONS

This nomogram can be used to quickly solve several types of cushioning problems, such as the following:

1. At the outset of a package design problem, it is often desirable to estimate the minimum possible thickness of cushioning material if the proper combination of bearing area and stiffness of material could be attained. This preliminary operation will show whether a pad-type cushion will provide a practical solution and will set a minimum thickness at which to aim.

PROCEDURE: Enter Part 2 with the G-factor and height of drop. Use the largest deflection factor of the available materials. Use the number 2.53 on the Selection Scale. Read the cushion thickness. (This is a preliminary operation and neither the material selected nor the thickness read should be considered final. Read the remaining instructions.)

2. One of the most common cushioning problems is to determine the required thickness of a given cushioning material, when the bearing area is fixed.

PROCEDURE: Enter Part 1 with the weight of the item, its bearing area, its G-factor, and the stiffness factor of the material. Read the number on the Selection Scale, and transfer this number to the Selection Scale in Part 2. Enter Part 2 with the G-factor, height of drop, and the deflection factor of the material. Read the cushion thickness.

3. Another common cushioning problem is to select a material which will provide a cushion of minimum thickness when the bearing area is fixed.

PROCEDURE: Enter Part 1 with the weight of the item, its bearing area, its G-factor, and the number 2.53 on the Selection Scale. Read the stiffness factor and select a material whose stiffness factor is close to this value. (Then determine the required thickness by the procedure described in Instruction 2.)

4. It is sometimes desirable, where practicable, to modify the package design to provide the bearing area that results in a cushion of minimum thickness of a given material.

PROCEDURE: Enter Part 1 with the weight of the item, its G-factor, the number 2.53 on the Stiffness Scale, and the stiffness factor of the material. Read the bearing area. (Then determine the required thickness by the procedure described in Instruction 2.)

Fig. 5 – Instructions for use of cushioning nomogram shown in Fig. 4

age. Added to this is the unknown material-handling service conditions. These service conditions must be defined by rational design parameters such as height of drop for different weights of packages, standardized testing methods and procedures, environmental tolerance, and length of time that the packaged system must operate satisfactorily. Although the development of fragility ratings for various products to be packaged is a major step in the right direction, its "development sheets" should be extended to include other basic methods of packaging besides the use of bulk or dunnage materials.

In this respect there is an economic limitation to the use of bulk cushioning materials when the weight of the package is sufficiently great such that the amount of cushioning and the size of package is against the economics of good packaging design. This may apply to some packages weighing as little as 50 lb.

Shock-Mounting Systems

Where new methods of packaging design must be employed, consideration must be given to the use of shock-mounting systems. It is very interesting to note that as packaging problems have increased in their importance, more and more technical men in the field of vibration and shock control have exchanged their views in an attempt to solve these problems.

While the use of cushioning materials has solved many problems in the package design for light weight items, their adaptability to items such as guided missile containers, electronic control systems, aircraft jet engines, business machines, com-

puters, and transit cases is quite limited.

The packaging should be designed to withstand the imposed shock and vibration loadings in the most economical manner. As the packaged weight increases, the loads resulting from transportation and handling must be controlled by an efficient shock-mounting design.

Design Considerations

The following design considerations are important:

1. Type of load-deflection curve for the resilient system.
2. Performance and damping.
3. Environmental tolerance.
4. Load tolerance.
5. Resistance to aging (re-usable containers).

A nonlinear type of deflection curve, recommended for bulk-cushioning, is also a requisite for good design in the case of shock-mounting systems.

Mounting systems having a wide load tolerance combined with overload capacity are most recommended. In this respect, the nonlinear load-deflection characteristic provides uniform performance throughout a wide load range without excessive deflection. In addition, such systems provide good overload capacity and reasonable performance characteristics at loads as great as three to four times the static load rating.

The curve of vibration transmissibility versus frequency ratio is a measure of the performance of any mounting system. Transmissibility is a measure of the force transmitted to the packaged equipment and is defined as the ratio of transmitted force to impressed force. Frequency ratio is the ratio of impressed frequency to the undamped natural frequency of the mounting system.

Damping efficiency is generally measured in terms of percent of critical damping where C/C_c is the ratio of the actual damping coefficient to the critical damping coefficient. A spring-supported mass system is critically damped when it does not oscillate after having been displaced from its equilibrium position. Here again, the simplest method for measuring the damping ratio is to record the wave form of the mounted system during oscillatory transients as noted in Fig. 2.

Types and Advantages

Mounting systems possessing at least 20% of critical damping at resonance are desirable. This value should not be affected by environmental changes such as pressure, temperature, or humid-

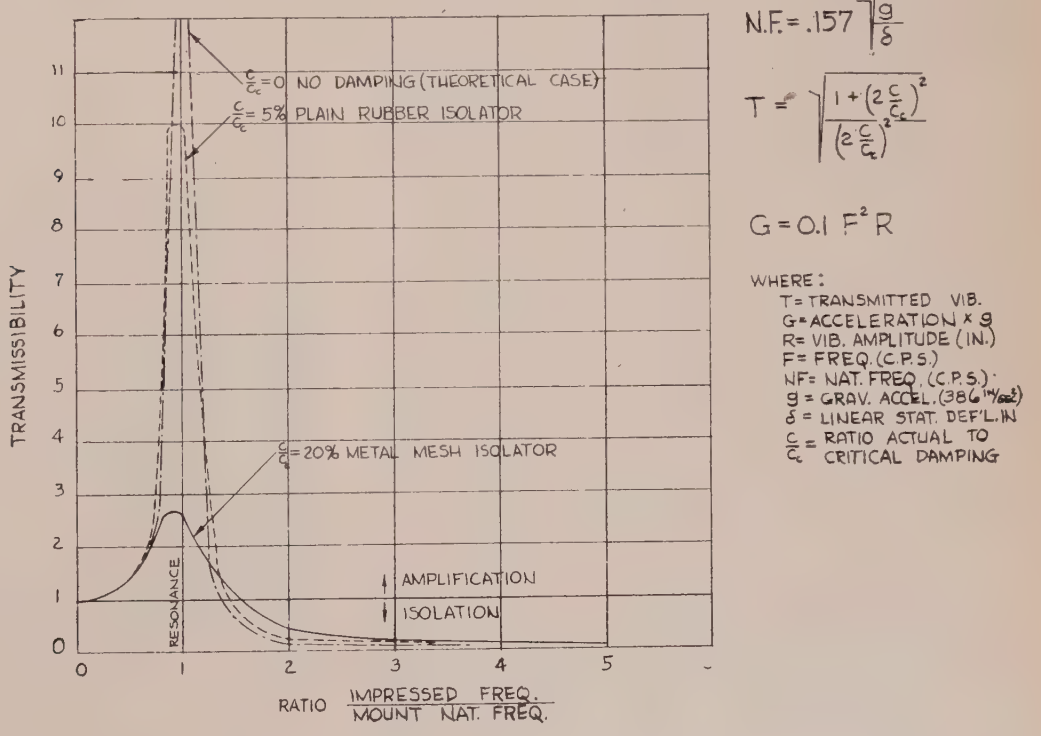

Fig. 6 – Comparative damping efficiencies of metal-mesh and plain rubber isolators

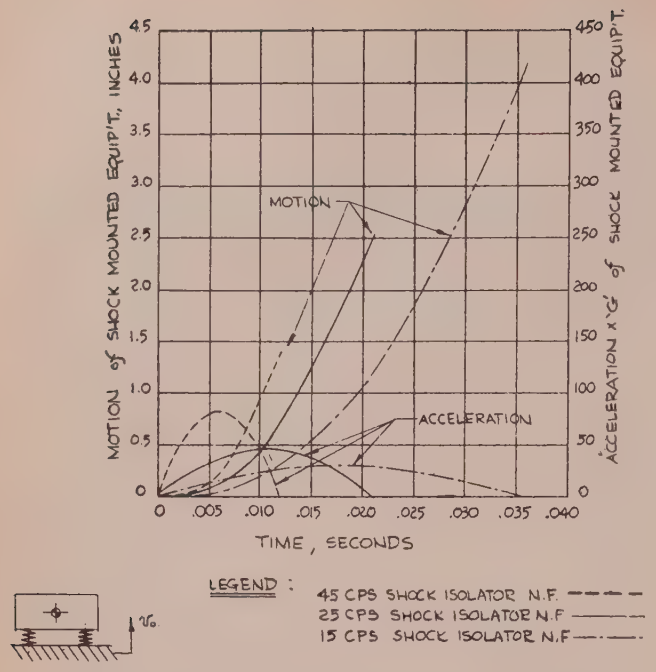

Fig. 7 – Comparison between mount natural frequencies, transmitted accelerations, and motion of isolated equipments for instantaneously applied velocity (V_o) of 10 fps (it is assumed that the mounts do not bottom out abruptly)

ity. In the case of vibration attenuation, to reduce the transmissibility to a minimum, the damping ratio should decrease in value for a frequency ratio greater than $\sqrt{2}$. Test results indicate that such behavior is possible with the knitted-wire load-carrying resilient element because of its nonlinear damping characteristics. The amount of damping varies with deflection, providing high damping at resonance and low damping at higher impressed frequencies. Fig. 6 points out the advantages of an all-metal system compared to mountings employing rubber or synthetic elements as the resilient members.

Utilizing springs alone results in excessive deflection at resonance and consequent abrupt snubbing. Such snubbing may amplify the initial shock load many times if no auxiliary means of damping is provided.

Fig. 7 shows a comparison between linear shock mounts of three stiffnesses, all subjected to 10 fps velocity applied instantaneously. The softest mount is best, but results in an undue deflection. The balance between mount frequency, allowable deflection, and transmitted acceleration forces is established by space limitations. Nonlinear mounts require less deflection than linear mounts for similarly reduced acceleration peaks.

Other methods of effective spring suspensions, such as torsion bars, have been applied in some applications. Here again, it is necessary to provide for adequate auxiliary damping. A torsion bar system may lend itself to specific applications where the item to be supported is long and heavy and inadequate space is provided for the use of supporting resilient elements.

There are many different types of mounting designs utilizing shock mounts. Since the packaging of modern equipment presents problems requiring mounting systems of specialized design, the importance of engineering the system to the configuration, weight and inertia characteristics of the equipment cannot be overemphasized. Unless an engineered mounting is used for such equipment it is unlikely that desired performance specifications can be met.

The designer should bear in mind that there are at least three basic types of mounting systems available. On the basis of certain ranges of geometrical ratios of equipment width and length, resilient mounting centers, and inertia characteristics, a base mounting combined with adequate stabilizing resilient elements may be satisfactory. If the parameters fall outside the first ranges, an effective center-of-gravity-type mounting system may be the answer to the problem. In this case, the mountings are located at the top and bottom of the equipment such that the diagonal lines of the top and bottom shock mounts intersect at the center of gravity of the equipment. Another system of this type utilizes designed-in mounting elements located at each end of the equipment and set at an angle to produce an effective center of gravity support. An example of this basic design is shown in Fig. 8.

Another excellent example, shown in Fig. 9, illustrates the method of multidirectional shock protection by providing four specially designed all-metal Robinson mounting beams located within

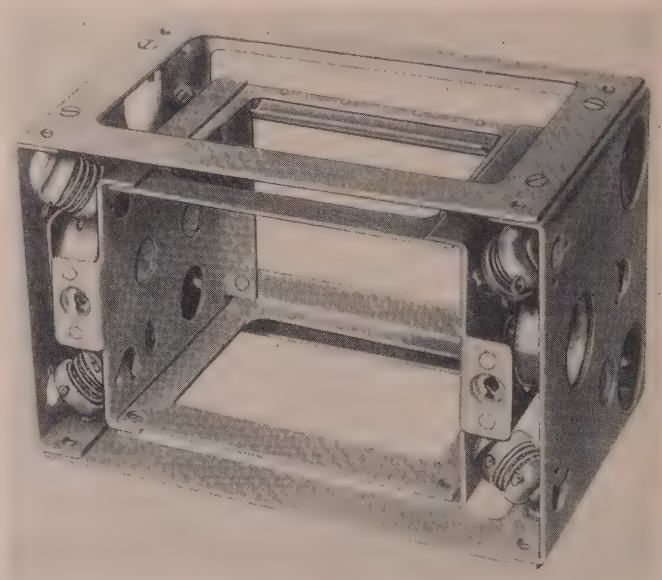

Fig. 8 – Illustration of effective center-of-gravity packaging mounting system

and around a cylindrical container. An effective center-of-gravity suspension is afforded after the equipment has been installed in place. Each beam is precompressed the correct amount for this equipment installation in order to provide for the number of degrees of freedom. Stiffnesses in all planes may be varied to suit the packaging requirements. For long pieces of equipment, the beam arrangement provides an excellent method of distributing the suspended load along the beams where convenient structural attachments may be made to the equipment. Being all-metal in design and employing resilient load-carrying cushions of knitted wire, this type mounting system lends itself particularly well to re-usable shipping container applications.

A true center-of-gravity-type mounting system may be required in which the resilient mountings not only lie in the plane of the center of gravity, but are located at distances from the center of gravity equivalent to the radii of gyration about the principal axes.

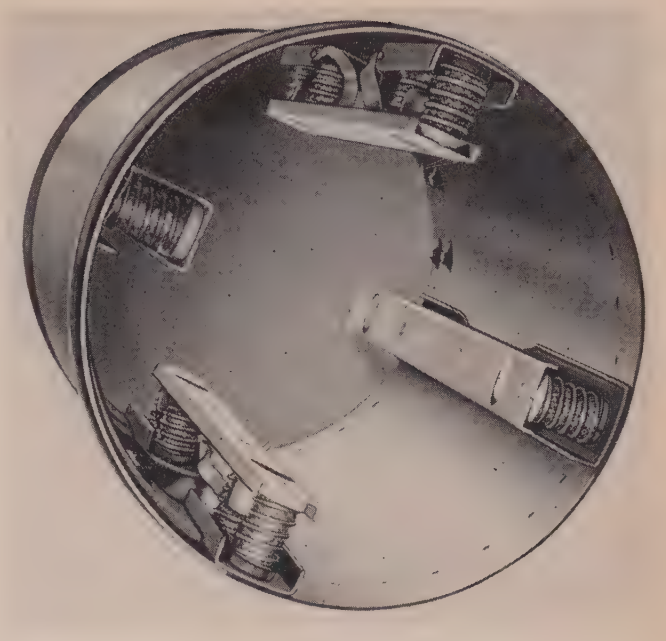

Fig. 9 – Illustration of multidirectional Robinson shock-mounting system

Package Within a Package

In many instances, it has been found that great care has been taken to design a shock-mounting system for a piece of equipment with little or no regard to items which might already be mounted within the equipment. Where the shock-mounting system has been carefully designed to protect a semirigid equipment mass, severe damage can occur to items within the equipment which are individually mounted for vibration protection only. In such cases, it has been found necessary to block out the vibration-mounting systems during transit to assure that no low-frequency resonant effects are present.

The same thinking applies to items within the equipment which, although not vibration-mounted, are attached to weak structural members whose natural frequencies are sufficiently low to result in similar resonant damage effects.

It is necessary, therefore, to look thoroughly at the complete picture of the many stiffnesses and masses which are being packaged before going ahead with a design.

Conclusions

The following conclusions can be drawn:

1. Coordination of technical information relating to packaging design is essential in ascertaining the type of packaging and the method of approach to be used.

2. The design characteristics of cushioning materials should be itemized with respect to a common set of parameters defining their characteristics.

3. Static and dynamic tests must be considered in evaluating the performance of cushioning materials.

4. New standards of environmental tolerance are necessary to establish the design requirements for modern and advanced packaging.

5. The energy concept for determining the characteristics and design application of cushioning materials is a good method to standardize on. Further study is required relative to the inclusion of the pulse-time parameter into the analysis and testing of cushion characteristics.

6. The fragility rating established for equipment to be packaged is the necessary design parameter required for making valuable the information accumulated to date on various types of cushioning materials.

7. In order to provide maximum vibration protection, the cushioned-package natural frequencies should be at least one-third of the lowest critical-component natural frequency in the equipment being shipped.

8. The use of shock-mounting systems becomes essential when the economic, performance, and environmental limitations of bulk-cushioning materials are exceeded.

9. To meet the design performance characteristics and provide for the necessary protection of the latest type of equipment mounted in guided missile containers, transit cases, and electronic system pods, an all-metal mounting system of nonlinear design combined with a damping ratio of 20% is recommended.

Evaluation of Reaction Kinetics

The M-Combustion

FROM the beginning of high-speed diesel development, mixture formation has been considered the key problem. The difficulty of achieving an effective mixture is appreciated by comparing the time available for mixing in a diesel and a carburetor engine. A diesel engine running at the same speed as a carburetor engine has only 1/6 of the time to produce its mixture of fuel and air. It is very difficult to measure the process of mixture formation accurately and thus obtain a standard for its quality. Diesel engineers have, therefore, been inclined to blame deficient mixture for all difficulties in diesel combustion such as steep pressure rise, poor air utilization, noise, and smoke. All the while they neglected another no less important aspect: the chemistry of diesel combustion.

Enormous improvements in the gasoline engine have been made possible only because we succeeded in getting sufficient insight into the nature of its combustion knock. This has enabled chemists to work out means to counteract the performance limitations it produces by changing the molecular structure of the fuel. Diesel fuel, on the other hand, is the same today as it was at the time of Diesel, and apart from some standardization of physical properties such as ignition quality, no attempt has been made to adapt it in any way to the requirements of diesel combustion. However, heat liberation in a diesel engine, and consequently, its performance, depend essentially on the combustion process; it is, therefore, almost more important to provide conditions which are favorable to the process itself than to ensure a thorough mixture. For many years, diesel engineers dogmatically held that the ideal is an instantaneous mixture of liquid-fuel spray and compressed air, and a large variety of designs have been evolved to achieve this end. In light of recent experience, this concept of an ideal air-fuel mixture can be refuted as fundamentally wrong because it ignores the reaction kinetics in the combustion of diesel fuels.

A large number of experiments have been necessary to arrive at this conclusion. One of the decisive

Eliminates Diesel Knock—

System of MAN

J. S. Meurer, Maschinenfabrik Augsburg Nürnberg (MAN)

This paper was presented at the SAE Golden Anniversary Summer Meeting, Atlantic City, June 14, 1955.

MIXTURE formation and combustion impose contradictory demands on the high-speed diesel engine. A study of reaction kinetics reveals rules for eliminating the resulting drawbacks, combustion noise, and exhaust smoke.

These rules were applied in developing the M-combustion system of MAN, in which a fuel film is sprayed on the combustion-chamber wall and drawn off by a high-speed air swirl. Deposition of fuel on the wall at the proper time reduces exhaust smoke and insures smooth operation and low sfc over a wide speed range.

Ready cold-starting is obtained even with high-octane gasolines which the M-engine is capable of burning without operating roughly. The multi-fuel characteristic of the M-system covers petroleum distillates with end points between 100 and 750 F. Indicator diagrams show a smooth pressure rise and absence of combustion knock.

experiments was the following: Direct-injection systems generally rely on the combination of two effects to create the air-fuel mixture, namely:

1. Atomization and distribution of fuel by the nozzle.

2. Motion of air in the combustion chamber.

The various systems differ in the degree to which they make use of these two effects. The atomization and dispersion qualities of a spray can be measured quantitatively with a more or less complicated test setup.[1, 2] This becomes impossible when air motion is introduced.

In order to find to what extent the performance characteristics of a diesel engine can be improved by better mixture formation, we selected an engine in which the mixture was produced essentially by the spray pattern without the help

[1] See Berichtsheft der 74 VDI-Hauptversammlung, Darmstadt 1936, Fachvorträge, pp. 242-249: "Neuere Mittel zur Untersuchung der Vorgänge im Motor," by J. S. Meurer.

[2] See *Automobiltechnische Zeitschrift*, Vol. 43, April, 1940, pp. 185-190: "Das neue MAN-Verfahren für schnellaufende Dieselmotoren," by J. S. Meurer.

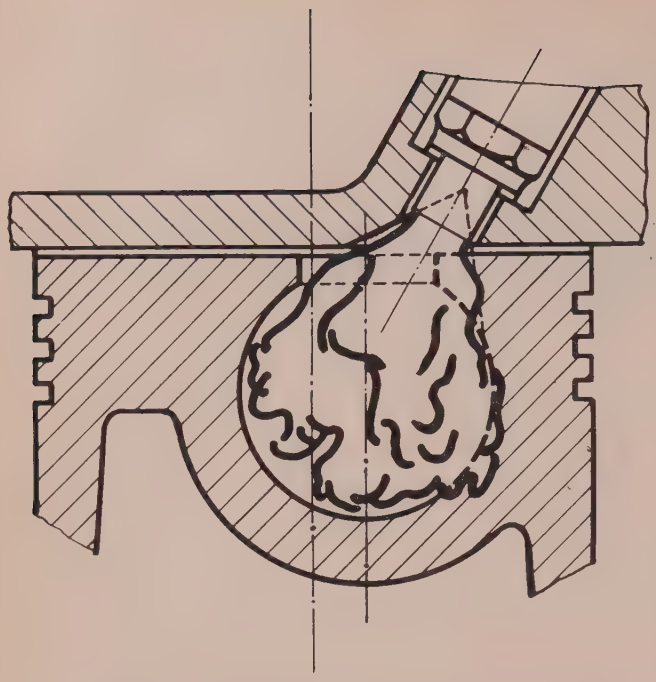

Fig. 1 – Former MAN spherical combustion chamber with air distribution of injected fuel

of any appreciable air movement. The combustion chamber was spherical as in previous MAN engines (Fig. 1). We developed a nozzle for this engine which would distribute the fuel in conformity with the air distribution in the combustion chamber, so that at the end of injection, every fuel particle should find in its immediate vicinity the quantity of air required for complete combustion. In this manner, we attempted to reduce to a minimum the diffusion distances of the vapor developed in the process. Since this kind of distribution could be achieved before ignition occurred, it would not be disturbed by any turbulence arising in the chamber due to localized ignition. Furthermore, the nozzle was designed to atomize the fuel as fine as possible.

High-speed photographs of the spray pattern and measurements of the fuel distribution in the spray by means of small collecting tubes provided numerical evidence that the nozzle produced the desired distribution. Development of the spray under atmospheric pressure, shown in the upper series of photographs in Fig. 2, indicates that the natural frequency of the needle valve was high enough to enable it to follow the fluctuations of the injection pressure without any appreciable delay and so avoid periods of insufficient atomization. For small injection quantities, under certain circumstances, the needle closes repeatedly during a single injection period. At an air density equivalent to that in the engine, the velocity of the spray was considerably lower as a result of fine atomization and absence of a spray core, but the hollow cone quickly filled up with well-atomized fuel. In the fourth photograph of the lower series it can be seen clearly that, as desired, the spray was geometrically well-adapted to the shape of the combustion chamber; furthermore, it could be proved that fuel distribution in the spray matched the distribution of air in the combustion chamber. The results of the nozzle development, which ensured a nearly ideal micro- and macromixture within the period of ignition lag at least up to 1200 rpm, were most satisfactory. However, tests in the engine were disappointing. The characteristic diesel-combustion knock was extremely loud, which was understandable, but contrary to all expectations the air utilization, in spite of good fuel distribution, was very poor and resulted in heavy exhaust smoke over the entire load and speed range. This result confirmed the paradoxical conclusion that an "ideal" mixture formation is a handicap to combustion, that is, during ignition lag, diesel fuel somehow cannot stand being mixed with air at all. Such a conclusion might have been inferred from other tests of a similar nature if numerical evidence had been available.

This conclusion made it necessary to look to reaction kinetics for the explanation of a phenomenon that obviously fetters mixture formation. Thus, attempts to produce a homogeneous mixture of fuel and air before ignition occurs, as in a gasoline engine, had only aggravated some very undesirable features of diesel combustion.

A similar handicap exists for other systems of mixture formation where air motion is introduced in the combustion chamber to mix air and fuel in a timed sequence to control heat liberation by progressive formation of air-fuel mixture during combustion. If, to improve mixture formation, either the air velocity or spray velocity or both were increased, combustion noise became louder. If the fuel rate at the beginning of injection was reduced, the engine ran smoother, but there was an increase in exhaust smoke. In this maze of effects and countereffects, diesel engineers have searched for the best way out. The best solution to be found was only a compromise between smooth operation, fuel consumption, and exhaust smoke – which again became questionable with every change in operating conditions, such as turning to a fuel of different ignition quality. An intensification or acceleration of mixture formation in most cases resulted only in a deterioration in performance. It became obvious that the defects of diesel combustion did not stem solely from the limitations on mixture formation, but there had to be some specific fuel reactions which hampered combustion.

Combustion Seen in Light of Reaction Kinetics

Although the phenomena of auto-ignition in the diesel engine and combustion knock in the gasoline engine are closely related, still there are significant differences with respect to sequence of events, tem-

peratures, and state of the charge, causing considerable variations in the chain of reactions.

In neither type of engine do we find that direct oxidation of the original fuel molecule into its final products could cause self-ignition. Oxidation takes place through intermediate products whose reaction is extremely rapid. After 64% of the charge has been burned in an otto-cycle engine, the temperature of the unburned gas is about 1250 F; that in a diesel engine is about 1100 F at the beginning of injection and rises very fast when reaction starts. Due to the heterogeneous mixture, local temperatures are much higher than the average thermodynamic temperatures. Local flame temperatures reach a constant maximum value of 3800 F[3] which is largely independent of the air-fuel ratio. This observation indicates, first, that the reaction in the diesel engine takes place with constituents that are still in the liquid or solid state (which particles form radiation centers), and, second, that the influence of local temperatures is still greater than would be obtained with homogeneous gas-phase reactions.

It is known that temperature exerts a predominant influence on the speed of chemical reactions. This is shown by the Arrhenius equation, which admittedly is exact only for a homogeneous gas-phase reaction of perfect gases.[4] The mechanism underlying that equation is explained by molecular motion dependent on temperature and the resulting collisions of molecules. If collisions of sufficient energy occur between fuel and oxygen molecules, then an exothermic reaction starts; if no oxygen is available changes will occur in the fuel molecule which manifest themselves as decomposition of the C-C and C-H bonds, especially the latter.

While the dependence of the latter process on temperature cannot be measured since there is no measurable variable as in an exothermic reaction, observations made in the engine suggest that a similar speed increase takes place as in the oxidizing reaction. In addition, it seems that such phenomena may also occur in the liquid phase, especially if evaporation is delayed, which, considering the finite velocity of molecular motions, is likely to happen in the high-speed engine.

In the gas phase and in the presence of oxygen, the path of disintegration is via peroxide into radicals, and consequently, corresponds to the knock reaction in a gasoline engine.[5, 6]

In the diesel engine, however, this process characterizes only the first step, for which the necessary conditions of oxygen concentration and fuel evaporation are prepared during ignition lag. The process cannot continue for it is impossible to feed enough oxygen for the rapidly-increasing reactivity caused by the temperature rise. The activating heat added by the pre-reaction now causes decomposition of the C-H and C-C bonds in the molecule, which clearly shows up in spectrographs in which C-C bands are seen developing immediately after ignition has started.[5, 6] To the degree that oxygen is supplied through mixture formation, reaction of the cracked products takes place, but the rising temperature soon widens the discrepancy between cracking rate and oxygen supply so that eventually only pure carbon remains. As the diesel exhaust smoke shows, burning this carbon early enough presents a problem which is likely to be solved only with the aid of the catalytic influence of water vapor produced during combustion according to the equation $C+H_2O \rightarrow CO+H_2$, and subsequent reoxidation.

This catalytic influence can be fully effective only if H_2O is formed close to the molecule, namely, if the H_2 and C reactions in the molecular compound commence at least simultaneously – the H_2 reaction always proceeds at a faster rate – and before disintegration to pure carbon has taken place. The only way to achieve this without starting the temperature-propelled avalanche of thermal disintegration is by means of pre-oxidation that proceeds sufficiently slow to enable the reactive surface of the molecule to be suitably transformed.

These phenomena are well exemplified in the gasoline engine, where diffusion time is enough to produce an almost molecular mixture and an exhaust practically free from smoke. But even here one can produce smoke without changing the air-fuel ratio or mixture formation, which proves that at high temperatures, the H_2O diffusion rate cannot keep pace with the rate of disintegration, even

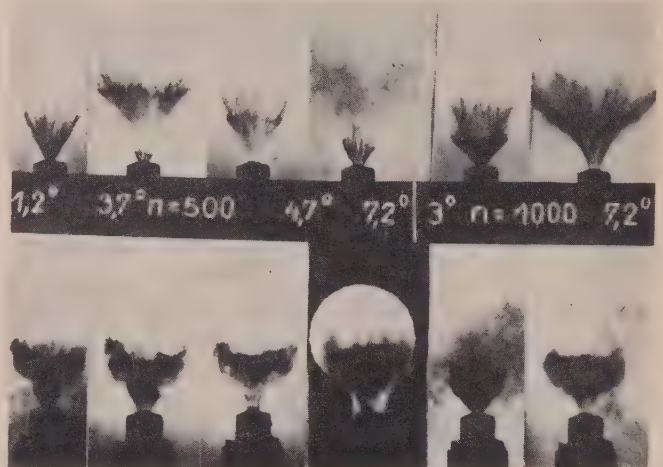

Fig. 2 – Fuel-spray patterns from nozzles producing best air distribution.
Numbers indicate injection timing in deg.
Upper row: Injection into atmosphere
Lower row: Injecton into compressed air with same density as in running engine

[3] See Vorbericht zur öffentlichen Sitzung der Deutsch en Akademie der Luftfahrtforschung, May, 1939, p. 17: "Fortschritte in der Erkenntnis der Dieselmotorischen Verbrennung," by K. Neumann.

[4] See Zeitschrift für physikalische Chemie, Abteilung A, Vol. 4, July, 1889, pp. 226-248: "Uber die Reaktionsgesgeschwindigkeit bei der Inversion des Rohrzuckers bei Säuren," by S. Arrhenius.

[5] See SAE Transactions, Vol. 63, 1955, pp. 253-264: "Some Concepts of Knock and Antiknock Action," by B. M. Sturgis.

[6] See SAE *Quarterly* Transactions, Vol. 3, July, 1949, pp. 490-515: "Combustion of Diesel Fuel," by M. A. Elliott.

over minimum distances. Thus, if the compression ratio of a gasoline engine burning paraffin-base fuels is increased so that knocking involves an ever-greater fraction of the charge, smoke will appear in the exhaust. In that case, the temperature and disintegation rate of unburned charge reach the point where the catalytic effect of H_2O begins to lag and fails to have any effect on the molecular changes.

Regarding the influence of temperature on the physical mixing process, we find there is very little acceleration due to temperature.[7, 8] Mechanical distribution by the nozzle and air motion is influenced by the temperature only as far as it affects air density; in the engine, however, temperature and pressure variations go together, so that no conditions accelerating distribution can arise. With evaporation this is different.

In short, we find ourselves confronted with the fact that the higher the temperature in the diesel engine, the less chance we have to produce a perfect mixture of air and vapor formed from the liquid particle. The fuel molecule disintegrates as described above, while the oxygen, being supplied at a relatively slow rate compared with molecular disintegration, is used up in a chain of auto-ignitions of activated fractions before a homogeneous mixture can form, leaving a carbon skeleton very difficult to oxidize in the time available. Certainly, the enormous acceleration which temperature imparts to all chemical processes insures self-ignition at the right time, but what helped to bring about ignition is very undesirable in the subsequent phases of reaction. From the view-point of reaction kinetics, the irresistible avalanche of disintegration deteriorates the fuel – namely, it places the most sluggish reaction at the end of combustion. This could be avoided if means were found to adapt the physical mixing process to the high rate of chemical reactions, even though not much would be gained thereby because of the resulting steep pressure rise which, being a source of noise, is to be avoided. However, one might try to achieve it in delaying the initial reaction by cutting down the oxygen supply, which would produce some improvement in this particular respect at the cost of more exhaust smoke. This is so because at the high local temperatures, the avalanche set off by self-ignition continues irresistibly until the fuel has broken down to pure carbon. This vicious circle explains the limitations of mixture formation mentioned earlier. Auto-ignition in itself is fine, but its consequences are less desirable; logically it should be limited to the smallest possible portion of the fuel.

On the other hand, this process of molecular disintegration is not the only one possible for combustion of gas oils. If gas oil is mixed with air prior to combustion – at low temperatures especially – as in a blowtorch, the flame spectrum will show bands in the ultra-violet range, indicating that oxidation proceeds via the radicals CH, C_2, and OH; only later does a continuous spectrum develop in the visible range of carbon monoxide.

In the engine, combustion starts with a continuous spectrum, indicating broken-up carbon compounds.

While the blowtorch operates without smoke, combustion in the engine tends to form soot, that is, the path of reaction is fundamentally different, and for complete combustion it is obviously essential that fuel and oxygen should be heated together, or that at least provision be made for starting oxidation gradually.

Attention should be paid to another observation. In 1908 Rieppel[9] advanced a theory stating that the supply of a little heat causes diesel fuels to form oil vapors, and it is these that burn in the engine. Wollers and Ehmcke[10] using an ignition-point tester found that these oil vapors have a much higher ignition point than the liquid fuel from which they are formed, and that the temperatures reached at the end of compression are too low to ignite them.

Evidently, the ignition point is influenced by the mechanism of mixture formation, being low for vapors formed by heating fuel droplets with hot air, and high for vapors formed by heating fuel in the absence of any appreciable amount of air or oxygen, and subsequent diffusion in air. This observation is confirmed in the M-engine, where it has been put to good use.

Application of Reaction Kinetics to Engine

There are two phenomena in diesel combustion that cause the most trouble and which we desire to eliminate:

1. Combustion noise, a more or less intense knocking depending on the fuel properties.

2. Exhaust smoke which develops before excess air is fully used up.

From reaction kinetic concepts we can derive a few rules to observe in order to eliminate these drawbacks:

1. Minimize the portion of fuel involved in auto-ignition.

2. Allow fuel to oxidize gradually and try to heat fuel and air together.

3. Mix fuel and hot air fast enough to effect a stoichiometric air-fuel ratio before ignition starts, and make sure no more fuel is mixed at any time

[7] See *Forschung auf dem Gebiete des Ingenieurwesens,* Ausgabe A, Vol. 3, March/April, 1932, pp. 94-98: "Wärme-Übergang von Drähten an strömende Luft," by J. Ulsamer.

[8] See *Forschung auf dem Gebiete des Ingenieurwesens,* Vol. 6, May/June, 1935, pp. 105-115: "Der Zündvorgang im Dieselmotor," by W. Wentzel.

[9] See *VDI-Forschungsheft,* 1955 (1908), pp. 1-35, "Versuche über die Verwendung von Teerölen zum Betrieb von Dieselmotoren," by P. Rieppel.

[10] See *Kruppsche Monatshefte,* Vol. 20, January, 1921, pp. 1-20: "Der Vergasungsvorgang der Treibmittel, die Ölgasbildung und das Verhalten der Öldämpfe und Ölgase bei der Verbrennung im Dieselmotor," by C. Wollers and V. Ehmcke.

than can burn with a permissible pressure rise.

These requirements cannot be met with conventional methods of mixture formation in diesel engines. Certainly, it might be quite possible to follow rule 1 by employing a fine pilot jet for ignition, although nozzle orifices of such a small diameter are undesirable in practice. The real difficulty lies in complying with rules 2 and 3 at the same time. Rule 2 calls for caution in bringing the fuel into contact with hot air, while rule 3 postulates: mix fuel with air in successive minute portions, the rate of mixture of each portion being many times faster than that of the preceding one. Furthermore, for those portions of the fuel entering the chamber later in succession, it seems impossible to observe rule 1, for it necessitates changing the properties of the same fuel from highest ignition quality to maximum anti-knock rating. To operate an engine on two fuels, which might be a solution, has never been desirable.

If we consider a diesel engine with direct injection and air motion of conventional design (Fig. 3) in light of the above rules, we find that rule 1 cannot be complied with, since even during a very short ignition lag, approximately one-half of the fuel is already finely sprayed into the hot air and the quantity involved in initial self-ignition can no longer be controlled. This also prevents compliance with rule 2.

In combustion chambers of such engines, a rotary air swirl is frequently employed which tears atomized fuel from the entering fuel jets at a right angle. Even if the spray is very coarse, this insures that maximum fuel surface is exposed to hot air. During this very period when rule 2 calls for slow pre-oxidation, the relative movement of air and fuel is at a maximum, for the fuel particles are being deflected from their original path by the force of the air. The air swirl is not really desirable at that moment, and in order to comply with rule 3, it should reach its maximum intensity only in the next phase. Actually, at that time the relative movement of air and fuel decreases because in the meantime fuel particles have been turned into the direction of the air stream.

We do not mean to say that such "air-distributing" engines are not practical. The fact is, they perform very well, but they suffer from the drawbacks mentioned previously and which become especially noticeable when fuels of varying ignition qualities are used.

We found that rule 1 could be fulfilled only by providing an external source of ignition for the remainder of the charge, or rather, an ignition that can be timed. A precondition is that an air-fuel mixture be formed which does permit ignition by external means before auto-ignition occurs, namely, the ignition point of the mixture must be as high as possible. As mentioned earlier, such mixtures are obtained by means of careful heating

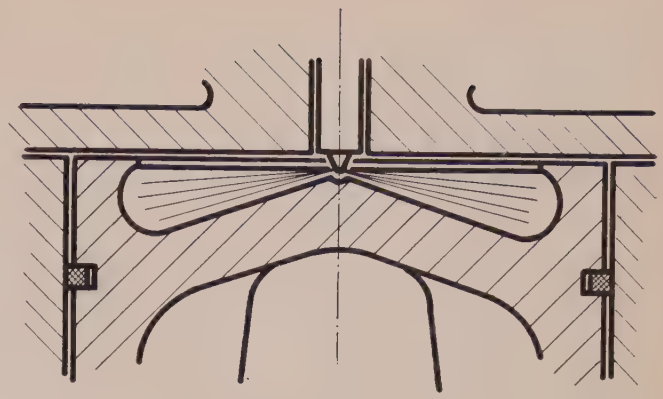

Fig. 3 – Cross-section of combustion chamber of standard direct-injection diesel engine

combined with gradual oxidation, prescribed by rule 2. It is clear that neither can be achieved with a droplet moving in hot air with tremendously-high heat-transfer rates.[8]

According to rule 2, the fuel must not be allowed to contact air in the first stage, and therefore, must not be atomized. Inasmuch as it is to be eventually burned in the combustion chamber, it must be kept there in a nonatomized form and at a temperature at which gradual pre-oxidation and progressive mixture according to rule 3 is possible.

The most suitable spot for this is the combustion-chamber surface, the temperature of which is sufficiently below the gas temperature to protect the fuel from rapid heating. Thus, at the beginning of mixture formation, a process has been adopted whose retarding effect on reaction is well known and dreaded: a fuel impingement on the wall. The only reason this is bad is because reaction has already begun while fuel was penetrating the hot air. Trouble experienced in conjunction with this latter condition has given the idea of wall contact a bad reputation, although it was actually applied in engines some 40 years ago.

The need for simultaneous cooling and evaporation implied by rule 2 could be met best by spreading a thin fuel film over a maximum area in the combustion chamber. It has to be thin in order to make cooling sufficiently effective right through the fuel film, and to prevent the top surface in contact with hot gases from being heated too fast as a result of the temperature gradient through a thick layer.

Slow and uniform pre-oxidation also requires a certain surface area. Certainly there is more turbulence in a fuel splash shooting along the wall of a combustion chamber than in a fuel droplet; thus, the fuel particles are partly exposed to the oxidizing effect and partly to the cooling effect of the wall. As a result, the combustion-chamber wall acts as an intermittent carburetor performing a very complex function. The fuel, already in a highly active state, is still under the control of the

wall. Through its specific properties, the wall is capable of exerting a catalytic effect on the course of reaction.

Finally, rule 3 must be complied with. So far the indispensable mixture with air has not yet taken place, and as we know, it should proceed at an extremely high rate. Without this rapid mixing process, the results of depositing fuel on the wall to such an extent would be entirely negative with respect to air utilization and fuel consumption, for the diffusion rate of fuel vapor which develops on the wall is much too low to insure mixing at the necessary high rate. The only suitable means remaining is an air motion, which, in view of the application of fuel in the form of a film, should be well-directed and maintained throughout combustion and be undisturbed by the latter. It is easier to provide a turbulent air motion by squish, but such a swirl is limited to a short period and breaks down due to expansion of the charge following ignition.

In order to peel off the fuel film in layers, a rotary air motion around the cylinder axis is most suitable. It should be produced during the suction stroke and maintained by inertia of the air long enough to be still noticeable during the exhaust stroke. Rotary air velocity in the decisive phase of mixture formation can be efficiently increased and a favorable distribution of air in the combustion chamber obtained, if the diameter of the latter is kept smaller than the cylinder diameter and if care is taken to insure a maximum portion of the air getting into the combustion chamber.

However, before we apply such a violent air motion, we must investigate whether we can reconcile it with the requirement of rule 2 for slow oxidation and minimum air contact. Breakup of the fuel jet occurs as a result of friction between the jet surface and air, which is at a minimum when the jet and air have the same velocity. The nearest approach to this state is obtained by directing the jet tangentially to the air motion and onto the wall. If the jet hits the wall at a distance from the nozzle sufficient only to start breakup, excessive atomization will be prevented, no matter whether it is injected tangentially, against, or in the direction of rotation. If fuel jet and air move in the same direction, the air will assist in spreading the fuel film.

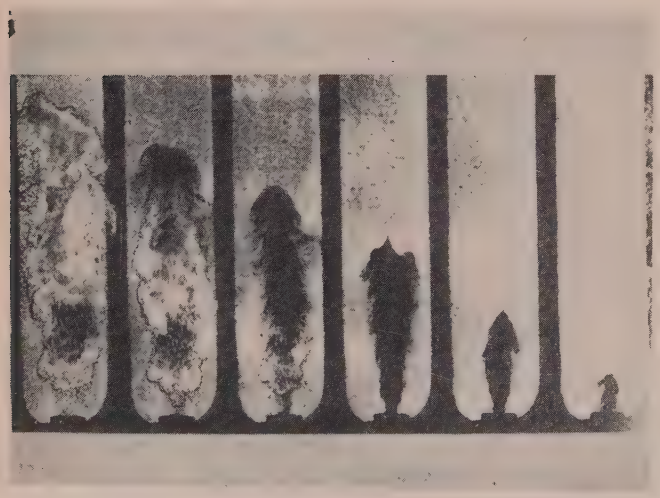

Fig. 4 – High-speed motion pictures of diesel fuel-spray ignition and combustion. Film speed: 445 frames per sec

At the same time, selecting the proper distance from nozzle tip to the combustion-chamber wall will help comply with rule 1. By means of high-speed photographs of fuel injection into a hot bomb,[8] it has been found that first ignition was always initiated by a small cloud which formed near the nozzle (Fig. 4). Obviously, this small fuel cloud develops at the very beginning of injection, and due to initial impact on the air, consists of very fine particles whose aerodynamic resistance is higher than their inertia. These particles, therefore, lag behind the jet. The nozzle tip is located at a point not directly exposed to the rotary air motion, thereby providing a distance between the tip and wall which enables the fine particles to separate before the fuel jet hits the wall. Thus it is possible to subject these particles to the normal auto-ignition of fuel distributed in air. In this manner, the small portion only of fuel which should self-ignite, according to rule 1, is obtained without an additional nozzle orifice. To achieve self-ignition of this portion, advantage is taken of the low ignition point of fine fuel-fog formed in the presence of oxygen. The details of these processes were brought to light by experiments, and as will be shown later, very convincing evidence was found that they really do take place in that manner.

According to rule 3 the function of air motion is to produce the mixture so rapidly that at least a stoichiometric air-fuel ratio is attained before ignition sets in. In addition, rule 1 requires that auto-ignition be avoided. The measures so far proposed create favorable conditions to meet both requirements:

1. Fuel which initially shoots across to the combustion-chamber wall at nearly the speed of the air is considerably retarded in the process, and as the mixture formation period approaches its end, the velocity difference between the rotating air and fuel increases progressively. In effect, this is the opposite of what happens in engines where fuel is injected at right angles to the air swirl. There, the velocity of air relative to fuel decreases as the droplet is reduced by evaporation in the course of mixture formation, so that its eventual velocity is in the direction of the air motion and it moves along enveloped in its own vapor cloud. Apart from that, each liquid droplet constitutes an undesirable accumulation of fuel which, for correct mixture under engine compression densities, requires approximately 6.5 times the air volume

required by fuel vapor of equal volume. Once deposited on the wall, the fuel hardly leaves it in the liquid state. Thus, the risk of wide differences in fuel concentration in the mixture is eliminated.

2. Evaporation of fuel on the combustion-chamber wall is not instantaneous but is controlled by wall temperature and the temperature difference between the wall and gas. The total kinetic energy stored in the air rotation affects only a fractional amount of vapor at a time and can achieve the prescribed rapid mixture followed immediately by combustion. Thus, the same process that takes place only once in the conventional methods of mixture formation, and which involves the complete fuel charge, is successively repeated many times here.

In selecting wall temperature, care must be taken to have it high enough to initiate evaporation, but not so high as to cause thermal decomposition of the fuel molecules to the point of formation of solid soot. Due to heat dissipation, the air temperature is lower, initially, near the wall than in the center of the combustion chamber, so that the desired slow oxidation takes place partly as a surface reaction in the boundary layer between the liquid and vapor phases and partly in the vapor phase.

The evaporating fuel particles consist of decomposition products of the first stage (aldehydes, ketones, olefins), that are formed under moderate heat and an extreme air deficiency; these ignite spontaneously at a temperature higher than vapor formed in the presence of hot air. Consequently, the induction time for these mixtures at the temperatures attained through compression in the diesel engine is now long enough to prevent auto-ignition within the period during which they are mixed with hot air. Therefore, external ignition and subsequent combustion are possible before the portion of the mixture involved can ignite spontaneously. The instant of ignition is evidently determined by the ignition limit set by the fuel concentration being passed. and the means of ignition are the incandescent fuel particles generated in the limited auto-ignition according to rule 1. This process is repeated in rapid succession in different places, and at any one time involves only that small mixture fraction which, depending on the rate of evaporation, passes the ignition limit at that time. Similar to the gasoline engine, where there is no knock if the last portion of the mixture can pass through the flame front before self-ignition occurs, knocking is prevented here by producing, igniting, and burning very small amounts of the mixture at a rapid rate. Thus it is possible to trick the high-compression ratio out of its traditional function of triggering self-ignition. This method is also adaptable to the gasoline engine.

What has been described in the foregoing is well confirmed by the engine in operation, although the

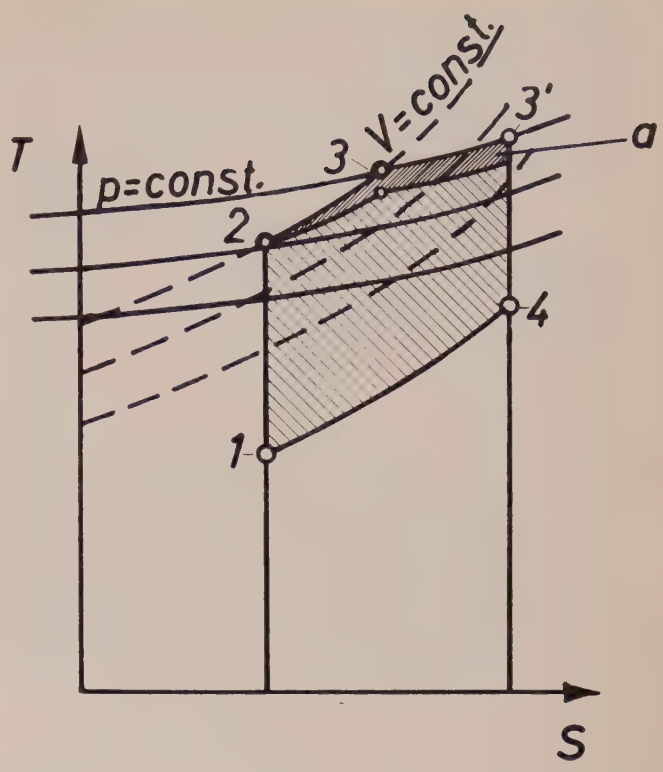

Fig. 5 – Temperature-entropy diagram of diesel cycle showing heat loss *a* due to evaporation of fuel

practical design suffers from a few compromises, especially that regarding the removal of fuel from the wall, which removal is effected at such a high rate that the increasing gas temperature tends to assist the decomposing reaction.

There is also an interesting thermodynamic advantage in evaporating fuel on the wall. If the liquid fuel is distributed in hot air in the combustion chamber, evaporation heat can be taken only from the heat of air produced by compression work. This constitutes a loss shown schematically in the temperature-entropy diagram (Fig. 5). If fuel is evaporated on the wall, heat of evaporation is drawn from the piston and not from the working medium. The heat in the piston, however, being essentially waste heat, can thus be partly recovered in order to avoid a loss of available energy in the working medium. Admittedly, this is a very small amount (approximately 1.8% of the heating value); nevertheless it is of some importance when it is desirable to obtain somewhat longer combustion with the same fuel consumption.

Combustion Chamber Design for M-System

There are several ways of translating into practice the rules and instructions given in the foregoing. One design is shown in Fig. 6.

The piston is designed with a combustion chamber in the center forming little more than a half-sphere. The throat of the chamber has a recess

Fig. 6 – Direction of fuel spray and formation of fuel film on combustion-chamber wall

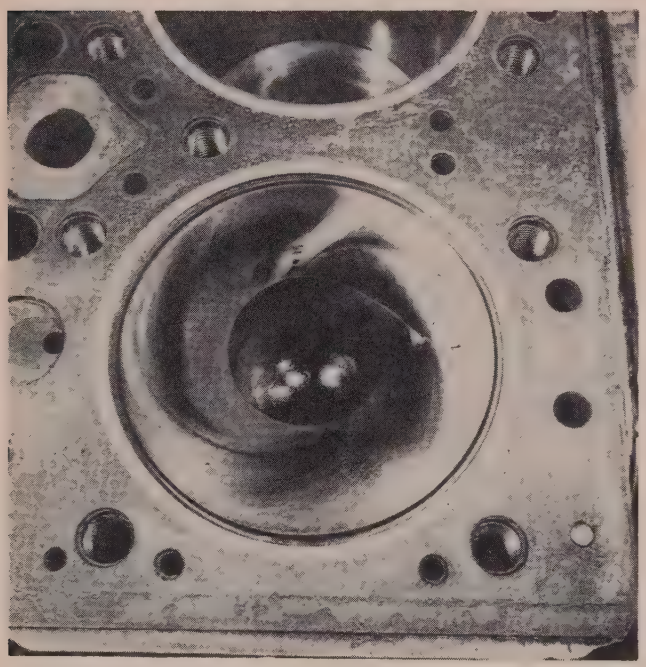

Fig. 7 – Appearance of piston top after short running time. Note clean strip on combustion-chamber wall due to fuel film deposited by injection spray

through which fuel jets reach the combustion-chamber wall at an acute angle. The nozzle has two orifices 0.015 in. in diameter and operates at a pressure of 2500 psi. During the suction stroke, rotary motion of the air is induced in the cylinder in the same direction as the fuel jets. The air swirl

Table 1 – Comparison of Mixing and Combustion Processes in Normal Diesel System and MAN M-System

Normal Diesel System		MAN M-System	
100% of injected fuel		100% of injected fuel	
1) Injection into air	of liquid fuel	1) Injection of liquid fuel	
		about 5% in the air	about 95% on the wall
2) Mixing with hot air.		same as in normal Diesel engine (see left)	2) Evaporation at low temperature under lack of oxygen Slow preoxydation.
3) Evaporation at high temperature in presence of oxygen.			3) Mixing of fuel vapor with air.
4) Autoignition of incontrollable quantities of fuel (low ignition temperature); decomposition to carbon.			4) Ignited by incandescent carbon particles produced by autoignition of air distributed droplets.
5) Combustion with high reaction rate at the start, increasingly inert toward the end.			5) Combustion before autoignition occurs.

rpm is considerably increased when its diameter at top dead-center is reduced from cylinder to combustion-chamber diameter. Fuel is applied to the wall of the combustion chamber in two splashes which spread rapidly and eventually flow together to form a continuous film which, as seen from the surface appearance of used pistons, covers half the combustion-chamber surface (Fig. 7). Assuming uniform film distribution, its thickness can be calculated from the quantity of fuel injected and is 0.006 in. at full load.

Combustion-chamber wall temperature is maintained at about 640 F at full load by an oil-cooling arrangement (Fig. 8). A nozzle in the crankcase throws up to 2 qt per min of oil against that side of the combustion chamber where the fuel film is deposited. Piston cooling might be effected without oil by suitably dimensioning the cross-sections of the material, but oil cooling makes the piston lighter and has the added advantage of keeping pistons very clean. When the engine is started cold, oil is instantly available at the piston rings and the engine oil supply warms up quickly. It is somewhat difficult to control oil consumption; a very satisfactory solution was found in the present case, however, in the form of wide return channels in the piston skirt.

All prerequisites for successful adoption of the described system are now fulfilled:

1. Deposition of fuel on the wall in the form of a film, with a small amount of fuel separated for distribution in the air and initial auto-ignition.

2. Direction of jets tangential to the direction of air so that undesirable mixture of liquid fuel and hot air is reduced to a minimum.

3. Vaporization in the presence of very little air at low temperature and gradual pre-oxidation,

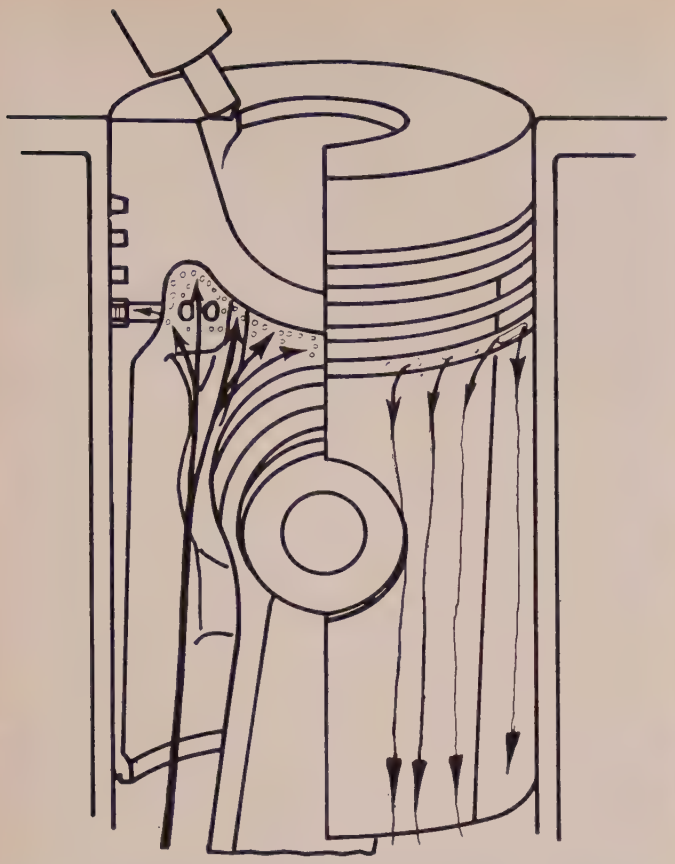

Fig. 8 – Oil cooling by jet directed toward combustion chamber from below

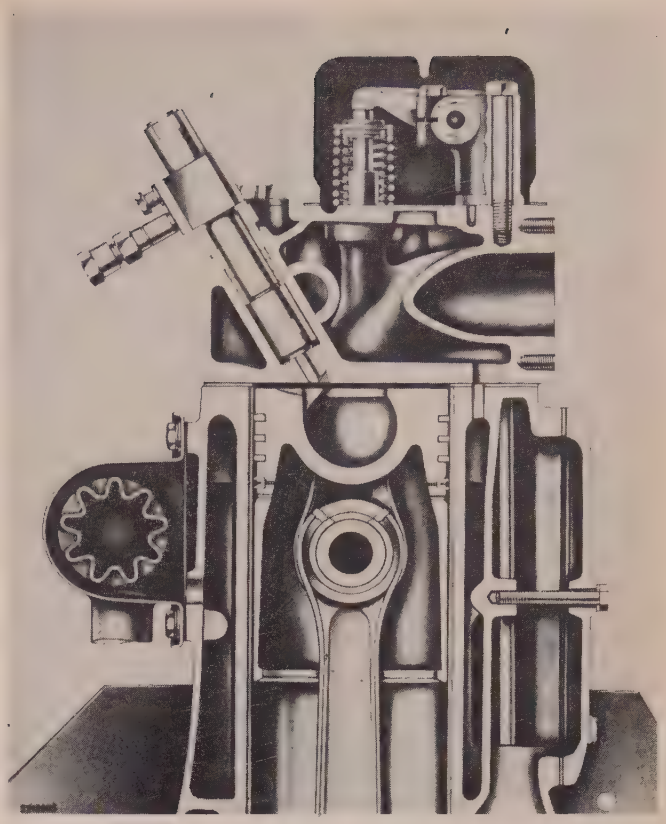

Fig. 9 – Cross-section of 6-cyl, 4.4 x 5.5-in. production engine. 200 hp max output (supercharged) at 2300 rpm (see Fig. 11)

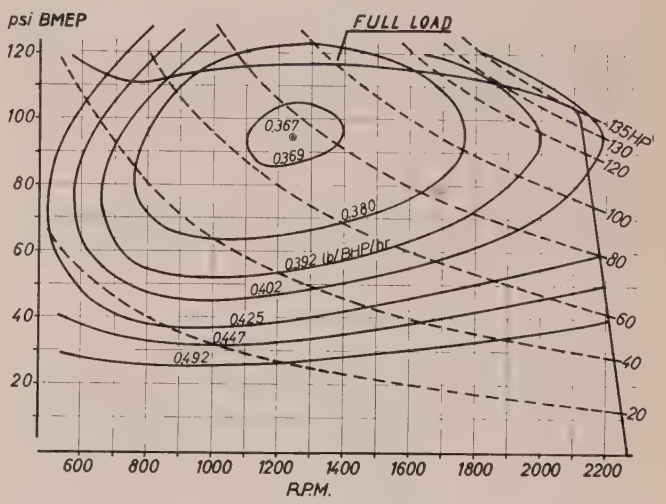

Fig. 10 – Sfc characteristics in relation to engine speed and mep and full-load power curve for 6-cyl, D 1246 M engine with natural aspiration

rapid mixture of the fuel vaporizing per unit time, and a properly-timed external ignition.

Although the individual phases overlap, it is possible without oversimplification to compare a conventional direct-injection engine and the M-system (Table 1).

It is seen clearly that for most of the fuel, the M-system interchanges points 2 and 3 of the standard diesel system shown in Table 1.

Test Results

Engine test results of the new system are amazing. In particular, the typical diesel knock has disappeared over the entire speed range, even during idling and starting of the cold engine, and this has been obtained without sacrifice in specific output or in fuel consumption. Moreover, within wide limits, these characteristics are independent of fuel characteristics, including cetane number.

It can be seen from Fig. 9, a cross-section of a 4.4 x 5.5-in. engine, that the M-system has not complicated the design in any way. It is essential to locate valves in the central plane of the cylinder where they can be designed with a maximum cross-section. This is of special importance for the intake valve because measures necessary to produce air rotation reduce the effective port area.

Sfc of a 6-cyl engine with the above dimensions is shown in Fig. 10. The curves of equal consumption extend over wide speed and mep ranges. There is no appreciable narrowing of the spacing in the region of high or low speeds, indicating that there is no definite point beyond which mixture forma-

tion is a limiting factor. A notable fact is the extent of the curves into the low-speed region. In road service, these engines show a surprising flexibility, and even at 300 rpm, combustion is uniform enough to permit full-load fuel quantity to be injected without trouble. Below 800 rpm, the governor-controlled injection pump supplies an extra starting charge for improved flexibility (Fig. 10, full-load curve).

The turbocharged version of the same engine has a peak output of 200 hp, and its consumption is less than 0.37 lb per hp-hr over wide speed and mep ranges (Fig. 11).

Comparison of Soot Formation

Interesting conclusions can be drawn with respect to the reactions during mixture formation from the amount of soot in the exhaust and the analysis of the oil used. If discoloration of the diesel exhaust smoke is measured, it will be found that there is a marked reduction when the mep decreases which is readily explained as the result of increased excess air. However, the influence of the air-fuel ratio must be eliminated if, in order to clarify the mechanism of combustion, we want to find what percentage of the carbon supplied in the fuel is obtained in solid form in the exhaust. This is done by relating the amount of soot not to the exhaust gas quantity but to the quantity of fuel injected; in other words, by making the amount of filtered exhaust proportional to the fuel quantity.

The investigation covered three different methods of mixture formation; the results are recorded in Fig. 12. It is surprising to find that independent of the air-fuel ratio, a pre-combustion chamber engine and a direct-injection engine transform nearly the same percentage of fuel into free carbon. This clearly indicates that soot formation in the diesel engine is essentially caused by reaction kinetics. Only in the power range above 75 bmep does the influence of mixture formation become noticeable. Soot formation in the M-system shows a different trend. In the range up to 50 bmep, soot formation is within the limits of a gasoline engine; it then approaches the characteristic of the diesel engine because the present design of the M-system still suffers from some compromises in the region of high mep.

This result agrees very well with the analysis of oils used in engines employing the M-system (Table 2). Column 1 shows data for direct-injection and M-system versions of the same engine under equivalent operating conditions. It can be seen that the percentage of constituents which are insoluble in standard benzene is much lower in the M-system engine, while – and this is of particular interest –

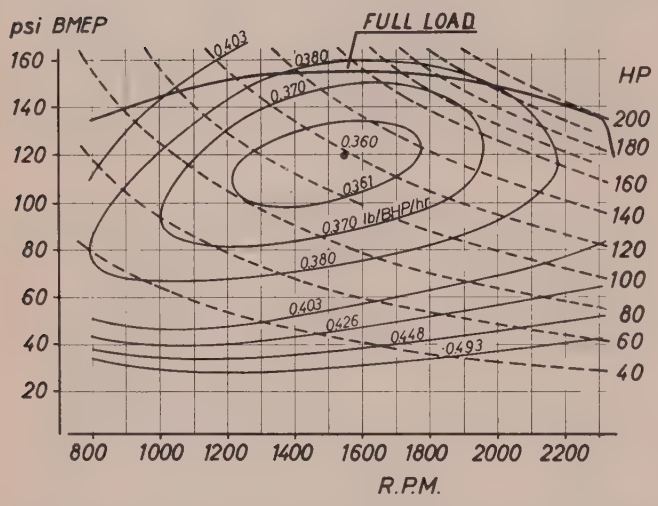

Fig. 11 – Sfc characteristics in relation to engine speed and mep and full-load power curve for 6-cyl, D 1246 M engine with exhaust turbo-supercharger

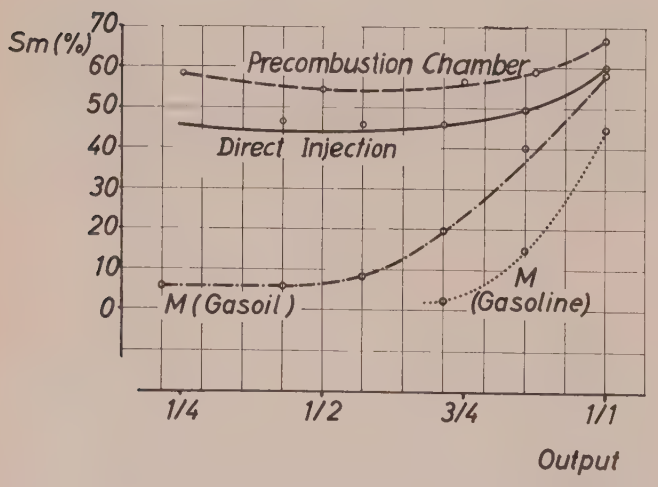

Fig. 12 – Exhaust smoke measured for same weight of injected fuel for several load conditions at 1400 rpm

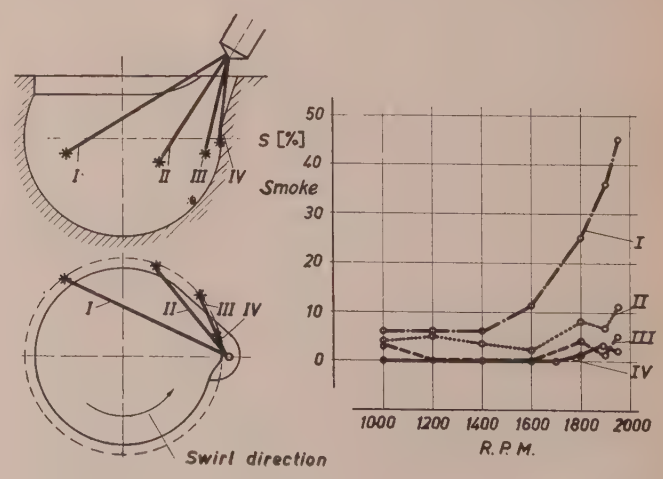

Fig. 13 – Influence of direction of fuel spray upon exhaust smoke. Injection well below plane of chamber throat

Table 2 – Chemical Analysis of Lube Oil in Direct-Injection and M-System Diesel Engines for Same Length of Service

Full Load - Endurance Test Run.		
Engine Type	8 × 4.53" × 5.51" 180 HP Direct Injection	8 × 4.53" × 5.51" 210 HP M - System
Hours of Test Run Equivalent Miles	60 2620	60 2620
Neutralization Number	0.3 %	0.0 %
Insolubles in Benzene	0.8 %	0.28 %
Specific Sludge Formation	2.3 oz./1000 Miles – 100 HP	1.1 oz./1000 Miles – 100 HP
Road Test (City Bus Service)		
Engine Type	6 × 4.41" × 5.51" 130 HP Direct Injection	6 × 4.41" × 5.51" 130 HP M-System
Stat Mile	2240	2240
Neutralization Number	0.83 %	0.53 %
Insolubles in Benzene	1.9 %	1 %
Specific Sludge Formation	6.0 oz./1000 Miles – 100 HP	3.1 oz./1000 Miles – 100 HP

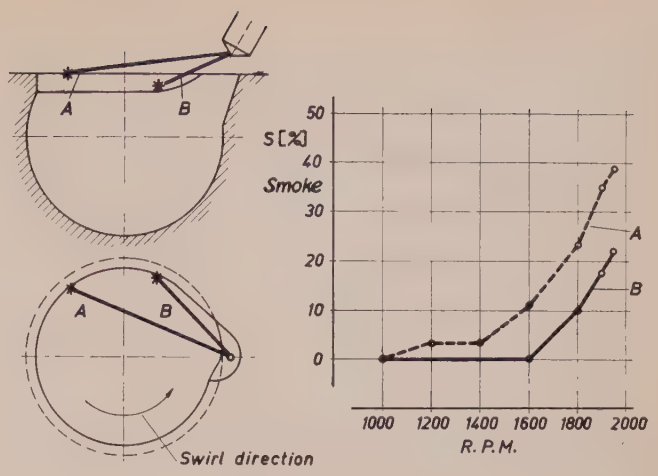

Fig. 14 – Influence of direction of fuel spray upon exhaust smoke. Injection in plane of chamber throat

the acidity of the oil in that engine is a fraction of that arising in the direct-injection engine. The latter result clearly suggests the different direction of reactions which no longer form acetic and formic acids, but take place via ketones, olefins and aldehydes. From the analysis one may calculate the "sludge rate", a value which indicates the amount of benzene insolubles produced in an engine per hp and mile. Whereas the "sludge rate" for orthodox diesel engines is 4.6 oz per 1000 miles and 100 hp, for M-engines it is as low as 1.1 oz per 1000 miles and 100 hp. In gasoline engines it is approximately 1.1 oz per 1000 miles and 100 hp. In other words, the M-engine equals the gasoline engine in low oil contamination.

Influence of Jet Direction in Combustion Chamber

If the concept of wall contact influencing smoke formation is correct, then it should be possible to vary the latter by modifying the direction of the jet in the combustion chamber which, in conjunction with air motion, controls degree of wall contact and area of the film. That this is so could be easily proved by rotating the nozzle in the combustion chamber. A three-hole nozzle was used with only one orifice open; thus, the amount of fuel injected was reduced to one-third. In Fig. 13, the alternate jet directions together with measured exhaust discoloration are given. According to the orthodox belief that rapid distribution of fuel in air is essential, jet I should have given better combustion than jets II and III, and especially better than IV, the latter directly hitting the wall. However, it was precisely jets III and IV which caused practically no discoloration of the exhaust, while jet I produced about 4 times more smoke at 1900 rpm. The differences in fuel consumption were small, but jet I produced a distinct noise which disappeared nearly entirely with jet III.

It has been pointed out frequently in the relevant literature that for favorable combustion, injection should be directed into the zone of air turbulence. No doubt this zone is in the plane of the combustion-chamber throat; but as seen in Fig. 14, at high speeds jet A fails to give the smokeless exhaust obtained by jets III and IV of the preceding illustration. The reason is that the squish pushes the jet off the wall and tears too much fuel out of it.

It should be added that there is an interaction between the circumferential velocity of air in the combustion chamber and the jet direction, inasmuch as a higher air velocity enables more fuel to be brought into contact with the wall. However, the heavier air drag then makes it necessary to place the jet more in direction III, otherwise the amount separated for initiating self-ignition would become too small.

Influence of Air Motion

It will be appreciated that the influence of air swirl in the M-system is very great and that the atomizing effect of the nozzle is secondary in importance to its directing effect. If air swirl is omitted and jet direction is retained, output, based on the same degree of exhaust discoloration will drop to approximately 57% of the optimum value and fuel consumption will rise substantially (Fig. 15). Even if the full force of the swirl is made to act in the reverse direction, output at the smoke limit will be somewhere between the optimum value and that of the test without air swirl.

The production of effective rotary air motion in the cylinder presents a rather difficult aerodynamic problem. For the air to enter the cylinder tangentially, it is necessary to throttle part of the airflow through the valve port. Any reduction of the flow coefficient in certain sections of the valve port tends

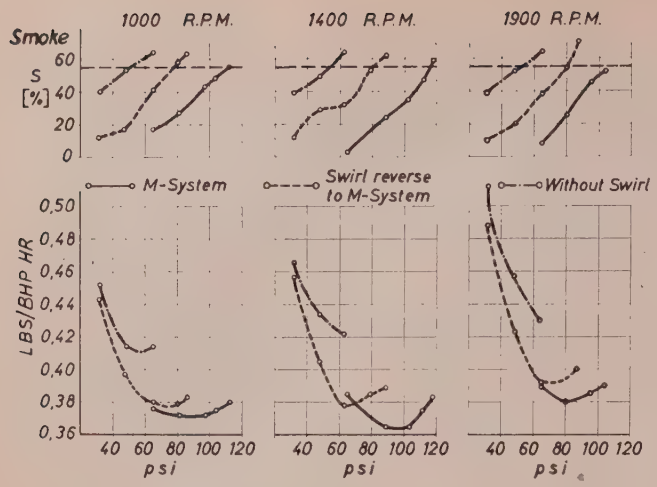

Fig. 15 – Sfc and percent smoke versus mep for different speeds and air swirl conditions

to increase flow resistance and limit volumetric efficiency of the engine, at the same time increasing the pumping losses of the gas change cycle. To compensate for increased flow resistance by means of a larger intake valve is very seldom practicable.

The loss in a well-designed intake is relatively low at moderate rotary air velocities. Results of static flow tests in intake ducts are reproduced in Fig. 16. Cylinder suction pressure was measured which, for a given valve lift, is required to draw air in at an axial velocity corresponding to a mean piston velocity of 2000 fpm. An anemometer was used to determine the circumferential velocity of the air swirl on a circle of 0.7 times the cylinder diameter. Another scale is shown in Fig. 16 indicating the ratio between anemometer and engine speed at a stroke of 5¾ in.

Curve *a* is plotted for a duct fitted with a masked valve, the mask angle increased in steps as indicated. Circumferential velocity increased proportionally and a higher cylinder suction pressure had to be produced. Mask angles employed in the M-system engine vary between 110 and 120 deg, and it is seen that anemometer speed then corresponds to about 8 times engine speed. Inlet pressure drop increased to approximately 1.5 times that for the unmasked valve.

Curve *b* is drawn for a similar test made with an unmasked valve where swirl was imparted by the special duct shape. It can be seen readily that this design produced the required rotary air velocity with less flow resistance, and the inlet pressure drop increased only to 1.3 times that for the unmasked valve. It is possible, therefore, to keep to a minimum the losses due to means for inducing air swirl.

A considerable increase in swirl speed is obtained by making the combustion-chamber diameter smaller than that of the cylinder. Allowing for friction losses, it is safe to assume that swirl speed in the *combustion chamber* will be at least 6 times the engine speed.

Cold-Starting Ability

It is essential for every automotive engine to be able to start quickly even at very low ambient temperatures. It is unlikely that fuel deposited on the cold combustion-chamber wall in the M-system will vaporize in time. Only the air-distributed fuel fraction separated from the jet for initial auto-ignition may do so, but being very small, the pressure rise attained by its combustion is insufficient to overcome the frictional resistance and so to start the engine.

To remedy this deficiency, two measures have been introduced:

1. Fuel pump injection was increased to 180% of full-load quantity in the range of starting speeds. Consequently, the air-distributed fuel fraction became large enough to insure sufficient heat liberation after ignition to start wall vaporization. Starting time nevertheless remained longer than that for conventional engines fitted with glow plugs and the exhaust showed unburned fuel vapor during the first 30 sec.

2. Perfectly reliable quick cold-starting was insured by means of a small compressed-air burner illustrated in Fig. 17. Compressed air is supplied from the air receiver of the brake system *a* or by means of a hand pump through a pressure regulating valve *b* to an air nozzle *d* blowing over a fuel nozzle. Some fuel is drawn from the nozzle, and after mixing with the air stream, is ignited by a spark plug *e*. The small flame developed reaches approximately into the middle of the intake pipe where it is met by an air stream emanating from nozzle *f* which is heated by the gases and is discharged through the filter element of the air cleaner into the open. The filter is heated and after about 20 to 30 sec the starter is operated and the

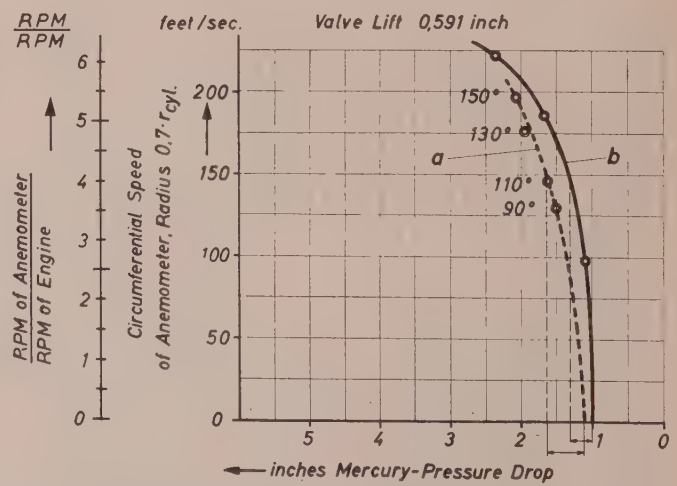

Fig. 16 – Results of static flow tests for required pressure drop to create given swirl

Table 3 – Cold-Starting Results Using Diesel Fuel and 80/86 Octane Gasoline

Test Nr.	Engine type	Temperature °F	Fuel	R.P.M.	Cold starting device	Time to run on its own sec.	Preheating time sec.	
1	6x44"x55"	13	D.F.	110	without	57	—	a)With a third fuel jet „air distributed"
2		"	"	"	a	28	—	b)Air swirl reversed
3		"	"	"	b	24	—	c)Manifold burner
4		"	"	"	a+c	4	30	
5		-4	D.F.	110	c	9	30	
6		"	"	"	b+c	9	30	
7		"	Gasoline 80/86	"	c	20.5	30	
8		"	"	"	b+c	17	30	

engine draws cold air through the highly preheated filter. Without any oxygen in the intake air being consumed, the latter is preheated about 110F, which is sufficient to enable the engine to start instantaneously. This cold-starting unit may be operated as long as the engine is warming up because the flame is nearly self-sufficient due to the compressed air supply and consumes scarcely any oxygen from the intake air. In case air pressure in the brake receiver is zero, there is a nonreturn valve which insures that during the first revolutions of the engine the brake compressor pumps air to the burner before any air is delivered into the brake system. The unit, operating on gas oil, is controlled by a pushbutton fitted on the dashboard. Using gas oil for fuel and allowing 30 sec preheating time and a 110 rpm, starter speed, the engine will run on its own within 9 sec at –4F. This arrangement provides very satisfactory cold-starting under normal service conditions.

If very low-cetane number fuels such as high-octane gasolines are used, another measure must be taken in addition to the cold-starting device. With the above-mentioned equipment it is not at all difficult to insure ignition and starting of the engine, but longer preheating time is required when fuels of low ignition quality are used in order to attain maximum speed and full power. But this difficulty, too, was successfully overcome. The cold-starting ability of a diesel engine is roughly proportional to the amount of fuel which is "air distributed", or able to undergo auto-ignition or at least participate in the preparatory stages. The more the wall application of fuel can be changed into air distribution, the better the cold-starting ability. A first attempt was made by providing an additional third fuel jet directed into the center of the combustion chamber to bring about "air distribution". The effect on the cold-starting ability of the engine was quite marked (see Table 3). However, under full-load service, that advantage was offset by increased exhaust smoke and rough engine operation.

Rotating the entire nozzle for low-temperature starts is also very effective, but it is simpler to

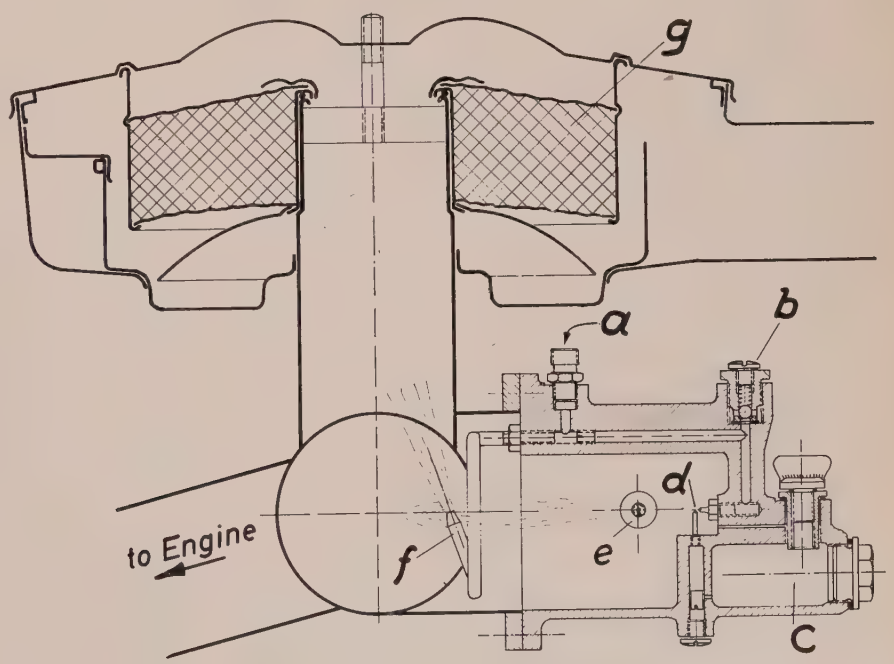

Fig. 17 – Cold-starting device in intake manifold showing *a*, compressed air inlet; *b*, automatic pressure control; *c*, fuel tank; *d*, air and fuel nozzles; *e*, spark plug; *f*, secondary air nozzle; *g*, metallic air filter insert

Table 4 – Fuel Characteristics and Results of Multifuel Tests for 60% Smoke

No	Fuel	Specific Gravity °API	Boiling Range °F	% Residues + Evaporation Loss	Heating Value LHV / 18270	H %	C %	S %	Cetane No	1900 RPM psi	1900 RPM lbs/BHP/hr Sm = 60%	1900 RPM lbs/BHP/hr Optim.	1900 RPM lbs/BHP/hr 35.5	1400 RPM psi	1400 RPM lbs/BHP/hr Sm = 60%	1400 RPM lbs/BHP/hr Optim.	1400 RPM lbs/BHP/hr 35.5	1000 RPM psi	1000 RPM lbs/BHP/hr Sm = 60%	1000 RPM lbs/BHP/hr Optim.	1000 RPM lbs/BHP/hr 35.5
1	Commercial Diesel Fuel	38.3	372 – 680	1.5	1.001	13.03	86.01	0.72		113.8	.389	.381	.455	118.0	.378	.367	.464	118.8	.378	.363	.434
2	Gasoil 428 - 644 °F	38.0	414 – 644		0.9935	12.38	86.89	0.59		118.8	.401	.372	.459	121.0	.381	.372	.452	118.8	.383	.369	.436
3	Gasoil 392 - 572 °F	39.0	399 – 563		0.998	12.99	86.56	0.39	54	113.6	.383	.372	.452	121.0	.376	.367	.430	113.9	.376	.363	.430
4	Diesel Fuel Imported from Austria	33.4	399 – 698	4.5	1.002	13.27	86.66	0.08	52	100.8	.387	.385	.466	119.5	.385	.374	.461	113.9	.385	.378	.443
5	Special Wide Range Diesel Fuel 104-752 °F	39.0	104 – 745	2.5	0.982	13.30	86.16	0.66	41	108.0	.385	.380	.463	114.8	.374	.365	.450	113.1	.376	.367	.434
6	Cracked Diesel Fuel	26.5	412 – 597	1.0	0.968	10.93	87.14	2.07	~25	110.2	.389	.385	.488	120.3	.385	.372	.461	120.3	.394	.378	.457
7	Diesel Fuel with High Sulphur Contents	36.0	363 – 662	2.0	1.005	12.74	82.25	5.00	46	111.9	.405	.401		110.3	.385	.383		111.8	.394	.383	
8	Aramco Crude Oil (purified)	34.6	153 – 680		0.994	12.40	84.27	1.63	51	101.7	.405	.398	.481	110.0	.394	.385	.472	(98.1)	.387	.385	.464
9	Mogasoline 80/86	54.5	95 – 392(680)	2.0	1.018	13.70	86.10	0.21	~16	108.1	.362	.354	.423	118.1	.338	.331	.406	123.1	.346	.333	.394
10	JP4	51.5	131 – 549	1.0	1.022			0.16	~35	115.0	.376	.352	.416	118.1	.353	.340	.400	120.9	.367	.349	.397
	max. } Values of Brake Mean Effective Pressure and Specific Fuel Consumption									118.8	.362	.352	.416	121.0	.338	.331	.400	123.1	.346	.333	.394
	min. }									100.8	.405	.401	.488	110.0	.394	.385	.472	111.8	.394	.385	.464
										+4% -11%	+12	+14	+17	+3% -7%	+6	+16	+18	+4% -7%	+14	+15	+18

vary the velocity or direction of air swirl in the combustion chamber. If the air swirl is reversed by turning the masked intake valve through an angle of 180 deg, the jet, being directed against the air stream, will be broken up considerably. Even a reduction of swirl velocity alone improves the cold-starting ability appreciably, as can be seen from Table 3. A combination of all three measures is most effective, and at a temperature of – 4 F, enables the engine to reach operating temperature and peak speed in a very short time, even when leaded gasolines of 80/86 octane are used.

The Multifuel Characteristic of the M-System

As noted previously, the successful elimination of combustion noise in the M-system is achieved by reducing to a minimum the portion of fuel involved in auto-ignition. The rate of mixture formation is controlled by the temperature in the combustion chamber, that is, by combustion itself, because it takes a rise in temperature to accelerate vaporization of the fuel film on the combustion-chamber wall.

These two features of the M-system result in another remarkable advantage in that they make it possible to operate on fuels having considerably lower ignition qualities than gas oil.

It is desirable to extend the fuel range of a compression-ignition engine to include low-boiling point fuels such as gasolines and all kerosene fractions between the gasolines and gas oils, and so obtain a multifuel engine capable of burning all distillation fractions with boiling points up to 750 F.

Modern refining processes yield gasolines of a high octane number and correspondingly low cetane number. If such gasoline is used in a diesel engine of the "air-distributing" type, combustion roughness will increase intolerably. The reason is that during the long ignition lag a large percentage of fuel particles suspended in air undergo the phases preparatory to auto-ignition, so that when the latter occurs in a favorable place, a small

amount of energy is sufficient to cause a large portion of the fuel to react rapidly.

The M-system itself does not reduce ignition lag, but in the course of longer ignition lag, it allows only a negligible amount of additional mixture to form since there is no temperature rise in the combustion chamber during that phase to act to accelerate vaporization of fuel on the wall.

Vaporization on the wall is speeded up only when the "air-distributed" fuel portion has overcome the ignition lag and begins to liberate heat. Then the higher vapor pressures of the low-boiling point fuels prove most effective in making up for time lost due to the long ignition lag. For subsequent combustion, it is actually better to have anti-knock fuels, for, as noted above, they are more likely to be ignited by initial ignition particles before they ignite spontaneously.

The real problem in burning low-boiling point fuels in the M-system lies in shortening ignition lag adequately. This can be effectively solved by either raising the compression ratio or applying supercharging. Thus, a compression ratio of 1/19 makes it possible (without any supercharging) to use gasolines of as much as 80/86 octane while obtaining the same peak output. It even allows idling for many hours without misfiring or any audible combustion noise. It follows that such an engine is capable of operating on all other petroleum fractions with a distillation temperature higher than gasoline.

Performance data and sfc at the smoke limit for a large number of widely different fuels are given in Fig. 18. Included are data for an SAE 10 lubricating oil. Because of the great differences in specific gravities and, therefore, in heating values per unit volume of fuels, it is necessary to adjust the injection quantity to obtain the same output. However, one fixed setting is sufficient for ignition timing without suffering much from the compromise. It is a remarkable fact that high-octane gasolines, particularly in the low-speed range, give better fuel consumption than gas oils. At high speeds this relationship is reversed, because in that range the ignition lag of gasolines can be sufficiently shortened only by retarding injection to some extent. Best results are obtained with JP-4 jet engine fuel. Table 4 compares sfc and mep obtained with 10 different fuels within the distillation range from 104 to 752 F. Part-load values at the most economical rating and at an mep of 35.5 psi are included. The two lower rows show the maximum and minimum bmep and sfc measured at the same exhaust discoloration of Sm = 60% and at part loads. This comparison shows that differences in mep at 60% exhaust discoloration decrease as the speed is reduced. The reverse holds for fuel consumption values, which diverge with decreasing speed, particularly at an mep of 35.5 psi. Taking into consideration the widely different characteristics of fuels tested, it can be said that the differences are not really significant. The multifuel capacity is emphasized by fuel No. 5 with a distillation range from 104 to 752 F, which contains all fractions distilled in the atmospheric tower of crude oil refineries. The good results attained with this type fuel prove the engine capable of operating on any mixture of the listed fuels. This enables the user of diesel power to operate most economically on any one of a wide range of distillation products.

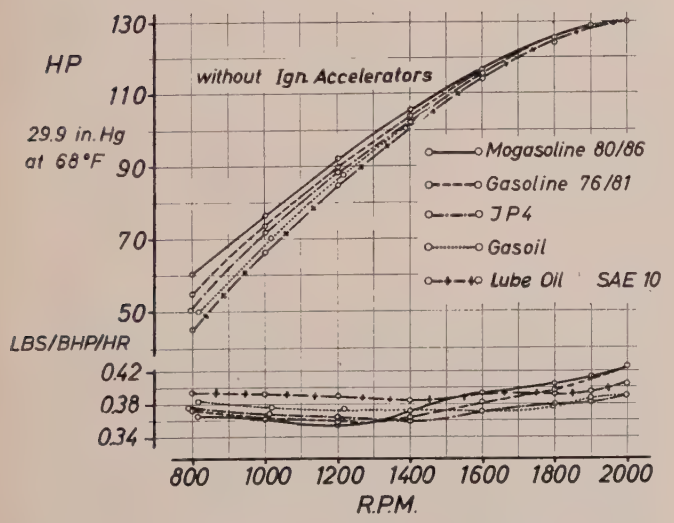

Fig. 18 – Output and sfc using different fuels in multifuel version of naturally aspirated, 6-cyl, 4.4. x 5.5-in. engine

Indicator Diagrams

In order to obtain distortion-free pressure diagrams, a cylinder head was drilled to accommodate the diaphragm of a quartz indicator placed flush with the cylinder head, thereby avoiding an additional clearance volume and indicator duct. A photograph of an actual diagram taken at 1900 rpm and 100 psi bmep is reproduced in Fig. 19. According to the needle lift diagram, injection begins 23.5 deg btdc and ends after a period of 33

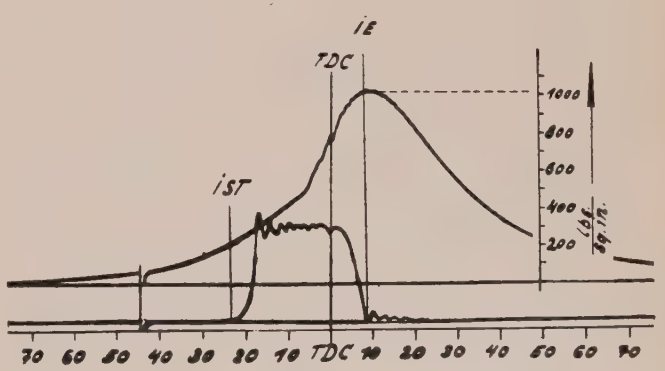

Fig. 19 – Pressure diagram at 1900 rpm and 100 psi mep

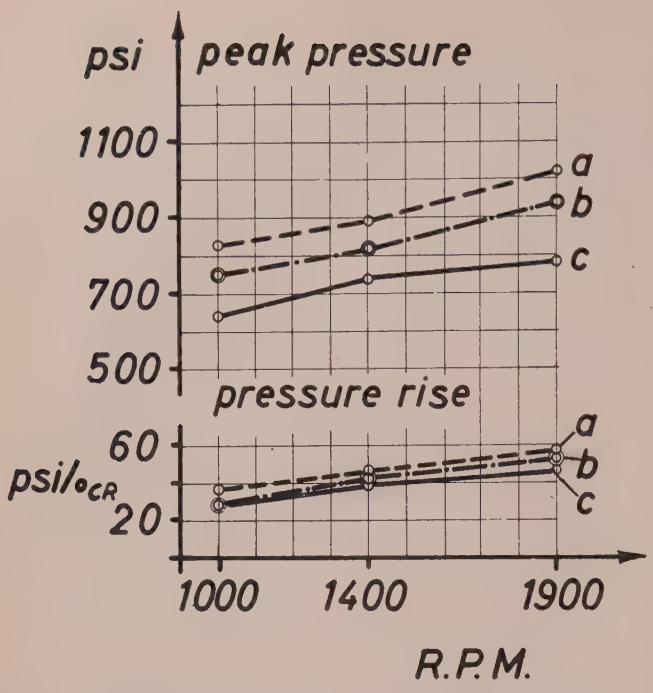

Fig. 20 – Peak pressure and pressure rise versus speed and mep. (a) 100-psi mep, (b) 77-psi mep, (c) 46.5-psi mep

deg of crank rotation, 9.5 deg atdc. Ignition takes place 7.2 deg btdc after an ignition lag of 16.3 deg of crank rotation. There is a constant rate of pressure rise of 57 psi per deg of crank rotation up to nearly the maximum pressure, which is attained 8.5 deg atdc. The pressure curve is free from modulating pressure oscillations. (The break interrupting the pressure slope was caused by the dead center mark.) The peak pressure is 1020 psi for injection timing resulting in the lowest fuel consumption. If the injection is retarded 4 deg of crank rotation, the peak pressure will drop to 920 psi, while fuel consumption and exhaust smoke deteriorate.

From the summary in Fig. 20 of results obtained from pressure diagrams, it is concluded that the rate of pressure rise required in the M-system to obtain optimum results is between 35 and 57 psi per deg of crank rotation. With increasing speed, the higher rate of pressure rise has to be accepted. Maximum combustion pressures are dependent on mep and speed. They range between 840 and 1020 psi according to the speed for an mep of 100 psi.

A good comparison between the combustion pattern in the M-system and in a diesel engine of the "air-distributing" type is afforded in Fig. 21, where two diagrams taken for the same mep are superimposed. The two ratings reproduced in the diagram correspond to the values at 1400 rpm given in Fig. 15 for test "M" and the test "without air swirl." It can be seen clearly that as a result of "air distribution," the pressure rises rapidly immediately after the beginning of combustion and causes the entire pressure pattern to shift upwards and towards the tdc position. With "air distribution," the reaction is very rapid initially, and as indicated by the unfavorable fuel consumption (see Fig. 15), must slow down considerably in the later stages. Conversely, the M-system succeeds in keeping the reaction rate low at the beginning of combustion, and increasing it towards the end of combustion. This is necessary in order to insure a low fuel consumption in spite of the retarded pressure peak (see Fig. 21), and the resulting low expansion ratio.

The very slow start of combustion is well-demonstrated by diagrams taken with a somewhat retarded injection or during idling (Fig. 22). Ignition takes place later, but transition into the combustion pressure rise is along a smooth curve without any sharp break indicative of the start of a very rapid reaction.

In order to ascertain the source of combustion noise which is audible outside the engine, the transmitted sound was recorded together with pressure in a manner such that the sound modulates the pressure curve. As shown in Fig. 23, in the M-system, no increase in noise amplitude is found after ignition and the beginning of combustion, and only at the moment of maximum pressure does a sound modulation appear. Contrary to the M-system, in the "air-distributing" engine, the

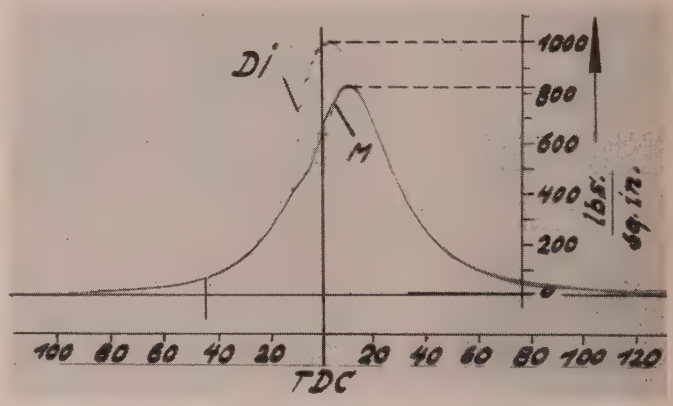

Fig. 21 – Comparison of pressure diagrams for different spray positions using same engine under identical operating conditions of 62 psi, mep and 1400 rpm. *D*, air-distributing, equivalent to direct-injection; *M*, M-system, wall-distributing

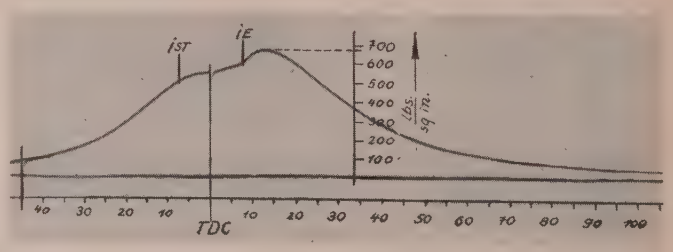

Fig. 22 – Pressure diagram with injection timing set 4 deg later than optimum

maximum amplitudes of sound modulation rise immediately after ignition and before the steep pressure rise is completed. This suggests that the source of sound is not only in the rapid pressure rise, but that similar to gasoline knock, the high rate of pressure rise is accompanied by pressure waves of high frequency which hit the combustion-chamber wall and cause metallic diesel knock.

An interesting test elucidating the ignition phenomena in the M-system can be made by relieving the spring load on the nozzle needle with the engine running, so that nozzle-opening pressure becomes zero. The same amount of fuel is injected into the cylinder as before, but the pressure is lower, particularly at the beginning of injection, so that no fine atomization takes place in the first phase of injection. Consequently, there is no self-igniting fuel fraction such as required in the M-system for pilot ignition, and in spite of the fact that fuel is injected, the charge must fail to ignite.

Actually, this can be observed at speeds up to about 1800 rpm even if the above test is made with maximum mep (and, therefore, maximum temperature in the combustion chamber). At higher speeds, the effect is not quite so clear because fuel velocity becomes high enough to form a small amount for initial ignition, although rather late.

Fig. 24 shows a diagram taken at 1400 rpm with an injection quantity corresponding to an mep of 100 psi. It closely resembles the compression diagram drawn below for comparison. The test confirms the three criteria of the M-system, namely:

1. Ignition is initiated by the "air-distributed" portion. If, as in the above test, there is no such portion, ignition must fail even with full injection.

2. Fuel rising from the combustion-chamber wall in the form of vapor is not ignited by the heat of compression, and if so, is ignited too late.

3. Mixture formation is accelerated essentially by the temperature rise during combustion. If this does not occur, as in the present case, vaporization will be negligible.

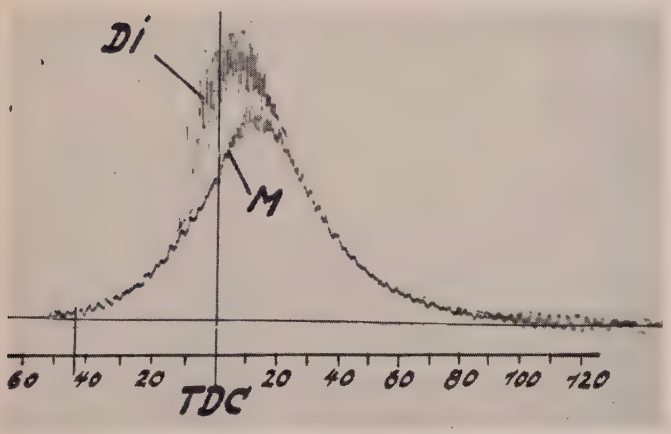

Fig. 23 – Pressure curve modulated by simultaneously recorded noise emanating from cylinder head in engine under same operating conditions as Fig. 21

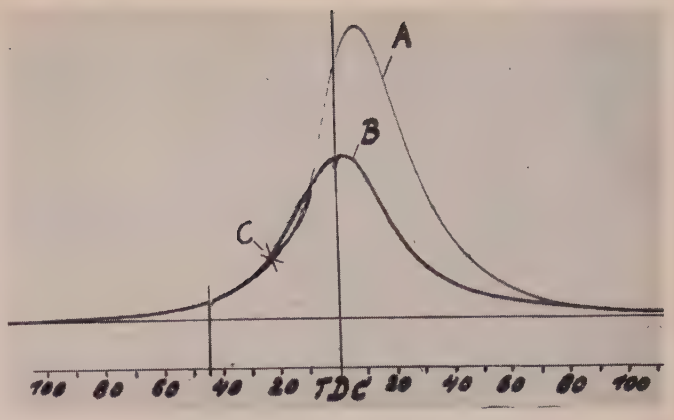

Fig. 24 – Comparison of pressure diagrams for following conditions:
A – Full-load injection with normal injector-pressure setting
B – Full-load injection with injector needle spring removed
C – Pre-ignition of fuel left from previous cycle

Evidence for a change in combustion pattern inferred from the disappearance of combustion noise and the variation of the oil analysis is supported by the indicator diagrams mentioned in the foregoing. They all support the contention that the M-system provides means for controlling combustion reactions in a high-compression engine and eliminates the drawbacks of conventional "air-distributing" diesel engines where control of reactions is effected by throttling the oxygen supply.

In the M-system, only a small portion of the fuel is allowed to undergo diesel-type auto-ignition, while combustion of the greater part of the fuel charge has the reaction characteristics of that in the gasoline engine.

Conclusion

The evaluation of reaction kinetics discussed in this paper has led to the M-system. The first realization of the M-system in the MAN truck-diesel engine still suffers from some compromises, but it shows clearly the following advantages over conventional combustion systems:

1. Diesel knock virtually can be eliminated even at very low speeds, resulting in a quiet engine with an extremely elastic torque characteristic.

2. Engines with the M-system can be operated as true multifuel engines on different fuels ranging from gasoline and jet fuels to diesel fuels without sacrificing engine performance.

3. M-system combustion produces less soot per pound of fuel than conventional systems at part load.

4. The path of reactions in M-system combustion

is similar to that in gasoline engines, resulting in lube oil contamination no greater than in gasoline engines.

Additional References

1. *Forschung auf dem Gebiete des Ingenieurwesens,* Ausgabe A, Vol. 7, March/April, 1936, pp. 51-65: "Kinetische Analyse des Verbrennungsvorganges in der Dieselmaschine," by K. Neumann.

2. *VDI-Forschungsheft,* March/April, 1936, pp. 1-31: "Spektraluntersuchung des Verbrennungsvorganges," by G. Beck and C. Erichsen.

3. *Automobiltechnische Zeitschrift,* Vol. 39, October, 1936, pp. 501-515: "Beitrag zum Verbrennungsvorgang in der Dieselmaschine," by K. Karde.

4. *Forschung auf dem Gebiete des Ingenieurwesens,* Vol. 6, September/October, 1935. Beilage Forschungsheft 375, 25 pp., "Zündung und Flammenbildung bei der Diesel-Brennstoff-Einspritzung," by O. Holfelder.

DISCUSSION

M-System Combustion Conditions Exist in All High-Speed, Solid-Injection Diesels

– Harry R. Ricardo
Ricardo & Co., Engineers (1927), Ltd.

IF I understand Dr. Meurer correctly, he contends that when combustion takes place on the fringes of the spray, as is usually the case – or at least as is usually supposed – the droplets are receiving heat at a greater rate than they are receiving oxygen, with the result that cracking takes place and things get out of control. On the other hand, when combustion takes place from the surface of a thin liquid film spread on the relatively cool combustion-chamber walls, it takes place mainly in the vapor phase and its rate can be controlled by the rate of evaporation and intensity of air swirl, whose function, in this case, I take it, is to peel off the burning vapor, layer by layer, and bring fresh oxygen to the next layer. There is still need, however, for a small – and apparently only a very small – proportion of free spray to initiate combustion. This is certainly a new line of thought to me, for from my earliest days, I was brought up to believe that on no account should liquid fuel be allowed to settle on the combustion-chamber wall. This new line of thought recalls, and somewhat explains, the results of our early experiments with compression ignition, for which I ask leave to go back a long time.

Around 1923 when we first set out to try to develop a really high-speed CI engine, we chose a sleeve-valve engine to start our experiments. Following Hesselman's early teaching, I believed – and still believe – that an organized air swirl is a highly desirable if not an essential feature if efficient high-speed operation is to be achieved. We knew we could both obtain and control air swirl within close limits using a sleeve-valve engine, and do so without curtailment of breathing capacity. Other reasons for our choice were that with no valves in the head, we had much greater freedom of maneuver as regards combustion-chamber shape. Last, but not least, we had become very fond of the sleeve for its own sake.

In these experiments we employed a cylindrical combustion chamber about one-half the diameter of the piston and about the same height, with a single orifice injector squirting directly downward towards the flat piston crown. The spray was in the form of a narrow angle cone; as a first approximation we located the injector at about the radius of gyration, far enough out from the center to encounter most of the rotating air, but not far enough to impinge against the surrounding walls. Once the rate of air swirl and fuel delivery had been correctly matched, this setup gave pretty good high-speed performance but with a very pronounced diesel knock. We tried relocating the injector, and somewhat to our surprise, we found we got both the best all-around performance and least diesel knock with the injector as far away from the center as we could get it, namely, about ⅛ in. from the side wall. Under these conditions nearly half of the total fuel injected must have impinged against the cold side wall. Indeed, this was proved by motoring the engine and injecting a noncombustible pigment for a few cycles. Unconsciously, then, we were working under somewhat the same conditions as Dr. Meurer advocates. Some years later, when our sleeve-valve diesels were in production and being marketed in the Far East, we were faced with the problem of getting them to run on a very low-cetane fuel from Borneo. To this end we fitted a heat-insulated austenitic steel liner inside the combustion chamber. This proved very effective, but we also found it necessary to greatly speed up the rate of air swirl (to the best of my recollection, from about 9 to 13:1), presumably because of the greater rate of evaporation of the liquid fuel sprayed on a much hotter surface.

Quite recently we have been developing a technique of combustion photography using a wide variety of combustion-chamber shapes including direct injection, "Comet" type, "Whirlpool," and others, and in all of these we have been a little surprised to find how considerable is the proportion of fuel which is actually deposited on and burned from the surface of the combustion-chamber walls. This, however, is an accidental, not a deliberately chosen condition, as in the MAN engine. In short I suggest that the combustion conditions Dr. Meurer advocates are present to some much lower degree in every high-speed, solid-injection diesel engine, but to Dr. Meurer and the MAN Co. is due the credit for recognizing, evaluating, and cultivating them.

Comparisons between M-System and Cummins Engine Combustion

– N. M. Reiners
Cummins Engine Co., Inc.

AT Cummins, we have always considered exclusive our combination of fuel metering, injection, and combustion. Now there is another exclusive combination based upon a new concept of diesel combustion, wherein Dr. Meurer focuses attention on the importance of reaction kinetics. We are prompted to re-examine our experience and to re-evaluate our thoughts and opinions.

In his conclusion, Dr. Meurer states that "the first realization of the M-system in the MAN truck-diesel engine still suffers from some compromises." For whatever aid it may give Dr. Meurer in refining his system or further developing his combustion concept, I should like to cite some comparable data and draw some comparisons between the M-system, as described in the paper, and the combustion characteristics in Cummins engines.

For this purpose, our Model NH 6-cyl engine is best

suited. It has approximately the same displacement, being just slightly larger, is rated at the same rpm, develops the same bmep when naturally aspirated.

The Cummins combustion system consists of direct injection into an open chamber located in the piston crown. The chamber is essentially of the quiescent type. No attempt is made to induce "swirl" and there is little "squish" from the piston rim. There is no controlled air movement other than the indiscriminate motion generated by air passing through the inlet ports.

The Cummins injector is basically a constant-stroke reciprocating positive-displacement pump. The plunger reciprocates along a controlled path which is fixed by the injector-cam shape. Engine speed and load are controlled entirely and completely by the quantity of fuel metered into the injector cup by the fuel pump during the time the plunger is retracted. The fuel charge never completely fills the cavity; the remaining portion of the cavity fills with heated compressed air from the engine cylinder during the compression stroke. Air enters the cup through the open spray holes. Thus, a mixture of heated air and fuel is prepared in the cup before actual injection. Therefore, in this phase of Cummins combustion, the fuel is being heated in the presence of little air, complying to a degree with Dr. Meurer's suggestion "that during ignition lag diesel fuel somehow cannot stand being mixed with air at all."

Because of the vaporous mixture within the injector cup of the Cummins system, actual injection does not commence when the cam starts the plunger downward. Injection cannot begin until pressure in the cup equals and then exceeds the pressure existing in the combustion chamber. At the beginning of injector-plunger movement, the plunger is compressing a mixture of air and fuel. Pressure rise in the cup follows the rules for compressible fluids, producing a relatively slow discharge of vapor and fuel or "pilot injection." Soon, however, the downward-moving plunger compresses the mixture to a substantially solid mass; then the rate of pressure rise in the cup increases sharply, producing the necessary propulsion force to inject the main charge. The rate of injector-plunger travel during injection of the main charge determines the degree of atomization, penetration, and distribution of the fuel emerging into the combustion chamber. Since the small pilot charge is displaced and arrives in the combustion chamber prior to the main charge, it passes through the usual ignition delay but has already started the fire when the main charge arrives. Thus, the condition for minimum ignition delay, and fast, smooth combustion of the main charge has been prepared by the initial injection characteristics of the injector system. The outstanding starting ability, performance, output, and service life established by actual field service are indicative of the degree to which the Cummins combustion system provides conditions favorable to the combustion process itself.

Dr. Meurer suggests that compliance with reaction kinetic concepts is imperative if the following objectionable phenomena which cause the most trouble in diesel combustion are to be eliminated:

1. "Combustion noise, a more or less intense knocking depending on fuel properties."

2. "Exhaust smoke which develops before the excess air is fully used up."

At full power, exhaust from the NH engine is commercially clean throughout the speed range to the extent that it is acceptable for city bus operation, and though combustion noise may be called audible, it is not considered objectionable to the ear and under normal conditions of operation can hardly be classified as knock.

At 2100 engine rpm and rated bmep of 101 psi, fuel injection begins 22 deg btdc and ends after a period of 37 deg of crank rotation, 15 deg atdc. Ignition begins 8 deg btdc after an ignition lag of 14 deg of crank rotation. Compression pressure is 525 psi, maximum rate of pressure rise is 78 psi per deg of crank rotation, and maximum cylinder pressure of 850 psi peaks 6 deg atdc.

With the exceptions of rate of pressure rise and maximum cylinder pressure, these characteristics are practically identical to those of the M-system at the same conditions of speed and load. True, the M-system gives a lower rate of pressure rise of approximately 60 psi per deg of crank rotation, compared to 78 in the Cummins engine, but with practically identical compression pressure, maximum cylinder pressure is higher – approximately 1060 psi compared to 850.

The Cummins NH engine tolerates a rate of pressure rise of 78 psi per deg of crank rotation, as evidenced by excellent record and service life where 500,000 miles or more of trouble-free service is obtained in many cases. Apparently injection and combustion characteristics are such that the uniformly increasing rate of pressure rise which exists permits exceptionally high maximum rates of pressure rise with no adverse effects. In fact, in the supercharged version of this engine, experience and engine life are good with a maximum rate of pressure rise of over 100 psi per deg of crank rotation. It seems that the maximum permissible rate of pressure rise is governed by the conditions generating and developing it as well as the ability of the working parts of the engine to withstand it without adverse effects.

Regarding fuel consumption, there appears to be no significant difference between the MAN and Cummins NH engines. At all comparable speeds and loads, the brake sfc is practically identical.

Regarding fuel spray impinging on metal in the combustion chamber, we agree with Dr. Meurer that it is permissible without detriment under certain conditions. Admittedly, we have made no evaluations taking into consideration Dr. Meurer's reaction kinetic concept, and we have felt it not desirable to do so as a general rule. However, we have indications that fuel caroms off the piston rims in our engines and is burned efficiently without smoke. At one time in our research work, we tried a comparatively flat-top piston with no rim. The angle of fuel spray was varied and the best performance was a few percent under that obtained with our conventional chamber. We noted that optimum performance was had with considerable fuel impingement on the top of the piston. At that time, tests were run to evaluate the effects of squish and the only significance attached to fuel impingement on top of the piston was that it could be tolerated to a degree.

From the information presented by Dr. Meurer, it appears the principal advantage of the M-system is that it can be operated as a true multifuel engine. In this connection, the ability of the Cummins combustion system to digest various grades of fuel is also considered good. Our range of laboratory testing has included light fuels such as kerosene and heavy fuels up to the equivalent of No. 4 fuel oil with cetane ratings ranging between 35 and 55. With all these fuels, we found no practical difference in performance or operation throughout the load and speed range of the engine. We officially approve the use of No. 1 or 2 diesel fuels in our engines; they are the commercial fuels readily available to the operators of our engines in the United States.

M-System Engine Performance Tested in United States

– Herbert H. Haas
Continental Motors Corp.

THERE is no doubt that Dr. Meurer has thoroughly upset conventional thinking on the diesel-combustion process, and we would like to substantiate the fact that the MAN

diesel engine demonstrates the practical result of the theory. The engine which we tested at Continental has performed exactly as Dr. Meurer has indicated. An excellent fuel consumption is combined with a very soft and smooth engine operation. No combustion noise is present, even when using 80-octane gasoline.

The multifuel aspects of the engine are also very interesting, and Fig. A shows the full-power performance obtained with several fuels. The only engine adjustment required to do this is a change in the fuel-injection pump stop to permit full power with lower sp gr fuels. Complete evaluation with all different fuels is not finished yet, and whether supplementary difficulties will develop is not known at this time. However, from the viewpoint of multifuel operation, engine performance has already been outstanding.

Speculation has occurred regarding the heat rejection of this engine in view of the high turbulence and the piston oil cooling required for such a relatively small-bore engine. Fig. B shows that the overall heat rejection which we

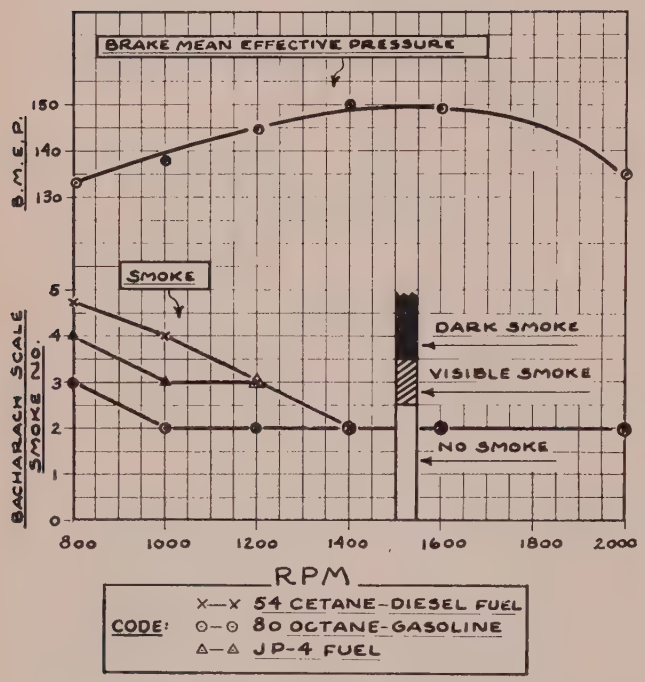

Fig. A – MAN diesel engine exhaust smoke at full load with various fuels

obtained appears to be of ordinary magnitude. A probable difference compared to other engines of this kind is the slightly higher heat rejection to the lube oil which is compensated by a proportionately lower heat rejection to the coolant.

Dr. Meurer's remarks regarding less smoke with more volatile fuels is substantiated by Fig. C, showing some smoke at low-speed "lugging" conditions when using diesel fuel, but no smoke under any conditions when using gasoline. Acceleration from idling also shows a period of smoke with diesel fuel, but none with gasoline.

Besides this short summary of our evaluation of the MAN engine, I would like to add a few considerations about some interesting coincidences which emerged from this meeting and which are probably worthwhile to mention.

In their excellent paper, Caris and coauthors reported new ways to improve the mechanical octane number of spark-ignition engines. However, the means used look very familiar to diesel engineers:

1. A compact combustion chamber formed by a spherical cavity in the piston crown.

2. Small clearance between piston top and cylinder head, minimizing the amount of air outside the combustion chamber.

3. Intensive squish action inherent with this configuration.

4. High turbulence created by a shrouded valve.

All these features are very similar to those used in open-chamber diesel engines for a long time.

It is rather likely that such a similarity of configurations generates somewhat similar effects with regard to the combustion process in the spark-ignition engine as well as in the diesel engine. Actually, this appears to be so to a fairly wide extent, despite the fact that both parties approach each other from opposite ends of the line. Looking closer at the specific combustion problems of both engine types, we recognize that they have become less different in the last years than we are wont to believe.

As regards the compression-ignition engine, the major reason for this change seems to be the continuing increase in speed which creates serious injection problems. In the earlier days of diesel engines, the injection rate performed combustion control and this is still the case on large, low-speed engines today. In modern, high-speed, compression-ignition engines, injection time had to be shortened so much (less than 0.002 sec) that the injection rate over the duration of injection runs out of control. This problem has been aggravated further by the continued increase in the quantity of fuel injected per stroke (reaching 200 cu mm and more on high-output engines), due to the rapid increase in supercharging ratio. Actually, we are driving fuel into the cylinder with a sledge hammer, creating dynamic pressures in the injection system of 8000 to 20,000 psi and more. On the other hand, ignition delay of our present commercial fuels is a somewhat constant factor of about 0.001 sec which has not improved very much during the last few decades. Consequently, a major portion of the fuel is already dispersed in the combustion chamber before ignition occurs. Instead of creating and maintaining a successively progressing combustion process, a rather instantaneous detonation-like combustion starts all over the charge, leading to a steep pressure rise and high peak pressure. This, of course, becomes more significant if low-cetane fuels like gasoline are to be used in spark-ignition engines.

Considering spark-ignition combustion, the problem of detonation of the rest charge is well-known and looks very similar to the aforementioned problem of diesel knock, the only difference being that it arises during the second half of spark-ignition combustion rather than at the beginning, as in compression-ignition engine. Likewise, in both systems, an ignitable air-fuel mixture exists in the combustion chamber and is exposed to high pressure and temperature, so that detonation is more likely than controlled combustion. I think the relationship between spark- and compression-ignition becomes very apparent at this point. Why should it not be possible to solve the same problem by the same method?

If we remember the Hesselman, Texaco, and finally the new MAN development – and in some ways, also, the pre-combustion chamber – we recognize that these systems tend to start combustion in a well-defined area of the combustion chamber and provide a successively progressive combustion rather than prepare and ignite the whole charge simultaneously all over the combustion chamber.

At this point I think that the excellent clarification of the combustion mechanism disclosed by Dr. Meurer, and the

successful application of theory in the new MAN engine is an important step forward in our knowledge of internal combustion, not only with regard to the diesel engine, but also with regard to every kind of combustion system, and offers an outstanding solution to the aforementioned problems. It makes the combustion process widely independent of the injection mechanism by successive controlled formation of ignitable mixture and its ignition by a few already burning particles (spark plugs) without additional mechanical complication. This has been accomplished mainly by the logical exploitation of chemical combustion reactions in the running engine.

It would exceed the scope of this discussion to go further into the fascinating aspects of the probable relationship between spark and ignition combustion and the applicability of Dr. Meurer's theory to the spark-ignition engine, but I am sure that a lot of thinking will go on along the lines established by Dr. Meurer's combustion theory.

M-System an Important Consideration In Future Diesel Development

– P. H. Schweitzer
Pennsylvania State University

AUTO-IGNITION of hydrocarbons is not merely an oxidation process, direct or indirect; thermal decomposition or breakdown of molecules due to pressure and temperature, in the absence of oxygen, is a decisive part of the process. The hard-to-burn solid carbon among the combustion products is not the result of oxidation at all but of thermal cracking when the latter is allowed to continue to its very end.

This much was already known before. What Dr. Meurer discovered is that the mere presence of an adequate amount of oxygen adjacent to fuel molecules will not, in itself, insure the oxidation of the hydrocarbon, because the diffusion of oxygen to the reaction cannot keep pace with the avalanche of thermal disintegration.

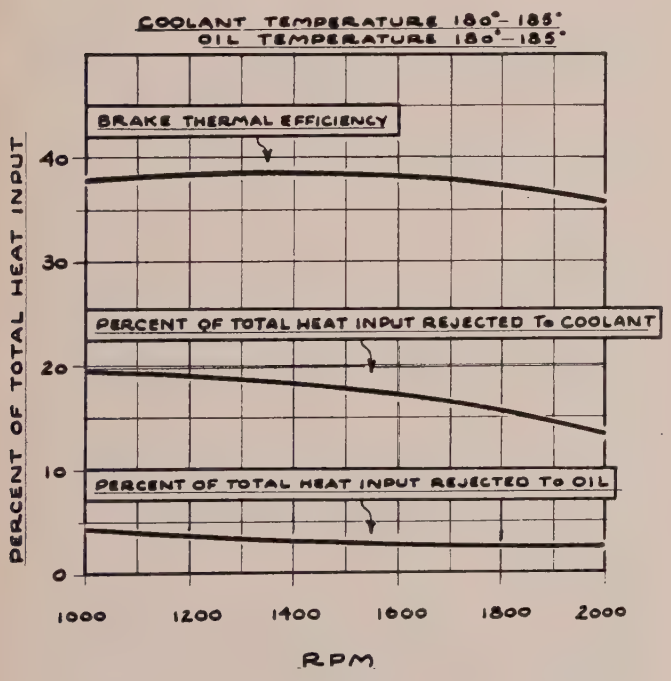

Fig. B – MAN diesel engine full-load heat rejection

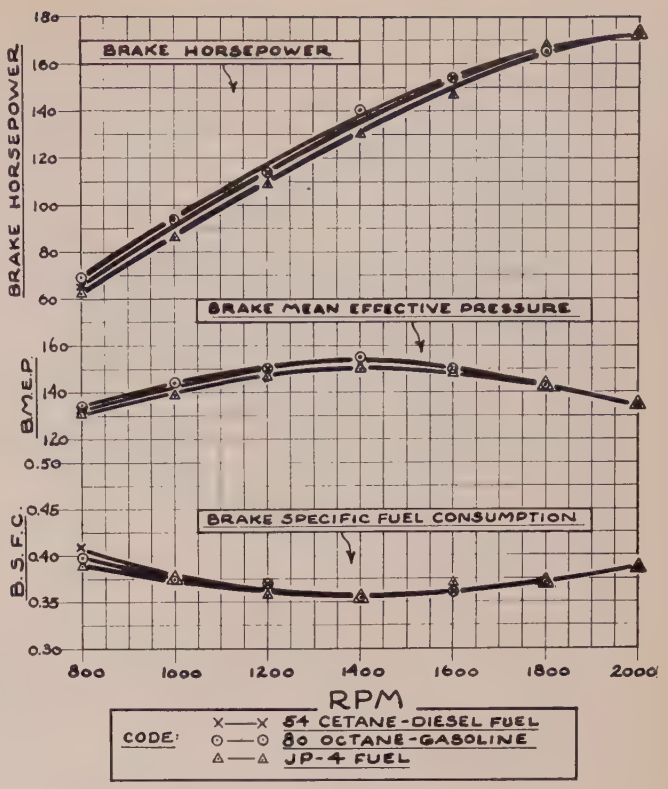

Fig. C – MAN diesel engine full-load performance

What we are faced with is a race between the thermal effect on reactivity, going up at an exponential rate, and the diffusion rate of oxygen, changing only gently with time. The latter is left hopelessly behind in the conventional diesel-combustion process. The result is that thermal breakdown of the hydrocarbon proceeds to its destructive end with pure carbon particles left over which are next to impossible to burn. Hence diesel smoke.

Dr. Meurer's solution to this unpleasantness follows logically from his theory and takes care of diesel knock at the same time, all without sacrificing either power or fuel economy. He slows down thermal decomposition and speeds up oxidation when it is really needed in the latter stages of combustion. When cracking and oxidation are brought to a semblance of balance, troubles related to diesel combustion begin to disappear.

Now the pieces of this jig-saw puzzle begin to fall into place. Seemingly unrelated observations can be understood. Air-injection engines had little smoke. In swirl-chamber engines, injection in the direction of air rotation is good for running, bad for starting. Poorly-atomized injection often resulted in a quieter engine. Introduction of fuel into intake air reduces exhaust smoke of a compression-ignition engine. The use of heavy oil in a high-speed engine causes excessive cylinder wear (carbon abrasion, Lyn.).

Besides such hindsight, Dr. Meurer created a truly outstanding engine able to burn a variety of fuels from gasoline to crude oil.

Of course, there are still wide gaps in our knowledge. The mechanism of the cracking process and the chemical and physical properties of intermediate combustion products are largely unknown. With such knowledge, engines and fuel could be designed to permit getting more ft-lb per Btu with less noise, smoke, stink, and wear than we are getting now.

Dr. Meurer's invention is an important step in that direction which it would be unwise to ignore in any future engine

development. While the M-system engine is already a commercial success, Dr. Meurer is the last person who would consider it the ultimate and not subject to further development.

Author's Closure To Discusssion

DR. Hass pointed out rightly that it may not be justified any more to speak of "diesel-engine combustion" and of "gasoline-engine combustion" as of two different things. With the M-system it is indeed possible to relinquish any mechanical octane-number requirement. Knocking will occur only if the fuel-air mixture stays a sufficiently long time under the influence of pressure and temperature. With the M-system the two components are in the combustion chamber initially not mixed and therefore essentially not influencing each other, so that any reactions which may further knocking cannot occur at all. The actual mixing process only takes place, dose after dose, immediately before combustion, and for each dose so rapidly that mixing and burning are already completed before any reaction leading to knocking can spread. This shows that the M-system is not only a way to avoid knocking at the beginning of combustion, but also during and at the end of combustion. If an engine with the compression ratio of a diesel engine is to be operated without fuel decomposition, then knocking must be avoided in each and every moment of the combustion process. In an engine with electric ignition, it is essentially the knocking at the end of combustion. For both cases, the M-system shows the way.

Mr. Reiners drew some parallels between the Cummins injection system and the M-system. In a Cummins engine, some preoxidation may be effected by air entering the injection cup, but its extent appears to be quite minimal due to the small heat content of the small quantity of air entering the cup. The main fuel charge is, undoubtedly, being air distributed, as in the conventional diesel engine, and combustion takes place along the usual lines through decomposition stages. It will hardly be possible to operate such an engine on gasoline, particularly of higher octane numbers.

ORAL DISCUSSION

Reported by W. E. Meyer

Pennsylvania State University

John Dickson, Detroit Diesel-Engine Division, GMC: The M-engine we have in our laboratory comes up to all its claims. This is something we could say about very few of our competitors' engines, which we have had occasion to test through the years. It is a pleasure to listen to this engine and to realize that it is a diesel.

I disagree with the author on the question of exhaust smoke and particularly on his contention that the smoke density of the M-engine begins to increase at a much higher load than that of other diesel engines. I believe that combustion begins to be incomplete with any good engine – the M-engine not excepted – at about 50 bmep. For 20 different engines a plot of log bhp or log ihp versus fuel per cycle gives straight lines that show a break at 50 bmep. The reason for this break is not fully understood, but it is evidence of incomplete combustion, which shows up in the exhaust as increased smoke.

Dr. Meurer: The causes of diesel smoke seem to lie in the conventional methods of mixing and burning fuel with air. I believe that smoke is due not so much to simple unavailability of oxygen as to reaction kinetics that prevent full utilization of the available oxygen. The importance of the M-system rests in its different mechanism of mixture formation, since this results in a different type of combustion. If, in a conventional engine, the mean temperature level of the cycle is lowered, the smoke will be increased, although the mixture formation has in no way been affected or changed. This clearly indicates that it is not mixing per se that controls smoke but the decomposition and combustion processes. These, however, can be influenced in the desired direction by choosing a different type of mixture formation, as is done in the M-engine.

I believe that Mr. Dickson did not look at Fig. 12 in the way in which it is presented. Fig. 12 shows, at constant rpm, smoke content versus mean effective pressure. However, the percentage scale of the abscissa does not refer to the volume of the exhaust gases, but it is proportionate to the quantity of fuel injected. Thus the curves apply always to the same quantity of injected fuel, and so they indicate what percentage of the carbon contained in the injected fuel reappears in the exhaust gases in the form of smoke. These curves are, therefore, not comparable with the usual exhaust smoke curves showing percentage of smoke relative to the volume of exhaust gases.

Only by this method of graphic illustration does it become clear that, in the conventional diesel engine, the formation of smoke is not at all influenced by the fuel-air ratio. It also shows that, with the M-system, within the range of low loads, a smaller percentage of the carbon contained in the injected fuel appears in the exhaust gases as smoke. Moreover, it becomes apparent that the more stable gasoline molecules indeed form less smoke. This fact is considered to prove the presented theory of the combustion mechanism in the conventional diesel engine which is characterized by decomposition of fuel molecules.

It is a task for the future to change the molecular structure of the fuel so as to prevent the occurrence of undesirable reaction chains. The key to the smoke problem lies in the temperature history of the fuel prior to burning. Since gaseous molecules are more temperature stable than liquid molecules, smoke will be reduced if the hydrocarbons are completely vaporized before burning is initiated. If this can be accomplished there will be less smoke. Such a course also reconciles the contradictory requirements of a high cetane rating for ignition, and a low one for burning, because the vapors of a diesel fuel have a much lower cetane number than the liquid.

C. G. A. Rosen, Caterpillar Tractor Co.: Is there any limit to the cylinder size to which the M-system can be applied?

Dr. Meurer: It is being used experimentally on an engine of 7-in. bore and, on the other end of the scale, on an engine of 3-in. bore. The shape of the combustion chamber may have to be varied in order to adapt the M-system to the cylinder size, however, in every case the three rules laid down in the paper must be obeyed.

A DESCRIPTION of ride analysis by experimental and mathematical methods is presented. Test facilities and instrumentation employed in experimental analysis are described, followed by presentation of actual test results.

The application of electronic analog computers to mathematical analysis is explained, and experimental results are correlated with mathematical analysis. Results of experimental and mathematical analyses are interpreted in terms of passenger comfort limits.

The authors cite the need for more extensive information regarding response of the human body to motion in passenger cars.

Passenger-Car Suspension Analysis

A. C. Bodeau, R. H. Bollinger, and L. Lipkin
Ford Motor Co.

This paper was presented at the SAE Golden Anniversary Summer Meeting, Atlantic City, June 15, 1955.

PASSENGER-CAR ride is an impression. In a broad sense, it can be defined as an impression of the comfort of the car. The impression is perceived through the senses of sight, touch, and hearing, in response to external stimuli by motions, forces, and sounds. We can relate the stimuli to the senses as follows:

1. Sight – Motions arising from:
   (a) Motion of the passenger with reference to the road.
   (b) Motion of the passenger relative to the car.
   (c) Relative motion between portions of the car.
2. Touch – Forces created by:
   (a) Accelerating the passenger or portions thereof.
   (b) Relative motion between portions of the body.
3. Hearing – Noise created by:
   (a) Road surface irregularities.
   (b) Relative motion between various portions of the car.
   (c) Powerplant, drive train, and other mechanical components.

As engineers we are not particularly equipped to discuss the psychological or physiological response of the human body. Thus, we deal primarily with the physical phenomena of motions, forces, and sounds, all of which are measurable and fall in the engineering domain. Ride, however, is a problem in human engineering, and wherever possible one must interpret the results of ride analyses in terms of the physiological and psychological response of the passengers.

Under this broad definition of ride there are three sources of stimuli. The first source involves the response of the vehicle to road surface irregularities. The jouncing a passenger is subjected to in driving over a railroad crossing and the drumming vibration encountered on brick roads are two very different though typical examples of stimuli from this source.

The second source of ride stimuli is the responsiveness and stability of the vehicle to the driver's maneuver commands. Feel of the steering wheel re-

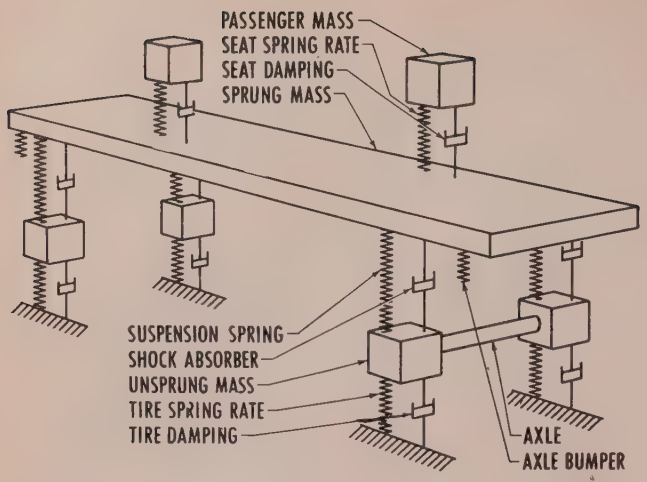

Fig. 1 – Ride analysis schematic diagram

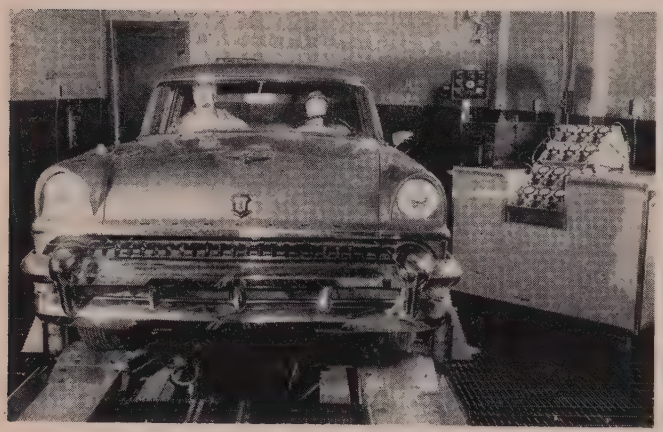

Fig. 2 – Car in position on "bump rig"

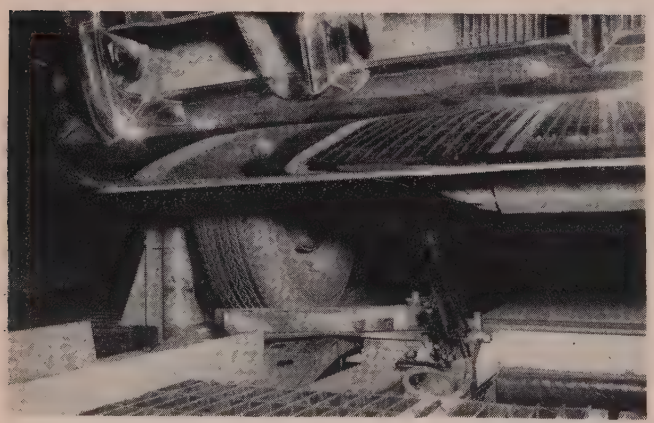

Fig. 3 – "Flying wedge" used to simulate transient problems

lated to turning of the car in response to steering commands is a typical example; feel of the brake pedal and deceleration of the vehicle in response to application of the brakes is another.

A third source of stimuli which falls under our broad definition of ride are noises and vibrations which emanate from the powerplant, power transmission system, and other such sources.

Engineers generally think of the three sources of disturbing stimuli separately and distinctly, realizing that there is frequently an interaction between disturbances from one source and those of another. For purposes of identification, the disturbing stimuli arising from the three sources are given names as follows:

1. *Ride:* Stimuli created by the vehicle in response to road surface irregularities.
2. *Controllability:* The response of the vehicle to maneuver commands.
3. *Noise and vibration:* Disturbances created by the powerplant and other parts.

Thus, the engineer's definition of "ride" is quite specific, and this definition of passenger-car ride will be used in this paper.

The objective of ride analysis is to improve passenger-car ride through an understanding of the mechanics of response of the car and interpretation of ride data in terms of response of the passenger. The steps which are generally involved in a ride analysis are:

1. Determine and compare the ride characteristics of cars.
2. Determine what changes should be made to improve the ride characteristics.

The three methods currently employed in ride analysis are called observation, experimental analysis, and mathematical analysis.

Observation Method

The most obvious method of determining ride characteristics of a car is to drive and ride in it over various types of roads and observe its performance. To determine what changes should be made, one makes the changes and observes their influence. The observation method is the oldest, quickest, and most widely used method of evaluation. It was largely through the application of the observation method, and the experience and calibrated posteriors of ride engineers, that the ride of our present cars was evolved.

Ride engineers recognize the following shortcomings of the observation method.

1. The method depends upon the observer's memory to make comparisons, because he cannot observe the ride characteristics of more than one car at a time. Observations rely on sharpness of the observer's perceptions, and are subject to the observer's moods and prejudices. In short, the observation method is a subjective method which does not supply numerical data which can be evaluated on an absolute basis and compared over long-time periods.
2. The observation method generally will detect disturbing ride characteristics, but will seldom determine the source of the disturbance or indicate corrective measures.

Experimental Analysis

Lord Kelvin, the renowned 19th century physicist, had similar shortcomings in mind when he said: "I often say that when you can measure what

you are speaking about, and express it in numbers, you know something about it; but when you cannot express it in numbers, your knowledge is of a meager and unsatisfactory kind."

When a ride analyst looks at a car he sees a problem in dynamics and thinks of the car as a collection of springs, masses, and dampers (Fig. 1). To determine ride characteristics, he must study the motions of the system and the interaction of the various components. It is important to interpret ride data in terms of the passenger's motion response, and to do this the passenger's body must be considered part of the system.

To create the motions of the system a great variety of test devices have been used. A device which we find very useful is an indoor test road which we call the "bump rig" (Fig. 2). The rig is comprised of a pair of 6-ft-diameter drums belted to an electric motor capable of driving or absorbing 75 hp from the drums at peripheral speeds up to 105 mph. Road surface irregularities are simulated by cams and cleats bolted to the drums. By varying the speed of the drums and number of lobes on the cams, excitation frequencies ranging from ten to several thousand cycles per minute can be obtained.

The rig is arranged to excite either the front or rear wheels, permitting the excitation of one end without excitation from the other end influencing the measurements. Drums are mounted so that one may be indexed with respect to the other, thus readily allowing changing the phase between bumps. This feature is useful when changing from in-phase excitation generating a pitching motion, to out-of-phase excitation producing a rolling motion.

The "flying wedge," a 2 x 4 beam pivoted to the structural members, is used for transient problems such as those encountered when hitting a small pot hole (Fig. 3). The beam is pulled between the wheel and drum, which then eject it rearward. Expansion joints are simulated by means of a ½ x 2 in. cleat bolted to the drum, and road noise is studied by means of cams with surface roughness of desired texture.

Instrumentation for ride studies has taken many different forms. One of the simplest devices is a masked flashlight bulb which projects a narrow beam of light on the lens of a camera (Fig. 4). The light is mounted on the car with modeling clay or a suction cup, and the camera is mounted on the floor of the room. The motions of the car are recorded on the film by opening the shutter at the desired test conditions.

Where it is desirable to correlate the motion of various parts of the system, modern electronic measuring instruments are most useful (Fig. 2). Such instruments generally consist of:

1. Transducers which produce an electric signal proportional to a function of the motion under study (Fig. 5).

2. Amplifiers which operate on the transducer

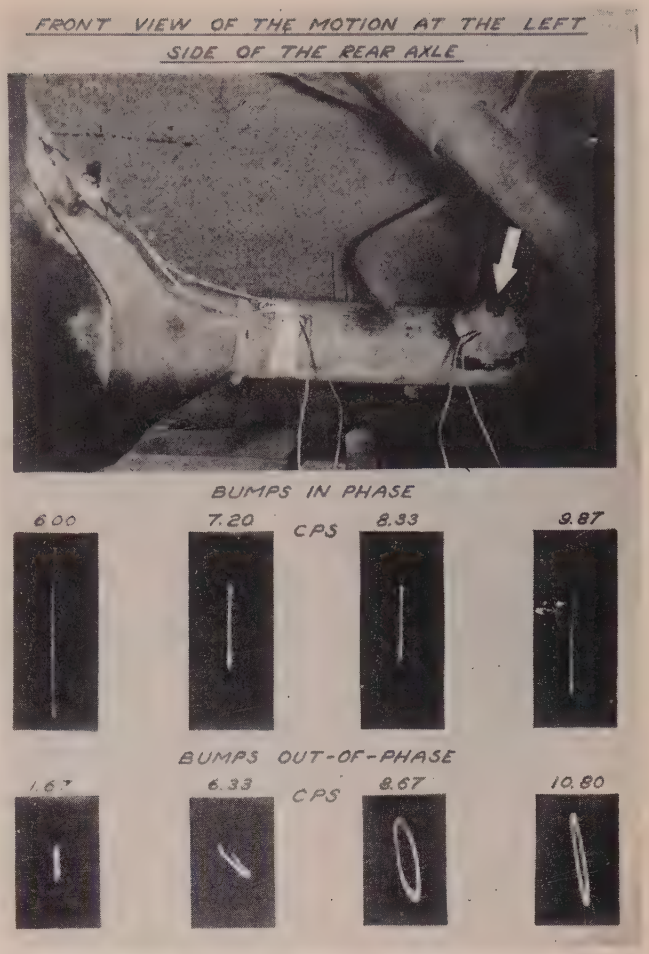

Fig. 4 – Illustrating results obtained with light-beam instrumentation

Fig. 5 – Transducers positioned on dummy placed in test car

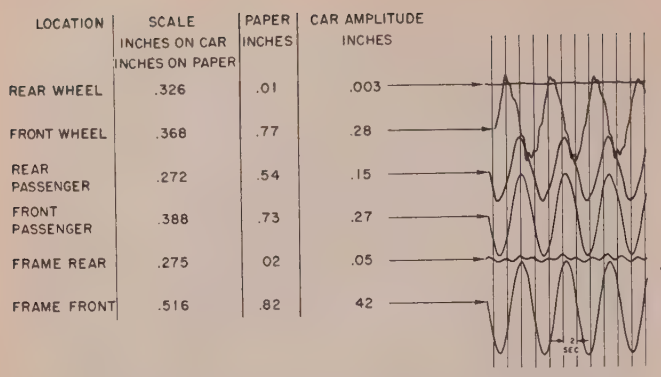

Fig. 6 – Sample oscillogram for front excitation at 9.4 cpm

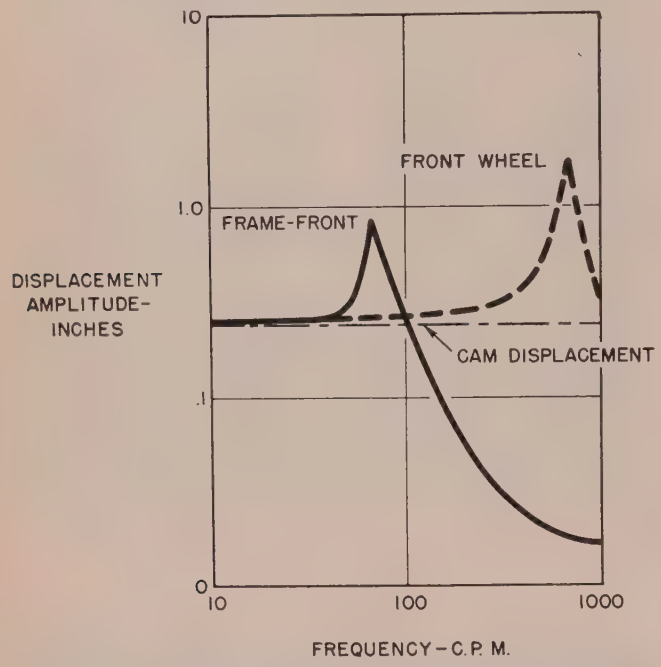

Fig. 7 – Vehicle frequency response to sinusoidal, front wheel, in-phase excitation

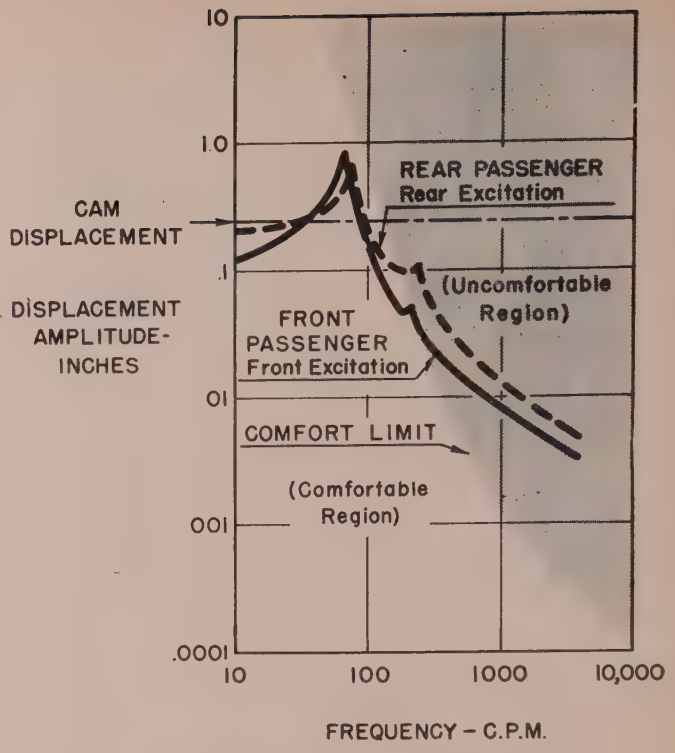

Fig. 8 – Passenger response and comfort limits

signal and prepare it for the multichannel recorder.

3. A multichannel recorder on which several signals can be recorded simultaneously.

The instruments produce an oscillogram, or a scaled reproduction of the function of the motions plotted against time (Fig. 6). The function of the motion may be displacement, velocity, acceleration, or the rate of change of acceleration, commonly called "jerk."

When the drum cams are sinusoidal, the displacement amplitudes of the motions at the desired points of the system are plotted against the cam frequency and define the familiar resonance curves (Fig. 7). With the front wheels on the drums, resonance measured near the front end of the car in the vicinity of 70 cpm is called the front pitch natural frequency, while that near 600 cpm measured on the front wheel is called the front-wheel hop natural frequency.

Similar measurements made with the rear wheels on the drums determine the natural frequencies of the rear pitch and rear-wheel hop. Indexing the drums so that cams alternately raise the left and right wheels permits the determination of the natural frequencies of the sprung mass in roll and the rear-axle assembly in tramp.

The responses of the passengers are plotted on a graph which also shows the comfort limits (Fig. 8). Small peaks in the vicinity of 200 cpm are the natural frequencies of the passengers on their seats. Large peaks in the vicinity of 70 cpm are reflections of the front pitch and rear pitch natural frequencies of the sprung mass. Examination of the data on the rear passenger indicates that his displacement at the rear pitch natural frequency (75 cpm) is nearly seven times that at the seat natural frequency (235 cpm). His motion at 75 cpm is about 70% of the comfort level, while at 235 cpm it is nearly four times the comfort limit. Despite much larger displacement at the pitch frequency, reductions of the displacement in the vicinity of the seat frequency are more beneficial to increased comfort.

In relating the stimuli to the senses, relative motion between passenger and car and portions of the passenger's body were outlined. These relative motions can be determined by further analysis of the data (Fig. 9) and can be considered relative motion between the passenger's body and the car body, as well as relative motion between the passenger's body and feet and/or hands. Here no comfort limit is indicated, as no generally-accepted comfort limits exist for this type of motion.

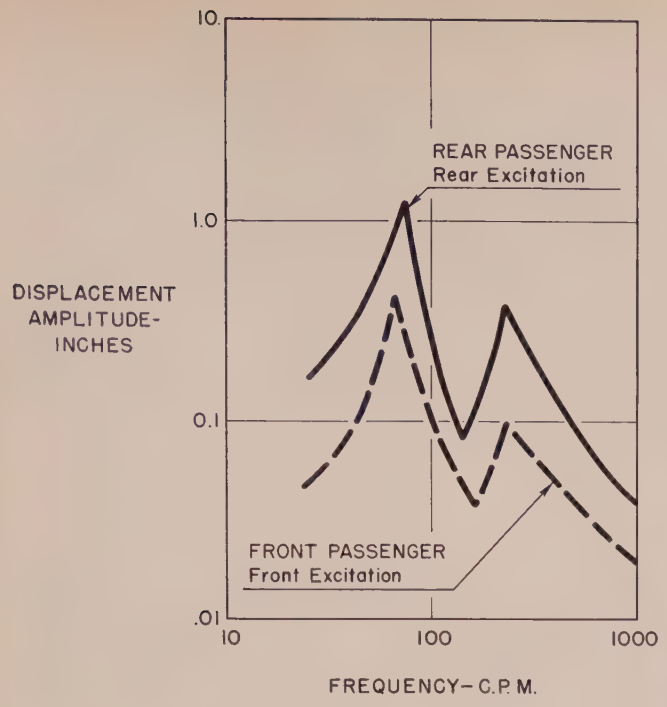

Fig. 9 – Relative motion between passenger and car

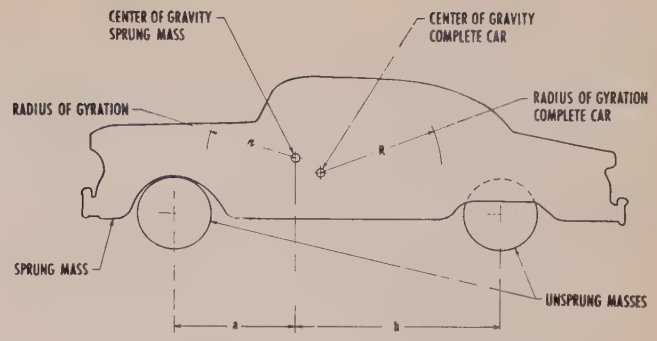

Fig. 10 – Inertia characteristics of passenger car

Fig. 11 – Test car on swing-type pendulum

Fig. 12 – Test car on test track

The sprung-mass pitch and bounce natural frequencies are generally determined by having several men push on the front and rear bumpers to produce the pitching or bouncing motion. Several cycles of the desired motion are counted and timed by stop watch, and the frequency calculated. Pitch and bounce natural frequencies can also be calculated from the sprung-mass front and rear pitch natural frequencies determined on the bump rig. Where $r^2/ab = 1$, the front and rear pitch natural frequencies are the sprung mass pitch and bounce natural frequencies. Where r^2/ab is other than 1, coupling is involved and the relationship is not so straightforward.

The parameter r^2/ab mentioned above is an important relationship in ride analysis (Fig. 10). It is an expression of the proximity of the front and rear wheels to the conjugate centers of percussion of the sprung mass about a pitching axis through the sprung mass center of gravity. Its numerical value is determined by first locating the center of gravity of the sprung mass (cgsm). This is located by weighing the car in various attitudes to determine the c.g. of the entire car, and then correcting for the unsprung masses. Having thus located the cgsm, the horizontal distances (a and b) from it to the wheels are easily determined.

The radius of gyration of the sprung mass, r, is determined in a similar manner on a swing-type pendulum (Fig. 11). The calibrated period of the pendulum is a function of the mass and radius of gyration, R, of the car. The radius of gyration of the sprung mass, r, is determined by correcting for the influence of the unsprung mass. The pendulum is designed so that the inertia of the car can be completely defined by rotating the car about three mutually perpendicular axes. Tests conducted with the unsprung masses removed show good agreement with the values obtained by the correction method.

Much of the testing connected with experimental analysis is done on the test track. One obvious reason is that many of the violent bumps and chuck holes available on the ride evaluation roads of our test track cannot be duplicated in the laboratory (Fig. 12). Also, we continually cross check on the road to verify the simulations employed in the laboratory.

Recent studies of shock absorbers are an excellent illustration of road-test methods. Along with the customary accelerometers, calibrated strain gages were applied to the shock absorbers to determine the loads they developed (Fig. 13). Deflection beams located on the suspension were used to determine characteristics of the relative motion between

Fig. 13 – Calibrated strain gages applied to shock absorbers

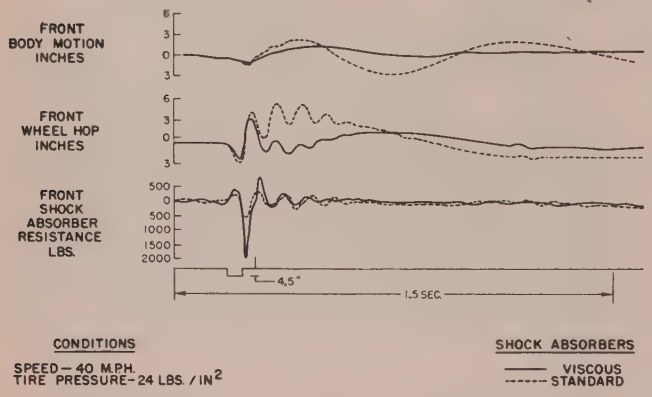

Fig. 14 – Front body and wheel movement and shock absorber resistance on driving over bump

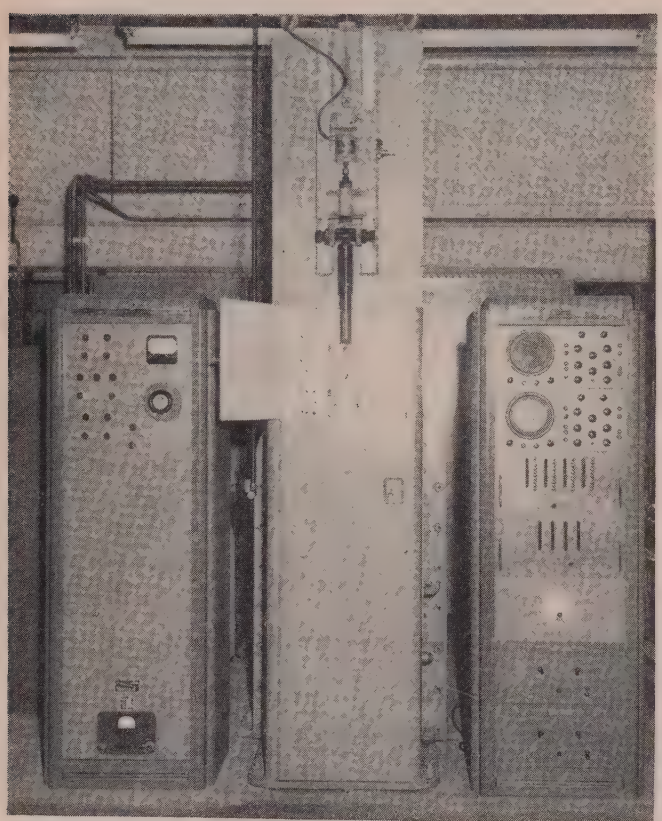

Fig. 15 – Calibrating machine for simulating severe road test conditions

Table 1 – Differential Equations

$$M_3\ddot{Y}_3 + C_3(\dot{Y}_3 - \dot{Y}_2) + K_3(Y_3 - Y_2) = P_3(t)$$

$$M_2\ddot{Y}_2 - C_3(\dot{Y}_3 - \dot{Y}_2) + C_2(\dot{Y}_2 - \dot{Y}_1) -$$

$$K_3(Y_3 - Y_2) + K_2(Y_2 - Y_1) = 0$$

$$M_1\ddot{Y}_1 - C_2(\dot{Y}_2 - \dot{Y}_1) + C_1\dot{Y}_1 - K_2(Y_2 - Y_1) + K_1Y_1 = 0$$

ends of the shock. Test cars were driven over the various test track ride roads, and the results were typical transient response-type oscillograms (Fig. 14). Analysis of the data clearly illustrated the superiority of one type of shock absorber and threw some light on an old ride problem.

Ride engineers have found that shock absorbers which perform identically on a shock absorber-calibrating machine sometimes influenced car ride quite differently. These measurements indicated that shock absorber loads and velocities were considerably higher than those developed by currently available shock absorber machines. Further study indicated that shocks which performed differently on the car frequently did so only at loads and velocities beyond those attainable in the calibrating machines. On this basis a new calibrating machine capable of simulating severe road test conditions has been designed and is now nearing completion. It will be another valuable tool in the study of improved ride (Fig. 15).

Mathematical Analysis

In addition to experimental analyses it is desirable to perform mathematical analyses, which are most useful to:

1. Obtain a fundamental understanding of the system which will indicate desirable design changes.
2. Predict the performance of proposed modifications or completely new designs.

Here, it appears, we have a very powerful tool which will permit us to analyze a system to determine what design changes should be made, and evaluate new designs without building a single experimental part. After so examining proposed designs, only the best need be built for evaluation and endurance tests.

The basic steps in a mathematical solution are:

1. Derive the differential equations for the system.
2. Solve the differential equations for algebraic equations in terms of the constants of the system and the frequency of the excitation.

Table 2 – Algebraic Equation – Sprung Mass

$$X_2 = \frac{P_E}{M_3}\left\{\frac{K_1K_3M_3 + K_2K_3M_3 - (K_3M_1M_3 + C_1C_3M_3 + C_2C_3M_3)\,W^2 + }{K_1K_2K_3 - (K_1K_2M_3 + K_1K_3M_3 + K_2K_3M_3 + K_3K_1M_2 + K_2K_3M_2 + K_2K_3M_1 +}\right.$$

$$\frac{J[(C_3K_1M_3 + C_3K_2M_3 + C_1K_3M_3 + C_2K_3M_3)W - (C_3M_1M_3)W^3]}{C_2C_3K_1 + C_1C_3K_2 + C_1C_2K_3)W^2 + (C_2C_3M_1 + C_1C_2M_3 + C_1C_3M_2 + C_2C_3M_2 +}$$

$$\frac{}{C_1C_3M_3 + C_2C_3M_3 + K_1M_2M_3 + K_2M_2M_3 + K_2M_1M_3 + K_3M_1M_3 + K_3M_1M_2)W^4 + W^6}$$

$$\frac{}{+ J[(K_1K_2C_3 + K_1K_3C_2 + K_2K_3C_1)W - (C_3K_1M_2 + C_2K_1M_3 + C_3K_1M_3 +}$$

$$\frac{}{C_3K_2M_2 + C_3K_2M_3 + C_3K_2M_1 + C_2K_3M_1 + C_1K_2M_3 + C_1K_3M_3 +}$$

$$\frac{}{C_2K_3M_3 + C_1K_3M_2 + C_2K_3M_2 + C_1C_2C_3)W^3 + (C_3M_1M_2 + C_2M_1M_3 +}$$

$$\left.\frac{}{C_3M_1M_3 + C_1M_2M_3 + C_2M_2M_3)W^5]}\right\}$$

$$W = 2\pi f$$

3. Obtain a number of numerical solutions to the algebraic equations to determine the response of the system.

A problem involving the influence of engine mounts on ride will illustrate the application of mathematical analysis to the "steady-state" ride problem (Fig. 16). Considering only vertical motions, a three-mass system, with dynamic characteristics of a simplified version of the car, gives rise to three differential equations of motion (Table 1). The differential equations are not too difficult to establish, but are frequently most difficult and tedious to solve. The solutions to the differential equations are three algebraic equations – one for each mass of the system – which express the motion of the system in terms of the components of the system and the frequency and magnitude of excitation (Table 2).

Approximately 1500 solutions of one algebraic equation were required to determine the frequency

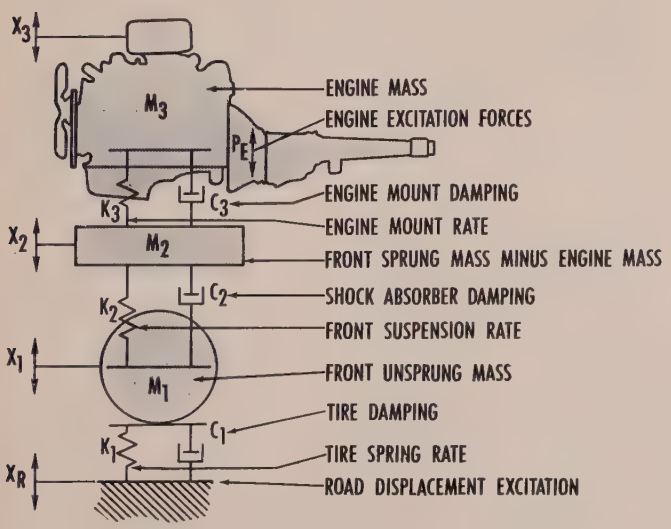

Fig. 16 – Schematic diagram of three-mass system at front end of car

Fig. 17 – Three-dimensional model illustrating frequency response of sprung mass for various engine mount spring rates

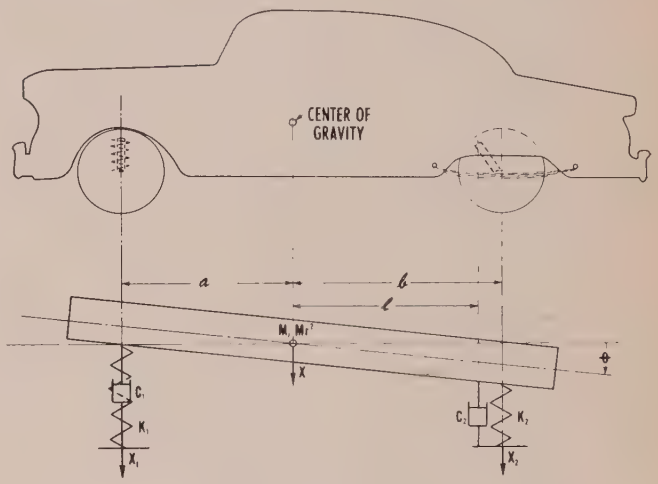

Fig. 18 – Standard suspension system of automobile

response of the sprung mass for various engine mount spring rates (Fig. 17). Calculating time employing conventional calculating machines would have been in excess of one man-year. The excessive man-hour requirement, illustrated by this very simple example, is the reason that mathematical analysis has found such limited use in those engineering fields which give rise to problems requiring such computational solutions.

With the advent of modern computing machines such as the electronic analog computer, computing times for such problems have been drastically reduced. These machines have permitted engineers to utilize mathematical analysis practically and economically. Computations for the three-dimensional

graph illustrated required less than one man-month, including time to set up the computer, compared to more than one man-year with conventional calculating machines.

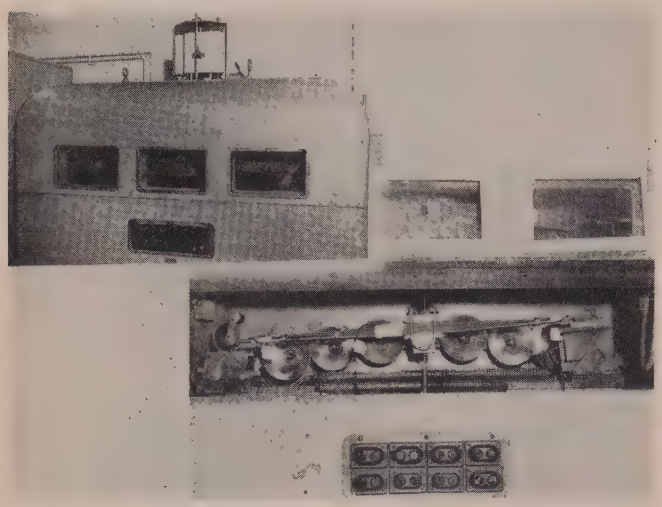

Fig. 19 – Equipment for determining dynamic damping coefficient and rate of rear spring

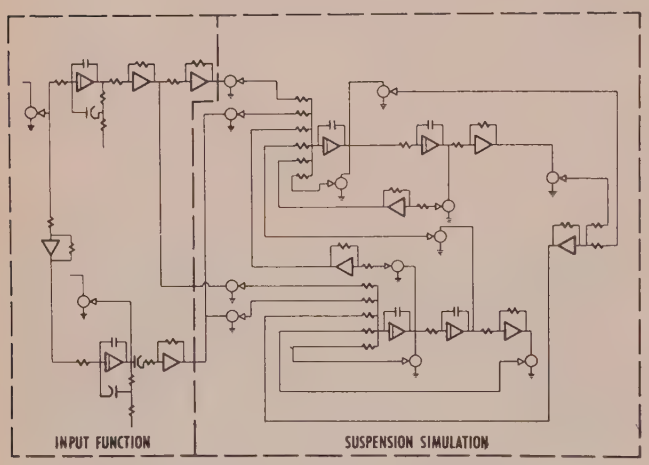

Fig. 20 – Analog computer wiring diagram

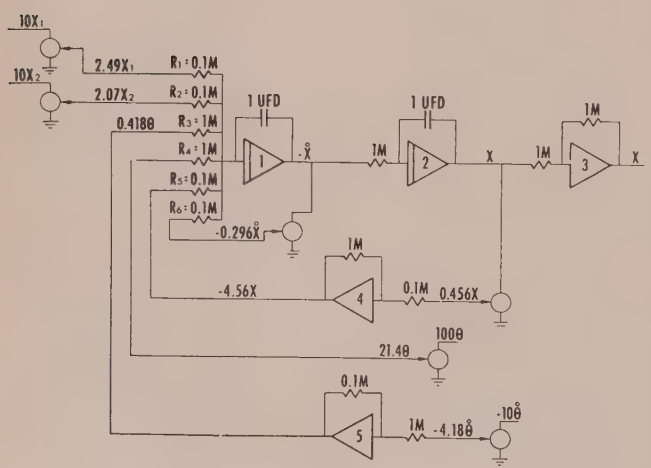

Fig. 21 – Simulation of bounce numerical equation

To illustrate the manner in which the analog computer is used to determine the transient ride motions of a car, let us consider the pitch and bounce of the car's sprung mass (Fig. 18). In this example the unsprung masses have been removed. This is reasonable for a first approximation since the unsprung masses have only minor effects on the system in the vicinity of pitch and bounce resonance. The equations of motion describing the simplified system are two simultaneous differential equations in terms of the forces and torques acting on the sprung mass in pitch and bounce (Table 3). The terms in X_1, $\dot{X}_1$, X_2, and $\dot{X}_2$ are the displacements and velocities of the front and rear axles, respectively, and reflect irregularities in the road profile. As such they represent the forcing functions, or excitation, to the system.

For this set of differential equations to apply to a particular system, coefficients of the variables must be determined and their respective numerical values substituted into the equations. The numerical values which describe the characteristics of the various components of the suspension are determined from controlled tests such as those performed to determine the dynamic damping coefficient and rate of the rear spring (Fig. 19). This machine subjects the leaf spring of an automobile to a prescribed load and initial deflection. The spring is then released and allowed to reach a new equilibrium point. Above the machine is a chart on which is traced a curve of instantaneous spring deflection as a function of time. With these data, a dynamic coefficient of friction and the rate for the spring are derived. During the test the spring is covered by an insulated enclosure wherein the ambient temperature can be maintained in the range from 0 to 130 F.

Numerical values determined for the coefficients of the physical components are substituted for the general coefficients in the original differential equation, and the numerical differential equation results (Table 4). With a rather rough estimate of the maximum values the dependent variables θ and X and their derivatives will attain, the numerical differential equation is then simulated in the computer.

The basis of simulation is that voltages in the computer are analogous to motions of the car and are described by identical differential equations – hence the term analog computer. The basic element of the computer is the stabilized, high-gain, direct-coupled amplifier. Amplifiers are used to multiply, change sign, sum, and integrate voltages. They are connected in a manner determined by the functions required by the differential equations and indicated by the wiring diagram (Fig. 20). Note that the wiring diagram is composed of two distinct parts – the car simulation and the input function. Numerical coefficients required by the numerical differential equation are provided by settings on voltage divid-

Table 3 – Equations of Motion for Standard Suspension

$$m\ddot{x} + 2C_1(\dot{X} - a\dot{\theta} - \dot{X}_1) + 2C_2(\dot{X} + \ell\dot{\theta} - \dot{X}_2)$$

$$+ 2K_1(X - a\theta - X_1) + 2K_2(X + b\theta - X_2) = 0$$

$$mr^2\ddot{\theta} - 2C_1a(\dot{X} - a\dot{\theta} - \dot{X}_1) + 2C_2\ell(\dot{X} + \ell\dot{\theta} - \dot{X}_2)$$

$$-2K_1a(X - a\theta - X_1) + 2K_2b(X + b\theta - X_2) = 0$$

Table 4 – Numerical Equations for Standard Suspension

$$\ddot{X} + 2.96\dot{X} + 45.6X - 0.418\dot{\theta} - 21.14\theta =$$

$$24.9X_1 + 20.7X_2 + 1.503\dot{X}_1 + 1.451\dot{X}_2$$

$$\ddot{\theta} + 3.25\dot{\theta} + 56.9\theta - 0.00015\dot{X} - 0.0076X =$$

$$-0.486X_1 + 0.476X_2 - 0.02935\dot{X}_1 + 0.0294\dot{X}_2$$

ers connected to the amplifiers.

For this work acceleration is the basic function of the motion which is studied. Where velocity-sensitive devices such as shock absorbers are simulated, it is necessary to integrate the voltage representing acceleration to arrive at a voltage proportional to velocity. The velocity voltage is then operated on by the voltage divider simulating the shock absorber coefficient. In Fig. 21, amplifier No. 1 receives an input voltage representing acceleration, $\ddot{X}$, and integrates it to an output voltage proportional to velocity, $\dot{X}$. This output voltage is then fed to voltage divider "A," which operates on the voltage as an ideal viscous shock absorber operates on the velocity.

Similarly, the output voltage of amplifier No. 1 is directed to amplifier No. 2, which integrates it from velocity, $\dot{X}$, to a voltage proportional to displacement, X. This output voltage from amplifier No. 2 is then fed to voltage divider "B," which operates on it as a spring operates on a displacement. The voltages developed by these operations are then fed back to the input of amplifier No. 1 to simulate the action of the suspension. The wiring diagram is developed in this manner, so that the computer will operate on the voltages just as the components of the car operate on the motions.

These aforementioned analog relationships can also be expressed mathematically. For the analog to be identical, the voltage equations must be the same as the equations of motion. At the input of amplifier No. 1 the following voltage appears:

$$2.49\,X_1 + 2.07\,X_2 + 0.418\,\dot{\theta} + 21.14\,\theta - 4.56\,X - 0.296\,\dot{X}$$

Since this amplifier functions as an integrator, the following relationship between the output and input voltages exists:

$$-\frac{d}{dt}(-\dot{X}) = \frac{1}{R_1C}(2.49\,X_1) + \frac{1}{R_2C}(2.07\,X_2) + \frac{1}{R_3C}(0.418\,\dot{\theta})$$

$$+ \frac{1}{R_4C}(21.14\,\theta) + \frac{1}{R_5C}(-4.56\,X) + \frac{1}{R_6C}(-0.296\,\dot{X})$$

Substituting for the resistances and capacitance their respective values and performing the indicated differentiation, we get:

$$\ddot{X} = 24.9\,X_1 + 20.7\,X_2 + 0.418\,\dot{\theta} + 21.14\,\theta - 45.6\,X - 2.96\,\dot{X}$$

This equation is identical with the first numerical equation of motion in Table 4, with the exception that the front- and rear-axle velocity terms have been omitted. The velocities were omitted in the example to simplify the mathematical analysis and the input function. It is a first approximation for the low speeds under consideration, but at higher speeds it would be necessary to include these terms in the input function. The input function which excites the system may be made to correspond to any type of road profile desired – chuck hole, railroad tie, curb, ramp, or even the profile of some particular stretch of test road. As far as the analog computer is concerned, it will solve the equations for whatever input function we specify. This is one of the tremendous advantages of the analog computer.

When considering any of the present-day computing machines, however, it is important to remember that computers are not "magic brains." They are nothing more than very-high-speed computing devices, and we must tell the computers all the important information concerning the simulation and the input function. We must tell them what information they are to have available, what to do, how it is to be done, and what answers are wanted. As it has been so appropriately put, "Computers are becoming so human that they can act without intelligence."

The analog computer in actual operation is shown in Fig. 22. The wiring diagram is directly above the problem board, which is a convenient mechanical means for interconnecting components in the analog computer to produce input function and suspension simulation. Coefficients of the numerical equation are set on voltage dividers appearing in rows on the center of the computer control panel. To the right of the computer is the pen recorder used to record solutions obtained by the computer.

To illustrate typical solutions obtained from the

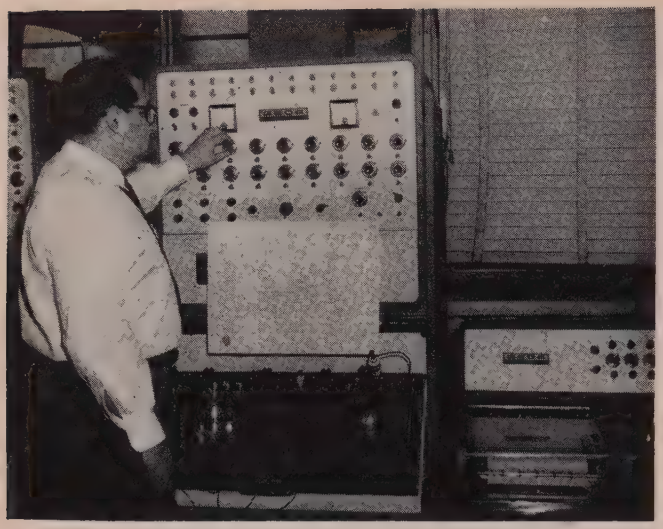

Fig. 22 – Analog computer in actual operation

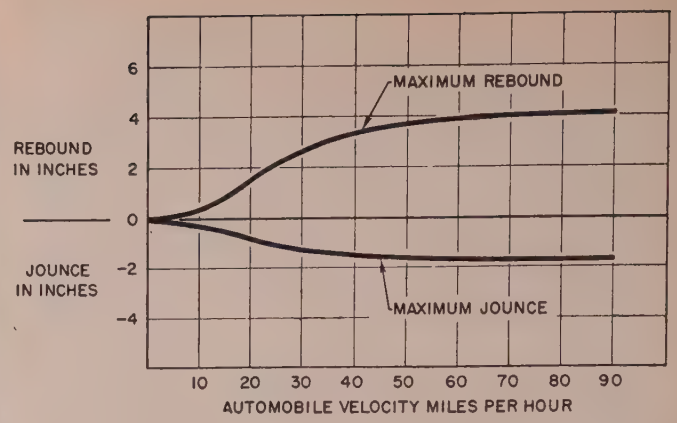

Fig. 25 – Simulated suspension rebound and jounce at c.g. for 4½-deg ramp with 9.7-in. rise

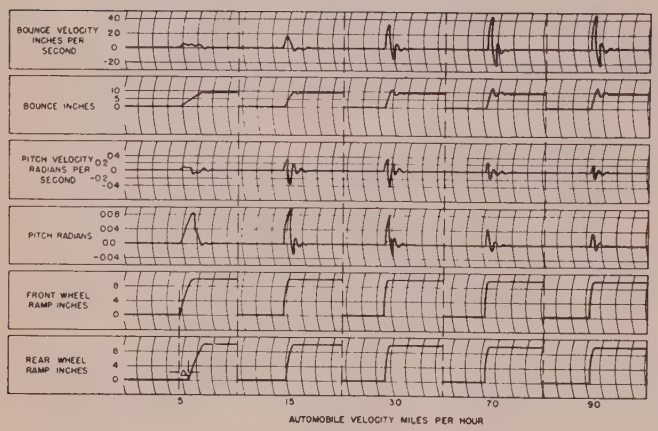

Fig. 23 – Simulated suspension traveling over 4½-deg ramp with 9.7-in. rise

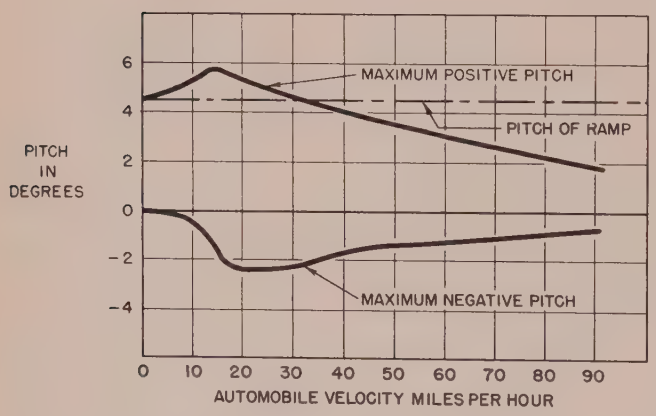

Fig. 24 – Simulated suspension pitch characteristic for 4½-deg ramp with 9.7-in. rise

computer and the type of analysis applied thereto, our "simplified" car was made to run up, in the computer, a 4½-deg ramp with a 9.7-in. rise. For purposes of analysis the pitch and bounce of the c.g. of the sprung mass were recorded from the computer (Fig. 23). From left to right are shown the computer solutions as the velocity of the car increased.

Fig. 24 is a graph of the manner in which the maximum positive and negative pitch angles vary with speed of the vehicle; note that the positive pitch angle is maximum at approximately 15 mph, whereas the negative pitch angle reaches its maximum at approximately 20 mph. Fig. 25 shows how the simulated suspension reacts to the ramp at various speeds in jounce and rebound.

Correlation between road tests and corresponding computer runs gives a measure of the accuracy of simulation. To illustrate the correlation, a car was driven over an actual ramp duplicating that used in the computer and the pitch and bounce of the center of gravity of the sprung mass was measured. These tests duplicated those performed on the simulated car in the computer, and Figs. 26 and 27 illustrate the correlation between the actual and simulated tests at 30 mph. Considering the number of simplifying assumptions that were made in the simulation, the correlation between the respective bounce characteristics is very good. In Fig. 27, the maximum and minimum amplitudes of the bounce curves are almost identical. The more rapid initial rise in bounce of the test automobile could be caused by bottoming on the suspension, which was not considered in the simulation. The simulated suspension curve would have a greater initial rate of rise had the vertical velocity portion of the ramp been included in the input function. Frequencies of the two responses differ slightly.

The pitch curve of the simulated suspension differs considerably from that of the test automobile. Examination of the pitch equation shows that the input is composed of differences of the quantities involving $\dot{X}_1$, X_1, $\dot{X}_2$, and X_2. In some cases, these differences are the result of subtracting two quantities of similar magnitude, so that small errors in these quantities could produce very large difference errors. In essence, the pitch equation is

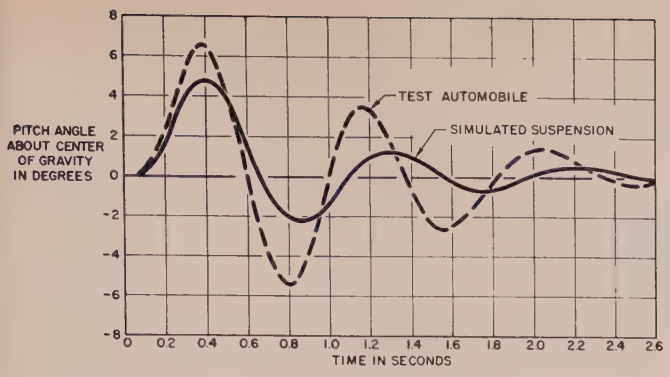

Fig. 26 – Comparison of pitch characteristics of simulated suspension and test automobile for 4½-deg ramp with 9.7-in. rise at 30 mph

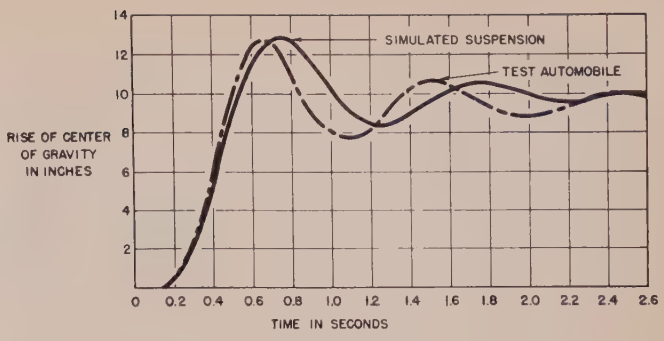

Fig. 27 – Comparison of bounce characteristics of simulated suspension and test automobile for 4½-deg ramp with 9.7-in. rise at 30 mph

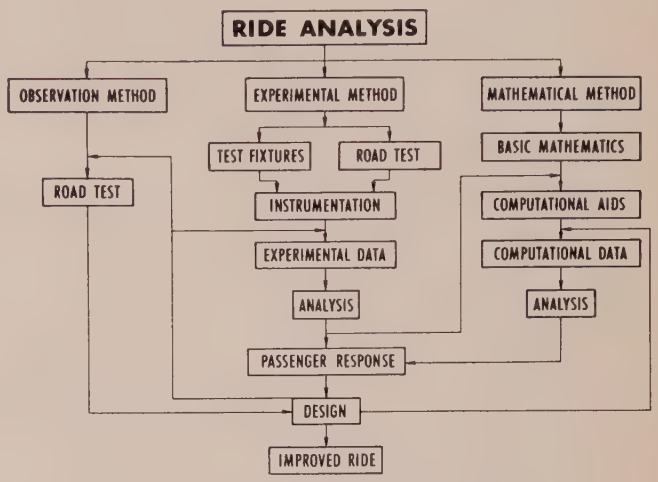

Fig. 28 – Flow chart of methods of ride analysis

much more sensitive to errors in input function than is the bounce equation.

When the correlation is not satisfactory, it can be improved by more accurately simulating the actual system. This involves re-examining simplifying assumptions, as in the example, and introducing such refinements as additional masses (wheels, engine), limits (axle bumpers), nonlinearities (variable spring rates and viscous damping coefficients), and friction damping. Such refinements complicate the problem, for they require the determination of detailed characteristics of various components, and introduce more quantities which can be varied. Such refinements also require more computer equipment.

To determine the influence of a change in the characteristics of the shock absorbers, for instance, the modified shock absorber coefficients are placed in the differential equation and result in modified numerical coefficients for the velocity terms. The different numerical coefficients are then introduced to the computer by setting the voltage dividers to new settings. Varying the coefficients of components of the system requires 5 to 10 min, and solutions such as those shown in Fig. 23 required approximately 1 hr of running time.

Literally, the computer simulates the physical system, and as such, has the same dynamic characteristics. To apply computer techniques one is forced to define the system under study and determine the characteristics of its components. The simulation principle and thorough knowledge of the system required to simulate the problem in the computer promote a fundamental understanding of the operation of the dynamic system. They lead to an understanding of the system's predominant characteristics, peculiarities, sensitivity to modification, and possibilities for improvement. These more subtle benefits accrue to, and are being utilized by, those who apply computer techniques.

In this paper we have endeavored to point out how an analyst makes measurements and/or computations which end up as "wiggles on a piece of paper." As such, the wiggles mean nothing. It is only when analyzed and correlated with test conditions, motions of the car, and response of the passenger, that they are meaningful.

The various methods of ride analysis have been outlined, and it has been demonstrated that there is considerable similarity and correlation between the methods (Fig. 28). In our opinion there is no one best method. In practice we frequently employ the observation method to evaluate a problem. Experimental methods are then used to define the problem and to determine the system to set up in computers. Solutions obtained from the computer are then re-evaluated by observation and experimental methods. It is through such integrated application of all three methods that the ride characteristics of our cars are studied and improved.

One area where further work will be very beneficial is in the determination of human response characteristics. In recent years there has been increased recognition of the problems associated with human engineering. We feel sure that as the application of available information increases, additional basic information on the response of the human body and mind will be forthcoming.

DISCUSSION . . .
. . . of this paper starts on p. 291

The New Packard Torsion

NEW automobile developments seem to appear in cycles. In the early thirties, introduction of helical gear transmissions and synchronizers marked a new era in transmissions. In the early and middle thirties, independent suspensions appeared on American automobiles, setting a new standard of riding comfort and vehicle control. From 1939 to 1953 automatic transmissions have been introduced on all makes of American cars. The second period of continued innovations followed from 1953 to the present, and apparently will continue for some time to come. We are all familiar with engine programs resulting in the change from straight-eights to V-8's which has swept the industry, and the rapid adoption of power steering.

In the 20 years prior to 1955 there has been no change in basic principle in the overall design of suspensions on American cars. It would seem that such a change is overdue.

Since 1935, we have analyzed many ideas in search for a new suspension principle that would be a step forward in improving ride of our cars. We hoped to provide an improvement that would be apparent to a customer before he had driven the car more than a few blocks.

It is general knowledge in the industry that better boulevard ride could be obtained by lowering spring rates, but at a sacrifice in road stability. As a result, car suspensions have been compromised to give a certain amount of each of these qualities, depending upon the maker's judgment of customer desires. A suspension improving both boulevard ride and road stability would be a step forward.

Packard has had patent coverage on torsion bars connecting front- and rear-wheel suspensions since the early thirties. Compensation for rear-passenger load was introduced by Daimler-Benz on the Mercedes car but operated manually and for two positions only. American experimental cars and buses have been equipped with automatic self-leveling devices. In 1947 we were exposed to the idea of combining torsion-bar suspension connecting front and rear wheels with an automatic load compensator or levelizer, which, in addition, gave necessary stability to the system. In 1951 an intensive development program started, culminating with the introduction of torsion-level suspension in the 1955 Packard. We feel this design represents

Level Suspension

Forest R. McFarland Studebaker-Packard Corp.

This paper was presented at the SAE Golden Anniversary Summer Meeting, Atlantic City, June 15, 1955.

PRINCIPLES of a new suspension utilizing torsion bars and a levelizing unit are presented. Among other things, it is claimed to provide a flat, level, and more stable ride on both the boulevard and open road.

Several design features are discussed, and it is concluded that this new design should probably initiate a cycle of development in automotive suspensions.

a step forward in accomplishing the objective of improving both boulevard and open road ride.

General Description

The suspension in general contains two features:

1. Long torsion bars connect front and rear wheels by a suitable linkage causing the car to ride level when passing over bumps and holes. These bars provide the "soft" ride.

2. Short torsion bars connect rear wheels to the frame, and together with an adjusting mechanism (called a compensator or levelizer), keeps the car level at all times, whether empty, or with six passengers and over 300 lb of baggage. These bars provide vehicle stability.

Long Torsion Bars and Suspension Structure

Let us describe the long bars in the general arrangement shown in Fig. 1. These bars run from the front to the rear of the vehicle, are 111 in. long on the Packard model, and have forged hexagonal sections at each end. The ends fit in hexagonal holes broached in levers mounted on needle bearings in brackets attached to the front cross-member and rear brackets welded to the outside of the frame.

The front levers bear upon the lower A-frames of the front suspension through struts shown in Fig. 2. The antifriction bearings will be described in detail later. The front suspension structure is the same as in our previous standard front suspension, except for a change in caster and camber adjustment and slightly looser fits in threaded bushings

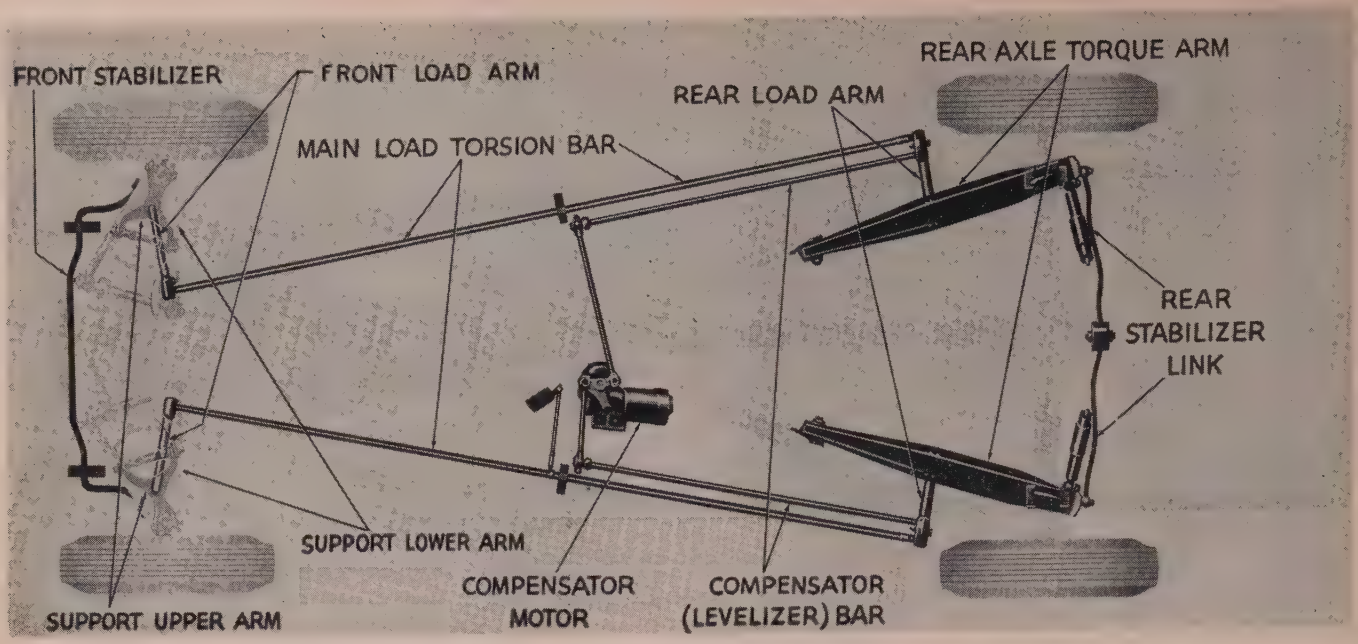

Fig. 1 – General arrangement of new Packard torsion-level suspension

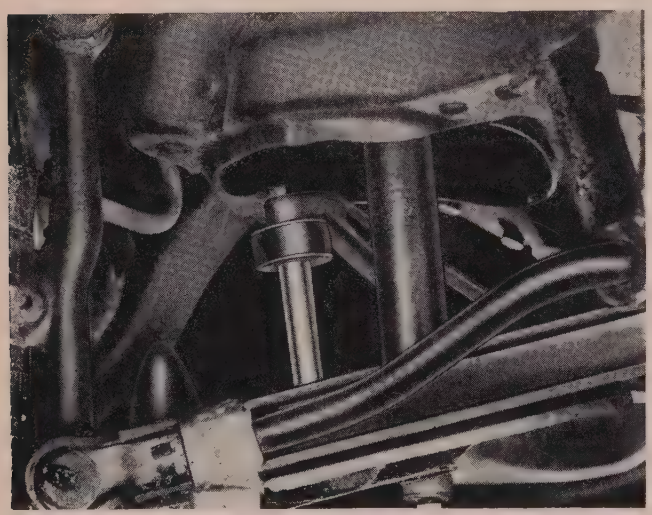

Fig. 2 – Front-suspension construction showing front-strut location

Fig. 4 – Rear-suspension construction showing rear-stirrup location

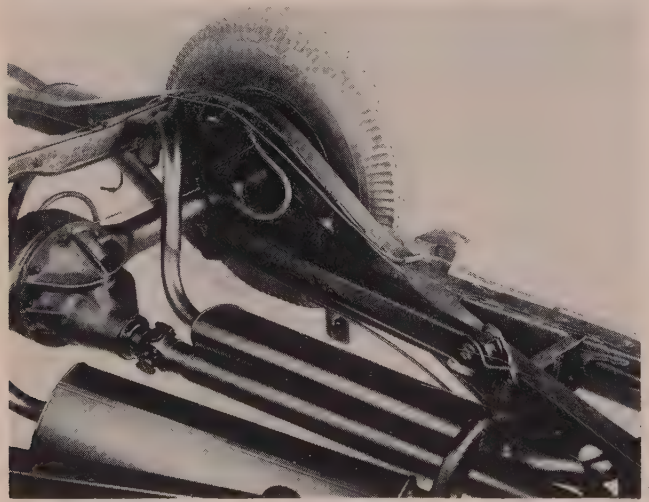

Fig. 3 – Rear-suspension construction showing rear-axle attachment to frame

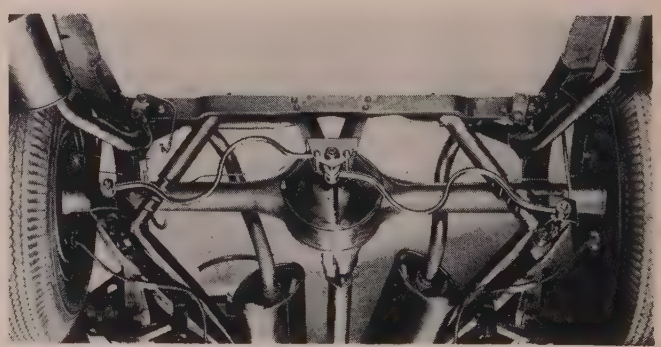

Fig. 5 – Rear-track linkage viewed from rear of chassis

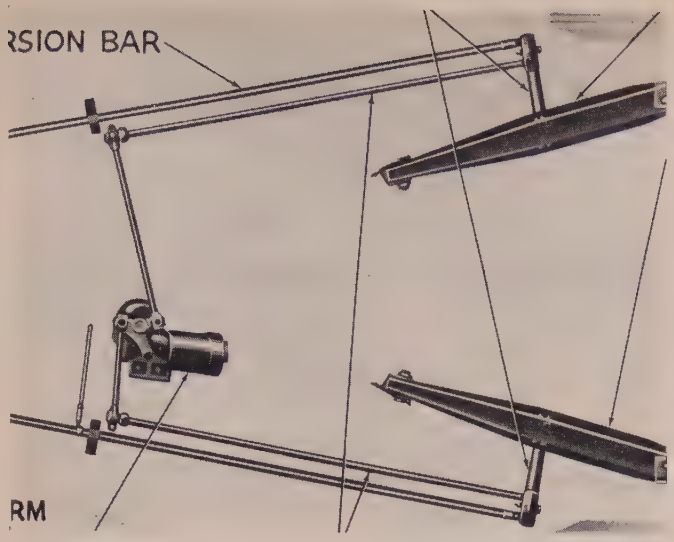

Fig. 6 – Enlarged section of Fig. 1 showing compensator construction

to minimize friction, particularly at small amplitudes.

The rear axle is located fore and aft and against rotation by torque arms shown in Fig. 3. Levers at the rear of the long torsion bars are attached to torque arms by the stirrups shown in Fig. 4. Antifriction bearings are located at the top and are the same as those on the front struts except that the upper and lower bearings are changed to satisfy the geometry.

The rear axle is located laterally by the stabilizer or tracking linkage construction shown in Fig. 5. Two links are fastened to the rear axle at the outer ends and to the equalizing lever at their inner ends by rubber bushings. The equalizing lever is mounted in rubber bushings to a bracket bolted on the rear channel. This construction provides vertical axle movement without feeding lateral movements into the rear of the frame, and so avoids harshness. It also ties the axle to the frame, in addition to the shock absorbers, as an added safety feature for unusual operating conditions.

Consider how this portion of the suspension operates. When the front wheel encounters a bump, it rises and twists the torsion bar through the front-suspension linkage, causing an increase in upward load at the torsion-bar lever bracket attached to the front frame channel. The increase in bar twist causes lever loading at the rear end of the bar to increase, thereby increasing rear-wheel loading on the ground. The net reaction of the rear torsion-bar lever and torque arm appears on the frame rear upward at the point the rear lever is attached. Simultaneously, there is an increase in upward loading at the front channel. The resultant of these two loads is applied near the car's fore and aft center of gravity and tends to lift the car without any appreciable pitch.

Since the spring rates are only slightly over half those of conventional front and rear springs, the total upward thrust is approximately equal to that at the front of the car with a conventional suspension. The inertia of the car in translation upward is high compared to the polar moment of inertia about a horizontal transverse axis in the vicinity of the center of gravity. Due to these facts, the upward movement of the car is small compared to pitch in a car with a conventional suspension.

The suspension acts in the same manner when the rear wheel goes over a bump.

In the description above the actions of rubber bushings on the front suspension, and of rubber bushings and compensator bars on the rear suspension have been omitted. Their rates will be given later when describing technical details.

Short Torsion Bars and Compensator or Levelizer Linkage

The compensator or levelizer functions to keep the car level for all normal passenger loading and furnish suspension stability.

Compensator construction is shown in Fig. 6. It consists of two short torsion bars attached to the rear axle linkage and frame, an electric motor, a gear-reduction unit and linkage for winding the bars in either direction to raise or lower the car, and a sensing unit to tell the levelizer when the car is out of level.

Torsion bars are clamped at their rear ends in hexagonal holes broached in the same levers that carry the rear ends of the long torsion bars. At their front ends, short bars are clamped in hexagonal holes in levers and located in brackets attached to the frame. Both left and right levers are attached to links through ball joints. These links are attached to ball joints on two arms of a central lever mounted on a shaft at the output of a total planetary and worm gear reduction of 2762/1 (86/1 reduction in the worm and worm-wheel unit). The electric motor driving the worm is a converted

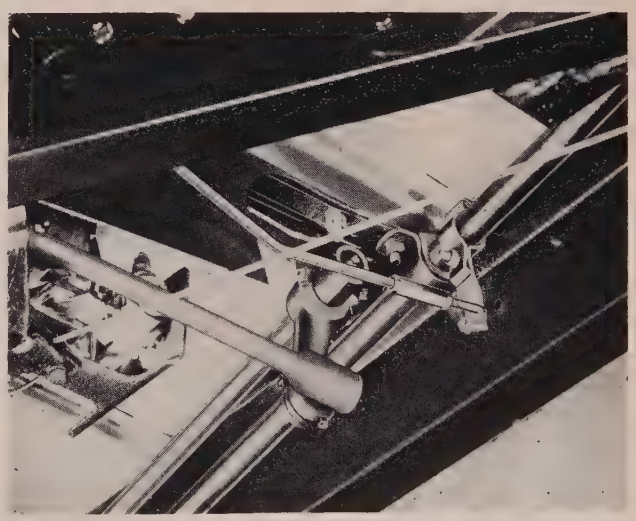

Fig. 7 – Lever and linkage between left main torsion bar and compensator control switch

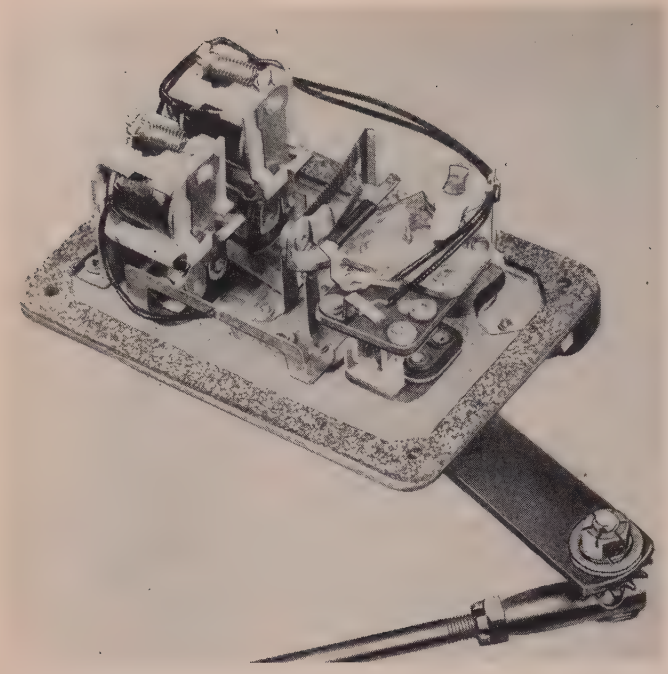

Fig. 8 – Compensator control switch with cover removed. Linkage shown connects to lever on main bar

high-production generator responsive through solenoids to a control switch which, in turn, is actuated by the sensing lever located on the long left torsion bar.

The detailed operation follows. The sensing lever is located at the left bar node at a 6-o'clock position (see Fig. 7). As long as the car is level, even though its height changes, the nodal point does not rotate and the lever remains at 6 o'clock. If the rear of the car is low the lever moves to a position slightly earlier than 6 o'clock (viewed from the rear). If the rear is high, the lever moves to a position slightly later than 6 o'clock. The moving lever on the long left bar then moves the lever in the control switch mounted on the front frame X-member. Fig. 8 shows this switch with cover removed and operating rod in position. When the car is out of level approximately $\frac{5}{8}$ in., contact is made inside the control switch (shown schematically in Fig. 9), which heats a bimetallic element. After a 5-7-sec delay, the bimetallic element closes and actuates a small relay supplying current to the motor-operating solenoid. The motor winds the two short bars in the proper direction through the reduction gears and linkage and brings the car back to level. When the car is within $\frac{5}{8}$ in. of level, the long torsion bar lever moves the control switch lever and cuts off current to the relay and solenoid, and the electric motor stops. Slight motor overrun brings the car close to ideal level.

The compensator operates in the opposite direction in the same manner, except that the opposite leg of the bimetallic switch is heated and makes contact with the switch operating the motor-reversing relay and solenoid, thereby lowering the car.

Fig. 9 is self-explanatory. One point of particular interest is the bimetallic element. Heating one leg causes motion in one direction, and vice versa. Ambient temperature differences act on both legs, rendering the unit substantially temperature insensitive with respect to the contact gaps. The bimetallic element solved a troublesome problem by eliminating most of the variation in time delay due to temperature variation. A switch combined with the stop-light switch opens the compensator control circuit when the brakes are applied, preventing compensator action during braking.

Lever travel is controlled by limit switches which cut off current when the levers have moved to their maximum desired positions. A dash switch is provided to cut out compensator action when changing tires. Within a few days after our mechanics had

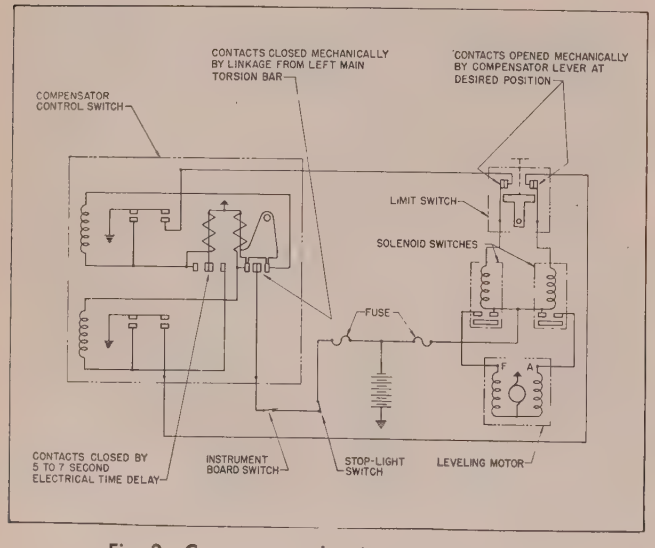

Fig. 9 – Compensator electric circuit schematic

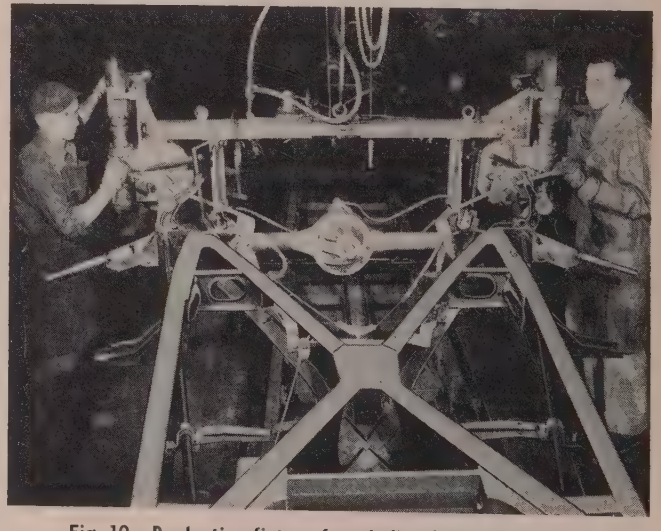

Fig. 10 – Production fixture for winding long torsion bars

been exposed to this mechanism, two of them found they could sit on the rear bumper, let the compensator level the car, then immediately turn off the compensator switch, leaving the rear of the car elevated and thereby saved themselves considerable work jacking up the rear of the car to change rear tires.

Technical Details of Construction

The long torsion bars are of one inch diameter SAE 5160 steel, precision-rolled. Straight hexagonal sections are upset to size at each end, with no further finishing operation. Considerable thought was given to crowning the ends or making the hexagon larger at its outer end to "flow" the stress more uniformly out of the bar. To date no hexagonal ends have failed, indicating the present method is satisfactory. The bars are shotpeened and pretwisted 100% to properly index the ends and to prestress the outer fibres to further insure against breakage. Bars are stressed to a maximum of 130,000 psi under full simultaneous bottoming of front and rear wheels, which is a rare condition. This compares very favorably with the combined stresses in front coil springs for the majority of present production cars under front-wheel bottoming loads only, which occurs more frequently.

Problems in the assembling of long torsion bars in the chassis were worked out during development. A winding fixture shown in Fig. 10 was designed and used to wind the bars on engineering cars as a pre-production procedure check. The fixture consists of two air motors, each driving a gear-reduction unit. The reduction-unit output shafts have pilots fitting into the holes broached in the rear levers carrying the hexagonal ends of the long torsion bars, and driving arms that bear against the torsion-bar levers. After assemblying the fixture to the bar in the free state, the bar is twisted approximately 120 deg, the stirrup dropped over the lever end, and the lever backed up, seating the lever bearing end into the stirrup bearing. Production now states assembly of these bars is preferred to the assembly of conventional coil and leaf springs. This was a happy ending to an element of the problem that concerned us from the start.

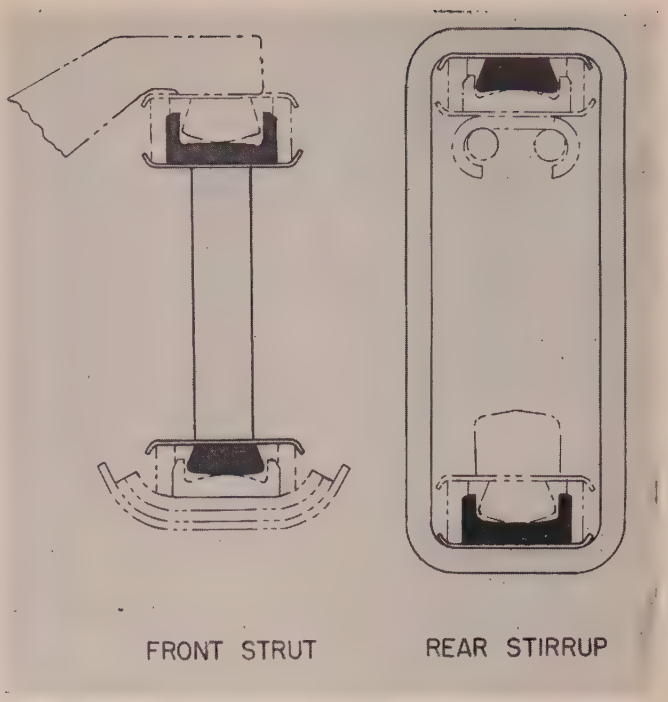

Fig. 12 – Cross-sections of front strut and rear stirrup

Compensator bars are assembled under no load and offer no assembly problem. These bars operate at comparatively low stresses, but are shotpeened for good measure.

Front struts between front torsion-bar levers and front-suspension lower A-frames come in four lengths in ½-in. increments. These vary the standing car height in ⅜-in. increments to handle manufacturing variations. Parts are coming through production uniformly enough so that one length has been used almost entirely. Experience to date indicates less loss in riding height in service than is present in standard suspensions.

The question has come up, "Why weren't the bars run directly off the pivot point of the front suspension?" The answer to that question is shown in Fig. 11, which represents our first design, and in which this was done. We found the present design using the extra arm in front better on several counts, besides permitting use of the present front suspension substantially as is.

One of the problems in this development was to minimize the system friction. Front-suspension structure inner bearings and all rear-suspension structure joints are of rubber. Torsion-shaft levers operate on needle bearings. Bearings in the front

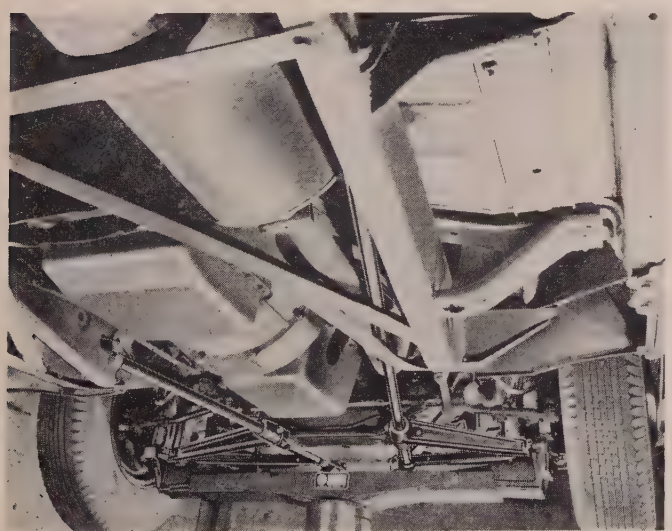

Fig. 11 – First design of torsion-level suspension, showing connection of long torsion bars and pivot points in front suspension

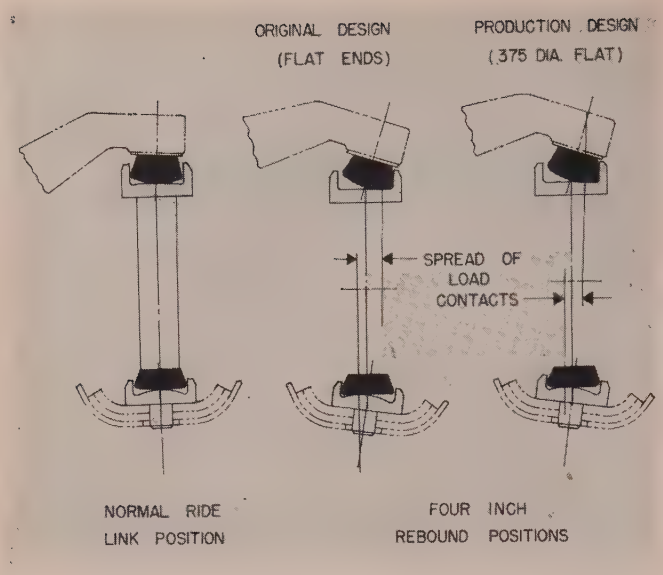

Fig. 13 – First and final designs of front-strut antifriction bearing geometry

struts and in the rear stirrups represented one of the development problems. These bearings had to operate substantially without friction. Various needle bearings, bronze ball seats, and nylon and rubber arrangements were tried, without success. The final design for front and rear is shown in Fig. 12. This design resembles one we had used previously to take friction out of a standard clutch linkage. Bearings in the ends of front and rear torsion-bar levers are spherical. Bearings in the plates cushioned in rubber in the lower front-suspension arms and bearings located in the stampings bolted into the rear torque arms are spherical too. Front struts originally had flat bearings which "clicked" under full jounce or rebound due to spread of the load contact lines, as shown in Fig. 13. This caused the bearings to slide under load and hit the cup sides. Addition of a radius tangent to the bearing flat at a 0.375-in. diameter reduced contact spread, and eliminated clicking under normal conditions. The rear arm angle was only approximately one-half that of the front arms, so these same bearings were first used in the rear stirrups. The stirrups, however, are tension members, whereas the struts are compression members. It was found desirable to alter the stirrup bearing design by suitable radii to control spread of load contact lines to eliminate clicking.

Maximum Hertz compressive stresses in full-loaded bearings are approximately 400,000 psi. Ball- and roller-bearing makers advised us these figures are in line with stresses in ball and roller bearings providing proper service life. Endurance testing on the bench and in cars has indicated this stress is satisfactory.

Bearings were run satisfactorily while dry and without rubber seal rings for many thousand miles. It was considered safer, however, to start with bearings sealed and filled with a molybdenum disulphide grease because of possible sliding of the cup sides.

Considerable time has been spent in describing a small detail of this design because it presented a real problem in its development.

Functioning of Design

Individual wheel rates on the Packard car are 66 lb per in. in front and 69 lb per in. in the rear. Ride rates are approximately 3 lb per in. less. When front and rear wheels are deflected equal amounts simultaneously, front-wheel rate is approximately 100 lb per in. and rear-wheel rate 104 lb per in. Ride rates are approximately 7 lb per in. less. Front-wheel and ride rates include 26 lb per in. due to front suspension and stabilizer rubber bushings. Rear-wheel and ride rates include 40 lb per in. due to rates of compensator bars, torque arms, and track-linkage rubber bushings.

These rates contribute toward pitch but are low compared to the equivalent standard suspension rates, making the car relatively pitch-free under most normal conditions. Pitch frequency is approximately 40 cpm and bounce frequency approximately 54 cpm for the Packard with a 4.5-passenger load.

Roll stability is higher than that of our standard cars due to location of the long torsion-bar lever attachment points at the rear and the fact that combined spring rates act on the body in roll.

The roll center is approximately at ground level at the front wheels and approximately 11.75 in. above the ground at the rear wheels.

Roll centers at the rear from 4 in. below standard to 4 in. above standard were evaluated by five engineers riding in a test car without knowing what was in the car. Four of the engineers preferred a higher roll center if a change from standard were to be made, and one preferred a lower roll center. Even experts disagree!

Rear-end steering has been given considerable attention. The design carries definite understeer due to geometric location of the torque arm front bearings. The torque arm-to-rear axle rubbers, by their own geometry, lessen overall understeer expected from the torque arms.

Measurement of understeer effect under roll shows a definite difference between understeer with reference to the body compared to that with reference to the front wheels because the front roll center is lower than that at the rear.

Rear-end lateral flexibility influences understeer. Some personnel have questioned the rear-end lateral softness with full passenger load although reaction from the field has been good. Proving ground drivers on a 25,000-mile run at an average speed of 104.7 mph stated they could drive cars with the new suspension approximately 5 mph faster than our standard cars with the same feeling of stabil-

ity. Several of our personnel have reported more than a 5 mph differential on country roads. Less flexibility is easily obtained to give less lateral movement, but at the cost of increased harshness.

A complete discussion of steering, including tire, wind, and other effects, will not be attempted here.

Summary

The advantages in the torsion-level suspension design over the standard type are:

1. Flat ride: The suspension remains more level than a standard suspension with a minimum of pitching, and results in a more comfortable, relaxed ride for the vehicle occupants.

2. Level ride: Whether the car is empty or carries six passengers and over 300 lb of baggage, it remains level. Overall height varies by a little over an inch. This is an answer to the stylist's prayer.

3. Soft boulevard ride with gain in stability on the highway: The ride is definitely softer than with conventional suspensions, for spring rates per wheel individually are only slightly more than half that of conventional suspensions. The great reduction in pitch which suspension engineers have been striving for and the lessened roll permit a softer ride with an attendant gain in open-road ride.

4. Headlights stay on the road: A valuable safety feature.

5. No rear-end squat on acceleration: Bottoming under this condition is absent due to torque-arm action.

6. Less dive on stopping: There is front-end dive, but torque arms tending to hold the rear down help lessen the overall dive effect.

7. Better wheel traction: Tests have indicated less wheel spin upon starting.

8. Reduced torsional stresses in the frame.

Conclusion

This discussion opened with mention of cycles of development of transmissions, engines, and steering. The time is ripe for a cycle of development in automotive suspensions. With the present knowledge of the various types of suspensions, including DeDion, rear independent, air, combination air and hydraulic, rubber, and others, it would seem that within the next 2 to 5 years, we should see some radical changes in suspension design.

It is hoped that introduction of the Packard torsion-level suspension will serve to stimulate more activity in this field, and result in a better, safer ride for all future car owners.

Acknowledgment

Acknowledgment is made of the contributions to this development by the personnel of Studebaker-Packard Advanced Engineering, and Packard Engineering and Proving Ground. In particular mention must be made of the contributions of George Joly and our associate, W. D. Allison. Several of our suppliers have contributed in the engineering of the products they are furnishing. The engineering, manufacturing, and corporate management of Studebaker-Packard Corp. have been very receptive and understanding in this development. The combined cooperation of all concerned has made this project possible.

DISCUSSION

of Bodeau, et al and McFarland papers

Let's Not Lose Sight Of Passenger Comfort

– Maurice Olley

Chevrolet Motor Division, GMC

AUTOMOBILE engineers have reason to be grateful for all new aids that assist them in providing fundamental ride improvements. The analog computer helps us to calculate more conditions than we were able to tackle in the past.

The only precaution is that we must not lose sight of the wood in counting the trees, or forget that the fundamental need is passenger comfort.

Mr. Bodeau will scarcely recall our 1930 passenger cars or the development around 1933 of the independent suspension on American cars.

The only instrumentation we had was our calibrated posteriors, with the occasional assistance of a bump-rig, to assist us in developing passenger comfort. We also had an experimental 7-passenger Cadillac limousine, fitted with outriggers fore and aft and with 720 lb of removable cast-iron weights which could be transferred from the center of the wheelbase to either end in such a way as to change the weight distribution and therefore the spring deflection at either end, and change the K^2/ab ratio through a wide range, in a matter of a few minutes. Thus, a wide variety of fundamental changes could be tried out by actual riding on a given stretch of road, as many as five or six times in a single day's running.

In the very earliest days we used a ride meter, which came close to giving really good results. This was a beaker filled up to a standard mark with water. The ride was measured by the amount of water which remained in the beaker after a given run on a given stretch of road.

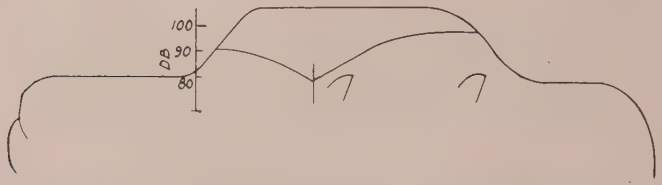

Fig. A – Form of cavity resonance that forms at about 100 cps

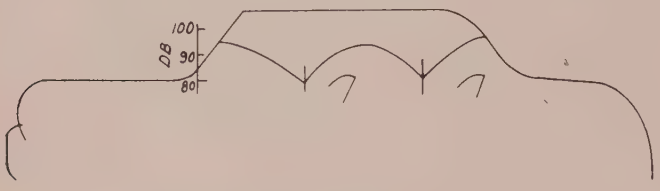

Fig. B – Sound pressure waves that form at about 200 cps

As a slight change of subject, but one which also reflects on passenger comfort, I would like to draw attention to Figs. A and B, which are typical curves of cavity resonance in our present cars.

Fig. A shows the form of cavity resonance which forms at about 100 cps. The rear passengers get the full force of this, whereas the driver's head is close to a node, so he does not worry about it.

Fig. B shows the sound pressure waves which form at frequencies of about 200 cps. In this case both the driver's ears and the rear passengers' are close to regions where the noise is at a maximum.

These sound waves produced in the body cavity can have disagreeable effects on the occupants, especially when driving with open windows.

Electronic Computer Handy To Study Passenger Motion

– Robert N. Janeway
Chrysler Corp.

MR. BODEAU and his coauthors have shown that the present method of riding cars for evaluation cannot be eliminated, but we have a new tool to enable us to obtain results in a shorter time.

Fig. 1 shows no less than 20 deg of freedom. For simplicity, let us consider only motions in vertical and longitudinal planes. This reduces the motions to 8 deg, including front and rear passengers.

To study these simultaneous motions, it is best to have an electronic computer, as illustrated by the authors' analyses. The ultimate objective we are after is minimum passenger disturbance. In an oversimplification, we can consider the passengers to have vertical and angular motion in the longitudinal plane. This longitudinal translation increases to a maximum at the passenger's head, which is unsupported above the neck. We have no criterion to judge this effect.

The unsprung mass is excited to resonance with large amplitude at about 700 to 800 cpm. These amplitudes must be absorbed by the sprung mass and the passengers through seat cushions. This resonance amplitude must be kept to a minimum for the wheels to stay on the ground. Effectively, this bypasses the spring and gives a resonance frequency of around 200 cpm. This frequency usually gives the passengers some amplified motion through the seat cushions. These residual free vibrations on the cushion must be absorbed quickly by effective cushion damping to maintain passenger comfort.

Our sprung mass with pitch and bounce oscillating centers is controlled by the effective deflection ratios of the front and rear springs, that is, K^2/ab.

With slightly different static deflections at front and rear, there is no coupling and less tendency to pitch between spring centers. Packard relies on mechanical coupling at front and rear, thus requiring a restoring force for stability. This tendency to pitch between wheel centers will result in resonance when long-wavelength disturbance is encountered.

Unitized Body Structure Offers Greater Torsional Rigidity

– R. H. Isbrandt
American Motors Corp.

MR. BODEAU and his coauthors highlight methods accepted in engineering design and engineering laboratories for evaluating passenger comfort in today's automobiles. The laboratory techniques developed give the ride engineer fundamental data with which to evaluate overall passenger comfort as affected by the tires, suspension springs, shock absorbers, and seat cushion springs, combined with disturbing forces resulting from road shock and such other secondary disturbances as may arise from the powerplant, steering gear, and suspension in their respective mountings.

In addition to laboratory or test techniques developed, mathematical methods for predicting the ride expected from a certain design have been discussed. It is recognized that much test time can be saved if the ride of the car as originally designed approaches the anticipated characteristics closely.

If these mathematical relationships are to represent accurately the effects of various elements that determine the car ride, the equations required become rather numerous and their solution cumbersome. In addition, many comparative solutions for different systems must be made. It is here that electronic computers are used to advantage to reduce the number of man-hours required.

Sometimes it appears as though the experimental engineer and the mathematical analyst compete with each other in attempting to see who can make his approach more unintelligible to the practical engineer. However, when these two groups work together, much time can be saved.

This reminds me of a story told some time ago by a test engineer who has been in the automotive industry since its inception. It seems a car was being tested on one of our modern proving grounds. The car was equipped with all the latest analytical recording devices and was instrumented to the nth degree. The old timer walked up to the car, looked it over, and then turned to the young engineer in charge. The conversation that took place went

somewhat as follows: Old Timer, "What are you testing this car for?" Young engineer, "For ride." Old timer, "How does the job ride?" Young engineer: "I really don't know. All the data have not been analyzed yet."

The young engineer unrolled yards and yards of paper, pointing out the curves plotted by the recording devices which had to be analysed. The conversation continued: Old timer, "Who determines how the car rides?" Young engineer, "My boss." Old timer, "What does he think of the ride?" Young engineer: "He doesn't know. He hasn't had an opportunity to analyze all the data. Analyzing it keeps him so busy he doesn't get a chance to ride the car." This is an example of what may happen if we permit instrumentation and analytical evaluation to go overboard.

Mr. McFarland's paper on Packard's new torsion suspension has brought to our attention some very interesting features. Torsion bars as such are not new to the automotive engineer, since they have been used extensively in European cars as well as by the military in this country for heavy vehicles such as tanks, trailers, and so forth.

Packard's application is unique in that a single torsion bar is used to carry both the front- and rear-wheel loads on one side of the vehicle by interconnecting the front- and rear-wheel positioning systems. Superimposed on the primary torsion bars are secondary compensator bars activated by a linkage system driven from an electric motor. This system is used not only to equalize the loads between the front and rear ends and thus keep the car level, but also to maintain the center of gravity a constant normal height above the ground for various loading conditions. Other manufacturing advantages appear to be that front-wheel positioning means is essentially the same as that employed with conventional coil springs, thus making it possible for this manufacturer to use conventional coil springs in the lower-priced cars.

Attaching the torsion bar to the linkage by upsetting the bar end into a hexagonal shape has obvious merits over some previous designs. While Packard has been able to take full advantage of the suspension in its advertising program by making the public conscious of a new suspension, it seems unfortunate that the customer is not able to realize all of the advantages claimed for this system. An exceedingly low wheel rate does not always produce a soft boulevard ride, and it appears that excessive damping of this suspension through the shock absorbers has been found necessary in order to approach accepted standards of stability and control.

Packard does deserve credit for attempting a different approach in the improvement of suspension systems. This phase of design probably will always bear improvement, and the Packard approach may be the beginning of some serious thought in this direction.

We have used a little different approach toward passenger-car comfort. Since 1940, Nash has employed unitized body construction. Hudson has used this type of construction since 1948.

A considerable advance in suspension technique is possible through the greater torsional rigidity of single-unit car design. With increased flexibility of the car as a whole, ride is adversely influenced and the suspension alone exercises less control. For the suspension designer to foretell automobile ride accurately, he must assume first that body and frame will not be flexible enough to contribute vibrations of their own.

Torsional stiffness of the car is important in its relation to the resisting force when one wheel passes over a road irregularity, which tends to cause a longitudinal twist. Excessive deflection of this type contributes to front-wheel tramp and other vibratory movements of the front end which affect steering and cause passenger discomfort.

With our single-unit car design, it is customary to obtain double the torsional rigidity of conventional separate-frame cars. One important factor in this connection is that use of flexible body mountings makes it impossible to take full advantage of the inherent rigidity of even a conventional type body.

When both front or rear wheels hit an irregularity together, the car is subjected to bending stresses. In a car with a conventional chassis the bending stresses are usually concentrated at the forward mounting point of the body to the frame, where an abrupt change in section height occurs. With a well-designed single-unit-type body, on the other hand, with its rugged A-structure joining the body dash to the front suspension, there is no such stress concentration or weak section.

A well-designed single-unit car feels more stable on the road and gives a better ride than a comparable conventional car with separate frame and flexibly mounted body.

With unitized body construction it is possible to take advantage of direct-acting front and rear springs. At the front end the spring transmits wheel load directly from the knuckle-support member to the front wheelhouse section of the body. This completely eliminates loading the wheel-positioning members, thereby reducing secondary vibrations of the front suspension to an absolute minimum. A similar arrangement is used at the rear end, where the spring is mounted directly to the rear-axle tube at its lower end and to the body-sill member at the upper end, the axle being positioned by the torque tube fore and aft and by the stabilizer linkage in a lateral direction.

McFarland's Closure To Discussion

WE appreciate Mr. Isbrandt's comments in which he states that the system holds the car at a constant normal height. Actually, there is approximately an inch difference in height between an empty car and one with normal passenger load, but the car does stay level, which we feel is particularly important.

Mr. Isbrandt states that excessive dampening is required by this suspension. We do not agree with this statement. Actually, the 1955 Clippers used the same shock absorbers with conventional or torsion level suspension. The 1955 Packards used softer shock absorbers with the torsion level suspension than were used with the standard suspension on the 1954 Packards. This suspension, in common with standard suspensions, does require more shock absorber control for all road conditions than is required for boulevard ride. We agree that reduction in spring rate is not the only factor that improves ride. We do feel, however, that it is one of the most important factors.

We are glad Mr. Olley has made a comparison between the work which he did on the early Cadillac with the present system on the Packard. Had he concentrated all of the mass of the vehicle equally at the front and rear wheels, the K^2/ab ratio would have equalled 1 for practical purposes. With the Packard torsion level suspension, an effect is obtained that could only be possible with a standard suspension system with a K^2/ab ratio considerably greater than 1. Evidence of this fact is the figures given of 54-cpm frequency in bounce and only 40-cpm frequency in pitch. This is due to the fact that only that portion of the springing of the front and rear wheels directly connected to the frame at the front and rear influences the car in pitch.

With regard to Mr. Janeway's comments, others have prognosticated that certain unusual road conditions would cause a Packard car to pitch. Any pitch that would occur with a torsion level suspension would be at from ½ to ⅔ the frequency of the pitch in a conventional car, so would be definitely less noticeable from that standpoint. It is true that, as stated in the paper, the compensator bar connected to the frame, together with the rubber bushing spring connections to the frame, do serve to give stability to the vehicle.

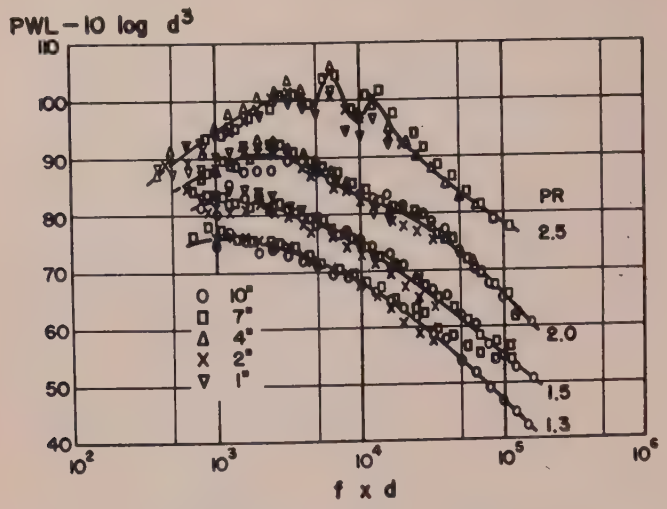

Fig. 1 – Generalized power spectra of bellmouth nozzles

A JET EXHAUST

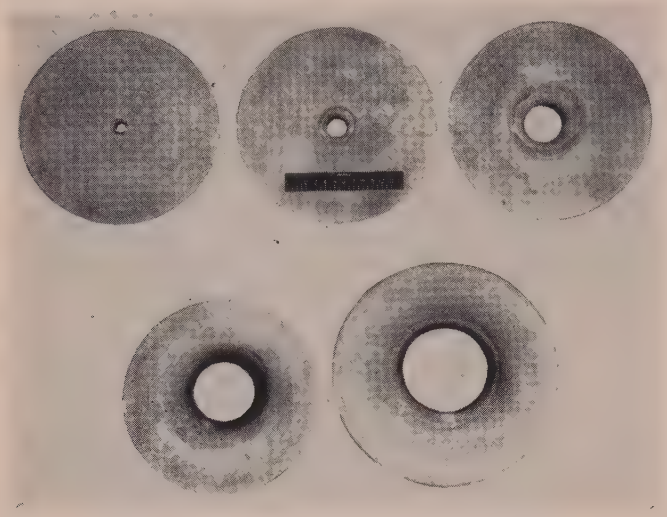

Fig. 2 – Five bellmouth nozzles

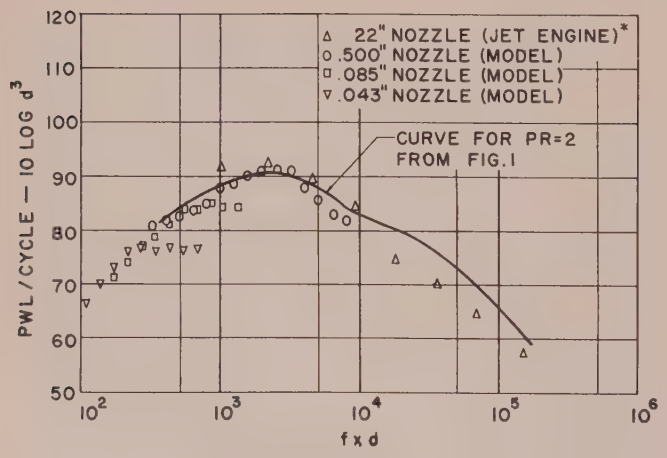

Fig. 3 – Generalized power spectra of variety of nozzles

A METHOD of reducing the audible noise to which airport neighborhoods are subjected by jet-powered aircraft is presented in this paper. As now conceived, such an exhaust silencer could conceivably quiet large jet aircraft exhaust noise to levels equal to or below that of present propeller-driven aircraft. This would involve added weight, loss in take-off thrust and the complication which goes with added gadgetry. Obviously, the optimum design will be a compromise among these variables.

The principle involved in this silencer design can be explained by reference to commonplace auditory experiences. For example, a large exhaust nozzle, such as that of a jet engine, produces a deep-throated or low-frequency roar. A small air jet, as used in the shop to blow chips out of cavities, when directed so that the airstream is not striking an obstruction, produces a hissing noise. So does the air vent valve in household hot water heating systems. These small jets have most of their noise energy in the high-frequency range

SILENCER

AN effective method for silencing, to an agreeable amount, the noise produced by a jet-engine exhaust system is described in this paper.

The principle employed is based on the fact that high-frequency noises are more rapidly attenuated with increasing distance from the source than low-frequency noises. Basically, the performances of the developed silencers are to reduce the amount of noise of a jet exhaust by increasing the frequency range of the noise produced.

Full-scale silencers have been developed for use as ground equipment. Scale models of airborne silencers have been studied and show promise for full-scale development, however, further studies are required to minimize disadvantages to airborne applications.

J. M. Tyler and G. B. Towle
Pratt & Whitney Aircraft, Division of United Aircraft Corp.

This paper was presented at the SAE Golden Anniversary Aeronautic Meeting, New York City, April 19, 1955.

as compared with the jet-engine exhaust, which has most of its energy in the low-frequency range. An example of the auditory effects of noises at various frequencies is the noise made by an electric generator going from a standstill to full speed. You hear it groan as it starts to turn over, then it growls through the low-speed range, then becomes more shrill as it goes faster and finally the shrill notes drop out of the noise pattern as they go above the audible range. Similarly, we find that as you make nozzles smaller and smaller the whole noise spectrum from the jet exhaust wake shifts upward in frequency until with very small nozzles the bulk of the noise energy is above the audible range. This high-frequency noise, including the audible portion, is attenuated very rapidly with distance from the source. The airport neighborhood, therefore, would be greatly benefited by the use of small nozzles instead of large ones.

Silencer Design Principle

The principle upon which the development is based was presented in Fig. 4 of the paper presented a year ago.[1] The same material is presented as Fig. 1 in this paper. It is a plot of the generalized power spectra of bellmouth nozzles and includes data from nozzles ranging from 1 to 10 in. in diameter, as shown in Fig. 2. This generalization[2] was obtained by plotting PWL/cycle – 10 log diameter[3] versus frequency times diameter. It indicates that the noise spectrum is an inverse function of the nozzle diameter and if the velocity remains constant, then the overall power is a function of the nozzle area. It was also shown that the overall power level of subsonic jets is an

[1] See SAE Transactions, Vol. 63, 1955, pp. 308-319: "Jet Noise," by J. M. Tyler and E. C. Perry.

[2] The PWL parameter is a measurement of total noise energy or power within a reverberation chamber, or it is the summation of the total noise emanating from a source.

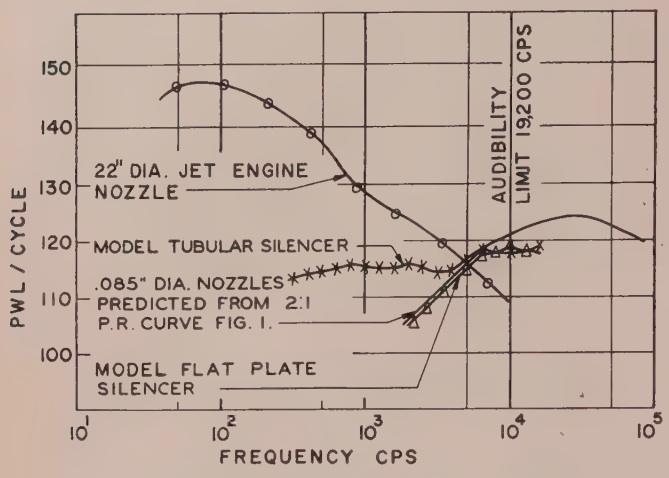

Fig. 4 – Power level per cycle spectra – jet-engine nozzle versus silencer

eighth function of the jet velocity to the power and additional material was presented to permit generalizations to account for the effect of pressure ratio and temperature. Thus we can reduce to a single spectrum the noise developed by any subsonic jet if we know these three primary variables, diameter, pressure ratio, and temperature. Fig. 3 presents noise spectra reduced in this manner for jets varying from 0.043 to 22 in. in diameter. The solid line shown is from the 2/1 pressure ratio curve of Fig. 1. The 22-in. nozzle data were taken from full-scale jet-engine measurements and are in good agreement with the curve. Extremely small nozzle data agree with the curve throughout most

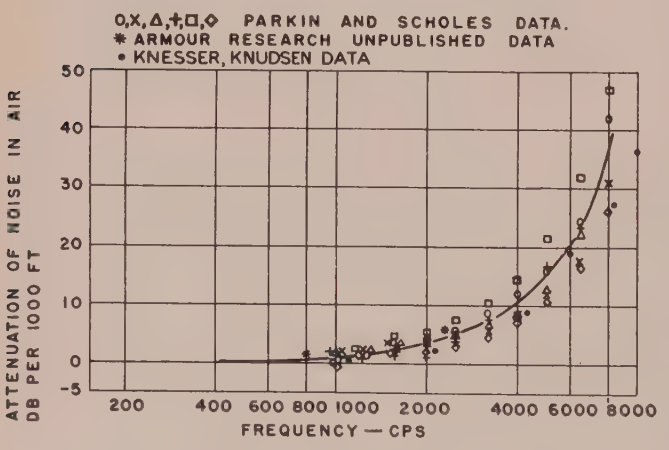

Fig. 5 – Air absorption of noise

of the frequency range but depart from the general curve at higher frequencies where accurate measurements are difficult to obtain.

It should be noted that PWL/cycle is a constant bandwidth unit whereas the usual unit, PWL/octave, increases in bandwidth with frequency and therefore, the plotted spectra using PWL/cycle appear to drop off sharply with frequency as compared with spectra plotted using the conventional unit.

The method of noise reduction discussed in this report depends on the frequency increase, as shown in Figs. 1 and 3, which can be obtained by using very small nozzles. Replacing a 22-in. nozzle by a vast number of small nozzles with an equivalent exhaust area may produce the results shown in Fig. 4. At the left, peaking at 87 cps, is the noise spectrum from a jet engine operating at rated thrust. To the right is a predicted spectrum to be obtained by replacing the 22-in. nozzle with a multiplicity of 0.085-in. nozzles. While the total noise power is identical for these two curves the latter curve peaks at 23,600 cps and much of the noise is above the audible range. The result is an appreciable reduction in audible noise.

Fig. 4 also includes curves of test data from model configurations, one having 0.085-in. diameter nozzles in a flat plate and another configuration having 0.085-in. diameter nozzles in the surface of a tube. Note that the 0.085-in. diameter nozzles in the flat plate agree with the curve predicted from the generalized spectra, except for the high-frequency points. The test data from the 0.085-in. diameter nozzles in the tube show an appreciable increase in the low-frequency portion of the spectrum. This increase in low-frequency noise is probably due to mixing of the jet streams as discussed in the next section.

Multiple Nozzle

Going from the individual nozzle to a large number of nozzles is not a simple step. A determination must be made as to how the nozzles should be arranged with respect to each other. It was discovered rather early in this study that if the spectrum for a multiple nozzle arrangement is to be the same as for a single nozzle of the same size, except for noise level, the wakes from the individual nozzles must be kept separate, at least throughout the wake volume in which the turbulence level is high enough to be contributing appreciably to the noise.

Tests conducted using sections of perforated sheet metal as the multiple nozzle showed that as the holes were arranged closer and closer together, the low-frequency end of the spectrum was raised, indicating that the dimensions of the turbulence involved a volume appreciably larger than a single wake. From these tests a hole spacing of three diameters apart in the perforated sheet was se-

lected as a reasonable compromise. It should be pointed out that with a fixed hole spacing the spectrum may change appreciably with changes in airflow either on the inside of the silencer or on the outside of the silencer. The three-diameter hole spacing was used in the silencer, the spectrum of which is shown in Fig. 4.

Attenuation of High-Frequency Noise Due to Air Absorption

The reduction of jet-engine noise as it radiates into the surrounding community is the result of (a) the dispersion of noise energy governed by the inverse square law, (b) the concentration or spreading of noise resulting from thermal and velocity gradients in the atmosphere above the community, (c) the scattering of noise due to turbulence in the atmosphere, and (d) the absorption of noise energy in the atmosphere. The inverse square relationship is well known and a considerable amount of data have been collected to indicate average noise levels at a distance in the presence of average thermal and velocity gradients and scattering due to turbulence. However, until recently little actual aircraft noise data had been obtained on noise absorption in the atmosphere. This latter effect depends to a large extent on the temperature and humidity of the atmosphere.

Data on air absorption of noise propagated by aircraft flying overhead are now available for average temperature and humidity conditions existing during the summer in Great Britain and northern United States which are of interest in connection with high-frequency noise spectra. Fig. 5 is a plot containing data presented in the *Acoustical Society Journal* for November, 1954, by Parkin and Scholes and data from Armour Research on the same subject. Data are also included for the 60% humidity, 68 F condition from a study by V. O. Knudsen and H. O. Kneser in 1933-1935. The average curve drawn through the aircraft noise test data indicates slightly more absorption than that predicted by the Knudsen-Kneser studies for frequencies between 1000 and 6000 cps and considerably greater absorption at frequencies above 6000 cps. The significance of these attenuations is shown in the plots in Fig. 6 where a conventional jet-engine spectrum is plotted together with a spectrum obtained from an experimental silencer utilizing miniature nozzles. The overalls are adjusted to be equal at 150 ft. Sound pressure levels were calculated at varying distances using only inverse square spreading and the air absorption indicated in Fig. 5. It will be noted that as the distance from the source is increased to 1000 ft, 3000 ft, and 7000 ft, the upper ends of both spectra drop out, and the noise levels at a distance are essentially a comparison of the low-frequency ends of the spectra. From this comparison the advantage of having low noise levels at low frequency is obvious.

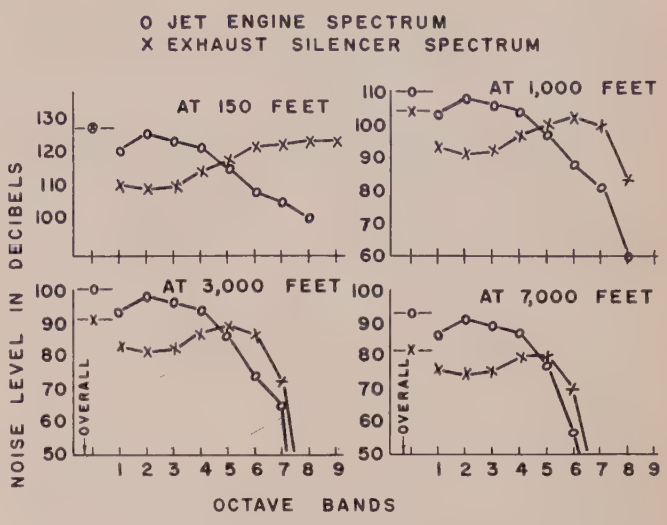

Fig. 6 – Comparison of changes in jet and silencer spectra due to absorption

Ground Silencer

A jet engine mounted on an outdoor test rig and equipped with a perforated sheet-metal exhaust silencer is shown in Fig. 7.

For some of the early tests a perforated sheet-metal tube was attached to the nozzle of the jet engine. The end of this tube was closed with a cone of the same perforated sheet metal, 0.085-in. holes, three diameters apart. When the engine exhausts into this tube the tube acts as a diffuser. The exhaust gas escaping through the holes allows the exhaust stream to expand as it flows rearward, thus providing pressure recovery and the development of a pressure head in the tube. By using the proper effective nozzle area for the tube, that is, the proper amount of surface area of perforated

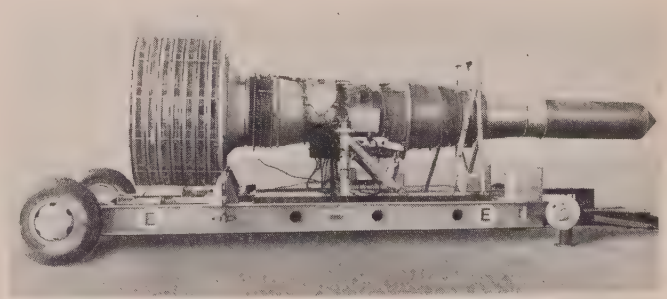

Fig. 7 – Jet engine with exhaust and intake silencers

sheet metal, the pressure rise through the diffuser may be adjusted to be equal to the pressure drop through the perforated sheet metal for a given exhaust flow, thus providing ambient pressure at the discharge of the engine nozzle. In practice this has been accomplished by the use of an unperforated sheet-metal band at the rear end of the tube. The tube was made slightly oversize and the band was adjusted forward and backward until the proper amount of perforated sheet-metal surface was exposed.

It should be explained that the addition of the silencer to the jet-engine nozzle changes the flow characteristics of this nozzle. The silencer area may be adjusted as described above so that at a given operating condition, say at take-off thrust, the engine operates the same with the silencer as without. At lower airflow the combination of nozzle and silencer will act like a nozzle of smaller diameter. However, this may be satisfactory for ground running purposes.

This engine was also equipped with an intake silencer to prevent the compressor noise from interfering with accurate measurements of exhaust noise. The intake silencer consisted of a solid disc in front and a series of washer-shaped sound-absorbing panels mounted on a bellmouth engine air inlet.

In Fig. 8 are patterns of take-off noise levels for (a) the jet engine in the standard configuration, (b) with both intake and exhaust silencer installed, (c) an estimated curve for the exhaust silencer only, and (d) for a DC-6 powerplant. A close inspection of this plot reveals a noise pattern for the silenced configuration which would be satisfactory for most jet-engine ground testing operations.

This perforated tube exhaust silencer should have a quick-disconnect clamping-ring for use in clamping it to the nozzle. In most airplane installations it would be necessary to provide a shroud around this silencer to collect the hot gases and give them an appreciable velocity rearward to blow them away from aircraft structure so as to prevent overheating of airplane parts. Such a shroud has a minor effect on the noise coming from the silencer.

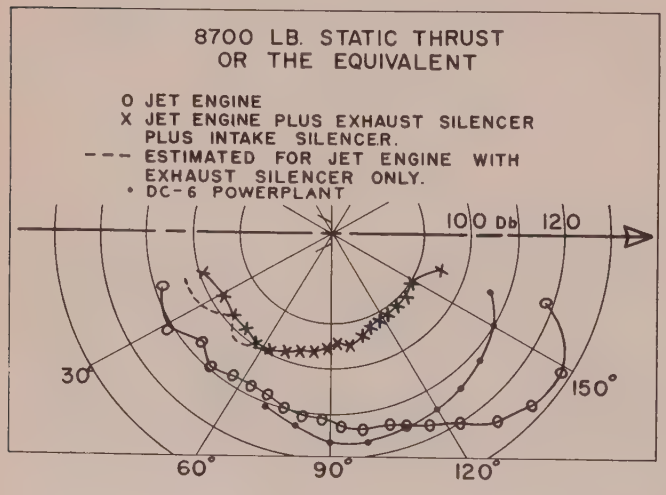

Fig. 8 – Contour plot of overall noise levels along 150-ft radius arc

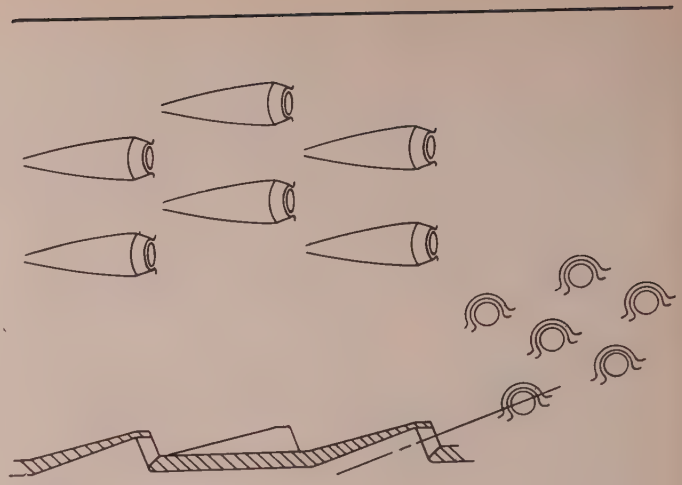

Fig. 9 – Thrust producing small nozzles in surface of cylinder silencer

The need for an engine air inlet silencer for ground running will depend on the degree of silencing required. The one shown in the photograph is 7 ft in diameter and weighs approximately 1000 lb. It was made oversize to insure no appreciable intake pressure drop when using square-cornered panels. If this type of intake silencer were to be built in production quantities, a much lighter and smaller construction could be built having the same pressure drop and noise attenuation.

Flight Silencer

While the perforated sheet-metal tube silencer described above provides a relatively high degree of exhaust silencing, it provides negligible thrust since the hot gases are exhausted in a radial direction with respect to the thrust axis. In order to produce thrust the gas must be exhausted rearward. In an effort to obtain a high degree of jet exhaust silencing and at the same time obtain as nearly full exhaust thrust as possible, exhaust nozzles have been built and tested which have an overall shape the same as the perforated sheet-metal tube described above, except that the gases are exhausted through a hole at the rear of small protrusions in the surface of the cylinder as shown in Fig. 9. Individual scale-model nozzles having this shape have been tested which have thrust coefficients the same as the full-scale conical nozzle on the engine. There are two factors, however, which tend to reduce the overall thrust from a multiple nozzle of this type. The individual nozzles

must be pointed slightly outward from the surface of the silencer, so that the jet wakes will not impinge on other nozzles immediately downstream and so that the wakes will not mix with the wakes from other miniature nozzles in the same area. Also, the flow patterns of these wakes and the induced secondary airflow at the surface of the silencer involve pressure distribution patterns on the surface of the silencer which affect the thrust. A great deal of work has been done using scale-model nozzles set in an angle of 20 deg to the thrust axis. Since the cosine of this angle is approximately 0.94, this would represent perfection for this arrangement. Actually, the test results scatter a few per cent below this value.

No noise patterns, noise power levels or spectra are presented for the flight-type silencer. It will be recognized that these values depend on the spacing and pattern of the miniature nozzles on the silencer surface as well as the size and shape of these nozzles. A delineation of the relationship between silencer performance noisewise and its performance thrustwise and weightwise must await the results of further studies.

In order to prevent the silencing thrust loss from affecting cruise economy, a silencer configuration as shown in Fig. 10 could be used. In this arrangement the silencer elements are stowed like sections of a collapsable drinking cup around the tailcone for the cruise condition. Thus, clean internal and external lines are provided for airflow through the exhaust duct and over the engine fairing for normal flight conditions. For take-off and climb the tailcone and silencer sleeves are extended rearward and the cruise nozzle is closed. This forces the exhaust to be ejected through the large number of small rearward pointing nozzles in the surface of the silencer sleeves. After the airplane has climbed to an altitude such that the noise will not be objectionable on the ground, the silencer is retracted and the climb is continued using the conventional nozzle. The airspeed at the time of retraction will probably be not over 200 mph.

The use of the silencer for take-off would be at the option of the pilot, of course. If the airplane takes off from an airport where high noise level is permitted or at a time of day or in a direction such that the noise is not objectionable, the take-off could be made without the use of the silencer and, therefore, without thrust loss. Some of these conditions might allow an airplane to make trans-oceanic flights at maximum gross weight without the silencer, whereas the bulk of the flying out of our busy airports could be with the silencer in use.

Summary

1. It is felt that an effective method of silencing exhaust noise has been developed. This method is adaptable to the silencing of jet engines running on the ground with some minor operational objections, that is, change in nozzle characteristics with airflow and ducting for the disposal of hot exhaust gases where they won't harm the airplane. The noise from the silenced jet engine will be at high frequency. This noise is easily attenuated by means of ear protectors, for the maintenance personnel who need to work on the engine. The noise is also attenuated by air absorption at appreciable distances from the airplane.

2. The application of this method of exhaust silencing to aircraft in flight is being studied. The problems confronting the designer are not as simple as those of the ground silencer. Penalties in weight, loss of thrust, and gadgetry are involved. Design compromises of this sort are not made without a great deal of serious study. However, the knowledge that it is possible to silence the roar of a jet engine should give courage to those who are concerned about the possibility of operating jet transports out of our domestic airports. It is an indication that either this or some other silencing method may become available in the future.

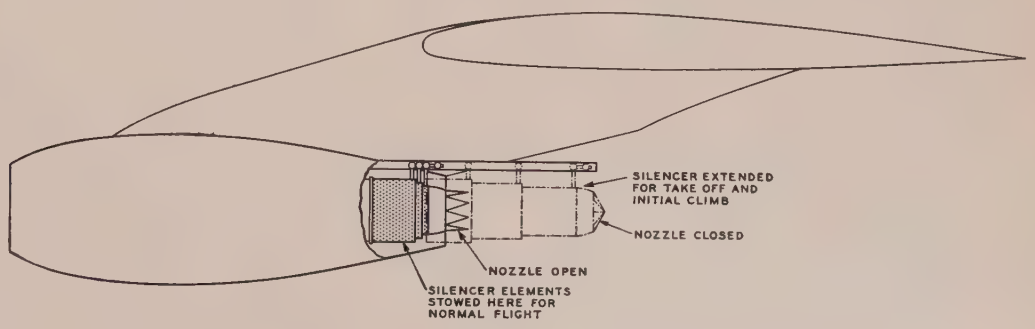

Fig. 10 – Jet-engine exhaust silencer – flight type

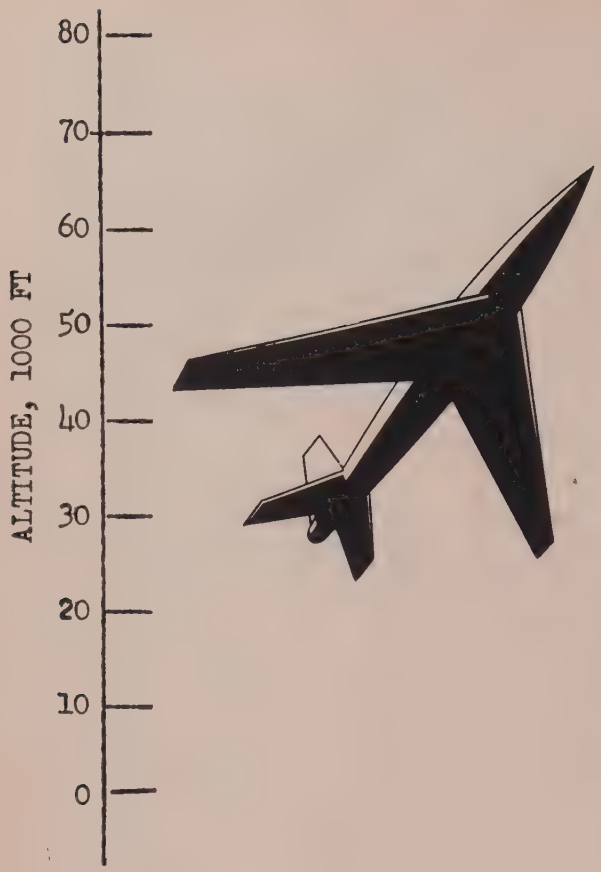

How High Should

As everybody knows, the atmosphere we live and fly in reduces in density and temperature as we go to higher and higher altitudes. Most people have had some experience at altitudes varying from sea level to about 10,000 ft if they have traveled in our western states. A much smaller number has had experience flying in airplanes up to altitudes of 25,000 ft. Only very few of us have had any real experience at altitudes above 25,000 ft. It is the purpose of this paper to discuss the effects of altitude on the various functions and systems of a modern jet transport airplane, to look at the many facets and glean from them a better and more intimate understanding of this new and improved airplane. By this method we hope to answer the question that forms the title of this paper.

The Atmosphere

For most people, the atmosphere is more or less taken for granted. They are occasionally reminded of its presence by clouds, wind, rain, or extremes of temperature. To another and more technical group, the atmosphere is a standardized medium with its temperature and pressure defined by a mathematical equation. Truly, it is all of these things and many more. While we do not have time to delve deeply into meteorology, some is necessary for an understanding of our problem.

Fig. 1 shows the average or standard temperature; Fig. 2, the pressure as it varies with altitude. As can be seen, the variation of pressure with altitude is uniform, and does not show much deviation. On the other hand, the variation in temperature is considerable. Fig. 3 shows some average seasonal lapse rates. Individual lapse rates often differ from these averages by as much as 20 F. Fig. 4 shows the variation of temperature and the height of the tropopause with latitude. It is worth noting that the tropopause is both higher and colder in the tropical latitudes.

A cross-section at any altitude averaged over a long period of time would show a distribution somewhat like that shown in Fig. 5. While most days are within 20 F of standard, there are a considerable number that are as much as 40 F from standard, and a few that are even 60 F. This is very important to our discussion, because airplanes must function normally in these extremes of temperature. Increasing the operating altitude of airplanes from 25,000 ft well into the stratosphere can be seen to have lowered the range of our operating temperatures by more than 50 F, and reduced

We Fly?

FLYING at altitude intensifies most problems, simplifies some, the author shows.

Increasing operating altitude from 25,000 ft to well into the stratosphere lowers temperature more than 50 F, and reduces pressure to one-fifth the sea-level value. This complicates structural problems. It affects the hydraulic and control systems, electrical systems, cooling, and air conditioning, and increases the danger from failure of any of these essentials. Gusts and turbulence, on the other hand, are lessened by flying high.

The author charts the extent of each of the problems, and shows how altitude economy gains make solutions imperative.

Schuyler Kleinhans, Douglas Aircraft Co., Inc.

This paper was presented at the SAE Golden Anniversary Aeronautic Meeting, Los Angeles, Oct. 13, 1955.

the pressure to less than one-fifth of the sea-level value.

Gusts and Turbulence

The extremes of temperature indicated in Fig. 3 can be expected to produce great variation in the density of the atmosphere which, in turn, due to the gravitational forces involved, produces both large and small mass movements in the air. If the mass of air affected is not too large, but the resultant velocities are considerable, these movements are called gusts. They obviously cause stress and strain in an airplane flying through them. Fig. 6 shows the variation of gust frequency with altitude in terms of the number of miles that must be flown to intercept a gust of any particular value. Fig. 7 shows the variation of gust intensity with altitude, with the gust frequency as a parameter.

The interesting thing about these two curves from our point of view is that we must fly about 10 times as far at 25,000 ft, and about 100 times as far at 40,000 ft, as we do at 10,000 ft, to intercept the same size and number of gusts.

Fig. 8 shows the result of these characteristics in terms of ride roughness for a number of different airplanes. As can be seen, the ride roughness

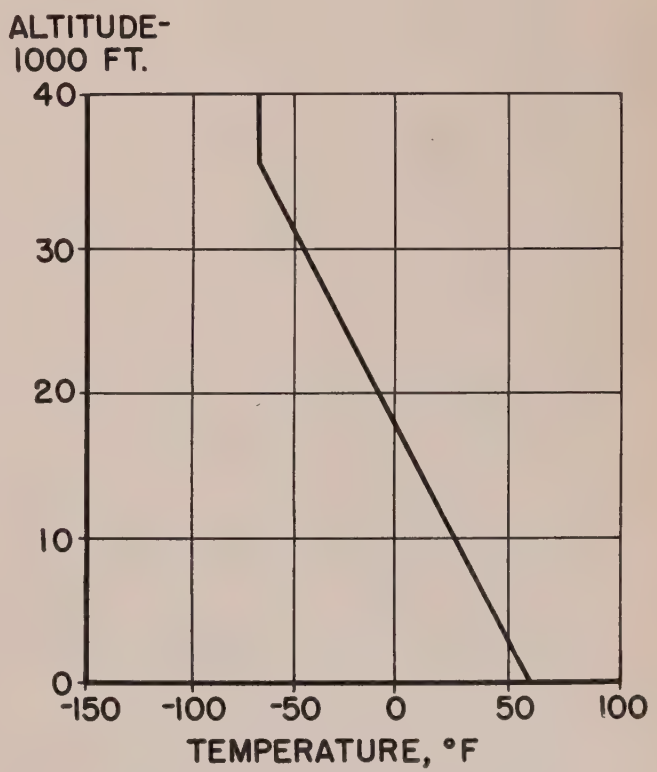

Fig. 1 – Average or standard temperature

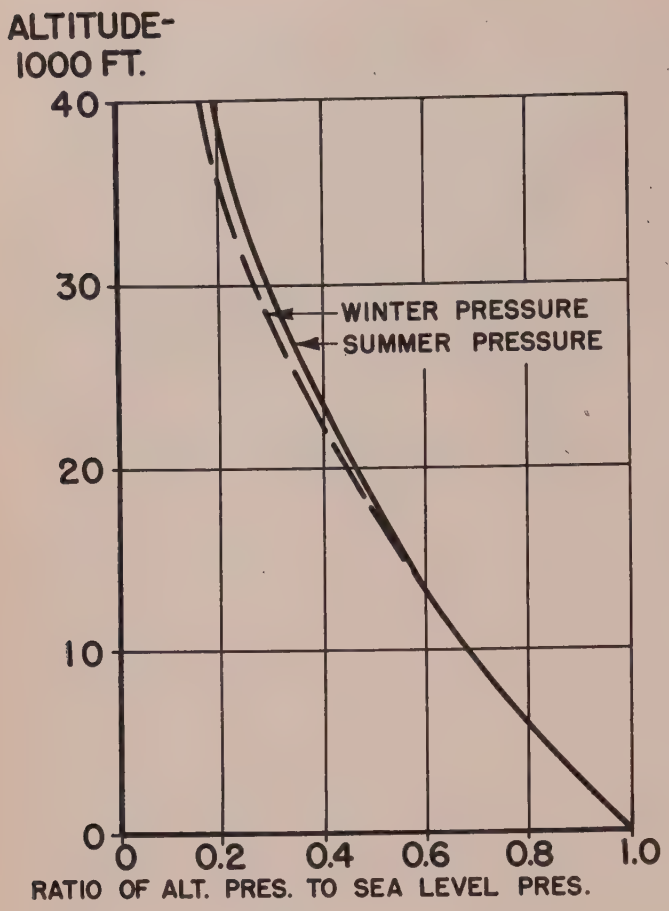

Fig. 2 – Pressure as it varies with altitude

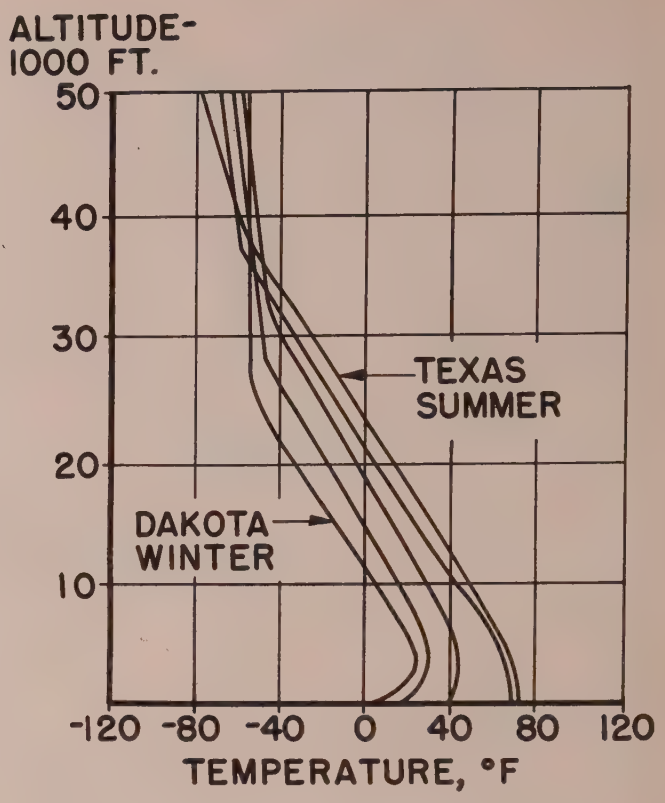

Fig. 3 – Some average seasonal lapse rates in temperature

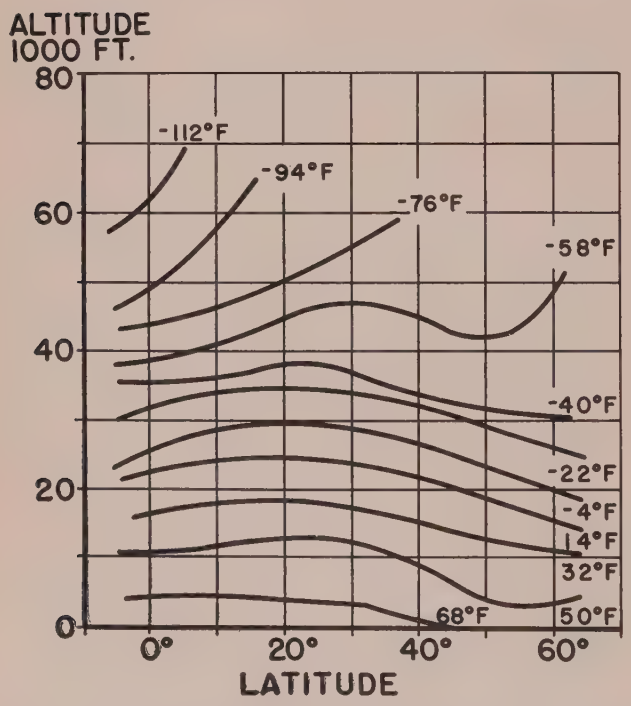

Fig. 4 – Variation of temperature and height of tropopause with latitude

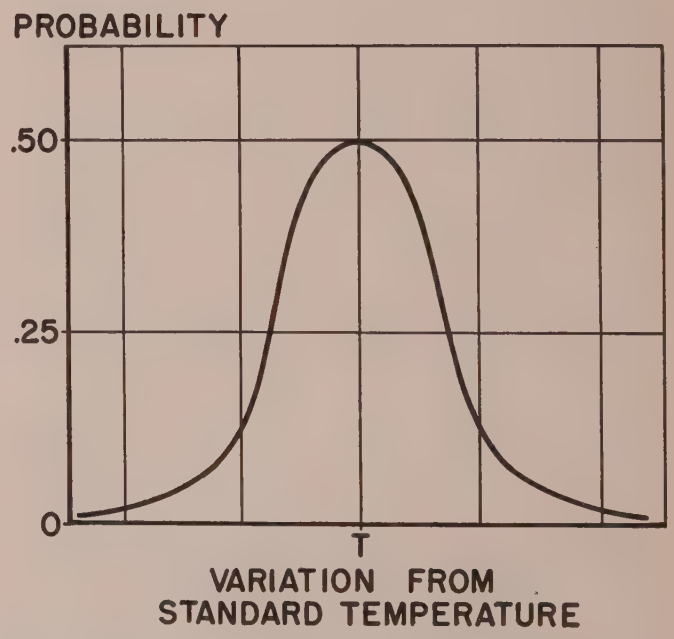

Fig. 5 – Probability of temperature variation at any altitude, averaged over long period of time

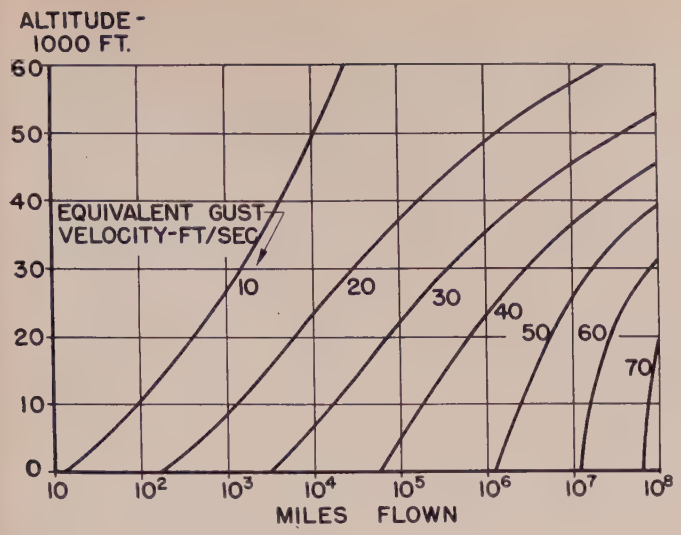

Fig. 6 – Variation of gust frequency with altitude in terms of number of miles that must be flown to intercept a gust of any particular value

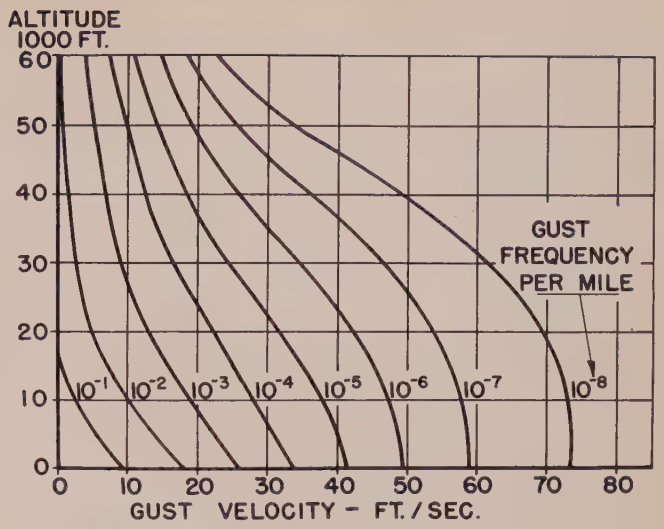

Fig. 7 – Variation of gust intensity with altitude, with gust frequency as parameter

is cut approximately in half for each 5000 ft increase in altitude. However, it should be remembered that all airplanes must fly through the lower altitudes when taking off or landing. In this case, if an airplane such as the DC-8 were flown at its normal operating speed, it would ride more roughly than a DC-7 but more smoothly than a DC-3. Of course its speed could be reduced, in which case it could be equal to the DC-7. Fig. 9 shows how the rough airspeed practically coincides with the cruising speed at altitude. This means that the pilot does not have to slow down when encountering rough air at high altitude.

Structural Considerations

Gusts, turbulence, and altitude immediately bring to mind questions of fatigue, cabin pressure, and general structural integrity. Experience has shown that if structural quality is maintained, and both the frequency and magnitude of the loads are carefully considered in the design, reliable and trustworthy structures can be provided.

The four main principles and their correlaries that have been found to provide safe structures are:

1. Structures of unlimited life.
   a. Stress levels.
   b. Frequency and magnitudes of loads.
   c. Quality of detail design.
   d. Fatigue evaluation.
2. Structures of limited life.
   a. Where unlimited life cannot reasonably be provided, the life must be determined by analysis and test.
   b. A scheduled periodic replacement should be made.
   c. Structural parts should be used in multiples.
3. Structural arrangement should be such as to minimize the risk of catastrophic failure.
   a. Multiple-member structures.
   b. Retain a large fraction of the initial strength after the failure of any one element.
   c. Restrict the extent of the failure.
   d. Provide tear-resistant and nonexplosive-type structure and details.
4. Inspection.
   a. To guarantee safety of the structure.

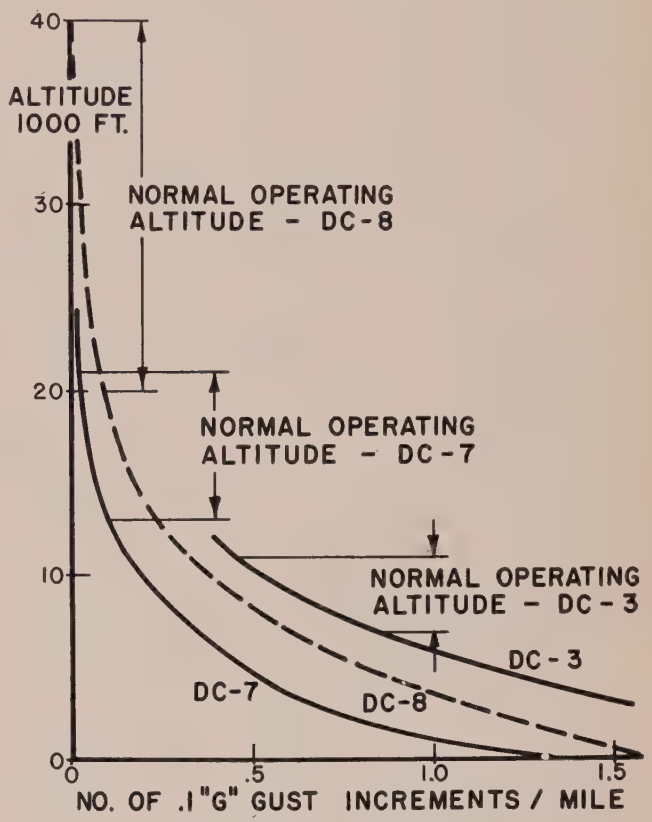

Fig. 8 – Results in terms of ride roughness

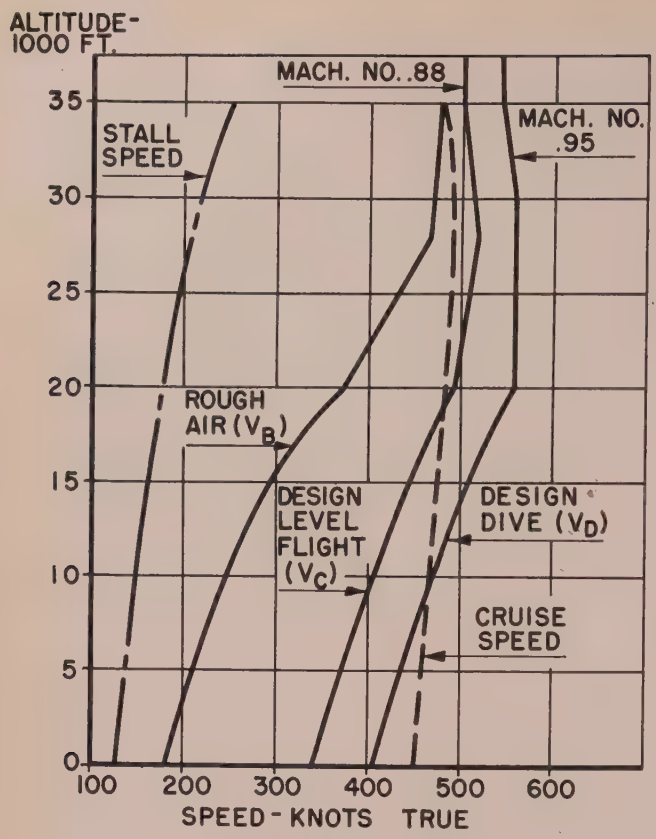

Fig. 9 – Design speeds, showing that rough airspeed practically coincides with cruising speed at altitude, so that there is no need for pilot to slow down when encountering rough air at high altitude

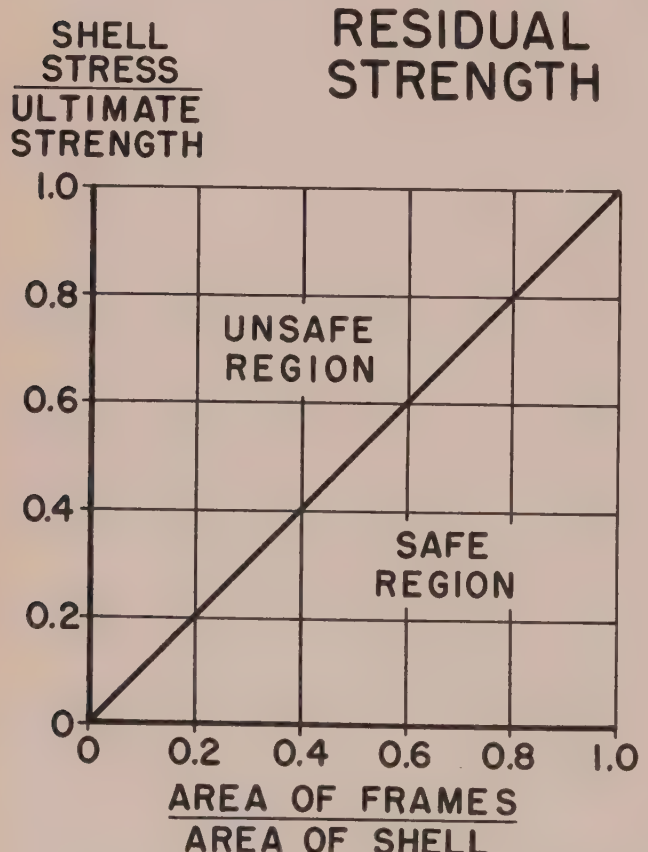

Fig. 10 – Effect of multiple structural arrangement, showing safe and unsafe areas

b. To discover accidental damage.
c. To discover incipient failures before they have developed.
d. To establish points where design improvements or life limits are required.

Fatigue tests have shown that at the stress levels used in modern American transports, the basic structure has a life of several hundred thousand hours. To be sure that the fittings and details have a similar life, it is necessary to make suitable adjustments in the stress levels and proper allowance for irregularities. This is best done by evaluating the detail designs by laboratory testing and matching them against the basic structure. If this work is conscientiously done, a reservoir of design information results, and the details are often equal to the basic structure to which they are attached.

Pressure cabins have received a great deal of attention by structural designers. The same principles apply to them as to the other structures. However, the tendency for a partial failure to grow into a catastrophic one is somewhat greater, so more care must be taken to provide a multiple structure, and special provisions must be made to limit the extent of failures. Fig. 10 shows the effect of multiple structural arrangement. The safe and unsafe areas are clearly shown.

At this point it might be well to point out that it is generally American practice to restrict the stress levels in pressure cabins at working pressure to the same general values that are used for the $1g$ or unit acceleration loads in the wings. Actual stress values of 10,000 to 15,000 psi are commonly used.

After all steps have been taken in the design and manufacture of any product, the continued suitability of the product is dependent on its maintenance and repair. Airplanes are no exception to this rule. It is practically impossible to exaggerate the importance of inspection. This is particularly true in guarding against fatigue and incidental structural damage.

Windows, doors, and other closures are affected by altitude, not only in that they must be designed for the loads imposed, but they must have additional factors of safety because the safety of the entire airplane and its contents is dependent on them. Fig. 11 shows a modern window design. Fig. 12 shows the arrangement of a double-glazed windshield. Fig. 13 shows the effect on cabin pressure

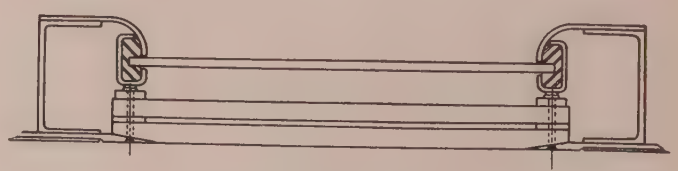

Fig. 11 – Typical cabin window

if a window were permitted to fail. Fig. 14 shows the effect on an average passenger under these circumstances. The need for absolute protection from such a mishap is obvious.

Air Conditioning System

The air conditioning system is actually made up of several such systems that work together to produce the overall result. The system is divided into:

1. The pressure-supply system.
2. The pressure-control system.
3. The flow control system.
4. The heating system.
5. The cooling system.
6. The ventilating system.
7. The distribution system.

Of these, the pressure-supply system and the pressure-control system are certainly the most vital.

These two systems are critical in an airplane designed for flight at high altitudes. Fig. 15 shows the small amount of time available before the crew or passengers would become victims of anoxia if the pressure were lost instantaneously.

To protect against this eventuality, the pressure-generating system is divided into several independent units. This division is such that any one of the units can maintain the pressure, and any two can provide reasonable ventilation. Under these conditions, it can be assumed that the pressure-producing system is as reliable as the main propulsion system.

Reliability of the pressure-regulating system must be of the same order; but more important, it must be of the fail-safe type of design, so that in case of failure it will continue the status quo until taken over by manual control.

Figs. 16 and 17 show the pressure and the range of altitude that this system must cover.

The ventilation control system becomes of great importance at altitude, because in case of smoke, noxious fumes, or similar emergency, the cabin cannot be depressurized until the airplane descends to a safe altitude.

Electrical System and Equipment Items

The effect of altitude operation on the electrical system, radio, radar, and instruments is primarily

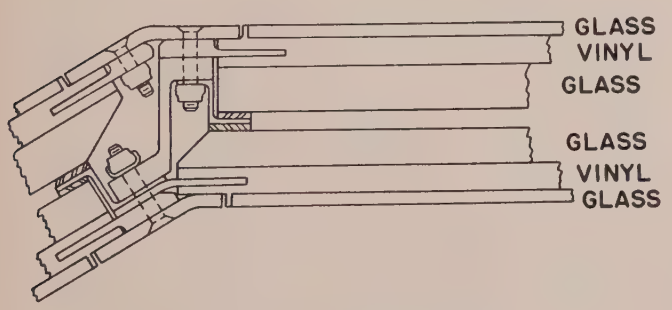

Fig. 12 – Double-glazed windshield

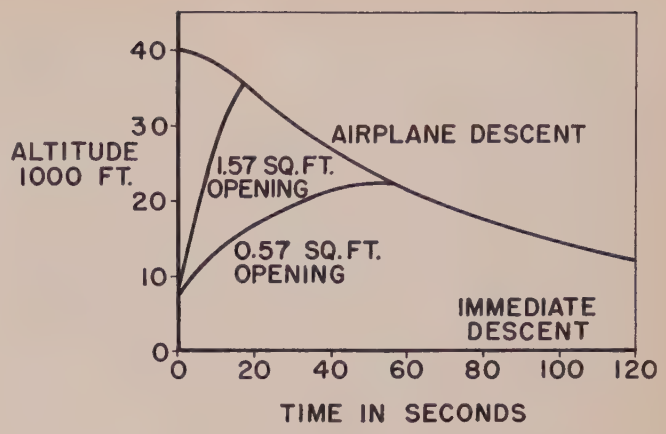

Fig. 13 – Effect of window failure on cabin pressure

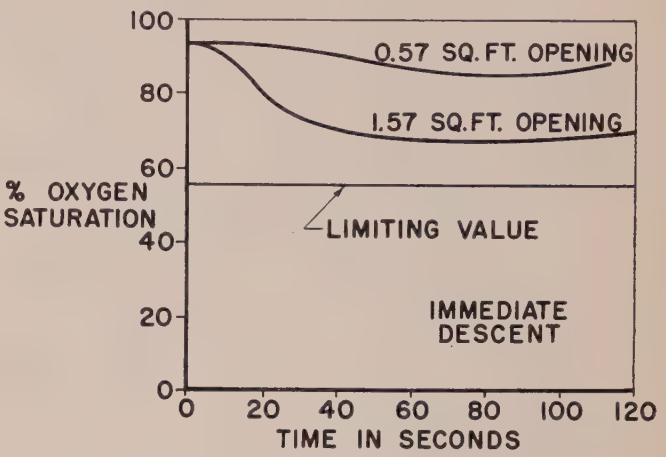

Fig. 14 – Effect of window failure on oxygen supply

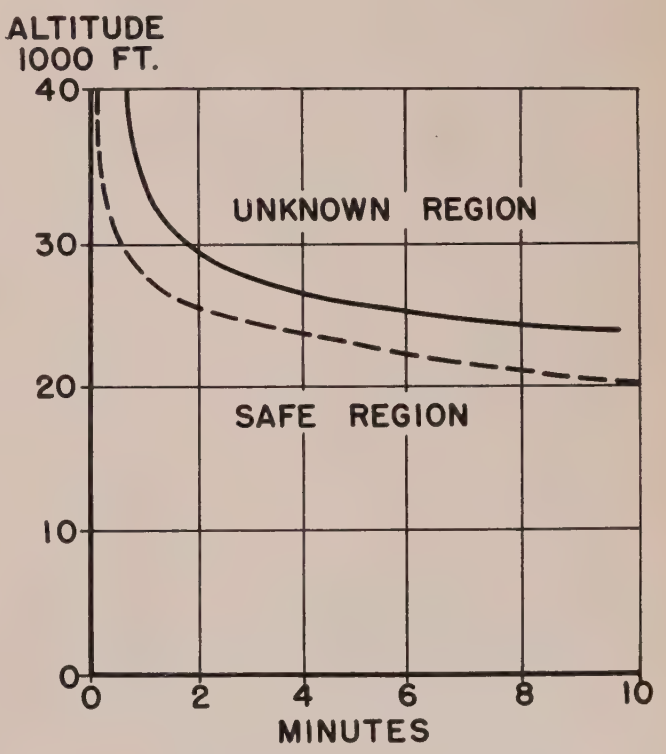

Fig. 15 – Time available before crew or passengers would become victims of anoxia after instantaneous pressure loss

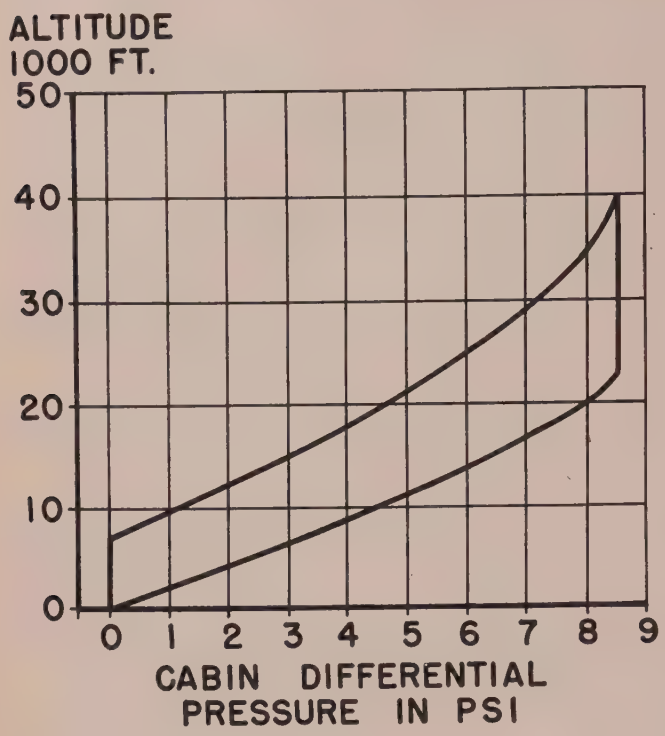

Fig. 16 – Range of cabin pressure

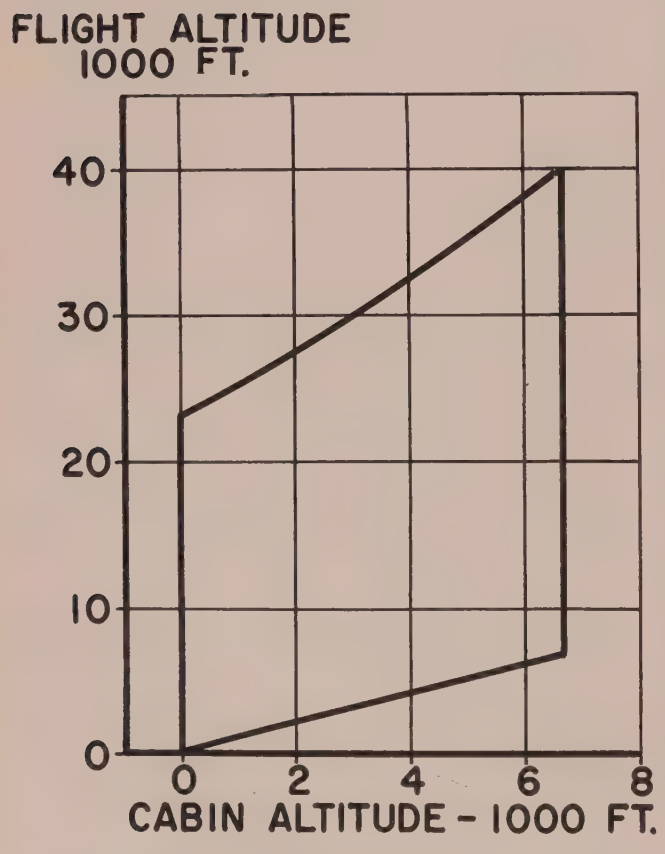

Fig. 17 – Range of cabin altitude

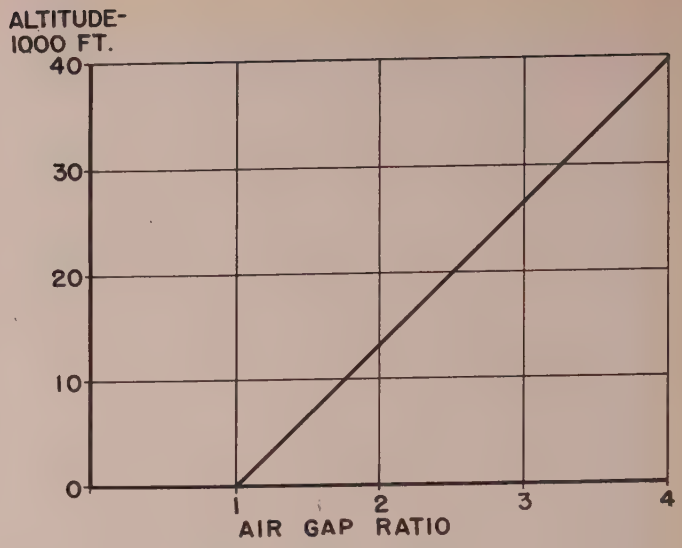

Fig. 18 – Ratio of air gap required to maintain equal sparking resistance at various altitudes

one of suitable insulation and satisfactory cooling.

The insulation of much of our electrical equipment is dependent on keeping the circuits separated so that a suitable air gap is maintained. As altitudes are increased, these air gaps must also be increased in inverse proportion to the density to maintain equivalent conditions, or the equipment must be insulated in some other way. Fig. 18 shows the ratio of gap that is required to maintain equal sparking resistance. Two other ways that have been proposed are pressurizing the individual units in hermetically sealed cases, or potting the units in some suitable insulating compound.

Increasing the gaps makes the equipment larger, nonstandard, and heavier. Hermetically sealing and pressurizing increases the weight and introduces serious maintenance problems. Potting increases the weight and makes maintenance virtually impossible except by outright replacement. At present, hermetically sealing and pressurizing seems to be the least evil choice.

The use of commutators, brushes, or slip rings is unsatisfactory under altitude conditions due to short life, and has resulted in the development of alternating current systems so that equipment without these elements may be installed.

The problem of cooling any kind of heat-releasing equipment has always been severe. Altitude operation aggravates this situation because the density of the cooling air decreases faster than the temperature difference increases due to the lower ambient air temperature at altitude. Fig. 19 shows the relative cooling capacity as a function of altitude drawn for an arbitrary equipment temperature of 100 C.

Landing Gear – Hydraulics Controls

The landing gear, hydraulic, and control systems are affected by altitude principally due to the low temperatures involved. Actually, it is the tempera-

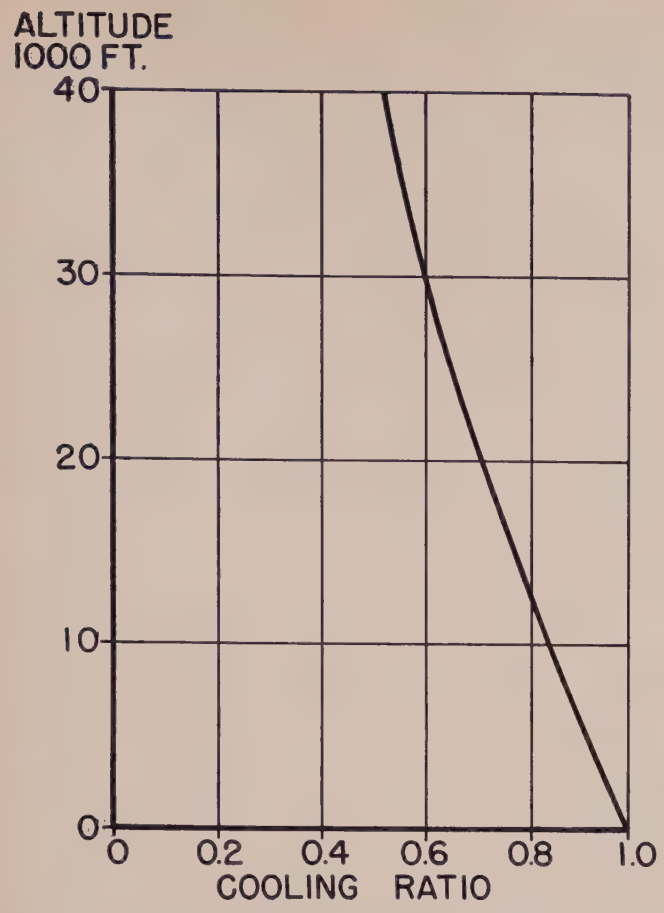

Fig. 19 – Relative cooling capacity as function of altitude, drawn for arbitrary equipment temperature of 100 C

ture range that produces the problems for these items. The thermal contraction and expansion of parts, the stiffening of elastomers, and the viscosity of hydraulic fluids must be provided for, or new materials must be developed. The addition of 50 F to the temperature range can be expected to produce a host of minor maintenance annoyances, but is not expected to introduce any new safety problems.

Powerplant

The effects of altitude on the powerplant are primarily a reduction in thrust with altitude, certain functional problems related to the low temperatures, and the usual cooling difficulties always associated with heat power machinery.

Fig. 20 shows the thrust from a typical jet engine plotted against altitude. Curves for 200 mph and 500 mph are drawn to show the small change in thrust with forward speed.

Fig. 21 shows the fuel consumption plotted against altitude. The specific fuel consumption is practically independent of altitude, but the total fuel flow decreases just as the thrust does.

The amount of fuel carried in a modern jet transport may be as much as one-half of its take-off weight. To pump such large quantities of fuel requires pumps, lines, valves, and fittings much

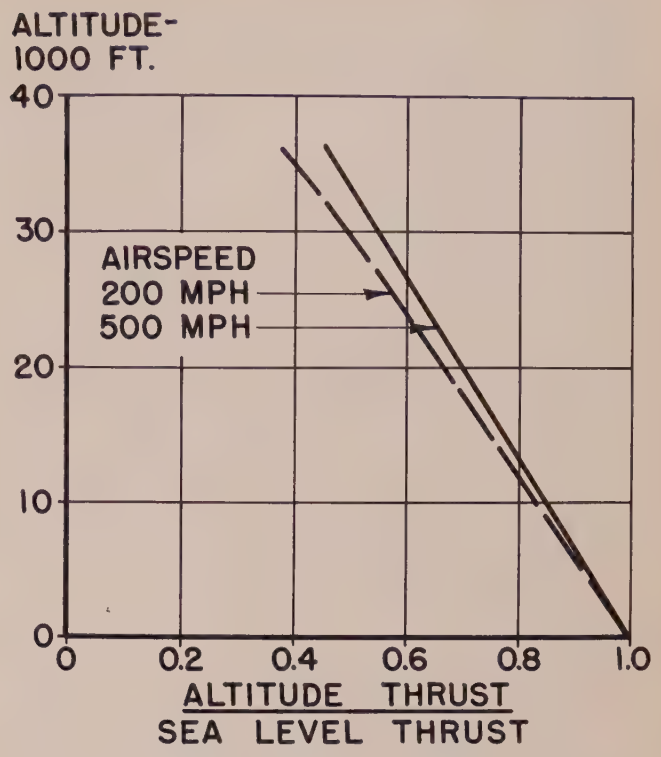

Fig. 20 – Thrust from typical jet engine plotted against altitude

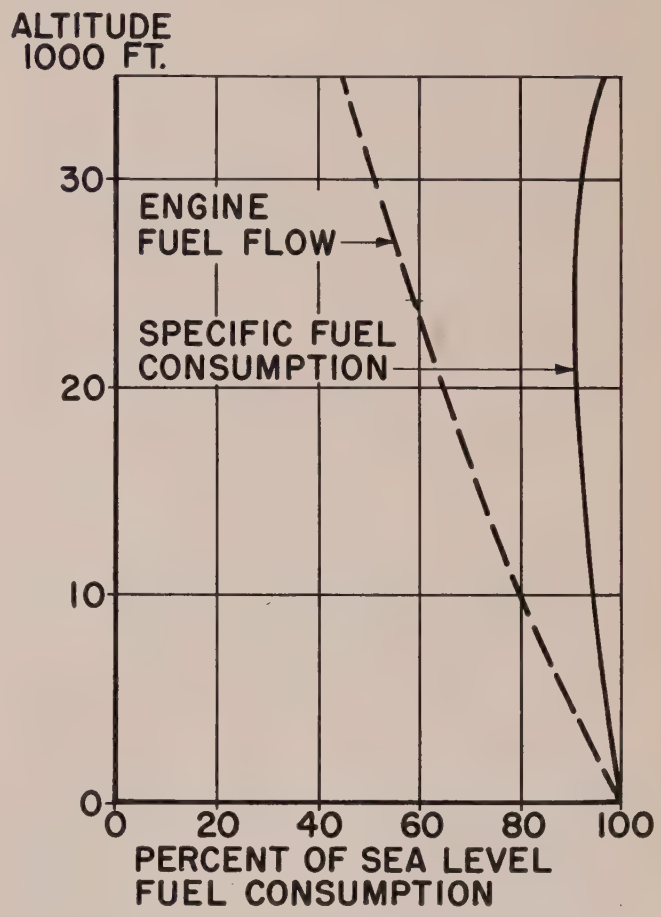

Fig. 21 – Fuel consumption plotted against altitude

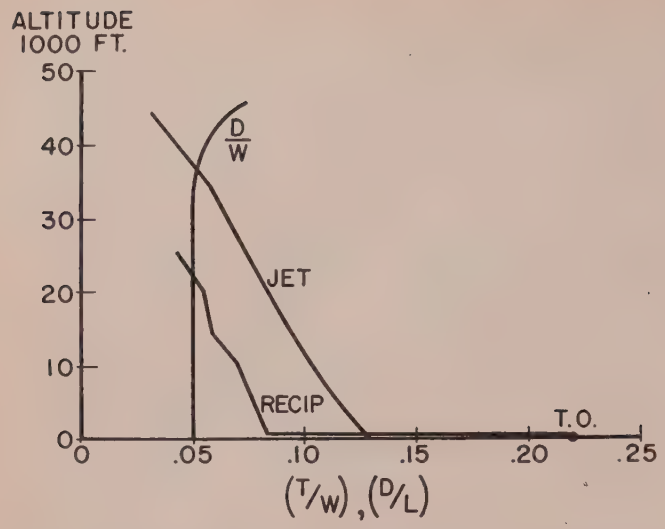

Fig. 22 – Thrust as fraction of weight for both types of airplane, plotted as function of altitude; drag of typical airplane at its best operating speed is also plotted

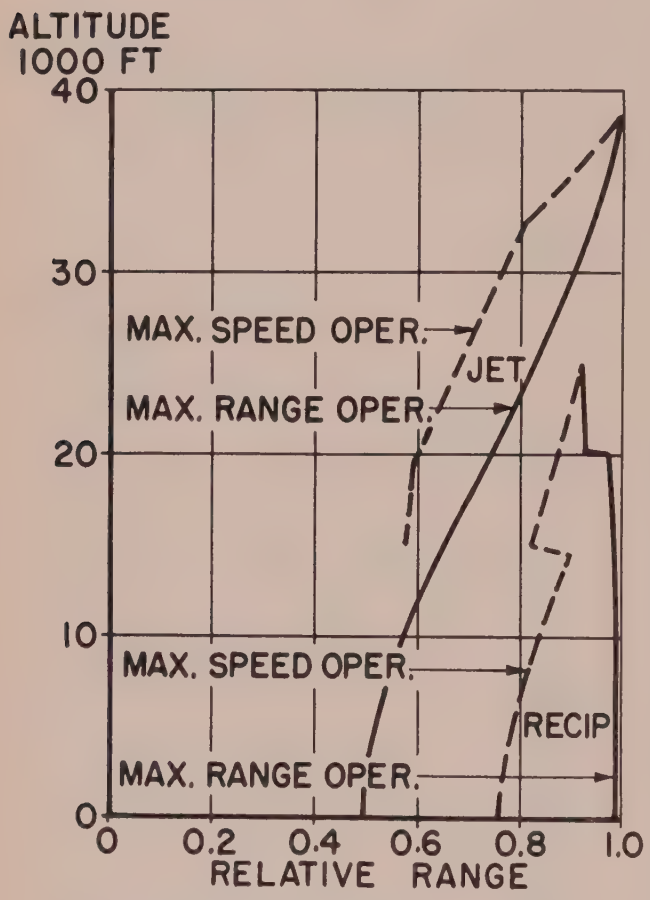

Fig. 23 – Speed-altitude characteristics of jet planes

larger than have been used in the past. The fuel may be cooled to a very low temperature due to the high altitude. This often results in the formation of a large quantity of ice in the system as the water is forced out of solution. Protection from this ice by filters and a fuel-heating system becomes imperative.

Cooling problems are always aggravated by altitude. In a jet engine installation the principal cooling requirement is to cool the oil. Since fuel heating is required, it is quite natural to use the fuel to cool the oil or use the oil to heat the fuel, depending on the point of view. In transport-type installations, it appears practical to do this without any additional air cooling.

Low temperatures associated with altitude introduce problems with organic materials such as rubber and various seals. New and improved types are constantly being developed.

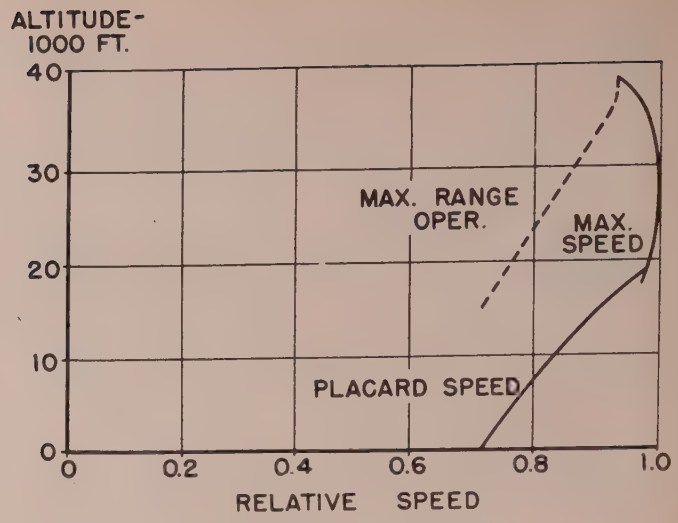

Fig. 24 – Effect of altitude on range

Performance

The principal items of performance and economy affected by extremes of altitude are speed, range, and operating cost.

For the same take-off distance, jet engine airplanes have much greater power installed. This is the principal reason that such airplanes are much faster and fly much higher. Fig. 22 shows the thrust as a fraction of the weight for both types of airplane, plotted as a function of altitude. Also plotted is the drag of a typical airplane at its best operating speed. The thing of interest is that these curves cross at about 25,000 ft for the reciprocating engine and about 37,000 ft for the jet, and that there is a much greater margin of thrust for the jet airplane at all altitudes.

Speed-altitude characteristics are shown in Fig. 23. There are three speeds shown: the maximum speed, the speed for maximum-range operation, and a structural limiting speed. The structural limiting speed is a designer's choice, and is used to restrict the loads that the airplane must be designed to withstand. The maximum speed is practically independent of altitude; however, the speed advantage of higher altitudes in both the maximum range and structural limit cases is clearly shown.

The effect of altitude on range is shown in Fig. 24. Two cases are plotted: one for maximum range

operation, and one for maximum speed operation. At the limiting altitude, these curves coincide and define the point where the maximum range can be accomplished at the maximum operating speed. Reducing the altitude decreases the maximum range, until at sea level only half the possible range can be made good. However, the shape of the curve is such that the altitude can be reduced about 10,000 ft at a cost of 10% of the range.

If a jet airplane is operated within its range limitations, it can be operated at any altitude without appreciable effect on its block speed or economy. Fig. 25 shows the direct cost in cents per 200 lb-mile as a function of altitude. The cost increases slowly down to 20,000 ft, then increases more rapidly due to the structural limiting speed. The structural speed limitations could be eliminated by designing for a greater speed at lower altitudes, but would result in a considerable increase in the structural weight. A compromise based on operating conditions is usually made.

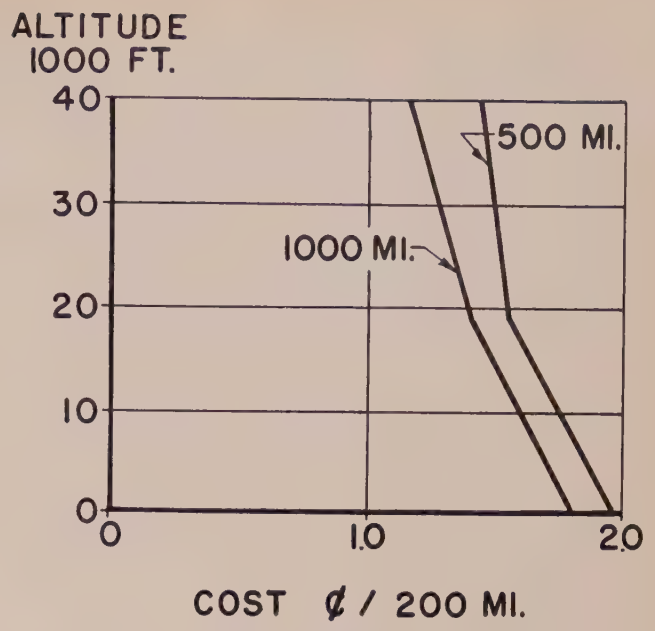

Fig. 25 – Direct operating cost in cents per 200-lb-mile as function of altitude

DISCUSSION

Calls Net Income Determining Factor

– Mark E. Kirchner

Boeing Airplane Co.

BASICALLY, the jet airplane wants to cruise at high altitudes for range reasons. This is pointed out in Mr. Kleinhans' Fig. 24, where he shows the relative range of jet airplanes and reciprocating-engined airplanes as a function of altitude. Although Mr. Kleinhans points out many effects of cruising at high altitude (such as pressurization problems, electrical problems, and so forth), the fact remains that the altitude for cruise will be that which yields the greatest net income per flight for any particular route. The incidental problems which naturally arise as a result of flying at these altitudes must then be solved, and, in fact, have been solved, as is evidenced by the many years that heavy, pressurized jet airplanes have been successfully operating in this country.

The net income per flight will be determined by two factors:

1. The direct operating cost of the airplane.
2. The passenger load factor attained.

The block-to-block speed will affect both the direct operating cost and the passenger load factor. The direct operating cost will be further influenced by the cruise fuel consumption. These are the factors which must be balanced in determining the optimum cruise altitude and resulting cruise speed for any flight segment. For long-range flights, the cruise altitude will, of necessity, be high.

Our evaluation of the structural considerations for the design of a modern airplane has led to the conclusion that a successful airplane must combine the two basic requirements of a high level of safety and a long, maintenance-free life. Attainment of either one of these two basic requirements does not necessarily mean that the other has also been accomplished.

Mr. Kleinhans' paper suggests that safety may be attained by scheduled replacement of parts or components. We believe that it is extremely difficult to predict the proper replacement period of a part or component on the basis of either analysis or laboratory tests, because of the unaccountable influence of such items as route variations, local aero-dynamic or sonic loadings, pilot technique, corrosion, or manufacturing variations.

We believe that safety may best be attained by means of multiple-path design. This is done by disposition of the material such as to give adequate strength with a member failed. But this also entails use of a material which has the properties of providing high residual strength after some damage, and a slow rate of crack propagation. Without these properties, it is believed that it will be extremely difficult to provide safety against failure of every critical element.

Since the revenue potential of this class of airplane is so enormous, it is more than ever imperative that the minimum amount of time be spent on the ground for purposes of structural maintenance. Our investigations have shown that the selection of the material and the detail design are the most powerful factors in attaining long life. These factors are far more important than the selection of stress level in obtaining the best structure with minimum weight. These considerations have been found to apply to both primary and secondary structure.

Author's Closure To Discussion

IT is self-evident that jet airplanes will be flown at altitudes that are most ideal for their operation. The purpose of the paper was to show the effects of variation from the ideal when jet airplanes were operated under other conditions. Actual experience has shown that such nonstandard operation is often required for a great variety of reasons.

It was not intended to imply that safety can be attained by scheduled replacement of parts or components. What was said was that if parts of limited life cannot be avoided, then such parts should be thoroughly tested, safe life established, and a scheduled replacement program followed. As everybody knows, this is common practice in the case of tension bolts when they are used anywhere near their real strength.

Mr. Kirchner apparently agrees that the quality of the detail design is the greatest single factor in providing a trouble-free, long-life structure.

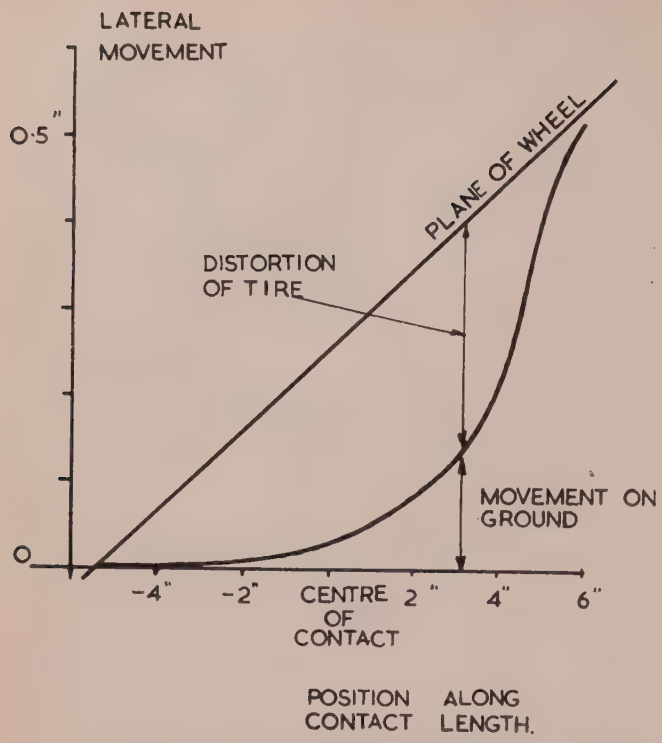

Fig. 1 – Distribution of lateral movement along contact length for a tire operating at a 3-deg. slip angle

Practical Tire

IN THIS paper the following researches are discussed:

1. Studies of distribution of force and movement within the tire-ground contact area with the tire operating at a slip angle.
2. Studies of buffing patterns observed on worn tire treads.
3. A new method of presenting cornering properties of tires, and its application.
4. A picture of a traction or standing wave in a tire on a flat road at high speed.

The first three are clearly related, and while the fourth may not be directly related, it comes within the scope of the paper and is thought of sufficient general interest to be included.

Tire-Ground Forces During Cornering

The ability of a tire to produce a large lateral force with only a relatively small angle of drift from the course it would take if it rolled freely without a side force, is fundamental to the production of a practical vehicle which must be maneuvered on land. The progressive relationship between drift, or slip angle and lateral force obtained with a tire is also of fundamental importance. Many devices could be made to carry load, maintain level motion, cushion the vehicle from effects of obstacles, or to stop or retard forward motion. But without a guiding action similar to that obtained with a tire, these devices will never seriously challenge the supremacy of the pneumatic-tired wheel. The gasoline engine was considered the indispensable feature of road transport, but its position has been threatened in turn by diesels, turbines, jets, and (maybe) atomic engines. But even the latter will need tires capable of producing controllable cornering forces!

The cornering properties of tires (that is, cornering properties under particular conditions of load, pressure, road camber, and surface condition), decide (a) the path the vehicle can achieve, or, its navigation, (b) stability of its course, and (c) "feel" or handling of the vehicle. That a tire must provide the centripetal force causing the vehicle to deviate from a straight course makes cornering one of the main factors influencing tire wear. All these aspects are interrelated, and it is difficult to select an order of discussion to best highlight the essentials. Accordingly, the mechanism producing cornering force will be discussed first.

Evans and others have stated a plausible mechanism for the development of a cornering force.

Research

TIRE-GROUND forces during cornering have been studied with the aid of an experimental device, and tire tread buffing patterns are correlated with tire position and use.

Tire characteristic curves are introduced and are shown to be helpful in interpreting the interrelations between cornering force, aligning torque, slip angle, and caster. An example is given of the use of characteristic curves to study an application of power steering.

A photo of a standing wave on a tire running at 100 mph is included as a matter of general interest.

V. E. Gough, Dunlop Rubber Co., Ltd.

This paper was presented at the SAE Golden Anniversary Summer Meeting, Atlantic City, June 15, 1955.

Namely, a tire lays its tread down along its line of progress (which is at an angle to the plane of the wheel), and because of the friction the tread remains at the point on the ground where it was laid until contact ends. Then the fall in contact force allows elastic forces in the casing (set up by the distortion), to return the tread to the plane of the wheel. How nearly true this idealized concept is is shown by comparing Figs. 1 and 2, which are based on hundreds of diagrams we have obtained on a device (Figs. 3 and 4), which records lateral movement and force within the tire-ground contact area under a tire rolling at a slip angle.

A one-inch-square bar whose top face is flush with the top surface of the plank is carried by two single leaf springs, one at each end of the bar. Edge-wise stiffness of the springs is sufficient to eliminate downward deflection of the bar, while their lateral stiffness is such that a small deflection ensues from a side-wise force acting on the bar. This small deflection is magnified by a lever which causes a stylus to trace a diagram on a smoked glass plate. The plate is moved at right angles by a spike passing through a slot in the bar and into the tire tread. The diagram produced represents intensity of side-wise force versus side-wise movement. Location through the contact area is obtained by lifting the stylus electromagnetically every inch the axle progresses.

Enlarged smoked-glass recordings are shown in Fig. 5. Figs. 1 and 2 are obtained from such recordings. Justification for using a bar covering the full tread width and a spike to record movement of one

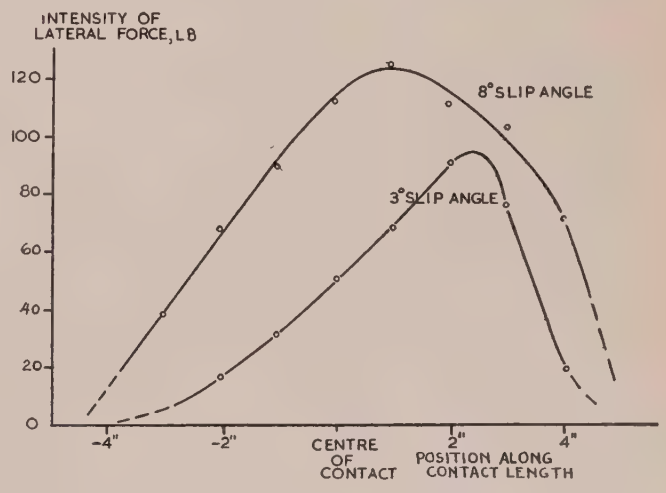

Fig. 2 – Distribution of lateral force compared for two different slip angles

rib resides in fairly extensive investigations of scratch records obtained by the use of grit on blackened metal plates.

At any significant slip angle, tire movements on the ground are primarily lateral and all ribs move a similar amount, Fig. 6. Small departures from this do not invalidate the apparatus of Figs. 3 and 4. At zero slip angle, movements are more complex and different for different ribs. They are all trivial, however, compared with the general lateral movement occurring in a cornering tire; even at a half-degree slip angle the lateral movements predominate.

Lateral movement and distribution of lateral force versus distance progressed through the contact area, Figs. 1 and 2, can be deduced from Fig. 5. They agree substantially with the original suggestions of Evans, Bull, Olley, and others. The only significant departure is in the slight creeping movement before peak intensity of lateral force develops. Area under the curve in Fig. 2 equals cornering force developed, and its first moment about the center of contact is approximately equal to the self-aligning torque, that is, the center of action of the lateral force is to the rear of the midpoint of the contact area an amount equal to the pneumatic trail or caster. The results check against values determined by other methods.

As expected at higher slip angles, lateral force reaches its limiting value earlier in the contact

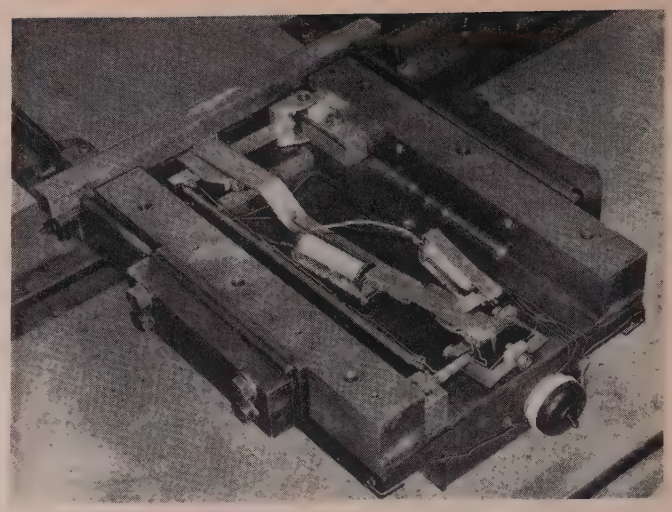

Fig. 3 – Closeup view of recording mechanism

area. Data of this kind suggest that side force intensity increases in proportion to the movement through the contact area until it cuts a curve representing the limiting intensity which can be resisted, and is dependent upon intensity of loading and friction. The diagrams are triangular at low slip angles and trapezoidal at high slip angles.

With both high and low slip angles, work done against lateral forces is mostly in the rear portion of the contact area, confirming the fact that abrasion occurs in the latter half of the contact area.

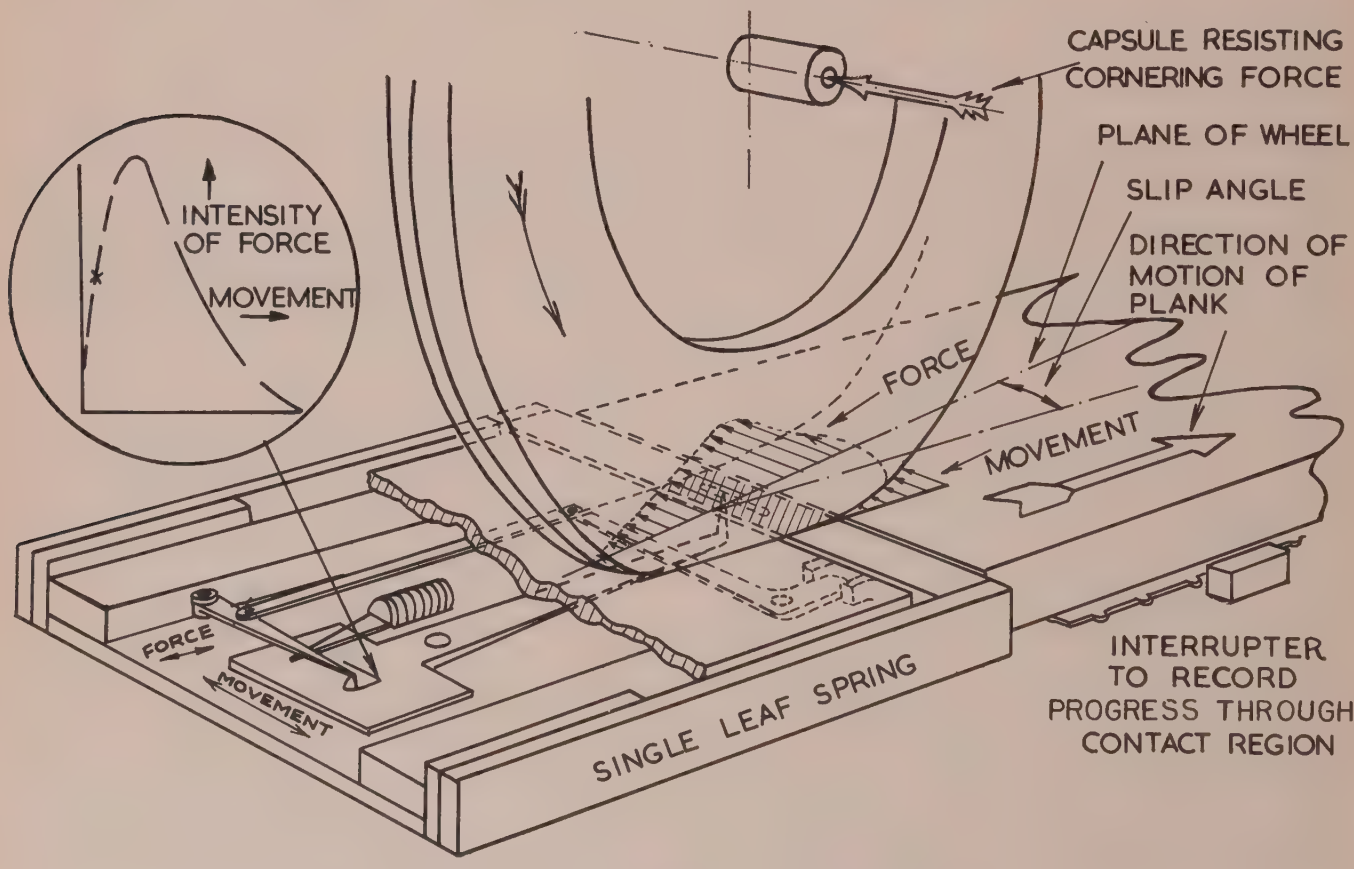

Fig. 4 – Apparatus used in study of tire-ground lateral forces

This is shown in Fig. 5 (in which midpoint of contact is indicated), for both low and high slip angles. Area under the diagram represents work done against ground friction in a lateral or side-wise direction. The creeping effect before peak frictional force develops is of fundamental importance, but its consequences would require a separate paper for adequate discussion. We shall not deal with it here except to point out that it explains why lateral forces, such as cornering and traction forces, develop in a manner depending on distance rolled and not on time as such. This is confirmed by experiment; the quantity defined by Lippman as the ...nd ...justment-rate constant is substantially identi... ...his when determined from simple curves of cornering force versus distance rolled with movement of the order of inches per minute and when determined using strain-gages at road speeds. The reciprocal of the adjustment-rate constant is about 20 in., and defines the intercept between the original gradient at the start of rolling movement and the limiting value of cornering force, which is exponentially approached. This corresponds approxim...tely to achieving 50% of the steady value in 1-1½ ft, and 90% in 3-4 ft.

Lateral movement and resulting work done increase rapidly with cornering force developed (as the square or cube of the cornering force), thus explaining the importance of cornering on tread wear. Joy and Hartley have shown that increase of power consumption when cornering is due mainly to the forward component of the cornering force.

For conventional tire construction, area under the curve in Fig. 5 is of the same magnitude as that deduced from this forward component of cornering force. It is possible, however, to make tires for which the diagram area is less, resulting in reduction in wear, but at the price in other tire properties.

Enough has been said to show that cornering is a vital factor in producing wear. It is agreed, of course, that acceleration and braking produce wear, but for most operating conditions, the following simple argument indicates that cornering wear outweighs braking or driving wear. $V^2 = 2fs$ applies for forward acceleration or braking, and $f = \frac{V}{r}$ gives the centripetal acceleration necessary to maintain a curve of radius r. It follows that forward braking force on a vehicle coming to rest from a speed V with constant retardation in a distance s equals cornering force on the same vehicle at constant speed V on a circle of radius Y, where $Y = 2s$. By executing a complete circle, a driver can cause a given lateral force to be exerted on the tires for a distance equal to 4π times the stopping distance obtained from a braking force equal to the lateral force. That is to say, for a given speed one right-angle turn is approximately equal to three full braking stops each in a distance equal to one half the turn radius and from the same given

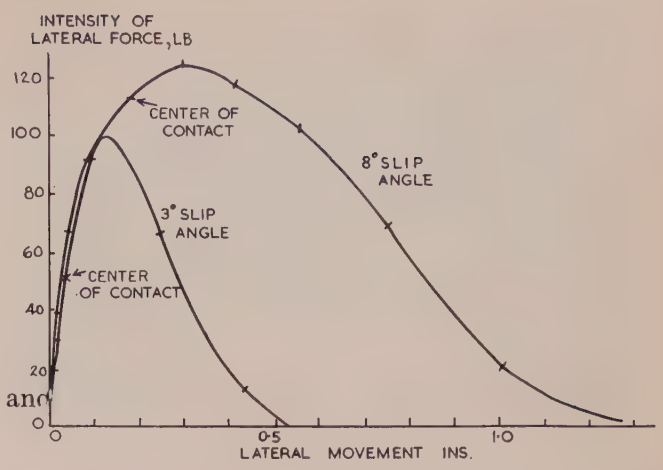

Fig. 5 – Lateral force versus lateral movement at high and low slip angles

Fig. 6 – Scratches recorded by tire operating at a slip angle

speed. Presence of road camber or crosswind requires continuous application of slip angle to produce the necessary counteracting cornering force. Although low in value, this force is always present even on the straightest road.

Buffing Patterns on Tire Treads

Practical evidence that cornering is important in tire wear is offered by what might be called the tire's fingerprints. A rapidly worn tread has innumerable ridges of fine sawtooth section over its whole surface. Overall slip during cornering is a major factor deciding local tire-ground movements recorded by those ridges.

At all places the line of the ridges is perpendicular to the relative motion between tire and road. We have used this fact to develop a system of interpretation enabling us to determine how the tire has been used and even something about the wheel position and the vehicle's mechanical condition.

A marked front-wheel wear pattern is visible on the tread shown in Fig. 7. Fig. 9 shows the directions of wear lines corresponding to (a) Fig. 7 (a

Fig. 7 – Coarse-textured buffing pattern on a tire continuously cornered

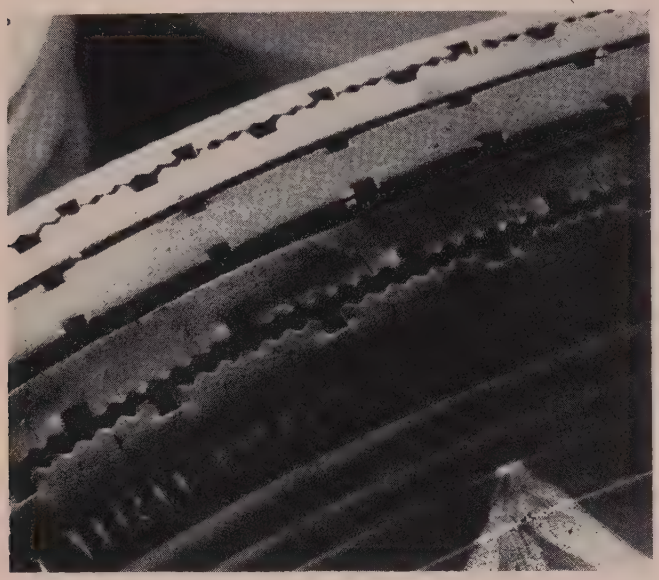

Fig. 8 – Type buffing pattern on tire resulting from irregular wear

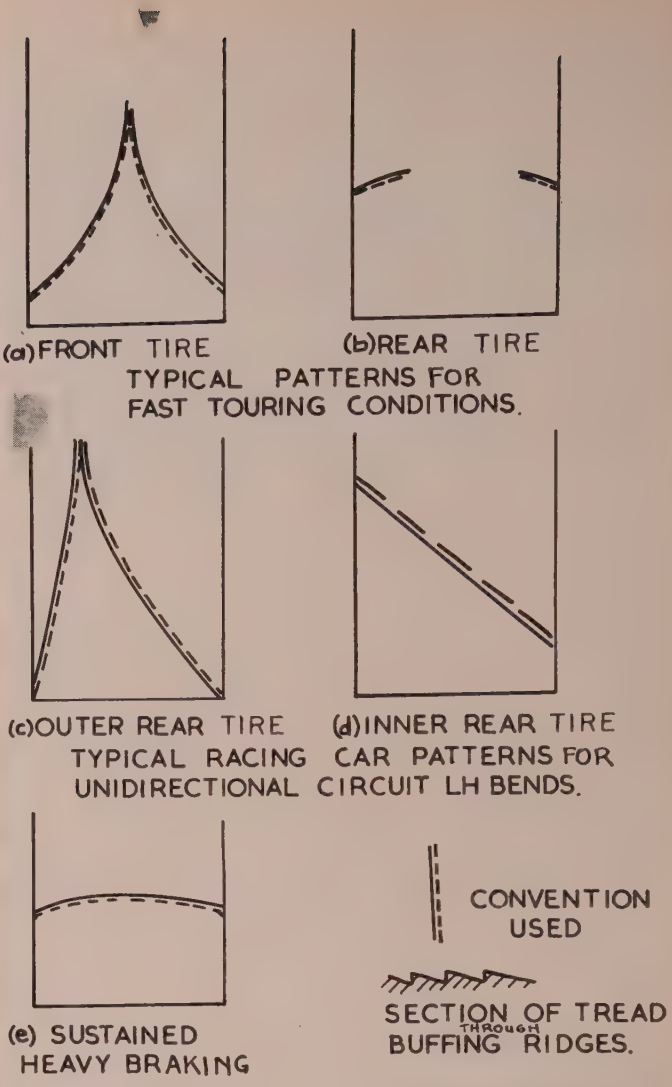

Fig. 9 – Typical buffing patterns on tires for different locations and types use. Tires are viewed coming toward the observer

front wheel), (b) a typical rear tire, (c) rear tire of a car driven hard or the outer rear tire of a racing car, (d) inner rear tire of a powerful racing car driven at full power on corners, showing wheel spin, and (e) those of a wheel continually under heavy traction or braking. The section in Fig. 7 also illustrates the importance of cornering; the tread was worn as shown in 32 miles of continuous cornering at 8 mph (0.3g).

Note that buffing ridges as coarse as those in Fig. 7 are unusual. More frequently they resemble those in Fig. 8, or they may be so fine as to require a magnifying glass to be seen. Fig. 8 also shows how the direction of the lines changes at spots of local wear. The explanation for this has been given in other papers by the author and his colleagues.

In the United States and Canada, the presence of road dust results in less sharp ridges than those observed on the other side of the Atlantic. In general, roads here are smoother and straighter, and buffing patterns are not so readily or frequently observed. When visible they exhibit the same patterns we see in England. Just as driver behavior tends to render them more common in Europe, I should expect "hot rods" to produce the most marked patterns. The more readily the pattern is seen the more rapidly the tire has been worn.

Tire Characteristic Curve

So far we have discussed the mechanism of tire cornering, how cornering forces are developed, and how they influence wear. Since many of the factors mentioned are more in the driver's hands or are settled by the route to be negotiated (decided by the highway engineer), they may be considered of less interest to the automotive engineer than the effects of tires on handling or vehicle stability.

The work of Evans, Olley and Bull is well known, so I shall devote more space to some of the recent additions by my colleagues and myself to the literature in England.

First of all we agree with Olley that understeer and oversteer relate to the state of stability of the vehicle's motion. It is not generally realized that

equality of front and rear slip angles corresponds precisely only to neutral steer on straight paths. This caused Hardman to re-define neutral steering in terms of effects of side force on the path radius. The difference between definitions is small in practical cases, and for many analyses, unimportant. Its presence must be borne in mind in more advanced stability studies which will surely come in due course.

There will be two kinds of studies: those of vehicle stability with locked steering, and those of stability with a human driver.

Both studies will need tire data. We have found the use of a characteristic curve a great help. This curve (Fig. 10), is a plot of cornering force versus aligning torque for several loads and slip angles. In effect it is a plot of what the driver applies – aligning torque – against what he gets – cornering force. Relegating slip angle to a subsidiary role is justified because the driver never knows the front tire slip angle. It does not prevent cornering power from being read off, for it is the ordinate of the curve for given load and slip angle.

The sloping straight lines allow pneumatic trail (caster or offset), to be read off directly. These lines follow from the relation: cornering force $\times$ trail = moment; or 600 lb $\times$ 1 in. = 50 lb-ft.

The relations between the characteristic curve of Fig. 10 and the distribution of lateral force intensity of Fig. 2 follow: area under the curve of Fig. 2 is the cornering force; moment of area under the curve about an axis through the center of contact is the aligning torque, and distance between the center of area of the curve and center of contact is the trail.

These characteristic curves have been discussed in other publications, where it is shown that curves of cornering force versus torque at the kingpin can be derived readily by shifting the curve by the correct amount of caster trail, while keeping the same cornering force. When this is done a set of curves shown in Fig. 11 is obtained for each load; or a new family of curves of the type of Fig. 10 (but for a given caster value), can be drawn.

It will be noted from Figs. 10 and 11 that in all cases at low slip angles, cornering force developed is roughly prorata with torque (with different slopes of course); that is, a progressive relation exists. At higher slip angles for both light loads and with negative or low caster, this progressive relation changes such that cornering force called for does not cause appreciable change of aligning or steering torque. This corresponds to a loss of feel as judged by the driver from his estimate of steering effort.

It is possible to show that reduction in the coefficient of friction of road surface causes loss of feel at a lower cornering force (Fig. 12). This occurs because the upper end of the curve becomes asymptotic to the limiting friction, and aligning torque decreases to negative values. This explains why an experienced driver can sense a slippery surface without losing control.

Using these characteristic curves, French and Gough have shown that instability of vehicle motion and loss of feel at the steering wheel do not necessarily go together. It is possible to show that the situation is complicated further by friction and compliance in the steering. For instance, it is not always right to assume that because more steering movement must be applied with one set of tires than with another, the vehicle is more understeered

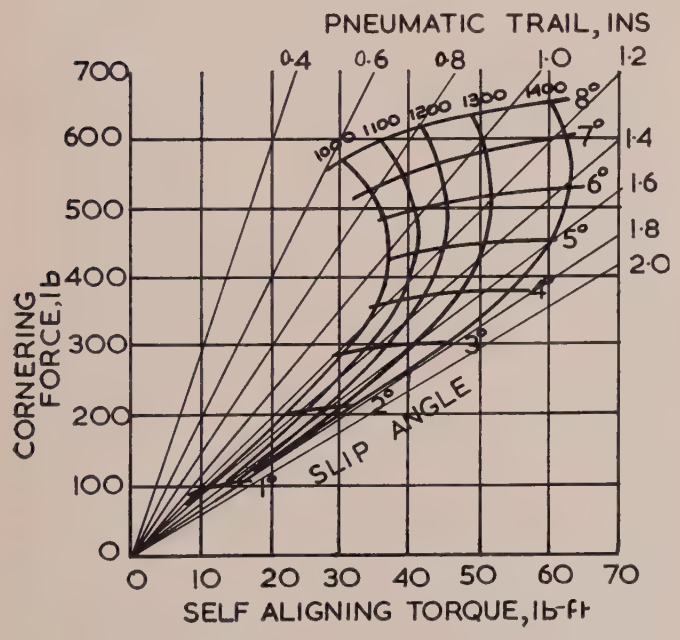

Fig. 10 – Characteristic curve of 7.60-15 tire with 24 psi inflation pressure

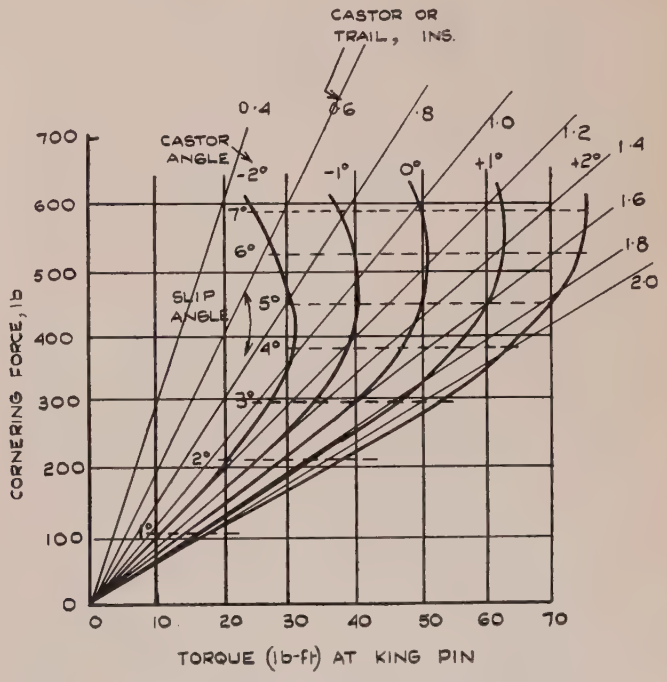

Fig. 11 – Effect of caster on kingpin torque

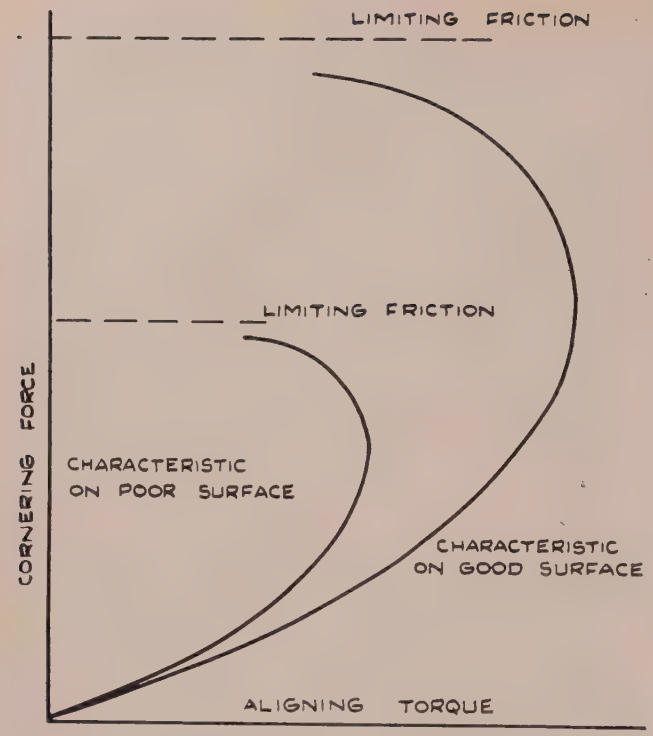

Fig. 12 – Influence of limiting friction on type characteristic curve

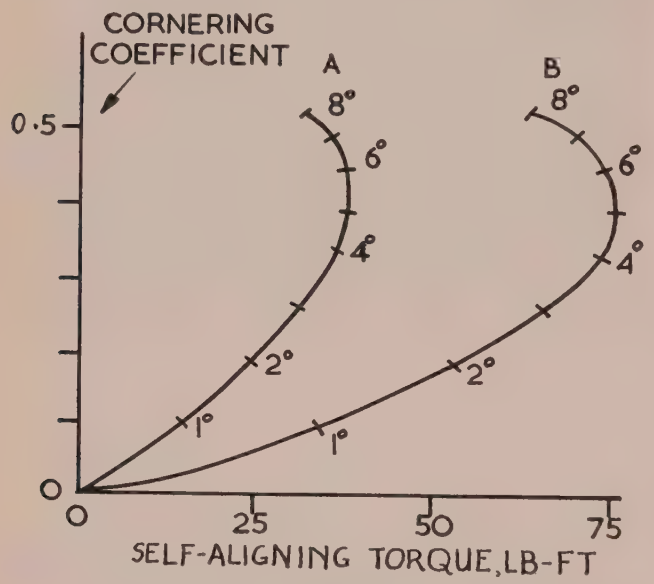

Fig. 13 – Characteristic curves illustrating effect of steering-mechanism compliance

with the first set.

Consider two types of tires, A and B, of equal cornering power, with similar shaped characteristics, but with different values of maximum self-aligning torque, 37.5 and 75 lb-ft (Fig. 13). These are used on a vehicle with zero caster whose steering mechanism is found to deflect such that when it exerts 100 lb-ft of torque at the kingpins the steering wheel rim moves 2 in. At 0.5 g, with tire A a steering-wheel movement of 1½ in. (with B, 3 in.) in addition to the steering angle needed at the kingpins would arise. Since steering-wheel movement needed for a 0.5 g corner at 90 mph is theoretically 1½ in. (with completely rigid links), it is seen that at high speeds, at least, tire B would require more steering-wheel movement than A. This may mislead those who try to judge under- or oversteer by steering wheel movements into claiming that tire B understeers compared with A, whereas stability as settled by slip angles (the true measure of under- or oversteer), is the same for both tires. The effect is present at lower speeds, but is masked by the fact that steering-wheel movements needed are proportionately larger than deflection of the mechanism.

A simple example of using characteristic curves to study the characteristics of power steering is illustrated by Fig. 14. Fig. 14A gives tire curve at zero caster and vehicle curve for +2 deg. To obtain the same maximum torque at the steering wheel without power steering, different steering box ratios would be needed for the +2 and −2 deg case. The latter case would need proportionately more movement of the steering wheel than the former and would lack progressive feel at all but the lowest slip angles. This is in accord with experience. However, with power steering both cornering force – torque curve for the required feel and the desirable gear ratio could be selected and the power system designed accordingly. In a power-steering system, if, and I say if, the system were merely manual up to a certain torque and then fully power with no feedback or proportional feel, then the response would be as in curve (i) of Fig. 14C. On the other hand, a true servomechanism with proportional feedback would produce curve (ii); the precise shape of (ii) could be modified by selection of caster. Obviously, practical power steering will be something different and probably intermediate, but it is the author's opinion that the ideal is nearer (ii) than (i). Curve (i) would enable navigation but not driving with good handling, for while it would enable the driver to tell which side of the road he was on (due to road camber), he would have no feel on corners, no information as to what cornering force he was inciting, and no warning of slippery roads. A vehicle with a response curve like (i) could be driven safely if, and only if, it was inherently understeered.

The tire characteristic curve and a plot of front and rear cornering force were used by French and Gough to discuss the relations between feel and stability. The same technique can be used to show how the location of a roll-bar can influence these phenomena. As seen from Fig. 15A, the characteristic curve can be obtained for a given load transfer by a simple averaging process. This has been done for several values of load transfer (Fig. 15B) (dotted lines). By assuming load transfer proportional to cornering force, the final steering characteristic (full line) is obtained. Using this characteristic and considering two cases, (A) with all load transfer at the front, (B) with all load transfer at the rear, we obtain four diagrams in

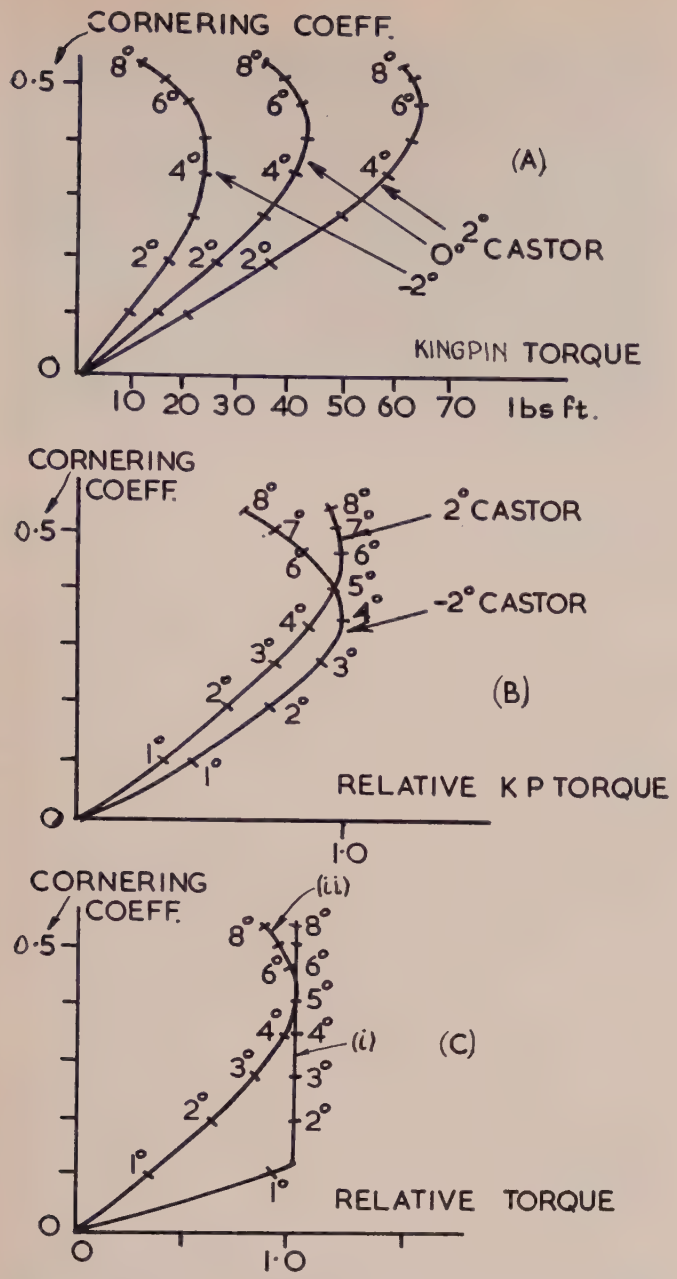

Fig. 14 – Characteristic curves used in analysis of power-steering application

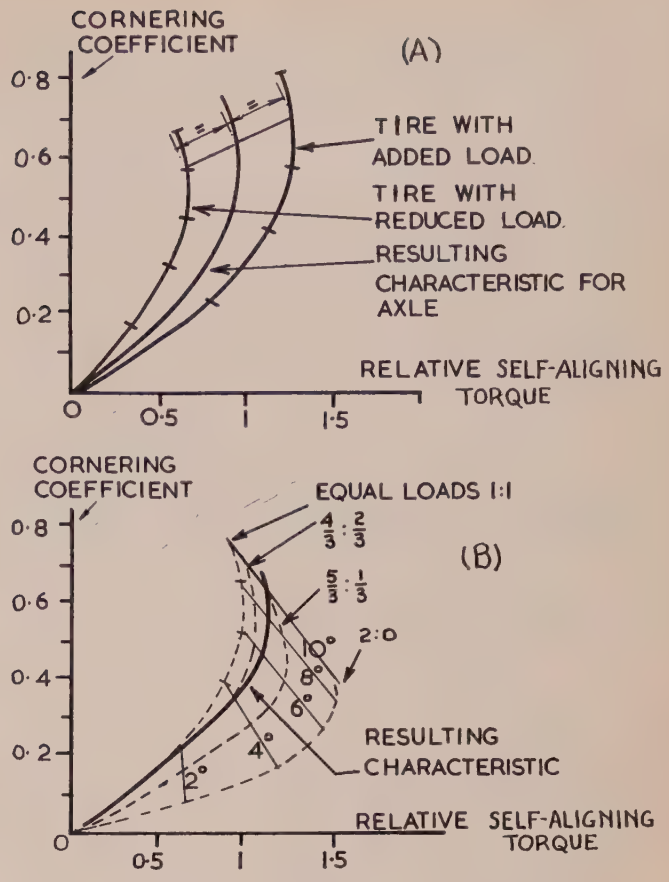

Fig. 15 – Effect of load transfer on characteristic curves

Fig. 16. These diagrams show that if load transfer is at the rear only (corresponding to the roll-bar at the rear), an inherently oversteer condition arises and rear slip angle will rise very rapidly without substantial increase of cornering force. Furthermore, as the load transfer cannot take effect until the roll-bar is twisted, namely, the body has rolled relative to the axle, this oversteer comes in late and makes the vehicle lunge into the oversteered state. Experiments support this finding. In the case of load transfer at the front a state of understeer will eventually set in, the delay in this case suggesting front-end breakaway to the driver. This effect is not one of tire lag. As mentioned earlier, tire lag is only 1½ to 2 ft, say 1/25 sec at 30 mph, which is small compared with the times of body roll on the suspension.

From this example it appears that delays, especially when they cause change from slight understeer to gross oversteer, are bad and probably worse than oversteer itself. This point has been made often by Hardman during discussions of stability problems.

I think that putting all cornering data on one chart – the characteristic curve – it is easier to interpret what is happening than when separate cornering and aligning curves are used.

Traction or Standing Wave

The land speed record has been increased gradually over the past quarter century to around 400 mph. This could be done only by mastery of the traction or standing wave which occurs at high speed. There have been papers on standing waves, so we will not discuss the phenomenon except to show a photo of a wave on a tire on a flat road at over 100 mph (Fig. 17). The method used to obtain this photo is of interest. If the camera and flash equipment is carried on the vehicle there are three major problems: (a) keeping the optical axis of the camera steady relative to the tire and ground, (b) weight, and (c) electric supply. The solution is simple if it is noted that the part of the tire on the ground is at rest, and that part which is of interest is moving slower than the vehicle. Hence, place the camera on the ground, use a photocell to trigger a microflash (which gives a sharp picture

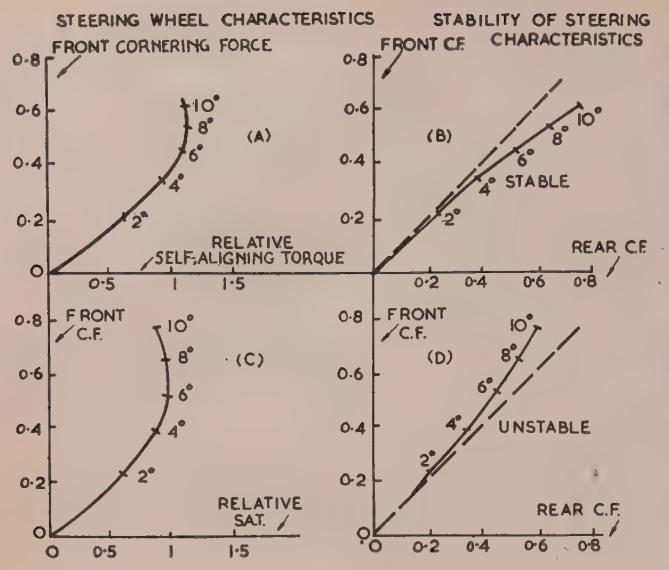

Fig. 16 – Effect of load transfer on vehicle characteristics. A and B: all load transfer at rear axle; none at front axles C and D: all load transfer at front axle; none at rear axle

even at the vehicle speed), and finally, get an extremely good driver who can place the car within ±2 in. of the correct "in-focus" position.

Conclusion

We have discussed conditions obtained between tire and ground during cornering, evidence obtainable from buffing ridges on tires, and characteristic curves of tire-cornering properties and their use in considering the tire's influence on the vehicle's motion and handling. Characteristic curves were obtained on the usual drum-type machine, but the evidence from both sources ties in quite well. We are progressing towards an understanding of the tire-ground region and the tire characteristics as presented to the vehicle, good enough to help design the tire. A picture of a tire exhibiting standing waves on a flat road was included as a matter of interest.

Acknowledgment

Acknowledgment for permission to publish this paper is made to the Dunlop Rubber Co., Ltd., in whose Research Center this work was carried out.

Thanks are due the author's colleagues for cooperation and assistance, and to Maurice Olley for advice and help in the selection of subjects discussed in the paper.

References

1. SAE Transactions, Vol. 34, 1939, pp. 344-350: "Tire Behavior in Steering," by A. W. Bull.

2. SAE Transactions, Vol. 30, 1935, pp. 41-49: "Properties of Tires Affecting Riding, Steering, and Handling," by R. D. Evans.

3. Proceedings of Institute of Motor Industry, Munich, 1954, pp. 21-39: "Role of Tires in Automobile Design and Performance," by T. French and V. E. Gough.

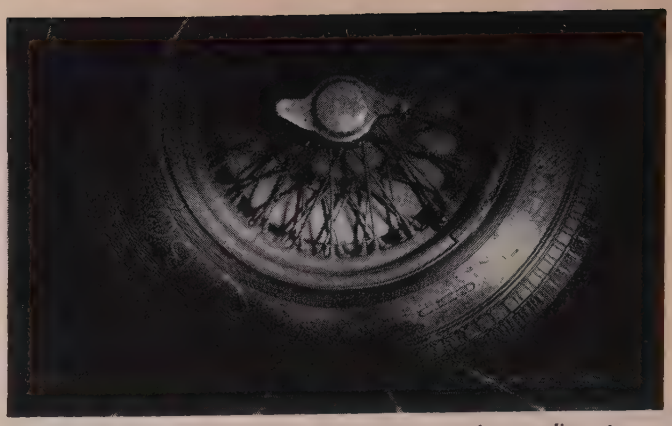

Fig. 17 – Photo of a traction or standing wave on tire traveling at over 100 mph on flat road

4. *Automobile Engineer,* Vol. 44, April, 1954, pp. 137-141: "Cornering Characteristics of Tires," by V. E. Gough.

5. *Automobile Engineer,* Vol. 39, March, 1949, pp. 97-106; April, pp. 139-145: "Tire and Vehicle Behavior," by V. E. Gough.

6. "Abraded Tire Threads," by V. E. Gough, J. H. Hardman, and R. J. Maclaren. To be pub. in Transactions of Institution of Rubber Industry, April, 1956.

7. *Automobile Engineer,* Vol. 42, January, 1952, pp. 17-23: "Tire Testing – Some Aspects in Relation to Vehicle Behavior," by V. E. Gough and P. W. B. Jones.

8. "Tire as Part of Steering System," by J. H. Hardman. Paper presented before Scottish Automotive Division of Institution of Mechanical Engineers, November, 1949.

9. Proceedings of Institution of Mechanical Engineers (Automotive Division), 1953/1954, pp. 113-133: "Tire Characteristics as Applicable to Vehicle Stability Problems," by T. J. P. Joy and D. C. Hartley.

10. *Kautschuk und Gummi,* Vol. 6, September, 1953, pp. 178-186: "Abrasion of Automotive Tires," by W. Kern. (Pub. in English in *Rubber Chemistry & Technology,* Vol. 27, July/September, 1954, pp. 549-568.)

11. "Car Stability and Transient Tire Forces," by S. A. Lippman. Paper presented at SAE National Passenger-Car, Body, and Materials Meeting, Detroit, March 4, 1954.

12. Proceedings of Institution of Automobile Engineers, Vol. 32, 1937/1938, pp. 509-572: "National Influences on American Passenger-Car Design," by M. Olley.

13. Proceedings of Institution of Automobile Engineers, Vol. 41, 1946/1947, pp. 147-182 + (disc.) 523-551: "Road Manners of Modern Car," by M. Olley.

14. Transactions of Institution of Rubber Industry, Vol. 28, October, 1952, pp. 256-268: "Abrasion Pattern on Rubber," by A. Schallamach.

DISCUSSION . . .
. . . of this paper starts on p. 344

Tires For High-Performance Cars

T. J. P. Joy, D. C. Hartley, and D. M. Turner, Avon India Rubber Co., Ltd.

This paper was presented at the SAE Golden Anniversary Summer Meeting, Atlantic City, N. J., June 15, 1955.

THIS paper reviews earlier work concerned with steering characteristics of tires and wave formation in tires revolving at high speeds. The authors describe various machines used in obtaining fresh, experimental evidence to support earlier theories.

A new approach is made to the problem of power consumption of tires. Equations relating wavelength to high-speed power consumption of tires are supported by new experimental evidence.

In order to examine changes in cornering force and self-aligning torque with speed, the authors use the suggestion that a forward movement of the center of pressure in the tire contact patch depends upon an increase in power consumption of the tire.

Variations in tire characteristics with extreme braking and traction forces are examined in parallel with suggested changes in the shape of the tire contact patch. Factors affecting the handling of a sports car at the point of tire breakaway are examined.

FROM the earliest days of passenger-car history there has existed a nucleus of car owners who have been interested in motoring, beyond the basic requirement of getting from A to B under a car's own power. This core of enthusiasts has formed the center of a demand for a type of car with a performance which generally outshines the normal family car, as far as speed and road holding are concerned.

Initially, superior attributes such as speed and road holding were obtained only at the expense of reliability and personal comfort, but such is progress that today certain cars provide sparkling performance with a high degree of reliability. Even passenger comfort has been studied.

In parallel with the improvements made in performance, the safety aspect has been considered and the slogan "Safety First" is now applicable to most high-performance cars.

Such interest has been aroused in the past eight years or so that every car-producing nation is manufacturing cars which fall into the sporting category. The competitive spirit is being fostered on every continent, and an ever-growing list of sports car competitive events, covering both rallies

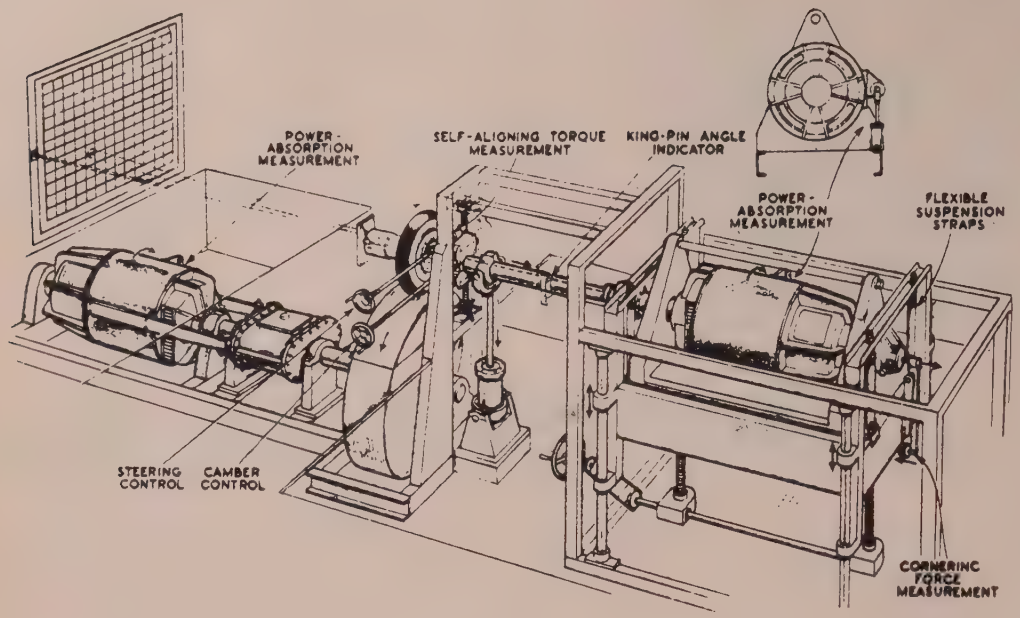

Fig. 1 – Diagram of stability machine

and endurance races, is attracting attention far beyond the realms of the car-owners themselves. These events are now being used to demonstrate the qualities of the cars, and they form a satisfactory proving ground for testing most components of the cars.

Whatever the final specification of the car, whether it be a light two-seater or a high-performance luxury limousine, its ultimate success can be marred by unsatisfactory tire performance. Tires whose characteristics do not suit the car concerned can seriously affect its handling, especially when being driven to its limit. Under critical conditions such tires can be dangerous.

Over the years, the improvements introduced by tire engineers have kept pace with the increase in overall car performance in spite of the adverse trend of wheel diameters, which, to the uninitiated, is associated with the forgetfulness of the car designers. They seem to begrudge the fitting of wheels and tires to a car. Considerable development work has been done by the tire engineers while overcoming the problems confronting them, and several papers have been published recording the manner in which the problems have been observed, analyzed and solved.[1-12]

In particular, the aspects of tire behavior at speeds associated with present-day high-performance cars have been examined. Attempts have been made to estimate car-handling characteristics from basic tire data obtained on indoor test machines.

In this paper a review is made of earlier work completed by the authors and their colleagues (most of it recorded in separate papers) with the ultimate objective of suggesting how this information may be of assistance in assuring satisfactory tire performance on the type of car outlined earlier.

Test Machines

The major part of the work dealt with in this paper was carried out on the stability machine (Fig. 1). The speed limitation imposed by this equipment is 125 mph maximum. All investigations at higher speeds were made on a simpler machine whose speed range enabled the investigations in straight running (of a tire on a surface) to be extended up to 240 mph (Fig. 2).

The stability machine has been adequately described in the technical journals[13-14] but reference to its general design will bear repeating.

A 50-bhp, variable-speed Heenan d-c dynamom-

[1] See SAE Transactions, Vol. 30, 1935, pp. 41-49: "Properties of Tires Affecting Riding, Steering, and Handling," by R. D. Evans.

[2] See Proceedings of Institution of Automobile Engineers, Vol. 33, November, 1938, pp. 211-274: "Tire Requirements for Modern Transport," by C. D. Law.

[3] See SAE Transactions, Vol. 34, 1939, pp. 344-350: "Tire Behavior in Steering," by A. W. Bull.

[4] See SAE Transactions, Vol. 36-49, 1941, pp. 81-93: "Car Control Factors and Their Measurement," by K. A. Stonex.

[5] See Proceedings of Institution of Automobile Engineers, Vol. 41. 1946/1947, pp. 147-182 + (disc.) 523-551: "Road Manners of Modern Car," by M. Olley.

[6] See Journal and Proceedings of Institute of Road Transport Engineers. Vol. 2, Part II, January, 1949, pp. 25-39: "Tires and Steering Geometry," by J. H. Hardman.

[7] See *Automobile Engineer*, Vol. 39, March, 1949, pp. 97-106; April, pp. 139-145: "Tire and Vehicle Behavior," by V. E. Gough.

eter capable of absorbing or delivering a recorded power is coupled to a steel test drum through a speed-reducing gearbox. The purpose of the gearbox is to assure that the motor works over its most efficient speed range. The drum has a circumference of 1/300th mile. The dynamometer gearbox and drum are sunk in a pit such that the upper surface of the drum, which forms the running surface for the tire, just clears ground level. This arrangement simplifies tire installation and observation.

A second dynamometer is carried by four steel straps swung in a cradle. This cradle may be raised or lowered to adjust the centerline of the dynamometer relative to that of the test drum. The steel straps allow the dynamometer to float horizontally along its major axis while resisting any lateral motion. This second dynamometer is connected to the hub, which is attached to the wheel and test tire. The test tire and wheel are connected to the hub through an axle equipped with Bendix-Weiss universal joints at each end. These joints assure a flexible connection between hub and dynamometer, permitting angular movement of one relative to the other.

Bendix-Weiss joints were chosen because of their constant angular velocity characteristics and high overall efficiency. These features are maintained over a wide angular-displacement range.

The axle itself is housed in a casing through which the wheel load can be applied by a hydraulic loading ram. Because of its ease of operation and its damping characteristic, this loading system was preferred to a dead-weight system.

The stability-machine arrangement therefore consists of a tire capable of being steered on a drum at measurable slip angles over a range of speeds and loads in such a manner that the cornering force, self-aligning torque, and power consumption may be measured. The machine may be operated in the following manner.

1. Load can be varied up to 2400 lb. The load values are set by loading arms located in the control room. The arms are hydraulically coupled to the loading gear on the axle casing. The mechanism has an auxiliary function: by reversing the hydraulic loading circuit the tire can be raised off the test drum. This reversal is controlled by an emergency switch. Use of this feature enables the rapid cessation of tests in cases of emergency, while preserving evidence if such an emergency is caused by incipient tire failure. Regenerative braking is introduced by the same operation, so that the tire is braked from maximum speed to rest in 15 sec. Tire temperatures influenced by a minimum of cooling can therefore be recorded.

2. Inflation pressure can either be controlled to a predetermined figure or close observation can be kept on pressure fluctuations. A Schrader rotating coupling is located on the nose of the hub; this coupling connects the rotating air line from the tube valve to the static inflation line and pressure-recording gage, the latter being located in the control room.

3. Drum speed range covers 36-125 mph.

4. Tire slip angle varies from 0 to 12 deg. This angle is obtained by steering the tire on the drum using a steering gear actuated from the control room. The angle itself is measured by a reflected light method. The light source projects crossed-

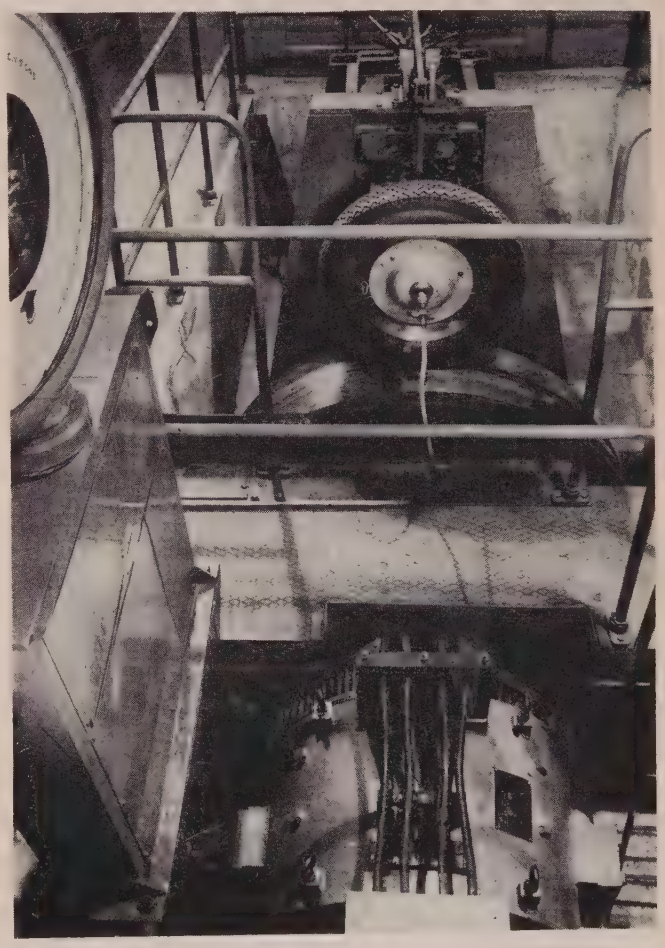

Fig. 2 – Photograph of high-speed machine

[8] See *Automobile Engineer*, Vol. 42, January, 1952, pp. 17-23: "Tire Testing – Some Aspects in Relation to Vehicle Behavior," by V. E. Gough and P. W. B. Jones.

[9] See *Journal of Institute of Motor Industry*, Vol. 2, August, 1951, pp. 3-14: "Tires, Steering, and Car," by J. H. Hardman.

[10] See Research Association of British Rubber Manufacturers Translation No. 401, "Tires and Driving Safety," by E. Bobeth.

[11] "Car Stability and Transient Tire Forces," by S. A. Lippman. Paper presented at SAE National Passenger-Car, Body, and Materials Meeting, Detroit, March 4, 1954.

[12] See *Automobile Engineer*, Vol. 44, April, 1954, pp. 137-141: "Cornering Characteristics of Tires," by V. E. Gough.

[13] See *Autocar*, Vol. 95, May 5, 1950, pp. 521-523: "Scientific Tire Testing."

[14] See *Automobile Engineer*, Vol. 40, April, 1950, pp. 137-139: "Tire Testing."

wire shadows onto a mirror carried on the front face of the test-wheel hub. The reflected beam falls onto a frosted screen, the surface of which is calibrated to indicate the actual slip-angle values. These are recorded by horizontal movement of the crossed wires.

5. Similarly the camber angle at which the tire runs can be varied and measured. These values, restricted to a ±5-deg range, are measured by vertical movement of the crossed wires.

6. Means are also provided for varying king-pin inclination and wheel offset.

7. Conditions of braking and acceleration can be reproduced on the machine. These effects are reproduced by alternative use of each of the two dynamometers. If the drive is taken directly to the drum through the gearbox, so that the drum drives the tire, then absorbing power in the tire dynamometer, the machine will simulate braking. Reversal of this procedure, so that the tire drives the drum, will reproduce accelerating conditions.

With the above variables, the following dependents can be measured:

(a) Power consumed by the tire may be obtained from the power balance in the system. The torques developed by both dynamometers are measured by Budenberg gages connected to the swinging stators of the motors. Knowledge of the speeds of each of the two motors enables the horsepower developed or absorbed by each to be determined. When due allowance has been made for the no-load losses of the system, absolute values for tire power consumption can be obtained.

(b) Under the influence of the enforced slip angle, the tire develops a cornering force. The component of this force acting along the axle causes the suspended motor to float horizontally and to increase its pressure on a Budenberg capsule housed in the framework of the suspending cradle. The thrust thus produced is measured on a suitably calibrated gage.

(c) The steering torque is applied to the tire by a steering arm loaded through a further pressure capsule. When the system is running at a steady slip angle, the reaction recorded by the capsule is a measure of the self-aligning torque of the tire.

The stability machine is capable of running tires whose overall diameters do not exceed 39 in. and whose rim diameters are at least 13 in. The overall diameter is limited by the vertical lift of the suspended motor, and the minimum rim diameter is limited by the size of the machine hub itself. This latter item is somewhat large since it contains the king-pin arrangement and wheel bearings.

Limits of accuracy imposed by the machine's design are as follows:

1. Cornering-force to 5 lb between limits 30 lb and 1500 lb.

2. Self-aligning torque to 1 lb-ft from 2 lb-ft to 250 lb-ft.

3. Horsepower consumption to 0.3 bhp to 50 bhp.

All measuring devices may be checked by using dead-weight loading. Routine checks are systematically made at regular intervals. Up-to-date correction charts are used for all work.

Finally, checks over a number of standard tires tested under the same conditions revealed that the mean cornering force of three nominally identical tires is within 4% of true mean and within 95% of confidence limits. A similar figure for self-aligning torque is 7%.

As indicated earlier, a simpler high-speed machine has been used to examine the straight-running characteristics of tires at speeds above 125 mph. In this application a 130-bhp dynamometer drives a steel drum of similar dimensions to the steel drum of the stability machine. A dead-weight loading mechanism imposes the test load, although the load may be applied through an inching device. By this means the tire may be spun up to test speed under a negligible load and then the test load applied in full as required. Similarly, the load may be removed at any time to enable tire observations or temperature checks to be made. Both tire and drum may be braked, the former mechanically and the latter by regenerative means. Measurements of power absorbed by the system may be observed, although additional braking or accelerating effects cannot be applied. The maximum load is 2240 lb.

High-Speed Wave Formation

Early work on tires running at high speeds on a drum led to the observation of the now well-known phenomenon of waves in tires, popularly known as "standing waves." As a result of their investigations, Gardner and Worswick[15] published a detailed description both of the characteristics of these waves and of some influential factors governing them.

In conventional car tires, the wave became apparent at speeds above 90 mph. It appeared that, owing to the high speed, the tire did not recover immediately from distortion originated by the deflection, and the residual displacement initiated a wave. The amplitude of the wave was greatest immediately on leaving the drum and was damped out in the normal exponential manner around the circumference of the tire. The authors emphasized that waves of this type are not a resonant vibration, and that every portion of the tire on the same

[15] See Transactions of Institution of Rubber Industry, Vol. 27, 1951, pp. 127-146: "Behavior of Tires at High Speed," by E. R. Gardner and T. Worswick.

circumferential line undergoes identical motion as the tire rotates.

It was observed that the amplitude increased with tire rotational speed, as did the wavelength and persistence of the wave around the normally undeflected portion of the tire. The amplitude depended directly on the load applied, but could be reduced considerably by higher inflation pressures. Increases in amplitude led directly to increases in power consumption. There was little difference in the appearance of waves associated with a limited range of tire sizes or with various rim widths. The investigation covered a range of tire sizes from 5.00-16 to 6.00-16 and rims from 3.50D to 4.50E. Each application was tested at a 30% overload (based on British standards) for the tire concerned.

Of the variants in the construction of the tires tested, neither the number of plies nor the degrees of unbalance of the tire, tube, and wheel assembly appeared to have any effect. However, a reduction in tread weight did tend to minimize the wave, as did a reduction in the cured cord angles of the tire casing.

It was indicated that the steeply rising power consumption of tires with increasing speed was associated with the formation of the wave. Such a high power consumption is not only a serious encumbrance to the performance of a high-speed car but also causes high heat generation in the tire, so as to incur the risk of tread separation. It was suggested that the high power consumption was due to a further loss, in addition to the normal hysteresis loss. The increase in power consumption was the result of the tire possessing an amount of residual energy at the point it left the drum, this energy being dissipated as the resulting wave was damped out.

When any phenomenon is examined, it is desirable to evolve a theory which elucidates the relationship between cause and effect demonstrated in the experimental investigations, and so bring some degree of order to the mass of evidence. The theory will have a greater value if it can be used to predict the most fruitful lines for further investigation and so enable unprofitable experiments to be bypassed or work on the more trivial aspects to be deferred until their investigation is warranted.

A tire is an exceedingly complex object, if one wishes to perform a mathematical analysis on its mechanics. Firstly, its irregular toroidal shape needs many dimensions for complete definition; secondly, the tensions in its casing vary with the cord angles, which change according to their position in the tire; and finally, there is the irregular distribution of mass across the tire section and through the tread contour. In order to carry out any analysis, it is necessary to make some sweeping assumptions and drastic approximations and to consider a "model" which is as simple as possible.

In the theory developed by Turner,[16] the model took the somewhat improbable form of a flat membrane, infinite in one direction and bounded by two rigid bars in the other. The membrane was considered to be in uniform tension. By a consideration of the propagation of diagonal waves in the membrane, similar in mechanism to electromagnetic waves in wave guides, formulas were developed relating the wavelength, the rate of flow of energy, and the rate of dampening of the waves to the physical properties of the membrane. Such wave formation is analogous to that in the tire and the formulas can be applied readily.

The first important result indicated that for a particular tire at a given inflation pressure a critical velocity exists and, before the wave can form, this velocity must be exceeded. This critical velocity (c) is the most important parameter governing the wave, and was shown to be determined by the simple expression $c = \sqrt{T/\rho}$ where T is the circumferential tension in the tire and ρ the tread density per unit area.

The circumferential tension is dependent on the tension in the cords of the tire casing and also on the cord angle. It may be increased by reducing the cord angle and increasing the inflation pressure. In addition, the design of the tire itself can be made to increase the value of T. If a squat tire is designed (that is, one with a standing section height to width ratio considerably less than unity), the circumference of the tire increases upon inflation, putting the tread into circumferential tension. Also, if the tire is constructed with an inextensible breaker unit, advantage of the centrifugal force can be taken to increase T.

A formula was derived for the wavelength λ which showed it to be proportional to

$$\frac{v}{c}\sqrt{1 - c^2/v^2}.$$

This relationship was verified on the high-speed machine. Fig. 3 shows the theoretical curves fitted to the experimental points. This is probably the best method of estimating the critical velocity.

The initial amplitude of the wave is proportional to the product of the wavelength and the angle of deflection ϕ. This angle ϕ is defined as the angle at which the undistorted tread surface intersects the line of the drum or ground. This is illustrated in Fig. 4. It follows that ϕ is proportional to the square root of the tire deflection D. Hence, the amplitude is connected with tire load and inflation pressure.

Probably the most important consequence of the wave is the high power consumption of the tire. In fact, the increase in power consumption is the first indication of the onset of the wave. In this manner, its influence may be detected from power-

[16] See Proceedings of Third Rubber Technology Conference, pub. by Heffer, London, 1954, "Wave Phenomena in Tires at High Speed," by D. M. Turner.

consumption curves obtained on the test machines at speeds 20 mph below those at which the wave is actually observed. The basic formula for the power consumption of the wave was calculated to be:

$$B\rho\phi^2\nu\ (\nu^2 - c^2)$$

where ν is the tire velocity, B is the length across the tire from rim to rim, ρ is the tread density per unit area, ϕ is the angle of deflection, and c is the critical velocity. Thus the power consumption has no real value below the critical velocity. Above it, the power consumption increases rapidly with rising speed. It was shown that by choosing suitable values for the terms, the formula produced results which, when plotted, closely followed a series of curves for power consumption obtained on a drum for 3.50-18 motorcycle tires. The formula emphasizes the need for as high a critical velocity value as possible.

Since the earlier work was published, further thought has been given to the information already available. Certain additional data have been produced to fortify the previous opinions. Some have already been dealt with by Hartley and Turner,[17] but since this paper has yet to be widely circulated certain details will bear complete reproduction.

That paper draws attention to a consequence of a tire having a high power consumption: namely, that there must be a forward movement of the center of pressure. If the tire is transmitting no tangential thrust and if it is consuming a certain power, then there must be a torque applied to the axle equivalent to this power. In order to balance the axle torque, the normal reaction between the tire and road must act at a point forward of the axle. For example, with a tire of radius 1.38 ft consuming 20 hp at 100 mph, the axle torque is 104 ft-lb. If the load on this tire is 1120 lb, the center of pressure must have moved forward 1.1 in. The questions now arising are what is the mechanism of this forward movement of the center of pressure, and how is it influenced by the formation of the wave.

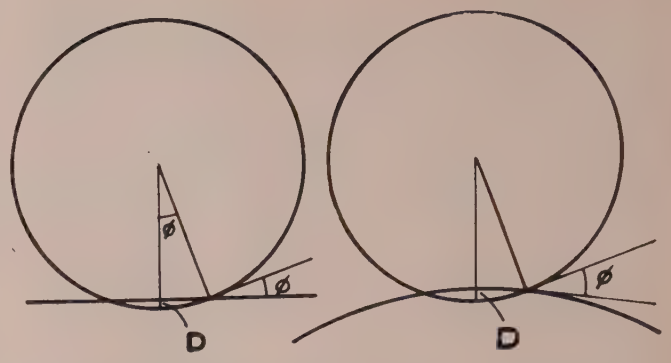

Fig. 4 – Diagrams illustrate dependence of angle of deflection ϕ on tire deflection and on curvature of surface. Left: tire on flat surface; right: tire on drum

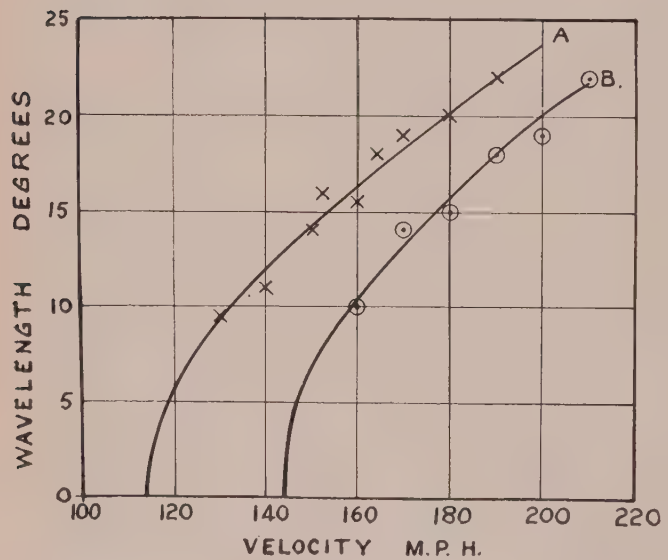

Fig. 3 – Graph of wavelength versus velocity for a 3.50-21 high-speed tire. Curves are calculated from formula: $\lambda \propto \nu \sqrt{1 - \frac{c^2}{\nu^2}}$

(A) Pressure is 20 psi and critical velociy is 114 mph. (B) Pressure is 60 psi and critical velocity is 144 mph

Now Fig. 5 shows a tire rotating at a velocity considerably higher than the critical velocity for wave formation. It is seen that the tread is completely undistorted until it actually hits the drum, whereas below the critical velocity a tire normally starts to distort at an appreciable distance before impact. The reason for this behavior is that at speeds above the critical velocity it is not possible for a signal to be transmitted through the tire against the direction of rotation, and so to inform the tread that it is about to hit the drum. Consequently, when the tread does hit the drum, there will be a considerable impact. The continuous effect of this impact gives rise to the retarding torque applied to the axle.

An analysis of this behavior results in an expression for the power consumption of the tire. Consider the tire in Fig. 6. The angle of deflection is ϕ and the radius is R. Let it be rotating with peripheral velocity ν. Let the effective density per unit area of the tread and casing be ρ, and the width of the tread be B. A length δx of the tread will contribute a downward momentum on hitting the road of: $B\rho\phi\nu\delta x$.

To oppose this continuous supply of momentum,

[17] "Racing Tire Design," by D. C. Hartley and D. M. Turner. Paper presented before Midland Section of Institution of Rubber Industry, Feb. 13, 1955.

an upward force P has to be applied to the tread. Then:

$$P = B\rho\nu\phi\delta\chi \times \nu/\delta\chi = B\rho\nu^2\phi$$

Not all this force has to be supplied by the road. Where the tire makes contact with the road there is an abrupt change in direction of the carcass, which is equal to the angle ϕ. The circumferential tension T in the carcass acting at this point contributes an upward force of $BT\phi$.

The reaction between the road and tire is therefore, $F = B\rho\phi\nu^2 - B\phi T$

The force acts at a distance ϕR from the axis of the tire, and therefore the couple C on the tire is:

$$C = B\rho\phi^2 R\ (\nu^2 - T/\rho)$$

Hence the power consumption is $B\rho\phi^2\nu\ (\nu^2 - T/\rho)$.

This is identical to the formula obtained earlier for the power consumption of the wave. These two formulas must obviously apply to the same source of power loss. Work is initially performed in distorting the tire to make it deflect on impact with the road. This energy is stored as potential energy when the deflection reaches its maximum, but the energy is not converted into a force helping the tire to rotate as the deflection is reduced. The energy is therefore present as kinetic energy when the tire leaves the road surface, and the energy manifests itself in the form of the wave.

The reaction at the leading edge of the contact area contributes a force between the tire and road which is additional to that carried by the inflation pressure. In the example quoted above of the tire consuming 20 hp, if the length of the contact patch is 9 in., then the reaction is 278 lb of weight. This is about 25% of the total load. As the speed increases and the power consumption becomes greater, so will this proportion increase. Eventually, at the highest speed all the load will be carried at the leading edge, and this in effect leads to a limit being reached in the rolling resistance of the tire.

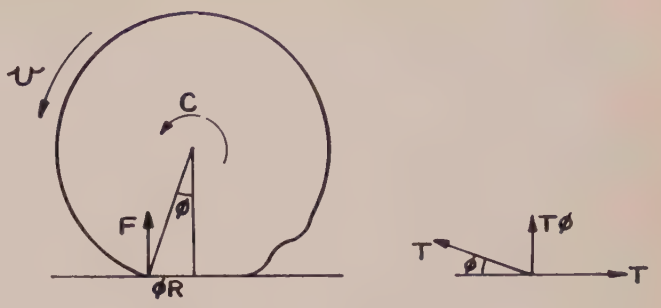

Fig. 6 – Diagrams illustrate derivation of equation for power consumption of tire from considerations of impact of tread surface on road. Left: forces acting on tire; right: action of tension

At high speeds the contact area is reduced both in width and in length by centrifugal force, making the tire into a peaked shape. This is described as the tire standing on tiptoe. As indicated above, the contact area must be reduced further by the effective load reduction due to high power consumption. Also, there is the forward movement of the center of pressure. These factors influence the cornering force and self-aligning torque, and are discussed later in this paper.

Fig. 5– Tire striking drum at angle

Cornering Characteristics of Tires

The work reviewed so far has been entirely associated with tires running in a straight path on a drum. Let us now turn to matters directly affecting the handling of a car when deflected from a straight path, either under the influence of its own steering ability or under the influence of superimposed side loads, and consider the additional tire characteristics involved.

Cornering force, self-aligning torque, and power consumption variations have been studied on the stability machine, the initial results being recorded in full detail by Joy and Hartley.[18] A summary of these findings is given in Table 1. This table shows the general picture of causes and effects, but in some particular instances the tests were not exhaustive enough. These points led to a further investigation in which the effects of some of the variables were ascertained in greater detail.

The effect of braking, as noted in the table, was originally investigated only on braking forces up to 35% of the vertical load. Occasions arise, however, for example in emergency braking on very good surfaces, when the braking forces attain as much as 80% of the vertical load. Thus it was desirable to know what would happen in such circumstances. Owing to the limitations in the power

[18] See Proceedings of Institution of Mechanical Engineers (Automobile Division), 1953/1954, pp. 113-133: "Tire Characteristics as Applicable to Vehicle Stability Problems," by T. J. P. Joy and D. C. Hartley.

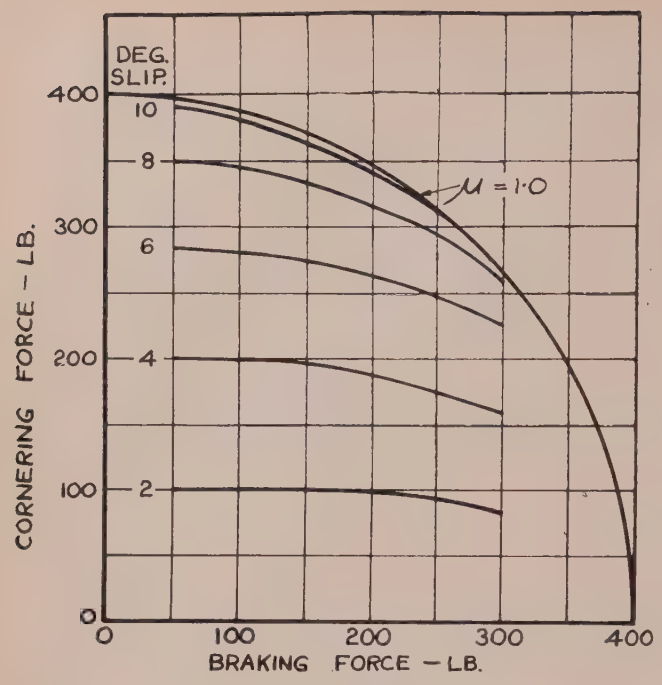

Fig. 7 – Effect of braking on cornering force; tire is 6.00-16, 4-ply; load is 400 lb; pressure is 28 psi

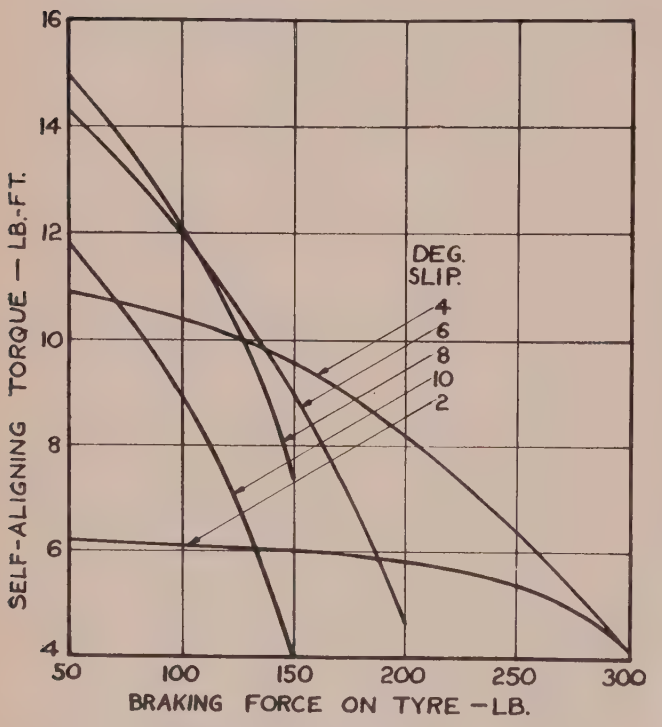

Fig. 8 – Effect of braking on self-aligning torque; tire is 6.00-16, 4-ply; load is 400 lb; pressure is 28 psi

of the stability machine motors, it was necessary to reduce the vertical load considerably to achieve this effect. How braking under these conditions influences cornering force and self-aligning torque is shown in Figs. 7 and 8, respectively.

The effect of braking on cornering force is very marked, especially at the higher slip angles and

Table 1 – Summary of Results of Joy and Hartley[a]

Increase in Factors Listed below Result in	Cornering Force	Self-Aligning Torque	Horsepower Consumption
Slip angle	Steady increase	Increase up to a maximum at about 6-deg slip, then decrease	Steady increase, slightly greater than expected increase of cornering force × sin α
Camber angle	Camber thrust proportional to tangent of camber angle; also proportional to load except at higher loads when increase becomes less (camber thrust and cornering force independent of each other)	No effect	Slight increase
Speed	No effect	No effect	Rapid increase
Pressure	Steady increase	Steady decrease	Slight decrease at slip angles less than 5 deg; slight increase above this
Braking	Below 4-deg slip, no effect noticeable; above 4-deg, decrease becomes marked	Decrease of both torque and slip angle at which it reaches a maximum	No effect
Traction	Slight decrease	Increase of both torque and slip angle at which it reaches a maximum	No effect
Rim width	Increase	No effect	No effect
Rim diameter	Increase	Increase	Slight increase resulting from higher cornering force
Section width	Increase	Increase	No effect
Number of plies	No effect	Decrease	No effect

[a] See footnote 18.

higher braking torques; in particular, at 10-deg slip and 70% braking the horizontal forces at the tire-drum interface are equal to the vertical forces. As the coefficient of friction of these two surfaces is just above unity, this implies that the tire has nearly reached the point of breakaway. It is reasonable to suppose that on surfaces with lower coefficients of friction, such as on a normal road surface, the curves start to fall rapidly at smaller braking forces corresponding to earlier breakaway points.

The reduction in cornering force is consequent upon the reduction of the adhesion region. Normally, at a point near the rear of the contact patch where the lateral distortion of the center line becomes too great, the adhesion breaks down, and from there to the rear of the contact patch the tire slides over the drum or road surface. If in addition there is superimposed a longitudinal force, as in braking, then the lateral displacement of the centerline will not be so great before slipping occurs. Following the reduction of the adhesion region and the lateral displacement, the cornering force diminishes.

The effect of braking on self-aligning torque is also very marked. Not only does braking reduce

the torque but it also reduces the slip angle at which the torque reaches a maximum. As the sliding region at the rear of the contact patch increases, so the rear portion contributes less to the cornering force. Therefore, the line of action of this force moves forward, thus reducing the self-aligning torque.

This effect of braking or self-aligning torque has an important bearing on the geometry of steering design. In the search for means to obtain lighter steering, without the expensive and complicated method of power steering, car designers have progressively reduced the caster angle of the front wheels, even making it negative in some cases, and have relied more and more on the self-aligning torque of the tires to keep the wheels straight. If the caster angle is made too negative, although the self-aligning torque is probably sufficient for normal running, under the action of heavy braking the torque becomes vanishingly small; then, owing to the inherent instability of the Ackermann steering system, the wheels will tend to turn strongly onto one lock or the other. As heavy braking usually occurs only in emergencies, this effect can be disastrous. The variation in self-aligning torque therefore sets a lower limit to the caster angle on cars with old-fashioned manual steering.

The effect of extreme traction is very important when considering the mechanism of breakaway of a vehicle. When a car is cornering fast, the inside rear-wheel load decreases considerably and so does the cornering force contributed by the tire; but in addition, the tire has to transmit half the total driving force. This generally has the effect of breaking down the adhesion, and in this context the effect of traction on cornering force is particularly important. Also, for the owners of front-wheel-drive cars, the effect on self-aligning torque is not without interest. The variations in the two dependents are shown in Figs. 9 and 10.

The effect of traction on cornering force is similar to that of braking, but until breakaway it is less in magnitude. The reason for this can be seen from the following consideration. When a tire is subjected to a driving torque, the portion of the tire immediately behind the contact patch is put into tension. This tension, acting at the surface of the tread, breaks down the adhesion at the rear of the patch, as in the braking case; but whereas in the braking case the lateral displacement of the tire would fall rapidly to zero in and beyond the sliding region, in the traction case the tension at the rear of the patch reduces any tendency for the displacement of the tire to return rapidly to zero. This has the effect of giving the lateral displacement curve a long tail (Fig. 11) which minimizes the decrease in cornering force.

Therefore the effect of traction on the driving axle of a car is such that it slightly increases the slip angle; but since the greatest effect is on the tire which is contributing the least cornering force, the resultant change in slip angle of both tires is small.

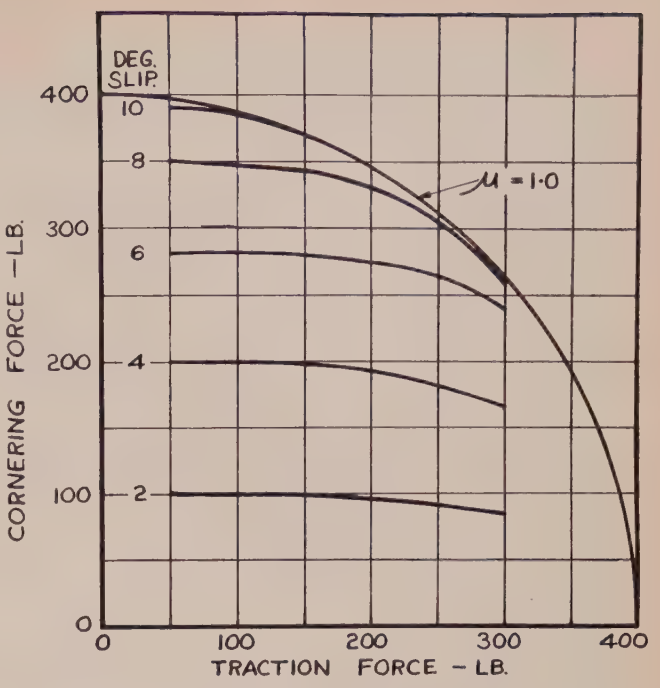

Fig. 9 – Effect of traction on cornering force; tire is 6.00-16, 4-ply; load is 400 lb; pressure is 28 psi

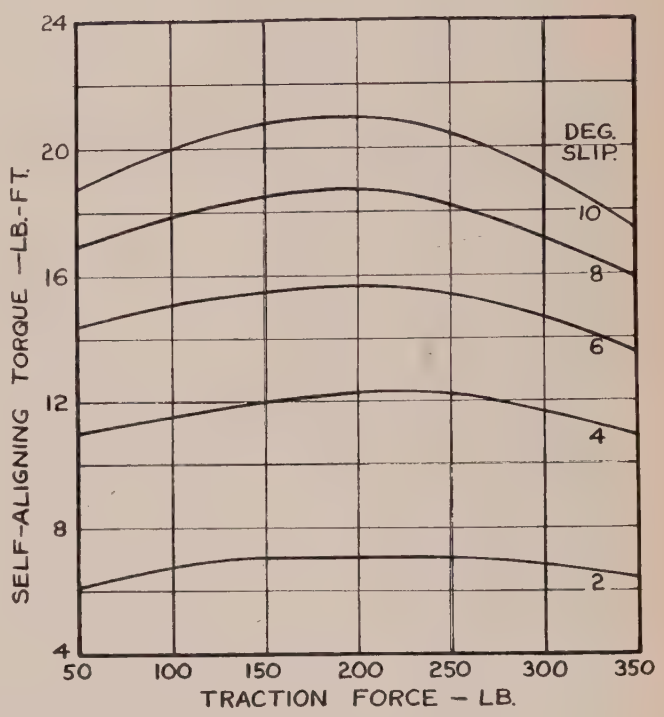

Fig. 10 – Effect of traction on self-aligning torque; tire is 6.00-16, 4-ply; load is 400 lb; pressure is 28 psi

The effect of traction on self-aligning torque is interesting since, at lower traction forces, say up to 40% of the vertical load, the torque increases; but

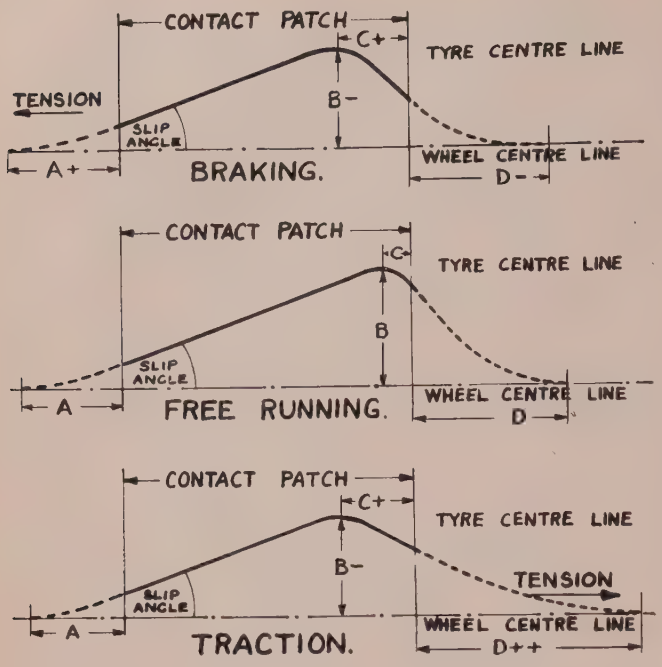

Fig. 11 – Action of traction and braking on centerline displacement

above this figure, the torque decreases steadily. The explanation is that initially the long tail mentioned above causes the line of action of the cornering force to move back, thus increasing the aligning torque; as the driving forces increase further, the lateral displacement becomes less, and the cornering force is reduced. This effectively causes the self-aligning torque to decrease.

Only driving forces up to 40% of the vertical load will normally be used with a front-wheel drive and thus the self-aligning torque will usually increase with driving torque. If the driver releases the accelerator in the middle of a bend in the road, the steering will immediately go light. The property of steering torque increasing with driving torque is probably the cause of the good reputation of this type of car, since the harder the car is driven around the corner, the firmer is the feel at the wheel; this sensation is also helped by the fact that, under traction, self-aligning torque does not have a maximum at a 6-deg slip angle, but is still steadily increasing at a 10-deg slip angle.

A third factor, investigated more closely, was the effect of speed on cornering force and self-aligning torque. Originally, it was stated that speed has no appreciable effect on these two variables within the range 40-80 mph, but subsequently some indirect tests indicated that there might be variations, especially at small slip angles. Tests were then made at higher speeds to determine this effect.

The results for cornering force (shown in Fig. 12) clearly indicate a maximum at about 70 mph, with an increase in fall-off at around 90 mph. A number of conflicting factors appear to effect this variation. Initially, the centrifugal force acting on the tread increases the tensions in the cords and makes the tire stiffer, thus encouraging a higher cornering force; but this stiffness tends to reduce the contact-patch length and hence reduces the cornering force. Also, as stated earlier, at speeds above the transverse critical velocity it is impossible for a signal to be transmitted against the rotation of the tire; this transverse critical velocity will probably be higher than the wave critical velocity. Therefore at the front end of the contact patch the centerline will be undistorted and will take the shape in Fig. 13b instead of the shape in Fig. 13a. This will reduce the total distortion and decrease the cornering force.

Finally, the center of pressure moves forward with the high power consumption associated with the wave, and points of low lateral displacement will now have a high vertical loading (and vice versa). This will also reduce the cornering force.

The effect on self-aligning torque (as shown in Fig. 14) is not so clearcut since the decrease tends to level off at 90 mph. As the speed rises and the tire stands on tiptoe the self-aligning torque increases with the cornering force. When the critical velocity is reached, although the line of displacement of the tire centerline has shifted toward the rear of the contact patch, the center of pressure has

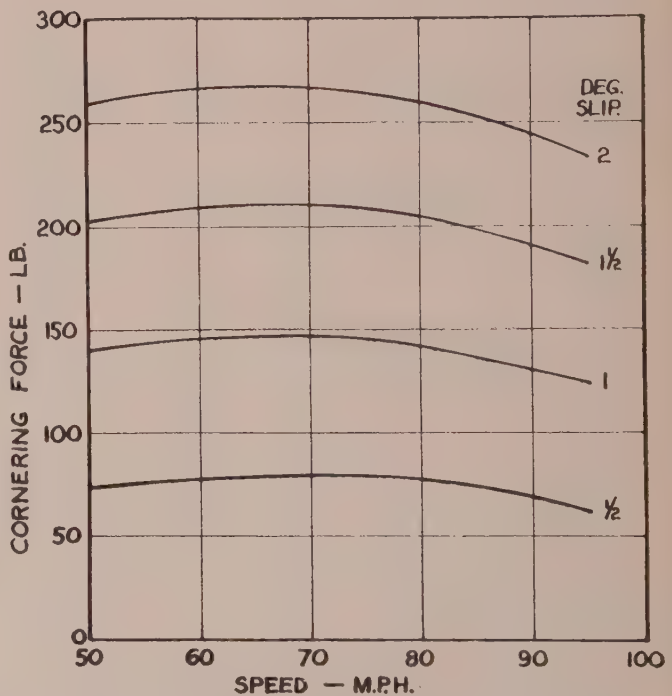

Fig. 12 – Effect of speed on cornering force; tire is 8.20-15, 6-ply; load is 1120 lb; pressure is 20 psi

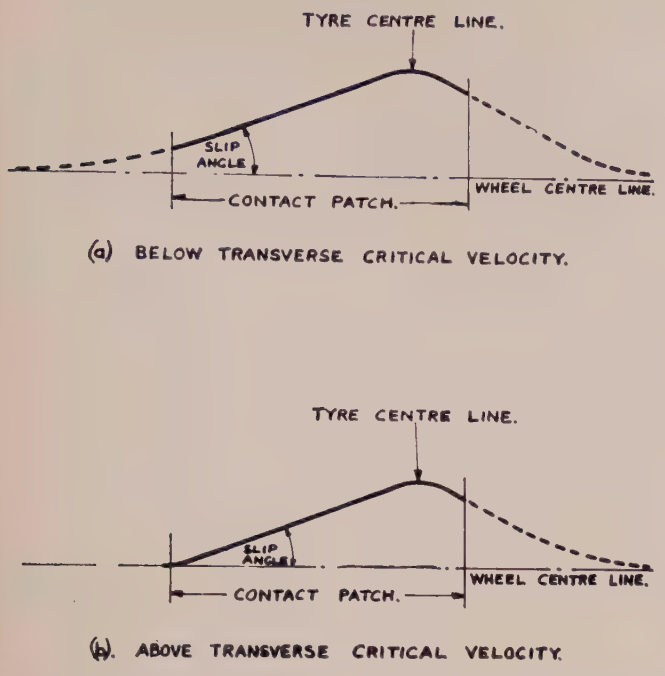

Fig. 13 – Effect of critical velocity on centerline distortion

moved forward; these two factors tend to cancel each other out and the self-aligning torque stays roughly proportional to the cornering force.

The variation is slightly different with a tire having an inextensible tread. The centrifugal force increases the tension in the tread considerably, and has the effect of increasing both the cornering force and the critical velocity. Also, the center of pressure will still move forward even if there is no wave, and this will offset the increase in self-aligning torque.

How is a car affected by these variations in tire characteristics with speed? If the ratio of cornering force to self-aligning torque increases, then the steering feels lighter, and vice versa. Now, with a conventional tire, according to the measurements made on the stability machine, this ratio increases slightly and the steering should feel a little lighter. When this effect is considered in parallel with the inherent decrease in car stability at high speeds, coincidentally with a greater necessity for even more accurate steering and a better feel at the wheel, this speed effect increases the uncertainty of the driver and thus diminishes the general stability of the car. This effect will only persist to approximately 90 mph; above this speed the critical-velocity effect becomes predominant and the steering should become firmer, or heavier. If, however, a tire with an inextensible tread is used, the reduction in the feel at the steering wheel is more marked, and furthermore persists to a higher speed. This reduction in feel will delay driver reaction and can be a dangerous factor in stability at high speeds.

The above raises the whole question of the extreme importance of self-aligning torque, which has been rather overshadowed in the past. A car is mainly driven by feel, and this feel at the wheel is the only indication to the driver of the action of the front tires. Also, because the front tires bear a definite relation to the rear tires, this feel is a considerable aid to appreciating rear-tire action. A typical example of greater stability being indicated by self-aligning torque is the marked reduction in feel on slippery surfaces. If one is driving along a straight road and the steering becomes very light, an immediate warning of a slippery surface is given and greater caution can be observed.

A car design feature affecting self-aligning torque is the weight transference on the front wheels. It is well known that weight-transference from an inside to an outside tire reduces the total cornering force of the two tires; this reduction calls for an increase in the slip angle and so increases the feel at the wheel. This feel is further increased since, for a given slip angle, the total torque is increased by weight transference from one tire to the other, owing to the convex nature of the self-aligning torque versus tire-load curves (Fig. 15).

The weight transference at the front end increases driver confidence by making the steering firmer. Therefore, it would be logical to assume that the faster the car, the greater should be the

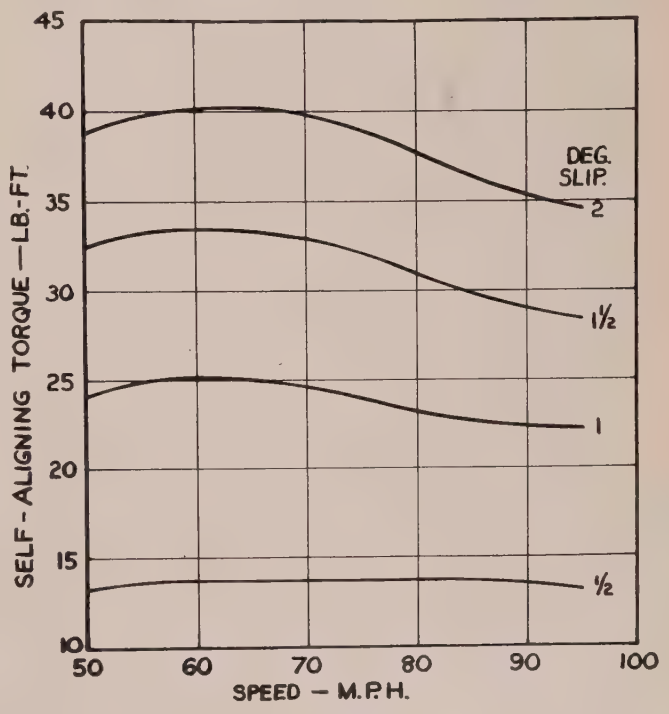

Fig. 14 – Effect of speed on self-aligning torque; tire is 8.20-15, 6-ply; load is 1120 lb; pressure is 20 psi

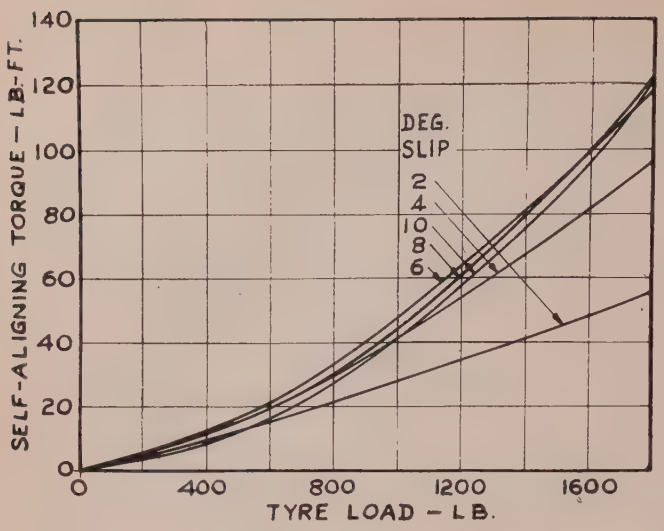

Fig. 15 – Effect of load on self-aligning torque; tire is 6.00-16, 4-ply; pressure is 28 psi

amount of weight transference on the front tires. Generally speaking this is so, and high-speed sports cars usually have well over half their total weight transference on the front end.

However, this distribution is used for a different reason than the one outlined above, since the effect (of firmer steering) is very small on this type of car. The tire pressures and loads used are such that the cornering-force versus tire-load curves are virtually straight, especially at the higher slip angles. The main need for increased weight transference at the front is due to the complementary effect of reduced weight transference on the rear tires. This becomes apparent when we consider the mechanism of breakaway.

Breakaway

Before this subject is dealt with in detail, it should be pointed out that, although all the arguments are applied to high-speed cornering and breakaway, they can be applied with equal validity directly to low-speed cornering and skidding. Thus any factor which improves the cornering power of a high-speed sports car should also reduce the tendency of more docile machines to skid on slippery surfaces, though possibly not to the same degree.

As the term breakaway is used frequently in this paper, it is advantageous at this stage to pause and consider exactly what the term means. If a car is driven with steadily increasing speed around a circle, a point will be reached when the car will no longer be able to maintain its course, and either the front wheels or the rear wheels will slide outwards. This is the breakaway point of the car and is usually expressed as the sideways acceleration in terms of the acceleration due to gravity. This breakaway of the car is initiated by the breakaway of one of the inside tires.

If an inside tire breaks away, its effective cornering force drops, thus putting a higher stress on the corresponding outer tire. This tire now breaks away and thus the whole car follows. Probably a more precise definition is that after breakaway, the only tire characteristic having any effect on the direction of the resultant horizontal force at the road surface is the coefficient of friction. This force acts against the direction of slippage.

The mechanism of breakaway at fairly high speeds is as follows. At a lateral acceleration a few per cent before breakaway, each of the four tires is contributing a cornering force roughly proportional to the tire's vertical load. To overcome the air resistance, the normal rolling resistance of the tires, and the rearward components of the four cornering forces, the driving wheels must transmit a forward thrust. Unfortunately, the action of a normal differential does not divide the thrust in proportion to the load on the two wheels but divides the thrust equally between them. Therefore the inside rear tire, which has a comparatively light load, has to sustain both a cornering force that is nearly enough to make it slide on its own and also the high driving force. Consequently, this tire breaks away first. Immediately, its cornering force drops considerably, and to maintain the position of the car on the curve the outside wheel has to generate more cornering force. Normally, it cannot sustain this extra force and the whole rear end breaks away. Then the car spins around unless rapid, reverse steering action is applied.

Since the inside, rear wheel is the first to slide, this is the wheel which should have the highest possible load. Two common ways of achieving this are as follows: the total weight transference from side to side can be reduced by lowering the center of gravity; or, the weight transference at the rear can be reduced by increasing that at the front. The first method is also beneficial for aerodynamic reasons and is probably nearing the limit in many sports cars today. One of the limitations on the second method is the need to be sure that the inside front wheel does not come off the ground when going around any corner (that is, at lateral accelerations below, say, approximately $0.9g$).

The effect of increasing the load on the inner rear wheel will become more influential as the speed increases because, although the cornering force changes only slightly with speed, the driving force varies rapidly. In a typical example, the driving force on the inner wheel is about 2/3 that of the cornering force at breakaway on a 1000-ft radius curve, while it is only about 1/3 at breakaway on a 100-ft radius curve. This fact makes it difficult to test calculations precisely, since the only available method of testing high-speed cornering characteristics is on a race track. This introduces the complicated human element, since one relies on the reactions and comments of a driver who is usually preoccupied with more exacting problems. In addition, at high speeds a number of aerodynamic effects become important. These include the forward

movement of the center of air pressure on the car, especially for cross-winds of low angular incidence, and sometimes a reduction in load due to aerodynamic lift. These considerations are beyond the scope of this paper but they are mentioned to indicate the difficulty of testing small differences in handling at high speeds. However, these differences, though small, may be vital and the aerodynamic effects should remain constant while the factors causing these variations still have the same relative effect.

Calculations on a typical high-performance sports car show that by changing the side-to-side weight-transference ratio front to rear from 1.3/1 (at which the inside front wheel comes off the ground at 1.18g sideways acceleration) to a ratio of 2.94/1 (at which the inside front wheel comes off the ground at 0.9g) the theoretical speed around a 1000-ft radius corner could be raised from 95 mph to 99 mph. This is a considerable improvement and should make the car appreciably more stable at all speeds.

Another advantage of the higher anti-roll rate at the front is that it increases the anti-roll rate of the whole car, which in turn reduces the roll angle, the camber angles of the front tires, and in turn their slip angles. This will make the car less prone to an extremely undesirable feature: breakaway at the front end.

Naturally, the disadvantages of having such a high anti-roll rate on the front are decreased comfort and also, when cornering fast, the inside front wheel might have such a light load on it that it could tend to bump off the ground, with disconcerting results.

Obviously, the breakaway point depends not only on the car design but on the tire design as well. Two of the characteristics of a tire which decide the breakaway point are its cornering-force versus slip-angle curve, and the coefficient of friction between the tread and the road. The effect of the coefficient of friction is obvious, and calculations similar to those carried out in the example above show that if the coefficient can be raised from 0.8 to 0.9 the speed of the car around the 1000-ft curve can be increased from 95 mph to 100 mph.

The effect of cornering force is not quite so direct. However, if the cornering forces of the tires on a car can be improved, the slip angles for a given sideways acceleration will be reduced together with the rearward components of the cornering forces. The necessary driving thrust is then diminished and breakaway is delayed. The effect will be much more marked at lower speeds where the power consumption of the tire due to the rearward components of the cornering forces is a larger factor in the total resistance to forward motion. But even in the examples quoted above, a 20% increase in cornering force should result in an increase in breakaway speed from 95 mph to 97 mph.

The effect of cornering force can be studied in practice, since it is comparatively simple to make tires with the same coefficients of friction but with different cornering characteristics and to test them on a standard 108-ft skid pad. This has been done and it was found that an increase of 15% in cornering force, as determined on the stability machine, gave an increase in breakaway speed of 7%.

Unfortunately, although the effect of coefficient of friction is nearly independent of speed, it is impracticable to produce tires which have the same cornering force but different coefficients. Consequently this effect cannot be completely isolated. To illustrate the magnitude of this factor, two sets of tires, identical except for the tread compositions, which were of approximately the same hardness, were tested on the skid pad. It was found that one gave a breakaway speed just over 3% faster than the other. To show that the effect of coefficient of friction is roughly independent of speed, the tires were further tested at the Silverstone race track on the same sports car. Once again, with the better tires the lap speeds were consistently slightly over 3% faster.

Most of the above arguments apply mainly to dry conditions on rough surfaces, and can be relevant only to a much smaller degree under wet or slippery conditions. Under these conditions, the coefficient of friction is not so much an interaction between rubber and road as it is a measure of the efficiency of the action of the wiping edges of the tire patterns. In these circumstances, coefficients can vary appreciably from one tread pattern to another with consequent influence on safety. This subject is outside the scope of this paper and probably the best account is to be found in Grime and Giles.[19]

Before leaving this subject, we should mention the possible warning of impending breakaway. Some tires, although they may have a later breakaway point than normal, appear to slide very suddenly without any warning. This is an extremely dangerous feature, and it is safer to have a tire with earlier breakaway which gives adequate warning. The problem is connected with the peaking of self-aligning torque with cornering force. For a normal tire this torque drops fairly sharply after 0.6g. Thus, when the slip angle increases above this value, the steering becomes lighter, which is a good indication of incipient breakaway. If the torque does not decrease much after the maximum, then little warning will be given of impending skidding; this induces a sense of false confidence. Nothing is more dangerous on the road.

Tire Noise

Quite early in its development, the high-performance car reached a stage when it could be driven

[19] "Skid-Resisting Properties of Roads and Tires," by G. Grime and C. G. Giles. Paper presented before Institution of Mechanical Engineers, Nov. 9, 1954.

Table 2 – Factors Affecting Tire Noise

Source	Road Conditions	Medium of Transmission	Component of Tire Generating Noise	Features in Tire Which Reduce Noise	Influence of Tread Compound	Influence of Inflation Pressure
Squeal	Cornering Smooth surface Hot and dry	Airborne	Relaxation-type oscillation of tread elements coupled to casing acting as resonating chamber	Irregularity in tread pattern and features to prevent independent vibration of ribs	Harder tread gives higher frequency and is more irritating	Higher pressure increases frequency but also increases critical cornering force for squeal
Hum	Straight running Smooth surface	Airborne	Impact of regularly placed features in tread pattern	(A) "Frequency modulation" of distance between similar pattern elements (B) Distribution of pattern elements to eliminate lower frequencies	Softer and lower resilience treads give slight improvement	Reducing pressure in a particular tire increases noise, as a result of greater deflection
Squelch	Straight running Smooth surface Hot and dry	Airborne	Squeal-type noise due to flattening of curved tread on impact with ground	Flatter tread surface	Same as for squeal	High pressure reduces noise by decreasing deflection
Rumble	Straight running Rough surface	Transmitted through chassis	Vibration of casing initiated by irregularities in road surface	Broken-up tread patterns have slight effect	Softer treads are better	Lower pressures reduce noise

around corners with complete safety at speeds which resulted in the tires producing intense squeals. While the enthusiast rather welcomed such a signal of his arrival, with the advent of the "silent" sports car it became imperative to take active steps in tire design to reduce squeal. In fact, the design of "silent" cars has progressed so far that the emission of any noise by tires during either straight running or cornering has been reduced to the absolute minimum.

Several classifications have been made of noise emitted by tires on the road.[2,20] The relative importance of these sources depends to a large extent on the type of car and on the road surface. Consequently, the conclusions of various investigators differ. Our observations have been limited to four types of noise: squeal, hum, squelch, and rumble.

Squeal is heard when the cornering or braking force on the tire exceeds a critical value. The factors affecting squeal and the three straight-running noises are detailed in Table 2.

As far as the tire designer is concerned, hum is the most important of the straight-running noises. Hum is widely recognized as being due to the regular impact on the road of regularly placed features in the tread pattern. A frequency analysis shows a series of peaks, the most readily audible peaks being found between 300 and 1000 cps.

Hum is characterized by four parameters:

1. The overall hum intensity, which is governed by the number of edges in the tire-pattern, the angle these make with the axis of the tire, and the width of the transverse grooves.

2. The fundamental frequency, which is inversely proportional to the length of each repeated pattern unit in the tire.

3. The distribution of harmonics of the fundamental frequency, which depends on the spacing of individual features with each repeated pattern unit.

4. The "frequency modulation." This term is borrowed from radio engineering and describes very adequately the practice of varying the length of pattern units around the tire. It is a very popular method of converting high peak frequencies which are readily discernible into broad bands which can hardly be distinguished from wind and other general noises. The mathematical analysis of frequency-modulated radio carrier waves is directly applicable here. The exact method of applying this analysis is given in the Appendix. It confirms the practical observation that there must be a certain minimum variation in lengths of pattern units to produce any appreciable spread of the main frequency peaks. It goes further by showing exactly what distribution of pattern lengths will give good results without involving too great a difference between the minimum and maximum lengths.

Squelch is a type of noise not previously reported. It is produced during straight running on very smooth surfaces by tires with comparatively small tread arc radii and plain, continuous ribs. The intensity is relatively low and can be heard only in high-quality cars. The mechanism of the squelch vibration in the tire is similar to that for squeal. In fact, the main frequency peaks of the two types coincide.

Rumble is mainly a function of road surface and is characteristically generated by the dressings of ½- to ¾-in. stone chips. These dressings are becoming increasingly prevalent in Britain. Rumble is transmitted through the suspension and chassis to the interior of the car. Consequently, the design and layout of the car have great influence. Rumble

[20] See *TBA News*, Vol. 14, September, 1951, p. 20: "Causes of Tire Noise," by W. F. Perkins and W. F. Billingsley.

Table 3 – Frequencies and Their Amplitudes

Frequency of Peak	Amplitude
p	$J_0(M)$
$p\left(1+\frac{1}{N}\right),\ p\left(1-\frac{1}{N}\right)$	$J_1(M)$
$p\left(1+\frac{2}{N}\right),\ p\left(1-\frac{2}{N}\right)$	$J_2(M)$
$p\left(1+\frac{3}{N}\right),\ p\left(1-\frac{3}{N}\right)$	$J_3(M)$

has been successfully eliminated from some modern, high-quality cars. Expansion-joint noise is governed by the same factor.

Conclusion

As with the majority of investigations into tire-performance matters, the subject of successful tire design is again shown to be a matter of considered compromise. Whether the high-speed characteristics are obtained by using low crown angles, stiff undertread constructions, or high inflation pressures, they are obtained only by sacrificing ride comfort. Even the restoration of tire deflections to values associated with conventionally constructed, low-pressure tires by the use of extremely flexible casings gives rise to directional instability at high speed. This instability is a direct consequence of the reduction in lateral stiffness of the tire casings.

In the main, the general performance characteristics outlined have been obtained under optimum, dry-road conditions. This type of road surface has a high coefficient of friction. The coefficient may be reduced many fold, however, when wet conditions prevail. In such circumstances the detailed design of tread patterns comes into its own, possibly for the only time as far as car handling is concerned. Here, the optimum performance is obtained by assuring the most intimate contact between the tire and road. This dictates that the water film normally present between tire and road must be completely broken down. The introduction of a multiplicity of drainage paths into the tire tread achieves this end, and may be accomplished either by using a studded pattern or by introducing a system of slots into a more fundamental, ribbed design.

Such features give rise to excessive, running tire noise, especially when the tires are partly worn, unless the patterns are designed to scramble the frequencies of the notes produced by the tire and so reduce their level to a nonirritating standard or to a condition where they are concealed by other noise sources.

It is recognized that this paper has, in the main, merely reviewed earlier published papers. An attempt has been made, however, to indicate how the work described in these papers has a direct application to current vehicles, and also to deal with particular aspects of tire performance in greater detail.

Acknowledgments

The authors wish to express their thanks to the directors of the Avon India Rubber Co., Ltd., for permission to prepare and present this paper. Thanks are also due to our many colleagues who have been most helpful in discussing our work.

APPENDIX

"Frequency Modulation" of Tire Patterns

The mathematical analysis of frequency modulation of radio carrier waves which is found in standard radio engineering textbooks[21] can be applied directly to the case of hum in tires. A systematic variation in length of studs or in distances between slots constitutes "frequency modulation" in tire patterns. It has the effect of converting the frequency spectrum from a large, single peak into a series of small peaks.

Let us consider a typical case, where the length of the pattern unit follows the scheme:

aaaa bbbb cccc bbbb aaaa bbbb

In one cycle of pitch variation, there are 16 units (N). If b is the mean of a and c, then the deviation ratio $r = \frac{c-b}{b}$

The modulation index M is the product Nr, and is the important parameter which determines the effectiveness of the "frequency modulation." In order to split the main peak into two smaller peaks, M should have a minimum value of 2. If p is the main frequency, the two smaller peaks are at frequencies $p\left(1+\frac{1}{N}\right)$ and $p\left(1-\frac{1}{N}\right)$. To give M a value of 2 in the above example (with $N = 16$), r must equal $\frac{2}{16} = \frac{1}{8}$. Therefore, $c = 1.25a$.

If a higher modulation index is used, a series of small peaks is obtained. The spectrum is symmetrical about the original frequency. The frequencies and their amplitudes are listed in Table 3.

$J_n(M)$ is the numerical value of the Bessel function of the first kind and n^{th} order with argument M. These values can be obtained in standard tables.

DISCUSSION . . .

. . . of this paper starts on p. 344

[21] See p. 483 of "Radio Engineering," by F. E. Terman. Pub. by McGraw-Hill, New York City, 1947.

THIS is a preliminary report of tire tests on cornering and self-alignment torque as they are affected by high-speed driving.

Made at 100 mph on a standard chassis and a 10-ft test wheel, the experiments confirmed most previous smaller-scale, lower-speed work; but, the author reports, they also showed that self-aligning torque does not drop off at higher speeds at normal slip angle, as previously believed, and in addition suggested areas of the alignment torque problem which need (and are currently getting) further study.

High-Speed

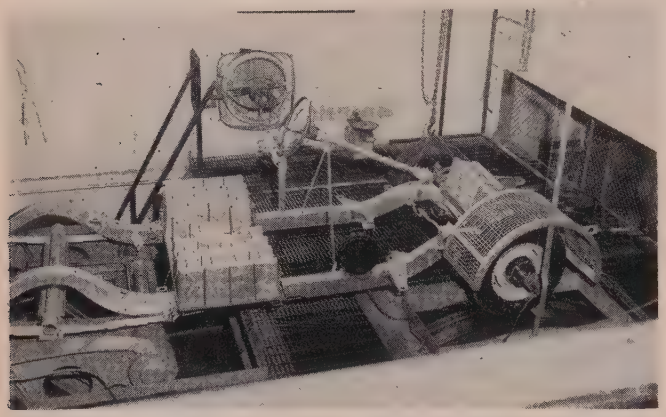

Fig. 1 – Passenger-car chassis mounted on 10-ft test wheel

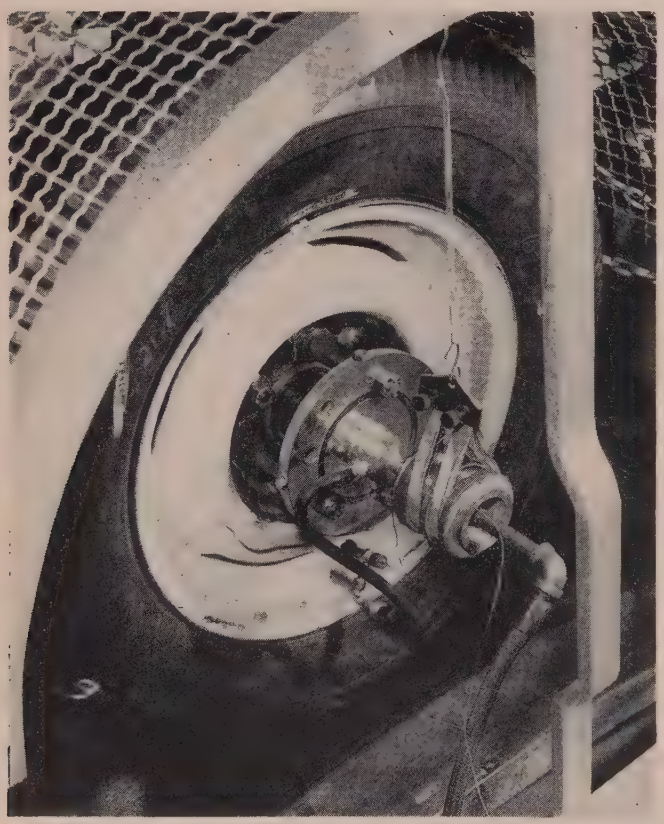

Fig. 2 – Tire in running position, with slip coupling to record inflation pressures and electrical slip-ring connections to record temperatures

THE handling characteristics of tires at high speeds have long been a source of great interest to tire engineers and automotive engineers alike. The ability to corner well and to maintain control easily are major factors in the overall performance of the car, and may contribute much to the safety and pleasure of the modern automobile.

In an effort to extend the knowledge of this subject, we have recently installed a new laboratory which we hope will closely simulate road conditions. This laboratory incorporates the following:

1. A standard automotive chassis – to utilize the flexible suspension of a car and to get the roll or feel of the car to at least a limited extent.

2. A 10-ft test wheel – to more nearly approximate a flat surface.

3. A 100-mph speed – to carry into speed ranges of the modern automobile.

This setup is indicated by Fig. 1, showing the chassis loaded and mounted, the right front tire on a 10-ft submerged test wheel. The left front wheel is slung in a cradle and hangs freely.

Cornering Forces

J. J. Robson, Firestone Tire & Rubber Co.

This paper was presented at the SAE Golden Anniversary Summer Meeting, Atlantic City, June 15, 1955.

Fig. 2 shows the tire in running position, equipped with a slip coupling to record inflation pressures, and electrical slip-ring connections to record temperatures.

Fig. 3 shows strain gage "A" recording fore-and-aft forces, strain gage "B" recording side thrust. These combine to furnish the cornering force produced by the tire.

Fig. 4 shows strain gage "C" recording forces in the tie-rod, giving us the self-aligning torque characteristics of the tire.

This system continuously records the observations in which we are interested – temperature and pressures of the tire, and the forces acting on the chassis and on certain chassis parts.

Our initial runs have just been completed, with emphasis on the cornering forces exerted on the vehicle and the self-aligning torque produced by the tire at various turning angles.

To simplify these data, we will show a series of results using a basic setup of: 6.70-15 tire; 925-lb load (T&R Rating); 24-psi cold inflation (increasing to 30-psi hot at higher speeds); 0-deg camber; and 0-deg caster.

First, let us look at the cornering forces produced by the tire.

Fig. 5 shows the cornering force produced by a regular original-equipment tire. This follows the established pattern we would expect of increasing cornering force in almost a straight line function in those turn angles which anyone might conceivably use. Cornering force in this tire indicated a tendency to decrease at higher speeds.

In Fig. 6 we record the cornering ability of a similar nylon tire with almost the same characteristics and little difference in the cornering force at higher speeds. Results at different speeds were so close a single line covers all runs.

Both of the above tires are of conventional compounds and constructions, and their similar response suggested that we try a high-performance racing tire designed and built for elevated speeds.

This racing tire (shown in Fig. 7) produced almost the same cornering-force characteristics as the previous standard tires, indicating that not a

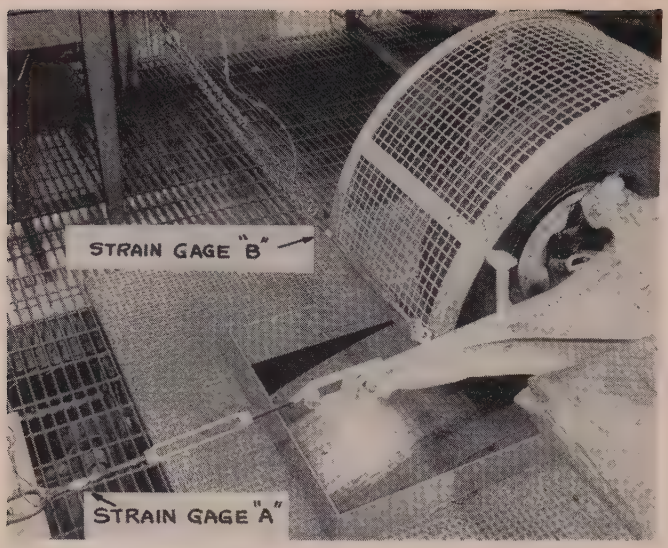

Fig. 3 – Strain gage "A" recording fore-and-aft forces, while strain gage "B" records side thrust

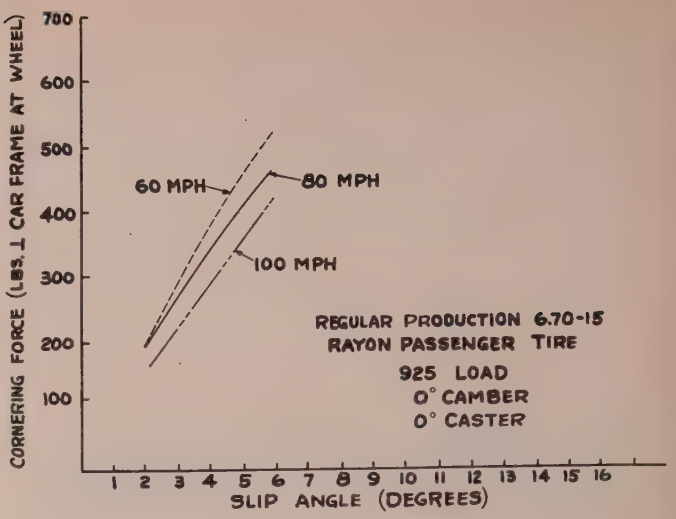

Fig. 5 – Cornering force produced by regular-production rayon passenger tire

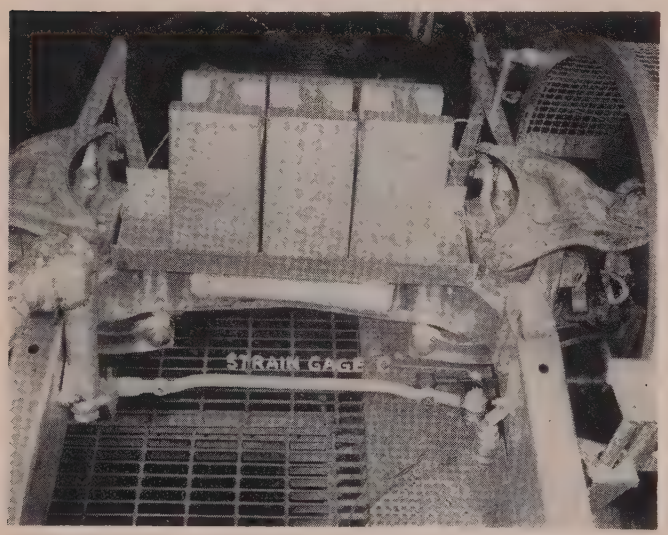

Fig. 4 – Strain gage "C" recording forces in tie-rod, giving self-aligning torque characteristics of tire

great difference exists in the cornering power of these three tires.

These data have been repeated under varying alignment conditions with little change in the general cornering-force characteristics of the tire, and it would appear at this time that little difference exists in this characteristic, even with tires having wide variations in cord angle and construction.

Self-Aligning Torque

We have also recorded the self-aligning torque as another basic characteristic, and here we find various tires displaying a little more individuality.

Fig. 8 shows the self-aligning torque – the factor which helps the tire to straighten up and maintain its direction of travel – for a regular-production rayon tire. This indicates a reasonably straight function in normal turning angles, and remarkably small difference at various speeds – probably within experimental error of these initial runs.

The nylon tire (in Fig. 9) again indicates a similar tendency, with a surprising increase at higher speeds.

Our racing tire (Fig. 10) shows a definite improvement in self-aligning torque at all speeds. This improvement goes as high as 65% in self-aligning characteristics in some cases, and thus confirms the good feel which we normally associate with high-performance tires of this type.

Certain indications have come out of this study at this time, and have a bearing on several questions which have been raised by previous observers and by automotive engineers. These are:

1. Cornering force seems to be an inherent characteristic of the pneumatic tire which will be diffi-

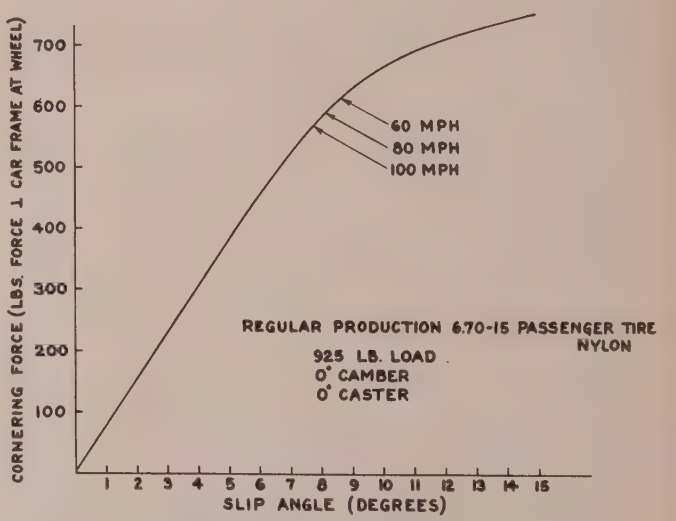

Fig. 6 – Cornering force produced by nylon tire

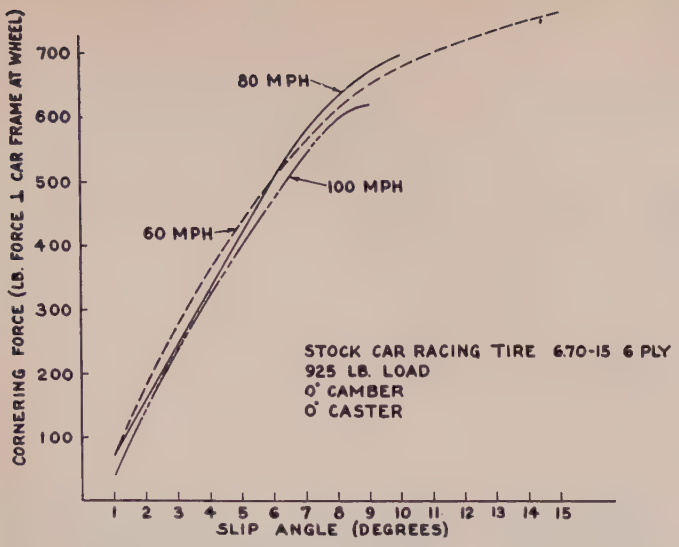

Fig. 7 – Cornering force produced by racing tire

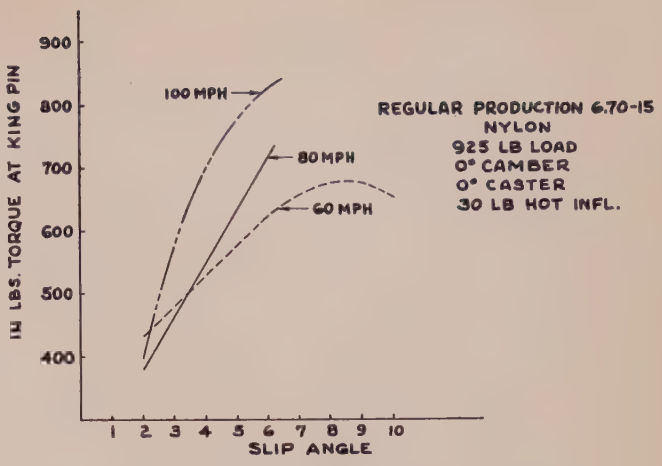

Fig. 9 – Self-aligning torque for nylon tire

cult to change greatly by tire construction.

2. Self-aligning torque did not drop off at higher speeds at normal slip angles, which tends to contradict previous findings and opinion.

3. Self-aligning torque can be improved through tire construction, but probably at a sacrifice in riding comfort.

4. Self-aligning torque drops off rapidly at higher angles – however, these are beyond normal turning angles used on the highway.

5. Our studies thus far show a reasonable correlation with previous work, which has generally been done on smaller test wheels at lower speeds.

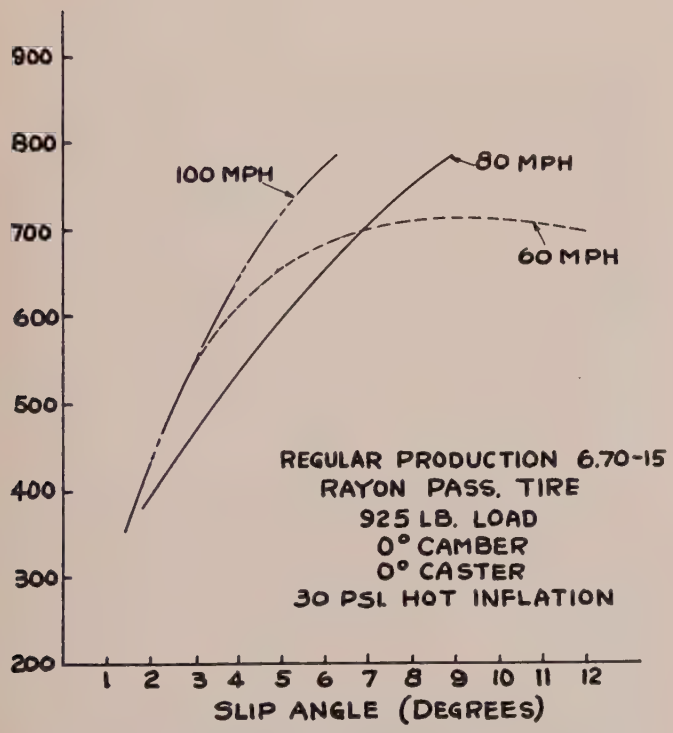

Fig. 8 – Self-aligning torque for regular-production rayon tire

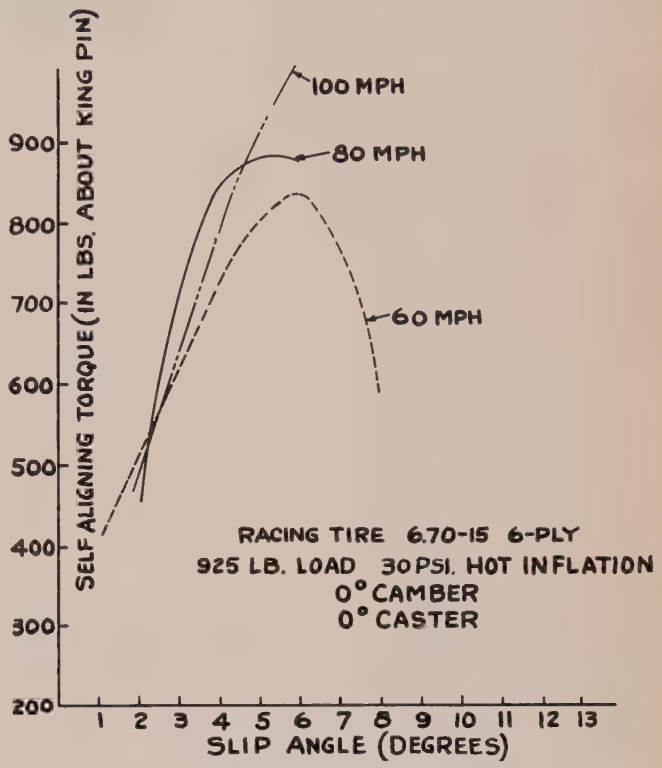

Fig. 10 – Self-aligning torque for racing tire

This is but a preliminary report. Certain peculiarities have shown up, particularly in the erratic behavior of the alignment torque which needs further work now in progress in our study.

In particular, we are gratified by the "feel" which this setup produces in the observers – closely simulating actual road experiences. We believe the technique affords an opportunity to improve tire-handling characteristics at higher speeds, an objective in which we are all interested.

DISCUSSION . . .

. . . of this paper starts on p. 344

Operation of Passenger

THE progressive nature of the tire industry can be seen in the performance record of today's passenger-car tire. Tread mileage has increased steadily over the years, until the national average in our 1954 survey was almost 30,000 miles. The danger of blowouts has been minimized, and skid and traction qualities improved. Even the reliability of the tire against "flats" from punctures has been improved by the move to tubeless construction. In spite of the trend to more severe tire service imposed by smaller-diameter wheels, higher engine horsepower, and super highways, the cost per mile of tires to the customer has been reduced to the lowest it has ever been.

Such a record of performance has been possible only because our engineers have kept the product ahead of the changing needs. Today, the tire engineer looks ahead at a new potential demand. The development of higher engine powers and super highways is creating a new set of requirements for passenger tire performance at high speeds.

The standard tire supplied on passenger cars at present does, with few exceptions, give satisfactory performance for all driving needs. One underlying reason is that the duration of travel at high speeds is generally insignificant. Cars seldom travel above 90 mph on the road. In those cases where the speed is greater, this rate is rarely sustained for long. There are few stretches of road in the United States where 100 mph can be driven for more than 35 miles. Even on these roads, high speeds must be reduced every few minutes because of traffic, crossroads, or curves. Even the super-highways (where speeding would be otherwise possible) have enforced speed limits.

To reiterate, then, for the type of speeding that prevails today, the tires that are now being produced perform quite well. Few tires are returned to us for damage incurred at high speeds. This is significant, for when there is a deficiency in the product, even a minor one, it is generally reflected in the returns.

Complacency, however, is not in order, for driving at high speeds is becoming more prevalent. The performance of tires on test tracks and high-speed courses indicates the nature of the impending prob-

Tires at High Speeds

E. H. Wallace and S. A. Lippmann, U. S Rubber Co.

This paper was presented at SAE Golden Anniversary Summer Meeting, Atlantic City, June 15, 1955.

THE standard tire will operate continuously at 94 mph without failing, but last only about 50 miles at 100 mph. This paper discusses means of counteracting the high power consumption and inertial effects that cause such deterioration of tire materials at high speeds.

The authors describe one special tire with tread ground away in such a manner as to lower power consumption and allow operation at 120 mph with very little distortion.

Whatever means are used to allow the higher speed operation sure to be required of future tires, the authors say, major improvements in physical properties will account for only a few mph speed improvement. Eventual requirements, they feel, will be met with compromises in tread wear and perhaps cost.

lem. At a sustained speed of 100 mph, the standard tire at normal inflation and load will fail in about 50 miles of running. This same tire does not fail in continuous operation at 94 mph. We are currently operating close to the limit of safety, and tomorrow may be beyond it.

Most of the failures at high speeds are of the type referred to as "separations." A section of the tread (or possibly the entire tread) may lift from the carcass. If the tire is not brought to rest soon after the separation occurs, the carcass will be damaged and a blowout will follow. The failure originates as a dual effect of centrifugal force and the deterioration of the strength of the rubber and cord materials at high temperatures. The high temperatures come about as a result of the conversion of mechanical energy to heat in the tire. We generally speak of this effect from the automobile engineer's viewpoint, and call it the power consumption of tires.

Let us look at a typical curve showing the power consumed in a standard tire in the range from 0 to 100 mph (Fig. 1). Apparently, two kinds of effects are taking place. The power consumed varies in an almost linear fashion with speed up to approximately 50 mph. It follows then that (in

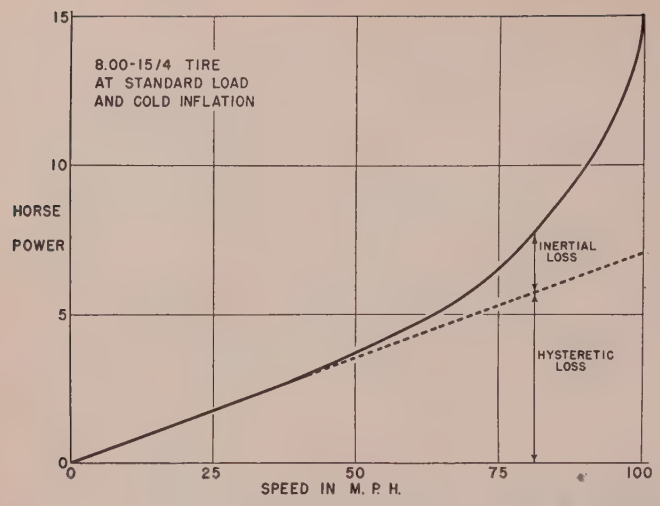

Fig. 1 – Power consumed in standard tire on 4-ft dynamometer roll-free rolling tire at equilibrium

this range of speeds) during each revolution about the same amount of mechanical energy is converted into heat regardless of the speed. This is a simple law of behavior that one would expect from the mechanical hysteresis of tire materials. The power or amount of energy lost per minute is, therefore, proportional to the number of flex cycles per minute. At high speeds, the power increases more than linearly. The energy lost per cycle increases with speed. This dependence on speed indicates that the process of energy loss is intimately tied up with the time. On casting around for possibilities, we find that time can be brought into the matter only through inertial effects, or through relaxation phenomena in the tire materials, and road friction.

We will jump ahead of the story at this point to say that very little of the loss is attributable to relaxation processes, and that inertia can be shown to play the major role.

In singling out these time-dependent losses, we first have to isolate the portion that is hysteretic

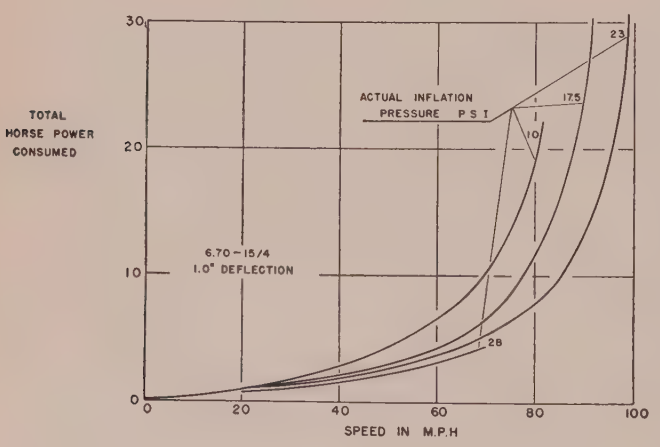

Fig. 2 – Power consumption of passenger tire at constant deflection and various inflation pressures

at higher speeds. This is done by extending the linear portion of the power curve, as illustrated by the dotted line of Fig. 1. For the analysis to be strictly valid, however, we must take a precaution. The deflection of the tire (on which the hysteretic losses depend) must be the same for all of the points on the power curve. This is an odd set of operating conditions for a passenger tire, but can be readily attained in the laboratory. The time-dependent losses can then be obtained by subtracting the extended linear power curve from the total power curve.

Fig. 2 displays the power data for a single tire at constant deflection and at various inflations. These curves tend to deviate further from the straight line than the more usual curves for constant load. The influence of the inflation pressure on the nonlinear portion is quite striking. We will shortly concern ourselves with this effect.

There is a speed at which the power curve first departs from the linear behavior, and we refer to this as the critical speed. The critical speed is often surprisingly slow, 30 to 40 mph. It is useful to employ the critical speed in defining a new variable, termed the speed index. The speed index is the ratio of the critical speed to the actual speed. For example, if the critical speed is 33 mph, then the speed index at 66 mph is 2. At 99 mph, the index is 3, and so forth.

The two derived variables, speed index and the time-dependent loss, are used in Fig. 3 to replot the data of the previous figure. We have also divided the time-dependent loss by the speed to obtain a quantity that represents the time-dependent loss per revolution of the tire. The resulting plot is remarkable in that all the inflations which produced the widely varying curves of Fig. 2 now fall on the same curve.

This curve is quite illuminating. It signifies that the time-dependent losses do not depend on the rate of flexing. Consequently, the losses cannot be due to relaxation effects. This leaves inertia as the remaining possibility. Furthermore, the time-dependent losses are determined by how many times larger the operating speed is than the critical speed. All in all, this has the character of a problem that is common in dynamic systems.

Let us suppose that there is a single inherent speed at which the structure of the tire will adjust from being deformed in contact with the road to be undeformed elsewhere. When the tire travels so that its parts move at a lesser speed, it is always in instantaneous adjustment. When the tire is moving excessively fast, however, the parts are not able to catch up. The speed of adjustment of the tire is too slow. There is consequently a buildup of compressions and distortions that eventually produces forces sufficient to accelerate the parts of the tire into place. There may be overshooting and other dynamic effects in addition. The compressions and erratic motions will result in large losses

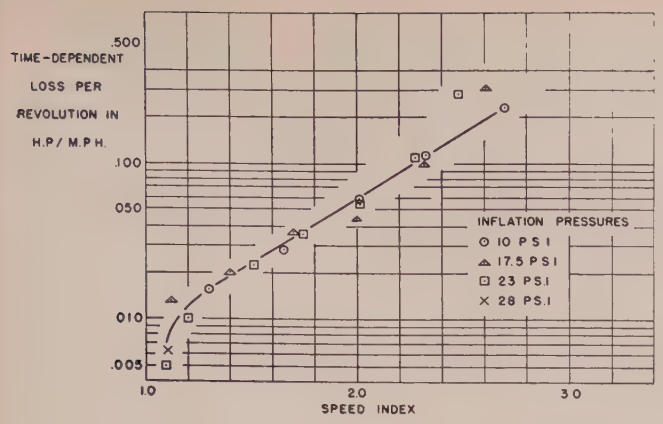

Fig. 3 – Effect of inflation on time-dependent losses

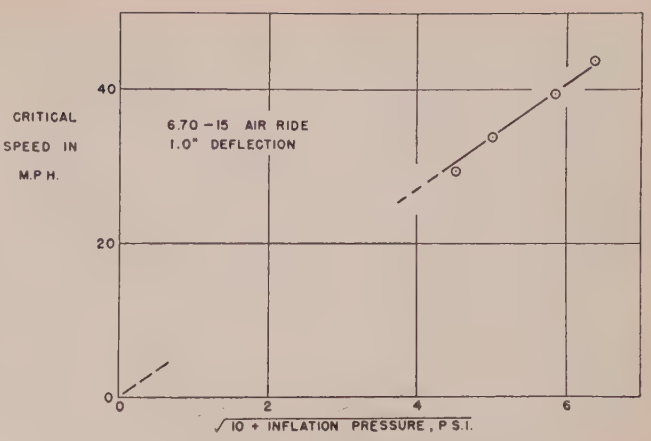

Fig. 4 – Relation of critical speed to inflation pressure

due to internal friction, phase effects, and so forth. This is admittedly a greatly simplified picture, but will serve to carry the idea.

Assume for the moment that the inherent speed of the parts of the tire is equivalent to the critical speed. The inflation pressure affects the rate of adjustment of the parts of the tire, since it and the structural stiffness are the motivating agents behind the adjustment. We would expect to find from the usual dynamic considerations that the critical speed is proportional to the square root of the spring rates of the structures of the tire. This spring rate is contributed to by the stiffness of the parts by an amount equivalent to 10 psi of inflation pressure. This can be determined from other studies. Fig. 4 confirms that the critical speed does follow the relationship that we expect. The critical speed is proportional to the square root of 10 psi plus the inflation pressure of the tire. Other data not presented here also show that the critical speed depends on the weight of the tire in the proper manner.

The time-dependent losses are then inertial, and behave as though they originate in the slow speed of adjustment of the parts of the tire structure.

I would like to comment on the magnitude of the total power lost by tires (Fig. 1). You will note that four standard tires will absorb 60 hp at 100 mph, and that the increase with speed is exponential. This is one reason that a substantial increase in engine power results in only an incremental increase in car speed at this range.

Another significant point follows from the previously mentioned observation that the safe maximum sustained operating speed for the standard tire is about 94 mph. This is equivalent to a power consumption of about 10 hp. We find in general that for all passenger tires made with the materials conventional to the industry at present, the critical level of power is 10 hp. This provides a convenient "rule of thumb" for gaging the limit of safe operation of a tire. Ten horsepower is about all the heat power a tire can dissipate without becoming dangerously hot.

Fig. 5 illustrates the appearance of a passenger-car tire at 110 mph on a dynamometer. The distortions have been loosely called "standing waves," and are manifestations of the inertial effects we have touched upon.

Tests run on a standard tire and a tire having a special construction against a 4-ft dynamometer roll up to speeds of 120 mph demonstrate that high-speed distortion is not confined to the radial plane but also occurs across the face of the tread.

One tire operated at 120 mph with very little distortion. As may be suspected, this tire consumes much less power at high speed. Let us now examine the construction features involved in the design of such a tire. Obviously, anything which reduces the weight at the crown of the tire will reduce the inertial effects. Fig. 6 demonstrates this point. In this case, the total power consumed for the tire of the upper curve is about 20 hp at 100 mph. By the

Fig. 5 – Passenger-car tire running at 110 mph on dynamometer

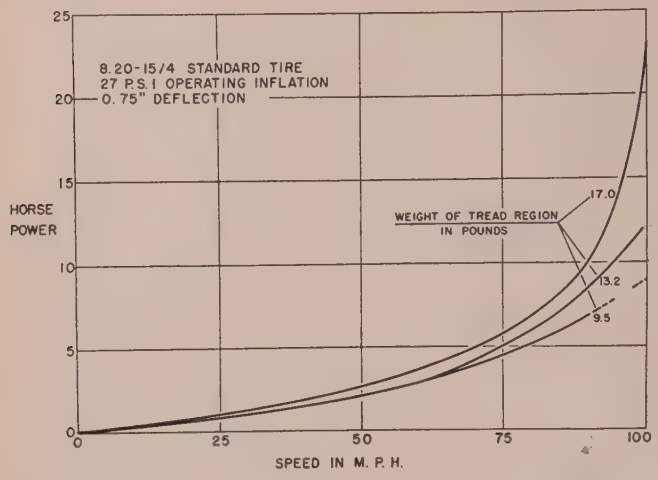

Fig. 6 – Effect of weight of tread region on power consumed

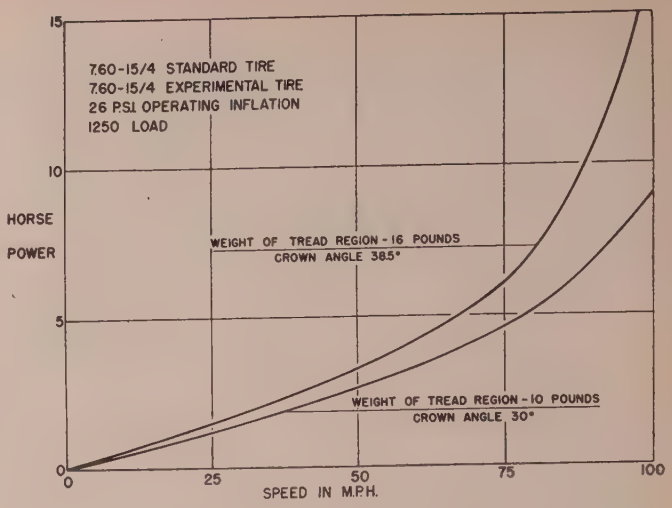

Fig. 9 – Effect of tread weight and cord angle on power consumed

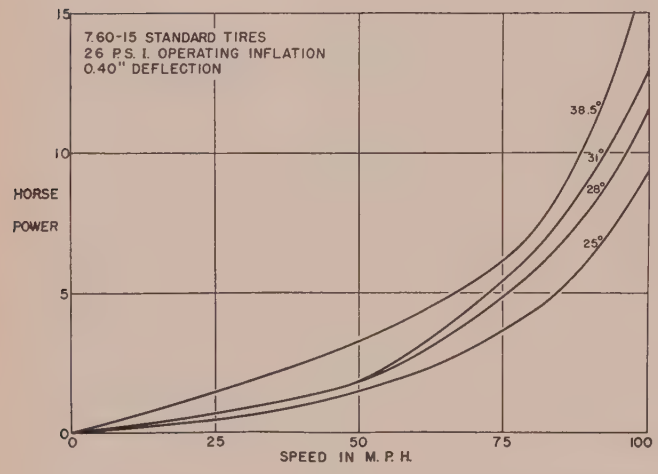

Fig. 7 – Effect of finished crown angle of cords on power consumption

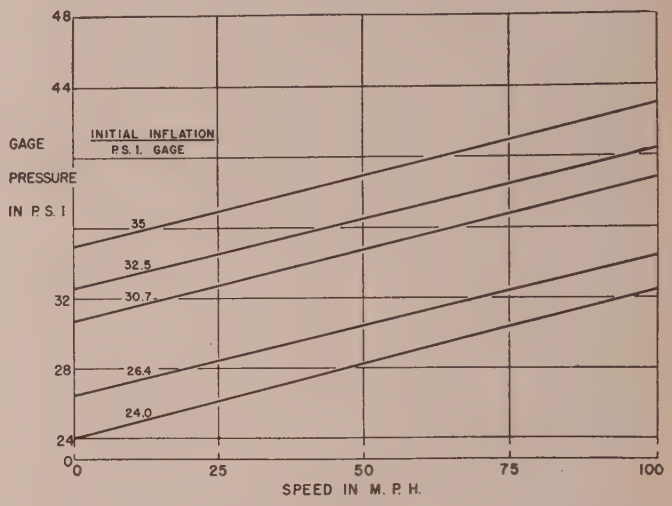

Fig. 10 – Inflation buildup at equilibrium for various initial pressures

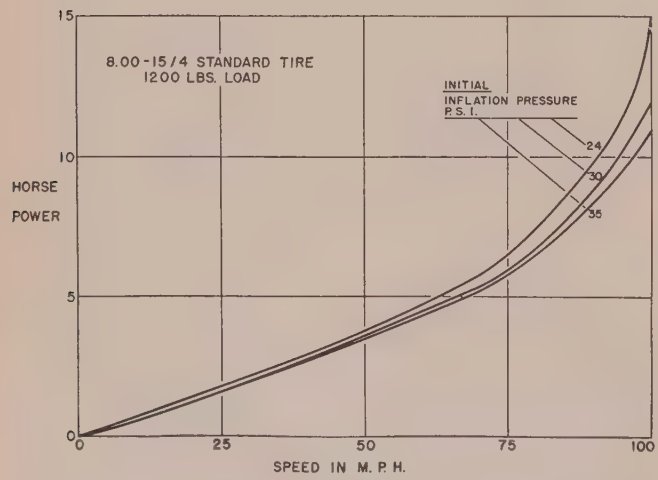

Fig. 8 – Effect of initial pressure on power consumed at equilibrium

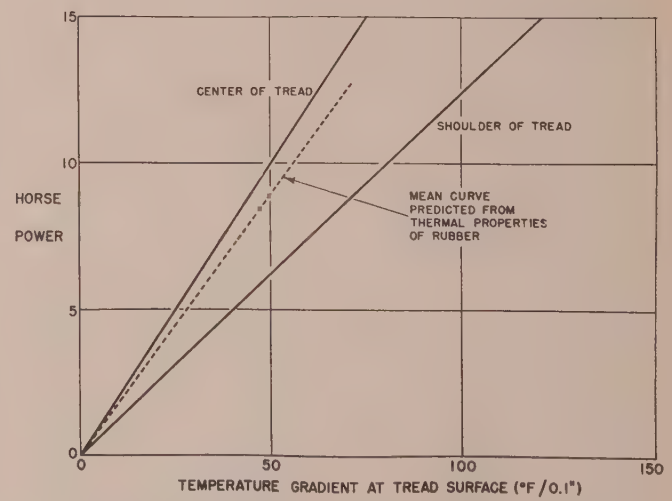

Fig. 11 – Relation of total power consumed to heat flow through tread

simple expedient of grinding tread rubber away in the amounts shown, the power consumed is lowered appreciably.

The thought must immediately occur to you that a worn tire is better for high speed operation than a new tire. This is true if the carcass of the worn tire has not been subjected to any unusual deteriorating effects. It also follows that a tire designed for high speed may carry a penalty with respect to tread mileage. We believe there will be a trend in the industry where the purchaser of premium tires will prefer to buy safety at high speeds rather than extra tread mileage.

We previously mentioned that a way to cut down on the inertial losses at high speed is to stiffen the tire to improve the rates of adjustment. This can be done two ways: first, by changing the carcass cord angle; and second, by increasing the inflation pressure. Figs. 7 and 8 give data showing the effect. An explanation of the term "carcass cord angle" may be desirable here. As you know, carcass cords extend diagonally from bead to bead. The cord angle is measured under the center of the tread, and is the acute angle that the cord makes with the center line of the tread.

The cord angle in standard tires is usually between 38 and 40 deg. The lower the angle, the more circumferentially the cords run. Lower angles result in greater readjustment forces in the tire. Reduction in cord angle over standard practice cannot be made without some change in other properties of the tire. Ride harshness is increased, while stability and steering response are improved. The improved handling characteristics which result, however, complement the other requirements for high-speed driving.

Fig. 8 shows that the standard tire can be made slightly safer at high speed by increasing the inflation. Using 10 hp as a maximum power loss for safe operation, we gain an increase in speed of safe driving from 93 mph to 97 mph upon changing the cold inflation from 24 to 35 psi. Unfortunately, even this minor achievement is accompanied by a considerable loss in riding comfort.

Weight of the tread and cord angle are then the major factors involved in design for high-speed operation. Fig. 9 shows the power-consumption-versus-speed curve for an experimental tire combining these features. Only moderate deviations in the construction of the standard tire were made to maintain good ride, handling, and wear characteristics. In fact, the data of this figure were obtained from the previously described experimental tire which operated with very little distortion at 120 mph. This tire represents one of the advanced designs for satisfying the possible trend in driving habits.

There are, of course, factors other than the two named which affect the power consumption and high speed operation of tires. Some of these are:

1. Hysteresis of rubber compounds.
2. Type of cord – rayon, nylon, others.
3. Tire size.
4. Tire load.
5. Break-in.

In general, the gains to be made by lowering the hysteresis of the rubber compounds must be accomplished with care, since they are often accompanied by major losses in one or more qualities, such as tread wear, cracking, and so forth. Nylon is the best carcass material for high-speed operation, principally because it results in a lighter tire. Tire size, load, and break-in are conditions limited by customer usage, and are not discussed at length here because they are not fundamental to the construction of the tire.

We have been concerned with the rather large increases in the horsepower consumed that underlie the generation of heat. The heat itself, however, is the primary problem. For our first look at the resulting temperatures, let us consider the matter of inflation buildup. Fig. 10 shows how the inflation pressure in the air chamber varies with speed. The data represent equilibrium conditions with various starting or "cold" inflations. We note that regardless of the initial inflation, there is approximately an 8-lb buildup under equilibrium conditions at 100 mph. We immediately notice another curious thing: The power consumed by the tire is a combination of linear and exponential functions of speed, and the inflation buildup is not. Obviously, the inflation buildup does not reflect the total power consumed by the tire. Analysis of these data, with inflation pressures restated in terms of temperature, is as follows:

According to the experimental data:

1. $P = P_o + KS$

where:

P_o = Initial inflation (absolute pressure)

P = Equilibrium inflation (absolute pressure)

S = Speed

K = Parameter of tire

According to the gas law, at constant volume:

2. $P/P_o = T/T_o$ from (1) and (2).

3. $(T - T_o) = T_o K \frac{S}{P_o}$.

The conclusion from this analysis is that temperature buildup is proportional to speed and inversely proportional to initial inflation pressure. We can view this as indicating that the temperature buildup in the air chamber is proportional to the deflection of the tire, and reflects hysteretic losses due to this deflection. Contrary to the thinking of many people, the inflation buildup in a tire during a high-speed run does not reveal the power consumed by the tire and the possibility of failure. Where then is the heat going that represents the major part of the power loss?

Fig. 11 shows the relation of heat flux through the tread surface to the total power consumed by

the tire. We also have superimposed a calculated curve showing the average heat flux if all the power consumed by the tire flowed out through the tread. The theoretical curve and experimental curves are sufficiently consistent with each other so that we can conclude that most of the heat produced by the tire, both through simple hysteresis and inertial processes, flows out through the tread.

As indicated earlier, heat is dangerous because of its degrading effect on the strengths of the materials from which the tire is constructed. Although tread-to-carcass bonds may be improved in the hot tire and the tear resistance of rubber stocks increased, we do not foresee improvements in the immediate future that will greatly influence the speed at which failure will occur. This follows from the fact that a major improvement in physical properties of the tire materials is equivalent to an increase of only a few mph in speed.

As we have attempted to point out in this short paper, large-scale improvements in high-speed operation, for the present, appear to be limited to constructional changes alone. There may be future demands for high-speed tires, and we believe tire manufacturers will be ready to meet the requirements. We further believe that this will be done with compromises only in tread wear and perhaps in cost.

DISCUSSION

of Tire Symposium Papers

Tire Tester Described

– David Whitcomb
Cornell Aeronautical Laboratory

I WOULD like to discuss some tire research activity at our laboratory. At the March, 1954, SAE meeting in Detroit, we discussed briefly the design of tire testing equipment which Cornell was developing for the Air Force. This machine has now been constructed and is in use on a variety of test programs for the Air Force and several of the tire manufacturers. This equipment was constructed as part of an Air Force program to develop a tire testing facility for measuring the cornering characteristics of a full range of aircraft tires. I think that a description of this device would be of interest particularly because of many similarities which it bears to Mr. Joy's "stability machine."

Fig. A shows that the basic configuration of the tire tester is that of a single test wheel and tire trailed behind a truck. This equipment, therefore, measures the tire's characteristics while running on a flat road surface. On the truck are mounted the necessary operating controls, the recording instrumentation and power supply. The equipment is normally operated by a crew of two or three people. The test wheel is mounted on an axle, which in turn is supported on two linear ball bearings, which permit the axle to float freely in a sidewise direction. Each end of the axle is secured by a strain-gaged balance, which permits the measurement of the vertical and horizontal load at each end of the axle. These measurements permit immediate determination of the vertical load on the tire, the rolling resistance, the aligning torque, and the cambering torque. An additional balance beam is mounted at the end of the axle and measures loads along the axle or the cornering force. The steering angle of the test wheel is hydraulically controlled and may be adjusted to any value between 0 and ± 30 deg. Camber angles are provided with a fixed adjustment in increments of 2 or 5 deg up to 30 deg. Maximum loads up to 3000 lb may be applied to test tires and the machine will accommodate tires up to a maximum of 32 in. outside diameter or tires with a minimum rim diameter of 13 in. The test data in the form of loads, angular positions, and the like, are continuously recorded on an oscillograph. This equipment is, therefore, designed to measure both the steady and dynamic characteristics of the tire on a flat road. Forces and moments are reported with reference to an axis system having its origin at the wheel center and aligned with the wheel plane and axle except when the wheel is cambered. Data can, of course, be transferred to any other axis system of interest, if desired. Maximum testing speeds are limited by those of the truck and the practical limit appears to be about 50 mph for the present configuration.

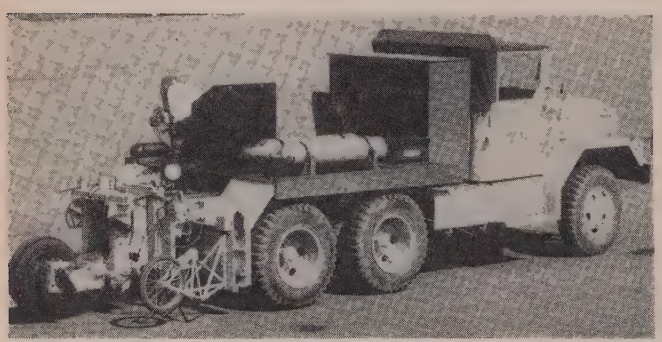

Fig. A – View of tire tester

Fig. B gives a closer view of the console mounted on the truck. From this point the test engineer operates the steering, loading, and recording controls and at the same time is provided with a full view of the test tire. Also seen in this view is the steering axis which is forward of the test wheel, thereby providing trail. The bounce axis is located horizontally at the bottom of the steering axis. The hydraulic

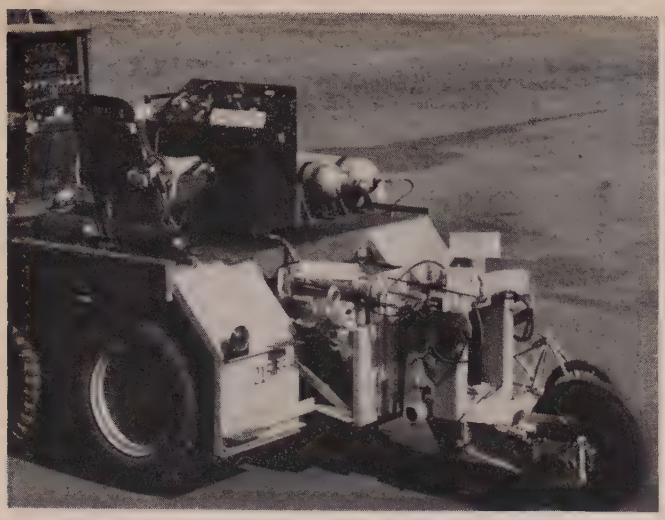

Fig. B – Closer view of console mounted on truck

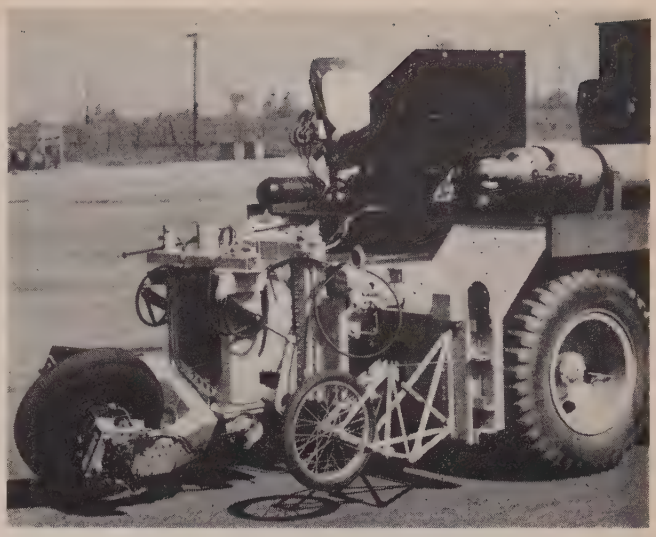

Fig. C – Close-up view of right-hand side of tire tester

steering actuator will also be noted. With this steering system it is possible to position the wheel at any desired angle or to vary the steering angle slowly at different rates, which may be as low as 0.1 deg per sec. It has been our practice to use these slow-speed sweeps for conducting tests at small slip angles in the range of ±3 to 5 deg. The console is also equipped with a steer angle indicator and a steering rate indicator to aid the engineer in the operation of the equipment.

Fig. C is a close-up view of the right-hand side of the tire test equipment and shows the test wheel in a typical cambered configuration. Of particular interest is the trailing fifth wheel. This is used to measure the slip angle of the truck with respect to its path which is applied as a correction to the measured steering angle of the test wheel to give true slip angle of the test tire. This fifth wheel was especially designed for this equipment after considerable development work in which a conventional fifth-wheel speedometer was extensively modified. A unique feature of this design is that the yaw and pitch axis are at different locations. This gives a satisfactory yawing response but at the same time permits the wheel to follow the variation in contour of the average road surface without undue bouncing.

Fig. D shows a close view of the test wheel, the balance boxes, side load beam, camber linkage, and loading cylinder. The vertical load on the test wheel is controlled by applying nitrogen under pressure to the load cylinders. A pressure regulator permits selection and adjustment of the load. The system is equipped with surge bottles and operates at constant pressure, thus providing constant load on the test tire, irrespective of any bouncing motion. No ballasting is thus required to vary the tire load. A loading range of 300-3000 lb is provided. The camber links permit manual adjustment of camber angle in 2- or 5-deg increments up to ±30 deg.

Fig. E shows the internal components of one axle strain-gage balance. It will be noted that there are two vertical and two horizontal beams constructed in the form of a cross. The test axle wheel floats in the center ring and the ends of the four beams are secured through flexures to the frame of the machine. The two vertical beams are thus placed in bending when subjected to a fore-and-aft load. The two horizontal beams respond similarly to vertical loads. The flexures and also the strain-gage circuitry tend to eliminate any interaction between vertical and horizontal beams. The strain-gaged beam which reads the side force is shown in the lower part of the figure. The axle attaches to the center of this beam, the ends of which are secured to the tire tester frame. Thus, this beam is placed in bending

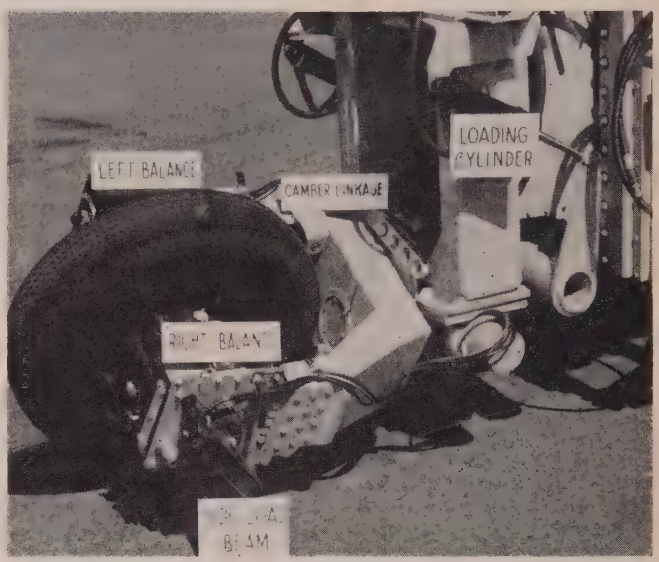

Fig. D – Close view of test wheel, balance boxes, side load beam, camber linkage, and loading cylinder

when subjected to a tire cornering force.

Various items of the recording instrumentation are seen in Fig. F. These are mounted at the forward end of the truck platform and include the strain gage bridge circuits which provide for bridge balancing, attenuator adjustments, controls, and filters; an 18-channel recording oscillograph, relay boxes, and associated electrical components.

This installation features direct recording of the strain-gage signals and no amplifiers are required. Recorded information includes the following: vertical and horizontal load on right-hand end of axle and vertical and horizontal load on left-hand end of axle, axle side force, steering angle, truck slip angle, attitude of the test wheel trailing arm with respect to the truck, test wheel revolutions, and miscellaneous voltages.

The use of a recording system of this type permits the continuous recording of the time history of the above quantities and thus enables the determination of either the steady or of the time variant characteristics of the tire.

Some typical data obtained with this machine are presented in Fig. G. This includes a plot of tire cornering

Fig. E – Internal components of one axle strain gage balance

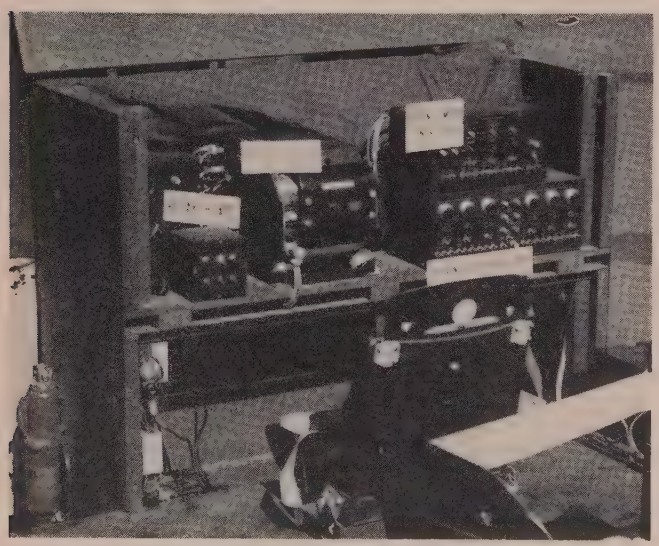

Fig. F – Various items of recording instrumentation

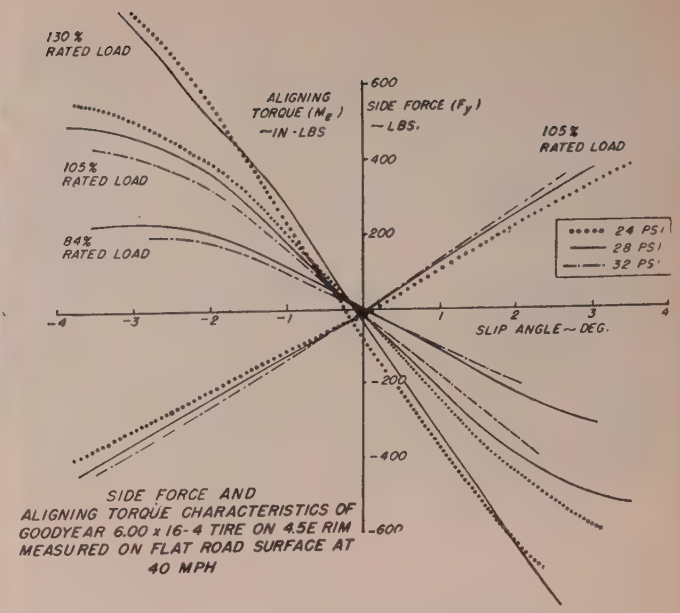

Fig. G – Typical data obtained from tire tester

forces versus slip angle for one load and three pressures. Aligning torque versus slip angle is shown for three loads and three different pressures. It has not been possible to include all of the cornering force data on these curves, as many are coincident and were removed from the graph for the sake of clarity. A tire characteristic worthy of note is the effect of pressure on aligning torque at constant load. The result is as would be expected, that is, an increase in pressure results in a reduction of aligning torque at constant slip angle. At constant pressure, the effect of load on aligning torque is most marked and, as would be expected, an increasing load results in an increase of aligning torque. The effect of load on cornering force (although not shown on this figure) is not particularly great at small slip angles. The effect of pressure on cornering force is as would be expected, that is, an increase in pressure gives a higher cornering force for the same slip angle.

It may be of interest to note that we have compared these data with some obtained by Mr. Joy for the same size tire. In comparing these data, it is important to note that there are probably differences in tire construction and that Mr. Joy's information was obtained from rolling drum tests whereas those which we report were obtained from a flat road surface. The principal difference that we found was that our data showed greater cornering stiffness, that is a steeper slope of the cornering force versus slip angle curve. This was found to be approximately 25% greater at rated load and 28 psi.

Our data showed a greater sensitivity of aligning torque to changes in load. The maximum aligning torque which we recorded for 85% load is lower than that recorded by Mr. Joy, whereas for 130% load it is higher.

Questions Several Points Discussed by Gough

– A. Schallamach
British Rubber Producers' Research Association

IT APPEARS from Mr. Gough's Fig. 4 that the method adopted for measuring side-force intensity introduces an additional deflection of the tire because of the finite deflec-

[a] See reference No. 14 of main paper.

[b] Paper by A. Schallamach, pub. by Kautschuk und Gummi, Sonderheft "Der Reifen," 1955.

[c] See reference No. 6 of main paper.

tion of the dynamometer bar. It would be helpful if Mr. Gough indicated the possible error involved.

As for buffing marks, I do not think that his Fig. 9(B) is a typical representation of the surfaces of rear tires. It is very often found that rear tires, or more generally driving tires, are marked similarly to the schematic sketch in his Fig. 9(A), with this difference that the direction of abrasion is reversed. Such a case has, for example, been shown in the first paper[a] published on this subject. In this paper, where the markings were called abrasion patterns, attention was also drawn to the important bearing abrasion patterns have on tire wear. It was demonstrated that their presence on an abraded rubber surface can increase the rate of abrasion, and it has since been concluded[b] that differences in the wear rating of tread compounds tested under varying conditions of severity can be ascribed to differences in the intensity of the abrasion patterns formed under such circumstances.

Gough Closure To Discussion

In the apparatus in Fig. 4, the bar deflects only 0.02 in. at 100-lb sideway force and this is trivial compared with the movements recorded. A zero method of measuring the force is, of course, a research man's ideal but it is not achievable with simple apparatus. In the present case this small deflection has not in any way invalidated the findings.

I cannot agree that, "It is very often found that rear tires, or more generally driving tires, are marked similarly to the schematic sketch in Fig. 9(A), with this difference that the direction of abrasion is reversed." We have searched through all our recordings and have also been on the lookout for such a case ever since Dr. Schallamach's paper was published, but we have not seen a single instance of an arrow-like pattern with the direction of abrasion from the crown of the tire on both halves of the tire. It arises on one-half of the tire in the case of a rear tire turning corners in one direction only, as in Fig. 9(C). The following argument, which is based on the paper by Gough, Hardman, and Maclaren,[c] shows that the reversed abrasion on both halves is unlikely to arise.

If there is an arrow-like buffing pattern on a tread, then the movement at the point of the arrow is sideways, either one or both directions. The most heavily laden half, and the one which develops the coarsest buffing ridges and which also wears most, is the half which the road meets first in the sideway movement. As shown in Fig. 9(C), this half has the sawtooth ridge direction the same as a front tire.

When a tire is cornered both ways, the pattern produced on a particular half of the tire, when that half is the lightly laden region, is masked by the pattern produced when that same half is in the heavily laden condition. Hence, under these conditions a buffing pattern like a front tire is produced. This has been observed many times on high-speed racing vehicles relatively lightly loaded when driven on a tortuous course.

I find it extremely difficult to make any useful comment on the influence of an abraded rubber surface on the rate of abrasion of a tire as they are inextricably related, but I would incline to the view that the pattern is merely an indication of the severity of the conditions causing a high rate of wear.

Oral Discussion

Reported by P. C. Bowser
Chevrolet Motor Division, GMC

Robert Schilling, GM Research Laboratories Division: There are two points about which we know very little:

1. We have to find the decrease in dynamic response of a tire due to hopping on the road. If a tire takes say 2 ft to build up full cornering force but loses it instantly when off the road, it can lose average cornering force appreciably when hopping even a little at 10 cps.
2. We need to measure the rapid fore-and-aft force reversals at the wheel spindle when a wheel is hopping, because of their excitation of wheel fight.

Maurice Olley, Chevrolet Motor Division, GMC: I enjoyed Mr. Gough's plots which cover the essential character of the tire in one diagram. I also agree with Mr. Gough that a car is steered by feel and not by sight.

I liked Mr. Joy's proof that the theory of high-speed performance holds true when tires are built with inextensible tread and resulting elimination of standing wave.

Forest McFarland, Studebaker-Packard Corp.: Before the war, we did some work on air resistance measurement. At that time, we were unable to get adequate rolling resistance data. However, with this new information, we will be able to revise our upper 30-mph figures.

I thought that the 10-hp rule of thumb mentioned by Mr. Lippmann was very significant.

I also thought that the cornering, aligning torque, and caster effect were very clarifying. I have been prodding the tire companies for such information for years.

Also, I might add that we have put 1-1¾-in. cleats on wheels to establish what happens to tire characteristics as a result of wheel hop.

A. W. Bull, U. S. Rubber Co.: It appears that we are beginning to get into the speed range where, instead of tire engineers, we are going to need fins to go around corners and stop.

The close agreement of the data reported here reminds me of some early data which we gathered on 30 makes of tires of the same size. We found as much as 30% difference of physical characteristics at some standard condition. I expect, therefore, that this apparent good agreement is perhaps coincidental.

Mr. Olley: I think it is also of interest that the flat testing results showed an increase of cornering force and aligning torque over the corresponding results from the conventional drum test.

Shaft Gas Turbines

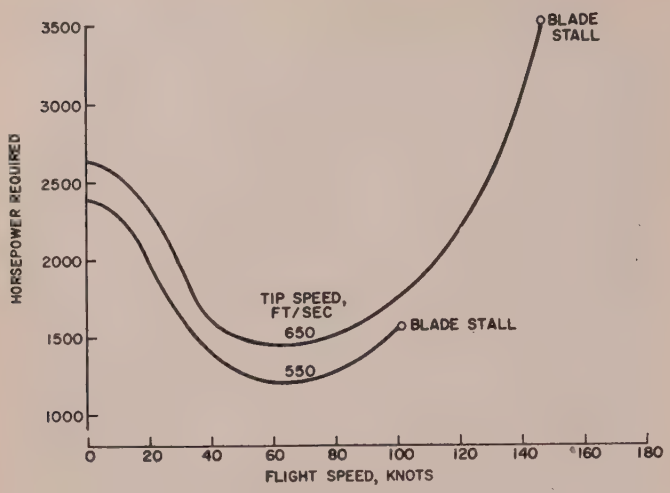

Fig. 1 – Helicopter power requirements

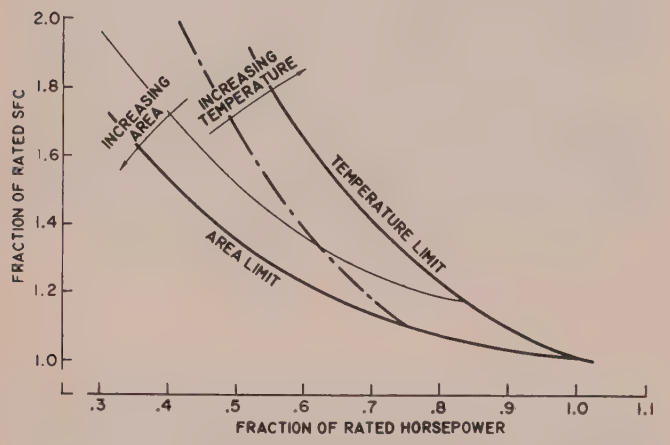

Fig. 2 – Fixed turbine specific fuel consumption (rated speed)

LIGHT weight, smooth power, and low vibration level are the undisputed and well-advertised virtues of the gas-turbine engine. These characteristics explain, to a large extent, the serious consideration given to the gas turbine as a powerplant for the larger and faster helicopters that will soon appear.

When such an installation is planned, however, and before the design is fixed, certain questions must be answered. For example, is the choice both clear and decisive between the single-shaft fixed turbine and the two-shaft free turbine? What are the effects of reserve power requirements and engine-rotor match points on powerplant size and operational efficiency? Which engine type, fixed or free, has the better characteristic from the standpoint of rotor-engine dynamics and control? These answers can often be found in a comparison of hovering duration, flight range, and payload capacity for an assumed helicopter powered, in turn, by the various engines under consideration. At other times a flight-performance comparison is unsatisfactory, and a complete picture is given only by a direct comparison of engine-performance characteristics.

Helicopter Power Requirements

The difficult demands made by a helicopter on its powerplant are illustrated in Fig. 1. Here, horsepower required by the helicopter is plotted against forward flight speed for two rotor-tip speeds, 550 and 650 fps. Values given are representative of a 30,000 lb, transport-type helicopter. The familiar droop in the power curves is a result of the changing profile and induced drags of the rotor and the increasing parasite drag of the fuselage as flight speed is increased. For a given tip speed, power required in hovering flight (represented by the intersection of the curves with the vertical axis at zero forward speed) is shown in Fig. 1 to be nearly twice the power at minimum-power, forward flight speed. Furthermore, for the rotor configuration represented in Fig. 1, power required during

For Helicopters

THIS paper on helicopter gas turbines is divided into two parts. The first compares the performances of two helicopters, one powered with a two-shaft free turbine and the other with a single-shaft fixed turbine. The second part considers the engine and rotor control problems associated with each type of powerplant.

Part one of the paper discusses helicopter performance advantages arising from the flexibility of the free turbine. Also, several modes of helicopter operation for each turbine are considered in two flight plans. Advantages in helicopter hovering time and range for various methods of turbine operation are assessed on the basis of steady-state engine performance.

Part two of the paper considers the transient behavior of the two types of powerplants under several control actions. Anticipated helicopter maneuvers during a flight plan are studied. Various combinations of powerplants, powerplant schedules of operation, control systems, and helicopter maneuvers, are used to indicate control problems.

W. S. Miller, Jr., R. P. Krebs, and T. C. Blaschke,
Lewis Flight-Propulsion Laboratory, NACA

This paper was presented at the SAE Golden Anniversary Aeronautics Meeting. New York, April 20, 1955.

any flight condition is higher for the higher tip speed. Retreating blade stall is, of course, delayed at the higher tip speed; also, maximum flight speed is greater as shown by comparison of the circled points.

Fig. 1 illustrates the aerodynamic advantage afforded by a variable tip-speed rotor. From the standpoint of rotor power required, it is best to hover at a low tip speed and to use a higher tip speed when high-speed forward flight is desired. Some of the performance characteristics of the fixed and free gas turbines that qualify them as variable shaft-speed helicopter powerplants are examined in the following sections.

Engine Characteristics

Specific Fuel Consumption of Fixed and Free Turbines – In Fig. 2, specific fuel consumption is plotted as a function of shaft horsepower for a single-shaft fixed turbine. The plot is valid for rated shaft speed. Lines of constant turbine-inlet temperature and constant exhaust-nozzle area are shown. Because of the comparatively low forward speed of the helicopter, no effort was made in the powerplant analysis to obtain useful thrust from the gas-turbine jet. A maximum exhaust-nozzle area was therefore assumed. Fig. 2 shows that this is the operational mode that gives best fuel economy. Nozzle area smaller than maximum – in this case 1.4 times the compressor area – give higher specific fuel consumptions. When the nozzle area is held constant, higher turbine-inlet temperatures increase the available power and reduce the specific fuel consumption. Turbine temperatures are limited to the specified, maximum allowable turbine temperature shown in Fig. 2.

Maps similar to Fig. 2 can be constructed for the case where the gas turbine is run at speeds lower than rated shaft speed. On these maps, specific fuel consumption, at a given percentage of rated power, is found to be slightly improved over the values shown on the rated shaft-speed plot. The temperature-limit line moves to the left, giving lower ob-

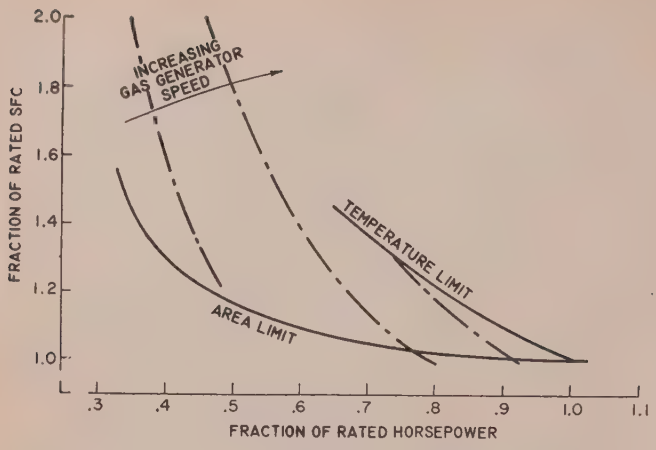

Fig. 3 – Free turbine specific fuel consumption (rated speed)

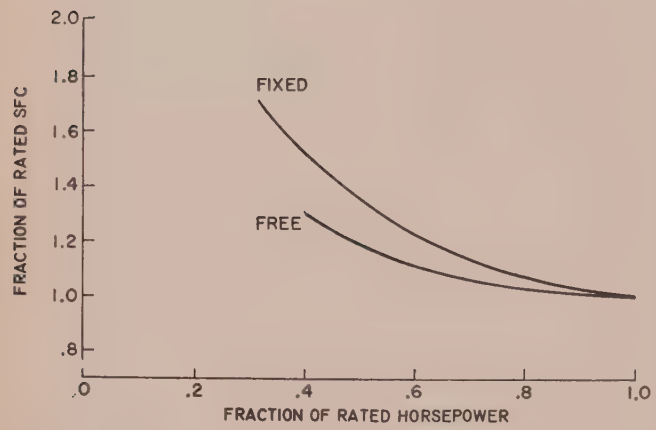

Fig. 4 – Comparison of specific fuel consumptions of fixed and free turbines (rated speeds)

tainable horsepowers for the maximum nozzle-area.

Fig. 3 is a plot of specific fuel consumption for the free turbine at rated shaft speed. Lines are shown giving nozzle-area limits, turbine-temperature limits for the gas generator, and constant gas-generator speed. Like the single-shaft fixed turbine, the free turbine gives best fuel economy when the exhaust-nozzle area is held at its maximum permissible value. The maximum horsepower obtainable from the free turbine is limited either by the temperature on the gas-generator turbine or by the speed of the gas generator. It is important to note that the power output of the free turbine, for fixed shaft speed, can be changed only by varying the rotational speed of the gas generator if the exhaust-nozzle area is held constant. Maps similar to Fig. 3, constructed for free turbine speeds less than rated, show small improvements in specific fuel consumption for a given horsepower.

The minimum specific fuel consumption curves for the fixed and free turbines shown in the two preceding figures have been replotted for comparison on Fig. 4. This plot shows that fuel consumptions for the two engine types are equal at rated power. However, as power is reduced from the rated value, the specific fuel consumption for the fixed turbine increases more rapidly than for the free turbine. At 0.5 of rated power, for example, the specific fuel consumption of the fixed turbine is 15% higher than for the free turbine.

Maximum Available Shaft Power – Maximum available shaft power is plotted in Fig. 5 as a function of shaft speed for the fixed and free turbine engines. It has been pointed out that maximum power, at a given speed, is determined by limiting turbine-inlet temperatures and exhaust-nozzle areas. Since the free turbine is choked at design point, and remains choked during power modulation because of the large nozzle area, changes in free turbine speed have little effect on the gas generator section. Power changes and free turbine speed variations, therefore, are due primarily to small changes in turbine efficiency. Because these differences in turbine efficiencies are small, the maximum available power curve for the free turbine is quite flat.

On the other hand, a change in the speed of the fixed turbine gives a simultaneous variation in both airflow and pressure ratios. Compared to the free turbine, shaft power drops off sharply as shaft speed is reduced. At 0.85 of rated speed, for example, the shaft power of the free turbine is 0.93 of rated while that of the fixed turbine has fallen to 0.75 of rated power. Overspeeding of the fixed turbine gives an increase in airflow and pressure ratios, and powers greater than rated values can be obtained.

With the free turbine, power cannot be increased beyond rated values by overspeeding unless the free turbine efficiency is increased. The shapes of the curves plotted in Fig. 5 are dependent upon the characteristics and matchings of the gas-turbine components.

Both engine types employed conservatively designed axial-flow compressors with low axial Mach numbers. Compressor efficiency peaked at about 0.93 of rated shaft speed. As far as possible, similar component characteristics were used for both the fixed and the free turbines.

Flight Performance

A convenient means of evaluating the combined effect of engine specific fuel consumption, power-speed relationship, and engine size is to compute the resulting performance which comes from installing several turbine engines in an assumed helicopter. The helicopter used in this study had a gross weight of 30,000 lb, carried a crew of two, and completed all its missions with a 10% fuel reserve on board.

Three missions were considered: ultimate range with no payload, 300 nautical miles at the forward speed corresponding to best range, and 3 hr of hovering at standard atmospheric conditions. Three

gas turbines were used as powerplants: one free turbine and two fixed turbine designs. All the engines were sized to have at least a 30% power reserve at sea level while hovering, and to be able to hover the helicopter at 6000 ft on a 95 F day. Forward flight was conducted with all engines at rated engine speed.

Fig. 6 shows how the engine size is determined. The flight condition and operating point at which engine speed and rotor speed are matched in the helicopter design are herein defined as the engine-rotor match point. The rotor power requirements in hovering flight are shown as a function of tip speed on both sides of Fig. 6 by the lower solid lines.

On the left side of Fig. 6, the match point for the free turbine was set at 550 fps tip speed, corresponding to 0.85 of engine rated speed. Since the reserve power requirement was 30% over the hovering power, the free turbine engine was sized to provide 3100 hp at 0.85 of rated speed. The dashed power-speed curve for the free turbine is relatively flat and shows that this engine, matched to the rotor at 0.85 of rated speed, will develop 3280 hp when its speed is raised to fully rated.

For the fixed turbine A which runs at constant shaft speed, the match point was set at a rotor tip speed of 650 fps, corresponding to rated engine speed. To provide the necessary reserve power at hovering tip speed, turbine A was sized to provide 3410 hp. Its power-speed characteristic is given by the lower dashed line.

In like manner fixed turbine B, which runs at variable speed, is matched in hovering at 550 fps and 0.85 of engine speed. To provide reserve power, it must develop 3100 hp at this speed. Because of its steep power-speed characteristic, turbine B will provide 4260 hp when its speed is raised to fully rated. Fig. 6 graphically demonstrates that fixed turbine B is a considerably larger engine than either the fixed turbine A or the free turbine.

The ultimate range given by the three engine designs is shown in Fig. 7 as a function of helicopter

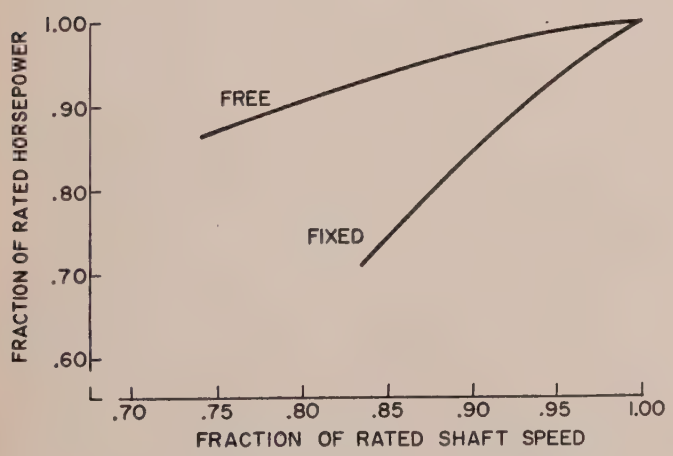

Fig. 5 – Power vs. speed, fixed and free turbines

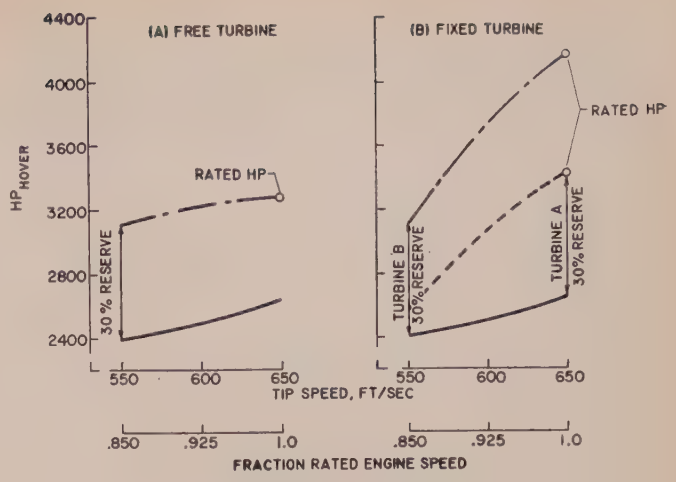

Fig. 6 – Engine-rotor match points, fixed and free turbines

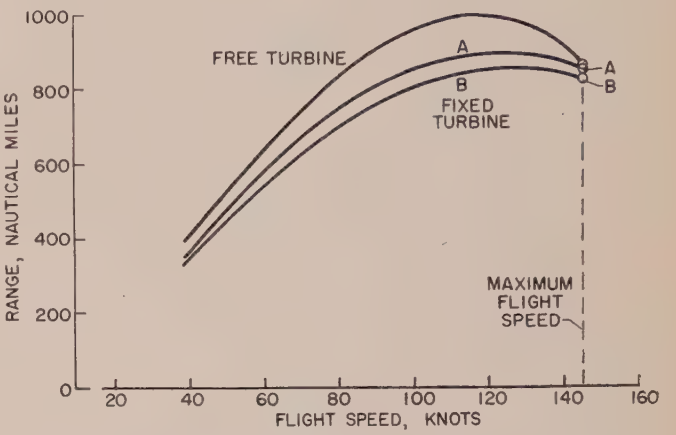

Fig. 7 – Range vs. flight speed at sea level, fixed and free turbines

flight speed. Because forward flight was carried out in each case at the same rotor tip speed – 650 fps – maximum flight speed is identical for the three helicopters and maximum range is obtained at about equal speeds.

Fig. 7 shows that the free turbine has the longest ultimate range. The constant-speed fixed turbine is next. In a mission of this type, which could possibly be a ferry flight, power requirements are reduced steadily as fuel is burned and the helicopter lightens. As the engine operates further from rated power, the specific fuel consumption of the fixed turbine engine becomes increasingly greater than that of the free turbine. It is apparent, therefore, that a mission of this type, involving considerable off-design operation of the powerplant, presents more unfavorable conditions for the fixed turbine than for the free.

If part of the initial fuel abroad is replaced by payload and the mission range is limited to 300 miles, the off-design requirements made on the powerplant are not so severe. In Fig. 8, the payload that can be carried on a 300-mile mission is used as a figure of merit for the three powerplants. The

free turbine is shown to carry the heaviest payload, 8860 lb, while the fixed turbine A, which operates at constant shaft speed, carries 8450 lb. The compromise engine (fixed turbine B, since it is a larger engine than turbine A) operates further off-design during the flight and its payload capacity is 8060 lb for the mission.

In a similar manner, hovering performance with payload was calculated for the three powerplant installations. Here a 3-hr hovering mission, such as might be required in anti-submarine warfare, was assumed. These results are summarized, along with the forward flight results, in Table 1. The free turbine again carried the heaviest payload for the 3-hr flight. Fixed turbine B, which was allowed to hover at a tip speed corresponding to 0.85 of engine speed, carried about 5.5% less payload than the free turbine. Fixed turbine A, hovering at the high tip speed, carried about 7.5% less payload than the free turbine.

This payload comparison in hovering flight gives rise to an interesting question: what happened to the appreciable rotor-power advantage that was predicted for the helicopter hovering at low tip speed? Although the helicopter with fixed turbine B was operated at a tip speed of 550 fps, it was found to have only a slightly better payload capactiy for the 3-hr flight than that for fixed turbine A, which hovered at 650 fps. The answer to this apparent anomaly is found primarily in the fact that all engines were sized to have 30% reserve power at sea-level hovering tip speed. To develop this reserve at 0.85 of rated shaft speed, turbine B had to be a larger engine than either turbine A or the free turbine. Since turbine B was therefore further off-design in sea-level hovering flight, its off-design fuel consumption was appreciably poorer than that of either of the other engines. Furthermore, since a rotor torque increase accompanied the tip speed decrease, the reduction gear required for turbine B was heavier than that used for turbine A, giving an additional payload penalty.

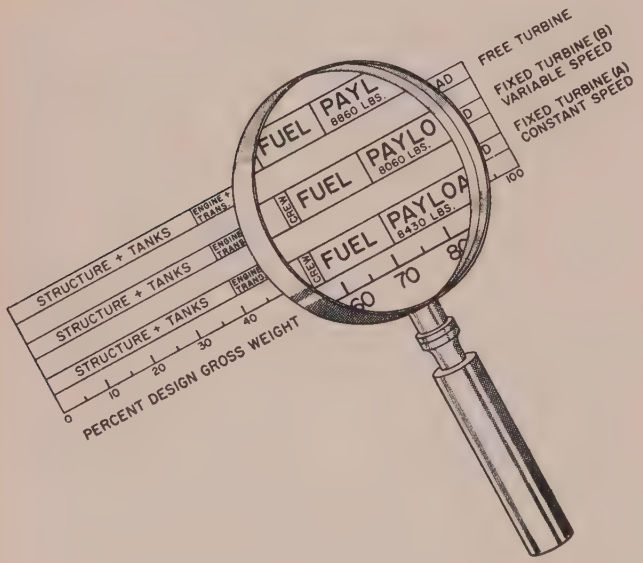

Fig. 8 – Payload comparison, fixed and free turbines

Table 1 – Performance Summary

	Ultimate Range, %	Payload for 300-Mile Mission, %	Payload for 3-Hr Hovering Mission, %
Free Turbine	100	100	100
Fixed Turbine A Constant Rotor Speed	90	95.5	92.5
Fixed Turbine B Variable Rotor Speed	85	91	94.5

The flight performance comparisons that have been given underline certain differences in the basic characteristics of fixed and free turbine powerplants. For example, when the fixed and free turbines are operated at the same fraction of rated power, the free turbine has the better specific fuel consumption, a fact reflected in its superior ultimate range. Furthermore, when either powerplant is designed to meet the requirement of low tip-speed hovering flight and high tip-speed forward flight, the free turbine engine results in a lighter powerplant because of its flatter horsepower-shaft speed characteristic. However, the performance advantages illustrated were not overwhelming. It was considered advisable to examine the control and stability characteristics of the fixed and free turbines to see if the advantage again lies with either one or the other engine type.

Control Characteristics

Two classes of such problems will be discussed. The first class is associated with large changes in operating variables, such as acceleration from idle to full power, recovery of rotor speed after a suddenly applied gust load, and the modulation of power level. The second class of problems deals with small changes in operating variables (such as are encountered in stability and control characteristics) which are studied in terms of frequency responses.

Maximum Power-Speed Characteristics – The most pertinent engine characteristics applicable to these problems are the horsepower versus rotor speed and torque versus rotor speed curves. The well-known maximum horsepower-rotor speed characteristic for the free-turbine engine was shown in Fig. 5. The oft-quoted operational advantage in a free-turbine engine of the rather flat horsepower versus rotor speed curve bears repeating. As already illustrated, this advantage allows a better choice of rotor speeds for the range that is required from hovering to maximum forward flight speed. It relaxes close control of rotor speed and provides restoring power should the rotor speed suddenly be reduced, as by a gust load.

On the other hand, the fixed turbine engine has

been pictured as having a steep, maximum horsepower versus rotor speed curve, requiring near maximum rotor speed for any appreciable horsepower and giving very little, if any, excess power at reduced rotor speeds – even to the extent of instability.

Our studies, in the main, do not bear out this gloomy picture. The calculated horsepower-rotor speed characteristic for the fixed turbine engine used in the foregoing performance studies is shown in Fig. 5. While the free-turbine engine is undeniably superior in this regard, showing a loss in power of only 4% for a 10% reduction in rotor speed, the fixed turbine engine shows a not too drastic loss of 15% in power for the same 10% rotor speed reduction. This more hopeful characteristic of the fixed turbine engine may be attributed in part to the use in our studies of an axial flow compressor which has a flatter air flow-compressor speed characteristic than that obtained using a centrifugal compressor.

Engine Acceleration and Thrust Modulation – The maximum available power curves for these engines do not reveal the ease or difficulty of realizing this power, of accelerating the engine or rotor, or of varying the thrust. For the free turbine engine, all power changes require changes in the gas generator speed. Thrust modulation is dependent on the acceleration of the gas generator rotor, and involves the very difficult problems of compressor stall and heat and combustion limits. The gas generator, like a turbojet engine, may require as much as 5-6 sec to go from idle to full speed.

It is interesting to note that the fixed turbine engine can be operated as a constant-speed machine since almost the full range of powers is available at constant rotor speed. This aspect of the fixed turbine engine may be utilized to simplify helicopter operation and control, to allow very rapid thrust modulation (as fast as the fuel flow rate and rotor blade angle can be varied), and to bypass the entire problem of rotor accelerations. Performance-wise, it has already been shown that a fixed turbine engine designed for constant rotor speed is better than one designed to hover at low speeds, because it is operated closer to its design point. For the foregoing reasons, it seems to us that the overheating problem for the free turbine engine is more critical.

Overheating is required for acceleration of the gas generator rotor in any reasonable time, and any inadvertent or emergency power overheating at maximum power would give simultaneously overspeeding. For the fixed turbine engine, overheating might be tolerated at reduced rotor speeds for transient bursts of power. Emergency power application would not involve any overspeeding.

Engine-Rotor Static Stability – So far we have discussed engine power availability in terms of engine speed and heating, and in terms of the relationship of the engine power availability to the power required by the rotor at constant flight conditions. For considerations of the stability of an engine-rotor system, the pertinent characteristics of the engine are the horsepower versus speed or, better, the torque versus speed curves at constant fuel flow. The pertinent characteristics of the rotor are the torque versus speed curves at constant blade angle. The expected characteristics of the free turbine engine are shown in Fig. 9. Static stability results when the slope of the load line is greater than that of the engine, as is the case here.

The corresponding torque versus speed curve for the fixed turbine engine has been represented in the literature as having a highly positive slope, sometimes even more positive than that of the load line. This curve implies that the fixed turbine engine rotor system is unstable. Furthermore, the performance line (constant temperature) and the stability line (constant fuel flow) are sometimes used interchangeably. Our studies of a fixed turbine engine are shown in Fig. 10 for the torque speed curves at constant fuel flow and constant temperature, along with the load line. No unstable tendency is indicated. Even where the temperature line has a positive slope, the fuel flow line may be flat or have a negative slope. There is no reason for suspecting the fixed turbine engine to have less stability than a turbine-propeller engine.

The stabilizing characteristic of the fixed turbine engine is an inherent feature of a compressor-burner-turbine combination. The free turbine engine has all its damping action in the power turbine and utilizes almost none of the gas generator damping. For the fixed turbine engine shown, the operating point chosen would influence the slope of the torque-speed curve at that point. It seems that the rotor can be matched to the engine for best per-

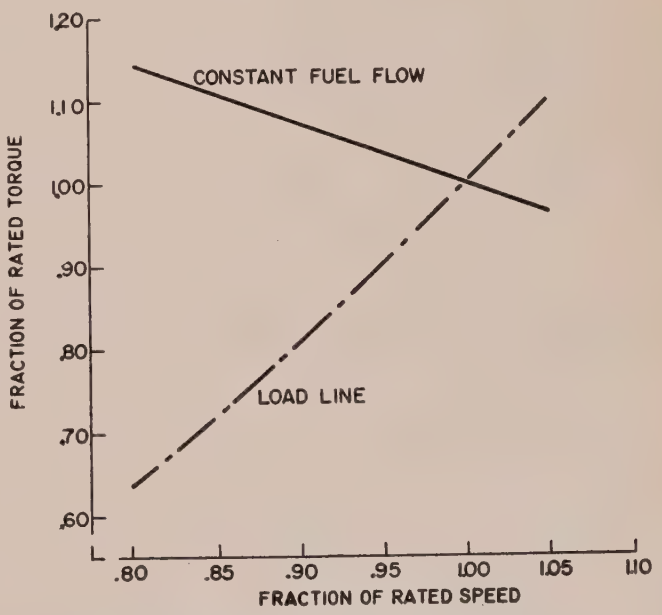

Fig. 9 – Rated torque vs. rated speed, free turbine

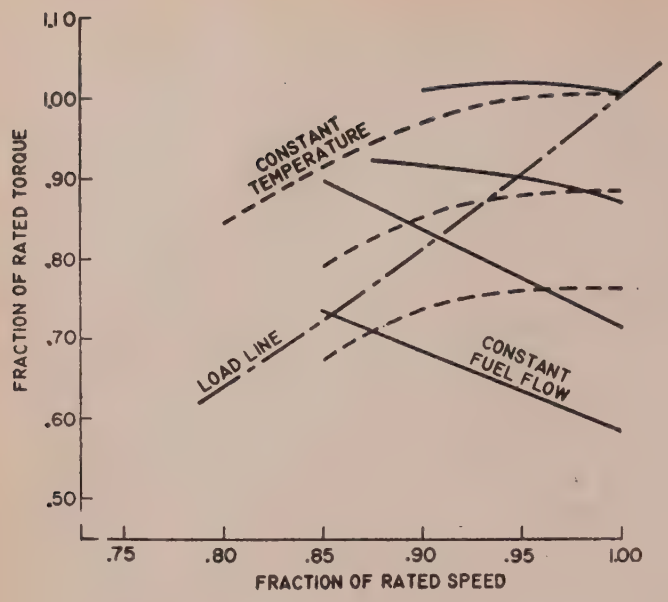

Fig. 10 – Rated torque vs. rated speed, fixed turbine

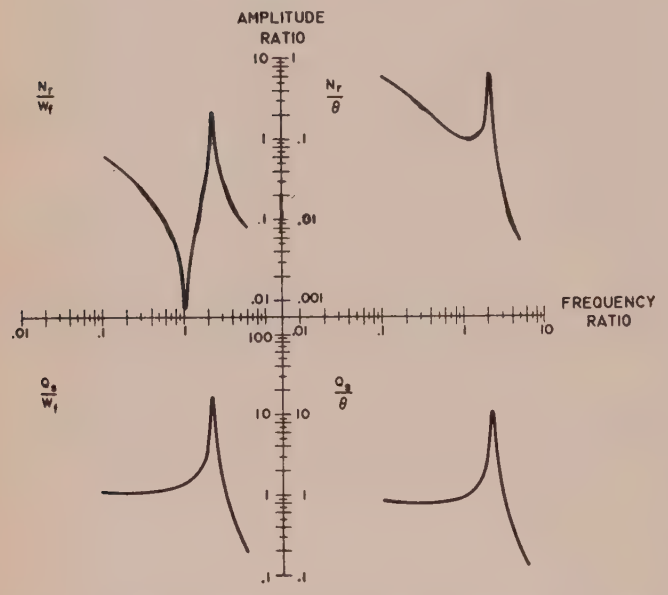

Fig. 11 – Frequency response of free turbine (undamped lag hinge)

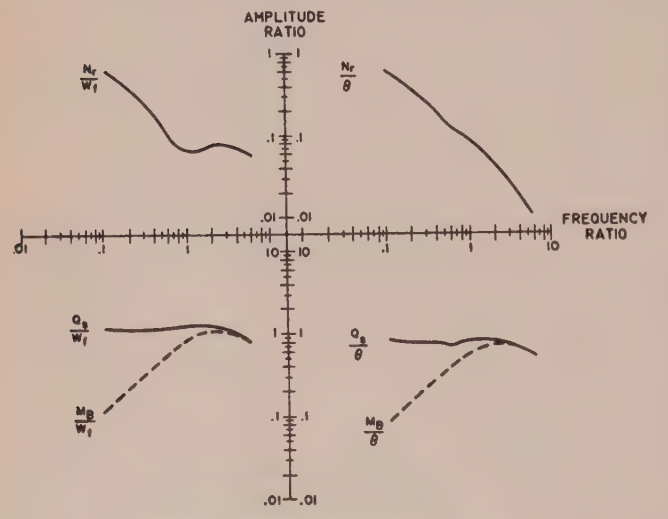

Fig. 12 – Frequency response of free turbine (damped lag hinge)

formance, as already discussed, without introducing static stability problems.

Engine-Rotor Frequency Responses – In order to further investigate stability and controllability of these engine-rotor combinations, some frequency response calculations were made. A lag-hinged rotor was assumed and a simplified case of hovering with neglected flapping was assumed. The question arises in a gas-turbine-driven rotor as to whether the lag resonance can be damped by the natural damping action of the engine in the presence of its high inertia.

Fig. 11 shows the frequency response characteristics of the free turbine system for the case of no damper on the lag hinge. Shown are the responses of rotor speed to fuel flow and blade angle, and shaft torque to fuel flow and blade angle. The system is quite resonant at a frequency ratio of 2.2/1 (the frequencies shown being relative to the undamped natural frequency of the lag-hinged rotor blade).

The speed responses show a corner frequency ratio of 0.08/1 (corresponding to a time constant of 2.5 sec for the configuration studied) and a resonant point at the frequency ratio of 2.2/1. The rotor speed to fuel flow response has an antiresonant point at the frequency ratio of 1/1. The shaft torque responses show a large resonant peak at the frequency ratio of 2.2/1.

When a damper is applied to the lag hinge and is set for a damping ratio of 1/2 on the characteristic equation for lagging, the results are as shown in Fig. 12. The resonance has been completely damped out. There now seems to be no stability or resonant problem here for this amount of damping. But the introduction of a lag damper causes a torque to appear at the blade root. This blade torque increases with increasing frequency and beyond a frequency ratio of 2/1 the entire shaft torque is transferred to the blade root. Both the shaft and blade moments, however, fall off at the still higher frequencies.

The frequency response curves for the fixed turbine system, shown in Fig. 13, are similar to those for the free turbine. For the sake of comparison, the slope of the torque-speed curve for the fixed turbine engine was made identical to that for the free turbine engine. Fig. 13 is the case of no damping on the lag hinge. The fixed turbine system is slower (that is, responds at lower frequencies) than the free turbine system. The time constant is 4.5 sec. These time constants are sensitive to the slope of the torque-speed curves and because of their variability, already discussed, the faster response (1.8/1) of the free turbine system may not be general. Resonance occurs at a frequency ratio of 1.4/1. The resonance is not as bad for the fixed turbine, probably because it occurs at a lower frequency where engine damping can be more effective.

When the same damper as was used for the free turbine system is applied to the fixed turbine en-

Table 2 – Control Summary

	Hp Loss, 10% Rotor Speed Decrease, %	Thrust Modulation	Over Temperature	Speed Control	Static Stability	Time Constant, sec	Lag Hinge Resonance	Shaft Torque Response
Free Turbine	4	Slow	Critical	Gas generator rotor speed and acceleration control required	Excellent	2.5	Requires more damping	—
Fixed Turbine	15	Constant-speed machine	Can be bypassed or used to advantage	—	Adequate	4.5	Requires damping	Sensitive to rotor loads

gine system the results are as shown in Fig. 14. Again the resonance is eliminated and the system with this much damping would give no stability or control problem. The blade torque becomes equal to the shaft torque beyond a frequency ratio of 1.5/1. The determination of the proper amount of damper action is beyond the scope of this paper.

From the foregoing frequency response characteristics we can surmise some of the transient response characteristics. For transients initiated by a step change in either fuel flow or blade angle, the time constants are 2.5 sec for the free turbine system and 4.5 sec for the fixed turbine system. The shaft torque will not overshoot for the free turbine engine. For the fixed turbine engine, the shaft torque will not overshoot in response to fuel flow but will overshoot about 100% in response to blade loads.

The frequency response curves for the free turbine engine assumed no coupling between gas generator speed and free turbine speed. A small amount of coupling would not affect these curves too much but would introduce a new problem for the free turbine engine: namely, that gas generator speed can be disturbed by the rotor. It seems that for this reason and for those previously mentioned, the gas generator would require at least an overspeed control.

Summary of Operational and Control Comparisons – Comparisons of the operations and controls herein discussed for the free and fixed turbine engines are summarized in Table 2. The loss in maximum available horsepower with reduced rotor speed for the fixed turbine engine may not be so drastic as to rule it out. The free turbine engine requires rotor accelerations with their attendant problems for thrust modulation, whereas the fixed turbine can, and probably should, operate as a constant-speed machine. It seems that overheating and overspeeding problems are more severe for the free turbine engine, probably requiring at least an overspeed governor on the gas generator rotor.

The stability characteristics of the free turbine may be superior to those of the fixed turbine. No unstable tendencies were discovered, however, for the several fixed turbine engines studied. Frequency response studies showed that the free turbine engine was faster and more resonant than the fixed turbine. The results showed that shaft torque response would be more sensitive to rotor loads for the fixed turbine engine. For both engines, lag hinge dampers would be required.

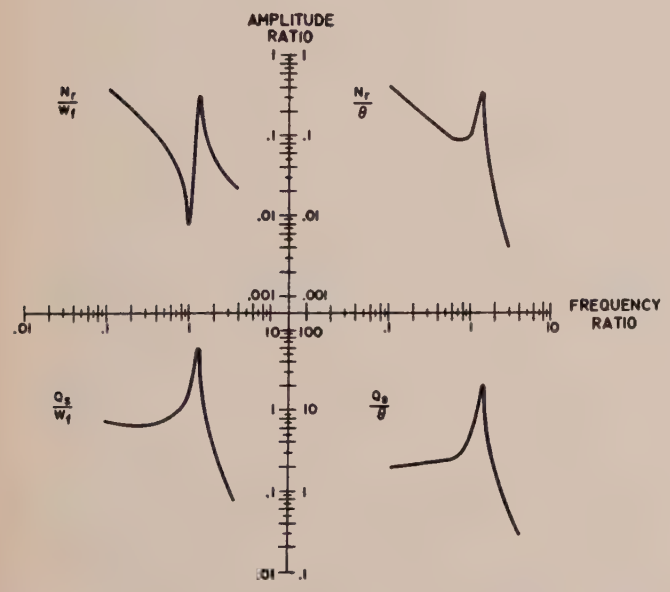

Fig. 13 – Frequency response of fixed turbine (undamped lag hinge)

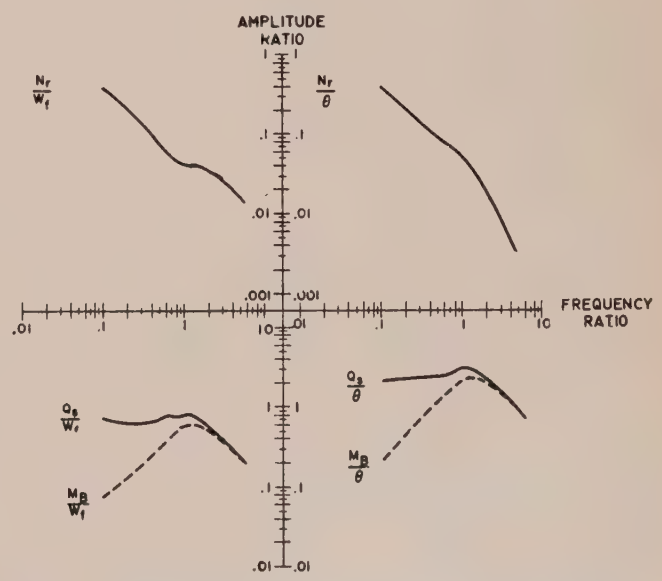

Fig. 14 – Frequency response of fixed turbine (damped lag hinge)

A NEW technique is described utilizing a dynamic micrometer to observe valve motion during actual operation under simulated highway conditions.

Using this instrumentation, studies were conducted on the effect on valve life due to dynamic sticking resulting from additive concentration, valve motion, and valve flexure. The test data indicate that exhaust-valve burning in passenger-car engines appears to be due principally to valve-face corrosion.

Instrumentation for

THE GENERAL trend toward high-performance overhead-valve engines in passenger automobiles has resulted in increased emphasis on proper exhaust-valve performance. Changes in valve-train design and materials and the increased use of additives in fuels and lubricants have introduced new variables in exhaust-valve studies. Published data on this subject have shown a lack of agreement among investigators as to the causes of and factors governing exhaust-valve burning.[1, 2, 3] Absence of correlation between road tests and dynamometer tests is particularly notable.

Studies in this laboratory indicate that exhaust-valve life of almost any duration can be obtained, depending on the average power level employed, as shown for engine A in Fig. 1. Realistic valve life in terms of road operation was achieved in a laboratory cyclic test designed to simulate power demands of highway driving recorded during a passenger-car road test in which valve burning was experienced. Valve burning was evident in engine A after 250 hr under simulated highway test conditions. This was in excellent agreement with the 15,000-mile (300-hr) valve life in this engine during the actual road test.

Theories advanced previously to explain the phenomenon of exhaust-valve burning include: (1) guttering and cracking of deposits on valve faces and seats, with resultant local leakage causing burning,[1] and (2) improper valve seating due either to distortion of valves and seats or accumulation of stem deposits, resulting in local leakage.[4] Inspection of failed valves from both actual and simulated highway tests did not substantiate the deposit-flaking mechanism because in many cases deposits were negligible on both faces and seats. Furthermore, deposits on valves from simulated highway tests showed evidence of being fluid at operating temperatures, as illustrated in Fig. 2. The presence of hard, black deposits with striations on the port ends of the valve stems (Fig. 3), indicating possible valve sticking, appeared to substantiate the improper seating hypothesis. The evidence was not conclusive, however, for no interference between valve stems and guides could be detected at room temperature.

---

[1] "Exhaust-Valve Burning as Affected by Engine Oil Composition," by H. C. Mougey. ASTM Symposium, June 28, 1949.

[2] "Road Test Investigation of Exhaust-Valve Burning," by W. E. Kuhn, P. A. Binda, and W. A. Pendergast. ASTM Symposium, June 28, 1949.

[3] "Exhaust-Valve Burning in Dynamometer and Road Tests," by M. M. Roensch and H. J. Chalk. ASTM Symposium, June 28, 1949.

[4] "Valve Burning as Affected by Material, Design, and Operating Conditions," by A. T. Colwell. ASTM Symposium, June 28, 1949.

Valve-Burning Studies

W. D. Sims, Shell Oil Co.

This paper was presented at the SAE Golden Anniversary Summer Meeting, Atlantic City, June 14, 1955.

The relative merits of the two hypotheses were further examined by means of single-cylinder engine tests. The deposit-cracking theory was invalidated by experiments in which a 1/32-in. saw cut across the valve face failed to induce burning. On the other hand, relieving the valve stem to minimize interference of stem deposits with the port end of the valve guide markedly extended valve life.

In order to investigate the effect of stem-deposit interference more fully, a study was made of means of observing valve motion during actual operation under simulated highway-test conditions.

Valve-Test Instrumentation

Two systems of instrumentation employed by other investigators were considered; mechanical lash-measuring techniques utilizing a strain gage, and high-speed cinematography similar to that applied to abnormal-valve-motion studies of valve-spring surging. Lash measurement was not applicable for use with hydraulic lifters. Experiments with high-speed motion pictures revealed severe limitations in discerning the true valve motion during the final 0.050 in. of closing.

The shortcomings of previously employed meth-

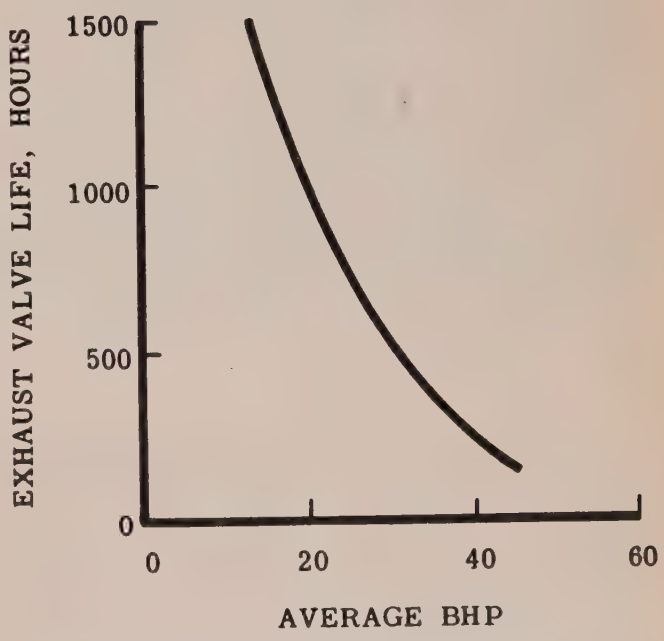

Fig. 1 – Variation of exhaust-valve life with average bhp output for 6-cyl ohv engine (engine A)

Fig. 2 – Example of exhaust-valve face deposit resulting from simulated highway test

Fig. 3 – Condition of exhaust valves after simulated highway test

ods made it necessary to consider a new approach. Emphasis was placed on selecting a system which would not influence valve motion and still permit the use of standard engine parts. It was necessary that the apparatus be rugged and easy to operate, applicable to the simulated highway-test procedure, and provide magnification of those portions of valve travel very near the closed position. Finally, it was desirable to use available equipment if possible.

The "dynamic micrometer" made by Electro

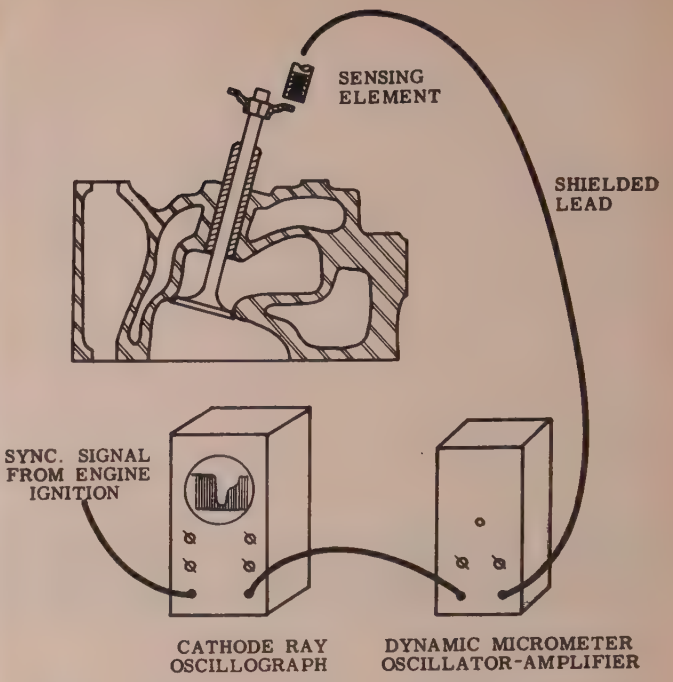

Fig. 4 – Schematic layout of dynamic micrometer instrumentation

Products was selected. This electronic device was designed for observation of shaft runout, turbine-wheel growth, or vibration in turbine-type equipment. A schematic layout of the instrument and accessories is shown in Fig. 4. The dynamic micrometer consists of a reluctance pickup or sensing unit mounted in a screw micrometer. It is supplied with a known signal from an oscillator furnished with the assembly. The output signal, varied by proximity of magnetic metal to the pickup, is observed on the screen of a cathode-ray oscilloscope.

In applying the instrument to engine A, the pickup is mounted on a bar fastened along the cylinder head (see Fig. 5). The support is machined to keep the axes of the pickup and exhaust-valve stems parallel. Six stations are established to allow locating the pickup adjacent to each exhaust valve. The metal face registering with the active end of the pickup is the valve-spring washer. The oscillograph pattern height changes with clearance between the washer and pickup, as shown in the calibration curve, Fig. 6. Oscillograph sweep is synchronized by the engine ignition, and motion can be related to crank angle.

The technique employed with the dynamic micrometer consists of observing the motion of all exhaust valves at 8- to 24-hr intervals. The engine is operated at simulated highway-test conditions during observation. At each station the pickup and micrometer assembly is bolted to the mounting bar, and the micrometer screw adjusted to obtain a maximum pattern height of 3 in. The oscilloscope

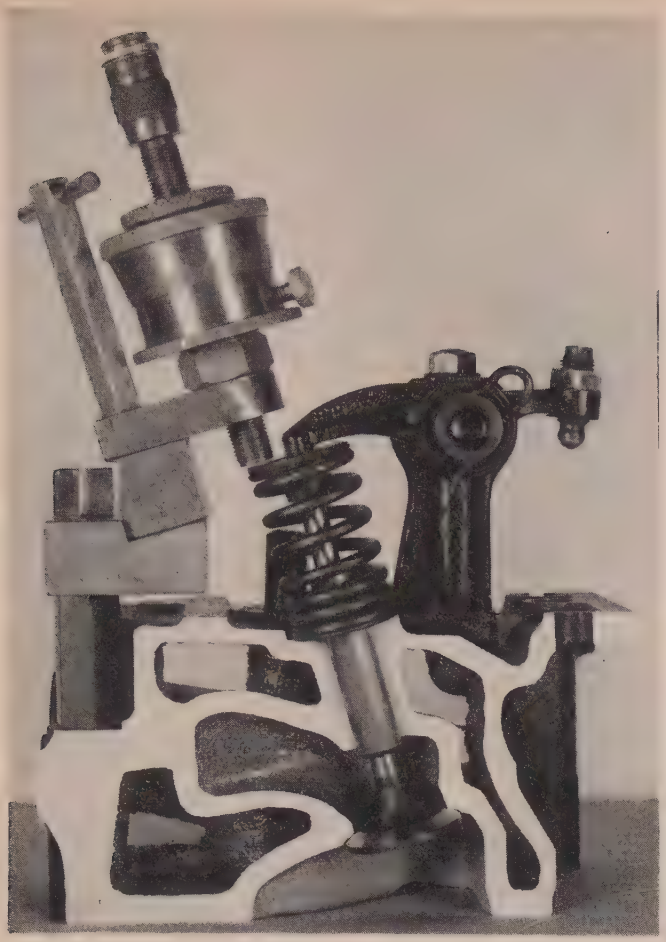

Fig. 5 – Cross-section of engine A cylinder head showing dynamic micrometer installation

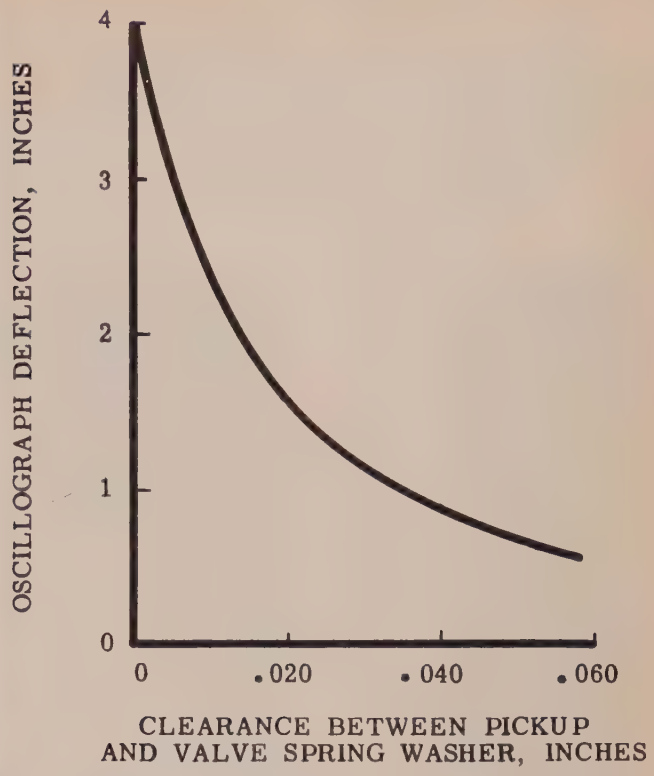

Fig. 6 – Calibration curve for dynamic micrometer as applied in valve-burning tests

gain is preset so as to provide this pattern height for a clearance of 0.005 in. Valve motion is related to the calibration curve (Fig. 6) for determination of axial displacements.

Reference to the calibration curve shows that the instrument is most sensitive with a small clearance between pickup and object. While this characteristic is highly desirable in permitting observation of movements as small as 0.0005 in., it requires extreme rigidity in the mounting. A smooth surface finish on the valve-spring washer was found necessary in order to obtain a reproducible pattern height versus clearance relationship.

In addition to observation of valve motion, any dimensional changes due to seat-deposit accumulation or valve stretch can be followed with the dynamic micrometer. A fixed reference point such as the pickup mounting bar is established before each reading to obtain such measurements.

Installation on engine B is shown in Fig. 7. Individual pickups are supplied for each valve in the left cylinder bank. An 8-point switch provides selection. The pickups are mounted through a rigid platform integral with the rocker cover and are adjusted to suitable clearances with the respective valves at the start of the test. Amplifier calibration

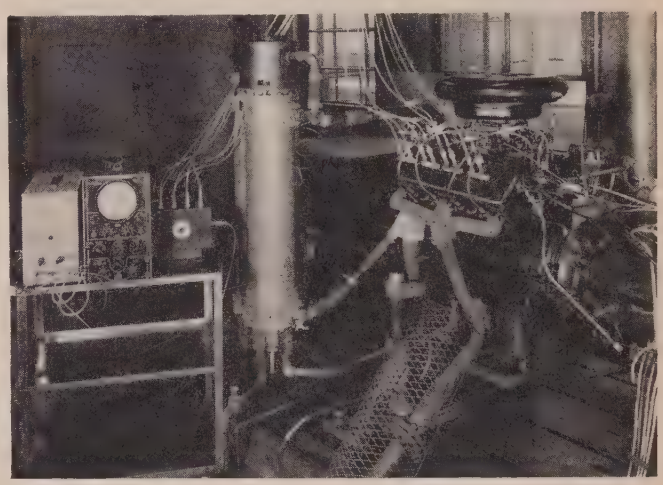

Fig. 7 – Installation of dynamic micrometer instrumentation in engine B

is maintained through the use of an external pickup and micrometer assembly.

Valve Motion Observations

Tests on engines A and B have shown the dynamic micrometer to be accurate, rugged, and dependable for the observation of valve motion. In addition to the necessity for rigid mounting and good surface finish mentioned above, the only caution found necessary with the instrument as used in these tests was to make observations at speeds

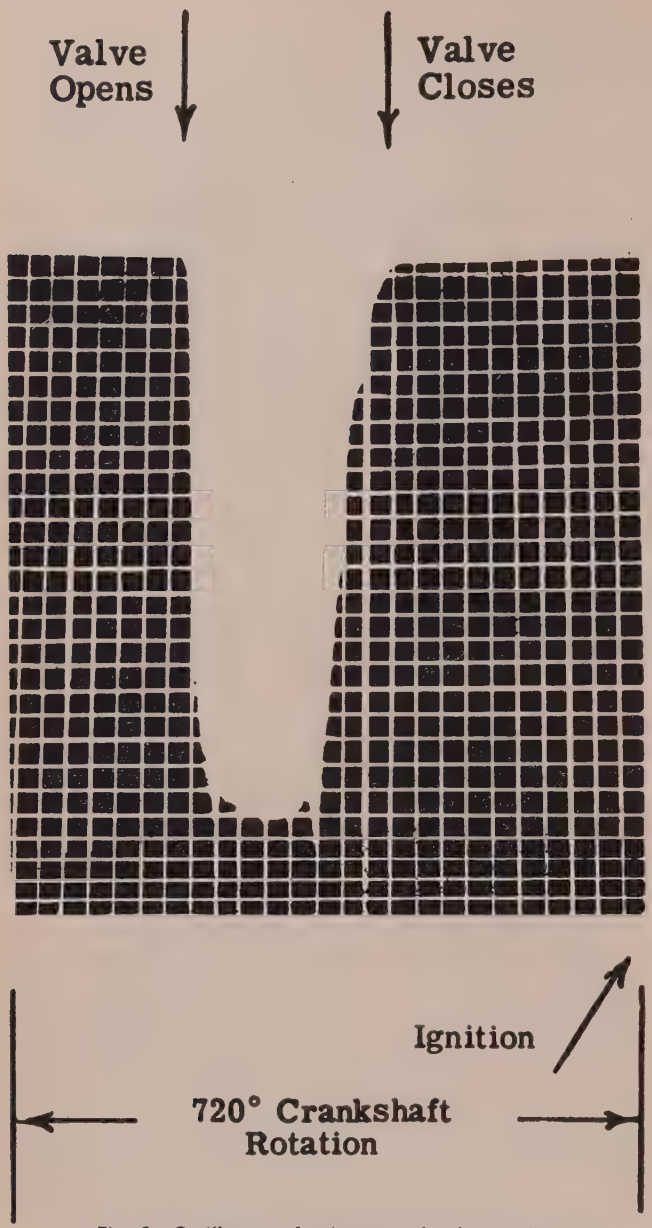

Fig. 8 – Oscillogram showing normal valve motion

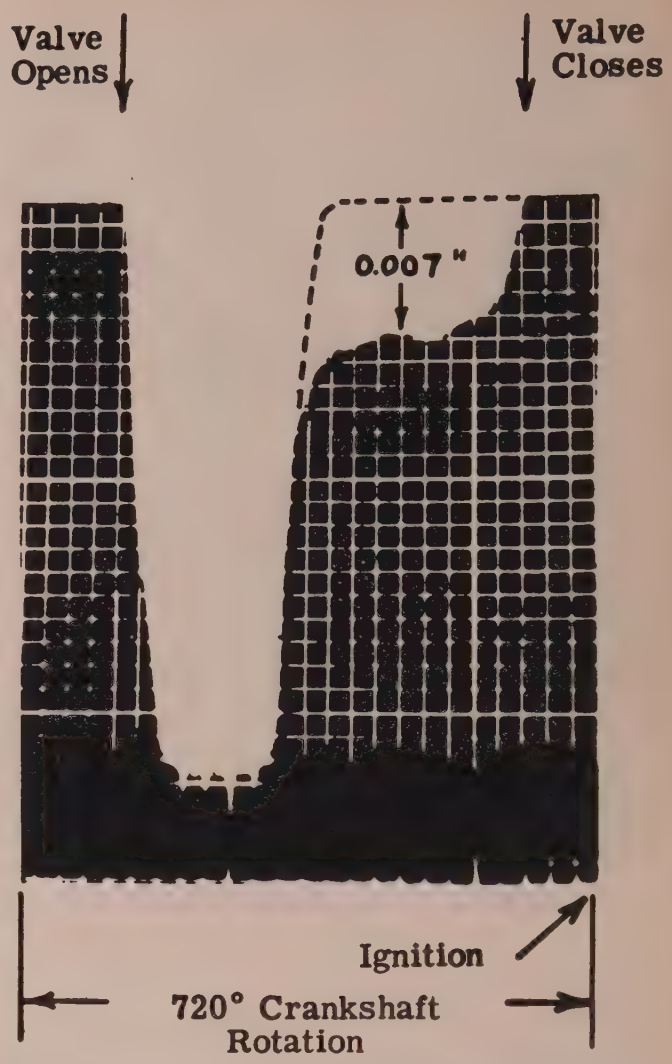

Fig. 9 – Oscillogram showing exhaust valve sticking 0.007 in. from seat until compression closes it. Dashed line indicates normal closing

below the resonant frequency of the valve springs. If spring surge is encountered, the motion of the valve-spring washer – which is the actual point of observation – is not the same as that of the valve.

Dynamic micrometer observations of typical exhaust-valve motion in engine A under simulated highway conditions are illustrated in photographs of the oscillograph trace, Figs. 8, 9, and 10. The pattern in Fig. 8 is for a properly operating valve. The sequence of events, from left to right, is as follows: (1) the trace originates at the point of ignition with the valve closed, (2) as the valve opens, the trace drops rapidly until the valve passes beyond the range of observation, (3) as the valve closes to full contact with the seat the trace rises smoothly to the original pattern height and remains so to the end of the cycle. The pattern for a sticking valve is similar in opening, but note in Figs. 9 and 10 that the valve does not return to its seat immediately in a smooth stroke. Instead, the valve essentially stops before reaching its seat. In the instances shown it remains off the seat throughout the intake stroke. Seating is accomplished by increased cylinder pressure during the compression stroke. In more severe instances compression pressure has been found to be insufficient to close the valve, closing then being induced by firing pressure. Occasionally the valve has remained off its seat during the entire cycle.

From the standpoint of engine roughness, sticking is not discernible until the phenomenon has progressed so far that a valve is off its seat at the time of ignition. Power loss is indicated by decreas-

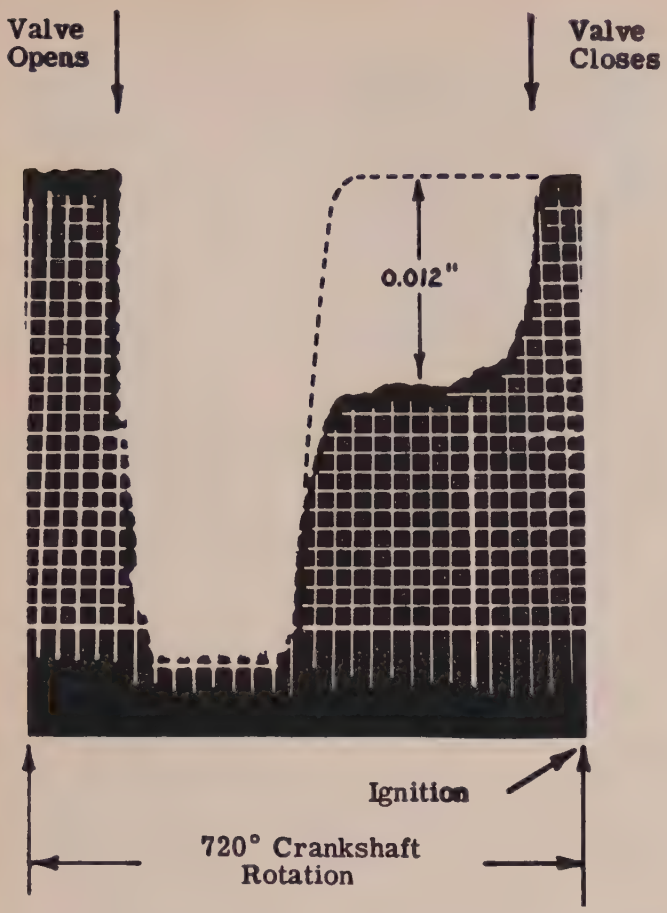

Fig. 10 – Oscillogram showing exhaust valve sticking 0.012 in. from seat until compression closes it. Dashed line indicates normal closing

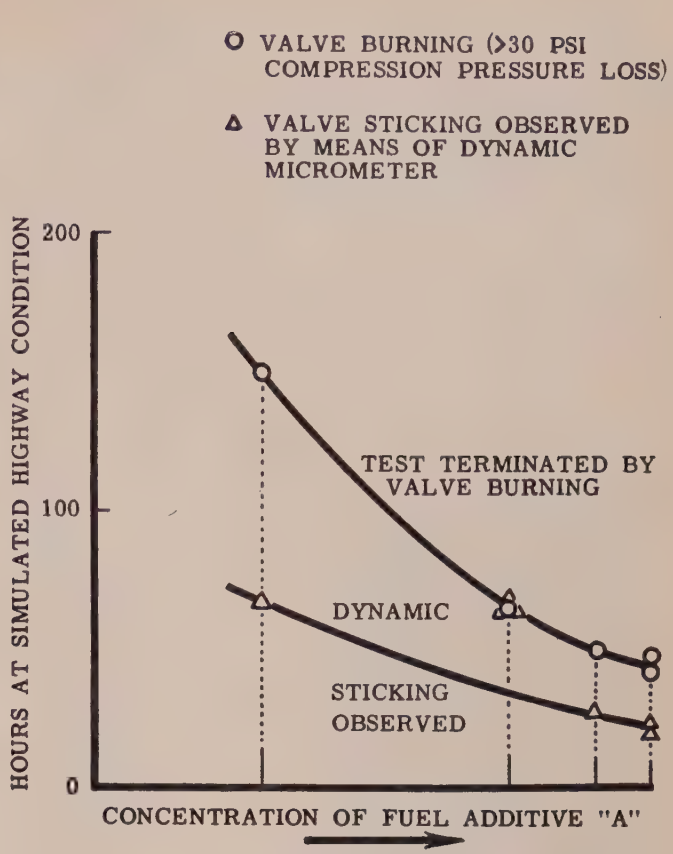

Fig. 11 – Variation of valve life as affected by dynamic sticking with concentration of fuel additive A under simulated cyclic highway tests

ing manifold vacuum whenever valves remain open until closed by combustion pressure.

Relation of Dynamic Sticking to Exhaust-Valve Life

The relation between dynamic sticking and exhaust-valve life in engine A operated under simulated highway conditions is shown in Fig. 11. Dynamic sticking and valve burning are shown as a function of the concentration of a commonly-used fuel additive A. It is seen that as concentration is increased, the test duration before observation of dynamic sticking and valve burning is reduced.

Additives can have a complex effect on valve life, necessitating the thorough evaluation illustrated in Fig. 12. Here it is seen that the concentration of commercial fuel additive B is critical with respect to valve life. Initial incremental additions of this material reduce test time before dynamic sticking and result in shortened valve life. Further increases in concentration, however, minimize deposits responsible for dynamic sticking, thereby prolonging valve life.

Applications of the dynamic micrometer technique to engine B have shown interesting differences in valve motion compared to engine A. Photo-

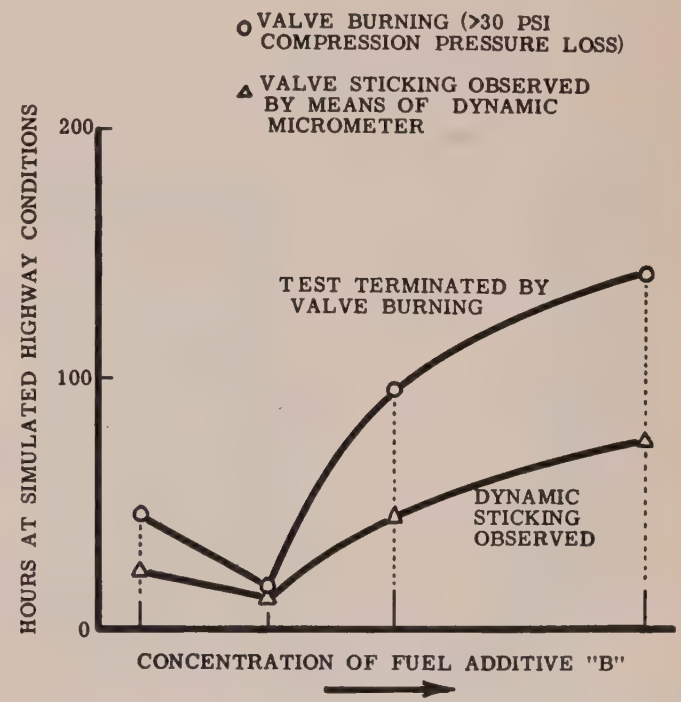

Fig. 12 – Variation of valve life as affected by dynamic sticking with concentration of fuel additive B under simulated cyclic highway tests

graphs of oscillograph patterns of inlet and exhaust valve traces with newly installed valves are shown as Figs. 13 and 14. A peak appears in each figure shortly after ignition. This peak is due to displacement of the valve stem toward the pickup resulting from flexure of the valve head under combustion pressure. The amplitude of this movement is of the order of 0.003 in. for the inlet valve and 0.001 in. for the smaller exhaust valve under high-output conditions. Similar flexure was not observed in the 6-cyl engine due mainly to the stiffer valve design used, and, to a lesser degree,

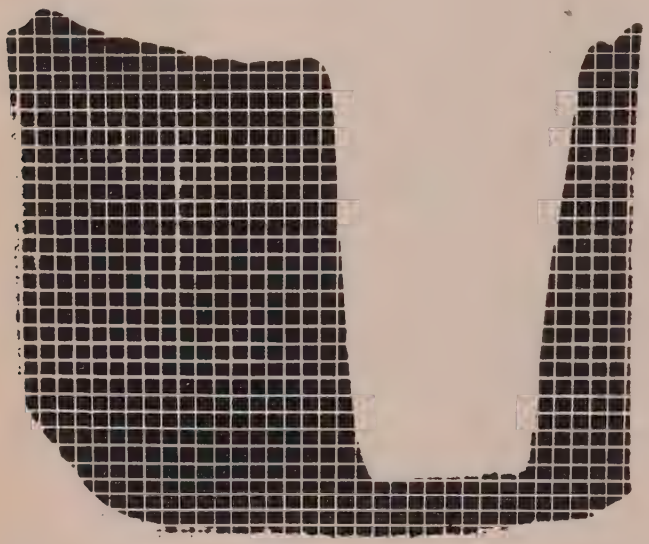

Fig. 13 – Oscillogram of normal inlet-valve motion in engine B under simulated highway test conditions

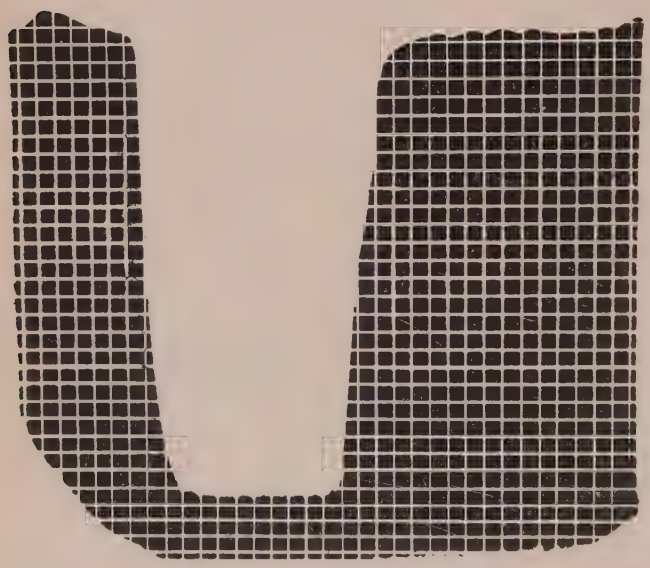

Fig. 14 – Oscillogram of normal exhaust-valve motion in engine B under simulated highway test conditions

Fig. 15 – Oscillogram of inlet-valve motion in engine B after 200 hr of operation under simulated highway test conditions

because of lower peak cylinder pressures resulting from lower compression ratio.

The manufacturer of the valves used in engine B claims that provision for flexure provides improved valve sealing by allowing conformance with the seat, with resulting extended valve life. No valve failures have been encountered in this engine in approximately 400 hr (or 26,000 equivalent miles), under simulated highway-test conditions. However, valve motion traces shown in Figs. 15 and 16 reveal loss of flexure in the exhaust valve, indicating that deposits on exhaust-valve stems can nullify benefits of flexible valve design by preventing valve-stem motion beyond the normal valve-closed position.

Mechanism of Valve Burning

As interpreted with the aid of the dynamic micrometer, the mechanism of exhaust-valve burning in passenger cars appears to be principally one of valve-face corrosion. It is known that most combustion-chamber deposits become markedly corrosive to metals at temperatures approaching their melting point. Under normal operating conditions with properly seating valves, valve-face temperatures are sufficiently below the melting points of the deposits and corrosion proceeds slowly. When dynamic sticking occurs valve cooling by seat contact is affected and valve temperature increases, highly accelerating valve-face corrosion.

Little valve corrosion is experienced in engine A operated at simulated highway conditions with normal valve seating. Use of valve rotators to prevent dynamic sticking resulted in valve life greater than 480 hr. Without rotators, however, dynamic sticking was observed after 24 hr of operation and valve-face corrosion was evident after 48 hr.

Valve temperatures in engine A measured by

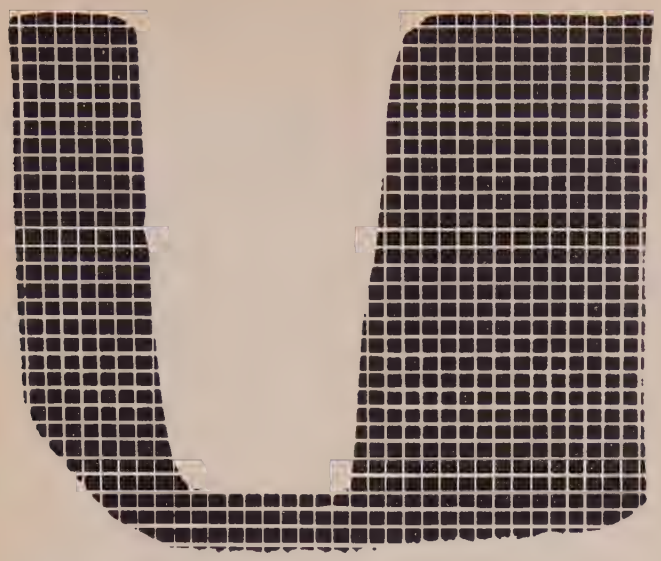

Fig. 16 – Oscillogram of exhaust-valve motion in engine B after 200 hr of operation under simulated highway test conditions

optical pyrometry are shown in Fig. 17. The temperatures at continuous high-power and simulated highway-test conditions are 1250 and 1150 F, respectively. Thus, the difference between satisfactory valve life and extremely short life is of the order of 100 F. The importance of this temperature difference is indicated by S. D. Heron,[5] who states that "50 F reduction in valve temperature is well-worth working for" (by the engine designer) in terms of valve life.

The process whereby valve temperature is increased by dynamic sticking is illustrated by Fig. 18. The temperature-distribution pattern in this figure was determined using a hardness-relaxation technique. (Measurements by Thornton Research Centre, Shell Research, Ltd.) Whereas optical pyrometry indicated a valve temperature of 1150 F under simulated highway-test conditions, it is seen that the face temperature was of the order of only 850 F because of cooling via the valve seat. With seat contact loss due to dynamic sticking, the valve-head temperature will become more uniform, the face temperature approaching that of the portion of the valve visible to the optical pyrometer. Combining the Thornton observation that 80% or more of valve cooling is accomplished by seat contact and the demonstrated reduction in seat-contact duration shown in Figs. 9 and 10 due to dynamic sticking – from 60% of the total cycle to 30% – it is obvious that the overall valve temperature will increase. In the case of engine A operated under simulated highway-test conditions, the resulting increase in face temperature was sufficient to subject the exhaust valves to accelerated corrosive attack by the deposits present.

[5] "Exhaust-Valve Temperature, a Study," by S. D. Heron, R. V. Kerley, and A. E. Felt. Ethyl Corp. Report AR-219, Aug. 20, 1953.

Conclusions

The dynamic micrometer has proved to be a simple, durable, and accurate device for observing valve motion in operating engines. Information

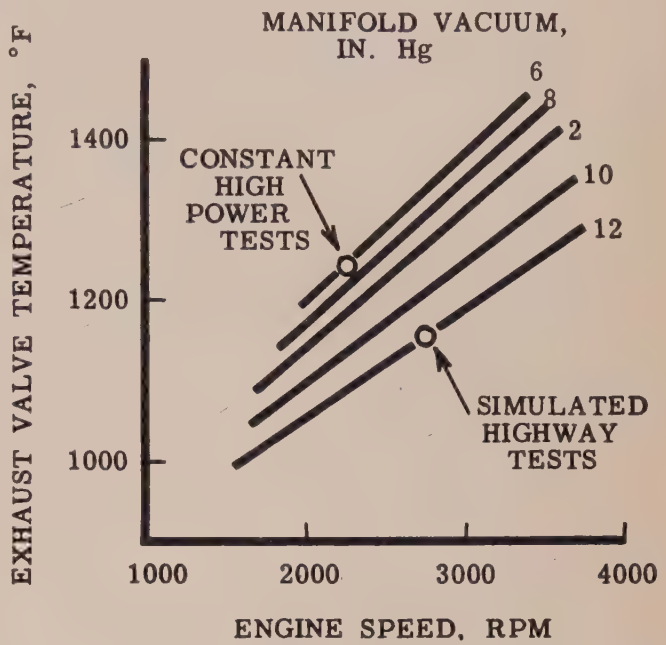

Fig. 17 – Exhaust valve temperature versus speed in engine A from optical pyrometer observations

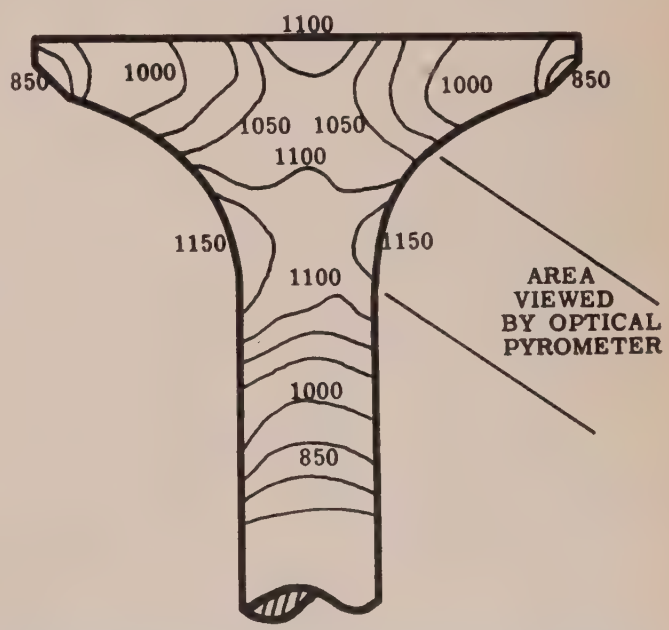

Fig. 18 – Approximate temperature distribution in exhaust valve in engine A. Valve motion is normal under simulated highway test conditions, and temperature field is in deg F

obtained with this instrument has contributed materially to the understanding of the mechanism of exhaust-valve burning and the factors which determine valve life. Data presented here have illustrated means of improving valve life through proper selection and application of fuel additives which minimize the effects of valve-stem deposits causing dynamic sticking.

Observation of exhaust-valve motion by means of the dynamic micrometer has demonstrated the value of valve-stem relief and valve rotators in prolonging valve life. The technique is also applicable to the study of other factors which may affect valve performance, such as dimensional changes during engine operation and intake valve-stem and -guide rusting. Its principal advantage is the ability to assay performance while the engine is operating, as opposed to the usual attempts at reconstructing the sequence of events by inspection of parts after test. In addition, information obtained during engine operation often permits termination of tests before destruction of parts. The simplicity of the installation on engine B, where a pickup was provided for each valve mounted in rigid rocker covers, can be extended to include engines installed in automobiles or trucks.

APPENDIX

Exhaust-Valve Test Procedure

Test Type	Simulated Highway Cam-Controlled	
Engine	6-cyl ohv	V-8 ohv
Cycle, min		
Idle Condition	1	1
Simulated Highway Condition	12	12
Idle Condition		
Rpm	500–550	450–500
Manifold Vacuum, in. of Hg	17–20	16–18
Simulated Highway Condition		
Rpm: max	3250	3400
min	1800	1600
average	2800	2900
control	3200	3200
Bhp: max	38	40
min	12	12
average	30	32
control	34	36
Manifold Vacuum, in. of Hg		
max	20	22
min	3	5
average	10	15
control	12	17
Oil Temperature, F	215	200
Coolant Out, F	145	143
Air/Fuel Ratio	[a]	[a]

[a] Carburetor setting standard for engine.

DISCUSSION

Valve Rotation Increases Valve Life

– R. V. Kerley and M. A. Remondino
Ethyl Corp.

WE HAVE not had experience with this instrumentation, hence we cannot comment directly on its application to valve studies. It does appear, however, that this paper serves to add another tool to the kit which the engine and petroleum industry laboratories uses in evaluation of their products.

Regarding valve burning and its causes, there are several areas in which we agree with the author's analysis, and some others in which our findings differ. We agree that the concentration of additive is very important. It has been conclusively demonstrated in our own laboratory engines, which were equipped with valve rotators, and in passenger-car road tests where valve rotators were not used, that concentration effects such as those shown in Fig. 12 are real[a].

We believe sufficient evidence has been accumulated to adequately support each of the following as an important mechanism leading to valve burning, and to indicate that no one of these mechanisms will explain all instances of valve burning:

1. Guttering and cracking of deposits on valve faces (or seats) with resulting local leakage and burning.
2. Improper valve seating due to distortion of the cylinder head (or block) which prevents proper seating[a].
3. Accumulation of valve-stem (or valve-guide) deposits preventing proper valve seating[b].
4. Chipping or cracking of the degradation products of valve-face material leading to local leakage and burning.
5. Loss of clearance in the valve-operating mechanisms due to valve recessing which leads to operation with partially open valves and consequent burning.
6. The "old-fashioned" type of advanced surface ignition termed preignition in aircraft circles[c].

Of course, overheating of the valves is the common denominator in all these mechanisms.

Figs. 13 and 14 are of considerable interest since the early peak indicates a displacement of the valve stem toward the pickup "due to flexure of the valve head under pressure of combustion." This peak does not exist after some engine operating time has elapsed, as shown in Fig. 16, and the author attributes this to deposits on the valve stem preventing the downward movement of the stem. While this explanation is a possibility, there are other explanations which might apply on the basis of existing data. Flexing of the valve which can result in movement of the stem as described can occur in two different manners:

1. The center of the valve head may move down while the face remains fixed. This is similar to the motion of a flexed diaphragm, as shown in Fig. A (left). The author implies this type of flexing.
2. The center of the valve head may move down while only one side of the valve head remains fixed by its seat and the other side of the valve head moves down until it contacts its seat (Fig. A, right).

Since the flexible valve's objective is to permit the valve face to contact its seat and seal the port, flexibility of the valve throat area is most important. As shown in

[a] "Fuel Additives and Engine Durability," by A. E. Felt, R. V. Kerley, and H. C. Sumner. Paper presented at SAE National West Coast Meeting, Los Angeles, Aug. 18, 1954.

[b] See SAE *Quarterly* Transactions, Vol. 1, April, 1947, pp. 252-265: "Light Aircraft Service Experience with All-Purpose Fuel," by R. V. Kerley.

[c] See SAE Transactions, Vol. 62, 1954, pp. 24-31: "Uncontrolled Combustion in Spark-Ignition Engines," by S. D. Heron.

Fig. A (right), the valve stem must bend for the port to be sealed when the cylinder head distorts. When valves are not rotated, it is quite common to find that valve heads have bent relative to the centerline of the stems to provide proper seating. Similarly, valve breakage in the throat area has been a real problem in some engines incorporating both rotation and stiff valves. It is obvious that the deflection peak noted in Fig. 14 would no longer exist once the valve had been permanently bent until good face-to-seat contact was complete.

Our experience parallels the author's in that very marked increases in valve life have been obtained by valve rotation. We have attributed part of this improvement to the elimination of valve-stem sticking. We believe it is equally important that deposits and scale are more effectively removed from the faces and seats due to movement of the face relative to the seat. These cleaner surfaces result in better heat transfer from valve face to seat.

Regarding the seating delay period illustrated in Figs. 9 and 10, this may very well indicate dynamic sticking as concluded by the author. It might also indicate a period during which deposits may be squished or crunched from between the valve face and seat. We are convinced, however, that valve-stem sticking in either dynamic or static form does not completely explain the results of the additive concentration effect similar to that in Fig. 12. Our conviction is based on data we have obtained in a single-cylinder laboratory test engine, in a multicylinder passenger-car engine on the dynamometer, and in another make of passenger car operated on the road.

Author's Closure To Discussion

WE are pleased to note that the results of exhaust valve performance tests employing the dynamic micrometer are in relatively good agreement with those obtained by other investigators employing traditional test techniques.

Regarding the mechanisms of valve burning enumerated by Messrs. Kerley and Remondino, we agree that valve failures may result from mechanisms other than dynamic sticking. However, we feel that in many instances valve burning has been ascribed to guttering and cracking of deposits on faces and seats, inadequate tappet clearance, and the like, when dynamic sticking of the valves due to the interference of stem deposits with proper seating was the actual precursor to failure. This is particularly true where valve temperatures are within the structural limitations of the valve materials, yet failure occurs after relatively short operating periods.

For example, as described in the paper, dynamic sticking followed by valve failure was observed after relatively short operating periods with engine A. The use of valve rotators on this engine permitted a tenfold increase in operating time with no evidence of valve sticking or burning being observed. Inspection of the valves at the conclusion of the test revealed a marked reduction in stem deposits, although the deposit accumulation on the valve faces was much heavier than that noted previously in the shorter tests without rotators. The cyclic test procedure employed (which included periodic stops) provided ample opportunity for flaking or chipping of the heavy face deposits to promote valve burning, yet no evidence of such behavior was detected. These results clearly emphasize the greater importance of the stem deposits (which cause dynamic sticking) over that of face and seat deposits in the valve burning mechanism.

Evidence of semifluid flow in valve face deposits also suggests that deposit cracking or flaking is not of major importance as a precursor of valve burning. This is shown in Fig. 2 of the paper, a photograph of a valve head, which has been operated at temperature levels which result in rapid face corrosion. The evidence of previous fluidity of the deposits is clearly visible.

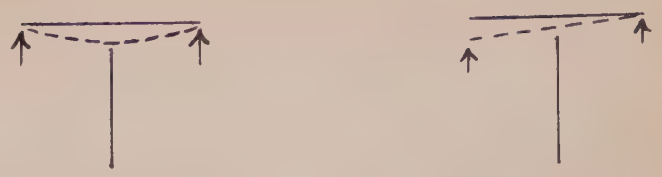

Fig. A – Left: diaphragm-type valve-head flexure; right: cantilever-type valve-head flexure

Such fluid deposits would be squeezed from between the valve and seat by gas and spring pressure (thus allowing the valve to regain contact with the seat and thereby obtain proper cooling) unless prevented by dynamic sticking. The presence of cracks in face deposits at lower temperatures, where the deposits are in the solid phase, has been demonstrated by compression pressure measurements. The harmless nature of such leakage at lower valve face temperatures, however, has been confirmed by the experiments with notched-face valves described in the body of our paper. Further evidence of harmless leakage through cracks or voids in valve face deposits may be found in the erratic single observations of low compression pressure frequently encountered in valve tests. This occurrence is so common, in fact, that most investigators require several consecutive low compression pressure readings before assuming that damage to the valves has occurred.

Valve head flexure in engine B (Figs. 13 and 14 of the paper) is indeed similar to that of a flexed diaphragm. The amplitude of the flexure has been observed to be proportional to the pressure in the engine cylinder in a continuous manner from nonfiring compression to full throttle with the engine firing. If serious tipping of the valve head were occurring the displacement of the valve stem with increasing cylinder pressure would be nonlinear with an inflection at the pressure required to obtain full seat contact. Since such an inflection was not observed, it is concluded that valve head tipping was not a factor in the patterns observed.

Regarding the effects of additive concentrations shown in Figs. 11 and 12 of the paper, our investigations of valve life in a number of full-scale engine dynamometer and road tests have indicated that the time required for the onset of dynamic sticking is a function of the rate of accumulation of stem deposits (which is dependent on the composition and physical characteristics of the deposits) and engine operating conditions. Once the deposits have reached the level where sticking begins to prevent proper seating, the valve temperatures increase and corrosion of the face is accelerated. The length of the interval between onset of sticking and failure of the valve is dependent, among other things, on the corrosive characteristics of the deposits on the face of the valve. The corrosive characteristics can, of course, be markedly influenced by the use of additives. The marked reduction in corrosivity of deposits with increased concentrations of additive B (suggested by the results in Fig. 12) has been confirmed in other laboratory engine and bench tests. Thus, we feel that the dynamic sticking mechanism (which involves sticking of the valve with subsequent overheating and accelerated corrosion) fully explains the results shown in Fig. 12.

In summary, previous work has demonstrated beyond question the importance of adequate cooling, dimension stability, materials selection, and maintenance of proper lash clearances on exhaust valve life. We feel that the demonstration of dynamic sticking, made possible through the instrumentation described in our paper, has provided a much needed reassessment of the role of deposits in the mechanism of exhaust valve burning. It is our belief that many (if not all) of the valve failures heretofore ascribed to deposit guttering were actually due to dynamic sticking with subsequent overheating and corrosion.

Application of High-Temperature in the Temperature

THE use of metals at temperatures in excess of 1200 F and up to temperatures in the vicinity of their melting points is a challenging and fascinating portion of the fight to pass the heat barrier in the design and performance of aircraft and their powerplants. The materials available for service in this temperature range are restricted. The problems in design of structural components involve many more considerations than the old criteria of strength-to-weight ratio and fabrication costs. Thermal expansion, heat conductivity, surface emissivity, and scaling resistance are as important in selection of materials for given applications as are the various measures of strength previously considered primary.

OUR aircraft industry is fast approaching the time when it will be hard-pressed to design and construct elevated-temperature structural components from engineering materials now available. This situation is particularly aggravated in afterburner, ramjet, and rocket engine design, where operating combustion temperatures may exceed the melting points of constructional metals developed to date.

Several applications of available alloys to combustion-chamber design are described, and it is concluded that new materials such as molybdenum, cermets, and ceramic coatings, together with refined cooling techniques, must provide the answer to the limitations imposed by the inadequacies of elevated-temperature materials available today.

This discussion will be limited to the fields of design and fabrication of turbojet afterburners, ramjets, and rocket engines. Turbojet engine design and development as affected by materials has been discussed extensively. Afterburner, ramjet, and rocket engine design, however, with higher operating temperatures and shorter lives, is a rather new subject that will command more and more attention from the materials engineer.

Types of Metals Used

1. Characteristics and Functions of Alloying Ele-

Materials to Aircraft Powerplants

Range 1200-2400 F

Alan V. Levy, Marquardt Aircraft Co.

This paper was presented at the Aircraft Research Seminar held by the SAE Southern California Section at the University of California, Los Angeles, Dec. 8, 1954.

ments – One of the primary requirements of metals and alloying elements used to produce high-temperature alloys is that they and the products of their combination have melting temperatures above the service temperature. In addition to this, requirements of strengthening the end-alloy, ability of elements to combine and produce ductile alloys, cost and availability of alloying elements, and many other important factors must be considered. Table 1 lists those metallic elements commonly found in high-temperature alloys, together with a brief description of their functions.

2. Classes of Alloys – Metals retaining sufficient strength to be used in the service temperature range above 1200 F are the alloys which have iron, nickel, or cobalt as the major constituent. Alloys based on all three of these elements, singly or in combination, are currently used in countless powerplant applications. New developments in metal technology are evolving alloys based on molybdenum, titanium, and possibly, chromium and other metals. But at this time iron, nickel, and cobalt are the foundation elements for the high-temperature alloy field. Table 2 lists some of the commonly used alloys and an insight into their characteristics, divided into classes based on their major constituent. In general, alloys of iron are used in the temperature range up to 1500 F, alloys of nickel in the range 1500-1800 F, and alloys of cobalt in the range

Table 1 – Functions of Alloying Elements

Element	Function
Iron	Foundation element for structural metals
Nickel	Austenitizer; improves oxidation resistance in stainless steels; adds high-temperature strength; improves corrosion resistance
Cobalt	Base metal for highest-strength high-temperature materials; improves high-temperature strength in mixed alloy materials (M-155)
Chromium	Primary source of oxidation resistance
Molybdenum	Improves high-temperature strength; adds corrosion resistance; has precipitation hardening potential in some alloys
Tungsten	Improves high-temperature strength
Columbium	Stabilizing element in austenitic stainless steels; adds high-temperature strength
Titanium	Same as Cb, but has precipitation-hardening value in some alloys
Aluminum	Primarily added as precipitation hardening agent (17-7 PH, Inconel "X")
Vanadium	Thought to improve creep resistance
Silicon	Added up to about 2% to improve oxidation resistance in some stainless steels

Table 2 – Some Common High-Temperature Alloys

Alloy[a]	Characteristics
Iron-Base Alloys:	
Type 321, 347, stainless steel	These materials are stabilized 18% chromium, 8% nickel basic nonhardenable stainless steel. They have excellent fabrication characteristics, are weldable and fully corrosion resistant. They are commonly used in elevated-temperature applications to 1500 F where medium strength and corrosion resistance are required
Type 310 stainless steel	Standard AISI steel which contains 25% chromium and 20% nickel. This material has excellent scaling resistance up to 2000 F, and over. It is used where high strength is not needed, at temperatures to 2200 F
19-9 DL, 19-9 DX	Low-alloyed (with molybdenum and tungsten) modified stainless steel. It retains strength comparable to most of the high-temperature alloys up to 1400–1500 F. It is an excellent low-critical-alloy-index material for general structural use up to 1500 F
16-25-6	Chromium, nickel, molybdenum alloy available in bars and forgings. This alloy has been a commonly used turbine wheel material for service up to about 1500 F
A-286	Age-hardenable stainless steel material that can be used up to the low end of the temperature range (around 1200 F)
17-4 PH, 17-7 PH	Age-hardenable stainless-steel materials that have high strength-weight ratios at lower temperatures, but that find some application in the temperature range around 1000 F
Discalloy 24	Age-hardenable stainless steel primarily used as a forged-wheel alloy up to 1300 F
Nickel-Base Alloys:	
Inconel	80% nickel, chromium, iron alloy that has seen much use as a low-strength, high corrosion-resistance material at elevated temperatures. It is hot-short (low ductility) at 1200 F and is not commonly used in powerplant structures today
Inconel X	Age-hardenable offspring of Inconel containing titanium and aluminum for age-hardening. Of all high-temperature alloys, it is tops in strength up to 1600 F. It is difficult to fabricate and must be heat-treated after forming. It has found wide-spread use as a combustion-chamber material for afterburners as well as many other applications
Incoloy	Version of Inconel X with somewhat lower properties and reduced critical alloy content
Nimonic 75, 80, 90	Series of British-developed alloys similar in composition and function to Inconel X
Hastelloy B	Haynes Stellite development that contains molybdenum as the major alloying element and no chromium. The absence of chromium and high percentage of molybdenum lowers its scaling temperature. It has excellent strength to 1600 F, and higher
Hastelloy C	Haynes Stellite product that contains chromium for increased scaling resistance. It has been used for high-strength applications to 1800 F, and above. However, its high critical-alloy content and fabrication characteristics limit its use
Hastelloy X	Critical-alloy-reduced version of other Hastelloys that combines excellent scaling resistance with good strength. It is being used more and more in combustion chambers and combustion component applications of all powerplants
Cobalt- and Mixed-Base Alloys:	
N-155 (Multimet)	Chromium, nickel, cobalt, iron mixed-base alloy that has become somewhat of a workhorse in the temperature range from 1200 F on up. It is considered a scrap-base alloy It has good high-temperature properties to 2000 F, compared to all other alloys, can be readily fabricated, requires no heat-treatments
S-816	Mixed-base alloy with 3% or higher of columbium, tungsten, and molybdenum. It is high on the critical-alloy list, has excellent strength at the higher temperatures. It has been used extensively for forged turbine blades.
Refractalloy 70	Mixed-base alloy with high molybdenum that has good elevated-temperature properties. It is not widely used
L-605 (H.S. 25)	Cobalt-base material that is the strongest of all high-temperature alloys above about 1600 F. It is only used where high stresses exist at the upper end of the temperature range (1700–2200 F). It has high critical-alloy content
H.S. 21, 23, 30, 31, etc.	Series of cobalt-base casting alloys. They are commonly used for cast turbine blades and other high-temperature applications requiring high strength

[a] All alloys are available in all shapes and forms unless specifically noted.

1600-2200 F. For the most part, the materials listed are generally available from material producers. Many major powerplant manufacturers have developed similar alloys primarily for their own products and are producing or having them produced to their own specifications.

Selecting the Metal

1. Mechanical and Physical-Property Requirements at Service Temperature – The strength of a metal at elevated temperature can take several forms, depending on the type and duration of loading. Short-time tension, compression, shear, and bearing strengths are of primary importance in the design of short service-life power plants. Creep and stress rupture properties are also important, especially as service-life increases. Fatigue strength, notch-impact, notch-tensile strength, and modulus of elasticity must be considered in most designs, and thermal shock and fatigue are also important strength factors.

The strength properties of metals generally decrease with increasing temperature. This fact is the result of different elevated temperature mechanisms, depending on the alloy considered. Age-hardenable materials overage and thereby lose strength. Work-hardened materials are annealed at operating temperature. Materials containing many different alloying elements form new phases at elevated temperature and can lose strength or become brittle. In addition, the atomic bonds that hold metals together and give them strength change when subjected to additional heat energy, and by various mechanisms, result in lowered strength.

Because metals lose strength at elevated temperature by several mechanisms, the service temperature and life of the component must be carefully considered before the material is chosen. The various measures of strength must be integrated to prevent selection of a material high in one strength property for an application where a high-temperature peculiarity of the metal will result in failure. Some metals have comparatively high short-time strength but considerably lower creep strength than others. Some metals have hot-short or brittle ranges at certain temperatures, while others precipitate constituents at grain boundaries at certain

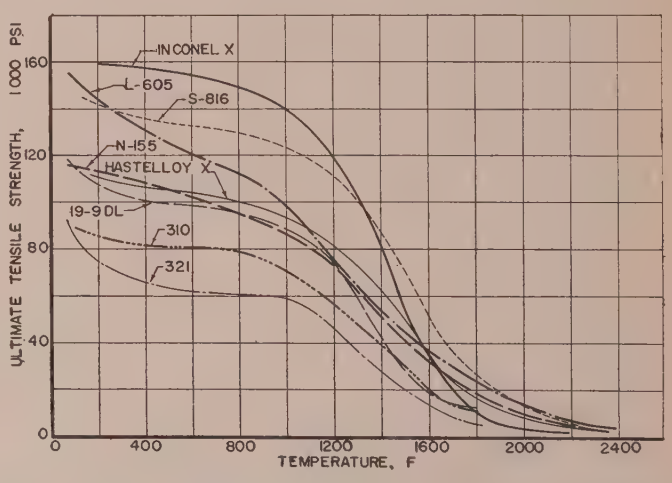

Fig. 1 – Variation of typical ultimate tensile strength with temperature for several high-temperature alloys

Table 3 – Summary of Short-Time Mechanical Properties

Alloy	Room Temperature			1000 F			1200 F			1400 F		
	Tensile Strength, psi	Yield Strength, psi	Elongation, % in 2 in.	Tensile Strength, psi	Yield Strength, psi	Elongation, % in 2 in.	Tensile Strength, psi	Yield Strength, psi	Elongation, % in 2 in.	Tensile Strength, psi	Yield Strength, psi	Elongation, % in 2 in.
19-9 DX	129,800	101,900	26	95,400	77,300	20	80,100	70,300	20	52,700	49,500	24
19-9 DL	118,250	89,000	58	89,000	42,000	43	75,000	39,000	34	42,625	35,500	36
16-25-6	114,000	68,000	42	93,000	42,000	35	88,000	40,000	36	53,000	33,000	42
Discalloy 24	145,000	106,000	19	125,000	94,000	16	104,000	91,000	19	73,000	60,000	14
321	92,200	39,300	55	80,900	26,800	35	46,200	25,400	34	27,800	15,000	70
310	82,400	40,000	55	66,750	26,000	50	48,000	23,000	24	42,000	21,000	27
L-605	155,000	70,000	55	100,000	35,000	67	74,500	35,000	25	53,000	37,000	14
Hastelloy B	135,000	63,000	44	109,000	41,500	31	94,000	42,000	16	77,000	39,700	16
Hastelloy C	129,500	54,000	38	97,000	54,500	22	86,700	49,800	23	63,000	47,100	32
Hastelloy X	113,200	55,800	44	94,000	41,500	45	83,000	40,700	37	63,100	37,800	37
Inconel X	162,000	92,000	24	140,000	84,000	22	120,000	82,000	9	80,000	62,000	—
Nimonic 75	92,000	60,000	50	—	—	—	—	—	—	46,000	20,000	28
Nimonic 80	—	—	—	108,000	73,000	41	87,500	72,500	15	67,000	63,000	7
Nimonic 90	148,000	90,000	39	123,000	82,000	27	111,000	77,000	24	90,000	63,000	14
N-155	116,000	57,000	43	85,000	—	37	72,300	39,700	35	50,000	35,000	33
S-590	118,000	72,000	—	128,000	79,000	—	100,000	70,000	—	65,000	50,000	—
S-816	140,000	62,750	31	121,000	46,000	27	112,000	45,000	22	87,750	40,000	26
Refract 26	153,000	98,000	18	142,000	91,000	17	134,000	95,000	14	108,000	90,000	13
Refract 70	133,000	—	—	117,000	—	—	104,000	—	—	83,000	—	—
Inconel	90,500	36,500	47	84,000	28,500	47	65,000	26,500	39	27,500	17,000	46
Inconel W	146,000	81,000	—	123,000	72,000	—	117,000	82,000	—	—	—	—

Alloy	1500 F			1600 F			1800 F			2000 F		
	Tensile Strength, psi	Yield Strength, psi	Elongation, % in 2 in.	Tensile Strength, psi	Yield Strength, psi	Elongation, % in 2 in.	Tensile Strength, psi	Yield Strength, psi	Elongation, % in 2 in.	Tensile Strength, psi	Yield Strength, psi	Elongation, % in 2 in.
19-9 DX	39,100	32,900	43	—	—	—	12,600	10,400	85	—	—	—
19-9 DL	32,500	29,500	53	18,000	—	56	12,600	—	61	—	—	—
16-25-6	41,000	30,000	49	30,000	—	57	18,000[a]	—	59[a]	—	—	—
Discalloy 24	—	—	—	—	—	—	—	—	—	—	—	—
321	22,000	13,000	73	14,000	11,000	82	5,000[a]	—	—	—	—	—
310	32,000	19,000	37	24,000	17,000	43	11,000	—	55	7,000	—	63
L-605	50,000	—	17	37,000	34,000	18	22,700	—	19	13,950	—	22
Hastelloy B	66,000	—	17	55,000	38,500	19	24,000	—	30	—	—	—
Hastelloy C	50,700	—	36	38,000	36,000	39	19,000	—	38	12,000[a]	—	30[a]
Hastelloy X	52,000	37,000	33	36,500	25,700	50	21,000	17,000	43	16,000 at 1900 F	—	—
Inconel X	52,000	44,000	22	34,000	24,000	47	9,000	5,500	89	—	—	—
Nimonic 75	36,000	15,000	33	—	—	—	—	—	—	—	—	—
Nimonic 80	60,000[a]	47,000[a]	9	—	—	—	—	—	—	—	—	—
Nimonic 90	64,000	52,000	8	—	—	—	—	—	—	—	—	—
N-155	36,700	32,800	39	32,000	24,000	42	17,000	12,400	38	12,000	7,200	30[a]
S-590	52,000	47,000	—	40,000	37,000	—	22,000	20,000	—	13,000	14,000	—
S-816	72,800	41,000	23	50,750	—	17	25,475	—	20	12,460	—	24
Refract 26	73,000	72,000	28	48,000	48,000	49	—	—	—	—	—	—
Refract 70	64,000	—	—	50,000	—	—	—	—	—	—	—	—
Inconel	—	—	—	15,000	9,000	80	7,500	4,000	118	—	—	—
Inconel W	—	—	—	—	—	—	—	—	—	—	—	—

[a] Extrapolated values.
Note: All values above are for material in annealed condition except:
19-9 DX, 19-9 DL, hot-rolled and stress-relieved. Inconel X, Inconel W – aged. Nimonic 80, 90 – aged. Discalloy 24 – aged. 16-25-6 – hot-rolled. Refract 26, 70 – aged. S-816 – aged. S-590 – aged.
Data source: Material producers.

temperatures which severely reduce their performance under load.

Fig. 1 shows the variation of ultimate tensile strength with temperature for several elevated-temperature alloys. The rate of change of strength with temperature varies with the alloys. Inconel X in its heat-treated condition is the strongest material up to about 1600 F. However, this material has low ductility at about 1200 F due to a hot-short phenomenon. L-605, a high critical-alloy content material retains the greatest strength at temperatures in excess of 1600 F. Other materials, combining wide variations of properties, fall below these materials in strength at elevated temperature. Table 3 is a summary of short-time tensile properties of typical materials in the four alloy-base classes.

Both Fig. 1 and Table 3 show that the strength level at 1800 F and up for all alloys is very low. However, many of the high-temperature components of afterburners and ramjets can be designed to function at temperatures up to 2200 F for short times. It is essential, however, that the strength be known at these temperatures so that compensating increased thicknesses can be used. Unfortunately, data at the higher temperature levels are rather limited. Some excellent work recently done by the Haynes Stellite Co. provides data on short-time tensile properties up to 2400 F, or just about up to the melting temperature of the alloys tested. (See Table 4.)

Tables 5 and 6 are compilations of short-time (to 1000 hr) creep and stress rupture strengths for alloys commonly used in afterburner and ramjet

Table 4 – Experimental Elevated-Temperature Properties

Temperature, F	Hastelloy X Ultimate Strength, psi	Hastelloy X Elongation, % in 2 in.	Multimet Ultimate Strength, psi	Multimet Elongation, % in 2 in.	No. 25 Alloy (L-605) Ultimate Strength, psi	No. 25 Alloy (L-605) Elongation, % in 2 in.
1800	15,320	42	19,200	61	22,300	43
1800	15,220	50	19,500	55	23,900	44
2000	9,280	41	9,425	45	12,800	31
2000	9,340	37	9,370	46	12,900	28
2200	4,688	43	4,600	29	6,770	17
2200	4,575	37	4,630	26	6,800	10
2300	3,360	21	3,350	18	4,580	16
2300	3,280	20	3,420	19	4,560	9.5
2350	2,500	2	2,545	8.5	—	—
2350	2,800	8	2,660	7	—	—
2400	685	1	439	0	3,030	6
2400	—	—	—	—	3,090	5

Note: All material in annealed condition sheet and held at test temperature for 15 min before loading.
Data source: Material producers.

construction. Much more work must be done in the shorter time range of creep and stress rupture strengths to obtain data satisfactory to the designers of guided missiles and guided missile powerplants.

In addition to mechanical properties, physical properties of metals, such as coefficient of thermal expansion, thermal conductivity, and emissivity, become very important factors in elevated-temperature service. Table 7 is a compilation of physical property data for several high-temperature alloys.

Thermal stresses due to differential expansion of parts subject to different temperatures or differential expansion at a joint between metals of different thermal expansive properties can impose as much as 50% or more of the total load applied to the part. Many cases of failure due to differential thermal expansion are on record. In general, a low expansion coefficient is desired. Equally as important in the case of dissimilar metal joints, however, are equal coefficients of thermal expansion, high or low.

Thermal conductivity is critical in applications such as combustion chambers, where heat must be rapidly distributed and dissipated. This is especially true where uneven combustion produces hot spots. Since most high-temperature alloys have comparatively low thermal conductivity, differential heating and hot spots can easily lead to severe distortion and actual burning through the metal. Thermal stresses causing failure often result from inability to distribute heat evenly throughout a part.

The property of emissivity has only recently been seriously considered by the powerplant designer. This property is a measurement of the amount of incident radiant heat that can be absorbed by or emitted from a surface. Properly speaking, emissivity is the ratio of heat radiated by a body to that radiated by a black body at the same temperature. Absorptivity is the ratio of heat absorbed relative to that absorbed by a black body at the same temperature. For common combustion-chamber materials, emissivity is numerically equal to absorptivity. An emissivity factor of 1 is for a black body absorbing or radiating the maximum amount of heat. It is important in combustion chambers to have the inside surface with the lowest possible emissivity in order to reflect the maximum growth of radiated heat from the combustion gases. On the other hand, the outer surface of a ramjet combustion chamber is open to the atmosphere and should have the highest emissivity factor possible to radiate the most heat to the atmosphere. The magnitude of the emissivity can mean hundreds of degrees in operating wall temperature. Table 8 lists various surfaces and their emissivity factors based on a true black body having an emissivity factor of one.

2. Critical Alloy Content – Many of the alloying elements that compose high-temperature alloys are in limited supply in the United States either because of the scarcity of the elements in the earth or because of the overseas source of the element,

Table 5 – Creep Data for Some Elevated-Temperature Alloys

Temperature, F	Elongation, % per hr	321	310	19-9 DL	Inconel X	Hastelloy C	Hastelloy X	N-155	S-816	L-605
1200	0.01	—	—	22,000	82,000	—	30,000	—	62,000	—
	0.001	9,500	—	21,000	73,000	—	—	—	52,000	—
	0.0001	8,000	8,600	20,000	64,000	—	—	—	42,000	—
1350	0.01	—	—	16,000	55,000	—	18,500	34,400	39,500	33,000
	0.001	—	—	13,000	47,000	—	9,500	25,000	26,800	26,000
	0.0001	3,000	4,000	10,000	38,000	—	—	18,400	18,000	—
1500	0.01	—	—	15,300	30,100	—	11,000	18,300	23,200	21,000
	0.001	—	—	10,400	19,600	—	7,000	13,800	16,400	17,000
	0.0001	1,000	1,000	7,100	12,300	—	—	10,300	11,500	—
1600	0.01	—	—	—	13,000	—	5,000	—	12,300	16,000
	0.001	—	—	—	11,000	—	3,200	—	8,500	12,500
	0.0001	—	—	—	9,000	—	2,400	—	5,800	—

Table 6 – Stress Rupture in psi of Several High-Temperature Alloys

Temperature, F	Time, hr	321	310	19-9 DL	Inconel X	Hastelloy C	Hastelloy X	N-155	S-816	L-605
1000	1	—	—	—	—	—	—	—	—	—
	10	—	—	—	122,000	—	—	—	—	—
	100	—	—	—	115,000	—	—	—	—	—
	1000	—	32,000	—	110,000	—	—	—	—	—
1200	1	33,000	38,300	—	—	—	—	—	100,000	—
	10	31,000	—	70,000	92,000	—	58,000	80,000	80,000	—
	100	25,000	27,000	60,000	80,000	53,000	45,000	60,000	62,000	45,000
	1000	17,500	13,700	40,000	55,000	35,000	30,000	46,000	50,000	—
1400	1	—	—	—	—	—	—	—	—	—
	10	—	—	45,400	52,000	—	30,000	33,000	45,000	40,000
	100	—	—	28,000	42,000	—	21,000	25,700	32,000	30,000
	1000	5,600	5,100	16,500	33,000	—	16,000	19,500	27,000	23,000
1500	1	20,000	—	—	—	—	—	—	43,000	—
	10	12,000	16,600	18,000	38,000	—	21,000	33,000	35,000	35,000
	100	3,800	8,300	13,000	30,000	15,000	14,000	20,000	29,000	22,000
	1000	3,700	3,500	10,500	18,500	9,500	10,000	15,000	22,000	18,000
1600	1	—	—	—	—	—	—	—	—	—
	10	—	—	—	17,000	—	16,000	18,000	20,000	24,000
	100	—	—	—	11,000	—	8,000	15,000	15,000	15,000
	1000	—	2,400	—	6,600	—	6,000	7,300 (1650F)	10,000	11,000
1800	1	—	6,300	—	—	—	—	10,000	—	—
	10	4,800	—	—	—	—	7,000	8,800	8,800	13,000
	100	2,900	—	—	—	4,000	3,400	3,300	5,500	7,000
	1000	—	1,000	—	—	1,400	—	2,800	3,100	4,500
1900	1	—	—	—	—	—	—	—	—	—
	10	—	—	—	3,200	4,500	3,000	—	5,700	—
	100	—	—	—	1,700	2,700	—	—	3,200	—
	1000	—	—	—	—	—	—	—	—	—

Note: All materials in annealed condition except: 19-9DL – stress relieved at 1200F, Inconel X – aged, and S-816 – aged.
Data source: Material producers.

or both. The amount and types of alloying element available to our country in a national emergency is of great strategic importance. Thus, the government has stressed the use of minimum critical-alloy content in powerplants designed for piloted aircraft and missiles. Since the end of the Korean War, the supplies of critical alloys have increased measurably. However, the criterion of minimum critical-alloy content must be continuously applied. Some of the elements used in high-temperature alloys that have been in critical supply in the past few years are: nickel, cobalt, columbium, molybdenum, chromium, and tungsten. The changing supply picture continues to modify the list, and

Table 7 – Physical Properties of Several Elevated Temperature Alloys

	321		310		19-9 DL		Inconel X		Hastelloy C		Hastelloy X		N-155		S-816		L-605	
Density, lb/cu in.	0.290		0.290		0.287		0.298		0.322		0.297		0.300		0.313		0.330	
Melting Point, F	2575		2600		2600		2540		2350		2400		2500		2400		2570	
	Temperature, F	Coefficient	Temperature, F	Coefficient	Temperature, F	Coefficient	Temperature, F	Coefficient	Temperature, F	Coefficient	Temperature, F	Coefficient	Temperature, F	Coefficient	Temperature, F	Coefficient	Temperature, F	Coefficient
Mean Coefficient of Thermal Expansion, in./in./F x 10^{-6}	32–212	9.3	32–212	8.0	70–212	8.2	100–200	7.6	70–600	7.02	79–200	7.70	70–600	8.70	70–600	6.6	70–600	7.61
	32–600	9.5	32–600	9.0	70–600	8.7	100–400	7.7	70–800	7.35	79–400	7.82	70–800	8.89	70–800	6.9	70–800	8.28
	32–1000	10.3	32–1000	9.4	70–1000	9.5	100–600	7.9	70–1000	7.44	79–600	7.90	70–1000	9.10	70–1000	7.1	70–1000	8.30
	32–1200	10.7	32–1200	9.7	70–1200	9.7	100–800	8.0	70–1200	7.73	79–800	8.15	70–1200	9.40	70–1200	7.4	70–1200	8.55
	32–1800	11.2	32–1800	10.6	70–1600	10.2	100–1000	8.2	70–1500	8.07	79–1000	8.39	70–1500	9.77	70–1400	7.7	70–1400	8.92
					70–1800	10.5[a]	100–1200	8.4	70–1600	8.20	79–1200	8.56	70–1600	9.90	70–1600	8.0	70–1600	9.30
					70–2000	11.0[a]	100–1350	8.7			79–1350	8.76			70–1800	8.3	70–1800	9.70
							100–1500	9.0			79–1500	8.92						
							100–1600	9.2			79–1650	9.07						
											79–1800	9.20						
Coefficient of Thermal Conductivity, Btu/ft²/in./hr/F	200	112	200	96	200	101	Room	85	—	—	—	—	392	101	302	101	Room	85
	600	—	600	—	600	117	600	137					572	110	572	119	600	91
	1000	152	1000	130	1000	134	1000	144					752	120	932	142	800	98
					1200	143	1200	156					932	129	1112	155	1000	100
					1400	150	1400	168					1112	139	1292	155	1200	102
					1600	163	1600	180									1400	103
							1800	195									1600	112
																	1800	116
Modulus of Elasticity, psi x 10^6	Room	29.0	Room	29.0	Room	29.4	Room	30.8	Room	28.5	—	—	Room	29.3	Room	35.2	—	—
	200	28.0	200	28.2	200	28.4	200	30.4	1200	26.8			200	—	300	33.8		
	600	25.2	600	25.7	600	25.5	600	28.1	1500	22.0			600	—	600	31.9		
	1000	22.5	1000	23.2	1000	24.5	1000	25.0	1800	18.7			1000	24.2	900	29.7		
	1200	21.1	1200	22.0	1400	20.5	1200	23.0					1200	—	1050	28.7		
	1400	19.8	1400	20.8	1600	19.3[a]	1400	20.2					1500	20.8	1200	27.6		
															1500	25.4		

[a] Extrapolated values. Data source: Material producers.

Table 8 – Surface Emissivity

Material	Temperature Range, F	Emissivity
Metallic Surface:		
Polished iron	800–1880	0.144–0.377
Cast-iron polished	392	0.21
Wrought-iron polished	100–480	0.28
Cast iron, newly turned	72	0 435
Polished steel casting	1420–1960	0.52–0.56
Ground sheet steel	1720–2010	0.55–0.61
Smooth sheet iron	1650–1900	0.55–0.60
Cast iron, lathe turned	1620–1810	0.60–0.70
Oxide Surface:		
Iron plate, pickled, then rusted red	68	0.612
Completely rusted	67	0.685
Rolled sheet steel	70	0.657
Oxidized iron	212	0.736
Cast iron, oxidized at 1100 F	390–1110	0.64–0.78
Steel, oxidized at 1100 F	390–1100	0.79
Smooth oxidized electrolytic iron	260–980	0.78–0.82
Iron oxide	930–2190	0.85–0.89
Rough ingot iron	1700–2040	0.87–0.95
Sheet steel, strong, rough oxide layer	75	0.80
Dense, shiny, oxide layer	75	0.82
Cast iron, rough, strongly oxidized	100–480	0.95
Wrought iron, dull oxidized	70–680	0.94
Other Alloys:		
18-8 stainless steel sandblasted	180–350	0.5
18-8 stainless steel oxidized at 1000 F	180–340	0.32–0.36
18-8 stainless steel oxidized at 1500 F	165–330	0.63–0.69
Inconel untreated	193–250	0.16–0.20
Inconel oxidized at 1400 F	185–340	0.19
Monel	1000	0.10
Monel – oxidized	1000	0.46
Pigments:		
Black lacquer	750	0.95
Black (CuO)	750	0.85
Red (Fe_2O_3)	750	0.70
Green (Cu_2O_3)	750	0.67
Yellow (PbO)	750	0.49
White (MgO)	750	0.84
White (ZrO_2)	750	0.77

stockpiling also has an effect on present and future critical-alloy supplies.

Obviously, practically all elements used in high-temperature alloys have been or are considered in critical supply.

3. Fabrication Characteristics – In general, high-temperature alloys present greater difficulties to the fabricator than either alloy steels or stainless steels. Fabrication characteristics of type 18-8 stainless steels have been fairly well documented, and it is common practice to compare the high-temperature alloys to stainless steels when considering the various fabrication methods.

Welding: All high-temperature alloys can be fusion welded satisfactorily. Heliarc welding is best for most of the alloys because it offers the least chance of contamination by carbon and oxides. Use of flux-coated rods or liquid or paste fluxes introduces the problem of complete flux removal prior to elevated-temperature service. The finish configuration of welds, especially in sheet material, has a great effect on elevated-temperature performance. For this reason, the optimum welded joint is a tight butt weld made automatically by the heliarc method, adding no filler metal and roll-leveling the resulting bead. Roll-leveling mechanically forces weld metal into the plane of the base metal, producing a flush, stress-relieved, cold-worked joint.

Resistance-welded joints are readily made using pressures somewhat greater than those necessary for stainless steel.

Forming: High-temperature alloys can be formed by all of the common forming techniques. They tend to work-harden rapidly and require roughly twice the number of intermediate anneals as do stainless steels. Minimum bend radii are somewhat larger than for stainless steels, and provision must be made for greater springback. Annealing is performed at temperatures generally above 2000 F, requiring high-temperature furnaces and special equipment for removing scale.

Machining: All the high-temperature alloys are hard to machine, though to varying degrees. In general, mixed- and cobalt-base materials are most difficult, nickel-base alloys less difficult, and iron-base alloys the easiest to machine. A good value for estimating the cutting speed for machining high-temperature alloys is ⅓ to ½ the speed of cutting stainless steels for normal operations such as milling, drilling, shaping, and so forth.

Forging: Forging is possible on practically all the high-temperature alloys. However, forging pressures must be higher and temperatures hotter than for stainless steels. Tolerances in the as-forged condition may not compare with those of stainless steel or alloy steel parts because of the more difficult working conditions.

Casting: Many high-temperature alloys are cast by several of the casting methods. Complicated parts of hard-to-machine alloys like Haynes Stellite 21, 23, or 31, are investment cast to finish shape. Turbine blades and afterburner nozzle segments are typical of parts cast to finish shape. Many cobalt-base alloys are fabricated only by casting.

4. Scaling and Corrosion Resistance – As the service temperature of a part climbs above 1500 F, scaling becomes an important factor in determining the choice of materials. In addition, the corrosion effects of hot combustion gases on burner components must be considered. Chromium content of a high-temperature alloy gives the best, but not the only, indication of scaling resistance.

Table 9 – Typical Cost of Sheet Materials

Material	Cost, $ per lb
Low-Alloy Steels	
AISI 1020	0.10
AISI 4130	0.20
Stainless Steels	
AISI 302	0.60
AISI 321	0.75
AISI 310	0.90
17-7 PH	0.85
High-Temperature Alloys	
19-9 DL	1.10
Multimet (N-155)	2.50
Hastelloy X	2.50
Inconel X	2.50
Hastelloy C	3.50
H.S. 25 (L-605)	5.50

Table 10 – Melting Points of Some of the More Common Metallic Elements

	Melting Point, F
Boron	4200
Chromium	3430
Cobalt	2723
Columbium	4380
Iron	2800
Manganese	2273
Molybdenum	4760
Nickel	2651
Palladium	2830
Platinum	3225
Rhenium	5740
Rhodium	3571
Tantalum	5425
Thorium	3300
Titanium	3300
Tungsten	6170
Uranium	2065
Vanadium	3150
Zirconium	3200

Chromium contents of 15-20% in high-temperature alloys will result in scaling resistance up to 1800-1900 F. As the chromium content is increased to the 25% level of AISI 310 stainless steel, the free-scaling temperature increases to 2200 F. At and above this temperature, all alloys have a decided scaling rate. However, since scaling is determined by temperature, atmosphere, and time, the short service lives of guided missile powerplants enable parts to function for periods up to several hours at temperatures of 2000 F and higher. The expected service life of afterburners limits their top metal temperatures to about 1900 F. The much shorter service life of ramjets extends their top operating temperatures to 2000-2200 F. Probably the two best scaling resistance materials available today are AISI 310 stainless steel and Hastelloy X, the scaling resistance primarily due in both cases to the high chromium content.

5. Cost – Cost of most high-temperature alloys is considerably above the cost of low service-temperature alloy steels and stainless steels. The expensive alloying elements used and the special melting and mill practices necessary to produce high-quality finished products contribute to the increased cost. However, the material needs of modern high operating temperature powerplants can be satisfied only by high-temperature alloys. Cost, therefore, is usually a minor consideration. Table 9 lists typical costs for some commonly used high-temperature alloys compared to stainless steel and low-alloy steels.

Limitations on Elevated-Temperature Performance

1. Strength – Usable strength levels for high-temperature alloys vary with the application. For short-time applications at low loads and with a simple stress pattern, service temperatures as high as 2200 F have been considered for structural components of ramjets. In other applications such as high-speed, long service-life turbine blades, temperatures of 1600 F and lower are considered top temperatures today. Each application must be rated with respect to load, service time, and other factors to determine a ceiling temperature of operation. Many times an alloy can be used for intermittent, short time service at temperatures considerably above the normal operating temperature. For these applications and ultra-high-temperature applications, it is important to know just how strength drops off with temperature. These data are just now becoming available. Work by Armour Institute, Haynes Stellite, and other organizations on short-time properties of alloys and Battelle Memorial Institute on creep and stress rupture data down to 0.1 min constitutes important contributions to missile powerplant design. Tables 4-6 summarize some of the newer data available.

2. Melting Point – Eventually, metal technology in the high-temperature field is going to meet a formidable foe in the periodic table of elements. (See Table 10.) Combustion temperatures using known fuels are already in excess of the highest-melting-point metals. Most of the refractory metals with melting temperatures over 3000 F are brittle and susceptible to rapid oxidation. The basic structural metal element, iron, melts at 2800 F. As alloying elements are added this temperature becomes lower. Cobalt and nickel melt below 2800 F; their alloys melt down in the range 2400-2600 F. In general, it can be stated that all present structural materials capable of unprotected operation at temperatures above 1500 F melt below 2700 F. To the combustion engineer, 2700 F is a low gas temperature.

Present efforts to produce ductile alloys of molybdenum, chromium, titanium, and zirconium for service at temperatures in excess of 2000 F is progressing slowly. The high melting points of these

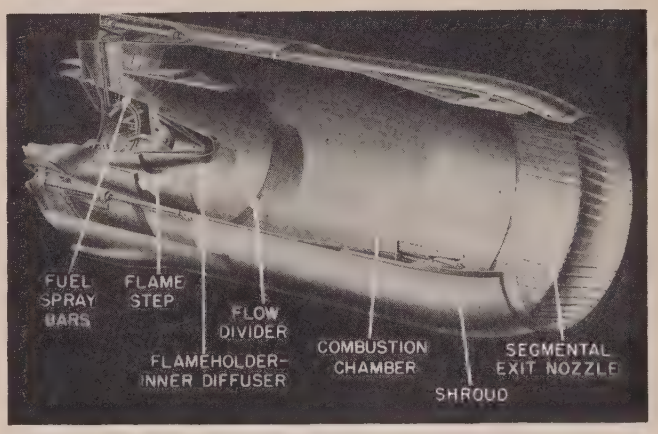

Fig. 2 – Illustration of typical afterburner

elements (above 3000 F) are offset by lack of oxidation resistance and strength, brittleness, and production or fabrication difficulties. Molybdenum (melting point: 4750 F) catastrophically oxidizes at about 1800 F, tends to produce brittle alloys and is very difficult to fabricate – and especially to weld. Titanium alloys (melting point: about 3100 F) presently produced drop off markedly in strength above about 1000 F and embrittle when exposed in air to temperatures above about 1400 F. Chromium and its alloys (melting point: about 3400 F) investigated to date are too brittle for structural applications.

While it is anticipated that molybdenum alloys will eventually be available having typical ultimate tensile strengths of 20,000 psi at 2400 F, much work must still be done before these alloys become a true reality.

Most of the other high melting-point metals are so brittle or so susceptible to scaling, or both, that development work on structural alloys of tungsten, rhenium, tantalum and other high-melting-point elements for high-temperature service is nonexistent. Therefore, it can be stated that we are nearing the ultimate in high-temperature structural metals at service temperatures considerably below the combustion gas temperatures known today. Cermets and refractory hard metals – silicides, borides, carbides, nitrides, and so forth – seem to be the principal hope of the future.

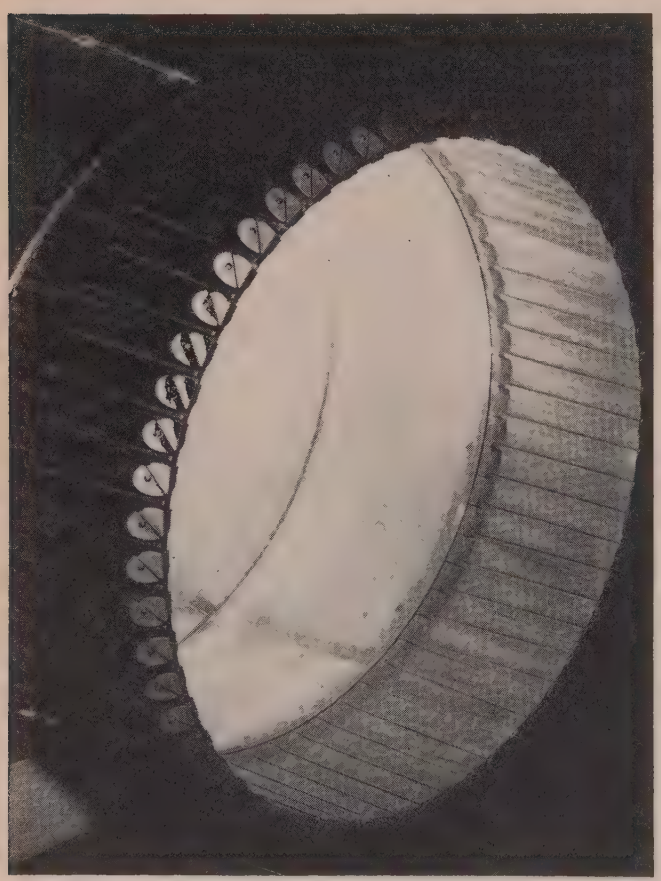

Fig. 3 – View of a segment-type afterburner exit nozzle

Applications in Turbojet Afterburners

Afterburners are presently being used in turbojet engines to obtain additional thrust for short periods during take-off and at other times when deemed necessary. Fundamentally, an afterburner works by injecting additional fuel into the turbojet exhaust to consume the excess oxygen present. It is composed of a fuel injector, a flameholding device, a combustion chamber, and a variable area exit nozzle. Fig. 2 shows a typical afterburner. The present military specification for afterburners requires that each model pass a qualification test consisting of 150 hr of operation and shall include 22 hr of afterburning.

A. Combustion Chambers – The combustion chamber of a typical afterburner is either a single- or double-wall cylinder of high-temperature alloy sheet material usually less than 0.1 in. thick. Dimensions range from 60-120 in. long and from 32-42 in. in diameter. In operation, the wall temperature of a single-wall chamber reaches temperatures from 1500 to 1650 F in the burning area. Service life and loads require that a material such as N-155 be used in the forward regions and L-605 in the exit area. These materials, in thicknesses ranging from 0.050-0.070 in., are rolled into cylinders or cones and fusion welded together. Welds must be near flush to prevent formation of hot spots due to weld bead projection into the hot combustion gases.

Double-wall chambers are usually corrugated to allow passage of cooling air between the walls. Several double-wall chamber designs have been fabricated from Inconel W or X. These materials have high strengths at the service temperatures encountered (1300 F for the outer wall, 1600-1800 F for the inner wall). Relatively high final aging temperatures and times required to put these alloys into their maximum strength condition create a heat-treating production problem because the chambers are comparatively large. Fabricating corrugations in these alloys is also a production problem. However, at the service temperatures, comparatively thin metal thicknesses can be used, resulting in a minimum weight chamber.

B. Flameholders – Flameholders of afterburners are subjected to the highest service temperatures in the unit, reaching temperatures during afterburning of 1800-1900 F at and near the flame step. Problems of differential heating inducing thermal stresses, radiation from one surface to another building up temperature, and high collapsing pressures for the service temperatures all tend to cause premature failure unless some cooling method is incorporated in the design.

A typical afterburner flameholder consists of two developed-surface truncated sheet metal cones with a flame step between them. (See Fig. 2.) The large cone is fabricated from 0.050 in. N-155. The smaller inner cone is fabricated from AISI 310 stainless steel. The cones are spun or rolled into shape and fusion welded together. The flame step is the hottest area of the flameholder and the point where scaling and differential thermal expansion resulting in high thermal stresses are critical design considerations. Present practice is to machine the step from an AISI 310 stainless steel rolled-ring forging into an annular cup shape to reduce thermal stresses. Cooling air from the turbine exhaust (at 1200 F) is passed along the inside walls of the sheet metal cones to keep them cool and at a more uniform temperature. The use of Hastelloy X is being considered for present AISI 310 stainless steel components of flameholders to take advantage of its greater strength at temperatures around 2000 F and scaling resistance equal to the 25% chromium AISI 310 stainless steel.

Fig. 4 – View of eyelid-type afterburner exit nozzle

C. Fuel Spray Bars – Fuel is introduced into an afterburner through a series of single- or multi-holed radial fuel spray bars placed upstream from the flameholder. These bars consist of AISI 321 or 310 stainless steel, or N-155 tubes with about a 0.060 in. wall thickness and 10 in. long that have been flattened into an elliptical cross-section. Small holes are drilled in the tube wall through the minor diameter of the ellipse. These holes usually range in diameter from 0.025 to 0.062 in. in diameter to produce the proper dispersion of fuel in the air stream. Drilling small diameter holes in high-temperature alloys through a small-radius surface that has been work-hardened is almost a science in itself! Methods for drilling these holes using high-speed steel drills have been developed. Ultrasonic and electronic methods for drilling small diameter holes in hard-to-machine alloys have also been tried. The individual tubes are welded or nicro-brazed (a process using a high-melting-point nickel-boron brazing alloy in a hydrogen-atmosphere furnace), to a central manifolding system.

Service conditions imposed upon the fuel spray bars are the exact opposite to those of any other component of the afterburner. When the afterburner is not operating, the turbine exhaust temperature keeps the fuel spray bars at 1200-1400 F. The moment fuel is introduced into the afterburner, the fuel spray bar wall temperature drops to 100-200 F. This thermal shock must be considered when the bars are designed, especially at the junction of the bar and the fuel manifold.

D. Exit Nozzles – (1) Segmental, iris-type nozzles: The segmental, iris-type exit nozzle design used in Marquardt afterburners has been one of the more fundamental advances in afterburner design from its beginning at the end of World War II. A variable-type nozzle is required to provide the optimum exit area for operation of the turbojet alone and of the turbojet and afterburner in combination. When the afterburner is operating, the exit area must be greater than for the turbojet operating alone. (See Fig. 3.)

Segments of an afterburner nozzle must be capable of withstanding operating temperatures of 1800-1900 F, with local hot-spots reaching 2000 F, of resisting oxidation by hot combustion gases, and of withstanding loads that can warp individual segments out of line with their neighbors and thereby affect the operation of the nozzle as a whole. The segments are investment cast of AISI 310 stainless steel. 310 is used primarily because of its high scaling resistance. The segments are hinged at one end and fit into a hinge ring connected to the combustion chamber. The segments are operated by the action of a shroud that moves fore and aft along the outside of the combustion chamber, pivoting the segments from the hinge ring into a smaller or larger diameter exit area.

At one stage in the development of these segments, the edge of each segment overlapped that of its neighbor to prevent pressure loss through the nozzle. The differential temperatures set up in this configuration caused warping and cracking of the overlapped edge. In the latest designs, the segments themselves do not overlap. Instead, an overlapping sheet-metal section of L-605 alloy is placed between each segment to prevent leakage. The L-605 is ceramic coated to prevent galling and to reduce scaling from high service temperatures and direct impingement of combustion gas.

(2) Eyelid-type nozzles: Most of the earlier afterburners had a clam-shell or eyelid-type of sheet-metal exit nozzle constructed from N-155 or

a similar material. Many present high-production afterburners still use the eyelid-type nozzle. (See Fig. 4.) In the open, or afterburning, position, the nozzle is at 1800-1900 F. In the closed position, the nozzle is at turbine exhaust temperature, 1200-1400 F. The eyelids rotate on bearings that have been moved far enough away from the high-temperature area to function reliably.

Under operating conditions, the bulbous shape of the nozzle wants to open up from its fabricated shape. To prevent this, a comparatively heavy, box-type structure must be built on the side of the nozzle components away from the flame to keep them round. This structure is costly in weight, fabrication time, and functional design considerations. For these reasons, the eyelid-type nozzle is being replaced in newer designs by segmental, iris-type nozzles.

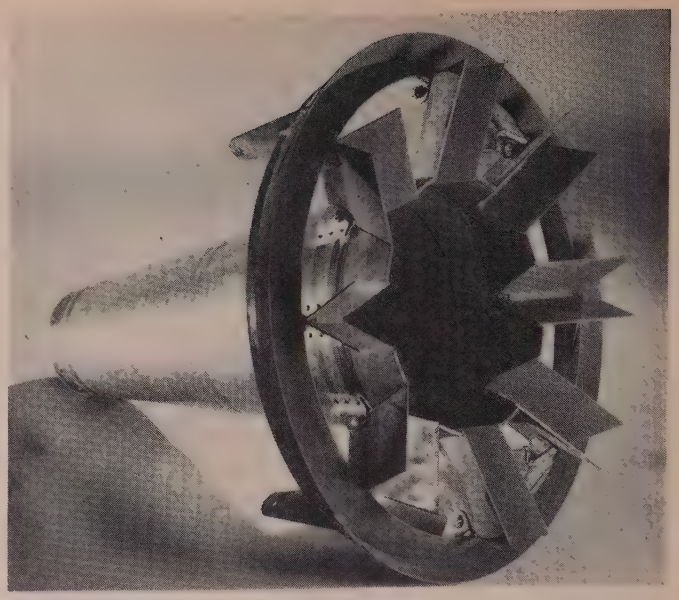

Fig. 6 – View of ramjet gutter-type flame holder

Ramjet Engines

A. Brief Description of Operation – Ramjets are air-breathing jet engines essentially containing no moving parts. Fig. 5 illustrates a typical supersonic ramjet with the various components labeled. The principle of operation is the same as that for any other air-breathing jet engine: compress air, introduce fuel into the compressed air, burn the mixture, and exhaust combustion gases in such a manner to produce a net forward thrust. Actually, the ramjet can be roughly compared to a turbojet in the following manner:

The ramjet depends upon its forward motion and the configuration of its inlet, or diffuser, to sufficiently compress incoming air. A turbojet requires a compressor to do this. The compressed air is then driven back into the fuel injector area, where fuel is sprayed into it. From there the fuel-air mixture enters the combustion chamber. The ramjet combustion chamber corresponds to the combustion chambers in a turbojet. Hot combustion gases are exhausted through the exit nozzle. The differences are these: Since the ramjet does not need a compressor to compress air, it requires neither a turbine to drive the compressor nor a compressor drive shaft which necessitates placing several small combustion cans about the shaft instead of using a single large-diameter combustion chamber. Therefore, all the ramjet has in common with the turbojet is an inlet, a fuel injector, and a combustion chamber. In addition, there is a flameholder in a ramjet creating a turbulence in the air stream within the combustion chamber such that it will support combustion. This layman's description of the ramjet gives one a quick picture of the basic principles of operation. We have been pioneers in ramjet development, initiating work on this type of heat engine over 10 years ago.

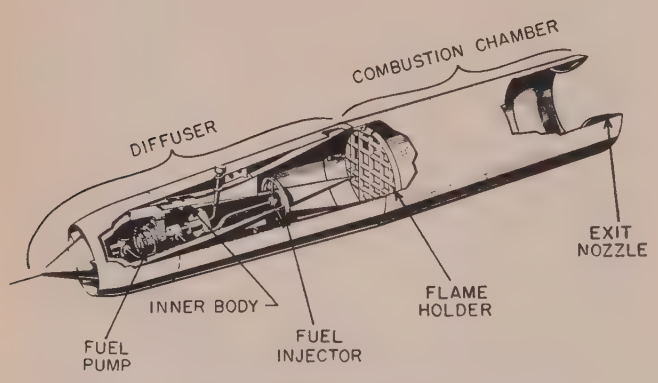

Fig. 5 – Cutaway of typical supersonic ramjet engine

B. Field of Application – The ramjet cannot produce static thrust. The principle of compression by ramming air into the engine requires that some means be provided to get the aircraft moving at speeds sufficient for it to sustain burning with usable thrust. For optimum engine performance, the versatility of this propulsion system is limited to a specific range of speeds and altitudes for which it has been designed. Ramjet propulsion is used in the guided missile field, with rocket boosters usually used to initially accelerate the missile. In the field of guided missile powerplants, the ramjet performs an essential job providing the most economical means of propulsion to several types of missiles for intermediate- and long-range applications at intermediate altitudes and Mach numbers. It occupies a niche all its own between the capabilities and limitations of turbojets on the low

speed and altitude side and rockets on the high speed and altitude side. It is particularly suited to single-shot missile applications because of its constructional simplicity and low fabrication costs. Its thrust-to-weight ratio of approximately 20/1 is also a salient feature.

C. Flameholders – The only components of ramjets that operate at service temperatures in excess of 1200 F are the flameholder, combustion chamber, and exit nozzle. The flameholders may be either the gutter- or can-type.

(1) Gutter-type flameholder: Gutter-type flameholders consist of radial and/or annular V-shape gutters fabricated from AISI 321 stainless steel sheet up to ⅛ in. thick painted with a fire-resistant, inorganic-base paint called pyrochrome. (See Fig. 6.) AISI 321 stainless steel is used primarily because of its availability. As flameholder design is refined, considerable advantage can be had, weightwise, from use of higher strength alloys. Operating gutter temperatures are high, reaching 1800-1900 F during normal operation. However, slight variations in performance that result in flame impingement on the flameholder components can result in actual burning of gutter edges at temperatures considerably above 2000 F. This is not detrimental to the functioning of the engine, for it is a momentary situation if and when it occurs.

There are several types of loading imposed upon the various parts of the flameholder. High thermal stresses are induced by large temperature differentials from the flame side to the back side of the gutters. This is due to combustion gas at 3500 F radiating heat to one side of the gutter and cooling diffuser air at 600-800 F hitting the opposite side of the gutter. In addition, a high differential pressure across the V gutter tends to collapse the V cross section of the gutter. Suspension of the unit in the center of the engine aft of the diffuser exposes it to extreme vibration loads generated by the combustion process.

Gutter-type flameholders are fabricated from formed sheet-metal joined by fusion and resistance welding, riveting, and bolting. A conical pilot can of AISI 321 stainless steel containing the engine ignition system is located at the forward side of the flameholder.

(2) Can-type flameholder: The can-type flameholder in a standard engine is a truncated cone several feet long, varying in diameter from about one foot to a diameter approaching the engine diameter, approximately three feet. The cone has holes of various sizes along its length ranging up to several inches in diameter. Diffuser air passes through these holes to the inside, where burning takes place. The pilot can containing the ignition system is attached at the small diameter (upstream) end of the can. The pilot can may be a truncated cone or a cylinder with a hemispherical head.

The high operating temperatures of both the pilot and perforated main can, which may reach temperatures over 2000 F in service, necessitate the use of a high scaling-resistant material. For this application, AISI 310 stainless steel and Hastelloy X have been considered. The high chromium content of both materials imparts high scaling resistance. The service loads on the can are collapsing loads for which a conical shape provides maximum resistance. The high modulus of elasticity of these materials also helps resist collapsing loads. In the hotter areas of the can, material 0.125-in. thick is used to resist collapsing.

Holes are punched in the sheet-metal before it is rolled into a conical shape and fusion welded. Finish of the holes is an important operation; improperly done, it may result in elevated-temperature radial fatigue cracks. The cans are painted with pyrochrome paint to reduce oxidation.

D. Combustion Chamber – The combustion chamber of a ramjet is a cantilevered, large-diameter, thin wall cylinder protruding aft several feet beyond its junction point with the diffuser. (See Fig. 7.) The combustion chamber and integral exit nozzle, together with the flameholder, account for approximately half the entire engine weight and compose the combustion temperature limiting components in ramjets. The chamber is, essentially, a thin-wall pressure vessel subject to varying pressures and cantilever loads creating large vibrations and fluctuations of the skin material.

The chamber is fabricated from 0.050-0.078 in. thick N-155 alloy into cylinders as large as 35 in. in diameter and 8 ft long. The exit nozzle portion of the chamber is formed from 0.078 in. sheet N-155 and is an integral, unfaired portion of the chamber. The service temperatures reach 1850-1950 F with local hot spots, the area at the nozzle throat reaching short-time temperatures up to 2200 F. The

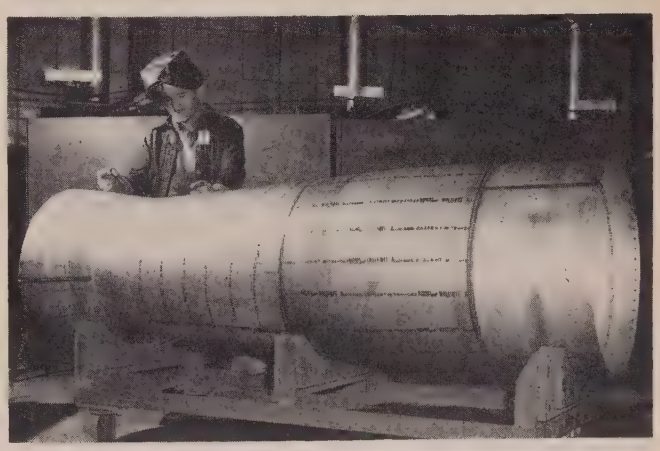

Fig. 7 – Welded ramjet combustion chamber

forward section, where the chamber is bolted to the diffuser, reaches temperatures only of about 1000-1200 F.

Fabrication of the chamber involves rolling and welding of cylinders and cones. The contoured sections forming the nozzle area are made on an expanding mandrel. The welds are a critical part of the assembly. Welds are made using heliarc welding with no addition of filler rod. The completed joint is roll-leveled to produce a flush, stress-relieved joint that will stand up at the high operating temperatures. The outside surface of the chamber is treated in a molten sodium dichromate bath to produce a black, highly emissive surface coating. No protection is given the inside surface of the chamber. A spot welded doubler is located at the throat of the chamber to strengthen the hottest part of the unit and stabilize fluctuation of the exit section during operation.

It has been found that the carbide precipitation characteristics of N-155 alloy used in the combustion chamber are an excellent indication of the top temperature the metal in a particular area of the combustion chamber has been subjected to. This tool has been very valuable in failure analysis work during the development of this chamber. Between temperatures of 1800 and 2300 F and for the service times involved in ramjets (of the order of several minutes), precipitation of carbides occurs in the grain boundaries of N-155 that will permit pinpointing the temperature within 25-50 F.

The chamber is cooled in flight by the convection of cool air along the outside surface and by radiation of heat from the outside surface to the atmosphere. For these reasons, the change in section near the throat cannot be made too severe, lest air layer separation occur and convective cooling lost. Radiation cooling is enhanced by the black, high emissivity coating on the outside surface.

Rockets

The use of metals in rockets at service temperatures above 1000 F and below the melting point of the metal is usually limited to three classes of rockets: liquid-propellant rockets whose service life is 0 to 4 sec, solid-propellant rockets, and regeneratively cooled rockets with service lives of several seconds to a minute or more. Uncooled rockets with intermediate service lives use ceramic materials to withstand combustion temperatures. Rocket components operating at elevated temperatures caused by the combustion process are the combustion-chamber liner and the exit nozzle.

A. 0-4 Sec, Uncooled, Liquid-Propellant Rockets – Mild steel and SAE 4130 alloy steel are used in the combustion-chamber area of short-life rockets. The rate of deterioration of these materials is calculated to be slow enough for the rocket life. The chambers are rolled plate, welded and machined to shape. The steel is painted to prevent rusting prior to service. Alloy or mild steels rather than high-temperature alloys are used in these applications primarily because the combustion temperatures in rockets are so much in excess of the melting temperatures of all constructional metals that the use of any metal is strictly a function of the amount of deterioration during its service life.

B. Regeneratively Cooled Rockets – Rocket engines that must operate for times of the order of a minute require a method of drastically cooling the combustion chamber walls. Even ceramic materials will deteriorate excessively under the operating conditions if uncooled. Therefore, double-wall rocket chambers are fabricated by one of several methods. Rocket fuel is passed through the area between the walls – thereby cooling the inner wall – before it passes into the combustion chamber to be burned.

Typical construction consists of an inner liner wall of ⅛-in. "A" nickel (of good thermal conductivity), mild steel, or SAE 4130 steel, and a 3/16-in. exit nozzle wall of the same materials. The cooling action keeps the liner and nozzle wall surfaces between 1200 and 1500 F for the expected service life. Again, it is seen that the tendency is to use a high-conductivity material or low-alloy steel rather than a high-temperature alloy. The weight per unit area of wall is not as critical as in afterburners and ramjets, where 0.050-0.070-in. thick combustion-chamber materials must be used to reduce weight. The relative size is an important factor here. Rockets are usually smaller in diameter and length than afterburners and ramjets.

C. Solid-Propellant Rockets – This type rocket is usually of short burning duration and is designed so that fuel is burned from the center out to the liner wall, thus keeping the wall as cool as possible. Typical solid-propellant liners and exit nozzles are rolled or forged cylinders of mild steel or SAE 4130, finish-machined to shape. Fiberglass laminates have even been used in a short-time application.

Conclusion

The application of high-temperature metals to afterburners, ramjets, and rockets is rapidly pushing the present constructional metals to their performance limits. A ramjet with hot spots at 2200-2300 F is operating within 200-300 F of the melting temperatures of the best high-temperature alloys. The ramjet designer must look forward to molybdenum, ceramic coatings, or cermets as future materials to withstand ever-increasing combustion temperatures. The place for the known construction materials in the combustion component picture has been set. We must await development of new materials and/or resort to cooling methods in order to take advantage of the greater performance attainable from higher combustion temperatures.

The Low Silhouette Drive Line

R. Burkhalter and P. J. Mazziotti, Dana Corp.

This paper was presented at the SAE Annual Meeting, Detroit, January 13, 1956.

PASSENGER-car styling considerations on new cars demand reduced height to produce the low silhouette now in vogue. To achieve this reduced height, there are several possibilities. The roof can be lowered closer to the seats; however, a practical limit has already been reached. Ground clearance can be reduced by reducing tire diameter or lowering engine and other mechanical parts closer to the ground. Some lowering at this point will probably be accomplished; however, cars must still be able to clear a reasonable ramp angle and clear obstacles without danger to the lower portions. Aside from reducing clearance, the drive line must be lowered to lower seats and floor line. A drive line configuration revised to allow a lower tunnel and floor can help lower the entire car.

This paper will review problems involved in accomplishing a lower drive line in a passenger car. The drive line must transmit torque from the engine located at the front of the vehicle to an axle located at the rear driving wheels if our present passenger-car configuration is to remain. This might, of course, be revised to a front-wheel-drive car or a rear-engine car at some time in the future; however, this paper will deal generally with problems in the conventional arrangement.

Today's typical passenger car uses a one-piece

PASSENGER-CAR styling considerations demand a low silhouette. The drive line must be lowered to provide reduced height. Several possible configurations could be used to achieve this, but each is limited by the excitation which can be absorbed without objectionable disturbances.

These effects are explored in so far as they vary with drive-line revisions and practical limits established. This permits comparison of possible drive-line arrangements as they affect lowering of the car.

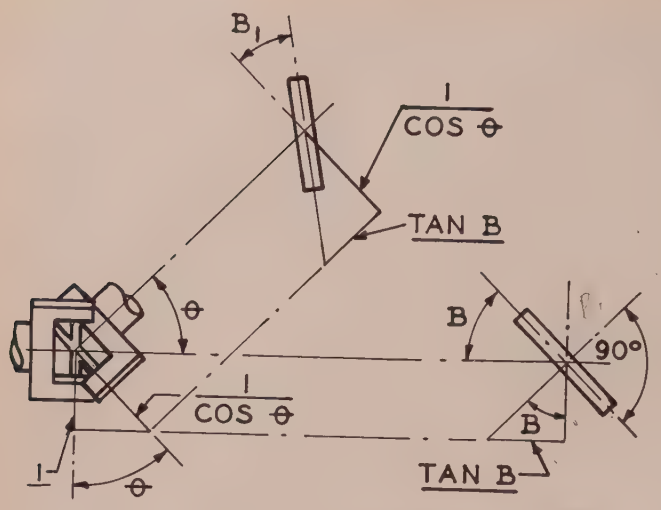

Fig. 1 – Angular relationships

propeller shaft equipped with two universal joints to connect transmission and rear-axle pinion. Universal joints generally are of the conventional Cardan- or cross-type, and operate through comparatively small joint angles while running. This type universal joint has unusual nonuniform motion characteristics which can present problems.

Present passenger cars with small joint angles and reasonably long propeller shafts keep resulting excitations down to a level where they are not usually troublesome. With this arrangement, satisfactory drive lines have resulted despite nonuniform motion characteristics. Under instantaneous conditions of metal-to-metal contact and full rebound, considerable excitation is often present; however, these are not usually noticeable.

Car height might be lowered a bit merely by using larger joint angles. This would allow tipping down the axle pinion and lowering the rear of the engine to provide lower tunnel height. This cannot usually be done due to higher excitation forces present with larger joint angles. A revised drive line configuration can provide desired lower tunnel and floor if proper consideration is given to maintaining excitation within reasonable limits. Many possibilities along this line will be discussed. To accomplish as much lowering as possible, excitation must be more carefully controlled to allow absorption of as much as possible without objectionable disturbances. This requires a more complete study of the various types of excitation and their effects. To this end, this paper is divided into three sections:

1. Review of equations of motion resulting from a Cardan-type universal joint operating at an angle. This will include an analysis of simplified equations used to aid in the analysis. These simplified equations allow use of conventional sine wave relationships to solve problems where the actual curve varies slightly from a sine wave.

2. Types of excitation resulting from nonuniform motion and their effects on the vehicle. This will include some maximum limits of excitation which generally have been found acceptable.

3. Comparison of some possible drive line configurations which can reduce car height. A hypothetical typical passenger car of today is proportioned showing heights resulting with present drive line. This is compared to the lowering possible with some other configurations which can be used.

Maximum reduction possible with a complete change in vehicle arrangement is shown in the concluding section of the paper.

Equations

Equations of motion of a Cardan-type joint are derived using the following notation:

ω = Angular velocity of drive yoke – assumed uniform in the analysis

ω_1 = Angular velocity of driven yoke

θ = Joint angle

β = Angle of rotation of drive yoke from position where it is normal to the plane of joint angle

β_1 = Angle of rotation of driven yoke from position where it is in the plane of joint angle

Γ = Torque on input yoke – assumed uniform in the analysis

Γ_1 = Torque on output yoke

C = Secondary couple on drive yoke

C_1 = Secondary couple on driven yoke

α = Angular acceleration of drive yoke – assumed zero in the analysis

α_1 = Angular acceleration of driven yoke

α_{1m} = Maximum value of α_1

σ = Angle of lag of driven yoke

A = Amplitude of torsional vibration

Fig. 1 shows the basic angular relationship of a joint operating at an angle. The illustration shows the fundamental relationship between β_1 and β:

$$\tan \beta_1 = \cos \theta \tan \beta \tag{1}$$

Differentiating (1) with respect to time:

$$\sec^2 \beta_1 \frac{d\beta_1}{dt} = \sec^2 \beta \frac{d\beta}{dt} \cos \theta$$

Since:

$$\frac{d\beta_1}{dt} = \omega_1, \frac{d\beta}{dt} = \omega$$

$$\sec^2 \beta_1 \omega_1 = \sec^2 \beta \, \omega \cos \theta$$

$$\omega_1 = \frac{\sec^2 \beta \, \omega \cos \theta}{\sec^2 \beta_1}$$

But:

$$\tan^2 \beta_1 = \cos^2 \theta \tan^2 \beta$$

And:

$$\sec^2 \beta_1 = 1 + \tan^2 \beta_1$$

Whence:

$$\omega_1 = \frac{\omega \cos \theta \sec^2 \beta}{1 + \cos^2 \theta \tan^2 \beta}$$

With:

$$\sec^2 \beta = \frac{1}{\cos^2 \beta}$$

$$\omega_1 = \frac{\omega \cos \theta}{(1 + \cos^2 \theta \tan^2 \beta) \cos^2 \beta}$$

With:

$$\tan^2 \beta = \frac{\sin^2 \beta}{\cos^2 \beta}$$

$$\omega_1 = \frac{\omega \cos \theta}{\cos^2 \beta + \cos^2 \theta \sin^2 \beta}$$

$$= \frac{\omega \cos \theta}{(1 - \sin^2 \beta) + \sin^2 \beta (1 - \sin^2 \theta)}$$

Finally:

$$\omega_1 = \frac{\omega \cos \theta}{1 - \sin^2 \beta \sin^2 \theta} \qquad (2)$$

Differentiate (2) with respect to time, to find angular acceleration, α:

$$\frac{d\,\omega_1}{dt} = \frac{-\omega \cos \theta \left(-\sin^2 \theta\, 2 \sin \beta \cos \beta \frac{d\,\beta}{dt}\right)}{(1 - \sin^2 \beta \sin^2 \theta)^2}$$

Since:

$$\frac{d\,\omega_1}{dt} = \alpha_1, \quad \frac{d\,\beta}{dt} = \omega$$

$$\alpha_1 = \frac{2\,\omega^2 \cos \theta \sin^2 \theta \cos \beta \sin \beta}{(1 - \sin^2 \beta \sin^2 \theta)^2} \qquad (3)$$

Amplitude of torsional vibration resulting from a Cardan joint operating at an angle, A, is the maximum difference between β and β_1.

If $\beta - \beta_1 = \sigma$, then:

$$\beta_1 = \beta - \sigma$$

$$\tan (\beta - \sigma) = \cos \theta \tan \beta$$

$$\frac{\tan \beta - \tan \sigma}{1 + \tan \beta \tan \sigma} = \cos \theta \tan \beta$$

$$\tan \beta - \tan \sigma = \cos \theta \tan \beta + \cos \theta \tan^2 \beta \tan \sigma$$

$$\tan \sigma = \frac{\tan \beta (1 - \cos \theta)}{1 + \cos \theta \tan^2 \beta}$$

Since σ is maximum and equal to A, when $\tan \sigma$ is maximum,

$$\frac{d\,(\tan \sigma)}{d\,(\tan \beta)} =$$

$$\frac{(1-\cos \theta)(1+\cos \theta \tan^2 \beta) - \tan \beta (1-\cos \theta)\, 2 \tan \beta \cos \theta}{(1 + \cos \theta \tan^2 \beta)^2}$$

$$= \frac{(1-\cos \theta)(1+\cos \theta \tan^2 \beta) - 2 \cos \theta \tan^2 \beta (1-\cos \theta)}{(1 + \cos \theta \tan^2 \beta)^2}$$

This is equal to zero where σ is maximum and equal to A.

$$(1 - \cos \theta)(1 + \cos \theta \tan^2 \beta) = 2 \cos \theta \tan^2 \beta (1 - \cos \theta)$$

$$\cos \theta \tan^2 \beta = 1$$

$$\tan \beta = \pm \left(\frac{1}{\cos \theta}\right)^{\frac{1}{2}}$$

$$\beta = \tan^{-1} [\pm (\cos \theta)^{\frac{1}{2}}] \qquad (4)$$

where σ is maximum.

For $\beta - \beta_1 = A$, and at the point which suits equation (4):

$$\beta_1 = \tan^{-1} (\cos \theta \tan \beta)$$

or: $$A = \tan^{-1} [(\cos \theta)^{-\frac{1}{2}}] - \tan^{-1} [\cos \theta (\cos \theta)^{-\frac{1}{2}}]$$

$$A = \tan^{-1} [(\cos \theta)^{-\frac{1}{2}}] - \tan^{-1} [(\cos \theta)^{\frac{1}{2}}] \qquad (5)$$

These are the equations for the actual motion, velocity and acceleration of a Cardan joint operating through an angle. As such, they are hard to handle. A much simpler set of equations can be obtained using the following:

θ = A small angle; if necessary the following approximations can be made:

$$(\cos \theta)^{\frac{1}{2}} \approx 1$$

$$\sin^2 \theta \approx 0$$

$$A = \tan^{-1} [(\cos \theta)^{-\frac{1}{2}}] - \tan^{-1} [(\cos \theta)^{\frac{1}{2}}]$$

This is exactly equation (5) for torsional amplitude.

This equation is a special condition for:

$$\sigma = \beta - \beta_1$$

in which:

$$\beta_1 = \beta_{1m} = \tan^{-1} [(\cos \theta)^{\frac{1}{2}}]$$

$$\beta = \beta_m = \tan^{-1} [(\cos \theta)^{-\frac{1}{2}}]$$

$$A = \beta_m - \beta_{1m}$$

$$\tan A = \tan (\beta_m - \beta_{1m})$$

$$= \frac{\tan \beta_m - \tan \beta_{1m}}{1 + \tan \beta_m \tan \beta_{1m}}$$

$$= \frac{(\cos \theta)^{-\frac{1}{2}} - (\cos \theta)^{\frac{1}{2}}}{1 + 1}$$

$$= \frac{1 - \cos \theta}{2 (\cos \theta)^{\frac{1}{2}}}$$

Since $(\cos \theta)^{\frac{1}{2}} \approx 1$ and $\tan A \approx A$ (in radians),

$$A \approx 1/2 (1 - \cos \theta) \qquad (6)$$

This can be expressed in another approximate form: cosine of the joint angle can be expressed by the trigonometric series:

$$\cos \theta = 1 - \frac{\theta^2}{2!} + \frac{\theta^4}{4!} - \frac{\theta^6}{6!} + \cdots\cdots$$

For small values of θ this is approximately

$$\cos \theta = 1 - \frac{\theta^2}{2!} = 1 - \frac{\theta^2}{2}$$

whence:

$$1 - \cos \theta = \frac{\theta^2}{2}$$

This gives another approximate equation:

$$A \approx \frac{\theta^2}{4} \qquad (7)$$

with A and θ in radians

Torsional amplitude of vibration due to joint angle can be approximated by either equation (6) or (7).

The approximate analysis can be applied to equations of motion, velocity, and acceleration as follows:

Actual equation of motion is:

$$\beta_1 = \tan^{-1} (\cos \theta \tan \beta)$$

$$\sigma = \beta - \beta_1$$

$$\sigma = \tan^{-1} \left[\frac{\tan \beta (1 - \cos \theta)}{1 + \cos \theta \tan^2 \beta}\right]$$

This equation of actual motion is expressed in terms of the relationship between torsional oscillation and angle of rotation of drive yoke.

Since:

$$A \approx \frac{1 - \cos \theta}{2} \qquad (6)$$

and for small angles:

$$\sigma \approx \tan \sigma \ (\sigma \text{ in radians})$$

$$\sigma = \frac{\tan \beta \, 2A}{-2A \tan^2 \beta + [1 + \tan^2 \beta]}$$

$$= \frac{\frac{\sin \beta}{\cos \beta} 2A}{-2A \frac{\sin^2 \beta}{\cos^2 \beta} + \frac{1}{\cos^2 \beta}}$$

$$= \frac{2A \sin \beta \cos \beta}{-2A \sin^2 \beta + 1}$$

$$-2A\sigma \sin^2 \beta + \sigma = 2A \sin \beta \cos \beta = A \sin 2\beta$$

$$\sigma = A \sin 2\beta + 2A\sigma \sin^2 \beta$$

Since $A\sigma$ is small (it is actually smaller than A^2, which itself equals $\frac{\theta^4}{16}$), ignoring this quantity in the equation results in $\sigma = A \sin 2\beta$.

Here σ represents an angle of lag of the driven yoke. To express driven yoke motion as a sine wave, the wave is in phase with output shaft motion if oscillation is represented as a lead of the driven yoke. Therefore σ is replaced by σ_1, which two have the same absolute value except for a phase shift equal to ½ wave length:

$$\sigma_1 = -A \sin 2\beta \qquad (8)$$

This is a negative sine wave of amplitude A with 2 oscillations per revolution of β.

Angular velocity is actually expressed by equation (2) as:

$$\omega_1 = \frac{\omega \cos \theta}{1 - \sin^2 \beta \sin^2 \theta}$$

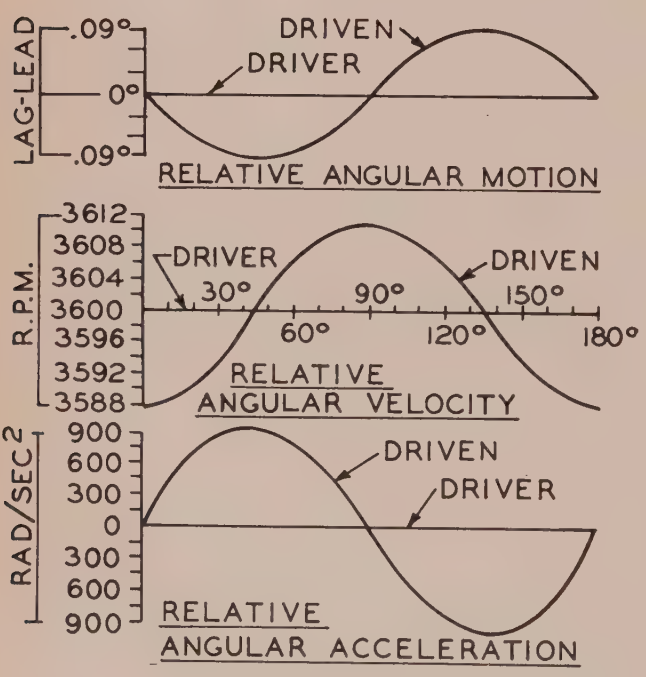

Fig. 2 – Motion characteristics for 4½-deg joint angle at 3600 rpm

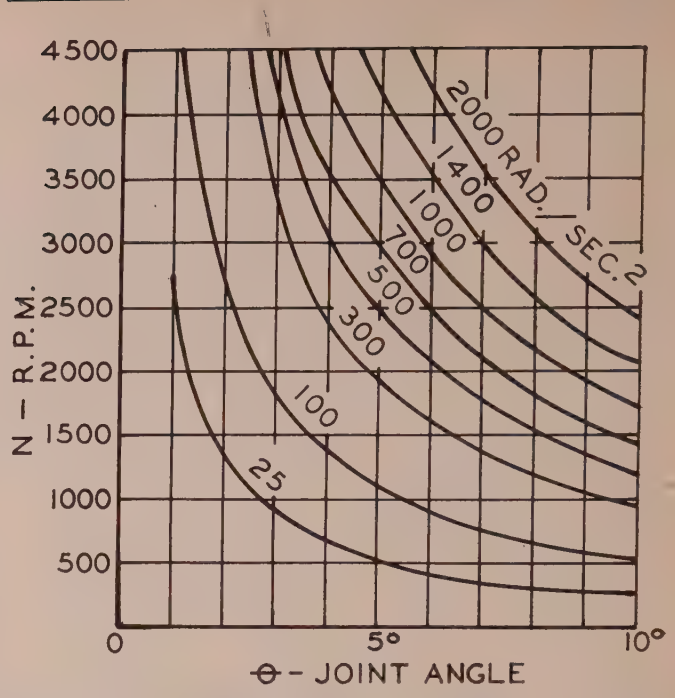

Fig. 3 – Maximum angular acceleration as function of joint angle and rpm

Which can also be expressed as:

$$\omega_1 = \omega + \frac{d\sigma_1}{dt}$$

$$= \omega - 2A \cos 2B \frac{d\beta}{dt}$$

Since:

$$\frac{d\beta}{dt} = \omega,$$

$$\omega_1 = \omega - 2A\omega \cos 2\beta \qquad (9)$$

The same solution can be used for acceleration.

$$\alpha_1 = \alpha + \frac{d\omega_1}{dt}$$

Since α is assumed to be zero:

$$\alpha_1 = \frac{d\omega_1}{dt} = +4A\omega \sin 2\beta \frac{d\beta}{dt}$$

$$\alpha_1 = 4A\omega^2 \sin 2\beta \qquad (10)$$

These characteristics are shown in Fig. 2. The maximum value of α_1 is:

$$\alpha_{1\,max} = 4A\omega^2$$

These maximum values are shown in Fig. 3.

The force relationships existing on a Cardan-type joint transmitting torque at an angle is shown in Fig. 4. Notation is the same as before, with the following additions:

τ = Angle between drive yoke and journal cross

μ = Angle between driven yoke and journal cross

Γ_0 = Torque on journal cross

$$\Gamma_0 = \Gamma/\cos \tau$$

$$\Gamma_1 = \Gamma_0 \cos \mu = \frac{\Gamma \cos \mu}{\cos \tau}$$

$$\cos \mu = \sin \theta \, (\text{ctn}^2 \theta + \cos^2 \beta)^{\frac{1}{2}} = \frac{\text{ctn } \theta}{(\text{ctn}^2 \theta + \cos^2 \beta)^{\frac{1}{2}}}$$

$$\Gamma_1 = \frac{\Gamma \, (\text{ctn}^2 \theta + \cos^2 \beta) \sin \theta}{\text{ctn } \theta}$$

$$\Gamma_1 = \Gamma \left[\frac{\cos^2 \theta}{\sin^2 \theta} + (1 - \sin^2 \beta) \right] \frac{\sin^2 \theta}{\cos \theta}$$

$$\Gamma_1 = \Gamma \frac{[\cos^2 \theta + \sin^2 \theta - \sin^2 \beta \sin^2 \theta]}{\cos \theta}$$

$$\Gamma_1 = \frac{\Gamma \, [1 - \sin^2 \beta \sin^2 \theta]}{\cos \theta} \qquad (11)$$

This relationship also follows from equation (2):

$$\omega \, \Gamma = \omega_1 \, \Gamma_1$$

This holds at all times since there is no change in power.

$$\Gamma_1 = \frac{\omega \, \Gamma}{\omega_1}$$

$$\Gamma_1 = \frac{\Gamma \, (1 - \sin^2 \beta \sin^2 \theta)}{\cos \theta} \qquad (11)$$

$$C = \Gamma \tan \tau = \Gamma \tan \theta \cos \beta$$

$$C = \Gamma \tan \theta \cos \beta \qquad (12)$$

This is a cosine wave with amplitude:

$$C_{max} = \Gamma \tan \theta \qquad (13)$$

$$C_1 = \Gamma_0 \sin \mu = \frac{\Gamma \sin \mu}{\cos \tau}$$

$$C_1 = \Gamma \frac{\sin \beta \sin \theta \, (\text{ctn}^2 \theta + \cos^2 \beta)^{\frac{1}{2}}}{\text{ctn } \theta}$$

$$C_1 = \Gamma \sin \theta \sin \beta \, (1 + \tan^2 \theta \cos^2 \beta)^{\frac{1}{2}}$$

Again, for θ small, $\tan^2 \theta$ is very small. $\cos^2 \beta$ cannot be more than 1, so we ignore the $\tan^2 \theta \cos^2 \beta$ term. Thus:

$$C_1 \approx \Gamma \sin \theta \sin \beta \qquad (14)$$

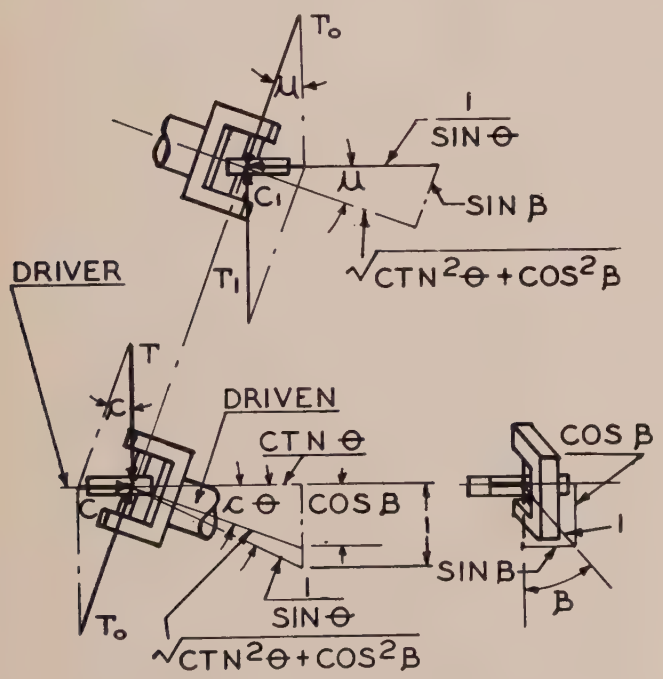

Fig. 4 – Force relationships

Table 1 – Per Cent Error for Approximate Values of A, A_1, and $\alpha_{1\,max}$

Joint Angle, deg	Error from True Value, % $A_1 = \frac{1}{2}(1 - \cos \theta)$	$A = \frac{\theta^2}{4}$	$\alpha_{1\,max} = 4A\omega^2$ *
2	....	....	....
4	0.13	0.15	0.17
6	0.27	0.22	0.23
8	0.46	0.29	0.50
10	0.77	0.50	0.75
12	1.12	0.76	1.06
14	1.52	1.04	1.42
16	1.94	1.23	1.81
18	2.43	1.67	2.86
20	2.97	1.96	2.72

* Based on practical maximum acceleration at 45-deg angle of rotation.

$$\alpha_{1\,max} = \frac{\cos \theta \sin^2 \theta}{\left(1 - \frac{\sin^2 \theta}{2}\right)^2} \omega^2$$

For small angles $\sin \theta \approx \tan \theta$, so that values of the couple on the drive and driven yokes are approximately equal.

Summary – The following equations can be used in solving practical joint angle problems when θ is small:

$$A = 1/2 \, (1 - \cos \theta) \qquad (6)$$

or

$$A = \theta^2/4 \qquad (7)$$

(A and θ in radians)

$$\alpha_1 = -A \sin 2\beta \qquad (8)$$

$$\omega_1 = \omega - 2A\omega \cos 2\beta \qquad (9)$$

$$\alpha_1 = 4A\omega^2 \sin 2\beta \qquad (10)$$

$$\alpha_{1\,max} = 4A\omega^2$$

$$C = \Gamma \tan \theta \cos \beta \qquad (12)$$

$$C_{max} = \Gamma \tan \theta \qquad (13)$$

$$C_1 = \Gamma \sin \theta \sin \beta \qquad (14)$$

$$C_{1\,max} = \Gamma \sin \theta \qquad (15)$$

Accuracy of these approximations is shown in Table 1.

Excitation and Effects

Nonuniform angular rotation characteristics of the Cardan-type joint produce fluctuating speeds and torques with resulting excitations on propeller-shaft assembly and supporting members. This excitation can be classified into three basic types, each with its own distinctive characteristics and effect. Disturbances resulting from these different excitations can be identified by these characteristics and general maximum limits of allowable excitation established based upon similar installations.

Torsional Excitation – The nonuniform velocity obtained when the universal joint operates at an

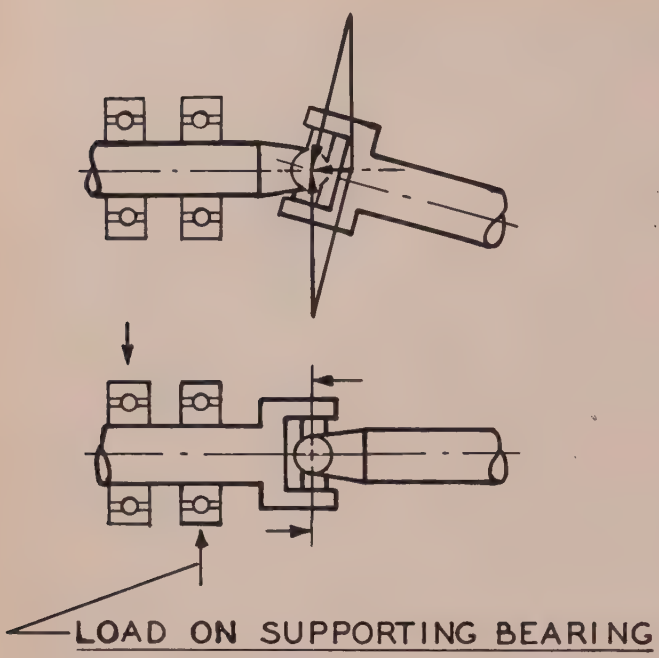

Fig. 5 – Secondary couple force on supporting bearing

angle produces torsional vibration. With a propeller shaft containing two universal joints, it is desirable to have equal angles on both joints and torsional oscillations in phase-opposition to each other so that the whole produces uniform velocity characteristics over the 2-joint system. Since absolutely equal angles are practically impossible throughout the operating range, it is necessary to determine some maximum limit of inequality of angles or torsional excitation which can be accepted. The effect of two universal joints on a propeller shaft operating through unequal angles can be combined and expressed as an equivalent single-joint angle producing the same torsional oscillation.

Amplitude of torsional oscillation acceptable without causing excessive disturbance depends upon operating speed and characteristics of mounts and other units in the drive line. It has been found that if this excitation is maintained within the effect of a maximum angular acceleration of 400 radians per sec^2 in any continuous operating position and speed, the drive line in a passenger car is satisfactory. This is equivalent to driving the system with a single universal joint at an angle of about 3 deg at 3600 rpm.

Excessive torsional excitation can be identified through its characteristics:

(a) Torsional vibration produces oscillating reaction torque on major supports. This can affect engine mounts and rear-axle spring supports, especially through any resonant frequency of these mountings. The disturbance is usually frequency- and torque-sensitive. Extreme peaks of vibration and noise will often show up through a short speed range under specific loading characteristics. This very often occurs under full-drive or full-coast, where mounts are fully deflected and have their highest vibration-transmitting characteristics.

(b) Torsional fluctuation of supporting shafts can cause load and unload cycles on driving parts, and thus tends to accentuate gear noises and clatter which otherwise may not be noticeable.

(c) Rotating parts not under load are often oscillated within their backlash limitations. This can be especially disturbing when the rotating part tends to have a resonant frequency and is excited by the torsional vibrations to produce objectionable noise.

Inertia Excitation – This excitation is produced by oscillating torque loads resulting from propeller-shaft inertia being accelerated through nonuniform motion. This exists with any propeller shaft operating at a joint angle, even when torsional excitation is eliminated by exactly equal angles producing complete cancellation. Inertia of the center member in a propeller shaft produces fluctuating torque loads due to changes in velocity. Amount of torsional fluctuations depends upon size of joint angle and inertia of the propeller-shaft center member. This type fluctuation limits choice of the maximum acceptable joint angle.

Passenger-car installations have been found extremely sensitive to this type excitation and to the disturbances it creates. Generally, for average installations with a relatively large propeller-shaft inertia, the excitation must be kept under a maximum acceleration of 1000 radians per sec^2 in any continuous operating position. This is equivalent to operating the shaft at 4½-deg joint angles at 3600 rpm. A conventional 2-joint propeller-shaft drive line falls into this class. With any small propeller-shaft inertia, acceleration can often be increased to 2000 radians per sec^2, which is equivalent to a 6½-deg joint angle at 3600 rpm. Extremely short, small-diameter propeller shafts used in some applications allow this increased acceleration due to small propeller-shaft inertia.

In multiple propeller-shaft installations, it is often possible to arrange the system so that acceleration of the shafts are in phase-opposition to each other and so reduce the effect on the overall system. This type arrangement will allow use of larger joint angles for those applications where cancellation can be achieved. The typical 3-joint installation in a passenger car with center bearing generally does not allow full advantage of this cancellation due to the arrangement required to cancel secondary couple loads.

Inertia excitation usually produces disturbances in the unloaded or very lightly loaded drive condition. Effects are similar to that of torsional excitation, except that they are usually identified with light load conditions. This shows up most

often during a float-down condition. Under these light loads, parts in the driving system are allowed to reverse and clatter through their backlash and clearance limitations. The resulting noise is usually extremely disturbing due to the generally low level of other noises under light load conditions. The disturbance is frequency-sensitive usually through the intermediate speed ranges.

Secondary Couple Excitation – Secondary couple force resulting from a Cardan-type joint operating at an angle produces excitation on the supports. Fig. 5 shows how this force is applied to a supporting bearing. It has been shown by equations (12) and (14) that this load has the characteristics of a sine or cosine wave with one complete oscillation per revolution. This couple load occurs in the plane of the yoke. With a rotating yoke, force on a supporting bearing changes direction with rotation. Since magnitude of the couple force also changes during rotation, complex excitation results.

Fig. 6 shows the characteristics of this force on a supporting bearing. The result is equivalent to a static force plus an oscillating force with frequency of two cycles per revolution. Generally, several yokes on a drive line produce excitation on a support. Magnitude of excitation depends on angles, bearing spans, and phase relationship of yokes.

A center-bearing mounting is very susceptible to this excitation since it has well-defined resonant frequency. Secondary couple loads excite the mounting at a rotating speed equivalent to one-half resonant speed. This is due to the "twice per revolution" characteristics of the oscillating force. With a low-frequency, low-damping mounting needed for low vibration transmission at high speed, resonant frequency occurs at low speeds (critical frequency usually 1000-1500 cpm). This will be excited twice per revolution at 500-750 rpm propeller-shaft speed. Actual joint angles in this speed range must be determined to calculate secondary loads on the mounting. These angles occur at a start, and since loads are torque-sensitive, full-throttle start angles are most important.

It has been found on installations of center bearings in passenger cars that oscillating load should be kept under 10 lb. When it exceeds this value there is a starting, shudder-type vibration due to couple loads. A good center-bearing installation will have to be studied primarily to obtain acceptable cancellation.

Additional Considerations – Installation of an automotive drive line requires consideration of some additional problems. These problems exist in all installations; however, their effect may be increased or reduced with a modified drive line to suit a low silhouette car.

1. Critical speed: The propeller-shaft assembly must be proportioned to have the relationship between bending stiffness and length provide a critical bending frequency in excess of maximum operating speed. A critical speed occurs at a rotating speed equal to the bending frequency. Critical speed of a rotating member is an unstable self-excited vibration which can build up to high amplitudes at any time. These high amplitudes can cause shaft failure. It has not been possible to produce commercially propeller-shaft assemblies adequately balanced to ensure safe operation at critical speeds for long periods of time. A new, well-balanced assembly may be capable of operating at its critical speed for some time without failure. However, as clearances increase with wear, unbalance will almost certainly become large enough so that failure can occur at critical speed.

This type of failure is potentially so dangerous at high-speed operation that it is avoided by providing a maximum operating speed always below critical speed. This requires that most passenger-car propeller shafts use a large-diameter tube in order to suit length requirements. This tube size possesses excess torsional strength and is used only for critical speed considerations. Because of this, it is possible often to reduce tube diameter at certain points where it has minimum effect on critical speed in order to obtain required clearance. In 3-joint installations where individual propeller shafts are quite short, tube diameter can be reduced to the size required for torsional strength.

2. Friction forces: Friction forces are present when length changes occur during operation. These forces are applied to the supporting units. Sup-

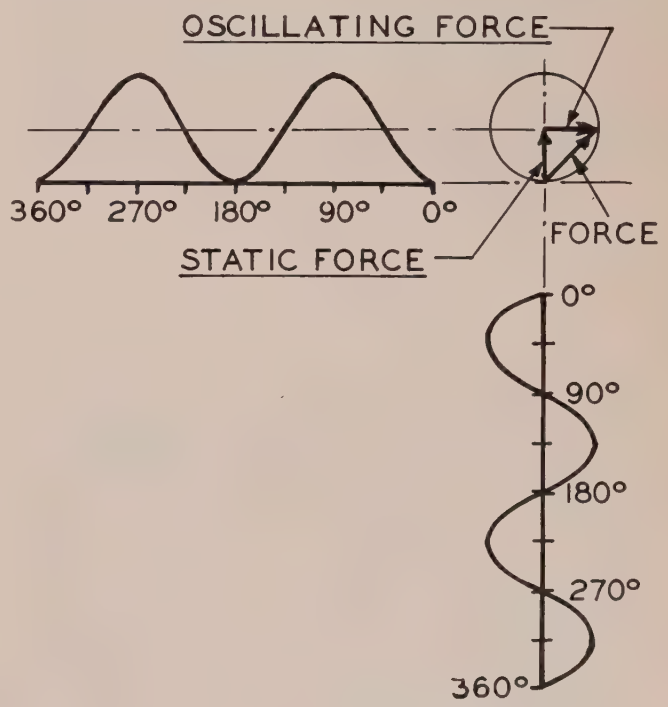

Fig. 6 – Characteristics of secondary couple force on supporting bearing

porting mountings must be designed to absorb the loads. Rolling or sliding friction can be used, depending on construction used.

Friction provides damping which limits amplitude of vibrations. This is observed often when a mount is excited by secondary couple forces at its resonant frequency.

3. Bearing capacity and torsional strength: The entire drive line must be proportioned so as to provide bearing capacity to transmit torque loads and obtain adequate life. In passenger-car installation torque requirements are selected according to vehicle weight and continuous and short-duration torques required in normal operation. Engine size and transmission ratio must be used as auxiliary considerations only since they are usually in excess of those required for normal performance.

4. Balance: A propeller shaft rotating at high speeds must be in good dynamic balance. Present standards of freedom from noise and vibration require that unbalance forces be kept at a minimum. These standards are being increased constantly as cars are improved.

Amount of unbalance which can be tolerated depends upon the sensitivity of the supporting mounts. A center bearing, in addition to engine and axle mounts, is another source for transmission of any disturbance present. The center bearing mounting characteristics must be designed to transmit as little disturbance as possible, especially at high speeds, where unbalance forces are high.

Lowering passengers closer to the drive line will necessitate improvements in present standards of unbalance limits. This, along with the higher standards, will require better and better balancing.

Comparison of Drive Line Configurations

A series of possible configurations which will result in a lower drive line is shown in Figs. 7-14. The first illustration shows a typical present drive line with a single-piece propeller shaft. This installation is used as a base line for determining the lowering possible with various arrangements. In this comparison, cars are made to clear a 15-deg ramp angle with a minimum of 6 in. ground clearance at the rear of the transmission.

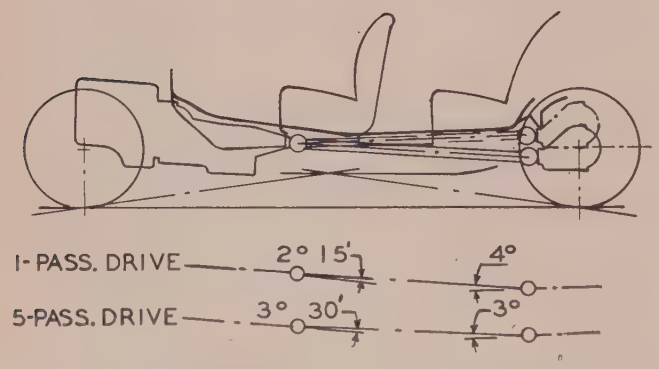

Fig. 7 – Typical passenger car with single propeller shaft

The arrangement shown is not designed to suit any particular car, but is typical present practice. In the revised arrangements, some liberties have been taken with engine angle, axle pinion angle, and length of propeller shaft in order to illustrate the points presented.

A. Typical passenger car with single propeller shaft: The arrangement shown uses a transmission extension to obtain a propeller-shaft length of 54 in., center to center. With this length a 3-in.-diameter tube is used to obtain a satisfactory critical speed.

Use of this type drive line requires a tunnel and seat height to clear the shaft as shown in Fig. 7. Joint angles are shown for 1- and 5-passenger drive positions.

The angles produce excitation as follows:

1. Torsional excitation:

1-passenger drive:

$TE_1 = (4.0^2 - 2.25^2)^{\frac{1}{2}} = 3.3$-deg equivalent joint angle

5-passenger drive:

$TE_5 = (3.5^2 - 3.0^2)^{\frac{1}{2}} = 1.8$-deg equivalent joint angle

2. Inertia excitation:

In this arrangement maximum inertia load is equivalent to the size of largest joint angle.

1-passenger drive:

$I_1 = 4$ deg

5-passenger drive:

$I_5 = 3.5$ deg

3. Secondary couple excitation:

Supporting members are excited by secondary couples resulting from torque transmitted at an angle. Amount of this excitation depends on torque transmitted and actual joint angles existing at various positions.

For joint angles shown, excitation on transmission and axle supports are as follows, based on 1000 lb-in. torque:

1-passenger drive:

Transmission end:

Couple = 1000 tan 2 deg 15 min = 1000 (0.039)
= 39 lb-in.

$$\text{Force at joint centerline} = \frac{39 + 70}{54} = 2 \text{ lb}$$

Axle end:

Couple = 1000 tan 4 deg = 1000 (0.070) = 70 lb-in.

Force at joint centerline same as at transmission end; 2 lb.

5-passenger drive:

Transmission end:

Couple = 1000 tan 3 deg 30 min = 1000 (0.061)
= 61 lb-in.

Force at joint centerline $= \frac{61 + 52}{54} = 2.1$ lb

Axle end:

Couple = 1000 tan 3 deg = 1000 (0.052) = 52 lb-in.

Force at joint centerline same as at transmission end; 2.1 lb.

B. Modifications of typical installations: Some reduction in tunnel height is possible by modifying the conventional installation. These modifications are those not changing the general angle setup and should not show much difference in excitation from the typical installation.

1. Increase pinion offset on the rear axle. This would lower the rear joint and allow the engine rear to be lowered. Problems arising with the axle in accomplishing this are outside the scope of this paper. Generally, it should be possible to lower tunnel and seats the same amount as axle offset is increased.

2. Reduce tube diameter in those locations where it has least effect on critical speed. This is possible on the ends of the propeller shaft with minimum effect. Often it is necessary to increase tube diameter in the center of the shaft to make up for reduction in critical speed from the reduced diameter at the ends.

Reduced diameter can provide increased clearance at a close point and allow for overall lowering of the car.

3. Indirect drive transmission: The drive line at the transmission end could be lowered if an indirect drive transmission is used. This requires driving through a set of transmission gears at all operating speeds. The drive line could be lowered at the transmission end by the amount of offset from the indirect drive.

The same type of modifications could be made on the revised drive line configurations. Modifications to the supporting units could lower the drive line in any of the arrangements shown. In order to eliminate repetition in exploring all possible combinations, the remainder of the paper will cover installations using more conventional units.

C. Increased joint angles: The conventional single-propeller-shaft installation uses joint angles slightly under the maximum possible. These angles could be increased to about 4 deg 30 min. Were this done, the angles would have to be maintained more equal to each other through the operating range. The lowering possible through these larger angles is quite small and is outside the accuracy involved in assumptions used here.

D. 3-joint installation with center bearing: This arrangement uses a conventional axle with the same motion as in a typical present car. Addition of the center bearing allows use of a longer drive line and eliminates need for the transmission extension. The longer drive line is also advantageous in that forces on mounts from secondary couples are reduced. Since each shaft is comparatively short, tube diameter can be selected based on strength requirements rather than on critical speed considerations. On this basis, a tube of 2-in. diameter is used.

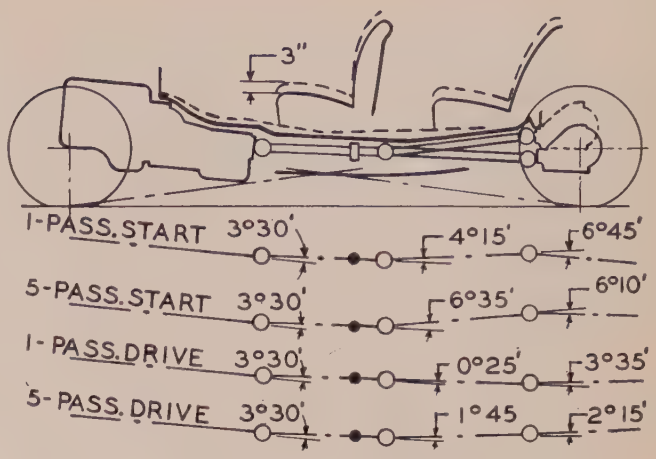

Fig. 8 – Three-joint installation with center bearing

The installation shown in Fig. 8 allows for a seat lowering of 3 in. This is based on the same height of seat above the tunnel as on the present installation. To accomplish this, engine angle has to be increased to provide proper angles required for effective cancellation of excitations. The lengths are:

Front shaft: 24 in. from joint centerline to center bearing

Rear shaft: 35 in. between joint centerlines

Excitations resulting from this setup are as shown below. Torsional and inertia excitations are calculated for drive angles, and secondary couple excitation on the center bearing is figured from starting angles.

1. Torsional excitation:

1-passenger drive:

$TE_1 = (3.6^2 - 3.5^2 - 0.4^2)^{\frac{1}{2}} = 0.8$-deg equivalent joint angle

5-passenger drive:

$TE_5 = (3.50^2 + 1.75^2 - 2.25^2)^{\frac{1}{2}} = 3.2$-deg equivalent joint angle

2. Inertia excitation: Due to the phase relationship required to cancel secondary couples, inertia excitation is higher than the minimum possible with the angles used. Inertia excitation must be figured from each end and the maximum value used in appraising the installation. Total inertia excitation is the sum of the excitation on each shaft as a function of its mass. For this installation, it is assumed that mass of the two shafts are equal and that total excitation is the average of the excitation in each individual shaft.

1-passenger drive:

$$I_1 = \left(\frac{(2)\,3.5^5 + 0.4^2}{2}\right)^{\frac{1}{2}} = 3.5\text{-deg equivalent joint angle}$$

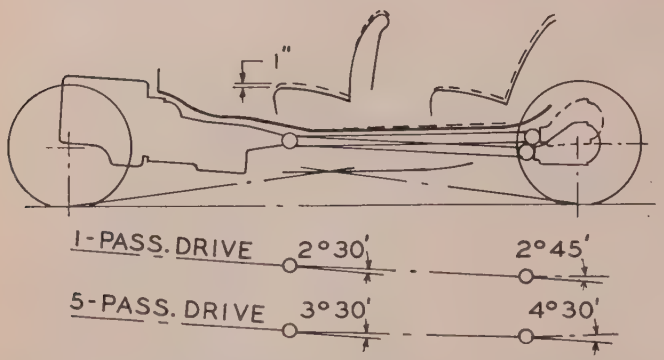

Fig. 9 – Axle motion controlled with radius-rod and single propeller shaft

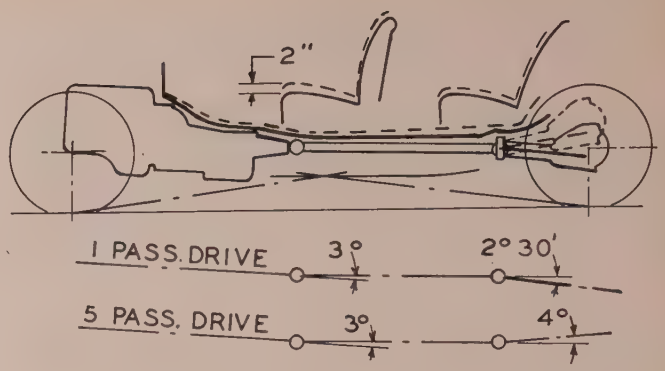

Fig. 10 – Extended-pinion controlled axle movement

$$I_1^1 = \left(\frac{(2)\,3.6^2 - 0.4^2}{2}\right)^{\frac{1}{2}} = 3.6\text{-deg equivalent joint angle}$$

$$I_{1max} = 3.6\text{-deg equivalent joint angle}$$

5-passenger drive:

$$I_5 = \left(\frac{(2)\,3.5^2 + 1.75^2}{2}\right)^{\frac{1}{2}} = 3.7\text{-deg equivalent joint angle}$$

$$I_5^1 = \left(\frac{(2)\,2.75^2 - 1.75^2}{2}\right)^{\frac{1}{2}} = 2.5\text{-deg equivalent joint angle}$$

$$I_{5max} = 3.7\text{-deg equivalent joint angle}$$

3. Secondary couple excitation: Load on center bearing at joint angles and during a full-throttle start; force at 1000 lb-in. torque:

1-passenger start:

$$F_1 = \frac{1000\ (\tan 3.5\ \text{deg} - \tan 4.25\ \text{deg})}{24} + \frac{1000\ (\tan 6.75\ \text{deg} - \tan 4.25\ \text{deg})}{35}$$

$$= (-0.54 + 1.25) = 0.71\ \text{lb}$$

5-passenger start:

$$F_5 = \frac{1000\ (\tan 3.5\ \text{deg} - \tan 6.6\ \text{deg})}{24} + \frac{1000\ (\tan 6.2\ \text{deg} - \tan 6.6\ \text{deg})}{35}$$

$$= (-2.25 - 0.2) = 2.45\ \text{lb}$$

These forces represent double amplitude of the oscillating part of the center bearing secondary couple load. Since it has been established to use a maximum oscillating force of 10 lb, this arrangement is within these limits up to:

$$\left[\frac{(2)\ (10)}{2.45}\right] 1000 = 8200\ \text{lb-in. torque}$$

This maximum allowable torque at rotating speed equals one-half the resonant frequency of the center bearing mounting.

Secondary couple excitation on transmission and axle supports at the drive angles are as follows:

1-passenger drive:

Transmission end:

Couple = 1000 (tan 3 deg 30 min) = 1000 (0.061)
= 61 lb-in.

$$\text{Force at joint centerline} = \frac{61 + 7}{24} = 2.2\ \text{lb}$$

Axle end:

Couple = 1000 (tan 3 deg 35 min) = 1000 (0.063)
= 63 lb-in.

$$\text{Force at joint centerline} = \frac{63 + 7}{35} = 2\ \text{lb}$$

5-passenger drive:

Transmission end:

Couple = 1000 (tan 3 deg 30 min) = 1000 (0.062)
= 61 lb-in.

$$\text{Force at joint centerline} = \frac{61 + 30}{24} = 1.3\ \text{lb}$$

Axle end:

Couple = 1000 (tan 2 deg 15 min) = 1000 (0.039)
= 39 lb-in.

$$\text{Force at joint centerline} = \frac{39 + 30}{35} = 2.0\ \text{lb}$$

These figures show that excitations are about equal to those on the conventional installation. Addition of the center bearing requires that excitation on it be kept within reasonable limits. The arrangement shown in Fig. 8 allows a silhouette 3 in. lower with the addition of a center bearing and a change in engine and axle pinion angle.

E. Axle motion controlled with radius-rod, single propeller shaft: Some lowering is possible by controlling axle motion. This reduces height of the propeller-shaft rear in the metal-to-metal position and allows an equivalent drop in the tunnel at this point. Fig. 9 shows an arrangement of this type and will allow about a 1-in. drop in seat height. Position of the center of rotation of the radius-rod affects the change in joint angles with load. Angles shown are based upon a geometry in which joint angle increases at axle end with increased load. This arrangement requires a slightly increased engine angle from that used in the conventional

installation and uses the same propeller-shaft proportions. Excitations resulting from this installation are as follows:

1. Torsional excitation:

1-passenger drive:

$TE_1 = (2.75^2 - 2.5^2)^{\frac{1}{2}} = 0.8$-deg equivalent joint angle

5-passenger drive:

$TE_5 = (4.5^2 - 3.5^2)^{\frac{1}{2}} = 2.8$-deg equivalent joint angle

2. Inertia excitation:

In this arrangement maximum inertia load is equivalent to the largest joint angle.

1-passenger drive:

$I_1 = 2.75$ deg

5-passenger drive:

$I_5 = 4.5$ deg

3. Secondary couple excitation: Secondary couple excitations on the supports based on a 1000 lb-in. torque are:

1-passenger drive:

Transmission end:

Couple = 1000 (tan 2 deg 30 min) = 1000 (0.044)
= 44 lb-in.

Forces at joint centerline $= \frac{44 + 48}{54} = 1.7$ lb

Axle end:

Couple = 1000 (tan 2 deg 45 min) = 1000 (0.048)
= 48 lb-in.

Forces at joint centerline same as at transmission end, 1.7 lb.

5-passenger drive:

Transmission end:

Couple = 1000 (tan 3 deg 30 min) = 1000 (0.061)
= 61 lb-in.

Forces at joint centerline $= \frac{61 + 79}{54} = 2.6$ lb

Axle end:

Couple = 1000 (tan 4 deg 30 min) = 1000 (0.079)
= 79 lb-in.

Forces at joint centerline same as at transmission end, 2.6 lb.

This arrangement allows for a slight lowering of the tunnel by controlling axle motion. Resulting joint angles are similar to those in a typical single-propeller shaft installation except, for a faster rate of change of angle with load at the axle end. Resulting excitations are equivalent to those in a typical installation.

F. Extended pinion with axle motion controlled around centerline of rear joint: This type of installation uses an extended pinion with axle motion controlled around the rear joint centerline. This setup requires no change in propeller-shaft height during rear-axle springing. Due to the axle setup, rather large changes in joint angle exist at the axle end. Fig. 10 shows this arrangement with a possible seat height lowering of 2 in. This arrangement uses a 46-in.-long propeller shaft and allows tube diameter to be reduced 2½ in. With this arrangement, the limitation on joint angles is established by the maximum allowable difference in angle. Excitations resulting from these angles are:

1. Torsional excitation:

1-passenger drive:

$TE_1 = (3.0^2 - 2.5^2)^{\frac{1}{2}} = 1.7$-deg equivalent joint angle

5-passenger drive:

$TE_5 = (4.0^2 - 3.0^2)^{\frac{1}{2}} = 2.6$-deg equivalent joint angle

A point exists between maximum and minimum load where axle joint angle equals zero. In this position $TE = 3$ deg equivalent joint angle.

2. Inertia excitation:

In this arrangement the maximum inertia load is equivalent to the largest joint angle.

$I_1 = 3.0$ deg

$I_5 = 4.0$ deg

3. Secondary couple excitation:

Joint angles shown produce the following excitation on the mounts at 1000 lb-in. torque:

1-passenger drive:

Transmission end:

Couple = 1000 (tan 3 deg) = 1000 (0.052) = 52 lb-in.

Force at joint centerline $= \frac{52 - 44}{46} = 0.2$ lb

Axle end:

Couple = 1000 (tan 2 deg 30 min) = 1000 (0.044)
= 44 lb-in.

Force at joint centerline same as at transmission end, 0.2 lb.

5-passenger drive:

Transmission end:

Couple same as for 1-passenger load

Force at joint centerline $= \frac{52 + 70}{46} = 2.8$ lb

Axle end:

Couple = 1000 (tan 4 deg) = 1000 (0.070) = 70 lb-in.

Force at joint centerline same as at transmission end, 2.8 lb.

The angles shown produce about the same excitation as the typical installation.

G. Axle motion controlled with radius-rod;

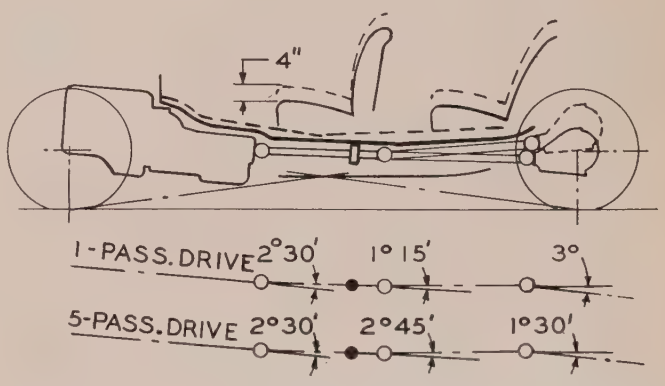

Fig. 11 – Axle motion controlled with radius-rod in 3-joint installation with center bearing

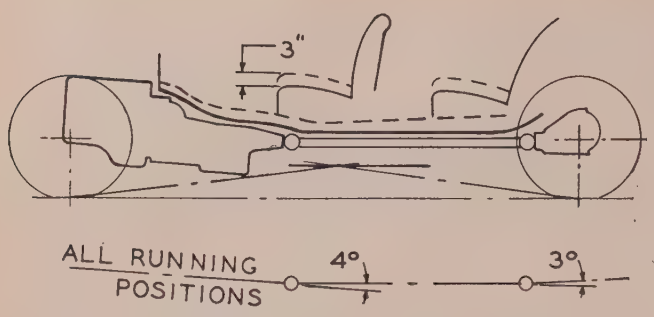

Fig. 12 – Independent rear suspension and single propeller shaft

3-joint installation with center bearing: When axle motion is controlled an even lower drive line is possible with a center bearing installation. Fig. 11 shows this type of installation and allows a lowering in seat height of 4 in.

It is necessary to tip the axle pinion up in order to obtain effective cancellation. Excitations resulting from this installation are:

1. Torsional excitation:

   1-passenger drive:

   $TE_1 = (3.0^2 - 2.5^2 - 1.25^2)^{\frac{1}{2}} = 1.1$-deg effective joint angle

   5-passenger drive:

   $TE_5 = (2.5^2 + 2.75^2 - 1.5^2)^{\frac{1}{2}} = 3.4$-deg effective joint angle

2. Inertia excitation:

   1-passenger drive:

   $$I_1 = \left[\frac{(2)\ 2.5^2 + 1.25^2}{2}\right]^{\frac{1}{2}} = 2.7\text{-deg effective joint angle}$$

   $$I_1^1 = \left[\frac{(2)\ 3.0^2 - 1.25^2}{2}\right]^{\frac{1}{2}} = 2.9\text{-deg effective joint angle}$$

   5-passenger drive:

   $$I_5 = \left[\frac{(2)\ 2.5^2 + 2.75^2}{2}\right]^{\frac{1}{2}} = 3.2\text{-deg effective joint angle}$$

   $$I_5^1 = \left[\frac{2.75^2 - (2)\ 1.5^2}{2}\right]^{\frac{1}{2}} = 1.8\text{-deg effective joint angle}$$

Load on center bearing based on starting joint angles the same as drive angles, force at 1000 lb-in. torque:

1-passenger start:

$$F_1 = \frac{1000\ (\tan 2.5\ \text{deg} - \tan 1.25\ \text{deg})}{24} + \frac{1000\ (\tan 3.0\ \text{deg} - \tan 1.25\ \text{deg})}{35}$$

$$= 0.92 + 0.86 = 1.78\ \text{lb}$$

5-passenger start:

$$F_5 = \frac{1000\ (\tan 2.5\ \text{deg} - \tan 2.75\ \text{deg})}{24} + \frac{1000\ (\tan 1.5\ \text{deg} - \tan 2.75\ \text{deg})}{35}$$

$$= -0.02 - 0.63 = 0.65\ \text{lb}$$

Based on a maximum of 10-lb excitation, this installation could be used up to a torque of:

$$\left[\frac{(2)\ (10)}{1.78}\right] 1000 = 11{,}200\ \text{lb-in.}$$

Secondary couple excitations on end supports are:

1-passenger drive:

Transmission end:

Couple = 1000 (tan 2 deg 30 min) = 1000 (0.044)
= 44 lb-in.

$$\text{Force at joint centerline} = \frac{44 - 22}{24} = 0.9\ \text{lb}$$

Axle end:

Couple = 1000 (tan 3 deg) = 1000 (0.052) = 52 lb-in.

$$\text{Force at joint centerline} = \frac{52 + 22}{35} = 2.1\ \text{lb}$$

5-passenger drive:

Transmission end:

Couple same as for 1 passenger

$$\text{Force at joint centerline} = \frac{48 - 44}{24} = 0.17\ \text{lb}$$

Axle end:

Couple = 1000 (tan 1 deg 30 min) = 1000 (0.026)
= 26 lb-in.

$$\text{Force at joint centerline} = \frac{26 + 48}{35} = 2.1\ \text{lb}$$

H. Independent rear suspension; single propeller shaft: The axle housing is mounted directly to the frame and drives each wheel independently through a wheel-drive propeller shaft. This arrangement is especially suitable to the lowered silhouette since no room need be allowed for axle and main drive propeller shafts during spring motion. Fig. 12 shows an arrangement of this type which produces a seat lowering of 3 in.

The arrangement shown has a 9-in. ground clearance under the axle housing in the 5-passenger load position. The angle setup for wheel drive shafts is shown in section J. Shaft length and diameter are the same as for the typical installation.

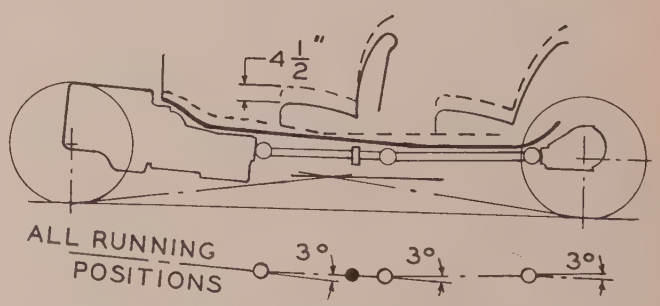

Fig. 13 – Independent rear suspension with 3-joint installation with center bearing

The excitation resulting from the angles are:

1. Torsional excitation in All Running Positions:

$TE = (4^2 - 3^2)^{\frac{1}{2}} = 2.6$-deg equivalent joint angle

2. Inertia excitation in All Running Positions:

$I = 4$-deg largest joint angle

3. Secondary couple excitation at 1000 lb-in. torque:

Transmission end:

Couple = 1000 (tan 4 deg) = 1000 (0.070) = 70 lb-in.

$$\text{Force at joint centerline} = \frac{70 + 52}{54} = 2.2 \text{ lb}$$

Axle end:

Couple = 1000 (tan 3 deg) = 1000 (0.052) = 52 lb-in.

Force at joint centerline same as at transmission end, 2.2 lb.

I. Independent rear suspension, 3-joint installation with center bearing: Additional lowering is possible with a 3-joint drive line to the axle housing. Fig. 13 shows this arrangement, which allows for a 4½-in. seat lowering. Propeller-shaft proportions are the same as in the other 3-joint installations.

The excitations resulting are:

1. Torsional excitation in All Running Positions:

$TE = (3^2 + 3^2 - 3^2)^{\frac{1}{2}} = 3$-deg equivalent joint angle

2. Inertia excitation in All Running Positions:

$$I = \left(\frac{2 \times 3^2 + 3^2}{2}\right)^{\frac{1}{2}} = 3.7\text{-deg equivalent joint angle}$$

$$I_1 = \left(\frac{2 \times 3^2 - 3^2}{2}\right)^{\frac{1}{2}} = 2.1\text{-deg equivalent joint angle}$$

3. Secondary couple excitation:

Loads on center bearing, assuming starting angles are the same as in the running position:

$$F = \frac{1000 (\tan 3 \text{ deg} - \tan 3 \text{ deg})}{24} + \frac{1000 (\tan 3 \text{ deg} - \tan 3 \text{ deg})}{35}$$

$F = 0$ (perfect cancellation)

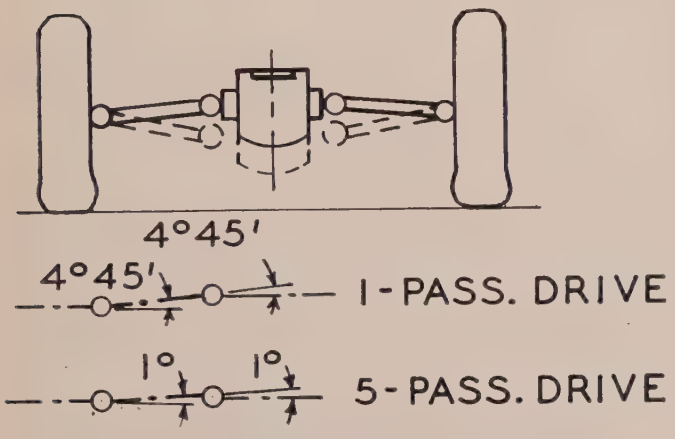

Fig. 14 – Independent rear suspension wheel drive angles

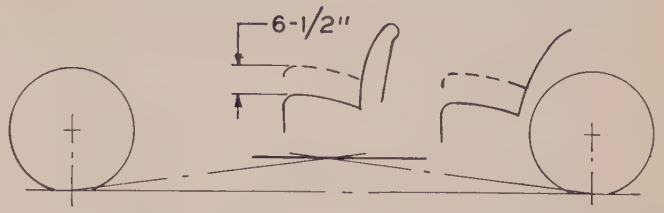

Fig. 15 – Maximum lowering of car with no drive line under body, possible with either rear-engine, rear-wheel or front-engine, front-wheel drive

Secondary couple excitation on supporting units:

Transmission end:

Couple = 1000 (tan 3 deg) = 1000 (0.052) = 52 lb-in.

$$\text{Force at joint centerline} = \frac{52 - 52}{24} = 0$$

Axle end:

Couple = 1000 (tan 3 deg) = 1000 (0.052) = 52 lb-in.

$$\text{Force at joint centerline} = \frac{52 - 52}{35} = 0$$

This arrangement provides excellent cancellation of secondary couple excitation because of equal angles. Any amount the angles change during a start would modify this setup and require additional study.

J. Independent rear suspension; wheel-drive angles: Fig. 14 shows a possible angle arrangement on a wheel-drive shaft. A setup is shown where angles are normally equal with parallel input and output shafts. With this arrangement torsional variations are completely canceled. Because of low-speed inertia, excitation should not be troublesome.

Secondary couple excitation is very critical because of the high torques on the wheel drive. Since the differential allows relative phase changes during operation, many combinations are possible. When the yokes at the differential end are at right angles to each other, the couples add up. When they are in line, the couples cancel. As long as angles are equal on both ends of the shafts, forces on the joint centerline cancel each other.

Rear-axle housing mountings must withstand this excitation. This may be very critical, especially through a resonant frequency of the installation.

Complete Change in Vehicle Configurations

The maximum lowering possible within clearances used here requires taking the drive line out from under the passenger section. This allows lowering the floor pan to the minimum ground clearance position. Fig. 15 shows this setup using the same proportions as on the other schemes. This shows a maximum possible lowering of 6½ in.,

keeping the same seat height above the floor.

This installation would require the use of either a front-engine, front-wheel-drive or a rear-engine rear-wheel-drive arrangement. These require additional consideration in setting up a satisfactory drive line. European cars are made with both arrangements; however, their application to larger, heavier American cars would require additional study. The long-range, lowered-silhouette program would indicate the need for a study of this type.

DISCUSSION

Application of 3-Joint Propeller Shafts

– P. C. Bowser
Chevrolet Motor Division, GMC

THE approximate formulas that the authors have derived and the accompanying table of accuracies are very pertinent and should serve as a valuable tool to others who seek to design installations of 3-joint propeller shafts. However, I feel that the formulas could be further simplified by using the angle in radians in place of the tangents without seriously affecting their accuracy.

Since I represent a using firm, I shall endeavor to summarize some of what I feel are the more important phases of the application of 3-joint propeller shafts to automobiles.

The authors stress the design sensitivity of the mid bearing support to vibration excited by secondary couple excitation. In our limited experience we have found that their suggested maximum unbalanced secondary couple excitation at the mid bearing support of 10 lb oscillating load is a very realistic value.

Although I have no such intimate check on the suggested maximum values of angular excitation (400 radians per sec^2) and of torsional inertia (1000 radians per sec^2), I assume that they have been determined experimentally and are equally realistic.

If these values have been determined experimentally I am surprised that the authors did not discover a sensitivity of the rear-axle resonant bending vibration excited by the secondary couple induced on the pinion yoke. While some cars may not be as sensitive as others to this vibration, it has proved to be more of a problem to us than the response by similar excitation of the mid bearing support.

As they pointed out, the secondary couple excitation at the mid bearing support can be virtually canceled by a proper design, but this fortunate set of circumstances cannot be employed to reduce the excitation from the rear universal joint on the rear-axle pinion yoke. In fact, this secondary couple excitation is a function only of the drive line torque and the rear universal joint angle and is directly proportional to each.

Since this is true, the rear universal joint angle should be kept at a minimum and, in general, should not exceed 3 deg during full driving torque. In other words, the secondary couple on the rear-axle pinion yoke should be limited to about 125 lb-in.

Needless to say, this requirement makes a satisfactory installation of a 3-joint propeller shaft on a Hotchkiss drive car difficult to accomplish because of the variations of rear universal joint angle caused by changes of passenger loading and driving torque. The solution to this problem is, at best, a compromise which will possibly require a slight sacrifice from our present-day drive line smoothness.

Another resonant system which can be readily excited by secondary couple excitation is the powerplant assembly, which when vibrating as a beam produces a very objectionable noise inside the car. This is usually not a problem on our modern V-8 engines because of their high stiffness-to-mass ratio. However, on a car in which the beaming resonance frequency of the powerplant assembly is low enough to be excited by the two per revolution secondary couple excitation, caused by the front universal joint angle, this can become a very serious problem. In this case, one must be very careful to limit the front universal joint angle to as low a value as is possible.

In general, as long as the powerplant beaming resonant frequencies are higher than 180 cps this vibration will not be excited by the propeller-shaft secondary couple.

It should also be mentioned that the rear-axle radius arms used in some of the examples toward the end of the paper are impractically short. The use of a radius arm much shorter than 30 in. will produce objectionable lift of the rear of the car in acceleration as well as a severe problem of brake hop and/or reverse power hop. In addition to these considerations, the use of short radius arms can produce excessive twist and resulting failures in the rear-axle housing and undesirable torsional fluctuations in the axle shafts and, as a result, in the drive line when running over rough road surfaces.

Indicates "Low Silhouette" Drive Line Preference

– Charles E. Cooney, Jr.
Mechanics Universal Joint Division, Borg-Warner Corp.

THE authors have been very conservative in setting forth the standards to be followed if satisfactory results are to be obtained.

The conservative standards have been qualified by the authors of this paper when they pointed out that the size of the angles could be increased to 4 deg, 30 min, but this would require closer control of joint angularity. This is a very important point for chassis designers. It is good practice to allow enough joint angularity tolerances to handle chassis variations and operating variables.

In the drive line configuration comparison the authors have not indicated their drive line preference.

My first selection for a low silhouette would be as illustrated in Fig. 13 with equal angles and independent rear suspensions.

My next selection would be a 3-joint application as illus-

trated in Fig. 8. With this configuration it may be necessary in some cases to control or restrict the rear-axle windup. A 3-joint drive line is generally smoother throughout the operating range of the vehicle, especially at higher shaft revolutions. It also is more easily adapted to the floor pan requirements with a lowered body design. This statement is made with reservations that unreasonable joint angles are not used.

However, it is felt that future styling demands, if present conventional chassis layouts are to be maintained, will force universal joint engineers into developing a drive line that will operate smoothly at greater angles. The requirement will be a system that will operate at 15-20-deg angularity without causing objectionable disturbances.

This prediction is made assuming that the demand for low silhouette models will continue and will not be limited by buyer rejection.

In lowering a drive line with the selection of a 3-joint application, the limiting condition to be encountered will be when an angularity is reached that will not permit a satisfactory compromise between inertia excitation and secondary couple excitation.

The secondary couple problem in a 3-joint application exists in most designs at the center bearing. A properly designed center bearing should handle this problem.

The center bearing mount should be designed with two stages. One stage should be capable of handling the low-speed secondary couple problem which usually exists over the range 0-30 mph. The other stage should have sufficiently low transmissability characteristics to handle the higher-frequency disturbance which exists as the shaft increases in speed and the secondary couple load decreases.

In developing a 3-joint drive line it will simplify the center bearing design if the secondary couple oscillating load is kept at a minimum.

However, future requirements are certain to produce a simplified center bearing mount which will handle higher secondary couple loads. An improved center mount would then permit taking more advantage of phasing with a corresponding increased angularity.

Torsional vibration characteristics of a drive line should be investigated very carefully in the experimental development of a new drive line configuration. Components coupled by the shaft should be assembled with parts representing expected production tolerances and observed under actual road conditions. Careful observation for variations in rear-axle gear noise level, transmission gear rattle, and noise level or objectionable vibration should be made.

To mold a satisfactory drive line under one of these future low silhouettes it may be necessary to give consideration to the engine mounts and rear suspension along with the center bearing mount.

3-Joint System Presents Some Problems

—G. E. Dunn
Universal Products Co.

IT APPEARS that in the immediate future the trend of drive lines for low silhouettes is toward the 3-joint system.

As pointed out in the paper, this system presents a number of problems. These may be solved satisfactorily only if the general configuration of the engine shaft, the propeller shafts, and the axle pinion shaft is within certain limits. These limits may be roughly defined by a summation of the three joint angles.

It has been shown that, because the center bearing is quite sensitive to excitation, it is essential to keep the forces imposed on it as low as possible. If the sum of the true angles in the two end joints can be made equal to, or somewhat greater than, twice the angle in the center joint, a suitable cancellation of forces can be found. As this condition, in general, cannot be maintained throughout the starting and driving range, various compromises are necessary. Because of present engine angle limitations, it is unfortunate, from the point of view of lowering the silhouette, that the best compromise frequently proves to be the raising of the center bearing.

When the axle windup is controlled, the situation is greatly relieved as the change in joint angles is reduced. This assists in finding better solutions for the 3-joint system and helps propeller-shaft performance. As has been shown, it can also be a significant factor in lowering the vehicle.

The use of a sprung differential with various types of rear suspensions poses a different set of problems. This is especially true in the large American passenger car. Secondary couples from high torque have been mentioned and these are aggravated by high angles in the short shafts connecting the wheels and differential. High couple forces produced in both the wheel mounts and differential can be troublesome. Again, however, a substantial lowering of the vehicle may be obtained by the use of this system.

ORAL DISCUSSION

Reported by L. H. White
Ford Motor Co.

A. B. MacIsaac, Ford Motor Co.: What are the advantages of the constant-velocity joint versus the Cardan joint.

Mr. Mazziotti: The constant-velocity joint eliminates the major sources of excitation, but some inertia excitations will still exist. Considerable cost is now involved, however, with the constant-velocity joint.

R. Bollinger, Ford Motor Co.: I have three questions:

1. How do you identify torque-sensitive torsional vibration from couple-load-excited vibration?

2. What was the effect of couple load on transmission and axle, especially through the bearing span on the supports?

3. Which vibration is the most troublesome: torsional, inertia, or couple?

Mr. Mazziotti: My comments are as follows:

1. It is extremely difficult at times to tell them apart. The only successful way is to make a series of changes in angles, denote the effect and from analysis determine what was changed to produce the results.

2. These characteristics are so different on various vehicles that it is impossible to generalize.

3. Generally, on a 3-joint installation, couple-load vibration is the most troublesome.

FARM TRACTORS

NO OTHER single change in farm tractor design has so improved their efficiency, increased their utility, and promoted their popularity as has the advent of low-pressure pneumatic tires. These tires made possible the transition from animal to tractor power in many areas where steel tires and high drive-wheel lugs were unacceptable. Higher working speeds and improved transportability resulting from the use of rubber opened new avenues for implement design, raised the overall level of tractor performance, and significantly increased the volume of work a tractor could do in a given time. On the other hand, this evolution was not without the incurrence of tire difficulties.

Since the first installation of rubber tires on drive wheels of farm tractors, there has been a continuing trend toward the use of larger and larger tires. In many instances, increase in tire size was accompanied by operating difficulties, including slipping of the tire on the bead seat, side wall buckling with resulting failures, and sidewise rolling. From the tractor and implement viewpoint, in many instances, this increase in drive-wheel tire size has resulted in an intolerable reduction in drawbar pull, decrease in clearance between integral implements and tractor parts, and poor implement performance due to changes in location of attaching points and hitch-linkage geometry. As the result of these acute problems which confront the entire tractor industry, the present Tractor Tire Subcommittee of the SAE Tractor Technical Committee was organized to investigate these problems and determine suitable corrective measures.

In the interest of holding tractor prices at the lowest level, tractors are tested at Nebraska and "commonly priced" with the smallest drive-wheel tires which can be satisfactorily used under so-called "average" or less severe operating conditions. In this discussion, this minimum tire is designated as the "basic" tire. In order to meet trade requirements arising where more severe conditions of traction and flotation are encountered, or those resulting from the activities of overzealous salesmen, generally tractor manufacturers have found it necessary to provide larger tires in one or more sizes, which optionally replace the basic tire. The practice involving the use of tires larger than the basic tire is termed oversizing. Conventional design makes availabe two methods of oversizing:

A. Use of oversize tires having the same bead-seat diameter as the basic tire, but with section widths, outside diameters, and rolling radii all

AND THEIR TIRES——————

F. C. Walters and W. H. Worthington, Deere Mfg. Co.

This paper was presented at SAE Golden Anniversary Tractor Meeting, Milwaukee, Sept. 14, 1955.

respectively larger than those of the basic tire. An example of this is the 11-12-13 x 38-in. series of tire shown in Fig. 1. This is the oversizing practice generally followed by all tractor manufacturers today. The figure shows that use of 12- and 13-in. tires as oversizes for the basic 11-in. tire results in a considerable increase in rolling radius accompanied by corresponding changes in the height of the rear axle, drawbar and integral implement attaching points, and alters the linkage geometry.

B. Use of oversize tires having increased section widths with respect to the basic tire, but with approximately the same outside diameter and rolling radius. An example of this practice is shown in Fig. 2, which again refers to the 38-in. tire as the basic size. This method provides a series of increasing section widths without disturbing the height of the rear axle, drawbar, implement-attaching points or linkage. It has the serious disadvantage of involving different rim diameters and mounting methods.

Providing oversize tires using method A (see Fig. 1) has resulted in difficulties mentioned earlier, and specifically:

1. Tire side-wall buckling.
2. Side-wise rolling when operating on a slanted hillside or with one wheel in a deep furrow.
3. Increased travel speed without corresponding increase in engine and power take-off shaft speed.
4. Reduction in drawbar pull.
5. Decrease in both lateral and longitudinal tractor stability.
6. Poorer integral implement performance.

From the viewpoint of tractor and implement performance, use of method B, which provides the desired increase in section width without departing

TWO methods of oversizing basic tires are available, each with advantages and disadvantages. Extensive field test data presented here correlate very well with laboratory work performed by others.

Based on data gotten from the tests and test conditions described, low section height tires provide the many advantages resulting from the use of basic and oversize tires with common outside diameters and rolling radii, without sacrificing tractive performance, when compared with oversize tires of conventional configuration.

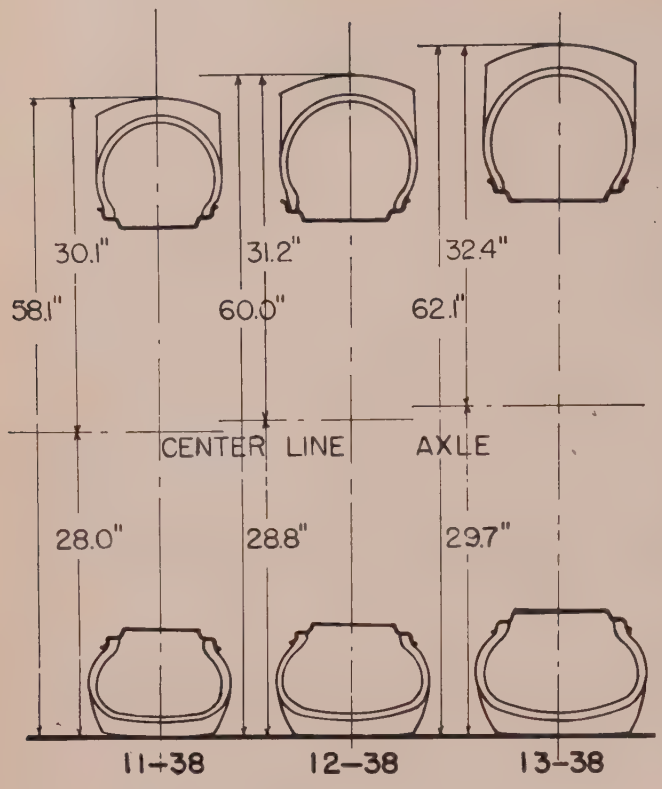

Fig. 1 – Oversizing tires by method A

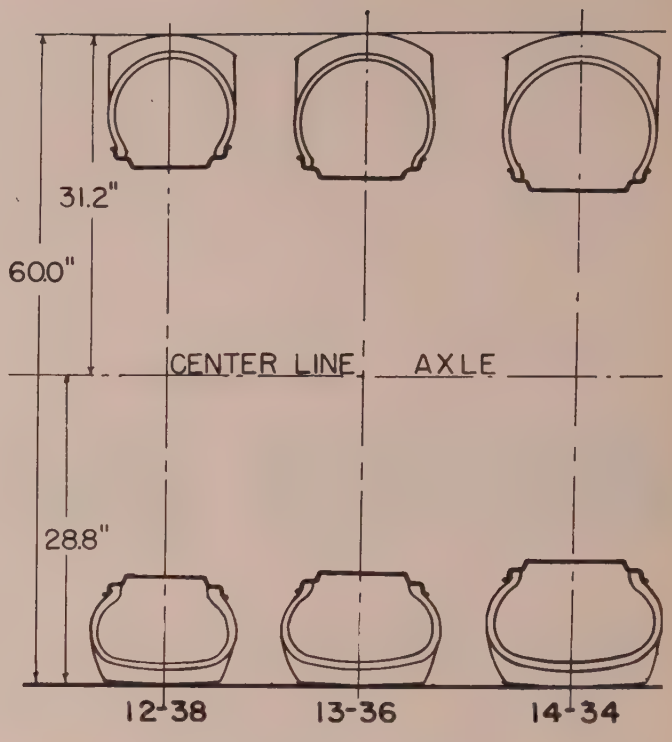

Fig. 2 – Oversizing tires by method B

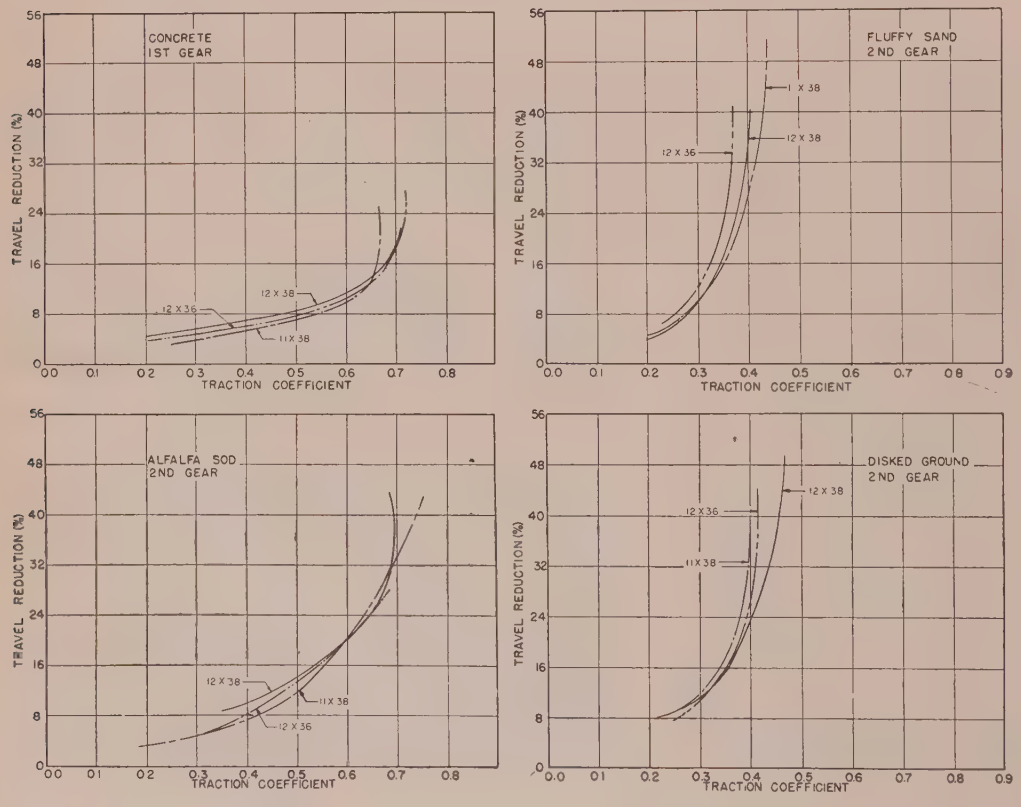

Fig. 3 – Comparison of oversizing by methods A and B. Tires weighted to capacity of basic tire

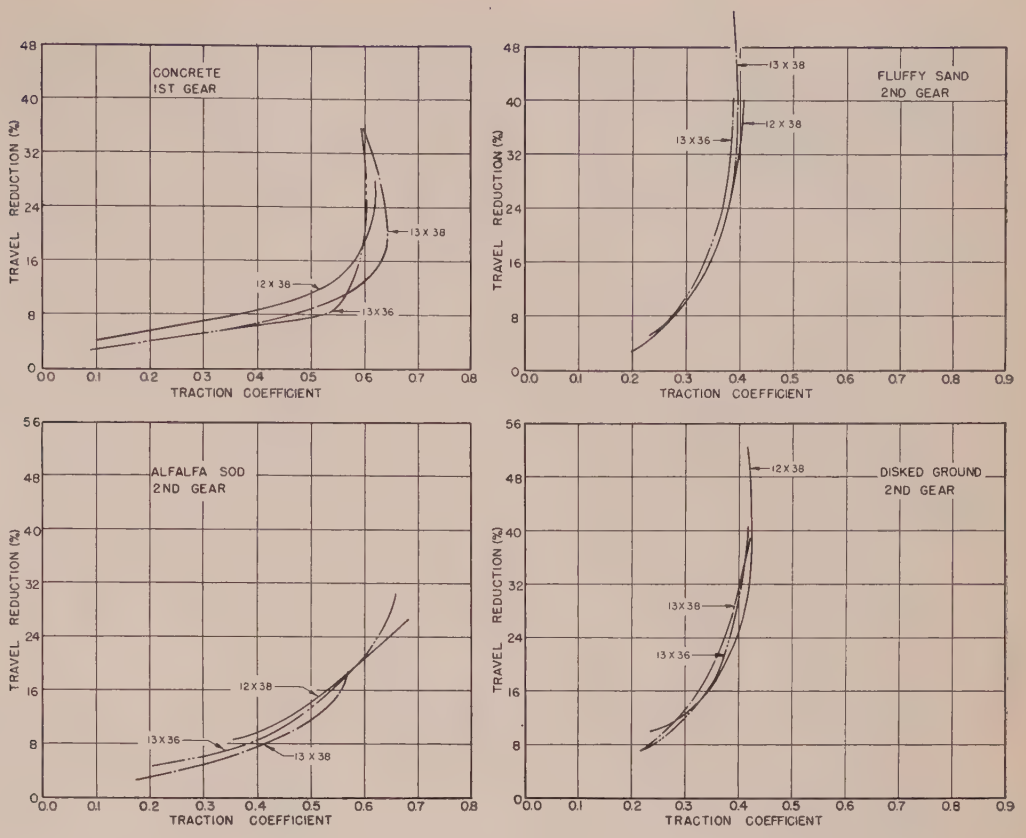

Fig. 4 – Comparison of oversizing by methods A and B. Tires weighted to capacity of basic tire

from the outside diameter and rolling radius of the basic tire, becomes very attractive. The principal advantages afforded by method B as compared with method A include:

1. Interchangeable use of basic and oversize tires, without significantly affecting travel speed and drawbar performance.

2. Distance of c.g. of rear-mounted implements from rear axle may be determined by the outside diameter of the basic tire rather than that of the largest oversize tire. This improves the longitudinal stability of the tractor-implement combination, improves maneuverability, lessens demand on the hydraulic system, and reduces the auxiliary front-end weight necessary to provide adequate stability under adverse field conditions.

3. Use of oversize tires does not disturb the geometric relationship between tractor, ground, and rear- or front-mounted integral implements.

4. Use of an oversize tire does not change the vertical location of the tractor's c.g. As a result, the tractor's safety against backward and sideways upsets is measurably improved.

However, the choice of oversizing method must be qualified by considerations of tire performance alone. Tests conducted in Arizona by the John Deere Waterloo Tractor Works and subsequently verified at the United States Department of Agriculture Tillage Laboratory at Auburn, Alabama – utilizing the equipment described in the SAE paper "Instrumentation For Evaluating the Operating Performance of Farm Tractor Tires" – indicated that where all tires of a series were loaded to approximately the same basic weight, method A resulted in slightly better traction performance than did method B. Again, other tests made in Arizona under similar conditions showed contradictory results with no advantage in performance resulting from the increase in outside diameter and rolling radius.

Figs. 3 and 4 show traction performance of tires tested, as determined on various soil surfaces. To minimize variables in condition of the traction surface, similar tests were always conducted on the same day and insofar as possible, under identical field conditions. It is evident from a study of these curves that the differences in performance follow no definite pattern and they intertwine. In any case, within the range of sizes investigated, advantages or disadvantages in performance of tires of different section widths but with constant diameters were in all cases slight compared with similar tires of variable diameters.

Because of the advantages afforded by method

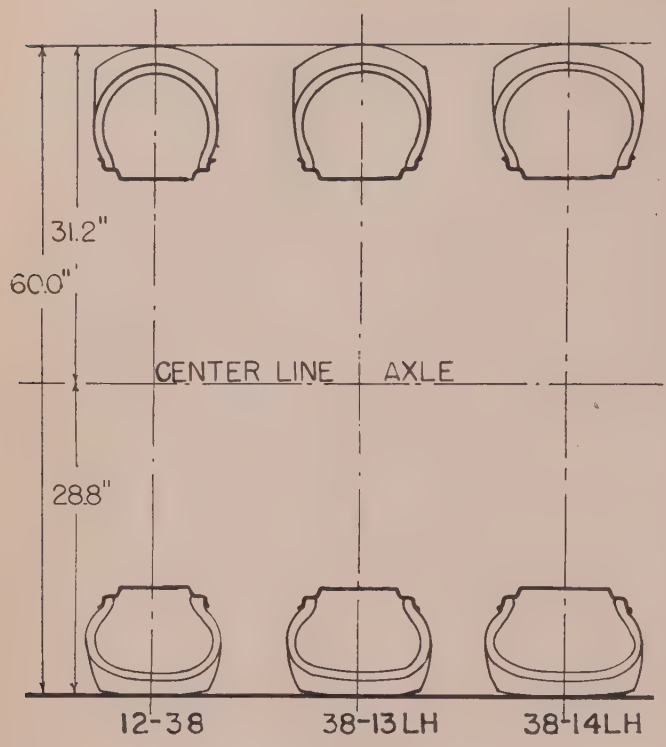

Fig. 5 – Low section tire cross-sections

B, other ways of attaining these benefits were investigated with a view toward avoiding some of the disadvantages of the practice. The following two methods were evolved:

1. Providing oversize tires having section widths greater than that of the basic tire, but maintaining the same rim diameter and approximately the same outside diameter and rolling radius. The ratio of section height to width is smaller on oversize tires, and they are hereafter referred to as "low section height" tires. These are shown in Fig. 5.

2. Providing oversize tires having section widths greater than that of the basic tire, while maintaining approximately the same outside diameter and rolling radius, but with varying rim diameter. (The ratio of section height to width of basic and oversize tires remains constant. This is accomplished with conventional tires as shown in Fig. 2).

A close review of Figs. 2 and 5 shows the following:

A. Both methods provide a range of section widths, all with approximately the same rolling radius. However, method 1, exemplified by Fig. 5, utilizes the same drive-wheel hub and rim-well diameter with all section widths. This is accomplished by varying the ratio of section height to width as tire width increases.

B. Method 2, exemplified by Fig. 2, required different drive-wheel hubs and rim diameters with increasing tire section widths; however it does maintain the same ratio of tire section height to width.

To evaluate the relative traction performance afforded by tires corresponding to methods 1 and 2, cooperative field test programs were undertaken at Colby, Kan., and Columbiana, Ohio. Popular sizes of tires, representative of those now in general use, may be divided into these two general classes:

1. General-purpose tractor tires were represented by the basic 28-in. and 38-in. tire groupings.

2. Standard tread tractor tires were represented by the basic 34-in. tire grouping.

Table 1 lists tire groupings, sizes, and weight capacities used in this test program. In addition to work at Colby and Columbiana, a separate program was conducted at the United States Department of Agriculture Tillage Laboratory at Auburn, Ala. Tests at Auburn were limited to groups 1 and 2.

Table 1 – Tire Dimensions at 12-Psi Inflation Pressure

Test Group	Tire Size	Ply Rating	Tire Source	Rim Width, in.	Section Width, in.	OD, in.	Loaded Radius, in., at Rated Load, lb	No. of Cleats per Tire	Liquid Capacity, gal[b]
1 and 2	12x38	6	Goodrich	11	13.2	61.5	28.5 at 2570	48	68
	38x13	6	Goodrich	12	13.9	61.84	28.47 at 2840[a]	48	74
	38x14	6	Goodrich	14	15.47	61.81	28.52 at 3090[a]	48	84
	13x36	6	Firestone	12	14.4	62.0	28.5 at 2970	46	81
	14x34	6	Goodrich	13	16.0	62.2	28.2 at 3530	44	95
3 and 4	14x34	6	Goodyear	14	16.23	62.28	27.74 at 3530	44	95
	34x15	8	Goodyear	16	18.22	62.49	28.05 at 3800[a]	44	115
	34x18	8	Goodyear	18	20.55	62.87	28.44 at 4150[a]	44	129
	15x30	6	Goodyear	14	17.87	61.38	27.03 at 3940	42	112
	18x26	8	Goodyear	20	23.17	62.51	27.02 at 5580	42	170
5 and 6	11x28	4	Firestone	10	11.9	49.8	22.8 at 1890	38	44
	28x12	4	Firestone	11	13.1	49.8	22.7 at 1725[a]	38	50
	28x13	4	Firestone	12	14.4	49.8	22.7 at 1775[a]	38	55
	12x26	4	Firestone	11	13.1	49.8	22.5 at 2150	38	51
	13x24	4	Firestone	12	14.4	50.0	22.5 at 2470	36	61

[a] The rated capacity of low section height tires are based on calculations, not on experimental data, and hence are not as reliableas the conventional tire capacities.

[b] 100% filled.

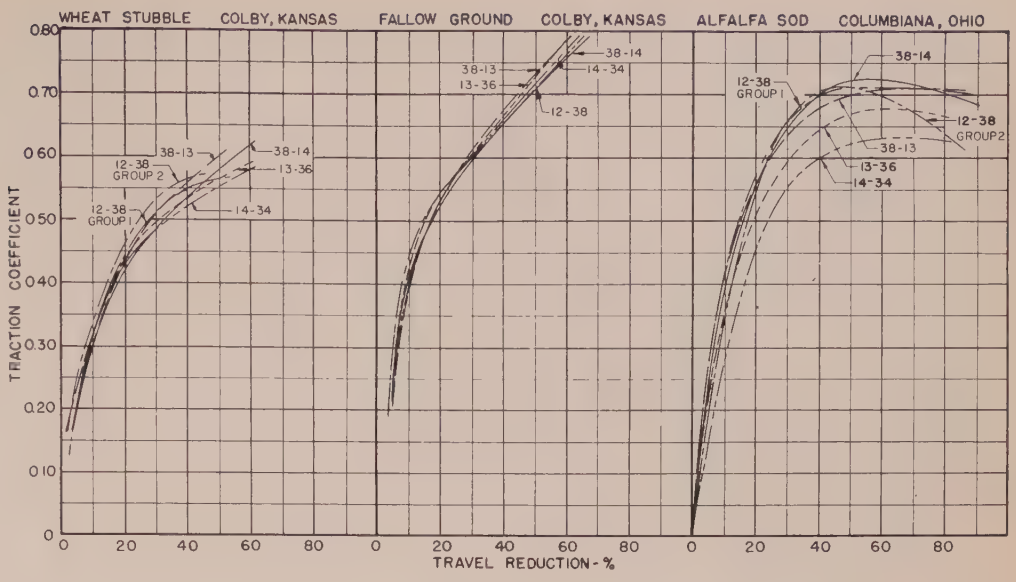

Fig. 6 – Traction coefficient versus travel reduction for group 1 and 2 tires for various soil conditions. Equal weighting test. Basic tire: 12 x 38 at 12 psi

Tractive surfaces for field work varied from light loam soil with wheat stubble and summer fallow surface to moist clay loam with an alfalfa sod covering from 12-18 in. tall. At Auburn, the tractive surface ranged from Lloyd clay to Lakeland sand.

To eliminate the variable represented by weight-carrying capacity of these tires, our comparative evaluation of tire performance is based on:

1. Traction coefficient.
2. Travel reduction.
3. Tire efficiency.

To provide a basis for comparison with much

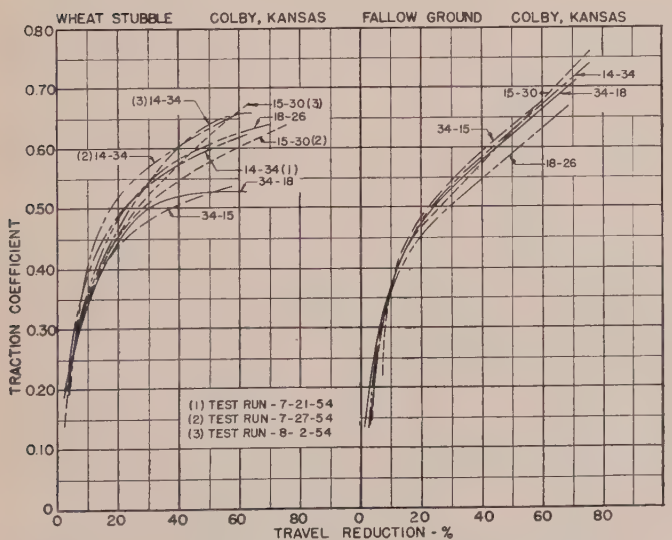

Fig. 7 – Traction coefficient versus travel reduction for group 3 and 4 tires for various soil conditions. Equal weighting test. Basic tire: 14 x 34 at 12 psi

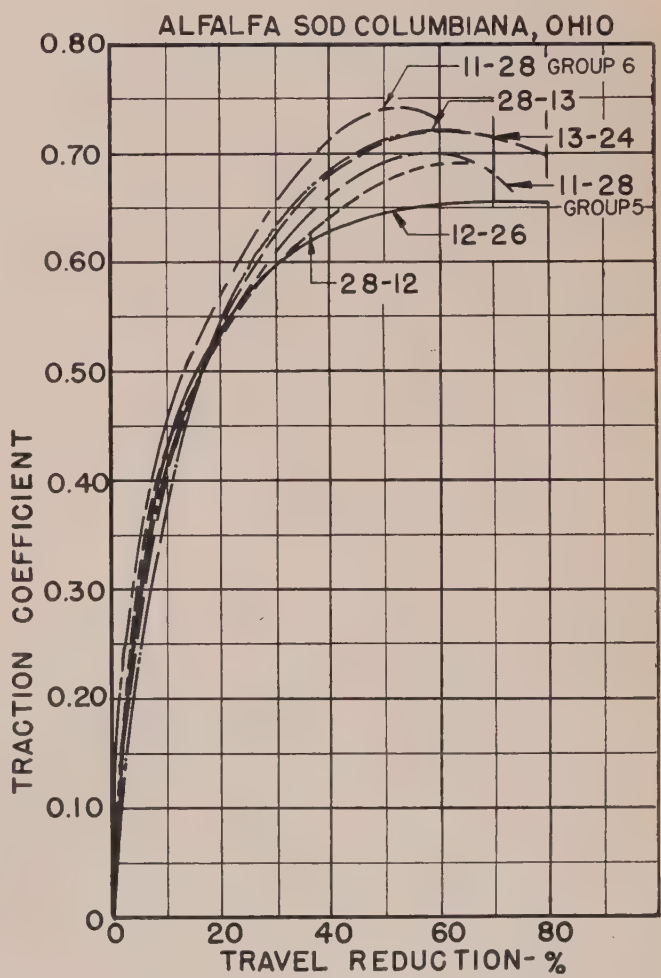

Fig. 8 – Traction coefficient versus travel reduction for group 5 and 6 tires in alfalfa sod. Equal weighting tests. Basic tire: 11 x 28 at 12 psi

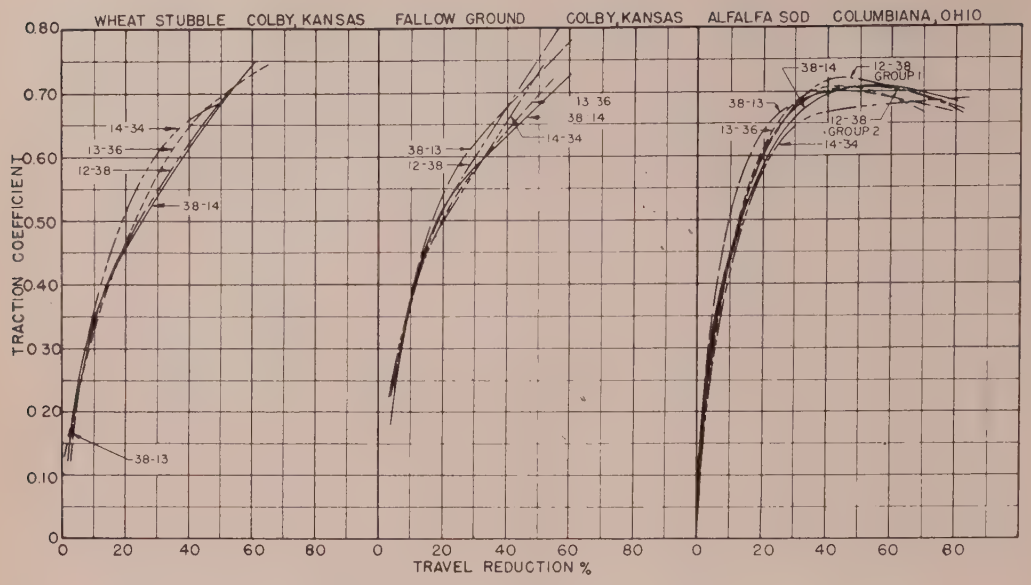

Fig. 9 – Traction coefficient versus travel reduction for group 1 and 2 tires for various soil conditions. Capacity weighting test. Basic tire: 12 x 38 at 12 psi

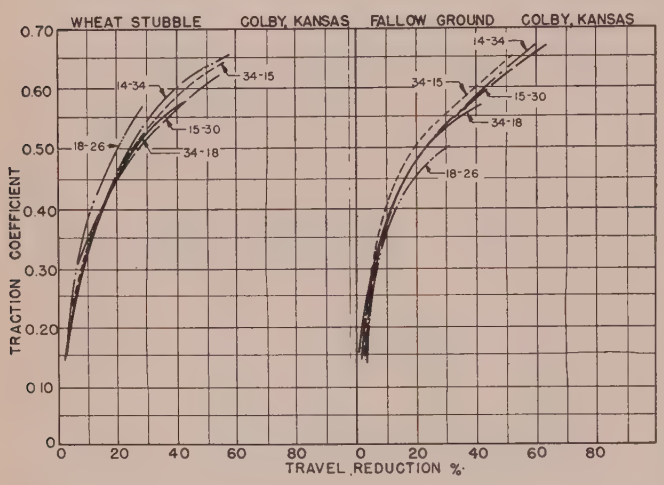

Fig. 10 – Traction coefficient versus travel reduction for group 3 and 4 tires for various soil conditions. Capacity weighting test. Basic tire: 14 x 34 at 12 psi

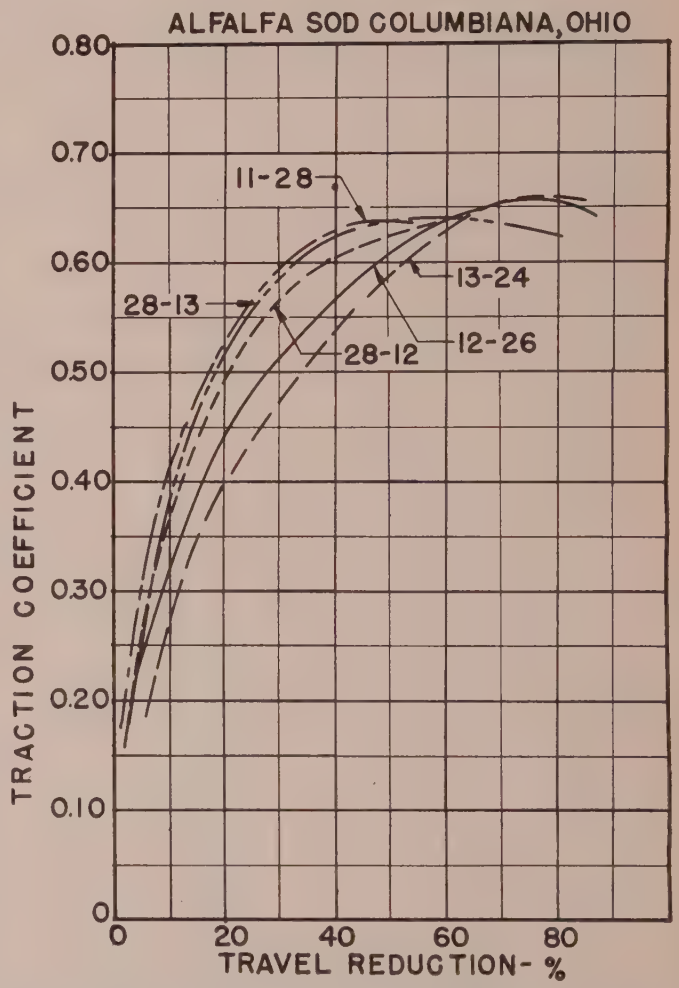

Fig. 11 – Traction coefficient versus travel reduction for group 5 and 6 tires in alfalfa sod. Capacity weighting tests. Basic tire: 11 x 28 at 12 psi

background information currently available, an additional evaluation was made on the basis of tire horsepower and tire net force output.

In conducting all tests involving any specific tire grouping, all tires were operated at the same rolling radius circumferential velocity. This was done purposely to eliminate any effect that a slight variation in rolling radius might have on tire horsepower. In this manner, variations in tire horsepower output would result directly from the difference in section width and not from travel speed. Further, all tests were conducted so that at all times sufficient engine power existed to produce traction stalls rather than power stalls. This was

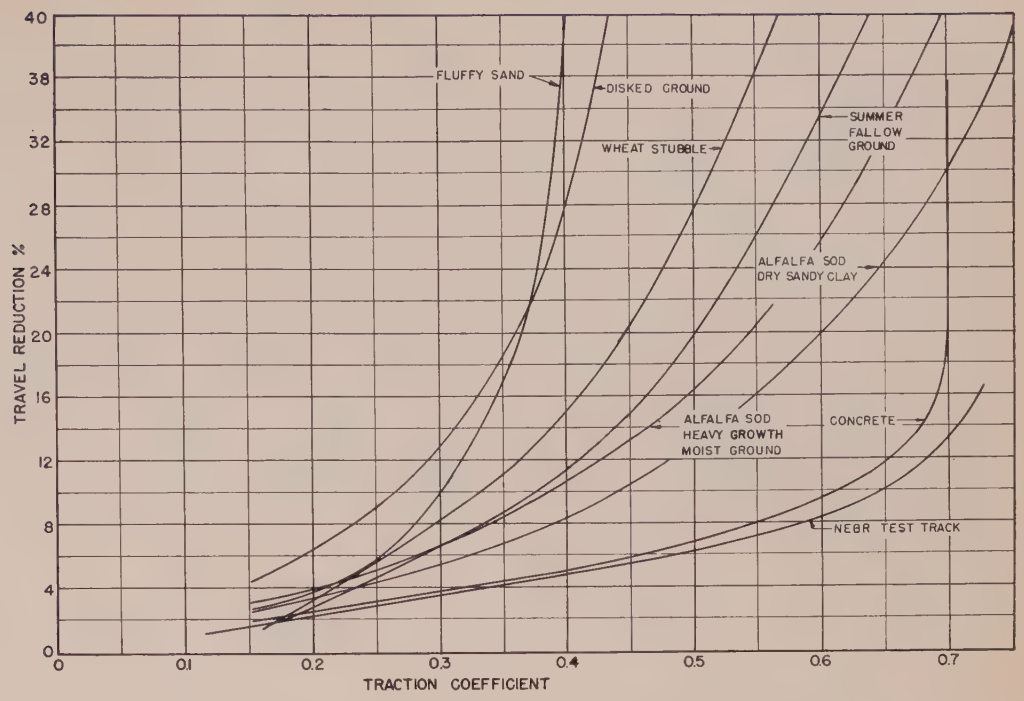

Fig. 12 – Travel reduction versus traction coefficient for various soil conditions tested

done to insure that resulting data reflected only tire performance and was not affected by available engine power.

Figs. 6, 7, and 8 show performance of these tires in tests conducted with all tires loaded to approximately rated capacity of the basic tire at 12-psi inflation pressure. Comparison of values of traction coefficient and travel reduction (slippage) shows that many of the curves intertwine, evidencing close conformity and lack of divergence in the performance characteristics afforded by various types and sizes of tires. Figs. 9, 10, and 11 show performance for each tire loaded to rated capacity at 12-psi inflation pressure. These figures also show close conformity and intertwining of the various curves. When one tire evidenced a slight improvement in performance under a given soil condition, a tire with different width of section afforded better performance under some other soil condition.

As expected of tests involving different types of

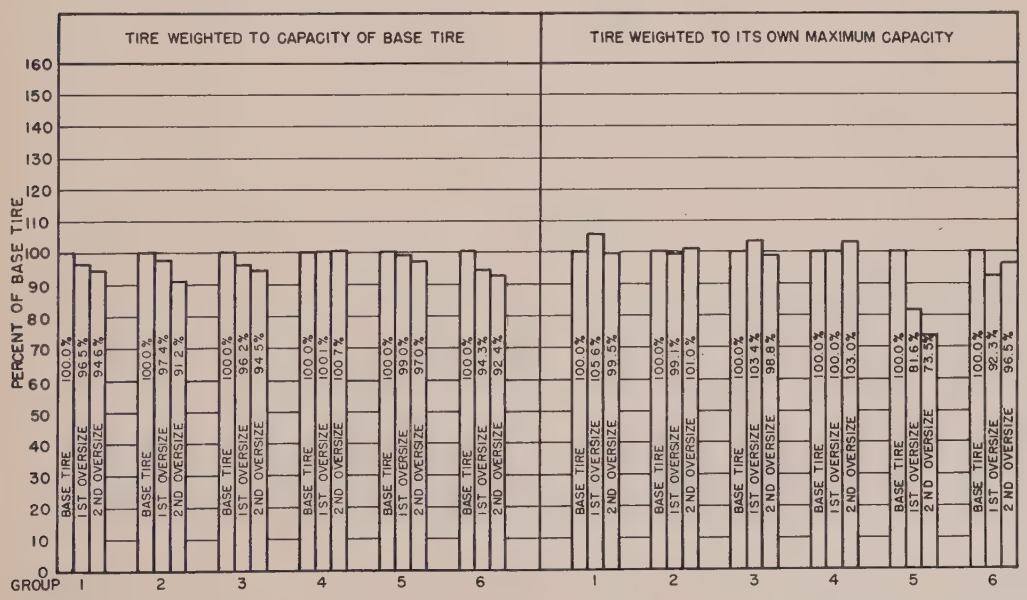

Fig. 13 – Traction coefficient in terms of basic tire for 16% travel reduction

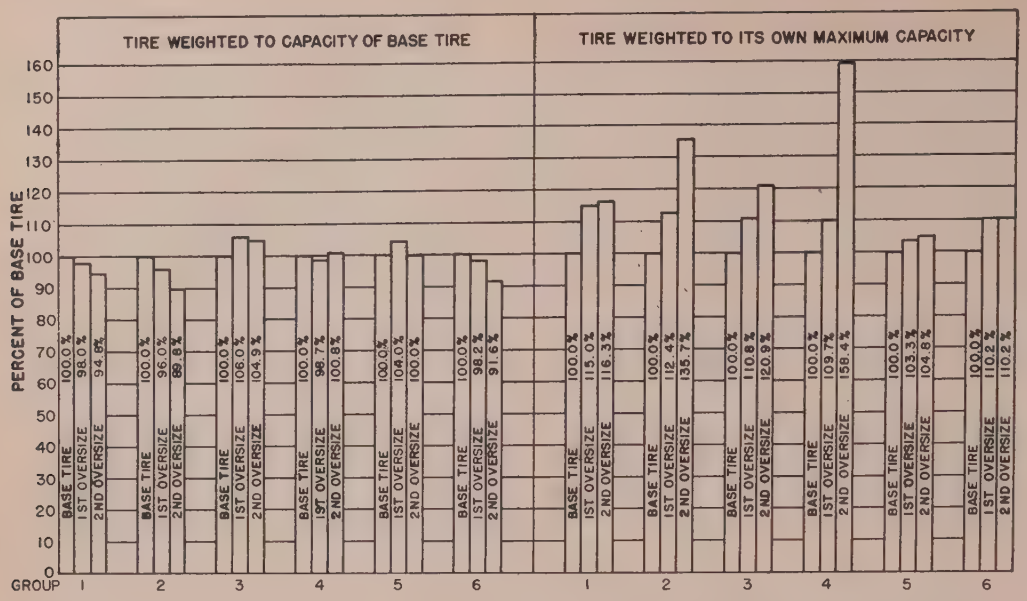

Fig. 14 – Tire net force output in terms of basic tire for 16% travel reduction

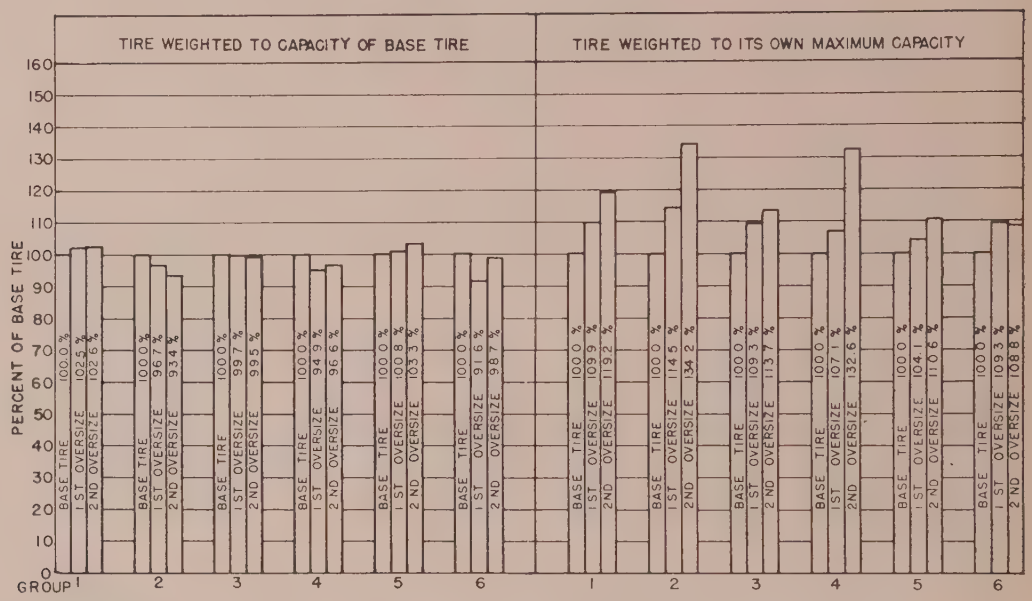

Fig. 15 – Tire net force output in terms of basic tire for 45% travel reduction

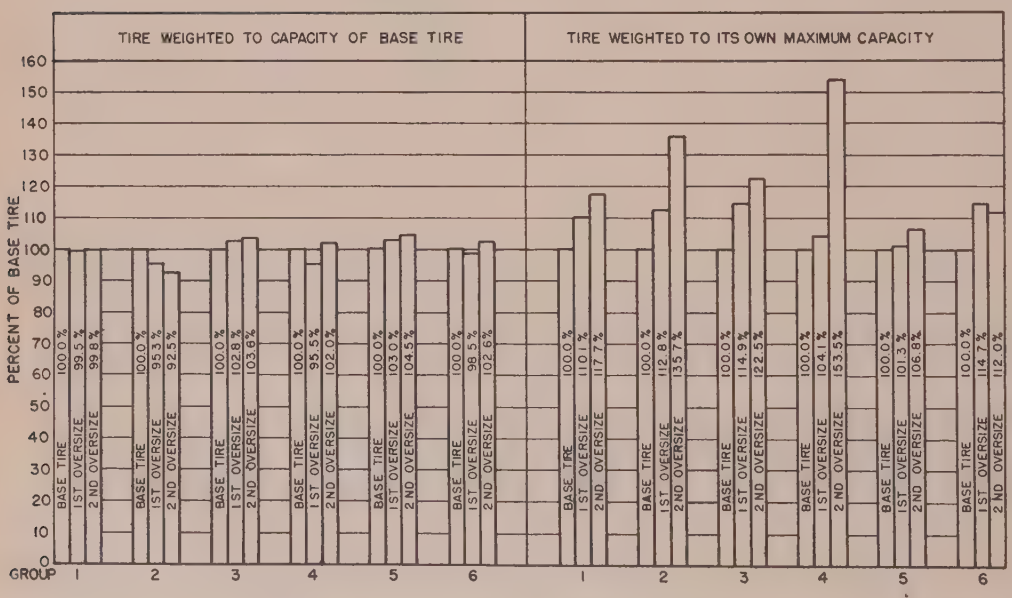

Fig. 16 – Tire horsepower in terms of basic tire for 16% travel reduction

soil and surface conditions, varying values of traction coefficient were found. A summary of all data secured throughout the entire series of tests led to curves which represent the overall performance characteristic for different types of surfaces. (See Fig. 12.) An interesting facet of this study is the close conformity of tractive performance applying to each soil and surface condition, irrespective of tire section width.

Observations of actual farming operations with tractors driven by their owners, together with much other field-test data, indicate that travel reduction in the order of approximately 15-16% is common, and is apparently acceptable to the users. Results of other tests indicate that when high tire slippage results in a tendency to "dig in," maximum traction output occurs at approximately 45-50% travel reduction. Using this as a basis for further analyzing performance data secured during these tests, the charts shown in Fig. 13 were prepared. This figure shows the effect of section width on traction coefficient. The left portion of the graph shows values of traction coefficient occurring when the oversize tire was carrying the same load as the basic tire. The right portion shows values of traction coefficient where each tire was loaded to its rated capacity at 12-psi inflation pressure. From these operations under closely controlled soil and surface conditions, three conclusions are evident:

1. When basic and oversize tires were loaded to rated capacity of the basic tire, basic tire performance was slightly better than that of either oversize. This probably results from the fact that under this condition, unit pressure of the basic tire against the soil is somewhat higher and holding action of the tire lugs is better.

2. With each tire loaded to its individual rated capacity, no significant difference was found among the values of traction coefficient of any of the tires tested.

3. When flotation is adequate, the traction advantages resulting from use of oversize tires are directly proportional to their loading. In other words, unless the greater load carrying capacity of the larger sections is utilized by adding ballast – either a liquid or cast iron – beyond the load capacity of the basic tire, no traction advantage results. On the contrary, oversize tires may not have the traction afforded by the basic tire under the same condition.

Figs. 14 and 15 show characteristic tire performance as tire net force output at 16 and 45% travel reduction. A study of these data reveals the following:

1. Considering all tires of any group tested with oversize tires loaded only to the capacity of the basic tire, little difference in tire net force output was observed. In general, any large difference found favored the basic tire.

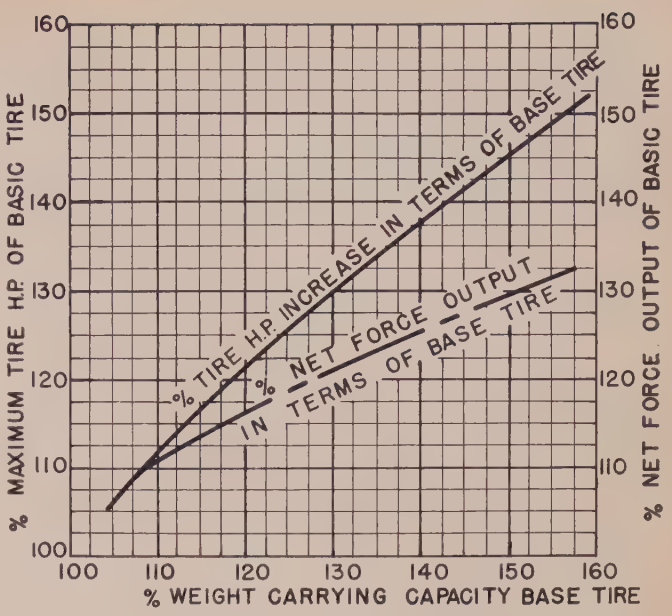

Fig. 17 – Tire horsepower and tire net force output versus weight-carrying capacity in terms of basic tire

2. When any oversize tire was loaded to its full rated capacity, the tire net force output was greater than that of the basic tire, and varied directly with the tire loading.

Referring to Fig. 16, the effects of oversize tires on tire horsepower become apparent. In general, the same trends exist as those characterized by a comparison of tire net force output. Where any difference in performance was found, it was magnified by the change in travel reduction (slippage) characteristics. Benefits gained from increased tire loading are very evident. Here again, no significant improvement in performance is gained through use of oversize tires unless advantage is taken of their greater weight-carrying capacity.

Summarizing all these charts, it is found that:

1. Section width has little effect on traction coefficient. What effect did exist favored the smaller section width tire.

2. Unless advantage is taken of the greater weight-carrying capacity of oversize tires, little to no advantage is gained through their use.

As has just been shown, with each tire operating at its capacity load, the effects of added weight are clearly evident in both its tire horsepower and tire net force output. Fig. 17 shows a comparison of basic and oversize tire performance in terms of gain in tire horsepower and tire net force output plotted against increase in tire loading. Basic tire power and weight are taken as 100% in both cases.

1. Tire sections with load-carrying capacity up to approximately 130% of the basic tire may be

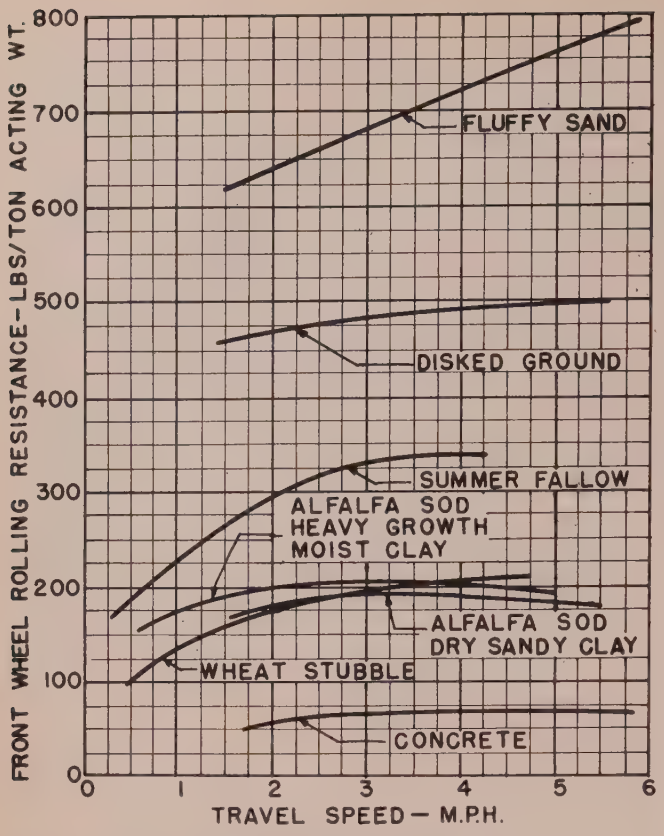

Fig. 18 – Front-wheel rolling resistance versus travel speed. 6.00 x 16 tire at 28 psi inflation pressure

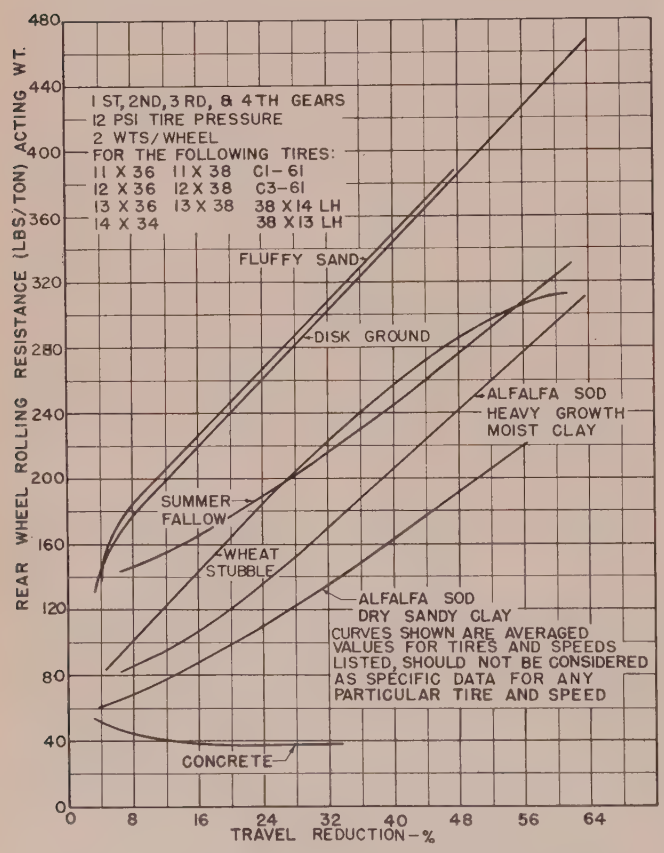

Fig. 19 – Travel reduction versus rear-wheel rolling resistance

loaded to develop a corresponding increase in tire horsepower, when compared with the basic tire. When loaded in excess of this amount, the rate of increase in tire horsepower is no longer proportional to the increased load.

2. Tire sections which allow up to 130% increase in load-carrying capacity of the basic tire have approximately a 120% increase in tire net force output in terms of the basic tire.

A byproduct of these tests was information concerning rolling resistance of both front and rear tires. As these tests were conducted under field operation, it was necessary to measure actual rolling resistance of the front wheels. Summarizing tests conducted at Tucson, Colby, and Columbiana, Fig. 18 shows the rolling resistance per ton of weight acting on the front wheels with 6.00 x 16 tires under four surface conditions and at various travel speeds. It might be added that these data were gathered from approximately 1000 actual field runs, and a broad scatter pattern resulted. The curve shown is determined by the mean points of groups of test results, each group based on similar travel speeds.

Rear-tire rolling resistance in all cases has been that defined by the expression:

$$\frac{\text{Rear-axle torque}}{\text{Rear-tire rolling radius}} - (\text{drawbar pull} + \text{front-wheel rolling resistance})$$

From a study of these data, the only definite pattern found to exist was that between rolling resistance and travel reduction. (See Fig. 19.) The curves plotted from the test of various tires intertwined, so that the curve again represents mean or characteristic results.

This analysis of the field performance of basic and oversize tires with common tread designs, outside diameters, and rolling radii operating under a wide variety of carefully controlled soil and surface conditions leads to the following conclusions:

1. Ability of an oversize drive-wheel tire to increase tractor performance is largely a function of any additional weight that can be carried safely by the tire and not the result of section size or configuration (as distinguished from type of tread).

2. When weights carried by various tires are nearly equal, there is no significant difference in performance characteristics of comparable low section height (method 1) and conventional-design oversize tires (method 2).

3. Traction coefficients and tire efficiencies of the narrowest or basic tire are generally equal to, or slightly better than, those of the corresponding oversize tires. This was found to be true for any soil conditions tested, regardless of rear-axle weight.

4. Because performance is directly dependent upon the weight carried by the tire, oversize tires with conventional section configuration have a performance (tractive effort) potential slightly greater than tires of low section height configuration. This is because the volume available for carrying liquid ballast and rated load capacity of the former are both greater than for the latter.

5. Based on data secured from these tests and test conditions, the many advantages resulting from the use of basic and oversize tires with common outside diameters and rolling radii may be secured with low section height tires (method 1) without sacrificing tractive performance, when compared with oversize tires of conventional section configuration.

DISCUSSION

Soil Compaction Needs Study

—H. L. Brock
Ford Motor Co.

AS HAS been proved before, little is gained in tractor performance by oversizing tires except where additional weight is added to the vehicle. Under many conditions of operation, where flotation is not the limiting factor, additional weight must be added to the vehicle with oversize tires to obtain performance equal to that with the basic size tire. This is particularly true when the ratio of weight to horsepower is less than 100.

Although drawbar performance of oversize tires does not substantiate their use, the factor of soil compaction may very well justify this ever-increasing trend. We should expend every effort in seeking the answer to this important question. Today as in the past, our group has been blessed with individuals who are constantly searching out the problems confronting the farmer, and in turn establishing programs to effectively bring about their solution. Compaction is one problem now being investigated.

The final statement of the author's paper, "the many advantages resulting from the use of basic and oversize tires with common outside diameters and rolling radii may be secured with low section height tires (method 1) without sacrificing tractor performance, when compared with oversize tires of conventional section configuration," answers the primary question involved in this investigation. Other questions of economics and customer acceptance must be answered before the program can be concluded.

In Proper Combinations, Existing Tires Will Do Same Job as Low Section Height Tires

—R. W. Sohl
Goodyear Tire & Rubber Co.

WE ARE glad to see the low-pressure pneumatic tire recognized as one of the major improvements in tractor performance and efficiency. This has been proved beyond doubt over the past 20 years.

Some of the operating difficulties attributed to tractor tires are, in many cases, the result of improper maintenance or use.

Sidewall buckling with resultant premature failure is caused by too low inflation pressure for the job being done.

Sidewise instability or tire rolling can be caused by underinflation, but narrow rims may also contribute to this.

The intolerable reduction in drawbar pull when oversize tires are used could be improved if the design were based on the first oversize instead of the basic tire size, in which case the variation in speed would be limited to $\pm$ 3% instead of the + 6% which results with the 11-12-13 $\times$ 38 series referred to.

If method B of oversizing (decreasing rim diameter as tire section increases) is used, rolling radius is maintained and some reduction in cost is realized.

We believe the rim and wheel problem in this system can be solved. Disc wheels with rims attached will work without question, but demountable rims offer more of a problem. The most difficult combination is with the power-adjusted tread width system where the rim well should be as wide as possible to support the spiral mounting rails which provide tread width variation.

The low section height tire has no advantage in traction performance over standard tires, as indicated in the various tests made with both kinds of tires. Actually, the standard tire is somewhat the better of the two.

There are also indications that the durability of the low section height tire will be inferior to the standard tire because of its reduced height.

The basic shape of this tire is contrary to good tire-design practice, for as tire size increases the ratio of section height to section width decreases. With tire flexing concentrated in a shorter sidewall area, fatigue failures are sure to give trouble. It will be necessary to operate these tires at higher inflation pressures to keep them seated on the rims, for the lateral force holding the bead seated decreases with reduced section height.

Actually what we are doing is making a tire with smaller air volume, and less efficient. No doubt, it would be expected to do the same work as its larger size counterpart of the wide base type.

The tire industry can not, therefore, find a sound basis for asking our managements to spend the millions of dollars required to provide low section height tires and rims for tractors when existing tires, if used in proper combinations, will provide the same constant rolling radius feature as low section height tires.

Excellent Correlation Between Field, Laboratory Test Data

—I. F. Reed
United States Department of Agriculture

WE APPRECIATE having had the opportunity to collaborate in the work by conducting the controlled laboratory tests referred to in the authors' paper and discussed

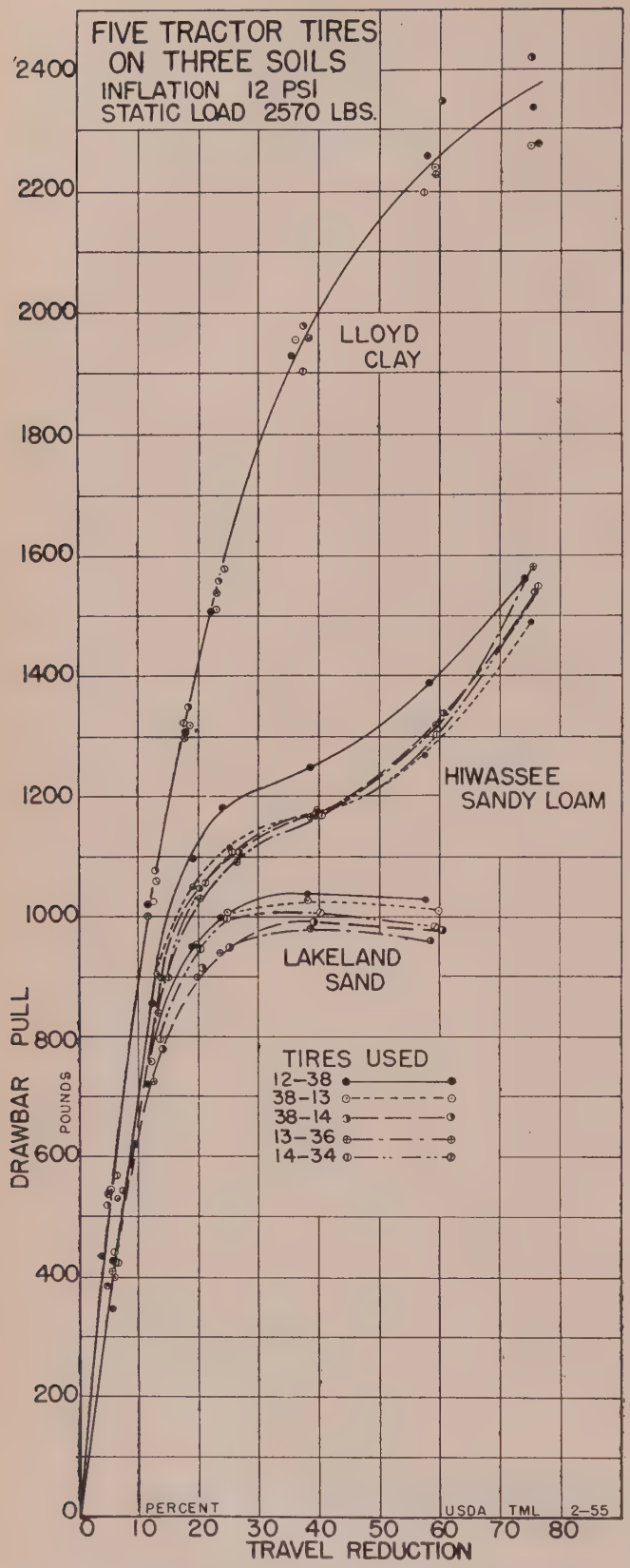

Fig. A – Relationship between drawbar pull and travel reduction for five tires in three soils through range zero-75% travel reduction

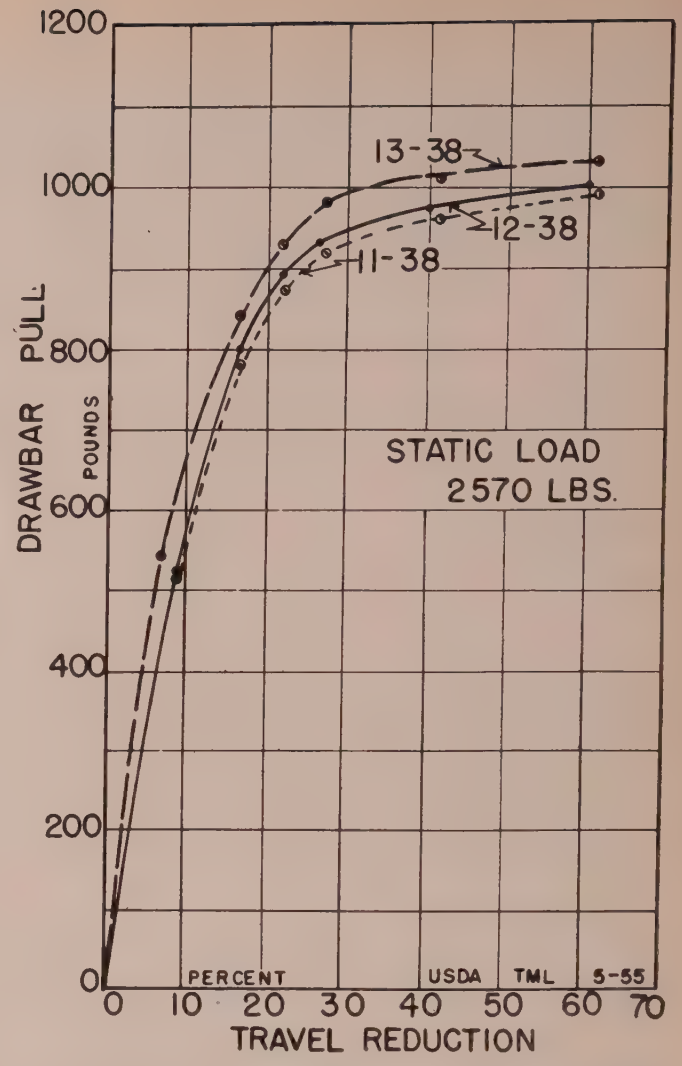

Fig. B – Relationship between drawbar pull and travel reduction in sand for three tires inflated to 12-psi pressure and carrying 2570-lb static load

more fully in our paper presented before the annual meeting of the American Society of Agricultural Engineers last June and published in the September issue of "Agricultural Engineering." We appreciate also the fact that field and laboratory data supplement each other so effectively. The careful and complete planning of equipment, procedures, and all other factors connected with the field work have paid off in that it enabled obtaining data that lack the fluctuations often found in field data. Duplicated tests produced like results. Let me repeat, however, that these results were obtained only because strict attention was paid to all details in carrying through a well thought out and organized program. Apparently, no needed expense was spared in providing needed instrumentation and other factors. In fact, we pay the highest compliment to this work by saying that results obtained approach the range of accuracy possible in laboratory tests.

The fact that field and laboratory data supplement each other so completely should strengthen all our beliefs in results obtained by each method. If anyone doubted the effectiveness and application of Tillage Machinery Laboratory findings or the possibilities of getting relatively exacting results from field tests, the results presented in this paper should remove these doubts.

In the presentation of results of field tests, the authors

Table A – Tire Information on 11-, 12-, and 13-In. Sizes Used in Lakeland Sand

Tire	Inflation Pressure, psi	Maximum Rated Load, lb	Rolling Radius, ft	Water for 85% Fill, lb	Number of Lugs
11x38	12	2185	2.371	405	24
12x38	12	2570	2.458	500	23
13x38	12	3050	2.544	600	23
11x38	14	2390	2.346	405	24
12x38	14	2810	2.454	500	23
13x38	14	3330	2.529	600	23

have steered away from talking about drawbar pull. The authors have purposely kept their discussion in rather abstract terms—to farmers at least—to enable comparing one factor against another without the influence of variation in weight-carrying capacity. This is good. We have made similar comparisons using data obtained by use of controlled tests at our laboratory. However, in working closely with farm operators, we often find it necessary to state results in terms with which they are familiar. The terms used in the paper describe exactly what the authors are trying to bring out if you are familiar with them. However, if not it is somewhat like the colored boy on trial. The judge asked: "Sam, are you the plaintiff or the defendant?" Sam replied: "How's that, judge? I's neither one. I's the one that stole the pig." So, though we come up with the same answers, let's look briefly at the Tillage Machinery Laboratory test data referred to by the authors by showing drawbar pull plotted against travel reduction, or, slippage in farmers' language.

Fig. A shows the results for the five tires classed as groups I and II when operated in three soils at slips varying from 5-75%. Note that in sand and sandy loam soils the basic tire outpulled the oversize tires by a small amount. However, only one curve is drawn for tests on the clay soil for the results for different tires were so nearly alike. Remember that all tires were inflated to the same pressure and were carrying the same static load, 2570 lb, the maximum load recommended for the basic 12 × 38 tire. These data show then that oversizing tires by either method, 1 or 2, which keep the outside diameter constant, does not pay off in increased drawbar pull if the user does not take advantage of the greater load-carrying capacity of the larger tires.

Data in Fig. B show that when tires were oversized by method B, the oversized tires pulled more. Note that the data are consistent. There is no intertwining of this set of curves. Again, the field test results are in line with these findings.

In the paper, the authors have brought out the fact that the traction coefficient-travel reduction relationship remains practically constant for a group of tires in each of the soil conditions. This means to us, then, that the tire with higher load-carrying capacity, if loaded to that capacity, will pull the greatest load.

Table A, similar to one used in the paper, shows the maximum recommended loads for three tire sizes, 11 × 38, 12 × 38, and 13 × 38.

Fig. C shows drawbar pulls for these three tires, each loaded to its maximum recommended carrying capacity, for 14-psi inflation pressure and operating at slippages varying from zero to 60%. For these tires inflated to the same pressure, the greater weight carried by the oversize tires enabled them to pull more. A comparison of data for the 12 × 38 tire in Figs. B and C shows that weight must be considered with inflation. For the most part, the 12 × 38 tire inflated to 12 psi and carrying 2570 lb pulled practically as much as this tire inflated to 14 psi and carrying 2870 lb. This indicates that there appears to be an interesting relationship between inflation pressure, load, and drawbar pull in sand. This point is being studied further.

The reports and papers cited show that the effectiveness and efficiencies of various sizes of rear tractor tires can be measured both in the field and at our laboratory. These papers do not, however, show what actions and reactions have taken place in the soil. Oversizing without increasing weight under some conditions may reduce compaction so as to take it outside of the critical range; that is, the range where the soil pores are closed or rearranged in a way that moisture and air movements are retarded to the detriment of root growth. We are working on this problem. It is a big job, but with everyone realizing the importance of the study and helping, our coordinated efforts should bear fruit.

The conclusions for all tire tests discussed are exactly the same whether we draw them from a study of all field test data, a study of laboratory data, or a study of all data combined. It was fortunate that this extensive coordinated study was made. As stated earlier in this discussion, if there was any doubt before, now all of us will be more willing to accept without reservation results obtained by comprehensive studies made either in the field or in the laboratory.

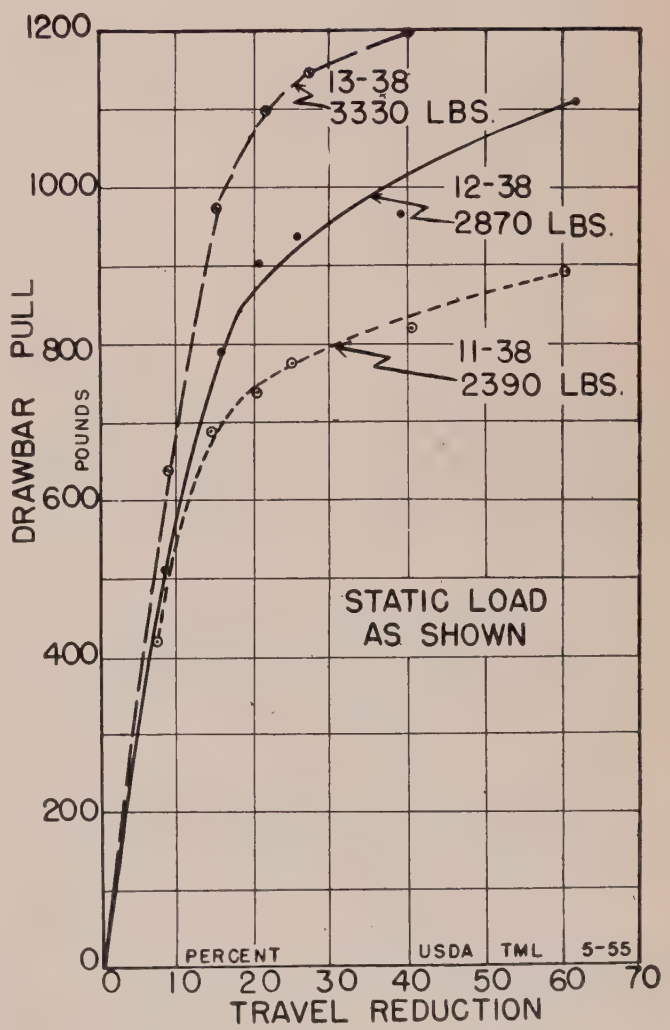

Fig. C – Relationship between drawbar pull and travel reduction in sand for the tires of Fig. B, but inflated to 14-psi pressure and each tire carrying its maximum recommended load

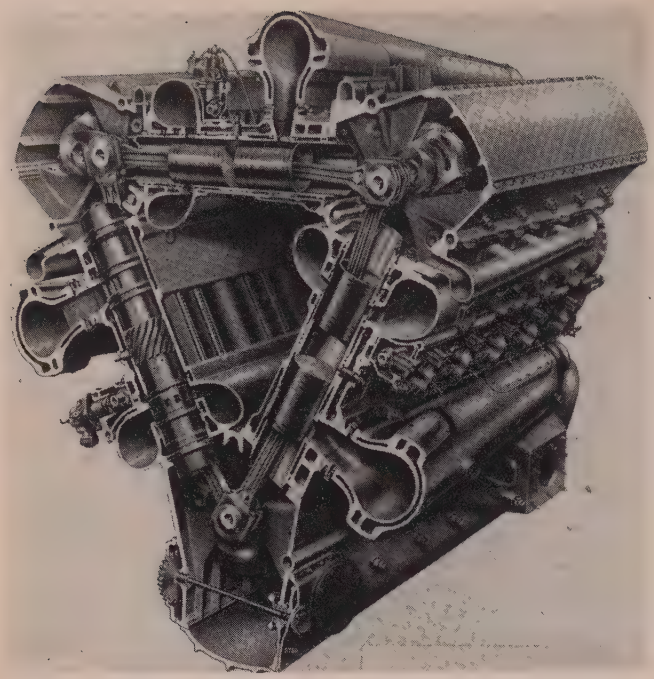

Fig. 1 – Pictorial cross-section of Napier Deltic diesel engine

The Napier Deltic

THE Napier Deltic is a diesel engine operating on the 2-stroke-cycle principle, which, by virtue of its unusual design configuration, demonstrates exceptional qualities of robustness and simplicity in operation coupled with a high degree of lightness and compactness.

Design of this engine began in 1946. After an intensive period of development sponsored by the British Admiralty, during which 20,000 hr of running time have been accumulated on the test bench and in service, the engine is now in production for both naval and commercial purposes.

Qualities demonstrated by the engine are believed to represent a technical advance in the field of diesel engineering, and for that reason provide a subject of sufficient interest for presentation here.

Basic Design Concepts – The two main factors which operate in combination to achieve the results stated are, first, use of opposed pistons, and second, disposition of cylinders in the form of an equilateral triangle. The engine consists essentially of three opposed-piston engines combined together, with common crankshafts at each corner of the triangle (see Fig. 1).

The opposed-piston principle is particularly attractive for high-speed operation for the following reasons:

(a) Efficient "end to end" scavenging of the cylinder is obtained.

(b) Generous port areas and gas flow passages are possible without undue sacrifice of effective stroke.

(c) Complexity and mechanical difficulties connected with design and operation of valve gear are avoided entirely.

(d) There are no cylinder-head sealing problems.

(e) Combustion-chamber walls consist to a large extent of hot piston crowns. Heat losses are thereby minimized and combustion processes are improved, with resulting gains in thermal efficiency.

When three sets of opposed-piston cylinders are combined together as in the Deltic, full advantage is taken of all these beneficial factors, which are enhanced still further by the following advantages derived directly from the triangular configuration:

(f) The triangular disposition of cylinders provides a structure of great inherent rigidity. When care is taken in design for transmission of all com-

Diesel Engine

Ernest Chatterton, D. Napier & Son, Ltd.

This paper was presented at the SAE Golden Anniversary Diesel-Engine Meeting, St. Louis, Nov. 3, 1955.

THE Deltic diesel engine, developed during the past few years in England by Napier is now in quantity production. The Deltic presents novel design features claimed to achieve a technical advance in current diesel-engine practice.

Some special features are discussed in the paper, and a description of the engine, its characteristics and performance is included. The general design philosophy behind the Deltic is outlined by the author, and some comments on reliability as applied to high-speed engines are set forth.

A survey is made of current applications of the Deltic, and a brief reference is made to future developments.

bustion loads through high tensile strength steel bolts, a very robust and light construction results, allowing use of light-alloy castings with no sacrifice in lift or reliability as compared with more conventional materials. The basic system of load transmission in the Deltic is shown in Fig. 2, which shows that there is direct load transmission from main bearing caps to the through-bolts, thereby relieving the cylinder blocks of all combustion loadings.

(g) It is a well-known design fact that use of multiple cylinders of small dimensions results in a lower weight per horsepower than a smaller number of larger cylinders. The triangular disposition makes it possible to group multiple cylinders very compactly, thus combining advantages of short length and compactness with low weight per horsepower.

(h) Ability to employ multiple cylinders reduces dimensions of main engine components to an extent which gives the greatest possible latitude in choice of materials, heat-treatment processes, and manufacturing techniques, thus enabling the most modern technical standards to be applied in the design. The components also become suitable for quantity production methods, thus ensuring com-

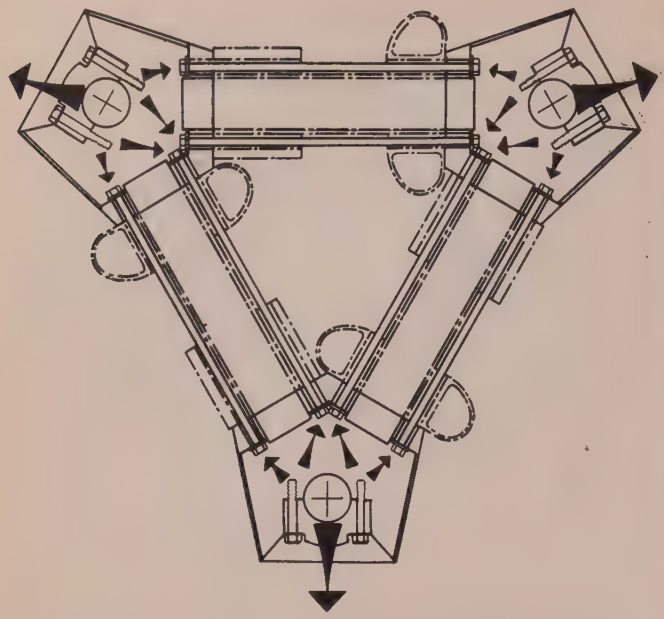

Fig. 2 – Diagram showing transmission of combustion loads

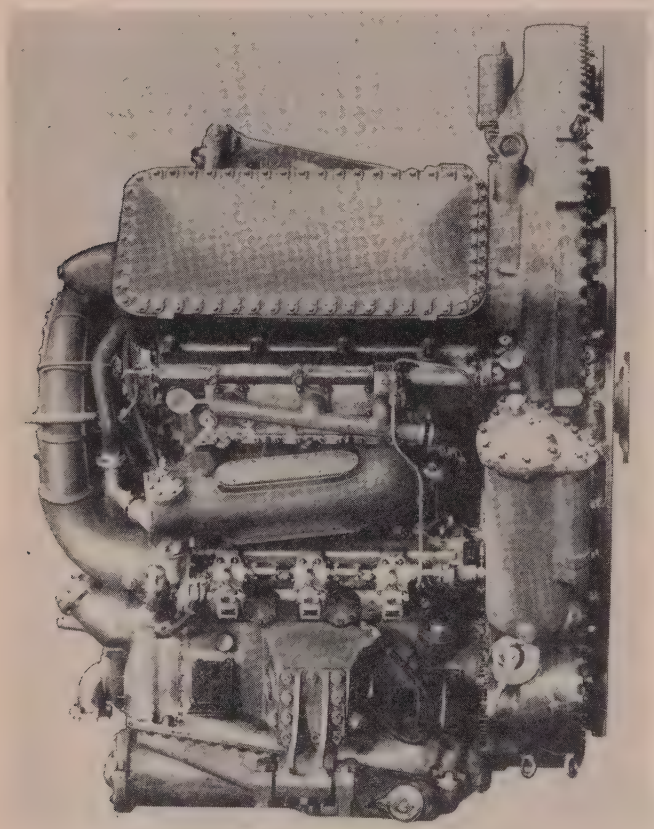

Fig. 3 – Side view of 9-cyl Deltic

plete interchangeability of all parts and low production costs.

Other important technical advantages will emerge later, but at this point it is desirable to state briefly the results demonstrated by the Deltic in practice.

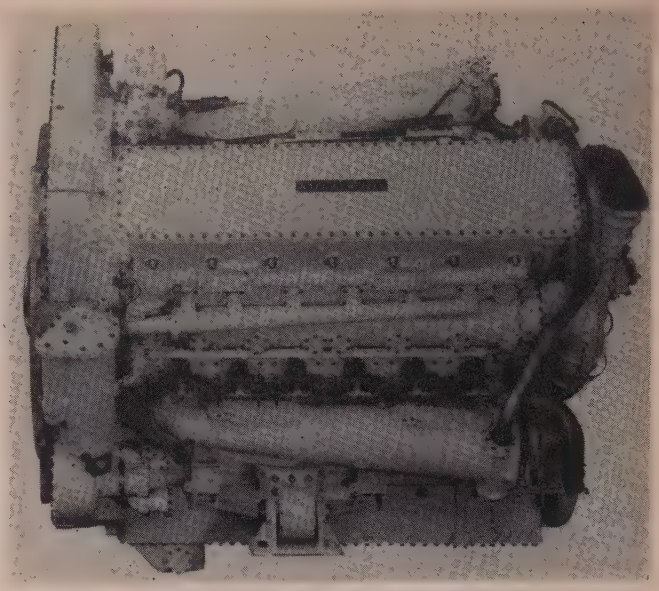

Fig. 4 – Side view of 18-cyl Deltic

The Deltic Engine in Practice – At present, Deltic engines are being produced in two forms, the first with 9 cyl and the second with 18. Designs have also been worked out for 15- and 24-cyl engines, but these are not yet being built.

A side view of the 9-cyl engine is shown in Fig. 3; the 18-cyl engine is shown in Fig. 4. For our immediate purpose, figures for the 18-cyl engine will be quoted as indicative of leading characteristics of the Deltic-type engine.

As supplied to the British Admiralty for use in fast patrol boats, which require a minimum period of 1000 hr between piston withdrawals, the stripped engine produces a maximum of 2730 bhp. Engine weight is 8860 lb, giving a specific weight of 3.24 lb per bhp. This low specific weight is achieved with a bmep of 100.4 psi and piston speed of 2416 fpm. Both bmep and piston speed are conservative, indicating clearly that the low specific weight results from engine design features and not from high cylinder ratings. Engine dimensions are: length=105 in., width=71¼ in., and height=80 in. Fuel consumption at maximum power is 0.380 lb per bhp-hr.

For commercial purposes, with a minimum 5000-hr period between piston withdrawals, the 1 hr rating of the stripped engine is 1950 bhp, giving a specific weight of 4.56 lb per bhp. Bmep at this condition is 95.5 psi and piston speed 1812 fpm. Again, these figures are extremely conservative. Fuel consumption at this rating is 0.360 lb per bhp-hr. Engine dimensions are identical with those quoted above.

These figures for performance, weight, and space occupied provide practical confirmations of technical advantages demonstrated by this type of engine.

Design Features

Geometrical Limitations – The triangular form

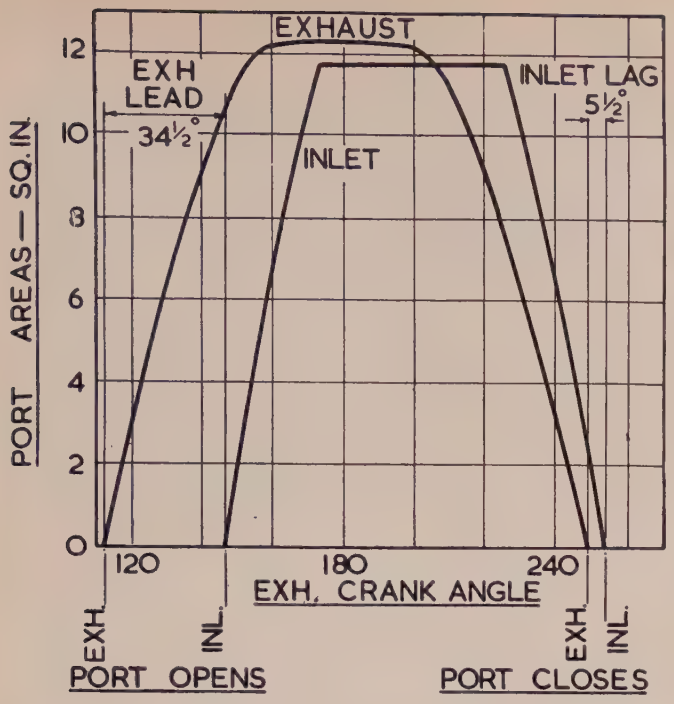

Fig. 5 – Porting diagram

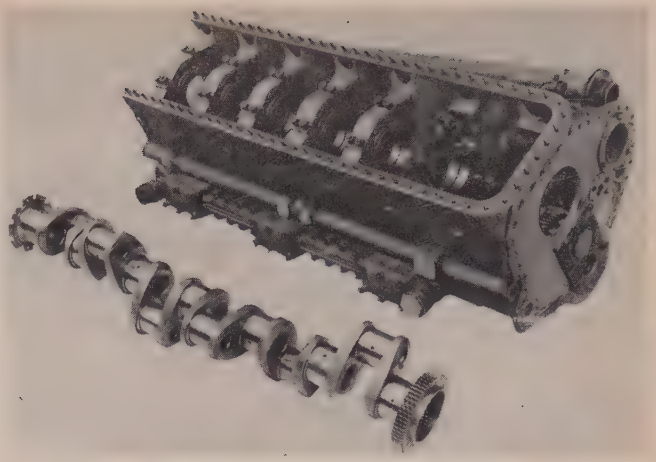

Fig. 6 – Crankcase and crankshaft

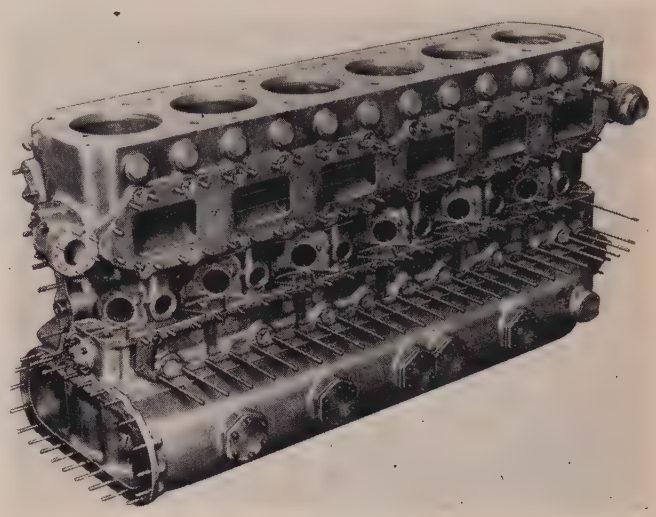

Fig. 7 – Cylinder block

imposes two design limitations, which arise directly from the geometry of the layout.

First, in order to obtain the correct sequence of cylinder firing, one crankshaft must run in a sense opposite to the other two. Second, a 20-deg phase difference between crankshafts at each end of one cylinder is unavoidable.

Neither limitation is disadvantageous. Crankshaft rotation can easily be taken care of in the gearing arrangements. Some phase difference between crankshafts is essential on the high-speed opposed-piston engine in order to obtain necessary displacement of port-opening diagrams to give a reasonable exhaust lead angle coupled with a smaller degree of inlet lag for cylinder filling. In the in-line opposed-piston engine, it is desirable to reduce this phase difference to a minimum, for as phase angle is increased, torque diagrams and power transmitted through the two crankshafts become widely different. This can be embarrassing and can lead to difficulties in the system coupling the two crankshafts.

In the Deltic, each crankpin carries one inlet piston and one exhaust piston, so that torque produced and power transmitted at each crankpin is identical. This further advantage of the triangular arrangement allows the 20-deg phase angle to be accepted without sacrifice. Resulting porting diagrams are shown in Fig. 5 and display characteristics desirable for high-speed operation.

Mechanical Features – Having referred briefly to the main points arising from the triangular arrangement of cylinders, components involved in the practical application may be considered. Illustrations and descriptions refer to the 18-cyl engine, but understand that the 9-cyl engine employs a large number of similar parts and effectively is one-half an 18-cyl engine.

(a) Crankcases and crankshafts: In the Deltic arrangement there is a crankcase housing a crankshaft at each corner of the triangle. Each crankshaft is supported by seven thin-wall lead-bronze type main bearings mounted directly in the light-alloy crankcases. The two top crankcases, one of which is shown in Fig. 6, are identical, while the bottom crankcase is extended both to provide an oil sump and to accommodate engine mount supports.

This illustration also depicts one of the three nitrided 6-throw crankshafts.

(b) Cylinder blocks: The three cylinder blocks (Fig. 7) are identical light-alloy castings, each held in the assembled engine by steel through-bolts passing through holes in the block and clamping it between the two adjacent crankcases. Coolant passages are cast in place and connected to water jackets surrounding the six removable steel cyl-

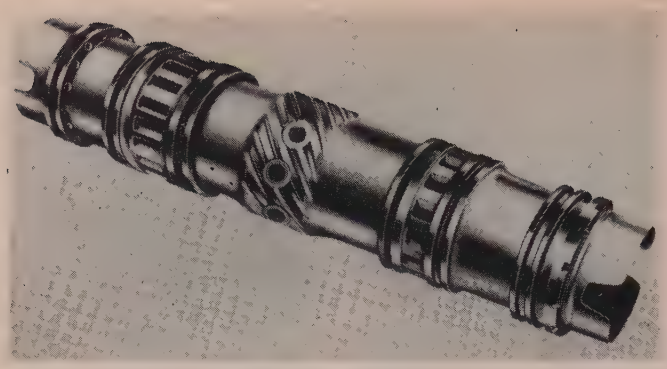

Fig. 8 – Cylinder liner

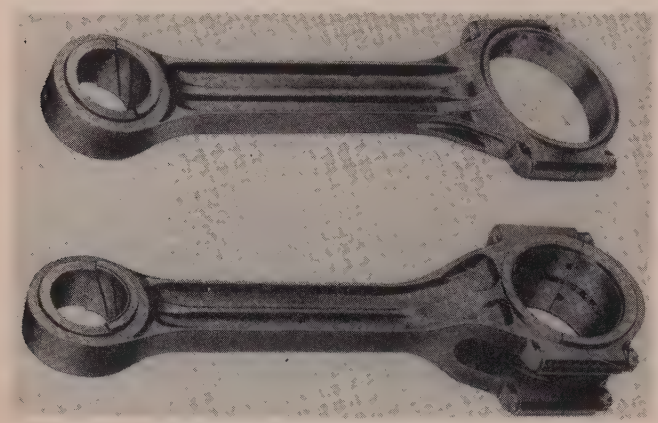

Fig. 9 – Connecting rods

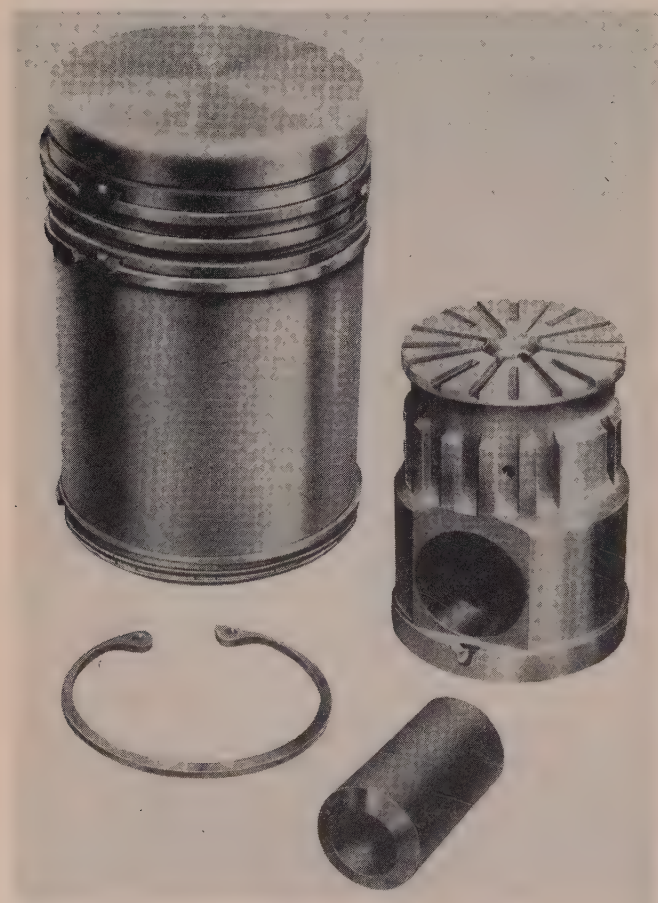

Fig. 10 – Piston components

inder liners. Triple-seal type rubber rings are provided between liner and block to effect coolant seals.

(c) Cylinder liners: All cylinder liners are identical (see Fig. 8). They are machined alloy-steel forgings, with a chromium-plated, lapped bore to resist wear. The major portion of working surface is covered with closely spaced etched dimples to retain lubricant and reduce ring and bore wear to a minimum. Nine exhaust ports are arranged around part of the circumference near one end of the liner and 14 inlet ports are placed around the complete circumference near the other end. Inlet ports are cut with a partial tangential entry to impart swirl to incoming air, thus assisting in scavenging the central core in the combustion chamber and also playing a vital part in fuel-air mixing.

(d) Connecting rods: Fig. 9 shows two high tensile strength, alloy steel, forged connecting rods, one plain and the other forked, which are mounted on each crankpin. The rods are drilled lengthwise to provide oil for lubricating the small end bearing and for piston cooling. The crankpin and plain rod bearings are of the thin-wall lead-bronze type, and that for the forked rod is housed in a steel shell hardened on the outside, which provides bearing surface for the plain rod bearing. Both bearings, therefore, run on hardened surfaces.

(e) Pistons: Piston components are illustrated in Fig. 10. Each piston comprises an outer piston body of cast aluminum and an inner member, which forms the gudgeon pin housing, machined from a Y-alloy forging. An annular space between these members, situated behind the gas rings and extended by grooves under the crown, is partially filled with oil. The oil is constantly replenished so that by reciprocation of the piston, heat is mechanically transported from the hot crown to the cool end of the piston skirt by means of the oil. The two members of the piston are secured by a spring circlip. Three compression rings are carried in grooves immediately below the flat crown, the two upper grooves being machined in a wear-resisting, austenitic iron insert bonded to the aluminum by the Alfin process. Two scraper rings at the bottom of the skirt provide oil control and seal against gas leakage into the crankcase.

(f) Phasing gear casing: The three crankshafts are connected to one another through the gear train depicted in Fig. 11, in which a separate tributary gear train from each crankshaft drives a common output gear at the center of the triangle. Observe that the two top crankshafts are connected through a single idler gear, while the bottom shaft drives through two idlers, thus accommodating the reversed direction of rotation of one shaft referred to previously. The gearing is housed in a thin triangular 2-piece casting designated as the phasing gear casing. By a different assembly of idler gears it is possible to reverse output shaft rotation, thus meeting a requirement for reversible

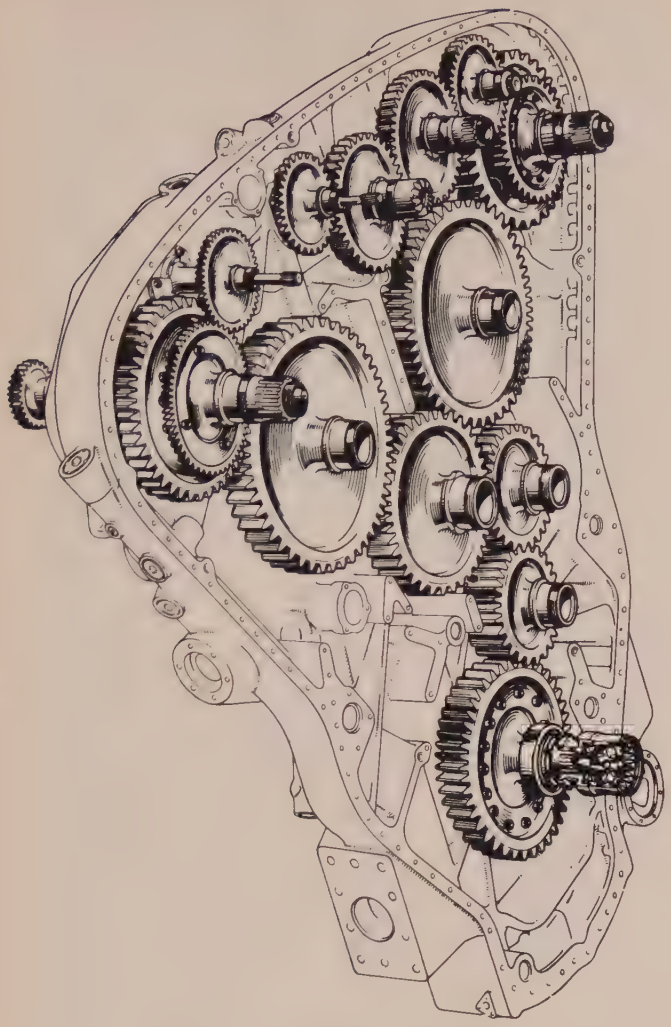

Fig. 11 – Crankshaft phasing gears

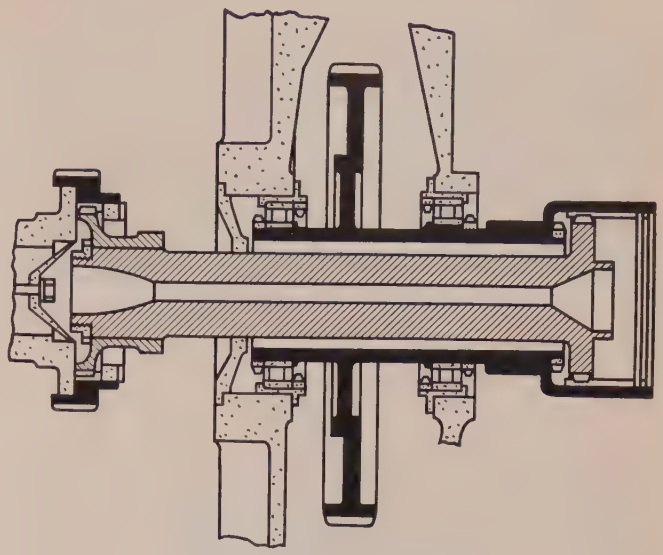

Fig. 12 – Crankshaft coupling

engines in marine applications.

(g) Coupling between crankshaft and gear system: Each crankshaft is connected into the phasing gear system through a flexible quill shaft (shown in Fig. 12). This not only provides a convenient device for assembly and dismantling, but also introduces a controllable degree of flexibility into the system which permits limited tuning of torsional vibration effects. This point will be discussed later.

(h) Camshaft casings: Each cylinder block has attached to it a casing containing the camshaft for operating six fuel injection pumps. These camshafts are driven by bevel gears from the crankshaft driving ends. Part of one camshaft casing, together with fuel injection pumps, is shown in Fig. 13. There are two injectors for each cylinder fed by one pump.

(i) Fuel injectors: Fuel injectors are of the type shown in Fig. 14, and are designed to be as short as possible to allow the maximum angle between nozzles within the space available.

(j) Fuel pumps: Fuel injection pumps are as shown in Fig. 15. They are of CAV manufacture and the normal "jerk" type, developed especially by Napier for the Deltic. Rack control is by a torsion shaft to eliminate differential expansion troubles. Each pump contains a built-in filter.

(k) Scavenge blower: The scavenge blower is shown in Fig. 16. This unit is mounted on the end remote from the phasing gear casings. Connection with air manifolds in the cylinder blocks is made directly through the bolted facing on which the blower is secured. The impeller is double-sided, this design providing high adiabatic efficiency and a diameter reduced sufficiently to permit well-shaped

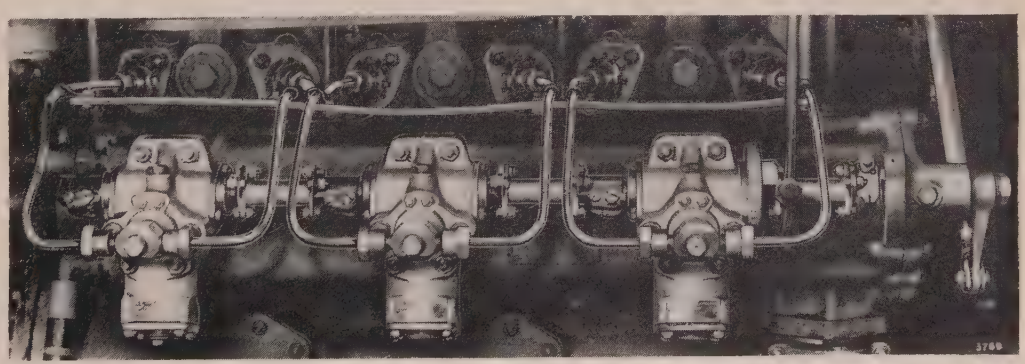

Fig. 13 – Fuel injection pump assembly

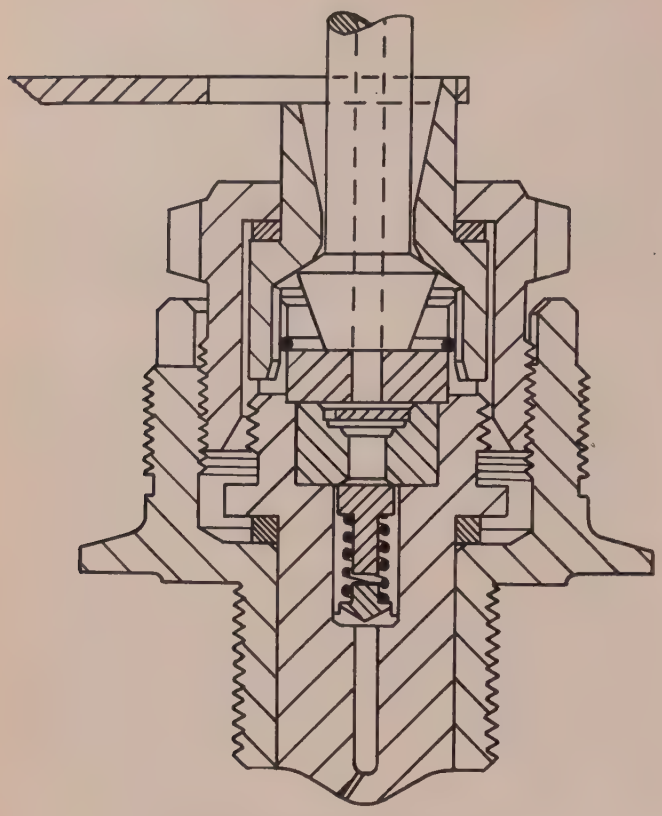

Fig. 14 – Cross-section of fuel injector

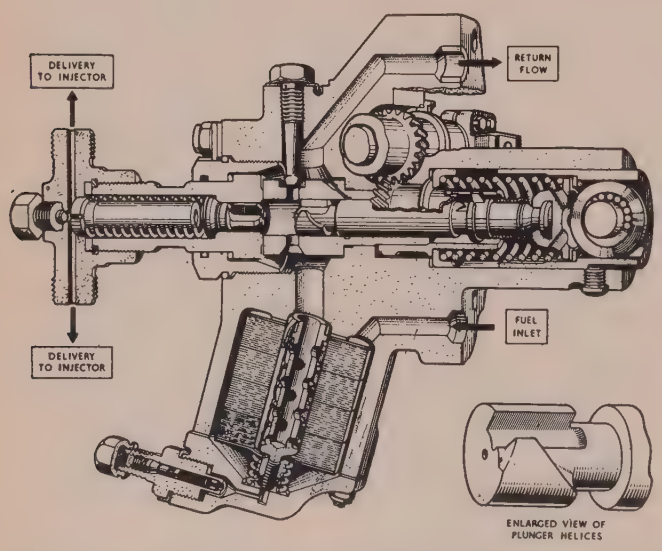

Fig. 15 – Fuel injection pump

air passages into the three cylinder blocks. End thrusts due to air loadings on the impeller are balanced. The blower is driven from the driving ends of the two top crankshafts by two long flexible shafts extending through the length of the two top crankcases.

(l) Governor: The engine is equipped with a hydraulic-type governor, providing control over the whole speed range from idling to maximum speed.

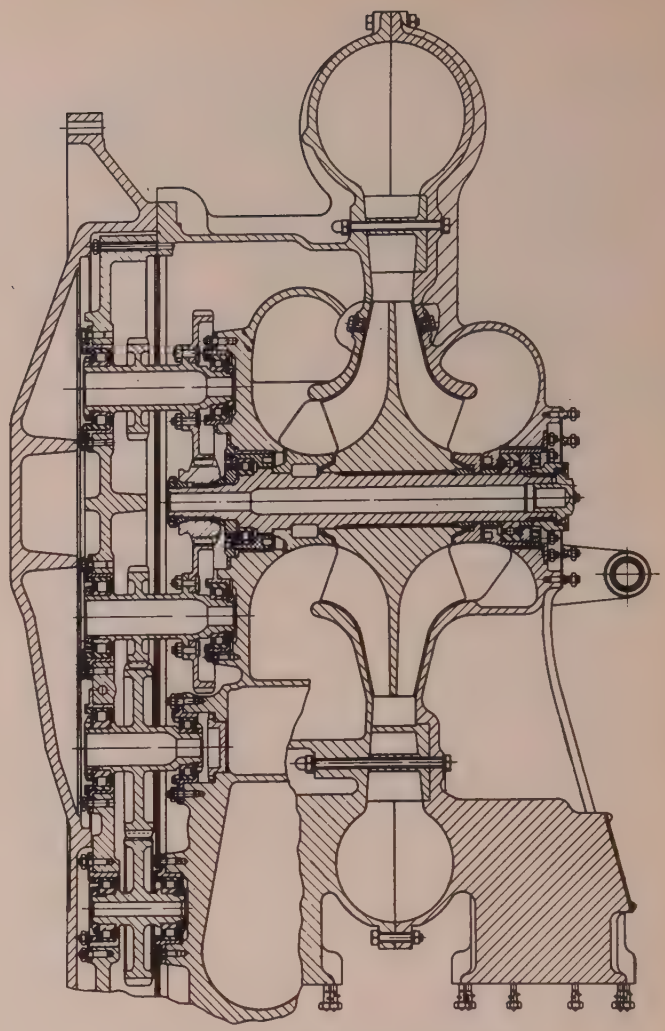

Fig. 16 – Cross-section of scavenge blower

(m) Starting: Alternative starting systems are available. For normal commercial purposes an air starting system has been developed to let timed air supply into one bank of six cylinders from an air reservoir. A connection into the cylinder is provided between the two fuel injectors. For naval use, starting is achieved by a "Plessey" cartridge-type starter firing cordite cartridge into a starter cylinder operating a Bendix claw. This constitutes a very light and effective starting system, but the necessity for a supply of cartridges makes it unsuitable for general commercial use.

Variations in Engine-Build Standards – Fig. 11 shows the engine output shaft at the center of the triangle. This output shaft position, with shaft running at crankshaft speed, is very convenient for many commercial applications. The engine arranged for this type output is illustrated in Fig. 17. This position is also suitable for driving a flange-mounted generator. In this case, the normal end cover is replaced by a short adapter interposed between engine and generator, as shown in Fig. 18.

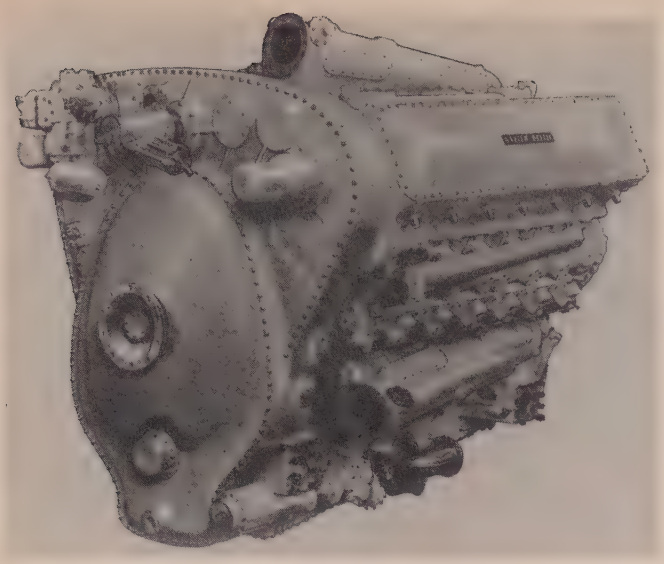

Fig. 17 – 18-cyl Deltic with central output shaft

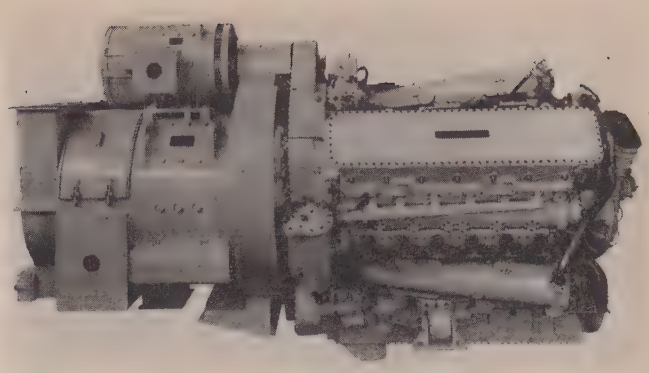

Fig. 18 – 18-cyl Deltic driving flange-mounted generator

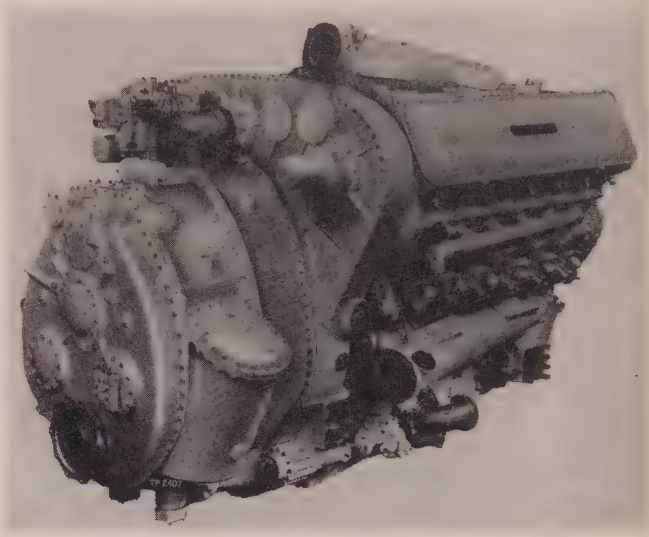

Fig. 19 – 18-cyl Deltic with marine reversing gearbox

The adapter is split horizontally, the upper half removable to permit access to the armature coupling bolts. The adapter has cast diffuser blades to improve characteristics of the generator cooling fan.

Where the central output shaft position is not suitable, it is a comparatively simple matter to provide a modified end cover and thereby arrange for different output shaft positions and speeds.

One particular case where this arises is in applications to marine propulsion, in which a low output shaft running at reduced speed is necessary, and a reversing gear is required. In this case the engine output shaft is taken into a reverse-reduction gearbox mounted on the phasing gear casing flange, as shown in Fig. 19. This reverse gear is of Napier design and consists basically of two constant-mesh gear trains, one for ahead and one for astern, with two oil-operated clutches to engage either train as desired.

In this form the engine constitutes a very compact, self-contained power unit for marine purposes complete with its own pumps, filters, and other auxiliaries, and with single lever control for both engine and reverse gear. This is the engine supplied to the Admiralty for naval craft.

Variations in build standards illustrated for the 18-cyl engine are also applicable to the 9-cyl engine.

General Engine Characteristics

Firing Intervals – Both 18- and 9-cyl engines have equally spaced firing, the 18-cyl engine producing impulses at 20-deg intervals and the 9-cyl engine at 40-deg intervals.

Output Torques – The output torque resulting from equally spaced multicylinder firing is remarkably smooth. The curve for the 18-cyl engine is shown in Fig. 20, in which maximum torque exceeds mean torque by only 2½%. A similar curve

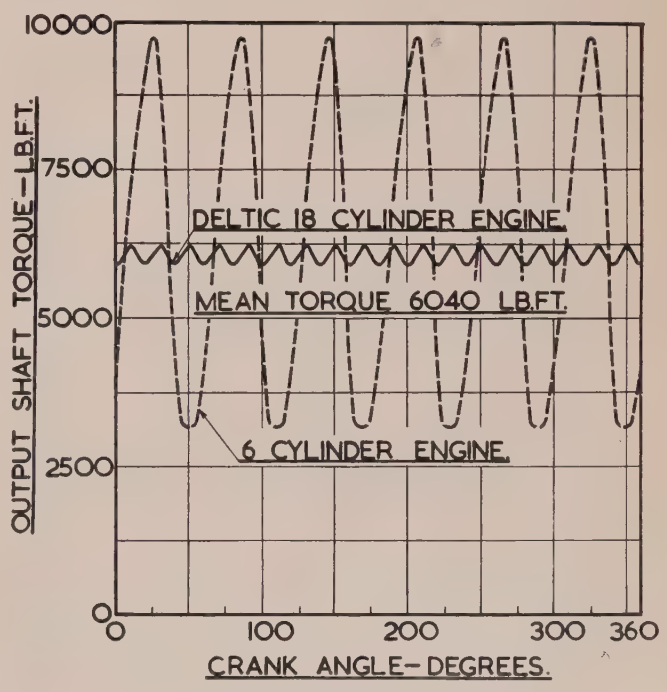

Fig. 20 – Torque curve for 18-cyl Deltic

Table 1 – Leading Particulars

	9 Cylinder		18 Cylinder	
	Commercial	High Power	Commercial	High Power
Bore, in.	5.125			
Stroke, in.	7.25 x 2			
Swept Volume, cu in.	2692	2692	5384	5384
Swept Volume per Min at Max Rpm, cu ft	2335	3115	4675	6230
Rated Speed, rpm	1500	2000	1500	2000
Piston Speed at Max Rpm, fpm	1812	2416	1812	2416
Max Power, shp	950	1250	1900	2500
Continuous Power, shp	860	937	1725	1875
Continuous Speed, rpm	1500	1700	1500	1700
Max Output Shaft Speed, rpm	1500	950	1500	950
Reduction Gear Ratio – Ahead	1:1	2.106:1	1:1	2.106:1
Reduction Gear Ratio – Astern	—	2.397:1	—	2.397:1
Output Shaft Rotation, Viewed from Free End	Ccw	Cw or ccw	Ccw	Cw or ccw
Auxiliary Power Take-off, hp	110	110	110	200
Scavenge Blower Type	Centrifugal			
Scavenge Blower Impeller	Single-sided		Double-sided	
Scavenge Blower Diameter, in.	15.5			
Scavenge Blower Gear Ratio	5.72 or 6.55	5.72	5.72 or 6.55	5.72
Nominal Compression Ratio	19.26			
Port Timing Referred to Exhaust Piston tdc				
Exhaust Opens, deg late	117	112	117	112
Inlet Opens, deg late	146½	146½	146½	146½
Exhaust Closes, deg early	117	112	117	112
Inlet Closes, deg early	106½	106½	106½	106½
Exhaust Period, deg	126	136	126	136
Inlet Period, deg	107	107	107	107
Exhaust Lead, deg	29½	34½	29½	34½
Inlet Lag, deg	10½	5½	10½	5½
Fuel Injection Timing, deg before exhaust tdc	32	30	32	30
Fuel Injection Rate, cu mm per deg	12.9			
Fuel Pump Plunger Diameter, mm	11			
Fuel Injector	Valve injector type			
Injector Opening Pressure, psi	525			
Injection Pipeline Pressure, psi	4500	6750	4500	6750
Lubricating Oil Consumption, pt per hr	4.25	5	8.5	10

for a 6-cyl two stroke engine is shown for comparison.

Engine Balance – Crankshafts in the 9-cyl engine are equipped with balance weights, but these are not necessary in the 18-cyl engine. There are no unbalanced forces on either engine, no unbalanced couples due to rotating masses, and no unbalanced primary couples due to reciprocating masses. There are small unbalanced secondary couples due to reciprocating masses, but these are not of sufficient magnitude to be observable even with very resilient engine supports.

Torsional Vibration – Both 9- and 18-cyl engines are fortunate from the torsional vibration point of view, for there is only one order of vibration producing effects of any significance, and this occurs at the extreme low end of the speed range. This is the sixth order, node at gears mode. By introducing a controlled degree of flexibility into the system in the form of quill shafts (illustrated in Fig. 12), critical speed for this order can be tuned to come below engine idling speed. Crankshafts are fitted at their free ends with dampers of the "viscous fluid" type, but these have only to deal with transient conditions occurring on starting and shutting down.

Any changes which are made outside the engine, such as the introduction of generators or alternators with widely different inertia values, have insignificant effects on the vibration frequency. There are, therefore, no critical speeds in the running range.

Operating Speed Range – Operating range of the 9- and 18-cyl commercial engines is from 1500 crankshaft rpm down to 350 rpm, a ratio of 4.3/1. High-performance engines have a range from 2000 crankshaft rpm down to 450 rpm, a ratio of 4.5/1.

Fuels – At commercial ratings both 9- and 18-cyl engines are at present cleared for operation on marine diesel fuels having a maximum sulfur content of 1.8%. Developments are at hand using residual fuels, but these have not yet progressed sufficiently to be of practical interest.

Engines with high performance ratings are usually required for applications in which power is of more importance than running costs, and at these ratings gas oil is used.

Major Technical Details – Leading technical particulars for both 9- and 18-cyl engines are given in Table 1.

Engine Performance

High-Performance Engines – In its original form developed for the Admiralty for use in fast patrol boats, the 18-cyl engine, equipped with reverse and reduction gear, produces a maximum of 2500 shp at 2000 crankshaft rpm with a specific fuel consumption of 0.415 lb per shp-hr. This power is subject to a ¼-hr limitation. The continuous power rating is 1875 shp at 1700 crankshaft rpm with a specific fuel consumption of 0.395 lb per shp-hr. At these conditions the running period between piston withdrawals was required by contract to be at least 1000 hr.

At least 80% of the total development time on the engine has been run at these ratings. An official Admiralty-type test of 1000-hr duration, based

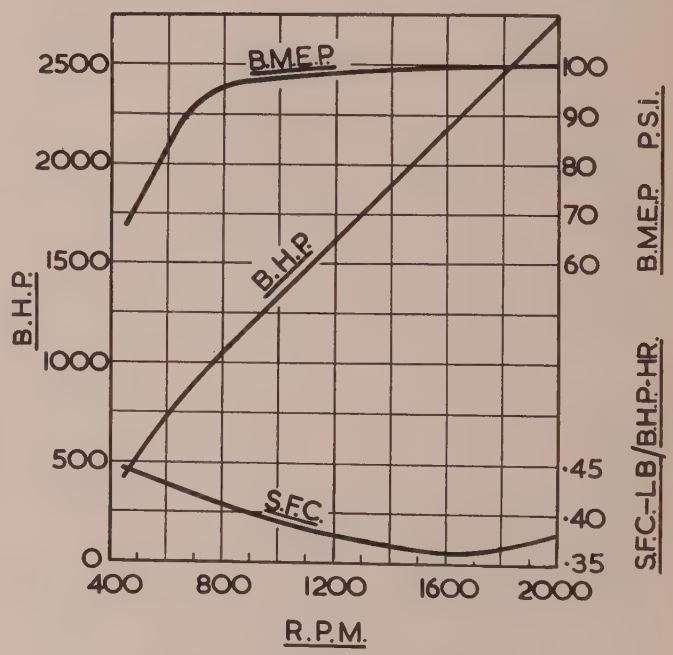

Fig. 21 – Power curves for 18-cyl Deltic

on a severe operating cycle, was successfully completed in 1953. Experience now indicates that under service conditions, running time which can be achieved between piston withdrawals will probably be 2000 hr.

Engine performances quoted above when related to a stripped engine (that is, the engine without reverse-reduction gear and without engine driven auxiliaries), are shown in Fig. 21. Under these conditions the maximum bhp is 2730, corresponding to a bmep of 100.4 psi at a specific fuel consumption of 0.380 lb per bhp-hr. The continuous rating is 2035 bhp with a bmep of 88 psi and a specific fuel consumption of 0.364 lb per bhp-hr. Air consumption figures are shown in Fig. 22, which shows that maximum power is obtained with a manifold pressure of 22.0 psia (44.8 in. of Hg), and an overall fuel/air ratio of 0.027/1. Continuous power is obtained with a manifold pressure of 20.0 psia (40.8 in. of Hg), and overall fuel/air ratio of 0.0238/1. Typical load range curves for the engine are illustrated in Fig. 23.

Commercial Engines – Commercial engines with a minimum 5000-hr period between piston withdrawals have a maximum 1-hr rating of 1900 shp at 1500 rpm. Referred to a stripped engine this power becomes 1950 bhp. This in only 71.5% of the maximum power at which the greater part of engine development has been run, so that actual load factor of the engine at commercial ratings is low.

Performances for engines at these ratings may also be taken from Figs. 21 and 22. Note that maximum power of 1950 bhp at 1500 rpm corresponds to a bmep of 95.5 psi and a specific fuel consumption of 0.363 lb per bhp-hr. This performance is maintained at an ambient air temperature of 85 F and a dry barometer reading of 29.5 in. of Hg (equivalent to an altitude of 500 ft), and is obtained with a manifold pressure of 19.0 psia (38.7 in. of Hg), and an overall fuel/air ratio of 0.023/1. Maximum cylinder pressure is 1500 psi and exhaust temperature 655 F.

Continuous rating of the commercial engine is

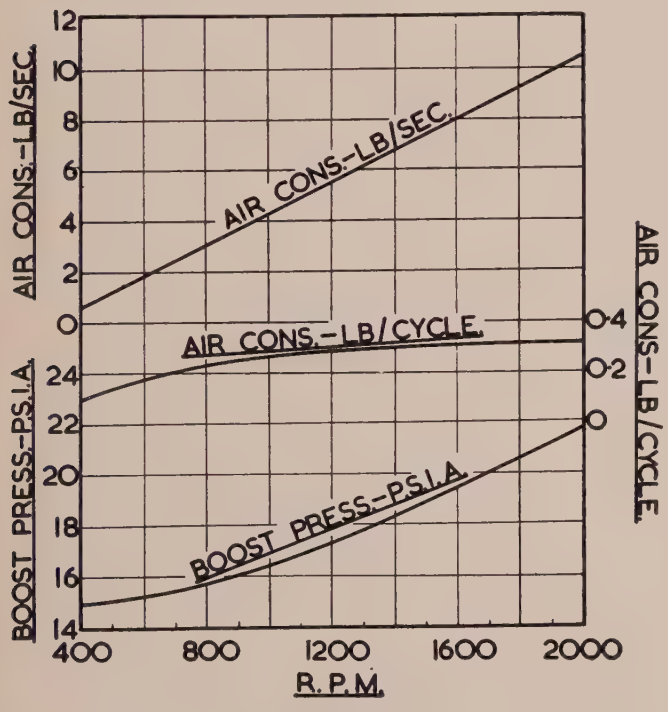

Fig. 22 – Air conditions for 18-cyl Deltic

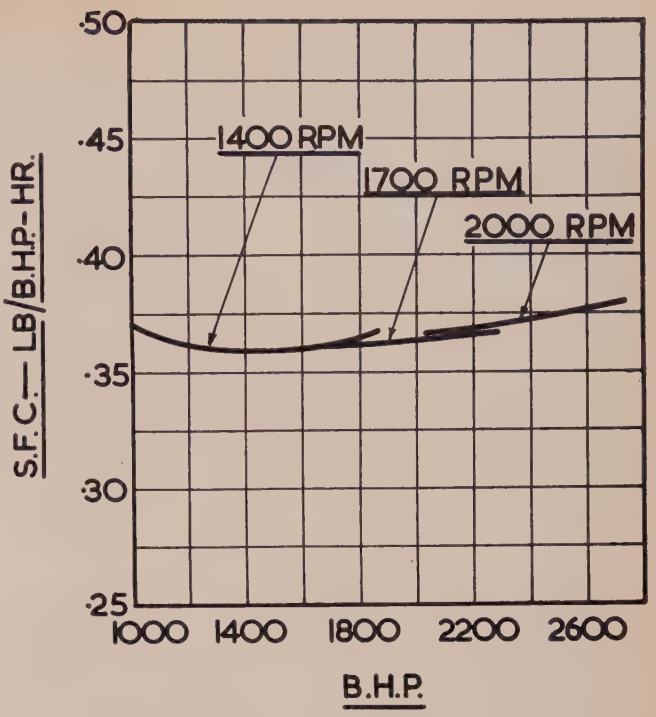

Fig. 23 – Load range curves for high-power 18-cyl Deltic

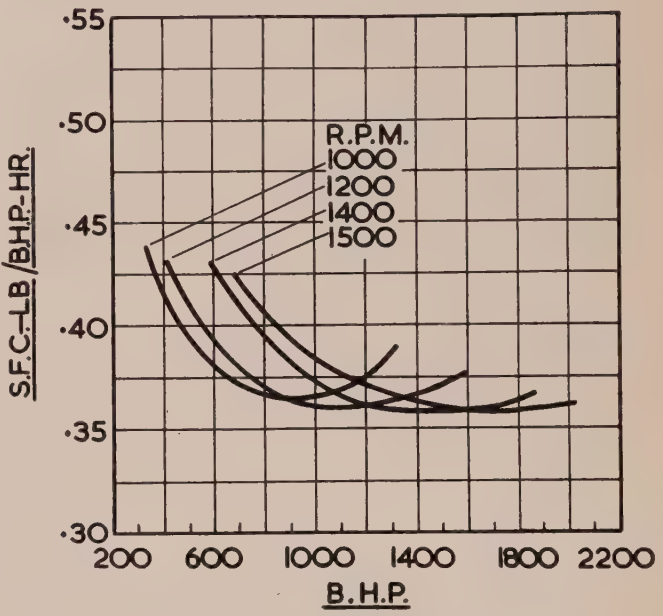

Fig. 24 – Load range curves for commercial 18-cyl Deltic

10% lower than the 1-hr rating at the same crankshaft speed.

Fuel consumption characteristics are shown in the form of load-range curves in Fig. 24, in which it is seen that best economy is maintained down to 50% load and 65% rpm.

Heat Losses – Fig. 25 shows heat losses to coolant and oil expressed as horsepower and as a ratio of engine brake horsepower. At full-load, heat loss to coolant is less than half the bhp, or 14% of fuel input.

Friction Losses – Fig. 26 shows the friction horsepower over the speed range. At 1500 rpm overall mechanical efficiency is 81%, while gross mechanical efficiency (bhp + compressor hp divided by ihp) is 86.5%.

At 2000 rpm, overall mechanical efficiency is 77% and gross mechanical efficiency is 85.5%.

Deltic Design Philosophy

The Deltic and the User – In the data presented so far, an attempt has been made to show that the design layout of the Deltic results in well-defined technical advantages in robustness, simplicity, light weight, and compactness.

From the user's point of view, demonstration of such technical advantages is only half the story. Reliability, serviceability, and overall economy in use are essential accompaniments of technical merit. The user's viewpoint was given serious consideration in design stages of the Deltic. As a result a clear-cut policy has been adopted in its design which should assure the user of the greatest possible degree of reliability, serviceability, and overall economy, whatever the engine applications.

Factors involved in the formulation of this policy are discussed next.

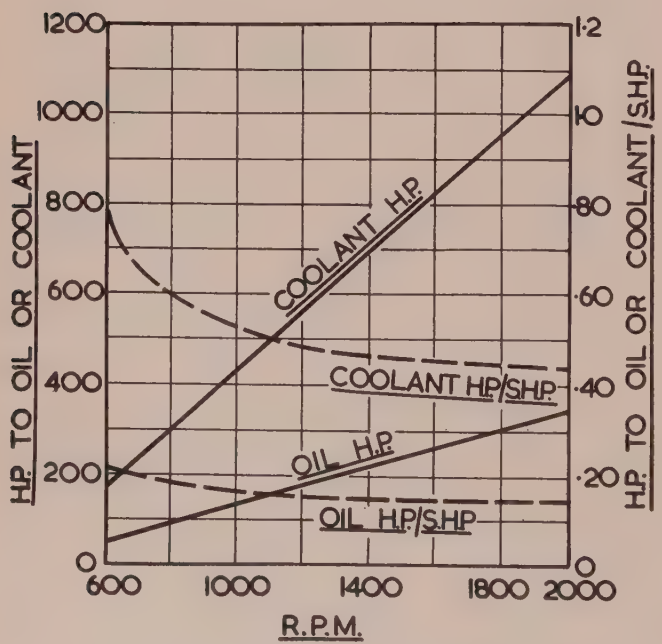

Fig. 25 – Heat losses for 18-cyl Deltic

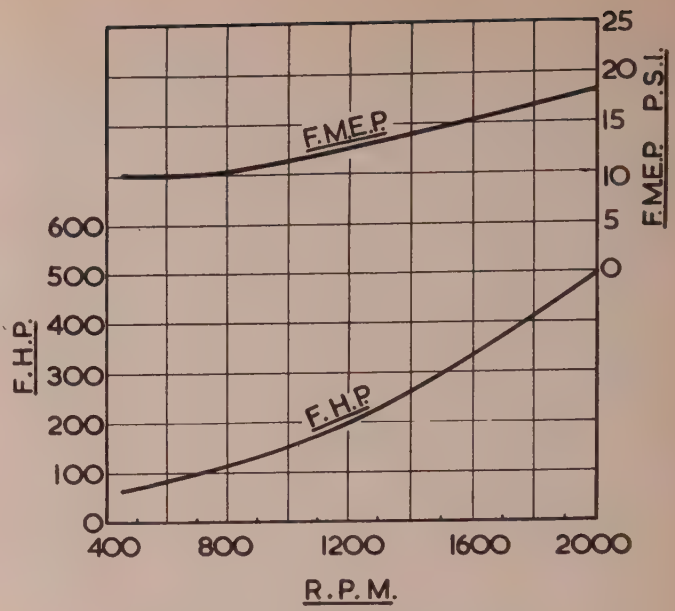

Fig. 26 – Friction losses for 18-cyl Deltic

Reliability and Serviceability – There is widespread acceptance of the idea that a high-speed engine having low specific weight must, of necessity, be less reliable than a heavier, slower moving engine.

The truth of this assumption must be assessed for each individual case, but as far as the Deltic is concerned it seems difficult to substantiate such a conclusion on any technical basis. In fundamental terms, reliability is a matter of safety factors, and those used in the Deltic design are at least as high, and probably higher, than in any other engine.

One reason for this is that the possibilities for considerable power development were foreseen in the early design stages and all stresses, bearing loads, and gear-tooth loads have taken such possibilities into account, resulting in safety factors on basic ratings that are higher than usual.

It may be true that design of a high-speed engine involves greater "factors of ignorance" than are encountered in design of slow-speed engines. But when sufficient development is done to disclose and eliminate such factors before the engine is put into service, as with the Deltic, this point has no significance.

Perhaps greatest criticism of the high-speed engine arises from the fact that, while users of diesel engines – for whatever purpose – lay great stress in a general sense upon reliability in operation, it is not generally appreciated that interpretations of reliability and serviceability vary widely in different fields of operation; thus actual requirements in particular cases are seldom clearly stated. For example, in heavy, slow-speed diesel machinery installed in ocean-going vessels, the engine becomes part of the ship's structure and is intended to remain in place for the whole life of the ship. Considerable work is done on such en-

gines during their lives, and by virtue of their general design they demand continuous engineering attention. In fact, to guard against emergencies, such engines demand continuous attendance of an engineering crew. When maintenance or repair work does become necessary it must be carried out under conditions not conducive either to effective or economical engineering; loss of serviceability in diesel-driven ships is, therefore, considerable.

Repair and maintenance carried out under such conditions imposes severe restrictions on design of such engines which effectively prevents any progress possible from use of improved materials or manufacturing techniques.

Provided such engines do not break down in service, or that the amount of time and money spent on them during repair and overhaul periods does not become excessive when viewed against the overall economic pattern of the ship's operation, the engines are regarded as reliable and the serviceability satisfactory.

Standards of reliability and serviceability in such cases are, therefore, assessed against the fact that engines remain installed and undergo continuous maintenance and repair the whole life of the ship.

At the other end of the scale is found an entirely different concept of the terms reliability and serviceability.

No form of transport demands a higher standard of reliability in operation than the passenger airline service. Many aircraft engaged in this service achieve a serviceability of 3000-4000 hr per year, with aircraft life between 15 and 20 years. Standards of effective reliability and serviceability are therefore extremely high. They are achieved with 4-stroke-cycle aircooled gasoline engines operating at bmep up to 250 psi and piston speeds up to 3000 fpm, with installed life between overhauls of 1000-1500 hr.

Specific weights of these engines are in the region of 1.2 lb per hp. This demonstrates clearly that for some applications at least the high-speed light-weight engine gives a good account of itself.

In aircraft applications work done on installed engines is extremely small and is limited to inspection, maintenance adjustments, and replacement of the simplest external parts. The underlying policy is repair by replacement. When engine overhaul life has expired, or major engineering work becomes necessary for other reasons, the engine is removed to a properly equipped workshop for repair and a replacement engine installed in its place, resulting in a minimum loss of aircraft operational time.

Results show that this system in aircraft service has proved both technically and economically sound.

Deltic Policy – Deltic policy has been formulated on the basis that requirements of most diesel-engine installations can be met most effectively by a system falling halfway between the two extreme methods above, and which takes full advantage of good points of both. Two factors are involved in practical application of this system.

First, running maintenance requirements have been reduced to a minimum and involve only removal and replacement of injectors at long intervals and very occasional renewal of oil and fuel filter elements.

Second, all engine components, both individual parts and assemblies, are built to rigid interchangeability standards, thus permitting application of repair by replacement system throughout the whole engine.

Any external accessory can be removed and replaced by a spare unit with minimum loss in serviceability time. This applies to all auxiliaries including fuel injection pumps. Spare pumps are supplied as calibrated units locked to a given setting, in which condition they can be assembled on the engine without adjustment. Correct alignment with other pumps is assured in the design.

The same applies to the main engine body itself, which is designed to be broken down into convenient, self-contained major assemblies (see Fig. 27). All these major assemblies are interchangeable between engines. Any one can be attached to the engine with no greater engineering skill than required in servicing an automobile.

It follows that most running repairs to the engine can be effected by a simple interchange of parts. It is submitted that cost of spare parts involved will be outweighed by savings resulting from the great reduction in down time.

When major engineering work, such as the resurfacing or renewal of cylinder liners becomes necessary, it is intended that the engine be removed from the installation and returned to a properly equipped workshop. It is considered that this is more satisfactory to the owner than any attempt on his part to undertake such major operations at the site. Where continuous operation is essential, a spare engine can be installed in a few hours; in

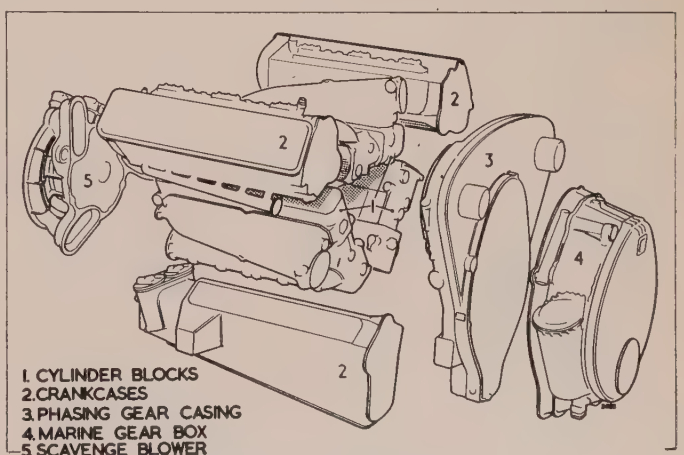

Fig. 27 – Major engine assemblies

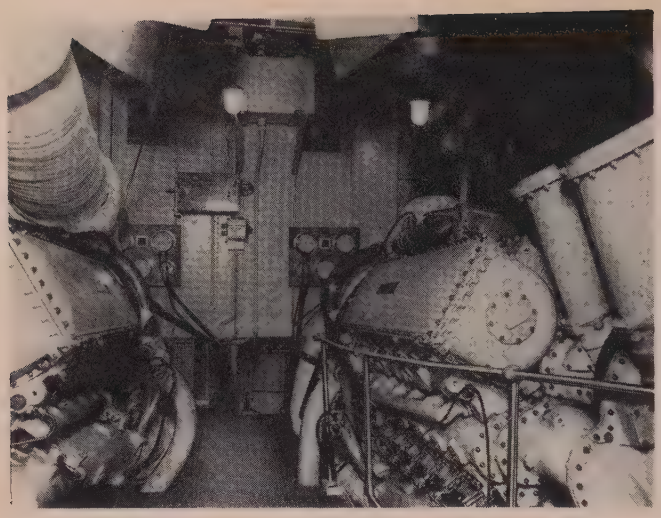

Fig. 28 – Engineroom of twinscrew Deltic installation

any case, such repairs can be more quickly and efficiently effected by this method. There is the added advantage in that opportunity is provided to replace worn parts throughout the engine, after which the engine is returned to the installation in an essentially new condition.

Space and equipment required to undertake such operations are small, and no high degree of engineering skill is required. For the benefit of owners operating a small number of engines, overhaul bases are being established at various locations throughout the world where such work can be undertaken.

It is claimed that the policy outlined above will result in the highest possible standards of reliability, continuity in service, and overall economy in operation.

Deltic Applications

Field of Application – Qualities of robustness and ease of maintenance, together with other features reviewed above, make the Deltic suitable to a wide range of applications, even when savings in weight and space are not of primary importance. Some more important fields of application are discussed next.

Naval Applications – The 18-cyl Deltic engines operating at high performance ratings are at present supplied to the British Admiralty and other navies for use in fast patrol boats and similar craft. Nine- and 18-cyl engines operating at conditions approximating commercial ratings are also being supplied for use in minesweepers, the low magnetic content of the engine conferring advantages in this type of service. A photograph illustrating the engine room with a twin-screw installation in this type of ship is shown in Fig. 28.

Fast Passenger Launches and Customs Vessels – Nine-cyl engines at commercial ratings are being supplied for propelling vessels in these two categories. Experience is showing that there is a wide range of commercial craft in which Deltic engines perform to advantage.

Multiengined Merchant Ships – Although no such installations are yet being made, a large number of design studies have been made. It will be interesting to consider some of the advantages accruing from a particular Deltic installation.

Fig. 29 shows six 18-cyl Deltic engines coupled through a gearbox to a single propeller shaft. In this installation in a cargo ship of 17,600 tons displacement, a 39-ft long engine room is required. Weight of engines and gearbox up to the propeller-shaft coupling is 65 tons. A slow-speed heavy diesel engine proposed for this ship would require an engine room 65 ft long and the comparable weight of 450 tons.

Considerable savings in weight and space result from the Deltic installation, and when these effects are added to increased serviceability time arising from the repair by replacement system, earning capacity of the ship is increased by an appreciable extent.

Rail Traction – Fig. 30 is an outline drawing of a locomotive powered by two 18-cyl Deltic engines, constructed by the English Electric Co., Ltd. A

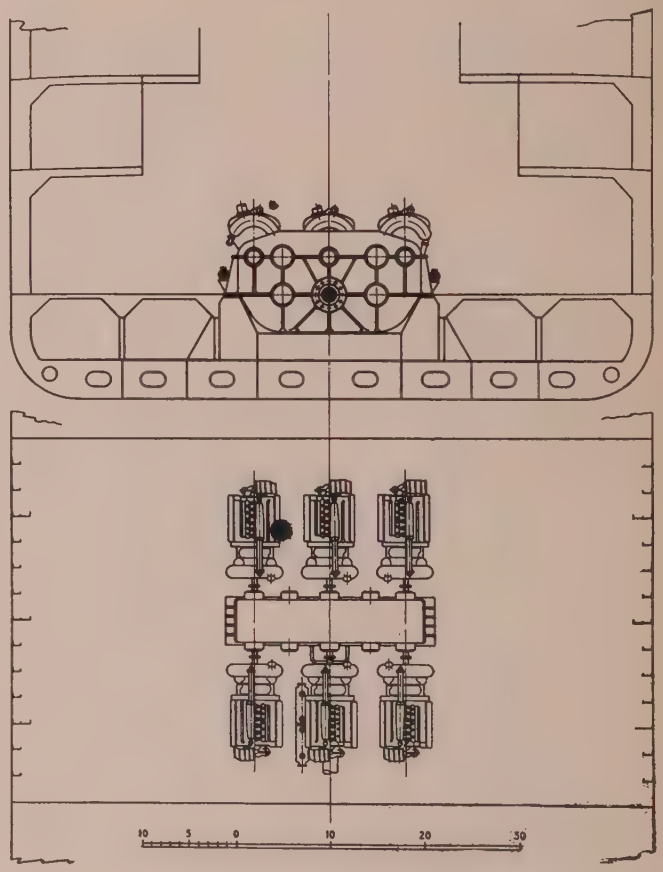

Fig. 29 – Diagram of 10,000-bhp marine Deltic installation

photograph of the complete vehicle is shown in Fig. 31. This locomotive is rated at 3400 hp and employs electric transmission with a Co-Co wheel arrangement. Axle load is less than 19 tons when ready for service (including car-warming equipment), and complete locomotive weight is 240,000 lb, or 71 lb per hp.

This locomotive was designed to take full advantage of increased serviceability achieved by the repair by replacement system. Total time necessary to effect an engine change, based on timed operations, is less than 8 hr.

A single-engine, 1700-hp Deltic locomotive, also with electric transmission, could be built weighing 168,000 lb, or 99 lb per hp.

It is believed that these figures are the best ever achieved and that they demonstrate practical merits of the Deltic for this type of service.

Mobile Equipment – An obvious field of application in which the Deltic's light weight and compactness can be exploited to advantage is in mobile equipment of various kinds.

Fig. 32 illustrates design of a completely self-contained 1200-kw generator set, totally enclosed, mounted on skids, and suitable for transportation by road, rail, or air. Full automatic engine protection is provided. Overall dimensions are 24 x 8 x 11 ft and total weight is 15¼ tons.

Similar applications for compressor and pumping sets are equally compact.

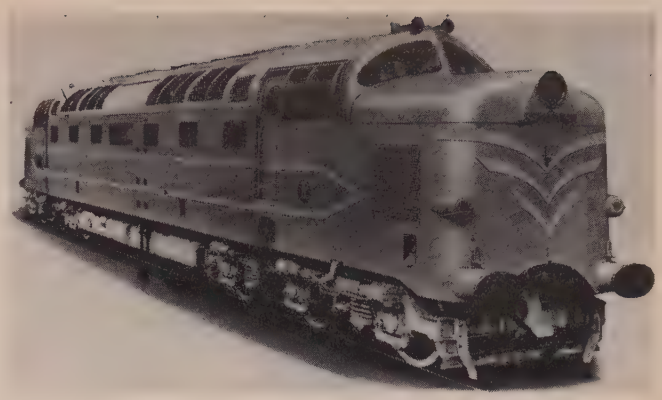

Fig. 31 – View of English Electric Co. 3400-hp Deltic locomotive

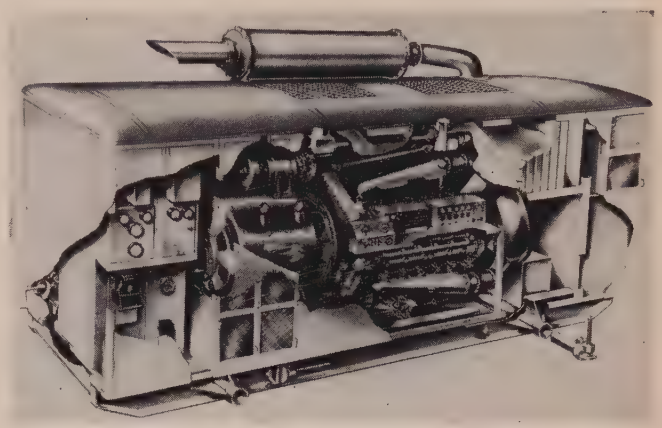

Fig. 32- Deltic installed in mobile 1200-kw generator set

Future Developments

Potentialities for Development – Technical merits of opposed-piston cylinders arranged in triangular form are of value also in providing potentialities for power development. These possibilities were considered in the early stages of Deltic design; in fact, to some extent, the design was influenced by them.

Turbocharging – In view of Napier's interest in the turboblower business, equipping Deltic engines with such units is an obvious possibility. The general layout of the Deltic does not lend itself easily

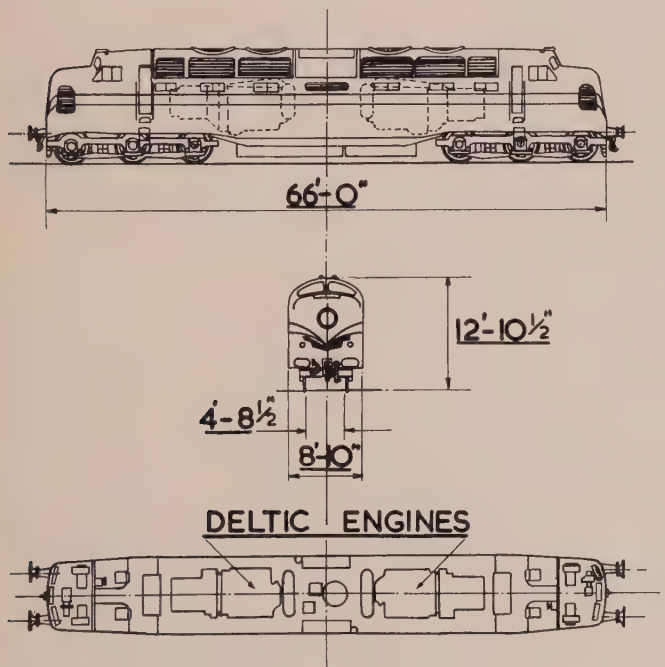

Fig. 30 – English Electric Co. 3400-hp Deltic locomotive

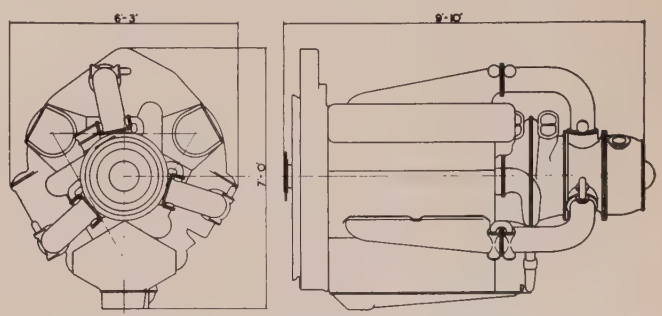

Fig. 33 – Overall dimensions of turbocharged 18-cyl Deltic

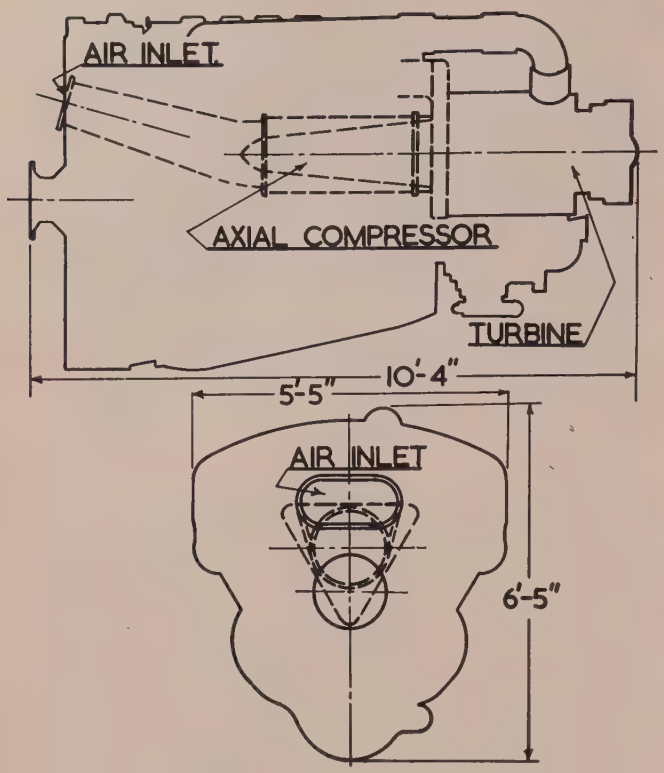

Fig. 34 – Overall dimensions of compound 18-cyl Deltic

to the pulse system, and development work is proceeding with a steady-pressure system. An outline of the 18-cyl engine equipped with a turboblower is shown in Fig. 33. As a first step, continuous commercial rating of this engine will be raised from 1725 hp to 2200 hp at the same 1500-rpm crankshaft speed. This represents 30% increase in power, engine specific weight at maximum power being reduced to 4.25 lb per hp with a very small increase in engine length. Increases in power above this are clearly possible with further development.

Compounding – The Napier Nomad engine,[1] an aircraft engine in which a diesel engine and gas turbine were compounded, has most successfully demonstrated the possibilities of such a combination, and its application to the Deltic is obvious.

First, application of compounding is much simpler on an engine operating only at sea level and thus not confronted with variations in operating conditions encountered in an aircraft engine. By coincidence the triangular space between Deltic cylinders is of the right size to accept an axial flow compressor. A compounded version of the 18-cyl Deltic would appear as shown in Fig. 34. This engine is only 20 in. longer than the original engine; other dimensions are unaltered.

Maximum power commercial rating of this engine for 5000 hr between piston withdrawals would

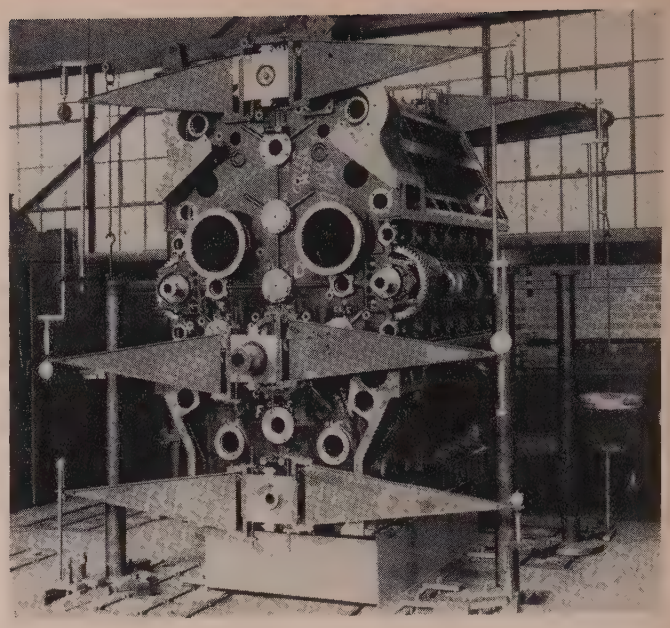

Fig. A – Six-bank 5¼ x 7¼ opposed-piston diamond engine under bend test

be 3850 hp and weight 10,700 lb, corresponding to 2.8 lb per hp.

Comparable increases in power could be expected at high-performance ratings.

Conclusions

It is hoped the information presented here will justify claims that present Deltic engines demonstrate desirable features which commend them for use in a wide range of applications, and that enough has been said to indicate future possibilities for this type of engine.

Acknowledgments

The writer thanks the directors of D. Napier & Son, Ltd. for their permission to present this paper, the English Electric Co., Ltd. for their permission to disclose information relating to locomotives of their design, and his colleagues who have rendered valuable help in the preparation of this paper.

DISCUSSION

Development of Diamond Opposed-Piston Diesel Engine

– R. H. Beadle
Fairbanks, Morse & Co.

I WISH to make the first public disclosure of some information relative to the development of a somewhat similar engine in this country.

Early in 1940, we undertook the design of the diamond

[1] See SAE Transactions, Vol. 63, 1955, pp. 107-131: "Napier Nomad Aircraft Diesel Engine," by H. Sammons and E. Chatterton.

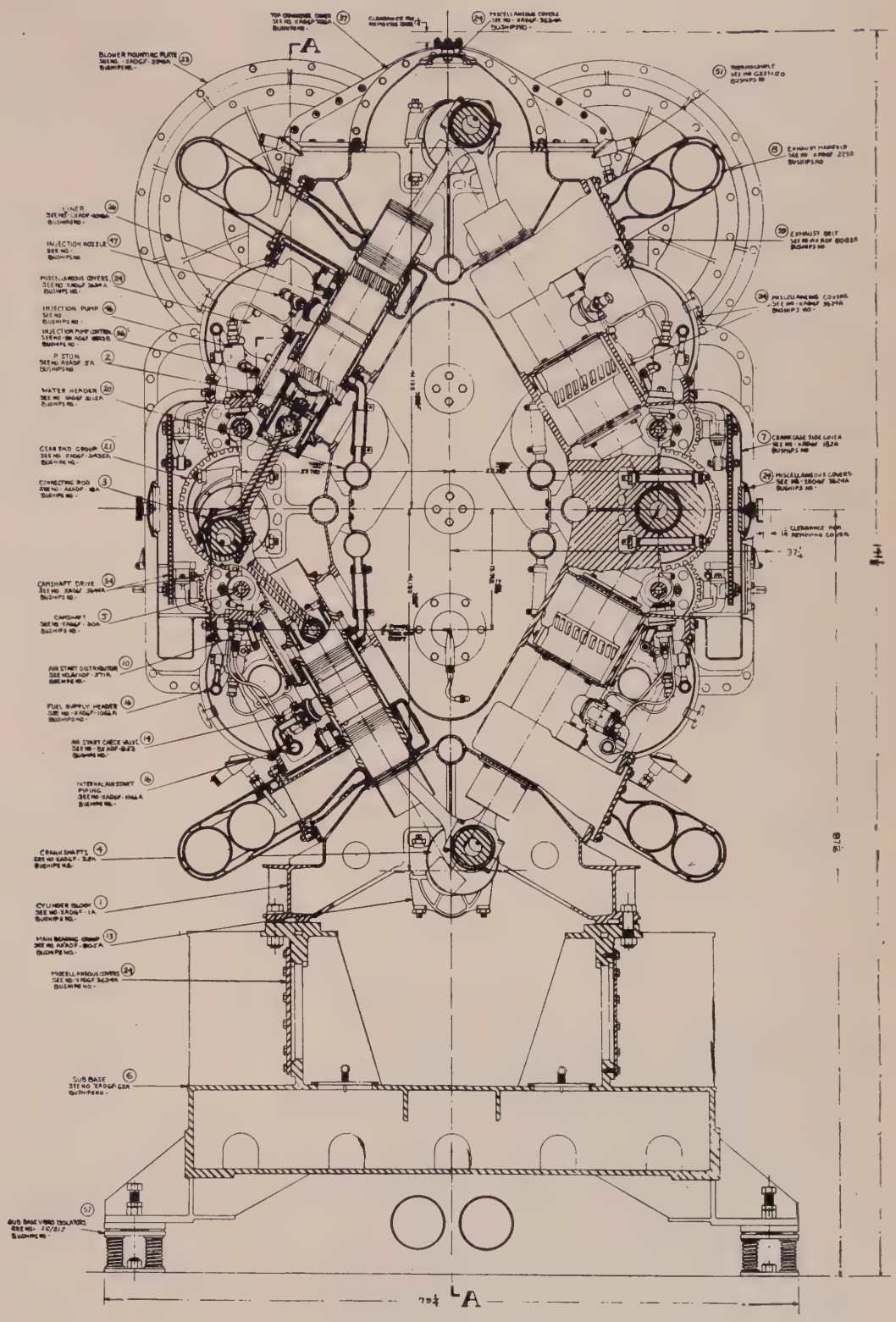

Fig. B – Cross-section of opposed-piston diamond engine

opposed-piston engine for the United States Navy. As an example of the magnitude of design problems encountered, over 6000 man-hr went into torsional vibration calculations alone. Stiffness values used in these calculations were checked during assembly of a 24-cyl prototype engine (shown in Fig. A). This figure also illustrates positioning of cranks at the points of a diamond in the welded-steel cylinder block. The centrally located shaft was the power takeoff and was connected to each of the four cranks through a herringbone gear train, – three idler gears to the upper crank and one idler gear to each of the side and bottom cranks.

Other constructional features of the engine are shown in Fig. B. Here, in cross-section, its diamond shape becomes evident. The forged-steel crankshafts were drilled to conduct oil from main bearings to rod bearings. The connecting rods, of rod and fork design, were also steel forgings finished and polished all over for increased strength, and drilled for pressure oiling of wristpins and to supply cooling oil to the underside of piston crowns. Pistons were cast iron with aluminum wristpin carriers. Forged steel cylinders had chromium plated bores and either steel or aluminum water jackets pressed on. Two gear-driven camshafts were located on each side of the engine to drive individual fuel injection pumps for each cylinder. Nozzles were of conventional multihole design, one per cylinder. The large cavity in the center of the engine served as air receiver, from which scavenging air entered the cylinder through ports designed to impart high swirl. Exhaust passed through ports at the opposite end of the liner and was carried away by four separate welded-steel water-cooled manifolds.

By 1942, manufacture of parts and assembly of the engine and test equipment was completed. (See Fig. C.) The entire power unit, engine, water-cooled alternator, and coolers were mounted on a single welded-steel subbase, which also served as an oil pan. The subbase in turn was mounted on six spring-type vibration isolators. Note twin air-intake silencers and gear-driven centrifugal compressors which supplied scavenging air. Exhaust from water-cooled manifolds was carried away through eight pipes connected to two large pipes close to the engine. These two pipes were joined to a single exhaust snubber mounted outside the test building.

Fig. D shows the results of a typical variable load test. The sfc at rated load and speed, 3000 bhp at 1500 rpm, was 0.420 lb per bhp-hr with 14 in. of Hg scavenging air pressure and approximately 775 F exhaust temperature. Two major problems, wear and port carboning, had not been corrected when this program was discontinued after a total of 2032 engine operating hours at the end of World War II.

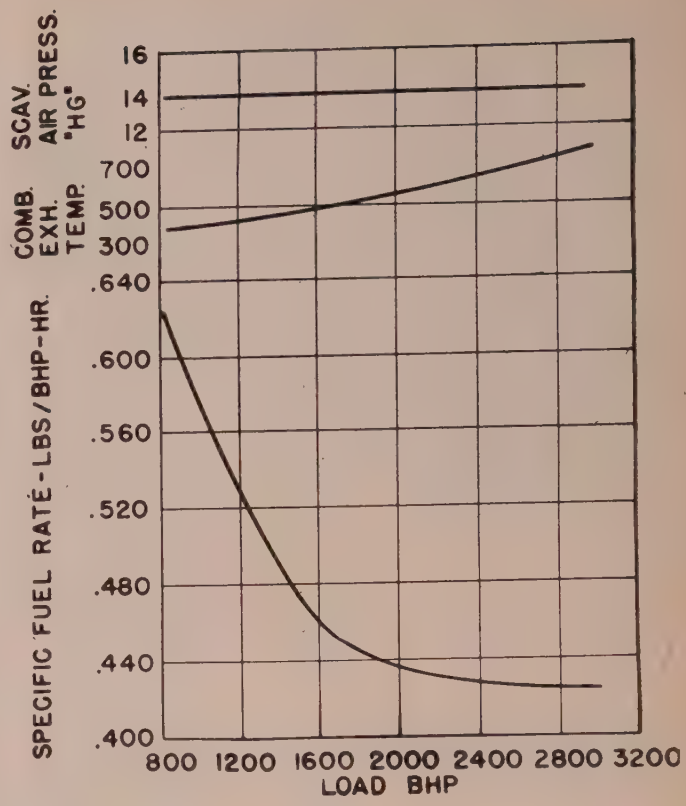

Fig. D – Variable load test – 1500 rpm – 5¼ x 7¼ opposed-piston diamond engine

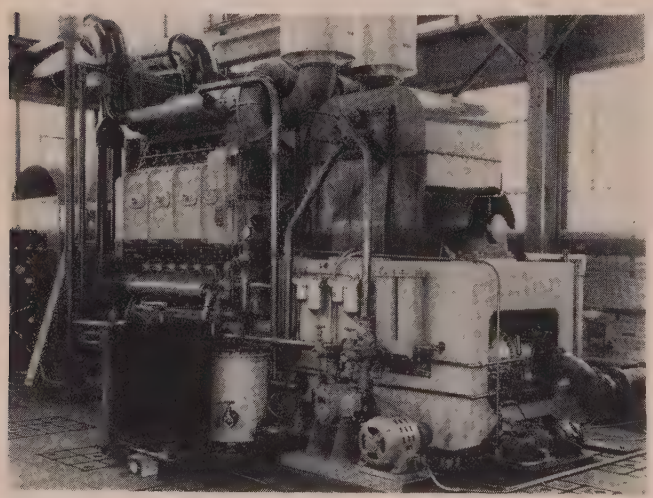

Fig. C – View of 6-bank 5¼ x 7¼ opposed-piston diamond engine

Some Performance Data for Junkers Aircraft Diesel Engines

– Klaus C. Karde
Harnischfeger Corp.

WITHOUT any doubt, the two-stroke opposed-piston engine allows the highest specific output (hp per cu in.) of any reciprocating engine. This principle has outstanding features such as best conditions for scavenging and supercharging, one combustion chamber for displacement of two pistons, any desirable rate of circular air motion for most effective injection and combustion, very moderate heat losses into the coolant, and most efficient cooling of the piston-ring area in the tdc position.

What can be achieved by applying the two-stroke opposed-piston principle may be best illustrated by some performance data for the Junkers Jumo 205-D and Jumo 207-D

[a] See pp. 125-127 of SAE Transactions, Vol. 63, 1955.

aircraft diesel engines, hitherto obviously not too well-known.

With a 105-mm bore (4.133 in.), a 2 x 160-mm stroke (2 x 6.30 in.), and a total displacement of 16.62 liter (1024 cu in.), the Jumo 205-D had the following performance data in 1938/39:

1000	hp at 3000 rpm
0.98	shp per cu in.
6.22	shp per sq in of piston area
1.50	lb per shp
0.336	lb per shp-hr
25.22	air/fuel ratio

The exhaust-turbocharged version of this engine, the Jumo 207-D was specified as follows in 1945:

1800	hp at 3200 rpm
2000	hp at 3200 rpm (with 197 lb per hr methanol injection into the inlet manifold)
1.80	shp per cu in.
12.44	shp per sq in. of piston area
1.1	lb per shp
0.330	lb per shp-hr for take-off power
0.336	lb per shp-hr for 60% take-off power
28.8	air/fuel ratio

In this case layout-point of the exhaust turbocharger was for an altitude of about 26,000 ft. Performance at sea level shows the flexibility of this powerplant with regard to changing ambient conditions. Eliminating the second-stage mechanically driven centrifugal blower would be the next step toward a simple high-output powerplant, as suggested by Rudolph Birmann in his discussion of the Napier Nomad engine.[a]

Author's Closure To Discussion

THE figures quoted by Mr. Karde for the Junkers aircraft engine are extremely interesting, the main point about them being that they do show what can be done with a 2-stroke diesel engine when associated with an exhaust-driven turbine.

The Junkers aircraft diesel engine was a very excellent engineering achievement, and it may not be generally known that about 1933 Napier manufactured a number of these engines under license from the Junkers company. The experience gained at this time was of great value when the Deltic design was undertaken.

Unfortunately, the Junkers engine suffered from one serious defect in its piston design, which affected its reliability. In spite of this it did a very successful job of work in airline service with Lufthansa and was, in fact, the only aircraft diesel engine to operate successfully in commercial aircraft service.

ORAL DISCUSSION

Reported by W. D. Sims
Shell Oil Co.

M. J. Berlyn, Dominion Engineering Works, Ltd.: Are the wristpin bearings caused to rotate in the manner used in the Napier Nomad?

Mr. Chatterton: Conventional wristpin bearings have proved adequate in the Deltic engine, so the more expensive design developed for the Nomad has not been considered.

Mr. Berlyn: Fuel injection pressures of only 4500-6000 psi are shown in the paper. If this is correct, what type of injector is used to obtain sufficient fuel atomization?

Mr. Chatterton: A single-hole outward-opening simple injection nozzle is used. Adequate atomization is obtained in the presence of air swirl as described earlier.

P. H. Schweitzer, Pennsylvania State University: The triangle is the most rigid structural shape devised by man. Employment of this shape greatly enhances the rigidity of the Deltic engine.

Does the outer portion of the Deltic piston rotate?

Mr. Chatterton: The Deltic piston does not rotate. In fact, the rings are pinned. This was done to preclude the possibility of ring gaps aligning with cylinder ports. Such alignment resulted in ring breakage in earlier engines.

Dr. Schweitzer: The 20 psi air-box pressure stated sounds very high. What is air delivery ratio at this pressure?

Mr. Chatterton: Air-box pressures quoted in the paper are absolute values. Air delivery ratios used in the Deltic engine are of the order of 1.32.

Dr. Schweitzer: In Napier parlance, what is the meaning of "compounded" engine versus turbocharged engine?

Mr. Chatterton: A compounded engine includes torque recovery from the turbine shaft. In a turbocharged engine there is no mechanical coupling between turbine shaft and engine output shaft.

E. R. Klinge, Continental Aviation & Engineering Corp.: Has a smaller engine of this design been considered?

Mr. Chatterton: No other size engine of this configuration has been built by Napier. The opposed-piston configuration demands a long stroke and scavenging dictates the corresponding bore size.

Mr. Klinge: Would a heavier piston, namely, cast iron versus aluminum, not be advantageous with regard to durability and reduced bearing loads?

Mr. Chatterton: Aluminum pistons employed offer two principal advantages: less catastrophic results from piston seizure and superior heat-transfer characteristics.

Mr. Klinge: How is oil transfer from rod to piston accomplished? Is piston pin bushing free to rotate or fixed?

Mr. Chatterton: Oil transfer to the piston is accomplished by an annular groove around the piston pin in the fixed pin bushing, then via a hole through the top of the rod to the collector cavity in the carrier piston.

Fatigue and Fail-Safe

UNTIL recently airframe designers proportioned aircraft structures to be strong enough to sustain certain ultimate-design loads without failure and certain limit-design loads without detrimental permanent set. Limit loads generally were the maximum loads expected in service and ultimate loads were limit loads multiplied by a safety factor, usually 1.5. A structure sustaining these discrete maximum loads had a tolerable service experience, and fatigue failures were usually confined to places subject to abnormal vibration or due to some substandard design detail.

More recently it became clear that an aircraft structure designed for strength only could very well experience failure from repeated loads during its otherwise useful lifetime. This situation came about as a result of many factors such as refined design to decrease excess weight, new materials with high static properties, greater daily utilization of aircraft, longer economic life, and many others. All this in spite of increased knowledge about stress concentrations, load statistics, and inspection methods.

Designers, therefore, frequently have been obliged to provide additional structural material, over and above that required for maximum onetime strength, to guard against fracture from repeated loads. This provision for fatigue has been a crude thing at best in view of the great difficulty in predicting actual service loads and great number of variables affecting the development of a fatigue crack.

The recent Comet accidents and subsequent splendid investigations by the Royal Aeronautical Establishment coupled with certain other accidents and near-accidents from fatigue on aircraft throughout the world have brought the whole subject of safety from catastrophic fatigue failure into very sharp focus.

Basically, two methods for preventing aircraft destruction from the effects of a fatigue crack present themselves. The first of these is the safe-life

Airframe Design

J. F. McBrearty, Lockheed Aircraft Corp.

This paper was presented at the SAE Golden Anniversary Aeronautic Meeting, Los Angeles, Oct. 14, 1955.

TWO principal methods for providing safety against catastrophic aircraft structural fatigue – safe-life and fail-safe – are treated. The author concludes that the safe-life method is generally inadequate, while the fail-safe method is practical and sound. Some test results of the fail-safe attributes of certain materials, stress levels, and design details are summarized, and some observations on fail-safe testing techniques are made.

From a fail-safe standpoint, it is concluded that 24ST aluminum alloy is superior to 75ST, that certain stress levels and design features will fail safe, and that underwater pressure testing is probably unnecessary because dynamic overstresses in fail-safe tests are probably small and fatigue cracks can be quickly simulated in the laboratory.

method, the other the fail-safe method.

Safe-Life Method

In the safe-life method the expected loading history of the structure is estimated or measured, the structure analyzed or tested for these loads, and a predicted or laboratory life determined. The safe life then chosen is this laboratory life divided by a safety factor to provide for test scatter or other variables not otherwise accounted for. The structure is retired or replaced when the safe life is reached in service. There are many variations of this method, including determination of a safe stress, in which the safety factor is applied to stress rather than life, equipping the aircraft with recording instrumentation and retiring the structure when a predetermined history of loadings is reached, and periodically sampling the service structure to measure its residual life. Still another variation is found in fatigue-warning devices designed to indicate consumption of fatigue life.

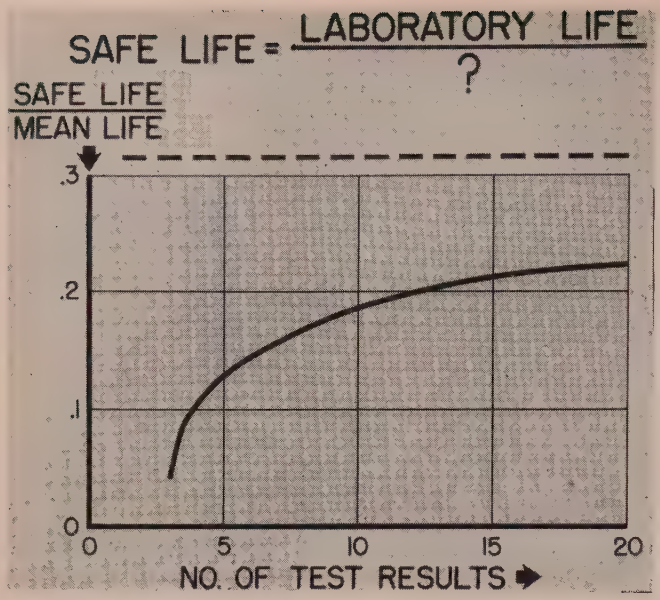

Fig. 1 – Ratio of safe life to mean life will increase as number of test result increases

All these methods have in common that safety depends on a serious fatigue crack not occurring within a certain safe period of service. Fundamentally, the method is an analytical one because, although many of its steps may be based on tests, the crucial one of determining the safe life itself requires the analytical or arbitrary provision for many variables. Put another way, the big question is:

$$\text{Safe Life} = \frac{\text{Laboratory (or Predicted or Record) Life}}{?}$$

On the determination of this "?" factor hinges the adequacy of the safe-life method. If the approach is based on a laboratory test of the structure under repeated loads, then the "?" factor must account for the following:

1. Statistical variation in specimens,
2. Loads omitted in test,
3. Thermal effects,
4. Corrosion- or time-dependent effects,
5. Repairs and service modifications,
6. Effects of high onetime loads, and
7. Statistical variations in loading experiences.

Undoubtedly there are many others. What must the factor be? A factor of three is not uncommon among laboratory specimens under controlled conditions. In the Comet tests fuselage laboratory life was 2.4 times that of the Elba failure and 3.4 times that of the Naples failure, hence the factor could not logically be less than three or four.

Fig. 1 and the following are reproduced from Tye.[1]

"Statistical methods had been used by Kennedy to determine the additional allowance which should be made when information was limited to a few specimens. His calculations had been used to obtain the example illustrated in the diagram (Fig. 1). Assuming the results of n tests, these indicated an average life represented by 1.0, and a scatter such that a life of 0.32 of average occurred once in 1000 occasions. It was possible that the true mean could be lower or higher, and the scatter greater or less than the experimental values, and so there was no certainty that the safe life would be 0.32. Using statistical methods we could say with 90% confidence (with 9 chances out of 10 of being right), the safe life indicated by the experimental results would be no lower than the curve shown in Fig. 1. Thus, if there were but six results from which a safe life of 0.32 were deduced, there was in fact a 1 in 10 chance that the life would be only 0.14.

"This very discouraging conclusion implied among other things that one could feel more confidence than was justified when a standardized degree of scatter was assumed, even when the experimental results supported the use of a standard value. It also meant that if the component indicated low scatter it would be unwise to accept this indication unless many results were available."

It is fairly obvious that we cannot test a great number of fuselages or wings or other components in order to pin down this effect accurately. Even so, there will remain at least the other variables in the list above. For example, acoustic vibrations from propeller, turbine, or jet efflux must be considered in either the test or in the factor chosen. Thermal stresses from changing temperature environment have their effect. Furthermore, it is known that specimens exhibit a longer lifetime when tested in a vacuum than when tested in air, indicating that actual consumption of fatigue life is a stress-corrosion process and is thus time-dependent. Repairs and modifications are a practical consideration; a fuselage or wing could hardly be retested under repeated loads each time a different window arrangement, new door, or practical alteration occurred. The question of what to do about a severe gust experience or a hard landing that produces limit loads or even minor damage in service presents itself.

Must tests be rerun? The aviation press reports the British feel two structures must be tested, one statically and one in fatigue, rather than one structure for both tests, because the static test would invalidate the fatigue results. A high static load in service would then presumably invalidate the safe life for the aircraft on which it occurred.

Thus, determination of the factor for relating laboratory life to safe life is a most difficult process, and if safety is to depend on this factor, it must be chosen conservatively. Again the aviation press reports the British feel the factor cannot safely be less than nine.

This same discussion applies and many of these

[1] See *Flight*, Vol. 67, March 18, 1955, pp. 347, 349, 352: "Airframe Fatigue." Report of Second Barnwell Lecture by W. Tye.

Table 1 – Examples of Fail-Safe Principle

1. Multiple engines.
2. Dual controls.
3. Alternate airports.
4. Automatic plus manual systems.
5. Morris Plan cosigners.

same variables enter the problem when any of the variations of this basic approach are followed. For example, if an instrument is installed to record the actual stresses or accelerations experienced in the aircraft, this can minimize the error in determining the load history but cannot account for the statistical variation in material lifetime, time-dependent effects on the material, repairs, and so forth to the structure. At the same time it introduces new variables in the form of instrument response, reliability, and decisive location.

A safe-life factor inherently means that when the safe-life point is reached in service all the structures have life remaining and many structures which have not actually experienced the effects provided for will have consumed only a small fraction of their useful life; yet they must be retired or replaced. This is wasteful, but the price which must be paid for safety with this method.

One point, in the author's opinion, constitutes the *coup de grâce* for the safe-life concept. Assuming a safe life could be established to guard completely against catastrophic fatigue failure, there are other sources of structural damage, trivial in themselves, which cannot be permitted to destroy the aircraft. For example, the fuselage must not be destroyed by a turbine bucket or even a thrown propeller blade. Certainly a pressurized cabin should not blow up if pierced by small arms fire from, say, a demented passenger. Similarly a wing should not be destroyed by the presence of unnoticed ground damage from a loading truck or some other source.

It is concluded that the safe-life method is impractical as a means *to provide safety from catastrophic failure.* In one form or another it must be used by the designer to provide a structure as free from fatigue cracking as the state of the art, the economics of the airplane, and the manufacturer's reputation for a reliable product will allow. In this function, methods available are *not* inadequate. Lundberg[2] has already delineated much of the fatigue design field. When viewed as a means to secure a generally serviceable structure, rather than a technique upon which lives depend, fatigue analyses and complimentary tests take on an altogether different significance. For such purpose safe life becomes some reasonable average figure not of profound importance, and important quantities become design stresses (or allowables), subject to minor scatter and comparatively easy to select, as shown clearly by Shanley.[3]

Consequently, the author concludes that fatigue analyses and tests must be pursued with vigor because the structure must indeed be as free from cracking as is practically possible. But this freedom from cracking cannot be guaranteed, indeed may never be, and is inadequate and impractical as a means to provide safety from catastrophic failure.

Fail-Safe Method

The fail-safe method appears to satisfy the need for a sound, practical safeguard against catastrophic failure from fatigue cracking or other reasonable damage. A fail-safe structure can carry an honorable service load even after one of its elements ruptures. (See Fig. 2.) The complete structure will sustain 150% of maximum expected (limit-design) loads as it does under present design philosophy, and a fail-safe design will sustain approximately limit loads when any one of its elements has failed.

This design philosophy is not new, but its application to aircraft structures is.[4, 5, 6] It is based on the assumption that mechanical and human failures will occur and the airframe system must be prepared to cope with them. Examination of this philosophy shows that the measure of safety in aircraft operation that has been achieved is due to a fail-safe philosophy. Multiple engines, dual controls, emergency systems, alternate airports, and so forth, are examples of this philosophy applied to similar problems. (Table 1).

In fact, the catastrophic fatigue failures that have occurred around the world can be traced to the absence of this feature. On the other hand, serious failures which occurred and were not catastrophical were certainly not the result of a safe-

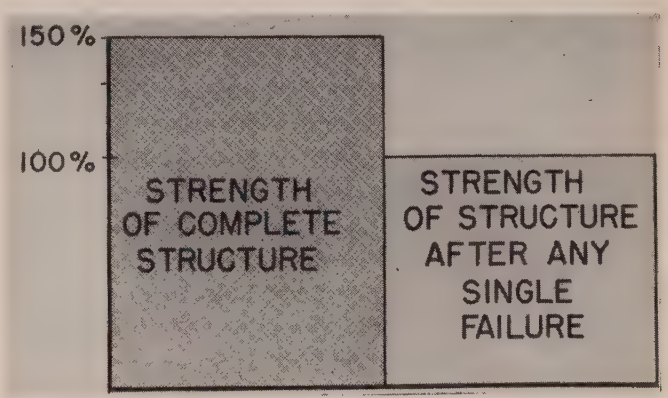

Fig. 2 – Strength requirements for fail-safe structure

[2] See *Journal of Aeronautical Sciences*, Vol. 22, June, 1955, pp. 349-413: "Fatigue Life of Airplane Structures," by Bo Lundberg.
[3] Rand Corp. Report RM-1439, March, 1955: "A Comparison of the FFA and Rand Methods of Fatigue Analysis," by F. R. Shanley.
[4] Fourth Anglo-American Aeronautical Conference, London, September, 1953: "Some Observations on Problem of Fatigue of Airplane Structures," by R. V. Rhode.
[5] See pp. 403-404 of footnote 2, discussion by W. Littlewood.
[6] See pp. 406-407 of footnote 2, discussion by J. F. McBrearty.

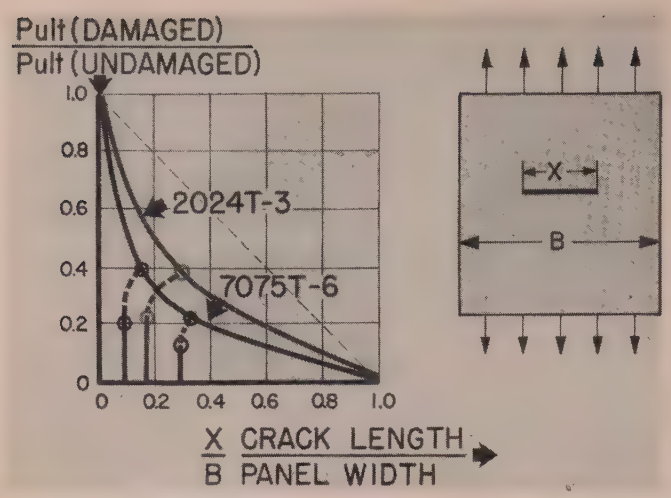

Fig. 3 – Comparison of strength of cracked sheet of two different alloys

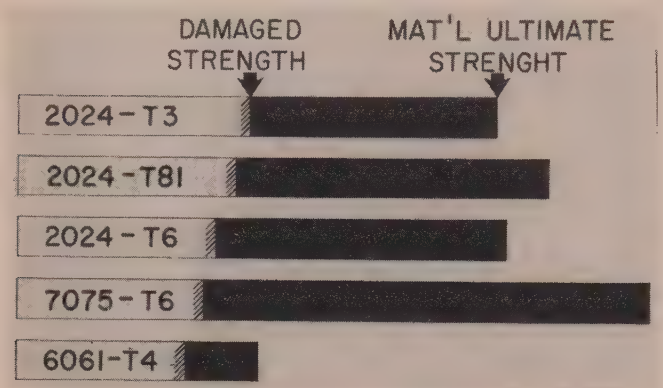

Fig. 4 – Damaged strength of some aluminum-alloy panels 0.040 x 9 x 20-in. with 3-in. crack cross-grain

Fig. 5 – Full-scale fuselage panel pressure test

life approach, but were due instead to the fact that those structures, intentionally or otherwise, were indeed fail safe. When a propeller blade failed and passed completely through a Constellation fuselage in pressurized flight at 20,000 ft, it was fail-safe ability that made this an incident rather than a catastrophe. Airline reports are full of cases of fractures from fatigue or other causes. The structures' ability to fail safe under the circumstances has been the reason serious consequences did not ensue.

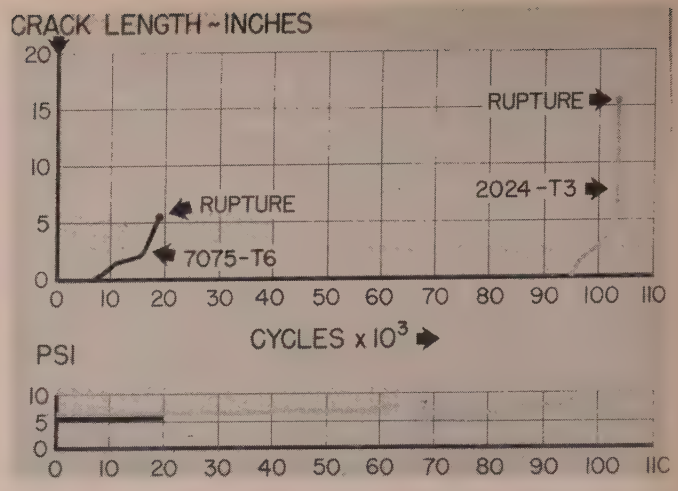

Fig. 6 – Crack length versus press cycles for 0.040-in. fuselage panel

The author concludes that the only practical answer to the safety problem generated by fatigue cracking and accidental damage is a fail-safe structure. Much of the structure of today's airplanes is fail-safe (perhaps not intentionally so), and it is believed that rather simple research, testing, and analysis will show the way to a completely fail-safe airframe.

It is felt that supplementary stress analyses and laboratory tests of typical structural details can satisfy the fail-safe objective. Final fail-safe demonstrations of the structure may or may not be required, depending to a great extent on the thoroughness of the prior analyses and tests. Analyses and tests of changes, repairs, or modifications can readily be made. In such tests and analyses static strength is the property sought, not a nebulous and elusive lifetime. The state of the art in static strength prediction and in laboratory testing is well developed and can be exploited in fail-safe design.

Much remains to be done but the problems lend themselves to straightforward research and proved stress-analysis methods. The remainder of this paper reports some of the progress we have made in this field.

Developments in Fail-Safe Airframe Design

This discussion covers highlights of some of our fail-safe structural developments. More thorough treatment of certain aspects of this work will be reported by others. It is now covered in unpublished reports.[7, 8]

Work in this field naturally divides itself into three parts: material, stress level, and detail design. Some results and observations on each of these aspects follow.

[7] Lockheed Report No. 10498, February, 1955 (unpublished): "Crack Propagation Tests for Some Aluminum-Alloy Materials," by P. J. Gurin.
[8] Lockheed Report No. 10655, May, 1955 (unpublished): "Tests of Crack Propagation Past Longitudinally Riveted Seams," by W. J. Conway and T. J. Stapleton.

The Material – Fig. 3 summarizes the results of static tension tests on sheets of aluminum alloy of width B with centrally located jeweler's saw cuts of length X normal to the load. Compared with 7075-T6, 2024-T3 aluminum alloy carried more load before initial cracking occurred, a longer crack was survived before rupture, and a greater load was sustained at rupture.

Similar tests for several materials tested cross-grain are shown in Fig. 4, which shows that absolute load-carrying strengths of severely cracked materials (3-in. crack length), arrange themselves roughly in this order of descending strength: 2024-T3, 2024-T81, 2024-T6, 7075-T6, and 6061-T4.

Some large-scale fuselage panel tests are illustrated in Fig. 5, in which pressure cycles were repeated until complete failure occurred. To speed the test, water pressure was used until a crack started; thereafter air was employed. Fig. 6 shows the results of such tests on identical 7075-T6 and 2024-T3 panels. The 7075 panel began cracking after about 7500 cycles at 5.7 psi and ruptured after a 6-in. crack developed at around 19,000 cycles. The 2024 panel, however, didn't start to crack until about 95,000 cycles (many of which were as high as 8.5 psi to accelerate the test), and ruptured only when the crack became 16 in. long.

Fig. 7 illustrates some comparative information on the strength developed by cracked sheet material at low temperatures. Strength of damaged 2024 sheet material is unaffected by temperatures as low as —60 F, while 7075 damaged sheet, weaker at room temperature than 2024, is further weakened about 15% at the low temperature. Comparative data from similar tests on ship steel[9] show an enormous reduction in strength of cracked material at low temperature.

Another significant property in a fail-safe design is the rate of crack growth. In Fig. 8 some data from tension fatigue tests of flat 9-in. wide strips have been plotted to show this property for 7075 and 2024 sheet material. This curve is plotted in *per cent* of total life; thus a greater fraction of life remains after perceptible cracking in 2024 than in 7075, at least under conditions of these tests.

There is a considerable difference in the fail-safe ability of different materials, and other things being equal, 2024 sheet appears to require a greater static load to produce initial cracking, to sustain a greater crack before rupture, to support a greater static load at rupture, to be less affected by low temperatures, and to have a slower rate of crack growth under repeated stresses than 7075 sheet.

Stress Level – The second variable the engineer controls in creating a fail-safe design is the stress level. No other quantity has as profound an effect not only in providing a fail-safe environment, but also in reducing susceptibility to fatigue. However, structure weight is a direct function of the design-stress level and the designer must choose a value which is just necessary and sufficient.

Fig. 9 summarizes some tension tests on panels composed of three parallel sheets joined along their edges by rivets. The center panels were grooved

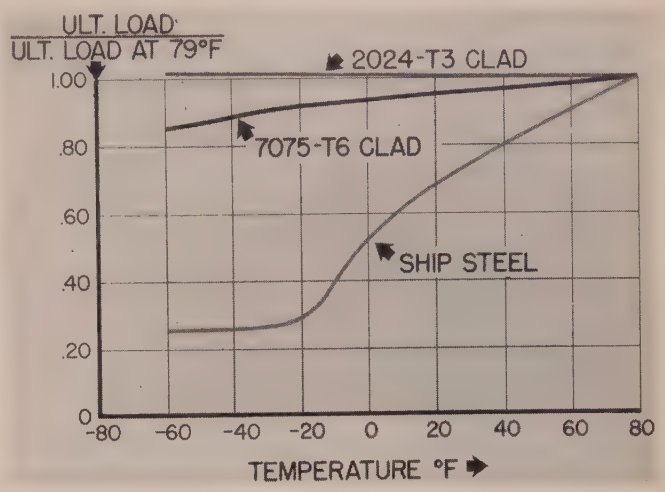

Fig. 7 – Variation of strength of cracked sheet with temperature

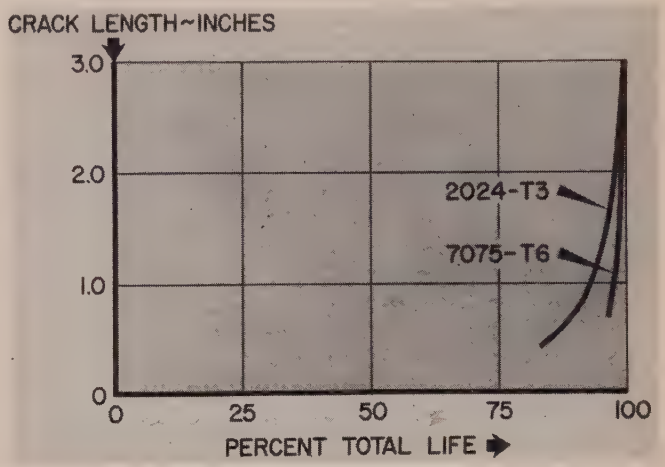

Fig. 8 – Crack growth versus time for cyclic loading from 1200-12,000 psi

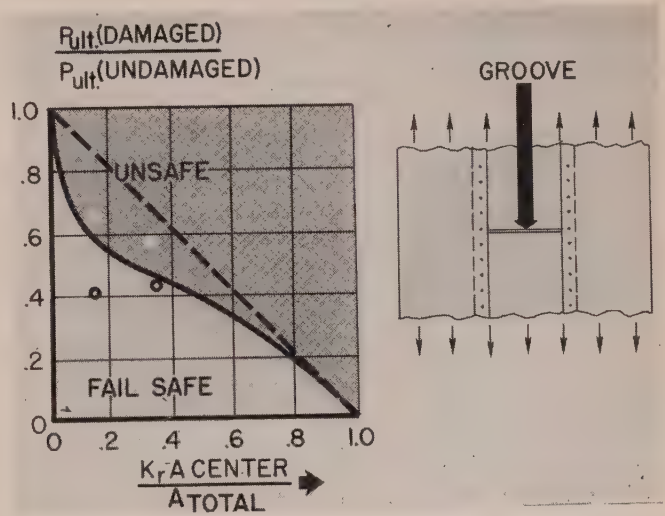

Fig. 9 – Fail-safe stress level for composite structure

[9] See *Welding Journal*, Vol. 33, February, 1954, pp. 99s-111s: "Report on Brittle Fracture Studies," by F. J. Feely, Jr., D. Hrtko, S. R. Kleppe, and M. S. Northup.

to varying depths to produce sudden tension failure of the center panels at various load levels. At loads – or stresses – above the shaded boundary the adjacent panels broke when the center panel failed; in other words, the panel did not fail safe. Below the shaded boundary, when the center panel failed the added load was supported by its neighbors; it failed safe. Strain concentration caused by local failure of the center panel reduces the strength of the side panels below their nominal P/A strength, which would simply be the dotted diagonal straight line between the corners of this diagram. The dynamic effect of sudden failure will be discussed later.

Information on the stress-level boundary between explosive and gradual failure in pressurized cylinder tests which also indicates that a stress level can be chosen to preclude a destructive failure has been published.[10, 11]

Fig. 10 is a plot of some Lockheed tests of full-scale fuselage pressure panels shown in Fig. 5. These two panels were identical except for skin-metal gage. The thinner panel ruptured under a pressure of 5.7 psi and a nominal hoop stress of 9200 psi when the crack had grown to about 6 in. The thicker panel, with a hoop stress of 5750 psi, did not rupture even when the crack had been extended to about 22 in. The test was stopped due to insufficient air supply. Absence of rupture in

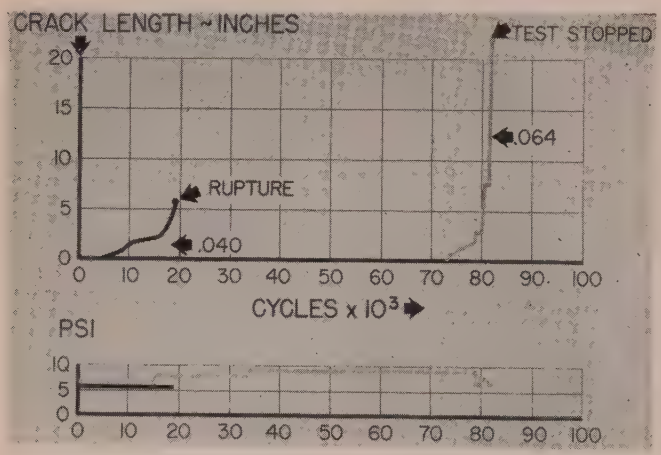

Fig. 10 – Crack length versus press cycles for 7075-T6 fuselage panel

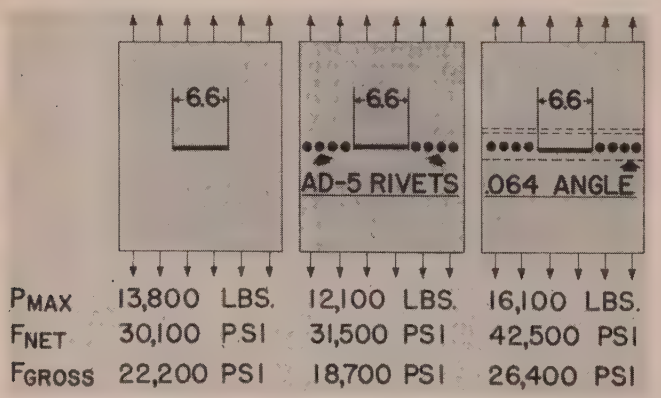

Fig. 11 – Effect of structural features on transmitted force

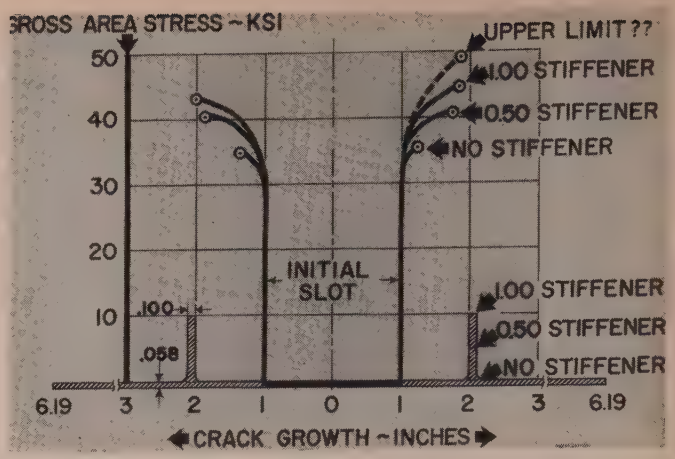

Fig. 12 – Effect of stiffener height on static crack growth and static strength

spite of such obvious damage indicates a fail-safe structure.

It appears that a properly chosen stress level can produce a fail-safe design in a multiload-path structure, and first indications are that this stress level is, as might be expected, below the nominal ultimate strength of the undamaged elements. A weight cost is indicated which research and design ingenuity must minimize.

Detail Design – A fail-safe structure must be composed fundamentally of multiple load-paths or several elements, such that when any one fails the structure suffers only to a degree unlike say, a simple truss, which is no structure at all when one member fails. This criterion does not rule out structures with large single members provided these *members* are composed of discrete elements whose individual failure leaves the member with reasonable strength and which failure can be detected immediately. Multiple elements present one form of crack- or failure-stopper; there is room for considerable design ingenuity to achieve a fail-safe structure by variations of this idea. Some design features under investigation at Lockheed are discussed briefly below.

One idea having merit seeks to exploit the fact that a round hole presents a lower-order stress raiser than the end of a crack. In application, for example, the fuselage skin might be composed of two layers, a thick inner skin containing an array of holes and a thin outer layer. It was thought that a crack would advance from one hole to the next, and for a given length of crack would provide more strength. Fig. 11 summarizes the results of some simple tests on sheet aluminum with holes aligned with an initial narrow saw cut. Contrary to expectations it tore along the perforations; the holes weakened rather than strengthened the initially damaged material. On the other hand a

[10] "Review of High-Altitude-Cabin-Pressurization Design Criteria Related to Future Transport Operations," by L. M. Hitchcock. Paper presented at 23rd Annual Meeting of IAS, New York City, Jan. 24-27, 1955.

[11] See NACA RM L55D15b (1955): "Preliminary Investigation of Failure of Pressurized Stiffened Cylinders," by N. F. Dow and R. W. Peters.

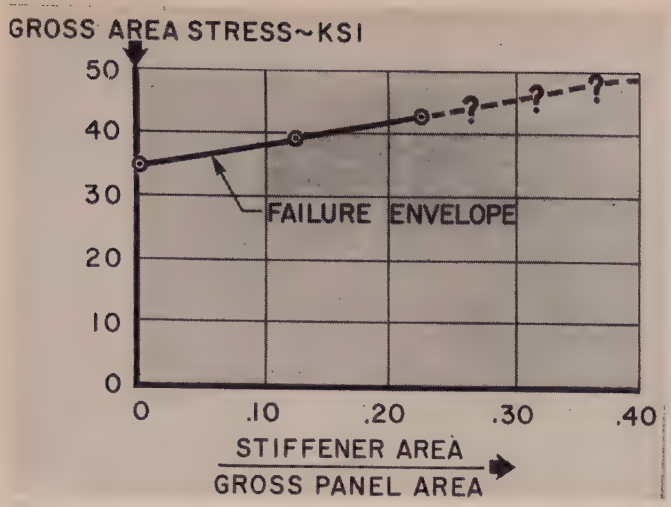

Fig. 13 – Effect of stiffener area on static strength

simple stiffener attached with rivets through this same arrangement of holes increased the strength of the cracked sheet almost 20%, as shown on the right of Fig. 11.

The behavior of longitudinal stiffeners in integrally stiffened structure is illustrated in Fig. 12, which summarizes some simple tests on 7075 extruded aluminum panels 12⅜ in. wide machined as shown and tested in static tension with an initial narrow saw cut in the skin. The integrally stiffened arrangement develops more strength (higher fail-safe ability) than the flat panel, the stiffeners serving, within limits, as crack stoppers. This is also shown in Fig. 13 as a function of the ratio of stiffener area to total cross-sectional area. Since *gross* area stress is plotted here, it is clear that by careful design, the weight cost for a fail-safe structure can be controlled.

Another design idea to provide a fail-safe characteristic, especially in a pressure cabin, consists of reinforcing strips which might be located at the fuselage rings and extend circumferentially to support hoop-pressure loads in the event of skin failure. Fig. 14 presents the results of some tests to simulate this arrangement. Panels of 2024-T3 alclad 35 in. wide were tested in longitudinal tension with two spacings and two thicknesses of reinforcing strips. Each panel was tested with an initial lateral cut made with a jeweler's saw. While cracking commenced at about the same gross stress as in the plain sheet, rupture did not occur until the failure had progressed beyond the reinforcing strips; and for the same extent of damage these panels developed at least 30% more strength. Again, the added elements served as crack- or failure-stoppers and provided a more efficient fail-safe arrangement from a weight standpoint.

Fig. 15 shows some further design features we are considering and evaluating. Fig. 15a illustrates a method to provide a crack stopper for a wing shear web. In this arrangement the stiffener operates in service at a very low stress and can prevent complete loss of the shear web in the event the lower spar cap ruptures for any reason. Fig. 15b illustrates an arrangement of integrally stiffened surface into segments proportioned and joined such that any segment can fail completely without major loss in total strength. Fig. 15c illustrates the pressure cabin hoop strips discussed more fully in connection with Fig. 14, and Fig. 15d indicates how this idea might be extended to a grid arrangement to avoid joggling or shimming the stiffeners.

Much can be done toward achieving a fail-safe structure by applying design ingenuity and so minimizing the weight price paid for this important feature.

Fail-Safe Testing Methods

Much can be done by straightforward stress analysis of a structure containing assumed damage, but until such time as our fund of knowledge about crack propagation, ductility, secondary effects, and so forth is much greater, there will be considerable dependence on subjective testing. Furthermore, it is believed that even after stress analysis methods for predicting the fail-safe capacity of aircraft structures are well established and designers have acquired more experience in cre-

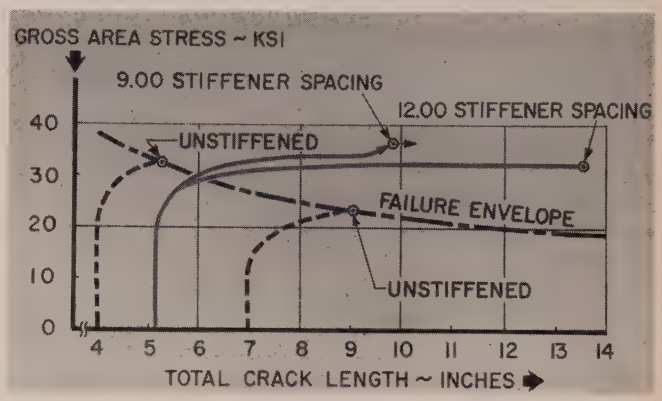

Fig. 14 – Effect of stiffener spacing on static crack growth and static strength

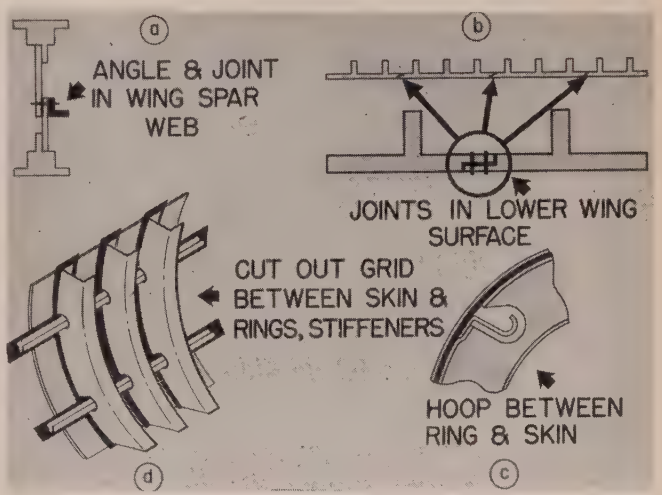

Fig. 15 – Examples of fail-safe structure

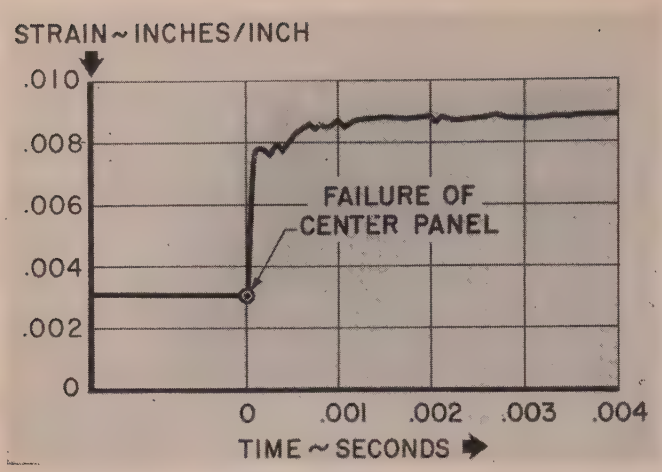

Fig. 16 – Strain-time record of side panel at 0.25 in. from center panel edge

ating optimum arrangements, there will be a continuing need for fail-safe tests of the demonstration variety. Consequently, before leaving the subject of fail-safe structures, some observations on testing methods and techniques are appropriate.

Of the many questions concerning techniques used in fail-safe structural tests this discussion will be confined to three:

1. Should air or water be used for pressure cabin testing?
2. Must the dynamic effects of sudden failure be provided?
3. Does artificial damage simulate a crack?

Pressure Cabin Testing – Water-pressure testing of submerged pressure cabins is advocated by some to provide safety, minimize the scope of failure, and accelerate pressure cycling in repeated load tests. The large volume of compressed air in a large transport fuselage may amount to several million foot-pounds of potential energy, which when suddenly released due to a major structure failure, can propel a large structure quite far. When using air safety precautions in some form, such as rope netting, stuffing with some suitable material, or adequate barricades must be provided. Results observed to date indicate that a water-pressure test is safe, while there have been several cases of near accidents in air-pressure tests. Whether water tests really minimize the scope of a failure, however, is open to question. In the Comet tests for example, failure extended about 18 ft in spite of the use of water pressure. In a test with air pressure on one panel similar to Fig. 5, complete rupture from end to end occurred in spite of the fact that the air volume is less than ¼% of total cabin volume. There is more than this much excess water volume in a complete pressure-cabin test due to elastic distension. This excess water volume must escape to relieve stresses. It is believed that strain energy in the structure determines the scope of rupture, and that rupture takes place before any appreciable material (air or water) escapes. This is so because fracture advances at a high fraction of the speed of sound in the metal, which for aluminum is about 16,000 fps. A simple home experiment will illustrate this phenomenon. A toy balloon distended with water and then punctured is destroyed as completely as it is when distended with air. In fact, rupture is so sudden that the eye can perceive the intact volume of water after the balloon departs.

However, it is believed that in air tests there are aftereffects over and beyond primary rupture due to flow, which effects may or may not be of interest, depending on the purpose of the test. In pressure tests of large vessels dynamic overtravel of decompression results in a following suction which may cause crushing failures with either air or water.

Water-pressure testing definitely speeds cyclic testing compared to air and is rather commonly employed at least during the initial stages of such tests.

The decision to use air or water hinges on the purpose of the test. Four kinds of tests of large cabins where this question may arise are:

(a) Pressure-cabin fatigue testing – If full-scale tests are necessary water may be used to speed the tests and provide safety. Ultimate primary failure should be as complete as with air but without aftereffects. However, the author questions the necessity of a full-scale cabin fatigue test in view of the discussion earlier in this paper. If a fail-safe structure is provided for safety, laboratory fatigue tests of fuselage components are better controlled and more economical.

(b) Pressure-cabin proof tests – Type proof tests should not be conducted with water since the fuselage must be a deliverable and saleable article. Water tests appear out of the question for production-line leakage testing.

(c) Pressure-cabin fail-safe tests and demonstrations – Water could be used to determine scope of failure but would not reveal aftereffects which may be important from a fail-safe standpoint. Air testing is more convincing, realistic, and simpler. Safety can readily be provided by other means.

(d) Pressure-cabin ultimate or destruction static tests – This is the kind of test for which there is, in the author's opinion, the best case for a water test due to hazard, the principal interest in the failure load itself, and the desire to minimize aftereffects for subsequent testing of the specimen.

It is the author's conclusion that a large tank for testing pressure cabins under water is justifiable only when ultimate pressure static tests are required.

Dynamic Effects in Fail-Safe Tests – The question of dynamic effects in sudden static failures is significant because the objective of a fail-safe design is to provide sufficient strength not only *after* a failure or crack has occurred but *while* it is formed. If a sudden failure imposes a dynamic effect over and above the external load to be supported, then

the structure must possess this added increment of strength. Proposed Civil Air Regulations contain a 15% additional factor for this effect if not accounted for in an actual test. However, first indications are that this effect may be small. In tests such as those illustrated in Fig. 9, specimens developed the same strength whether tested under sudden rupture of the center panel or tested statically with the center panel initially severed. Fairly high-speed instrumentation was unable to detect any dynamic overstrain above the static strain. (See Fig. 16.)

It is believed that a dynamic effect can be significant only if there is substantial momentum to be arrested by the surviving structure. In structural failures considered of reasonable scope for a fail-safe design the local velocities of movement may be large but the moving masses are small. For example, in the rupture of a single tension element in the lower surface of a fail-safe wing, the added deflections are local and leave the bulk of the wing structure unaffected over the span. Since overall deflections are a function of the integrated deformations over the entire span, beam deflections are suspected to be virtually unchanged. This effect must be established with certainty through further research, for it is important both in testing – whether the structure must fail under load or not – as well as in design.

Crack Simulation in Fail-Safe Tests – Perhaps the most difficult aspect of fail-safe structural design is to determine the size or scope of the damage which should reasonably be provided for. In the case of discrete elements this decision is relatively simple, but in a fuselage skin it must – for the present – be based on practical judgment. Whatever the extent of crack or damage to be considered, some fair simulation is necessary in tests.

One device has been tried with no success. It is similar to an ax but requires tremendous forces, provides little control over the extent of damage produced, and usually simply bounces off the structure without producing any damage at all.

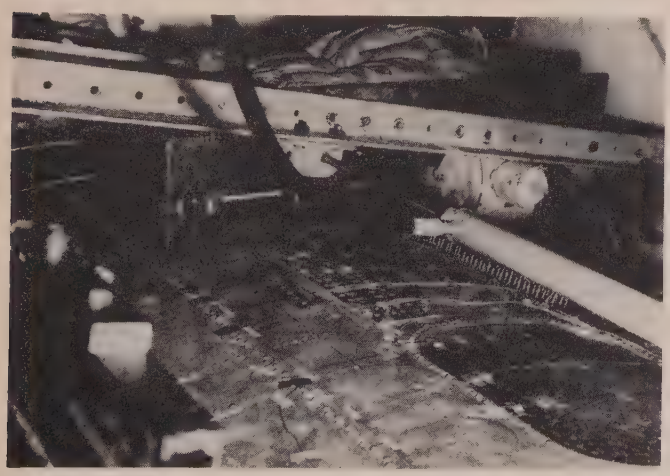

Fig. 17 – Mechanism for sawing slot in fuselage panel while under pressure

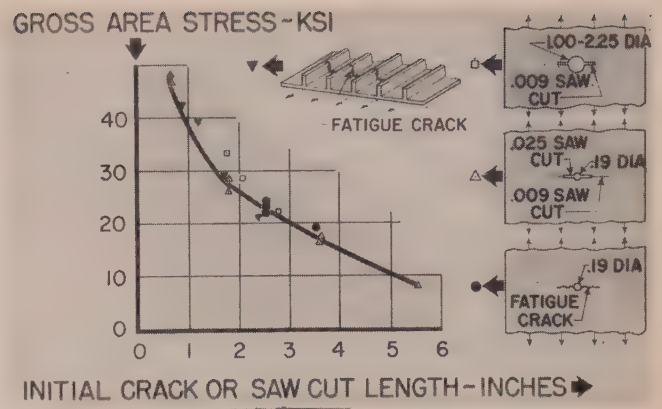

Fig. 18 – Static strength of fatigue-cracked and saw-slotted panels of 7075-T6 Alclad sheets machined to shape

Saw cuts (for example, Fig. 17) have been used with some success in producing controlled damage quickly. This is certainly a more attractive means than laborious cyclic testing, which requires a great deal of time, is expensive, usurps facilities and, more often than not, fails to produce cracks where simulated damage is sought.

To determine whether a saw cut of given length produces an equivalent reduction in static strength as a fatigue crack of the same length, a series of simple specimens were tested in tension. They consisted of assorted fatigue-cracked and artificially damaged (saw cut) pieces. Static strength of these specimens are plotted against length of fatigue crack or slot in Fig. 18. Note that, in the case of these specimens at least, no difference in static strength results whether the damage is a narrow saw cut or a fatigue crack of the same length.

Further work is contemplated to improve these techniques, but it appears that fatigue cracks can be rather faithfully simulated in a simple fashion for fail-safe static testing.

Conclusions

The following conclusions appear warranted on the basis of the foregoing discussion and available laboratory observations:

1. The safe-life method in any of its forms is impractical as a means to prevent catastrophic failure from fatigue and inadequate to prevent catastrophic failure from other reasonable causes.
2. The fail-safe method of structural design is a sound, practical means to provide reasonable safety against complete failure from fatigue or other sources of damage.
3. From the fail-safe standpoint 2024 aluminum alloy is superior to 7075 aluminum alloy.
4. For a given crack or damage the stress level in the undamaged elements is below the ultimate strength of the material, as expected, but the indicated weight penalty can be minimized by suitable design practices.
5. Water testing of submerged pressure cabins may be desirable for ultimate strength testing when required or for fatigue testing when neces-

sary, but is undesirable for fail-safe tests and impractical for proof tests.

6. Dynamic effects in fail-safe tests appear to be small.

7. Fatigue cracks can be simply and faithfully simulated in fail-safe tests and demonstrations.

ORAL DISCUSSION

Reported by W. J. Oakes
Northrop Aircraft, Inc.

J. Keys, Naval Research Laboratories: During wartime operations, considerable structural damage results from small-arms fire and shrapnel, resulting in numerous laid-up aircraft. Effective size of the Air Force could be increased by using fail-safe procedures and allowing pilots to take up lightly damaged airplanes. I question the feasibility of using the fail-safe approach for this purpose.

Studies at NRL indicate that it depends upon the size of test specimen whether water or air should be used for pressure testing. The amount of stored energy in the structure is an important parameter.

Some equations and simplifications applicable to integrally stiffened panels were listed.

Mr. McBrearty: With regard to scale effects, fail-safe panels tested as shown in this paper had vastly less strain energy than the actual fuselage. Fracture extended 16 ft (full length) even in such a reduced strain-energy fuselage specimen, and it thus was felt that the scale was of proper order.

C. Riparbelli, Convair Division, General Dynamics Corp.: Results of recent tests indicated that a multi-element 75ST structure has fail-safe properties at least as good as those of 24ST. Would you agree that there are some local areas in an aircraft structure where it is economical and advantageous from a design standpoint and safe to follow the safe-life policy? With particular reference to control surfaces, might it not be just as good to have two heavier hinges rather than three light ones?

Mr. McBrearty: 75ST structures may be made fail-safe. However, if the structural criteria specifies a fail-safe design, then 24ST will give a lighter structure. Airplanes as a whole may be fail-safe even with the loss of a control surface. This is up to the fail-safe criteria. The use of multiple hinges is a way to make a control surface fail-safe. It would certainly be unwise to use too few hinges, especially on a door.

P. R. Strohm, Trans World Airlines, Inc.: How does fail-safe design philosophy affect maintenance of aircraft structure? Could it increase the probability of minor structural failure, and so dictate increased inspection frequency and increased unscheduled structural repair?

Mr. McBrearty: We don't think so. Fail-safe philosophy should not result in a structure with more cracks than one designed for a specific lifetime. But a bad job using fail-safe criteria could be just as bad as using a non-fail-safe philosophy. No relaxation on the prevention of cracking can be tolerated, fail-safe design or not.

Mr. Strohm: What weight penalty will accrue in achieving complete structural redundancy for all primary structure?

Mr. McBrearty: We feel there will be no weight penalty for designing to a fail-safe philosophy, although there may be a slight penalty at first due to inexperience. We have a lot to learn about making fail-safe structures with no increase in weight. We recommend using reduced allowables in order to give a high maintenance cycling time. At the present we predict an increase in empty weight of ¼% to provide for a fail-safe structure.

A. L. Klein, Douglas Aircraft Co.: The DC-2 and -3 had highly redundant structures; even so, the tension-side-bolting wing flange was the only one which needed maintenance. In the DC-4, as the design progressed, this wing joint was made fail-safe. There are no wing joints on the DC-8. By eliminating joints which must be made fail-safe, the structure can be made stronger by putting the weight saved from the joint into the structure.

Mr. McBrearty: Many design details are indeed fail-safe, whether intentionally or otherwise. It is quite likely that designers will be able to provide a fail-safe design without any net weight penalty.

G. N. Mangurian, Northrop Aircraft, Inc.: The fail-safe design philosophy should have some sort of degree or rating of importance added to it where military aircraft are considered. Military aircraft companies are very competitive and performance figures must be met. If one company employs fail-safe design philosophy, resulting in a weight penalty, it would not be able to compete with other military airplane companies.

D. M. Badger, Northrop Aircraft, Inc.: With regard to fail-safe criteria as applied to control surfaces, it may be that the optimum structure requires two hinges, but three are required for a fail-safe design. In this case deflection criteria might call for three hinges.

Mr. McBrearty: It is quite probable that there will remain some places on the airplane where our current level of ingenuity will fail to make the structure fail-safe. In this region the only criteria to use is that of safe life.

Regarding making a fail-safe landing gear, it is not intended to apply the fail-safe philosophy to the landing gear for the following reasons:

1. The airplane is on the ground when you need to consider it.

2. Crash structures and so forth are provided should failure of the landing gear occur.

The landing gear is not a problem and need not be made redundant for fail-safe reasons alone.

J. Bussey, Civil Aeronautics Authority: It has been my experience with some airline operations that, in regard to wings and their use as fuel tanks, the fuel tank areas will not be inspected unless it can be proved that something is amiss. Since you can't physically inspect all areas of the airplane, some sort of fail-safe criteria should be utilized, especially in these areas.

R. Matlock, Zenith Plastics Co.: Weight of the structure designed to the fail-safe criteria should be more correctly compared to the weight of the structure which is overstrength by the amount to provide the same stresses as in the fail-safe structure.

R. S. Sutton, North American Aviation, Inc.: Could you design a fail-safe all-movable tail? Please comment on the recent fail-safe bolt design which has one bolt inside another bolt.

Mr. McBrearty: It should be possible to design a fail-safe horizontal tail. The double bolt is an example of design to make a single member fail-safe. The fail-safe criteria cannot be achieved with a single pin.

W. R. Slagg, Northrop Aircraft, Inc.: Please tell us about the stringers added to the fuselage.

Mr. McBrearty: Stringers aren't always needed in the fuselage structure. I suggest that if there are stringers, the rings have cutouts and these rings can be made more fail-safe by inserting a strip behind them. In general, a monocoque fuselage skin must be heavier if there are no stringers.

Dr. Klein: It is not necessary to have fuselage frames with notches.

Mr. Mangurian: Comparing crack propagation between 0.040- and 0.064-in. thick material, there is a large increase in the 0.064 material. Is there some kind of thickness factor here that should be considered?

Mr. McBrearty: No. During the cycling period pressures were increased to accelerate the onset of cracking, so direct comparison of cycles to failure is not warranted. However, after cracking started the pressures used were the same. Crack propagation difference appears to be attributable to the stress difference.

Human Problems in Jet Air Transportation

Dr. Ross A. McFarland, Harvard School of Public Health

This paper was presented at the SAE Golden Anniversary Aeronautic Meeting, New York City, April 18, 1955.

THE human problem with jet aircraft begins even before take-off, the author points out, with discomfort and loss of efficiency from noise, and ground injuries on the field or in repair shops.

In the air, although noise and vibration in the jet plane are less than with the reciprocating engine, human tolerance is matched against other extreme forces of acceleration, direction changes, temperature and pressure variations.

Through detailed examination of what happens to passengers and crew in the many situations that can arise to challenge human limitations, the author shows why he believes there is need for closer cooperation between the biologist and the engineer, and for better education of crewmen in the effective use of their equipment and in their own physical limitations.

OUR concepts of time and space are being revolutionized with the advent of jet air transports. The stresses imposed on airmen in flying some of this equipment are reaching tolerance limits in all realms of human behavior. Altitudes so high that human life is no longer possible may now be reached within a few minutes, and the full range of tolerable temperatures is met within a single flight. Extremes in accelerative forces leading to loss of consciousness or to death may be encountered during maneuvers and in the sudden impact of crash landings. Currently, the aeronautical engineer is solving many of the problems of high-altitude, high-speed flying by means of cabin pressurization and other advances. Much remains to be accomplished, however, even if altitudes of 40,000 ft are not exceeded, and if speeds remain below Mach 1. Airmen and passengers must be protected from the adverse influences of the physical environment, not only in the event of failure of equipment, but also in extending the operational efficiency of the newest types of aircraft.

Operational Aspects Influencing Comfort and Safety

1. Advantages Relating to Speed – One of the

distinctive features of contemporary air transportation is the continuing emphasis on one of its greatest assets – namely, speed of transit. Now that limits have been reached with conventional reciprocating propeller-driven engines, research is being directed toward jet-powered transport aircraft in an effort to increase maximum speeds. The jet transports now being tested cruise at about 500 mph. Even higher speeds are anticipated in the future. Decreasing the flight time results in certain advantages in the comfort and contentment of passengers. The shorter the time to complete a journey, the less attention must be given to providing escape from boredom, food service aloft, and sleeping accommodations. Also, the faster the aircraft, the greater is its speed of disposition; thus, fewer standby planes are required. The greater premium on quick turnarounds at terminals, however, requires not only improvement in design, but also simplification of procedures for ground handling of equipment, sanitation, and maintenance. Since human errors are more apt to occur under the pressure of time limits, increased efficiency of the aircraft must be matched by adequate safety procedures and special equipment.[1]

Air transports equipped with turbojet engines may become quite flexible with regard to range and speed. Essentially, the range and speed factors mean that, despite somewhat higher direct operating expenses, the total costs will be decreased because of reduction in such indirect items as fuel and lubricating oil, number of personnel, training, and special ground equipment and facilities. Although taxiing in jet planes takes the same amount of time as in piston aircraft, starting and checks are reduced about 50%. Greater speed not only results in a saving of passenger time, but permits a reduction in the number of night operations in domestic service. Flights could be scheduled to arrive no later than midnight at all major airports, while permitting multiple choice of departure times.

2. Safety Factors in Jet Transports – Safety factors include a reduction in fire risks because of the use of kerosene or fuels of lower volatility than gasoline and slower spread of fire. Three-engine operation at altitude is practical; hence the failure of an engine in flight is not very critical in jet airliners. The absence of propellers permits the aircraft to be designed closer to the ground, allowing the use of shorter and sturdier landing gear and greater ease and speed in loading and unloading passengers. The plane's landing gear and flaps can be serviced from the ground without ladders or stands. Higher margins of safety should result from simpler cockpit instrumentation, and the need for a flight engineer may be eliminated. The lower levels of noise and vibration in the cockpit should improve radio communication and reduce operational fatigue.

3. Disadvantages and Operational Problems – The greatest disadvantages of the turbojet engine are its large fuel consumption and inability to carry out extensive holding procedures in bad weather or heavy traffic patterns. Fuel reserves for turbine aircraft will remain proportionately higher than for conventional aircraft for a considerable time to come. Thus a high ratio of aircraft take-off weight and a place to store the fuel for satisfactory range are required. The large-scale adoption of jet transports will depend greatly on the extent to which operational difficulties associated with relatively high-density traffic can be minimized. It will be necessary to improve traffic procedures, and to eliminate the factor of weather through successful blind-landing systems. Longer runways may be necessary without the use of reversible-pitch propellers or thrust reverses for jet engines. Airport approach and landing procedures must be readjusted to permit rapid descents and straight-in approaches. It must be kept in mind that the pilot is a human being whose reflexes and physiology cannot be changed.

Jet-powered aircraft are most efficient at altitudes of 30,000 ft or more. This raises the important question of the effect of pressure failure on the crew and passengers. It is essential that the design of cabin windows and doors be equal in reliability to the primary aircraft structures, since pressure failures at 35,000-40,000 ft would have very serious effects on the occupants. Unless this possibility is eliminated, the airlines might be required to carry excessive weights of emergency oxygen and equipment and provide methods of dispensing it. This latter problem is a serious one, since the period of useful consciousness is less than 1 min at 30,000 ft. Other aspects of cabin pressurization must also be perfected. Because of the substantial increase in rates of climb and descent, the pressurization equipment must be more reliable as compared with present standards. Unusual heating, cooling, and humidification problems are known to exist for high-speed aircraft at high altitude, and must be considered by the designer to increase comfort for the passengers and reduce stresses on the air crews. Once these problems are solved, the future of the turbojet transport seems assured.

Safety Problems in Ground Operations

Some information on the ground operation of jet aircraft is available from the manufacturers and military services. But more data on the pressure, velocity, and temperature distribution of the jet tailpipe wake are required for airline and air-

[1] See *Aeronautical Engineering Review*, Vol. 9, No. 5, 1950, pp. 34-44: "Looking Ahead with Air Transport," by Charles Froesch.

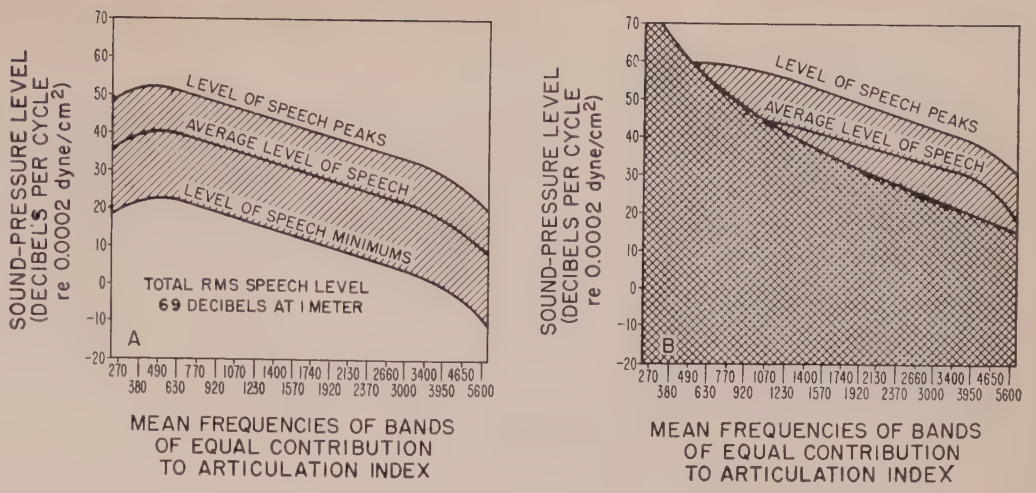

Fig. 1 – Effect of aircraft noise on speech intelligibility. A (left) – Shaded area indicates area of speech sounds that can be heard with normal intelligibility by a listener at 3 ft. B (right) – Cross-hatched area shows extent to which aircraft noise interferes with hearing spoken voice. Reduction in articulation index is about 44% in front seat of DC-3B, where speaker was 1 ft away from listener[9]

port engineers. The blast effects from the jet exhausts must be considered during engine idling, taxiing, and at maximum take-off power in regard not only to the personnel but also to runway surface materials. Concrete ramp pads are essential because of high blast temperatures and because kerosene dissolves asphalt. The influence of the noise and blast effects on the spectators at airports must also be considered. The pressure patterns and velocity of the engine air inlets while the engines are running must be understood by the servicing personnel to avoid unusual hazards. The spacing between aircraft lined up for clearance might have to be greater because of jet blast. Also, the air inlets must be protected against the ingestion of water, snow, mud, or stones thrown rearward by the landing-gear wheels. Their location should be such as to minimize the possibility of swallowing birds in flight, if such a choice is possible!

A passenger arriving at an airport to embark on a turbojet airliner may find that his plane is located some distance from the terminal building. He may be conveyed to it by a station wagon or, if he boards the plane nearby, submit to the passage of time while the plane is towed out to the runup and take-off area. He may also observe that, when the engines are started, the ground crew will be wearing helmets with large ear pads, will receive instructions via walkie-talkie, and stay away from areas in front and in back of the engines.[2] The safety and comfort problems involved are those relating to (1) noise, (2) jet blast, and (3) air intakes.

A. The Problem of Noise from Jet Engines – The sound levels generated in the vicinity of jet engines constitute a serious problem. This fact is brought out very vividly on the flight deck of an aircraft carrier. In tests made aboard the carrier "Coral Sea," for instance, flight deck personnel were found to be exposed to sound levels of 140 db while a plane was turning up on the catapult. When the engine included an afterburner, overall decibel levels of 159 were recorded. A level of 125 db was reached even at the flight bridge on the island, halfway back along the deck, when a single-engine plane was on the catapult.[3]

It has been suggested that there are three distinguishable signs that noise may be approaching dangerous levels. For example, the threshold of discomfort is about 120 db, and at about 130 db discomfort is supplemented by an unpleasant tickle in the ear. At 140 db, the response may be further complicated by sharp pains in the ear, and above 140 db the noise is usually too intense to be accepted voluntarily.[4] At this intensity, eardrums have been ruptured. The noise levels which give rise to temporary or permanent deafness following prolonged exposure have not been precisely determined. A survey of published data led Kryter to suggest that tones of 85 db above 0.0002 dynes per sq cm may cause some deafness following exposure applied intermittently over months or years. The intensities necessary to cause deafness after brief exposures lasting up to an hour appear to be in the range of 100 db for any frequency or critical band.[5] It has been stated that about 2% of the ground personnel working close to the noise of the Comet engines complained of dizziness and lack of concentration. These complaints have been occasional, and transient. They did not occur among the personnel wearing ear plugs or protective pads.[6]

A second consideration relates to communication by voice in the vicinity of jet-engine noise. This involves not only the overall loudness, but the frequency components of noise. The noise from piston engines is considerably more intense at the

[2] See "Jet Aircraft Operation Problems," by J. B. Fornesaro. In "Air Safety Forum," reports presented at First Annual Air Safety Forum, Airline Pilots Association, Chicago, April, 1953.

[3] See *Journal of Aviation Medicine*, Vol. 25, No. 5, 1954, pp. 485-491: "Jet-Engine and Other Noise Problems Aboard Aircraft Carriers," by R. L. Christy.

[4] See "Hearing and Deafness," by H. Davis. Pub. by Murray Hill Books, Inc., New York, 1947.

[5] See *Journal of Speech and Hearing Disorders*, Supplement 1, September, 1950: "Effect of Noise on Man," by K. D. Kryter.

[6] See *Journal of Aviation Medicine*, Vol. 25, No. 5, 1954, pp. 440-450: "Aero Medical Problems of Jet Passenger Aircraft," by H. E. Wittingham.

frequencies below 600. The noise spectrum of jet engines is more even throughout. Compared to piston engines, it is relatively less intense at low frequencies, and relatively more intense in the frequency band from 600 up.[7, 8] With greater intensity in the speech range, further masking of the human voice is to be expected. Without the use of devices which attenuate the higher frequencies, communication by voice is impossible among workers near a jet engine. These relationships as applied to the effect of aircraft noise on speech intelligibility may be seen in Fig. 1.[9]

B. Accidental Injury to Ground Personnel or Passengers – Other safety considerations in the preflight operations of jet transports relate to the hazards of jet blast and of air intakes. While the blast from a turbojet engine dissipates with distance, the problem created for ground personnel can be illustrated by the following information on one jet engine. The blast 15 ft behind the tailpipe was traveling at a speed of 450 knots, at a temperature of 430 F. At 35 ft, the force of the blast was still 160 knots, and the temperature 250 F.[10] Not only is there danger of injury from the blast itself, but the hazards of injury to persons in the vicinity and of danger to planes from flying debris picked up by the blast are real.

Jet blast is not the only source of potential injury to those working or standing near jet engines. Personnel may also run the risk of accidental injury if they approach too closely to the air intakes of jet engines. A report of the injuries sustained by 15 men who had been sucked into the air intakes of jet engines was made at the meeting of the Aero Medical Association in Brussels in September, 1953, by Major Evrard of the Belgian Air Force. The incidents reported occurred in the Belgian, French, Dutch, British, Danish, and United States Air Forces.

The men involved were sucked into the air-intake openings from distances of less than 1 ft up to 5 or 6 ft away. Some escaped serious injury when their shoulders prevented their being completely drawn in. However, eight of the accidents resulted in the death of the person. In most of these fatalities the men were sucked completely into the air chamber, usually headfirst. A few men who were drawn completely in survived, but with rather severe injuries. One 19-year-old mechanic, for instance, had been working on an F86 engine turning up at about 70% normal rpm. He was sucked in from a distance of about 1½ ft, and was pulled out by rescuers only after 4-5 min. Although he survived, he was unconscious for 72 hr, and sustained a complete amnesia for the accident.

C. Accidents in Aviation Line Maintenance and Base Repair Shops – Since the initial stages of air transport operations, emphasis has been placed on flying safety, or the prevention of accidents during routine flight operations. An enviable record has been achieved by means of excellent training programs, precise operational techniques, and exacting specifications for new equipment. Greater attention should now be given to reducing accidents among ground employees in the shops and hangars and on the ramps. A program leading to these objectives is presented in Chapter 11, "Prevention of Industrial Accidents in Ground Operations," of my recent work.[9]

A study of frequency and severity rates of different airline employee groups indicates that no unusual problems are present (a) in the general office and traffic personnel and (b) in stations and office personnel. The frequency rates of line maintenance and base repair shops remain high, however, and the severity rates are high for the flight crews.

Some of the more important factors that may underlie the high frequency of industrial accidents in airline maintenance units are (a) high turnover and low continuance rates in the work force, with a substantial number of new employees whose lack of experience is reflected in higher accident rates; (b) nonrepetitive nature and wide variety of jobs; (c) need for high utilization of aircraft, requiring a high concentration of plane service crews in a limited space, often at night and under adverse weather conditions; (d) inherent maintenance and servicing hazards, such as height of the aircraft off the ground with landing gear extended, rounded and polished exterior surfaces, close working quarters in the interior of the plane, and propellers and other projections; (e) fire hazards from volatile fuels and liquids required for servicing and cleaning the accessory equipment, air frame, and engines; and (f) inadequate managerial support. An attempt should be made to anticipate the problems which may arise in the maintenance of jet air transports.

Safety and Comfort in Flight

The chief advantages for passenger comfort other than speed itself are less vibration and a smoother ride. Noise remains a problem, especially in the rear of the cabin. Improvements can be brought about only by powerplant relocation or sound treatment of the cabin. The reduction in vibration gives rise to less maintenance trouble, and it is estimated that the equipment and instrument life is 30-40% longer.[11] The smoother ride is attributable to the higher wing loadings, swept-wing design, and higher aspect ratio. In addition, the frequency and magnitude of gusts may be less

[7] See "Human Factors in Air Transport Design," by R. A. McFarland. Pub. by McGraw-Hill, New York, 1946.

[8] See USAF Manual 160-30 (1953), "Physiology of Flight."

[9] See "Human Factors in Air Transportation – Occupational Health and Safety," by R. A. McFarland. Pub. by McGraw-Hill, New York, 1953.

[10] See Naval Special Devices Center Navexos P-960 (1951) (restricted), "High-Speed Flight Information for Pilots."

[11] See Report of Fourth Anglo-American Aeronautical Conference, 1953, pp. 265-288, "Indoctrination of Comet into Service," by A. C. C. Orde.

at the optimal operating altitudes of 35,000-40,000 ft. The Comet encountered only one case of clear air gusts at high altitudes in 250 hr, and there was sufficient warning to prepare for severe turbulence. Each of these problems will be discussed below.

A. Noise and Vibration in Flight – Comfort and safety problems involving noise and vibration are less intense in jet transports than in contemporary piston-powered crafts. Maximum noise levels at any frequency during take-off and climb in the Comet, for instance, did not exceed 90 db in the rear of the main cabin and, while cruising, the levels in the frequency range of speech varied from 62 to 79 db.[6] That still greater gains are desirable can be seen from Fig. 2, if conversation at 3 ft is the criterion. The noise levels inside the cabin of the Comet are included in this illustration.

The most distinctive improvement noticeable to the passenger in a jet transport is the marked reduction of vibration. As a result of the continuous rather than intermittent firing in jet engines and the relative lack of moving parts, less low-frequency vibration is transmitted to crew and passengers in jet craft. It has been well established that low-frequency vibrations give rise to discomfort.[7] Jet engines produce vibrations even beyond 200 cps, however, and the effects of these frequencies are not clearly understood. The fact remains that no sensation of vibration is experienced by the passenger in a jet transport, and it is possible to balance a coin on its edge on a table while cruising.[6]

B. Problems Relating to the Speed and Direction of Motion – Flights at very high but uniform speeds and without change of direction have no adverse effects on man as long as he is protected against wind blast. Any considerable deviation in speed or direction, however, is immediately sensed. Accelerative forces may become limiting factors in performance or even survival in high-speed aircraft, however, during maneuvers, crashes, and related situations. Higher landing speeds will place a greater premium on the reflex coordination and reaction times of the pilot as well as on his ability to think ahead and attend to the many elements of a complex traffic pattern at a busy airport.

1. Influence of acceleration and motion. Acceleration is defined as a change in speed or direction of a moving body. It is designated as positive $(+g)$ or negative $(-g)$, that is, whether the change of direction results in forces acting from head to seat or seat to head. Forces may also act in the horizontal or transverse direction, that is, from front to back, or vice versa (T_g). There are three general types of acceleration: (1) linear, as in take-offs, landings, and crashes; (2) radial, as in turns; and (3) angular, as in spins and certain types of acrobatics. The first involves a change in rate, the second a change in direction, and the third a change in both.[7, 8]

Linear accelerations, which are best tolerated in the usual seated position, will ordinarily present few difficulties on transport planes. The exact tolerance of man to positive g when he is fully stretched out is not known. Thus, possibly the passenger on sleeper planes reclining with his head toward the cockpit might have excessive positive g forces imposed on him, especially during highly accelerated take-offs. The problem of linear acceleration will become important in the positioning and protection of the air crews and passengers when future transports are equipped with jet or rocket-type propulsion. As speeds increase and flight durations are greatly reduced, however, sleeping accommodations may not be necessary. Seated passengers may be expected to complain if accelerations during landing or take-off exceed 10 ft per sec per sec.[9]

Radial acceleration in aircraft is an acute problem in military combat planes. Since aerial combat may require completion of extreme maneuvers at very high speeds, the planes must be highly stressed. In certain instances the personnel, even though highly selected for physical fitness, must be given personal protective equipment and indoctrination in the methods of increasing their tolerance.[12]

The relation of airspeed to the production of various magnitudes of g should be considered for human tolerance to radial acceleration.[7] If speed is held constant, the number of g's increases as the radius of turn decreases. For example, at a speed of 300 mph, g increases from 3 to 6 as the radius of turn decreases from about 2000 ft to approximately 1000 ft. This problem is becoming increas-

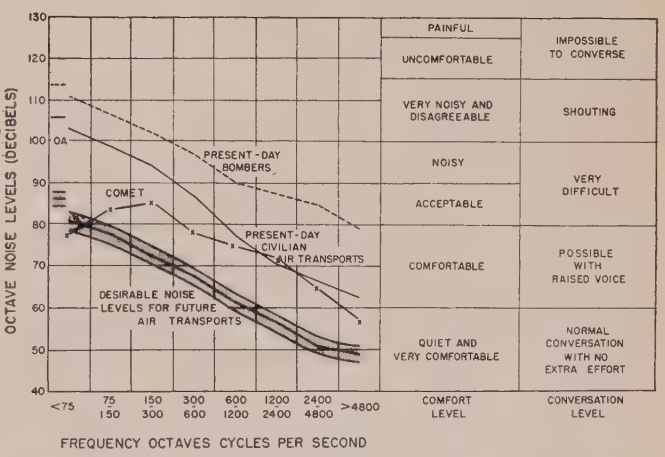

Fig. 2 – Average noise levels for contemporary aircraft compared with desirable levels. At 3 ft, comfort and conversation levels of military and civilian aircraft are much higher than desirable levels for commercial air transports. Note that noise levels within Comet cabin have been indicated[7, 9]

[12] See *Federation Proceedings*, Vol. 5, No. 3, 1946, pp. 327-344: "Effect of Acceleration in Relation to Aviation," by E. H. Wood, E. H. Lambert, E. J. Baldes, and C. F. Code.

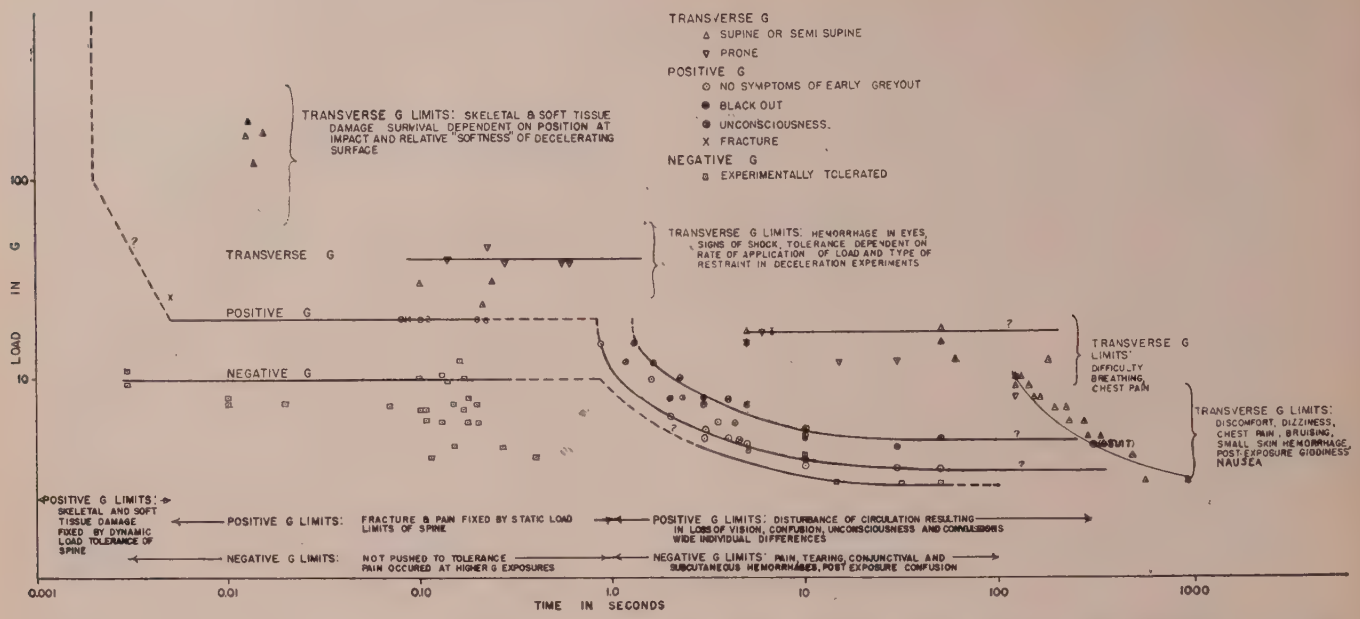

Fig. 3 – Human tolerance to accelerative forces. Experimental data from various studies for positive, negative, and transverse *g* have been plotted in this composite chart in terms of load in *g* and time in sec[15]

ingly important with jet-propelled aircraft.

2. Human tolerance to acceleration. Numerous experiments have been carried out to determine human tolerance to sustained accelerations of 10 sec or more duration. The data indicate that body position has an important influence on tolerance.[13] The subjective effects of positive accelerations can be summarized as follows: At 2*g*, the subject is pressed firmly into the cockpit seat; at 3-4*g*, upward movements of the extremities become difficult or impossible, and the soft tissues of the face and body begin to sag. At a force of only 3*g*, a pilot will be immobilized in his seat and will need assistance or some kind of propulsive device if he is to escape from his plane. At 3.5-5*g*, visual disturbances begin, characterized by dimming of vision. When the forces are relatively small, as 3-5*g*, marked physiological effects are not produced for about 5 sec, and a continuance of the force beyond 10 sec probably will not increase the severity of the symptoms. At or above 5 or 6*g*, unconsciousness may result within 5 sec. As accelerative force arises to about 7-9*g*, the time required for blackout or unconsciousness to occur is as low as 2 sec.

The dimming or complete loss of vision and consciousness that may result from exposure to high positive accelerations in aircraft or on the human centrifuge is caused by reduced amounts of oxygen in the retina and brain. The effects are the result of the marked decrease in arterial pressure at the level of the head produced by the centrifugal force. Since extreme oxygen want produces temporary functional or permanent histological damage to the brain and certain other tissues, the question has been raised whether test pilots or combat airmen might suffer permanent neurological damage. Many of the personnel of human centrifuge laboratories have served repeatedly as subjects in such tests. It has been found that repeated exposures of 5-10 sec duration have no untoward effects, and that pilots have nothing to fear from the residual effects of repeated blackouts or similar episodes experienced in flight.[14] An extensive review of this subject has recently been made by White, and the results of the survey are shown graphically in Fig. 3.[15]

The limit of man's tolerance to negative acceleration is reached at the comparatively low values of –2 to –3*g*. The flow of blood toward the head results in congestion and a sharp rise in blood pressure; gritting sensations occur in the membranes of the eyelids, and throbbing pains are felt in the head. At –3*g*, the visual field may be colored red, retinal function may be impaired, and a persistent headache may develop. At values exceeding

[13] "Human Requirements for Design of Supersonic Aircraft," by A. P. Gagge. Paper presented at meetings of American Association for the Advancement of Science, Boston, Mass., December, 1946.

[14] See *Journal of Aviation Medicine*, Vol. 18, No. 5, 1942, pp. 471-482: "Do Permanent Effects Result from Repeated Blackouts Caused by Positive Acceleration?" by E. H. Wood, E. H. Lambert, and C. F. Code.

[15] See "Biological Tolerance to Accelerative Forces," by C. S. White. Lovelace Foundation for Medical Education and Research, Albuquerque, N. Mex., June 10, 1954.

$-3g$, such serious complications as retinal and cerebral hemorrhages can be anticipated.

In both positive and negative acceleration, with the forces acting along the long axis of the body, the chief effects are on the cardiovascular system. The heart, which acts as a pump, must work against an excess pressure of about 120 mm of Hg to force blood to the head during a positive acceleration of $5g$. The heart is unable to compensate for this added force, however, and the brain is deprived of its blood flow. If the deprivation is sustained, unconsciousness intervenes. In negative acceleration, the blood is forced into the head, and pressure may rise greatly since the bony structure of the head does not permit a ready expansion of the blood vessels. The effects on the nervous system are secondary to those resulting from changes in blood pressure and flow, and have not been of as much concern to investigators.[16, 17]

C. Accidental Injuries to Passengers in Flight – Another aspect of the safety and comfort in air transportation relates to the possibility of injury to passengers during any phase of flight. The possibility of injury from debris flying in the blast of jet engines warming up prior to take-off, previously mentioned, is one illustration. Thus far no attempt has been made to classify and record systematically the accidents that occur to passengers during the course of a flight, or on the ramps. In the absence of C.A.B. records for this type of accident, the author surveyed the insurance files of several companies to obtain the information reported[9] in Table 1. Most of the injuries to passengers occurred in turbulent air and on the ramps. If such data were compiled from all the carriers, the overall importance of the problem could be appraised more thoroughly. Injuries on the ramps remain an important problem in ground operations.

1. Injuries caused by turbulence. If sudden and extreme turbulence is encountered, and the seat belts are not fastened or the anchorages of the belts or seats fail, minor and often severe injuries may result. For example, in 1946 a civilian transport encountered severe turbulence while flying through the Newhall Pass in California. The weather was clear and the ceiling unlimited, and there was no reported turbulence along the route. Without warning, the aircraft dropped suddenly about 200 ft and was then thrown up about 1000 ft. The passengers were thrown against the ceiling and then to the floor of the plane. Six passengers suffered lacerations, moderate shock, and sprains. Of three passengers wearing seat belts, two sustained sprains, and the other was torn clear of his belt and fell to the floor uninjured. Other incidents are known in which fractures and spinal injuries were sustained by passengers when sudden turbulence has been encountered.[9]

Table 1 – Incidence of In-Flight Accidents to Passengers

	Airline A		Airline B					Airline C
	1946	1947	1943	1944	1945	1946	1947	1946-1947
Injuries Due to Turbulence	40	10	0	4	0	13	5	2
Barotrauma Involving Ear	1	2	0	0	2	0	0	0
Other In-Flight Accidents	13	9	6	1	3	4	0	2
Ramp Injuries	51	28	0	0	2	6	0	9
Total	105	49	6	5	7	23	5	13

Accident reports during a 20-month period from March, 1952, through December, 1953, show that in air carrier operations, six crew members and 51 passengers were injured when flights encountered turbulent air. Although the seat belt sign was "on" in most instances, all passengers had not fastened their seat belts when the severe turbulence was encountered. (From CAA Air Carrier Bulletin No. 39, March 16, 1954.) Preventing such accidents is complicated on long flights by the operator's desire to afford the passenger as much freedom of movement as possible. A few airlines wisely encourage passengers to keep their seat belts loosely attached at all times, thus affording some protection if a sudden gust is encountered. It may be assumed that there will be no danger of seat and belt fixture failure if they are designed to meet the loads suggested for the protection of passengers during crashes.

Although at the cruising height of jet transports turbulence is not as frequently encountered, it occasionally occurs, and ascent or descent must still be considered in this respect. Problems also can be anticipated when in the vicinity of, or entering and leaving, jet streams. An additional source of protection may be afforded if the correlation between atmospheric gustiness and meteorological conditions is known, and with advancement in instruments to detect turbulence. Further development of radar may aid in this regard.

2. Injuries to passengers in sudden maneuvers. In the discussion on human tolerance to accelerative forces it was indicated that passengers may be submitted to excessive forces when circumstances dictate abrupt, perhaps even violent, maneuvers, as to avoid a collision. For example, one scheduled flight was proceeding routinely when a military plane suddenly appeared in the flight path of the airliner. Although a collision was prevented by a sharp maneuver, several passengers were injured quite seriously when flung to the ceiling. In 1946, the first-aid station at one large airport

[16] See USAF Manual 160-5 (1954), "Flight Surgeon's Manual."

[17] See Navy Special Devices Center Report 151-1-9, "Bibliographic Evaluation of Effects of Acceleration on Control and Safety of High-Speed Aircraft," by E. Girden, J. E. Barmack, and J. D. Coakley.

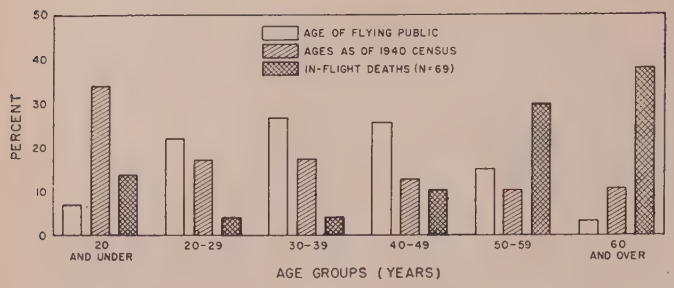

Fig. 4 – Age of passengers who died in flight on United States airlines. Chart compares age distributions by per cent of 69 passengers who died on United States transports from 1930 through 1949 with that of flying public and general population. Approximately 68% of all deaths occurred in passengers over 50, and 38% in those over 60 years of age[9]

treated 10 passengers who had been injured under similar conditions. In two instances in which eight persons were injured, the aircraft successfully avoided collision; in a third, the planes actually collided in mid-air, but neither plane crashed. With increasing traffic between cities, and with the greater closing speeds involved in high-speed flight, improved traffic control to prevent mid-air collisions and near collisions will be essential. Abrupt maneuvers also may be experienced if a pilot has to position his craft for landing under instruments or in breaking through an overcast. Rough landings and crosswind landings also require protecting the passenger from injury occasioned by unexpected changes in the motion of the craft.

Because of high landing and take-off speeds, the design of passenger cabins should provide maximum safety in the case of serious impact. An attempt should be made in the original design of jet transports to take advantage of the tolerance of the human body to high rates of deceleration. This can be done most effectively by incorporating rearward-facing seating so that impact loads can be evenly distributed over the body area. Adequate protection for the head must be included. Seats and structures should be capable of absorbing high decelerative forces without an excessive weight penalty. It may be necessary to keep passengers belted in at all times in planes traveling at such high rates of speed.

3. Injuries to passengers resulting from faults in the design of cabin interiors. A survey of minor in-flight accidents indicated that many of them could have been prevented if more attention had been given to details in the interior design of the plane. For example, carpets that are not securely fastened, or outside steps not flush with the cabin threshold, present a continuous hazard of tripping or falling. In the toilets, fixtures and containers which are installed so they extend out from the walls rather than being recessed may result in injury during unstable flights. Handles should be provided for bracing during turbulence, and the doors of overhead compartments should not open downward. Typical notations from first-aid reports of in-flight injuries suggest that the accidents closely resemble those in any similar confined area. Therefore, emphasis should be placed on designing of smooth, rounded surfaces, level, continuous floors and ramps, adequate handcords, and similar features to minimize the occurrence of minor injuries.

D. Transportation of Patients by Air – The volume of airline passenger traffic has been increasing steadily in recent years. Approximately 36,000,000 revenue passengers are using this form of transportation on United States scheduled airlines each year. On a worldwide basis, the number of revenue passengers in 1954 amounted to 58,000,000. The question naturally arises as to how many may be flying with some physical defect or illness who should not travel by air. At present there are no accurate estimates of the number of people with defects or illnesses who are traveling by air. There are many reasons for believing that a fairly substantial number of such individuals has flown and is flying constantly, and that air travel is the preferred method of transporting patients. In fact, if patients or casualties can be moved by any means whatsoever, they can probably be transported by air with greater facility and safety than by any other method.

The most common stresses in air transportation are associated with turbulent or rough air, oxygen want at high altitude, and changes in barometric pressure during ascents and descents. Therefore, certain patients with illnesses that might be adversely influenced by these variables can be expected to encounter the greatest difficulty in using this mode of travel. The high incidence of circulatory and respiratory disorders in the middle and older age groups, and the relatively high incidence of ear trouble in children, would suggest that (1) the majority of difficulties in operating experience would center about these diseases, and (2) travel by air would most likely be contraindicated for people suffering from them.

1. Survey of passenger deaths on civilian transports. Case histories of all deaths that have occurred in flight during the 17-year period from 1930 through 1946 were obtained by the author from the medical and traffic departments of the airlines. Since 1947, the operating companies have been required to report all in-flight nonaccident deaths to the CAA. The total number of fatalities was surprisingly low in comparison with the volume of traffic. Only 91 deaths occurred in flight during the 22-year period 1930 through 1951. The in-flight death rate was 0.6 per million revenue passengers and 1.1 per billion revenue passenger-

miles. Of 69 cases up to 1950, 53, or 77%, were males, and 16, or 23%, were females. During the 3-year period 1948-1950, all cases of loss of consciousness in flight on scheduled airlines were reported to the medical department of the CAA. There were 201 cases, including 44 passengers suffering from chronic and acute illness, 25 reported to have cardiovascular disease, and 41 who were under severe emotional strain, acutely fatigued, or intoxicated.

The age distribution of those individuals who died in flight is compared with that of the flying public and that of the general population in Fig. 4. Approximately 68% of all deaths occurred in those over 50 years of age, and 38% in those over 60 years of age. Fourteen per cent were under 20 years of age and 6% under 1 year of age. Many of the deaths occurred in elderly persons in the advanced stages of their illness; they were being transported to another locality for treatment or to be with relatives at the time of death. Thus, many of the patients were so ill that they might have died during the interval of the flight regardless of where they were or their mode of travel. It is unlikely that altitude or pressure changes played a contributory role except in the case of those tuberculous patients under treatment by pneumothorax and in certain of the cardiovascular cases. Most of the flights were made at moderate altitudes. Since 1947, with the advent of pressurized cabins, only 12 passenger deaths have been reported at altitudes greater than about 7000 ft.

In general, it may be concluded that the stresses imposed on passengers in routine operations rarely aggravate a pre-existing illness to the extent of causing a fatality except in severely ill or decompensated cases. Because of the speed, comfort, and safety of jet air transportation, an unusual opportunity will be afforded the airlines not only to expand their volume of traffic, but also to meet the specific needs of this component of the flying public.

Cabin Pressure Failure in High Altitude Operations

It is a well-established fact that jet aircraft are most efficient at very high altitudes. The design of air transports with pressurized cabins is a very significant improvement, not only making flights at high altitude possible, but also bringing about a greater degree of comfort for crew and passengers. This type of equipment, however, has created certain difficulties because of the possibility of a sudden loss of pressure during flight. In such instances, very rapid rates of descent must be possible, or oxygen must be administered immediately because of the limited time of useful consciousness at high altitude.

A. Effects of Rapid Decompression in Flight – The first hazard in rapid decompression is the fact that, if an astrodome, emergency hatch, or window fails, the pressure gradient is equalized rapidly and with great force. In such an event, an individual sitting or standing near the opening might be swept out of the plane. Such cases are on record in both civilian and military operations. Thus, the importance is emphasized of indoctrinating the crew members in the necessity of keeping their safety belts fastened and their essential instruments and equipment securely attached at all times.

A second hazard results from the direct effects of a very rapid rate of decompression. There are at least four important physical variables that must be considered: (1) the volume of the pressurized compartment, (2) the size of the opening, (3) the pressure differential, and (4) the flight altitude at which the decompression takes place.[18] Naturally, the most drastic decompression possible would be that occurring in the smallest cabin with the lowest cabin altitude at the highest possible flight altitude. Experiments have been made at Wright Field to test very extreme conditions in small military aircraft in flight at 35,000-40,000 ft.[8] The results indicated that the average subject experienced a sense of inflation in the chest and abdomen as a result of expanded gas, and about 20% suffered "bends" during the first 5 min at high altitude.[19] These conditions were much more acute than would be experienced in transports with larger pressurized areas.

1. The effects of acute oxygen want. By far the greatest and most serious hazard of a rapid decompression is that of acute oxygen want, since useful consciousness can be maintained no longer than about 1 min at 40,000 ft.[20, 21] The response of an airman to the oxygen want encountered at high altitude depends on (1) absolute height attained, (2) rate of ascent, (3) length of exposure, (4) amount of physical exertion, and (5) certain individual factors, such as degree of acclimatization, physical fitness, emotional adaptation, and degree of fatigue. The effects of a sudden and extreme, that is, acute, oxygen want are very different from those of repeated or prolonged exposures, that is, chronic oxygen want.[9, 22] The compensatory mechanisms of the body begin to fail when the arterial oxygen saturation approaches 70%; this stage occurs in most subjects at about 15,000-18,000-ft altitude. When it falls as low as 60% or the altitude is approximately 20,000 ft, collapse may be imminent. The critical stage for short exposures occurs be-

---

[18] See *Journal of Aeronautical Science*, Vol. 13, No. 3, 1946, pp. 143-150: "Aeromedical Aspects of Cabin Pressurization for Military and Commercial Aircraft," by W. R. Lovelace, II, and A. P. Gagge.

[19] See "Decompression Sickness, Caisson Sickness. Diver's and Flier's Bends and Related Syndromes," edited by J. F. Fulton. Pub. by Saunders, Philadelphia, 1951.

[20] See USAF (Wright-Patterson Air Force Base) Technical Report 5970 (1950), "Some Factors Affecting Time Consciousness at High Altitudes," by E. Comfort and J. W. Wilson.

[21] See "Times Available for Protective Measures in Emergencies at High Altitude," by B. G. King and J. J. Swearingen. Medical Division, Civil Aeronautics Administration, Washington, D. C., April, 1951.

[22] See CAA Technical Development Report 11 (1941), "Effects of Oxygen Deprivation (High Altitude) on Human Organism," by R. A. McFarland.

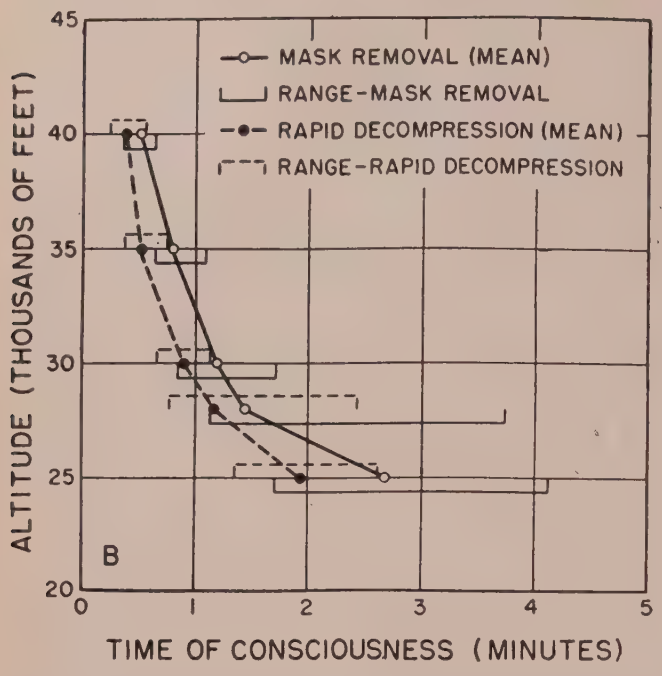

Fig. 5 – Duration of useful consciousness in relation to acute oxygen want at high altitude. Time of useful consciousness is greater in mask-removal experiments than following rapid decompression. Note wide range of individual reactions compared with mean response of subjects[20]

tween 20,000 and 23,000 ft while breathing air, and between 44,800 and 45,500 ft while breathing 100% oxygen with special pressure breathing devices.[16]

2. The times of useful consciousness following loss of pressure. At very high altitudes, the time for the onset of symptoms is very rapid, and the effects on the body are extreme. The relationship between altitude and the time for the onset of symptoms in healthy young males was investigated in mask-removal experiments. Such tests as card sorting and handwriting were used as criteria of the time of useful consciousness, using subjects in low-pressure chambers following removal of their masks. In addition to mask removal, the investigation made at Wright Field employed the tests following explosive decompression from 8000 or 10,000 ft to altitudes above 25,000 ft while breathing air.[20] It was found that the time reserve is 29-49% longer in the mask removal than in the rapid-decompression series. These latter findings are significant because they simulate more realistically the type of response that would occur during loss of pressure in an air transport while in flight at high altitude. Such data have been used to plot the rate of descent necessary for pilots breathing oxygen to avoid unconsciousness in the event of rapid decompression at various altitudes.[21] The report of SAE Committee A-9, "Air Conditioning of Aircraft at High Altitudes," should be consulted.[23, 24]

The time that useful consciousness can be maintained in the acute oxygen want associated with various altitudes is an important consideration above 25,000 ft. The data are summarized in Fig. 5. The indicated time reserves would be less for an active pilot carrying out a certain amount of emergency action than for subjects at rest. The air crews should don oxygen masks immediately on reaching an altitude of 8000 ft, and should be thoroughly familiar with their use and accessibility. The masks should be of the oral-nasal type with a built-in intercommunication system to avoid loss of consciousness, which might occur if an airman talks while using a nasal-type mask. Until the possibility of pressure failure has been completely eliminated, at least one crew member should wear an oxygen mask at all times as an added safety measure. A potentially more serious problem of acute oxygen want exists (1) if a plane should be forced because of weather or terrain to remain at altitudes over 25,000 ft after loss of pressure and (2) if sufficient oxygen is not available for all crew members and passengers.[7]

The seriousness of the effects of acute hypoxia in military flying may be illustrated from the AAF experience with regard to high-altitude missions during World War II. From August, 1942, to May, 1945, there were 388 nonfatal and 77 fatal cases attributable to oxygen want in the Eighth Air Force alone. Analysis of the circumstances surrounding each incident revealed that most of the causes were directly related to a lack of, or failure in, indoctrination. An examination of the hypoxic death rates in November, 1943, indicated an incidence of 21.6 deaths per 100,000 man-missions.[25] With improved and expanded indoctrination programs, the death rate due to oxygen want declined to a level of 2 per 100,000 man-missions by the end of the war. The aircraft manufacturing companies maintain an indoctrination program for their personnel who fly at high altitudes. In one company no serious hypoxic incident has occurred in more than 1300 hr of operations above 25,000 ft, despite the occasional failure of oxygen or of pressurization equipment in flight.

3. The effects of aeroembolism. In case of failure of pressurization, acute oxygen want is more likely to be the limiting factor than aeroembolism. However, aeroembolism cannot be lightly dismissed. It has been shown that men resting quietly can with-

[23] See SAE AIR No. 33A (1953), "Air Conditioning of Aircraft at High Altitude."

[24] See IAE Preprint No. 536 (1955), "Review of High-Altitude-Cabin Pressurization Design Criteria Related to Future Transport Operations," by L. M. Hitchcock.

[25] See *Air Surgeon's Bulletin*, Vol. 2, No. 3, 1945, p. 83: "Trend of Anoxia Accidents in Eighth Air Force Heavy Bombardment. October, 1943, to November, 1944."

[26] See "Neurocirculatory Collapse at Altitude," by H. F. Adler. Special Project, USAF School of Aviation Medicine, Randolph Field, Tex., June, 1950.

stand exposures of 35,000 ft for upwards of 30 min before such symptoms as "bends" become manifest. Under conditions of explosive decompression with 0.1 sec at 35,000 ft, however, about 20% of subjects suffered bends within the first 5 min of altitude. It is important to note that the subjects in such experiments have been healthy men.[8, 20]

A more serious aspect of aeroembolism in decompression than "bends" or "chokes" is the danger of severe neurocirculatory collapse involving either the neurological or circulatory systems or both. In the low-pressure chamber indoctrination and testing program of the Air Force, there have occurred some 400 cases of collapse, of which about 150 were severe. Seven of these resulted in death.[26] The incidence of collapse was greater in the earlier years, when subjects typically remained at pressures simulating high altitudes for protracted periods. However, fatal collapse has resulted from an exposure as short as 10 min at 40,000 ft. Primary shock in collapse cases may not become manifest immediately, but may be delayed. In a small proportion, shock was reached without being preceded by any of the common symptoms of aeroembolism.

Two cases of fatal decompression sickness were presented at a recent meeting of the Aero Medical Association. In both instances these individuals were relatively young men. However, they were judged to be in poor physical condition. They were obese, weighing close to 250 lb with a height of under 6 ft. The incidents occurred while flying as passengers in a 2-place Lockheed Jet Trainer (T-33). Cabin pressures were below 30,000 ft, and duration of flight at this altitude was under 1 hr. Oxygen equipment was adequate and functioning properly. Symptoms were those of confusion and inability to comply with commands given by the pilot. On landing, the individuals were unconscious. Intensive treatment failed and death occurred within 12 hr after landing. The diagnosis of acute aeroembolism (fatal decompression sickness) was confirmed at autopsy.[27, 28] A third case was presented by Dr. A. Frykholm of the Swedish Air Force. In this instance, difficulty was encountered during a chamber flight. Acute onset of paralysis of all four limbs occurred. Immediate hospitalization and treatment followed. Within several months this individual has made almost complete recovery.

Another feature of the response to changes in barometric pressure relates to the expansion of gases trapped within the body cavities. Distension of the stomach and intestines might give rise to considerable discomfort and pain, and passengers afflicted with certain diseases of the heart or lungs and with abdominal or intestinal conditions would experience severe reactions.[9]

There are other variables in addition to oxygen want and aeroembolism which must be considered in decompression effects in civil aircraft. The effects of cold would undoubtedly be serious in some instances. Glasses and windshields would fog up due to condensation of moisture. Obviously, the air crews should be thoroughly indoctrinated to handle all phases of emergency situations.[9]

4. Operating experience with pressurized transports. Ten rapid-decompression failures had occurred on U. S. scheduled transports up to Jan. 1, 1950, in approximately 1,000,000 hr of flying. Four occurred on the Constellation in 511,038 hr of operation, five in the DC-6 in 441,262 hr, and one in the B-377 in 23,501 hr. Thus, the rate of sudden compression failures was about 1 in 96,000 hr of flying. All the incidents listed for the DC-6 were confined to door-latch mechanism failures. In the case of the L-49, one failure was caused by the loss of an astrodome, one by an incident in which a propeller went through the fuselage, and two by failure in the door mechanism.

From 1950 to 1954, 17 additional decompression incidents have occurred on scheduled air transports.[29] Several of those occurring at high altitudes are described below. Three involved the B-377; in two instances the main cabin door blew open due to a failure of the lock, and in the other, cabin pressurization was lost when a piece of the propeller ruptured the fuselage. Two incidents on Constellations involved failure of the windows, and two on DC-6's resulted from the failure of a door and rupture of the fuselage by a propeller blade. A similar incident also took place on a CV-240.[9] In one airline recently a plane ascended to 27,000 ft to avoid a storm. The plane encountered severe hail, and a drift sight cover was broken, resulting in a partial loss of cabin pressure. The plane was unable to descend for 12 min, and the administration of oxygen to passengers became necessary. This review of the operating experience with pressurized transports indicates that a marked improvement is taking place. It should be kept in mind, however, that if failure occurs at 40,000 ft or above, serious consequences will result to the crew and passengers. Stated in the words of one aeronautical engineer, "If a pressure problem exists, there will be no jet air transports operating at very high altitudes." (See Fig. 6.)

Problems Primarily Related to Cabin Atmosphere

The efficiency of flight crews and the comfort of passengers may be adversely influenced if certain stimuli in the cabin atmosphere are not maintained within reasonable limits. Probably the most important variables in air transport operations are (1) ventilation, temperature, and humidity and

[27] "Fatal Decompression Sickness in Flight," by W. Haymaker and V. M. Downey. Paper presented at 26th Annual Meeting, Aero Medical Association, Washington, D. C., March 23, 1955.

[28] See "The Biophysical and Pathological Effects of Explosive Decompression," by D. A. Vavala. Report of U. S. Air Force School of Aviation Medicine, Randolph Field, Tex., June, 1954.

[29] See "Decompression Accidents." Bureau of Safety Investigation, Civil Aeronautics Board, Washington, D. C., March 25, 1955.

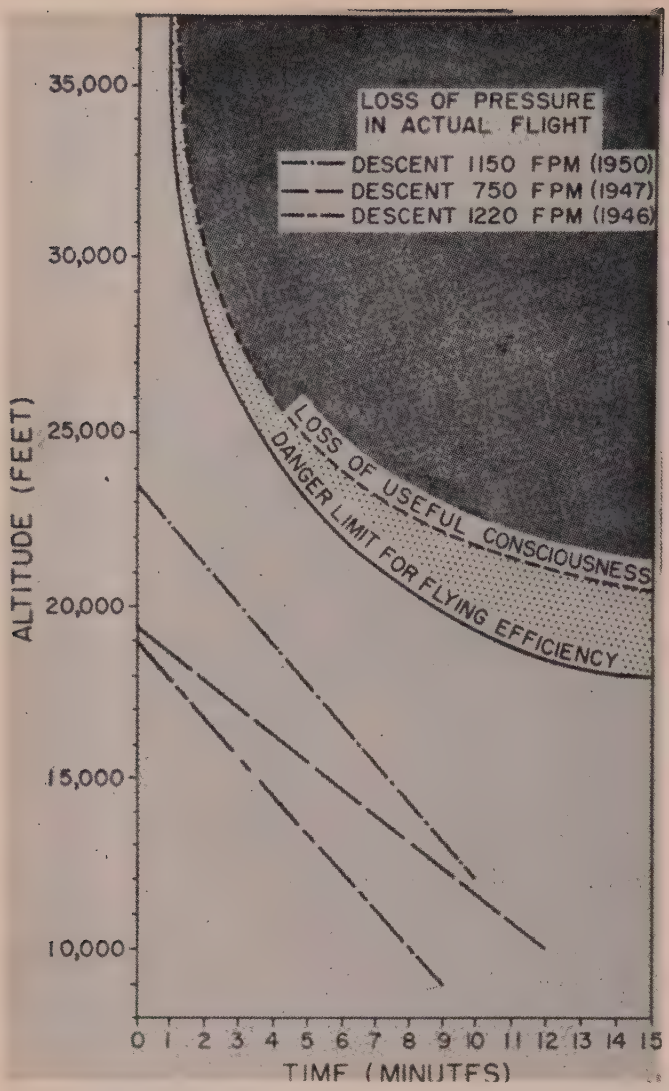

Fig. 6 – Examples of forced descent patterns. Chart shows patterns of descent from approximately 20,000 ft following sudden loss of pressure on commercial air transports in relation to time for loss of flying efficiency and useful consciousness. No serious symptoms were experienced in these incidents by flight crews or passengers, although it is obvious from chart that loss of pressure at 30,000-40,000 ft would be very serious[9]

(2) noxious gases and vapors. Very cold or hot temperatures may be encountered in a forced landing in arctic or tropical regions. A failure of the heating system, window, or door would create an unusually cold environment in flight at even moderate altitudes.

A. Temperature and Related Variables – A significant factor in the operation of high-speed aircraft is the high temperatures generated by (a) the frictional impact of air on their outer surfaces, (b) the powerplant, (c) the compression of air for the ventilating system, and (d) solar radiation. This aerodynamic heating is in part a function of the number of molecules of air encountered by the plane's surfaces during a given time period. Hence, both high speeds and/or dense air will increase temperatures within the plane. In the absence of refrigeration, the temperature within the cabin of an aircraft traveling at 650 mph at sea level could be as much as 70 F above the outside ambient air temperature. Temperatures as high as 160 F have been recorded in the cockpits of jet aircraft, and 275 F on the skin of a V2 rocket.

In general, this problem is somewhat alleviated by the fact that jet aircraft normally operate at fairly high altitudes, for there is a general decrease of temperature with altitude, equalling approximately a drop of 1 F in every 300 ft. A jet plane taking off at sea level in a temperature of 59 F, for example, will be in an external temperature range of –67 F at 36,000 ft. In spite of the decrease of temperature with altitude, however, the dominant factor of aerodynamic heating at high speeds is adequate to maintain sufficiently high temperatures so that the problem is one of refrigeration rather than of heating. It should be noted, however, that even under the worst temperature conditions of high-speed flight, that is, low altitude, hot day, failure of air conditioning, the anticipated temperatures would still be within the physiological limits of tolerance. Air Force tests at the University of California have revealed that, under conditions of low humidity, temperatures of 160 F can be tolerated for over 1 hr, and even as high as 240 F for 23 min. Even if practical limits for pilots were one-half of these tolerance times, there would presumably be ample time for remedial action.[8]

Performance is impaired well below the limits which can be tolerated by man. When ambient temperatures rise above about 85 F, errors are more frequent and concentration is impaired. When humidity is also high, the effects are greater. On the other hand, air containing too little moisture gives rise to irritating sensations due to drying of membranes, such as those of the eyes and respiratory passages. Due to the drying effects of temperature during compression, the air in cabins is more likely to contain insufficient moisture for comfort. Criteria for the air conditioning of cabins have been determined on the basis of the limits of human comfort and discomfort, so that passengers and crew may not be exposed to extremes in these respects.[23, 30, 31]

B. Toxic Gases and Atmospheric Contaminants – Hazardous situations occasionally arise from the least suspected sources in spite of extensive flight tests of new equipment and careful appraisal of all fluids and other substances. The concentration of a gas expressed in terms of percentage or parts per million does not adequately describe the con-

[30] See "Heating, Ventilating, Air Conditioning Guide," Vol. 24, American Society of Heating and Ventilating Engineers, New York, 1946.

[31] See AAF Report TSEAA-694-16A (1947), "Annotated Bibliography on the Psychological Aspects of Orientation as They Relate to Aviation," by T. G. Hermans and R. B. Loucks.

Table 2 – Incidence of Smoke or Fumes in Scheduled Air Carrier Aircraft in Two Selected Periods

	July, 1951 – Dec., 1952					July, 1953 – Dec., 1954				
	Number	% of Total	Number on Ground	Number in Air	Number of Unscheduled Landings	Number	% of Total	Number on Ground	Number in Air	Number of Unscheduled Landings
Radio and Electrical Equipment	105	36	19	86	13	36	29	5	31	11
Other Electrical Equipment	83	29	28	55	22	37	30	11	26	11
Ventilation or Pressurization System[a]	16	5	6	10	6	20	16	1	19	13
Heaters	23	8	7	16	8	11	9	2	9	5
Hydraulic Fluid	10	3	1	9	6	5	4		5	2
Gas	16	5	4	12	1	3	2	1	2	
Oil	4	1		4	2					
Batteries	3	1	3							
Miscellaneous	18	6	9	9	2	12	9	2	10	7
Unidentified	12	4	1	11	5					
Total	290	—	78	212	65	124	—	22	102	49

Source: Bulletins of the Committee on Toxic Gases, Aero Medical Association, and Aviation Toxicology Bulletins, Office of Aviation Safety, Medical Division, CAA.

[a] Includes compressor/supercharger.

ditions encountered in aviation. The amount of bodily absorption can be accurately determined only when all the following factors are known: (1) the percentage concentration of gas in the ambient air, (2) the barometric pressure, (3) the temperature and humidity of the air in direct contact with absorptive surfaces of the body, and (4) the magnitudes of any gaseous exchange affecting concentrations in air in contact with the body. Representative incidents have been reviewed by the Committee on Aviation Toxicology of the Aero Medical Association in air transportation, and similar reports are available from the Military Services.[8, 32]

Of the various hazards, smoke from insulation or overheated electrical equipment as well as carbon monoxide from cabin internal-combustion heaters and engine exhausts have been the most common sources of trouble. Table 2 shows the incidents reported to the CAA in two representative periods. While the total number of such incidents appears to be on the decrease, it is to be noted that unscheduled landings have been necessary in a considerable proportion when the trouble occurred during flight. Also, the ventilation and pressurization systems are more frequently involved.[33]

Adverse effects from exposure to fumes and vapors from fuel have been observed when the cabin or cockpit atmosphere has been contaminated by (1) leaking tanks or piping connections, (2) fuel transfer, and (3) fuel dumping. Pipes and gages carrying hydraulic fluid under pressure may be a source of contamination should leaks develop. Sometimes, harmful fumes are produced when leaking oil comes in contact with hot surfaces. In military jet flying some accidents have been attributed to CO taken in from the exhaust of preceding planes through ventilating system.[34]

In some pressurization systems of jet aircraft, cabin air is bled off from the compressors. Contamination from the lubricants has been reported, resulting especially in irritation of the eyes and other serious complaints.[35]

In setting up standards for atmospheric contaminants such as carbon monoxide, it should be kept in mind that a single numerical value is inadequate because of the problems peculiar to aviation. The generally accepted standard of carbon monoxide in the ambient air is 0.005%. This figure may be satisfactory for a person sitting quietly at sea level, but it should be reduced if the amount of exercise, degree of ventilation, or the length of time increases. An additional complication is introduced while in flight because of the combined effect of carbon monoxide and the oxygen want associated with high altitude. For example, if there is 0.005% carbon monoxide in the ambient air at 9000 ft, the resultant physiological altitude is 15,000 ft. For an example, see Fig. 7.[36]

Special Problems for Pilots Flying at High Altitudes at High Speeds

Flight at high altitudes and high speeds imposes additional stresses on pilots and air crew. A number of the more important ones are briefly discussed below.

A. Sky Brightness and Illumination Levels – There are interesting changes in the visual sur-

[32] See "Aviation Toxicology," prepared under the direction of the Committee on Aviation Toxicology, Aero Medical Association. Pub. by Blakiston, New York, 1953.

[33] See "Aviation Toxicology Bulletin." Office of Aviation Safety, Medical Division, Civil Aeronautics Administration, Washington, D. C.

[34] See USAF Office of Inspector General (Norton Air Force Base) Report M-19-52 (1952) (restricted), "Human Factors in Jet Fighter Accidents, Period 1, January 1950 through June 1952."

[35] "Cabin Air Contamination Problems in Jet Aircraft," by S. Kitzes. Paper presented at 26th Annual Meeting, Aero Medical Association, Washington, D. C., March 22, 1955.

[36] See *Journal of Aviation Medicine*, Vol. 15, No. 6, 1944, pp. 381-394: "Effects of Carbon Monoxide and Altitude on Visual Thresholds," by R. A. McFarland, F. J. W. Roughton, M. H. Halperin, and J. I. Niven.

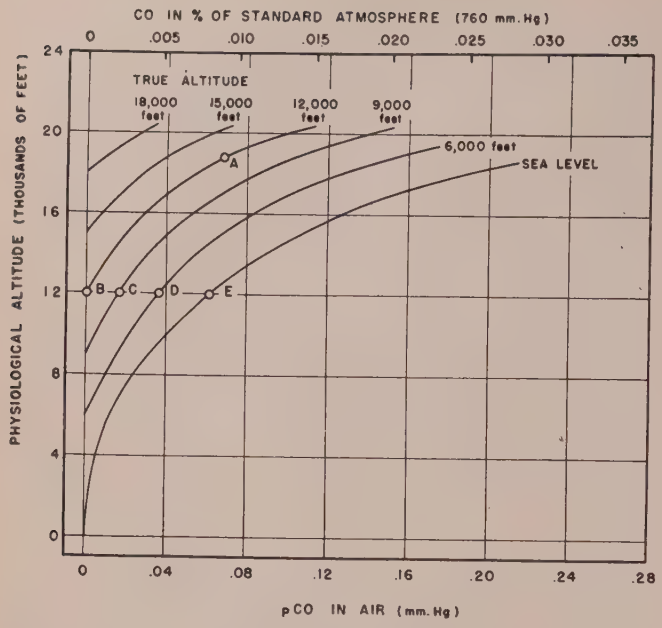

Fig. 7 – Effects of carbon monoxide on altitude tolerance. Chart shows relation between physiological altitude and partial pressure of carbon monoxide in air at various true altitudes when equilibrium with blood has been reached. For instance, if pilot at true altitude of 12,000 ft is exposed to air containing 0.07% carbon monoxide, physiological reaction he experiences would correspond more nearly to that of approximately 19,000 ft (point A)[36]

roundings in flight at very high altitudes. The sun's rays become more intense and contain a higher proportion of ultraviolet light, the sky becomes darker, and there is less haze.[37, 38, 39] The use of sunglasses becomes more necessary as protection against the ultraviolet radiation and the increased light intensities. However, because of the darkened sky and the lack of diffusion of the sun's rays, shadows become darker, instruments and shaded areas of the cockpit are darker, but sunlit areas are more glaring. The reading of instruments may become especially difficult where there are small windshields and glare shields over the panel. On such occasions, white artificial lighting may be used or, on some occasions, sunglasses of graded density.[8]

B. Visual Perception Times at High Speed – In high-speed aircraft, additional demands are placed upon the pilot in so far as vision and reaction time are concerned. With high closing speeds, only a few seconds may elapse between the sighting of another aircraft and its passing. Often the decision for action must be made, and the correct control response initiated and carried out, in a matter of seconds. Flight obstacles must be picked up at greater distances in order for the proper evasive action to be taken. Mid-air collisions, especially in the neighborhood of airports, are currently a serious problem. In recent years there have been 11 mid-air collisions involving scheduled air transports with other planes resulting in 130 fatalities. Such hazards naturally increase while operating at greater speeds.[7, 40]

The extent to which a lag in visual perception and reaction times may have been involved is not known, but pilots flying high-speed aircraft must be indoctrinated in regard to this problem. At 600 mph, a plane travels a mile every 6 sec, or about 880 fps. If a pilot is flying at 600 mph on a collision course with a fixed object, about 2 to 3 sec might be involved in taking evasive action. The latent period of the pilot involves 0.8 sec for recognition, 0.5 sec for visual accommodation, 0.07 sec for foveal perception, 0.05 sec for eye movements, and 0.175 sec for reaction time. In addition, the time required for the response of the plane itself must be considered. Thus, a distance of 2000-3000 ft might be traversed before evasive action could be taken.[39, 41, 42, 43]

While pilots of high-speed aircraft carry out many of the same activities as they would in slower planes, there is often much less time, and a high premium is consequently put upon reaction time. A moment's hesitation can have serious implications. However, it is under such conditions of stress requiring instantaneous decisions that human errors are most likely to occur in reading instruments or operating controls. A pilot may often do what seems "natural" rather than what he has been trained to do. For this reason, all of the pilot's operational activities should be designed, in so far as possible, to coincide with what his natural reactions would be. Significant progress has been made along these lines in recent years.

C. Visual Illusions in Flight – The designer should keep in mind the fact that visual illusions may be accentuated during high-speed flight. Illusory responses result from a wide variety of causes, and are frequently classified according to whether they are visual or nonvisual in origin. The former are primarily related to the visual mechanism, while the latter arise from stimulation of the vestibular mechanism in the inner ear and the muscles, tendons, and joints. Misinterpretations may be caused by the conflict of one visual cue with another or by various combinations of visual and nonvisual stimuli. A brief summary of representative illusions most commonly reported by airmen may be found in my most recent book[9] and a com-

[37] See Naval Medical Research Institute Research Report, Project NM 001 056.07.01 (1953), "Brightness of Atmosphere," by N. L. Barr, J. E. Murray, R. D. Murray, J. A. Hussman, and J. F. Parker.

[38] See Naval Medical Research Institute Research Report, Project NM 001 056.07.02 (1953), "Brightness of Atmosphere; Effect of Cloud Conditions," by N. L. Barr, J. F. Murray, R. D. Murray, J. A. Hussman, and J. F. Parker.

[39] See Office of Naval Research Report No. 151-1-14, Project 20-M-16 (1948), "Estimates of Visibility from High-Altitude Aircraft," by J. D. Coakley, L. Festinger, H. H. Kelley, and J. Orlansky.

[40] See "Growing Problem of Mid-Air Collision," Flight Safety Foundation, Inc., New York, 1955.

[41] See *American Journal of Ophthalmology*, Vol. 34, February, 1951, p. 2: "Visual Problems of Supersonic Speeds," by V. A. Byrnes.

plete bibliography, including abstracts of experimental studies, has been compiled by the U. S. Air Force.[31] It is obvious that pilots should be indoctrinated in regard to the recognition of these and other illusory responses in high-speed flying.[9]

D. Control Forces and the Performance of the Pilot – The present concepts of flying have incorporated within them a need for the application of human proprioceptive senses. That is, the pilot receives a good deal of information about his aircraft's attitude and speed through position and pressure stimuli presented to him through his controls.

As is well known to aeronautical engineers, the tremendous forces required to move the control surfaces of high-speed aircraft are so great as to necessitate the introduction of boost systems between the controls and the control surfaces. Jet pilots, therefore, do not have the same direct pressure feedback or "feel" on the stick that is present in slower aircraft. In addition, control force reversals may occur at very high airspeeds, such as right aileron pressure causing the plane to roll to the left. Pilots must thus continually sample aircraft response and sense changes in stick forces, because at very high speeds instability of control may cause the aircraft to disintegrate in a few seconds. In certain recent models, however, which are of such great weight or designed to fly at such high speeds, the forces are too great to allow for any feedback. In such irreversible systems, the pilot no longer flies his aircraft but adjusts a hydraulic metering valve which directs the desired forces. Attempts have been made to develop an artificial "feel" system to duplicate the positions and forces in the control system of the older type of aircraft. In this way the previously learned flying habits of the pilot are unimpaired. This requires a knowledge of human response characteristics when the pilot is considered as a part of the total servo-boost control system. Further research is indicated in regard to whether such systems should comprise "feel" alone, position or pressure alone, or simple visual stimuli.[7, 44]

E. Problems of Pilot Fatigue – One source of stress which has been prominent in conventional aircraft as they have been developed was the complexity of instrumentation and controls. Simpler controls and fewer instruments for the operation of the powerplant reduce this problem for the jet pilot. Fig. 8 compares the Boeing Stratocruiser and the 707 jet transport in this regard.[44] Similar changes made it possible for Comet operations without the need for a flight engineer in the crew. However, certain other aspects of jet transport flight may offset this gain. Orde, for instance, has pointed out that activities relating to navigation and traffic control which have to be carried out in a particular segment of flight are compressed in jet flights within a shorter space of time, a situation which favors the introduction of errors.[11] Capt. Martin of the Lockheed Aircraft Corp. has indicated that additional monitoring duties will be involved with the development of "fail-safe" and "standby systems" for insuring the integrity of cabin pressurization, and raises the question of the efficiency of humans as monitors of equipment and of resistance to boredom and fatigue in such duties. Human subjects are notoriously poor as monitors of equipment.

Long-range flights at speeds close to 600 mph may involve moving through several time-zones, so that pilots must adjust to a time change of as much as 12 hr in one day. There may thus be a complete inversion of the sleep and diet rhythm in a single trip.[45] Air crews should attempt to keep the sleep rhythm of their own country, and their flight schedules should not be shifted too frequently. It may take as long as one week to become fully adjusted to a marked alteration in the sleep cycle and new physiological rhythms. Insufficient rest may constitute a more severe hazard for fliers than for members of other occupations because of the environment in which they operate; tolerance for altitude is progressively lowered by loss of sleep. This has been verified experimentally.[9] These time-zone changes naturally present similar difficulties for passengers.

F. Health Maintenance Problems – In addition to the influences already discussed, certain other

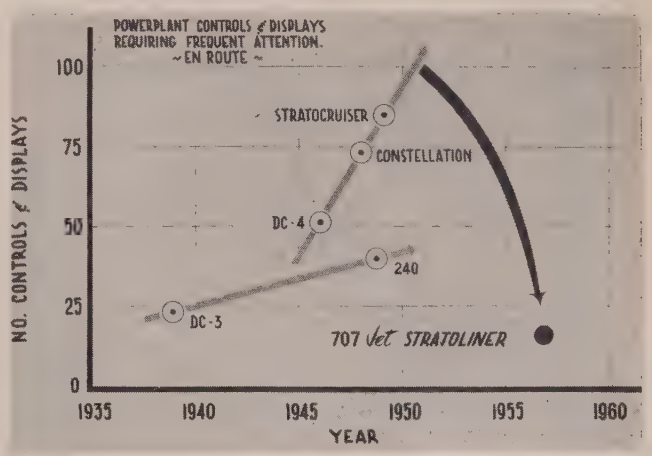

Fig. 8 – Cockpit complexity trend. Chart indicates cockpit complexity trend in recent years for representative 2-engine and 4-engine aircraft. Note reverse in trend for jet air tanrsport[44]

[42] See "The Human Time Factor in Flight: I. The Latest Period of Optical Perception and Its Significance in High-Speed Flying," by H. Strughold. Unnumbered project, USAF School of Aviation Medicine, Randolph Field, Tex., January, 1951.

[43] See "The Human Factor in Flight: II. Chains of Latencies in Vision," by H. Strughold, Unnumbered project, USAF School of Aviation Medicine, Randolph Field, Tex., November, 1950.

[44] "Design Safety of the Boeing 707 Jet Transport," by E. W. Norris. Paper presented at Annual Meeting of the Institute of the Aeronautical Sciences, New York, Jan. 26, 1955.

[45] See *Journal of Aviation Medicine*, Vol. 23, No. 5, 1952, pp. 464-473: "Physiological Day-Night Cycle in Global Flights," by H. Strughold.

features of high-speed, high-altitude flight have implications for the continued health and efficiency of the air crew engaged in jet transportation.

The primary particles which make up cosmic radiation are protons, neutrons, alpha particles, and heavy nuclei. These particles come from outer space and travel at high velocities. These cosmic "rays" are much more penetrating than other radiations. Cosmic radiation can be measured by its ionizing effect with the aid of the same device used to measure other ionizing rays such as X-rays. Such measurements have been made by Millikan and his associates. On the basis of fairly extensive research with X-rays and radium, the biological effects of cosmic radiation can now be estimated. Accurate predictions are not possible, however, since the densely ionizing cosmic radiation, consisting of neutrons and heavy primary particles, may differ in biological effect from the less densely ionizing X-rays. Nevertheless, careful analysis of cosmic radiation data indicates that its biological effectiveness will definitely be less than 10 times that of X-rays.

It has been calculated that an aviator spending 1000 hr a year at 55,000 ft would receive in an average week only 0.015 roentgen units of exposure. For the medical profession and Atomic Energy Commission, 0.3 roentgen units of exposure per week is considered safe, or a dosage 20 times that received by the pilot mentioned above. Even if the biological effects of cosmic radiation were 10 times that of X-rays, he would still receive only one-half of the dosage considered safe for indefinitely continued exposure.[8]

Ultraviolet light energy ranges from 80 microwatts per sq cm at ground level to 222 at 40,000 ft. However, the wavelengths which have an adverse physiological effect are mainly those below 320 mμ; these waves are efficiently absorbed by the ocular media, and do not reach the retina in injurious amounts. Exposure to even moderate amounts of ultraviolet of wavelengths as long as 365 mμ will, however, affect dark adaptation thresholds adversely.[9]

Summary and Conclusions

The objective of this paper has been to review several of the more important human factors which are involved in the safety and comfort of travel in high-speed, high-altitude transports. Emphasis was placed on a better understanding of the aircraft environment, and the related limitations imposed on human performance. The functional limitations of the brain and sense organs are important considerations in this context, as illustrated by an analysis of the noise problem created by jet engines during servicing and preflight operations.

Although cabin pressurization and pressure breathing equipment provide satisfactory solutions to problems encountered in ascent to altitudes in the stratosphere, much remains to be done in improving the comfort and reliability of such advances. Sudden losses in pressure were discussed, with emphasis upon the acute oxygen want created, and the problems associated with rapid change in barometric pressure. A discussion of human tolerance to accelerative forces indicates that transport operating forces approaching or surpassing human limits are likely to be encountered chiefly in abrupt emergency maneuvers, or in crashes. Data on the effects of acceleration were then reviewed. High-altitude flight involves visual problems for the pilot because of the changes in the illumination of the sky and the absence of reference points for judging distance and direction. With increasing speeds of travel, the latent time of visual perception becomes of increasing importance, and the danger of mid-air collision requires special emphasis.

Data on the effects of cosmic radiation and ultraviolet exposure were presented to evaluate the importance of these influences on the health and efficiency of air crews engaged in high-altitude operations. The need for air-crew indoctrination in the effective use of equipment was demonstrated throughout, as well as the need for airmen to understand their own physical limitations in flight. The need for more effective collaboration between the biological and engineering sciences has been stressed as an approach to increasing the safety and comfort of the coming form of air transportation.

Additional References

1. "Effect of Heat upon Performance of Men in High-Speed Aircraft. A Critical Review," by J. S. Coakley, J. Orlansky, and L. Connell. Report No. 151-1-17, Project 20-M-lb. Human Engineering Board, Special Devices Center, Office of Naval Research, June 30, 1948.

2. *Journal of Industrial Hygiene and Toxicology,* Vol. 31, No. 6, 1949, pp. 365-375: "High Concentrations – Short Time Exposures and Toxicity," by B. G. King.

3. "Human Problems Associated with High-Speed and High-Altitude Flight," by R. A. McFarland. Preprint 54-A-230, American Society of Mechanical Engineers, New York, 1955.

4. "Synopsis of Aero Medical Aspects of Jet-Propelled Aircraft." Engineering Division, Aero Medical Laboratory, Air Materiel Command, Wright-Patterson Air Force Base, Dayton, Ohio, January, 1949.

5. "Turbine Transports." Report by the CAA Turbine-Powered Transport Evaluation Team, Civil Aeronautics Administration, Washington, D. C., January, 1954.

Lightweight Springs for Limited Life

E. H. Spaulding, Lockheed Aircraft Corp.

This paper was presented at the SAE Golden Anniversary Aeronautic Meeting, Los Angeles, October 13, 1955.

WEIGHT-REDUCTION efforts have caused aircraft designers to seek means of weight reduction that few other industries would find necessary. Some springs in aircraft mechanisms may operate only a few times each flight and, therefore, a life limited to 300,000 cycles may be entirely satisfactory. A method of spring design is presented that cuts spring weight to as little as ¼ of the value obtained from standard spring design handbooks.

For example, a spring in the Constellation (749) main landing, gear drag, strut damper was redesigned as shown in Fig. 1 to save 17 lb. Being smaller, the housing weight was reduced and, with two required, a total weight saving of 55 lb per airplane was realized. Since then these springs have served well for over 20,000 service hr. This unusual weight saving was achieved by increasing the working stress more than 50%. Such a high working stress was made possible through the use of preset and stresspeen techniques applied to springs of unusually high quality.

It may not be economical to apply this method to small springs unless there are a sufficient number per airplane to justify the effort.

The following design principles can be used to reduce the weight of any spring, but service life may be greatly affected if the spring isn't used in the

A SPRING in the Constellation (749) main landing-gear drag-strut damper was redesigned to save 17 lb. The smaller spring required a reduced-size housing, and the overall weight saving per airplane using two such units totaled 55 lb. These springs have served well for over 20,000 hr.

This unusual weight saving was achieved by increasing the working stress more than 50% over conventional design practice. A high working stress was made possible through the use of preset and stresspeen techniques on springs of unusually high quality.

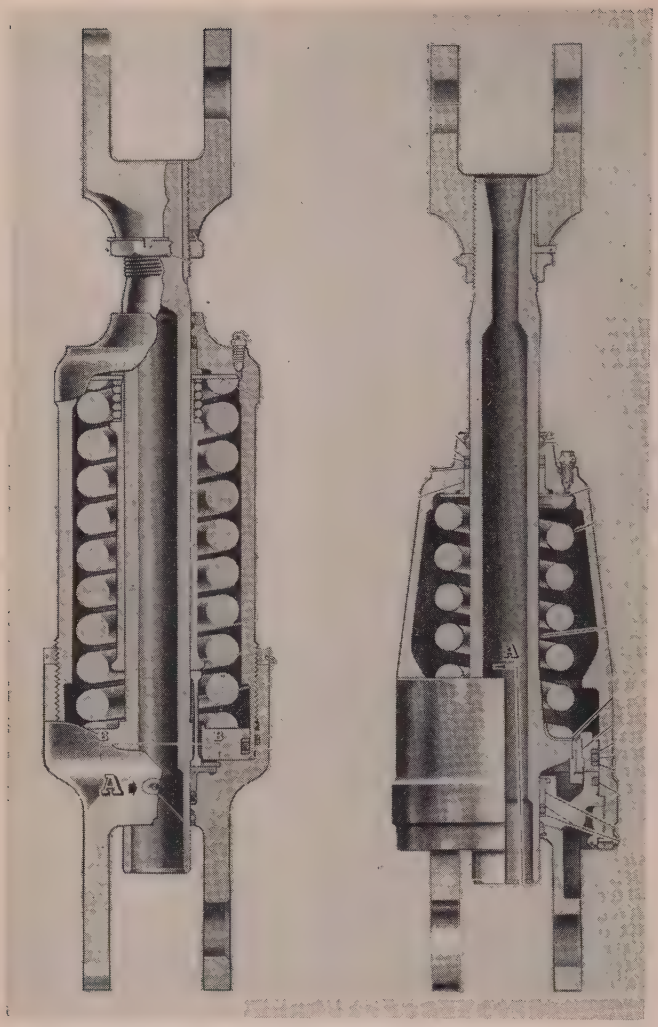

Fig. 1 – Original design (left) and revised design (right) of Constellation drag-strut damper. Revised design resulted in a weight saving of 55 lb per airplane

exact manner assumed in this analysis. An example is presented for a spring with the following requirements:

1. Service life is limited to less than 300,000 cycles.
2. Spring load at top of stroke must be ½ the load at bottom of stroke.
3. Spring is loaded only in compression.

Definitions

Wound height – Height of spring as originally wound and heat-treated.

Installed height – Height of spring at the top of working stroke.

Compressed height – Height of spring when compressed to bottom of working stroke. The spring is intended to operate between its installed and compressed heights.

Solid height – Height of spring when all coils are bottomed.

Set deflection – Distance the spring must be compressed from wound height for appreciable permanent set to begin. This travel causes an average surface stress slightly higher than the yield stress in shear.

Set height – Height of spring when relaxed after preset.

Stresspeen height – Deflected height while the spring is shotpeened.

Wahl factor, ψ – This curved torsion-bar stress-correction factor is found in any standard spring handbook.

Optimum Spring

Relationship of Working Stroke to Total Deflection – A spring that holds a given load at its installed height is of minimum weight when the working stroke is ½ the total deflection between relaxed and compressed heights. Thus, load at the bottom of the working stroke is twice that at the beginning of the working stroke.

Volume of Active Steel Required – Volume of active steel required may be determined by equating internal and external energy.

$$\text{Total external energy} = \frac{PL}{2}$$

(including installed energy + operating energy)

$$\text{Total internal energy} = \frac{VF_s^2}{4G}$$

where:

P = Spring load at bottom of stroke, or Maximum operating load

L = Total spring deflection from relaxed to compressed position, or deflection required to develop load P

V = Volume of active steel required

F_s = Allowable change in shear stress from relaxed to compressed height

G = Shear modulus of elasticity

The volume becomes:

$$V = \frac{2PLG}{F_s^2}$$

Wire and Coil Diameter – Wire diameter is determined from the shear stress equation:

$$F_s = \frac{Tr}{J}$$

where:

T = Torsional moment in wire

r = Wire radius

J = Polar moment of inertia of wire

Since T is a function of the mean coil diameter (D):

$$T = P\frac{D}{2}$$

and wire diameter $d = 2r$, this final relationship becomes:

$$d = \frac{4JF_s}{PD} = 2\sqrt[3]{\frac{PD}{\pi F_s}}$$

Number of Active Coils – Knowing wire diameter, (d), mean coil diameter (D), and the volume of active steel required (V), we find it a simple matter to compute the number of active turns, (N), to give the required volume:

$$N = \frac{4V}{\pi^2 d^2 D}$$

Preset Operation

The purpose of presetting is to induce favorable residual stresses that will allow a greater range of working stress without producing permanent set. The spring is wound longer than desired in its final configuration. It is then deflected to its compressed height, producing a strain approximately double the yield strain and causing a permanent set. After presetting, the relaxed spring has the desired length called its set height.

It is recommended that preset deflection be twice that causing appreciable permanent set. Preset greater than this is permissible and will lock in higher beneficial residual stresses, but there is little further to be gained and the physical problems of performing the more extensive operations makes it impractical.

The spring will buckle and fly out of the press if not restrained and guided during presetting. It is imperative that the spring be well guided by a close-fitting tube or mandrel; otherwise it won't set evenly and will be crooked. Short of breaking the spring, it is not possible to preset too much.

Referring to Fig. 2 and using the assumed stress-distribution consisting of two straight lines *oab*, we find the internal moment within the torsion-bar under preset load is:

$$T_q = \int_{r/2}^{r} 2\pi X^2 F_{ps}\, dx + \int_{o}^{r/2} 2\pi X^3 \frac{F_{ps}}{r/2}\, dx$$

$$T_q = \frac{7}{12} \pi r^3 F_{ps} + 1/16\ \pi r^3 F_{ps}$$

$$T_q = 0.64\ \pi r^3 F_{ps}$$

Removing preset load reduces the internal moment to zero. However, since the recovery is elastic, the condition is equivalent to applying an equal and opposite moment producing a linear stress distribution, represented in Fig. 2 by the straight line *oc*. The ordinate *cr*, representing the change in surface stress due to removal of preset load can be found by equating the internal moments produced by the two stress-distributions. Thus:

$$0.64\ \pi r^3 F_{ps} = 1/2\ (F_{ps} + F_{rs})\ \pi r^3$$

and:

$$F_{rs} = 0.28\ F_{ps}$$

Algebraic addition of stress distributions oab and oc in Fig. 2 gives the residual stress-distribution shown in Fig. 2, with 0.28 F_{ps} the surface residual stress.

When the spring is compressed again it can now move a distance to cause an average stress change on the surface equal to 1.28 F_{ps} without surface material yielding. This is the gain from the preset operation.

Effect of Wahl Factor

Stress distribution within the wire cross-section shown in Fig. 2 is only an average condition. Since the wire is wound into a coil, more stress is concentrated on wire surface nearest the axis of the coil. The factor by which this stress is increased is known as the Wahl factor, ψ, a sort of a stress-concentration factor. Fig. 3 illustrates the stress condition on the most highly stressed portion of the wire during and after preset.

Stresspeening

Almen says[1] that shotpeening leaves the surface in a state of biaxial compression equal to about ½ the yield strength of the material. This affects the surface material to a depth of only one or two thou-

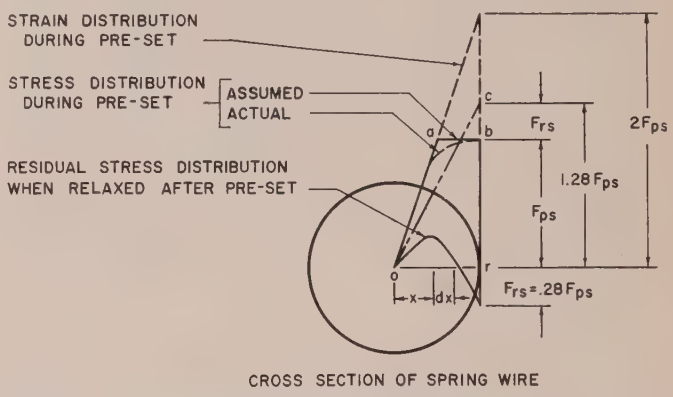

Fig. 2 – Average stress distribution within wire during and after preset. Wahl factor neglected

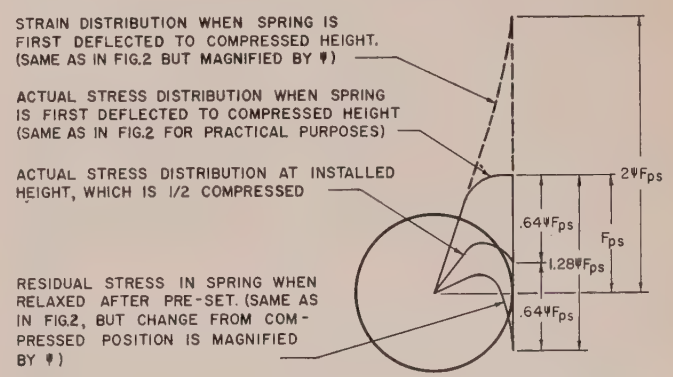

Fig. 3 – Stress distribution at inner face of coils during and after preset, including effects of Wahl factor

[1] See *Product Engineering*, Vol. 21, November, 1950, pp. 117-140: "Fatigue Weakness of Surfaces," by J. O. Almen.

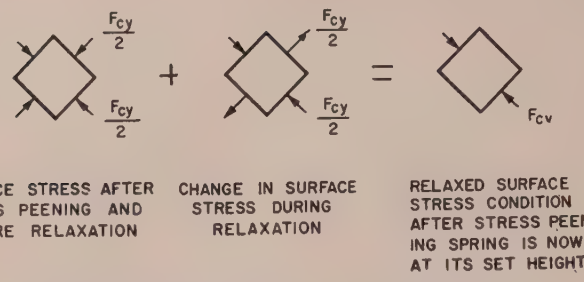

Fig. 4 – Inner surface stress conditions after stresspeening, after relaxation, and at set height

sandths of an inch.

If the spring is compressed somewhat beyond the shear yield stress (F_{ps}), on the most highly stressed inner face and is then shotpeened while held in that position, the surface stress condition is changed to biaxial compression equal to ½ the compression yield stress, as shown in Fig. 4. Since the yield stress in shear is usually greater than ½ the tension (or compression) yield stress, it is conservatively assumed that $F_{ps} = F_{cy}/2$.

When the spring is removed from the jig and relaxed, the surface stress changes by F_{ps}, assumed equal to $F_{cy}/2$. The final stress in the relaxed state is compression equal to F_{cy}, shown in Fig. 4.

When the spring is compressed to its installed height, the surface stress changes by 0.64 ψ F_{ps}, equal to 0.32 ψ F_{cy}. This is the beginning of the working stroke. The resulting stresses at the installed height are shown in Fig. 5.

When the spring is compressed through its working stroke to its compressed height, the change in surface stress is again 0.32 ψ F_{cy}. This operation is shown in Fig. 6.

Under the above conditions the spring surface will never be in tension unless the Wahl factor exceeds 1.56. This is improbable, for a good spring design will maintain dimensions to keep the factor much lower. This is a desirable condition for fatigue because a failure can't start from the surface. Evidence indicates that fatigue strength of subsurface material is higher than for surface material.

During relaxation after stresspeening the spring will not quite return to its original set height because of the change in surface stress condition during peening. About 2-5% of the stresspeen stroke will be lost. Allowance for this must be provided for in design if spring load at its installed height is a critical value.

Design Summary

Allowable Stress – Allowable stress to use in spring formula $F_s = \frac{8PD}{\pi d^3}$ can be as high as 1.28 F_{ps} (see Fig. 2). The Wahl factor (ψ) need not be considered when choosing the allowable stress. Assuming $F_{cy} = 0.8\ F_{tu}$, then $F_{ps} = F_{cy}/2 = 0.4\ F_{tu}$, and the allowable stress becomes $F_s = 0.51\ F_{tu}$. Assuming heat-treatment to 320,000 psi, the allowable shear stress that can be used becomes $F_s = 163{,}000$ psi.

Wire and Coil Diameter – Wire and mean coil diameter are found from the relationship:

$$d = 2\sqrt[3]{\frac{PD}{\pi F_s}}$$

Number of Active Coils – Number of active coils is found from:

$$N = \frac{8PLG}{F_s^2 \pi^2 d^2 D}$$

Solid Height – Solid height = d (N + inactive coils).

Compressed Height – Compressed height should be no less than solid height + $\frac{Nd}{10}$ but may be greater. This additional length beyond solid height allows for slight unevenness in winding the coil and prevents coils from touching one another during the working stroke. If coils touch one another, unequal stresses are induced which seriously shorten life.

Installed Height – Installed height = compressed height = working stroke.

Set Height – Set height = compressed height + 2 (working stroke).

Wound Height—Wound height = compressed height + 3.12 (working stroke). By reference to Fig. 2, working stroke is proportional to 1.28 $F_{ps}/2$. (Wound height − compressed height) is proportional to 2 F_{ps}. Thus:

$$\frac{2\ F_{ps}}{1.28\ F_{ps}/2} = 3.12$$

Stresspeen Height—Stresspeen height = set height − $\frac{1.56}{\psi}$ (working stroke). By reference to Fig. 3, working stroke ≈ 1.28 ψ $F_{ps}/2$. (Set height − stresspeen height) ≈ F_{ps} (by defini-

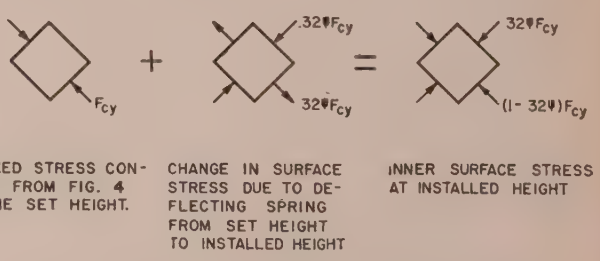

Fig. 5 – Inner surface stress conditions at installed height

tion). Thus:

$$\frac{F_{ps}}{1.28\,\psi\,F_{ps}/2} = \frac{1.56}{\psi}$$

Special Notes

1. Satisfactory springs have been made from SAE 9260 steel heat-treated to 320,000 psi.

2. Ends may be squared and ground after heat-treatment. Under no circumstances can other grinding or cutting be performed beyond this stage.

3. Springs must be guided during presetting to prevent buckling. Adequate guides will permit uniform set along the length of wire.

4. Load at installed height before stresspeening should be about 5% greater than finally desired after stresspeening. Stresspeening will cause load at installed height to drop about 5%. Some "cut and try" with heat-treatment may be necessary in order to raise or lower the load at installed height to the desired value.

5. Fixtures to hold spring compressed during stresspeening must allow shot to get to all parts of the spring. The inner face of the coils must have complete coverage as well as the rest of the wire.

6. No plating or electrolytic treatment is permissible. Corrosion protection can be obtained if spring runs in oil or is covered by heavy grease.

7. Spring steel must be of high quality with no laps, seams, or gouges. Care must be taken during winding not to gouge the wire, or early service failures will result.

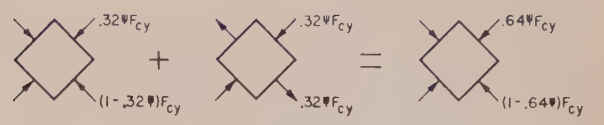

STRESS CONDITION AT INSTALLED HEIGHT FROM FIG. 5

CHANGE IN SURFACE STRESS DUE TO DEFLECTING SPRING THROUGH ITS WORKING STROKE TO ITS COMPRESSED HEIGHT.

INNER SURFACE STRESS CONDITION AT COMPRESSED HEIGHT.

Fig. 6 – Inner surface stress conditions at compressed height

8. Decarburization cannot be permitted if a 300,000-cycle service life is desired. Decarburization has a very harmful effect on fatigue life.

9. Carburization of the surface cannot be tolerated because it causes cracking or failure during presetting. There is some danger that spring fabricators may carburize the surface in their efforts to avoid decarburization during heat-treatment.

10. Spring manufacturers may not be easily convinced of the soundness of this design. It may be necessary to relieve them of any responsibility for the spring before they agree to such specifications. It will be difficult to find a manufacturer who is able to produce such high-quality springs, but it has been and is being done.

DISCUSSION

Infinite Life Possible at Reduced Nominal Stress

by J. O. Almen

General Motors Corp.

I AM pleased to learn from this paper that Lockheed is continuing its progress in the application of prestressed hard steel in highly loaded, dynamically stressed structural parts. This work is additional confirmation of theories advanced in an earlier paper.[a]

Mr. Spaulding's title implies that the springs he describes are useful only in the finite region of fatigue. I see no reason why they cannot have an infinite life by operating at slightly reduced nominal stress.

The springs described were heat-treated to 320,000 psi, which corresponds to a Rockwell C hardness of 58-59. Tests of even harder coil springs[b, c] (RC 61-63) were made a number of years ago. They also showed that by avoiding brittleness (surface weakness) through prestressing it is possible to utilize the potential strength of very hard steel. These harder springs were not strainpeened because that process[d] was not applied until some time after the spring tests.

Regarding the precautions listed by Mr. Spaulding under "Special Notes," I offer the following:

1. I doubt the necessity for prohibiting all electroplating, and particularly soft plating commonly used for corrosion protection, provided cleaning by grit blasting follows plating.

2. Cracking or failure during presetting can be mitigated by (a) presetting at an elevated temperature, perhaps not greater than tempering temperature, and/or (b) shot-peening before presetting to reduce surface-fracture vulnerability.

3. Carburizing is not necessarily bad. Buick has long formed its "Crown" clutch spring from low carbon sheet carburized to develop spring quality steel in the highly stressed surfaces. Carburizing can, no doubt, be beneficial in restoring lost carbon, provided the process is properly applied. But until carburizing is better understood, I will support Mr. Spaulding in prohibiting its use.

[a] See SAE Transactions, Vol. 51, (July) 1943, pp. 248-268: "Shotblasting to Increase Fatigue Resistance," by J. O. Almen.

[b] See National Defense Committee of OSRD, War Metallurgy Division, Final Report, Part 1, OSRD No. 3274 (1944), pp. 46-47: "Effect of Shot-peening on the Physical Properties of Steel," by R. L. Mattson and J. O. Almen.

[c] See *Product Engineering*, Vol. 24, July, 1953, pp. 189-191: "Residual Compressive Stress Strengthens Brittle Materials," by J. O. Almen.

[d] See National Defense Committee of OSRD, War Metallurgy Division, Final Report, Part 2, OSRD No. 4825, 1945, pp. 108-109: "Effect of Shot-peening on Physical Properties of Steel," by R. L. Mattson and J. O. Almen.

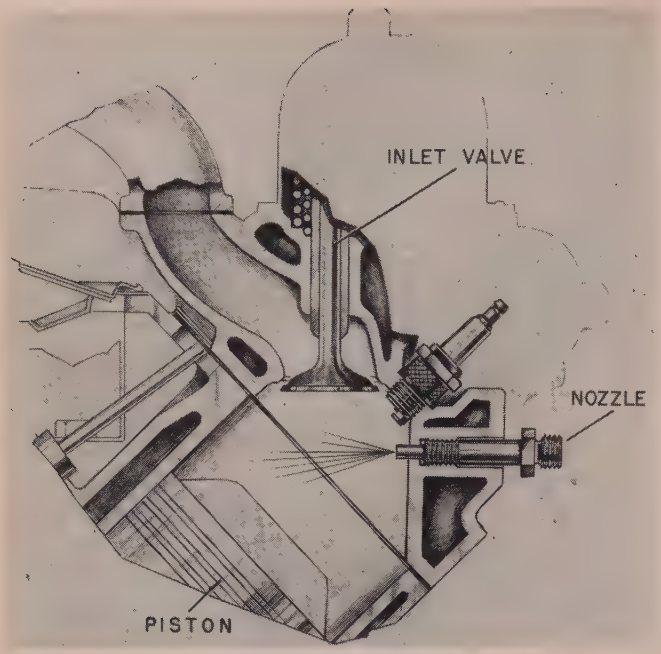

Fig. 1 – Direct injection

Automotive

ONE of the principal problems in connection with the design of 4-stroke-cycle gasoline engines is that of providing equally distributed fuel-air mixtures to the various cylinders under all of the many operating conditions that the engines are called upon to meet.

Carburetors have been improved constantly over the years and will, with proper intake manifold designs, provide excellent engine flexibility over the operating range. However, a properly designed manifold for use with the conventional carburetor must have the branch areas sized to maintain a certain minimum velocity at idle airflows in order that liquid fuel will not settle out and prevent proper mixture distribution to the individual cylinders. This condition, of course, imposes an important limitation on high-speed, full-throttle operation because of the excessive inlet manifold pressure drop at the higher airflows. In addition, a hot spot is required to assist carburetor vaporization under some conditions. This hot spot, fed generally by the exhaust manifold, heats up the inducted air and reduces the mass airflow. Thus it will be seen that the use of a carburetor imposes two major penalties in inlet manifold design which limit the efficiency and maximum output of the engine.

In order to avoid the problem of area-limited branches, methods of pressure carburetion in which a very rich mixture is formed and distributed through tubes to the separate cylinder inlets where it is further diluted by manifold air have been tried with rather indifferent success. Likewise, cold carburetion systems having both fuel and mixture distributing devices have been developed but to date have lacked the essential flexibility required by the automotive application. It is therefore natural that the attention of gasoline engine designers should be directed toward a fuel system similar to that of the diesel engine in order that the two limitations on manifold design may be avoided.

For a great many years designers in many countries have adapted diesel-fuel injection equipment to handle gasoline in the gasoline injection engine. In general, excellent results have been obtained and complete freedom in inlet manifold design has been achieved. The cost of such equipment, however, has

Gasoline Injection

Sidney E. Miller, American Bosch Division, American Bosch Arma Corp.

This paper was presented at the SAE Golden Anniversary Fuels & Lubricants Meeting, Philadelphia, Nov. 10, 1955.

APPLICATION of injection equipment, especially designed for gasoline, to the stock V-8 passenger-car engine is described here.

The port-injection system tested basically consists of an injection pump driven at half crankshaft speed, a mixture control governing the pump setting, a motor-driven fuel supply pump maintaining fuel pressures above the vapor pressure of gasoline, and the associated nozzles and fuel filter.

Advantages of converting a stock carbureted engine to gasoline injection include 10% greater full-throttle horsepower output, a minimum decrease of 500 rpm in torque peak position, 5-15% more miles per gallon, and the use of fuels having higher vapor pressures and end points.

presented a very real and important restriction to its widespread use. We at American Bosch have made adaptations of diesel equipment to the gasoline engine on many occasions; but realizing that the system cost must be drastically reduced, we have in the past few years developed injection pumps, nozzles, and other accessories specifically for use with gasoline and for the automotive engine. Since the injection pressures and mechanical loadings are appreciably lower than in most of the diesel automotive engine applications, a considerably simpler and cheaper mechanical design has been reached.

The Europeans in their adherence to the principle of the diesel injection system have in general continued their use of direct injection with the gasoline engine (Fig. 1). The fuel is, however, injected on the intake stroke so that the mixture is compressed as usual preparatory to firing. In this country most of the proposals have been of a port-injection type in which fuel is sprayed toward the back of the inlet valve and is carried into the cylinder by the air during the intake stroke (Fig. 2). We have been un-

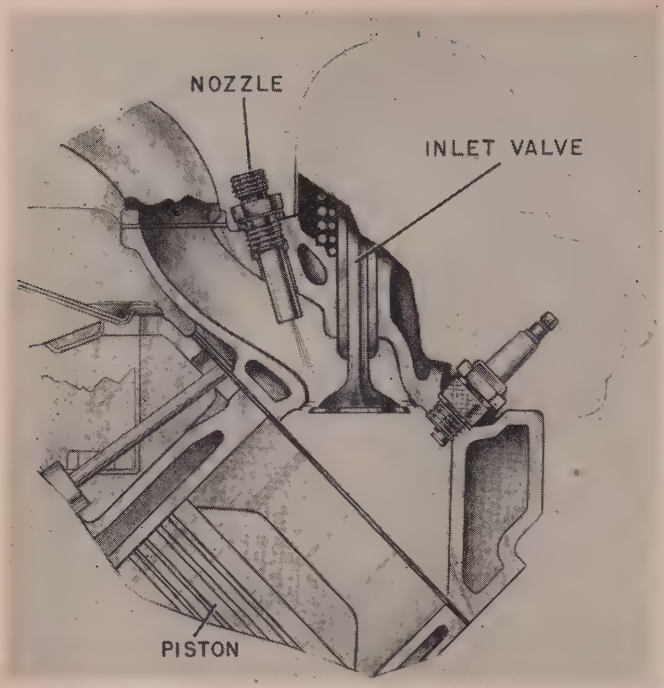

Fig. 2 – Port injection

able to detect any difference in engine performance below 5000 rpm with either system. However, as the engine speed is raised to some figure of 5500 to 6000 rpm the inlet valves are open such a short time that injection timing and duration must be extremely accurate and short with port injection. At these high engine speeds the direct-injection engine has an advantage since the full time of piston intake stroke and some part of the compression stroke may be utilized for fuel injection. However, since most automotive engines in this country operate at speeds below 5000 rpm the extra cost involved in the direct-injection system may be avoided with no penalty by the use of the port-injection system.

The complete gasoline port-injection system which has now been field tested for well over one year on several well-known automotive engines consists of an injection pump driven at half crankshaft speed, a mixture control governing the pump setting, a motor-driven fuel supply pump maintaining fuel pressures well over the service vapor pressure of gasoline, and the associated nozzles and fuel filter. The system schematic is shown in Fig. 3.

Injection Pump (8-Cylinder)

The injection pump shown in Fig. 4 is comprised of an integral 8-lobe face-cam and plunger *A* reciprocating and rotating within housing *B*. A metering sleeve *C* is fitted to the plunger to control the fuel spill point and is adjusted for metering position by eccentric shaft *D*.

In operation, supply fuel enters sump *E* and during the suction stroke fills the internal volume of the plunger through radial ports *F* in the plunger and sleeve. As the plunger turns, the fill ports are covered at the end of the suction stroke and distributing port *G* registers with one of the outlets *H*. At the start of the pumping stroke, fuel trapped in the internal volume of the plunger is forced out through spill ports *K* to sump *E* for that part of the stroke determined by the metering sleeve position. As the plunger lifts further, the spill ports are cov-

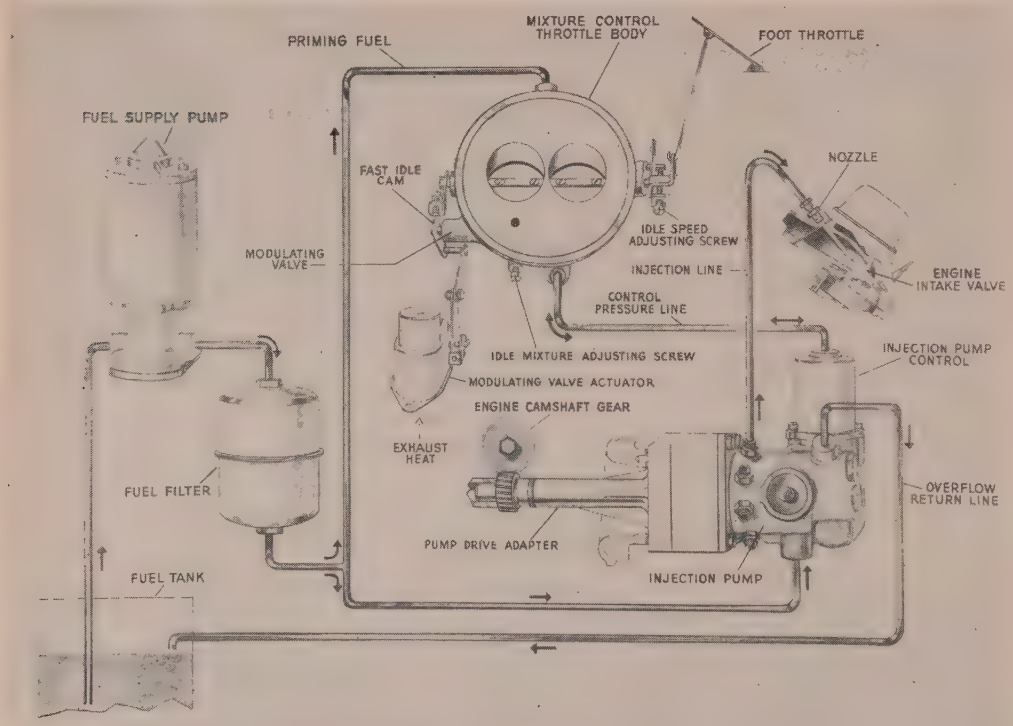

Fig. 3 – Gasoline injection system

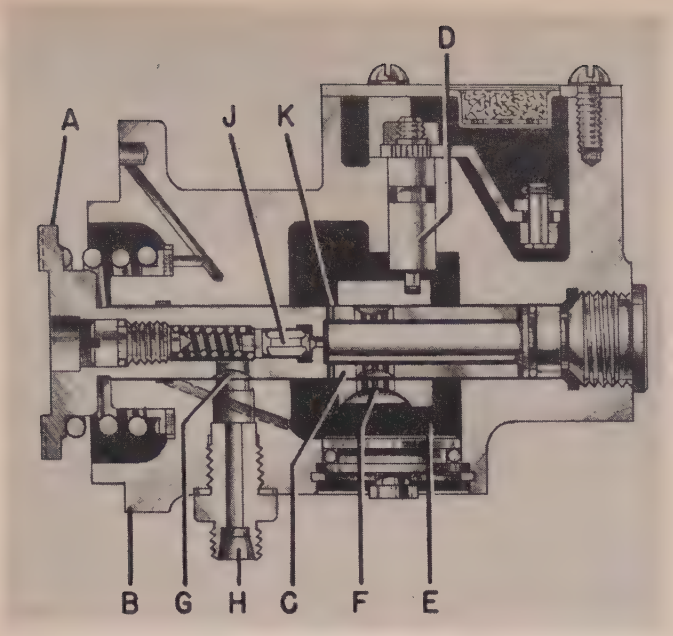

Fig. 4 – Injection pump

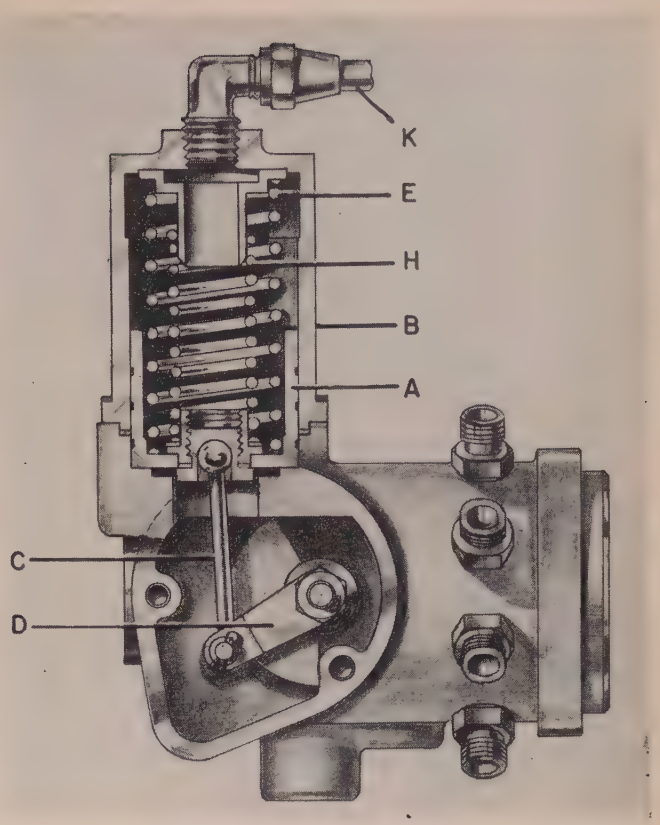

Fig. 5 – Injection pump control

ered by the sleeve, and fuel is then forced through delivery valve *J* and out through distributing slot *G* to a nozzle line. Injection continues to the end of the stroke, and the cycle repeats for an adjacent outlet.

The injection pump therefore has variable beginning and constant ending of injection.

Injection Pump Control

This control (Fig. 5), mounted directly on the injection pump, receives control pressure from the mixture control through tube *K* and translates it into an angular movement at the metering shaft of the injection pump. The control consists of a piston *A* operating in cylinder *B* and biased against control pressure by springs *E* and *H*. Piston *A* is connected to metering control lever *D* by link *C*. At high control pressure corresponding to low manifold vacuum (wide open throttle) piston *A* is moved down toward maximum fuel position (shown) by outer spring *E*. As engine speed increases, the control pressure is reduced, and piston *A* is forced upward against spring *E* at a constant rate until free inner spring *H* reaches its seat, at which time spring *H* adds its effect to spring *E* and the rate of piston travel with change in control pressure is reduced.

Since piston *A* is mechanically linked to pump metering control lever *D*, the fuel quantity injected per pump stroke is a function of control pressure applied to the piston. The relation of this control pressure to injected quantity per stroke required by a particular engine is shown in Fig. 6.

Injection Pump Drive

Although any one-half-engine-speed drive may be used, we have found it both practical and expedient on the stock engine to obtain the injection pump drive from the ignition distributor driveshaft.

As shown in Fig. 7, an adapter *A*, housing a right-angle gear drive *B*, is interposed between the camshaft drive and the ignition distributor. The ignition distributor *C* mounts on the top of the adapter, and the injection pump *D* mounts on the side. The injection pump is driven by the cross-shaft through coupling *E*. The face-cam fixed roller *H* is also carried by the adapter.

Lubrication of the injection pump drive gears and the face-cam and roller is with engine oil, the

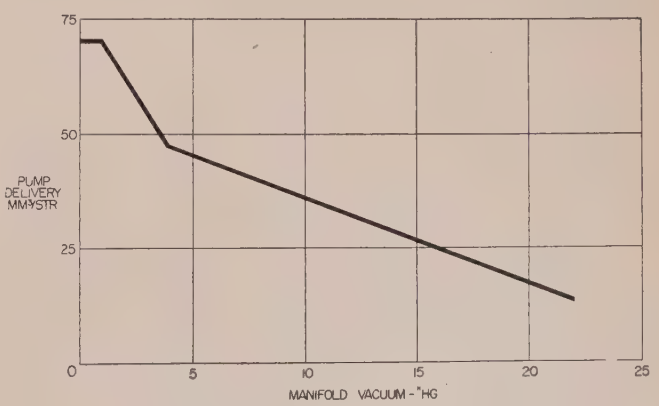

Fig. 6 – Injected quantity per stroke versus control pressure

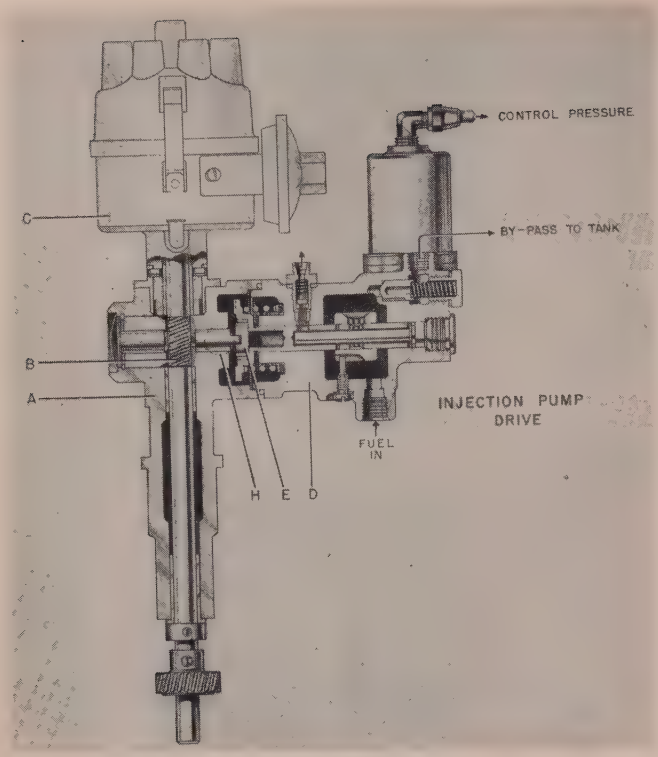

Fig. 7 – Injection pump drive

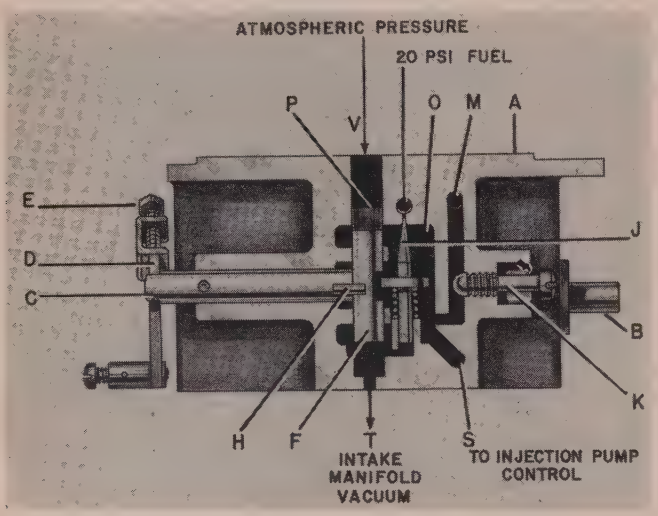

Fig. 8 – Mixture control

return being through the adapter to the engine cam section.

Mixture Control

The mixture control in its basic and simplest form is merely a manifold pressure control and throttle-body with a chamber feeding a modified manifold pressure to the injection pump control during cold starting and idling.

A section of the mixture control is shown in Fig. 8. In this view the throttle plates mounted on shaft *B* are not shown but are of conventional design with an idling port just above the closed throttle position and connected to passage *M*. The valve positions shown correspond to a cold engine condition. Since a cold engine requires excess fuel during the warmup period and since the injection pump meters to a control pressure curve, the control pressure must be raised during warmup to increase the pump delivery. This enrichment is accomplished as follows:

A control chamber *O* is formed in the throttle-body casting and is connected at *S* with the injection pump control. A vertically slidable valve *F* operates within a passage between upper- and lower-deck pressures. When the valve *F* is in its lower position as shown, the pressure in chamber *O* is between that of *V* and *T*. When the valve *F* is in its upper or normal running position *P*, the chamber pressure is that of *T* or manifold pressure. The injection pump therefore delivers additional warmup fuel to the engine until valve *F* reaches position *P*.

Valve *F* is operatively connected through pin *H* and eccentric shaft *C* to a lever which also carries a fast-idle cam *D* cooperating with a throttle idle adjustment screw *E*. The lever itself may be actuated by a manual choke wire or an automatic operator responsive to exhaust or water temperature.

In order to insure good cold starting of the engine, a fuel flow considerably greater than the full-load quantity is required. This quantity of two to three times full-load value could be provided by using an injection pump large enough to supply it. The size and cost, however, of such a double- or triple-sized pump makes it necessary to use other means of cold priming. Since supply fuel at a pressure of 20 to 30 psi is available as soon as the ignition key is turned on, a convenient source of pressurized fuel is at hand and may be used for priming. A spring-loaded priming valve *J* mounted adjacent to warmup valve *F* is held normally closed on its seat against fuel supply pressure by a spring. An extension on valve *J* engages in a slot in valve *F* so that in the cold position a slight additional movement of shaft *C* allows valve *F* to engage priming valve *J* and open it. Fuel then is discharged into the

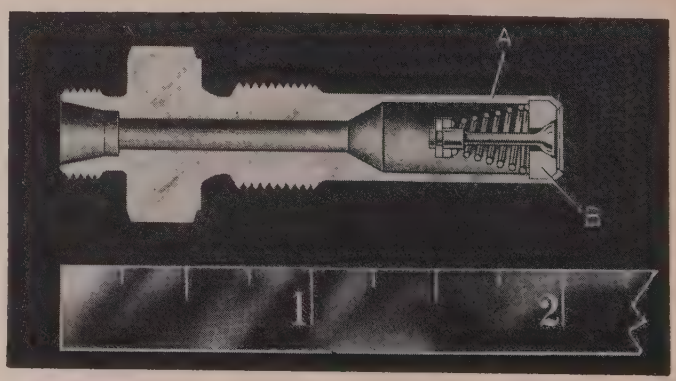

Fig. 9 – Spray nozzle

control chamber and enters the intake manifold through passage *T*. The additional movement of shaft *C* necessary to actuate the primer valve *J* may be furnished conveniently by a small solenoid acting through the heat-responsive element and energized by the electric starter circuit. By having the primer solenoid act through the heat-responsive element, priming is prevented on any hot restart.

The idle airflow is adjusted in the usual manner by screw *E*. The idle mixture is adjusted by screw *K* which at idle receives inlet air pressure through idle slot *M* and modifies the control-chamber pressure. Above the idle setting the throttle plate edge rises above the idle port, the idle port becomes manifold pressure, and the screw *K* has no effect on engine mixture.

Nozzle

The spray nozzle used is a simple outwardly opening poppet type as shown in Fig. 9. It consists of a valve assembly *B* rolled into a holder *A* which is available in several lengths to satisfy the various engine and manifold requirements. Opening pressure is a nominal 70 psi, and atomization is very good at all quantities due to the floating and self-aligning pintle action.

Fuel Filter

The fuel filter, Fig. 10, is especially designed for gasoline use and consists of a steel enclosure *A* and filter element *B*. The filter element is built up of alternate layers of high-wet-strength paper and fiber spacers and provides 2-micron filtering of the fuel. Service life is approximately 30,000 miles of normal car operation.

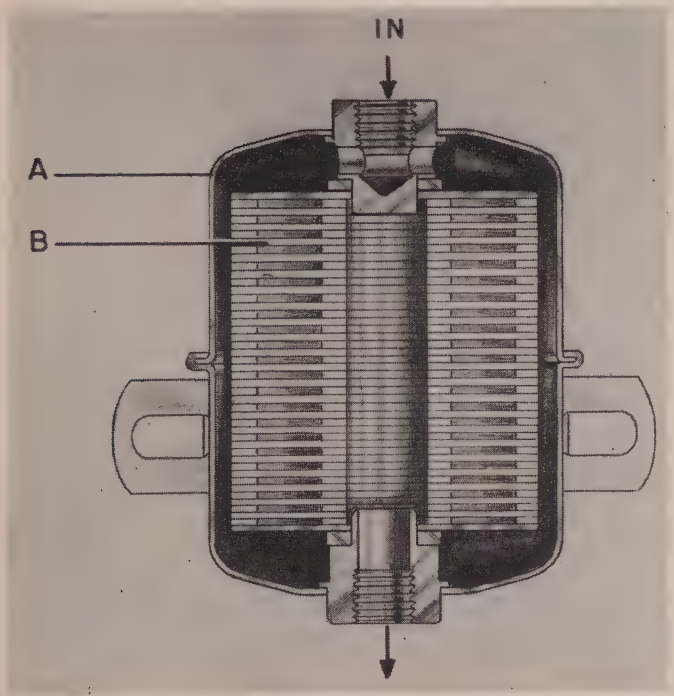

Fig. 10 – Fuel filter

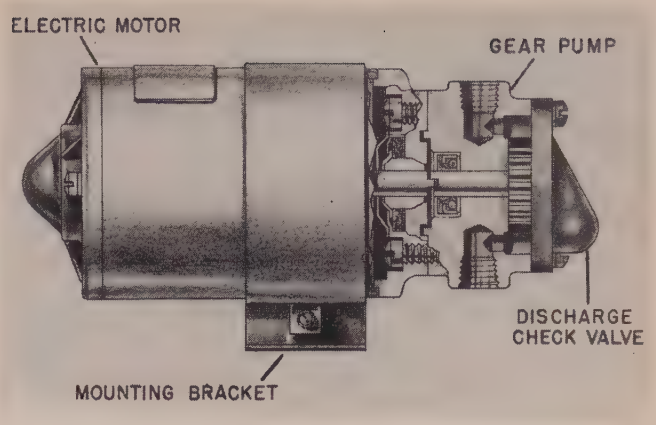

Fig. 11 – Fuel supply pump

Fuel Supply Pump

The fuel supply pump, Fig. 11, consists of an electric-motor-driven gear-type pump with a discharge check valve which retards the decay of pressure in the system during a temporary engine shutdown. A pressure-regulating valve built into the injection pump holds system pressure to a nominal 20 psi.

Performance

Because gasoline injection can increase styling freedom, as by allowing lower hood lines, and because in other respects it will have value as a sales feature, there are those who say that its performance need only equal that of a carburetor. As engineers, we will appreciate that performance must be better than a carburetor if gasoline injection is to have any wide acceptance over a long period. There have been many claims made of startling economies to be realized by the use of gasoline injection on a stock engine. We have not yet had an engine specifically designed to take the greatest advantage from the use of gasoline injection for our testing. We can say, however, that with the stock carbureted engine which has been converted to gasoline injection the following important advantages are realized:

1. Full-throttle horsepower output is increased 10% at rated speed.
2. A decrease of at least 500 rpm in the torque peak position is obtained.
3. An improvement of 5 to 15% in miles per gallon can be realized in road-load performance, as shown in Fig. 12.
4. Higher-vapor-pressure fuels may be used because of the pressurized fuel system. The use of such fuels with their higher octane rating reduces the tel requirement and promotes cleaner burning and a reduction in combustion-chamber deposits.
5. Higher-end-point fuels may also be used be-

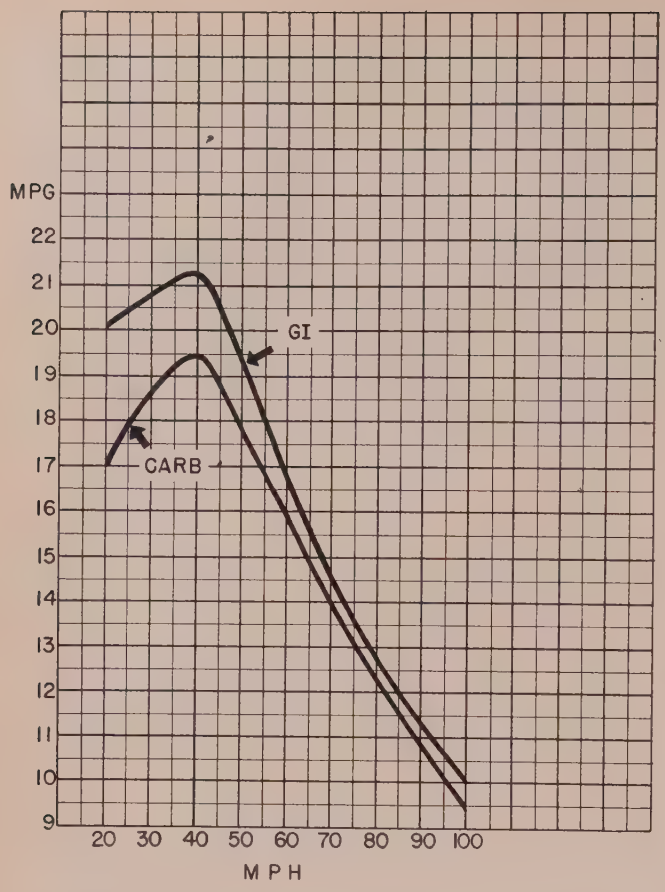

Fig. 12 – Road-load performance of 300 cu in. V-8 engine

cause atomization and distribution are not dependent on the induction air.

In addition, the intangible performance factor which might be labeled "liveliness" is improved because of the instant response of the engine to fast or slow throttle movements. Because of the absence of heat on the intake manifold some mechanical octane advantage is gained and the spark

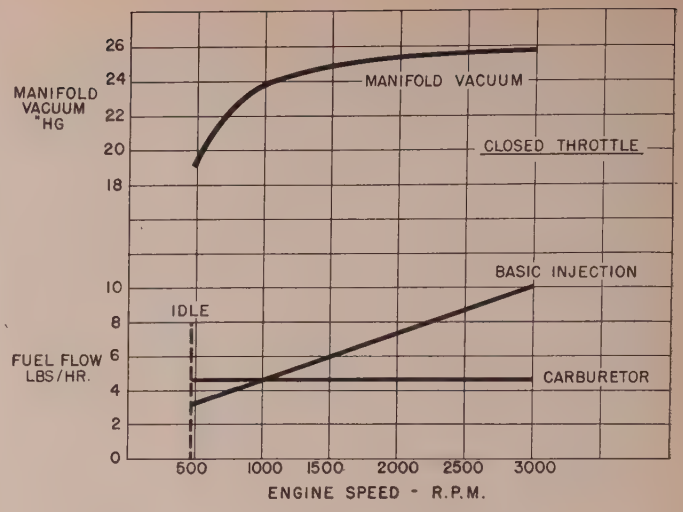

Fig. 13 – Basic deceleration fuel flow, engine 14

timing may be advanced considerably without any detonation occurring in the engine.

System Modifications

Deceleration Fuel Controls – Attention has recently been directed to the unburned hydrocarbons present in the exhaust of a decelerating engine. There is considerable evidence to indicate that these exhaust products may contribute to the formation of smog. Certainly these unburned gases are wasteful of fuel.

Full or partial cutoff of fuel flow during deceleration can be automatically accomplished in the gasoline injection system by several methods.

A well-adjusted carburetor will maintain idle fuel flow during deceleration regardless of engine speed or manifold pressure (Fig. 13). A basic injection pump, however, is set to deliver idle fuel of X cu mm per stroke at idle manifold pressure. Therefore under deceleration conditions and with quantity per stroke held constant, the *total* fuel flow is a function of engine speed. Since deceleration manifold pressures can only reduce the injec-

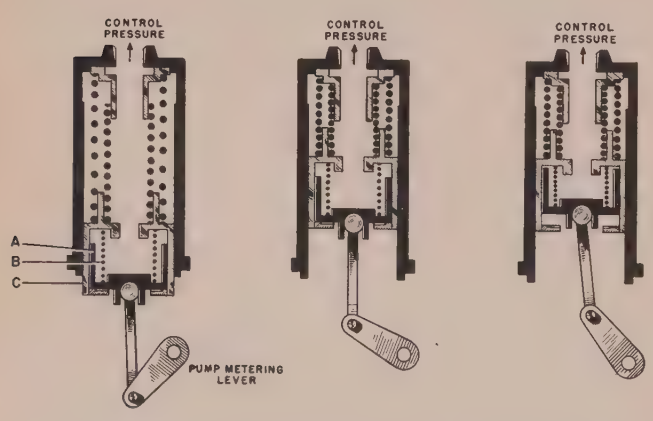

Fig. 14 – Fuel cutoff device; (left) full throttle, maximum fuel, 0 in. of Hg manifold vacuum; (center) idle, idle fuel, 21 in. of Hg manifold vacuum; (right) deceleration, no fuel, 25 in. of Hg manifold vacuum

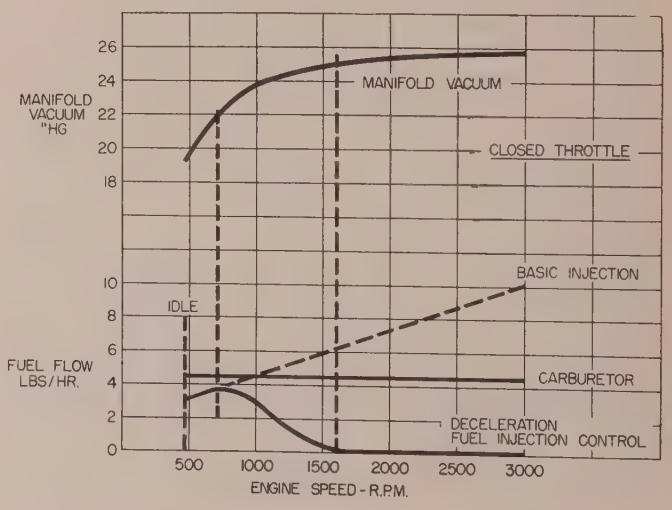

Fig. 15 – Deceleration fuel flow control, engine 14

tion pump quantity per stroke to a little below idle quantity, a curve of the basic pump delivery in total flow will be somewhat as shown.

In order that total deceleration fuel flow be reduced, it is therefore necessary to reduce the pump setting by some means which will move the pump metering control toward cutoff in the 22 to 25 in. of Hg manifold vacuum range. One such device is shown in Fig. 14 and represents complete fuel cutoff at 25 in. of Hg manifold vacuum. It consists of an auxiliary piston *A* biased by a low-rate spring *B* which balances the piston force at 22 in. of Hg manifold vacuum. Piston *A* is mechanically linked to the pump metering lever and is carried within pump control piston *C*. During normal operation from idle to full throttle, piston *A* moves with piston *C* as a unit. When engine deceleration occurs and manifold vacuum exceeds 22 in. of Hg, piston *A* moves upward within piston *C*, and the fuel pump metering lever is moved into the fuel cutoff position. A curve of fuel flow under this deceleration fuel control condition is shown in Fig. 15.

Density Corrections – Since the force required to move the pump metering control is extremely low, altitude and temperature compensation can be obtained by the insertion of capsules in the link joining the pump control piston and the pump metering lever. It is planned, at present, to specify these inputs only on the truck engine application where economy is the most important factor in vehicle operation.

The gasoline injection system described has been used only on "stock" engines. It is probable that with engines designed for use with a fuel system of this type at least 25% more output horsepower can be obtained from the same displacement. In addition, the mechanical octane improvement may be used further to increase compression ratios for still better output and economy.

The advantages to the fuel producer in the event of widespread use of gasoline injection are definite and important, since fuels of higher Reid vapor pressures or higher end point or both may be properly used in the gasoline injection engine.

DISCUSSION

Discusses Fuel Injection Control in Detail

– H. M. Gammon
Thompson Products, Inc.

THIS discussion will deal primarily with the subject of control with emphasis on the speed-density system or the general type of control described by Mr. Miller. As a preliminary to more detailed discussion of fuel injection control, the control problem is defined:

Supply fuel on the basis of engine air consumption:

1. By direct effect (venturi, pitot, and the like).
2. By use of operating parameters associated with air consumption (engine speed and manifold pressure).

Provide extra fuel for:

1. Starting and warmup.
2. Idling.
3. Maximum power.
4. Acceleration.

Provide less fuel or cutoff for:

1. Deceleration.
2. Downhill braking.

How does the venturi carburetor fulfill these requirements of control? Fig. A shows that the basic response of the simple venturi will not provide a constant air/fuel ratio over a range of airflow rates. There is a distinct tendency to enrich at higher airflows and, hence, the necessity for air bleeds to push up the end of the curve. In order to provide for maximum power enrichment, idling enrichment, starting enrichment, and acceleration enrichment, various compromise devices are superimposed on the venturi to bias the signals or venturi characteristics. However, to modify or bias the venturi signal or the signal linkage, and still have sufficient control force to regulate properly the injection pump, involves expense that seems quite high.

Fig. B shows how two production carburetors supplied fuel to a modern V-8 engine with respect to the engine fuel requirements. These carburetors were picked at random; and while it is recognized that they could be modified to match the engine more precisely, this is what was found in laboratory tests. Note the overrichness below 2400 rpm and lean mixtures above 2400 rpm. At 20 in. of Hg manifold pressure, at 1600 rpm, the enrichment is 5 lb per hr.

It appears that the speed-density control offers improved control in fuel injection at low cost. Further, if a venturi is used to measure airflow in order to control a fuel injection system, the induction system may possibly be compromised. There is an appealing promise of substantial power increases from pressure-wave reinforcement in air ducts that do not have to carry fuel as well as air. Hence, if the venturi is eliminated, the way will be opened for greatly improved air ducting without complication in the design.

But just how well will a speed-density system do the job?

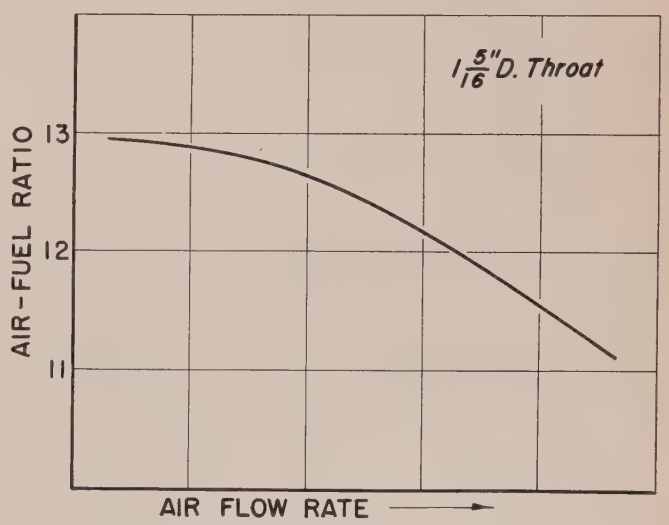

Fig. A – Effect of airflow rate on air-fuel mixture, using simple venturi

First of all an injection pump is required that will provide, at a given setting, the same fuel charge regardless of speed. Fig. C shows how two different types of injection pumps compare. One type was most excellent while the other was fairly satisfactory up to about 55% of capacity. A second requirement for a good speed-density system is an engine that has characteristics of a good air pump, if manifold pressure is to be used as a control parameter. Fig. D shows the volumetric efficiency of a modern overhead-valve engine compared with an older L-head V-8. Note that the modern engine has a volumetric efficiency curve that is almost a straight line. Hence, it is shown that the present V-8 has the characteristics needed for good speed-density control. But air consumption should be some dependable straight-line function of manifold pressure in the engine operating range. In Fig. E are actual air-consumption curves from a very excellent modern V-8 engine. Note that the straight-line function does exist. From these curves, it is concluded that a speed-density or speed-manifold pressure control is a most reasonable choice.

A major question in answering the fuel injection control problem is whether or not compensation should be made for altitude and air temperature. From an engineering standpoint we would recommend compensation, but from a cost standpoint, the engine builders may be forced to forego the advantages of compensation. Fig. F shows how air/fuel ratio is influenced by altitude. In the East we tend to scoff at altitude effects, but in the western part of the country a very definite problem exists. At 10,000 ft the air/fuel ratio can become rich by 3½ ratios without altitude compensation. As a matter of fact between 28 and 30 in. of Hg atmospheric pressure, there is ¾ of a ratio change. As for temperature, we see in Fig. G that the air/fuel ratio goes rich by 2 ratios in about 60 F with saturated air.

The acceleration problem deserves special attention be-

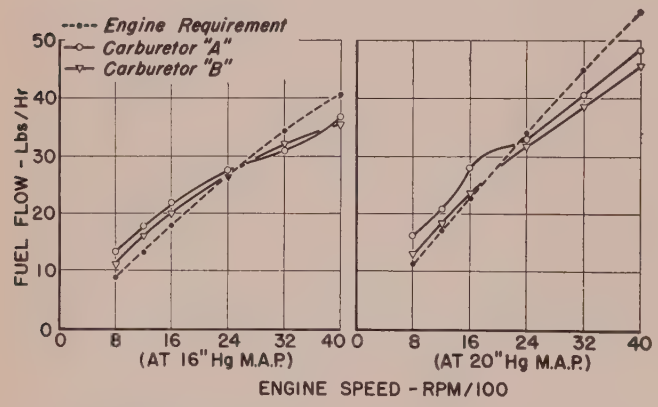

Fig. B – Carbureted fuel delivery contrasted with ideal requirements

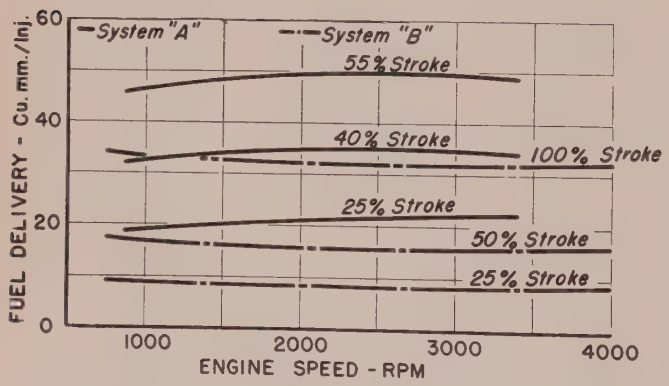

Fig. C – Delivery characteristics of two fuel injection metering distributors at several load conditions

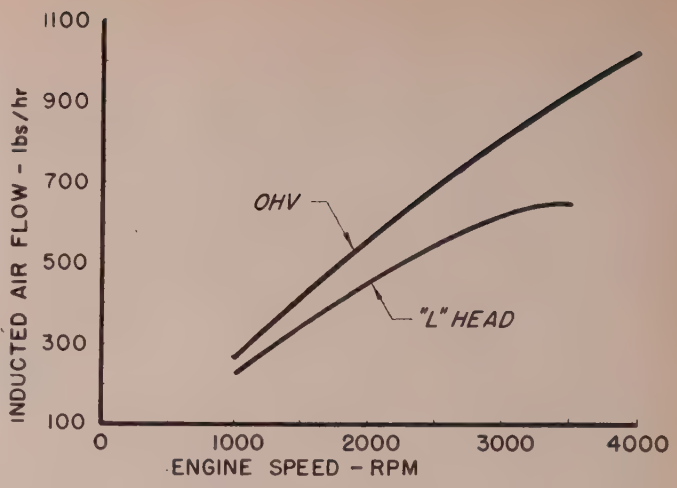

Fig. D – Air-breathing characteristics of overhead-valve versus L-head engine

cause if there is one characteristic that today's engine builder must retain, it is stoplight performance. Fundamentally, if the control system has zero time lag, there is no requirement for an accelerating device. When the throttle plate is opened, the intake port mixture goes to a lean condition unless full power fuel is provided instantly. An enriching bias may very well be needed with fuel injection systems because zero time response may not be commercially practical. Time will tell just how much lag the public will accept. We have had direct experience in this area and have found that an accelerating device can be simple and inexpensive – possibly less expensive than the cost of low inertia control.

One of the outstanding advantages of fuel injection is the ease of providing fuel cutoff for coasting and deceleration. Mr. Miller has described a simple and effective method in his paper. With carburetors it does not appear practical to cut off the fuel during deceleration because of the restarting problem with a dry manifold.

In review, experience in this field leads to the following statements:

1. Manifold pressure is a practical approach to fuel injection control.
2. Atmospheric pressure compensation is needed and can be provided at small expense.
3. Air temperature compensation is desirable.
4. A means will probably be required to offset the control system lag for proper acceleration response.
5. Deceleration fuel cutoff is necessary and can be provided in a practical manner.

Hopes for General Adoption Of Gasoline Injection Engine

– W. S. Dack
C. A. V. Division of Lucas Electrical Services, Inc.

FOR a number of years, I have been a great enthusiast for gasoline injection and was, in fact, responsible for the development of the Thornycroft truck-type gasoline injection engine in England in 1946. This engine received considerable publicity, not only in Europe but also in the United States.

Mr. Miller's paper concerns a new design of injection pump, coupled with its accessories for use with a gasoline engine; therefore, engine problems have been excluded, and my comments will concern only the injection equipment.

Earlier efforts by various people not only in the United States but in Europe have all died an unnatural death.

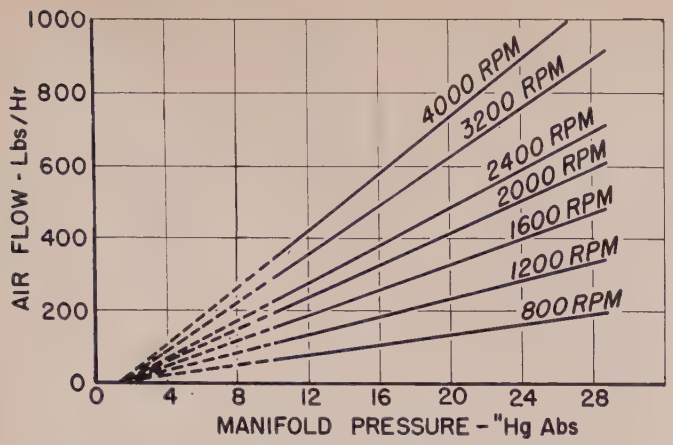

Fig. E – Airflow versus manifold pressure for typical V-8 engine

While being so very successful technically, all have eventually failed commercially because of the high cost of the injection equipment, which has always been based upon designs suitable for diesel engines. For myself, I have never agreed that the high cost of the equipment should have been a deterrent to its development since, based upon results which I have obtained, such cost would have paid for itself by lower running costs in one to two years based on mileages in England. In this country such mileages would be covered in a very much shorter time. I had always hoped that some farsighted engine manufacturer would have put out a number of engines in the field to gain experience and to promote its general adoption.

The author's company is to be congratulated on its efforts to manufacture a gasoline injection package at a much lower cost than hitherto and will thus promote the adoption of the gasoline injection engine which is so long overdue.

On Fig. 5 it will be noted that there are two springs in the injection pump control, the outer spring being in operation only at full injection. It is not until there is a manifold vacuum of approximately 4 in. of Hg that the second spring comes into operation, so that there is a quick relative weakening of the mixture just below full throttle opening.

This is shown very well on Fig. 6 where at full throttle there is a relatively rich mixture to give full power, but when the throttle is closed there is a very considerable weakening of mixture at about 4 in. of Hg which continues right down through the throttle range of what could possibly be known as the cruising range. This curve extends down to approximately 22 in. of Hg where idling takes place. This control is very similar to the one which was used by my own company on the Thornycroft engine, but we found that it was necessary to enrich the mixture slightly at about 19 in. of Hg manifold vacuum in order to get more stable idling. This, of course, is quite a common feature with carburetors.

In starting from cold, the gasoline injection engine has a particular advantage over the carburetor engine. Since fuel is injected near the inlet valve, deposition on manifold walls is minimized; therefore, the overall fuel/air ratio to give an ignitable mixture in the cylinder can be much less than that required with a carburetor. Furthermore, the carburetor engine relies on manifold heat to assist vaporization which is nonexistent under cold-starting conditions. The gasoline injection engine is not dependent upon these conditions and atomizes the fuel mechanically assisted by greater heat derived during the compression stroke by reason of such engines being able to run on a higher compression ratio. Therefore, the starting conditions on a gasoline injection engine conform much more closely to running conditions. In my previous experience, I did not find it necessary to use any device for excess fuel for cold-starting purposes since full-load injection could take place with the butterfly closed during the early cranking period. It must be admitted, however, that the cold-starting conditions were not very low and took place at about 32 F. I note that the author requires two to three times the full-load value to provide starting under conditions of extreme cold. This is probably because priming takes place at the same position on the intake manifold as a carburetor with all the disadvantages which go with it.

I notice that the spray nozzle is a simple outwardly opening poppet type but that the needle does not have any guide. I would imagine that the spray could possibly be directed mainly to one side because of irregularities in the spring action. We have found it necessary to guide this needle valve to insure uniformity of spray, and we make quite a feature of the needle oscillating rapidly during the injection period in order to insure good pulverization of the spray.

In my study of the author's paper, I should like to raise a few questions.

Calibration

I have run out a few rough calculations using the diameter of the plunger at ⅝ in. With such a plunger 0.001-in. stroke would correspond to a displacement of about 5 cu mm. Taking the case of an 8-cyl engine of about 305-cu in. capacity, the full-load requirements would be some-

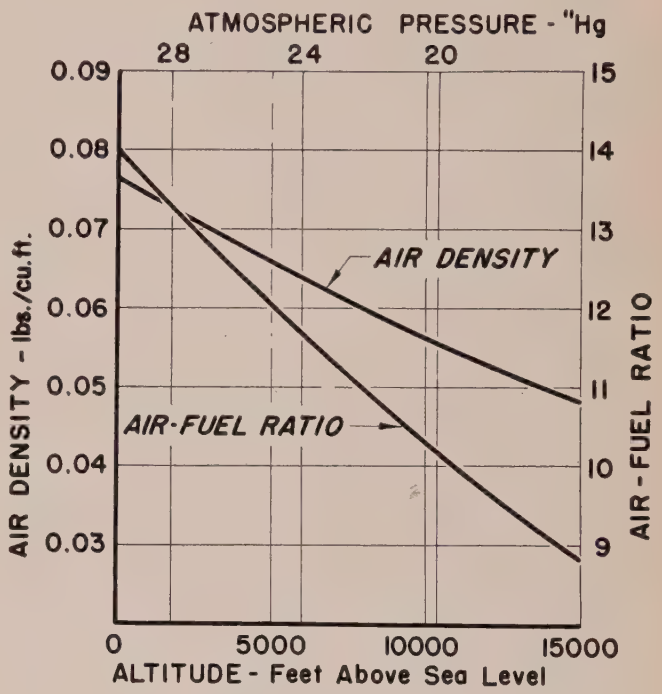

Fig. F – Effect of altitude on air/fuel ratio

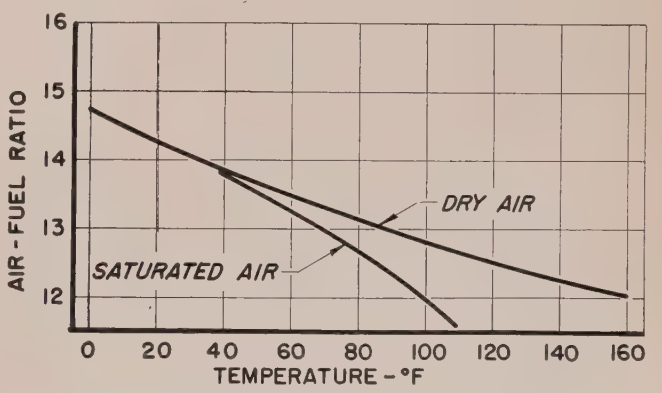

Fig. G – Injected engine without temperature compensation

where in the region of 60 cu mm per stroke. From this it can be seen that a variation of 0.001 in. in the lift of the cam or a corresponding variation in the squareness of the control sleeve end would immediately be responsible for variations in delivery of 8% of the full-load quantity. At light loads the situation would become correspondingly worse, and at idling the variation might amount to as much as 40% of the delivery.

It would be interesting to know the line-to-line variation over the speed and load range. Also, what are the delivery characteristics of the pump? Does it have a rising or lowering delivery characteristic as speed increases? Is it possible to produce whatever characteristic is required, and have any difficulties been experienced in matching the full-load output curve to the volumetric efficiency of the engine?

Injection Period

One of the problems of any distributor pump, especially in the case of an 8-cyl engine, is the very short injection period at the pump. In the case of an 8-cyl pump this can never be more than 22½ deg and in practice is more likely to be between 10 and 15 deg (30 deg flywheel). My own experience with gasoline injection indicates that a very much longer injection period is beneficial, something in the order of 80 deg flywheel; but, of course, this may be subject to variation because of engine characteristics.

Should the engine characteristic require a long injection period, how would the author overcome this problem? Could the author tell us whether the discharge from the nozzle is deliberately throttled in order to extend the injection period; if so, what is the variation in this period over the operating speed range?

Lubrication

In Fig. 4 there does not appear to be any provision made to lubricate the plunger shaft where it rotates in the pump housing. I notice that the plunger is provided with a relief groove back to the fuel supply sump, but since this is under pressure at 20 psi from the electrically driven feed pump, it would appear that this has been done purposely to provide lubrication with gasoline to the plunger shaft within the pump body. There appears to be no provision to seal against this pressure, and I would imagine that appreciable leakage past the plunger at the drive end would take place. If this does happen, it will find its way into the ignition distributor drive and could have disastrous results. This could be further aggravated by the use of a single roller for operating the cam which must produce a side thrust on the plunger.

Could the author enlarge on the subject of the lubrication of the pump and what provision is made to prevent excess leakage into the engine and whether there is adequate lubrication against the side thrust produced by the single roller? Alternatively, is leakage allowed to take place along the plunger shaft but is trapped and returned to the tank, although such is not shown in the diagram?

Delivery Valve

Fig. 4 shows a delivery valve interposed between the pumping chamber and the distributor port. Fig. 7, on the other hand, shows a valve in each delivery line.

Could the author say which is the later construction and what were the reasons which led to the necessity for the delivery valve?

Cold Starting

In describing the starting arrangements, the author states that the priming valve is opened by a temperature-responsive element so as to give a direct supply of gasoline to the manifold with cold starting. As described in the paper, this would result in an uncontrolled discharge of gasoline into the manifold in the event the ignition is left switched on with the engine stationary.

Would the author say how this possibility is prevented, and is there some further connection in the electrical circuit not shown on the slides which insures that this is only operative during cranking or engine rotation? Could the author give us a direct comparison between gasoline injection and the carburetor when starting under conditions of extreme cold?

Mixture Control

It is noted that the author has employed a piston as the pressure-responsive member in the pump control unit, whereas in similar designs a diaphragm is usually used. Because troubles are frequently experienced on carburetors containing such sliding parts, there would appear to be danger of sticking which could result in the mixture to the engine becoming totally upset.

Could the author give his reasons for the choice of a piston for this purpose and indicate whether any special materials are employed or lubrication arrangements made to prevent trouble in service because of sticking?

Cost

The system as described by the author, while undoubtedly being cheaper than some other efforts we have seen in the market, would appear nevertheless to be still quite a costly piece of apparatus. This is made particularly so by the necessity for a motorized feed pump.

Would the author be prepared to indicate the relative cost of the system he has described with an equivalent carburetor installation for a similar type of engine?

General

Undoubtedly the author has applied his scheme to various engines in this country, and, therefore, he must have amassed a considerable amount of technical data as to the reaction to gasoline injection from both large and small engines. Furthermore, in order to sell engine makers on this gasoline injection system, substantial gains in power output and in improved consumption must be made in order to offset the increased cost over the carburetor.

Could the author give us some examples of power curves in various sizes of engines showing extra power obtained for lower consumption? Also, do injection characteristics change substantially when engine size or differences in combustion-chamber shape or both are encountered?

Need Better Utilization Of Petroleum Resources

– H. S. Kelly
Socony Mobil Oil Co., Inc.

FROM the point of view of its effect on the petroleum industry, the development of a practical method of gasoline injection for passenger-car engines should present definite advantages, provided injection permits more flexibility in gasoline vapor pressure and end point than carburetion.

It is the purpose of these comments to present two facts bearing on gasoline refining which must be recognized in any automotive development which meets the objective of continued and, if possible, increased efficiency in the utilization of our petroleum resources.

Vapor-pressure specifications affect the amount of butane which the refiner can incorporate into gasoline. The properties of butane may be of interest. They are 60 lb Rvp, over 100 octane number, and favorable stability and combustion characteristics. Table A illustrates how higher vapor pressure affects gasoline quality and quantity. An increase of only 1.5 lb Rvp increases production by about 3% and octane number of a typical regular grade gasoline by 0.4 octane number. This increase in octane is in addition to all other methods of improving octane by tel or by more expensive refining.

The supply of butane is increasing steadily both through refining and as a byproduct from natural-gas production.

Both catalytic cracking and catalytic reforming, the two basic refinery processes for increasing octane number, produce more butane than can be directly utilized in today's gasoline. The efficient utilization of butane is one of the keys to efficient utilization of our petroleum resources.

Higher end points are also important to the gasoline refiner because of the connection between end point and octane number of catalytically reformed gasolines. Catalytic reformers of one type or another are being installed at most United States refineries. They offer the most practical means of increasing motor gasoline octane number above today's levels.

Table B shows the yield-octane distribution of a typical catalytically reformed gasoline. The highest octane portion, by far, is that boiling over 320 F. The proper utilization of these higher boiling portions of catalytic reformate is another key to future quality trends in motor gasoline. However, any trend in this direction for greater power and economy will have to be balanced against possible adverse effects on combustion-chamber deposits. Even in the absence of developments in gasoline injection, this subject will warrant considerable study during the coming few years.

Summarizing, there is a real engineering need for higher-vapor-pressure and end-point gasoline specifications for efficient utilization of our petroleum resources. Gasoline injection may be the answer to this need. However, any advantage to the petroleum industry along these lines will be realized only very gradually, since commercial brands of gasoline will have to continue to meet the needs of the 50 or more million carburetor-equipped cars now on the road.

Table A – Importance of Vapor Pressure

	Average Gasoline	With Additional Butane
Reid Vapor Pressure, psi	11.0	12.5
Volume, %	100	103
Distillation Temperature, F		
10% Evaporated	115	108
50% Evaporated	210	207
90% Evaporated	340	338
Octane Number (with 3 cc tel per gal)	90.0	90.4

Table B – Yield-Octane Relationship of Typical Catalytic Reformate

Boiling Range, F	Yield, %	Octane Number (with 3 cc tel per gal)
Below 200	20	94
200 to 320	60	98
Over 320	20	104

Dirt, Corrosion are Important Problems in Injection Systems

– C. J. Livingstone
Gulf Oil Corp.

THERE has been a great deal of discussion regarding the merits of fuel injection in regard to its effect on automotive gasoline production. It has been pointed out many times that the end point and vapor pressure of gasoline can both be significantly increased with a saving in octane numbers and a reduction in tel content, while at the same time engine octane requirements can be reduced with the use of fuel injection. From an oil company standpoint, these are all very desirable objectives, but I am rather skeptical as to how much direct advantage we can gain from them. In regard to the reduction in octane requirement, from past experience we would expect that the automotive designer would take advantage of any such reduction by increasing compression ratio until the octane requirement of the engines approximated the octane quality of the best commercial fuels available. Consequently, we would not expect the lead content of the fuel to be reduced because of fuel injection engines as suggested by Mr. Miller. However, if compression ratios were increased, the car owner would benefit either by improved performance or better fuel economy.

Mr. Miller has pointed out the improvement in vapor-handling characteristics in the Bosch fuel injection system over the normal carbureted engine. However, it should be borne in mind that in the system described by Mr. Miller, fuel is fed to the injectors by an electric-motor-driven gear pump which recirculates fuel back to the gasoline tank. When a similar method of supplying fuel to the carburetor is applied to the carbureted engine, considerable improvement in vapor-handling potential can be expected. Consequently, we would appreciate the author's comments as to how much of the improvement in vapor-handling characteristics is due to fuel injection itself or to the method of delivering the fuel from the tank. While recirculating-fuel systems have been quite successful in reducing vapor lock when applied to carbureted engines, our experience indicates that part of their efficiency results from weathering the gasoline in the fuel tank because of agitation and heat. We know of one instance where gasoline in the main fuel tank of 13 lb vapor pressure was reduced to 5 lb within a half hour of operation. It would not make sense to add extra butane to gasolines unless the consumer could expect to burn it in his engine, and I feel it would be undesirable to supply him a gasoline that would be quickly weathered in his fuel tank, with resultant loss in economy and air pollution. We do feel that a fuel injection system would minimize the hot-fuel handling problems, such as hard hot starting and hot stalling, which are associated with overrich conditions in a carbureted engine.

The reason for maintaining the 90% point and end point of present-day gasolines at relatively low levels is not primarily because of distribution problems in the carbureted engine. Engine deposits, spark-plug fouling, and crankcase dilution are serious problems with high-boiling-range fuels, and not until it is demonstrated that a fuel injection engine with or without deceleration fuel control will handle the higher boiling fuels as well as, or better than, the carbureted engines, will we be able to decide whether or not the end points of gasoline can be significantly increased.

Fuel injection could affect the midrange volatility of automotive gasolines to a significant extent. Since engine warmup problems will probably be reduced considerably with fuel injection, it is quite possible that the 50% distillation point can be increased significantly, allowing the refiner to use components now restricted by the 50%-point limitation. Regardless of the 50% distillation point range, one definite advantage of fuel injection would be the elimination of the carburetor icing problem.

I would also like to point out that in order to take advantage of possible decreased volatility requirements of fuel injection engines, such fuels cannot be made available until the number of engines on the road is adequate to justify the distribution of the fuel. Of course, as the overall car requirements move in a certain direction, the oil industry can take advantage of any trend either in higher vapor pressures or higher boiling requirements, whether with fuel injection engines or carbureted engines. Due to the large number of cars involved and the large quantities of gasoline used, these trends should be slow rather than revolutionary.

While Mr. Miller does not anticipate any difficulty in handling dirt from contaminated gasolines in fuel injection systems, it is a matter about which we feel some concern. Our experience with aircraft and other engines using fuel injection leads us to believe that a great deal of care will

have to be taken in order to keep dirt out of the fuel injection equipment. Automotive gasolines are not dispensed through the same type of filtering equipment that is used in aircraft tenders, and the chances of contamination of the fuel tank itself by dirt and dust is much greater in automotive vehicles than in aircraft. There is also the matter of corrosion of the injection equipment, and it is believed corrosion here is much more serious than it is in carbureted systems. However, the increasing use of antirust agents in automotive gasoline should be beneficial in protecting the injection system against rusting, as well as providing a cleaner gasoline to the automobile tank through the control of rust in the distribution system of the fuel supplier.

Increased Fuel Necessary During Warmup and Driveaway

– E. W. Downing
Joseph Lucas Ltd.

MOST pump engineers will agree that their problem is rarely an inability to deliver liquid but always to get it into the working chamber where work can be done upon it. This point has obviously been appreciated in the pump design described here, and I shall be interested to know up to what maximum speed the pump will operate satisfactorily with the 20 psi input fuel pressure. The mixture control is clearly of a very simple type, and with continued development it may be possible to build in certain other desirable characteristics.

The excess fuel control of Fig. 8 is almost identical with the type that we used initially in our experiments, but we found this to be unsatisfactory during the warmup and driveaway period because it cannot deliver to the engine any more fuel than is available at full throttle. We consider it essential for an excess of fuel above normal full-throttle fuel to be available during the driveaway period when, because of friction horsepower of the engine and transmission is high, full-throttle operation is required. Can the author state what their experience is on cold starting and driveaway with this device?

The author has suggested that higher end-point fuels may be used, but in our experience which was with kerosenes on vaporizing oil tractor engines, so much heat had to be added to the incoming air to assist in the final vaporization of the fuel (in addition to the "pressure atomization") that we were still down on power output of the engine. Did the tests referred to on the stock carbureted engine show any improvement in power or economy when higher-end-point fuels were used?

Finally, I feel that Mr. Miller is too optimistic in suggesting that at least 25% more output can be obtained from the same size engine by the use of a gasoline injection system. In our experience, if the engine is well carbureted and has a reasonably sized induction tract, we should not expect the improvement in power to be more than 8-10%.

No Marked Improvement in Vapor-Handling Properties

– N. R. McManus
Ford Motor Co.

THE development work being conducted by our company on various gasoline injection systems has indicated general concurrence with the existence of many of the combustion and control problems discussed. The often-expressed theory that the condition and form of the fuel fed to an engine cylinder by a spray nozzle was unimportant has repeatedly been proven false. Likewise, the adaptation of gasoline injection to a carbureted engine involves much more than the mere substitution of an injector pump for the carburetor. Results indicate that comparatively small gains in performance and economy can be realized by such a substitution. The greatest gains will be achieved only after an engine is designed around a flexible and reliable injection system. Considering the state of development of current V-8 engine carburetion systems, the development of such an injection system alone presents quite a challenge.

Our experience indicates that an injection-equipped engine exhibits some marked differences in fuel requirements from those of a carbureted engine. Tests show that both the shape of the octane requirement curve over the speed range and the engine response to commercial-type sensitive gasoline are different. Appreciable gains in mechanical octane number have not been evident, but should such gains occur, they will be used to permit higher compression ratios.

We have not been able to substantiate any marked improvement in the vapor-handling properties of injection systems. The requirement for maintaining solid fuel in the injection pump, lines, and nozzles, all located in a hot engine compartment, is difficult to achieve with present fuels. Higher-vapor-pressure fuels would only aggravate this condition. Most injection systems also require a tank return line for spill and excess delivery pump fuel. This creates a problem of retention of the light ends when this fuel is returned to the tank. A check of the fuel in the tank of an injection-equipped car, tested on a chassis dynamometer at 80 F air temperature, indicated that the 9-lb rvp fuel used was lowered to 8 lb rvp after less than three-quarters of the tank fuel was consumed.

The automobile industry is currently investigating various means of reducing the amount of unburned fuel in car exhaust because of the possible smog-forming potential of hydrocarbons in the atmosphere of the Los Angeles area. The possibilities that fuel injection systems designed to permit fuel cutoff during deceleration can aid in this effort are indeed hopeful, and further effort in this field of endeavor is to be encouraged.

In summation, it would appear that it is impossible at this time to draw any definite conclusions concerning the impact of fuel injection upon future fuel requirements. Items currently under development such as injection pumps, nozzles, intake and exhaust manifolds, combustion chambers, valve events, and many others, all may affect the fuel used. Injection systems under consideration by our company are being developed around current gasolines.

Author's Closure To Discussion

MR. GAMMON is quite right in stating that the temperature and pressure compensation of the fuel metering curve must be carefully studied to make sure that the system will perform satisfactorily within the range of temperature and pressure normally encountered. An analysis of performance at altitudes of –100 ft to +10,000 ft and temperatures of –10 F to +150 F is being made on the basis of test vehicle data. Preliminary indications are that even without temperature and pressure compensation the gasoline injection system is far superior to the carburetor in its performance under extreme conditions. It is, however, quite possible that both forms of compensation will be required on the truck and bus engine, although some doubt still remains as to the necessity in regard to the passenger-car engine.

The pump control spring system mentioned by Mr. Dack is designed to meet the requirements of the particular engine to which the control is to be applied. It should be pointed out that the idling mixture is not a function of this pump control spring system but is separately controlled by

an idling bleed quite similar to that used in the conventional carburetor.

In regard to cold starting and cold driveaway, Mr. Dack is quite correct in stating that under driveaway conditions the throttle position will correspond roughly to one-half or three-fourths load and that unless additional fuel is supplied the engine during cold warmup, insufficient power will be developed to supply both acceleration and increased engine friction load. For this reason, later versions of the control insure a greater than full-load fuel quantity during the cold warmup part of the control cycle.

I am sure Mr. Dack will agree that, in respect to the spray nozzle, no requirement of good atomization exists much beyond the idle range, and indeed nozzle position will have a much greater effect on both idling and acceleration than will the degree of atomization. The problem of providing a long duration injection period is apparently not present in port-injection-type engines but may be a real factor in the proper performance of a direct injection system. In this regard it may be noted that there are several means of increasing the injection duration within the cam limits available, one very good way being the use of a small displacement piston in the delivery portion of the pump.

The lubrication of the pumping elements is in fact fully accomplished by the fuel being used with the exception of the face cam and roller combination, which is lubricated by engine oil. Fuel leakage to the engine compartment consists of a slight "weep." This leakage, which is controlled by the lapped fit of the plunger in its bore, is so small that we have been unable to measure it and certainly in the many thousands of miles of road testing it has been both completely satisfactory and safe.

In regard to the pump control and the use of a piston responsive to the control pressure, diaphragms and other flexible members are of course to be preferred, provided a material having satisfactory hysteresis forces and the desired flexibility, particularly in the low-temperature range, can be found. Sticking of the piston in its bore has been no problem since the proper bore and piston treatment was developed.

In regard to cost it is felt that when the gasoline injection system is produced in the same quantities as 4-barrel carburetors, the cost may well be equal to two such carburetors.

In reply to Mr. Kelly, in the use of a higher percentage of butane in the fuel, it is possible that the supply pressure of the system may need increasing. It is also probable that a pressure-type supply tank in pressures much above 12 psi Rvp will be required. The higher end-point fuels do offer certain advantages in combination with the higher Rvp fuels. We certainly agree, however, that any change in the current gasoline specifications must be a gradual one and much of the evaluation of the future trends in fuels must be done by the oil companies themselves.

Mr. Livingstone is quite correct in his comments relative to the efficiency of a circulating fuel system in eliminating many of the vapor lock problems encountered with carburetors. A great deal of work has been accomplished in the use of electric fuel pumps mounted either in the fuel supply tank or immediately adjacent to it in the carburetor application. Weathering of the fuel will unavoidably be present with any circulating fuel system including an open or vented fuel tank.

We have found that even with the higher end-point fuels the increase in plug fouling and crankcase dilution with the gasoline injection system is not a limitation on the end-points within the range reported on. We feel that this insensitivity of the engine to these fuels is probably due to the more perfect distribution of the fuel to the various cylinders under all conditions and the absence of unburned fuel in the cylinder during deceleration. The idle fuel flow of an injection engine will always be at least 25% less than with a carburetor, and in reference to a particular cylinder this fuel flow may be as much as 60% less.

The handling of dirty fuel has not been a problem due to the efficiency of the fuel filter used as an integral part of our system. I believe Mr. Livingstone will agree that many of the problems in aircraft fuel filtering in the plane arise from the formation of ice crystals, which tend to blanket any filter used and reduce or stop the flow of fuel.

The question of maximum pump speed permissible with complete filling at the 20-psi supply pressure, as mentioned by Mr. Downing, is one that has not been fully investigated since the engines with which we have worked do not operate at speeds above 6000 rpm. In an engine of this speed rating the supply pressure is ample at the supply pressure mentioned.

Mr. Downing is in agreement with both Mr. Dack and myself on the point of cold driveaway fuel and we may agree that a fuel delivery of greater than full load quantity must be provided.

Mr. Downing is probably correct in that an increase of 25% more output cannot be obtained with every engine by the use of gasoline injection. We agree that some engines are better than others and the improvement to be noted with the gasoline injection system must reflect the degree of success achieved originally in the marriage of the engine to the carburetor. We do feel, however, that there is a great deal of work to be done in combustion-chamber design, valve timing, the induction system, and other engine variables. The completion of the development work on the engine itself will, we feel, result in a general improvement approaching 25% in output per cubic inch.

In reply to Mr. McManus, we do not agree that the form of fuel fed to the engine cylinder by the spray nozzle is important in the power range of the engine. We feel that the characteristic of the spray produced is important only in the idle range. Nozzle position, however, is most important and any impingement of the spray on the manifold wall or valve port wall may make necessary the use of an accelerating device providing extra fuel during snap-throttle operation.

The substitution of a good gasoline injection system, such as described, for a commercial carburetor will leave the driver of the vehicle in no doubt that a considerable improvement in performance has been achieved. Economy will also be measurable and in several instances has amounted to as much as two miles per gallon improvement.

In regard to vapor locking it is impossible for this system to vapor lock in operation within the range of temperatures and pressures encountered in American operation. The circulating supply pressure automatically purges itself of any vapor formed in the supply lines. Residual pressure in the nozzle lines amounting to about 60 psi is sufficient to maintain solid column in the discharge lines to the nozzle under the most severe engine operating conditions. If for any reason this residual pressure should be lost, as for instance during a hot-soak on shutdown, the system cannot be said to vapor lock even under this condition since the supply line will be full and the pump will definitely fill up the discharge lines on cranking. Under this condition, it may require as much as 10 sec for the pump to fill a boiled-out line to the nozzle but the system is not vapor locked and will function as soon as the pump delivery is sufficient to charge the nozzle line.

We agree with Mr. McManus that any development of a gasoline injection system must at this time be based on currently available gasoline since any change in available fuel must be a gradual one. We believe, however, that the additional freedom given the engine designers because of the insensitivity of the gasoline injection system to manifold configuration, mixture control position, and valve porting can result in much better engines for the motoring public.

THE role of pneumatics as a computing medium for engine control in high-speed flight is indicated, and use of pressure ratio as the logical pneumatic control parameter is discussed. The Microjet concept of pressure ratio control, operating without springs and evacuated references, is introduced and compared to conventional means.

This principle is expanded to demonstrate various computing and function-generating operations with respect to theoretical and practical design criteria. Typical present and projected applications to the control of turbojet and ramjet engine cycles are illustrated.

This paper received the SAE Wright Brothers Medal for 1955.

A New Approach to Turbojet

TRENDS in aircraft and engine control component design indicate a compelling need to develop pneumatic actuating and computing components to overcome many problems associated with high-speed flight. In this regard, use of pneumatic pressure ratios as control parameters for turbojet and ramjet engine cycles is particularly attractive in view of our recent development of a versatile, highly simplified computing element known as the Microjet Control. The purpose of this discussion is to familiarize the industry with basic principles of this new control element, and to demonstrate the versatility with which this principle can be applied to pneumatic control of turbojet and ramjet engines.

Scarcely more than half a century has passed since the Wright brothers demonstrated the feasibility of powered flight, and yet men are boldly contemplating extraterrestial flight at astounding speeds of 18,000 to 25,000 mph. The metamorphosis of man, as he emerges from his cocoon-like existence on this planet, is confronted with many barriers, not the least of which is man himself. The most widely publicized, of course, are the so-called sonic barrier and, more recently, the thermal barrier.

In the aircraft of 1960, which are on the drawing boards today, the pilot of a Mach 2.5 airplane would roast in a torrid 450 F atmosphere were the ship not equipped with an elaborate refrigeration system to keep him cool and comfortable (see Fig. 1). At more than twice sonic speed, the aircraft structure becomes a problem necessitating the exclusive use of high-temperature alloy steels. Steel melts at Mach 6 and the most temperature-resistant material known to man, diamond, vaporizes at Mach 10. Unless atomic research leads to an entirely new type of metallurgy, man shall probably be confined in flight within his atmosphere and at speeds less than five times sonic speed.

At Mach 3, the lowest air temperature found anywhere in the aircraft is 650 F. Engine and associated control components must operate at temperatures much higher than this. Ambient operating temperature requirements for engine control components in the forthcoming generation of engines will range from 800 to 1000 F.

By contrast, as seen in Fig. 2, many presently available electronic components required for control systems are limited to operating temperatures of less than 250 F. Even highly developed electro-

and Ramjet Engine Control

Wendell E. Reed, Solar Aircraft Co.

This paper was presented at SAE Golden Anniversary Aeronautic Meeting, Los Angeles, Oct. 14, 1955.

mechanical components, such as electric motors and solenoids, are marginal above 500 F. At 500 F the best-known hydraulic fluids begin to decompose, and the most advanced types of plastic materials used for seals become unsatisfactory at temperatures exceeding 600 F. Obviously the technology of control design and control component materials has not kept pace with military requirements.

While the electronics industry has made great strides in improving the reliability of components, this effort is largely offset by higher ambient operating temperatures required. On the other hand, use of hydraulics is also limited. Since the fluid itself is nonexpendable, and small leaks present a serious fire hazard, highly reliable sealing methods must be used. Both seal material and hydraulic fluid are critically limited by temperatures they can tolerate.

Advantages of the Pneumatic Approach

Pneumatics may be a solution. Turbojet and ramjet engines are basically air pressure producing machines. Small amounts of leakage present no problem, and certainly no fire hazard. For this reason, seal design is less critical and not necessarily limited to the use of temperature-limited resilient materials.

In addition to these advantages, use of pneumatics eliminates the necessity for storage tanks,

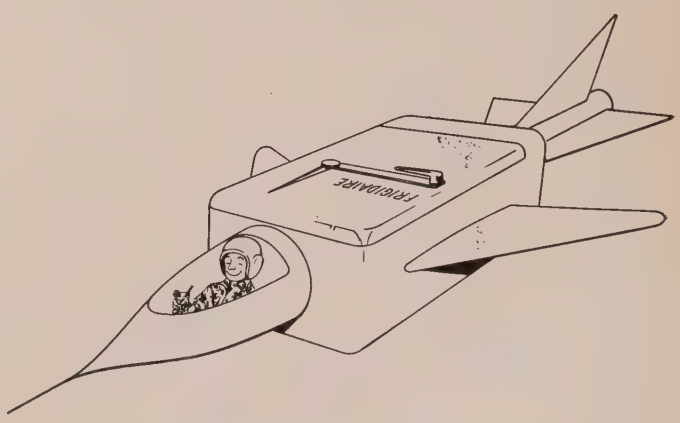

Fig. 1 – The heat barrier in high-speed flight

pumps, and power supplies normally required for electric or hydraulic systems. The source of fluid in the pneumatic system is assured as long as the engine is operating. In general, pneumatic systems are regarded as highly reliable. Certain other features of pneumatic systems make them attractive from the standpoint of simplicity. For example, single-sided systems may be used, in which return fluid is vented overboard. Elimination of return lines and fittings results in savings in weight and complexity.

There are certain disadvantages with pneumatic systems, such as problems of achieving desired stability and response. These problems, however, are not insurmountable and can be solved within the capabilities of experienced control engineers.

Merely substituting compressed air for electric power or hydraulic fluid as the operating medium for a control system does not, however, permit full realization of the potential advantages of an all-pneumatic control system. Not only the muscles or actuating elements, but also the brains or computing elements of the system must undergo considerable face-lifting to exploit conversion to pneumatics. For example, in controlling the variable area jet nozzle of a turbojet engine, it is conventional practice to utilize turbine inlet or turbine discharge temperature as the primary control parameter. Selection of this parameter inherently demands the use of electronics in the system. Thermocouples used to measure temperature generate weak electric signals which must be amplified electronically before they are usable.

Nonelectronic means for measuring temperature are available. These, however, are eliminated from practical consideration on the basis of response time. A well-designed thermocouple has a time constant of 1-5 sec, which is considerably faster than the best-known devices of the differential expansion, vapor pressure, or gas bulb types. Even the response rate of the thermocouple is totally inadequate in light of system transient operating requirements resulting from igniting or extinguishing an afterburner flame.

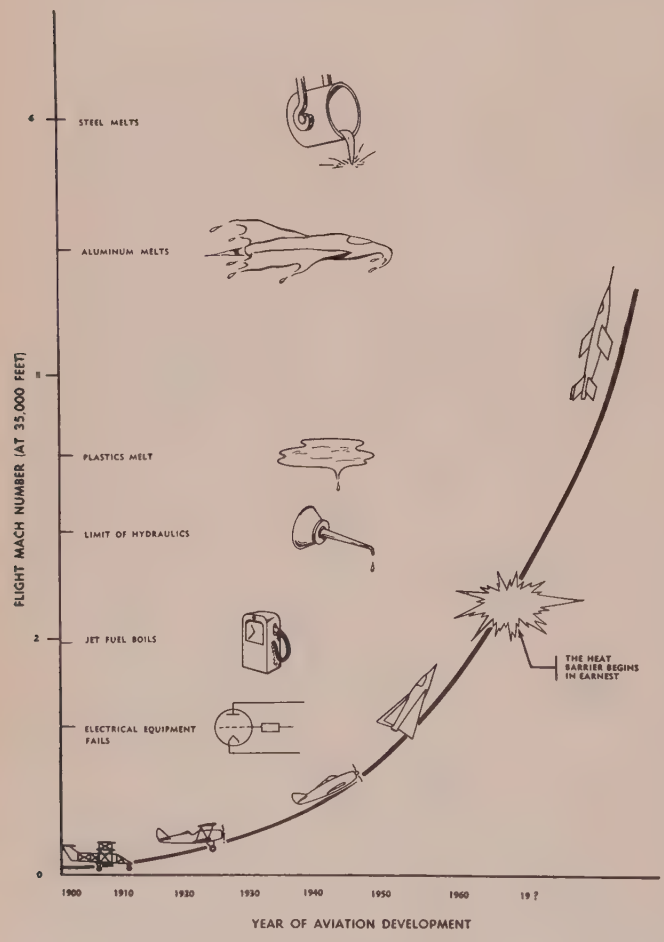

Fig. 2 – Limiting temperatures reached with increased speed over the years of aviation development

Use of Pressure Ratio Parameters

Benefits of a pneumatic system can be realized to a greater extent if pneumatic control parameters are used in place of temperature parameters. A new criterion for selection of control parameters must be evolved, and a simple pneumatic method of sensing these parameters and computing the required relationship between them must be provided.

Sufficient pneumatic parameters are available to control the turbojet engine cycle, (see Fig. 3). It is significant that engine matching characteristics can be controlled using three engine pressure ratios. If rpm and two pressure ratios are known, actual turbine inlet temperature can be controlled. It is possible merely by sensing pressure ratio parameters to control the variable area jet nozzle, afterburner fuel flow, engine fuel, compressor air bleed, variable inlet guide vanes, and variable inlet geometry, in order that engine variables may be maintained within prescribed mechanical and thermodynamic limits required of a high-performance engine.

A significant advance has been made possible using pneumatics and applying pressure ratio as a control parameter, both through development of a new type pneumatic computing control. This development has provided a simple, reliable method for sensing pressure ratios and absolute pressures, separately, in combination with each other, or in relation to other engine parameters such as rpm and fuel flow.

Conventional pressure ratio sensing and computing devices rely heavily on the use of evacuated bellows, springs, and complicated linkages. These entail considerable complexity and provide doubtful reliability under conditions of severe vibration and high temperature. Microjet Control, so named because its underlying principles are analogous to those of the engine for which it was designed, establishes an absolute plane of reference without resorting to the usual evacuated chambers and in-

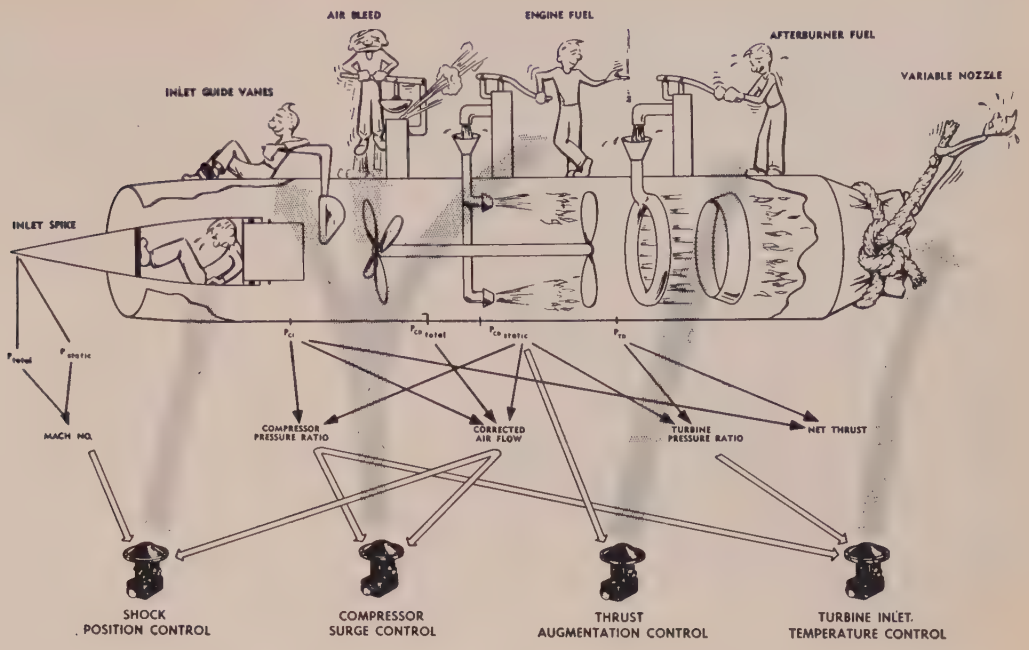

Fig. 3 – Use of pneumatic parameters for jet-engine control

dependent of spring calibration. This plane of reference is created by bleeding air through a pair of orifices in series.

Operation and Theory of the Microjet Principle

The Microjet principle has been successfully applied to a variety of jet engine control problems, including afterburner light-off and blow-out detection, turbine-inlet temperature control, overspeed control, and afterburner fuel control. Several component configurations have been accepted as standard equipment on late design aircraft and engines. Numerous other applications also have been found for controlling ramjet engines. The impressive versatility of the device for use in computing engine cycle parameters indicates a possible wide variety of uses in controlling temperature, cruise matching, compressor surge, and shock wave position.

A simplified illustration of the operating principle of Microjet Control is shown in Fig. 4. Primary purpose of the device is to provide a mechanical displacement output signal indicating magnitude of the ratio between two pressures. One of two pressures is applied to the upper side of a flexible diaphragm; the other generates a controlled reference pressure which is applied to the lower side of the diaphragm. This reference pressure is generated by bleeding air – generally from the compressor discharge in jet engine applications – through two orifices in series, the area of one being controlled by a tapered needle attached to the diaphragm.

In operation, the flexible diaphragm, being substantially free to move in response to pressure differences, operates in a manner to maintain the reference pressure always exactly equal to the pressure applied above the diaphragm. Increase in the upper pressure results in a downward movement of the diaphragm, resulting in a corresponding decrease in area of the second orifice. This raises reference pressure and retards diaphragm movement until equilibrium is reestablished and the diaphragm displaced to a new position at which the two pressures are equal. This position is directly related to the new value of ratio between the two applied pressures.

Three basic equations define the steady-state characteristics of the device: the force balance equation, which states that the sum of all forces acting on the diaphragm and needle assembly as a free body equals zero; the orifice flow equation,

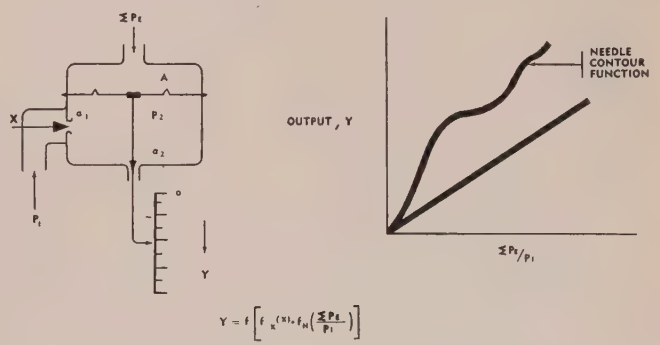

Fig. 4 – General equation for Microjet pressure ratio control

which states that weight flow through the first and second orifices is equal; and an equation for needle contour which establishes characteristics of the output displacement signal.

For the orifice:

$$W = K \frac{aP}{\sqrt{T}} N \tag{1}$$

(See Nomenclature at end of paper for meaning of symbols.)

For two orifices operating in series:

$$W_1 = W_2 \tag{2}$$

Equating airflows through the two orifices:

$$K_1 \frac{a_1 P_1}{\sqrt{T_1}} N_1 = K_2 \frac{a_2 P_2}{\sqrt{T_2}} N_2 \tag{3}$$

Assuming an isothermal throttling process with no heat transfer:

$$T_1 = T_2 \tag{4}$$

Thus:

$$\frac{P_2}{P_1} = \frac{K_1}{K_2} \frac{a_1}{a_2} \frac{N_1}{N_2} \tag{5}$$

If the second orifice is operating at critical discharge (P_2/P_o greater than 0.53), $N_2 = 1$. Since N_1 is a function of the ratio of pressures P_2/P_1, this ratio is substantially a function only of the effective nozzle areas, or:

$$\frac{1}{N_1}\left(\frac{P_2}{P_1}\right) = f_N\left(\frac{P_2}{P_1}\right) = \frac{K_1}{K_2}\frac{a_1}{a_2} \tag{6}$$

If the diaphragm and attached movable mechanism is considered as a free body, and if the reference pressure is applied to one side of the diaphragm and other arbitrarily selected forces are applied to oppose it, an equation for equilibrium of this free body can be written. Assuming all these forces colinear, this equation is:

$$P_2 A = \sum F \tag{7}$$

Whence:

$$P_2 = \sum \frac{F}{A} \tag{8}$$

$\sum F/A$ has dimensions of pressure, (force per unit area), and is defined here as the "applied pressure equivalent," $\sum P_E$.

Substituting in equation (8):

$$P_2 = \sum P_E \tag{9}$$

Two additional equations must be considered before the final general equation can be derived. The first relates area of the second orifice to displacement of the movable needle attached to the diaphragm:

$$\frac{1}{a_2} = f_Y(Y) \tag{10}$$

A similar equation relates area of the first orifice

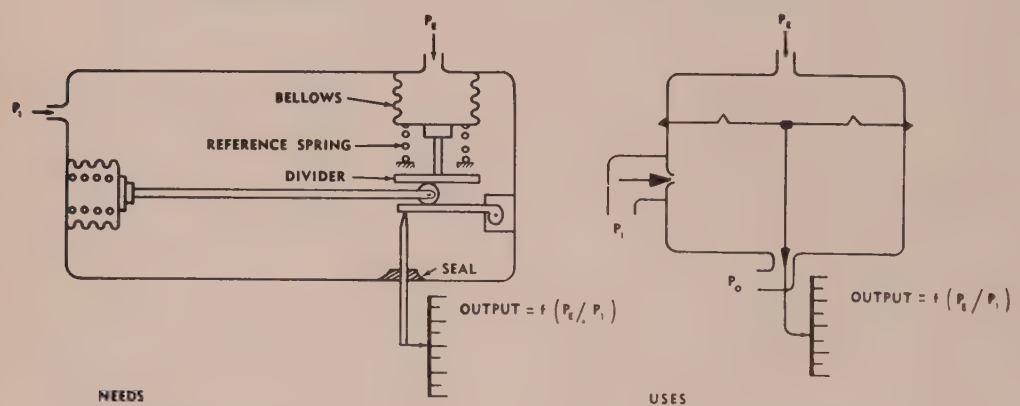

NEEDS

1. PRECISION EVACUATED BELLOWS
2. PRECISION TEMPERATURE COMPENSATED REFERENCE SPRINGS
3. COMPLICATED AND PRECISION DIVIDING LINKAGE
4. DELICATE INSTRUMENT-TYPE CONSTRUCTION
5. SKILLED SERVICING REQUIRED
6. OUTPUT FUNCTION NON-LINEAR UNLESS COMPENSATED BY ADDITIONAL CAMS, ETC.

USES

1. SINGLE NON-RESILIENT DIAPHRAGM SIZE NOT CRITICAL
2. EASILY CALIBRATED AND ADJUSTED
3. NO FRICTION OR WEARING PARTS
4. SIMPLE YET RUGGED CONSTRUCTION
5. EASILY SERVICED BY ANY TRAINED TECHNICIAN
6. CONTOURED NEEDLE PROVIDES ANY OUTPUT FUNCTION

Fig. 5 – Comparison of pressure ratio sensing devices

to displacement of an adjustable input needle:

$$\frac{1}{a_1} = f_X(X) \tag{11}$$

Relationships $f_Y(Y)$ and $f_X(X)$ are determined by shapes of the respective contoured elements and requirements of the particular application.

General Microjet Equation

Substituting equations (9), (10), and (11) in equation (6) and rearranging terms gives the following:

$$Y = f\left[f_X(X) \cdot f_N\left(\frac{\sum P_E}{P_1}\right)\right] \tag{12}$$

For the special case when both orifices are choked:

$$Y = f\left[f_X(X) \cdot \frac{\sum P_E}{P_1}\right] \tag{13}$$

Equation (12) is the general equation describing the Microjet principle, which states in effect that output displacement Y is a function of the product of the pressure ratio function, $f(\Sigma P_E/P_1)$, and input displacement function, $f_X(X)$. In this general equation, $f_X(X)$, and $f(\Sigma P_E)$ are not specifically defined. They are general terms for which specific values may be selected according to requirements of the application.

In following paragraphs, it will be shown that virtually any type characteristic equation involving pressure ratios can be solved by substituting appropriate values for the terms in the general equation. By utilizing various type mechanical inputs such as throttle position or displacement from some pressure- or speed-sensing device, Microjet Control can perform a wide variety of sensing and computing functions. Additional computing functions can be achieved by applying various type forces to the movable element. These forces may include pressures acting on diaphragms or pistons, spring forces, inertia forces, and so forth. By these methods, various type linear and nonlinear schedules may be obtained, and various pressure ratio parameters can be combined by addition, subtraction, multiplication, or division.

Comparison with Conventional Pressure Ratio Controls

Significant advantages of Microjet pressure ratio control over the conventional pressure ratio sensor shown on the left in Fig. 5 stems from the latter's use of precision bellows to measure differential pressures. One bellows must be evacuated to provide a reference for absolute pressure. Displacement of each bellows is calibrated against a temperature-compensated reference spring and is mechanically divided by a complicated precision linkage, so that output becomes a function of pressure ratio.

This type device involves very delicate instrument-type construction, utilizes precision instrument bearings, and requires some form of precision, low-friction seal. Manufacture of component parts must be controlled within very tight tolerances. In service, highly skilled personnel are required to make repairs or adjustments.

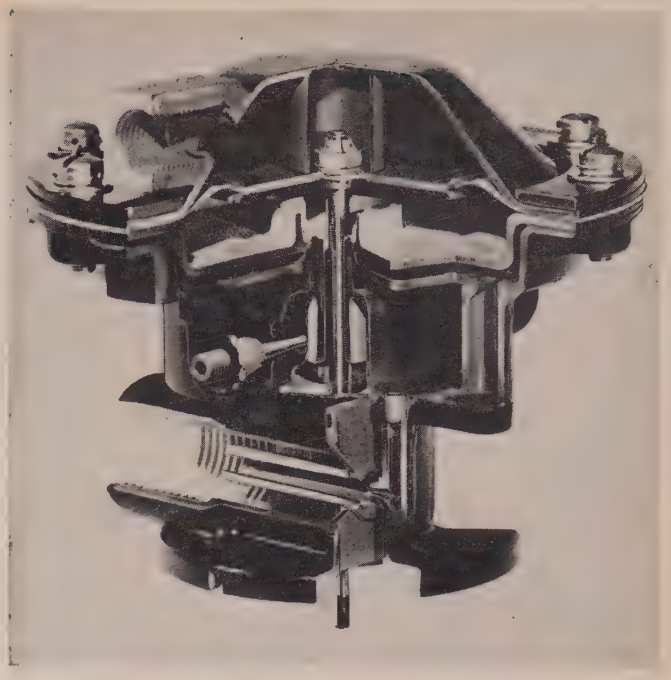

Fig. 6 – Cutaway of typical microjet pressure ratio control

By comparison, the Microjet type control is relatively simple and more versatile, as illustrated on the right in Fig. 5. It utilizes one nonresilient diaphragm, whose size is not critical. It contains no springs, so the difficult problem of close control of spring rates is eliminated. Its simple construction is essentially friction-free since it has no wearing parts. The need for a precision, low-friction seal is eliminated by virtue of the fact that the needle extends through the second orifice to the region of ambient pressure, where it is connected to the output indicating or control device. The simple, rugged construction is apparent from the cutaway shown in Fig. 6.

Simple Jet Nozzle Control

A simple illustration of a typical application of Microjet pressure ratio control is the variable area jet nozzle control shown in Fig. 7. Early turbojet engines were designed for use with a fixed jet nozzle. This resulted in operation at essentially fixed turbine pressure ratio. When afterburners were applied to these engines, it became necessary to provide a variable area jet nozzle in order to compensate for increased volume of exhaust gas resulting from afterburner combustion, and to maintain "balanced cycle" control; that is, maintain the constant turbine pressure ratio for which the engine and associated control system were designed.

It was for this purpose, in conjunction with afterburner development, that we initially conceived

the Microjet principle, but only after considering virtually every other possible means of obtaining required response and reliability. In 1949 Microjet Control was first applied to a Westinghouse J34-WE-34 engine and flight-tested in a Chance Vought XF7U airplane at Dallas, Tex. Initial ground and flight tests proved so successful that numerous other engine models were equipped with similar systems. Those early systems utilized a 2-position control, but the underlying concept of pressure ratio sensing was the same as described above. Referring to Fig. 7, the system consists of a Microjet pressure ratio sensing element, the output needle of which controls an integrating servo valve and actuator combination to move the jet nozzle. Successful systems have been developed utilizing all the various media (electricity, hydraulics, or pneumatics), but for purpose of this discussion the pneumatic type system only is discussed.

Microjet Control senses two engine pressures: turbine discharge pressure, applied to the upper side of the diaphragm, and compressor discharge pressure, applied to the two orifices to produce an intermediate reference pressure at the lower side of the diaphragm.

Making appropriate substitutions in equation (12), there results:

$$Y = f\left[f_X(X) \cdot f_N\left(\frac{P_{TD}}{P_{CD}}\right)\right] \qquad (14)$$

Output needle position can have only one value of displacement Y for a prescribed value of turbine pressure ratio. In a null-balance-type system, this results in the relationship:

$$K_Y = f\left[K_X f_N\left(\frac{P_{TD}}{P_{CD}}\right)\right] \qquad (15)$$

wherein turbine pressure ratio is maintained constant at a value determined by the adjustment, $K_X = f_X(X)$.

In operation a decrease in turbine pressure ratio such as caused by afterburner light-off causes turbine discharge pressure to rise, displacing the Microjet Control diaphragm downward. As the contoured needle decreases size of the second orifice, it raises reference pressure until the diaphragm reaches a new equilibrium position corresponding to the error in turbine pressure ratio. As the needle moves downward, it operates the pneumatic servo valve which ports compressor discharge air to one side of the pneumatic actuator, moving the jet nozzle in the open direction. This reduces turbine discharge pressure, restoring it toward its original value. Conversely, in the event the afterburner flame is extinguished, sudden increase in turbine pressure ratio will cause the Microjet Control to return the jet nozzle toward the closed position.

Control of Turbine Discharge Temperature

With the next generation of jet engines, the afterburner was incorporated as an integral part of the engine. The next logical step was to utilize the variable jet nozzle to improve the nonafterburning performance of the engine by maintaining maximum permissible turbine blade temperature. This resulted in a general requirement for constant turbine-inlet-temperature control. Since it proved impractical to utilize thermocouples in the high-temperature zone ahead of the turbine, use of turbine discharge temperature was universally accepted as a compromise substitution.

In order to maintain constant turbine discharge temperature at constant military rpm, it is necessary to increase turbine pressure ratio by opening the jet nozzle as compressor inlet temperature rises. In initial attempts at utilizing Microjet Control to maintain constant temperature, turbine pressure ratio setting was biased as a function of compressor inlet temperature. This was done by utilizing a temperature compensating element which biased the turbine pressure ratio setting of the Microjet by changing position of the adjustable needle in the first orifice. This was not the most desirable solution because of the slow response of this type of temperature element.

The system was reevaluated on the basis of substituting other engine parameters for compressor inlet temperature. With engine operating at constant military rpm, compressor pressure ratio varies almost linearly with compressor inlet temperature. Therefore, by establishing a scheduled relationship between turbine pressure ratio and compressor pressure ratio, constant turbine discharge temperature operation can be achieved. Further analysis indicated that a very close approximation

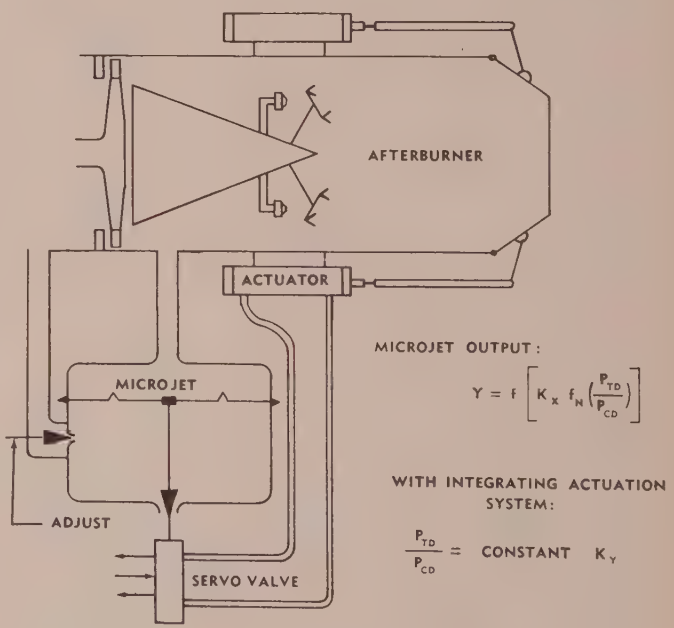

Fig. 7 – Pneumatic variable nozzle control to effect constant turbine pressure ratio

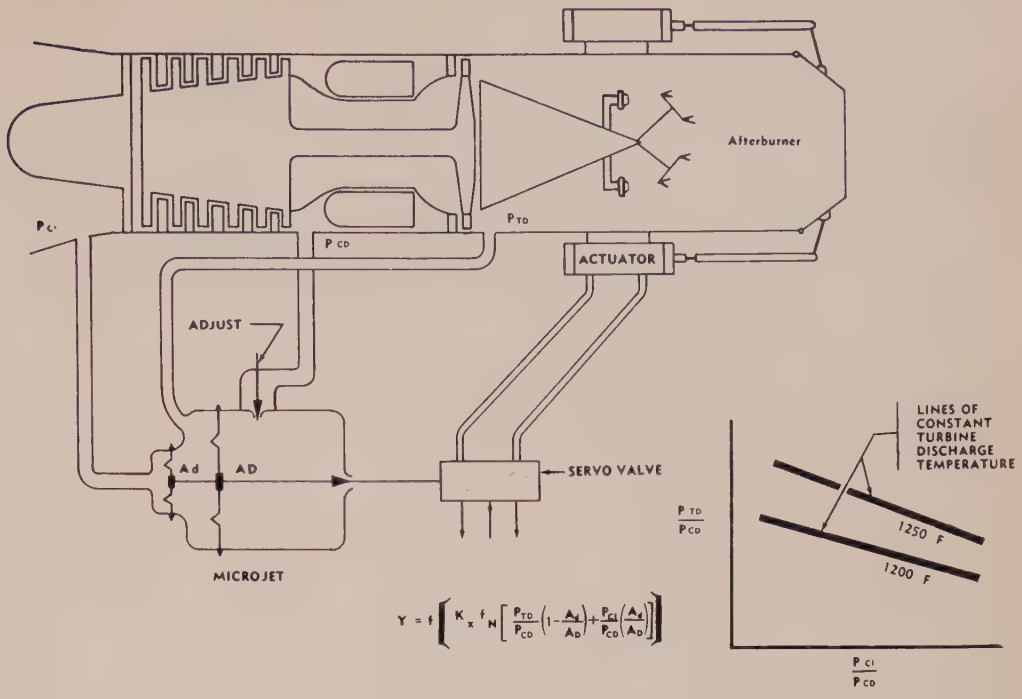

Fig. 8 – Pneumatic variable nozzle control to effect constant turbine discharge temperature

could be achieved by utilizing a linear sum of the pressure ratio reciprocals. Utilizing two diaphragms of different sizes in the Microjet Control, a schedule of the type shown in Fig. 8 was established. Applying compressor inlet pressure to the top cavity above the small diaphragm and turbine discharge pressure to the intermediate diaphragm cavity, equation (12) takes the form:

$$Y = f\left\{K_X f_N\left[\frac{P_{TD}}{P_{CD}}\left(1-\frac{A_d}{A_D}\right)+\frac{P_{CI}}{P_{CD}}\left(\frac{A_d}{A_D}\right)\right]\right\} \quad (16)$$

This type system was first test-flown in an F-86 airplane powered by a General Electric J47-GE-27 engine. In more than a year of flight-testing involving approximately 130 flights, the control gave highly satisfactory and reliable operation.

Effects of Reynolds Number

Repeated flight tests to altitudes above 50,000 ft indicated that still another factor had to be taken into consideration. Above 40,000 ft, decreased air density has a marked effect on engine compressor efficiency. This is the result of wide variation in Reynolds number. As compressor efficiency falls off at high altitude, it takes relatively more work to turn the compressor. To maintain constant turbine discharge temperature, this additional work can be obtained only by increasing turbine pressure ratio; thus, as altitude increases it is necessary to raise turbine pressure ratio by opening the jet nozzle slightly to hold temperature constant, as illustrated in Fig. 9.

It was found that a very close approximation to this schedule requirement could be achieved by addition of an inverse function of compressor discharge pressure. Incorporating a small, low-rate spring, acting downward on the diaphragm assembly of the Microjet Control, equation (12) takes the form:

$$Y = f\left\{K_X f_N\left[\frac{P_{TD}}{P_{CD}}\left(1-\frac{A_d}{A_D}\right)+\frac{P_{CI}}{P_{CD}}\left(\frac{A_d}{A_D}\right)+\frac{F_S}{P_{CD}\,A_D}\right]\right\} \quad (17)$$

Through addition of an extra diaphragm and a small spring, the control computes the algebraic sum of terms involving compressor pressure ratio, turbine pressure ratio, and compressor discharge pressure.

Subtraction can be performed just as easily by applying forces in the upward direction. Systems of the type described were flight-tested at Edwards Air Force Base on a General Electric J47 engine. Similar systems were tested later on a Curtiss-Wright J65 engine in the altitude facility at Dain-

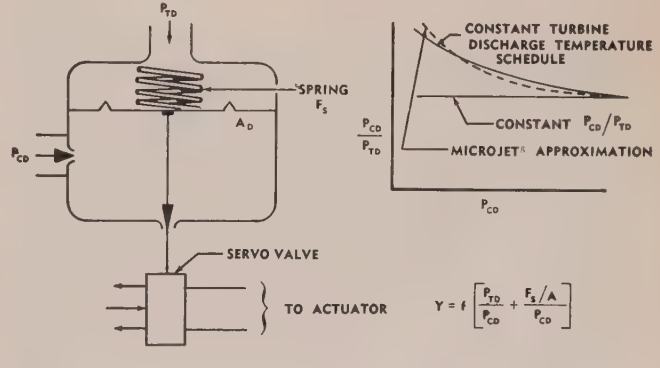

Fig. 9 – Effect of Reynolds number on pressure ratio schedule

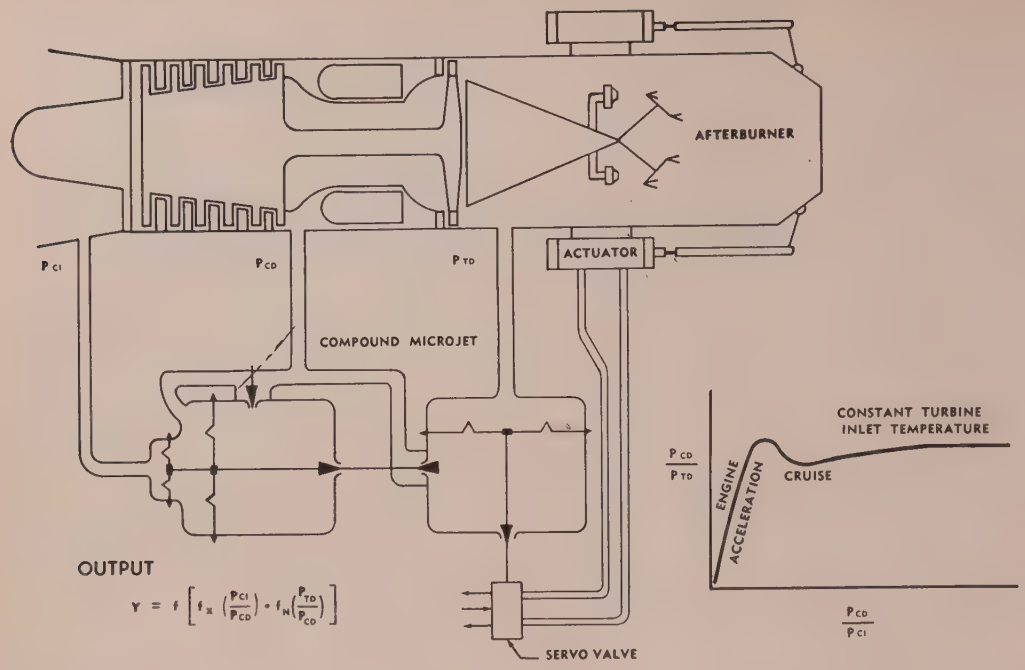

Fig. 10 – Pneumatic variable nozzle control for complex functions

gerfield, Tex. These tests demonstrated conclusively the feasibility of maintaining constant turbine discharge temperature by the use of pneumatic parameters, and with an accuracy comparable to the best electronic systems. Flight-test data for a Microjet variable nozzle control system indicates that turbine discharge temperature was held to within 10 C of a constant value over a range of altitudes up to 60,000 ft.

Application to Nonlinear Schedules

In the foregoing illustrations, selection of schedules was made on the basis of close linear approximations. Not all schedules, however, can be reduced to this degree of simplicity. High pressure ratio engines in particular tend toward greater nonlinear characteristics. Furthermore, a modern nozzle area control must provide not only constant temperature at military rpm, but ideally must provide an appropriate nozzle area for cruise operation and maintain a preselected nozzle position during engine acceleration. A schedule of this type is shown in Fig. 10. By compounding two Microjet elements into a single control, this or virtually any other type nonlinear schedule can be achieved.

As illustrated in Fig. 10, the compound Microjet Control consists of two units combined into one. The primary unit senses turbine pressure ratio and the secondary unit senses compressor pressure ratio. The output needle of the secondary unit changes position of a contoured element in the first orifice of the primary unit, thus biasing the turbine pressure ratio setting as a function of compressor pressure ratio. Letting the input, $f_X\ (X)$, become a function of compressor pressure ratio, equation (12) now takes the form:

$$Y = f\left[f_X\left(\frac{P_{CI}}{P_{CD}}\right) \cdot f_N\left(\frac{P_{TD}}{P_{CD}}\right)\right] \qquad (18)$$

The relationship between the two pressure ratio functions depends entirely on shape of the contoured needle in the primary control inlet. For the case illustrated in Fig. 10, the contour is established on the basis of nonlinear schedule requirements.

The compound Microjet principle was applied first to the Solar T-300J-1 gas turbine ground starter cart shown in Fig. 11, where it was used to regulate bleed airflow for starting large jet engines. The control maintained limiting turbine inlet temperature by sensing air bleed flow and compressor pressure ratio.

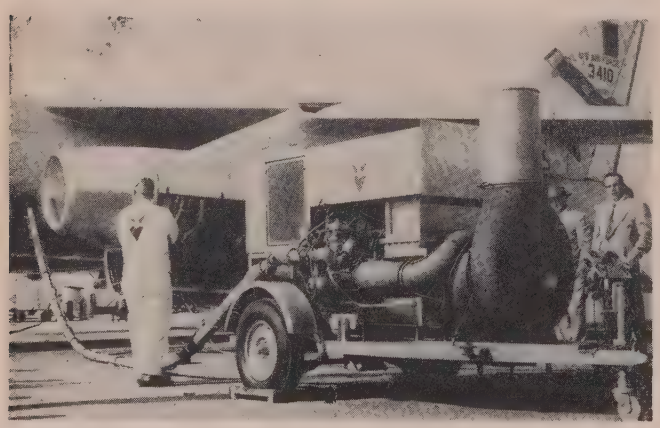

Fig. 11 – Solar T-300J-1 gas turbine ground starter cart equipped with Microjet air bleed control

Snap Action Feature

A unique characteristic is achieved if taper on

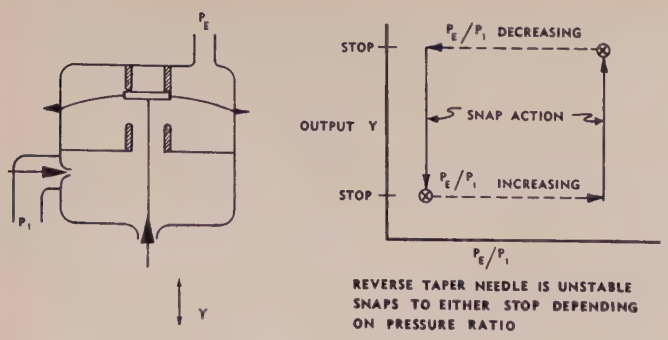

Fig. 12 – Snap action for 2-position output

the needle of the basic Microjet Control is reversed, as shown in Fig. 12. With this configuration, the diaphragm assembly becomes unstable and snaps to either stop, depending on the pressure ratio level. In other words, whereas the basic unit normally produces an output signal that is a continuous proportional function of the error, the reverse taper introduces a discontinuous characteristic, analogous to the action of a simple toggle switch, except that it is pneumatic rather than mechanical. In operation, this type unit maintains full displacement in one direction until pressure ratio is increased to a specific value depending on adjustment of the inlet orifice. When the predetermined pressure ratio is reached, the needle snaps to the other extreme of its displacement and remains there until pressure ratio is reduced to another value considerably below the first. This type control is used with 2-position jet nozzles, where it is desired to establish and maintain the jet nozzle in the full-open position when the afterburner ignites and to return it to the closed position when the after burner is extinguished. This type of Microjet Control eliminates the necessity of elaborate holding circuits otherwise required.

Versatility of Microjet Principle

Various modifications and adaptations of the basic elements described illustrate the impressive versatility of the Microjet principle. As shown in Fig. 13, by using various types of pistons, springs, or diaphragms to produce coacting forces on the movable needle, algebraic addition or subtraction of pressure ratio functions can be achieved. By selecting appropriate needle contours in the compound Microjet, various types of linear or nonlinear schedules are possible. Similarly, if these contours have the proper relationship to displacement, the compound unit can be used for multiplication and division.

Design Considerations

The general equation (12) is based on the assumption that the second orifice of the Microjet Control operates at the critical discharge or choked condition. Actually, the use of the control is not limited strictly to this condition. Numerous applications exist where it is desirable to operate in the unchoked range, to match some particular engine characteristic. This is true, for example, of the simple constant turbine pressure ratio control described earlier; in actual practice constant turbine pressure ratio is desired only at or near military rpm of the engine. At reduced power settings, characteristics of the control operating at subcritical discharge will duplicate performance of the jet nozzle operating with fixed effective area.

In most other applications it is necessary to operate with a choked second orifice. If pressure ratio across the second orifice drops below the critical discharge, then output displacement becomes a function not only of input pressures but also of ambient pressure. In most cases, supply pressure (P_1) is compressor discharge pressure P_{CD} of the engine, and even at idle rpm is sufficient to maintain choked operation of the second orifice.

Choked range of the control can be increased substantially by utilizing a convergent-divergent rather than a convergent second orifice. The convergent-divergent orifice will maintain sonic flow at its throat even though pressure ratio across it is subcritical. Constant pressure ratio characteristics can be extended to second orifice pressure ratios as low as 1.2 by this method. Numerous variations in configuration of diaphragms and orifices make it possible to use the device to measure pressure ratios over an unlimited range.

Use as Net Thrust Indicator

Application of Microjet Control is not necessarily limited to pressure ratio functions involving compressor discharge pressure of the engine, nor is it necessary to bleed air through pressure sensing lines. An example is shown in Fig. 14 where the compound Microjet is used to measure engine pressure ratio (P_{TD}/P_{CI}), which is a function of net thrust.

Neither turbine discharge nor compressor inlet pressure is suitable for an orifice system. If turbine

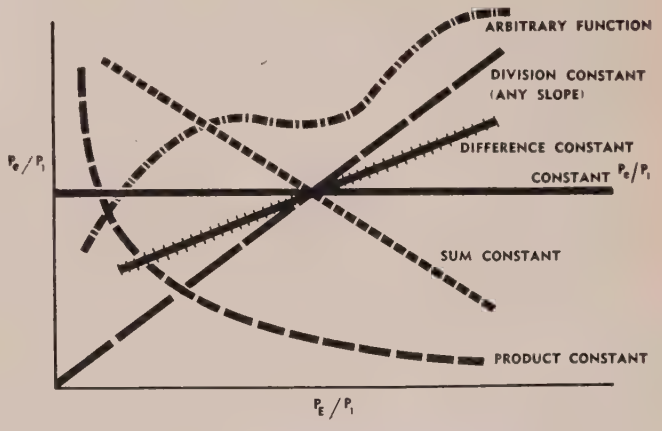

Fig. 13 – Typical pneumatic computing functions possible with Microjet control

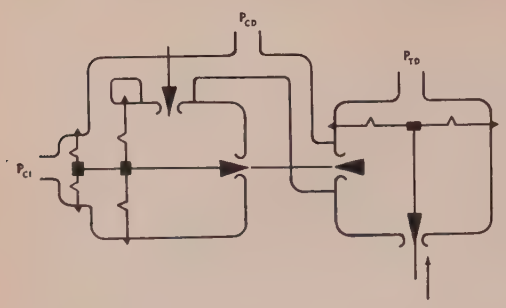

$$Y = f\left[\frac{P_{TD}}{P_{CD}} \Big/ \frac{P_{CI}}{P_{CD}}\right] = f\left[\frac{P_{TD}}{P_{CI}}\right] = f\left[\frac{F_N}{S}\right]$$

OUTPUT IS A FUNCTION OF P_{TD}/P_{CI} OR NET THRUST

P_{TD} AND P_{CI} SENSING LINES REQUIRE NO FLOW.

OPERATES INDEPENDENT OF COMPRESSOR DISCHARGE PRESSURE.

Fig. 14 – Measurement of net thrust with Microjet control

discharge pressure were bled through the orifices, high temperatures would be imposed on the control and excessive combustion products might be precipitated. Compressor inlet pressure, on the other hand, is sometimes lower than ambient pressure and is not high enough to assure critical discharge. Knowing that engine pressure ratio is equal to the compressor pressure ratio divided by the turbine pressure ratio, we can overcome the problem quite satisfactorily. A compound Microjet is used, in which the primary unit senses turbine pressure ratio and the secondary unit senses compressor pressure ratio. By appropriate shaping of the contoured needle, and operating the primary Microjet unit with both orifices choked, the quotient of these two parameters is computed pneumatically such that output displacement of the primary unit is a function only of engine pressure ratio P_{TD}/P_{CI}. This eliminates the need for bleeding air through either of the two critical lines sensing turbine discharge pressure and compressor inlet pressure. As before, compressor discharge air is utilized for the orifice system, yet output of the device is completely independent of compressor discharge pressure.

Airflow Requirement

Airflow requirements of the Microjet Control are relatively small compared to the availability of compressor discharge air. Standard units generally require less than 0.05 lb per sec at sea-level conditions, or less than 0.05% of engine airflow.

Insensitivity to Dirt

Service experience on over 2,000 Microjet Controls indicates that the units are relatively free from malfunction caused by dirt or impurities in the air supply. This can be attributed to several design factors. In most installations the compressor discharge bleed port can be designed so that heavier particles are carried past the opening by the high-velocity air stream. Most smaller particles that may be carried into the Microjet Control are separated by centrifugal action resulting from the unique housing design. Furthermore, orifices are selected large enough so that plugging is virtually impossible. Cases are on record where some of these control systems were subjected to large quantities of ground walnut shells, passed through the engine to clean the engine compressor, without perceptible shift in calibration.

Permissible Operating Temperatures

Suitability of the control under high operating temperatures has been demonstrated by the successful completion of military environmental qualification tests in accordance with Specification MIL-E-5009A, in an ambient temperature of 350 F using compressor discharge air at 925 F. Other units have been operated successfully at ambient temperatures as high as 600 F. Operation at these temperatures is made possible by a unique self-induced cooling arrangement utilizing a small amount of compressor discharge air to induce flow of cooler ambient air around the lower side of the diaphragm cavity. In this way the silicone-coated fiberglass diaphragm is maintained at a temperature several hundred degrees below that in the orifice chamber.

Operating temperature limit is determined only by physical properties of the plastic diaphragm material. Plastic is used to provide a diaphragm with no spring rate. This is required for devices having a scheduled output displacement. Null devices, on the other hand, can use metallic diaphragms for very high-temperature applications. Current research into new types of material and diaphragm configurations promises to eliminate operating temperature as a limitation.

Allowable Pressures

Maximum pressure limit of the control is determined primarily by strength of the housing mate-

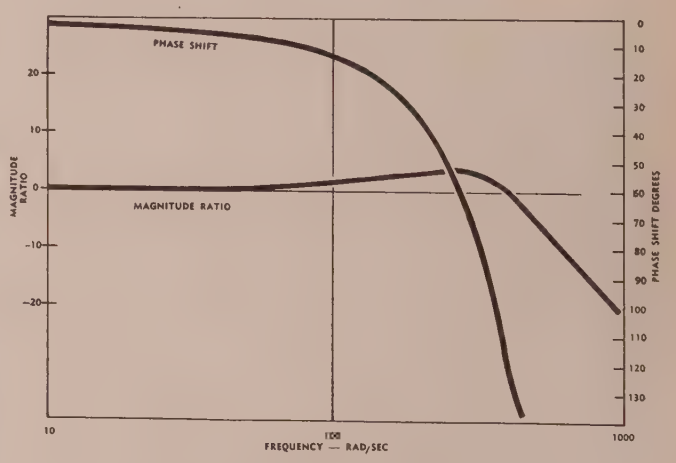

Fig. 15 – Theoretical Microjet frequency response

rials. Most present applications require operating pressures as high as 300 psig. Operating pressure level, however, is not a limiting factor, since diaphragms generally operate with very low pressure differential.

Accuracy

A design consideration contributing to the high degree of accuracy of the control is that large diaphragm areas – of the order of 5-6 sq in. – are generally selected, so that even at high-altitude operating conditions, significant actuating forces are available. Relatively large displacements of the order of 0.125-0.500 in. are used, thus minimizing inaccuracies due to manufacturing tolerances. Pilot valves or other control devices operated by the Microjet sensing element ordinarily require extremely small operating forces of the order of a few grams. As a result, an accuracy of approximately 0.3% is achieved over a wide range of altitude operation. For applications requiring large force outputs, conventional servo-positioning techniques are used.

Response

Transient characteristics of Microjet Control lend themselves well to application in high-performance systems. A theoretical frequency response characteristic is shown in Fig. 15. Crossover frequency is 300 radians per sec with a resulting phase shift of 5 deg at 20 radians per sec. Consistent with high crossover frequency is a high permissible internal gain which results in a minimum of following error on ramp inputs. These theoretical characteristics are borne out in actual test results which demonstrated time constants of from 0.001-0.005 sec and following error so low as to be negligible.

Afterburner Light-Off and Blow-Out Detection

Use of pressure ratio parameters for control is becoming more widespread. In large measure this is attributable to faster response characteristics of the pressure ratio system. As a result, in numerous applications of Microjet Control the system's primary purpose is to overcome slow response of an existing control.

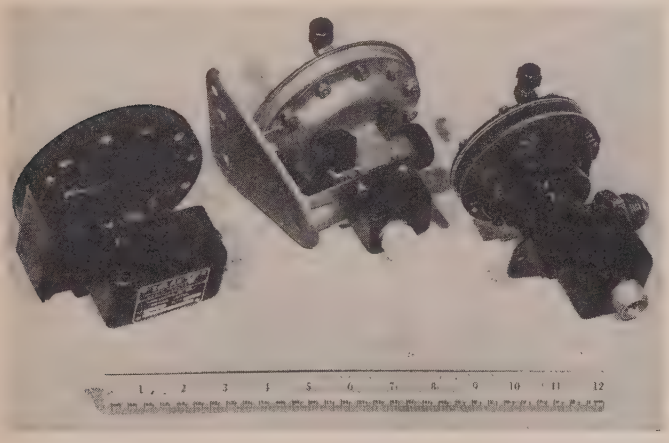

Fig. 16 – Typical production models of Microjet afterburner light-off and blow-out detectors

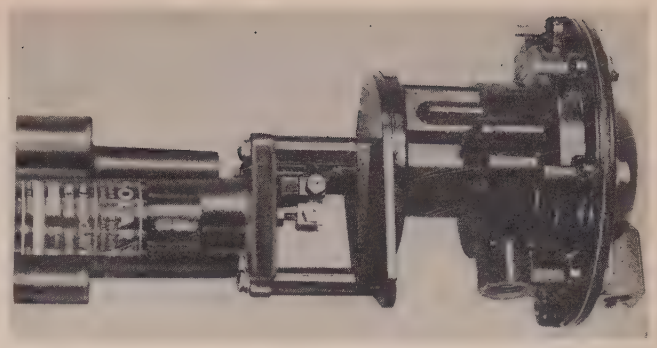

Fig. 17 – Overspeed control for 2-spool engine

In some current production engines equipped with conventional electronic temperature-sensing variable nozzle controls, slow thermocouple response has created problems associated with afterburner ignition. Transient effects of afterburner ignition are so severe that compressor surge can result if the jet nozzle is not opened quickly enough. Response of the temperature-sensing system is limited further by the fact that the time constant of the entire engine control loop is added to that of slow-response thermocouples. When the afterburner ignites, engine speed must first change, causing the governor to increase engine fuel flow and subsequently to increase the turbine discharge temperature, before thermocouples begin to detect error. Only then is the nozzle area correction initiated. Turbine pressure ratio, on the other hand, changes instantaneously when the afterburner ignites. As a result, Microjet Control is used in several applications as an afterburner light-off and blow-out detector to initiate rapid nozzle opening or closing. Several typical production models are pictured in Fig. 16.

Overspeed Control

In another application of afterburner light-off and blow-out detection, a Microjet Control of the type shown in Fig. 17 is used for preventing overspeed in a 2-spool engine. In this case afterburner blow-out transient causes the low-pressure compressor spool to overspeed severely. Because of mechanical limitations of the actuators it is impossible to close the nozzle rapidly enough to prevent overspeed. In this application, Microjet Control reduces engine fuel flow when a sudden change in turbine pressure ratio indicates that afterburner blow-out has occurred, thus preventing overspeed. Over 500 hr of extensive ground testing has demonstrated the success of this approach.

Jet Nozzle Control

Use of the Microjet principle to maintain constant turbine inlet temperature by controlling the variable jet nozzle has already been successfully demonstrated in ground tests, altitude tank tests,

and actual flight tests. Fig. 18 illustrates two typical controls of this type, one hydraulic, the other pneumatic. Use of pressure ratio for fully variable control of the jet nozzle is being given serious consideration by many major engine manufacturers because of the significant weight reduction, increase in reliability, and faster response. Fig. 19 compares a typical electronic temperature-sensing system weighing 30 lb and a pneumatic system weighing one-tenth as much. Some systems under development are wholly pneumatic, using pneumatic actuators and sensing pressure ratio parameters.

Ramjet or Afterburner Fuel Control

An application of the Microjet Control that has not been mentioned and which is currently the subject of an extensive development program is a fuel metering control for afterburners or ramjet engines. The basic fuel control of the ramjet engine is quite similar to that required for an afterburner. In both cases, the primary purpose of the control is to establish and maintain a basic fuel schedule at least roughly proportional to engine airflow. For the ramjet this fuel schedule is required mainly for ignition, the schedule being trimmed or overridden thereafter by a shock-wave positioning control.

Fig. 20 illustrates a Microjet Fuel Control applied to a ramjet engine. The pneumatic section of the fuel metering control senses pressure at the diffuser discharge. This pressure, for practical purposes, is roughly proportional to engine airflow. Full diffuser discharge pressure is applied to the upper side of the diaphragm of a Microjet Control, and a fraction of this pressure is applied to the lower side of the diaphragm. This fraction is determined by the area ratio of the two orifices in series. As a result, force produced by the differential pressure across the Microjet diaphragm is proportional to the absolute diffuser discharge pressure, thus providing the proper fuel-air ratio for ignition.

Shock-Wave Position Control

Once ignition of the ramjet has been established, the basic fuel schedule is modified by a secondary Microjet Control controlling the first orifice of the fuel metering control. The secondary control maintains proper position of the normal shock wave at the diffuser inlet. Some systems accomplish shock-wave positioning by controlling inlet diffuser pressure ratio as a scheduled function of flight Mach number. Others, as illustrated in Fig. 20, maintain a constant ratio between two pressures, one before and one behind the normal shock wave. Considerable success is indicated in numerous tests conducted by the NACA using both these methods for controlling shock-wave position.

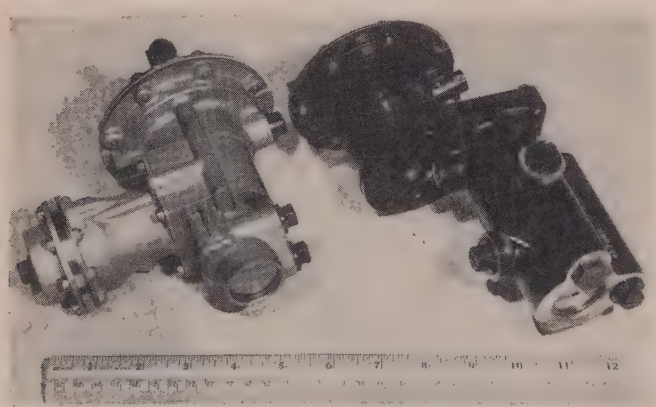

Fig. 18 – Two models of Microjet variable nozzle controls; pneumatic output (left), and hydraulic output (right)

There are many other methods by which position of the diffuser shock wave can be controlled. In the case of a ramjet engine with a fixed exit nozzle it is accomplished by trimming the basic fuel schedule. In other cases, it can be accomplished by varying the exit nozzle area. In supersonic fighters shock-wave control is generally achieved by changing inlet geometry with a ramp or movable spike. For the most part, any one of these methods utilizes pressure ratio as the basic parameter for control, and as such are projected applications of the Microjet principle.

Engine Fuel Control

Fuel flow control in the turbojet engine is a much more difficult problem than the control of ramjet or afterburner fuel flow. It is conventional practice to schedule engine acceleration fuel as a function of rpm, compressor inlet temperature, and compressor discharge pressure. Schedule accuracy is extremely critical and must take into account many factors of uncertainty. Variations in thermodynamic and aerodynamic characteristics of engines in production, slight changes in sp gr of fuels with age, grade, and source, differences in fuel heating value, and variations in combustion efficiency make it necessary to allow considerable margin between acceleration schedule and actual compressor surge limit.

In the interest of reducing compressor surge margin and eliminating the effect of variations in fuel characteristics, we have made engineering studies to determine if a new concept utilizing closed loop control of compressor pressure ratio might provide an answer to control of engine acceleration. These studies reveal many interesting possibilities, among them being that engine acceleration fuel as well as inlet guide vane position and compressor bleed airflow could be controlled by the use of pressure ratio parameters.

The compressor surge line may be defined as a function of compressor pressure ratio and corrected airflow:

$$\text{Surge} = f\left[\frac{P_{CD}}{P_{CI}}, \frac{W\sqrt{T_{CI}}}{P_{CI}}\right] \qquad (19)$$

Corrected airflow could be expressed as a function of axial Mach number at compressor inlet,

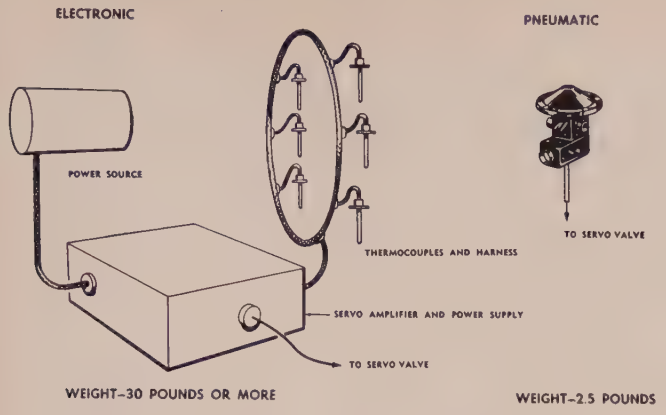

Fig. 19 – Comparison of weight of computing media

which in turn could be measured as ratio of compressor inlet and total static pressures. However, recent investigations by NACA and some major engine manufacturers indicate that wide variations in velocity distribution at the compressor inlet make accurate measurement of total to static pressure ratio at the compressor inlet virtually impossible. As air passes through the compressor, velocity distribution becomes considerably more uniform. Measurement of Mach number at the compressor discharge rather than at the compressor inlet is worthy of consideration.

Thus it may be possible to modulate the supply of engine acceleration fuel with a closed-loop type of control, sensing compressor pressure ratio and compressor discharge total to static pressure ratio. Control would permit engine acceleration at a limiting value of compressor pressure ratio as determined by corresponding value of corrected airflow. Utilizing these principles, it would be possible to simplify the engine fuel control system considerably, eliminating much fuel scheduling apparatus including complicated 3-dimensional cams, bellows, linkages, and so on. Modulating rather than scheduling fuel flow would result in complete independence from effects of variations in specific gravity, fuel heating value, and combustion efficiency, thus making it possible to reduce the margin between acceleration limit and surge limit so that faster engine accelerations could be achieved.

Conclusion

The foregoing illustrates that pressure ratio parameters will play an important role in control of virtually all phases of engine cycle performance, particularly in view of the high-temperature problems associated with supersonic flight. Use of pressure ratio has heretofore been limited because of lack of simple, highly accurate, reliable pressure ratio sensing and computing elements. Development of the Microjet principle has brought the use of pressure ratio parameters into the realm of practical reality.

Nomenclature

A = Effective area of diaphragm
a = Effective area of orifice
f = Arbitrary function
F = Force
K = Dimensional constant
N = Flow factor from Omega flow equation, where:

$$N = \sqrt{\frac{\left(\frac{P_0}{P}\right)^{\frac{2}{\gamma}} - \left(\frac{P_0}{P}\right)^{\frac{\gamma+1}{\gamma}}}{\frac{\gamma-1}{\gamma+1}\left(\frac{2}{\gamma+1}\right)^{\frac{2}{\gamma-1}}}}$$

P = Pressure
T = Total temperature
W = Weight of airflow
X = Input displacement
Y = Output displacement
γ = Ratio of specific heats, C_P/C_V

$\sum F$ = Summation of forces acting on needle

$\sum P_E$ = Summation of applied pressure equivalents = $\sum F/A$

Subscripts:

$_0$ = Ambient
$_1$ = First orifice inlet
$_2$ = Second orifice inlet
$_{CD}$ = Compressor discharge
$_{CI}$ = Compressor inlet
$_d$ = Small diaphragm
$_D$ = Large diaphragm
$_N$ = Pertaining to flow factor from Omega flow equation
$_S$ = Spring
$_{TD}$ = Turbine discharge
$_X$ = Pertaining to input displacement
$_Y$ = Pertaining to output displacement
$_{E,\,e}$ = Pressures applied to diaphragms

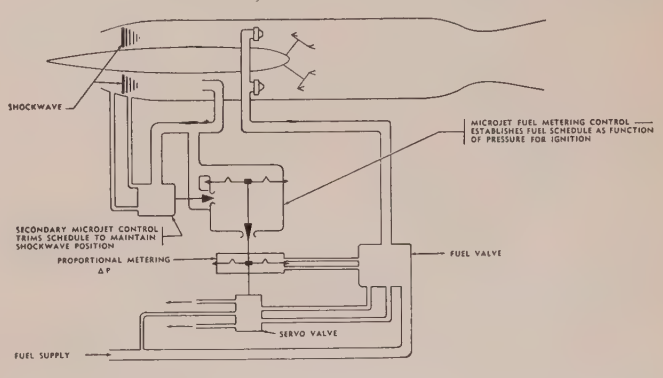

Fig. 20 – Microjet principle applied to control of ramjet fuel supply

Principles and Applications

THE principal objective of this paper is to demonstrate in the simplest manner possible the principles, general characteristics, and merits of "bypass" or "ducted-fan" engines. No attempt will be made to cover in detail the wide range of possible thermodynamic and gas dynamic variations of this type of aircraft powerplant. Attention will be focused on simplifying the basis of this analysis sufficiently to avoid blurring the overall picture. No consideration will be given to the innumerable details essential for the successful development of such an engine, but not essential for understanding its overall characteristics. Results obtained, therefore, can in no way be considered final, but serve to indicate the direction in which detailed analyses and development appear to be most necessary and promising.

This presentation shall aim also to call attention to the thoughts and developments devoted to ducted-fan engines almost 10 years ago, for the increasing interest in this form of aircraft powerplant appears to make such a review a timely one.

In pursuit of the general objectives stated, this presentation will be subdivided as follows:

(a) Considerations of propulsive efficiency.

(b) Overall efficiency and effectiveness of bypass engines.

(c) General arrangement of bypass or ducted-fan engines.

(d) Some considerations of boundary-layer intake.

Attention will be focused throughout exclusively on the problems of subsonic transport planes. Specifically, results will be quoted for a 435 knot cruising speed (500 mph) at an altitude of 30,000 ft and for a flight distance of about 3000 miles. While one reason for this choice of speed and altitude is the availability of dependable engine performance data for this set of flight conditions,[1] it is also believed that these conditions are of practical interest to commercial aviation of the near future.

Considerations of Propulsive Efficiency

The principles of the bypass or ducted-fan engine can best be discussed on the basis of so-called propulsive efficiency, defined as the thrust produced by a jet engine times the velocity of flight divided by the difference in kinetic energy between the air

[1] See NACA TR 891 (1947), "Thermodynamic Study of Turbojet Engine," by B. Pinkel and I. M. Karp.

# of Bypass Turbojet Engines

George F. Wislicenus, Pennsylvania State University

This paper was presented at the SAE Golden Anniversary Aeronautic Meeting, New York, April 18, 1955.

THE bypass or ducted-fan turbojet engine is a highly controversial aircraft powerplant. It is hoped that this presentation of its operating principles will lead to a more rational understanding of the pros and cons of the issue. Discussion is explicitly limited to transport aircraft applications at speeds in the neighborhood of 500 mph.

Noise, duct losses, boundary-layer intake, and structural considerations are all shown to be important.

It appears that a comprehensive design development of bypass or ducted-fan engines in connection with aircraft aerodynamics and structure poses a serious problem in the field of high-subsonic-speed transport aircraft.

stream entering and leaving the engine. Propulsive efficiency, η, can be written:

$$\eta = \frac{1}{1 + \frac{\Delta V}{2V_1}} \qquad (1)$$

where:

ΔV = Difference in velocity between discharging and incoming streams (thrust per unit mass flow passing through the engine)

V_1 = Velocity of incoming air relative to the engine (presumed here to be equal to the forward velocity of the airplane)

It is immediately evident that propulsive efficiency diminishes with increasing velocity change, ΔV, of the stream through the engine, as shown graphically by the curve marked $k = 0$ in Fig. 1. (The significance of the parameters k and of the other curves in Fig. 1 will be discussed later.) Since ΔV is also the absolute velocity of the jet behind the moving airplane, it is seen that change in propulsive efficiency with ΔV simply reflects the changes in lost kinetic energy left in the air behind the aircraft. The fact that thrust per unit of mass flow changes with the first power of ΔV, whereas kinetic energy of the jet follows a quadratic law also suggests the advantage, efficiency-wise, of low jet velocities.

At subsonic flight velocities considered here, present jet engines have a rather high $\Delta V/V_1$ ratio,

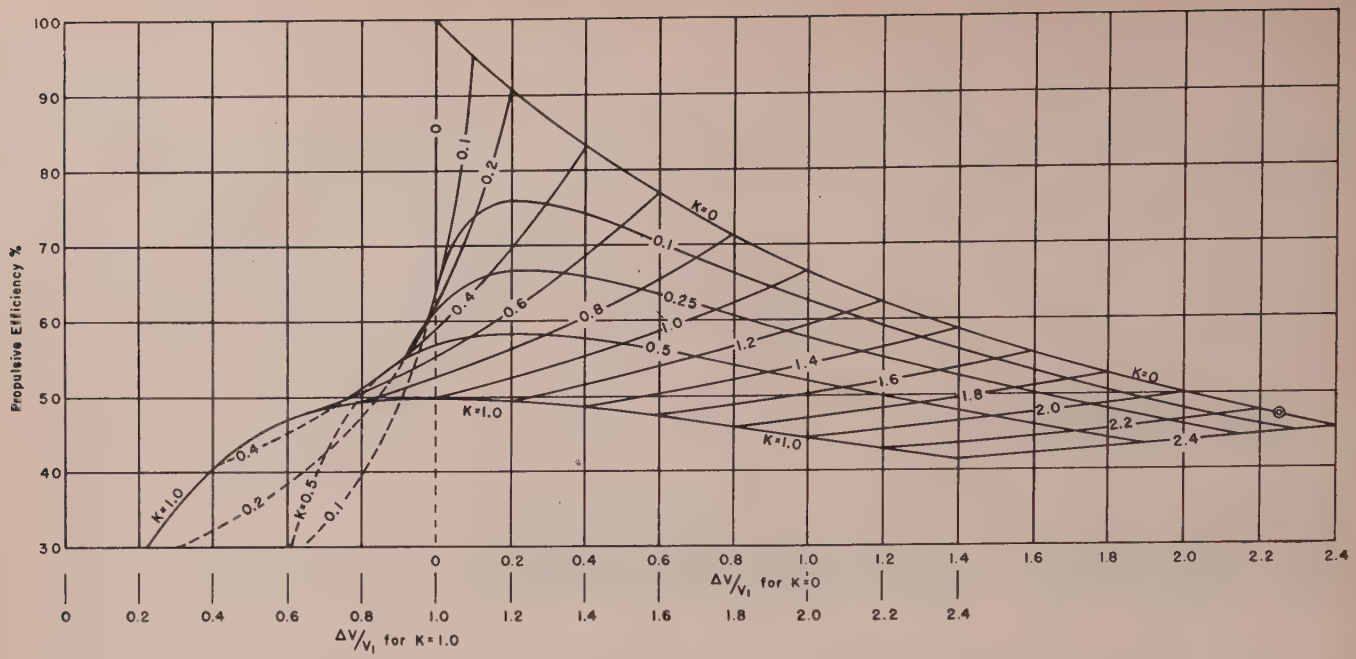

Fig. 1 – Carpet plot of $\Delta V/V_1$ versus propulsion efficiency for several values of duct-loss coefficient k

and therefore a rather low propulsive efficiency. On the other hand, at the same flight velocity standard propellers have rather low $\Delta V/V_1$ ratios with correspondingly high propulsive efficiencies, and would be preferable were it not for prohibitive propeller-blade losses, vibrations, and noise, as well as the high weight of reduction gears and propellers. These considerations lead to the use of jet engines in preference to propellers at flight velocities approaching or exceeding 500 mph.

Thus in the range of flight speed considered here, one is compelled to accept the low propulsive efficiencies of standard jet engines unless he can use a powerplant having general characteristics somewhere between the propeller and the standard jet engine. This will avoid the shortcomings of the propeller at high subsonic speeds, while allowing for operation with a lower jet velocity and, therefore, a better propulsive efficiency than obtainable from standard jet engines. This combination of requirements leads to the consideration of bypass or ducted-fan engines.

To illustrate this point, consider a modern jet engine operating at these flight conditions:

Airplane velocity $V_o = V_1 = 733$ fps $= 500$ mph

Ambient absolute temperature, $T_o = 412$ R (standard for 30,000-ft altitude)

From reference 1, the following representative engine characteristics for a modern jet engine operating at the flight conditions stated are selected:

Turbine-inlet temperature, $T = 1960$ R $= 1500$ F

Compressor pressure ratio $= 12{:}1$

Thrust per unit mass flow of air, slugs/sec, $F/M_a = \Delta V = 1630$ fps

Jet velocity at 500 mph, $V_2 = 2363$ fps

This thrust and jet velocity correspond to a "specific impulse" of approximately 50 lb thrust per lb of air per sec.

For these flight conditions, reference 1 gives a sfc of 1.03 lb of fuel per lb of thrust per hr, corresponding to an overall propulsion efficiency of about 17.8%.

From the data above, $\Delta V/V_1 = 2.225$, and equation (1) gives propulsive efficiency $= 47.4\%$.

These two efficiencies lead to a thermal efficiency for the powerplant of approximately 37.5%, which is representative for modern gas turbines operating at altitude temperatures.

It is evident from the foregoing that low propulsive efficiency renders jet engine performance at moderate speeds somewhat questionable as to overall economy. An attempt to improve this part of the overall efficiency is natural.

Before discussing the solution of this problem by the bypass or ducted-fan engine, consider briefly the use of more nearly standard jet engines at reduced pressure ratios and turbine-inlet temperatures. This would reduce jet velocity increase, ΔV, and improve the propulsive efficiency, but at the same time would reduce thermal efficiency in accordance with the reduced turbine temperature and pressure ratio. This opposite trend of propulsive and thermal efficiencies manifests itself in a very slow and insignificant change in overall efficiency, or sfc, for varying turbine-inlet temperatures when using optimum pressure ratios. The greater simplicity, ruggedness, and reduced cost of a jet engine designed for lower turbine temperature and reduced pressure ratio makes this solution significant from a practical point of view, but is not regarded as part of the subject of this paper since the principal idea behind the development of by-

pass or ducted-fan engines is to obtain the desired increase in propulsive efficiency *without* a corresponding reduction in thermal efficiency.

A simple and natural way of realizing this principle of a bypass or ducted-fan engine is to increase the flow capacity of the engine compressor or of the low-pressure stages of this compressor beyond the flow capacity of the compressor-driving turbine, thus bypassing part of the compressor stream and forming a cold jet of correspondingly reduced velocity. With this arrangement the compressor-driving turbine must furnish more power to the compressor than without bypassing. It is evident that the hot turbine-discharge jet has a reduced kinetic energy and thereby a reduced velocity, satisfying the *before-mentioned* objective for obtaining lower values for the jet velocity ratio $\Delta V/V_1$. This simple bypass principle satisfies the requirement for increased propulsive efficiency without necessarily involving major sacrifices in thermal efficiency, for the turbine operates at undiminished temperature and pressure ratio.

A jet engine designer will readily appreciate that an increase in compressor flow rate of the type just described is limited to fairly small values unless one makes major revisions in the engine arrangement, particularly changes in the rotative speed of the enlarged portion of the compressor. However, the substantial increases desired in propulsive efficiency demand correspondingly substantial increases in the flow rate through the enlarged part of the compressor. For this reason, earlier engines employing this principle incorporated a separate turbine-driven compressor element called a "fan," and were called "ducted-fan engines." In spite of its title, a part of the objective of this paper is to review the principles behind these earlier attempts. It will direct slightly more attention to "ducted-fan engines" with fairly large relative increases in the flow rate than on engines bypassing small parts of the compressor flow, although the entire spectrum of possible or likely increases in airflow will be investigated.

The earliest known engine to incorporate the

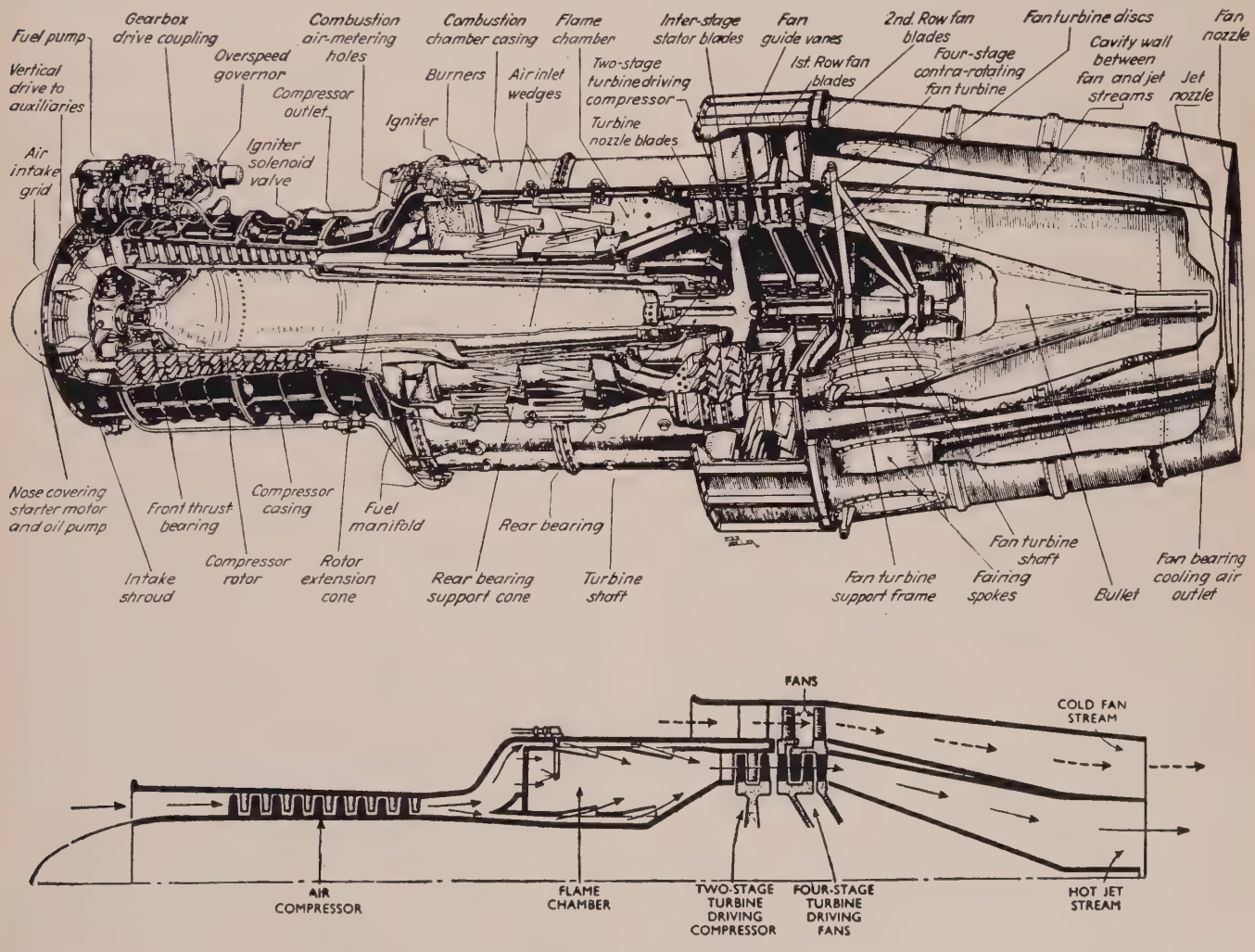

Fig. 2 – Early Metro-Vickers engine incorporating ducted-fan principle

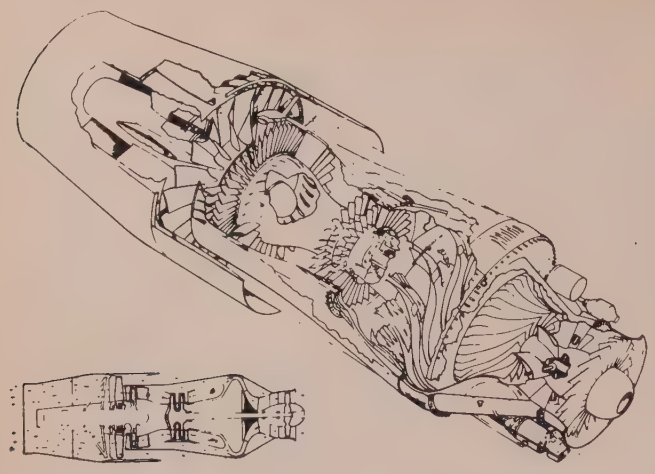

Fig. 3 – Packard ducted-fan turbojet engine (model XJ49-V-1)

"ducted-fan" principle is the Metro-Vickers engine shown in Fig. 2. In this engine the two-stage counterrotating "fan" is driven by a four-stage counterrotating turbine behind the compressor-driving turbine in the direction of the engine stream. Cold airflow through the augmenting fan in this case exceeded airflow through the high-pressure or "primary" part of the engine; the latter will be referred to subsequently as the "hot stream."

A feature of this engine still regarded as of great potential significance lies in the fact that the augmenting turbine and fan were added to an existing jet engine, thus substantially reducing the development cost and time of the ducted-fan engine as such. (Later in this paper we shall consider how this principle would apply to a modern turbojet engine.) Between 1946 and 1948, the aircraft division of the Packard Motor Car Co. worked on a ducted-fan engine with essentially the same characteristics. (See Fig. 3.) The Packard engine also added a fan part to an essentially existing jet engine, requiring only slight modification of the compressor-driving (primary) turbine to reduce gas velocity at the primary turbine discharge. This was necessary to permit utilizing energy of this gas stream to drive the fan turbine. The Packard engine was designed for approximately three times the take-off thrust of the English ducted-fan engine shown in Fig. 2, and was simpler by virtue of the use of a single-stage fan driven by either a two-stage or single-stage turbine, thus taking advantage of some significant advancements in the stage pressure ratio of axial compressors initiated by the Packard Aircraft Engine Division of those days.

To be more precise in discussing the principles of bypass or ducted-fan engines, it is necessary to recall briefly the essential gas-dynamic reason why jet engines are better suited than propellers for high flight speeds. The reason lies in the fact that the rotating elements of jet engines – in particular the first compressor stages – are operating in a closed duct, thereby making the flow velocities through the rotating elements of the jet engine essentially independent of the forward velocity of the aircraft. It follows that the rotating elements of the bypass or ducted-fan engine must remain "ducted" in order to avoid the speed limitations of the open propeller. Such ducting, however, necessarily includes flow losses, internally as well as externally, at least in proportion to the added skin-friction area of the duct. These flow losses must be considered in any realistic appraisal of the efficiency advantages of bypass or ducted-fan engines over standard jet turbines.

The duct flow losses may be regarded as proportional to the velocity head, $V_1^2/2g$, of the stream approaching the engine. Designating this proportionality factor as k, the corrected propulsive efficiency of an engine with duct losses $kV_1^2/2g$ can be written:

$$\eta = \frac{\Delta V \cdot V_1}{\frac{V_2^2 - V_1^2}{2} + K\frac{V_1^2}{2}} \tag{2}$$

which simplifies to:

$$\eta = \frac{1}{1 + \frac{\Delta V}{2V_1} + \frac{K}{2}\frac{V_1}{\Delta V}} \tag{3}$$

Equation (3) reduces to equation (1) when $k = 0$. Curves for progressively increasing values of duct-loss coefficient k are shown in the "carpet plot," Fig. 1, where curves for various degrees of duct loss are separated from each other by a horizontal shift of the $\Delta V/V_1$ scale towards the left in direct proportion to the duct-loss coefficient k. Lines of constant $\Delta V/V_1$ ratio are also entered on the "carpet," and represent cross-plots of the family of curves k = constant, thus showing the effect of increasing duct loss for given constant values of jet velocity ratio $\Delta V/V_1$.

It is noted that the effect of duct losses on the propulsive efficiency of the engine is a very significant one.[2] Indeed, for the extreme case of losing one full velocity-head by the presence of ducting ($k = 1.0$), no significant efficiency advantage can be derived from reducing the ratio $\Delta V/V_1$. This is seen by comparing the propulsive efficiency of the reference jet engine previously described and marked by a double circle on the $k = 0$ curve above $\Delta V/V_1 = 2.225$. Even small duct losses, characterized by $k = 0.1$, result in a maximum obtainable propulsive efficiency of about 0.75; or substantially less than the propulsive efficiencies obtained with unducted propellers, which may well exceed 90%. Furthermore it is seen that with duct losses, the propulsive efficiency curves have maxima at some finite value of $\Delta V/V_1$ which is higher with increased duct-loss coefficient k.

[2] Private communication from Calvin A. Gongwer, Aerojet Corp.

As explained above, the desired reduction in jet velocity ratio $\Delta V/V_1$ is obtained in the bypass or ducted-fan engine by adding a cold stream of weight flow W_c lb/sec to the hot stream through the primary part of the engine of weight flow W_h lb/sec. The general relationship between $\Delta V/V_1$ and the "ratio of augmentation" W_c/W_h was considered a little too complicated for presentation in this paper. However, a simple form is obtained by assuming that the cold jet velocity equals the hot jet velocity. This assumption does not exactly correspond to the actual conditions likely to be encountered, wherein the two velocities are unequal. However, it is believed that the effect of this velocity difference between these two parts of the jet is not sufficient to affect the significance of the results obtained assuming a single resultant jet velocity V_3.

In the bypass or ducted-fan engine the kinetic energy of the jet in the basic unaugmented engine (with propulsive efficiency $\eta_{i0} = 0.474$), is divided between the hot and cold parts of the jet in the augmented engine by means of a turbine-driven compressor or fan with a combined turbine and fan efficiency $= \eta_{tf}$. In this part of the paper this combined efficiency is assumed uniformly $= 0.72$, corresponding to turbine and fan efficiencies $= 85\%$. (For reasons not discussed here, it is of no consequence whether the efficiencies be either polytropic or adiabatic.)

This division of jet energy in the basic engine over the two streams in the augmented engine is expressed analytically as:

$$\frac{V_2^2 - V_1^2}{2g} \cdot W_h = \frac{V_3^2 - V_1^2}{2g}\left[W_h + W_c \frac{1}{\eta_{tf}}\right] \qquad (4)$$

where:

$V_2 =$ Jet velocity in the basic engine constituting the primary part of the augmented engine

$V_3 =$ Uniform velocity of the jets in the augmented engine

Let $\Delta V_2 = V_2 - V_1$ and $\Delta V_3 = V_3 - V_1$. Then equation (4) becomes:

$$\frac{\Delta V_2}{V_1}\left(2 + \frac{\Delta V_2}{V_1}\right) = \frac{\Delta V_3}{V_1}\left[2 + \frac{\Delta V_3}{V_1}\right]\left[1 + \frac{W_c}{W_h}\frac{1}{\eta_{tf}}\right] \qquad (5)$$

Let $\Delta V_2/V_1 = 2.225$, the previously assumed value for the basic engine. The relationship between $\Delta V_3/V_1$ and the augmentation ratio W_c/W_h is represented by the corresponding curve in Fig. 4.

Corresponding values of propulsive efficiency for the augmented engine may be calculated from $\Delta V_3/V_1$ and in accordance with equations (3). These have been plotted in Fig. 4 for various values of the loss coefficient k. No significant increase in efficiency is obtained over the basic engine if k is of the order of unity. As expected, propulsive efficiency increases significantly with augmentation ratio.

[2] Private communication from Richard J. Rossbach and Curtis L. Walker, NACA.

Overall Efficiency and Effectiveness of the Bypass Engine

The relative advantage of the augmented engine is not directly proportional to its propulsive efficiency as compared to that of the "basic engine" because of loss in thermodynamic efficiency resulting from addition of the "fan" (or augmenting part of the compressor), and its driving turbine.[3] At this point it is no longer possible to use any of the foregoing simplifications because the approximations involved will decisively influence the results obtained. Instead, it is necessary to consider the true thermodynamic engine cycle and derive engine performance directly therefrom. In doing so the previous assumption of equal velocities in the hot and cold parts of the jet is replaced by the more realistic condition of equal static pressures immediately behind the fan and behind the fan-driving turbine runner. Under this condition it is unnecessary to require a solid partition between the hot and cold parts of the jet, as employed in the original British ducted-fan engine. (See Fig. 2). Rather, a certain degree of mixing between these two streams can be assumed which resulted in a slight increase in overall efficiency.

Furthermore, the thermodynamic analysis expresses internal duct losses in the form of polytropic efficiencies of fan and turbine streams, assumed to be 85 and 90% respectively, rather than

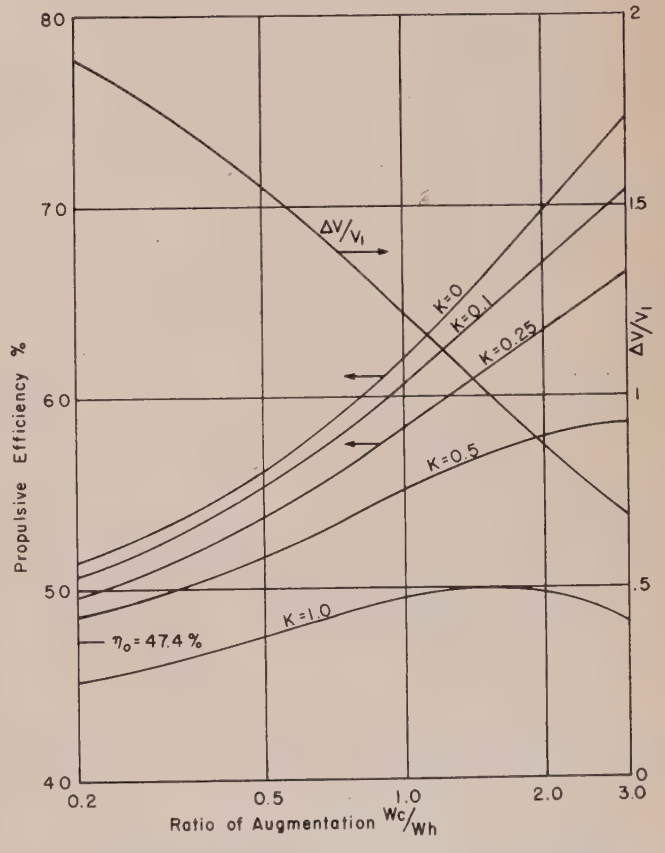

Fig. 4 – Variation of augmentation ratio with propulsive efficiency for several values of k

in terms of a duct-loss coefficient k. The polytropic jet efficiency was assumed to be about 97%. It is felt that these assumptions may be equivalent to a duct-loss coefficient k of about 0.1, although no direct comparison seems possible between this coefficient and the thermodynamic cycle efficiencies. It must be remembered that neither form of calculation reflects actual conditions of engine flow, since in reality the losses are concentrated in certain limited regions (boundary layers and mixing zones); that is, losses are not distributed uniformly throughout the gas streams as assumed by either form of analysis employed here.

The lower curve in Fig. 5 gives the results of this thermodynamic analysis plotted as thrust ratio increase at the specified flight conditions versus augmentation ratio of the engine. This thrust ratio, F/F_o, is also the ratio in overall efficiency η/η_o of the augmented engine to the basic engine. This is so since the fuel-consuming parts and flow conditions in the engine are assumed unaffected by the addition of the cold augmenting stream.

Generally speaking, one can conclude from these curves that thrust and overall efficiency may be increased by about 20% if the cold part of the augmenting flow is about twice the hot flow through the "primary" part of the engine.

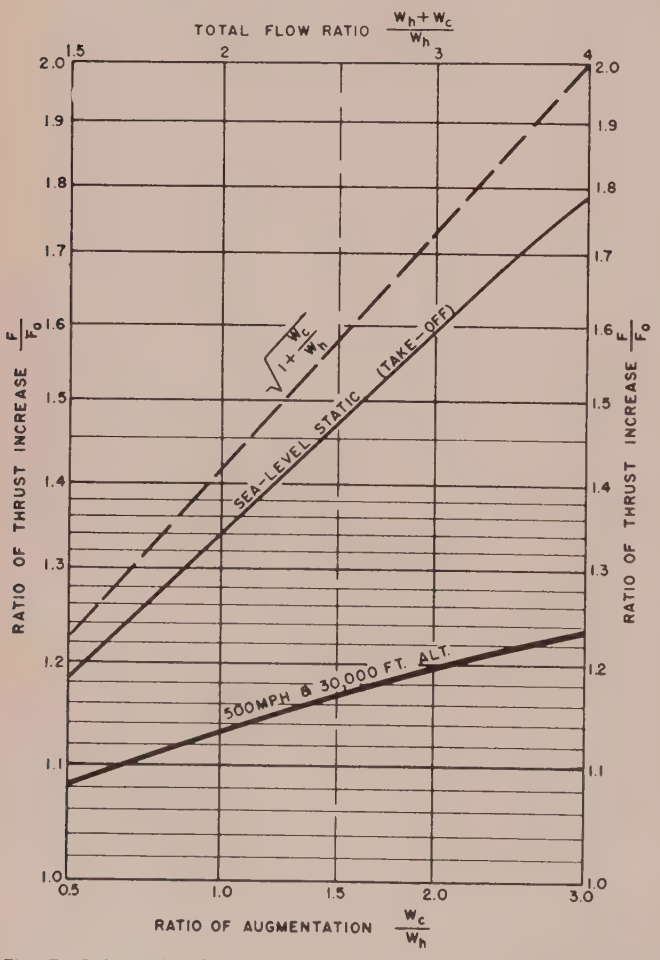

Fig. 5 – Relationship between ratio of thrust increase, augmentation ratio, and total flow ratio for different operating conditions

Beside the effect of augmentation on thrust and efficiency at normal flight conditions, it is of interest to consider the effects of augmentation at take-off and landing. For this reason, ratio of thrust increase at sea-level static conditions (zero speed) was calculated for the same type engine and plotted as the upper solid curve in Fig. 5. Note that ratio of thrust increase at zero speed is much greater than at 500 mph, indicating that the practical value of such augmentation is not completely described by the increased thrust and efficiency at normal speed. For a bypass or ducted-fan engine with an augmentation ratio of $W_c/W_h = 2$, and for the case considered here the thrust increase from flight at altitude to zero-speed conditions is 31% greater than for the "basic" jet engine, a significant improvement in that particular area of operation in which standard jet engines are notoriously poor. The advantage of the augmented engine at take-off can be increased to 50% by supplementary burning between the compressor-driving and the fan-driving turbine stages. In doing so, the sfc remains somewhat lower than for the basic jet engine at take-off, in marked contrast to augmentation by a conventional afterburner.

Efficiency increases plotted as the lower curve in Fig. 5 are recognized as representing only part of the complete story involved in the application of bypass or ducted-fan engines to transport aircraft. Obviously, the addition of a fan and its turbine or an increase in rate of flow through part of the compressor will increase engine weight over that of the basic jet engine used for comparison.

The effect of engine weight on efficiency can only be evaluated in definite form by reference to a specific flight schedule. For this purpose, consider flight at 500 mph and a 30,000-ft altitude for a duration of 7 hr. The sfc calculated in reference 1 for the basic engine under these flight conditions is 1.03 lb fuel per lb thrust per hr.

We shall assume further that the basic jet engine weight is 1.15 times its thrust at altitude and at 500 mph.

The sfc of the augmented engine is, then,

$$f = f_0 \frac{\eta_o}{\eta} = 1.03 \frac{\eta_o}{\eta} \qquad (6)$$

where efficiency ratio η_o/η is the reciprocal of thrust ratio F/F_o at 500 mph plotted in Fig. 5.

Weight of the augmented engine is related to basic jet engine weight by a coefficient a defined as the percentage increase in engine weight divided by the percentage increase in weight of airflow through the engine.

This relationship is expressed analytically as:

$$(EW) = (EW)_o \left(1 + a \frac{W_c}{W_h}\right) \qquad (7)$$

where:

(EW) = Engine weight

Subscript o refers to basic jet engine without augmentation

Total fuel weight, (WF) divided by total thrust

F is related between engines by the efficiency ratio η_o/η. Combined with equations (6) and (7), this leads to:

$$\frac{(WF)+(EW)}{F} = \frac{\eta_o}{\eta}\left[\frac{(WF)_o}{F_o} + \frac{(EW)_o}{F_o}\left(1 + a\frac{W_c}{W_h}\right)\right] \quad (8)$$

This applies only to the one particular length of flight assumed previously. For our specific example the significant numerical values are $(WF)_o/F_o = 7.2$ and $(EW)_o/F_o = 1.15$. With these values, equation (8) becomes:

$$\frac{(WF)+(EW)}{F} = \frac{\eta_o}{\eta}\left[7.2 + 1.15\left(1 + a\frac{W_c}{W_h}\right)\right] \quad (9)$$

The efficiency ratio appearing in the last equation is also a function of the augmentation ratio W_c/W_h. It follows that fuel weight plus engine weight per unit of thrust (for a flight duration of 7 hr at the specified flight conditions), can be plotted as a function of augmentation ratio W_c/W_h, with the weight increase factor a as the independent parameter. This is done in Fig. 6 in terms of percent of fuel plus engine weight in relation to that same weight in the basic jet engine.

The physical significance of $a = 1$ means that doubling the total airflow through the engine by augmentation would also double the total engine weight. This, of course, is an extremely unfavorable assumption leading to no significant weight savings; indeed, a weight increase would result as shown by the upper broken curve in Fig. 6.

The solid curves in Fig. 6 represent the results obtained for $a = 0.5$ and 0.25, that is, doubling the total airflow ($W_c/W_h = 1$) will increase total engine weight by 50 and 25%, respectively. Under these assumptions the fuel plus engine weight for a 7-hr flight is reduced by 5.5 and 11%, respectively. The designer and user of modern aircraft will appreciate the practical significance of such weight reductions by virtue of the effects of weight reduction either on the payload for an aircraft of given size, or on the gross weight of the aircraft required to handle a given payload on the given flight schedule.

It is of interest to note the difference in augmentation ratio at which the fuel plus engine weight is a minimum under the different assumptions made. For $a = 0.5$ this minimum lies between $W_c/W_h = 1$ and $W_c/W_h = 1.5$, whereas for $a = 0.25$ the minimum occurs at about $W_c/W_h = 2.3$. This leads to the conclusion that an augmentation ratio greater than $W_c/W_h = 2$ can hardly ever be justified on this basis alone. It should be considered, however, that installed engine weight may not be dictated entirely by normal flight conditions, but rather by take-off requirements. In this case larger augmentation ratios could be justified on the basis of the upper solid curve in Fig. 5, but the real answer to this question demands more detailed investigations which are beyond the scope of this paper.

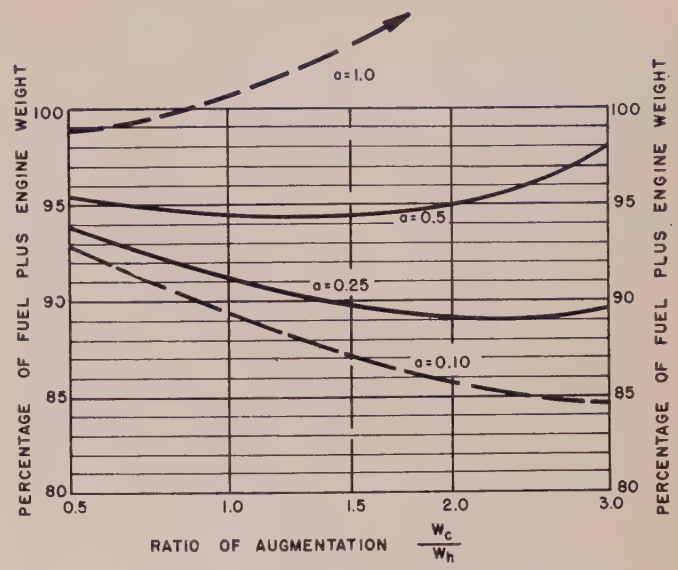

Fig. 6 – Percent of fuel plus engine weight versus augmentation ratio for different values of a

The broken curve for $a = 0.10$ is given in Fig. 6 only to show the trend of overall weight for reduced fan and fan-turbine weights. It is not believed that $a = 0.1$ represents a practicable possible value at the present time.

Before closing the discussion on general principles and characteristics of bypass and ducted-fan engines, it seems advisable to call attention to the problems of engine noise that may well become a major, if not decisive, factor in the selection of this type of powerplant for commercial aircraft.

It is dangerous to talk about noise and the desirability of its reduction without reference to specific frequencies and the corresponding noise attenuation to be expected between source and either passengers or residents neighboring airfield. Such detailed consideration is, perhaps, premature in this field and lies outside the scope of this paper. At this time it will suffice to state that the propelling jet itself appears to be a major source of jet engine noise. The origin of much of this noise is probably somewhere behind the engine, and appears to be connected with the mixing process between the jet and the surrounding air stream. It is safe to say that intensity of this noise will diminish very rapidly with jet velocity (possibly as the 8th power). Thus a reduction in jet velocity as contemplated for bypass or ducted-fan engines is almost certain to reduce jet noise in a very significant manner. This may be another important reason why this type engine occupies an important place between standard jet engines and turboprop engines.

General Arrangement of Engines

Changes in engine design and arrangement necessary to obtain various augmentation ratios are

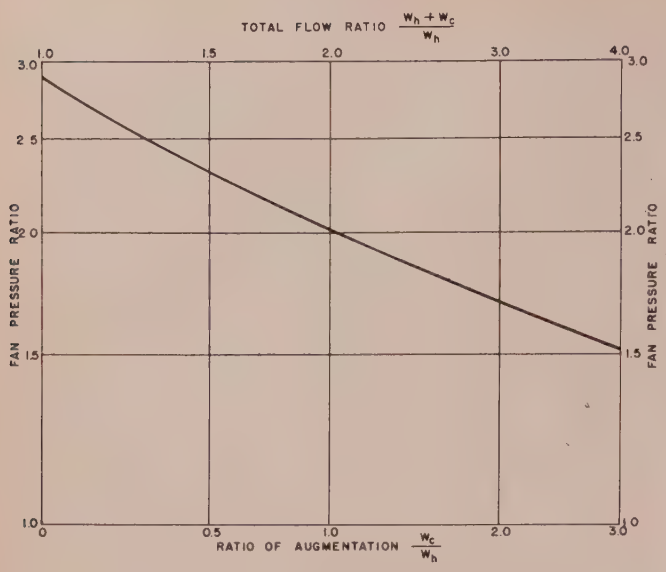

Fig. 7 – Relationship between fan pressure ratio, augmentation ratio, and total flow ratio

dictated not only by the varying airflow rate but also by the pressure ratio of the augmenting part of the compressor, or the "fan." For this reason the fan pressure ratios used in the thermodynamic analysis which lead to the curves in Fig. 5 are plotted in Fig. 7 as a function of augmentation ratio.

Only for augmentation ratios exceeding unity can one expect to produce the necessary fan pressure ratio in two stages, and at the highest augmentation ratios, possibly in one stage. At augmentation ratios of appreciably less than unity, the fan becomes a multistage axial-flow compressor, and would be most naturally the low-pressure part of the main-engine compressor slightly increased in diameter to take care of the increased airflow rate. For augmentation ratios of less than unity, therefore, it is appropriate to use the term "bypass engine" in the more limited sense of the word, whereas for augmentation ratios exceeding unity the term "ducted-fan engine" may be more appropriate. Generally, no such distinction is made in this paper, for the operating principles in both ranges of augmentation ratios are the same.

Focusing attention on the high-flow end of the scale of augmentation (characterized by low pressure ratios of the augmenting stream), one thinks of a turboprop engine as an extreme case. Since the next step towards a ducted-fan engine necessarily involves ducting the fan in order to realize its principal advantages at high speeds, a natural form of ducted-fan engine appears to be similar to a turboprop engine. The main difference lies in replacing the propeller by a shrouded fan wheel or an axial compressor with very few stages. Fig. 8 is a diagrammatic view and section of such a unit.

In the lower half of Fig. 8 a single-stage fan having a rather large flow area is shown incorporating a very short shroud. Its cold jet passes over the streamlined exterior of the primary part of the engine. Obviously, skin-friction losses resulting from the fan jet passing over this nacelle must be charged against the overall efficiency of the unit and its effect included in the losses expressed by the duct-loss coefficient k. Extending the shroud and so enclosing the fan over the entire length of the engine, as shown in the upper half of Fig. 8, is resorted to to avoid this type of loss. In this case flow velocities between the engine housing and the primary engine casing can be kept sufficiently low to minimize flow losses in this part of the stream. The external friction drag of this arrangement, obviously, is a significant factor in its overall efficiency.

It may be mentioned in passing that the flow arrangement in the upper half of Fig. 8 may conceivably be used to cool the primary engine air stream between the two major portions of the main compressor. The feasibility of this scheme is quite uncertain until such time as the size and aerodynamic resistance of the necessary heat exchanger has been fully explored.

An alternate arrangement for a ducted-fan engine is shown in Fig. 9. This arrangement follows rather closely that of the early British ducted-fan unit in Fig. 2 as well as that of the Packard Engine in Fig. 3, except for substitution of a modern jet engine as the primary part of the unit.

In comparison with the arrangement shown in the lower half of Fig. 8, the design in Fig. 9 has an advantage in that the stream *approaching* the fan has to pass over the nacelle containing the engine. In this case no additional friction losses should arise from the fan stream. It is expected that this fan arrangement will have a favorable influence on both the general aerodynamics of the airflow over the nacelle and the propulsion efficiency. A further exploitation of this manner of utilizing the fan flow will be discussed later.

The arrangement in Fig. 9 is regarded favorably because:

(a) Duct-flow losses may be regarded as low, justifying a low value of duct-loss coefficient k (probably not over 0.1).

(b) Increase in engine weight over the primary engine weight certainly would be low compared to the weight flow increase obtained with the fan, justifying the values of weight factor a assumed for the solid curves in Fig. 6.

(c) A thrust-augmenting fan such as shown in Fig. 9 probably can be added to an existing jet engine with minimum modification of the engine. Such modifications probably would be limited to structurally reinforcing the primary engine casing surrounding the last stage of the primary turbine, since the weight of the fan, its casing, and the fan-

driving turbine probably would have to be supported from this part of the casing.

(d) A slight increase in distance between primary and fan-driving turbines may allow the use of intermediate burning between the two turbines, thus providing for a more efficient increase in engine performance for take-off or climbing as compared to that possible with simple tail pipe burning.

With reference to item (c), note that the arrangement shown in Fig. 9 (internal structural elements indicated by broken lines), puts minimum requirements on the structural strength and rigidity of the shroud surrounding the fan and the fan and turbine discharge nozzles. Compare this to the older classical arrangements shown in Figs. 2 and 3, in which the structural support for the fan and fan-driving turbine came from behind the fan and its turbine, requiring a fan casing strong enough to support this structure. The reason for this seeming round-about method of structural support is that it was desired to keep the space between the primary and fan-driving turbines free of structural elements because the gas dynamics problems of flow in this region were insufficiently explored at the time this design was chosen. In the case of the British engine of Fig. 2, the primary turbine discharges directly into the fan-driving turbine, thus minimizing the distance between the primary part of the engine and the fan. This arrangement precludes the possibility of locating any structural parts between the primary and fan turbines. However, preliminary studies carried out at the Packard Aircraft Division indicated the feasibility of the arrangement in Fig. 9, which employs a strong cooling stream between structural elements and guide-vane surfaces (relatively few, large hollow vanes), between the two turbines.

Another significant practical problem encountered with the arrangement of Fig. 9 lies in the structural design of the rotating shroud between the fan and fan-driving turbine, and in the radial fairing between the fan blades and the turbine blades below the fan. This problem received much attention during the Packard ducted-fan development, and it was indicated clearly that a practical solution to this problem, though difficult, is definitely feasible. A detailed presentation of the solution is not included here.

Boundary-Layer Intake

Any discussion of aircraft or ship propulsion efficiency would be incomplete without some consideration of improvements possible by suitable interaction between the engine stream and the general flow about the propelled craft.

To be more specific, aerodynamic or hydrodynamic propulsion is brought about primarily by producing a rearward jet whose rate of momentum flow relative to the stationary atmosphere is equal and opposite to the total drag on the moving craft. This drag, however, manifests itself by an equivalent forward momentum flow of the air dragged along by the moving craft. Thus in normal propulsion schemes there are two streams of equal and opposite momenta left behind the craft; the friction wake and the propelling jet(s). The dynamic conditions of propulsion could be equally well satisfied if the engine streams would just fill in the friction wake, leaving the air behind the airplane undisturbed except for the vertical momentum of the "downwash" necessary to sustain flight of any heavier-than-air craft. Thus this ideal flow configuration would minimize the kinetic energy left behind the airplane and thereby reduce propulsion work to its lowest possible value.

A complete study of ways to approach this ideal is not known to the writer. The solution that suggests itself immediately is that of boundary-layer intake to the engines. Only this well-known scheme will be explored here with respect to bypass or ducted-fan engines.

The merits of boundary-layer intake have been examined repeatedly. The results with respect to overall flight efficiency are usually somewhat disappointing. This is due in part to the fact that production of a friction wake is itself a very inefficient process. The bulk of the total friction work is dissipated in viscous or turbulent shear motion, so that recovery of energy or momentum in the friction wake can never be expected to affect more than a fraction of the total friction work. However, another reason usually exists why recovery of friction momentum is incomplete, namely, the fact that for a standard jet engine, the rate of flow through the engine for a given thrust is determined by the specific impulse of the engine, a quantity which usually does not vary over wide limits. With

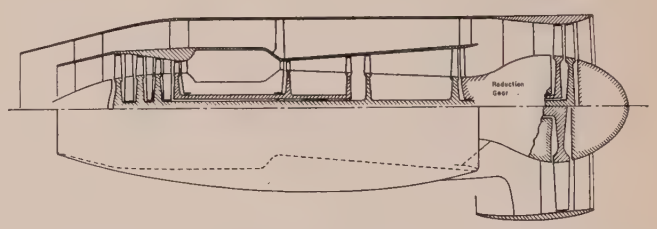

Fig. 8 – Sections of two possible arrangements of ducted-fan engines

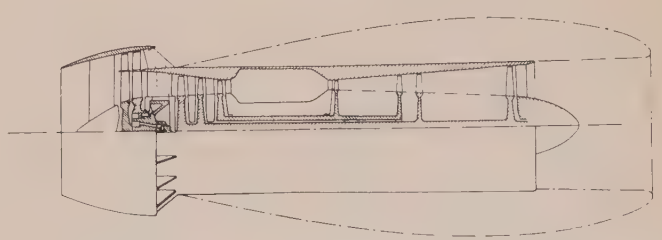

Fig. 9 – Alternate arrangement for a ducted-fan engine

a bypass or ducted-fan engine, however, specific impulse becomes a design variable depending primarily on the augmentation ratio W_c/W_h. It seems reasonable, therefore, to inquire into the possibility of increased efficiency by boundary-layer intake when using ducted-fan engines.

It becomes necessary now to distinguish between the airplane velocity V_o and the mean air velocity V_1 at the engine intake. With boundary-layer intake, $V_1 < V_o$ (relative to the moving airplane), whereas static pressure may be regarded to be unaffected by this friction effect on intake velocity.

Under these conditions, propulsive efficiency assumes the form:

$$\eta = \frac{(V_3 - V_1) \cdot V_o}{\frac{V_3^2 - V_1^2}{2} + K\frac{V_o^2}{2}} \qquad (10)$$

where: k is the duct-loss coefficient (defined previously).

Substituting $\Delta V = V_3 - V_1$ for the difference between engine discharge (jet) and inlet velocities, equation (10) simplifies to:

$$\eta = \frac{1}{\frac{V_1}{V_o} + \left[\frac{\Delta V}{2V_o} + \frac{K}{2}\frac{V_o}{\Delta V}\right]} \qquad (11)$$

Referring to equation (3), this expression may be rewritten in the form:

$$\eta = \frac{1}{\frac{1}{\eta_o} - \left[1 - \frac{V_1}{V_o}\right]} \qquad (12)$$

where:

η_o = Efficiency as given by equation (3) for intake from the unaffected stream *outside* of the boundary layer, for which $V_1 = V_o$

Subscript $_o$ refers here to any jet or ducted fan engine with intake from outside the boundary layer and *not* to the basic jet engine. It describes reference conditions with respect to boundary-layer intake or no boundary-layer intake *only*.

With boundary-layer intake velocity V_1 at the engine inlet is not uniformly distributed over the intake opening. The single value for this velocity used in equations (10) to (12) requires some explanation. Indeed, upon further examination, the mean intake velocity does not seem to have a definable single value because in the numerator of equation (10), V_1 expresses momentum of the incoming stream given by:

$$V_1 = \int_0^{\Delta y} V(y)^2 dy \Big/ \int_0^{\Delta y} V(y) dy$$

where Δy = depth of the flow layer entering the engine inlet, whereas in the denominator it expresses the kinetic energy, given by:

$$V_1^2 = \int_0^{\Delta y} V(y)^3 dy \Big/ \int_0^{\Delta y} V(y) dy$$

For a normal boundary layer these two values of V_1 are so close that their difference can be neglected.

The curves for:

$$\int V(y)dy, \quad \int V(y)^2 dy, \quad \text{and} \quad \int V(y)^3 dy$$

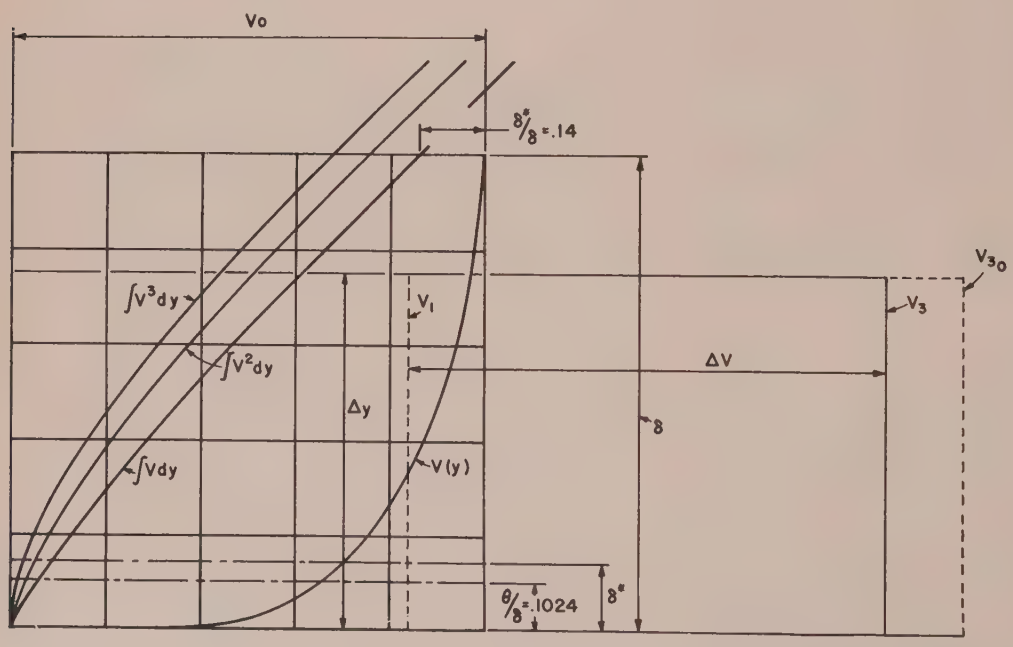

Fig. 10 – Boundary-layer, characteristics for a boundary-layer velocity-distribution factor, H, of approximately 1.35

are shown in Fig. 10 for a boundary-layer velocity-distribution $V(y)$ with a form factor H of approximately 1.35, which is characteristic for a normal turbulent boundary layer at a high Reynolds number and after a very slight pressure increase. This value may be regarded valid for a region of flow slightly behind the pressure minimum on the surface of an aircraft wing or fuselage, a likely location for a boundary-layer intake. Fig. 10 also indicates the mean inlet velocity V_1 and the discharge or jet velocity V_3 for a ducted-fan engine with a velocity ratio $\Delta V/V_1 = 1$, assuming a depth of flow layer entering the engine intake, Δy, equal to ¾ of the total boundary-layer thickness.

Were the engine to receive an inlet stream with full aircraft velocity V_o, a higher jet velocity V_{3_o} would be required to obtain the same momentum increase per unit mass flow, ΔV, as in the previous case. The increase in kinetic energy from V_o to V_{3_o} however, would be greater than that from V_1 to V_3, which is required with boundary-layer intake. This reduction in jet energy is directly responsible for the efficiency increase given by equation (12), and is represented graphically in Fig. 11 for the case in which reference propulsive efficiency, $N_o = 0.65$ for the same engine at the same flight conditions, but with intake from outside the boundary layer. (The flight conditions assumed here obviously require a bypass or ducted-fan engine.)

Efficiency increases suggested by the curves in Fig. 11 are subject to considerable revisions if only a part of the total engine flow, that is, the cold stream, is taken from the boundary layer. Furthermore, the efficiency advantage is reduced by virtue of the ram efficiency for boundary-layer intake being naturally somewhat less than for free-stream intake. On the basis of data given in reference 4 and discussed briefly at the end of this section, the losses total about 17% of the incoming stream energy, which may be equivalent to about 4% of the entire engine work. However, even the most ideal intake is penalized with some measurable losses.

Fig. 11 shows that efficiency increase obtainable with boundary-layer intake is a function of the relative portion of boundary layer, $\Delta y/\delta$, admitted to the engine, for this ratio determines the effective inlet velocity:

$$V_1 = \int_0^{\Delta y} V(y)^2 dy \Big/ \int_0^{\Delta y} V(y) dy$$

in relation to V_o for a given boundary-layer velocity-distribution.

It becomes necessary, then, to determine the ratio $\Delta y/\delta$ for a given aircraft-engine configuration.

It is assumed that the relative proportions of boundary-layer intake $\Delta y/\delta$ are determined largely by the aerodynamic requirements for an efficient intake opening and duct. This question was experimentally and theoretically investigated and is

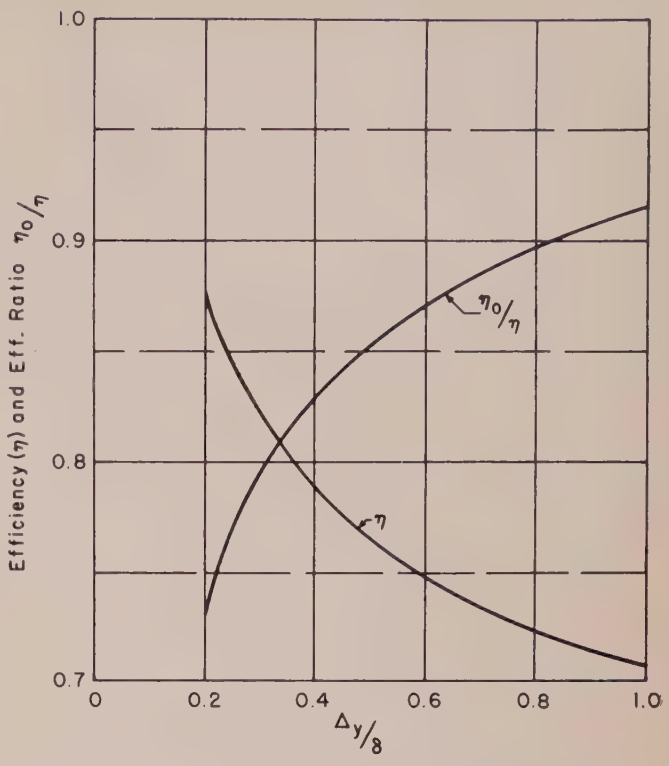

Fig. 11 – Effect of boundary-layer intake on propulsive efficiency. $H = 1.35$ and free-stream intake propulsive efficiency $\eta_o = 0.65$

described briefly below. The result showed that efficient intake under these conditions is not only possible, but surprisingly unaffected by the relative intake depth $\Delta y/\delta$.

This result leaves the ratio $\Delta y/\delta$ to be determined from the fact that boundary-layer thickness δ is closely related to the aircraft drag, and that the depth Δy, or cross-section, of the inlet stream is related to engine thrust, the latter being equal and opposite to the drag during level flight. This relates $\Delta y/\delta$ to the specific impulse, or to $\Delta V/V_o$, and in turn, for a bypass or ducted-fan engine, to the augmentation ratio W_o/W_h, as shown below.

Friction drag D_f ahead of a certain location on the wing or fuselage is related to the boundary-layer thickness there by the relation:

$$D_f = \rho b \theta V_o^2 \qquad (13)$$

where:

$$\theta = \int_0^{\delta} \frac{V}{V_o}\left(1 - \frac{V}{V_o}\right) dy$$

is the "momentum thickness" of the boundary layer, defined as thickness of a flow layer with free stream velocity V_o having the same momentum as that lost in the boundary layer due to frictional retardation

b = Total width of friction surface measured normal to the flow

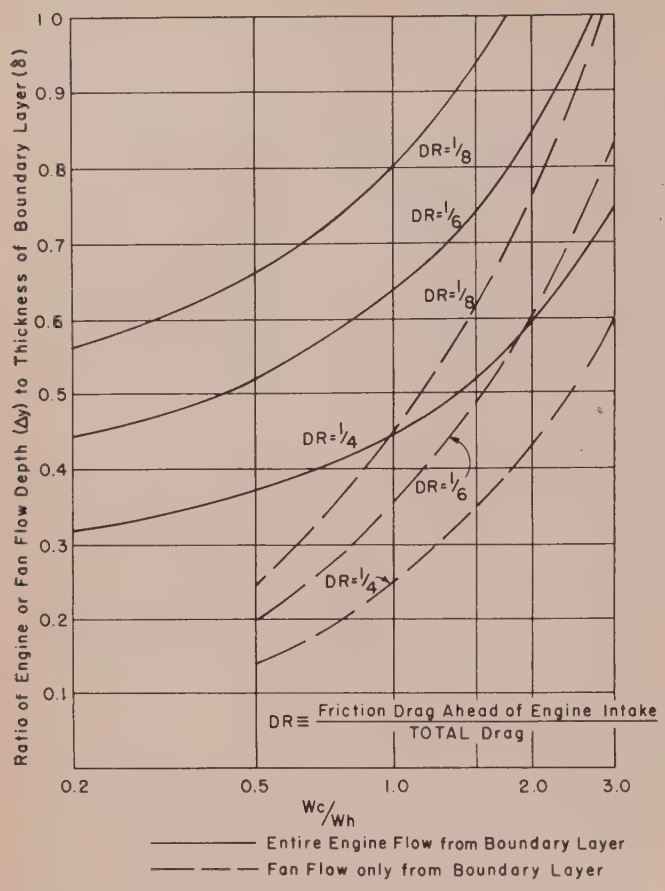

Fig. 12 – Variation of boundary-layer intake depth ratio with augmentation ratio for several values of drag ratio, *DR*

Let β be the ratio of the friction drag ahead of a given location on wing or fuselage (the location of the intake slot), to the total aircraft drag or engine thrust. Then:

$$\rho b \theta V_o^2 = \beta \left[\rho b_E \Delta y \overline{V}_1 \right] \cdot \Delta V \qquad (14)$$

where:

b_E = total width of engine intake slots normal to flow

$\Delta y V_1 = \int_0^{\Delta y} V(y)dy = \rho b_E \Delta y \overline{V}_1$, the mass flow entering the engine

Dividing both sides of (14) by the boundary layer thickness δ results in:

$$\frac{\Delta y}{\delta} = \frac{\theta/\delta}{\left[\beta \frac{b_E}{b}\right] \frac{\overline{V}_1}{V_o} \frac{\Delta V}{V_o}} \qquad (15)$$

where the combination $\beta \frac{b_E}{b}$ can be designated (with some reservations) as the ratio *DR* of friction drag ahead of the engine intake to total drag of the aircraft. The results of equation (15) are presented in Fig. 12 as solid lines for various values of drag ratio *DR*, plotted against the augmentation ratio W_c/W_h, which determines $\Delta V/V_o$ through equation (5).

The broken lines plotted in Fig. 12 are values of $\Delta y/\delta$ for the case when only fan flow W_c (Fig. 9) is taken from the boundary layer. In that case, equation (15) becomes:

$$\frac{\Delta y}{\delta} = \frac{\theta/\delta}{\left[\beta \frac{b_E}{b}\right] \left(\frac{\overline{V}_1}{V_o}\right) \left(\frac{\Delta V}{V_o}\right) \left[1 + \frac{W_h}{W_c}\right]} \qquad (16)$$

It should be understood that when fan flow only is taken from the boundary layer, the efficiency advantage is substantially less than shown by equation (12) and Fig. 11, being roughly in proportion to fan flow, W_c divided by flow through the primary part of the engine, W_h. For example, for $W_c/W_h = 1$, the efficiency increase indicated in Fig. 11 is cut approximately in half, depending on several variables not considered here. However, this efficiency increase is not the only reason for boundary-layer intake. It may help also to improve the overall characteristics of the aircraft, aerodynamically as well as structurally. Because of this the percentage of the boundary layer ($\Delta y/\delta$ in Fig. 12) that should be withdrawn in any particular case cannot be stated generally. Figs. 11 and 12 simply give the relations between the few variables considered here, and a general picture of the situation, without permitting general conclusions regarding optimum conditions.

Fig. 13 shows a hypothetical arrangement of two engines of the type shown in Fig. 9 in one nacelle taking fan flow from a suction wing. This is discussed in detail in reference 5. The twin-engine arrangement was selected to indicate the possibility of maintaining adequate boundary-layer suction in case of failure of one engine.

The hypothetical arrangement shown in Fig. 13 also serves to illustrate a well-known and very real difficulty connected with boundary-layer suction. Even by limiting boundary-layer intake to a fraction (say ⅔) of the boundary-layer thickness δ, it is apparent that the ducting necessary to efficiently conduct this flow to the engines occupies the entire wing cross-section. In fact, the entire wing cross-section at the juncture of wing and engine nacelle is barely sufficient to carry the suction flow of a span of two wing-chord lengths. It is hardly possible to use anywhere near the entire wing-section as duct area. It follows, then, that boundary-layer suction probably must be limited to those wing portions joining the engine nacelles and to the nacelles themselves. This is a serious limitation but should not be regarded as prohibitive. Perhaps marked aerodynamic advantages can be derived by improving the flow condition around nacelles and near the wing roots at the fuselage – usually not more than one wing-chord away from the nearest engine – by using boundary-layer suction.

An alternate application of boundary-layer suc-

tion may be the admission of *fuselage* boundary layer to the engine. Obviously, this will require a highly unconventional engine arrangement. The engines would have to be placed at the tail end of the fuselage, resulting in a problem of weight distribution. Some departures from conventional practice are worthy of serious study in order to realize some potential advantages of bypass or ducted-fan engines and boundary-layer suction.

Any consideration of boundary-layer intake raises the question of efficiency of the flow-intake process. Air admitted through an intake slot must be ducted to the engine so it is expected that flow velocity after intake must be reduced below the velocity ahead of the intake in order to minimize duct losses. The intake process, then, involves a retardation of the incoming stream.

It is known that with free-stream, or nose, intake this retardation can be accomplished very efficiently. With nose intake a significant part of this retardation can take place in the free stream ahead of the intake, thus partly avoiding the retardation of flow along a solid boundary. This retardation in the free stream ahead of the intake will be called prediffusion.

For boundary-layer intake, retardation of the incoming stream involves retardation of a stream of non-uniform velocity and energy distribution. Difficulties involved in this particular flow process are so well-known as to throw serious doubt on the feasibility of efficient boundary-layer intake.

To this end the Office of Naval Research, through a sponsored contract with Johns Hopkins University, conducted an investigation of boundary-layer intake through a slot.[4] The most general characteristics of these results will be outlined here to answer the question regarding feasibility of boundary-layer intake.

(a) Boundary-layer intake seems feasible provided the intake-duct form receives the most careful consideration. With a straight duct behind the intake slot, overall intake efficiencies in the neighborhood of 83% were consistently measured. There is no known reason why curved inlet ducts cannot be developed successfully if available information on turbulent flow in curved channels is used effectively.

(b) Prediffusion in connection with boundary-layer intake is not only feasible, but appears to be preferable to intake without any prediffusion. Pressure rise obtainable by prediffusion is calculable on the basis of existing theories of boundary-layer flow in the presence of a pressure gradient, and test results were found to be in good agreement with theoretical predictions.

(c) The process of boundary-layer intake with prediffusion does not appear to be unduly sensitive to changes in operating condition, so that it seems possible to develop boundary inlets capable of meeting a reasonable range of off-design conditions.

The results above were obtained at rather low Mach numbers, so that possible compressibility effects in the subsonic flight range still require systematic investigation.

Conclusions

Some general conclusions drawn from the foregoing considerations are:

1. Bypass or ducted-fan engines seem to offer sufficient promise for improved overall efficiency of transport aircraft to warrant serious investigation. However, overall improvements in economy of flight can be expected only if efficiency of the augmenting components is quite high and the increase in engine weight due to augmentation quite low. Improvements in take-off performance are significant and must be considered in judging the potential value of this type engine.

2. To realize substantial advantages in overall efficiency, reconsideration of augmentation ratios (W_c/W_h) between one and three (attempted by earlier investigations in this field) are indicated.

3. For commercial aircraft, the reduction in jet noise resulting from reduced jet velocities of bypass or ducted-fan engines may seriously be worth considering.

4. Development of bypass or ducted-fan engines may be economically feasible when treating the fan as an addition to an existing jet engine.

5. With respect to boundary-layer intake, bypass or ducted-fan engines offer the advantage of wide design variations in the specific impulse, that is, in the rate of flow available for boundary-layer control.

6. Efficiency advantages obtainable by boundary-layer intake, as far as can be predicted on the basis of engine propulsive efficiency are not spectacular, unless very far-reaching changes in aircraft design

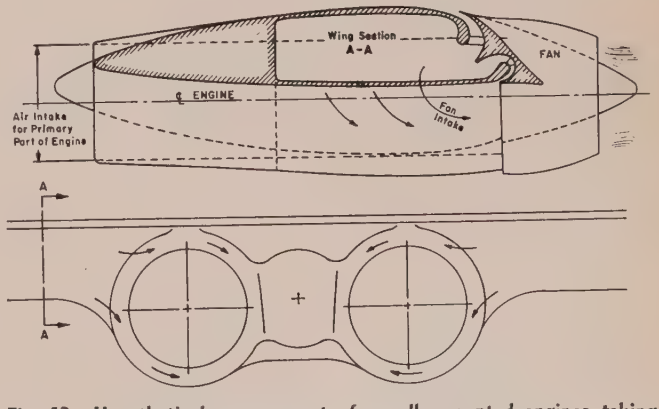

Fig. 13 – Hypothetical arrangement of nacelle-mounted engines taking fan flow from a suction wing

[4] See Johns Hopkins University (Mechanical Engineering Department) Report I-6, Part B (March 21, 1952), "Problem in Retardation of Turbulent Boundary Layer." (Contract N ONR-24312 and 248 (32), Office of Naval Research.)

[5] See *Journal of Aeronautical Sciences*, Vol. 15, April, 1948, pp. 189-220: "Low-Drag and Suction Airfoils," by S. Goldstein.

are considered. They may be significant, however, since they add to the advantages of the bypass or ducted-fan engine. The merits of boundary-layer intake are known to go well beyond those of increased engine propulsive efficiency.

7. Good theoretical and experimental evidence exists that the ram efficiency of a boundary-layer intake slot can be sufficiently high for practical application, and that an intake slot can meet off-design conditions.

DISCUSSION

Bypass Engines Offer Performance, Installation, and Noise Advantages

– H. Pearson
Rolls-Royce, Ltd.

THE most useful contribution I can make to this discussion is to give our considered opinion of the merits of the bypass engine after several years of experience in carrying design and development of such an engine to the type-test stage.

Dr. Wislicenus has adequately described the principles of the engine as a device for improving propulsive efficiency while allowing engine temperature to remain high, thus preserving a high basic-cycle efficiency. Of course the jet velocity of a simple jet engine may also be reduced by operating at a lower temperature. This will improve the propulsive efficiency too, but will reduce the basic-cycle efficiency, so that the overall result is not as good.

This efficiency advantage of the bypass engine can be obtained only at the expense of extra weight. The paper emphasized that this factor must be allowed for when considering the relative advantages of the two types of powerplant. For an aircraft mission involving high subsonic speed at around 40,000 ft and a 6-8-hr flight duration, the relative importance of fuel consumption to weight may be expressed as roughly four to one. Thus, an improvement of 1% in engine weight is worth ¼% gain in sfc. This is a useful basis for assessing the result of our investigations.

Consider a bypass engine of around 12/1 compression ratio with a bypass ratio of 0.5 (flow through the combustion chamber is twice that through the bypass), consisting essentially of two separate compressors on independent shafts. It is a relatively simple design exercise to scale the high pressure section up in size so that all the flow passes through the hot part of the engine and so convert the engine into a high pressure ratio simple jet engine. By this means quite accurate figures for the weights of the two engines may be obtained. Because the components are so similar, the performance of the two engines may be similarly compared. A temperature for the bypass engine very close to the optimum sfc is obtained at a turbine inlet temperature of 1040 K (1412 F). For the same sfc from a simple jet engine the temperature must be reduced to 920 K (1197 F). Both engines may be scaled to give the same cruising thrust when we obtain the following results given in Table A.

Table A – Test Results

Ratio	Bypass / Simple Jet
Altitude Cruise Thrust	1.000
Altitude Cruise Sfc	1.000
Compressor Tip Diameter	1.037
Altitude Cruise Airflow	1.074
Engine Weight	0.860
Installed Weight	0.830

A gain of 17% in installed engine weight results from the bypass engine. This is equivalent to a reduction of 4-5% in fuel consumption, or about a 5% increase in range.

If both engines are speeded up to give the same take-off temperature, the simple jet engine gives 13% more thrust at the expense of 6% more overspeed. This latter could not be done without a further compromise in engine weight.

Another, and perhaps better, method of comparison is to design the two engines for the same take-off temperature, pressure ratio, and thrust. Then, assuming the bypass engine cruises at approximately its optimum temperature of 1040 K, the simple jet engine may be compared under a variety of conditions – either at the same temperature, the same thrust, or the same sfc. Results are tabulated in Table B.

Cruising at equal combustion temperatures the bypass is 7% better in sfc, but 7.5% heavier for the same thrust. Effectively, it is 5% better in sfc and range.

Cruising at the same thrust and installed weight the bypass shows a direct gain of 4.5% in sfc and range.

Cruising at the same sfc bypass shows a thrust gain of 33%, or a 25% reduction in specific weight. Effectively it shows a 6% improvement in sfc and range.

It is seen that under all conditions a bypass engine provides an improvement in range of around 5%. Perhaps this will be regarded as small, but nevertheless it is an important advantage and one which can be achieved only by fairly radical measures such as this. It must not be thought that this 5% gain is compared with existing jet engines, where the gain is greater, but is compared with the best that can be obtained by similar design practice.

A very attractive feature of the engine is its lower noise-level for given take-off thrust as compared to normal jet engines. Tests carried out with an actual engine have shown a reduction of approximately 7 db, a significant gain indeed. Urgent work is in progress to reduce jet-engine noise by various methods. These same reductions, however, are obtained when applied to the bypass engine.

There are significant gains in installation that have not been accounted for in the above calculation. It will be appreciated that the bypass engine consists of the usual jet engine components surrounded by a complete sheath of relatively cool air. From the fire-hazard point of view, and as regards engine compartment ventilation and fire precautions, a significant reduction in weight should be realized. For commercial aircraft such reductions are difficult to specify since they are subject to agreement by the certifying authority for an actual installation. For military use at least we can foresee a reduction in engine weight of some 3-4% and a gain in engine thrust of 1-2% due to reduced ventilation drag.

On the debit side, the bypass engine's greater size and airflow will incur a weight penalty in a buried installation because spar construction becomes less economic. In the podded installation more popular in your country the weight

Table B – Test Results

	Ratio	Bypass	
		Simple Jet	
Take-off Thrust		1.000	
Compressor Tip Diameter		1.135	
Installed Weight		1.000	
Cruising Conditions	Combustion Temperature	Thrust	Sfc
Thrust	0.925	1.000	1.33
Sfc	0.930	0.955	1.00
Temperature of Simple Jet, K	1040	995	885

penalty would be negligible, but a slight increase in drag due to greater engine diameter may result.

In concluding, it can be stated that the bypass engine offers a small but definite improvement in performance, and a simpler and safer engine installation. It has a marked advantage in jet noise, which we understand is so important for civil aircraft in your country.

Turboprops Have Edge on Bypass Engines For Subsonic Transport Aircraft

– Bernard J. Mezger
Curtiss-Wright Corp.

THIS thought-provoking paper deals with a subject whose controversial aspects are beginning to approach those prevailing in the pre-World War II era on the subject of air-cooled versus liquid-cooled engines. And just as in that previous debate, still unsettled academically but settled practically, there are both theoretical and practical viewpoints to consider. At the moment the bypass engine appears to have the questionable distinction of being one of the oldest, most discussed, and least used of all types of aircraft gas turbine. There are more known or theoretically possible variations and combinations of bypass and ducted fan engines than all other engine types and combinations put together. This profusion of configurations has not helped to solve the questions of the true position and value of the bypass or ducted fan engine in the overall spectrum of aircraft powerplants. Moreover, confusion of data arising from detailed numerical analysis has tended to impede rational discussion and logical conclusions related to these questions.

Noting in particular the following assumptions limiting the area of engine operation in the author's study, it is difficult to argue the sound conclusions he draws:

1. Transport aircraft operation at fixed altitude and speed.
2. Entirely subsonic flight speed.
3. Operation at design point only.
4. Comparison with a straight turbojet.

With these simplifying assumptions the author shows some convincing calculations in favor of and about the bypass engine. Attention is drawn to the rather clever method employed to show the very strong effect of inlet losses on the redefined "propulsive efficiency," which, in this case is not a simple overall momentum-energy relationship but is adjusted to include consideration of inlet loss, one of the internal cycle losses. While not rigorous, it is most revealing. The greatest risk in using a bypass engine appears to be its great sensitivity to small changes in the efficiency of the inlet, and perhaps, other components. Extending this method of presentation to include similar effects regarding any bypass engine component such as the compressor, combustion chamber, turbine, or nozzle will show that a performance advantage becomes a disadvantage if component efficiencies are not up to par. This also largely serves to explain why off-design performance of bypass or ducted fan engines can become so poor. As components move off their efficiency peaks the sensitive overall performance changes drastically.

The mention of off-design performance is not in accordance with the author's assumptions but is one of the most important exceptions that can be mentioned. Off-design performance becomes most important in full-operational use of a bypass engine and suggests that variable blading or the introduction of an additional control variable may be a prerequisite to successful development and utilization of potential efficiency advantages theoretically available with a bypass or ducted fan engine. In this sense it is not unlike the propeller, to which it is related by evolution. The propeller did not become a really successful propulsion device until introduction of variable pitch to allow off-design operation without catastrophic reduction in performance.

Some fringe benefits offered by the bypass or ducted fan engine such as noise reduction and boundary-layer intake appear to hold promise for the serious consideration of this type engine. Difficulties in understanding bypass application added to the practical development position of the variable-pitch propeller – with its reverse thrust advantage – tend to make bypass engine application an uphill battle in relation to turboprop application for use in subsonic air transports.

Possibility for Compressor Supercharging With Ducted-Fan Engine

– S. G. Hooker
Bristol Aeroplane Co., Ltd.

I have been interested in the ducted-fan principle ever since seeing the Metro-Vickers engine run in 1944. British engines have operated on bypass ratios of 50 to 60% (cold-air flow to hot-gas flow), and it is evident that much higher ratios will really be required to enable them to "cash in" on this principle. The ducted-fan portion of the engine should definitely be at the front end of the engine to take advantage of possibilities for supercharging the compressor, and to retrieve somewhat the inevitable loss in power per lb of airflow per sec which the ducted-fan suffers.

Author's Closure To Discussion

THE author would like to thank the discussers for their constructive contributions which form a gratifying justification for the presentation of a paper on this subject. Particularly Mr. Pearson's contribution is of considerable interest as it reflects the thinking connected with perhaps the most advanced development along these lines.

The author also finds himself in agreement with most of Mr. Mezger's comments, although his comparison with the turboprop engine deserves a more detailed analysis regarding the full engine plus fuel weight (including prop and reduction gear) of the turboprop engine as compared with bypass engines before this comparison assumes a definite meaning. It is also to be considered whether gas-dynamic as well as mechanical limitations of the propellers with respect to speed of flight might weigh the balance in favor of the bypass engine.

In answer to Mr. Hooker's comments, it should be considered that a fan "supercharging" the engine has to handle the entire weight flow whereas a fan arranged at the aft end of the engine handles the cold part of the flow only. It is thus possible that the effect Mr. Hooker seeks to achieve is also obtainable by simply adding a stage or two to the main compressor.

Fig. 1 – Conventional (left) and tubeless (right) truck tire sections

Tire Design—

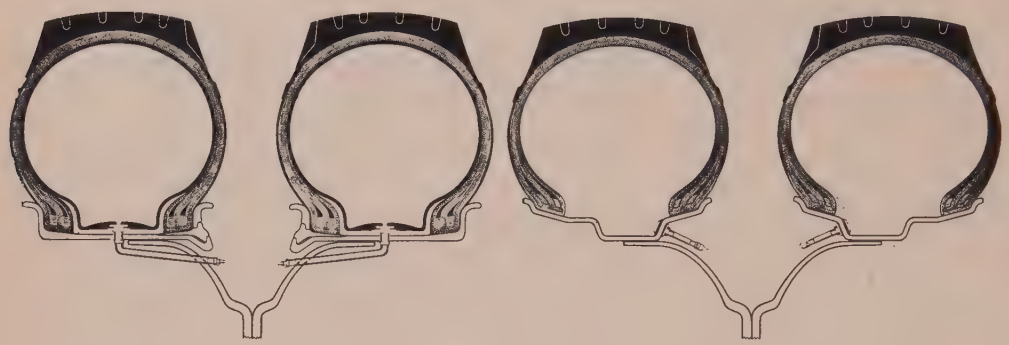

Fig. 2 – Weight comparison of tubeless and conventional tires with disc wheels (left) and cast spoke wheels (right)

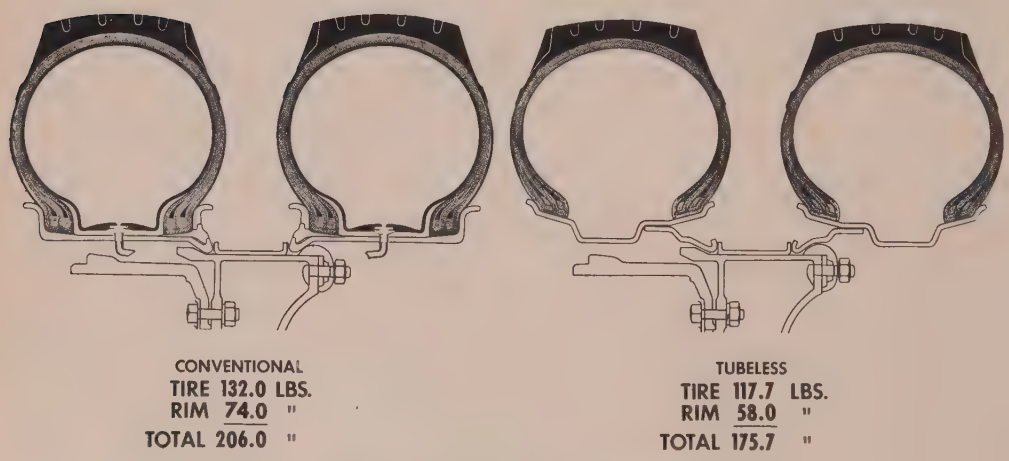

Present and Future

L. L. Baldwin, Firestone Tire and Rubber Co.

This paper was presented at the SAE Golden Anniversary Transportation Meeting, St. Louis, Nov. 2, 1955.

AS we look into the crystal ball of the future, we can see this nation crisscrossed with ribbons of fine highways, turnpikes, and thruways. These will increase the speed of travel for all vehicles. Tire engineers fully realize that much improvement will have to be made in design to build tires to withstand the increased speed, higher heat, and more abrasive surface conditions. Highway truck-tire construction and design are already going through some radical and interesting changes.

Tubeless Truck Tires

As predicted in at least two earlier papers presented to SAE meetings, the tubeless truck tire is now a production reality.

This is without question the most radical change in truck-tire design since the invention of the pneumatic tire.

The industry has now standardized on highway tubeless truck tires of the 15-deg-bead, drop-center-rim type in all sizes up to and including replacement for the conventional 11.00-22 size (12-24.5 in tubeless). A comparison between present conventional and new tubeless tire and rim cross-sections is shown in Fig. 1.

Because of its many advantages over present tires, the tubeless drop-center tire has been adopted by all major truck manufacturers, beginning with 1956 models, and will unquestionably be adopted by trailer manufacturers as well. Also, these new tires and rims are rapidly being incorporated into commercial fleets. Millions of miles already run on such fleets have indicated very satisfactory service.

The principal advantages of tubeless truck tires are:

1. Simplified assembly: Only two pieces (compared to five or six), less maintenance, less capital invested, less space in inventory and spare racks involved.

2. Weight savings (Fig. 2): It will be noted, for example, that when a pair of 10.00-20 tires on demountable rims is replaced with 11-22.5 tubeless on demountable drop-center rims, a weight saving

AS use of tubeless truck tires increases, new methods and new materials constantly are being developed to make them better and better.

The author tells what is being contributed by better, stronger synthetic cords such as rayon, nylon, steel or wire, fortisan 36, and dacron; improved compatible adhesives; and new treads and tread patterns.

Design innovations and steady advances in repairing and retreading procedures add their part to the constantly brightening picture for tubeless tires.

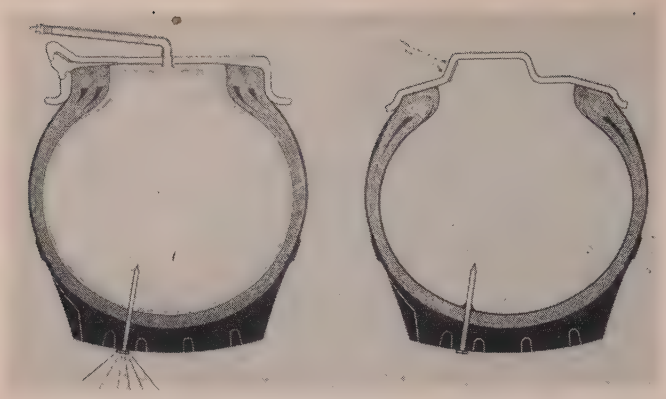

Fig. 3 – Puncture and blowout resistance of conventional (left) and tubeless (right) tires

of approximately 121.2 lb per axle is realized. The same sizes of tires on disc wheels save even more weight, approximately 162.0 lb per axle. This means more payload and revenue.

3. Mounting and demounting tubeless tires is quite easily done when instructions are followed and proper tools used. Fundamentally, the procedure is the same as for any drop-center passenger or farm tire, except that longer tools, rubber lubricant, and vise-grip pliers are employed.

4. Safety: Safer because no air pressure can be inserted unless beads go into place properly. Safer because no loose rim parts exist to be mismatched, or misapplied or distorted in service; and safer on the road if the tire should lose air.

5. Puncture protection: Because the relatively relaxed innerliner does not allow rapid loss of air, down time on the road is reduced, changing and repairing can be down at a garage or terminal. (See Fig. 3.) A regular tube has 20-25% stretch in a tire. When punctured it rips, and air rushes out. In a tubeless tire, the puncturing object must displace the innerliner. The liner hugs or clings to the puncturing object, minimizing air loss.

6. Blowout resistance: Because of the same relaxed innerliner, integral with the body of the tire, the sudden concussion of a blowout as caused by highly stretched inner tubes is minimized. The inner tube tends to "explode" when pinched into a small fabric break, resulting in a large, violent rupture. An integral innerliner if ruptured has an opening which remains small, a slow loss of air.

7. Cooler running: Up to 25 F less running temperature by reason of rapid heat loss through the steel rim, and a more flexible tire. This results in better, longer tire life and fewer body failures commonly caused by too much heat.

8. Better ride: Because of better flexing sidewall and bead construction and rounder shape, the tire actually rides better, reducing driver fatigue and costly front-end maintenance.

9. Elimination of tube and flap is self-explanatory. Suffice it to say, tubes and flaps have been a serious source of trouble in conventional tires.

Repairing and Retreading Tubeless Truck Tires

This involves some different methods, but will be no particular problem.

Small nail holes or punctures up to 3/16 in. in diameter will be repaired by an inside patch, curing the patch to the inside of the tire by heat and pressure, or by use of a self-curing patch. Injuries repaired by these methods must be filled with a filler gum.

There is also a good probability that many smaller holes can be repaired by insertion of a plug (with chemical self-curing surface) from the outside, thus making unnecessary the removal of the tire from the rim or vehicle. Advantages of such a repair would be obvious.

There are one or more kits on the market to provide the above material.

Larger injuries (more than 3/16 in.) in tubeless tires will require a built-up or ready-built repair. For the time being, these are cured in heated section molds which, because of the change in tire shape, will require new curing bags and bead plates. In the future we are hopeful that successful chemical curing section patches will be available. Experimentation and testing is under way and looks good. Innerliner gum is available for replacing on surface of section repairs to restore the liner seal.

Retreading and recapping will continue to be done in the same matrices, but instead of outside curing rims, we recommend *inside* curing rims with the proper curing bag.

New equipment will be available from several sources.

Design Innovations in Tubeless Truck Tires

The big difference in design is in the bead area. (See Fig. 1.) Because of the tight 15-deg wedge fit of the tire on the rim, the bead wire is now located in the natural position – in the circle of structure. The new bead is constructed of more flexible or pliable material, as also is the whole tie-in of plies around and above the bead-wire

Table 1 – Tubeless Truck Tire Sizes – Nomenclature

Present	Tubeless	Present	Tubeless
7.00–15 15-in. heavy duty	7–17.5	8.25–20	9–22.5
7.00–16 7.50–15 7.50–16	8–17.5	9.00–20 10.00–20 10.00–22	10–22.5 11–22.5 11–24.5
7.00–17 7.50–17	8–19.5	11.00–20	12–22.5
6.50–20 7.00–20	7–22.5	11.00–22	12–24.5
7.50–20	8–22.5	—	—

Table 2 – Rayon Cord Strength Ratings

	Cord Strength, lb	Fatigue Resistance Rating, %
Super Strength	32.50	135
Improved Strength	28.75	100
Regular Strength	26.25	85

groups. The old-style high flanges supported most of the load, but the new tubeless tire load is supported on the base of the bead – the 15-deg taper. The low flange serves as a stop and centering device, reducing any lever action to a minimum. The air seal between tire and rim is under the bead on the 15-deg taper.

It can be noted in this slide that the distance from the point of contact with the flange to the edge of tread is about the same for each tire.

Present chafers in conventional tires are mostly square woven cotton fabric. A different material or different treatment of the chafer is required in tubeless tires, because air seepage or wicking can not be permitted. Problems in the treatment of the chafer fabric or its replacement, such as type of material, dip solution, or friction coverings, have involved many new ideas and inventions.

The innerliner of a tubeless tire seals the air inside. It replaces the tube. It is cured to the tire as an integral part. Penetrating objects generally cause only a slow leak – and sometimes no leak at all.

Because the tires are not interchangeable with conventional types on the same rim, size markings are different. (See Fig. 1 and Table 1.) For example, a 10.00-20 on its recommended rim measures the same cross-section and the same overall diameter as the 11-22.5 tubeless on its recommended rim. Correspondingly, other sizes of conventional tires are replaced by tubeless.

Other than the points discussed above, the tubeless tire is essentially the same as a conventional tire. So much for the tubeless tire.

Tire Body Changes – Cord

Truck-tire body construction has been undergoing a steady evolution, especially cord material for plies.

Rayon cord has been greatly improved. This improvement was badly needed, as requirements in speed and load are always increasing. The new cord is called super-rayon. The regular rayon and the super-rayon tire cord may be better understood by comparing a photomicrograph section of each. (Fig. 4.) Note the highly oriented super-filament with little or no amorphous area. Whereas regular rayon is about 50% tough "skin" and 50% soft core, super-rayon is 100% tough skin throughout.

Rayon tire cord of 1650 denier is most popular in the industry. Today it can be classified as super-strength, improved-strength, and regular-strength. (See Table 2.)

As tire engineers, we look forward to further improvement in rayon:

1. Higher strength (1650/2 cord with 40 lb strength).
2. Higher impact resistance.
3. Higher fatigue resistance.
4. Greater resistance to moisture.
5. Improved resilience of basic material.

Nylon, a synthetic polyamide, is fast becoming a most popular truck tire cord. It is excellent for tires – with the advantages of impact strength, high-speed performance, flexing resistance, moisture resistance, flexibility, and heat resistance.

At present, nylon is standard production material in off-the-highway, road grader, airplane, premium-priced passenger and truck tires, and special military applications.

Nylon used to date is known as "Nylon 66." There

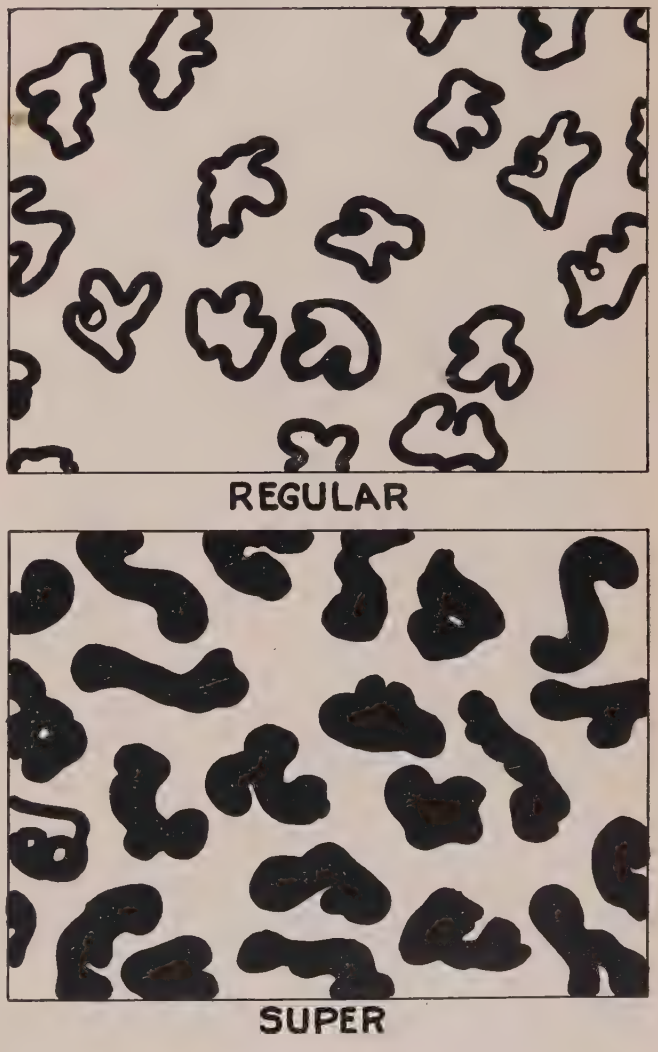

Fig. 4 – Regular rayon and super-rayon cord (original photographs taken at 3000X)

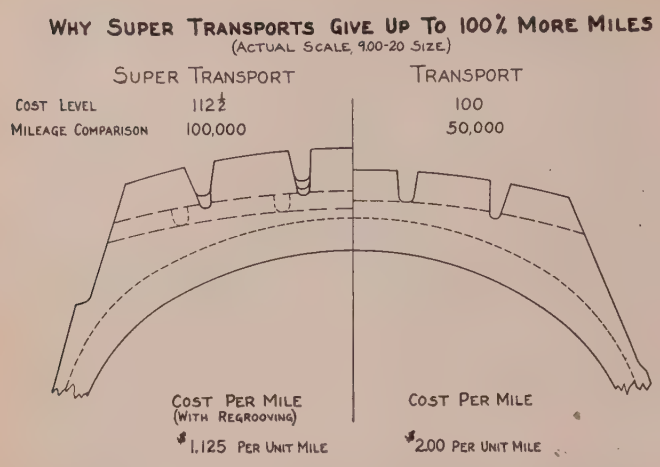

Fig. 5 – Mileage and cost comparison of extra-tread and regular-tread tires

is another nylon called "Nylon 6." The latter has a somewhat lower melting point and is somewhat different in chemical formula. If Nylon 6 works out in tires satisfactorily, it could become popular, as its cost may be less.

Steel or wire cord has been used for many years as a premium tire cord. It is gaining in popularity. Tires made with this material have amazing strength, lower running temperature, no growth or cracking, excellent high-speed and load-carrying qualities, and give good tread wear. Because of its inherent strength and resistance to body breaks, it is being used on front wheels of buses. It is without question the safest tire; however, its cost is high.

The strength of currently used production tire cord materials in the tire can be summed up as shown in Table 3.

Possible new materials for future use in tire bodies are:

Fortisan 36: A new type, high-tenacity yarn for tires, called Fortisan 36, is under consideration. It has very high strength, but appears low in fatigue resistance. The cost is high at present, and only time will determine if it will become competitive.

Dacron: Dacron is a synthetic polyester which offers possibilities as a tire cord. Production now is used in wearing apparel, curtains, and industrial products such as filter cloths, dye bags, ropes, high-pressure hose, fan belts, conveyor belts, and elec-

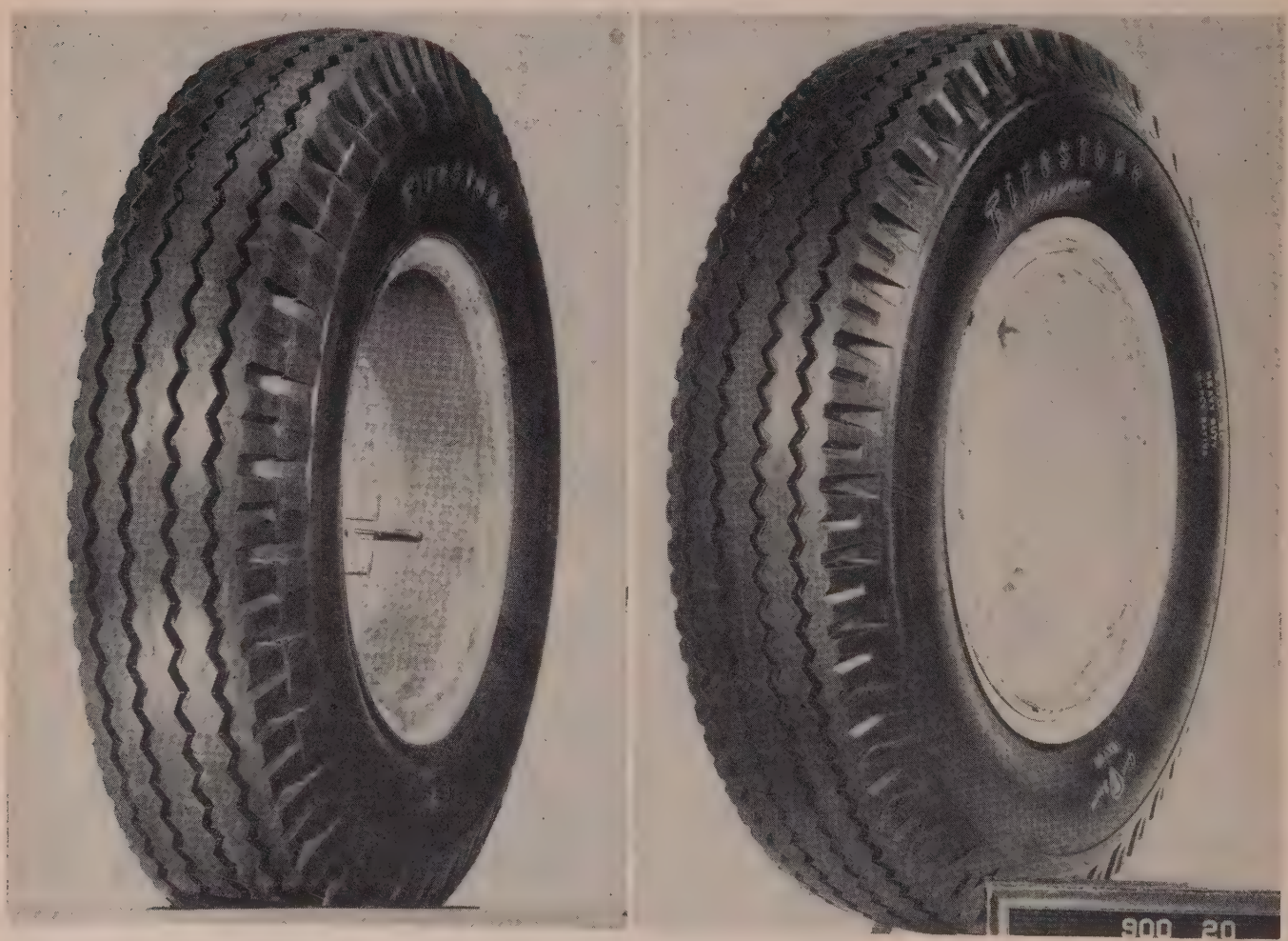

Fig. 6 – Rib-type highway tires – extra-tread (left) and regular tread (right)

Fig. 7 – Combination highway and traction tread

Fig. 8 – Crossbar tread – traction and sideskid resistance

trical applications. Tires made of dacron show very little growth, less than rayon. It has high impact resistance. Only time will tell if dacron is some day to replace nylon in tires.

Other possible tire materials which have been considered or tested include aluminum, glass, teflon and orlon. These materials do not show promise.

Adhesives, that is, cements and dips, used to condition the separate components making up tires, are continually being improved. New cord discoveries demand new dip and cement solutions. This is a constant problem in chemical compounding.

Conditioning of cord by stretch and heat is currently going through much experimentation. Certainly we can expect improved factory methods along these lines.

Rubber compounds: Synthetic rubber as used in tires has increased in quantity. In 1954 about 51.5% of the total tonnage consumed was synthetic, and in 1955 it will be 59%. This is because of improvement in quality, and also because of cost comparison with natural rubber. Present synthetics have been entirely satisfactory for passenger-car tires, but due to too much heat generation were unsatisfactory for large heavy-gage truck tires unless mixed with natural rubber.

A new synthetic with physical properties equivalent to natural tree rubber at normal and elevated temperatures has been recently discovered. This improved synthetic may be satisfactory in a greater percentage of large truck tires and military tires. The new synthetic is easier to process because it has an inherent tackiness which was lacking in the former GRS. Resistance to tread cracking and better tread wear are indicated. It is cooler running than GRS.

Still another newer synthetic rubber, a polyurethane type, is under test. It looks very promis-

Table 3 – Tire Body Strength Comparison

			Wire	
	1650/2 Rayon	Nylon	A	B
Gage, in.	0.029	0.021	0.036	0.048
Cord Strength, lb	28	28	200	385
Cords per in.	28	35	20	14
Number of Plies	10	12	4	4
Tire Strength, %	100	150	200	280

ing because it has exceptional abrasive resistance in tire treads. Tests indicate up to 100% improvement. It has this quality without depending upon carbon-black reinforcement to the extent as does present GRS or natural rubber. There is definitely a production problem to be solved before it can be in widespread use.

Tread designs: Use of premium extra-tread truck tires is becoming more popular. These tires give lower-cost operation. Improved body fabric, compounds, and construction described above have made it possible to use these tires on long, hot runs with almost no heat failures.

A sketch of regular-tread tires as compared to extra-tread is shown in Fig. 5.

Note that original tread mileage (not taking recaps into consideration) can result in almost 50% cost reduction.

The most practical tread pattern for highway use is basically a rib design. Typical of these are the Firestone "transport" and "super-transport" (Fig. 6).

Fig. 9 – Extra traction – on-and-off-highway design

Fig. 10 – Cross siping traction treatment

Where extra traction is required for on-and-off-the-road service, or winter snow or mud, compromise patterns incorporating ribs and cross-bars are sometimes used. Typical of such is the Firestone "all-traction" design (Fig. 7); or crossbar pattern (Fig. 8); or "super-all-traction" (Fig. 9).

A number of plain-rib, front-wheel tires have been put on the market in the past two years. While theoretically these would be good front tires, I have noted many of them badly wiped or irregularly worn after becoming about half worn. It appears this design tread is not successful.

Extra traction on slippery, wet pavement can be provided by special treatment known as "siping." This is done by molding or hand cutting. An example of this is shown in Fig. 10. Traction may be increased also by curing steel wire coils or other metallic particles in the treads. Examples of such are shown in Fig. 11. As a rule, traction is improved by such methods as long as the wires stay in. They have a tendency to work loose when about half worn through.

Tread compounding is ever on the upward grade

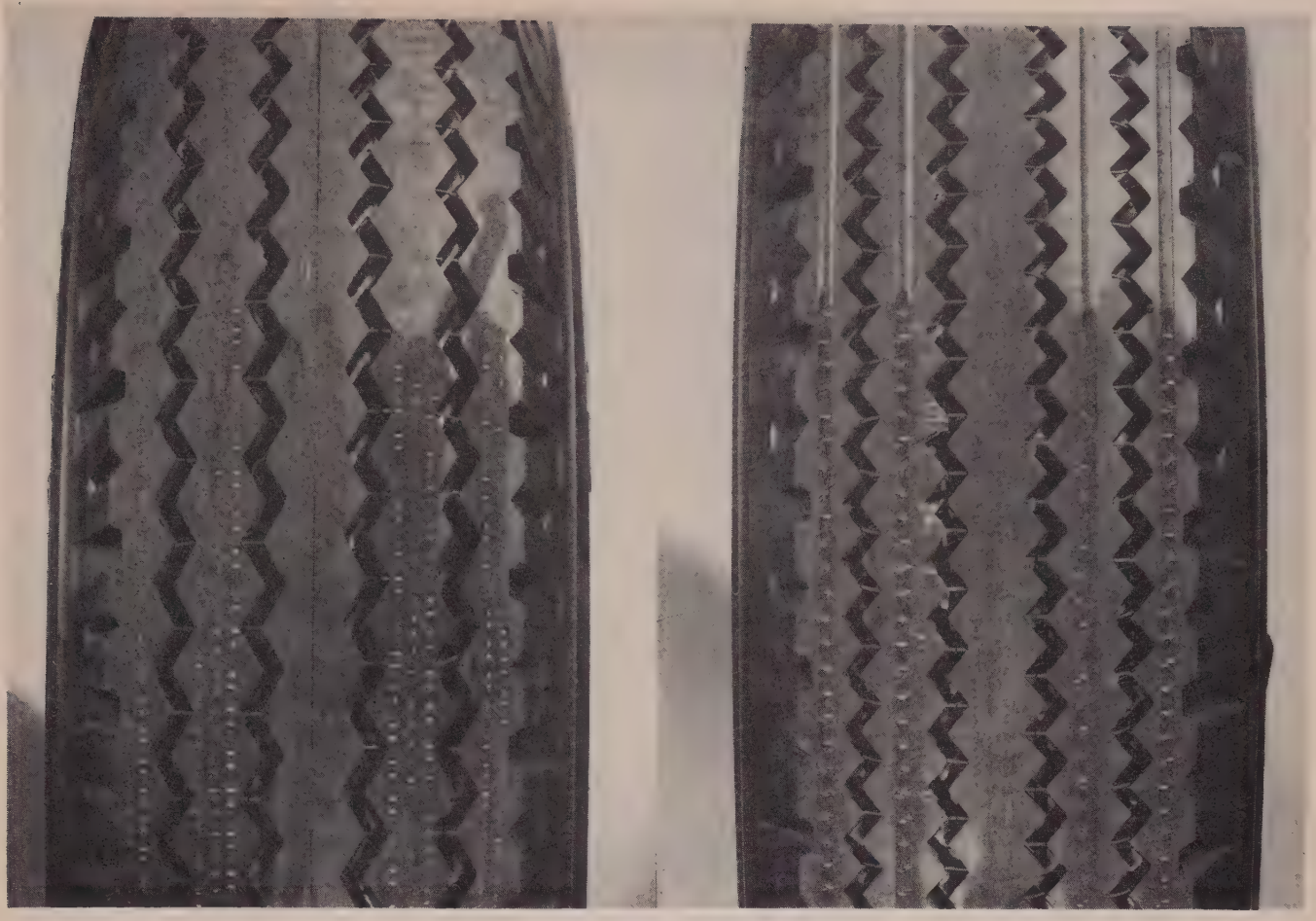

Fig. 11 – Two types of wire-insert tread

to provide better service. Most improvements have been brought about by improved blacks known as super-abrasion types. Fundamentally, they are blacks consisting of finer, smaller particles. A comparison of new versus old black particle sizes is shown by photomicrographic means in Fig. 12.

Safety diaphragms now being used to some extent in passenger tires could possibly be incorporated in tubeless-type truck tires, a thought for the future.

Summarizing, recent changes in tire construction and use of improved materials are making a product which will meet the toughest operating conditions and do so at less cost to the motor carrier. Tubeless tires, drop-center rims, weight savings, stronger cord bodies, better cements and dips, treatment of cord, improved synthetic rubber, better traction treads, practical premium treads, specialized tread patterns, and better compounding, all are already here. The future certainly will bring more perfection in each of the above, and possible discovery of new materials and methods of construction to improve tire design further.

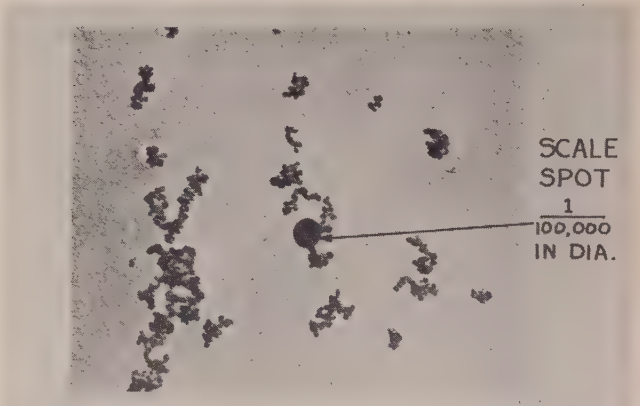

Fig. 12 – Carbon-black particles (original photographs taken at 159,000X)

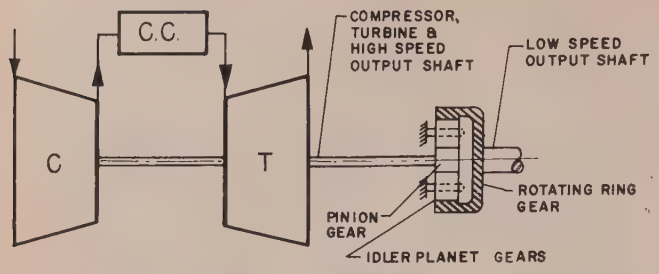

Fig. 1 – Schematic of single-shaft gas turbine

The Differential

THE information concerning the differential gas turbine contained in this paper is a result of research directed toward improving the performance of gas-turbine powerplants by improving the internal relationships between the compressor and turbine components. In most cases, the benefits gained by improving the internal relationships will be additive to benefits gained by improving the performance of the components themselves.

The use of a differential as an interconnection between the compressor, turbine, and output shafts establishes entirely new equations relating their torques and speeds. These new relationships enable the differential gas turbine to maintain higher component efficiencies and better thermal efficiency than conventional powerplants while operating over the wide torque and speed ranges required in transportation applications. The differential gas turbine, therefore, offers many advantages in transportation applications, including better part-load fuel economy, quicker acceleration, lower idling fuel consumption, and a broader operating range.

The information contained in this report is in three parts:

1. A discussion of the fundamental differences between differential and conventional powerplants.
2. Comparison of the overall performance of the basic differential and conventional two-turbine powerplants.
3. Two-turbine differential gas turbines for transportation applications.

Fundamentals

It seems appropriate to begin a discussion of the fundamental differences between the differential and conventional powerplants with a review of the basic operating characteristics of conventional powerplants.

The Single-Shaft Gas Turbine – Fig. 1 is a schematic representation of the earliest form of a gas turbine, a single-shaft machine, having a compressor and turbine on a common shaft which also serves as the high-speed output shaft. The reduction gearing shown in Fig. 1 is typical of that used in many gas turbine powerplants. This gearing utilizes a number of planet gears meshing with both a small pinion on the high-speed output shaft and a large internal ring gear on the low-speed

Gas Turbine

BETTER part-load fuel economy, quicker acceleration, lower idling fuel consumption, and a broader operating range are among advantages claimed for the differential gas turbine.

Differentially connecting the turbine to the compressor and output shafts, the author explains, gives up to 50% more turbine power at low output speeds than a two-turbine powerplant operating at the same compressor speed and fuel flow, and fuel savings up to 65% over a two-turbine unit operating at the same compressor speed and output power.

The two-turbine differential combination in particular, he says, offers a valuable opportunity to vary relationships between the components to achieve, in one powerplant, the optimum combination of performance features required for a particular application.

David W. Hutchinson, Turbex Corp., Mamaroneck, N. Y

This paper was presented at the SAE Golden Anniversary Transportation Meeting, St. Louis, Nov. 1, 1955.

output shaft. The centers of the planet gears are stationary, so that they serve as idlers, causing the direction of rotation of the low-speed output shaft to be opposite to that of the high-speed output shaft. The output speed reduction is proportional to the diameter ratio of the ring and pinion gear.

The use of a single shaft to serve as the compressor, turbine, and high-speed output shaft requires that the compressor and turbine speeds be equal to each other and also equal to the speed of the high-speed output shaft. Fig. 2 shows the relationship between compressor, turbine, and output speed. The torque exerted on the output shaft is equal to the difference between the compressor and turbine torques, and the net power of the machine is equal to the difference between the compressor and turbine powers.

Assuming this powerplant is operating at the maximum compressor and turbine speed, the output speed will be at its maximum value. Further assume this powerplant is operating at its maximum turbine inlet temperature, providing the maximum turbine power, and hence the maximum net power. Let us then see what happens when the output speed is reduced. In order to reduce the output speed, it is necessary to reduce the compressor and turbine speeds, causing a reduction in airflow and pressure ratio. Therefore, even if the turbine inlet temperature of this machine is maintained at its maximum value, the available output torque and output power decreases rapidly as the output speed is reduced. By the time the output speed is reduced to about 40% of its maximum value, the turbine will cease to provide more power than is required to drive the compressor, and the output torque and output power will be equal to zero, as shown in Fig. 3. This figure also shows the reduction in fuel flow caused by the decreased airflow at the low output speeds.

In summary, then, having a common compressor, turbine, and output shaft causes a rapid decrease in the output torque and output power as the output speed is reduced, with zero torque and zero power occurring at about 40% of the maximum output speed. These characteristics are obviously not suited to transportation applications requiring operation over a wide range of output speeds.

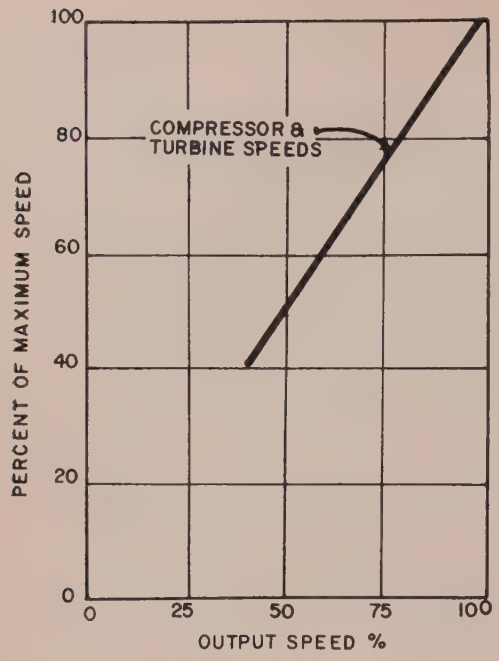

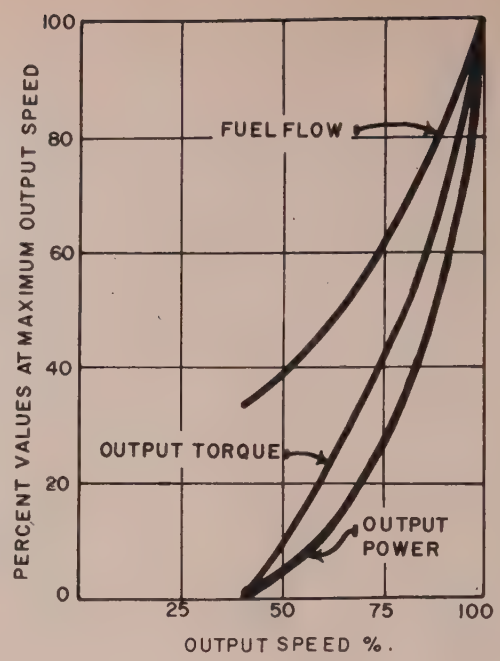

Fig. 2 (left) – Shaft speed relationships for single-shaft gas turbine

Fig. 3 (right) – Performance of single-shaft gas turbine at maximum turbine temperature

The above curves for the single-shaft machine assume that all of the turbine power is being transmitted to the output shaft except for that power required to drive the compressor. If additional power were needed to accelerate the compressor and turbine, a larger proportion of the turbine power would have to be transmitted to the compressor shaft, reducing the output torques and output powers shown in Fig. 3.

The single-shaft gas turbine has the advantage that the output torque is equal to the difference between the compressor and turbine torques, and therefore may be either positive or negative. At any output speed, the fuel flow may be reduced, causing the turbine torque to be less than the compressor torque, whereby the machine wll act as a brake.

The Two-Turbine Gas Turbine – Fig. 4 is a schematic representation of a two-turbine gas turbine, also referred to as a split-turbine or free-turbine machine, which can provide increased torques and powers at reduced output speeds, enabling its use in transportation applications. This powerplant has the turbine divided into two portions. One portion of the turbine is mounted on the compressor shaft, which has no mechanical connection with the output shaft. The other portion is mounted on a high-speed output shaft. The portion of the turbine in the compressor shaft is designed to provide exactly that power required to drive the compressor at its maximum speed when the turbine inlet temperature is at its maximum value. The output-shaft portion of the turbine is designed to extract the remaining available power from the combustion products in the most efficient manner when the output speed is at its maximum value.

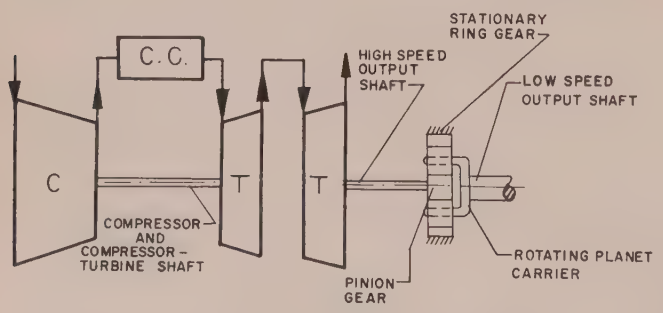

Fig. 4 – Schematic of two-turbine gas turbine

The reduction gearing shown in Fig. 4 has rotating planet centers and a stationary ring gear. This type of reduction gearing, used in several recent gas-turbine powerplants, provides a larger speed reduction for the same pinion and ring-gear diameter than the gearing having stationary planet centers, shown in Fig. 1.

The elimination of the mechanical connection between the compressor and output shafts permits the speed of the compressor and compressor-shaft portion of the turbine to be independent of the output speed, but still requires that the speed of the output portion of the turbine be equal to the output speed. It also requires that the torque of the compressor and compressor-turbine be equal in order to maintain any compressor speed, and furthermore prevents the output turbine portion from assisting the compressor-turbine to accelerate the compressor at low output powers.

Let us now consider what occurs when the output speed of a two-turbine machine is reduced while operating at its maximum turbine-inlet tem-

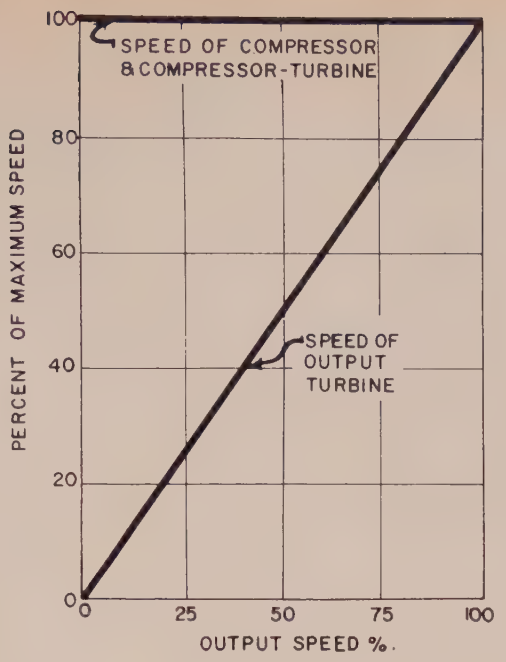

Fig. 5 (left) – Shaft speed relationships for two-turbine unit at maximum compressor speed

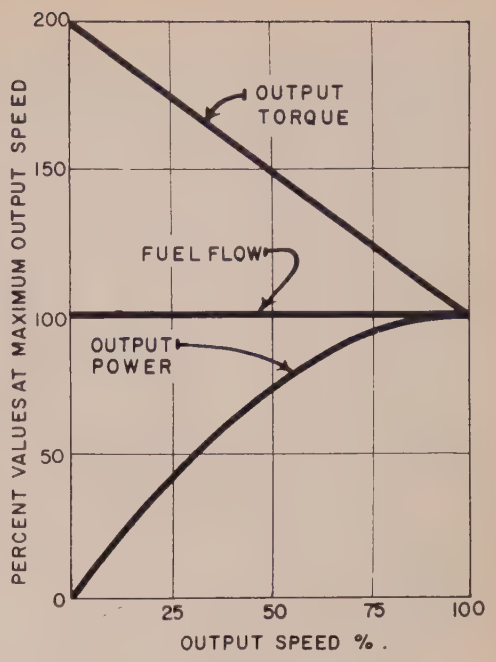

Fig. 6 (right) – Performance of two-turbine unit at maximum compressor speed and maximum turbine inlet temperature

perature. As shown in Fig. 5, the speed of the output portion of the turbine is reduced in a manner similar to that of a single-shaft machine; but the portion of the turbine in the compressor shaft is not affected, and continues to provide exactly that power required to maintain the compressor at its maximum speed, maintaining the airflow and pressure ratio at their maximum values. The fuel flow and the inlet conditions of the power turbine are, therefore, maintained constant as the output speed is reduced.

The reduction in the power-turbine speed with constant inlet pressures and temperatures causes a reduction in the velocity of the rotor blades at constant gas velocities, reducing the velocity ratio and the turbine efficiency. The output power decreases as the output speed is reduced until, as in any kinetic machine, the efficiency of the output turbine becomes zero at zero output speed. However, the reduction in the blade velocity at constant gas velocities provides an increase in the turbine torque at reduced turbine speeds. As is shown in Fig. 6, the two-shaft machine, therefore, succeeds in providing large output torques at all speeds between zero and the maximum speed, but does so at the cost of requiring as much fuel to operate at zero power as that required to operate at full load.

In summary, the two-turbine powerplant is capable of operating over the wide speed ranges required for transportation applications, but has very poor fuel economy at output speeds other than the narrow output speed range at which the power turbine is operating at high efficiency.

It should also be noted at this time that due to the mechanical separation of the two portions of the turbine, the portion of the turbine connected to the output shaft cannot assist the compressor-turbine in driving the compressor even if there was little or no load on the output shaft. The rate of compressor acceleration and the idling fuel consumption of the two-turbine powerplant are thereby both impaired.

The Basic Differential Gas Turbine – Let us now examine Fig. 7, showing a schematic representation of the differential gas turbine in its most basic form. This differential machine has its compressor and turbine mounted on separate shafts, and utilizes differential gearing to connect these shafts to each other and to an output shaft. This is the same gearing arrangement used in all automobiles to enable the motor to transmit torques to both wheels while allowing their speeds to differ. In a differential gas turbine, differential gearing enables a single turbine to transmit torque to both the compressor and output shafts, while allowing the speeds of the compressor and output shafts to differ.

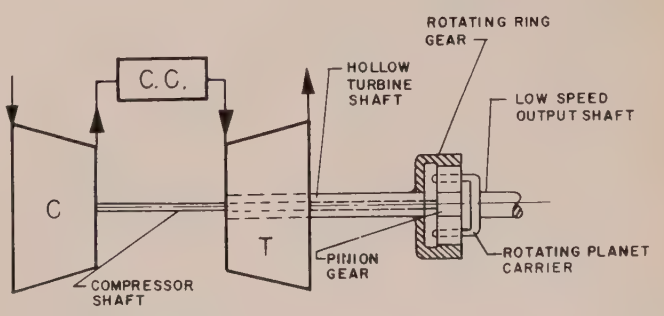

Fig. 7 – Schematic of basic differential gas turbine

In the particular example shown in Fig. 7, the turbine is designed for rotation in a direction opposite to that of the compressor, and has a hollow shaft surrounding a compressor shaft extension. The differential gearing of Fig. 7 is mechanically very similar to the reduction gearing shown in Figs. 1 and 4. However, in the case of the differential gear, both the planet centers and ring gear are free to rotate, combining the features of reduction gearing shown in Figs. 1 and 4. The ring gear of the differential is connected to the turbine shaft, and the pinion or sun gear is connected to the compressor shaft. The planetary gears are free to rotate about their centers and as a unit to cause rotation of the low speed output shaft. This particular differential gearing arrangement has the advantage of also providing the initial stage of speed reduction whereby the high speed output shaft is eliminated.

When the output shaft is held stationary, the planet centers are stationary and the planet gears act as idlers as in Fig. 1, whereby the turbine drives the compressor at the maximum compressor speed while rotating in the opposite direction at about half the compressor speed. When the turbine speed is increased to equal the compressor speed, still rotating in the opposite direction, the planetary centers and low-speed output shaft are caused to rotate in the direction of the turbine shaft at about one-third the turbine speed.

The planetary member may be considered as tending to rotate in the direction of the turbine because of the rotation of the ring gear, and also tending to rotate in the opposite direction due to the rotation of the sun gear. Because the diameter of the ring gear is larger than that of the sun gear, the planet centers and output shaft will rotate in the direction of the turbine when the compressor and turbine speeds are equal. A reduction in the turbine speed at constant compressor speed will reduce the output speed until the pitch-line velocities of the ring and sun gear become equal, effectively canceling each other and providing zero output speed when the turbine is rotating at about one-half the compressor speed, as shown in Fig. 8. The output speed of a differential gas turbine is, therefore, a function of the difference between the compressor and turbine speeds, whereby a small change in turbine speed will provide a large change in output speed.

In this typical example, the differential gearing serves to exert half of the turbine torque on the compressor shaft and the other half, multiplied by the torque multiplication of the gearing, on the low-speed output shaft. The differential, therefore, causes an approximately equal distribution of turbine power between the compressor and output shafts at the maximum output speed when the compressor and turbine speeds are equal. As the output speed is reduced, a progressively larger portion of the turbine power is transmitted to the compressor shaft, until at zero output speed all of the power of the turbine is transmitted to the compressor shaft. This automatic variation in the division of turbine power between the compressor and output shafts has several advantages, as will be shown.

Appendix I compares the equations relating the torques and speeds of the compressor and turbine of a differential gas turbine with the equations relating the compressor and turbine torques and speeds in conventional powerplants.

Let us now examine what happens to the differential powerplant when the output speed is reduced

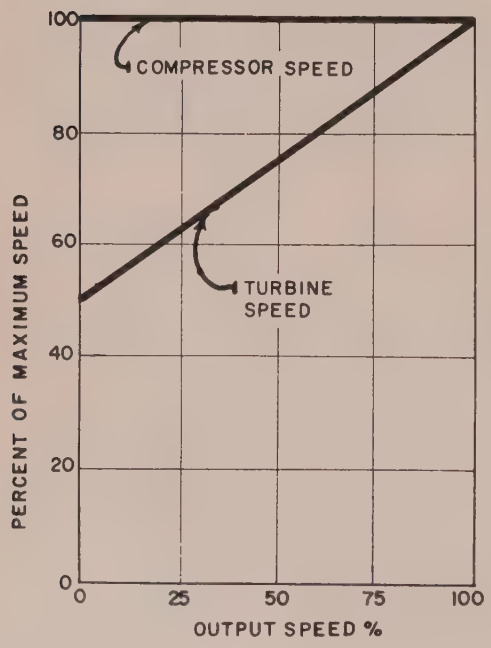

Fig. 8 (left) – Shaft speed relationships for differential powerplant at maximum compressor speed

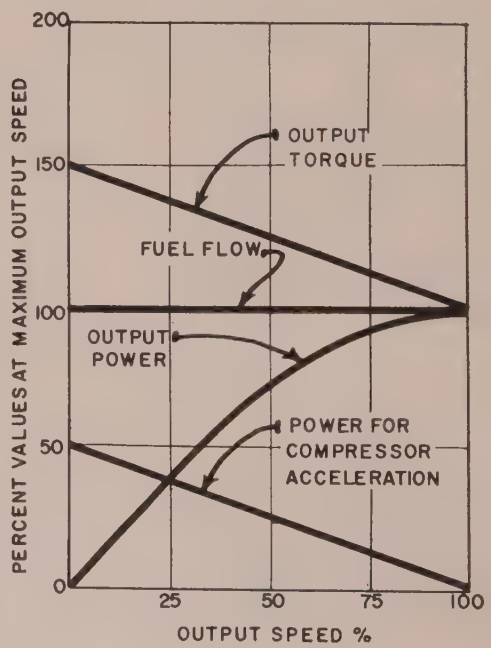

Fig. 9 (right) – Performance of basic differential powerplant at maximum compressor speed and maximum turbine temperature

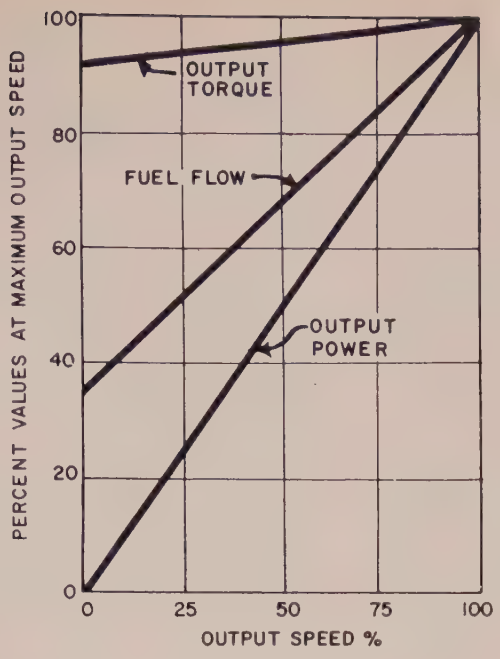

Fig. 10 (left) – Performance of differential gas turbine at maximum compressor speed with no compressor acceleration

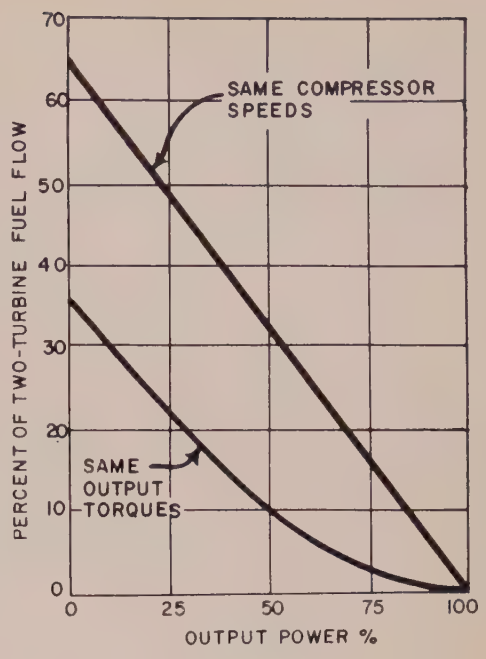

Fig. 11 (right) – Fuel savings of differential gas turbine compared to two-turbine unit providing same output power

at maximum compressor speed, maximum turbine-inlet temperature, and maximum fuel flow. As the output speed is reduced, the turbine speed will reduce more gradually than the turbine of a single-shaft machine or the output turbine of a two-turbine powerplant, decreasing to about 50% speed when the output speed is zero, as shown in Fig. 8.

At one-half its maximum speed, the turbine is still operating in its efficient range, and is capable of providing 75% of its maximum power at 150% of its maximum torque. The torque on the output shaft is, therefore, increased by 50% at zero output speed, and there is a similar increase of 50% in the torque exerted on the compressor shaft. Therefore, reducing the output speed to zero provides a 50% increase in the power available to drive the compressor, which would result in rapid acceleration of the compressor shaft. Fig. 9 plots the output torque, fuel flow, and output power of the differential powerplant versus output speed at maximum compressor speed and maximum turbine-inlet temperature. You will note that these curves are quite similar to those of the two-turbine shown in Fig. 6. However, the differential gas turbine provides large powers to accelerate the compressor and turbine, in addition to providing these large output torques and output powers. An additional curve showing the power available to accelerate the compressor is, therefore, plotted in Fig. 9.

In the case of the single-shaft gas turbine, the output power curve shown in Fig. 3 may be considered the sum of the turbine power available for driving the load and accelerating the compressor so that it would be necessary to reduce the output powers below the values shown in order to accelerate the compressor. In the case of the two-turbine, no power is available for acceleration of the compressor at the fuel flow shown in Fig. 6. A higher turbine inlet temperature and a higher fuel flow than that shown in Fig. 6 would be required to accelerate the compressor of the two-turbine powerplant. The higher efficiency, and hence higher turbine power, of the differential powerplant is shown by the fact that the sum of the output power and the power available to accelerate the compressor is larger than the output powers of the two-turbine powerplant at all but the maximum output speeds.

As the turbine of a differential powerplant operating at reduced output speeds and the maximum fuel flow transmits more power to the compressor shaft than is required to drive the compressor, the fuel flow of a differential powerplant may be reduced as the output speed is reduced, and the turbine will still provide sufficient power to maintain the maximum compressor speed. Fig. 10 shows the performance of a differential powerplant operating at the maximum compressor speed at the reduced fuel flows providing no compressor acceleration.

You will note that when the compressor is not being accelerated, the differential gas turbine provides up to a 65% reduction in fuel flow as the output speed is decreased, while still providing an output torque closely approximating the output torque at maximum fuel flow. As the two-turbine powerplant requires 100% fuel flow at the maximum compressor speed at all output speeds and powers, as shown in Fig. 10, the differential gas turbine offers fuel savings up to 65% compared to a two-turbine operating at the same compressor speed and output powers.

These large fuel reductions are made possible by the fact that the turbine power is reduced as the output speed is reduced, but the turbine is

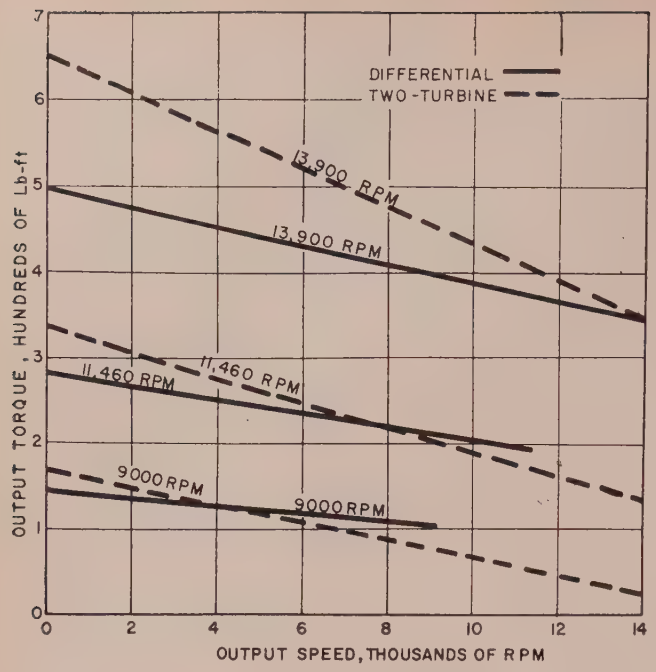

Fig. 12 – Torque-speed characteristics of two-turbine and basic differential powerplants at turbine inlet temperature of 1700 F

maintained in its highly efficient operating range. The turbine efficiency of a differential powerplant operating at the low output speeds with no compressor acceleration is even higher than its turbine efficiency when providing compressor acceleration, because the gas velocities are reduced as the turbine speed is reduced, maintaining the ratio of gas velocity to the turbine-blade velocity very near the ratio providing optimum turbine efficiency. In the powerplant shown by way of example here, the turbine efficiency only dropped from 84% at maximum power to 77% at zero output speed. A similar reduction of output speed of the two-turbine powerplant caused the efficiency of the output turbine to decrease to zero.

The differential powerplant is capable of maintaining a large output torque at the large fuel reductions at low and zero output speeds, because the differential can exert a torque on the output shaft due to the reaction forces of the gearing without requiring the expenditure of any of the powerplant's available energy. The large standstill torques of the two-turbine, on the other hand, require the expenditure of approximately half of the available turbine power in a stationary output turbine operating at zero efficiency. The elimination of the loss of available energy and the high turbine efficiency of the differential gas turbine makes possible the large fuel reductions shown in Fig. 10.

The fuel savings of the differential gas turbine, when not providing compressor acceleration and operating at the same compressor speed as the two-turbine, are shown in Fig. 11. These fuel savings are achieved at lower output torques than those of the two-turbine at low output speeds, as shown in Fig. 10. Fig. 11 also plots the fuel savings of the differential powerplant while providing the same output torque and output powers as the two-turbine powerplant. In the latter case, the compressor speed of the two-turbine powerplant is reduced as the output speed is reduced, providing a reduction in the fuel flow of the two-turbine.

In summary, differentially connecting the turbine to the compressor and output shafts enables the basic differential gas turbine to provide large output torques at low and zero output speeds, and maintains a high turbine efficiency at low output speeds, whereby the differential gas turbine will provide the following:

1. Up to 50% more turbine power at low output speeds than a two-turbine powerplant operating at the same compressor speed and fuel flow, thereby enabling faster compressor acceleration than a two-turbine powerplant providing the same output power.

2. Fuel savings up to 65% of the fuel flow of a two-turbine powerplant operating at the same compressor speed and output power, or up to 35% of the fuel flow of a two-turbine powerplant operating at the same output torque and output power.

The above demonstrates the operational flexibility and improved powerplant performance gained by differentially connecting the turbine to the compressor and output shafts.

Comparison of the Overall Performance

The performance of both basic differential and conventional two-turbine powerplants has been calculated using the same compressor, burner, and turbine performance. Appendix II provides infor-

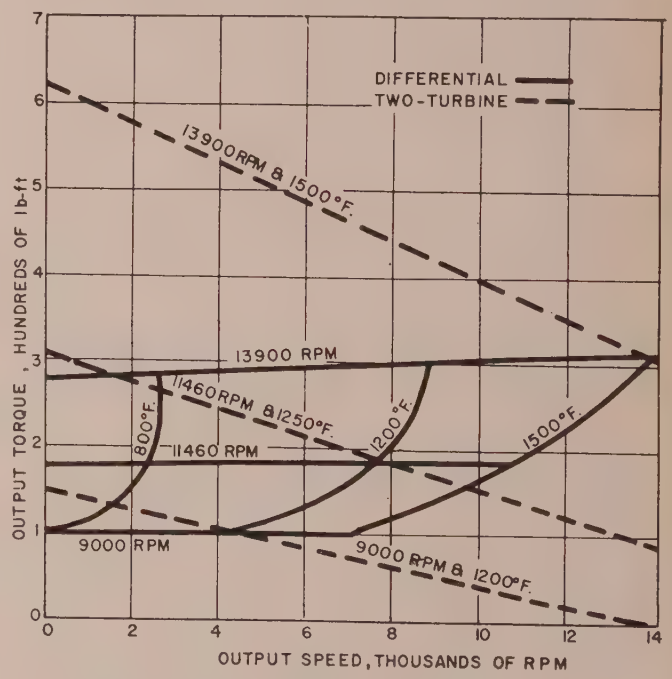

Fig. 13 – Torque-speed characteristics of two-turbine and basic differential powerplants with no compressor acceleration

mation concerning the performance of the components used in these calculations. It will suffice to say here that the component data were the tested performance of actual compressors and turbines published in NACA reports. These calculations were also the source of data shown in the previous illustrations.

Each powerplant was investigated for both steady-state and transient performance at three or more compressor speeds over a wide range of output speeds and output powers. The steady-state performance was calculated, assuming the fuel flow to be metered by a governor on the compressor shaft to maintain the compressor speed constant at each of the compressor speeds investigated. The transient performance was calculated, assuming the fuel flow to be metered by an acceleration control to provide a constant turbine-inlet temperature of 1700 F during acceleration of the compressor.

The results of these calculations are plotted in Figs. 12 through 14, and are discussed in the following paragraphs.

Fig. 12 shows the transient torque-speed characteristics of the two-turbine and basic differential powerplants at a constant turbine inlet temperature of 1700 F. The two-turbine powerplant provides up to 30% more output torque at low output speeds, but the differential gas turbine provides much higher powers for acceleration at the low output speeds.

At this temperature, the two-turbine requires 7.1 sec to accelerate the compressor from 9000 to 13,900 rpm. As the output turbine of the two-turbine powerplant does not contribute to this compressor acceleration, the time required to accelerate the compressor of the two-turbine is constant at all output speeds. At low output speeds, most of the turbine power of the differential is utilized for compressor acceleration. At zero output speed, the differential powerplant will accelerate the compressor from 9000 to 13,900 rpm in 2.5 sec, a reduction in accelerating time of 65%.

The accelerating time of the differential powerplant increases as the output speed is raised, increasing the portion of the turbine power transmitted to the output shaft. At the compressor speeds below the maximum, the differential powerplant provides more output power than the two-turbine powerplant at the higher output speeds. In the region in which the differential gas turbine provides more output power than the two-turbine powerplant, its rate of compressor acceleration is less than that of the two-turbine powerplant.

Fig. 13 plots the steady-state torque-speed characteristics of the two-turbine and basic differential powerplants. The fundamental difference between their performance is that the two-turbine provides increasing output torques at a constant turbine inlet temperature, as the output speed is reduced, while the differential gas turbine provides approximately constant output torques at decreasing

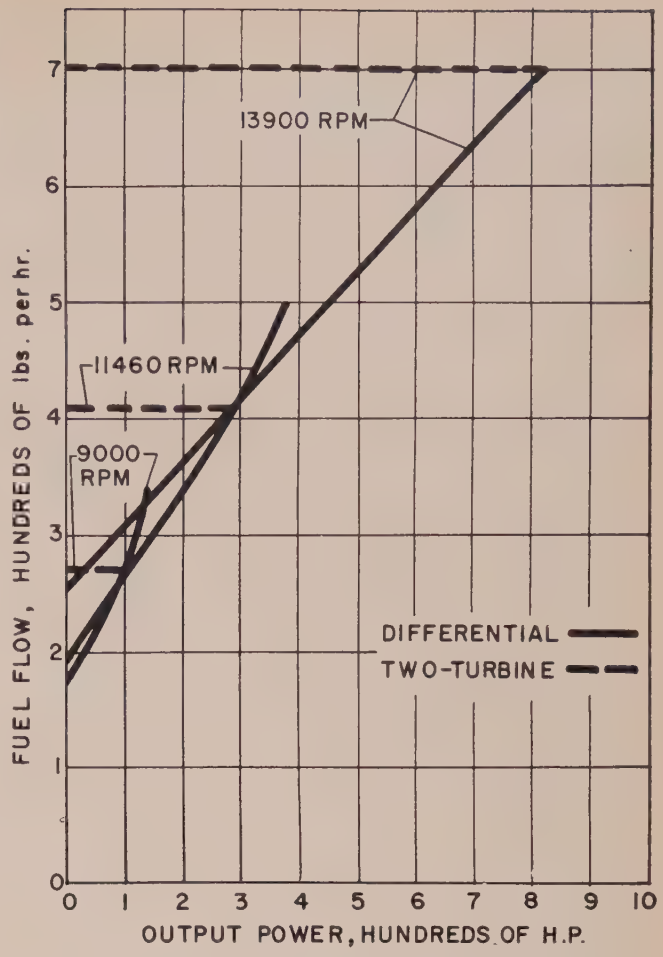

Fig. 14 – Fuel consumption of two-turbine and basic differential powerplants with no compressor acceleration

turbine-inlet temperatures as the output speed is reduced. At the maximum compressor speed, the two-turbine provides 100% more standstill torque than the differential powerplant. At lower compressor speeds this torque advantage is reduced to 50% at zero output speed, and the differential gas turbine will provide larger powers. This comparative improvement in differential performance at low compressor speeds is due to the two-turbine's progressive decrease in turbine inlet temperature as the compressor speed is decreased. The reduced turbine inlet temperature of the two-turbine at reduced compressor speeds is due to the necessity of maintaining the balance of compressor and compressor-turbine power at the reduced compressor powers. Although the differential powerplant provides larger output powers than the two-turbine at low compressor speeds, these larger output powers are provided at lower output speeds than with the two-turbine powerplant.

Fig. 14 plots the steady-state fuel consumption of the two-turbine and basic differential powerplants versus output power. The two-turbine requires a constant fuel flow at each compressor speed independent of the output power, while the

fuel consumption of the differential powerplant decreases rapidly at the reduced output powers. At the maximum compressor speed, the differential powerplant offers fuel savings up to 65% compared to the two-turbine. Due to the reduction in turbine inlet temperature of the two-turbine at the reduced compressor speeds, the maximum fuel savings of the differential powerplant are reduced to 35% of the fuel flow of the two-turbine, but the maximum output powers of the differential powerplant are 40% greater than those of the two-turbine.

It is significant that the higher maximum turbine inlet temperatures of the differential powerplant at reduced compressor speeds also enable it to provide a 10% reduction in specific fuel consumption when operating at these higher maximum output powers.

In summary, the comparison of the overall performance of the basic differential and conventional two-turbine powerplants shows that the differential powerplant provides reductions in compressor accelerating time of up to 65% in combination with good transient torque-speed characteristics. Under steady-state conditions, the basic differential gas turbine provides fuel savings up to 65% compared to the conventional two-turbine providing the same output power. However, under steady-state conditions the differential powerplant does not provide the large output torques at low output speeds, or the low output torques at high output speeds provided by the two-turbine powerplant.

As a single-shaft machine operates well at low output torques and high output speeds, the differential powerplant can also be made to operate in this region, by mounting an overrunning clutch between the compressor and turbine shafts. At high output speeds, the compressor and turbine speeds of the differential powerplant become equal and the clutch will automatically engage, forming a single-shaft powerplant. At low output speeds, the clutch automatically disengages. This arrangement also enables the differential powerplant to act as a brake. Of course, by similar means, the two-turbine powerplant could be made to operate as a single-shaft machine at low output torques and high output speeds, and would also provide braking action.

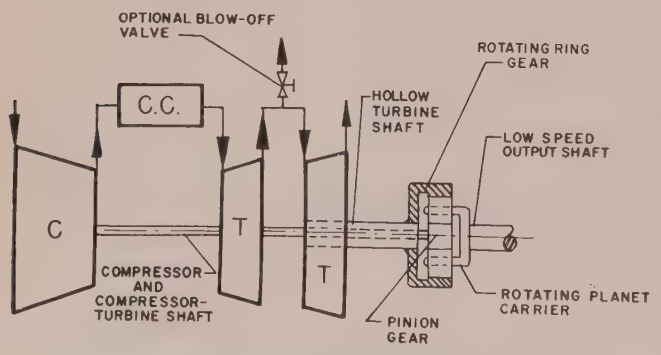

Fig. 15 – Schematic of two-turbine differential gas turbine

Transportation Applications

As their different mechanical arrangements provide the basic differential powerplant with better fuel economy and faster acceleration, and the two-turbine with better torque-speed characteristics, an investigation was made of the two-turbine differential powerplant which combines their mechanical features, schematically shown in Fig. 15. This powerplant has the turbine divided into two portions, with one portion mounted on the compressor shaft. The other portion of the turbine is mounted on a separate hollow turbine shaft surrounding a compressor-shaft extension. A differential serves to connect the compressor and separate turbine shafts to each other and to the output shaft.

In this type of differential powerplant, the portion of the turbine mounted on the compressor shaft is designed to provide only part of the power required to drive the compressor. The separate turbine assists in driving the compressor, and also provides the output power. The operation is similar to the basic differential gas turbine, except that the torque of the compressor shaft is equal to the difference of the torques of the compressor and compressor-turbine, and is, therefore, increased by a reduction in the compressor-turbine torque. The equations relating the torques and speeds of the components of a two-turbine differential gas turbine are shown in Appendix I. Fig. 15 also shows an optional blow-off valve.

A number of powerplants of this type could be built, each having modified turbines providing a different distribution of power between the compressor-turbine and output turbine under the maximum power conditions. The performance of these powerplants would be similar, but each would provide modified torque-speed, fuel economy, and accelerating characteristics.

Fig. 16 plots the steady-state torque-speed characteristics of a two-turbine differential gas turbine having component performance equal to that of the previous powerplants. In this case, the compressor-turbine is designed to provide exactly one-half the power required to drive the compressor at its maximum compressor speed and the maximum turbine-inlet temperature. These torque-speed characteristics combine the features of the two-turbine and basic differential powerplants, providing increasing output torques with decreasing turbine inlet temperatures as the output speed is reduced. This differential powerplant has extended areas of operation in the high-torque, low-speed and high-speed, low-torque ranges compared to the basic differential gas turbine. Although the maximum steady-state output torque at zero output speed has been

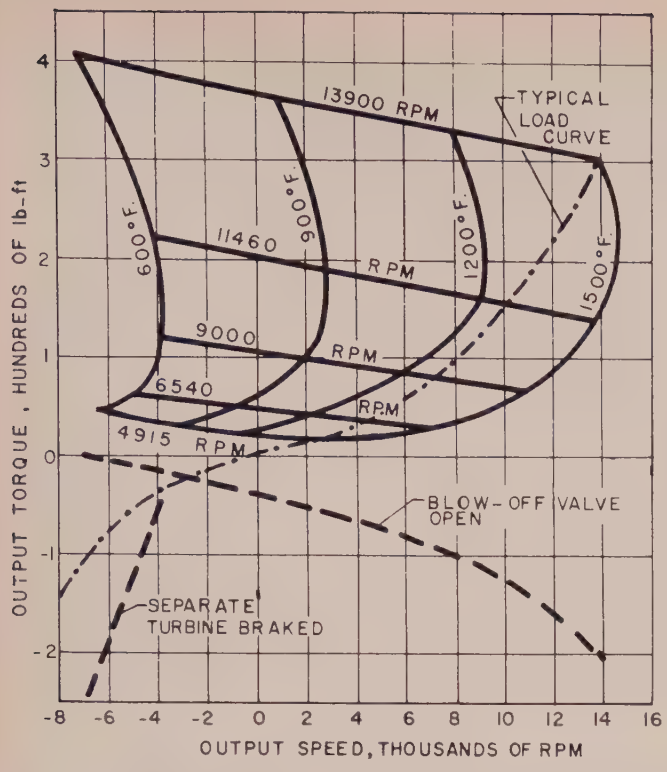

Fig. 16 – Torque-speed characteristics of two-turbine differential gas turbine with no compressor acceleration

differential powerplant offers fuel savings up to 50% at the same compressor speeds and output powers. Fuel savings up to 30% are achieved at the same torques and output powers. These data also show the reduction of over 60% in the idling fuel consumption.

Therefore, the two-turbine differential gas turbine provides improved torque-speed characteristics compared to the basic differential powerplant, and still maintains large advantages in accelerating times and part-load fuel economy. The conventional two-turbine powerplant provides larger output torques at low output speeds, but the differential powerplant can operate over a wider speed range along a typical load line.

Operation in the small area of low torques at high speeds not included in the operating range of the two-turbine differential gas turbine, and operation as a brake, can be provided by means of an overrunning clutch, or optional blow-off valve, shown in Fig. 15.

The opening of the optional blow-off valve reduces the back pressure of the compressor-turbine, increasing its torque and decreasing the torque required to drive the compressor shaft. If the compressor-turbine back pressure is decreased to increased from 275 to 375 lb-ft, it still falls far short of the 620 lb-ft of the conventional two-turbine.

The area of operation of the two-turbine differential powerplant includes lower compressor speeds than the conventional two-turbine powerplant. The minimum compressor speed for this powerplant is 4915 rpm, compared to 9000 rpm for the two-turbine previously shown. These lower compressor speeds enable the differential powerplant to operate at lower output torques at low output speeds. The minimum output torque of the differential powerplant is 30 lb-ft, compared to 150 lb-ft for the conventional two-turbine. These torque-speed characteristics enable the two-turbine differential powerplant to operate along a propeller or road-load curve anywhere between 16 and 100% of the maximum output speed. The conventional two-turbine powerplant can only operate between 50 and 100% of the maximum output speed along such a load curve.

When the two-turbine differential powerplant is operating at 1700 F during compressor acceleration, it provides a maximum output torque at zero output speed of 525 lb-ft, compared to 650 lb-ft for the conventional two-turbine powerplant. The two-turbine differential powerplant also provides reductions in compressor accelerating time of up to 50%.

Fig. 17 plots the steady-state fuel consumption of the two-turbine differential gas turbine. Comparison of these data with those of the conventional two-turbine powerplant of Fig. 14 shows that this

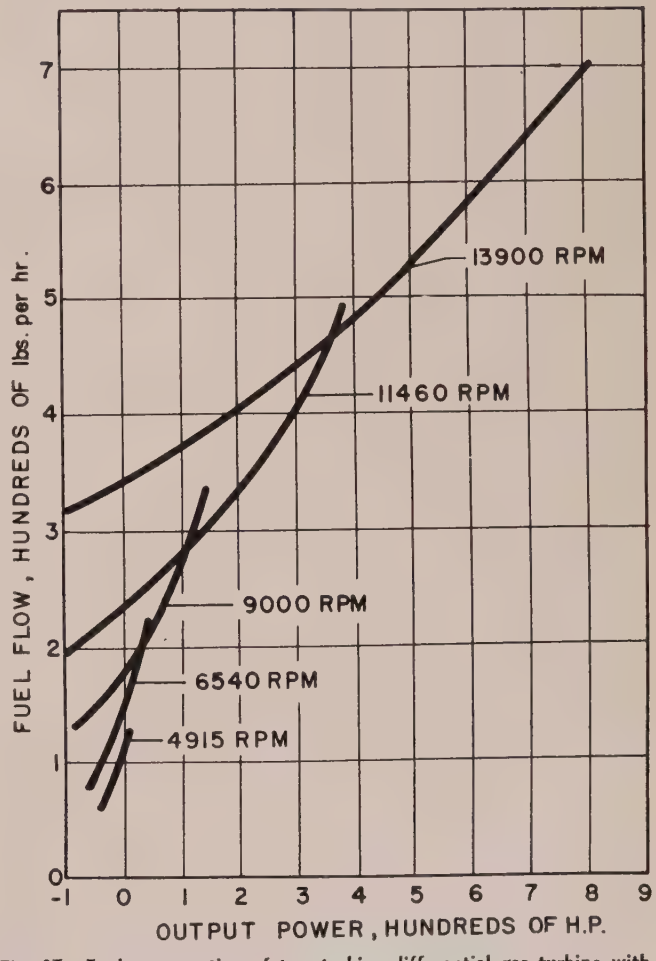

Fig. 17 – Fuel consumption of two-turbine differential gas turbine with no compressor acceleration

atmospheric pressure, the compressor-turbine will provide more torque than is required to drive the compressor, and the compressor shaft torque will have been reversed. Opening the blow-off valve will also decrease the torque of the separate turbine, and reducing the inlet pressure to atmospheric pressure will cause the separate turbine to act as a brake due to its windage losses. Therefore, opening the blow-off valve reverses the torques of the compressor shaft and turbine shaft, and hence reverses the torque on the output shaft, whereby the powerplant acts as a brake. Fig. 16 plots the estimated steady-state braking torques as determined by the windage losses of the separate turbine at maximum compressor speed.

Partial opening of the blow-off valve enables operation at any torque between the maximum braking torques shown and the maximum driving torques achieved with the blow-off valve closed.

With the blow-off valve open, this differential powerplant can provide negative output torques at zero output speed, because the separate turbine rotates at about one-third speed when the output shaft is stationary. These negative torques can be utilized to drive the output shaft in the reverse direction, further reducing the turbine speed. If the separate turbine is then held stationary by a brake, the compressor and compressor-turbine will act as a single-shaft gas turbine, and will provide the large negative output torques and negative output speeds shown in Fig. 16. Reverse powers up to 45% of the maximum power result in this example. This means of providing power in the reverse direction is particularly suitable for large marine applications, and offers many advantages compared to reversible pitch propellers or reverse gearing. A conventional with a blow-off valve does not provide as large braking torques, and does not provide reverse powers.

Before closing, it should be pointed out that it is not necessary that the compressor-turbine of a two-turbine differential gas turbine provide exactly half the power required to drive the compressor under the maximum power conditions, as was the case in the example shown. Two-turbine powerplants having compressor turbines providing more than half the compressor requirement at the maximum power conditions will have larger output torques at low output speed, greater areas of operation in the high output speed, low output torque range, and larger reverse powers than the example shown. Such differential powerplants, however, will have reduced fuel economy and accelerating advantages at the low output speeds.

It should also be pointed out that at reduced compressor speeds all differential gas turbines provide larger maximum output powers than conventional two-turbine powerplants operating at the same compressor speed, and that these larger powers are achieved at specific fuel consumptions lower than any achieved by the conventional two-turbine powerplant at the same compressor speed. These advantages result from the ability of the differential powerplant to operate at higher turbine-inlet temperatures at the reduced compressor speeds than the conventional two-turbine powerplant, and would enable a two-turbine differential powerplant having a compressor pressure ratio of about 6/1 to provide very good part-load fuel economy.

Conclusion

The use of a differential as an interconnection between the compressor, turbine, and output shafts establishes entirely new equations relating their torques and speeds. These new relationships enable the differential gas turbine to provide better part-load fuel economy and quicker acceleration than conventional powerplants having the same component performance. In the two-turbine differential gas turbine, these advantages are combined with torque-speed characteristics very suitable for transportation applications. This powerplant is particularly attractive because it provides the powerplant designer with the unique opportunity of varying the relationships between the components to achieve in one powerplant the optimum combination of the performance features required for a particular application.

References

1. *Mechanical Engineering,* Vol. 66, June, 1944, pp. 373-383: "Basic Gas-Turbine Plant and Some of Its Variants," by J. K. Salisbury.

2. Institute of Marine Engineers Transactions, Vol. 64, May, 1952, pp. 79-122: "Epicyclic Gears," by H. N. G. Allen and T. P. Jones.

3. SAE Transactions, Vol. 63, 1955, pp. 72-82: "Pinwheels or Pistons? – Progress Report on Automotive Gas Turbines," by W. A. Turunen.

4. ASME Transactions, Vol. 77, May, 1955, pp. 561-590: "British Naval Gas Turbines," by G. F. A. Trewby.

5. Society of Naval Architects and Marine Engineers Transactions, Vol. 59, 1951, pp. 811-834: "Theoretical Study of Stopping of Ships," by H. J. Chase and A. L. Ruiz.

6. NACA TN 1459 (1947) "Analysis of Performance of Jet Engine from Characteristics of Components," by A. W. Goldstein.

Appendix I

Steady-State Torque and Speed Equations

Conventional Gas Turbine Arrangements

	Single-Shaft Unit	Two-Turbine Unit
Torque equations	$T_o = T_t - T_c$	$T_c = T_{t1}$ $T_o = T_{t2}$
Speed equations	$N_c = N_t = N_o$	$N_c = N_{t1}$ $N_o = N_{t2}$

Differential Gas-Turbine Arrangements

	Basic	Two-Turbine Unit
Torque equations	$T_0 = K_1T_t = K_2T_c$	$T_0 = K_1T_{t2}$ $= K_2(T_c - T_{t1})$
Speed equations	$N_0 = K_3N_t - K_4N_c$	$N_0 = K_3N_{t2} - K_4N_c$

where:

T_o = Output torque
T_c = Compressor torque
T_t = Total turbine torque
N_o = Output speed
N_c = Compressor speed
N_t = Turbine speed
T_{t1} = Torque of compressor-turbine
T_{t2} = Torque of output-turbine
N_{t1} = Speed of compressor-turbine
N_{t2} = Speed of output-turbine

K_1, K_2, K_3, and K_4 are constants established by the construction of the differential

Appendix II

Component Performance

The compressor performance used in both powerplants was the test performance of an experimental 8-stage axial-flow compressor described in NACA Report 758 and in Fig. 12, in particular.

The burner was assumed to have a combustion efficiency of 95% and a pressure ratio $P_4/P_3 = 0.95$. The average heating value of the liquid fuel, referred to 400 R, was 18,840 Btu per lb.

The turbine power for each powerplant was provided by two 2-stage axial-flow turbines, each having performance similar to the tested performance of the 2-stage axial flow turbine described in NACA Report 878 and in Figs. 14 and 15 in particular. The turbines were arranged for series flow of the combustion products through all four stages. The two-turbine powerplants had the first two stages on the compressor shaft, and the third and fourth stages mounted on the output shaft. The single-shaft and basic differential powerplants had all four stages mounted on the same turbine shaft.

The design point compressor pressure ratio was 3.0/1 at a compressor efficiency of 86.5%. The maximum turbine efficiency was 84%.

The particular differential selected for use in the calculation of the basic differential powerplant established the following torque and speed equations, neglecting the speed reduction provided:

$$T_o = 0.512\,T_t = 1.05\,T_c$$
$$N_o = 1.95\,N_t - 0.95\,N_c$$

The particular differential selected for use in the calculation of the two-turbine differential powerplant established the following torque and speed equations, neglecting the speed reduction provided:

$$T_o = 0.67\,T_{t2} = 2.01\,(T_c - T_{t1})$$
$$N_o = 1.5\,N_{t2} - 0.5\,N_c$$

DISCUSSION

Suggests Better Bases For DGT Comparison

– P. F. Martinuzzi
Stevens Institute of Technology

IN the last years there have been very few new ideas in the gas-turbine field. The differential gas turbine is a welcome new concept which shows that there are still interesting new possibilities for the gas turbine.

Final judgment on the differential gas turbine must be left to detailed studies and to experiment, and this will take time. It would seem, however, that in some cases the author has not done justice to all the possibilities of his idea. For instance, in his discussion of the two-turbine differential gas turbine for transportation applications, the author states that the maximum steady-state output torque at zero speed of 375 ft-lb falls far short of the 620 ft-lb which could be obtained from a comparable conventional split-shaft turbine. This statement, if true in general, would put the differential gas turbine at a heavy disadvantage relatively to the conventional split-shaft turbine. High torque at zero output speed is one of the most pressing requirements for a transport gas turbine, because it allows a simple and cheap gear shift to be used.

However, the above statement is not true in general; it is only true for the case examined by the author, in which the two-turbine differential gas turbine and the conventional split-shaft turbine have the same performance at design point (1500 F, 13,900 rpm for the compressor). A look at Figs. 13 and 16 shows immediately that this is the basis of comparison. But it does not have to be, nor is it the best.

In a conventional split-shaft turbine, the compressor cannot absorb any greater power than at design point, unless the turbine inlet temperature is increased above the design-point value. But in a two-turbine differential gas turbine, the compressor can easily absorb more power than at design point without increasing the design-point turbine-inlet temperature. Provided compressor and compressor turbine are designed so as to permit overspeeding above the design-point value, the extra power is provided at low and zero output speeds by the second turbine through the differential. If the author will provide a curve for a two-turbine differential gas turbine in which compressor and compressor turbine are capable of overspeeding, plotting torque

against output speed at constant maximum turbine inlet temperature, the results will be quite different and very much more interesting than those shown in Fig. 16.

It is obvious that, if and when a differential gas turbine will be built, specially designed components will have to be used. Once this is done, provision for overspeeding of the compressor and compressor turbine can easily be made. The design criterion should be that component efficiency should be a maximum at design point, but the mechanical and flow characteristics should permit overspeeding. The amount of overspeeding is not large, because the power absorbed increases with the cube of the overspeed ratio.

If this is done, and if the machine is operated at maximum turbine-inlet temperature throughout the whole output speed range, the fuel consumption will be much higher than that shown in Fig. 17. But, if the overspeeding two-turbine differential gas turbine is operated through the whole speed range at the temperatures indicated in Fig. 16, then the economy will be the same as that shown in Fig. 17. In other words, by allowing compressor and compressor turbine to overspeed, all the advantages claimed by the author can be obtained and, in addition, the torque at low and zero output speed can be very much increased in case of necessity, so that the transmission can be very much simplified.

It is also unfortunate that in all comparisons the components described in Appendix II have been used. These are machines of very old design, and they are jet engine components. Had the characteristics of more modern and less heavily loaded components been used, the results would probably have been better.

It is to be hoped that a further study on this very interesting concept will soon be published, in which specially designed components with modern characteristics will be used.

Describes Tests with Turbine-Powered Truck

– R. C. Norrie
Kenworth Motor Truck Corp.

IT appears as though the basic thought behind Mr. Hutchinson's proposed turbine is to provide a means of improving part-load and idling fuel consumption characteristics on the turbine; also, in one of his proposed turbines, to improve the braking or retarding characteristics. This should, then, give the turbine similar characteristics to engines in present use on automotive equipment.

Our experience with turbine engines has only been with an experimental unit tested in conjunction with the Bureau of Ships, Boeing Airplane Co., and the West Coast Fast Freight Co. The turbine-powered truck was put in initial testing on April 10, 1950. One of the purposes of installing the engine in a truck was to provide another means of testing the engine and possibly finding deficiencies in truck service which would not appear in test cell checking. Blade rubbing and minor failures were evident within a very few miles of operation.

The truck and loaded semi-trailer continued in test operation and test running in the state of Washington until June, 1952, when a 3000-mile load run was made from Canada to Mexico and back on U. S. Highway 99. In August, 1952, the unit was put into service and operated by West Coast Fast Freight Co., hauling freight from Seattle to Spokane, Wash., and way-points. It continued in service until November, 1953, when all companies agreed to discontinue testing.

We found that it had extremely desirable characteristics as far as the driver was concerned. There was a complete absence of vibration and the noise level was low. The fuel consumption on this unit, operating at 68,000 lb gross combination weight, was approximately three times that of a diesel engine of comparable horsepower operating in the same service. In some instances, the consumption would run as high as four times. The engine developed 175 hp and weighed 230 lb installed.

Mr. Hutchinson's paper indicated that in his calculations he used a specific fuel consumption of approximately one pound per brake horsepower. Therefore, I would like to know if I understood this figure correctly and what style and size of turbine gave this consumption figure?

Two Questions For the Author

– Robert Cass
White Motor Co.

WHAT do you think of the two roads, heat exchanger versus high compression ratio, as the most effective ways of meeting the fuel consumption picture?

Also, how much progress has been made with the carbide ceramic turbine blades?

Asks About Ways to Improve Fuel Consumption

– F. R. Nail
Mack Mfg. Corp.

DID your research and development work include actual vehicle applications of the differential gas turbine so that a fuel consumption comparison could be made with a single-shaft gas turbine on a miles-per-hour basis, and if so, what was the comparison?

Also, are there any developments which might be under way to improve the fuel consumption of a gas turbine?

Size, Fuel Economy, And Cost Questions

– C. A. Lindblom
International Harvester Co.

WILL the differential gas turbine provide a powerplant of smaller dimensions than a modern internal-combustion engine of equivalent power, say in the 200- or 300-hp category?

With the requirements for regeneration in order to obtain optimum fuel economy as implied by Mr. Hutchinson, will there be much of a weight advantage over modern internal-combustion engines?

Granting that an efficient engine can be built, will the initial cost be comparable to modern combustion engines?

Author's Closure To Discussion

DR. MARTINUZZI is to be congratulated on his very thoughtful comments which indicate his thorough understanding of the concept advanced and on his extension of

the area of discussion by his suggestion that the output torque of the two-turbine differential gas turbine at low output speeds be increased by increasing the compressor speed under these conditions. This indeed provides a means of increasing the output torque of the two-turbine differential gas turbine at low output speeds without increasing the maximum turbine inlet temperature.

Actually, Dr. Martinuzzi's suggestion is one of several means to improve the torque at low output speeds which have been investigated. I would like to point out that the advantages gained by overspeeding the compressor are not restricted to the two-turbine differential gas turbine of Fig. 15 but also can be achieved in the basic differential powerplant of Fig. 7, in which case the maximum turbine speed is not increased. In the basic differential machine, overspeeding the compressor provides a torque multiplication where none would exist without such overspeeding. In the case of the two-turbine differential machine, overspeeding the compressor provides torque multiplications larger than those normally achieved by a two-turbine differential gas turbine.

The result of having the compressor speed vary 21% over the output speed range from 13,900 rpm at the maximum output speed to 16,800 rpm at zero output speed can be estimated from the performance curves included in this paper. The torque multiplications provided by this 21% variation in compressor speed would approximate that resulting from a 21% variation in compressor speed from 11,460 rpm at the maximum output speed to 13,900 rpm at zero output speed. As can be seen from the curves, this latter compressor speed variation provides a 1.6 torque multiplication for the basic differential machine of Fig. 13, and a 2.7 torque multiplication for the two-turbine differential powerplant of Fig. 16. Hence, at 16,800 rpm the basic differential machine would provide about 495 lb-ft of standstill torque or 80% that of the conventional two-turbine powerplant, and the two-turbine differential machine would provide approximately 810 lb-ft of standstill torque or approximately 130% that of the conventional two-turbine powerplant. During compressor acceleration both these differential powerplants would provide standstill output torques considerably higher than the figures just mentioned.

If the compressor efficiency were not seriously impaired by increasing the compressor speed to 16,800 rpm at standstill, the steady-state turbine inlet temperature of both differential machines would remain low, in the order of 800-1000 F. It seems unlikely that the compressor efficiency would be sufficiently impaired by overspeeding within structural limits as to require the use of the maximum turbine inlet temperature at standstill because of the high turbine efficiency and zero output power of differential powerplants under these conditions.

Thus the torque multiplication of differential powerplants can be greatly improved by overspeeding the compressor at low output speeds. This can be achieved without increasing the maximum turbine inlet temperature and even without increasing the maximum turbine speed in the case of the basic differential powerplant. However, such overspeeding would require either increasing the centrifugal stresses and loadings on the differential gearing and other powerplant components or derating the powerplant, either alternative resulting in an increase in the size, weight, and cost of a powerplant of a given power. Designing a compressor for overspeeding would likewise mean compromising to some extent its performance. As pointed out previously, this is one of several means by which the torque multiplications of differential gas turbines can be improved and it is too early to say which is the most appropriate means to increase the output torques of differential gas turbines at low output speeds.

The performance data included in the paper were calculated from tested compressor and turbine performance, but no complete experimental powerplants were tested. The compressor performance was that of the NACA eight-state axial-flow compressor described in detail in NACA Report 758. This compressor provided an airflow of 10 lb per sec at a pressure ratio of 3.0/1 and an efficiency of 86.5% at the design point. The data were also based on the tested performance of a two-stage axial-flow turbine described in detail by Goldstein.[a] Two two-stage turbines were used in series to provide a total of four turbine stages in all powerplants. Each turbine had a maximum efficiency of 84% at the design point. Both the compressor and turbines had a tip diameter of about 14 in. and had a maximum speed of 13,900 rpm. The performance of these components together with the assumed burner performance described in Appendix II provided a full-load specific fuel consumption of 0.86 lb per hp-hr at 820 hp.

As Dr. Martinuzzi points out, our performance data were derived from compressor and turbine tests made more than 10 years ago. It, therefore, does not indicate the performance that a differential gas turbine could achieve today using contemporary components. Modern gas turbines in the larger powers, the Allison T-56,[b] for example, provide sea level specific fuel consumptions less than 0.6 lb per **shaft** hp-hr without heat exchangers, and modern experimental automotive gas turbines with centrifugal compressors are using rotary heat exchangers to enable these small gas turbines to provide fuel economy approximating that of modern automobile piston engines. These experimental automotive gas turbines, with heat exchangers, are about the same size as our present automobile engines but are about 200 lb lighter. The results of the performance studies included in this paper indicate that differential gas turbines using similar modern components would be about the same size and weight and would have the same full-load fuel economy as modern conventional gas turbines, but would provide improved torque response and improved part-load and idling fuel economy.

Many government and industrial gas turbine research programs are directed towards developing improved components, materials, and methods. These development programs are also aimed at reducing the present excessive cost of gas turbine powerplants. The improvement of compressor and turbine efficiency, or the development of improved materials or cooling means to enable the use of higher turbine inlet temperatures, would greatly improve the efficiency of the gas turbine, and further reduce its size and weight. As a 1% increase in compressor or turbine efficiency can provide a 2 or 3% increase in powerplant efficiency, and as increasing the turbine inlet temperature from 1400 to 1800 F can double the output power and provide a 20% increase in powerplant efficiency, it seems very likely that today's gas turbine powerplants will seem large and inefficient 10 years from now.

Ten years from now there will probably be three types of gas turbines in operation:

1. High-pressure-ratio (10/1 to 15/1), high-temperature (2000-2500 F) powerplants without regenerators.

2. Low-pressure-ratio (5/1), low-temperature (1500 F) powerplants with regenerators.

3. Low-pressure-ratio, low-temperature powerplants without regenerators.

The first type will probably be restricted in application to the larger, more costly installations unless inexpensive cooling means are developed or the present price of high-temperature (carbide) materials is drastically reduced. The second type will probably be the more numerous and available in smaller powers. Both these types will probably provide fuel economies as good as any non-gas turbine powerplants in their power ranges. The third type will be restricted to applications where simplicity and first cost are more important than fuel economy.

[a] See reference No. 6 of main paper.

[b] "Allison T-56 Turboprop Aircraft Engine," by J. B. Wheatley, D. G. Zimmerman, and R. W. Hicks. Paper presented at SAE Golden Anniversary Aeronautic Meeting, New York, April 18, 1955.

SOME structural design problems produced by aerodynamic heating are examined to determine design approaches that may help alleviate undesirable effects. Loss of strength and creep of structures at uniform elevated temperatures are discussed, and the probable effect of creep on design of airplane structures is indicated.

Nonuniform temperature distributions produced by changing flight conditions are discussed to introduce the subject of thermal stresses and their possible effects on the structure, thermal buckling, and severe loss of stiffness at stress levels well below those producing buckling. Design approaches that can be used to prevent thermal stresses and consequent adverse effects are then indicated.

Some Elevated Temperature Effects of High-Speed

THE various structural effects of aerodynamic heating have been discussed in many papers in the recent literature.[1] Such papers have made it clear that the resulting structural design problems are numerous, complex, and so severe that performance capabilities of high-speed aircraft may be limited by aerodynamic heating effects. The purpose of this paper is to consider the nature of a few such problems and indicate design approaches that may help alleviate the undesirable effects. Maximum temperatures experienced by high-speed aircraft are indicated and loss of strength and creep of structures at uniform elevated temperatures are discussed. Nonuniform temperature distributions produced by changing flight conditions then lead to consideration of thermal stresses and their effects on the structure, thermal buckling, and severe loss of stiffness at stress levels well below those required for buckling.

Uniform Elevated Temperatures

Maximum Temperatures Encountered in Flight – Maximum temperatures attainable on the surface of an aircraft structure during sustained flight are given in Fig. 1. This is the familiar plot of temperature against Mach number for altitudes in the stratosphere (35,000-105,000 ft). The upper curve labeled "no radiation" gives the adiabatic wall temperature; that is, the surface temperature at which no heat flows from boundary layer to the structure. The structure loses heat by radiation, however, and at high Mach numbers this effect becomes significant, as indicated by the lower equilibrium temperatures given by the dashed lines for altitudes of 40,000 and 80,000 ft. Alleviating effects of radiation become increasingly beneficial as altitude is increased.

Curves such as those in Fig. 1 show that temperatures are beyond human endurance at Mach 2 and that failure of common aircraft materials such as plexiglas and rubber poses a serious problem. At higher speeds, structural materials lose strength, and sustained flight for even pilotless aircraft is possible only either with substantial cooling or at very high altitudes.

Strength and Creep of Structures at Elevated Temperatures – Loss of strength of structural materials at elevated temperatures is the most obvi-

[1] "Symposium on Thermal Barrier," nine papers presented at ASME Annual Meeting, New York City, Nov. 28-Dec. 3, 1954.

Temperature Structural Problems Aircraft

Richard R. Heldenfels, NACA Langley Aeronautical Laboratory

This paper was presented at the SAE Golden Anniversary Aeronautic Meeting, Los Angeles, Oct. 13, 1955.

ous, and probably the most serious, of the structural problems encountered by high-speed aircraft. Some resulting design problems will be considered now by discussing strength of aluminum alloys at moderate elevated temperatures; similar problems exist with other structural materials at higher temperatures.

Variation of strength with temperature is illustrated in Fig. 2. (Materials data for this and subsequent figures were taken from the literature.[2]) Stress is plotted against temperature for tensile and compressive loadings of 2024-T3 aluminum alloy exposed to temperatures for ½ hr before loading. The dashed curve gives ultimate tensile strength and the solid lines give compressive strength of simply-supported plates for width-thickness ratios (b/t) of 20, 30, 45, and 60. For the plates, the maximum average stress the plate will support is given. This maximum stress is approximately equal to the buckling stress for $b/t = 20$ and 30, but is substantially higher than the buckling stress for $b/t = 45$ and 60. The curves in Fig. 2 show a significant decrease in strength at temperatures above 400 F. The plate curves show a slight increase in strength at 400 F due to artificial aging of this alloy.

In addition to loss of strength at elevated temperatures, time spent under load and temperature also has an effect, as shown in Fig. 3. Stress is plotted against time in hours, with left-hand curves for tensile loads and right-hand group for compressive loads. These particular data are for a temperature of 500 F where the effect of time at temperature is large, but similar effects are observed at other temperatures.

In the case of tension, the curves show ultimate tensile stress and tensile yield stress as dashed lines and creep rupture stress as a solid line. There is a significant difference between the load-temperature-time combinations that give the dashed and solid curves. To get the dashed lines (static strength test results), the specimen is exposed to temperature alone for the specified number of hours and then is loaded to failure. The solid curves (creep test results) are obtained by applying the load and then exposing the specimen to both load and temperature until failure occurs.

[2] See NACA RM L55E11b (1955), "Preliminary Investigation of Compressive Strength and Creep Lifetime of 2024-T3 (formerly 24S-T3), Aluminum-Alloy Plates at Elevated Temperatures," by E. E. Mathauser and W. D. Deveikis.

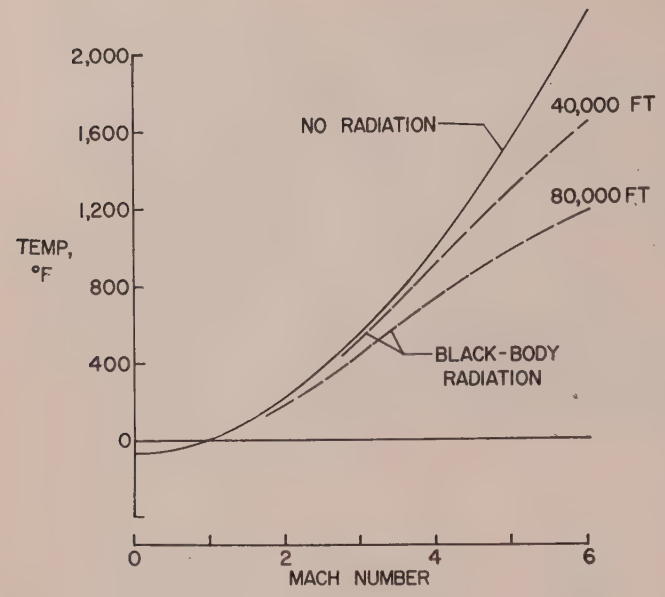

Fig. 1 - Temperatures attained by aircraft during sustained flight in stratosphere (altitude from 35,000-105,000 ft), including effects of radiation at altitudes of 40,000 and 80,000 ft

A similar set of curves is shown for compression loads on plates with $b/t = 20$ and 45. Again, the dashed curve is the maximum load carried in a static strength test and the solid curve is for creep collapse of the plate.

All curves show a substantial decrease of stress with increasing time. This characteristic is expected in creep curves, but the large effect of exposure time on static strength is a characteristic of aluminum alloys not so pronounced in most other structural materials.

Comparison of static strength of the material in tension with compressive strength of a plate with $b/t = 20$ indicates that maximum strength in tension is higher in this range of exposure times. On the other hand, creep curves show that this plate is capable of carrying slightly higher stresses in compression than in tension for creep lifetimes up to 100 hr.

Data presented here cover two extreme types of load and temperature histories; that is, in the static strength test the structure is exposed to temperature for a time and then loaded to failure, whereas in the creep test the structure is loaded and then exposed to both load and temperature until failure occurs. The airplane structure, however, does not experience such simple histories. It experiences a number of heating cycles of variable duration and temperature, and during any such cycle experiences a somewhat random application of load that varies in duration and magnitude. Behavior of materials and structures under such conditions is not yet established, but is being studied.

Effect of Creep on Design of Aircraft Structures – Data such as those in Fig. 3 indicate that creep would be the primary consideration when designing an aluminum-alloy structure for a temperature of 500 F. The creep curves lie below the static strength curves, indicating a lower allowable stress and thus more weight. This is not necessarily true for an airplane structure, however, for as previously mentioned, an airplane experiences a variety of temperatures and loads and spends only a small part of its life at temperature and load combinations that produce significant creep. Conse-

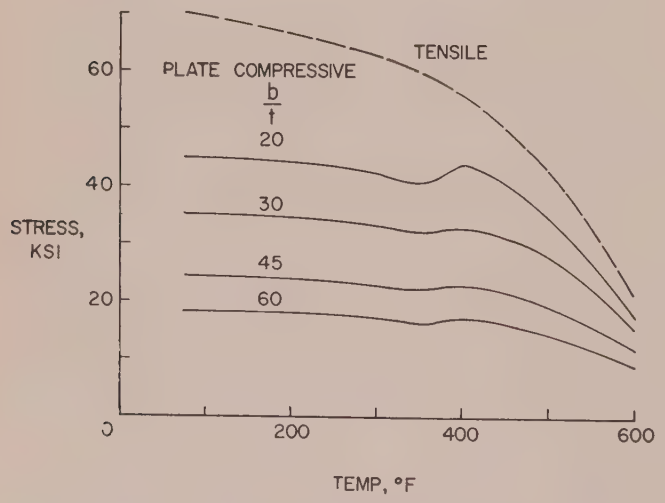

Fig. 2 – Strength of 2024-T3 aluminum alloy at elevated temperatures for tensile members and plates in compression

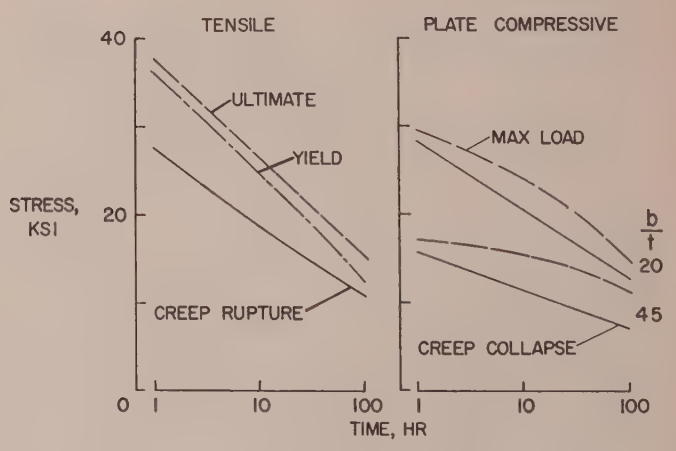

Fig. 3 – Effect of time at temperature of 500 F on strength and creep behavior of 2024-T3 aluminum alloy

quently, creep lifetime of an airplane structure at design load and temperature could be substantially less than exposure time used to establish the static strength.

Fig. 4 compares the weight required to support a given tensile load for several different design conditions. Weight required (in arbitrary units) is plotted against temperature. Solid curves give weight required when creep rupture is used as the design criterion for lifetimes of 10, 100, and 1000 hr, respectively. The two dashed curves give weight required for static strength after 1000 hr exposure; the upper curve (dash-dot) is for yield strength, and the lower curve (dash-dash) is for ultimate strength. Since creep rupture curves fall both above and below the strength curves, weight required will be determined by the particular combination of loads and times used for a design criterion.

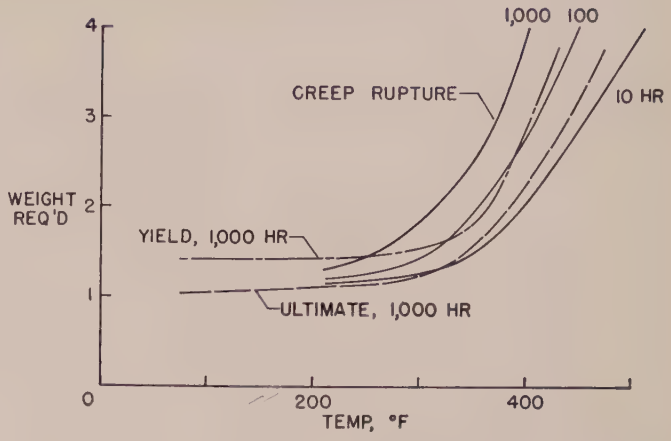

Fig. 4 – Weight of 2024-T3 aluminum alloy required to support equal tensile loads at elevated temperatures as determined by some strength and creep design criteria

Total time a high-speed airplane will spend at supersonic speed – and thus at elevated temperatures – might be conservatively estimated as 1000 hr. During this period the airplane will probably spend less than 10% of the time at load levels high enough to produce creep of the structure. In this case, then, a reasonable design approach is to require the structure to have sufficient strength to support the design limit load without yielding after 1000 hr exposure to temperature or to have the ability to support the design-limit load at temperature for 100 hr without rupturing, whichever requires the greater weight. This approach indicates that static strength governs design up to about 325 F; above this temperature the two criteria require approximately equal weights. Such considerations then indicate that creep may have little effect on design of aluminum-alloy-aircraft structures. The situation is somewhat different for other materials, however.

Fig. 5 is a similar comparison for three structural materials. Weight (in arbitrary units) is plotted against temperature for 2024-T3 aluminum alloy, RC-130A titanium, and Inconel X, materials which cover the temperature range in which metals are usable. Stainless steels generally fall between RC-130A and Inconel X, but nearer RC-130A.

Weight required to support the load on the basis of yield strength after 1000 hr at temperature is given by the dash-dot lines. Weight required to meet the creep criterion of rupture after 100 hr at load and temperature is given by the solid lines. At each temperature the higher line for a given material determines the governing design criterion. For the aluminum alloy, the creep criterion requires less weight than the strength criterion, as shown previously, so that creep is no problem under these conditions. Similarly, creep is no problem for Inconel X up to 1200 F, but above this temperature creep would govern the design. For the titanium alloy, the creep criterion governs design throughout the temperature range. This particular titanium alloy has poor creep characteristics; others have better creep properties than RC-130A, but less tensile strength. Perhaps further development of titanium alloys will improve this situation.

From such considerations it appears that creep may or may not have a significant effect on design of structures for high-speed airplanes, depending on both materials involved and design criteria used. In some cases where creep may influence design, conversion to another material or alloy may remove creep from consideration and increase structural efficiency of the design.

The effect of creep depends largely on the design

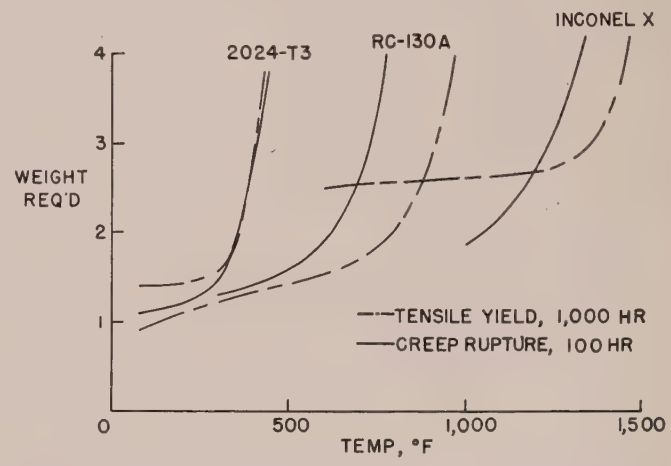

Fig. 5 – Weights of three materials required to support equal tensile loads at elevated temperatures as determined by a strength and a creep criterion

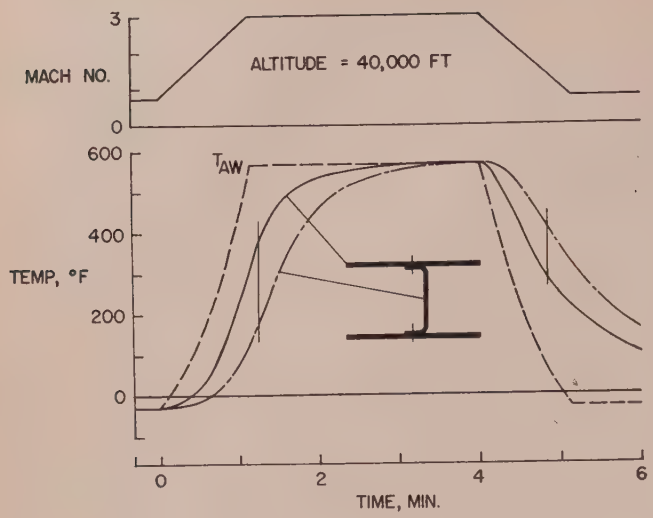

Fig. 6 – Variation of Mach number and temperature with time for representative structural element during short supersonic flight at 40,000-ft altitude

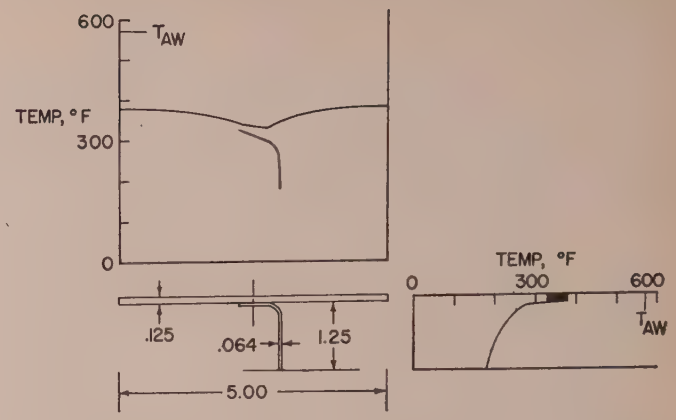

Fig. 7 – Temperature distribution in structural element of Fig. 6 at time of maximum thermal stress following acceleration to supersonic speed (1.23 min)

criteria used. The criterion used in this example is believed conservative in view of probable load-temperature-time experience of high-speed airplanes. A design creep lifetime less than 100 hr probably could be used safely, in which case creep would be even less of a problem than indicated here.

Creep rupture in a specified time was used as the creep design criterion in this analysis because of the obvious significance of this type failure. Another design criterion, such as a limiting amount of permanent creep strain or deformation might have been used, but its validity in aircraft design appears doubtful. This doubt arises from experimental investigations of creep behavior of aluminum-alloy structural elements and box beams,[2, 3] in which measured deformations followed no simple pattern that could be used to establish a reasonable limiting strain. Although a limiting strain may not be a suitable creep design criterion, designs susceptible to creep failure will have to be checked nevertheless for excessive creep deformation and, if necessary, revised to correct any deficiencies.

Other factors requiring some consideration are effect of prior creep strain on ultimate strength and effects of intermittent or cyclic heating and loading on creep of the structure. The latter was previously mentioned and is an open subject at present, since existing data show both alleviating and aggravating effects, depending on the material and combinations of load, time, and temperature. Regarding the effect of creep on strength, exploratory tests on aluminum-alloy plates indicate that creep strains approaching those expected at collapse cause at most a slight reduction in maximum strength below that expected from a static test following an equally long exposure to temperature.

Thus it is too early to state how these many factors will combine to determine the true influence of creep on design of structures for high-speed airplanes. It appears, however, that creep may well be a major design criterion only at high temperatures where all available materials experience significant creep. For the time being, a conservative design approach combined with proper selection of materials will avoid creep problems. However, static strength of light alloys cannot be utilized to the fullest in high-speed airplanes, nor can the maximum usable temperatures be determined for other metals until a realistic creep design criterion is established for aircraft structures. A realistic creep criterion must take into account fully the particular types of load and temperature histories experienced by high-speed airplanes or needless weight may be added to the structure.

Nonuniform Temperature Distributions

Temperature Distribution in a Structural Element – The discussion thus far has concerned maximum possible temperature, but a structure may not experience this maximum because of the structure's heat capacity and time required for heat to be transferred from boundary layer to the structure. This temperature lag is very beneficial since short flights are possible at high Mach numbers without excessively high temperatures. Times involved depend on flight path and structure configuration. An example of the temperature history of part of an airplane wing structure is given in Fig. 6. Mach number and two structural temperatures are plotted against time in minutes for a

[3] See NACA TN 3310 (1954), "Investigation of Static Strength and Creep Behavior of an Aluminum Alloy Multiweb Box Beam at Elevated Temperatures," by E. E. Mathauser.

short supersonic flight at 40,000-ft altitude. The airplane, initially cruising at Mach 0.75, accelerates at 1 g to Mach 3.0, flies steadily at this speed for a few minutes, and then decelerates at 1 g to its original cruising speed. The structure considered is a skin and web combination forming a multiweb wing. Temperature is shown for a point on the skin and for a point on the web centerline. The variation of adiabatic wall temperature (T_{AW}) with time is also included. The curves show that considerable time is required for the skin to stabilize at T_{AW}, and that web temperature lags skin temperature. During acceleration the skin is hotter than the interior, whereas the interior is hotter during deceleration.

These curves show that the structure may be required to withstand high temperatures for a portion of its flight and also experience considerable nonuniform temperature distribution during heating and cooling periods. Elevated temperatures lead to loss of strength and structural creep, as discussed previously, whereas nonuniform temperature distributions lead to thermal stresses and some associated structural effects.

During acceleration, the largest temperature differences occur at $t = 1.23$ min, 0.10 min after the constant Mach number phase begins. The largest temperature differences experienced during deceleration occur at $t = 4.83$ min, 0.83 min after the beginning of deceleration and 0.30 min before the final constant Mach number phase is reached. Temperature distributions at these times are given in Figs. 7 and 8, respectively. Each figure gives details of the structural component, temperature distribution along the surface, and temperature variation down to the web centerline. A small temperature drop across the riveted joint between skin and web is indicated by the two lines in that region. Comparison of Figs. 7 and 8 shows that temperature distribution during deceleration is opposite to that encountered during acceleration; that is, the skin is cooler than the interior during deceleration.

Rates of acceleration and deceleration used in this example are somewhat high for most airplanes but were selected arbitrarily for the example since maximum thermal stresses are rather insensitive to large changes in acceleration.

Thermal Stresses in the Structural Element – Thermal stresses arise from restraint of thermal expansion and may occur when a structure is subjected to a nonuniform temperature distribution. In general, the hot parts try to expand and develop compressive stresses while the cool parts develop the combination of tensile and compressive stresses necessary to make thermal stress distribution a self-equilibrating system.

Fig. 9 shows thermal stress distribution (produced by the temperature distribution of Fig. 7) in the structural element following acceleration to supersonic speed. Stress is plotted against distance measured along the upper skin to the web, down through the web to the lower skin, and then along the lower skin, as indicated by dimensions A, B, and C. The solid curve gives thermal stress distribution and the dashed curves give load stresses due to an applied bending moment. Overlapping portions of each curve give stresses in the skin and web flange where the two are in contact. The difference in thermal stresses at the joint is due to the temperature drop across the connection. As usual in wing structures, load stresses are compressive in the upper skin and tensile in the lower skin. Thermal stresses (produced by the temperature distribution of Fig. 7) consist of compression in the hot skins and tension in the web. Compres-

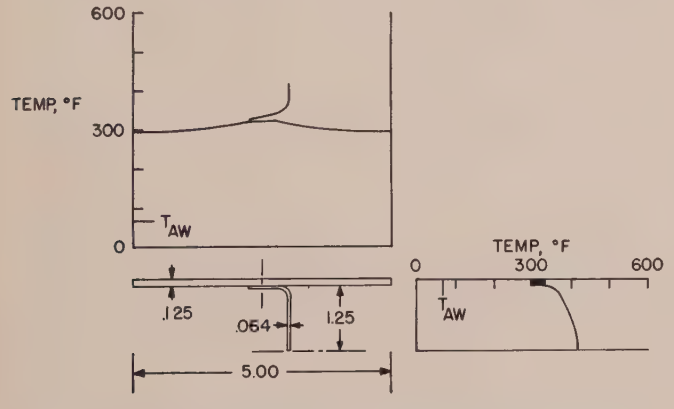

Fig. 8 – Temperature distribution in structural element of Fig. 6 at time of maximum thermal stress during deceleration from supersonic speed (4.83 min)

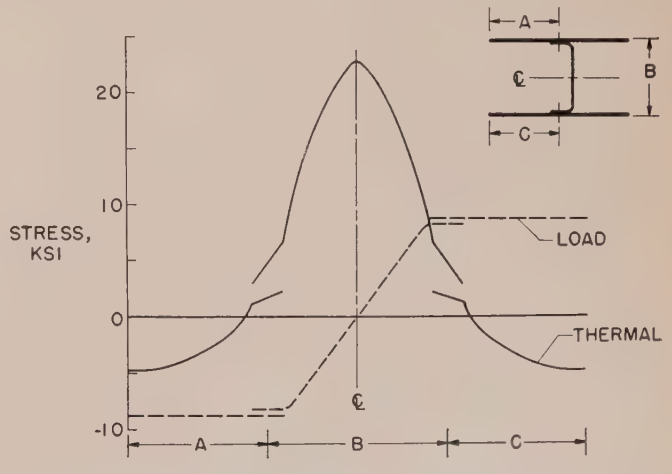

Fig. 9 – Stress distribution in structural element showing stresses due to applied bending moment and thermal stresses due to temperature distribution of Fig. 7

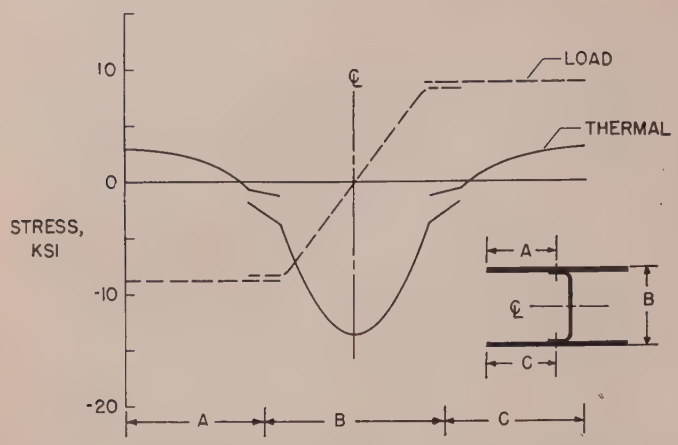

Fig. 10 – Stress distribution in structural element showing stresses due to applied bending moment and thermal stresses due to temperature distribution of Fig. 8

sive stresses in the skin are the maximum resulting from acceleration to supersonic speed. It is evident in this case that thermal stresses increase compression in the upper surface and decrease tension in the lower surface. They also add large tensile stresses to the web, which may influence design of this member.

The results above are for maximum thermal stresses resulting from acceleration to supersonic speed. The situation is somewhat different during deceleration, as shown in Fig. 10, which gives thermal stresses produced by the temperature distribution of Fig. 8. The presentation is similar to Fig. 9, but here thermal stresses are smaller in magnitude and reversed in direction; that is, there is tension in the skin and compression in the web. Tensile stresses in the skin are the maximum resulting from deceleration. Thus for this phase of flight, compression in the upper surface is relieved and tension in the lower surface increased. In addition, there is compression in the web.

The fact that thermal stresses increase stresses in some part of the structure each time the flight condition is changed could be a serious design problem. The appearance of web compression during deceleration and increased skin compression during acceleration may be of particular significance because these stresses may cause buckling. Such problems would be eliminated if the structure could be designed free of thermal stresses. Several approaches can be used to reduce the magnitude and alter the distribution of thermal stress. For example, altering the area ratio of skin and web, reducing coefficients of thermal expansion, using different materials for skin and web, or by lowering extensional stiffness of the web. Each of these approaches can result in a reduction of restraint between skin and web and thus lower skin stresses. Of these approaches, changing web stiffness seems to offer the best remedy for general use. Thermal stresses can be substantially reduced if the web is designed to expand and contract freely with the skin while continuing to perform its functions of stabilizing the skin and carrying shear. Webs with closely spaced vertical corrugations or pin-jointed trusses are types of construction that meet these requirements.

Thermal Buckling of Multiweb Beams – It may not be necessary or feasible in many cases to use construction that reduces thermal stresses to a negligible level. The structure may then be designed to withstand thermal buckling; hence it is appropriate to examine some factors that influence thermal buckling of multiweb structures. Obviously, buckling should be prevented to avoid deformation of aerodynamic surfaces and lower structural stiffness of a buckled structure.

In order to study thermal buckling of structures, web spacings required to prevent buckling of a multiweb beam were calculated for various load stresses in combination with maximum thermal stresses produced by an instantaneous acceleration from rest to a given Mach number. In this analysis, temperature distribution was calculated by an approximate method and these temperature distributions were then used to determine maximum thermal stresses in the skin. Web spacing was found by equating thermal stresses in the skin to the elastic buckling stress of a simply-supported plate. Throughout the analysis, it was assumed that all stresses were elastic and that material properties did not vary with temperature. These two assumptions about material properties give rise to errors in the analysis but they do not invalidate trends indicated. Variation of some material properties with temperature could have been included but the analysis would have been much more complex. Plasticity effects were excluded because effects of plasticity on thermal stresses have not been established. Thermal buckling in the elastic range is well defined,[4, 5, 6] but has not been investigated when thermal stresses are in the plastic range. Similar considerations apply to the interaction of load and thermal stresses. Since all these factors could not be included, the analysis was restricted to the simplest approach that would yield trends.

Fig. 11 shows some combinations of dimensions of a simplified aluminum-alloy multiweb beam that make it susceptible to thermal buckling under symmetrical aerodynamic heating conditions. Required web spacing (on a logarithmic scale) is plotted against Mach number for several values of applied load stress. For web spacing above a line, the combination of load and thermal stresses will

[4] See NACA TN 2771 (1952), "Thermal Buckling of Plates," by M. L. Gossard, P. Seide, and W. M. Roberts.

[5] See NACA TN 3474 (1955), "Rapid Radiant-Heating Tests of Multiweb Beams," by J. N. Kotanchik, A. E. Johnson, and R. D. Ross.

buckle the skin, whereas below a line buckling will not occur.

When no load stresses are present, skin buckling can be prevented easily because thermal stresses produced by these flight conditions are very small. Addition of load stresses requires substantial reductions in web spacing, but thermal stresses have a smaller effect on web spacing as load stresses are increased. At Mach 1, there are negligible thermal stresses in the structure and the web spacing given is essentially that required to support the load without buckling. At higher Mach numbers, thermal stresses become significant, and at Mach 4, require reductions in web spacing ranging from 40% for a load stress of 2 ksi to a reduction of only 9% for a load stress of 40 ksi. Thus, thermal stresses have only a small effect on web spacing of an efficient load-carrying multiweb beam; that is, one designed to carry high load stresses. Skin thermal stresses are large due to close web spacing, but are relatively small compared to load stress and buckling stress.

Fig. 12 shows similar results for a stainless-steel structure. Again, web spacing (on a logarithmic scale) is plotted against Mach number for several values of load stress. The same general trends are observed as for the aluminum structure, but required changes in web spacing are larger than for the aluminum alloy. Reductions in web spacing required by thermal stresses at Mach 6 range from 64% at 10 ksi to 28% at 100 ksi. With a steel structure one might expect that larger web spacings could be used to prevent thermal buckling because the coefficient of expansion is smaller than that of aluminum alloy. However, thermal conductivity is much lower for steel, with the result that larger temperature differences, and thus thermal stresses, are produced by aerodynamic heating.

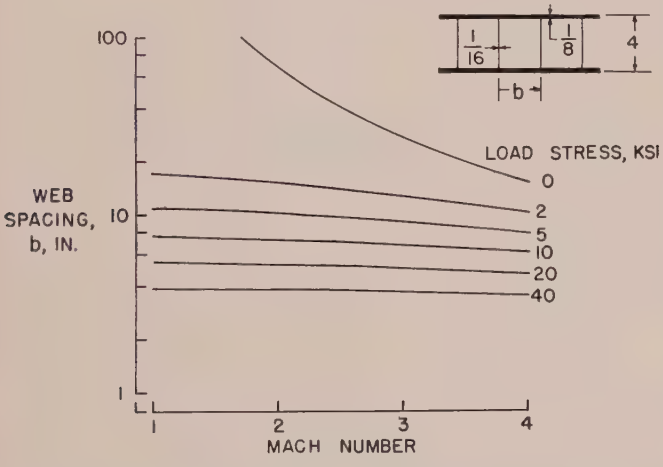

Fig. 11 – Web spacing required to prevent thermal buckling of skin of aluminum-alloy multiweb beam for various combinations of thermal and load stresses. Thermal stresses are maximum obtained following instantaneous acceleration to given Mach number at 40,000-ft altitude

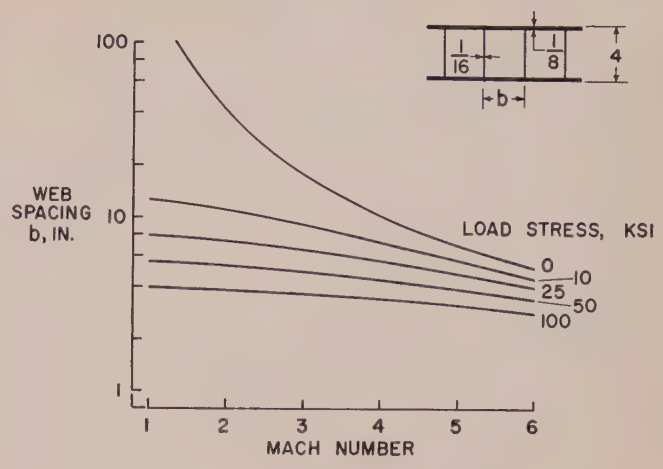

Fig. 12 – Web spacing required to prevent thermal buckling of skin of stainless-steel multiweb beam for various combinations of thermal and load stresses. Thermal stresses are maximum obtained following instantaneous accceleration to given Mach number at 40,000-ft altitude

Figs. 11 and 12 are based on several simplifying assumptions and thus indicate only approximate combinations of dimensions and Mach number that produce buckling of one series of beams. Similar charts are easily prepared for other configurations, but an actual design should be checked by a more exact analysis. In addition, to make trends more evident, the curves of Figs. 11 and 12 have been carried to Mach numbers at which skin temperature of the multiweb beam would be above the usable temperature range of the material.

Reductions of Stiffness Caused by Thermal Stresses – The foregoing discussion has been concerned with thermal buckling and its prevention, but thermal stresses well below those required for buckling can reduce stiffness of structures very significantly. These reductions in stiffness are similar to reduction of bending stiffness of a beam produced by an axial load, but the reductions in stiffness produced by thermal stresses can take many forms and range from reductions in local panel stiffness to reductions in overall stiffness of a wing or tail surface. Various types of stiffness changes produced by thermal stresses and the manner in which they influence design are a new subject of research,[6, 7] but the nature of these effects can be illustrated by the reduction of torsional stiffness experienced by solid-section airfoils. Solid sections were selected because they are most affected by this phenomenon.

[6] See NACA RM L55E20c (1955), "Behavior of a Cantilever Plate Under Rapid Heating Conditions," by L. F. Vosteen and K. E. Fuller.

[7] See IAS Preprint No. 579: "Influence of Aerodynamic Heating on the Effective Torsional Stiffness of Thin Wings," by B. Budiansky and J. Mayers. (Paper presented at Twenty-fourth Annual Meeting of Institute of Aeronautical Sciences, January, 1956.)

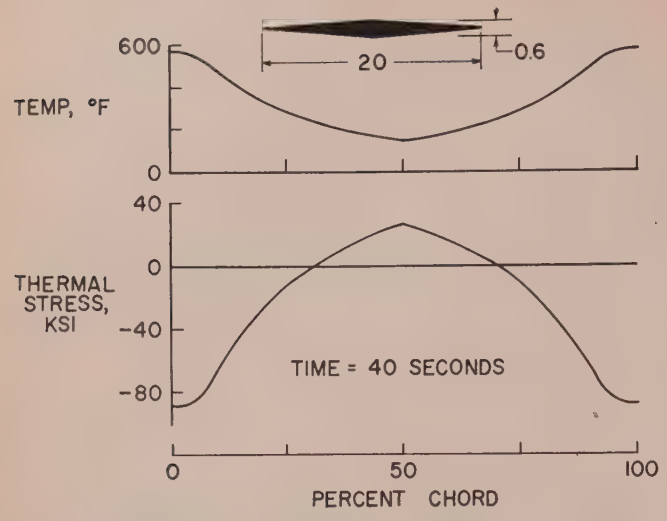

Fig. 13 – Temperature and thermal stress distributions in 3% thick, stainless-steel, double-wedge airfoil 40 sec after instantaneous acceleration to Mach 3 at 40,000-ft altitude

Fig. 13 shows temperature and thermal stress distributions in a 3% thick, solid, stainless-steel, double-wedge airfoil section with a 20-in. chord. Temperature and stress are plotted against percent chord at a particular time during flight at Mach 3 at 40,000-ft altitude. The airfoil was assumed instantaneously accelerated to the flight condition and temperature and stress distributions were calculated by neglecting heat conduction in the airfoil and by using a heat-transfer coefficient assumed constant across the chord. Temperatures and thermal stresses thus arise solely because of chordwise variation of airfoil mass.

Note that large compressive stresses are present near leading and trailing edges and that there are tensile stresses in the midchord region. If the wing is twisted by an applied torque, compressive stresses will act to increase twist while tensile stresses will resist the torque, but compressive stresses will produce the larger twisting moment. Consequently, the wing twists more under the action of these thermal stresses than it would due to applied torque alone. Thermal stresses thus reduce torsional stiffness of the section.

A history of effective stiffness of the airfoil is given in Fig. 14, where the ratio of effective torsional stiffness (GJ) to initial torsional stiffness (GJ_o) is plotted as a function of time in minutes. Stiffness drops very rapidly as the airfoil is heated. In less than a minute, the section has lost over 80% of its original stiffness. Then as temperature distribution becomes more uniform, the section gradually returns to its initial stiffness. Temperature and stress distribution shown in Fig. 13 are those existing at about the time of minimum torsional stiffness.

Loss of torsional stiffness illustrated above can be very serious in that it could cause loss of aileron effectiveness or lead to bending-torsion wing flutter. It is well to examine the factors that influence the amount of stiffness lost. For a solid airfoil, the significant factors are shape, coefficient of thermal expansion, airfoil thickness ratio, and maximum possible temperature difference. This temperature difference is a function of Mach number and ambient temperature. For a given material and shape, thickness ratio producing a given loss of stiffness can be plotted as a function of Mach number, as in Fig. 15. These curves give maximum loss of torsional stiffness and have been drawn to indicate thickness ratios that may retain only ¾, ½, or none of the initial torsional stiffness. The condition of zero stiffness is somewhat misleading in that an actual wing would possess some stiffness but would be buckled in a twisted or torsional mode. Zero stiffness is a consequence of the small-deflection theory used to calculate these curves. The net result, however, is that thin airfoils may experience substantial reductions in torsional stiffness at high speeds.

Loss of torsional stiffness can be avoided by any means that reduces thermal stresses. One factor at the designer's disposal is the shape of the airfoil section, which may be altered to minimize this problem. Since the curve for zero torsional stiffness in Fig. 15 is a basic one from which others can be easily derived, it will be used to illustrate the effect of airfoil shape on loss of stiffness. The case of theoretical zero stiffness is also significant because it corresponds to torsional buckling of the airfoil.

Fig. 16 is another plot of thickness ratio against

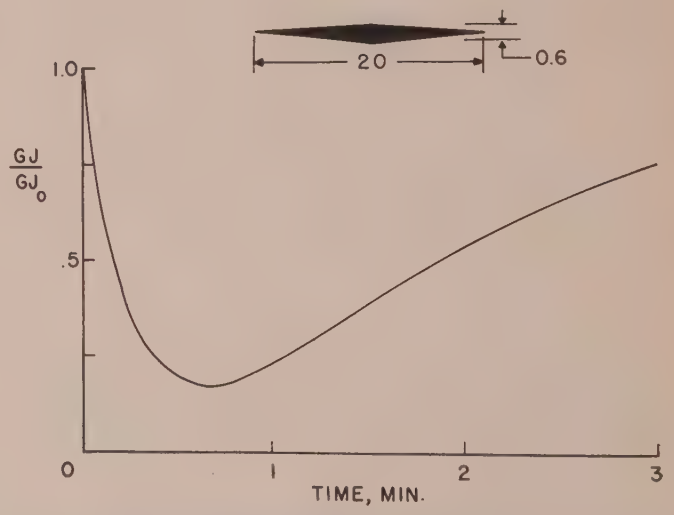

Fig. 14 – Variation of torsional stiffness with time for 3% thick, stainless-steel, double-wedge airfoil following instantaneous acceleration to Mach 3 at 40,000-ft altitude

Mach number. Two curves are shown; the upper one is the zero stiffness curve for the double wedge given in Fig. 15, the lower one is a comparable curve for a modified double wedge of uniform thickness for half the chord. For each section, thickness ratios on or below the line may lead to complete loss of stiffness, and thus to torsional buckling, due to thermal stresses. At any Mach number, the modified section can be used at a lower thickness ratio than the double wedge and still retain the same percentage of its initial torsional stiffness. Hollow sections are even less susceptible to loss of torsional stiffness than solid sections and it is theoretically possible to design a hollow airfoil that will lose a negligible amount of stiffness.

Both Figs. 15 and 16 are limited to a particular range of altitudes so that Mach number can be related to temperature, but altitude has only a small effect on location of the curves shown. It is significant that maximum possible percent loss of stiffness is independent of rate of heat transfer to the wing or to the absolute size of the wing. Size and heat-transfer coefficient do, however, determine the rate at which stiffness is lost and time required to reach the point of minimum stiffness. Increasing airfoil size or flight altitude reduces the rate at which stiffness is lost.

Other factors influencing the amount of stiffness lost are aspect ratio and rate of acceleration, both of which were assumed infinite in the preceding examples. Finite values of either aspect ratio or acceleration, however, give a loss of stiffness that is only slightly less than that indicated in Figs. 15 and 16, except when aspect ratio or acceleration is very small. The principal effect of a finite acceleration is to reduce the rate at which stiffness is lost.

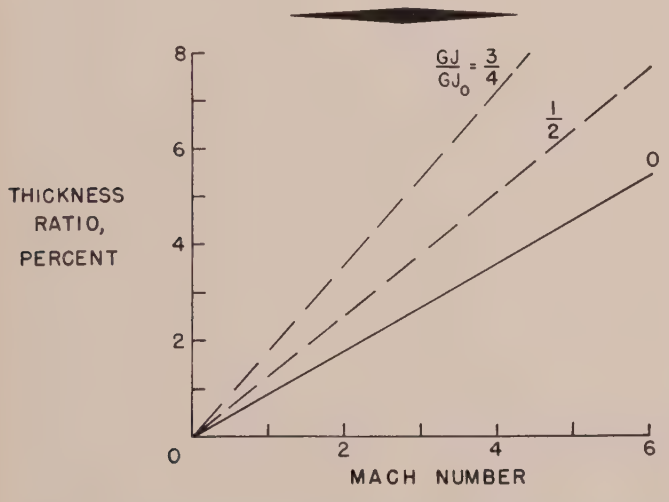

Fig. 15 – Thickness ratios of stainless-steel, double-wedge airfoils giving various maximum reductions in torsional stiffness during stratosphere flights (altitude of 35,000-105,000 ft)

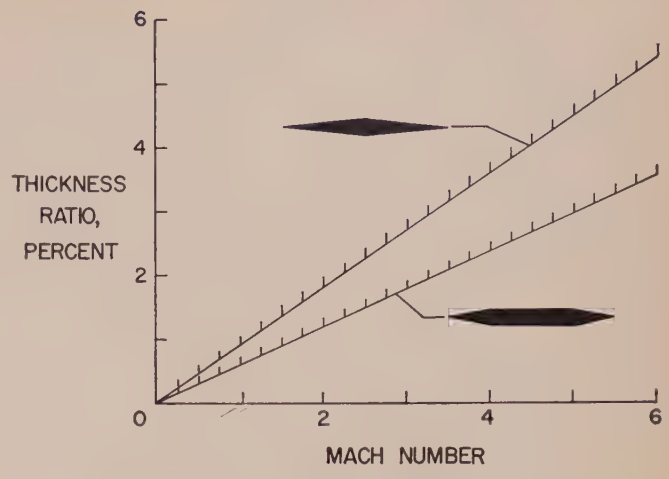

Fig. 16 – Thickness ratios resulting in torsional buckling of stainless-steel, double-wedge and modified double-wedge airfoils during stratosphere flight

The above examples and observations apply to loss of torsional stiffness of solid airfoils and the conclusion drawn may not be applicable to other configurations or types of stiffness loss. However, in any case, designs that minimize thermal stresses will avoid all such problems.

Conclusions

Some structural problems resulting from aerodynamic heating of high-speed aircraft have been discussed and the manner in which they may influence design has been indicated. The examples did not account for means of alleviating heating effects, such as insulation and cooling. Successful high-speed aircraft will undoubtedly incorporate both these means of reducing the severity of aerodynamic heating and resulting structural design problems. However, it is unlikely that a practical protective system will completely eliminate the undesirable effects.

Results presented are based on the present limited knowledge of a relatively new flight regime. Many new structural design problems will be encountered as speeds increase and much more must be learned about existing problems. At first glance, many problems appear insurmountable, but further study usually reveals that careful design can overcome or circumvent most troublesome effects. Loss of material strength at elevated temperatures, however, will always constitute a limit that the designer cannot exceed, but insulation and cooling provide the designer with some control over maximum structural temperatures the aircraft will experience.

Effect of Rapid Load Changes

THE excavating industry is becoming more and more aware of the advantages offered by torque converters and there is an increasing demand for converters on excavators such as shovels, draglines, and dragshovels. The variety of converters offered for excavator service is also on the increase.

Application of torque converters to excavating machinery presents certain problems which differ from those usually encountered in other industrial applications in that the loads imposed by an excavator on its powerplant vary rapidly over a wide range. For instance, when digging blasted rock, the load increases sharply when the dipper meets a large boulder, and then decreases to near zero if the dipper slides over it or the boulder breaks loose. Rapid load changes can also be imposed by severe clutch application. It is important, therefore, that excavator design engineers should recognize the factors which affect transient torque-converter performance so as to exploit the favorable factors and to minimize the others.

It is highly desirable to obtain maximum power output during the time the excavator is digging in the bank, for it is during this relatively short period that peak power is required. Most other excavator operations require less than full power. During digging operations, output power losses may result from any or a combination of the following factors:

1. Decrease in engine efficiency during periods of deceleration.
2. Slow governor action.
3. Decrease in torque-converter efficiency due to changes in loads and speeds.
4. Power from burning fuel going into engine acceleration during transient periods.

Performance is also affected by inertia of rotating masses on both sides of the converter. It will be shown that WR^2 of the input and output sides can be chosen to obtain optimum performance following rapid application of load.

Manufacturers of engines and torque converters usually furnish only steady-state performance data for the power package. Since transient performance of a power package is very hard to predict and to present in a general fashion, a test program was set up to explore the possible effects of transient loads on excavator performance. In these tests the power package was subjected to transient conditions corresponding closely to actual service requirements and performance was established experimentally by recording input and output

on Torque-Converter Performance

P. J. Swanson and J. H. Meier, Bucyrus-Erie Co.

This paper was presented at SAE Golden Anniversary Tractor Meeting, Milwaukee, Sept. 13, 1955.

DESIGNERS of excavating machinery such as shovels, dragshovels, and draglines are confronted with the problem of selecting powerplant components which will give maximum performance during rapid load changes. To obtain design data, an engine alone and an engine torque-converter package were subjected to rapidly applied loads, and torques and speeds were recorded until steady-state conditions were reached.

Analysis of test records indicates that significant losses in output power following rapid application of load are caused by the energy required for engine acceleration and by lower torque-converter efficiency during transient periods. Proper selection of components exploits the favorable factors and minimizes the others.

speeds and torques.

Test Equipment

General arrangement of the test setup is shown in Figs. 1 and 2. Engine and torque converter are mounted on a Bucyrus-Erie 22-B Excavator with the cab removed. (The test setup was arranged so that future field tests could be made with a minimum of changes.) Loads were applied by means of an air-actuated disc brake. Manually operated valves permitted quick change of brake actuating pressure from atmospheric to that of Tank Nos. 1 or 2. Because of heat generated at the brake, time during which loads were applied was limited to between 10 and 20 sec, depending on output horsepower.

Brake inertia was almost exactly equal to the corresponding inertia of the rotating machinery parts. Thus the dynamic behavior of the test rig was the same as that encountered in an actual machine.

The recorder shown in Fig. 1 is an Offner Dynagraph which writes on current-sensitive Teledeltos paper. It has six channels for continuous recording and ten styli for recording on-off functions.

Input torque to the converter was measured by a special input shaft which separated engine and torque converter, carrying a strain-gage torquemeter and four cast silver slip rings. Copper-graphite brushes riding the slip rings established

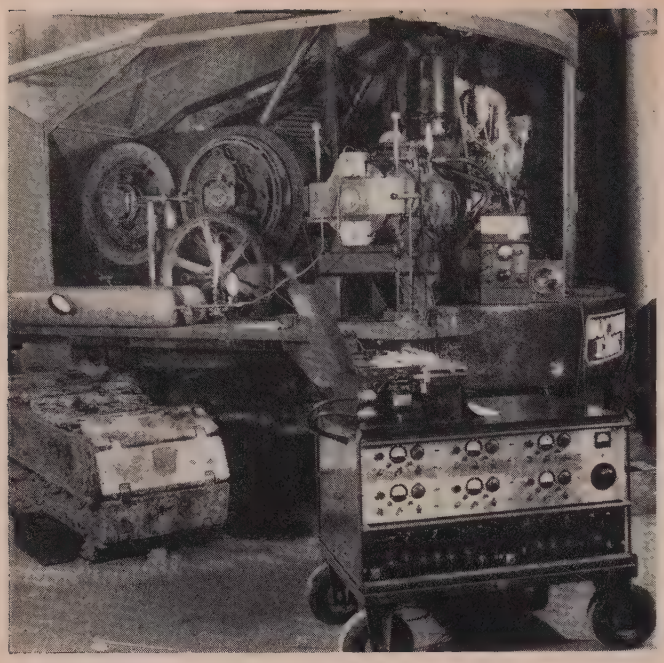

Fig. 1 – General arrangement of test

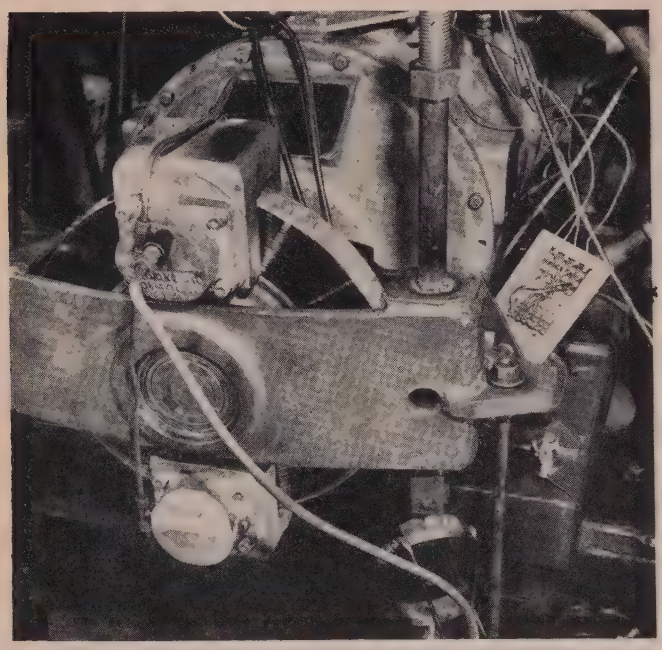

Fig. 2 – Close-up view of disc brake

electrical connection to the rotating torque-meter. Output torque was determined by strain-gage measurement of brake reaction at a known distance from the center of the output shaft. This setup was calibrated by applying known static torques.

Input and output speeds were obtained by two methods:

a) Drag-cup generators mounted on the input and output sides gave signals directly proportional to speed and were used to record speeds during transient conditions.

b) Intermittent marks on the test records were produced by contactors engaging shafts and correspond to input and output revolutions. They were used to determine the input and output speeds for steady-state conditions and to obtain an accurate calibration of the signals from the drag-cup generators.

A potentiometer connected to the linkage from governor to fuel racks was used to record governor action. The pressure in the brake air lines was recorded from an SR-4 pressure cell; however, these data were not used in analyzing the records.

A sample test record is shown in Fig. 3.

Test Program

The first phase of the test program was to determine the performance of the engine alone when subjected to controlled transient loads. Loads varying from 20-200% of full-load engine torque were rapidly applied to investigate engine and governor performance under these conditions. In this process steady-state engine performance was obtained for loads up to full load.

The second phase of the test program consisted of determining performance of the engine and torque converter package in a similar manner. Steady-state performance of the engine and torque-converter package was obtained for loads up to 250% of full-load engine torque (output shaft stalled). Loads varying from 20-250% of full-load engine torque were then rapidly applied to the output side of the torque converter. Tests also included rapid increases and decreases in load starting from partial load.

Steady-State Performance

Steady-state engine performance alone is shown in Fig. 4, and steady-state performance of the

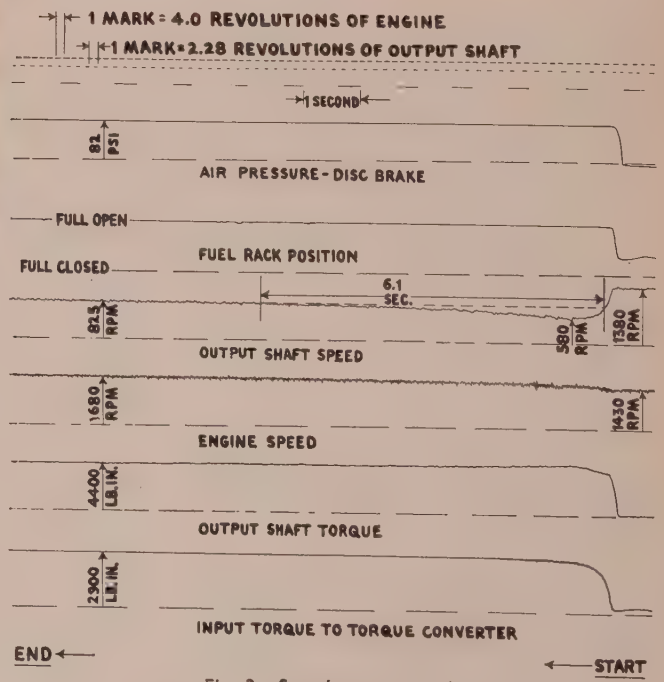

Fig. 3 – Sample test record

engine and torque-converter package is shown in Fig. 5. Further investigation of engine or engine and torque converter performance will be based on these experimentally obtained steady-state performance characteristics.

Transient Performance of Engine Only

Test records for engine performance alone when subjected to transient loads were examined closely to determine brake torque at various speeds when the engine was subjected to various rates of deceleration.

Total engine torque output (developed from burning fuel and from deceleration) and engine speed were recorded. Deceleration rate was calculated from the speed record at two arbitrarily selected speeds (1140 and 1000 rpm through which the engine speed passed in many tests). Total output torque is plotted against deceleration rate in Fig. 6. The curves are straight lines within the range of experimental accuracy. These lines were extrapolated to zero deceleration to obtain steady-state torque for the respective engine speeds. Steady-state torques so obtained are plotted on the steady-state torque-speed curve in Fig. 7. Agreement is considered satisfactory. From the slopes of the straight lines of Fig. 6, WR^2 of the engine was calculated as 14,600 lb-in.^{2} The WR^2 values furnished by the respective manufacturers are:

Engine	910 lb-in.^{2}
Flywheel	11,010 lb-in.^{2}
Clutch	897 lb-in.^{2}
Disc Brake	1,185 lb-in.^{2}
Total	14,002 lb-in.^{2}

Agreement is within 4.2% and is considered satisfactory.

From these tests on the engine alone, it was concluded that the combustion and fuel efficiency of the engine appear to be unaffected by rapid transients, and that the total torque available from the engine during transient conditions can be calculated as the sum of steady-state torque at the particular engine speed and deceleration torque.

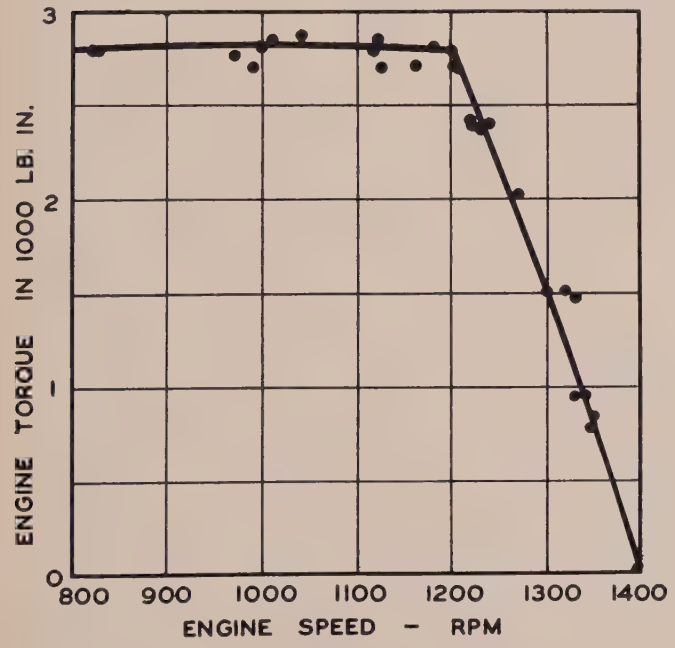

Fig. 4 – Steady-state performance of engine only

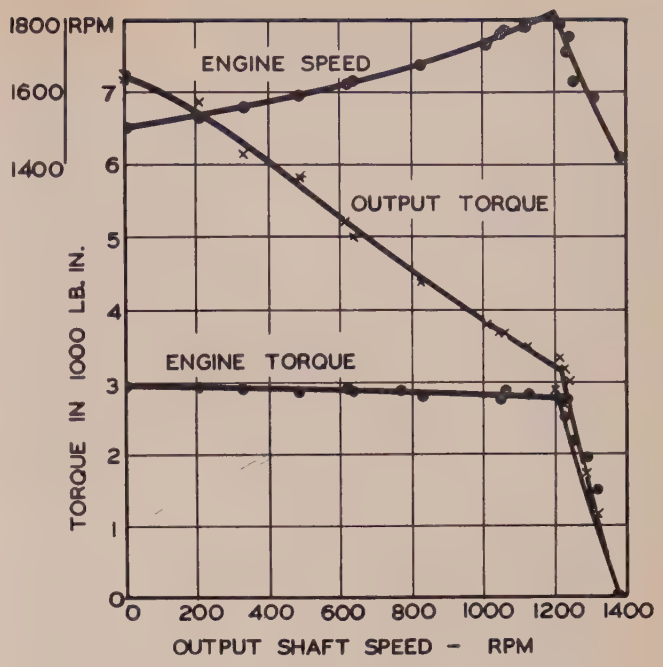

Fig. 5 – Steady-state performance of engine and torque-converter package

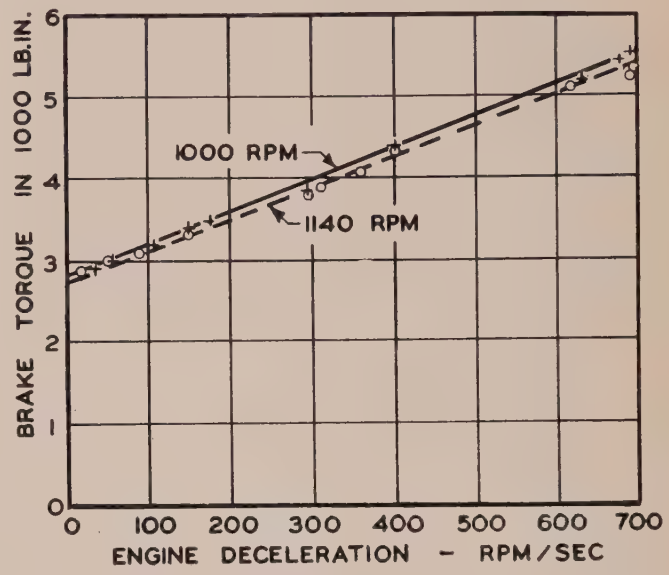

Fig. 6 – Brake torque at two engine speeds versus engine deceleration

Transient Performance of Engine Governor

On a direct-drive machine, the diesel engine governor causes the engine to idle at the selected high-idle speed and to deliver full-load torque when the speed drops a certain amount below high idle. The gear ratio to the machinery is selected to

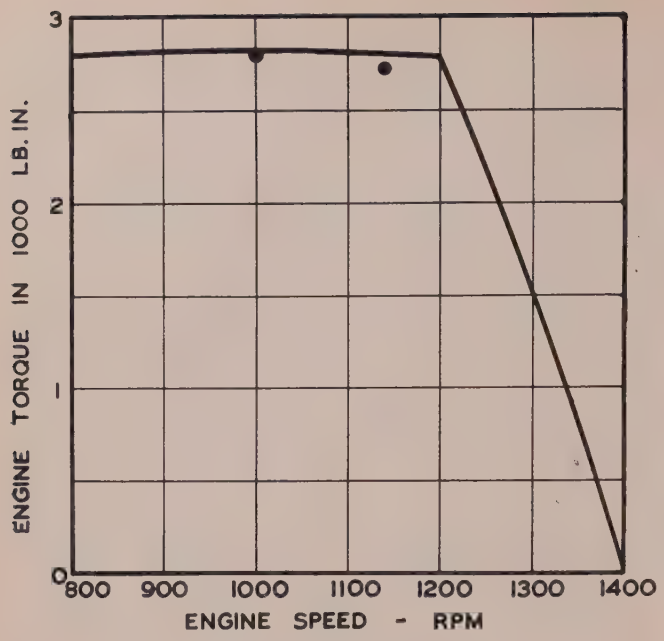

Fig. 7 – Comparison of engine torque extrapolated to zero deceleration with steady-state performance

develop desired machinery torque at full engine throttle. High-idle engine speed is selected to limit top machinery speed to the desired level.

On a similar machine with torque-converter drive, the gear ratio between converter and machinery must be changed in order to keep machinery torques at converter stall within acceptable limits. This may cause very high machinery speeds at high idle of the engine and no load on the converter. It is frequently necessary, therefore, to provide an output-shaft governor which reduces engine speed whenever converter output speed reaches a certain value. The engine thus goes slower at idling speed of the converter output than when the converter is under load. This feature deserves careful study, for if engine speed at idle is very much lower than at full load, some lag will occur, as seen from the following consideration: When substantial loads are suddenly applied following a period of idling, the engine has to accelerate itself against increasing torque demand from the converter. Some time is required for the engine to come up to speed and to deliver the required horsepower.

In order to protect the engine during times when the main power take-off clutch (which is ahead of the output-governor drive) is disengaged, an engine top-speed governor is provided. This governor is set somewhat higher than the maximum speed at which the engine can drive the loaded converter. Hence, it does not come into play in normal operation.

The output-shaft governor can affect the overall performance if it fails to react to a minimum drop in speed, or if it does not act sufficiently fast. If its action is slow following rapid load application, engine speed (and with it output-speed) drops too low, and it is hard for the engine to accelerate under load up to the normal speed. It is very important, therefore, that the governor open as rapidly as possible following application of load.

The governor used for this test series was a dual hydraulic type with drives from the converter output and the engine.

Test records show that this governor acts very fast and that no appreciable loss in performance can be attributed to governor lag. For instance, Fig. 3 shows that fuel-rack position changes from high-idle to full-open positions in less than 0.10 sec.

Internal Losses in Torque Converter During Changes in Loads

Internal losses in the torque converter during transient operation could not be measured directly, and were determined by comparison of calculated and observed performance. To determine losses during the transient period, output speed was calculated for a rapidly applied load using the experimentally obtained steady-state performance characteristics of the engine and torque converter package. At each instant it was assumed that the package performed exactly as under steady-state conditions for the same input and output speeds. Excess engine torque over converter demand was balanced by engine acceleration and deficiency or excess of converter output torque as compared with brake load was balanced by output deceleration or acceleration, respectively. WR^2 of the con-

Table 1 – Sample Step-By-Step Calculation for Determining Engine and Torque-Converter Performance Following Rapid Load Application

		Input Side (WR^2 = 8615 Lb-In.^{2}; Rpm/Sec = 0.428, Δ Torque)							Output Side (WR^2 = 2942 Lb-In.^{2}; Rpm/Sec = 1.253, Δ Torque)					
Time, sec	Interval, sec	Input Speed, rpm	Output Speed, rpm	Speed Ratio	$\left(\frac{\text{Input Speed}}{1000}\right)^2$	F_2,[a] lb-in.	T.C. Input Torque, lb-in.	Engine Torque, lb-in.	Δ Torque, lb-in.	Acceleration, rpm/sec	Δ Rpm	F_3,[b] lb-in.	T.C. Output Torque, lb-in.	External Torque, lb-in.	Δ Torque, lb-in.	Acceleration, rpm/sec	Δ Rpm
0.11	0.01	1447	1155	0.798	2.094	763	1598	2850	+1252	+536	+5	745	1560	4000	−2440	−3057	−31
0.12		1452	1124	0.774	2.108												

[a] F_2 = Input torque at 1000-rpm input speed, as a function of speed ratio.
[b] F_3 = Output torque at 1000-rpm input speed, as a function of speed ratio.
Note: For any given speed ratio, input and output torque varies as the square of the speed.

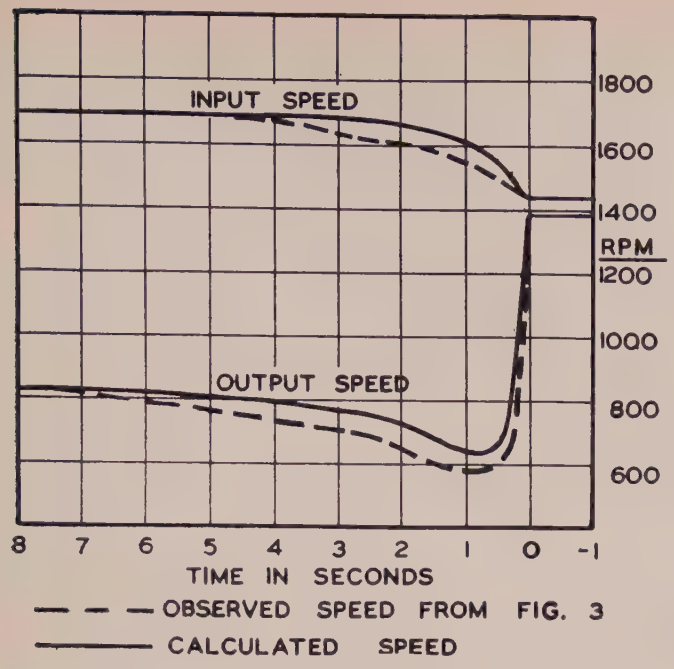

Fig. 8 – Comparison of observed and calculated torque-converter speeds following application of load

verter fluid was neglected in the calculation. Applied loads and governor reaction for the calculation were taken from the actual test record in order to introduce proper conditions. The calculation was made by the finite difference method (see Table 1), and small time increments were used.

Results so calculated are compared with observed data in Fig. 8, wherein the difference between calculated and observed output speeds must be attributed to transient losses in the converter. Since the calculation is based on steady-state data obtained with the same instrumentation, a possible small calibration error has only a negligible effect on the comparison. With this method of investigation, the resulting effect of transients does not depend on perfect agreement between steady-state performance predicted by the manufacturer and that observed in tests.

Converter transient losses may affect performance of the package in two separate ways or in a combination of the two; namely, lower output speed or higher input torque as compared to steady-state operation for a corresponding combination of input speed and output torque.

Reduced output speed is a direct effect and concerns the converter only. Increased input-torque demand is an indirect effect and concerns the entire package. As the converter demands more torque from the engine, less torque is available to accelerate the input side and the engine is slower in developing the required horsepower. This effect carries over to the output side and causes a further drop in output speed. Examination of Fig. 8 indicates that both types of effect are present. Observed engine speed lags behind calculated speed, but observed output speed lags behind calculated speed even more.

Transient performance of the engine and converter package is of greater importance than the detailed action of the converter alone. Hence, no attempt has been made to separate the transient converter losses into the direct effect of reduced output speed and the indirect effect of increased input torque. Considerable study was made of the total loss, however, for various transient conditions.

In the test of Fig. 3, the suddenly applied load amounts to about 65% of steady-state stall-torque. Output speed dropped below steady-state speed and it took about six seconds to recover this speed. During this time the output shaft made 7.3 revolutions less than it would have made had the steady-state speed prevailed from the moment of sudden load application. Steady-state output speed for this load is 825 rpm, or 13.75 rps. Total transient loss of the package is thus equivalent to $7.3/13.75 = 0.53$ sec of steady-state operation.

Fig. 9 shows total transient loss of the package when high-idle condition is followed by suddenly applied loads of various magnitude. The loss is expressed in the equivalent time of steady-state operation for the corresponding output torque. Greatest total transient loss occurs when the suddenly applied load corresponds to maximum steady-state engine speed. In this case the engine has to accelerate through the maximum range from high idle to top speed.

Effect of Rotating Masses on Transient Performance

The greater the input-side rotating mass, the

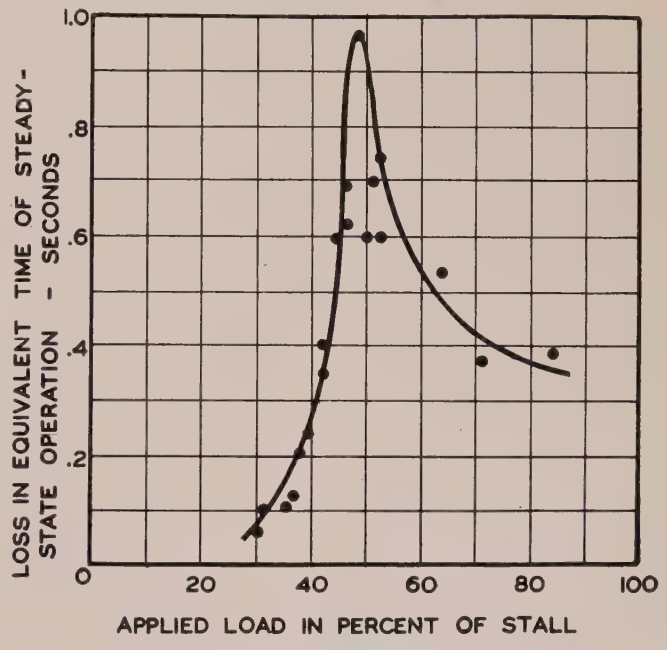

Fig. 9 – Total transient loss of engine and torque-converter package following rapid application of load

greater time required for the engine to come to steady-state speed following a change in load. For quick response, the input-side rotating mass should be as small as possible. A certain minimum flywheel inertia must be maintained, however, in order to absorb firing strokes.

The greater the output-side rotating mass, the less transient loss following a sudden increase in load and the greater transient loss following a sudden decrease in load. In excavating service, transient loss following a sudden increase in load is more objectionable than the transient loss (or slower speed-up) following a sudden decrease in load. Hence, in this particular respect, a large output-side rotating mass would be desirable. On the other hand, a large output-side mass causes higher impact torques when the dipper is suddenly stopped. There is a practical limit, therefore, to the rotating mass on the output side; this limit can be established by the following consideration: maximum steady-state torque occurs at stall and the machinery must be sufficiently sturdy to withstand this torque repeatedly. Maximum impact torques generally occur at high output-shaft speeds, that is, when the converter output torque is relatively low. Hence, output-side rotating mass may be increased to the point where the sum of steady-state and impact torques approaches stall torque. Field tests are required to establish the necessary calculation factors.

Conclusions

Results of this investigation bring to light problems the design engineer has to consider to obtain best transient performance of excavators equipped with torque converters.

There are many types of torque converters as well as engines, flywheels, governors and clutches offered for excavator service, and best transient performance will be obtained through proper selection of components. Ideas and methods presented in this paper may help in arriving at a proper selection. It is hoped that this paper will stimulate further research into transient characteristics of engines and converters and thus lead to even better performance and longer life of excavators.

DISCUSSION

Close Regulation Not Feasible at Both Low and High Engine Speeds

by J. W. Lusch
Caterpillar Tractor Co.

INFORMATION such as the authors have presented is invaluable, and it can be obtained only after the engine-converter unit has been installed on a unit in the field. In our lab, we can simulate the conditions with which our engines must cope, but it is not realized to the fullest extent just what the actual conditions are which are imposed on the engine when it is powering an excavator until field tests are conducted by competent people in the excavator field.

We are in total agreement with the information given in the paper. We would like to elaborate on one point: namely, slow governor action.

The trend is toward 10% regulation, mainly because of the tendency of close-regulation governed engine-converter units to have a very definite surge. This surge can usually be controlled when the excavator is not digging; but when loads are imposed on the power unit, a surging condition will be encountered at some point during the work cycle. Three per cent regulation is commonly used on Cat units with good results, but it must be remembered that this close regulation, in most cases, is encountered only in the range of speed (usually limited to approximately 200 rpm), at the high-speed end of the engine power curve. In other words, if 3% governor regulation is available at 2000 rpm engine speed, then regulation may be up to 15% at the speed at which an output-shaft governor holds the engine during no-load or light-load periods. As a heavy load is imposed on the output shaft and the engine must accelerate to meet this power demand, governor regulation is off at the low speed and, consequently, a noninstantaneous engine response is observed.

Now consider if there were no output-shaft governor restricting engine speed and the engine were permitted to run at maximum speed. Were a load imposed on the converter output shaft under these conditions, then the engine reaction time would be faster because of absolute 3% governing available at high speeds.

Under present setups it is not feasible to have 3% or close regulation at both low and high engine speeds, so the point to consider is a drive design problem in the application of the engine-converter power unit.

I would like to take this opportunity to ask excavator designers to carefully consider application of engine and converter power units when excavator machinery and drives are being designed.

Some converter manufacturers are giving a great deal of thought to design of the converter circuit so that an inherent speed cut-off point can be reached with the converter, thus permitting the engine to be run at full throttle without the need of an output-shaft governor. It appears that for the immediate future the only possible means of achieving this end is through machinery and drive design.

We agree with the authors that torque-converter application on excavators is not a simple engineering problem. This is a complex problem in which the engine, converter, and excavator manufacturers have a vital interest. We pledge ourselves to keep the interest of the excavator manufacturer in mind whenever a decision must be made involving application of converters to our engines.

Authors' Closure To Discussion

AS to the elimination of the output shaft governor, we fully agree that this is a most desirable feature. We are prevented from doing this at present because we do not have converters with a sufficiently low torque ratio. To give an example: If our calculations show that we can live with a peak shaft torque in our machinery that is twice as high as the engine at maximum steady-state torque can provide with direct drive, we must limit the torque provided by a converter drive to the same value. Now if we choose a converter with a stall ratio of 2.5 and we use the same engine, we must change our drive ratio from the converter to the machinery by a factor of $2.5/2.0 = 1.25$. If our chain reduction ratio for direct drive was 1/7.5, it should be changed to 1/6. We are now all right for the maximum torque, when the converter is stalled. On the other hand, under no-load condition, or when swinging at full speed, our machinery goes 25% faster. This is undesirable and means have to be employed to keep top speed within acceptable limits. Hence, the output governor.

ORAL DISCUSSION

Reported by John J. Treutelaar
Heil Co.

A. J. Hill, Corps of Engineers, U. S. Army, Engineer Research & Development Laboratories: Is control of the load maintained on torque-converter-equipped shovels if the ratio is not over 2/1? Will it reverse at low engine speeds and cause dropping of the load?

Mr. Meier: We have made tests as to the possibility of controlling the position and motion of a load from the throttle of a crane equipped with a single-stage converter. It was found that heavy loads could be handled readily and accurately. With light loads, on the other hand, we encountered difficulties. In order to lower a light load, particularly at a worth-while speed, we had to throttle the engine to very low speed. On several occasions the engine stopped, or was even driven backward, by the converter. In such cases, the only means of preventing the load from dropping is to apply the hoist brake, and in order to start the engine and continue operation, the hoist clutch must be disengaged. We understand that this type of operation is better achieved with a 3-stage converter, but we have not tried this yet.

E. W. Spannhake, Le Tourneau-Westinghouse Co.: Engine power losses during acceleration are due to loss of fuel. For the most part, however, the actual losses are due to circulation around the converter blades.

Mr. Meier: Acceleration does cause loss of fuel. Closer cooperation of torque converter users and manufacturers is desirable. Extreme application of load causes rapid deceleration and results in circulation around the converter blades. In many cases of actual practice, application of the load is slower and results in smaller losses.

E. F. Farrell, Products Development Laboratories, Borg-Warner Corp.: We have not conducted research in connection with acceleration. All of our work has been in deceleration, with output checks from 0 to 1400 ft-lb in 0.3 sec. We have found no difference in steady state and transient state. Transient checks have been made to the extent of seven times engine torque. The output torque was measured by strain gages on the output shaft. Use has been made of a differential speed recorder to obtain more consistent results. Minor changes in input torque have considerable effect on output performance. With a 2-stage converter, units can be designed to handle a given torque in a smaller diameter.

Mr. Meier: Our test records include acceleration and deceleration, going from no load or partial load to higher loads or full load, and vice versa. We have analyzed the deceleration portions in greater detail and have presented the results of this study because this feature is of greatest interest in excavating service. It is realized, of course, that in other fields, notably for automobile transmissions, the acceleration phase is of greatest interest. However, our records indicate that the general conclusions drawn for the decelerating phase also hold for the accelerating phase.

The brake discussed in our test had a rotating inertia coming very close to that of the machine on which the converter was tested. This was done so as to duplicate the actual condition on the excavator. It should be realized, however, that all our calculations take care of the inertia factors with the exception of the fluid in the converter itself. Since the rate of deceleration is known to a considerable degree of accuracy, the deceleration torque of the brake disc can be calculated accurately. If this torque is subtracted from the external brake torque, the actual torque on the converter itself is obtained. Our records would permit us to establish the behavior of the converter with driven parts of negligible inertia.

We realize that speed records must be very accurate to yield proper data on converter performance. Our calculations are based on the widely accepted hypotheses that, for each speed ratio, there is a corresponding torque ratio and that, for any given speed ratio, input and output torques increase with the square of the absolute speeds. We were thus interested in the absolute input and output speeds as well as the difference between them. Our instrumentation was aimed at getting both speeds accurately, so that we could cover the entire range of speed ratios, whereas an accurate measure of the speed differential would have been attractive primarily for the higher speed ratios, notably, operation in the coupling range. By means of the dots recorded on the paper we could account for every revolution of the engine and the converter output shaft. We could thus calibrate and check our speed records to a high degree of accuracy and we believe that our results truly represent the behavior of the converter under test.

NACA Investigation

THRUST reversers have been receiving considerable attention of late, and probably before long many operational airplanes will be equipped with such devices. One reason for this is shown in Fig. 1, which presents a comparison of the landing-run or ground-roll distances when using wheel brakes alone, in combination with a drag chute, and with various amounts of thrust reversal. As noted in the chart, the landing run is reduced 40% by the use of the drag chute and about 55 and 70%, respectively, by the use of 40 and 80% thrust reversal. Although these numbers will vary depending upon the specific airplane and ground conditions under consideration, the important thing to remember is that whenever a ground roll problem is encountered, the thrust reverser merits serious consideration.

In addition to ground roll reduction, the thrust reverser has other potentialities or auxiliary functions such as dive brake or landing approach applications.

Because of the interest and apparent need for thrust reversers, a research program was inaugurated to investigate the performance and problems of thrust reversers. It was the purpose of this program to isolate the more promising types, investigate their potentialities, and obtain design and performance information rather than end up with a specific reverser designed for a specific application. Most of this work was done on a small-scale unheated air-duct setup equipped with a 4-in.-diameter exhaust nozzle, although some experience was obtained on a full-scale installation.

The configurations investigated were selected on the basis of their being able to meet most of the items in the following list of practical requirements:

1. There is the requirement of reliability, which is greatly enhanced if the device is kept simple; that is, there should be a minimum of hot-exhaust gas seals, complicated mechanisms and controls, and the actuating forces should be kept as small as possible.

2. It is desirable that engine performance be unaffected.

3. It has been found to be desirable to set some target value of reversal to shoot for. As will be recalled, the first figure indicated that 40% produces a significant change in landing roll, so a minimum requirement of 40% was set.

4. The installation should have both a low external and internal drag when not in use.

In addition to the aforementioned practical re-

# of Thrust-Reversal Techniques

John H. Povolny and Jack G. McArdle, Lewis Flight-Propulsion Laboratory, NACA

This paper was presented at the SAE Golden Anniversary Aeronautic Meeting, Los Angeles, Oct. 13, 1955.

quirements, it is desirable that the reverser also exhibit the following desirable characteristics:

1. As in all aeronautical considerations, minimum weight is of extreme importance.
2. The device must fail safe in the event of power or actuator failure.
3. It should be quick-acting in order to satisfy the emergency requirements of a wave-off or similar occurrence. Two seconds is considered a maximum permissible actuation time.
4. Attachment of the reversed gases to the fairing (nacelle or fuselage) is to be avoided if this results in overheating of the structure or ingestion of the hot gases and consequent overheating of the engine inlet air.
5. It is essential that the airplane control forces be relatively unaffected when the reverser is used in flight.

In addition to the above general requirements, there are also several other considerations that may influence the selection of a reverser. One of these has to do with whether or not the engine is equipped with an afterburner, and the other with whether or not the engine is equipped with a complicated variable-geometry back end. In either case, it may be undesirable to have the reverser installed in the vicinity of the exhaust nozzle.

Target-Type Thrust Reversers

Two groups of configurations were experimentally investigated. One group was designated as

INCREASING importance of the thrust reverser for ground-roll reduction, for dive brake and landing approach applications, or both, led to this NACA survey of design and performance potentialities of the more promising types.

Target- and cascade-type devices were judged with an eye to reliability, simplicity, speed, minimum weight, lack of effect on engine performance and control forces, low external and internal drag when out of use, fail-safe characteristics, and a minimum of 40% effectiveness.

The authors show that reversals up to 80% can be achieved under certain conditions.

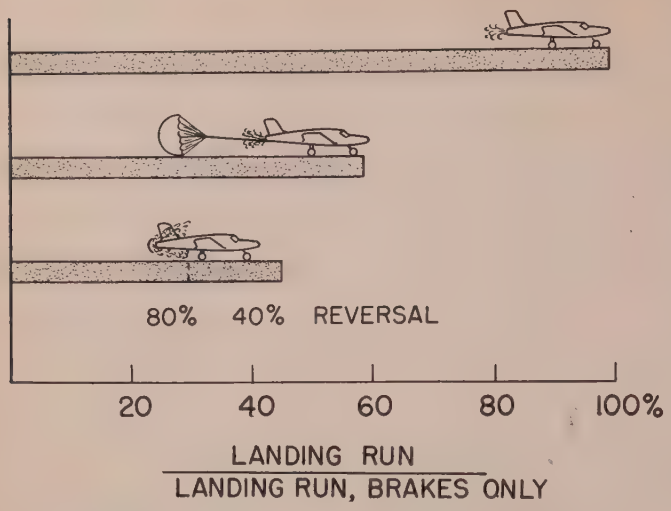

Fig. 1 – Landing run required for jet aircraft using wheel brakes alone, in combination with a drag chute, and with various amounts of thrust reversal

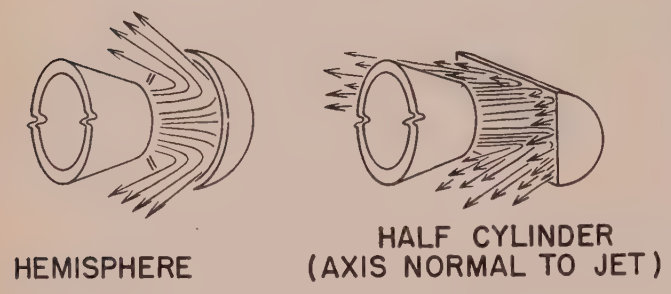

Fig. 2 – Two target-type thrust reversers

target-type reversers, because the jet is turned by a target positioned behind the exhaust nozzle. The other group was designated as cascade reversers, because the gas is turned by means of a cascade. Two target-type reversers which appeared to have promise are illustrated in Fig. 2. The hemisphere, shown on the left, can be designed similar to a clam shell nozzle, so that the gas forces acting on the reverser segments are balanced during actuation. This results in low actuation forces. The cylindrical or circular arc reverser shown on the right was expected to have desirable jet directional qualities with respect to avoiding control surfaces because of the longer flow path of the gases along the length of the cylinder.

The investigation of the target-type reversers was conducted on the small-scale rig, and consisted of a determination of the effects of the various geometrical design variables on the performance and external flow fields of the reverser. The variables considered included reverser spacing, size, and exit angle, and also several attempts at shape simplification.

Effect of Spacing Ratio

As might be expected, the position of the target with respect to the exhaust nozzle will have a considerable influence on the performance. If the target is positioned too close to the exhaust nozzle the engine operation will be affected, and if it is positioned too far away the reverse thrust will be reduced. This is illustrated in Fig. 3, which shows a plot of reverse thrust against spacing ratio when employing a fixed-area exhaust nozzle. The data presented are for the hemispherical reverser illustrated in Fig. 2; similar effects were obtained for the half cylinder.

Reverse-thrust ratio is defined as the ratio, in per cent, of the resultant reverse jet thrust of the reverser at a given exhaust nozzle pressure ratio to the forward jet thrust of the exhaust nozzle at the same pressure ratio. Spacing ratio is defined as the ratio of the distance, G, between the exit of the exhaust nozzle and the leading edge of the reverser, divided by the exhaust nozzle diameter, D_N. Curves are presented for hemispheres having diameters approximately 1.5, 1.7, 1.8, and 1.9 times the nozzle-exit diameter, and for an operating pressure ratio of 2.0. This pressure ratio was selected as being typical of that which will probably be used for full-power ground-roll reduction.

Examination of the curves reveals that they are fairly flat, with each one reaching a maximum within the range of spacings investigated. The marks on the curves indicate the minimum spacing at which 100% of normal airflow is obtained. To the left of the mark, a reduction in spacing ratio results in a reduction in airflow or an overtemperature condition if the reverser is installed

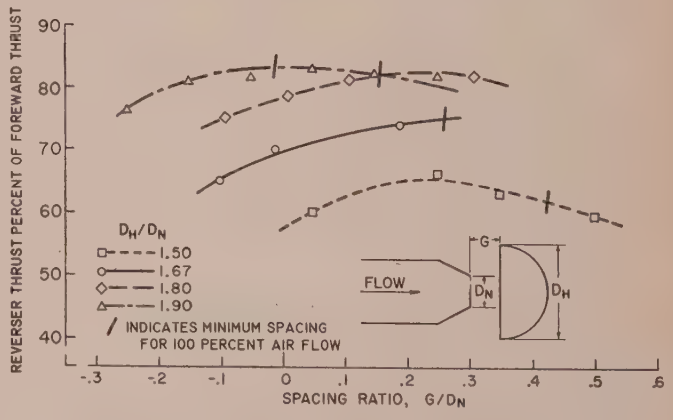

Fig. 3 – Hemispherical thrust reverser with fixed-area exhaust nozzle (nozzle pressure ratio, 2.0)

on an engine. To the right of the mark, an increase in spacing ratio has no effect on airflow.

Operation to the left of the marks is possible on an engine if a variable-area exhaust nozzle is used to keep the effective flow area and the tail-pipe gas temperature constant. Investigation of this mode of operation, however, revealed that the gains to be realized were small.

The minimum spacings allowing 100% of normal airflow range from about zero for the largest hemisphere investigated to about 0.4 for the 1.5-diameter-ratio model. In general, the minimum spacing for a target-type reverser is a function of the cross-sectional or frontal area of the target. This is illustrated in Fig. 4, which shows a plot of minimum-spacing ratio versus frontal-area ratio for several hemispherical and cylindrical targets. The data for the cylinder with a length-to-width or aspect ratio of 1.0 and a lip angle of 180 deg fall on the same (lower) curve as those for the hemisphere. Modifications to the cylinder resulting in departures from these values of aspect ratio and lip angle result in increases in the minimum spacing. This is illustrated by the data for a cylinder with an aspect ratio of 2.4 and lip angles of 180 deg and 146 deg.

Effect of Reverser Size

The effect of the size of the target-type reversers on performance is illustrated in Fig. 5, which shows reverse thrust plotted against frontal-area ratio of the reverser. Data are presented for half cylinders of length-to-width ratios ranging from about 1.0 up to 2.50, and also for the hemisphere. These data were all obtained at the minimum spacing required for 100% airflow, and full end plates were used on the cylinders. It is to be noted that length-to-width ratio of the cylinder has only a small effect, and the effect of cross-sectional area ratio is about the same for both the hemisphere and cylinder. It is emphasized that reduction in size or cross-sectional area has only a small effect until a value equal to about 2½ times the nozzle area is reached. Below this, the fall-off in reversal is quite rapid.

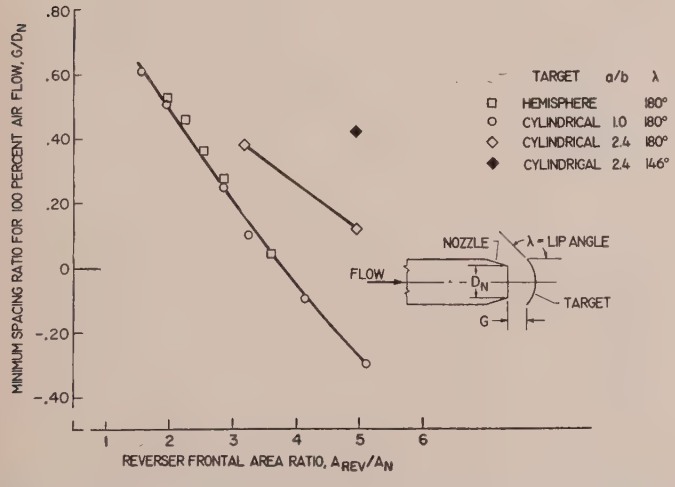

Fig. 4 – Minimum spacing ratio versus frontal area ratio for several hemispherical and cylindrical target-type reversers (nozzle pressure ratio, 2.0)

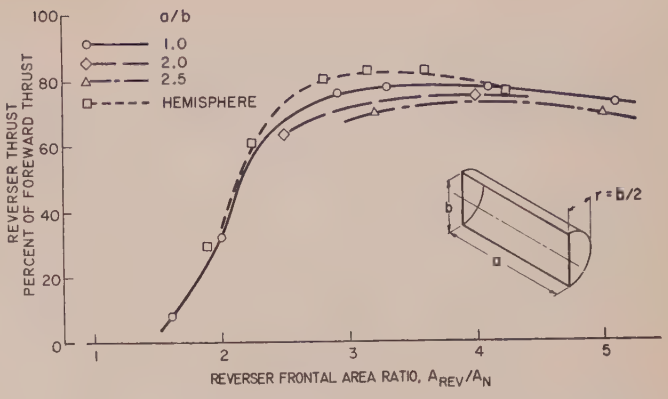

Fig. 5 – Effect of frontal area on performance of target-type thrust reverser (nozzle pressure ratio, 2.0; 100% airflow)

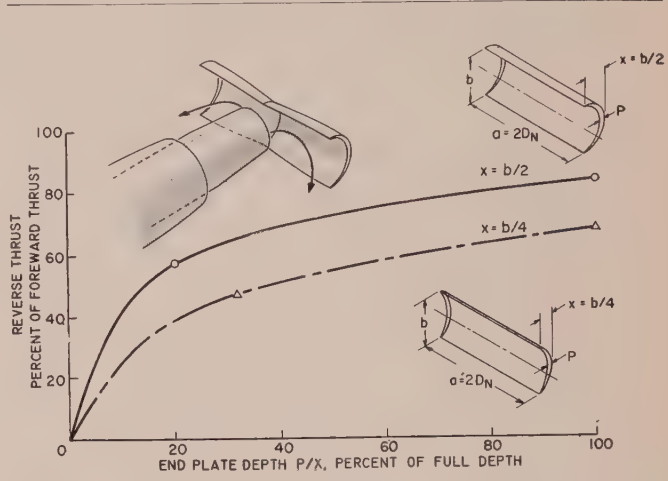

Fig. 6 – Effect of target and end plate depths on performance of cylindrical reverser (nozzle pressure ratio, 2.0; 100% airflow)

Effect of Shape Simplification

Following the investigation of some of the basic design considerations, attempts were made to simplify the shapes of the target-type reversers, and thereby reduce the installation and actuation problems. Typical of these were the attempts to reduce both the depth of the reverser and also the depth of the end plates of the cylindrical reversers. The results obtained are illustrated in Fig. 6, which presents reverse thrust versus end-plate depth for a full half cylinder ($X = b/2$) and also for one with only half the depth of the former ($X = b/4$).

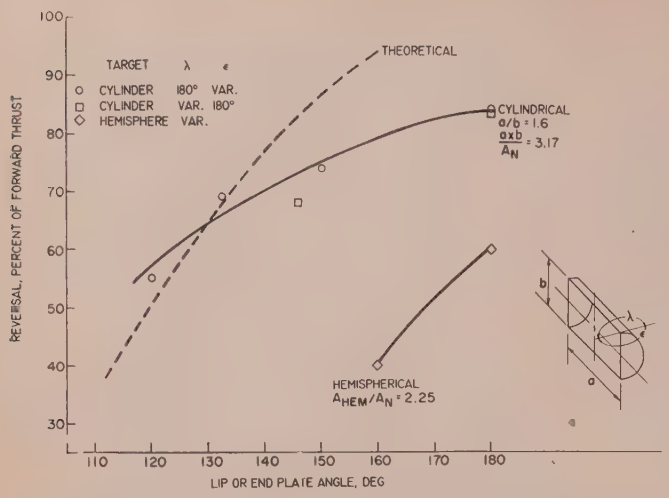

Fig. 7 – Effect of lip and end-plate angle on performance of target-type thrust reverser (nozzle pressure ratio, 2.0; 100% airflow)

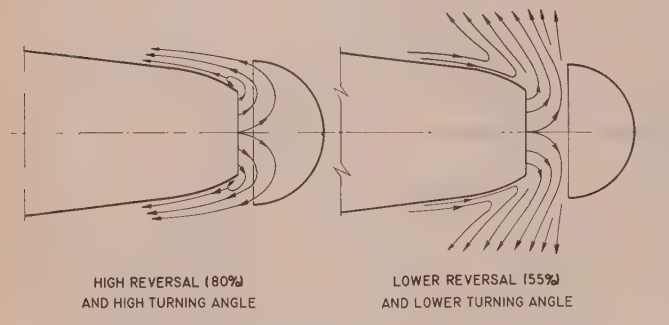

Fig. 8 – External flow fields for hemispherical reverser

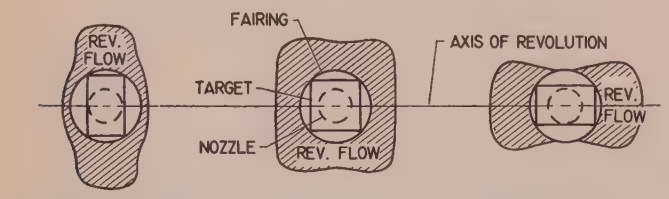

Fig. 9 – Effect of aspect ratio on envelope of reversed jet (cylindrical reversers with full end plates; nozzle pressure ratio, 2.0; 100% airflow)

The per cent end-plate depth is defined as being equal to 100 times the distance P divided by X as indicated on the chart.

The effects of both reductions in the performance of the cylindrical reverser were not too great for, as indicated on the chart, over 40% reversal was obtained with a configuration having only half the depth of a full half cylinder, and with an end-plate depth of slightly over 30% of a full end plate. Thus, considerable simplification of the cylindrical reversers can be made, which will greatly alleviate installation problems. Similar modifications were also made to the hemispheres, with similar results.

Effect of Reverser Exit and Gas Turning Angle

As might have been expected, it was established early in the investigation that for each reverser a unique relationship existed between the amount the gas was turned and the reverse thrust that was obtained, such that high gas turning angle resulted in high thrust reversal. Moreover, this effect was independent of how the gas angle was varied, whether by changing target size, spacing ratio, or lip or end-plate angle. In general, the trends were similar to that of the theoretical cosine variation, except that the experimental curves were displaced varying amounts lower than the theoretical curve, the displacement being a function of the total pressure losses in each case.

The thrust reversal variations resulting from changes in gas angle as determined by changes in target size and spacing ratio have already been presented. The variations resulting from changes in target lip or end-plate angle are presented in Fig. 7. Data obtained on both a cylindrical and hemispherical reverser are included, as well as the theoretical cosine curve. The lip angle of the cylinder and hemisphere and the end-plate angle of the cylinder are defined by the sketches on the chart.

It is to be noted that the effects on the performance of the cylinder of changing either lip angle or end-plate angle are about the same, but that the slope of the curve defined by these data is less than that for the hemisphere or the theoretical curve. The reason for this is that only part of the gas was affected when one of these angles was varied, whereas all of the gas is affected when the hemisphere lip angle is varied. The significant thing to note in this chart is that if you want high thrust reversal you will require a high lip or end-plate angle, and this will result in a high gas-turning angle. This may introduce other problems, for if the gas-turning angle is high there is a possibility of jet attachment to the fairing or nacelle, and even possibly reingestion of the hot gases into the engine inlet.

External Flow Fields and Jet Attachment

Some information on external flow fields and jet attachment has been obtained on models by means of tuft and rake measurements. Fig. 8 shows typical flow patterns for a relatively low gas-turning angle, low reversal (about 55%) hemisphere, and a high gas-turning angle, high reversal (about 80%) hemisphere. The mean angle of flow for the former was about 150 deg, and for the latter about 170 deg. As illustrated in the chart, the low-angle flow actually induced secondary flow instead of attaching to the fairing. The high-angle flow, on the other hand, attached itself to the fairing and

remained attached for a considerable distance. Whether or not this is undesirable depends on the application, for in many cases of ground-roll reduction the reverser will be used for periods of only 15 sec duration.

As might be expected, the flow is discharged from the hemispherical reverser in a continuous circumferential sheet. In many instances this may cause difficulty because of flow impingement on wings or control surfaces. This impingement can be remedied by blanking out or blocking the undesired flow regions by means of plates or fairings installed at the reverser, but this usually results in a reverse-thrust reduction. One way of avoiding this impingement without loss of reverse thrust is to employ an elongated cylindrical target reverser which discharges the flow in the form of a lobed pattern. This is illustrated in Fig. 9, which presents the external flow fields obtained (four nozzle diameters upstream) with the cylindrical reverser; also shown is the effect of aspect ratio on these flow fields. It can be seen that for an aspect ratio of 1.0, that is, a square cylindrical target, the flow is discharged in an approximately square pattern, but that for values of aspect ratio greater or less than one the lobed pattern is obtained. A more distinct separation of the flow into lobes is noted for the case of aspect ratio greater than one. In all the cases illustrated, the flow was attached to the back end fairing; this is consistent with the high values of thrust reversal obtained and noted on the figure.

Detachment of the reversed flow from the fairing is possible if the effective gas turning angle is reduced. Unfortunately, as previously noted, the thrust reversal will also be reduced. An illustration of this is presented in Fig. 10, which shows the variation in reversal and flow patterns that was obtained with a cylindrical reverser by varying the depth of the end plates. The top sketch shows the attached flow pattern and high reversal (75%) that were obtained with a high gas-turning angle when using full-depth end plates. The bottom sketch shows the unattached flow pattern and lower reversal (55%) that was obtained with a reduced gas-turning angle when using end plates with a depth equal to 20% of the full depth.

Attempts were made with the target reversers to obtain values of thrust reversal higher than 55% without jet attachment. One of these, which was not successful, consisted of extending the long dimension of the reverser to length-width ratios as high as 2½. Another, which permitted an additional 10% reversal before encountering jet attachment, consisted of decreasing the angle between the two cylinder halves from 180 deg to about 120 deg. This is illustrated in Fig. 11. As the angle between halves was decreased, a considerable amount of flow escaped through the V-gap at the top and bottom, and it was necessary

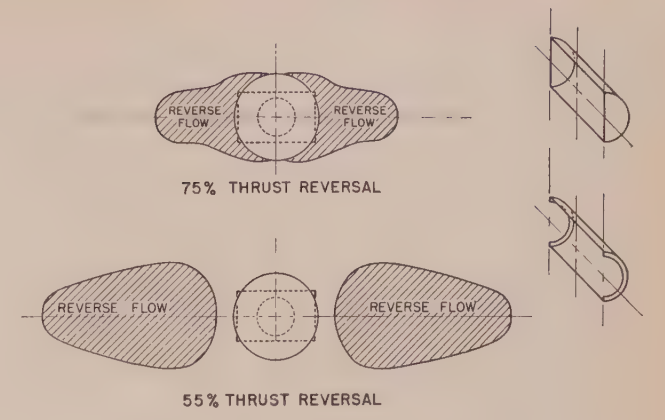

Fig. 10 – Variation in reversal and flow patterns obtained with cylindrical reverser by varying depth of end plates

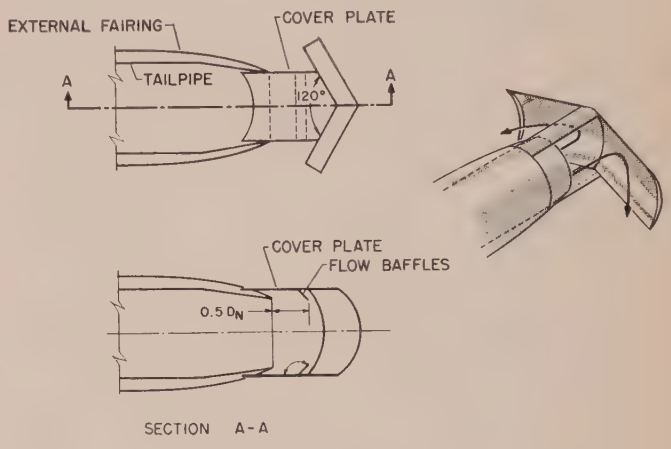

Fig. 11 – Angled cylindrical reverser, giving 65% reversal without jet attachment

to install plates to prevent this. The installation of the plates, however, caused an intolerable flow instability. Further investigation showed that this could be eliminated by installing flow baffles at the locations indicated on the figure.

To recapitulate, if jet attachment must be avoided when using a target reverser, 55% thrust reversal can be obtained fairly simply. Higher reversals without attachment are possible, but only at the expense of additional complication.

Effect of Hot Gas Reingestion

Obviously, one of the disadvantages of reversed flow attachment to the back end fairing is that it results in overheating of the structure in that region. A more serious aspect, however, would be reingestion of the reversed gases by the engine inlet, with consequent overheating of the inlet air. This would not only result in considerably reduced thrust, but could also result in destruction of the

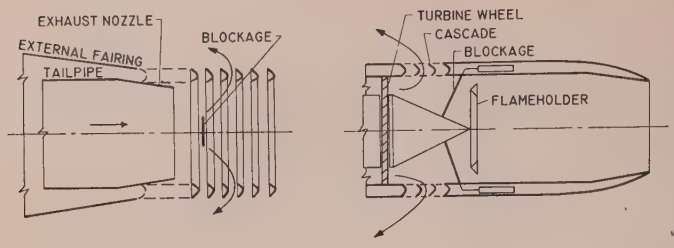

Fig. 12 – Two types of cascade thrust reverser. Left: ring cascade reverser; right: tail-pipe cascade reverser

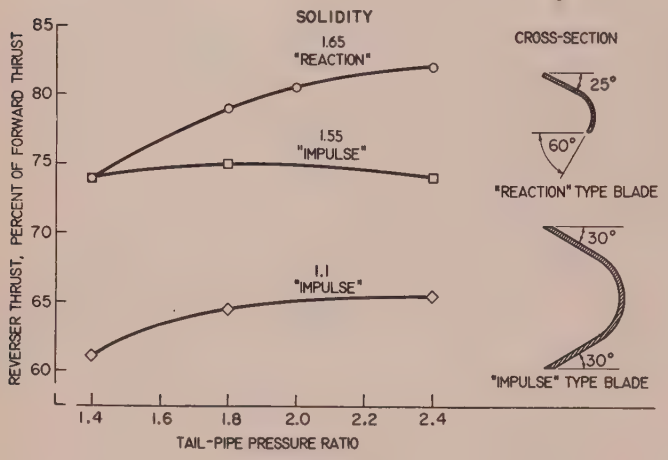

Fig. 13 – Performance of tail-pipe cascade thrust reverser (100% airflow; 100% mechanical blockage in tail pipe; tail-pipe Mach number, 0.22)

engine. Full-scale tests indicated that this can occur when using a high reversal target device on a short nacelle while operating under static ground conditions, and that increases of 300-400 F or more in inlet air temperature are possible. It is possible, however, that for most installations the forward velocity of the airplane during ground roll may be sufficient to prevent the reingestion. This was actually demonstrated on the same short full-scale nacelle, wherein it was determined that reingestion did not become serious until the ground speed had been reduced to about 60 mph. It is expected that on a nacelle with a more realistic value of length-diameter ratio this effect would occur at much lower ground roll speeds, if at all.

Cascade-Type Reverser

As previously mentioned, the second group of thrust reversers that was investigated is the cascade group. Fig. 12 illustrates two types of cascade thrust reverser for which scale model data were obtained. The sketch on the left illustrates a ring cascade installed in the region of the exhaust nozzle, and the one on the right shows a proposed installation of a tail-pipe cascade-type reverser installed just behind the turbine wheel. The operation of the ring reverser requires the extension of the rings from the fairing and the location of a small amount of blockage, as indicated, to trigger the gas into the rings. The blockage can be a bar or a circular disc, depending on the type of ring used, or even an air blast. Most success was obtained with the mechanical blockage triggers. When the gas is triggered it is all picked up and turned by the rings, provided there are enough of them and the trigger blockage is sufficient. Obviously, one can be traded for the other.

Another method that has been successfully employed by Dr. Ackeret of the Swiss Federal Institute of Technology makes use of swirl or centrifugal force for directing the gas into the rings. This is accomplished by rotating a set of vanes installed in the tail pipe upstream of the exhaust nozzle.

The operation of the tail-pipe cascade reverser requires that the cascade be unblocked and the tail pipe blocked, thus forcing the gas into the cascade. The ring reverser is felt to have the advantages of simplicity and low actuating forces, and the tail-pipe cascade reverser has the advantage of being readily adaptable to afterburning engines.

Tail-Pipe Cascade

Typical performance of several of the tail-pipe cascade reversers obtained with the tail pipe completely blocked is illustrated in Fig. 13. Curves of reverse thrust versus tail-pipe pressure ratio are presented for sheet-metal cascades using a "reaction type" (minimum area at blade exit) blade of

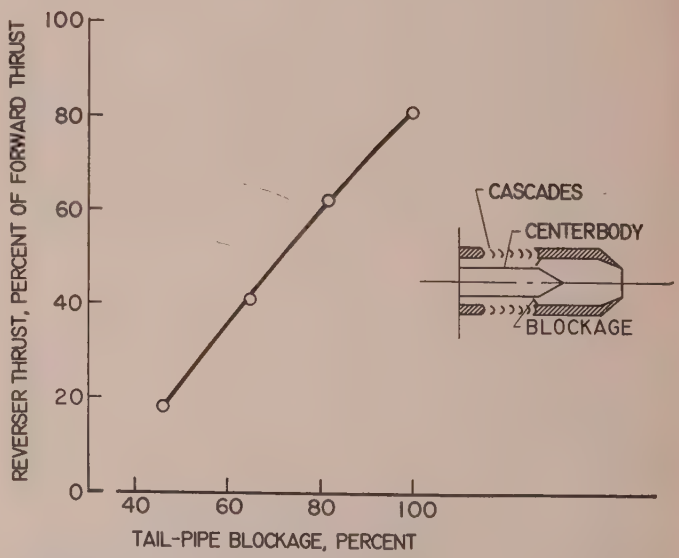

Fig. 14 – Effect of varying tail-pipe blockage on reverse thrust obtained with tail-pipe cascade reverser (tail-pipe pressure ratio, 2.0; 100% airflow)

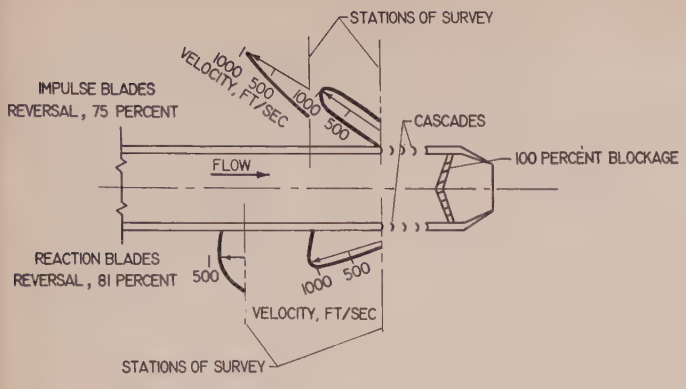

Fig. 15 – External flow fields for cascade thrust reverser (pressure ratio, 2.0)

1.65 solidity and an "impulse" (minimum area at blade inlet) type blade of 1.5 and 1.1 solidity. Sketches showing cross-sections through the blades are also included. The Mach number in the tail pipe just ahead of the cascades was about 0.22 in this case.

The tests with these cascades indicated that high reversal (over 80%) and gas-turning angles close to design are obtainable with these simple sheet-metal blades. Modification of the blade shape from "reaction" to "impulse" type had negligible effects on performance, as the difference between the two top curves at the higher pressure ratios can be accounted for by the difference in blade exit angle. Changing the cross-section of the blade from that indicated to an airfoil shape with increased thickness likewise had only a small effect on performance, and at no time increased the reversal more than 5%. Relocation of the cascade to a high Mach number region (about 0.50) comparable to that immediately downstream of the turbine resulted in a drop in reversal of no more than 5 points. Size and shape (length-to-width ratio) of the cascade, likewise, appeared to have negligible effect, as long as it was correctly sized to pass the desired airflow.

Effect of Tail-Pipe Blockage – The effect of varying the tail-pipe blockage on the reverse thrust obtained with a typical cascade reverser is illustrated in Fig. 14. The reverse thrust is evaluated on a unit airflow basis, which assumes that the overall hardware is scaled down to keep the airflow constant as the blockage is decreased. As expected, the reverse thrust decreases as the tail-pipe blockage is decreased. Of interest is the fact that 40% thrust reversal can be obtained with a blockage of 64%. Thus, it is not necessary to completely block the tail pipe to obtain a reasonable value of thrust reversal.

External Flow Fields – As with the target-type reversers, the external flow fields of the cascade reversers are of considerable interest, and thus typical external velocity patterns are presented in Fig. 15. The profiles at the top of the figure were determined for an "impulse" type cascade that produced 76% reversal at a pressure ratio of 2.0, whereas those at the bottom were determined for a "reaction" type cascade that produced 81% reversal at the same pressure ratio. The essential difference between the two is that although the reverse thrust was high and about the same value, the flow from the "reaction" type blades was attached to the external fairing, whereas that from the "impulse" type blades was not. Although the exact reason for this phenomenon is not known, it is suspected that the location of the minimum flow area of the blade row is the main contributing factor. It will be recalled that the "reaction" type cascade has its minimum area at the exit of the blade row, whereas the "impulse" type has its minimum area at the entrance.

A brief investigation was undertaken to determine if the flow from the "reaction" type blades could be made not to attach, and the following information was obtained. It was learned that the following tended to enhance separation of the flow (see Fig. 16):

1. Increasing length- (along the tail-pipe axis) to-width ratio of the cascade.
2. Parallel blade end plates rather than radial blade end plates.
3. The presence of external doors, either bombay or cowl flap type, that would cover the cascade when the reverser is not in use.

The following had no effect on separation:

1. External obstruction upstream of the cascade.
2. Boundary layer trippers in the flow passage of the first blade.

It is felt that with the optimum combination of the above mentioned factors favorable for separation, it should also be possible to achieve complete nonattachment of the flow when using a "reaction"-type cascade. In any event, the significant fact to note is that with a cascade reverser it is possible to obtain higher values of thrust reversal

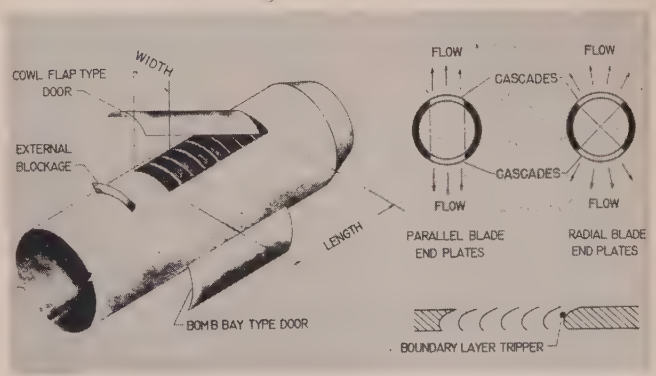

Fig. 16 – Influence of geometrical factors on flow attachment with reaction cascade reversers .

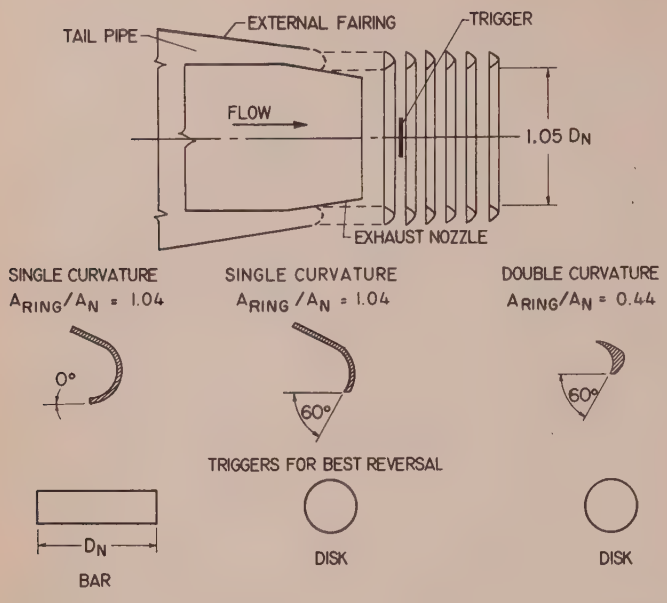

Fig. 17 – Some successful combinations of ring shape and flow trigger

without flow attachment than it is with the target-type reversers. (This difference may be partly accounted for by the fact that the external fairing for the target-type reversers made an angle of 7 deg with the tail-pipe axis, whereas the fairing for the cascade made an angle of 0 deg.)

Ring Cascade

The development of the ring-type reverser with mechanical flow trigger initially involved a considerable amount of trial and error. Early attempts using "impulse" type rings with a circular arc cross-section were unsuccessful. Modification of the ring cross-section so that it resembled a turbine nozzle diaphragm in cross-section, and thus became a "reaction" type ring, resulted in considerable improvement in reversal. Fig. 17 shows some of the combinations of ring shape and flow trigger that were successful. At the top of the figure is a sketch showing the relative positions of the exhaust nozzle, the flow trigger, and the reverser rings. For all of the configurations investigated, the inside diameter of the rings was equal to 1.05 exhaust nozzle diameters, and there was no device for guiding the flow from the nozzle into the rings. As indicated, the single curvature ring with zero entrance angle performed best with a bar-type trigger, whereas the same ring with a 60-deg entrance angle gave its best performance with a disc-type trigger. The double-curvature blade investigated likewise gave optimum performance with a disc trigger. As will be illustrated subsequently, more of these double-curvature blades were required because of the smaller size of the individual blades.

Effect of Spacing Ratio – Typical reversal performance obtained with a 6-ring reverser of the large-ring type is presented in Fig. 18 as a function of ring-spacing ratio for trigger blockages of 16, 25, and 50% of the nozzle area. Ring-spacing ratio is defined as the distance between adjacent rings divided by exhaust nozzle diameter, D_N. The data are presented for the 60-deg inlet angle, single curvature rings with a disc trigger. The sensitivity of the rings to spacing is clearly evident in the figure, there being a very sharp fall-off in reversal as the spacing is varied from the optimum. The maximum reversal obtained was slightly over 60%, obtained with a trigger blockage of 50%. Reducing the blockage to 16% resulted in a drop in maximum reversal of about 15 points. The reversal was found to be relatively insensitive to first ring spacing within a reasonable range of spacings. The optimum spacing of the trigger was found to be close to the minimum distance required for 100% airflow, and for the data presented was approximately equal to 0.5 D_N.

Effect of Number of Rings – The effect of the number of rings on reverse thrust is illustrated in Fig. 19. The curve at the left is for the single-curvature large-ring cascade with 60-deg entrance angle and a trigger blockage of 25%. The one at the right is for the double-curvature small-ring cascade, also with a trigger blockade of 25%. It can be seen that increasing the number of the larger blades from 2 to 6 resulted in an increase in reverse thrust from —30 to +60%, whereas increasing the smaller blades from 4 to 10 increased the reverse thrust from —10 to +55%. Although approximately the same peak perform-

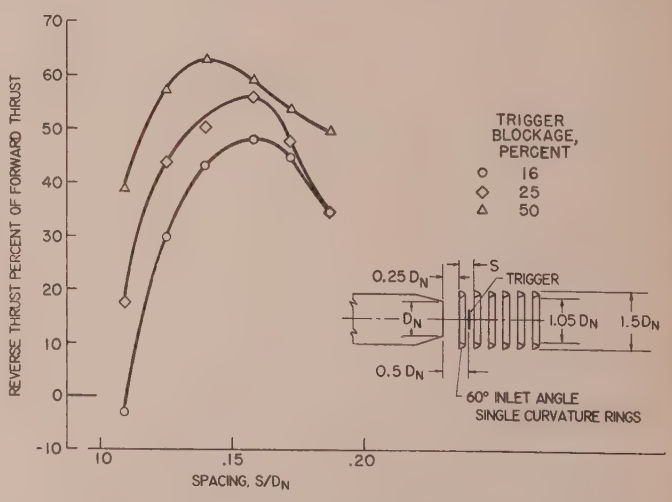

Fig. 18 – Effect of ring spacing on performance obtained with 6-ring reverser of large-ring type (nozzle pressure ratio, 2.0; 100% airflow; disc triggers)

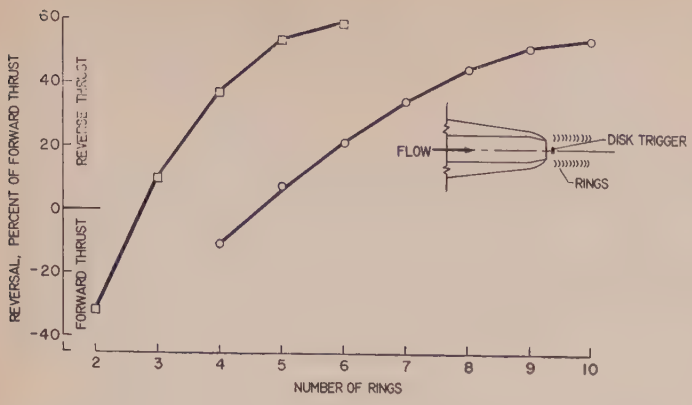

Fig. 19 – Effect of number of rings on reverse thrust of ring cascade reverser (nozzle pressure ratio, 2.0; 100% airflow; trigger blockage, 25%)

ance was obtained in each case, the double-curvature cascade required more blades. As previously mentioned, this is because the cross-sectional area of each of the double-curvature blades is considerably less than that of the single-curvature blades (0.44 times the nozzle area compared to 1.04 times the nozzle area). A comparison of the total projected cross-sectional area of these rings with that for a high reversal target-type reverser reveals that the rings have about twice as much turning area. This is a possible indication that there may still be room for refinement of the ring reverser in the direction of reducing ring projected area.

A brief recapitulation of the performance of cascade-type reversers would be as follows:

1. Investigation of the tail-pipe cascade revealed that it is possible to obtain high reversal without flow attachment by the use of simple blade shapes and reverser geometries.

2. Forty per cent reversal can be obtained with a tail-pipe cascade when using a physical blockage in the tail-pipe of 64%.

3. The performance of ring cascade reversers is sensitive to ring shape spacing and the type of trigger, and the ring reverser requires at least twice as much turning cross-sectional area as the target type.

External Flow Fields – As with the hemisphere target-type reversers, the ring reversers discharge the reversed gas in a circumferential sheet. This is undesirable, of course, for the same reason that it was for the targets. Attempts were therefore made to interrupt the flow and provide an essentially two-lobed pattern. The results of these attempts are illustrated in Fig. 20, which shows some of the flow patterns that were measured at a station four nozzle diameters upstream of the nozzle exit. Included for each sketch is the thrust reversal obtained, the type of trigger used, and the blockage of the trigger in terms of the nozzle area.

The figure at the upper left shows that it was possible to obtain a two-lobed pattern with 90-deg top and bottom shrouds installed at the outside of the rings. Unfortunately, it was possible to obtain only 25% reversal with a 50% blockage bar trigger, and thus this arrangement is considered unsatisfactory. It is of interest to note that this same arrangement with a 50% disc trigger produced only 8% thrust reversal. This is typical of the performance obtained with disc trigger plus shrouds, and it may be concluded that this combination is undesirable. The remaining configurations considered all used bar triggers.

The flow pattern at the upper right was obtained with 90-deg top and bottom shrouds installed at both the inside and outside of the rings. In addition to producing a well defined two-lobed pattern, this arrangement also produced higher reversal (42%) than the preceding one when using a 50% blockage trigger. The reversal with a 25% trigger, however, was insignificant. Improvement in the reversal with a 25% trigger was obtained by cutting down the shroud angle from 90 deg to 60 deg. The flow pattern and reversal obtained is indicated by the sketch at the lower left. Although in this case the reversal was increased to 32% with the 25% trigger and 58% with the 50% trigger, the flow pattern was somewhat altered so that two distinct lobes were no longer obtained. The reversed flow out of the top and bottom was not too great, however, and could probably be tolerated in some cases.

Another method of producing a two-lobed reversed-flow pattern that may be satisfactory in some cases consists of providing the rings in the top and bottom quadrants with a 90-deg exit angle instead of blocking off these quadrants with a shroud. The reversed-flow pattern and reversal

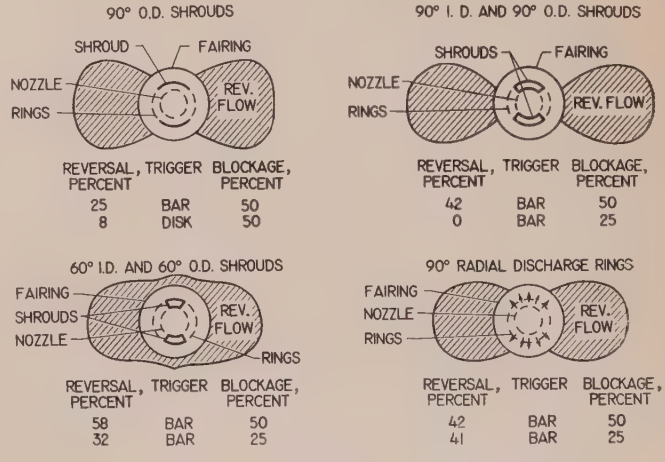

Fig. 20 – Some flow patterns measured at a station 4 nozzle diameters upstream of nozzle exit (nozzle pressure ratio, 2.0; 100% airflow)

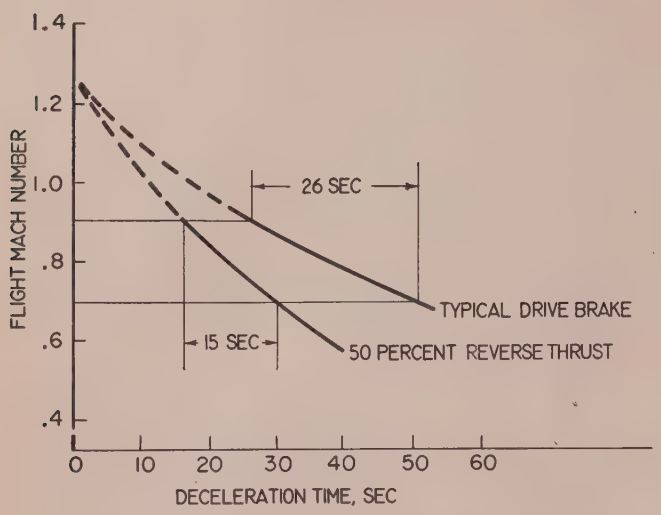

Fig. 21 – Effectiveness of thrust reversal as an in-flight brake (20,000-lb airplane; 25,000-ft altitude)

obtained are indicated in the lower-right-hand corner. This is the only one of the lobed flow configurations tested that produced over 40% thrust reversal with a 25% trigger.

Thrust Modulation

Regardless of application, thrust reversers may be classified into one of two categories:

1. An on-off device that provides either full forward or full reverse thrust.
2. A modulating device that, in addition to the above, will also provide desired intermediate values of thrust.

Devices falling into the first category would probably be used mainly for reducing landing ground roll, whereas those falling into the second category would, in addition to ground-roll reduction, also be used for landing approach and in flight-braking applications.

The effectiveness of the thrust reverser for reducing the ground roll was illustrated earlier in this paper. The effectiveness of the thrust reverser as an in-flight brake is illustrated in Fig. 21, which shows a comparison of the time required for decelerating a 20,000-lb airplane at an altitude of 25,000 ft when it is equipped with a conventional aerodynamic dive brake, with that required when the same airplane is equipped with a thrust reverser providing 50% reverse thrust. For a reduction in flight Mach number from 0.9 to 0.7, the time required for the dive brake was 26 sec, whereas that required for the thrust reverser was only 15 sec. Thus, it appears that the thrust reverser will have some advantages as an in-flight brake.

A consideration of the engine-thrust reverser relationship indicates that the thrust-reversal devices previously considered may be broken down into two classes:

1. Those that have no effect on engine performance, and
2. Those that affect engine performance.

Examples of the former are the target-type reversers with spacings greater than the minimum required for 100% airflow, the ring reverser, and the tail-pipe cascade with scheduled blockage. Examples of the latter are the target-type reverser with spacings less than the minimum, and the tail-pipe cascade with combined cascade cover and blockage.

Obviously, if the reverser has no effect on engine performance, or, in other words, if the effective nozzle flow area remains unchanged, then no new engine control problems are introduced. On the other hand, if the device affects engine performance (as a result of changes in the effective nozzle flow area) then either a variable-area exhaust nozzle and/or an engine overspeed regulator may be required. This is no problem, inasmuch as these devices are currently in operation on existing airplanes.

Thus, with respect to engine control no obvious problems are introduced, for the thrust reverser will either require no changes in the engine control system or make use of existing controls.

As previously mentioned, for ground roll reduction the reverser may be simply used as an on-off device or it may be used as a thrust modulator too. There are probably many cases where the on-off application will provide satisfactory ground roll reduction; however, further gains may be realized if the modulating feature is incorporated. These gains are accomplished in two ways. First, if the reverser is used to modulate thrust during the landing approach, the airplane is able to land with a lower thrust, at a lower speed, with a faster thrust recovery time than is presently possible. Second, the time required to produce the full braking force (reverse thrust) is considerably shortened, because the engine is maintained at rated conditions and does not have to be accelerated to produce full reverse thrust.

Several reversers have been examined for modulation characteristics, and four of those considered are illustrated in Fig. 22. The sketch at the top left shows a possible method of modulating thrust with a cylindrical target-type reverser. In this case, the two halves of the cylindrical target have been actuated only part way, so that a portion of the exhaust gas is reversed and the remainder is discharged through the opening in the rear.

The sketch at the top right shows a method of modulating thrust using a tail-pipe cascade with the tail-pipe blockage and cascade cover scheduled so that the total flow area is kept constant at all times. During modulation, part of the gas passes

through the cascades and the rest is discharged through the exhaust nozzle.

The sketch at the lower left shows another method of modulating thrust with a tail-pipe cascade, but in this case the total flow area is not maintained constant during modulation because the blockage and cascade cover are combined into one unit. Modulation is obtained the same as before, with part of the gas being discharged through the exhaust nozzle and part through the cascade. In this case, the modulated thrust obtained will be a function not only of the reverser position but also of the engine on which it is installed.

The sketch at the bottom right shows a method that could be employed to modulate thrust when a ring reverser is installed. In this case, a bar trigger is employed and modulation is obtained by setting the two halves of the bar at various intermediate positions.

The modulation characteristics of the four configurations just described are presented in Fig. 23. The performance is shown as a plot of reverse thrust against per cent actuation, wherein the latter is defined as the ratio of the reverser position to the final position. The performance of the cylindrical, the cascade with scheduled blockage, and the ring-type reversers is independent of the engine used, but that of the cascade with combined blockage and cascade cover is not. For this latter case, the reverser was assumed to be installed on a typical current single-spool turbojet engine. In each case, the performance curve is continuous and has sufficient slope so that it should not be difficult to set any desired value of thrust. Thus, all of these configurations have desirable modulation characteristics. The reduced value of forward thrust of the ring reverser at zero per cent actuation is a result of the rings' picking up a small amount of air and reversing it. Full forward thrust is regained when the rings are retracted.

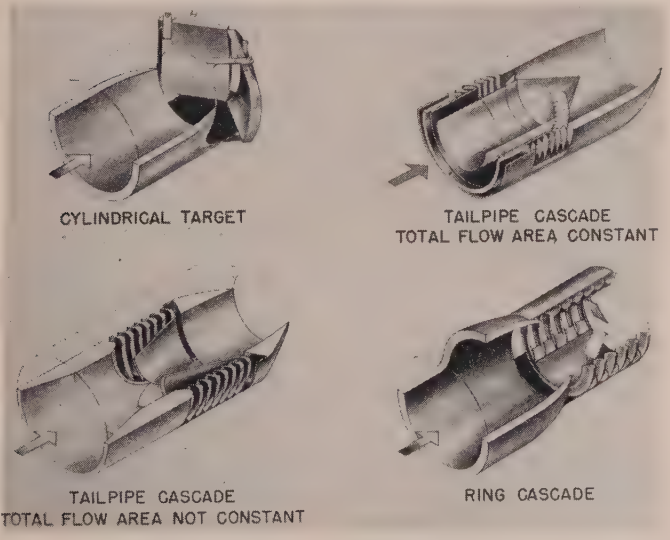

Fig. 22 – Four modulating thrust reversers

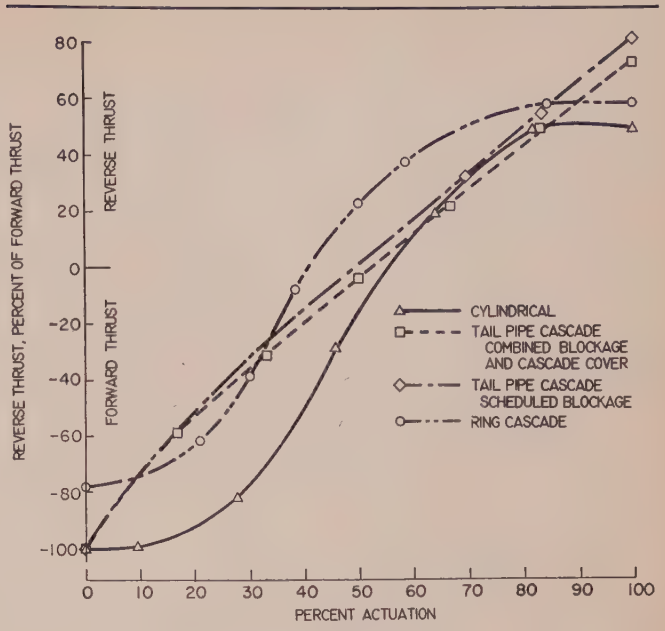

Fig. 23 – Modulation characteristics of thrust reversers

Summary

The results of the NACA investigation of thrust reversers may be summarized as follows: The tests of the target-type reversers indicated that:

1. High thrust reversal (up to 80%) is possible with several types of simple devices, but jet attachment limits thrust reversal to about 55%.
2. Thrust reversal is largely a function of reverser size and/or gas turning angle with reverser lip angle being highly critical.

The tests of the cascade-type reversers indicated that:

1. High thrust reversal (about 75%) without jet attachment is possible with a tail-pipe cascade.
2. Cascade aspect ratio, blade design, and external doors have small effect on thrust reversal but a considerable effect on reversed flow attachment.
3. The performance of the ring cascades is sensitive to ring shape and spacing.

The modulation tests of thrust reversers indicate that those investigated have desirable characteristics.

References

1. "Performance Characteristics of Hemispherical Target-Type Thrust Reversers," by Fred W. Steffen, J. G. McArdle, and J. W. Coats. NACA RM E55E18 (1955).

2. "Preliminary Performance Data of Several Tail-Pipe-Cascade-Type Model Thrust Reversers," by J. G. Henzel, Jr. and J. G. McArdle. NACA RM E55F09 (1955).

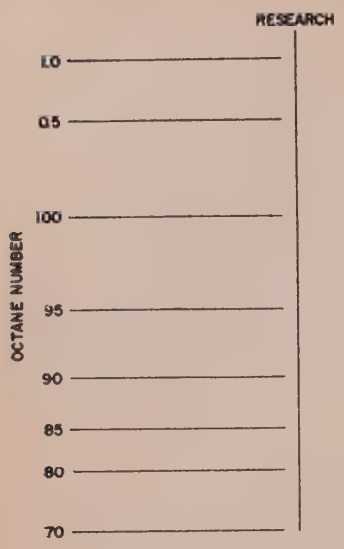

Fig. 1 – Research Method fuel ratings

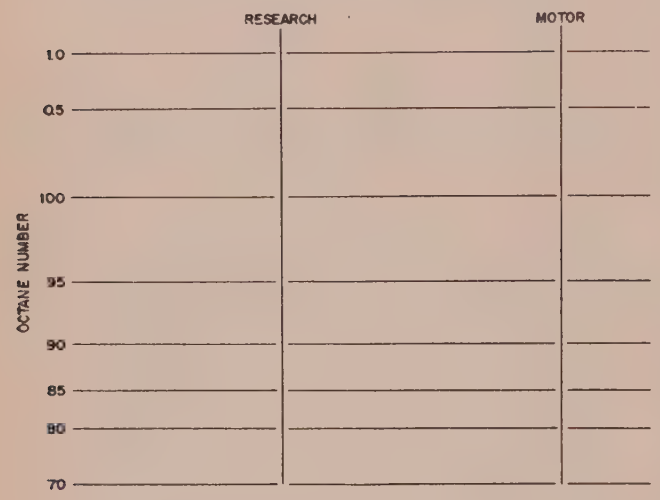

Fig. 2 – Research Method and Motor Method ratings

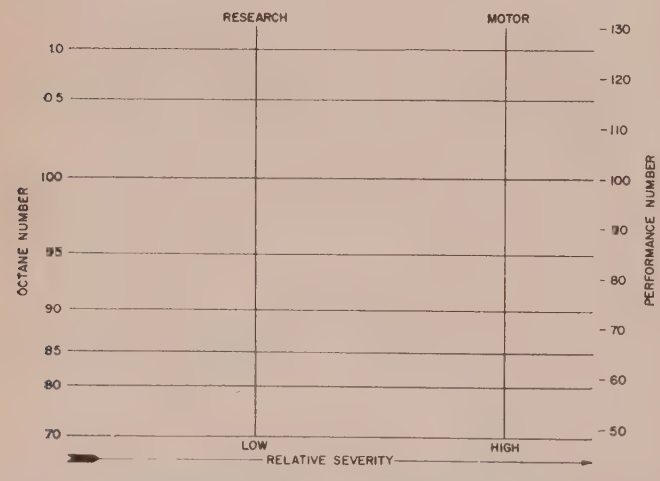

Fig. 3 – Octane numbers plotted to the AN Performance Number scale

Knocking Behavior

THE correlation of full-scale engine knock test results with the results obtained in single-cylinder fuel quality control engines such as the Motor and Research Method engines has been a continuous problem. As a result of the apparent lack of correlation existing between quality control methods and the automotive engines as installed in vehicles, a great deal of confusion has existed, and much time and money have been spent in attempts to develop new knock test methods. Our laboratories have developed a nomographic method[1, 2] which has assisted materially in understanding the mutual relationship of engines and fuels, and it is the suggested applications of this graphic method which are presented in this paper.

Fuel Sensitivity and Engine Severity

This graphic method is, in part, the result of inability to prepare mathematical formulas which will permit calculation of the fuel requirements of an engine. The general use of terms such as "fuel sensitivity" and "engine severity," neither of which can be defined with precision, also results

[1] "Knock Testing of Aircraft Engine Fuels," by Robert V. Kerley. Presented at the Panel on Fuels for Air-Breathing Powerplants, Research and Development Board Committee on Fuels and Lubricants, New York, Dec. 18, 1951. Unpublished.

[2] "The Relative Severity of Knock Test Engines," by Robert V. Kerley. Presented at the CFR Motor Fuels Division, Coordinating Research Council, Detroit, Sept. 26, 1952.

# of Fuels and Engines

R. V. Kerley and K. W. Thurston, Ethyl Corp.

This paper was presented at the SAE Golden Anniversary Fuels & Lubricants Meeting, Philadelphia, Nov. 10, 1955.

from the lack of knowledge permitting the calculation of engine requirements or fuel ratings. If the octane number of the test fuel varies over a wide range, depending on what engine is used in making the rating, the fuel is said to be "sensitive." Thus, the "sensitivity" of the fuel is determined in terms of the behavior of the test fuel relative to the primary reference fuels. An engine which gives a low rating to a sensitive fuel is generally called a "severe" engine. On the other hand, an engine which gives a high rating to a sensitive fuel is said to be a "mild" engine. In contrast to the term "sensitive," as applied to fuels and which, by general use, is relative to a specific primary reference fuel system, the term "severe," as applied to engines, has not been generally defined relative to specific reference engines. This paper suggests that the severity of many types of engines may be defined relative to the Research and Motor Method engines.

Graphic Method

It is generally thought that current automotive passenger-car engines rate fuels in about the same order and at about the same level as the Research Method. The vertical line shown in Fig. 1 will be used to represent any fuel rating obtained by the Research Method from 70 octane number at the low end to octane + 1.0 ml tel per gal at the high end. This line can, of course, be extended to include higher or lower values, but the portion shown covers the current fuel quality range with some room to spare.

The octane number scale used on this sheet is nonlinear. The authors have arbitrarily plotted fuel quality in proportion to AN Performance Numbers.

THIS paper represents a method by which the knocking characteristics of automotive engines may be compared in relation to the Research Method and Motor Method engines.

The effects of many engine variables on the ratings of sensitive fuels in passenger-car engines are illustrated. These variables include compression ratio, engine speed, air density, distributor tolerances, and temperature.

Direct comparisons are made of the manner in which 1955 passenger cars utilize fuel antiknock quality. It is indicated that two knock test methods must be used to achieve fuel quality control as fuel quality is recognized by engines operated in passenger cars.

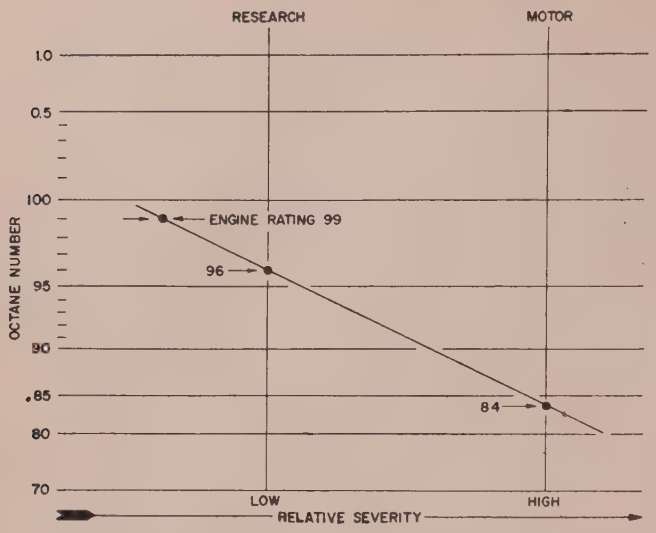

Fig. 4 – Research and Motor Method ratings locate fuel sensitivity line

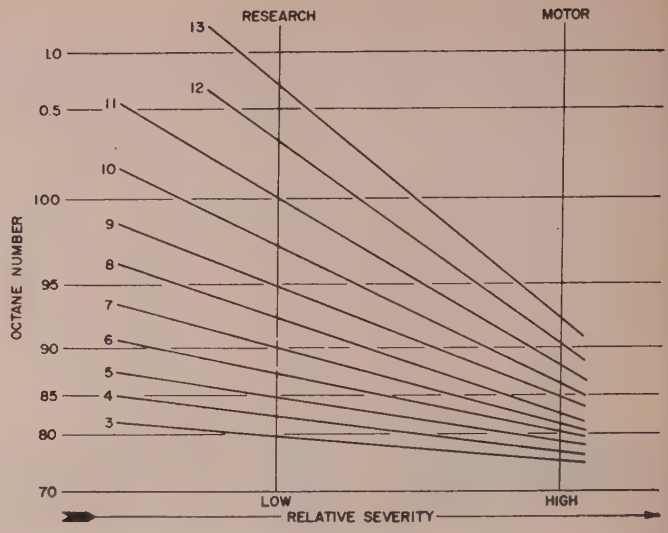

Fig. 5 – Sensitive reference fuel series formed by blends of isooctane, n-heptane, and diisobutylene

Although it might have been possible to use a linear octane number scale, the scale shown is convenient because values above and below 100 are often involved.

The second laboratory quality control method often used by refineries is the Motor Method. This method is shown in Fig. 2 as a second vertical line. It should be understood that the location of this line is completely arbitrary as is the choice of a line parallel to the Research Method. The distance separating the Research Method line from the Motor Method line is unimportant. In this figure the octane number lines have been extended as horizontal lines across the sheet to include ratings obtained by the Motor Method. This is justified since these lines represent primary reference fuels, and these are constant in all engines by definition. In other words, 80% octane in 20% heptane is always 80 octane number regardless of the engine or engine conditions used to make it knock.

In Fig. 3 the Performance Number scale has been added along the right-hand margin for orientation. Across the bottom of this figure is the arbitrary phrase "Relative Severity." Most commercial fuels have a lower octane number when rated by the Motor Method than when rated by the Research Method, and the Motor Method is therefore said to be "more severe" than the Research Method.

If a fuel is rated by both methods this fuel may be represented by a line connecting the Motor Method rating value with the Research Method rating value. For convenience this line has been called a fuel sensitivity line.[3] This is shown in Fig. 4. In this case the fuel had a rating of 84 octane number by the Motor Method and 96 octane number by the Research Method. The choice of a straight fuel sensitivity line is arbitrary, but no serious disadvantages have been noted as a result of the assumption that all fuels can be represented by straight lines.

When this fuel is rated in any other engine the value obtained in the other engine can be represented by a point on the fuel line. For example, if

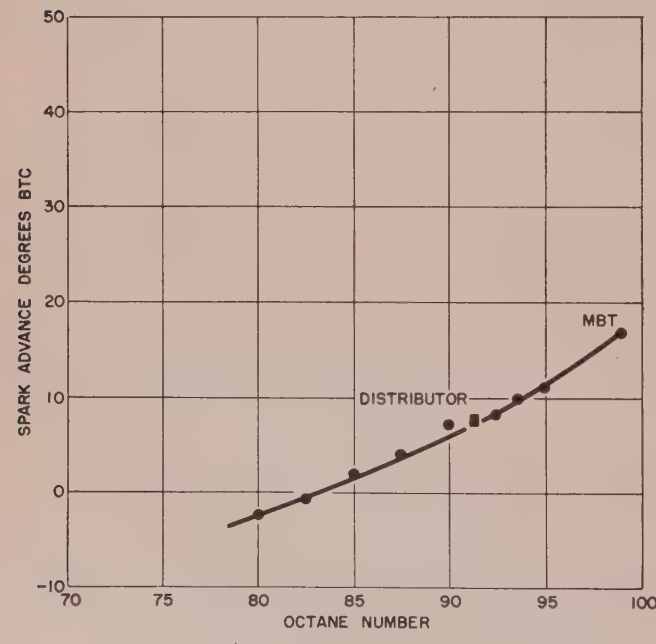

Fig. 6 – Effect of spark advance on primary reference fuel requirement for engine make D at 1000 rpm

[3] Representing a fuel by means of a straight line connecting a rating obtained at a severe condition to a rating obtained at a mild condition is not new. See footnote 6.

Table 1 – "S" Reference Fuel Composition and Laboratory Ratings

Fuel	Composition, %			Octane Rating	
	Diisobutylene	n-Heptane	Isooctane	Motor Method	Research Method
1-S	15.3	35.0	49.7	72.9	75.0
2-S	22.9	36.4	40.7	74.4	77.5
3-S	32.2	38.0	29.8	76.0	80.0
4-S	36.2	36.7	27.1	77.2	82.5
5-S	38.9	34.5	26.6	78.7	85.0
6-S	41.8	32.2	26.0	80.0	87.5
7-S	44.9	29.7	25.4	81.4	90.0
8-S	46.1	26.5	27.4	82.9	92.5
9-S	43.6	21.9	34.5	85.0	95.0
10-S	40.8	16.9	42.3	86.6	97.5
11-S	37.9	11.6	50.5	88.3	100.0
12-S	34.9	5.9	59.2	90.4	110.0 PN
13-S	32.8	1.8	65.4	92.3	120.0 PN

a rating of 99 octane number is obtained in the third engine there is only one place where 99 octane number will intersect the fuel sensitivity line. This is shown in this figure. The fuel shown changes its rating rather quickly in terms of primary reference fuels as engine conditions are altered and for this reason it would be called a "sensitive" fuel. Fuel sensitivity for automotive fuels is commonly expressed in terms of "jump," meaning the difference between the Research Method rating and the Motor Method rating. In this instance the fuel sensitivity is 12 octane numbers.

"S" Reference Fuel Series

By rating a series of sensitive fuels in terms of primary reference fuels in a third engine, it is possible to represent the third engine in its relation to the Motor Method engine and the Research Method engine. For this purpose we have found the "S" reference fuel series[4] shown in Fig. 5 to be quite useful. The "S" reference fuels are all blends of three pure hydrocarbons: isooctane, n-heptane, and diisobutylene.[5] The amounts of the three components are adjusted to give the desired Research octane number and the desired sensitivity for each fuel blend. The sensitivity is approximately the same as the average commercial fuel of the same Research octane number. The composition and laboratory ratings of the fuels shown are included in Table 1.

Automotive Engine Ratings of Fuels

In order to rate automotive fuels of different octane numbers in the Research and Motor Method laboratory test engines the compression ratio is increased until knock occurs. This is done while maximum knock fuel/air ratio and a specified spark advance are maintained.

Various methods resembling the Modified Borderline Method, or the Modified Uniontown Method, all of which require a change in spark advance to cause the fuel to knock, are normally used for automotive engine testing of the antiknock properties of fuels. The same general procedure was followed in dynamometer calibrations of some 1955 passenger-car engines in Ethyl Corp. Research Laboratories. The details of the calibration at 1000 rpm are illustrated in Fig. 6. Using the carburetor supplied with the engine, speed was held constant, and the engine was operated at full throttle on various blends of primary reference fuels. For each blend the spark was manually adjusted until the fuel knocked and the degrees of actual spark advance required to cause knock for each blend of isooctane in n-heptane are shown in this figure. The spark advance which would have been obtained, if the distributor had been set at the manufacturer's recommended basic setting and had followed the standard distributor advance curve, is also marked. Reading along the horizontal scale it is indicated that the engine requirement at 1000 rpm is 91 octane number at this speed. Dynamometer calibration also permits the determination of maximum power spark advance. If the distributor had been set to give the minimum spark advance required to produce maximum power (a spark advance commonly referred to as "minimum for best torque" and hereafter indicated simply mbt) the engine would have required 99 octane primary reference fuel.

In actual test work the spark advance for knock on a single primary reference fuel is determined at each of several speeds before changing to the next reference fuel. The results of the complete calibration over the speed range for engine make D is shown in Fig. 7. The primary reference fuel requirements for this engine at the standard distributor setting and at the minimum spark advance for best torque are shown at each of five speeds.

Fig. 8 indicates the spark advance required to cause knock for seven of the sensitive reference fuels at each of five engine speeds.

Since Fig. 7 related octane-number requirement to spark advance and engine speed, it is possible by superimposing Figs. 7 and 8 to determine the octane number ratings of each of these sensitive fuels at each engine test condition. This is illustrated in Fig. 9 where, for example, it may be seen that S-7 which knocked at 7 deg at 1000 rpm is found to rate 91 octane number. At 3000 rpm it knocked at 30 deg spark advance, and it is therefore 85 octane number.

Relative Severity of Passenger-Car Engine, Make D

Referring again to Fig. 4, it is indicated that if a straight line is drawn through the Research Method rating and the Motor Method rating for a given fuel, the octane number rating of the same fuel in a third engine could be plotted at the proper location on this line. The ratings obtained in engine make D at 1000 rpm for all seven of the sensitive reference fuels have been plotted on the proper fuel

[4] Adopted as "Severity Reference Fuels" by the CRC Field Equipment Survey Panel in 1951.

[5] The diisobutylene (fuel SR-10) is actually a mixture of two isomers. It contains about 80% by volume 2,4,4-trimethyl-1-pentene and 20% by volume 2,4,4-trimethyl-2-pentene.

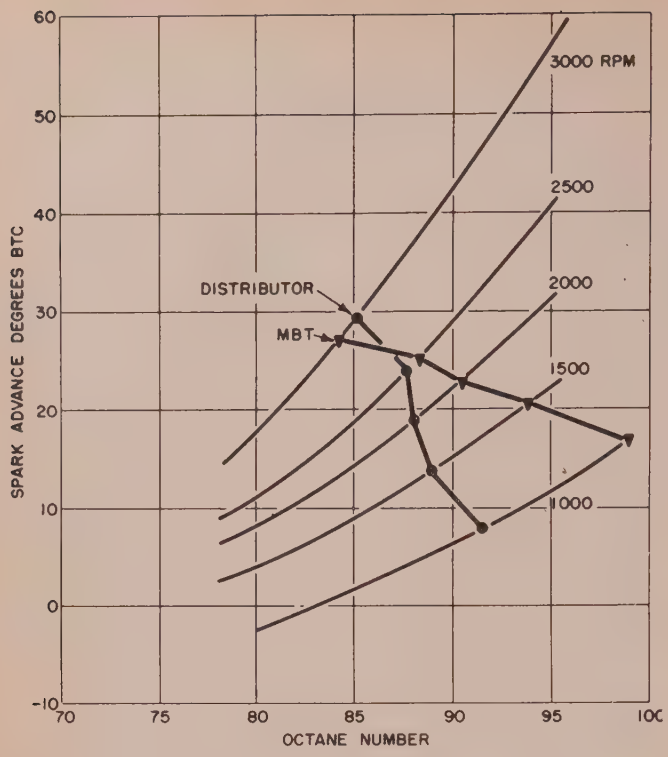

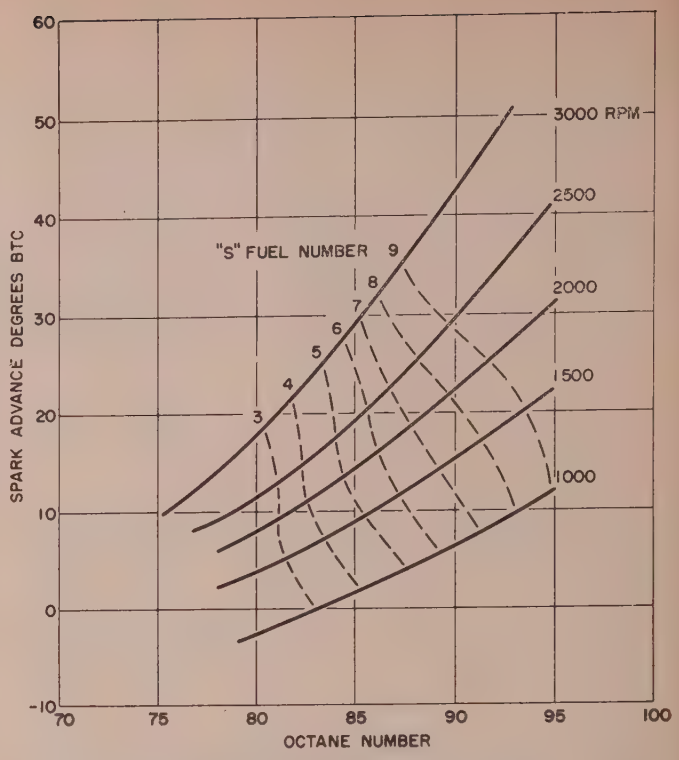

Fig. 9 – Primary reference fuel ratings of the "S" series of sensitive reference fuels in engine make D

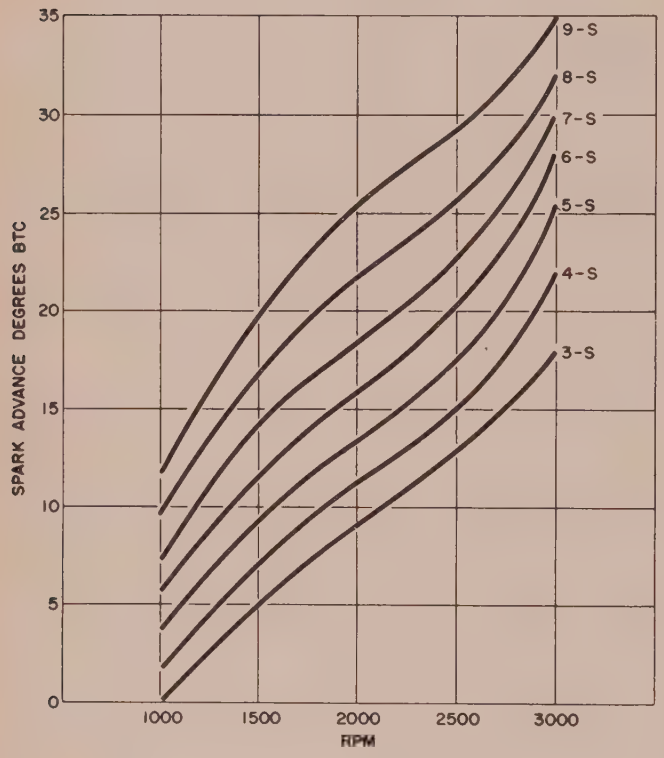

Fig. 7 – (upper) Effect of spark advance on primary reference fuel requirement for normal operating speeds of engine make D

Fig. 8 – (lower) Knock-limited spark advance for "S" series of sensitive reference fuels in engine make D

sensitivity lines in Fig. 10. The approximate spark advance in degrees causing four of these fuels to knock is indicated just to the right of the line connecting these points. This line represents the "severity" of this engine at 1000 rpm relative to the Research Method and to the Motor Method. It will be noted that sensitive fuels are rated relatively lower as spark advance is increased. Stated in another way, fuel 3-S rates 3 octane numbers above the Research octane number when spark occurs at top dead-center, while fuel 9-S rates slightly below its Research rating with the spark advanced to 12 deg btdc.

Effect of Spark Advance on Severity – When all the speed lines are constructed in this same manner for engine make D they form the engine severity pattern shown in Fig. 11. Each speed line follows the same trend noted previously. As spark advance is increased to cause the better fuels to knock, fuel ratings become relatively lower and approach the Motor Method octane number of the fuel. For example, at 3000 rpm 3-S knocked at 18 deg and rated at Research rating level, while 9-S knocked at 35 deg and rated only 3 octane numbers higher than its Motor Method ratings.

Effect of Engine Speed on Severity – Just as increased spark advance normally increases engine severity (or lowers sensitive fuel ratings), engine speed also increases engine severity. Increasing engine speed from 1000 to 3000 rpm has almost as much effect on fuel ratings as the difference between Research and Motor ratings.

Determination of Fuel Requirement – The fuel requirement of this engine is readily transposed to the engine severity pattern. Fig. 7 showed the pri-

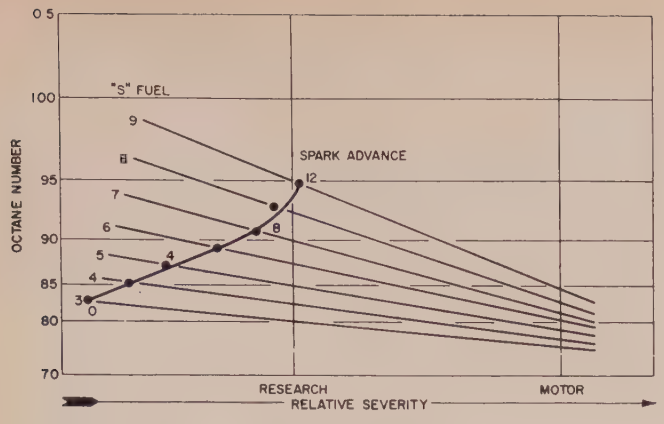

Fig. 10 – Engine make D severity line established by ratings of sensitive reference fuels at 1000 rpm

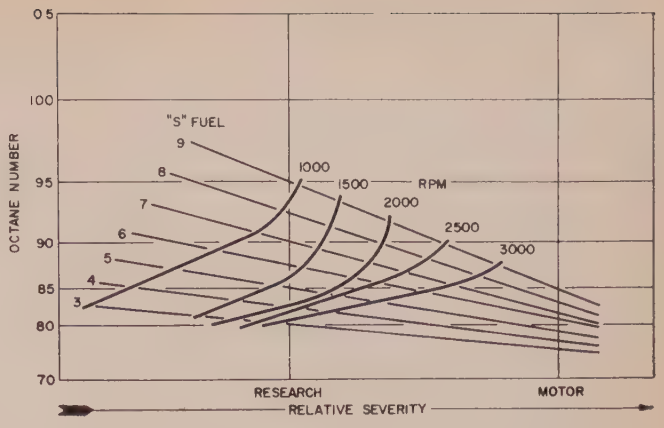

Fig. 11 – Engine make D severity pattern established by ratings of sensitive reference fuels at normal operating speeds

mary reference fuel requirement for the distributor setting at each speed. Since the speed lines have been constructed the reference fuel requirement may be shown as indicated in Fig. 12. It will be seen that fuel 7-S is likely to knock at low speed between 1000 and 1500 rpm. Knock would then be expected to die out and start again between 2000 and 3000 rpm.

Effect of Distributor Tolerance on Requirement – It has been assumed in Figs. 6, 7, and 12 that all distributors follow the standard spark advance curve. This is unlikely since tolerances are permitted during production. The effect of these spark-advance tolerances on knocking behavior will also depend on the speed at which the basic timing is set. If the distributor basic timing is set at a higher rpm, say at 1000, with the manifold vacuum advance mechanism disconnected, the fuel requirements are as indicated in Fig. 13. Both upper- and lower-limit requirements are shown, and two hypothetical fuels are indicated. An engine equipped with either distributor would require a fuel of 91 Research octane number. However, an engine equipped with the upper-limit distributor would require 91 Research octane number in conjunction with 85 octane number by the Motor Method. Such a fuel is considerably less sensitive than the average commercial fuel. A fuel of normal sensitivity which would just avoid knock in the high-speed range would have a Research rating of 93 and a Motor rating of 83. The same engine equipped with the lower-limit distributor requires a fuel having a

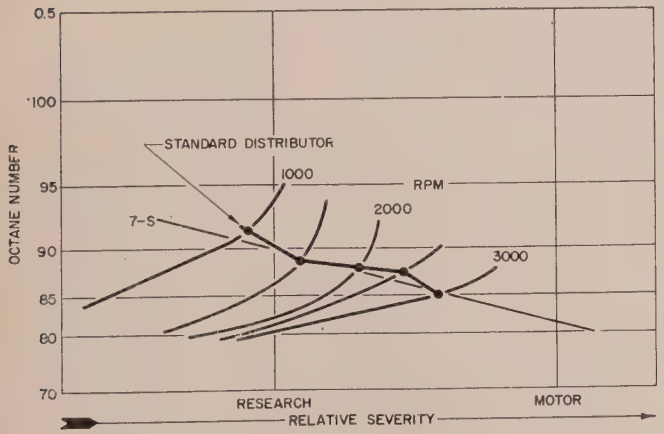

Fig. 12 – Engine make D fuel requirement at standard distributor spark advance

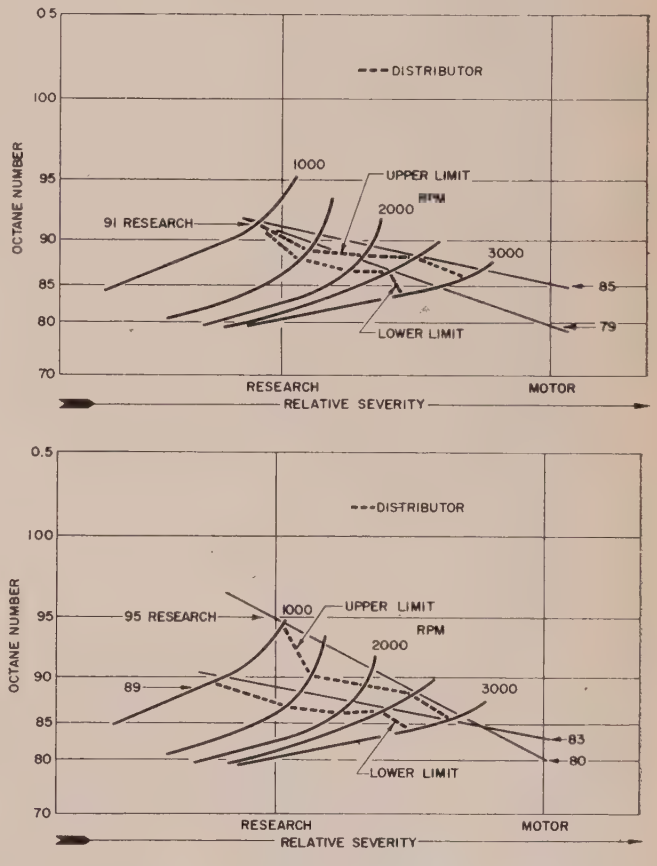

Fig. 13 – (upper) Fuel requirement of engine make D as influenced by distributor tolerances when basic timing is set at 1000 rpm

Fig. 14 – (lower) Fuel requirement of engine make D as influenced by distributor tolerances when basic timing is set at idle

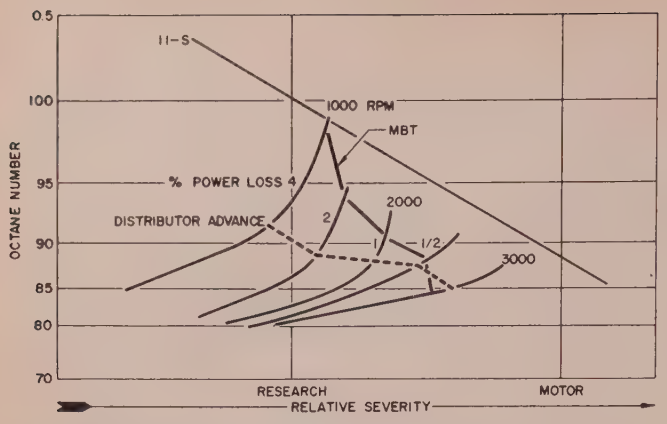

Fig. 15 – Reduction in fuel requirement for engine make D resulting from choice of distributor advance below that which results in best torque

Research Method rating of 91 in conjunction with a Motor Method rating of only 79. This combination is readily satisfied by most commercial fuels of 91 Research octane number.

If the basic timing is set at idle with the vacuum disconnected, as is standard procedure for most makes of automotive engines, a completely different fuel requirement will be obtained as is shown in Fig. 14. This figure indicates that a fuel of 89 Research and 83 Motor will be required to avoid knock with the lower-limit distributor. A fuel of 95 Research and 80 minimum Motor must be used to avoid knock with the upper-limit distributor. Figs. 13 and 14 indicate the necessity for determining the characteristics of the particular distributor being used in a knock-rating vehicle. They also indicate that the vehicle manufacturer should give very careful consideration both to the control of distributor tolerances and to the instructions for proper setting of distributor basic timing. Distributor tolerances and the method used for setting basic timing both markedly influence the knocking behavior of the engine.

Effect of Power Loss on Requirement – In Fig. 7 the distributor spark advance and the minimum spark advance for best torque were shown. The octane-number requirements for these spark-advance values have been transferred to the engine severity plot in Fig. 15. If the engine builder had decided to set the distributor to obtain maximum performance, the engine would have required a fuel of 100 Research octane number. This is illustrated by the 11-S fuel line. The distributor curve actually chosen results in a power loss of 4% at 1000, 2% at 1500, and essentially no loss from there up to 3000 rpm. These are all full-throttle values. By making this compromise on power, the fuel requirement is reduced by about 8 Research octane numbers. With a 92 Research octane number fuel, however, knock could be expected at high speed if the Motor Method octane number fell below about 82.

Effect of Basic Spark Advance on Requirement – By utilizing the information given in Fig. 7 relating spark advance, octane-number requirement, and distributor setting, the effects of basic-spark-advance changes on fuel requirements of the engine may be shown graphically as in Fig. 16. The standard distributor set at the manufacturer's basic recommended timing will follow the zero line as has been discussed. If the basic setting is retarded 4 deg the fuel requirement will follow the line "minus 4." If the basic setting is advanced 4 deg, the fuel requirement will follow the line "plus 4." With the Modified Uniontown technique the basic distributor setting might be advanced by 8 deg. Under these conditions the engine would knock at low speed on a fuel of 98 Research and 85 Motor. If retarded by 8 deg the engine would knock on any fuel lower than 83 Research and 83 Motor. For example, it would knock at high speed on fuel 4-S.

Relative Severity and Fuel Requirements of Engine Make A

It may be noted that a great deal of time has been spent in discussing the various attributes of engine make D. Data from this engine were chosen only to illustrate a few of the many factors which can be shown graphically. In Fig. 17 the same type of engine severity data are shown for a 1955 passenger-car engine make A. The fuel requirement resulting from the basic distributor setting chosen is approximately 90 Research, 79 Motor. Fig. 18 indicates that a power loss of approximately 1% was accepted from the minimum spark advance for best torque in order to drop the fuel requirements in the speed range below 2500 rpm. This engine at mbt would have required a fuel of 93 Research with normal fuel sensitivity (about 84 Motor). A saving of about 3 Research octane numbers was therefore achieved for a slight sacrifice in power in the low-speed range.

Relative Severity and Fuel Requirements of Engine Make B

Passenger-car engine make B shown in Fig. 19 is apparently satisfied with a fuel of about 84

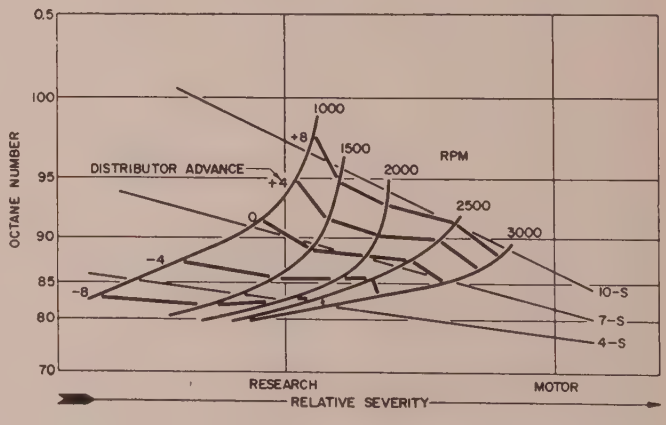

Fig. 16 – Effects of basic spark-advance changes on fuel requirements of engine make D

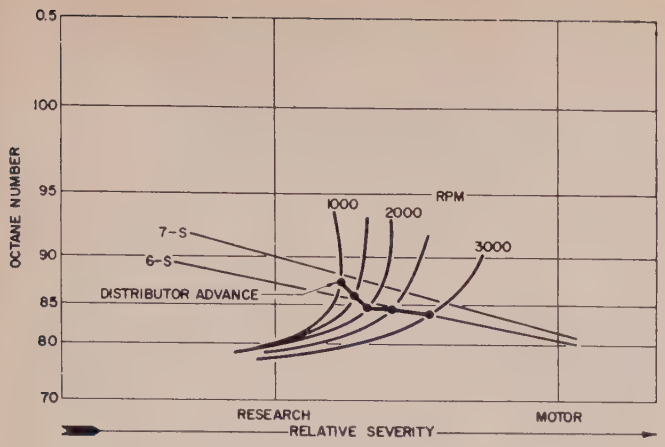

Fig. 17 – Engine make A fuel requirement at standard distributor spark advance

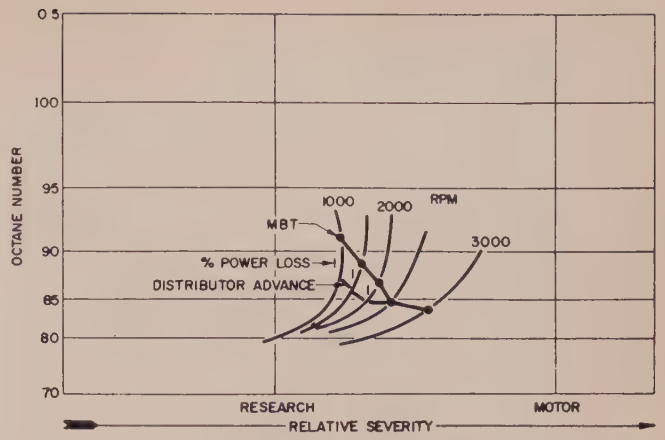

Fig. 18 – Reduction in fuel requirement for engine make A resulting from choice of distributor advance below that which results in best torque

Research and 80 Motor. The dynamometer data obtained on this engine indicated the fuel requirements shown in Fig. 20 at minimum spark advance for best torque. In choosing the distributor curve, power losses of 5% at 1000 rpm, 4% at 1500 rpm, and about 1% at the higher speeds were accepted. The fuel requirement for mbt in terms of a normally sensitive fuel would have been about 91 Research. This is not changed for higher fuel sensitivity since the Motor Method requirement at mbt is only 70. In this instance, the reduction in fuel requirement from mbt to the standard distributor curve amounts to 7 Research octane numbers.

Engine Dynamometer Ratings Compared to Road Ratings

There are several factors which must be considered when applying engine dynamometer calibration data to vehicles on the road. The calibration data discussed for passenger-car engines A, B, and D were obtained while operating at constant conditions after temperatures had reached equilibrium. On the chassis rolls or on the road, ratings are made during a series of level-road accelerations. Equilibrium temperatures are unlikely to be reached under these conditions. It would be expected that the temperature lag of combustion-chamber parts would favor higher fuel ratings or lower engine requirements under road-rating conditions. The engine on the dynamometer does not have the acoustical barriers such as normally exist to some degree in a passenger car. The effect of the general noise level on the ability of the operator to detect light knock is not well defined. During full-throttle accelerations on the road, the accelerator pump fuel slug modifies the fuel/air ratio obtained from the carburetor. This does not occur in the constant-speed dynamometer engine. The transient condition of the fuel-air mixture in the manifold during acceleration is most likely to affect knocking characteristics at the lowest speed at which full-throttle operation is permitted by the type of transmission installed on the particular make of vehicle. Few automatic transmissions will currently permit wide-open throttle below 1000 rpm, and the tendency is for the lowest full-throttle rpm to be increased with newer designs.

With these factors in mind, it is of interest to compare ratings of the "S" reference fuel series

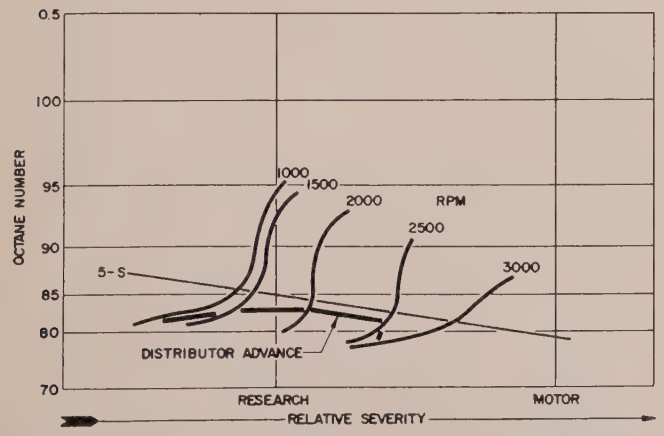

Fig. 19 – Engine make B fuel requirement at standard distributor spark advance

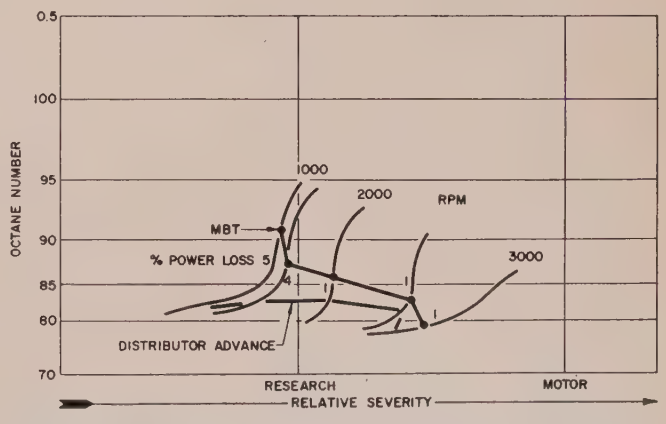

Fig. 20 – Reduction in fuel requirement for engine make B resulting from choice of distributor advance below that which results in best torque

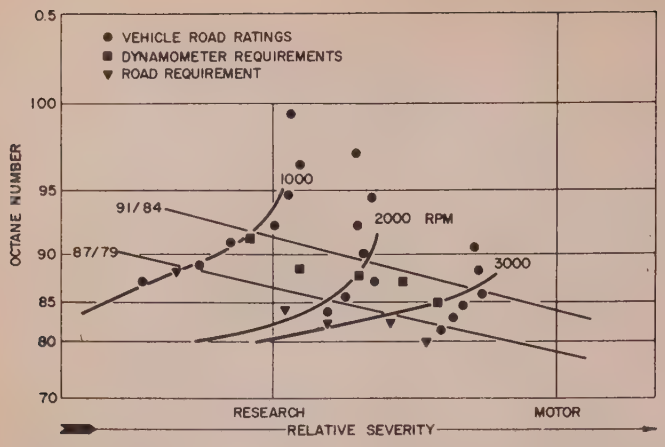

Fig. 21 – Comparison of sensitive reference fuel ratings and engine requirements of engine make D obtained on the engine dynamometer with those obtained on the road

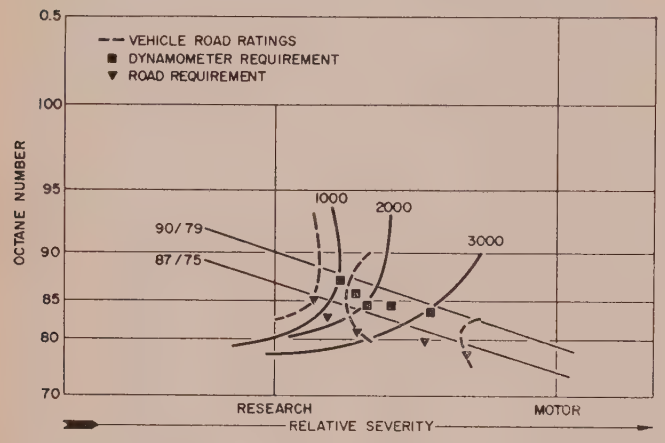

Fig. 22 – Comparison of sensitive reference fuel ratings and engine requirements of engine make A obtained on the engine dynamometer with those obtained on road

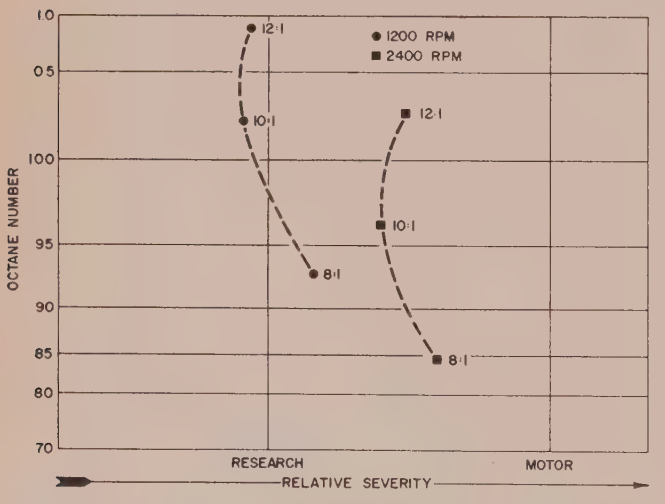

Fig. 23 – Effect of engine compression ratio and engine speed on engine severity and fuel requirement for a 36-cu in. single-cylinder engine; 100 F air temperature, 180 F jacket temperature, "S" fuels, minimum spark advance for best torque

Table 2 – Test Conditions for 36-Cu In. Single-Cylinder Engine

Cylinder Dimensions, in.	3¾ bore × 3¼ stroke
Compression Ratios	8/1, 10/1, 12/1
Engine Speeds, rpm	1200, 2400
Jacket Temperature, F	180
Intake Air Temperature, F	100
Fuel/Air Ratio	0.080

obtained in 1955 passenger car make D with the ratings obtained from the same make and model engine on the dynamometer. Fig. 21 shows that road ratings of each of the sensitive reference fuels were almost identical to those obtained on the dynamometer. The maximum difference was obtained at 3000 rpm on the lowest "S" reference fuels. Since the relative engine severity is essentially unchanged, it is somewhat surprising that the dynamometer engine requirement is higher by three to four octane numbers for the standard distributor spark advance. In this figure the squares and the triangles at any one engine speed represent the same spark advance in degrees btc. On the road 88 octane primary reference fuel knocked at 9 deg btc while it required 91 octane to permit the same 9 deg advance on the dynamometer engine. The same tendency for primary reference fuels and "S" reference fuels to knock at lower spark advance in the constant-speed dynamometer engine continues to hold at the higher engine speeds.

A similar comparison is made in Fig. 22 for 1955 passenger-car engine A. Again the agreement is good for actual fuel ratings of the "S" reference fuels. In this engine the fuel requirement indicated by the dynamometer engine is again about three to four octane numbers higher than the requirement obtained in the road vehicle tests.

Effects of Compression Ratio on Severity

The effect of compression-ratio change on engine severity has been the subject of considerable conjecture. In those cases in which vehicle engines have been increased in compression ratio, some decrease in severity has been indicated. However, considerable study would be required to separate the change due to compression-ratio increase from the changes due to volumetric-efficiency increase, compromises in distributor settings, and cooling changes in the cylinder head and jacket. In order to obtain a more independent study of compression ratio as such, a 36-cu in. single-cylinder engine having a combustion chamber similar to the Oldsmobile was operated at two different speeds under carefully controlled conditions which are indicated in Table 2. Three different compression ratios were used, and the same cylinder head was used by milling first to obtain a change from 8/1 to 10/1 and finally to 12/1. The results of these tests are shown in Fig. 23. At each compression ratio and test speed a series of "S" reference fuels were rated in terms of primary reference fuels by changing

Table 3 – Test Conditions for 27-Cu In. Single-Cylinder Engine

Cylinder Dimensions, in.	3¼ bore × 3¼ stroke
Compression Ratio	7/1
Engine Speeds, rpm	1200
Jacket Temperature, F	150 and 250
Intake Air Temperature, F	150 and 250
Fuel/Air Ratio	0.080

spark advance, while the absolute manifold pressure was maintained at 28 in. of Hg. The points shown in this figure indicate the fuel requirements at the minimum spark advance for best torque.

Fig. 23 indicates that changing compression ratio from 8 to 10 to 12 resulted in no significant change in relative severity. A fuel quality increase of 10 to 12 Performance Numbers for each compression ratio was required. Since both the Research Method and the Motor Method engines rate fuels by varying the compression ratio and since these methods were arbitrarily used as a basis for measuring relative severity, it might be expected that varying the compression ratio of the third engine would have a parallel effect on severity.

Effect of Cylinder Air Density on Severity

The effect of changing cylinder air density by opening or closing the throttle of a 1951 passenger-car engine make F on sensitive fuel ratings is shown in Fig. 24. This engine was also operated on the dynamometer. In these tests, both fuel/air ratio and spark advance were adjusted to maintain maximum power for each fuel rating. Various blends of diisobutylene and n-heptane were rated in terms of primary reference fuels by opening the throttle just sufficiently to obtain knock. In this figure it will be noted that increasing the air density decreases engine severity relative to the Research and Motor Methods. The very marked effect of engine speed on engine severity is again indicated.

In order to study further the effect of increased cylinder air density on relative engine severity, a 27-cu in. single-cylinder engine was operated on various blends of diisobutylene in n-heptane. Two test conditions, both at 1200 rpm were chosen. These conditions are given in Table 3. This engine was equipped with a jacketed inlet manifold through which cylinder jacket water was circulated. For convenience, the cylinder jacket temperature, inlet manifold temperature, and intake air temperature were maintained at the same values. Controlling in this manner also tended to insure that the temperature of the mixture entering the inlet port was reasonably close to the controlled value. Fig. 25 indicates that at 250 F the engine was quite severe. Fuel ratings were almost identical to the 3600-rpm ratings obtained in passenger-car engine make F. At 150 F the ratings are almost identical to those obtained at 1000 rpm in passenger-car engine make F. At both conditions, increasing charge density results in relatively higher ratings on sensitive fuels, indicating again that increasing cylinder charge density decreases relative engine severity.

Fuel Requirements of Four 1955 Passenger Cars

It is unlikely that one make of vehicle will determine both octane number level and fuel sensitivity for a commercial fuel. The fuel requirements at standard distributor timing for four 1955 passenger cars have been shown in Fig. 26. The fuel sensitivity line shown is 95.8 Research and 86 Motor. This line represents the weighted average premium fuel quality sold in the United States in midsummer of this year. The two cars, makes E and Q taken together, appear to limit both Research octane number level and fuel sensitivity. With the average quality fuel shown it is likely

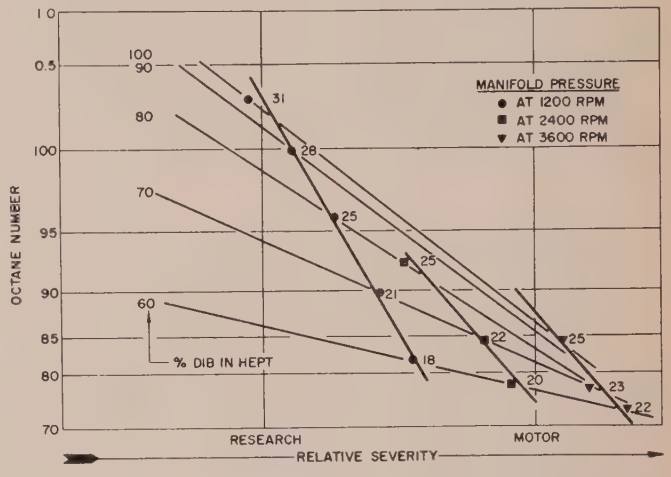

Fig. 24 – Effect of changing absolute manifold pressure and engine speed on engine severity and fuel requirement for engine make F at 8/1 compression ratio

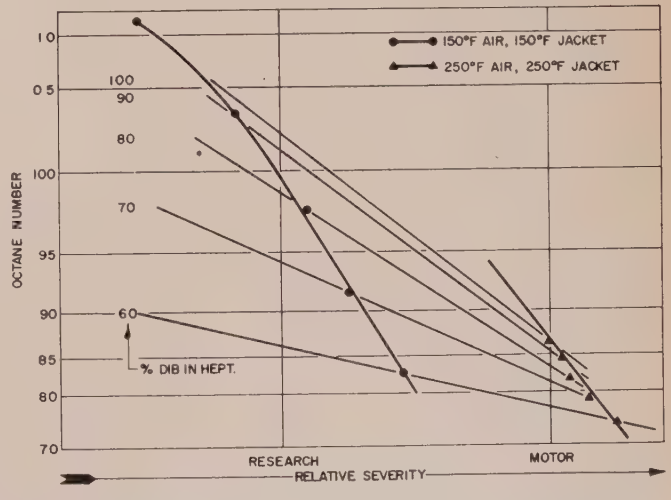

Fig. 25 – Effect of intake manifold pressure and engine temperatures on engine severity and fuel requirement; 27-cu in. engine, 7.2/1 compression ratio, 0.080 fuel/air ratio, 1200 rpm

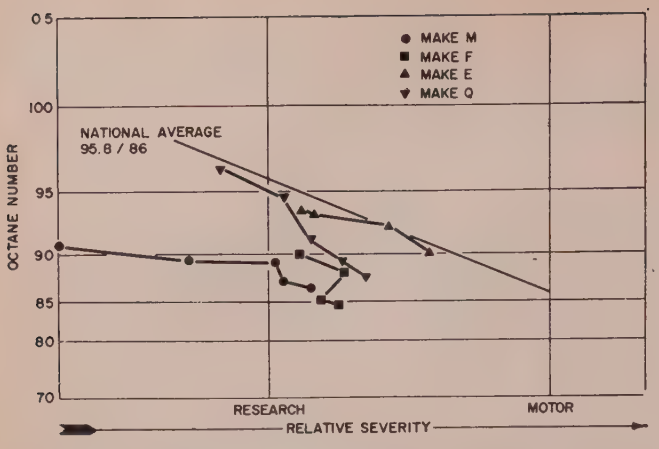

Fig. 26 – Fuel requirements at standard distributor timing for four 1955 passenger cars at normal operating speeds

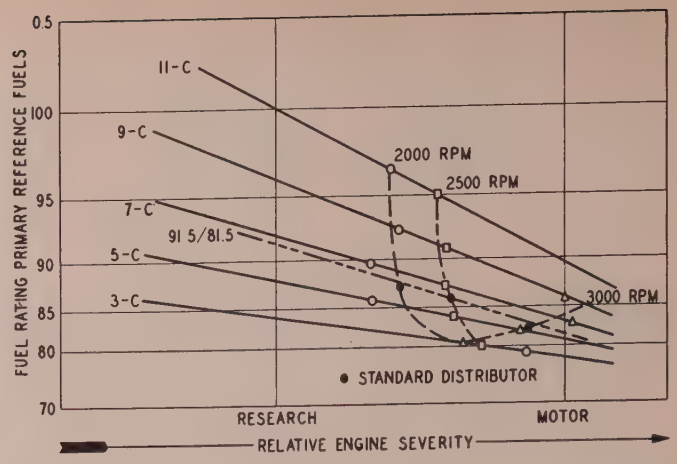

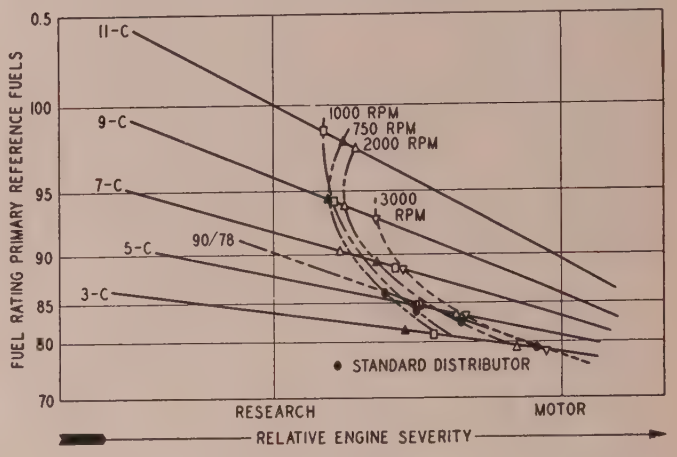

Fig. A (upper) – Knock behavior and fuel requirement for 1955 car make DA

Fig. B (lower) – Knock behavior and fuel requirement for 1955 car make DM

that knocking complaints would be received on make E. If the Research octane number is held constant and Motor Method quality is increased, engine make Q will knock at low speed (1000 to 1500 rpm). If the Research quality is held constant and the Motor Method quality is decreased, engine make E will knock at high speed (2500 to 3000 rpm).

Conclusions

It may be said that the general concept of the nomographic approach was first published by Dr. W. J. Sweeney.[6] Dr. Sweeney, however, did not propose that ratings of sensitive fuels be used to relate the knocking behavior of engines.

There are many other ways in which relative engine severity can be calculated or plotted, and other fuel measuring or numbering scales can be used. It is possible to apply relative severity numbers to the engines. None of these alternative methods appears to give a clearer representation of either engine or fuel behavior, and none is easier to use.

The authors have established the basic engine severity pattern for a given knock-rating vehicle engine and from this have predicted the ratings of a group of test fuels in the same engine. The Research octane number and Motor octane number must, of course, be known for the test fuels. The authors believe that predicted ratings for the majority of the fuels have about the same accuracy as vehicle test-fuel knock ratings which are obtained with average precision. This experience has indicated that an occasional fuel blend will rate consistently higher or lower than would have been predicted. No specific illustration of fuel-rating prediction has been included in this paper.

It is important that the refiner know by actual tests which stocks give better results in critical vehicle makes than would be indicated by the relative severity graphs. It is believed that the best dividends are obtained when these graphs are used concurrently with the execution of knock-rating programs. Used at this time, any change in the engine behavior becomes immediately apparent when check fuels are rerun. This concurrent use also permits immediate rechecks of fuels which give higher or lower ratings than might be expected.

The results of the studies substantiate the use of automotive engines mounted on dynamometers for fuel ratings as a valuable supplement to the use of knock-rating vehicles. It is indicated that the severity of one engine can be compared with the severity of other engines just as the ratings of one fuel can be compared with the ratings of other fuels. The application of the graphic method to the study of speed, spark advance, cylinder air density, compression ratio, and temperatures has been demonstrated. Many other engine variables are subject to study in this same manner.

Passenger-car engine fuels are rapidly approaching the 100-octane level. Since this paper has dealt with the general subject of fuel sensitivity and engine severity, it seems appropriate to borrow a

[6] See *Petroleum Refiner*, Vol. 23, October, 1944, pp. 383-387: "Relation of Aviation Fuel Quality to Engine Performance," by Dr. W. J. Sweeney.

concluding paragraph from a paper[7] presented almost ten years ago.

"In conclusion, it may be remarked that if all fuels had the same temperature sensitivity there would be no performance-number (or octane-number) controversy either technical or commercial. Alternatively, if all engines had equal severity there would be no octane-number controversy, and an accurate rating in any one engine would be valid for all engines with, of course, the proviso that fuel distribution effects within the fuel-air induction system of multicylinder engines would modify the validity of this one rating."

Acknowledgments

Many of the ideas incorporated in this paper were undoubtedly obtained during discussions with those of you who have pondered the multiplicity of octane numbers which may be obtained on a single sensitive test fuel. The authors are indebted to many of their colleagues in the Ethyl Corp. Research Laboratories for a considerable amount of the data used in this paper. They are particularly indebted to A. E. Felt and H. A. Toulmin for constructive criticism and suggestions.

DISCUSSION

Lab Results Will Never Agree with Road Ratings

– J. B. Duckworth
Standard Oil Co. of Indiana

ONE phase of this paper that appeals to me greatly is the recognition of the significance of engine design factors and operating conditions on fuel ratings.

The paper demonstrates that there is no single number which will adequately express road antiknock performance. This in itself serves to emphasize the futility of developing a single laboratory engine test method which will correlate with fuel ratings on the road.

Use of Other Test Fuels Effects Engine Severity Results

– Harold M. Trimble
Phillips Petroleum Co.

WHILE this idea for describing the knocking behavior of engines with fuels has been discussed in committee circles, it was surprising how little of the available data were directly applicable to a discussion of this paper. As a result, I called upon friends in du Pont and American Motors for permission to use some of their data to supplement our own for this discussion.

The bulk of the authors' data are concentrated on engine make D, so it seemed advisable to concentrate on data obtained on this make. In the studies I will discuss, the data were obtained on the road and with a different series of fuels than were used by the authors. The results obtained in one car equipped with engine make D are shown in Fig. A. This car was equipped with an automatic transmission. It will be noted that the points do not fit the curves as closely as they did for the authors, but it should be remembered that these data were obtained on the road where the same conditions throughout a complete test are more difficult to attain than on a test stand. However, none of the points deviates by more than one octane number from the corresponding speed line. The more important thing seems to be that the 2000- and 2500-rpm lines are more perpendicular and slope to the right instead of the left as they do in the authors' studies (see Fig. 11). It will be noted that the fuel requirement I have indicated for this car is similar, though, to that indicated by the authors for this engine make in their Fig. 21. In their figure they indicated a requirement of 91/84 on the dynamometer and 87/79 on the road. While my requirement of 91.5/81.5 indicates a more sensitive fuel is required, this is true only on the basis of making the maximum use of the fuel, as a fuel with a 90/83 rating will also satisfy the distributor requirements shown.

Now let us look at another car equipped with this same make of engine. This car had a manual transmission, and the data obtained are shown in Fig. B. The points again are all within one octane number of the lines. The various speed lines this time are all bunched quite closely together and again slope to the right instead of the left. The requirement again indicates a more sensitive fuel but at about the same level as indicated by the authors. In this case this sensitivity could also be reduced by giving away octane number

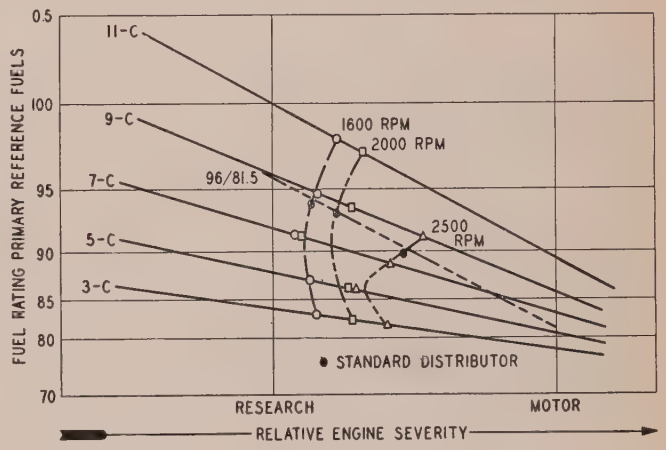

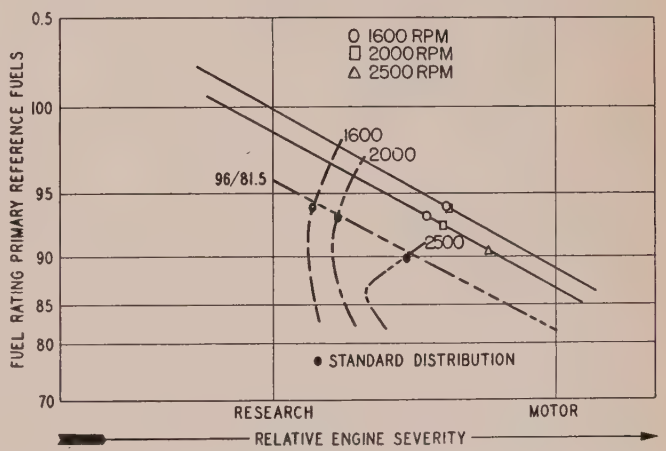

Fig. C (upper) – Knock behavior and fuel requirement for 1955 car make MA

Fig. D (lower) – Knock behavior and fuel requirement for 1955 car make MA

[7] See SAE Transactions, Vol. 54, 1946, pp. 511-512: "Fuel Sensitivity and Engine Severity in Aircraft Engines," by S. D. Heron.

at the higher speeds. The distributor requirements shown indicate fuels with 89/81 and 88/83 ratings would also be satisfactory. These data plots do raise some questions that I would like to pose to the authors. In their work and studies on this idea, have they encountered this wide variation in the speed lines for various engines of the same make? Do they have an explanation of it? Do they have any idea of the significance of the variation?

In studying this idea further, we analyzed the data from another car with a different make of engine. The results are shown in Fig. C. In general, the points fit the speed lines very well with the lower-speed lines being essentially vertical. Now in this car we also tested two different fuels not related to the series of fuels on which the speed lines in Fig. C were developed. In Fig. D, the speed lines from Fig. C have been reproduced and the data on the two new fuels added. It will be noted that the points for the various speeds have moved considerably to the right of their respective speed lines. These same two fuels were also tested in the first two cars, so in Fig. E I have shown the speed lines for car DA from Fig. A and the data for the two new fuels. Again the points have shifted to the right of the speed lines except in the case of the 3000-rpm speed. In Fig. F, the same treatment has been given car DM, and again most of the points have shifted to the right with the only exception being the 750-rpm point on the lower-rating fuel. This raises some more questions for the authors. Have they had any indications that different series of fuels give different speed lines? If so, how does this affect the fuel requirements as determined from the standard distributor requirements? If not, do they have any idea as to an explanation of these data or their significance?

Give Nomograph Representation Of Military Engine Data

– Dale E. Woomert and Charles F. Schwarz
Aberdeen Proving Ground

AT Aberdeen, we are primarily concerned with the octane rating of engines and not the rating of fuels. The procedure generally followed is to check only that spark setting specified by the manufacturer. Successively lower octane fuels (primary and severity reference fuels) are flowed until one is found that causes a given knock level. By this method, it is not possible to plot in the exact manner presented by the authors, but by interpolating fuels the engine requirement curve can be plotted on the nomograph.

Since 1951 many tests on a wide variety of engines and engine-vehicle combinations have been conducted by this laboratory. These covered the full range of military vehicles

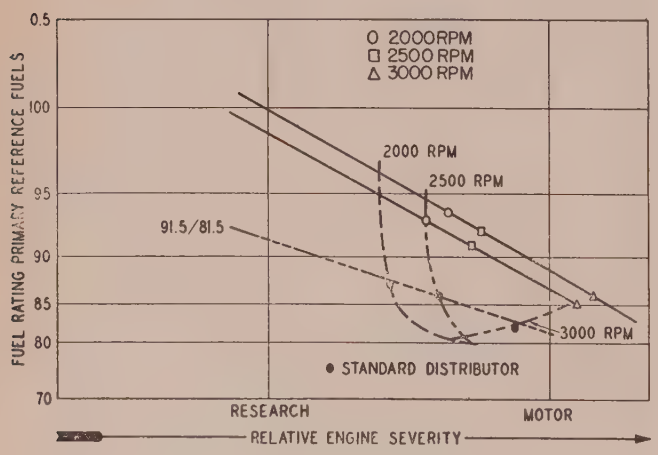

Fig. E – Knock behavior and fuel requirement for 1955 car make DA

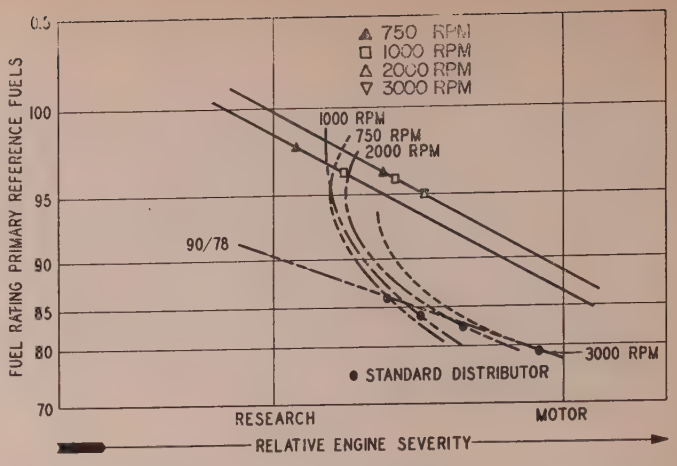

Fig. F – Knock behavior and fuel requirement for 1955 car make DM

and to some extent may be indicative of the octane pattern for commercial trucks.

The plots for these engines, shown in Figs. G and H, do not in any way resemble those obtained by the authors; fish-hooks and loops are quite common. However, this does not impair the use of the nomograph for evaluating the engine and fuel. Without exception, the engines tested had a straight centrifugal ignition advance. The lack of vacuum advance undoubtedly accounts for some of the difference in the shape of the curves. The loops and fish-hooks are a result of the engines' having their maximum rating approximately at the midpoint of the speed range.

We believe the nomographic method to be the best means yet suggested for presenting octane data and that it is equally valuable to the engine engineer and petroleum engineer. The possibility of a third method of rating fuels, supplementing or replacing the current Motor and Research Methods, seems to lead only to confusion. It is possible that adopting this nomographic method of presenting data might eliminate this need for new test methods.

In the work described by the authors, an attempt was made to compare data obtained on a dynamometer stand with those obtained in the field. A great many of the tests conducted at Aberdeen Proving Ground were engine calibrations, that is, the engine was power checked and octane rated on the test stand and then installed in the vehicle for field tests. These data show that the test-stand operation is more severe than acceleration tests, the difference being in the order of 3 octane numbers. This fact, of which I am sure the authors are well aware, should be emphasized: The spread of octane numbers between two engines of the same model would probably mask any correlation between test stand and field tests. It has been shown by many investigators that this spread may be 3 to 15 octane numbers for passenger cars, and data from this laboratory show it to be 4 to 11 octane numbers for military vehicles.

Asks About Spark-Advance Effect on Octane Number

– Charles S. Gilbert, Jr.
Sun Oil Co.

FROM the curves presented in this paper, it would appear that advancing the distributor settings from manufacturer's recommendations to mbt resulted in an engine appetite (octane requirement through the speed range) for a fuel of greater sensitivity (Research minus Motor rating). Conversely, as the spark was retarded from mbt to manu-

• 134.2 cu. in. displacement, 7.4 compression ratio, 4 cylinder
× 141.5 cu. in. displacement, 7.5 compression ratio, 4 cylinder
△ 302 cu. in. displacement, 7.2 compression ratio, 6 cylinder
⊙ 531 cu. in. displacement, 7.6 compression ratio, 6 cylinder
⊡ 844 cu. in. displacement, 6.7 compression ratio, 8 cylinder

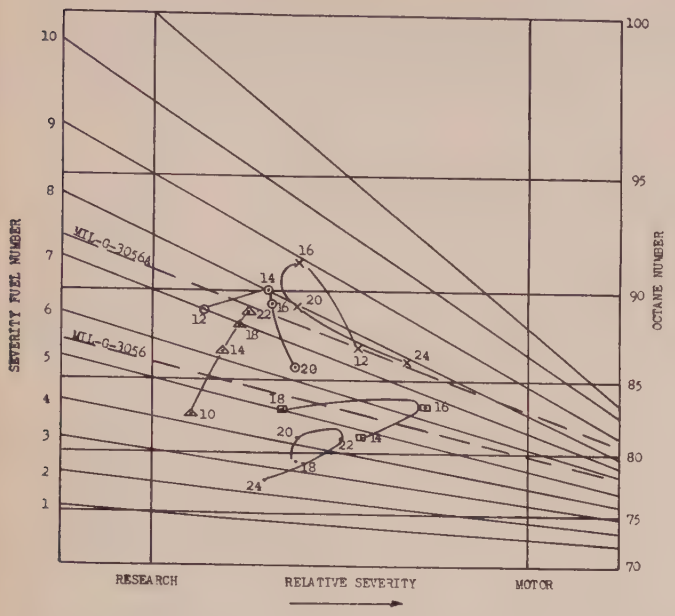

Fig. G – Maximum octane requirement with manufacturer's specified ignition timing; numbers on curves indicate engine speed in rpm/100

× 1790 cu. in. displacement, 6.5 compression ratio, 12 cylinder
⊙ 895 cu. in. displacement, 5.5 compression ratio, 6 cylinder, supercharged

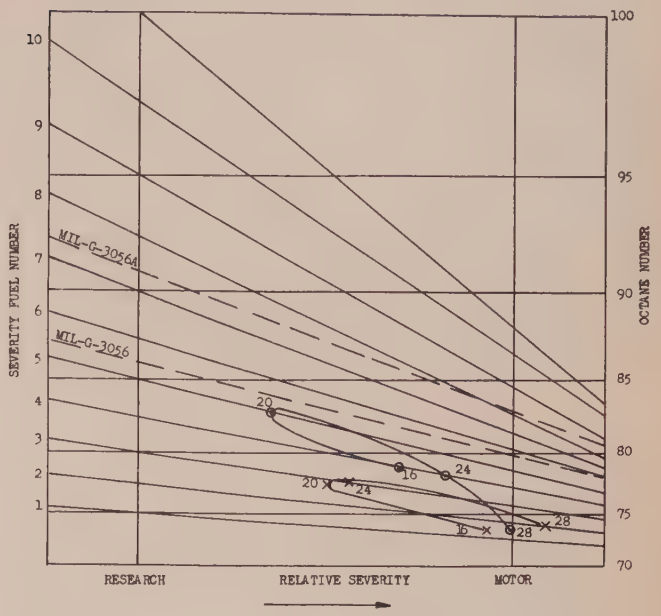

Fig. H – Maximum octane requirement with manufacturer's specified ignition timing; numbers on curves indicate engine speed in rpm/100

facturer's specification, the curve seemed to indicate an appetite for a fuel of lower sensitivity.

Am I correct, therefore, in interpreting the data to show that advancing the spark to mbt results in the engine's being more appreciative of the sensitive-type fuels?

Discusses Density, Temperature, And Time Exposure Factors

– Otto Enoch
Ford Motor Co.

WE think the Ethyl nomograph presents one of the best methods which have yet been published to show the relationships of engine octane requirement, fuel sensitivity, and engine severity in a single graph. We certainly need a good picture of these relationships, because fuel sensitivity and engine reaction to fuel sensitivity have become increasingly important in evaluating knock-limited engine performance.

We have plotted some of our road-test data in such a nomograph (see Fig. I). It shows octane requirements and, at the same time, fuel ratings for some full-boiling-range sensitive reference fuels for two engines at various speeds. We see how the octane requirements as well as the fuel octane ratings decrease at higher speeds and how the "relative severity" moves towards the F-2 abscissa. It is an excellent picture. However, we believe the authors will agree with us that this nomograph is still not the last answer to the questions involved. In particular it seems to us that engine "severity" needs a more accurate definition.

We can better show what we mean in a D-T (density-temperature) diagram as known from publications by Rothrock, Siegel, and others (see Fig. J). A fuel is supposed to autoignite under various end-gas density-temperature conditions along a definite density versus temperature curve. It will autoignite at high-density, low-temperature,

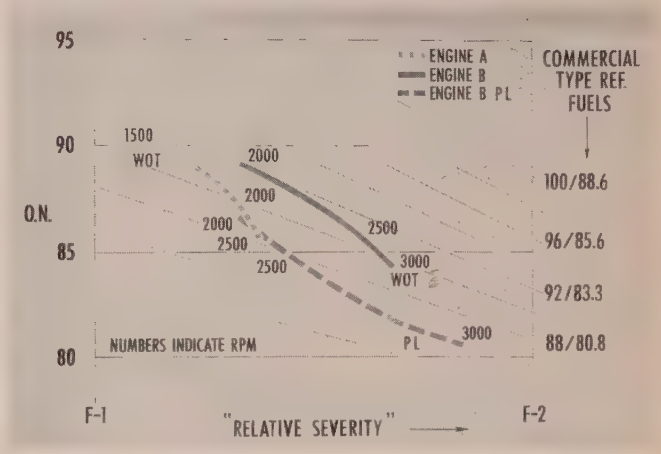

Fig. I – Octane requirements and fuel ratings for some full-boiling-range reference fuels in two engines at various speeds

and also at low-density, high-temperature conditions of the end gas. The latter conditions we use to define more "severe" conditions. Fuel A in our graph might represent a primary reference fuel mix, fuel B a more sensitive fuel type, as indicated by the sharper drop of its autoignition curve. Each curve divides the density-temperature field into two regions, the region above the curve in which the fuel will autoignite (knock) and the region below the curve in which the fuel will not knock.

The graph also shows two lines which indicate the gas density-temperature combinations of the CFR engine at F-1 and F-2 operation conditions. At the density-temperature condition at which the two fuel curves intersect, both fuels are on the verge of autoignition. Since fuel A is a primary reference fuel mix, we can say that at its intersection with fuel B it represents the octane rating of fuel B. Furthermore, the location of the intersection relative to the F-1 and

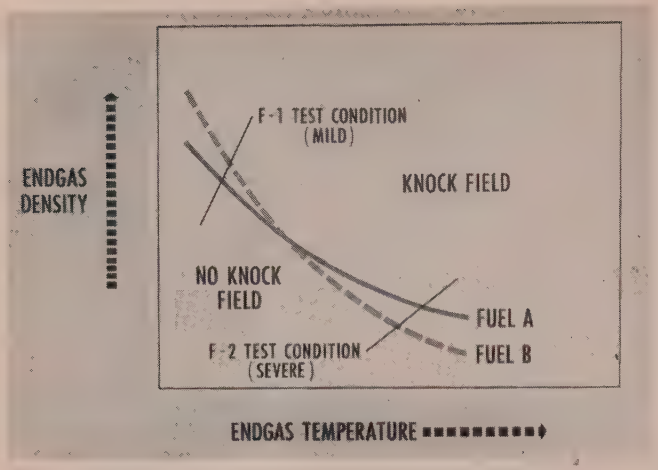

Fig. J – Fuel D-T borderline knock curves with fuel B more sensitive than fuel A

F-2 lines represents the "relative severity" as defined by the Ethyl nomograph. Thus, "relative severity" could be defined as a **definite** point in the end-gas density-temperature field if each fuel has a **definite** autoignition curve in this field.

However, this definite-point-and-curve concept might not be quite true. A number of researchers have shown that precombustion reactions have a significant effect on the autoignition tendency of a fuel, and that not only end-gas density and temperature but also the **time element** during which the fuel is exposed to density and temperature can greatly affect the total combustion mechanism and, thus, the autoignition tendency of the fuel. If the time factor is important, it could mean that curves A and B do not intersect or that they do intersect at another point in the D-T field if the data are obtained in another engine or at other operating conditions for which the time factor involved has a different magnitude. Fuel ratings as well as "relative severity" might change, which could mean that for the same fuel rating in two engines the "relative severity" might be different, or that for the same "relative severity" the fuel ratings might differ.

When sometime in the future we will be able to pick up end-gas density, temperature, and time of fuel exposure, we might be in the position to define more accurately engine severity conditions as affecting fuel ratings by three- instead of two-dimensional plots of autoignition D-T graphs or Ethyl nomographs.

We bring these questions into the discussion without being able to offer a satisfactory solution at the present time.

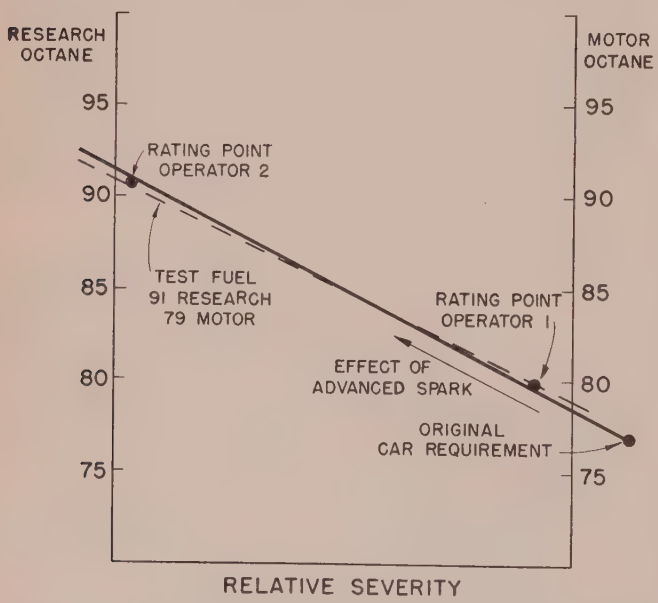

Fig. K – Precision of Modified Uniontown road ratings for car make A

Authors' Method Explains An Apparent Discrepancy

– G. W. Pusack
Socony Mobil Oil Co., Inc.

AS the result of working extensively with the type of severity analysis presented by these authors, I would like to emphasize the great utility of this method of analysis in systematizing results obtained on fuels and engines. In our experience we have also found discrepancies with various types of fuels, as pointed out by other discussers. We believe, however, that in trying to determine the source of these discrepancies one can learn a great deal about the performance of a fuel. To illustrate the value of this technique, I would like to relate an unusual occurrence which was not explained until this severity analysis was brought to bear on the problem.

Several years ago, while rating a certain test fuel by the Modified Uniontown Method, we discovered a discrepancy of approximately 11 octane numbers between two operators in the rating of this fuel in one car. Check tests substantiated the original results that each operator obtained. By use of this severity analysis a much greater understanding was obtained of conditions which were being obtained on the road. It was found that the test car had a normal octane-number requirement and severity very close to the Motor Method engine and only slightly below that of the Motor octane rating of the test fuel (see Fig. K). In advancing the spark to make this test fuel knock, it was found that the test-engine severity moved toward that of the Research engine. Similar to the authors' diagram for a sensitive fuel, the rating of the test fuel likewise increased at approximately the same rate. Eventually both operators advanced the spark enough to cause the requirement of the car to exceed the quality of the fuel, resulting in trace knock. One operator, however, who could not detect knock at quite as low a level as the other operator, found he had to advance the spark considerably more. As a result, the fuel was found to have a much higher rating since the rating point was found to be much closer to the severity of the Research engine.

While this is a peculiar and unusual instance, it was chosen as being illustrative of the powerful tool that this severity analysis has turned out to be. I would recommend strongly that anyone associated with fuel and engine octane performance acquaint themselves intimately with this analysis technique. Mr. Kerley and Mr. Thurston should be thanked for making this information available to the petroleum and automotive industries in general.

Authors' Closure To Discussion

THE authors appreciate the interest shown by all the discussers. We are in complete agreement with Mr. Duckworth's statement that no single laboratory engine test method can be expected to correlate with fuel ratings on the road. It is our belief that reasonable fuel quality control can be achieved by using both the Motor Method and Research Method engines. Further development of quality control

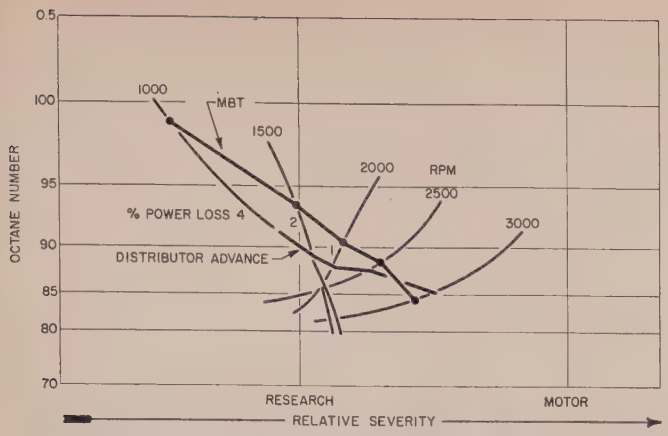

Fig. L – Severity pattern for engine make D, established by ratings of 1954 "C" series CRC full-boiling-range fuels, differs from that shown in Fig. 10

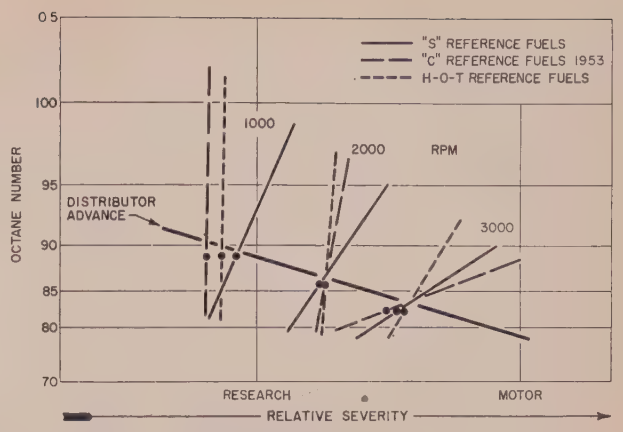

Fig. M – Differences in severity patterns established by ratings of three series of sensitive reference fuels in 1953 passenger car of make Q

methods, including equipment, should be directed toward more accurate and more reproducible ratings. This development is particularly urgent in the range above 100 octane number.

The authors are indebted to Mr. Trimble for his very pertinent discussion. The choice of a different group of sensitive fuels does change the appearance of the engine behavior graphs.

The degree to which this behavior pattern may be changed is illustrated in Fig. L showing the engine severity for passenger-car engine make D which was obtained using the 1954 CRC full-boiling range "C" series fuels. Since these ratings were made in the same dynamometer engine, Fig. L and Fig. 12 are directly comparable. The contrast is quite great. The converging engine severity lines in the lower-octane-number range, using "C" series fuels, has been noted for many different makes of engines. It has been suspected that this may be due partially to the fact that all three blending gasolines are not used in each fuel of the "C" series.

Engine severity lines were determined in one 1953 vehicle, make Q, for three different series of sensitive fuels. These three series included the CRC 1953 full-boiling-range fuels, the CRC "S" series, and a series composed of blends of n-heptane, isooctane, and toluene (H-O-T series). The three groups of engine severity lines are shown in Fig. M. It is interesting that the same fuel-requirement line is obtained at standard distributor setting regardless of which sensitive fuel series is chosen. This is not necessarily significant, since the divergence of the three lines for the high-spark-advance ratings indicates that fuel quality requirement for mbt might be quite different for the three series of fuels.

Tests of the "S" reference fuel series, the H-O-T series, and the 1953 "C" series were run in a 36-cu in. single-cylinder laboratory engine equipped with a hemispherical combustion chamber. The results indicated only slight differences in the engine severity lines obtained, although comparisons were made at fuel/air ratios from 0.070 to 0.10 for each fuel.

The authors prefer the use of the "S" reference fuel series or the heptane-octane-toluene series for comparing engine makes and models. This is due to the fact that all the components have similar boiling points and each cylinder is likely to have the same proportion of each component though fuel/air ratios may be different from cylinder to cylinder. Preference is given to these two series for the additional reason that they can be reproduced from year to year.

The authors believe that some passenger-car fuel-rating problems do relate to distribution characteristics. These problems might be better understood if more single-cylinder laboratory engine tests were used to explore fuel behavior.

Mr. Gilbert's question is in reference to Figs. 15, 18, and 20. In each of these figures an advance in spark would result in an increase in octane requirement. Since movement of ratings to the right indicates **increased** engine severity, engine make D, Fig. 15, increases in severity as spark is advanced from the normal distributor setting to mbt at all speeds except 3000 rpm. This increase in severity is particularly marked at 1000 rpm. Engine make A, Fig. 18, increases in octane-number requirement with no real change in severity as spark is advanced to mbt. Engine make B, Fig. 20, increases in severity at all speeds except 2000 rpm as spark is advanced to mbt.

For all three of these engines, advancing the spark to mbt increases the octane-number requirement at low speed much more than at high speed. This would be expected because the standard distributor setting on these engines was at or near mbt at the higher speeds. If mbt spark advance is used at all speeds, all three engines would utilize very sensitive fuels, but the Research rating of these fuels would be very high.

We have attempted to answer Mr. Gilbert's question without using the term "appreciate" since "appreciate" is commonly used to indicate that a passenger-car engine rates fuels higher than the Research Method rating.

We wish to thank Mr. Enoch for his discussion of the temperature-density-time relationship. We are in agreement with Mr. Enoch that some absolute scale for measurement of fuel and engine knocking behavior is desirable. Numerous attempts have been made to measure the effects on fuel ratings of engine variables such as spark advance, engine speed, coolant temperatures, absolute manifold pressure, and compression ratio in terms of another engine variable such as inlet air temperature or inlet mixture temperature. While a large amount of useful information has been obtained, it may also be added that these measurements have left much to be desired.

Changes in combustion-chamber shape which result in less spark advance being required to obtain maximum power generally result in higher ratings on sensitive fuels. Because of this, we believe that the residence time of the charge in the combustion chamber is quite important. When it becomes possible to make simultaneous records of end-gas temperatures, densities, and residence time, the complex relationship may be more clearly defined.

In closing, we again wish to emphasize that all fuel blends having the same Motor Method and the same Research Method ratings do not always behave in the same manner in a multicylinder engine. Further investigations are required to indicate why this is true. Comparisons of fuel ratings in a carbureted engine with the ratings of the same fuels in the same engine equipped with a proper fuel injection system should indicate whether cylinder-to-cylinder distribution of antiknock components can explain this discrepancy.

Flight Research at High Altitudes with Rocket-

AS ALMOST everyone knows, the research airplane program has been under way since late in 1944, when contracts were let for the X-1 and D-558-I airplanes. These airplanes were built at a time when model test facilities could not furnish information in the transonic speed range. They were built to bridge the gap in the research information available. The X-1, as is well known, was the first airplane to accomplish flight in excess of Mach number 1 in October, 1947. With the success of these airplanes, additional airplanes were manufactured for the series, either to increase speed range available for tests, or to check generalized configurations. The research airplanes have included the X-1 through the X-5 and XF-92A, which were contracted for by the Air Force, and the D-558-I and D-558-II, contracted for by the Navy. The X-1 series actually involves three different series of airplanes, the original X-1 series, the X-1A, B, and D series, and the X-1E. The discussion in this paper will be limited to the rocket-propelled airplanes of the group. It is with these airplanes that we have made the large advances in Mach number and altitude. The other machines, powered by turbojets, were for the most part capable of supersonic flight. However, they have not reached the extensive performance that the rocket-propelled airplanes have.

Planes Used in Program

Fig. 1 shows three of the rocket research airplanes which are being used in the program. The airplane on the left is the X-1B airplane. This machine is basically the same as the original X-1 series with the 8% thick wing, except that it has a longer fuselage with higher fuel capacity, which gives greater performance, and a more normal cockpit canopy. This type of airplane has been flown to Mach numbers approaching 2½, and to altitudes in excess of 90,000 ft.

The center airplane is the D-558-II. Two versions of this airplane have been used in the program, one with both a turbojet engine and rocket power, and the other an all-rocket version. The all-rocket version, the fastest of the two, is shown in the photograph. This airplane has a swept-back wing and swept-back tail surfaces. This machine was the first to reach a Mach number of 2, and at one time held an altitude record of 82,000 ft.

The airplane at the right is the X-1E. This is

and High Speeds

Propelled Research Airplanes

Walter C. Williams, National Advisory Committee for Aeronautics

This paper was presented at the SAE Golden Anniversary Aeronautic Meeting, Los Angeles, Oct. 14, 1955.

actually one of the original X-1 airplanes, but now has a modified fuel system, a new cockpit arrangement, and a wing which has a thickness of only 4%.

The X-2, which is not shown, is another one of the rocket-propelled airplanes. It has swept-back wing and tail surfaces. It has higher performance capabilities than the airplanes shown. It differs from these machines primarily in that it has a stainless-steel structure, rather than aluminum alloy. This airplane is at present undergoing demonstration by the manufacturer, Bell Aircraft Corp. All these machines are launched from the B-29 or B-50-type mother ships, conserving all the rocket fuel for test work at altitude and not consuming it in climbing from the ground to 35,000 ft. In addition, the air-launch method offers a very important safety factor. The air-launch system was originated by Bell Aircraft for the X-1, and resulted in further exploitation of the D-558-II, which was originally a ground take-off machine. The X-2 is also air-launched.

Exploratory Program

Of course, one of the basic aims of the program

AMONG outstanding problems facing designers of high-speed, high-altitude planes, the author says, are:

1. Deterioration of directional stability with Mach number.

2. Loss in damping and increase in airplane natural period with altitude.

3. Coupling of effects of inertia and aerodynamic characteristics of planes.

4. Aerodynamic heating.

These and many other specific problems are being investigated in the 12-year-old program reported here. Its value, the author feels, lies chiefly in the confidence it gives designers and operators of high-speed planes, the backlog of data it builds up for use in future investigations, and the added focus it lends to the work of research scientists in the field.

Fig. 1 – X-1B, X-1E, and D-558-II rocket research airplanes

is the exploration and exploitation of the maximum performance capabilities of these airplanes. This phase of the program has led to one of the more important results of the program which is the confidence given by knowledge of repeated flight in the speed regime that will be entered by our new operational airplanes. I might add that this phase of the program is always the most interesting to those directly concerned. The first step in this direction, of course, was Major Yeager's first supersonic flight back in 1947, showing that supersonic flight was feasible. These limits, of course, have been stretched from his original flight slightly in excess of Mach number 1 through Mach number 2 with the D-558-II, and on up to almost 2.5 with the X-1A. The altitude range in the same manner has been stretched from the order of 50,000 to 60,000 ft to in excess of 90,000 ft. Actually, we do not consider reaching a high Mach number alone as sufficient to obtain useful information for the airplane designer, but we find that it is necessary to obtain information up to a practical maximum lift of the configuration at any given Mach number.

Fig. 2 shows the limiting normal-force coefficient as a function of Mach number for the X-1, D-558-II, and X-1A. The chart illustrates somewhat the difficulty in obtaining information at supersonic speeds. It should be noted that maximum lift actually was not reached at Mach numbers in excess of 1 because of insufficient longitudinal control power, although the full-moving stabilizer is used in maneuvering. If the control power were available, the lift coefficient reached would be limited actually by the structural strength of the airplane, even at the altitudes at which we are flying. It should also be noted that as the speed is increased, the normal force reached decreases, until at a maximum speed the normal-force coefficient shown is only that equivalent to level flight. This simply indicates that in operation near maximum speed the speed decreases rapidly as angle of attack is increased, which means that the steady speed for maneuvering is possibly well below the maximum speed. As can be seen, the higher speed capabilities of the D-558-II and then the X-1A permit exploration at higher values of normal-force coefficient than was possible with the X-1. By the same token, we will need a much faster airplane than the X-1A in order to obtain data at high lift coefficients at a Mach number of 2.5. Now, of course, the high thrust of the rocket engines at altitude has helped appreciably in this exploration, since it has been possible to cover larger lift coefficients and also reach higher lifts without exceeding the structural strength of the airplane.

This chart also illustrates the limits of our exploratory programs with the airplanes. It defines the range of lift coefficients and Mach numbers within which we will operate. It should be noted that in any exploratory program we have always, in addition to increasing the Mach number progressively, increased the lift coefficient that was explored. We rarely increase Mach number without first having increased lift coefficient at a lower Mach number, since many of the phenomena which may manifest themselves will show up at a slightly elevated lift coefficient at a lower Mach number before they are encountered at the high Mach number in straight flight. This is particularly true for the transonic case, but has also been borne out in supersonic flight.

Detailed Flight Research Programs

Having the test limits established during the exploratory phase of the investigation, we then enter upon our detailed flight-research programs. We will not be able to discuss these in detail here, but rather will just cover some of the high points. Actually, it's the detailed evaluations that are the backbone of the program. The subject matter studied falls into three categories. Some of these subjects are established at the start of the program; in fact, in some cases they are the reason for building the particular airplane. In addition, however, there are other subjects which force themselves upon us which have to be investigated, and the third category of subject matter is that of an operational nature about which we just nat-

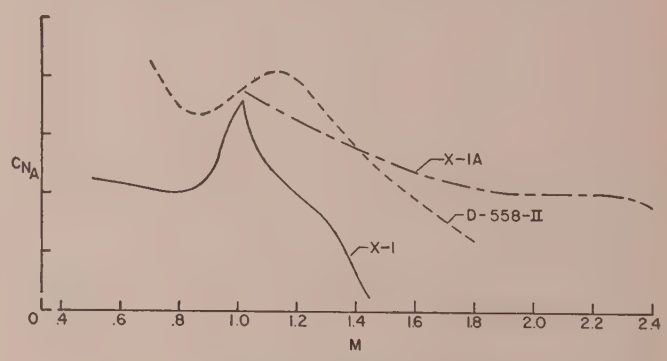

Fig. 2 – Variation of normal-force coefficient with Mach number for three high-speed research airplanes

urally accumulate information by flying. These subjects are shown in Table 1 under four general headings: aerodynamics, loads, stability and control, and operations.

Under aerodynamics have been listed the validation of tunnels, interpretation of wind-tunnel data, and aerodynamic heating. The first, validation of tunnels, of course refers to the fact that when new experimental equipment for research is put into operation, it is necessary to have some basic information for comparison to determine whether there are errors that may have been unforeseen in the basic development. The research airplane data in the vicinity of Mach number 1.0 have been very useful in validating the transonic tunnels with ventilated throats that have been developed by the NACA. Models of several of the research airplanes were constructed for this purpose. The interpretation of tunnel data has been concerned primarily with the field of stability and control where the tunnel yielded static results that had to be interpreted in terms of the dynamic system represented by an airplane in flight. Aerodynamic heating is, of course, one of the newer problems which we are now just encountering. As the adiabatic temperature rises as the square of velocity, it is easy to see that the problem is much more serious for the X-1A at a speed of Mach 2.5, than for the original X-1 at Mach 1.5, and this problem will increase in severity as the speed of airplanes is increased further.

Under loads, we listed distribution, meaning relative to the wing and also between the wing and other parts of the airplane. Load distribution data in the supersonic regime for these various airplane configurations are one of the major phases of the exploratory work being done with the research airplanes. However, it is a back-breaking, tedious job that is frequently overlooked but results in a considerable amount of systematic data. The gust research has concerned itself primarily with air turbulence at extreme altitudes, and is actually an example of the type of work that can be obtained during the normal course of operation. Buffeting was one of the first problems encountered in transonic flight, and is still somewhat of a problem, although it has been reduced to a marked extent by the use of sweep and reduced wing thicknesses. Aeroelastic effects actually go hand-in-hand with load distribution, and require repetition of certain loads work at different altitudes simultaneously with the measurement of the structural deformation of the surfaces. Also, some of our research airplanes have had serious stability deficiencies which have resulted in large uncontrolled motions. Means of alleviation have been studied. It is possible, however, that certain deficiencies may have to be accepted in production airplanes until satisfactory characteristics are obtained. Structural as well as aerodynamic loads of the wing and tail surfaces have been documented with the research airplane during maneuver in flight in the regions of reduced stability.

Table 1 – Operational Flight-Research Program

Aerodynamics	Stability and Control
Validation of tunnels	Longitudinal control
Interpretation of tunnel data	Blunt trailing edge control surfaces
Aerodynamic heating	Alleviation of pitchup by wing devices
	Effect of principal inertia axis on lateral stability
	Inertia effects
	Jet effects on control surfaces
	Directional divergence
Loads	**Operations**
Distribution	High-speed flight exploration
Gustiness at extreme altitudes	Speed loss in maneuvers
Buffeting	High-altitude problems
Aeroelastic effects	Pressure suit use
Effect of reduction of stability	Airspeed measurement

Stability and Control

Under stability and control, we have listed longitudinal control, that is, the loss of control effectiveness in the transonic and supersonic region which, coupled with increase in static longitudinal stability, has made control over the complete angle-of-attack range difficult and has led first to the adoption of adjustable stabilizers and now, as a standard on all supersonic airplanes, all-moving control surfaces. Blunting the trailing edge of a control surface by decreasing the angle between the two sides is a means of avoiding some of the large reduction in control effectiveness that occurs in the transonic regime. It does, however, cost somewhat in drag. The problem of pitch-up and its alleviation was one of the problems forced on us by the swept-back plan forms used on research airplanes, particularly the D-558-II, to alleviate the high drag associated with transonic flight. As you are aware, the straight-wing airplanes with moderate aspect ratio used during World War II had linear variations of pitching moment with lift coefficient or angle of attack as measured in the wind tunnel which gave straight lines, and it was only necessary for the slope of these lines to be negative for satisfactory stable airplanes. With the swept-wing configurations, however, variation of pitching moment with angle of attack is not necessarily linear, and has abrupt changes in slope. Obviously, if the slope became positive, indicating static instability, it was apparent that stability difficuties would be encountered and the airplane would not fly satisfactorily. In addition to the clear-cut case of very large changes in stability, some configurations gave wind-tunnel pitching-moment curves with varying degrees of nonlinearity and varying degrees of abruptness to these nonlinearities. Which of these pitching-moment variations would be satisfactory or tolerable was a moot question which could only be answered by tests of

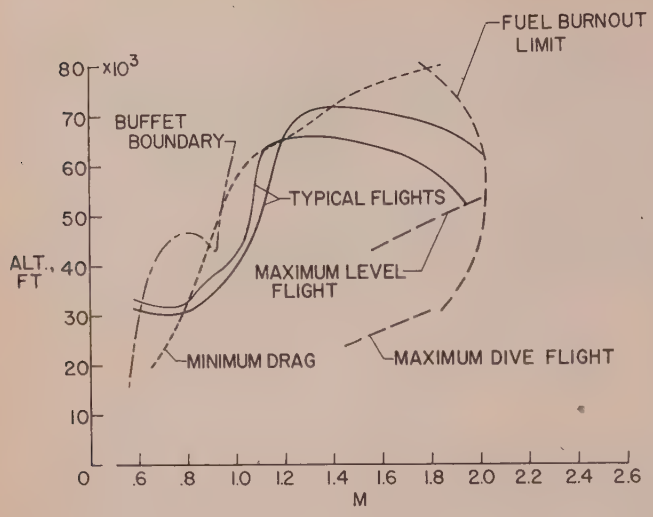

Fig. 3 – Operational boundaries of high-speed research airplane

various devices in flight, each of which successively appeared to give better wind-tunnel pitching-moment variations. It should be noted that we have tried in flight only wing devices, because it has not been possible economically to try different tail locations which are known to have an appreciable effect on the pitch-up tendency of airplanes. Incidentally, it would be just as difficult to change tail location appreciably on an operational airplane. The effect of principal inertia axis on lateral stability has been rather serious in that rather drastic reductions in dynamic lateral stability occur as a result of inclination of the principal axis in a nose-down direction, and have caused rather serious lateral oscillations at low angles of attack.

Under heading of inertia effects, we have studied the problems involved in dynamic conditions where the airplane mass is distributed primarily along the fuselage axis with light loading along the wings. In these cases, the aerodynamic effects are offset somewhat by the mass effects with the result that, although a specific motion may be primarily about one axis, a resultant motion occurs about the other axes. Typical of problems studied have been rolling instabilities where rolling caused motion in pitch and yaw, and lateral oscillations that have resulted in pitch motions. Jet effects on the empennage control surfaces are another problem that came up unexpectedly as a result of the flights of the research airplanes. Another problem partially in the same category, and also particularly one where flight tests were required to interpret wind-tunnel results, has been that of directional divergence. This directional divergence occurs at high angles of attack because the wing-tip vortices on a low aspect ratio or swept-wing airplane interfere so much with the flow at the vertical tail that even with small amounts of sideslip, the tip vortex might cause reverse flow at the tail and result in essentially static directional instability. Vortices shed from the fuselage can also cause this difficulty.

Operations

The operational problems and studies are self-evident. It should be mentioned that we have not participated in the actual development of the pressure suit until recently. The Air Force Aero-Medical group foresaw the problem and had developed a usable suit. The first use of such suits, however, was in the research airplanes, and credit for the first emergency use of the pressure suit goes to Lieutenant-Colonel Everest, who experienced a canopy failure and consequent loss of cabin pressure while flying the X-1 at high altitude.

In leaving the detailed results, this then generally illustrates the type of subject matter we have covered. It will not be possible to discuss any of the results of the program in detail because of the unclassified nature of this paper. However, I would like to cover some of the generalized results.

Typical Flight Plans

Fig. 3 illustrates typical flight plans accomplished with the airplanes. This chart illustrates performance characteristics of the airplane, and the problem involved in obtaining the maximum Mach number, as limited somewhat by the total drag of the airplane and also the amount of fuel carried aboard. In this chart the dash line indicates the point of minimum drag. However, it is rather difficult to fly this line because of other characteristics such as buffeting or pitch-up, which has a boundary much like that shown for buffeting. The pilot will fly at higher speeds than that for mini-

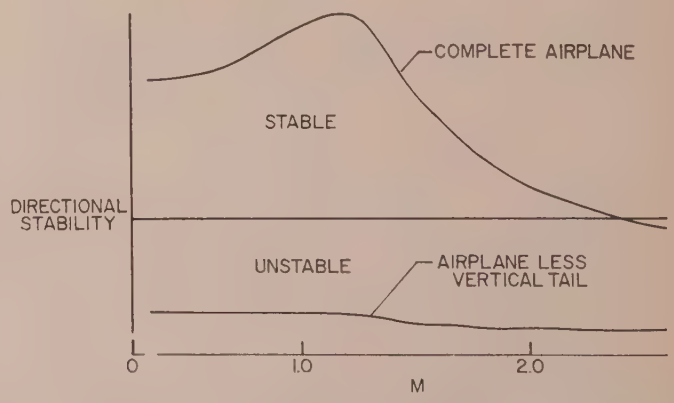

Fig. 4 – Variation of directional stability with Mach number for high-speed research airplane

mum drag at a given altitude in order to avoid buffeting or pitch-up, since entering this regime of flight usually results in increases in drag which further decrease the speed of the airplane, resulting in increased buffeting as well as higher drag and very large increases in fuel consumption in order to climb. The plots of typical flights flown are shown. The pilot, as noted, climbs at higher speeds than for minimum drag and then, instead of continuing to climb, to realize the maximum performance, he dives somewhat in order to reach higher Mach numbers before fuel burnout is reached. As can be seen, there is an optimum altitude for these speed runs where sufficient fuel is left to reach the point where thrust equals drag, and two typical flights are shown: one where fuel burnout was reached before maximum level flight speed, and the other case where maximum level flight speed actually was reached before burnout. This, of course, is not the whole story on the performance of these machines, but it illustrates the difficulty of flight plan of these airplanes for maximum performance. Of course, maneuvers along the flight path will increase the fuel consumed and decrease the maximum performance reached.

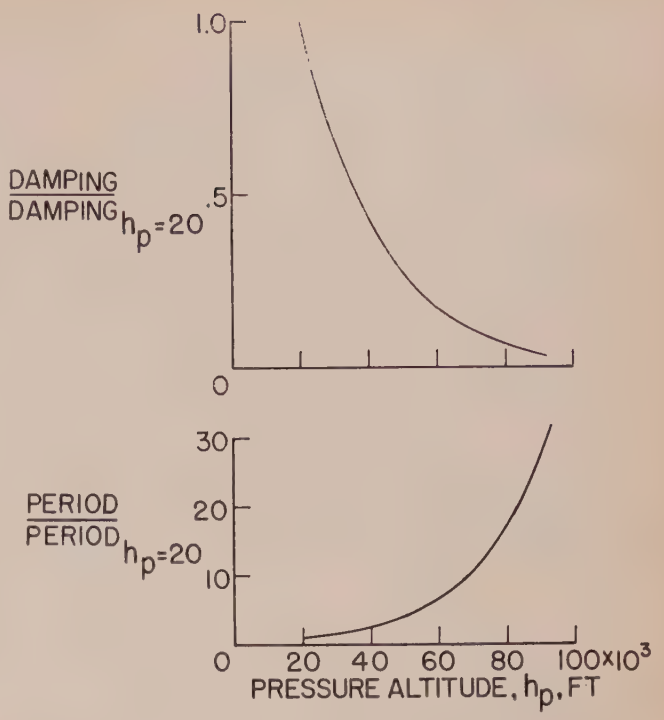

Fig. 5 – Effect of altitude on period and damping relationships

Directional Stability Problems

It might be well now to discuss some of the outstanding problems facing not only the research airplane program but the designer of any high-speed, high-altitude machine. One of the most serious problems that has arisen is the deterioration of directional stability with Mach number. This is illustrated in Fig. 4, which shows the variation of directional stability parameter, C_{n_β}, with the Mach number. As can be seen, subsonically and transonically there is little change, in fact somewhat of an increase in the directional stability. Then, as the Mach number increases above 1, the directional stability begins to decrease at a rather alarming rate, and as the Mach number approaches 2, it is quite a bit lower than at Mach number 1. The main reason for this decrease is the decrease in lifting effectiveness of the vertical tail. The tail is balancing the unstable yawing moments of the fuselage which are essentially unchanged with speed, and since the tail effectiveness decreases, there is an overall decrease in the directional stability of the airplane.

Actually, it is not necessary for the directional stability to go completely to zero in order to have difficulties with these machines since, in the dynamic case, depending on the relationships of directional stability to lateral stability as well as inertia effects, violent oscillations in roll and yaw can occur as well as possible divergent motions. Some of the loss in directional stability can of course be handled by mechanical or electronic devices, and the stability can be augmented artificially. However, studies are under way to find means of accomplishing increases in directional stability by aerodynamic means.

Another factor which, coupled with the loss of directional stability, has resulted in unsatisfactory stability and control characteristics is the loss of damping and increase in airplane natural period as the altitude is increased. A typical case is shown in Fig. 5, where the variation of period and damping with altitude is shown for a constant Mach number normalized to that existing at 20,000 ft. It can be seen in this chart that damping decreases seriously as the altitude increases and the period becomes quite long. This does mean, as far as the long period is concerned, that it could be easier for the pilot to control with the longer time involved. However, for such a long period, the pilot has difficulty in determining whether he is encountering a divergent motion or an oscillatory motion. In addition, the long period of the airplane, coupled with low damping, results in a response characteristic that gives the pilot an impression of little control, although the effectiveness might be quite high. The damping is so very light at the higher altitudes that there is little doubt it will be necessary for the airplane to have automatic or artificial damping.

Coupling Effects

Another factor which has been causing increasing difficulties is the coupling of the effects of the inertia characteristics of the airplane and the aerodynamic characteristics. An illustration of one type

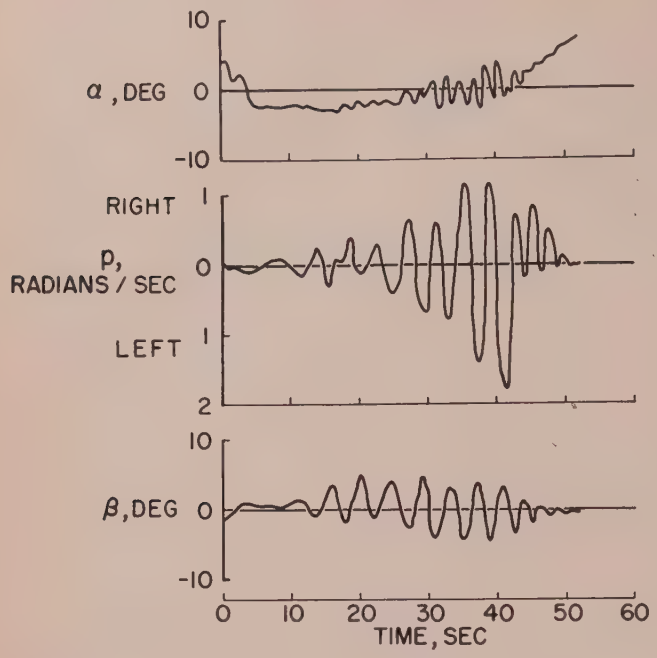

Fig. 6 – Time history of lateral oscillation of high-speed research airplane

of this coupling is shown in Fig. 6, which is a time history of an oscillation experienced at high Mach numbers with one of the research airplanes, and shows the change in angle of attack, angle of sideslip, and rolling velocity with time. As can be seen from the time history, the airplane is undergoing a typical Dutch roll oscillation; that is, rolling and yawing is coupled. However, as can be seen, there is also an oscillation in pitch as shown by the angle of attack trace. It should be noted that this pitch oscillation is of an appreciable magnitude that occurred at twice the frequency of the rolling oscillation, and the phasing is such that as the airplane changes direction of bank angle, it begins a pitch cycle.

Aerodynamic Heating

Another problem we face as we increase speed will be that of aerodynamic heating. We are just getting into this problem. We've had some experience with the D-558-II and are engaged now in a program using the X-1B airplane to study the effects of aerodynamic heating on the aircraft structure and the distribution of heat through the structure. A typical example of some of the results with the D-558-II is shown in Fig. 7, a time history of the Mach number, the stagnation temperature, and the nose and wing-skin temperatures. The maximum stagnation temperature was 200 F; as expected, the nose and skin temperatures did not reach this value because of the heat transfer time and recovery factor. As you will notice, the highest temperature reached on the nose and wing skin occurred after the maximum Mach number was reached and the speed was decreasing. Actually, the temperature as shown is of no great concern, but it does show that we are getting the speeds of appreciable temperature rise, in this case 170 F above free-air temperature.

Conclusion

In conclusion, it might be stated that we feel the program has been extremely useful and will continue to be of value in the future. We have given you examples of the work being done with the research airplanes and have pointed out that there are still a number of problems remaining within the speed range we have tested. The extreme speeds we have reached have been at high altitudes, and there are still a number of problems that will have to be overcome before such speeds are feasible at moderately low altitudes. However, we have been able to outline problem areas and experiences to the point that as unusual conditions are encountered with newer type operational airplanes, it has been possible to draw on this backlog and contribute directly to the development of these machines.

Probably one of the most important contributions is the fact that the research airplane program has acted as a means of focusing the research scientist's attention on specific problems of high-speed flight, and in this way has had considerable influence upon the direction of research. In other words, it is a great help to those studying the problems of flight to have someone come along every so often to indicate which problems are important and which problems exist only on paper.

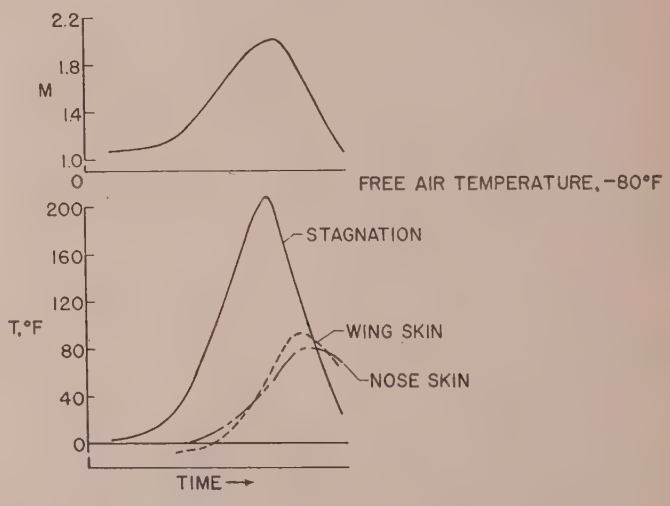

Fig. 7 – Time history of structural temperatures and Mach number in high-altitude flight of high-speed research airplane

A Radioactive Method for Measuring Engine Deposits

J. G. Mingle, H. W. Sigworth, and B. A. Fries, California Research Corp.

This paper was sponsored by the SAE at the Nuclear Engineering and Service Congress, Cleveland, Dec. 12, 1955.

THE problem of conveniently and accurately measuring deposits has confronted many researchers. In research using automotive engines many methods have been applied, such as:

1. Extracting deposits with a solvent, evaporating the solvent, and weighing;
2. Using other indexes to measure deposits, for instance, octane requirement increase to indicate buildup of combustion chamber deposits; and
3. Weighing engine parts before and after deposition.

These methods usually require a long running time to reach equilibrium deposit level or to accumulate a weighable amount of deposit, and they require extensive disassembly of the engine.

A rapid and sensitive method has been devised for measuring engine deposits using radioactivity[1] which has reproducibly measured deposits as thin as 10 millionths of an inch, and can be employed without engine disassembly. Because of its sensitivity, this method can indicate deposition rate after only a few hours, compared to tens or hundreds of hours by conventional methods.

Radiation attenuation techniques employing beta, gamma, and X-rays for the measurement of thickness or density are well known. For example, the "beta-ray gage" has broad industrial use in the measurement of thicknesses of foils, plastic films, rubber sheet, and so forth. The same principle is employed for the measurement of deposits in relatively inaccessible portions of internal-combustion engines. The end surface of a removable plug is made radioactive and inserted into the chamber of the engine where deposition is to be observed (see Fig. 1). Count rates are determined before and after the test. The quantity of deposit is obtained by comparing the attenuation by the deposits with

THE RADIOACTIVE deposition plug technique is a rapid and sensitive method of measuring engine deposits. The authors report it eliminates hours of engine operation and extensive engine disassembly.

Deposits accumulate on the radioactive surface of a removable plug, and are measured by comparing the attenuation of the radiation by the deposits with that obtained from absorbers of known thickness. Sulfur-35 and cobalt-60, the authors say, have been found to be the most suitable radioisotopes.

[1] United States Patent 2,660,678.

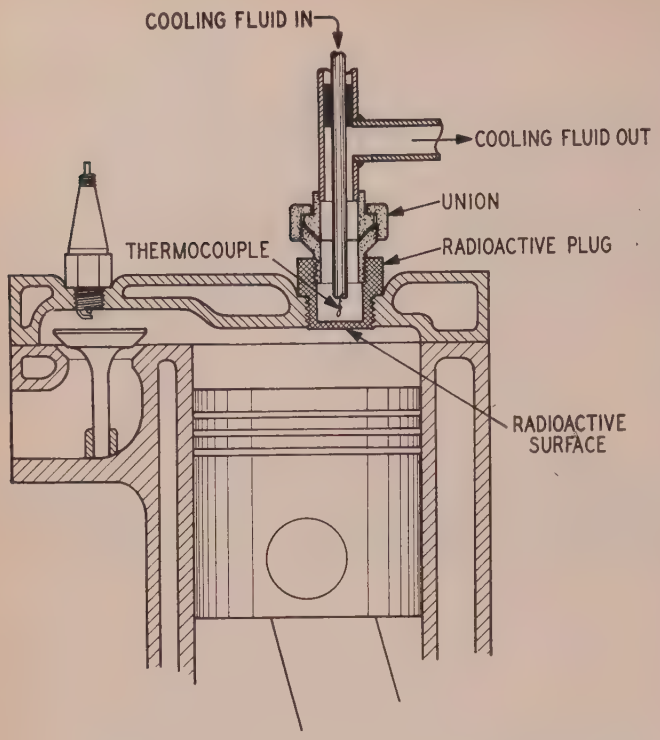

Fig. 1 – Schematic of radioactive plug installation in combustion chamber of L-head engine

that obtained from absorbers of known thickness. (As used in this paper, the term "thickness" refers to surface density, mg/cm².)

These radioactive deposition plugs have been used to measure the rate of combustion-chamber deposit buildup in a firing engine, and to observe changes in deposit level in gasoline engine induction systems. It is the purpose of this paper to describe the radioactive deposition plug and its use.

Preparation of Radioactive Plugs

Selection of Radioisotopes – Suitable radioisotopes should have the following properties:

1. The half-life should be sufficiently long so that the plugs can be used repeatedly over an extended period of time;

2. The energy of the radiation should be such that suitable sensitivity and accuracy can be obtained for the deposit thicknesses encountered; and

3. The material should be convenient to apply as a radioactive surface, superimposed on the surface of the plug, and not be subject to chemical or physical deterioration in the environment of its use.

For the beta-ray measurement of engine deposit, sulfur-35 and cobalt-60 have been found most suitable. Sulfur-35 has an 87-day half-life and emits only 0.17 Mev beta rays. It is useful for deposit thickness measurements up to about 15 mg/cm². Cobalt-60 has a 5.2-year half-life, and emits 0.31 Mev beta rays together with two gamma rays with energies of 1.17 and 1.33 Mev. Although the maximum beta-ray range of cobalt-60 is considerably greater than that of sulfur-35, the associated gamma rays limit the usefulness of cobalt-60 to thicknesses of about 30 mg/cm².

Preparation of Radioactive Surface – Sulfur-35 surfaces were formed on mild steel plugs by treatment either with elemental sulfur dissolved in hot mineral oil or with dilute ammonium sulfide solution. In both methods, high specific activity sulfur was employed to avoid appreciable thicknesses of iron sulfide. With sufficiently high specific activity, the sulfide film need be only a few molecular layers thick.

In the first experiments, plugs were lacquered on all surfaces except the desired end surface, and were immersed for 10 to 20 min at 400 F in 10 ml of mineral oil containing 21 mg of sulfur labeled with 5 mc sulfur-35. About 0.1 microcurie of sulfur-35 was deposited using this procedure. This gave a convenient counting rate, about 200-300 c/s, when measured with a thin-window Geiger tube held close to the plug. In a later method, a dilute solution of ammonium sulfide with high specific activity sulfur-35 (prepared by absorbing hydrogen sulfide in concentrated ammonium hydroxide) was applied directly to the end surface of the plug. A convenient amount of activity was deposited within one minute at room temperature.

The surface produced was stable toward hot organic solvents and gentle wiping. Engine tests showed that the sulfur-35 was stable even in the combustion chamber. However, a protective coating of nickel was electroplated over the radioactive surface. This eliminated any deterioration of the surface; and deposits subsequently formed on the plug could be removed, the nickel surface repolished, and the plug reused repeatedly. A convenient plating bath consists of 1.1 g $NiSO_4 \cdot 6H_2O$, 10 g $(NH_3)_2SO_4$, 50 ml concentrated NH_3OH, and 100 ml water heated to 50 C. Using a platinum anode, a current of 0.1 amp at 3 v for 1 min deposited a coating a few microns thick. This coating attenuates the beta radiation by only a few per cent.

Cobalt-60 surfaces were prepared by electroplating. An equivalent amount of labeled cobalt sulfate was substituted for nickel sulfate in the above bath. The specific activity was selected so as to deposit 0.1 microcurie in 20 to 30 sec. A protective nickel plating was then applied over this surface.

Counting Technique and Calibration – The radioactivity of the plug is measured using a thin-end mica-window Geiger tube, such as Amperex 200 CB, and a scaler. To ensure reproducible positioning of the plug surface just under the tube window, the plug is screwed into a tray which slides in a rack of the tube holder (Fig. 2). The plug is counted prior to use, then again after the deposit has formed. If both counts are made the same day, there is no decay correction for sulfur-35; otherwise, the correction amounts to about 1% per

Fig. 2 – Counting apparatus, as used (left) and disassembled (right)

day. Usually no decay correction is required for cobalt-60.

To establish the relationship between deposit thickness and radiation attenuation, a series of absorbers of known thickness (determined by weighing) was interposed between the plug and counter tube. For carbonaceous deposits, such as those from unleaded gasoline, chemically similar materials such as polystyrene and cellophane foils, about 0.001 in. thick, were used. A plot of the logarithm of the count rate against absorber thickness is the calibration curve. The curves shown in Fig. 3 were normalized to 100% for the bare plug. Window and air path thicknesses need not be included, because these are constant for all measurements.

The absorption curve for sulfur-35 is nearly a straight line over the whole range. With cobalt-60, the curve deviates from a straight line after 20 mg/cm² because of the associated gamma activity. The counter tube has about 100% efficiency for beta rays which enter it, but only a few per cent efficiency for hard gamma rays. For the thinnest deposits, the activity measured is principally beta radiation; but as the deposit increases, the beta radiation is greatly attenuated, and a larger fraction of the activity measured is gamma radiation.

Referring to Fig. 3, the slope for sulfur-35 is considerably steeper than for cobalt-60; this corresponds to a greater sensitivity. A change of 1% in count rate, which is about the practical limit of counting accuracy, represents a thickness change of 0.05 mg/cm² with sulfur-35, and 0.2 mg/cm² with cobalt-60. Consequently, sulfur-35 is used for

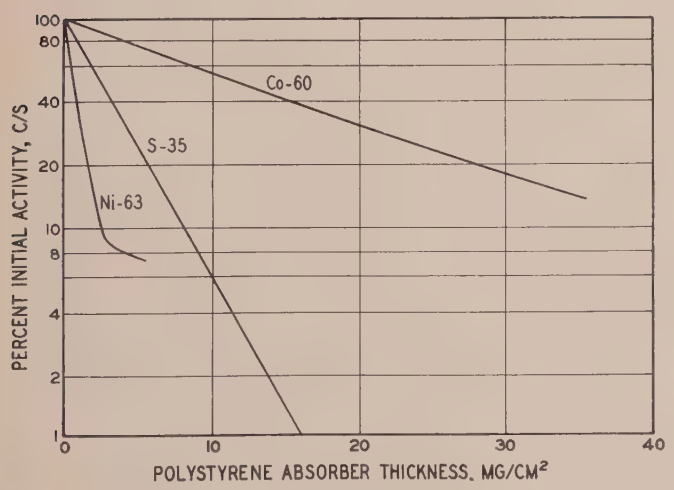

Fig. 3 – Experimental absorption curves

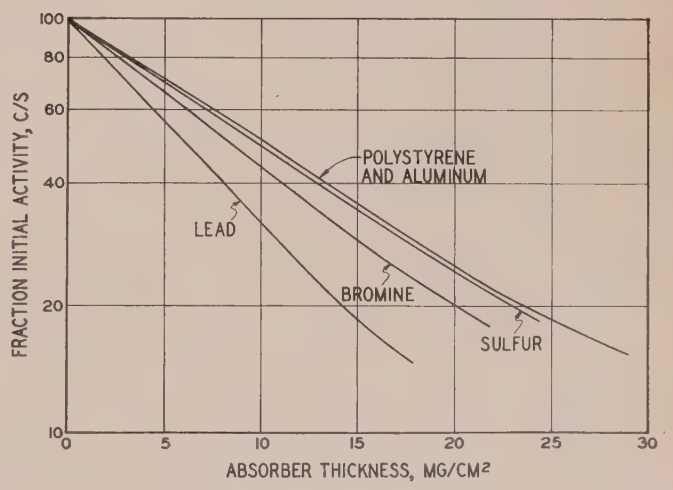

Fig. 4 – Co-60 absorption curves for different absorbers

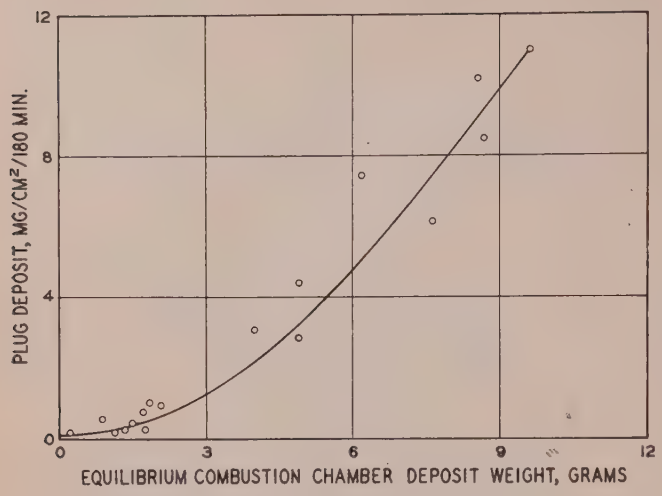

Fig. 5 – Correlation of radioactively measured deposit with weighed deposit

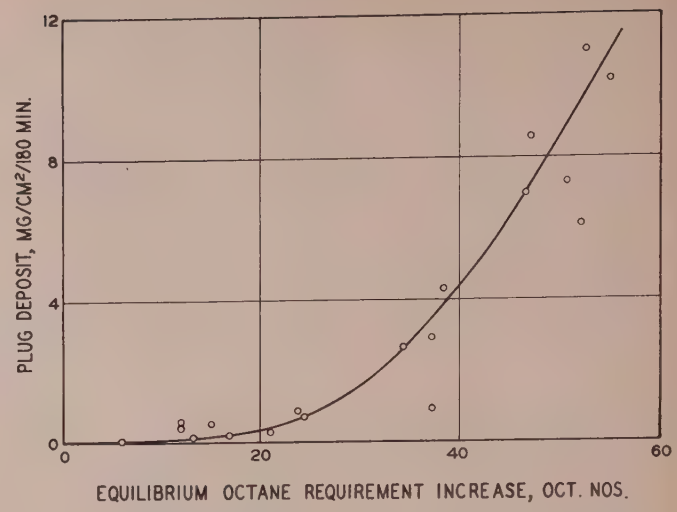

Fig. 6 – Correlation of radioactively measured combustion-chamber deposit with octane requirement increase

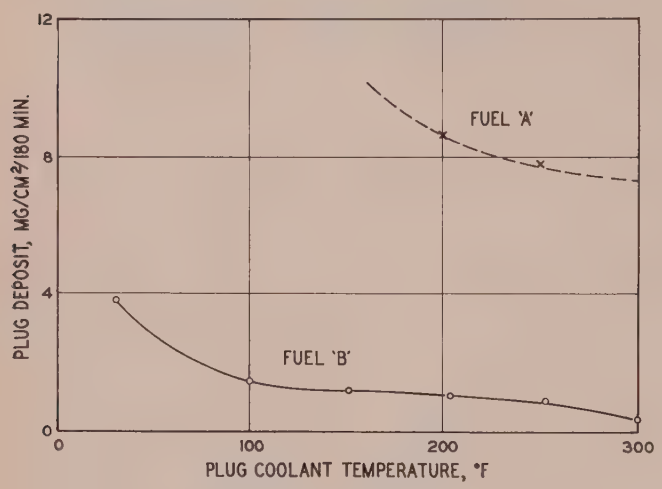

Fig. 7 – Effect of plug coolant temperature on combustion-chamber deposit

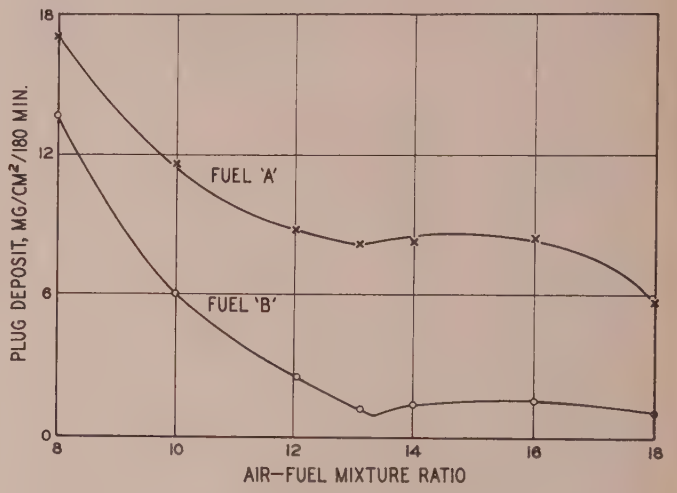

Fig. 8 – Effect of air-fuel mixture ratio on combustion-chamber deposit

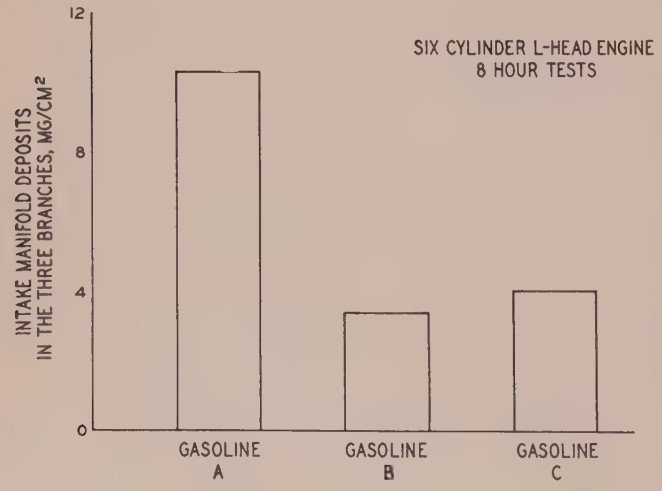

Fig. 9 – Buildup of deposits in intake manifold branches using radioactive plug technique

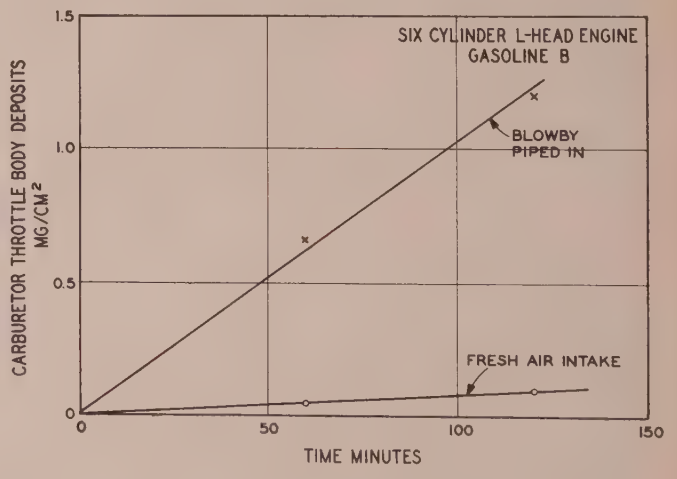

Fig. 10 – Buildup of throttle body deposits using radioactive plug technique

the lightest deposits, such as in the engine induction system, and cobalt-60 is used for heavier deposits, such as those in the combustion chamber.

In a few instances, 85-year nickel-63 was used. Because of its extremely soft beta radiation, 0.067 Mev, it is most convenient to count nickel-63 within a windowless, gas-flow proportional counter. A 1% change in count rate corresponds to 0.01 mg/cm^2 thickness. The calibration was made with 0.00025-in. Mylar film. The tail at the end of the absorption curve is probably due to cobalt-60 impurity in the nickel-63.

For deposits which are not strictly carbonaceous, such as combustion-chamber deposits using leaded gasoline, the attenuation at a given thickness (mg/cm^2) is sensitive to the chemical composition. This is illustrated in Fig. 4, where cobalt-60 absorption curves are shown for several elements commonly found in the deposits. These curves were estimated from experimental curves obtained with aluminum, nickel, and tantalum absorbers. The absorption coefficients of sulfur and chlorine are nearly equal to that of polystyrene, but those of bromine and lead are considerably greater. If the chemical composition of the deposit is known, or can be estimated, the deposit thickness can be determined.

Test Procedure

Combustion-Chamber Deposits – The engine used to develop the test method was a standard CFR engine crankcase, fitted with a 6.8 to 1 compression ratio, L-head cylinder. The plug with the radioactive surface was installed in the cylinder head, as shown in Fig. 1, and was maintained at constant temperature by a circulating fluid. Using a dummy plug, the engine and the circulating fluid of the plug were brought to an equilibrium temperature. Meanwhile, the initial count rate of the clean, radioactive deposition plug was determined. After equilibrium temperatures were reached, the test plug was exchanged for the dummy plug, and the engine operated for 3 hr with a test gasoline on a predetermined schedule of operating conditions. At the conclusion of the test period, the radioactive plug was removed from the engine, the final radioactive count rate determined, and the deposit rate calculated. Duplicate tests were made on each fuel. If the two results differed by more than 10%, a third or referee test was made, and the two closest values averaged. The results of this test procedure are expressed in terms of deposit thickness per unit time.

Induction System Deposits – A 6-cyl, L-head passenger-car engine was used for induction-system deposit tests. Radioactive deposition plugs were located at the throttle-plate section of the carburetor, in the heat riser or stove section of the intake manifold, and in the three branches of the manifold. The plugs were counted prior to the test, installed in the engine, and the engine operated for various times up to 8 hr. When testing various gasolines, the engine was operated on a stop-start cycle to simulate around-town driving. The radioactive deposition plugs were removed and counted at various points during the test run.

Application of the Method

In the field of combustion-chamber deposit research, the problems are usually associated with gasoline composition, additives, and engine operating conditions. The radioactive deposition plug test procedure has been found very useful in exploring all three of these variables. Fig. 5 shows the validity of the method by the correlation of the radioactively measured deposit with the weighed equilibrium combustion-chamber deposit where gasoline composition was the major variable. Each equilibrium deposit weight data point represents at least 200 hr of engine operation and 100 gal of gasoline. Each corresponding radioactive plug data point represents 6 hr of engine operation and 3 gal of gasoline. Fig. 6 shows a similar correlation of the radioactively measured combustion-chamber deposit with equilibrium octane requirement increase. Fig. 7 shows the effect of the coolant temperature of the radioactive plug on combustion-chamber deposit. The plug coolant temperature is analogous to the engine-jacket temperature. Deposit data from two gasolines are shown as another example of the usefulness of the method. Fig. 8 shows the effect of mixture ratio on the radioactive plug deposit, and is an example of one of the engine operating conditions that may be explored.

Induction system deposits are difficult to measure because of their inaccessibility and nonuniform coverage of a large area. Plugs were placed in the carburetor throttle body, intake manifold heater area, and at the three branches of the intake manifold on a 6-cyl passenger-car engine. An example of deposit buildup observed in the manifold branches is shown in Fig. 9. The influence of blowby on throttle body deposits is shown in Fig. 10. The radioactive plug reduced the time required for both these tests from about 40 hr to 2 to 3 hr.

Summary

The radioactive method for measuring engine deposits is employed as follows:

1. The end surface of a removable plug is made radioactive and inserted into the chamber of the engine where deposition is to be measured.
2. The quantity of deposit is computed by comparing the attenuation of the radiation by the deposits with that obtained from absorbers of known thickness.
3. Sulfur-35 and cobalt-60 have been found to be the most suitable radioisotopes.

The test method has been used to measure the rate of deposition in gasoline engine induction systems and combustion chambers.

New Alloys

Table 1 – Alloy Costs of an Automotive Turbine

Type	Usage	Finished Weights, lb	Estimated Maximum Unit Cost, ¢ per lb	Maximum Cost per Engine, $
A. Very thin ferritic stainless sheet	Heat exchanger	55	65 (0.002-in. sheet)	35.75
B. Ferritic stainless sheet	Moderate-temperature, high-stress ducts; high-temperature, low-stress parts	48	30 (sheet)	14.40
C. Austenitic stainless sheet	High-temperature, high-stress ducts	45	45 (sheet)	20.25
D. Austenitic high-temperature alloy forgings	Compressor turbine[a] rotor, etc.	14	85 (forging billet)	11.90
E. High-temperature alloy castings	Compressor turbine[a] blading, etc.	10	90 (into the mold)	9.00
F. Stainless alloy castings	Power turbine, etc.	30	20 (into the mold)	6.00
	Total	202		97.30

[a] Hypothetical engine assumed has two turbines: one to drive the engine's compressor and one to develop power for the output shaft.

IN order to establish the gas turbine as an automotive powerplant, whole new classes of high-temperature alloys will have to be developed. The necessity for new alloys for the automotive gas turbine arises almost exclusively from considerations of cost. High-temperature alloys used by aircraft turbine builders would be largely satisfactory for the contemplated stresses and temperatures in automotive turbines, except that they are too costly.

This paper should be considered a progress report on new alloys for automotive turbines. Large-scale commercial production of most of the materials to be described has not been accomplished. Also, the amount of operating experience to date on automotive turbines is so limited that material development is largely incomplete.

Table 1 shows a breakdown of weights for a hypothetical regenerative gas turbine of 300 hp. Also shown on Table 1 are estimated upper limits of alloy costs for the various categories. The costs are only approximate, but they were established with some regard for the alloy composition that will probably serve the purpose, and at production volumes large enough to minimize the price.

The total manufacturing cost of the automotive gas turbine should come close to that for the passenger-car piston engine of today. For any conceivable application, it cannot be more than four times such cost. The alloy total cost shown in Table 1 would fit the upper limit of engine costs and looks just possible for the lower limit. One can readily see, however, how hopeless it would be to meet the low cost figure with austenitic high-temperature forging and casting alloy costs of $4 per pound – this being representative of aircraft alloy costs. At $4 per pound, their usage (24 lb) in the hypothetical 300-hp turbine would alone amount to about the projected total alloy cost for the engine.

In order to proceed with the development of needed high-temperature alloys, limits to alloy usage were established:

1. Cobalt not to exceed 5% in the compressor turbine blading alloys and none elsewhere in the engine.

2. Nickel not to exceed 50% in the compressor turbine blading and not to exceed 5% in other hot rotating parts. None elsewhere in the engine.

3. Tungsten, vanadium, and molybdenum not to exceed 2% in hot rotating parts and none elsewhere in the engine.

These limitations were established by considering the present and predicted future cost and availability or strategic character of the alloying elements.

Table 2 shows representative alloying element costs. It is clear that the use of cobalt-base alloys for the 10 lb of austenitic high-temperature alloy castings shown in Table 1 (category E) is prohibitive in cost. The use of 50% nickel in the same application is about the limit to meet the projected

Table 2 – Alloying Element Costs

Alloying Element	Unit Cost, $ per lb contained
Cobalt (97–99%)	2.60–2.67
Nickel, electrolytic	0.645
Molybdenum	1.46
Vanadium	3.10
Tungsten	3.45
Manganese, electrolytic	0.30
Aluminum, pig	0.225
Chromium	0.365

for Automotive Turbines

Donald N. Frey, Ford Motor Co.

This paper was presented at the SAE Annual Meeting, Detroit, Jan. 10, 1956.

alloy cost.

Assuming 50% nickel in item E of Table 1 and 5% in items D and F, 7.2 lb of nickel per engine would be used. The free world's production of nickel in 1954 was around 380,000,000 lb. Volume production in the millions-per-year of gas turbines, each containing a maximum of 7.2 lb of nickel per engine, could apparently be sustained with foreseeable nickel production rates.

Three classes of alloys are being developed to fall within the above listed limitations – iron-base Cr-Mn-N austenitic alloys; iron-aluminum ferritic alloys containing up to 16% Al; and cast ferritic alloys with up to 12% Cr and minor amounts of Ti, V, Mo, and W.

Manganese Austenitic Alloys

Present gas turbine design calls for forging, sheet, and casting alloys capable of high-stress service within the 1150 to 1400 F temperature range. These alloys correspond to categories C, D, and E of Table 1. Ferritic steels are inadequate, generally, for service above 1150 F. Alloys currently employed in this temperature range usually contain a minimum of 8% nickel and as much as 75% nickel. The search for a substitute for the nickel has occupied the attention of numerous investigators, particularly in Germany and Russia, where nickel was in short supply in the late thirties and the forties.

An obvious substitute, manganese, immediately suggests itself, although it is common knowledge that the austenite-forming capacity of manganese is weak compared with nickel. Nitrogen, whose solubility in manganese-bearing austenites is higher than in nickel-bearing austenites, is a powerful austenite former. Therefore, the combination of Mn and N has long been attractive as a substitute for nickel.[1] Recent work[2] also indicates that nitrogen contents of ½% or more allow the addition of several per cent of ferrite-forming hot strengtheners such as molybdenum, without subsequent austenite decomposition at elevated temperatures.

The room-temperature properties of such alloys are characterized by high yield and tensile strengths with excellent ductility, even after cold working, as shown in Tables 3 and 4. The 1350 F creep-rupture properties of Cr-Mn-Mo-N steels are comparable to those of commercial alloys such as

THIS paper reports on progress to date in the development of high-temperature alloys for automotive gas turbines.

Strict limitations have been set on the alloying elements in order to keep costs down – the cost factor being the main reason for this alloy search.

The materials discussed here, which meet the alloy limitations and the temperature and stress requirements, fall into three classes:

1. Iron-base chromium - manganese - nitrogen austenitic alloys.
2. Iron-aluminum ferritic alloys.
3. Cast ferritic alloys with up to 12% chromium and some titanium, vanadium, molybdenum, and tungsten.

[1] See *Stahl and Eisen*, Vol. 61, 1941, pp. 1073-1078: "Applications of Stainless and Heat-Resisting Steels Alloyed with Nitrogen," by F. Rapat.

[2] "High Nitrogen Austenitic Cr-Mn Steels," by V. F. Zackay, J. F. Carlson, and P. L. Jackson. To be published in ASM Transactions, Vol. 48, 1956.

Table 3 – Room Temperature Tensile Tests of Wrought Cr-Mn-Mo-N Steels

Nominal Composition	Tensile Test Data		
	Yield Strength, psi	Tensile Strength, psi	Elongation, %
16 Cr, 14 Mn, 2 Mo, 0.5 N	61,400	119,000	70
16 Cr, 14 Mn, 2 Mo, 0.5 N	59,100	121,250	68
16 Cr, 14 Mn, 2 Mo, 0.6 N	61,500	120,000	65
17 Cr, 13 Mn, 2.5 Mo, 0.75 N	75,000	140,000	50

Table 4 – Tensile Properties of Cold-Worked Austenitic Steels

Nominal Composition	Type				
	301	302	CM[a]	Cr, Mn, N	Cr, Mn, N
Cr	17	18	16	16	17
Ni	7	9	1	—	—
Mn	—	—	15	14	13
Mo	—	—	—	2	2.5
N	—	—	—	0.6	0.75
Cold work, %	40	60	40	33	25
Yield Strength, psi	150,000	180,000	145,000	183,000	176,000
Tensile Strength, psi	200,000	195,000	185,000	207,000	205,000
Elongation, %	10	3	5	13	11.5

[a] A commercial Cr-Mn steel.

Table 5 – Creep-Rupture Properties of Wrought Cr-Mn-Mo-N Steels

(Water Quenched from 2150 F)

Nominal Composition	100-Hr Rupture Life at 1350 F, psi
16 Cr, 13 Mn, 3 Mo, ½ N	28,000
16 Cr, 14 Mn, 2 Mo, ½ N	26,000
16 Cr, 25 Ni, 6 Mo	27,000

Table 6 – Creep-Rupture Life of Centrifugally Cast Cr-Mn-Mo-N Steels

(Water Quenched from 2150 F)

Nominal Composition	100-Hr Rupture Life at 1350 F, psi
16 Cr, 18 Mn, 2 Mo, 0.73 N[a]	
Radial Test Specimen	28,000
Circumferential Test Specimen	28,000

[a] Actual nitrogen value.

Table 7 – Creep-Rupture Life of Wrought Cr-Mn-Mo-N Austenitic Steels

(All specimens water quenched from 2150 F)

Nominal Composition[a]	Casting Condition	100-Hr Rupture Life at 1350 F, psi
15 Cr, 16 Mn, 4 Mo, 0.50 N	Gassy, Pressure Melt	25,000
16 Cr, 15 Mn, 3 Mo, 1 Ni, 1 Si, 0.46 N	Gassy, Pressure Melt	26,000
16 Cr, 12 Mn, 2 Mo, 0.60 N	Gassy, Pressure Melt	29,000
16 Cr, 16 Mn, 2 Mo, 0.62 N	Gassy, Air Melt	29,000
16 Cr, 16 Mn, 2 Mo, 0.61 N	Gassy, Air Melt	26,000
16 Cr, 14 Mn, 2 Mo, 0.55 N	Gassy, Mechanically Capped	26,000
16 Cr, 14 Mn, 2 Mo, 0.56 N	Gassy, Mechanically Capped	26,000

[a] Actual nitrogen values.

the popular 16-25-6, containing 16% chromium, 25% nickel, and 6% molybdenum, as shown in Table 5.

Heliarc (or argonarc) welding tests were made on the Cr-Mn-Mo-N steels, and gas porosity, doubtlessly due to N evolution, was found. By making the welds under either a partial or complete atmosphere of nitrogen, sound and ductile welds were obtained. The weldability, in fact, with the atmosphere modification appears excellent.

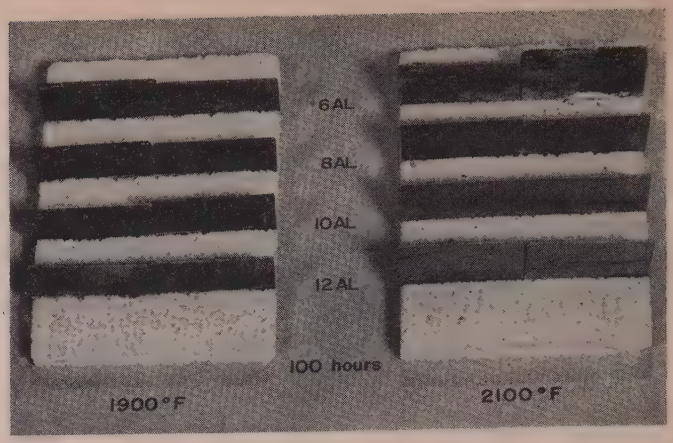

Fig. 1 – Effect of varying aluminum content on oxidation resistance of iron-aluminum alloys

Chromium-manganese steel containing ½% nitrogen must be made under pressure if ingot gassing is to be avoided.[2] However, there are difficulties attendant to this practice. Pressure melting restricts the ingot size, and the equipment required is costlier and more complicated than comparable air-melting facilities. An effort was made, therefore, to determine more economical methods of adding nitrogen.

The pressures generated in centrifugal casting usually range from 5 to 10 atmospheres and are sufficient to prevent the gassing of high-nitrogen chromium-manganese steels. A centrifugal casting was made of an alloy containing 16% Cr, 18% Mn, 2% Mo, and 0.73% N. A disc, 8 in. in diameter and 1½ in. thick, was cast at 1000 rpm. It has been calculated that a pressure of 9 atmospheres was developed at the periphery of the disc at this speed. Metallographic inspection of specimens taken from the disc revealed no gas holes or other defects. The elevated-temperature properties of radial and circumferential specimens taken from this casting are given in Table 6. The creep-rupture life of this cast, nickel-free, austenitic steel was equivalent to that of the wrought Cr-Mn-Mo-N steels.

Although centrifugal casting appears to lend itself to the manufacture of high-nitrogen austenitic steels, its applicability is limited to relatively small sizes.

A process applicable to the production of large ingots of high-nitrogen steels is suggested by low-carbon rimming steel practice. Gas holes formed during ingot solidification are not detrimental so long as they weld shut during hot rolling. An eco-

[3] See *Journal of Iron and Steel Institute*, Vol. 130, No. 2, 1934, pp. 389-418: "Physical Properties of Iron-Aluminum Alloys," by C. Sykes and J. W. Bampfylde.

nomic advantage of gassing ingots is the increased ingot-to-slab yield, especially if the ingots are mechanically capped. Also, it is probable that higher nitrogen levels can be achieved with mechanically capped ingots than with hot-topped ingots.

A series of gassy heats was made under both atmospheric and higher pressures, as indicated in Table 7. Several of the air-melted ingots were mechanically capped by chilling the molten ingot tops with a steel plate. The ingots were allowed to freeze in steel molds without hot-tops unless otherwise indicated.

A comparison of Table 5 with Table 7 shows no significant difference in creep-rupture properties of the gassy and the nongassy ingots after hot working, nor between the gassy ingots produced under different conditions. Commercial-size heats are currently being produced and evaluated using "rimming" or gassy ingot practice. The results are most encouraging.

In summarizing the findings for high-nitrogen manganese austenitic steels, it appears that the properties of the rather simple alloys shown are adequate for sheet of category C, Table 1, and turbine rotors of category D. The properties are inadequate for compressor turbine blading, however, and further development on stronger, more complex alloys is needed.

Iron-Aluminum Alloys

A definite need exists in the automotive turbine for an alloy possessing very high oxidation and corrosion resistance and only low to moderate high-temperature strength (category B of Table 1). It would be used in burner can assemblies and nozzle guide vanes. It must, therefore, be amenable to conventional fabricating techniques such as cold forming and welding. As usual, economic and strategic considerations rule out the nickel- and cobalt-base materials presently employed in many aircraft turbines.

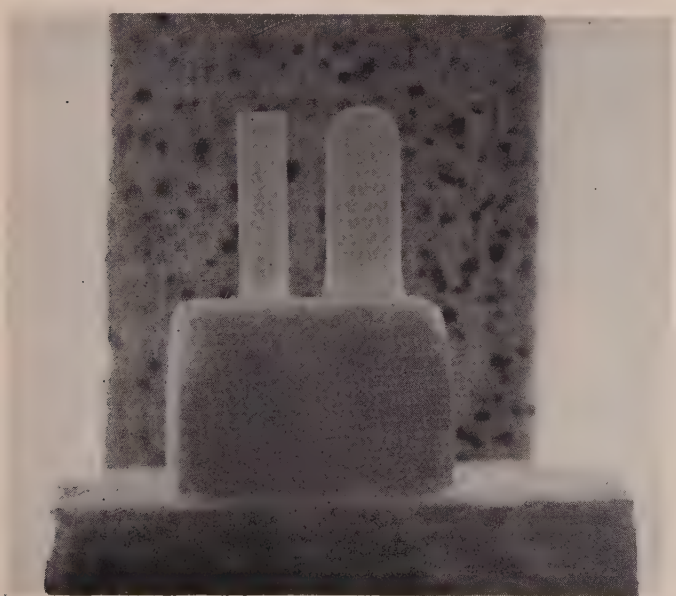

Fig. 2 – Cylinders of iron-aluminum (14% Al) alloy (left) and Type 316 stainless steel (right) after 80-hr exposure to air at 2300 F

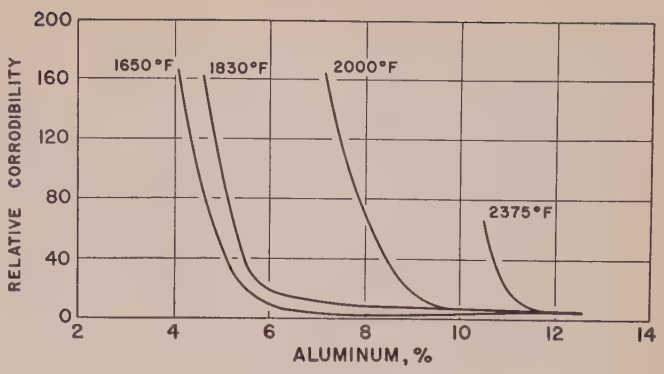

Fig. 3 – Relative oxidation resistance of iron-aluminum alloys

Iron-base alloys of relatively high aluminum content are known to have excellent oxidation resistance.[3] The effect of varying aluminum content can be judged visually from the samples shown in Fig. 1. At the 6% aluminum level, significant scaling is apparent at both 1800 and 2100 F, but the 8% aluminum alloy is relatively unattacked. Above this aluminum level, the iron-aluminum alloys are superior to most commercial austenitic steels, and this superiority increases with increasing service temperature. A typical example is shown in Fig. 2. A cylinder of 14% aluminum alloy and a similar specimen to Type 316 were exposed side-by-side in air at 2300 F for 80 hr. The severe swelling and blistering of the stainless steel occurred in the first few hours, while the iron-aluminum alloy was practically unaffected at the end of the test.

At least 8% aluminum is required for appreciable oxidation resistance at 1800 F or more (see Fig. 3). Unfortunately, alloys containing more than 5% aluminum have, in the past, been brittle at room temperature. This lack of ductility has seriously retarded the use of these alloys.

The extreme brittleness of early iron-aluminum alloys was attributed to the presence of impurities, principally oxygen. Although such alloys were melted under protective slags, the oxygen content was believed sufficient to cause embrittlement.

The first step was to develop a simple and effective technique to reduce the oxygen level significantly below that obtained by vacuum melting alone. Two conventional methods of deoxidation appropriate to vacuum melting – carbon and hydrogen reduction – were evaluated. Hydrogen should be the more effective of the two, but it is potentially explosive, especially at elevated temperatures, and the process is relatively slow and costly. It requires 4 hr to reduce oxygen content to 0.0015% with hydrogen. By contrast, carbon additions supplemented by high vacuum can reduce the oxygen level to about 0.001% in 10 min.

The simplicity, efficiency, and safety of carbon reduction had led to its adoption as standard pro-

cedure. A maximum carbon content of 0.03% had proved adequate for efficient deoxidation while still retaining high impact strength and ductility.

Careful control of alloy composition, melting procedure, and fabrication techniques has led to much improved ductility. A measure of the progress made in improving the ductility is illustrated in Fig. 4. The variation of elongation with aluminum content is shown for the alloys prepared by Sykes and Bampfylde and those of the present author. In the earlier work, the sharp drop in ductility occurred at about 5% aluminum. An analogous decrease in ductility appears in the alloys of the present investigation at about 10% aluminum. At this level of aluminum, adequate oxidation resistance up to 2150 F is obtained. This is sufficient oxidation resistance for the applications cited.

From a cost standpoint, vacuum-melted alloys appear marginal. Therefore, the air melting in conventional equipment of iron-aluminum alloys have been extensively investigated. By careful control of melting procedure, results similar to Fig. 4 have been attained.

The hot-strengthening effect of many elements has been evaluated for iron-aluminum alloys, principally by creep-rupture tests. It would be desirable to build in sufficient high-temperature strength to use the Fe-Al alloys in the form of forgings or sheet up to temperatures of at least 1100 F.

The results may be briefly summarized by stating that titanium and silicon produce the best increase in creep-rupture life. For example, the creep-rupture characteristics of 8 and 14% aluminum alloys with 3% titanium are shown in Fig. 5 on a Larson-Miller plot, where stress is plotted against a parameter involving temperature and time to rupture. For convenience, vertical lines are shown defining the 100-hr rupture life at the indicated temperature. The creep-rupture life of Type 302 austenitic stainless steel is included for comparison.

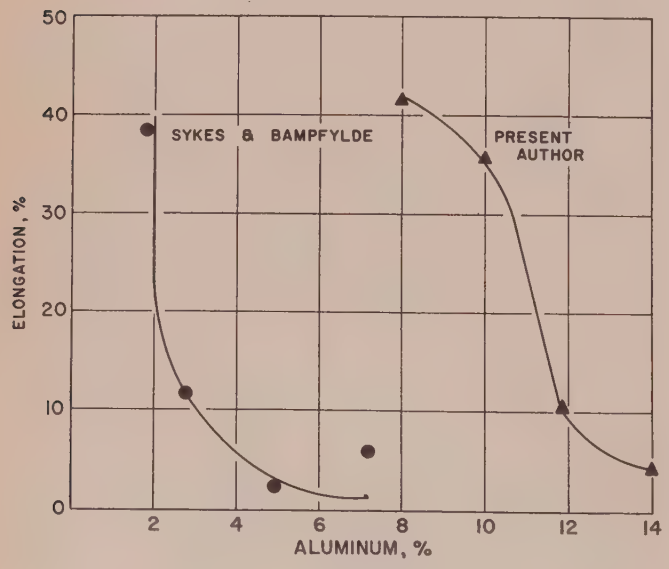

Fig. 4 – Effect of aluminum on ductility

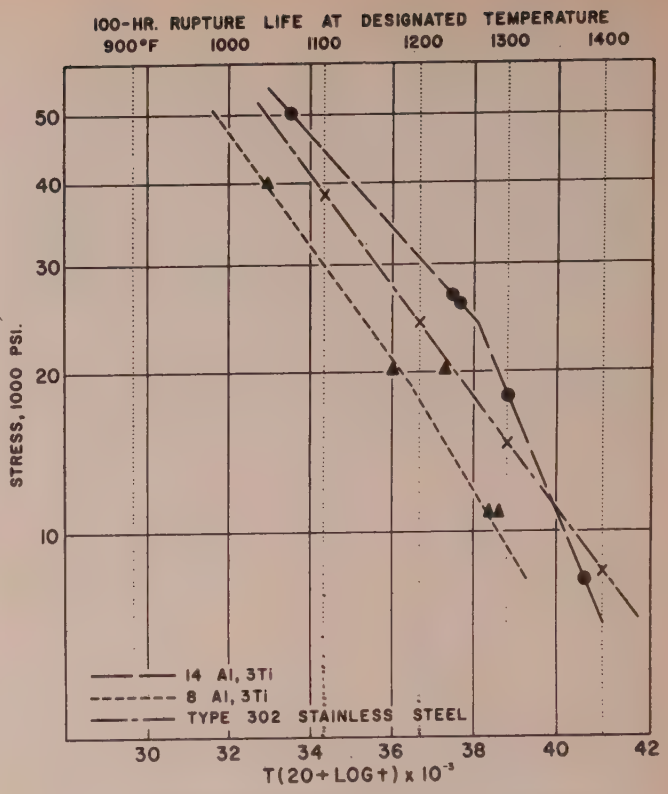

Fig. 5 – Stress-rupture properties of two Fe-Al-Ti alloys

It appears probable, therefore, that ductile and workable simple iron-aluminum alloys with about 10% aluminum can be economically produced in sheet form for very high-temperature, low-stress parts as combustor can liners. It should be appreciated, however, that the use of aluminum-coated plain carbon steel is another possibility. Cost will probably be the deciding factor.

It also appears probable that high-stress parts operating at temperatures up to 1100-1150 F can also be made of Fe-Al alloys. Paradoxically, the aluminum content must be at least 10% in order to achieve adequate hot strength.

Cast Ferritic Alloys

In addition to the development of the wrought materials for high-temperature use, it is advisable also to carry on a cast-alloy development program for applications in the moderate-temperature range (up to 1150 F). Such alloys would meet the requirements of category F in Table 1.

In the last decade a number of high-creep-strength low-alloy ferritic wrought steels have been developed for service in the 900 to 1150 F range. A review of the literature for the most promising steels was made, and Table 8 shows the commercial designations. These same compositions were melted and tested in the cast form along with a few minor composition variations also shown in Table 8. The heats were made in a 50-lb induction furnace. Commercial melting materials were used with ingot

Table 8 – Ferritic Cast Alloy Compositions

Designation	C	Cr	Mo	V	Ti	W	B	Commercial
W-7	0.25	1.25	0.5	0.85	—	—	—	17-22 V
W-8	0.25	1.25	0.5	0.85	—	—	0.02	—
W-9	0.25	1.25	0.5	0.85	0.25	—	0.02	—
W-10	0.25	2.25	0.5	0.85	—	0.65	—	H-40, HGT-3, Hykro V-80
W-11	0.15	—	0.5	0.35	0.25	—	—	Mo-V-Ti (Glen's alloy)
W-59	0.15	1.25	0.8	0.35	0.15	—	—	—
59	0.15	1.25	0.8	0.35	0.15	(Al 0.8)	—	—
W-60	0.28	12.0	2.5	0.5	—	1.5	—	422 M

Table 9 – Typical Stress-Rupture Values at 1100 F and 45,000 Psi, for 422 M with B and Ti Additions

(Solution Treated 2100 F, Oil-Quenched, 1200 F Temper)

	Time, hr	Elongation, %	RA, %
A. Cast 422 M	1050	24	46
B. A plus 0.01 B	510	10	13
A plus 0.04 B	173	2	8
C. A plus 0.01 B and 0.5 Ti	360	23	38
A plus 0.04 B and 0.5 Ti	130	3	2

iron as the base material and the alloy additions made as ferroalloys. Specimens were made from sections cut from 1½-in. keel block. All specimens were heat-treated in a protective atmosphere before machining. Testing was performed on 0.250-in. diameter specimens.

The creep- and stress-rupture properties of the various compositions were determined, and the stress-rupture data of those representative alloys given in Table 8 are shown in Fig. 6. For comparative purposes, the stress-rupture data of the wrought alloys are also included. Because of the area of interest, testing was done at 1100 and 1200 F. The heat-treatment usually consisted of normalizing at 2100 F, oil quenching from 1950 F, and then tempering at 1200 to 1290 F. This generally represented the best heat-treatment investigated.

In the temperature range investigated, it will be noted that the cast alloys have stress-rupture properties similar to those of the wrought alloys. The one exception is the Cr-Mo-V material (heat W-7) where cast properties are inferior. Heat-treatment may be responsible, as will be demonstrated later.

Of those alloys containing less than 4 to 5% total alloy content, it was found that the Mo-V-Ti compositions (represented by heat W-11) possessed the greatest strength. Since the desired temperature of operation is high, and hence oxidization a factor, alloy additions to improve oxidization resistance were made. Chromium was increased to as much as 3%. With 1.25 Cr (heat W-59), a slight decrease in strength was noted. Increased Cr additions further decreased strength. Small aluminum additions, when carefully made, had little effect on strength (heat 59). Increasing the Al content further, however, brought about a marked decrease in strength.

Boron additions were made to the Cr-Mo-V steels (heat W-7) to increase strength. It was found that B alone gave improved strength and that the further addition of titanium, as indicated in the literature, is not necessary. The strengthening effect was probably associated with a transformation product having an increased resistance to tempering or to the dispersion hardening of a precipitated boride such as molybdenum boride.

In the 12% Cr group of alloys the most promising was 422 modified. The cast properties, with those of the wrought material, are given in Fig. 6, D. Again, it will be noted that the cast and wrought materials have similar stress-rupture properties over the temperature range investigated.

Strengthening with B and with B plus Ti was tried with this composition also. Additions of 0.01 and 0.04% B to this alloy gave decreased stress-rupture properties as the amount of boron increased. Titanium additions had little effect (see Table 9).

Throughout the testing program, tempering was carried out at 1250 F. This temperature is in the general range for development of optimum strength by tempering and is sufficiently above the proposed maximum operating temperatures to insure a reasonably stable structure. Normalizing and solution temperatures were varied and were found to have a large effect on the stress-rupture properties. This effect is shown in Fig. 7 for the materials containing a maximum of 4 to 5% total alloy. All normalizing

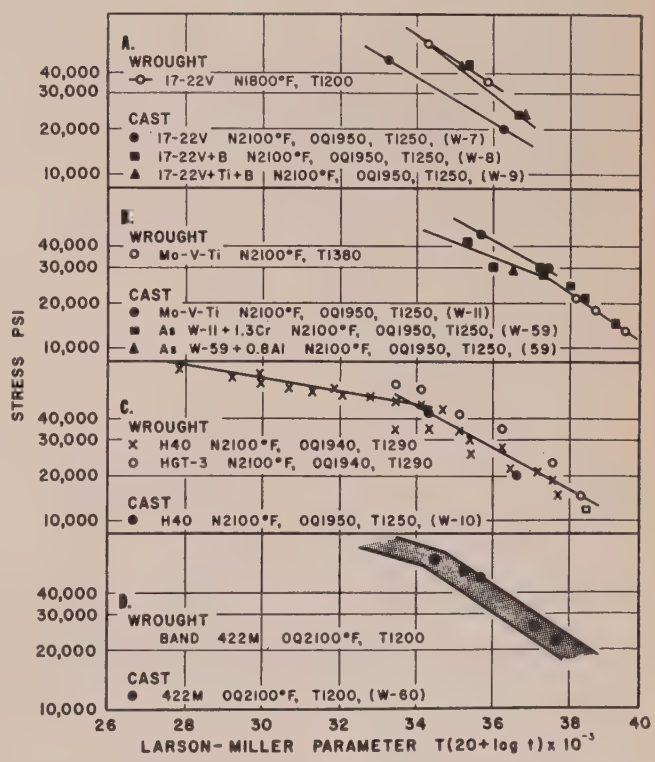

Fig. 6 – Rupture strength of low-alloy steels

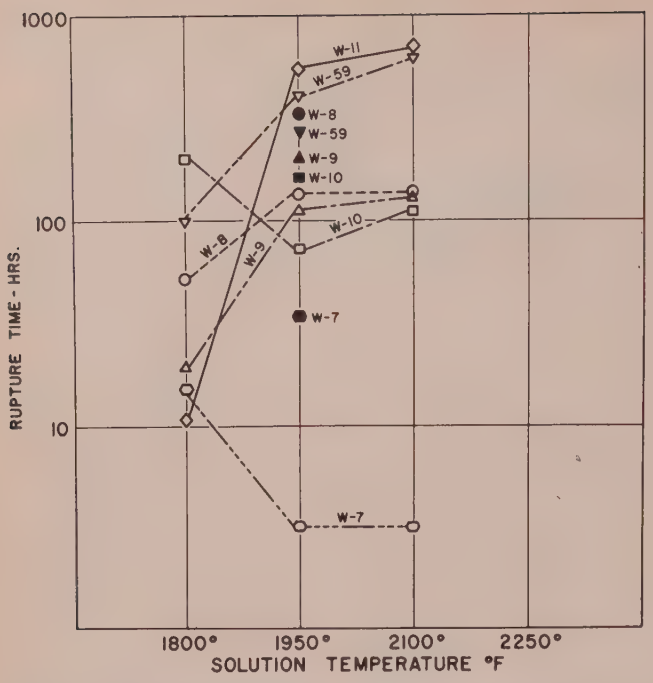

Fig. 7 – Effect of solution temperature; rupture tests at 42,000 psi and 1100 F; open points not normalized; filled points given 2100 F normalizing prior to 1950 F solution treating; all specimens tempered 6 hr at 1250 F

and solution treatments were followed by a temper of 6 hr at 1250 F, and the tests were run at 42,000 psi and 1100 F. It will be noted that generally the best treatment for these alloys was to normalize at 2100 F and to follow with a solution treatment at 1950 F. With the high-temperature normalizing treatment, a more homogeneous alloy was obtained; and upon further treatment, a better distribution of the carbide was obtained. High-temperature solution treatments gave a more acicular ferrite, a structure which is often associated with improved creep resistance. The high solution and normalizing temperatures are particularly important in the titanium and/or boron bearing alloys.

Similar results were obtained in tests run at 1200 F and 20,000 psi.

An increase in solution temperature results in improved stress-rupture properties of the 12% cast Cr alloy investigated. Table 10 presents these data and shows that 2100 F is about optimum. No measurable difference was noted in properties as a result of tempering at either 1200 or 1275 F.

Table 10 – Effect of Solution Temperature on Stress-Rupture Properties of Cast 422 M (Heat W-60)[a]

Test Condition	Solution Temperature, F	S-R, hr	Elongation, %	RA, %
1100 F and 47,500 psi	2200	500	—	—
	2100	488	28	62
	2000	—	—	—
	1900	234	32	56
1200 F and 22,500 psi	2200	251	9	15
	2100	431	33	41
	2000	255	32	55
	1900	171	50	84

[a] All samples drawn 4 hr at 1200 to 1275 F

In conclusion, then, it appears that cast and heat-treated Mo-V-Ti has excellent strength properties up to 1100 F but would have marginal oxidation resistance in many turbine applications. The less economical 422 M has about the same strengths at 1100 F but better oxidation resistance. The blades of a power turbine could perhaps be made of 422 M and the hub of Mo-V-Ti. The prime disadvantage of both of these alloys appears to be the rather difficult and expensive heat-treatments required to obtain the good high-temperature properties.

Conclusions

A start has been made in developing the new alloys needed for the automotive turbine. It appears that the stringent limitations on cast or strategic alloy content can be met at least in part with the types of alloys described. Further extension of this work should lead to meeting all of the high-temperature alloy requirements for the mass-produced automotive turbine of the future.

Acknowledgment

The developments outlined have been carried out by almost the entire staff of the metallurgy department of the Scientific Laboratory. In particular, the writer wishes to acknowledge the contributions of Drs. E. Morgan, V. Zackay, and W. Kiessel.

ORAL DISCUSSION

Reported by R. H. Briggs
Eaton Mfg. Co.

Question: Relative to the Fe-Al type alloy, you remarked that one air-melted heat had given results as good as a vacuum-melted heat. What was the size of the heat? How much to process?

Dr. Frey: We have made about 50 heats of 100 lb each. The melting practice information is not available.

The Fe-Al type alloy was not shown with respect to price. One large Fe-Al heat was made of the ductile type and has processed well.

Question: Do you still feel that the brittleness is due to oxygen?

Dr. Frey: No. The evidence has become less clear, and the variables are not clearly separated. For example, an optimum carbon content was found and nitrogen has an effect.

O. W. McMullan, Bower Roller Bearing Co.: I recall that, many years ago, we once added up to 5% aluminum to the ingot iron which produced hot shortness and brittleness to the degree that we had to drop the forging temperature to 1500 F. A yellow tinge was noted in the grain boundaries. Now silicon appears to reduce oxidation. Will you comment on these?

Dr. Frey: If the temperature is high (say 2100 F) grain growth occurs, giving poor workability. The Fe-Al and the Fe-Si systems are similar, but the ductility of the Si-Fe system changes to brittleness at about 3%. Further work may eliminate this brittleness with silicon.

Nuclear Power and the Machinery Builder

R. C. Allen, Allis-Chalmers Mfg. Co.

This paper was presented at a meeting of the SAE Central Illinois Section, Springfield, Ill., Oct. 24, 1955.

IN LIGHT of the world's continually increasing demand for electric power and the attendant decrease in economically recoverable fossil fuels, the need for nuclear powerplants becomes all the more pressing.

The author briefly covers in a general way several developments in design of different reactor types. Some problems inherent in generating power from fissionable isotopes are mentioned, together with the solutions which will enable the realization of electric current generation from the "burning" of nuclear fuels.

Some startling theoretical schemes are mentioned which bid fair to making the generation and transmission of electric current in the future so different from our present methods as to mark the coming of age of yesterday's and today's science fiction.

FEW of us appreciate, as we flick an electric light switch, turn on a TV set, or operate any of the numerous electrically driven conveniences in our homes, that electric power is inseparable from the comforts and advantages of our American way of life, and that an ever-increasing supply of cheap power is essential to the advance of civilization all over the world.

With the present total central station generating capacity in the United States above the 100-million-kw mark, and as predicted a few decades ago, estimates of fossil fuel reserves for well over 1000 years, one might question the degree of activity in development of generating plants to derive power from energy released from fissionable material. Recent estimates of fuel reserves are quite different, as shown later.

Further questions arise after a brief review of various estimates which have been prepared to indicate the economics of nuclear powerplants designed for electric power generation. Cost studies of power generated from a nuclear heat source have come up with figures all the way from six mils to several cents per kilowatt-hour. Additional questions are raised when it is stated that raw fuel costs in a nuclear powerplant are almost negligible.

Further review of nuclear powerplant cost studies shows that operation of such plants is intricately intermeshed with government controls and that builders of these plants are depending on the government to perform certain essential operations and assume some costs. This is so because of special facilities owned by the government which are too expensive for any single utility or group of

utilities to own and operate.

Another strong reason for close association with the government is the need of defense regulations covering nuclear fuels. Because of their weapons value, fissionable materials must be under government control for an indefinite future period. Today as never before civilization is faced with the possibility of widespread annihilation from a small amount of material in the hands of a subversive or unfriendly group.

Fissionable materials are elements which can be made to split into their component atoms when they are bombarded, under suitably controlled conditions, with fundamental particles called neutrons. Three such elements now known can be employed in reactor heat sources operating with a controlled chain reaction: uranium 233, uranium 235, and plutonium 239.

Numbers following the elements indicate the particular isotope, each isotope being a different form of the same chemical element. All isotopes of an element have the same number of protons in the nucleus and the same number of electrons. They cannot be separated chemically.

Uranium 233 differs from uranium 235 in that it has two less neutrons in the nucleus, or core, of each atom. Plutonium 239 is different from uranium, although it is "man-made" from uranium 238, a so-called "fertile" material. Plutonium can be separated from uranium by the process of wet chemistry.

Uranium 235 is the only natural fissionable material known to exist in sufficient quantities to be useful. It is present in ordinary uranium to the extent of 0.7%.

Uranium 233 is a man-made fissionable isotope derived from thorium. Thorium oxide is the main constituent of the "gas-mantle" common in our homes until Edison's electric light bulbs were no longer luxury items.

Uranium 238 is the common and most plentiful isotope of uranium. It does not support a chain reaction under controlled conditions as do the fissionable isotopes. The great value of uranium 238 lies in its capability of being converted into plutonium under reactor conditions.

Control of fissionable materials involves the problem of strict accountability at all times in a manner comparable to that employed at Fort Knox with our gold reserves, but very much more complex and more difficult. This problem is not encountered in conventional powerplant operation and confronts the nuclear powerplant operator as well as the designers and manufacturers of the reactor, fuel elements, apparatus, and machinery for chemical processing of fuel and fabrication of fuel elements.

The importance of fissionable materials in the national defense program may, from time to time, place restrictions on the amount of material which may be available for the enrichment of natural uranium containing 0.7% of the fissionable uranium 235, to higher percentages, as may be required to suit the economics of a specific reactor system.

For example, uranium 235 is separated from natural uranium in government-owned gaseous diffusion plants operated by various contractors for the Atomic Energy Commission. In those plants, natural uranium is converted to gaseous uranium hexafluoride. The tendency for the lighter isotope to pass more readily through porous material is employed for the production of highly concentrated uranium 235, requiring thousands of porous barriers and compressor stage to accomplish this. In an extreme emergency, limitations may be placed on the use of uranium 235 because of defense requirements. The degree of commercial hazard in this regard can be determined only with the passage of time.

Plutonium is another source of fissionable material, produced in huge reactors at Hanford, Wash., and Savannah, Ga. Here again, the weapons phase of production operations might have to come first in the event of a national emergency. Conversely, the increasing probability of international peace makes these tremendous installations available for production of fissionable materials for electric power generation.

In operating a coal-burning powerplant, the main objective is to burn fuel as completely as possible. The residue, or ash, presents a disposal problem usually solved either by employing ash for fill or dumping it in some unused area.

In the nuclear powerplant, a different problem is encountered. In the first place, only a small part of the nuclear fuel can be economically fissioned, or "burned," each time the fuel elements are used, after which an expensive chemical process is required to remove generally unusable elements resulting from fission and to reclaim unfissioned uranium for refabrication into new fuel elements. At this point new complications enter, because used fuel elements are dangerously radioactive. All chemical processing must be handled by remote control, requiring heavy shielding and complex mechanical devices to carry out the operation without exposing personnel to dangerous radiation.

Another problem confronts the designer in processing fuel elements. Most reactors in which controlled fission is carried out are of the so-called thermal-neutron type, in which neutrons released by fission are slowed down to an energy level most conducive to fission. In such reactors, it has been found possible to employ blanket elements in which a certain amount of natural uranium is converted, through neutron capture and radioactive decay, into plutonium 239, a fissionable material suitable for weapons and for use as nuclear fuel.

At this point, the breeder reactor enters the picture. Here the core operates in the fast neutron range. Such reactors will convert a quantity of uranium 238, not ordinarily fissionable, into plutonium 239 in an amount greater than the quantity

of fissionable material burned in the core. In some nuclear powerplants, the value of byproduct plutonium as weapons material may equal the income from electric power generated by the same reactor as a heat source. Here again, physicists, chemical engineers, and metallurgists enter the picture in order that the maximum amount of extremely valuable plutonium may be produced and later separated by chemical processing.

If the plutonium is not sold to the Defense Department, it has great value as new fuel.

Another radically different problem is involved with respect to the safety of a nuclear powerplant. Many fear that under some combination of events, a reactor may become an atomic bomb. It is considered that factors entering into the probability of an occurrence of this kind are well understood, and likelihood of such an event can now be dismissed.

Almost equally serious might be a "melt-down" of a reactor and vaporization of dangerous isotopes which then could be dispersed over large fall-out areas. Factors governing such a possibility are now capable of control, and means are provided for the complete containment of all radioactive material which might be released in any accident involving mechanical or electrical failure of control apparatus. Thus, full protection of personnel inside and outside the plant is assured.

A basic principle is employed in securing a negative temperature coefficient, which means that as reactor temperature rises, its energy output is automatically reduced. Reactors being built today are carefully designed and tested to insure that this inherently self-regulating characteristic is achieved. This self-regulation is separate and distinct from normal controls, which themselves provide adequate protection.

Insurance considerations have not yet been formulated into a definite policy. If insurance were required to cover the possibility of a devastating burst, it is hardly reasonable to expect that such coverage could be underwritten. Looking at the other side of the picture, it is understood that some reactor insurance has already been purchased. The ability of scientists and engineers to adequately handle the safety problem is well illustrated by present plans for building nuclear powerplants relatively close to thickly populated areas.

Present Power Situation

In 1902, installed electric generating capacity in the United States totaled 1,212,000 kw. In 1925, this figure had grown to 21,472,000 kw. In December, 1954, electric utility generating capacity in the United States passed the 100-million-kw mark.

Apparently the industry is far from reaching its saturation point. Industrial economists agree that installed capacity of the country's central station generating plants will be doubled by 1965, thus bringing their total capacity up to 200 million kw. Power generated by fossil-fuel burning plants is presently close to 76% of the total, 24% generated in hydroelectric plants.

This tremendous growth in the generated power output sharply calls attention to the question of fuel reserves and indicates the need for a precise re-evaluation with today's yardsticks. Results of these re-evaluations are disturbing.

Remember that modern economists base their pessimistic views on data much more precise than that available a few years ago.

Palmer Putnam, and other economists have concluded that world supplies of fossil fuels total approximately eighty Q, where Q is defined as an amount of fuel with a total heat content equal to 10^{18} Btu. Expressed in another way this quantity represents the quantity of heat liberated by the combustion of 40 billion tons of coal having a calorific value of 12,500 Btu per lb.

Putnam's economic studies indicate that the world's consumption of fossil fuels up to the year 1947 was approximately 12 Q, and that annual consumption as of 1947 was of the order of 0.1 Q.

Extension of these studies in connection with Bureau of Mines data has led to a further downgrading of total world resources. Of the approximately 70 Q now thought to represent the world's coal resources, some authorities conclude that as little as six Q is economically recoverable. Taking the average rate of use for the next few decades as 0.2 Q, it appears that our supplies of high-grade fuels will be consumed in something like 30 years.

Studies by Dr. J. E. Hobson, director of the Stanford Research Institute, support the views of other economists. As he points out, "The coal beds of thickest veins, of highest quality, and of greatest accessibility are being worked first – and, therefore, exhausted first."

Hobson predicts that the time when consumption of petroleum and natural gas will exceed the ability of wells to produce is one or two dozen years away, or, as he mentioned in one of his talks, "a mere watchtick away."

With regard to other sources of energy, there is an approximate total capacity of 86 million kw of undeveloped hydroelectric power in our country, of which only about 40 million kw are considered economically recoverable. At the present rate of construction, these sites will be developed in the next 32 years.

Power from tides has been studied extensively. The Passamaquoddy development on the northeastern boundary of Maine is probably the largest project of its kind ever seriously considered. Some 20 years ago, work was started on a power system which would have included ten 11,000-kw generating units. The high cost of low-speed, low-head generating machinery, together with the large number of emptying and filling gates and their controls, appeared to point toward an overall project cost excessively high in relation to corresponding investments for competitive sources of power. The

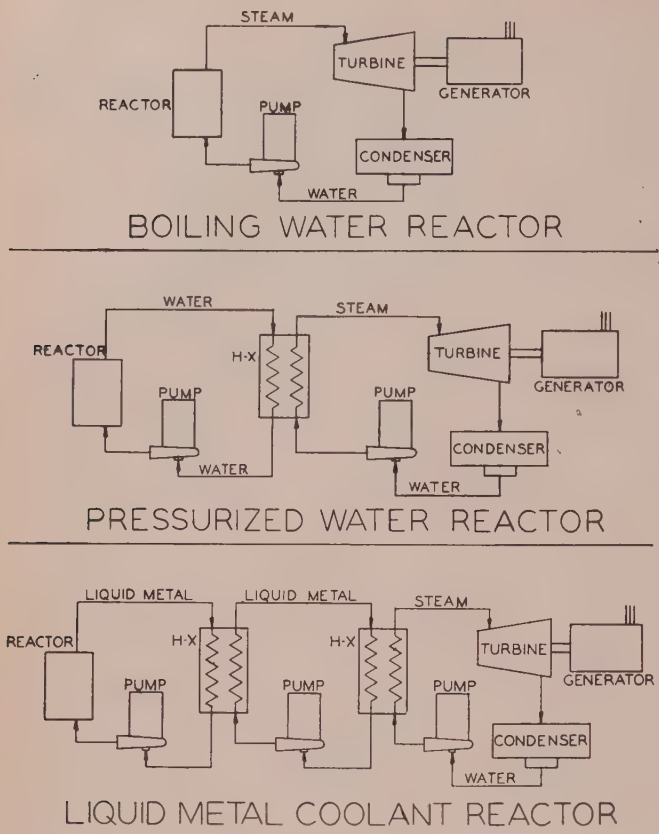

Fig. 1 – Typical nuclear powerplant cycles

project was abandoned after a limited amount of construction.

While many authorities still question the commercial justification of tidal power for a long time to come, a recent press release announced a substantial government appropriation to support a further study of the Passamaquoddy development.

Wind power has also been intensively investigated in recent years. A 1250-kw generating unit with a two-bladed propeller 175 ft in diameter was constructed and operated on a mountain top in Vermont during the years 1941-45. It was estimated that further units could be built at a cost of about $191 per kw, a figure some 50% higher than the engineers of the utility considered could be paid, due to the intermittent nature of the source of power. While wind power does not seem a likely candidate for application to large power systems, there is considerable activity, particularly in Europe, in the development of wind-power-driven generators of a few hundred kilowatts capacity.

Studies of solar heat as a source of energy are being undertaken at increasing rates. After deducting for transmission losses through the atmosphere, it appears possible to recover approximately 220 kw of electrical energy per acre of exposed black body surface.

The Port Washington plant of the Wisconsin Electric Power Co. now has coal-burning generating equipment currently loaded at its rated output of 400,000 kw. Some 1800 acres of black-absorbing surfaces, completely housed, would be required to equal the output of this plant. This refers only to peak generating capacity. No practical proposal has been made as yet for storing large amounts of energy for availability at night or when the sun is obscured by clouds.

While an increasing number of eminent scientists and engineers have become optimistic over the possibility of power from the sun, use of solar heat for extremely large blocks of power does not seem to offer promise for the near future.

With the immediate future outlook for large-scale power generation somewhat discouraging with respect to wind, tidal, and solar power sources, coupled with the rapid depletion of our highest grades of fossil fuels, utilization of nuclear energy offers the greatest promise as a potential power source.

Compared to the estimated total 70 Q and 6 Q of economically recoverable thermal energy from high-grade coal, nuclear fuel sources have been estimated to have a 1500 Q theoretical potential. This figure is based on the practical development of breeder reactors to convert fertile materials into fissionable isotopes, so that, theoretically, all fertile materials such as uranium 238 and thorium 232 may be consumed.

The 1500 Q potential for nuclear fuels can be expected to suffer some reduction after accumulating experience with chemical processing of used fuels and cost of separating contaminating isotopes.

The comments immediately preceding are intended to bring out reasons why the great activity in development of nuclear powerplants can be justified. Work must go on at an increasing tempo if we are to continue to use increased amounts of power for national defense, individual security, and personal comforts.

It must be recognized that present estimated costs of power generation are bound to drop as experience is gained. A significant example is the sharp downward trend in electric power costs in the United States from the start of the century until about ten years ago, together with the substantially constant average cost of power since that time. This has been accomplished in spite of great increases in labor and material costs. A similar future trend can be expected in the nuclear power area.

The earlier statement of present estimated power costs of six mils to several cents per kilowatt-hour requires specific comment. The high investment costs in present estimates of nuclear plants reflect high contingencies necessary to satisfy investors. Elaborate safeguard precautions call for added expense in today's figures. Research and development expenses are extremely high. Further contingencies reflect lack of experience with the life of reactor components during long operating cycles. On the other hand, the low estimates reflect what can be

done with standardization of designs and processes and an accumulation of operating experience.

Actually, there are many places where fuel is costly, water scarce, and where the cost of power, under present-day conditions, is such that nuclear powerplants are economically sound. For example, consider a remotely situated defense installation.

A striking difference between coal-burning plants and stations using nuclear fuels is that coal costs are now running up to half the cost of energy generated and are increasing, whereas raw nuclear fuel costs are presently in the neighborhood of 1/10-1/15 the cost of coal on a unit power cost basis.

General Types of Nuclear Powerplants

Fig. 1 is a diagram of three of the principal types of plants. The first is a boiling water reactor. Steam is generated within the reactor core where heat is released by nuclear fission and then piped directly from reactor vessel to steam turbine.

Water in the reactor acts as a moderator to slow the neutrons to the most effective energy level. This promotes a self-regulating characteristic in the event of loss of control. If water is removed, the loss of moderating effect will stop the chain reaction. Removal of water is automatically accomplished when an excessive amount of steam bubbles form in the core cooling passages.

While steam becomes radiocative in its passage through the core, its half-life is comparatively short, so that if there are no long half-life contaminants lodged in the turbine, only a relatively short shutdown is necessary prior to servicing the steam turbine, condenser, and auxiliaries.

The second diagram shows a pressurized water reactor similar to that employed on the submarine U.S.S. Nautilus. In this cycle, water under 2000 psi pressure is employed as a coolant for the reactor core. High-pressure water from the reactor is passed through a heat exchanger, where it produces steam at approximately 400 psi in an independent water and steam circuit. Saturated steam from the heat exchanger is not radioactive. Steam turbine generating equipment is of relatively standard design.

The third diagram shows a liquid-metal-cooled reactor, the primary coolant being liquid sodium because of its low neutron-capturing capacity. Sodium, however, becomes radioactive. Sodium transmits heat to a second coolant through a heat exchanger. The second coolant may be a eutectic alloy of sodium and potassium called NaK. This alloy is liquid at room temperature. Heat from the NaK generates steam in the second heat exchanger to operate the turbine.

Another type reactor is termed homogeneous because the fuel is in liquid form and is thus capable of acting both as the heat carrier as well as fuel. One such fuel is a water solution of uranyl sulphate. When this liquid is pumped into a spherical container of the right dimensions, fission takes place in the fissionable isotope throughout the material in the vessel. Heat thus generated is carried away by continuously pumping the fuel solution out of the reactor vessel, through a heat exchanger, and then back into the reactor vessel. Chain reaction of the fuel solution stops immediately after it leaves the reactor vessel because the mass assembly in pipes and other containers is of a geometric form such that chain reaction is not sustained. A manifest advantage is the possibility of a continuous chemical processing of fuel, avoidance of the problem of fabricating fuel elements, and eliminating some stages of chemical processing.

Another type reactor employs a liquid metal solution of fuel, such as a mixture of metallic uranium in liquid bismuth. The liquid-metal type of fuel reactor is believed by its developers to offer promise in the power field.

Still other reactor types are under development, one of which is the sodium-cooled graphite-moderated reactor.

Reactor Developments

A manufacturer entering into reactor development preferably should organize a staff which will include the services of nuclear physicists, chemical engineers, and metallurgists trained in Atomic Energy Commission laboratories. This becomes a difficult problem because of the limited number of high-level personnel in these categories. Alternately, the services of specialists in this field may be employed, such as Nuclear Development Associates, who are well equipped to handle the work in theoretical physics.

Another problem involved in entering this field is the necessity of working closely with the AEC, which in turn requires access to classified material and the obtaining of "Q" clearances for personnel.

Quite apart from the nuclear physics phase of reactor development, there are advanced problems of fluid flow and heat transfer. It appears that heat output, and therefore investment cost of a reactor heat source, depend largely on fluid flow and heat transfer developments in areas outside of past experience in steam powerplants.

The reactor builder finds himself in a new world of metallurgy involving such materials as beryllium, zirconium, and boron steels, to say nothing of the metallurgy of uranium itself. Research and development information on materials of construction and for use in fuel elements is now becoming generally available, and the store of knowledge is being added to from many fast-moving programs.

Another new area of experience is that of radiation damage to reactor materials. Published accounts show that natural uranium will grow to an almost unbelievable extent when exposed to the neutron flux in a reactor. Certain alloys have been developed which greatly improve the stability of fuel elements during their life in the reactor core.

At this time, a word on fuel elements is in order.

The reactor core in a heterogeneous reactor is a geometric assembly of chunks of fuel which must be carefully arranged in a theoretically determined pattern, with coolant spaces between fuel elements to carry away heat. The geometric pattern is necessary for the establishment and safe control of the fission chain reaction, while at the same time permitting coolant space for the heat to be carried away to serve a useful purpose. A fuel element is composed primarily of a certain quantity of fissionable material enclosed in a protective casing. The fuel itself may be natural uranium or natural uranium enriched with a greater amount of uranium 235 obtained from the diffusion plants. Similarly, plutonium or uranium 233 may be the active component.

Uranium must be protected against the action of any oxidizing agent such as water. A still more important reason for enclosing the fuel element in a liquid- and gas-tight shell is the positive need for preventing the escape of radioactive fission products.

The next problem is to design fuel containers so that there will be thermal bonds of high conductivity between fuel cores and inner walls of the protective containers, so that heat can escape from fuel elements without generating excessive temperatures.

Fuel must be suitably alloyed and burn-up time regulated so that radiation damage will not distort or burst fuel containers.

Design of fuel elements, therefore, requires intimate knowledge and direct experience with the effect of radiation damage on different fuel element combinations, as well as development of processes for manufacture of gas-tight containers which will withstand both mechanical and chemical action obtained during the burn-up time employed.

Construction of the reactor itself will vary widely, depending on the type. The main vessel, where used, will be in the form of a cylindrical tank, which, for a pressurized water reactor, may be several inches thick. Present construction favors the use of an 18-8 type stainless steel. Such vessels are extremely expensive, and present attention is being directed toward the use of less highly alloyed materials.

These vessels are fabricated by welding processes presently well established.

Other types of reactors may employ thinner vessels because of lower internal pressures.

In reactor component construction as well as with fuel elements, the ever-present problem of radiation damage requires actual exposure of proposed materials to a neutron flux. The presently available facility is the materials testing reactor (MTR) at Arco, Idaho. The problem will arise wherein a manufacturer must decide whether his development of reactor materials can await its place in the MTR schedule at Arco, or whether he will build his own MTR.

The control system is an important part of the reactor, active components of which are control rods. These rod assemblies are arranged to slide in and out of holes at appropriate locations in the core. The effective section of the rod is made of material having an extremely high affinity for neutrons. Boron is such a material. A compound or alloy of boron is contained in the control rod normally poised outside the core when full heat output is required. When it is desired to reduce the reactivity of the assembly or make the reactor go noncritical, control rods may be moved, or, in case of emergency, projected rapidly into the core, where neutron absorption operates to reduce energy output. Other control rods called shim rods have a fuel assembly at one end and a quantity of neutron absorber at the other.

There are design problems in connection with control rods with respect to mechanisms with which rods may be adjusted from a remote point into the desired positions to regulate reactor output and match power demand. In the pressurized water reactor, electrical and mechanical devices must operate in the pressurized water. In the sodium-cooled reactor, where liquid metal will have a blanket of inert gas on its upper surface, the control-rod operating mechanisms may be outside the reactor, although development of seals to conserve the blanket gas becomes a nice technical problem.

Under emergency or "scram" conditions, control rods must be quickly projected into the core to check the increase of heat output in the event of a runaway or "prompt excursion." A secondary problem is the development of retarding dashpots at the bottom of the stroke of each control rod to prevent mechanical damage to the parts themselves.

There are numerous tests involved, such as checking nuclear physics computations to determine the correctness of assumptions in proportioning the core assembly. It appears that at present, a manufacturer must depend on the reactor testing station at Arco, Idaho, for carrying out such experiments.

It is not the intention to amplify or unduly stress the magnitude of problems involved in the development and construction of reactors. In this brief review, it is possible only to touch on some highlights of the overall job. When stripped down to the fundamental elements of each specific problem, the procedure is generally straightforward. However, at the present time it is difficult to conceive that any reactor, not a duplicate of one previously constructed, can be built without an extensive program of research, development, and testing on the nature of core assembly, fuel elements, and their process of manufacture. Broad problems involved in fuel processing must also be thoroughly checked.

The homogeneous reactor has been mentioned along with its advantages with respect to fuel processing. With the heterogeneous reactor and

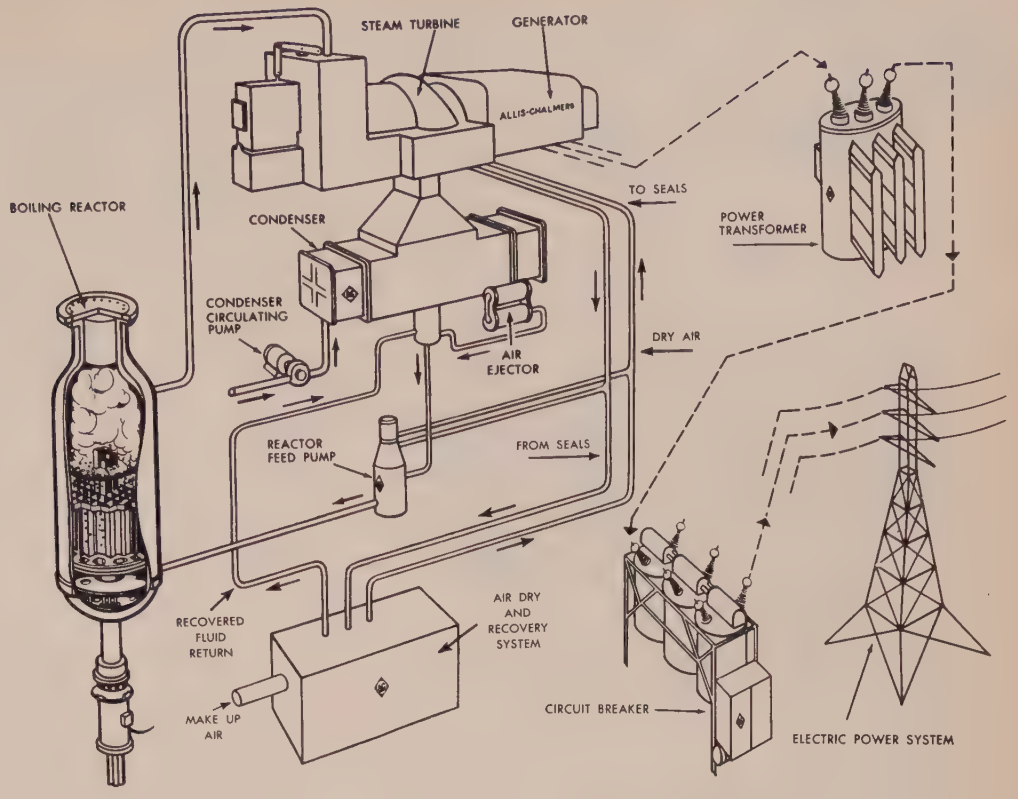

Fig. 2 – Flow diagram of 5000-kw nuclear powerplant

fuel elements in which fuel slugs are contained in gas-tight wrappers, the usual process employs aqueous chemistry to dissolve fuel elements and their casings in acid, after which waste fission products are separated and suitably disposed of, and unused fuel fabricated again into fuel elements. In like manner, if it is desired to separate the plutonium, this is also done by wet chemistry.

In contrast, the homogeneous reactor starts with a liquid solution of fuel. Means have been devised whereby fuel may be continuously processed as it circulates from reactor vessel through the heat exchanger and back to the reactor again. The homogeneous reactor, therefore, avoids the problem of fuel element fabrication.

As usual, there are difficulties. If the fuel solution is sufficiently concentrated to reduce fuel investment and to keep the reactor of moderate size, corrosion presents a problem. Good progress, however, has been made in the direction of practical solutions.

Advocates of the liquid-metal fuel reactor have encountered corrosion difficulties and have likewise made good progress in solving these problems.

5000-Kw Boiling Water Reactor Powerplant

Fig. 2 shows the arrangement of apparatus to be installed in a 5000-kw electric output nuclear powerplant now under construction at the Argonne National Laboratory near Chicago. Construction of this plant was preceded by construction of test reactors which underwent extensive trials at Arco with respect to demonstrating self-regulating characteristics. Simplicity of the present cycle is manifest from the diagram. Dry saturated steam at 600 psig is produced.

The plant will be placed in operation with ordinary water as the cycle fluid. Equipment is designed for operation with heavy water as a possible future service condition. Heavy water has desirable characteristics because of the low neutron capture cross-section of heavy hydrogen. Heavy water presents two problems, however, one being the high cost of any water lost through gland or joint leakage. For example, in a normal steam plant steam leakage of 50 lb per hr might not be considered an excessive total loss from turbine shaft glands and various seals on valve stems, condensate pumps, and so forth. At the present cost of heavy water, this amount of leakage would cost about $1500. At one cent per kilowatt-hour, the total value of electrical output would be only $50 per hour. These rough figures indicate the nature of the seal problem involved where heavy water is used.

A second problem is avoiding contamination of the heavy water supply with light water from the atmosphere, which might result from intermixing engine room air with leakage steam.

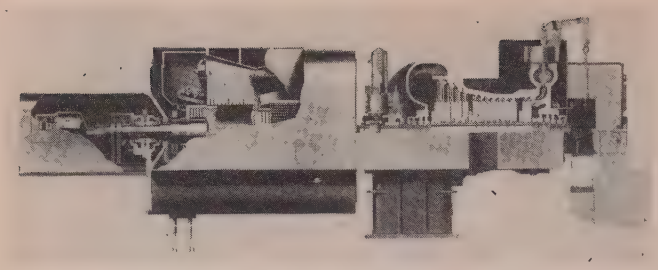

Fig. 3 – Cross-section of turbine and generator for 5000-kw boiling-water-reactor plant

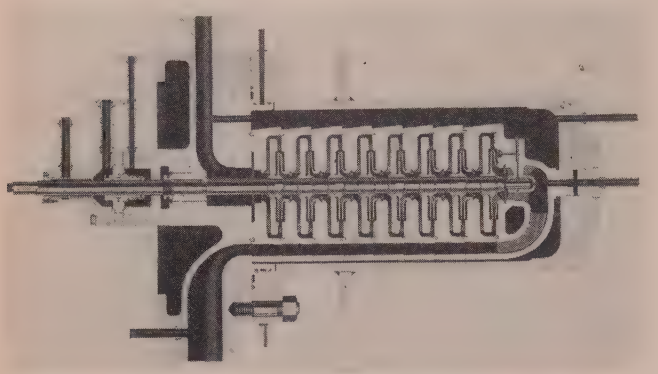

Fig. 4 – Cross-section of combined condensate and feed pump

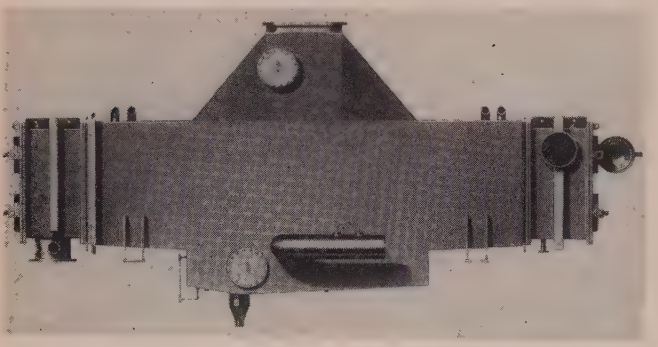

Fig. 5 – Outside view of condenser for 5000-kw boiling-water reactor plant

These problems are solved by sealing all outer gland spaces with chemically dried air and extracting heavy water vapor from the air-ejector offtake by cooling the vapor-air mixture, followed by passing discharge air through chemical dryers. The design is based on means for limiting heavy water leakage loss to an amount not exceeding one pound per day, and for limiting contaminating light water infiltration to half this amount.

The horizontal turbine casing joint and various valve bonnet covers are provided with welded covers designed to catch and prevent vapor leakage to the atmosphere and, similarly, in-leakage of engine room air.

All valve stem seals and corresponding seals on auxiliary pumps are provided with superdried air seals.

Fig. 3 is a cross-section of the steam turbine and generator for this plant.

Tests of this installation will demonstrate how much radioactive contamination will find its way into the turbine as the result of material eroded from the turbine casing or blades, or which may result from corrosion. Ion exchangers and filters are provided to remove such impurities from feedwater to the desired degree.

Detailed design of other turbine parts follows substantially standard lines.

Special controls are involved in which a rapid change in load will permit immediate discharge of excess steam to the condenser, after which output will be established at the demand level by adjustment of reactor controls.

Fig. 4 is a section of the combined condensate and feed pump for the above boiling water reactor. The combination of two pumps in one casing avoids the second shaft seal required if a second pump were used.

Fig. 5 is an outside view of the condenser for the 5000-kw boiling-water reactor plant. Aluminum tubes are rolled into steel tube sheets. Double tube sheets are used, with the space between connected to a suitable leakoff system. This is to prevent light water leakage from the circulating system from contaminating the heavy water charge, which might take place with a standard tube sheet arrangement.

100,000-Kw Fast Breeder Reactor Generating Plant Under Development by APDA

Fig. 6 shows a model of the Atomic Power Development Associates (APDA) plant as now planned for installation in the area served by the Detroit

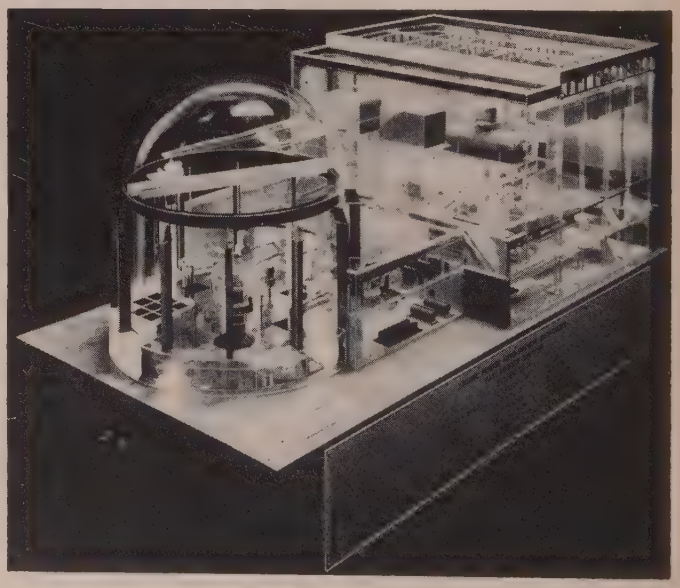

Fig. 6 – Plastic model of APDA nuclear powerplant

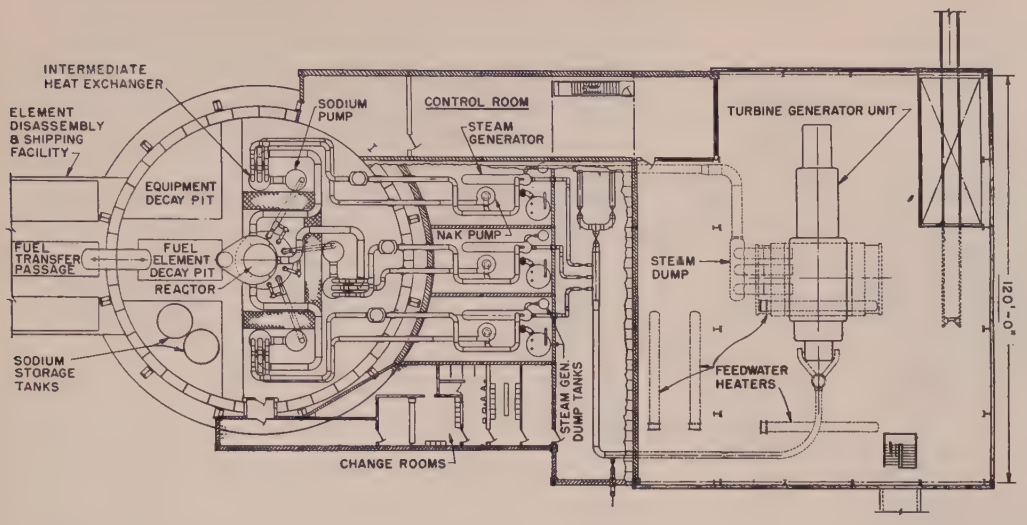

Fig. 7 – Plan layout of APDA nuclear powerplant

Edison system. This program has been developed by the above group which includes 33 companies representing utilities and manufacturers. Allis-Chalmers is a member of this group.

The structure at the left with the hemispherical top is a steel tank 84 ft in diameter which will house the reactor and primary heat exchanger. This structure is designed to withstand safely the maximum pressure which can result from any accident presently thought possible under the worst combination of operating misadventures and control failures.

The building at the right houses the steam turbine and the power generating machinery, distribution equipment, and control apparatus.

Fig. 7 shows a plan layout of the APDA plant. The circular enclosure housing the reactor is at the left, together with heat exchangers to transfer heat from the primary sodium coolant to the secondary coolant, NaK. Note that the reactor enclosure does not contain water which might increase the containment problem should a heat exchanger failure occur.

The view shows the secondary heat exchangers or steam generators outside the main enclosure. Initial steam conditions are 600 psig and 730 F.

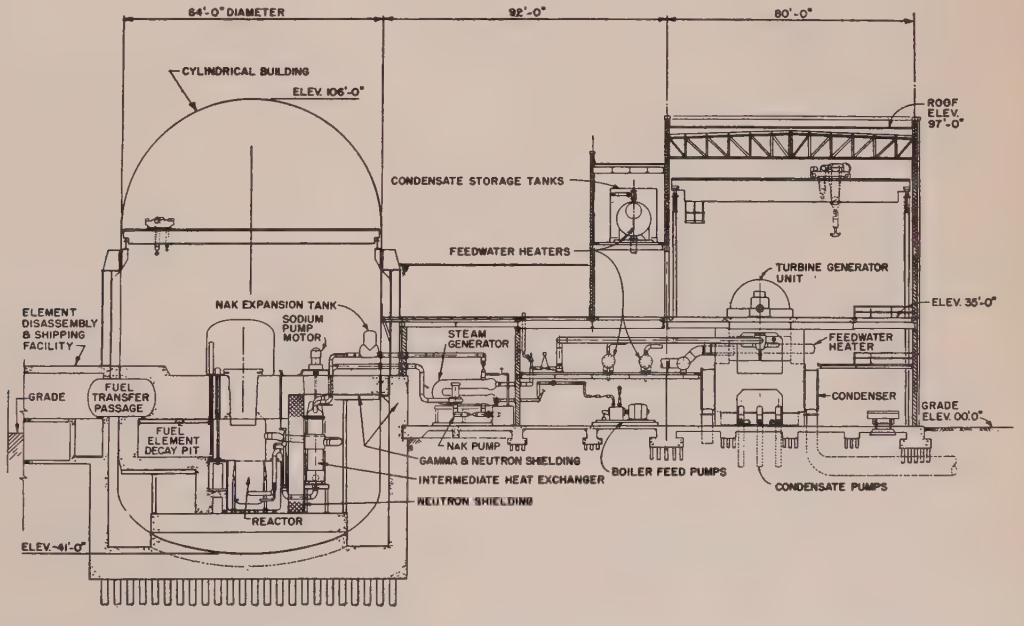

Fig. 8 – Elevation of APDA nuclear powerplant

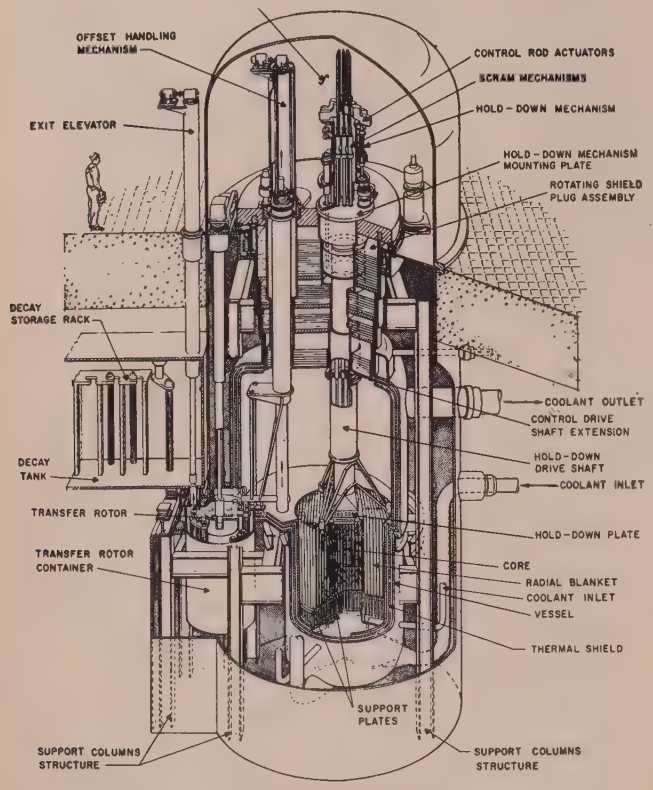

Fig. 9 – Perspective section of APDA nuclear reactor

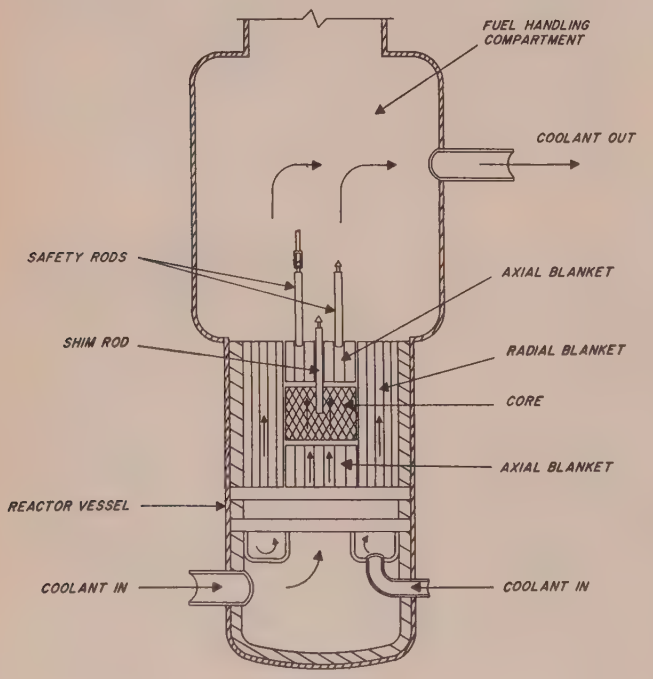

Fig. 10 – Arrangement of APDA nuclear reactor

At the extreme right is the steam turbine generating unit, of conventional design except that inlet steam pressure and temperature will be quite low as far as modern practice is concerned. This will result in a turbine larger for its nameplate capacity than would be the case were it designed for the pressures and temperatures common today in coal-burning plants.

This plant will be operated by two companies. The reactor company will own and operate the reactor building and its contents. Income will come from sale of steam to the power company and plutonium to the government. Processing of fuel elements will be performed in government installations at an appropriate charge to the reactor company.

The steam turbine generating plant will be owned and operated by the Detroit Edison Co. It will purchase steam from the reactor company at rate previously agreed on which will enable the turbine plant to generate power at an acceptable rate comparable to power costs of other stations of the Detroit Edison system.

Fig. 8 is an elevation of this plant, illustrating the containment structure around the reactor itself.

While the layout indicates spaces for fuel element decay, transfer, and storage, the space required for these facilities is vanishingly small compared to the reserve coal storage of a conventional plant.

Fig. 9 is a perspective section of the reactor itself. The central core is approximately three feet in diameter and three feet high. Core elements are approximately 2½ in. square and are arranged for removal by a handling procedure designed to transport spent fuel elements while they are still highly radioactive.

At the top of the reactor, there is a rotating structure approximately 10 ft in diameter and 12 ft high which is a shield to prevent harmful radiation from reaching the upper floor. This plug can be rotated on a ball-bearing track into indexed positions for removal of fuel or blanket elements.

The vertical shaft left of center is part of the handling mechanism also indexed around its axis, so that it can pick up particular elements when they are to be replaced or moved into other desired positions in the fuel and blanket assemblies. Removal of a fuel element consists in lifting it out of the reactor assembly. The handling mechanism is next rotated, and the element is lowered into a space in the transfer rotor. The transfer rotor is then indexed to bring the element under a vertical opening, where the exit elevator picks it up and puts it in the decay storage rack.

All operations just mentioned must be carried out with the used elements fully submerged in liquid sodium coolant. This is because the heat generated by decay of the radioactive isotopes would result in fusion of the elements if the cooling were not continued for a considerable time after removal from the reactor vessel.

The following brief review of the remote-controlled refueling procedure has been included to show that the mechanism designer has a splendid opportunity to contribute to the handling mechanism construction. The extreme limit in reliability must be achieved because of the obvious cost of completely deactivating and decontaminating the reactor for intimate servicing of the kind associated with conventional equipment. Design of shielding to prevent escape of dangerous radiation is an ever-present problem.

The free upper surface of liquid sodium and of NaK must be prevented from coming in contact with atmospheric air. An inert gas, preferably helium, will be used as the nonoxidizing blanket. While today helium is a relatively plentiful commodity, the many possible points of leakage require careful design consideration, as there might otherwise be an excessively high annual expenditure for blanket gas.

Fig. 10 is a diagram of the reactor arrangement for the APDA plant. The rectangular space in the center with diagonal cross-hatching is the core. Elements above, below, and around the core are blanket elements. Coolant is arranged to flow upward through both blanket and core, two circuits being provided because of different quantities of heat to be removed and the various resistances to fluid flow. The head against which coolant pumps operate will be the static head plus flow resistance through core and blanket elements.

Auxiliary Apparatus

Fig. 11 shows a typical design of coolant pump employed for circulating either water or liquid metal through reactor vessels. This particular illustration shows a 16,500-gpm coolant pump for the pressurized water reactor to be installed in the Shippingport Plant of the Duquesne Light Co. near Pittsburgh. Note that the pump and its driving motor are hermetically sealed against leakage. The fluid is pumped through the motor air gap itself. Rotor and stator iron are fully enclosed in stainless steel "cans" which protect the punchings against attack and avoid contamination of coolant.

Journals of the rotating element of such a unit must be effectively supported by the fluid pumped. This is accomplished by the use of fluid piston bearings usually in the form of four equally spaced support pads with containment areas on opposite sides of the shaft filled with cycle fluid at a pressure higher than the background pressure of the system. Two orifices in each support pad make possible the automatic control of shaft position. One orifice leads into each fluid support cavity. Leakage area around each bearing support pad forms the second orifice. A moment's study will show that deflection of the shaft off its center will reduce pressure in the cavity on the side of greatest clearance and increase pressure in the opposite cavity, thus introducing a restoring force tending

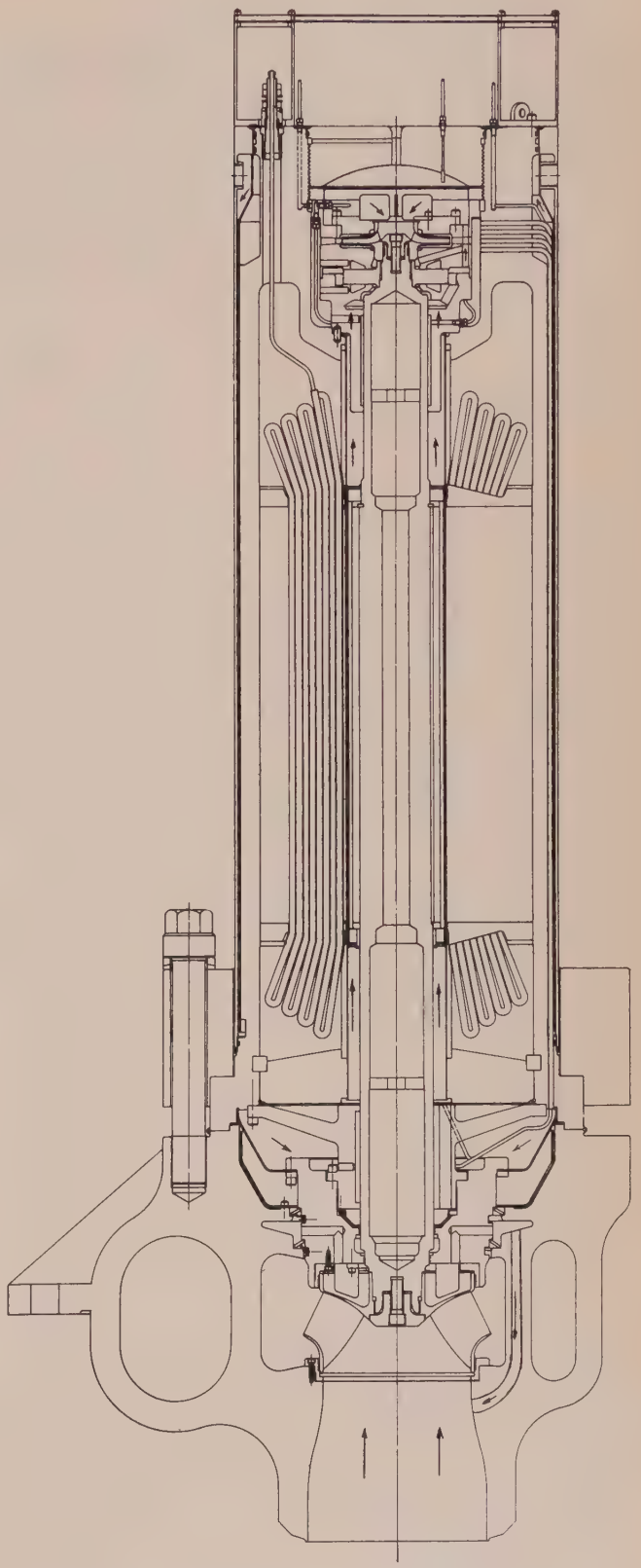

Fig. 11 – Section of coolant pump for circulating water or liquid metal through reactor vessels

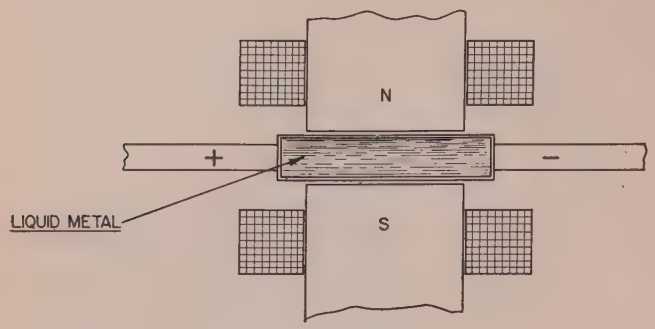

Fig. 12 – DC linear Faraday-type pump

to bring the shaft back to its central position. These bearings are an extremely important feature of hermetically sealed pumps.

Other means of pumping fluids have been developed when the material pumped is electrically conducting. Fig. 12 shows an electromagnetic-type pump designated as the Faraday pump. The diagram shows a rectangular tube with a magnetic flux passing in a vertical direction through the tube and its contents. From the usual right-hand rule of flux, current, and force, a pumping traction is imposed on the fluid at right angles to the plane of the diagram. A direct-current source is applied to the opposite sides of the tube. The difference in conductivity between stainless steel and conventional liquid metal coolants makes it possible to operate such pumps at acceptable efficiencies. The most interesting feature of pumps in this class is the absence of seal problems or moving parts of any kind in contact with the material being pumped.

Fig. 13 is a section of the Einstein-Szillard pump which operates on the same principle as an induction motor. Instead of the magnetic flux rotating around an axis, the three-phase pattern of consecutive poles moves lengthwise down the liquid metal tube. This type pump has the advantage of employing alternating current. The general type is somewhat limited to efficiencies of about 45%, whereas the direct-current Faraday pump is considered capable of operating at higher efficiency. The Faraday pump, on the other hand, requires a large quantity of low-voltage direct current.

Fig. 14 shows a low-voltage direct-current generator designed for operation with Faraday-type pumps. The output of this particular unit is 100,000 amp at one volt.

Advanced liquid metal techniques made possible the collection of extremely high current output in a unit of small dimensions. The rotor is approximately 8 in. in diameter and two feet long. The rotor is completely submerged in NaK, current being collected at the center and ends of the rotor. Stainless steel sleeves of low conductivity act as insulators on portions of rotor and stator iron.

A word on heat exchangers may be of interest. Where sodium or NaK is employed as the heat carrier to transfer heat to water, great care must be taken in design to secure the most reliable construction and, as an emergency safety measure, to provide for pressure jumps which will occur in the event of a leaking tube. Considerable development has been directed toward this problem, and good answers have been found.

Another procedure is to use double tubes, with a liquid between the two tubes which is an effective heat carrier, but which, at the same time, is compatible with both water and sodium or NaK.

The great potential of nuclear fission as a source of power is ample justification for development of apparatus and machinery necessary for generation of electric power from this source to supply rapidly increasing needs of our civilization. Reduced to practical terms, the actual potential is over 20 times the total energy that can be made available by consuming the world's remaining stores of fossil fuels.

Admiral Strauss, Chairman of the AEC, in a recent press release, indicated that the controlled fusion reactor is under study by several groups in the United States. Statements made in this press release indicate a tremendously greater potential source of power from materials found in nature which can be employed in the fusion reactor than is presently estimated as being available from the world supplies of fertile and fissionable isotopes. This development of a controlled fusion reaction, which involves elements at the low end of the periodic table, is not ready for immediate use. The remarks of Admiral Strauss indicate that serious research is being directed toward the future achievement of a power generation process in the atomic fusion field.

Speculation on the possibility of direct generation of electric power without employing customary heat cycles and rotating machinery is gaining greater attention. The knowledge of the fuel cell goes back over 100 years. This reversal of the electrolytic process is being revived and studied, although promise of a power generation cycle for

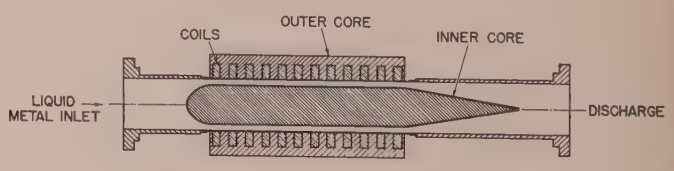

Fig. 13 – AC Einstein-Szillard-type pump

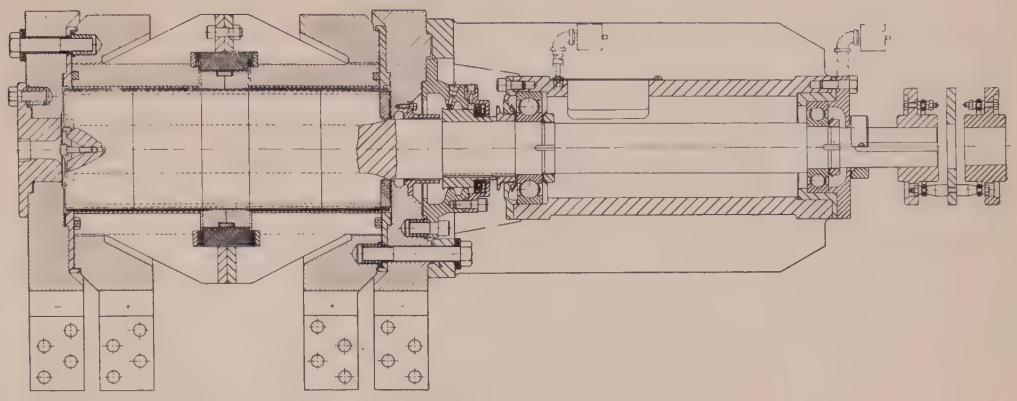

Fig. 14 – Low-voltage, unipolar, dc generator for use with Faraday-type pump

large systems is not presently predictable.

The Bell "Beta" battery has been given wide publicity. This interesting gadget may well find use as a power source for signalling and other similar applications.

Use of thermocouple elements has been advanced by the discovery of certain partial conductors which make possible efficiencies of the order of 8%.

Investigators are still not content with new fields already under intensive research. Brief press releases indicate promise of a new kind of electric power generation at some future date following advanced and highly theoretical studies now in progress. Scientists believe that at temperatures above 20,000 C matter is ionized, and that if passed through a series of magnetic fields, might be accelerated to extremely high velocities. This was mentioned by Dr. Gerhard Piel in his presentation at M.I.T. in 1954.

Recent press releases mention temperatures of 100 million C as the temperature at which matter is completely ionized.

Dr. Arthur Kantrowitz, in his *Scientific American* article of September 1954, said, ". . . at these temperatures a gas becomes a very good conductor of electricity because the heat produces a large number of free electrons. . . . Because of its high conductivity, a filament of very hot gas behaves like a wire in an electric or magnetic field. . . . It is plain that an electric current will be generated in a highly conducting gas moving across the lines of force of a magnetic field just as it is in the armature of an electric generator."

These extremely interesting and intriguing fields of investigation point toward new types of equipment for electric power generation. It must be recognized, however, that there is much to do before achieving the fundamental requirements necessary for such cycles, particularly with regard to the problem of containing quantities of matter at temperatures far above the vaporization temperature of any known substance.

There is little doubt that manufacturers may be puzzled and uncertain about how the apparatus required for the new technology can be built in their plants at a profit. This situation has been helped by the government in many instances by cost-plus-fixed-fee contracts. These are admittedly not desirable, because such work ties up engineering facilities without much production output to keep manufacturing plants busy. On the other hand, this type contract does permit industry participation in new and unknown areas of development.

Industry is gaining steadily in the development of recognized types of nuclear powerplant designs. Established features of construction are being recognized in various areas, which, on the other hand, leave plenty of opportunity for individual manufacturers to achieve outstanding quality by unique and original design. The trend of industrial participation during the last year shows a marked movement in the direction of fixed price contract commitments with definite guarantees.

Never before has industry been faced with such a tremendous opportunity for development of machinery and apparatus intended for production of low-cost power.

The most important phase of our present situation is that the development of nuclear power has accomplished a great deal toward bringing together peoples from remote corners of the earth. There was exhibited at the Geneva Conference this summer a friendliness among scientists and engineers of the many nations represented that helped immeasurably toward bringing together the thinking of representatives of these countries. The common interest in the subject of low-cost power, so necessary to raise living standards of people throughout the world, has stimulated the advance of personal friendships that will go far toward the common objective of world peace.

Relationship of Low-Temperature to Viscosity Characteristics

THE history of the multigrade engine oil development has been brief and interesting. A need for an engine oil permitting good low-temperature cranking and yet retaining high-temperature performance and economy has been evident for many years. Light oils treated with sufficient polymer to meet high-temperature viscosity demands were known to be quite satisfactory, but the needs evidently were not considered pressing enough for production. However, when it was shown that by the use of the same polymer-treated oils the octane requirements of an automobile engine could be reduced by an average of 3 octane numbers,[1] production of multigrade oils was not long following.

Public acceptance of the multigrade oils has been comparatively rapid. These oils began to appear on the market in quantity in 1953 and today account for nearly 50% of the crankcase oil sales in some areas according to C. M. Heinen of Chrysler Corp.[2] An overall sales figure of about 20% has been mentioned. In 1955 ten American car manufacturers representing 70% of the market recommended such multigrade oils.[3]

A difficulty that faced these manufacturers (and still faces them today) was the problem of recommending the correct multigrade oil for the temperature ranges previously served by the single-grade oils, especially for low-temperature operation.

Logically, a multigrade oil should be equal to any of the single grades it encompasses. Following this line of reasoning, one automobile manufacturer gave recommendations as shown in Table 1. This table is typical of the recommendations of the other manufacturers. Here a 10W-30 multigrade oil is considered equivalent to a 10W grade oil for use at temperatures as low as 0 F. But are they equivalent? Without actual tests one can only say "they should be."

Such general acceptance as has been mentioned could easily be interpreted as positive evidence that these oils are well meeting the needs for which they

Table 1 – Manufacturer's Crankcase Oil Recommendations

Anticipated Lowest Atmospheric Temperature, F	Recommended SAE Viscosity Number	Recommended Viscosity Range if Multiviscosity Oils Are Used
32	SAE 20 or SAE 20W	SAE 10W-30 or SAE 10W-20
0	SAE 10W	SAE 10W-30 or SAE 10W-20
Below 0	SAE 5W	SAE 5W-20

HOW well are multigrade oils performing at low temperatures?

An investigation has shown that the low-temperature properties of multigrade oils are often not equivalent to the single-grade oils – 10W in a multigrade oil may actually be 20W.

One phase of this investigation, a full-scale cranking study using commercial 10W and 10W-30 oils in cars at 0 F, is discussed in detail in this paper.

Cranking Resistance of Multigrade Engine Oils

G. K. Malone and T. W. Selby, General Motors Corp.

This paper was presented at the SAE Annual Meeting, Detroit, Jan. 13, 1956.

were designed, especially in regard to the low-temperature starting requirements.

But in the late summer of this year rumors were heard that "all was not what it seemed." More specifically, it was suggested that some of the 10W-30 oils were being manufactured from base stocks which were more viscous at 0 F than the finished oil. It was somewhat difficult to understand how several per cent of an extremely viscous polymer solution could be blended with a light or fluid base stock and yield a product of lower viscosity at 0 F than that of the base stock. In view of the wide use of the multigrade oils, an investigation into the low-temperature characteristics of these fluids was clearly desirable.

A three-pronged attack was made on the problem. The first was a full-scale cranking study using commercial 10W and 10W-30 oils in cars at 0 F, supported by low-temperature viscometric laboratory analysis. The second was a dolly-mounted engine study using oils blended at General Motors Research and again supported by laboratory analysis. The third was a low-temperature viscometric study of several systems of polymer-treated oils.

Only the full-scale cranking study will be discussed in detail in this paper. The authors would like at this point to express their appreciation to William L. Foster for his efforts in conducting the cold-room tests and to thank Thomas M. Verdura and Jack W. Zimmerman for their contributions to the viscometric studies.

The first step was the logical one of establishing whether further work was necessary. Cranking speeds using various commercial brands of 10W-30 oils were compared to one another and to the cranking speeds obtained using each brand's respective 10W oil. The cars were filled with the oil to be tested, run for 1 hr, drained, refilled, run for 15 min (at which time an oil sample was taken for viscometric analysis), and then put into the cold room at 0 F for a period of either 17 or 35 hr. The longer cold exposure seemed to have little or no effect on cranking speed. Cranking power was derived from the car battery which went into the test with the car.

Results of one series of cranking tests on four brands of oil are shown in Table 2, Column 3. The

[1] "Effects of Lubricating Oil on Octane Requirements of Cars in Customer Service," by P. A. Bennett and J. R. Landis. Presented at SAE Cleveland Section Meeting, Cleveland, Jan. 18, 1954.

[2] "Our Mutual Problems from Additives to Zzmog," by C. M. Heinen. Presented before SAE Metropolitan Section, New York, April 7, 1955.

[3] "Trends in Passenger-Car Lubrication Recommendations 1941-1946-1951-1955," Chek-Chart Corp., 1955.

Fig. 1 – Brookfield LVT viscometer

maximum difference in this analysis between 10W-30 oils is 11 rpm. However, even larger differences than those evident in Table 2 have been found between different brands of 10W-30 multigrade oils. A maximum difference of 30 rpm has been obtained. This difference in cranking speed corresponds to a temperature difference of about 15 deg. In other words, where the oil yielding the low cranking speed might just start the car at 5 F, the oil yielding the high cranking speed might start some 15 deg colder. Or, from another point of view, if we consider 40 to 50 rpm a critical cranking speed for a car in average condition, then using one brand of SAE 10W-30 the car might not start, while using another it would start easily. It is also apparent in Table 2 that marked differences may exist between the 10W and the 10W-30 oils of the same brand. A maximum difference of 19 rmp has been found. The 10W oil is usually the better of the two, viscometrically.

There is no doubt that these differences are significant, and the immediate question that arises is why such differences exist in oils with the same

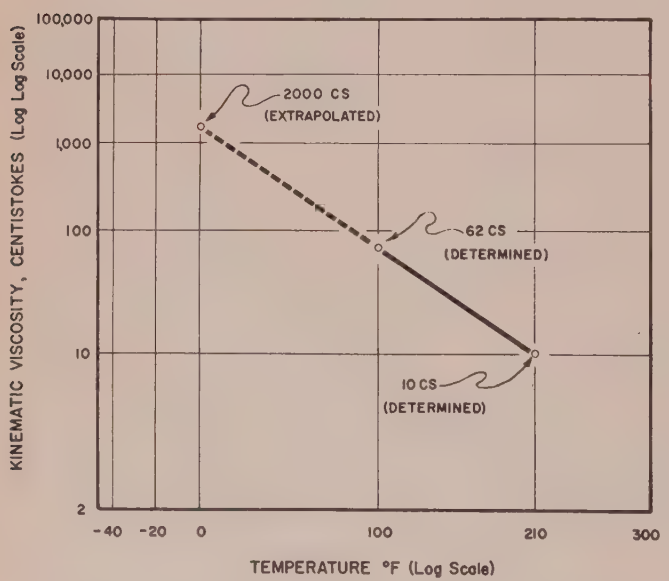

Fig. 2 – Extrapolated method of determining 0 F viscosity

Table 2 – Commercial Oil Analysis at 0 F

Brand	SAE Grade	Cranking Speed	Brookfield Viscosity	Extrapolated Viscosity
A	10W-30	54	3620	2273
	10W	66	2400	2285
B	10W-30	65	2540	2217
	10W	73	1820	2016
C	10W-30	61	2940	1936
	10W	74	1920	1498
D	10W-30	58	3070	2266
	10W	64	2430	2184

SAE 0 F classification.

In view of the known relationship between engine cranking speed and viscosity, it was thought that the differences in rpm might be explained by differences in viscosity.

The first viscometric analysis of the eight commercial oils at 0 F was performed on a Brookfield LVT viscometer shown in Fig. 1. This is a rotational viscometer of simple, rapid operation and a sensitivity of $\pm$ 0.2% of full scale. Results of this analysis of the commercial oils in Table 2, are shown in Column 4.

Analysis of the oils was a relatively rapid process. Approximately 15 ml of the oil to be tested was poured into a cell carrying its own spindle (see the dissembled cell in the foreground of Fig. 1). The cell was placed in the cold box forming the background of the picture for 2 hr at 0 $\pm$ 0.3 F. After this time of cold exposure the cell was encased in the balsa block shown and immediately analyzed. At 0 F the influence of ambient air temperature on the analysis was not evidenced for 3 or 4 min because of the insulating qualities of the balsa block. This allowed more than sufficient time for the determination of viscosity. One of the major advantages of this method is that a number of analyses may be made in a short period of time using a group of cells.

The facts to be observed from a comparison of cranking speed to viscosity in Table 2 are:

1. The viscosity values are markedly different.
2. The cranking rates inversely correspond to these viscosity values.

A more important observation should be made from Table 2. The SAE 10W grade oil must have a maximum viscosity at 0 F no greater than 2606 centistokes (12,000 SUS) which is equivalent to approximately 2400 centipoises. Only three of the eight oils tested are, therefore, within the 10W classification according to the viscometric analysis, and these three are 10W single-grade oils. How then do the other five oils qualify as 10W oils?

The answer to this question may be found in the SAE Handbook.[4] In this handbook an extrapolation technique is recommended for the determination of low-temperature viscosities. According to this method a straight line is drawn through two points on an ASTM viscosity-temperature chart as in Fig.

2. The chart and extrapolation technique are based on the empirical Walther equation:[5]

$$\log \log (v + a) = m \log T + b$$

where:

v = Viscosity, centistokes
a = Constant equal to 0.6 (above 1.5 centistokes)
m = Slope constant
T = Absolute temperature, K
b = Intercept constant

Walther found that mineral oils in general obeyed this equation through the temperature range in which these oils behaved as simple single-phase or Newtonian liquids. Below this temperature range the oil becomes complex or non-Newtonian and the Walther equation no longer applies. The viscosity-temperature curve then departs from the equation as in Fig. 3.

Since this method was most likely the one used in classifying the commercial oils investigated, the 0 F viscosities of these fluids were determined by extrapolations from their viscosities at 100 F and 210 F. The extrapolated values are given in Column 5 of Table 2. Most of the extrapolated values fall below the determined values; and, by such extrapolation, all eight oils now fall within the 10W classification. It appears, then, that at 0 F these fluids have entered the temperature region in which they are no longer Newtonian, the zone in which the Walther equation obviously no longer applies and thus the zone in which extrapolated values are no longer valid. This departure from the equation is markedly expressed by the 10W-30 oils in Table 2. Considering brand C, for example, the determined value of the 10W-30 oil is about 60% higher than the extrapolated value.

Such behavior by the multigrade oils provides the answer to the original paradox which initiated this investigation – the problem of how it is possible to manufacture a multigrade oil of less viscosity at 0 F than the base stock from which it is made by adding several per cent of syrupy polymer solution. The answer is that the extrapolation technique is responsible for this contradiction to nature. Fig. 4 shows both the extrapolated and determined viscosity temperature curves of the multigrade oil and its base stock.

It will be noted that it is possible for the oil-polymer curve to intersect the oil curve at temperatures *below* 0 F due to another phenomenon known as "pour-point depressance." But, this in no way may be considered as a justification for the use of the extrapolated viscosity values.

On the basis of these facts, it may be of some interest to compare engine cranking speeds at 0 F with the extrapolated and the determined viscosity data. From this comparison it should then be possible to determine which viscosity has the greater correlation to engine cranking speed.

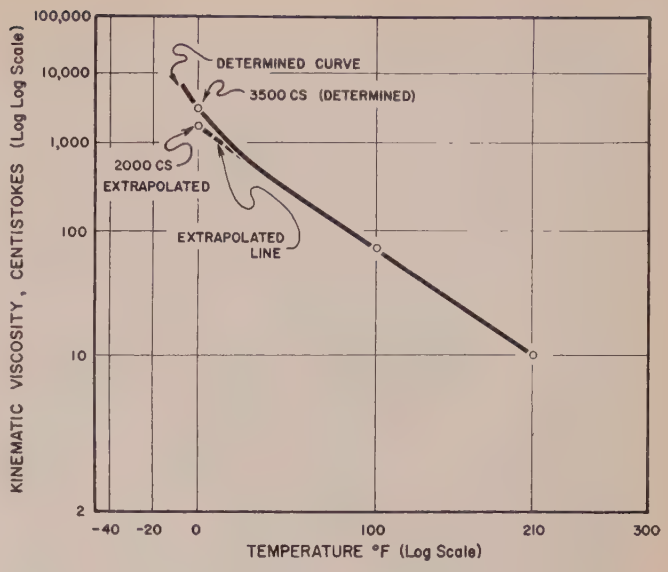

Fig. 3 – Comparison of determined and extrapolated viscosity-temperature curves at 0 F

Cranking speed versus *extrapolated* viscosity is shown in Fig. 5. The points seem almost randomly dispersed. By drawing the best straight line through the points (by the method of least squares) and calculating the correlation coefficient, it may be shown that the extrapolated values show only 5.3% correlation to the cranking speeds. In other words, this indicates that the viscosity of the oil at 0 F influences a cranking speed of, say, 50 rpm by only 2 or 3 rpm – certainly a negligible effect, contrary to experience. The band shown in Fig. 5 represents the standard deviation of points about the line.

The same oil samples were analyzed by the Brookfield viscometer at 0 F and are plotted versus the cranking speed in Fig. 6. Again drawing the best straight line through the points, the correlation between viscosity at 0 F and cranking

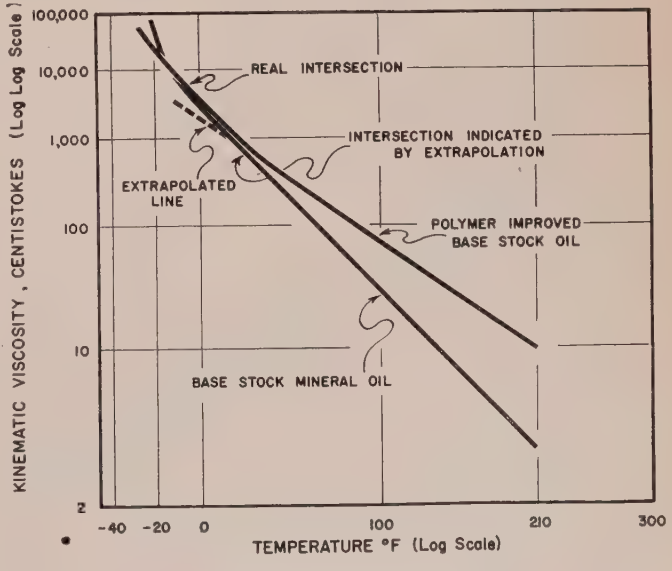

Fig. 4 – Extrapolated viscosity error in the comparison of a multigrade oil to its base stock

[4] See 1954 SAE Handbook, pp. 360-361: "Extrapolated Oil Viscosities."
[5] See *Oel und Kohle*, Vol. 1, December, 1933, pp. 71-74: "Evaluating Lubricating Oils," by C. Walther.

speed is found to be 32%; or, restating this relationship, 32% of the cranking-speed variation at 0 F is due to the viscosity of the oil in the engine. This is certainly a much more significant effect than that indicated by the extrapolated values.

A Fenske-Ostwald reverse-flow capillary viscometer was also used to investigate these oil samples. This viscometer, shown inside the cooling bath in Fig. 7, is common in most oil laboratories. The results of this analysis are shown in Fig. 8. More scatter is found in the points since this instrument, when operated under its own hydrostatic head, is sensitive to structures which some oils form at these temperatures. The correlation between these viscosity values and the cranking speed, found to be 16.3%, is about half that of the Brookfield analysis but about three times that indicated by extrapolation. Undoubtedly, this correlation would be improved by using a greater pressure to move the oil through the capillary than that developed by the hydrostatic head since this would tend to eliminate the influence of fragile oil structures on the determined values.

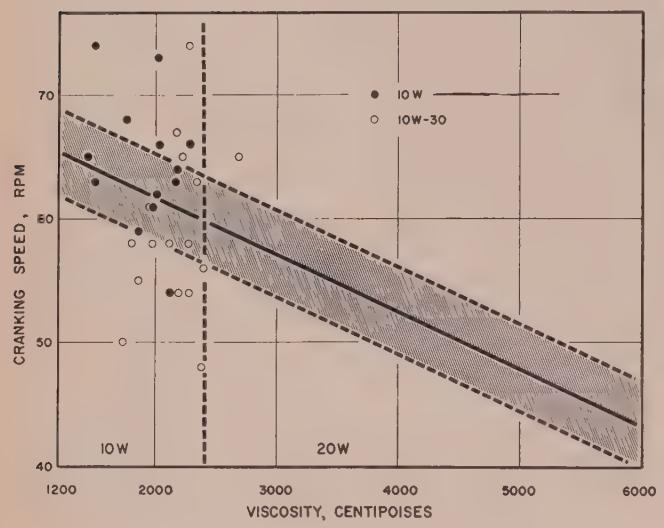

Fig. 5 – Cranking speed versus extrapolated viscosity

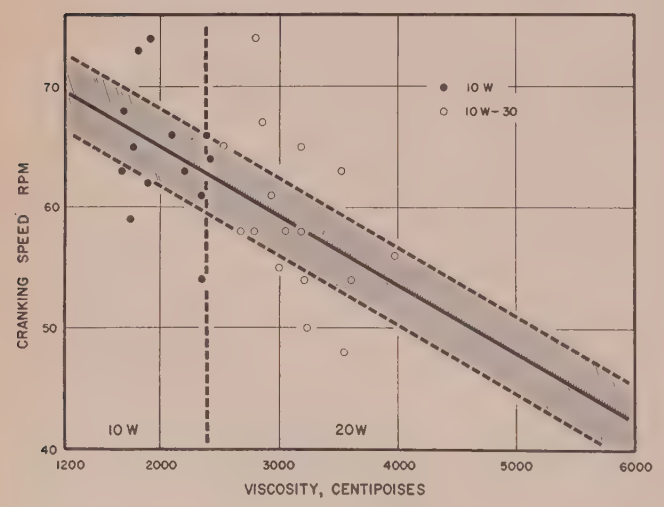

Fig. 6 – Cranking speed versus Brookfield viscosity

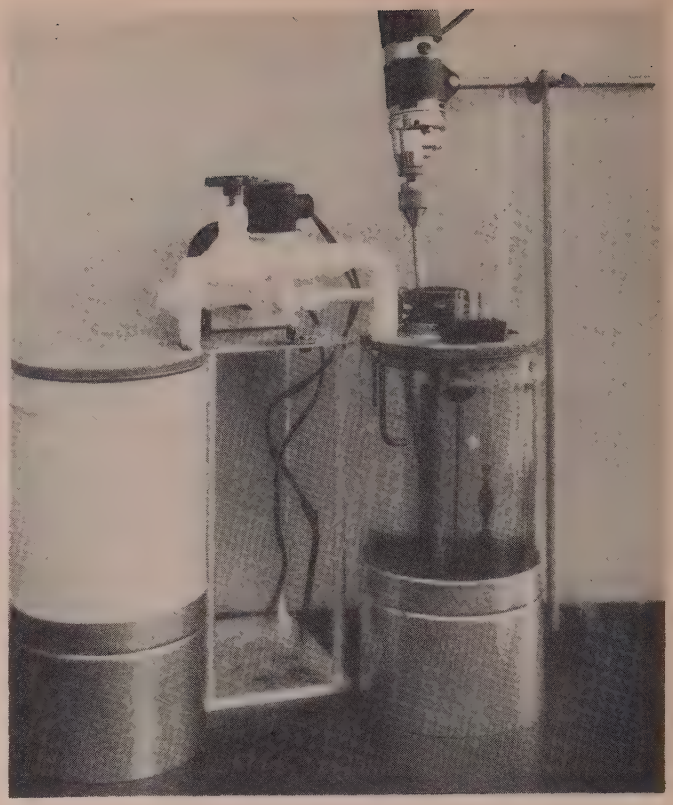

Fig. 7 – Fenske-Ostwald reverse-flow capillary viscometer

This dependence of the capillary values on the flow rate leads to an important fact concerning mineral oils in a non-Newtonian state. When a fluid is non-Newtonian, the actual viscosity value becomes dependent on how fast the molecules are pushed past one another, the so-called shear rate. If the fluid is a mineral oil, it has been found that, in general, as the shear rate becomes greater, the viscosity decreases.[6]

The average shear rate imparted in the Model LVT Brookfield viscometer using a No. 4 spindle in a 25-mm diameter cell is about 1.6 reciprocal sec. The average shear rate found in the Cannon-Fenske No. 500 capillary viscometer is about 0.3 reciprocal sec. On the cylinder walls of an engine cranking at 50 rpm, the rate of shear is about 2500 reciprocal sec. If the shear rate is high enough, it is *conceivable* that the viscosity *may* approach the extrapolated value as a limit.

The evidence indicates that, at least with the multigrade oils, such a decrease in viscosity with the high shear rates is not to be expected. One point of evidence is the better correlation of *determined* viscosity with cranking speed. For, if at high rates of shear the viscosity of the oil in the engine became quite similar to that predicted by extrapolation, then the extrapolated data would have the closer relationship to cranking speed; this we have seen is not the case.

[6] See "Viscosity Characteristics of Motor Oils," by C. Georgi. Preprint No. 8, Section VI/C in Proceedings of Fourth World Petroleum Congress, Rome, Italy, 1955.

A second point of evidence lies in the results given by a viscometer developed by General Motors Research for the low-pressure analysis of mineral oils at shear rates up to about 3000 reciprocal sec. This viscometer, shown in Fig. 9, is called the forced-ball viscometer and is based on the viscometric principles of a falling sphere of high artificial density.

The results of this viscometric analysis are plotted against cranking speeds in Fig. 10. Correlation between these viscosity values and cranking speeds was found to be 43% or about eight times better than the correlation found using the extrapolation data.

It is to be noted that the slope of the best straight line is steepest for the forced-ball analysis (slope $= -7.89 \times 10^{-3}$) less steep for the Brookfield analysis (slope $= -5.68 \times 10^{-3}$) and still less for the capillary analysis (slope $= -1.77 \times 10^{-3}$). This should be the expected relationship since the 10W-30 oils were shown to be more non-Newtonian than the 10W oils (cf Table 2) and thus would be more shear susceptible. The best lines then would tend to shift very slightly in the 10W regions and considerably in the 10W-30 region, thus rotating the lines clockwise under increasing shear.

The conclusions from this study in conjunction with the two studies not included may be stated briefly.

1. The low-temperature performance of multigrade oils in engines is often not equivalent, grade for grade, to the single-grade oils. In other words, a 10W in a multigrade oil is often really a 20W.

2. Classification of an engine oil for low temperature should be based on its determined viscosity at these temperatures and at a specified shear rate – preferably at rates comparable with those adjacent to the principal moving parts in the engine.

3. The use of the empirical Walther equation in oil analysis should be restricted to that portion of the temperature spectrum where it is known to apply.

Fig. 9 – Forced-ball viscometer

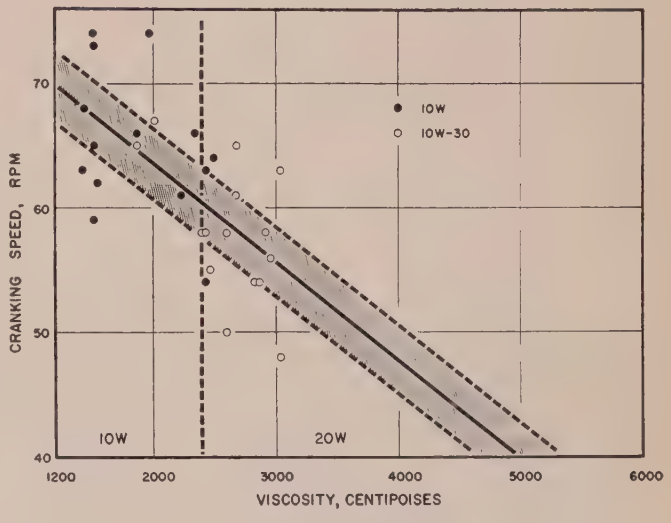

Fig. 10 – Cranking speed versus forced-ball viscosity

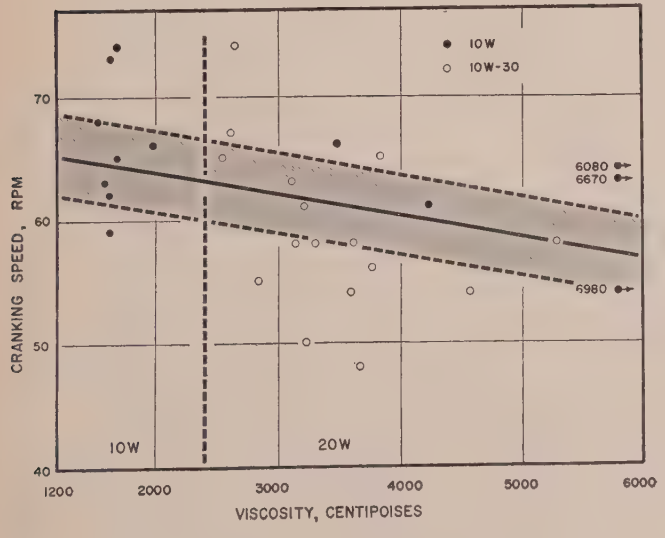

Fig. 8 – Cranking speed versus capillary viscosity

It should be emphasized that the multigrade crankcase oil, as it was conceived, is a definite advance, viscometrically. But a portion of the advantages of such a system should not be forfeited because methods of classification have not kept pace with development.

When it is considered that the automotive engineers have constantly endeavored to increase the winter-weather usability of the automobile, it may be time for them to be more specific in classifying the materials which provide one of the chief hindrances to low-temperature starting.

DISCUSSION . . .

. . . of this article starts on p. 621

Cold Starting with V.I.

IN recent years, the trend in passenger-car engine lubrication has been toward year-round multiviscosity-grade oils. These oils are formulated with large amounts of polymeric V.I. improvers in order to provide maximum viscosities at high temperatures for good oil consumption and minimum viscosities at low temperatures for easy starting in cold weather. However, it is well known that the viscosities of oils containing polymers change with temperature and shearing conditions in a manner that is quite unlike the behavior of conventional mineral-oil lubricants. In this study, the cold-starting performance of polymer-thickened oils was evaluated in full-scale engine cranking tests with a view toward determining the effects of these unique viscosity properties. It was found that multigraded oils of identical viscosities at 210 F and ASTM extrapolated viscosities at 0 F cranked faster or slower than conventional mineral oils of the same 0 F viscosities, depending on the particular combination of V.I. improver and base oil used in their formulation. The observed differences in cranking performance can be explained in the following way: (1) The capillary viscosities of V.I. improved oils at low temperatures are much higher than the ASTM chart predicts, and (2) temporary losses in viscosity occur during engine operation to reduce this high value in some cases. Both of these factors can be estimated so that it is now possible to calculate the cold-starting behavior of a V.I. improved oil from its measured high-temperature viscosities, provided the high-temperature viscosities of the base oil and the composition of the V.I. improver are also known.

Introduction

Multiviscosity-Grade Oils – The SAE winter grades of motor oils, designated as 5W, 10W, or 20W, are classified according to their viscosities at 0 F. These viscosities are not determined experimentally but are obtained by extrapolation on the ASTM viscosity-temperature chart (D 341-43) from measured viscosities at 100 and 210 F. The low-temperature viscosities, as determined from this chart, correlate very well with the cranking speeds obtained during cold starting in an automobile engine with oils containing no V.I. improver. However, over the last several years, there has been a growing trend toward the use of V.I. improved motor oils. At present about one-fifth of the premium grade automotive lubricants sold in this country are multiviscosity graded, and this figure is increasing rapidly. Multiviscosity-graded oils, such as the 5W-20's, the 10W-30's, and the 20W-40's, are

Improved Multigrade Oils

F. B. Fischl, H. H. Horowitz, and T. S. Tutwiler,
Esso Research and Engineering Co.

This paper was presented at the SAE Annual Meeting, Detroit, Jan. 13, 1956.

formulated with large concentrations (5-15%) of various V.I. improvers in order to reach the high V.I. levels (120-150 V.I.) required to meet the specification limits imposed by the multiple grading (see Table 1).

Since the presence of V.I. improver in a lubricant imparts unique physical properties, there is no assurance that the low-temperature viscosities of such oils predicted by the ASTM chart will correlate with observed cranking speeds. A 10W-30 oil, for example, may or may not perform at low temperatures as well as a conventional 10W mineral oil. The cold-starting tests described here are designed to clarify this situation.

SAE System for Defining Low-Temperature Viscosities – Before discussing the experimental results, it will be well to consider why the SAE system for defining winter-grade oils is based on

LARGE differences in cold-starting behavior have been found in engine cranking tests on 10W-30 oils formulated with different V.I. improvers. Oils of identical viscosities at 210 F and ASTM extrapolated viscosities at 0 F cranked faster or slower than conventional 10W mineral oils, depending on the particular V.I. improver-base oil combination used in their formulation.

It has been found that a substantial portion of the viscosity imparted to the oil by the V.I. improver is temporarily lost under the high shearing stresses encountered in cold engine startup. Thus, the cold-starting performance of a V.I. improved oil approaches that of the base oil from which it is blended.

It appears from this work that the SAE system for defining the limits of winter-grade oils, while adequate for mineral oils, needs improvement for polymer-thickened multigraded oils. Laboratory viscosity measurements under high shearing stresses are now being conducted in an effort to obtain a simple technique for estimating the cold-starting performance of polymer-thickened oils.

Table 1 – SAE Viscosity Limits for Multigraded Oils

SAE Grade	At 0 F Max	At 210 F Min	At 210 F Max	Minimum Viscosity Index
5W-20	4,000	45	58	140
10W-30	12,000	58	70	134
20W-40	48,000	70	85	121

ASTM extrapolated viscosities at 0 F instead of on measured low-temperature viscosities. The principal reason for this is that wax precipitation prevents meaningful capillary tube measurements at 0 F if the cloud points are above 0 F. ASTM extrapolated viscosities for conventional oils generally agree well with values measured in capillary viscosimeters if the oil is free of wax at the test temperature. However, conventional high V.I. oils contain appreciable amounts of paraffin wax and generally have cloud points considerably above 0 F, so that the observed results at 0 F are often manyfold higher than the chart predicts. Early work with such oils[1] showed that the ASTM viscosities correlated much better with engine cranking speeds at low temperature than did the measured capillary viscosities. The reason for this is that even relatively mild shear stresses almost completely eliminate the contribution of wax and bring the viscosity back to the ASTM value. Gavlin, Swire, and Jones,[2] for example, found that when as little as 10 ergs per cc of work were done on a Pennsylvania 150 Neutral below its pour point, at any shearing stress, its viscosity would fall to the ASTM value. Similarly, Georgi, in a recent paper given before the World Petroleum Congress,[3] indicated that the viscosities of all mineral oils follow the ASTM extrapolation at low temperatures if they are measured under high rates of shear. In this connection, previous work at Esso Research and Engineering Co.[4] has shown that two oils that required equal cranking torques in an engine at temperatures above and below their pour points also cranked equally fast at a temperature where one oil was above its pour point and the other below. The only effect of wax is to increase ordinary capillary viscosities; since the ASTM chart gives the viscosities that would exist if the wax did not contribute, it is considered the more reliable indication of the cold-starting performance of waxy mineral oils than is a direct viscosity measurement in a capillary instrument.

In the case of V.I. improved oils, however, there are factors other than wax that invalidate the use of the chart for predicting low-temperature startup. One is the fact that the viscosity-temperature relationships of V.I. improved oils do not extrapolate as straight lines on the ASTM chart but have a concave upward curvature. For example, when a straight-line extrapolation is attempted, the ASTM chart will very often predict that a blend of a mineral oil thickened with V.I. improver will have a low-temperature viscosity below that of the mineral oil itself. This is obviously incorrect, since a V.I. improver, a high molecular weight polymer, will always thicken a mineral oil at all temperatures. Secondly, even if the chart accurately predicted the low-temperature capillary viscosities of V.I. improved oils, it still would not correctly predict their engine performance because the ASTM chart neglects temporary viscosity loss which occurs during engine operation. The term "temporary viscosity loss" refers to an apparent drop in the viscosity of polymer-thickened oils during the application of high shearing stresses to the oil. On release of the shearing stress, the oil reverts immediately to its original viscosity. This phenomenon was found to be extremely important in determining the startup performance of V.I. improved oils as was clearly established by data obtained from the low-temperature cranking tests described in the following sections.

Low-Temperature Engine Cranking Tests

In these tests, a 1955 V-8 engine was calibrated as a low-temperature viscosimeter by cranking it with its own starting motor, using mineral oils of known low-temperature viscosities in the crankcase. A relation between cranking speed and viscosity was obtained. The engine was then used to measure the "engine" or actual viscosities of a series of 10W-30 oils of identical high temperature and 0 F ASTM extrapolated viscosities. In this way it was possible to obtain the following information: (1) a comparison of multigraded V.I. improved oils with mineral oils of SAE 5W, 10W, and 20W grades and (2) a comparison of different V.I. improver blends.

Test Procedure – The engine, which had been broken in by driving it in mild service for 2500 miles, was housed in a cold box where its temperature could be controlled automatically to ±0.5 F. The engine was fully equipped except that no transmission or power accessory equipment was attached. The engine was only cranked, not fired. There was no gasoline in the carburetor, to avoid possible dilution of the test oil.

The low-temperature performance of the test oils was obtained at 0, –10, and –20 F by two independent measurements:

1. The engine was cranked with its own starting motor powered by an externally mounted 12-v

[1] See *SAE Journal*, Vol. 28, February, 1931, pp. 234-239: "Cold-Starting Characteristics of Automobiles," by A. J. Blackwood and N. H. Rickles.

[2] See *Industrial and Engineering Chemistry*, Vol. 45, October, 1953, pp. 2327-2335: "Pour-Point Depression of Lubricating Oils," by G. Gavlin, E. A. Swire, and S. P. Jones, Jr.

[3] "Viscosity Characteristics of Motor Oils at Higher Rates of Shear," by C. W. Georgi. Section VI/C, Reprint No. 8, Proceedings of Fourth World Congress, Rome, Italy, 1955.

[4] See *ASTM Bulletin*, No. 198, May, 1954, pp. 70-77: "Lubricating Oil Requirements of Modern Automotive Engine," by J. P. Hamer, T. S. Tutwiler, and C. A. Weisel.

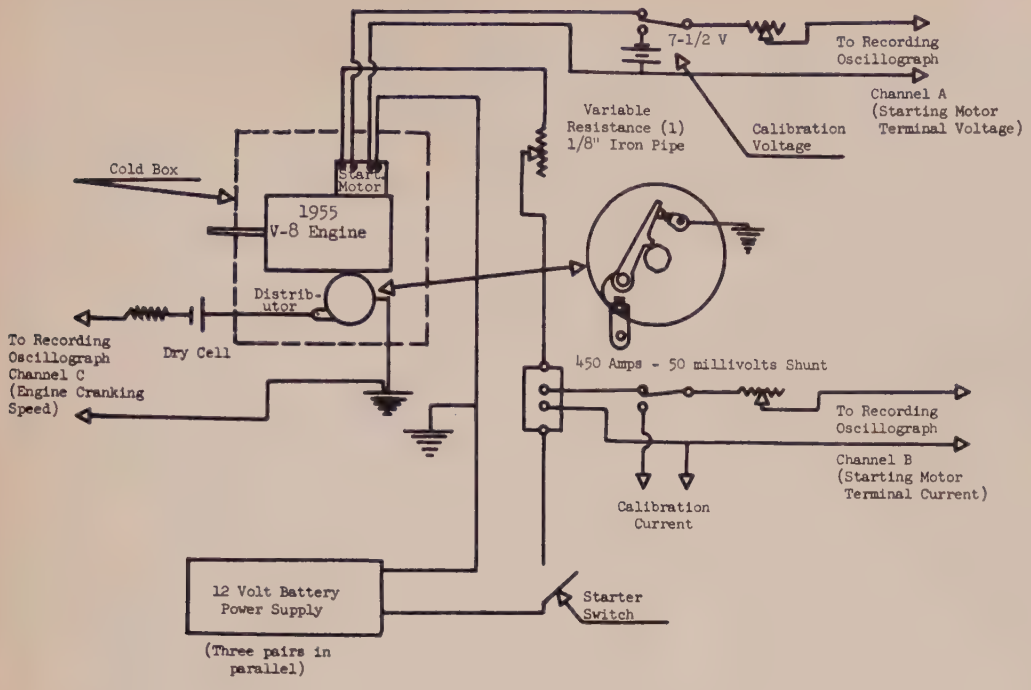

Fig. 1 – Schematic arrangement for low-temperature cranking with engine starting motor

(1) Adjusted to duplicate output of a fully charged battery at test temperature.

source operated in series with a resistance bar to simulate the characteristics of a standard battery at the test temperatures. The cranking speed and the starting-motor terminal current and voltage were recorded. Fig. 1 illustrates the electrical circuits used to obtain these measurements. Duplicate tests were run on each oil at each temperature. Since it was still necessary to compensate for minor variations in battery output, the observed speeds at each temperature were corrected to the output of the standard battery in a fully charged condition. These corrections are based on the property

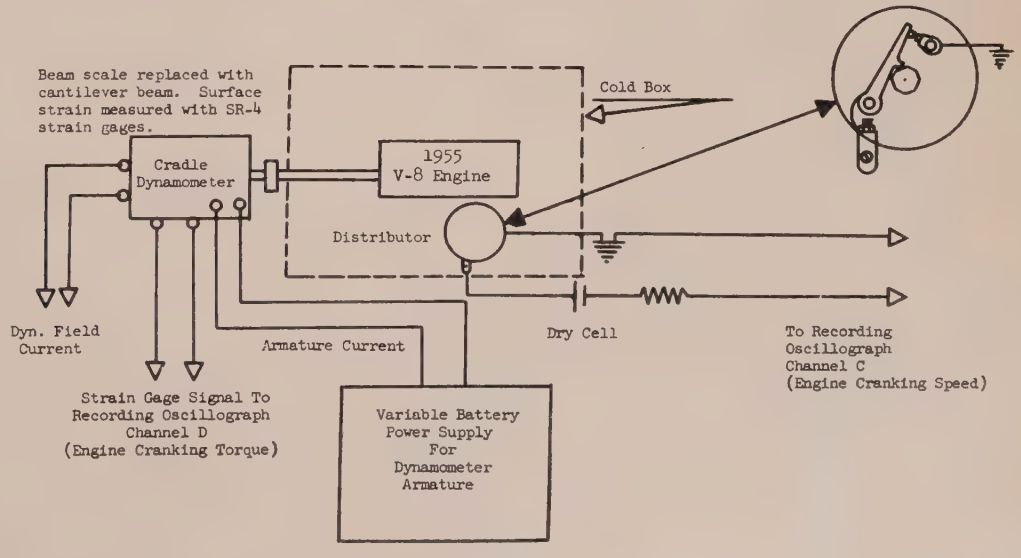

Fig. 2 – Schematic arrangement for low-temperature cranking with dynamometer

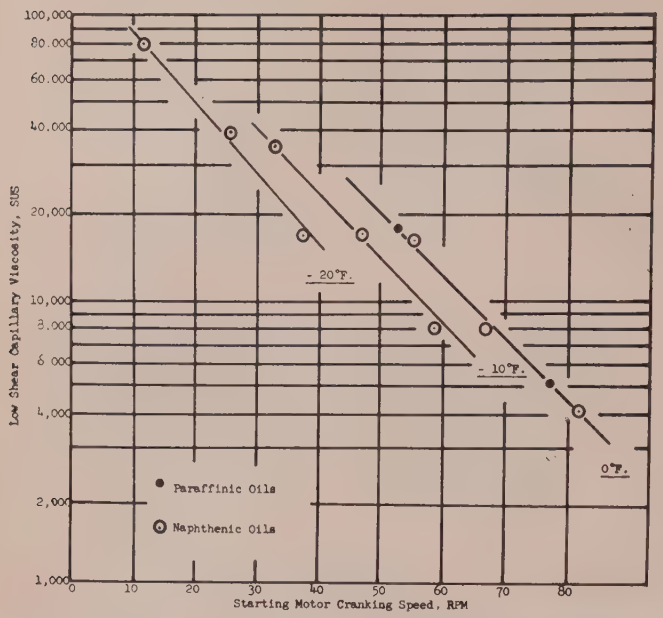

Fig. 3 – Calibration of V-8 engine as a low-temperature viscosimeter

of series-wound motors that the rotational speed at a given torque level is proportional to the counter emf. In general, the speed corrections ranged from 0 to ±5 rpm.[5] After applying these corrections, the average of the duplicate tests was reproducible to ±2 rpm.

Table 2 – Low-Temperature Viscosities of Calibration Oils

SAE Grade	5W	10W	20W
Measured (Capillary) Viscosities at 0 F, SUS	4120	8080	16,500
ASTM Extrapolated Viscosities at 0 F, SUS	3900	7600	16,500

2. The engine was also cranked with a cradle-mounted dynamometer, and the applied torque was computed from strain-gage measurements at different speeds. A schematic diagram showing the arrangement used is presented in Fig. 2.

Each oil was evaluated using a standard test sequence to avoid errors due to differences in cooling rates and soaking periods. All torques, speeds, voltages, and currents were recorded on a multichannel recording oscillograph.

Oils Tested – 1. *Calibration Oils* – The V-8 engine was calibrated as a viscosimeter with three nonwaxy mineral oils of SAE grades 5W, 10W, and 20W, respectively, on which capillary viscosities at the three test temperatures (0, –10, and –20 F) could be measured accurately. For these oils, the ASTM extrapolated and laboratory measured viscosities were essentially identical as shown in Table 2.

[5] These corrections do not take into account the rise in torque with increasing speed observed in the dynamometer cranking tests. This causes the corrections used here to be slightly high, but the differences are small and do not materially affect the conclusions.

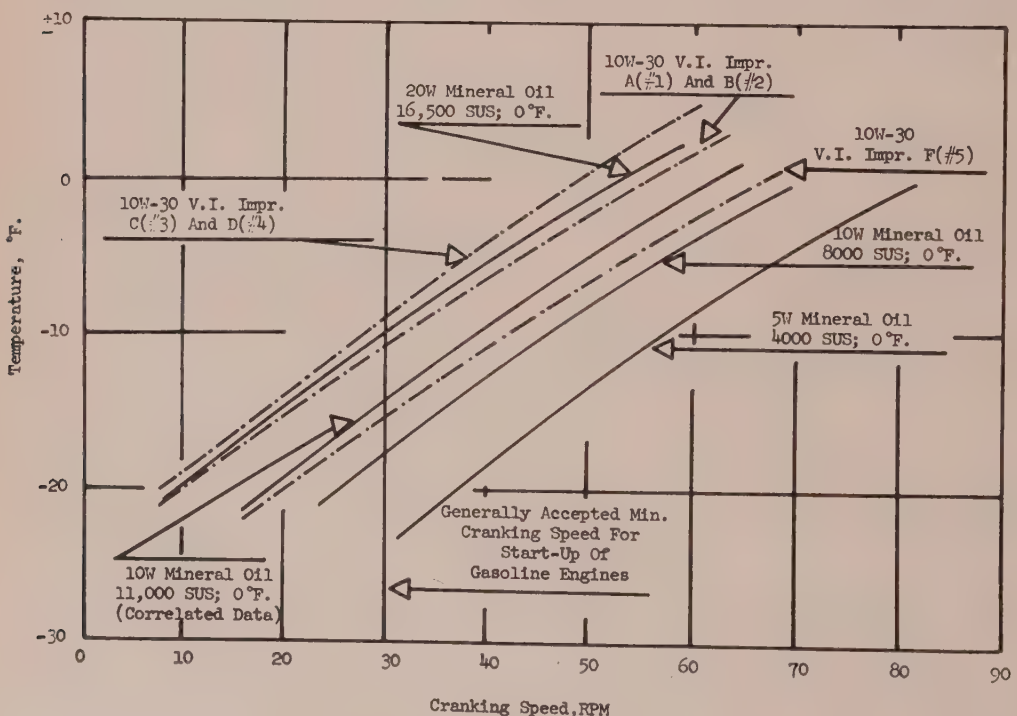

Fig. 4 – Effect of engine oil type on starting-motor cranking speed

Table 3 – Comparison of Cranking Speeds at 0 F of 10W-30 Oils with Conventional Mineral Oils

SAE Grade	10W[a]	10W-30			20W
V. I. Improver	None	F	B	C	None
Starting-Motor Cranking Speed at 0 F, rpm	62	66	57	49	52
ASTM Extrapolated Viscosity at 0 F, SUS	11,000	11,000	10,500	11,500	18,000

[a] Interpolated from data in Fig. 3.

In addition, two of the base oils from which finished 10W-30 oils were blended through the addition of V.I. improver were included. Since the oils were waxy, their viscosities could not be checked at 0 F, but measurements at +20, 100, and 210 F showed that they followed the ASTM extrapolation (Appendix Table 12). The relationship between cranking speed and viscosity for the calibration oils is given in Fig. 3, which shows that the speed is related to the logarithm of the viscosity.

2. *Test Oils* – The test oils were formulated with one experimental and five commercial V.I. improvers that differed widely in molecular type, molecular weight, V.I. improving effectiveness, and shear stability. A polyisobutylene and two types of esterified vinyl polymers were included. With the exception of three oils, all V.I. improved test lubricants were blended to have the same viscosities at 210 F (about 64 SUS), the same viscosity indexes (138), and the same ASTM extrapolated viscosities at 0 F (11,000 SUS) (Appendix Table 14). To accomplish this, different viscosity base oils were required for each V.I. improver. These were obtained by blending different percentages of two base oils of 90-95 V.I. having viscosities at 100 F of 90 and 300 SUS, respectively. These formulations represent the most economical use of each V.I. improver. The test oils also contained the necessary detergent-inhibitor additives to make them typical of commercial oils in all respects.

Discussion of Test Results – Significant differences have been found in engine cranking speed among 10W-30 oils formulated with different V.I. improvers. Some of these oils, depending on their formulation, exhibited the startup qualities expected of 10W mineral oils, whereas others performed like 20W mineral oils. This is shown in Table 3.

More detailed data are presented graphically in Figs. 4 and 5 by data derived from both the cranking speed and torque measurements. Fig. 4 shows the effect of oil composition and temperature on starting-motor cranking speed, while Fig. 5 shows

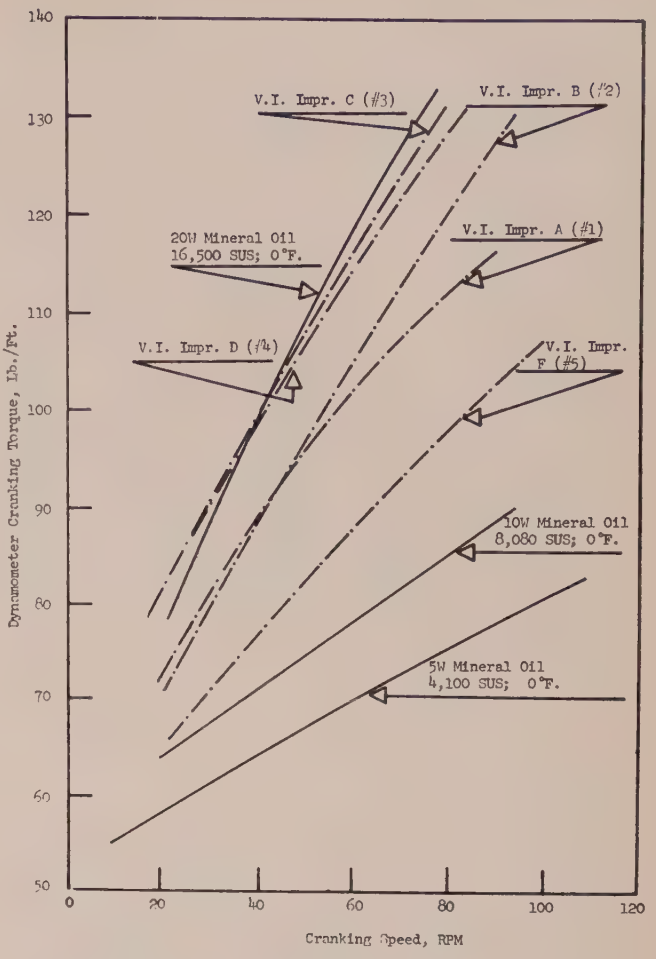

Fig. 5 – Dynamometer speed-torque relation at 0 F for mineral and 10W-30 oils

the magnitude of torque that has to be applied to crank the engine with a dynamometer to maintain different levels of speed at 0 F. It will be noted that only the 10W-30 blends of V.I. improver F could be classified as 10W oils. The others definitely behaved like 20W oils. As will be explained later, the startup qualities of multiviscosity oils are related to the viscosity of the base oil from which they are prepared. They are not related to the ASTM extrapolated viscosities. The actual engine viscosities of the multiviscosity oils, as determined from the mineral oil-cranking speed calibration curve (Fig. 3), are illustrated in Table 4 and graphically in Fig. 6 in direct comparison with their respective ASTM extrapolated viscosities. These data emphasize that the viscosity of V.I. improved oils in engines deviates very appreciably from the ASTM extrapolated viscosity.

The observed differences in actual engine viscosities of V.I. improved oils, formulated to identical ASTM extrapolated viscosities, have considerable practical application in terms of modern engine startup. Earlier studies[6] have shown that

[6] "Motor Oil Viscosity and Cold Starting," by J. K. Appeldoorn. Paper presented at API meeting, Chicago, Nov. 6, 1948.

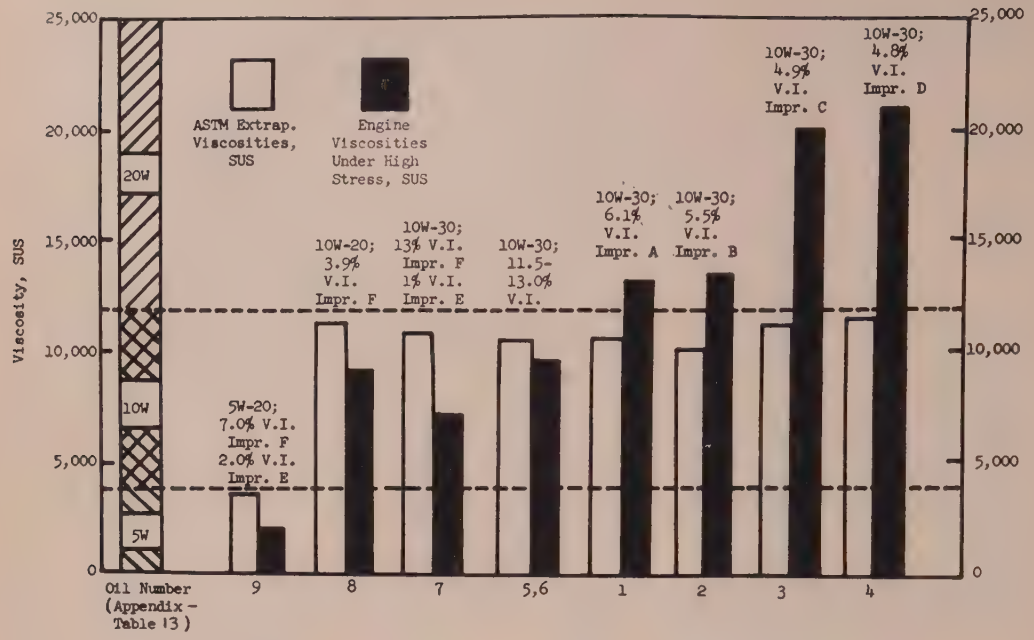

Fig. 6 – Viscosities at 0 F of multiviscosity oils blended with V.I. improvers of different molecular types

there is a critical cranking speed in the range of 20-30 rpm below which an automotive gasoline engine will not start, regardless of temperature. A few rpm can mean the difference between start and no-start. Popular auxiliary equipment, such as power steering and automatic transmissions, increase the load on the starting motor to the extent of 20-25%.[7] A picture of the significance of the cranking-speed variations cited above may be obtained by considering that the difference between oils containing V.I. improvers F and C is roughly equivalent to the effect of adding these automatic devices to the load on the starting motor.

Explanation of Differences Between V.I. Improved Oils

The above data demonstrate how V.I. improved oils of equal viscosities at 210 F and V.I.'s, each having an ASTM extrapolated viscosity at 0 F of about 11,000 SUS, can have engine viscosities as far different as 9500 and 20,000 SUS. Such variation is due to:

1. Differences in the low shear viscosities of the V.I. improved oils not predicted by the ASTM chart.

2. Temporary viscosity loss, which affects the oils to varying degrees.

A method has been devised for estimating these two factors from viscosity measurements at 100 and 210 F. Thus, it becomes possible to predict the engine viscosity during cold cranking of V.I. improved oils.

Estimation of Low-Temperature Capillary Viscosities – A new system has been devised for the estimation of the capillary (low shear) viscosities of V.I. improved oils at low temperatures. It is based on the general observations (1) that mineral oil base stocks follow the ASTM chart fairly well and (2) that the contribution of the polymeric V.I. improvers to the lubricant viscosity varies regularly with temperature. This contribution of V.I. improvers to the blend viscosity can be expressed as the specific viscosity, S, defined as:

$$\frac{V_B - V_O}{V_O}$$

where:

V_B = Viscosity of the blend, centistokes

V_O = Viscosity of the base oil, centistokes

It has been found through a large number of measurements on wax-free blends that the specific viscosities from +20 to –20 F may be calculated

Table 4 – Engine Viscosities Under High Shearing Stress of 10W-30 Oils at 0 F

	V. I. Improver F	V. I. Improver B	V. I. Improver C
Engine High Stress Viscosity, SUS	9,500	14,000	20,000
ASTM Extrapolated Viscosity, SUS	11,000	10,500	11,500
Mineral Base Oil Viscosity, SUS (ASTM Extrapolated)	5,000	11,800	18,000

[7] "Our Mutual Problems from Additives to Zzmog," by C. M. Heinen. Presented at SAE Metropolitan Section, New York, April 7, 1955.

Table 5 – Calculation of Low-Temperature Viscosities of V. I. Improved Oils at 0 F

% V. I. Improver	Viscosity at 0 F, centistokes		
	Calculated	Measured	ASTM Extrapolated
8% B	1220	1160	750
4% C	730	707	440
9% F	1950	1960	1250

from the specific viscosities at 100 and 210 F using the following empirical formulas, one for each type of V.I. improver.[8]

V.I. Improvers A, B, and E $$S_T = \frac{S_{100}}{80+T}\left(111.4\frac{S_{100}}{S_{210}} + T - 41.4\right)$$

V.I. Improvers C and D $$S_T = \frac{S_{100}}{80+T}\left(63\frac{S_{100}}{S_{210}} + T\right)$$

V.I. Improver F $$S_T = \frac{S_{100}}{80+T}\left(163\frac{S_{100}}{S_{210}} + T - 94.2\right)$$

where:

T = Temperature between +20 and –20 F,
S_{100} and S_{210} = Specific viscosities at 100 and 210 F, respectively.

These equations hold regardless of the concentration of the V.I. improver, or the viscosity, V.I., or chemical nature of the base oil. Even blends in synthetic oils may be treated in this way.

Once the specific viscosity at the low temperature has been determined, it is a simple matter to compute the capillary viscosity of the V.I. improved lubricant using as the viscosity of the base oil the ASTM extrapolated value. One multiplies the base oil viscosity by $1 + S$. Examples of the use of this method with blends in highly dewaxed stocks whose viscosities could be measured at low-temperatures are given in Table 5 and in more detail in Appendix Table 15.

The agreement between calculated and measured values is good, as compared to the ASTM extrapolated viscosities which are grossly in error in most cases.

The largest part of the observed errors in this method of calculation is due to errors in the estimation of the base stock viscosities with the ASTM chart. The errors in the estimations of S are almost always less than 5%, which causes an error of only 2-3% in the final calculated viscosities. This is true because the variation of S with temperature is relatively small. Between 210 and 0 F, S varies only threefold at most (and the quantity $1 + S$ varies only about 50%), while the viscosity itself may increase some one-thousandfold. Indeed, it is this relative constancy of thickening power with temperature that accounts for the V.I. improving powers of these polymeric materials, as contrasted, for example, to petroleum bright stocks, whose thickening power increases rapidly with decreasing temperature.

It should be emphasized that S is positive at all times, which means that the viscosity of a V.I. improved blend can never be calculated to be lower than that of the base oil. This provides a distinct advantage for the new method over the ASTM extrapolation technique for V.I. improved oils and alone is probably sufficient justification for its use.

Using this system described here, the low shear or capillary viscosities of the oils used in the cold-starting tests have been calculated and found to vary considerably. These have been compared with the actual engine viscosities and the base oil values as shown in Table 6 (taken from Appendix Table 13).

It will be seen that the engine viscosities generally are lower than the calculated capillary viscosities. These differences can be explained by taking into account the occurrence of temporary viscosity loss. This phenomenon is caused by the elongation and alignment of the coiled polymer molecules in the direction of the high shearing stresses prevailing in the engine during low-temperature startup. As soon as the stress is removed, the viscosity of the oil returns to its low shear value. This is the first time, as far as can be ascertained, that temporary viscosity loss has been demonstrated to occur during cold starting.

Extent of Temporary Viscosity Loss in Low-Temperature Engine Cranking – The extent of the temporary change in viscosity that occurs depends on (1) the amount of viscosity that is contributed by the polymer at the given temperature and (2) the percentage of the viscosity due to polymer that is lost as a result of shear. The first factor is controlled by the V.I. improving effectiveness of the polymer. For example, V.I. improver F requires a

Table 6 – Viscosities of 10W-30 Test Oils at 0 F

Oil No.	V. I. Improver	Calculated Low Shear Viscosity, SUS	Engine Viscosity, SUS	Base Oil Viscosity, SUS
2	B	16,600	14,000	11,800
3	C	22,000	20,000	18,000
5	F	16,700	9,500	5,900

[8] By using a slightly more complex formula, all these V.I. improvers may be accommodated in one equation, which is offered here for further consideration:

$$S_T = \frac{S_{100}}{80+T}\left[42\left(\frac{S_{100}}{S_{210}}\right)^3 + T + 28.2\right]$$

where T is between +20 and —20 F. This equation is of a preliminary nature and has not been tested extensively.

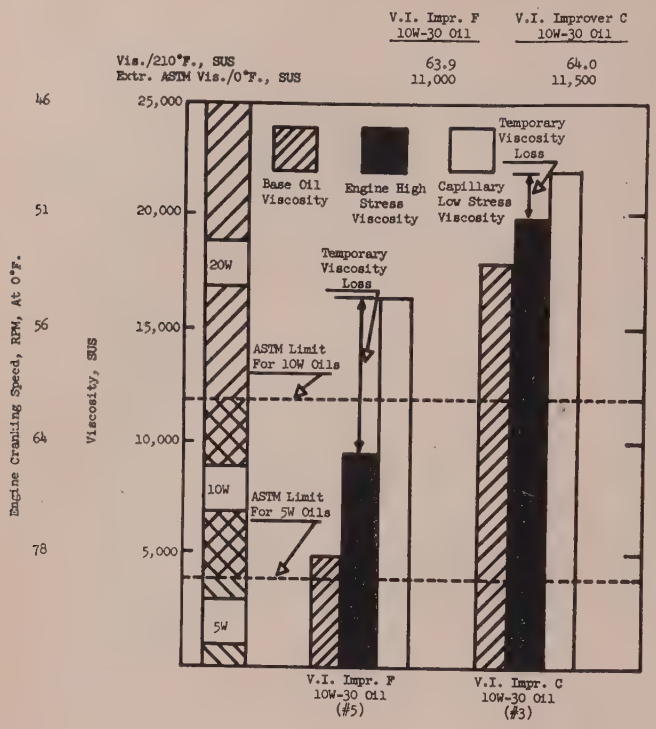

Fig. 7 – Viscosities of 10W-30 oils blended with V.I. improvers C and F

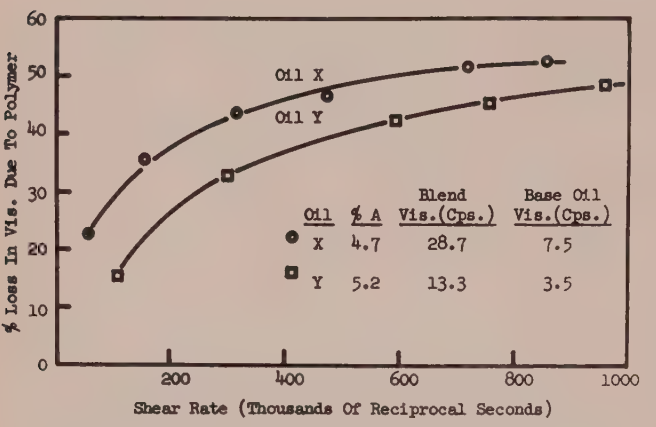

Fig. 8 – Temporary viscosity loss of V.I. improver A blends at 100 F

base oil of 41 SUS at 210 F to prepare a 64 SUS 138 V.I. oil, while V.I. improver C uses a 48 SUS base oil to prepare a blend of the same viscosity and V.I. At 0 F, as shown in Appendix Table 15, V.I. improver F contributes 70% of the finished oil viscosity, whereas V.I. improver C contributes only 18%. (Mathematically, the fraction of viscosity due to polymer is given by $S/(S+1)$, where S refers to the specific viscosity defined in the preceding section.) It is apparent then that the blends containing V.I. improver F can lose more of their

Table 7 – Comparison of Starting-Motor Cranking Speeds of 10W-30 Oils with Their Respective Base Oils

Starting-Motor Cranking Speed, rpm	V. I. Improver C		V. I. Improver F	
	Base Oil without V. I. Improver	Finished Blend	Base Oil without V. I. Improver	Finished Blend
At 0 F	53	49	77	66
At −20 F	12	11	29	21

overall viscosity due to temporary viscosity loss.

The accuracy of the cranking tests was such that the percentage of temporary viscosity loss due to the polymer could be determined with confidence only for V.I. improver F. This V.I. improver showed 45-65% temporary loss at all three test temperatures. With the other V.I. improvers, the amount of polymer thickening in these 10W-30 formulations is too small to permit an accurate estimation of their temporary viscosity loss characteristics. However, because only a small portion of their overall viscosity is due to polymer, it is not important, as far as cranking is concerned, whether 0 or 100% temporary viscosity loss due to polymer occurs.

On the other hand, it should be pointed out here that temporary viscosity loss during engine cranking does not appear to eliminate completely the contribution of polymer to the blend viscosity. The base oils from which two of the 10W-30 oils were blended through the addition of V.I. improver cranked faster at all test temperatures than the finished blends. This is illustrated in Table 7.

The behavior of the blends of V.I. improvers C and F, representing the extremes in cranking speeds, is also summarized in the bar graph of Fig. 7. This graph and Table 7 emphasize the importance of a light base stock for good cold-starting performance with V.I. improved oils and the desirability of temporary viscosity loss.

Laboratory high shear viscosity measurements are being conducted to determine what factors affect the percentage of temporary loss in viscosity due to polymer that occurs during cold starting. Some measurements were obtained in the Pennsylvania State University pressure capillary viscosimeter at shear rates[9] up to 10^6 reciprocal seconds.[10]

The most important fact uncovered in these studies so far is that the shearing stress determines the amount of temporary viscosity loss,

[9] "Shear rate," is a measure of the difference in velocity of layers of a moving liquid. The "shearing stress" is a measure of the force required to bring about this difference in velocity. Viscosity is defined as the ratio of shearing stress to shear rate. A simple explanation of these terms is given in the book "Viscosity of Liquids," by E. Hatschek, London, 1928.

[10] See *Lubrication Engineering*, Vol. 11, March/April, 1955, pp. 101-108: "Some Viscosity-Shear Characteristics of Lubricants," by E. E. Klaus and M. R. Fenske.

rather than the traditionally used shearing rate. For example, Fig. 8 shows temporary viscosity loss-shear rate plots at constant temperature for two blends of the same V.I. improver in different viscosity base stocks. When the plots are redrawn with shearing stress as abscissa rather than shearing rate, the curves become superimposable (Fig. 9). Measurements made on one V.I. improved blend at different temperatures (+100 and –40 F) also show that shearing stress is the better parameter to use (Table 8). Equal shearing stresses produced approximately equal overall percentage viscosity losses (and approximately equal per cent viscosity losses based on polymer) despite the fact that the shearing *rates* differed by several orders of magnitude.

The graphs of viscosity versus shear rate at different temperatures given by Georgi[3] can also be made nearly superimposable by replotting against shearing stress.

The dependence of temporary viscosity loss on shearing stress rather than rate is highly significant with regard to cold-starting performance. The shearing rates encountered in the various lubricated parts of an engine, the bearings, cylinder walls, and so forth, are quite low during cold starting where the engine speed may be about 30 rpm as compared to the shear rates under running speeds of the order of 2000 to 3000 rpm. But the shearing *stresses* are just as large or perhaps even larger during cold starting due to the very high viscosity of the oils at low temperatures. A reasonable estimate of these quantities is presented in Table 9.

The relatively large amount of temporary viscosity loss that occurs during cold cranking is therefore not surprising if considered in terms of shearing stress.

Factors other than shearing stress that affect the percentage of temporary viscosity loss *due to polymer* are now being studied in a high-pressure viscosimeter. These factors include:

1. Polymer type. The currently available commercial V.I. improvers vary somewhat in their susceptibility to viscosity loss but are all of the same order of magnitude.

2. Polymer molecular weight. The amount of viscosity loss at a given shear stress appears to be directly proportional to the molecular weight.

3. Polymer concentration. The higher the concentration the lower the viscosity loss at a given shearing stress.

4. Temperature. The variation of viscosity loss with temperature is slight, but the losses appear to be somewhat higher at low temperatures than at high temperatures.

The aim of this laboratory work is to enable the prediction of the amount of temporary viscosity loss that occurs under any condition with any commercial V.I. improver blend. Until these studies are completed, it is felt that 50% temporary viscosity loss due to polymer is a good first-order approximation for estimating the cold-starting performance of 10W-30 oils in the temperature range of –20 to 0 F. This represents the average value for V.I. improver F obtained in the cold-cranking tests described in a preceding section. Limited laboratory high shear viscosity data[11] on one of the test blends containing V.I. improver F at +20 F indicate that a shearing stress of close to 10^6 dynes per cm^2 is necessary to produce this amount of temporary viscosity loss. This is the best estimate now available of the average effective shearing stress obtained in this particular test

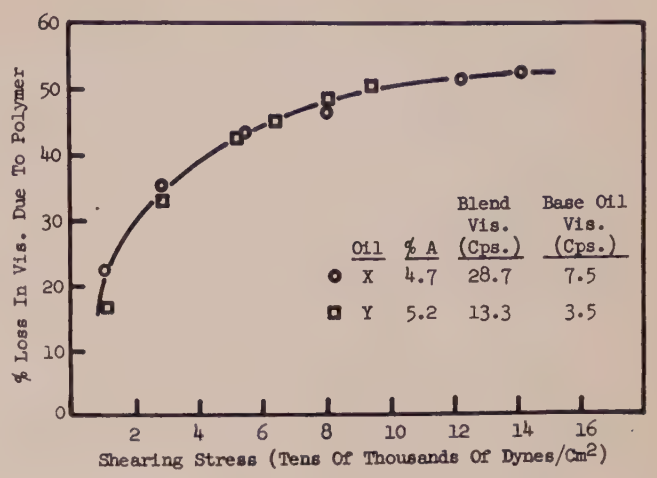

Fig. 9 – Temporary viscosity loss of V.I. improver A blends at 100 F

Table 8 – Temporary Viscosity Loss at –40 and +100 F; 4.5% V. I. Improver A in a Base Oil of 7.5 Centipoise at 100 F

Temperature, F	Low Shear Viscosity, centipoise	High Shear Viscosity, centipoise	Shearing Stress, dynes/cm²	Shear Rate, sec⁻¹	Viscosity Loss, %
–40	4615	4077	6,500	160	12
100	25.5	22.5	6,750	30,000	11.5
–40	4615	3596	18,000	500	22
100	25.5	20.2	18,200	90,000	21
–40	4615	3423	30,800	900	26
100	25.5	18.5	31,400	170,000	27.5

Table 9 – Relative Engine Shear Rates and Stresses

Engine Operation	Oil Temperature, F	Speed, rpm	Shearing Rate,[a] sec⁻¹	Oil Viscosity,[b] centipoise	Shearing Stress,[c] dynes/cm²
Running	210	3000	100×10^4	0.1	1×10^5
Cold Starting	0	30	1×10^4	25	2.5×10^5

[a] Average effective shear rate generally estimated for critical engine parts (bearings, cylinder walls, etc.).

[b] Typical of 10W-30 oils.

[c] Equals product of shearing rate and viscosity.

[11] From private communication with M. R. Fenske.

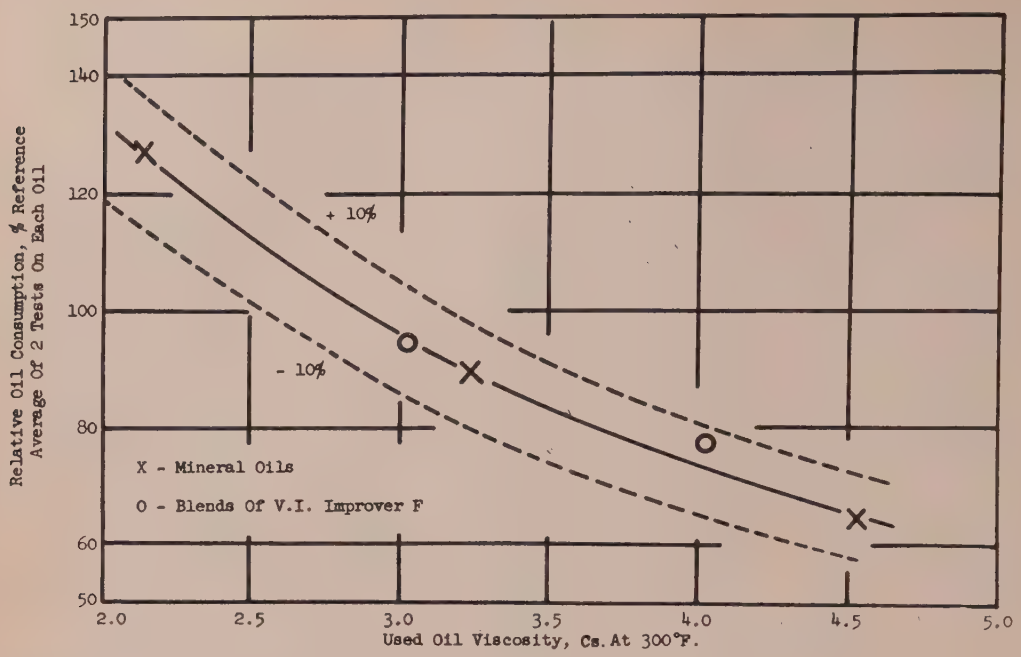

Fig. 10 – Oil consumption versus viscosity at 300 F (laboratory engine hill-cycle; test reproducibility ±10%)

engine during cold starting and is the range in which future laboratory viscosity loss measurements will be made.

Temporary Viscosity Losses at Higher Temperatures

It is not the purpose of this paper to cover in detail the high-temperature performance of V.I. improved oils. However, the discussion would be incomplete if it were not pointed out that temporary viscosity loss also occurs under high-temperature engine operating conditions with multigraded oils and produces definite beneficial effects. It causes a reduction in engine friction horsepower and thus a reduction in fuel consumption as compared to mineral oils of the same or even lower viscosity at the possible operating temperatures. This is shown in Table 10.

Addition of bright stock to a 5W mineral oil resulted in sizeable increases in engine friction horsepower at two speed levels. Thickening the same 5W oil with V.I. improver F in place of the bright stock resulted in a 40% smaller increase in friction horsepower in each case. These reductions in friction were reflected in corresponding decreases in fuel consumption.

Other investigators[12, 13, 14] have reported field test results showing even greater decreases in fuel consumption (up to 15%) with multigraded oils as compared to mineral oils of the same summer grade. However, these improvements are due to more than temporary viscosity loss alone. They also include the benefits afforded by the high viscosity index of these oils, which reduces the engine viscosity under the moderate temperatures prevailing during engine warmup and under urban driving conditions.

In the cases so far studied, temporary viscosity loss does not appear to cause any increase in oil consumption. In controlled laboratory weighed sump engine tests, 5W-20 and 10W-30 oils blended with V.I. improver F showed the same oil consumption as mineral oils of equal used oil viscosity at 300 F (Fig. 10). Extensive field test work[15] has shown that the low shear viscosity at 300 F of a lubricant determines the rate of its consumption, provided, of course, that the base oil is nonvolatile under engine operating conditions. This indicates that most of the oil consumption takes place under conditions where the shear stresses are relatively low, such as down the intake valve stems and around the rear of the piston rings. This premise is substantiated by data presented by Sanders[16] showing that decreasing the intake manifold vacuum from 26 to 20 in. of Hg decreased the oil consumption of his laboratory engine eightfold when operating under conditions simulating steady downhill driving. He also found that prevention of the axial displacement of one of the piston rings

[12] "Multigrade Crankcase Lubricants," by J. A. Miller and L. M. Hartmann. Presented at SAE Summer Meeting, Atlantic City, June 9, 1954.
[13] "Multigrade Oils for Improved Performance," by C. C. Moore, W. L. Kent, and W. P. Lakin. Presented at SAE National West Coast Meeting, Los Angeles, Aug. 17, 1954.
[14] See SAE Transactions, Vol. 63, 1955, pp. 349-361: "New Look in Lubricating Oils," by J. B. Bidwell and R. K. Williams.
[15] See SAE *Quarterly* Transactions, Vol. 4, July, 1950, pp. 410-421, 454: "Performance of High V.I. Motor Oils," by C. L. Fleming, Jr., B. W. Geddes, N. V. Hakala, and C. A. Weisel.

Table 10 – Effect of Temporary Viscosity Loss on Engine Friction and Fuel Consumption

Block-Mounted 6-Cyl Engine; 200 F Oil Sump

Lubricant	Viscosity, SUS		Friction Horsepower		Fuel Consumption, hp-hr/gal	
	210 F	300 F	3150 rpm[a]	2000 rpm[b]	3150 rpm[a]	2000 rpm[b]
5W Mineral	44.3	35.0	18.2	6.6	8.6	20.7
5W Mineral Oil + Bright Stock	70.7	43.0	23.3	9.9	8.2	19.7
5W Mineral Oil + V.I. Improver F	71.4	45.0	21.4	8.6	8.4	20.2

[a] Part throttle.
[b] Full throttle.

Table 11 – V. I. Improver Permanent Viscosity Loss

V.I. Improver	Permanent Loss in Viscosity Due to Polymer,[a] %
A	25
B	40
C	50
E	15
F	15

[a] The viscosity loss was obtained by passing 630 cc of a 77 SUS blend of V.I. improver in a 57 SUS base oil through a pressure-relief valve at 1000 psig at a rate of 2700 cc per min for 1 hr at 200 F.

in its groove markedly reduced oil consumption under high vacuum. Both these pieces of information complement the visual observations of Beaubien and Catteneo[17] that oil enters into the combustion chamber around the rear of the piston rings, where shear rates and stresses are very low, rather than between the rings and the cylinder wall.

In all this discussion, the effect of *permanent* viscosity loss due to polymer degradation in V.I. improved oils under turbulent conditions has not been considered. The permanent viscosity losses vary for different V.I. improvers as is shown in Table 11.

This type of viscosity loss, in contrast to temporary viscosity loss, does increase oil consumption, since it is irreversible and reduces the low shear viscosities.

As far as passenger-car engine wear is concerned, millions of miles of field tests carried out by the Esso Research and Engineering Co. indicate that properly compounded 10W-30 oils have excellent wear characteristics and are at least equivalent to single-graded SAE 30 premium motor oils. Published information by other investigators[12] also confirms this. At the present time, one can only theorize about the way in which V.I. improver blends can temporarily lose viscosity and yet not increase wear. In the case of cylinder liner and piston rings, wear occurs mostly at the ends of travel where the shear stress is close to zero and the oil is at its nominal viscosity. The reduction in viscosity, on the other hand, occurs in the center of piston travel where the shear stress is high. Bearing wear is a function of the eccentricity ratio (which is a measure of the clearance between the lubricated surfaces under operating conditions), all other things being equal. According to the theory of short bearing lubrication (see NACA Report No. 1157[18] for example) the eccentricity ratio is a function of the viscosity in the endwise direction of the bearing, while the friction loss is a function of the viscosity in the circumferential direction. The average shear stress in the circumferential direction is relatively high. Therefore, temporary viscosity loss occurs to a large extent with V.I. improved oils, thus reducing the friction. In the endwise direction, on the other hand, the average shear stress is relatively low, and little temporary viscosity loss occurs. Thus, the eccentricity ratio and consequently the wear should not be affected by the presence of V.I. improvers.

Conclusions and Recommendations

The cold-starting test data presented here demonstrate that 0 F viscosities as determined by extrapolation on the ASTM chart are inadequate for classifying V.I. improved oils into the proper SAE winter grades. Not only is the chart inadequate for predicting the low shear wax-free viscosities of these oils, but it also fails to take into account the occurrence of temporary viscosity loss under high shearing stresses.

The SAE grade viscosity limits appear to be satisfactory, since they insure sufficient cranking-speed differences between oils of the various grades. However, the means of determining the necessary viscosities need improvement. It would be necessary to devise an apparatus that would measure low-temperature viscosities at 0 F under the same shearing stresses that prevail in typical engines during cold starting. Based on the results with the particular engine used in these tests, the required shear stress appears to be in the range of 10^6 dynes per cm^2. The standard shearing stress, however, would have to be established by determining the average temporary viscosity loss that occurs in various engines and comparing this value with the shear stress necessary to achieve the same amount of viscosity loss in laboratory instruments. Vis-

[16] See SAE Transactions, Vol. 63, 1955, pp. 400-419: "New Chevrolet V-8 Engine," by R. F. Sanders.
[17] See *SAE Journal*, Vol. 54, October, 1946, pp. 60-67: "Piston Lubricating Phenomena in Motored Glass Cylinder Engine," by S. J. Beaubien and A. G. Cattaneo.
[18] See NACA Report 1157 (1954), "Analytical Derivation and Experimental Evaluation of Short-Bearings Approximation for Full Journal Bearings," by G. B. Dubois and F. W. Ocvirk.

cosity measurements under the established shearing stresses could then be used along with the present SAE viscosity limits to define the winter grades.

The authors acknowledge with appreciation the assistance of the Southwest Research Institute in conducting the low-temperature engine cranking tests. Recognition is also expressed for the helpful comments from our many friends in the automotive and petroleum industries.

APPENDIX

Table 12 – Calibration Oils for Low-Temperature Cranking Study

	Naphthenic Oils			Paraffinic Oils	
	SAE 5W	SAE 10W	SAE 20W	10W[a]	20W[b]
Low Shear Capillary Viscosities, SUS					
At 210 F	36.9	38.8	42.1	40.8	48.3
At 100 F	86.1	113	165	120	233
At +20 F	1,340	2,390	4,580	1,675	5,130
At 0 F	4,120	8,080	16,500	—	—
At −20 F	17,170	39,400	80,000	—	—
ASTM Extrapolated Viscosity, SUS					
At +20 F	1,300	2,400	4,600	1,750	5,100
At 0 F	3,900	7,600	16,500	5,000	18,000
Viscosity Index	20	15	35	92	96
Pour Point, F	−40	−35	−25	−25	−20
Cloud Point, F	−40	−30	−20	+15	+15

[a] Base oil for V.I. improver F blended 10W-30 oil (No. 5) plus 0.1% pour depressant.
[b] Base oil for V.I. improver C blended 10W-30 oil (No. 3) plus 0.1% pour depressant.

Table 13 – Engine Viscosities at 0 F of Cold-Starting Test Oils

No.	Oil Type	% V. I. Improver	Calculated Low Shear Viscosity, SUS	Engine Viscosity, SUS	Base Oil Viscosity,[a] SUS
1	10W-30	6.1 A	16,600	13,000	11,800
2	10W-30	5.5 B	16,600	14,000	11,800
3	10W-30	4.9 C	22,000	20,000	18,000
4	10W-30	4.8 D	23,600	21,500	20,000
5	10W-30	13.0 F	16,700	9,500	5,000
6	10W-30	11.5 F + 0.9 A	16,700	9,700	5,000
7	10W-30	13.0 F + 1.0 E	13,900	6,000	4,100[b]
8	10W-20	3.9 F	12,200	9,700	8,500[b]
9	5W-20	7.0 F + 2.0 E	3,900	2,300	1,700[b]

[a] Obtained from ASTM chart except as noted.
[b] These blends were made up in 110 + V. I. base stocks whose viscosities at 0 F are approximately 15% lower at 0 F than the ASTM chart predicts (based on measurements made at temperatures as low as +20 F). The values in the table have been corrected for this deviation.

Table 14 – Tests Oils for Low-Temperature Cranking Study

No.	Oil Type	% V. I. Improver	Low Shear Viscosities, SUS 210 F	100 F	20 F	V. I.	Pour Point, F	ASTM Extrapolated Viscosity at 0 F, SUS	Base Oil Viscosity at 210 F, SUS
1	10W-30	6.1 A	64.2	333	5600	138	−35	11,000	—
2	10W-30	5.5 B	62.1	314	5260	137	−35	10,500	45.4
3	10W-30	4.9 C	64.0	333	6150	137	−30	11,500	48.0
4	10W-30	4.8 D	63.8	331	—	137	0	11,500	48.3
5	10W-30	13.0 F	63.9	330	5400	138	−25[a]	11,000	40.7
6	10W-30	11.5 F + 0.9 A	65.2	339	5510	138	−25	11,500	—
7	10W-30	13.0 F + 1.0 E	69.4	363	—	141	−25	11,000	41.5
8	10W-20	3.9 F	53.3	257	—	124	−25	11,500	46.6
9	5W-20	7.0 F + 2.0 E	51	173	—	153	−25	3,700	38.1

[a] Contains 0.7% pour depressant.

Table 15 – Calculation of Low-Temperature Viscosities of V. I. Improved Oils
(All viscosities are in centistokes)

% V. I. Improver	Base Oil Type[a]	Base Oil Viscosity at 210 F	Base Oil Viscosity at 100 F	Blend Viscosity at 210 F	Blend Viscosity at 100 F	Test Temperature, F	Viscosity at Test Temperature: Calculated	Measured (Capillary)	Extrapolated
8 B	M	3.10	16.07	9.21	46.72	0	1840	1890	970
6 B	M	3.10	16.07	7.36	37.68	0	1520	1540	850
8 B	N	3.12	15.31	8.68	39.78	+10	688	670	435
8 B	O	4.29	22.24	9.88	46.25	0	1220	1160	750
8 B	P	5.91	37.0	15.86	84.94	+15	1410	1260	900
6 C	M	3.09	16.04	7.49	36.63	0	1270	1400	730
6 C	N	3.10	15.15	6.96	30.22	0	853	819	455
4 C	N	3.10	15.15	5.47	24.50	0	730	707	440
6 C	O	4.27	22.24	8.27	35.96	+20	378	352	255
12 F	M	3.10	16.07	8.45	49.34	0	2580	2580	1540
9 F	M	3.10	16.07	6.72	38.28	0	1950	1960	1250
12 F	N	3.12	15.31	8.31	46.05	+10	1100	1090	780
7 F	O	3.23	14.14	5.41	25.53	+15	324	312	280

[a] (M) Acid-treated low cold test oil from Columbian crude.
(N) Solvent-extracted low cold test oil from Coastal crude.
(O) Solvent-extracted and dewaxed oil from a paraffinic distillate.
(P) Solvent-extracted, dewaxed, and clay-treated oil from a paraffinic distillate to which a small amount of bright stock was added.

DISCUSSION

of Malone-Selby and Fischl-Horowitz-Tutwiler papers

Reports on Previous Low-Temperature Starting Tests

by F. S. Wood

Standard Oil Co. of Ind.

WE were gratified to learn that the data in the paper by Messrs. Fischl, Horowitz, and Tutwiler support work on low-temperature starting carried out in our laboratory some five years ago. Our work was conducted in a car housed in a cold room. Instruments were provided to measure engine rpm by counting valve openings, current flow from the battery, voltage drop across the battery, and accurately time the test. Continuous readings of the instruments were assured by means of 16-mm motion pictures taken at a speed of 32 frames per sec. Thus, in the course of a 20-sec test, 640 photographs of the instruments were taken for later study.

In each test, the engine was flushed with test oil and run until the oil temperature reached 150 F to minimize fuel dilution. The car then was driven into the cold room and allowed to soak at the test temperature for 16 hr. We also chose 0, –10, and –20 F for our tests. Actual engine viscosities of the multigraded oils were obtained from a correlation we developed between the viscosities of straight mineral oils and engine cranking speeds.

Fig. A is a bar graph of these derived engine viscosities and the ASTM extrapolated viscosities of multigraded

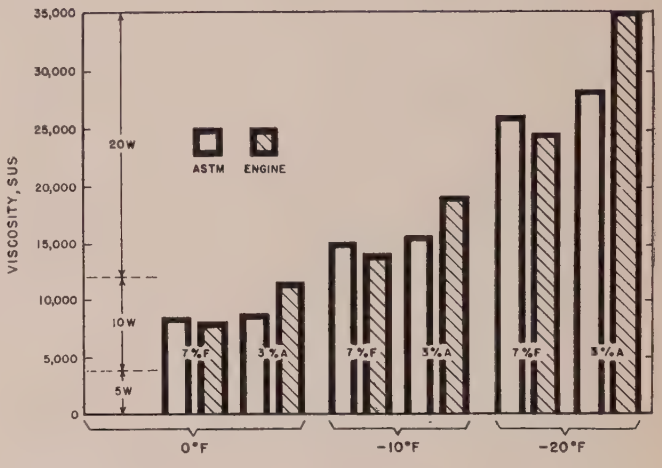

Fig. A – ASTM versus engine viscosity for 10W-20 motor oils

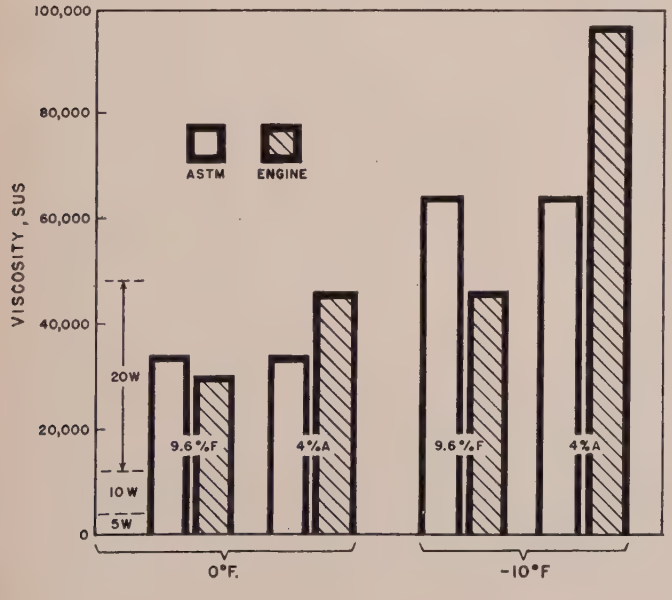

Fig. B – ASTM versus engine viscosity for 20W-40 motor oils

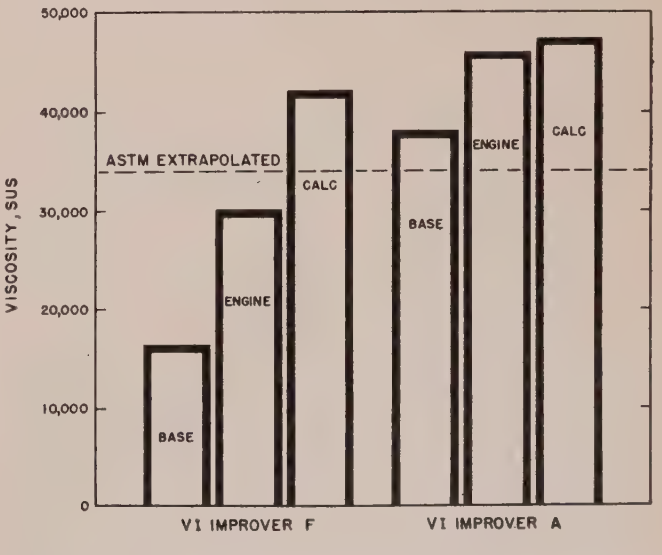

Fig. C – ASTM versus calculated and engine viscosities for 20W-40 motor oils at 0 F

10W-20 test oils; 10W-30 oils had not yet come onto the scene. V.I. improvers F and A were used. At each temperature, the engine viscosity is less than the ASTM extrapolated viscosity with F and greater with A. The differences were not as great as found in the Esso work but were proportional to the amounts of V.I. improvers used in the two test oils.

Fig. B shows that the differences in engine and ASTM extrapolated viscosities were greater in a series of tests on 20W-40 oils containing slightly larger amounts of V.I. improver. It is interesting to note that at –10 F the difference between the oils was large enough so that the engine in excellent conditions was able to start with F and failed to start with A.

Fig. C compares the two 20W-40 oils at 0 F and shows the relative positions of calculated viscosities, engine viscosities, ASTM extrapolated viscosities, and base-oil viscosities. If we compare the difference between the calculated viscosity and the engine viscosity with the amount of viscosity that is contributed by the V.I. improver, we find that F presumably had a temporary shear loss of 50% under these test conditions, and A a loss of 15%. Under other test conditions, losses ranged from 40 to 70% for F and 10 to 50% for A. For any given oil, the losses became greater as the temperature decreased, and the starting effort and shearing forces became greater.

Needless to say, we heartily agree with the authors that ASTM extropolated viscosity does not indicate the ease or difficulty the motorist may have in starting his engine with any given motor oil. Likewise, because of the principles involved in engine friction, ASTM viscosities cannot be used to determine the effect a motor oil has on gasoline consumption. These factors certainly should be considered in developing or evaluating a multigraded motor oil.

Cold-Start Viscosities Depend on Choice of V.I. Improver

by W. P. Lakin

Union Oil Co. of Calif.

THE work on cold starting certainly provides an excellent explanation of differences which have been noted in the performance of lubricants in both laboratory and field tests. For example, it is apparent that cold-starting viscosities in the engine are nearly the same as ASTM extrapolated viscosities when certain V.I. improvers are used. In this case the temporary viscosity loss is just about equal to the difference between the measured and extrapolated viscosity figures. This appears to be a lucky coincidence but nevertheless true. On the other hand, an experimenter who had pulled a different V.I. improver off the shelf would be convinced that engine viscosities were much higher than extrapolated viscosities. He could also be right.

These papers recommend the measurement of viscosities under shearing conditions. It certainly seems logical to adopt such a method as soon as it can be made available.

The data on lube-oil consumption in the paper by Messrs. Fischl, Horowitz, and Tutwiler are in line with our data and experience, but those in the paper by Overcash et al.[a] seem at first glance to be contradictory. However, there are several factors which may explain these differences. A few of the neutrals used in this work were much lighter than any we have ever used even in the laboratory, and several were lighter than any ever used in service testing. In addition, the engine test conditions were very severe and this probably emphasized the effect of volatility. In the test work on multigrade oils, the contradiction may possibly be explained by a comparison of the viscosities of the used oils. The SAE 10W-30 oil tested had a new oil viscosity which was below that of the SAE 30. It appears possible that the used viscosity of this particular 10W-30 may have been below that of the used SAE 20.

Just What Is a Properly Compounded Multigrade Oil?

by V. W. Ware

Rohm and Haas Co.

WE note with pride the statement in the paper by Messrs. Fischl, Horowitz, and Tutwiler that there is a growing trend toward the use of V.I. improved motor oils, that one-fifth of the premium oils sold today are multigraded and that this figure is increasing rapidly. There must be good reasons for this rosy outlook. Could it be that there are important reasons other than low-temperature starting which might account for it?

In connection with the modest differences shown between the starting temperatures of oils based on V.I. improver F, on the one hand, and V.I. improver A, as a representative of all the others, let's consider the poor guy who is condemned to exist in an area where the temperature may drop to 15 or 20 deg below zero. He goes out to start his modern 200-hp juggernaut. Its crankcase is filled with virgin multigrade motor oil, with its high content of virgin V.I. improver. Or is it so pure and undefiled? Did the man have his crankcase filled the night before right

[a] "How Do Volatility, Viscosity, and V.I. Improvers Affect Oil Consumption?" by R. L. Overcash, W. Hart, and D. J. McClure. Presented at SAE Annual Meeting, Detroit, Jan. 13, 1956.

where the car now stands or was the oil changed at the service station several blocks away and perhaps many days ago? If the temperature is now —20 F it certainly has been fairly chilly around those parts for several days —usually the roads have ice or snow at such temperatures, so neither the man, his wife, nor even his mother-in-law has been driving that car at 60-70 mph for any length of time. So doesn't it follow that that crankcase will be loaded with fuel? And isn't it a fact that with 5-10% gasoline in the oil these modest differences in startup will become indistinguishable, regardless of the type of V.I. improver used? These data would have been much more practical and perhaps of real value to the oil industry if a few per cent of fuel had been included in all of the finished blends.

There are other requisites of a multigrade oil which are in direct opposition to the low-viscosity base stock required with V.I. improver F, in spite of the fact that this particular stock gives a 5-6 deg lower starting temperature than do the stocks which are required with, for instance, V.I. improver A and B. Three primary considerations are (1) oil consumption, (2) wear, particularly valve-train wear, and (3) valve deposits. I think it is pretty generally recognized that, in order to keep these three manifestations at a satisfactory minimum, it is desirable, if not imperative, to blend a 10W-30 oil with a base stock of the highest possible viscosity.

We note the statement, "as far as passenger-car engine wear is concerned, millions of miles of field tests indicate that **properly compounded** 10W-30 oils have excellent wear characteristics and are a least equivalent to single-graded SAE 30 premium motor oils." For confirmation, they refer to a paper by Miller and Hartman.[b] May I suggest the possibility that the oils studied by Miller and Hartman and the data presented by them were not based on stocks such as would be used with V.I. improver F but rather with the much higher viscosity stock that could be used with V.I. improvers A, B, C, or D.

What do the authors of this paper consider a properly compounded oil to be? Obviously, from the standpoint of low-temperature starting they feel that V.I. improver F and a light volatile neutral give the best oil. But can they honestly say that, from the overall viewpoint and including consideration of oil consumption, wear, and valve deposits, all three of which are known to undergo improvement as the base stock increases in viscosity, the F type of blend is the better, when it is possible at lower cost to blend an oil with V.I. improver A, B, C, or D with all the improved performance that goes with a much heavier neutral? So I ask, what is a properly compounded multigrade oil?

But we do agree with the authors of this paper that, "the startup qualities of a multigrade oil are related to the viscosity of the base oils from which they are prepared" and that it basically deals with the cold-starting properties of stocks of varying viscosities and not with the starting properties of V.I. improvers as such. Without any supporting data at hand we would speculate that kerosene, if you cared to go to such a light stock, would, as long as it remained in the crankcase, give startup at lower temperatures than any shown here with any V.I. improver, regardless of the position of that V.I. improver in the alphabet.

Now let's take a look at Fig. 5 of the paper. You see the curve for the 10W straight mineral oil. The authors have been very circumspect and have chosen a viscosity of 8000 SUS at 0 F right in the middle of the range. But let's look at the curve for the 20W mineral oil. They have chosen a viscosity of 16,500 SUS at 0 F as typical.

We had never seen a straight 20W non-V.I. improved oil with a viscosity, either extrapolated or determined, as low as 16,500 SUS. So just to doublecheck, we picked up samples of the straight non-V.I. improved 20W oils of all the major marketers around Philadelphia. Among these the lowest 0 F viscosity was 27,000 SUS, the highest was about 40,000, and the average was 32,000. Why then did the authors of this paper choose a viscosity of 16,500 SUS at 0 F to represent a 20W oil? Perhaps they chose the low value because the average of 32,000 would barely show in the top left corner of Figs. 5 and 6. The only solution to that problem would be to extend the ordinates on the charts to include higher values. Under these conditions it would be seen that, in reality, the low-temperature starting properties of all the 10W and 10W-30 oils discussed fall in a very close group and that the straight 20W non-V.I. improved oil is away off in left field all by itself.

Messrs. Malone and Selby gave the clearest explanation of some of the low-temperature phenomena connected with the use of V.I. improvers that we have yet seen. It is obvious that much fundamental work is being done here. We note that in these papers there is some agitation for a better correlation of SAE extrapolated limits of a multigraded oil with actual determined viscosities. We have long favored such a step but feel that it must not be taken precipitately. Unless there is an overwhelming need for such a change, and we have heard no reports of serious starting difficulties with 10W-30 oils, we must bear in mind that to require an actually determined maximum viscosity of 12,000 SUS at 0 F will involve some extreme changes in the base stocks used in many of these multigraded oils. Such a requirement will force a large drop in the viscosity of the neutral base. This will involve greater oil consumption, more wear, and increased intake-valve deposits. Such a step must be taken only if necessary, not just for fun, and after serious consideration of the one factor against the several.

Malone and Selby Closure to Discussion

IN view of the fact that several points of the discussion will be treated in a forthcoming paper, it is felt that there is no need for a reply at this time.

Fischl, Horowitz, and Tutwiler Closure to Discussion

IT is very gratifying to us that the comments of Messrs. Lakin and Wood and the results presented by Messrs. Malone and Selby in their paper on cold starting agree so well with our own data. The cold-starting tests described by Mr. Wood showed the same differences between V.I. improved oils that we did in our tests. Using the same method of calculating the low-temperature viscosities, he obtained the same type of deviations from the ASTM extrapolated viscosities and the same amount of temporary viscosity loss. This indicates that the methods of correlating the data that were developed for our own base oils are also applicable to other types of base stocks. This gives us further confidence in our equations and our predictions of the extent of temporary viscosity loss. It also suggests that the variation in average shear stress from engine to engine is small.

The paper by Messrs. Malone and Selby gives us a very good idea of the wide differences in cranking speed

[b] See footnote 12 of main paper.

Table A – Effect of Dilution on Cold-Starting Viscosities of 10W-30 Oils at 0 F

V. I. Improver	Original Engine Viscosity, SUS	Cranking Speeds,[a] rpm	Viscosity after 5% Dilution, SUS	Cranking Speeds after Dilution,[a] rpm
F	9,500	65	4140	82
C	20,000	50	7360	70
Difference	111%	15	78%	12

[a] Read from Fig. 3 of our paper.

that can be obtained with so-called 10W-30 oils. We believe we have explained the reason for these differences. Excellent agreement was also obtained in the actual cranking speeds obtained in their and our cold-starting tests (about 60 rpm with an oil of 12,000 SUS viscosity at 0 F). We believe, however, that several points in the paper by Messrs. Malone and Selby need clarification. One statement they make is that, "If the shear rate is high enough, it is conceivable that the viscosity may approach the (ASTM) extrapolated value as a limit." This is generally true for mineral oils within the accuracy of the ASTM chart. In the case of V.I. improved oils, however, at very high rates of shear the viscosity approaches that of the **base oil** from which the blend was made. This, as we have explained, may be higher or lower than the ASTM extrapolated viscosity.

Once this is understood, a misconception by Messrs. Malone and Selby becomes obvious. They state, "The evidence indicates that at least with the multigrade oils such a decrease in viscosity with high shear rate is not to be expected. One point of evidence is the better correlation of determined viscosity with cranking speed. For if at high rates of shear the viscosity of the oil in the engine became quite similar to that predicted by extrapolation, then the extrapolated data would have the close relationship to cranking speed; this, we have seen, is not the case." We say that even though a fall in viscosity occurs the engine viscosity approaches the base-oil viscosity rather than the ASTM value.

Their own data, in fact, indicate that temporary viscosity loss **does** occur under high shearing rates. The viscosities they obtained using the forced-ball high shear viscometer (Fig. 10) are consistently lower than the viscosities obtained with the Brookfield low shear viscometer (Fig. 6) with the 10W-30 oils. With the straight 10W oils, on the other hand, the viscosities are almost the same in both viscometers. It is unfortunate that Messrs. Malone and Selby did not have any information on the base oils and the V.I. improvers that were used to formulate the 10W-30 oils that they were testing. Otherwise they might have been able to obtain valuable information on the extent of temporary viscosity loss from their viscometer data.

The comments of Dr. Ware are most provocative but are not substantiated by data. His first point is that the cold-cranking tests should have been run with a few per cent of fuel in the finished blends, and that, if they had been run that way, the difference between the various 10W-30 oils would have disappeared. This is definitely not correct. It is true that there are many factors affecting cold starting that an average driver would experience with his car that were not included in our tests. We were interested in the basic concepts involved and did not wish to confuse the data by introducing a large number of variables simultaneously. Of course dilution of the oil with fuel will make the cranking speeds higher and starting easier. On the other hand, using an older battery or an engine with leaky piston rings and valves will make cranking more difficult. We assumed that while all of these factors will change the cranking speeds the relative differences between the oils will remain about the same. Thus, the point to be resolved is whether dilution tends to eliminate the relative differences between the oils. It is possible to calculate the effect of adding 5% of gasoline to lube oils at 0 F. Consider two oils like the 10W-30 oils containing V.I. improvers F and C having engine viscosities of 9500 and 20,000 SUS at 0 F, respectively. The effects of dilution are shown in Table A.

It will be noted that even after dilution there is still a large difference in the viscosities of the two oils and that most of the cranking-speed difference is still apparent. In other words, dilution reduces the differences between the oils only to a small extent.

A second way to look at the question of dilution is to remember that 10W oils came into being in the first place because it was found that, despite dilution, 20W oils did not give good enough cold-starting performance in certain areas. Now that specially balanced high-volatility gasolines carefully adjusted for seasonal temperature variations are in common use, we can count even less on dilution to provide easy starting. Cold-starting ease must be built into the lubricating oil.

In regard to the high-temperature properties of V.I. improved oils, such as oil consumption and engine wear, our paper explains that V.I. improved 10W-30 oils made with light, nonvolatile base oils are equivalent to 30 grade mineral oils. Dr. Ware misinterprets our paper when he ascribes the "millions of miles of field tests" proving this point to Miller and Hartmann. As stated in our paper, they were our own field tests. Some of the results were reported in a previous paper, "A Field Approach to Engine Wear," by Yowell, Weisel, and Risher, SAE Summer Meeting (1954). Other data from these tests are still unpublished. In fact, as far as the effect of the V.I. improver on oil consumption is concerned, perhaps we did not emphasize strongly enough that this feature depends on the amount of **permanent** polymer breakdown. Here, again, there is a significant difference between V.I. improvers.

Basically, however, a discussion of the relative merits of the 10W-30 oils described in our paper at high temperatures is out of order, for they are not all true 10W-30's. We feel that by definition a 10W-30 oil should be equivalent in cold starting to a 10W mineral oil. The SAE winter grading system should be based on this premise. Otherwise there is no advantage for a 10W-30 over a 20W-30 oil. 20W-30 oils have been on the market for many years and can be blended with a relatively small amount of any V.I. improver. Why go to the trouble of making a high-priced super-premium motor oil if it still starts like a 20W-30? "True" 10W-30 oils can be compounded with any one of today's commercially available V.I. improvers, provided it is used in conjunction with the right base stock. It is only within this framework that the relative merits of different formulations can be compared. The SAE winter grading system should be modified so that multigrade oils are compared on the basis of 0 and 210 F engine viscosities rather than on the basis of V.I. or ASTM extrapolated viscosities.

The same reasoning applies to Dr. Ware's suggestion that we compare our 10W-30 oils to commercial 20W mineral oils. In our opinion a 10W-30, to be worthy of its grade, must show an advantage in cold starting over a 20W-30 oil, not merely over a straight 20W mineral oil. There are several 20W-30 oils on the market that have viscosities near 20,000 SUS at 0 F, much lower than the 32,000 SUS considered average by Dr. Ware. A true 10W-30 oil should have a significant cold-starting advantage over such an oil. It should have a viscosity at 0 F of less than 12,000 SUS under engine shearing conditions. It should not achieve this by fooling the ASTM chart.

Human and Environmental Factors of Automobile Safety

Dr. Ross A. McFarland, Harvard School of Public Health

This paper was presented at the SAE Golden Anniversary Summer Meeting, Atlantic City, June, 16, 1955.

THE integration of motor vehicles into our way of life has become very costly in terms of fatalities, injuries, and damaged equipment. As miles traveled, passengers carried, and tons conveyed have increased, traffic has become more dense, speed levels have risen, and there has been, as a direct result, an increase in deaths, injuries, and monetary costs. Highway safety has become a matter of pressing national concern.

In spite of the enormous increase in volume of traffic mentioned above, there has been a significant change in accident rates during the past 25 years. For example, in 1954 the fatality rate per 100,000,000 miles of travel was only 6.5, in comparison to a rate of 15 about 20 years ago. These trends are clearly portrayed in Fig. 1, which shows the improvement in accident rates in comparison with the large increases in the numbers of vehicles on the roads and in the miles traveled.[1]

Nevertheless, the *actual number of persons killed* or disabled, and the direct and indirect costs to the nation's economy, have been increasing from year to year with fair regularity. The only exception was during the period of restricted travel during the war years. The total number of fatalities each year is shown in Fig. 2. In 1954 there were approximately 36,000 deaths, and over 1,000,000 injuries disabling beyond the day of the accident. In addition, the direct costs of these accidents approximate 1½% of the national income, or about

BIOLOGY, engineering, and the social sciences must work together, the author says, toward preventing passsenger-car accidents. He compares deaths and injuries from motor-vehicle accidents with the effects of mass disease – and calls the epidemiological approach used in disease study the most logical way of analyzing complex causes of accidents in terms of the interactions between the driver, the vehicle, and the environment of driving.

The author reports the many exhaustive studies of what makes an accident, then points out that efforts to improve driver, vehicle, or roads must always begin with human physical and mental characteristics and limitations firmly in mind.

[1] See "Accident Facts," Annual Publication, National Safety Council, Chicago, Ill.

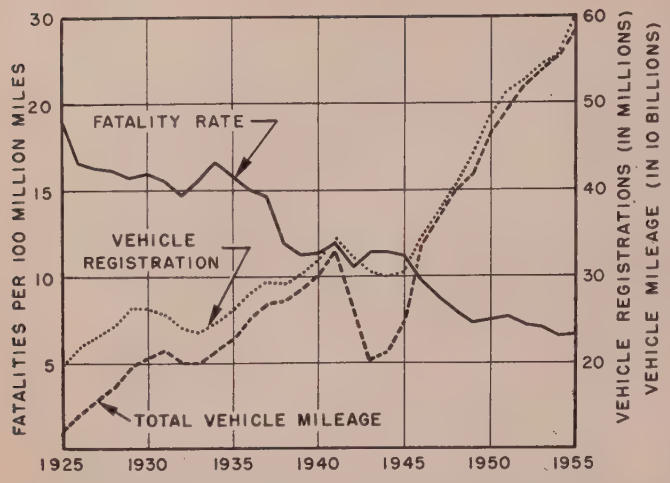

Fig. 1 – Fatality rates in motor vehicle accidents compared with vehicle registrations and total vehicle mileage, 1925-1955[2]

$4,500,000,000. The indirect costs may be five times larger.[1, 2]

Automobile accidents constitute a very serious problem for the Armed Services. In all three branches, vehicular accidents are currently the leading cause of death, and are responsible for greater noneffectiveness in the defense effort than any other single cause. In 1952, 388,025 man-days were lost by Air Force personnel from injuries sustained in vehicular accidents, while 810,000 man-days were lost in the Army from the same cause that year. In 1953, noneffectiveness in the Navy and Marine Corps due to injuries from motor vehicle accidents reached 366,000 days. The major problem in all services is the off-duty accident, incurred while personnel are in private vehicles, off-base. In 1954 the loss to the Armed Forces from off-duty, private-vehicle accidents comprised 1610 deaths, 10,360 nonfatal injuries, and 536,600 man-days away from duty. The cost to the government for these automobile accidents alone was more than $64,000,000.[2]

Accidents of all kinds have now replaced diseases as the leading cause of death in the age range of 1-40 years. Approximately one-third of the accidental deaths, and one-seventh of the accidental injuries, result from motor vehicles. The fact that most of these victims are in the younger age groups in contrast to those whose deaths are attributable to certain degenerative diseases implies an enormous cost to the productive resources of the country in terms of "life-years" lost. Measurement of the fact that a death has occurred is less meaningful than the measurement of how much "life-time" has been lost prematurely.[3]

It has been estimated on the basis of present trends that one person out of every 10 in this country may be killed or injured in a motor-vehicle accident within a period of 15 years.[4] It is clear that intensified efforts are needed in order to gain a better understanding of the basic causes of vehicular accidents to provide a foundation for improved methods of accident prevention. Many contend that the complexity of modern equipment and the density of traffic on the highways can only be expected to result in many accidents. There is general agreement, however, that a substantial reduction can be made, provided careful research is carried out on the basic causes of accidents.

There is general agreement that accidents, especially those occurring on the highway, have taken on the characteristics of a mass disease of epidemic proportions. Accidental injuries do, in fact, provide frequency distributions in time and place which are comparable to those of certain mass diseases. In this approach, causation is viewed as a disequilibrium between man and his environment, with a multiplicity of causes. The results are principally an action of the *agent or vehicle* because of some particular characteristic of the *host or driver,* and as a function of the *environment.* Accidents usually occur through some combination of circumstances involving all three variables – namely, the vehicle, the driver, and the environment. Attempts at control must consider all three factors. The driver is of greatest psychological and medical concern; the vehicle is of engineering concern; the environment is a concern of highway engineering and many other specialized fields. A team approach is a basic requirement in taking adequate preventive measures.

A broad research program in the field of highway safety has been in progress at the Harvard School of Public Health during the past 8 years. These studies were initiated by the American Trucking Associations, Inc., the National Association of Motor Bus Operators, and the National Association of Automotive Mutual Insurance Companies. The facilities of the Harvard medical center are being used by a team of scientists representing various engineering, medical, and biological sciences to study the most important human variables and their relation to accidents.

Since 1951, the Commission on Accidental Trauma of the Armed Forces Epidemiological Board, Department of Defense, has sponsored research on the human factors in vehicular accidents at Harvard and at a number of other universities and research institutions. Thus far the research program has stressed basic causes in the areas of (1) identifying traits of personality and behavior

[2] See "Human Factors in Vehicular Accidents – A Survey of the Literature," by R. A. McFarland, R. C. Moore, and A. B. Warren. Pub. by Harvard School of Public Health, Boston, 1955.

[3] "Human Variables in Design and Operation of Highway Transport Equipment," by R. A. McFarland. Presented at SAE Annual Meeting, Detroit, Jan. 16, 1952.

[4] See "Field of Highway Safety Research." Pub. by Committee on Highway Safety of National Academy of Sciences, National Research Council, Washington, D. C., August, 1952.

which lead to repeated errors, (2) defects in the design of equipment (human engineering), (3) injuries and fatalities resulting from vehicular crashes, and (4) mathematical studies of the various interrelationships of contributory causes in accidents.[5] An extensive review of these and other studies of human factors in highway safety has recently been completed as a part of this project.[2, 5]

Role of Human Factors in Automobile Safety

A logical starting point in the analysis of human factors in automobile safety is the driving situation itself. Although the task may appear at first hand to be a simple one, many influences may be brought to bear which may result in a hazardous situation. An analysis of driving has been well stated in a report by the Highway Safety Research Committee of the National Research Council as follows:

"The driver must first learn to coordinate both hands, both feet, vision, and hearing. This coordination must be learned to a point where it becomes semiautomatic before he can hope to operate in traffic with any degree of safety. He must also learn to make judgments of changing space-time relationships. He must operate in close proximity to other vehicles of different sizes and speeds, going in the same and opposite directions, and on crossing courses. He must operate on highways and streets which require passing other vehicles with a clearance of only 1 ft or 10 or 20 ft. When the time intervals within which he must react, even at relatively low speeds, are considered, it will be seen that he must learn to anticipate conditions and situations. If two cars are approaching at 30 mph and one driver loses control when they are 45 ft apart, each driver has 0.5 sec to react. This means, in the light of our present knowledge, that he would just have time to get his foot on the brake, but there would be no possibility of stopping the car in time to prevent a collision. Thus the factors of foresight, planning, and appreciation of hazards must be involved to a major extent. Actually, it seems probable that *more continuous attention* from moment to moment is required of the motor vehicle driver than of the operator in any other type of transportation including the airplane."[4]

Obviously any factor which may distract attention, diminish alertness, or decrease consciousness will place the driver and his vehicle in jeopardy.

The causes of automobile accidents are usually attributed to failure on the part of drivers in from 80 to 90% of the cases. In other words, most accidents on the highway result from some unsafe driving habit or procedure.[1, 6] However, even when one classifies such unsafe practices and errors, and finds some more important than others, little has been gained in understanding the basic causes. It is necessary to obtain additional information. Why did the drivers carry out the unsafe practices or commit the errors? What are the characteristics of man himself which may predispose him to errors? What are the influences, both within and without the driver, which affect his efficiency and enhance the possibilities of errors? Under what circumstances are mistakes more likely and safety compromised?

It is becoming increasingly clear that the causes of automobile accidents are rarely found in any one specific human characteristic, in a certain aspect of the equipment, or in one particular environmental feature. More often the interrelationships among all three factors are combined to create the accident potential of a given situation.

Thus the human factors in automobile accidents can be fully understood only when the basic physical, physiological, and psychological characteristics of drivers are associated with the characteristics of vehicles under given environmental conditions and at specified times and places. The preventive measures which emphasize the role of human factors in safety should be focused upon the characteristics of the driver, upon the interrelation between the driver and his equipment, and upon the interaction between the driver and his environment.[7]

A. *The Role of the Accident Repeater* – The observation in industry that a relatively small proportion of the workers is responsible for a large proportion of the accidents led to the theory that certain individuals are inherently predisposed to accidents. The view became widely held that accident-proneness was a major cause of motor-vehicle accidents, and a great deal of research has been directed toward the detection of the accident-prone driver.[6]

1. Statistical considerations: The word "proneness" has been used to imply a series of personality traits which, as yet, have not been precisely identi-

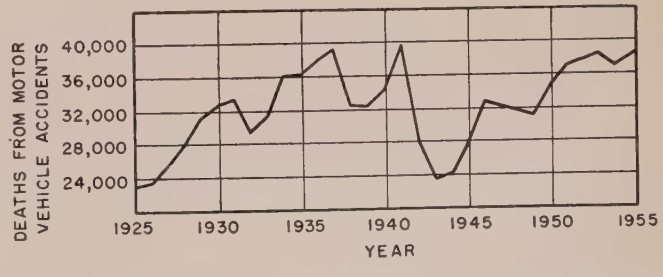

Fig. 2 – Deaths resulting from motor vehicle accidents, 1925-1955[3]

[5] See "Annual Report, 1954-1955," Commission on Accidental Trauma, Armed Forces Epidemiological Board. Department of Defense, Washington, D. C., 1955.

[6] See "Human Factors in Accidents, with Special Reference to Aircraft Accidents," by R. L. Thorndike. Project 21-30-001, Final Report, USAF School of Aviation Medicine, Randolph Field, Tex., February, 1951.

[7] See SAE Transactions, Vol. 62, 1954, pp. 335-345: "Human Engineering: New Approach to Driver Efficiency and Transport Safety," by R. A. McFarland.

Table 1 – Chance and Obtained Distribution of 7288 Accidents for 17,952 Pilots during an Eight-Year Period

Number of Accidents	Number of Pilots Associated with Number of Accidents	
	Chance Distribution	Obtained Distribution
0	11,962	12,475
1	4,856	4,117
2	986	1,016
3	133	289
4	14	53
5	1	14
6	0	6
7	0	2

fied. It is necessary to make a distinction between accident-proneness and accident liability. Accident liability results from all the circumstances present at a given time – accident proneness would be but one of the factors influencing the probability of an accident under the total set of circumstances.[8, 6] The term accident-proneness implies the consistent tendency of a person to have accidents as a result of his basic response tendencies. For example, two taxi drivers may drive the same cab under approximately identical circumstances. Thus, they would have the same situational probability of having an accident. One, however, may be inherently poor in coordination, and because of this lack of proficiency, he would be more apt to have an accident in circumstances requiring coordination. He would then be called an accident-prone driver – and his accident proneness would be but one of the conditions of accident probability. Other conditions of liability, which are not included in proneness, are the temporary or transient characteristics of drivers, for instance, fatigue, illness, emotional states, and all of the factors not under direct control of the individual.

In demonstrating statistically the presence of accident proneness, it is first necessary to show *that certain individuals had more accidents than might be expected on the basis of chance alone.* The classical method is through use of the Poisson equation,[9] and is illustrated by Table 1 which presents the distribution of 7288 accidents of 17,952 Air Force pilots during an 8-year period, together with the mathematically derived chance distribution.

A common fallacy in discussions of accident proneness can be illustrated by referring to the column headed "Chance Distribution" in Table 1. If having multiple accidents is taken as the definition of accident proneness, some 35% of the accidents could be so classified, involving 16% of the group, but this is precisely the distribution expected if chance alone determined who would have the accidents. The mere finding that a small proportion of the people have had a high proportion of the accidents cannot be accepted as evidence of accident proneness.[10]

The significant point in Table 1 is that more pilots had no accidents at all, and more had repeated accidents, than would have been expected from chance alone. Clearly, something other than chance is operating in distributing these accidents; whether this is personal accident proneness is another question. Findings similar to those in Table 1 have been reported for the highway accidents of several groups of drivers.

Another method has been to correlate the frequency of accidents sustained by the same individuals in different periods of time. Small but apparently significant correlations have been found in some studies made on drivers.[6] Many others have been negative.

The difficulty with the evidence from the two statistical methods outlined above is that the effect demonstrated is not necessarily due to the stable characteristics within individuals. Other conditions of liability may exist continuously with the individual, but quite apart from his own personal response tendencies. For instance, two drivers with the same inherent accident tendencies may drive in situations which require reactions of quite different complexity, or which involve quite different frequencies of exposure. The accident susceptibility of the two drivers would differ, and would result in "a something-beyond-chance effect," even though the drivers do not differ in proneness. Without strict controls over the kind and amount of exposure, and of all the other conditions of liability, inferences about the presence and extent of accident proneness are inconclusive. Accident records usually do not contain such controls, and the net result of the attempts to demonstrate and measure accident proneness in motor vehicle accidents is that proneness may be an influence in some sets of records, but conclusive evidence is usually lacking. Furthermore, if the effect noted is due to proneness, the phenomenon is a relatively restricted one in proportion to the total numbers of accidents and in relation to other conditions of liability.[2, 5, 6, 8]

2. The clinical approach: Another method of studying accident proneness has been the clinical appraisal of individuals who have sustained repeated accidents. This approach has led to the concept that certain individuals have unconscious emotional needs which give rise to accidents through impulsive or aggressive behavior. Thus, injuries may resolve emotional tensions associated with

[8] See *Biometrics*, Vol. 7, No. 4, 1951, pp. 340-432: "Accident Statistics and Concept of Accident Proneness," by A. G. Arbous and J. E. Kerrich.

[9] The mathematical model for the distribution of accidents purely by chance among the members of a group is the well-known Poisson distribution. This refers to events unlikely to occur on any given occasion, equally likely on all occasions, and with many opportunities for occurring. By means of the Poisson equation it is possible to determine the way the total accidents for a group would be divided up among its members if chance alone were the determining factor. Thus for 500 people having a total of 300 accidents the chance division would be 275 with no accidents, 165 with one apiece, 49 with two, 10 with three, and 1 with four. In this example (see footnote 6) 12% of the group would be expected to have 44% of the accidents, on the basis of chance alone.

[10] See *Psychological Bulletin*, Vol. 50, 1953, pp. 133-136: "Some Relations between Two Statistical Approaches to Accident Proneness," by W. B. Webb and E. R. Jones. See also "Repeater Pilot Accidents in the USAF," by W. B. Webb and E. R. Jones. Human Resources Research Laboratory, Report No. 30, Air Research and Development Command, USAF, 1952.

feelings of guilt or desire for attention.[11, 12] However, these concepts have been developed on a *post hoc* basis, without reference to suitable control groups. It would be an unimaginative psychologist or psychiatrist who could not find emotional conflicts and tendencies which are consistent with the clinical concept of proneness *after* an accident has occurred. With suitable controls, however, and with the development of methods which limit subjective judgments, the clinical approach is regarded by many as especially well suited to reveal the *nature* of accident proneness, although less adaptable to measuring its extent.[13]

3. Summary: It is apparent from the above discussion that the only certain way at present of identifying the accident-prone individual is through a history of repeated accidents. However, not all accident-repeaters are accident-prone, and various circumstances may result in a truly accident-prone driver remaining accident free. Difficulties such as these, and a recognition of the multiple influences which affect the probability of accidents, have resulted in the proposal that the term accident-repeater is more accurate than the term accident-prone.

Accurate records and careful research should reveal those individuals who have had repeated accidents, and provide a starting point for licensing bureaus or companies to set up control measures through medical or training aids. Also, more fruitful research on the causes of accidents can be accomplished by the analysis of accident-repeaters in relation to the circumstances of their accidents than through efforts to prove the existence of proneness and to relate a measure of proneness to a general accident index. Furthermore, if a large percentage of accidents are caused by a small percentage of the population, no one has thus far demonstrated adequate methods of identifying and controlling them.

B. *The Significance of Specific Psychological Characteristics and Physical Defects* – A wide variety of sensory, psychomotor, and mental characteristics have been investigated in relation to the accident rates in various groups of drivers. In spite of the fact that highway accidents are usually attributed to human limitations, close relationships between the frequency of accidents and specific human variables have not been revealed. Some factors are of greater importance in causing accidents than others, but the studies are essentially negative. Some typical findings are as follows: The correlation between visual acuity and accident rate in a group of over 3000 drivers was only –0.04. In another study, high accident rates were reported for those drivers who failed to see cars approaching from side streets because of more limited visual fields than the average for the group as a whole. Correlations between a wide variety of psychomotor tests and accident indexes range from zero to 0.11. In some studies, a *knowledge of safe driving principles* was associated with freedom from accidents, but the reverse finding was observed in other investigations.[2, 6]

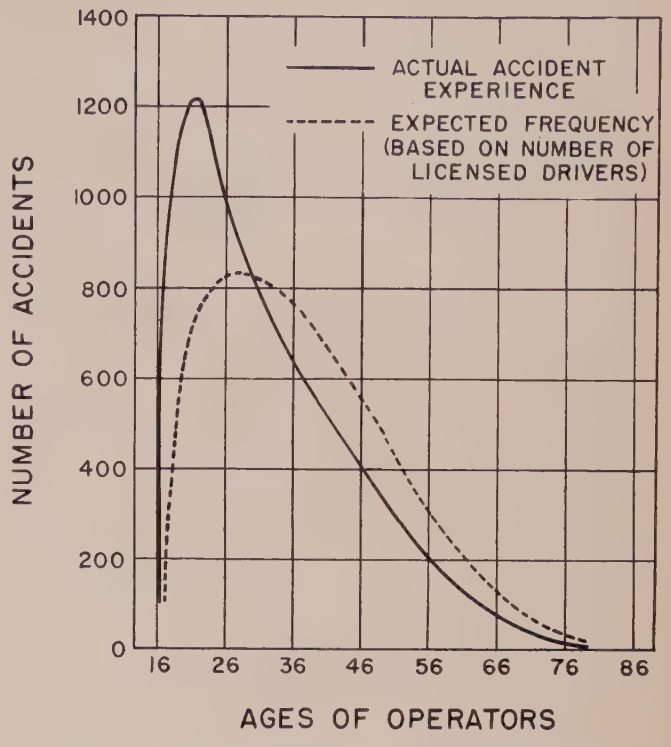

Fig. 3 – Expected and actual frequency of vehicle accidents for drivers of various age groups. Expected frequency is based on the number of licensed drivers[13]

There is agreement among several studies that accident rates for younger drivers are higher than would be expected if age was of no influence. This is shown in Fig. 3, where the number of accidents for a large group of Connecticut drivers is given in proportion to the age composition of the driving public. Youthful drivers showed an excessive number of accidents, while drivers over 30 had fewer accidents than would have been expected. A large sampling of drivers in Iowa has been studied more recently, with similar results in regard to the effects of age on accident rates.[2, 14]

The attributes of drivers having the highest statistical relationship to accident frequencies include *low intelligence, youthfulness, and a personality*

[11] See *Public Health Reports*, Vol. 64, No. 12, 1949, pp. 357-362: "Accident-Prone Individual," by F. Alexander.

[12] See *Medical Clinics of North America*, Vol. 28, No. 3, 1944, pp. 653-662: "Susceptibility to Accidents," by H. F. Dunbar.

[13] See "Human Factors in Air Transportation – Occupational Health and Safety," by R. A. McFarland. Pub. by McGraw-Hill, New York, 1953.

[14] See *Bulletin de L'Association International de Psychotech.* (*Psychol. Appl.*), Vol. 3, No. 1, 1954, pp. 43-58: "Contributions by Psychologists to Reduction of Highway Traffic Accidents in the United States of America," by T. W. Forbes.

make-up in which social responsibility is limited or lacking.[2]

The most recent studies have indicated that temperamental factors and personal adjustments are of greater significance in highway safety than are sensory, psychomotor, or mental abilities. In one Canadian study it was found that accident-repeaters as a group could be clearly distinguished from accident-free drivers on the basis of *personal-social adjustments as revealed in the number of contacts with the courts, credit agencies, social service agencies, and public health clinics.*[15] Also, studies of truck drivers suggest that certain personality traits and types of adjustment are associated with preventable accidents.[16] A study of fatal ground accidents among Air Force personnel has indicated similar trends.[2] Currently, the Armed Forces Epidemiological Board is sponsoring a research project at the University of Colorado Medical Center on the personal and interpersonal factors in automobile accidents among military and civilian populations.[5]

There are frequent newspaper accounts of drivers who have experienced serious accidents because of advanced physical disabilities, such as heart failure, diabetes, or epilepsy. For example, the *New York Times* recently reported the case of a man who died of heart disease while driving. He killed two boys standing near their bicycles at the side of the road, and the car finally stopped in the lobby of a moving picture theater which fortunately was empty at the time.

Limiting those drivers with certain advanced illnesses presents a serious problem, however, because of the difficulty in establishing a reliable diagnosis in advance of the accident or in setting up adequate criteria for cut-off points within various diseases or physical limitations. The American public is very reluctant to accept a limitation of its freedom, especially of the right to drive. Most would agree that a diabetic who needs insulin should not drive a school bus or a public conveyance. Some states have dealt with this problem satisfactorily through close collaboration between the medical profession and the licensing bureaus. Carefully controlled studies are urgently needed in regard to these problems.

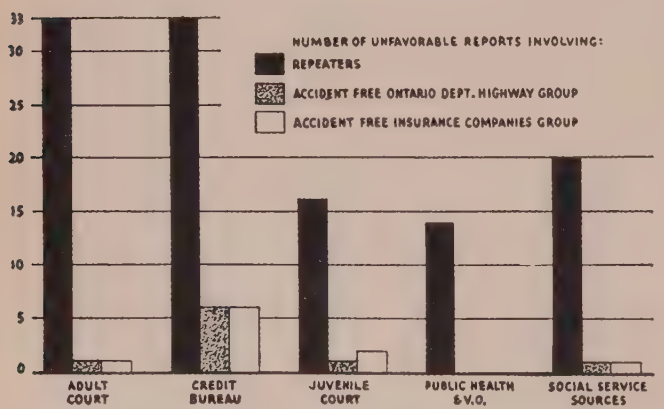

Fig. 4 – Social background of accident-repeater and accident-free taxi drivers as determined through case histories and confidential interviews[15]

The general trend is toward excluding from driving those individuals with severe sensory and perceptual defects; those with amputations or disturbances of motility which would interfere with the normal operation of controls; those with conditions leading to possible lapses of awareness or periods of unconsciousness; those with drug or alcohol addiction; and those with severe mental defect or disorder. An individual diagnosis is needed in such instances, and arbitrary regulations cannot be satisfactorily set regarding disqualifying conditions.[17]

C. *The Prevention of Accidents through the Selection and Training of Drivers*—Although individual tests have limited value in predicting accident rates, the use of a battery or group of tests offers greater promise. Also, training programs have resulted in a reduction in highway accidents. Such methods are especially applicable to educational institutions, companies, and military installations.

1. The role of job analysis in selection: A basic requirement in selection is that measures used to predict subsequent performance should be functionally related to the critical requirements of the performance. This involves an analysis of the task to determine its critical components.[13] In general, the procedures used in selecting drivers have not been based on such a process.

More effective procedures and standards for psychological and physical selection can be developed when the critical human requirements of the driving task have been established. Only a beginning has been made in this direction in the field of vehicular operation.[16] Factual information is urgently needed, not only in regard to the initial selection of drivers, but also for its usefulness in evaluating changes in abilities and driving skill with the passage of time and with changes in physical fitness or health. The most satisfactory procedures of study include the analysis of driver activity, the recording of driving errors, and the analysis of behavior in critical incidents, near-accidents, and accidents.

2. The results of studies on the selection of drivers: Several studies of commercial drivers have reported favorable results in safety when drivers have been selected on the basis of a variety of physical and psychological measures.[6] The evidence is

[15] See *American Journal of Psychiatry*, Vol. 106, No. 5, 1949, pp. 321-331: "Accident-Prone Automobile Driver; Study of Psychiatric and Social Background," by W. A. Tillmann and G. E. Hobbs.

[16] See "Human Factors in Highway Transport Safety," by R. A. McFarland and A. L. Moseley. Pub. by Harvard School of Public Health, Boston, 1954.

[17] See "Health, Medical and Drug Factors in Highway Safety." Publication 328, National Academy of Sciences – National Research Council, Washington, D. C., September, 1954.

limited, however, and only a few followup studies have been made of the professional driver. Also, little is known of the effect of driver-licensing programs on accident rates. There are indications that safer drivers, on the whole, tend to have average or better than average intelligence, to be relatively free from sensory and physical defects, and to be free from emotional conflicts or maladjustments.[2, 6]

One of the most promising procedures for the detection of accident repeaters prior to employment relates to the quality of personal-social adjustments. The method is based on the concept that *"a man drives as he lives,"* and employs objective indexes of social and personal adjustments.[15] Fig. 4 presents the findings from a study in which 97 accident repeaters were compared with two groups of 100 accident-free drivers on the basis of numbers of contacts with the courts, credit agencies, social service agencies, and public health clinics. This same concept has been used in a study of accident-free and accident-repeater truck drivers. A new scoring system was developed for weighting the significant items.[16] When tried in a new group, this scoring system differentiated the drivers as accident repeaters or accident free, with 85% of the cases studied accurate.

3. The results from training programs: A second method proposed for reducing accidents is that of adequately training drivers. Evidence for the effectiveness of training comes from studies made on students who have received formal driver-training compared with others who learned to drive more casually. The data from 12 investigations carried out in the United States have been combined into Table 2 (From Glanville[18]).

A few adequately designed studies have been made on the effectiveness of re-training commercial drivers. The findings support the view that training is a method of great potential value in reducing highway accidents.[6]

Further research is needed to determine the most important subject matter to be taught and the most effective methods of training. In this regard it has been shown that training in the recognition of dangerous situations, and practice in carrying out emergency maneuvers, have been of value for the safe operation of aircraft. An application of this approach should be worth while in the vehicular field. There is a need for the development of more adequate driving simulators to (1) permit sufficient behind-the-wheel practice so that responses may be automatic in routine operating practices, and (2) permit practice in the operation of vehicles under adverse conditions and emergency situations without attendant danger of injury.

Analyses of near accidents, critical situations,

Table 2 – Ratio of Accident Rates of Untrained to Trained Drivers in Comparable Periods of Time

	Exposure in Driver Months	Accidents	Accident Rate per 1000 Drivers per Month	Ratio of Accident Rates
Men and Boys				
Untrained	123,865	979	7.9	1.8
Trained	61,818	265	4.3	...
Women and Girls				
Untrained	42,581	110	2.6	2.2
Trained	62,272	72	1.2	...

and accidents have implications for the content and emphasis of driver-training and safety-education programs. For example, in an analysis of bad-weather accidents on the Pennsylvania Turnpike, it was observed that the driving practices employed sometimes precipitated, or prolonged, skidding which resulted in accidents. The conclusion was reached that important factors in the cause of these accidents were (1) inexperience in preventing skids and in handling slipping vehicles, and (2) lack of training in respect to this aspect of driving.[19]

A study carried out on bus drivers indicated that the frequency of errors in performing routine operating procedures was closely related to the accident records of the drivers. The bulk of these errors could be classified as errors in complex maneuvers, and as inattention to the task at hand. Studies such as these are needed to relate training to the operation of vehicles in the interests of safety.[16]

Another study was made of near accidents during routine vehicular operations at night and during the day to discover (1) the number of variables involved in emergencies, (2) how the driver determines the nature of an emergency, (3) how the driver reacts to prevent an accident, (4) the variety of critical situations and their relative frequency, and (5) the relationship between near and real accidents. The study revealed that, as a rule, critical situations develop very rapidly and are of short duration. Of the 66 near accidents observed, 53, or 80% of them, were closely related to the three most common types of accident which actually occur on the highway; namely, side-swipe, rear-end, and head-on collisions. The most important variables contributing to the critical situations were: (1) following too closely; (2) following too closely while approaching to pass, that is, cornering; (3) operator inattention, that is, dozing at the wheel; (4) vehicle running off the road; (5) intersection errors; (6) errors in passing; (7) operating in wrong lane of traffic; (8) leaving and entering the roadway; and (9) pedestrian errors.

It is possible that some of the near accidents are related to the personality and aptitude of the drivers, or that certain drivers have a tendency to become involved in the same type of situation repeat-

[18] See *Journal of the Royal Society of Arts*, Vol. 102, No. 4426, 1954, pp. 496-519: "Safety on the Road," by W. H. Glanville.

[19] See "Accident Causation," ed. by P. K. Echardt, Pennsylvania Turnpike Joint Safety Research Group. Pub. by Westinghouse Air Brake Co., Swissvale, Pa., 1954.

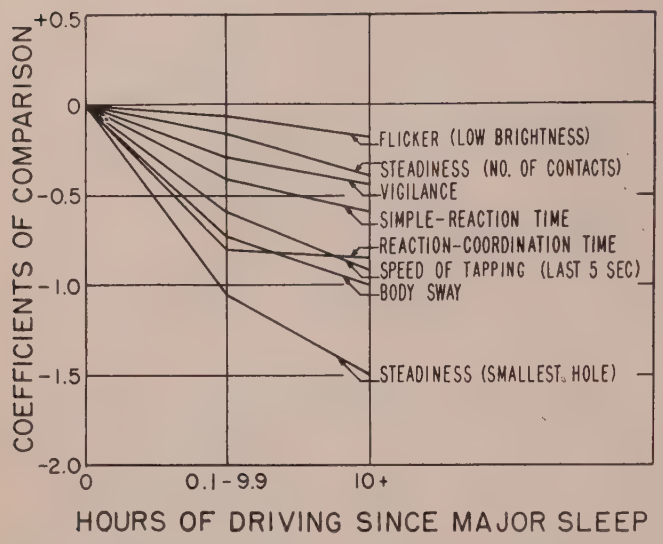

Fig. 5 – Influence of prolonged driving on visual and psychomotor reactions. Note general decrease in performance with increasing hours of driving[13]

edly. Observations thus far indicate a characteristic failure of the driver to take "defensive" action, that is to say, there is a tendency to wait for the other driver to allow for margins of safety. This occurred in 95% of the 66 incidents observed.[16]

4. The role of defensive driving in training programs: A study of near accidents thus affords an ideal opportunity for training the driver. In locations, or under conditions, where a given type of *near* accident is common, it may reasonably be expected that similar types of *real* accidents will occur. When the driver knows where accidents are most likely to occur he can be especially cautious at such locations. When he knows what types of accidents can occur, and the appropriate defensive measures, he can be prepared to meet such occasions without hesitation or bad judgment.

A potential accident situation arises very quickly, and the time elapsed before it has passed may be a few seconds or only a fraction of a second. To drive *defensively* is to remove all possibility of accident by preventive action. It implies that the driver knows where the hazardous locations are along the road, what hazardous situations are likely to arise, how fast he must react, and what action he should take in each of the anticipated concrete situations, and, finally, what general principles he should follow where specific measures cannot be predetermined. This concept of safe driving is directly opposed to the all-too-common practice in which one driver gambles on the fact that the other driver will take the necessary corrective action to prevent a collision.

D. *The Significance of Temporary States and Conditions of the Driver in Accidents* – A wide variety of temporary states and conditions also influences highway safety through their effect upon the behavior and efficiency of drivers. The influence of such states is usually difficult to determine statistically, although they are believed to be responsible for many accidents.

1. Fatigue: The effects of fatigue are most pronounced in driver-asleep accidents. In most other situations it is difficult to determine the loss of efficiency due to fatigue. It has been demonstrated that subjects do less well on a variety of psychological and psychomotor tasks after prolonged driving. The results have been interpreted to indicate reduced efficiency, and, hence, increased liability to accidents.[6, 13] For example, Fig. 5 shows the changes found on various psychological tests in relation to the length of time since the last major rest period for drivers operating trucks on the highways. Such findings provide some evidence for the regulations governing hours of driving and intervening rest periods which have been adopted by the Interstate Commerce Commission.

Evaluating the role of fatigue in highway safety is, however, not simply a matter of relating hours of driving to accident frequencies. Actually, in the case of truck drivers, the greatest frequency of accidents (about 60%) is found within the first 3 hr of driving rather than near the end of the day's run. The amount and quality of previous rest, time since last rest, the nature of activities prior to driving, and concurrent emotional stress are some of the numerous complicating factors.[16]

A clearer understanding of the effects of fatigue on driving performance can be gained from the concept of "skill fatigue" suggested by Bartlett.[20] A complex skilled performance such as driving has been shown to deteriorate in characteristic ways under protracted operation, or under other fatigue-producing conditions. One initial effect concerns the timing of reactions. While in later stages gross mistakes may appear, at first it is more likely that the right response is made, but at the wrong time. As fatigue increases, the field to which the operator is responding as a whole loses its integrated quality, and the operator reacts to individual aspects of it. Certain stimuli predominate, while others are ignored, and important responses are omitted. Standards of performance deteriorate, and the operator thinks he is doing as well as previously while he is actually operating less skilfully, and no longer recognizes or appreciates his errors. There may be loss of insight into the seriousness of the situation.

Under conditions of extreme fatigue, drivers

[20] See *British Journal of Industrial Medicine*, Vol. 8, No. 4, 1951, pp. 209-217: "Bearing of Experimental Psychology upon Human Skilled Performance," by F. C. Bartlett.

have been known to experience hallucinations, and to have accidents through maneuvers to avoid collision with obstacles perceived but not actually present on the highway. Confidential interviews with drivers have indicated that such experiences are most likely to occur on long-distance runs, at night, and when driver activity level is low and he feels a need for sleep. An example is given in the following case report:

"The operator of a semitrailer was traveling on a flat straight stretch of roadway during the middle of the night. There was no moon, but the weather was clear. Suddenly the driver 'saw' a calf standing in the road ahead in such a position that it was difficult to avoid hitting the animal. The driver turned his vehicle sharply to the left, and it was overturned in the roadway. A second vehicle belonging to the same company was following close behind, and the driver stopped to render assistance. Separate reports were made by both drivers, but the second driver did not indicate the presence of a calf in the roadway. An interview with the driver revealed that when extremely sleepy while driving he frequently sees 'things that are not there.' One of the indications of his sleepy state is that he sees herds of mules in bright shining harness crossing the roadway in front of him. This requires him to stop suddenly. After stopping he realizes that the mules are really nonexistent and that he has been 'dreaming.' " Similar kinds of reactions were reported in a series of 50 cases. The information was obtained during confidential interviews with commercial drivers.[16]

2. Alcohol: Alcohol also has a temporary effect on the driver, and is known to be an influence in causing highway accidents. Measuring the extent of the influence of alcohol in accidents presents statistical difficulties, however, because of the necessity of having control data. One study in which controls were observed is summarized in Table 3 (from Thorndike and Habstead[6]), which indicates that the likelihood of accident increases even at low levels of alcohol in the blood. Higher levels are characterized by a sharply increasing likelihood of accidents.

Various laboratory investigations have also shown that the effects of alcohol, although subject to wide variations in individual susceptibility, are always in a deleterious direction on a variety of sensory, psychomotor, and psychological functions.[13] Of particular importance for driving is the effect involving reduced standards of performance and a loss of insight into the quality of performance.[21]

3. The influence of emotional disturbances: More information is needed in regard to the influence of emotional disturbances and temporary emotional states in causing accidents. Isolated vehicular accidents have been attributed to emotional stress or preoccupation with anxieties. Further research on this problem needs to be carried out. It is well known that emotions influence our behavior during periods of stress. Incorrect and incompatible responses frequently replace more appropriate ones. Military establishments and large commercial fleets represent situations where the collection of data for investigations of this kind would be feasible.

4. The influence of drugs and medications: More needs to be known regarding the principal action or the side effects of commonly used medications and drugs on the safety and efficiency of performance at the wheel. It is not always realized, for instance, that a sedative effect persists up to 24 hr after the ingestion of some preparations ordinarily prescribed for relaxation and sleep. Disturbances of vision and of equilibrium, and episodes of drowsiness, have also been reported in some persons after self-medication with over-the-counter preparations to relieve pain or the symptoms of colds. Research at the University of Rochester has suggested that a number of medicinal preparations have effects upon attitudes and behavior which may be of importance in safety as reflected in the driving practices displayed by persons while influenced by such substances.[13, 17]

Application of Human Engineering Principles to Automobile Design

A. *The Design of Equipment in Relation to Human Requirements* – One means of improving highway safety is to design automotive equipment in terms of human capabilities and limitations. Mechanical design should be intimately related to the biological and psychological characteristics of the driver. It is reasonable to expect, therefore, that machines should be designed from the man outward, with instruments and controls considered as extensions of his nervous system and body appendages. This implies that the automobile should be built around the operator, rather than placing him in a setting without due regard for his requirements and capacities. Unless this is done, it is hardly fair to attribute so many accidents to human failures. If this point of view is carried out in practice, fewer accidents should result, and extensive

Table 3 – Relative Frequency of Automobile Accident Cases for Different Alcohol Concentrations

% Alcohol in Blood	Number of Accident Cases per 100 Control Cases
None	9
Less than 0.04	45
0.04–0.07	21
0.08–0.11	53
0.12–0.15	146
0.15 and over	577

[21] See *Quarterly Journal of Studies on Alcohol*, Vol. 11, No. 1, 1950, pp. 1-30: "Effect of Alcohol Ingestion on Driving Ability: Results of Practical Road Tests and Laboratory Experiments," by K. Bjerver and L. Goldberg.

redesigning of equipment after it is put into use should be eliminated.

It was commonly, and sometimes tragically, observed during World War II that machines do not fight alone. Radios do not hear; radar doesn't see; sonars don't detect; guns don't aim; nor do automobiles drive themselves. Difficulties arise when mechanization becomes too complicated for human operators. Since there appears to be little possibility in the near future that the drivers of automobiles will be eliminated by automatic control, as may be the case with pilots of aircraft, everything must be done to design the equipment and to set up the operating procedures to facilitate the greatest possible efficiency and safety.[3]

More directly stated: First, the engineer must have an understanding of the sense organs and the characteristics of human perception if satisfactory information is to be supplied from signals and lights in the operation of equipment. *In general, man is a poor monitor of equipment.* Second, the engineer must not place unreasonable demands upon the worker in regard to the physical responses involved, that is, in reaching and operating controls or levers or in clearly differentiating between them. Otherwise an inadvertent or delayed operation of a switch or control may occur. Third, the engineer must consider that the operator of equipment is frequently suffering from a temporary impairment of his functions causing inefficiency, such as fatigue or minor illness, and that there may be changes in function as a result of aging. Finally, the physiological and environmental conditions such as temperature, humidity, toxic gases, noise and vibration, and other factors must be considered.[7]

The major areas of automotive design in which the biological and engineering sciences can collaborate most effectively are as follows: (1) the layout of the driving area for comfort and efficiency of operation, including allowances for variations in human body size; (2) the design and arrangement of visual displays to provide information for operating under normal and emergency conditions; (3) the design of controls and their arrangement; (4) the control of toxic factors in the environment, and (5) the protection of the driver in the event of a sudden deceleration or collision.

B. *The Role of Advance Analysis in Accident Prevention.* Improvements in automotive design influencing safety can be brought about only by an *advance analysis* of all possible faults in the equipment. Advance analysis assumes several considerations. The first involves an operational job analysis, which should include a survey of the nature of the task, the work surroundings, the location of controls and instruments, and the way the operator performs his duties. The second implies a *functional concept of accidents,* that is, it anticipates the errors which may occur while the operator is driving the machine. A third consideration relates to *human limitations;* it should be assumed that no driver is perfect. He may, in fact, be far below the ability assumed by the designer. Finally, a *wide margin of safety* should be provided to eliminate any possible situations which place the driver near his maximum ability in terms of aptitude or effort, especially when adverse factors enter the picture.[22]

A few examples may help to clarify the concept of advance analysis in relation to human limitations. If an acoustical engineer designs any device in which a person must hear a signal, it would be important to know something about the receptivity of the human ear to such stimuli, otherwise the signal might be placed in the range of frequencies hardest to hear. This would be especially true for those in the age ranges that have difficulties in hearing higher frequencies.

Why should colors be used on maps or signaling devices which penalize those with borderline color vision? In regard to taking advantage of tinted windshields in reducing glare and controlling temperature within the car, why not use tints in the frequency bands less apt to influence the transmission of light or colors outside the car? Also, careful consideration should be given to the density of the tinting in relation to sitting eye level height, and especially to the reduced ability of the older person to see at low levels of illumination on the highway at night. Furthermore, it should be kept in mind that older persons require more time to make complicated responses, and all operations should be kept within their range of abilities.

Many examples can be given of the way in which automotive engineers have made advances to meet human requirements. Four-wheel brakes, power steering, and automatic shifting are excellent examples. However, carefully controlled mockup studies, in which the nature and range of human abilities can be tested, might aid in making the most of these advances. How fast should the brakes operate in relation to the age, sex, size, and strength of the driver? How much "feedback" should be present in the power-steering system, and how should the automatic shifting device be designed for greatest ease of operation and standardization? If the biological scientist were present during the mockup stages, he might aid the engineer in regard to the ranges of abilities and limitations of the driving population.

The concept of design failure is relatively new and unexplored in the automotive field, partly because accident reports have failed to identify this source as a cause of accidents. Design failures may be so subtle that those responsible for reporting accidents may not even be aware of them, particularly if they are not trained to recognize such failures.

It is fully realized that design problems of this

[22] See "Human Factors in Air Transport Design," by R. A. McFarland. Pub. by McGraw-Hill, New York, 1946.

nature are not the source of all, or even most, vehicular accidents. Such factors as mental state, morale, and intoxication are probably of greater importance. Nevertheless, if a major design deficiency exists it is only a matter of time before some operator has an accident because of it. Even minor inconveniences and discomforts will add up, in the presence of increasing fatigue, to situations in which it becomes easier for an accident to happen. Furthermore, even though the driver may compensate for design failures under normal conditions, he may be at a disadvantage in emergencies. For these reasons, advance analysis of operator error in relation to design offers a field in which specific and immediate gains may be made in reducing accidents.[16]

C. *Safety Factors in the Design of the Driver's Area* – It has often been stated that automobiles do not cause accidents, but that the people who operate and maintain them are the primary sources of error. The view presented here is that either the operator *or* the equipment may be at fault unless the instruments and controls are effectively integrated with the operator. Many errors may be inherent in the automobile, truck or bus: (a) if the controls cannot be easily reached, or rapidly differentiated and operated; (b) if visual links introduce reading errors because the gages or dials are illegible; (c) if the operation of a control or lever is beyond the range of the operator's visual, tactual, or kinesthetic cues, or (d) if the position and design of the seat is inadequate. Human capabilities and body size must, therefore, be considered in the original design of controls, visual displays, window areas, and seats if errors are to be prevented by the operator.[3]

1. Human body size and the location of seats and controls: In order to determine the minimum size of a vehicle seat (height, width, and depth), and the effective location of controls, pedals, and switches, it is necessary first to determine the full range of size of the driving population. Once this has been established, by means of anthropometric techniques, the equipment must be evaluated in terms of the following sort of questions: (a) Is there sufficient horizontal adjustment in the seat to allow a small woman to reach the pedals and still give a tall man enough space so that his legs won't be cramped under the steering wheel? (b) Is there sufficient vertical adjustment in the seat to allow the short woman to have her eye level several inches above the top of the steering wheel, and still permit the tall man to bring his eye level below the top of the windshield? (c) Are all controls within easy reach of the driver, once the seat has been adjusted? (d) Is the inside of the car or cab high enough so that the tall driver can avoid striking his head on the roof?[23]

If answers to the above conditions are unsatisfactory, the equipment is poorly adjusted to the extremes of the size distribution of drivers. A lack of adequate horizontal seat adjustability will force the short driver to sit forward on the seat with no brace for her back, and she may have trouble in steering or in applying the brakes. Moreover, without adequate vertical adjustment, she will have a limited field of vision, and thus will have difficulty in seeing people or objects close to the vehicle. Inadequate vertical and/or horizontal seat adjustment for the tall man may cause him to strike the steering wheel when moving his leg to the brake, and may prevent him from braking in time. An accident may occur when a control is so far from the driver that he must lean out of the normal driving position to operate it.[16]

The measurements of the human body necessary for establishing the dimensions of the working space and locating controls have been outlined by King[24, 25] and are as follows: (a) The maximum arm reaches attainable without altering the position of the body. (b) The extension of these reaches which can be attained by the movement of the trunk or body. (c) The eye level of the man in the operating position. (d) Body dimensions in the operating position, that is, sitting heights, fore and aft and lateral measurements at various levels. (e) The leg reaches attainable without altering or disrupting posture. With such information available, the engineer can design machinery that will accommodate a very large percentage of the driving population with regard to comfort, efficiency, and safety.

Many of the newer designs of automobiles, trucks, and buses are meeting the requirements outlined above in regard to human body size and capabilities. Design recommendations have been formulated through the SAE Riding Comfort Research Committee. Also, manuals have been prepared which give the distributions for a wide range of physical measurements in both civilian and military populations.[16, 26] Marked improvements are being achieved in many types of vehicular equipment.

2. The design of controls and displays: Many errors can be prevented if controls are designed and placed so that rapid and accurate movements can be made. Some of the important factors relating to the design and operation of controls are: (a) their location for ease and accuracy of reaching; (b) the direction of movement for greatest efficiency; (c) the amount of force that must be

[23] See "Human Factors in the Design of Highway Transport Equipment: Summary Report of Vehicle Evaluation," by R. A. McFarland et al. Pub. by Harvard School of Public Health, Boston, 1953.

[24] See "Cockpit Studies – Boundaries of Maximum Area for Operation of Manual Controls," by B. S. King, O. J. Morrow, and E. P. Vollmer. Project X-651, Report No. 3, Naval Medical Research Institute, National Naval Medical Center, Bethesda, Md., July, 1947.

[25] See *American Journal of Physical Anthropology*, Vol. 6, 1948, pp. 341-351: "Measurements of Man for Making Machinery," by B. S. King.

[26] See "Human Body Size and Capabilities in Design and Operation of Vehicular Equipment," by R. A. McFarland et al. Pub. by Harvard School of Public Health, Boston, 1953.

applied for operation; (d) rate of movement from point to point; (e) speed and amount of rotary or wrist movement required in wheels or knobs; (f) size and shape; (g) frequency of use; and finally, (h) the degree to which the control performs a critical function. Many data of this nature are currently available and may be applied to problems of automotive design.[26]

One promising area is that of the various pedal relationships. The brake and accelerator pedals are sometimes placed so that they force the driver's foot to make lengthy movements in three directions before the brake can be activated, that is, up, over, and then down. Undoubtedly a feature such as this must have been responsible for many near accidents, and a contributing factor in a certain proportion of real accidents as well. However, recent changes in the pedal design of some cars with power brakes have considerably reduced this foot-travel distance.

Visual displays can contribute directly to troublesome situations if an operator does not clearly perceive the location or movement of the indicators or dials. Factors having a significant effect on ease of instrument reading include size and spacing of critical detail, contrast between object and immediate background, amount of illumination including the use of color, and contrast between the objects to be seen and their surroundings. Design criteria for the shape, size, scale markings, and numbering of instruments as well as the most legible width and length of pointers have been determined experimentally, and are currently available.[27] Drivers sometimes spend too much time looking for a specific control or instrument because it is surrounded by others of the same size, shape, and general design. At other times, the instrument may be behind the steering wheel or too far away to be read easily. Such factors as these may seem trivial in that improvements may result in the saving of only 1/10 sec. At 40 mph, however, 1/10 sec means 6 ft, and 6 ft can well mean the difference between life and death to a driver in a critical situation.

In general, it may be said that any control unnecessarily difficult to reach and operate, any instrument difficult to read, any seat inducing poor posture or discomfort, or any unnecessary obstruction to vision, may contribute directly to an accident because of the difficulty of proper operation on the part of the driver. In addition, the cumulative effects of such difficulties are sure to induce fatigue, resulting in the overall deterioration of driver efficiency and perhaps leading to an eventual accident.

D. *Automotive Design in the Light of Crash Injury Research* – The decelerative forces involved in sudden stops will result in bodily injury to the occupants if they are thrown forward against the windshield, dashboard, or other structures or projections. The degree of safety is in large part dependent upon the rate at which the vehicle stops. Ideally, the brakes of a modern vehicle are capable of producing a deceleration of up to 1 g (32 ft per sec^2)[28] but in practice it has been found that 20 ft per sec^2 is the maximum that can be expected under most circumstances without skidding or sliding the wheels.[29] Nevertheless, this figure is still considerably higher than those determined by Starks for the points at which a person riding in a vehicle feels discomfort, or must prepare to avoid bodily injury. A series of controlled braking stops were made from a speed of 70 mph, and the subjective responses of the drivers and passengers were recorded. On the basis of these data obtained, the maximum limits of deceleration for comfort can be set slightly below 11 ft per sec^2. However, as these forces approached 14 ft per sec^2, the reaction was judged severe and the passengers had to prepare to avoid injury.[28] Since high decelerative forces will occur only during conditions of emergency, they cannot be completely controlled through driver choice. The ultimate solution, then, is in so far as is possible to prevent injury to the occupants of the vehicle once such conditions occur. Research by Stapp, De Haven, Dye, and others on the ability of the human body to withstand sudden deceleration and impact forces has indicated that the force of many accidents that are now fatal may be within the physiological limits of survival.[30, 31]

It was found, for example, that a human being can withstand very high accelerative forces without injury if he is properly restrained. On the other hand, a speed of 15 mph can cause death if the momentum of the head is not checked during rapid deceleration of the vehicle. If a 10-lb object, the approximate weight of a human skull, falls 1 ft and strikes an area 1 in. square the deformation would be very slight. On the other hand, under the same conditions, if an object 1 cm square is struck, a puncture fracture would result.[32]

Controlled research in this area should define not only the tolerances which the human body can stand, but the variables within a decelerating vehicle which result in injury as well. This requires a uniform system of obtaining and recording data on the causes of injury *within* automobiles in crashes. At the Automotive Crash Injury Project at Cornell Medical College, case histories are being accumulated at a rate soon to reach 2000 per year, from seven states. This study is being sponsored by the Commission on accidental trauma of the AFEB, Department of Defense, and the U. S. Public Health Service.[5] Some of the findings which have resulted from the correlation of injuries with data

[27] See "Psychological Aspects of Equipment Design," by P. M. Fitts. Technical Report No. 5829, Air Materiel Command, USAF, Wright-Patterson Air Force Base, Dayton, Ohio, August, 1949.

[28] See *Motor Industries Research Association Bulletin*, Second Quarter, 1950, pp. 17-33: "Factors which Influence Braking Performance of Vehicles," by H. J. H. Starks.

[29] See *SAE Transactions*, Vol. 61, 1953, pp. 623-639: "Safe Brakes for Passenger Cars," by G. T. Ladd and S. B. Dew.

on the portion of vehicle structure involved or the nature of forces involved are as follows: One or more front doors opened in from 44 to over 50% of the injury-producing accidents. Rolling over of the car significantly increased the frequency with which front doors opened. When front doors opened, one out of four occupants was completely ejected from the car. Complete ejection through opened doors approximately doubled the risk of sustaining moderate through fatal injuries.[5]

An interesting sidelight on crash injury data from two different studies was the finding that in at least two instances, attempts to commit suicide by driving head-on at high speed into an embankment or a wall were rendered ineffective because the design of the steering-wheels and steering posts was such that impact forces were absorbed through deformation and were dissipated over relatively wide areas, so that serious injury was prevented.

Studies of the specific features of vehicular designs that cause injuries in crashes offer considerable promise in reducing fatalities. Automotive engineers can obviously make a great contribution to this area of injuries and fatalities, which we have compared to a mass epidemic, if preventive action can be taken at the source, namely the vehicle itself. The role of restraining devices also offers a promising field for all those concerned with automobile safety.[5]

E. *Human Factors in the Design of Equipment in Relation to Environmental Variables* – The comfort, efficiency, and safety of the driver are also influenced by the extent to which design features in the car are able to modify or control the physical variables of the environment. These variables include temperature, humidity, ventilation, carbon monoxide, noise, vibration, and deceleration. For each of these factors there are reasonably well defined ranges of comfort, discomfort, and harmfulness.

1. Temperature, humidity, and ventilation: A change in any one of these variables will affect the other two in so far as they determine comfort, and hence all three must be considered as a unit. Fig. 6, developed by the American Society of Heating and Ventilating Engineers, shows the various comfort zones and the typical subjective responses to heat, cold, and humidity.[33]

The winter comfort zones range from a dry-bulb temperature of approximately 65 to 78 F, and summer from 68 to 85 F, depending on the relative humidity. The optimum range for the winter is 68 to 72 F (dry bulb), and for summer 74 to 78 F. For these comfort zones, a relative humidity of 30 to 70% is quite acceptable. Excessively high humidities are uncomfortable owing to the lack of body cooling through evaporation at high temperatures, and a sensation of coolness or dampness at low temperatures. Humidities below 15% may result in a drying out of the eyes, nose, and throat.[22]

One of the most important requirements for driver and passenger comfort relates to air movement and the amount of fresh air that must be used in ventilating the car. Very low rates of air movement will produce a feeling of stuffiness, and body odors and tobacco smoke may become very irritating. Optimally, 35 to 40 cfm of fresh air should be supplied per individual at velocities of between 20 and 60 fpm in order to maintain a sense of freshness without creating undesirable drafts.[22] It should be remembered that increased air velocities tend to have a greater cooling effect which may be advantageous in summer but uncomfortable in winter.

The most important implication of the atmospheric variables, however, is the fact that human performance has been shown to deteriorate significantly at temperatures of about 83 E.T. and above,

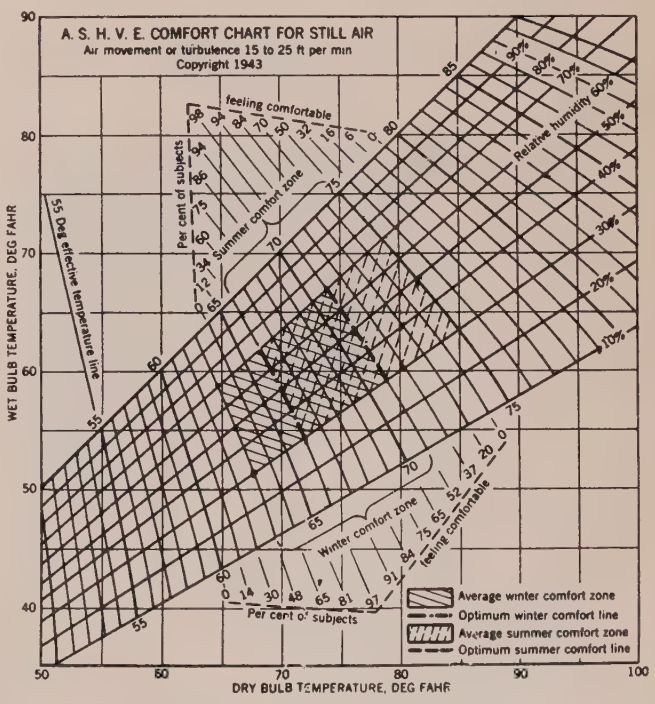

Fig. 6 – Winter and summer comfort zones as related to temperature and humidity. Winter zone applies to rooms heated by convection method, while summer zone applies to air conditioned areas to which occupants become fully adapted[33]

[30] See "Accident Survival – Airplane and Passenger Automobile," by Hugh DeHaven, Crash Injury Research Project, N60NR 264-12, Cornell University Medical College, New York, January, 1952.

[31] See "Human Exposures to Linear Deceleration: I. Preliminary Survey of Aft-Facing Seated Positions (1949); II. Forward-Facing Position and Development of a Crash Harness (December, 1951)," by J. P. Stapp. Technical Report 5915, Air Materiel Command, USAF, Wright-Patterson Air Force Base, Dayton, Ohio.

[32] See *Mechanical Engineering*, Vol. 66, April, 1944, pp. 264-268: "Mechanics of Injury under Force Conditions," by Hugh DeHaven.

[33] See "Heating, Ventilating, Air Conditioning Guide, Vol. 22." Pub. by American Society of Heating and Ventilating Engineers, New York, 1944.

(the equivalent of 83 F at 100% humidity).[34] Of the different types of activity which show deterioration some are traceable, at least in part, to many of the types of activity having direct implications for safe driving. Fortunately, many of these atmospheric variables have been controlled in the modern automobile by the use of adequate heating, air conditioning, and ventilating equipment, thus insuring not only increased comfort and efficiency for the driver, but also the likelihood of a small attendant decrease in accidents resulting from deterioration in driver performance and skill.[35]

2. Carbon monoxide: The possibility of carbon monoxide poisoning can rarely be completely eliminated in the operation of motor vehicles. Quite small amounts of this gas will be rapidly absorbed by the blood stream, resulting in an oxygen deficiency which may at first be unnoticed by the individual. The initial reaction to carbon monoxide poisoning consists primarily of lowered attention, difficulty in concentration, slight muscular incoordination, sleepiness, and a mental and physical lethargy. These first symptoms are not permanently injurious, but, owing to their nature, could easily involve a driver in hazardous situations. With higher concentrations, severe headaches, dizziness, nausea, and vomiting may result, followed by a loss of consciousness and, ultimately, death.[22]

In motor vehicles, dangerous concentrations of carbon monoxide may result from leaks in the exhaust system. The use of a carbon monoxide tester will easily reveal whether the levels are

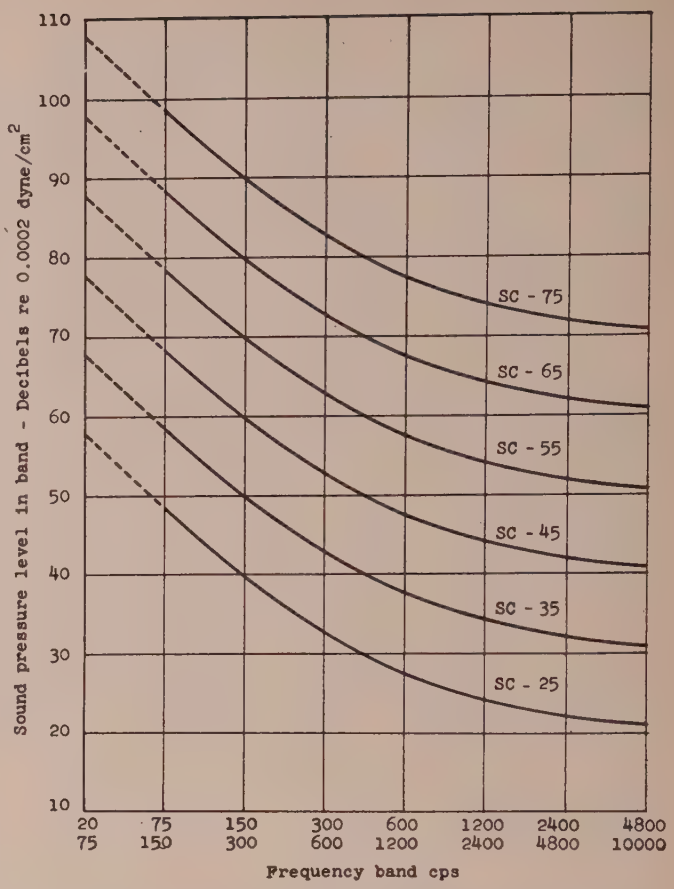

Fig. 8 – Speech communication (SC) levels. Curves indicate various degrees of speech interference at different frequencies[36]

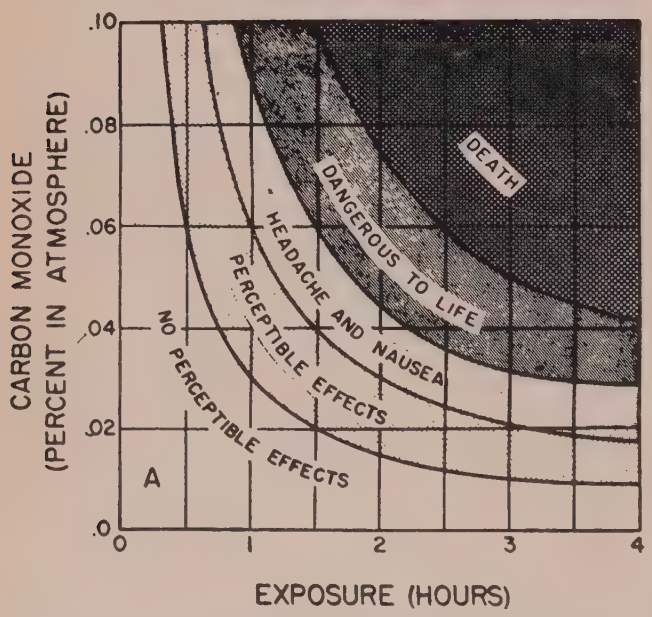

Fig. 7 – Human tolerance limits for carbon monoxide in terms of concentration and exposure[13]

within any of the danger zones indicated in Fig. 7. It will be noted that exposure to 0.10% carbon monoxide can be dangerous to life after 1 hr. Exposure to even as small a concentration as 0.01%, although having no perceptible effects for several hours, should not be permitted over long periods of time. In general, exhaust systems have been made resistant to the loss or leakage of fumes. Drivers of commercial vehicles should be well indoctrinated into the procedures of airing vehicles left standing with idling motors.[23]

3. Noise and vibration: The noise and vibration levels in most passenger automobiles are of a sufficiently low degree to require virtually no design changes from the point of view of driver health and safety. This is in marked contrast to the situation of some commercial vehicles where overall sound level readings of as much as 95 db have been

[34] See "Researches on Measurement of Human Performance," by N. H. Mackworth. Medical Research Council, Special Report Series No. 268, His Majesty's Stationery Office, London, 1950.

[35] See "Physical Variables Influencing Driver Comfort, Efficiency, and Safety," by R. A. McFarland and H. W. Stoudt. Pub. by Harvard School of Public Health, Boston, 1955.

recorded. This figure is within or approaching the limits for hearing loss set by some investigators.[35] Noise reduction in commercial vehicles constitutes a real challenge to automotive engineers, and something should be done about it to answer mounting public protests.

The most satisfactory criterion for comfort in regard to noise levels is the ease at which ordinary conversation can be carried on without exerting great effort. Referring to the *speech communication* (SC) criterion in Fig. 8, if the SC-55 curve is not exceeded for any of the frequency bands, conversation will be intelligible at a distance of several feet.[36] This is probably the maximum sound level that should be considered acceptable for passenger-car operation. Noise levels may be reduced by the use of soft mounts, vibration damping compounds, silencers, mufflers, and so forth, some of which will also aid in reducing vibration.[26]

4. Limits of physical variables for driver comfort and safety: A schematic interpretation of the various stimuli encountered in driving is given in Fig. 9 in terms of limits for comfort, discomfort, and physiologically harmful zones. The values indicated in the figure cannot always be considered as rigid standards because of the interdependence of one variable with another. The difficulty of giving a single numerical value as a standard is exemplified in the limits for carbon monoxide. The generally accepted maximum value is 100 ppm of carbon monoxide in circulating air for prolonged exposures. This figure may be satisfactory for a person sitting quietly at sea level, but it should be reduced if the amount of exercise, degree of ventilation, or the length of time increases. The permissible amplitudes for vibration, on the other hand, apply only at frequencies of 8 cps or less. Frequencies higher than this are probably not a major factor in automobile operation. The same complexity characterizes almost every other function that has been discussed.[16] Linear scales or straight line functions are not so adaptable to the study of human variables as nomograms in which one can ascertain the effects of altering any one of the variables upon the others.

Driver-Environment Interrelationships in Accident Causation

An understanding of the causes of accidents may also be clarified through a consideration of the relationships between the capabilities and limitations of drivers and their environment. Such studies have implications for highway safety through (a) an understanding of the variables in the environment which influence drivers, such as illumination and weather, (b) the design of highways in relation to driver capabilities and limitations, and (c) the effect of social forces, attitudes, and enforcement programs.

A. *Environmental Factors Influencing Visibility* – It has been reported by the National Safety Council that night driving is considerably more hazardous than day driving, and that the hazard is considerably greater in rural than in urban areas. Based on a national average, the ratio is about 3 to 1 between the rates at night and during daylight hours.[1, 19] This observation emphasizes the importance of the relationship between visual perception and the level of illumination. A reduction of accident rates at night has been brought about when artificial lighting has been increased.[6] Improvements have also resulted from better taillights, especially an increase in intensity, and also in reference to the number and location of taillights.[2, 18]

The design of lighting systems for both vehicles and highways should give adequate consideration to the basic characteristics of human vision. An activity analysis of how the eyes will be used should be included in vehicular and highway planning. A few relevant factors are mentioned below. At low illumination, the acuity of vision suffers, color values change, and relatively greater contrasts between object and background are necessary for perception. Age is also of importance, with greater intensities of light required as individuals

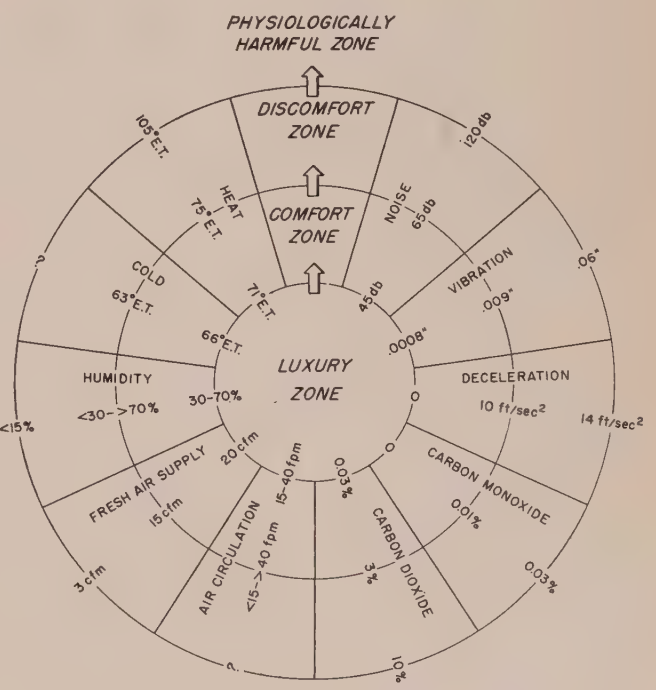

Fig. 9 – Physical variables of environment influencing driver comfort, health, and safety. These values must be considered approximations, since each variable is interdependent on one or more additional factors[35]

[36] See "Handbook of Acoustic Noise Control." Vol. II: "Noise and Man," by W. A. Rosenblith, K. N. Stevens et al. WADC Technical Report 52-204, Wright Air Development Center, Wright-Patterson Air Force Base, Dayton, Ohio, 1953.

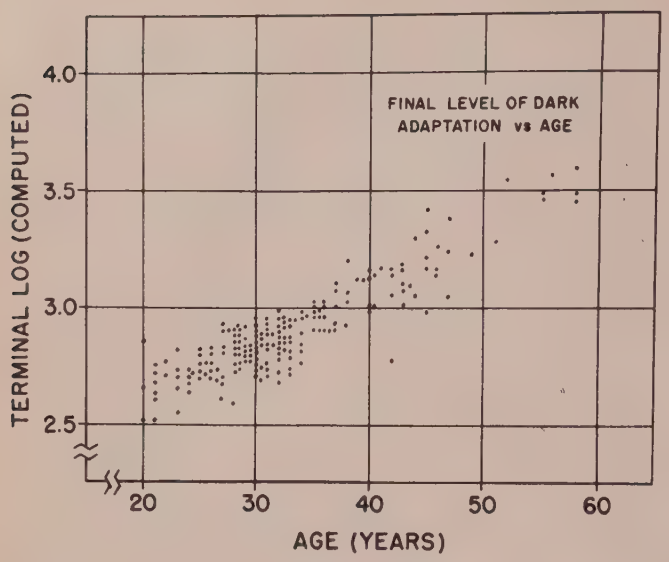

Fig. 10 – Scatter plot showing relationship between age and final level of dark application. Coefficient of correlation is 0.895[37]

progress beyond 40 or 50 years of age.[13] The results of a study of dark adaptation in relation to age are shown in Fig. 10. A high negative correlation (0.89) was found between age and maximum dark adaptation.[37]

It was observed during the war that pilots who spent long periods of time on sunlit beaches subsequently experienced difficulties in night flying. Wearing colored glasses during exposure to bright sunlight proved effective in preserving night vision. This finding has implications for automobile drivers at night who have previously been driving in bright sunlight.[2]

Operational research has demonstrated that brightness-contrast is of prime importance in perception during nighttime driving. Important variables are the intensity and color of lighting, the uniformity in brightness of the road surface, and the color and reflectance characteristics of the road surface. Objects on the roadway are perceived as darker silhouettes against a lighter background.[4]

On unlighted roads, objects tend to be perceived directly by the reflected light from headlights. Rough-textured road surfaces of light color have been recommended to enhance silhouette perception of objects having low reflectance.[18] Several other studies have also shown that light colors and reflecting materials increase the distances objects and various kinds of highway markers are visible at night.[2, 4]

The perceptual abilities of drivers in regard to signs and markers are also relevant to the proficiency and safety of driving. Design criteria based on visibility and legibility distances have resulted from a number of studies in which such factors as size, shape, color, letter characteristics, and length of legend have been investigated. Whether sufficient attention has been paid to the range of perceptual abilities in the driving population is not always clear, and applications of the data may require additional information in regard to the portion of the driving population with poorer than "normal" vision.[2, 4, 6]

B. *The Role of Weather in Highway Safety* – The atmospheric conditions outside the vehicle also have an influence upon highway safety. Rain and snow tend to be accompanied by a lower volume of travel, but with increased accident rates per unit of travel.[1, 4, 18, 38] Reduced visibility due to lower illumination and obstructions to vision is probably a human-related variable in this complex. Other human variables include the driving practices employed in relation to the reduced traction of wet or icy surfaces. Control measures involve both the use of materials in highway construction which provide adequate friction under poor weather conditions, and the indoctrination and training of drivers with respect to procedures for driving under all adverse conditions.

The automotive engineer should not disregard the need for continuing to improve the reliability and efficiency of braking systems simply because many studies have shown that a large majority of highway accidents have occurred in good weather, during the daytime, and on roads in good repair.[16]

C. *Driver Capabilities in Relation to Highway Design and Traffic Engineering* – When highways have been designed to eliminate known hazards, such as sharp curves, narrow bridges, and opposing or crossing streams of traffic, accident rates are usually lower as compared to rates on unimproved roads bearing comparable traffic. Data on human characteristics have influenced some of these advances.[4, 14] For example, observations on the swerving practices of drivers while passing led to recommendations for highway design in terms of the width of the lanes.[4] Data are needed on sight distances, perception, decision, and reaction times at different rates of travel to be correlated with engineering data on acceleration and deceleration in determining preference paths and the geometrical design of highways. Other observations determined the time required by drivers to decide to carry out a passing maneuver. This time was then included with speed and distance data to determine safe passing zones.[14]

The location of accidents by means of statistical quality control affords a method of identifying

[37] See *Journal of Gerontology*, Vol. 10, No. 4, 1955, pp. 424-428: "Alterations in Dark Adaptation as Function of Age," by R. A. McFarland and M. B. Fisher.

[38] See *British Journal of Physiological Optics*, Vol. 10, No. 2, 1953, pp. 63-85: "Some Factors Affecting Visibility from Driver's Seat and Their Effect on Road Safety," by R. J. Smeed.

those highway sites and features where analysis in terms of human variables may contribute to a solution of accident problems. Studies of this kind have been made by Dunlap and Associates on several modern highways under the sponsorship of the Commission on Accidental Trauma of the Armed Forces Epidemiological Board, Department of Defense.[5]

Sometimes when improvements have been introduced in the design of highways, accident problems of a new sort have resulted because sufficient analysis has not been made of driver behavior. Lack of awareness of speed may result from continuous driving on modern high speed throughways. For example, an important psychological factor in driving may be the mechanism of adaptation. This factor has been proposed as a possible explanation of incidents and accidents at the terminal end of a well-known toll road in which drivers failed to stop soon enough at the toll booths. The drivers, traveling close to 60 mph on the throughway for some time, had become adapted to the speed so they were no longer aware of how fast they were moving, and were unalert to the implications of their speed. The introduction of warning signs did not have the desired effect.

D. *The Role of Social Forces in the Driving Environment* – Not only are the physical variables in the environment important, but forces of a social nature may also influence driver behavior and safety. Little is known of this area, which numerous writers consider the most important one in highway accidents. The basic human variables relate to attitudes which underlie the specific behaviors exhibited during driving – attitudes toward traffic, toward the presence of other drivers, toward vehicle laws and regulations, toward enforcement activities, and toward society. Since attitudes cannot be observed or measured directly, the evidence is indirect as to what the attitudes of drivers are, how and under what circumstances attitudes and behavior are modified, and what their effects upon highway safety may be. There is great need for the development of better methods of assessing attitudes, and for studies on the effect of various social influences on the attitudes of drivers and on trends in accident rates.

Observation of the driving behavior of motorists under various traffic conditions, or in relation to specific kinds of maneuvers, has been one source of inference about driver attitudes. A common attitude among drivers seems to be that other drivers will take action to prevent accidents when insufficient time or distance has been allowed for the completion of a traffic maneuver. Another common attitude involves the assumption of a clear pathway or unobstructed roadway beyond the limit of immediate visibility for the road ahead, as at curves and hilltops.[4, 16]

An attitude of overconfidence may also be responsible for accidents. When a series of accidents on the Pennsylvania Turnpike was analyzed, drivers in many instances could offer no explanation for their mishaps. It has been concluded that driving beyond one's abilities of attention and capacity for alertness to all the conditions of travel may well result from the reinforcement that each mile of safe travel, or travel without a critical incident, exaggerates the estimate a driver has of his own driving ability.[19] It is a psychological axiom that repeated success in an activity results in its being more firmly fixed as a habit. Poor as well as good driving practices tend to become habitual when they have not resulted in an accident. The relative infrequency, in the experience of any driver, of near accidents and accidents compared to the number of miles driven can thus easily lead to the belief that one is driving very well indeed.

The taking of risks is another aspect of driver behavior which is dependent upon attitudes. An interesting set of observations in this regard comes from the Dunlap studies mentioned above. Taking certain kinds of risks on the highway seems more likely if the traffic previously encountered has been relatively light. Also, driving practices at any one time seem to be adapted, not to the existing conditions, but rather to previous traffic conditions.[5] Studies are needed in this connection to determine the communication values of different kinds of driver behavior and the various cues which may influence the determination of what a driver will do in a particular situation.

The control of drivers through *socio-legal channels* represents another aspect of the influence of the social environment on driving. For example, there are marked variations from state to state in motor-vehicle fatality rates. In 1954, the national motor-vehicle fatality rate was 6.5 per 100,000,000 miles. Two states, Connecticut and Rhode Island, had rates less than 3, and in two others, Massachusetts and New Jersey, the rates were less than 4. The poorest records characterized Nevada, New Mexico, and Arizona, with rates respectively of 10.5, 9.9, and 9.6.

It is reasonable to believe that in states where the rates have been appreciably below the national average, favorable results have come from the efforts of vehicle administrators and highway safety officials. It would be difficult to single out specific features of the various programs as responsible for the results in safety. However, it has been shown that in states requiring a periodic safety-check of vehicles, accident rates tend to be low. At the same time, states requiring periodic vehicle inspection also turn out to be the same ones in which other measures to improve highway safety are also emphasized.

A number of studies have shown that increasing the quantity, or improving the quality, of the enforcement of vehicle laws, results at least tempo-

rarily in an improvement in accident rates. There are no controlled investigations, however, which indicate the relative effectiveness of methods used to control driver behavior by such means. One of the difficulties in making such studies is the lack of uniformity in the regulations concerning driving and in the practices regarding enforcement, court actions, and the control of driving licenses by motor-vehicle administrators. At present there is a trend toward the use of demerit systems in the regulation of drivers. These involve a series of warnings and corrective interviews which are specifically designed to clarify the attitudes of drivers, and to foster safer attitudes and practices under the implicit threat of loss of the privilege to drive.

Summary

It has been shown that highway accidents are a major problem to the nation, even though fatal accident rates have been improved over a span of 20 years. The numbers of persons killed, and the disabilities resulting from injuries incurred in motor-vehicle accidents, have reached epidemic proportions, and constitutes a serious problem of public health, in many ways similar to the effects of mass disease.

A better understanding of the basic causes of accidents is clearly needed if adequate preventive measures are to follow. Most accidents have multiple causes. An analysis of the complex interrelations in the causes of accidents can be advanced if the framework of the epidemiological approach to mass disease is adopted. This approach is particularly suitable for analyzing the complex causes of accidents in terms of the interactions between the driver, his vehicle, and the environment in which driving is carried out. This conception also requires a team approach to the study and prevention of accidents, and fosters the integration of findings from the biological, engineering, and social sciences.

A review of the attempts to relate specific characteristics of individuals to their safety records has indicated that only low intelligence, youthfulness, and an attitude in which social responsibility is lacking are appreciably related to having highway accidents. Sure ways of identifying those relatively few drivers who are accident repeaters have not been found. A promising method in this connection is based on the concept that "a man drives as he lives." The method uses objective indexes of the quality of adjustments in meeting the demands of life, and has proved useful in differentiating between accident-free and accident-repeater drivers.

Attempts to decrease motor-vehicle accidents by selecting drivers have not yielded impressive results. If modern methods of job analysis are applied to the task of driving, it is possible that more appropriate procedures for selecting safe drivers may be developed. At present, the results from studies on the training of drivers suggests that emphasis upon training in safe driving practices and in the principles of defensive driving does significantly reduce the frequency of accidents. Such training should include practice in recognizing dangerous situations as they develop, and in handling vehicles under adverse conditions.

Drivers also should be indoctrinated with respect to the effects of various temporary conditions and states upon their safety and efficiency. The characteristic effects of fatigue upon skilled performance were outlined, as they might become apparent in the tired driver. Alcohol was shown to have a deleterious effect upon driving skill even at relatively low concentrations in the blood, and the risk of accident was shown statistically to increase markedly as the levels of blood alcohol increased. Emotional disturbances also were discussed in relation to their adverse effects upon the safety of driving. Attention was also called to the deleterious effects upon skilled performance of side-action of various drugs and medications commonly used by the public.

The vehicle and the environment must also be considered in effective measures to prevent highway accidents. An important way of advancing highway safety is to increase the integration of the driver with his automobile. It was pointed out that mechanical design should be based upon the biological and psychological characteristics of the drivers, and that vehicles should, therefore, be designed from the man outward, with instruments and controls considered as extensions of his nervous system and body appendages. The importance of advance analysis was stressed, whereby all possible faults in the machine can be anticipated and avoided before the vehicle is put into production. This can be done only in conjunction with (a) an operational job analysis, (b) a functional concept of accidents, (c) an awareness of human limitations, and (d) the provisions of a wide margin of safety.

Some general principles were discussed for the arrangement and design of the equipment in the driver's working area. These include the use of human body size data to indicate the location and relationships of various foot and hand controls, the design features of the controls, and factors to be considered in the design of instruments. In general any control that is difficult to reach or operate, any instrument that is difficult to read, any seat inducing discomfort, or any obstruction to vision may contribute directly or indirectly to decreased driver efficiency and eventually to accidents.

Attention was directed to the fact that the decelerative forces of many fatal accidents theoretically have been within the physiological limits of survival when the individuals can be given the proper protection. Current research in the relation of crash injury to design was then briefly reviewed.

Such environmental variables as temperature, humidity, ventilation, noise, and vibration were discussed with reference to the comfort, health, and efficiency of the driver. Data were presented to show the desirable and undesirable limits of these factors as an aid to the designers of automotive equipment. The engineering profession has an unusual opportunity at this time to make contributions to automotive safety.

The interaction between the driver and his environment was also discussed as a basis for understanding the causes and control of accidents. Factors affecting visibility were reviewed in relation to the basic characteristics of human vision, and the implication of a knowledge of man's capabilities and limitations for the design of safer highways was stressed.

Also considered were the effects of a variety of social forces upon the attitudes and behavior of drivers. Inferences about attitudes were drawn from observations made on driver behavior, and the variations in the accident records of the different states were discussed from the standpoint of differences in the methods used to control the behavior of drivers and to increase safety.

In summary, there is multiple causation in most accidents, and attempts at control should involve consideration of the interaction among the driver, his equipment, and the environment. Attempts should be made first to set forth the basic physical, physiological, and psychological characteristics of the driver. When such facts are associated with the vehicle under given environmental conditions and at specific times and places, information can be obtained so as to understand and prevent accidents. Factual information of this type can be discovered only by carefully controlled experimental studies, epidemiological surveys, and statistical analysis. A dynamic and continuous safety program can produce positive results only by the constant application of the fundamental principles resulting from such studies.

Special Note

This program was sponsored by the Commission on Accidental Trauma of the Armed Forces Epidemiological Board, Department of Defense, and supported by funds from the Research and Development Division, Office of the Surgeon General, Department of the Army.

Additional References

1. "Annotated Bibliography on Human Factors in Engineering Design." Project X-651 (Av-340-a), Aviation Branch, Research Division, Bureau of Medicine and Surgery, Department of the Navy, February, 1946.

2. "Applied Experimental Psychology – Human Factors in Engineering Design," by A. Chapanis, W. R. Garner, and G. T. Morgan. Pub. by Wiley, New York, 1949.

3. *Mechanical Engineering,* Vol. 71, 1949, pp. 811-816: "Human Factors in Design of Manual Machine Controls," by L. E. Davis.

4. Proceedings of Ergonomics Research Society, Vol. II, 1954. Pub. by H. K. Lewis & Co., London: "Symposium on Human Factors in Equipment Design," edited by W. F. Floyd and A. T. Welford.

5. "Handbook of Human Engineering Data." Tufts College Institute for Applied Experimental Psychology, Medford, Mass., Tufts College Bookstore, 1951.

6. "Survey in Seating," by E. A. Hooten et al. Pub. by Heywood-Wakefield Co., Gardner, Mass., 1945.

7. "Human Factors in Undersea Warfare." Panel on Psychology and Physiology, Committee on Undersea Warfare, National Research Council, Washington, D. C., 1949.

8. *Electrical Manufacturing,* Vol. 49, No. 3, 1952, pp. 90-95: "Introduction to Human Engineering in Product Design," by A. E. Javitz.

9. *Psychological Bulletin,* Vol. 43, No. 6, 1946, pp. 489-532: "Detection and Treatment of Accident-Prone Drivers," by H. M. Johnson.

10. "Driver Control: Achieving Greater Traffic Safety through Efficiency at Wheel," by M. A. Kraft. Eno Foundation for Highway Traffic Control, Saugatuck, Conn., 1954.

11. *Journal of Gerontology,* Vol. 9, No. 3, 1954, pp. 338-348: "Age and Problems of Professional Truck Drivers in Highway Transportation," by R. A. McFarland, M. B. Fisher, and A. L. Moseley.

12. "Yearbook of Physical Anthropology, 1947," Vol. 3, 1948, pp. 197-203: "Anthropometric Problems in the Royal Air Force," by G. M. Morant.

13. *British Journal of Industrial Medicine,* Vol. 4, 1947, pp. 77-83: "Some Anatomical Problems in Naval Warfare," by A. G. M. Weddell and H. D. Darcus.

14. "Human Engineering Guide for Equipment Designers," by W. E. Woodson. Pub. by University of California Press, Berkeley, Calif., 1954.

DISCUSSION . . .
. . . of this article starts on p. 654.

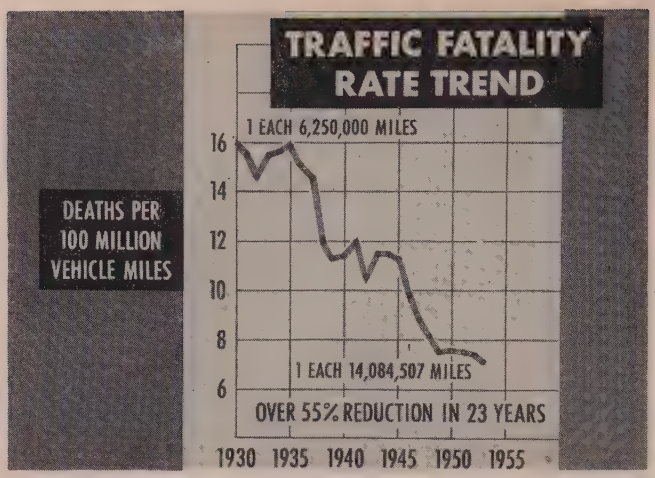

Fig. 1– Rate trend in traffic fatalities for past 25 years

DESIGN FACTORS

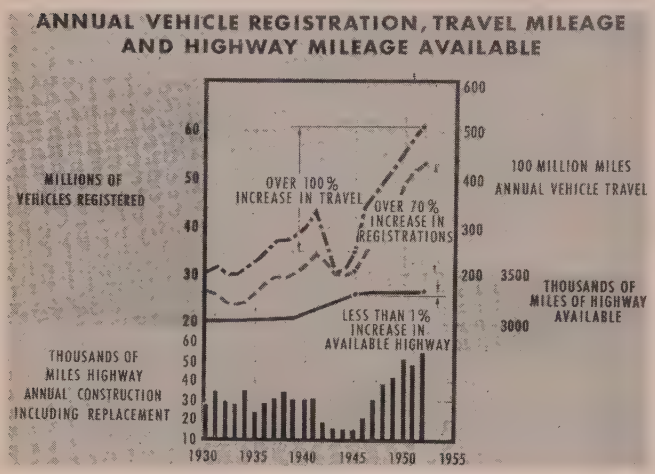

Fig. 2 – Growth in vehicle population, increase in total annual travel, and miles of available highway facilities

VEHICLE design is but one of many factors involved in safe automotive transportation. The assurance of human safety has two aspects – the prevention of accidents, and the reduction of injuries and fatalities.

Accident prevention has been the most logical and direct line of approach for improving human survival in traffic. The statistics[1] for the past quarter century, as shown in Fig. 1, clearly illustrate that considerable progress has been made toward this objective on a national scale.

The preliminary 1954 statistics indicate the traffic fatality rate has continued its downward trend. With a new figure of 6.4 deaths per 100 million miles of travel, a 60% reduction in the traffic toll has been achieved during the last 24 years.

This accomplishment is all the more remarkable when we consider how the traffic load per mile of highway constantly has increased. Fig. 2 shows the growth in vehicle population, increase in total annual travel[1], and miles of available highway facilities[2, 3]. Since the end of World War II, during the period from 1945 to 1952, vehicle registrations increased over 70%, and the total miles of annual travel increased two-fold, while the available highway mileage increased less than 1%.

Obviously, beneficial influences must have operated during this period to improve human survival in spite of the greater apparent hazards of increased traffic congestion. There can be no doubt that driver education, better traffic management, and improved highway design have made important

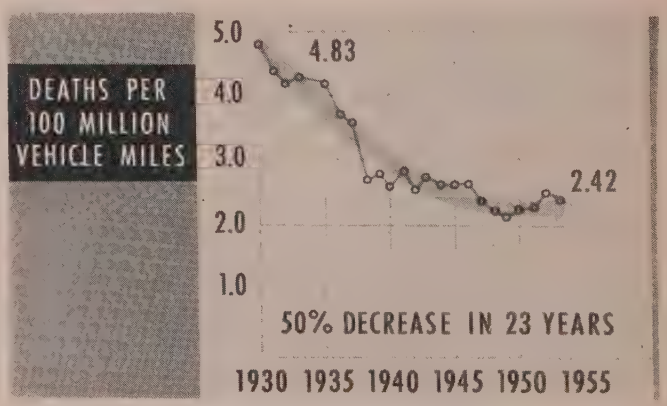

Fig. 3 – Declining death rate from accidents involving only one vehicle for past 25 years

IN AUTOMOTIVE SAFETY

A. L. Haynes, Ford Motor Co.

This paper was presented at the SAE Golden Anniversary Summer Meeting, Atlantic City, June 16, 1955.

TWENTY-FIVE-YEAR statistics, detailed in this paper, show declining accident and fatality rates despite radical increase in vehicle registrations and annual vehicle miles.

The author shows how the passenger-car industry has built safety into vehicles to the point where – as an example – only 14% of accidents on the Pennsylvania Turnpike over its 13-year history were attributed to vehicle failures.

Paralleling these efforts and the increasing emphasis on safer highways, better traffic management and driver education, are extensive studies aimed at bypassing the human factor and increasing human safety in automotive vehicles. Among those described here are crash investigations, laboratory tests of safety devices, and establishment through various other means of design criteria for human impact tolerance.

contributions to vehicle operating safety. However, it must be realized that the automobile industry, through continual improvements in design, also has done much to promote this safety accomplishment.

The facts become more apparent when the information on total fatalities per mile of travel are separated into accident types. The steadily declining death rate from accidents where only one vehicle is involved (Fig. 3) shows how better highway and vehicle designs have reduced the possibilities of the driver losing control of the vehicle.

During the same period, the pedestrian fatality risk (Fig. 4) also has been reduced. This four-fold improvement in human survival reflects the effects of safety education, and the vehicle improvements for better driver vision, braking response, and overall vehicle control.

The subject of vehicle and highway safety has come to the forefront of public attention in recent months, both through the press and public statements. Various charges have been made and numer-

[1] See "Accident Facts." Published by National Safety Council, Inc.
[2] See "Highway Statistics." Published by U. S. Department of Commerce, Bureau of Public Roads, Washington.
[3] See "Automobile Facts and Figures." Published by Automobile Manufacturers Association, Detroit.

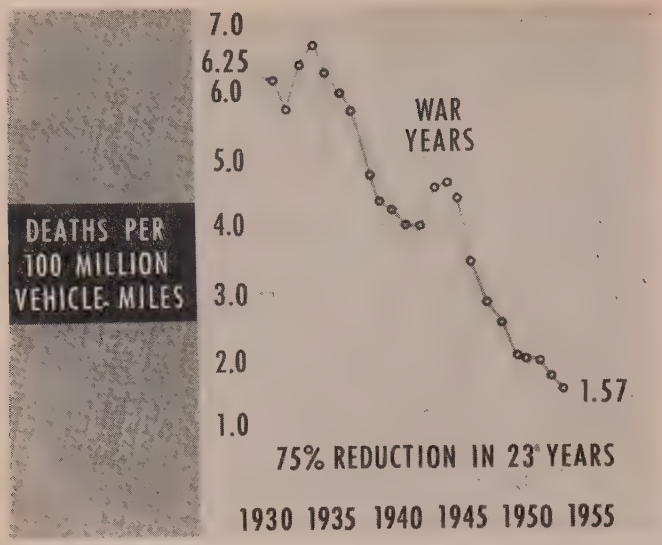

Fig. 4 – Reduction in pedestrian fatality rate for past 25 years

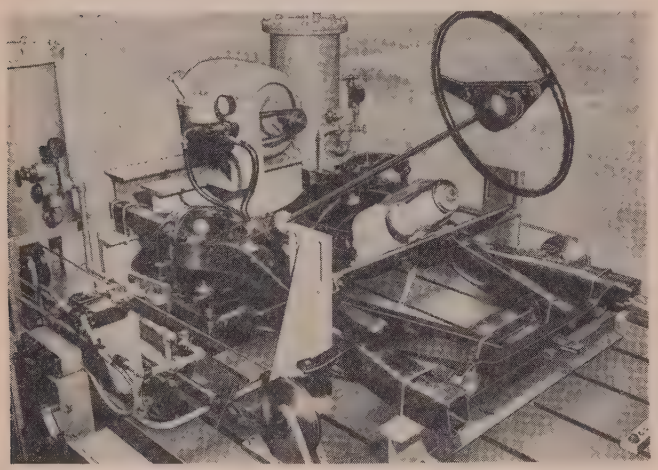

Fig. 5 – Test setup designed to guard against vehicle failures. Steering mechanism is submitted to repeated shock loads and turning to make sure adequate safety is provided

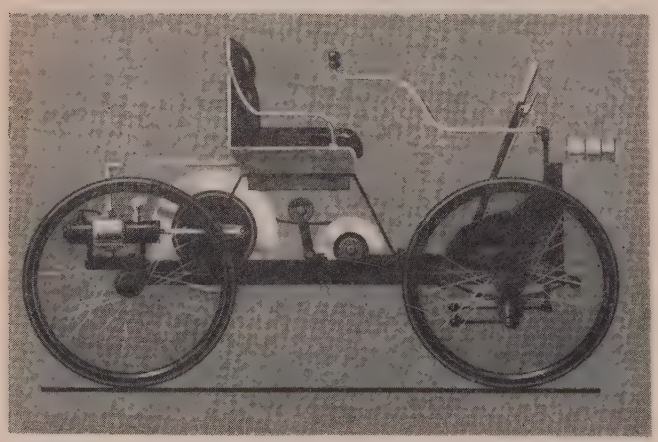

Fig. 6 – Horseless carriage, with wooden body; no top, doors, or windshields; and hand tiller for steering

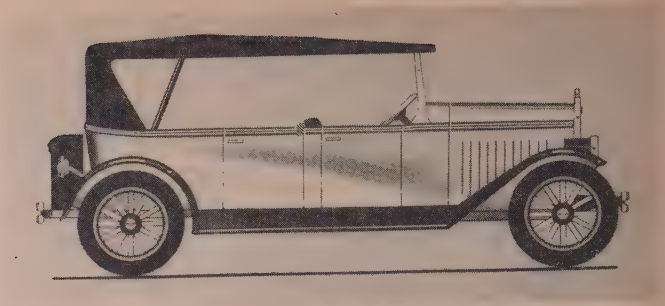

Fig. 7 – Better roadability, driver vision, and packaging of occupants designed into passenger cars of early 20th Century through left-hand drive, steering wheels, progressive-shift transmissions, electric headlamps and tail-lights, and better positioning of driver controls

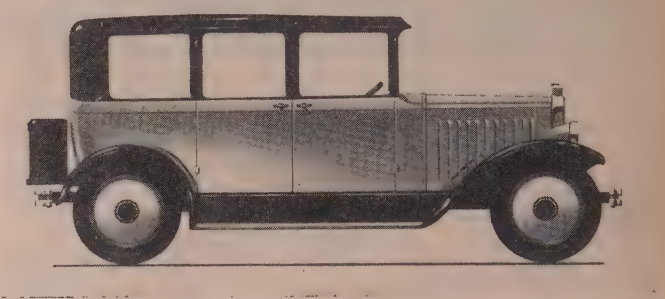

Fig. 8 – Increased safety built into passenger cars of 1920's through such innovations as safety-glass windshields, automatic windshield wipers, heaters, defrosters, 4-wheel brakes, and shock absorbers

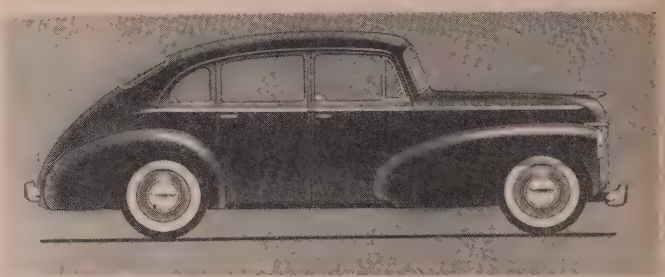

Fig. 9 – Prewar safety improvements, including all-metal body with integral roof structure, low-pressure tires, smaller, sturdier wheels, and sealed-beam headlamps

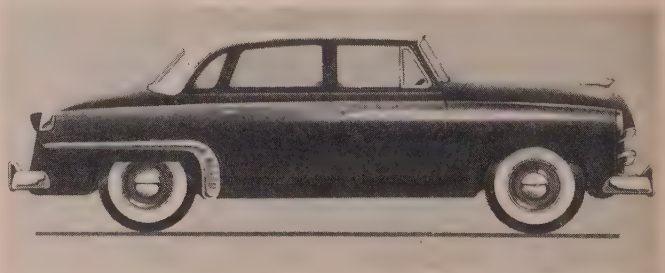

Fig. 10 – Additional safety features introduced by 1950, despite wartime interruption, included windshield washers, direction signals, and automatic transmissions

ous proposals suggested for mitigating the problem. The impetus from the interest of the many individuals and groups that have become concerned cannot but encourage further improvements in traffic safety.

The automobile industry has been deeply concerned with the complex problem of vehicle safety for many years. During the last few years, our activity in this field has been greatly accelerated. In addition to our own research investigations, we are working with highway, traffic management, and safety foundation groups, and contributing to driver education programs with training films, textbooks, and the provision of vehicles for high school driver-training courses. We believe these cooperative efforts are paying rewarding dividends in achieving better highway safety.

Vehicle and components testing for performance reliability is one area where the manufacturer can have direct control over the behavior of his product in the hands of the user. We conduct extensive test programs, which simulate the extremes of actual operating requirements, to guard against vehicle failures. One such test setup is shown in Fig. 5. The steering mechanism is installed in this rig as it would be in an actual vehicle. Shock loads on the wheel spindles and constant turning of the steering wheel to the right and left are endlessly repeated to assure that an adequate safety factor is provided in the design.

Numerous similar performance tests are made on components, assemblies, and the complete vehicle. Particular emphasis is on primary structure details. That this attention to primary structure is successful is demonstrated by the fact that we rarely hear of any failure in these components during actual operation.

The expenditure for scientific, research, and engineering talent constantly has been increased through the years so that the best and safest possible product will be manufactured and offered for sale at any given period in the progress of the automotive art.

To place this discussion in the proper frame of reference, the historical background of the modern automobile and the evolution of some of today's safety features should be reviewed.

As shown in Fig. 6, the first cars had wooden bodies and were almost identical with the horse-drawn conveyances of the period. The primitive bodies rarely had tops; doors and windshields were nonexistent, and steering usually was accomplished by means of a hand tiller. Roadability was little, if any, better than for the horse and buggy.

During the first two decades of the 20th Century, many of the design innovations (Fig. 7) contributed to safety through better vehicle roadability, driver vision, and packaging of the occupants. The left-hand drive was adopted for safer passing of on-coming traffic. Steering wheels and progressive-shift transmissions were incorporated for better and safer vehicle control. Electric headlamps and tail lights replaced oil and gas equipment for reliable night-driving illumination. Driver controls were positioned for greater convenience and operating safety.

The evolution of safety features became even more apparent during the 1920's (Fig. 8). The safety-glass windshield was adopted, followed by shatter-proof glazing of all vision area for greater occupant protection. Automatic windshield wipers assured driver visibility during inclement weather. The heater and defroster offered additional comfort and clearer visibility during cold-weather operation. The introduction of the vastly superior 4-wheel brake system was followed by the adoption of hydraulic actuation for safer, better-controlled stopping ability. All-metal wheels, of both spoke and disc designs, became standard equipment for greater strength and durability. Shock absorbers bettered the car's riding quality and significantly improved steering control.

Important safety improvements in the next 10 years (Fig. 9) included the all-metal body with integral roof structure. Low-pressure tires reduced shock to the chassis, and were less subject to frequently disastrous sudden failure. The wheels for these larger cross-section tires were reduced in diameter, and the spoke structure became short and wide to provide a considerably sturdier base for the tire. The foot-operated headlamp-dimmer switch permitted night-time driving with convenient courtesy, and undoubtedly prevented many an accident that could have been caused by glare-blinding of on-coming drivers. Even the feature of indirect lighting for the instruments had important safety overtones, since the operator could keep informed of vehicle performance without reducing his vision acuity. Sealed-beam headlamps assured prolonged reflector efficiency and better controlled illumination pattern on the road.

By 1950 (Fig. 10), even with the production interruption of World War II, several additional safety features had been introduced. Automatic windshield washers became available for improved driver vision during adverse driving conditions. Direction-indicator signals were another courtesy feature with safety significance that quickly prompted the whole industry to adopt them as standard equipment. The introduction of the automatic transmission into practically all car lines simplified the act of driving still further, and permitted the beginner to master the routine driving skills more quickly. Further tire improvements brought about the extra-low-pressure design for added comfort and blowout protection.

Fig. 11 shows some of the latest developments that have contributed to safer vehicle operation during the past five years. The introduction of air conditioning for better driving comfort will im-

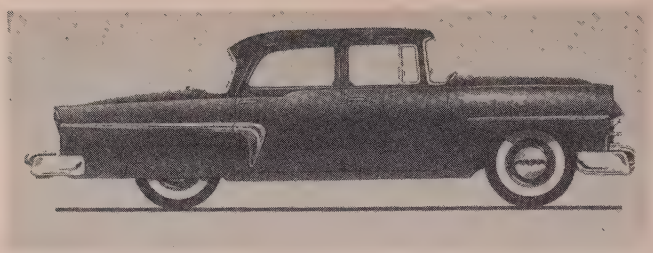

Fig. 11 – Air conditioning, expanded windshields, power brakes and steering, tubeless tires, and improved engine capacity have added to safe vehicle operation during past five years

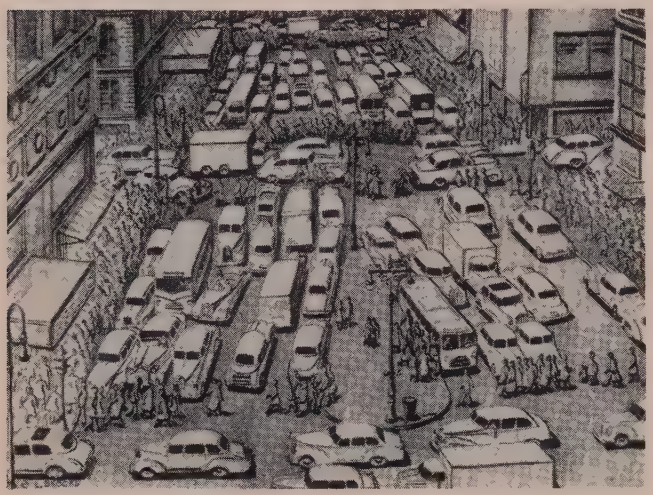

Fig. 12 – One busy intersection where thousands of cars make stops that depend on consistent tire and brake performance

prove operator alertness during adverse weather conditions. Driver vision has been vastly improved with the wider field of view through the expansive windshield and rear window and the reduced obstruction of body structure and sheet metal. Power steering makes the handling of the car almost effortless in traffic and parking maneuvers, and, in addition, provides steering stability when running off the road, passing over chuck holes, or driving through snow, sand, or mud. The greater capacity of the high-torque engine permits better acceleration for safer maneuvering through congested traffic, and passing highway obstacles with less time and distance spent on the wrong side of the road. Power brakes reduce the energy demand on the operator during stopping, and shorten the interval between the decision to stop and the actual deceleration of the vehicle. The new-type sealed-beam headlamps, introduced in 1955, provide a higher-intensity low-beam illumination pattern on the road, and also reduce both glare into the eyes of oncoming drivers and stray light reflections when driving through dust, snow, rain, or fog. The 4-way adjustable power seat simplifies the positioning of the driver for comfort, vision, and vehicle control. The new tubeless tires not only make a blowout highly improbable, but also tend to reseal against the loss of air when punctured.

The refinement of any one component or mechanism usually has been gradual, but through the

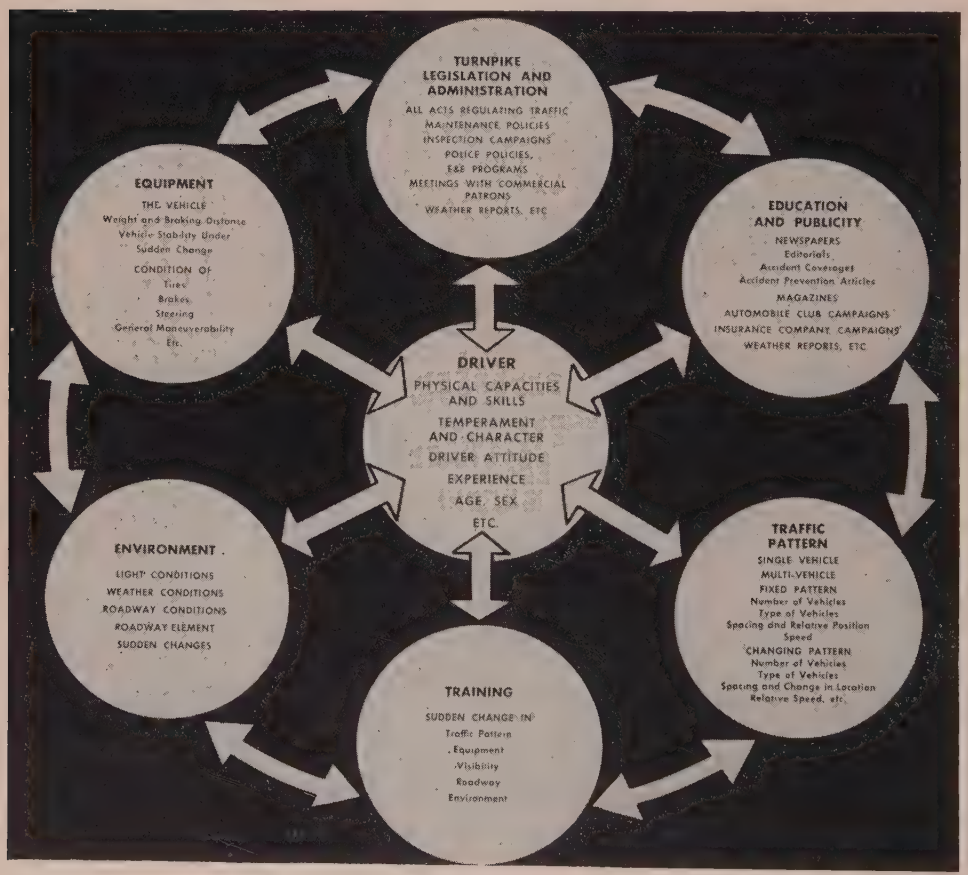

Fig. 13 – Diagram showing complexity of factors involved in safe vehicle operation

years operation has progressed from critical behavior to accepted reliability. The development of durable and reliable tire equipment is one example of progress in the automotive art, and the continuing improvement in vehicle brakes is another. The scene in Fig. 12 is not uncommon in many of our larger cities. As many as 40,000 vehicles may be required to stop at a busy intersection during the course of a day's normal traffic. Similarly, vehicles of all types, with all kinds of people driving them, make repeated stops day-in-day-out, year-in-year-out. We take such consistent performance for granted. But this high degree of reliability has actually been the outgrowth of many years of continuous engineering refinement. Similarly, we rarely think about the numerous engineering design achievements where, all through the automobile, research and development unceasingly have striven to provide a maximum in safety and reliability.

The interrelationship of many factors becomes apparent whenever vehicle accidents are investigated. The Pennsylvania Joint Safety Research Group[4] developed the chart shown in Fig. 13, which illustrates the complexity of the problem in safe vehicle operation. Although a considerable number of factors influence the total picture, it will be observed that they are all modified by the behavior and motivation of the driver.

Through research and experience, automotive engineers have gained an extensive understanding of the components that make up a modern automobile. We know the characteristics of servomechanisms, the permissible stresses in primary structure, and the control problems as they affect the vehicle. Highway designers, traffic engineers, and law enforcement agencies have collected a wealth of data from which they have learned how to build safer highways and better manage traffic. The one important field where there is insufficient knowledge is that of human behavior. We cannot predict how a driver will respond to any given set of conditions. However, we are progressing toward some answers to that many-sided problem.

With our new methods of analysis and the use of high-speed electronic computing machines and analog equipment (Fig. 14), we consider the driver as the feed-back in a closed-loop servomechanism.

As shown by the block diagram, Fig. 15, this feed-back is used in our control and stability equations. The feed-back, of course, is a function of the reaction time of the individual, his psychological makeup, his anticipatory reactions, and similar factors. We still need further data on these human factors, and have enlisted the resources of the various sciences, particularly the human engineering biological and psychological sciences, to furnish this information.

The previously mentioned Pennsylvania Joint Safety Research Group issued an Accident Causa-

[4] See "Accident Causation." Published by Pennsylvania Turnpike Joint Safety Research Group.

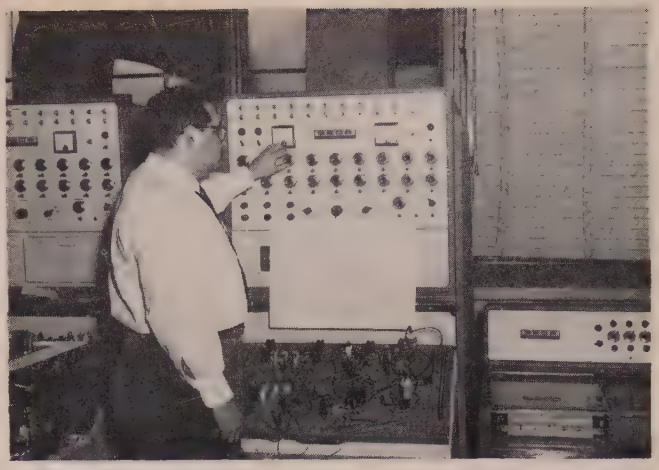

Fig. 14 – Electronic computing machines and analog equipment, which help in analyzing driver behavior and motivation

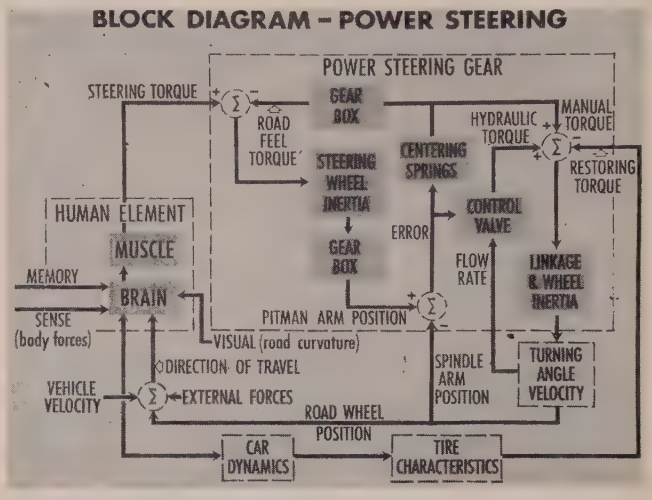

Fig. 15 – Block diagram – power steering

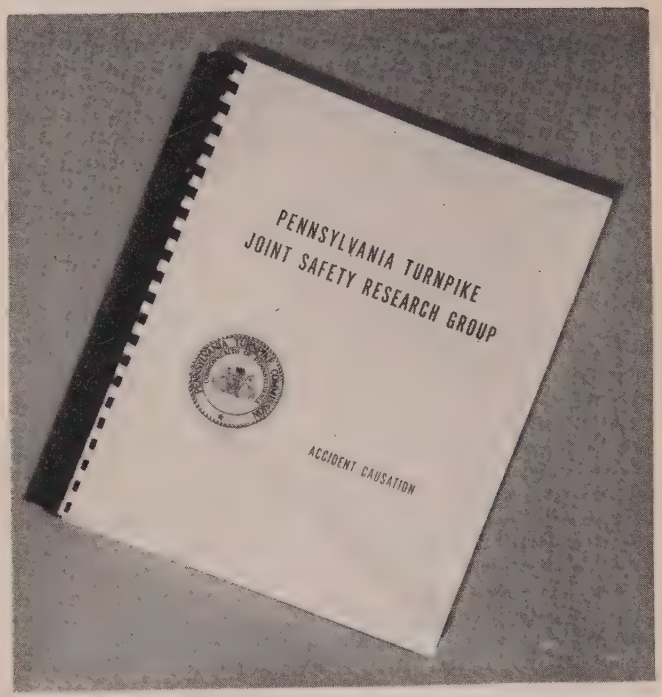

Fig. 16 – Accident causation report issued by Pennsylvania Joint Safety Research Group for first 13 years of Turnpike operation

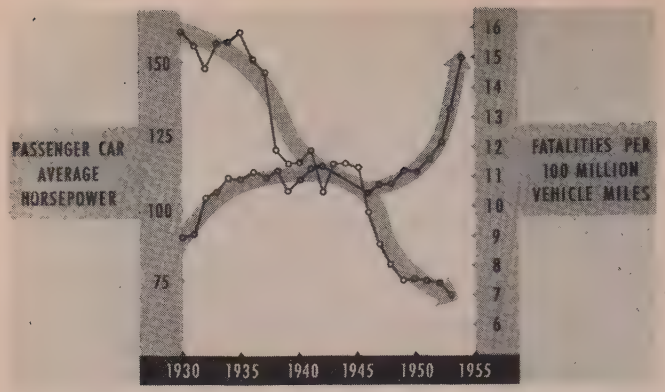

Fig. 17 – Statistics show that since 1930 passenger car average horsepower increased 65%, total traffic fatality rate decreased over 55%

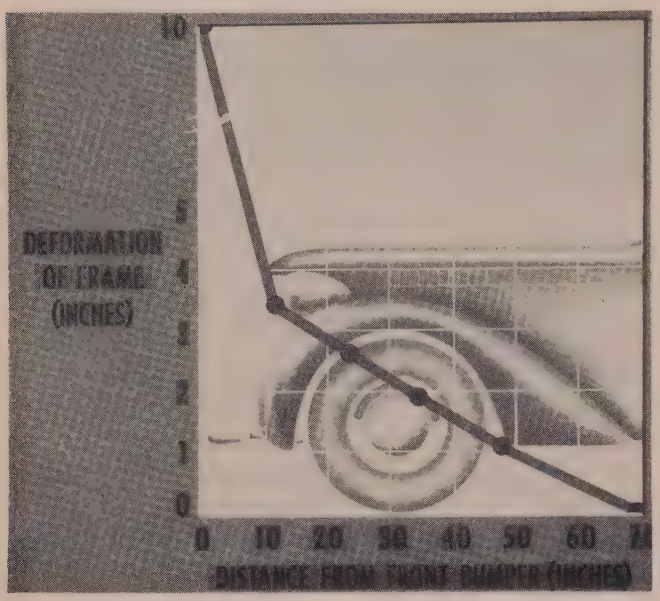

Fig. 18 – Decrease in frame deformation with distance from front bumper in 25-mph barrier impact

tion Report (Fig. 16) for the first 13 years of Turnpike operation. Perhaps hard-and-fast conclusions cannot be drawn from this report, since it represents operation under a special set of conditions. However, these records are practically the only complete and consistently maintained volume data available at the present time. Since accident patterns are repeated year after year in these tabulations, it appears logical to assume they represent some of the general conditions experienced on any highway.

The data from this impartial survey (Table 1) showed that 86% of the accidents and 97% of fatalities were caused by driver incompetence, carelessness, recklessness, inattention, or incapability of judging distance. Only 14% of the accidents were attributed to vehicle failures. We can assume that this 327 miles of high-speed highway imposes a higher-than-normal strain on vehicles, and these were not all new, late-model cars and trucks by any means. Tire failures alone accounted

Table 1 – Pennsylvania Turnpike Data
(October 1940 – December 1953)

Total Number of Accidents	13,426
Total Number of Fatalities	486
Driver Causation:	
Accidents, %	86
Fatalities, %	97
Type of Accident:	
Personal Injuries, %	34.4
Fatalities, %	3.9
Property Damage Only, %	61.1
Majority of Accidents Occurring:	
Speed Range	Weather – Road
41 – 50	Clear – Dry
31 – 40	Wet, Snow, Slush, Ice

for about half of the vehicle failures leading to accidents. It must be realized that, during the period covered by the report, the tire shortage of World War II forced many operators to continue with the use of tires that, in normal times, would have been discarded as unsafe. The vehicle failures also included the results of inadequate maintenance, improper truck loading, and swaying trailers which, in the final analysis, are really caused by human neglect or inexperience.

The highest accident frequency occurred in the 41-50 mph bracket during favorable weather, and in the 31-40 mph range when there was rain, snow, slush, or ice. Less than $15 expense was incurred in 85% of the property damage cases. This low loss figure would indicate that high-speed collisions were not prevalent; in fact, less than 2% of accident-involved cars were traveling in excess of 70 mph.

Statistics such as these clearly reveal that much more information is needed to evaluate the human factor in our equation. Unfortunately, well-meaning people are sometimes led to erroneous conclusions when they consider means of improving traffic safety. One such example is the insistent fallacy that engine power and accident frequency are directly proportional; therefore, engine power should be limited by legislation. This reasoning is as shortsighted as the highways law in England, which early in the 19th Century stifled progress in the development of self-propelled, over-the-road transportation. A steam coach service between London and Bath was maintaining a traveling speed of 15 mph as early as 1829. Agitation against this means of transportation became so vehement that even though a Parliamentary investigation disagreed, a law was enacted which compelled the coach to be preceded by a man on foot carrying a red flag. Of course, the coach line could not continue when so restricted, and further progress in self-propelled highway vehicles was abandoned for many years.

While it is true that engine power can be mis-

[5] See "Brief Passenger-Car Data." Published by Ethyl Corp.

[6] See "Automobile Barrier Impacts," by D. M. Severy and J. H. Mathewson. Highway Research Bulletin No. 91, published by National Academy of Sciences, National Research Council, Washington.

used by an irresponsible driver, the statistics[5] (Fig. 17) show that the traffic fatality rate has continued to fall while the average vehicle horsepower has risen through the years. All of us are familiar with the pros and cons of high-torque engines, but the arguments for accelerating ability, improved middle-speed performance, increased operating economy, and reduced engine wear cannot be disregarded.

It also must be realized that while each accessory improves the convenience and safety of car operation, it absorbs a portion of the engine power. Consequently, the growing popularity of automatic transmissions, power steering, power brakes, power-operated windows and seats, and electrical accessories such as radios, heaters, air conditioners, and so forth, calls for added engine output to maintain operating efficiency.

Up to this point, the efforts made to prevent vehicle accidents have been emphasized. This first aspect of the problem always must receive highest priority in vehicle and highway designing. However, it is apparent that human performance failures will continue to precipitate accidents, regardless of accident prevention features. The introduction of safety glass and the development of all-metal bodies are examples of some of the important measures already adopted in connection with the second aspect of the problem – the reduction of human injuries and fatalities. During the past few years, research investigation of crash injury has been intensified to learn what additional provisions will increase human safety in automotive vehicles.

It has been found necessary to stage full-scale collisions to determine the behavior of the vehicles and occupants during impact. Many complex reactions, which require careful evaluation of numerous factors, have been observed during these investigations.

Here again, there is no dearth of voluntary suggestions from the public at large and well-intentioned, self-styled experts. However, the problem is considerably more involved, and the forces generated during collisions are much greater than

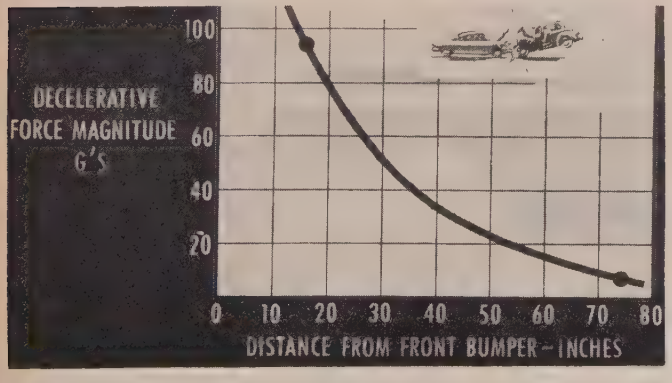

Fig. 19 – Reduction in impact reaction and injury to vehicle occupants with distance from front bumper in 30-mph impact

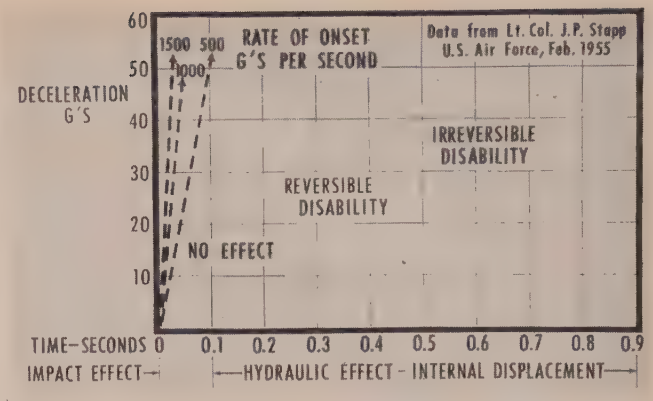

Fig. 20 – Human tolerance to dynamic forces (seated position, forward motion)

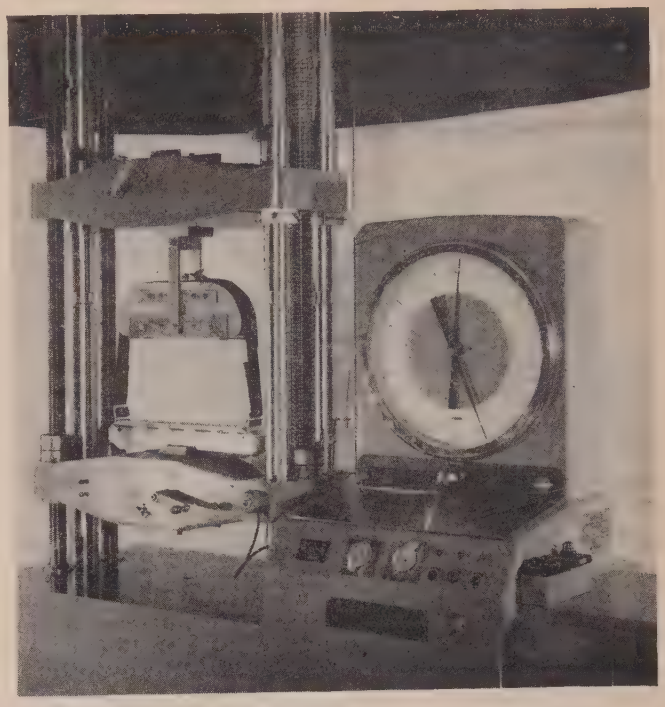

Fig. 21 – Tension-testing machine and body block used in testing seat belts and hardware

usually assumed. For instance, we frequently are criticized for not providing greater structural strength in our vehicles to withstand collisions with less damage. However, when the laws governing inertia, deceleration, and the dissipation of kinetic energy are considered, it becomes obvious that structural bending and yielding forward of the driving compartment (Fig. 18)[6] greatly moderate the force of the impact. Fig. 19 demonstrates how effective the structure of the modern car is in reducing the impact reaction and injury to the vehicle occupants.

The subject of seat belts for automotive use has been receiving considerable attention for some time. Properly installed and used, such equipment should improve the chance of human survival and reduce collision injuries. For one thing, the driver

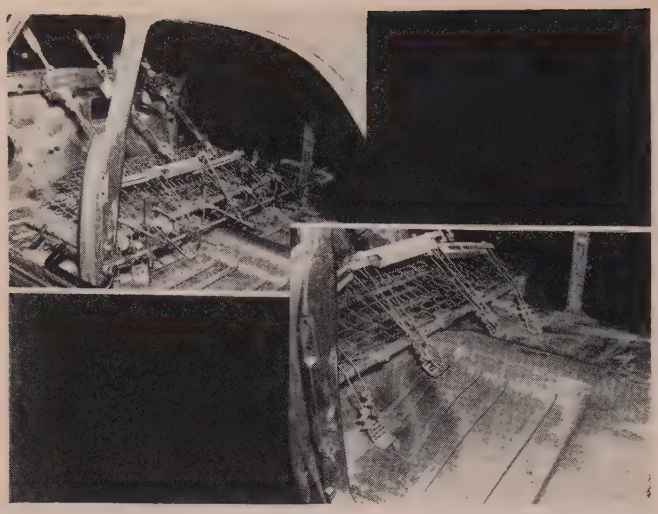

Fig. 22 – Pull tests on body floor to establish structural requirements for adequate seat-belt installation

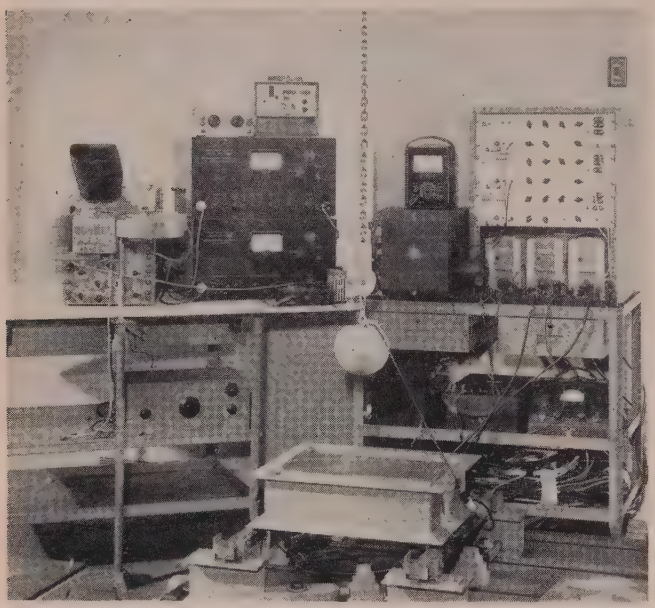

Fig. 23 – Laboratory setup for investigating energy-absorbing characteristics of various configurations and materials as they apply to instrument panels

will be less likely to lose control of the vehicle during a minor accident, and be injured because the vehicle subsequently went out of control. We also know that the probability of injury-reception is reduced when the occupants are retained within the protective enclosure of the vehicle. However, we do not know the tolerance of the human body under various impact conditions. Considerable work has been done on the human tolerance to dynamic forces by Lt.-Col. J. P. Stapp[7] of the U. S. Air Force. Stapp's preliminary chart (Fig. 20) indicates that, during ideal conditions of body restraint, appreciable deceleration can be tolerated.

Crash investigations using instrumented anthropomorphic dummies and seat belts have supplied the range in loading developed under various impact conditions. Laboratory tests (Fig. 21), using a tension-testing machine and a body block, have assisted in the qualification of belts and hardware. Pull tests on the body floor (Fig. 22) have established the structural requirements for adequate seat-belt installation. In short, investigations to date have broadly determined the physical conditions which the seat-belt installation must meet to withstand the forces developed during collisions.

The other half of the problem, the determination of the human impact tolerance, also is under investigation. The values, preliminarily established by Stapp's work, cannot be translated directly into automotive practice, since the elaborate restraints used in the Air Force investigations could not and would not be acceptable to automotive users. However, such information provides relative values which, along with the work of medical researchers and the examination of accident statistics, assist in the establishment of design criteria for human impact tolerance.

Fig. 23 illustrates a laboratory setup for investigating the energy-absorbing characteristics of various configurations and materials as they apply to instrument panels. Similar techniques are used to evaluate various other components. Again, only relative values can be established by these means. But when these are correlated with full-scale crash studies and medical observations on human subjects, practical values which will be effective in reducing human injury can be determined.

Fig. 24 is a schematic of the test setup used to conduct full-scale crash studies. The crashed car is instrumented to determine the impact forces developed, and in some tests an immovable barrier is substituted to simulate a collision with a tree or

[7] See "Human Tolerance to Dynamic Forces," by Lt.-Col. J. P. Stapp. Published by Aero Medical Field Laboratory, Holloman Air Development Center.

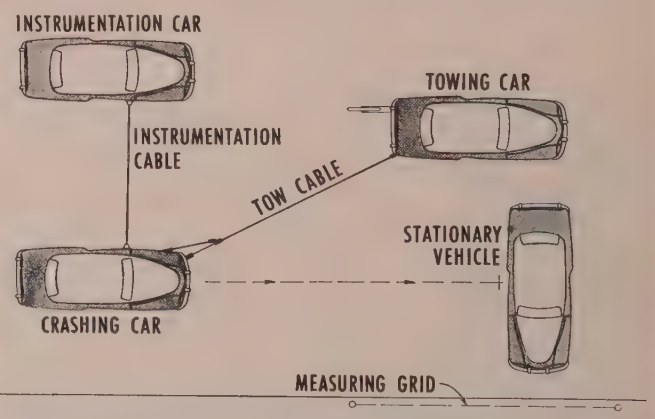

Fig. 24 – Schematic of test setup used to conduct full-scale crash studies

Fig. 25 – Human-size dummies which can be instrumented and set to simulate human reaction and reveal injuries from collision

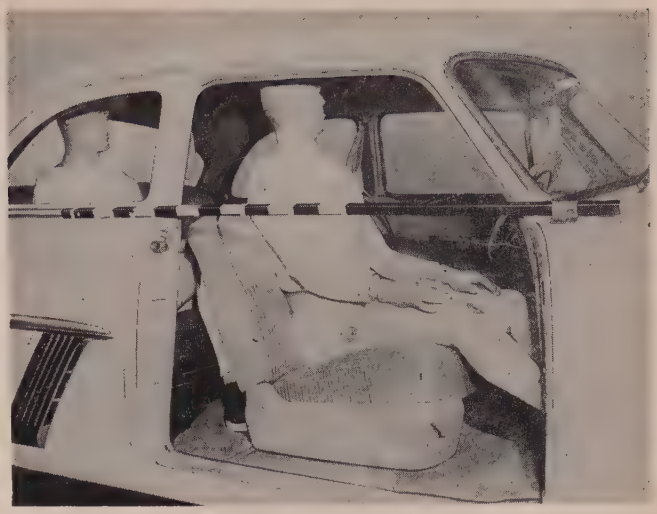

Fig. 26 – Dummies installed in a test vehicle. Crashes are conducted with dummies both free to move and held by restraining devices

bridge abutment. The anthropomorphic dummies shown in Fig. 25 approximate humans in size, weight distribution, and skeletal articulation. They can be instrumented to determine the history of the collision events, joint tensions can be preset to simulate human anticipatory reaction, and their "skin response" will disclose injury-producing contacts with the interior of the vehicle.

Fig. 26 shows the dummies installed in a test vehicle. Crashes are conducted with the dummies both free to move and held by restraining devices. High-speed motion pictures are taken as the crash occurs, and these are analyzed frame-by-frame (Fig. 27) to provide a complete time-motion history of the collision, and determination of those areas with the highest injury-producing index. These observations are guiding us in our research studies and design development programs for safer vehicles.

We are working with numerous recognized groups in the vehicle accident field in our attempts to determine facts which accurately reflect actual operating conditions. Besides Stapp's group at Holloman Air Base, we are cooperating with the Crash Injury Research Group at Cornell University Medical School, various medical groups, and police officials.

In summary, automotive history demonstrates the willingness of the industry to adopt new ideas and keep abreast of technological developments. The engineer incorporates safety features into the

Fig. 27 – Frame-by-frame analysis of motion pictures taken of crashes to determine highest injury-producing areas

automobile as rapidly as they can be developed and proved effective. The complexity of the safety problem is realized by everyone seriously participating in crash injury research. We all agree that the progressive development of safer vehicles must continue, but it must be understood that the cooperative efforts of all agencies and individuals concerned with improving vehicular operating safety will be required to further improve the traffic accident statistics.

DISCUSSION

of R. A. McFarland and A. L. Haynes papers

Foresees Continued Progress in Safer Passenger-Car Design

by P. C. Ackerman

Chrysler Corp.

SAFETY in travel on our streets and highways is commanding a greater share of the public's interest . . . and alarm. The fact that each year, over the past 25 years, has seen the national highway safety record steadily improve, has not had the impact on public thinking that other phases of the problem have.

Perhaps this is as it should be. Certainly, the automobile industry has long taken a strong, positive interest in improving its products to reduce the likelihood of accident in so far as possible and to reduce the severity of accidents, should they occur.

Progress has been substantial on all fronts. Vehicles are better; streets and highways improved; traffic engineering is contributing more and more; driver education has helped and will help more in the future; and the American motorists, themselves, are driving better. All of these factors have contributed to safety. If they had not, we should not have seen the highway toll cut more than in half in terms of vehicle miles, or even better when based on the use and numbers of vehicles, over the past quarter-century.

But this does not erase the seriousness of the remaining problem, nor the earnestness with which the automobile industry regards it. Neither has it mitigated the highly vocal alarm and demands for action from groups of members of medical associations, large segments of the nation's press, lawmakers the country over, and many other institutions and groups.

Neither have the facts shielded the automobile industry from broadly unjust accusations, attributing the accident toll in an unrealistic measure to alleged intrinsic defects of the automobile. One could be philosophical about this, and remind himself that it is human nature to blame the inanimate, in this case the machine, for shortcomings that are essentially human. It is easy to point the finger at such mute mechanisms as automobiles, or to such intangibles as horsepower races, when the fault lies largely within ourselves that we kill each other on the highways.

But being philosophical does not grapple with the problem. The automobile industry traditionally comes to grips with situations that call for action. It considers this situation as a challenge worthy of its best efforts.

These efforts have been continuous, and they have borne good fruit. The problem has been attacked on three fronts: First, to design cars that can be driven in a manner to reduce the likelihood of accidents happening; second, to design cars that will minimize the effect of an accident on the occupants of the car should an accident take place; and third, to promote highway construction on a national scale that will reduce the number of accidents and the severity when accidents do occur.

In each category, important progress has been made. We all know that significant new developments to improve the vehicle in these respects are under way in the automotive laboratories and proving grounds. The President's Highway Advisory Committee's recommendation to spend $101,000,000,000 for roads in the next 10 years is certainly proof that this phase of the problem is getting serious attention.

But we cannot design automobiles that will make up for all the ineptness, carelessness, or selfishness of which human beings are capable. We cannot produce an automobile proof against a head-on collision without developing a vehicle of such grotesque appearance, and completely unrealistic cost, as to be unacceptable on a variety of important counts to almost any car buyer. I say this mindful of the lay suggestions that continue to arise from people, often competent in other fields, which suggest an incredible lack of information about the technology and economics of automobile design and manufacture.

But we know that we can continue the progress we have already made in the design and development of better, safer automobiles for all people. We will continue to improve the agility of cars, to better their stopping ability; to make them more maneuverable and more responsive to controls; and to enhance even more the day and night-time visibility enjoyed by their drivers.

And we shall continue to improve the protection offered to occupants of our cars, should accidents happen, both through the structure itself and through an ever increasing number of inherent features and accessories designed primarily for passenger protection and safety.

A Billion Engine Hours On Aluminum Bearings

R. S. Frank and W. J. Lux, Caterpillar Tractor Co.

This paper was presented at the SAE Annual Meeting, Detroit, Jan. 9, 1956.

NO one knows better than the engineer that to achieve the best design of a product means finding the best compromise possible. The design of main and connecting-rod bearings for a diesel engine is certainly a prime example of this fact. As in all engineering problems, bearings must be designed to provide the best compromise of the requirements of the customer, the serviceman, the bearing manufacturer, and the engine builder, and still satisfy the engine itself. A bearing should be hard and strong for one reason, and at the same time should be soft and conformable for other reasons.

For several years, we have used both solid-aluminum and steel-backed, aluminum-lined bearings in our diesel engines with excellent results. The purpose of this paper is to describe some of our experiences in the production use of these bearings, and to show how a bearing material and its characteristics are adapted to engine requirements.

This experience covers engines with ratings of 50-500 bhp, and operating speeds of 700-2000 rpm. On engines rated at 2000 rpm, overspeeds to 3000 rpm are common, rubbing speeds under this condition reaching 3350 fpm. These engines have been used in all kinds of service from variable-speed tractor operation to continuous-duty marine applications, and range from engines driving electric generators to engines powering excavators or oil-well drill rigs.

To appreciate better the use of aluminum bearings, we might briefly review the characteristics of a material which make it suitable for use as a bearing. Load-carrying ability, fatigue strength, hardness, wear resistance, embeddability, conformability, seizure resistance, and corrosion resistance are all important properties to be considered.

Load-carrying ability is logically the first consideration. Often space problems and high unit loadings occur together, forcing the designer to rely on bearing materials with higher load-carrying ability instead of making larger bearings. Load-carrying ability is closely related to several material characteristics.

Because main and connecting-rod bearing loads are cyclic, bearing failures are often of a fatigue nature. Fatigue strength therefore must be considered in bearing design. Hardness and wear resistance are important in determining bearing life, and are closely related to strength.

Since close clearances are maintained between the journal and its bearing, foreign material, such as chips in the lube oil, can cause havoc with the

HIGH load-carrying ability and fatigue strength, good embeddability and conformability, and resistance to wear, seizure, and corrosion are factors that sold them on aluminum for bearings, the authors report.

Bonded steel backing, they say, makes aluminum bearings even better. Retaining aluminum's good properties, it improves some of its bad points and gives such advantages as:

- **Reduced bearing clearances, compared with those used with solid-aluminum bearings.**
- **No life limit in operation below 5000 psi fatigue stress value.**
- **Less sensitivity to high oil temperatures.**
- **Negligible wear (after 29,000 hr in one test).**
- **Simpler and less expensive bearing-locating designs.**
- **Special excellence for high-load, high-speed applications.**

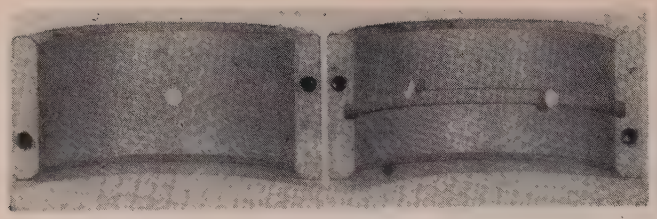

Fig. 1 – Typical solid-aluminum bearing

bearing and journal surfaces and often lead to bearing seizure. A bearing material's ability to resist seizure and to embed small particles before they can score the journal or destroy the bearing is vital. Because manufacturing processes result in a certain amount of dimensional inaccuracy, and during engine operation distortion and flexing occur in the journals and bearing supports, the bearing should be able to conform to some misalignment and motion. The alternate requirement, of course, is rigid design and extremely close tolerances. However, no structure can be completely rigid and no parts can be made without some dimensional tolerances.

High temperatures and other conditions in the lube oil can contribute to rapid bearing deterioration and wear. Chemical action as well as physical action can make a bearing unfit for a specific application.

It is apparent that a good bearing design must take into account many factors; the bearing must be a compromise which provides those features considered most important.

The early Caterpillar diesel engines, 20 years ago, used steel-backed, 1/16-in.-thick babbitt for the main and connecting-rod bearings. These bearings were adjusted to control bearing clearance by the addition or removal of shims. This design was dropped long ago to use precision bearings, eliminating the need for shims and bearing adjustment at installation.

Because thick babbitt has a rather low load-carrying ability due to poor fatigue strength, progress brought along a better design using a thin layer of babbitt on the backing, thus getting more advantage from the strong backing material. Here again, a compromise was necessary, and the final choice resulted in a layer of babbitt 0.012 in.-0.016 in. thick on a bronze back. Bronze was used in place of steel for the backing material, to give better seizure resistance should the babbitt layer be damaged by operating without oil or by foreign material in the oil.

We have tested various other bearing materials, including copper-lead, silver, microbabbitt, and trimetal bearings. Economic considerations, manufacturing problems, and the results of extensive testing led to our ultimate choice of aluminum for our engine bearings. Our design and development energy has since been concentrated on engine designs to make the best possible use of aluminum's bearing qualities in the heavy-duty jobs our engines perform.

Solid Aluminum Bearings

We elected to introduce solid aluminum-alloy bearings only after six years of testing, developing, and retesting. The war years were years of practically frozen design, when manufacturers made few changes in equipment for civil consumption. When hostilities ceased, we were ready with a thoroughly tested bearing improvement.

Solid aluminum bearings were first used in our engines after the end of World War II, and since that time, a large number of them have been put into service. Some certainly have upwards of 40,000 hr of service on them. Fig. 1 shows a typical solid-aluminum bearing.

The results with solid-aluminum bearings were amazing to us. No longer did we have to restrict our bearing loading to the 2000-psi peak value of babbitt. Corrosion, which often plagues other types of bearing, had no effect on aluminum-alloy bearings; they were not fussy about the chemical actions of lube oil. Our new aluminum bearings had high fatigue strength and excellent load-carrying ability. Their embeddability was quite good, hardness fair, seizure resistance above average, and conformability good. Wear of the bearing itself was practically nonexistent, and wear on the crankshaft journal was small. Even though the aluminum bearing under test conditions was made to seize due to abnormal load or lack of lubricant, we found that the aluminum adhering to the crankshaft journal could be removed with crocus cloth and a new bearing could be run against this journal without difficulty.

For a numerical comparison of the increase obtained in load-carrying ability, the results obtained on our Underwood-type rotating weight-fatigue machine give us the best illustration. While we were able to build our rotating loads up to only 2000 psi with thin babbitt bearings before fatigue failure occurred, the solid-aluminum-alloy bearings handled 5000 psi, 2½ times as great, without failure. Such an increase in bearing capacity either offered us a larger margin of safety in our existing size bearings, or offered our engineers much more freedom in designing the cylinder center spacing, the crankshaft outline, and the supporting bearing structure. Therefore, changing existing babbitt bearings to aluminum for service replacement at that time took care of any fatigue failures suffered previously. Also, newly designed engines could be shortened, and rotating parts such as crankshafts and connecting rods materially strengthened. In some cases we were able to raise crankshaft stiffnesses to a point where further cost savings might result from elimination of a vibration damper. As the designer approaches a new model, he knows that engine length means pounds of iron added – pounds of iron mean added cost – and the profit from the use of smaller bearings becomes great.

Aluminum has been sometimes overlooked as a bearing material because of its coefficient of expansion. The coefficient for aluminum is 12.3 x 10^{-6} in./in./F, steel is 6 to 7 x 10^{-6}, cast iron is 5.87 x 10^{-6}. Since the aluminum bearing is retained in a steel or cast-iron housing, differences in thermal expansion complicate the bearing design somewhat. Aluminum has a low modulus of elasticity and a poorly defined yield point, so to evaluate the temperature effects properly, the designer must follow a thorough calculation of the bearing loading and dimension changes, taking into account temperatures, crush, and the different physical characteristics of the two materials. We evolved a formula using basic theories of elasticity and thermal expansion to calculate these thermal effects on bearing clearance, and confirmed our formula assumption with laboratory test work. Calculations on a 3½-in.-diameter journal with a ⅜-in. bearing wall show bearing clearance decreases between 0.0009 in. and 0.0013 in. when bearing temperatures are raised from room level to 260 F. This figure represents the net change in clearance due to changes of both the bearing and the journal. Thus, to be safe, we have found it necessary to run solid aluminum bearings with slightly more clearance than with babbitt bearings. A typical bearing might have 0.002 in. of diametral clearance per inch of shaft diameter.

To provide proper seating in the bearing support and to prevent bearing rotation within the support, "crush" height is added to both halves of the bearing shell at the joint face. The purpose of the crush is to prestress the bearing by assembling it in a bore which is smaller in diameter than the bearing shell. Since the main and connecting-rod bearings are assembled as halves in a removable bearing cap, the provision of the added height to each half is the practical way to secure the bearing shell.

We determine the crush height added to each half of the bearing shell in this manner:

Crush per half shell = (0.0004 x OD of the bearing in inches times $\pi/2$) plus manufacturing tolerances. Fig. 2 shows the effect of crush on a bearing

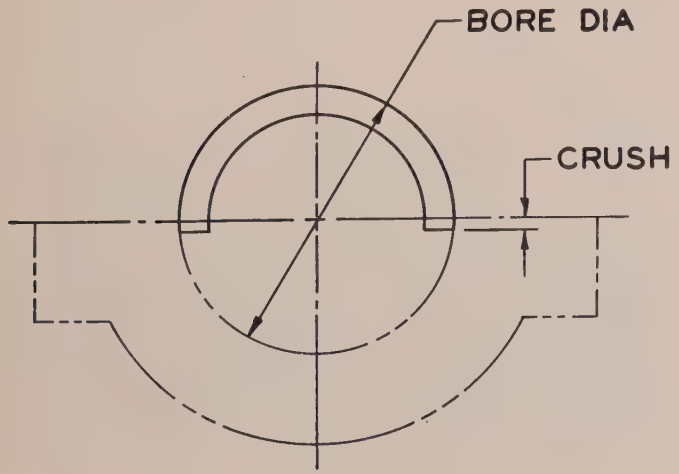

Fig. 2 – Effect of crush on bearing shell

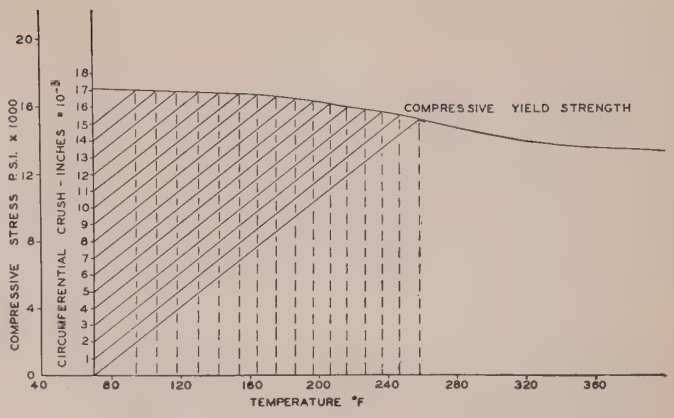

Fig. 3 – Compressive stress and circumferential crush versus temperature—750-T101 aluminum alloy—based on 3-in. OD bearing

shell. For the 3½-in. bearing (4¼ in. outside diameter) considered previously, the crush would be 0.0027 to 0.0045 per half shell, or a maximum of 0.009 per bearing assembly.

Fig. 3 interrelates the effects of crush and temperature on the bearing shell. The outer scale on the vertical axis is compressive stress, while the inner scale is the circumferential crush which corresponds to the compressive stress. Bearing temperature is shown in the horizontal scale.

Starting at an initial crush figure, stress increases along the diagonal lines as temperature increases. The upper limit of the stress is the yield strength of the material. If, for example, a minimum crush of 0.004 is needed for proper retention of the bearing shell, the maximum operating temperature which will permit retention of the 0.004 minimum crush at 90 F would be 216 F. The diagonal lines may also be extrapolated to intersect the base line, indicating the temperature at which the bearing would come loose in the housing.

Recognizing that aluminum is a low modulus material, and to control the stresses formed in the bearing shell, we chose to use a relatively thick wall. A ⅜-in. wall on a 3½-in. bearing journal, for example, distributes the crush load in such a manner that when the operating loads of the engine are added, excessive stresses will not result. Rule-of-thumb figures for calculated stresses in bearing design are as follows:

1. Radial stress – bearing against restraining wall – 800 psi mean stress.
2. Circumferential stress at bearing ID – 7600 psi mean stress.

In order to be sure that the solid aluminum bearings stay tight under operating temperatures, we set 18,000 psi compressive yield strength as our minimum specification for these bearings. This minimum is reached either by control of cooling rates during casting or by cold-working and/or heat-treating the rough castings. Note that because aluminum doesn't have a well defined yield point, 0.2% offset is taken as the yield point. Refer to Fig. 4 for explanation of this term. The cold-working process (Fig. 5), when used, consists of

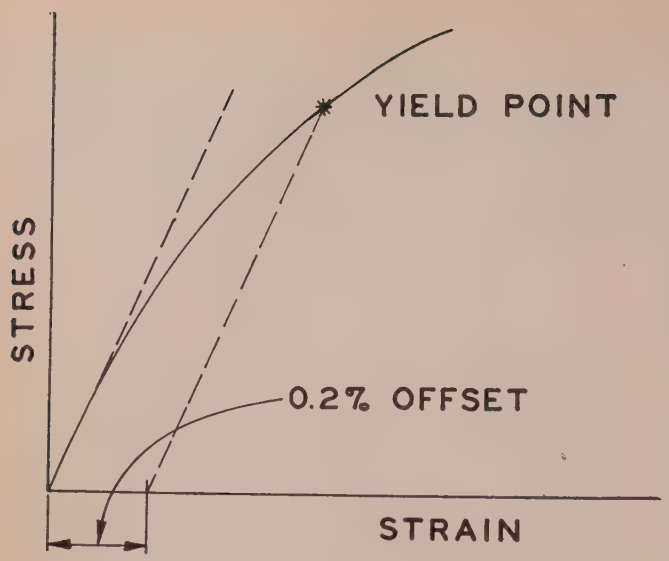

Fig. 4 – Aluminum yield point

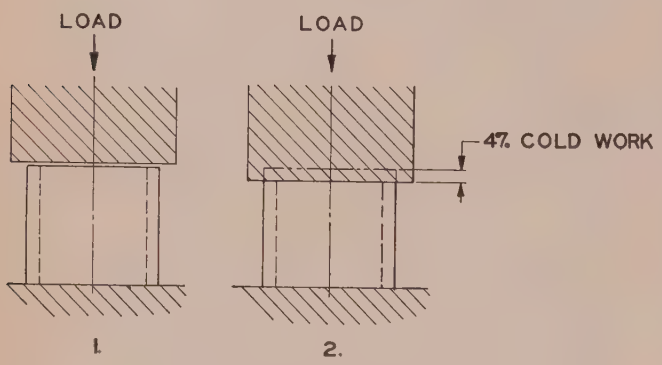

Fig. 5 – Cold-working process

cold-pressing the bearing axially to shorten it about 4%. This is done without supporting the circumference of the bearing.

The use of aluminum for engine bearings has not been widespread. We do not know the reason behind this. Why have we been able to accomplish trouble-free operation with them? Perhaps the following factors may be contributory.

We build rigid crankshafts, bearing caps, and connecting rods into our engines. Various design features shown in Fig. 6 contribute to crankshaft strength and rigidity, and consequently provide a straighter journal for the bearing. They include large overlap between the main and rod journals, thick crankshaft cheeks, and large radii, in addition to simply making the shaft journals larger. Also, our bearing-supporting structures are extremely heavy, providing adequate support with minimum flexure even under high peak loading of the cylinders and rough operation of the vehicle into which the engine may be installed. Fig. 7 shows a typical massive bearing cap and block support used on our V8 and V12 industrial engines. Rigid supporting structure, plus relatively thick-walled bearings, keep bearing stresses within safe limits and assure us of good bearing operation.

We have used hardened crankshaft journals for many years. Is it essential that aluminum-alloy bearings must be mated with hardened journals to be successful? While we would answer "no" to this question, we do believe that they help aluminum bearings to perform better. Note Fig. 8, which shows a bearing run on a soft crank journal (Rockwell C25) after 2000 hr of operation in one of our diesel engines. Comparison of journals on a hard and a soft crankshaft will show slight scratching on the soft journals, while the hardened shaft is usually unaffected.

How about oil filtering and general engine cleanliness during manufacture? Since every engine has a certain amount of foreign material which even the best cleaning processes do not remove, and certain "mating" between the bearing and journal must be accomplished during initial running, some softer plating on the bearing proves to be of value. Our solid-aluminum bearings are given an inexpensive 0.00015-in. plating of tin by a nonelectrical immersion process. We do not expect this very thin layer of tin to remain throughout the life of the bearing, but it does give valuable assistance during break-in.

We provide full-flow filters on most of our engines, and we feel this has contributed greatly to the success of aluminum bearings. Ordinary fine dirt may not cause seizure, but it certainly contributes to wear on a bearing journal regardless of the bearing material used. Large steel chips or other foreign material can lead to seizure, however, and they must be kept out of any bearing. We have run many aluminum bearings with bypass filters, and found the wear rate of the journals in dusty conditions to be 7-10 times the rate with full-flow filtering. This fact makes us heartily recommend full-flow filtering for use with any type of bearing.

The temperature of the bearing has been discussed previously along with crush. The temperature at which solid-aluminum bearings can be successfully used is limited by the amount of crush and the yield strength at that temperature. Looseness of the bearing will result if it is operated at some temperature where its yield strength is ex-

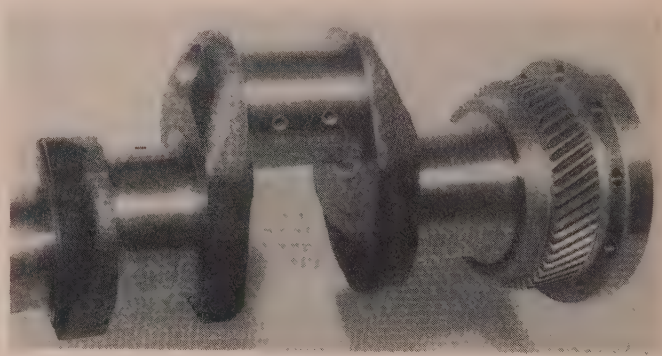
Fig. 6 – Strong, rigid crankshaft designed to provide straighter journal for bearing

Fig. 7 – Typical massive bearing cap and block support used on V8 and V12 industrial engines

A solution which showed promise of removing both these limitations was an aluminum bearing material bonded to a steel backing. Such a bearing would give the advantage of a high-strength material with a larger modulus of elasticity which could retain its crush at higher temperatures. At the same time, the steel backing provides us with a material having a coefficient of expansion about the same as the cylinder block or connecting-rod material.

We worked very closely with Johnson-Bronze Co. and Bohn Aluminum and Brass Corp. in the development of a bonded-aluminum-on-steel bearing. This bearing soon became a production reality. Fig. 11 is a cross-section of a steel-backed aluminum bearing. Many failures and difficulties were met and overcome before a successful bearing was developed, but both our collaborators produced successful steel-backed bearings after considerable

ceeded, and successful bearing operation from then on is limited. Solid-aluminum bearings must be kept tight in their restraining bores. Correct control of the lubricating-oil temperature thus becomes important and sometimes necessary for good bearing life, since the oil acts as a coolant for the bearing surfaces. The oil temperature depends upon general engine design, ambient air temperatures, heat dissipation to the oil, and speed and loads to be encountered. Therefore, tests are generally needed to determine whether external oil cooling is necessary.

The heavy loads encountered by most of our diesel engines require that we use lube oil coolers. This is done by using either oil-to-air or oil-to-jacket water-heat exchangers.

Steel-Backed Aluminum Bearings

Success with solid aluminum led us to look for further ways of bearing improvement. As we gained production experience with solid-aluminum bearings, we found two major limitations confronting us. First, at high speeds and corresponding high temperatures and loads, the thinner-walled connecting-rod bearings sometimes tended to lose its crush and become loose in its bore. Even when the bearing was doweled to the rod, such a design would not prevent rotation, since the dowel would cut into the soft aluminum and allow it to rotate, cutting off the oil supply, and seizure would result (Fig. 9). The design of better bearing-retention devices was difficult, since bearing retention depended for the most part on the crush between the bearing halves and the corresponding radial stress of the bearing against the bearing wall. The second limitation was the tendency for solid-aluminum bearings sometimes to fail in fatigue in a peculiar manner under high-load conditions. Such failures, which were rare and caused by extreme conditions, resulted in bearings broken into many pieces as shown in Fig. 10.

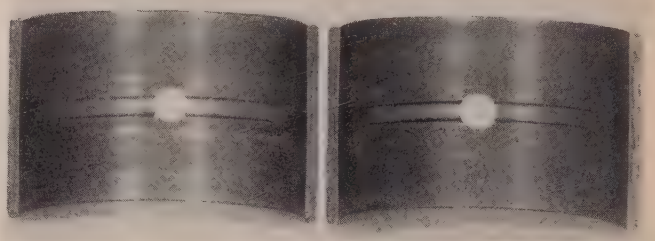

Fig. 8 – Bearing run on a soft crank journal after 2000 hr operation, resulting in slight scratching of journal

Fig. 9 – Seizure in solid-aluminum bearing resulting from poor bearing retention

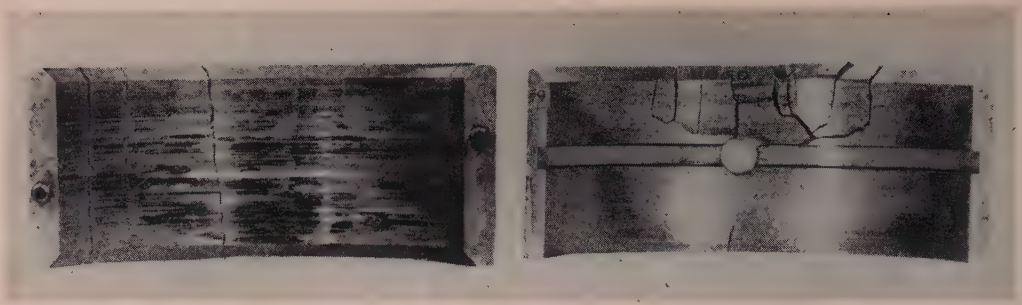

Fig. 10 – Broken bearing, a rare result of fatigue failure under high-load conditions

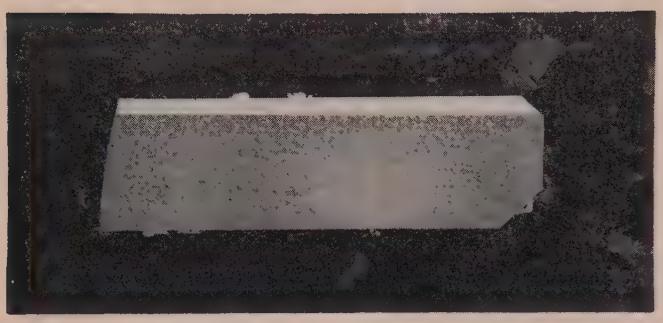

Fig. 11 – Cross-section of steel-backed aluminum bearing

Fig. 12 – Flanged thrust-carrying main bearing of aluminum on-steel

expenditure of time, money, and effort. We certainly owe them every credit for overcoming many obstinate difficulties to reach the production stages of such a bearing.

As an example of one of the difficult problems of manufacturing these bearings, forming the flanged thrust-carrying main bearings stands out (Fig. 12). We wanted to maintain interchangeability between our solid-aluminum-alloy bearings and the newer steel-backed ones, so the same wall thicknesses had to be maintained. Remembering that the solid-aluminum version had relatively thick walls, you can understand the problems of flanging such steel sections without rupture of the bond or splitting of the steel. We found that the bond was extremely ductile, and would stand all of the stress imposed on it in flanging without failure. Fig. 13 shows the ductility of the aluminum-to-steel bond. The aluminum itself seemed to stretch readily, but the steel sometimes tended to split at the parting line, as shown in Fig. 14. We found that our geometry of wall thickness to diameter was such that an economical flanged bearing could not be made in some sizes, so we turned to thinner walls to facilitate manufacturing and keep down costs. This destroyed the advantage of interchangeability with solid-aluminum bearings, but it was considered worth this disadvantage.

Steel-backed aluminum bearings (Fig. 15) were added to some of our diesel engine designs a few years back. We estimate some of these bearings have now piled up over 25,000 hr, and we have a large number of them in successful operation in our machines.

On the steel-backed bearings, we use Alcoa XB80S aluminum alloy, which is essentially the same chemistry as the Alcoa 750 or Bohn MB7

Fig. 13 – Example of ductility of aluminum-to-steel bond

Fig. 14 – Steel backing split at parting line, an early manufacturing problem

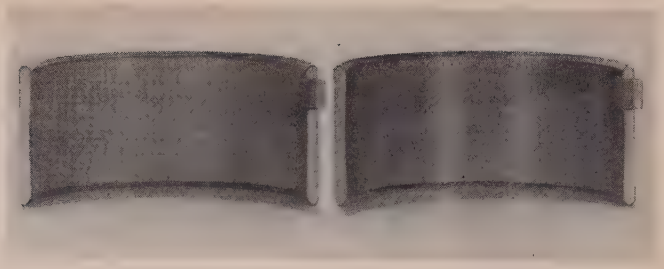

Fig. 15 – Steel-backed aluminum bearings, some of which have run 25,000 hr in diesel engines

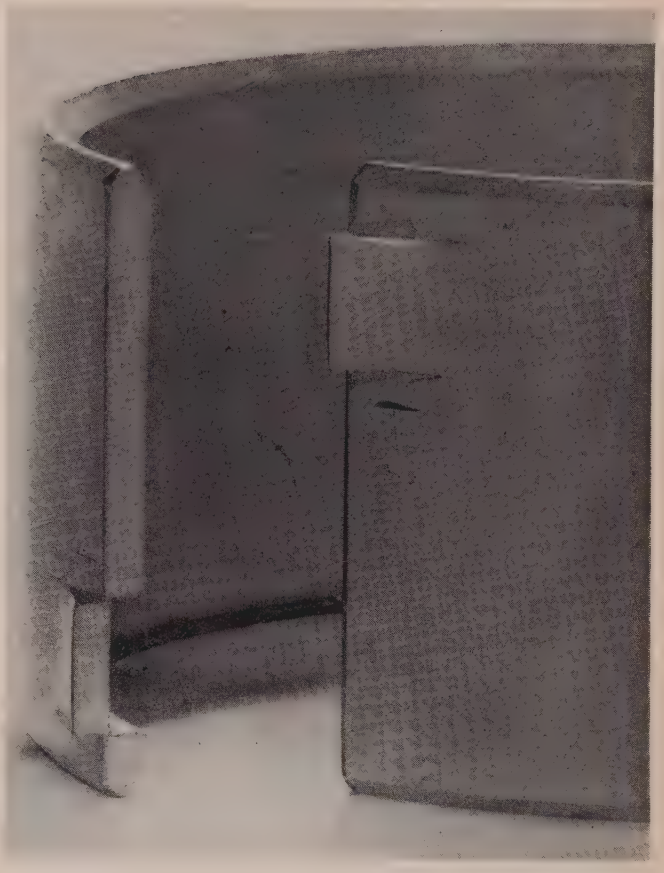

Fig. 16 – Tabs substituted for dowels to prevent both rotary and axial motion of bearing shell

materials used in our solid-aluminum bearings. As expected, we found the same good bearing properties in the new bearings as we had in the solid-aluminum bearings. In addition, we had eliminated the two major shortcomings of the solid-aluminum bearings. Furthermore, the bearing clearances could be reduced 37% over those used with solid aluminum. On steel-backed aluminum bearings, we use clearances of 0.0012 in. per in. of journal diameter. To some engine manufacturers who might consider such clearances excessive, we can suggest eccentric bearing walls, which provide a closer clearance in the vertical plane. We are interested in reducing the large amounts of oil which flow through our bearings, as such reductions offer advantages in smaller oil pumps and filter design. Eccentric bearing walls are being studied as a means of reducing oil flow on our engines for this reason.

Because wear on the aluminum bearing material is negligible, operation below the 5000-psi fatigue stress value gives us a bearing without a life limit. Bearings of some other materials have to be replaced at definite intervals. The steel backing makes the bearing less sensitive to high oil temperatures. Where 215 F was the maximum oil temperature that could safely be used with solid-aluminum bearings, steel-backed aluminum bearings may be safely run at oil temperatures up to 250 F. We do not recommend these high oil temperatures for other reasons, but the improvement relieves one of the limits on aluminum bearings. Recently we examined a set of steel-backed aluminum bearings with 29,000 hr. Wear was negligible, and there were no surface defects which would prevent the bearings from being re-assembled for further use.

Another advantage with steel backing is that it allows simpler and less expensive bearing-locating designs. Dowels can be eliminated and tabs, illustrated in Fig. 16, substituted to provide a simple method of preventing both rotary and axial motion of the bearing shell.

To evaluate properly the merits of the many

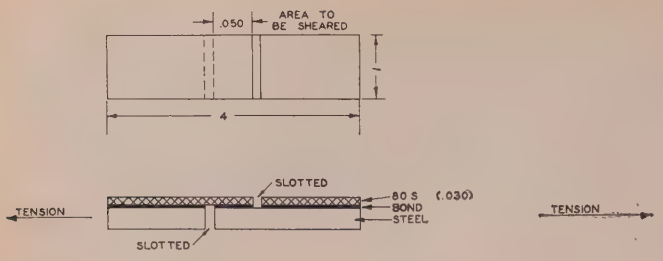

Fig. 17 – Specimen of clad bearing prepared for bond-shear test

bearing materials and designs considered, we use several different testing procedures. These tests vary widely in form, but each discloses important information about the test bearing, and together they tell a complete story of how the bearings will work in our diesel engines.

Bond-strength tests for clad bearings have always been difficult to devise. Bearing manufacturers use chisel tests for this, and we have likewise resorted to this somewhat crude evaluation. Being engineers, we wanted to hang a numerical value on bond strength, and so we devised a bond-shear test in which a specimen of the clad bearing is prepared, as shown in Fig. 17. Note that a given depth of machining is specified, and a given length of bonded alloy is stressed in combined tension and twist. With this setup we have a destructive test procedure, but we are able numerically to rate the strengths of various bonding techniques and/or alloys.

One laboratory test procedure for bearings entails the use of a modified Underwood fatigue machine, in which extremely heavy (8000 psi) loads can be placed on the test bearing. Fig. 18 shows this machine. Weights can be adjusted so that loading on the bearing can be varied to build up high unit stresses. We well realize that such a test is not exactly simulating the engine cyclic loads, and therefore warn the reader not to judge anything but relative fatigue strengths of various types of bearings from such data. It is, however, extremely valuable to cull out those bonding processes or weak materials which should be given no further considerations in our bearings. To obtain the high test loads desired, it was necessary that the test bearings be cut down to reduce the bearing area. Fig. 19 shows such a test bearing. This also represents a compromise in testing, since oil flows and temperature distributions in the test bearing are different than in a full-width bearing.

A bearing property machine built in our research laboratory is used to evaluate the running friction properties of different materials. This machine (Fig. 20) consists of a variable loading device, an electric motor which drives the test journal, and a controlled lubricating supply. The loading device acts on the test bearing and journal as shown in Fig. 21. The motor is cradle-mounted on ball bearings, and the driving force of the motor on the journal is measured on a small balance scale. Oil

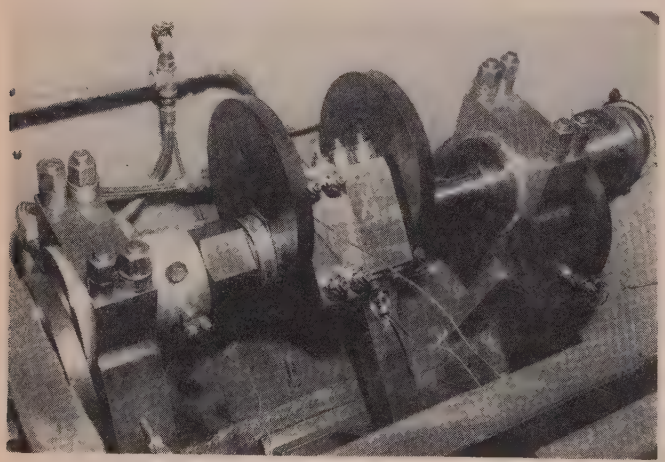

Fig. 18 – Modified Underwood fatigue machine for heavy-load bearing tests

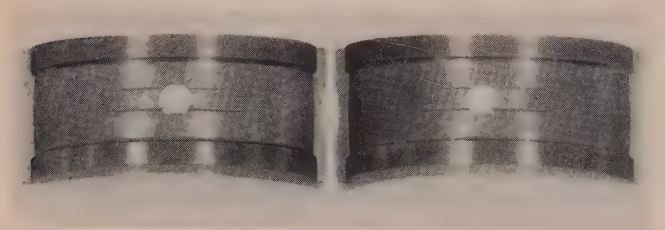

Fig. 19 – Test bearing with reduced area to obtain high test loads

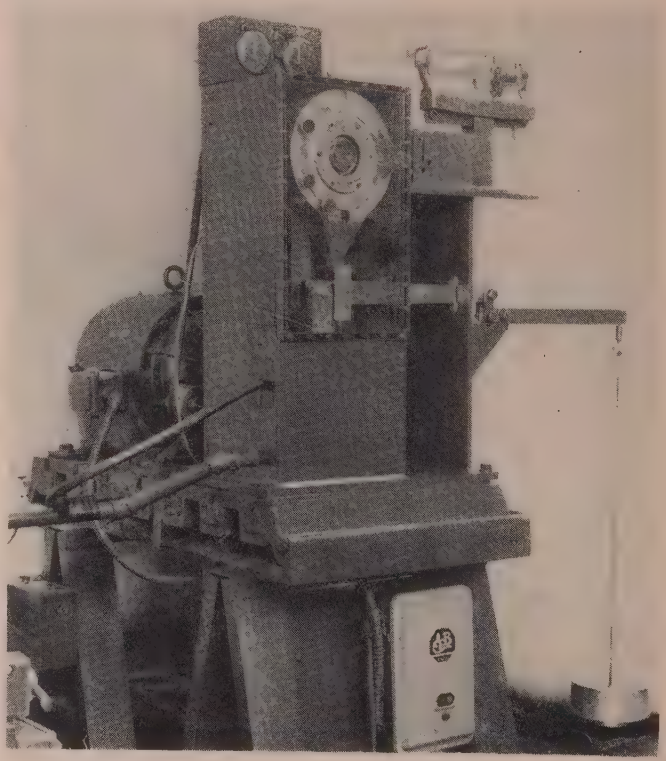

Fig. 20 – Bearing property machine for evaluating running friction properties of different materials

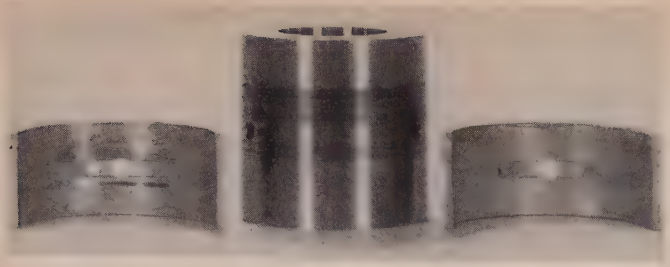

Fig. 21 – Bearing and journal used in bearing property tests

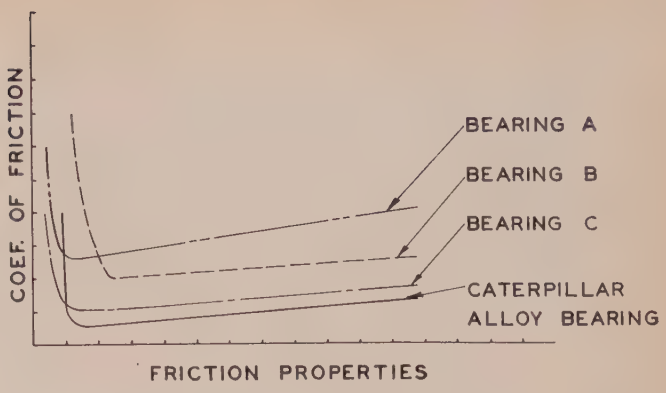

Fig. 22 – Friction properties of several materials tested on friction machine

pressure and temperatures are controlled, thus eliminating two of the variables which can affect friction. This machine can discern small differences in running friction properties. Fig. 22 shows Zn/p curves of several materials tested on the friction machine. They illustrate how materials differ in running properties, and support data obtained from engine tests.

When preliminary testing has shown a bearing material to be promising, engine tests subject the bearing to loadings, temperatures, lubricating conditions, and other factors as they occur in the actual engine design. These engine tests, in addition to loading the bearing under normal operating characteristics, may be modified to test the bearing under all kinds of adverse conditions. Overspeed testing is a rule in any bearing development program. Such running may detect shortcomings in the bearing, and point out exactly where speed limitations are. The usefulness of such testing in future development is obvious. Design variations can be studied here; for example, the effect of an unbalanced crankshaft versus a balanced crankshaft can only be evaluated by the engine. Oil temperature, bearing clearances, and many other factors may be quickly and accurately evaluated in the test engine.

After these steps, field testing will provide still more data on the proposed bearing. The ultimate user sometimes does things to the engine that the test engineer cannot anticipate. Often the conditions under which the engine will run, such as severe overspeeding, cycle loading, or dusty operation, cannot be exactly duplicated in the laboratory or on one's proving-ground location. The customer can veto a new development quickly if the product is marginal or bad from a practical standpoint. They have, however, given wholehearted approval to our solid and steel-backed aluminum bearings.

We are pleased with our success with steel-backed aluminum, and to date we haven't found any other material that fully satisfies our requirements. We know there are still factors of aluminum bearing design which can be improved, and we are continuing to concentrate our efforts to develop these improvements.

Cost reduction is a primary objective, since lower cost will make steel-backed aluminum bearings more adaptable to small, low-cost engines. Much work can and will certainly be done in this area, not only by our company but by the bearing manufacturers.

Steel-backed aluminum bushings (Fig. 23) are beginning to find many uses in heavy-load applications where babbitt or bronze bushings cannot handle the load or speed. The same features which make steel-backed aluminum excellent for main and rod bearings make it useful for gear-train bearings and other small bushing applications.

Other uses will also be found. Our most recent application of a steel-backed aluminum bearing is in a turbocharger, where a bearing 0.800 in. in diameter carries a shaft turning 48,000 rpm. This results in a surface running speed in excess of 10,000 fpm. By comparison, a 4-in. main bearing

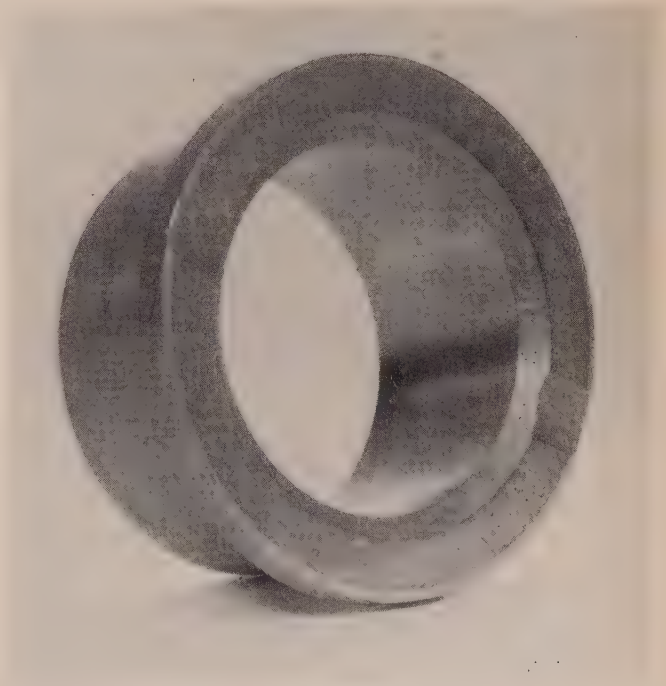

Fig. 23 – Steel-backed aluminum bushing, designed for heavy-load applications

running 2000 rpm has a surface running speed of 2090 fpm.

We do not offer aluminum alloy as the only good bearing material. Babbitt, bronze, and other bearing materials have their own uses and applications. Our success does prove that steel-backed aluminum bearings are excellent for high-load, high-speed applications; and we hope that this paper in some way furthers and improves its development as a truly useful tool for engineers.

DISCUSSION

Discusses Advantages Of Solid-Aluminum Bearings

—D. B. Wood
Aluminum Co. of America

AS a partial explanation for the lack of widespread use of aluminum bearings mentioned by the authors, we would state that aluminum-alloy bearings are relatively new. Caterpillar production with these bearings started in 1945, after six years of test work. Caterpillar was more fortunate than some other engine builders in that it was aware of and able to test aluminum bearings during the war years. Many other companies are adopting aluminum bearings as their test work is completed, and there are clear indications that a change should be made. Among companies in production with solid-aluminum bearings are Fairbanks-Morse, Ingersoll-Rand, Morgan Construction Co., John Deere, Witte, International Harvester, Nordberg, Waukesha, Harnischfeger, Cooper-Bessemer, and Clark Brothers. Steel-backed aluminum bearings manufactured by Moraine Products Division, GMC, and sold under the trade name "Moraine 400," are used in production by Cadillac, Buick, Detroit Diesel, and GMC Truck.

We believe at present, based upon laboratory data and experience from production use, that solid-aluminum bearings offer some definite advantages over any other bearings now in commercial production. This does not mean that they can be used in all applications indiscriminately. Sufficient bearing-wall thickness must be provided or be present in the existing design. This wall thickness is roughly 0.04 times the shaft diameter plus 0.020 in.

The major disadvantage of solid-aluminum bearings cited by the authors is the problem presented by differential expansion between bearing metal and housing metal. In most cases this can, by design and calculation, be solved by adjustment of bearing dimensions and tolerances. Where exceptional conditions (for solid-aluminum bearings) are encountered, the use of full-floating bearings or a nonferrous housing eliminates the problem.

Solid-aluminum bearing materials are unique in that they present a metal capable of operating under heavy-duty requirements without benefit of any supporting or lining material.

In the automotive field, which is of special interest to this group, it might be possible to increase the large end of the connecting rod to provide sufficient bearing-wall thickness for solid aluminum and still not be limited in overhaul, since most engines today are large-bore, small-stroke compared with those of years gone by.

Although aluminum bearings are new, a lot of useful information has been accumulated in the past 10 years that gives a potential user a good start toward successful operation. For any particular type of application, reasonably accurate recommendations can be made that incorporate knowledge on such subjects as load, crush, running oil clearance, locking, grooving, hardness and finish of mating parts, lubrication, dirt control, and general bearing design.

Praises Properties Of Aluminum-on-Steel

—J. W. Butler
Johnson Bronze Co.

FIRST I should like to ask the authors' opinion of their stated safe maximum aluminum-on-steel bearing operating temperature of 250 F, in view of the fact that recent publications have recommended that babbitts can be safely used up to that temperature, ignoring the obvious difference in unit loads involved.

Secondly, I should like to add a few thoughts to this paper.

Aluminum bearing alloys are one of the few bearing alloys to fulfill the widely accepted classical ideal bearing-metal theory based upon a structure consisting of small particles of undissolved constituents, both soft and hard, dispersed throughout a soft matrix. They also have another very important property in addition to those listed by the authors: their high thermal conductivity, which helps prevent local hot spots, and consequently prevents any seizure due to the lack of ability to distribute the heat over the entire bearings surface.

Notice the lack of a seam or split in that aluminum-on-steel bushing shown in Fig. 23. It is approximately 1⅛ in. long, 1⅝ in. ID, 0.150 in. wall thickness, with a 3/16-in. flange on one end. This particular type of bushing is drawn from flat aluminum-on-steel strip material, which vividly illustrates the amazing ductility of this bimetallic material.

We feel the operation of an aluminum-on-steel bearing for 2000 hr on a relatively soft shaft, Rockwell C25 (Bhn 255 at 500 g), is quite significant in view of the fact that the aluminum had only a thin tin overplate. This, along with the fact that aluminum-on-steel bearings are operating in a turbocharger at a speed of 10,000 surface fpm, seemingly could open an entire new realm of applications for this bearing material.

Other Tests Reported On Steel-Backed Aluminum

—W. E. McCullough
Bohn Aluminum & Brass Corp.

IT is customary to apply heavy pressure through bearing cap studs and nuts to assure proper fitting of the bearings in connecting rods and crankcases. The bearing must be able to resist such pressures without permanent deformation or loss of crush resistance.

Whereas certain makers of cast-aluminum bearings achieved the required compressive yield strength in the bearing by cold compression of the nonheat-treated casting, we have used a slightly different alloy, and always have produced the required yield strength through heat-treatment. We understand that both treatments are satisfactory, but believe our method is simpler.

Concerning fatigue endurance of the steel-backed, aluminum-lined bearing, we made comparative flexure tests in which flat strips of steel coated with aluminum and others with copper-lead bearing alloys were alternately bent across opposed convex steel anvils, and found that whereas the copper-lead linings cracked before the steel-backs, the reverse was true with aluminum-alloy linings, which developed no fatigue cracks before steel-back failure.

Concerning corrosion resistance of aluminum-bearing alloys under engine service conditions, we have yet to receive a single complaint of corrosion failure with this type of bearing.

We are greatly encouraged by performance reports covering tests of steel-backed aluminum bearings in various other engines than are covered by this paper.

New Instrumentation for Engine Combustion Studies

J. A. Warren and J. B. Hinkamp, Ethyl Corp.

This paper was presented at the SAE Annual Meeting, Detroit, January 12, 1956.

RESEARCH and development of fuels and lubricants for engines has depended considerably upon instrumentation for engine evaluations and has occasionally marked time until the necessary instruments were devised. The earliest engine research instruments were wholly mechanical in nature and were quite adequate for slow-speed engines of the day. It was not long, however, before many instruments included combinations of mechanical and electrical components. Even today the most precise cylinder-pressure sensing instruments are of this type. However, birth of the so-called electronic age brought about a radical change in instrumentation. Within a few years it became possible to follow precisely on an oscilloscope the instantaneous pressure changes in an engine cylinder, to "sense" electronically the presence of a flame front, or to photograph the actual combustion process at speeds of many thousands of frames per second. These techniques are of invaluable aid in

A NEW research tool, the crank angle-time recorder, is described. This instrument conveniently obtains a permanent record of the time at which various combustion phenomena occur in the engine cycle. Use of the recorder in studies of normal and abnormal combustion (deposit-ignited surface ignition) has provided information of interest to both engine designer and petroleum refiner.

Studies include determinations of those deposit-ignited flame fronts which result in knock, effect of fuel antiknock quality and additives on surface ignition, and resistance of fuels to surface ignition. The records obtained show that considerable variability exists in the time at which normal flame fronts arrive at an ionization gap. Some factors affecting magnitude of this variability are ignition timing, fuel-air ratio, engine throttling, changes in manifolding, and fuel type.

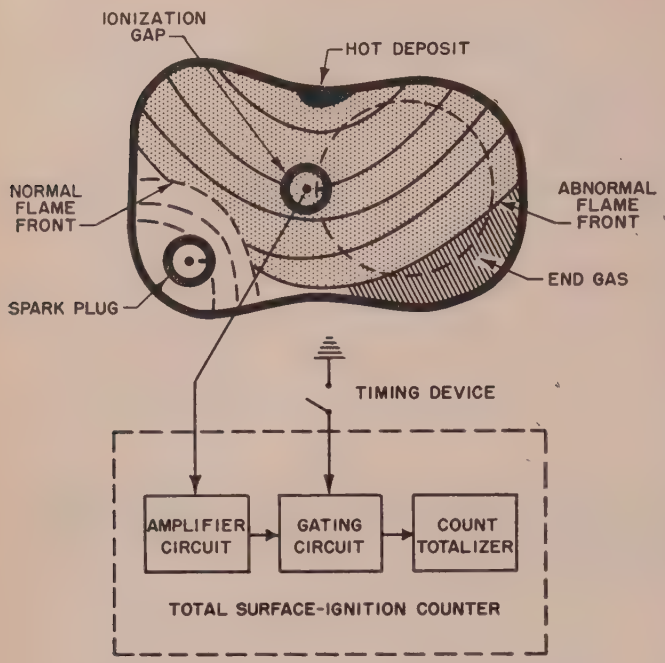

Fig. 1 – Illustration of surface ignition and means by which it is detected and counted

studying reproducible engine phenomena such as ignition, flame propagation, and spark knock, but have not been completely satisfactory for investigating erratic combustion processes such as surface ignition or wild ping. An instrument was desired to provide a conveniently obtained permanent record of the time in the cycle at which erratic engine phenomena occur. Such an instrument has now been developed by combining a number of previously perfected principles into a device which should find many applications. This paper describes its design, operation, and use.

Otto-Cycle Engine Combustion and Spark Knock

Normal combustion in the Otto-cycle engine[1] is initiated solely by a timed spark followed by movement of a flame front across the combustion chamber in a uniform manner at a normal velocity. In such a process there is no sudden release of energy from the fuel-air mixture, nor are there any auxiliary sources of ignition from combustion-chamber deposits, hot spark plugs, overheated valves, or other hot sources within the combustion chamber.

Abnormal combustion will occur if the fuel-air charge inducted is not of sufficient antiknock quality. In this type combustion part or all of the charge may be consumed at extremely high rates. Generally, end-gas, the last portion of charge to burn, spontaneously ignites and gives rise to a sharp metallic noise referred to as spark knock. This type knock is recurrent and repeatable in terms of audibility and is controllable by spark advance; advancing the spark increases knock intensity and retarding the spark reduces knock intensity.

Deposit-Ignited Combustion

The combustion chamber often contains deposits of such nature that a portion of them may become sufficiently heated to initiate chemical reactions, causing them to glow during one engine cycle and to remain glowing during intake and compression strokes of the following cycle. If enough heat energy is available in the glowing deposit, it may act as an ignition source and start an abnormal flame front in the combustion chamber, shown schematically in Fig. 1. This occurrence is referred to as surface ignition, defined by CRC[1] as "the initiation of a flame front by any hot surface other than the spark discharge prior to the arrival of the normal flame front." The abnormal or deposit-ignited flame front may be started before ignition occurs at the spark plug, or it may start sometime after the regular or normal flame is already in motion. In addition, a number of ignition centers caused by hot deposits may be present simultaneously in the combustion chamber either as attached deposits or as loose particles floating about.

Occurrence of the extra flame front or fronts in the combustion chamber may or may not result in knock. Possibility of knock will be determined generally by antiknock quality of fuel in the end-gas and time in the cycle at which extra flame fronts were started. If fuel antiknock quality is just sufficient to satisfy the engine under normal conditions, presence of an additional flame front may cause autoignition of end-gas, resulting in a sharp crack similar to that associated with spark knock. An abnormal flame front started very early in the cycle may also result in knock in a manner similar to that caused by advancing ignition timing. Both of these are examples of knocking surface ignition.

Glowing deposits and consequent erratic combustion may persist for only a single engine cycle, or may last for a number of cycles. This is followed by normal combustion, and the noise heard previously is referred to as wild ping, defined[1] as "knocking surface ignition characterized by one or more erratic sharp cracks." However, if fuel antiknock quality is sufficiently high, no knock would occur and the only manifestation of surface ignition, without special instrumentation, would be momentary engine roughness. This would be caused by the abnormal rate of pressure rise resulting from more rapid charge consumption as a result of additional flame fronts in the combustion chamber.

Instrumentation

Total Surface-Ignition Counter – We have developed electronic equipment (described in a previous

[1] See Coordinating Research Council Report No. 278, New York, June 1954: "Terms for Use in Otto-Cycle Engine Combustion."

paper[2]) which detects and counts uncontrolled deposit-ignited combustion (surface ignition). This equipment, referred to as the total surface-ignition counter, and which has been used with both single and multicylinder engines, employs an ionization gap in the combustion chamber, as shown in Fig. 1. The ionization gap has a voltage impressed across it which is a small fraction of that necessary to produce a spark. When a flame front passes the gap, the gas ionizes, gap resistance is reduced, and a current pulse is permitted to flow. This pulse triggers an electronic circuit and actuates a digital counter. When surface ignition is being studied a camshaft-driven switch or timing device is used to ground the electronic surface-ignition counter, making it inoperative just prior to the time of arrival of the normal flame front. The earliest normal flame fronts, in the CFR L-head engine, usually arrive at the ionization gap at about 15 deg atdc, if ignition timing is at tdc and fuel-air ratio is 0.077. For this condition, the timing device is set to automatically close at 10 deg atdc, hence none of the normal flame fronts will trigger the counter. The timing device automatically opens at 70 deg btdc, thus making the counter operate over an 80 deg period of crankshaft rotation. At other ignition timings, the timing device is set to close 5 deg before the normal flame fronts arrive at the ionization gap.

Surface ignition illustrated in Fig. 1 resulted in initiation of an abnormal flame front in the combustion chamber prior to ignition by the timed spark. In this instance, the abnormal flame front has moved across the ionization gap prior to 10 deg atdc and will automatically be registered on the counter. If antiknock quality of the fuel is too low, or if the hot deposit ignited the charge very early in the cycle, end-gas knock may occur. This would be a case of audible or knocking surface ignition. The total surface-ignition counter does not discriminate between knocking and nonknocking surface ignitions, but records all flame fronts, provided they arrive at the ionization gap within the specified period. Surface ignitions determined by this electronic equipment are referred to as total surface ignitions.

Audible Surface-Ignition Counter – Our laboratories have also developed an audible surface-ignition counter (described in a previous paper[3]) which can be used to count spark knock or knocking surface ignitions. Briefly, this counter consists of a microphone suspended above the engine head, necessary electrical components, and an electromechanical recording counter. The microphone is isolated from external noises by an acoustical baffle. An electrical filter is incorporated which results in the counter being actuated only by high-frequency disturbances resulting from knocking surface ignitions or from spark knock. When fuels of sufficient antiknock quality to prevent spark knock are used, this counter supplies an accurate count of knocking surface ignitions only. An acoustical device is provided which permits sensitivity of the audible counter to be adjusted periodically to a standard. This audible surface-ignition counter supplements the total surface-ignition counter and provides additional information regarding surface-ignition effects.

Crank Angle-Time Recorder – The total surface-ignition counter detects and counts uncontrolled combustion arising from ignition by deposits and differentiates it from normal combustion in the manner discussed previously. However, this instrument gives no information about the time in the cycle at which the gap is ionized by abnormal flame fronts caused by surface ignition. Others[4, 5, 6] have developed test techniques generally making use of a cathode-ray oscilloscope in conjunction with suitable pickups to obtain a visual representation of time in the cycle at which surface ignitions occur. A permanent record of oscilloscope patterns may be made by photographic or other means.[6] However, an on-the-spot permanent record of the transient phenomenon of surface ignition is highly desirable. In order to obtain this record an electromechanical device, referred to as the crank angle-time recorder (CATR), was designed and constructed. This instrument can be used to make a permanent record of time in crank-angle degrees at which a number of engine phenomena take place, including arrival of normal or surface-ignited flame fronts at the

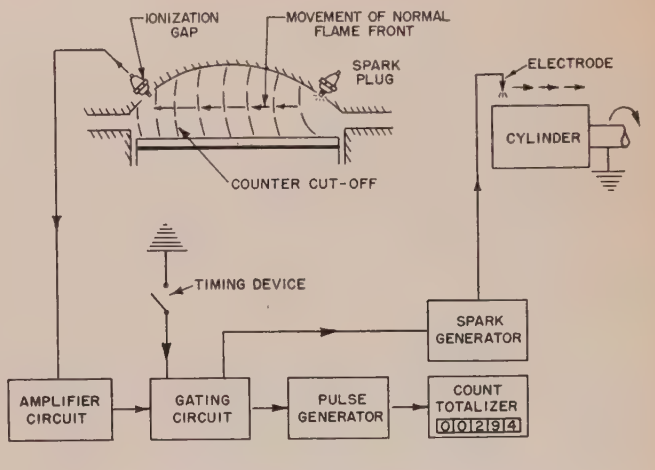

Fig. 2 – Block diagram of electric circuits for crank angle-time recorder

[2] See SAE Transactions, Vol. 62, 1954, pp. 40-49: "Deposit-Induced Ignition, Evaluation in Laboratory Engine," by D. A. Hirschler, J. D. McCullough, and C. A. Hall.

[3] See SAE Transactions, Vol. 63, 1955, pp. 53-62: "Practical Yardsticks for Deposit Effects," by C. A. Hall, J. A. Warren, and J. D. McCullough.

[4] See SAE Transactions, Vol. 61, 1953, pp. 453-468: "Method for Identifying Preignition," by R. F. Winch and F. M. Mayes.

[5] "New Engine Analyzer," by E. A. Martin and J. H. Goffe. Paper presented at SAE Summer Meeting, Atlantic City, June 10, 1954.

[6] "Observation of Automotive Preignition and Knock," by R. C. Bowers and A. R. Isitt. Paper presented at SAE Summer Meeting, Atlantic City, June 10, 1954.

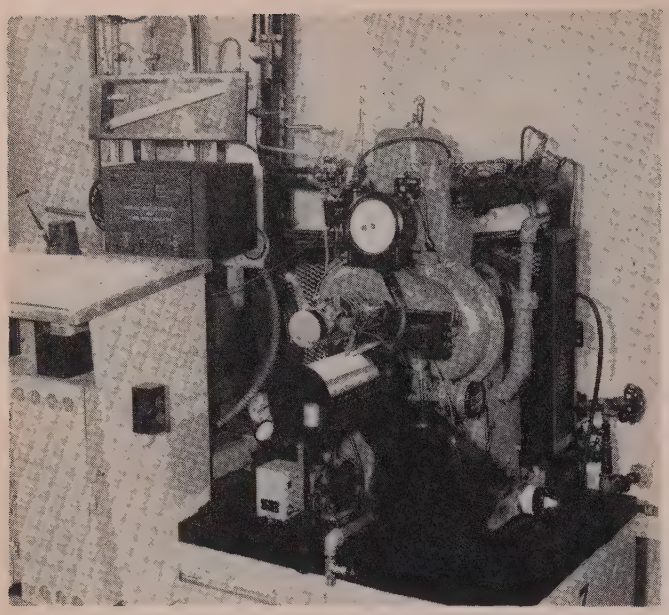

Fig. 3 – CATR unit connected to single-cylinder engine

ionization gap.

The CATR can make use of the ionization signal received by the total surface-ignition counter to trigger a spark generator which jumps a spark between an electrode and crankshaft-driven cylinder covered with sensitized paper. Fig. 2 is a block diagram of the electrical circuits involved. A photograph of the CATR connected to a single-cylinder engine is shown in Fig. 3. Electronic equipment is installed in the cabinet designated surface-ignition counter and flame-front indicator. It is possible to show each ionization as a dot on sensitized paper at the instant ionization occurred by moving the electrode along the longitudinal axis of the cylinder. Visual inspection of the paper record gives the

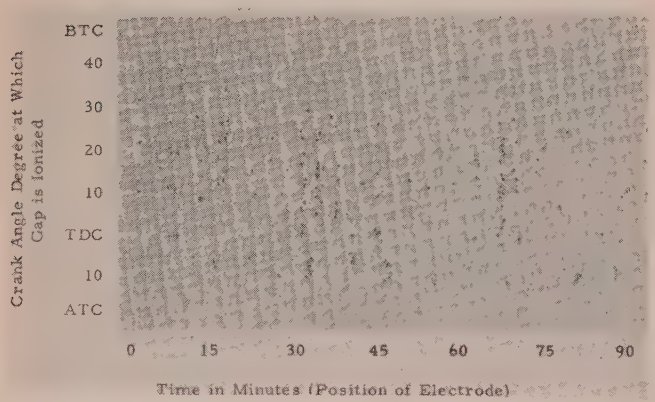

Fig. 4 – Typical CATR record of surface ignitions for CFR L-head engine with deposits. Ignition timing: tdc. Fuel: 2-A. Oil: 1-A. Each dot indicates period at which a deposit-ignited flame front arrived at ionization gap

Table 1 – Cycling Deposit-Accumulation Schedule for Single-Cylinder Engine Procedure

	Idle	Full Throttle
Cycle Duration, sec	50	150
Speed, rpm	600	900
Fuel-Air Ratio	0.087	0.077
Ignition Timing	Tdc	
Compression Ratio	7.0:1	
Jacket Coolant Temperature, F	150	
Oil Temperature, F	160	
Intake Air Temperature, F	112	
Test Duration, hr	165	

crank-angle degree in the cycle at which the gap was ionized. Regulation of the camshaft-driven timing device allows a record to be made of either surface ignitions or normal combustion. The CATR can also be used with the audible surface-ignition counter to record time in the cycle at which audible manifestations of both knock and knocking surface ignitions occur. Unless otherwise specified the CATR was used in conjunction with the total surface-ignition counter.

A CATR unit was connected to a CFR L-head engine operated on a special cycling schedule summarized in Table 1. The engine was run with a premium-grade automotive-type fuel containing 3 ml tel per gal, coded as fuel 2-A, and a high-V.I., straight mineral, nonadditive oil, coded as oil 1-A. Fig. 4 shows a paper record of surface ignitions taken after the engine had reached an equilibrium deposit condition. Each dot is the result of an abnormal flame front reaching the ionization gap. The data show the cyclic nature of surface ignition and indicate that, for the given fuel-oil combination under the particular test conditions, a large portion of surface ignitions ionized the gap before the spark plug ignited the charge, since ignition was at tdc. Hence, these are preignitions. Only surface ignitions are recorded in Fig. 4, since the special timing device grounded the counter prior to arrival of normal flame fronts.

Fig. 5 illustrates another method of presenting data obtained with the CATR. This plot shows distribution of surface ignitions with regard to crank-angle position of piston over a two-hour period. While these data are not from the same test as those of Fig. 4, it is obvious that in this instance also a majority of surface ignitions occurred before ignition by the spark plug. A special modification of the CATR is now being tested in which the paper record showing occurrence of surface ignitions is replaced by a number of digital counters. Each digital counter is connected in the electronic circuit in such a manner that only flame fronts arriving at the ionization gap during a certain crank-angle period are registered on a particular counter. Thus, data similar to those in Fig. 5 are obtained directly.

The special cycling schedule summarized in Table

1 was used to accumulate deposits in all tests discussed in this report unless otherwise noted. Used with the CFR L-head engine, this procedure increases both rate of deposit accumulation and tendency of deposits to produce knock, thus increasing sensitivity of the test method and magnifying effects of test variables. Fuel, oil, and additive factors have given test results using the above procedure which, although magnified, are in relative agreement with results obtained in modern engines operated in passenger-car road service.

Application of CATR

Studies of Surface Ignition – A. Which surface ignitions result in knock?: Two CATR units were used simultaneously to determine both period in the cycle at which each deposit-ignited flame front reached the ionization gap in the head of a CFR L-head engine, and those surface ignitions which resulted in knock. One CATR unit was triggered by the pulse occurring in the electronic circuit when a flame front arrives at the ionization gap. The second unit was triggered by an audible surface-ignition counter at the period in the cycle when the microphone from this counter picked up the audible effect of a knocking surface ignition. Each CATR unit included a separate electrode from which a spark could jump to the cylinder containing the sensitized paper. The two electrodes were a fixed distance apart at all times, for they were moved in the same plane parallel to the longitudinal axis of the cylinder. Thus, for a knocking surface ignition, both a record of period in the cycle at which the gap was ionized by the deposit-ignited flame front, and a record of period in the cycle at which resulting knock triggered the second CATR unit were recorded on the same piece of paper.

By superimposing records from both CATR units, it is possible to tell not only which surface ignitions resulted in knock, but also period in the cycle at which flame fronts of knocking surface ignitions arrived at the ionization gap. Fig. 6 is a representative record of surface ignitions taken after the engine had reached an equilibrium deposit condition on fuel 2-A. The antiknock quality of this fuel was about eight octane numbers higher than the minimum required to satisfy the engine at tdc ignition timing under which the investigation was made. The lower portion of Fig. 6 shows period in the cycle during which spark knock, with tdc ignition, triggered the CATR unit actuated by the audible surface ignition counter. To obtain these latter data, a primary reference fuel blend which knocked at tdc ignition timing was used. Results in Fig. 6 and similar data show that for this particular engine:

1. With tdc ignition timing, microphone response to knocking surface ignitions was recorded earlier in the cycle than response from spark knock.

2. Knocking surface ignitions were predominantly preignitions, since flame fronts from these surface ignitions generally arrived at the ionization gap before ignition by the main spark plug.

3. Surface ignitions which occurred late in the cycle were predominantly inaudible.

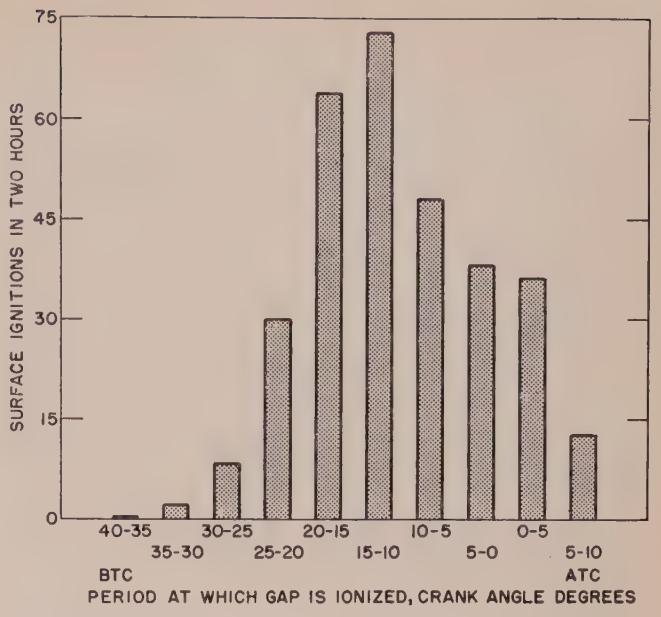

Fig. 5 – Typical distribution of surface ignitions for CFR L-head engine with deposits. Ignition timing: tdc. Fuels: leaded primary reference fuel blend containing 30 ml of oil 1-A per gal. Oil: 1-A

B. Effect of fuel antiknock quality on surface ignition: Influence of fuel antiknock quality on surface ignition was investigated in the CFR

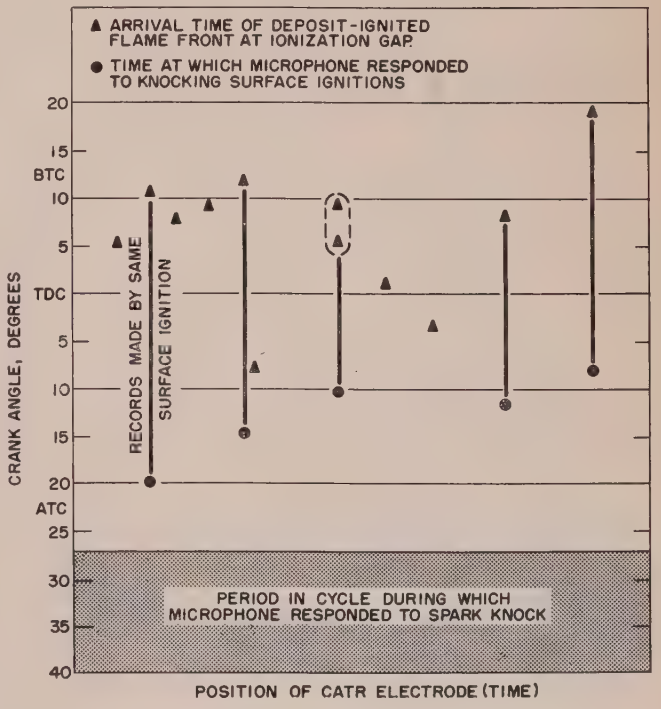

Fig. 6 – Period in engine cycle at which knocking surface ignitions originate for CFR L-head engine with deposits. Ignition timing: tdc. Fuel: 2-A. Oil: 1-A

L-head engine. The engine was equipped with both an audible and a total surface ignition counter. The latter instrument was connected to a CATR unit. This made possible recording of total and audible surface-ignition counts as well as providing a CATR paper record of time in the cycle at which deposit-ignited flame fronts reached the ionization gap.

Using the cycling procedure outlined in Table 1, the engine was run on a 90 Research-octane fuel until deposit equilibrium was reached. This fuel was a blend of primary reference fuels to which 3 ml tel and 30 ml of oil 1-A were added per gal of fuel. Unlike a full-boiling gasoline, volatile, paraffinic reference fuel blends do not produce a reasonable surface-ignition rate unless a small quantity of heavy material, such as lubricating oil, is added. A 2-hr paper record of surface ignitions that occurred was made with the CATR after deposit equilibrium was reached. Both total and audible surface-ignition counts were recorded. Fuel was then switched to a different octane number reference fuel blend containing the same amounts of tel and oil. The same records were made with this new fuel and the engine then changed back to the original fuel and run until an equilibrium deposit-ignition condition was reestablished. This procedure was repeated until fuels from 86-98 Research-octane number had been investigated. Each new fuel blend contained the same amounts of tel and oil.

Audible and total surface-ignition counts obtained with various blends are shown in Fig. 7. Although only one set of data is shown for each test fuel, the results were verified in two additional observations on each fuel blend. Knock-limited spark advance for most blends is included in the figure. These latter data were obtained by advancing the spark with each fuel blend until a steady trace-knock condition existed. Audible and total surface-ignition counts were not influenced by variations in fuel quality above 91 octane. However, both total and audible surface-ignition rates were influenced to a high degree by fuel antiknock quality below 91 octane. In this region antiknock quality of fuel blends was approaching that just sufficient for knock-free operation at tdc timing at which the engine was operated. Thus, as knock-limited spark advance obtained on fuel blends came closer to tdc, the number of total and audible surface ignitions increased very rapidly. It is possible that an incipient-knock condition may have existed in the engine during some cycles without audible manifestations when the engine was cycled at tdc ignition timing on fuels below 91 octane. This could be expected as a result of cycle-to-cycle variation in flame movement that existed in the combustion chamber. (See section of this paper entitled, "Studies of Normal Flame Movement.") An incipient-knock condition in one cycle may lead to hotter deposit surfaces which might set off deposit-ignited flame fronts in the following cycle. Such knock-induced surface ignitions would be expected to occur in bursts, each succeeding surface ignition being caused by heating or dislodging of deposits as a result of knock that occurred in the previous cycle. CATR paper records showed that this tendency for surface ignitions to occur in bursts actually happened more often in runs in which fuel was below 91 octane.

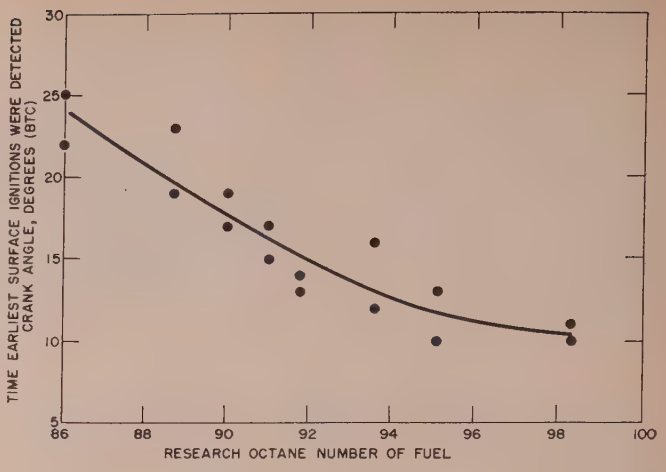

Fig. 8 – Effect of fuel quality on time earliest surface ignitions were detected for CFR L-head engine with deposits. Fuels: various blends of primary reference fuels + 3 ml tel + 30 ml of oil 1-A per gal. Oil: 1-A. Two-hour periods of operation at tdc ignition timing

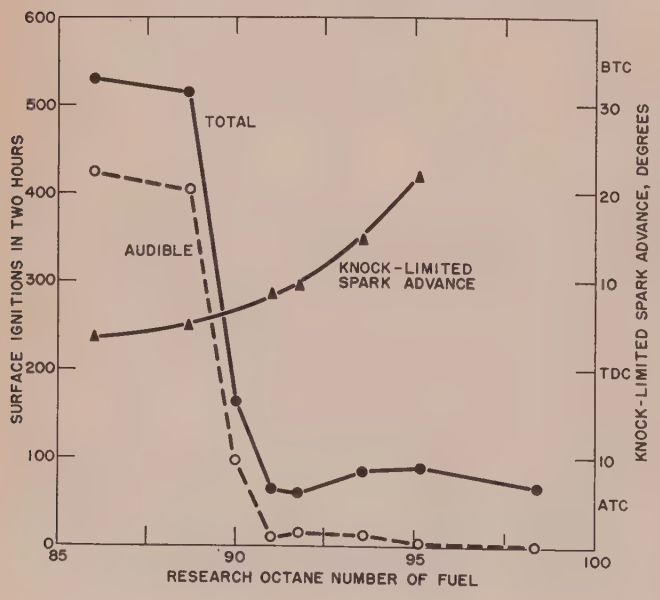

Fig. 7 – Effect of fuel quality on surface ignition for CFR L-head engine with deposits. Fuels: various blends of primary reference fuels + 3 ml tel + 30 ml of oil 1-A per gal. Oil: 1-A. Two-hour periods of operation at tdc ignition timing

[7] "Detection of Abnormal Flame Fronts in Road Tests with Engine Using Independent Ionization Gaps," by J. R. Landis. Paper presented at SAE Summer Meeting, Atlantic City, June 10, 1954.

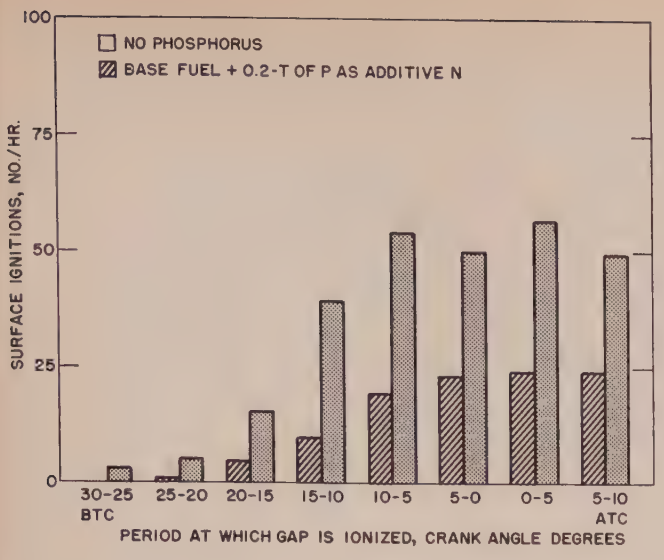

Fig. 9 – Effect of phosphorus additive on surface ignition for CFR L-head engine run to deposit equilibrium in individual tests on each of two fuels. Ignition timing: tdc. Compression ratio: 8.5/1. Base fuel: fuel 2-D with 3 ml tel per gal. Oil: 1-A

These results agree with road data[7] which showed that number of scattered or isolated surface ignitions was independent of fuel octane number, while sustained or continuous surface ignitions were affected by fuel antiknock quality.

An examination of CATR paper records of surface ignitions for each fuel blend indicated that fuel octane number had an effect on time in the cycle at which earliest surface ignitions occurred. Fig. 8 shows such data plotted against Research-octane number of the various fuel blends. These results suggest that increasing fuel octane number increased resistance of the fuel to being ignited by hot deposits, since earliest surface ignitions occurred nearer tdc, or later in the cycle, as fuel octane number was increased. This increased resistance to ignition may also have had some influence on the decrease in total and audible surface ignitions that occurred as fuel octane number was increased. However, the degree of change in crank angle at which earliest surface ignitions occurred does not appear to correlate directly with observed changes in total and audible surface-ignition rates. Further discussion of surface-ignition resistance of fuels is included in a later section of this paper.

C. Fuel additive effects: The CATR has been used to obtain information on effectiveness of fuel additives in controlling surface ignition. This equipment makes it possible to determine the relative degree of effectiveness of additives at different periods in the engine cycle. An example of this type of work is presented in Fig. 9, which shows distribution of surface ignitions with regard to crank-angle position of the piston for a test with leaded full-boiling gasoline 2-D, and a test with the same fuel containing 0.2 theories of phosphorus as additive N. Oil 1-A was used as crankcase lubricant for both tests run in a CFR L-head engine using cycling procedure outlined in Table 1, except that engine compression ratio was increased to 8.5/1.

Fig. 9 shows that phosphorus additive reduced surface-ignition rate during all portions of the cycle investigated, particularly earliest surface ignitions – those most prone to result in knock.

D. *The Surface-Ignition Resistance of Fuels* – Surface-ignition characteristics of fuels depend upon two distinctly different phenomena. First, fuels may form deposits which have widely different tendencies to undergo glowing oxidation, and second, these same fuels may exhibit various degrees of resistance to ignition by glowing deposits. Fuel-air ratio has been observed to influence both these factors. It was shown in an earlier paper[3] that deposits formed during prolonged rich-mixture operation using the cycling procedure outlined in Table 1 were more prone to cause surface ignition than those accumulated under prolonged lean-mixture conditions. It was also reported that short-term operation at an enriched fuel-air ratio reduced audible or knocking surface ignitions from a given set of deposits. This latter work has been repeated in a CFR L-head engine equipped with a CATR used in conjunction with a TS-IC.

The engine was run with premium-grade automotive-type fuel 2-A and non-additive high-V.I. oil 1-A to an equilibrium deposit condition using the same cycling procedure with a fuel-air ratio of 0.077. Full-throttle fuel-air ratio was varied for two-hour periods and records were made with the CATR of surface ignitions which occurred. These records showed that surface-ignition rate changed

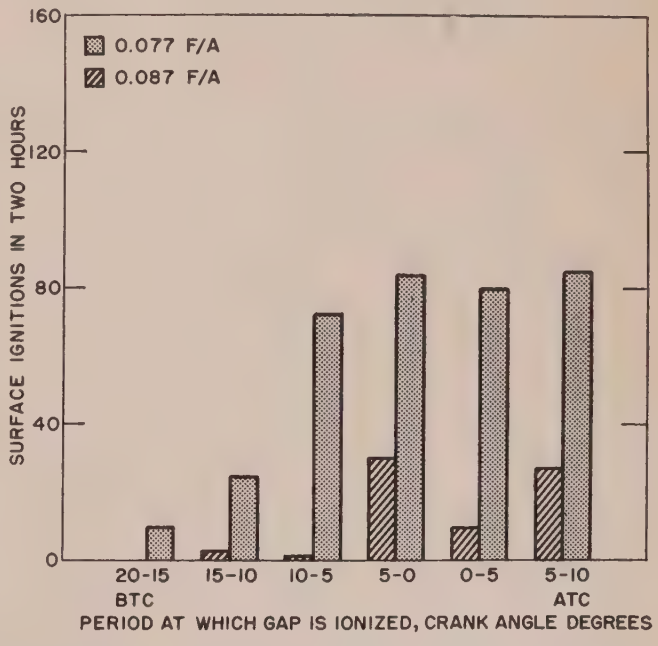

Fig. 10 – Distribution of surface ignitions at two fuel-air ratios for CFR L-head engine containing deposits formed at 0.077 fuel-air ratio. Ignition timing: tdc. Fuel: 2-A. Oil: 1-A

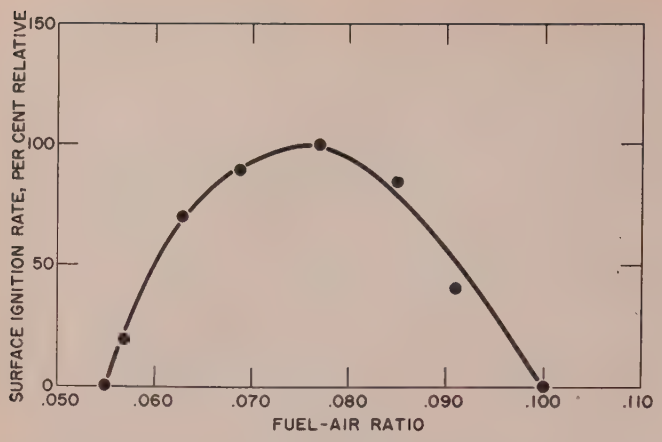

Fig. 11 – Effect of fuel-air ratio on surface-ignition rate for CFR L-head engine with deposits. Ignition timing: tdc. Fuel: 2-A. Oil: 1-A. Minimum of five 15-min wide-open throttle observations at each fuel-air ratio

at the same time that fuel-air ratio was varied. Fig. 10 shows distribution of surface ignitions for two different fuel-air ratios and indicates that enriching the mixture from a ratio near that resulting in maximum power decreased surface-ignition rate and also caused earliest surface ignitions to occur later in the cycle. Surface-ignition rate may have been reduced as the mixture was enriched because either the rich mixture was more resistant to hot-deposit ignition or deposits were cooler at the rich-mixture condition. (A combination of these two factors may have been involved.) However, deposits formed under prolonged rich-mixture conditions were found more prone to cause surface ignition than those accumulated under prolonged lean-mixture conditions. The deposit-cooling effect of the rich mixture would

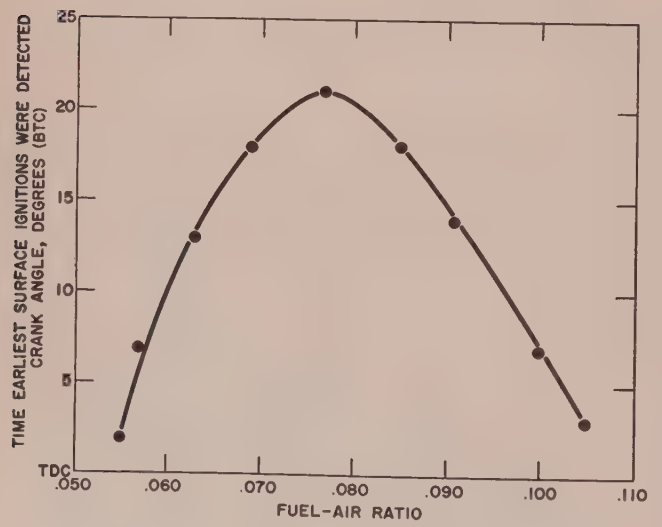

Fig. 12 – Effect of fuel-air ratio on time earliest surface ignitions were detected for CFR L-head engine with deposits. Ignition timing: tdc. Fuel: 2-A. Oil: 1-A. Minimum of five 15-min wide-open throttle observations at each fuel-air ratio

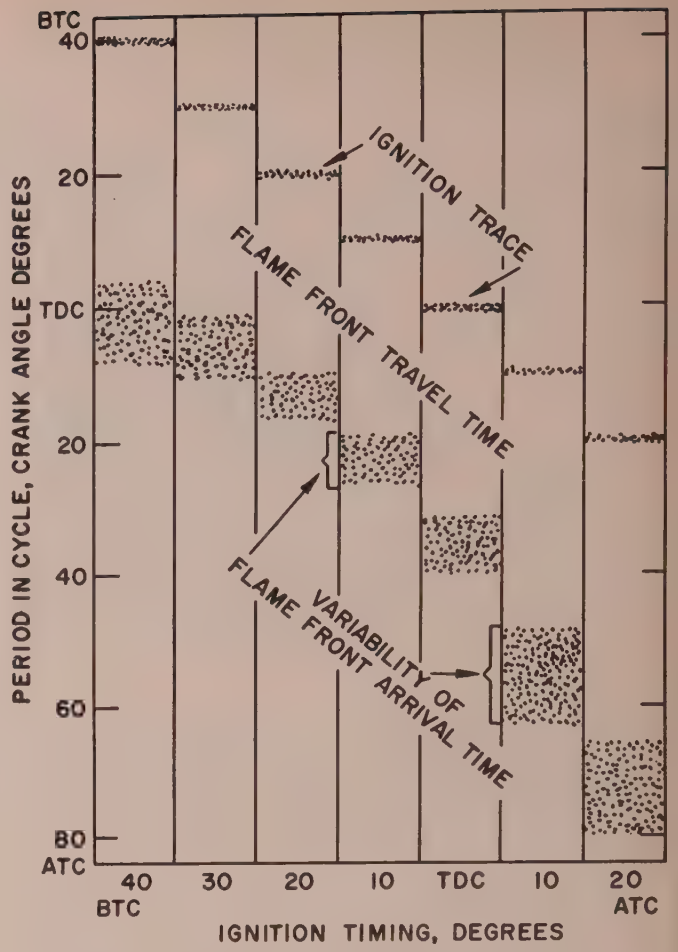

Fig. 13 – CATR record of effect of ignition timing on arrival time of normal flame fronts at ionization gap for single-cylinder code Q engine with deposits. Compression ratio: 9.5/1. Speed: 1200 rpm. Wide-open throttle. Fuel-air ratio: 0.077. Fuel: Isooctane + 3 ml tel per gal

be expected to be the same for both short and long-term operation at such a mixture. Although these data are not conclusive proof, it would appear that reduction in surface ignition shown in Fig. 10 was due largely to increased resistance of the fuel to ignition by hot deposits as the mixture was enriched.

Results of a more complete investigation of the effect of fuel-air ratio on surface-ignition resistance of fuel 2-A are included in Figs. 11 and 12. These data were obtained in a manner similar to that used for the data in Fig. 10 except that a shorter period of operation was used at each fuel-air ratio. Also, each point represented in the figures is the average of a minimum of five observations. Although variations existed in results obtained in different observations for a given fuel-air ratio, the results are believed to be representative, at the given conditions, of effects of changes in fuel-air ratio on the surface-ignition resistance of fuel 2-A. Number of surface ignitions was reduced at both very lean and very rich fuel-air ratios. Also, earliest surface ignitions occurred much later in

the cycle for those same lean and rich ratios. These two facts indicate that after deposit equilibrium, operation for short periods at fuel-air ratios richer or leaner than about 0.077 probably caused considerable increase in resistance of the given fuel to being ignited by hot deposits.

Effect of fuel-air ratio on surface-ignition resistance of a number of pure hydrocarbons and full-boiling fuels has been investigated using the above procedure. Results in all cases have shown the same trends as indicated for fuel 2-A in Figs. 11 and 12. However, degree of resistance to ignition by hot deposits has been found to be different for various fuels, isooctane having a very high resistance, benzene a much lower resistance, and full-boiling fuels falling between these two pure hydrocarbons.

Studies of Normal Flame Movement – A. Effect of ignition timing: In addition to showing the point in the engine cycle when abnormal flame fronts caused by surface ignition reached the ionization gap, the CATR may also be used to record time of arrival at the ionization gap of flame fronts from normal combustion. Fig. 13 is a copy of such a record, taken with a CATR connected to a single-cylinder engine equipped with a 9.5/1 compression ratio combustion chamber similar to that of a modern high-compression V-8 code Q engine (hereinafter referred to as the single-cylinder code Q engine). Leaded isooctane was used in this investigation. Both an ignition trace and normal flame front data, not taken simultaneously, are shown for a number of engine cycles at each of several ignition timings. Arrival of each normal flame front at the ionization gap, located in the end-gas region of the combustion chamber 2⅞ in. from the spark plug, is shown by a single dot in Fig. 13. Considerable variability of normal flame front arrival time, and hence flame front travel time, is observed at a given ignition timing. Both flame front travel time and its variability are influenced by ignition timing. The magnitudes of these two effects are shown in Fig. 14. Minimum flame front travel time at minimum variation in flame front travel time for a given ignition timing occur at a timing close to that required for maximum power. The flame front travel time includes both time required to start the flame after the spark occurs and that required for the flame front to move from spark plug to ionization gap. The relative degree to which each of these two factors is influenced by operating conditions is not known at this time.

Data similar to that shown in Figs. 13 and 14 have been obtained from a single cylinder of a 1953 V-8 code M engine connected to a dynamometer. Test results, with a full-boiling gasoline were of similar nature as those shown in Fig. 14, although the degree of variability appeared to be slightly greater.

B. Effect of fuel-air ratio – Results of an investigation of effect of fuel-air ratio on travel time of

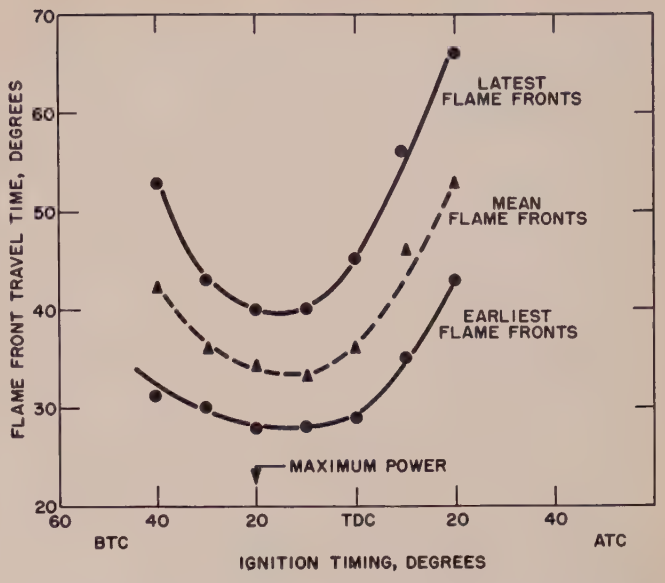

Fig. 14 – Effect of ignition timing on travel time of normal flame fronts for single-cylinder code Q engine. Compression ratio: 9.5/1. Speed: 1200 rpm. Wide-open throttle. Fuel-air ratio: 0.077. Fuel: isooctane + 6 ml tel per gal. Oil: 1-A

normal combustion flame fronts from spark plug to ionization gap are shown in Fig. 15. These data were obtained on the same single-cylinder code Q engine operated at maximum-power ignition timing with leaded isooctane and with fuel-air ratio varied over a wide range. Fuel-air ratio is observed to have a considerable influence on cycle-to-cycle variability of normal flame front travel time. At lean and rich fuel-air ratios, the line representing

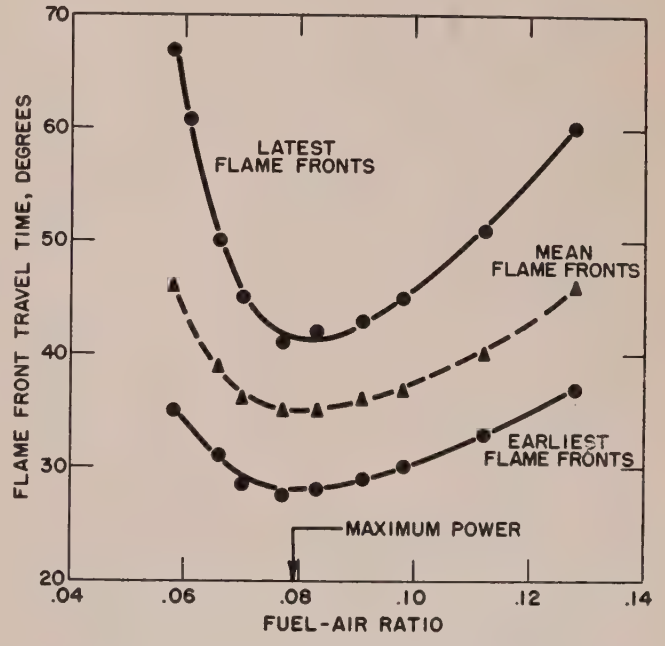

Fig. 15 – Effect of fuel-air ratio on travel time of normal flame fronts for single-cylinder code Q engine. Compression ratio: 9.5/1. Speed: 1200 rpm. Wide-open throttle. Ignition timing: 20 deg btdc. Fuel: isooctane + 6 ml tel per gal

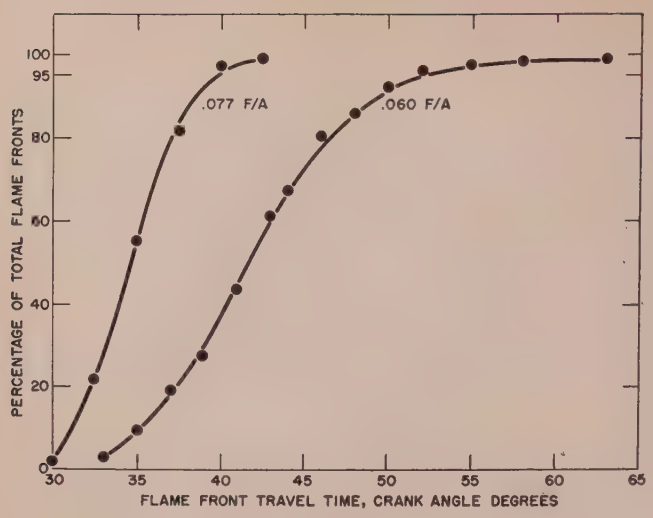

Fig. 16 – Cumulative frequency distribution of travel time of normal flame fronts for single-cylinder code Q engine. Compression ratio: 9.5/1. Speed: 1200 rpm. Wide-open throttle. Ignition timing: 20 deg btdc. Fuel: isooctane + 6 ml tel per gal

travel time of mean normal flame fronts in Fig. 15 follows the pattern of earliest flame fronts more nearly than that of latest flame fronts. This indicates that at these mixture conditions, the last 50% of flame fronts to arrive at the ionization gap had a greater cycle-to-cycle variability than the first 50%. This is shown in another manner in Fig. 16. This figure shows the cumulative frequency distribution of cycle-to-cycle normal flame front travel time for a fuel-air ratio of 0.060, close to the lean limit of combustion, and for a ratio of 0.077, close to that necessary for maximum power. Pressure-time cards and flame front travel time records taken simultaneously at the lean ratio indicated an inverse relationship between power and normal flame front travel time.

Cycle-to-cycle variation of such factors as charge density, fuel-air ratio, degree of turbulence, degree of fuel vaporization prior to ignition, and shape of flame front may have contributed to the observed variability of travel time of normal flame fronts at a given set of conditions. With leaded isooctane, neither varying speed of the single-cylinder code Q engine from 900 to 1800 rpm nor heating the mixture appeared to influence the variability. However, throttling caused considerable increase in the variability factor and in travel time of earliest flame fronts, possibly as the result of increased clearance-gas dilution of the inducted charge. Degree of variability was reduced considerably, especially at lean and rich fuel-air ratios, when a cylindrical manifold of about 50 cu in. capacity was inserted between carburetor and intake port of the same code Q engine after the compression ratio was changed to 11.5/1. This effect is shown in Fig. 17 for a lean fuel-air ratio of 0.061 and for one of 0.077, near the maximum-power ratio. Note also the effect of a special full-boiling type fuel made up of a mixture of pure hydrocarbons. This fuel resulted in further reduction of the variability factor at the lean fuel-air ratio but had little influence at the richer ratio. Arrival time of earliest flame fronts was not affected appreciably by fuel type or induction system manifolding. Cyclopentane, a pure hydrocarbon considerably more volatile than isooctane, gave essentially the same results as isooctane when run with the conventional induction system.

Such factors as engine throttling, changes in manifolding, and variations in ignition timing and fuel-air ratio were found to have considerable influence on variability of travel time of normal flame fronts. Full-boiling fuels also appear to have less variability than pure hydrocarbons tested. These effects have been observed in both the single-cylinder code Q engine and the CFR L-head engine.

Since from among a group of pure hydrocarbons benzene had shown the least resistance to being ignited by hot deposits, it was of interest to determine the influence of fuel-air ratio on flame travel time for this hydrocarbon. Results of an investigation in the 11.5/1 compression ratio single-cylinder code Q engine are shown in Fig. 18. The engine had been run for a short time on leaded isooctane prior to operation with benzene. Although antiknock quality of benzene was believed more than sufficient for knock-free engine operation, the engine went into violent autoignition for fuel-air ratios between about 0.075 and 0.105. Inspection of the CATR paper record showed the existence of surface ignitions for this range of fuel-air ratio. This is indicated in Fig. 18 by the zone marked "surface-ignition-limited zone." Engine operation on leaded

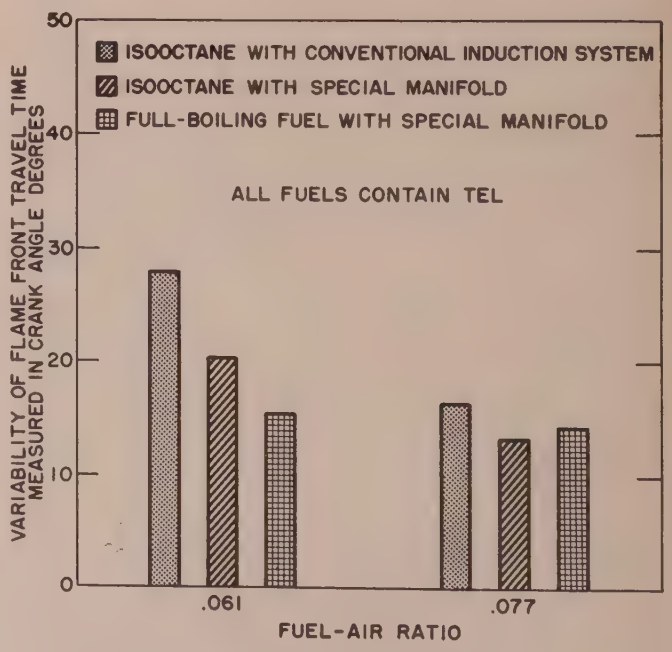

Fig. 17 – Influence of engine and fuel factors on variability of flame front travel time for single-cylinder code Q engine. Compression ratio: 11.5/1. Speed: 1200 rpm. Wide-open throttle. Ignition timing: 16 deg btdc

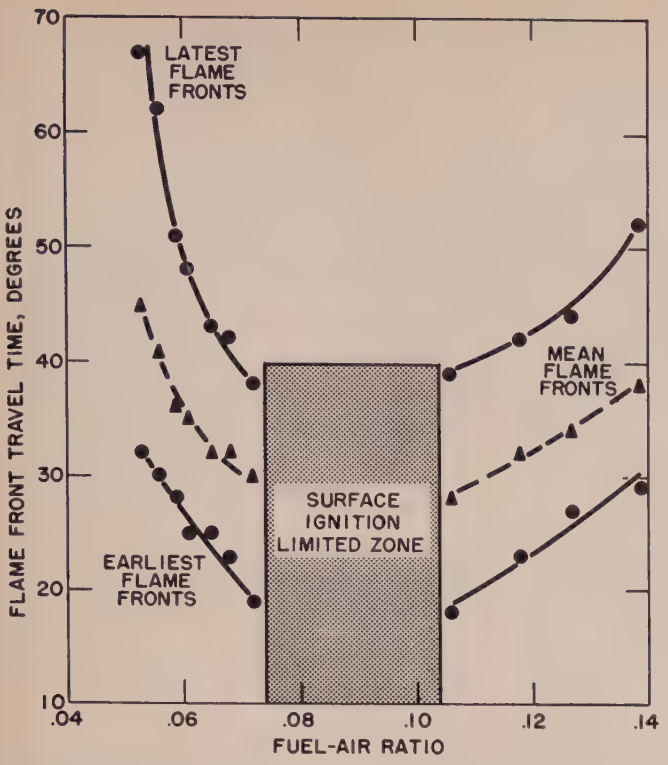

Fig. 18 – Effect of fuel-air ratio on travel time of normal flame fronts for single-cylinder code Q engine. Compression ratio: 11.5/1. Speed: 1200 rpm. Wide-open throttle. Ignition timing: 16 deg btdc. Fuel: benzene

isooctane did not result in a similar surface-ignition-limited zone. A colder spark plug had no influence on the results obtained with benzene. These results are additional evidence that benzene is less resistant to surface ignition than isooctane.

Power Loss from Surface Ignition – Surface ignition is so erratic that it is impossible to predict which engine cycles will produce it. Hence, the problem of measuring influence of surface ignition on engine power output, either in a car on the road or when connected to a dynamometer, is most difficult. However, the CATR makes it possible to obtain an indirect evaluation of the influence of surface ignition on power.

In order to make this evaluation use was made of the relation between time of arrival of flame fronts from normal combustion at an ionization gap in the combustion chamber and power output, as the ignition timing was varied. Such data are shown in Fig. 19 for a 7.5/1 compression ratio single-cylinder code Q engine. These data may be used to determine relative power output of a given engine cycle if time of arrival of flame fronts at the ionization gap is known, provided the origin of flame fronts was in the vicinity of the firing spark plug. Paper records made with a CATR have shown that about 10% of deposit-ignited flame fronts arrived at the ionization gap between 10 deg btdc and tdc. If these flame fronts originated from hot deposits located near the spark plug, data in Fig. 19 indicate that for these cases loss of power of individual cycles, based upon optimum spark-setting performance, would range between 8 and 29%. Some deposit-ignited flame fronts arrived at the ionization gap as early as 20 deg btdc. For these cases loss of power, on the same basis as before, would be significant. With the basic timing of the engine retarded to tdc, some surface ignitions were recorded, which, when analyzed using data contained in Fig. 19, resulted in an increase in power compared to that developed by normal combustion at this retarded timing. These surface ignitions caused flame fronts to arrive at the ionization gap earlier than those which were spark ignited. Hence, the effect was similar to advancing ignition timing. Evaluations of loss of power caused by surface ignition, determined by means of data in Fig. 19, agree well with those reported by other investigators using a simulated surface-ignition source.[8]

Occurrence of end-gas knock as a result of early ignition by hot deposits, if octane quality of fuel is too low, is a factor that might cause power loss from such surface ignitions to be greater than that indicated in Fig. 19 for a given flame front arrival time.

Although power loss resulting from deposit ignition in a single engine cycle may not be significantly high, the persistence of such surface ignition

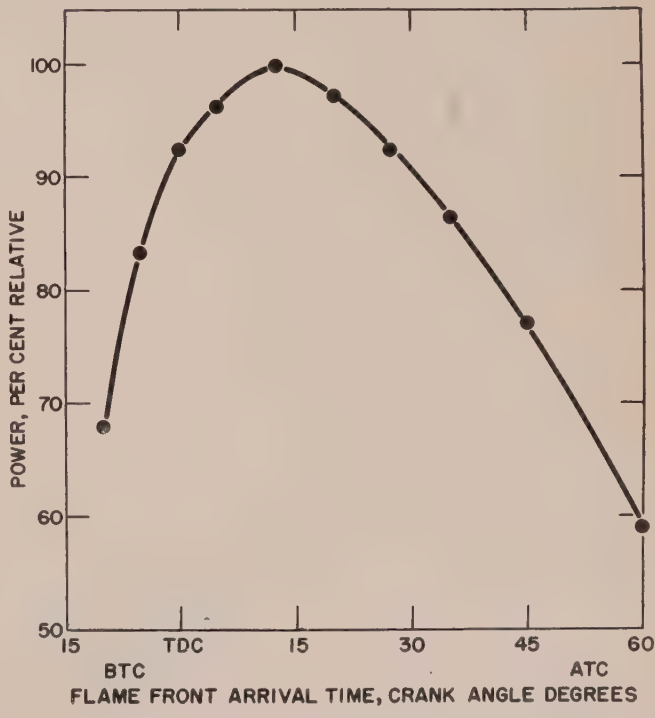

Fig. 19 – Relation between power and arrival time of spark-ignited flame fronts at the ionization gap for single-cylinder code Q engine without deposits. Compression ratio: 7.5/1. Speed: 1200 rpm. Wide-open throttle. Fuel-air ratio: 0.077. Fuel: leaded isooctane. Oil: 1-A

[8] "Effect of Simulated Surface Ignition on Engine Performance," by L. B. Shore and J. F. Kunc, Jr. Paper presented at SAE Summer Meeting, Atlantic City, June 10, 1954.

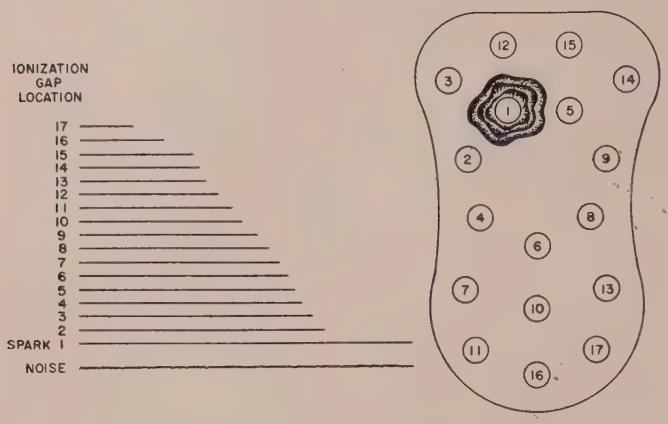

Fig. A – Normal combustion – L-head CFR engine

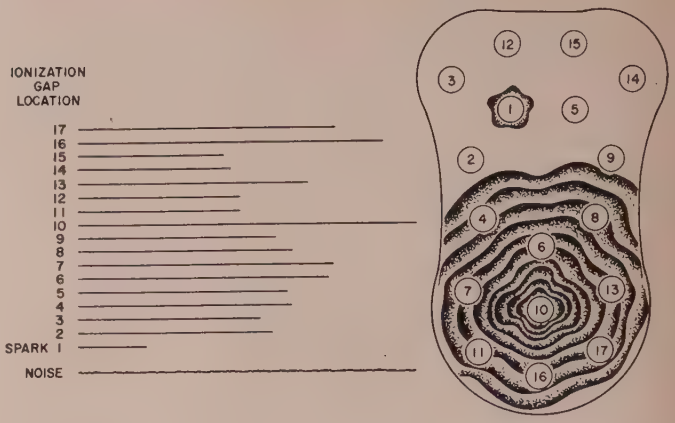

Fig. D – Very advanced preignition – no noise – L-head CFR engine

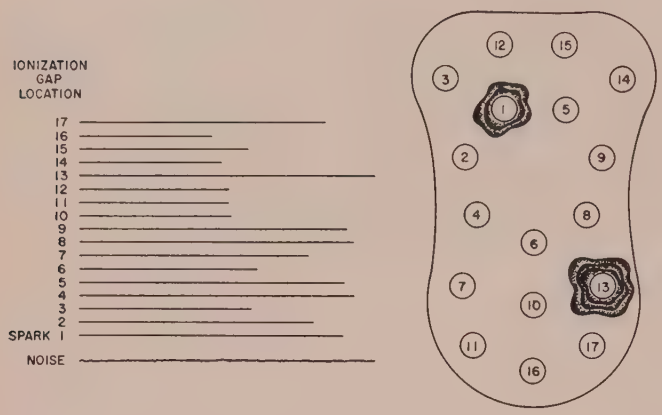

Fig. B – Slightly advanced preignition – no noise – L-head CFR engine

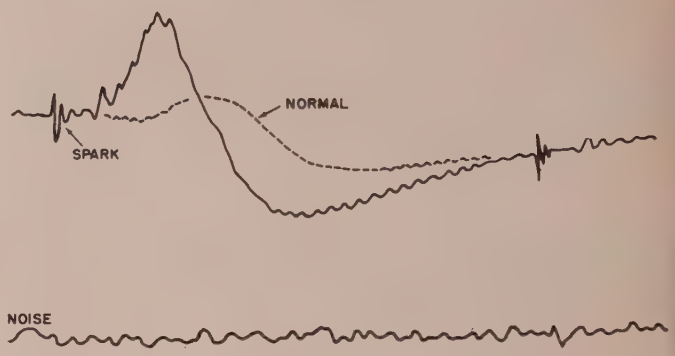

Fig. E – Slightly advanced preignition – no noise – multicylinder V-8 engine

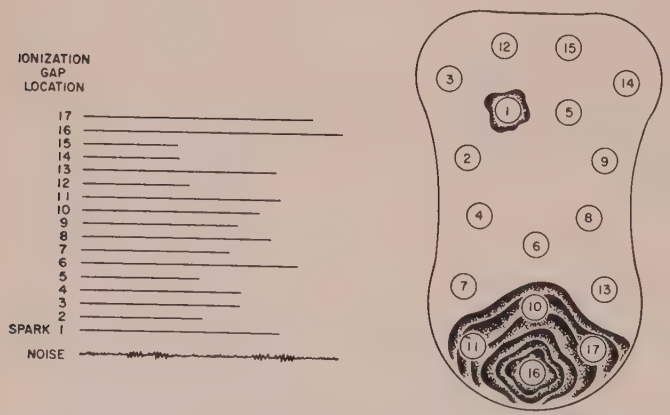

Fig. C – Moderately advanced preignition – heavy noise – L-head CFR engine

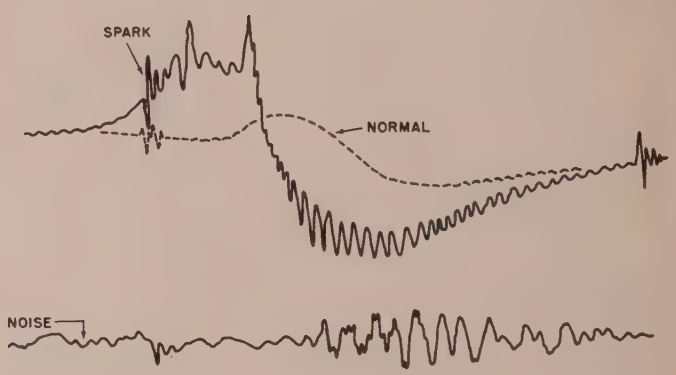

Fig. F – Moderately advanced preignition – heavy noise – multicylinder V-8 engine

in any cylinder can readily lead to destructive effects on engine parts such as piston top, valves, and spark plug.

Summary

A new research tool, the crank angle-time recorder, has been presented which makes possible conveniently obtaining a permanent record of time in the cycle at which various engine phenomena occur. Use of the crank angle time recorder in studies of normal and abnormal combustion has provided information of interest to both engine designer and petroleum refiner.

Application of the instrument has included studies to determine those deposit-ignited flame fronts which resulted in knock, effect of fuel anti-knock quality and additives on surface ignition, surface-ignition resistance of fuels, and studies of effect of a number of factors on normal flame movement.

DISCUSSION

Describes Other Methods For Studying Engine Combustion

– M. W. Corzilius

E. I. du Pont de Nemours & Co.

I WOULD like to describe briefly two methods which have been found particularly useful at our laboratory for studying combustion phenomena and to compare the results obtained by these methods with those described by the authors.

The first of these methods shows not only the crank angle when surface or spark ignition occurs, but also the ignition location in the combustion chamber and the path of the flame as it travels across the combustion chamber. Sixteen ionization gaps as well as the firing spark plug were located in the head of an L-head, CFR engine. Each of the ionization gaps and the firing spark plug were connected through suitable electronic circuits to neon bulbs which were illuminated when a flame passed the gaps. The time sequence of illumination of the neon bulbs was recorded by means of high-speed streak photography, while engine noise was sensed by a microphone and displayed on an oscilloscope which was photographed at the same time.

Fig. A shows a typical record for normal combustion. On the right is a plan view of the engine head showing the location of the 17 plugs. The No. 1 plug is the firing spark plug. On the left are the streak records of the neon bulbs. Advancing time is from right to left. The oscillographic record of noise accompanying the combustion is shown underneath the streak records. In the case of normal combustion the streak records clearly show that the flame was initiated by the firing spark plug and passed smoothly across the combustion chamber. The noise trace is representative of normal combustion.

Fig. B shows the case of surface ignition which occurred only slightly before spark. Again the ionization gap locations are shown along with the streak and noise records. A second flame front has appeared at gap No. 13. A glance at the streak records shows that this flame was initiated slightly before spark and, therefore, is the result of preignition. Since the noise trace is similar to that recorded during normal combustion, this was a "silent" preignition. This is in agreement with the authors' results. They reported that late surface ignitions were generally inaudible.

We are also in agreement that early surface ignitions frequently result in knock. Fig. C shows an example of this. Here we see preignition originating in the vicinity of gap No. 16, an appreciable time before spark. Note that this preignition is followed by heavy knock, shown on the noise trace.

Early surface ignition does not necessarily result in knock, however, though it may be extremely harmful to the engine. For example, Fig. D shows very advanced preignition but no noise. In this case the preignition occurred in the vicinity of gap No. 10. The streak records show that the flame traversed most of the combustion chamber before spark. Since no knock occurred, this very early preignition apparently is equivalent to advancing the spark beyond the maximum octane requirement with the spark-plug location changed to the opposite end of the combustion chamber.

To confirm the single-cylinder data, rate of pressure change pickups, commonly known as *dp/dt* pickups, were installed in each cylinder of a 9/1 compression ratio, multicylinder, V-8 engine. Using the *dp/dt* pickups it was possible to detect quite accurately the occurrence of preigni-

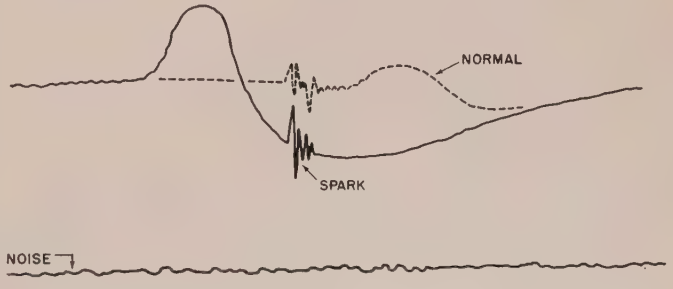

Fig. G – Very advanced preignition – no noise – multicylinder – V-8 engine

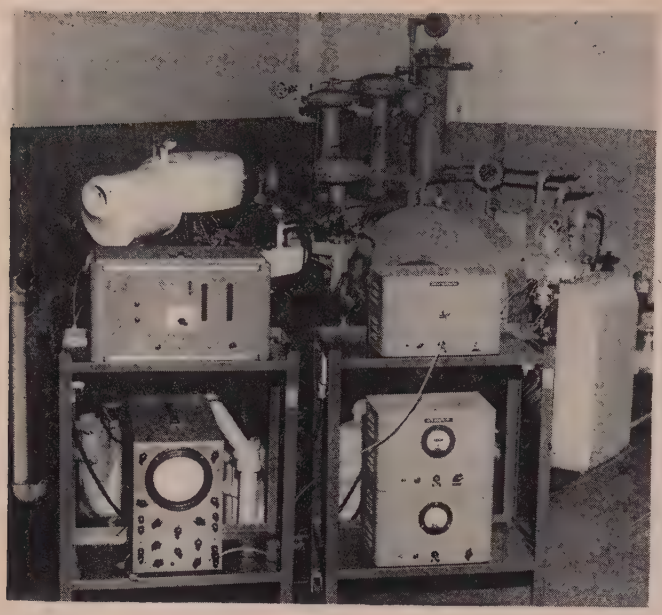

Fig. H – Electronic surface ignition detector

tion, postignition, knock, or other abnormal combustion phenomena. By photographing simultaneously several oscilloscope screens showing the dp/dt signal from each of the engine cylinders, together with the noise signal from a sensitive microphone placed near the engine, the abnormal noises produced by the engine were correlated with the combustion patterns.

Fig. E shows the dp/dt pattern and noise signal for the case of slightly advanced preignition. In this figure, and in Figs. F and G, the normal combustion pattern is superimposed on the diagram as a dotted line, while the preignition pattern is shown as a solid line. The noise pattern is shown as the bottom trace in each figure. For the engine cycle shown in Fig. E, preignition occurred just ahead of spark and caused the pressure to peak slightly before it normally would have. The preignition advance in this case was 7 crank angle deg ahead of spark. No indication of knock is observed on either the dp/dt or the noise trace.

Going now to a moderately advanced preignition, Fig. F shows preignition which occurred some 24 crank angle deg before spark. Again the characteristic rapid pressure rise is evident but now pressure fluctuations resulting from knock are observed on the downward sweep of the dp/dt trace, while the microphone signal furnishes additional evidence that knock occurred.

With very advanced preignition, as shown in Fig. G, the

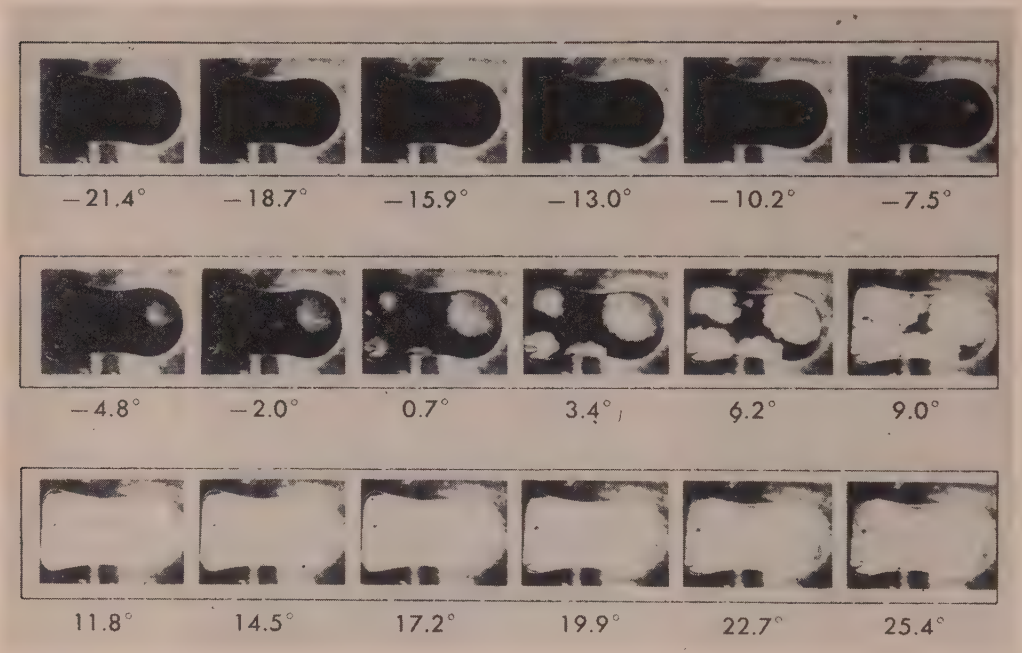

Fig. I – Engine explosion in which both preignition and postignition occurred

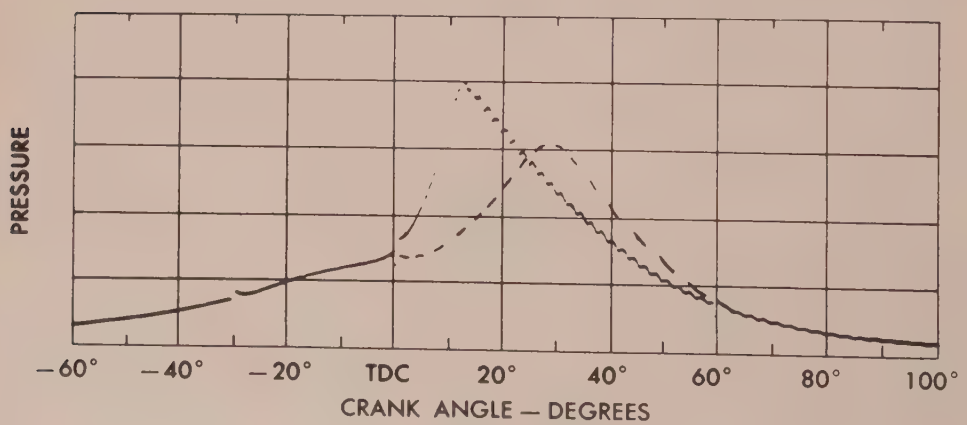

evidence of knock is again absent, just as it was for the single-cylinder engine. In this case, preignition occurred about 40 crank angle deg before spark.

The two methods just described are not applicable to all types of engines because of space limitations. On the other hand, the ionization gap technique, such as described by the authors, can be used with practically any engine. All that is required in addition to the ionization gaps is a device for gating-out the signal from the normal flame and an instrument for registration of the preignition signal. These functions can be performed mechanically, as the authors have done, or they can be performed electronically by means of an electronic gate circuit and an electronic counter such as pictured in Fig. H. Shown are the electronic gate units, the oscilloscope for monitoring the signals, an electronic counter for recording the preignition count, and a sweep generator for synchronizing the trace with changing engine speed. The gate unit is nothing more than an electronic breaker point, which prevents the signals from the normal flame from being counted. Both the time at which the gate prevents further signals from recording and the length of time during which surface ignitions are recorded are variable by means of potentiometers located on the front panel. These adjustments make it possible to adjust the unit for different engine designs, different flame travel distances, and so forth. The only connections required are a single shielded wire from the ionization gaps and a lead from the spark primary to trigger the electronic gate. Because it is triggered by the spark, the electronic gate can be used with any engine, regardless of the number of cylinders. In fact, these units are being used at the present time with both single and multicylinder engines.

Favors Use of Pressure-Time Cards

– F. W. Bowditch
Research Laboratories Division, GMC

I BELIEVE that in the main the separate ionization gap will show a suitable indication when a flame front passes through it. I can therefore agree that instrumentation such as the authors have shown does indeed mean a case of surface ignition has occurred where the ionization gap signal occurs earlier than the signal which is produced by a normal combustion process under similar engine conditions. However, since the time of ionization bears little relation to the **severity** of surface ignition, I do not believe that any further significance can be given to the time of ionization. The point is best explained by reference to Fig. I. Here we have one engine explosion in which both preignition and postignition have occurred. In the flame pictures, time increases from left to right and from top to bottom. The intake valve is at the upper left in each flame photograph, the exhaust valve and the extended spark plug leads in the lower left. The engine was running at 900 rpm with a primary reference fuel in the presence of leaded engine deposits and with a spark advance of 5 deg btc. The spark discharge can be seen in the first photograph of the second row in the lower left-hand corner. This frame was taken at 4.8 deg btc, as shown.

The first case of deposit-induced surface ignition occurred at 10 deg btc over the far edge of the piston – a case of preignition. Subsequent cases of postignition occurred around the periphery of the combustion chamber. Had an ionization gap been placed in the center of the chamber, as was the case with the authors' gap, it is doubtful if any early ionization signal would have been produced. Similarly, an explosion producing too early an ionization signal can be readily visualized.

Under the flame photographs, I have shown two pressure-time cards. The dashed curve is the average normal card obtained under these same engine conditions but with no surface ignition. Peak pressure occurs at about 30 deg atc. The other card is the pressure-time card for the engine explosion shown in the photographs. In this instance peak pressure occurs at about 12 deg atc, or 18 deg earlier than the normal case.

In our own studies of surface ignition, we have considered the ionization gap instrumentation but have rejected it for two reasons. First, because it does not show all cases of surface ignition. Secondly, because we feel that the **severity** of surface ignition is the criterion which should be used in measuring the surface ignition phenomenon and, since the ionization instrumentation does not furnish the requisite time base, it is therefore unsuitable.

We have adopted a pressure card technique and in doing so have used the fact that the pressure records, by their very nature, show the cumulative effects of any abnormal ignitions. We are, therefore, allowing the engine to tell us how adversely the combustion process is affected when surface ignition occurs. By noting the deviation of the time of peak pressure from the time of peak pressure under nonsurface-igniting conditions (18 deg in the case shown in Fig. I), we have then a measure of the severity of surface ignition.

Authors' Closure To Discussion

THE method described by Mr. Corzilius, in which neon bulbs were used in conjunction with multiple ionization gaps, is somewhat similar to the one that was used at Ethyl in the preliminary studies of the surface-ignition problem which finally resulted in the development of the total surface-ignition counter. Results of the early studies and of more recent work with the crank angle-time recorder, used in conjunction with multiple ionization gaps in the CFR L-head engine, indicate that deposit-ignited surface ignition originates predominately in the area above the piston, although occasional instances of deposit ignition have been detected in all parts of the combustion chamber. It has also been determined from these studies that a single ionization gap centrally located in the combustion chamber gives a reliable indication of the amount of deposit ignition which occurs over a period of engine operation and thereby provides a simple, convenient basis for comparing different oil-fuel-additive combinations.

Mr. Bowditch states that the time of ionization bears little relation to the severity of surface ignition. However, additional studies in the L-head engine and new studies in the Code Q engine confirm the statement in the paper that those surface-ignited flame fronts which arrive at the ionization gap earliest in the cycle are the ones most likely to result in knock. Furthermore, Mr. Corzilius has presented experimental data in his discussion which also indicate that early surface ignitions frequently result in knock.

While pressure-time cards are an invaluable aid in fundamental studies of combustion, their use to obtain data on all abnormal engine cycles in long-term studies of the surface-ignition problem is quite impractical. The simple, more convenient ionization-gap technique has made it possible to obtain continuous information during the 175,000 hr of testing that have been completed in single-cylinder engines as part of the studies of the surface-ignition problem.

Further evidence of the value of the ionization-gap technique has been the application of data, so obtained in single-cylinder engines, to predict successfully the relative performance of oil-fuel-additive combinations in modern engines operated in passenger-car road service.

DIESEL SMOKE

(Progress Report of the Smokemeter Group of the Diesel Fuels Division,

PRIOR to 1940, when the Full-Scale Procedure and Instrumentation Group of the CFR Committee's Automotive Diesel Fuels Division undertook the development of a smokemeter, there had been many versions of the lamp-and-photocell instrument in use by the Navy, various engine manufacturers, oil company research laboratories, and educational institutions. The design suggested by the Naval Engineering Experiment Station was executed in modified form by the Standard Oil Development Co. and tested cooperatively by the oil and engine laboratories participating in the CFR Committee project. This design was adopted in the form made commercially by the Photovolt Corp. of New York, and became known as the CRC Smokemeter (Fig. 1).

IN response to numerous complaints against the CRC (photoelectric) smokemeter, the CFR Diesel Fuels Division in 1952 set up a project (1) to consider the objections raised, and (2) to review other instruments for measuring smoke in diesel exhaust. Its objective was to recommend a more suitable type of instrument, which would overcome some operational objections to the CRC smokemeter.

Of the several makes of commercial instruments considered, one make has been tested cooperatively and found superior in several respects to the CRC smokemeter. An interim report on the CRC project is presented in which directions for its use and precautions to be observed in order to get optimum satisfaction from the continuous, filtering-type, tape-recording smokemeter are given.

Many of these instruments have been used by various organizations throughout the world. However, there has been wide dissatisfaction with this direct-reading, light-extinction (photoelectric) type of instrument. Dissatisfaction has been based on its erratic performance, caused by uneven sensitivity over the range of smoke density it is designed to measure, sensitivity to sampling line conditions, susceptibility to corrosion by diesel exhaust gas, and failure to correlate with the density of visible exhaust smoke.

It is hard to explain exactly why the direct-reading, light-extinction instrument should give such unsatisfactory results as a smokemeter, but the following observations may give some idea why the filtering type is preferable. First, the characteristic of the light-extinction meter is an exponential curve, as illustrated in Fig. 2. This means that at either end of the meter scale, a slight change in smoke density causes a disproportionate change in meter reading. Hence, instrument sensitivity is excessively high at one end of the scale and very low at the other end. The filtering-type instrument, on the other hand, at any given tape speed, has a straight-line characteristic of trace density versus

MEASUREMENT

Coordinating Fuel and Equipment Research Committee, CRC)

H. C. Hunter, Gulf Oil Corp.

This paper was presented at the SAE Golden Anniversary Diesel-Engine Meeting, St. Louis, Nov. 3, 1955.

smoke concentration. Second, according to Coolidge and Schulz (reference 17), it is theoretically impossible to measure true smoke-particle density with a light-extinction instrument.

Continuous Filtering Recording Smokemeter

Current investigations carried out by the Smokemeter Group of the Diesel Fuels Division, Coordinating Fuel and Equipment Research Committee have shown a continuous filtering-type tape-recording smokemeter to have certain points of superiority over the light-absorption-type, nonrecording meter now recommended by CRC.

In the continuous filtering-type tape-recording smokemeter, exhaust gas is sampled at a uniform rate through a moving tape of specially prepared filter paper, which is guided between orifices in the "head" of the instrument. Adjustment of sampling rate and selection of both tape speed and orifice size (area and shape) are possible, giving a wide range of sensitivity. This permits matching the instrument range to particular operating con-

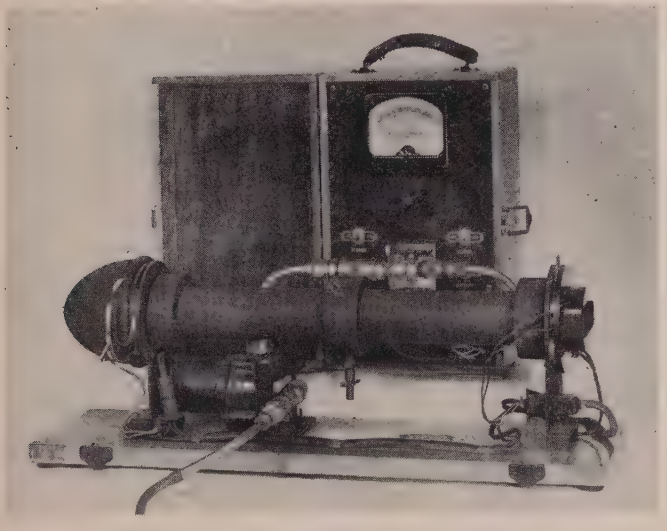

Fig. 1 – CRC Smokemeter (photoelectric)

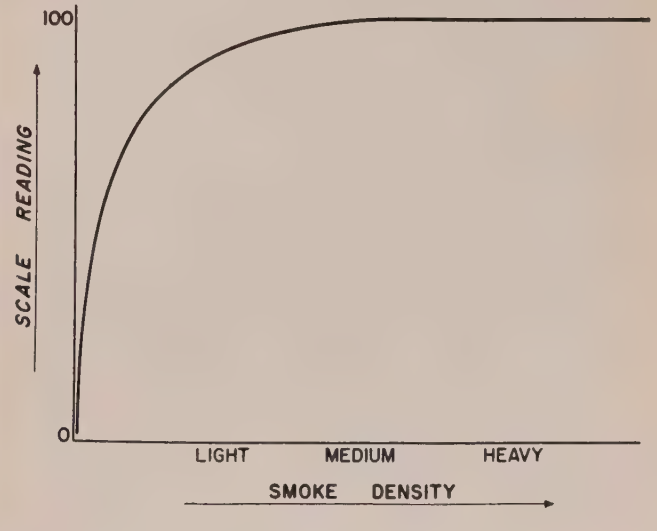

Fig. 2 – Characteristic of photocell smokemeter

ditions and facilitates calibration. Time interval marks are embossed on the tape as the test progresses. A fixed rate of flow through the tape is maintained by adjusting the vacuum on the suction side of the head. Tape advance and vacuum pump are operated by separate motors. The smoke record appears as a trace on the 1⅜-in. wide filter tape, lighter or darker, gray to black, depending upon concentration of smoke in the exhaust gas. A commercial instrument of this type is illustrated in Fig. 3. Fig. 4 shows a continuous filtering-type smokemeter.

In comparison with the CRC Smokemeter, which is a direct-reading, light-extinction instrument, the continuous filtering-type tape-recording meter has shown superiority in the following respects:

1. It is insensitive to sampling line conditions over wide limits.

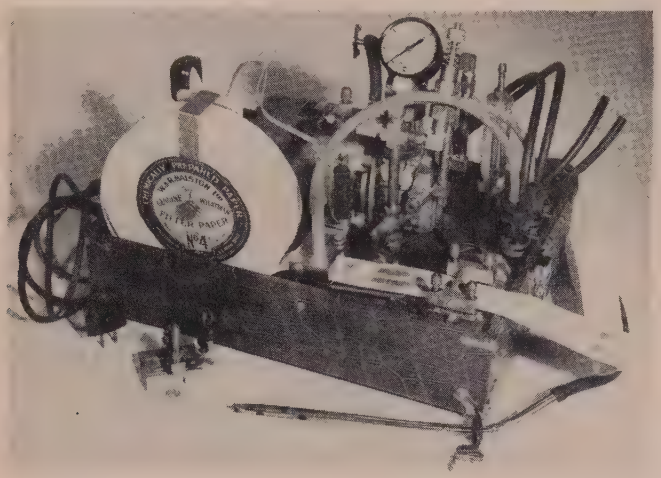

Fig. 3 – Von Brand filtering recorder (continuous gas sampler)

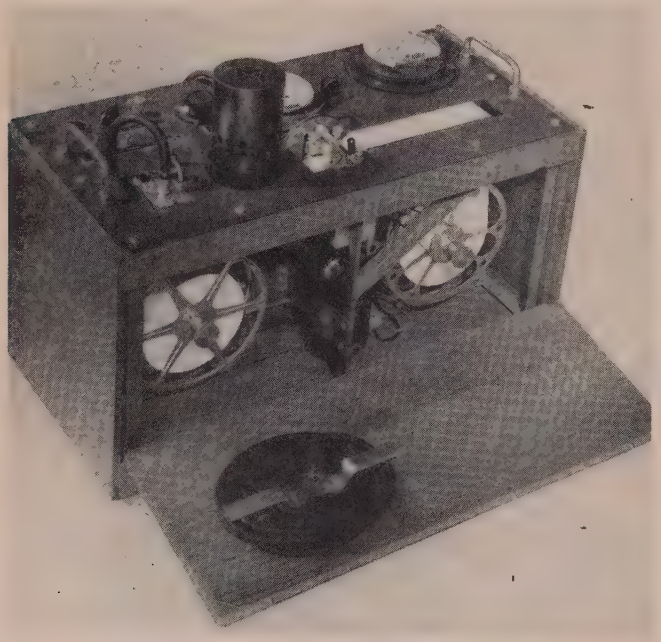

Fig. 4 – International Harvester Co. continuous filtering-type smokemeter

2. It has relatively little change in sensitivity at different ranges of smoke density. (By changing tape speed, sensitivity can be adjusted to smoke density range as required.)

3. A visual record of smoke density is automatically obtained.

4. Graphic comparison of recorded smoke density, and changes in smoke with operating conditions during a test period, can be made instantly while the test is in progress.

5. Correlation between recorded and visible smoke from diesel engine exhaust can be obtained under some conditions.

6. Stop-start operation may yield records of greater utility in studying transient conditions, as during acceleration of moving vehicles, than is possible with a photoelectric (nonrecording) meter.

7. Recording of smoke density can be continuous or intermittent, as desired.

8. It is not susceptible to undetected error resulting from failure to clean optical glass surfaces as often as necessary.

9. It does not suffer from corrosion of internal parts from exhaust gas condensate.

10. It is insensitive to small changes in line voltage and to vibration.

11. Recent experience in the application of the continuous filtering-type tape-recording instrument in tests on interurban buses has demonstrated its utility on moving vehicles and brought out the important feature that exhibition of the tape records has a more convincing effect than meter readings upon persons who have to interpret smoke readings.

Discussion of Operating Characteristics

Instructions for operation, adjustment, and maintenance are supplied with each instrument by the manufacturer. The following details of operating technique are offered for the guidance of users as a result of the Group's investigation to date, with the object of avoiding certain pitfalls into which an inexperienced operator could fall.

A. Sampling line: In the work done by members of the Smokemeter Group, location of sampling point was not found to be critical between 3 and 40 ft from engine exhaust ports. Under some conditions it is probably satisfactory to locate the sampling point closer to, or even farther from, the exhaust ports.

Length and diameter of sampling line are not critical, except that, for practical considerations, it should be no smaller than ¼-in. tubing to avoid plugging for an extended period of time. Three-

eighth-inch tubing makes a quite satisfactory sampling line. The sampling line should be as short as possible to reduce lag, but not so short as to allow hot gas to reach the instrument.

Traps for condensate do not remove smoke. Low spots in the line should be avoided, however, to prevent collection of water and soot in the line itself.

In general, it is better not to arrange the sampling tube probe with its open end facing the flow of gases in the exhaust pipe, but to use a closed-end tube with several small holes drilled through at right angles to its axis. This may be put lengthwise or crosswise into the exhaust pipe, as circumstances permit.

In sampling dust- or smoke-laden gas from a flowing stream, optimum conditions for obtaining a truly representative sample result when velocity in the sampling line is two or three times higher than velocity in the exhaust line.

B. Sensitivity: The continuous filtering-type tape-recording smokemeter is inherently quite sensitive. For example, at low tape speed, cigarette smoke in room air leaves a plainly visible brown trace. Sensitivity of this type of instrument is adjustable over an almost infinite range simply by varying the tape speed. When smoke to be measured is in the plainly visible, dense, or heavy range, a high tape speed is selected. Normal tape speed furnished is 4 in. per min. By changing the drive motor (and gearing if necessary), tape speeds of from less than one-half to 60 in. per min are available. Low tape speeds, one-half to 2 in. per min, produce plainly visible smoke traces from diesel exhaust which does not produce visible smoke from the end of the tailpipe.

For some purposes it is of advantage to obtain intermittent smoke records by stopping the tape for definite intervals and advancing it periodically. Stop-start or spot records may be obtained by advancing the tape manually, or by use of a cycle timer in the tape-drive motor circuit. Some users have modified their instruments by addition of a mechanical linkage or an interrupted-gear drive to produce stop-start records. This technique is helpful in reading records for rapidly changing conditions, since the whole area of each spot is of uniform density instead of changing continuously. This facilitates matching against a standard smoke-spot scale, or measuring with a photometer. Two-second cycle intervals have been found good for acceleration test runs on motor coaches. For extremely tenuous smoke samples, the dwell period in the stop-start cycle may be made very long, greatly increasing *effective sensitivity*.

When very heavy (dense) smoke is to be encountered, smokemeter sensitivity can be adapted to the condition by using high tape speed. It should be possible always to choose a tape speed such that the tape never has an appreciable thickness of soot piled up on its surface, thus avoiding the necessity of trying to distinguish between a dead black trace and one which is "heavier than dead black."

C. Effect of operating conditions: Compared to the CRC meter, the continuous filtering-type tape-recording smokemeter is relatively insensitive, within limits, to variations of pressure, flow, and so forth, both in the sampling system and in the instrument itself. Tests made in laboratories of Group members have demonstrated that there was little or no difference in smoke trace density when the sample was taken from different points in the exhaust pipe, or when tape suction (vacuum gage reading), was varied over a range of 3.0-6.0 in. of Hg. Variation of tape suction below 3.0 in. of Hg did affect smoke trace density. One laboratory has determined, for a single instrument, correction factors to be applied to photoelectric density readings when top-side tape pressure, bottom-side tape vacuum, or tape speed is varied from predetermined standard values.

It is self-evident that sampling system leaks and maladjustments such as loose or uneven fitting of recorder head on either side of the tape, marred surfaces of the recorder head working faces, improper flush fit of orifice inserts in the head, or loose drive roll tension, are to be avoided.

D. Accuracy and precision: The continuous filtering-type tape-recording smokemeter is not an absolute measuring instrument, in the sense that a certain density of the recorded trace always means a certain "smokiness" in the gas sampled (see section on Correlation). It is an "absolute" instrument, however, in that all particulate matter, or smoke, fed to it is filtered out and retained on the filter tape, provided the instrument is in proper condition and is correctly operated. Since density of the filter "trace" formed is a direct function of *volume* of smoke sample passed through a given area of paper, the meter will give valid indications only as long as *rate* of flow of gas passing through the filter strip is constant for a given rate of forward strip motion. This is obtained by assuring that tape suction (pressure drop across the tape), porosity of tape paper, tight fit of head surfaces against tape, and leakage in the whole system do not exceed permissible limits. Trials reported in the previous section show that allowable tolerances in sampling line length, location of sampling point, and tape suction are generous, and should be easily maintained. Different samples of tape tested were found to vary only slightly (not over 2%), in porosity and light transmission or reflectance.

Any doubt as to drawing equal volumes every time through a filtering-type smokemeter can be removed by using a one-shot (single-sample filtering-type) smokemeter,[1] but the Group favors the

[1] For example, the Bacharach true-spot smoke tester, or Bacharach smokemeter, model RXB; Bacharach Industrial Instrument Co., 7000 Bennett St., Pittsburgh 8, Pa.

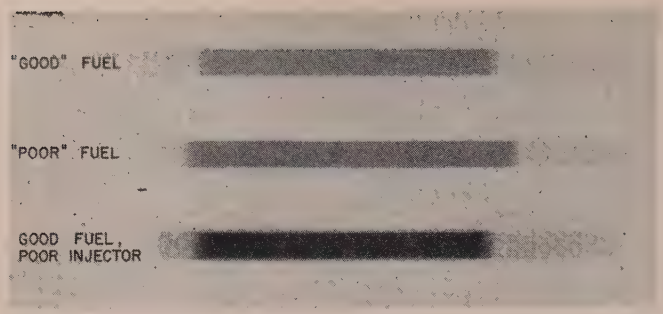

Fig. 5 – Representative smokemeter tapes – tests in interurban bus on dynamometer; 30 mph, full throttle, tape speed 6 in. per min

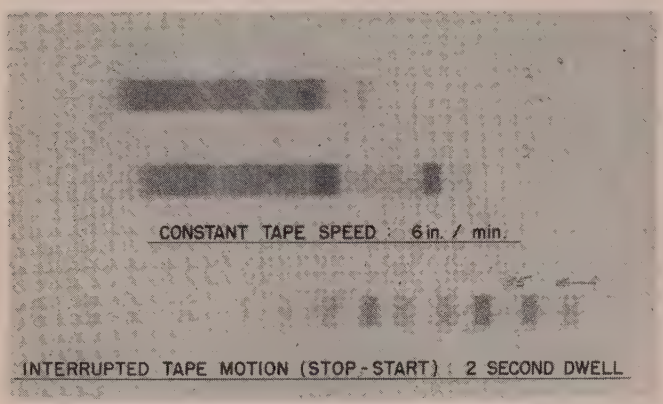

Fig. 6 – Representative smokemeter tapes from highway tests of interurban bus

continuous filtering-type meter because it is more rapid, continuous, and more versatile.

Precision, or repeatability, of readings obtainable with this type of smokemeter has not been established experimentally by the Group (its proof would require a source of smoke of unvarying density), but experience of users indicates it is of a satisfactory order. It would depend, of course, upon maintenance of the instrument and its auxiliary apparatus.

Accurate rendition of exhaust smoke density on the filtering tape will depend upon selection of a tape speed appropriate to the operating conditions being studied. Tape speed should not be so fast as to give only traces of very light density, and not so slow that at any condition encountered the trace will reach full dense black. Within the range of grays, from clean "white" paper to full black, tape traces can be measured to one part in 100 by a suitable photometer.

E. Quantitative measurement: Changes in smokiness resulting from changes in engine operating conditions are plainly visible on the smokemeter tape and can easily be followed by mere visual inspection. For some purposes, this is all that is necessary. The tape can be marked with pencil to indicate the time of beginning a test, speed used, date, and all other data of interest. The time of events in the test can be correlated with the same portions on the trace from time pips and starting marks. Fig. 5 shows the effect of a rather extreme difference in fuel quality on smoke from a 6-cyl bus engine, and the greater effect of one faulty injector when operating on the same good fuel. Fig. 6 shows how the continuous filtering-type smokemeter is capable of detecting the transient changes in smoke density with gear changes during acceleration of a vehicle from a standing start.

Measurement of smoke-trace density can be made by visual matching against a "gray-scale" standard, such as the smoke-spot scale.[2] This is a scale of 10 units, from zero for white to 9 for dead black, in increments varying by 10% of the light reflection from the No. 9 spot. Tape traces can easily be read to fractions (½ or even ¼) of the interval between adjacent spots. It is somewhat easier to match uniform-density traces made by the stop-start technique than the continuous trace when using the smoke-spot scale on smoke traces made when the smoke density is varying rapidly. Fig. 7 shows the correspondence of readings of typical smokemeter tapes by reflectance photometer and by comparison with the gray-scale comparator. Displacement of the actual curve from the theoretical one may be due to the difference between actual light-reflectance value of the No. 9 spot on the comparator scale and the dead-black reference point on which the photometer is standardized.

If the expense is justified, it is preferable to use a photoelectric photometer for measuring the smokemeter trace density. Measurements have been made both by light transmitted through the tape, and by light reflected from the tape face. Either method gives similar, if not identical, results as long as the trace is completely dry. Under those conditions which give wet traces from presence of incompletely vaporized, unburned fuel oil, or lubricating oil mist, transmitted light readings are very misleading. Wet traces give much lower readings by transmitted light (due to the grease-spot photometer effect), than true "blackness" of the trace should indicate. Reflected-light photometer readings give relatively little or no error in this condition, compared with readings obtained by matching against a gray scale. (Visual matching against a gray scale is, of course, by reflected light.)

Two types of photoelectric photometers have been used by members of the Group for measuring density of smoke traces made by the continuous filtering-type tape-recording smokemeter. Two meters using light *transmitted* through the tapes were used; one an adaptation of the present CRC Smokemeter, the other a standard commercial instrument.[3] Reflectance readings of smokemeter tape traces were made by light *reflected* from the smoke

[2] For example, the Bacharach true-spot smoke tester comparator scale No. RR776 (Bacharach-Shell smoke spot scale).
[3] Photovolt transmission densitometer, model 525; Photovolt Corp., 95 Madison Ave., New York City 16.
[4] Photoelectric reflection meter, model 610; Photovolt Corp.

Table 1 – Smokemeter Tape Readings with Printed Comparator Scale (Four Observers)

Observer	Tape Reading: Bacharach-Shell Scale Number						
Ht	4	5	5½	6	3½	5	8
Hn	4	5	5+	6–	4–	5	8
Gm	3	4	5	5½	2½	5	8
Ma	4	4½	5	5½	4	5½	8

trace surface, using a reflectance photometer made by the same manufacturer.[4]

When a series of smokemeter tapes was evaluated independently by each member of the Group by visual matching against the smoke-spot scale, agreement was quite good (maximum spread = 0.5 spot number), among all but one member, he being consistently low by 0.5 to 1 number, except on the darkest spot. (See Table 1.) Photometer measurements are free from errors due to individual characteristics, and ability to measure small differences in trace density is of the order of five times as great as by visual observations.

Filter tape traces from the continuous filtering-type tape-recording smokemeter can be kept and used for some time after the tests are run, for purposes of study, reference, and data analysis. They are not permanent, however, and should be evaluated numerically by photoelectric readings or by matching against a standard scale as soon as practicable. Perfectly dry traces, of light to medium shade, are stable for considerable periods of time, and may even be reliable, for reference purpose only, for some years, if carefully preserved. But heavy traces, even if dry, are subject to change as they lighten in shade. This occurs immediately if carelessly handled, folded against themselves, bound between paper as in a report, or sent by mail. Traces that are the least bit wet are subject to gradual and fairly rapid change in either light transmittance or reflectance value. Traces can be photographed successfully, and true comparisons can be made between traces in pictures made by photoreproductive processes as long as traces of known value are included in the same print as reference points.

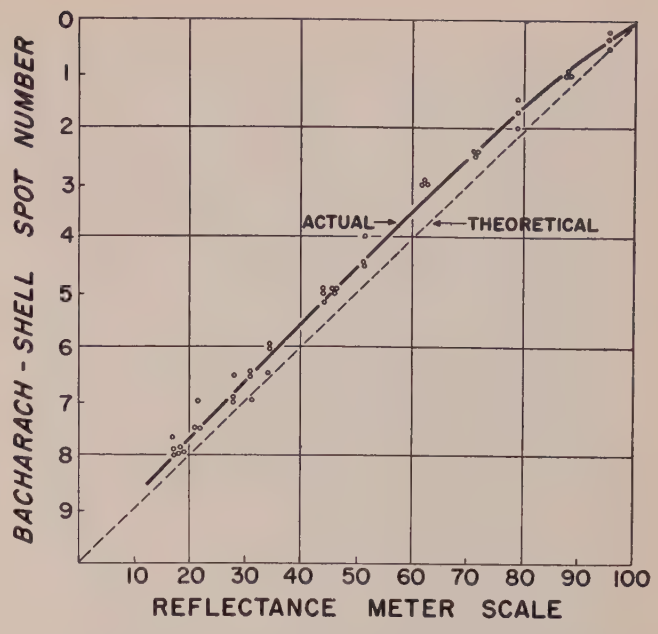

Fig. 7 – Smokemeter tape recordings; reflectance photometer versus gray scale readings

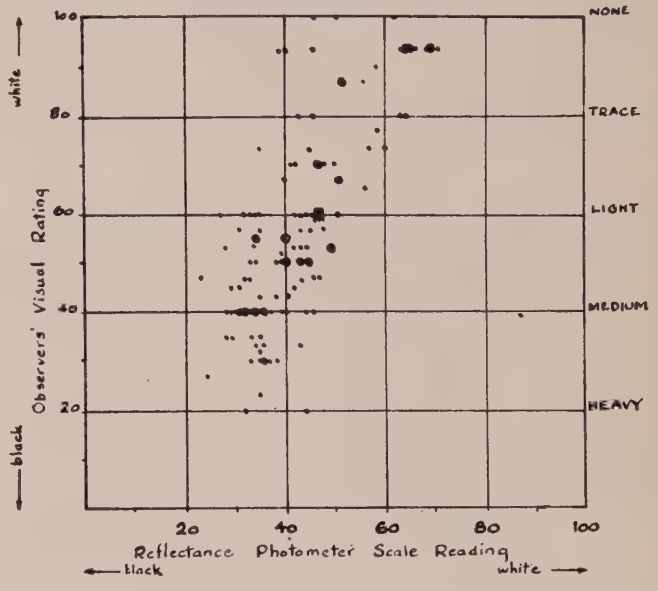

Fig. 8 – Reflectance readings of smokemeter tape versus observed smoke at tailpipe for Greyhound bus on chassis dynamometer

Correlation with Visible Smoke

Correlation between smokemeter readings and appearance of visible smoke discharged from diesel-engine exhaust pipes is a matter which has to be dealt with by each investigator to suit the conditions he is employing. There is no such thing as a reading of 50 on the photometer scale, or 4½ on the smoke-spot scale of 9, that will mean "50% visible smoke"; that is, half as dense as it can be, under all operating conditions of any and all diesel engines. A moment's reflection will show that the same visible appearance of exhaust can result from a variety of conditions: engine size, load and speed, fuel, lighting, background, and so on. Conversely, the same smoke density measured by a sample withdrawn from the exhaust can give different appearances to the exhaust out in the atmosphere, depending upon background, lighting, wind, vehicle motion, and so forth.

No scale of "per cent visible smoke" can be established for the continuous filtering-type tape-recording smokemeter. The same can be said for the intermittent-sampling type or any light-extinction type meter. In fact, it has been shown mathematically that, "no true indication can be obtained

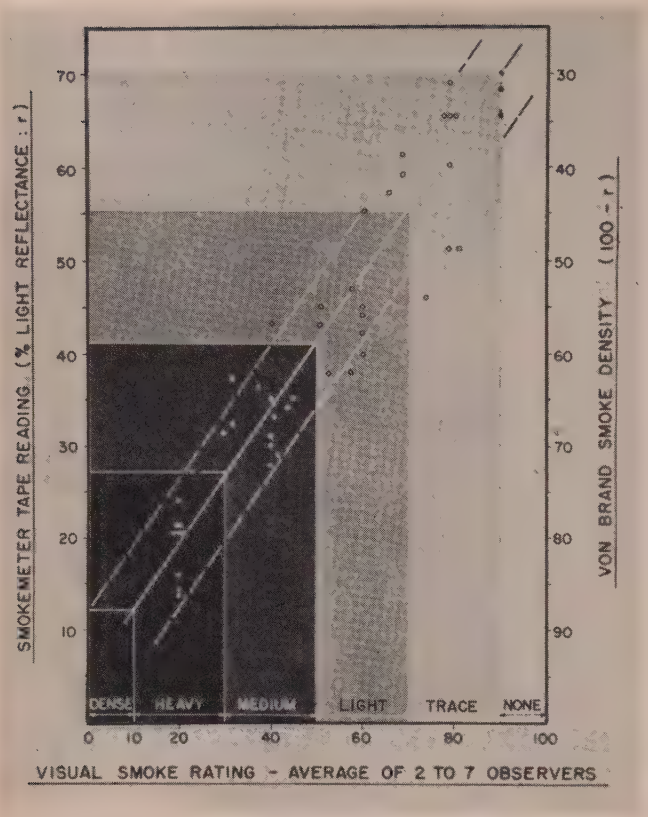

Fig. 9 – Comparison of smokemeter rating with visible smoke ratings for Greyhound bus with GM 6-71 engine on chassis dynamometer

by these means."[5] All that can be done is to establish a numerical scale in terms of the blackness, optical density, or light-reflecting value of the *filter paper surface* itself. Any scale of "per cent smoke" will depend upon the density taken as "100%" for the particular setup from which the smoke was being sampled. Each investigator must therefore establish his own reference points and scale of values appropriate to the kind of job being undertaken. The scale may be fine or coarse, as required by the magnitude of differences in smoke density thought to be important or significant. For some work a scale of five points (none, trace, light, medium, and heavy) may be adequate. For many purposes, in engine or fuel development, trouble-shooting and complaint settling, a scale of 10 full points between white and black is sufficient. In some research and development work a scale of 100 may be desired.

Fig. 8 is a plot of 134 points taken during fuel tests in a Greyhound bus running on a chassis dynamometer. Reflectance photometer readings of the smokemeter tape are plotted against density of visible smoke issuing from the tailpipe as judged by from one to five observers. Smokemeter tape speed was 6 in. per min, tape suction 5 in. of Hg. Different test fuels were run at 20, 30, 40, and, in some cases, 50 and 60 mph rear wheel speed, all at full throttle. Observers viewed smoke from different angles and against different backgrounds, the lighting of which changed throughout each day. Smoke appraised as "heavy" was in no case dense and black, but rather a medium shade of gray, the judgment of "heavy" being really the observer's rating of an objectionable amount of smoke from a vehicle operating on the public highway. Individual observers also tended to apply a mental correction, rating smoke which could be seen as "trace" or "none" considering (correctly) that if the vehicle had been running on the road instead of being stationary on the dynamometer the smoke would have been imperceptible. These facts account for the wide spread of "observed smoke" values at similar values of actual smoke density in the exhaust pipe as measured by the meter. In the narrow range of actual smoke density represented by meter readings of 40-50, different observers judged visible smoke all the way from none to heavy. The "error" is not in the smokemeter but in the individual observers' points of view.

Bearing out the previous statement that correlation with visible smoke can be obtained under some conditions, however (see point No. 5 listed under the subhead, "Continuous Filtering Recording Smokemeter"), Fig. 9 has been prepared from selected points from the same series of tests described above. Here, average smoke ratings of only those observers who consistently viewed exhaust discharge from the same locations are plotted against smokemeter tape readings. All single ratings of individuals (which are plotted in Fig. 8) are discarded. This graph would not apply to other investigations in which engines of different size, type, or speed range were used, nor if smokemeter tape speed and vacuum were different from those used in the bus tests.

Conclusion

The continuous filtering-type tape-recording gas sampler is capable of measuring relative smoke density, in the visible and invisible range, in exhaust gases from diesel or spark-ignition internal-combustion engines. It makes a visible record, either continuous or intermittent as desired, which is capable of indicating changes or differences in smoke density too small to be detectable by the eye alone. The useful recording range of the instrument can be adapted to any range of smoke density to be measured.

Investigation is continuing with the object of establishing its limits of application and test-proving the proposed improvements in the mechanism as now manufactured, which have been developed by the Group and by individuals using the filtering-type meter during the period of this investigation.

This investigation will culminate in a recommendation by CRC which will define the construc-

[5] Smoke or dust concentration by light-extinction measurement. (See *Instruments*, Vol. 24, May, 1951, pp. 534, 544, 578-580: "Photoelectric Measurement of Dust," by J. E. Coolidge and G. J. Schulz.)

tion and mechanism of a continuous filtering-type tape-recording smokemeter believed to be most usefully adapted to quantitative measurement of exhaust gas smoke from compression-ignition internal-combustion (diesel) engines. The recommendation for the smokemeter and auxiliary apparatus will not restrict construction of the instruments to any one source. All work done by the CFR-DFD Smokemeter Group has been with a single type of continuous filtering-type tape-recording smokemeter[6] and with different types of photometers made by a single manufacturer.[7]

I would draw your attention particularly to the limitations of this sampling type of exhaust smoke measuring device. It is eminently suitable for use in laboratory testing and development, and for service work where conditions permit drawing exhaust gas samples from the exhaust pipe. It is *not* intended nor recommended for use in smoke abatement control or enforcement.

References

1. U. S. Patent 2,667,779 to Ernest Kurt Von Brand (Feb. 2, 1954), "Analytical Apparatus for Smokes and Gases." Describes Von Brand continuous, filtering, gas sampling recorder.

2. Bulletins of Bacharach Industrial Instrument Co., Pittsburgh, Pa. In particular: Leaflet 610: "Diesel Exhaust Smoke Measurements"; Leaflet 746: "Bacharach Smokemeter"; Bulletin 762: "Smoke Rating Analysis" (reprint from *Fuel Oil and Oil Heat,* February, 1949); Bulletin 777: "Fyrite Combustion-Testing Utility Kit"; Bulletin 795: "Portable Combustion Testing Instruments."

3. Bulletins of Photovolt Corp., New York. In particular: No. 605: "Description of Photoelectric Reflection Meter, Model 610"; No. 660: "Instructions for Operating Photoelectric Reflection Meter Model 610."

4. "Applications of Portable Continuous Smoke Recorder," by E. K. Von Brand. *Mechanical Engineering,* Vol. 72, June, 1950, pp. 479-481. Has 11 references.

5. "Smoke and Its Measurement," Department of Scientific and Industrial Research, Great Britain; Fuel Research Board Technical Paper No. 53; London, H. M. Stationery Office (1946). 20 pp., including illustrations and graphs; description of optical apparatus, light-extinction-type comparator; details of tests on coal-fired boiler.

6. "AISI Automatic Smoke Filter," Research Appliance Co., Pittsburgh, Pa. Bulletin describes construction and results obtained with a noncontinuous-filtering-type meter similar in construction to the Von Brand continuous gas sampler, but adapted especially for air pollution study.

7. Combustion Control Corp., Cambridge, Mass. Bulletin CM 506 describes "fireye" smoke indicators and recorders (light-extinction type), applications, and installation.

8. "Filter-Paper Method for Obtaining Dust-Concentration Results Comparable to Impinger Results," by C. E. Brown, U. S. Bureau of Mines RI 3788 (1944).

9. Coordinating Research Council, New York: "Use of CRC-Photovolt Smokemeter in Measuring Smoke from Diesel Engines." CRC Report No. 238 (1948); "Interim Report on Operation of Continuous-Filtering, Recording Smokemeter." CRC Report No. 285 (1954).

10. "Handbook on Aerosols," Atomic Energy Commission, Washington, D. C., (1950). See Chap. 7: "Optical Properties of Aerosols"; Chap. 8: "Measurement of Particle Size Distribution"; and Chap. 10: "Methods of Testing Smoke Filters."

11. SAE SP-101, "Diesel Smoke Symposium." Comprises six papers on various phases of diesel-engine exhaust smoke presented at the SAE 1948 Annual Meeting (out of print).

12. "Fuels and Combustion Handbook," by A. J. Johnson and G. H. Auth. Pub. by McGraw-Hill, New York, 1951. See especially Chap. 14: "Smoke, Fine Particles, and Other Combustion Rejects, including Slags."

13. "Requirements of Smokemeter," by K. M. Brown. SAE Transactions, Vol. 36-49, 1941, pp. 188-192. Description of forerunner of CRC (photoelectric) smokemeter; relationship between smoke density and "per cent smoke."

14. "Smoke-Density Measurement," by W. F. Stoecker. *Mechanical Engineering,* Vol. 72, October, 1950, pp. 793-798.

15. "Measurement of Smoke," by K. O. Beatty, Jr., and J. E. Deas. *Heating, Piping, and Air Conditioning,* Vol. 22, October, 1950, pp. 107-115.

16. "Smoke Measurement in Fuel Oil Test Unit," by D. W. Locklin and G. V. Parmelee. *Heating, Piping, and Air Conditioning,* Vol. 22, November, 1950, pp. 107-111.

17. "Photoelectric Measurement of Dust," by J. E. Coolidge and G. J. Schulz. *Instruments,* Vol. 24, May, 1951, pp. 534, 544, 578-580. Good for theory; shows why CRC (photocell type) smokemeter doesn't work very well.

18. "Air Pollution and How to Measure It," by J. W. Shaw and B. J. Linsky. *American City,* Vol. 65, October, 1950, pp. 116-117.

19. "Diesel-Engine Exhaust – Developments for Accurate Evaluation of Appearance," by A. L. Wachal. *Automobile Engineer,* Vol. 43, July, 1953, pp. 303-305.

DISCUSSION ON FOLLOWING PAGES

[6] Von Brand continuous filtering gas sampler; E. K. Von Brand, Hopewell Junction, N. Y.
[7] Photovolt Corp.

DISCUSSION

Continuous Filtering-Type Tape-Recording Gas Sampler Gives Satisfactory Repeatability

– E. K. Von Brand
Von Brand Filtering Recorders

THIS paper bears out the fact that the continuous filtering-type tape-recording gas sampler can be used to advantage in various applications. Some reasons leading to its design merit brief mention, particularly in view of modifications and new adaptations.

The tape is conditioned with respect to (a) humidity by means of a heated recording head, and (b) improvement of surface uniformity (nap) by passage between polished surfaces under sufficient but not excessive pressure. Clamping or gaskets for obtaining a seal around the tape filtering area are not employed because such means subject the tape to varying strain and deformation. The combined effect of these features makes for uniform permeability, equally important for a continuous trace record or for spot sampling. Tape vacuum tends to maintain a satisfactory seal between tape and recording head surfaces. Holding the sampling line closed and then lifting the head demonstrates this inherent beneficial effect. Leakage at this point is insignificant for practical purposes (vacuum range 4-8 in. of Hg), and moreover is nearly constant for small changes in vacuum, as verified by operating the sampler in a gastight case. A small change in vacuum is accompanied by a relatively much smaller change in flow produced by a positive displacement pump. Metering action of such a pump is effectively sustained by continuous uninterrupted feeding of clean tape into the sample stream (at a speed sufficient to avoid excessive loading or clogging, or with sampling rate reduced for the same reason). The resulting straight line characteristics, in this application of trace density versus smoke concentration, is very valuable in the economical planning and interpretation of tests.

These features, together with use of high-quality filter paper, facilitate production of records with a satisfactory repeatability.

More Information On Correlation Needed

– G. C. Wilson
Ethyl Corp.

MR. HUNTER and his CFR Diesel Fuels Division Group have made a thorough investigation of the requirements for a good smokemeter, and their report points out several advantages of a continuous filtering-type tape-recording instrument. However, the problem of correlation was touched upon rather lightly. It seems likely that many users of any smokemeter will attempt correlation of its determinations with visible smoke. The purpose of this discussion is to urge the smokemeter group to furnish additional information by enlarging item No. 5, which states that correlation can be obtained under some conditions.

It would seem most desirable to prevent, so far as possible, any misuse of a smokemeter capable of making repeatable relative ratings. It is a well-known fact that smoke ratings from visual observations can be inaccurate, even though made by an experienced observer.

Disputes Superiority of Continuous Filtering-Type Tape-Recording Smokemeter

– P. H. Schweitzer
Pennsylvania State University

THIS paper contains a number of inaccuracies and misstatements calling for comment. The paper is based on the "Interim Report on the Operation of the Continuous Filtering Recording Smokemeter" (CRC Project No. CFD-36-52), October, 1954. The writer has called attention to several inaccuracies in that report. Some have been corrected in the paper, while others have been added. The following comments pertain to the paper.

As to history, the first published record of a diesel smokemeter, as the writer is able to establish, appeared in *Automotive Industries*, Aug. 20, 1938, p. 238. The smokemeter described there, developed by the writer, operated on the sampling and light absorbing principle and used a commercial General Electric lightmeter as the sensing element. Foot-candles were read directly and per cent smoke was set proportional to the number of foot-candles of light prevented from reaching the photocell. Incorporating improvements developed by the Naval Engineering Experiment Station and Esso Laboratories, this smokemeter was redesigned and described in *Instruments*, September, 1942. The "Improved Penn State Smokemeter," with a "few features added to make the instrument more universally applicable," was then marketed by the Photovolt Corp. and adopted by the CRC. Hundreds of these instruments have been built here and abroad and neither the Photovolt Corp. nor the writer is aware of dissatisfaction by the users.

The author found it "hard to explain why the direct-reading light-extinction smokemeter should give . . . unsatisfactory results," but it was not for lack of trying. First he mentions that the "characteristic curve of the light-extinction meter is exponential," as shown in Fig. 2. The writer does not know what is plotted against what in Fig. 2. The photocell is being used to measure lightness or opaqueness in millions of photographic and commercial lightmeters. Furthermore, the CRC smokemeter is empirically calibrated. Its 100% point corresponds to complete extinction of light, its zero to clean air in the smokemeter tube, and its x% point to the shielding of x% of the photocell surface area with clean air in the tube. Therefore, x% smoke on the CRC smokemeter means that (100-x)% light reaches the photocell and x% is extinguished by the smoke. In spite of this the CRC smokemeter has an almost linear scale.

In his reference 17 the author appends: "Good for theory; shows why the CRC (photocell type) smokemeter doesn't work well." The cited article says nothing of the sort, nor does it support the statement at the end of the introduction.

The author lists 11 points of superiority of the continuous filtering-type smokemeter over the CRC smokemeter. Some of these are arguable, others clearly false, to wit:

1. "It is insensitive to sampling line conditions over wide limits." In his laboratory the writer did not find the CRC smokemeter more sensitive to sampling line conditions than the continuous recording filtering type, nor does he see any reason why it should be. No such claim should be made.

2. Adjustable sensitivity of the filtering type smokemeter is an advantage if the instrument is also to be used for other purposes, but is of no importance in measuring diesel exhaust smoke. On the other hand, this very feature prevents interchange of results obtained between separate laboratories.

7. According to its maker, the light-extinction-type

smokemeter can also be made continuous or intermittent.

8. Since the smokemeter scale is zeroed before making a measurement, the CRC smokemeter is not susceptible to undetected error, even if the glass surfaces are not cleaned often.

9. No corrosion of internal parts from exhaust gas condensate has been noted.

10. It was news to the Photovolt Corp. that CRC smokemeter indications are affected by line voltage changes. The writer withholds opinion.

Regarding correlation of visible smoke with meter reading, the writer agrees that no perfect correlation can be expected with either instrument. It is useful, however, to point out that while condensed water vapor or "cold smoke" consisting of liquid fuel ("Must Diesel Engines Smoke?" by P. H. Schweitzer, SAE Quarterly Transactions, July, 1947) tends to block out light in a light-extinction type of smokemeter, it will leave little or no mark on the filter paper. It is good to realize that to engineers interested in combustion, the smokemeter reading is often more enlightening than the visual impression of the smoke. For instance, a long hot stack can burn up smoke and make it almost invisible without affecting combustion in the cylinder or the sample taken near the cylinder. Dilution smoke by an air aspirating ejector will make it less visible but not less existent. What kind of smokemeter should be given preference depends largely on what the objectives and circumstances are. For laboratory use, we prefer the CRC smokemeter, although we use the Von Brand type, for instance, when we want to take two simultaneous records from two cylinders equipped with different spray nozzles. For use in a moving vehicle the continuously recording filtering-type smokemeter is more convenient.

I am unable to go along with the suggestion that the filtering-type smokemeter is more accurate or less sensitive to external circumstances than the light-absorption type.

Author's Closure To Discussion

PROFESSOR Schweitzer's role in the development of the CRC Smokemeter, and in the art of diesel smoke measurement is acknowledged. Omission of his name from the paper, where the Navy's version of his meter is cited, was by no means intended to minimize it. References he gives should be added to the list given in the paper; but by no means do these list all publications on measurement of engine smoke.

The present CFR Smokemeter Group was formed and assigned the project of investigating other types of smokemeter because of dissatisfaction expressed by users of the CRC smokemeter, particularly with respect to its apparent sensitivity to sampling conditions and the inability to obtain correlation with diesel exhaust smoke as viewed in the atmosphere. Whereas this progress report on the Group's work to date might infer that the filtering-type meter should replace the photoelectric type, such is not the case. In work planned since the presentation of the report, a study to establish proper sampling technique for both types of smokemeter when used with diesel engines is the item of first importance.

The meter scale point reading "100%" does not correspond to complete extinction of light, in the instrument as manufactured. In test work with one instrument (Serial No. 210) in perfect operating condition, a 100% scale reading was obtained with "light" cigarette smoke in the light tube, which allowed a great deal of the light from the lamp to reach the photocell, as checked by direct observation. Also, the CRC Smokemeter scale is not linear, but throughout the full range from bright light to dark it follows the characteristic output curve for the photronic cell shown – purposely without scale values – in Fig. 2.

As to the Coolidge and Shulz reference, the author thinks it does tend to explain a shortcoming of the light-extinction type meter for measuring smoke-particle density; however, it is preferable to delete the comment in reference 17.

In reference 17 Coolidge and Shulz say, under "Theory" on p. 579: "Photoelectric measurements can be accomplished by measuring either the absorption of light by the dust-laden air, or the scattering produced by the dust. In either case, the measurement depends on the wavelength of the light, the particle - size distribution of the material, and the surface properties of the particles. Theoretical expressions for the light absorption in dust-laden gases **cannot be derived** except for the simplest conditions, and parameters obtained by experiments have to be employed in practice . . . (formulas given) . . . The dust loading (m) can be expressed in terms of the measured light intensities because $m = (1/\alpha) \ln (I_o/I)$. Therefore, a knowledge of α would enable a calculation of the dust loading. However, a theoretical determination of this lumped 'constant' is very difficult, and in most cases impossible because the distribution function is unknown. Thus it appears that the absorption-type photoelectric smokemeter is a qualitative instrument, unless the constant α can be obtained by other means." They go on to say that in their laboratory work it was possible to find the constant for their particular setup and thus to use the photelectric smokemeter as a quantitative instrument. "It should be noted that the values for the lumped 'constant' obtained in this way are valid only for this particular system, dust, and wavelength of light." Under "Sampling Characteristics," p. 579, they state: "The following conclusions can be drawn from this study:

1. A true loading indication cannot be obtained . . .

2. An optimum indication is obtained at higher sampling velocity . . .

3. No true indication can be obtained by these means."

With reference to the 11 points in which the Smokemeter Group found the tape-recording type of meter superior, for one reason or another, to the light-extinction type, all five members of the Group are unanimous in their agreement on them, in particular:

"(1) It is insensitive to sampling line conditions over wide limits." This is a statement of experimentally determined fact. The Group members agree that in their experience the CRC Smokemeter is sensitive to conditions in the sampling line (for reasons unknown).

"(9) It does not suffer from corrosion of internal parts from exhaust gas condensate." This was one of the major complaints against the CRC Smokemeter.

"(10) It is not sensitive to small changes in line voltage, nor to vibration." The author and other users have repeatedly observed the CRC Smokemeter needle to jump 2-5 scale divisions with no sample in the instrument, just standing on the bench. Sometimes this could be correlated with turning lights on or off, or starting or stopping pumps, or motors in the building. The small-size voltage-regulating transformer in the control box appears not altogether adequate to level out appreciable line voltage fluctuations. The CRC Smokemeter microammeter is, of course, quite susceptible to vibrations; this is, in fact, one reason why that meter is not usable on moving vehicles. The tape-recording smokemeter does not have this objectionable feature. In addition, the photronic-type photoelectric cell used in the CRC Smokemeter has a rather large temperature coefficient of output.

Professor Schweitzer's comments on the inability of the filtering-type smokemeter to detect and measure white, blue or "cold" smoke are quite correct. For thorough study of factors producing visible exhaust products (smoke), whether on the engine or fuel side, use of both types of smokemeter is desirable.

Physical and Chemical Ignition Delay

Using the Hot-

EVER since the diesel engine first assumed its role as one of the primary sources of power, the phenomena of ignition delay have been observed and studied. That these studies have been helpful is evidenced by the constant improvement in efficiency and flexibility of diesel engines. However, in spite of these many studies the details of phenomena that occur during the ignition-delay period are missing. Any detailed information on events occurring during ignition delay are of interest.

THE present work uses the hot-motored technique to compare a hot, motored pressure diagram with a fired, pressure-time diagram. This technique is applied to a diesel engine to study the small pressure changes after injection and before rapid inflammation. The data resulting from these studies show a relationship between the magnitude of these pressure changes and cetane number of the fuel. Data for selected fuels are presented to show the relative magnitude of different phenomena causing ignition delay.

Studies of combustion flame temperatures in diesel engines at the University of Wisconsin had not shown much difference between fuels.[1, 2, 3] Thus, it was decided to make a detailed study of the pressure change occurring during ignition delay. It was hoped that such a study would provide useful additional information about the phenomena occurring.

Information most helpful in understanding details of events during ignition delay are pressure, temperature, and composition of compressed gases, rate of injection and of vaporization of injected fuel, and rates of chemical reaction of vaporized fuel. To the best of the authors' knowledge, no measurements of diesel-engine compression temperatures have been made. Although instrumentation is still in the development stage, two different techniques[4, 5] have been used to make preliminary mea-

[1] See ASME Transactions, Vol. 68, Jan., 1946, pp. 17-30: "Flame Temperature Measurements in Internal-Combustion Engines," by O. A. Uyehara, P. S. Myers, K. M. Watson, and L. A. Wilson.

[2] See ASME Transactions, Vol. 69, July, 1947, pp. 465-477: "Diesel Combustion Temperatures – Influence of Operating Variables," by O. A. Uyehara, P. S. Myers, K. M. Watson, and L. A. Wilson.

[3] See SAE *Quarterly* Transactions, Vol. 3, Jan., 1949, pp. 178-199: "Diesel Combustion Temperatures – Influence of Fuels of Selected Composition," by O. A. Uyehara and P. S. Myers.

[4] See *Journal of Acoustical Society of America*, Vol. 26, Sept., 1954, pp. 824-830: "Ultrasonic Temperature Measurement in Internal-Combustion-Engine Chamber," by J. C. Livengood, T. P. Rona, and J. J. Baruch.

[5] See SAE Transactions, Vol. 62, 1954, pp. 503-513: "Compression and End-Gas Temperatures from Iodine Absorption Spectra," by S. K. Chen, N. J. Beck, O. A. Uyehara, and P. S. Myers.

in an Operating Diesel Engine

Motored Technique

T. C. Yu, O. A. Uyehara, and P. S. Myers,
University of Wisconsin

R. N. Collins,
Continental Oil Co.

K. Mahadevan,
Indian Institute of Science

This paper was presented at the SAE Golden Anniversary Diesel Engine Meeting, St. Louis, November 4, 1955.

surements of compression and end-gas temperatures in spark-ignition engines. Both techniques are applicable to diesel engines and undoubtedly eventually will be used for measurements of gas temperatures during compression in diesel engines. Work has already been done on rate of fuel injection.[6] Studies of rates of fuel vaporization are in progress.[7, 8] Rates of chemical reaction are not yet available but information like that obtained by a rapid-compression machine should be helpful.

While a complete understanding of the events occurring during ignition delay will undoubtedly await the results of the above and other studies, it was believed that detailed studies of pressure changes occurring during ignition delay would be useful. Interest in this approach was increased by the pressure decrease presumably due to vaporization that was observed in a combustion bomb. The hot-motored technique was developed to study small pressure changes occurring during ignition delay in an operating engine using selected fuels.

Apparatus

A single-cylinder, GM 1-71 diesel engine donated by the Detroit Diesel-Engine Division of General Motors was used for these studies. Principal specifications and engine dimensions are shown in Table 1.

An experimental head with an additional opening beside the customary valve and injector opening was obtained from the manufacturer. A second additional opening was machined to take a Li-Draper indicator.[9]

To provide complete control over the inlet-air temperature and pressure, the blower normally sup-

[6] See SAE Transactions, Vol. 61, 1953, pp. 542-552: "Measuring Rate of Fuel Injection in Operating Engine," by R. J. Wehrman, H. R. Mitchell, and W. A. Turunen.

[7] See NACA TN 3179 (1954), "Theoretical Investigation of Heating-Up Period of Injected Fuel Droplets Vaporizing in Air," by M. M. El Wakil, O. A. Uyehara, and P. S. Myers.

[8] See NACA TN 3870 (1956), "Experimental and Calculated Temperature and Mass Histories of Vaporizing Fuel Drops," by M. M. El Wakil, R. J. Priem, H. J. Brikowski, P. S. Myers, and O. A. Uyehara.

[9] See *Journal of Aeronautical Sciences*, Vol. 16, October, 1949, pp. 593-610: "New High-Performance Engine Indicator of Strain-Gage Type," by C. S. Draper and Y. T. Li.

Table 1 – Specifications of GM 1-71 Diesel Engine

Bore, in.	4.25
Stroke, in.	5.00
Rated Brake Horsepower at 1200 Rpm	15
Compression Ratio	16/1

Table 2 – Engine Operating Conditions

Engine Speed, rpm	800 ± 5
Engine Load – Injector rack set to give approximately constant weight of fuel injected per cycle. Engine load varied with fuel	
Inlet-Air Temperature, F	90 ± 5
Inlet-Air Pressure, in. of Hg	40 ± ¾
Inlet-Jacket Water Temperature, F	140 ± 5
Point of Injection, deg btdc	12 ± 1½

plied with the engine was removed and the inlet-air chamber connected to an external air supply whose temperature and pressure could be controlled at will.

The fuel system was modified by disconnecting the governor and adding a micrometer and solenoid to the injector rack. The micrometer enabled tests to be run with the rack in a known fixed position while the solenoid, when properly actuated, would rapidly move the rack to the no-fuel position. Means were also provided for accurately measuring engine fuel rate.

The output of strain gages installed on the rocker arm actuating the injector was used to indicate the beginning, rate, and end of injection. A reasonable correlation between the results obtained with this technique and with a strain gage around the injector tip was found by Wehrman et al.[6]

A slotted disc, 30 in. in diameter and solidly coupled to the engine, together with a light and photocell arrangement, produced timing marks every two crank-angle degrees.

A special drum camera using a film strip approximately 5 x 30 in. coupled to the engine by a pair of selsyns provided a time base as well as a photographic record of data displayed on oscillograms.

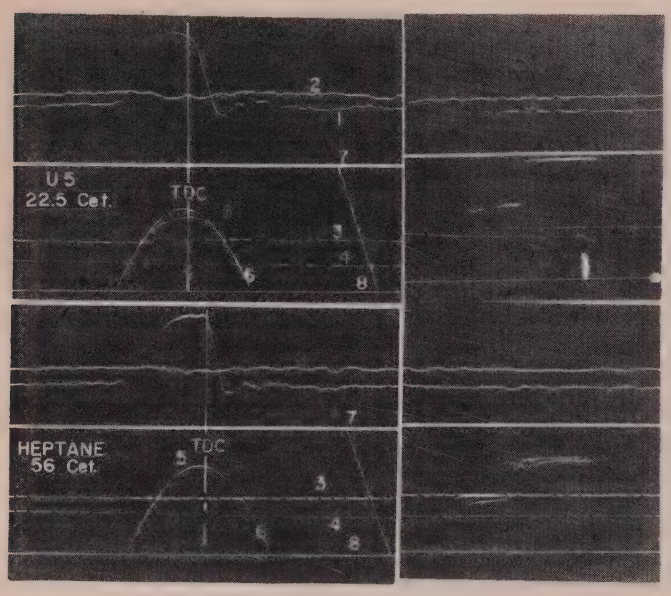

Fig. 1 – Typical oscillogram photographed when using hot-motored technique

Experimental Procedure

Since it was desired to study very small pressure changes occurring during ignition delay, the hot-motored technique was devised. A description of this technique follows:

With the engine operating normally on the test fuel (except for the inlet-air and governor modifications previously noted), a pressure-time record for a single fired cycle was obtained. On the next cycle, the solenoid pulled the injector rack back to the no-fuel position and the drum camera also recorded this hot-motored cycle on the same film as the fired cycle. Thus two successive cycles – the first fired and the second unfired – were obtained on a single film. In both cases the vertical pressure scale was expanded so that only the high-pressure portion of the compression stroke showed on the oscilloscope and was recorded.

Typical oscillograms are shown in Fig. 1. Pressure difference between the fired and unfired cycle will be denoted by ΔP_{fv}.

The events shown on this oscillogram are:

1 and 2: Voltage output of the strain gage on the rocker arm during fired and hot-motored cycles respectively.

3 and 4: Timing marks for fired and hot-motored cycles, respectively. These timing marks were automatically shifted downwards on the hot-motored cycle by means of a relay to prevent overlap.

5 and 6: A much-expanded, pressure-time record for the fired and unfired cycle, respectively. The step functions shown on the right-hand side after the break in the film are caused by two calibration resistors being successively inserted into the pressure-pickup circuit. The pressure corresponding to the step shown is 50 psi.

7 and 8: Alignment lines for scaling purposes.

The hot-motored technique provides a reference cycle in which, except for the question of cyclic reproducibility, all conditions are exactly the same as in the fired cycle except that no fuel is injected, that is, hot clearance gases are present, walls are

Table 3 – Fuels

Fuel	Approximate Cetane Number								
	22.5	33	40	50	56	59	71	77	100
Laboratory Fuel			x						
Primary Reference Fuels[a]	x		x			x			x
Secondary Reference Fuels									
U5 and T12	x	x	x			x	x		
33-Cetane Commercial[a]		x	x[b]			x[c]			
40-Cetane Commercial[a]			x						
54-Cetane Commercial					x				
59-Cetane Commercial			x[d]	x[e]		x			
n-Heptane-Iso-Octane[a]			x						
n-Heptane[a]				x					
Decane								x	

[a] Supplied by Ethyl Corp.
[b] Cetane number increased by addition of 0.3% amyl nitrate.
[c] Cetane number increased by addition of 1.8% amyl nitrate.
[d] Cetane number decreased by addition of 3.85 cc/gal tel.
[e] Cetane number decreased by addition of 1.55 cc/gal tel.

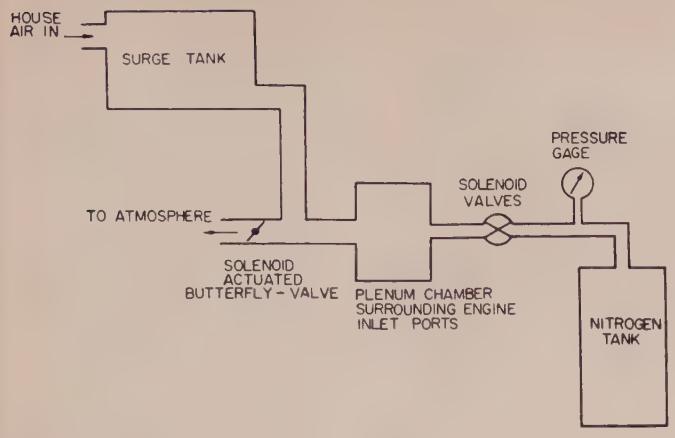

Fig. 2 – Schematic arrangement of equipment for introduction of nitrogen

hot, incoming air is heated by the walls and piston, and so forth. Thus any differences in pressure between the two cycles must be due either to the fuel injected or to irreproducibility of engine and instrumentation.

Except where specifically varied, engine operating conditions shown in Table 2 were held constant. Fuels run are shown in Table 3. Characteristics of commercial fuels are shown in Table 4.

To maintain weight of fuel injected more nearly constant, the injector-rack setting was changed slightly for different fuels. This explains in part the $\pm 1\frac{1}{2}$ deg variation in the point of injection. A portion of the $\pm 1\frac{1}{2}$ deg variation, however, is caused by the irreproducibility of the determination of the injection point. This point is mentioned in the discussion of data reproducibility.

To study fuel vaporization with no oxidation reactions present, a nitrogen tank was connected by two solenoid valves to the plenum chamber surrounding the inlet-air ports. This nitrogen tank was connected on the side of the plenum chamber opposite the entrance from the blower. The entrance to the blower normally connected to the atmosphere was connected to a 50-gal drum fed with house air. This same entrance could be connected to atmosphere by means of a 2-in., solenoid-operated butterfly valve. The arrangement used is shown schematically in Fig. 2. In operation, a pressure-time record was obtained with the engine firing normally and solenoid valve closed. Just after the ports were closed on this fired cycle the solenoid valves were opened, flooding the plenum chamber with nitrogen. On the next cycle the cylinder was scavenged and filled with nitrogen. When fuel was injected a pressure-time record with vaporization, but no oxidation reactions, was obtained. For comparison a hot-motored cycle using nitrogen but with no fuel injected was obtained. This technique is in the development stage

Table 4 – Inspection Data for Commerical Fuels Used

	33-Cetane Commercial Fuel	40-Cetane Commercial Fuel	40-Cetane Laboratory Fuel	54-Cetane Commercial Fuel	59-Cetane Commercial Fuel	U5 Fuel	T12 Fuel
API	32.2	37.4	30.0	39.5	44.4	51.0	43.7
Viscosity at 100 F	2.45 (centistokes)	—	—	34 (sec)	32 (sec)	—	—
Pour Point, F	−70	−55	—	−5	−25	—	—
Cloud Point, F	−70	−40	—	0	−24	—	—
Flash Point, F	150	—	150	160	—	—	—
Initial Boiling Point, F	350	348	420	350	367	364	398
10% Point, F	409	398	476	412	405	380	456
50% Point, F	454	404	520	481	450	392	494
90% Point, F	526	502	598	587	516	490	540
End Point, F	623	576	620	660	546	604	586
Cetane No.	33.4	40.1	40	54	59.3	22.5	71.5

but two cycles are presented to indicate the possibilities of the technique and the type of results obtained.

Experimental Data

Because of the small magnitude of pressure changes being studied (a maximum of 13 psi with peak firing pressure around 1000 psia), the reproducibility of the engine, instrumentation, and technique was of special interest. Consequently reproducibility data using 40-cetane laboratory fuel were taken on two different days. Data are shown in Fig. 3, where curves of ΔP_{fv}, quantity of fuel actually in the cylinder (see Appendix I), and per cent of maximum injection pressure are plotted as a function of crank-angle degrees after start of injection. Data are presented as a function of crank-angle degrees after start of injection rather than of crank angle *per se* because of the small

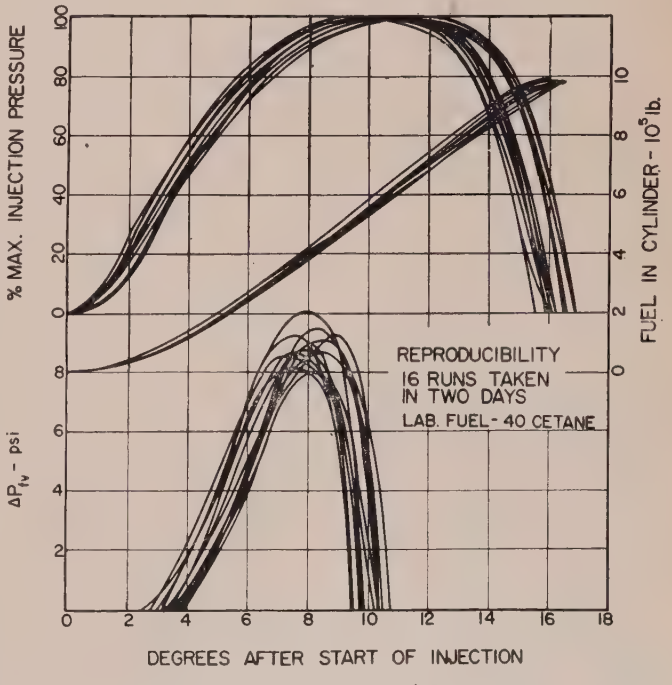

Fig. 3 – Data showing reproducibility of ΔP_{fv}, per cent maximum injection pressure, and fuel in cylinder

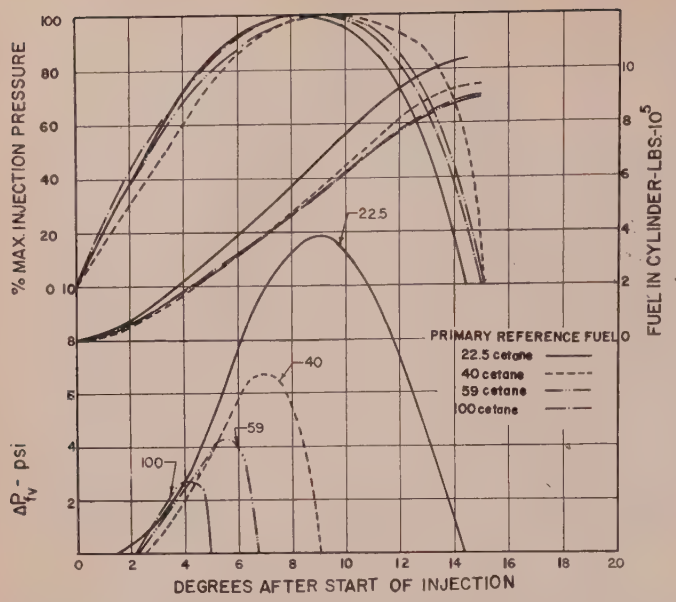

Fig. 4 – Data showing ΔP_{fv}, per cent maximum injection pressure, and fuel in cylinder for primary reference fuels

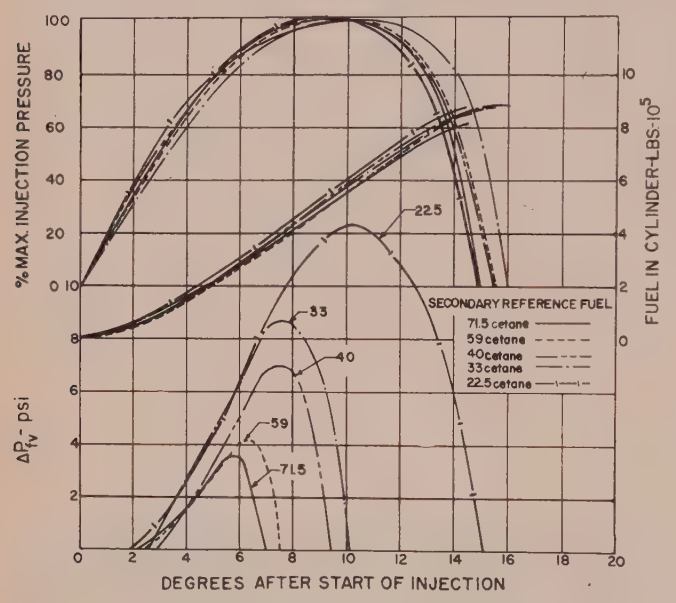

Fig. 5 – Data showing ΔP_{fv}, per cent maximum injection pressure, and fuel in cylinder for secondary reference fuels

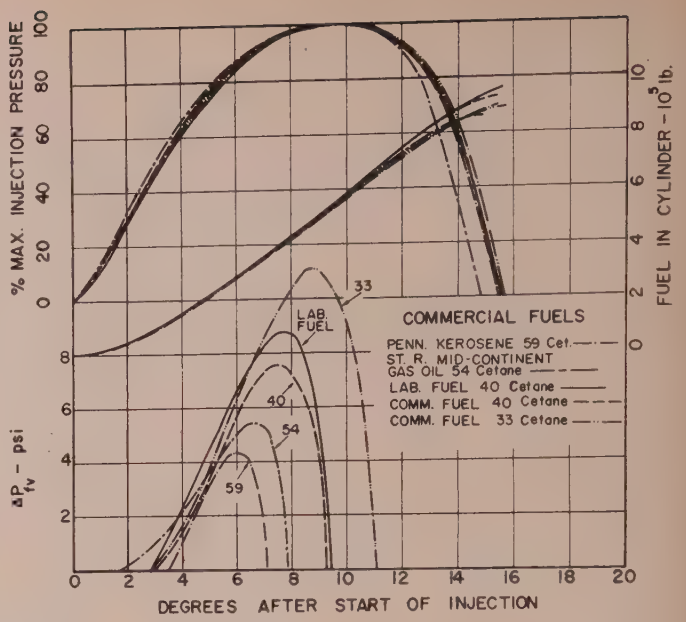

Fig. 6 – Data showing ΔP_{fv}, per cent maximum injection pressure, and fuel in cylinder for selected commercial fuels

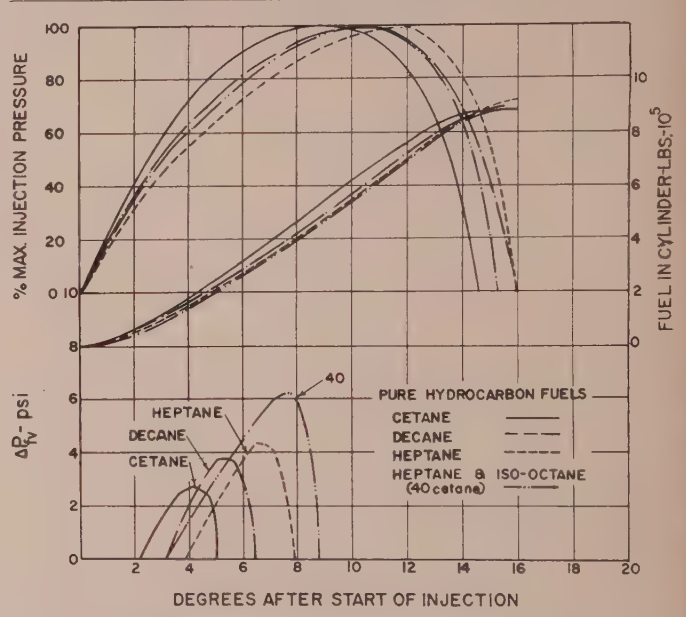

Fig. 7 – Data showing ΔP_{fv}, per cent maximum injection pressure, and fuel in cylinder for selected pure fuels

variation in the point of injection (as noted in Table 2), and because this permits a direct comparison of fuels. A portion of Table 5 shows the average value of point of injection for each fuel. Top dead-center will be at $12 \pm 1\frac{1}{2}$ crank-angle degrees after start of ignition.

Considering the magnitude of the pressure changes involved, reproducibility was considered fairly good. It was decided, however, that because of the variation shown in Fig. 3 average curves rather than individual cycles should be compared. Accordingly, the remaining data presented will represent the average of six or more individual cycles.

Data were gotten next for mixtures of the primary reference fuels, cetane and alpha-methyl naphthalene. The resulting curves are shown in Fig. 4. Note that ΔP_{fv} varies appreciably with cetane number.

For comparison, data were also gotten using secondary reference fuels U5 and T12. The resulting curves are shown in Fig. 5. Note that here, too, ΔP_{fv} varies with cetane number.

It was thought of interest to compare ΔP_{fv} for commercial fuels of different cetane number. Accordingly, data for five commercial fuels of dif-

[10] See "Fuel Vaporization and Ignition Lag in Diesel Combustion," by M. M. El Wakil, P. S. Myers, and O. A. Uyehara, on pp. 712-726 of this issue.

Table 5 – Average Injection Timing

	Start of Injection deg btdc	End of Injection deg atdc
100-Cetane Primary Reference Fuel	11.7	3.0
59-Cetane Primary Reference Fuel	11.0	3.8
40-Cetane Primary Reference Fuel	12.0	3.5
22.5-Cetane Primary Reference Fuel	10.5	3.7
71.5-Cetane Secondary Reference Fuel	11.3	3.9
59-Cetane Secondary Reference Fuel	11.8	3.6
40-Cetane Secondary Reference Fuel	11.9	3.2
33-Cetane Secondary Reference Fuel	12.6	2.9
22.5-Cetane Secondary Reference Fuel	11.4	3.2
Heptane	13.6	2.2
Decane	12.6	2.6
Iso-Octane and Heptane (40-Cetane)	13.1	2.4
Pennsylvania Kerosene	12.0	3.4
Pennsylvania Kerosene + 1.55 Cc/gal Tel	11.5	3.1
Pennsylvania Kerosene + 3.83 Cc/gal Tel	11.5	3.0
33-Cetane Commercial	12.0	3.7
33-Cetane Commercial + 0.3% Amyl Nitrate	11.0	3.7
33-Cetane Commerical + 1.8% Amyl Nitrate	11.3	3.6
54-Cetane Commercial	11.2	3.6
40-Cetane Commercial	12.0	3.4
Laboratory Fuel	12.0	3.7

Injection Timing for Reproducibility Runs

Run No.	Start of Injection deg btdc	End of Injection deg atdc
1	12.0	3.5
2	12.1	3.7
3	12.0	3.8
4	12.3	3.9
5	12.2	3.7
6	11.9	3.5
7	12.0	3.5
8	12.1	3.7
9	12.3	3.5
10	12.4	3.7
11	13.0	3.5
12	11.7	3.9
13	11.8	3.5
14	11.9	3.7
15	12.0	3.5
16	12.2	3.6

ferent cetane numbers were obtained. The resulting curves are shown in Fig. 6.

Computations of rate of vaporization of drops of pure fuels were available,[7, 8, 10] so it was decided to obtain data for pure fuels. In addition to the data shown in Fig. 7 some runs were made using iso-octane. With iso-octane the engine misfired and ran so rough that no data were obtained.

In an attempt to obtain data that would permit estimation of the magnitude of the chemical delay portion of the total ignition period, it was decided to add amyl nitrate and tel to the 33- and 59-cetane commercial fuels, respectively. These data are shown in Figs. 8 and 9.

It was desired to obtain vaporization rates without oxidation reactions present. Accordingly nitrogen was introduced as described above. Preliminary data obtained using this technique are shown in Fig. 10. Note that these data were taken at 400 rpm while all other data shown were taken at 800 rpm.

Discussion of Results

Reproducibility of data is shown in Fig. 3. Considering the order of magnitude of peak pressure changes being studied (2-12 psi out of 1000-psi firing pressure, or about 0.2-1.2% of peak pressure), reproducibility seems as good as could be expected with present equipment and techniques. Note that this reproducibility was obtained through the use of a drum camera which gave a greatly expanded time scale, a greatly expanded pressure scale to show only the high-pressure portion of the compression cycle, use of stable d-c amplifiers, and use of the hot-motored technique. It is doubtful if perfect reproducibility could be expected considering the small variation in heat transfer required to cause a variation in compression pressure and the randomness of the atomiza-

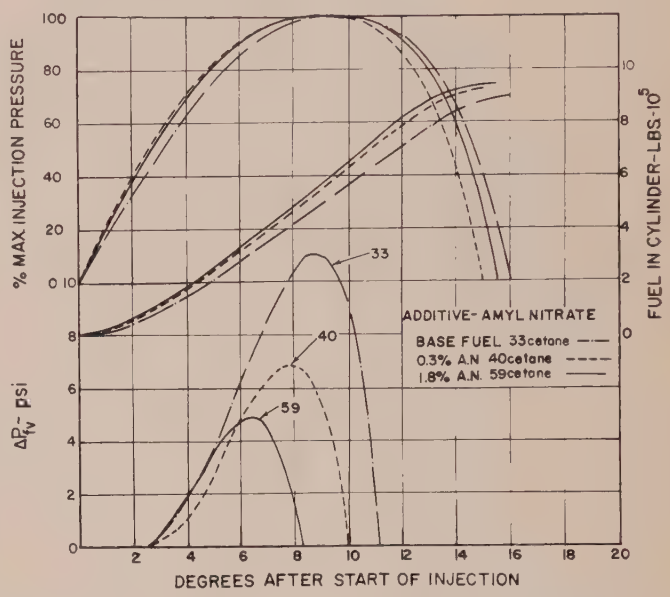

Fig. 8 – Data showing $\triangle P_{fv}$, per cent maximum injection pressure, and fuel in cylinder for 33-cetane fuel with amyl nitrate added

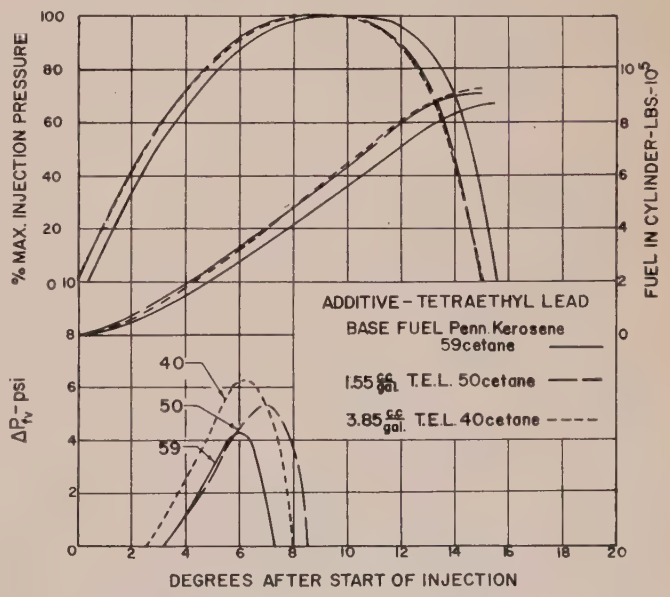

Fig. 9 – Data showing $\triangle P_{fv}$, per cent maximum injection pressure, and fuel in cylinder for 59-cetane fuel with tel added

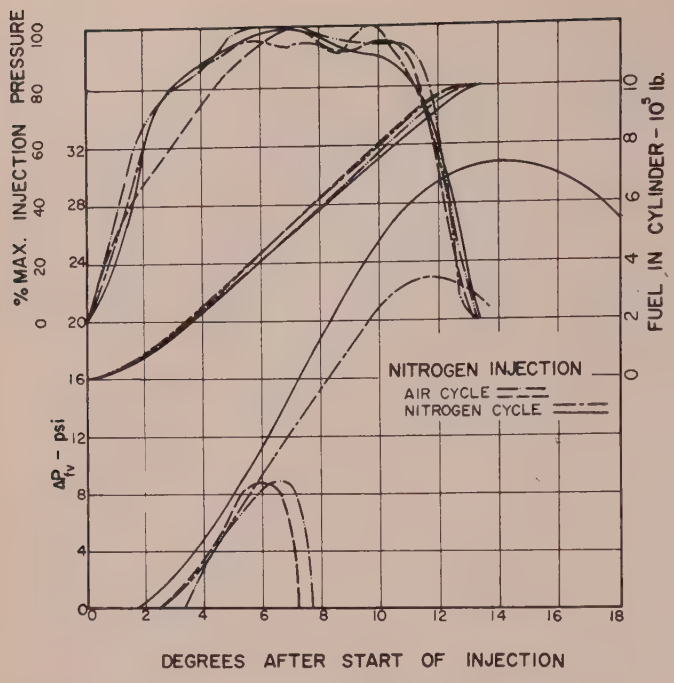

Fig. 10 – Data showing ΔP_{fv}, per cent maximum injection pressure, and fuel in cylinder with nitrogen and with air in cylinder

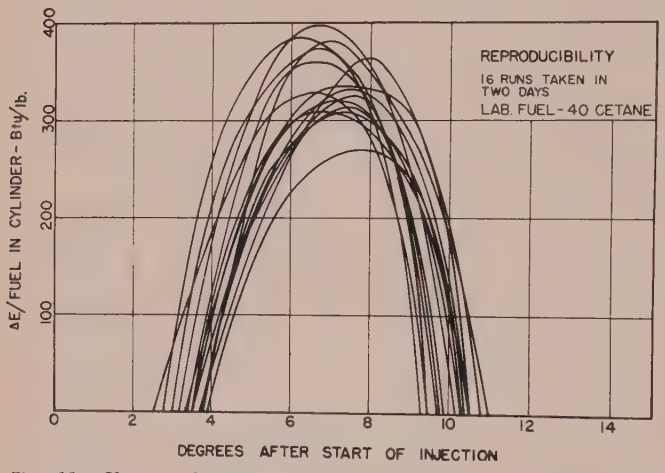

Fig. 11 – Change of specific internal energy in reproducibility runs

tion and vaporization processes.

Regarding factors causing irreproducibility, determinations of point of injection from the same film by different individuals varied by as much as 0.5 crank-angle deg.

Variations in point of injection for the individual reproducibility runs are shown in Table 5, as well as average values of point of injection for different fuels studied.

Scaling accuracy was estimated at 0.25 psi. Determinations of ΔP_{fv} from the same film by different individuals varied by 0.25 psi. This value represents not only scaling error but also any small misalignments between fired and hot-motored cycles with respect to both crank angle and pressure scale.

Data on primary reference fuels in Fig. 4 show very clearly the trend in peak value of ΔP_{fv} with cetane number. The trend is not unexpected for with lower cetane-number fuel more fuel is injected, and if no evolution of heat occurred more cooling of air would be expected. The trend towards higher values of ΔP_{fv} with lower cetane-number fuel may have been accentuated slightly by the somewhat greater quantity of low-cetane fuel injected. It is of interest to note that ΔP_{fv} approaches zero more rapidly – the slope of the curve has a larger negative value – for high-cetane fuel than for low-cetane fuel. This trend is reversed, of course, soon after ΔP_{fv} passes through zero and the rapid pressure rise accompanying combustion of low-cetane fuels is experienced.

Similar data and results for secondary reference fuels are shown in Fig. 5. The same trend for peak value of ΔP_{fv} to increase with a decrease in cetane number is evident here. With the exception of the 71.5-cetane fuel the trend for a greater negative slope with increased cetane number is also evident in Fig. 5.

Commercial fuels of varying cetane number, data for which are shown in Fig. 6, also show the same trend in ΔP_{fv}. They do not seem to show the increased negative slope with increased cetane number as did the primary and secondary reference fuels. The significance of this disagreement is not clear. Fig. 7 shows the data for pure fuels. Again the trend for the peak value of ΔP_{fv} to increase with cetane number is evident. Heptane, the lower-cetane fuel, is also more volatile. It is not clear from Fig. 7 whether the higher peak value of ΔP_{fv} is due to increased volatility of heptane, its lower cetane number, or a combination of the two.

Addition of amyl nitrate and tel to a low- and high-cetane fuel respectively (see Figs. 8 and 9) results in the same relationship between ΔP_{fv} and cetane number. With amyl nitrate, however, the negative slope of the curve decreased with in-

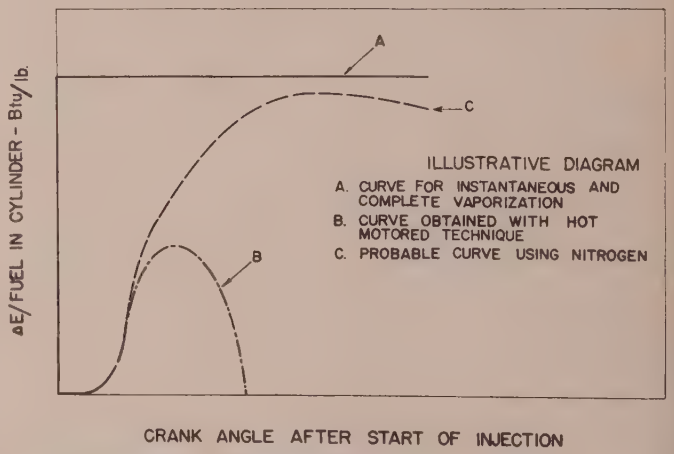

Fig. 12 – Illustration of significance of curves for change in specific internal energy

creased cetane number rather than increasing as it did for the primary and secondary reference fuels. With tel there was no pronounced change in slope.

One of the basic aims of the study was to determine the relative importance of events occurring during ignition delay. If combustion is considered to occur only in the vapor phase then vaporization and subsequent chemical reactions in the vapor phase are the two important events during ignition delay. Consequently, considerable thought was given to ways in which the data might yield information on these events.

It was decided to compute and plot curves of change of internal energy E of fuel actually present in the combustion chamber, that is, ΔE per pound of fuel injected up to a particular crank angle. Details are given in Appendices I and II. Briefly, the procedure is as follows: weight of fuel injected up to any crank angle (designated W_{fCA}), is obtained from published data,[6] oscillograms of rocker-arm strain gages driving the injector, and measured fuel rates. Total change of internal energy of the fuel is obtained by writing the general energy equation for fired and hot-motored cycles from the crank angle corresponding to the start of injection to the crank angle in question. Assuming the two cycles identical up to the start of injection, that heat transfer from the gases to the wall (or vice versa) is the same for the fired and hot-motored cycles, and that the perfect gas law is applicable to the air, exhaust gases, and fuel vapor, the resulting two equations can be solved for change of internal energy, E_{fCA}, of the fuel. The ratio of the two quantities, $\Delta E_{fCA}/W_{fCA}$, is the desired figure.

Considering the assumptions involved, remember that the range of crank-angle degrees covered is small (a maximum of 13 deg), that for most fuels tested only about half of the fuel was injected during the ignition delay period (impingement on the walls should be small), and that fuel vapor pressure was comparatively low.

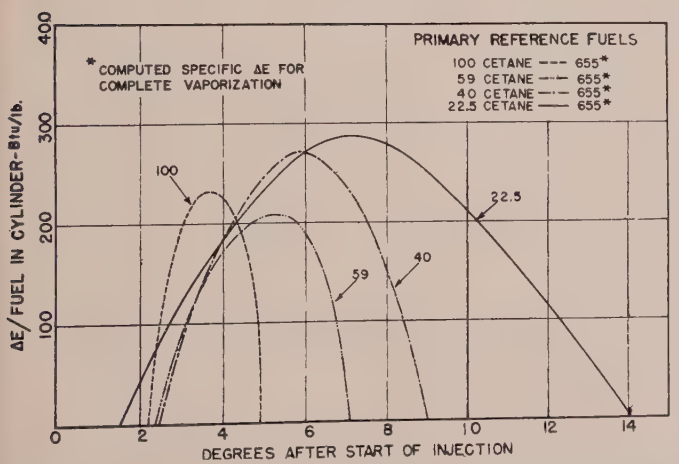

Fig. 13 – Change in specific internal energy for primary reference fuels

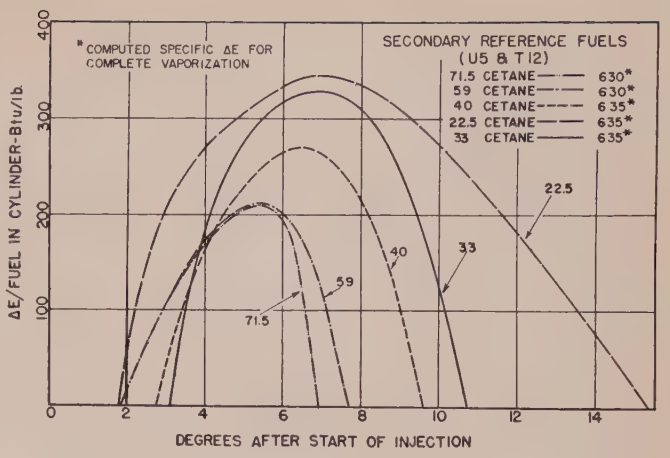

Fig. 14 – Change in specific internal energy for secondary reference fuels

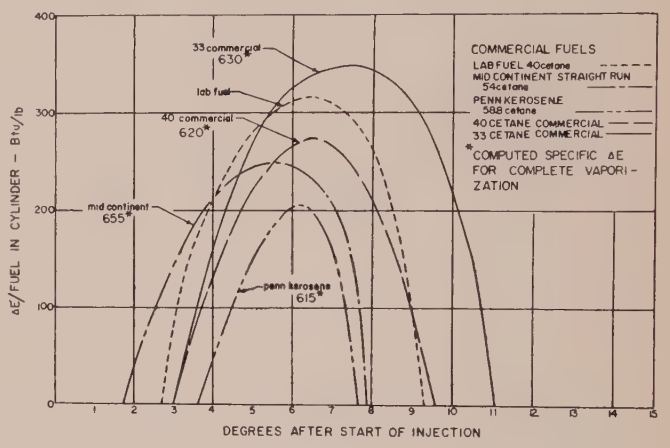

Fig. 15 – Change in specific internal energy for commercial fuels

Curves of $\Delta E_{fCA}/W_{fCA}$ were computed for the reproducibility runs in Fig. 3. The resulting curves are shown in Fig. 11. Note in Fig. 11 that the variations in $\Delta E_{fCA}/W_{fCA}$ under the same operating conditions are of the same order of magnitude as the variation in ΔP_{fv}.

Fig. 12 will help in explaining the significance of the curves of Fig. 11. Fig. 12 shows three curves. The first curve shows values for the change in specific internal energy if vaporization were instantaneous and complete as soon as fuel is injected, assuming a constant temperature and no chemical reaction. The second curve is a typical experimental curve. As expected the fuel does not vaporize completely and instantaneously, especially at first when injection pressures are low. As injection pressure increases the extent of vaporization increases but soon exothermic chemical reaction occurs. When the rate of heat evolution exceeds the rate of heat absorption due to vaporization the curve begins to decrease in value and soon becomes negative. Thus while some chemical reaction is undoubtedly occurring prior to the maxi-

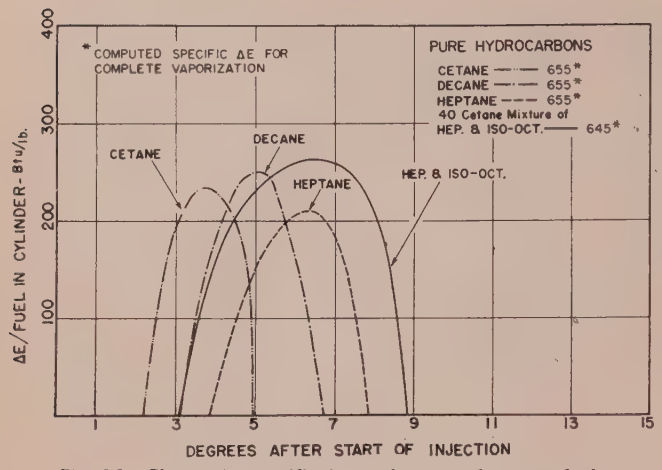

Fig. 16 – Change in specific internal energy for pure fuels

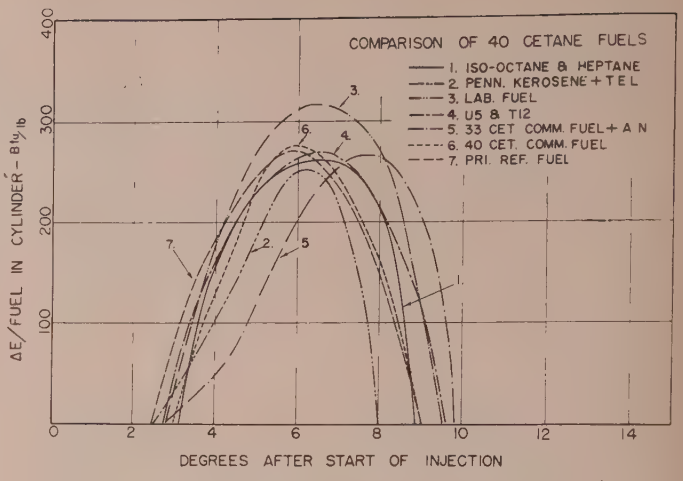

Fig. 19 – Change in specific internal energy for 40-cetane fuel

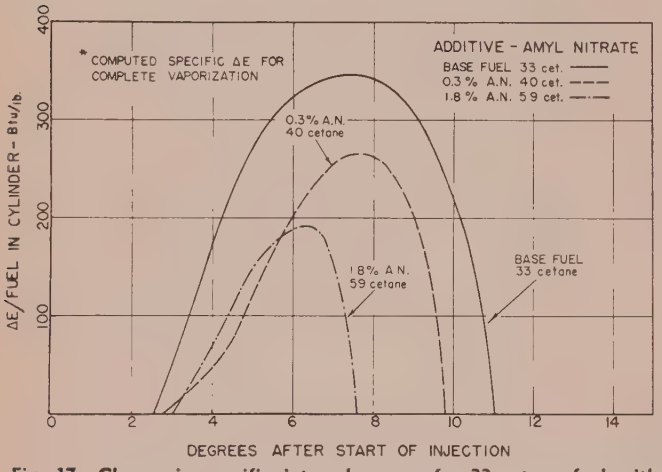

Fig. 17 – Change in specific internal energy for 33-cetane fuel with amyl nitrate added

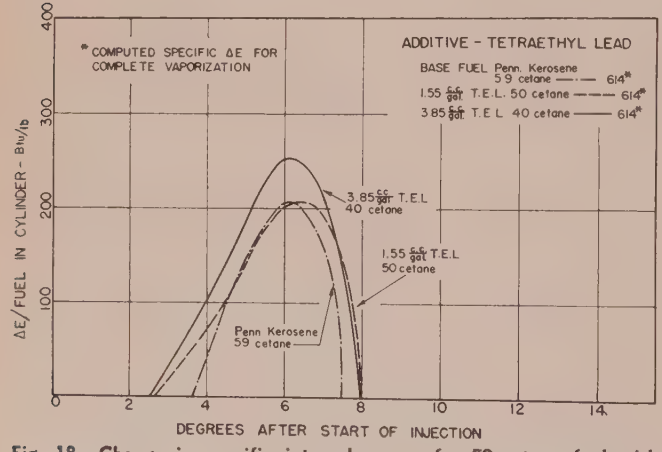

Fig. 18 – Change in specific internal energy for 59-cetane fuel with tel added

mum value of $\Delta E_{fCA}/W_{fCA}$ it seems certain that the portion of delay after this maximum value is entirely due to the time required for chemical reaction to build up to explosive values. The third curve is a probable curve that would result were the fuel injected into an inert gas such as nitrogen rather than air.

Curves of $\Delta E_{fCA}/W_{fCA}$ for the data of Figs. 4-9 were computed and are shown in Figs. 13-18. In order to give an indication of the extent of vaporization, estimates were made of $\Delta E_{fCA}/W_{fCA}$ for complete and instantaneous vaporization. In these computations fuel was assumed to enter the combustion chamber at 200 F, vaporized, and heated to 1000 F. Because of uncertainties in these figures and in the physical constants used, the values shown may be in error by as much as 10-15%. No particular accuracy is claimed for these estimates.

Fig. 13 presents data for primary reference fuels. The negative slope of the curves is greater for the higher-cetane number fuel. As defined, ΔE includes energy changes due to vaporization and chemical reaction; the curves shown are the sum of these two opposing effects. There seem to be no large differences in the rate of injection and vaporization between the high- and low-cetane fuels, so one must conclude that during early reactions the rate of exothermic reaction is appreciably higher for high-cetane fuel than for low-cetane fuel. On an overall basis, at least, as soon as the reaction becomes explosive this situation is reversed.

It is of interest that peak values of ΔE are appreciably less than the values estimated for complete vaporization.

Values of ΔE for secondary reference fuels are shown in Fig. 14. Statements made concerning primary reference fuels seem equally applicable to secondary reference fuels.

Similar data for commercial fuels are shown in Fig. 15. The change in value of the negative slope with cetane number is not as apparent as for the primary and secondary reference fuels. This may be due in part, however, to the fact that the range of cetane numbers covered was appreciably less.

The data for the pure hydrocarbons (Fig. 16) are of interest in that peak values of ΔE for volatile heptane differ but little from peak values of ΔE for comparatively nonvolatile cetane.

The addition of amyl nitrate (Fig. 17) shows a decrease in ΔE with an increase in cetane number. This was also the case with primary and secondary reference fuels. The inflection in the early part of the curve for 0.3% amyl nitrate is of questionable significance since this portion of the curve is not too accurate.

Decreasing cetane number by adding tel (Fig. 18) does not seem to produce as much of an increase in maximum value of ΔE per pound as was evidenced with the reference fuels.

Values of ΔE per pound for all the 40-cetane fuels are plotted in Fig. 19. Both pure and commercial fuels are included and a wide range of volatility and viscosity are covered. Disregarding the data for fuels containing additives, the spread between 40-cetane fuels is no greater than the spread between the reproducibility runs.

Curves previously presented help illustrate the factors causing ignition delay. Speaking of the ΔP_{fv} curves, in general there is a lag of 2-3 crank-angle deg between beginning of injection and beginning of measurable ΔP_{fv}. Since ΔP_{fv} must be caused either by vaporization or by endothermic reactions (and more probably the former), and heat transfer to the spray is small until breakup occurs, this must mean either an injection delay or a spray breakup delay. In considering this delay it must be remembered that it is difficult to determine with precision the crank angle at which ΔP_{fv} first ceases to be zero.

Injection delay might result from the open nozzle used, and if so, would be expected to be more important for volatile fuels. Data for pure hydrocarbons show that cetane, a viscous fuel, has fewer degrees before the start of ΔP_{fv} than heptane, a nonviscous fuel. This would seem to indicate that injection lag caused by outrush of fuel as the ports started to close or by leakage past the plunger might be contributing to this portion of the delay. Data for other fuels seem to be random and no conclusions can be drawn at this time. It would be of interest to determine the precise instant at which fuel first entered the cylinder in each case.

Once the fuel is in the chamber and spray breakup has started it is of interest to compare behavior of fuels. To make this comparison curves of ΔE were plotted against crank-angle degrees after the start of ΔP_{fv}.

Comparison for primary reference fuels is shown in Fig. 20 while comparison for secondary refer-

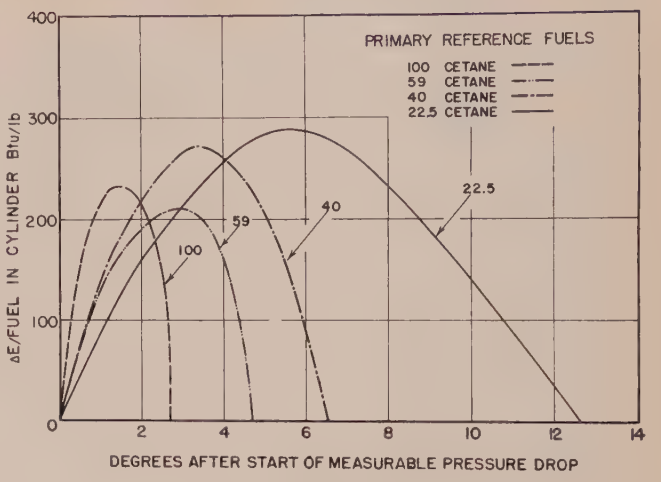

Fig. 20 – ΔE as function of degrees after start of ΔP_{fv} for primary reference fuels

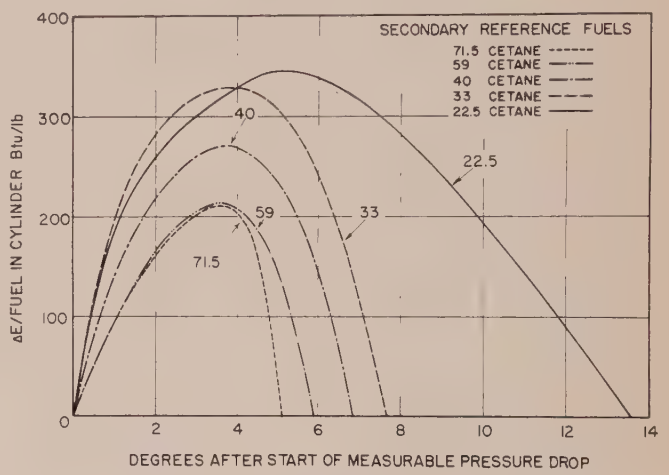

Fig. 21 – ΔE as function of degrees after start of ΔP_{fv} for secondary reference fuels

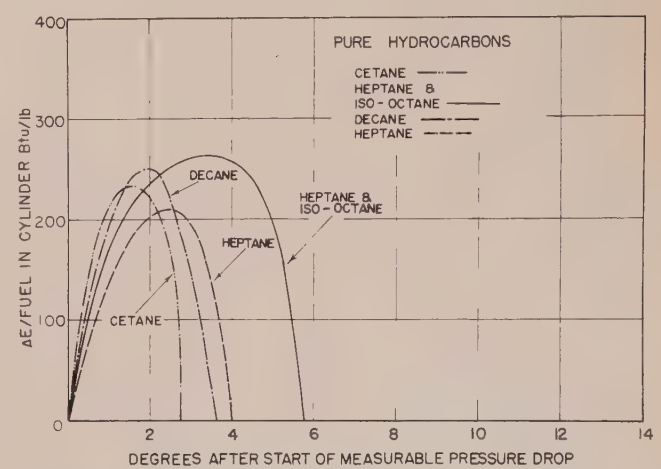

Fig. 22 – ΔE as function of degrees after start of ΔP_{fv} for pure fuels

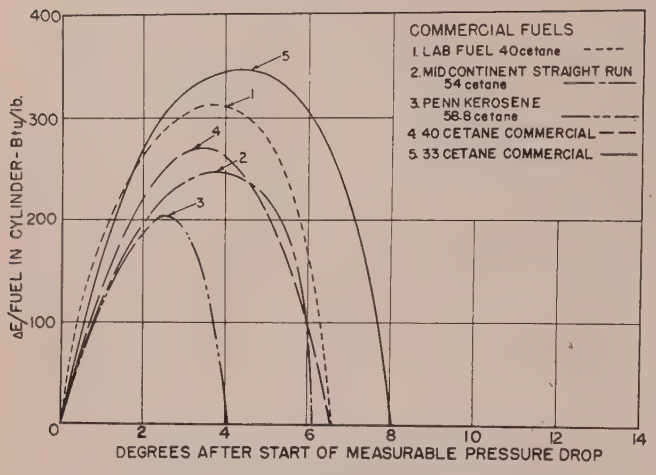

Fig. 23 – $\triangle E$ as function of degrees after start of $\triangle P_{fv}$ for commercial fuels

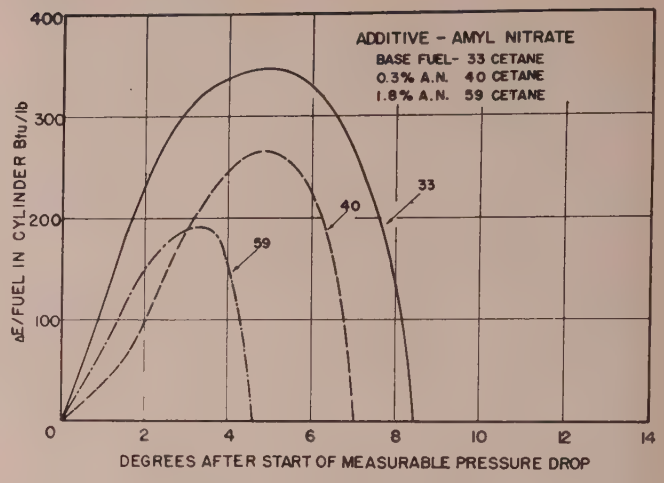

Fig. 24 – $\triangle E$ as function of degrees after start of $\triangle P_{fv}$ for 33-cetane fuel with amyl nitrate added

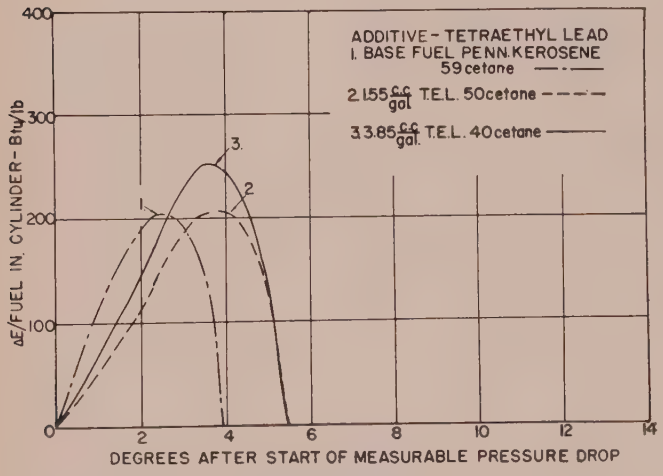

Fig. 25 – $\triangle E$ as function of degrees after start of $\triangle P_{fv}$ for 59-cetane fuel with tel added

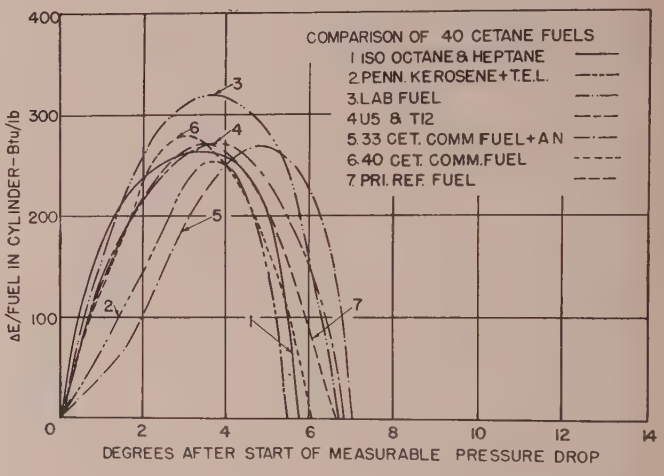

Fig. 26 – $\triangle E$ as function of degrees after start of $\triangle P_{fv}$ for 40-cetane fuel

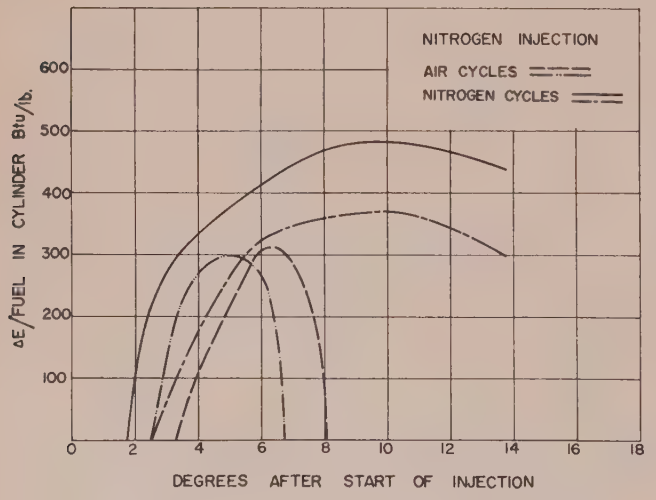

Fig. 27 – Change in specific internal energy when using nitrogen

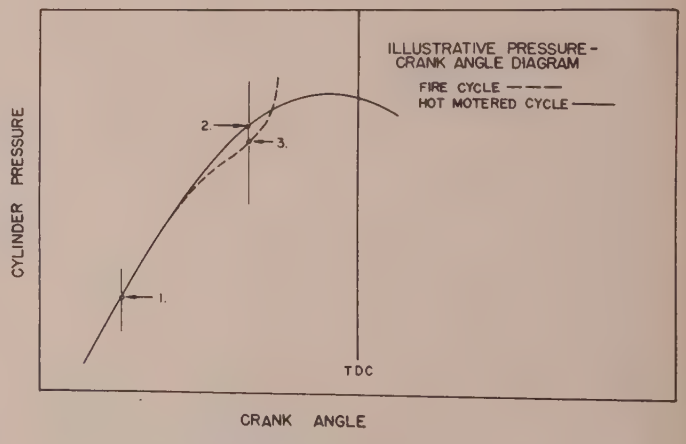

Fig. 28 – Diagram illustrating thermodynamic analysis of hot-motored cycle

ence fuels is shown in Fig. 21. Data for primary reference fuels show a larger positive slope for higher cetane number while secondary reference fuels show the reverse trend. On the portion of the curve with a positive slope, 40- and 59-cetane-number primary reference fuels seem to be in reverse order as well as the 33- and 40-cetane secondary reference fuels. In spite of these anomalies it is indicated that fuels differ either in the rate at which the spray receives heat from the air or during very early reactions.

Fig. 22 shows similar data for pure hydrocarbons. Cetane, decane, and heptane show a consistent trend. The heptane-iso-octane mixture is not quite consistent with heptane. This mixture should not differ too much in volatility from heptane, which would indicate that some effect other than that due to volatility was important. It should be emphasized, however, that the initial portion of these curves is in a region where results are affected very much by scaling errors in ΔP_{fv} and errors in determining rate of fuel injection.

Corresponding curves for commercial fuels is shown in Fig. 23, in which no particular trend is noticeable.

Data for the two additives used are shown in Figs. 24 and 25. Data for tel do not show a consistent trend. Data for amyl nitrate do not show a consistent trend as plotted. As mentioned previously the inflection in the early part of the 0.3% amyl nitrate curve is questionable. Were the curve drawn to the base line without this inflection a consistent trend would obtain.

Fig. 26 shows data for all the 40-cetane fuels. Were the data for doped fuels omitted, there would be remarkably little variation in the curves considering the wide range of fuels and fuel properties dealt with.

An attempt was made to obtain data with everything the same except that air in the cylinder was replaced by nitrogen for a single cycle. This technique is still in the development stage. Some difficulties encountered are that at higher rpm, although the engine would misfire completely, apparently there was enough oxygen mixed with the nitrogen to allow a small amount of reaction. Even this small amount of reaction is not permissible since it might mask vaporization effects. Another associated problem was that in spite of the large air volume and a 2-in., solenoid-operated, butterfly valve opening to atmosphere, compression pressure was around 30-50 psi higher with nitrogen.

Some data were obtained at 400 rpm. Two cycles are presented in Fig. 10. The ΔP_{fv} curve for nitrogen was obtained by comparing two nitrogen cycles, one with fuel injected, the other without fuel injected. Obviously, these cycles were not consecutive although they were taken only 30 or 40 sec apart. The ΔP_{fv} for air was obtained in the usual manner, the only difference being that engine speed was 400 instead of 800 rpm.

There is an appreciable difference between both the ΔP_{fv} curves for nitrogen and for air and between the two ΔP_{fv} curves for nitrogen. The difference between the nitrogen and air curves is expected. The difference between the two nitrogen curves may be due to the time difference between taking data for the curves, or it may be due to the difference in compression pressures (about 50 psi) for the two resulting curves. This higher compression pressure might indicate better air-box scavenging and thus more nitrogen (and less oxygen) in the cylinder and less reaction. It is emphasized again that those data are preliminary only and the technique is still under development.

Change of specific internal energy for the nitrogen data is shown in Fig. 27. The two curves show considerable disagreement as to the extent of vaporization. It is not clear whether this is a result of different compression pressures, of the incomplete development of the technique, or cycle irreproducibility.

In conclusion, the following points seem important:

1. There are small differences between fuels either in injection lag or in spray-breakup time.
2. Once spray breakup is accomplished there are small differences in the rate at which fuel sprays receive heat from the air. A volatile fuel does not seem to receive heat more rapidly than a nonvolatile fuel.
3. The larger the cetane number the smaller the peak value of ΔP_{fv}.
4. Once spray breakup has occurred there is appreciably more variation in the rate of early chemical reactions than there is in rate of fuel vaporization.
5. Vaporization of fuel on a weight basis does not seem to be much more than half completed by the time rate of heat evolution due to chemical reaction exceeds the absorption of heat due to vaporization.

Acknowledgment

The authors wish to acknowledge the support of the following organizations: equipment from the Research Laboratories, General Motors Corp.; fellowship support and supply of test fuels from the Research Laboratories, Ehyl Corp.; fellowship support, equipment, and salary support from the College of Engineering, University of Wisconsin and the Wisconsin Alumni Research Foundation; and the interest and assistance of the Continental Oil Co.

Appendix I

Recent work by Wehrman et al.[6] has established that even in pulsating flow the flow rate through the nozzle of the GM-71 unit injector for all practical purposes is proportional to the square root of the pressure. Although this relationship was established using a strain gage around the injector tip

it was also established that a strain gage mounted on the rocker arm gave reasonably good correlation with the strain gage in the tip. The present experiments use a strain gage on the rocker arm.

In order to translate rocker-arm strain-gage reading to rates of fuel injection the following assumptions were made:

1. Flow rate is proportional to the square root of pressure.

2. Rocker-arm strain-gage reading is directly proportional to nozzle pressure. In this connection no signal was observed from the strain gage during the hot-motored cycle, indicating inertia effects were negligibly small.

3. Fuel injected per cycle is the same for each cycle with all conditions held constant during the test run.

4. Cylinder pressure has a negligible effect on flow rate. Both theory and data of Wehrman et al.[6] show that this is not a completely valid assumption during the very first part of injection but the effect of this assumption on the computed results was negligible.

The following procedure was used: From the experimental oscillogram record of strain-gage reading versus crank angle, a curve of square root of strain-gage reading versus crank angle was plotted and the area under this curve measured. The ordinate of this plot was proportional to the flow rate while area under the curve was proportional to weight of fuel injected per cycle. Weight of fuel injected per cycle was obtained from the measured fuel rate. This measurement, together with the measured area under the curves, established the proportionality constant between area and flow rate. Measurement of an incremental area under the curve of square root of strain-gage reading together with this proportionality constant gave an average value of fuel-flow rate for the crank angle at the center of the incremental area.

Appendix II

Fig. 28 illustrates the hot-motored cycle from which change in internal energy of the fuel during ignition delay is determined. The assumptions made are:

1. Up to the time fuel was injected (point 1, Fig. 28), the two cycles were identical. They were identical during the period 1 to 2 except for the injection of fuel. This implies:

(a) Heat transferred to the walls was the same in both cases. This assumes no impingement of fuel on the wall.

(b) There was negligible chemical reaction in the gases during the hot-motored cycle.

(c) Change in internal energy of fuel in the nozzle tip during the hot-motored cycle was negligible.

2. During the fired cycle the chemical reaction was small enough not to alter the thermodynamic properties of the gases.

3. Gases and fuel vapor in the cylinder obeyed the perfect gas law. Gases were assumed to have the thermodynamic characteristic of air.

4. Change in total pressure due to increase in partial pressure of fuel during vaporization is a negligible percentage of ΔP_{fv}. Computations justifying this assumption have been made by Collins.[11]

Let us define our thermodynamic system as the engine cylinder plus the volume of fuel injected. The notation used is:

F = Fired cycle
HM = Hot-motored or nonfired cycle
a = Air
f = Fuel
w = Weight of gases trapped in cylinder
W = Work
E = Internal energy
Q = Heat transferred

Writing the First Law for the two cycles gives:

$$Q_{HM} = E_{a2} - E_{a1} + W_{1-2} \tag{1}$$

$$Q_F = E_{a3} - E_{a1} + W_{1-3} - E_{f3} - E_{f1} + W_f \tag{2}$$

Subtracting (2) from (1) gives:

$$0 = E_{a2} - E_{a3} + W_{1-2} - W_{1-3} - W_f \tag{3}$$

$$E_{f3} - E_{f1} = E_{a2} - E_{a3} + W_{1-2} - W_{1-3} - W_f \tag{4}$$

The quantity $W_{1-2} - W_{1-3}$ represents area under a curve of ΔP_{fv} versus cylinder volume. The difference between these terms was quite small. The quantity W_f represents work done in injecting fuel. This quantity was also found to be quite small.

The quantity $E_{a2} - E_{a3}$ represents the change in internal energy of the air. It can be evaluated by:

$$\begin{aligned} E_{a2} - E_{a3} &= wC_v\,(T_{a2} - T_{a3}) \\ &= wC\,\frac{(PV)}{(wR)_{a2}} - \frac{(PV)}{(wR)_{a3}} \\ &= \frac{VC_v}{R}\,(P_{a2} - P_{a3}) \end{aligned}$$

All quantities except C_v and R can be experimentally determined. Both C_v and R are specified by assuming the gases have the thermodynamic properties of air and assuming a compression temperature estimated as 1500 R in this case.

[11] See "Pressure Study of Injection Cooling Effect in Diesel Engine," by R. N. Collins. M. S. Thesis in Mechanical Engineering, University of Wisconsin, 1954.

DISCUSSION . . .
. . . of this article starts on p. 726

Fuel Heat Gain and Release in Bomb Autoignition

R. W. Hurn, J. O. Chase, C. F. Ellis, and K. J. Hughes,
Bureau of Mines

This paper was presented at the SAE Golden Anniversary Diesel-Engine Meeting, St. Louis, Nov. 4, 1955.

NET interchange of heat between injected fuels and the atmospheres into which they were injected has been studied in a constant-volume combustion-bomb. These studies were undertaken to gain more information on the factors that govern the heating of injected fuels and the release of chemical energy in the autoignition process.

The data show that chemical heat release occurs only after an appreciable interval of time during which the fuel is heated and may be partly or wholly vaporized. The rapidity of this heating – and associated ignition delay – are influenced markedly by the physical properties of the surrounding gas. Fuel volatility and chemical structure have relatively little influence on the rate of heat transfer to the fuel in the pre-reaction period. It is also shown that the delay period before release of chemical energy and the rate of chemical energy release are influenced both by the chemical composition of the fuels and by gas-to-fuel heat-transfer rates during the pre-reaction period.

THE work reported was done in collaboration with investigators at the University of Wisconsin to obtain the time history of heat transfer between fuels and air (or other gases) when fuels were injected into a heated and pressurized bomb-type vessel. These heat-transfer data were expected to yield information indicating how fuel heating, vaporization, and subsequent heat release are influenced by the physical and chemical properties of both the fuel and the atmosphere into which the fuel is injected. Engine data pertinent to this subject and a theoretical treatment of the problem have been presented by University of Wisconsin investigators.[1, 2] It is intended that the data in this paper be used in conjunction with the data and theoretical discussion in the Wisconsin papers.

It is the purpose of this paper to present data with a minimum of interpretation. Following presentation of the data, it is hoped that these findings may be correlated with those of other investigators, and that they may be critically reviewed for agreement with the theoretical concepts presented by others.

Experimental Procedure

All data reported were obtained in a constant-volume combustion-bomb chosen for this work because of the high degree of precision that may be obtained in both temperature and pressure control

[1] See "Physical and Chemical Ignition Delay in Operating Diesel Engine Using Hot Motored Technique," by T. C. Yu, R. N. Collins, K. Mahadevan, O. A. Uyehara, and P. S. Myers, on pp. 690-702 of this issue.

[2] "Fuel Vaporization and Ignition Lag in Diesel Combustion," by M. M. El Wakil, P. S. Myers, and O. A. Uyehara, on pp. 712-729 of this issue.

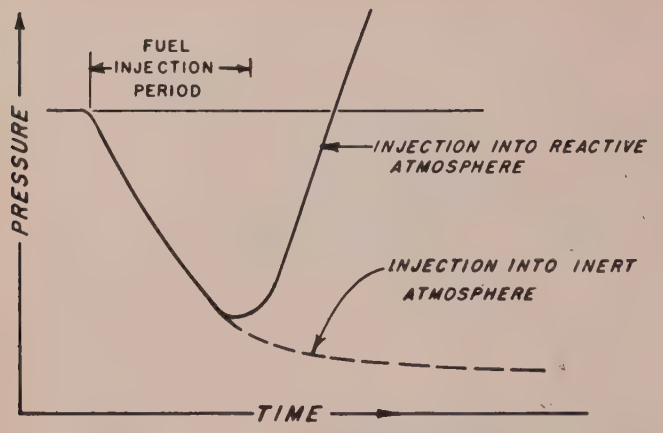

Fig. 1 – Typical pressure record

and because of the flexibility with which conditions of operation may be chosen. The apparatus has been described previously.[3] Briefly, it consists of a heated stainless-steel cylinder approximately 2½ in. in internal diameter by 4 in. in internal length. Temperature may be controlled within the range of 400 to 1300 F. Fuel is introduced by means of a conventional plunger-type injection pump, modified to permit injection of a single charge of fuel. Pressure changes that accompany injection and combustion of the fuel are sensed by means of a strain-gage pickup and associated electronic circuitry. These pressure signals are generated on a cathode-ray oscillograph, and may be photographed for study.

The heat transfer between injected fuel and the

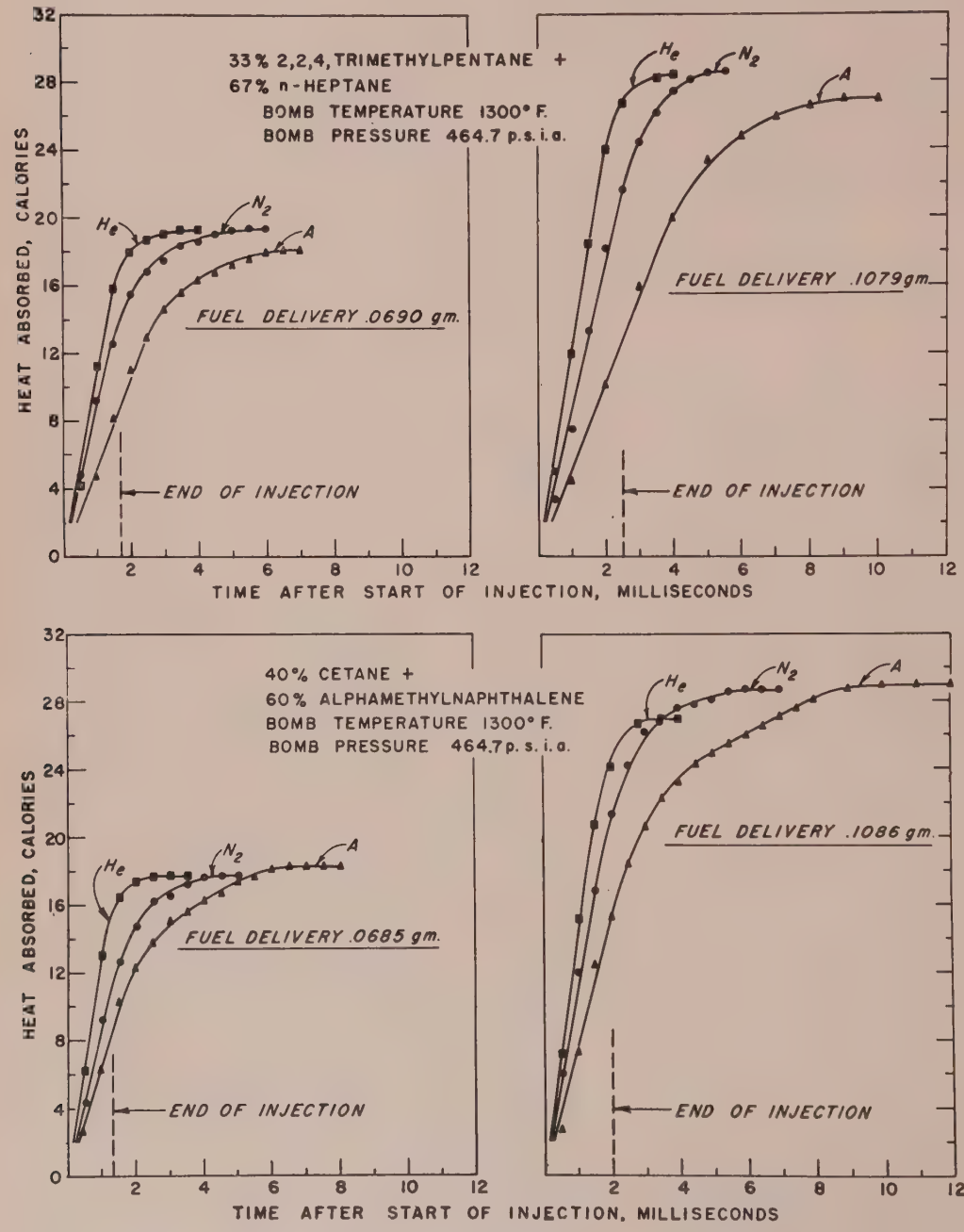

Fig. 2 – Influence of different gases on heat absorbed by injected fuel. (Bomb temperature 1300 F)

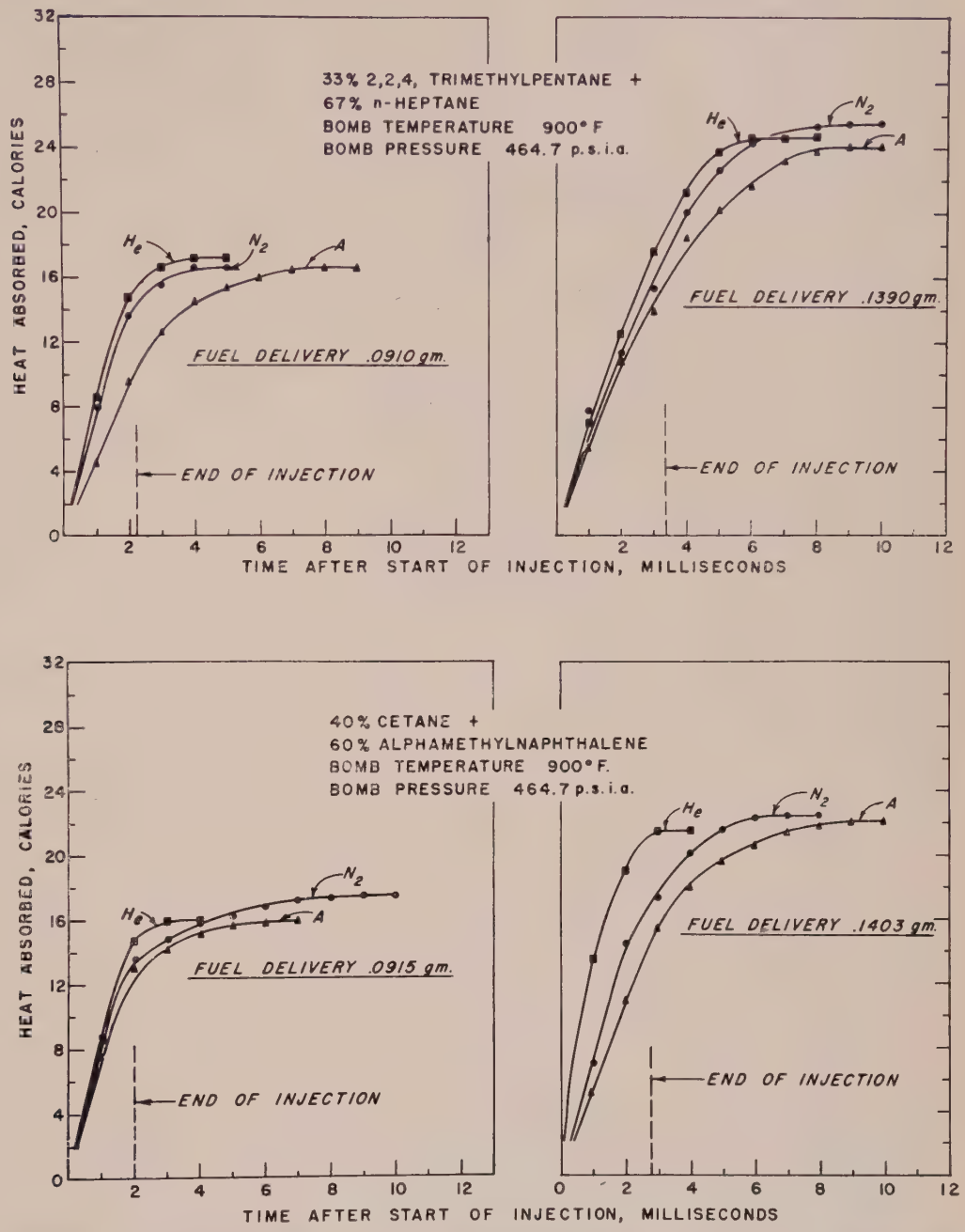

Fig. 3 – Influence of different gases on heat absorbed by injected fuel. (Bomb temperature 900 F)

gas medium in the bomb was calculated from the pressure data by use of well-known thermodynamic relationships. Heat-release data were calculated by comparing the pressure-time curve that resulted from injection of the fuel into an oxidizing atmosphere to the pressure-time curve obtained when the fuel was injected into an inert atmosphere. Heat released in the oxidation reaction was presumed to result in deviation of the reactive curve from the inert curve. Representative curves are shown in Fig. 1.

A primary objective of these experiments was to determine how fuel volatility affects vaporization and heating of the fuel. Two fuels of widely different volatility, but of approximately equal cetane number, were chosen, and the bulk of the study was made on these two fuels. Both fuels were of 40 cetane number, one a relatively volatile mixture of 33% isooctane (2,2,4, trimethyl pentane) and 67% normal heptane, and the other a low-volatility mixture of 40% normal cetane and 60% alphamethylnaphthalene. Data were taken at bomb temperatures of 900 and 1300 F, using inert bomb

[3] See Proceedings, American Petroleum Institute, Vol. 30M [III], 1950, pp. 227-237: "Constant-Volume Combustion of Diesel Fuels," by R. W. Hurn and K. J. Hughes.

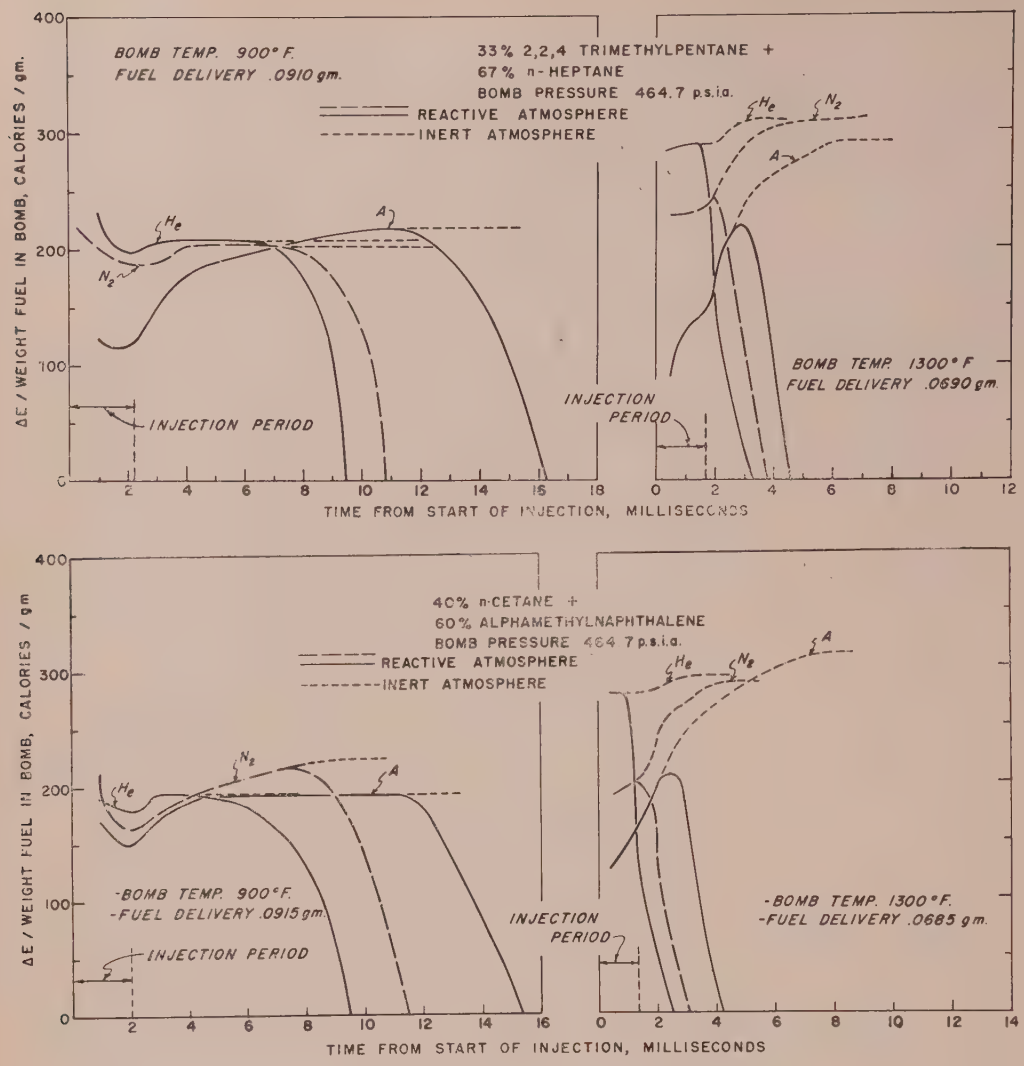

Fig. 4 – Effect of inert gas on heat absorbed per unit weight of fuel in bomb – nominal F/A ratio = 0.02. ($F/O_2 = 0.09$)

atmospheres of helium, nitrogen, and argon, and reactive atmospheres of each of these inert gases plus 20.4 mol per cent oxygen. For each of the test conditions, fuel delivery was adjusted to give each of two fuel/oxygen ratios that corresponded to nominal F/A ratios of 0.02 and 0.03.

Some pertinent data on the gases and fuels are given in Tables 1 and 2.

Additional data were obtained for fuels containing an ignition inhibitor or an ignition improver, and for blends of different cetane-number mixtures. This was done to determine how a change in ignition quality might influence the course of early heat absorption and release.

Table 1 – Comparative Values of Thermal Conductivity and Density of Gases at 0 C[a]

Gas	Thermal Conductivity, cal/(cm)(sec)(deg C)	Density, 1 Atmosphere, g/liter
He	33.60×10^{-5}	0.1785
N_2	5.68×10^{-5}	1.2506
A	3.88×10^{-5}	1.7824

[a] From "Handbook of Chemistry," by N. A. Lange, 1952 edition. (Comparative rates of mass diffusion and heat transfer also are pertinent. The Lewis Number, which is the dimensionless ratio of thermal conductivity to the coefficient of self diffusion, is 1.2 for monatomic gases and 1.0 for diatomic gases.)

Experimental Results

Figs. 2 and 3 show heat absorbed by the isooctane-heptane and cetane-alphamethylnaphthalene blends in three different inert atmospheres. From a study of these data, the following conclusions are made:

1. The heat absorbed within a given time interval increases in the same order as the thermal conductivities of the gases, and decreases with the

increase of gas densities. By the same token, it may be said that the rate of heat absorption increases with increased diffusivity of the gas;

2. The rate of heat absorption is not materially influenced by the quantity of fuel injected except during the terminal period of heat transfer;

3. Higher gas temperatures result in higher rates of heat transfer.

The curves of Fig. 2 are reasonably well defined by the empirical equation:

$$Q = Q_{max}\left[1 - B\,[1 - e^{-B(t_f - t)}]\,[t_f - t]^{1.5}\right]$$

where:

Q = Heat absorbed from inert atmosphere, cal

Q_{max} = Total heat absorbed from inert atmosphere at final equilibrium, cal

t_f = Time to attain final equilibrium, msec

t = Elapsed time from beginning of fuel injection (between the limits where $Q = 0$ and $t = t_f$)

Dependence of the factor *"B"* has not been established. For the curves of Fig. 2 for isooctane-heptane (0.1079 g fuel) the factors are:

Argon, B = 0.08
Nitrogen, B = 0.175
Helium, B = 0.225

Although the equation is empirical, it has a theoretical basis in that the exponential function, $1\text{-}e^{-B(t_f - t)}$, which it contains, is similar to heat-transfer expressions that are derived from known physical laws. The addition of fuel mass during the interval $t_0 - t_f$ enormously complicates the heat-transfer process, and probably precludes complete rationalization of any equation defining the process. Nevertheless, something may be learned by studying the nature of the mathematical elements that fit the data.

The data for the lower fuel/oxygen ratio are shown in another manner in Fig. 4, in which the quantity of heat absorbed per unit weight of fuel in the bomb is shown as a function of time. For the first ¼ msec the accuracy of calculation of the ratio, $\triangle E$/weight fuel suffers, since the weight of fuel injected is assumed to be proportional to the elapsed time after the start of fuel injection, and therefore small time-measurement errors introduce gross percentage errors in calculated fuel weights. There is a characteristic dip in the curves at about the end of the injection period that may or may not be significant, since the precise time at the end of injection is unknown, and there may be some error in estimating the cumulative quantity of fuel injected to this point.

In these curves, the behavior most immediately apparent is rapid absorption of heat by the helium atmosphere upon first contact with injected fuel and, conversely, the exceptionally slow absorption

Table 2 – Laboratory Values for Some Physical Properties of the Hydrocarbon Blends

Blend	Boiling Range, F	Specific Gravity, 60 F d——— 60 F	Kinematic Viscosity, 100 F, centistokes
33% isooctane 67% n-heptane	209.3-210.7	0.6919	0.571
40% n-cetane 60% α-methylnaphthalene	467.6-549.5	0.9257	2.17

Table 3 – Calculated Net Specific Heat of Absorption, g-cal Fuel Injected (to equilibrium temperature between inert gas and injected fuel)

Composition of Bomb Atmosphere	Blend: 33% isooctane, 67% n-heptane; Initial Temperature of Bomb Atmosphere, F: 1300 Low Injection	1300 High Injection	900 Low Injection	900 High Injection	Blend: 40% n-cetane, 60% α-methylnaphthalene; 1300 Low Injection	1300 High Injection	900 Low Injection	900 High Injection
He	446	443	269	267	394	383	239	243
N_2	421	399	259	249	374	359	246	235
A	422	405	259	251	374	354	239	229
Fuel Injected, g	0.069	0.1079	0.0910	0.1390	0.0685	0.1086	0.0915	0.1403

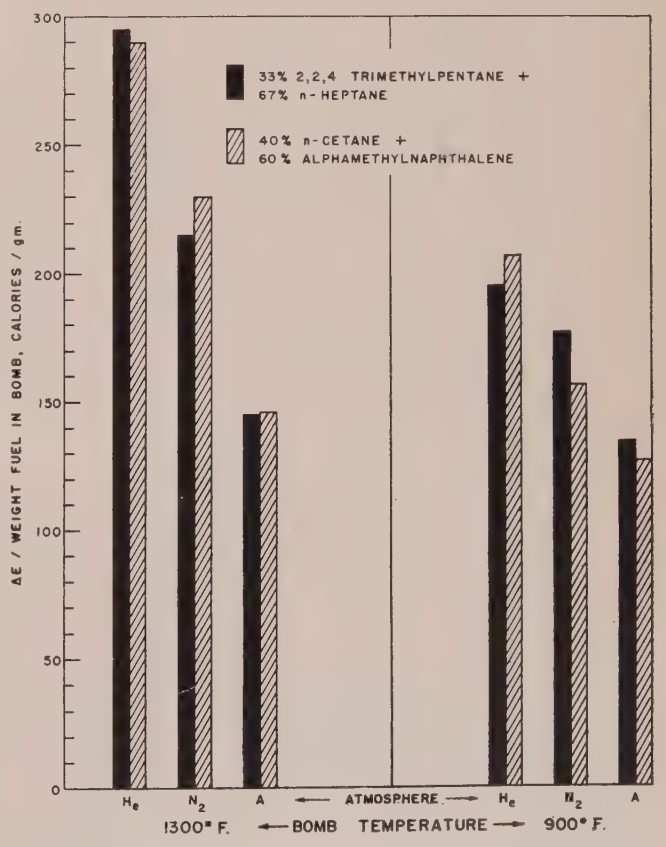

Fig. 5 – Comparison of heat absorbed by fuels with different volatilities. (Values are cumulative to 1.35 msec after start of injection)

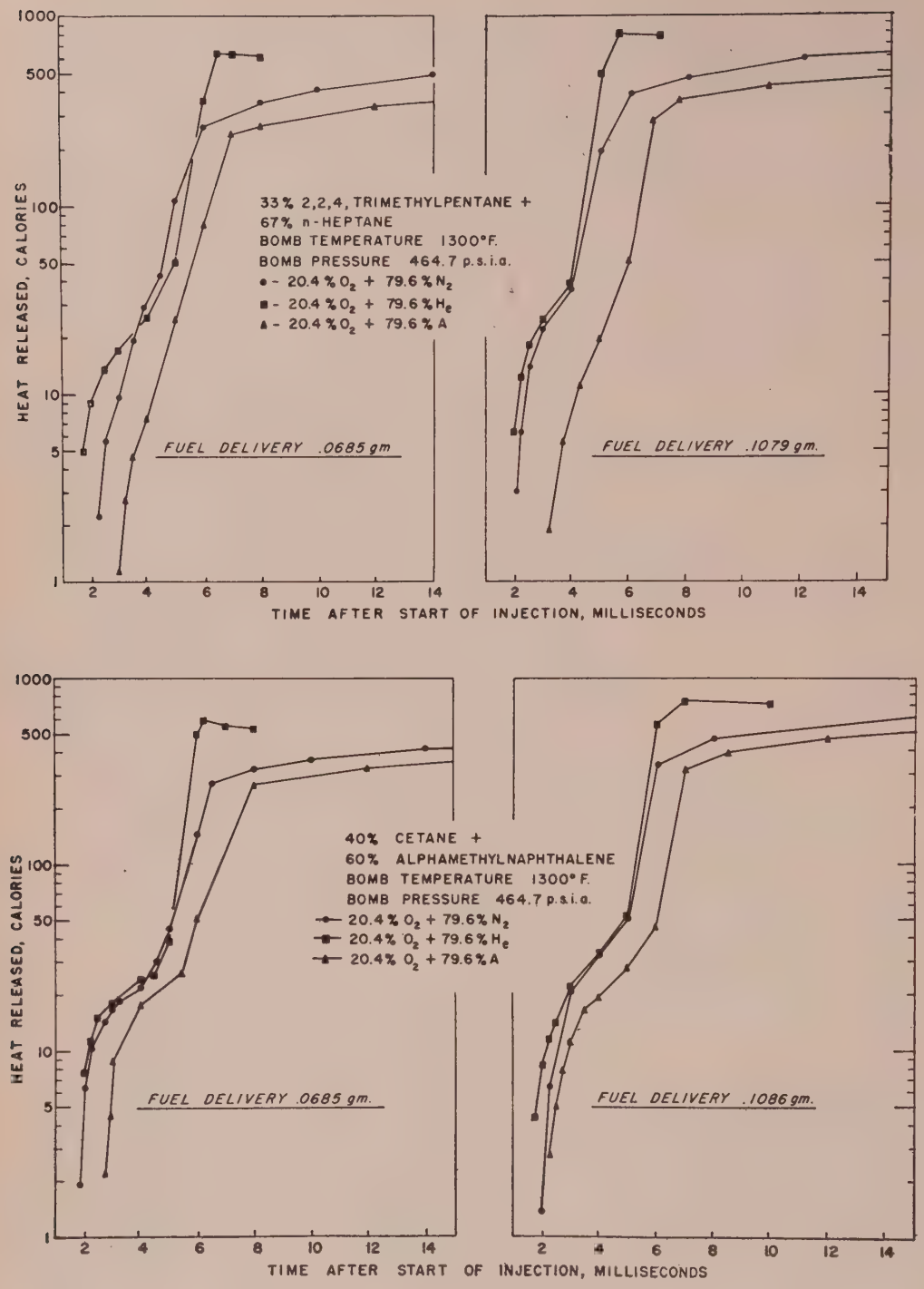

Fig. 6 – Influence of inert gas constituent on heat released during autoignition. (Bomb temperature 1300 F)

of heat by the argon atmosphere. This difference at the beginning of the heat-transfer process appears to be caused solely by differences in thermal conductivity. The point of beginning of heat release is shown as the departure of the reactive atmosphere curve from the curve for inert atmosphere. Release of heat thus is indicated as a negative absorption of heat by the fuel.

The calculated amounts of heat theoretically required to result in temperature equilibrium and complete evaporation following injection of the fuel into the bomb are given in Table 3.

The measured values are roughly three-fourths of the theoretical values. Since the quantity of the fuel injected may be estimated with reasonable accuracy, there was some expectation that measured

values would approach theoretical more closely. It can be presumed that the fuel was injected at an actual temperature higher than that assumed, or that the fuel received an appreciable quantity of heat from the bomb walls.

The average of the data for both 0.02 and 0.03 nominal fuel/air ratio are shown in another manner in Fig. 5. This figure was constructed to permit comparison of the heat absorbed within a given interval of time by two fuels of different volatility. The height of the solid bar represents data for the higher volatility mixture of isooctane-n-heptane, while height of the cross-hatched bar represents data for the low volatility normal cetane-alpha-methylnaphthalene mixture. At neither temperature is there a significant difference between the specific heat absorption of the two fuels. These experimental data show that higher volatility does not result in faster transfer of heat to the fuel. Portions of these data and experimental observations not reported herein suggest that under some conditions the reverse may be true; however, more experimental data are required for verification of these observations.

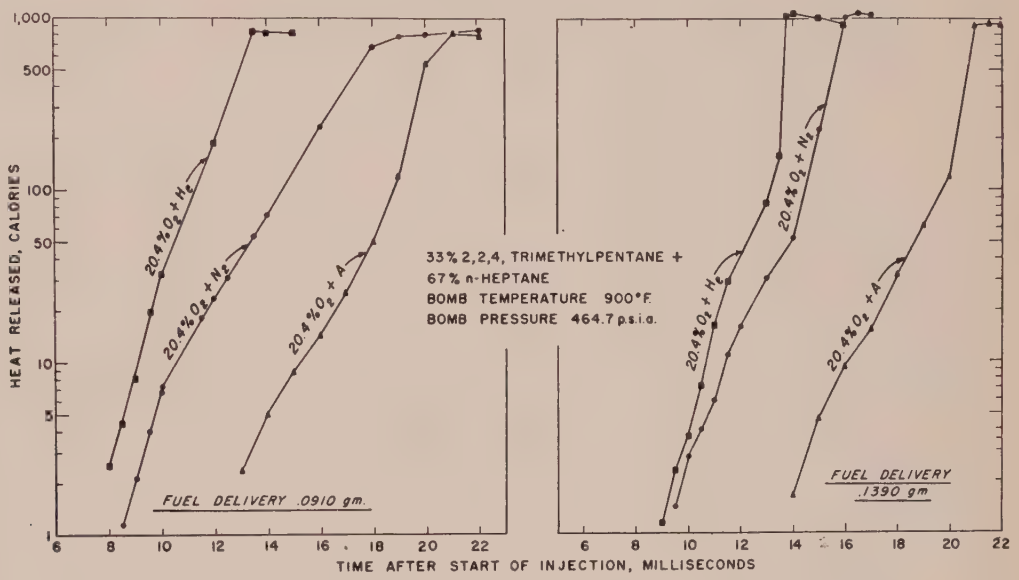

Fig. 7 – Influence of inert gas constituent on heat released during autoignition. (Bomb temperature 900 F)

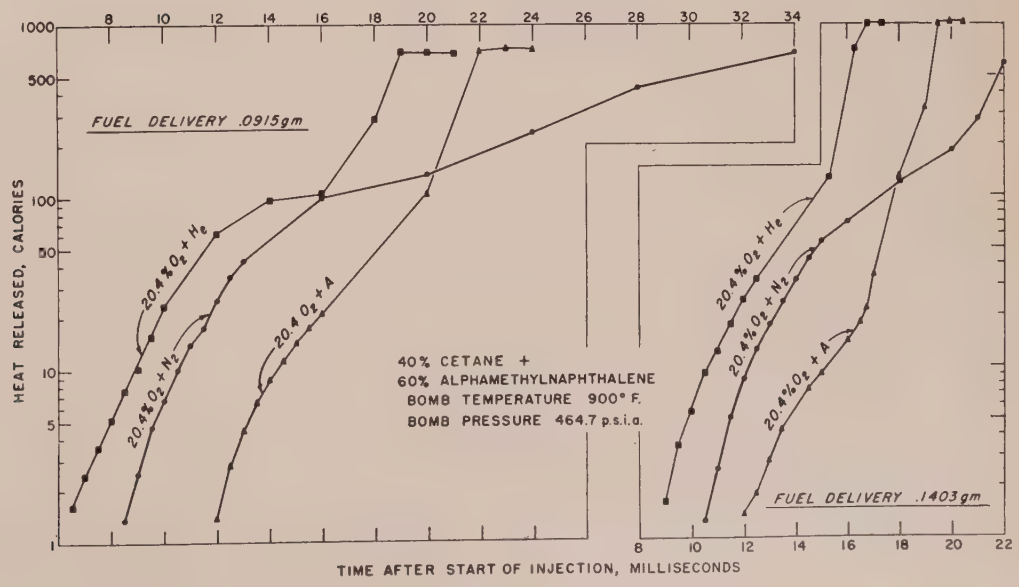

These bar-graph data show another interesting comparison that may be significant. In the helium atmosphere, the two fuels show approximately 50% greater specific heat absorption at 1300 F than at 900 F; in the nitrogen atmosphere, the fuels show approximately 30% greater heat absorption at 1300 F, while in the argon atmosphere the increase in specific heat absorption at 1300 F is only 10% over that at the lower temperature. This suggests that the effect of increased temperature is much more pronounced in the atmospheres that have higher heat conductivity and diffusivity.

Calculated values of heat release following autoignition of the fuels are given in Figs. 6 and 7. Study of these data leads to the following observations:

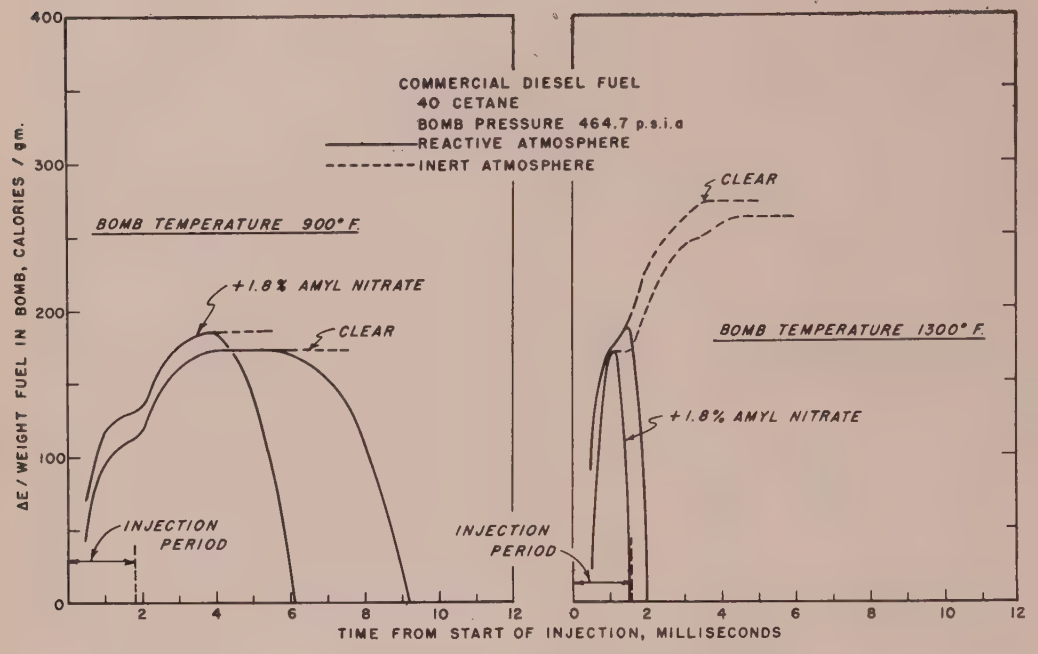

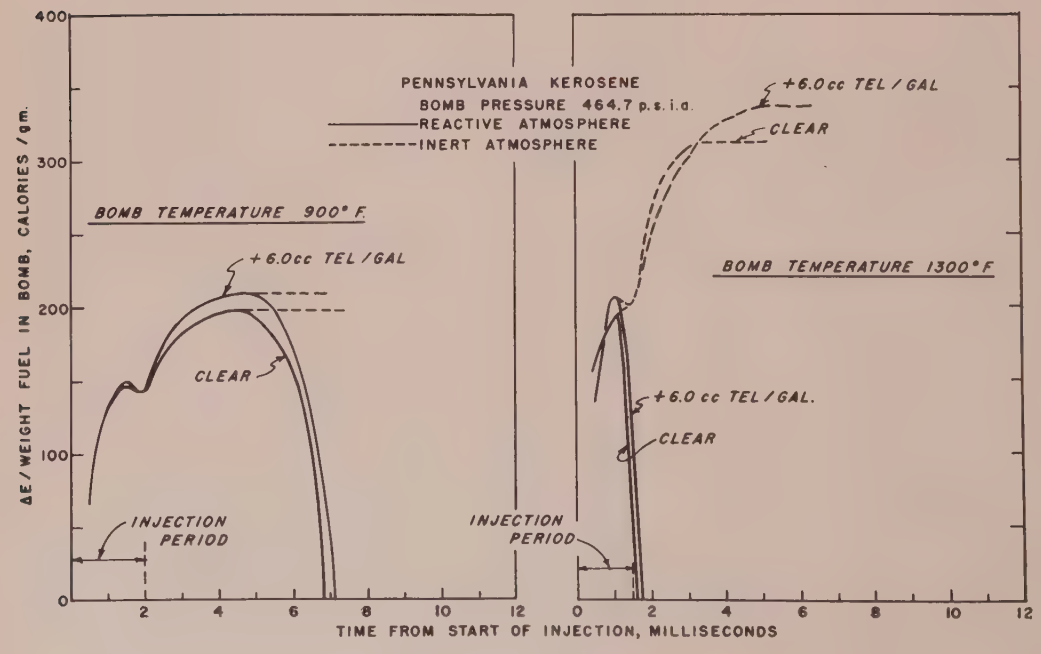

Fig. 8 – Influence of additive on specific heat absorption and release

1. The helium atmosphere is conducive to the earliest heat release. Probably this can be explained on the basis that its higher heat conductivity causes faster heating of the fuel and earlier attainment of an equilibrium high temperature.

2. The argon atmosphere is least conducive to early heat release. Since argon and helium have identical specific heats, these differences are probably explained on the basis of differences in heat conductivity. This effect is particularly pronounced in the earlier phases of fuel injection. For later phases, diffusivity factors may be controlling.

3. The data for the isooctane-heptane mixture show greater differences between atmospheres than the data for the lower volatility cetane-alphamethylnaphthalene mixture.

4. Lower temperatures accentuate the differences between different atmospheres.

5. The staged heat-release phenomenon is more pronounced for the cetane-alphamethylnaphthalene mixture than for the isooctane-heptane mixture.

At 900 F, the combustion of cetane-alphamethylnaphthalene mixture in the nitrogen-bearing atmosphere shows a marked reduction in rate of heat release shortly after autoignition begins. This results in a very slow combustion compared with combustion in the helium and argon atmospheres. The authors offer no explanation, but since the data are believed to be reproducible, comment by others would be interesting.

To obtain information regarding the influences of additive materials on heat transfer during the pre-reaction period, data were taken on a commercial diesel fuel treated with amyl nitrate-type ignition improver and on a high-quality kerosene to which tel had been added as an inhibitor. Comparable data also were taken on three different blends of normal cetane and alphamethylnaphthalene. Curves for these data are presented in Figs. 8 and 9. Curves for specific heat absorption of the commercial diesel fuel clear and with the ignition improver indicate that there is no significant difference between heat transfer to the additive-bearing material and to the clear fuel. However, there is a significant difference between the time of beginning of heat release for the two fuels. Furthermore, the fuel with the ignition improver releases heat more rapidly early in the autoignition process.

The effect of tel in the Pennsylvania kerosene is also shown clearly. However, the difference between combustion curves for the clear and tel-bearing kerosene is not as great as might be expected from the difference in cetane number. The effects of amyl nitrate and tel are sharply contrasted. Whereas the amyl nitrate has a marked effect at the lower temperature of 900 F, tel has little more effect at 900 F than it does at 1300 F. The influence of the tel at low test temperatures is therefore relatively minor,

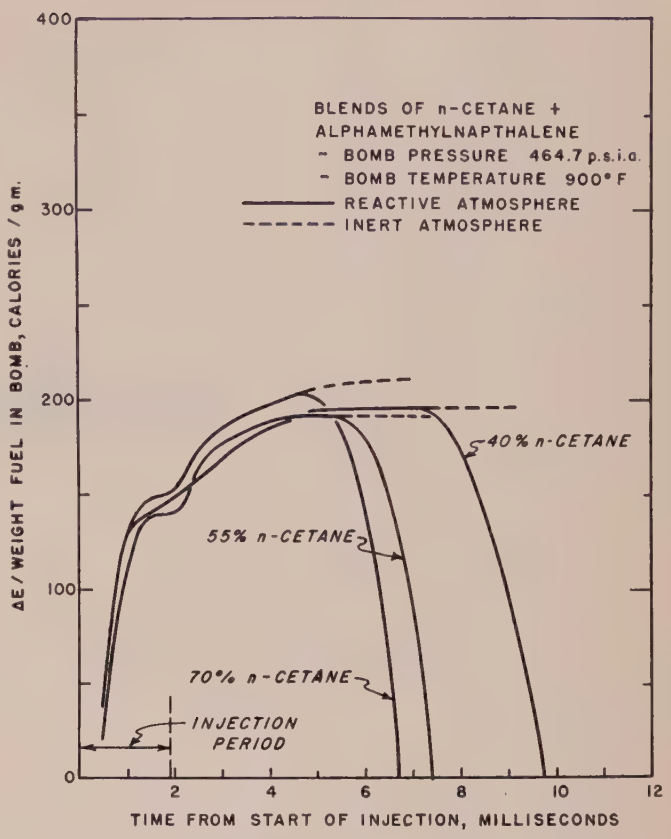

Fig. 9 – Specific heat absorption and release for reference fuel blends

whereas it does show a significant influence at the high temperature.

The differences between combustion curves for the several different cetane-alphamethylnaphthalene blends were very similar to the differences between the commercial diesel fuel clear and that fuel with amyl nitrate ignition improver. There are no significant differences in rates of heat transfer to the several blends during the pre-reaction period, and the only material difference in the curve for the different blends is in the time at which heat release begins. From these data it appears that the greatest difference between the autoignition behavior of fuels is in those factors that affect chemical reaction, rather than in those that affect physical processes. However, it must be kept in mind that fuel atomization, spray formation, turbulence, contact cooling, and other mechanical factors may markedly affect temperatures and, in turn, the course and time-history of chemical reaction.

DISCUSSION . . .

. . . of this article starts on p. 726.

Fuel Vaporization and Ignition

ALTHOUGH early experimenters held different views it is now generally accepted that combustion of liquid fuels occurs in the vapor phase rather than the liquid phase. If this concept is accepted it follows immediately that ignition lag experimentally observed in the diesel engine may be due in part at least to the time required to get fuel into the vapor phase.

It has also been demonstrated experimentally[1] that completely vaporized fuels do not burn instantaneously even under conditions of high temperature and pressure. From these and other data, the concept of chemical delay arises. Thus for purposes of discussion, ignition lag in a diesel engine is sometimes divided into physical and chemical delay. It is realized, of course, that some chemical reactions probably take place during vaporization and that at times the two phenomena may take place simultaneously. The concept is helpful, however, and will be used.

While it is common to divide ignition lag into these two different parts, to date there has been no determined effort to determine the relative magnitude of the two components, that is, which one is rate determining. Wentzel[2] in a pioneering paper computed time required to vaporize fuels. He concluded that small droplets vaporized very rapidly (one-half millisecond), while larger droplets vaporized much more slowly. Schmidt[3] recognized Wentzel's calculated results but suggested a formula for ignition lag based on chemical reaction rates alone. Rothrock and Waldron[4] photographed fuel in a diesel combustion chamber. After reviewing previous work they concluded there was considerable vaporization of injected fuel and that this vaporization affected the course of combustion. Miller's high-speed photographs[5] show that combustion begins long before vaporization is complete. On the other hand it was shown[6] that rate of pressure drop in a constant volume bomb due to fuel cooling was directly proportional to estimated rate of fuel injection. The preceding data are confusing but it seems certain that vaporization has not been entirely completed when combustion starts.

This paper will discuss factors entering into ignition delay. Before doing so it might be well to summarize known experimental facts concerning ignition lag. These are:

1. An increase in inlet air pressure and temperature, in fuel temperature, and in jacket water

[1] See SAE *Quarterly* Transactions, Vol. 4, April, 1950, pp. 232-274: "Ignition of Fuels by Rapid Compression," by C. F. Taylor, E. S. Taylor, J. C. Osgood, W. A. Russell, and W. A. Leary.

[2] See NACA TM 797 (1936), "Ignition Process in Diesel Engines," by W. Wentzel.

[3] See NACA TM 891 (1939), "Theoretical and Experimental Study of Ignition Lag and Engine Knock," by F. A. F. Schmidt.

[4] See NACA TR 435 (1932), "Fuel Vaporization and Its Effect on Combustion in High-Speed Compression-Ignition Engine," by A. M. Rothrock and C. D. Waldron.

Lag in Diesel Combustion

M. M. El Wakil, P. S. Myers, and O. A. Uyehara, University of Wisconsin

This paper was presented at the SAE Golden Anniversary Diesel-Engine Meeting, St. Louis, Nov. 4, 1955.

temperature all decrease ignition lag to varying degrees.

2. Ignition lag decreases with engine speed. This is generally attributed to an increase in turbulence with speed. However, Small[7] found that in a bomb, increased turbulence did not give decreased ignition lag. Probably, actual compression temperature increases with speed.

3. There is a reasonably good inverse relationship between the cetane and octane scales. Since ignition delay in a spark-ignition engine is predominantly chemical, octane number would presumably be related to chemical delay. This would indicate that the chemical delay was rate-determining.

4. While fuel volatility seems to affect ignition lag, the accompanying change in fuel structure seems more important. For example, isooctane and n-heptane have markedly different ignition lags but about the same volatility, while cetane and isooctane are markedly different in both volatility and ignition lag.

5. Small concentrations of additives affect ignition lag. Although possibly these small concentrations (0.5-1.0% or less), affect spray formation and physical delay, it seems more likely that they act in a chemical manner.

6. In a constant-volume bomb with everything else held constant, an increase in quantity of fuel injected increases ignition lag if combustion begins near the end of ignition. This would indicate a fuel cooling or a concentration effect.

With these experimental facts in mind, discussion of phenomena occurring during the ignition

AN analysis of phenomena occurring during the ignition delay period is presented. Vaporization of atomized fuel is shown to take place under conditions ranging between single droplet and adiabatic saturation from edge to center of the spray. Mechanisms of vaporization and combustible mixture formation are presented for both cases.

Correlation of theoretical analysis with experimental data from both a combustion bomb and diesel engine is presented to establish actual conditions existing during vaporization. Estimates of physical and chemical delays for the engine and bomb are given.

[5] See SAE Transactions, Vol. 53, December, 1945, pp. 719-735: "Slow-Motion Study of Injection and Compression of Fuel in Diesel Engine," by C. D. Miller.

[6] See Coordinating Research Council Diesel Bomb Advisory Group Progress Report, February, 1951, "Combustion Characteristics – Ignition Delay Bomb."

[7] See *Engineer*, Vol. 164, Dec. 10, 1937, p. 668: "Vagaries of Internal Combustion," by J. Small.

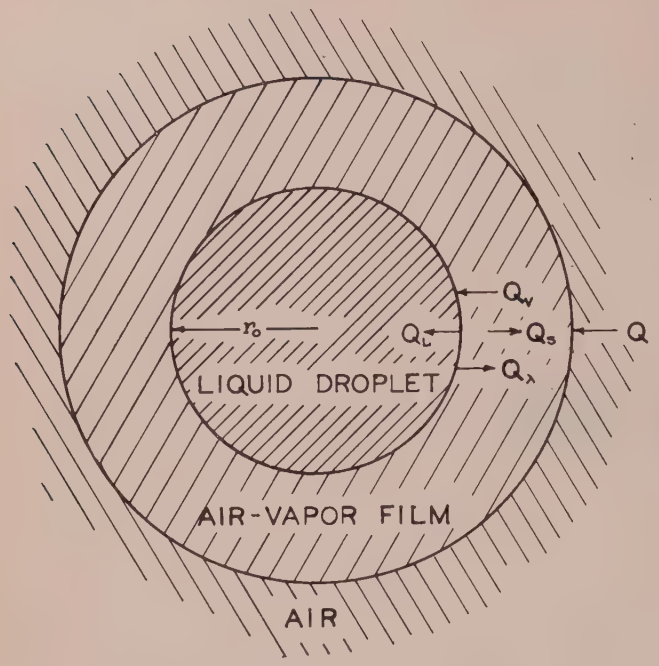

Fig. 1 – Heat-transfer from air to droplet

delay period follows.

The Jet Breakup

As fuel is introduced into the combustion chamber it leaves the nozzle initially as a sheet or ligament which ultimately breaks up into a spray of different size droplets. Since the surface/volume ratio is not large for sheets and ligaments, vaporization is usually considered negligible until breakup occurs. Any delay in jet breakup contributes to ignition delay.

The mechanism of jet breakup has been studied by a number of different investigators[8-16]. For intermittent sprays used in diesel engines the picture formed from a study of these references is as follows: fuel initially leaves the injector at low pressure (and thus, low velocity), relative to the air. Under these conditions aerodynamic forces play but little part in jet breakup. However, ever-present surface disturbances are amplified until the fuel column breaks up into fragments which assume a spherical shape due to surface tension. These spherical droplets are relatively large and slow-speed. As injector pressure increases, jet velocity increases, influence of aerodynamic forces and liquid turbulence increases, and size of droplets formed decreases. If turbulence is high enough the jet breaks up into droplets a short distance from the orifice. Since air density also decreases jet breakup distance, it is probable that fully developed spray in a diesel engine has a very short breakup distance.

As injector pressure rises, average size of droplets decreases while their velocity increases. The first relatively large, slow droplets formed start at the center of the spray but are pushed sideways by the incoming rush of succeeding smaller, higher velocity droplets. Thus, unless the combustion chamber is deliberately designed to provide high turbulence, a developed spray will ultimately consist of a concentrated core of high-velocity small droplets surrounded by larger droplets injected early in the process. These larger droplets will have low velocity relative to the air both because of their low initial velocity and the fact that air is swept along with the jet.

Experimentally measured dispersion patterns[11] show that in the vicinity of the nozzle fuel is concentrated largely in the center of the spray at low injection pressures. As pressure and distance from the nozzle increase, fuel is spread more uniformly throughout the spray. Studies also show that the lower the fuel viscosity the more uniform the distribution throughout the spray.

This picture is important in understanding later events. However, all evidence obtained outside engines suggests that spray breakup is not an important part of the physical delay period. Confirmation of this statement will be found in the literature and by Hurn's observation[6] that pressure drop due to fuel vaporization started almost simultaneously with injection. Data taken in an engine by Chow[17] and Yu[18] indicate that neither injection lag nor spray breakup are negligible in an engine.

Drop Vaporization

The discussion above has pointed out factors affecting formation of droplets of different sizes and velocities. These droplets might be considered to vaporize under either of two conditions: (1) they are so far removed from each other that there is no influence of one droplet on another and on air between them, or (2) under conditions where droplets are very close to each other with a consequent large effect on both temperature and fuel-vapor concentration in the surrounding air. At first thought the second condition would seem more likely, but Pilcher[19] has deduced that in atmospheric sprays there is little interaction between drops. Since it is not clear which viewpoint is correct, let us consider both cases and compare conclusions reached from them with experimental results.

[8] See NACA TM 659 (1932), "Disintegration of Liquid Jet," by A. Haenlein.

[9] See *Bureau of Standards Journal of Research*, March, 1931, pp. 369-376: "Mechanism of Atomization of Liquids," by R. A. Castleman, Jr.

[10] See NACA TR 440 (1932), "Mechanism of Atomization Accompanying Solid Injection," by R. A. Castleman, Jr.

[11] See Pennsylvania State College Engineering Experiment Station Bulletin No. 40, August, 1932, "On Formation and Dispersion of Oil Sprays," by K. J. DeJuhasz, O. F. Zahn, and P. H. Schweitzer.

[12] See NACA TR 425 (1932), "Effect of Nozzle Design and Operating Conditions on Atomization and Distribution of Fuel Sprays," by D. W. Lee.

[13] See NACA TR 454 (1933), "Photomicrographic Studies of Fuel Sprays," by D. W. Lee and R. C. Spencer.

[14] See NACA TR 438 (1932), "Experiments on Distribution of Fuel in Fuel Sprays," by D. W. Lee.

[15] See NACA Report 565 (1936), "Measurements of Fuel Distribution within Sprays for Fuel-Injection Engines," by D. W. Lee.

Vaporization without Interaction between Drops – Considering the first case we shall assume that droplets do not affect each other and the air between and that spherical symmetry exists both for the droplet and the air-vapor film surrounding it. This last assumption is necessary for mathematical solutions to be possible. It is also assumed that thermal conductivity of the liquid is quite high, which is justified by the rate of circulation experimentally observed in drops.[20] It will be considered that combustion does not occur during this period. The physical model used is shown in Fig. 1.

Three phenomena will determine the history of the droplet itself under these conditions:

1. Slowing down of the droplet by aerodynamic drag forces.

2. Heat-transfer to the droplet from the air.

3. Mass-transfer (vaporized fuel) away from the droplet.

A complete derivation of formulas applicable to these phenomena are given in the literature.[20, 21, 22]

The equation expressing decrease in droplet velocity relative to the air is:

$$\frac{dU}{d\theta} = -\frac{3}{8} C_D \frac{\rho_m}{\rho_L} \frac{U^2}{r_o} \qquad (1)$$

where:

U = Velocity

θ = Time

C_D = Drag coefficient. There is some evidence that the drag coefficient for vaporizing drops is not the same as that for solid spheres.

ρ_m = Average density of air-vapor mixture in film surrounding the droplet

ρ_L = Density of liquid droplet

r_o = Radius of droplet

Basically, equation (1) says that according to Newton's first law, the aerodynamic drag force slows down the droplet. Mathematically the equation shows that a droplet with higher velocity and smaller diameter has a higher deceleration.

The final formulation for mass transfer is:

$$w = dm/d\theta = A_o K_g P_{fL} \alpha \qquad (2)$$

where:

w = Rate of vaporization of droplet

m = Mass of droplet

A_o = Surface area of droplet

K_g = Mass-transfer coefficient (analogous to heat-transfer coefficient)

P_{fL} = Partial pressure of fuel-vapor at the surface of the droplet (the driving force for mass transfer because partial pressure in the air is assumed zero)

α = Dimensionless correction factor to account for the fact that the film is semipermeable

Like the heat-transfer coefficient, the mass-transfer coefficient is a function of Reynolds see below number. Thus equations (1) and (2) are related.

Referring to Fig. 1, heat-transfer from air to the droplet, Q may be divided into three parts: (a) sensible heat Q_L to heat up the liquid droplet, (b) latent heat of vaporization Q_λ, and (c) superheat Q_S to raise temperature of the diffusing vapor from that of the droplet itself T_L to the air or boundary temperature T_B.

Thus, $Q = Q_L + Q_\lambda + Q_S$

Heat-transfer is given by the standard equation with a correction factor z to account for the effect of mass-transfer on heat-transfer:

$$Q_V = h A_o (T_B - T_L) z \qquad (3)$$

where:

Q_V = Heat transferred to the liquid surface of the drop = $Q_L + Q_\lambda$

h = Heat-transfer coefficient

T_B = Temperature of air surrounding the droplet

T_L = Temperature of liquid droplet

z = Dimensionless correction factor for the effect of mass-transfer on heat-transfer

The concept requiring introduction of z is a very important one and requires explanation. Experimentally it is found impossible to boil a liquid droplet when the droplet receives heat from a gas by convection only. This statement can be explained as follows: heat is transferred to the droplet by the surrounding gas. If the droplet boiled, that is, if partial pressure of the liquid equalled total pressure, there would be no air next to the liquid surface to conduct heat to it. In addition, flow of fuel vapor away from the droplet surface is so rapid that no heat can be conducted in. Under these conditions z would be zero and the droplet would cool down. As temperature – and thus vapor pressure – of the liquid varies from a very low temperature – and thus low vapor pressure – to boiling, z varies from 1 to 0.

This concept is of obvious importance during the physical delay period, for it means that regardless of how hot the air is, in the absence of radiation the droplet temperature will always be below its boiling temperature at the existing gas pressure. It also means that as air temperature becomes very high and droplet temperature approaches its boiling temperature, the driving force for mass-transfer, P_{fL}, approaches the total pressure irrespective of the

---

[16] See ASME Transactions, Vol. 74, 1952, pp. 1157-1162: "Photographic Analysis of Sprays," by J. L. York and H. E. Stubbs.

[17] "Effects of Additives on Diesel Combustion Process," by W. Chow, O. A. Uyehara, and P. S. Myers. Paper presented at SAE National Diesel-Engine Meeting, St. Louis, Oct. 31, 1952.

[18] See paper by Yu, Collins, Mahaderan, Uyehara, and Myers on pp. 690-702 of this issue.

[19] "Characteristics of Sprays and Droplets," by J. M. Pilcher. Paper presented at Conference on Atomization, Sprays, and Droplets, September, 1953, Technological Institute, Northwestern University.

[20] "Experimental and Calculated Temperature and Mass Histories of Vaporizing Fuel Drops," by M. M. El Wakil, R. J. Priem, H. J. Brikowski, P. S. Myers, and O. A. Uyehara. To be published as TN by NACA.

[21] See NACA TN 3179 (1954), "Theoretical Investigation of Heating-up Period of Injected Fuel Droplets Vaporizing in Air," by M. M. El Wakil, O. A. Uyehara, and P. S. Myers.

[22] See "Experimental and Calculated Temperature and Mass Histories of Vaporizing Fuel Drops – Part II," by R. J. Priem, G. L. Borman, M. M. El Wakil, O. A. Uyehara, and P. S. Myers. Report prepared under NACA Contract Naw-6358, August, 1955.

fuel. This means that differences in fuel volatility will be less important at high air temperatures than at low air temperatures.

Note that P_{fL} is a function of T_L and that h is a function of Reynolds number, so that equations (1), (2), and (3) are related and must be solved together. Simultaneous solution of the three equations yields the temperature and mass history of a droplet. Because of the complicated relationships a stepwise integration using a Model II, IBM card-programmed, electronic calculator was used. As a matter of interest calculations for a single point take almost two hours using this machine or a week using a desk calculator. Several references[20, 21, 22] present the method of calculation. They also compare calculated and experimental histories at atmospheric pressure and show that agreement between the two is within the accuracy of physical properties used.

Typical vaporization histories calculated by this method are shown in Figs. 2, 3, and 4 for droplets of n-hexadecane (100 cetane), n-decane (76 cetane), and n-heptane (56 cetane), all of 0.00075 in. initial radius, 150 F initial temperature, and 10,000 in. per sec initial velocity relative to the air, vaporizing in air under constant ambient conditions of 500 psia and 1000 F. These histories have been carried through the first millisecond of the droplet's lifetime.

Figs. 2, 3, and 4 show the temperature, mass, radius, velocity, penetration or distance traveled through air, rate of mass-transfer, rate of heat-transfer from air to the liquid (sensible heat), and latent heat of vaporization histories for each case.

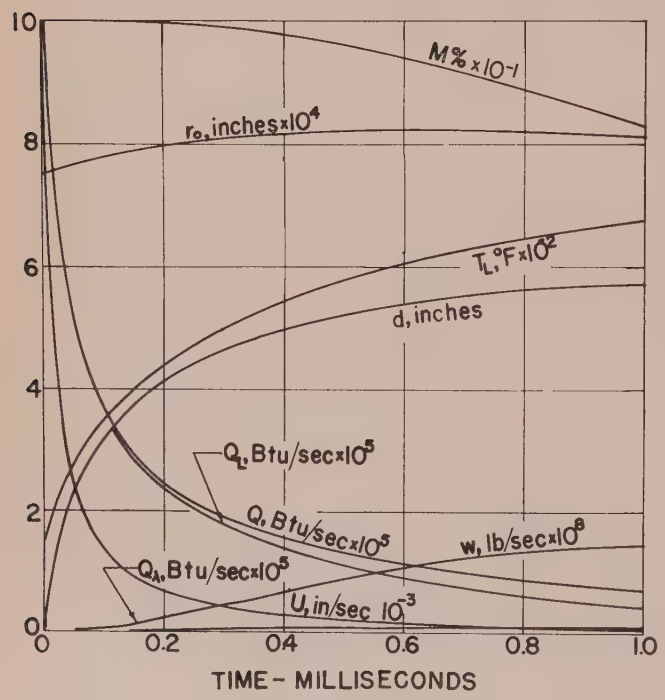

Fig. 2 – Vaporization history of cetane droplet. Initial radius 0.00075 in. Initial temperature 150 F. Initial velocity relative to air 10,000 in. per sec. Air pressure 500 psia, air temperature 1000 F

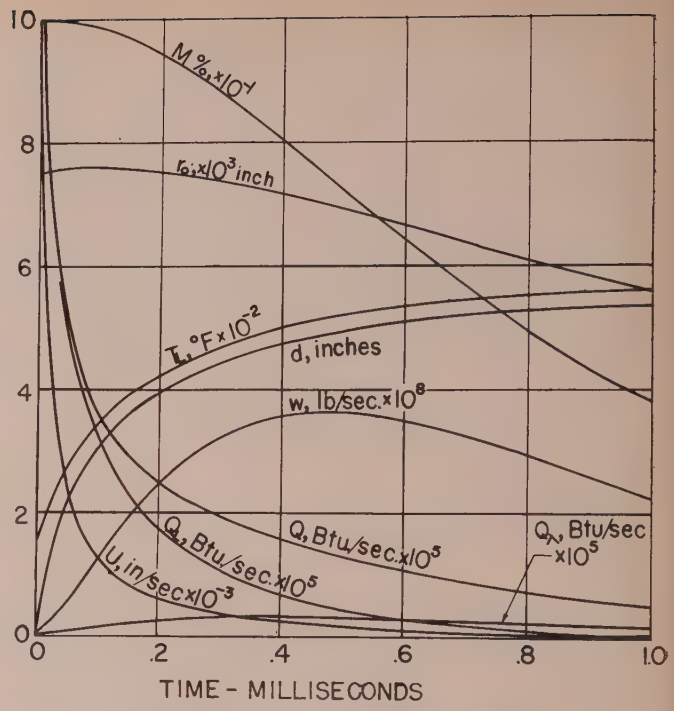

Fig. 3 – Vaporization history of decane droplet. Conditions same as those for Fig. 2

The computed histories show that temperature of each droplet rises rapidly as soon as it comes into contact with air. Then it gradually levels off and asymptotically approaches the wet-bulb temperature corresponding to the particular fuel used and ambient air conditions. Wet-bulb conditions are those when the heat-transfer from air to the droplet is carried away entirely by the mass-transfer. Under these conditions droplet temperature has reached a value where its vapor-pressure and mass-transfer are so high that latent heat of vaporization Q_λ, and diffusing vapor superheat Q_S, balance heat-transfer from the air, Q. For this condition, heat to the liquid Q_L, approaches zero and the droplet remains at its wet-bulb condition until it vaporizes completely. Roughly, then, the lifetime of each droplet can be divided into two portions: the unsteady-state, or time spent by the droplet in heating up to its wet-bulb conditions, and the steady-state, where the droplet remains at its wet-bulb conditions until complete vaporization takes place. The unsteady-state has been found to be an appreciable portion of the droplet's lifetime in most cases.

It is interesting to note from Figs. 2, 3, and 4 that the radius of an injected droplet initially increases before diminishing to zero. This reflects the fact that initially thermal expansion rate is higher than mass-transfer rate. This effect is more pronounced the lower the liquid volatility and the initial liquid temperature.

Another interesting fact is that immediately after a droplet has been formed, and during most

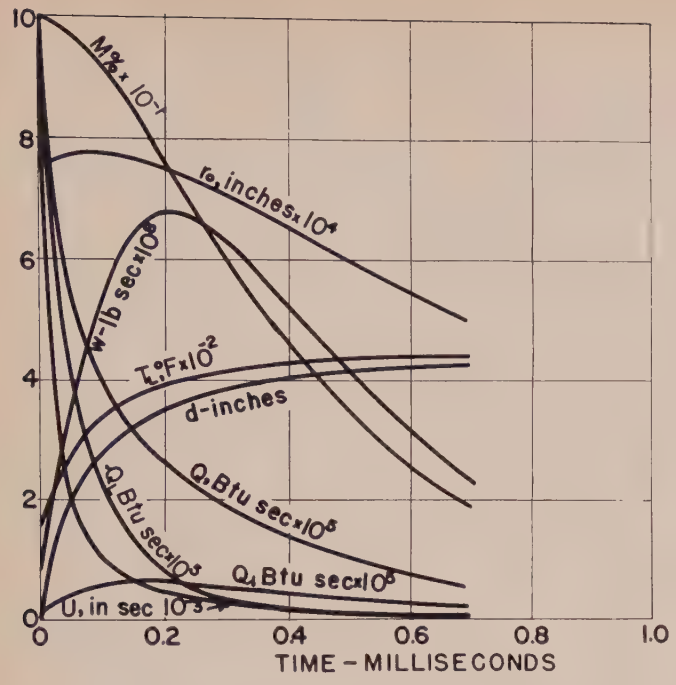

Fig. 4 – Vaporization history of heptane droplet. Conditions same as those for Fig. 2

of the unsteady-state period, heat transferred from the air to supply sensible heat to the liquid fuel far exceeds the amount it loses to supply latent heat of vaporization. Again, the effect is more pronounced the lower the volatility of the fuel and its initial temperature. This may be important in thinking of the pressure drop occurring during the ignition delay period in diesel combustion.

Both computations and experimental data for a variety of pure compounds and under different ambient conditions lead to the following conclusions:

1. For any one fuel the higher the air temperature or pressure, the higher the wet-bulb temperature. (A droplet can cool down to its wet-bulb temperature if ambient conditions are right.)

2. The higher the wet-bulb temperature or the lower the initial droplet temperature, the greater the fraction of its lifetime the droplet spends in the heating-up or unsteady-state.

3. The more volatile the fuel the lower the wet-bulb temperature and the shorter the droplet's lifetime.

4. The higher the air temperature the smaller the differences between a volatile and nonvolatile fuel with respect to the droplet's lifetime.

All these conclusions seem fairly logical. The last is especially important in considerations of self-ignition, for all our thinking concerning volatile and nonvolatile fuels is related to behavior of these fuels at room temperature. For example, at room temperature the ratio of lifetimes of two drops of different fuels might be 8 to 1, while at temperatures in the order of 1000 F or more the ratio of lifetimes may be only of the order of 2 to 1.

Air-Vapor Film Surrounding the Droplet – If it is considered that combustion occurs only in the vapor phase, then from the standpoint of initiating combustion the history of the droplet itself is of interest only insofar as it determines history of the air-vapor film surrounding it (see Fig. 1). Thickness of this film, B_o, varies from infinity at zero velocity of the drop relative to air, to values smaller than the droplet radius drop at normal relative velocities.[20]

Across this air-vapor film, temperature varies from air temperature, T_B, to droplet temperature, T_L. Partial pressure of fuel, P_f, varies from zero at the outer edge to the vapor pressure P_{fL} corresponding to T_L at the inner edge. (Film width for heat-transfer may differ from film width for mass-transfer.[23]) It follows then that a wide range of air-fuel ratios exists across the film.

From the discussion of history of the droplet itself it is obvious that T_L and P_{fL} vary with time, and that temperatures and partial pressures throughout the film vary with both distance and time. This situation is shown in Fig. 5, where different lines represent the values of fuel-vapor partial pressure and air-vapor mixture temperature at equal intervals of time in the film. The situation is obviously idealized but the concepts are valid.

It is recognized that combustion occurs only between fairly narrow limits of air-fuel ratio, the exact values depending on the pressure and tem-

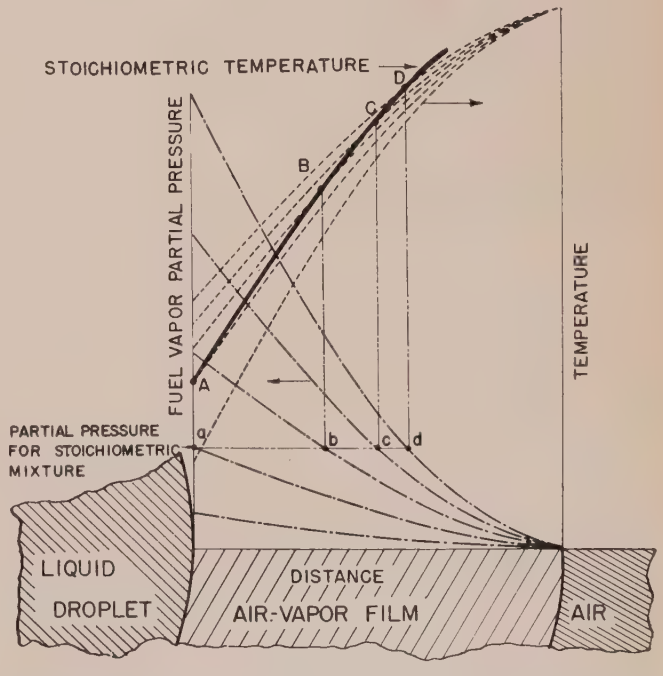

Fig. 5 – Development of stoichiometric-mixture temperature history in air-vapor film from lines of fuel vapor partial pressure and lines of temperature plotted at equal time intervals

[23] See Forschungsheft 382, Beilage zu Forschung auf dem Gebiete des Ingenieurwesens, January-February, 1937: "Wärmeübergang und molekulare Stoffübertragung im gleichen bei grossen Temperatur und Partialdruckdifferenzer," by G. Ackerman.

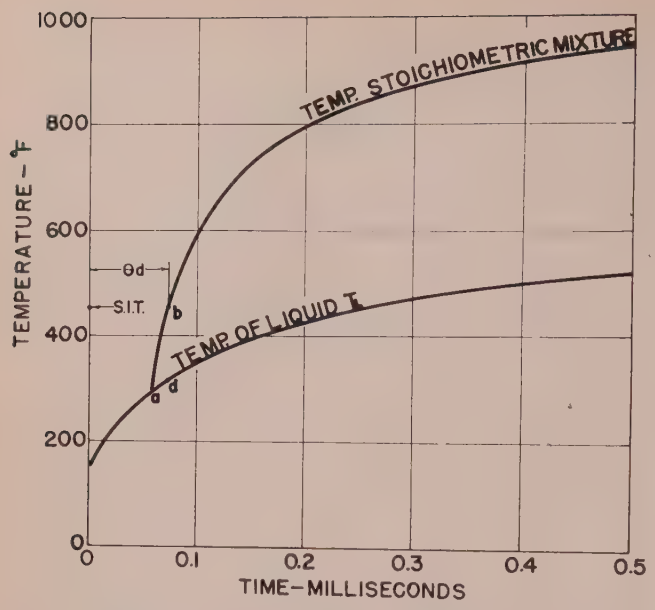

Fig. 6 – Liquid droplet and stoichiometric air-fuel-vapor mixture temperature histories for decane droplet vaporized under conditions of Fig. 3. θ_d = physical ignition delay; SIT = self-ignition temperature

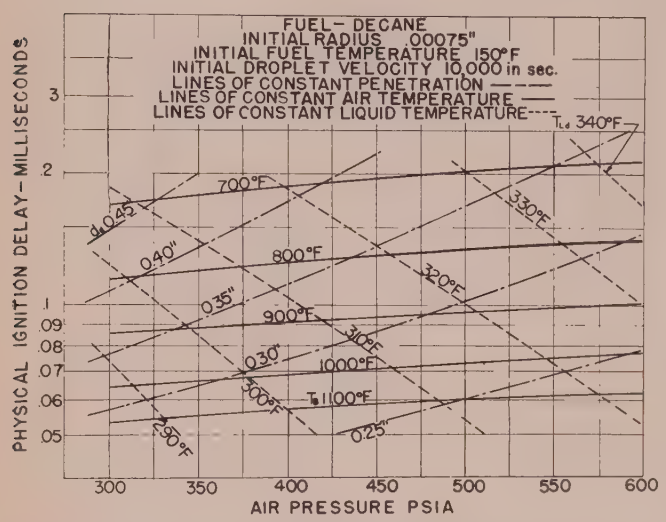

Fig. 7 – Physical ignition delay chart for a decane droplet at different ambient air conditions. Lines of constant penetration and constant droplet temperatures are for end of physical ignition delay

perature involved. If one picks some particular air-fuel ratio such as the stoichiometric value and determines corresponding partial pressure of the fuel, Fig. 5 will show that this mixture will be formed first at the liquid surface and then as time passes on it will move out through the film to regions of higher temperatures. For example, at time-increment 2 in Fig. 5 the partial pressure would have the value corresponding to point a at the liquid surface and would be at the temperature A. At time increments 3, 4, and 5 the same partial pressure (and therefore the same air-fuel ratio), would be at the temperatures B, C, and D respectively. The heavy solid line represents different temperatures encountered by the particular air-fuel ratio selected. The equation for the line is developed by Priem et al.[22], as:

$$T = \left[\left(\frac{C_0}{C_3} + T_L\right)\left(\frac{P_T - p_f}{P_T - p_{fL}}\right)^{\frac{C_3}{C_1}} - \frac{C_2}{C_3}\right] \qquad (4)$$

where:

T = Temperature of mixture required

p_f = Partial pressure of fuel vapor in the mixture at the required strength

C_1, C_2, C_3 = Constants depending upon the instantaneous heat- and mass-transfer to the drop

In order to establish the magnitude of physical ignition delay of single droplets, delay was defined as time required for a stoichiometric mixture to reach its self-ignition temperature in the film. Fig. 6 presents such a history for a droplet of decane. The stoichiometric mixture is not formed, of course, until the droplet itself has reached a sufficiently high temperature (and consequently partial pressure), to form the stoichiometric mixture at the liquid surface. The physical ignition delay is marked θ_d.

It should be noted that temperature of the stoichiometric mixture (or any other mixture), reaches a constant value at the same time the droplet temperature does. It follows, then, that for a single droplet physical delay is infinite, that is, the droplet will not burn if the self-ignition temperature is not reached by the air-vapor mixture during the unsteady-state history of the droplet.

A large number of computations for physical

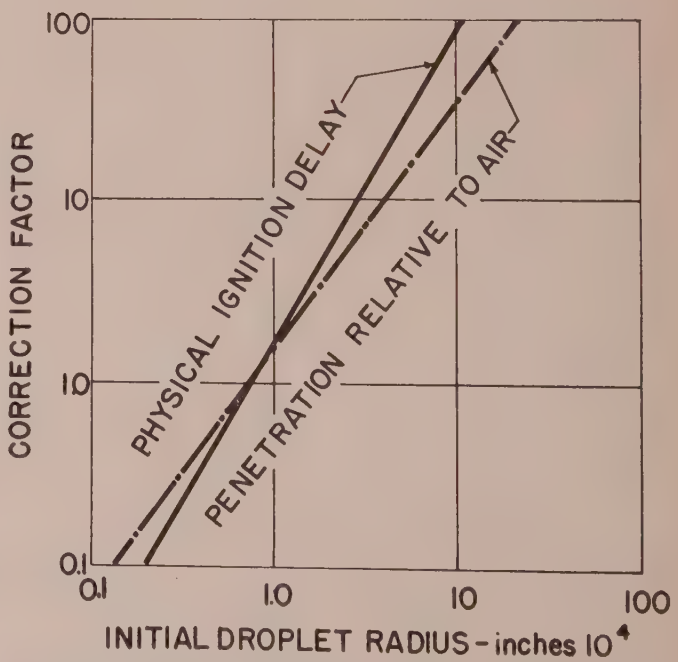

Fig. 8 – Correction factors for Fig. 7 with initial droplet radii other than 0.00075 in.

ignition delay θ_d were performed for decane. Results are summarized in Fig. 7, where θ_d is plotted against air pressure. Fig. 7 also shows liquid temperature and penetration at the end of the physical delay period. Fig. 7 and other computations reveals the following generalizations:

1. θ_d increases slightly with air pressure. This is due to the fact that the droplet must reach a higher temperature to form a higher partial pressure in the film to give a stoichiometric mixture at the higher air pressure. This may be of interest from the standpoint of smoke formation.

2. θ_d decreases with air temperature.

3. θ_d increases rapidly with droplet size, Fig. 8. The exact relationship varies only slightly with air temperature, but the following has been found satisfactory for all conditions of interest:

$$\theta_d \propto (r_{oi})^{1.75} \qquad (5)$$

where r_{oi} is the initial droplet radius.

4. θ_d decreases with initial liquid temperature, T_{Ll}, Fig. 9. Within the range of interest in diesel combustion, the relationship between θ_d and T_{Ll} can be described by a straight line with negative slope. θ_d becomes zero if the droplet is injected with T_{Ll} equal to or exceeding that of point d, Fig. 6.

5. θ_d decreases rapidly with initial droplet velocity relative to air at the lower velocity range, while an increase in droplet velocity at the higher range has little effect on θ_d, Fig. 10.

6. θ_d increases with fuel boiling point, Fig. 11,

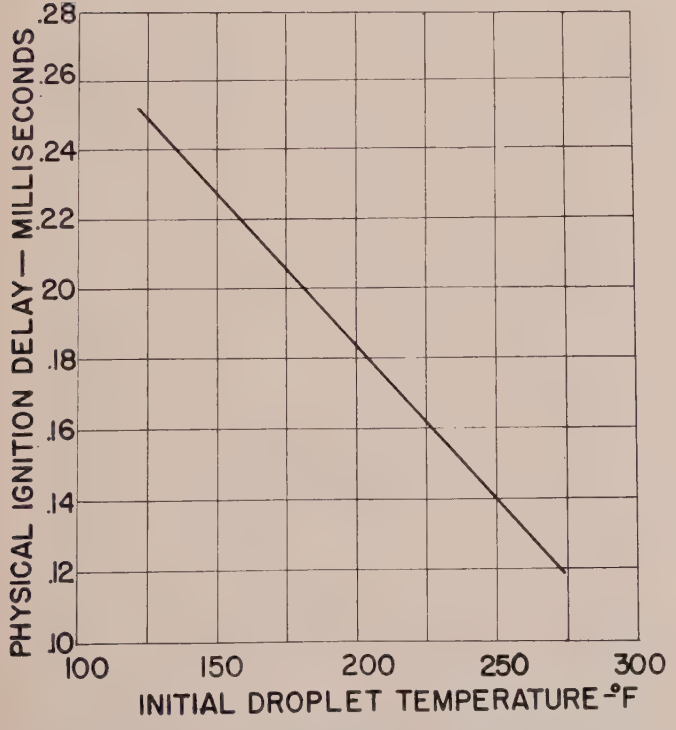

Fig. 9 – Effect of initial liquid temperature on physical ignition delay of single cetane droplets. Conditions other than initial liquid temperature same as for Fig. 2

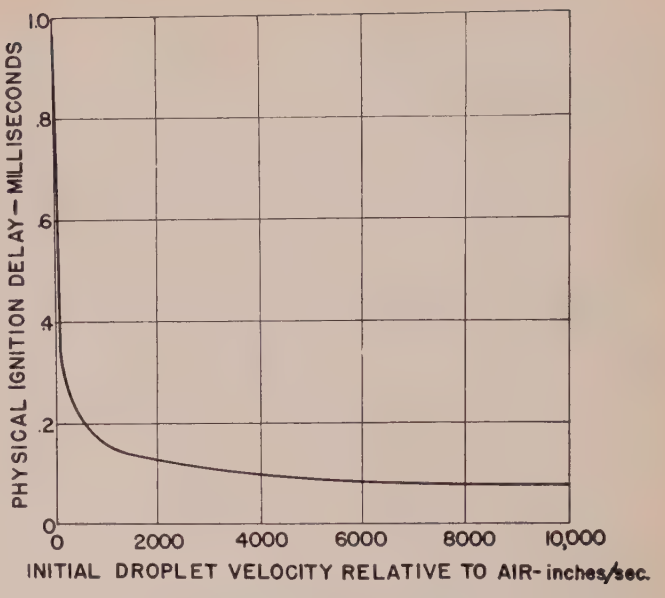

Fig. 10 – Effect of initial droplet velocity relative to air on physical ignition delay of single decane droplets. Conditions other than velocity same as for Fig. 3

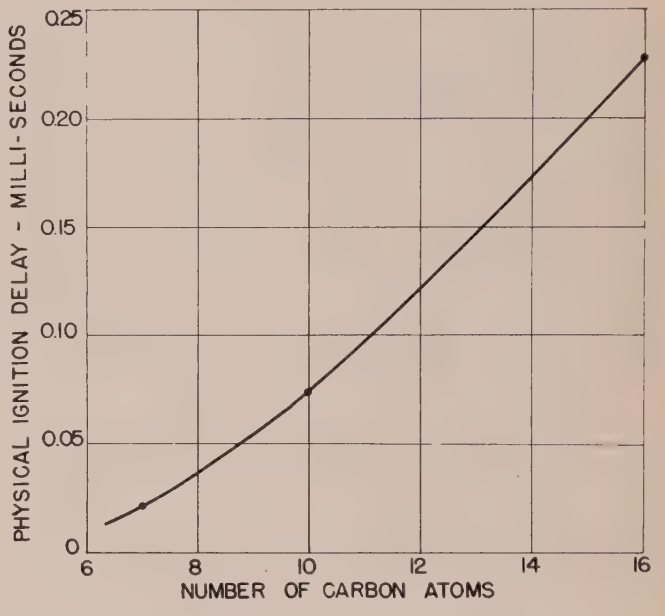

Fig. 11 – Effect of number of carbon atoms in normal paraffin fuels on physical ignition delay of single droplets under conditions identical to those in Figs. 2, 3, and 4

for fuels of the same hydrocarbon family. The heavier fuels have a higher molecular weight, slightly lower self-ignition temperature, and require lower partial pressures to form the same mixture strength in the film, but require much higher droplet temperatures to form these partial pressures due to their low volatility.

Vaporization with Interaction Between Droplets – Previous discussion illustrated expected variations in physical delay if there is no interaction between spray droplets. Validity of this assumption can be checked only by comparison with ex-

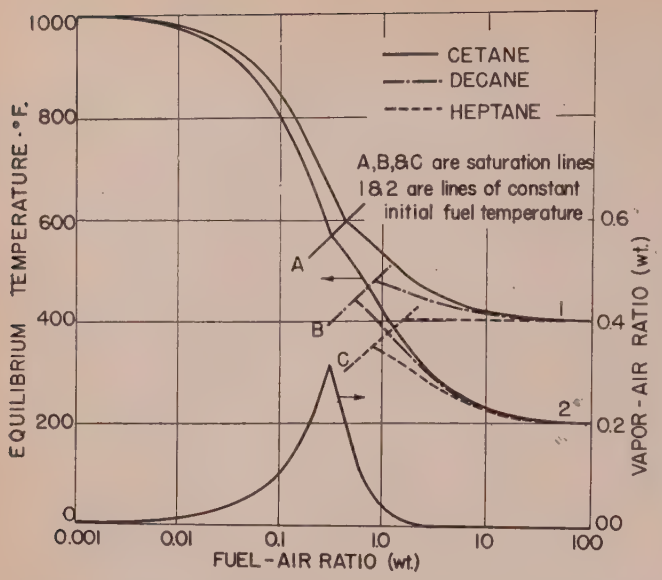

Fig. 12 – Adiabatic saturation temperatures for different overall fuel-air ratios by weight for heptane, decane, and cetane with initial liquid temperatures of 200 and 400 F. Air pressure 500 psia. Initial air temperature 1000 F. Vapor-air ratio versus overall fuel-air ratio at adiabatic saturation conditions for cetane with initial liquid temperature of 200 F is also shown

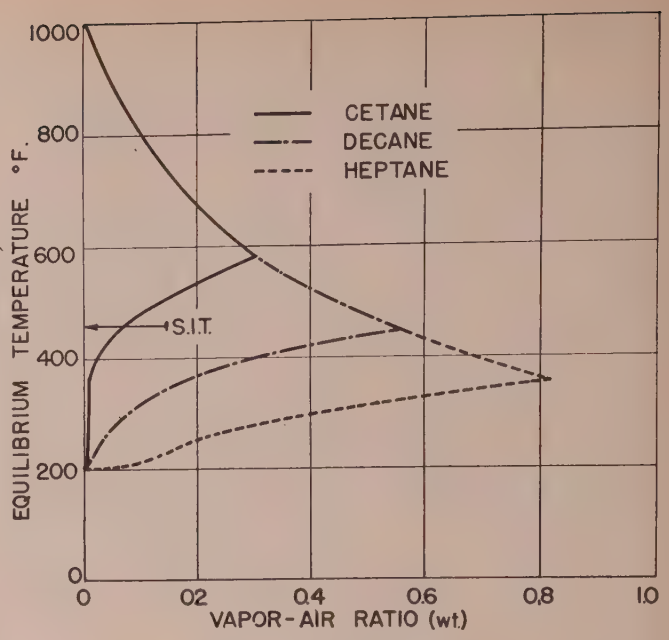

Fig. 13 – Adiabatic saturation temperature versus vapor-air ratio by weight at adiabatic saturation conditions. Air pressure 500 psia. Initial liquid temperatures 200 F. Initial air temperature 1000 F

perimental data. Before making this comparison let us consider what happens when a large amount of interaction between droplets is assumed to take place.

In the previous section wet-bulb temperatures were mentioned, and it was noted that these were temperatures of the liquid when dynamic equilibrium existed between heat transferred in and mass transferred out. Implicit in the discussion was the fact that surrounding air temperature was essentially unchanged by droplet vaporization.

Another type of equilibrium may exist in the spray, namely, thermodynamic equilibrium. This condition is usually called adiabatic saturation. Experimentally, adiabatic saturation as applied to the diesel spray would be realized by sealing a gas and a liquid that would not absorb the gas in an insulated container and allowing them to sit for a period of time until they reached thermodynamic equilibrium.

It should be noted that there is a difference between adiabatic saturation as applied here and in air conditioning work. In air conditioning the liquid is customarily assumed initially at adiabatic saturation temperature and of sufficient quantity to completely saturate the air. In the spray, fuel is obviously not initially at adiabatic saturation temperature and may not be of sufficient quantity to saturate the air. Thus for fixed conditions adiabatic saturation temperature in air conditioning has a single value. In the spray, however, it has an infinite number of values ranging from air temperature to initial temperature of the liquid fuel and depends upon fuel-air ratio and initial liquid temperature.

Equations used in computations for conditions of air adiabatically saturated follow. They are derived in a report prepared for the NACA.[22]

$$\int_{T_2}^{T_{B1}} C_{pa}\,dT = \frac{F}{A}\int_{T_{L1}}^{T_2} C_{pL}\,dT + \frac{P_{fL2}}{T_2}\left(\frac{T_{B1}}{P_{T1}}\cdot\frac{M_f}{M_a}\right)\lambda_2 \qquad (6)$$

and

$$\int_{T_2}^{T_{B1}} C_{pa}\,dT = \frac{F}{A}\left[\int_{T_{L1}}^{T_i} C_{pL}\,dT + \lambda_i + \int_{T_i}^{T_L} C_{pf}\,dT\right] \qquad (7)$$

where:

T_{B1} = Initial air temperature
T_2 = Final saturation temperature
C_{pa} = Specific heat of air at constant pressure
F/A = Fuel-air ratio by weight
T_{L1} = Initial fuel liquid temperature
C_{pL} = Specific heat of liquid fuel
P_{fL2} = Vapor pressure of fuel at temperature T_2
P_{T1} = Initial total pressure
M_f = Molecular weight of fuel
M_a = Molecular weight of air
λ_2 = Latent heat of vaporization at temperature T_2
λ_i = Latent heat of vaporization at temperature T_i
T_i = Intermediate temperature at which fuel will vaporize in the superheat range
C_{pf} = Specific heat of fuel vapor at constant pressure

Equation (6) is for the "wet" region in which the final equilibrium mixture contains air, fuel vapor, and liquid fuel in equilibrium with its vapor.

Equation (7) is for the "superheat" region where all fuel has been vaporized and the vapor superheated to the equilibrium temperature T_2.

Results of computations for three different fuels

are presented in Fig. 12, in which adiabatic saturation temperature is plotted against initial liquid-air ratio. Lines A, B, and C represent points where all the liquid has just vaporized. Below them liquid is present; above them there is none. (No lines for decane and heptane are shown in the superheat range because they are almost identical with those for cetane.)

Fig. 12 shows that adiabatic saturation temperature depends upon initial liquid-air ratio. For example, if an almost infinite amount of liquid were present the gas would be cooled down to the liquid temperature almost immediately with but little change in overall temperature.

Fig. 12 also shows a surprisingly large cooling effect for mixtures having fuel-air ratios that may well be formed in the spray core. As expected, adiabatic saturation temperatures approach initial air temperature at very lean mixtures and initial liquid temperatures at very rich mixtures. These and other similar computations show:

1. Adiabatic saturation temperatures are higher with higher air pressures.
2. Adiabatic temperatures are higher with both higher initial air and liquid temperatures.
3. Differences between fuels are negligible in the superheat region. In the wet region where there is some difference, the lower the fuel volatility, the higher the adiabatic saturation temperature.

When adiabatic saturation conditions are reached, the temperature and partial pressure of fuel vapor in the resulting mixture are fixed. This fixes the vapor-air ratio at adiabatic saturation conditions. Fig. 13 is a plot of vapor-air ratio at adiabatic saturation conditions as a function of adiabatic saturation temperature for cetane, decane, and heptane. Considering the heptane curve, an infinite fuel-air ratio would give an adiabatic saturation temperature equal to the fuel temperature; in this case, 200 F. As fuel-air ratio decreases, adiabatic saturation temperature increases, amount of liquid decreases, and vapor-air ratio increases. When fuel-air ratio is such that all the liquid is vaporized, the curve reverses itself and temperature increases while vapor-air ratio decreases. In this superheat region a single curve is obtained for all fuels.

Note in Fig. 13 that the same vapor-air ratio can be obtained at two different temperatures. The higher temperature represents the condition where fuel-air ratio was low, and consequently not much cooling of air occurred. The lower temperature represents the condition where fuel-air ratio was high and liquid fuel was still present when adiabatic saturation occurred. Energy required to heat this liquid must come from the air, resulting, of course, in a low air temperature.

The next question concerns how long it takes for a mixture of fuel droplets and air to reach adiabatic saturation. Previous equations for the case of a single droplet can be used to provide a close estimate of this time if air temperature T_B and the vapor concentration are considered to vary with time because of the cooling effect of fuel. Such computations were performed. Results are shown in Fig. 14, where air and liquid temperatures are plotted against time. Computations were performed for a spray of uniform-size droplets. The time for air and actual spray with a certain droplet-size distribution would probably be shorter because of very rapid evaporation of small droplets.

Fig. 15 shows that the expected rapidity with which adiabatic saturation is reached is a function of air-fuel ratio. Times are shorter the richer the original mixture.

Two other items should be noted in considering

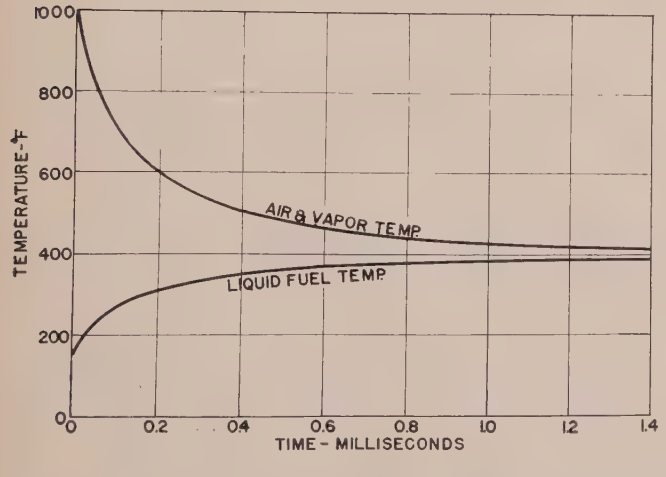

Fig. 14 – Temperature-time relationship for air and vapor and for liquid fuel system proceeding to adiabatic saturation conditions. Cetane spray with uniform droplet size of 0.000965 in. Fuel-air ratio 1/1 by weight. Initial air temperature 1000 F. Other conditions same as for Fig. 3

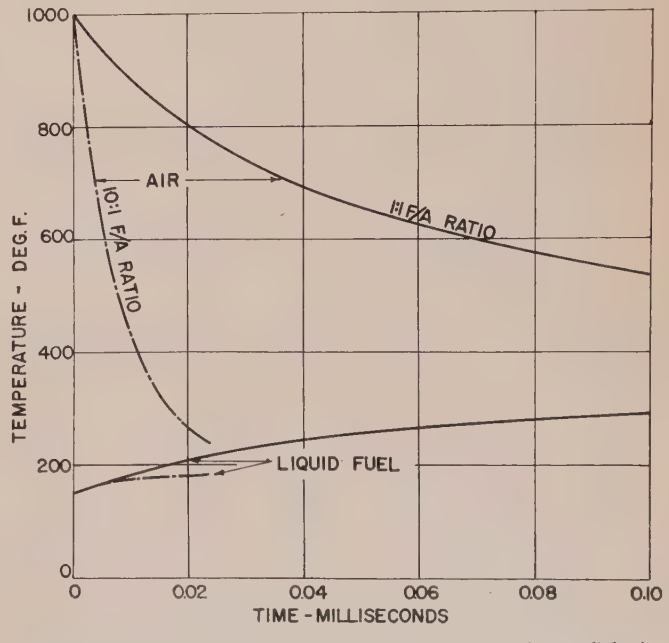

Fig. 15 – Effect of fuel-air ratio on rapidity of approach to adiabatic saturation conditions. Decane with fuel-air ratios 1/1 and 10/1 by weight. Other conditions same as for Fig. 14

adiabatic saturation. It was mentioned above that the less viscous the fuel the more uniform its distribution in the spray envelope.[11] Thus if adiabatic saturation exists in the spray a volatile fuel such as heptane would have a spray uniformly cool throughout except at its very edge. Since combustion usually begins at the spray edge this item might be significant.

The other item to be noted is that in thinking of the air-fuel ratios involved it should be remembered that delay period is under consideration, and consequently volume close to the nozzle is of interest. Furthermore, additional fuel is constantly being introduced into this volume by the continual injection. Thus the fuel-air ratio of interest is undoubtedly markedly richer than the overall fuel-air ratio.

With our present knowledge of theory, it is impossible to determine the exact conditions prevailing in a spray. It will be well, however, to consider experimental data in an attempt to infer what does happen in the spray and therefore the factors that influence physical delay.

Correlations with Experimental Data

Conditions Existing in the Spray – Before proceeding with a discussion of factors affecting ignition delay it seems wise to attempt to decide whether single droplet or adiabatic saturation conditions exist in the spray. In choosing between these two alternatives the authors have drawn heavily on the experimental data of Hurn et al,[24] and Yu et al.[18]

The authors believe that one must picture diesel engine spray as proceeding to adiabatic saturation at the spray center and changing with distance from spray center single droplets on the extreme edge. Manner and rate at which this transition takes place will be discussed later. The authors believe the above conditions represent diesel engine spray because:

1. Both Hurn and Yu show that for fuels of the same cetane number both initial rate of heat-transfer from air to fuel and physical delay is nearly independent of fuel volatility with a nonvolatile fuel having – if anything – a slightly higher rate of heat-transfer than a nonvolatile fuel. Although higher air temperatures minimize differences in fuel volatility for a single droplet there would still be a difference in physical ignition delay between fuels in the case of a single droplet.

Assuming adiabatic saturation, Fig. 13 explains why a volatile fuel may not form a combustible mixture at the proper temperature more readily than a nonvolatile fuel. Consider the curve for heptane in Fig. 13. If the vapor-air mixture is to be in the range of inflammability, the temperature must be in the neighborhood of either 200 F or 850-900 F. A temperature of 850-950 F is high enough to cause self-ignition but requires a local fuel-air ratio of around 0.04. This value would be highly improbable at full load, for it would require almost perfect distribution and vaporization. On the other hand 200 F is much lower than self-ignition temperature. Thus with a volatile fuel under adiabatic saturation conditions it is more difficult to obtain a mixture both in the region of inflammability and at a temperature high enough to cause ignition.

With a nonvolatile fuel such as cetane this problem is minimized, for with adiabatic saturation and liquid present, the vapor-air temperature of cetane reaches the self-ignition temperature (see Fig. 13). Thus with adiabatic saturation in diesel engine spray, physical delay of cetane would probably be shorter than that of heptane.

The above discussion concerns only droplets receiving heat by convection, as is customarily desired in diesel combustion. In a recent engine,[25] however, spray was directed on the piston-head and received heat by conduction from the metal. This technique would eliminate z in equation (3) as a factor in the heat-transfer relationship, and under certain conditions at least, can improve atomization following impingement on the piston. From theoretical considerations this should (a) increase rate of heat-transfer to the spray, (b) minimize possibility of adiabatic saturation, (c) minimize differences in physical delay between fuels, and (d) because of higher temperature of vapor-air mixture, would decrease absolute values of chemical delay of all fuels and thus minimize delay differences. Note that these explanations are not the same as those published;[25] nevertheless they seem theoretically sound.

2. Using different inert atmospheres it was found that helium gave appreciably higher heat-transfer rates than nitrogen and argon during the vaporization period.[24] Shorter ignition delays were also found using an artificial atmosphere replacing helium with nitrogen. Thermal conductivity and diffusion coefficient of helium are higher than those for nitrogen and argon. Higher thermal conductivities and diffusion rates increase heat-transfer rates for the single droplet case and have an even more marked effect in the case of adiabatic saturation, where an increase in thermal conductivity can eliminate the extremely cool center core of the spray.

3. It has been shown[6] that if combustion starts at about the end of injection, ignition delay in the diesel combustion bomb is increased by decreasing duration of injection. Presumably this occurs because of increased cooling due to increased quantity of fuel injected. If the single droplet view were correct, ignition delay would be independent of quantity of fuel injected. Again this would seem

---

[24] See paper by Hurn, Chase, Ellis, and Hughes on pp. 703-711 of this issue.

[25] See SAE *Journal*, Vol. 63, September, 1955, pp. 18-25: "Hear No Noise, See No Smoke with New German Diesel," by J. S. Meurer.

to prove that spray conditions closely approach adiabatic saturation conditions.

4. Were the single droplet view correct, an increase in turbulence should have but little effect on ignition delay because of initially high fuel droplet velocity relative to air (see Fig. 10). Turbulence would be expected to have an appreciable effect under adiabatic saturation conditions, however, because it would distribute fuel more evenly throughout the combustion chamber, thus decreasing local fuel-air ratio and markedly increasing air-vapor mixture temperature. Data on two identical fuels show appreciably longer ignition delays in a combustion bomb even at a bomb temperature of 1300 F.[18, 24] A compression ratio of 16:1 and ratio of specific heats $k = 1.4$ gives a compression temperature of approximately 1340 F. Actual compression temperature would probably be less than 1340 F because of heat transfer, decrease of k with temperature, and due to fuel being injected approximately 12 deg btdc with compression ratio somewhat less than 16:1. Turbulence presumably existing in the engine is a very logical explanation for shorter delay observed with presumably lower temperatures.

5. High-speed motion pictures[4, 13, 26] all show that visible combustion first starts at the spray edge. This would result naturally if adiabatic saturation were present at the spray center.

Ignition Delay and Its Components – With this picture of the spray center core approaching or reaching adiabatic saturation conditions, let us try to evaluate the magnitude of factors causing ignition delay. We arbitrarily define ignition delay as the time interval between start of injection and time the pressure decrease caused by the cooling effect of injected fuel has just been recovered.

Start of injection is a logical, accepted choice for start of the ignition delay period. Choice of end of the delay period is not so clear-cut. Hurn et al.[24] define end of delay as time at which pressure rose to 10 lb above charging pressure. Yu et al.[18] define ignition delay as defined here. The F-5 cetane rating procedure defines end of delay as occurring when rate of pressure rise due to combustion exceeds the maximum rate of pressure rise during compression. There might be merit in defining end of delay as occurring when a certain amount of energy has been released by the chemical reactions. In any event definition of the end of ignition delay involves an arbitrary specification of either rate or extent of chemical reaction. In this paper we define ignition delay as indicated and discuss the relative magnitude of factors involved in light of this definition.

Fig. 16 schematically presents definitions used for engine data. It is quite probable that start of chemical delay occurs before the specific ΔE reaches its peak value. Since no more accurate technique

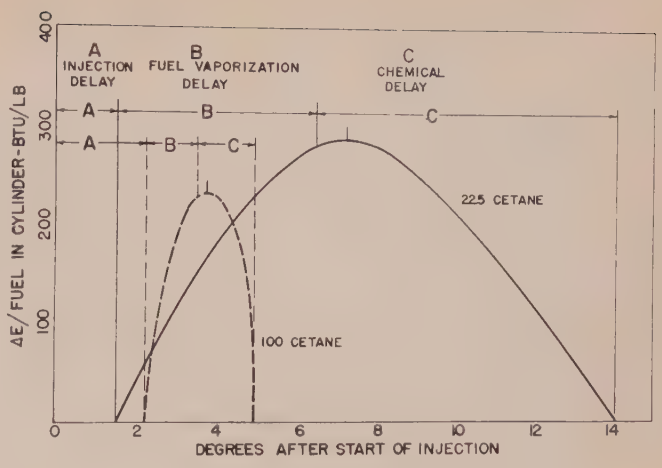

Fig. 16 – Heat-transfer per pound of fuel in cylinder after injection, showing components of ignition delay in diesel engine for two cetane number fuels. Engine: GM 1-71 at 800 rpm. Data from Yu et al.[18]

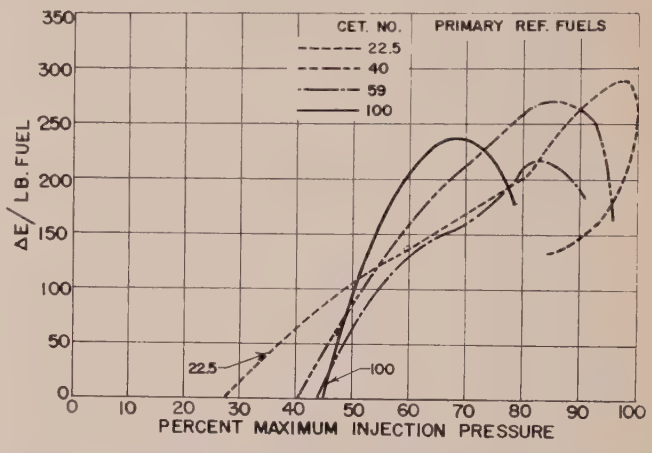

Fig. 17 – Heat-transfer per pound of fuel in cylinder versus per cent maximum injection pressure for primary reference fuels. Engine: GM 1-71 at 800 rpm. Data from Yu et al.[18]

was available the procedure indicated was used.

Injection Delay – The first factor discussed is injection delay. There may be some question whether this is properly included in the ignition delay period. Data in reference 18 show that time between beginning of injection (measured by a strain gage on the rocker arm), and time of measurable pressure drop due to cooling effect of fuel is not negligible. Yu's data for primary reference fuels are replotted in Fig. 17, where specific change in internal energy is plotted as a function of percent maximum injection pressure. Similar plots for secondary reference fuels and pure fuels are shown in Fig. 18. In these curves injection pressure reached 30-40% or more of its maximum value before measurable pressure drop occurred. Maximum injection pressure was probably of the order of 20,000 psi, so that an injection pressure of 6000-7000 psi had been achieved before appreciable heat-transfer to the spray occurred.

Several explanations seem possible. The injector

[26] See NACA TM 790 (1936), "Ignition and Flame Development in Case of Diesel Fuel Injection," by O. Holfelder.

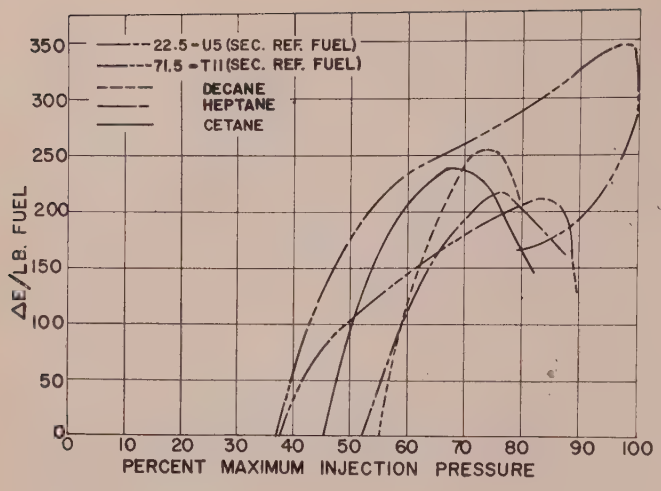

Fig. 18 – Heat-transfer per pound of fuel in cylinder versus per cent maximum injection pressure for secondary reference fuels and pure hydrocarbons. Engine: GM 1-71 at 800 rpm. Data from Yu et al.[18]

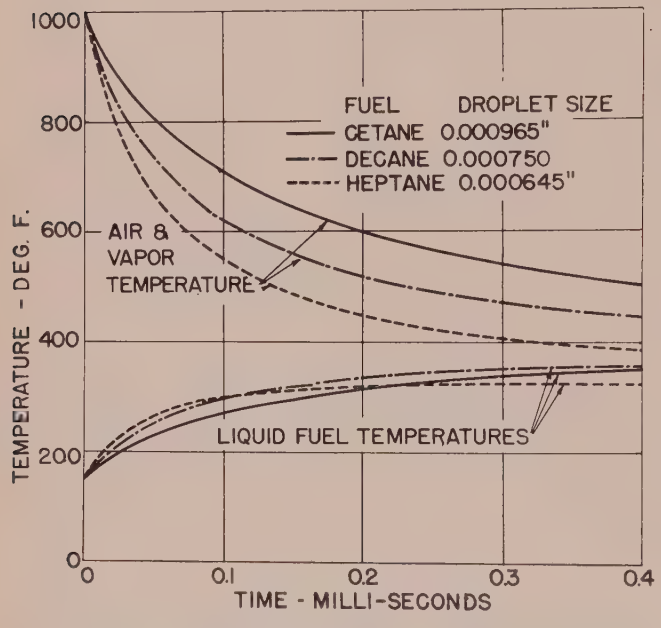

Fig. 19 – Effect of volatility and fineness of atomization on rapidity of approach to adiabatic saturation conditions for heptane, decane, and cetane. Other conditions same as for Fig. 14

used had an open nozzle. Fuel vaporization in this open nozzle might occur between injections, producing the effect shown. Another explanation would be due to spray breakup. Data in reference 24 indicate that pressure drop occurs as soon as fuel is introduced. However, there was some evidence of a small delay between injection and decrease in pressure due to fuel cooling when argon was used. Fuel compressibility might cause a time difference between injection (measured by a strain gage on the rocker arm), and beginning of measurable pressure drop. However, because of short distances involved and low opening pressure of the nozzle valve, this explanation does not seem too plausible.

Fuel Vaporization Lag – Once spray breakup begins and spray starts to form, data in reference 18 indicate that while there is some difference between fuels in rate of heat absorption from air, these differences are not large. Here differences in fuel distribution within the spray and during atomization become important. De Juhasz et al, state that as oil viscosity increases, mean droplet diameter decreases.[11] It is also stated that fuel dispersion in a given cross-sectional area becomes more even as fuel viscosity decreases and distance from the orifice increases.

Fig. 19 presents results of computations similar to those presented in Figs. 14 and 15, except that in Fig. 19 effect of fuel viscosity on drop size has been taken into account.[11] Lower viscosity fuel spray will have smaller average droplets than fuel of high viscosity. Further, a less viscous fuel is likely to be more volatile. Both these factors will cause the less viscous fuel to approach adiabatic saturation more rapidly.

Fig. 20 schematically presents the relationship between fuel distribution, estimated temperature distribution, and distance for two fuels of different viscosity.

The middle left-hand curve in Fig. 20 suggests a better possibility of self-ignition occurring because of the more gradual change in temperature and fuel-air ratio with distance. It is no coincidence then that ignition usually starts at the spray edge and not in the center or tip of the spray.

Fig. 20 also illustrates why ignition delays obtained in a combustion bomb are longer than those obtained in operating engines. Macroscopic turbulence (as opposed to microscopic turbulence) tends to bring fresh air into the spray center and thus aids in eliminating adiabatic saturation conditions

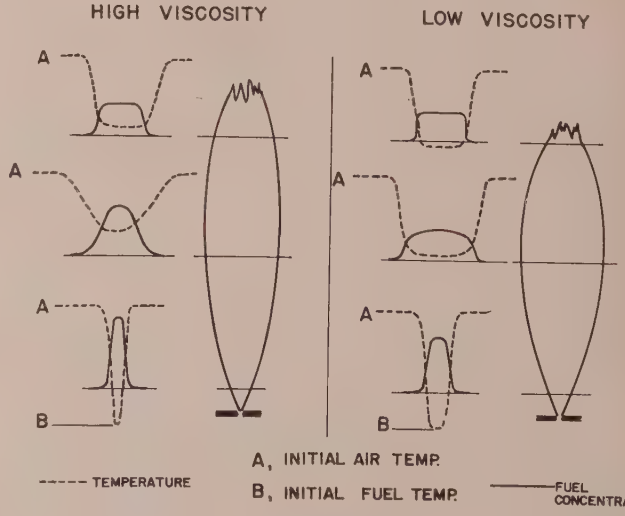

Fig. 20 – Fuel and temperature distribution for sprays of different viscosity fuels

and increasing possibilities of achieving a combustible mixture at self-ignition temperature. This same reasoning also explains decrease in ignition delay with increase in engine rpm, although compression temperature undoubtedly increases somewhat with rpm.

Chemical Delay – Having established conditions within the spray that lead to formation of a combustible mixture at its self-ignition temperature, the next thing to consider is time required for the reactions to become explosive, namely, chemical delay. Here there is a marked difference between fuels, as shown by the data in reference 18, where curves of change in internal energy per pound of fuel versus crank angle are given. Those data show very clearly that before the reactions became explosive, chemical energy is released at different rates for different fuels, and that additives effect this rate. This correlates well with the inverse relationship between the cetane and octane scales. If physical conditions are fixed physical delay would not be zero or even negligible, but would be approximately constant for fuels whose physical properties do not vary widely. Thus differences between fuels would result largely in differences in chemical delay.

Magnitudes of Components of Delay – The conclusions above were based primarily on engine data. In order to compare these conclusions with those based on data from a combustion bomb, data in reference 24 were replotted as illustrated in Fig. 21. Early pressure changes in the bomb occurring with nitrogen and air are plotted on the same graph. Hurn's data show essentially no injection lag, except possibly with argon. Thus physical delay in the bomb data consists primarily of time

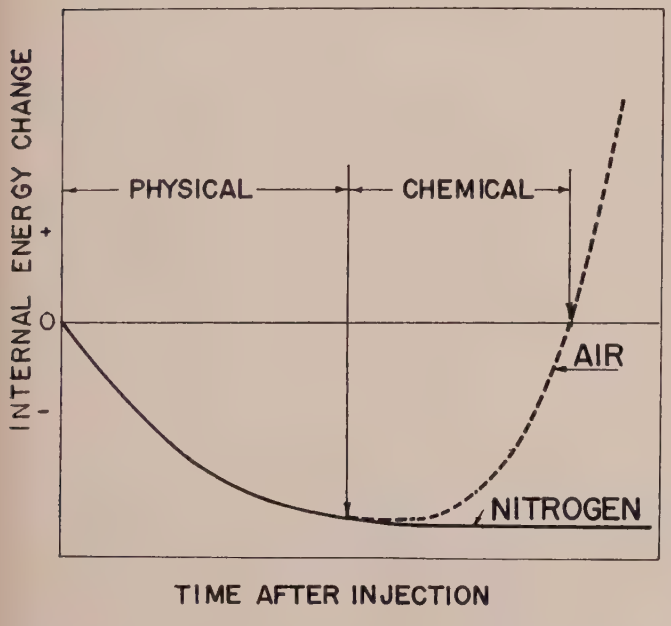

Fig. 21 – Heat-transfer due to vaporization and reaction, showing components of ignition delay in combustion bomb. Data from Hurn et al.[24]

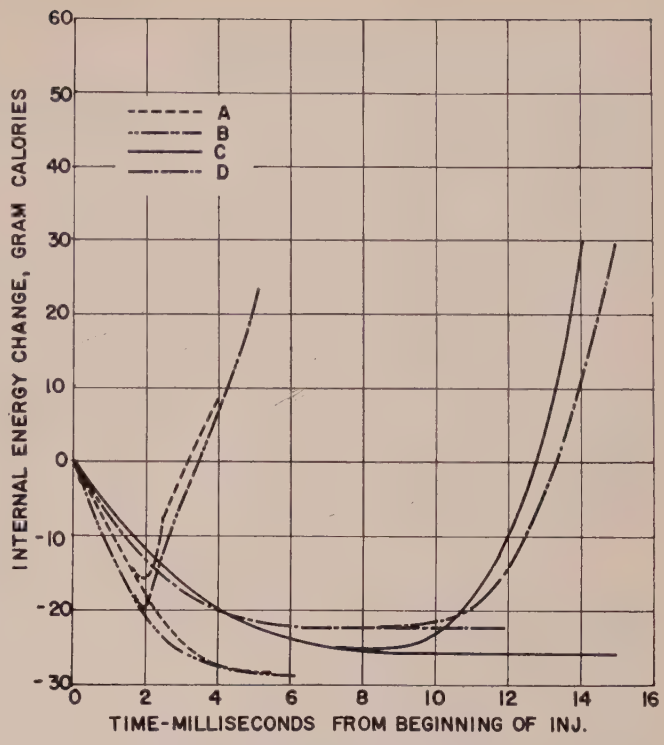

Fig. 22 – Heat-transfer due to vaporization and reaction in combustion bomb. Data from Hurn et al.[24]

(A) 40-cetane mixture of isooctane and heptane at 1300 F. 0.1079-gram fuel

(B) 40-cetane mixture of cetane and alpha-methyl naphthalene at 1300 F. 0.108-gram fuel

(C) 40-cetane mixture of isooctane and heptane at 900 F. 0.139-gram fuel

(D) 40-cetane mixture of cetane and alpha-methyl naphthalene at 900 F. 0.1403-gram fuel

required to form a combustible mixture. The end of physical delay and beginning of chemical delay was defined as time at which the first detectable difference occurred between curves for nitrogen and air atmospheres. Chemical delay was defined as ending when pressure had reached the original charge pressure; that is, when change in internal energy is zero. Note that the definition of start of chemical delay used for bomb data may not agree with the definition used for engine data.

Fig. 22 presents data for two fuels and two temperatures considered in reference 24. It is evident that both fuels receive heat more rapidly at higher temperatures. Furthermore, at a particular temperature, differences in rates at which fuels receive heat is not large, especially when large differences in volatility are considered.

Since data for two fuel mixtures (cetane-alpha methyl naphthalene and isooctane-heptane) of the same cetane number were available from both bomb and engine, it was decided to compare the magnitude of delays. See Table 1.

Table 1 shows that physical and chemical delays are both much longer in the bomb than in the engine, even at 1300 F. The lower value of physical

Table 1 – Comparison of Ignition Delay Data

		Condition	33% Isooctane 67% n-Heptane[b]	40% Cetane 60% Methyl Naphthalene[b]
Bomb	Total	1300 F	3.22	3.45
	Physical	0.108 gram[a]	1.70	1.75
	Chemical	450 psi	1.52	1.70
	Total	1300 F	3.42	3.00
	Physical	0.069 gram	1.75	1.50
	Chemical	450 psi	1.67	1.50
	Total	900 F	12.8	13.4
	Physical	0.140 gram	7.2	8.5
	Chemical	450 psi	5.6	4.9
	Total	900 F	11.75	11.5
	Physical	0.091 gram	6.75	7.0
	Chemical	450 psi	5.0	4.5
Engine[c]	Total		1.83	1.88
	Injection		0.64	0.50
	Heating Up		0.65	0.71
	Total Physical		1.28	1.21
	Chemical		0.54	0.67

[a] Weight of fuel injected.
[b] Delay in milliseconds.
[c] Conditions: 800 rpm, injection at 12.5 deg btdc.

delay in the engine is not unexpected because of engine turbulence, but decrease in chemical delay is larger than would be expected, unless the compression temperature were much higher than is normally considered. Possibly some of the discrepancy is attributable to the different techniques used in determining end of physical delay and beginning of chemical delay.

Unfortunately bomb data for fuels of different cetane numbers are not available. Such data, however, are available for the engine. The range of magnitude of the different components is summarized in Table 2.

Conclusions

The following statements can be made concerning ignition delay and factors causing it:

1. It seems almost certain that adiabatic saturation is approached very closely in the spray core. As distance from the spray center increases, the air-fuel mixture becomes leaner with consequently higher air-vapor temperatures. Under these conditions adiabatic saturation is approached less rapidly. At the extreme edge of the spray a few single droplets will almost certainly be found.

2. The closeness and rate of approach to adiabatic saturation conditions varies with distance from the spray core in a different manner for fuels of different viscosities and volatilities.

3. A volatile fuel does not receive heat that much more rapidly than a nonvolatile fuel, as would be expected from differences in their volatility.

4. Under adiabatic saturation conditions a nonvolatile fuel has as good or a better chance as a volatile fuel to achieve the combination of temperature and vapor-air ratio required for self-ignition and rapid combustion.

5. Physical delay is not a negligible portion of total ignition delay. In fact, for the conditions shown it may be as large or larger than chemical delay.

6. Injection delay may not be of negligible magnitude in an operating engine.

7. While there are some differences in the way in which different fuels receive heat following spray breakup, major difference between fuels of varying cetane number lies in the manner in which they release chemical energy during very early reactions.

8. For the same fuel, total, physical, and chemical delays are smaller in an operating engine than in a combustion bomb operated at the highest temperature estimated to exist in the engine.

Acknowledgment

The authors acknowledge with thanks assistance of the Wisconsin Alumni Research Foundation and the College of Engineering, both with respect to salary and equipment. The cooperation of the Bureau of Mines, Bartlesville, Okla., in securing and exchanging data is appreciated. The indirect aid provided by the NACA in sponsoring much of the basic research that guided thinking about the problem is also acknowledged.

DISCUSSION
of Diesel Combustion Research Papers

More Fundamental Studies Are Needed

– G. C. Wilson
Ethyl Corp.

THE results of the painstaking efforts taken in the Yu et al. and El Wakil et al. papers furnish stepping stones on the way toward an ultimate solution of the question as to exactly what changes take place in the injected fuel prior to the time that it becomes involved in rapid combustion. It will require more studies, such as these before there will be enough pieces to fit together and thus obtain the final answer. Such fundamental studies are neither easy nor glamorous, but they do hasten the day when a complete history of the "delay period" will be known. This minute period of time (± 0.001 sec) is of the greatest importance, since upon its duration depends the nature of the rapid combustion which follows.

Every designer of automotive diesel engines would appreciate having longer delay periods for mixing fuel and air if it were not for the fact that such delays are followed by an

Table 2 – Summary of Delays for Different Cetane-Number Fuels. GM 1-71 Engine, 800 Rpm.
Range of Cetane Number of Fuels Used: 22.5 – 100

Delay	Approximate Range for Delay, millisec
Injection	0.41 – 0.63
Heating	0.31 – 0.83
Chemical	0.21 – 2.70

Table A – ASTM Cetane Numbers for a Coastal Straight-Run Distillate with Additives

Fuel No. 907	DB-1, weight %	Tetraethyl Lead, weight % 0	0.1	0.25	0.50	1.0	2.0
	0	33.0	27.2	24.4	23.0	21.2	20.0
	0.25	38.5	—	—	—	—	—
	0.50	40.7	—	—	—	—	—
	1.00	45.8	36.5	32.2	29.3	25.7	23.0
	2.00	50.6	42.0	37.2	33.5	30.6	25.7
	2.75[a]	54.0	43.7	39.1	35.8	33.0	27.7
	3.00	54.8	—	—	—	—	—

[a] All data for 2.75 weight % n-butyl nitrate (DB-1) were read from curves.

Table B – Combustion Data for a Coastal Straight-Run Distillate with Additives (Data are the average for four oscillograms)

	TEL, weight %	DB-1, weight %	Ignition Delay, millisec	Maximum Pressure, psi	Rate of Pressure Rise, psi/deg
Clear Fuel	0	0	1.05	955	33.3
Fuel + Tel	1.0	0	1.60	1020	91.5
Fuel + DB-1	0	2.00	0.06	950	19.5
Fuel + Tel + DB-1	1.0	2.75	1.00	960	31.5

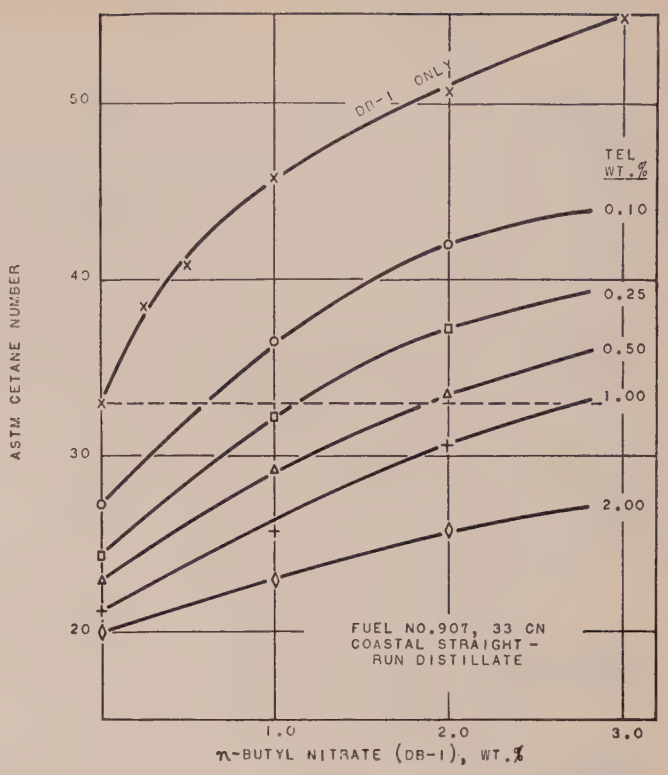

Fig. A – Effect of tel and n-butyl nitrate on fuel ignition quality

explosive type of combustion. It is known that the fuel goes through a series of changes in the presence of hot air in the combustion chamber. After the details of these changes during the delay period are known, the necessary basic information will be at hand for developing methods of controlling these changes so that combustion shock may be avoided even though the delay period may be relatively long. A continuation of these investigations should be encouraged.

Results of Full-Scale Engine Tests Reported

– C. Walcutt and G. C. Wilson
Ethyl Corp.

HURN and his coauthors have contributed toward a better knowledge of the exchange of heat between a fuel spray and the medium into which it is sprayed. This study included several different types of hydrocarbons; these combustibles showed appreciable differences in the time factor for heat release. This may account for some of the differences in the early stages of autoignition that are known to occur with different types of diesel fuels in full-scale engines.

The concept that the steps in the heat-release curves after fuel injection is evidence of a 2-stage combustion process is supported by investigations of combustion in a rapid compression machine and in a motored engine operating on premixed charges. Both of these studies showed a close agreement between the extent of the heat of precombustion reactions and the heat release at the time of the steps in the curves.

Oscillograms for combustion in full-scale diesel engines, under certain conditions, show definite increases in pressure at a slow rate for a period preceding the rapid rise in pressure. This slow rate of combustion can be shown to occur during a critical set of conditions such that a change of either fuel properties or engine operating temperatures will alter the extent of this type of precombustion.

The authors report that a lower temperature resulted when fuel was injected into an engine operated on helium-oxygen than that which occurred when argon-oxygen was used. We obtained the same lower temperature with a helium-oxygen mixture, either with or without a premixed fuel charge in a motored engine. We support their conclusion that this effect is due to the much greater thermal conductivity of helium as compared with argon.

The measured value of heat required to result in temperature equilibrium following injection of fuel into the bomb was only three-fourths of the calculated amount. This figure seems reasonable since the bomb is essentially an isothermal apparatus, and since heat conduction from the walls could mask the cooling effect from fuel evaporation.

The tests of kerosene containing 6.0 cc tel are of interest. The reason that tel in the injected fuel did not increase the ignition delay at a low bomb temperature (900 F) but did at a high temperature (1300 F) is readily explained by the fact that tel cannot decompose during so short a period as a few milliseconds before combustion occurs at the low temperature (900 F).

An interesting point with regard to the effects of tel on combustion in a diesel engine may be shown from the data in Tables A and B and the graph shown in Figs. A and B. Fig. A shows ASTM cetane-number ratings for a distillate containing both tel and an ignition improver (DB-1). From these ratings it appeared that 2.75 weight % of DB-1 would just offset the effect of 1.00 weight % of tel. That is, the addition of 1.00 weight % tel to a distillate fuel reduced the cetane number from 33 to 21.2, and the addition of 2.75 weight % of an ignition accelerator (DB-1) brought the final blend back to the same cetane-number rating as that of the clear fuel.

In order to explore further the indication that the two additives were counteractive in their effects, tests were made in a full-scale single-cylinder diesel engine. The load and speed were held constant at 65 bmep and 1800 rpm by varying the amount of fuel injected. The combustion diagrams are shown in Fig. B. Each of the four diagrams shows

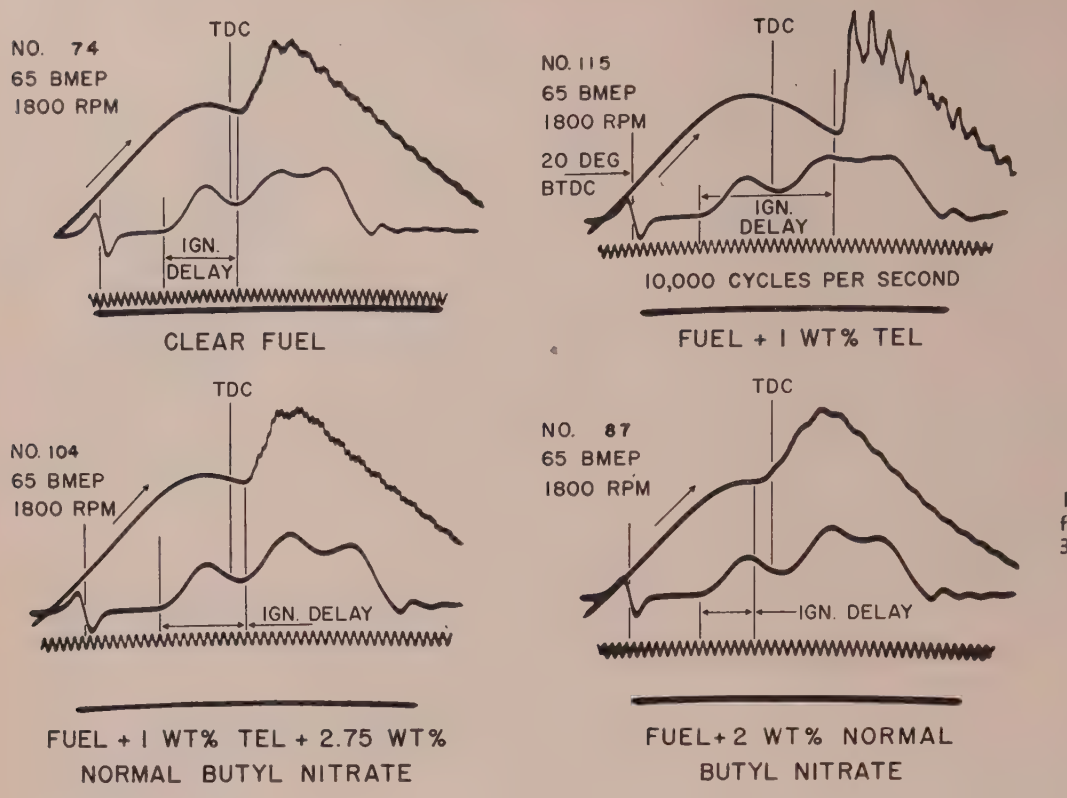

Fig. B – Combustion diagrams for single-cylinder, prechamber, 3¾x5-in., 4-stroke diesel engine

a pressure graph, a fuel-injection timing graph, and a timing wave. It is of interest to observe the effectiveness of tel for delaying autogeneous combustion and also the sharp pressure rise which follows a long delay period in a diesel engine, as shown in Fig. B, diagram No. 115. Also, it is of special interest that diagram No. 104 for fuel containing the balanced amounts of the two additives closely resembles the combustion diagram, No. 74, for the clear fuel.

Cycling Combustion Chamber Used To Observe Ignition Delay Phenomena

– Klaus C. Karde
Harnischfeger Corp.

IN discussing factors influencing ignition delay, the authors mention some discrepancies in comparing experimental results obtained in a bomb with those found in a diesel engine.

More comparable results may probably be obtained by applying a combustion chamber which is equipped with inlet and outlet valves, a high-pressure air supply, and an ordinary injection pump. Such a chamber allows operating the diesel cycle under actual engine conditions. Two such cycling combustion chambers, which for further observations were equipped with diametrally located quartz windows have been used at the Technical University, Hanover, Germany, for studying the diesel cycle. Their design and test results are described in *"Automobiltechnische Zeitschrift,"* Vol. 39 (1936), No. 20, pp. 501-515 and *"Motortechnische Zeitschrift,"* Vol. 6 (1939), pp. 181-190 and Vol. 2, No. 1 (1940), pp. 7-15.

Test results show that combustion-chamber pressure drop occurs without any delay from the beginning of injection. The end of ignition lag (physical and chemical), is defined as the point of lowest pressure (equilibrium between endothermal and exothermal reaction), between beginning of injection and the sudden pressure rise of combustion. Different combustion rates lead to dividing it into three phases: precombustion, main combustion, and afterburning.

All test results and observations indicate that such a cycling chamber is the most versatile instrument which can be used to gain more intimate knowledge about the different physical and chemical phenomena taking place in a diesel engine.

Points Out that Cracking Must Not Be Ignored

– P. H. Schweitzer
Pennsylvania State University

ON the technique used by El Wakil and his coauthors I have no comment except that the cycle-to-cycle variation of the injection quantity and timing is probably responsible for some of the scatter in the points.

I believe, however, that in the interpretation of the results an important factor was ignored, due consideration of which would have changed some of the conclusions.

Pyrolysis, or thermal decomposition, commonly called cracking, is an important part of both preflame and postflame reactions. In fact one probably must have some cracking to have autoignition at all. Unless ignition nuclei are present in the gas-air or vapor-air mixture, self-ignition

would probably not take place without cracking of the hydrocarbon molecules creating free radicals which initiate ignition.

The important thing to realize is that cracking is endothermic. How much so can be seen from the bond strengths:

Single-bond carbon: C — C 80 Kcal per mole
Double-bond carbon: C = C 150 Kcal per mole
Triple-bond carbon: C ≡ C 200 Kcal per mole
C — H 100 Kcal per mole

So cracking, like vaporization, absorbs heat from the mixture.

Slow oxidation which also precedes ignition in the firing cycle (and lasts from the time of ignition to the point explosive reaction) is, on the other hand, exothermic. Our tests show that the heat generated by the preflame oxidation of hexane, heptane, and high-cetane fuel is amazingly large, while that of isooctane and alcohol is next to zero.

Before ignition occurs cracking and slow oxidation counteract each other although in engines where injection takes place close to top center, the latter is necessarily small.

In any case, in an energy balance cracking must not be ignored. In nitrogen, atmosphere oxidation is absent but cracking is very much present and it no doubt influences curve C in Fig. 12.

For numerical evaluation of the cracking Btu's, one, of course, would have to know how many and what kind of molecules crack. This could, perhaps, be determined experimentally by injecting fuel into hot nitrogen saturated with fuel vapor which should be at high pressure because pressure promotes cracking as much as temperature.

By accepting the foregoing, the authors probably will modify some of their conclusions. The endothermic reactions cannot be dismissed, while the "spray breakup delay" is probably unimportant.

While some cracking is generally necessary to initiate ignition, the cracking goes on cheerfully even after ignition has set in and then does a lot of mischief. It is responsible for the exhaust smoke and for the carbonaceous deposits in the cylinder.

Yu et al. and El Wakil et al. Closure to Discussion

THE authors appreciate the comments of the discussers and the fact that they have taken the time to read through the papers in such detail.

The possibility that cracking may influence the early pressure changes, as suggested by Prof. Schweitzer, certainly cannot be ignored. Computations show, however, as illustrated below, that its effect is negligibly small during the delay period unless cracking is markedly accelerated by either the oxygen or the nitrogen.

Concerning the engine data, the average interval between the beginning of injection and the peak pressure drop is about 6 crank angle deg or 1.25 millisec at 800 rpm. The average temperature and pressure during this period are estimated to be 1150 F and 450 psia, respectively.

Let us assume complete vaporization at the beginning of the period of all the fuel injected during this 6-deg period (the worst possible case) and a first-order reaction.[a] Using the Arrhenius equation, and reaction velocity constants from the literature,[b-e] we are able to estimate the rate of cracking. The energy absorbed (and therefore the resulting pressure change) depends upon the cracking reaction assumed. In general, the pressure change is smaller for the cracking of a heavier molecule and for a given molecule is larger the smaller the resulting molecules (in the limit H and C).

Table C summarizes the results, considering always the worst possible case, that is, complete, instantaneous vaporization and small molecules as the end result.

Table C – Summary of Results

	Fuel	
	Heptane	Cetane
(1) Maximum Measured ΔP, psi	6.5	4.5
(2) Maximum ΔP, assuming All Fuel Injected Cracked, psi	4.4	2.8
(3) Fraction of Fuel Cracked (from Reaction Rate Computations)	0.00017	0.00032
(4) ΔP due to Cracking (from Computations), psi	0.0035	0.0065
(5) Ratio of Item 4 to Item 1, %	0.08	0.23

The conclusion is reached, therefore, that, due to the brief time available, the amount of cracking is negligible for the present studies unless the temperature estimation is in major error or it is accelerated very markedly by the presence of oxygen or nitrogen.

This conclusion may not be, and in fact probably is not, correct after the start of rapid combustion.

ORAL DISCUSSION

Reported by Ernest W. Landen

Caterpillar Tractor Co.

E. W. Landen, Caterpillar Tractor Co.: The type of engine instrumentation used by Yu et al. seems to give information which engine people are eager to have. There is a time element involved in ignition and combustion in an operating engine which is difficult to reproduce by other methods. For example, small diesel engines have been operated up to 5000 rpm; here the entire combustion process is over within one or two millisec. Differences observed in the primary and secondary reference fuels indicate that there are still some things in an operating engine which need explaining.

E. R. Kling, Continental Motors Co.: Two people have told us we do not make our combustion chambers and atomization equipment properly. M. G. Fiedler injects large droplets and J. S. Meurer injects the fuel on the piston surface. Does the technique described here help in studying these combustion systems?

Prof. Myers: Mr. Kling's question is, we feel, partly answered by the El Wakil et al. paper.

H. F. Bryan: The forerunner of the type of work covered by El Wakil et al. was the measurement of ignition quality in different types of engines. The "Front End Volatility Group" of CRC worked several years in determining what the front end did so far as ignition delay was concerned without much progress. The work reported today indicates that composition influences ignition more than the volatility. Anomalies have been observed in experimental data which have not been explained. The study of vaporization will help us understand these anomalies.

[a] See Proceedings of Royal Society of London, Vol. A 203, 1950, pp. 486-501: "Kinetics of Thermal Decomposition of Normal Paraffin Hydrocarbons. III – Activation Energies and Possible Mechanisms of Molecular Reactions," by K. U. Ingold, F. J. Stubbs, and C. N. Hinshelwood.

[b] See Proceedings of Royal Society of London, Vol. A 214, 1952, pp. 471-481: "Activation Energies and Frequency Factors in Thermal Decomposition of Paraffin Hydrocarbons," by M. G. Peard, F. J. Stubbs, and C. N. Hinshelwood.

[c] See Proceedings of Royal Society of London, Vol. A 214, 1952, pp. 20-35: "Kinetics of Thermal Decomposition of Normal Paraffin Hydrocarbons. V – Order of Reaction over Extended Ranges of Pressure," by F. J. Stubbs, K. U. Ingold, C. B. Spall, C. J. Danby, and C. N. Hinshelwood.

[d] See p. 2099 of "Science of Petroleum." Vol. III. "Theory of Cracking," by P. K. Frolich and S. C. Fulton. Pub. by Oxford Press, London, 1938.

[e] See "Selected Values of Physical and Thermodynamic Properties of Hydrocarbon and Related Compounds." Pub. by American Petroleum Institute and Carnegie Press, 1953.

Human Factors in Highway

THE extensive use of some kind of motor vehicle is now generally accepted as the primary means of trransportation. The marked increase in the number of automobiles, trucks, and buses in recent years constitutes the most outstanding development in our economy. One of the most important implications of the above change in the national scene relates to safety in transit. As miles traveled, passengers carried, and tons conveyed have increased, traffic has become more dense, speed levels have risen, and there has been, as a direct result, an increase in deaths, injuries, and monetary costs. Thus, the integration of motor vehicles into our way of life has become very costly, and highway safety has become a matter of pressing national concern.

A BROAD research program in the field of highway safety has been in progress at the Harvard School of Public Health during the past six years. These studies were initiated by the American Trucking Associations, Inc., the National Association of Motor Bus Operators, and the National Association of Automotive Mutual Insurance Companies.

Since 1951 the Commission on Accidental Trauma of the Armed Forces Epidemiological Board, Department of Defense has sponsored research on the human factors in vehicular accidents at Harvard and at a number of other universities and research institutions. Thus far the research program has stressed basic causes in the areas of:

1. Identifying traits of personality and behavior which lead to repeated errors.
2. Defects in the design of equipment (human engineering).
3. Injuries and fatalities resulting from vehicular crashes.
4. Mathematical studies of the various interrelationships of contributory causes in accidents.

An extensive review of these and other studies of human factors in highway safety, which has recently been completed as a part of this project, is given here.

Transport Safety

Dr. Ross A. McFarland, Harvard School of Public Health.

This paper was presented at the SAE Golden Anniversary Transportation Meeting, St. Louis, Nov. 2, 1955

The Bus Industry – The number of persons using buses each year is far greater than for any other form of public transportation. There are 25,000 buses which operate over an estimated 400,000 route miles, providing service for a billion revenue passengers a year and employment for more than 65,000 persons. The above figures for volume of traffic do not include the use of transit lines within urban areas. If such transport systems are included, it is estimated that over 9 billion revenue passengers use some form of bus transportation each year.[1, 2]

In many areas of the country buses provide the only form of public transportation. The attractiveness of bus service is based upon the relative economy, frequency and flexibility of service, and safety in transit which characterizes this industry. Safety is one of the most important points in the choice of a mode of transportation. The record achieved by the bus industry exceeds that of railroad passenger trains, scheduled air transport, passenger autos, and taxis, in the order indicated.[3, 4, 5] The number of deaths involving buses each year amounts to less than 1% of the total number of vehicular deaths on the highways.

The Trucking Industry – In recent years the trucking industry has assumed major proportions. In fact approximately 50% of the nation's freight is transported over the highways.[6] In many areas of the United States all movement of goods is carried out by highway transport vehicles, while many cities and towns which have rail service available also depend upon the trucking industry for more frequent schedules. Other large areas would be on a starvation diet after a week if the supplies brought in by truck were stopped.

The basic reasons for the extensive use of truck services are essentially the same as for buses, and all sections of the United States depend upon trucks for cargo hauling. The service is flexible, economical, dependable, and rapid. Truck service makes possible faster movement of raw materials to the manufacturer and to the wholesale and retail outlets by eliminating unnecessary handling of materials. This faster movement of goods plays an important role in the national economy. One of the very significant aspects of the trucking industry is the transportation of agricultural products to market: 89% of these products are hauled from the farm to market by truck; the remaining 11%

[1] See "Bus Facts." Pub. annually by National Association of Motor Bus Operators, Washington, D. C.

[2] "Human Variables in Design and Operation of Highway Transport Equipment," by R. A. McFarland. Presented at SAE Annual Meeting, Detroit, Jan. 16, 1952.

[3] See "Accident Facts." Pub. annually by National Safety Council, Chicago.

[4] See 1942-1951 editions of "Accident Rates in Transportation Industries." Pub. by National Safety Council, Chicago.

[5] See "Human Factors in Air Transportation: Occupational Health and Safety," by R. A. McFarland. Pub. by McGraw-Hill, New York, 1953.

[6] See "Trucking Trends." Pub. annually by American Trucking Associations, Inc., Washington, D. C.

is moved either by truck or wagon to a railroad or to a dock for further shipment.[7]

In 1950 there were approximately 9,000,000 registered vehicles which were involved in the great volume of trucking operations mentioned above. It is estimated that 424,000 trailers aided in this task. The industry provided employment for 5,714,000 persons, the majority being drivers. According to the American Trucking Associations there are over 5,000,000 truck drivers, constituting one of the largest job classifications in the country. Thus approximately 1 out of every 11 persons employed in the United States is employed in the trucking industry.[8]

In recent years, the use of trucks has accounted for about one-fifth of the total annual vehicular mileage. In regard to the safety record in these operations, data from the National Safety Council indicate that trucks were involved in about 4-5% of the traffic deaths last year.[3]

Role of Automotive Engineer in Highway Safety

Human failure of one kind or another has usually been given as the chief cause in from 80 to 90% of motor vehicle accidents. This has frequently led automotive engineers to be pessimistic about the effect improvements in design might have in reducing accidents. It could be expected that drivers would continue to make errors and have accidents, despite changes in design which made the vehicle fundamentally safer. Nevertheless, such improvements have undoubtedly played a part in the reduction which has been made in the fatal accident rates over the past 30 years. From 1925 to 1930, the fatality rates for motor vehicle accidents averaged about 17 per 100 million vehicle-miles. In 1954, the fatality rate had dropped to 6.5.

With careful research on the causes of accidents, further advances can be made to bring these rates still lower and to reduce the annual totals of death and injury from highway transport accidents. In 1955 there were approximately 38,300 deaths and more than one million disabling injuries. The direct cost of these accidents approximated about one and one-half per cent of the national income, and estimates of the indirect cost run many times larger. Automotive engineers can contribute especially in those areas where, in the combination of circumstances of the driver, the vehicle, and the environment, the design of equipment has an important relationship to how well the driver will be able to operate. One of the primary purposes of this study is to outline ways in which the automotive engineer can develop more effective integration between driver and vehicle. Improvements both in operating efficiency and in safety should result.

Designing to Meet Human Requirements – Established methods of controlling accidents, such as driver selection and education, and the socio-legal measures, stress the role of factors within the driver. There is also a relatively new discipline which can reduce accidents by relating the mechanical design of equipment to the biological and psychological characteristics of the operator. This approach, called human engineering, engineering psychology, or biotechnology, is from the point of view that machine controls are basically but extensions of the body appendages, and that instruments and other devices which supply man with the information he needs for the satisfactory operation of his equipment serve as extensions of his nervous system. This implies that the capabilities and limitations of human operators should be basic considerations in the design of equipment to be operated by persons. Unless this is done, design features may be conducive to operating errors, or may place undue burdens upon the operator leading eventually to "human failure" incidents.[7, 9, 10]

The above concept was developed chiefly in the field of aviation. There have been significant results in terms of reduced training time and costs, improved operator efficiency, and fewer accidents. The role of faulty design in driver-errors, and in highway accidents, however, has not as yet been determined. Attention has been given to their possible influence in only very few of the attempts to analyze the accident causes. However, the general principles can be applied in all situations in which humans operate mechanized equipment, whether in aviation, in industry, or in highway transport. The design of displays, that is, devices and signals to supply the operator with the information he needs, requires an understanding of the sense organs and of the characteristics of human perception. Data on the ranges of human size and dimensions are important for the overall layout, seating, and the location of controls. Information on biomechanics, that is, range and position, is required for the proper design of controls. Furthermore, margins of safety are necessary because the capacities of operators are not always at a maximum. The driver may be influenced by fatigue, minor illness, and the like, or noxious features of the environment. The biological scientists can assist the engineer with respect to human requirements both in an advance analysis of equipment

---

[7] See "Human Factors in Highway Transport Safety," by R. A. McFarland and A. L. Moseley. Pub. by Harvard School of Public Health, Boston, 1954.

[8] See reference in footnote 6.

[9] See "Applied Experimental Psychology – Human Factors in Engineering Design," by A. Chapanis, W. R. Garner, and G. T. Morgan. Pub. by Wiley, New York, 1949.

[10] See "Human Body Size and Capabilities in Design and Operation of Vehicular Equipment," by R. A. McFarland et al. Pub. by Harvard School of Public Health, Boston, 1953.

[11] See Air Materiel Command, Wright-Patterson Air Force Base, Dayton, Ohio, USAF Technical Report No. 5829, August, 1949: "Psychological Aspects of Equipment Design," by P. M. Fitts.

[12] See "Human Factors in Undersea Warfare." Pub. by Panel on Psychology and Physiology, Committee on Undersea Warfare, National Research Council, Washington, D. C., 1949.

[13] See "Human Factors in Air Transport Design," by R. A. McFarland. Pub. by McGraw-Hill, New York, 1946.

in the early stages of design, and at the mockup stage.[11-13]

A few examples may illustrate this point of view. If an auditory warning signal such as a tone is proposed to indicate the malfunction of equipment, would it not be best to select a frequency in the bands to which the ear is most sensitive, and which lies below those frequencies which older people hear less well? If muscular "feedback," as well as vision, is of importance in the control of the directional stability of a vehicle, might not the resistances in a power-steering system be related to information about the human "muscle senses"? If two control knobs are located close together, might not designing them so that they can readily be differentiated by touch help prevent confusing the controls and operating the wrong one?

Analysis of Driver Activities and Critical Incidents

One of the basic procedures in obtaining important information concerning the design of equipment for human use is to analyze driver activities and near accidents.[14] As an initial step in the research program at the Harvard School of Public Health an attempt was made (a) to describe precisely what is involved in driving, or to analyze driver activities, (b) to determine the critical component of the operator's job, and (c) to analyze those types of reactions which may contribute to emergency situations or real accidents.[7]

When the task of driving itself is employed as the logical starting point, a rational analysis indicates that anticipation, foresight, and continued alertness on the part of each driver are required to avoid accidents.[15] Thus, any feature which may distract attention, interfere with perception, lengthen reaction times, or hinder the completion of required responses may directly compromise safety. Other features, in themselves less critical, may however result in reduced efficiency if they force the driver to operate near, or beyond, the limits of his normal capacities. Such features may also accumulate in their effects, adding to fatigue.

A. *Methods of Analysis* – A wide variety of techniques are required to obtain reliable information for a thorough understanding of driving duties and possible sources of error. These techniques require well-trained analysts skilled in psychological and research procedures. The chief methods which can be applied to the driving of trucks or buses are as follows:

1. Interviews and confidential reports: By means of interviews and confidential reports from drivers, it is possible to obtain accurate accounts of critical situations which have been experienced and emphasize those occurring most frequently. This approach is important not only from the point of view of understanding the critical components of the job but also in outlining areas in which the design of equipment can be improved. An example may be taken from the field of airline piloting. Based on confidential interviews it was found that *inattentive manipulation* or *mistaken identity* of controls accounted for 229 of 460 errors, or about 50% of the specific acts attributed to pilot error.[16] Such studies provide important information for standardization in the design and locations of controls to prevent inadvertent use. Similar studies have been made by carrying out confidential interviews with drivers concerning their accident reports.[7]

2. Sampling of activities: The time-sampling method of analyzing activities of drivers at work provides relevant information in the field of job analysis and near accidents. Samples of activity are recorded at regular intervals by means of a system of codes and symbols. This method reveals a precise description of how much time the operator devotes to each of many tasks, the order in which they are performed, and potential sources of error and observed error as will be shown later.[17]

3. Time and motion study: Another technique for determining the skill requirements of a job is time and motion study.[18] The activity patterns and sequence of operations are clearly revealed in the frame by frame analysis of motion pictures. These studies are particularly useful in studying eye movements while reading instruments on the panel of an aircraft, truck, or bus.[7, 19] Link values as well as the amount of time spent on different instruments can be determined precisely.[20]

4. The study of critical incidents and near accidents: The critical-incident technique, or study of near accidents, offers promise in the analysis of operating techniques, habits, and errors of truck and bus drivers. By an *incident* is meant any observable type of driver activity which is sufficiently complete in itself to permit description and inference.[21] To be *critical,* situations must have developed in such a way that they leave little doubt that an accident is impending. The description of incidents and critical situations can be accomplished by direct observation of drivers during usual roadway operations. Critical incidents may be observed

---

[14] See CAA, Division of Research, Washington, D. C., Report No. 73, November, 1947: "Airline Pilot – Survey of Critical Requirements of His Job and of Pilot Evaluation and Selection Procedures," by T. Gordon.

[15] See "Field of Highway Safety Research." Pub. by Committee on Highway Safety Research of the National Academy of Science – National Research Council, Washington, D. C., August, revised, 1952.

[16] See Wright-Patterson Air Force Base, Aero Medical Laboratory, Psychology Branch, Dayton, Ohio, Memorandum Report TSEAA-694-12, July 1, 1947: "Analysis of Factors Contributing to 460 'Pilot Error' Experiences in Operating Aircraft Controls," by P. M. Fitts and M. L. Jones. See also TSEAA-694-12A of Oct. 1, 1947.

[17] See *Personnel Psychology,* Vol. 3, No. 3, 1950, pp. 361-368: "Sampling Technique for Use in Activity Analysis," by J. M. Christensen.

[18] See "Time and Motion Study," by R. M. Barnes. Pub. by Wiley, New York, 1946.

[19] See Air Materiel Command, Wright-Patterson Air Force Base, Dayton, Ohio, USAF Technical Report No. 5839, October, 1949: "Eye Fixations of Aircraft Pilots. II: Frequency, Duration, and Sequence of Fixations when Flying USAF Instrument Low Approach System (ILAS)," by J. L. Milton, R. E. Jones, and P. M. Fitts.

[20] See Boeing Aircraft Co., Engineering Division, Seattle, Doc. D-7192, September, 1945: "Preliminary Time-Motion Study of Flight Deck Technique of B-29 Copilot During and After Landing," by R. B. Harlan.

[21] See *Personnel Psychology,* Vol. 2, No. 5, 1949, pp. 419-425: "Critical Requirements: New Approach to Employee Evaluation," by J. C. Flanagan.

Table 1 – Activity Analysis of Bus Drivers in Long-Haul Operations[a] – The Frequency of Observed Items and the Percentage of Time That Each Occurred

	Frequency	%
Vehicle		
Straightaway	1243	73.7
Right turn	94	5.6
Left turn	86	5.1
Stopped in traffic	154	9.1
Passing	58	3.4
Pickup	37	2.2
Discharge	14	0.8
Total	1686	99.9
Eyes		
Front	1153	78.0
Right front	68	4.5
Left front	81	5.4
Right	21	1.4
Left	23	1.5
Left mirror	95	6.4
Right mirror	25	1.7
Instruments	8	0.5
Down	9	0.6
Total	1483	100.0
Right Hand		
Wheel	1200	80.9
Shift	161	10.8
Rest	97	6.5
Hand brake	4	0.3
Instruments	6	0.4
Fares	3	0.2
Signals	0	0.0
Horn	13	0.9
Waving	0	0.0
Total	1484	100.0
Left Hand		
Wheel	1465	98.8
Rest	17	1.1
Hand brake	0	—
Instruments	0	—
Fares	0	—
Signals	0	—
Horn	0	—
Waving	2	0.1
Total	1484	100.0
Right Foot		
Accelerator	1286	87.0
Brake	198	13.0
Rest	0	—
Total	1484	100.0

[a] See reference in footnote 7.

and recorded by the driver trainer, or the safety supervisor, or by some other trained observer.

B. *Analysis of Activities, Distribution of Work Load, and Errors of Professional Drivers* – In the sections which follow a study is first reported on the activities and work load of bus drivers during long- and short-range operations. A study is then reported on the most frequent type of errors and near accidents in long-haul trucking operations.

1. Activity analysis of bus drivers: The objectives of this study were to observe the concurrent actions of the operator's hands, feet, and eyes while driving a vehicle and to determine not only the peak loads on each part of the body but also to study the critical components of each task. One method involved photographing, and another involved interval sampling of the head, body, hand, and foot movements used in turning, decelerating, accelerating, shifting, stopping suddenly, and braking. The data were obtained by a trained observer who recorded the frequency and time of each activity carried out by the drivers. Instances of driver errors were also recorded. This information was used to describe the requirements of the job, the proportion of time spent in different activities, and the number of errors made by each operator. Unusually complicated activities were photographed by the use of an electrically operated 16-mm motion picture camera.

Trips were made between Boston and New York on a scheduled interstate carrier. Observations were recorded during 7 of the 9½ hr required for each trip; the route involved both city traffic and open highway conditions over varying terrain. The frequency distributions shown in Table 1 were based on approximately 1500 observations for the vehicles and the various parts of the body mentioned above. The data in this table indicate that the bus was operating in the straightaway position 74% of the time and that the driver had his eyes to the front 78% of the time. The left hand was kept almost continuously on the wheel (99%), while the activity of the right hand was divided between the wheel (81%) and the gear shift (11%). The right foot was on the accelerator 87% of the time and on the brake 13%.

An analysis of the activities of the drivers of buses used in intercity operations revealed that the automatic transmission makes possible a reduction of from 5 to 25% of the total amount of activity per minute in a normal passenger run. Any simplification of the driving routine gives the operator more time to react properly to other aspects of driving and the care of passengers.

Micromotion studies of each activity show the link value of various controls, the time necessary to do these activities, and the critical components of various tasks. The data collected on the methods of shifting, vision from the cab, and the use of switches and instruments are also of value in considering improvements in the design of equipment.[22]

The results may be helpful in improving the design and location of various controls and switches in that the relative frequency of use is indicated. Data on the use of the eyes suggest that attention is devoted primarily to the roadway ahead. More extensive use of side and rear vision may be encouraged by mirrors of improved design. Individual muscle groups may become acutely fatigued from holding a steady position. The lower right leg and foot, for example, may react slowly in emergency situations after maintaining steady, continuous pressure against the accelerator pedal. With only intermittent use required, the left leg can be exercised to some extent in transit. Since the driver is seated almost continually while at work, the seat should be made as adjustable, comfortable, and

[22] See Chapter 10 of reference in footnote 7.

free from road shock and vibration as possible. In some situations, as on runs in mountainous country, continuous turning and shifting are required. Mechanized or hydraulic aids to steering will continue to reduce the possibility of errors during these combined maneuvers.

2. A study on the proficiency of bus drivers in operating their equipment: In evaluating the proficiency of individual drivers in handling their equipment and appraising their errors and susceptibility to errors or accidents, direct observation was made of 30 bus drivers throughout routine scheduled runs in New England. The route was approximately 23 miles long and the scheduled time 55 min. Detailed recordings of the drivers' activities were made during each minute. An objective numerical score for 22 possible errors was obtained for each driver. It was found that both frequency and types of errors differentiated between the good and poor drivers. The eleven kinds of errors of greatest value in this respect are shown in Table 2. Correlations of 0.71 and 0.61 were obtained between the "error" score and the safety director's rankings and the operator's past accident records, respectively. Study of the detailed records indicate that these experienced drivers made few errors in the elementary skills of their task but made many in the more complex aspects of maneuvering. One possibility of reducing such errors is through improvement in the design of the equipment to simplify the more complicated operations.[22]

3. Analysis of near accidents in bus operations: A study was made of near accidents during 4000 miles of routine long-haul bus operations in the far west. The analysis revealed that as a rule critical situations develop very rapidly and are of short duration. Of the *66 near accidents* observed, 53, or 80%, of them were closely related to the three most common types of accidents which actually occur on the highway, namely, sideswipe, rear-end, and head-on collisions. The most important variables contributing to the critical situations were as follows: (1) following too closely; (2) following too closely while approaching to pass, that is, cornering; (3) operator inattention, that is, dozing at the wheel; (4) vehicle running off the road; (5) intersection errors; (6) errors in passing; (7) operating in wrong lane of traffic; (8) leaving and entering the roadway; and (9) pedestrian errors.

It is of interest to note the speed with which defensive driving operations must be carried out if accidents are to be avoided. For example, the maximum value observed in decelerating for an emergency ahead was 7.2 sec, passing a second vehicle from 13.2 to 29 sec, and passing a semitrailer at road speed 13.2 sec. Errors were noted in the use of headlights and in the allowance for adequate braking distance. Emergency situations may have a total duration of less than a second.[22]

4. Analysis of near accidents in long-haul truck operations: Very similar findings resulted when an observer obtained detailed descriptions of 48 near accidents which occurred during 20 long-haul truck trips totalling 5000 miles. Most of the incidents were precipitated through operational errors or errors in judgment on the part of drivers. Even though the maneuvers leading into a near accident may have consumed a half a minute or more, as when lengthy vehicles overtake and pass at a low speed differential, the elapsed time of a near accident was of the order of a second or two, often less than one second. Critical situations with such limited time relations were most frequent when visibility of the roadway ahead was restricted, as at blind curves and intersections, at the crests of hills, and in fog. Under such circumstances, the limits of human reaction time and physical braking distance may be exceeded, and safety is dependent upon the design features which reduce perception and reaction time even fractionally and reduce the time and effort of emergency maneuvers in controlling heavy equipment.[22]

5. Areas suitable for collaboration between engineering and biological scientists: The view which is being emphasized throughout this report is that the integration of the driver and his equipment is essential in the prevention of accidents. Either the operator *or* the equipment may be at fault unless the instruments and controls are effectively integrated with the operator.

An operator may be much more likely to make errors if (a) he cannot easily reach, or rapidly select and operate a control, (b) gages or dials cannot easily be read at a glance, (c) sensory cues fed to him are outside the range of his maximum sensitivity, (d) seating does not provide him a position suitable for carrying out all the operations of driving while at the same time preserving the best conditions for continuous, clear vision of the roadway.

Information developed by the biological sciences on the limitations and capabilities of human operators can be effectively applied by the engineer in

Table 2 – Discrimination Value of Types of Errors Observed in Bus Drivers[a]

Type of Error	Discrimination Value (X^2)
Follows vehicle too closely	5.6
Errors at stoplights and signs	3.8
In wrong lane of traffic for conditions	3.8
Writing on day card in motion	2.8
Improper passing	2.3
Improper turn	2.3
Excessive speed	2.3
Collecting equipment for relief in motion	2.3
Attention not on road	1.4
Errors at intersection	1.1
Miscellaneous inattentions	1.1

[a] See reference in footnote 7.

the design of vehicular equipment to prevent errors arising from the faulty integration between man and his machine. Specific areas where such a collaborative approach is important include: (a) layout of the working space, (b) the visual, auditory, and kinaesthetic displays intended to provide the operator with information about his equipment and his performance, (c) design, location, and operating characteristics of controls, (d) control of toxic or harmful environmental factors associated with driving, and (e) the protection of vehicle occupants against impact and decelerative forces in the event of accident.[7, 11, 13]

Human Body Size and Design of Seats and Controls

If an engineer is to design a seat which will accommodate any given proportion of drivers in height, width, and depth, he must know the full size range of the driver population.[23-25] The same consideration obtains for the effective location of controls, pedals, and switches. Anthropometric techniques can be used to obtain distributions of the body dimensions of driver populations, and these distributions can be applied in the design and evaluation of vehicular equipment in terms of practical questions of the horizontal and vertical adjustment of seats, and of clearances and allowances within the layout and overall working space provided for driving.[26]

Equipment which will accommodate a large proportion of the driving population can also be designed if dimensions of the human body important for the location of controls, and for defining the limits of the working space, are considered. The most important dimensions in this regard have been indicated by King.[27] These are: (a) the maximum arm reaches which can be obtained without a change in the position of the body; (b) the extension of these reaches which can be obtained by movement of the trunk or body; (c) the eye-level of the man in the operating position; (d) body dimensions in the operating position, that is, sitting heights, fore and aft and lateral measurements at various levels; (e) the leg reaches which can be obtained without altering or disrupting posture. The application of such data will help in preserving the comfort, efficiency, and safety of a greater proportion of the driving population under consideration.

The Bodily Dimensions of Bus and Truck Drivers – In order to carry out evaluations of trucks and buses, it was necessary to know not only the dimensions of the vehicles themselves but also the body dimensions of the operators. A great deal of human sizing data has been obtained for pilots in connection with cockpit design, but until recently little specific information has been available on truck and bus drivers.[9, 24] To remedy this situation, an anthropometric team, consisting of members of our staff, conducted surveys in the field to assemble the necessary raw data. Thirty-two measurements, including the important body segments, were taken on 100 bus drivers, 100 New England truck drivers, 70 Texas truck drivers, and 100 Champion truck drivers. Only those measurements were taken which are specially pertinent to vehicle design.[10]

The data are *not* presented in terms of averages, for the use of average values may account for many defects in vehicle design.[2] The average value should not be employed directly, since, by definition, arrangements based upon an average would be suitable for only 50% of the operators in a normally distributed group. Provision for 90 or 95%, or any other predetermined per cent of potential operators, will require identifying the correct cutoff point. For example, where arm reach for the operation of manual controls is under consideration, the cutoff point should be well below the average reach. Due consideration must be given to the 25% of the drivers whose dimensions exceed the average values as well as to the 25% whose measurements are below the average.

Table 3 – Percentile Distributions of Anterior Arm Reach, Knee Height, and Sitting Eye Height for Professional Bus and Truck Drivers[a]

Percentiles	Anterior Arm Reach, in.	Knee Height, in.	Sitting Eye-Level Height, in.
5	32.95	20.08	27.72
10	33.46	20.43	28.11
15	33.94	20.63	28.39
20	34.33	20.83	28.58
25	34.65	20.98	28.74
30	34.88	21.18	28.98
35	35.12	21.30	29.13
40	35.32	21.42	29.29
45	35.51	21.58	29.45
50	35.75	21.69	29.61
55	35.94	21.81	29.72
60	36.14	21.93	29.88
65	36.38	22.05	30.00
70	36.58	22.16	30.16
75	36.85	22.24	30.43
80	37.13	22.36	30.55
85	37.44	22.56	30.75
90	37.87	22.84	30.98
95	38.42	23.50	31.61
	Number: 312 Range: 30.66-41.67 Median: 35.75	Number: 301 Range: 19.29-25.98 Median: 21.69	Number: 309 Range: 26.38-32.68 Median: 29.61

[a] See reference in footnote 23.

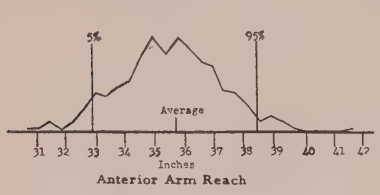

Anterior Arm Reach

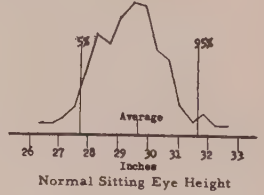

Normal Sitting Eye Height

[23] See "Human Factors in Design of Highway Transport Equipment: Summary Report of Vehicle Evaluation," by R. A. McFarland, J. W. Dunlap, W. A. Hall, and A. L. Moseley. Pub. by Harvard School of Public Health, Boston, 1953.

[24] See *Yearbook of Physical Anthropology*, Vol. 1947, No. 3, 1948, pp. 197-203: "Anthropometric Problems in Royal Air Force," by G. M. Morant.

[25] See *British Journal of Industrial Medicine*, Vol. 4, 1947, pp. 77-83: "Some Anatomical Problems in Naval Warfare," by A. G. M. Weddell and H. D. Darcus.

[26] See SAE Transactions, Vol. 62, 1954, pp. 335-345: "Human Engineering: New Approach to Driver Efficiency and Transport Safety," by R. A. McFarland.

[27] See *American Journal of Physical Anthropology*, Vol. 6, 1948, pp. 341-351: "Measurements of Man for Making Machinery," by B. S. King.

Table 3 gives the percentile distributions of three body dimensions found to be important in regard to the location of the seat and controls in cabs. Two of the distributions are also shown graphically.

Two manuals have been developed in the Highway Safety Research Project at the Harvard School of Public Health, one entitled "Human Body Size and Capabilities in the Design and Operation of Vehicular Equipment,"[10] and the other "Human Factors in the Design of Highway Transport Equipment: A Summary Report of Vehicle Evaluation."[23] The second report was based upon our evaluation of 12 trucks and 4 buses. All of them were 1950-1951 models, and they represented various types, such as light and heavy tractors, straight trucks with cab-over-engine design, both gas and diesel, and sleeper cabs.

Several examples are given below to illustrate errors which the designer might avoid by using data such as given above:

1. Marked variations were found to occur in the *overall working space* provided for the drivers of trucks and tractors. In one instance, it was estimated that only the drivers representing the smallest 40% of the group could be accommodated. However, if, as was usually the case, the manufacturer had given consideration to the driver rather than solely to cab weight, this was not true.

2. Many errors were observed in regard to *human sizing*. In several models, for example, only 5% of the drivers could comfortably reach and operate the hand brake. In others, only 60% could be accommodated for knee height between the pedals and the steering wheel. Many of the drivers were unable to adjust their sitting position to obtain maximum visibility with regard to their instruments and the road ahead.

3. Failure to provide for adequate *seat adjustment to allow for variations* in human size was frequently noted both in the comments of drivers interviewed and from the objective studies on working areas. Probably the most striking defect is that the front of the seat cannot be lowered for shorter individuals to enable them to operate the pedals without excessive pressure under the knees. Some of the medical problems frequently observed in truck drivers are believed to be related to poor seat design and to failure to provide adequate shock absorbers.

4. In many instances, it is necessary to *observe the driver at work* in order to reveal limiting factors in the layout of the cab and controls. In one extreme case – a 1950 truck cab – it was impossible for a driver to put his foot on the brake pedal without first shifting gears. For 80% of the drivers the distance between the brake pedal and the bottom of the steering wheel was too short to permit the leg to move high enough to put the foot on the pedal. Furthermore, the gearshift in either of the left positions was too close to the wheel to allow the leg to slip between. As a result, the foot was trapped on the floor until the driver could shift gears.

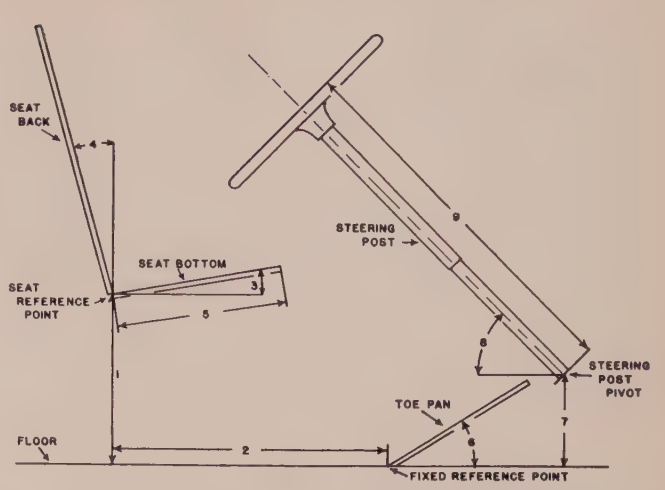

Fig. 1 – Schematic diagram of mockup truck cab, showing various adjustments available to subject and manner in which each was measured

The static human dimensions discussed above cannot always be applied to the dynamic driving situation without additional study.[28] However, mockups can be built to aid in determining the optimum placement and design of the various controls and seats in both static and dynamic situations, and human subjects representing selected sizing characteristics can be used effectively to evaluate the space provisions.[13, 29]

An apparatus to test the adequacy of fitting men to the machines was developed at the Harvard School of Public Health, and an experiment was carried out by Dunlap with this equipment. The different components of the device shown in Fig. 1 could be adjusted in terms of the range of human size in order to find the optimum compromise arrangements. It was also possible to determine the dependence of one functional variable upon another, thus permitting the establishment of an order of importance of the dimensions and angulations involved. Such variables include seat adjustment, pedal location, steering-wheel dimensions, and the like. The concept of the dynamic nature of the job is inherent in this approach. The results of the study indicated that subjects made fewer errors in a simulated driving task after using the nine possible adjustments in the seat, steering wheel, and pedals to find the most comfortable arrangement.[29, 30]

Several sources of data on the body size dimen-

[28] See ASME Transactions, Vol. 67, 1945, pp. 167-175: "Locomoter Mechanics and Occupation," by A. Steindler.

[29] See "Human Factors in Design of Vehicle Cab Areas," by N. C. Kephart and J. W. Dunlap. Pub. by Purdue University, Occupational Research Center, Psychology Department, Lafayette, Ind., 1955.

[30] See Commission on Accidental Trauma, Armed Forces Epidemiological Board, Annual Report, 1954-1955. Pub. by Department of Defense, Washington, D. C., 1955.

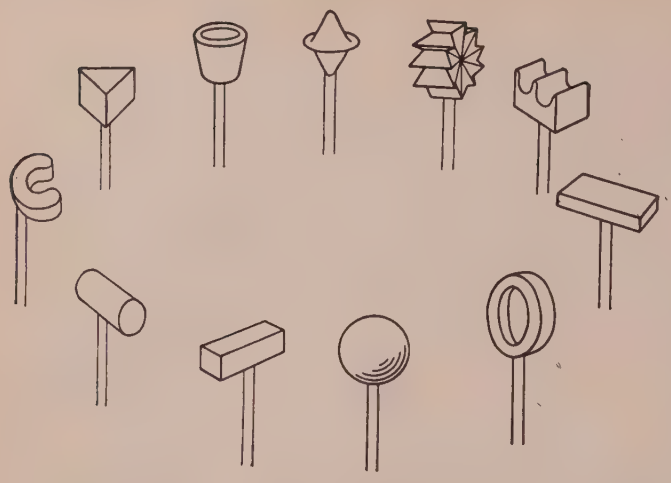

Fig. 2 – Shape coding of controls: 11 knob shapes shown were found to be most easily distinguishable from each other by touch (from Jenkins, see footnote 10)

sions of driver populations are now available. A number of manuals have been prepared which include distributions for a wide range of physical measurements, made on both military and civilian truck driver groups.[10, 31-33] Committees of the SAE are currently developing design recommendations,[34] and in a number of recent model vehicles consideration has been given to many of the principles outlined in the foregoing.

Design of Controls to Meet Human Requirements

In addition to considerations which involve the body size range of vehicle operators, the design of controls also should be related to data on the dynamics of human movement, that is, biomechanics. Many of the basic principles in this area have been worked out in regard to aircraft controls, and many of the data available can be applied to problems of design in vehicles.[10, 13, 35-37] Speed of movement, the forces which can be exerted by foot or hand from the seated operator position, the accuracy of reaching movements, and the most natural type or direction of movements, are illustrations of areas where integration between human factors and design may influence efficiency and safety.

This principle may be understood through a consideration of brake and accelerator pedal relationships. In a number of vehicle models evaluated, to activate the foot brake the driver is forced to make lengthy movements with his foot – up, across, and down. The vertical portion alone of this movement was as much as 9 in. in some cases, thus vitiating to a considerable extent the rapidity of the driver's basic reaction time and extending emergency stopping distance significantly.

In reviewing the material mentioned previously in regard to the evaluation of 16 vehicles, several generalizations can be made. For instance, there was *no standardization of shift patterns* in the various models studied. This predisposes the driver to error in the event that he is transferred from one model or type to another. Many errors in selecting the correct gear have been observed during normal runs. The location of the shift levers is not standard, with the exception that they are all for right-hand operators.

Another area which may be the source of errors or accidents relates to the *location and design of switches and knobs,* especially with respect to headlamps, fog lamps, marker lights, and cigarette lighters. In two instances, the dimmer switch was found to be located directly beneath the foot pedals, behind the steering post. In these models, the driver may inadvertently operate the air horn or fog lights while attempting to dim his headlamps. Even when he operates correctly, more complex motions and longer reaction times are required to avoid the pedals. Since many accidents occur when approaching another vehicle, the location of the switch underneath the pedal may cause undue delay in pedal operation. Adequate shape coding for the accurate identification of knobs and switches by feel or touch might be used to greater advantage (see Fig. 2). Also, greater standardization in the location of switches might aid in the reduction of accidents which are attributed to the inadvertent operation of a wrong control.[23]

Design of Visual Displays

Visual displays usually refer to devices, for example, gages, dials, and signal lights, which convey to an operator information about the way his equipment is performing. If the operator cannot clearly or quickly perceive the indicators, pointers, markers, or numerals, errors of either commission or omission may result, perhaps at times eventuating in accidents. Such factors as the size and spacing of instrument markings, contrast between object and background, and color and illumination are important in regard to the ease with which instruments are read.[11, 13] A number of manuals are now available which give design criteria for ease of reading in terms of shape, size, location, illumination, and scale, numeral, and pointer design.[11, 32, 38] Fig. 3 illustrates some of these principles.

---

[31] See *American Journal of Physical Anthropology,* Vol. 13, No. 4, 1955, pp. 711-742: "Physique of Bus and Truck Drivers, including Review of Occupational Anthropology," by A. Damon and R. A. McFarland.

[32] See "Handbook of Human Engineering Data." Pub. by Tufts College Institute for Applied Experimental Psychology, Tufts College Bookstore, Medford, Mass., 1951.

[33] See "Survey in Seating," by E. A. Hooten et al. Pub. by Heywood-Wakefield Co., Gardner, Mass., 1945.

[34] See SAE SP-6, "Ride and Vibration Data," 1950.

[35] See *Mechanical Engineering,* Vol. 71, 1949, pp. 811-816: "Human Factors in Design of Manual Machine Controls," by L. E. Davis.

[36] See *Psychological Review,* Vol. 56, 1949, pp. 9-17: "Application of Operational Analysis to Human Motor Behavior," by D. G. Ellson.

[37] See *Electrical Manufacturing,* Vol. 49, No. 3, 1952, pp. 90-95: "Introduction to Human Engineering in Product Design," by A. E. Javitz.

[38] See "Human Engineering Guide for Equipment Designers," by W. E. Woodson. Pub. by University of California Press, Berkeley, Calif., 1954.

One of the most important considerations in the design of the visual display in vehicles is the length of time the operator must divert his attention from the roadway in order to comprehend the meaning of his instruments. Thus the recommendation has been made that instrumentation for vehicles be designed especially for rapid check reading, keeping the direct reading of numerals and interpretation of scale markings to a minimum, except for instruments of infrequent, noncritical function.

A. *A Study of the Eye Movement of Drivers in Relation to the Location and Design of Instruments* – A study was made of the eye movements and fixations made by drivers. With a Bell-Howell A-7 Eyemo 35-mm camera, eye movements were photographed as reflected in a mirror. The camera field also included a portion of the roadway ahead. Analysis of the films is in terms of (a) frequency of fixations, (b) duration of fixations, (c) point of fixation (such as, instrument, mirror, forward field), and (d) link values. Sample findings from a bus run are as follows: viewing straight ahead, 87.6% of the time; looking in left rear-vision mirror, 0.3% of the time; looking in right mirror, 0.4% of the time; viewing extreme right field, 1% of the time; passenger mirror, 0.01% of the time. Average fixation time for left mirror was 0.45 sec; for the right mirror, 0.7 sec; and for the passenger mirror, 0.5 sec. Link values were equally strong for right and left mirrors. In this particular run, no fixations were observed for dashboard instruments. The detailed study, which will be reported later, may prove to be of interest not only in showing the marked differences in time required to obtain the necessary information from instruments but in determining the interrelationships most important for safe driving.[30]

B. *The Design of Windshields and Mirrors* – The design of windshields, side windows, and rear-vision mirrors represents one aspect of the visual display. Studies of accidents in the truck and bus field indicate that additional research should be carried out in these areas. Adequate vision from the cab remains a serious problem in some models, although marked improvements have been made in others.

The frequency of pedestrian accidents involving trucks operating in residential and busy areas suggests the need for improvements. This contention was supported by an analysis of 57 light delivery truck accidents which indicated that 50% of the cases involved pedestrians. When operating during bad weather, the range of forward vision was reduced approximately 50%, and visibility from the side was reduced even more because of no provision for cleaning or defogging. Although the areas of the side windows are approximately the same, there are marked variations in the ability to see pedestrians on the right because of the distance of the driver from the right-hand windows.[7]

1. An analysis of backing accidents and rear-vision mirrors: The importance of more adequate provisions for vision to the side and rear has been brought out in an analysis of backing accidents in trucks. In a thorough investigation by our research staff at the Harvard School of Public Health, all of the accidents in one large trucking company during a single year were analyzed. Of the 258 collisions, 65 were backing accidents occurring primarily at locations related to loading and unloading activities, dock areas, driveways and alleys, usually in business districts but away from streams of traffic. Provision for side and forward vision was shown to be poor. Inadequate provision for rear vision was a characteristic of practically all the vehicles involved. Thus, present mirrors place undue burdens on drivers in carrying out backing operations and in operating in spaces with small clearances.[39]

2. Man's area of vision in relation to windshield design: The range and field of view for drivers from all types of vehicles is an area where engineering and biological scientists can collaborate in research. Methods are being developed for the objective rating of each automobile, truck, bus, and all types of military vehicles such as tanks and weapon carriers. The principle involved is the geometry of vision from the eye position of drivers in relation to the supporting structures of the windows. King and Sutio have developed an instrument which per-

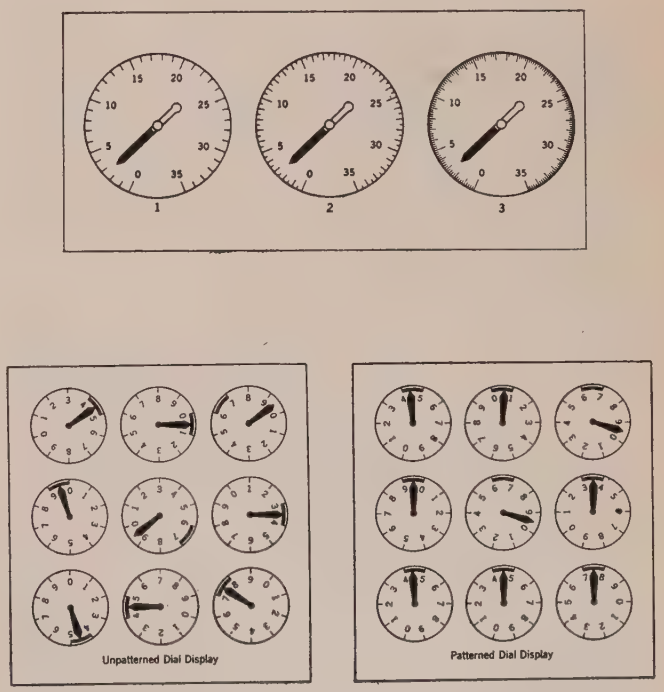

Fig. 3 – Principles of instrument design and dial marking. Upper view: Fewest reading errors were made with dial on left having fewest markings. Lower view: It is demonstrated that if a group of instruments is oriented so that normal operating range is in same direction, a single glance can tell which are incorrect (right), instead of examining each dial individually (left) (from footnote 9)

[39] See Chapter 11 of reference in footnote 7.

mits numerical comparison of the outside physical area visible through various arrangements of windshield and windows with the total area man is capable of viewing (see Fig. 4). It is specifically concerned with improving the design provisions for seeing other vehicles and stationary objects in time to avoid a collision. Current emphasis in this research project is concerned with possible improvements from windshield-wiper patterns and installations. Those interested in this field of research should consult the original papers which are available on request.[27, 30, 40]

3. Implications for safety in the use of tinted windshields: The use of tinted windshields has been widely accepted, and certain advantages may be obtained in reducing the glare from bright sunlight and aiding in the control of temperature within the car. The same principle has been applied to buses, especially for passenger windows, and is being considered for use in various types of trucks. Since the National Safety Council reports that accident rates are three times higher at night than in the daytime, the use of tinted windshields at night deserves careful consideration in order to utilize the principle to the greatest advantage without introducing additional hazards.[3, 7, 41]

In our research project in this area, the first step involved the precise measurement of the per cent of transmission of light with various types of tinted windshields currently in use. The tinted glass absorbs from 25 to 30% of the light as compared to about 12% for ordinary safety glass. The next step was to obtain dark adaptation curves and test recovery from light shock, with and without the tinted windshield. Tests were also made for visual acuity and depth perception under both conditions.[30] The next step was to obtain dark adaptation curves on subjects varying in age from 20 to 70 years. A correlation of −0.89 was obtained between final, or best, point of dark adaptation and age. In practical terms, this finding indicated that for a very dim light or object to be just seen by an eye in the dark, a doubling of the intensity of illumination was required for each increase of 13 years in age.[42] Fig. 5 illustrates these findings.

Dark adaptation curves are now being obtained on subjects varying in age from 18 to 80 both without and through tinted windshield glass. The final step of our project will be to run tests on the highway at twilight and at night with and without the tinted windshields. The objects to be seen by the subjects will be located at places unknown to them. Although the evidence from these and other studies may indicate that subjects over 55 or 60 may experience difficulty in driving at night with tinted windshields, certain precautions may be developed which might limit the hazards and retain the advantages of this design feature. Obviously, the relative density of the glass at the eye-level height of drivers and the spectral transmission characteristics of the filter are both important considerations.

Fig. 4 – Goniometer in place to measure areas of clear vision available from eye position of driver

Automotive Design in Relation to Crash Injury and Rapid Deceleration

The ability of the human body to withstand sudden decelerative and impact forces is extremely important for the operator's safety in case of collision. It has been demonstrated that, as far as the physiological limits are concerned, the force of many accidents which now are fatal can be tolerated without serious injury.[43-46] The limiting factors relate to the control of the body's momentum when the vehicle is decelerated at a rapid rate, and

---

[40] See Commission on Accidental Trauma, Annual Report, 1951-1952: "Man's Area of Vision as Basis for Design of Windshields and Side Windows," by B. G. King and P. J. Sutio. Pub. by Armed Forces Epidemiological Board, Department of Defense, Washington, D. C.

[41] See *Journal of Optical Society of America*, Vol. 45, No. 6, 1955, pp. 413-419: "Safety Hazard of Tinted Automobile Windshields at Night," by H. Haber.

[42] See *Journal of Gerontology*, Vol. 10, No. 4, 1955, pp. 424-428: "Alterations in Dark Adaptation as Function of Age," by R. A. McFarland and M. B. Fisher; see also *Journal of Gerontology*, Vol. 9, No. 3, 1954, pp. 338-348: "Age and Problems of Professional Truck Drivers in Highway Transportation," by R. A. McFarland, M. B. Fisher, and A. L. Moseley.

[43] See Cornell University Medical College, Crash-Injury Research Project, N 6ONR, 264-12, January, 1952: "Accident Survival – Airplane and Passenger Automobile," by H. DeHaven.

[44] See Cornell Aeronautical Laboratory, Buffalo, Internal Research Project Report OM596-J-1, November, 1949: "Kinematic Behavior of Human Body during Crash Deceleration," by E. R. Dye.

[45] See SAE *Quarterly* Transactions, Vol. 6, April, 1952, pp. 357-364: "Tractor Ride Research," by A. K. Simons. See also "Health Hazards of Rough-Riding Vehicles," by A. K. Simons. Presented to Commission on Accidental Trauma, Armed Forces Epidemiological Board, Department of Defense, Washington, D. C., July 8, 1955.

[46] See *Journal of Aviation Medicine*, Vol. 26, No. 4, 1955, pp. 268-288: "Effects of Mechanical Force on Living Tissues. I. Abrupt Deceleration and Windblast," by J. P. Stapp.

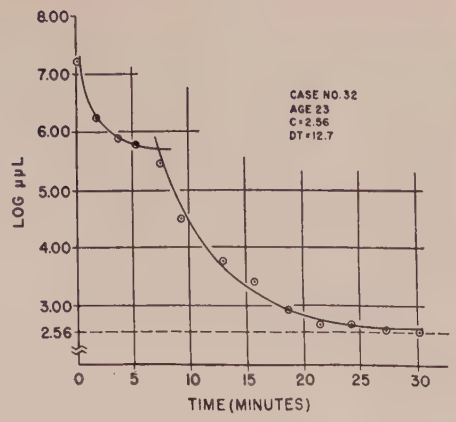

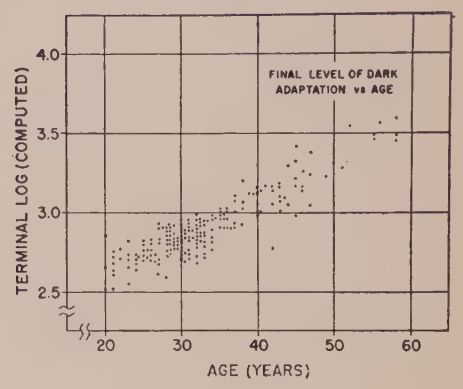

Fig. 5 – Left: Dark adaptation curve for individual subject, indicating computed final level of adaptation, 2.56. Right: Scatter diagram showing relationship between age and final level of dark adaptation for a large number of subjects[42]

the dissipation of impact forces. Many needless injuries, both fatal and serious, result from the unfortunate design and location of various objects and structures in the vehicle's occupant compartment. Moreover, it has been calculated that, if an individual in a motor vehicle is properly restrained, as by a shoulder harness, he should be able to survive uninjured a head-on collision with a brick wall, in which the vehicle is stopped in 2 ft from a contact velocity of 57.4 mph.[47]

Auto crash injury research has been undertaken at Cornell University Medical College as an extension of a similar program in aviation. A uniform system of collecting data on the causes of injury within automobiles in crashes has been developed, and case histories from seven states are being received and analyzed.[30] Some of the preliminary findings of this research program have already been translated into specific design modifications by some automobile manufactures.[48,49] For example, it was ascertained that the greatest single risk of moderate through fatal injury in crashes was associated with the ejection of occupants through doors which "popped open" under the impact force. This led to the design of improved latches so that doors would remain closed during crashes and keep the occupants inside the vehicles. Another illustration is the steering wheel with the recessed hub, and the rim designed to bend and dissipate the momentum of the driver thrown against it. The top of the steering post had been identified as one of the most important sources of severe injury to the driver in crashes.

An acceleration and expansion of this program for identifying the design features within vehicles which are associated with injury has been made possible by a substantial research grant from two major manufacturers in the past year.

Studies like the above are very promising as a basis for reducing injuries and fatalities through a coordination of the biological data and engineering design. While perhaps the frequency of injury to the occupants of trucks and buses may be less than in automobiles, the eventual results of crash injury research should be valuable to the transportation industry as well, and particularly when studies are specifically oriented to the solution of crash injury problems in commercial vehicles.

Human Factors in Design of Equipment in Relation to Environmental Variables

The designers of trucks and buses can also contribute to the comfort, efficiency, and safety of the drivers through design features related to the known effects of environmental variables upon human performance, well being, and health. Temperature and humidity, carbon monoxide, noise, and vibration illustrate such variables.

A. *Temperature, Humidity, and Ventilation* – Excessive temperatures in vehicle cabs can have detrimental effects on the efficiency and well being of the driver. It is known that heat not only reduces the willingness to work but the capacity for work as well. Several studies have indicated that as temperatures rise into the 90's and 100's a given kind of work is judged to be progressively difficult and finally impossible.[32] In an investigation to determine the limits of heat stress at which performance begins to deteriorate, Mackworth found, rather surprisingly, that the point on the temperature scale at which performance began to deteriorate was exactly the same for a variety of types of activity, namely when the effective temperature

[47] Air Materiel Command, Wright-Patterson Air Force Base, Dayton, Ohio, Technical Report 5915, 1949: "Human Exposures to Linear Deceleration. I. Preliminary Survey of Aft-Facing Seated Positions," by J. P. Stapp; and December, 1951: "II. Forward-Facing Position and Development of Crash Harness."

[48] See "Study of Crash-Injury Patterns as Related to Two Periods of Vehicular Design," by J. O. Moore. Pub. by Cornell University Medical College, Automotive Crash-Injury Research, Department of Public Health and Preventive Medicine, New York, March, 1955.

[49] See "Sample Reliability Study. Evaluation of Automotive Crash-Injury Research Sample of Injury-Producing Automobile Accidents in Maryland," by J. O. Moore, B. Tourin, and I. D. Bross. Pub. by Cornell University Medical College, Automotive Crash-Injury Research, Department of Public Health and Preventive Medicine, New York, January, 1955.

rose from 83 to 87.5 deg. A rise from 79 to 83 deg effective temperature on the other hand produced no significant deterioration in performance.[50] Eighty-three degrees on the eective temperature scale is equivalent to that combination of any temperature and humidity at which the individual feels an equal sensation of heat as he would at 83 F with a humidity of 100%. Equivalents of 83 deg effective temperature, for example, would be 88 deg at 70% humidity, 92 deg at 50%, or 98 deg at 30%, and so on. As the effective temperature rises above the 83-87.5-deg range there is a further marked decrease in performance. Since some of the elements of safe driving were included, at least in part, in the above tests it seems reasonable to conclude that a deterioration in driving efficiency will take place somewhere in the range of 83-87.5 deg effective temperature and will become more marked with greater extremes of temperature. In addition, the more subjective factors of discomfort and irritability must also be considered.

The optimum indoor summer temperature at which 98% of the population are comfortable has been determined at 71 deg effective temperature by the American Society of Heating and Ventilation Engineers; 75 deg effective temperature has been defined as the limits of the upper range of the summer comfort zone.[51] Intolerable temperatures, on the other hand, would be those corresponding to approximately 105 deg effective temperature or 120 deg at humidities below 40%. It should be remembered that the temperature of the cab is likely to be 1-3 deg effective temperature higher than that of the outside air, owing to the addition of radiant heat from the metal panels and heat from the engine. In addition, sunlight falling directly upon a part of the driver's body may substantially increase his sense of discomfort.[52]

In view of such conditions, the advantages of air conditioning should be seriously considered for all commercial vehicles operating for any length of time in regions of high temperatures. The requirements of passenger comfort necessitate air conditioning equipment for many intercity buses. In trucks, however, the driver must sometimes perform his job under conditions of intense heat.

In areas of relatively cool summers, air conditioning will be unnecessary but in other regions such as those where long-distance desert operations are required, the overall advantages of this equipment could well justify the initial financial outlay.

With regard to comfort, air conditioning seems advisable at temperatures over 75 deg effective temperature; with regard to safety and efficiency it appears desirable whenever protracted operations are necessary in temperatures in excess of 83 deg effective temperature.

Extremes of cold can be usually avoided by the use of cab heaters to be found in many commercial vehicles. If necessary, however, warmly clothed individuals can be subjected to temperatures of approximately 0 F for several hours with little or no effect on manual coordination, reaction time to audition and vision, difficult task performance, or area of the field of vision.[32] Where heating is available such heavy clothing need not be worn and hence a minimum temperature must be maintained to ensure comfort. The optimum winter temperature may be considered as approximately 66 deg effective temperature with a minimum at 63 deg effective temperature. These temperatures may be lowered somewhat if heavy clothing is normally worn.

The normal, comfortable range of relative humidity is generally considered to be about 30-70%.[51] Only variations above this maximum figure and below the minimum have significant implications for discomfort. High humidities will have an undesirable effect on the comfort of the individual at both high and low temperatures. With high temperatures and humidities there is usually an increased feeling of warmth because of the decrease of heat loss from the body by evaporation in the already moist air. When combined with low temperatures, high humidities may give rise to an added sensation of coolness. More important is the likelihood that such conditions may undermine the general vitality of the individual, weaken resistance to diseases of the upper respiratory tract, and accentuate neuralgia and rheumatic disorders.

Low humidities on the other hand (below 15%) have a similar adverse effect at both high and low temperatures, namely the drying out of the mucous membranes of the eyes, ears, nose, and throat, thus rendering them more susceptible to infection.[13] Low humidities in combination with high temperatures, rapid air velocities, and quantities of tobacco smoke make for the worst possible conditions for the eyes.[5] Where humidity control is possible, minimums should be set at 30% and maximums at 70%.

For commercial vehicles two or three cubic feet of air per minute per person will suffice in so far as the oxygen supply is concerned. This requirement can usually be satisfied without special arrangements for ventilation. Odors, on the other hand, such as those resulting from oil vapors from the engine, exhaust fumes, human bodies, or smoking, may become very unpleasant and possibly give rise to a feeling of stuffiness and headache or loss of appetite. In air conditioned buses where the passenger may have as little as 35 cu ft of space,

---

[50] See Medical Research Council, Special Report Series No. 268: "Researches on Measurement of Human Performance," by N. H. Mackworth. Pub. by His Majesty's Stationery Office, London, 1950.

[51] See "Heating, Ventilating, Air Conditioning Guide," Vol. 22. Pub. by American Society of Heating and Ventilating Engineers, New York, 1944.

[52] See "Heat Stress Effects on Motor-Vehicle Operators," by H. P. Roth and W. V. Blockley. Pub. by University of California, Institute of Transportation and Traffic Engineering, September, 1950.

[53] See Publication 328: "Health, Medical, and Drug Factors in Highway Safety." Pub. by National Academy of Sciences – National Research Council, Washington, D. C., September, 1954.

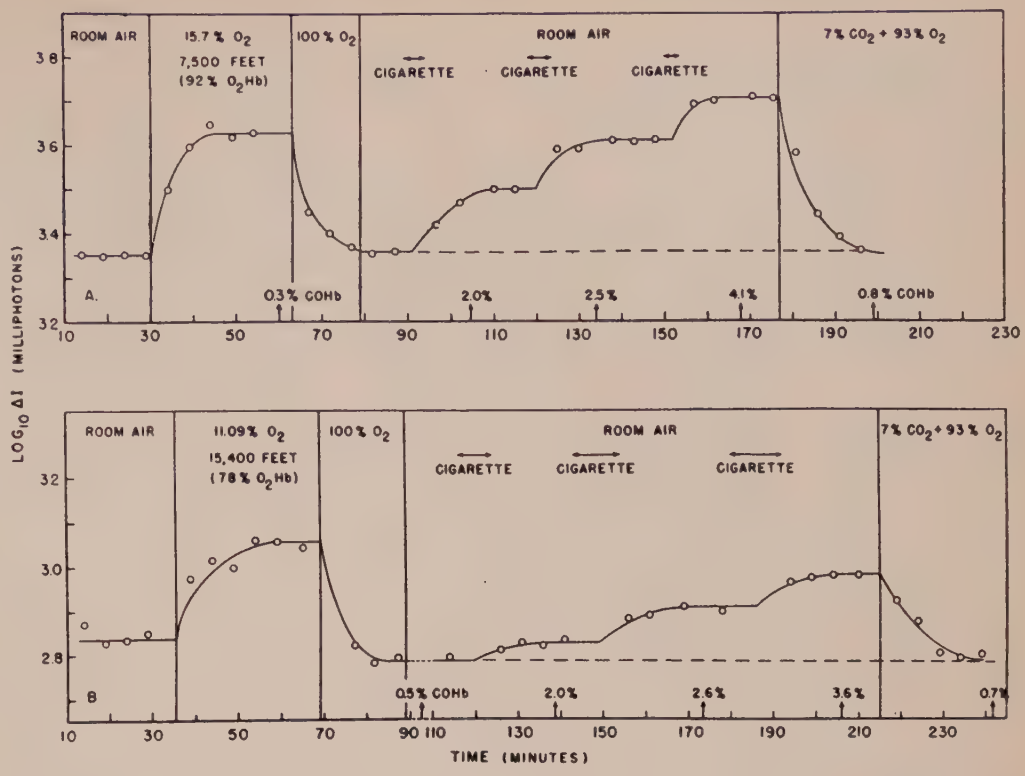

Fig. 6 – Effect of carbon monoxide from smoking on light sensitivity of two subjects compared with effect from high altitude. In panel at left, light sensitivity was measured in room air. One subject was then exposed to simulated altitude of 7500 ft (above) and the other to 15,400 ft (below). Rise in visual thresholds is apparent. After normal sensitivity was restored by breathing 100% oxygen, three cigarettes were smoked by each subject. A distinct rise in visual threshold can be observed after each cigarette, effect of three being comparable to that of 7500-ft altitude. Note rise in carboxyhemoglobin indicated at bottom of charts[5]

it is usually considered desirable to supply him with about 30 cfm of air during summer operations. Of this total some 8-10 cfm may be outside air and the remainder recirculated. Where smoking is involved there should be at least 15 cfm of outside air.[51] In trucks the supply of outside air is usually never critical since this can be more than adequately supplied by opening the air vents or ventilating windows.

Air velocities of below 15-25 fpm in the circulating air should be avoided since they may result in a feeling of stuffiness or stagnancy. On the other hand, velocities above 40 fpm are very likely to give rise to a sensation of drafts.[51] While causing discomfort in winter these higher velocities may be acceptable in summer since they supply an added cooling factor.

B. *Carbon Monoxide* – Carbon monoxide poisoning is an ever-present possibility in the operation of motor vehicles. The automotive engineer should consider this problem not only in relation to the presence of carbon monoxide within the cab, but also in the ambient air surrounding the vehicle. The concentration of carbon monoxide in areas of heavy traffic is being reduced by improved engine, carburetor, and muffler design. The problem is becoming increasingly important, however, in relation to smog, and heavy deceleration and idling in traffic in metropolitan areas.[53] The influence of carbon monoxide on health from this source is known to be serious and it is a health hazard in areas of high traffic density. Also, there are large amounts of hydrocarbons which are discharged into the air from the use, storage, and transportation of gasoline. Here again the automotive engineer can make an important contribution to the health of the public.

The severity of symptoms and the degree of incapacitation from carbon monoxide are dependent not only on the concentration of the gas in the air, but also on the duration of exposure.[54] A concentration as low as 1000 ppm can be dangerous to life in an hour, and continued exposure even to 100 ppm should not be permitted over long periods of time. Holding the concentration of carbon monoxide to only 30 ppm would be desirable, since oxygen deficiencies develop which are often not perceptible by persons exposed to quite small amounts of the gas. Reduced attention, drowsiness, and reduced night vision on such a basis may be of considerable significance in quite a number of highway accidents. Fig. 6 illustrates the effect upon night vision of the carbon monoxide inhaled in the smoke of three cigarettes.

When trucks stand with motor idling, concentrations of carbon monoxide in the cabs quickly build up to dangerous levels. In the Harvard study, concentrations of this order were found in almost all of the truck models evaluated, after all windows

[54] The time-concentration relationships in reference to symptoms of carbon monoxide poisoning are given in Fig. 7 of the paper, "Human and Environmental Factors in Automobile Safety," by R. A. McFarland, and appears on p. 638 of this issue.

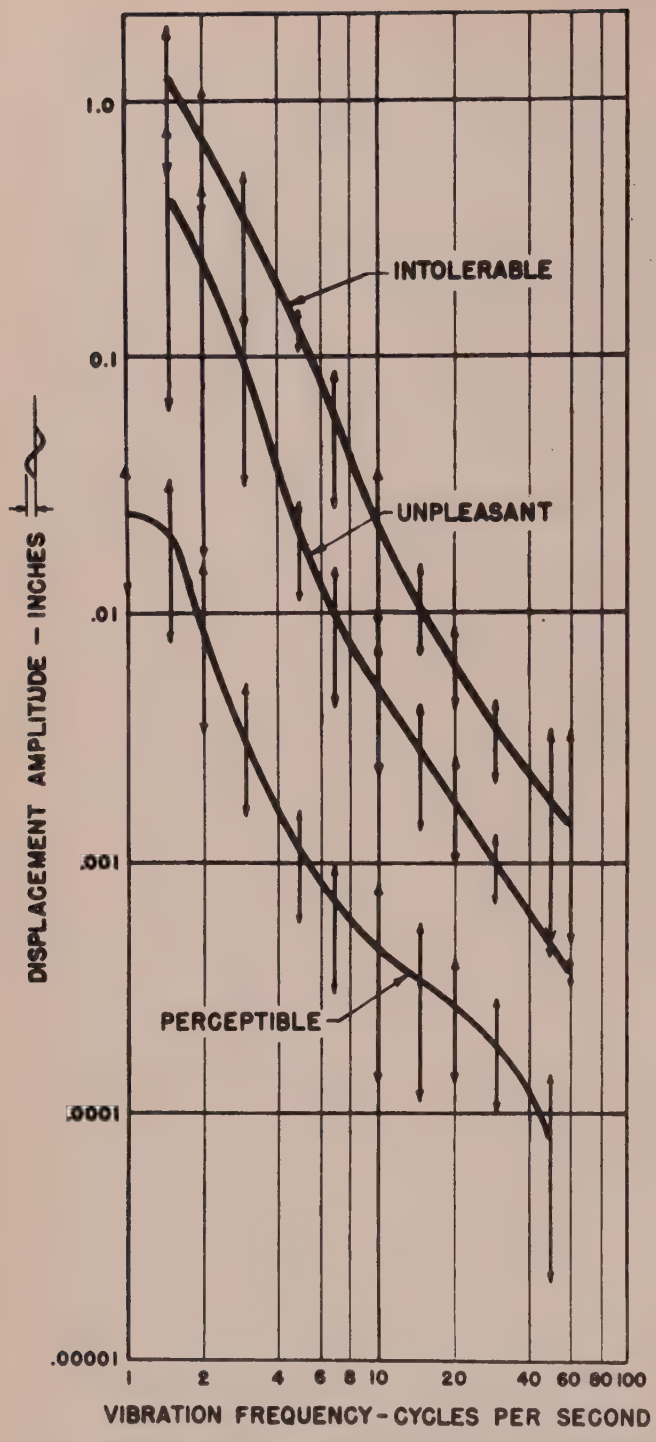

Fig. 7 – Subjective responses to sinusoidal vibration of short duration at various frequencies and amplitudes. Range of vertical arrows include reactions of about two-thirds of all subjects above or below mean (from footnote[60])

and vents were closed and the motor allowed to idle for 15 min. Tests made in the same vehicles in motion indicated that, under normal operating conditions, there was sufficient air leakage to keep the carbon monoxide concentration within safe limits.[23] Such findings, along with reports of drivers found dead at the wheel in standing closed cabs, indicate the importance of indoctrinating drivers in procedures for flushing the air of standing cabs, as well as the need for continued efforts on the part of designers to eliminate the possibility of combustion and exhaust gases entering or being drawn into vehicle interiors.

C. *Noise* – High noise levels, including those found in some commercial vehicles, are capable of producing a detrimental effect upon the subjective reaction and efficiency of the individual. For example, it is known that work carried out under noisy conditions requires a considerable increase in human energy expenditures even though the output of work may remain the same. Hearing is, of course, seriously affected by noise, and there is evidence that both mental performance and motor processes are adversely influenced, at least temporarily. In addition, annoyance, fatigue, discomfort, and irritability are frequently reported as subjective reactions.[32]

The noise levels in most passenger automobiles are sufficiently low, in marked contrast to the situation in some commercial vehicles. In seven current truck models, which were tested for overall noise levels *within* the cab by our research group, it was found that the range was from 49 to 89 db with the cab closed and the engine idling. On those models which were road tested under normal operating conditions, the second- and third-gear noise levels were between 80 and 95 db and just below 90 db in fourth gear.[23] It will be noted that this is within or approaching the limits for hearing loss set by several investigators.[55]

An octave-band analysis of the noise *outside* heavy and medium trucks made by Callaway revealed heavy trucks to reach a peak of 93 db in the 75-100 cps frequency band, dropping to 80 db in the 600-4800 cps band. These figures may be contrasted with those taken on a passenger automobile during the same investigation, which reached a maximum of only 64 db in the 150-300 cps band.[56, 57] Only in the latter vehicle has a sufficiently low noise level been maintained. Admittedly the economic function of commercial vehicles may preclude a comfort level such as that attained in the family pleasure car. The noise from trucks, however, is a serious problem to residents of many communities. It should be pointed out that the wide range of differences in noise levels from the quietest and noisiest trucks indicate that some designers, at least, have been able to make a more effective compromise than others. Noise reduction in commercial vehicles constitutes a real challenge

[55] See Wright Air Development Center, Wright-Patterson Air Force Base, Dayton, Ohio, WADC Technical Report 52-204, 1953: "Handbook of Acoustic Noise Control. Vol. II. Noise and Man," by W. A. Rosenblith, K. N. Stevens, and others.

[56] See SAE Transactions, Vol. 62, 1954, pp. 151-162: "Measurement and Evaluation of Exhaust Noise of Over-the-Road Trucks," by D. B. Callaway.

[57] See Proceedings of Second Annual Noise Abatement Symposium, Chicago, Oct. 5, 1951: "Instrumentation and Techniques for Measurement and Evaluation of Industrial Noise," by D. B. Callaway.

[58] See Dept. of Navy, Bureau of Ships, Code 371, Reprint 371-N-12, July, 1952: "Criteria for Setting Airborne Noise Level Limits in Shipboard Spaces," by M. Strasberg.

to automotive engineers to meet the mounting public protests over the present situation. Suggested criteria for the designer in this respect are shown in Table 4.[38, 58]

D. *Vibration* – The human body is quite sensitive to the various types of vibration encountered in motor vehicles and is usually much less capable of tolerating it than is the mechanical structure of the vehicle itself. There is mounting evidence that drivers of commercial vehicles are often subjected to levels of vibration which exceed the limits of tolerance. In general, there is no doubt that such excessive vibration adds substantially to discomfort and fatigue in driving operations. In addition, vibration of excessive degree may constitute a health hazard and result in serious physical disorders.[45] There is also evidence that vibration causes a considerable reduction in visual acuity.[9] It is thus essential that the physiological limits of tolerance to vibration be clearly recognized. Collaborative medical and engineering studies are especially needed to study the effects of vibration on health, safety, and efficiency beyond the subjectively intolerable limits, in order to improve vehicle suspension and driver seat design.[45]

Vibration may be defined simply as a movement involving a specific amplitude or distance of travel, occurring at a specific frequency. As such it consists of three types, vertical, longitudinal, and transverse, the latter two being the most objectionable from the individual's point of view.[59] However, the subjective reaction varies with the frequency and amplitude of the vibration. In cases where vibrations composed of varying frequencies and amplitudes are superimposed, the ones with the higher values should be chosen in determining comfort criteria since these will be the more unpleasant, that is, the higher the frequency, the lower the amplitude must be to maintain a given level of comfort and vice versa. In addition, as frequencies increase, the effect tends to become more localized. At the highest frequencies, only the parts in direct contact with the source of vibration are affected; while for slow frequencies, the whole body may be involved. For the most part the frequencies encountered in motor vehicles are relatively slow, that is, roughly 8 cps or less.[34]

The results of various investigations have shown the subjective responses of the human body to vibratory motion (see Fig. 7). Taking the 8-cps range as an example, it can be seen that vibration becomes perceptible at a displacement amplitude of 0.0008 in., unpleasant at 0.009 in., and intolerable at 0.06 in.[60] By referring to the chart, similar limits may easily be determined for any given amplitude or frequency. In general, where one is excessively high the other must be made correspondingly low. Ideally, of course, both amplitude and frequency should be reduced as much as possible.

Table 4 – Limits for Deafness-Avoidance and Comfort

	Maximum Permissible Sound Pressure Level, db above 0.0002 microbar			
	Deafness-Avoidance Criterion		Comfort Criterion	
Octave Band	Occasional Exposure (1 Hr or Less)	Repeated Exposure (Period of Months)	Noisy (People Expect Noise)	Quiet (People Expect Quiet)
38– 75	125	115	100	80
75– 150	120	110	95	70
150– 300	120	110	90	60
300– 600	120	105	85	55
600–1200	115	100	75	50
1200–2400	110	95	65	50
2400–4800	105	90	60	50
4800–9600	110	95	55	45

E. *Interrelationship among Environmental Variables and Limits for Driver Comfort and Safety* – In the foregoing discussion of the influence of various physical variables of the environment, the attempt has been to define limits at which discomfort or threat to health may be expected to occur. The values cited, however, represent approximations, rather than precise limits, because of the complex nature of any one variable, and because of the interdependence among various variables. For example, if a person is moving briskly or carrying out a physically active task, the effects of exposure to a given concentration of carbon monoxide will be manifest earlier than would be the case if he were sitting quietly while breathing the same air. Similarly, the effects of humidity are influenced by such other variables as the temperature and rate of circulation of the air. Thus the designer will find nomograms developed to account for the relationship between variables more useful than simple linear scales for the separate factors.[13] A schematic interpretation of the variables affecting driver comfort and efficiency has been presented in another paper by the present author in terms of the ranges for comfort and discomfort, and limits at which the danger of physiological harm arises.[61, 62]

Summary and Conclusions

It has been shown that highway accidents are a major problem to the nation, even though fatal accident rates have been improved over a span of 20 years. The number of persons killed and the disabilities resulting from injuries constitute an important problem for the transportation indus-

[59] See USAF School of Aviation Medicine, Air University, Randolph Field, Tex., Project No. 21-1203-0002, January, 1953: "Physiological Effects of Mechanical Vibration," by V. Guillemin and P. Wechsberg.

[60] See Naval Medical Research Institute, Report No. 1, March 16, 1943: "Review of Subjective Responses to Vibratory Motion of Human Body," by D. E. Goldman.

[61] See "Physical Variables Influencing Driver Comfort, Efficiency, and Safety," by R. A. McFarland and H. W. Stoudt. Pub. by Harvard School of Public Health, Boston, 1955.

[62] This diagram has also been reproduced as Fig. 9 of the paper, "Human and Environmental Factors in Automobile Safety," by R. A. McFarland, and appears on p. 639 of this issue.

tries. Since it is known that human factors play such a predominant role in the causation of accidents, it logically follows that control measures should be broadened to include contributions from both the biological and engineering sciences. In this broadened sense safety in transit falls within the province of preventive medicine and public health, and the automotive engineer can assume increased responsibility in the prevention of accidents through consideration of the human factors in the design of equipment.

Since most accidents have multiple causes, a successful approach to the prevention of accidents requires consideration of the relationships and interactions between the driver, his equipment, and his environment as a basis for control. Experimental studies, epidemiological surveys, and statistical analyses are necessary, in which basic human variables – physical, physiological, and psychological – are related to structural and operational features of vehicles at specific times and places and under known environmental conditions. The fundamental principles emerging from such studies would have important implications for the development of measures in a continuous and effective program to reduce and prevent accidents.

A new concept has been developed in this investigation which emphasizes the collaboration between the biological and engineering sciences. This may be referred to as biotechnology, or human engineering. Thus it is proposed that an important way of advancing highway safety is to increase the integration of the driver with his vehicle. It was stressed throughout that mechanical design should be based upon the biological and psychological characteristics of the drivers, and that vehicles should therefore be designed from the man outward with instruments and controls considered as extensions of his nervous system and body appendages.

Methods of analyzing driver activity to gain information which would be relevant for the design of vehicular equipment in terms of the capabilities and limitations of operators were reviewed. Illustrative findings were then cited from studies carried out in the Harvard project, and the areas outlined which seemed most suitable for improvements through collaboration between biological and engineering approaches.

It was pointed out that anthropometric data on the range and variation of human size are of importance in the design of seating, the location of controls, and cab layout. Principles important in designing to accommodate the middle 90% of the drivers of trucks and buses were outlined, and illustrations of faulty design in this regard were presented from an evaluation study made on a series of trucks and buses.

Consideration was also given to the role of the design of instruments, and the operating controls in the prevention of operating errors and in preserving the comfort, efficiency, and safety of drivers. The importance of an advance analysis of equipment to detect and eliminate all possible faults in the vehicle was emphasized.

A brief review was given of recent studies on the relationship of crash injury to structural features of vehicles and the kinematic behavior of the human body under the influence of decelerative forces. Design features to protect the occupant of vehicles against decelerative and impact forces offer considerable promise toward the reduction of fatal and serious injury now resulting from collisions and accidents.

The effects of a variety of environmental variables upon human performance and health were reviewed, and data pertaining to temperature, humidity, ventilation, noise, vibration, and carbon monoxide were presented to aid the automotive engineer in designing to preserve the efficiency, comfort, and safety of drivers.

Finally, it is important to recognize that many remarkable achievements in the field of safety have resulted from the efforts of automotive engineers. It is submitted that in making the most of these advances and in developing additional requirements for safety in line with the concepts presented above, the engineering profession has an unusual opportunity. The implication of these advances are far reaching, not only in terms of the safety of the traveling public but also of all the communities in which automotive equipment is operated.

Additional References

1. "Annotated Bibliography on Human Factors in Engineering Design," Project X-651 (Av-340-a), Aviation Branch, Research Division, Bureau of Medicine and Surgery, Dept. of the Navy, February, 1946.

2. Motor Industries Research Association Bulletin, Second Quarter, 1950, pp. 17-33: "Factors Which Influence Braking Performance of Vehicles," by H. J. H. Starks.

3. "Human Factors in Motor-Vehicle Accidents: Survey of Literature," by R. A. McFarland, R. C. Moore, and A. B. Warren. Pub. by Harvard School of Public Health, Boston, 1955.

4. Proceedings of Ergonomics Research Society, Vol. II, "Symposium on Human Factors in Equipment Design," ed. by W. F. Floyd and A. T. Welford. Pub. by H. K. Lewis & Co., London, 1954.

5. SAE Transactions, Vol. 61, 1953, pp. 623-639: "Safe Brakes for Passenger Cars," by G. T. Ladd and S. B. Dew.

6. Highway Research Board, Proceedings of

Thirty-second Annual Meeting, Washington, D. C., Vol. 32, 1953, pp. 421-436: "Braking Distances of Vehicles from High Speeds," by O. K. Normann.

7. "Analysis of Transport Aircraft Cabin Air Conditioning Requirements with Special Reference to Air Freshness, Temperature, and Humidity Control," by B. E. Del Mar. Presented at SAE National Aeronautic Meeting, Los Angeles, Oct. 3, 1946.

8. Wright Air Development Center, Wright-Patterson Air Force Base, Dayton, Ohio, AF Technical Report 6569, July, 1951: "Discussion of Scale-Reading Habits," by W. E. Kappauf.

DISCUSSION

Current and Proposed Laws Recognize Need for Driver Control

– Roy Haeusler
Chrysler Corp.

ALTHOUGH Dr. McFarland has covered human factors as they affect vehicle and highway design as well, I will direct my attention in this discussion toward those portions of his study that deal with the driver.

In that respect I will be right in line with our Governor in Michigan and with our state legislature. A special session of the legislature has just begun. Its major program will consist in appraising and adopting such proposals as seem to offer promise of reducing our highway death and injury toll. Apparently agreeing with Dr. McFarland that driver mistakes and unsafe driving practices may account for the large majority of all accidents, our lawmakers are giving special consideration to the many proposals that would further control the driver.

The driver may be required to be better qualified before receiving his license. A school subsidy may be offered for high school driver training to help him in this respect. A more thorough examination may be set up, and the examiners may be required to be more adequately qualified and trained. Even so, the driver may lose his license more readily through revocation based on a bad driving record, as revealed by an adequately maintained central records file. Or he may lose his license through inability to meet the standards when he is reexamined. New maximum speed laws may restrict him; and if he chooses not to cooperate, additional enforcement officers and additional enforcement equipment, including more radar, may serve to oblige him to cooperate, or else.

As these and other proposals are considered, there will immediately be a need for related information. What are the circumstances under which drivers are most likely to make mistakes or become careless? How would such controls influence the driver, directly and indirectly? What will be the effect on driver characteristics, either through stiffer licensing requirements, or more training, or both?

These are the very sorts of questions for which Dr. McFarland and his team have been searching for answers.

While admittedly there is yet a great deal more to learn, such answers as have already begun to take form are very interesting.

For example, let us look at driver characteristics and their relationship to accidents. Are these characteristics such that we can attribute most accidents to a small group of drivers? Are accidents caused primarily by a minority among us who are accident-prone? Essentially, the answer is no. It is true that some drivers have more accidents than average and others have none, but the laws of chance will produce much the same result.

A careful and thorough study of the data available thus far indicates that accident-proneness plays only a small part. Accidents are caused by you and me and not just by the other fellow. If we tend to be smugly satisfied with our record, let us recognize that the million driver deaths and injuries per year are distributed among sixty million drivers.

In keeping with the finding that accident involvement is widespread among our drivers, Dr. McFarland also notes that there is little or no significant correlation between accident records and such driver characteristics as visual acuity, visual field, or reaction time. The driver's likelihood of making a mistake or engaging in unsafe practices seems rather to be related to characteristics and to influences and circumstances that may vary from time to time, as well as from driver to driver. This supports the picture that most people are temporarily accident-prone from time to time, and that chance combines with such momentary accident-proneness to scatter the accidents among us.

Prof. Rowbotham of Durham University, Great Britain, must have had somewhat the same thoughts in mind when he summarized the situation by saying that accidents result from small risks taken a great many times.

As we realize that the driver characteristics that predispose toward accidents are themselves variables, we see our problem in all its formidable complexity. The influences within and exterior to the driver that affect his efficiency and thus enhance his chances to make mistakes are additional variables. So are the circumstances under which the driver errors are likely to occur.

In trying to relate cause and effect while dealing with such a mass of variables, we recognize the need for analyzing large masses of data on actual accidents. We have altogether departed from the field in which rationalizing can be of much help, nor will we gain much from clinical studies or from the analysis of 17 or 39 cases. This is a problem of the same order as that of determining the causes of injury in automobile accidents. The Cornell University Medical College Automotive Crash-Injury Research Project, under the sponsorship of the Defense Department, the U. S. Public Health Service, the Ford Motor Co., and the Chrysler Corp., and with the full cooperation of medical societies and state police in each of a number of states, is now in the process of stepping up its activities to reach a goal of 10,000 accident cases per year. It appears that the determination of the causes of the accidents, themselves, will require much the same sort of teamwork between doctors, engineers, and law enforcement personnel or other accident investigators. Add to this team the psychologists and the psychiatrists who will be concerned with the visual

and the emotional problems, the attention and fatigue factors, and the attitudes and their origins, and you have faced the immensity of the job ahead of us.

It would seem altogether fitting that Dr. McFarland's painstaking ground work lead on into just such a project as this.

Describes Truck Features Providing Operating Safety

– Edgar L. Hollifield
Ford Motor Co.

TRUCK manufacturers will always be highly competitive in providing progressive designs and features which promote the sale of their products. Not the least of these progressive developments has been along the lines of operating safety. After all, a truck usually is a professional tool; it represents vital capital investment and generally is more carefully evaluated before it is purchased than a passenger car. I am sure that you can recount the step-by-step progress that has resulted in the highly efficient, reliable, durable, and safe-operating workhorse of today. Since these achievements largely have been industry-wide, I will but mention a few particular progressive improvements in our product that have and will contribute to greater operating safety.

Power steering, which has obvious safety advantages for maneuvering ease and lessening of driver fatigue, is available as optional equipment on many truck lines.

Seat-spring snubbers have been standard equipment on our trucks for several years. These devices damp the seat jounce, which means the operator does not continue to bounce on the seat for an extended period after the vehicle has passed over a road irregularity.

Tubeless tires, which were introduced on practically all passenger cars in the 1955 models, now have been extended to truck use and are standard equipment in the 1956 model Ford trucks. The tubeless tire runs cooler, which promotes longer tire life and is less subject to blowouts

Adequate power capacity, for varying highway conditions, is a **must** for truck operation, especially where long hauls over mountainous roads can make an underpowered truck a traffic hazard. Our trucks not only are available with extrapowered engines for such conditions, but for 1956, a new type fan drive is available as optional equipment on the larger models. This device is referred to as the dynamatic fan and combines thermostatic control with an electric clutch.

Designing for accident prevention always has been a major concern of the automotive engineer and it will continue to be. Ford has conducted extensive research and development for the reduction of injuries which can occur during highway accidents.

Most of our work in this research and development program has been in connection with passenger cars where the bulk of injuries and fatalities occur. Using highway accident statistics and guided largely by the work of Cornell University Medical College findings in their automotive crash-injury group, we have been able to pinpoint the areas in the vehicle responsible for driver and passenger injuries. On our own test areas and in our laboratories, we have been able to confirm these findings and develop truck designs which, we are convinced, will minimize the injury and fatality potential in highway accidents.

In some respects, the injury reduction problem in connection with trucks is considerably simplified. To begin with, the truck driver is usually a professional. He does not get involved in accidents as frequently as a passenger-car operator. His vehicle is usually heavier, and he generally travels at a lower rate of speed. The forces developed in the operator compartment during a truck collision are of a lower level than experienced in passenger-car conditions.

The basic principle of injury reduction is to realize that the structure of the vehicle provides a highly effective container which, when properly used, will protect the driver and occupant from injury.

Obviously, the human must be retained within the package for greatest protection. Accident statistics show that the chances of receiving injury are twice as great when ejected from the vehicle during an accident. One method of assuring retention within the vehicle is to keep the doors from popping open during a collision. To accomplish this, all 1956 Ford trucks are equipped with double-grip door latches designed to provide protection against the possibility of doors springing open during accidents.

Another method for keeping occupants within the vehicle is by the use of a seat belt, and for 1956, all Ford trucks have seat belts available as optional equipment. Of course, the seat belt has several other important advantages.

The seat belt will keep the driver behind the wheel, his feet on the pedals, and the vehicle under control. But supposing this is more or less a violent collision. The driver's chest is going to impact the steering wheel.

With a wheel of conventional design, the rim will collapse and the driver will be impaled by the steering column. This condition can happen with or without a seat belt. However, with a seat belt, only a third to half of the driver's body weight is going to come in contact with the steering wheel. The force of impact is still enough to break the conventional wheel and injure the driver.

The telescoping steering column is one of the devices frequently suggested as a solution to this problem. We actually built and tested some of these assemblies. In this design, splined elements permitted the column to retract against a spring load, and shock absorbers were added to control the recoil after compression.

When this design was tested in our impact rig, it was found that the problem still had not been solved, because the steering wheel rim collapsed prematurely and the weight of the body contacted and was supported over a small area by the steering wheel hub.

We next considered the possibility of designing the collapsible distance into the wheel itself by recessing the hub. It was believed that the rim could be provided with sufficient strength to support the driver's chest, and the spokes could be designed to absorb energy as they yielded under impact. Testing of these wheels has shown that up to 20 g force can be absorbed without the body contacting the hub. Such a recessed-hub safety wheel is standard equipment on the 1956 Ford truck line.

Seat belts, which I have previously mentioned, must meet certain definite specifications to be effective. We have investigated various types of restraining harnesses and belts and believe that the lap belt is at present the most acceptable design.

The full effectiveness of the seat belt could not be obtained if the seat were not prevented from running off the track. For this reason, we developed a seat track stop which restrains the seat from exceeding the maximum forward adjustment position.

Another item, which in crash statistics showed itself to be responsible for about 4% of injuries, was the rear-view mirror. Our new rear-view mirror uses a double pivot attachment which allows it to move out of the way easily. In addition, the glass of the mirror is backed with a plastic material to which the fragmented glass adheres, in the event of fracture, and thereby prevents the release of jagged pieces of glass. Even the edge of the mirror is surrounded by a plastic ring to prevent accidental contact injury.

As time goes by, we hope to have other important developments which we will make available in production as

rapidly as possible. We believe we have made a good beginning toward the eventual solution to this problem, and I can assure you we intend to continue our efforts constantly to improve transportation safety in all its aspects.

Discusses Additional Truck Safety Items

– C. A. Lindblom
International Harvester Co.

DR. McFARLAND'S valuable research work to date on the relationship of human factors to highway transport safety brings to light the immense scope of the project and the tremendous range of human variables involved in the operation of vehicular equipment.

Obviously much remains to be done. The problem involves three important factors: (1) the vehicle, (2) the highway, and (3) the driver – all of which must be integrated with safety maintenance for effective solution.

Widespread headlines of recent truck accidents have focused attention on the **vehicle.**

What are the truck engineers doing about it?

The answer is, "Safety has been and always will be a major design consideration in motor trucks."

In truck engineering, the intimate association with all of the elements that go into a vehicle makes the engineer conscious of the fact that **safety is a personal responsibility** – rather than just the other fellow's obligation.

The slogan, "Remember, the life you save may be your own," is a reminder of profound significance.

This same realization of individual responsibility is evidenced when truck manufacturers, truck operators, and public officials work together to improve safety in truck transportation. As a result, much has been accomplished through the diligent and cooperative efforts of organizations such as SAE, the Automobile Manufacturers Association, Truck Trailer Manufacturers Association, American Trucking Associations, Interstate Commerce Commission, American Association of State Highway Officials, Bureau of Public Roads, Highway Research Board, National Council of Safety, to mention only a few.

Truck engineers are striving continually to design "a second chance" into the vehicle to cope with the fallibility of human behavior.

One striking example is quoted from the AMA press release of Oct. 27, 1955:

DETROIT, Oct. 27—"A new auxiliary braking system designed to provide positive emergency stopping for truck-trailer combinations has been developed cooperatively by the truck, trailer, and brake manufacturing industries," Automobile Manufacturers Association announced today.

"The system enables the vehicle operator to make at least one controlled stop in case the regular service brakes fail." It may be applied to service brakes of all types, the AMA said.

"The new system was developed by a special brake committee organized in the Motor Truck Division of the AMA in December of 1954.

"On August 23, a proving-ground demonstration of the new brake was held for interested groups, including officials of the Section of Safety, Bureau of Motor Carriers, Interstate Commerce Commission. The ICC now is in the process of formulating new regulations governing braking systems for vehicles in interstate commerce."

There is no shortcut to developing a safe, dependable truck. Rather, it is an evolution of refinements in the many vital components that comprise the vehicle.

Certainly, safety consideration must start with the man behind the steering wheel – the driver. To be alert and in complete control of the truck, he must be comfortable, have good vision, be able to reach all controls, and be able to hear well.

For driver comfort, quality seats with proper cushion and back angle with adjustment for different sized men must be provided. The steering wheel must be located at a natural angle for easy steering and be made in the right diameter for the least steering effort consistent with accurate steering control. For the ultimate in steering ease and control, under adverse conditions, power steering has been developed. Besides reduced steering effort, clutches now require less pedal pressure. Hydraulic, vacuum, and air brakes need but a minimum of driver energy to operate.

Cab ventilation comes in for a great deal of attention in truck design. For safer, comfortable winter driving, efficient fresh-air heaters and defrosters are being improved all the time.

Studies to place the operating controls and instruments within the sight and easy reach of the driver are continuous, seeking the best arrangement to require the least amount of distraction from driving.

For the driver's vision, larger glass areas have been designed into cabs. Vacuum, electric, and air-operated windshield wipers are much more dependable and efficient today as a result of progressive developments in these important safety accessories. More attention is being given to serviceability of windshields as recommended in the recent ATA-RCC meeting in Washington, D. C., Oct. 21, 1955.

The adoption of the very latest sealed-beam headlights now enables truck drivers to see further down the road at night and still not blind the oncoming traffic.

Modern exhaust systems have been developed to provide quieter operation so that truck drivers can use their ears as well as their eyes for safe driving. The 125-sone requirement for mufflers is being met by most manufacturers today.

For overall safety, it is possible to crawl out of the window openings in the doors or, if necessary, kick out the windshield. Thus, in an emergency, the driver is assured he can get out of the cab.

Many other safety features are incorporated to make trucks safe to operate. To reduce fire hazards to a minimum, all fuel systems – gas, diesel, and LPG – are inspected and approved by the Underwriters' Laboratories. Safety tanks that meet ICC regulations, also UL approved, are available. All gas tanks are equipped with caps conforming to ICC regulations so as not to leak more than 1 oz per min when upset. All fuel lines are connected to the engine with flexible connectors to avoid vibration breakage and fuel fires. All electric wiring is approved by UL and meets ICC regulations.

Adequate fuses and circuit breakers are in separate electric circuits. The headlight circuit is isolated from the others, so a short in another circuit does not affect the headlights.

The things mentioned above are but a few of the many associated with safety in trucks.

Today, reduction in hazards in motor truck design is no longer the "cut-and-try" operation of a few years ago. Modern laboratory fatigue testing techniques and experimental stress measurements have taken the hocus-pocus out of many of the old fashioned engineering practices. Furthermore, millions of miles of testing on proving grounds and selected customer operations, under all conceivable conditions are required to prove the integrity of the product.

To keep pace with the accelerating trend in highway transportation will be a continuing challenge to engineering ingenuity. However, you may rest assured, the precept of safety and dependability will always pervade the minds of the truck engineers.

ORAL DISCUSSION ON NEXT PAGE ——→

ORAL DISCUSSION

Reported by Eugene E. Wallace
Wagner Electric Corp.

F. K. Glynn, American Telephone and Telegraph Co.: In the crash studies made with dummies and collapsible steering wheels, motion pictures show that the driver dummy collapses the steering wheel and glances to the side. I feel that the human would not do this but would have the torso rested by the collapsed lower half of the wheel and the face or forehead would contact the still intact upper portion, with resultant severe facial injury. Have studies or data on such wheels with humans been made?

Mr. Hollifield: Little actual evidence is available, but facial injuries appear preferable to being impaled on the steering post under severe crash conditions.

Dr. McFarland: Dummies do not give complete solutions in crash research, but human beings are not available nor expendable for such tests. Dummies do provide valuable data, however, for evaluation of designs and for establishing design criteria.

C. L. Burton, Aluminum Co. of America: Trucks and operator controls should be able to be made more functional from the safety viewpoint than passenger cars where styling is deemed so important. Truck designers could better control such features as better driver visibility or standardization of control positions and method of operation.

Mr. Lindblom: Styling demands cannot be neglected on trucks. Most pickups, for example, are sold for family use to the farm market, and improved styling has been reflected in sales appeal. Larger trucks can be more functional. Obtaining the best combinations of style and function has been an evolutionary process, and progress continues to be made as better knowledge of the problems and solutions for them are attained.

Mr. Haeusler: The introduction of 4-way seats has been very helpful in providing better visibility for each driver. Too often, however, purchasers will not pay for the safety equipment that is now available at additional cost.

John Hulse, Truck-Trailer Manufacturers' Association, Inc.; Seat belts seem most suitable for preventing vertical motion, but since the impacts in vehicles would be in a horizontal plane, shouldn't the belts be across the shoulders?

Dr. McFarland: The design and specifications of seat belts are now being studied by an SAE and ASA committee. Belts across the lap do permit "whipping over" from the hips, but this is still appreciably different from the impact of an unrestrained body. Practical studies as to the value of seat belts are also underway in large fleets.

Mr. Haeusler: Aircraft seat belts are only incidentally used to protect against vertical accelerations which normally do not exceed 2 g in commercial aircraft; their major load requirement is for possible horizontal impacts, just as on cars or trucks. In addition, there is considerable study in process on the problem of possible "whiplash" neck injuries if shoulder straps are used in vehicles with seat backs too low to restrain the head upon rebound from an impact.

Mr. Hollifield: Seat belts are very useful in accidents such as glancing impacts by keeping the driver in position at the controls where his actions may help to control and stop the vehicle.

H. M. Gammon, Thompson Products, Inc.: Won't use of seat belts tend to result in spinal injuries by causing lateral bending of the unrestrained upper torso under the effect of sideways acceleration?

Dr. McFarland: Light-plane accident studies have not indicated that this is too serious a problem, and the same should hold true in automotive use.

J. O. Sibley, U. S. Fidelity & Guaranty Co.: Insurance groups are generally not ready to endorse seat belts until standards are established and seat belts on the market are found to meet such standards.

Dr. McFarland: I understand that one insurance group has now announced support for use of seat belts, although I agree that there may be unfavorable public reaction due to some of the inadequately designed or constructed belts that are available.

Mr. Hollifield: Both my company and Mr. Haeusler's have set up stringent requirements for belts including such things as ease of usage, corrosion resistance, and resistance to deterioration, as well as failure strength.

Henry Jennings, Fleet Owner: Has there been any solution to the problem of the split-back seat flying up and hitting the driver or passenger on the back?

Dr. McFarland: Although work has been done on this, no direct solutions have been offered, as far as we know.

R. Gardner, American Trucking Associations, Inc.: What are the effects of the new windshields on effective wiper areas and distortion through the unwiped surface?

Dr. McFarland: No general answer can be given, but such problems appear to be directly solved by studies made to provide the best visibility for each particular case.

E. R. Klinge, Continental Aviation & Engineering Corp.: Since steering wheels cause driver injury, why not eliminate them and use steering levers or similar means such as those used in military tanks and various tracked vehicles?

Mr. Haeusler: The newer military vehicles are returning to the use of steering wheels in order to obtain better driver control and steering accuracy, which might, from a safety viewpoint, override the danger of driver injuries from the wheel.

Fred Lautzenhiser, Pierce Governor Co.: Safety is still based on the "Three E's" of Education, Engineering, and Enforcement.

Robert Norrie, Kenworth Motor Truck Corp.: Has any work been done to determine whether audio or visual warnings are the best for obtaining quick reaction from the driver for such things as loss of air pressure or engine overheating?

Dr. McFarland: Visual warnings may be the most simple to obtain, but a study has indicated that auditory warnings are most quickly discerned and reacted to by the driver. However, any appreciable number of auditory warnings might cause confusion since the driver would then have to determine which warning the sound referred to before taking action.

Stop Sludge and Go Clean

R. H. Albrecht and R. I. Potter, Standard Oil Co. (Ohio),
and Kent Hyatt, E. I. du Pont de Nemours & Co., Inc.

This paper was presented at the SAE Golden Anniversary Fuels & Lubricants Meeting, Philadelphia, Nov. 9, 1955.

MECHANICAL removal of engine sludge is one of the most expensive jobs encountered by the motorist with a modern V8 engine. Such a job usually necessitates cylinder-head removal, hydraulic cam follower replacements, removal of oil pan and screen, and replacement of rocker arms and shafts. In many cases a ring or valve job and other replacements are made at this time while the engine is disassembled.

Engine sludging is an old problem which has been with us for a good many years. In the Great Lakes and Coastal areas where weather consists of low-temperature, high-humidity conditions over a large portion of the year, formation of harmful engine sludge is one of the major problems facing the automotive and petroleum industries.

During the past 13 years much progress has been made by the petroleum industry in improving resistance of motor oils to high-temperature oxidation and top ring-groove filling in diesel engines. The advent of wide-spread use of solvent-extracted motor oils together with oxidation inhibitors and detergents effective at high engine-oil temperatures has in most cases overcome the problem of engine deposits in heavy-duty service.

It is common knowledge, however, that the most severe service for passenger cars and light trucks is stop-and-go driving encountered by the great majority of drivers in congested areas. It has been pointed out that about half the cars in the country average less than four miles per trip.[1] Many trips in an urban area are of necessity only one or two miles long. It is also of interest that about 70% of all automotive oil is used in passenger cars.[2]

The automotive industry has done a great deal to aid this severe low-duty oil sludging problem in their vehicles by providing superior oil filters of full-flow design, and in many cases by recommend-

THIS paper describes the background, operation, and results of a series of 50,000-mile low-duty service tests on motor oils. Comparisons of engine cleanliness and wear are presented in oils ranging from base oil to Series 2 level, using several different additive types, and a common base oil.

Large differences were found in the ability of additive types and concentrations to combat harmful low-temperature engine sludge.

Some observations are made on the correlation between full-scale laboratory engine tests and results of this field test.

[1] "Fuel Economy with Multigrade Oils," by C. C. Moore, W. L. Kent, S. P. Lakin, and R. W. Mattson. Paper presented at SAE Summer Meeting, Atlantic City, June 9, 1954.

[2] "'New' Motor Oil Properties," by J. R. Griffin, Jr. Paper presented at Independent Oil-Compounders Assn. Annual Meeting, Chicago, September, 1955.

Fig. 1 – Sludge problem

ing a high-temperature thermostat for winter operation. On the other hand, they may have added to the problem by recommending 2500-5000-mile oil drains. This has given the motorist the impression that oil changes are not important, and that he can follow this procedure throughout the year, even though automobile manufacturers are very careful to point out that frequent oil changes in cold

weather are necessary.

The motorist becomes thoroughly disillusioned after about two years operation with "normal" oil and filter changes when he finds that constipated cars do exist and that he has one of them. This owner and car thus become a number one nuisance problem to both the automotive and petroleum industries. Random examples of engines which encountered heavy sludging in actual service are shown in Fig. 1.

A possible explanation for the above engine sludging is that under severe low-duty driving conditions a lightly loaded engine condenses considerable water in the crankcase oil system. This water robs much of the dispersancy characteristics from high-temperature detergents and permits agglomeration of the sludge-forming particles.[3]

Obviously there is very little the engine manufacturers and petroleum companies can do to prevent formation of unburned fuel particles and water under these severe low-duty driving conditions. Hence it was proposed that perhaps the best attack on the problem would be to keep the engine clean by some further improvements in lubricating oils.

Since basic data of a comprehensive nature were not available on which to base experiments, it was decided that fundamental field data should be obtained which would give background information on the performance of a range of motor oils extending from base oils up to and including Series 2 level lubricants.

Objectives of Test

The primary objectives of the 50,000-mile severe low-duty field test were outlined as follows:

1. To obtain basic field information on various oil types for correlation with laboratory low-duty operation.

2. To evaluate the performance of a mid-continent solvent-extracted base oil when treated with various types and concentrations of motor oil additives.

General Test Program

Program for Severe Low-Duty Field Test – One of the most practical approaches to severe low-duty operation was found in utilizing standard 4-door sedans of a popular make, operated in taxicab service in the outskirts of a metropolitan city. Thirty new 1953 6-cyl engines of 235-cu in. displacement, from the same manufacturing lot, each carefully measured and inspected, were installed in taxi sedans equipped with standard transmissions. A single regular grade gasoline was used in all cabs throughout the test. Ten different motor oils were used and three cabs were supplied with each test oil – a desirable concept from a statistical standpoint. The test was run from May, 1953, through June, 1954.

Table 1 – Test Oils Used in 50,000-Mile Severe Low-Duty Field Test

Identification Letter	API Service Classification	Additive Content Identification
A	ML	Base Oil
B_1	MM	Inhibitor F
B_2	MM	Inhibitor G
C_1	MS-DG	Inhibitor F – Detergent H
C_2	MS-DG	Inhibitor-Detergent J
D_1	"MS-LD"	Inhibitor G – Dispersant K
D_2	"MS-LD"	Inhibitor G – Dispersant K – Detergent L
D_3	"MS-LD"	Inhibitor G – Dispersant 2 K
E_1	DS	Inhibitor-Detergent M
E_2	DS	Inhibitor-Detergent N

Motor oil was changed at 4500-mile intervals and the entire drain retained for analysis. No oil filters were used. Accurate records of fuel and oil consumption were maintained daily. The new engines normally came equipped with conventional solid cam followers or valve lifters. One of the three engines operated on each test oil was modified to take 1952 hydraulic valve lifters (chilled cast iron), and corresponding camshaft (forged steel). Thus twenty vehicles were operated with solid lifters and ten with hydraulic lifters. In accordance with standard practice of this fleet, governors were used to limit vehicle speed to 35-40 mph. These governors left insufficient room for the standard air cleaner. Consequently, the use of a small, dry, mesh-type air filter was standard in this operation.

At the end of 25,000 miles of operation, one engine on each of the ten oils was inspected and returned to service. At the end of 50,000 miles, engines were removed from all vehicles, brought to the laboratory, torn down, rated, and measured at the same time.

Test Fuel – Fuel used was a commercial type, regular grade gasoline of 88.5 Research Octane Number using 2.0 to 2.5 cc tel/gal. Fuel was a blend of catalytic cracked, thermal cracked, straight run, and catalytic polymer gasolines. Volatility was changed seasonally.

Test Oils – All ten test oils were SAE 10W-30 grade, made from the same solvent-extracted, mid-continent base oils of low carbon residue, to which a methacrylate-type VI improver was added. Viscosities of the finished oils were held between 65 and 66 SUS at 210 F, and viscosity index ranged between 137 and 140. Finished oils were classified as shown in Table 1 for type differentiation and identification in this report.

In order to best describe oils used in this test, they have been identified under the API Service Classification wherever possible. Some oils did not conform to the popular usage of the API Service Classification, and so liberties have been taken with the system to describe these oils. They are

[3] See SAE Transactions, Vol. 63, 1955, pp. 777-786: "Control of Low-Temperature Sludge in Passenger-Car Engines," by R. L. Willis and E. C. Ballard.

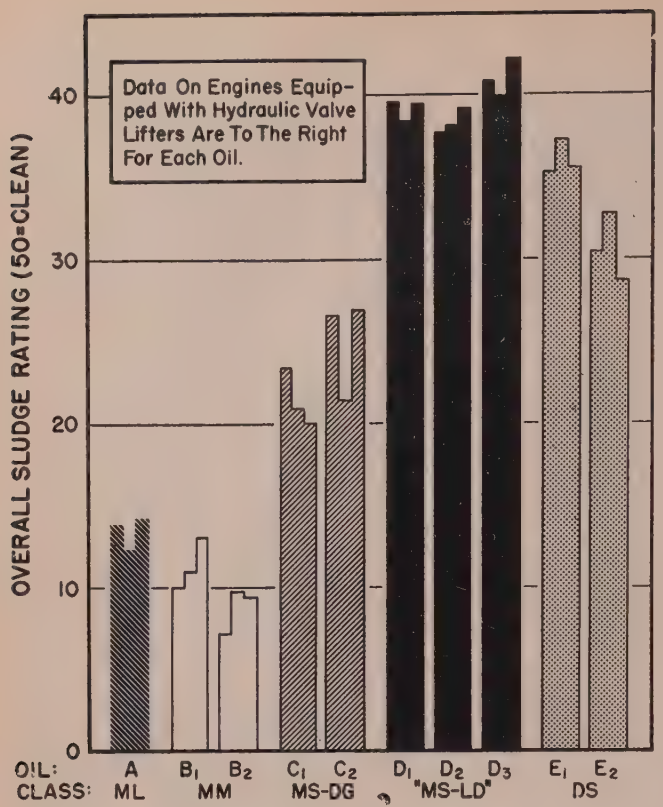

Fig. 2 – Sludge ratings from field test

identified as "MS-LD," meaning "Motor-Severe Low Duty." The need for some such service designation may become necessary if severe-low-duty oils are gradually accepted.

It might be well to state also that oils blended for this program were "type" oils only and not "production" oils of any kind or designation. However, only commercially used additives were employed.

Performance of Test Oils in Severe Low-Duty Field Service

A – Engine Cleanliness – After 50,000 miles of operation all engines were evaluated for cleanliness, the specific items being sludge, varnish, oil-ring plugging, intake valve tulip deposits, and oil screen ratings. Oil-ring plugging was evaluated by means of a photoelectric ring rater, a standard instrument for Ex-3 Test oil-ring deposit rating. Oil-screen plugging was evaluated visually. A clean screen was given a merit rating of 10.

In order to facilitate rating engines for varnish and sludge deposits, half of each pushrod cover, oil pan, and rocker arm was tin plated before the new engines were assembled. The other half of these surfaces was left in new factory condition to show any rusting which might occur during use.

1. Field sludge ratings: Sludge ratings were made on the same eight engine parts rated by the CRC Engine Varnish and Sludge Group in their Ex-3 engine test work. These ratings are presented in Fig. 2, and show the individual result for each engine, grouped according to oil service classification. A rating of 50 represents a perfectly clean engine.

There were two items in particular which stood out in the inspection of these engines:

a. Uniform appearance of each group of three engines run on the same oil.

b. Large differences in engine sludge between oils.

MM class oils gave extremely dirty engines; dirtier in fact than the base oil. The sludge in some places was up to ½-in. thick. Oil lines to rocker arms were cleaned on an average of twice during the test for each engine in order to correct oil starvation to rocker arms.

MS-DG oils showed improvement, but considerable amounts of sludge were still formed. They averaged about ⅔ oil-line cleaning per engine.

DS oils gave moderately clean engines in this service. No oil line cleaning was required.

"MS-LD" oils gave superior cleanliness ratings, engine parts being almost as free from any sludge as those normally found after 1000-2000 miles of operation with a new engine. In other words, parts were clean but covered with dirty oil, with a few light sludge ripples in some spots.

Figs. 3 and 4 show visual evidence of this cleanliness and contrasting engine filthiness with MM type oils.

2. Field cover sludge ratings: The CRC group working on development of the Ex-3 Test Technique has found the ratings on the rocker arm cover, pushrod cover, and timing gear cover to be particularly sensitive with respect to sludge deposits. They combined the ratings on these three parts into a rating called "cover sludge." Fig. 5 shows cover sludge ratings for field test engines, 50 indicating a perfectly clean engine. Cover sludge ratings approximate quite closely the total sludge ratings. Both ratings show that differences between oil types are greater than differences between engines on a single oil; hence, oil types are significantly different.

3. Field varnish ratings: Total engine varnish ratings (shown in Fig. 6) indicate relatively small differences between oils. All engines rated between 13 and 25 out of a possible 50. What improvement there was occurred in the direction of increased additive content of the respective oils.

Perhaps one of the reasons for this small difference in varnish ratings was the formation of so much sludge in the A, B, and C class oils that varnish deposits did not have as much chance to

Table 2 – Piston Varnish Ratings

A – 3.5	B_1 – 3.2 B_2 – 3.2	C_1 – 3.7 C_2 – 3.9	D_1 – 4.0 D_2 – 4.2 D_3 – 5.2	E_1 – 5.9 E_2 – 5.2

Fig. 3 – Pushrod covers and chambers from field test

accumulate with these oils, and hence drop even lower in rating.

Maximum spread in total piston varnish ratings themselves, which included ratings of piston skirts and piston pin area varnish deposits, was 2.7 out of 10, shown in Table 2, where 10 = perfect.

These ratings tended to follow the trend of total engine varnish ratings, too.

4. Field oil-ring plugging: Oil rings used in all engines were conventional, wide-slot, cast-iron rings originally obtained from the same manufactured lot. After removal from engines, all rings

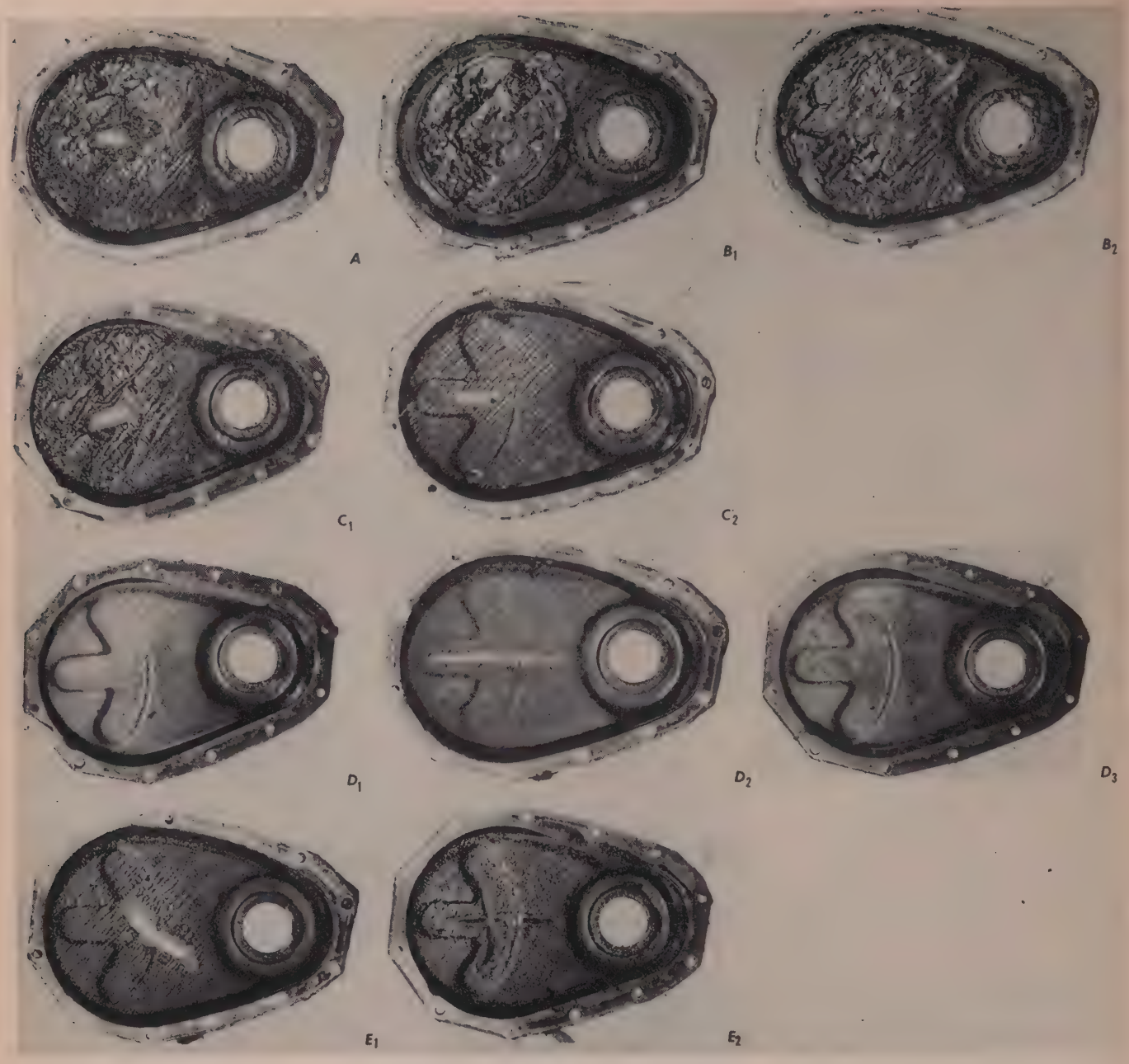

Fig. 4 – Timing gear covers from field test

were rated for percent plugging on the photoelectric ring rater.

Average oil-ring slot plugging for individual engines has been plotted in Fig. 7.

In general, there was not much variation in oil-ring slot plugging as might have been expected from (1) range of types of oils tested, or (2) effect of these same oils on engine sludging.

It is interesting to observe that only 7 of 30 engines showed ring plugging over 55%, which indicates that partial oil control was still being obtained even after 50,000 miles of operation.

From results shown in this plot not too much can be summarized, but it is evident that ring plugging within any particular oil group was somewhat erratic. The most consistent group performance with the least plugging was found with D oils.

5. Field intake valve tulip deposits: At the conclusion of the final engine inspection program, valve tulips were photographed, and deposits removed and weighed. In general intake valve tulip deposits showed considerable variation between individual valves in a given engine. There were also large differentials in tulip deposits between three engines using the same oil.

Results of intake valve deposits expressed in average grams per valve for each engine are shown in Fig. 8.

The greatest deposits were found in one engine each on oils C_1, C_2, and D_1. These deposits were

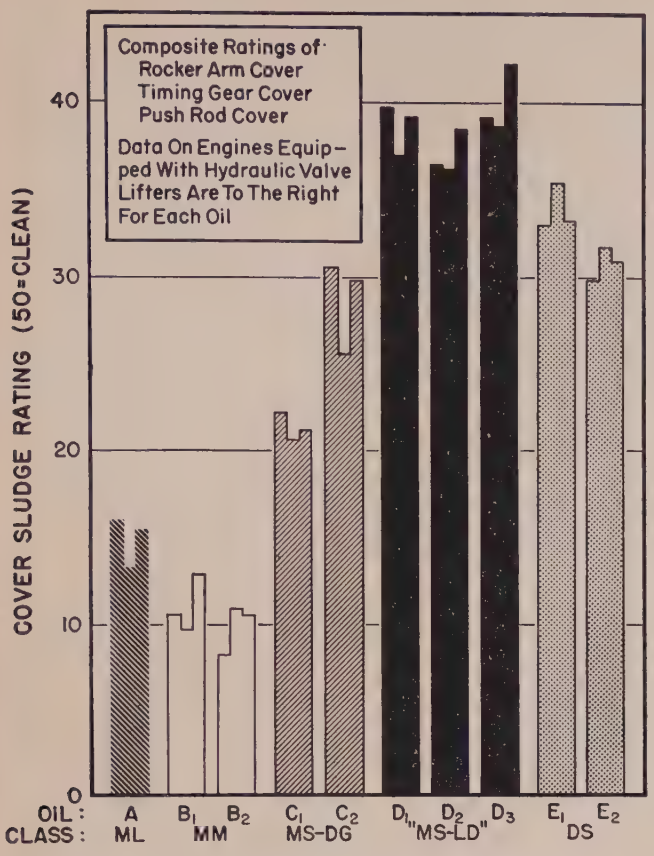

Fig. 5 – "Cover sludge" ratings from field test

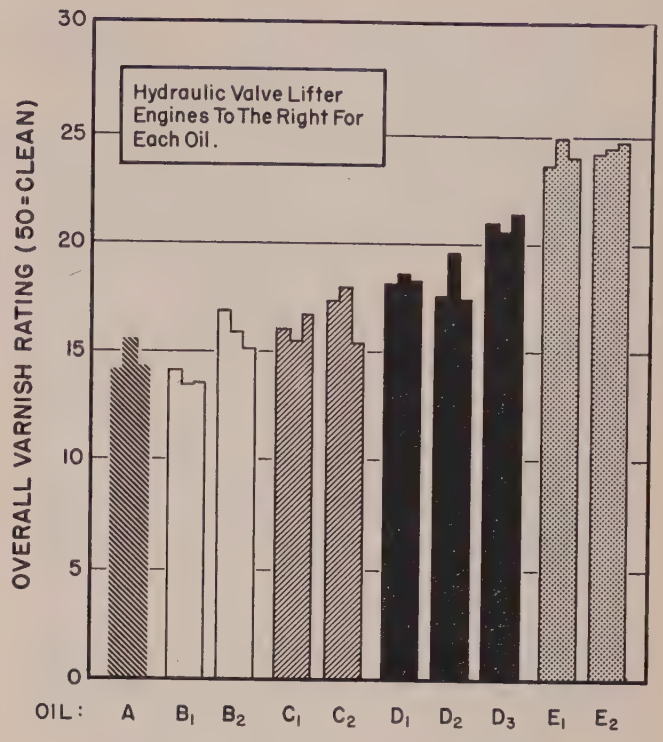

Fig. 6 – Varnish ratings from field test

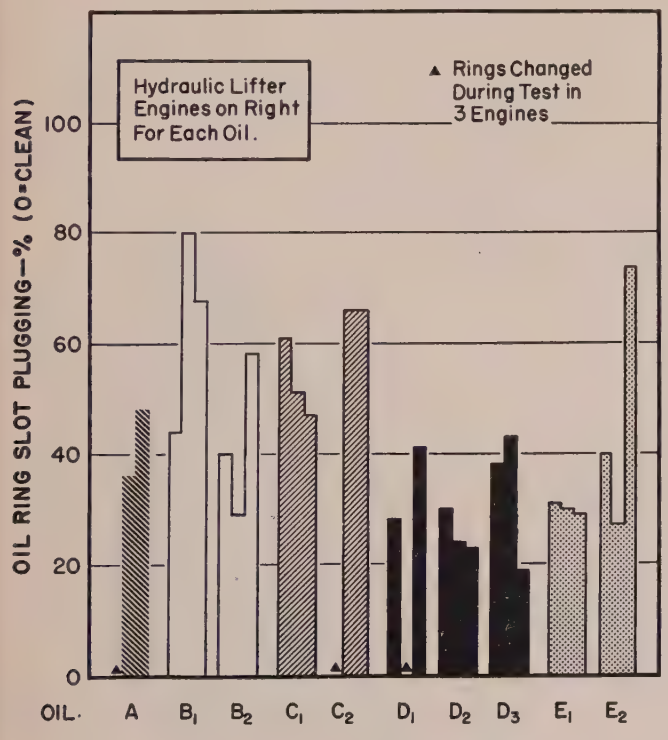

Fig. 7 – Oil-ring slot plugging in field test

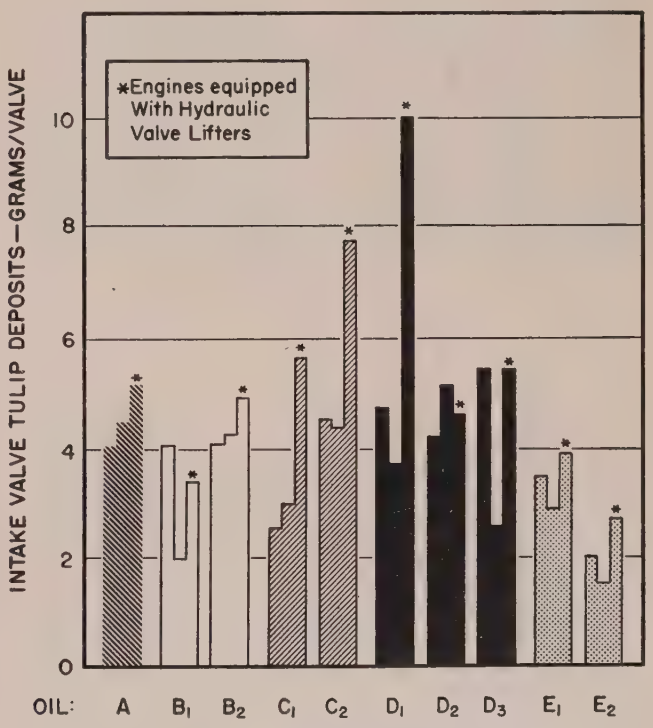

Fig. 8 – Intake valve tulip deposit weights in field test

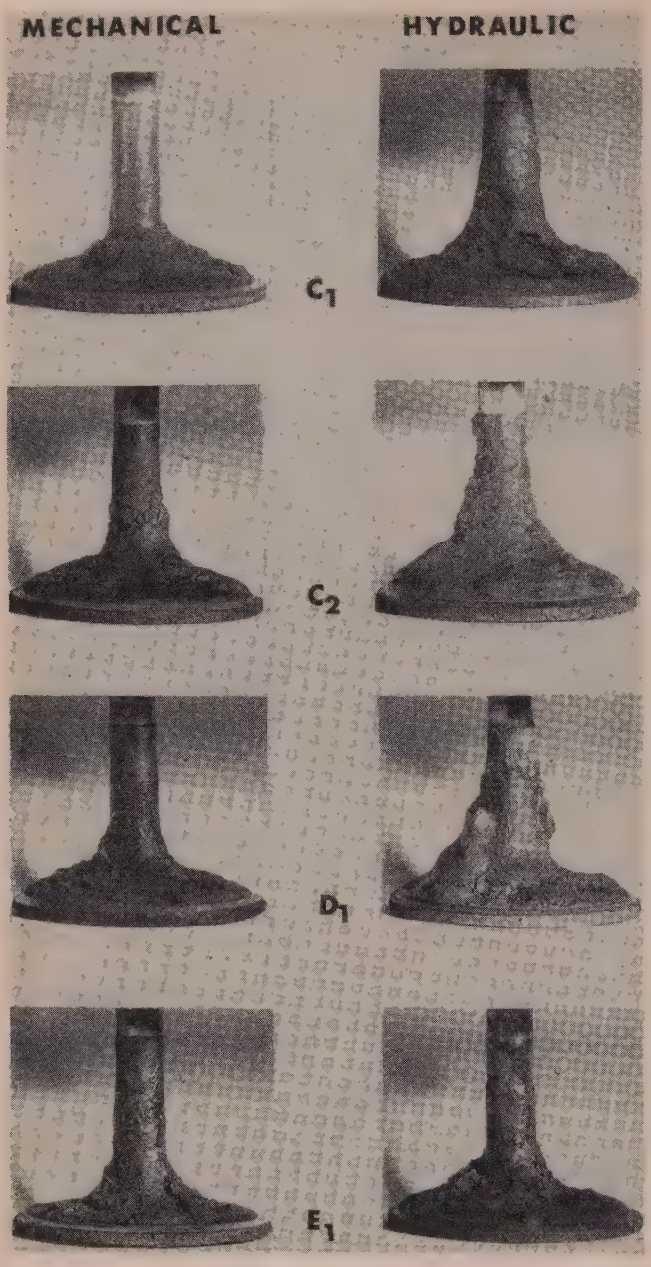

Fig. 9 – Comparison of intake valve tulip deposits formed with mechanical and hydraulic valve-lifter equipped engines

unusually large relative to the other two engines on the same oil, giving values as high as 10 g per valve. On the other hand, the lowest amounts of deposits were found with oil E_2, found to be statistically superior in this property to six of the nine other oils.

One of the most interesting points highlighted in this project was the discovery that hydraulic valve lifters may have a startling effect on several engine performance criteria. One such effect was on inlet valve tulip deposits. Bar graphs marked with an asterisk indicate engines equipped with hydraulic cam followers and corresponding camshafts. As previously stated, cylinder heads, valves, and valve operating linkages were identical for all 30 engines, the only change being that 10 were equipped with hydraulic followers and cams. Observe that in 8 of 10 oils the largest amount of intake valve tulip deposits occurred with these engines, and in several cases the increase was quite substantial. A comparison between deposits formed with standard and hydraulic lifters with oils C_1, C_2, D_1, and E_1 is shown in Fig. 9. Whether this difference is caused by a variation in mixture distribution, higher volumetric efficiency, more consistent manifold vacuum, or increased oil consumption through intake valves with engines using hydraulic cam followers, is not known at this time. At least the phenomenon is an interesting one and perhaps deserves more than just passing comment.

6. Field oil screen ratings: One of the best engine indicators of oil performance under severe low-duty engine sludging conditions is oil pump inlet screen plugging.

Large differences were found in performance of the several oil types tested with regard to oil screen ratings. (See Fig. 10.) Oil types A and B gave very badly coated screens. As a matter of record, two engines with zero ratings on oil A required screen replacements at 25,000 and 32,000 miles respectively. Similarly, zero rating screens with oils B_1 and B_2 required replacement at 25,000 miles, as they were completely blocked.

C oils gave only fair screen performance with approximately 20-50% area remaining open for oil flow. D oils gave excellent screens with almost new appearance after 50,000 miles. E oils gave

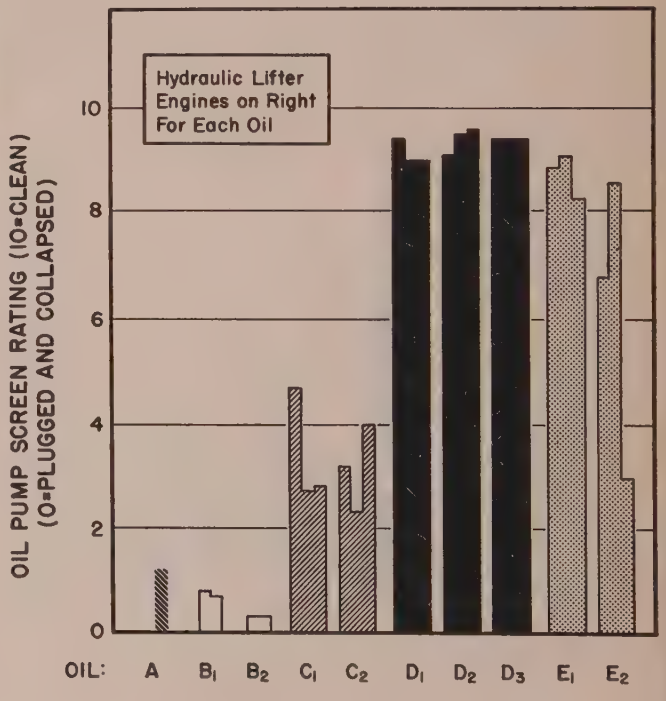

Fig. 10 – Oil screen ratings from field test

Fig. 11 – Oil screens from field test

variable performance ratings, with from 30-93% of their area being open.

Typical screens on each oil are shown in Fig. 11.

7. Rusting and lifter sticking: Essentially no rusting was found on any engine parts at the time of engine disassembly for rating.

As previously mentioned, 10 of 30 engines used in the test were equipped with hydraulic valve lifters. Throughout 1.5 million miles of test operation, even though heavy sludging was encountered with many test engines, there was surprisingly little lifter trouble. For the entire test, replacement of only 8 of 120 lifters in operation was required. This might be attributed to the fact that cabs were generally out of service but four hours a day and were stored in a heated garage for this period.

B – Field Wear – Wear is the primary factor in engine life, and it is at least one of the major factors in determining when engines are overhauled. Wear as observed in this field test is discussed below under various headings.

1. Cylinder bore wear: Cylinder bore wear was measured with two different types of instruments: one, a dial gauge checked against a micrometer to measure bore diameter, the other a dial gauge measuring the change in profile along the bore above and below ring travel.

Average increase in bore diameter at the top of ring travel for each engine, computed from both sets of measurements, is shown in Fig. 12.

Data on the three engines which had ring replacements at 25,000 miles are omitted since the results are not comparable. Wear was found highly concentrated in the top ¾ in., giving a flare-shaped bore.

Considering the wide variation in oil types,

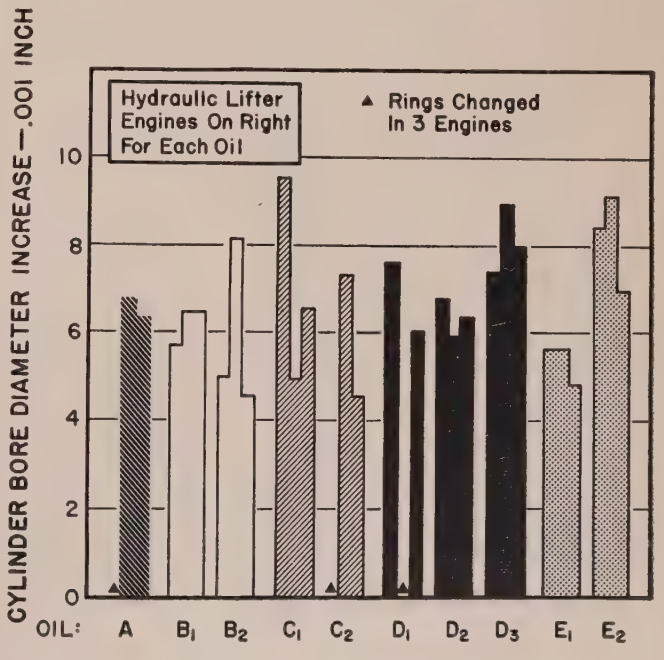

Fig. 12 – Bore wear at top of ring travel in field test

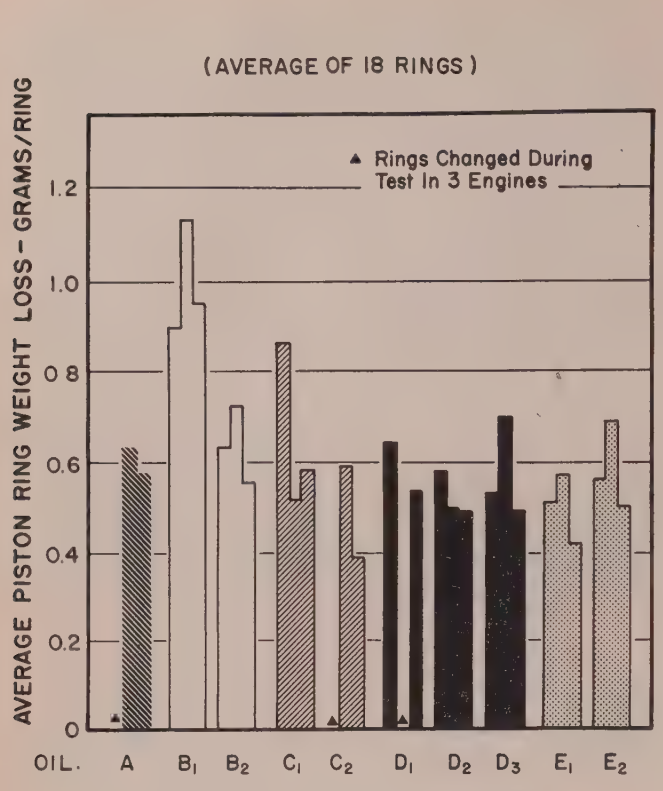

Fig. 13 – Piston ring weight loss in field test

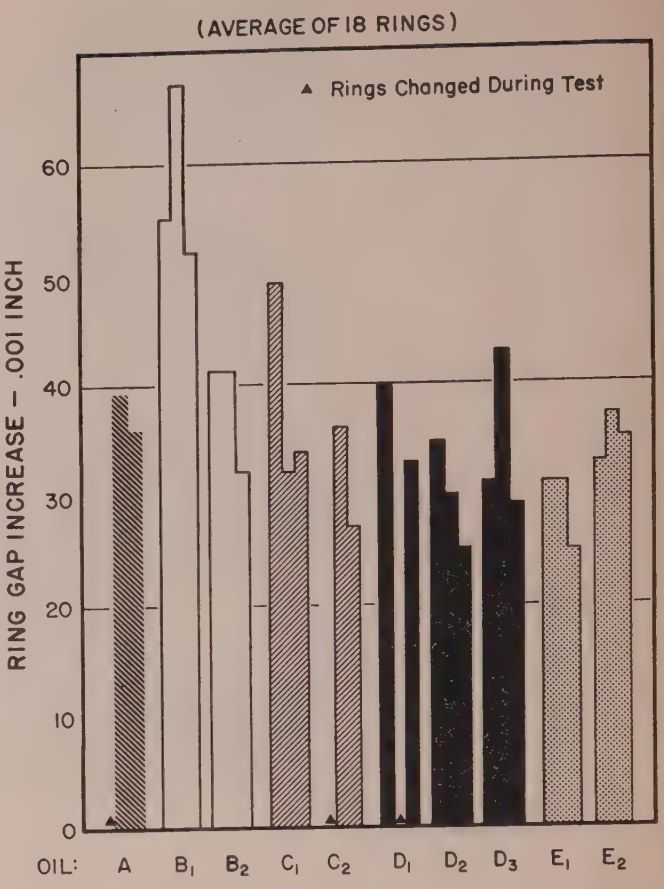

Fig. 14 – Piston ring gap increase in field test

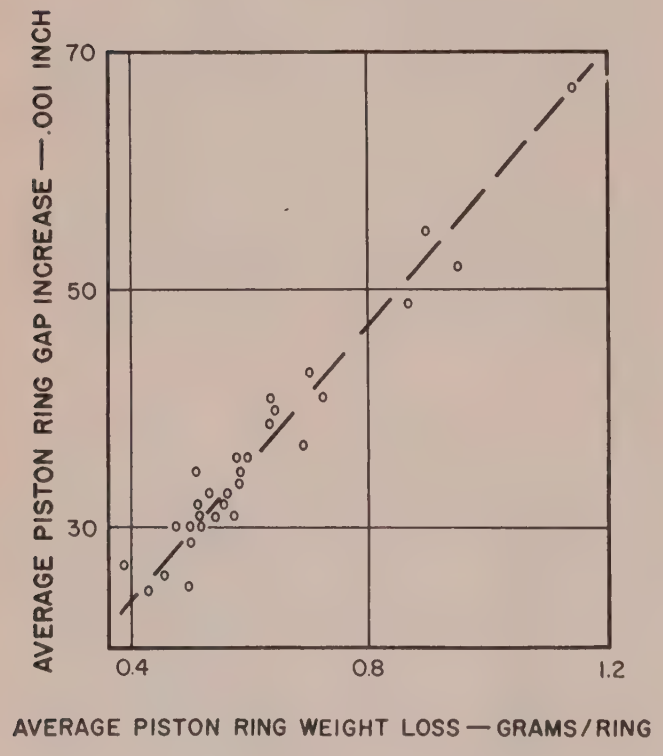

Fig. 15 – Piston ring weight loss versus gap increase

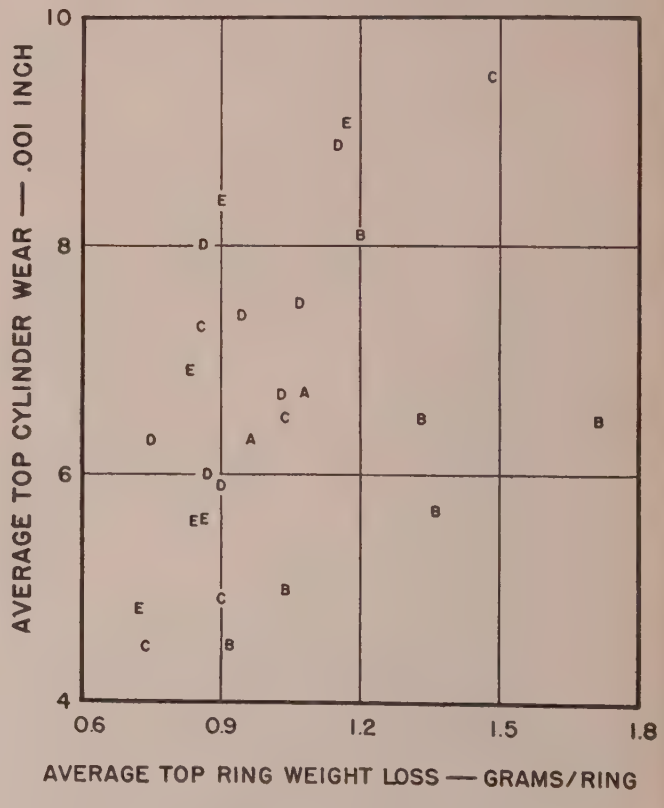

Fig. 16 – Cylinder bore wear versus ring weight loss

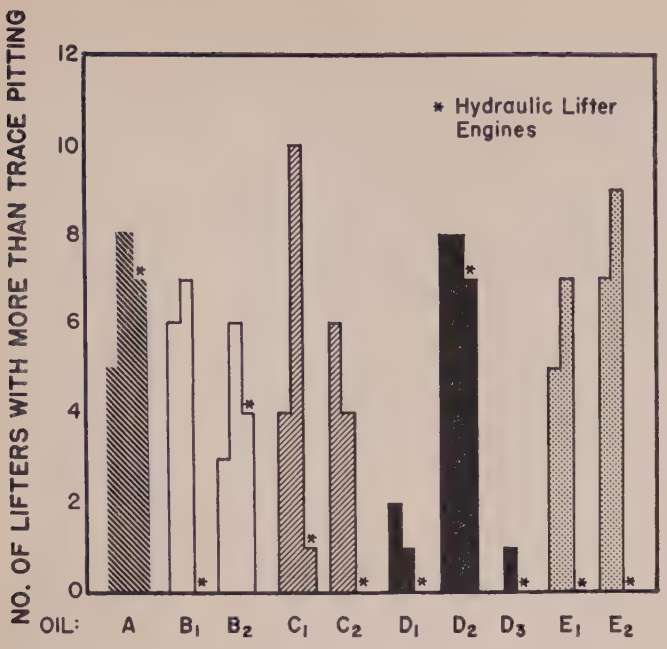

Fig. 17 – Valve lifter pitting in field test

spread in bore wear from the best engine to the worst was surprisingly small. The variation was as great among the engines on oil C_1 as it was among the other 24 engines. No oil type was consistent. It is interesting to note that average bore wear on oil E_1 was the lowest (0.0054 in.), while on oil E_2 it was equal to the highest (0.0081 in.).

Although a vague correlation was found between bore wear and oil consumption, analysis of the data indicates that bore wear, within the limits found in this test, was not a primary factor in oil consumption.

2. Piston ring wear: All piston rings were weighed and gaps measured in a standard bore both before and after the field test. Average weight losses for all rings in each engine are presented in Fig. 13, and similarly, average ring gap increases are presented in Fig. 14. These two figures agree fairly well as indicated by the correlation curve in Fig. 15. Similar data for top, second, and oil control rings, taking each group separately, although not shown, give the same general wear pattern.

With the exception of oil B_1, which gave very high wear, there was surprisingly little difference in average ring wear among the various oils. Oils C_2 and E_1 tended toward low wear, while oils B_2 and C_1 tended toward high wear.

Fig. 16, a plot of bore wear against top ring weight loss, shows that little correlation exists. Apparently factors causing high ring wear do not necessarily cause high bore wear.

3. Valve train wear – lifter pitting: Valve lifter pitting was quite severe and erratic in many engines. The number of lifters in each engine with more than a trace of pitting is shown in Fig. 17. As a base line, oil A, containing only a VI improver, permitted more than a trace of pitting on 5 to 8 of the 12 lifters in each engine.

In looking at this plot there are two points that stand out:

a. In general hydraulic valve lifters showed considerably less pitting than mechanical lifters.

b. With the exception of oils B_2 and D_2, all additive combinations essentially eliminated pitting on hydraulic valve lifters, but only oils D_1 and D_3 gave relatively good performance on mechanical lifters.

Actual lifter wear was not measured, but many severely pitted lifters were obviously "dished." No indication of internal lifter wear was obtained, nor was there any indication of the mileage at which lifter pitting occurred.

Cam lobe wear: No measurements were made of camshafts before the test, but cam lobe major diameters were measured at the end of the test and compared to the engine manufacturer's specifications. As would be expected from lifter pitting, and as may be seen from Figs. 18 and 19, cam lobe wear varied widely. By far the worst wear occurred with oil C_1, where half of all cam lobes showed wear of over 0.020 in. Severe lobe wear also occurred with several other oils although not so consistently.

Summarizing the above figures, it is seen that:

a. Cam lobe wear was generally less severe in engines equipped with hydraulic valve lifters.

b. Exhaust cam lobes generally showed more

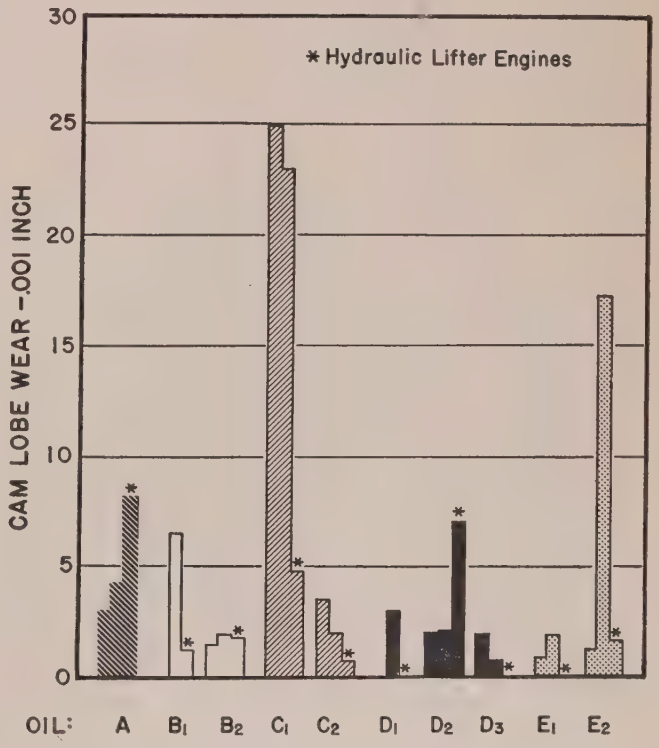

Fig. 18 – Camshaft intake lobe wear in field test

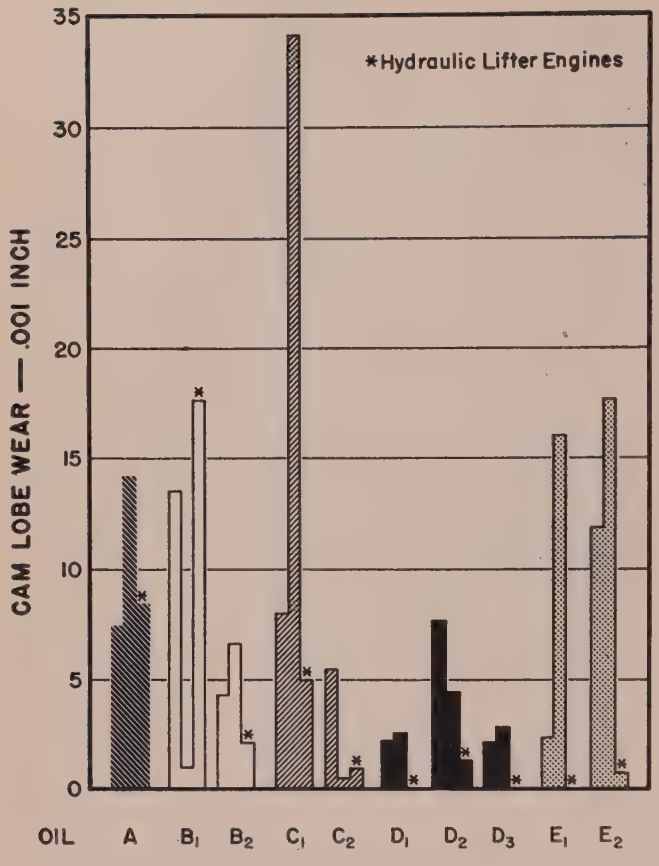

Fig. 19 – Camshaft exhaust lobe wear in field test

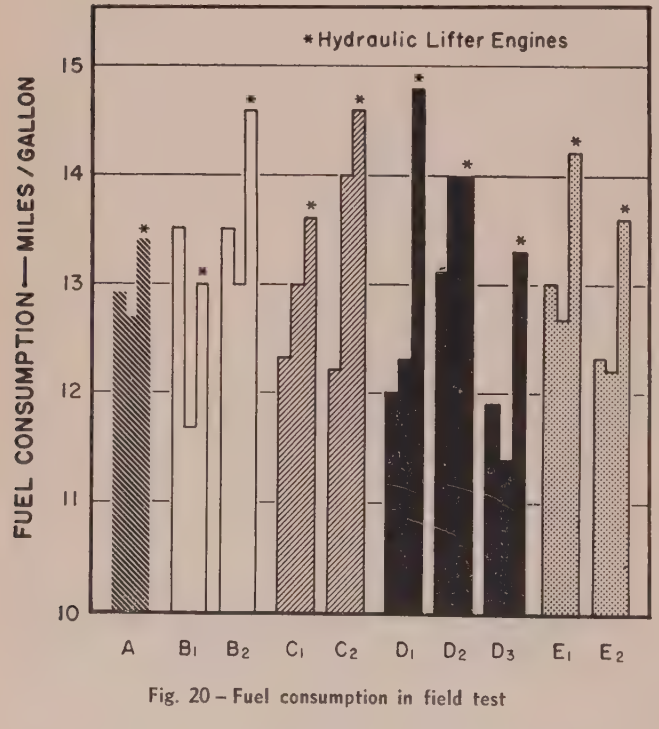

Fig. 20 – Fuel consumption in field test

wear than intake cam lobes.

c. Oils D_1 and D_3 gave the most consistent low wear.

While pitted lifters undoubtedly were an important factor in cam lobe wear, it did not necessarily follow that engines with the higher number or more severely pitted lifters also had more cam lobe wear. For example, oil D_2 permitted the highest total number of pitted lifters, but more than half the other oils gave higher average cam lobe wear. On the other hand, the one engine on oil C_1 that had the most severe lifter pitting in the whole fleet also had the highest average cam lobe wear, with individual lobes giving up to 0.050 in. wear.

Rocker arm shaft wear: Rocker arm shafts were measured before the test, but at the end of the test many rocker arms were so badly scored due to lack of lubrication from oil line plugging that no accurate measure of relative wear could be obtained with an ordinary micrometer.

A visual examination of rocker arm shafts showed all shafts run on oil types A and B to be in bad condition. Bearing surfaces were badly scored and pronounced shoulders had formed on the shafts. Rocker arm shafts on other oils appeared to be in satisfactory condition with the exception of one shaft operated on oil C_2. Wear on these shafts was generally less than 0.001 in.

4. Miscellaneous wear: With the exception of

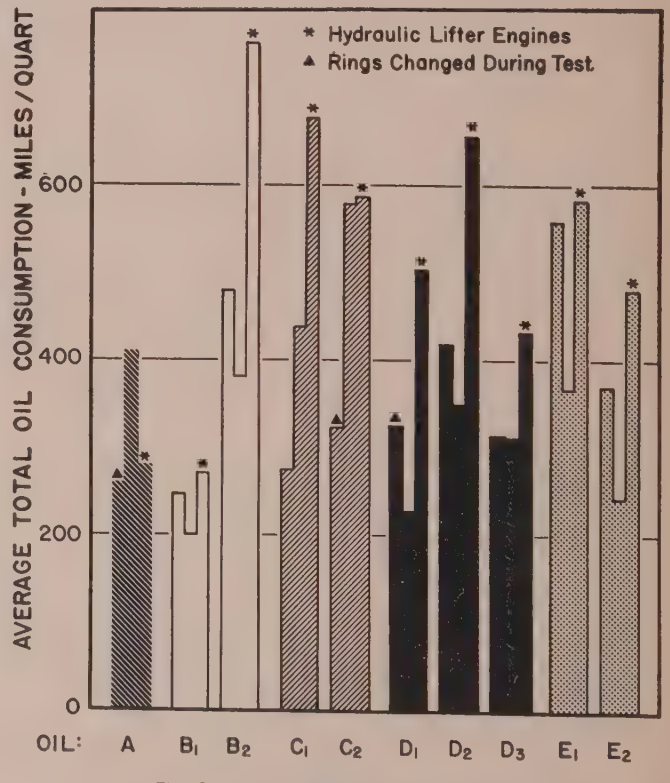

Fig. 21 – Oil consumption in field test

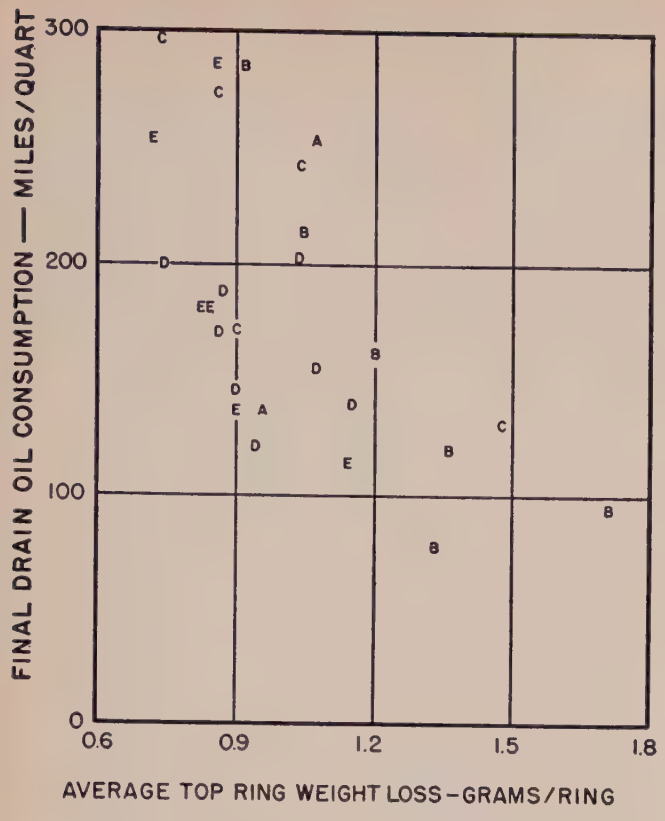

Fig. 22 – Oil consumption versus piston ring wear

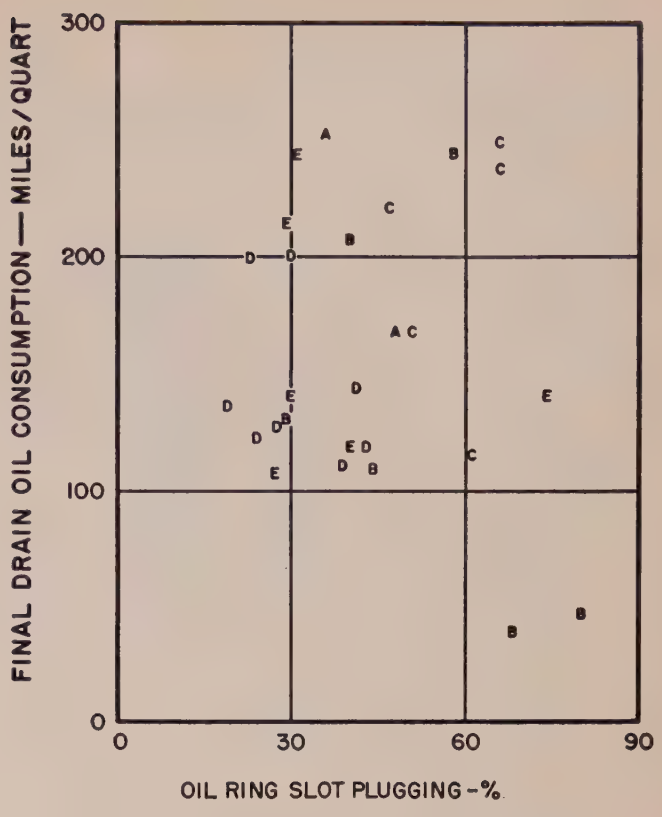

Fig. 23 – Oil consumption versus oil-ring slot plugging

one engine wrecked at about 48,000 miles due to a connecting-rod cap nut coming off, the main and connecting rod bearings were in satisfactory condition in all engines. Journal wear was negligible in all engines. Only one connecting-rod journal showed wear as much as 0.001 in.

Piston wear was measured, but no significant differences were found.

Piston pins and bushings were not measured for wear, but inspection disclosed none that was excessively loose.

No particular note was taken of valve stem clearance or valve guide dimensions either before or after the test.

For record purposes, pistons and rings in all engines were cast iron; the rings nonplated. Piston-ring side wear was less than 0.001 in., and there was no evidence of excessive groove wear.

C – Fuel Consumption – There was considerable variation in gasoline consumption from cab to cab throughout the test, (see Fig. 20), ranging from 11.4 to 14.8 mpg. Variation in mileage between cabs on the same oil is so great that it is impossible to show any differences between oils if they exist.

Upon further examination of the data, however, it is noted that with only one exception, the highest mileage cab on each oil was the one with hydraulic valve lifters. For the overall test cabs with hydraulic lifters averaged 13.9 mpg, while the others averaged 12.7 mpg. The number of theories proposed to explain this phenomenon is greater than the number of authors, with little unanimity displayed.

D – Oil Consumption – A record was maintained for each cab as to quantity of all oil added and drained throughout the test period. Fig. 21 shows overall oil consumption in mpq for the entire test. While variation in consumption between cabs on the same oil makes it difficult to distinguish between oils, it is interesting to note that with the exception of oil A, cabs containing hydraulic lifters gave the best oil consumption. Average figures were approximately 520 mpq compared to 350 mpq.

Correlation with bore wear: Fig. 22 shows a correlation between oil consumption during the final drain period and top piston-ring weight loss. In this range an increase in average top ring weight loss of ½ g indicated roughly an increase in oil consumption of 150 mpq.

A number of other possible correlations dealing with oil consumption were investigated but none was found to be significant. One of these is the relationship between oil ring plugging and final oil consumption, Fig. 23.

E – Octane Requirements – Octane requirements were determined at the beginning, during, and at the completion of the test on most cabs. In Fig. 24 are shown final octane requirements of 27 of 30 cabs. Cabs operating on oil E_2 had, on the average, final octane requirements significantly lower (ap-

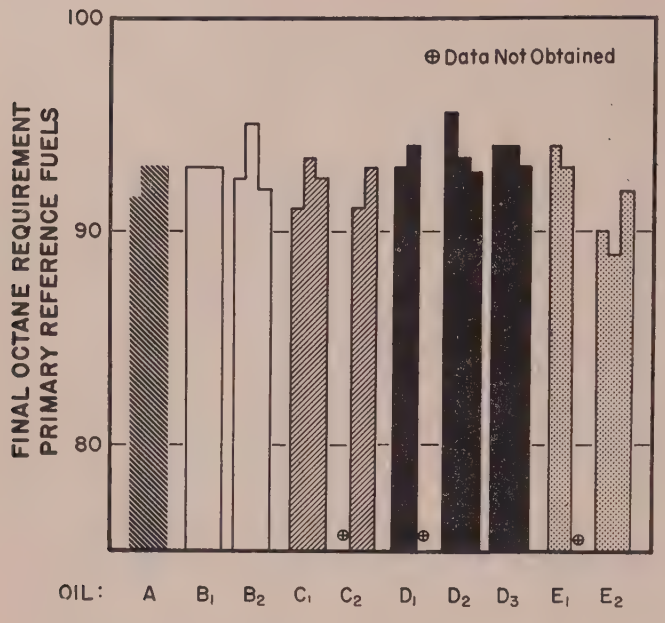

Fig. 24 – Final octane requirements in field test

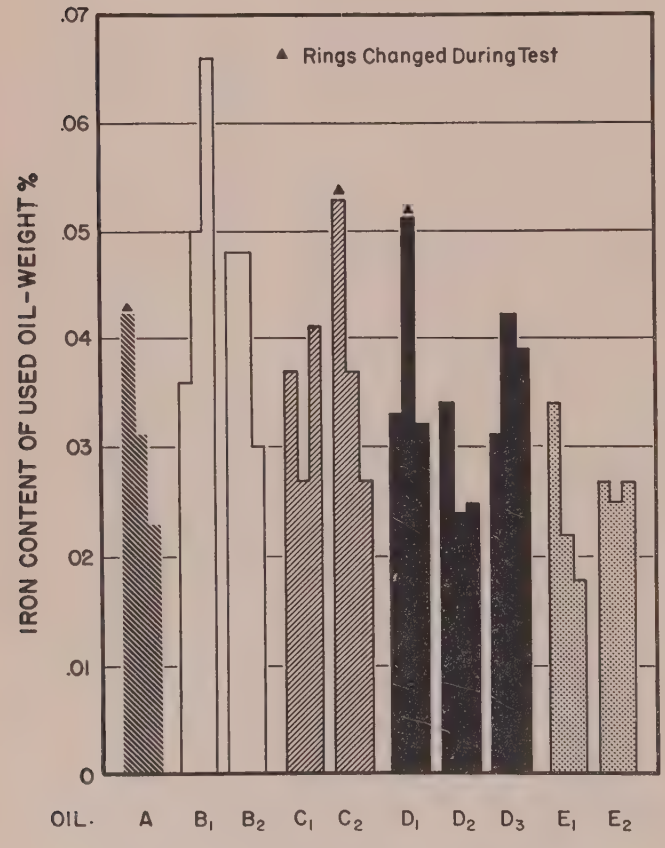

Fig. 25 – Iron content of used oils from field test

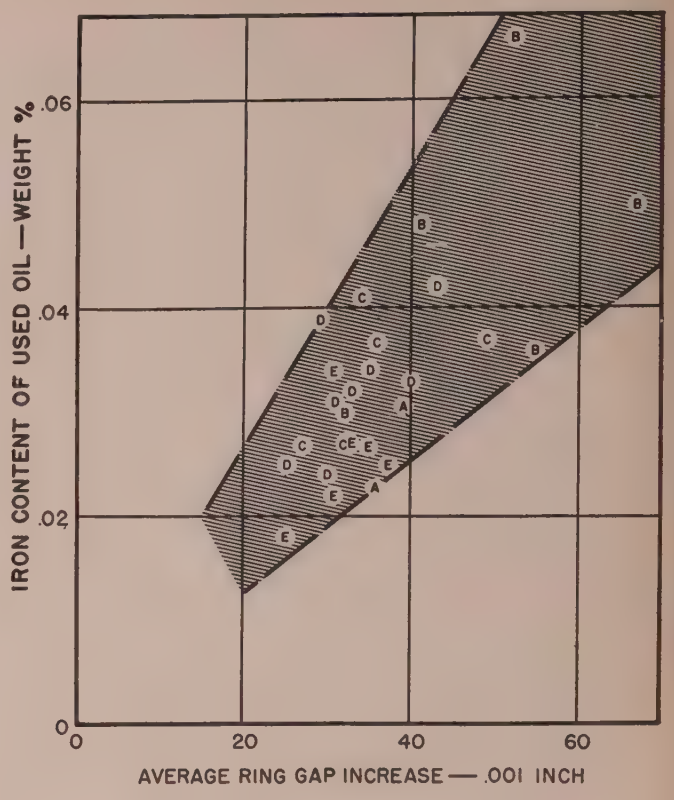

Fig. 26 – Ring wear versus iron in used oils

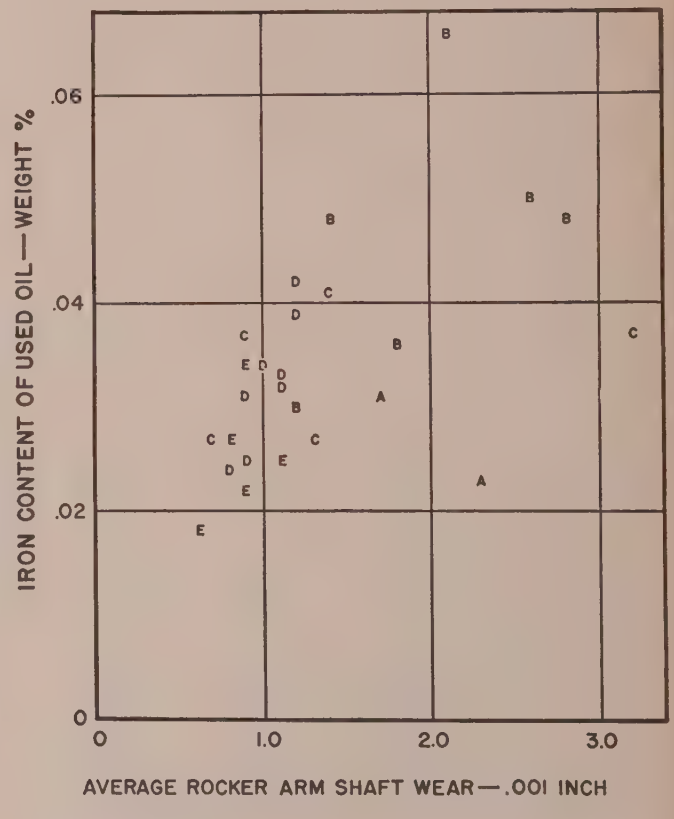

Fig. 27 – Rocker arm shaft wear versus iron in used oils

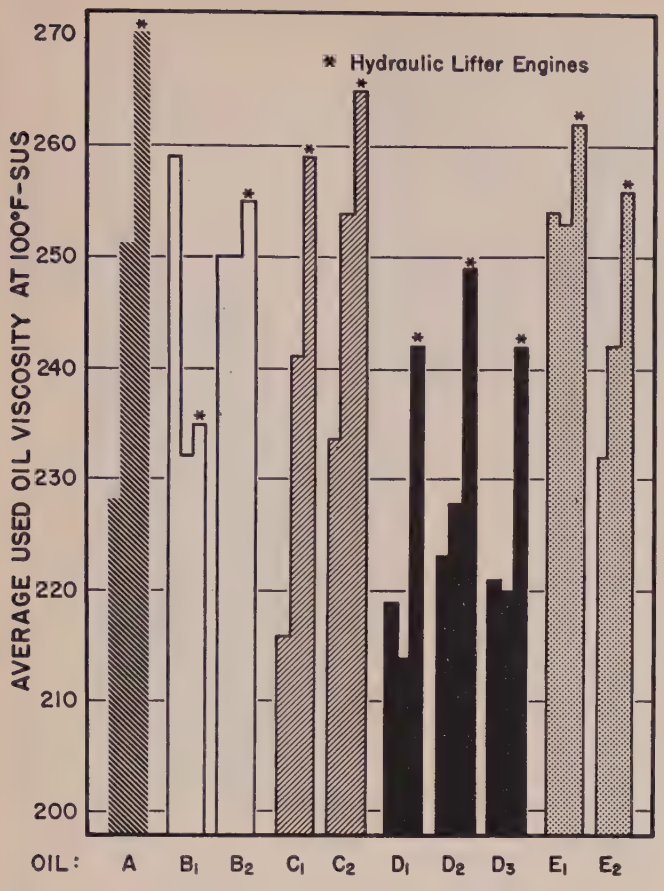

Fig. 28 – Viscosity at 100 F of used oils from field test

when put together with the proper factors. Such a multiple regression analysis to determine these factors has not been made. None of the other spectrographic analyses was found to be significant in regard to any performance factors.

Physical analysis: The following physical inspection tests were run on all used oil samples:

1. Viscosity at 100 F } viscosity index.
2. Viscosity at 210 F }
3. Dilution.
4. Acid number.
5. Base number.
6. Pentane insolubles.
7. Benzene insolubles.

In addition, naphtha insolubles and MEK insolubles, using the high-speed centrifuge, were run on about two-thirds of the samples.

1. Viscosity at 100 F: Average viscosity at 100 F of 11 samples from each of the cabs is shown in Fig. 28. The large differences between cabs on the same oil leave little significance between oils. One interesting thing is that with one exception, highest viscosities were encountered in used oils from cabs with hydraulic lifters. There was also some semblance of correlation between average viscosity at 100 F and overall oil consumption, as shown in Fig. 29.

2. Viscosity at 210 F: Similar data at 210 F are shown in Fig. 30. Here the reproducibility is much better between cabs on the same oil. Series D oils all seem to be lower than the other oils. However, in proximately 2 O.N.), than the rest of the oils. No other significant differences were shown.

F – Used Oil – During the progress of the test, particular care was taken to have oil drains made with the engine hot, as soon after coming off the road as possible. The entire drain was collected, shaken, and sampled within a short period of time. These samples were sent to the laboratory for physical and spectrographic analyses.

Spectrographic analysis: Quantitative results by spectrographic analysis were obtained showing amounts of iron, silica, tin, antimony, and several other elements in the used oil samples. Average iron content in weight percent for the eleven drains from each cab are shown in Fig. 25. The large variation between cabs on the same oil prevents seeing any difference between oils. In trying to correlate these data with wear data, it was found that piston-ring wear and rocker arm shaft wear were the only two items that showed much promise, (see Figs. 26 and 27). No correlation was found between iron in the used oil and cylinder bore wear. It is possible that iron content represents total wear taking place in the engine and would correlate with combined wear of pistons, piston rings, cylinder bores, rocker arm shaft, camshaft, valve train, and bearings

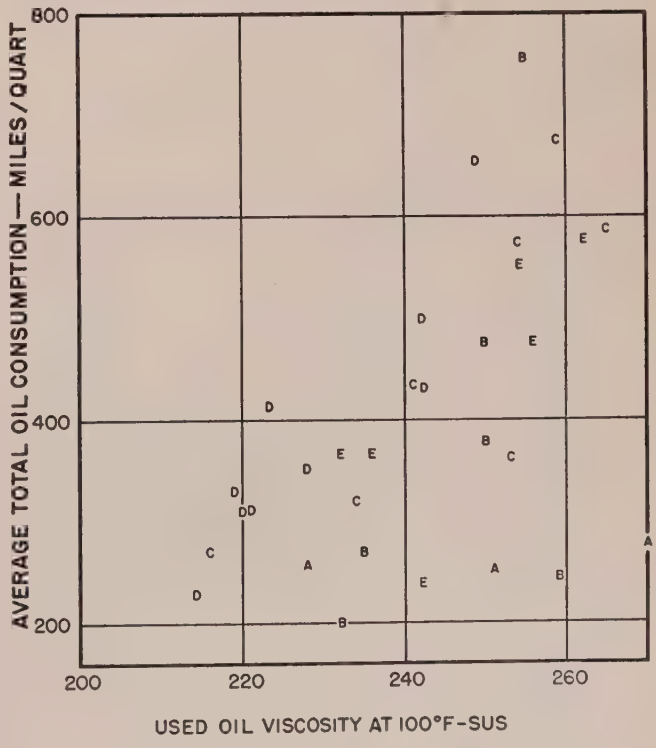

Fig. 29 – Oil consumption versus used oil viscosity at 100 F

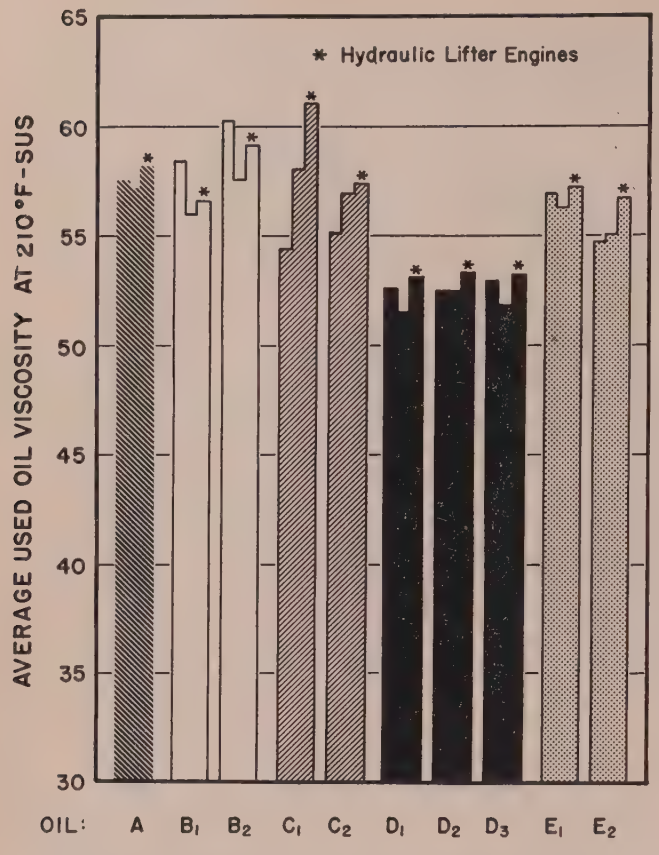

Fig. 30 – Viscosity at 210 F of used oils from field test

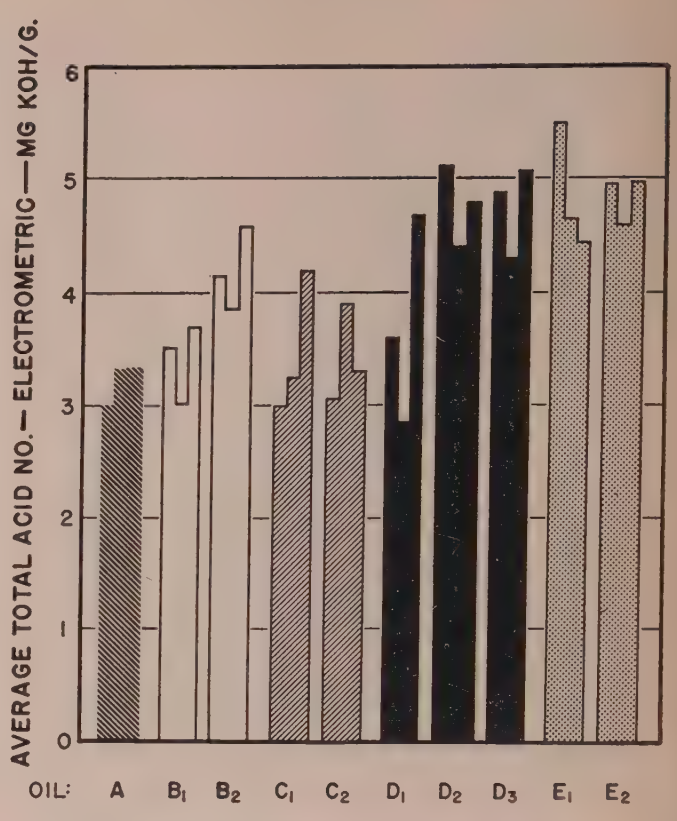

Fig. 31 – Total acid numbers of used oils from field test

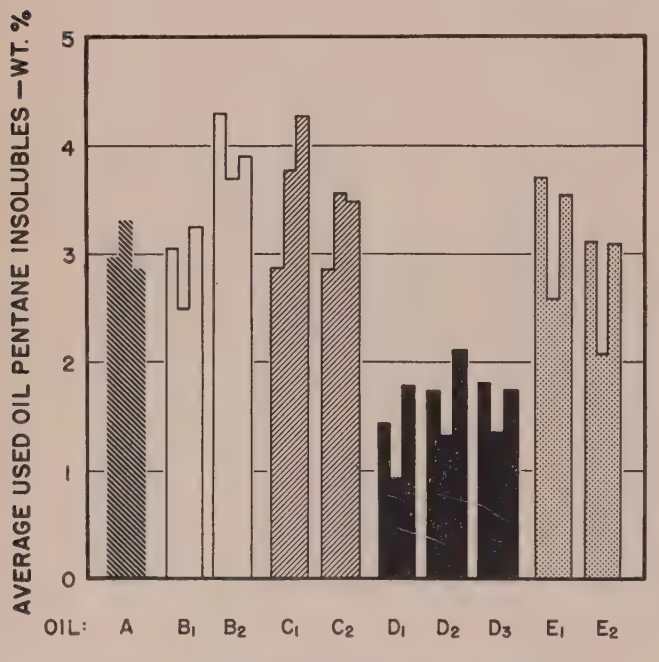

Fig. 32 – Pentane insolubles in used oils from field test

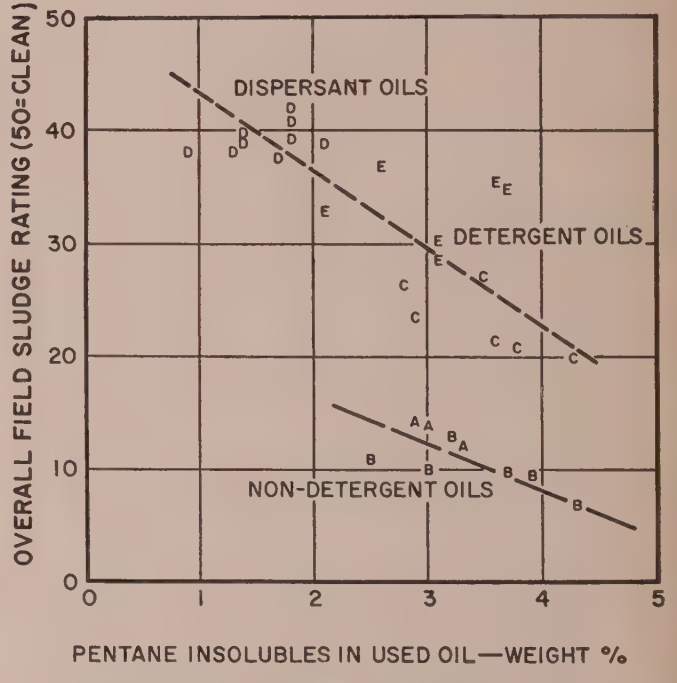

Fig. 33 – Pentane insolubles versus sludge ratings

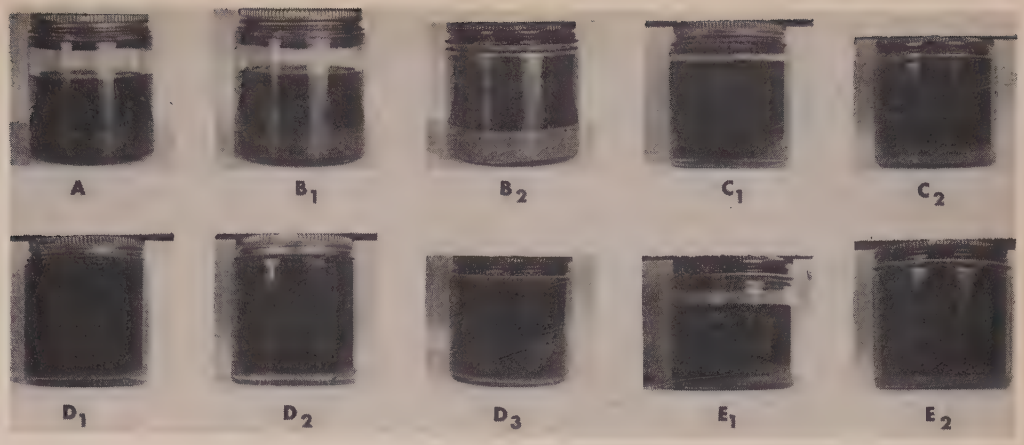

Fig. 34 – Used oils from field test after extended settling

trying to relate this fact to performance, no correlation was found between used oil viscosity at 210 F and oil consumption.

During the progress of the test, the apparent shear instability of D oils was noted. However, it was found that these differences were due almost entirely to solid materials in used oils which were more finely dispersed in the D group. Larger particles in the other used oils increased viscosity as measured by the kinematic viscosimeter. Evidence of this was the fact that the 210 F viscosities of used oils after centrifuging all fell within a narrow band of about two seconds.

3. Dilution: Dilution, which averaged about 2%, appeared to bear no relation to any performance factor.

4. Acid number: Average acid numbers of the 11 drains on each oil are shown in Fig. 31. Here, while there was some variation between cabs on the same oil, no correlation with performance could be found.

5. Base number: Only three of the oils showed any base number on the used oil samples. These oils were C_1, E_1, and E_2.

6. Pentane insolubles: The average pentane insolubles in the used oils are shown in Fig. 32. D series oils are definitely lower in this regard than all others. One of the reasons for this is that dispersion of sludge particles was sufficient to maintain them in suspension during the low-speed centrifuge operation used in this test method. A plot of pentane insolubles versus sludge appearance rating, Fig. 33, presents an interesting picture. The oils appear to fall into two groups: (a) dispersant and detergent oils, and (b) nondetergent oils. Within each group a fair degree of correlation exists between these two factors.

Further evidence of the differences in dispersancy characteristics among the 10 oils is shown in Fig. 34. These are samples of used oils after 4500 miles of service which have been allowed to settle for 15 months. Note the marked differences in amounts of settled insolubles. Essentially no separation occurred with the "MS-LD" oils in spite of the long drain periods and the fact that water is nearly always present in this type service.

7. Benzene insolubles: About the same picture exists with benzene insolubles as with pentane insolubles.

During World War II the FL-2 Test was developed to evaluate effects of fuels and crankcase oils on engine deposits under low-temperature operating conditions. There has always been considerable dissatisfaction with this test for several reasons.

1. Sludge deposits produced were not as heavy nor did they look the same as those occurring in the field.[4]

2. Oil variations were much more likely to affect

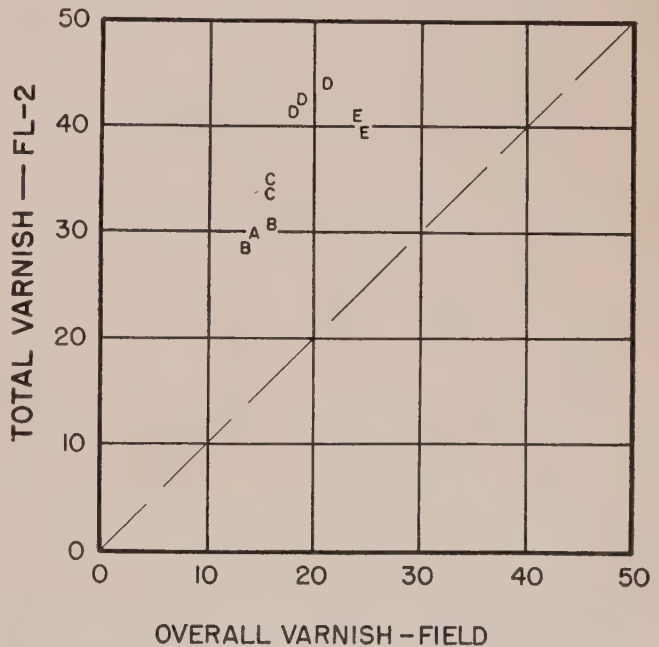

Fig. 35 – FL-2 versus field test varnish ratings

[4] "Oil-Ring Plugging – Missing Link in Laboratory Tests," by L. J. Test and C. A. Hall. Paper presented at SAE Fuels and Lubricants Meeting, St. Louis, Nov. 4, 1949.

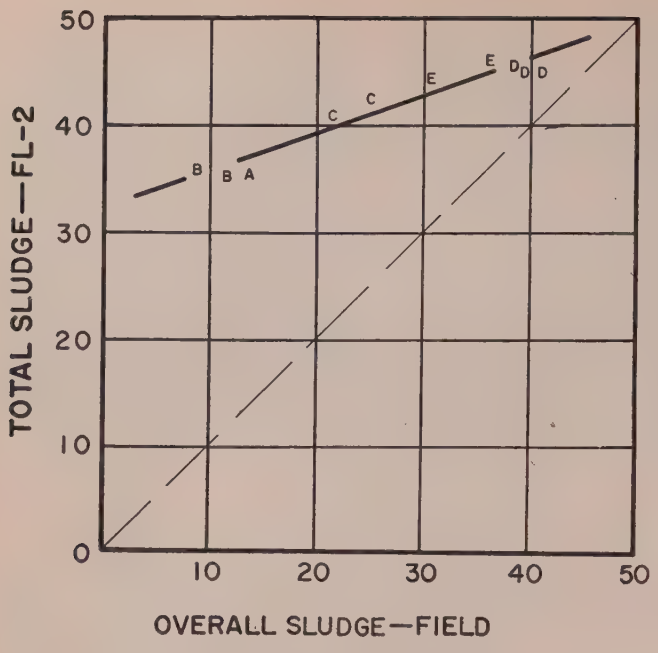

Fig. 36 – FL-2 versus field test sludge ratings

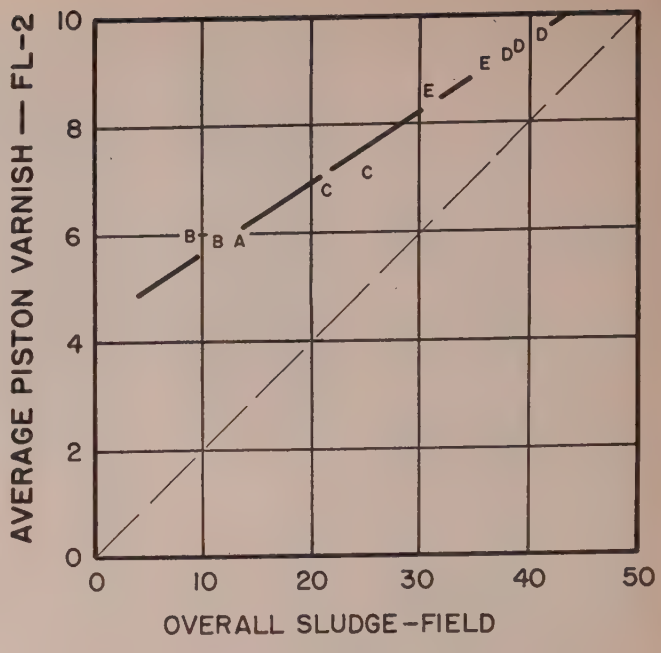

Fig. 38 – FL-2 piston ratings versus field test sludge ratings

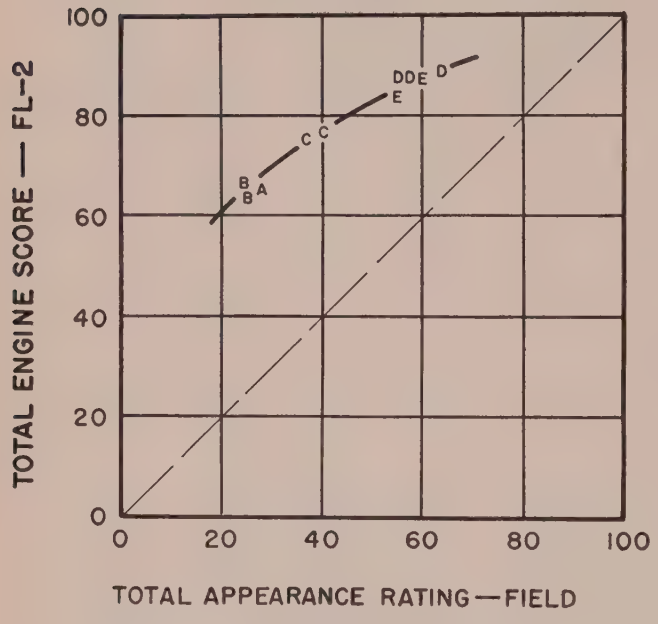

Fig. 37 – FL-2 versus field test total engine ratings

varnish deposits than sludge deposits in the FL-2 Test, while the converse was generally found in the field.

3. Many claim that lubricating oil additives which showed improvement in field service did not show similar improvement in the FL-2 Test.

However, since the FL-2 Test probably has been used more widely than any other single procedure to attempt to evaluate low-temperature performance of crankcase oils, duplicate tests were run on each of the 10 oils evaluated in the field test. A moderately dirty leaded thermal reformate was used in these FL-2 Tests.

As might be expected, differences in total varnish deposits between oils was somewhat greater in FL-2 Tests than had been found in field tests, and while the general trend was the same in both, the correlation left much to be desired. Average data for each oil are presented in Fig. 35.

Again, as expected, differences in FL-2 sludge were considerably smaller than in the field sludge. However, correlation was fairly good, as shown in Fig. 36. It is seen that with poor oils FL-2 engines were not nearly as dirty as field engines.

When varnish and sludge ratings are added together for a total rating, we get a very consistant relationship between FL-2 and field tests, although the FL-2 Test was less sensitive than field engines (see Fig. 37).

It has generally been recognized that piston deposits in the FL-2 Test are most sensitive to variations in fuel or oil. Fig. 38 shows that for these oils in this service, FL-2 piston varnish gives a good measure of general engine cleanliness.

There is undoubtedly a strong feeling among many people against adding varnish and sludge ratings together as was done in Fig. 37, and again comparing varnish ratings in one engine to sludge in another engine as in Fig. 38, but the fact remains that a good correlation is indicated.

Correlation of EX-3 Type Test Results

In 1948 the CLR Division of CRC authorized setting up a new group known as "Engine Deposits and Wear Group." The objective was to develop lab-

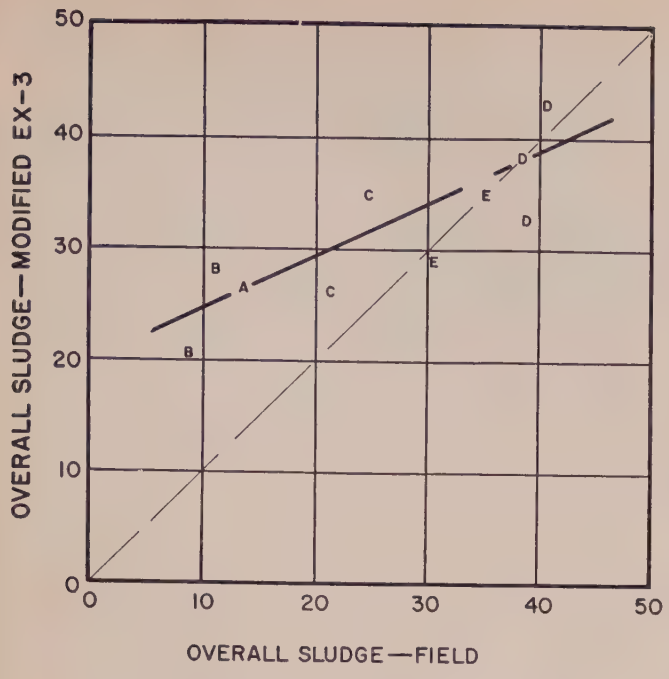

Fig. 39 – Modified EX-3 versus field test sludge ratings

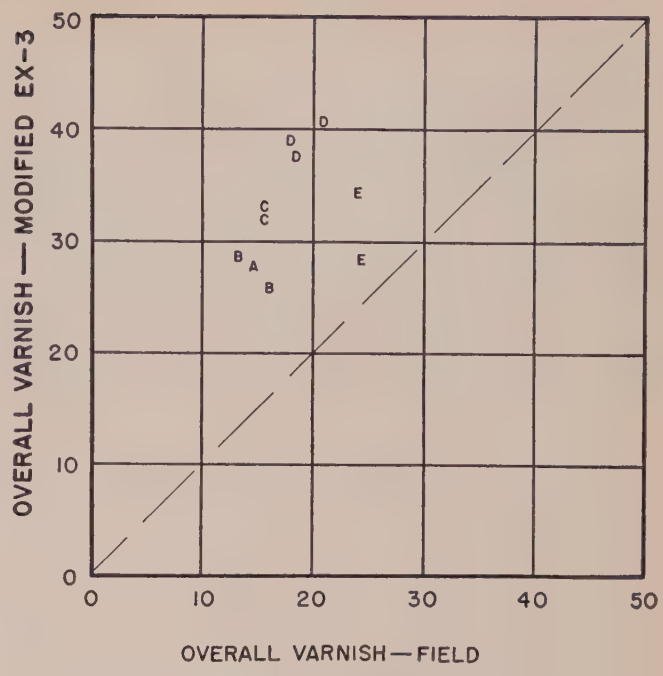

Fig. 40 – Modified EX-3 versus field test varnish ratings

oratory engine tests which reproduce deposits and wear typical of field service, with specific emphasis on cold sludge type engine deposits, piston-ring plugging, inlet oil screen plugging, and piston-ring and liner wear.

This group has evolved several tentative procedures, the latest of which is known as EX-3. The test consists of running a multicylinder laboratory engine for 96 hr under cyclic operation. Sludge and varnish deposits are formed which are similar in appearance to those found in stop-and-go field service. Further work is being done to improve the test in general.

The 10 oils in this 50,000-mile field test have been evaluated in duplicate in a modified form of the EX-3 Test. Commercial gasoline similar to that used in the field test was used in the laboratory tests. Results in Fig. 39 indicate that this test is more sensitive to sludge formation than the FL-2 Test. Although the spread was not as great as that found in the field, a reasonably good correlation is shown.

Varnish ratings from the laboratory have been compared to the field ratings in Fig. 40. It can be seen that very little correlation exists. However, correlation does exist between modified EX-3 and FL-2 varnish as shown in Fig. 41 and indicates that while neither test correlates with the field in this respect, both laboratory procedures have the same deficiency.

Again, liberties have been taken with the data in adding varnish and sludge ratings together for a total appearance rating shown in Fig. 42. With the exception of oil E, a reasonable correlation exists.

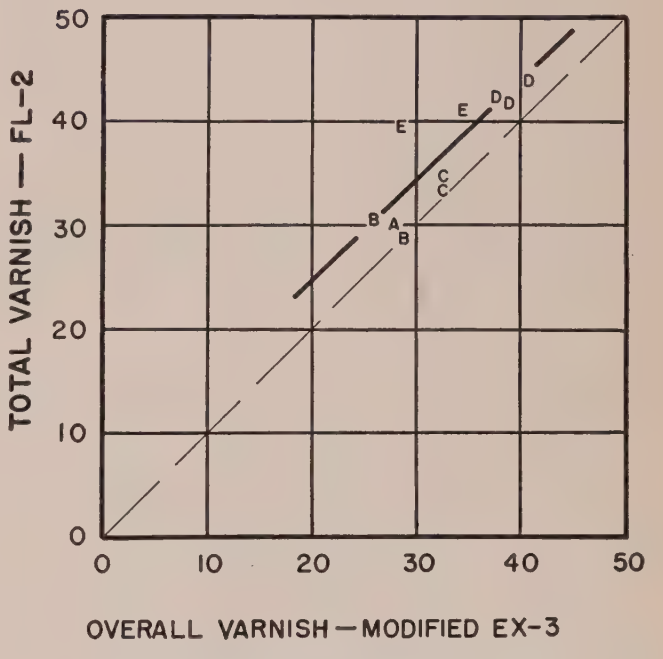

Fig. 41 – Modified EX-3 versus FL-2 varnish ratings

Fig. 43 shows there is a semblance of correlation on oil screen ratings, although the modified EX-3 test is relatively insensitive in this respect.

Summary and Conclusions

The performance of 10 oils containing a variety of additive types and concentrations in the same base oil in 30 taxicabs driven 50,000 miles each has

been presented. The following conclusions may be drawn:

1. The three engines on each oil were remarkably similar in appearance.

2. Oils varied widely in their ability to prevent sludging under severe low-duty operation. Service classification ML and MM oils gave extremely dirty engines. MS-DG oils gave only small improvement. DS oils gave moderately clean engines in this service. "MS-LD" oils gave superior cleanliness.

3. Differences in field varnish ratings were small, but generally higher additive concentrations gave somewhat less deposits.

4. Oil-ring plugging was generally erratic, and variation between oil types was not as great as might have been expected. The most consistent group performance with least plugging was found with "MS-LD" oils.

5. Large differences were found in performance of several oil types with regard to oil screen plugging. "MS-LD" and DS oils were markedly superior in this respect to the ML, MM, and MS-DG oils.

6. Valve train wear in the field as observed in valve lifter pitting and cam lobe wear was consistently low with "MS-LD" oils D_1 and D_3 in engines equipped with mechanical lifters. In engines equipped with hydraulic valve lifters, all additive combinations except those in oils B_2 (MM), C_1 (MS-DG), and D_2 ("MS-LD") gave good performance with respect to valve lifter pitting and corresponding cam lobe wear.

7. Unexpected differences were found between engines equipped with hydraulic valve lifters and those equipped with mechanical lifters with respect to several performance criteria as follows:

a. In general, engines equipped with hydraulic valve lifters had considerably less lifter pitting and cam lobe wear than those with mechanical lifters.

b. With 8 of 10 oils, the heaviest intake valve tulip deposits occurred in engines equipped with hydraulic lifters.

c. With 9 of 10 oils best gasoline mileage was obtained with cabs equipped with hydraulic lifters.

d. Oil consumption was lowest with the hydraulic lifter-equipped engine with 9 of 10 oils.

e. In 8 of 10 cases the highest used oil viscosities, as drained, were found with oils from hydraulic valve lifter engines.

8. The differences between oils with regard to cylinder bore wear were surprisingly small. With the exception of oil B (MM), the same is true with regard to piston-ring wear.

These same 10 oils have also been evaluated in duplicate FL-2 and modified EX-3 Tests.

Good correlation existed between FL-2 Tests and the field with regard to sludge, total appearance rating, and FL-2 piston varnish versus field sludge.

Good correlation existed in the modified EX-3 Test in regard to engine sludging, total appearance rating, and fair correlation on oil screen plugging.

The modified EX-3 Test was more sensitive to oil sludging differences as measured in the field than the FL-2 Test.

It was found both helpful and necessary to modify the API Service Classifications as popularly used in order to differentiate between MS-DG and "MS-LD" oils.

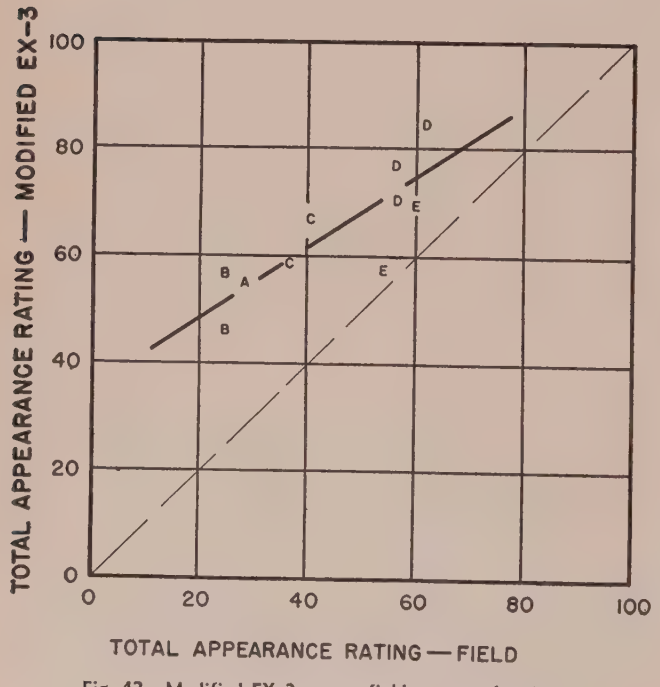

Fig. 42 – Modified EX-3 versus field test total ratings

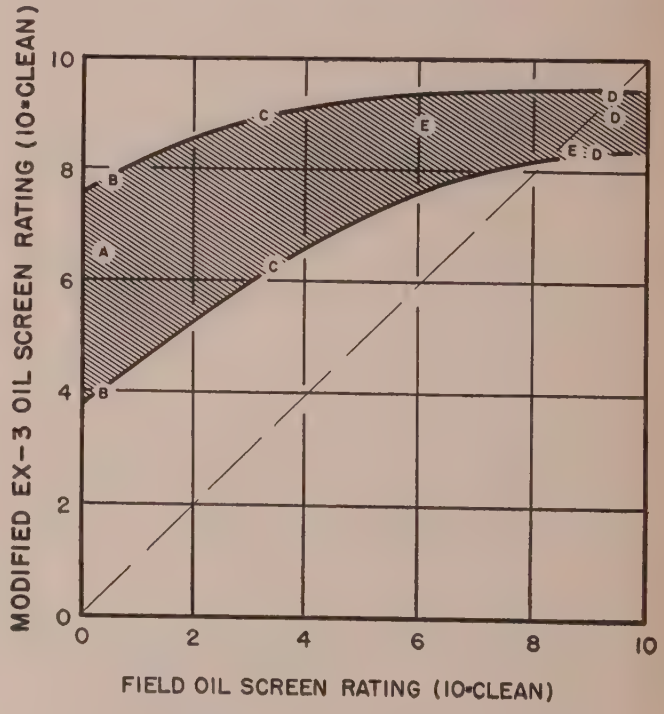

Fig. 43 – Modified EX-3 versus field test oil screen ratings

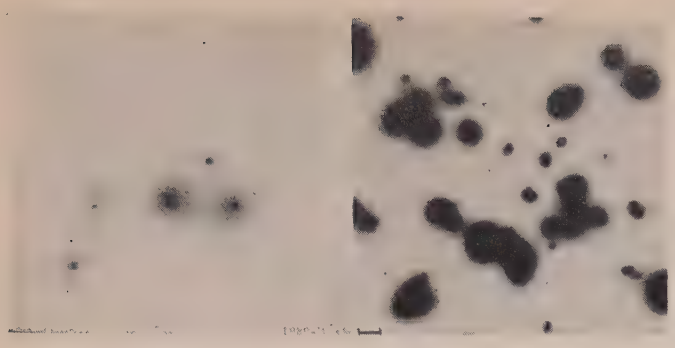

Fig. A – Used oil A – API classification ML – left: supernatant; right: mixed

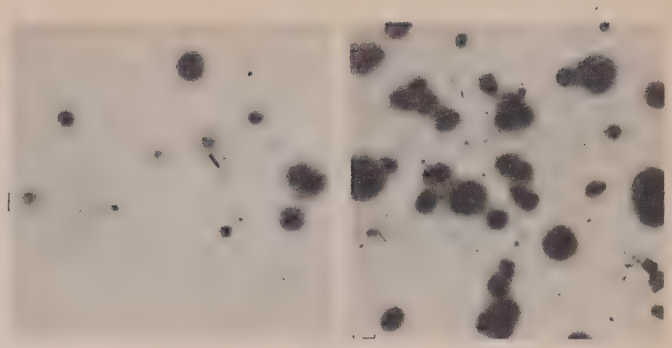

Fig. B – Used oil B_2 – API classification MM – left: supernatant; right: mixed

DISCUSSION

Study of Lube Oil Detergency By Electron Microscopy

– W. L. Grube, S. R. Rouze, and F. A. Forster
General Motors Corp.

THE authors have demonstrated quite conclusively by their work that an engine exhibits a remarkable sensitivity to detergency level in the lubricating oil it uses. This sensitivity manifests itself in many ways, as the authors have shown, but the amount of sludge deposited upon various interior engine surfaces appears to be the most significant measure of detergency level. Since detergent oils are effective in preventing sludge deposition, it follows that sludge particles must remain suspended in the oil. If this is so, then electron microscope examination of particles suspended in used oil should provide a measure of the oil's effectiveness in preventing sludge deposits. It has been demonstrated previously[a] that this can be done under certain conditions, and we have undertaken to examine oils that have been so thoroughly investigated by the authors to determine whether or not appearance under the electron microscope can be correlated with engine performance on a 50,000-mile low-duty test.

Samples of all oils examined were drawn at the end of a 4500-mile oil drain period in the neighborhood of 30,000 total miles.

Two types of specimen of each used oil were examined. One specimen was drawn from the whole used oil after thorough mixing. This specimen represents the condition of the oil as it is drained from the crankcase. Another specimen was withdrawn from the top of the oil sample after it had been allowed to stand undisturbed for several days. This specimen from the supernatant liquid provides an estimate of the oil's effectiveness in keeping solids suspended upon standing. It is pointed out that both types of specimens must be examined in order to evaluate oils under the electron microscope. This is necessary because the relative amount of solid material found in the supernatant liquid, with respect to the mixed oil, is one of the factors considered in the evaluation.

[a] See footnote 3 of main paper.

Specimens for electron microscope examination were prepared by the "printing" method. In this method, a thin film of the oil is spread on a clean microscope glass. A portion (the top layers) of this film is then transferred to a plastic film floating on water. The plastic film containing the thin deposit of oil is then picked up on an electron microscope specimen screen in the customary manner and placed in the electron microscope for examination. Magnifications of the order of 5000-10,000 diameters are used to examine and evaluate the oils. The list of oils examined is the same as that given as Table 1 in the authors' paper. All 10 oils were examined under the electron microscope without knowing the exact identity of any of them, so that electron microscopic examination was completely unbiased.

Fig. A illustrates the type electron micrograph obtained from examination of a nondetergent oil. Shown in this figure are micrographs of the supernatant liquid and the whole, mixed base oil (without additives), investigated by the authors. First, note that there is considerably more solid material present in the mixed oil than there is in the supernatant liquid, indicating that this oil is unable to keep solid material suspended. Furthermore, solid particles present in the mixed oil are aggregated in dense clumps and may be expected to precipitate and create sludge deposits on the interior engine surfaces. The mark in the lower portion of the micrograph is one micron in length, and indicates the magnification of the illustration.

Fig. B shows electron micrographs of an MM service classification oil, B_2, investigated in the taxicab test. These micrographs indicate that this is a nondetergent oil since solids present exhibit a tendency to aggregate into dense masses. In addition, relatively little solid material appears in the micrograph of the supernatant liquid – another characteristic of a nondetergent oil.

Fig. C shows micrographs of the supernatant liquid and mixed specimen of an MS-DG oil, C_1. Appearance of this oil under the electron microscope indicates the presence of a detergent, although the actual amount remaining after 4500 miles of use may be small. Solids in the mixed sample are not as densely aggregated as they were in the nondetergent oil and more solid material appears in the micrograph of the supernatant liquid.

Essentially the same results are obtained with the other MS-DG oil tested by the authors (C_2). Micrographs of this oil are shown in Fig. D. Dense masses occur in the mixed

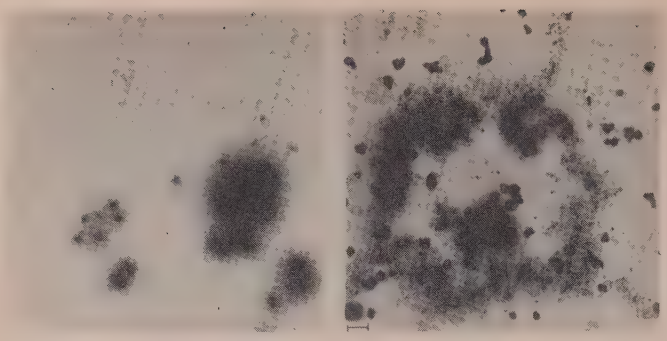

Fig. C – Used oil C_1 – API classification MS-DG – left: supernatant; right: mixed

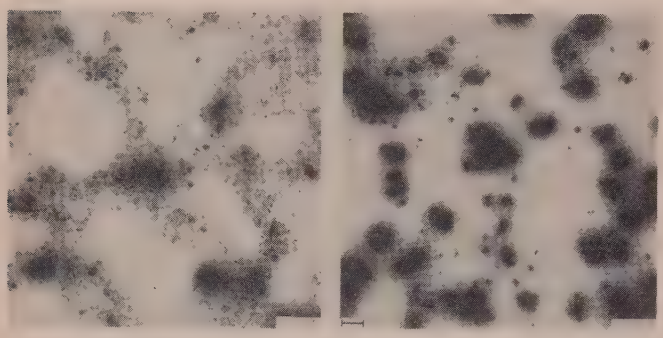

Fig. D – Used oil C_2 – API classification MS-DG – left: supernatant; right: mixed

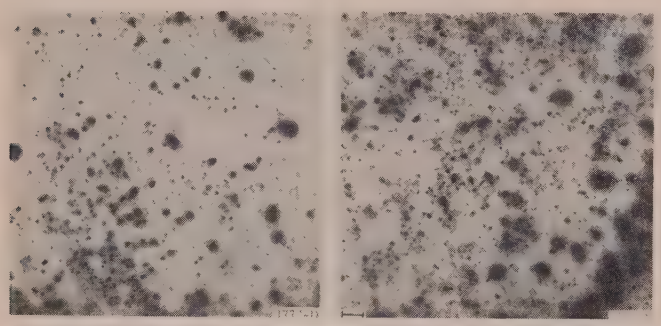

Fig. E - Used oil D_3 – API classification "MS-LD" – left: supernatant; right: mixed

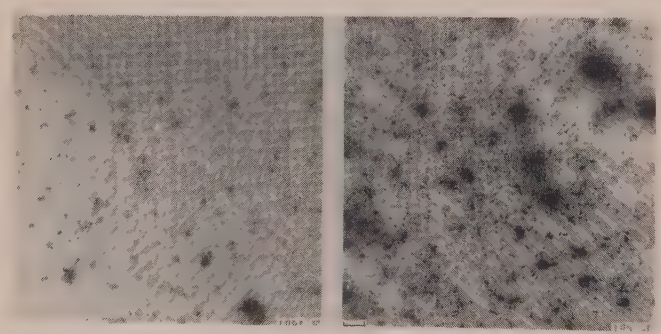

Fig. F – Used oil D_1 – API classification "MS-LD" – left: supernatant; right: mixed

specimen of this oil, but close examination reveals that they are more loosely aggregated than those in a nondetergent oil. Also, as shown in the supernatant liquid micrograph, a large amount of solid material is held in suspension in this oil. If it were necessary to choose the better oil of the two MS-DG grades (C_1 and C_2), on the basis of their appearance under the electron microscope, C_2 would be chosen. It is interesting to note that on the basis of field test sludge ratings discussed by the authors, the engine is of the same opinion.

Continuing to the series of MS-LD oils tested, Fig. E shows micrographs of oil D_3. These micrographs show that solid material is exceptionally well-dispersed and that a large amount of finely divided solid particles remain in suspension in the upper portion of the sample upon standing. In fact, the differential between the amount of solid material suspended in these two specimens is very small. On the basis of these micrographs it would be expected that very little sludge will appear in an engine using this oil. Results discussed by the authors show this to be the case. In field sludge ratings this oil, D_3, scored an average of 42 out of a possible 50 – the highest rating of any of the oils tested.

Micrographs of another MS-LD oil, D_1, are shown in Fig. F. Again, this oil exhibits exceptional dispersing ability. Even though a large amount of solid material is present in the mixed used oil, it remains well-dispersed, and the differential between the amount of solids in the mixed oil and that in the supernatant liquid is relatively small when compared with nondetergent oils.

The DS oils tested were also examined and micrographs of one of them, E_1, are shown in Fig. G. These micrographs are characteristic of a detergent oil, but on the basis of the appearance exhibited these oils do not rate significantly better than the MS-DG oils. Reference to the author's paper shows that the engine rates DS oils better than MS-DG oils, but still poorer than MS-LD oils.

Fig. H shows a comparison between electron micrographs of three of the oils tested. Represented in this figure are

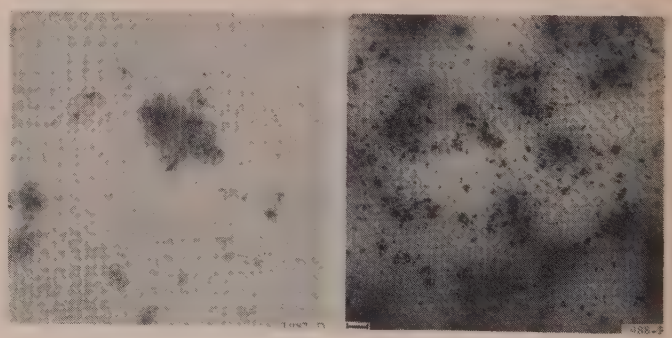

Fig. G – Used oil E_1 – API classification DS – left: supernatant; right: mixed

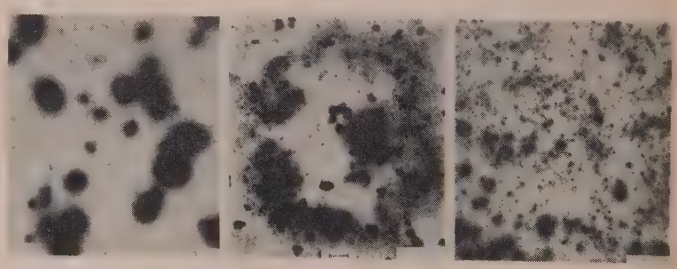

Fig. H – Used oils (whole oil) – left: oil A – API classification ML; center: oil C_1 – API classification MS-DG; right: oil D_3 – API classification "MS-LD"

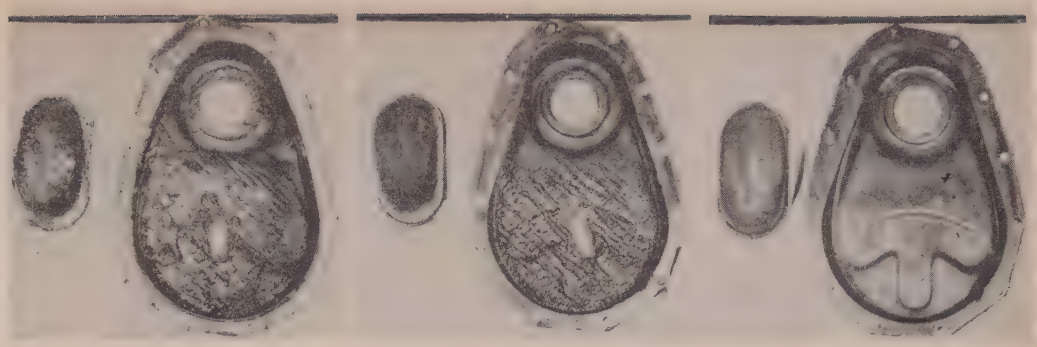

Fig. I – Oil screens and timing gear covers from 50,000-mile taxicab service test (4500-mile drain period) – left: Oil A – API classification ML; center: oil C_1 – API classification MS-DG; right: oil D_3 – API classification "MS-LD"

the base oil (ML classification), an MS-DG level oil, and an MS-LD oil that contains a polymeric dispersant. On the basis of these micrographs it could be predicted that engine cleanliness in a performance test of these oils will vary in direct proportion with detergency level. Fig. I shows timing gear covers and oil screens from engines using the three oils shown in Fig. H, and it can be seen that there is good correlation between appearance under the electron microscope and the amount of sludge deposited upon these parts during the low-duty performance test.

Thus, it appears that detergent oil performance, from the standpoint of its ability to prevent sludge deposits on low-duty service, can be predicted by electron microscopic examination of an oil sample after 4500 miles of operation. It remains to be shown whether or not this can be done with fewer miles of operation, and also whether or not it can be done during the **first** 4500 miles with a new engine.

Type of Field Test Important In Devising Laboratory Test

– L. A. McReynolds
Phillips Petroleum Co.

RESULTS of work discussed in this paper indicate that an unusually well controlled field test program has been conducted. Particularly interesting is the extremely good agreement in deposit ratings among three different cars operated on each test oil. The excellent reproducibility obtained is positive indication that careful attention was given to minimizing the many variables which can influence test results.

For several years I have been serving as leader of a Program and Analysis Panel of a group of the Coordinating Lubricants Research Committee working on engine varnish and sludge. Information presented in the paper was of particular interest, since it will provide additional data for the group to consider. Interest and support for this work have come from the automotive, petroleum, and military people. The objective of the project has been to develop know-how to permit one to obtain, in laboratory engine tests, the type deposits encountered in various type engines in actual field service. Principal attention has been focused on the problem of deposits as they accumulate under stop-and-go, moderate-temperature operating conditions. Generally, it has been found that operating conditions, engine type, and fuels and lubricants all play a very significant part in type and amount of engine crankcase deposits formed. The group has developed one engine test technique. While results obtained using this technique have been helpful in defining certain problems involved, the group feels that the technique must be improved further to more clearly differentiate between various levels of crankcase deposits obtained as a function of fuels, lubricants, and operating conditions.

The significance of any laboratory technique can best be tested by comparing results against actual field tests. However, one must regard with caution the field tests against which such comparisons are to be made. Two different field operations designed to test sludging characteristics of oils, for example, might be different from the standpoint of such important variables as type engine, mechanical condition of engines, type fuel used, or other variables that could significantly affect results. It is for this reason that the CLR group working on the problem is reluctant to accept as reference oils for laboratory work products tested in only one field operation. Reference oils are desired which have been tested in at least two different field operations.

The authors have pointed out that engine sludging is an old problem and have referred in particular to those areas of the country where low-temperature, high humidity conditions result in a situation that causes formation of engine sludge. I agree with the authors' viewpoints, but would like to add that sludge can certainly be a problem even in areas of low humidity, due partially to condensation of water resulting from the combustion of fuel. Part of such condensed water, along with other combustion products, can escape past the ring area into the crankcase, where they all can add to the likelihood of sludge formation. It appears to me that this is an important point to keep in mind, since current engine design is in the direction of larger, more powerful engines, with a chance for more combustion product debris to escape to the crankcase, where oil capacity is not being increased. It can be concluded that the potential problem of engine sludge appears to be increasing. The paper just presented is important in that it increases our knowledge of this problem.

MS-LD Oils Prove Economical

– Glenn Shaw
Yellow Cab Co.

IN discussing a paper by Round and Mount,[b] D. K. Wilson of New York Power & Light Corp. said, "One of our major problems is that of low-temperature operation . . . we would like to suggest that, some day, a paper on 'What the Fleet Owner Should Know about Fuels and Lubricants under Low-Temperature Conditions' would be of wide interest." Provided we interpret "low-temperature conditions" as meaning low engine operating temperatures due to light-duty operation, I believe the paper just presented does an excellent job of fulfilling Mr. Wilson's request as far as motor oils are concerned.

As taxicab operators, we, along with probably most other

[b] See SAE *Quarterly* Transactions, Vol. 5, April, 1951, pp. 236-258: "What the Fleet Operator Should Know about Fuels and Lubricants," by G. A. Round and W. S. Mount.

operators of light-duty fleets, have had the engine sludge problem as a constant thorn in our side. For many years, we used nothing but straight mineral oil on the basis of price. Our first change from this policy came about in 1946 when we tried using oil meeting the old 2-104B classification. This oil increased engine life to about 60,000 miles from the 30,000-mile life we had encountered previously. While this switch helped reduce ring and bore wear, it did not help the sludge problem to a great extent. It was still necessary periodically to drop the oil pans and clean out sludge and oil lines.

We next changed to an oil of the Mil-L-2104 type which would fall into the present API MS-DG classification. With this oil we were again able to increase engine life from a bore wear standpoint to about 90,000 miles. While we did notice a small decrease in sludge formation, it was far from that which we had hoped for. It was still necessary to drop the pan every six months to clean sludge from the oil screen and oil lines on our overhead valve engines.

In early 1955, we changed to an oil falling into the service designation described in the paper as MS-LD. While insufficient time has elapsed since we started using this oil to get any engine life figures for it, we have noted several things upon which I would like to comment. In spite of increased oil price, we have realized considerable cost savings to date using this oil, both from a consumption and a maintenance standpoint. Indications to date are that our sludge problem has been eliminated, relieving us of periodically dropping the pan and cleaning oil lines. With all previous oils used we had a considerable expense replacing badly worn rocker arms and shafts on overhead valve engines due to lack of lubrication when oil lines plugged up with sludge. This expense has been eliminated. While most of our operation does not use oil filters, the one fleet which does, normally changed filters at 4,000 to 5,000 miles. The "MS-LD" oil has increased oil filter life to 20,000-25,000 miles.

In closing, let me say that over the years we have run a test similar to the one described in the paper. In general, I believe our results agree with those just presented. "MS-LD" oil has brought us closer to our ultimate objective than we have ever been before; namely, to keep cabs on the road in good operating condition, with minimum down time in the shop, and at the lowest cost.

MS-LD Oils Have Outstanding Sludge Rating

– W. Schreiber
Atlantic Refining Co.

SOME of the results in this paper appear most interesting in the light of our own experience.

On the basis of overall sludge rating there is a definite advantage for increasing the detergent or dispersant power of oils. Oils designated as MS-LD appear outstanding in this respect.

On oil-ring plugging the spread between various oils was not as great as might have been expected. The author explains this on the basis of engine design, and this seems logical. I would like to add another possible explanation. Our test work has demonstrated that you must have a certain amount of hot as well as cold operation in order to obtain appreciable plugging. The laboratory engine tests such as the EX-3 procedure, for example, are based on this concept. Perhaps under the test conditions described in the paper there was not enough hot operation to give the expected degree of plugging with low detergency oils.

On piston ring and cylinder wear the differences between oils were not too great. One of the factors in reducing this kind of wear is oil alkalinity. We know that this is gradually depleted in service, so that on a 4500-mile oil change basis the benefits from alkalinity are greatly reduced. Also, with this infrequent change practice and no oil filters, abrasive wear becomes a major factor. According to our data abrasive wear is not affected by oil composition. In a recent road test where we changed both oil and oil filter every 5,000 miles, it was found that abrasive wear comprised about 50% of the total. With oil filters out of the system this figure would have been much higher, perhaps 80% of the total.

[c] See SAE Transactions, Vol. 61, 1953, pp. 154-164: "Can All Engine Wear Be Trapped in a Can?" by R. J. Pocock.

Alleviate Sludging By Engine Design

– C. H. Ruth, Jr.
Evening-Star-Sunday-Star, Washington, D. C.

THIS paper serves to accentuate continuing efforts made by petroleum refiners to meet the increasing problem of sludge formation in engines used in "city service," where the general nature of the operation could be termed "stop-and-go" driving. My own experience confirms in general the findings of those presenting the paper, though my experience has not covered the difference between hydraulic and mechanical lifters and valve tulip deposits.

As I read this paper, I could not help but recall a paper by Robert J. Pocock of Ford.[c] Fig. 5 of his paper indicates that the use of additive oils possibly caused more rapid wear at the lower end of the cylinder bore than did oils of the nonadditive type, because the additive oils were carrying abrasives in suspension. The SAE has spent much time and money on this subject regarding the cures. Apparently what we are after is the elimination of sludge to lengthen engine life by reducing wear. It appears to me that we accept the creation of sludge as inevitable and constantly seek new cures for the disease rather than search for a healthier environment which would either eradicate it or reduce its prevalence.

There is no lack of information as to what causes sludge, nor do I know of any studies which indicate that use of additive oils will eliminate raw gasoline and condensed water from the crankcase. Most studies reported, based on both laboratory and field tests, indicate the need for adequate ventilation at low road speeds and the desirability of reaching crankcase oil temperatures in excess of 140 F in the shortest possible time.

The operator of a city fleet of approximately 120 vehicles consisting primarily of light delivery trucks was plagued with sludge. Sludge formation was markedly reduced by:

1. Ventilation of crankcase with a small electric blower.
2. Installation of high-temperature thermostat in cooling system.
3. Installation of a ⅜-in. ID helical finned coil submerged in crankcase oil and circulation of hot cylinder-head water through the coil to the suction side of water pump.
4. Coating of crankcase pan, oil filter can, and overhead valve covers with a ground cork insulating material held by a plastic binder.

The theory behind the above was not original with the operator. He only followed the recommendations of oil refiners and studies reported in SAE publications.

Sludge is still a problem for refiners. However, it need not be if, based on remedies already well known and tested, corrective action were taken by the makers of popular small truck engines.

The SAE is a failure in this particular instance if it cannot obtain more cooperation from engine manufacturers in creating engines designed not to produce sludge. Unused knowledge is worse than no knowledge.

Learning Curve Theory as Applied to Production Costs

Robert H. Lundberg, Chance Vought Aircraft, Inc.

This paper was presented at the SAE Annual Meeting, Detroit, Jan. 12, 1956.

AIRCRAFT costs, like those of many other manufactured articles, are determined to a great degree by the magnitude of direct labor hours required to manufacture the article. Not only are direct labor costs a substantial portion of the total cost, but also they are directly responsible for incurring a major portion of overhead expense. Direct labor cost, together with the overhead expense it controls, account for the major portion of aircraft cost, and because of this, particular attention is directed to its control.

An extensive study of aircraft production in many companies throughout the country established some definite patterns for reduction of direct labor time. This study was started by T. P. Wright as early as 1922 and presented to the aircraft industry as a theory in 1936. During World War II, this theory was applied by the War Production Board as a tool to measure and compare production efficiencies of aircraft plants. This application fairly well established the "80% curve" as being average performance for the aircraft industry. In addition, this application brought to light some interesting behavior patterns of direct labor variations which are discussed here.

While learning curves have been established based on aircraft production, principles controlling them are common to any "custom-made" production, medium-quantity production, or even mass production itself. Indeed, a knowledge of factors influencing learning curves is the key to understanding production labor costs.

A series of cumulative average production labor costs of a particular product (that is, the cost found by dividing the cumulative cost of production labor by the number of units produced), plotted on linear graph paper against number of articles produced results in a curve similar to that shown in Fig. 1. This hyperbolic curve approximates a straight line when plotted on logarithmic graph paper, as shown in Fig. 2. For all practical purposes this curve is considered a straight line, (over the normal range of aircraft production quantities), and its equation is of the general form $y = bx^m$. The mathematics of this curve will be discussed later.

The most impressive features of this curve are the very high initial cost and rapid rate of reduction in the early portion, with a gradual tapering off in the latter portion until a fairly stable condition exists. A number of factors cause this behavior, and for the sake of convenience, we divide them into two groups: (1) those due to certain conditions

FOR a number of years the aircraft industry has employed a very worth-while tool in dealing with labor costs. This tool is popularly known as the "learning curve."

The learning curve traces the reduction in labor hours required for consecutive units produced. This paper discusses the various factors affecting production labor expenditure that determine the pattern of these curves, the mathematics of learning curves, and how learning curves can be used for estimating costs, forecasting labor requirements, predetermining production trends for control, and analyzing actual hour variations and trends.

While these curves are based on aircraft experience, the author believes that the factors involved, and therefore the application of the theory, might well be adapted to any type of production.

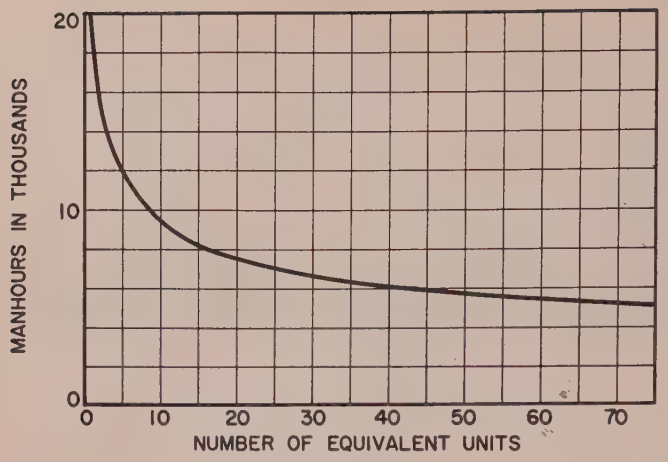

Fig. 1 – Cumulative average of cost trends in direct manufacturing labor. Typical 80% learning curve plotted on linear graph paper

that the quantity of units produced permits, and (2) those due to normal improvements made in cost performance during production of any given quantity.

By way of investigating these reasons, consider the article whose production cost performance establishes the curve. That article has designed into it a certain complexity and a number of things to be done by some combination of men, tools, and machines.

The relationship of work allocation between men, tools, and machines can vary within a wide latitude for any given quantity to be produced. Generally, increased tooling reduces man-hours of work. However, increased tooling also requires a sizeable initial cost which must be prorated over the articles produced. If only a few articles are produced, savings in labor most frequently do not offset increase in total cost.

A similar situation is involved as high-quantity production is approached and special purpose machines are considered to replace tooling and further reduce manpower requirements. Obviously, costs cannot be controlled without some degree of administration in the way of planning and scheduling. Here again, the matter of degree is important. It is possible through planning to predetermine the minimum cost for which a certain operation can be performed, and through further planning and scheduling, to assure that it will be attained. This is a very involved and expensive procedure for even the simplest part, and is economical only for very large quantities. The minimum quantity warranting such action is a function of the complexity of the article, its ultimate intended cost, and time permitted for such planning and scheduling. As quantity decreases, complexity increases, and time permitted for such planning and scheduling decreases, a more general approach is necessary. As a result, work performed by men becomes more complex and costly. Further, without rigid cost control, higher cost is certain.

In the case of small-quantity production, only a few articles bear tooling and administrative costs. To keep cost from becoming excessive, tooling and master planning must be held to a minimum. Therefore, complexity of the article must be coped with by shop labor, and a substantial portion of actual production must be accomplished by men rather than tools and machines. Further, since it is not economical to master plan and put rigid controls into effect, inefficiencies of production labor, tooling, machine use, and so on are bound to occur, thus resulting in a fairly high cost.

On the other hand, assuming the delivery schedule for the first production article permits, as the quantity of articles produced increases, more tools can be employed during production, thereby affecting a reduction in complexity of work performed, as well as reducing amount of production labor required. As more master planning is allowed, a system of controls is developed to assure more efficient use of labor, materials, machine, tools, work routing, and so on, thus affecting a further cost reduction. The approximate curve for ratio of master planning cost to average labor cost per unit follows a trend similar to that shown in Fig. 3, but of course has a lower ratio value.

As illustrated above, quantity of articles produced is one of the main factors in determining the shape of the progress curve for labor cost versus quantity by controlling the effort and means employed to reduce complexity and place the production burden on machines and tools rather than men.

It is known that cost performance can always be improved *during* production of any given quantity of articles. For a very large quantity, this improvement may be slight over the entire production run, while on a small or medium quantity, cost reduction can be very noticeable early in production, and will

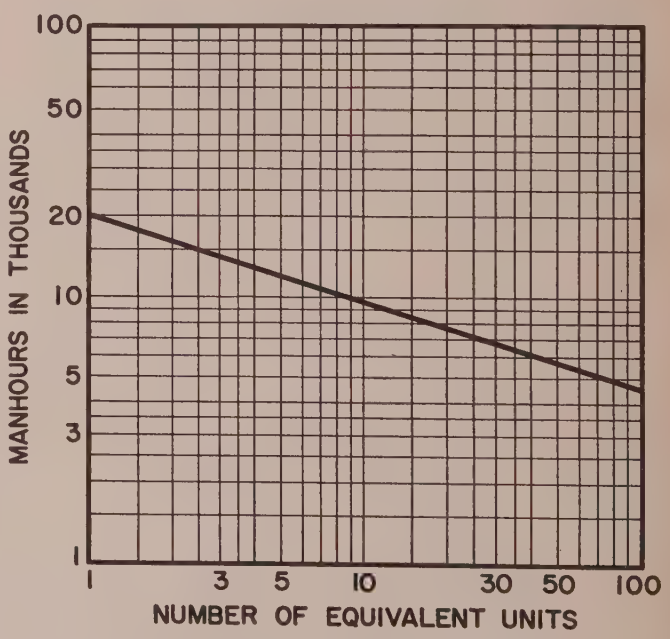

Fig. 2 – Cumulative average cost trends in direct manufacturing labor. Typical 80% learning curve plotted on logarithmic graph paper

taper off gradually until a stable cost is attained. In any case, this reduction is due to learning which takes place during production and involves improvement of job knowledge by shop personnel, improvement in manpower allocations by management, design changes, corrections of tools, improvement of shop methods, and a general adjustment which takes place throughout the organization. Thus, the amount of learning which takes place *during* production of the article also has a controlling influence on the shape of the learning curve for labor cost versus quantity.

Fig. 4 shows a series of curves approximating the effect of learning on cost of successive units for production runs of various quantities of aircraft. Because of difficulty in securing sufficient reliable cost information necessary to prove these curves, they should be considered only as showing cost trends. Curves in Fig. 4 show cost trends for individual quantities under the following conditions:

1. Production engineering and operational planning is consistent with the quantity involved.
2. Proved tooling is available, based on curve of Fig. 3.
3. Manpower and work flow is scheduled in accordance with the curve.
4. Turnover of shop personnel is stabilized so they become familiar with their work by repetition and relearning is held to a minimum.

If the above conditions are not met in small production runs, the initial cost will continue at a rate and for a time dependent on the amount of deviation. Only after corrections and adjustments are made will costs begin to be reduced according to the applicable rate. In the case of mass production, such deviation will invariably cause an appreciable increase in early costs as well. Corrections will cause cost reductions at an increased rate until the proper rate is approached and levelling off occurs. Deviation from these basic principles during intermediate production runs may cause a combination of both the above conditions and results.

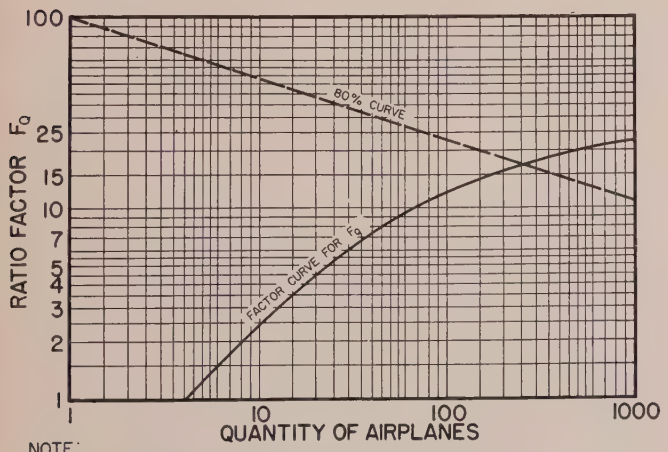

Fig. 3 – Ratio of aircraft tool labor to manufacturing labor

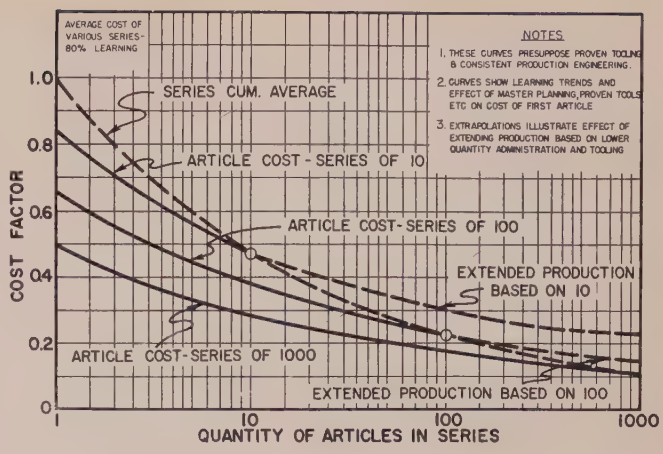

Fig. 4 – Learning curves for cost of successive articles in a series plotted on semilogarithmic graph paper

In aircraft production, time between receipt of contract and delivery of the first article generally does not permit a complete production engineering and planning treatment. Frequently, it becomes necessary to begin production with minimum tooling and to supplement this program with more production tools. The importance of meeting the delivery schedule for succeeding articles and coping with design changes makes it difficult to schedule manpower and work flow and to stabilize shop labor. As a result, learning curves showing average cost of succeeding units of a given contract do not follow the trends shown by the solid lines in Fig. 4, but approach the learning curve pattern for aircraft contracts of various quantities as shown by the dotted line in Fig. 4, which is the same curve as that in Fig. 1.

When aircraft production proceeds as described above, and the cumulative average direct manufacturing labor costs are plotted against corresponding unit numbers as in Fig. 1, a definite pattern is observed. This pattern is about the same for all aircraft, and is the basis for the theory of the 80%-learning curve, which states: "each time the quantity of planes is doubled, the cumulative average cost will be 80% of the cumulative average cost at the quantity which was doubled." Thus, if the first 10 aircraft were produced at an average cost of 10,000 man-hr, average cost for the first 20 will be 8000 man-hr each, the first 40 will average 6400 man-hr each, and so on. The curve would be expected to level off after a certain quantity. A certain amount of levelling off is embodied in the theory itself, for a 20% reduction between 500 and 1000 units is extremely small when investigated on a unit-to-unit basis. Reference to the right-hand portion of the 80% curve in Fig. 1 illustrates the tendency to level off. Similarly, for a 90% learning curve, each time the number of units is doubled, cumulative average cost becomes 90% of the cumulative average cost at the quantity which was

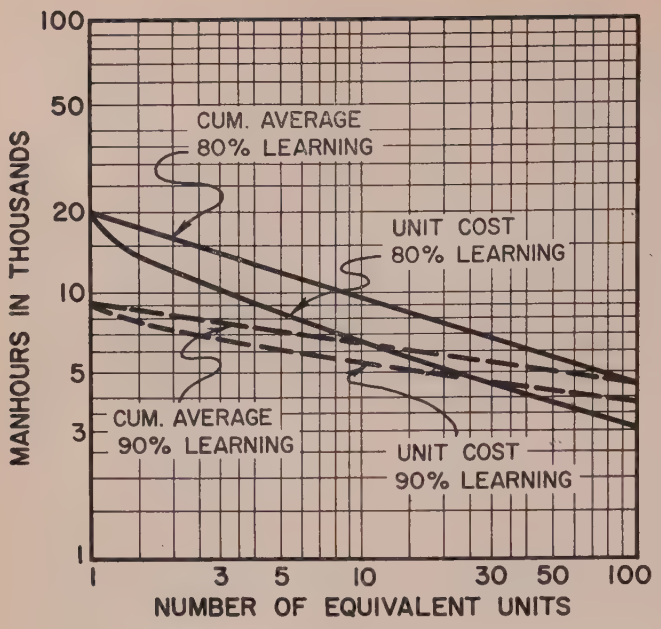

Fig. 5 – Curves of cumulative average and unit cost trends in direct manufacturing labor

doubled. Corresponding relationships exist for other percentages.

While the 80% curve is a good, practical, average learning curve for aircraft production, relative design complexity generally results in a slightly different actual performance. As might be expected, the more complex the article, the higher the initial cost and the faster the rate of reduction, since more learning is involved and there is more opportunity for tools to simplify production as the quantity permits. Conversely, the simpler the article, the lower the initial cost and the slower the rate of reduction. As an example, a fighter aircraft of given weight may require 35 man-hr per lb for the first unit, but reduce along a 76% curve. On the other hand, a simple trainer may require only 20 man-hr per lb for the first unit, but reduce along a much flatter 84% curve.

Although learning curves discussed above are set up to show cumulative average cost trends, it is possible to plot a curve of unit costs necessary to produce the particular percentage of progress expected. When plotted on logarithmic graph paper, the approximate formula for the unit cost curve plots as a straight line and is parallel to the cumulative average cost curve from the third unit on at a given distance below it, depending on the per cent reduction of the cumulative average cost. Fig. 5 shows the relationship between cumulative average cost and unit costs of an 80% and a 90% curve, resulting in the same cumulative average at the hundredth unit. Note that from the third unit on, each time the quantity is doubled, unit cost is a certain percent of unit cost at the unit which was doubled. This percent unit cost reduction is the same as the cumulative average cost percent reduction.

The following mathematical treatment of learning curves is included in this paper to provide better understanding of their behavior and to develop a background for factors and curves used in dealing with production costs.

Mathematics of Learning Curves

Before treating the mathematics of learning curves, it is necessary to review briefly some principles of graphic representation.

In any type of graphing, there is a particular relationship between distance from the origin to a point on an axis and the label, or unit value, assigned to that point. For a linear scale, as on linear graph paper, the distance and label bear a constant relationship expressable by:

$$\overline{X} = K\,x \tag{1}$$

$$\overline{Y} = K\,y \tag{2}$$

where:

$\overline{X}$ and $\overline{Y}$ = Distance
x and y = Labels
K = A constant

Obviously, when distance is doubled, value of the label is doubled. In other words, if value of the first label is \$50 at a measured distance of 2 in. from the origin, and if value of the second label is \$100, the distance from the original to the second label also will be doubled and will measure 4 in.

On a logarithmic scale, distance bears a constant relationship to the logarithm of the label. This relationship may be expressed as:

$$X = K\log_{10}x \tag{3}$$

$$\overline{Y} = K\log_{10}y \tag{4}$$

Putting equations (3) and (4) in exponential form, we have:

$$10^{\overline{X}} = x^{\overline{K}} \tag{5}$$

$$10^{\overline{Y}} = y^{\overline{K}} \tag{6}$$

From equations (5) and (6) it is apparent that values of the labels increase in powers of 10 as distances increase in units. Thus, if distance is one unit the label is \$10, when distance is two units, the label is \$100, and so on.

Remember that linear graph paper has linear scales on both vertical and horizontal axes, logarithmic graph paper has logarithmic scales on both vertical and horizontal axes, and semilogarithmic graph paper has a logarithmic scale along one axis and a linear scale along the other.

The general equation for a straight line on linear,

logarithmic, or semilogarithmic graph paper is:

$$\overline{Y} = m\,\overline{X} + \overline{B} \tag{7}$$

where:

$\overline{B}$ = Distance from origin to intercept of the line with the y axis
m = Slope of the line

A straight line on linear graph paper is of the form:

$$y = m\,x + b \tag{8}$$

A straight line on logarithmic graph paper is of the form:

$$\log_{10} y = m \log_{10} x \log_{10} b \tag{9}$$

From equations (3) and (4):

$$\overline{Y} = K \log_{10} y$$

$$\overline{X} = K \log_{10} x$$

$$\overline{B} = K \log_{10} b$$

where:

b = Label

Changing equation (9) from logarithmic to exponential form, we obtain the general form of the equation of a straight line on logarithmic graph paper:

$$y = b\,x^m \tag{10}$$

With m positive, equation (10) describes a parabola, and the straight line plotting this function on logarithmic paper has an ascending slope. With m negative, equation (10) describes a hyperbola, and the straight line plotting this function on logarithmic paper has a descending slope. The exponent m is the tangent of the angle between the straight line and the x-axis. Semilogarithmic paper is logarithmic along the y-axis, and linear along the x-axis. The straight line equation is:

$$\mathrm{Log}_{10} y = mx \log_{10} b \tag{11}$$

or, changing to exponential form:

$$y = 10^{mx} b \tag{12}$$

When the logarithmic scale is along the x-axis and the linear scale along the y-axis, the equation becomes:

$$x = 10^{my} b \tag{13}$$

Cumulative Average Cost Curves – As discussed previously, studies of aircraft production statistics lead to the theory of learning curves, which states: "Each time the quantity of planes is doubled, the cumulative average cost will be a certain percentage (generally taken to be 80%), of the cumulative average cost at the quantity which was doubled."

By assuming a value for the percentage reduction and selecting a cost for the first unit, a cost curve representing this theory may be plotted. When this curve is plotted on logarithmic paper, it is a straight line. Thus, the equation must be of the form:

$$y = b\,x^m \tag{14}$$

where:

y = Cost of airplane
x = Airplane number
b = Cost of the first airplane
m = Slope of curve on logarithmic paper

To find various values for the exponent, take equation (9) and let the y-intercept equal unity. If the intercept is one, then:

$$x = 1 \tag{15}$$

$$y = 1 \tag{16}$$

$$b = 1 \tag{17}$$

Also, when:

$$x = 2 \tag{18}$$

y = Decimal value of percentage, or $y = 0.8$ for 80% (19)

and equation (17) is still true.

By substituting equations (17), (18), and (19) in equation (9) and solving for m, we get:

$$m = 3.32 \log_{10} \left(\frac{\%}{100}\right) \tag{20}$$

From this may be calculated the various values of m. Table 1 lists these values for the most frequently used percentages and the corresponding slope angles in degrees.

Unit Cost Curves – Mention has been made regarding the unit cost trend necessary to obtain a given progress of the cumulative average cost curve. A study of this curve and its equation follows.

Consider a cumulative average curve with an 80% progress. Assume a cost of 100 man-hr at the first unit. From equation (9) can be calculated the cumulative average cost for succeeding units. Thus, average cost at unit one is 100 man-hr, at unit two, 80 man-hr, at unit three, 70.2 man-hr, and so on. Obviously, the cumulative average cost and the unit cost are the same for the first unit. Cost at any unit must equal the difference between total cost at that

Table 1 – Learning Curves – Table of Exponents, Slopes, and Factors for Cumulative Average and Unit Cost Curves

Percentage of Curve	Exponent m	Slope	Factor F	Percentage of Curve	Exponent m	Slope	Factor F
50	−1.000	45°	0.000	77	−0.376	20°42′	0.624
55	−0.851	40°30′	0.149	78	−0.358	19°48′	0.642
60	−0.737	36°0′	0.263	79	−0.340	18°54′	0.660
61	−0.713	35°6′	0.287	80	−0.322	18°0′	0.678
62	−0.689	34°12′	0.311	81	−0.304	17°6′	0.696
63	−0.666	33°18′	0.334	82	−0.286	16°12′	0.714
64	−0.643	32°24′	0.357	83	−0.269	15°18′	0.731
65	−0.621	31°30′	0.379	84	−0.251	14°24′	0.749
66	−0.599	31°30′	0.379	85	−0.234	13°30′	0.766
67	−0.577	29°42′	0.423	86	−0.217	12°36′	0.783
68	−0.556	28°48′	0.444	87	−0.201	11°42′	0.799
69	−0.535	27°54′	0.465	88	−0.184	10°48′	0.816
70	−0.514	27°0′	0.486	89	−0.168	9°54′	0.832
71	−0.494	26°6′	0.506	90	−0.152	9°0′	0.848
72	−0.474	25°12′	0.526	91	−0.136	8°6′	0.864
73	−0.454	24°18′	0.546	92	−0.120	7°12′	0.880
74	−0.434	23°24′	0.566	93	−0.105	6°18′	0.895
75	−0.415	22°30′	0.585	94	−0.089	5°24′	0.911
76	−0.395	21°36′	0.605	95	−0.074	4°30′	0.926

General Form of Equation $y = bx^m$
Slope Formula $m = 3.32 \log \%/100$
Unit Cost Factor $F = (1 + m)$

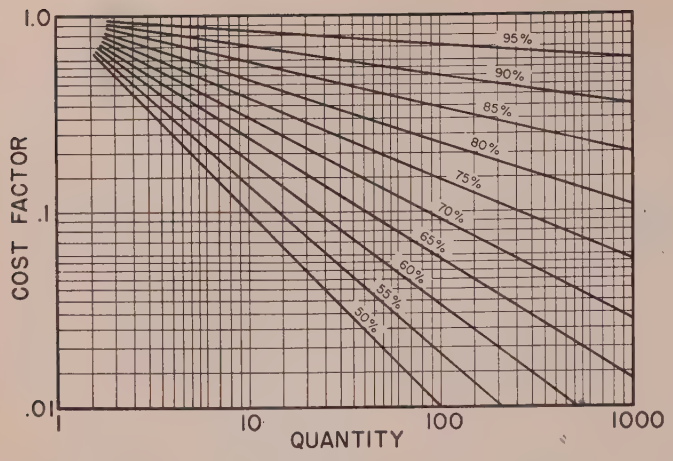

Fig. 6 – Cost factors for 50-95% learning curves in 5% increments

unit and total cost of the preceding unit. Thus, total cost at the first unit is 100 man-hr and total cost at the second unit is 2 x 80, or 160 man-hr. The difference of 60 man-hr is the cost of the second unit.

In a similar fashion unit cost at any unit number is calculated.

For ease in calculating, the development of the formula for the actual unit cost curve follows:

Let:

x = Unit number

$(x - 1)$ = Preceding unit number

y = Unit cost at x

C_1 = Total cost at x

C_2 = Total cost at $(x - 1)$

From the discussion above:

$$y = C_1 - C_2 \tag{21}$$

To put equation (21) into a more workable form, from equation (14), let:

y_1 = Cumulative cost at $x = bx^m$

y_2 = Cumulative cost at $(x - 1) = b\ (x - 1)^m$

Total cost at any unit is the product of the cumulative average cost and the cumulative unit number, so that:

$$C_1 = xy_1 \tag{22}$$

This may be expressed as:

$$C_1 = x\ b\ x^m, \text{ or}$$
$$C_1 = b\ x^{m+1} \tag{23}$$

and:

$$C_2 = (x - 1)\ y_2 \tag{24}$$

which becomes:

$$C_2 = b\ (x - 1)^{m+1} \tag{25}$$

Substituting equations (22) and (24) in equation (21):

$$y = xy_1 - (x - 1)\ y_2 \tag{26}$$

Substituting equations (23) and (25) in equation (21) we get:

$$y = b\ x^{m+1} - b\ (x - 1)^{m+1}$$

or:

$$y = b\ (x^{m+1} - (x - 1)^{m+1}) \tag{27}$$

Study of this formula discloses that it does not represent a straight line, but rather a curve with decreasing curvature approaching the x-axis asymptotically as x increases.

Equation (27) may also be written as:

$$y = bx^{m+1}\left[1 - \left(1 - \frac{1}{x}\right)^{m+1}\right] \tag{28}$$

Remembering that m is negative with a numerical value between zero and 1, we apply Cauchy's test ratio and find that the series $\left(1 - \frac{1}{x}\right)^{m+1}$ is convergent. Finding the sum of this series and substituting in equation (28), we have:

$$y = b\ x^m\ (m + 1) + R \tag{29}$$

where R becomes very small as x increases. Disregarding R, and making a substitution from equation (14), results in the approximate formula for the unit cost curve to attain a predetermined cumulative average cost progress.

$$y = (m + 1)\ b\ x^m \tag{30}$$

The form of equation (30) is changed to:

$$y = (m + 1)\ y_2 \tag{31}$$

from which unit cost at any unit can be found when the cumulative average cost is known.

Investigation of equation (30) reveals this approximate formula is correct to within 2% from unit three on. To obtain a satisfactory value for the second unit we need only to join the unit cost from equation (30) at unit three to the cumulative average cost at unit one with a straight line.

Further development of equation (29) results in deriving a more accurate formula, which applies from the first unit to any number of units. At the tenth unit this curve is accurate to within 0.03%.

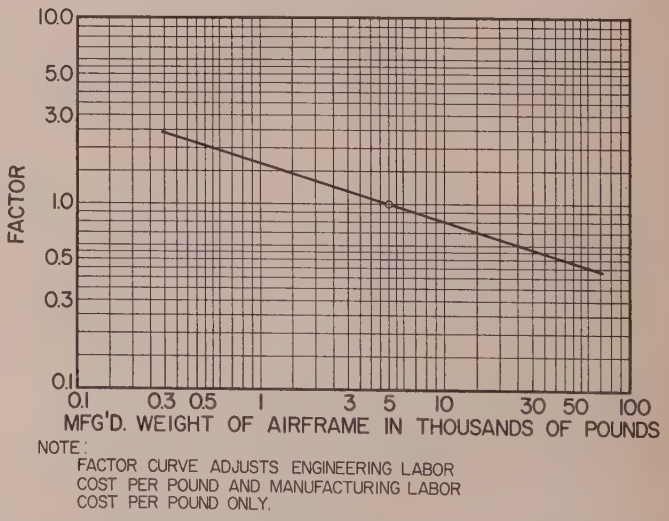

Fig. 7 – Learning curve for cost versus weight. Correction factors for change in cost per pound with change in weight adjust cost to 5000-lb base manufactured weight

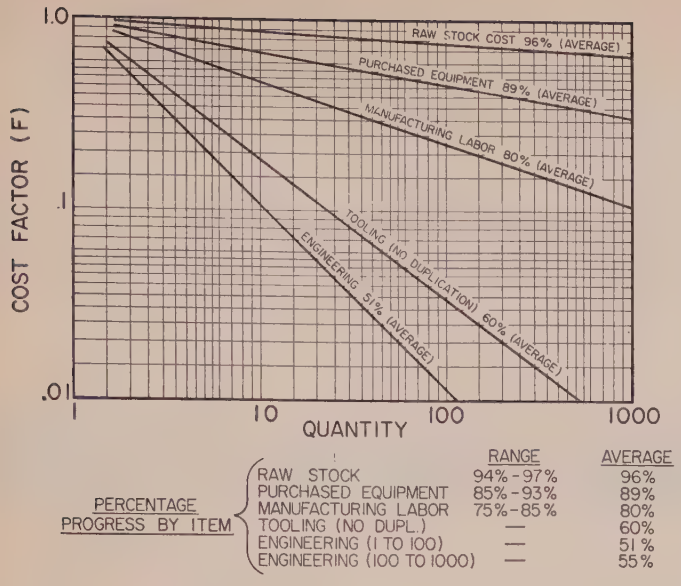

PERCENTAGE PROGRESS BY ITEM	RANGE	AVERAGE
RAW STOCK	94%-97%	96%
PURCHASED EQUIPMENT	85%-93%	89%
MANUFACTURING LABOR	75%-85%	80%
TOOLING (NO DUPL.)	—	60%
ENGINEERING (1 TO 100)	—	51%
ENGINEERING (100 TO 1000)	—	55%

Fig. 8 – Progress curves for item cost versus quantity

This second approximate formula is:

$$y = b\left(x - \frac{1}{2}\right)^m (m + 1) \tag{32}$$

Cumulative Cost Curves – As the name implies, cumulative cost curves are curves representing cumulated costs at any unit. Cumulated cost at any unit is the product of the cumulative average cost and the unit number.

Let:

x = Unit number

y = Cumulative average cost at x

y_3 = Cumulative cost at x

Then:

$$y_3 = xy \tag{33}$$

Substituting from equation (14):

$$y_3 = x\, b\, x^m$$

or:

$$y_3 = b\, x^{m+1} \tag{34}$$

This curve is a straight line of ascending slope passing through $y = b$.

Fig. 6 contains learning curves based on Table 1 for quickly obtaining adjustment factors and trends of these curves in 5% increments. Also listed on Fig. 6 are percentages for learning curves for raw stock, purchased equipment, and tooling and engineering costs, as well as aircraft production labor. These curves were established when it was discovered that they plotted as hyperbolas on linear graph paper.

Another interesting use for learning curves is shown in Fig. 7. It has been recognized for some time that per pound costs of aircraft are affected by size, measured as manufactured weight of the airplane. Some of the more important reasons for this variation are:

1. Number of parts does not increase in proportion to weight increase.

2. There are less parts of minimum size and gage in a larger airplane.

3. A large airplane has a greater spread of such items as crew, electronics, hydraulic systems and components, fuel systems, and other equipment.

4. A large airplane generally provides better access to parts and equipment than a smaller aircraft.

In determining the trend of these items, again a hyperbolic tendency was observed. When plotted on logarithmic graph paper it resulted in the progress curve shown on Fig. 7.

There are many other practical applications of learning curves. (See Figs. 8 and 9.) Once the trends have been established by putting historical data in the mathematical expressions above, they can be used in formula, chart, or slide rule form for estimating labor costs for submitted bids, forecasting shop labor loads, planning manpower needs, scheduling work flow, and many other purposes. Another particularly important use for the learning curve of labor costs during a given production quantity is that of a running guide to compare actual performance against estimated performance to locate and correct causes of malperformance when they occur, rather than when the production run is completed and money has been lost.

References

1. "Production Engineering in Air Industry," by A. B. Berghell. Pub. by McGraw-Hill, New York, 1944.

2. "Projecting Labor Loads in Aircraft Production" by P. B. Crouse. *Aero Digest,* Vol. 43, October, 1943, pp. 216-218, 242-243.

3. "Graphic and Mechanical Computation," by J. Lipka. Pub. by Wiley, New York, 1921.

4. "Factors Affecting Cost of Airplanes," by T. P. Wright. *Journal of Aeronautical Sciences,* Vol. 3, February, 1936, pp. 122-128.

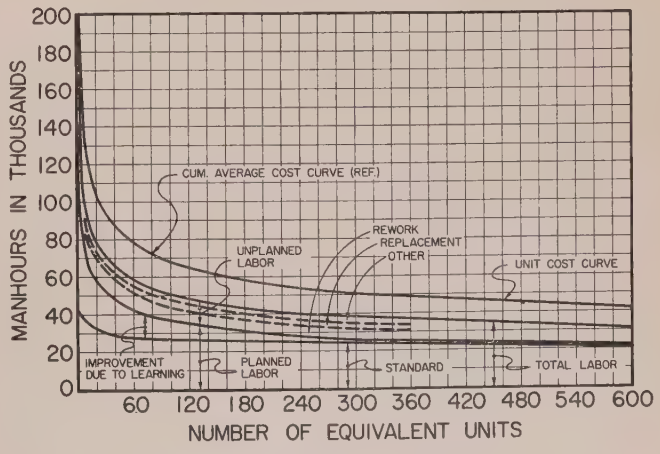

Fig. 9 – Analysis of learning as compared to standard

Mechanism of Engine Sludge

IT IS now generally recognized that sludge formed in gasoline engines *under low-temperature operating conditions* is largely associated with fuel combustion residues when high quality lubricants are employed.[1] Extensive studies by the petroleum and automotive industries have shown that (a) changes in engine design and operating conditions, (b) use of gasolines of high volatility and improved cleanliness, (c) application of oil filters, (d) utilization of motor oil detergent additives, and (e) employment of high solvency synthetic oils are successful in varying degrees in reducing gasoline engine sludge deposits. For example, operating at theoretical air/fuel ratios rather than above or below this level and increasing jacket, crankcase, and intake mixture temperatures were found to be effective in reducing sludge deposits. Mechanical improvements such as piston-ring design and crankcase ventilation were also found beneficial. Fuel quality was found highly important. Volatile gasolines were substantially less prone to sludge formation. Certain reactive components found in cracked naphthas appeared to promote sludge formation, particularly those in the high boiling gasoline fractions. Fortunately, these components could be either removed or modified by conventional treating methods. Improvement through use of more viscous crankcase oils, motor oil additives, and synthetic oils was ascribed by previous investigators to the ability of these oils to retain a greater quantity of deposit-forming contaminants in the oil, although more viscous oils were also considered to contribute to deposit reduction through improved piston-cylinder seal.

In early work on low-temperature sludge, reactions leading to sludge formation were usually considered as taking place in the combustion chamber. Blowby products contaminating the oil were listed as water, unburned fuel, resinous materials from the oxidation and polymerization of certain high boiling fuel fractions, fuel soot, and lead residues. Water and oil containing these contaminants were thought to emulsify to form a mayonnaise-like sludge which rapidly dropped out of the oil and deposited on engine parts. These earlier conclusions were based for the most part on visual examination of engine sludge deposits and upon conventional used oil analyses.

Basic studies on the mechanism of sludge formation have been in progress at these Laboratories for a number of years. These studies were con-

[1] See SAE *Quarterly* Transactions, Vol. 2, January, 1948, pp. 132-147: "Factor Affecting Low-Temperature Engine Deposits," by E. J. Bowhay and E. F. Koenig.

Formation and Additive Action

D. T. Rogers, W. W. Rice, and F. L. Jonach,
Esso Research and Engineering Co.

This paper was presented at the SAE Golden Anniversary Fuels & Lubricants Meeting, Philadelphia, Nov. 9, 1955.

THE bulk of low-temperature gasoline engine sludge is formed from the fuel rather than the lubricant, according to tests performed by the authors. Their tests indicate that most of this sludge is formed in the crankcase lubricant from oil-soluble, low molecular weight fuel oxidation products. They report that oil-soluble, sludge-forming intermediates have been isolated from used crankcase oils.

Reduction in low-temperature engine sludge deposits by commercial "detergent - inhibitor" additive combinations is seen to be due mainly to an inhibition mechanism rather than a "detergency - dispersion" mechanism, as previously assumed.

Ability of some synthetic lubricants containing oxygen to minimize sludge deposits appears, according to the authors, to result from their ability to dissolve a substantial proportion of the sludge component which normally acts as a precipitating agent for the total sludge.

A cyclic laboratory engine test is described which produces the same type and yield of sludge deposits as obtained under very severe field conditions; namely, stop-and-go light-duty delivery trucks.

cerned primarily with determining the origin of sludge deposits; that is, to what extent reactions leading to sludge formation take place in the combustion chamber and in the crankcase lubricant and, where possible, to define chemical reactions leading to formation of these deposits. In addition, studies have been made to determine the mechanism by which motor oil additives and synthetic lubricants help maintain engine cleanliness. Results of these studies are presented in this paper.

Mechanism of Low-Temperature Sludge Formation

A. *Composition of Sludge* – Engine sludge is an extremely complex mixture. In this paper, engine sludge refers to engine deposits in the crankcase, push-rod, rocker arm, and timing gear areas. It

Table 1 – Composition of Engine Sludge
(High deposit-forming fuel, 2 cc tel; uncompounded mineral oil)

Insoluble Components, 20%			Oil
Organic		Inorganic	+
Acetone-Soluble	Acetone-Insoluble	Lead Salts	Oil –
Low molecular weight resins	High molecular weight resins	Engine metals	soluble products, 80%
Emulsifying agents	Trace carbon	Road dirt	
Precipitating agents	High molecular weight hydrocarbons	Water	

Table 2 – Composition of Low-Temperature Sludge
(Lubricant: uncompounded SAE 10 mineral oil)

	Oil- and Metal-Free Deposits	
	Acetone-Soluble	Acetone-Insoluble
% Carbon	71.3	85.0
% Hydrogen	8.0	3.0
Carbon/Hydrogen Ratio	8.9/1	28/1
% Oxygen	12.8	9.5
% Nitrogen	1.7	1.0
% Sulfur	2.4	1.5
Neutralization No.[a]	40.0	—
Saponification No.[b]	200.0	—
Molecular Weight	1500	>2000

[a] ASTM Method D-664-54.
[b] ASTM Method D-94-52T.

does not include those in the intake system, combustion chamber, and on pistons. Overall composition of a typical low-temperature sludge obtained from a light-duty truck engine is shown in Table 1. Note that sludge is an emulsion of about 20% insolubles by weight and about 80% oil. Appearance of sludge varies depending to a considerable extent upon crankcase temperatures. At very low temperatures sludge contains appreciable quantities of water, is highly emulsified, and has the consistency of mayonnaise. At higher temperatures insolubles are less highly emulsified and sludge is of the coffee-grounds type. Although the mayonnaise and coffee-grounds types of sludge appear greatly different, composition of the oil-insoluble materials in both is quite similar. Approximately 1½ lb of sludge are obtained from a relatively dirty engine.

The insoluble organic portion of the sludge, which makes up 10% by weight of the total sludge, may be separated into two fractions of different properties by extraction with acetone. The acetone-soluble fraction, which has an average molecular weight of 1000-2000, contains low molecular weight resins of the same type as found on piston skirts, valve lifter plungers, and so forth. This fraction also contains materials which appear to act as precipitating agents for the total sludge. The proportion of organic insolubles which is soluble in acetone varies with fuel composition and engine operating conditions and is altered by some motor oil additives.

The inorganic portion which is also present in about 10% concentration by weight of the total sludge is composed mainly of lead salts when leaded fuels are used. Because of high density of these materials, they do not contribute appreciably to sludge volume.

Ultimate analyses for the acetone-soluble and -insoluble fractions of the sludge are given in Table 2. Note that the insoluble fraction is more aromatic (higher C/H ratio), than the soluble fraction. Both fractions are highly oxidized and contain appreciable quantities of nitrogen and sulfur.

The method used to recover and work up engine deposits and used oil insolubles is given in Appendix I. Briefly, this consists in washing all engine parts except the intake system, combustion chamber, and pistons with heptane. Tightly adhering deposits are removed with acetone. Washings are diluted further with heptane and filtered through a sintered glass funnel. The heptane-insoluble materials obtained are referred to as "engine deposits" in this paper. Drain oil is similarly diluted with an excess of heptane and filtered. Insoluble products obtained are referred to as "drain oil insolubles" in this work. Amount of oil insolubles obtained by heptane dilution and filtration agrees closely with values obtained by isopentane dilution and centrifuging (ASTM Designation ES-42), for uncompounded oils. For some additive-containing oils, however, ES-42 values are considerably lower than those obtained by filtration.

The acetone-soluble fraction of the engine deposits and drain oil insolubles appears to be the most important component. When per cent of this fraction is low, the remainder of the insolubles is readily dispersed even by uncompounded oils. It will be shown later that amount of acetone-soluble resins produced in an engine is influenced by fuel type and engine operating conditions. Amount of these soluble resins can be reduced by use of synthetic lubricants and certain additives.

Table 3 – Low-Temperature Sludge
(High-deposit fuel: A[a]; lubricant: SAE 10 mineral oil; 6-cyl overhead valve engine; approximately 400 gal of gasoline consumed)

		Organic Insolubles		
Type of Operation	No. of Stuck Lifters/Engine	Yield, g/Gal Gasoline	% Acetone-Soluble	Oxygen, %
Passenger car	12	0.25	75	18.5
Delivery truck	0	0.28	48	13.5

[a] Four test fuels have been used in this work. Fuels A, B, and C are high deposit-forming fuels; D, a commercial gasoline. Fuel A contains thermally cracked naphtha; B and C, catalytically cracked naphtha. All fuels except C contain tel.

B. *Development of Low-Temperature Sludging Tests* –

1. Effect of engine operating variables on sludge

yield and composition: In studies of the mechanism of sludge formation and additive action, it would be extremely difficult and time consuming to carry out the work in field equipment because of the high degree of control required. It was necessary, therefore, to develop a laboratory engine test which would produce the same type and quality of deposits obtained in the field. Since previous work had indicated that low-temperature sludge formation was very severe in light-duty truck engines engaged in door-to-door delivery operation, the laboratory engine test should simulate this type of operation. Development of this test is described in the following paragraphs.

During the course of field-test evaluations of sludge and varnish-forming tendency of fuels and lubricants, it was found that deposits formed in light-duty delivery trucks differed from those produced in passenger cars engaged in urban and suburban driving. With the same fuel, lubricant, and engine, passenger car engines were more highly varnished and the tendency for hydraulic valve lifter sticking was more pronounced than in delivery trucks. Overall yield of oil-insoluble products (engine deposits + drain oil insolubles), however, was approximately the same in both cases. Analysis of these insoluble products showed that those from passenger car engines were more soluble in acetone and more highly oxidized than those from trucks. This is shown in Table 3.

Examination of operating conditions in the two field tests showed that delivery trucks spent a greater proportion of the time on idle, and that air/fuel ratios generally were lower than in passenger cars. In laboratory test engines it has also been found that by changing air/fuel ratio and proportion of time spent on idling, it is possible to produce sludge ranging in type from that found in low temperature stop-and-go delivery trucks to that obtained in passenger car engines in urban and suburban driving.

In studies on the development of laboratory engine test methods for measuring low-temperature sludge formation, the basic pattern of cyclic operation shown in Table 4 was employed. This consisted of 1½ hr of idle, 2 hr of power operation at an oil sump temperature of 175 F, and 2 hr of power operation at an oil sump temperature of 225 F.

Tests were carried out in a 6-cyl, overhead valve (216 cu in.), engine. Total test time in each case was 110 hr which, on the basis of gasoline consumption, corresponds to approximately 4000 miles of operation in light-duty delivery trucks or 6200 miles of passenger car operation in urban and suburban driving.

In this cyclic laboratory test, increasing the air/fuel ratio during idle from 9.5 to 11.0 and during load operation from 11.5 to 14.0 markedly increased the proportion of low molecular weight sludge component (acetone-soluble), but did not alter yield of total organic insoluble products. Illustrative data are given in Table 5.

With the idling period eliminated from the laboratory cycle test, yield of insolubles drops off sharply, and proportion of deposits soluble in acetone increases, indicating that deposit formation is more rapid during idling, and that the major part of acetone-insoluble deposits is formed at that time. (See Table 6.)

Similar results have been obtained with a somewhat dirtier fuel than the test fuel A.

Thus, by changing air/fuel ratios and proportion of time spent idling in the cyclic laboratory engine test, it is possible to simulate deposits produced under a wide range of field conditions.

2. Comparison of laboratory and field tests: As shown in Tables 3 and 4, the laboratory engine test with the idling cycle and lower air/fuel ratios gave the same yield and type oil-insoluble organic products as obtained in the delivery truck engines with test fuel A. Similar results have been obtained with three other test fuels. Elemental analysis of organic oil-insolubles as well as average yields for the four

Table 4 – Cycle Test Conditions

	Step 1	Step 2	Step 3
Rpm	500	2000	2000
Jacket Temperature, F	115	160	160
Oil Sump Temperature, F	115	175	225
Hp	0	40	40
Hr	1½	2	2

Table 5 – Effect of Air/Fuel Ratio on Deposits Formation
(110 hr; test fuel: A; lubricant: SAE 10 mineral oil)

Air/Fuel Ratio		
Idle	9.5	11.0
Load	11.5	14.0
Total Organic Insolubles (Engine + Oil), g	104	110
% Organic Soluble in Acetone	48	75

Table 6 – Effect of Idling on Deposit Formation
(Air/fuel ratios: 9.5/1 at idle and 11.5/1 under power operation; test fuel: A)

	80 Hr Power Operation 30 Hr Idling	80 Hr Power Operation No Idling
Total Organic Insolubles (Engine + Oil), g	104	54
Acetone-Soluble (Organic), %	48	70
Yields of Organic Insolubles, g organic/gal gasoline		
Idle	1.31 (calculated)	—
Load	0.16	0.16
Overall	0.28	0.16

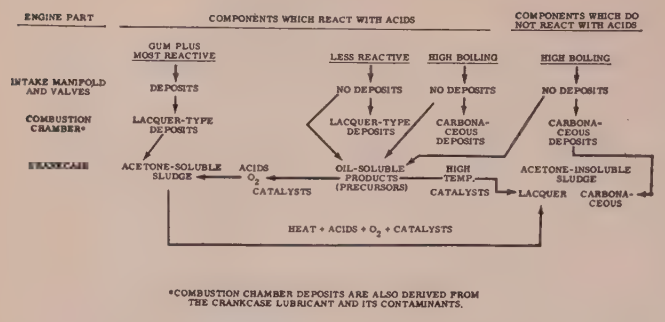

Fig. 1 – Mechanism of engine sludge formation

test fuels are given in Table 7.

Although there are some variations in the amount and composition of deposits between laboratory engine test and field test, variations are no greater than obtained among different trucks operating on the same fuel in the field test.

While engine sludge deposits from laboratory engines and field test engines had similar ultimate analyses and were obtained in the same yield, there were some differences in distribution of other deposits in the two tests. In general, laboratory engines had less oil-ring plugging than field test engines. With very dirty fuels, some compression ring sticking was obtained in the laboratory engines. Piston skirt varnish was slightly higher in the laboratory test, but in no case, even with high varnish-forming fuels, did this varnish build up to the point where it interfered with operation. Engine demerits are given in Table 8.

Ratio of drain oil insolubles to engine deposits was higher in the laboratory than in the field. This appears to be due mainly to higher dilution obtained in the field and to some extent to absence of repeated long-time shutdowns in the laboratory. In both laboratory and field test engines, there appears to be a direct relationship between quantity of drain oil insolubles and compression-ring groove deposits; the greater the amount of used oil insolubles, the greater the amount of groove deposits. This may explain heavier ring zone deposits in the laboratory test and tendency to ring sticking with dirty fuels. Oil consumption and piston-ring wear are also lower in the laboratory than in the field. Low oil consumption may be due to lack of repeated acceleration and deceleration and to lower piston-ring wear and oil ring plugging. Low piston-ring wear in the laboratory is expected since there are no repeated low temperature starts and no road dirt, and dilution is quite low.

The 110-hr laboratory engine test employing lower air/fuel ratios and idling step has been designated the ER 4-45 test. Details are given in Appendix II. Note that the pattern of cyclic operation is similar to that described in a previous paper from this Laboratory.[2]

The major portion of mechanism studies on sludge formation and additive action has been carried out using the ER 4-45 test and the 216 cu in. displacement engine. Similar tests have been carried out in more recent models of the same engine and in other makes of engines with equally satisfactory results. Related tests of the 4-45 type have been carried out using higher air/fuel ratios and less idling. Deposits obtained here represent those of passenger car operation.

C. *Origin of Sludge Deposits* – In earlier work on the mechanism of sludge formation reported in the literature, it was assumed, probably because of the black soot-like appearance of sludge, that it formed in the combustion chamber and was then blown as solids into the crankcase. In more recent work[3] the following conclusion was reached: "Tests have shown that lubricating oil is probably the medium through which deposit-causing agents from the fuel travel to form engine deposits." However, it was not shown in what form contaminants reached the crankcase.

In contrast to previous assumptions, this work indicates that the major portion of deposit-causing agents or precursors enter the crankcase lubricant as low molecular weight, volatile materials completely soluble in mineral oil. In the crankcase lubricant, favorable conditions for oxidation and polymerization reactions exist. Acids, oxygen, emulsifying agents, catalysts, and promoters such as metals and metal salts, and oxides of sulfur and nitrogen are present, with the result that oil-soluble products are converted into insoluble products.

Evidence pointing to liquid and gaseous blowby products rather than solids as the main source of sludge is as follows: Exhaust from 4-45 test engines (taken from exhaust manifold), during the power cycle contains only small amounts of solids, and liquid products are completely soluble in mineral oil. Under idling conditions, more carbonaceous material is obtained which is, however, still minor compared to the quantity of soluble products. Gases withdrawn from the combustion chamber (throughout the entire cycle), likewise contain only traces of solids. In tests on additive-containing oils, it has been found that some additives almost completely repress sludge formation during early test stages, thus indicating that no appreciable quantity of solid organic material reaches the crankcase. That increasing crankcase temperature or increasing crankcase ventilation markedly reduces sludge formation may also be taken as evidence that volatile blowby products are involved to a large extent. Further, condensable materials in blowby gases escaping from the breather pipe have been condensed and added to fresh oil, in

[2] "Low-Temperature Sludging Test," by J. G. McNab, M. E. Conn, D. S. McArthur, and K. L. Stehle. Presented at SAE Annual Meeting, Detroit, Jan. 16, 1953.

which they are completely soluble. Upon heating, deposits are formed. Steam distillate obtained from filtered crankcase drainings, when added to unused oil and heated, forms deposits. Precursors of sludge have also been isolated from filtered crankcase drainings by adsorption on silica gel. These low molecular weight, oil-soluble materials are readily converted into oil-insoluble products by heating. It has further been demonstrated that even unburned, thermally-reformed gasoline, when added to crankcase lubricant of an engine operating on very clean fuel, produces engine sludge and varnish. In the laboratory, black sludge can be produced simply by treating cracked naphthas with hydrogen chloride at room temperature.

Based on the work completed, mechanisms leading to formation of engine deposits from fuel can be postulated. An outline of the possible mechanisms involved is shown schematically in Fig. 1. As indicated, the bulk of engine sludge is derived from high boiling fractions of gasoline. Unburned gasoline and partially burned products are forced into the crankcase lubricant, where they are converted into oil-insoluble materials. When gasoline contains untreated, cracked naphthas, deposit-forming tendency is greater than for virgin naphthas of comparable boiling range. Greater deposit-forming tendency of cracked naphthas appears due to presence of materials readily converted into highly colored, oil-insoluble products by mineral acids. These reactive materials probably include phenols, conjugated diolefins, aromatic olefins, oxygen, nitrogen and sulfur compounds, and gum. The rate at which these various compounds react with mineral acids (as indicated by laboratory bench tests), apparently determines location of engine deposits. For example, the most reactive materials, which include existent gum, form deposits in the intake manifold, on intake valves, in the combustion chamber, and to some extent in upper parts of the ring zone. Less reactive components do not form deposits in the intake manifold but may form combustion chamber deposits. Components of naphtha which react with acid at a slow rate, especially those having high boiling points, may pass through the combustion chamber largely unchanged, and in the crankcase lubricant be converted principally to acetone-soluble deposits. The acetone-insoluble deposits appear to be produced mainly from naphtha components nonreactive to mineral acids. Some polynuclear hydrocarbons and soot-like materials may be formed in the combustion chamber.

Varnish deposits found on pistons and hydraulic valve lifter plungers may result from reactions occurring on these surfaces and from plating out of preformed low molecular weight resins. Insoluble lacquers found in hotter areas such as the upper ring zone may result from further polymerization of low molecular weight resins or may be formed directly from oil-soluble resins.

D. *Isolation of Sludge Precursors* – Used crankcase oils which have been diluted with heptane or pentane and carefully filtered to show no "Tyndall Effect," continue to form deposits on standing at room temperature. This suggests that oil contains products which react slowly to form insoluble products; that is, the change is chemical rather than physical in nature. These oil-soluble reactive materials can be removed by extraction with silica gel, Attapulgus clay, or alumina from heptane solution (desorption with acetone). The product obtained from silica gel is an intensely red-colored liquid completely soluble in lubricating oil. This is not derived from gasoline dye or gasoline additives. Gasolines were not dyed and infrared analyses indicate absence of gasoline inhibitors in precursors. Upon gentle heating, alone or in oil, "red oil" is rapidly converted into a brown resinous solid insoluble in oil but largely soluble in acetone. "Red oil" or resins obtained from it when heated at high temperature, are converted into a hard lacquer insoluble in organic solvents. Conversion of "red oil" into oil-insoluble products is accelerated by mineral acids. Organic peroxides and sol-

Table 7 – Yield and Composition of Sludge
(Laboratory engine test versus delivery truck fleet test[a]; lubricant: uncompounded SAE 10 mineral oil)

	Fuel A		Fuel B		Fuel C		Fuel D	
	Laboratory Test	Field Test	Laboratory Test	Field Test	Laboratory Test	Field Test	Laboratory Test	Field Test
Organic Insolubles, g	125	150	105	125	92	116	65	65
% Carbon	73.8	72.0	76.2	71.9	73.3	73.4	69.5	—
% Hydrogen	7.0	6.1	4.8	5.8	5.8	5.4	5.1	—
% Oxygen	15.6	15.5	12.0	13.5	15.4	16.1	20.2	18.3
% Nitrogen	1.4	1.5	2.3	2.7	2.7	3.0	1.6	2.2
% Sulfur	1.9	1.9	3.2	2.4	2.7	3.3	3.3	3.3

[a] Laboratory test: 110 hrs, low air/fuel ratio; field test: average of four trucks, 4000 miles of operation without oil change.

Table 8 – Comparison of Engine Condition in Laboratory and Field Tests[a]
(Lubricant: Uncompounded SAE 10 mineral oil)

	Engine Demerits[b]							
	Fuel A		Fuel B		Fuel C		Fuel D	
	Laboratory Test	Field Test	Laboratory Test	Field Test	Laboratory Test	Field Test	Laboratory Test	Field Test
Oil Ring Plugging	1.7	3.8	1.5	2.8	0.8	2.2	1.0	1.4
Ring Sticking	2.9	0.0	0.6	0.0	1.5	0.0	0.0	0.0
Piston Skirt Varnish	9.3	8.7	8.0	7.5	7.5	7.7	7.6	6.9

[a] Laboratory test: 110 hr, low air/fuel ratio; field test: average of four trucks, 4000 miles of operation without oil change.

[b] 0 = clean, 10 = maximum possible.

uble organic derivatives of metals such as iron and copper do not appear to increase tendency to form insoluble compounds. Gamma radiation has only a slight catalytic effect, which suggests that principal reactions do not involve free radical mechanisms.

Concentration of precursors in lubricating oil is roughly 5-10% when fairly high deposit-forming fuels have been employed. This is shown by extracting successively with silica gel, Attapulgus clay, and alumina (desorption with acetone in each case). These results are shown in Table 9.

Those precursors removed by chromatographic extraction probably represent the most stable or least reactive sludge precursors, the more reactive precursors having formed sludge during the course of the engine test. Concentration of precursors in used oil is higher when dirty fuels are used.

Chemically, precursors contain polynuclear aromatics, alkylaromatics, carbonyl linkages (aldehydes, ketones, and carboxylic acids), and a fair degree of unsaturation. They also contain a substantial amount of nitrogen and sulfur. Typical analytical values for silica gel extracts of ER 4-45 test oils after operation with high deposit-forming fuels are given in Table 10.

Similar precursors have been isolated from field test lubricants. This is further evidence that deposit formation in laboratory and field test engines follows the same mechanism.

E. *Role of Lubricant* – It has been quite generally accepted that high quality crankcase lubricants do not themselves contribute chemically to low-temperature sludge formation. This conclusion was reached on the basis of used oil analyses which showed that drain oils from low-temperature service contained little or no acidic materials soluble in the lubricant. In contrast, lubricants which had been subjected to high-temperature oxidizing conditions (L-4 engine tests or laboratory oxidation tests), contained relatively large quantities of high molecular weight, oil-soluble acids. This evidence, however, did not preclude the possibility that mineral acids (hydrohalogen, sulfurous, sulfuric, nitrous, and nitric), or reactive materials such as aldehydes, ketones, and fatty acids present in blowby gases from dirty fuels, could react with the lubricant to form insoluble products.

Table 9 – Isolation of Sludge Precursors from Used Engine Oil

Fraction	Appearance	Weight % of Original Oil	V.I.	Forms Deposits on Heating
Silica gel extract	Red oil	5.4[a]	−60	Yes
Attapulgus clay extract	Dark brown tar	2.4[a]	Low	Yes
Alumina extract	Yellow oil	3.5	106	No
Final filtrate	White oil	89.0	118	No
Silica gel extract of unused oil	—	4.3	27	No
Original unused oil	—	—	115	No

[a] Sludge precursors.

Table 10 – Elemental Analysis of Silica Gel Extracts of Filtered Used Oils (Straight Mineral Oils), from ER 4-45 Tests

	Fuel A	Fuel B
% Carbon	83.50	84.77
% Hydrogen	10.05	9.51
% Nitrogen	0.30	0.51
% Sulfur	3.27	3.07
% Oxygen	2.52	2.70
% Halides	0.30	0.30
Bromine No., cg Br/cc	29.4	18.7
Neutralization No.	25.9	33.0
Saponification No.	33.6	42.6
% Iron	0.007	0.004
% Lead	0.04	0.08
Iodide No., g I/100 g	63.1	77.9
Hydroxyl No., mg KOH/g acetylated sample	14.8	20.0
Molecular Weight	310	276-243
V.I.	—	−61

To determine the possibility of this latter point, two 4-45 engine tests were carried out with the same fuel but using two radically different type lubricants. In the first test, synthetic oil consisting mainly of polypropylene glycol was used; in the second test, a high quality SAE 10 straight mineral oil was used. With both lubricants, total quantity of hydrocarbon insolubles produced in the system (engine + drain oil), was essentially the same; 168 g total organic deposits for the synthetic oil, and 160 g for the mineral oil.

Thus it appears that where reasonably high quality lubricants are used, there is no material contribution to deposit formation from the lubricant itself under conditions of low-temperature service.

F. *Role of Acetone-Soluble Resins in Engine Sludge Deposit Formation* – In engines where low-temperature sludge is formed, quantity of deposits which separates out on the engine compared to amount of oil-insolubles suspended in the lubricant appears to depend on viscosity of the used oil (including dilution), and on amount and type of insoluble organic products in the system (engine + drain oil). As amount of organic insolubles increases, the proportion of insolubles, both organic and inorganic, retained by the lubricant decreases. In addition, as quantity of acetone-soluble resins increases in the system, tendency for oil-insoluble products to precipitate on engine parts increases.

Quantity of insoluble low molecular weight resins can be decreased by using a lubricant in which resins are partially soluble; as for example, a polypropylene glycol, or by using fuel with low concentration of active components. The overall result in each case is for the lubricant to retain a greater proportion of insolubles in suspension, providing a cleaner engine. These points are illustrated by the data in Table 11.

[3] "When and Why of Engine Deposits," by R. S. Spindt and C. L. Wolfe. Presented at SAE National West Coast Meeting, Seattle, Aug. 14, 1951.

[4] See U.O.P. Research and Development Laboratories Report, June 15, 1947, "Effects of Phenols in FL-2 Tests."

Table 11 – Effect of Fuel and Lubricant Type on Engine Cleanliness in ER 4-45 Tests

	Test Fuel A		Test Fuel A	Hydrofined Test Fuel A
	Mineral Oil	Synthetic Lubricant	SAE 10 Mineral Oil	
Sludge Demerit	2.0[a]	0.4	1.4[a]	0.6
Piston Skirt Varnish Demerit	10.0	7.6	9.8	6.5
Weight % Organic Materials Insoluble in Lubricant but Soluble in Acetone	43	18[b]	49	19
Weight % Total Solids Suspended in Drain Oil	53	93	64	85
Total Organic (Engine + Drain Oil), g	160	168	103	62

[a] Difference in sludge demerits due to engines of different severity level.

[b] 25% of total organic is soluble in lubricant and can be precipitated from lubricant by heptane. This fraction is soluble in acetone.

Laboratory studies indicate that acetone-soluble resins when dissolved in the synthetic lubricant also assist in dispersing the remainder of the deposits.

It is of interest that the same type and quantity sludge precursor is obtained with synthetic motor oil as with mineral oil.

G. *Chemistry of Sludge Formation* – Although the mechanics of sludge formation are fairly well understood, little is known about the chemistry of sludge formation because of the complex nature of sludge and because deposit-forming components in gasoline itself are present in small concentrations and are difficult to isolate unchanged.

Three types of compounds appear to be major contributors to engine sludge formation: (a) sulfur compounds, (b) conjugated diolefins (probably cyclic), or aromatic olefins, and (c) phenols (acid oils).

Although engine sludge from commercial cracked fuels invariably contains sulfur compounds, percentage of sulfur in engine deposits does not appear to be related to amount of sulfur in gasoline. Thus, it is possible that type of sulfur compound, or of other compounds with which sulfur-containing materials can react, is important, for example, diolefins or phenols.

Conjugated diolefins and certain aromatic olefins have been shown to increase low-temperature engine sludge formation.[3] In ER low-temperature engine tests, it has been found that dicyclopentadiene, when added to a moderately high deposit-producing gasoline, produces a marked increase in both sludge formation and piston deposits.

Phenols and related compounds (amino-phenols and aromatic diamines), have been reported by various investigators as contributing to low-temperature sludge. For example, Universal Oil Products Laboratory[4] found that addition of petroleum phenols to a thermally-cracked gasoline resulted in a tremendous increase in engine sludge deposits. When thermal gasoline alone was tested, used oil contained a very high concentration of insolubles, whereas in the test with phenols added, nearly all used oil insolubles were precipitated as engine deposits.

Reactions through which deposit precursors in gasoline are converted into oil-insoluble deposits involve principally oxidation and polymerization. These reactions in turn are facilitated by presence of acids, oxides of nitrogen and sulfur, and by some oil-insoluble materials which have not as yet been identified.

Formation of low-temperature sludge appears to involve reactions of acids. This was shown in an ER 4-45 test in which an emulsion of NaOH in an uncompounded mineral oil was used as the test lubricant (3% NaOH added as a 35% aqueous solution). Although the alkali did not reduce amount of organic insolubles in the system (engine + drain oil), approximately half the organic insolubles was water soluble. In the test with no alkali present (uncompounded mineral oil), only trace amounts of water-soluble products are obtained. When oil-insolubles from the test on mineral oil were heated with dilute NaOH, only small amounts were dissolved. Thus, it seems that the alkali prevented conversion of water-soluble products into higher molecular weight water-insoluble form. It is of interest also that a much larger amount of precursors (extraction with silica gel and clay), was obtained in the NaOH test than with straight mineral oil.

Considerable quantities of nitrogen are found in engine deposits, the major source of which appears to be from air rather than fuel. It is known that considerable quantities of nitric oxide (NO) and ammonia (NH_3) are produced in gasoline engines during combustion.[5] In one ER 4-45 test in which a careful material balance was made, 3% of the sulfur and 7% of the lead in gasoline are found in the engine system, whereas the equivalent of 38% of the nitrogen is recovered. Thus, it seems that some nitrogen in the deposits must be obtained from air as the result of reactions between NO and NH_3 and gasoline compounds. This has also been reported recently by other investigators.[6]

The role of sulfur compounds in deposit formation is not as well understood as that of nitrogen compounds. Judging from studies on diesel engines, it would seem that sulfonation and sulfation reactions are involved and that formation of sulfone and sulfoxide polymers is not precluded. Conversion of sulfur dioxide into more reactive sulfur trioxide may be promoted by oxides of nitrogen. In gasoline engines reactions of sulfur compounds appear to be modified by tel.

There are indications that sludge formation is catalyzed by oil-insoluble materials. This was

[5] See Stanford Research Institute Third Interim Report, 1950: "Smog Problem in Los Angeles County."

[6] See *Science*, Vol. 121, June 10, 1955, p. 836: "Role of Nitrogen Oxide in Formation of Engine Deposits," by R. S. Spindt, C. L. Wolfe, and D. R. Stevens.

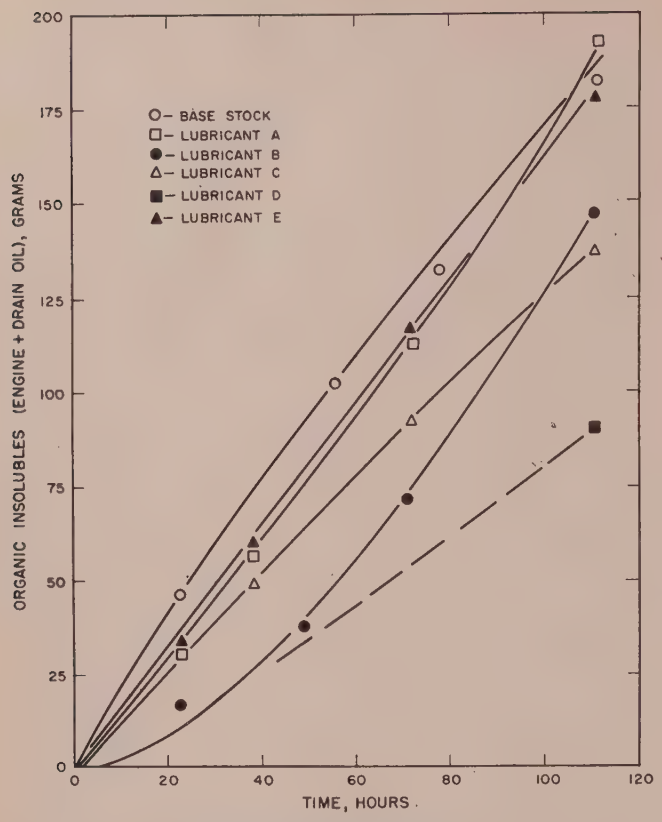

Fig. 2 – Formation of organic insolubles versus time in ER 4-45 engine tests with various lubricants

shown in ER 4-45 tests in which a full-flow type filter was employed. The cartridge was a commercial hard paper type from which sludge could be readily removed, replaced at the end of each 22 hr of operation. As shown by the data in Table 12, when the oil filter was used, only about one-third as much deposits was obtained in the system (engine + drain oil + filter), as when no filter was used.

Reduction in total deposits through use of the filter may be due to two factors: (1) removal of oil-insoluble catalysts, and (2) decreased blowby resulting from decreased piston ring wear. With decreased wear, quantity of catalytic materials such as engine metals getting in the lubricant is also decreased. In this connection it has been found that use of chrome-plated compression rings in place of unplated cast-iron rings in the 4-45 test reduces both sludge formation and compression ring wear by approximately 30%.

H. *Summary* – Based on laboratory engine tests, it appears that low-temperature sludge deposits are derived almost exclusively from fuel degradation products. These degradation products arrive in the crankcase lubricant mainly as low molecular weight oil-soluble products which then undergo further reactions and are converted into oil-insoluble form. Lubricating oil containing these insolubles, on circulating over engine parts, may deposit them as the result of physical separation and chemical reactions taking place on metal surfaces. Reactions whereby oil-soluble precursors are converted into sludge have not been defined but appear to involve acid-catalyzed oxidations and polymerizations. These reactions will be the subject of further study.

Mechanism of Motor Oil Additives Action

To determine the mechanism by which additives reduce low-temperature engine deposits, a series of five ER 4-45 tests was carried out in which two commercial detergent-inhibitor additives and two experimental additives were evaluated, using a solvent-extracted mid-continent SAE 10 oil as the base stock. The first commercial additive was used in two concentrations: to give a MIL-O-2104 type lubricant (lubricant A), and a Series 2 type lubricant (lubricant B). The second additive was used to give a MIL-O-2104 type oil (lubricant C). Both additives contained alkaline earth metals, phosphorus, and sulfur. The first experimental additive contained phosphorus and sulfur (lubricant D), and the second, oxygen and nitrogen (lubricant E). Both experimental additives did not contain metals.

Standard 110-hr 4-45 tests were conducted with the following exceptions:

1. Cast-iron rather than the chrome-plated compression rings, specified in Appendix II, were used to magnify piston-ring wear values.

2. During each test the engine was stopped three times to obtain sludge demerit ratings.

3. At each shutdown time a pint sample of crankcase oil was taken for analysis and replaced with an equivalent amount of fresh oil.

At the end of the test, engine deposits were removed by washing with heptane as previously described.

A. *Engine Test Results* – Overall engine sludge demerit ratings obtained in the additives study are presented in Table 13. Note that relative performance of the additive depends to a considerable extent on the time at which the comparison is made. At shorter test times improvement obtained through use of additives is considerably greater. This results from the fact that a high deposit fuel

Table 12 – Effect of Oil Filter

(ER 4-45 tests; lubricant: SAE 10 mineral oil; test fuel: A)

Filter Employed	No	Yes[a]
Overall Sludge Demerit	1.2	0.4
Total Insolubles Weight (Engine + Drain Oil), g	235	85[b]

[a] Filter changed every 22 hr in 110-hr test, corresponding to 800 miles of operation between filter changes.

[b] Includes deposits on filter.

was employed, and toward the end of the test excessive deposits were present in the engine system. With less effective additives, ring sticking, oil consumption, and additive depletion are obtained during the last stages of the test (greater than 75 hr).

Since rate of deposit formation with test fuel A is approximately twice that of commercial gasoline, results obtained at the 50-hr point in the 4-45 tests, given in Table 13, are more nearly representative of normal field experience.

Overall sludge ratings for lubricant E are somewhat lower than warranted by engine condition. Throughout the test, bottom crankcase sludge demerits for this lubricant were considerably higher than obtained even with the base stock. With usual visual rating systems, crankcase condition in this case is not properly reflected in the overall sludge rating. Although lubricant E reduced sludge deposits, with the exception of the oil pan, ring zone deposits were heavy and ring sticking was obtained. Used oil from this test was very viscous and contained an unusually high amount of oil-insoluble material. As pointed out previously, there appears to be a direct correlation between used oil insolubles and ring zone deposits in engines engaged in low-temperature service.

B. *Rate of Sludge Formation* – Rate at which insoluble products build up in the engine system (engine + drain oil), during the course of the 4-45 test has been determined for uncompounded oil and for the same oil containing various additives. This was done to determine if the additives did or did not reduce insoluble formation and to provide information on the mechanism by which additives function.

Estimation of quantity of engine deposits during the course of tests (without disturbing engine deposits), was possible as the result of two observations: (1) although composition of engine sludge and drain oil insolubles changes somewhat throughout the test, at any point during the test they are both the same; thus, composition of the oil-insoluble portion of engine deposits (both organic and inorganic), is the same as that of drain oil insolubles at each intermediate inspection, and (2) there is a linear relationship between overall sludge demerit and weight of organic engine deposits which holds for all lubricants except lubricant E (with lubricant E an unusually large amount of crankcase sludge was obtained). The relationship between sludge demerit and organic deposit weight is independent of weight of inorganic components present. As mentioned previously, inorganic salts, because of their high density, do not contribute appreciably to deposit volume.

In all tests amount of drain oil insolubles was adjusted for the amount withdrawn during sampling. In two tests (lubricants A and B), oil consumption during the last 25 hr of test was unusually high and a correction was applied for difference in consumption in these tests as compared to the remainder of the tests.

With uncompounded oils as well as additive-containing oils, buildup of insolubles appears to be approximately linear with time; thus, it appears that in the 4-45 test there is no appreciable induction period or breakpoint in the formation of oil-insoluble products in the engine system. The significant difference between base stock and compounded oils is that all additives give a lower rate of organic insolubles formation than the uncompounded oil, lubricant D being the most effective in this respect. Reduction with lubricants A and E is small however. These points are illustrated in Fig. 2 and are summarized in Table 14.

Reduction in amount of organic deposits obtained through use of additives could be due to (1) inhibition or repression of deposits formation, or (2) solubilization of the deposits. It will be shown later in this paper that additives in lubricants A, B, C, and D appear to repress deposits formation, whereas the additive in lubricant E does not repress deposits formation but does have a slight solubilizing effect.

Although additives reduced the amount of organic insolubles formed, a slight increase in inorganic insolubles was obtained. This increase is due

Table 13 – Effect of Additives on Engine Sludge
(ER 4-45 tests; test fuel: A; base oil: SAE 10 mineral oil)

	Time, hr			
	25	50	75	110
Overall Sludge Demerit for Base Oil	0.6	1.1	1.6	2.5
Relative Reference Rating Compared to Base Oil as 100% and Based on Overall Sludge Demerit				
Base Stock	100	100	100	100
Lubricant A	38	41	47	71
Lubricant B	9	16	22	42
Lubricant C	38	35	37	41
Lubricant D	—	—	8 (estimated)	12
Lubricant E	13	15	16	21

Table 14 – Effect of Additives on Formation of Organic Insolubles
(ER 4-45 tests; test fuel: A)

	Time, hr		
	25	50	75
Total Organic Insolubles (Engine + Drain Oil), with Indicated Lubricants, g			
Base Stock	54	95	132
Lubricant A	40	81	122
Lubricant B	17	39	76
Lubricant C	34	67	98
Lubricant D	—	35[a]	57
Lubricant E	40	80	122

[a] Estimated, assuming linear relationship with time.

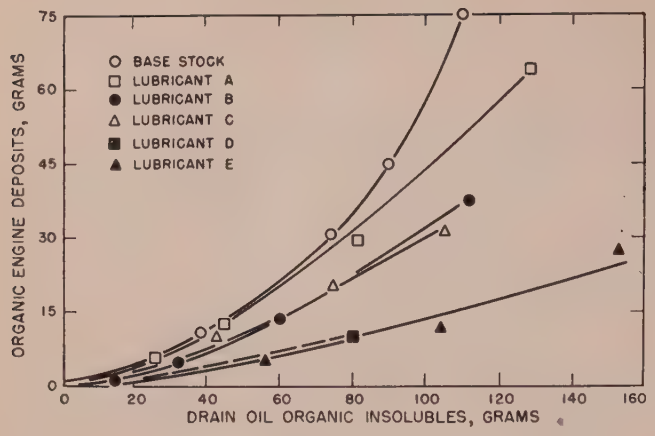

Fig. 3 – Organic engine deposits versus organic drain oil insolubles in ER 4-45 engine tests with various lubricants

Table 15 – Calculation of Extent of Inhibition and Dispersion

	50-Hr Data		Base Oil at 41 G Level
	Base Oil	Lubricant B	
Total Organic Insolubles (Engine + Drain Oil), g	95.0	41.0	41.0
Drain Oil Insolubles, g	67.5	35.3	33.2
Engine Insolubles, g	27.5	5.7	7.8
Reduction in Engine Deposits Due to Additive			
Grams	= 27.5 − 5.7 = 21.8		
%	= 21.8/27.5 = 79.4		
Reduction in Engine Deposits Due to Inhibition			
Grams	= 27.5 − 7.8 = 19.7		
%[a]	= 19.7/21.8 = 90.4		
Reduction in Engine Deposits Due to Dispersion			
Grams	= 7.8 − 5.7 = 2.1		
%[a]	= 100 − 90.4 = 9.6		

[a] Proportion of total reduction by additive.

in part to the metal component of the additive which is associated with oil-insoluble material, and in some instances to a greater quantity of lead salts resulting from differences in wear and blowby. Difference in amount of inorganic deposits, however, was not large.

C. *Distribution of Insolubles; Drain Oil versus Engine* – Distribution of organic insolubles between engine and drain oil for various lubricants is shown in Fig. 3. Note that all additive-containing lubricants retain a greater proportion of organic insoluble products in the drain oil than uncompounded oil. At first glance it would appear that reduction in engine deposits by additives is due to a dispersancy mechanism. But as will be shown in the following sections of this paper, this apparent dispersancy results, for the most part, from the inhibiting action of additives in lubricants A through D. In contrast, lubricant E does not repress insolubles formation.

When quantity of organic insolubles in the system (engine + drain oil), is high, drain oil retains a lower percentage of both organic and inorganic deposits. This relationship for organic deposits is shown in Fig. 4. Inorganic deposits show the same distribution as obtained for organic deposits, and for that reason the data are not presented. When an additive decreases amount of insoluble organic products in the system, it is not surprising that additive-containing oil retains a higher proportion of insolubles in drain oil than uncompounded oil. Extent to which inhibition or solubilization and dispersion contribute to engine deposits reduction can be calculated using the data in Figs. 2 and 4. Here it has been assumed that when additive reduces the total amount of insoluble organic materials in the system, there will be an increase in percentage of these materials retained in drain oil, as indicated by the base stock curve in Fig. 4. If reduction in engine deposits by the additive is greater than that calculated as being due to inhibition or solubilization, the remainder is assumed due to dispersancy. A sample calculation follows.

After 50-hr operation with base oil, amount of organic insolubles in the system (engine + drain oil), was 95 g, as indicated in Fig. 2. From Fig. 4, at this organic insolubles level for base oil (95 g), insolubles retained in drain oil = 71%. The value of 71% x 95 g gives 67.5 g of organic insolubles retained in drain oil, and 95 — 67.5 = 27.5 g on the engine. With lubricant B, for example, at the 50-hr point, amount of organic insolubles in the system obtained from Fig. 2 = 41 g. From Fig. 4 organic

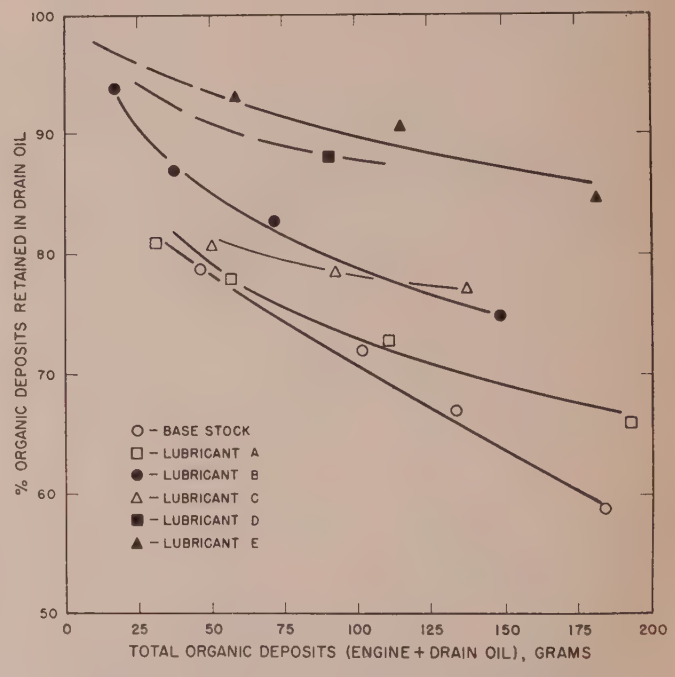

Fig. 4 – Variation of per cent of total organics in drain oil versus total organic deposits in ER 4-45 engine tests with various lubricants

Table 16 – Mechanism of Additive Action
(ER 4-45 tests; test fuel: A)

	Time, hr		
	25	50	75
Reduction in Engine Organic Deposits by Additive, %			
Lubricant A	33	29	27
Lubricant B	92	80	71
Lubricant C	58	54	55
Lubricant D	—	90[a]	87
Lubricant E	77	72	75
Reduction in Engine Organic Deposits Due to Additive Inhibition, %			
Lubricant A	33	25	16
Lubricant B	92	72	58
Lubricant C	50	43	41
Lubricant D	—	79[a]	72
Lubricant E	28[b]	15[b]	11[b]
Reduction in Engine Deposits Due to Dispersion, %			
Lubricant A	0	4	11
Lubricant B	0	8	13
Lubricant C	8	10	13
Lubricant D	—	11[a]	15
Lubricant E	49	57	64

[a] Estimated.
[b] Appears to be solubilization rather than inhibition.

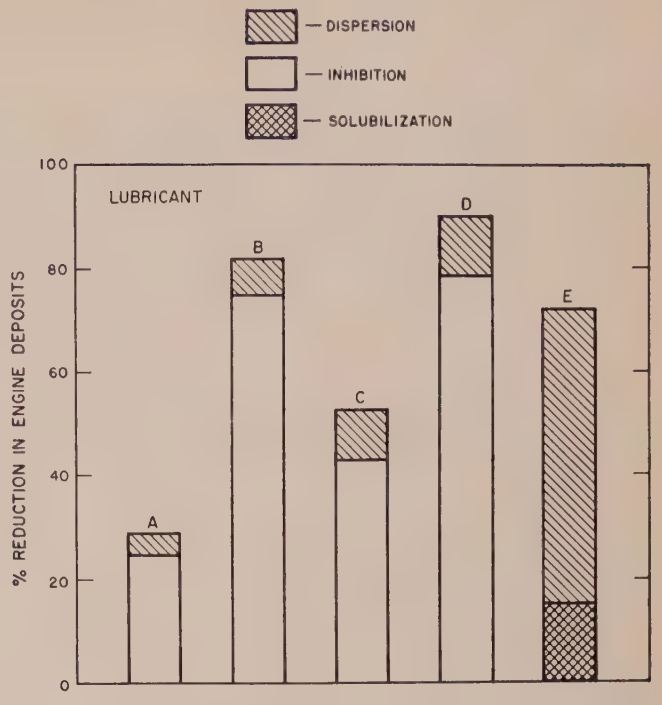

Fig. 5 – Mechanism of additive action in 50-hr ER 4-45 engine tests with various lubricants

deposits retained in drain oil for lubricant B at the 41-g level = 86%. The value of 41 g x 86% gives 35.3 g insolubles retained in drain oil and 41 — 35.3 = 5.7 g of organic deposits on the engine; therefore, total reduction in organic engine deposits by lubricant B compared to the base stock = 27.5 (base stock) — 5.7 (B) = 21.8 g, or 21.8/27.5 = 79.4%. Part of this reduction is due to additive inhibition and part to dispersancy. The proportion due to inhibiting action can be calculated from Fig. 4 by determining organic engine deposit weight for base stock at the total organic level obtained with lubricant B at the 50-hr point; namely, 41 g. Using the base stock curve in Fig. 4 at the total organic level of 41 g, amount retained in drain oil = 81%. This value of 81% x 41 g gives 33.2 g organic insolubles in drain oil and the remainder, or 7.8 g, on the engine. Therefore, reduction in organic engine deposits due to additive inhibition = 27.5 — 7.8 = 19.7 g. Total reduction by the additive in lubricant B = 27.5 — 5.7 = 21.8 g. The proportion of this reduction due to inhibition is 19.7/21.8 = 90.4%. The remainder, 9.6%, is due to dispersion. The calculation data are given in tabular form in Table 15.

Table 17 – Distribution of Deposits in ER 4-45 Tests

	Insolubles Retained in Drain Oil, %	
Lubricant	Organic	Inorganic
A	66	67
B	75	72
C	77	80
D	88	88
E	85	88

Summary results of these calculations are given in Table 16 and presented graphically in Fig. 5.

Note that for additives in lubricants A through D, the major portion of engine deposit reduction is due to either a repression of deposit formation or to solubilization. Chromatographic extraction of filtered used oils from these tests showed that amount of oil-soluble products (fuel derived), was either the same or less than obtained with uncompounded oil. This indicates that no solubilization of deposits had occurred, and therefore reduction must be due to inhibition. In the case of the additive in lubricant E, some solubilization of deposits occurs, but the major effect results from dispersancy. Dispersancy appears to result from an interaction of the additive with deposits, resulting in deposits being converted into more easily dispersed form.

When the relationship between total acetone-soluble resins in the system and per cent organic insolubles retained in drain oil is used as a basis for calculations similar to those discussed, the same general conclusions are reached. Dispersancy activity of additive-containing lubricants, except E, however, appears to be slightly greater when this method of calculation is employed.

It has not been possible to calculate the extent to which additive inhibition of the organic insolubles influences distribution of inorganic deposits between drain oil and engine, since with all additives a greater quantity of inorganics is obtained than with the base stock. This is not important, since

Table 18 – Effect of Additives on Deposits Composition
(ER 4-45 tests; test fuel: A)

	Time, hr		
	25	50	75
Reduction in Acetone-Solubles Relative to Base Stock, %[a]			
Lubricant A	0	7	11
Lubricant B	70	61	44
Lubricant C	0	12	20
Lubricant D	—	—	33[b]
Lubricant E	67	64	60
Reduction in Acetone-Insolubles Relative to Base Stock, %[a]			
Lubricant A	31	27	21
Lubricant B	60	64	53
Lubricant C	56	50	35
Lubricant D	—	—	76[b]
Lubricant E	37[c]	31[c]	30[c]

[a] For engine + drain oil.
[b] 110-hr value.
[c] Increase.

as already discussed, inorganics contribute only slightly to engine sludge volume. However, since distribution of organic insolubles between engine and drain oil appears to be almost exactly the same as distribution of inorganic insolubles in all tests, it would seem that reduction in engine inorganics by the additive is also due to reduction in the amount of organic insolubles. This is shown in Table 17.

Reduction in engine deposits by an inhibition mechanism for additives in lubricants A through D is consistent with the observation that degree of inhibition varies directly with quantity of additive remaining dissolved in the lubricant. There is also some question as to whether these same additives *per se* exhibit detergency, since dispersancy increases with test time, and additive concentration in the lubricant decreases. It appears rather that dispersion is the result of interaction of additives with fuel degradation products.

D. *Effect of Additives on Deposits Composition* – It appears that commercial additives used in this study and the experimental additive in lubricant D inhibit formation of acetone-insolubles to a greater extent than acetone-solubles. With the additive in lubricant E, however, large reduction in amount of acetone-solubles is accompanied by a large increase in amount of acetone-insoluble materials. Since acetone-insoluble products are more easily dispersed, this would appear to explain the high dispersing activity of this additive. These data are given in Table 18.

In the laboratory it has been found that acetone-soluble sludge from a 4-45 test on a nonadditive oil is largely converted into acetone-insoluble form by heating with lubricant E.

E. *Effect of Additives on the Production of Oil-Soluble Materials* – Silica gel extraction of filtered used oils from 4-45 tests shows that commercial additives have no marked effect on quantity of oil-soluble materials produced. This suggests that no solubilization of sludge had occurred. With the experimental additive in lubricant D, there is a marked reduction in quantity of oil-soluble resins produced. It appears that with this additive, reactions of fuel degradation products to form oil-insoluble materials are stopped at the stage where fuel degradation products are sufficiently volatile to be removed from the crankcase. With the additive in lubricant E, there was a large increase in quantity of oil-soluble materials which can be extracted by silica gel, compared to the base stock. These data are listed in Table 19.

In the laboratory it was found that lubricant E would partially solubilize deposits obtained with nonadditive oils in the ER 4-45 test. This type material may be present in the silica gel extract.

F. *Summary* – Although previous investigators have assumed that conventional motor oil additives – "detergent-inhibitor additives" – reduce low-temperature gasoline engine deposits by a dispersing mechanism, the present study indicates that their primary function is one of inhibition or repression of deposits formation. An effective experimental additive (containing phosphorus and sulfur) with increased inhibiting potency has been prepared.

Since the additive which has strong inhibiting potency does not contain metals and has an acidic reaction, it appears that inhibition of some sludge-forming reactions is possible without having acid-neutralizing capacity.

An experimental additive (containing oxygen and nitrogen), has been studied which reduces engine deposits in certain engine areas. Reduction in sludge by this additive appears to be the result of dispersion and solubilization. Dispersing power apparently results from ability of the additive to convert normal low-temperature sludge into easily dispersed form.

In development of improved motor oil additives for low-temperature service, the inhibitor route appears to be the most desirable; that is, it appears advantageous to prevent deposits formation rather than to disperse them after they have been formed.

Acknowledgment

The authors gratefully acknowledge the cooperation of their associates at the Products Research Division of the Esso Research & Engineering Co. in this work. In particular, the authors wish to thank A. E. Michaels, K. L. Stehle, and R. V. High,

Table 19 – Sludge Precursor Formation in ER 4-45 Tests

	Oil-Soluble Sludge Precursor in Filtered Drain Oil at Indicated Time, %[a]			
Time, hr	20	40	80	110
Lubricant				
Base stock	0.5	2.0	5.0	6.4
A	0.7	2.2	4.8	6.1
D	—	—	—	<2.0
E	0.9	6.8	9.2	10.3

[a] Values corrected for weight of silica gel extract on unused lubricants.

Jr., for aid in carrying out the fleet test work and laboratory studies. Thanks are also due to G. W. Duncan and J. G. McNab for suggestions on the preparation of this manuscript.

APPENDIX I

Procedure for Obtaining Engine Deposits and Drain Oil Insolubles

A. Engine deposits:

1. Method of collection: After disassembling and inspecting the engine, all covers and parts are placed in a metal tray so that no deposits will be lost. A second large metal tray is then set in a well-ventilated hood and the parts individually wiped off with a piece of fiberglass cloth and heptane. It has been found that if the fiberglass cloth is moistened with water prior to use, it will not entrain the deposits. All parts are wiped clean and rinsed in the heptane, and drainings collected in the tray. An air-heptane spray gun is used to loosen tightly adhering deposits. In some instances it may be necessary to remove varnish deposits with acetone. It has been found convenient to first wash all side and cover plates, then the push rod and rocker arm assemblies, connecting rods and camshafts, cylinder-head top and crankcase pan. Another large pan is set beneath the portable engine test stand and the engine block, crankshaft and timing gear assembly wiped and washed. Residual deposits are again removed with an air-heptane spray gun. The engine should be turned upside down on the test stand and washed from both upper and lower positions. About three gallons of washings are obtained from this work.

2. Engine deposit workup: Heptane washings are filtered through sintered glass vacuum-filter funnels (medium porosity), yielding a filtrate of oil and oil-soluble products in heptane. The filter cake is washed with heptane and permitted to dry. At this stage, this cake still contains some oil which cannot be removed by heptane washing. The cake is broken into small pieces and stirred for five minutes in acetone. It is refiltered yielding a filtrate containing acetone-soluble organics. The procedure of grinding, stirring with acetone, and refiltering is repeated until the filtrate is nearly colorless. Acetone-insoluble solids are dried and weighed. Acetone filtrate is evaporated and the residue ground and washed with heptane to remove residual lubricating oil. Acetone-soluble deposits are dried and weighed.

Table 20 – Breakin Schedule

Time, min.	Rpm	Bhp	Jacket Outlet Temperature, F	Oil Sump Temperature, F
10	1000	5	135–145	—
10	1250	10	135–145	—
10	1500	15	135–145	145–155

Table 21 – Test Conditions

	Cycle 1 500 Rpm	2 2000 Rpm	3 2000 Rpm
Jacket Water Outlet Temperature, F	115±5	160±5	160±5
Oil Sump Temperature, F	115±5	175±5	225±5
Intake Air Temperature, F	Room	Room	Room
Brake Horsepower	0	40	40
A/F Ratio	9.5/1	11.5/1	11.5/1
Cycle Length, hr	1½	2	2
Exhaust Back Pressure, in. of Hg	[a]	1.0	1.0

[a] See section B, part 6 of Appendix II.

B. Drain oil insolubles: Total drain oil from the engine at shutdown is collected and a 50-g sample submitted for neutralization number, saponification number, and ASTM Designation ES-42 sludge determinations. The remainder is diluted with seven volumes of heptane and filtered. The insoluble materials are then treated in the same manner as engine deposits.

For uncompounded oils, results from the ASTM Designation ES-42 method for used oil insolubles have agreed very closely with those obtained by heptane dilution and filtration. For some additive oils (lubricants D and E), however, ES-42 values have been considerably lower than those obtained by filtration. Coagulating agents have not been employed in either method.

Amount of organic material present in engine deposits and drain oil insolubles is calculated by subtracting weight of sulfated ash from the weight of acetone-insoluble fraction and adding weight of the acetone-soluble fraction.

APPENDIX II

ER 4-45 Engine Test Procedure

A. Engine breakin:

1. Charge 4 qt of test oil to engine for breakin.

2. The breakin schedule is given in Table 20.

3. Drain oil at the end of breakin to 60 drops per min. Recharge engine with 4 qt of test oil.

B. Cycle test conditions:

1. The conditions are given in Table 21.

2. Start test on 500 rpm cycle.

3. If engine is shut down during 2000 rpm cycle and must later continue under 2000 rpm cycle conditions, follow the breakin schedule for engine warmup. For a 500 rpm cycle shutdown, when continuing at 500 rpm conditions, bring engine up to conditions under the 500 rpm cycle conditions; that is, no subsequent warm up schedule is required.

4. Test duration will be 110 hr.

5. Use carburetor with adjustable jet.

6. The criterion of proper carburetor setting is to be the A/F ratio as determined by Orsat anal-

ysis. Automatic gas analyzer readings are taken but are used as a directional indication of mixture strength. During A/F ratio determinations on the 500 rpm cycle, a positive pressure of from 0.5-3 in. of water (measured at sampling line), is maintained on the exhaust system. If more than 1.2% oxygen is obtained, A/F ratio is lifted to 10.3. Calculations are made on basis of CO and CO_2 only. It is desirable that O_2 content does not exceed 2.5%.

C. Data recorded at end of each cycle period:

1. Date
2. Time
3. Hours on test
4. Jacket water inlet temperature, F
5. Jacket water outlet temperature, F
6. Oil sump temperature, F
7. Scale pull, lb
8. Brake horsepower
9. A/F ratio

(a) Use Automatic exhaust gas analyzer once on each cycle.

(b) Take three Orsat analyzer readings per day, one on each cycle.

10. Blowby, cu ft per hr. Take one per 2000 rpm cycle.
11. Exhaust back pressure, in. of Hg during power cycles or in. H_2O during A/F measurements on idle cycle.
12. Exhaust temperature, F
13. Intake manifold pressure, in. Hg
14. Oil pressure, psig
15. Barometric pressure (in. of Hg) and ambient temperature (F); once per day.
16. Record fuel consumption on data sheet.
17. Oil dipstick reading (after second power cycle).

D. Oil procedure for fuels testing:

1. Add oil when level drops to 3-qt level.

E. Oil procedure for lubricating oil testing:

1. Take 1 pt sample of crankcase oil at 22, 38½, and 71½ hr. Read dipstick and sump temperature just before removing sample. After each sample is taken, add 1 pt of fresh oil to engine.

2. It is desired to keep oil level at or above the 4-qt level. Therefore, add test oil in 8 oz increments at end of every second power cycle when needed. If sample period comes at same time as an 8 oz make-up addition is needed, sample first, add 1 pt to replace sample, and then add the 8 oz of make-up oil.

F. Engine Tolerances and Specifications to be Maintained at Each Turnaround:

1. Ring gaps: set to 0.050 in. in engine cylinders at position of top ring travel (9/16 in. down from top of cylinder).
2. Ring side clearance:
   (a) Compression rings: 0.0015-0.0030 in.
   (b) Oil ring: 0.0020-0.0035 in.
3. Valve lash (hot):
   (a) Intake: 0.006 in.
   (b) Exhaust: 0.013 in.
4. Spark-plug gap: 0.035 in.
5. Valve specifications:

(a) Stem Diameters: Intake: 0.3410-0.3417 in. Exhaust: 0.3400-0.3407 in.

(b) Stem to Guide Clearance: Intake: 0.002-0.004 in. Exhaust: 0.002-0.004 in.

6. Connecting rod bearing tolerances:
   (a) Radial clearance: 0.0015-0.0025 in.
   (b) End play: 0.004-0.012 in.
7. Valve seat angle: Inlet 30 deg. Exhaust 45 deg.
8. Ignition timing (crankshaft deg): 5 deg btdc

G. Cleaning procedure:

1. Clean all engine parts.
2. Remove crankshaft and clean oil gallery lines.
3. Remove cheek plate at rear of timing gear.

H. Turnaround schedule:

1. Install chrome-plated, compression rings with gaps as above. Install new standard oil ring. Weigh rings before and after test.
2. Grind valves.
3. Check timing gear case oil seal for satisfactory mechanical condition.
4. Clear all oil lines and passageways through engine.
5. Check thermocouples.
6. Install new spark plugs. Use hot plugs.
7. Set breaker point clearance at 0.018 in. Check distributor characteristics.
8. Install new gaskets.
9. Measure and record the following:

(a) Longitudinal and transverse diameters of all cylinders at 9/16, 4 3/16, and 5⅜ in. from top of cylinder block.

(b) Ring gaps at start and end of each test in cylinder block, 9/16 in. down from top of cylinder block in transverse position.

(c) Ring side clearance at start of each test.

(d) Ring weights before and after each test.

(e) Valve stems and guides.

10. Install new tin-plated pistons.
11. Install new spring on exhaust manifold hot spot.
12. If fuel filter is used, clean out bowl and install new filter element.

DISCUSSION . . .

. . . of this article starts on p. 807

Nitrogen Oxides, Combustion, and Engine Deposits

R. S. Spindt, Court L. Wolfe, and Donald R. Stevens,
Gulf Research & Development Co.

This paper was presented at the SAE Golden Anniversary Fuels & Lubricants Meeting, Philadelphia, Nov. 9, 1955.

ENGINE deposits generally have been pictured as being a result of hydrocarbon oxidation reactions accompanied by polymerization and condensation and as involving both fuel and lubricant. This paper introduces evidence that reactions of unsaturated fuel constituents with oxides of nitrogen, formed during combustion, also play an important part in formation of these deposits. Supporting evidence for this hypothesis has been obtained by evaluating influence of engine operating variables on fixation of nitrogen and by experiments devised to show effect of these oxides on formation of engine deposits.

That nitrogen oxides are formed in an engine is not a new observation. Hanson and Egerton[1] studied formation of nitrogen oxides during combustion. Observing formation of resins when fresh lubricating oils were treated with dilute nitrogen dioxide, they assumed that this gas acted as an oxidation catalyst. Graefe[2] found nitro-hydrocarbons in used lubricating oils; Ehlers[3] made similar

REACTIONS of unsaturated fuel constituents with oxides of nitrogen, formed during combustion, play an important part in formation of engine deposits. Engine varnish, the organic binder in engine deposits, results in large part from reactions of nitrogen dioxide with gasoline constituents.

Simplified kinetic studies indicate that nitrogen fixation and amounts of nitric oxide present in exhaust gases could be predicted. Tests have demonstrated that only under conditions leading to appreciable nitrogen fixation does heavy engine varnishing occur.

Because commercial engine oils are fairly resistant to oxidation, it is likely that current deposit problems result from the nature of fuel and prevailing operating conditions. Under average driving, low-temperature operation, lean mixtures with consequent high nitrogen oxide content contribute much to varnish formation.

[1] See Proceedings of Royal Society of London, Series A, Vol. 163, November, 1937, pp. 90-100: "Nitrogen Oxides in Internal-Combustion-Engine Gases," by T. K. Hanson and A. C. Egerton; pp. 334-340: "Influence of Catalysts on Oxidation of Oils," by T. K. Hanson and A. C. Egerton, in Vol. 2, Group IV, "Proceedings of General Discussion on Lubrication and Lubricants." Pub. by Institution of Mechanical Engineers of London, 1938.

[2] See *Petroleum* (Berlin), Vol. 28, No. 23, 1932 (*Motorenbetrieb u. Maschinen-Schmierung,* Vol. 5, No. 6, pp. 5-6), "Über die Bildung von Nitrokohlenwasserstoffen im Motor," by E. Graefe.

[3] See *Petroleum* (Berlin), Vol. 28, No. 41, 1932 (*Motorenbetrieb u. Maschinen-Schmierung,* Vol. 5, No. 10, p. 8), "Über die Bildung von Nitrokohlenwasserstoffen im Motor," by K. Ehlers; *Petroleum* (Berlin), Vol. 31, No. 15, 1935 (*Motorenbetrieb u. Maschinen-Schmierung,* Vol. 8, No. 4, pp. 2-3), "Salpetersäure in Gebrauchten Motorenölen," by K. Ehlers: *Petroleum* (Berlin), Vol. 34, No. 19, 1938 (*Motorenbetrieb u. Maschinen-Schmierung,* Vol. 9, No. 5, pp. 2-3), "Der Einfluzz der Salpetersäure auf die Alterung des schmieröles in Verbrennungsmotoren," by K. Ehlers.

observations and recognized nitric acid in oils removed from heavy duty trucks. Diamond, Kennedy, and Larson[4] found that nitrogen dioxide, as such, did not induce formation of varnish in a motored engine in the absence of fuels. Walker and O'Hara[5] have used a mass spectrometer to study nitric oxide content of engine exhaust gas and its variation with speed.

It has long been known in the coke oven gas industry that one type gum deposit which forms in meters and burner orifices results from the reaction of nitrogen dioxide with unsaturated constituents in the gas (vapor phase gum).[6] This type gum contains 3-5% nitrogen, and it has many of the chemical characteristics of engine varnish.

Recognition of Nitrogen Compounds in Deposits

The idea that oxides of nitrogen could play a part in deposit formation came first from a rather broad study of the composition of a wide variety of engine deposit materials. Nitrogen analysis of some hundreds of engine deposits of various types showed this element was always present, sometimes in amounts as high as 4%. It was also observed that deposits formed at high operating temperatures showed a lower nitrogen content (maximum 2%), than those formed at lower temperatures. Some typical figures for nitrogen contents are given in Table 1.

Analyses of representative low-temperature engine resins indicate that there is approximately one atom of nitrogen per molecule of varnish. Neither original fuels nor oils contain enough nitrogen to account for the amount found in these deposits. There are, however, sufficient oxides of nitrogen available from the combustion process to be a potential source for nitrogen found in engine resins.

With development of an analytical procedure[7] for aliphatic nitro-compounds, data were obtained which indicated the nitro-group was present in most engine resins. Averaged results given in Table 2, based on deposits from the laboratory test engine, show how both total nitrogen and nitrogen in nitro-groups (as determined by the method mentioned), vary with engine operating conditions.

Table 1 – Nitrogen Content of Engine Resins

High-Temperature Deposits	Nitrogen, %
Diesel	
Piston	2.0
Intake Valve	1.4
Aircraft	
Piston	1.2
Intake Valve	0.3
Truck	
Piston	0.3
Oil Screen	1.3
Laboratory L-4 Test	
Piston	0.6
Pentane (Insoluble from Oil)	1.3
Low-Temperature Deposits	
Passenger Car	
Piston	2.7
Intake Port	3.5
Ring Groove	2.2
Pentane (Insoluble from Oil)	2.4
Laboratory FL-2 Test	
Piston	1.8
Crankcase	2.4
Pentane (Insoluble from Oil)	2.7

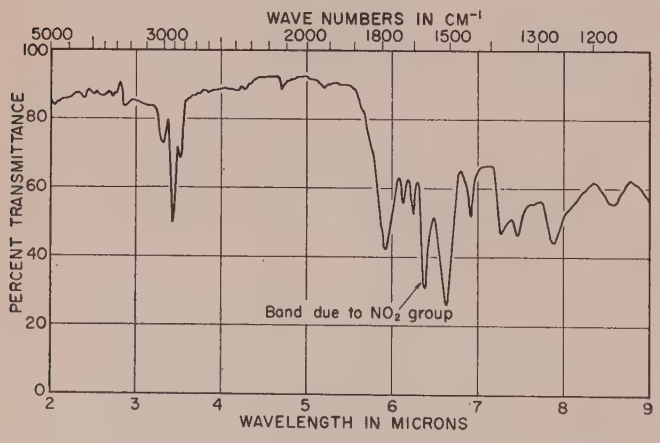

Fig. 1 – Infrared absorption spectrum of characteristic low-temperature engine deposits

Further proof of existence of the nitro-groups in engine resins was obtained from infrared spectra. A characteristic absorption peak is observed at about 6.4-6.5 microns, which has also been identified in spectra of aliphatic nitro-compounds. An example is given in Fig. 1.

Engine Production of Nitrogen Oxides

To understand better the formation of oxides of nitrogen in an engine, two approaches to the problem were followed.

a. A theoretical study of the reaction kinetics was made to show that amounts of nitric oxide actually found were predictable. Further calculations were used to interpret effects of different variables.

b. Experimental studies were conducted with both single- and multiple-cylinder engines to determine how the concentration of nitrogen oxides in exhaust gas varied with conditions. Chemical analysis of exhaust gas verified the theoretical conclusions that appreciable nitric oxide should be formed in the combustion process.

Theoretical Studies – The theoretical study of nitrogen fixation, details of which are given in Appendix I, may be described briefly as an evaluation

[4] See American Chemical Society, Petroleum Division, Preprints of General Papers, New York, September, 1947, p. 147: "Investigation of Deposition and Oil Deterioration Phenomena in Motored Engine," by H. Diamond, H. C. Kennedy, and R. G. Larson.

[5] See *Analytical Chemistry*, Vol. 27, May, 1955, pp. 825-828: "Analysis of Automobile Exhaust Gases by Mass Spectrometry," by J. H. Walker and C. L. O'Hara.

[6] See *Industrial & Engineering Chemistry*, Vol. 24, September and November, 1932, pp. 969-977 and 1238-1247: "Gum Deposits in Gas Distribution Systems, Liquid-Phase Gum," by C. W. Jordan, A. L. Ward, and W. H. Fulweiler; *Industrial & Engineering Chemistry*, Vol. 26, September and October, 1934, and Vol. 27, October, 1935, pp. 947-955, 1028-1038, and 1180-1190: "Gum Deposits in Gas Distribution Systems, Vapor-Phase Gum," by C. W. Jordan, A. L. Ward, and W. H. Fulweiler.

[7] See American Chemical Society, Petroleum Division, Preprints of General Papers, Minneapolis, September, 1955, pp. 33-39: "New Method for Determination of Aliphatic Nitro Compounds," by R. L. Sweet, R. S. Spindt, and V. D. Meyer.

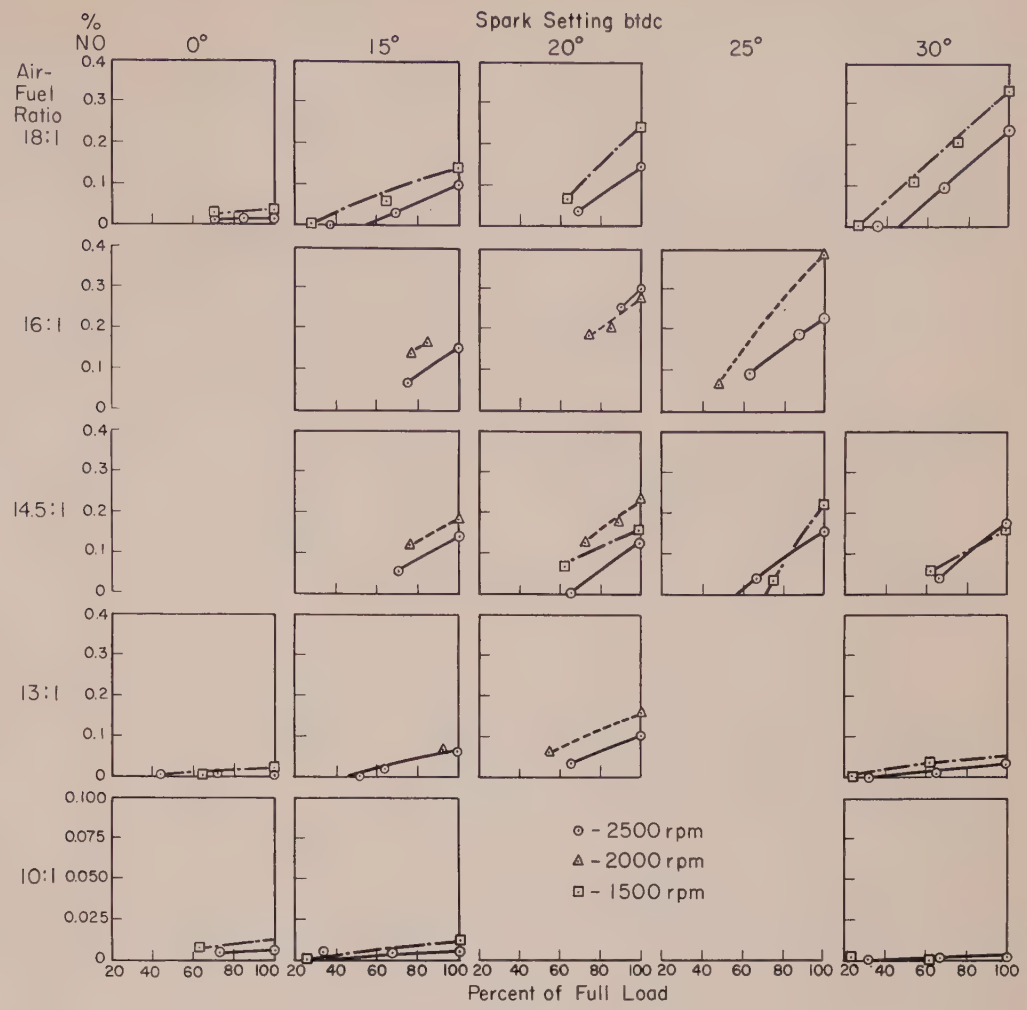

Fig. 2 – Effect of operating conditions on content of nitric oxide in exhaust gas

of the time, temperature, and pressure relations acting on the reactants, nitrogen and oxygen, according to the following equation:

$$N_2 + O_2 \underset{k_2}{\overset{k_1}{\rightleftarrows}} 2NO \qquad (1)$$

A knowledge of intake pressure, (a measure of engine load), air-fuel ratio, and engine compression ratio makes it possible to compute the gas concentration and a theoretical average flame temperature. Reaction rate constant can be computed from flame temperature. It is possible, therefore, to estimate nitric oxide concentration from equation (2). (A discussion of this equation is given in Appendix I.)

$$(NO) = K\sqrt{(N_2)(O_2)} \cdot \tanh k_2 K t \sqrt{(N_2)(O_2)} \qquad (2)$$

where:

(NO), (N_2), (O_2) = Concentrations of nitric oxide, nitrogen, and oxygen, respectively

K = Square root of equilibrium constant of equation (1), obtained from thermodynamic data

k_2 = Rate constant for decomposition of NO, cc/mole/sec

t = Time, sec

By varying intake pressure and keeping air-fuel ratio and compression ratio constant, a family of curves can be obtained for different time intervals. (See Figs. 6 and 7.) From these curves, comparisons can be made with experimentally found nitric oxide concentrations in order to determine whether the time factor for the reaction is of the same order of magnitude as that estimated to be available in the engine. Results of these calculations show that

Table 2 – Average Nitrogen Content of Piston Deposits from Two Types of Operation[a]

	L-4 Test Conditions	FL-2 Test Conditions
Total Nitrogen, % (Dumas)	1.00	3.78
Nitrogen in Nitro-Groups, %	0.09	0.65
Ratio Nitro-Nitrogen to Total Nitrogen, %	9	17

[a] Deposits obtained from the 2-cyl Gulf test engine.

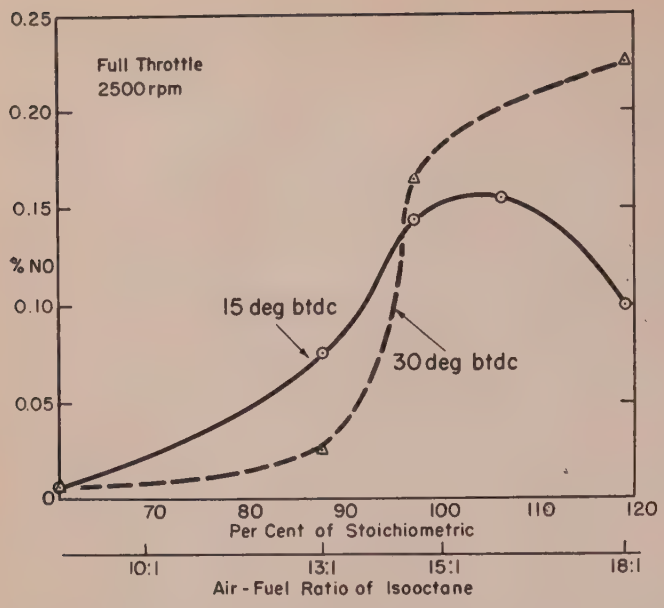

Fig. 3 – Correlation of nitric oxide in exhaust with air-fuel ratio at two spark settings

flame temperature is adequate to bring about nitrogen fixation, that the reaction will take place if oxygen is present in excess, and that sufficient time is available to account for the nitrogen oxides actually found.

Experimental Engine Studies – In a gasoline engine combustion can occur successfully over a wide range of air-fuel ratios. Maximum power is produced at about 12.5:1, while ratios theoretically correct for complete combustion lie at about 14.5:1, depending on the fuel. Since gasoline economy is achieved at high air-fuel ratios, manufacturers have endeavored to improve engine performance under lean conditions. As early as 1941 air-fuel ratios had reached an average of 15.5:1.[8]

Experimental data on nitrogen oxide content of exhaust gases were obtained by operating the test engine (Appendix III), under systematically varied conditions of speed, torque, spark timing, and air-fuel ratio. Exhaust gases were sampled and analyzed for nitrogen oxides as described in Appendix II. Isooctane was used to eliminate complications that might arise from engine knock. This is justified, since fuel type has been found to have little effect on the extent of nitrogen fixation.

The data in Fig. 2 show conditions employed and trend of results. These data are difficult to analyze due to complex interrelations of variables. One important conclusion drawn from Fig. 2 is that nitric oxide always increases with increasing intake pressure, as reflected in engine load, and is independent of any other fixed variable. In general, the effect of increasing speed is to reduce the amount of nitric oxide formed because of decrease in reaction time.

Some data contained in Fig. 2 are also the basis for Figs. 3 and 4. Fig. 3 correlates per cent nitric oxide with air-fuel ratio for two spark settings which bracket optimum engine performance. At rich mixtures, little fixation occurs because of lack of oxygen. At 15 deg btdc and 84% of stoichiometric mixture, (13/1 air-fuel ratio), nitrogen fixation occurs in spite of the slightly reducing atmosphere, whereas at 30 deg btdc the increased time available results in loss of nitric oxide as a result of reduction. At 100% of stoichiometric mixture, both curves indicate that appreciable fixation has occurred. Above 100% stoichiometric mixture, the 15 deg btdc curve reaches a maximum and starts to decrease because of lower flame temperatures occurring at lean mixtures, with resulting lower reaction rate. Increased time available at 30 deg btdc results in a continuing mild increase in amount of nitric oxide formed.

Fig. 4 correlates nitric oxide in exhaust gas with spark timing at three air-fuel ratios. Spark timing affects both time available and temperatures to which combustion-chamber gases are subjected. At rich mixtures, as exemplified by the curve for 13/1 air-fuel ratio, there is a gradual increase in nitric oxide production up to optimum spark timing; at more advanced timing the reducing atmosphere tends to destroy nitric oxide previously formed.

At slightly lean mixtures, as illustrated by a 16/1 air-fuel ratio, the amount formed has increased rapidly near optimum spark timing. It is in this range that rate of fixation is greatest. At lean mixtures, 18/1 and greater, rate of formation is slower because of lower flame temperatures. However, production continues at the more advanced timing because of excess oxygen and increased time available.

While experimental results on effect of compression ratio were not obtained, theoretical studies show that increasing this variable should result in higher combustion temperatures, and consequently a greater extent of nitrogen fixation would be expected.

A preliminary dynamometer test was run using a passenger car to evaluate concentration of nitrogen oxides in exhaust gas under simulated field conditions. Data were obtained at two car speeds for several different manifold vacua, and engine torque and air-fuel ratios were also measured. Air-

Table 3 – Effect of High and Low Nitric Oxide Production on Fuel Deposit Formation

	Piston Deposit			
	Low Nitric Oxide Production 11/1 A/F		High Nitric Oxide Production 17/1 A/F	
	CRC Color	Acetone Soluble Deposit, mg/in.²	CRC Color	Acetone Soluble Deposit, mg/in.²
Straight-Run Gasoline	10	0.05	10	0.01
Thermally Cracked Gasoline	10	0.10	7	3.85
Catalytically Cracked Gasoline	9.5	0.10	7	2.06

fuel ratio was found to be approximately 16/1 under part throttle conditions; and 12.5/1 at full throttle. Fig. 5 illustrates these data for nitric oxide content of exhaust gases.

Amount of nitric oxide present is controlled by throttle setting and air-fuel ratio. It is low at full throttle, rich mixture conditions, but increases at part throttle due to leaning out of the mixture. After passing through a maximum, it decreases with increasing engine manifold vacuum. At 50 mph, where road load is appreciably greater than at 30 mph, more nitric oxide is found than at the lower speed. Although these data were obtained from only one vehicle, they suggest that many cars may be operating under conditions of high nitric oxide formation much of the time.

It is concluded that engines operating under normal spark timings with mixtures on the lean side of stoichiometric mixture will produce appreciable nitric oxide, the amount formed depending most directly on applied load. There appears to be little hope for reduction in nitrogen oxides from changes in engine conditions, since optimum economical operation seems to be in the range of high nitrogen fixation. That these oxides of nitrogen can lead to piston and crankcase deposits has been shown by repeated engine tests.

Engine Experiments with High and Low Nitric Oxide Production

Low temperature tests were run using equipment described in Appendix III to evaluate engine conditions set to produce high and low nitrogen fixation, for their effect on deposits from different fuels. Fuels used were clean, nondepositing straight-run gasoline, and thermally and catalytically cracked distillates known to be deposit-forming. Typical inspection data for fuels used are given in Appendix IV.

The results in Table 3 indicate it is difficult to distinguish between these fuels when operating at rich mixtures, (11/1), or low nitrogen fixation. On the other hand, when operating at lean mixture, (17/1), with approximately 0.25 per cent nitric oxide in the exhaust (well within the range of that produced in practical operation), the cracked gasolines give significantly more deposits. It is clear that there is a large difference in the amount of deposits accumulated when using operating procedures that result in the formation of significantly different amounts of nitric oxide. (See Appendix III for a discussion of deposit weights.)

Effect of Added Nitrogen Dioxide on Engine Deposits

A series of engine tests was run to demonstrate that nitrogen dioxide can effect an increase in piston varnish.

This gas was chosen because it is known that nitric oxide reacts with oxygen to produce the dioxide. Residence time in the crankcase is sufficiently long for appreciable conversion, according to the following equation:

$$2NO + O_2 \rightarrow 2NO_2$$

It has been observed that exhaust gas, colorless when initially collected, changes on standing as colored nitrogen dioxide is formed. Further, lab-

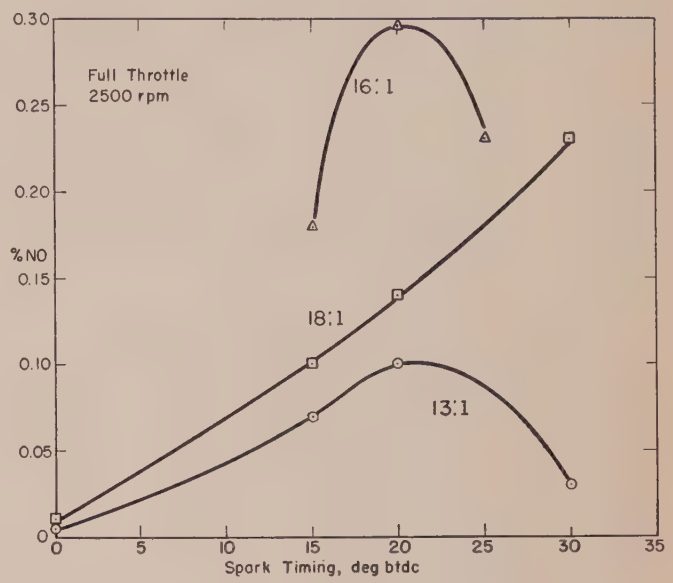

Fig. 4 – Correlation of nitric oxide in exhaust with spark timing at three air-fuel ratios

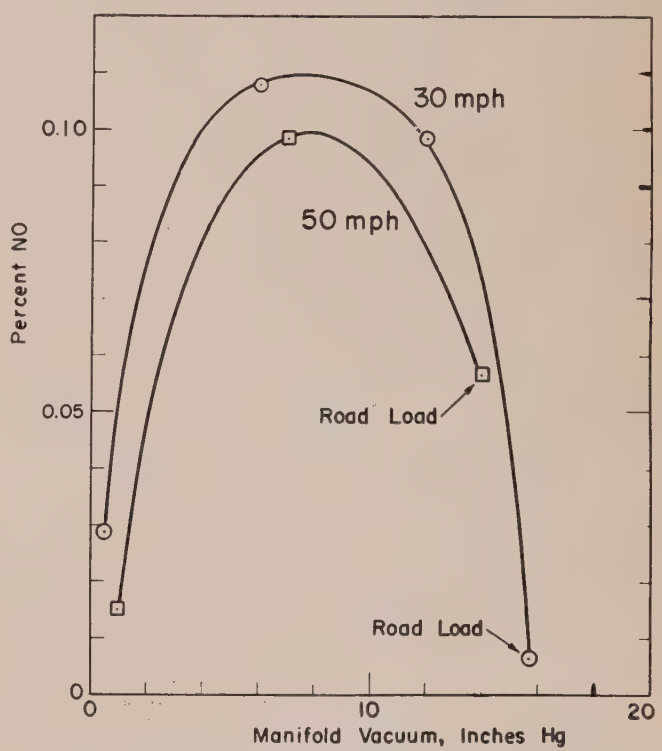

Fig. 5 – Nitric oxide in exhaust gas from conventional automobile engine as function of manifold vacuum

[8] See SAE Transactions, Vol. 36-49 (April) 1941, pp. 160-164: "13-Year Improvement in Mixture Ratios," by W. G. Lovell, J. M. Campbell, B. A. D'Alleva, and P. K. Winter.

oratory experiments have shown that reaction products of nitrogen dioxide and gasoline are similar to engine varnish. Because of these factors, and the difficulty in handling nitric oxide without introducing unknown amounts of the dioxide, it is believed that experiments using nitrogen dioxide lead to significant information.

A control run using low nitric oxide producing conditions (rich mixture) confirmed the fact that fuel contributed little to engine deposits under these conditions (See Table 4.) A second test was run under the same conditions except that nitrogen dioxide was added to the intake manifold at a rate of approximately 10 g/hr (0.03% of intake charge), in an attempt to simulate higher rates of nitrogen fixation. In spite of this small addition, there resulted a significant increase in piston varnish. In a third test, nitrogen dioxide was added to the engine crankcase; again, a notable increase in deposits was observed.

Engine Operation with a Nitrogen-Free Atmosphere

In order to eliminate formation of nitrogen dioxide during engine operation, test runs were made with an essentially nitrogen-free atmosphere in which air was replaced by a mixture of oxygen and carbon dioxide. Commercial gases available gave a mixture which still contained 0.1-0.5% nitrogen, but resulting exhaust gas analysis showed only 0.0004% nitric oxide, about 1/1000 that formed when operating with normal air under conditions conducive to high nitrogen fixation. Because of higher specific heat of carbon dioxide these tests were made with the artificial air containing 30-35% oxygen; this was necessary in order to provide flame temperature close to that calculated for normal air. Carburetion was controlled to yield about 5% oxygen in the exhaust. Under these conditions fuel consumption is 1.5 times that with normal air, indicating high concentrations of both fuel and oxygen. At the end of 39 hr of low-temperature operation on thermally cracked gasoline, the engine remained very clean, as shown in Table 5.

Adding nitrogen dioxide at an average rate of 130 g/hr (0.4%), to the engine intake running on artificial atmosphere resulted in heavy varnishing after only 10 hr of operation. The results in Table 6 as well as those in Table 4 indicate that nitrogen dioxide in the engine does increase deposits.

Table 4 – Effect of Added Nitrogen Dioxide on Deposit Formation

	Piston Deposit	
	CRC Color	Acetone Soluble Deposit, mg/in.^{2}
Reference	9	0.04
NO_2 Added to Intake (10 g/hr)	3	0.6
NO_2 Added to Crankcase (51 g/hr)	2	1.9

Table 5 – Effect of an Artificial Nitrogen-Free Atmosphere on Fuel Deposits (Thermally Cracked Gasoline)

	Piston Deposit	
Atmosphere	CRC Color	Acetone Soluble Deposit, mg/in.^{2}
Normal	3	2.4
Artificial	9	0.1

Precontaminated Oil Studies

Earlier studies[9] have shown that oil contamination by resin-forming materials usually accompanies deposit formation. For example, when oil was changed frequently, or when an abnormally large oil supply was used, very little engine deposit developed, presumably because in both cases only a low concentration of oil contaminants had accumulated. Moreover, if used oil from a previous varnish-forming run was charged to a clean engine operating under deposit-forming conditions with a nondepositing fuel, contaminants in the used oil deposited out as varnish or sludge.

These observations suggested the possibility of precontaminating an oil to yield low-temperature engine deposits under conditions where none would be obtained from the fuel employed. Such precontaminated oils were prepared by diluting the lubricant with 10% by weight of various hydrocarbons or special fuels with and without the addition of nitrogen dioxide. These oils were then engine tested to observe their effect on development of deposits; results are given in Table 7. Nitrogen dioxide-gasoline addition products greatly increase the amount of resin formed. This result suggests that no reactants other than nitrogen dioxide and olefins are necessary to account for at least a portion of the resins found in engines.

Proposed Mechanism of Varnish and Resin Formation

We have confirmed that appreciable nitric oxide may be formed during combustion, and that most of this gas will be eliminated with the exhaust. However, there is always some unscavenged gas remaining to mix with the fresh intake charge. While it is not known whether nitric oxide will react with organic material there is abundant evidence that nitrogen dioxide will. When the small amount of nitrogen dioxide, formed in the combustion chamber from nitric oxide and oxygen, reacts with unsaturated fuel constituents, the resin formed may account for the binder in deposits in this area. Unusual, soft, gummy combustion-chamber deposits have been found which still con-

[9] "Where and Why of Engine Deposits," by R. S. Spindt and C. L. Wolfe. Presented at SAE National West Coast Meeting, Seattle, Aug. 14, 1951.

[10] See Proceedings of Second National Air Pollution Symposium, 1952, pp. 62-70: "Composition and Nature of Blowby and Exhaust Gases from Passenger-Car Engines," by J. Q. Payne and H. W. Sigworth.

tain nitro-compounds formed by this reaction. Combustion-chamber resins are usually subjected to such intense heat that nitro-compounds are pyrolyzed into more resistant resins generally found in such locations.

Deposits on intake valves and ports also have been found to contain nitrogen. It is postulated that nitro-resins in the induction system might result from reactions of gasoline with nitrogen oxides present in either blowback from the combustion chamber or in exhaust gases from a preceding vehicle.

Blowby gas passing the piston appears to be the carrier for contaminants which lead to fuel-formed crankcase deposits. The fact that these gases contain 10-15% oxygen in addition to hydrocarbon material and oxides of nitrogen shows their marked difference from exhaust gases.[10] This difference occurs because amount of blowby passing the rings is greatest at the time of maximum cylinder pressure when the piston is near tdc but before all the charge adjacent to the piston crown has burned.

The low temperature, high oxygen concentration, and appreciable residence time in the crankcase are conducive to formation of nitrogen dioxide and its reaction products with unsaturated organic material. These latter products, which may form either in the vapor phase or in the oil, are carried by the oil to deposit out as resins throughout the crankcase area.

Summary and Conclusions

This paper has attempted to show that engine varnish, the organic binder in engine deposits, results in large part from reactions of nitrogen dioxide with gasoline constituents. Typical deposits from many types of service were found to contain an appreciable amount of nitrogen, of which at least a part was present in aliphatic nitro-compounds.

The problem of nitrogen fixation in gasoline engines was investigated. It was found that amounts of nitric oxide approaching thermodynamic equilibrium at the calculated flame temperature may be present in engine exhaust gases. Kinetic studies on a simplified basis indicate that these results could be predicted.

With respect to low-temperature, fuel-formed deposits, tests have demonstrated that only under conditions leading to appreciable nitrogen fixation does heavy engine varnishing occur. Operation at rich mixtures or with a nitrogen-free atmosphere results in very little engine deposition.

It is possible to precontaminate an oil by adding unsaturated gasoline diluent and reacting a part of it with nitrogen dioxide. The reaction products, dispersed in the oil, will plate out as a typical piston varnish when the mixture is used as a lubricant. This result suggests that nitrogen dioxide can react with gasoline hydrocarbons alone to give products yielding varnishes.

Since, in general, commercial engine oils are fairly resistant to oxidation, it is likely that current deposit problems result from the nature of fuel and prevailing operating conditions. At the low-temperature characteristic of average driving, it appears that lean mixtures with consequent high nitrogen oxide content contribute much to varnish formation.

Table 6 – Effect of Adding Nitrogen Dioxide to an Artificial Atmosphere (Thermally Cracked Gasoline)

Atmosphere	CRC Color	Acetone Soluble Deposit, mg/in.^{2}
Artificial (39 hr)	9	0.11
Artificial + 0.4% NO_2 (10 hr)	2	1.9

Table 7 – Deposits from Precontaminated Oil[a]

Oil Contaminant[b]	Piston Deposit	
	CRC Color	Acetone Soluble Deposits, mg/in.^{2}
Thermally cracked gasoline	10	0.1
Thermally cracked gasoline + 1.4% NO_2	2	1.6
Catalytically cracked gasoline	9	0.1
Catalytically cracked gasoline + 1.0% NO_2	4	1.2
Oxidized gasoline[c]	8	0.2
Oxidized gasoline[c] + 1.0% NO_2	4	2.3

[a] Low-temperature (90 deg coolant) tests of 15-hr duration with a clean fuel at stoichiometric air-fuel ratio and ¾ throttle.

[b] Gasoline diluent at 10% concentration in the oil.

[c] Thermally cracked gasoline highly oxidized in a static oxygen stability apparatu before adding to oil.

Acknowledgment

The authors wish to acknowledge the continuing interest and encouragement of W. A. Gruse of the Mellon Institute. Thanks are due to J. E. Taylor of Gulf Research & Development Co. for his active interest in this problem. Special thanks are also extended to J. E. Baily, H. T. Edwards, and A. N. Jones for their valuable assistance in conducting the tests.

APPENDIX I

Kinetic Calculations of Nitrogen Fixation

In attempting to estimate rate of nitric oxide formation in an engine from theoretical considerations, nitrogen is considered to react with oxygen according to a bimolecular reaction at high temperatures, as given in equation (1).

$$N_2 + O_2 \underset{k_2}{\overset{k_1}{\rightleftarrows}} 2NO \qquad (1)$$

Though some authorities believe the reaction may proceed through a chain mechanism, it is not considered desirable to include any consideration

of such reactions in this study, because of the critical simplifying assumptions which had to be made. Therefore, the following simplified rate equation accounts for the nitric oxide formation:

$$\frac{d\,(NO)}{dt} = k_1\,(N_2)\,(O_2) - k_2\,(NO)^2 \qquad (2)$$

In this equation nitrogen concentration has been assumed essentially constant. Further, since there is no practical way to determine initial oxygen concentration, this concentration is also assumed to remain constant and is calculated from the percentage of oxygen remaining in the final exhaust gas. A more rigorous derivation leads to an integrated equation of the same form, so that errors in computations are of degree rather than kind. Integration leads to an expression for nitric oxide concentration in terms of oxygen and nitrogen concentration, time, and reaction equilibrium and rate constants, which are functions of temperature.

$$(NO) = K\sqrt{(N_2)\,(O_2)}\,\tanh\, k_2 K t\sqrt{(N_2)\,(O_2)} \qquad (3$$

Additional simplifying assumptions required are:

A. Using the perfect gas law, gas concentrations are computed from intake gas pressure and temperature, residual exhaust gas temperature and pressure, and compression ratio for the condition with piston at tdc.

B. Combustion is assumed to occur instantaneously throughout the mixture, so that the gas is at a uniform temperature for the time intervals under consideration.

C. No account is taken of self-heating in the first portion of the gas to burn.[11]

D. No account is taken of dissociation in the burned gas.

With these restrictions, the following equations define oxygen and nitrogen concentrations and flame temperature:[12]

$$(O_2) = \frac{\%O_2 P_i}{100RT_i}\left[CR - (P_i/P_e)^{-1/\gamma}\right] \text{ mole/cc} \qquad (4)$$

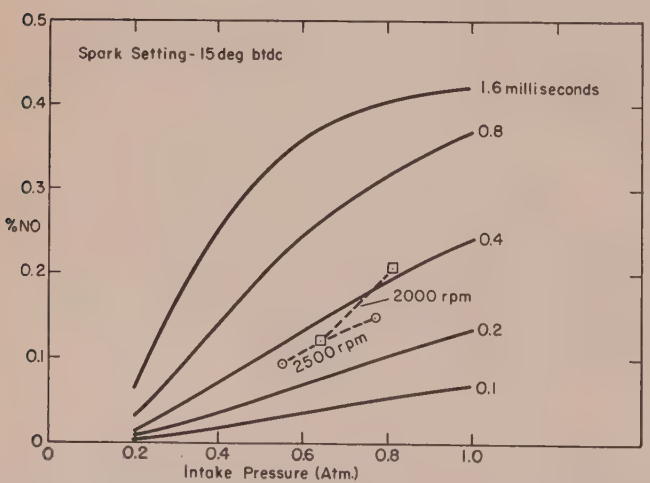

Fig. 6 – Theoretical nitric oxide formation as function of pressure and time with oxygen concentration in exhaust gas = 0.5%

$$(N_2) = \frac{\%N_2 P_i}{100RT_i}\left[CR - (P_i/P_e)^{-1/\gamma}\right] \text{ mole/cc} \qquad (5)$$

$$T_f = \frac{\left(\frac{T_e}{T_i}\right)\left(\frac{P_i}{P_e}\right)\left[CR - \left(\frac{P_i}{P_e}\right)^{-\frac{1}{\gamma}}\right]\left[T_i \cdot CR^{\gamma-1} + \frac{\Delta H}{C_v M_e}\right]}{\left(\frac{T_e}{T_i}\right)\left(\frac{P_i}{P_e}\right)\left[CR + \left(\frac{P_i}{P_e}\right)^{-\frac{1}{\gamma}}\right] + 1} + \frac{T_e \cdot CR^{\gamma-1}}{\left(\frac{T_e}{T_i}\right)\left(\frac{P_i}{P_e}\right)\left[CR - \left(\frac{P_i}{P_e}\right)^{-\frac{1}{\gamma}}\right] + 1} \qquad (6)$$

where:

P_e = Exhaust gas pressure, atmospheres

P_i = Intake gas pressure in cylinder, atmospheres

T_e = Residual exhaust gas temperature, K

T_i = Intake gas temperature, K

CR = Engine compression ratio

R = Gas constant, ml-atm

γ = Ratio of specific heats at constant pressure and constant volume

C_v = Specific heat at constant volume, cal/mole/K

ΔH = Heat of combustion of one mole of fuel, cal

M_e = Total moles of gas per mole of fuel

The temperature equation is derived from the following expression in terms of mixing temperatures, compression temperature, and heat released on combustion:

$$T_f = \frac{mi\,T_i + me\,T_e}{mi + me}\,(CR^{\gamma-1}) + \frac{mi}{mi + me}\cdot\frac{\Delta H}{C_v \cdot M_e} \qquad (7)$$

If V_c is the combustion-chamber volume, V_d is the piston displacement, and V_x the additional volume into which the residual exhaust gas expands to bring its pressure down to that of the intake gas, as defined by the relation,

$$P_i\,(V_c + V_x) = P_e V_c$$

then:

$$me = \frac{V_c P_e}{RT_e} = \text{moles unscavanged exhaust} \qquad (8)$$

$$mi = \frac{(V_d - V_x)\,P_i}{RT_i} = \frac{V_c}{RT_i}\left[CR - (P_i/P_e)^{-1/\gamma}\right]P_i \qquad (9)$$

= moles of intake charge.

Substituting these values for *mi* and *me* into equation (7), eliminating the volume term, and

[11] See SAE Transactions, Vol. 30 (April) 1935, pp. 125-136: "Flame Temperatures Vary with Knock and Combustion-Chamber Position," by G. M. Rasweiler and L. Withrow.

[12] Developed from equations presented in, "Combustion, Flames, and Explosions of Gases," by B. Lewis and G. von Elbe. Pub. by Academic Press, New York, 1951.

[13] See p. 748 of "Selected Values of Physical and Thermodynamic Properties of Hydrocarbons and Related Compounds," by F. D. Rossini. API Research Project 44, Carnegie Press, Pittsburgh, Pa., 1953.

[14] See pp. 393-402 of "New Shock Tube Technique for Study of High-Temperature Gas-Phase Reactions," by H. S. Glick, W. Squire, and A. Hertzberg, in "Fifth Symposium on Combustion." Pub. by Reinhold, New York, 1955.

[15] See *Journal of Chemical Physics*, Vol. 21, 1953, pp. 1904-1905: "Kinetics of Fixation of Atmospheric Nitrogen at Elevated Temperatures," by H. Wise and D. I. Baker.

[16] See *Journal of American Chemical Society*, Vol. 77, No. 8, 1955, pp. 2033-2036: "Kinetic Study of Oxidation of Nitric Oxide with Oxygen in Pressure Range 1-20 Mm," by J. C. Tracy and F. Daniels.

rearranging yields equation (6). Having evaluated the theoretical flame temperature, T_f, the rate constants required in equation (2) are obtained from equations (10)[13] and (11)[14]

$$K = 4.36e^{-21500/RT} \quad (10)$$

$$k_2 = 3.40 \times 10^{12}e^{-40000/RT} \text{ cc/mole/sec} \quad (11)$$

Rate of temperature change in an Otto-cycle engine due to expansion is of the order of 10^5 C per sec at about 2000 rpm, sufficiently rapid to freeze the reaction and retain most of the nitric oxide formed.[15] Time required to expand the charge to the point where this rate of temperature drop occurs is of the order of 0.5-5 millisec, depending on engine speed.

Using equation (3), nitric oxide concentration can be evaluated at constant air-fuel ratio and compression ratio for different values of intake pressure. A family of curves is obtained, as shown in Figs. 6 and 7 for various time intervals. Superimposed on these curves are experimental results which indicate that at high intake pressures, or high engine torque, apparent reaction time is truly of the order of 1-2 millisec. Further, these data show that at high intake gas pressures formation of nitric oxide approaches thermodynamic equilibrium for the calculated flame temperature. At low intake gas pressures several factors, such as less turbulence and slower burning velocities, may be operative to reduce rate of fixation from that predicted for a constant reaction time.

It is realized that calculations presented here involve assumptions that may have been oversimplified and results should be considered tentative only. The principal justification for considering them lies in the fact that the experimentally found concentrations are in accord with theoretical values at time intervals expected to occur in the engine.

APPENDIX II

Analysis of Nitrogen Oxides

As exhaust gas leaves an engine, the principal oxide of nitrogen present is nitric oxide, NO. This gas at atmospheric temperature slowly forms nitrogen dioxide[16] by reaction with oxygen. Direct determination of either of these gases is difficult. However, a satisfactory indirect chemical analysis has been worked out for total nitrogen oxides. It depends on reacting a sample of the gas, still containing principally nitric oxide, with oxygen and an alkaline solution. Oxides of nitrogen are recovered as nitrous acid.

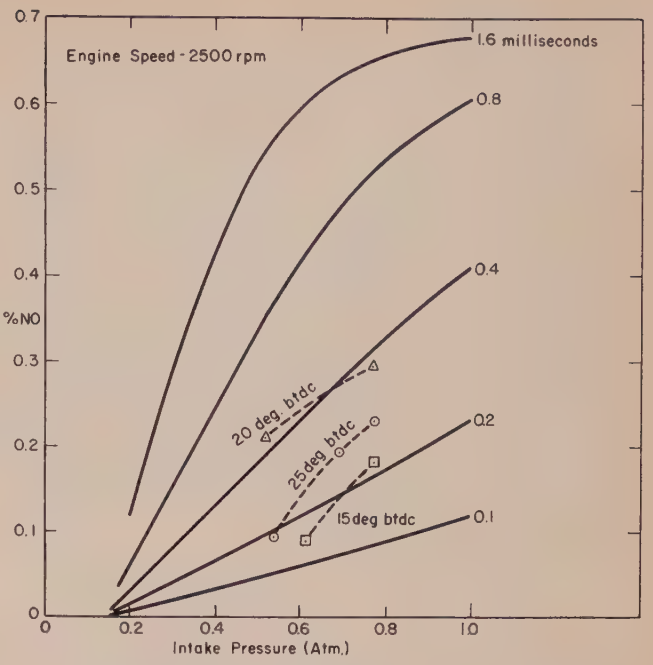

Fig. 7 – Theoretical nitric oxide formation as a function of pressure and time with oxygen concentration in exhaust gas = 2%

As long as nitric oxide is in excess, the reaction

$$NO + NO_2 + H_2O \longrightarrow 2HNO_2 \quad (12)$$

appears to be sufficiently rapid[17] to control the absorption. If, however, nitric oxide is first allowed to be converted into nitrogen dioxide, the reaction

$$2NO_2 + H_2O \longrightarrow HNO_2 + HNO_3 \quad (13)$$

occurs. It is, therefore, important to treat the sample with the alkaline solution soon after sampling.

The nitride ion formed is then determined colorimetrically by synthesizing a diazo dye.[18, 19, 20] The method is very sensitive; amounts as low as 1×10^{-9} mole/ml are easily detected. Therefore, the procedure can be applied to analysis of gases containing extremely small quantities of nitrogen oxides.

The method has been checked against synthetic gas mixtures of nitrogen and nitric oxide, and the results given in Table 8 obtained.

The procedure finally adopted in this laboratory is discussed below.

Analytical Procedure

A 100-ml gas sample, dried over phosphorous pentoxide, is collected over mercury in a gas burrette and transferred quantitatively to a clean, dried, evacuated 150-ml separatory funnel contain-

[17] See *Journal of Chemical Physics*, Vol. 19, January, 1951, pp. 41-47: "Kinetics of Rapid Gas-Phase Reaction between NO, NO_2, and H_2O," by L. G. Wayne and D. M. Yost.

[18] See *Journal of Industrial Hygiene and Toxicology*, Vol. 25, 1943, pp. 361-365: "Nitrite Field Method for Determination of Oxides of Nitrogen (Except N_2O and N_2O_5)," by F. A. Patty and G. M. Petty.

[19] See *Industrial & Engineering Chemistry* (Analytical Edition), Vol. 8, May, 1936, pp. 162-167: "Determination of Nitric Oxide in Coke-Oven Gas," by J. A. Shaw.

[20] See "Gas Chemists' Manual of Dry Box Purification of Gas," by G. E. Seil. Pub. by American Gas Association, New York, 1943.

Table 8 – Concentration of Nitric Oxide, volume %

In Gas Mixture	Found
0.107	0.115
0.25	0.255
0.567	0.505, 0.505

ing 25 ml of 10% sodium hydroxide solution. Oxygen is added to 1 in. of mercury pressure. The funnel is then shaken for 15 min on a wrist-action shaker to remove the nitric oxide by reaction (12).

An aliquot of this solution is treated with Greiss reagent[20] to develop the diazo dye. For concentrations of nitrogen oxides in the gas above 0.2%, 10 ml of the alkaline solution are first diluted to 100 ml with distilled water. The determination is completed by measuring the absorbance of the dye solution and comparing it with a solution prepared with standard sodium nitrite. Because sodium ion concentration was found to affect the development of the dye color it is necessary to determine the absorbance of the solution containing standard nitrite at the same sodium ion concentration employed with the sample.

Calculations for concentration in the gas are:

$$\% NO_2 = \frac{A_s}{A_{st}} \cdot \frac{C_{st} \cdot D \cdot V_s \times 22{,}400 \times 100}{V_g} = \frac{A_s \cdot C_{st} \cdot D \cdot V_s \times 2.24 \times 10^6}{A_{st} \cdot V_g} \quad (14)$$

where:

A_s = Absorbance of sample
A_{st} = Absorbance of standard solution
C_{st} = Concentration of standard in moles/ml
D = Dilution factor = ml of dye solution/ml of alkaline solution
V_s = Volume of alkaline solution, ml
V_g = Volume of gas corrected to standard conditions, ml

APPENDIX III

Apparatus

Most engine experiments were conducted using a 2-cyl Gulf Test Engine. A typical test unit, shown in Fig. 8, has been described in detail by others.[9, 21, 22] Briefly, this engine is a 2-cyl, V-type, 4-stroke-cycle gasoline engine especially designed for research purposes. Two separate lubricating systems are employed, one for the valve train and the other for the piston, connecting rod, and crankshaft bearings. For the research program described, only phenomena occurring in the crankcase oiling system are considered.

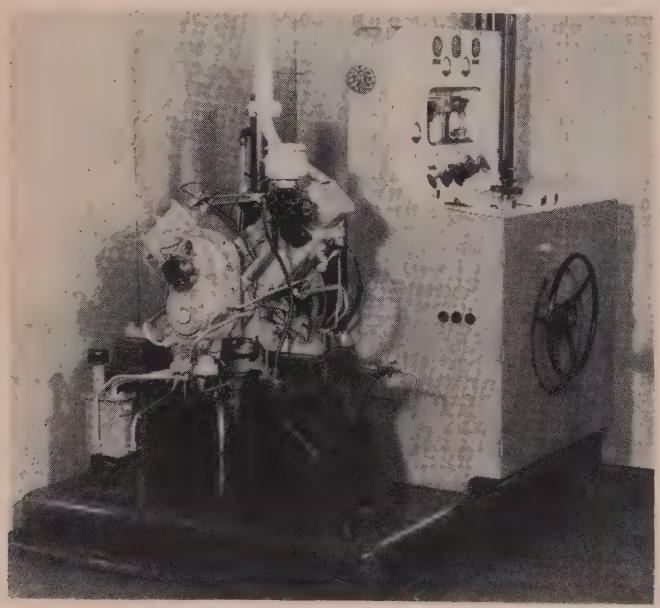

Fig. 8 – Setup of typical test equipment

Table 9 – Engine Variables

Speed, rpm	1500-2500
Torque, lb-ft	0 – maximum
Air-Fuel Ratio	10/1 – 18/1
Spark advance, deg btdc	0 – 30
Coolant Temperature, deg F	90
Oil Temperature, deg F	160
Oil Charge, g	500
Test Duration, hr	10 – 40
Compression Ratio	6.5/1 – 8.5/1

To gain additional data, one piston has been replaced by a balancing assembly shown in the schematic diagram, Fig. 9. This balancing member is made from a standard piston except that the head is cut out and ring grooves eliminated. Oil-laden vapors from the crankcase pass back and forth through this unit. The end of this assembly is closed with a conventional head. A heavy coating of varnish builds up on both the sliding unit and cylinder wall. In other respects, the engine is quite conventional, relative to control and instrumentation.

Engine displacement is 42.1 cu in. Compression ratio may be varied by changing heads. Engine variables were controlled within the ranges given in Table 9.

All engine tests were conducted with uncompounded lubricating oils to eliminate any effects attributable to use of additives. Unleaded refinery distillates, typical of commercial gasoline base stocks, were employed. Work in this laboratory had previously indicated that tetraethyl lead does not significantly change the amount of resin formed.

Upon completion of each test, both power and balance pistons were rated visually following standard CRC procedure. However, to obtain an objective measure of the deposits, varnish was removed with acetone and separated into insoluble and soluble fractions by centrifuging. Both fractions were then recovered, weighed, and reported in terms of mg/in.^{2} Relatively little insoluble material is obtained when operating on these base fuels and oils; therefore, they were not considered in this paper. Even though deposits from all collecting surfaces were evaluated, only data from the power piston are reported.

APPENDIX IV

Table 10 gives the inspection data on typical gasoline distillates used in this study.

[21] See *Petroleum Engineer*, Vol. 15, May, 1944, pp. 196-198: "Oil Test Engine Passes Initial Development Stage," by E. W. Jacobson.

[22] See pp. 23-41: "Gulf 2-Cyl Test Engine," by C. W. Butler, in "CRC Symposium on Laboratory Oil Test Engines," Nov. 3, 1949.

Table 10 – Inspection Data on Typical Gasoline Distillates Used in This Study

	Mid-Continent Raw, Thermally Cracked	Raw Fluid Catalytically Cracked	Mid-Continent, Straight-Run	Aviation Alkylate
Specific Gravity 60 deg/60 deg	0.7389	0.7559	0.7121	0.6998
Sulfur, (D1266) %	0.069	0.041	0.025	—
Oxygen Stability, (D525) min	>1440[a]	1260[a]	>1440	>1440
Bromine Number, (D1159) g/100 g	70.8	92.8	0.0	—
Olefins, (D875) %	50.2	63.2	0.0	—
Aromatics, (D875) %	1.5	8.8	—	—
Vapor Pressure, (D323) lb	10.3	5.3	—	3.5
Distillation, (D86) % Distilled, F				
Initial	92	116	94	125
10%	142	146	139	180
50%	260	246	212	220
90%	355	388	290	251
End	425	428	314	323
FL-2 rating	75	50	—	98

[a] Gasoline inhibited with di-t-butyl-p-cresol.

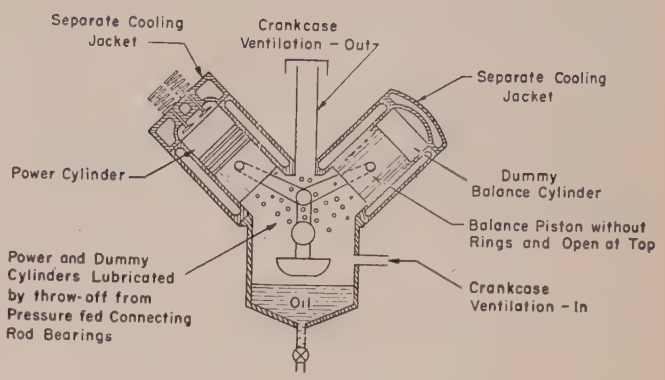

Fig. 9 – Schematic diagram of 2-cyl test engine

DISCUSSION

Nitric Oxide Mechanism Fails to Account For High Oxygen Content of Deposits

– E. A. Oberright
Socony Mobil Laboratories

ACTION of oxides of nitrogen in promoting piston deposits is a very interesting mechanism and a step forward in our knowledge of deposit formation.

With this mechanism and two previously proposed methods, one can account for the major chemical elements in deposits from different types of engines operated under varying conditions. The two former methods are (1) formation and condensation of oxyacids from oil to form lacquer, and (2) oxidation of sulfur compounds in the fuel to sulfur oxides which react with hydrocarbons to form deposits. The first was proposed for high-temperature operation and the second for high-sulfur diesel operation.

The major chemical elements found in deposits are carbon, hydrogen, oxygen, sulfur, and nitrogen. Carbon and hydrogen are introduced into deposits by all three methods. Oxyacids add oxygen, fuel sulfur contributes sulfur and oxygen, and nitrogen in the air introduces nitrogen and oxygen, via the method just presented. It appears that we have reached the end of the line and now are able to account for everything in deposits. But I am sure that as investigations of engine deposits progress, other mechanisms will be found, due to the great complexity of the problem.

The question naturally arises: How much does each of the mechanisms contribute to the deposit under a given set of engine conditions? Under low-temperature, FL-2 conditions, commercial engine oils are quite resistant to oxidation, and it is unlikely that oxyacids from oil oxidation contribute much to these deposits. Likewise, it is quite easy to argue that the sulfur mechanism plays a minor part. Sulfur content of gasoline is small, 0.1% or less, and our analyses of FL-2 deposits show very little sulfur, about 0.3%. However, the nitrogen content of gasoline is even smaller than sulfur, but deposits by the analyses made by Messrs. Spindt, Wolfe, and Stevens contain 1.8% nitrogen, which agrees with our values of 1-2%. The authors' mechanism adequately accounts for this nitrogen and possibly a good deal of the deposit.

The nitric oxide mechanism, however, fails to account for the high percentage of oxygen in deposits. Our analyses indicate 11-14% oxygen. If all the nitrogen were present as nitro-groups, which it definitely isn't, there is still oxygen in the deposit that must be attached to carbon. Infrared analyses in our laboratories have shown the presence of C = O carbonyl groups. Presence of these groups led to the belief that partially oxidized fuel products were carried along with blowby gases into the oil and were deposited as piston varnish. Some such reasoning in combination with the nitrogen oxide method could account for the high ratio of oxygen to nitrogen in deposits.

The authors' data, however, say that this is not so. One of their runs made with thermally cracked gasoline and artificial air gave very little deposits showing that oxidized fuel components **alone** do not form appreciable deposits. Addition of NO_2 to the artificial air did give deposits, showing the dependency of deposit formation on this component. As a suggestion without any facts, the high ratio of oxygen to nitrogen might be the result of oxidation promoted by oxides of nitrogen or, perhaps, the oxides of nitrogen act as polymerization catalysts for oxidized fuel components.

Another point of interest is the relationship of the amount of deposit to the amount of olefins in the gasoline. If the deposit-forming reaction is that of olefins with oxides of nitrogen, one would expect, that under the same engine operating conditions, deposits would increase with increasing amounts of olefins. However, the catalytically cracked gasoline of 63% olefin content produced less deposits than the thermally cracked gasoline containing 50% olefins. I am wondering if the discrepancy could be explained by the types of olefins present in the two gasolines.

This investigation is an excellent piece of fundamental work. Starting with the general idea that nitrogen in the engine deposit must get there some way, it proceeds in a

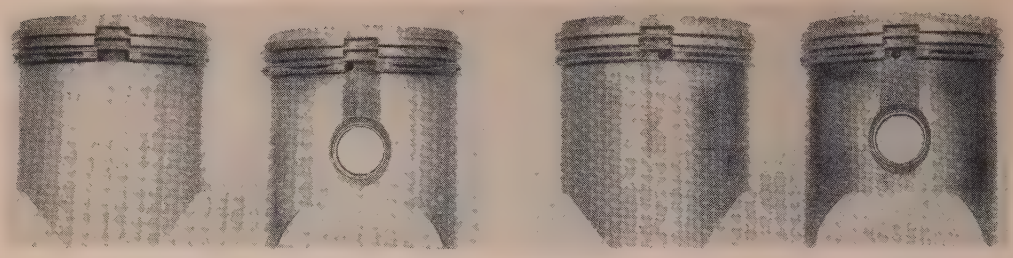

Fig. A – Effect of 20% prediluted oil with thermally cracked naphtha – left: base run; right: 20% prediluted oil

logical and orderly fashion to eliminate different variables and to convincingly prove that oxides of nitrogen and olefins are at least partially responsible for engine deposits.

Olefins Sometimes Contribute To Engine Deposits

– M. W. Savage
California Research Corp.

THERE is one point I should like to discuss briefly. Messrs. Spindt, Wolf, and Stevens showed that under test conditions where higher amounts of nitrogen oxides are present, the cracked fuels they used gave more piston deposits than straight-run fuel. This they attributed, at least in some cases, to the olefin content of the fuel. They also concluded that no reactants other than nitrogen oxides and olefins are necessary to account for at least a portion of the resins found in engines.

Our experience confirms that some fuels containing olefins, such as certain cracked stocks, do indeed contribute to engine deposits; but this is not always true. We have conducted engine tests with diisobutylene, which is 100% olefin, and have found clean deposit conditions. In the same tests, a straight-run fuel also gave low deposits, but other fuels, including some with less than 1% olefins, gave heavy deposits. These tests were conducted at low jacket temperatures and at an air-fuel ratio of 14.5/1, which the authors show to be conducive to formation of relatively large amounts of nitrogen oxides.

These data show that all olefins do not necessarily react with nitrogen oxides to form engine deposits. As the authors point out, there are other factors which influence engine deposits as well.

A fuller understanding of the mechanisms of gasoline engine deposit formation will eventually be attained, and the author's work is a valuable accomplishment in this field.

Diolefins Particularly Objectionable From Standpoint of Engine Deposits

– W. N. Fenney
Texas Co.

FORMATION of engine deposits has been a very complexing problem. The Spindt-Wolf-Stevens theory is a very interesting and significant contribution to the subject and may answer some pertinent questions concerning formation of engine deposits. However, many other factors undoubtedly contribute to this problem. For example, partial roles have also been assigned to other materials that are at hand during deposit-forming reactions such as trace metals, peroxides, sulfur compounds and other unstable hydrocarbons.

The authors indicate that engine deposits, particularly under low-temperature conditions, contain an appreciable amount of nitrogen compounds which cannot be attributed to the fuel. We have analyzed many engine deposits and Table A shows typical results obtained under low temperature S-II conditions. Note that nitrogen content of 2.6% checks reasonably well with the 3.78% obtained by the authors under FL-2 conditions. However, we wonder if the authors have available an extremely sensitive method for nitrogen analysis which would support their statement that nitrogen in engine deposits cannot be attributable to the fuel. We use the Kjeldahl Procedure having a lower limit of about 0.001%. A quick calculation shows there could be 5.9 g of nitrogen available from the fuel during an FL-2 test even though the fuel analysis failed to indicate any nitrogen. One component of engine deposits which does cause us some concern is the high oxygen content which, for the analysis shown, would be 22.8%. This is considerably more than could be accounted for from NO or NO_2. What part oxygen takes in this reaction is open to much speculation.

The authors conducted a series of low-temperature deposit runs with the crankcase lubricant precontaminated with 10% of various gasolines. Their data show that irrespective of the type diluent used, acetone soluble piston deposits were extremely low and the CRC piston rating in the 8-10 range. Fig. A shows some FL-2 data obtained by our laboratories using a 20% prediluted oil. This figure shows that 20% dilution with a thermally cracked naphtha will appreciably increase piston deposits. Admittedly, this predilution is twice that used by the authors. It does indicate that some deposits can originate from fuel dilution in the absence of artificially introduced NO_2, but perhaps if additional NO_2 were added, even greater deposits would have been obtained. Incidentally, since no runs are shown for the addition of NO_2 to a "clean" fuel, what do the authors feel is possible with this combination?

The authors also indicate that engine deposits are formed by the reaction of NO_2 with olefins from the fuel. Fig. B

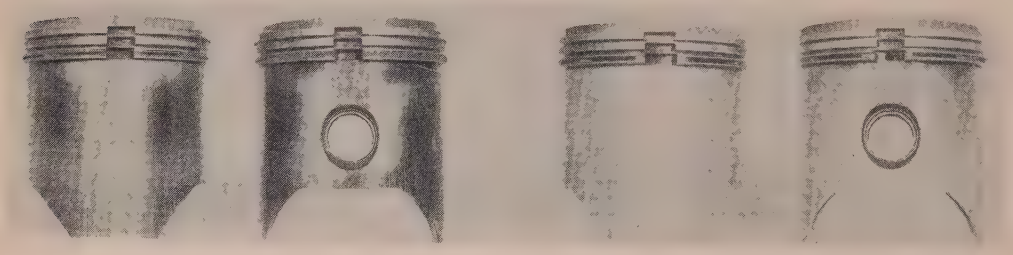

Fig. B – Effect of olefin content on engine deposits – left: high olefin content fuel; right: low olefin content fuel

Fig. C – Effect of diolefins on engine deposits

shows some FL-2 pistons obtained using a fuel of relatively high olefin content as compared with the same fuel hydrogenated to convert the olefins in the higher boiling 15% cut. These data would indicate that only some of the olefinic material contributes to piston deposit formation. However, we wonder if it is primarily the olefins that are the controlling factor in these reactions. We are of the opinion that the diolefins are particularly objectionable from the standpoint of engine deposits. It is known that highly olefinic fuels such as diisobutylene or C_3-C_4 polymer are very satisfactory with respect to low-temperature deposits. On the other hand, when we selectively hydrogenated a fuel to convert only the diolefins as indicated by the diene number, results as shown in Fig. C were obtained in an FL-2 test. You will note, particularly in the ring band area, that elimination of diolefins completely eliminated ring plugging. Table B reduces visual deposits to actual weight, and these data further confirm the large reduction in deposits resulting from elimination of fuel diolefins.

Table A – Analysis of Undissolved Sludge in Used Oil

	Acetone Soluble Portion of Undissolved Sludge, Weight %
Halogen	—
Sulfur	1.5
Carbon	66.1
Hydrogen	7.0
Nitrogen	2.6
Oxygen by Difference	22.8

Table B – Reduction of FL-2 Engine Deposits by Selective Hydrogenation

Engine Run Fuel	66–70 Thermal Cracked	66–73 Selective Hydrogenated
Deposit Weights, g		
Pistons		
Skirt	1.23	0.41
Rings	1.89	0.33
Pans and Covers		
Soluble	14.0	3.8
Insoluble	27.1	6.5
CRC Rating		
Piston	3.8	7.5
Total	28.8	47.5

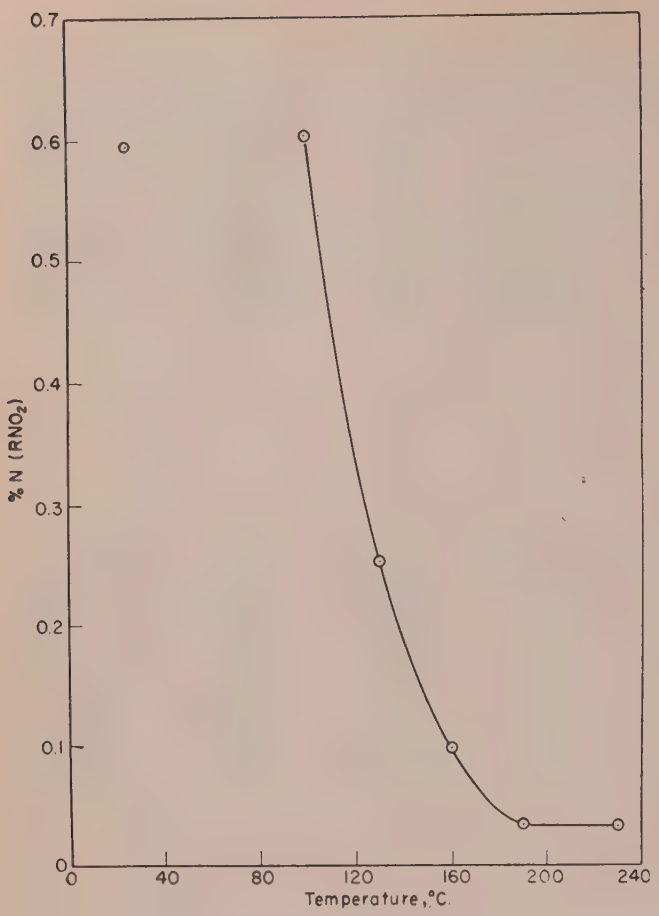

Fig. D – Change in nitro nitrogen in engine resins on heating

Some Condensed Ring Aromatics Also Aid Sludge Formation

– W. Schreiber
Atlantic Refining Co.

AS Messrs. Rogers, Rice, and Jonach have stated, and as other investigators have also found, engine sludge comes mainly from the higher boiling fractions of the gasoline. This is understandable when you consider that the compounds mentioned in the paper, namely, aromatic olefins, diolefins, and phenols, probably boil near the end of the gasoline range or even above it. In addition to these compounds, we have also found certain condensed ring aromatics to be bad, especially in the presence of sulfur compounds. These materials boil at 350 F and higher, which would put them in the heavy ends of the fuel.

Table C – Relationship of Inhibition and Oil Ring Plugging

Lubricant	% Reduction in Organic Insolubles by Additive[a]	Oil Ring Plugging, %
Base stock	—	32
A	15	16
B	59	5
C	30	7
D	63	2

[a] At 50-hr point in ER 4-45 Tests.

In operations involving low temperature we are concerned with deposits on functional parts of the engine because of their effect on performance and maintenance. One of these is oil ring plugging. In Table 13, which gives comparisons between the various additives, no mention is made of this property. I would like to ask if there were any differences between the oils with respect to ring plugging, and if so, did they line up with degree of inhibition.

Another question I would like to raise pertains to the mechanisms discussed in the paper. The question is "What is the role of water both in the mechanism of sludge formation and in the action of the inhibitors."

Motor Oil Additives Won't Rapidly Become Simplified

– W. A. Wright
Sun Oil Co.

I WAS particularly interested in the low-temperature cycling tests and the apparently good correlation with field experience presented by Messrs. Rogers, Rice, and Jonach.

We have not conducted work along the particular analytical lines used by the authors, but have drawn similar conclusions, at least to some degree, from our own work. For many years, we have operated some refinery vehicles on propane on an extended experimental basis. These engines have excellent service histories. Engine deposits and drain oil analyses are more than satisfactory. This is not a very practical solution to the general problem, however.

For 15 years or more we have made routine determinations of oil-soluble resinous materials in oil drain samples. This is done by an adsorption procedure. Average operation frequently shows oil-soluble resinous materials which appear to come from the fuel. This can happen even when the oil itself shows no really significant deterioration.

It would appear logical to take steps to prevent continued degradation of fuel byproducts. I assume the authors do not imply that inhibition alone is the path to follow. Top grade motor oils must be adaptable to high temperature as well as stop-and-go service. This, together with other desirable properties, would not seem to indicate that motor oil additives will rapidly become simplified.

Rogers, et al. Closure To Discussion

MR. SCHREIBER has asked if there were any differences between the oils with respect to ring plugging and if ring plugging lines up with the degree of inhibition. If the quantity of organic insolubles (engine plus drain oil) at the 50-hr point in the ER 4-45 test is taken as an indication of the average degree of inhibition during the test, there appears to be a fair correlation with the extent of oil ring plugging. This relationship is shown in Table C.

Mr. Schreiber has also asked what the role of water was in the mechanism of sludge formation and in the action of the inhibitors. The role of water is not clear. It is always present in small amounts in low-temperature engine tests. The rate of sludge formation is not increased by adding additional water to the crankcase. The amount of sludge, however, appears to be reduced if carefully dried air is used for crankcase ventilation. The water may provide the environment for emulsion-type polymerization, although this does not appear to be a major effect. In the presence of water, a portion of the oil additives may be precipitated during the first few minutes of engine operation and, as a

consequence, that portion would not be available for inhibition reactions. The most desirable inhibitors, therefore, would appear to be those which are not precipitated from oil solution by water.

Mr. Stevens has asked whether the time factor has an influence on the yield of deposits during idle as compared to load operation. It has not been possible to eliminate this factor since, in the test in which idling was attempted for 30 hr, crankcase dilution was excessive. It does appear, however, from spot samples taken during idling and load operation, that there is no appreciable interaction of the deposits produced during idling and under load.

Spindt et al. Closure To Discussion

IT IS well known that engine resins are complex materials derived from several different sources. Ultimate analyses have been made on many engine resins, and we find them to be highly variable irrespective of whether we are dealing with piston varnish, with the pentane-insolubles from a used oil, or with crankcase sludge. Table D shows the range of compositions found.

It is generally observed that even the acetone-soluble products have an appreciable ash content, which is principally iron. There must be a marked concentrating effect to achieve sulfur concentrations of 3%.

We also have observed "red oils" similar to those mentioned by Messrs. Rogers, Rice, and Jonach, and we found them to have properties like those reported. Chemical analysis indicates that this material is rich in nitro compounds, probably formed by reactions of nitrogen oxides with olefins. Examination of the steam distillates from used oils and the hydrocarbon blowby condensate shows that these materials also contain nitro compounds.

We find that the nitro compounds formed by reacting at room temperature nitrogen dioxide and gasoline yield, on heating, resins similar to those in an engine. Further, engine resins formed at low temperatures are changed, by heating, to typical lacquers.

Fig. D shows the effect heat has on the nitrogen present in nitro groups contained in a low-temperature deposit. There is a marked reduction in nitro groups, part of which is due to loss of nitrogen from the molecule and part to conversion into other types of nitrogen-containing compounds. Internal oxidation-reduction reactions can account for an increased oxygen content and the loss of nitro groups.

While many olefins will react with nitrogen dioxide to yield "red oils" that may be converted into resins, the ease of this conversion at low operating temperatures depends on the type of olefin involved. We also have run engine tests on heptenes and diisobutylene and have obtained very little piston varnish. However, with styrene we obtained heavy engine deposits typical of a gasoline varnish. These results support the conclusion of others that aromatic olefins can contribute to engine deposits. These three hydrocarbons were free of phenols and sulfur compounds and the results indicate that these latter do not need to be present to obtain engine deposits. This does not imply that phenols and sulfur compounds cannot contribute to deposits, however.

It is clear why crankcase ventilation helps. If the blowby gases are swept out of the crankcase there is a marked reduction in gasoline vapor, oxides of nitrogen, and other crankcase contaminants. On the other hand, the higher the boiling point of the fuel, the more crankcase dilution will occur and the more complex will be the hydrocarbons retained and subjected to reactions with nitrogen oxides.

We also believe that diolefins in the heavy ends may be the chief factor in gasolines that contribute to deposits. However, while low molecular weight olefins do not stay in the crankcase (or oil) long, because of their high volatility, our evidence indicates that they can contribute to deposits. Engine tests have been made where butadiene, isoprene, and butene-1, in separate runs, were fed into the crankcase under conditions where the fuel did not contribute to deposits. Even though these are gaseous hydrocarbons, their presence resulted in heavy piston varnish. This again is due to the reactions of the olefin with nitrogen dioxide, as shown by the analysis of the resins. Further, when butadiene was passed with exhaust gases into a 5-liter flask, a typical deposit formed on the walls, thus indicating that vapor-phase reactions can lead to resins just as well as can reactions occurring in the oil.

While it is possible that all of the nitrogen in deposits could have come from the fuel, a simple calculation shows that to obtain the concentration of nitrogen which we observe in the deposits, all of the nitrogen from the gasoline would have to be localized in the deposits and none of it passed out the exhaust. It is hard for us to believe that the small concentration of nitrogen compounds present in gasoline, mostly heterocyclic amines, could be that selectively separated from the combustion zone and pushed into the crankcase. The blowby gases seldom, if ever, exceed 5% of the total charge.

Precombustion reactions of gasoline may also contribute to deposits but we suggest that they may not be as important to this phenomenon as they may be to knock. A small contribution from this source could account for some of the oxygen content of engine resins. Among the oxygen-containing functional groups that we observed in the deposits are hydroxyl, carbonyl, and carboxcylic acids. These may be present in various combinations and they may be derived either from the precombustion reaction products or from oxidation-reduction reactions of nitroparaffins.

Our lack of deposits from an oil prediluted with gasoline has been questioned. Past experience had indicated that a 15-hr run would remove sufficient contaminants from a reused oil to give significant deposits. Therefore, all of our precontaminated oil studies were conducted on a 15-hr basis. Predilution of an oil with gasoline and then running the oil in an engine under lean mixture conditions should result in a deposit just as if the diluent had been used as a fuel. The oxides of nitrogen from combustion can react with the diluent to yield typical deposits. This takes time, however. In the 15-hr test the concentration of contaminants built up in this way does not yield significant deposits.

The question of what a clean-burning gasoline would do, if an oil solution were treated with nitrogen dioxide, was not investigated because a bench test had indicated that the clean gasoline with nitrogen dioxide did not yield resins. Upon evaporation the treated fuel yielded a clean dish while, under the same conditions with a cracked gasoline, heavy gummy deposits are obtained. We suggest that a clean gasoline used as an oil diluent, whether or not treated with nitrogen dioxide, should give no more deposit than when used as a fuel.

Undoubtedly, there are many reactions of several different types that contribute to deposit formation. We believe that those involving oxides of nitrogen are very important and accounted for many phenomena observed in engines.

Table D – Range of Compositions Found

Carbon, %	60–80
Hydrogen, %	3–11
Oxygen, % (diff.)	15–25
Nitrogen, %	0.5–4
Sulfur, %	0.5–3
Ash, %	0.5–2

Index to SAE Transactions

Volume 64—1956

Page

ACCIDENTS AND ACCIDENT PREVENTION (AIRCRAFT)
- Fatigue and Fail-Safe Airframe Design, J. F. McBrearty ... 426
- Human Problems in Jet Air Transportation, Dr. Ross A. McFarland ... 437

ACCIDENTS AND ACCIDENT PREVENTION (NONAIRCRAFT)
- A Practical Stopping-Ability Regulation, Carl C. Saal ... 229
- Design Factors in Automotive Safety, A. L. Haynes. 644
- Human and Environmental Factors of Automobile Safety, Dr. Ross A. McFarland ... 625
- Human Factors in Highway Transport Safety, Dr. Ross A. McFarland ... 730

ACKERMAN, P. C.
- Discussion of "Design Factors in Automotive Safety" by A. L. Haynes ... 654
- Discussion of "Human and Environmental Factors of Automobile Safety" by Dr. Ross A. McFarland.... 654

ADDITIVES, FUEL
- New Instrumentation for Engine Combustion Studies, J. A. Warren and J. B. Hinkamp... 665

ADDITIVES, OIL
- Cold Starting with V. I. Improved Multigrade Oils, F. B. Fischl, H. H. Horowitz, and T. S. Tutwiler.. 608
- Mechanism of Engine Sludge Formation and Additive Action, D. T. Rogers, W. W. Rice, and F. L. Jonach ... 782
- Nitrogen Oxides, Combustion, and Engine Deposits, R. S. Spindt, Court L. Wolfe, and Donald R. Stevens ... 797
- Relationship of Low-Temperature Cranking Resistance to Viscosity Characteristics of Multigrade Engine Oils, G. K. Malone and T. W. Selby..... 602
- Stop Sludge and Go Clean, R. H. Albrecht, R. I. Potter and Kent Hyatt... 751

AERODYNAMICS
- Flight Research at High Altitudes and High Speeds with Rocket Propelled Research Airplanes, Walter C. Williams ... 570
- How High Should We Fly? Schuyler Kleinhans.... 300
- Some Experiments in the Application of Boundary-Layer Control, Joseph Flatt... 101
- Wing-Lift Augmentation Methods for the Improvement of Low-Speed Performance of High-Speed Aircraft, John S. Attinello... 108

AIR CARGO
- Cushion Design From Fragility Rating, H. E. Nietsch ... 241
- Flexible Suspension Systems for Equipment in Transit, John J. Goodill... 41

AIRCRAFT ACCESSORIES AND EQUIPMENT
- A New Approach to Turbojet and Ramjet Engine Control, Wendell E. Reed... 472
- High-Temperature Problems Associated with the Use of Rubber in Aircraft, Frederick E. Clark..... 24
- NACA Investigation of Thrust-Reversal Techniques, John H. Povolny and Jack G. McArdle..... 542

AIRCRAFT DESIGN AND PERFORMANCE
- Application of High-Temperature Materials to Aircraft Powerplants in the Temperature Range 1200-2400 F, Alan V. Levy... 366
- Application of Metallic Materials for Aircraft Structures in the Temperature Range 600 to 1100 F, James W. Huffman ... 5
- Fatigue and Fail-Safe Airframe Design, J. F. McBrearty ... 426
- Flight Research at High Altitudes and High Speeds with Rocket Propelled Research Airplanes, Walter C. Williams ... 570
- How High Should We Fly? Schuyler Kleinhans 300
- NACA Investigation of Thrust-Reversal Techniques, John H. Povolny and Jack G. McArdle..... 542
- Some Elevated Temperature Structural Problems of High-Speed Aircraft, Richard R. Heldenfels..... 524
- Some Experiments in the Application of Boundary-Layer Control, Joseph Flatt ... 101
- The Selection of Metals for Airframe Components as Affected by Operation at Elevated Temperatures up to 600 F, M. Tiktinsky..... 131
- Wing-Lift Augmentation Methods for the Improvement of Low-Speed Performance of High-Speed Aircraft, John S. Attinello..... 108

AIRCRAFT LANDING GEAR
- Lightweight Springs for Limited Life, E. H. Spaulding ... 453

AIRCRAFT, ROTATING WING
- Shaft Gas Turbines For Helicopters, W. S. Miller, Jr., R. P. Krebs, and T. C. Blaschke..... 348

AIR TRANSPORT
- Human Problems in Jet Air Transportation, Dr. Ross A. McFarland ... 437

ALBRECHT, R. H.
- Stop Sludge and Go Clean (Co-authors R. I. Potter and Kent Hyatt) ... 751

ALLEN, R. C.
- Nuclear Power and the Machinery Builder..... 589

ALMEN, J. O.
- Discussion of "Lightweight Springs for Limited Life" by E. H. Spaulding..... 457

ALUMINUM AND ALLOYS
- A Billion Engine Hours on Aluminum Bearings, R. S. Frank and W. J. Lux..... 655
- Fatigue and Fail-Safe Airframe Design, J. F. McBrearty ... 426
- Some Elevated Temperature Structural Problems of High-Speed Aircraft, Richard R. Heldenfels..... 524
- The Selection of Metals for Airframe Components as Affected by Operation at Elevated Temperatures up to 600 F, M. Tiktinsky..... 131

ARNOLD, JOHN E.
- Creativity in Engineering ... 17

ATOMIC ENERGY
- Nuclear Power and the Machinery Builder, R. C. Allen ... 589

ATTINELLO, JOHN S.
- Wing-Lift Augmentation Methods for the Improvement of Low-Speed Performance of High-Speed Aircraft ... 108

AVIATION, MILITARY
- Some Experiments in the Application of Boundary-Layer Control, Joseph Flatt..... 101
- Wing-Lift Augmentation Methods for the Improvement of Low-Speed Performance of High-Speed Aircraft, John S. Attinello ... 108

B

BALDWIN, L. L.
- Tire Design – Present and Future ... 502

BEADLE, R. H.
- Discussion of "The Napier Deltic Diesel Engine" by Ernest Chatterton ... 422

Page

BEARINGS AND BEARING ALLOYS
A Billion Engine Hours on Aluminum Bearings, R. S. Frank and W. J. Lux 655
BLASCHKE, T. C.
Shaft Gas Turbines For Helicopters (Co-authors W. S. Miller, Jr. and R. P. Krebs) ... 348
BODEAU, A. C.
Passenger-Car Suspension Analysis (Co-authors R. H. Bollinger and L. Lipkin) 273
BODIES
A Study of Nonprotective Rust Formation On Auto-Body Sheet Steel, J. C. Holzwarth, R. F. Thomson, and A. L. Boegehold 221
Automobile Body Loads, Philip O. Johnson 12
BOEGEHOLD, A. L.
A Study of Nonprotective Rust Formation On Auto-Body Sheet Steel (Co-authors J. C. Holzwarth and R. F. Thomson). 221
BOLLINGER, R. H.
Passenger-Car Suspension Analysis (Co-authors A. C. Bodeau and L. Lipkin) 273
BOWDITCH, F. W.
Discussion of "New Instrumentation for Engine Combustion Studies" by J. A. Warren and J. B. Hinkamp 679
BOWSER, P. C.
Discussion of "The Low Silhouette Drive Line" by R. Burkhalter and P. J. Mazziotti 392
BRAKES
A Practical Stopping-Ability Regulation, Carl C. Saal 229
BROCK, H. L.
Discussion of "Farm Tractors and Their Tires" by F. C. Walters and W. H. Worthington 405
BURKHALTER, R.
The Low Silhouette Drive Line (Co-author P. J. Mazziotti) 379
BUS DESIGN AND PERFORMANCE
Human Factors in Highway Transport Safety, Dr. Ross A. McFarland 730
BUTLER, J. W.
Discussion of "A Billion Engine Hours on Aluminum Bearings" by R. S. Frank and W. J. Lux 664

C

CAMS AND CAMSHAFTS
Camshaft-Tappet Problems in Ford Overhead Valve Engines, J. S. Laird, C. L. Stevens, and V. L. Iles .. 153
Considerations Affecting the Life of Automotive Camshafts and Tappets, M. F. Garwood, D. R. Kinker, and J. J. Manganello 138
Interrelationship of Design, Lubrication, and Metallurgy in Cam and Tappet Performance, E. B. Etchells, R. F. Thomson, G. H. Robinson, and G. K. Malone 161
CARBURETORS AND CARBURETION
Mechanical Octanes for Higher Efficiency, D. F. Caris, B. J. Mitchell, A. D. McDuffie, and F. A. Wyczalek 76
CARIS, D. F.
Mechanical Octanes for Higher Efficiency (Co-authors B. J. Mitchell, A. D. McDuffie, and F. A. Wyczalek) 76
CHASE, J. O.
Fuel Heat Gain and Release in Bomb Autoignition (Co-authors R. W. Hurn, C. F. Ellis, and K. J. Hughes) 703
CHATTERTON ERNEST
The Napier Deltic Diesel Engine 408
CLARK, FREDERICK E.
High-Temperature Problems Associated with the Use of Rubber in Aircraft 24
COLD WEATHER OPERATION
Cold Starting with V. I. Improved Multigrade Oils, F. B. Fischl, H. H. Horowitz, and T. S. Tutwiler .. 608
Relationship of Low-Temperature Cranking Resistance to Viscosity Characteristics of Multigrade Engine Oils, G. K. Malone and T. W. Selby 602
COLLINS, R. N.
Physical and Chemical Ignition Delay in an Operating Diesel Engine Using the Hot-Motored Technique (Co-authors T. C. Yu, O. A. Uyehara, P. S. Myers, and K. Mahadevan) 690
COMBUSTION
Evaluation of Reaction Kinetics Eliminates Diesel Knock – The M-Combustion System of MAN, J. S. Meurer 250
Fuel Heat Gain and Release in Bomb Autoignition, R. W. Hurn, J. O. Chase, C. F. Ellis and K. J. Hughes 703
Fuel Vaporization and Ignition Lag in Diesel Combustion, M. M. El Wakil, P. S. Myers, and O. A. Uyehara 712
Mechanism of Engine Sludge Formation and Additive Action, D. T. Rogers, W. W. Rice, and F. L. Jonach 782
New Instrumentation for Engine Combustion Studies, J. A. Warren and J. B. Hinkamp 665
Nitrogen Oxides, Combustion, and Engine Deposits, R. S. Spindt, Court L. Wolfe, and Donald R. Stevens 797
Physical and Chemical Ignition Delay in an Operating Diesel Engine Using the Hot-Motored Technique, T. C. Yu, O. A. Uyehara, P. S. Myers, R. N. Collins, and K. Mahadevan 690
COMBUSTION CHAMBERS
Application of High-Temperature Materials to Aircraft Powerplants in the Temperature Range 1200-2400 F, Alan V. Levy 366
Mechanical Octanes for Higher Efficiency, D. F. Caris, B. J. Mitchell, A. D. McDuffie, and F. A. Wyczalek 76
Pneumatic and Sonic Measurement of Combustion-Chamber Volume, G. A. Weinert 50
The New Packard V-8 Engine, W. E. Schwieder 205
The New Plymouth V-8 Engine, H. L. Welch 195
COMPRESSORS, TURBINE ENGINE
New Alloys for Automotive Turbines, Donald N. Frey 582
The Differential Gas Turbine, David W. Hutchinson. 510
The Supercharged Turboprop, S. G. Hooker 185
CONSTRUCTION AND INDUSTRIAL MACHINERY
Effect of Rapid Load Changes on Torque-Converter Performance, P. J. Swanson and J. H. Meier 534
COONEY, CHARLES E., JR.
Discussion of "The Low Silhouette Drive Line" by R. Burkhalter and P. J. Mazziotti 392
CORROSION
A Study of Nonprotective Rust Formation On Auto-Body Sheet Steel, J. C. Holzwarth, R. F. Thomson, and A. L. Boegehold 221
Instrumentation for Valve-Burning Studies, W. D. Sims 356
Steels and Protective Treatments For Use up to 1000 F, H. J. Noble and W. H. Sharp 59
CORZILIUS, M. W.
Discussion of "New Instrumentation for Engine Combustion Studies" by J. A. Warren and J. B. Hinkamp 677
CRC
Diesel Smoke Measurement (Progress Report of the Smokemeter Group of the Diesel Fuels Division, Coordinating Fuel and Equipment Research Committee, CRC), H. C. Hunter 680

D

DACK, W. S.
Discussion of "Automotive Gasoline Injection" by Sidney E. Miller 466

Page

DARBY, R. A.
Discussion of "Some Experiments in the Application of Boundary-Layer Control" by Joseph Flatt.... 119
Discussion of "Wing-Lift Augmentation Methods for the Improvement of Low-Speed Performance of High-Speed Aircraft" by John S. Attinello 119

DAY, W. E., JR.
Discussion of "Camshaft-Tappet Problems in Ford Overhead Valve Engines" by J. S. Laird, C. L. Stevens, and V. L. Iles 183
Discussion of "Considerations Affecting the Life of Automotive Camshafts and Tappets" by M. F. Garwood, D. R. Kinker, and J. J. Manganello.... 183
Discussion of "Interrelationship of Design, Lubrication, and Metallurgy in Cam and Tappet Performance" by E. B. Etchells, R. F. Thomson, G. H. Robinson, and G. K. Malone..... 183

DEPOSITS, ENGINE
A Radioactive Method for Measuring Engine Deposits, J. G. Mingle, H. W. Sigworth, and B. A. Fries 577
Mechanism of Engine Sludge Formation and Additive Action, D. T. Rogers, W. W. Rice, and F. L. Jonach 782
Nitrogen Oxides, Combustion, and Engine Deposits, R. S. Spindt, Court L. Wolfe, and Donald R. Stevens 797
Pneumatic and Sonic Measurement of Combustion-Chamber Volume, G. A. Weinert..... 50
Stop Sludge and Go Clean, R. H. Albrecht, R. I. Potter, and Kent Hyatt 751

DETONATION
Evaluation of Reaction Kinetics Eliminates Diesel Knock – The M-Combustion System of MAN, J. S. Meurer 250
Knocking Behavior of Fuels and Engines, R. V. Kerley and K. W. Thurston 554
New Instrumentation for Engine Combustion Studies, J. A. Warren and J. B. Hinkamp..... 665

DIGGS, D. R.
Discussion of "Mechanical Octanes for Higher Efficiency" by D. F. Caris, B. J. Mitchell, A. D. McDuffie, and F. A. Wyczalek..... 97

DOWNING, E. W.
Discussion of "Automotive Gasoline Injection" by Sidney E. Miller 470

DUCKWORTH, J. B.
Discussion of "Knocking Behavior of Fuels and Engines" by R. V. Kerley and K. W. Thurston..... 565

DUNN, G. E.
Discussion of "The Low Silhouette Drive Line" by R. Burkhalter and P. J. Mazziotti 393

E

ELLIS, C. F.
Fuel Heat Gain and Release in Bomb Autoignition (Co-authors R. W. Hurn, J. O. Chase, and K. J. Hughes) 703

EL WAKIL, M. M.
Fuel Vaporization and Ignition Lag in Diesel Combustion
(Co-authors P. S. Myers and O. A. Uyehara).... 712

ENGINEERS AND ENGINEERING
Creativity In Engineering, John E. Arnold..... 17

ENGINES, AIRCRAFT (JET AND TURBINE)
A Jet Exhaust Silencer, J. M. Tyler and G. B. Towle. 294
A New Approach to Turbojet and Ramjet Engine Control, Wendell E. Reed 472
Application of High-Temperature Materials to Aircraft Powerplants in the Temperature Range 1200-2400 F, Alan V. Levy 366
Human Problems in Jet Air Transportation, Dr. Ross A. McFarland 437
Principles and Applications of Bypass Turbojet Engines, George F. Wislicenus 486
Shaft Gas Turbines For Helicopters, W. S. Miller, Jr., R. P. Krebs, and T. C. Blaschke 348
The Supercharged Turboprop, S. G. Hooker..... 185

ENGINES, DIESEL
A Billion Engine Hours on Aluminum Bearings, R. S. Frank and W. J. Lux..... 655
Evaluation of Reaction Kinetics Eliminates Diesel Knock – The M-Combustion System of MAN, J. S. Meurer 250
Fuel Heat Gain and Release in Bomb Autoignition, R. W. Hurn, J. O. Chase, C. F. Ellis, and K. J. Hughes 703
Fuel Vaporization and Ignition Lag in Diesel Combustion, M M. El Wakil, P. S. Myers, and O. A. Uyehara 712
Physical and Chemical Ignition Delay in an Operating Diesel Engine Using the Hot-Motored Technique, T. C. Yu, O. A. Uyehara, P. S. Myers, R. N. Collins, and K. Mahadevan 690
The Napier Deltic Diesel Engine, Ernest Chatterton. 408

ENGINES, JET AND TURBINE (NONAIRCRAFT)
New Alloys for Automotive Turbines, Donald N. Frey 582
The Differential Gas Turbine, David W. Hutchinson. 510

ENGINES, PASSENGER CAR
A Radioactive Method for Measuring Engine Deposits, J. G. Mingle, H. W. Sigworth, and B. A. Fries 577
Automotive Gasoline Injection, Sidney E. Miller.... 458
Camshaft-Tappet Problems in Ford Overhead Valve Engines, J. S. Laird, C. L. Stevens, and V. L. Iles.. 153
Considerations Affecting the Life of Automotive Camshafts and Tappets, M. F. Garwood, D. R. Kinker, and J. J. Manganello..... 138
Instrumentation for Valve-Burning Studies, W. D. Sims 356
Interrelationship of Design, Lubrication, and Metallurgy in Cam and Tappet Performance, E. B. Etchells, R. F. Thomson, G. H. Robinson, and G. K. Malone 161
Knocking Behavior of Fuels and Engines, R. V. Kerley and K. W. Thurston 554
Mechanical Octanes for Higher Efficiency, D. F. Caris, B. J. Mitchell, A. D. McDuffie, and F. A. Wyczalek 76
New Alloys for Automotive Turbines, Donald N. Frey 582
The New Packard V-8 Engine, W. E. Schwieder.... 205
The New Plymouth V-8 Engine, H. L. Welch..... 195

ENGINES, ROCKET
Application of High-Temperature Materials to Aircraft Powerplants in the Temperature Range 1200-2400 F, Alan V. Levy 366
Flight Research at High Altitudes and High Speeds with Rocket Propelled Research Airplanes, Walter C. Williams 570

ENOCH, OTTO
Discussion of "Knocking Behavior of Fuels and Engines" by R. V. Kerley and K. W. Thurston..... 567
Discussion of "Mechanical Octanes for Higher Efficiency" by D. F. Caris, B. J. Mitchell, A. D. McDuffie, and F. A. Wyczalek 98

ETCHELLS, E B.
Interrelationship of Design, Lubrication, and Metallurgy in Cam and Tappet Performance
(Co-authors R. F. Thomson, G. H. Robinson, and G. K. Malone) 161

EXHAUST SYSTEMS AND EXHAUST GASES
A Jet Exhaust Silencer, J. M. Tyler and G. B. Towle. 294
Diesel Smoke Measurement (Progress Report of the Smokemeter Group of the Diesel Fuels Division, Coordinating Fuel and Equipment Research Committee, CRC), H. C. Hunter 680

Page

Nitrogen Oxides, Combustion, and Engine Deposits, R. S. Spindt, Court L. Wolfe, and Donald R. Stevens 797

F

FARM MACHINERY
Farm Tractors and Their Tires, F. C. Walters and W. H. Worthington 394
FENNEY, W. N.
Discussion of "Nitrogen Oxides, Combustion, and Engine Deposits" by R. S. Spindt, Court L. Wolfe, and Donald R. Stevens 808
FINISHES (PROTECTIVE COATINGS)
Steels and Protective Treatments For Use up to 1000 F, H. J. Noble and W. H. Sharp..... 59
FISCHL, F. B.
Cold Starting with V. I. Improved Multigrade Oils (Co-authors H. H. Horowitz and T. S. Tutwiler).. 608
FLATT, JOSEPH
Some Experiments in the Application of Boundary-Layer Control 101
FLINN, R. A.
Discussion of "Considerations Affecting the Life of Automotive Camshafts and Tappets" by M. F. Garwood, D. R. Kinker, and J. J. Manganello.... 181
FOREIGN DESIGN AND OPERATION
The Napier Deltic Diesel Engine, Ernest Chatterton 408
The Supercharged Turboprop, S. G. Hooker..... 185
FORSTER, F. A.
Discussion of "Stop Sludge and Go Clean" by R. H. Albrecht, R. I. Potter, and Kent Hyatt..... 771
FRANK, R. S.
A Billion Engine Hours on Aluminum Bearings (Co-author W. J. Lux) 655
FREY, DONALD N.
New Alloys for Automotive Turbines 582
FREY, KURT P. H.
Discussion of "Some Experiments in the Application of Boundary-Layer Control" by Joseph Flatt..... 122
Discussion of "Wing-Lift Augmentation Methods for the Improvement of Low-Speed Performance of High-Speed Aircraft" by John S. Attinello..... 122
FRIES, B. A.
A Radioactive Method for Measuring Engine Deposits (Co-authors J. G. Mingle and H. W. Sigworth).. 577
FUELS, DIESEL
Diesel Smoke Measurement (Progress Report of the Smokemeter Group of the Diesel Fuels Division, Coordinating Fuel and Equipment Research Committee, CRC), H. C. Hunter 680
Fuel Heat Gain and Release in Bomb Autoignition, R. W. Hurn, J. O. Chase, C. F. Ellis, and K. J. Hughes 703
Fuel Vaporization and Ignition Lag in Diesel Combustion, M M. El Wakil, P. S. Myers, and O. A. Uyehara 712
Physical and Chemical Ignition Delay in an Operating Diesel Engine Using the Hot-Motored Technique, T. C. Yu, O. A. Uyehara, P. S. Myers, R. N. Collins, and K. Mahadevan 690
FUELS, MOTOR
Knocking Behavior of Fuels and Engines, R. V. Kerley and K. W. Thurston 554
Mechanical Octanes for Higher Efficiency, D. F. Caris, B. J. Mitchell, A. D. McDuffie, and F. A. Wyczalek 76
Mechanism of Engine Sludge Formation and Additive Action, D. T. Rogers, W. W. Rice, and F. L. Jonach 782
New Instrumentation for Engine Combustion Studies, J. A. Warren and J. B. Hinkamp..... 665
Nitrogen Oxides, Combustion, and Engine Deposits, R. S. Spindt, Court L. Wolfe, and Donald R. Stevens 797

Page

G

GAMMON, H. M.
Discussion of "Automotive Gasoline Injection" by Sidney E. Miller 465
GARWOOD, M. F.
Considerations Affecting the Life of Automotive Camshafts and Tappets (Co-authors D. R. Kinker and J. J. Manganello).. 138
GEYER, LEO A.
Discussion of "Some Experiments in the Application of Boundary-Layer Control" by Joseph Flatt.... 121
Discussion of "Wing-Lift Augmentation Methods for the Improvement of Low-Speed Performance of High-Speed Aircraft" by John S. Attinello..... 121
GILBERT, CHARLES S., JR.
Discussion of "Knocking Behavior of Fuels and Engines" by R. V. Kerley and K. W. Thurston..... 566
GOHN, GEORGE R.
Fatigue and Its Relation to the Mechanical and Metallurgical Properties of Metals..... 31
GOODILL, JOHN J.
Flexible Suspension Systems for Equipment in Transit 41
GOUGH, V. E.
Practical Tire Research 310
GRUBE, W. L.
Discussion of "Stop Sludge and Go Clean" by R. H. Albrecht, R. I. Potter, and Kent Hyatt..... 771

H

HAAS, HERBERT H.
Discussion of "Evaluation of Reaction Kinetics Eliminates Diesel Knock – The M-Combustion System of MAN" by J. S. Meurer..... 269
HAEUSLER, ROY
Discussion of "Human Factors in Highway Transport Safety" by Ross A. McFarland..... 747
HARTLEY, D. C.
Tires For High-Performance Cars (Co-authors T. J. P. Joy and D. M. Turner)..... 319
HAVELY, T. W.
Discussion of "Camshaft-Tappet Problems in Ford Overhead Valve Engines" by J. S. Laird, C. L. Stevens, and V. L. Iles..... 182
Discussion of "Considerations Affecting the Life of Automotive Camshafts and Tappets" by M. F. Garwood, D. R. Kinker, and J. J. Manganello..... 182
HAYNES, A. L.
Design Factors in Automotive Safety 644
HAZEN, DAVID
Discussion of "Some Experiments in the Application of Boundary-Layer Control" by Joseph Flatt..... 119
Discussion of "Wing-Lift Augmentation Methods for the Improvement of Low-Speed Performance of High-Speed Aircraft" by John S. Attinello..... 119
HELDENFELS, RICHARD R.
Some Elevated Temperature Structural Problems of High-Speed Aircraft 524
HINKAMP, J. B.
New Instrumentation for Engine Combustion Studies (Co-author J. A. Warren)..... 665
HOLLIFIELD, EDGAR L.
Discussion of "Human Factors in Highway Transport Safety" by Ross A. McFarland..... 748
HOLZWARTH, J. C.
A Study of Nonprotective Rust Formation On Auto-Body Sheet Steel (Co-authors R. F. Thomson and A. L. Boegehold). 221
HOOKER, S. G.
The Supercharged Turboprop 185
Discussion of "Principles and Applications of Bypass Turbojet Engines" by George F. Wislicenus..... 501
HOROWITZ, H. H.
Cold Starting with V. I. Improved Multigrade Oils (Co-authors F. B. Fischl and T. S. Tutwiler)..... 608

Page

HUFFMAN, JAMES W.
Application of Metallic Materials for Aircraft Structures in the Temperature Range 600 to 1100 F.... 5

HUGHES, K. J.
Fuel Heat Gain and Release in Bomb Autoignition (Co-authors R. W. Hurn, J. O. Chase, and C. F. Ellis) 703

HUMAN ENGINEERING
Design Factors in Automotive Safety, A. L. Haynes. 644
Human and Environmental Factors of Automobile Safety, Dr. Ross A. McFarland..... 625
Human Factors in Highway Transport Safety, Dr. Ross A. McFarland 730
Human Problems in Jet Air Transportation, Dr. Ross A. McFarland 437

HUNTER, H. C.
Diesel Smoke Measurement (Progress Report of the Smokemeter Group of the Diesel Fuels Division, Coordinating Fuel and Equipment Research Committee, CRC) 680

HURN, R. W.
Fuel Heat Gain and Release in Bomb Autoignition (Co-authors J. O. Chase, C. F. Ellis, and K. J. Hughes) 703

HUTCHINSON, DAVID W.
The Differential Gas Turbine 510

HYATT, KENT
Stop Sludge and Go Clean (Co-authors R. H. Albrecht and R. I. Potter).... 751

I

ILES, V. L.
Camshaft-Tappet Problems in Ford Overhead Valve Engines (Co-authors J. S. Laird and C. L. Stevens)..... 153

INJECTION, FUEL
Automotive Gasoline Injection, Sidney E. Miller.... 458
Evaluation of Reaction Kinetics Eliminates Diesel Knock – The M-Combustion System of MAN, J. S. Meurer 250
Fuel Heat Gain and Release in Bomb Autoignition, R. W. Hurn, J. O. Chase, C. F. Ellis, and K. J. Hughes 703
Fuel Vaporization and Ignition Lag in Diesel Combustion, M. M. El Wakil, P. S. Myers, and O. A. Uyehara 712
Physical and Chemical Ignition Delay in an Operating Diesel Engine Using the Hot-Motored Technique, T. C. Yu, O. A. Uyehara, P. S. Myers, R. N. Collins, and K. Mahadevan 690

INSTRUMENTS
Diesel Smoke Measurement (Progress Report of the Smokemeter Group of the Diesel Fuels Division, Coordinating Fuel and Equipment Research Committee, CRC), H. C. Hunter 680
Instrumentation for Valve-Burning Studies, W. D. Sims 356
New Instrumentation for Engine Combustion Studies, J. A. Warren and J. B. Hinkamp..... 665
Passenger-Car Suspension Analysis, A. C. Bodeau, R. H. Bollinger, and L. Lipkin..... 273

IRON AND STEEL
A Study of Nonprotective Rust Formation On Auto-Body Sheet Steel, J. C. Holzwarth, R. F. Thomson, and A. L. Boegehold 221
Application of High-Temperature Materials to Aircraft Powerplants in the Temperature Range 1200-2400 F, Alan V. Levy..... 366
Application of Metallic Materials for Aircraft Structures in the Temperature Range 600 to 1100 F, James W. Huffman 5
Camshaft-Tappet Problems in Ford Overhead Valve Engines, J. S. Laird, C. L. Stevens, and V. L. Iles.. 153

Page

Considerations Affecting the Life of Automotive Camshafts and Tappets, M. F. Garwood, D. R. Kinker, and J. J. Manganello 138
Fatigue and Its Relation to the Mechanical and Metallurgical Properties of Metals, George R. Gohn.. 31
Interrelationship of Design, Lubrication, and Metallurgy in Cam and Tappet Performance, E. B. Etchells, R. F. Thomson, G. H. Robinson, and G. K. Malone 161
Lightweight Springs for Limited Life, E. H. Spaulding 453
New Alloys for Automotive Turbines, Donald N. Frey 582
Some Elevated Temperature Structural Problems of High-Speed Aircraft, Richard R. Heldenfels..... 524
Steels and Protective Treatments For Use up to 1000 F, H. J. Noble and W. H. Sharp..... 59
The Selection of Metals for Airframe Components as Affected by Operation at Elevated Temperatures up to 600 F, M. Tiktinsky..... 131

ISBRANDT, R. H.
Discussion of "Passenger-Car Suspension Analysis" by A. C. Bodeau, R. H. Bollinger, and L. Lipkin.. 292
Discussion of "The New Packard Torsion Level Suspension" by Forest R. McFarland 292

J

JANEWAY, ROBERT N.
Discussion of "Passenger-Car Suspension Analysis" by A. C. Bodeau, R. H. Bollinger, and L. Lipkin.. 292
Discussion of "The New Packard Torsion Level Suspension" by Forest R. McFarland..... 292

JOHNSON, PHILIP O.
Automobile Body Loads 12

JONACH, F. L.
Mechanism of Engine Sludge Formation and Additive Action (Co-authors D. T. Rogers and W. W. Rice)..... 782

JOY, T. J. P.
Tires For High-Performance Cars (Co-authors D. C. Hartley and D. M. Turner).... 319

K

KARDE, KLAUS C.
Discussion of "Fuel Vaporization and Ignition Lag in Diesel Combustion" by M. M. El Wakil, P. S. Myers, and O. A. Uyehara..... 728
Discussion of "The Napier Deltic Diesel Engine" by Ernest Chatterton 424

KELLY, H. S.
Discussion of "Automotive Gasoline Injection" by Sidney E. Miller 468

KERLEY, R. V.
Knocking Behavior of Fuels and Engines (Co-author K. W. Thurston) 554
Discussion of "Instrumentation for Valve-Burning Studies" by W. D. Sims 364

KINKER, D. R.
Considerations Affecting the Life of Automotive Camshafts and Tappets (Co-authors M. F. Garwood and J. J. Manganello) 138

KIRCHNER, MARK E.
Discussion of "How High Should We Fly?" by Schuyler Kleinhans 309

KLEINHANS, SCHUYLER
How High Should We Fly?..... 300

KOPITUK, RAYMOND C.
Discussion of "Steels and Protective Treatments For Use up to 1000 F" by H. J. Noble and W. H. Sharp 75

KREBS, R. P.
Shaft Gas Turbines For Helicopters (Co-authors W. S. Miller, Jr. and T. C. Blaschke). 348

Page

L

LAIRD, J. S.
Camshaft-Tappet Problems in Ford Overhead Valve Engines
(Co-authors C. L. Stevens and V. L. Iles) 153

LAKIN, W. P.
Discussion of "Cold Starting with V. I. Improved Multigrade Oils" by F. B. Fischl, H. H. Horowitz, and T. S. Tutwiler 622
Discussion of "Relationship of Low-Temperature Cranking Resistance to Viscosity Characteristics of Multigrade Engine Oils" by G. K. Malone and T. W. Selby 622

LaQUE, F. L.
Discussion of "A Study of Nonprotective Rust Formation On Auto-Body Sheet Steel" by J. C. Holzwarth, R. F. Thomson, and A. L. Boegehold..... 228

LEGISLATION
A Practical Stopping-Ability Regulation, Carl C. Saal 229

LEVY, ALAN V.
Application of High-Temperature Materials to Aircraft Powerplants in the Temperature Range 1200-2400 F 366

LINDBLOM, C. A.
Discussion of "Human Factors in Highway Transport Safety" by Ross A. McFarland..... 749

LIPKIN, L.
Passenger-Car Suspension Analysis
(Co-authors A. C. Bodeau and R. H. Bollinger).. 273

LIPPMANN, S. A.
Operation of Passenger Tires at High Speeds
(Co-author E. H. Wallace)..... 338

LIVINGSTONE, C. J.
Discussion of "Automotive Gasoline Injection" by Sidney E. Miller 469

LUBRICANTS AND LUBRICATION (NONAIRCRAFT)
Cold Starting with V. I. Improved Multigrade Oils, F. B. Fischl, H. H. Horowitz, and T. S. Tutwiler.. 608
Interrelationship of Design, Lubrication, and Metallurgy in Cam and Tappet Performance, E. B. Etchells, R. F. Thomson, G. H. Robinson, and G. K. Malone 161
Mechanism of Engine Sludge Formation and Additive Action, D. T. Rogers, W. W. Rice, and F. L. Jonach 782
Nitrogen Oxides, Combustion, and Engine Deposits, R. S. Spindt, Court L. Wolfe, and Donald R. Stevens 797
Relationship of Low-Temperature Cranking Resistance to Viscosity Characteristics of Multigrade Engine Oils, G. K. Malone and T. W. Selby..... 602
Stop Sludge and Go Clean, R. H. Albrecht, R. I. Potter, and Kent Hyatt 751

LUNDBERG, ROBERT H.
Learning Curve Theory as Applied to Production Costs 775

LUSCH, J. W.
Discussion of "Effect of Rapid Load Changes on Torque-Converter Performance" by P. J. Swanson and J. H. Meier 540

LUX, W. J.
A Billion Engine Hours on Aluminum Bearings
(Co-author R. S. Frank)..... 655

M

McARDLE, JACK G.
NACA Investigation of Thrust-Reversal Technique
(Co-author John H. Povolny) 542

McBREARTY, J. F.
Fatigue and Fail-Safe Airframe Design..... 426

Page

MacCOULL, NEIL
Discussion of "Mechanical Octanes for Higher Efficiency" by D. F. Caris, B. J. Mitchell, A. D. McDuffie, and F. A. Wyczalek 100

McCULLOUGH, W. E.
Discussion of "A Billion Engine Hours on Aluminum Bearings" by R. S. Frank and W. J. Lux..... 664

McDUFFIE, A. D.
Mechanical Octanes for Higher Efficiency
(Co-authors D. F. Caris, B. J. Mitchell, and F. A. Wyczalek) 76

McFARLAND, FOREST R.
The New Packard Torsion Level Suspension..... 284

McFARLAND, DR. ROSS A.
Human and Environmental Factors of Automobile Safety 625
Human Factors in Highway Transport Safety..... 730
Human Problems in Jet Air Transportation..... 437

McMANUS, N. R.
Discussion of "Automotive Gasoline Injection" by Sidney E. Miller 470

McMANUS, R. L.
Discussion of "Some Experiments in the Application of Boundary-Layer Control" by Joseph Flatt..... 121
Discussion of "Wing-Lift Augmentation Methods for the Improvement of Low-Speed Performance of High-Speed Aircraft" by John S. Attinello..... 121

McREYNOLDS, L. A.
Discussion of "Stop Sludge and Go Clean" by R. H. Albrecht, R. I. Potter, and Kent Hyatt..... 773

MAGNESIUM AND ALLOYS
The Selection of Metals for Airframe Components as Affected by Operation at Elevated Temperatures up to 600 F, M. Tiktinsky..... 131

MAHADEVAN, K.
Physical and Chemical Ignition Delay in an Operating Diesel Engine Using the Hot-Motored Technique
(Co-authors T. C. Yu, O. A. Uyehara, P. S. Myers, and R. N. Collins) 690

MALONE, G. K.
Interrelationship of Design, Lubrication, and Metallurgy in Cam and Tappet Performance
(Co-authors E. B. Etchells, R. F. Thomson, and G. H. Robinson) 161
Relationship of Low-Temperature Cranking Resistance to Viscosity Characteristics of Multigrade Engine Oils
(Co-author T. W. Selby) 602

MANAGEMENT
Learning Curve Theory as Applied to Production Costs, Robert H. Lundberg 775

MANGANELLO, J. J.
Considerations Affecting the Life of Automotive Camshafts and Tappets
(Co-authors M. F. Garwood and D. R. Kinker).... 138

MARTINUZZI, P. F.
Discussion of "The Differential Gas Turbine" by David W. Hutchinson 521

MATERIALS (NONMETALLIC)
Tire Design – Present and Future, L. L. Baldwin.. 502

MAZZIOTTI, P. J.
The Low Silhouette Drive Line
(Co-author R. Burkhalter) 379

MEIER, J. H.
Effect of Rapid Load Changes on Torque-Converter Performance
(Co-author P. J. Swanson) 534

METALS
Application of High-Temperature Materials to Aircraft Powerplants in the Temperature Range 1200-2400 F, Alan V. Levy 366

Page

Fatigue and Its Relation to the Mechanical and Metallurgical Properties of Metals, George R. Gohn 31
New Alloys for Automotive Turbines, Donald N. Frey ... 582
The Selection of Metals for Airframe Components as Affected by Operation at Elevated Temperatures up to 600 F, M. Tiktinsky ... 131

MEURER, J. S.
Evaluation of Reaction Kinetics Eliminates Diesel Knock – The M-Combustion System of MAN ... 250

MEZGER, BERNARD J.
Discussion of "Principles and Applications of Bypass Turbojet Engines" by George F. Wislicenus ... 501

MILLER, SIDNEY E.
Automotive Gasoline Injection ... 458

MILLER, W. S., Jr.
Shaft Gas Turbines For Helicopters (Co-authors R. P. Krebs and T. C. Blaschke) ... 348

MINGLE, J. G.
A Radioactive Method for Measuring Engine Deposits (Co-authors H. W. Sigworth and B. A. Fries) ... 577

MITCHELL, B. J.
Mechanical Octanes for Higher Efficiency (Co-authors D. F. Caris, A. D. McDuffie, and F. A. Wyczalek) ... 76

MYERS, P. S.
Fuel Vaporization and Ignition Lag in Diesel Combustion (Co-authors M. M. El Wakil and O. A. Uyehara) 712
Physical and Chemical Ignition Delay in an Operating Diesel Engine Using the Hot-Motored Technique (Co-authors T. C. Yu, O. A. Uyehara, R. N. Collins, and K. Mahadevan) ... 690

N

NIETSCH, H. E.
Cushion Design From Fragility Rating ... 241

NOBLE, H. J.
Steels and Protective Treatments For Use up to 1000 F (Co-author W. H. Sharp) ... 59

NOISE
A Jet Exhaust Silencer, J. M. Tyler and G. B. Towle 294
Human Problems in Jet Air Transportation, Dr. Ross A. McFarland ... 437

NORRIE, R. C.
Discussion of "The Differential Gas Turbine" by David W. Hutchinson ... 522

O

OBERRIGHT, E. A.
Discussion of "Nitrogen Oxides, Combustion, and Engine Deposits" by R. S. Spindt, Court L. Wolfe, and Donald R. Stevens ... 807

OLLEY, MAURICE
Discussion of "Passenger-Car Suspension Analysis" by A. C. Bodeau, R. H. Bollinger, and L. Lipkin ... 291
Discussion of "The New Packard Torsion Level Suspension" by Forest R. McFarland ... 291

P

PACKAGING
Cushion Design From Fragility Rating, H. E. Nietsch ... 241
Flexible Suspension Systems for Equipment in Transit, John J. Goodill ... 41

PASSENGER CAR DESIGN AND PERFORMANCE
Design Factors in Automotive Safety, A. L. Haynes 644
Human and Environmental Factors of Automobile Safety, Dr. Ross A. McFarland ... 625
The Low Silhouette Drive Line, R. Burkhalter and P. J. Mazziotti ... 379

PEARSON, H.
Discussion of "Principles and Applications of Bypass Turbojet Engines" by George F. Wislicenus ... 500

PILGER, A. C.
Discussion of "Considerations Affecting the Life of Automotive Camshafts and Tappets" by M. F. Garwood, D. R. Kinker, and J. J. Manganello ... 182

POTTER, R. I.
Stop Sludge and Go Clean (Co-authors R. H. Albrecht and Kent Hyatt) ... 751

POVOLNY, JOHN H.
NACA Investigation of Thrust-Reversal Technique (Co-author Jack G. McArdle) ... 542

PRODUCTION (AIRCRAFT)
Learning Curve Theory as Applied to Production Costs, Robert H. Lundberg ... 775

PRODUCTION (NONAIRCRAFT)
Nuclear Power and the Machinery Builder, R. C. Allen ... 589

PROPELLER SHAFTS (NONAIRCRAFT)
The Low Silhouette Drive Line, R. Burkhalter and P. J. Mazziotti ... 379

PUMPS
Automotive Gasoline Injection, Sidney E. Miller ... 458

PUSACK, G. W.
Discussion of "Knocking Behavior of Fuels and Engines" by R. V. Kerley and K. W. Thurston ... 568

R

RADIOACTIVITY
A Radioactive Method for Measuring Engine Deposits, J. G. Mingle, H. W. Sigworth, and B. A. Fries ... 577

RAZAK, KENNETH
Discussion of "Some Experiments in the Application of Boundary-Layer Control" by Joseph Flatt ... 121
Discussion of "Wing-Lift Augmentation Methods for the Improvement of Low-Speed Performance of High-Speed Aircraft" by John S. Attinello ... 121

REED, I. F.
Discussion of "Farm Tractors and Their Tires" by F. C. Walters and W. H. Worthington ... 405

REED, WENDELL E.
A New Approach to Turbojet and Ramjet Engine Control ... 472

REINERS, N. M.
Discussion of "Evaluation of Reaction Kinetics Eliminates Diesel Knock – The M-Combustion System of MAN" by J. S. Meurer ... 268

REMONDINO, M. A.
Discussion of "Instrumentation for Valve-Burning Studies" by W. D. Sims ... 364

RICARDO, HARRY R.
Discussion of "Evaluation of Reaction Kinetics Eliminates Diesel Knock – The M-Combustion System of MAN" by J. S. Meurer ... 268

RICE, W. W.
Mechanism of Engine Sludge Formation and Additive Action (Co-authors D. T. Rogers and F. L. Jonach) ... 782

RIDING QUALITY
Passenger-Car Suspension Analysis, A. C. Bodeau, R. H. Bollinger, and L. Lipkin ... 273
The New Packard Torsion Level Suspension, Forest R. McFarland ... 284

ROADS AND STREETS
Human and Environmental Factors of Automobile Safety, Dr. Ross A. McFarland ... 625

ROBINSON, G. H.
Interrelationship of Design, Lubrication, and Metallurgy in Cam and Tappet Performance (Co-authors E. B. Etchells, R. F. Thomson, and G. K. Malone) ... 161

Page

ROBSON, J. J.
High-Speed Cornering Forces 334
ROGERS, D. T.
Mechanism of Engine Sludge Formation and Additive Action
(Co-authors W. W. Rice and F. L. Jonach)..... 782
ROUZE, S. R.
Discussion of "Stop Sludge and Go Clean" by R. H. Albrecht, R. I. Potter, and Kent Hyatt..... 771
RUBBER AND ELASTOMERS
High-Temperature Problems Associated with the Use of Rubber in Aircraft, Frederick E. Clark... 24
New and Improved Synthetic Elastomeric Materials for Automotive Use, W. J. Simpson 123
Tire Design – Present and Future, L. L. Baldwin.... 502
RUTH, C. H., Jr.
Discussion of "Stop Sludge and Go Clean" by R. H. Albrecht, R. I. Potter, and Kent Hyatt 774

S

SAAL, CARL C.
A Practical Stopping-Ability Regulation 229
SAVAGE, M. W.
Discussion of "Nitrogen Oxides, Combustion, and Engine Deposits" by R. S. Spindt, Court L. Wolfe, and Donald R. Stevens 808
SCHALLAMACH, A.
Discussion of "Practical Tire Research" by V. E. Gough 346
SCHREIBER, W.
Discussion of "Mechanism of Engine Sludge Formation and Additive Action" by D. T. Rogers, W. W. Rice, and F. L. Jonach 810
Discussion of "Stop Sludge and Go Clean" by R. H. Albrecht, R. I. Potter, and Kent Hyatt..... 774
SCHWARZ, CHARLES F.
Discussion of "Knocking Behavior of Fuels and Engines" by R. V. Kerley and K. W. Thurston..... 566
SCHWEITZER, P. H.
Discussion of "Diesel Smoke Measurement (Progress Report of the Smokemeter Group of the Diesel Fuels Division, Coordinating Fuel and Equipment Research Committee, CRC)" by H. C. Hunter.... 688
Discussion of "Fuel Vaporization and Ignition Lag in Diesel Combustion" by M. M. El Wakil, P. S. Myers, and O. A. Uyehara 728
Discussion of "Evaluation of Reaction Kinetics Eliminates Diesel Knock – The M-Combustion System of MAN" by J. S. Meurer 271
SCHWIEDER, W. E.
The New Packard V-8 Engine 205
SELBY, T. W.
Relationship of Low-Temperature Cranking Resistance to Viscosity Characteristics of Multigrade Engine Oils
(Co-author G. K. Malone) 602
SHARP, W. H.
Steels and Protective Treatments For Use up to 1000 F
(Co-author H. J. Noble) 59
SHAW, GLENN
Discussion of "Stop Sludge and Go Clean" by R. H. Albrecht, R. I. Potter, and Kent Hyatt..... 773
SHOCK ABSORBERS
Passenger-Car Suspension Analysis, A. C. Bodeau, R. H. Bollinger, and L. Lipkin 273
SIGWORTH, H. W.
A Radioactive Method for Measuring Engine Deposits
(Co-authors J. G. Mingle and B. A. Fries)..... 577
SIMPSON, W. J.
New and Improved Synthetic Elastomeric Materials for Automotive Use 123
SIMS, W. D.
Instrumentation for Valve-Burning Studies 356

Page

SOHL, R. W.
Discussion of "Farm Tractors and Their Tires" by F. C. Walters and W. H. Worthington..... 405
SPAULDING, E. H.
Lightweight Springs for Limited Life 453
SPINDT, R. S.
Nitrogen Oxides, Combustion, and Engine Deposits
(Co-authors Court L. Wolfe and Donald R. Stevens) 797
SPRINGS AND SUSPENSIONS
Lightweight Springs for Limited Life, E. H. Spaulding 453
Passenger-Car Suspension Analysis, A. C. Bodeau, R. H. Bollinger, and L. Lipkin..... 273
The New Packard Torsion Level Suspension, Forest R. McFarland 284
STEVENS, C. L.
Camshaft-Tappet Problems in Ford Overhead Valve Engines
(Co-authors J. S. Laird and V. L. Iles) 153
STEVENS, DONALD R.
Nitrogen Oxides, Combustion, and Engine Deposits
(Co-authors R. S. Spindt and Donald R. Stevens) 797
STRESSES
Automobile Body Loads, Philip O. Johnson 12
Fatigue and Fail-Safe Airframe Design, J. F. McBrearty 426
Some Elevated Temperature Structural Problems of High-Speed Aircraft, Richard R. Heldenfels..... 524
SUPERCHARGING
The Supercharged Turboprop, S. G. Hooker..... 185
SWANSON, P. J.
Effect of Rapid Load Changes on Torque-Converter Performance
(Co-author J. H. Meier) 534

T

THOMSON, R. F.
A Study of Nonprotective Rust Formation On Auto-Body Sheet Steel
(Co-authors J. C. Holzwarth and A. L. Boegehold) 221
Interrelationship of Design, Lubrication, and Metallurgy in Cam and Tappet Performance
(Co-authors E. B. Etchells, G. H. Robinson, and G. K. Malone) 161
THURSTON, K. W.
Knocking Behavior of Fuels and Engines
(Co-author R. V. Kerley) 554
TIKTINSKY, M.
The Selection of Metals for Airframe Components as Affected by Operation at Elevated Temperatures up to 600 F 131
TIRES AND RIMS
Farm Tractors and Their Tires, F. C. Walters and W. H. Worthington 394
High-Speed Cornering Forces, J. J. Robson 334
Operation of Passenger Tires at High Speeds, E. H. Wallace and S. A. Lippmann 338
Practical Tire Research, V. E. Gough 310
Tire Design – Present and Future, L. L. Baldwin... 502
Tires For High-Performance Cars, T. J. P. Joy, D. C. Hartley, and D. M. Turner 319
TITANIUM
Application of Metallic Materials for Aircraft Structures in the Temperature Range 600 to 1100 F, James W. Huffman 5
The Selection of Metals for Airframe Components as Affected by Operation at Elevated Temperatures up to 600 F, M. Tiktinsky 131
TOULMIN, H. A., Jr.
Discussion of "Mechanical Octanes for Higher Efficiency" by D. F. Caris, B. J. Mitchell, A. D. McDuffie, and F. A. Wyczalek 96

Page

TOWLE, G. B.
A Jet Exhaust Silencer
(Co-author J. M. Tyler) 294

TRANSMISSIONS, AUTOMATIC
Effect of Rapid Load Changes on Torque-Converter Performance, P. J. Swanson and J. H. Meier..... 534

TRIMBLE, HAROLD M.
Discussion of "Knocking Behavior of Fuels and Engines" by R. V. Kerley and K. W. Thurston..... 565

TRUCK DESIGN AND PERFORMANCE
Human Factors in Highway Transport Safety, Ross A. McFarland 730

TURNER, D. M.
Tires For High-Performance Cars
(Co-authors T. J. P. Joy and D. C. Hartley)..... 319

TUTWILER, T. S.
Cold Starting with V. I. Improved Multigrade Oils
(Co-authors F. B. Fischl and H. H. Horowitz)... 608

TYLER, J. M.
A Jet Exhaust Silencer
(Co-author G. B. Towle) 294

U

UYEHARA, O. A.
Fuel Vaporization and Ignition Lag in Diesel Combustion
(Co-authors M. M. El Wakil and P. S. Myers)... 712
Physical and Chemical Ignition Delay in an Operating Diesel Engine Using the Hot-Motored Technique
(Co-authors T. C. Yu, P. S. Myers, R. N. Collins, and K. Mahadevan) 690

V

VALADE, MERLE F.
Discussion of "Steels and Protective Treatments For Use up to 1000 F" by H. J. Noble and W. H. Sharp 75

VALVES AND GEAR
Camshaft-Tappet Problems in Ford Overhead Valve Engines, J. S. Laird, C. L. Stevens, and V. L. Iles 153
Considerations Affecting the Life of Automotive Camshafts and Tappets, M. F. Garwood, D. R. Kinker, and J. J. Manganello 138
Instrumentation for Valve-Burning Studies, W. D. Sims 356
Interrelationship of Design, Lubrication, and Metallurgy in Cam and Tappet Performance, E. B. Etchells, R. F. Thomson, G. H. Robinson, and G. K. Malone 161

VON BRAND, E. K.
Discussion of "Diesel Smoke Measurement (Progress Report of the Smokemeter Group of the Diesel Fuels Division, Coordinating Fuel and Equipment Research Committee, CRC)" by H. C. Hunter.... 688

W

WALCUTT, C.
Discussion of "Fuel Heat Gain and Release in Bomb Autoignition" by R. W. Hurn, J. O. Chase, C. F. Ellis, and K. J. Hughes 727

WALLACE, E. H.
Operation of Passenger Tires at High Speeds
(Co-author S. A. Lippmann) 338

WALTERS, F. C.
Farm Tractors and Their Tires
(Co-author W. H. Worthington) 394

WARE, V. W.
Discussion of "Cold Starting with V. I. Improved Multigrade Oils" by F. B. Fischl, H. H. Horowitz, and T. S. Tutwiler 622

Page

Discussion of "Relationship of Low-Temperature Cranking Resistance to Viscosity Characteristics of Multigrade Engine Oils" by G. K. Malone and T. W. Selby 622

WARREN, J. A.
New Instrumentation for Engine Combustion Studies
(Co-author J. B. Hinkamp) 665

WEINERT, G. A.
Pneumatic and Sonic Measurement of Combustion-Chamber Volume 50

WELCH, H. L.
The New Plymouth V-8 Engine 195

WHITCOMB, DAVID
Discussion of "Tires For High-Performance Cars" by T. J. P. Joy, D. C. Hartley, and D. M. Turner 344

WILLIAMS, WALTER C.
Flight Research at High Altitudes and High Speeds with Rocket Propelled Research Airplanes 570

WILSON, G. C.
Discussion of "Diesel Smoke Measurement (Progress Report of the Smokemeter Group of the Diesel Fuels Division, Coordinating Fuel and Equipment Research Committee, CRC)" by H. C. Hunter.... 688
Discussion of "Fuel Heat Gain and Release in Bomb Autoignition" by R. W. Hurn, J. O. Chase, C. F. Ellis, and K. J. Hughes 727
Discussion of "Fuel Vaporization and Ignition Lag in Diesel Combustion" by M. M. El Wakil, P. S. Myers, and O. A. Uyehara 726
Discussion of "Physical and Chemical Ignition Delay in an Operating Diesel Engine Using the Hot-Motored Technique" by T. C. Yu, O. A. Uyehara, P. S. Myers, R. N. Collins, and K. Mahadevan... 726

WISLICENUS, GEORGE F.
Principles and Applications of Bypass Turbojet Engines 486

WOLFE, COURT L.
Nitrogen Oxides, Combustion, and Engine Deposits
(Co-authors R. S. Spindt and Donald R. Stevens) 797

WOOD, D. B.
Discussion of "A Billion Engine Hours on Aluminum Bearings" by R. S. Frank and W. J. Lux..... 664

WOOD, F. S.
Discussion of "Cold Starting with V. I. Improved Multigrade Oils" by F. B. Fischl, H. H. Horowitz, and T. S. Tutwiler 621
Discussion of "Relationship of Low-Temperature Cranking Resistance to Viscosity Characteristics of Multigrade Engine Oils" by G. K. Malone and T. W. Selby 621

WOOMERT, DALE E.
Discussion of "Knocking Behavior of Fuels and Engines" by R. V. Kerley and K. W. Thurston..... 566

WORTHINGTON, W. H.
Farm Tractors and Their Tires
(Co-author F. C. Walters) 394

WRIGHT, W. A.
Discussion of "Mechanism of Engine Sludge Formation and Additive Action" by D. T. Rogers, W. W. Rice, and F. L. Jonach 810

WYCZALEK, F. A.
Mechanical Octanes for Higher Efficiency
(Co-authors D. F. Caris, B. J. Mitchell, and A. D. McDuffie) 76

Y

YU, T. C.
Physical and Chemical Ignition Delay in an Operating Diesel Engine Using the Hot-Motored Technique
(Co-authors O. A. Uyehara, P. S. Myers, R. N. Collins, and K. Mahadevan) 690

DATE DUE

FEB 2 77 UIC

JAN 14 19

JAN 16 78 FAC

FEB 06 UIC

GAYLORD

PRINTED IN U.S.A.